



# ANTIMICROBIAL RESISTANCE AS A GLOBAL PUBLIC HEALTH PROBLEM: HOW CAN WE ADDRESS IT?

EDITED BY: Ilana L. B. C. Camargo, Leonardo Neves de Andrade, Thierry Naas,  
Luciene Andrade Da Rocha Minarini, Raffaele Zarrilli,  
Eliana De Gregorio and Filipa Grosso

PUBLISHED IN: *Frontiers in Microbiology*, *Frontiers in Public Health* and  
*Frontiers in Medicine*



# frontiers

## Frontiers eBook Copyright Statement

The copyright in the text of individual articles in this eBook is the property of their respective authors or their respective institutions or funders. The copyright in graphics and images within each article may be subject to copyright of other parties. In both cases this is subject to a license granted to Frontiers.

The compilation of articles constituting this eBook is the property of Frontiers.

Each article within this eBook, and the eBook itself, are published under the most recent version of the Creative Commons CC-BY licence.

The version current at the date of publication of this eBook is CC-BY 4.0. If the CC-BY licence is updated, the licence granted by Frontiers is automatically updated to the new version.

When exercising any right under the CC-BY licence, Frontiers must be attributed as the original publisher of the article or eBook, as applicable.

Authors have the responsibility of ensuring that any graphics or other materials which are the property of others may be included in the CC-BY licence, but this should be checked before relying on the CC-BY licence to reproduce those materials. Any copyright notices relating to those materials must be complied with.

Copyright and source acknowledgement notices may not be removed and must be displayed in any copy, derivative work or partial copy which includes the elements in question.

All copyright, and all rights therein, are protected by national and international copyright laws. The above represents a summary only. For further information please read Frontiers' Conditions for Website Use and Copyright Statement, and the applicable CC-BY licence.

ISSN 1664-8714

ISBN 978-2-88966-284-5

DOI 10.3389/978-2-88966-284-5

## About Frontiers

Frontiers is more than just an open-access publisher of scholarly articles: it is a pioneering approach to the world of academia, radically improving the way scholarly research is managed. The grand vision of Frontiers is a world where all people have an equal opportunity to seek, share and generate knowledge. Frontiers provides immediate and permanent online open access to all its publications, but this alone is not enough to realize our grand goals.

## Frontiers Journal Series

The Frontiers Journal Series is a multi-tier and interdisciplinary set of open-access, online journals, promising a paradigm shift from the current review, selection and dissemination processes in academic publishing. All Frontiers journals are driven by researchers for researchers; therefore, they constitute a service to the scholarly community. At the same time, the Frontiers Journal Series operates on a revolutionary invention, the tiered publishing system, initially addressing specific communities of scholars, and gradually climbing up to broader public understanding, thus serving the interests of the lay society, too.

## Dedication to Quality

Each Frontiers article is a landmark of the highest quality, thanks to genuinely collaborative interactions between authors and review editors, who include some of the world's best academicians. Research must be certified by peers before entering a stream of knowledge that may eventually reach the public - and shape society; therefore, Frontiers only applies the most rigorous and unbiased reviews. Frontiers revolutionizes research publishing by freely delivering the most outstanding research, evaluated with no bias from both the academic and social point of view. By applying the most advanced information technologies, Frontiers is catapulting scholarly publishing into a new generation.

## What are Frontiers Research Topics?

Frontiers Research Topics are very popular trademarks of the Frontiers Journals Series: they are collections of at least ten articles, all centered on a particular subject. With their unique mix of varied contributions from Original Research to Review Articles, Frontiers Research Topics unify the most influential researchers, the latest key findings and historical advances in a hot research area! Find out more on how to host your own Frontiers Research Topic or contribute to one as an author by contacting the Frontiers Editorial Office: [researchtopics@frontiersin.org](mailto:researchtopics@frontiersin.org)

# ANTIMICROBIAL RESISTANCE AS A GLOBAL PUBLIC HEALTH PROBLEM: HOW CAN WE ADDRESS IT?

Topic Editors:

**Ilana L. B. C. Camargo**, University of Sao Paulo, Brazil

**Leonardo Neves de Andrade**, University of São Paulo, Brazil

**Thierry Naas**, Assistance Publique Hopitaux De Paris, France

**Luciene Andrade Da Rocha Minarini**, Federal University of São Paulo, Brazil

**Raffaele Zarrilli**, University of Naples Federico II, Italy

**Eliana De Gregorio**, University of Naples Federico II, Italy

**Filipa Grosso**, University of Porto, Portugal

**Citation:** Camargo, I. L. B. C., De Andrade, L. N., Naas, T., Da Rocha Minarini, L. A., Zarrilli, R., De Gregorio, E., Grosso, F., eds. (2020). Antimicrobial Resistance As a Global Public Health Problem: How Can We Address It?. Lausanne: Frontiers Media SA. doi: 10.3389/978-2-88966-284-5

# Table of Contents

- 08 Editorial: Antimicrobial Resistance as a Global Public Health Problem: How Can We Address It?**  
Luciene Andrade Da Rocha Minarini, Leonardo Neves de Andrade, Eliana De Gregorio, Filipa Grosso, Thierry Naas, Raffaele Zarrilli and Ilana L. B. C. Camargo
- 14 Counter Clinical Prognoses of Patients With Bloodstream Infections Between Causative *Acinetobacter baumannii* Clones ST191 and ST451 Belonging to the International Clonal Lineage II**  
Eun-Jeong Yoon, Dokyun Kim, Hyukmin Lee, Hye Sun Lee, Jong Hee Shin, Young Uh, Kyeong Seob Shin, Young Ah Kim, Yoon Soo Park, Jeong Hwan Shin and Seok Hoon Jeong
- 23 Synergistic Microbicidal Effect of Auranofin and Antibiotics Against Planktonic and Biofilm-Encased *S. aureus* and *E. faecalis***  
Pengfei She, Linying Zhou, Shijia Li, Yiqing Liu, Lanlan Xu, Lihua Chen, Zhen Luo and Yong Wu
- 35 Genomic Characterization of Prevalent *mcr-1*, *mcr-4*, and *mcr-5* *Escherichia coli* Within Swine Enteric Colibacillosis in Spain**  
Isidro García-Meniño, Dafne Díaz-Jiménez, Vanesa García, María de Toro, Saskia C. Flament-Simon, Jorge Blanco and Azucena Mora
- 49 In vitro Activity and Heteroresistance of Omadacycline Against Clinical *Staphylococcus aureus* Isolates From China Reveal the Impact of Omadacycline Susceptibility by Branched-Chain Amino Acid Transport System II Carrier Protein, Na/Pi Cotransporter Family Protein, and Fibronectin-Binding Protein**  
Bing Bai, Zhiwei Lin, Zhangya Pu, Guangjian Xu, Fan Zhang, Zhong Chen, Xiang Sun, Jinxin Zheng, Peiyu Li, Qiwen Deng and Zhijian Yu
- 61 Increasing Frequencies of Antibiotic Resistant Non-typhoidal *Salmonella* Infections in Michigan and Risk Factors for Disease**  
Sanjana Mukherjee, Chase M. Anderson, Rebekah E. Mosci, Duane W. Newton, Paul Lephart, Hossein Salimnia, Walid Khalife, James. T. Rudrik and Shannon D. Manning
- 73 Constructing and Characterizing Bacteriophage Libraries for Phage Therapy of Human Infections**  
Shelley B. Gibson, Sabrina I. Green, Carmen Gu Liu, Keiko C. Salazar, Justin R. Clark, Austen L. Terwilliger, Heidi B. Kaplan, Anthony W. Maresso, Barbara W. Trautner and Robert F. Ramig
- 90 Characterization of Lytic Bacteriophages Infecting Multidrug-Resistant *Shiga* Toxigenic Atypical *Escherichia coli* O177 Strains Isolated From Cattle Feces**  
Peter Kotsoana Montso, Victor Mlambo and Collins Njje Ateba
- 103 Is Meropenem as a Monotherapy Truly Incompetent for Meropenem-Nonsusceptible Bacterial Strains? A Pharmacokinetic/Pharmacodynamic Modeling With Monte Carlo Simulation**  
Xiangqing Song, Yi Wu, Lizhi Cao, Dunwu Yao and Minghui Long



- 118** *Multiple Klebsiella pneumoniae KPC Clones Contribute to an Extended Hospital Outbreak*  
Carolina Ferrari, Marta Corbella, Stefano Gaiarsa, Francesco Comandatore, Erika Scaltriti, Claudio Bandi, Patrizia Cambieri, Piero Marone and Davide Sassera
- 129** *Over-Expression of ISAbal-1-Linked Intrinsic and Exogenously Acquired OXA Type Carbapenem-Hydrolyzing-Class D- $\beta$ -Lactamase-Encoding Genes is Key Mechanism Underlying Carbapenem Resistance in Acinetobacter baumannii*  
Marcus Ho-yin Wong, Bill Kwan-wai Chan, Edward Wai-chi Chan and Sheng Chen
- 138** *Antibiotic Susceptibility, Virulence Pattern, and Typing of Staphylococcus aureus Strains Isolated From Variety of Infections in India*  
Shifu Aggarwal, Smrutiti Jena, Sasmita Panda, Savitri Sharma, Benu Dhawan, Gopal Nath, N. P. Singh, Kinshuk Chandra Nayak and Durg Vijai Singh
- 156** *Baicalin Inhibits Biofilm Formation and the Quorum-Sensing System by Regulating the MsrA Drug Efflux Pump in Staphylococcus saprophyticus*  
Jinli Wang, Haihong Jiao, Jinwu Meng, Mingyu Qiao, Hongxu Du, Miao He, Ke Ming, Jiaguo Liu, Deyun Wang and Yi Wu
- 167** *Increasing Prevalence of ESBL-Producing Multidrug Resistance Escherichia coli From Diseased Pets in Beijing, China From 2012 to 2017*  
Yanyun Chen, Zhihai Liu, Yaru Zhang, Zhenbiao Zhang, Lei Lei and Zhaofei Xia
- 179** *Down-Regulation of Flagellar, Fimbriae, and Pili Proteins in Carbapenem-Resistant Klebsiella pneumoniae (NDM-4) Clinical Isolates: A Novel Linkage to Drug Resistance*  
Divakar Sharma, Anjali Garg, Manish Kumar, Faraz Rashid and Asad U. Khan
- 188** *Effect of Dietary Copper on Intestinal Microbiota and Antimicrobial Resistance Profiles of Escherichia coli in Weaned Piglets*  
Yiming Zhang, Jian Zhou, Zhenglin Dong, Guanya Li, Jingjing Wang, Yikun Li, Dan Wan, Huansheng Yang and Yulong Yin
- 199** *Clinical Impact of Antibiotics for the Treatment of Pseudomonas aeruginosa Biofilm Infections*  
Elodie Olivares, Stéphanie Badel-Berchoux, Christian Provot, Gilles Prévost, Thierry Bernardi and François Jehl
- 211** *Colistin Resistance Gene mcr-1 Mediates Cell Permeability and Resistance to Hydrophobic Antibiotics*  
Baiyuan Li, Fang Yin, Xuanyu Zhao, Yunxue Guo, Weiquan Wang, Pengxia Wang, Honghui Zhu, Yeshe Yin and Xiaoxue Wang
- 218** *CRISPR-Cas System in Antibiotic Resistance Plasmids in Klebsiella pneumoniae*  
Muhammad Kamruzzaman and Jonathan R. Iredell
- 231** *Linezolid and Rifampicin Combination to Combat cfr-Positive Multidrug-Resistant MRSA in Murine Models of Bacteremia and Skin and Skin Structure Infection*  
Yu-Feng Zhou, Liang Li, Meng-Ting Tao, Jian Sun, Xiao-Ping Liao, Ya-Hong Liu and Yan Q. Xiong

- 242 Topical Therapeutic Efficacy of Ebselen Against Multidrug-Resistant Staphylococcus aureus LT-1 Targeting Thioredoxin Reductase**  
Chuanjiang Dong, Jingxuan Zhou, Peng Wang, Tao Li, Ying Zhao, Xiaoyuan Ren, Jun Lu, Jun Wang, Arne Holmgren and Lili Zou
- 254 New Tetramic Acids Comprising of Decalin and Pyridones From Chaetomium olivaceum SD-80A With Antimicrobial Activity**  
Xinzhu Wang, Liya Zhao, Chao Liu, Jun Qi, Peipei Zhao, Zhaoming Liu, Chunlei Li, Yingying Hu, Xin Yin, Xin Liu, Zhixin Liao, Lixin Zhang and Xuekui Xia
- 265 COL<sup>R</sup> Acinetobacter baumannii sRNA Signatures: Computational Comparative Identification and Biological Targets**  
Viviana Cafiso, Stefano Stracquadano, Flavia Lo Verde, Veronica Dovere, Alessandra Zega, Giuseppe Pigola, Jesús Aranda and Stefania Stefani
- 274 Reducing the Consumption of Antibiotics: Would That Be Enough to Slow Down the Dissemination of Resistances in the Downstream Environment?**  
Christophe Merlin
- 278 Evaluation of Machine Learning Models for Predicting Antimicrobial Resistance of Actinobacillus pleuropneumoniae From Whole Genome Sequences**  
Zhichang Liu, Dun Deng, Huijie Lu, Jian Sun, Luchao Lv, Shuhong Li, Guanghui Peng, Xianyong Ma, Jiazhou Li, Zhenming Li, Ting Rong and Gang Wang
- 285 Ectopic Expression of Rv0023 Mediates Isoniazid/Ethionamide Tolerance via Altering NADH/NAD<sup>+</sup> Levels in Mycobacterium smegmatis**  
Shailesh Kumar Gupta, Rajendra Kumar Angara, Suhail Yousuf, Chilakala Gangi Reddy and Akash Ranjan
- 299 Radezolid is More Effective Than Linezolid Against Planktonic Cells and Inhibits Enterococcus faecalis Biofilm Formation**  
Jinxin Zheng, Zhong Chen, Zhiwei Lin, Xiang Sun, Bing Bai, Guangjian Xu, Junwen Chen, Zhijian Yu and Di Qu
- 313 Analysis of Identification Method for Bacterial Species and Antibiotic Resistance Genes Using Optical Data From DNA Oligomers**  
Ryan L. Wood, Tanner Jensen, Cindi Wadsworth, Mark Clement, Prashant Nagpal and William G. Pitt
- 328 Essential Metabolic Routes as a Way to ESKAPE From Antibiotic Resistance**  
Angélica Luana C. Barra, Lívia de Oliveira C. Dantas, Luana Galvão Morão, Raíssa F. Gutierrez, Igor Polikarpov, Carsten Wrenger and Alessandro S. Nascimento
- 336 In vitro Activity of a New Fourth-Generation Cephalosporin, Cefoselis, Against Clinically Important Bacterial Pathogens in China**  
Jing-Wei Cheng, Jian-Rong Su, Meng Xiao, Shu-Ying Yu, Ge Zhang, Jing-Jia Zhang, Yang Yang, Si-Meng Duan, Timothy Kudinha, Qi-Wen Yang and Ying-Chun Xu
- 343 Metadata Analysis of mcr-1-Bearing Plasmids Inspired by the Sequencing Evidence for Horizontal Transfer of Antibiotic Resistance Genes Between Polluted River and Wild Birds**  
Yufei Lin, Xiaohong Dong, Jiao Wu, Dawei Rao, Lihua Zhang, Yousef Faraj and Kun Yang

- 355** *Molecular Analysis of Selected Resistance Determinants in Diarrheal Fecal Samples Collected From Kolkata, India Reveals an Abundance of Resistance Genes and the Potential Role of the Microbiota in Its Dissemination*  
Rituparna De, Asish Kumar Mukhopadhyay and Shanta Dutta
- 370** *In vitro Activity of Apramycin Against Carbapenem-Resistant and Hypervirulent Klebsiella pneumoniae Isolates*  
Mingju Hao, Xiaohong Shi, Jingnan Lv, Siqiang Niu, Shiqing Cheng, Hong Du, Fangyou Yu, Yi-Wei Tang, Barry N. Kreiswirth, Haifang Zhang and Liang Chen
- 377** *Gastrointestinal Carriage of Vancomycin-Resistant Enterococci and Carbapenem-Resistant Gram-Negative Bacteria in an Endemic Setting: Prevalence, Risk Factors, and Outcomes*  
Alexandra Vasilakopoulou, Polyxeni Karakosta, Sophia Vourli, Aikaterini Tarpatzi, Paraskevi Varda, Maria Kostoula, Anastasia Antoniadou and Spyros Pournaras
- 386** *Inactivation of Glutamine Synthetase-Coding Gene glnA Increases Susceptibility to Quinolones Through Increasing Outer Membrane Protein F in Salmonella enterica Serovar Typhi*  
Ana R. Millanao, Aracely Y. Mora, Claudia P. Saavedra, Nicolás A. Villagra, Guido C. Mora and Alejandro A. Hidalgo
- 396** *Confronting Tigecycline-Resistant Acinetobacter baumannii via Immunization Against Conserved Resistance Determinants*  
Ming-Hsien Chiang, Ya-Sung Yang, Jun-Ren Sun, Yung-Chih Wang, Shu-Chen Kuo, Yi-Tzu Lee, Yi-Ping Chuang and Te-Li Chen
- 409** *Prevalence, Characterization, and Drug Resistance of Staphylococcus Aureus in Feces From Pediatric Patients in Guangzhou, China*  
Xiaolan Ai, Fei Gao, Shuwen Yao, Bingshao Liang, Jialiang Mai, Zhile Xiong, Xiantang Chen, Zhuwei Liang, Hongling Yang, Zhiying Ou, Sitang Gong, Yan Long and Zhenwen Zhou
- 419** *Resistance of Klebsiella pneumoniae Strains Carrying bla<sub>NDM-1</sub> Gene and the Genetic Environment of bla<sub>NDM-1</sub>*  
Tianxin Xiang, Chuanhui Chen, Jiangxiong Wen, Yang Liu, Qi Zhang, Na Cheng, Xiaoping Wu and Wei Zhang
- 428** *Prevalence, Genetic Diversity, and Temporary Shifts of Inducible Clindamycin Resistance Staphylococcus aureus Clones in Tehran, Iran: A Molecular–Epidemiological Analysis From 2013 to 2018*  
Mehdi Goudarzi, Nobumichi Kobayashi, Masoud Dadashi, Roman Pantůček, Mohammad Javad Nasiri, Maryam Fazeli, Ramin Pouriran, Hossein Goudarzi, Mirmohammad Miri, Anahita Amirpour and Sima Sadat Seyedjavadi
- 446** *Exploring the Potential of CRISPR-Cas9 Under Challenging Conditions: Facing High-Copy Plasmids and Counteracting Beta-Lactam Resistance in Clinical Strains of Enterobacteriaceae*  
Thaysa Leite Tagliaferri, Natália Rocha Guimarães, Marcella de Paula Martins Pereira, Liza Figueiredo Felicori Vilela, Hans-Peter Horz, Simone Gonçalves dos Santos and Tiago Antônio de Oliveira Mendes

- 457** *Characterization of KPC-Producing Serratia marcescens in an Intensive Care Unit of a Brazilian Tertiary Hospital*  
Roumayne L. Ferreira, Graziela S. Rezende, Marcelo Silva Folhas Damas, Mariana Oliveira-Silva, André Pitondo-Silva, Márcia C. A. Brito, Eduardo Leonardecz, Fabiana R. de Góes, Emeline Boni Campanini, Iran Malavazi, Anderson F. da Cunha and Maria-Cristina da Silva Pranchevicius
- 471** *Prediction of Antimicrobial Resistance in Gram-Negative Bacteria From Whole-Genome Sequencing Data*  
Pieter-Jan Van Camp, David B. Haslam and Aleksey Porollo
- 484** *Hospital-Associated Multidrug-Resistant MRSA Lineages are Trophic to the Ocular Surface and Cause Severe Microbial Keratitis*  
Paulo J. M. Bispo, Lawson Ung, James Chodosh and Michael S. Gilmore
- 494** *Amoxicillin Increased Functional Pathway Genes and Beta-Lactam Resistance Genes by Pathogens Bloomed in Intestinal Microbiota Using a Simulator of the Human Intestinal Microbial Ecosystem*  
Lei Liu, Qing Wang, Huai Lin, Ranjit Das, Siyi Wang, Hongmei Qi, Jing Yang, Yingang Xue, Daqing Mao and Yi Luo
- 508** *Glycosmis pentaphylla (Rutaceae): A Natural Candidate for the Isolation of Potential Bioactive Arborine and Skimmianine Compounds for Controlling Multidrug-Resistant Staphylococcus aureus*  
Natarajan Murugan, Ramalingam Srinivasan, Athiappan Murugan, Myunghee Kim and Devarajan Natarajan
- 519** *Extended-Spectrum Beta-Lactamase-Producing Escherichia coli in Drinking Water Samples From a Forcibly Displaced, Densely Populated Community Setting in Bangladesh*  
Zahid Hayat Mahmud, Mir Himayet Kabir, Sobur Ali, M. Moniruzzaman, Khan Mohammad Imran, Tanvir Noor Nafiz, Md. Shafiqul Islam, Arif Hussain, Syed Adnan Ibna Hakim, Martin Worth, Dilruba Ahmed, Dara Johnston and Niyaz Ahmed
- 533** *Molecular Mechanisms and Epidemiology of Fosfomycin Resistance in Staphylococcus aureus Isolated From Patients at a Teaching Hospital in China*  
Wenya Xu, Tao Chen, Huihui Wang, Weiliang Zeng, Qing Wu, Kaihang Yu, Ye Xu, Xiucui Zhang and Tieli Zhou
- 543** *Alternative Therapeutic Options to Antibiotics for the Treatment of Urinary Tract Infections*  
Paul Loubet, Jérémy Ranfaing, Aurélien Dinh, Catherine Dunyach-Remy, Louis Bernard, Franck Bruyère, Jean-Philippe Lavigne and Albert Sotto
- 561** *Coexistence of the Oxazolidinone Resistance-Associated Genes cfr and oprA in Enterococcus faecalis From a Healthy Piglet in Brazil*  
Lara M. Almeida, Anthony Gaca, Paulo M. Bispo, François Lebreton, Jose T. Saavedra, Rafael A. Silva, Irinaldo D. Basílio-Júnior, Felipe M. Zorzi, Pedro H. Filsner, Andrea M. Moreno and Michael S. Gilmore





# Editorial: Antimicrobial Resistance as a Global Public Health Problem: How Can We Address It?

Luciene Andrade Da Rocha Minarini<sup>1</sup>, Leonardo Neves de Andrade<sup>2</sup>, Eliana De Gregorio<sup>3</sup>, Filipa Grosso<sup>4</sup>, Thierry Naas<sup>5</sup>, Raffaele Zarrilli<sup>6</sup> and Ilana L. B. C. Camargo<sup>7\*</sup>

<sup>1</sup> Department of Pharmaceutical Sciences, Federal University of São Paulo, Diadema, Brazil, <sup>2</sup> School of Pharmaceutical Sciences of Ribeirão Preto, University of São Paulo, Ribeirão Preto, Brazil, <sup>3</sup> Department of Molecular Medicine and Medical Biotechnology, University of Naples Federico II, Naples, Italy, <sup>4</sup> Faculty of Pharmacy, University of Porto, Porto, Portugal, <sup>5</sup> Assistance Publique Hopitaux De Paris, Paris, France, <sup>6</sup> Department of Public Health, University of Naples Federico II, Naples, Italy, <sup>7</sup> Laboratory of Molecular Epidemiology and Microbiology (LEMiMo), São Carlos Institute of Physics, University of São Paulo, São Carlos, Brazil

**Keywords:** antimicrobial resistance, CRISPR-Cas, oxazolidinone-resistant *Enterococcus faecalis*, carbapenem-resistant *A. baumannii*, colistin-resistant *E. coli*, antibiotic-resistant non-typhoidal Salmonella, MRSA, VRE

## OPEN ACCESS

## Editorial on the Research Topic

### Antimicrobial Resistance as a Global Public Health Problem: How Can We Address It?

Misuse of antibiotics in agriculture, food production, and especially among humans and animals is the predominant factor in the emergence and spread of antimicrobial resistance, which might further lead to deaths from infections worldwide (1). More specifically, in the European Union, attributable deaths due to antimicrobial-resistant microorganisms were estimated to be 33,110 per year (2). At the same time, it is now easier to isolate and characterize antimicrobial-resistant bacteria in clinical settings or the environment (1). In 2017, the WHO described the most critical multidrug-resistant bacteria for which novel therapeutics are urgently needed (3). Without surprise, they belonged to the already known group, ESKAPE (*Enterococcus faecium*, *Staphylococcus aureus*, *Klebsiella pneumoniae*, *Acinetobacter baumannii*, *Pseudomonas aeruginosa*, and *Enterobacter* spp.) (4), which causes most of the healthcare-associated infections nowadays.

On the top of the WHO list are the critical priorities: carbapenem-resistant *A. baumannii*, *P. aeruginosa*, and Enterobacteriaceae, plus ESBL-producing Enterobacteriaceae (3). As high priorities are vancomycin-resistant *E. faecium*, *Staphylococcus aureus* (methicillin-resistant, vancomycin-intermediate and resistant), clarithromycin-resistant *Helicobacter pylori*, fluoroquinolone-resistant *Campylobacter* spp., fluoroquinolone-resistant *Salmonellae*, *Neisseria gonorrhoeae* (cephalosporin-resistant, fluoroquinolone-resistant) (3). The third part of the WHO list ranked as medium priority consists of penicillin-non-susceptible *Streptococcus pneumoniae*, ampicillin-resistant *Haemophilus influenzae*, and fluoroquinolone-resistant *Shigella* spp. (3). In addition to the hospital (patients and healthcare workers) (5–8), bacteria of this list can also disseminate through the community (causing infections in humans or pets) (9–11), food chain (10, 12–14), and environment (15, 16).

Overuse of antibiotics prescribed to humans and animals plus the improper use in agriculture can select resistant bacteria that emerge after a spontaneous mutation or after acquiring resistance genes through horizontal transfer mediated by mobile genetic elements (17). This selection can occur in both the human and non-human gastrointestinal tracts as well as in contaminated environments. Once they become resistant to antibiotics, clonal bacterial cells are selected in

#### Edited by:

Marc Jean Struelens,  
Université Libre de Bruxelles, Belgium

#### Reviewed by:

Sergey Eremin,  
World Health  
Organization, Switzerland

#### \*Correspondence:

Ilana L. B. C. Camargo  
ilanacamargo@ifsc.usp.br

#### Specialty section:

This article was submitted to  
Infectious Diseases - Surveillance,  
Prevention and Treatment,  
a section of the journal  
Frontiers in Public Health

**Received:** 30 September 2020

**Accepted:** 21 October 2020

**Published:** 12 November 2020

#### Citation:

Minarini LADR, Andrade LNd,  
De Gregorio E, Grosso F, Naas T,  
Zarrilli R and Camargo ILBC (2020)  
Editorial: Antimicrobial Resistance as a  
Global Public Health Problem: How  
Can We Address It?  
Front. Public Health 8:612844.  
doi: 10.3389/fpubh.2020.612844

the microbial population and disseminates its daughter cells. Alternatively, plasmids carrying resistance genes are transferred to other bacteria through conjugation or transformation (17). In Switzerland, a recent study on freshwater samples from rivers, inland canals, and streams showed environmental dissemination of high-risk carbapenemase-producing Enterobacteriaceae with plasmids composed of elements identical to those of resistance plasmids retrieved from clinical and veterinary isolates locally and worldwide (15). The authors concluded that these plasmids carrying carbapenemase genes replicate and evolve pollutants of river ecosystems and represent a threat to public health and environmental integrity (15). ESBL-producing Enterobacteriaceae were isolated from a Tunisian semi-industrial pilot plant with biological treatment (WWPP) and its receiving river with high rates of CTX-M-15 and high genetic diversity (16). Therefore, the water treatment and appropriate use of antibiotics may represent important infection control measures to avoid antimicrobial resistance spread in hospitals and communities (1, 18).

Bacteria may grow planktonically but most often form biofilms in nature or human body infections (19). These biofilms are common in the hospital environment, especially in polymeric clinical devices, such as catheters and cardiac pacemakers. The inhibition of biofilm growth is of great importance in infection control and treatment of healthcare-associated infections owing to their inherent tolerance and “resistance” to antimicrobial therapies (19). In addition, biofilms constitute a great challenge in clinical settings since there is no “gold standard” available to reveal the presence of microbial biofilms.

The prevention of bacterial resistance spread is a significant challenge among healthcare professionals, especially in hospital settings. Surveillance of clones and lineages spread in a hospital environment or among patients, and the knowledge of their susceptibility to antimicrobials are crucial data to initiate a proper empiric treatment of hospital-acquired infections and infection prevention and control.

In many cases, precision medicine is the key to therapy since different microbes are prone to different remedies. New antimicrobials might seem more effective and promising, but some traditional compounds, such as beta-lactamase or efflux pump inhibitors that could prevent enzymatic action on known antibiotics or efflux pump activity, respectively, are also beneficial.

This Research Topic harbors 48 published manuscripts, including original research, review, opinion, and brief research reports addressing these subjects. The 443 involved authors focused on tackling antimicrobial resistance in bacteria. According to Merlin, although the increasing occurrence of antibiotic resistance among bacteria due to the antimicrobial agent consumption has been recognized for decades, only recently, the seriousness of the situation has been considered by international, national, and local health agencies. Some recommendations were defined in order to educate and improve the practices of health professionals and consumers. Most recommendations proposed coordinated actions in public health and veterinary/agricultural domains, limiting the inappropriate exposure of bacteria to antibiotics, in order to delay the

natural evolution toward resistance and its propagation in the downstream environment, in a One Health context.

The chapters of this Research Topic show that it is crucial to pay attention to antimicrobial resistance in microorganisms from wild animals, pets, livestock, food, and the environment, in addition to those isolated from humans, to understand how antimicrobial resistance spreads. Lin et al. used a genomic approach to study the horizontal transfer of colistin resistance between polluted rivers and wild birds. Metadata analysis of *mcr-1*-positive multidrug-resistant *E. coli* strains, which were isolated from the environment of egret habitat (polluted river) and egret feces, showed highly homologous *mcr-1*-bearing IncI2 plasmids among isolates from different regions along the East Asian-Australian Flyway, suggesting that migratory birds may mediate the intercontinental transportation of colistin resistance.

Mahmud et al. call the attention to the prevalence and characterization of MDR and ESBL-producing *E. coli* in drinking water samples collected from Rohingya camps, Bangladesh. The authors described that 66 out of 384 *E. coli* isolates in this study were ESBL-producers, of which 71% (47/66) were MDR. Sixty-four percent (42/66) of the ESBL-producing *E. coli* carried one to seven plasmids ranging from 1 to 103 MDa. Only large plasmids with antibiotic resistance properties were found transferrable via conjugation. This study shows that drinking water samples could foster exposure and dissemination of MDR, ESBL-producing, and pathogenic *E. coli* lineages, posing a health risk to the people residing in the densely populated camps of Bangladesh.

Chen et al. investigated the antimicrobial resistance trends and characteristics of ESBL-producing *E. coli* isolates from pets and whether this correlates with antibiotic usage in the clinic. The authors observed high rates of resistance to  $\beta$ -lactams and fluoroquinolones and resistance to >3 antibiotic classes. ESBL-encoding genes *bla*<sub>CTX-M</sub> ( $n = 44$ , 34.65%) and plasmid-mediated quinolone resistance genes *qnrB* ( $n = 119$ , 93.70%) were most common in 36 PFGEs types and 28 different sequence types (STs), including ST405 (7, 15.9%), ST131 (3, 6.8%), ST73, ST101, ST372, and ST827 (2, 4.5% each). Additionally, *bla*<sub>NDM-5</sub> was detected in three isolates ( $n = 3$ , 2.36%, two ST101 and one ST405), and *mcr-1* was also observed in three colistin-resistant *E. coli* (ST6316, ST405, and ST46).

García-Meniño et al. performed molecular characterization of 35 prevalent strains of colistin-resistant *E. coli* from swine enteric colibacillosis in Spain. The resistome analysis showed six different *mcr* variant genes. In seven of them, the authors observed an association with ESBL. The summative presence of mechanisms associated with high-level resistance to quinolone/fluoroquinolones and colistin could confer adaptive advantages to prevalent pig *E. coli* strains. The authors also reported the co-occurrence of double colistin-resistance mechanisms in a significant number of *E. coli* isolates.

Mukherjee et al. observed increasing frequencies of antibiotic-resistant non-typhoidal Salmonella (NTS) infections in Michigan, which is not part of the FoodNet surveillance system in the USA. A total of 198 isolates, from 2011 to 2014, belonged to 35 different serovars with the predominance of Enteritidis (36.9%), followed by Typhimurium (19.5%), and Newport (9.7%). A total of 30 (15.2%) NTS isolates were resistant to  $\geq 1$  antibiotic,

and 15 (7.5%) were resistant to  $\geq 3$  antimicrobial classes. They demonstrated the importance of surveillance, resistance frequency monitoring, and identification of risk factors that can aid in the development of new prevention strategies.

Almeida et al. described the coexistence of oxazolidinone resistance genes *cfr* and *optrA* in a MDR *E. faecalis* isolate belonging to ST29, obtained from a healthy piglet in Brazil in the context of surveillance study. Whole-genome sequencing revealed that the *cfr* gene was in a transposon-like structure of 7,759 nucleotides flanked by *IS1216E* and capable of excising and circularizing, distinguishing it from known genetic contexts for *cfr* in *Enterococcus* spp., while *optrA* was in an Inc18 broad-host-range plasmid of >58 kb. Both genes were able to conjugate. This study highlights the need for monitoring the use of antibiotics in the Brazilian swine production system to control the spread and proliferation of antibiotic resistance.

This Research Topic also presents studies reporting the mechanisms of resistance and lineages of bacteria of clinical importance. Carbapenem-resistant *A. baumannii* (CRAB) often causes fatal infections among seriously ill patients. Wong et al. used whole-genome sequencing, gene expression studies, and enzyme kinetics analyses to investigate the underlying carbapenem resistance mechanisms in 14 clinical *A. baumannii*. A large majority of isolates belonged to the International Clone II (IC-II), ST208. CRAB harbored *bla*<sub>OXA-23</sub>/*bla*<sub>OXA-72</sub>, or overexpression of the *bla*<sub>OXA-51</sub> gene upon *ISAbal* insertion, and had strong carbapenem-degrading activities. Over-production of carbapenem-hydrolyzing-class D- $\beta$ -lactamases (CHDLs) is the key mechanism of carbapenem resistance in the isolates studied.

Fosfomycin exhibits significant antimicrobial activity against a broad spectrum of pathogens, including *S. aureus*. Although widely described in gram-negative bacteria, fosfomycin's resistance mechanism is rarely reported among gram-positive bacteria (Xu et al.). The molecular mechanisms of 11 fosfomycin-resistant *S. aureus* isolates from a Teaching hospital in China were determined. The authors showed that the mutations in the *uhpT*, *glpT*, and *murA* genes and the overexpression of the efflux pump gene *tet38* under a subinhibitory concentration of fosfomycin might play a major role in conferring fosfomycin resistance in these isolates. In contrast, none of the resistant strains carried the *fosA*, *fosB*, *fosC*, *fosD*, and *fosX* genes, indicating that these genes might not be the primary factors mediating the resistance of *S. aureus* against fosfomycin. Furthermore, MLST analysis identified ST5708, a novel sequence type of *S. aureus* (Xu et al.).

The possible transference of resistance genes among different species and the consequences that these genes may cause in the cells were covered in this Research Topic, for instance, in the study by Xiang et al., which described the presence of *bla*<sub>NDM-1</sub> in 54 out of 1,735 carbapenem-non-susceptible strains, including *K. pneumoniae*, *A. baumannii*, and *E. coli*. After analyzing the *bla*<sub>NDM-1</sub> gene and its genetic environment, the authors hypothesized that, due to the presence of the *ble* and *tnpA* genes, *bla*<sub>NDM-1</sub> originates from *A. baumannii*, which is retained in *K. pneumoniae* over a long period by transposition of mobile elements.

Mobile genetic elements harboring resistance genes, in certain cases, may reduce bacterial fitness. In this Research Topic, Li et al. investigated the physiological function of the *mcr-1* gene, which encodes an LPS-modifying enzyme, in *E. coli* K-12. The removal of the *mcr-1* gene not only reduced resistance to colistin, but also increased cell viability under high osmotic stress conditions and led to increased resistance to hydrophobic antibiotics. Increased expression of *mcr-1* also resulted in a decreased growth rate and changed the cellular morphology of *E. coli* (Li et al.).

Sharma et al. used a proteomic approach to study the growth and fitness of a carbapenem-resistant NDM-4-producing *K. pneumoniae* clinical isolate under meropenem stress. The authors showed the downregulation of flagellar, fimbriae, and pili proteins by mass spectrometry and system biology analysis of networking pathways. Sharma et al. suggested that these proteins might be used as targets for the development of novel therapeutics against antimicrobial-resistant *K. pneumoniae* infections.

This Research Topic also brings the search and analysis of the CRISPR-Cas system, a microbial adaptive immune system involved in defense against different types of mobile genetic elements, in whole plasmid and chromosomal sequences of multidrug-resistant *K. pneumoniae* from GenBank (Kamruzzaman and Iredell). The authors found a putative CRISPR-Cas system in 44 plasmids from *Klebsiella* species and identified an identical system in three plasmids from other *Enterobacteriaceae*, with CRISPR spacers targeting different plasmids and chromosome sequences. Additionally, the authors showed that plasmid type IV CRISPR may depend on the chromosomal type I-E CRISPRs for their competence (Kamruzzaman and Iredell). Different aspects are involved in the acquisition and transference of resistance determinants, and the presence of CRISPR-Cas in plasmids just showed us we still have a lot to understand.

In this Research Topic, several manuscripts described the diversity of the most important pathogenic bacterial species and their susceptibility profiles. For instance, in India, the antibiotic susceptibility and typing of 109 *S. aureus* strains isolated from a variety of infections showed that all *S. aureus* isolates were multidrug-resistant, virulent, and diverse irrespective of sources and place of isolation being assigned to 46 *spa*-types, 33 STs and eight clonal complexes (Aggarwal et al.).

Ai et al. studied the prevalence, characterization, and drug resistance of *S. aureus* fecal carriage among pediatric patient feces in Southern China and found that the fecal carriage rates were 20.0% for *S. aureus* and 4.5% for methicillin-resistant *S. aureus* (MRSA). Among the 76 STs, the authors found 25 new STs, and the most prevalent were ST188, ST6, and ST15 for methicillin-sensitive *S. aureus* (MSSA) and ST59 and ST45 for MRSA. The authors described high rates of penicillin, erythromycin, and clindamycin resistance among the isolates. However, CC59 (ST338 and ST59) and CC45 exhibited different antibiotic resistance patterns. Ai et al. indicated an urgency for strengthening the surveillance programs in China that could contribute to *S. aureus* infection prevention and treatment.

Bispo et al. analyzed the population structure of ocular MRSA isolates using a combination of MLST analysis, SCC*mec* typing,

and detection of the panton-valentine leukocidin (PVL) coding gene. The 68 isolates (2014–2016) belonged to 14 different sequence types (STs) that grouped within two predominant clonal complexes: CC8 (47.0%) and CC5 (41.2%). Although the isolates were associated with lineages with community and hospital origins, the authors suggested that the niche specialization could act as a driver for the community structure observed.

In Iran, Goudarzi et al. conducted a study from August 2013 to July 2018 to investigate the prevalence and molecular epidemiology of inducible macrolide-lincosamide streptogramin B (MLS<sub>B</sub>) resistance in *S. aureus*. The prevalence of inducible MLS<sub>B</sub> (iMLS<sub>B</sub>) *S. aureus* increased from 7.5 to 21.7% during the study period. The authors observed a replacement of the CC22, predominant in 2013–2014, by CC8 in 2017–2018. Goudarzi et al. described for the first time the temporal shifts of iMLS<sub>B</sub> *S. aureus* isolates in Iran that identify predominant clones and treatment options for iMLS<sub>B</sub> *S. aureus*-related infections.

Vasilakopoulou et al. described the prevalence and risk factors of antimicrobial resistance by studying the gastrointestinal carriage of vancomycin-resistant enterococci (VRE) and carbapenem-resistant gram-negative bacteria (CRGN) in the fecal flora of the inpatients of a tertiary university hospital in Greece. The authors found high prevalence rates for VRE and CRGN carriage. Prolonged hospitalization and age were independent risk factors for VRE carriage, while CRGN carriage was associated with an increased risk of acquiring a resistant pathogen, prolonged hospital stay, and increased mortality.

In South Korea, Yoon et al. showed that most (84.5%) of the *A. baumannii* blood isolates belonged to the international clonal lineage II (ICLII), and 89.5% of the isolates were either multidrug- or extensively drug-resistant. The patient's old age, the sequential organ failure assessment score, and causative *A. baumannii* ST191 belonging to ICLII were risk factors for 30-day mortality (Yoon et al.).

Ferrari et al. identified the circulation of three distinct genome clusters of carbapenem-resistant KPC-producing *K. pneumoniae* in an intensive care unit in a hospital in Northern Italy. The authors described two clusters, one linked to ST512 and one to ST258; the ST258 isolates were also colistin-resistant and responsible for a high number of clinical infections (Ferrari et al.).

Ferreira et al. characterized KPC-producing *Serratia marcescens* strains isolated during an outbreak involving patients hospitalized in the intensive care unit (ICU) and neonatal intensive-care-unit (NIUC) of a Brazilian tertiary hospital. All isolates carried KPC-carbapenemase (*bla*<sub>KPC</sub>) and extended-spectrum beta-lactamase *bla*<sub>TEM</sub> genes. In addition to the MDR profiles exhibited by almost 25% of isolates, 98.2% of the isolates had the genes codifying to the pore-forming toxin (Sh1A), phospholipase with hemolytic and cytolytic activities (Ph1A), flagellar transcriptional regulator (FlhD), and positive regulator of prodigiosin and serratomolide production (PigP).

Due to increasing resistance to multiple antibiotics classes, the search for molecules displaying potent activity against multidrug-resistant (MDR) bacteria is mandatory. Additionally, the discovery of new therapeutic approaches and/or new

pathways to be inhibited is an open door for a directed search for bioactive compounds. As an example, Barra et al. discussed the possibilities, using an *in silico*-based analysis, of enzyme inhibition of two new possible druggable biosynthesis pathways present in most bacteria, fungi, and plants but incomplete in humans: the thiamine (vitamin B1) and the pyridoxal 5'-phosphate and its vitamers (vitamin B6).

Loubet et al. discussed alternative therapies and preventative strategies for urinary tract infections caused by multidrug-resistant uropathogens, focusing on the following phases of the pathogenesis: colonization, adherence of pathogens to uroepithelial cell receptors, and invasion. In this review, the authors discussed vaccines, small compounds, nutraceuticals, immunomodulating agents, probiotics, and bacteriophages, highlighting the challenges each of these approaches face Loubet et al.

Zhang et al. investigated the effects of pharmacological doses of copper, an essential microelement for animals, on the microbial communities in the hindgut, and the antimicrobial resistance profiles of *E. coli* in weaned piglets. The pharmacological dose of copper affected the composition of the microbial community (affected the microbial metabolic functions of energy metabolism, protein metabolism, and amino acid biosynthesis), increased antimicrobial resistance (to chloramphenicol and ciprofloxacin) of intestinal *E. coli*, and was most likely harmful to the health of piglets at the early stage after weaning (Zhang et al.).

The new anti-biofilm or antimicrobial agents' analysis, as well as their mode of action, were assessed in some studies. Murugan et al. described that arborine and skimmianine compounds from ethyl acetate extract of *Gycomis pentaphylla* harbor a high antibacterial activity against MDR *S. aureus*. Wang et al. showed that the flavone glycoside baicalin inhibits biofilm formation and the quorum-sensing system in *Staphylococcus saprophyticus*, thus suggesting that it might be a potential therapeutic agent for *S. saprophyticus* biofilm-associated infections.

She et al. described the potent antimicrobial activity of auranofin against MRSA/MSSA and *E. faecalis*, both planktonic cells and biofilms, with minimum inhibitory concentrations ranging from 0.125 to 0.5 mg/L. Auranofin, in combination with linezolid or fosfomycin, showed synergistic antimicrobial activities against MSSA and MRSA both *in vitro* and in a mouse infection model. There was also a synergistic effect with chloramphenicol against *E. faecalis*. Additionally, auranofin improved the antibiofilm efficacy of chloramphenicol and linezolid, even on biofilms grown on a catheter surface. Therefore, they showed that the combination of auranofin with linezolid, fosfomycin, and chloramphenicol provides a synergistic microbicidal effect *in vitro* and *in vivo*, which rapidly enhances antimicrobial activity.

Lytic bacteriophage therapy is a potential antibacterial therapy. Montso et al. characterized lytic *E. coli* O177-specific bacteriophages isolated from cattle feces. A total of 31 lytic *E. coli* O177-specific bacteriophages were isolated and 71% of these phage isolates produced large plaques on 0.3% soft agar. Selected phage isolates had a similar morphology (an icosahedral



head and a contractile tail) and were classified under the order Caudovirales, *Myoviridae* family. Montso et al. demonstrated that lytic *E. coli* O177-specific bacteriophages isolated from cattle feces are highly stable and can infect different *E. coli* strains.

Among the papers, the authors analyzed new antimicrobials and different compounds against MDR bacteria. Cefoselis, a fourth-generation cephalosporin, was evaluated by Cheng et al. against bacterial pathogens in China. The authors observed that cefoselis showed good activity against non-ESBL-producing *E. coli*, *K. pneumoniae*, and *P. mirabilis*, MSSA, and was also potent against Enterobacteriaceae, *P. aeruginosa*, and *Streptococcus*.

Omadacycline, a new tetracycline-class broad-spectrum aminomethylcycline, exhibited excellent *in vitro* activity against both MRSA and MSSA clinical isolates (Bai et al.). Omadacycline susceptibility in *S. aureus* may be affected by efflux pump proteins (i.e., a branched-chain amino acid transport system II carrier protein and a Na/Pi cotransporter family protein) (Bai et al.).

Zheng et al. compared the effects of radezolid and linezolid on planktonic and biofilm cells of *E. faecalis*. After analyzing 302 *E. faecalis*, they observed that the MIC<sub>50</sub>/MIC<sub>90</sub> values of radezolid (0.25/0.50 mg/L) were eight-fold lower than those of linezolid (2/4 mg/L). They observed that the radezolid MICs against the high-level linezolid-resistant isolates (linezolid MICs  $\geq 64$  mg/L) increased to  $\geq 4$  mg/L with mutations in the four copies of the V domain of the 23S rRNA gene. In addition, they showed the involvement of OG1RF\_12220 (mdlB2, multidrug ABC superfamily ATP-binding cassette transporter) in the alteration of radezolid and linezolid susceptibility. Zheng et al. described that Radezolid inhibited *E. faecalis* biofilm formation to a greater extent than linezolid. Therefore, radezolid is more effective than linezolid against *E. faecalis*.

Hao et al. showed a potent *in vitro* activity of apramycin, an antibiotic with good activity against a range of multidrug-resistant pathogens, against clinical carbapenem-resistant, and hypervirulent *K. pneumoniae* (CR-hvKp) along with carbapenem-resistant non-hvKp (CR-non-hvKp) isolates, including those resistant to amikacin or gentamicin.

Dong et al. demonstrated that ebselen, an organo-selenium with well-characterized toxicology and pharmacology, has high bactericidal activity against multidrug-resistant (MDR) *S. aureus* based on taking TrxR as a major target and disruption of the

redox microenvironment. The authors showed that ebselen is an effective topical antibacterial agent in animal model of MDR *S. aureus* LT-1 skin infection, reducing the bacterial load and the expression of pro-inflammatory cytokines.

Murugan et al. focused on the isolation and structural characterization of bioactive compounds from the ethyl acetate extract of *Gycosmis pentaphylla*. The isolated compounds identified as arborine and skimmianine have high bactericidal effects against MDR *S. aureus* clinical isolates. These compounds induced intracellular molecular imbalance and cell membrane disturbances that caused cell death of all MDR *S. aureus* strains and the reference standard *S. aureus* MTCC-96 strain.

A bottleneck in clinical microbiology, the incubation time necessary to the susceptibility test is ready for the antibiotic decision by the clinician is something to overcome. Genomics and technology can work together to improve the turnaround time in the clinical laboratory. Liu et al. used 2 genotype-based machine learning methods named Support Vector Machine (SVM) and Set Covering Machine (SCM) to predict the resistance to tetracycline, ampicillin, sulfisoxazole, trimethoprim, and enrofloxacin. The correlation results between the phenotype and the model predictions of the five antimicrobial agents indicated that both SVM and SCM models could significantly discern the resistant isolates of the sensitive isolates and could be potential tools in antimicrobial resistance surveillance and clinical diagnosis in veterinary medicine.

Resistance mechanisms, surveillance of antimicrobial-resistant bacteria, and new drug discovery studies offer different views of the antimicrobial resistance, which became a public health problem. There are more articles dedicated to the community focused on antimicrobial resistance in this Research Topic, and we hope you enjoy it.

## AUTHOR CONTRIBUTIONS

All authors wrote about the manuscripts they edited in the Research Topic. IC also compiled and edited the complete text.

## ACKNOWLEDGMENTS

We are grateful to all reviewers who put their efforts during the COVID-19 pandemic to analyze all the manuscripts.

## REFERENCES

- McEwen S, Collignon P. Antimicrobial resistance: a one health perspective. *Microbiol Spectrum*. (2018) 6. doi: 10.1128/microbiolspec.ARBA-0009-2017
- Cassini A, Högberg LD, Plachouras D, Quattrocchi A, Hoxha A, Simonsen GS, et al. Attributable deaths and disability-adjusted life-years caused by infections with antibiotic-resistant bacteria in the EU and the European Economic Area in 2015: a population-level modelling analysis. *Lancet Infect Dis*. (2019) 19:56–66. doi: 10.1016/S1473-3099(18)30605-4
- World Health Organization. *Global Priority List of Antibiotic-Resistant Bacteria to Guide Research, Discovery, and Development of New Antibiotics*. Available online at: <https://www.who.int/news-room/detail/27-02-2017-who-publishes-list-of-bacteria-for-which-new-antibiotics-are-urgently-needed2017> (accessed July 03, 2017).
- Rice LB. Federal Funding for the Study of Antimicrobial Resistance in Nosocomial Pathogens: No ESKAPE. *J Infect Dis*. (2008) 197:1079–81. doi: 10.1086/533452
- Souza RC, Dabul ANG, Boralli C, Zuvanov L, Camargo I. Dissemination of blaKPC-2 in an NTEKPC by an IncX5 plasmid. *Plasmid*. (2019) 106:102446. doi: 10.1016/j.plasmid.2019.102446
- Merlo TP, Dabul AN, Camargo IL. Different VanA elements in *E. faecalis* and in *E. faecium* suggest at least two origins of Tn1546 among VRE in a Brazilian hospital. *Microb Drug Resist*. (2015) 21:320–8. doi: 10.1089/mdr.2014.0077
- Zarrilli R, Bagattini M, Esposito EP, Triassi M. Acinetobacter infections in neonates. *Curr Infect Dis Rep*. (2018) 20:48. doi: 10.1007/s11908-018-0654-5
- Okado JB, Bogni SC, Fleck Renato LA, Martinez R, Gir E, Baratella da Cunha Camargo IL. Molecular analysis of methicillin-resistant *Staphylococcus aureus* dissemination among healthcare professionals and/or HIV patients from a

- tertiary hospital. *Revista da Sociedade Brasileira de Medicina Tropical*. (2016) 49:51–6. doi: 10.1590/0037-8682-0284-2015
9. Loncaric I, Mistic D, Szostak MP, Künzel F, Schäfer-Somi S, Spersger J. Broad-spectrum cephalosporin-resistant and/or fluoroquinolone-resistant enterobacteriales associated with canine and feline urogenital infections. *Antibiotics*. (2020) 9:387. doi: 10.3390/antibiotics9070387
  10. Hendriksen RS, Fricke WF, Ceyskens PJ, Gomart C, Billman-Jacobe H, Holt KE, et al. Global phylogenomics of multidrug-resistant *Salmonella enterica* serotype Kentucky ST198. *Microb Genom*. (2019) 5:e000269. doi: 10.1099/mgen.0.000269
  11. van Duin D, Paterson DL. Multidrug-resistant bacteria in the community: an update. *Infect Dis Clin North Am*. (2020) 30:377–90. doi: 10.1016/j.idc.2020.08.002
  12. Diaconu EL, Carfora V, Alba P, Di Matteo P, Stravino F, Buccella C, et al. Novel IncFII plasmid harbouring bla<sub>NDM-4</sub> in a carbapenem-resistant *Escherichia coli* of pig origin, Italy. *J Antimicrob Chemother*. (2020) dkaa374. doi: 10.1093/jac/dkaa374
  13. Garcia-Graells C, Berbers B, Verhaegen B, Vanneste K, Marchal K, Roosens NHC, et al. First detection of a plasmid located carbapenem resistant bla(VIM-1) gene in *E. coli* isolated from meat products at retail in Belgium in 2015. *Int J Food Microbiol*. (2020) 324:108624. doi: 10.1016/j.ijfoodmicro.2020.108624
  14. Liu X, Geng S, Chan EW, Chen S. Increased prevalence of *Escherichia coli* strains from food carrying bla (NDM) and mcr-1-bearing plasmids that structurally resemble those of clinical strains, China, 2015 to 2017. *Euro Surveill*. (2019) 24:1800113. doi: 10.2807/1560-7917.ES.2019.24.13.1800113
  15. Bleichenbacher S, Stevens MJA, Zurfluh K, Perreten V, Endimiani A, Stephan R, et al. Environmental dissemination of carbapenemase-producing *Enterobacteriaceae* in rivers in Switzerland. *Environ Pollut*. (2020) 265(Pt B):115081. doi: 10.1016/j.envpol.2020.115081
  16. Hassen B, Abbassi MS, Benlabidi S, Ruiz-Ripa L, Mama OM, Ibrahim C, et al. Genetic characterization of ESBL-producing *Escherichia coli* and *Klebsiella pneumoniae* isolated from wastewater and river water in Tunisia: predominance of CTX-M-15 and high genetic diversity. *Environ Sci Pollut Res Int*. (2020). doi: 10.1007/s11356-020-10326-w. [Epub ahead of print].
  17. Botelho J, Grosso F, Peixe L. Antibiotic resistance in *Pseudomonas aeruginosa* - Mechanisms, epidemiology and evolution. *Drug Resist Updat*. (2019) 44:100640. doi: 10.1016/j.drug.2019.07.002
  18. World Health Organization. *Water, Sanitation and Hygiene in Health Care Facilities: Practical Steps to Achieve Universal Access* (2019).
  19. Jiang Y, Geng M, Bai L. Targeting biofilms therapy: current research strategies and development hurdles. *Microorganisms*. (2020) 8:1222. doi: 10.3390/microorganisms8081222
- Conflict of Interest:** The authors declare that the research was conducted in the absence of any commercial or financial relationships that could be construed as a potential conflict of interest.
- Copyright © 2020 Minarini, Andrade, De Gregorio, Grosso, Naas, Zarrilli and Camargo. This is an open-access article distributed under the terms of the Creative Commons Attribution License (CC BY). The use, distribution or reproduction in other forums is permitted, provided the original author(s) and the copyright owner(s) are credited and that the original publication in this journal is cited, in accordance with accepted academic practice. No use, distribution or reproduction is permitted which does not comply with these terms.



# Counter Clinical Prognoses of Patients With Bloodstream Infections Between Causative *Acinetobacter baumannii* Clones ST191 and ST451 Belonging to the International Clonal Lineage II

## OPEN ACCESS

### Edited by:

Marc Jean Struelens,  
European Centre for Disease  
Prevention and Control  
(ECDC), Sweden

### Reviewed by:

Kwan Soo Ko,  
Sungkyunkwan University School of  
Medicine, South Korea  
Raffaele Zarrilli,  
University of Naples Federico II, Italy

### \*Correspondence:

Seok Hoon Jeong  
kscpjsh@yuhs.ac

### Specialty section:

This article was submitted to  
Infectious Diseases - Surveillance,  
Prevention and Treatment,  
a section of the journal  
Frontiers in Public Health

**Received:** 15 April 2019

**Accepted:** 02 August 2019

**Published:** 16 August 2019

### Citation:

Yoon E-J, Kim D, Lee H, Lee HS,  
Shin JH, Uh Y, Shin KS, Kim YA,  
Park YS, Shin JH and Jeong SH  
(2019) Counter Clinical Prognoses of  
Patients With Bloodstream Infections  
Between Causative *Acinetobacter*  
*baumannii* Clones ST191 and ST451  
Belonging to the International Clonal  
Lineage II. *Front. Public Health* 7:233.  
doi: 10.3389/fpubh.2019.00233

Eun-Jeong Yoon<sup>1</sup>, Dokyun Kim<sup>1</sup>, Hyukmin Lee<sup>1</sup>, Hye Sun Lee<sup>2</sup>, Jong Hee Shin<sup>3</sup>,  
Young Uh<sup>4</sup>, Kyeong Seob Shin<sup>5</sup>, Young Ah Kim<sup>6</sup>, Yoon Soo Park<sup>7</sup>, Jeong Hwan Shin<sup>8</sup> and  
Seok Hoon Jeong<sup>1\*</sup>

<sup>1</sup> Department of Laboratory Medicine and Research Institute of Bacterial Resistance, Yonsei University College of Medicine, Seoul, South Korea, <sup>2</sup> Biostatistics Collaboration Unit, Yonsei University College of Medicine, Seoul, South Korea,

<sup>3</sup> Department of Laboratory Medicine, Chonnam National University Medical School, Gwangju, South Korea, <sup>4</sup> Department of Laboratory Medicine, Yonsei University Wonju College of Medicine, Wonju-si, South Korea, <sup>5</sup> Department of Laboratory Medicine, Chungbuk National University College of Medicine, Cheongju-si, South Korea, <sup>6</sup> Department of Laboratory Medicine, National Health Insurance Service Ilsan Hospital, Goyang-si, South Korea, <sup>7</sup> Department of Internal Medicine, National Health Insurance Service Ilsan Hospital, Goyang-si, South Korea, <sup>8</sup> Department of Laboratory Medicine and Paik Institute for Clinical Research, Inje University College of Medicine, Busan, South Korea

This study was conducted to evaluate the possible clinical and bacteriologic features associated with 30-day mortality from *Acinetobacter baumannii* (*A. baumannii*) bloodstream infections (BSIs). We conducted a prospective, multicenter, observational study of 181 entire episodes of *A. baumannii* BSI from six general hospitals between May 2016 and April 2017 in South Korea. Cox proportional-hazards regression model was used to estimate risks of the primary endpoint, i.e., all-cause mortality within 30 days from the initial blood culture. Most (84.5%) of the *A. baumannii* blood isolates belonged to the international clonal lineage II (ICLII) and 89.5% of the isolates were either multidrug- or extensively-drug resistant. We identified three risk factors including the old age of patient {hazard ratio, 1.033; [95% Confidential Interval (CI), 1.010–1.056]}, the sequential organ failure assessment score [1.133 (1.041–1.233)], and causative *A. baumannii* sequence type (ST) 191 belonging to ICLII [1.918 (1.073–3.430)], and three protective factors including causative *A. baumannii* ST451 belonging to ICLII [0.228 (0.078–0.672)], platelet count [0.996 (0.993–0.999)], and definitive therapy within 72 h [0.255 (0.125–0.519)]. Differing 30-day mortality rate in the dominant ICLII was observed by ST, which was much high in ST191 and low in ST451 and it was likely associated with the molecular traits, rather than the drug resistance.

**Keywords:** *Acinetobacter baumannii*, bloodstream infection, international clonal lineage II, ST191, ST451

## INTRODUCTION

*Acinetobacter baumannii* is dominant in clinical settings primarily targeting immunocompromised patients in intensive care units (ICUs) and has the potential to cause healthcare-associated infections (1). Infections caused by *A. baumannii* have repeatedly been reported to have grave clinical outcomes (2, 3). *A. baumannii* has an epidemic potential of emerging diseases because of its ability to persist in hospital environments by resisting desiccation and disinfectants (1). A propensity toward rapid acquisition of foreign DNA, including antimicrobial resistance determinants and virulence determinants, also contributes to its effective dissemination (4).

Previous studies have demonstrated that *A. baumannii* infections are accompanied by serious morbidity and mortality associated with a high sequential organ failure assessment (SOFA) score (5), comorbidities (6), immunosuppression (3), and antimicrobial treatment failure, mainly due to the multidrug resistance (MDR) of the causative *A. baumannii* (5, 7, 8). The rates of resistance to the major anti-*Acinetobacter* agents are increasing (9). In particular in South Korea, predominance of the multidrug-resistant international clonal lineage II (ICLII) in hospital settings is of great concern (10–12).

This study was performed to evaluate the possible clinical and bacteriologic features associated with 30-day mortality from *A. baumannii* bloodstream infection (BSI) for the entire 1-year incidence of *A. baumannii* BSI cases of multiple general hospitals in South Korea.

## METHODS

### Study Design

A prospective, multicenter, observational study was designed to monitor the entire *A. baumannii* BSI episodes between May 2016 and April 2017 occurring in six general hospitals with 715–1,050 beds participating in a national surveillance study of antimicrobial resistance in South Korea (13). Local ethics committee approvals were expedited or waived at each participating hospital since the study had a purely observational nature. The *A. baumannii* BSI cases were detected through reviewing daily blood culture results. One authorized investigator at each hospital reviewed patients' medical records, all of the raw data were recorded in a pre-formatted spreadsheet, and the datasheet was submitted via email to an analysis center without monitoring. Prognoses of patients were followed for at least 30 days and the cases of transfer and hospital discharge were recorded as they were. The Charlson comorbidity index (14) and the SOFA score (15) were calculated in the analysis center using the collected raw data for the day of initial blood culture. For the sequential isolation of *A. baumannii* from one patient, the first isolate was used for analyses and the ensuing isolates were discarded. Among a total of 67,803 patients subjected to blood culture, *A. baumannii* isolates were recovered from blood specimens of 188 patients, and following the elimination of 7 episodes of death on the day of the initial blood culture, 181 cases were included in the analysis. The microbiological assessment was carried out in the analysis center.

## Definitions

Laboratory-confirmed *A. baumannii* BSI was defined as an *A. baumannii*-positive blood culture from one or more blood specimens (16). Hospital-originated (HO) infection was specified by  $\geq 2$  calendar days of hospitalization at the day of initial blood culture, including the time spent at a previous health care facility before transfer. The 30-day mortality was defined as all-cause mortality within 30 days from the initial blood culture. Non-susceptibility (NS) to a drug class was defined as NS to at least one drug in a class and resistance phenotypes were categorized following Magiorakos et al. (17): MDR (NS to three or more drug classes), extensively drug resistance (XDR, NS to at least one agent in all but one or two drug classes), and pan-drug resistance (NS to at least one agent in all drug classes). An empirical antimicrobial therapy was defined as an initial antimicrobial treatment before the susceptibility testing results for the causative pathogen. A definitive antimicrobial therapy was defined as prescribing a revised antimicrobial regimen based on the antimicrobial susceptibility testing results and, if the revised regimen was administered after 72 h, it was deemed to be a delayed definitive therapy. Adequate antimicrobial therapy must include at least one antimicrobial agent active *in vitro* and both the dosage and route of administration should meet current medical standards.

## Microbiological Assessment

Bacterial species were initially identified by matrix assisted laser desorption/ionization time-of-flight mass spectrometry using a Bruker Biotyper™ system (Billerica, MA, USA) and the detailed species of *Acinetobacter* spp. were confirmed by PCR and sequencing the *rpoB* gene. For *A. baumannii*, multilocus sequence typing was followed through the Oxford scheme (18). Antimicrobial susceptibility was tested following the Clinical and Laboratory Standards Institute (CLSI) guidelines (19). Antimicrobial susceptibilities to 13 anti-*Acinetobacter* agents belonging to seven drug classes were tested by the disk diffusion method. For carbapenem-resistant isolates, the *bla*<sub>OXA-23</sub> gene and the IS*Aba1-bla*<sub>OXA-51-like</sub> were identified by PCR and direct sequencing (20). Colistin MICs were determined by the broth microdilution method (21). Twenty-six virulence genes associated with eight virulence characteristics (22) were investigated by real-time PCR using gene-specific primers (23) and a KAPA SYBR Fast quantitative PCR master mix (Kapa biosystems, Inc., Wilmington, MA, USA). The resistance islands AbaR and AbGRII were specified by PCR using a set of primers, comMtr3\_145-126F (5'-CAAGCGTTGGCGTAAGACT-3') and reverse primers tniB\_546-525R (5'-CAAGTACATGCTCTGCAAGATG-3') only for the full *tniB* gene and tniB\_37-16R (5'-CAGACTCAATTCATTGCTGAGG-3') for both the full and the truncated *tniB* genes.

## Statistical Analysis

Statistical analyses were performed in SPSS statistics (version 23, IBM Corp., Armonk, NY, USA). Data are expressed as



the mean ± standard deviation if no special description is indicated. Categorical variables were compared by Pearson’s X<sup>2</sup> test, and continuous variables were compared by an independent two sample *t*-test. Associations between 30-day mortality and risk factors were evaluated using univariable and multivariable Cox proportional hazard regression models. The proportional hazards assumption was evaluated by including an interaction term between variables, and variables were natural-log transformed by follow-up time and by log-minus-log survival plots. For multivariable analyses, variables with a *P* value <0.1 in univariable analyses were considered to include any possible variables. Multicollinearity between variables was diagnosed by calculating the variance inflation factors, and a multivariable analysis was conducted by the backward stepwise method. All tests of significance were two-tailed; *P* values <0.05 were considered to be significant.

## RESULTS

### Characteristics of Enrolled Patients

A total of 181 laboratory-confirmed *A. baumannii* BSI cases were enrolled from the six participating hospitals and the number of cases was ranged from 22 to 52 by hospital (Figure 1). Among patients with *A. baumannii* BSIs, the sex ratio of male vs. female was 115:66, and their mean age was 67.7 ± 14.3 years (Table 1). The mean Charlson comorbidity index score was 4.1 ± 2.2. Solid tumors (26.5%, 48/181), diabetes mellitus (23.2%, *n* = 42), cerebrovascular diseases (18.2%, *n* = 33), kidney diseases (13.8%, *n* = 25), and chronic pulmonary diseases (6.6%, *n* = 12) were the five most observed underlying diseases and dementia (*n* = 9) and chronic liver diseases (*n* = 7) were followed. Of the total, 88.4% (*n* = 160) of cases were HO infections, 95.0% (*n* = 172) were inpatients, and 68.0% of those (117/172) stayed

in ICUs. The SOFA score had a mean value of 5.9 ± 3.5. Secondary BSIs were identified in 44.2% (80/181) of cases, and the majority (86.3%, 69/80) were originated from a pulmonary tract infection.

### The BSI-Causative *A. baumannii* Isolates Sequence Types

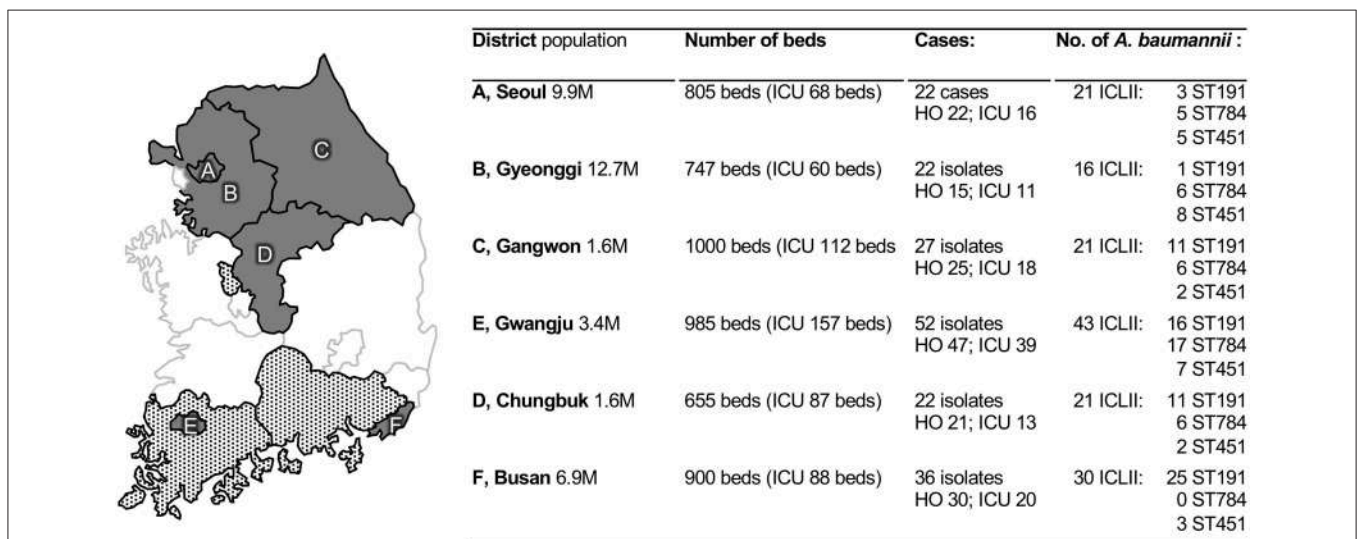
The majority of the *A. baumannii* blood isolates belonged to ICLII (84.5%, 153/181) and the ICLII mostly comprised sequence type (ST) 191 (allele numbers of *gltA-gyrB-gdhB-recA-cpn60-gpi-rpoD*, 1-3-3-2-2-94-3; 47.7%, 73/153), ST784 (1-3-3-2-2-107-3; 20.3%, *n* = 31), and ST451 (1-3-3-2-2-142-3; 19.0%, *n* = 29). The 30-day mortality rate of patients with *A. baumannii* ICLII BSIs was 1.83-fold higher than that with *A. baumannii* BSIs by non-ICLII strains (45.8 vs. 25.0%); and among the ICLII BSIs, the 30-day mortality rate with ST191 BSIs was the highest and, the lowest for ST451 BSIs (60.3 vs. 17.2%).

### Antimicrobial Resistance

Majority of the *A. baumannii* blood isolates (89.5%, 162/181) were either MDR or XDR, and the proportion was markedly greater in *A. baumannii* ICLII (98.7%, 151/153; 18 MDR and 133 XDR) than in non-ICLII (39.3%, 11/28; 5 MDR, and 6 XDR). All of the tested isolates were susceptible to colistin, and no pan-drug resistant isolate was observed. All but one carbapenem-NS *A. baumannii* harbored the *bla*<sub>OXA-23</sub> gene (99.4%, 159/160) and the remaining one carried an insertion sequence IS*AbaI* upstream from the *bla*<sub>OXA-51-like</sub> gene. Two thirds and one-quarter of *A. baumannii* possessed AbGRI1 (63.0%, 114/181) and AbaR (26.5%, 48/181), respectively.

### Virulence Factors

Factors for adhesion and membrane integrity, biofilm formation, carbohydrate metabolism, quorum sensing, and siderophore



**FIGURE 1 |** Participating sentinel hospitals and collected *Acinetobacter baumannii* blood isolates. Locations of the hospitals (in gray) and covering parts (in gray patterns) are indicated in a map of the South Korean peninsula, respectively, and the associated table represent information regarding blood isolates from each hospital including demographic information from 2016. HO, hospital-origin; ICLII, international clonal lineage II; ST, sequence type.

**TABLE 1 |** Thirty day mortality-associated factors for patients with an *Acinetobacter baumannii* BSI.

Variables	Total* n = 181	Survival n = 104	30-day death† n = 77	P‡	Univariate model HR [95%CI]§	P
<b>Demographic information</b>						
Male	115 (63.5%)	67 (64.4%)	48 (62.3%)	0.876	0.883 [0.557–1.400]	0.596
Age	67.7 ± 14.3	64.5 ± 15.5	72.1 ± 11.1	<0.001	1.033 [1.014–1.054]	<0.001
Inpatients	172 (95%)	98 (94.2%)	74 (96.1%)	0.735	1.355 [0.427–4.298]	0.606
Hospital origin	160 (88.4%)	87 (83.7%)	73 (94.8%)	0.033	2.808 [1.026–7.685]	0.044
Intensive care unit	117 (64.6%)	63 (60.6%)	54 (70.1%)	0.210	1.342 [0.824–2.187]	0.238
<b>Underlying disease¶</b>						
Charlson index	4.1 ± 2.2	3.9 ± 2.2	4.4 ± 2.2	0.108	1.086 [0.981–1.202]	0.112
Solid tumor	48 (26.5%)	27 (26.0%)	21 (27.3%)	0.866	1.183 [1.109–1.261]	<0.001
Diabetes mellitus	42 (23.2%)	28 (26.9%)	14 (18.2%)	0.213	0.049 [0.000–7.177]	0.620
Cerebrovascular disease	33 (18.2%)	23 (22.1%)	10 (13.0%)	0.125	0.597 [0.307–1.161]	0.129
Kidney disease	25 (13.8%)	15 (14.4%)	10 (13.0%)	0.831	1.043 [0.631–1.722]	0.870
Chronic pulmonary diseases	12 (6.6%)	7 (6.7%)	5 (6.5%)	>0.999	6.176 [0.840–45.40]	0.074
Chronic liver diseases	7 (3.9%)	2 (1.9%)	5 (6.5%)	0.137	2.182 [0.878–5.420]	0.093
Dementia	9 (5.0%)	5 (4.8%)	4 (5.2%)	>0.999	1.069 [0.432–2.649]	0.885
Other#	5 (2.8%)	2 (1.9%)	3 (3.9%)	0.652	1.019 [0.372–2.787]	0.971
<b>Severity variables</b>						
SOFA score	5.9 ± 3.5	4.8 ± 3.2	7.4 ± 3.5	<0.001	1.183 [1.109–1.261]	<0.001
<b>Lab data</b>						
WBC	11.5 ± 7.8	12.2 ± 6.9	10.6 ± 8.8	0.185	0.967 [0.934–1.000]	0.052
Hb	10.4 ± 7.8	10.9 ± 10.4	9.6 ± 1.6	0.262	0.910 [0.788–1.051]	0.201
Platelet	169.7 ± 132.1	206.9 ± 138.3	119.5 ± 104.8	<0.001	0.994 [0.991–0.997]	<0.001
<b>Origin of infection¶</b>						
Pulmonary tract	69 (38.1%)	36 (34.6%)	33 (42.9%)	0.281	1.259 [0.801–1.978]	0.317
Wound	7 (3.9%)	5 (4.8%)	2 (2.6%)	0.700	0.653 [0.160–2.662]	0.553
Urinary tract	4 (2.2%)	4 (3.8%)	0 (0%)	0.138	0.048 [0.000–18.92]	0.319
<b>Causative pathogen</b>						
Polymicrobial infection	44 (24.3%)	30 (28.8%)	14 (18.2%)	0.116	0.636 [0.356–1.135]	0.125
ICLII††	153 (84.5%)	83 (79.8%)	70 (90.9%)	0.060	2.083 [0.958–4.533]	0.064
ST191 (1-3-3-2-2-94-3)	73 (40.3%)	29 (27.9%)	44 (57.1%)	<0.001	2.630 [1.671–4.139]	<0.001
ST784 (1-3-3-2-2-107-3)	31 (17.1%)	17 (16.3%)	14 (18.2%)	0.842	0.983 [0.551–1.755]	0.954
ST451 (1-3-3-2-2-142-3)	29 (16.0%)	24 (23.1%)	5 (6.5%)	0.004	0.293 [0.118–0.727]	0.008
<b>Virulence factors</b>						
Bacterial lipocalin, Blc	145 (80.1%)	79 (76.0%)	66 (85.7%)	0.132	1.540 [0.813–2.916]	0.185
Pro-apoptotic porin, PorB	146 (80.7%)	79 (76.0%)	67 (87.0%)	0.086	1.839 [0.946–3.575]	0.073
Small protein A, SmpA	177 (97.8%)	101 (97.1%)	76 (98.7%)	0.638	1.773 [0.247–12.75]	0.569
Pili, Csu	73 (40.3%)	45 (43.3%)	28 (36.4%)	0.363	0.781 [0.491–1.243]	0.297
PNAG, Pga	173 (95.6%)	96 (92.3%)	77 (100%)	0.022	22.02 [0.307–1579]	0.156
Polysaccharide exporter, EpsA	9 (5.0%)	7 (6.7%)	2 (2.6%)	0.305	0.425 [0.104–1.730]	0.232
Capsule protein, MviM	7 (3.9%)	4 (3.8%)	3 (3.9%)	>0.999	1.047 [0.330–3.322]	0.938
Lipopolysaccharide, VipA	16 (8.8%)	9 (8.7%)	7 (9.1%)	>0.999	1.021 [0.469–2.220]	0.959
Lipopolysaccharide, Wzx	48 (26.5%)	26 (25%)	22 (28.6%)	0.613	1.144 [0.698–1.875]	0.595
Glyconokinase, GntK	179 (98.9%)	102 (98.1%)	77 (100%)	0.508	20.54 [0.004–93770]	0.482
Quorum Sensing, LuxR	159 (87.8%)	91 (87.5%)	68 (88.3%)	>0.999	1.000 [0.499–2.004]	0.999
Motility and secretion, PiliA	18 (9.9%)	12 (11.5%)	6 (7.8%)	0.460	0.723 [0.314–1.664]	0.446
Siderophore, BasD	179 (98.9%)	102 (98.1%)	77 (100%)	0.508	20.54 [0.004–93770]	0.482
<b>Antimicrobial resistance</b>						
Penicillins NS	157 (86.7%)	82 (78.8%)	75 (97.4%)	<0.001	7.352 [1.804–29.96]	0.005
3-, 4- gen. cephalosporins NS	162 (89.5%)	85 (81.7%)	77 (100%)	<0.001	25.33 [1.463–438.6]	0.026

(Continued)

TABLE 1 | Continued

Variables	Total* n = 181	Survival n = 104	30-day death <sup>†</sup> n = 77	P <sup>‡</sup>	Univariate model HR [95%CI] <sup>§</sup>	P
Carbapenems NS	160 (88.4%)	84 (80.8%)	76 (98.7%)	<b>&lt;0.001</b>	13.15 [1.828–94.63]	0.010
Aminoglycosides NS	141 (77.9%)	76 (73.1%)	65 (84.4%)	0.073	1.515 [0.818–2.805]	0.187
Fluoroquinolones NS	162 (89.5%)	85 (81.7%)	77 (100%)	<b>&lt;0.001</b>	25.33 [1.463–438.6]	0.026
Tetracyclines NS	13 (7.2%)	11 (10.6%)	2 (2.6%)	0.045	0.284 [0.070–1.156]	0.079
Drug susceptible	18 (9.9%)	18 (17.3%)	0 (0%)	<b>&lt;0.001</b>	0.040 [0.002–0.743]	0.031
MDR/XDR	162 (89.5%)	85 (81.7%)	77 (100%)	<b>&lt;0.001</b>	25.33 [1.463–438.6]	0.026
<b>Treatment</b>						
Adequate empirical therapy	49 (27.1%)	30 (28.8%)	19 (24.7%)	0.613	0.744 [0.443–1.249]	0.263
Definitive therapy within 72 h	49 (27.1%)	39 (37.5%)	10 (13.0%)	<b>&lt;0.001</b>	0.246 [0.124–0.488]	<0.001

\*The percentage was calculated from the total number of AB-BSI.

<sup>†</sup>All-cause mortality within 30 days from the initial blood culture.

<sup>‡</sup>P value is either from Pearson's  $\chi^2$  test for categorical data or from the t-test for continuous data. Bonferroni corrected significance level from 32 hypotheses was considered to be  $P < 0.0016$ , and the significant P values are indicated in bold.

<sup>§</sup>Cox proportional hazards regression model was applied to calculate the hazard ratio (HR) and the 95% confidence interval (CI).

<sup>¶</sup>Underlying disease and primary site of infection could be multiple by patient.

<sup>#</sup>Ulcer (n = 2), connective tissue disease (n = 2), congestive cardiac insufficiency (n = 2), and leukemia (n = 2) are included.

<sup>††</sup>Multilocus sequence typing profiles are indicated with the combination of alleles (gltA-gyrB-gdhB-recA-cpn60-gpi-rpoD).

SD, standard deviation; ICLII, the international clonal lineage II.

were detected in *A. baumannii* blood isolates (Table 1). The acinetobactin-associated *basD* (98.9%, 179/181), the glyco kinase *gntK* (98.9%, n = 179), the adhesion-associated *ompA* (97.8%, n = 177), and the biofilm formation-associated *pga* genes (95.6%, n = 173) were harbored by most of the *A. baumannii* blood isolates, while the capsule protein *mviM* (3.9%, n = 7), the polysaccharide exporter *epsA* (5.0%, n = 9), lipopolysaccharide *vipA* (8.8%, n = 16), and the type IV pili *pilA* (9.9%, n = 18) genes were occasionally identified. Among the virulence factors tested, the *pga* gene was significantly associated with 30-day death and the adhesion-associated *porB* had a tendency of 30-day mortality-associated.

A different frequency of each gene by ST was occasionally identified (Table 2). The *psaB* gene, formerly the *pab2* gene (24), was identified in all but one (96.6%, 28/29) ST451 isolates.

### Antimicrobial Treatment

The majority (95.0%, 172/181) of patients with *A. baumannii* BSIs received an empirical antimicrobial therapy with anti-*Acinetobacter* drugs and 28.5% (49/172) of those were adequate (Table 3). The other nine patients received either not-for-*Acinetobacter* drugs (n = 7) or none due to refusal of treatment (n = 2). Among the 132 patients who received an inadequate empirical therapy, 37.1% (n = 49) of patients were treated with a definitive antimicrobial therapy within 72 h and 20.4% (10/49) of those patients met death within 30 days, much less than that of patients who received a delayed definitive therapy (57.9%, 48/83).

### Risk Factors for 30-Day Mortality

Risk and protective factors associated with the 30-day mortality in patients with *A. baumannii* BSIs were searched for among the variables of  $P < 0.1$  through a Cox-regression univariable analysis. Most of the variables were omitted by

stepwise selection procedure, and each three of risk factors and protective factors associated with the 30-day mortality in patients with *A. baumannii* BSIs were identified through a Cox-regression multivariable analysis (Table 4): the age of patients of hazard ratio (95% CI), 1.033 (1.010–1.056); the SOFA score of 1.133 (1.041–1.233); and the BSI-causative *A. baumannii* ST191 of 1.918 (1.073–3.430). Three protective factors were also identified: the platelet count of 0.996 (0.993–0.999), the BSI-causative *A. baumannii* ST451 of 0.228 (0.078–0.672), and the definitive therapy within 72 h of 0.255 (0.125–0.519).

## DISCUSSION

During the surveillance study period, the overall incidence of *A. baumannii* was the third-highest (1.1/10,000 patient-days) BSI-causative Gram-negative bacteria followed by *Escherichia coli* and *Klebsiella pneumoniae*. Besides, the incidence was strikingly higher in ICUs (6.6/10,000 patient-days) than in general wards (0.4/10,000 patient-days) (25). The 30-day mortality rate of patients with *A. baumannii* BSIs is pretty varied by study depending on the subjected patients, and we observed 42.5% of 30-day mortality for entire *A. baumannii* BSI cases.

Among the variables studied, the old age and the high SOFA score were identified as the patient-associated risk factors. Those were reasonable hazardous factors since both factors pronounced the severity of illness directly or indirectly. A patient-associated protective factor, platelet counts in peripheral blood reflecting the patients' condition also made sense. As well, a treatment-associated protective factor, a proper definitive therapy within 72 h was comprehensible.

Curiously among the causative-pathogen-associated variables, the *A. baumannii* ST191 was a risk factor, while the ST451, another ICLII member, was a protective factor. *A. baumannii*

**TABLE 2** | Characteristics of the *A. baumannii* ICLII blood isolates.

Characteristics	ICLII n = 153	P*	ST191 n = 73	P*	ST451 n = 29	P*
Death within 30 days	70 (45.8%)	0.002	44 (60.3%)	0.000	5 (17.2%)	0.013
SOFA score (mean ± SD)	5.9 ± 3.6	0.005	6.2 ± 3.9	0.031	6.4 ± 3.6	0.161
Pulmonary tract of primary site of BSI	61 (39.9%)	0.000	24 (32.9%)	1.000	17 (58.6%)	0.002
<b>Drug resistance</b>						
MDR/XDR	151 (98.7%)	0.821	72 (98.6%)	0.003	29 (100%)	0.545
Penicillins NS	146 (95.4%)	0.000	70 (95.9%)	0.000	27 (93.1%)	0.004
3-, 4- gen. cephalosporins NS	151 (98.7%)	0.000	72 (98.6%)	0.000	29 (100%)	0.000
Carbapenems NS	149 (97.4%)	0.000	70 (95.9%)	0.000	29 (100%)	0.000
Aminoglycosides NS	136 (88.9%)	0.000	58 (79.5%)	0.006	29 (100%)	0.000
Fluoroquinolones NS	151 (98.7%)	0.000	72 (98.6%)	0.000	29 (100%)	0.000
Tetracyclines NS	11 (7.2%)	0.354	3 (4.1%)	0.553	6 (20.7%)	0.003
Polymyxin	0		0		0	
<b>VIRULENCE FACTORS</b>						
<b>Drug resistance</b>						
AbGRI1 (Tn6022)	112 (73.2%)	0.000	69 (94.5%)	0.000	5 (17.2%)	0.000
AbaR (Tn6019)	38 (24.8%)	0.164	2 (2.7%)	0.000	24 (82.8%)	0.000
OXA-23	148 (96.7%)	0.000	70 (95.9%)	0.000	28 (96.6%)	0.001
AdeC	32 (20.9%)	0.857	10 (13.7%)	0.110	6 (20.7%)	1.000
<b>Adhesion/Membrane Integrity</b>						
Blc	123 (80.4%)	0.002	56 (76.7%)	0.521	22 (75.9%)	1.000
PorB	124 (81%)	0.000	64 (87.7%)	0.001	23 (79.3%)	0.505
SmpA	149 (97.4%)	0.000	72 (98.6%)	0.002	27 (93.1%)	0.747
<b>Biofilm formation</b>						
Csu	133 (86.9%)	0.000	62 (84.9%)	0.000	29 (100%)	0.000
Pga	153 (100%)	0.000	73 (100%)	0.000	29 (100%)	0.002
<b>Capsule protein</b>						
EpsA	7 (4.6%)	0.742	1 (1.4%)	0.107	3 (10.3%)	0.160
MviM	6 (3.9%)	0.440	0 (0%)	0.099	2 (6.9%)	0.228
<b>Lipopolysaccharide</b>						
PsaB	36 (23.5%)	0.000	2 (2.7%)	0.000	28 (96.6%)	0.000
VipA	12 (7.8%)	0.448	7 (9.6%)	0.808	0 (0%)	0.084
Wzx	42 (27.5%)	0.129	17 (23.3%)	0.869	10 (34.5%)	0.172
<b>Carbohydrate metabolism</b>						
GntK	153 (100%)	0.000	73 (100%)	0.000	29 (100%)	0.003
<b>Quorum sensing system</b>						
LuxR	138 (90.2%)	0.000	65 (89%)	0.175	27 (93.1%)	0.183
<b>Motility and secretion</b>						
PilA	14 (9.2%)	0.808	2 (2.7%)	0.015	5 (17.2%)	0.164
<b>Siderophore</b>						
BasD	153 (100%)	0.000	73 (100%)	0.000	29 (100%)	0.010
<b>Treatment</b>						
Adequate empirical therapy	31 (20.3%)	0.000	16 (21.9%)	0.003	3 (10.3%)	0.002
Definitive therapy within 72 h	46 (30.1%)	0.013	20 (27.4%)	0.624	11 (37.9%)	0.109

\*P value is either from Pearson's  $\chi^2$  test for categorical data or from the t-test for continuous data. The Bonferroni corrected significance level from 33 hypotheses was considered to be  $P < 0.0015$ , and the significant P values are indicated with asterisks.

ICLII, is a well-known multidrug resistant clone (26, 27). The treatment options for patients infected by the clone are often limited to the very last resorts, such as carbapenems, tigecycline, minocycline, and polymyxins. For the infections cause by

multidrug-resistant *A. baumannii*, the use of combination antimicrobial therapy is recommended (28) and two thirds (66.3%, 120/181) of the patients were treated empirically by antimicrobial combinations. Carbapenem resistance is already



common in ICLII, and the remaining choices are always risky because tigecycline (29) and minocycline (30) have a bacteriostatic activity, which requires a combinational treatment; colistin has a severe dose-dependent neuro- and nephrotoxicity (31); and the colistin resistance is easily developed by prior use of the drug (32). The importance of an adequate antimicrobial therapy (33), including the proper use of colistin (34), has been addressed to diminish the 30-day mortality rate caused by *A.*

*baumannii* infections. The present results confirmed the notion through a significant protective effect of the definitive therapy including colistin. Among ICLII members, ST191 was the most and both ST784 and ST451 are recently emerging ICLII clones (27, 32). In this study, ST784 and ST451 were the second and third most ICLII clones and the clones were evenly recovered from the six hospitals (Figure 2).

In this study, all but two (98.7%) ICLII blood isolates, one ST191 and the other ST357, exhibited MDR/XDR. Since drug resistance is one of the noted hazardous factors obstructing an adequate antimicrobial therapy (7, 8), similar mortality rates were presumed for BSIs caused by any STs belonging to the ICLII. However, a marked difference in 30-day mortality was observed in the three dominant STs: 60.3% in ST191 BSIs, 45.2% in ST784 BSIs, and 17.2% in ST451 BSIs. Curiously, the least proportion of patients with ST451 BSIs (10.3%) were treated by an adequate empirical therapy (Table 2), indicating that the drug resistance and the relevant adequacy of treatment were not related to the 30-day mortality rate at least to BSIs caused by ST191 and ST451. ST451 was more associated with a primary pulmonary tract infection (58.6%) than ST191 (32.9%), however the primary site of infection

**TABLE 3 |** Antimicrobial regimens for the patients with *A. baumannii* BSIs.

Regimen	No. of cases	Proper	Improper
Ampicillin	1 (0.6%)	1	0
Piperacillin/tazobactam	26 (14.4%)	5	21
comb.w/ciprofloxacin	12 (6.6%)	1	11
comb.w/tigecycline	2 (1.1%)	1	1
comb.w/colistin	2 (1.1%)	2	0
3-, 4- gen. cephalosporins	20 (11.0%)	5	15
comb.w/ciprofloxacin	8 (4.4%)	0	8
comb.w/aminoglycosides	2 (1.1%)	0	2
Carbapenems	55 (30.4%)	5	50
comb.w/aminoglycosides	2 (1.1%)	0	2
comb.w/co-trimoxazole	2 (1.1%)	1	1
comb.w/ciprofloxacin	9 (5.0%)	1	8
comb.w/colistin	10 (5.5%)	10	0
Tigecycline	6 (3.3%)	5	1
comb.w/co-trimoxazole	1 (0.6%)	1	0
comb.w/fluoroquinolones	2 (1.1%)	2	0
Colistin	4 (2.2%)	4	0
Ciprofloxacin	6 (3.3%)	4	2
Aminoglycosides	1 (0.6%)	0	1
Co-trimoxazole	1 (0.6%)	1	0
Not treated*	9 (5.0%)	0	9
	181	49	132

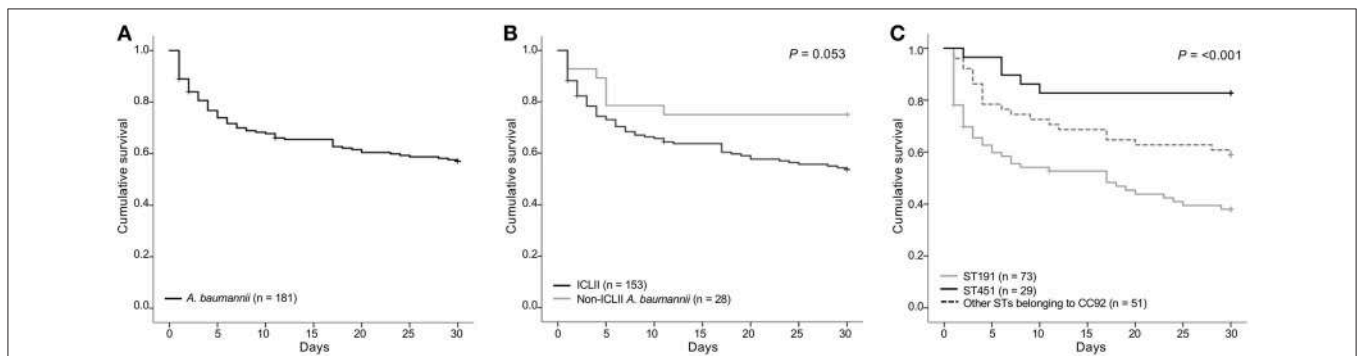
\*Patients received drugs not-for-*Acinetobacter* (n = 7) or none due to refusal of treatment (n = 2).

**TABLE 4 |** Risk factors associated with the 30-day mortality in patients with *A. baumannii* BSI.

Variables	VIF*	HR [95%CI]†	P
Age	1.058	1.033 [1.010–1.056]	0.005
SOFA score	1.335	1.133 [1.041–1.233]	0.004
Platelet	1.290	0.996 [0.993–0.999]	0.016
ST191	1.245	1.918 [1.073–3.430]	0.028
ST451	1.255	0.228 [0.078–0.672]	0.007
Definitive therapy within 72 h	1.094	0.255 [0.125–0.519]	<0.001

\*VIF, variance inflation factor. The collinearity was diagnosed for the variables including the multivariate analysis.

† A Cox-regression multivariate analysis was conducted by the backward method using the Wald model.



**FIGURE 2 |** Mortality of BSI patients by causative pathogen. (A) Mortality of patients with BSIs by *A. baumannii*, (B) comparison of mortality of BSI patients by ICLII and by non-ICLII *A. baumannii*, (C) comparison of mortality of BSI patients by ST191, ST451, and other STs belonging to CC91. The Kaplan-Meier plot illustrated survival in patients with AB-BSI infected with the indicated bacterial clone. Differences between groups were compared by the Log-Rank test of the Mantel-Cox model, and the P values are presented. ICLII, international clonal lineage II; ST, sequence type.

was insignificantly associated with a 30-day death (**Table 1**). Similarly, ST451 harbored the Tn6019-associated AbaR (82.8%) more frequently than the Tn6022-associated AbGRI1 (17.2%) differently from ST191 (2.7 vs. 94.5%), however no difference was expected since both may harbor the *bla*<sub>OXA-23</sub> gene (12). The lipooligosaccharide biosynthesis-associated *psaB* gene was harbored strikingly more by ST451 than by ST191 (96.6 vs. 2.7%). The *psaB* gene is a part of the oligosaccharide gene clusters generating an ordinary side-branch sugar Gal, differing from the *A. baumannii* ST191 often carries the gene cluster producing FucNAc sugar composing the oligosaccharide (24). Since the lipooligosaccharides of pathogenic bacteria have long been recognized as a major virulence factor (35), the difference in oligosaccharides between the two clones is possibly associated with the 30-day mortality rate and the detailed impact should be further studied.

This study should be considered with the following caveats in mind. First, the enrolled cases had a lack of external validation due to a distinct epidemiology of *A. baumannii* clinical isolates in South Korea in terms of high carbapenem resistance, mostly conferred by OXA-23. Second, analyses of bacterial lipooligosaccharides differed by the clones are remained for further study. However, to the best of our knowledge, this is the first notification of the counter clinical prognoses of the patients with a BSI by dominant ICLII clones, drawing an attention to a further follow-up for the clonal exchange and expansion of ICLII clones in clinical settings.

This delicate prognosis assessment combined with an evaluation of the molecular epidemiology for the causative *A. baumannii* blood isolates confirmed (i) the predominance of ICLII in clinical settings, (ii) the hazardousness of antimicrobial resistance and the importance of an adequate antimicrobial therapy, and finally, (iii) we highlighted

the differing 30-day mortality rates in patients with BSIs between causative multidrug-resistant *A. baumannii* clones ST191 and ST451 belonging ICLII probably due to the differing lipooligosaccharides.

## DATA AVAILABILITY

The raw data supporting the conclusions of this manuscript will be made available by the authors, without undue reservation, to any qualified researcher.

## ETHICS STATEMENT

The research, which has no involvement of human subject but the clinical isolates, does meet the exempt category without approval from Ethics Committee on Human Research of the Health Ministry in South Korea and the study design has not been reviewed by the committee.

## AUTHOR CONTRIBUTIONS

SJ conceived the study. E-JY and SJ designed the study. E-JY, HSL, and SJ analyzed the data. E-JY and SJ wrote the manuscript. DK, HL, JongS, YU, KS, YK, YP, JeongS, and SJ collected the clinical data and bacterial isolates.

## FUNDING

This study was supported by the Research Programme funded by the Korea Centers for Disease Control and Prevention (2017E4400101#). We would like to thank to Yena Oh for technical support for microbiological experiments.

## REFERENCES

- Dijkshoorn L, Nemec A, Seifert H. An increasing threat in hospitals: multidrug-resistant *Acinetobacter baumannii*. *Nat Rev Microbiol.* (2007) 5:939–51. doi: 10.1038/nrmicro1789
- Seifert H, Strate A, Pulverer G. Nosocomial bacteremia due to *Acinetobacter baumannii*. Clinical features, epidemiology, and predictors of mortality. *Medicine (Baltimore).* (1995) 74:340–9. doi: 10.1097/00005792-199511000-00004
- Gu Z, Han Y, Meng T, Zhao S, Zhao X, Gao C, et al. Risk factors and clinical outcomes for patients with *Acinetobacter baumannii* bacteremia. *Medicine.* (2016) 95:e2943. doi: 10.1097/MD.0000000000002943
- Vallenet D, Nordmann P, Barbe V, Poirol L, Mangenot S, Bataille E, et al. Comparative analysis of *Acinetobacters*: three genomes for three lifestyles. *PLoS ONE.* (2008) 3:e1805. doi: 10.1371/journal.pone.0001805
- Falagas ME, Karveli EA, Siempos II, Vardakas KZ. *Acinetobacter* infections: a growing threat for critically ill patients. *Epidemiol Infect.* (2008) 136:1009–19. doi: 10.1017/S0950268807009478
- Chopra T, Marchaim D, Johnson PC, Awali RA, Doshi H, Chhalana I, et al. Risk factors and outcomes for patients with bloodstream infection due to *Acinetobacter baumannii*-calcoacetatus complex. *Antimicrob Agents Chemother.* (2014) 58:4630–5. doi: 10.1128/AAC.02441-14
- Chopra T, Marchaim D, Awali RA, Krishna A, Johnson P, Tansek R, et al. Epidemiology of bloodstream infections caused by *Acinetobacter baumannii* and impact of drug resistance to both carbapenems and ampicillin-sulbactam on clinical outcomes. *Antimicrob Agents Chemother.* (2013) 57:6270–5. doi: 10.1128/AAC.01520-13
- Freire MP, de Oliveira Garcia D, Garcia CP, Campagnari Bueno MF, Camargo CH, Kono Magri ASG, et al. Bloodstream infection caused by extensively drug-resistant *Acinetobacter baumannii* in cancer patients: high mortality associated with delayed treatment rather than with the degree of neutropenia. *Clin Microbiol Infect.* (2016) 22:352–8. doi: 10.1016/j.cmi.2015.12.010
- Talbot GH, Bradley J, Edwards JE Jr, Gilbert D, Scheld M, Bartlett JG, et al. Bad bugs need drugs: an update on the development pipeline from the antimicrobial availability task force of the infectious diseases society of America. *Clin Infect Dis.* (2006) 42:657–68. doi: 10.1086/499819
- Heo ST, Oh WS, Kim SJ, Bae IG, Ko KS, Lee JC. Clinical impacts of a single clone (sequence type 92) of multidrug-resistant *Acinetobacter baumannii* in intensive care units. *Microb Drug Resist.* (2011) 17:559–62. doi: 10.1089/mdr.2011.0087
- Selasi GN, Nicholas A, Jeon H, Lee YC, Yoo JR, Heo ST, et al. Genetic basis of antimicrobial resistance and clonal dynamics of carbapenem-resistant *Acinetobacter baumannii* sequence type 191 in a Korean hospital. *Infect Genet Evol.* (2015) 36:1–7. doi: 10.1016/j.meegid.2015.09.001
- Yoon EJ, Kim JO, Yang JW, Kim HS, Lee KJ, Jeong SH, et al. The *bla*<sub>OXA-23</sub>-associated transposons in the genome of *Acinetobacter* spp. represent an epidemiological situation of the species encountering carbapenems. *J Antimicrob Chemother.* (2017) 72:2708–14. doi: 10.1093/jac/dkx205

13. Lee H, Yoon EJ, Kim D, Jeong SH, Shin JH, Shin JH, et al. Establishment of the South Korean national antimicrobial resistance surveillance system, Kor-GLASS, in 2016. *Euro Surveill.* (2018) 23:1700734. doi: 10.2807/1560-7917.ES.2018.23.42.1700734
14. Charlson ME, Pompei P, Ales KL, Mackenzie CR. A new method of classifying prognostic comorbidity in longitudinal studies: development and validation. *J Chronic Dis.* (1987) 40:373–83. doi: 10.1016/0021-9681(87)90171-8
15. Vincent JL, Moreno R, Takala J, Willatts S, de Mendonca A, Bruining H, et al. The SOFA (Sepsis-related Organ Failure Assessment) score to describe organ dysfunction/failure. On behalf of the Working Group on Sepsis-Related Problems of the European Society of Intensive Care Medicine. *Intensive Care Med.* (1996) 22:707–10. doi: 10.1007/BF01709751
16. CDC Bloodstream Infection Event (2018). *Central Line-Associated Bloodstream Infection and Non-Central Line Associated Bloodstream Infection*. Device-associated Module.
17. Magjorakos AP, Srinivasan A, Carey RB, Carmeli Y, Falagas ME, Giske CG, et al. Multidrug-resistant, extensively drug-resistant and pandrug-resistant bacteria: an international expert proposal for interim standard definitions for acquired resistance. *Clin Microbiol Infect.* (2012) 18:268–81. doi: 10.1111/j.1469-0691.2011.03570.x
18. Bartual SG, Seifert H, Hippler C, Luzon MA, Wisplinghoff H, Rodriguez-Valera F. Development of a multilocus sequence typing scheme for characterization of clinical isolates of *Acinetobacter baumannii*. *J Clin Microbiol.* (2005) 43:4382–90. doi: 10.1128/JCM.43.9.4382-4390.2005
19. CLSI. *Performance Standards for Antimicrobial Susceptibility Testing*. 25th Informational Supplement. Wayne, PA: Clinical and Laboratory Standards Institute (2016).
20. Poirel L, Walsh TR, Cuvillier V, Nordmann P. Multiplex PCR for detection of acquired carbapenemase genes. *Diagn Microbiol Infect Dis.* (2011) 70:119–23. doi: 10.1016/j.diagmicrobio.2010.12.002
21. EUCAST. *Recommendations for MIC Determination of Colistin (Polymyxin E) As Recommended by the Joint CLSI-EUCAST Polymyxin Breakpoints Working Group*. (2016). Available online at: [http://www.eucast.org/fileadmin/src/media/PDFs/EUCAST\\_files/General\\_documents/Recommendations\\_for\\_MIC\\_determination\\_of\\_colistin\\_March\\_2016.pdf](http://www.eucast.org/fileadmin/src/media/PDFs/EUCAST_files/General_documents/Recommendations_for_MIC_determination_of_colistin_March_2016.pdf)
22. Wong D, Nielsen TB, Bonomo RA, Pantapalangkoor P, Luna B, Spellberg B. Clinical and pathophysiological overview of *acinetobacter* infections: a century of challenges. *Clin Microbiol Rev.* (2017) 30:409–47. doi: 10.1128/CMR.00058-16
23. Lannan FM, O'conor DK, Broderick JC, Tate JF, Scoggin JT, et al. Evaluation of virulence gene expression patterns in *Acinetobacter baumannii* using quantitative real-time polymerase chain reaction array. *Mil Med.* (2016) 181:1108–13. doi: 10.7205/MILMED-D-15-00437
24. Hu D, Liu B, Dijkshoorn L, Wang L, Reeves PR. Diversity in the major polysaccharide antigen of *Acinetobacter baumannii* assessed by DNA sequencing, and development of a molecular serotyping scheme. *PLoS ONE.* (2013) 8:e70329. doi: 10.1371/journal.pone.0070329
25. Lee H, Yoon EJ, Kim D, Jeong SH, Won EJ, Shin JH, et al. Antimicrobial resistance of major clinical pathogens in South Korea, May 2016 to April 2017: first one-year report from Kor-GLASS. *Euro Surveill.* (2018) 23:1800047. doi: 10.2807/1560-7917.ES.2018.23.42.1800047
26. Diancourt L, Passet V, Nemeč A, Dijkshoorn L, Brisse S. The population structure of *Acinetobacter baumannii*: expanding multiresistant clones from an ancestral susceptible genetic pool. *PLoS ONE.* (2010) 5:e10034. doi: 10.1371/journal.pone.0010034
27. Zarrilli R, Pournaras S, Giannouli M, Tsakris A. Global evolution of multidrug-resistant *Acinetobacter baumannii* clonal lineages. *Int J Antimicrob Agents.* (2013) 41:11–9. doi: 10.1016/j.ijantimicag.2012.09.008
28. Durante-Mangoni E, Utili R, Zarrilli R. Combination therapy in severe *Acinetobacter baumannii* infections: an update on the evidence to date. *Future Microbiol.* (2014) 9:773–89. doi: 10.2217/fmb.14.34
29. Karageorgopoulos DE, Kelesidis T, Kelesidis I, Falagas ME. Tigecycline for the treatment of multidrug-resistant (including carbapenem-resistant) *Acinetobacter* infections: a review of the scientific evidence. *J Antimicrob Chemother.* (2008) 62:45–55. doi: 10.1093/jac/dkn165
30. Ritchie DJ, Garavaglia-Wilson A. A review of intravenous minocycline for treatment of multidrug-resistant *Acinetobacter* infections. *Clin Infect Dis.* (2014) 59(Suppl. 6):S374–380. doi: 10.1093/cid/ciu613
31. Falagas ME, Kasiakou SK. Toxicity of polymyxins: a systematic review of the evidence from old and recent studies. *Crit Care.* (2006) 10:R27. doi: 10.1186/cc3995
32. Qureshi ZA, Hittle LE, O'hara JA, Rivera JI, Syed A, Shields RK, et al. Colistin-resistant *Acinetobacter baumannii*: beyond carbapenem resistance. *Clin Infect Dis.* (2015) 60:1295–303. doi: 10.1093/cid/civ048
33. Lemos EV, de La Hoz FP, Einarson TR, Mcghan WF, Quevedo E, Castaneda C, et al. Carbapenem resistance and mortality in patients with *Acinetobacter baumannii* infection: systematic review and meta-analysis. *Clin Microbiol Infect.* (2014) 20:416–23. doi: 10.1111/1469-0691.12363
34. Liu CP, Shih SC, Wang NY, Wu AY, Sun FJ, Chow SF, et al. Risk factors of mortality in patients with carbapenem-resistant *Acinetobacter baumannii* bacteremia. *J Microbiol Immunol Infect.* (2016) 49:934–40. doi: 10.1016/j.jmii.2014.10.006
35. Moran AP, Prendergast MM, Appelmelk BJ. Molecular mimicry of host structures by bacterial lipopolysaccharides and its contribution to disease. *FEMS Immunol Med Microbiol.* (1996) 16:105–15. doi: 10.1111/j.1574-695X.1996.tb00127.x

**Conflict of Interest Statement:** The authors declare that the research was conducted in the absence of any commercial or financial relationships that could be construed as a potential conflict of interest.

Copyright © 2019 Yoon, Kim, Lee, Lee, Shin, Uh, Shin, Kim, Park, Shin and Jeong. This is an open-access article distributed under the terms of the Creative Commons Attribution License (CC BY). The use, distribution or reproduction in other forums is permitted, provided the original author(s) and the copyright owner(s) are credited and that the original publication in this journal is cited, in accordance with accepted academic practice. No use, distribution or reproduction is permitted which does not comply with these terms.



# Synergistic Microbicidal Effect of Auranofin and Antibiotics Against Planktonic and Biofilm-Encased *S. aureus* and *E. faecalis*

Pengfei She, Linying Zhou, Shijia Li, Yiqing Liu, Lanlan Xu, Lihua Chen, Zhen Luo and Yong Wu\*

Department of Clinical Laboratory, The Third Xiangya Hospital of Central South University, Changsha, China

## OPEN ACCESS

### Edited by:

Ilana L. B. C. Camargo,  
University of São Paulo, Brazil

### Reviewed by:

Mariusz Stanislaw Grinholc,  
Intercollegiate Faculty  
of Biotechnology of University  
of Gdańsk and Medical University  
of Gdańsk, Poland  
Airat R. Kayumov,  
Kazan Federal University, Russia

### \*Correspondence:

Yong Wu  
wuyong\_zn@csu.edu.cn

### Specialty section:

This article was submitted to  
Antimicrobials, Resistance  
and Chemotherapy,  
a section of the journal  
Frontiers in Microbiology

**Received:** 12 July 2019

**Accepted:** 11 October 2019

**Published:** 24 October 2019

### Citation:

She P, Zhou L, Li S, Liu Y, Xu L,  
Chen L, Luo Z and Wu Y (2019)  
Synergistic Microbicidal Effect  
of Auranofin and Antibiotics Against  
Planktonic and Biofilm-Encased  
*S. aureus* and *E. faecalis*.  
*Front. Microbiol.* 10:2453.  
doi: 10.3389/fmicb.2019.02453

Methicillin-resistant/susceptible *Staphylococcus aureus* (MRSA/MSSA) and *Enterococcus faecalis* strains are often found in community- and hospital-acquired infections. The single use of conventional antibiotics hardly completely kills the bacterial cells of interest, especially in the form of biofilms. Thus, drug repurposing and antimicrobial combination are promising ways to solve this problem. Antimicrobial susceptibility assays against cocci in a suspension and in a biofilm mode of growth were performed with broth microdilution methods. Checkerboard assays and the cutaneous mouse infection model were used to examine the activity of auranofin and conventional antibiotics alone and in combination. In the present study, auranofin possesses potent antimicrobial activities against both planktonic cells and biofilms with minimum inhibitory concentrations ranging 0.125–0.5 mg/L. Auranofin in combination with linezolid or fosfomycin showed synergistic antimicrobial activities against *S. aureus* MSSA and MRSA both *in vitro* and *in vivo*. Similarly, auranofin also behaved synergistic effect with chloramphenicol against *E. faecalis*. Additionally, auranofin improved the antibiofilm efficacy of chloramphenicol and linezolid, even on the biofilms grown on a catheter surface. Though, *S. epidermidis* showed significant susceptibility to AF treatment, no synergistic antimicrobial effects were observed with antibiotics we tested. In all, the use of a combination of auranofin with linezolid, fosfomycin, and chloramphenicol can provide a synergistic microbicidal effect *in vitro* and *in vivo*, which rapidly enhances antimicrobial activity and may help prevent or delay the emergence of resistance.

**Keywords:** auranofin, biofilm, combination therapy, subcutaneous abscess model, *Staphylococcus aureus*, *Enterococcus faecalis*

## INTRODUCTION

*Staphylococcus aureus* and *Enterococcus faecalis* have been known to be responsible for most of healthcare- and nosocomial-associated infections. *S. aureus* could cause polymicrobial infections with many pathogens, such as enterococcus (Reyes et al., 2010; Hayakawa et al., 2013), *Pseudomonas aeruginosa* (Radlinski et al., 2017; Alves et al., 2018),



*Peptostreptococcus anaerobius* (Yamagishi et al., 2017), *Streptococcus pyogenes* (Gilmer et al., 2013), and even *Candida* species (Nash et al., 2015; Todd et al., 2019), which are hard to be eradicated and finally led to a striking mortality rate. According to the report by the SENTRY antimicrobial surveillance program (North America), the main pathogens isolated from skin as well as soft tissue infections (SSTIs) now include 45.9% *S. aureus* and 8.2% *Enterococcus* sp. (Rennie et al., 2003). SSTIs abscesses, for instance, create fluid, pus-filled pockets infiltrated by bacteria as well as inflammatory cells, and are frequently extremely resilient to conventional antibiotic therapy (Ki and Rotstein, 2008). In addition, abscesses are the utmost common sign for high-dose, recurrent and long-term intravenous broad-spectrum antibiotic administration (Ramakrishnan et al., 2015).

Biofilms are a widespread problem in healthcare facilities and hospitals. Indeed, the United States National Institutes of Health reported that 80% of chronic infections are related to biofilms (Monroe, 2007). The attachment of *S. aureus*, *S. epidermidis*, and *E. faecalis* onto tissues or the surface of medical apparatuses contributes to the pathogenesis of infection (Archer, 1998). The bacterial cells living in a biofilm are responsible for a number of chronic infections and become resilient to antibiotics as well as host-defense mechanisms (Gomes et al., 2009).

Recently, many studies have been conducted to address the repurposing of FDA-approved drugs as new antimicrobial agents. Auranofin (AF) is a gold-containing compound and prescribed for the treatment of rheumatoid arthritis (Glennas et al., 1997). The study of AF for its antimicrobial effects and inhibition of biofilm formation is an attractive possible treatment approach (Natsis and Cohen, 2018). Researchers found its antimicrobial efficacy against cocci (including *Staphylococcus* sp. and *E. faecalis*) and *Mycobacterium tuberculosis*. AF employs its effects via a distinctive process comprising the prevention of TrxR, and it maintains action against current antibiotic-resistant strains (Cassetta et al., 2014; Harbut et al., 2015; Fuchs et al., 2016). In addition, AF compared with most of the conservative medications available might be an appropriate feature in the fight against a dynamic as well as quickly altering microbial community such as biofilms.

AF shows good antimicrobial effects on cocci and AF in combination with topical antibiotics (mupirocin, retapamulin, and fusidic acid) exhibits additive antimicrobial activity against MRSA (Thangamani et al., 2016). However, to the best of our knowledge, there is no research reporting combinatory therapy with conventional systemic administration associated antibiotics in a subcutaneous abscess infections model. In the present study, we showed the antimicrobial and antibiofilm activities of AF alone or in combination with conventional antibiotics against *S. aureus* and *E. faecalis* strains *in vitro* and *in vivo*.

## MATERIALS AND METHODS

### Bacterial Strains

AF and antibiotics [fosfomycin (FOF); ciprofloxacin (CIP); tetracycline (TET); linezolid (LZD); chloramphenicol

(CHL); levofloxacin (LVX); teicoplanin (TEC); clindamycin hydrochloride (CLI) hydro; gentamicin (GEN); vancomycin (VAN)] were purchased from the MedChemExpress company (Monmouth Junction, NJ, United States). *E. faecalis* ATCC 29212, *S. aureus* ATCC25923 and ATCC29213 were kindly provided by Juncai Luo (Tiandiren Biotech, Changsha, China).

**TABLE 1** | Antimicrobial susceptibility testing of AF and VAN toward bacterial strains (mg/L).

Organism	AF		VAN	
	MIC	MBC	MIC	MBC
<b><i>S. aureus</i></b>				
ATCC 29213	0.25	4	1	8
ATCC 25923 <sup>b</sup>	0.25	2	0.5	1
ATCC 43300 <sup>a</sup>	0.25	2	1	1
Newman	0.125	4	2	4
LZB1 <sup>b</sup>	0.5	4	1	2
RJ-2	0.125	2	1	8
SA1401	0.25	1	1	1
SA1414 <sup>b</sup>	0.5	2	1	2
SA1418 <sup>a</sup>	0.5	2	1	2
SA1419	0.25	2	1	4
SA1422 <sup>a</sup>	0.25	1	1	2
SA1423	0.5	1	2	2
SA1427 <sup>a</sup>	0.25	2	1	1
SA1435 <sup>a,b</sup>	0.25	1	2	4
<b><i>E. faecalis</i></b>				
ATCC 29212 <sup>b</sup>	0.25	>32	2	>32
EF1401	0.25	>32	1	>32
EF1402	0.25	>32	1	>32
EF1403	0.5	32	1	>32
EF1405 <sup>b</sup>	0.5	>32	2	>32
EF1407 <sup>b</sup>	0.5	>32	2	>32
EF1410	0.5	>32	2	>32
EF1411 <sup>b</sup>	0.25	>32	1	>32
EF1412	0.5	>32	1	>32
EFF01	0.5	>32	1	>32
EFF09 <sup>b</sup>	0.5	>32	1	>32
EFF11	0.5	>32	1	>32
<b><i>S. epidermidis</i></b>				
RP62A <sup>b</sup>	0.125	2	2	8
ATCC 12228	0.125	4	1	4
SE1801	0.125	1	2	2
SE1802	0.125	1	2	2
SE1803	0.125	0.5	2	2
SE1804	0.125	0.5	1	1
SE1805	0.125	1	2	4
SE1806	0.125	2	1	1
SE1807	0.125	1	2	2
SE1808	0.125	1	2	2
SE1809 <sup>b</sup>	0.125	0.5	2	4
SE1810 <sup>b</sup>	0.125	1	2	4

<sup>a</sup>Methicillin resistant *Staphylococcus aureus* (MRSA). <sup>b</sup>Biofilm formation positive strains determined by CV staining method.



*S. epidermidis* RP62A and ATCC 12228 were given by Di Qu (Shanghai Medical College of Fudan University), *S. aureus* ATCC43300 (MRSA), Newman, and RJ-2 were given by Min Li (Renji Hospital, Shanghai Jiao Tong University School of Medicine). Other clinical strains were isolated from the wound secretion or sputum of inpatients at the Third Xiangya Hospital of Central South University. *Staphylococcus* spp. were grown in tryptic soy broth (TSB) broth medium (Solarbio, Shanghai,

China), and *E. faecalis* was grown in brain heart infusion (BHI) broth medium (Solarbio, Shanghai, China) at 37°C.

## Susceptibility Testing of Planktonic Bacteria

Bacterial strains were cultured in cationic corrected Mueller–Hinton (MH) broth (BD/Difco, United States). Susceptibility

**TABLE 2** | The combinational antibacterial activities of AF and different antibiotics.

Organism	Agent	MIC (μg/mL)		MIC <sub>Incombination</sub> /MIC <sub>Singly</sub>	FICI	Outcome		
		Singly	In combination					
<i>S. aureus</i> LZB1	FOF	0.5	0.125	0.25	0.375	Synergy		
	AF	0.5	0.0625	0.125				
	LZD	4	1	0.25				
	AF	0.5	0.0625	0.125	1	No interaction		
	CLI Hydro	0.125	0.0625	0.5				
	AF	0.5	0.25	0.5				
	GEN	4	2	0.5				
	AF	0.5	0.25	0.5				
	LVX	0.25	0.25	1			2	
	AF	0.5	0.5	1			1	
VAN	1	0.5	0.5					
AF	0.5	0.25	0.5	0.75			No interaction	
<i>E. faecalis</i> ATCC29212	LZD	2	0.5					0.25
	AF	1	0.5		0.5			
	CHL	4	0.5		0.125	0.375		
	AF	1	0.25		0.25			
	TET	16	4		0.25	0.5		
	AF	1	0.25		0.25			
	TEC	0.25	0.031		0.125	0.625		
	AF	1	0.5		0.5			
	CIP	0.5	0.125		0.25	0.75		
	AF	1	0.5	0.5				
LVX	1	0.25	0.25	0.5				
AF	1	0.25	0.25	0.531	No interaction			
CLI Hydro	32	1	0.031					
AF	1	0.5	0.5					
VAN	2	0.5	0.25			0.75		
AF	1	0.5	0.5					
<i>S. epidermidis</i> RP62A	FOF	1	1			1	2	No interaction
	AF	0.25	0.25			1	1	No interaction
	CIP	0.25	0.125			0.5		
	AF	0.25	0.125			0.5		
	TEC	2	2			1		
	AF	0.25	0.25	1				
	LZD	2	1	0.5	0.625			
	AF	0.25	0.0313	0.125				
	CHL	16	8	0.5	0.516			
	AF	0.25	0.004	0.015				
	LVX	0.25	0.25	1	2			
AF	0.25	0.25	1					
TET	0.25	0.25	1	2	No interaction			
AF	0.25	0.25	1					

tests were performed by twofold regular broth microdilution of the test compounds, as recommended by the Clinical and Laboratory Standards Institute (CLSI) (Harbut et al., 2015). After 16–18 h of incubation at 37°C, the nominal concentration necessary to stop the development of test bacteria was defined as the MIC, and the minimum bactericide concentration (MBC) was identified depending on the lowermost concentration of antimicrobials that killed 99.9% of the test bacteria by spreading the bacterial culture out onto a suitable agar plate (CLSI, 2005).

## Susceptibility Testing of Biofilms

For *S. aureus* biofilm determination. The culture was grown overnight in TSB and successively diluted 1:50 in TSB to achieve an absorbance at 630 nm of ~0.1. Two hundred microliter aliquots of the diluted culture were added to every well of a microtiter plate and incubated at 37°C for 24 h. For *E. faecalis* biofilm determination, bacterial suspensions (18 µL) from overnight cultures were mixed with 162 µL of BHI in the wells, and biofilms were allowed to form on the plates for 24 h (Lee et al., 2012).

Following the incubation, the contents were removed and rinsed, 50 µL of medium and 50 µL of the specified drug were added to every well, and incubated at 37°C for 24 h. Then, the contents were removed and the remaining biofilms were determined by crystal violet (CV), XTT staining or live cell count as follows:

- (1) CV staining (Holmberg et al., 2012). Each well was stained with 100 µL of 0.25% CV for 15 min. The wells were rinsed and dissolved with ethanol for 20 min. The absorbance was determined at 570 nm.
- (2) XTT staining. One hundred microliters of a solution comprising 200 mg/L of XTT and 20 mg/L of phenazine methosulfate (MACKLIN, Shanghai, China) was mixed in each well, and the incubations were performed and incubated for 3 h at 37°C in the dark. The absorbance was determined at 490 nm (Nesse et al., 2015). The definition of

MBEC30/MBEC50/MBEC70 were defined as the minimal concentration of the particular antimicrobial's ability to inhibit 30/50/70% growth of the biofilms, respectively, compared to the control group (Gomes et al., 2009).

- (3) Biofilm viable count (Mataraci and Dosler, 2012). One hundred microliters of 1 × PBS was aliquoted into each well, and the contents were scrapped and mixed thoroughly with pipette tips. A sample volume of 100 µL was plated onto blood agar and successively diluted with a saline solution before plating onto additional agar plates.

## Checkerboard Assays for Planktonic Bacteria

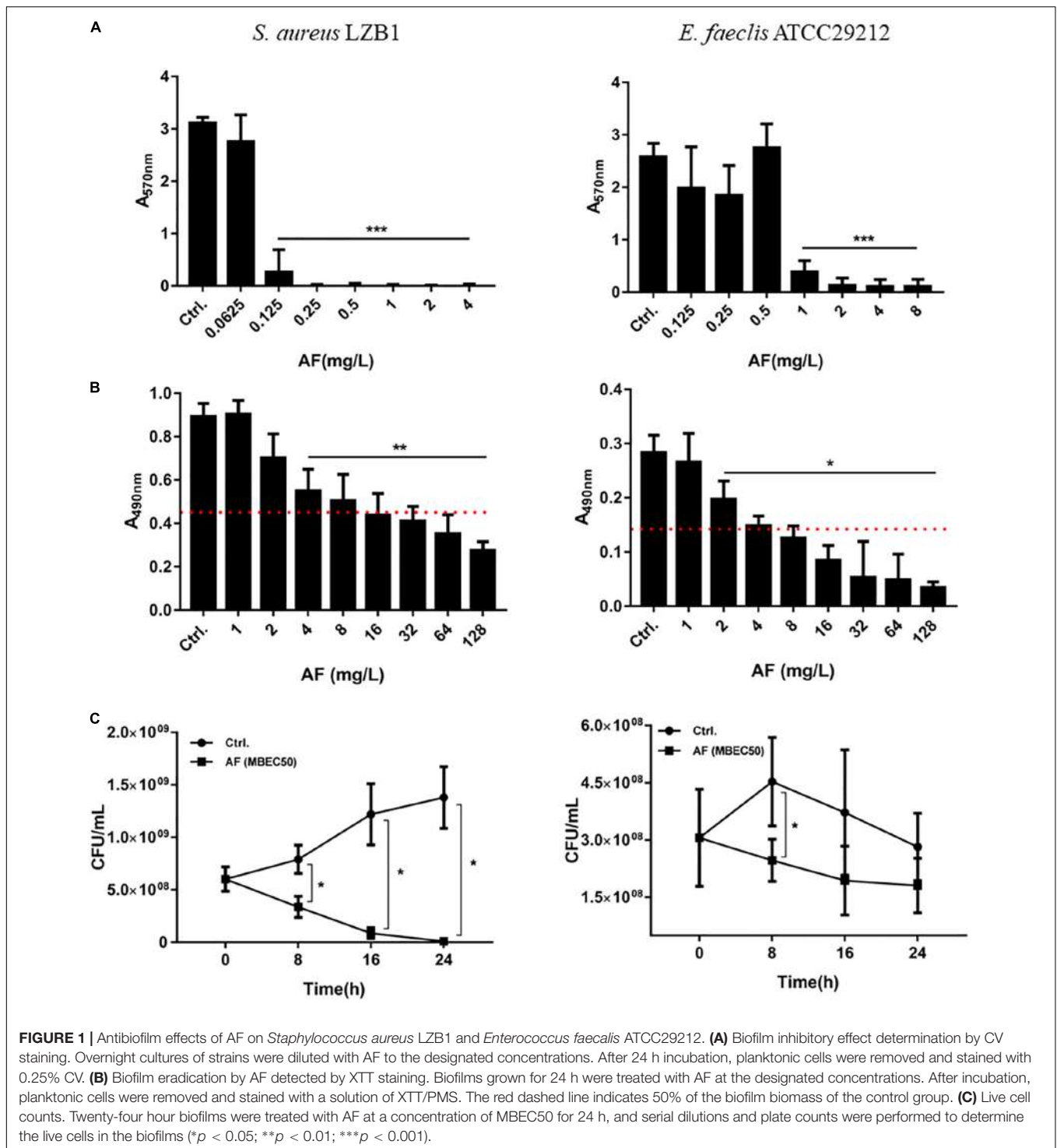
The impacts of individual antibiotics and in combination with AF were evaluated using the broth microdilution checkerboard technique (Odds, 2003; Flamm et al., 2019). Each microtiter well-comprising the designated combination of antibiotics was inoculated with an overnight culture diluted to provide an absolute concentration of  $\sim 5 \times 10^5$  CFU/ml. Following incubation, the optimal fractional inhibitory concentration index (FICI) was measured as the minimal inhibitory concentration of the combination divided by that of the single antibiotic (Odds, 2003):  $FICI \leq 0.5$  designates synergy;  $0.5 < FICI \leq 4.0$  designates no interaction;  $FICI > 4.0$  designates antagonism.

## Checkerboard Assays for Preformed Biofilms

The preparation of overnight biofilms was the same as explained earlier in this study. The biofilms were rinsed, twofold sequential dilutions of antibiotics and AF in a 96-well microtiter plate were prepared, and 100 µL of these mixtures were added to the biofilms. Concentration ranges, as recognized with susceptibility testing, were utilized for the antibiotics as well as the AF. Following an incubation for 24 h at 37°C, the medium containing antimicrobials was removed, and 100 µL of XTT with PSM was

**TABLE 3 |** The antibacterial activity and combined effects of AF and selected antibiotics alone or in combination against MRSA and other clinical isolates.

Organism	Agent	MIC (mg/L)		MIC <sub>Incombination</sub> /MIC <sub>singly</sub>	FICI	Outcome
		Singly	In combination			
<b><i>S. aureus</i></b>						
ATCC43300 (MRSA)	LZD	2	0.25	0.125	0.375	Synergy
	AF	0.25	0.0313	0.25		
SA1435 (MRSA)	LZD	4	0.5	0.125	0.375	Synergy
	AF	0.5	0.125	0.25		
ATCC43300 (MRSA)	FOF	8	2	0.25	0.375	Synergy
	AF	0.25	0.0313	0.125		
SA1435 (MRSA)	FOF	32	8	0.25	0.5	No interaction
	AF	0.5	0.125	0.25		
<b><i>E. faecalis</i></b>						
EF1402	CHL	8	1	0.125	0.375	Synergy
	AF	0.25	0.0625	0.25		
EF1403	CHL	16	0.25	0.016	0.266	Synergy
	AF	0.5	0.125	0.25		



added as described above (Koppen et al., 2019). The MBEC50 values were quantified.

### Antibiofilm Effect of AF on Catheters

To study the efficacy of AF combined with antibiotics against biofilms on catheters, overnight cultures of the biofilm-forming strains were diluted 1:40 in TSB (*S. aureus*) or BHI (*E. faecalis*)

containing 5% rabbit plasma. Catheter (Jerry infusion set, Shandong, China) pieces (1 cm in size) were cut, divided into two halves, and added to the culture. Next, they were incubated at 37°C for 24 h. Afterward, the catheters were removed and washed. The biofilms on catheters were challenged with AF alone or in combination with antibiotics for 24 h. The catheters were scratched by an inoculation loop and sonicated for 15 min. Then,

**TABLE 4** | Activity of AF in combination with conventional antibiotic against preformed biofilms (mg/L).

Organism	Agent	Singly MBEC50	In combination MBEC50	Fold decrease of MBEC50 in combination
<i>S. aureus</i> LZB1	AF	16	8	2
	LZD	>128	16	>8
	AF	16	16	–
	FOF	>64	>64	–
<i>E. faecalis</i> ATCC 29212	AF	8	2	4
	CHL	64	8	8

the samples were vortexed carefully and plated on blood agar plates (Nair et al., 2016).

### Confocal Laser Scanning Microscopy (CLSM)

The above-treated bacteria were cultured on glass cover slides and incubated with 10  $\mu$ L of 1000-fold diluted SYTO9 fluorescent staining solution and propidium iodide at a ratio of 1:1 (vol/vol) for 15 min in the dark. After rinsing, the stained biofilm was examined with a CLSM (Zeiss LSM 800, Jena, Germany) (Nair et al., 2016).

### Cutaneous Mouse Infection Model

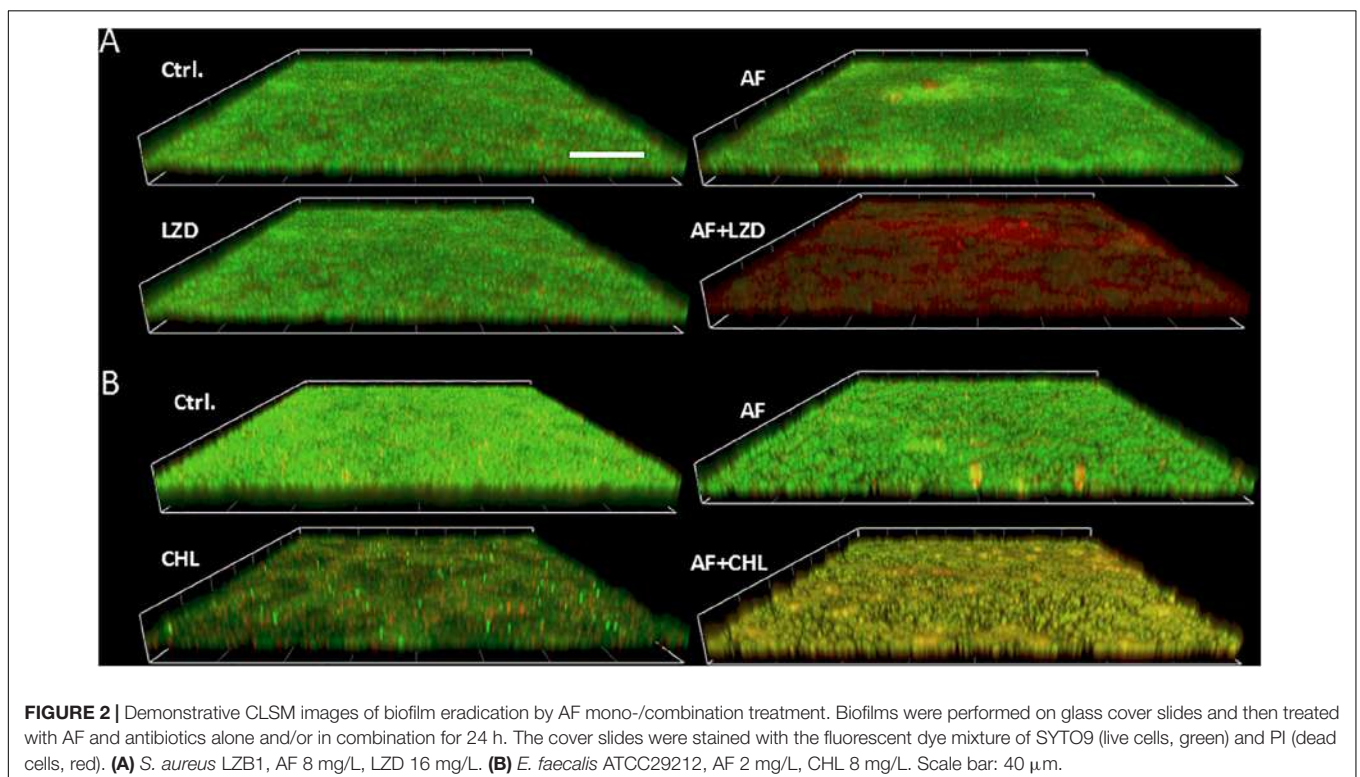
Seven-week-old female mice CD-1 were purchased from Hunan Slake Jingda Experimental Animal, Co., Ltd. (Hunan, China). They weighed approximately  $25 \pm 3$  g at the time of the experiments.

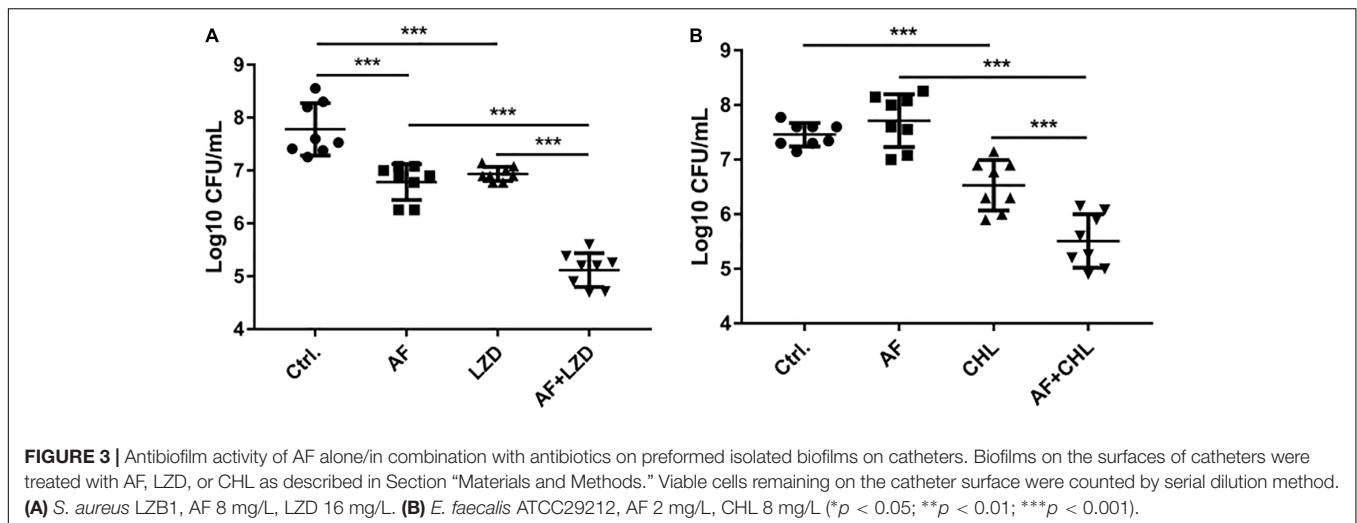
The high bacterial load abscess infection model was performed as defined earlier with slight adaptations (Pletzer et al., 2018).

Before the injection, bacterial cells were rinsed resuspended in  $1 \times$  PBS. An injection of bacterial suspension was given to the dorsum to achieve the concentrations to generate reproducible abscesses and bacterial counts: *S. aureus*,  $1 \times 10^8$  CFU/mice; and *E. faecalis*,  $1 \times 10^9$  CFU/mice. Antimicrobial administration was given directly into the subcutaneous space of the infected area at 1 h post-infection. The development of the infection was observed every day. Abscesses were determined on day 2 using a caliper. Skin abscesses were removed (comprising all accrued pus) and regimented in sterile PBS by an automatic tissue homogenizer (Servicebio KZ-II, Wuhan, China). Bacterial counts were quantified by serial dilution. For histopathological analyses, hematoxylin and eosin (H&E) staining was performed.

### Statistical Analysis

Statistical evaluations were performed using GraphPad Prism 7.0. Checkerboard methods were performed at least in biological duplicates, and other experiments were performed in triplicate.





## RESULTS

### Determination of the Susceptibility of Planktonic Cells

The MICs of AF and VAN against type strains and clinical isolates of *S. aureus* (MSSA/MRSA), *S. epidermidis*, and *E. faecalis* were 0.125–2 mg/L. The MBCs against *S. aureus* and *S. epidermidis* were 0.5–4 and 1–8 mg/L for AF and VAN, respectively. And the susceptibility of AF against MRSA and MSSA strains showed no difference. However, the MBCs of *E. faecalis* were > 32 mg/L for both AF and VAN (Table 1). In all, the strains we tested were more sensitive to the AF treatment than the VAN treatment.

### Synergistic Effect Between AF and Antibiotics Against Planktonic Cells

The synergistic effects of AF were investigated with some conventional systemic antibiotics (antibiotics with MIC values greater than 256 mg/L were excluded). The results of the combination screening assay are presented in Table 2. Synergistic interactions between AF and FOF (FICI = 0.375) or LZD (FICI = 0.375) were observed against *S. aureus* LZB1. For *E. faecalis* ATCC29212, synergistic interactions were observed between AF and CHL (FICI = 0.375). But no interactions between AF and antibiotics were observed against *S. epidermidis* RP62A (FICI > 0.5). Combinations with the lowest FICI values were selected for other representative strains. As shown in Table 3, the combination of AF and CHL still showed synergistic effect against the *E. faecalis* clinical isolates; combinations of AF + LZD/FOF still showed synergistic effects against *S. aureus* ATCC43300 (MRSA) and most of the clinical isolates, except for strain SA1435 which showed no interaction between AF and FOF with FICI of 0.5.

### Determination of the Susceptibility of Biofilms

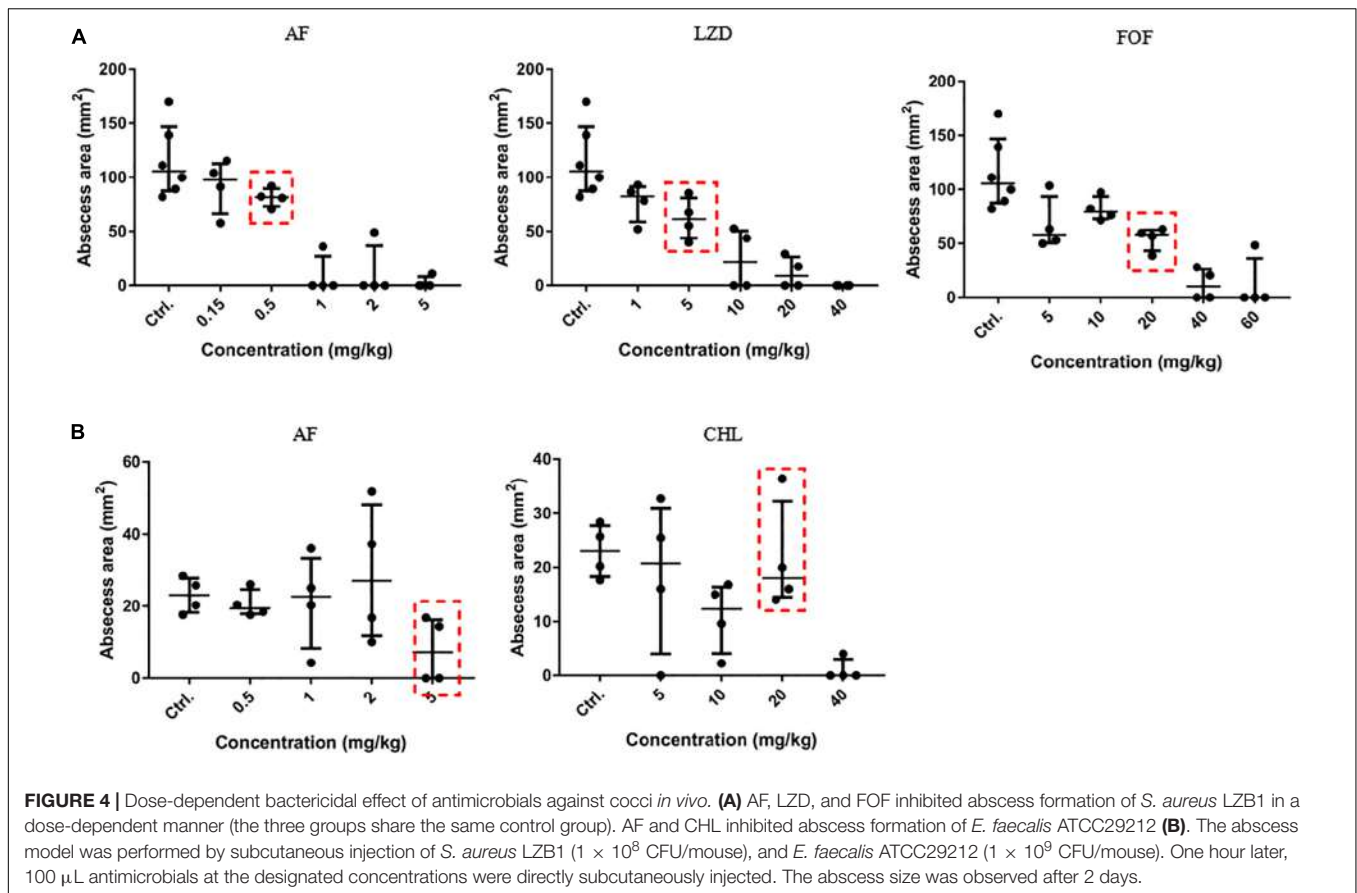
*Staphylococcus aureus* LZB1 and *E. faecalis* ATCC29212 were selected to test the antibiofilm activities of AF due to their strong

biofilm formation abilities (Kart et al., 2017). AF showed strong biofilm inhibitory effects against *S. aureus*, and *E. faecalis* at concentrations of 0.125 and 1 mg/L ( $p < 0.05$ ), respectively, in a dose-dependent manner (Figure 1A), which were very close to its MICs, indicating that the biofilm inhibitory effect of AF could be mainly due to its bacteriostatic or bactericidal activity by targeting thiol-redox homeostasis (Harbut et al., 2015). Because biofilm formation strongly increased the antimicrobial resistance to AF, the lowest concentrations needed to eradicate preformed biofilms were up to 4 and 2 mg/L for *S. aureus* and *E. faecalis*, respectively (Figure 1B). MBEC50 was selected to detect the time kill efficacy of AF against biofilms. AF showed significant biofilm killing activity against these strains in a time-dependent manner. Compared to the control group, AF reduced the live biofilm cells of *S. aureus* from  $(1.38 \pm 0.29) \times 10^9$  CFU/ml to  $(1.13 \pm 0.90) \times 10^7$  CFU/ml ( $p < 0.001$ ). Although statistical significance was only observed at 8 h after treatment ( $p < 0.05$ ), AF killed *E. faecalis* ATCC29212 biofilm cells throughout the 24 h period (Figure 1C). In addition, AF could also effectively eradicate clinical isolates with low MBEC50 values (Supplementary Table S2).

### Synergistic Effect Between AF and Antibiotics Against Biofilms

Antibiotics that showed a synergistic effect on planktonic cells were tested against preformed biofilms in combination with AF (Table 4). AF significantly promoted the antibiofilm efficacy of CHL against *E. faecalis* ATCC29212 (4- and 8-fold decrease of MBEC50 for CHL and AF, respectively). Meanwhile, AF also increased the antibiofilm activity of LZD against *S. aureus* LZB1 and exhibited a 2- and > 8-fold decrease of MBEC50 for AF and LZD, respectively, but showed no interaction with FOF (Supplementary Figure S1). Similar observations were made by visualization of AF and/or antibiotic-treated biofilms by CLSM, when AF used in combination with FOF (*S. aureus* LZB1, Figure 2A) or CHL (*E. faecalis* ATCC29212, Figure 2B), the live cells in the biofilms were significantly reduced, although some intact patches of biofilm could still be visualized.



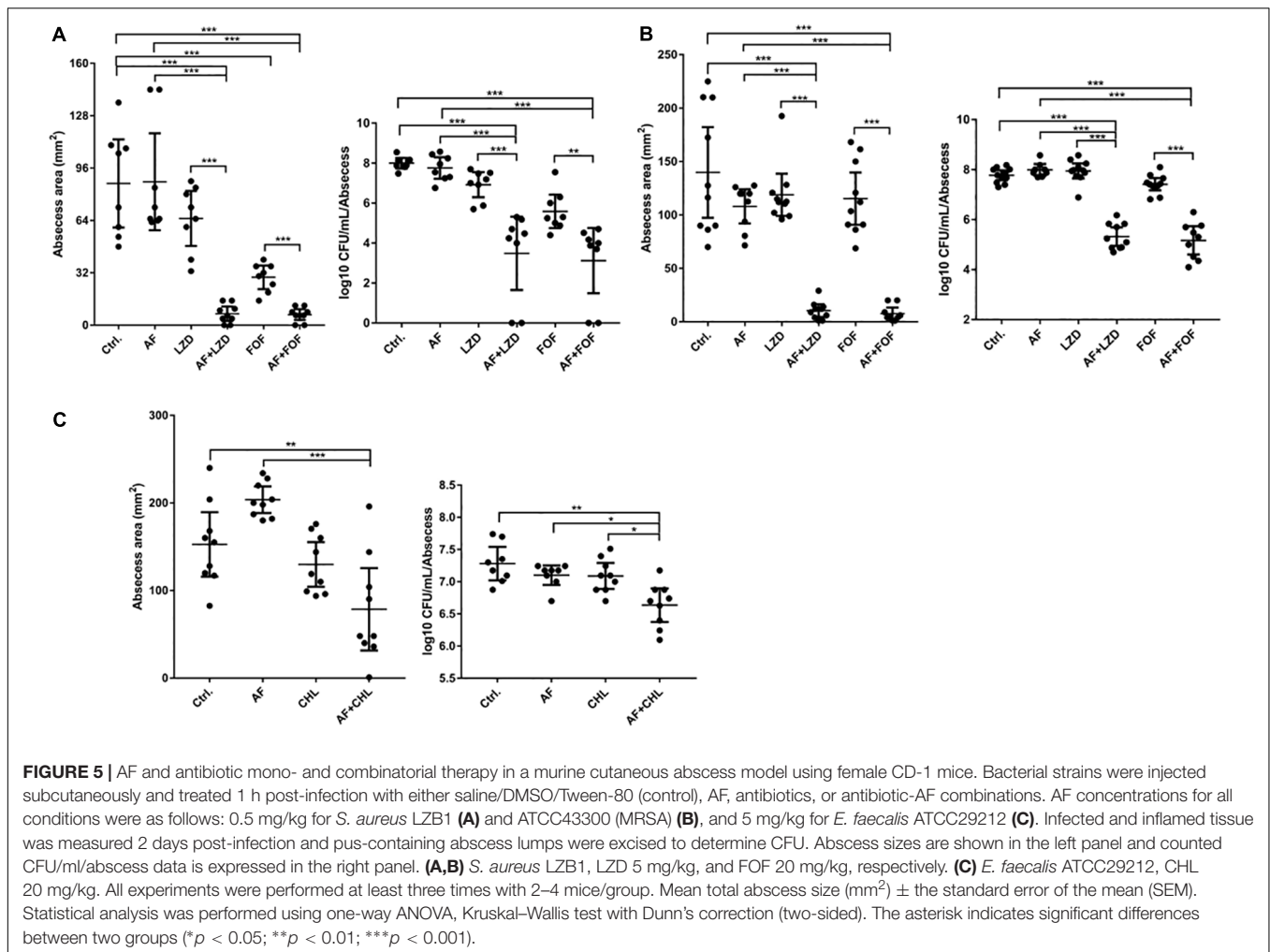


To simulate the *in vivo* conditions for biofilm formation in device-associated infections, we allowed strains to form biofilms on the surfaces of catheters. Treatment of biofilms with AF and in combination with antibiotics led to their synergistic eradication (Figure 3). A single dose of AF or antibiotics only showed moderate antibiofilm effects; however, combination treatment led to a 4.96- and 1.95-log reduction in CFUs for *S. aureus* (AF + LZD, Figure 3A) and *E. faecalis* (AF + CHL, Figure 3B), respectively, confirming that AF possesses antibiotic-promoting activity against preformed biofilms on catheters.

### Therapeutic Efficacy of AF Combined With Conventional Antibiotics *in vivo*

To optimize the treatment strategy, antimicrobials were chosen based on their moderate *in vivo* pharmacodynamics (Figure 4), and the concentrations used in the present study were equal or less than those empirically tested *in vivo* (CHL, 10 mg/kg; LZD, 60 mg/kg; and FOF, 100 mg/kg) (Shibl, 1982; Guo et al., 2013; Zykov et al., 2018) to determine an appropriate concentration that reduces abscess sizes just enough to observe the synergy between the AF and the antibiotics (Figure 4, red dashed line). A significant reduction in the mean bacterial load was observed for each combined treatment condition compared with the control (receiving DMSO or Tween-80) or single dose group.

Except for FOF, which reduced the abscess area of *S. aureus* LZB1 57.38 mm<sup>2</sup>, single use of AF (0.5 mg/kg), LZD (5 mg/kg) or FOF (20 mg/kg) showed no statistical significance in reducing abscess area or bacterial loads of *S. aureus* LZB1 (MSSA) (Figure 5A) and ATCC43300 (MRSA) (Figure 5B) infections; however, AF combined with LZD significantly decreased the abscess area and reduced the bacterial load for 4.51- (*S. aureus* LZB1,  $p < 0.01$ ) and 2.45-fold log<sub>10</sub> (*S. aureus* ATCC43300,  $p < 0.001$ ). Similarly, AF or CHL could not inhibit the abscess growth of *E. faecalis* ATCC29212 individually, but when combined, the area of abscess was reduced by 74.14 mm<sup>2</sup> ( $p < 0.01$ ). Single use of AF or CHL had no impact on bacterial load; however, combined therapy reduced the bacterial load by 0.61-fold log<sub>10</sub> ( $p < 0.01$ ) (Figure 5C). For *in vivo* observations, the abscesses caused by *S. aureus* were more obvious than those caused by *E. faecalis*. The ulcers were formed when infected with *S. aureus* LZB1 or ATCC43300 (Figures 6A,B); however, infection with a high load of *E. faecalis* ATCC29212 (Figure 6C) only caused subcutaneous lumps. In accordance with the *in vitro* observations, the representative pictures of abscesses and histological examinations showed that single use of AF, LZD, or FOF showed no/moderate activity against infections caused by *S. aureus* LZB1 (Figure 6A) or ATCC43300 (Figure 6B), and extensive inflammation with leukocyte infiltration emerged; however, drug combination (AF + LZD or AF + FOF) significantly reduced the size and inflammation of the abscesses,



which even eventually disappeared. The single use of AF or CHL had no influence on the abscesses caused by *E. faecalis* ATCC29212, the drug combination significantly diminished the abscess size and inflammation infiltration (Figure 6C). These important observations highlight that antimicrobial monotherapies are often ineffective when bacteria form high-density infections for *S. aureus* and *E. faecalis*. In addition, drug combinations could significantly improve the efficacy.

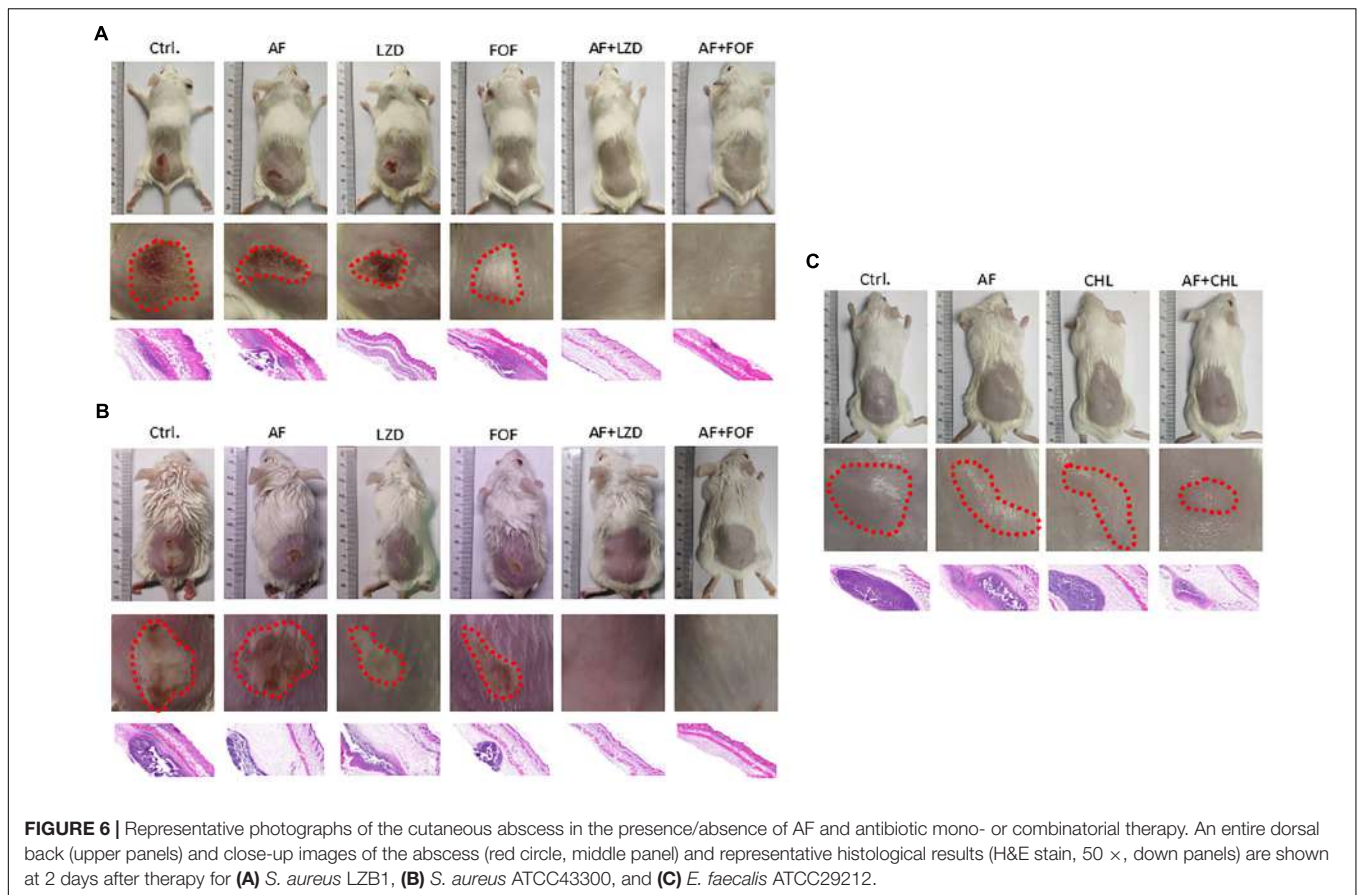
## DISCUSSION

In the present study, the antimicrobial activity of AF was assessed against a panel of type strains and clinical isolates of *Staphylococcus* spp. and *E. faecalis*. In accordance with the previous studies reported by Cassetta et al. (2014), Harbut et al. (2015), Fuchs et al. (2016), the MICs for *S. epidermidis*, *S. aureus* (including MSSA and MRSA), and *E. faecalis* were 0.125–0.5 mg/L, which showed more susceptibility than with VAN treatment, with MICs ranging from 0.5 to 2 mg/L.

Drug combination is a promising way to improve the efficacy of drugs and reduce side effects and cytotoxicity. In

our study, highly synergistic interactions between AF and CHL were observed against *E. faecalis*. CHL is a broad-spectrum antibiotic against many gram-positive/negative bacteria (Civljak et al., 2014). However, CHL is an old antimicrobial agent that is rarely used today mainly due to its most significant adverse effect of dose-related bone marrow suppression, according a meta-analysis by Eliakim-Raz et al. (2015), CHL is as safe a treatment alternatives as short antibiotic courses. In this way, drug combination could significantly diminish the dose required but achieve better antimicrobial efficacy, so that AF combined with CHL could be a better choice than CHL used alone in clinical therapy. Moreover, *E. faecalis* has shown many different metabolic responses from anaerobic to aerobic circumstances; these main metabolic cascades are related to the response to nutrients and may change the susceptibility of this bacterium to bactericidal drugs (Portela et al., 2014). However, even in the anaerobic condition, AF still showed a highly synergistic effect with CHL (Supplementary Table S1).

Highly synergistic interactions between AF and LZD/FOF were also observed against MSSA or MRSA strains of *S. aureus*. LZD has a wide spectrum of action against the mainstream of common gram-positive cocci. However, due to the development



of resistance to antibiotics as well as their unwanted side effects, combination therapy has evolved as an imperative novel treatment approach (Yang et al., 2018). FOF by itself has a bactericidal impact both *in vitro* as well as *in vivo*. Nevertheless, MRSA can easily develop tolerance, making utilization of FOF unattainable for medical situations (Roussos et al., 2009). FOF displays positive synergistic impacts on MRSA and its biofilms when utilized in combination with other antibiotics (Shi et al., 2014). Similarly, in our study, AF showed an excellent synergistic effect with FOF against MSSA and MRSA planktonic cells. In addition, different clinical isolates showed outcomes of different drug combinations, which indicates the importance of an *in vitro* synergistic test before clinical use.

Biofilms are easily formed on indwelling medical apparatus surfaces (Francolini and Donelli, 2010). During implantation of catheters, tissue damage might occur due to the buildup of platelets as well as fibrin at the suture site as well as on the devices. Microbial cells have enhanced capability to colonize these sites (Jamal et al., 2018). The formation of biofilms increases the antibiotic resistance and leads to persistent infections posing major healthcare challenges. AF showed modest biofilm inhibitory and eradicating effects against *Staphylococcus aureus* and *E. faecalis* both in type strains and clinical isolates with high values of MBEC70. Thus, our favorable outcomes of synergy among AF and antibiotics encouraged us to inspect the action of drug combinations against biofilms. AF

combined with CHL showed synergistic antibiofilm effects for *E. faecalis* on cover slides or infusion catheters (**Supplementary Figure S1**), AF significantly improved the antibiofilm effects of LZD against *S. aureus*. As numerous antibiotics have diverse antibacterial mechanisms and several bacteria have diverse resistance mechanisms, to entirely eliminate the whole biofilm-bacteria is a difficult challenge. Combination therapy comprising two or more antibiotics with diverse bactericidal mechanisms could synergistically eliminate biofilms (Simoes, 2011).

A high bacterial load-containing abscess model has rarely been studied for AF efficacy evaluation. In our *in vivo* subcutaneous abscess model study, single use of antimicrobials showed an extremely modest effect on abscess area or bacterial load. However, AF combined with LZD or FOF synergistically inhibited abscess and inflammation formation and reduced the bacterial load for both MSSA and MRSA strains. The safety of AF in *in vivo* animal studies and clinical use is well-documented. AF is widely used in clinical settings for long-term treatment at the daily dosage at 6 mg/day, and a average blood concentration of 3.5  $\mu\text{M}$  ( $\sim 2.38$   $\mu\text{g}/\text{ml}$ , which is far beyond the value of MICs) is reached in 12 weeks. Besides, the effectiveness and safety of AF at an dose of 12 mg/day is under Phase II clinical trial (Harbut et al., 2015). As reported by Aguinagalde et al. (2015), the dosage of AF used for murine model even reach to 10 mg/kg due to its safe toxicity profile and well-known pharmacokinetic/pharmacodynamic characteristics.

Similarly, the safety of antibiotics of FOF and LZD is well-studied and documented. As reported by Pachón-Ibáñez et al. (2011) and Guo et al. (2013), the dosages of FOF and LZD used are reached to 100 and 60 mg/kg in murine models, respectively. And the FOF and LZD used in our study are only 20 and 5 mg/kg, respectively. Therefore, the inflammation caused in our animal models is not caused by the antimicrobials we used. In all, the combination therapy of AF plus LZD/FOF might be an effective option for treating patients with *S. aureus*-related subcutaneous abscess infection. Similarly, AF combined with CHL also showed synergistic antibacterial effects on *E. faecalis* abscesses and partially reduced inflammation formation.

## CONCLUSION

The present study provides a valuable effect of antimicrobial combination therapy against cocci in subcutaneous abscess infections. This type of synergistic combination of two medications is likely preferred in clinical situations. The rationality of the outcomes should be validated by future clinical trials.

## DATA AVAILABILITY STATEMENT

All datasets generated for this study are included in the article/**Supplementary Material**.

## ETHICS STATEMENT

Ethical approval was obtained from the Animal Ethics Committee (certificate number 2017-S139), the Third Xiangya Hospital, Central South University, China.

## REFERENCES

- Aguinalde, L., Díez-Martínez, R., Yuste, J., Royo, I., Gil, C., Lasa, I., et al. (2015). Auranofin efficacy against MDR *Streptococcus pneumoniae* and *Staphylococcus aureus* infections. *J. Antimicrob. Chemother.* 70, 2608–2617. doi: 10.1093/jac/dkv163
- Alves, P. M., Al-Badi, E., Withycombe, C., Jones, P. M., Purdy, K. J., and Maddocks, S. E. (2018). Interaction between *Staphylococcus aureus* and *Pseudomonas aeruginosa* is beneficial for colonisation and pathogenicity in a mixed biofilm. *Pathog. Dis.* 76:fty003. doi: 10.1093/femspd/fty003
- Archer, G. L. (1998). *Staphylococcus aureus*: a well-armed pathogen. *Clin. Infect. Dis.* 26, 1179–1181. doi: 10.1086/520289
- Casetta, M. I., Marzo, T., Fallani, S., Novelli, A., and Messori, L. (2014). Drug repositioning: auranofin as a prospective antimicrobial agent for the treatment of severe staphylococcal infections. *Biometals* 27, 787–791. doi: 10.1007/s10534-014-9743-6
- Civljak, R., Giannella, M., Di Bella, S., and Petrosillo, N. (2014). Could chloramphenicol be used against escape pathogens? A review of in vitro data in the literature from the 21st century. *Expert Rev. Anti. Infect. Ther.* 12, 249–264. doi: 10.1586/14787210.2014.878647
- CLSI. (2005). *Performance Standards for Antimicrobial Susceptibility Testing, Fifteenth Informational Supplement. Approved Standard. M5100-S15*. Wayne, PA: Clinical and Laboratory Standards Institute.

## AUTHOR CONTRIBUTIONS

PS and YW designed and performed the experiments and wrote the manuscript. PS, YW, and LZ performed the experiments and data collection. SL, YL, LC, and ZL performed the experiments and revised the manuscript. All authors read and approved the final manuscript.

## FUNDING

This study was funded by the Hunan Provincial Natural Science Fund, China (Grant No. 2019JJ80029).

## ACKNOWLEDGMENTS

We are particularly grateful to the staff of the Department of Clinical Laboratory of the Third Xiangya Hospital of Central South University, Changsha, China.

## SUPPLEMENTARY MATERIAL

The Supplementary Material for this article can be found online at: <https://www.frontiersin.org/articles/10.3389/fmicb.2019.02453/full#supplementary-material>

**FIGURE S1** | Representative CLSM images of biofilm eradication by AF and FOF mono-/combination treatment. *S. aureus* LZB1 biofilms on the surfaces of cover slides were treated with AF (16 mg/L) and/or FOF (128 mg/L) as described in Section “Materials and Methods,” the stained with the SYTO9/PI fluorescent dye mixture.

**TABLE S1** | The combinational antibacterial activities of AF and different antibiotics against *E. faecalis* ATCC29212 in anaerobic conditions.

**TABLE S2** | Biofilm eradication activities of AF against other type and clinical strains (mg/L).

- Eliakim-Raz, N., Lador, A., Leibovici-Weissman, Y., Elbaz, M., Paul, M., and Leibovici, L. (2015). Efficacy and safety of chloramphenicol: joining the revival of old antibiotics? Systematic review and meta-analysis of randomized controlled trials. *J. Antimicrob. Chemother.* 70, 979–996. doi: 10.1093/jac/dku530
- Flamm, R. K., Rhomberg, P. R., Lindley, J. M., Sweeney, K., Ellis-Grosse, E. J., and Shortridge, D. (2019). Evaluation of the bactericidal activity of fosfomycin in combination with selected antimicrobial comparison agents tested against gram-negative bacterial strains by using time-kill curves. *Antimicrob. Agents Chemother.* 63:e02549-18. doi: 10.1128/AAC.02549-18
- Francolini, I., and Donelli, G. (2010). Prevention and control of biofilm-based medical-device-related infections. *FEMS Immunol. Med. Microbiol.* 59, 227–238. doi: 10.1111/j.1574-695X.2010.00665.x
- Fuchs, B. B., RajaMuthiah, R., Souza, A. C., Eatemadpour, S., Rossoni, R. D., Santos, D. A., et al. (2016). Inhibition of bacterial and fungal pathogens by the orphaned drug auranofin. *Future Med. Chem.* 8, 117–132. doi: 10.4155/fmc.15.182
- Gilmer, D. B., Schmitz, J. E., Euler, C. W., and Fischetti, V. A. (2013). Novel bacteriophage lysin with broad lytic activity protects against mixed infection by *Streptococcus pyogenes* and methicillin-resistant *Staphylococcus aureus*. *Antimicrob. Agents Chemother.* 57, 2743–2750. doi: 10.1128/AAC.02526-12
- Glennas, A., Kvien, T. K., Andrup, O., Clarke-Jenssen, O., Karstensen, B., and Brodin, U. (1997). Auranofin is safe and superior to placebo in elderly-onset



- rheumatoid arthritis. *Br. J. Rheumatol.* 36, 870–877. doi: 10.1093/rheumatology/36.8.870
- Gomes, F. I., Teixeira, P., Azeredo, J., and Oliveira, R. (2009). Effect of farnesol on planktonic and biofilm cells of staphylococcus epidermidis. *Curr. Microbiol.* 59, 118–122. doi: 10.1007/s00284-009-9408-9
- Guo, Y., Ramos, R. I., Cho, J. S., Donegan, N. P., Cheung, A. L., and Miller, L. S. (2013). In vivo bioluminescence imaging to evaluate systemic and topical antibiotics against community-acquired methicillin-resistant staphylococcus aureus-infected skin wounds in mice. *Antimicrob. Agents Chemother.* 57, 855–863. doi: 10.1128/AAC.01003-12
- Harbut, M. B., Vilcheze, C., Luo, X., Hensler, M. E., Guo, H., Yang, B., et al. (2015). Auranofin exerts broad-spectrum bactericidal activities by targeting thiol-redox homeostasis. *Proc. Natl. Acad. Sci. U.S.A.* 112, 4453–4458. doi: 10.1073/pnas.1504022112
- Hayakawa, K., Marchaim, D., Bathina, P., Martin, E. T., Pogue, J. M., Sunkara, B., et al. (2013). Independent risk factors for the co-colonization of vancomycin-resistant *Enterococcus faecalis* and methicillin-resistant *Staphylococcus aureus* in the region most endemic for vancomycin-resistant *Staphylococcus aureus* isolation. *Eur. J. Clin. Microbiol. Infect. Dis.* 32, 815–820. doi: 10.1007/s10096-013-1814-z
- Holmberg, A., Morgelin, M., and Rasmussen, M. (2012). Effectiveness of ciprofloxacin or linezolid in combination with rifampicin against enterococcus faecalis in biofilms. *J. Antimicrob. Chemother.* 67, 433–439. doi: 10.1093/jac/dkr477
- Jamal, M., Ahmad, W., Andleeb, S., Jalil, F., Imran, M., Nawaz, M. A., et al. (2018). Bacterial biofilm and associated infections. *J. Chin. Med. Assoc.* 81, 7–11. doi: 10.1016/j.jcma.2017.07.012
- Kart, D., Kustimur, A. S., Sagioglu, M., and Kalkanci, A. (2017). Evaluation of antimicrobial durability and anti-biofilm effects in urinary catheters against enterococcus faecalis clinical isolates and reference strains. *Balkan Med. J.* 34, 546–552. doi: 10.4274/balkanmedj.2016.1853
- Ki, V., and Rotstein, C. (2008). Bacterial skin and soft tissue infections in adults: a review of their epidemiology, pathogenesis, diagnosis, treatment and site of care. *Can. J. Infect. Dis. Med. Microbiol.* 19, 173–184. doi: 10.1155/2008/846453
- Koppen, B. C., Mulder, P. P. G., de Boer, L., Riool, M., Drijfhout, J. W., and Zaat, S. A. J. (2019). Synergistic microbicidal effect of cationic antimicrobial peptides and teicoplanin against planktonic and biofilm-encased staphylococcus aureus. *Int. J. Antimicrob. Agents* 53, 143–151. doi: 10.1016/j.ijantimicag.2018.10.002
- Lee, Y. S., Jang, K. A., and Cha, J. D. (2012). Synergistic antibacterial effect between silibinin and antibiotics in oral bacteria. *J. Biomed. Biotechnol.* 2012:618081. doi: 10.1155/2012/618081
- Mataraci, E., and Dosler, S. (2012). In vitro activities of antibiotics and antimicrobial cationic peptides alone and in combination against methicillin-resistant staphylococcus aureus biofilms. *Antimicrob. Agents Chemother.* 56, 6366–6371. doi: 10.1128/AAC.01180-12
- Monroe, D. (2007). Looking for chinks in the armor of bacterial biofilms. *PLoS Biol.* 5:e307. doi: 10.1371/journal.pbio.0050307
- Nair, S., Desai, S., Poonacha, N., Vipra, A., and Sharma, U. (2016). Antibiofilm activity and synergistic inhibition of staphylococcus aureus biofilms by bactericidal protein p128 in combination with antibiotics. *Antimicrob. Agents Chemother.* 60, 7280–7289. doi: 10.1128/AAC.01118-16
- Nash, E. E., Peters, B. M., Fidel, P. L., and Noverr, M. C. (2015). Morphology-independent virulence of *Candida* species during polymicrobial intra-abdominal infections with *Staphylococcus aureus*. *Infect. Immun.* 84, 90–98. doi: 10.1128/IAI.01059-15
- Natsis, N. E., and Cohen, P. R. (2018). Coagulase-negative staphylococcus skin and soft tissue infections. *Am. J. Clin. Dermatol.* 19, 671–677. doi: 10.1007/s40257-018-0362-9
- Nesse, L. L., Berg, K., and Vestby, L. K. (2015). Effects of norspermidine and spermidine on biofilm formation by potentially pathogenic *Escherichia coli* and *Salmonella enterica* wild-type strains. *Appl. Environ. Microbiol.* 81, 2226–2232. doi: 10.1128/AEM.03518-14
- Odds, F. C. (2003). Synergy, antagonism, and what the checkerboard puts between them. *J. Antimicrob. Chemother.* 52:1. doi: 10.1093/jac/dkg301
- Pachón-Ibáñez, M. E., Ribes, S., Domínguez, M. A., Fernández, R., Tubau, F., Ariza, J., et al. (2011). Efficacy of fosfomycin and its combination with linezolid, vancomycin and imipenem in an experimental peritonitis model caused by a *Staphylococcus aureus* strain with reduced susceptibility to vancomycin. *Eur. J. Clin. Microbiol. Infect. Dis.* 30, 89–95. doi: 10.1007/s10096-010-1058-0
- Pletzer, D., Mansour, S. C., and Hancock, R. E. W. (2018). Synergy between conventional antibiotics and anti-biofilm peptides in a murine, sub-cutaneous abscess model caused by recalcitrant escape pathogens. *PLoS Pathog.* 14:e1007084. doi: 10.1371/journal.ppat.1007084
- Portela, C. A., Smart, K. F., Tumanov, S., Cook, G. M., and Villas-Boas, S. G. (2014). Global metabolic response of enterococcus faecalis to oxygen. *J. Bacteriol.* 196, 2012–2022. doi: 10.1128/JB.01354-13
- Radlinski, L., Rowe, S. E., Kartchner, L. B., Maile, R., Cairns, B. A., Vitko, N. P., et al. (2017). *Pseudomonas aeruginosa* exoproducts determine antibiotic efficacy against *Staphylococcus aureus*. *PLoS Biol.* 15:e2003981. doi: 10.1371/journal.pbio.2003981
- Ramakrishnan, K., Salinas, R. C., and Agudelo Higueta, N. I. (2015). Skin and soft tissue infections. *Am. Fam. Physician* 92, 474–483.
- Rennie, R. P., Jones, R. N., Mutnick, A. H., and Group, S. P. S. (2003). Occurrence and antimicrobial susceptibility patterns of pathogens isolated from skin and soft tissue infections: report from the sentry antimicrobial surveillance program (united states and canada, 2000). *Diagn. Microbiol. Infect. Dis.* 45, 287–293. doi: 10.1016/s0732-8893(02)00543-6
- Reyes, K., Malik, R., Moore, C., Donabedian, S., Perri, M., Johnson, L., et al. (2010). Evaluation of risk factors for coinfection or cocolonization with vancomycin-resistant enterococcus and methicillin-resistant *Staphylococcus aureus*. *J. Clin. Microbiol.* 48, 628–630. doi: 10.1128/JCM.02381-08
- Roussos, N., Karageorgopoulos, D. E., Samonis, G., and Falagas, M. E. (2009). Clinical significance of the pharmacokinetic and pharmacodynamic characteristics of fosfomycin for the treatment of patients with systemic infections. *Int. J. Antimicrob. Agents* 34, 506–515. doi: 10.1016/j.ijantimicag.2009.08.013
- Shi, J., Mao, N. F., Wang, L., Zhang, H. B., Chen, Q., Liu, H., et al. (2014). Efficacy of combined vancomycin and fosfomycin against methicillin-resistant *Staphylococcus aureus* in biofilms in vivo. *PLoS One* 9:e113133. doi: 10.1371/journal.pone.0113133
- Shibl, A. M. (1982). Subcutaneous staphylococcal infections in mice: the influence of antibiotics on staphylococcal extracellular products. *Chemotherapy* 28, 46–53. doi: 10.1159/000238059
- Simoes, M. (2011). Antimicrobial strategies effective against infectious bacterial biofilms. *Curr. Med. Chem.* 18, 2129–2145. doi: 10.2174/092986711795656216
- Thangamani, S., Mohammad, H., Abushahba, M. F., Sobreira, T. J., and Seleem, M. N. (2016). Repurposing auranofin for the treatment of cutaneous staphylococcal infections. *Int. J. Antimicrob. Agents* 47, 195–201. doi: 10.1016/j.ijantimicag.2015.12.016
- Todd, O. A., Fidel, P. L. Jr., Harro, J. M., Hilliard, J. J., Tkaczyk, C., Sellman, B. R., et al. (2019). *Candida albicans* augments *Staphylococcus aureus* virulence by engaging the Staphylococcal agr quorum sensing system. *mBio* 10:e00910-19. doi: 10.1128/mBio.00910-19
- Yamagishi, Y., Mikamo, H., Kato, H., Nishiyama, N., Asai, N., Koizumi, Y., et al. (2017). Efficacy of tedizolid against methicillin-resistant *Staphylococcus aureus* and *Peptostreptococcus anaerobius* in thigh mixed-infection mouse model. *J. Infect. Chemother.* 23, 368–373. doi: 10.1016/j.jiac.2017.02.013
- Yang, W., Liu, J., Blazekovic, B., Sun, Y., Ma, S., and Ren, C. (2018). In vitro antibacterial effects of tanreqing injection combined with vancomycin or linezolid against methicillin-resistant staphylococcus aureus. *BMC Complement Altern. Med.* 18:169. doi: 10.1186/s12906-018-2231-8
- Zykov, I. N., Samuelsen, O., Jakobsen, L., Smabrekke, L., Andersson, D. I., Sundsfjord, A., et al. (2018). Pharmacokinetics and pharmacodynamics of fosfomycin and its activity against extended-spectrum-beta-lactamase-, plasmid-mediated ampc-, and carbapenemase-producing *escherichia coli* in a murine urinary tract infection model. *Antimicrob. Agents Chemother.* 62:e02560-17. doi: 10.1128/AAC.02560-17

**Conflict of Interest:** The authors declare that the research was conducted in the absence of any commercial or financial relationships that could be construed as a potential conflict of interest.

Copyright © 2019 She, Zhou, Li, Liu, Xu, Chen, Luo and Wu. This is an open-access article distributed under the terms of the Creative Commons Attribution License (CC BY). The use, distribution or reproduction in other forums is permitted, provided the original author(s) and the copyright owner(s) are credited and that the original publication in this journal is cited, in accordance with accepted academic practice. No use, distribution or reproduction is permitted which does not comply with these terms.



# Genomic Characterization of Prevalent *mcr-1*, *mcr-4*, and *mcr-5* *Escherichia coli* Within Swine Enteric Colibacillosis in Spain

Isidro García-Meniño<sup>1†</sup>, Dafne Díaz-Jiménez<sup>1†</sup>, Vanesa García<sup>1†</sup>, María de Toro<sup>2</sup>, Saskia C. Flament-Simon<sup>1</sup>, Jorge Blanco<sup>1</sup> and Azucena Mora<sup>1\*</sup>

<sup>1</sup> Laboratorio de Referencia de *Escherichia coli*, Departamento de Microbiología y Parasitología, Facultad de Veterinaria, Universidad de Santiago de Compostela, Lugo, Spain, <sup>2</sup> Plataforma de Genómica y Bioinformática, Centro de Investigación Biomédica de La Rioja, Logroño, Spain

## OPEN ACCESS

### Edited by:

Luciene Andrade Da Rocha  
Minarini,

Federal University of São Paulo, Brazil

### Reviewed by:

Darren Trott,  
The University of Adelaide, Australia  
Maite Muniesa,  
University of Barcelona, Spain

### \*Correspondence:

Azucena Mora  
azucena.mora@usc.es

<sup>†</sup> These authors have contributed  
equally to this work

### \*Present address:

Vanesa García,  
Department of Veterinary and Animal  
Sciences, Faculty of Health and  
Medical Sciences, University of  
Copenhagen, Frederiksberg, Denmark

### Specialty section:

This article was submitted to  
Antimicrobials, Resistance  
and Chemotherapy,  
a section of the journal  
Frontiers in Microbiology

**Received:** 26 August 2019

**Accepted:** 15 October 2019

**Published:** 01 November 2019

### Citation:

García-Meniño I, Díaz-Jiménez D,  
García V, de Toro M,  
Flament-Simon SC, Blanco J and  
Mora A (2019) Genomic  
Characterization of Prevalent *mcr-1*,  
*mcr-4*, and *mcr-5* *Escherichia coli*  
Within Swine Enteric Colibacillosis  
in Spain. *Front. Microbiol.* 10:2469.  
doi: 10.3389/fmicb.2019.02469

Antimicrobial agents are crucial for the treatment of many bacterial diseases in pigs, however, the massive use of critically important antibiotics such as colistin, fluoroquinolones and 3rd–4th-generation cephalosporins often selects for co-resistance. Based on a comprehensive characterization of 35 colistin-resistant *Escherichia coli* from swine enteric colibacillosis, belonging to prevalent Spanish lineages, the aims of the present study were to investigate the characteristics of *E. coli* clones successfully spread in swine and to assess the correlation of the *in vitro* results with *in silico* predictions from WGS data. The resistome analysis showed six different *mcr* variants: *mcr-1.1*; *mcr-1.10*; *mcr-4.1*; *mcr-4.2*; *mcr-4.5*; and *mcr-5.1*. Additionally, *bla*<sub>CTX-M-14</sub>, *bla*<sub>CTX-M-32</sub> and *bla*<sub>SHV-12</sub> genes were present in seven genomes. PlasmidFinder revealed that *mcr-1.1* genes located mainly on IncHI2 and IncX4 types, and *mcr-4* on ColE10-like plasmids. Twenty-eight genomes showed a *gyrA* S83L substitution, and 12 of those 28 harbored double-serine mutations *gyrA* S83L and *parC* S80I, correlating with *in vitro* quinolone-resistances. Notably, 16 of the 35 *mcr*-bearing genomes showed mutations in the PmrA (S39I) and PmrB (V161G) proteins. The summative presence of mechanisms, associated with high-level of resistance to quinolones/fluoroquinolones and colistin, could be conferring adaptive advantages to prevalent pig *E. coli* lineages, such as the ST10-A (CH11-24), as presumed for ST131. SerotypeFinder allowed the H-antigen identification of *in vitro* non-mobile (HNM) isolates, revealing that 15 of the 21 HNM *E. coli* analyzed were H39. Since the H39 is associated with the most prevalent O antigens worldwide within swine colibacillosis, such as O108 and O157, it would be probably playing a role in porcine colibacillosis to be considered as a valuable subunit antigen in the formulation of a broadly protective Enterotoxigenic *E. coli* (ETEC) vaccine. Our data show common features with other European countries in relation to a prevalent clonal group (CC10), serotypes (O108:H39, O138:H10, O139:H1, O141:H4), high plasmid content within the isolates and *mcr* location, which would support global alternatives to the use of antibiotics in pigs. Here, we report for first time a rare finding so far, which is the co-occurrence of double colistin-resistance mechanisms in a significant number of *E. coli* isolates.

**Keywords:** *Escherichia coli*, colistin, *mcr*, ESBL, fluoroquinolones, ST10, colibacillosis, swine

## INTRODUCTION

Multidrug-resistant Enterobacteriaceae, such as *Escherichia coli*, represent a threat to both human and veterinary health. *E. coli* has a great capacity to accumulate resistance genes, mostly through horizontal gene transfer. The major problematic mechanisms correspond to the acquisition of genes coding for extended-spectrum beta-lactamases (ESBL), carbapenemases, 16S rRNA methylases, plasmid-mediated quinolone resistance (PMQR) and *mcr* genes conferring resistance to polymyxins (Poirel et al., 2018).

Colistin has been widely used in Spain for the control of neonatal and post-weaning diarrhoea (PWD) in pigs caused by certain *E. coli* pathotypes: Enterotoxigenic *E. coli* (ETEC), defined by the presence of genes encoding enterotoxins (*eltA*, and/or *estA*, and/or *estB*); atypical Enteropathogenic *E. coli* (aEPEC), carriers of *eae* but negative for *bfpA* (aEPEC); Shiga toxin-producing *E. coli* (STEC), positive for *stx<sub>2e</sub>*; STEC/ETEC, positive for both shiga toxin type 2e and enterotoxin-encoding genes (*stx<sub>2e</sub>* and *estB* and/or *estA*) (García-Meniño et al., 2018). PWD results in significant economic losses for the pig industry due to costs derived of treatment and handling, decreased weight gain, and mortality. These circumstances have promoted the use and abuse of antibiotics in intensive farming (Luppi, 2017; Rhouma et al., 2017). However, specific regulations have been set up in Europe due to the concern that colistin resistance could be transmitted from food-production animals to humans which makes necessary the investigation of sustainable alternatives to antimicrobials (EUROPEAN COMMISSION, 2018).

In Spain, the rates of antibiotic resistance in pig farming were recently analyzed in a collection of 499 *E. coli* isolates from 179 outbreaks of enteric colibacillosis occurred during a period of 10 years (2006–2016) (García et al., 2018; García-Meniño et al., 2018). The results revealed a prevalence of colistin-resistant *E. coli* implicated in PWD in Spanish farms as high as 76.9% within 186 ETEC, STEC and STEC/ETEC isolates. Besides, PCR and sequencing identified the presence of *mcr-4* in 102 isolates, *mcr-1* in 37 isolates and *mcr-5* in five isolates. Interestingly, almost all *mcr-4* isolates belonged to the clonal group ST10-A (CH11-24) (García et al., 2018), which was shown to be highly present (more than 50%) within the *mcr-1* diarrheagenic isolates of a second study (García-Meniño et al., 2018). Both studies reinforced other countries' findings that the pig industry is an important reservoir of colistin-resistant *E. coli*, as well as being carriers of other additional risk genes such as *bla<sub>ESBL</sub>* genes (García et al., 2018; García-Meniño et al., 2018; Magistrali et al., 2018; Manageiro et al., 2019). Based on reported evidences (Beyrouthy et al., 2017; Gilrane et al., 2017), there is great concern about the *in vivo* acquisition of *mcr*- and *bla<sub>ESBL</sub>*-bearing plasmids by human *E. coli* isolates following treatment with colistin, or via animal transmission through direct contact or via food chain. Particular attention is given to those named as high-risk clones of (ESBL)-producing bacteria, worldwide spread within humans and animals, including *Escherichia coli* sequence types ST10, ST131, ST405, and ST648 (Mathers et al., 2015; Sellera and Lincopan, 2019).

The aims of this study were (i) the characterization of resistances and plasmid profiles of successfully spread *mcr-1*, *mcr-4*, and *mcr-5* *E. coli* in Spanish pig farming; (ii) the assessment of WGS-based approaches for the characterization of pathogenic *E. coli*, through the correlation of the *in vitro* results with *in silico* predictions using the bioinformatics tools of the Center for Genomic Epidemiology (CGE).

## MATERIALS AND METHODS

### *E. coli* Collection

Thirty-five swine *E. coli*, positive by PCR for *mcr*-genes, were fully sequenced. Specifically, the 35 *E. coli* were selected from 499 diarrheagenic isolates of different geographic areas of Spain (2006–2016) (García et al., 2018; García-Meniño et al., 2018), taking into account the results of prevalence and significant association observed between pathotypes, presence of *mcr* and certain serogroups. In brief, the serogroups O108, O138, O141, O149, O157 were found significantly associated with ETEC; serogroups O26, O49, O80, O111 with aEPEC; serogroups O138 and O141 with STEC/ETEC; serogroup O139 with STEC; and serogroups O2, O15, O26, O45, O111, O138, O141, O157 with *mcr*-positive isolates (García-Meniño et al., 2018). Therefore, the collection analyzed here included 27 ETEC isolates (of serogroups O7, O8, O15, O45, O108, O138, O141, O149, O157, ONT); four STEC (O2, O139); three STEC/ETEC (O138 and O141) and one aEPEC (O111). The 35 representative isolates were carriers of the three *mcr*-types (*mcr-1*, *mcr-4*, and *mcr-5*) detected so far in our *E. coli* collection of porcine origin. Conventional pheno- and geno-typing was performed to complete classical characterization of serotypes, phylogroups, pathotypes and resistance profiles.

### Conventional Typing

The H antigen was established for motile isolates by serotyping using H1 to H56 antisera, while non-motile isolates (HNM) were analyzed by PCR to determine their flagellar genes as described elsewhere (García-Meniño et al., 2018). The phylogroup was assigned by means of the quadruplex PCR of Clermont et al. (2013). Antimicrobial susceptibility was determined by minimal inhibitory concentrations (MICs) using the MicroScan WalkAway®-automated system (Siemens Healthcare Diagnostics, Berkeley, CA, United States) according to the manufacturer's instructions for: amikacin, ampicillin-sulbactam, aztreonam, cefepime, ceftazidime, ciprofloxacin, colistin, fosfomicin, gentamicin, imipenem, levofloxacin, meropenem, minocycline, nitrofurantoin, piperacillin-tazobactam, ticarcillin, tigecycline, and tobramycin. Additionally, resistance to ampicillin, amoxicillin/clavulanate, cefazolin, cefotaxime, ceftiofur, cefuroxime, chloramphenicol, doxycycline, nalidixic acid and trimethoprim-sulfamethoxazole was determined by disk (Becton Dickinson, Sparks, MD, United States) diffusion assays. All results were interpreted according to the CLSI break points (Clinical and Laboratory Standards Institute, 2019). Genetic identification of the ESBLs was performed by PCR using



the TEM, SHV, CTX-M-1 and CTX-M-9 group-specific primers followed by amplicon sequencing (García-Meniño et al., 2018).

## Whole Genome Sequencing (WGS) and Sequence Analysis

The libraries for sequencing were prepared following the instructions provided by the TruSeq Illumina PCR-Free protocol. Mechanical DNA fragmentation was performed with Covaris E220, and the final quality of the libraries assessed with Fragment Analyzer (Std. Sens. NGS Fragment Analysis kit 1-6000 bp). Lastly, the libraries were sequenced in an Illumina HiSeq1500, obtaining 100–150 bp paired-end reads which were trimmed (Trim Galore 0.5.0) and filtered according to quality criteria (FastQC 0.11.7). The reconstruction of the genomes and plasmids in the genomes was carried out using the methodology PLASmid Constellation NETwork (PLACNETw)<sup>1</sup> (Lanza et al., 2014). The assembled contigs, with genomic size ranging between 4.9 and 5.9 Mbp (mean size 5.5 Mbp), were analyzed using the bioinformatics tools of the Center for Genomic Epidemiology (CGE)<sup>2</sup> for the presence of antibiotic resistance (ResFinder V2.1.), virulence genes (VirulenceFinder v1.5.), plasmid replicon types (PlasmidFinder 1.3./PMLST 1.4.), and identification of clonotypes (CHTyper 1.0), sequence types (MLST 2.0) and serotypes (SerotypeFinder 2.0). All the CGE predictions were called applying a select threshold for identification and a minimum length of 95 and 80%, respectively. Phylogroups were predicted using the ClermonTyping tool at the iame-research center web<sup>3</sup>. The *mcr* gene location was determined using PlasmidFinder/ResFinder prediction, together with PLACNETw references, and automatic annotation with Prokka v1.13 (Seemann, 2014).

## RESULTS AND DISCUSSION

The phenotypic and genotypic traits of the 35 *mcr*-positive *E. coli* of swine origin, as well as their resistome and mobilome are summarized in **Table 1**. ResFinder confirmed that all genomes were *mcr* carriers. Likewise, VirulenceFinder predicted the acquired virulence genes encoding for the enterotoxins (*stx1*, *stx2*, *stx3*, *stx4*, *stx5*, *stx6*, *stx7*, *stx8*, *stx9*, *stx10*, *stx11*, *stx12*, *stx13*, *stx14*, *stx15*, *stx16*, *stx17*, *stx18*, *stx19*, *stx20*, *stx21*, *stx22*, *stx23*, *stx24*, *stx25*, *stx26*, *stx27*, *stx28*, *stx29*, *stx30*, *stx31*, *stx32*, *stx33*, *stx34*, *stx35*, *stx36*, *stx37*, *stx38*, *stx39*, *stx40*, *stx41*, *stx42*, *stx43*, *stx44*, *stx45*, *stx46*, *stx47*, *stx48*, *stx49*, *stx50*, *stx51*, *stx52*, *stx53*, *stx54*, *stx55*, *stx56*, *stx57*, *stx58*, *stx59*, *stx60*, *stx61*, *stx62*, *stx63*, *stx64*, *stx65*, *stx66*, *stx67*, *stx68*, *stx69*, *stx70*, *stx71*, *stx72*, *stx73*, *stx74*, *stx75*, *stx76*, *stx77*, *stx78*, *stx79*, *stx80*, *stx81*, *stx82*, *stx83*, *stx84*, *stx85*, *stx86*, *stx87*, *stx88*, *stx89*, *stx90*, *stx91*, *stx92*, *stx93*, *stx94*, *stx95*, *stx96*, *stx97*, *stx98*, *stx99*, *stx100*), for fimbriae (*fedF*, *k88*), verotoxin (*stx2*) and intimin (*eae*), correlating in all cases with the pathotype assignment previously determined by PCR (García et al., 2018; García-Meniño et al., 2018).

### Serotype Identification

In most studies, there is lack of information on *E. coli* serotypes since serotyping is performed by very few laboratories worldwide, hindering epidemiological comparisons. Here, we not only proved that there is a very good correlation between serotyping and SerotypeFinder predictions, but also the advantage of *in silico* H-antigen identification for those non-mobile (HNM) isolates. It is of note that 15 of the 21 HNM isolates were predicted

as H39 (**Table 1**), namely O108:H39, O157:H39 and O45:H39 (five genomes, each). Given that the H39 is associated with the most prevalent O antigens within swine colibacillosis, such as O108 and O157, as well as ONT (García-Meniño et al., 2018), it would be probably playing a role in porcine colibacillosis to be considered as a valuable subunit antigen in the formulation of a broadly protective ETEC vaccine (Roy et al., 2009). The remaining six HNM isolates showed different O:H combinations: O138:H14, ONT:H5, O8:H20, O50/O2:H32, and O182:H19. SerotypeFinder also allowed the O45-antigen determination of two non-typeable (ONT) isolates (LREC-141 and LREC-146) and O182 of LREC-172; while LREC-147, belonging to O157 serogroup (**Table 1**), was predicted as ONT, probably due to the limitation of the assembly based on Illumina short reads (100–150 bp paired-end reads here) (Wick et al., 2017).

### Phylogroups, Sequence Types and Clonotypes

The phylogroups established for the 35 genomes were the common ones reported for porcine *E. coli* isolates (A, B1, D-E) (Shepard et al., 2012; Bosak et al., 2019). However, we found discrepancies in the assignment obtained with the quadruplex PCR of Clermont et al. (2013) in comparison with that predicted by ClermonTyping for seven isolates: phylogroup E by PCR, while phylogroup D *in silico* (**Table 1**).

MLST and CHTyper tools determined 12 different STs, but mostly belonging to CC10 (21 genomes) and clonotype CH11-24 (18 genomes) (**Table 1**). The predominance of CC10, and specifically ST10, is in accordance with published data on *E. coli* isolates of swine origin, independently of the pathogenicity or antibiotic-resistance/susceptibility status (Shepard et al., 2012; Kidsley et al., 2018; Magistrali et al., 2018).

### Resistome, Plasmidome and Phenotypic Expression of Resistances

The resistome analysis revealed that 34 of the 35 genomes encoded mechanisms of antibiotic resistance for  $\geq$  three different antimicrobial categories (**Table 1**). Seven *E. coli* were carriers of *bla*<sub>ESBL</sub>, namely *bla*<sub>CTX-M-14</sub> (four genomes), *bla*<sub>CTX-M-32</sub> (one) and *bla*<sub>SHV-12</sub> (two). Besides, six different *mcr* variants were identified within the 35 *E. coli*: *mcr-1.1* (in 18 genomes, including two *mcr-4.2* carriers); *mcr-1.10* (one); *mcr-4.1* (one); *mcr-4.2* (13 genomes, including the two *mcr-1.1* carriers); *mcr-4.5* (two) and *mcr-5.1* (two).

PlasmidFinder revealed a high plasmid diversity based on the identified replicons, with two to seven different plasmid types per genome (**Table 1**). Within this heterogeneity, *mcr-1.1* genes were found mainly on plasmids of the IncHI2 and IncX4 types (six and four of the 12 *mcr-1.1* plasmid-located genes, respectively); however, *mcr-1.1* was also found integrated in the chromosome of LREC-145, LREC-148, LREC-149 and LREC-164 genomes. The *mcr-1.10* gene of LREC-151 was located on the chromosome, while *mcr-4* and *mcr-5* variants were on Col8282-like (*mcr-4.1*), ColE10-like (for all 13 *mcr-4.2* and two *mcr-4.5* carriers) and pKP13a-like (*mcr-5.1*) plasmids. Furthermore, we found that

<sup>1</sup><https://castillo.dicom.unican.es/upload/>

<sup>2</sup><https://cge.cbs.dtu.dk/services/>

<sup>3</sup><http://clermontyping.iame-research.center/>



**TABLE 1** | Features of the 35 colistin-resistant *E. coli* genomes of swine origin based on *in silico* characterization (light columns) and on conventional typing (gray columns).

Code	Year of Isolation <sup>1</sup>	Serotype <sup>2</sup>	Phylo Group <sup>3</sup>	CHType <sup>4</sup>	ST <sup>5</sup> (CC)	Plasmid content Inc group (pMLST) <sup>6</sup>	Acquired resistances (in black) and point mutations (in blue) <sup>7</sup>	<i>mcr</i> /location <sup>8</sup>	Virulence genes <sup>9</sup>	Phenotypic resistance profile <sup>10</sup>	Pathotype-associated VF <sup>11</sup>
LREC-144	2010	O141:H4	A	11-24	5786 (10)	IncF (F30:A-:B-) IncX1 IncHI2 (ST4)	<i>aadA1</i> , <i>aph(3')-Ib</i> , <i>aph(6)-Ic</i> ; <i>mdf(A)</i> ; <i>sul1</i> ; <i>tet(A)</i> , <i>tet(B)</i> ; <i>dfrA1</i> ; <b><i>mcr-1.1</i></b> <i>gyrA</i> D87G	<i>mcr-1.1</i> / IncHI2	<b><i>sta1</i></b> , <b><i>stb</i></b> , <b><i>fedF</i></b> , <i>astA</i> , <i>fedA</i> , <i>iha</i> , <i>iroN</i> , <i>iss</i>	NAL*, SXT, MIN*, DOX, FOF, CST	STa, STb, F18
LREC-145	2014	O50/O2:H32	A	11-23	10 (10)	IncF (F89:A-:B56) IncI1 (ST80) IncI2 pO111-like	<i>bla</i> <sub>TEM-1B</sub> ; <i>aadA1</i> , <i>aadA2</i> , <i>aadA24</i> , <i>aph(3')-Ia</i> ; <i>cmlA1</i> ; <i>erm(B)</i> , <i>mdf(A)</i> ; <i>sul3</i> ; <i>tet(A)</i> ; <i>dfrA1</i> ; <b><i>mcr-1.1</i></b> <i>gyrA</i> S83L	<i>mcr-1.1</i> / chromosome	<b><i>stx2</i></b> , <i>iha</i>	TIC, AMP, SAM, NAL, SXT, MIN, DOX*, CHL, FOF, CST	VT2e
LREC-147	2008	*ONT:H5	B1	29-38	156 (156)	IncF (F110:A-:B42) IncHI2 (ST4)	<i>aadA1</i> , <i>aadA2</i> , <i>acc(6')-Ib3</i> ; <i>catA1</i> , <i>catB3</i> , <i>cmlA1</i> ; <i>acc(6')-Ib-cr</i> ; <i>mdf(A)</i> ; <i>sul1</i> , <i>sul3</i> ; <i>tet(B)</i> ; <i>dfrA1</i> ; <b><i>mcr-1.1</i></b> <i>gyrA</i> S83L, <i>gyrA</i> D87N, <i>parC</i> S80I, <i>parC</i> E84G	<i>mcr-1.1</i> / IncHI2	<b><i>stb</i></b> , <i>astA</i> , <i>iss</i> , <i>lpfA</i> , <i>gad</i>	TIC, AMP, SAM, AMC, TOB*, NAL, CIP, LVX, SXT, MIN, DOX, CHL, CST	STb
LREC-148	2013	O157:H39	A	11-24	10 (10)	IncF (F12/08:A-:B42) IncB/O/K/Z Col156-like	<i>bla</i> <sub>CTX-M-14</sub> ; <i>bla</i> <sub>TEM-1A</sub> ; <i>mdf(A)</i> ; <i>tet(B)</i> ; <b><i>mcr-1.1</i></b> <i>gyrA</i> S83L; <b><i>pmrB</i> V161G</b>	<i>mcr-1.1</i> / chromosome	<b><i>itcA</i></b> , <b><i>stb</i></b> , <b><i>K88</i></b> , <i>astA</i> , <i>cba</i> , <i>celB</i> , <i>cma</i> , <i>gad</i> , <i>iha</i> , <i>sepA</i>	TIC, AMP, SAM, AMC*, CFZ, CXM, CTX, FEP, NAL*, MIN*, DOX, CST	LT, STb, K88
LREC-149	2010	O138:H10	A	27-0	100 (165)	IncF (F110/108:A-:B42) IncI1 (STunknown) IncI2 IncQ1	<i>bla</i> <sub>TEM-1B</sub> ; <i>aadA1</i> , <i>aac(3)-IIa</i> ; <i>mdf(A)</i> ; <i>tet(A)</i> ; <i>dfrA1</i> ; <b><i>mcr-1.1</i></b>	<i>mcr-1.1</i> / chromosome	<b><i>itcA</i></b> , <b><i>stb</i></b> , <b><i>K88</i></b> , <i>astA</i> , <i>capU</i> , <i>iha</i>	TIC, AMP, SAM, AMC, GEN, TOB, NAL*, CIP, MIN*, DOX, NIT, CST	LT, STb, K88
LREC-164	2009	O111:H9	B1	4-24	29 (29)	IncHI2 (STunknown) IncX1 Col8282-like	<i>aadA1</i> , <i>aadA2</i> , <i>aph(3')-Ib</i> , <i>aph(6)-Ic</i> ; <i>catA1</i> , <i>cmlA1</i> ; <i>mdf(A)</i> ; <i>sul1</i> , <i>sul3</i> ; <i>dfrA1</i> ; <i>tet(A)</i> ; <b><i>mcr-1.1</i></b> <i>gyrA</i> S83L	<i>mcr-1.1</i> / chromosome	<b><i>eae</i></b> , <i>espA</i> , <i>espB</i> , <i>espF</i> , <i>espJ</i> , <i>tccP</i> , <i>tir</i> , <i>cif</i> , <i>efa1</i> , <i>astA</i> , <i>celB</i> , <i>iha</i> , <i>lpfA</i> , <i>nleA</i> , <i>nleB</i>	TIC, NAL, SXT, DOX*, CHL, CST	Eae-β1
LREC-165	2006	O8:H20	A	7-0	398 (398)	IncF (F2:A-:B71) IncHI2 (ST4) IncI2 IncY	<i>aadA1</i> , <i>aadA2</i> ; <i>catA1</i> , <i>cmlA1</i> ; <i>mdf(A)</i> ; <i>sul3</i> ; <i>tet(A)</i> ; <b><i>mcr-1.1</i></b>	<i>mcr-1.1</i> / ND	<b><i>stb</i></b> , <i>astA</i> , <i>capU</i> , <i>gad</i>	DOX*, CHL, CST	STb

(Continued)

TABLE 1 | Continued

Code	Year of Isolation <sup>1</sup>	Serotype <sup>2</sup>	Phylo Group <sup>3</sup>	CHType <sup>4</sup>	ST <sup>5</sup> (CC)	Plasmid content Inc group (pMLST) <sup>6</sup>	Acquired resistances (in black) and point mutations (in blue) <sup>7</sup>	mcr/location <sup>8</sup>	Virulence genes <sup>9</sup>	Phenotypic resistance profile <sup>10</sup>	Pathotype-associated VF <sup>11</sup>
LREC-166	2010	O7:H4	A	11-27	93 (168)	IncF (F2:A-:B-) IncHI2 (STunknown) IncN (ST1) IncX1	<i>bla</i> <sub>SHV-12</sub> , <i>bla</i> <sub>TEM-1B</sub> ; <i>aph(3')-Ila</i> , <i>aph(3'')-Ib</i> , <i>aph(6)-Id</i> ; <i>catA1</i> ; <i>mdf(A)</i> ; <i>sul3</i> ; <b><i>mcr-1.1</i></b>	<i>mcr-1.1</i> /ND (plasmid localization)	<b><i>stb</i></b> , <i>astA</i> , <i>iss</i>	TIC, AMP, SAM, CFZ, CXM, CTX, CAZ, ATM, CHL, CST	STb
LREC-167	2007	O141:H4	A	11-24	7323 (10)	IncF (F30:A-:B-) IncI2 IncX1 IncX4	<i>bla</i> <sub>CTX-M-14</sub> , <i>bla</i> <sub>TEM-1A</sub> ; <i>aadA2</i> , <i>aph(3'')-Ib</i> , <i>aph(6)-Id</i> ; <i>catA1</i> ; <i>erm(B)</i> , <i>mdf(A)</i> ; <i>sul1</i> ; <i>tet(B)</i> ; <b><i>mcr-1.1</i></b> <i>gyrA</i> S83L; <b><i>pmrA</i> S39I</b>	<i>mcr-1.1</i> /ND (plasmid localization)	<b><i>sta1</i></b> , <b><i>stb</i></b> , <b><i>fedF</i></b> , <i>fedA</i> , <i>gad</i> , <i>iha</i> , <i>iroN</i> , <i>iss</i>	TIC, AMP, AMC*, CFZ, CXM, CTX, FEP, NAL, MIN*, DOX, CHL, CST	STa, F18
LREC-169	2015	O141:H4	A	11-24	7323 (10)	IncF (F30:A-:B-) IncHI2 (ST4) IncI1 (STunknown) IncN (ST1) IncQ1 IncX1	<i>bla</i> <sub>TEM-1B</sub> ; <i>aac(3)-IV</i> , <i>aadA1</i> , <i>aadA2</i> , <i>aph(3')-Ia</i> , <i>aph(3'')-Ib</i> , <i>aph(6)-Id</i> ; <i>floR</i> ; <i>qnrS1</i> ; <i>mdf(A)</i> , <i>inu(F)</i> ; <i>sul1</i> , <i>sul2</i> ; <i>tet(A)</i> ; <i>dfrA1</i> ; <b><i>mcr-1.1</i></b> <i>gyrA</i> S83L, <i>parC</i> S80R; <b><i>pmrA</i> S39I</b>	<i>mcr-1.1</i> /IncHI2	<b><i>sta1</i></b> , <b><i>stb</i></b> , <b><i>fedF</i></b> , <i>fedA</i> , <i>gad</i> , <i>iss</i>	TIC, AMP, GEN*, NAL, CIP, LVX, SXT, CHL, CST	STa, STb, F18
LREC-170	2015	O139:H1	*D	2-54	1	IncF (F14:A-:B-) IncX1 IncX4	<i>mdf(A)</i> ; <b><i>mcr-1.1</i></b>	<i>mcr-1.1</i> /IncX4	<b><i>stx2</i></b> , <b><i>fedF</i></b> , <i>eilA</i> , <i>fedA</i> , <i>gad</i> , <i>lpfA</i>	TIC, AMP, SXT, MIN*, DOX, CST	VT2e, F18
LREC-171	2008	O138:H14	*D	28-65	42	IncF (F111:A-:B42) IncX1 IncX4	<i>bla</i> <sub>TEM-1B</sub> ; <i>aadA1</i> , <i>aph(3')-Ia</i> , <i>aph(3'')-Ib</i> , <i>aph(6)-Id</i> ; <i>mdf(A)</i> ; <i>sul1</i> ; <i>tet(B)</i> ; <b><i>mcr-1.1</i></b> <i>gyrA</i> S83L, <i>gyrA</i> D87Y, <i>parC</i> S80R	<i>mcr-1.1</i> /ND	<b><i>itcA</i></b> , <b><i>sta1</i></b> , <b><i>stb</i></b> , <b><i>fedF</i></b> , <i>air</i> , <i>astA</i> , <i>cba</i> , <i>cma</i> , <i>fedA</i> , <i>gad</i> , <i>lpfA</i> , <i>iss</i>	TIC, AMP, SAM, AMC*, NAL, CIP, LVX, MIN, DOX, CST	LT, STa, STb, F18
LREC-172	2014	O182:H19	A	11-94	10 (10)	IncF (F4:A-:B56*) IncB/O/K/Z IncHI2 (ST4)	<i>bla</i> <sub>CTX-M-14</sub> ; <i>aadA1</i> ; <i>catA1</i> ; <i>mdf(A)</i> ; <i>sul1</i> ; <i>tet(A)</i> ; <i>dfrA1</i> ; <b><i>mcr-1.1</i></b> <i>gyrA</i> S83L	<i>mcr-1.1</i> /IncHI2	<b><i>sta1</i></b> , <b><i>stb</i></b> , <b><i>fedF</i></b> , <i>capU</i> , <i>etpD</i> , <i>gad</i> , <i>iha</i>	TIC, AMP, SAM, CFZ, CXM, CTX, FEP, GEN*, TOB*, ATM, NAL, CIP, LVX, SXT, DOX*, CHL, CST	STa, STb, F18
LREC-174	2010	O15:H45	*D	4-331	118	IncHI2 (ST4) IncX4 ColE10-like	<i>bla</i> <sub>TEM-1B</sub> ; <i>aadA1</i> , <i>aadA2</i> ; <i>catA1</i> , <i>cmlA1</i> ; <i>mdf(A)</i> ; <i>sul3</i> ; <b><i>mcr-1.1</i></b> <i>gyrA</i> S83L	<i>mcr-1.1</i> /IncX4	<b><i>stb</i></b> , <i>air</i> , <i>astA</i> , <i>eilA</i> , <i>gad</i>	TIC, AMP, SAM, GEN, TOB, NAL, MIN, DOX*, CHL, CST	STb
LREC-175	2009	O45:H45	E	550-400	4247	IncF (F72/2:A-:B71) IncX4 Col156-like ColE10-like	<i>mdf(A)</i> ; <b><i>mcr-1.1</i></b> <i>gyrA</i> S83L	<i>mcr-1.1</i> /IncX4	<b><i>stb</i></b> , <i>air</i> , <i>astA</i> , <i>celB</i> , <i>eilA</i> , <i>gad</i>	NAL, NIT*, CST	STb

(Continued)

TABLE 1 | Continued

Code	Year of Isolation <sup>1</sup>	Serotype <sup>2</sup>	Phylo Group <sup>3</sup>	CHType <sup>4</sup>	ST <sup>5</sup> (CC)	Plasmid content Inc group (pMLST) <sup>6</sup>	Acquired resistances (in black) and point mutations (in blue) <sup>7</sup>	<i>mcr</i> /location <sup>8</sup>	Virulence genes <sup>9</sup>	Phenotypic resistance profile <sup>10</sup>	Pathotype-associated VF <sup>11</sup>
LREC-178	2009	O141:H4	A	11-24	10 (10)	IncF (F30:A-:B-) IncHI2 (ST9*) IncI1 (STunknown) IncX1 IncX4	<i>bla</i> <sub>TEM-1B</sub> ; <i>aadA1</i> , <i>aadA2</i> ; <i>cmlA1</i> ; <i>mdf(A)</i> , <i>mph(B)</i> ; <i>sul1</i> , <i>sul3</i> ; <i>dfrA1</i> ; <b><i>mcr-1.1</i></b> <i>gyrA</i> D87G; <b><i>pmrB V161G</i></b>	<i>mcr-1.1</i> / IncX4	<b><i>sta1</i>, <i>stb</i>, <i>stx2</i>, <i>fedF</i></b> , <i>cma</i> , <i>fedA</i> , <i>iha</i>	TIC, AMP, GEN, TOB*, SXT, CHL, CST	STa, STb, VT2e, F18
LREC-151	2013	O139:H1	*D	2-54	1	IncI1 (STunknown) IncX1	<i>aph(3')-Ia</i> ; <i>mdf(A)</i> ; <b><i>mcr-1.10</i></b> <i>gyrA</i> S83L	<i>mcr-1.10</i> / chromosome	<b><i>stx2</i>, <i>fedF</i></b> , <i>eilA</i> , <i>fedA</i> , <i>gad</i> , <i>lpfA</i>	NAL*, CST	VT2e, F18
LREC-136	2012	O149:H10	A	27-0	100 (165)	IncF (F108:A-:B54) IncI1 (STunknown) IncR Col8282-like	<i>bla</i> <sub>TEM-1B</sub> ; <i>aadA1</i> , <i>aadA2</i> ; <i>aph(3')-Ia</i> ; <i>cmlA1</i> ; <i>mdf(A)</i> ; <i>sul3</i> ; <b><i>mcr-4.1</i></b> <i>gyrA</i> S83L	<i>mcr-4.1</i> / Col8282	<b><i>sta1</i>, <i>stb</i></b> , <i>astA</i> , <i>capU</i> , <i>iha</i>	TIC, AMP, SAM, AMC, NAL, DOX*, CHL, CST	LT, STa, STb, K88
LREC-131	2011	O108:H39	A	11-24	10 (10)	IncF (F111:A-:B42) IncI1 (ST3) IncI2 Col156-like ColE10-like	<i>bla</i> <sub>SHV-12</sub> ; <i>aadA2</i> , <i>aph(3')-Ia</i> ; <i>cmlA1</i> ; <i>mdf(A)</i> ; <i>sul3</i> ; <i>tet(B)</i> ; <i>dfrA12</i> ; <b><i>mcr-4.2</i></b> <i>gyrA</i> S83L, <i>gyrA</i> D87G, <i>parC</i> S80I	<i>mcr-4.2</i> / ColE10	<b><i>itcA</i>, <i>sta1</i>, <i>fedF</i></b> , <i>celB</i> , <i>fedA</i> , <i>iha</i>	TIC, AMP, CFZ, CXM, CTX, CAZ, ATM, NAL, CIP, LVX, SXT, MIN*, DOX, CHL, CST	LT, STa, F18
LREC-132	2016	O108:H39	A	11-24	10 (10)	IncF (F111:A-:B42) IncHI2 (ST9) IncI1 (ST48) IncI2 ColE10-like	<i>bla</i> <sub>TEM-1B</sub> ; <i>aac(3)-IIa</i> , <i>aac(3)-IV</i> , <i>aadA1</i> , <i>aph(3')-Ia</i> , <i>aph(3')-Ib</i> , <i>aph(4)-Ia</i> ; <i>catA1</i> ; <i>mdf(A)</i> , <i>mph(B)</i> ; <i>sul1</i> ; <i>tet(B)</i> ; <i>dfrA1</i> ; <b><i>mcr-4.2</i></b> <i>gyrA</i> S83L, <i>gyrA</i> D87G, <i>parC</i> S80I; <b><i>pmrB V161G</i></b>	<i>mcr-4.2</i> / ColE10	<b><i>itcA</i>, <i>sta1</i>, <i>stb</i>, <i>fedF</i></b> , <i>astA</i> , <i>cma</i> , <i>gad</i> , <i>iha</i>	TIC, AMP, AMC, GEN, TOB, NAL, CIP, LVX, SXT, MIN, DOX, CHL, CST	LT, STa, STb, F18
LREC-133	2006	O138:H14	*D	28-41	42	IncF (F14:A-:B-) IncX1 ColE10-like	<i>mdf(A)</i> ; <b><i>mcr-4.2</i></b> <i>gyrA</i> S83L, <i>parC</i> S80R	<i>mcr-4.2</i> / ColE10	<b><i>sta1</i>, <i>stb</i>, <i>stx2</i>, <i>fedF</i></b> , <i>air</i> , <i>eilA</i> , <i>fedA</i> , <i>gad</i> , <i>iha</i> , <i>iss</i> , <i>lpfA</i>	NAL, CIP, SXT, MIN, DOX, CST	Sta, STb, VT2e, F18
LREC-134	2013	O139:H1	*D	2-54	1	IncI1 (STunknown) IncX1 ColE10-like	<i>aac(3)-IVa</i> , <i>aph(3')-Ib</i> , <i>aph(4)-Ia</i> , <i>aph(6)-Id</i> ; <i>mdf(A)</i> ; <b><i>mcr-4.2</i></b> <i>gyrA</i> D87N	<i>mcr-4.2</i> / ColE10	<b><i>stx2</i>, <i>fedF</i></b> , <i>eilA</i> , <i>fedA</i> , <i>gad</i> , <i>lpfA</i>	GEN, TOB, CST	VT2e, F18
LREC-137	2009	O157:H39	A	11-24	10 (10)	IncF (F2:A-:B42) IncI2 Col156-like ColE10-like	<i>bla</i> <sub>TEM-1B</sub> ; <i>aadA1</i> ; <i>mdf(A)</i> ; <i>sul3</i> ; <i>tet(B)</i> ; <i>dfrA1</i> ; <b><i>mcr-4.2</i></b> <i>gyrA</i> S83L; <b><i>pmrB V161G</i></b>	<i>mcr-4.2</i> / ColE10	<b><i>itcA</i>, <i>stb</i>, K88</b> , <i>astA</i> , <i>cba</i> , <i>cma</i> , <i>gad</i> , <i>iha</i> , <i>sepA</i>	TIC, AMP, GEN, TOB, NAL, CIP*, SXT, MIN, DOX, CHL*, CST	LT, STb, K88

(Continued)

TABLE 1 | Continued

Code	Year of Isolation <sup>1</sup>	Serotype <sup>2</sup>	Phylo Group <sup>3</sup>	CHType <sup>4</sup>	ST <sup>5</sup> (CC)	Plasmid content Inc group (pMLST) <sup>6</sup>	Acquired resistances (in black) and point mutations (in blue) <sup>7</sup>	<i>mcr</i> /location <sup>8</sup>	Virulence genes <sup>9</sup>	Phenotypic resistance profile <sup>10</sup>	Pathotype-associated VF <sup>11</sup>
LREC-138	2008	O157:H39	A	11-24	10 (10)	IncF (F2/111:A-:B42) IncI1 (ST154) IncI2 ColE10-like	<i>aac(3)-IV</i> , <i>aph(3'')-Ib</i> , <i>aph(4)-Ia</i> , <i>aph(6)-Id</i> ; <i>floR</i> ; <i>mdf(A)</i> ; <i>tet(B)</i> ; <b><i>mcr-4.2</i></b> <i>gyrA</i> S83L, <i>gyrA</i> D87G, <i>parC</i> S80I; <b><i>pmrB V161G</i></b>	<i>mcr-4.2</i> /ColE10	<b><i>itcA</i></b> , <b><i>sta1</i></b> , <b><i>stb</i></b> , <i>astA</i> , <i>cba</i> , <i>cma</i> , <i>iha</i>	NAL, CIP, LVX, MIN*, DOX, CHL, CST	LT, STa, STb, F18
LREC-139	2009	O108:H39	A	11-24	10 (10)	IncF (F89*C2:A-:B42) IncN (ST1) IncI2 Col156-like ColE10-like	<i>aadA2</i> ; <i>mdf(A)</i> , <i>inu(F)</i> ; <b><i>mcr-4.2</i></b> <i>gyrA</i> S83L, <i>gyrA</i> D87N, <i>parC</i> S80I	<i>mcr-4.2</i> / ColE10	<b><i>itcA</i></b> , <i>astA</i> , <i>celB</i> , <i>gad</i> , <i>iha</i>	NAL, CIP, LVX, CST	LT
LREC-140	2015	O108:H39	A	11-24	10 (10)	IncF (F111:A-:B42) IncHI2 (ST9) IncI1 (ST80) IncN (ST1) IncI2 ColE10-like	<i>bla</i> <sub>CTX-M-32</sub> , <i>bla</i> <sub>TEM-1B</sub> ; <i>aac(3)-IV</i> , <i>aadA1</i> , <i>aph(3'')-Ib</i> , <i>aph(4)-Ia</i> ; <i>catA1</i> ; <i>erm(B)</i> , <i>mdf(A)</i> , <i>mph(B)</i> ; <i>sul1</i> ; <i>tet(B)</i> , <i>tet(M)</i> ; <i>dfrA1</i> ; <b><i>mcr-4.2</i></b> <i>gyrA</i> S83L, <i>gyrA</i> D87G, <i>parC</i> S80I; <b><i>pmrB V161G</i></b>	<i>mcr-4.2</i> / ColE10	<b><i>itcA</i></b> , <b><i>sta1</i></b> , <b><i>stb</i></b> , <b><i>fedF</i></b> , <i>astA</i> , <i>fedF</i> , <i>cma</i> , <i>fedA</i> , <i>iha</i>	TIC, AMP, CFZ, CXM, CTX, CAZ, FEP, GEN*, TOB*, ATM, NAL, CIP, LVX, SXT, MIN, DOX, CHL, CST	LT, STa, STb, F18
LREC-142	2010	O45:H39	A	11-24	10 (10)	IncF (F89*C2:A8*:B42) IncHI1 (ST2*) IncX1 Col156-like ColE10-like	<i>bla</i> <sub>TEM-1B</sub> ; <i>aadA1</i> , <i>aadA2</i> , <i>acc(3)-IV</i> , <i>aph(3'')-Ia</i> , <i>aph(3'')-Ib</i> , <i>aph(4)-Ia</i> , <i>aph(6)-Id</i> ; <i>cmlA1</i> , <i>catA1</i> ; <i>mdf(A)</i> , <i>inu(G)</i> ; <i>sul1</i> , <i>sul3</i> ; <i>tet(B)</i> ; <i>dfrA1</i> ; <b><i>mcr-4.2</i></b> <i>gyrA</i> S83L, <i>gyrA</i> D87G, <i>parC</i> S80I; <b><i>pmrB V161G</i></b>	<i>mcr-4.2</i> / ColE10	<b><i>itcA</i></b> , <b><i>stb</i></b> , <b><i>K88</i></b> , <i>astA</i> , <i>gad</i> , <i>iha</i>	TIC, AMP, GEN*, TOB, NAL, CIP, LVX, SXT, DOX*, CHL, NIT*, CST	LT, STb, K88
LREC-143	2006	O138:H14	*D	28-41	42	IncF (F14:A8:B-) IncHI1 (ST2*) IncX1 ColE10-like	<i>aadA1</i> , <i>aph(3'')-Ia</i> ; <i>mdf(A)</i> ; <i>catA1</i> ; <i>sul1</i> ; <i>tet(B)</i> ; <i>dfrA1</i> ; <b><i>mcr-4.2</i></b> <i>gyrA</i> S83L, <i>parC</i> S80R	<i>mcr-4.2</i> / ColE10	<b><i>sta1</i></b> , <b><i>stb</i></b> , <b><i>stx2</i></b> , <b><i>fedF</i></b> , <i>air</i> , <i>fedA</i> , <i>gad</i> , <i>iha</i> , <i>lpfA</i> , <i>iss</i>	NAL, CIP, SXT, MIN, DOX, CHL, CST	STa, STb, VT2e, F18

(Continued)



TABLE 1 | Continued

Code	Year of Isolation <sup>1</sup>	Serotype <sup>2</sup>	Phylo Group <sup>3</sup>	CHType <sup>4</sup>	ST <sup>5</sup> (CC)	Plasmid content Inc group (pMLST) <sup>6</sup>	Acquired resistances (in black) and point mutations (in blue) <sup>7</sup>	<i>mcr</i> /location <sup>8</sup>	Virulence genes <sup>9</sup>	Phenotypic resistance profile <sup>10</sup>	Pathotype-associated VF <sup>11</sup>
LREC-156	2011	O108:H39	A	11-24	10 (10)	IncF (F111:A8*:B42) IncHI1 (ST2*) IncI1 (STunknown) IncI2 IncY Col156-like ColE10-like	<i>bla</i> <sub>CTX-M-14</sub> ; <i>bla</i> <sub>TEM-1B</sub> ; <i>aac</i> (3)-IV, <i>aadA1</i> , <i>aadA2</i> , <i>aph</i> (3')-Ia, <i>aph</i> (3')-Ib, <i>aph</i> (4)-Ia, <i>aph</i> (6)-Ic; <i>cmlA1</i> , <i>catA1</i> ; <i>mdf</i> (A); <i>sul1</i> , <i>sul3</i> ; <i>tet</i> (B); <i>dfrA1</i> ; <b><i>mcr-4.2</i></b> <i>gyrA</i> S83L, <i>gyrA</i> D87G, <i>parC</i> S80I; <b><i>pmrB V161G</i></b>	<i>mcr-4.2</i> / ColE10	<b><i>itcA</i>, <i>sta1</i>, <i>fedF</i>,</b> <i>astA</i> , <i>celB</i> , <i>fedA</i> , <i>gad</i> , <i>iha</i>	TIC, AMP, CFZ, CXM, CTX, FEP, GEN*, TOB, NAL, CIP, LVX, SXT, MIN, DOX, CHL, CST	LT, StA, F18
LREC-135	2008	O45:H39	A	11-24	10 (10)	IncF (F89*C2:A-:B42) IncI1 (ST202*) IncX1 ColE10	<i>bla</i> <sub>TEM-1A</sub> ; <i>aac</i> (3)-IVa, <i>aph</i> (3')-Ib, <i>aph</i> (4)-Ia, <i>aph</i> (6)-Ic; <i>mdf</i> (A); <b><i>mcr-4.5</i></b> <i>gyrA</i> S83L, <i>gyrA</i> D87G, <i>parC</i> S80I, <i>parE</i> L416F; <b><i>pmrB V161G</i></b>	<i>mcr-4.5</i> / ColE10	<b><i>itcA</i>, <i>stb</i>, <i>K88</i>,</b> <i>astA</i> , <i>iha</i> , <i>sepA</i>	TIC, AMP, GEN*, TOB, NAL, CIP, LVX, CST	LT, Stb, K88
LREC-146	2008	O45:H39	A	11-24	10 (10)	IncF (F89*C2:A-:B42) IncI1 (ST202*) IncX1 ColE10-like	<i>bla</i> <sub>OXA-1</sub> , <i>bla</i> <sub>TEM-1A</sub> ; <i>aac</i> (3)-IV, <i>aadA1</i> , <i>aph</i> (3')-Ib, <i>aph</i> (4)-Ia, <i>aph</i> (6)-Ic; <i>floR</i> ; <i>mdf</i> (A); <i>sul1</i> , <i>sul2</i> ; <b><i>mcr-4.5</i></b> <i>gyrA</i> S83L, <i>gyrA</i> D87G, <i>parC</i> S80I; <b><i>pmrB V161G</i></b>	<i>mcr-4.5</i> / ColE10	<b><i>itcA</i>, <i>stb</i>, <i>K88</i>,</b> <i>astA</i> , <i>iha</i> , <i>sepA</i>	TIC, AMP, SAM, AMC, GEN, TOB, NAL, CIP, LVX, SXT, CHL, CST	LT, Stb, K88
LREC-152	2008	O157:H39	A	11-24	10 (10)	IncF (F108:A-:B42) IncI1 (ST290*) IncX1	<i>bla</i> <sub>TEM-1A</sub> ; <i>aac</i> (3)-IV, <i>aph</i> (3')-Ia, <i>aph</i> (3')-Ib, <i>aph</i> (4)-Ia, <i>aph</i> (6)-Ic; <i>mdf</i> (A); <b><i>mcr-5.1</i></b> <i>gyrA</i> S83L; <b><i>pmrB V161G</i></b>	<i>mcr-5.1</i> / ND (plasmid reference pKP13a)	<b><i>itcA</i>, <i>stb</i>, <i>K88</i>,</b> <i>astA</i> , <i>gad</i> , <i>iha</i>	TIC, AMP, SAM, GEN, TOB, NAL, CST	LT, Stb, K88

(Continued)

TABLE 1 | Continued

Code	Year of Isolation <sup>1</sup>	Serotype <sup>2</sup>	Phylo Group <sup>3</sup>	CHType <sup>4</sup>	ST <sup>5</sup> (CC)	Plasmid content Inc group (pMLST) <sup>6</sup>	Acquired resistances (in black) and point mutations (in blue) <sup>7</sup>	<i>mcr</i> /location <sup>8</sup>	Virulence genes <sup>9</sup>	Phenotypic resistance profile <sup>10</sup>	Pathotype-associated VF <sup>11</sup>
LREC-177	2007	O157:H39	A	11-24	10 (10)	IncF (F2/111:A-:B42) IncI2 Col156-like	<i>aadA1</i> , <i>aph(3')-Ia</i> ; <i>mdf(A)</i> ; <i>tet(B)</i> ; <i>dfrA1</i> ; <b><i>mcr-5.1</i></b> <i>gyrA</i> S83L; <b><i>pmrB</i> V161G</b>	<i>mcr-5.1</i> / ND (plasmid reference pKP13a)	<b><i>itcA</i></b> , <b><i>sta1</i></b> , <b><i>stb</i></b> , <b><i>fedF</i></b> , <i>astA</i> , <i>cba</i> , <i>celB</i> , <i>cma</i> , <i>fedA</i> , <i>gad</i> , <i>iha</i>	NAL, SXT, MIN, DOX, CST	LT, STa, STb, F18
LREC-141	2007	O45:H39	A	11-24	10 (10)	IncF (F89*C2:A-:B42) IncHI2 (ST4) IncQ1 IncX1 Col156-like ColE10-like	<i>bla</i> <sub>TEM-1A</sub> ; <i>aac(3)-IIa</i> , <i>aadA1</i> , <i>aph(3')-Ia</i> , <i>aph(3')-Ib</i> , <i>aph(6)-Id</i> ; <i>mdf(A)</i> ; <i>sul1</i> , <i>sul2</i> , <i>sul3</i> ; <i>tet(A)</i> ; <i>dfrA1</i> ; <b><i>mcr-1.1</i></b> , <b><i>mcr-4.2</i></b> <i>gyrA</i> S83L, <i>gyrA</i> D87G, <i>parC</i> S80I, <i>parE</i> L416F; <b><i>pmrB</i> V161G</b>	<i>mcr-1.1</i> / IncHI2; <i>mcr-4.2</i> / ColE10	<b><i>itcA</i></b> , <b><i>fedF</i></b> , <i>astA</i> , <i>celB</i> , <i>fedA</i> , <i>iha</i>	TIC, AMP, SAM, AMC*, GEN, TOB, NAL, CIP, LVX, SXT, DOX*, CST	LT, F18
LREC-163	2011	O45:H39	A	1	10 (10)	IncF (F89*C2:A-:B42) IncHI2 (ST4) IncX1 pO111-like Col156-like ColE10-like	<i>bla</i> <sub>TEM-1B</sub> ; <i>aadA1</i> , <i>aadA17</i> , <i>aph(3')-Ib</i> , <i>aph(6)-Id</i> ; <i>inu(F)</i> , <i>mdf(A)</i> ; <i>sul1</i> , <i>sul3</i> ; <i>tetA</i> ; <i>dfrA1</i> ; <b><i>mcr-1.1</i></b> , <b><i>mcr-4.2</i></b> <i>gyrA</i> S83L, <i>gyrA</i> D87G, <i>parC</i> S80I; <b><i>pmrB</i> V161G</b>	<i>mcr-1.1</i> / IncHI2; <i>mcr-4.2</i> / ColE10	<b><i>itcA</i></b> , <b><i>fedF</i></b> , <i>astA</i> , <i>celB</i> , <i>fedA</i> , <i>gad</i> , <i>iha</i>	TIC, AMP, SAM, AMC*, GEN, TOB*, NAL, CIP, LVX, SXT, CST	LT, F18

<sup>1</sup>Year of isolation of the WGS isolates recovered from pig colibacillosis. <sup>2</sup>Serotypes, <sup>4</sup>clonotypes, <sup>5</sup>sequence types, <sup>6</sup>replicon/plasmid STs, <sup>7</sup>acquired antimicrobial resistance genes and/or chromosomal mutations, <sup>9</sup>virulence genes were determined using SerotypeFinder 2.0, CHType 1.0, MLST 2.0, PlasmidFinder 2.0, pMLST 2.0, ResFinder 3.1 and VirulenceFinder 2.0 online tools at the Center of Genomic Epidemiology (<https://cge.cbs.dtu.dk/services/>), respectively; while <sup>3</sup>phylogroups were predicted using the ClermonTyping tool at the lame-research Center web (<http://clermontyping.iame-research.center/>). <sup>2</sup>Serotypes: underlined those antigens that were non-typeable (ONT or HNM) by conventional serotyping but determined by SerotypeFinder. \*LREC-147 was solved as O157 by conventional typing. <sup>3</sup>Phylogroups: "D" indicates that LREC-133, LREC-134, LREC-143, LREC-151, LREC-170, LREC-171, LREC-174 revealed discrepancies between the assignment obtained with the quadruplex PCR of Clermont et al. (2013) and the in silico assignment using ClermonTyping tool, showing phylogroup E by PCR, but phylogroup D in silico. <sup>6</sup>Plasmid STs: "\*" indicates alleles with less than 100% but >95% identity and 100% coverage; "/" indicates alleles with multiple perfect hits found. <sup>7</sup>Resistome: chromosomal and plasmid mechanisms associated to colistin resistance are highlighted in bold. Genes coding for ESBLs appear underlined. Acquired resistance genes: *beta-lactam*: *bla*<sub>TEM-1B</sub>, *bla*<sub>TEM-1A</sub>, *bla*<sub>OXA-1</sub>, *bla*<sub>CTX-M-14</sub>, *bla*<sub>CTX-M-32</sub>, *bla*<sub>SHV-12</sub>, *aminoglycosides*: *aac(3)-II/IV*, *acc(6)-Ib3*, *aadA*, *aph(3')-I/IIa*, *aph(3')-Ib*, *aph(4)-Ia*, *aph(6)-Id*; *phenicols*: *catA1*, *catB3*, *cmlA1*, *floR*; *fluoroquinolones*: *aac(6)-Ib-cr*, *qnrS1*; *macrolides*: *erm(B)*, *inu(F)*, *inu(G)*, *mdf(A)*, *mph(B)*; *sulfonamides*: *sul1*, *sul2*, *sul3*; *tetracycline*: *tet(A)*, *tet(B)*, *tet(M)*; *trimethoprim*: *dfrA1*, *dfrA12*. Point mutations: *quinolones and fluoroquinolones*: *gyrA* S83L: TCG-TTG, *gyrA* D87G: GAC-GGC, *gyrA* D87N: GAC-AAT, *gyrA* D87Y: GAC-TAT, *parC* S80I: AGC-ATC, *parC* S80R: AGC-AGG, *parC* E84G: GAA-GGA, *parE* L416F: CTT-TTT; *colistin*: *pmrB* V161G: GGG-GTG, *pmrA* S39: AGC-ATC. <sup>8</sup>The *mcr* gene location was determined using PlasmidFinder/ResFinder predictions, together with PLACNETw building and references (<https://castillo.dicom.unican.es/upload/>), and Prokka annotations. <sup>9</sup>Highlighted in bold, those features defining *E. coli* pathotypes (STEC, ETEC, EPEC). Virulence genes: *itcA*, coding for heat labile enterotoxin A subunit; *sta1*, heat stable enterotoxin ST-1a; *stb*, heat stable enterotoxin II; *fedF*, fimbrial adhesin AC precursor; *K88*, *K88/F4* protein subunit; *air*, enteroaggregative immunoglobulin repeat protein; *astA*, EAST-1; *capU*, hexosyltransferase homolog; *cba*, colicin B; *celB*, endonuclease colicin E2; *cif*, type III secreted effector; *cma*, colicin M; *eae*, intimin; *efa1*, EHEC factor for adherence; *eilA*, Salmonella HliA homolog; *espA*, type III secretions system; *espB*, secreted protein B; *espF*, type III secretions system; *espJ*, prophage -encoded type III secretion system effector; *etpD*, type II secretion protein; *fedA*, F107; *gad*, glutamate decarboxylase; *iha*, adherence protein; *iroN*, enterobactin siderophore receptor protein; *iss*, increased serum survival; *lplA*, long polar fimbriae; *nleA*, non-LEE encoded effector A; *nleB*, non-LEE encoded effector B; *sepA*, *Shigella* extracellular protein A; *tccP*, Tir cytoskeleton coupling protein; *tir*, translocated intimin receptor protein. bp, base pairs; CHType, clonotype (*fumC-fimH*); ST (CC), sequence type and clonal complex according to Achtman scheme; pMLST, plasmid sequence type. <sup>10</sup>Phenotypic resistances interpreted according to the CLSI (intermediate resistance is indicated with an asterisk \*). AMC, amoxicillin/clavulanate; AMP, ampicillin; AMP/SAM, ampicillin-sulbactam; ATM, aztreonam; CAZ, ceftazidime; CHL, chloramphenicol; CIP, ciprofloxacin; CST, colistin; CTX, cefotaxime; CXM, cefuroxime; CFZ, cefazolin; DOX, doxycycline; FEP, cefepime; FOF, fosfomicin; GEN, gentamicin; LVX, levofloxacin; MI, minocycline; NAL, nalidixic acid; NIT, nitrofurantoin; SXT, trimethoprim/sulfamethoxazole; TIC, ticarcillin; TOB, tobramycin. <sup>11</sup>Pathotype of the isolates, established by conventional PCR, based on specific genes encoding toxins (LT, STa, STb, Stx1, Stx2, Stx2e), fimbriae (F4, F5, F6, F18, F41) and intimin (*Eae*).

there was no *mcr* plasmid co-occurrence in LREC-141 and LREC-163, but rather the *mcr-1.1* and *mcr-4.2* genes were located in independent plasmids (IncHI2 and ColE10-like types, respectively). The *mcr* location remained undetermined for four isolates.

Since the *mcr-1* plasmid gene was first described (Liu et al., 2016), it has been identified in members of the Enterobacteriaceae family encoded in different plasmid types, including IncI2, IncX4, IncHI1, IncHI2, IncFI, IncFII, IncP, IncK (Sun et al., 2018). Different authors corroborate that large conjugative plasmids of types IncHI2, IncX4 and IncI2 would be the maximum responsible for the dissemination of the *mcr-1* gene among *E. coli* isolates from different sources and geographical locations (Doumith et al., 2016; Li et al., 2017; Manageiro et al., 2019). To date, other *mcr* genes (2–9) have been described (Carroll et al., 2019); among them, the *mcr-4* and *mcr-5* genes appear mostly encoded in small and non-conjugative ColE-like type plasmids (Sun et al., 2018). Here we found similar results, since *mcr-1.1* genes were located mainly on IncHI2 and IncX4 types, and *mcr-4* on ColE10-like plasmids. It is of note that the *mcr-5.1* gene, predicted in LREC-152 and LREC-177, was linked to a Kp13-like plasmid (CP003996.1), location previously described by Hammerl et al. (2018) for one *mcr-5* isolate recovered from a fecal pig sample at farm. Chromosomally-encoded *mcr-1* location remains rare, however, it was described soon after the discovery of this plasmid-borne gene (Falgenhauer et al., 2016; Veldman et al., 2016). Here, we determined chromosomal location in five genomes by means of PLACNETw, and according to the predictive annotation of the *mcr*-contigs, the only common element flanking the *mcr-1* was a putative ORE, *pap2*, which is part of the Tn6360 and encodes a Pap2 superfamily protein. Thus, Pap2 was detected in LREC-145, LREC-148, LREC-149, and LREC-164, while the IS*ApI1* element typically associated with the initial mobilization of *mcr-1*, was missing within the five contigs (Snesrud et al., 2018).

Overall, our findings are in accordance with those reported by Magistrali et al. (2018) on 13 *mcr*-positive *E. coli* isolated from swine colibacillosis in Belgium, Italy and Spain. Both studies show common features in relation to a prevalent clonal group (CC10), serotypes (O108:H39, O138:H10, O139:H1, O141:H4), and *mcr*-plasmid types. The confirmation of these similarities are of interest for the global design of alternatives to antibiotics that would curb the dissemination of specific clones in the pig farming.

The *in vitro* analysis of resistances showed that 30 of the 35 *E. coli* were multidrug-resistant (MDR) according to Magiorakos et al. (2012) definition (Table 1). Phenotypic results corresponded broadly to those predicted by ResFinder (Supplementary Table S1) as detailed below.

The quinolones/fluoroquinolones (FQ), together with polymyxins and 3rd–4th-generation cephalosporins, all are included in Category B of restricted antimicrobials in the EMA categorization, considering that the risk to public health resulting from its veterinary use needs to be mitigated by specific restriction (EMA/CVMP/CHMP, 2019). Two major mechanisms are implicated in the resistance to FQ, namely, mutations in the genes for DNA gyrase and topoisomerase IV, and decreased

intracellular drug accumulation. In addition, plasmid-mediated quinolone resistances also play a role but usually conferring low-level FQ resistance (van Duijkeren et al., 2018). Phenotypically, 17 of the 35 isolates showed resistance to both nalidixic acid and ciprofloxacin, and other eight resistance to nalidixic acid only (Supplementary Table S1). In the majority of cases, phenotypic results correlated with those predicted by ResFinder. Particularly, 28 of the 35 genomes carried the *gyrA* S83L substitution, with 12 of those 28 showing double-serine mutations (*gyrA* S83L and *parC* S80I). An additional substitution (*gyrA* D87N) was detected in two of the 12 *gyrA* S83L/*parC* S80I genomes. Thus, nalidixic acid resistance *in vitro* corresponded to one single substitution (*gyrA* S83L), and FQ resistance to double or triple substitutions (*gyrA* S83L/*parC* S80I/*gyrA* D87N). Plasmid-mediated quinolone resistant genes *acc(6′)-Ib-cr* and *qnrS1* were also present together with chromosomal mutations in LREC-147 and LREC-169, respectively. Double-serine mutations in specific positions of the *gyrA* and *parC* genes have been reported as a dominant feature of MDR lineages within *E. coli*, *S. aureus* and *K. pneumoniae*, with favorable fitness balance linked to high levels of resistance to FQ (Fuzi et al., 2017). This finding, in 12 out of the 28 *in silico* predicted FQ-resistant could be conferring adaptive advantages to certain widely spread pig pathogenic clonal groups of *E. coli*, such as the ST10-A (CH11-24) (García et al., 2018). This hypothesis is presently assumed for ST131 and other risk clones linked to high FQ-resistance (Johnson et al., 2015; Fuzi et al., 2017).

On the other hand, colistin has been widely used for the control of enteric diseases, mainly in swine and poultry (Rhouma et al., 2016; Hammerl et al., 2018). Several mechanisms of resistance due to chromosomal mutations or acquired resistance genes have been described so far (Olaitan et al., 2014; Poirel et al., 2018). The 35 colistin-resistant *E. coli* of this study showed MIC values > 4 mg/L. As detailed above, ResFinder confirmed that all the analyzed genomes were *mcr*-carriers. In addition to the plasmid mechanism (*mcr*) of resistance, polymyxin resistance in *E. coli* can be due to genes encoding LPS-modifying enzymes, particularly to mutations in the two-component systems PmrAB and PhoPQ, or in the MgrB regulator. Quesada et al. (2015) detected two colistin-resistant *E. coli* recovered in 2011 and 2013 from the stools of two pigs, which showed mutations in PmrB V161G and PmrA S39I, reporting the finding as a rare event. Subsequently, Delannoy et al. (2017) analyzed 90 strains of *E. coli* isolated from diseased pigs: 81 were phenotypically resistant to colistin and 72 *mcr-1* carriers (including two colistin-susceptible). Although different mutations were found in the amino acid sequences of the MgrB, PhoP, PhoQ, and PmrB proteins of eight isolates, only two of them were *mcr-1* positive (but colistin-susceptible). Surprisingly, we found here the double mechanism of colistin resistance in 16 *E. coli*, harboring *mcr*-genes together with one amino acid substitution: PmrB V161G (14 genomes) or PmrA S39I (two genomes). In a recent study on Parisian inpatient fecal *E. coli* (Bourel et al., 2019), the authors found 12.5% of colistin-resistant *E. coli* carriers among 1,217 patients; however, *mcr-1* gene was identified in only seven of 153 isolates, while 72.6% harbored mutations in the PmrA and PmrB proteins. According to the authors, their findings

indicate two evolutionary paths leading to colistin resistance in human fecal *E. coli*, one corresponding to a minority of plasmid-encoded *mcr-1* isolates of animal origin, and a second corresponding to a vast majority of human isolates exhibiting chromosomally encoded mechanisms (Bourrel et al., 2019). Thus, and given the limited data regarding the co-occurrence of double resistance mechanism, it is of note that 16 of the 35 *mcr*-bearing genomes of our study showed mutations in the PmrA and PmrB proteins. Furthermore, two *E. coli* (LREC-141 and LREC-163) shown to be carriers of two different *mcr*-bearing plasmids together with PmrB V161G mutation. An explanation for this rare finding is that these isolates would be reflecting a cumulative evolution to antibiotic pressure and, as a consequence, enhancing the transmission (vertical and horizontal) of colistin resistance. In any case, further investigation is needed to evaluate the implication of chromosomal mutations and *mcr* co-occurrence regarding colistin resistance phenotype.

In this study, 22 out of the 25 isolates showing phenotypic resistance to beta-lactams (Supplementary Table S1), were positive in the analysis *in silico* for the presence of *bla*<sub>TEM-1</sub> genes, alone (14 genomes), or in combination with other *bla* genes (*bla*<sub>CTX-M-14</sub>, *bla*<sub>SHV-12</sub>, *bla*<sub>CTX-M-32</sub> and *bla*<sub>OXA-1</sub>); additionally, two genomes showed the presence of *bla*<sub>CTX-M-14</sub> and *bla*<sub>SHV-12</sub>, respectively. With the exception of LREC-147, LREC-164, and LREC-170, which were phenotypically resistant to narrow-spectrum beta-lactamases but negative for the presence of genes, a good correlation was observed between genes predicted and resistance shown *in vitro*. It is of note that *bla*<sub>TEM-135</sub>, determined in LREC-156 by conventional typing, was not identified *in silico*. Beta-lactams are the most widely used family in current clinical practice. Numerous genes in *E. coli* confer resistance to this group, being some of them, such as *bla*<sub>TEM-1</sub> widespread in *E. coli* from animals coding for narrow-spectrum beta-lactamases that can inactivate penicillins and aminopenicillins. However, genes encoding ESBLs/AmpCs have increasingly emerged in *E. coli* from humans and animals, including food-producing animals (Cortes et al., 2010).

Thirty out of the 35 genomes showed high frequency of resistance genes to aminoglycosides, specifically encoding AAC(3)-II/IV and AAC(6)-Ib, which are the most frequently encountered acetyltransferases among *E. coli* of human and animal origins. The subclass AAC(3)-II, which is characterized by resistance to gentamicin, netilmicin, tobramycin, sisomicin, 2'-N-ethylnetilmicin, 6'-N-ethylnetilmicin and dibekacin (Shaw et al., 1993), and AAC(6') enzymes that specify resistance to several aminoglycosides and differ in their activity against amikacin and gentamicin C1 (Ramirez and Tolmasky, 2010) seemed to correlate with the phenotypic detection of resistance to gentamicin and/or tobramycin (12 of the 17 resistant isolates) (Supplementary Table S1). We also detected high prevalence of genes encoding nucleotidyltransferases (*aadA*), which specify resistance to spectinomycin and streptomycin, alone or together with phosphotransferases (APHs) (Ramirez and Tolmasky, 2010), but they were not tested in the phenotypic antimicrobial susceptibility tests.

It is noteworthy that the 35 genomes of our study were carriers of *mdfA*. Edgar and Bibi (1997) described that cells

expressing MdfA from a multicopy plasmid are substantially more resistant to a diverse group of cationic or zwitterionic lipophilic compounds. Besides, the authors found that MdfA also confers resistance to chemically unrelated, clinically important antibiotics such as chloramphenicol, erythromycin, and certain aminoglycosides and fluoroquinolones. This capability could correlate with the *in vitro* resistance observed for some isolates to tetracyclines and aminoglycosides, in absence of other specific genes. In our collection, of the 24 isolates showing phenotypic resistance to minocycline and, or doxycycline (Supplementary Table S1), 20 showed carriage of *tet* genes: 12 *tet(B)*, six *tet(A)*, one *tet(A) + tet(B)* and one *tet(B) + tet(M)*. However, two *tet(A)* isolates were susceptible to those antibiotics (LREC-163, LREC-169). Additionally, *tet* genes were not detected *in silico* in four phenotypically resistant isolates. In general, *tet(A)* and *tet(B)* are the most prevalent tetracycline resistance genes in *E. coli* of animal origin, and specifically in isolates from pigs (Tang et al., 2011; Holzel et al., 2012; Jurado-Rabadan et al., 2014).

Although the use of chloramphenicol was banned in the European Union in food-producing animals in 1994, fluorinated derivative florfenicol is allowed for the treatment of bacterial infection in these animals (Schwarz et al., 2004; OIE, 2019). In the present study, all 19 chloramphenicol-resistant isolates (Supplementary Table S1) correlated with the presence of genes *catA1* (12 genomes), *catB3* (one genomes), *cmlA* (ten genomes) or *floR* (three genomes) detected *in silico*. Travis et al. (2006) showed that chloramphenicol resistant genes are frequently linked to other antibioresistance genes. Thus, through transformation experiments conducted with *E. coli* from pigs demonstrated that *aadA* and *sul1* were located with *catA1* on a large ETEC plasmid, and plasmids carrying *cmlA* also carried *sul3* and *aadA*. According to the authors, this linkage might partly explain the long-term persistence of chloramphenicol resistance in ETEC despite its withdrawal years ago. In our study, ResFinder also showed an association of genes *cmlA*, *sul3* and *aadA* present in the same contig (7 of the 10 genomes positive for *cmlA*), and *cmlA/aadA* in all cases. Additionally, *aadA* and *sul1* were located with *floR* in LREC-146.

In *E. coli* from food-producing animals, sulfonamide resistance is mediated by *sul* genes (*sul1*, *sul2*, *sul3*), widely disseminated, and frequently found together with other antimicrobial resistance genes, while *dfr* genes confer trimethoprim resistance in *E. coli* and other gram-negative bacteria (van Duijkeren et al., 2018). Within our collection, 20 of the 35 isolates were *in vitro* resistant to trimethoprim/sulfamethoxazole (Supplementary Table S1), and most of them correlated with the presence of *sul + dfrA* genes in their genomes, with the exception of LREC-133 and LREC-170 (negative for the *in silico* detection of *sul*, *dfrA* genes) and LREC-146 (in which only *sul1* and *sul2* genes were predicted). Besides, ResFinder showed that *sul1* (present in 16 genomes), *sul3* (14 genomes) and *sul2* (three genomes) were located together with *dfrA*, and other resistance genes, as mentioned previously.

The fosfomycin resistance showed *in vitro* by two isolates of the study collection, was not predicted for LREC-144 and LREC-145 (Supplementary Table S1) by ResFinder, which



analyzes the presence of *fos* genes encoding for fosfomycin-modifying enzymes. The use of this antibiotic has been limited to the treatment of infections by Gram-positive and negative pathogens, included *E. coli*, mainly in pig and poultry farming (Poirel et al., 2018). However, phosphonic acid derivatives such as fosfomycin, have been recently categorized by the EMA (EMA/CVMP/CHMP, 2019) as Category A (antimicrobial classes not currently authorized in veterinary medicine in EU).

## CONCLUSION

Swine colibacillosis control has been traditionally managed through the extensive use of antibiotics. Our results are a reflection of the situation within the industrial pig farming, where global hygiene procedures and vaccinations are essential for improvement in antimicrobial stewardship. The summative presence of antibioresistances could be conferring adaptive advantages to prevalent pig *E. coli* lineages, such as the ST10-A (CH11-24). Based on the different replicons identified by PlasmidFinder (up to seven), it is of note the high plasmid diversity found within these isolates; further research is needed to know mechanisms of maintenance and advantages conferred to them.

Here, we report for first time a rare finding so far, which is the co-occurrence of double colistin-resistance mechanisms (*mcr*-genes and chromosomal mutations in the PmrA and PmrB proteins) in a significant number of *E. coli* isolates. This fact could be increasing the risk of colistin resistance-acquisition by means of food transmission. Globally, we found a very good correlation between resistances determined *in vitro* and genes predicted using CGE tools, and the same observation applies to the *E. coli* pathotype determination.

## DATA AVAILABILITY STATEMENT

The nucleotide sequence of the 35 LREC genomes have been deposited in the NCBI sequence databases with accession codes

SAMN11523829 to SAMN11523863. These sequences are part of BioProject ID PRJNA540146.

## AUTHOR CONTRIBUTIONS

IG-M, DD-J, and SF-S undertook the laboratory work. AM and JB conceived and designed the study. IG-M, DD-J, VG, MT, and AM performed the data analysis. IG-M, DD-J, VG, MT, JB, and AM drafted the manuscript. All authors provided critical input and approved the final version.

## FUNDING

This study was supported by projects PI16/01477 from Plan Estatal de I+D+I 2013–2016, Instituto de Salud Carlos III (ISCIII), Subdirección General de Evaluación y Fomento de la Investigación, and FEDER; AGL2016-79343-R from the Agencia Estatal de Investigación (AEI, Spain) and FEDER; ED431C 2017/57 from the Consellería de Cultura, Educación e Ordenación Universitaria (Xunta de Galicia) and FEDER. IG-M and VG acknowledge the Consellería de Cultura, Educación e Ordenación Universitaria, Xunta de Galicia for their pre-doctoral and post-doctoral grants (Grant Numbers ED481A-2015/149 and ED481B-2018/018, respectively). SF-S acknowledges the FPU programme from the Secretaría General de Universidades, Ministerio de Educación, Cultura y Deporte, Gobierno de España (Grant Number FPU15/02644).

## SUPPLEMENTARY MATERIAL

The Supplementary Material for this article can be found online at: <https://www.frontiersin.org/articles/10.3389/fmicb.2019.02469/full#supplementary-material>

## REFERENCES

- Beyrouthy, R., Robin, F., Lessene, A., Lacomat, I., Dortet, L., Naas, T., et al. (2017). MCR-1 and OXA-48 *in vivo* acquisition in KPC-producing *Escherichia coli* after colistin treatment. *Antimicrob. Agents Chemother.* 61:e2540-16. doi: 10.1128/AAC.02540-16
- Bosak, J., Hrala, M., Pirkova, V., Mícenková, L., Cizek, A., Smola, J., et al. (2019). Porcine pathogenic *Escherichia coli* strains differ from human fecal strains in occurrence of bacteriocin types. *Vet. Microbiol.* 232, 121–127. doi: 10.1016/j.vetmic.2019.04.003
- Bourrel, A. S., Poirel, L., Royer, G., Darty, M., Vuillemin, X., Kieffer, N., et al. (2019). Colistin resistance in parisian inpatient faecal *Escherichia coli* as the result of two distinct evolutionary pathways. *J. Antimicrob. Chemother.* 74, 1521–1530. doi: 10.1093/jac/dkz090
- Carroll, L. M., Gaballa, A., Guldimann, C., Sullivan, G., Henderson, L. O., and Wiedmann, M. (2019). Identification of novel mobilized colistin resistance gene *mcr-9* in a multidrug-resistant, colistin-susceptible *Salmonella enterica* serotype Typhimurium Isolate. *MBio* 10:e853-19. doi: 10.1128/mBio.00853-19
- Clermont, O., Christenson, J. K., Denamur, E., and Gordon, D. M. (2013). The Clermont *Escherichia coli* phylo-typing method revisited: improvement of specificity and detection of new phylo-groups. *Environ. Microbiol. Rep.* 5, 58–65. doi: 10.1111/1758-2229.12019
- Clinical and Laboratory Standards Institute, (2019). *Performance Standards for Antimicrobial Susceptibility Testing*, 29th Edn. Wayne, PA: CLSI.
- Cortes, P., Blanc, V., Mora, A., Dahbi, G., Blanco, J. E., Blanco, M., et al. (2010). Isolation and characterization of potentially pathogenic antimicrobial-resistant *Escherichia coli* strains from chicken and pig farms in Spain. *Appl. Environ. Microbiol.* 76, 2799–2805. doi: 10.1128/AEM.02421-2429
- Delannoy, S., Le Devendec, L., Jouy, E., Fach, P., Drider, D., and Kempf, I. (2017). Characterization of colistin-resistant *Escherichia coli* isolated from diseased pigs in France. *Front. Microbiol.* 8:2278. doi: 10.3389/fmicb.2017.02278
- Doumith, M., Godbole, G., Ashton, P., Larkin, L., Dallman, T., Day, M., et al. (2016). Detection of the plasmid-mediated *mcr-1* gene conferring colistin resistance in human and food isolates of *Salmonella enterica* and *Escherichia coli* in England and Wales. *J. Antimicrob. Chemother.* 71, 2300–2305. doi: 10.1093/jac/dkw093
- Edgar, R., and Bibi, E. (1997). MdfA, an *Escherichia coli* multidrug resistance protein with an extraordinarily broad spectrum of drug recognition. *J. Bacteriol.* 179, 2274–2280. doi: 10.1128/jb.179.7.2274-2280.1997

- EMA/CVMP/CHMP (2019). *Answer to the Request From the European Commission for Updating the Scientific Advice on the Impact on Public Health and Animal Health of the Use of Antibiotics in Animals - Categorisation Of Antimicrobials Ema/Cvmp/Chmp/682198/2017*. London: European Medicines Agency.
- EUROPEAN COMMISSION (2018). *Overview Report on Measures to Tackle Antimicrobial Resistance (Amr) Through the Prudent Use of Antimicrobials in Animals*. Brussels: European Commission.
- Falgenhauer, L., Waezsada, S.-E., Gwozdziński, K., Ghosh, H., Doijad, S., Bunk, B., et al. (2016). Chromosomal locations of *mcr-1* and *bla<sub>CTX-M-15</sub>* in fluoroquinolone resistant *Escherichia coli* ST410. *Emerg. Infect. Dis.* 22, 1689–1691. doi: 10.3201/eid2209.160692
- Fuzi, M., Szabo, D., and Cserssik, R. (2017). Double-serine fluoroquinolone resistance mutations advance major international clones and lineages of various multi-drug resistant bacteria. *Front. Microbiol.* 8:2261. doi: 10.3389/fmicb.2017.02261
- García, V., García-Meniño, I., Mora, A., Flament-Simon, S. C., Díaz-Jiménez, D., Blanco, J. E., et al. (2018). Co-occurrence of *mcr-1*, *mcr-4* and *mcr-5* genes in multidrug-resistant ST10 enterotoxigenic and shiga toxin-producing *Escherichia coli* in Spain (2006–2017). *Int. J. Antimicrob. Agents.* 52, 104–108. doi: 10.1016/j.ijantimicag.2018.03.022
- García-Meniño, I., García, V., Mora, A., Díaz-Jiménez, D., Flament-Simon, S. C., Alonso, M. P., et al. (2018). Swine enteric colibacillosis in Spain: pathogenic potential of *mcr-1* ST10 and ST131 *E. coli* isolates. *Front. Microbiol.* 9:2659. doi: 10.3389/fmicb.2018.02659
- Gilrane, V. L., Lobo, S., Huang, W., Zhuge, J., Yin, C., Chen, D., et al. (2017). Complete genome sequence of a colistin-resistant *Escherichia coli* strain harboring *mcr-1* on an IncHI2 plasmid in the United States. *Genome Announc.* 5:e1095-17. doi: 10.1128/genomeA.01095-17
- Hammerl, J. A., Borowiak, M., Schmogger, S., Shamoun, D., Grobbel, M., Malorny, B., et al. (2018). *mcr-5* and a novel *mcr-5.2* variant in *Escherichia coli* isolates from food and food-producing animals, Germany, 2010 to 2017. *J. Antimicrob. Chemother.* 73, 1433–1435. doi: 10.1093/jac/dky020
- Holzel, C. S., Harms, K. S., Bauer, J., Bauer-Unkauf, I., Hormansdorfer, S., Kampf, P., et al. (2012). Diversity of antimicrobial resistance genes and class-1-integrins in phylogenetically related porcine and human *Escherichia coli*. *Vet. Microbiol.* 160, 403–412. doi: 10.1016/j.vetmic.2012.06.010
- Johnson, J. R., Johnston, B., Kuskowski, M. A., Sokurenko, E. V., and Tchesnokova, V. (2015). Intensity and mechanisms of fluoroquinolone resistance within the H30 and H30Rx subclones of *Escherichia coli* sequence type 131 compared with other fluoroquinolone-resistant *E. coli*. *Antimicrob. Agents. Chemother.* 59, 4471–4480. doi: 10.1128/AAC.00673-615
- Jurado-Rabadan, S., de la Fuente, R., Ruiz-Santa-Quiteria, J. A., Orden, J. A., de Vries, L. E., and Agero, Y. (2014). Detection and linkage to mobile genetic elements of tetracycline resistance gene *tet(M)* in *Escherichia coli* isolates from pigs. *BMC Vet. Res.* 10:155. doi: 10.1186/1746-6148-10-155
- Kidsley, A. K., Abraham, S., Bell, J. M., ÓDea, M., Laird, T. J., Jordan, D., et al. (2018). Antimicrobial susceptibility of *Escherichia coli* and *Salmonella* spp. isolates from healthy pigs in Australia: results of a pilot national survey. *Front. Microbiol.* 9:1207. doi: 10.3389/fmicb.2018.01207
- Lanza, V. F., de Toro, M., Pilar Garcillan-Barcia, M., Mora, A., Blanco, J., Coque, T. M., et al. (2014). Plasmid flux in *Escherichia coli* ST131 sublineages, analyzed by plasmid constellation network (PLACNET), a new method for plasmid reconstruction from whole genome sequences. *PLoS Genet.* 10:e1004766. doi: 10.1371/journal.pgen.1004766
- Li, R., Xie, M., Zhang, J., Yang, Z., Liu, L., Liu, X., et al. (2017). Genetic characterization of *mcr-1*-bearing plasmids to depict molecular mechanisms underlying dissemination of the colistin resistance determinant. *J. Antimicrob. Chemother.* 72, 393–401. doi: 10.1093/jac/dkw411
- Liu, Y. Y., Wang, Y., Walsh, T. R., Yi, L. X., Zhang, R., Spencer, J., et al. (2016). Emergence of plasmid-mediated colistin resistance mechanism MCR-1 in animals and human beings in China: a microbiological and molecular biological study. *Lancet. Infect. Dis.* 16, 161–168. doi: 10.1016/S1473-3099(15)00424-4
- Luppi, A. (2017). Swine enteric colibacillosis: diagnosis, therapy and antimicrobial resistance. *Porcine Health Manag.* 3:16. doi: 10.1186/s40813-017-0063-64
- Magiorakos, A. P., Srinivasan, A., Carey, R. B., Carmeli, Y., Falagas, M. E., Giske, C. G., et al. (2012). Multidrug-resistant, extensively drug-resistant and pandrug-resistant bacteria: an international expert proposal for interim standard definitions for acquired resistance. *Clin. Microbiol. Infect.* 18, 268–281. doi: 10.1111/j.1469-0691.2011.03570.x
- Magistrali, C. F., Curcio, L., Luppi, A., Pezzotti, G., Orsini, S., Tofani, S., et al. (2018). Mobile colistin resistance genes in *Escherichia coli* from pigs affected by colibacillosis. *Int. J. Antimicrob. Agents.* 52, 744–746. doi: 10.1016/j.ijantimicag.2018.08.008
- Manageiro, V., Clemente, L., Romão, R., Silva, C., Vieira, L., Ferreira, E., et al. (2019). IncX4 plasmid carrying the new *mcr-1.9* gene variant in a CTX-M-8-producing *Escherichia coli* isolate recovered from swine. *Front. Microbiol.* 10:367. doi: 10.3389/fmicb.2019.00367
- Mathers, A. J., Peirano, G., and Pitout, J. D. (2015). The role of epidemic resistance plasmids and international high-risk clones in the spread of multidrug-resistant *Enterobacteriaceae*. *Clin. Microbiol. Rev.* 28, 565–591. doi: 10.1128/CMR.00116-14
- OIE (2019). *List of Antimicrobial Agents of Veterinary Importance*. Available at: [https://www.oie.int/fileadmin/Home/eng/Our\\_scientific\\_expertise/docs/pdf/AMR/A\\_OIE\\_List\\_antimicrobials\\_July2019.pdf](https://www.oie.int/fileadmin/Home/eng/Our_scientific_expertise/docs/pdf/AMR/A_OIE_List_antimicrobials_July2019.pdf) (accessed October 23, 2019).
- Olaitan, A. O., Morand, S., and Rolain, J. M. (2014). Mechanisms of polymyxin resistance: acquired and intrinsic resistance in bacteria. *Front. Microbiol.* 5:643. doi: 10.3389/fmicb.2014.00643
- Poirel, L., Madec, J. Y., Lupo, A., Schink, A. K., Kieffer, N., Nordmann, P., et al. (2018). Antimicrobial resistance in *Escherichia coli*. *Microbiol. Spectr.* 6:ARBA-0026-2017. doi: 10.1128/microbiolspec.ARBA-0026-2017
- Quesada, A., Porrero, M. C., Tellez, S., Palomo, G., García, M., and Dominguez, L. (2015). Polymorphism of genes encoding PmrAB in colistin-resistant strains of *Escherichia coli* and *Salmonella enterica* isolated from poultry and swine. *J. Antimicrob. Chemother.* 70, 71–74. doi: 10.1093/jac/dku320
- Ramirez, M. S., and Tolmasky, M. E. (2010). Aminoglycoside modifying enzymes. *Drug Resist. Updat.* 13, 151–171. doi: 10.1016/j.drug.2010.08.003
- Rhouma, M., Beaudry, F., Theriault, W., and Letellier, A. (2016). Colistin in pig production: chemistry, mechanism of antibacterial action, microbial resistance emergence, and one health perspectives. *Front. Microbiol.* 7:1789. doi: 10.3389/fmicb.2016.01789
- Rhouma, M., Fairbrother, J. M., Beaudry, F., and Letellier, A. (2017). Post weaning diarrhea in pigs: risk factors and non-colistin-based control strategies. *Acta Vet. Scand.* 59:31. doi: 10.1186/s13028-017-0299-297
- Roy, K., Hamilton, D., Ostmann, M. M., and Fleckenstein, J. M. (2009). Vaccination with EtpA glycoprotein or flagellin protects against colonization with enterotoxigenic *Escherichia coli* in a murine model. *Vaccine* 27, 4601–4608. doi: 10.1016/j.vaccine.2009.05.076
- Schwarz, S., Kehrenberg, C., Doublet, B., and Cloeckaert, A. (2004). Molecular basis of bacterial resistance to chloramphenicol and florfenicol. *FEMS Microbiol. Rev.* 28, 519–542. doi: 10.1016/j.femsre.2004.04.001
- Seemann, T. (2014). Prokka: rapid prokaryotic genome annotation. *Bioinformatics* 30, 2068–2069. doi: 10.1093/bioinformatics/btu153
- Sellera, F. P., and Lincopan, N. (2019). Zoonanthropotic transmission of high-risk multidrug-resistant pathogens: a neglected public health issue. *J. Infect. Public Health.* 12, 294–295. doi: 10.1016/j.jiph.2018.12.013
- Shaw, K. J., Rather, P. N., Hare, R. S., and Miller, G. H. (1993). Molecular genetics of aminoglycoside resistance genes and familial relationships of the aminoglycoside-modifying enzymes. *Microbiol. Rev.* 57, 138–163.
- Shepard, S. M., Danzeisen, J. L., Isaacson, R. E., Seemann, T., Achtman, M., and Johnson, T. J. (2012). Genome sequences and phylogenetic analysis of K88- and F18-positive porcine enterotoxigenic *Escherichia coli*. *J. Bacteriol.* 194, 395–405. doi: 10.1128/JB.06225-6211
- Snesrud, E., McGann, P., and Chandler, M. (2018). The birth and demise of the ISAp11-*mcr-1*-ISAp11 composite transposon: the vehicle for transferable colistin resistance. *MBio* 9, e2381-17. doi: 10.1128/mBio.02381-17
- Sun, J., Zhang, H., Liu, Y. H., and Feng, Y. (2018). Towards understanding MCR-like colistin resistance. *Trends Microbiol.* 26, 794–808. doi: 10.1016/j.tim.2018.02.006
- Tang, X., Tan, C., Zhang, X., Zhao, Z., Xia, X., Wu, B., et al. (2011). Antimicrobial resistances of extraintestinal pathogenic *Escherichia coli* isolates from swine in China. *Microb. Pathog.* 50, 207–212. doi: 10.1016/j.micpath.2011.01.004
- Travis, R. M., Gyles, C. L., Reid-Smith, R., Poppe, C., McEwen, S. A., Friendship, R., et al. (2006). Chloramphenicol and kanamycin resistance among porcine *Escherichia coli* in Ontario. *J. Antimicrob. Chemother.* 58, 173–177. doi: 10.1093/jac/dkl207

- van Duijkeren, E., Schink, A. K., Roberts, M. C., Wang, Y., and Schwarz, S. (2018). Mechanisms of bacterial resistance to antimicrobial agents. *Microbiol. Spectr.* 6, 51–82. doi: 10.1128/microbiolspec.ARBA-0019-2017
- Veldman, K., van Essen-Zandbergen, A., Rapallini, M., Wit, B., Heymans, R., van Pelt, W., et al. (2016). Location of colistin resistance gene *mcr-1* in *Enterobacteriaceae* from livestock and meat. *J. Antimicrob. Chemother.* 71, 2340–2342. doi: 10.1093/jac/dkw181
- Wick, R. R., Judd, L. M., Gorrie, C. L., and Holt, K. E. (2017). Completing bacterial genome assemblies with multiplex MinION sequencing. *Microb. Genom.* 3:e000132. doi: 10.1099/mgen.0.000132

**Conflict of Interest:** The authors declare that the research was conducted in the absence of any commercial or financial relationships that could be construed as a potential conflict of interest.

Copyright © 2019 García-Meniño, Díaz-Jiménez, García, de Toro, Flament-Simon, Blanco and Mora. This is an open-access article distributed under the terms of the Creative Commons Attribution License (CC BY). The use, distribution or reproduction in other forums is permitted, provided the original author(s) and the copyright owner(s) are credited and that the original publication in this journal is cited, in accordance with accepted academic practice. No use, distribution or reproduction is permitted which does not comply with these terms.



# *In vitro* Activity and Heteroresistance of Omadacycline Against Clinical *Staphylococcus aureus* Isolates From China Reveal the Impact of Omadacycline Susceptibility by Branched-Chain Amino Acid Transport System II Carrier Protein, Na/Pi Cotransporter Family Protein, and Fibronectin-Binding Protein

## OPEN ACCESS

### Edited by:

Rustam Aminov,  
University of Aberdeen,  
United Kingdom

### Reviewed by:

Agnese Lupo,  
ANSES Site de Lyon, France  
Eliana De Gregorio,  
University of Naples Federico II, Italy

### \*Correspondence:

Qiwen Deng  
qiwendeng@hotmail.com  
Zhijian Yu  
yuzhijiansmu@163.com

† These authors have contributed  
equally to this work

### Specialty section:

This article was submitted to  
Antimicrobials, Resistance  
and Chemotherapy,  
a section of the journal  
Frontiers in Microbiology

Received: 24 May 2019

Accepted: 22 October 2019

Published: 08 November 2019

### Citation:

Bai B, Lin Z, Pu Z, Xu G, Zhang F,  
Chen Z, Sun X, Zheng J, Li P, Deng Q  
and Yu Z (2019) *In vitro* Activity  
and Heteroresistance  
of Omadacycline Against Clinical  
*Staphylococcus aureus* Isolates From  
China Reveal the Impact  
of Omadacycline Susceptibility by  
Branched-Chain Amino Acid  
Transport System II Carrier Protein,  
Na/Pi Cotransporter Family Protein,  
and Fibronectin-Binding Protein.  
*Front. Microbiol.* 10:2546.  
doi: 10.3389/fmicb.2019.02546

Bing Bai<sup>1,2†</sup>, Zhiwei Lin<sup>1,2†</sup>, Zhangya Pu<sup>3†</sup>, Guangjian Xu<sup>1,2†</sup>, Fan Zhang<sup>1,2</sup>, Zhong Chen<sup>1,2</sup>, Xiang Sun<sup>1</sup>, Jinxin Zheng<sup>1</sup>, Peiyu Li<sup>1,2</sup>, Qiwen Deng<sup>1,2\*</sup> and Zhijian Yu<sup>1,2\*</sup>

<sup>1</sup> Department of Infectious Diseases and Shenzhen Key Lab of Endogenous Infections, Shenzhen Nanshan People's Hospital and the 6th Affiliated Hospital of Shenzhen University Health Science Center, Shenzhen, China, <sup>2</sup> Quality Control Center of Hospital Infection Management of Shenzhen, Shenzhen Nanshan People's Hospital, Guangdong Medical University, Shenzhen, China, <sup>3</sup> Key Laboratory of Viral Hepatitis of Hunan Province, Department of Infectious Diseases, Xiangya Hospital, Central South University, Changsha, China

Omadacycline (Omad), a new tetracycline (Tet)-class broad-spectrum aminomethylcycline, has been reported to exhibit excellent potency against Gram-positive bacteria, including *Staphylococcus aureus* and Enterococci. The aim of this study was to evaluate the *in vitro* activity and heteroresistance characteristics of Omad in clinical *S. aureus* isolates from China and investigate Omad resistance mechanisms. A sample of 263 non-duplicate clinical *S. aureus* isolates [127 methicillin-resistant (MRSA) and 136 methicillin-sensitive (MSSA)] were collected retrospectively. Our data indicated that Omad exhibited excellent *in vitro* activity against both MRSA and MSSA. Omad heteroresistance frequencies were 3.17% (4/126) in MRSA and 12.78% (17/133) in MSSA. No mutations in Tet target sites, (five 16SrRNA copies and 30S ribosomal protein S10) were present in heteroresistance-derived clones, whereas Tet target site mutations contribute to induced Omad resistance in *S. aureus in vitro*. RNA sequencing (RNA-Seq) revealed that overexpression of branched-chain amino acid transport system II carrier protein and Na/Pi cotransporter family protein contributes to Omad heteroresistance emergence. Whole-genome sequencing demonstrated that the



genetic mutation of fibronectin-binding protein (FnBP) could increase the Omad MIC. In conclusion, Omad heteroresistance risk should be considered in clinical isolates with MICs  $\geq 0.5$  mg/L and Omad susceptibility in *S. aureus* may be affected by efflux pump proteins (i.e., a branched-chain amino acid transport system II carrier protein and an Na/Pi cotransporter family protein), and FnBP.

**Keywords:** omadacycline, *Staphylococcus aureus*, antimicrobial activity, multilocus sequence typing, tetracycline specific resistance genes

## INTRODUCTION

*Staphylococcus aureus* is a pervasive human pathogen that causes infectious diseases ranging in severity from superficial skin abscesses to bacteremia and septic shock (Calfee, 2017). Although the incidence of methicillin-resistant *S. aureus* (MRSA) infection appears to be declining worldwide, the incidence of bacteremia and severe community-acquired infection caused by methicillin-susceptible *S. aureus* (MSSA) continues to be an important human health threat (Bal et al., 2017). Both MRSA and MSSA infections remain a major clinical problem exacerbated by the ongoing evolution and transmission of traits engendering resistance or reduced susceptibility to current last-line antimicrobial agents, including linezolid, daptomycin, tigecycline (Tig), and vancomycin. Thus, there remains an urgent need for the development of new antimicrobial agents (Bal et al., 2017; Calfee, 2017).

Omadacycline [7-dimethylamino, 9-(2,2-dimethylpropyl)-aminomethylcycline; Omad] is a recently developed semisynthetic aminomethylcycline belonging to the tetracycline (Tet) family (Pfaller et al., 2017a). It has extraordinarily broad-spectrum antimicrobial activity against Gram-positive and -negative bacteria, including difficult-to-treat multidrug resistant bacteria, such as MRSA and vancomycin-resistant *enterococci* (Pfaller et al., 2017a). Like other Tet drugs, Omad is a potent inhibitor of the bacterial ribosome that inhibits bacterial protein synthesis by binding 30S ribosomal subunits during translation (Draper et al., 2014; Honeyman et al., 2015; Heidrich et al., 2016; Villano et al., 2016). Omad has the advantage of being minimally affected by classical Tet resistance mechanisms, including efflux pumps and ribosomal protection mechanisms. Omad also exhibits lower minimum inhibitory concentration (MIC) values against multidrug resistant bacteria than minocycline and Tig (Draper et al., 2014; Honeyman et al., 2015; Heidrich et al., 2016; Villano et al., 2016), making it a novel potential last-resort antibiotic for difficult-to-treat bacteria infections (Noel et al., 2012; Macone et al., 2014; Pfaller et al., 2017b; Zhang et al., 2018).

Heteroresistance means that there are population-wide variable responses to antibiotics. Several reports, including the earliest studies describing the phenomenon, applied this definition without specifying a particular antibiotic concentration range (El-Halfawy and Valvano, 2013, 2015). Previously, we obtained MICs and heteroresistance occurrence data for the new generation Tet-class drug erevacycline in clinical *S. aureus* isolates from China, underscoring the importance and necessity of investigating the characteristics of new-generation Tet derivatives (Zhang et al., 2018; Zheng et al., 2018). There are

limited data regarding Omad activity against clinical *S. aureus* isolates from China. Heteroresistance development in last-resort antibiotics can hinder efficacy and, ultimately, lead to treatment failure (Claeys et al., 2016; Zhang et al., 2018; Zheng et al., 2018). Thus, it is important to establish potential factors associated with Omad heteroresistance development.

Reduced susceptibility to Tig, an archetype new-generation Tet-class drug, in several species of bacteria has been associated with genetic mutations affecting 30S ribosomal subunits, including altered copy numbers of genes encoding 16S rRNA and 30S ribosomal proteins S3 and S10 (Nguyen et al., 2014; Lupien et al., 2015; Grossman, 2016; Argudin et al., 2018). Tig resistance has been related to regulators of cell envelop proteins, including efflux pumps (e.g., SoxS, MarA, RamA, and Rob) in Gram-negative enterobacteria and MepR/MepA in *S. aureus* (Nguyen et al., 2014; Grossman, 2016; Linkevicius et al., 2016; Dabul et al., 2018). The possible influences of 30S ribosomal subunit mutations and the overexpression of efflux proteins on Omad heteroresistance and resistance in *S. aureus* has not been resolved and needs to be further studied.

The main purpose of this study was to investigate the *in vitro* antimicrobial activity of Omad and to use population analysis profile (PAP) analysis to evaluate the occurrence of Omad heteroresistance in *S. aureus* isolates from China. We examined Omad heteroresistance mechanisms in *S. aureus* by conducting polymerase chain reaction (PCR) experiments to detect genetic mutations in 30S ribosome units, administering efflux protein inhibitors (Zhang et al., 2018; Zheng et al., 2018), and conducting RNA sequencing (RNA-Seq) studies. Furthermore, we used *in vitro* induction of resistance under Omad pressure and next generation sequencing (NGS) to compare Omad-sensitive and -resistant isolates and uncover molecular factors involved in Omad resistance.

## MATERIALS AND METHODS

### Bacterial Isolates

A total of 263 non-duplicate clinical *S. aureus* isolates (127 MRSA and 136 MSSA) were collected from Shenzhen Nanshan People's Hospital, a tertiary hospital with 1,200 beds in China, between 2008 and 2016. The specimen sources are summarized in **Supplementary Figure S1**. *S. aureus* ATCC29213 was used as a quality control organism. All procedures involving human participants were performed in accordance with the ethical standards of Shenzhen University and the 1964 Helsinki

declaration and its later amendments, or comparable ethical standards. For this type of study, formal consent is not required.

## Antimicrobial Susceptibility

*Staphylococcus aureus* antimicrobial susceptibilities to a panel of antibiotics (i.e., amikacin, erythromycin, ciprofloxacin, rifampicin, Tet, tobramycin, vancomycin, linezolid, nitrofurantoin, amoxicillin/clavulanate, and quinupristin) with the VITEK 2 system (BioMérieux, Marcy l'Etoile, France) and susceptibility breakpoints based on CLSI guidelines (2016). Omad was obtained from The Medicines Company (Med Chem Express, Monmouth Junction, NJ, United States). Omad MICs were determined with the agar dilution method according to CLSI guidelines (Klionsky et al., 2016). We employed three Omad MIC levels ( $\leq 0.25$  mg/L, 0.5 mg/L, and  $\geq 1$  mg/L) in our antimicrobial susceptibility analysis. The following Acute Bacterial Skin and Skin Structure Infections Omad susceptibility breakpoints recommended by FDA criteria were adopted:  $\leq 0.5$  mg/L for susceptibility, 1 mg/L for intermediate status, and  $\geq 2$  mg/L for resistance.

## PAP Development

Omad heteroresistance in *S. aureus* was determined by PAP development as described previously (Zhang et al., 2018; Zheng et al., 2018) with a MIC cut-off criterion of  $\leq 0.5$  mg/L. Briefly, 50- $\mu$ L aliquots (108 bacterial colony forming units) were spread onto Müller-Hinton broth plates containing serial dilutions of Omad (in mg/L): 0.5, 1, 2, and 3. Colonies were counted on Omad-containing plates after 24 h of incubation at 37°C. According to the criteria described above, we defined 2 mg/L as the susceptibility breakpoint for PAP determination of *S. aureus*. For Omad-resistant subpopulations detected among Omad-susceptible *S. aureus* isolate colonies grown on agar plates with 2 mg/L Omad with a detection limit of  $\geq 5$  colony forming units/ml, the parental isolates were considered to have Omad heteroresistance. Two heteroresistance-derived colonies were selected randomly from plates and their Omad and Tig MICs were measured by agar dilution according to CLSI guidelines and then subjected to PCRs, efflux inhibition, and transcriptional analysis (Zhang et al., 2018).

## Polymerase Chain Reaction

Genomic DNA was extracted from isolates with Lysis Buffer for Microorganisms to Direct PCR (Takara Bio Inc., Japan). Tet resistance genes encoding Tet(K), Tet(L), Tet(M), and Tet(O) were detected by PCR analysis as described previously (Bai et al., 2018). The presence of 30S ribosomal subunit mutations, including five separate copies of the 16S rRNA gene, the genes encoding the 30S ribosomal proteins S3 and S10, and the genes encoding recombinase (RecB) and fibronectin-binding protein (FnBP) were analyzed by PCR and sequence alignment (primer sequences listed in **Supplementary Table S1**). Multi-locus sequence typing (MLST) was conducted to identify the distributions of sequence types (STs) among MRSA

and MSSA isolates. PCR conditions recommended for locus amplification<sup>1</sup> were employed.

## Efflux Inhibition

The role of efflux pumps in Omad heteroresistance was evaluated with the efflux pump inhibitors phenylalanine-arginine- $\beta$ -naphthylamide (Pa $\beta$ N) and carbonyl cyanide-chlorophenylhydrazine (CCCP; both from Sigma). Omad MICs were determined by the agar dilution method in the presence and absence of 50 mg/L PA $\beta$ N or 16 mg/L CCCP. Inhibition was confirmed based on a  $\geq 4$ -fold MIC reduction (Osei Sekyere and Amoako, 2017; Zhang et al., 2018).

## *In vitro* Induction of Omad-Resistance Under Omad Pressure

Seven parental *S. aureus* isolates, including six clinical isolates (MSSAs: CHS221, CHS165, and 149. MRSAs: CHS759, CHS810, and CHS820) and a well-characterized antibiotic-susceptible MS4 strain, were used to select Omad-resistant isolates. These isolates were subcultured serially in Mueller-Hinton broth containing gradual increasing Omad concentrations with the initial concentration being MIC equivalents followed by successive increases to 2 $\times$ , 4 $\times$ , 8 $\times$ , and 16 $\times$  MICs (Yao et al., 2018), with four passages at each concentration. Isolates from the passages of each concentration were stored at  $-80^{\circ}\text{C}$  in Mueller-Hinton broth containing 40% glycerol for subsequent Tet-target site genetic mutation detection, subsequent MIC assays, next generation sequencing, and PCR analysis. Killing curves were performed on the CHS221 (wild-type MSSA strain), CHS221-O (Omad heteroresistance MSSA strain), CHS221-1 $\Delta$ : (Omad resistance MSSA strain), CHS759 (wild-type MRSA strain), CHS759-O (Omad heteroresistance MRSA strain), and CHS759-1 $\Delta$ : (Omad resistance MRSA strain). Tubes containing Omad at concentrations corresponding to 0 and 4 mg/L were inoculated with a suspension of each test strain, yielding to a final bacterial density of  $8 \times 10^6$  cfu/ml. The killing curves shown Omad-resistant strain could grow well at concentrations corresponding to 4 mg/L (**Supplementary Figure S2**).

## RNA-Seq

Wild-type strain CHS221 (S221) and its heteroresistance-derived *S. aureus* isolate CHS221-O (S221-O1) were grown and prepared for total RNA extraction with TRIzol reagent (Invitrogen, Carlsbad, CA, United States) as described previously (Zheng et al., 2018). RNA-Seq of the aforementioned parental and heteroresistance-derived isolates was performed as reported previously (Lin et al., 2017). Raw data (raw reads) of fastq format were firstly processed through in-house perl scripts. In this step, clean data (clean reads) were obtained by removing reads containing adapter, reads containing ploy-N and low quality reads from raw data. All the downstream analyses were based on the clean data with high quality. The raw data from the samples were analyzed in Subread software; raw counts for each group

<sup>1</sup><http://www.mlst.com/server>

were normalized and processed in the EdgeR Bioconductor software package. 1.3-fold differences in expression level by RNA-Sequencing were considered to be differentially expressed genes (DEGs). The RNA sequencing outcomes for two strains were deposited in the NCBI database (BioProject accession number PRJNA505108).

## Quantitative Real Time (qRT)-PCR Analysis

We selected 30 DEGs based on our RNA-Seq results and employed qRT-PCR to compare transcriptional expression levels between the parental and heteroresistance-derived strains as described in detail previously (Zheng et al., 2018). The transcriptional expression levels of the eight candidate genes (USA300HOU\_RS00705, USA300 HOU\_RS03535, USA300 HOU\_RS01625, USA300 HOU\_RS00550, USA300HOU\_RS13205, USA300HOU\_RS13945, USA300HOU\_RS10505, and USA300HOU\_RS00660) were further analyzed and compared among the CHS165 (MSSA), 149 (MSSA), CHS759 (MRSA), CHS810 (MRSA), and CHS820 (MRSA) parental strains and their derivative heteroresistant and resistant strains. Total RNA of bacteria was extracted using the RNeasyH Mini Kit (QIAGEN, Hilden, Germany) following the manufacturer's instructions. The extracted RNA was reverse transcribed into cDNA using iScript reverse transcriptase (Bio-Rad, Hercules, CA, United States) with incubation for 5 min at 25°C, followed by 30 min at 42°C and 5 min at 85°C. Subsequently, qRT-PCRs were performed using SYBR green PCR reagents (Premix EX Taq™, Takara Biotechnology, Dalian, China) in the Mastercycler realplex system (Eppendorf AG, Hamburg, Germany) with amplification conditions of 95°C for 30 s, 40 cycles of 95°C for 5 s and 60°C for 34 s, followed by melting curve analysis. The control gene *gyrB* was used to normalize gene expression. Threshold cycle (Ct) numbers were determined by detection system software and analyzed with the  $2^{-44}\text{Ct}$  method and three replicates have been made. The qRT-PCR primers used are listed in **Supplementary Table S2**.

## Next Generation Sequencing

An Omad resistant *S. aureus* strain, MS4O8, was derived from an Omad-susceptible isolate, MS4. Chromosomal DNA was extracted from MS4O8 cells for NGS. Nextera shotgun libraries and whole genome sequencing were performed by Novogene Company (Beijing, China). Illumina PE150 sequencing data were mapped against the CP009828 *S. aureus* MS4 strain reference genome in bwa mem software (v0.7.5a)<sup>2</sup> with standard parameters. Small nucleotide polymorphisms and small insertions/deletions were detected in MS4O8 cells, relative to MS4, in MUMmer (version 3.23). A custom script was used to detect substitutions, insertions, and deletions that might be impacting protein coding regions. Binary alignment/map files of the sequenced strains were deposited in the NCBI database (BioProject accession number PRJNA511962).

<sup>2</sup><http://biobwa.sourceforge.net/>

## Gene Overexpression

Full-length candidate genes, including USA300HOU\_RS00550 (encodes a Na/Pi cotransporter family protein), USA300HOU\_RS01625 (encodes a branched-chain amino acid transport system II carrier protein), USA300HOU\_RS03535, USA300HOU\_Tet(K), NI36\_12460 (FnBP), and NI36\_00170 (RecB), were amplified with extra double enzyme sites from total DNA extracted from USA300HOU and MS4 isolates. RecB-M is RecB with a mutation (R10R, I23V, I23N, H24N, H24Q, V29L, and V35M) and FnBP-M is FnBP with a mutation (T672S and I665V). RecB-M and FnBP-M DNA fragments were amplified from MS4O8 by PCR. The candidate gene fragments were each integrated into separate pIB166 vectors, and their encoded target protein were induced with 2 mM chromium chloride (Wu et al., 2012). The primers used for vector constructs in this study are listed in **Supplementary Table S3**. Positively vector transformed *S. aureus* clones were selected with chloramphenicol and verified by PCR and Sanger sequencing. The overexpression plasmids were transformed separately into three to five Omad-sensitive isolates and their integrations was confirmed by PCR and Sanger sequencing. Candidate gene transcriptional levels were measured by qRT-PCR, as described above. Omad and Tig MICs for these derivatives were determined and heteroresistance occurrence in these derivatives was tested by PAP analysis under Omad pressure as described above.

## Statistical Analysis

Continuous data were analyzed with Student's *t*-tests and one-way factorial analyses of variance (ANOVAs) in SPSS software package (version 17.0, Chicago, IL, United States). *P*-values < 0.05 were regarded as statistically significant.

## RESULTS

### *In vitro* Activity of Omad Against Clinical *S. aureus* Isolates

Of the 127 MRSA isolates examined, 46 (36.22%), 80 (62.99%), and 1 (0.78%) were found to have Omad MIC levels of  $\leq 0.25$  mg/L (sensitive), 0.5 mg/L (sensitive), and 1 mg/L (intermediate), respectively. Of the 136 MSSA isolates examined, 23 (16.91%), 110 (80.88%), and 3 (2.20%) were categorized into these levels, respectively. Thus, there were higher frequencies of MSSA isolates than MRSA isolates with Omad MICs in the 0.5 and  $\geq 1$  mg/L levels. We analyzed the distribution of the above three Omad MIC levels among strains with sensitive and intermediate status relative to other common antibiotics (amikacin, erythromycin, ciprofloxacin, rifampicin, Tet, tobramycin, nitrofurantoin, quinupristin, and amoxicillin/clavulanate, vancomycin, and linezolid). The frequencies of isolates at each Omad MIC level found to be resistant to these antibiotics are reported in **Table 1**, together with the resistance breakpoints used. All *S. aureus* isolates in this study were susceptible to vancomycin and linezolid, and all of the MSSA isolates were susceptible to

**TABLE 1** | *Staphylococcus aureus* antibiotic resistance and correspondence to Omad MIC level.

Class	Drug	Resistance rate (%)	Total N	MIC breakpoint (mg/L)	N	Omad MIC level (mg/L), N		
						≤0.25	0.5	1
MRSA	Total		127	–	127	46	80	1
	Amikacin	51.61	124	≤16	60	24	36	0
				32	3	0	3	0
				≥64	61	20	42	1
	Erythromycin	99.21	127	≤0.5	1	1	0	0
				1–4	1	1	0	0
				≥8	125	44	80	1
	Ciprofloxacin	52.84	123	≤1	58	24	34	0
				2	1	0	1	0
				≥4	64	19	44	1
	Rifampicin	15.87	126	≤1	106	39	66	1
				≥4	20	6	14	0
	Tet	69.29	127	≤4	39	20	19	0
				8	15	6	9	0
≥16				73	20	52	1	
Tobramycin	52.84	123	≤4	58	23	35	0	
			≥16	65	21	43	1	
			≤32	122	43	78	1	
Nitrofurantoin	3.17	126	64	2	1	1	0	
			≥128	2	1	1	0	
			≤1	117	42	74	1	
Quinupristin	2.50	120	2	1	0	1	0	
			≥4	2	1	1	0	
			–	136	23	110	3	
MSSA	Total		136	–	136	23	110	3
	Amikacin	5.30	132	≤16	124	21	100	3
				32	5	0	5	0
				≥64	2	0	2	0
	Erythromycin	83.58	134	≤0.5	22	1	21	0
				1–4	3	0	3	0
				≥8	109	21	85	3
	Ciprofloxacin	10.76	130	≤1	116	21	93	2
				≥4	14	0	13	1
				≤1	127	21	104	2
	Rifampicin	4.51	133	≥4	6	1	4	1
				≤4	68	21	47	0
	Tet	50	136	8	9	0	8	1
				≥16	59	2	55	2
≤4				68	14	52	2	
Tobramycin	45.60	125	8	1	0	1	0	
			≥16	56	5	51	0	
			≤32	133	22	108	3	
Nitrofurantoin	0.74	134	64	1	0	1	0	
			≤1	116	20	94	2	
Quinupristin	2.5	120	2	1	0	1	0	
			≥4	2	0	2	0	

amoxicillin/clavulanate. Interestingly, as reported in **Table 1**, Tet-resistant MRSA were more frequent than Tet-resistant MSSA, and Omad MICs  $\geq 0.5$  mg/L were more frequent among MSSA isolates than among MRSA isolates, suggesting a non-conformity in the antimicrobial susceptibility dynamics of Tet and Omad. The characteristics of *S. aureus* with

Omad MICs of 1 mg/L are summarized in **Supplementary Table S4**. Briefly, no genetic mutations in 30S ribosome units were detected and efflux pump inhibition reversed Omad resistance, as evidenced by significant reductions in MICs to  $\leq 0.03$  mg/L with CCCP and to 0.25–1 mg/L with PAβN.



## Omad MICs of *S. aureus* Isolates Harboring Tet-Resistance Genes

The frequencies of genes encoding the Tet-resistance factors Tet(M), Tet(L), Tet(K), and Tet(O), alone and in combination, in MRSA and MSSA isolates are reported in **Supplementary Table S5**. There were 109 *S. aureus* isolates harboring at least one Tet-resistance factor gene; their MIC<sub>90</sub> values were consistently 0.5 mg/L. Omad exhibited excellent *in vitro* activity against both Tet-resistance gene carrying and non-carrying *S. aureus* isolates. Omad MICs for both MRSA and MSSA harboring Tet-resistance factors were  $\leq 0.5$  mg/L for all isolates, with the exception of three Tet(K) gene-carrying isolates (1 MRSA and 2 MSSA), indicating that overexpression of Tet(K) might impact Omad susceptibility. It is noteworthy that the Omad MIC values obtained for all 46 MSSA isolates carrying the Tet(K) gene, Tet(L) gene, or both were  $\geq 0.5$  mg/L. Meanwhile, of the 63 MRSA isolates with the Tet(M) gene, Tet(K) gene, Tet(L) gene, or some combination of these genes, just 47 (74.60%) had Omad MIC values  $\geq 0.5$  mg/L.

## Clonality of Omad MIC Distribution in Clinical *S. aureus* Isolates

MLST results for the 263 isolates are summarized in **Supplementary Figure S3**. To evaluate the relationship of ST clonality with Omad MIC distribution, we examined ST distributions relative to Tet and Omad MICs (**Supplementary Table S6**). Omad MICs  $\geq 0.5$  mg/L were found for 72.58% (45/62) of ST239-MRSA, 57.5% (23/40) of ST59-MRSA, and 57.14% (4/7) of ST1-MRSA isolates. Meanwhile, Omad MICs  $\geq 0.5$  mg/L were found for 89.66% (26/29) of ST7-MSSA, 89.47% (17/19) ST59-MSSA, 76.92% (10/13) of ST398-MSSA, 85.71% (6/7) of ST88-MSSA, and 71.43% (5/7) of ST120-MSSA isolates. Hence, Omad sensitivity differed between MRSA and MSSA of the same ST (e.g., ST59-MRSA vs. ST59-MSSA). MLST indicated that 72/81 (88.89%) MRSA isolates with Omad MICs  $\geq 0.5$  mg/L belonged to the top three MRSA STs (ST239, ST59, and ST1), whereas only 52/113 (46.12%) of MSSA isolates with Omad MICs  $\geq 0.5$  mg/L belonged to the top three MSSA STs (**Supplementary Table S6** and **Table 1**), revealing a more pronounced clustering of Omad MIC creep in the top three MRSA STs than in the top three MSSA STs (nearly 90% vs. less than half).

## Omad Heteroresistance Frequency and Mechanism in *S. aureus*

Omad heteroresistance was identified in 0.0% (0/46) of MRSA with an Omad MIC  $\leq 0.25$  mg/L and 3.75% (3/80) of MRSA with an Omad MIC of 0.5 mg/L. Omad heteroresistance was identified in 0.0% (0/30) of MSSA with an Omad MIC  $\leq 0.25$  mg/L and 17.48% (18/103) of MSSA with an Omad MIC of 0.5 mg/L. We determined the Omad and Tig MICs of two clones from each heteroresistant subpopulation and found that their Omad MICs were in the range of 1–8 mg/L and their Tig MICs were in the range of 2–8 mg/L (shown in **Supplementary Table S7** and data for six isolates subjected to *in vitro* resistance induction are shown in **Table 2**). Moreover, no genetic mutations were found in 30S ribosomal subunit genes (five 16SrRNA gene copies, 30S

ribosomal protein S3 and S10 genes) in heteroresistance-derived clones (**Table 2** and **Supplementary Table S7**). In efflux pump inhibition experiments, Omad MICs in heteroresistance-derived *S. aureus* clones were reduced to  $\leq 0.03$  mg/L by CCCP and reduced to 0.25–1 mg/L by PA $\beta$ N (**Supplementary Table S7**).

## Association of Selected Candidate Genes With Omad Heteroresistance

Efflux pump inhibition experiments indicated that efflux pumps or membrane proteins might participate in the development of heteroresistance. Therefore, RNA-Seq was performed and unigene transcription levels were compared between the parental strain CHS221 (S221) and its heteroresistant derivative CHS221-O1 (S221-O). Ninety six DEGs were found by this approach between S221 and S221-O, including 58 upregulated and 38 down-regulated genes in the derivative strain (**Supplementary Figure S4**). KEGG pathway analysis showed that the pathways most frequently linked to DEGs were related to phosphate ion transport (3 DEGs), inorganic anion transport (3 DEGs), dihydrofolate reductase activity (2 DEGs), and glycine biosynthesis process (2 DEGs).

Subsequent qRT-PCRs for 30 candidate genes were carried out to test the accuracy of our transcriptomic analyses implicated eight efflux-pump encoding DEGs in heteroresistance. The expression levels of these eight candidate genes determined by RNA-Seq and qRT-PCR are shown in **Table 3**. The results of qRT-PCRs performed to quantitate transcription in six *S. aureus* strain groups—inclusive of parental strains, their heteroresistance derivatives, and resistant isolates (**Table 2**)—enabled us to probe the relationship of their expression levels with Omad susceptibility (**Figure 1**). The data suggest that transcription levels of the three candidate genes USA300HOU\_RS03535, USA300HOU\_RS01625 (encodes a Na/Pi cotransporter family protein), and USA300HOU\_RS00550 (encodes a branched-chain amino acid transport system II carrier protein) may impact heteroresistance occurrence.

## Mechanism of Omad-Induced Resistance in *S. aureus* Under Omad Pressure

To evaluate Omad resistance mechanisms and Omad-Tig cross-resistance, *in vitro* induction experiments were carried out under Omad pressure with the following Omad-resistant *S. aureus*: CHS221 (MSSA), CHS165 (MSSA), 149 (MSSA), CHS759 (MRSA), CHS810 (MRSA), CHS820 (MRSA), and MS4. The Omad-resistant isolates were characterized with respect to MICs and resistance mechanisms (**Table 2**). Importantly, increasing Omad MICs were accompanied by increasing Tig MICs in Omad-resistant *S. aureus* isolates, indicating that Omad-Tig cross-resistance can be induced under Omad pressure. Moreover, upregulation of Omad MICs was related to increasing numbers of 16SrRNA copies with a genetic mutation. The mutation sites varied among the five 16SrRNA copies, with high frequencies of the T170G polymorphism in RR1, A1124G in RR2, C810T in RR3, and G1036A in RR4. Leu47His and Tyr87His amino acid

**TABLE 2** | Antimicrobial susceptibility and resistance mechanism of seven groups of parental, heteroresistant, and Omad-induced resistant strains.

Strain	MIC (mg/L)		Mutation(s)								
	Tig	Omad	RR1	RR2	RR3	RR4	RR5	S3	S10	RecB	FnBP
CHS221 (S221)	0.5	0.5	W	W	W	W	W	W	W	W	W
CHS221-O (S221-O*)	4	8	W	W	W	W	W	W	W	W	W
CHS221-1Δ	32	32	W	A1124G	C810T	G1036A	G1248C	W	MeT48Ile	W	W
CHS221-2	32	32	G848T	A1124G	C810T	G1036A	A854C	W	MeT48Ile	W	W
					A1281G						
CHS165	0.5	0.5		W	W	W	W	W	W	W	W
CHS165-O*	4	8	W	W	W	W	W	W	W	W	T672S,
CHS165-1Δ	32	32	T170G	G848A	C810T	G1036A	G1248C	W	LeT47His	W	T672S, I665V
				A1124G							
CHS165-2	32	32	T170G	G77A	C810T	G1036A	G742A	W	LeT47His	W	T672S, I665V
				A1124G	G848C		C1247T				
149	0.25	0.5	W	W	W	W	W	W	W	W	W
149-O*	8	4	W	W	W	W	W	W	W	W	W
149-1 Δ	64	64	W	A1124G	C810T	G1036A	W	W	LeT47His	W	W
149-2	>64	128	W	A1124G	C810T	G1036A	C1247T	W	LeT47His	W	W
					G848C						
CHS759	0.25	0.5	W	W	W	W	W	W	W	W	W
CHS759-O*	4	4	W	W	W	W	W	W	W	W	W
CHS759-1Δ	32	32	G1036A	A1124G	C810T	G185A	G1248C	W	Met48Thr	W	I665V
				G1036A	G848C	G1036A	G1036A				
CHS759-2	32	32	W	A1124G	C810T	G185A	C1036T	W	Let47Let Tyr87His	W	I665V
				G1036A	A1281G	G1036A					
CHS810	0.25	0.5	W	W	W	W	W	W	W	W	W
CHS810-O*	4	4	W	W	W	W	W	W	W	W	W
CHS810-1Δ	32	32	T170G	A1124G	C810T	G185A	T1257C	W	Tyr87His	W	W
						G1036A	G1248C				
CHS810-2	32	32	T170G	A1124G	C810T	G185A	A79G	W	Tyr87His	W	T672S,
						G1036A	T1257C				
CHS820	0.25	0.5	W	W	W	W	W	W	W	W	W
CHS820-O*	4	2	W	W	W	W	W	W	W	W	W
CHS820-1Δ	64	128	T170G	A1124G	C810T	G185A	A79G	W	Tyr87His	W	W
						G1036A					
CHS820-2	64	128	T170G	A1124G	C810T	G185A	A79G	W	Tyr87His	W	W
			G848C		A1281G	G1036A	G848C				
MS4	0.125	0.125	W	W	W	W	W	W	W	W	W
MS4-O2	4	4	T170G	W	C810T	W	T1257C	W	W	W	T672S,
			G783A		A1281G						
MS4-O8	4	4	T170G	G848A	C810T	W	W	W	Asp60Tyr	RecB-M	T672S, I665V
			C1041T	T1124C	T1281C						

Parental isolates are isolated with shading; \* and Δ represent heteroresistant and Omad-induced resistant strain, respectively (see qRT-PCR in **Figure 1**); RR1-7 are 16s rRNA gene copies; S3 and S10 are 30S ribosome proteins; W, wild-type (no mutation).

substitutions in the 30S ribosomal protein S10 were relatively frequent in Omad-resistant bacteria.

## Candidate Genes Related to Omad Resistance in NGS

To identify the genetic mutations that correlate with Omad resistance, whole genome sequencing of MS4O8 was performed and variants relative to MS4 were detected by NGS in MUMmer, version 3.23 (Supplementary Table S8 and Table 4). Non-synonymous mutations were found in NI36\_11090 (encodes 30S ribosomal protein S10), NI36\_12460 (*fnbp* encoding FnBP protein), and NI36\_00170 (*recB* encoding recombinase). Mutations affecting these three genes also emerged in our induced Omad-resistance experiment above (Table 2). Notably, 30S ribosomal protein S10 has been widely reported to be associated with Tet-class resistance and the impact of FnBP and RecB protein on Omad susceptibility need to be further verified.

## Relationship Between Candidate Genes Overexpression and Omad Susceptibility

The impacts of following candidate genes on Omad susceptibility in Omad-sensitive *S. aureus* isolates was conducted: USA300HOU\_RS03535, USA300HOU\_RS01625 (encodes a branched-chain amino acid transport system II carrier protein), USA300HOU\_RS00550 (encodes a Na/Pi cotransporter family protein), *tet(K)*, NI36\_12460/NI36\_12465 (*fnbp*), and NI36\_00170 (*recB*). The former three were candidate implicated in Omad heteroresistance in our qRT-PCR experiments. Meanwhile, *tet(K)* was found frequently among *S. aureus* isolates with an Omad MIC of 1 mg/L, and the proteins

encoded by *fnbp* and *recB* have been hypothesized to participate in antimicrobial resistance evolution.

The overexpression plasmids pRS00550, pRS01625, pRS03535, pTet(K), pRecB, pRecB-M, pFnBP, and pFnBP-M, where -M suffix indicates a mutated variant, were transformed into clinical isolates with low expression of the target gene (Supplementary Tables S9, S10). Stable overexpression of the candidate genes was confirmed by qRT-PCR (Supplementary Figure S5). The influence of the overexpression of these six genes on Omad susceptibility was reported in Table 5. Briefly, although RS00550, RS01625, and RS03535 did not elevate Omad or Tig MICs in the absence of antibiotic pressure, PAP experiments showed that RS00550 or RS01625 overexpression could lead to Omad heteroresistance compared with negative findings in controls (Table 5). RS00550 and RS01625 homology analysis results are reported in Supplementary Tables S11, S12.

Overexpression of *tet(K)* did not elevate Omad or Tig MICs and had no apparent contribution to heteroresistance development in *S. aureus*. The overexpression of *fnbp* (NI36\_12460) and its mutated type led to MIC creep (Table 5), supporting the possibility that FnBPs may participate in Omad resistance development. Homology analysis results for *fnbp* are shown in Supplementary Table S13. Overexpression of *recB* and its mutants did not impact Omad susceptibility in *S. aureus*.

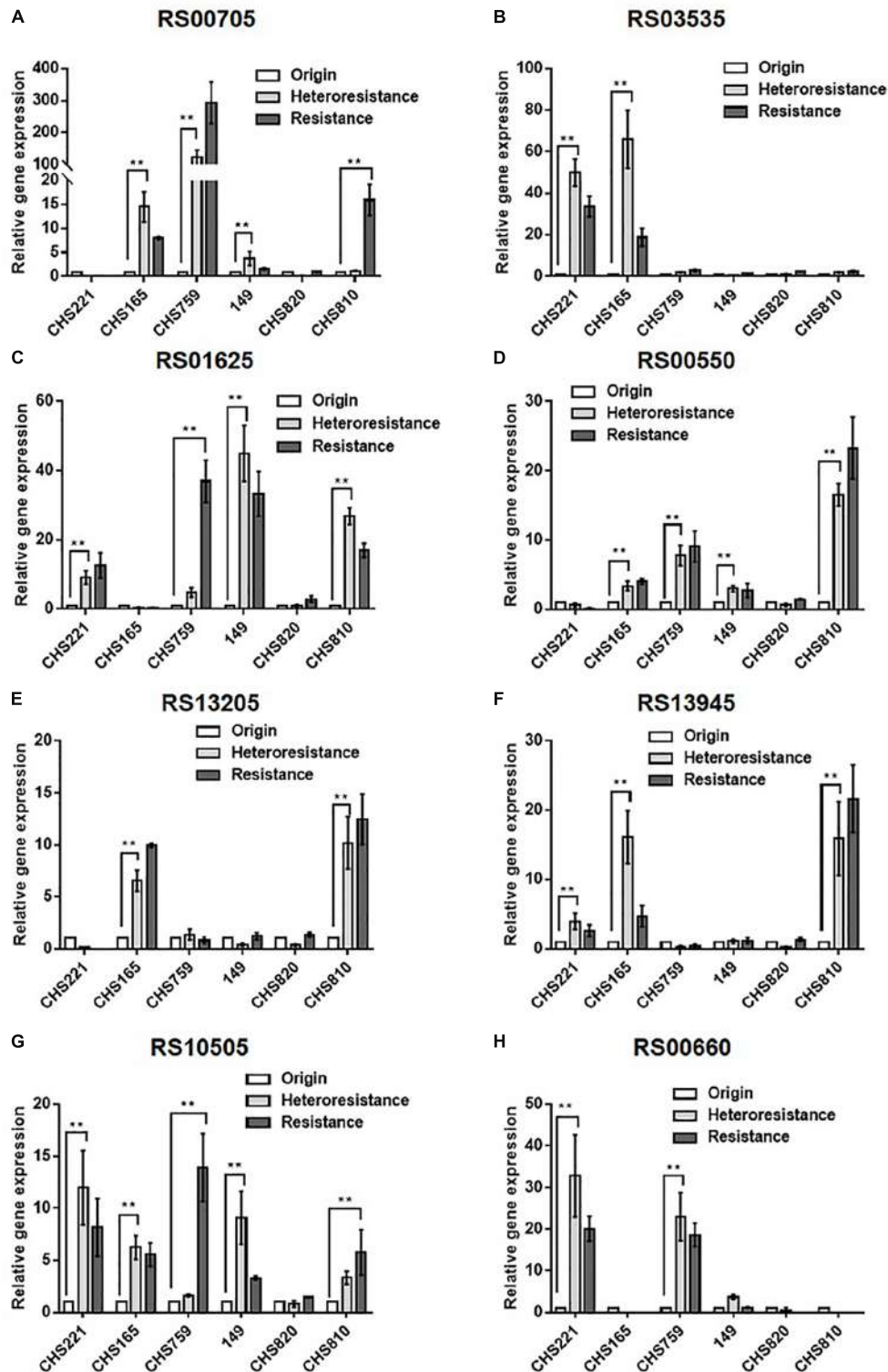
## DISCUSSION

The presently observed low Omad MICs in this study support the supposition that Omad should be considered a prospective preferential choice for *S. aureus* infection treatment. Omad MICs  $\geq 0.5$  mg/L were more frequent among MSSA than MRSA in this study, and moreover, Tet-specific resistance genes, particularly *tet(K)* and *tet(L)*, were found to be more common among MSSA than MRSA isolates, indicating that Omad may have greater efficacy against MRSA than MSSA. Our Omad MICs were higher than previously reported, perhaps due to regional variation and environmental factors (Villano et al., 2016; Pfaller et al., 2017a). We also obtained higher MICs for the new-generation Tet-class drug eravacycline in isolates from China than had been reported for isolates from the United States and Europe, suggesting that Tet-class drug MIC dynamics should be monitored across global regions with particular attention to MIC creep in China (Zhang et al., 2018; Zheng et al., 2018).

Major mechanisms of Tet resistance in both Gram-positive and -negative microorganisms have been linked to ribosomal protection proteins and efflux pumps, most of which can be overcome with new generation tetracyclines, including Tig and Omad (Jones et al., 2006; Noel et al., 2012; Draper et al., 2014; Macone et al., 2014; Honeyman et al., 2015; Grossman, 2016; Heidrich et al., 2016; Villano et al., 2016; Pfaller et al., 2017b; Argudin et al., 2018; Zhang et al., 2018). In this study, we obtained low Omad MICs for *S. aureus*, even among isolates harboring a ribosomal protection protein, namely Tet(M), or an efflux pump factor, namely Tet(K) and Tet(L), uncovering an apparent advantage of using Omad to overcome Tet-specific resistance mechanisms, particularly those mediated by Tet(M), Tet(K), and

**TABLE 3 |** Transcriptional expression levels of eight DEGs between S221-O and S221 analyzed by RNA-Seq and qRT-PCR.

Gene_ID	Gene description	Relative increase in transcription in S221-O compared to S221	
		qRT-PCR	Fold change in RNA-Seq
USA300HOU_RS00705	Cell wall-anchored protein SasD	1.42 ± 0.12	2.73
USA300HOU_RS03535	Membrane protein	1.73 ± 0.14	2.83
USA300HOU_RS01625	Branched-chain amino acid transport system II carrier protein	2.77 ± 0.21	2.84
USA300HOU_RS00550	Na/Pi cotransporter family protein	1.18 ± 0.06	2.90
USA300HOU_RS13205	Amino acid permease	1.32 ± 0.11	2.97
USA300HOU_RS13945	PTS transporter subunit IIC	1.42 ± 0.07	3.29
USA300HOU_RS10505	hypothetical protein	5.73 ± 0.65	3.42
USA300HOU_RS00660	MFS transporter	3.27 ± 0.22	3.43



**FIGURE 1** | Comparison of the relative transcription of eight candidate DEGs among parental, heteroresistant derivative, and resistant isolates. Relative expression of USA300HOU\_RS00705 (A), USA300HOU\_RS03535 (B), USA300HOU\_RS01625 (C), USA300HOU\_RS00550 (D), USA300HOU\_RS13205 (E), USA300HOU\_RS13945 (F), USA300HOU\_RS10505 (G), and USA300HOU\_RS00660 (H) were demonstrated by qRT-PCR analysis. The housekeeping gene *gyrB* was used as the endogenous reference gene. The original strain was used as the reference strain (expression = 1.0). All qRT-PCRs were carried out in triplicate. \*\* $p < 0.01$ , \* $p < 0.05$ . Parental strains are identified below the X axis and the relative folds increased are shown on the Y axis. The parental, heteroresistant, and resistant isolates are described in Table 2.



**TABLE 4 |** Non-synonymous mutations of candidate proteins correlated with Omad resistance found between MS4 and MS4O8.

Gene_ID	Gene description	Amino acid mutations (non-syn) between MS4 and MS4O8
NI36_11090	30S ribosomal protein S10	D60Y
NI36_12460	FnBP	T672S, I665V
NI36_00170	RecB	R10R, I23V, I23N, H24N, H24Q, V29L, V35M

**TABLE 5 |** Omad and Tig MICs in *S. aureus* derivatives with overexpression of candidate genes and their impact on PAPs.

Vector	Strain	MIC (mg/L)				PAP test positivity
		Parental isolates		Derivative isolates*		
		Omad	Tig	Omad	Tig	
pRS00550	SE7	0.25	0.5	0.25	0.5	10
	CHS545	0.5	0.5	0.25	0.5	12
	CHS569	0.25	0.5	0.25	0.5	5
pRS01625	SE4	0.25	0.5	0.25	0.5	3
	SE7	0.25	0.5	0.25	0.5	5
	CHS569	0.25	0.5	0.25	0.5	9
pRS03535	SE4	0.25	0.5	0.25	0.5	0
	SE7	0.25	0.5	0.25	0.5	0
	SE13	0.25	0.5	0.25	0.5	0
	CHS545	0.5	0.25	0.5	0.25	0
	CHS569	0.25	0.25	0.25	0.25	0
ptet(K)	SE4	0.25	0.5	0.5	0.5	0
	SE7	0.25	0.5	0.25	0.5	0
	SE13	0.25	0.5	0.25	0.5	0
	CHS545	0.5	0.25	0.25	0.5	0
pRecB	SE4	0.25	–	0.25	–	–
	SE4	0.25	–	0.25	–	–
pRecB-M	SE4	0.25	–	0.25	–	–
pFBP	SE4	0.25	0.5	0.5	1	–
pFBP-M	SE4	0.25	0.5	1	1	–

FBP-M has T672S and/or I665V mutations. RecB-M has R10R, I23V, I23N, H24N, H24Q, V29L, and/or V35M mutation. Positive PAP results are highlighted with shading.

Tet(L). Notwithstanding, Tig MICs were shown recently to be increased by a high transcriptional level of tet(M) and tet(L) in *Enterococcus faecium* (Fiedler et al., 2016). Because we observed a higher frequency of Tet-specific genes in MSSA than in MRSA from China and three isolates with MICs  $\geq 1$  mg/L harbored tet(K) in this study, we hypothesize that tet(K) overexpression may elevate Omad MICs, as was found in *E. coli* (Linkevicius et al., 2016). Our data demonstrate that tet(K) overexpression does not impact *S. aureus* susceptibility to Omad *in vitro*, and thus indicate that Omad can overcome the Tet(K)-mediated resistance in *S. aureus*.

Prior epidemiological data have revealed ST239 and ST59 to be predominant MRSA STs internationally, with MSSA ST predominance being more variable across regions (Atshan et al., 2013; Leon-Sampedro et al., 2016; Recker et al., 2017). *S. aureus*

clonality of drug-resistance and virulence factors has been reported (Atshan et al., 2013; Leon-Sampedro et al., 2016; Recker et al., 2017). The present examination of the relationship of ST clonality with Omad susceptibility revealed a far higher frequency of the top-three MRSA STs with MICs  $\geq 0.5$  mg/L than of the top-three such MSSA STs. Although a definite relationship of ST clustering with Omad MICs has not been established, it is noteworthy that ST59-MSSA were much more likely to have Omad MICs  $\geq 0.5$  mg/L than were ST59-MRSA.

Heteroresistance frequency is an important harbinger of last-resort antibiotic resistance risk (Zhang et al., 2018; Zheng et al., 2018). The present findings of heteroresistance in 16.98% of MSSA and 3.75% of MRSA with Omad MICs  $\geq 0.5$  mg/L suggest a need to be alert to selection resistance under Omad pressure for *S. aureus*, especially in strains from China. Moreover, we observed relatively high Tig MICs for Omad heteroresistance-derived clones (2–8 mg/L), indicating a potential risk of Omad-Tig cross-resistance. Mutations affecting 30S ribosomal subunits, which have been reported to participate in Tet or Tig resistance, were not found in our heteroresistance-derived clones or clinical isolates with Omad MICs  $\geq 1$  mg/L, indicating that 30S ribosomal subunit mutations cannot explain Omad MIC creep and heteroresistance occurrence (Nguyen et al., 2014; Grossman, 2016; Argudin et al., 2018).

The progression of reduced Tig susceptibility in *S. aureus* has been linked with *mepR/mepA* encoded efflux pumps (Lupien et al., 2015). However, the possible role of efflux pumps and cell envelopes in Omad heteroresistance in *S. aureus* is unclear. Multiple reports have shown that protonophore efflux pump inhibitors (e.g., CCCP and Pa $\beta$ N) can be used to evaluate interactions between antibiotics and cell envelope components in bacteria (Klionsky et al., 2016; Bai et al., 2018; Yao et al., 2018). Here, we found that the efflux pump inhibitor PA $\beta$ N and the cell envelope component inhibitor CCCP reduced Omad MICs of heteroresistance-derived *S. aureus* clones to as low as  $\leq 0.03$  mg/L and 0.12–1 mg/L, respectively, pointing to involvement of efflux pumps or cell envelopes in the progression of Omad heteroresistance in *S. aureus* (Klionsky et al., 2016; Bai et al., 2018). Omad MICs of isolates with Omad MICs  $\geq 1$  mg/L could also be reduced by CCCP and PA $\beta$ N, supporting the notion that efflux pumps or cell envelopes may play an important role in reducing susceptibility to Omad. Our findings showing that overexpression of RS00550 or RS01625 can lead to Omad heteroresistance occurrence, despite having no impact on Omad MICs in the absence of Omad pressure, indicate that expression of genes can facilitate the formation of Omad resistance under antibiotic exposure. Our phylogenetic analysis showed that both RS00550 and RS01625 encode efflux pump family proteins, supporting our hypothesis that efflux pump or membrane proteins contribute to Omad heteroresistance.

Crystallographic studies of the *Thermus thermophilus* 30S ribosomal subunit revealed at least one high-occupancy Tet-binding site and five other minor binding sites in 16S rRNA (Draper et al., 2014; Honeyman et al., 2015; Heidrich et al., 2016). Crystallographic studies with Tet, Tig, and Omad showed that, although they produced slightly different patterns of RNA cleavage and dimethylsulfate modification, all three antibiotics

associated with the same binding site, albeit in somewhat different orientations. In several bacterial species, Tig and Omad have been shown to exhibit higher binding affinities and greater antitranslational potencies than Tet or minocycline, and 16SrRNA mutations have been shown to affect Tet binding sites in the 30S ribosomal subunit, which may confer Tet/Tig resistance (Nguyen et al., 2014; Grossman, 2016; Zheng et al., 2018). Consistent with previous reports, we found that greater numbers of 16S rRNA copies with genetic mutations were associated with higher levels Omad/Tig resistance in *S. aureus* isolates with Omad-resistance induced under Omad pressure (Nguyen et al., 2014; Grossman, 2016). This finding implicates the participation of 16SrRNA mutations in the development of the Omad resistance. Additionally, our finding of frequent 30S ribosomal protein S10 mutations in Omad-derived resistant isolates indicates that such mutations may be an important factor in Omad resistance evolution. It will be important to examine the unknown mechanism(s) underlying MIC elevation during Omad resistance evolution in *S. aureus*. In this study, NGS was performed to identify candidate genes that may be involved in Omad resistance development and FnBP was identified as a novel membrane molecule that may contribute to Omad MIC elevation. Mechanistically, we hypothesized that the overexpression of FnBP could alter the penetration potential of cell membranes.

## CONCLUSION

Omad exhibited excellent *in vitro* activity against clinical *S. aureus* isolates from China and might represent a preferential choice for the treatment of *S. aureus* infections. However, we must be alert to the potential risk of Omad heteroresistance in *S. aureus*, especially in strains with MICs  $\geq 0.5$  mg/L. Compared with MRSA, MSSA had relatively low MICs with a more facile tendency for the occurrence of Omad heteroresistance. Omad heteroresistance in both MSSA and MRSA could be reversed by CCCP and Pa $\beta$ N, indicating involvement of efflux pumps in Omad heteroresistance development in *S. aureus*. Furthermore, both RS01625 and RS00550, which encode efflux pump family proteins (a branched-chain amino acid transport system II carrier protein and an Na/Pi cotransporter family protein, respectively),

## REFERENCES

- Argudin, M. A., Roisin, S., Dodemont, M., Nonhoff, C., Deplano, A., and Denis, O. (2018). Mutations at the ribosomal S10 gene in clinical strains of *Staphylococcus aureus* with reduced susceptibility to tigecycline. *Antimicrob. Agents Chemother.* 62:e01852-17. doi: 10.1128/AAC.01852-17
- Atshan, S. S., Nor Shamsudin, M., Lung, L. T., Sekawi, Z., Pei Pei, C., Karunanidhi, A., et al. (2013). Genotypically different clones of *Staphylococcus aureus* are diverse in the antimicrobial susceptibility patterns and biofilm formations. *Biomed. Res. Int.* 2013:515712. doi: 10.1155/2013/515712
- Bai, B., Hu, K., Li, H., Yao, W., Li, D., Chen, Z., et al. (2018). Effect of tedizolid on clinical *Enterococcus* isolates: in vitro activity, distribution of virulence factor, resistance genes and multilocus sequence typing. *FEMS Microbiol. Lett.* 365:fnx284. doi: 10.1093/femsle/fnx284
- Bal, A. M., David, M. Z., Garau, J., Gottlieb, T., Mazzei, T., Scaglione, F., et al. (2017). Future trends in the treatment of methicillin-resistant *Staphylococcus*

were found to contribute to Omad heteroresistance. FnBP emerged as a novel molecule to be associated with Omad resistance and Omad MIC elevation in *S. aureus*. The present data contribute to understanding potential resistance mechanisms that may impact clinical applications of Omad.

## DATA AVAILABILITY STATEMENT

All datasets generated for this study are included in the article/**Supplementary Material**.

## AUTHOR CONTRIBUTIONS

QD and ZY initiated and designed the project. BB, ZP, and ZL performed the molecular biological experiments with bacteria. GX, XS, JZ, and ZC performed the PCRs. FZ, PL, and GX performed the bacterial culturing and MIC testing. All authors participated in the data analysis. QD, ZY, and BB wrote the manuscript incorporating comments from all authors.

## FUNDING

This work was supported by grants from the National Natural Science Foundation of China (Nos. 81170370 and 81601797); Science, Technology, and Innovation Commission of Shenzhen Municipality of basic research funds (No. JCYJ20170412143551332); Shenzhen Health and Family Planning Commission (SZXJ2018027 and SZXJ2017032); Sanming Project of Medicine in Shenzhen; the Shenzhen Nanshan District Scientific Research Program of the People's Republic of China (No. 2018010, 2018011, and 2018021); and provincial medical funds of Guangdong (No. A2018163).

## SUPPLEMENTARY MATERIAL

The Supplementary Material for this article can be found online at: <https://www.frontiersin.org/articles/10.3389/fmicb.2019.02546/full#supplementary-material>

- aureus* (MRSA) infection: an in-depth review of newer antibiotics active against an enduring pathogen. *J. Glob. Antimicrob. Resist.* 10, 295–303. doi: 10.1016/j.jgar.2017.05.019
- Calfee, D. P. (2017). Trends in community versus health care-acquired methicillin-resistant *Staphylococcus aureus* infections. *Curr. Infect. Dis. Rep.* 19:48. doi: 10.1007/s11908-017-0605-6
- Claeys, K. C., Lagnf, A. M., Hallesy, J. A., Compton, M. T., Gravelin, A. L., Davis, S. L., et al. (2016). Pneumonia caused by methicillin-resistant *Staphylococcus aureus*: does vancomycin heteroresistance matter? *Antimicrob. Agents Chemother.* 60, 1708–1716. doi: 10.1128/AAC.02388-15
- Dabul, A. N. G., Avaca-Crusca, J. S., Van Tyne, D., Gilmore, M. S., and Camargo, I. (2018). Resistance in in vitro selected tigecycline-resistant methicillin-resistant *Staphylococcus aureus* sequence type 5 is driven by mutations in mepR and mepA genes. *Microb. Drug Resist.* 24, 519–526. doi: 10.1089/mdr.2017.0279
- Draper, M. P., Weir, S., Maccone, A., Donatelli, J., Trieber, C. A., Tanaka, S. K., et al. (2014). Mechanism of action of the novel aminomethylcycline antibiotic

- omadacycline. *Antimicrob. Agents Chemother.* 58, 1279–1283. doi: 10.1128/AAC.01066-13
- El-Halfawy, O. M., and Valvano, M. A. (2013). Chemical communication of antibiotic resistance by a highly resistant subpopulation of bacterial cells. *PLoS One* 8:e68874. doi: 10.1371/journal.pone.0068874
- El-Halfawy, O. M., and Valvano, M. A. (2015). Antimicrobial heteroresistance: an emerging field in need of clarity. *Clin. Microbiol. Rev.* 28, 191–207. doi: 10.1128/CMR.00058-14
- Fiedler, S., Bender, J. K., Klare, I., Halbedel, S., Grohmann, E., Szewzyk, U., et al. (2016). Tigecycline resistance in clinical isolates of *Enterococcus faecium* is mediated by an upregulation of plasmid-encoded tetracycline determinants tet(L) and tet(M). *J. Antimicrob. Chemother.* 71, 871–881. doi: 10.1093/jac/dkv420
- Grossman, T. H. (2016). Tetracycline antibiotics and resistance. *Cold Spring Harb. Perspect. Med.* 6:a025387. doi: 10.1101/cshperspect.a025387
- Heidrich, C. G., Mitova, S., Schedlbauer, A., Connell, S. R., Fucini, P., Steenbergen, J. N., et al. (2016). The novel aminomethylcycline omadacycline has high specificity for the primary tetracycline-binding site on the bacterial ribosome. *Antibiotics* 5:32. doi: 10.3390/antibiotics5040032
- Honeyman, L., Ismail, M., Nelson, M. L., Bhatia, B., Bowser, T. E., Chen, J., et al. (2015). Structure-activity relationship of the aminomethylcyclines and the discovery of omadacycline. *Antimicrob. Agents Chemother.* 59, 7044–7053. doi: 10.1128/AAC.01536-15
- Jones, C. H., Tuckman, M., Howe, A. Y., Orlowski, M., Mullen, S., Chan, K., et al. (2006). Diagnostic PCR analysis of the occurrence of methicillin and tetracycline resistance genes among *Staphylococcus aureus* isolates from phase 3 clinical trials of tigecycline for complicated skin and skin structure infections. *Antimicrob. Agents Chemother.* 50, 505–510. doi: 10.1128/AAC.50.2.505-510.2006
- Klionsky, D. J., Abdelmohsen, K., Abe, A., Abedin, M. J., Abeliovich, H., Acevedo Arozena, A., et al. (2016). Guidelines for the use and interpretation of assays for monitoring autophagy (3rd edition). *Autophagy* 12, 1–222. doi: 10.1080/1548627.2015.1100356
- Leon-Sampedro, R., Novais, C., Peixe, L., Baquero, F., and Coque, T. M. (2016). Diversity and evolution of the Tn5801-tet(M)-like integrative and conjugative elements among *Enterococcus*, *Streptococcus*, and *Staphylococcus*. *Antimicrob. Agents Chemother.* 60, 1736–1746. doi: 10.1128/AAC.01864-15
- Lin, Z., Cai, X., Chen, M., Ye, L., Wu, Y., Wang, X., et al. (2017). Virulence and stress responses of *Shigella flexneri* regulated by PhoP/PhoQ. *Front. Microbiol.* 8:2689. doi: 10.3389/fmicb.2017.02689
- Linkevicius, M., Sandegren, L., and Andersson, D. I. (2016). Potential of tetracycline resistance proteins to evolve tigecycline resistance. *Antimicrob. Agents Chemother.* 60, 789–796. doi: 10.1128/AAC.02465-15
- Lupien, A., Gingras, H., Leprohon, P., and Ouellette, M. (2015). Induced tigecycline resistance in *Streptococcus pneumoniae* mutants reveals mutations in ribosomal proteins and rRNA. *J. Antimicrob. Chemother.* 70, 2973–2980. doi: 10.1093/jac/dkv211
- Macone, A. B., Caruso, B. K., Leahy, R. G., Donatelli, J., Weir, S., Draper, M. P., et al. (2014). In vitro and in vivo antibacterial activities of omadacycline, a novel aminomethylcycline. *Antimicrob. Agents Chemother.* 58, 1127–1135. doi: 10.1128/AAC.01242-13
- Nguyen, F., Starosta, A. L., Arenz, S., Sohmen, D., Donhofer, A., and Wilson, D. N. (2014). Tetracycline antibiotics and resistance mechanisms. *Biol. Chem.* 395, 559–575. doi: 10.1515/hsz-2013
- Noel, G. J., Draper, M. P., Hait, H., Tanaka, S. K., and Arbeit, R. D. (2012). A randomized, evaluator-blind, phase 2 study comparing the safety and efficacy of omadacycline to those of linezolid for treatment of complicated skin and skin structure infections. *Antimicrob. Agents Chemother.* 56, 5650–5654. doi: 10.1128/AAC.00948-12
- Osei Sekyere, J., and Amoako, D. G. (2017). Carbonyl cyanide m-chlorophenylhydrazone (CCCP) reverses resistance to colistin, but Not to Carbapenems and tigecycline in multidrug-resistant *Enterobacteriaceae*. *Front. Microbiol.* 8:228. doi: 10.3389/fmicb.2017.00228
- Pfaller, M. A., Huband, M. D., Rhomberg, P. R., and Flamm, R. K. (2017a). Surveillance of omadacycline activity against clinical isolates from a global collection (North America, Europe, Latin America, Asia-Western Pacific), 2010–2011. *Antimicrob. Agents Chemother.* 61:e00018-e17. doi: 10.1128/AAC.00018-17
- Pfaller, M. A., Rhomberg, P. R., Huband, M. D., and Flamm, R. K. (2017b). Activities of omadacycline and comparator agents against *Staphylococcus aureus* isolates from a surveillance program conducted in North America and Europe. *Antimicrob. Agents Chemother.* 61:e02411-16. doi: 10.1128/AAC.02411-16
- Recker, M., Laabei, M., Toleman, M. S., Reuter, S., Saunderson, R. B., Blane, B., et al. (2017). Clonal differences in *Staphylococcus aureus* bacteraemia-associated mortality. *Nat. Microbiol.* 2, 1381–1388. doi: 10.1038/s41564-017-0001-x
- Villano, S., Steenbergen, J., and Loh, E. (2016). Omadacycline: development of a novel aminomethylcycline antibiotic for treating drug-resistant bacterial infections. *Future Microbiol.* 11, 1421–1434. doi: 10.2217/fmb-2016-0100
- Wu, Y., Wang, J., Xu, T., Liu, J., Yu, W., Lou, Q., et al. (2012). The two-component signal transduction system ArlRS regulates *Staphylococcus epidermidis* biofilm formation in an ica-dependent manner. *PLoS One* 7:e40041. doi: 10.1371/journal.pone.0040041
- Yao, W., Xu, G., Bai, B., Wang, H., Deng, M., Zheng, J., et al. (2018). In vitro-induced erythromycin resistance facilitates cross-resistance to the novel fluoroketolide, solithromycin, in *Staphylococcus aureus*. *FEMS Microbiol. Lett.* 365:fny116. doi: 10.1093/femsle/fny116
- Zhang, F., Bai, B., Xu, G. J., Lin, Z. W., Li, G. Q., Chen, Z., et al. (2018). Eravacycline activity against clinical *S. aureus* isolates from China: in vitro activity, MLST profiles and heteroresistance. *BMC Microbiol.* 18:211. doi: 10.1186/s12866-018-1349-7
- Zheng, J. X., Lin, Z. W., Sun, X., Lin, W. H., Chen, Z., Wu, Y., et al. (2018). Overexpression of OqxAB and MacAB efflux pumps contributes to eravacycline resistance and heteroresistance in clinical isolates of *Klebsiella pneumoniae*. *Emerg. Microbes Infect.* 7:139. doi: 10.1038/s41426-018-0141-y

**Conflict of Interest:** The authors declare that the research was conducted in the absence of any commercial or financial relationships that could be construed as a potential conflict of interest.

Copyright © 2019 Bai, Lin, Pu, Xu, Zhang, Chen, Sun, Zheng, Li, Deng and Yu. This is an open-access article distributed under the terms of the Creative Commons Attribution License (CC BY). The use, distribution or reproduction in other forums is permitted, provided the original author(s) and the copyright owner(s) are credited and that the original publication in this journal is cited, in accordance with accepted academic practice. No use, distribution or reproduction is permitted which does not comply with these terms.



# Increasing Frequencies of Antibiotic Resistant Non-typhoidal *Salmonella* Infections in Michigan and Risk Factors for Disease

Sanjana Mukherjee<sup>1</sup>, Chase M. Anderson<sup>1</sup>, Rebekah E. Mosci<sup>1</sup>, Duane W. Newton<sup>2</sup>, Paul Lephart<sup>2</sup>, Hossein Salimnia<sup>3</sup>, Walid Khalife<sup>4</sup>, James. T. Rudrik<sup>5</sup> and Shannon D. Manning<sup>1\*</sup>

<sup>1</sup> Department of Microbiology and Molecular Genetics, Michigan State University, East Lansing, MI, United States, <sup>2</sup> Clinical Microbiology Laboratory, University of Michigan, Ann Arbor, MI, United States, <sup>3</sup> Microbiology Division, Detroit Medical Center University Laboratories, Wayne State University, Detroit, MI, United States, <sup>4</sup> Microbiology, Immunology & Molecular Laboratories, Sparrow Hospital, Lansing, MI, United States, <sup>5</sup> Bureau of Laboratories, Michigan Department of Health and Human Services, Lansing, MI, United States

## OPEN ACCESS

### Edited by:

Ilana L. B. C. Camargo,  
University of São Paulo, Brazil

### Reviewed by:

Angelo Berchieri Junior,  
São Paulo State University, Brazil  
Rafael Antonio Casarin Penha Filho,  
São Paulo State University, Brazil

### \*Correspondence:

Shannon D. Manning  
mannin71@msu.edu

### Specialty section:

This article was submitted to  
Infectious Diseases - Surveillance,  
Prevention and Treatment,  
a section of the journal  
Frontiers in Medicine

**Received:** 31 July 2019

**Accepted:** 17 October 2019

**Published:** 08 November 2019

### Citation:

Mukherjee S, Anderson CM,  
Mosci RE, Newton DW, Lephart P,  
Salimnia H, Khalife W, Rudrik JT and  
Manning SD (2019) Increasing  
Frequencies of Antibiotic Resistant  
Non-typhoidal *Salmonella* Infections in  
Michigan and Risk Factors for  
Disease. *Front. Med.* 6:250.  
doi: 10.3389/fmed.2019.00250

Non-typhoidal *Salmonella* (NTS) are important enteric pathogens causing over 1 million foodborne illnesses in the U.S. annually. The widespread emergence of antibiotic resistance in NTS isolates has limited the availability of antibiotics that can be used for therapy. Since Michigan is not part of the FoodNet surveillance system, few studies have quantified antibiotic resistance frequencies and identified risk factors for NTS infections in the state. We obtained 198 clinical NTS isolates via active surveillance at four Michigan hospitals from 2011 to 2014 for classification of serovars and susceptibility to 24 antibiotics using broth microdilution. The 198 isolates belonged to 35 different serovars with Enteritidis (36.9%) predominating followed by Typhimurium (19.5%) and Newport (9.7%), though the proportion of each varied by year, residence, and season. The number of Enteritidis and Typhimurium cases was higher in the summer, while Enteritidis cases were significantly more common among urban vs. rural residents. A total of 30 (15.2%) NTS isolates were resistant to  $\geq 1$  antibiotic and 15 (7.5%) were resistant to  $\geq 3$  antimicrobial classes; a significantly greater proportion of Typhimurium isolates were resistant compared to Enteritidis isolates and an increasing trend in the frequency of tetracycline resistance and multidrug resistance was observed over the 4-year period. Resistant infections were associated with longer hospital stays as the mean stay was 5.9 days for patients with resistant isolates relative to 4.0 days for patients infected with susceptible isolates. Multinomial logistic regression indicated that infection with serovars other than Enteritidis [Odds ratio (OR): 3.8, 95% confidence interval (CI): 1.23–11.82] as well as infection during the fall (OR: 3.0; 95% CI: 1.22–7.60) were independently associated with resistance. Together, these findings demonstrate the importance of surveillance, monitoring resistance frequencies, and identifying risk factors that can aid in the development of new prevention strategies.

**Keywords:** non-typhoidal *Salmonella*, antimicrobial resistance, epidemiology, risk factors, Michigan



## INTRODUCTION

The gram-negative pathogen, *Salmonella enterica*, is an important public health concern resulting in 93.8 million cases of foodborne infections globally each year (1). In 2015, infection with non-typhoidal *S. enterica* (NTS) serovars was a leading cause of death, with 90,300 deaths reported (2). Infections with NTS can cause nausea, vomiting, abdominal pain, myalgia (muscle pain) and arthralgia (joint pain), while hepatomegaly (liver enlargement), and splenomegaly (spleen enlargement) can develop in some cases (3). Systemic infections can also occur in immunocompromised patients (4). Because of these complications, NTS infections were estimated to contribute to 70 disability-adjusted life years (DALY) lost/100,000 persons worldwide in 2010 (5). In the U.S., the number of NTS infections was estimated to be 1.2 million per year with 23,000 hospitalizations and 450 deaths (6). *Salmonella* infections were also reported to have the highest mean cost of illness among all foodborne infections (7). Geographical differences in serovar prevalence have been documented as well (8). In Europe and Asia, for instance, *S. Enteritidis* was the leading cause of clinical infections in 2002, whereas *S. Typhimurium* was the highest in North America followed by *S. Enteritidis*, *S. Newport* and *S. Heidelberg*. The *Typhimurium* and *Enteritidis* serovars, however, have been reported to cause the greatest number of enterocolitis and bacteremia cases (3).

NTS has been frequently isolated from commercially raised chickens and other poultry, and contact with cattle, pigs, horses, and other domestic animals are important risk factors for NTS infections (9). In addition, 74,000 *Salmonella* infections have been attributed to reptile and amphibian exposures in the U.S. each year (10); contact with reptiles and cats was associated with salmonellosis in a prior Michigan study (11). Other studies have identified serovar-specific risk factors as well. A study in the Netherlands, for example, found consumption of raw eggs and products containing raw eggs to be linked to *Salmonella* Enteritidis infections, while exposure to raw meat and playing in a sandbox were risk factors for *S. Typhimurium* infections (12). Prior history of antibiotic use, living on a livestock farm, and international travel were also identified as risk factors for *S. Typhimurium* infections in Canada (13). NTS isolates have been recovered from environmental sources including water and soil and can often survive in these environments for extended periods of time (14, 15). Taken together, these studies indicate the importance of the environment as a reservoir for *Salmonella*.

Antibiotic-resistant NTS infections have also emerged and are increasing in frequency in the U.S. resulting in high hospitalization rates and ~\$365,000,000 in medical costs every year (16). Fluoroquinolones, third generation cephalosporins, penicillins, macrolides, and trimethoprim-sulfamethoxazole are commonly prescribed for the treatment of salmonellosis, particularly in patients with immunocompromising conditions, young children and the elderly (17). Importantly, antibiotic resistant *Salmonella* infections have been linked to more severe disease outcomes including bloodstream infections as well as hospitalization (18) and multidrug resistance has emerged.

Resistance to ampicillin, chloramphenicol, streptomycin, sulfonamides and tetracycline, previously defined as ACSSuT isolates, for instance, has been reported in multiple NTS serovars in different geographical regions (19–22). In addition to ACSSuT, resistance to ampicillin, streptomycin, sulfonamides, and tetracycline (ASSuT) has been observed in *S. Typhimurium* from humans, food animals and retail meats in the U.S. (23). The emergence of these multi-drug phenotypes in *Salmonella* are of great concern since alternative antibiotics that can be used to treat *Salmonella* infections are limited.

Emergence of widespread resistance in *Salmonella* is attributed to the overuse of antibiotics and limits the effectiveness of these antibiotics for the treatment of human infections. Michigan is not included in the CDC FoodNet surveillance network, which monitors the incidence of foodborne illnesses and collects case information from 10 states in the U.S., covering 15% of the U.S. population. Consequently, we sought to examine the distribution of NTS serovars causing disease in Michigan and evaluate risk factors for infection using an active surveillance system at four hospitals. We also calculated the frequency of antibiotic resistance in NTS isolates and identified factors associated with resistance and NTS infections. This study highlights the importance of enhanced surveillance for resistant pathogens to ensure that the most appropriate drug targets are used, and to identify risk factors for infection and patients with an increased risk of more debilitating conditions.

## MATERIALS AND METHODS

### Strain Source and Collection

From 2011 to 2014, 198 NTS isolates were collected as part of the Enterics Research Investigational Network (ERIN), which was set up in collaboration with the Michigan Department of Health and Human Services (MDHHS) and four major hospitals in southern Michigan. Serovar classification was conducted at the MDHHS using traditional serotyping protocols as recommended by the Association of Public Health Laboratories (24); serovar data was extracted from the Michigan Disease Surveillance System (MDSS) for each case. To ensure that the ERIN surveillance network was representative of enteric infections occurring in Michigan, the frequency of ERIN cases was shown to be similar to those identified throughout the state of Michigan during the same time period (25). Isolates were stored in Luria-Bertani broth with 10% glycerol at  $-80^{\circ}\text{C}$  until further testing.

### Antimicrobial Susceptibility Profiling

For NTS, susceptibilities to 24 antibiotics were determined by broth microdilution using Sensititre GN4F Trek plates (Trek Diagnostic Systems, Cleveland, OH, USA) according to the manufacturer's instructions. Nine antibiotic classes were tested and included: aminoglycosides (amikacin, gentamicin, tobramycin);  $\beta$ -lactam antibiotics [penicillins (ampicillin, piperacillin);  $\beta$ -lactam/ $\beta$ -lactamase inhibitor combinations (ampicillin/sulbactam 2:1 ratio, piperacillin/tazobactam constant 4, ticarcillin/clavulanic acid constant 2); cephalosporins (cefazolin, ceftazidime, ceftriaxone, cefipime)];

carbapenems (imipenem, doripenem, ertapenem, meropenem); tetracyclines (tetracycline, minocycline); fluoroquinolones (ciprofloxacin, levofloxacin); glycolcyclines (tigecycline); nitrofurans (nitrofurantoin); monobactams (aztreonam); and anti-folates (trimethoprim/sulfamethoxazole). The minimum inhibitory concentration (MIC) was determined by identifying the lowest concentration of antibiotic that prevented visible bacterial growth. *Escherichia coli* ATCC 25922, which is susceptible to all antibiotics evaluated, was used as the quality control strain. The results of the susceptibility tests were interpreted as resistant or susceptible in accordance with published guidelines (26) and isolates were classified as multidrug resistant if they were resistant to three or more antimicrobial classes.

## Data Analysis

Epidemiological, demographic, and clinical data were obtained from the MDSS and managed using Microsoft Access and Excel. Season was classified as spring (March, April, and May), summer (June, July, and August), fall (September, October, and November) and winter (December, January, and February) based on the sample collection date; for those cases with a missing collection date, the stool arrival date and/or onset dates were used. Counties in Michigan were classified as urban or rural based on the classification scheme devised by the National Center for Health Statistics; only 10 Michigan counties were designated as urban (27). Based on the published rates of antibiotic prescription use in adults and children in Michigan (28), counties were classified as having high or low prescribing rates. High rates were defined as those counties where hospital service areas had >30% higher use rates relative to the state average. A dichotomous variable was created for length of hospital stay by defining a long hospital stay as one that was greater than 4 days.

SAS version 9.4 (SAS Institute, Cary, NC, USA) and Epi Info™ version 7.0 were used for all statistical analyses.  $\chi^2$  test and Fisher's exact test were used for dichotomous variables to identify significant associations between the dependent and independent variables; a  $p$ -value  $\leq 0.05$  was considered significant. A univariate analysis was first conducted, and those variables found to have strong associations with the outcome ( $p$ -value  $\leq 0.20$ ) were included in the multivariate analysis unless the variable contained >15 missing values. Multivariate analysis using forward logistic regression was performed to build a model containing significant variables ( $p$ -value  $\leq 0.05$ ) along with potentially confounding factors such as age and sex. The Mantel-Haenszel  $\chi^2$  test was used to test for trends and the student's  $t$ -test was used for testing statistical significance between means. Finally, the  $\chi^2$  test for equality of proportions was used for comparing sample proportions.

## RESULTS

### Characteristics of Cases With Non-typhoidal *Salmonella* (NTS) Infections

A total of 198 NTS cases were identified and roughly half were male (53.1%;  $n = 104$ ) and between 18 and 52 years of age ( $n =$

81; 40.9%). Forty-four (22.2%) cases were younger than 10 years of age and 14 were younger than 2 years. More cases self-reported as Caucasians ( $n = 125$ ; 74.0%) than as African Americans ( $n = 33$ ; 19.5%) or other races ( $n = 11$ ; 6.5%); race was not known for 29 cases. Diarrhea ( $n = 172$ , 97.2%), abdominal pain ( $n = 135$ , 80.4%), and fever ( $n = 106$ , 69.3%) were commonly reported symptoms, though 70 (41.9%) patients also reported bloody diarrhea. Sixty-five patients (34.6%) were hospitalized between 1 day and 17 days; the average duration of hospitalization was 4.4 days.

No significant difference in the proportion of cases was observed by year ( $p$ -value = 0.075), though a higher number was reported in the summer and fall ( $n = 139$ ; 70.2%) compared to the winter and spring months ( $p$ -value < 0.0001). Differences were also observed among the four participating hospitals, which represented 10.6, 23.2, 29.3, and 36.9% of the 198 cases. When stratified by county, 56.2% ( $n = 108$ ) of the cases lived in rural counties and 43.7% ( $n = 84$ ) resided in urban counties; the residence was not known for one case. A subset of five cases resided in other states (Colorado, Georgia, Illinois, Ohio, and South Dakota), though each patient developed symptoms and were diagnosed with salmonellosis while visiting Michigan. Of the 166 cases with travel information available, a significantly higher proportion of patients had not traveled in the past month ( $n = 103$ , 62.0%) when compared to those who reported travel ( $n = 63$ ; 37.9%) ( $p$ -value = 0.0019).

Patients reporting contact with animals ( $n = 95$ ; 61.3%) were also more likely to be affected when compared to those reporting no animal contact ( $n = 60$ ; 38.7%) ( $p$ -value = 0.0049). Among these 95 cases, 12 (12.6%) had contact with reptiles such as turtles and lizards, and nine (9.5%) reported contact with livestock including cattle, horses, goats, or pigs. Contact with domestic animals (e.g., cats, dogs, and small mammals) was also reported in 83 of the 95 (87.4%) cases.

Because more cases resided in rural counties, we conducted a case-case analysis between the rural and urban cases to further detect differences in disease frequencies (Table S1); the five cases from other states were excluded from this analysis. Notably, any animal contact was more common in patients living in rural vs. urban counties (OR: 1.8; 95% CI: 0.95–3.57), however, the association was not statistically significant. Contact with "other" animals including small mammals, fish and/or amphibians was also more common in rural cases (Fisher's exact  $p$ -value = 0.0095), though only one case from the urban counties reported "other" contact. No significant difference was observed by season or for well water consumption in rural ( $n = 18$ , 19.8%) vs. urban ( $n = 7$ , 11.9%) cases; however, pork consumption was significantly lower (OR: 0.1; 95% CI: 0.02–1.12) and peanut butter consumption was significantly higher (OR: 2.1, 95% CI: 1.06–4.35) in rural vs. urban cases.

### Risk Factors for More Severe NTS Infections

To identify predictors of hospitalization, a marker for more severe infections, we used hospitalization as the dependent

variable among the 165 cases with data available. In the univariate analysis, patients self-reporting nausea (OR: 2.0; 95% CI: 1.05–3.91) and vomiting (OR: 1.9; 95% CI: 0.99–3.64) were significantly more likely to be hospitalized as were patients over the age of 59 years ( $n = 16$ ; 51.6%). Patients from urban counties were also more likely to be hospitalized ( $n = 34$ ; 41.9%) than cases from rural counties ( $n = 29$ ; 27.9%). No associations were identified with specific serovars.

Multivariate logistic regression using forward selection identified urban residence (OR: 2.1; 95% CI: 1.06–4.04) and vomiting (OR: 1.9; 95% CI: 0.99–3.78) to be the strongest predictors of hospitalization while controlling for age and sex. Because vomiting and nausea were associated with each other ( $p$ -value  $< 0.0001$ ), only vomiting was included in the model. Age over 59 years met the  $p > 0.25$  significance level for entry into the model but despite the positive association (OR: 2.0; 95% CI: 0.87–4.78), it was not statistically significant.

## Distribution of *Salmonella enterica* Serovars in Michigan Cases

The 198 NTS isolates were classified into 35 different *S. enterica* serovars; the serovar could not be determined for three isolates (Table S2). Among the 195 typed isolates, the predominant serovar was Enteritidis ( $n = 72$ ; 36.9%) followed by Typhimurium ( $n = 38$ ; 19.5%), Newport ( $n = 19$ ; 9.7%), Hartford ( $n = 6$ ; 3.1%), Saintpaul ( $n = 5$ ; 2.6%), and Heidelberg ( $n = 4$ ; 2.1%). The remaining 51 isolates represented 28 different serovars with fewer than three isolates per type. Nine isolates were classified as I 4, [5], 12:i:- / I 4, 5,12:i:- ( $n = 3$ ), I 4, 12:b- ( $n = 3$ ), I 4, 12:i:- ( $n = 3$ ), and III 50:Kz ( $n = 1$ ), which likely represent variants of known serovars.

A significant difference in the proportion of Enteritidis cases was observed by hospital ( $p$ -value = 0.02). The highest proportion was observed at two sites with 24 (33.3%) and 25 (34.7%) Enteritidis cases, though 12 (16.7%) and 11 (15.3%) additional cases were identified at the remaining two sites. The proportion of Typhimurium cases also differed at the four hospitals ( $p$ -value=0.003) with frequencies of 44.7% ( $n = 17$ ), 34.2% ( $n = 13$ ), 13.2% ( $n = 5$ ), and 7.9% ( $n = 3$ ) per site. *S. Heidelberg* was recovered from only one case at each hospital, but significant differences were observed in the proportion of Newport cases across hospitals ( $p$ -value = 0.009) as well as cases with all other serovars combined ( $p$ -value = 0.0003).

Differences were also observed in the proportion of specific serovars by year. In 2011 and 2012, for instance, 21.1% ( $n = 12$ ) of the 57 cases and 35.2% ( $n = 18$ ) of the 51 cases, respectively, were classified as Enteritidis, whereas higher frequencies were observed in 2013 ( $n = 20$  of 34; 58.8%) and 2014 ( $n = 22$  of 53; 41.5%). The proportion of Typhimurium cases was similar in years 2011, 2012, and 2014 (average = 16.2%), though a greater proportion of cases ( $n = 12$ ; 35.3%) were recovered in 2013. Of the 19 Newport cases, the proportion of Newport cases decreased in 2013 ( $n = 2$ ; 10.5%) and 2014 ( $n = 3$ ; 15.8%) relative to 2011 ( $n = 7$ ; 36.8%) and 2012 ( $n = 7$ ; 36.8%), however, the difference between each period was not significant ( $p$ -value =

0.22). Only four Heidelberg cases were identified and three of these cases were from 2014. Among all other serovars reported, it is notable that the highest frequencies were recovered in 2011 ( $n = 28$ ; 49.1%) followed by 2014 ( $n = 17$ ; 32.1%) and 2012 ( $n = 17$ ; 33.3%). A more diverse serovar population was reported in 2011 as well given that infections were caused by 26 different serovars, while 15 and 17 serovars were reported in 2012 and 2014, respectively. Only Enteritidis, Typhimurium and Newport were recovered in 2013.

Because the number of cases differed by season with the highest proportion of cases occurring in summer than in other seasons ( $p$ -value  $< 0.0001$ ), we also examined seasonal variation by serovar (Figure 1). The number of Enteritidis cases was significantly higher in the summer months ( $n = 34$ ; 47.2%) when compared to the fall ( $n = 11$ ; 15.3%), winter ( $n = 10$ ; 13.9%), and spring ( $n = 17$ ; 23.6%) months ( $p$ -value = 0.0001). Similar trends were observed for Typhimurium in the summer ( $n = 16$ , 42.1%) vs. fall ( $n = 10$ ; 26.3%), winter ( $n = 6$ ; 15.8%), and spring ( $n = 6$ ; 15.8%) months. The majority ( $n = 14$ ; 73.7%) of the 19 Newport cases were reported in the summer as were most cases infected with other serovars ( $n = 31$ ; 46.9%). During the summer months, the greatest proportion of cases were caused by Enteritidis ( $n = 34$ , 35.8%), Typhimurium ( $n = 16$ , 16.8%), and Newport ( $n = 14$ , 14.7%).

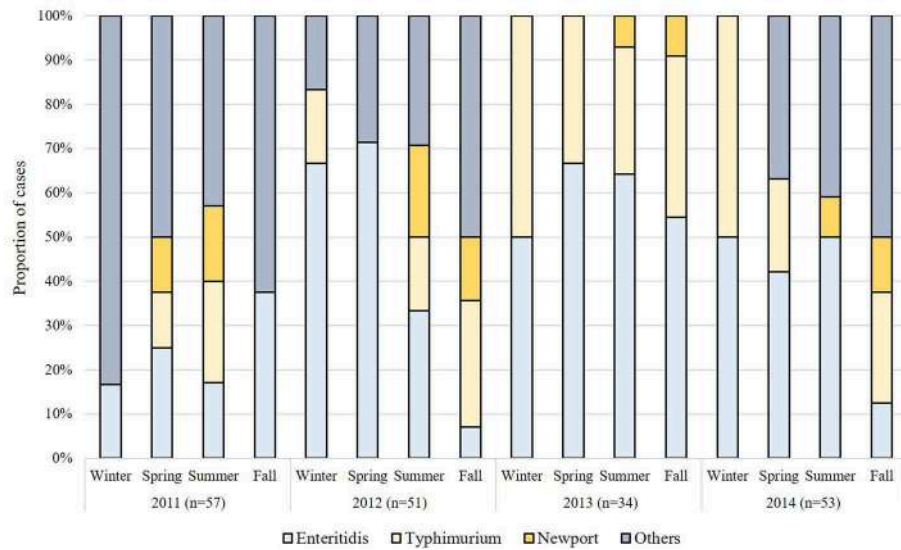
## Risk Factors for Infection With Specific *Salmonella* Serovars

Several serovar-specific factors were identified. In the univariate analysis, significantly more Enteritidis cases were reported in urban ( $n = 40$ ; 57.9%) vs. rural counties ( $n = 31$ ; 37.3%) ( $p$ -value = 0.011). Enteritidis was also associated with consumption of bottled water at home ( $n = 11$ ; 64.7%) relative to municipal ( $n = 30$ ; 37.0%) ( $p$ -value = 0.03) or well water ( $n = 10$ , 52.6%) ( $p$ -value = 0.21) as well as pork consumption (OR: 7.2; 95% CI: 0.85–61.5). The small sample sizes and missing data records for these variables, however, may have skewed the associations and prevented their inclusion into the multinomial regression analysis.

By contrast, Typhimurium infections were more common in the 95 patients reporting animal contact ( $n = 24$ ; 25.3%) than those without animal contact ( $n = 7$ ; 12.1%) ( $p$ -value = 0.078). Contact with livestock (Fisher's exact  $p$ -value = 0.0002) and other animals such as amphibians, small mammals, and fish (OR: 3.8; 95% CI: 1.41–9.97) were more common in Typhimurium cases relative to cases infected with other serovars.

A multinomial logit model using forward selection was used containing the following three outcomes: (1) Enteritidis infection; (2) Typhimurium infection; and (3) infection by all other serovars. When controlling for age and sex, residence was found to be a significant predictor of Enteritidis but not Typhimurium infections. Specifically, cases living in rural areas were significantly less likely to have infections caused by Enteritidis (OR: 0.4; 95% CI: 0.23–0.85;  $p$ -value = 0.01) but not Typhimurium (OR: 1.2; 95% CI: 0.52–2.71;  $p$ -value = 0.69); only the former association was significant.





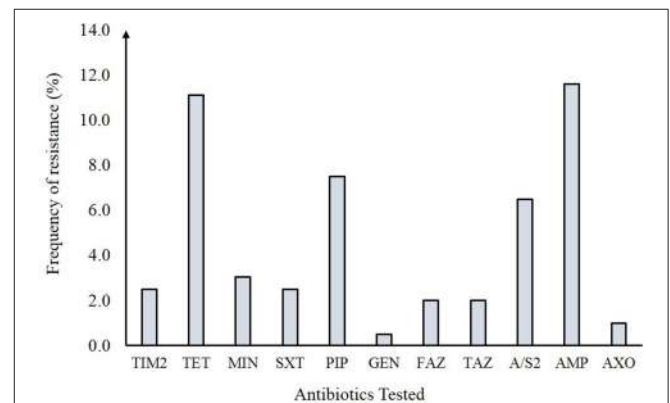
**FIGURE 1** | Seasonal variation in the distribution of non-typhoidal *Salmonella* (NTS) serovars in Michigan by year.

Because of missing data and too few cases per outcome, however, no additional variables could be examined in the multivariate analysis.

### Antibiotic Resistance Profiles in 198 Non-typhoidal *Salmonella* (NTS) Isolates

Resistance to at least one antibiotic was observed among 30 of the 198 (15.1%) NTS isolates (Figure 2). Resistance to the  $\beta$ -lactam, ampicillin (11.6%), and tetracycline (11.1%) predominated followed by resistance to trimethoprim-sulfamethoxazole (2.5%), gentamicin (0.5%), and other  $\beta$ -lactams including cephalosporins like cefazolin (2.0%), ceftazidime (2.0%), and ceftriaxone (1.0%). No resistance was observed to 13 of the 24 antibiotics tested. Overall, 19 distinct antibiotic resistance patterns were observed among the 30 resistant NTS isolates (Table S3). Multidrug resistance (MDR) to  $\geq 3$  antimicrobial classes was observed in 15 (7.5%) isolates while four (2.0%) isolates were resistant to  $\geq 4$  antimicrobial classes; nine (4.5%) isolates were resistant to only one antimicrobial class. When stratified by serovar (Figure 3), only 10 of the 35 NTS serovars contained isolates that were resistant to at least one antibiotic. Among these 10 serovars, Enteritidis was significantly less likely to comprise resistant isolates than Typhimurium (Fisher's exact  $p$ -value = 0.022) as well as the other eight serovars combined (Fisher's exact  $p$ -value < 0.0001). In all, four *S. Enteritidis* ( $n = 72$ ; 5.6%) and eight *S. Typhimurium* ( $n = 38$ ; 21.0%) isolates were resistant to at least one antibiotic.

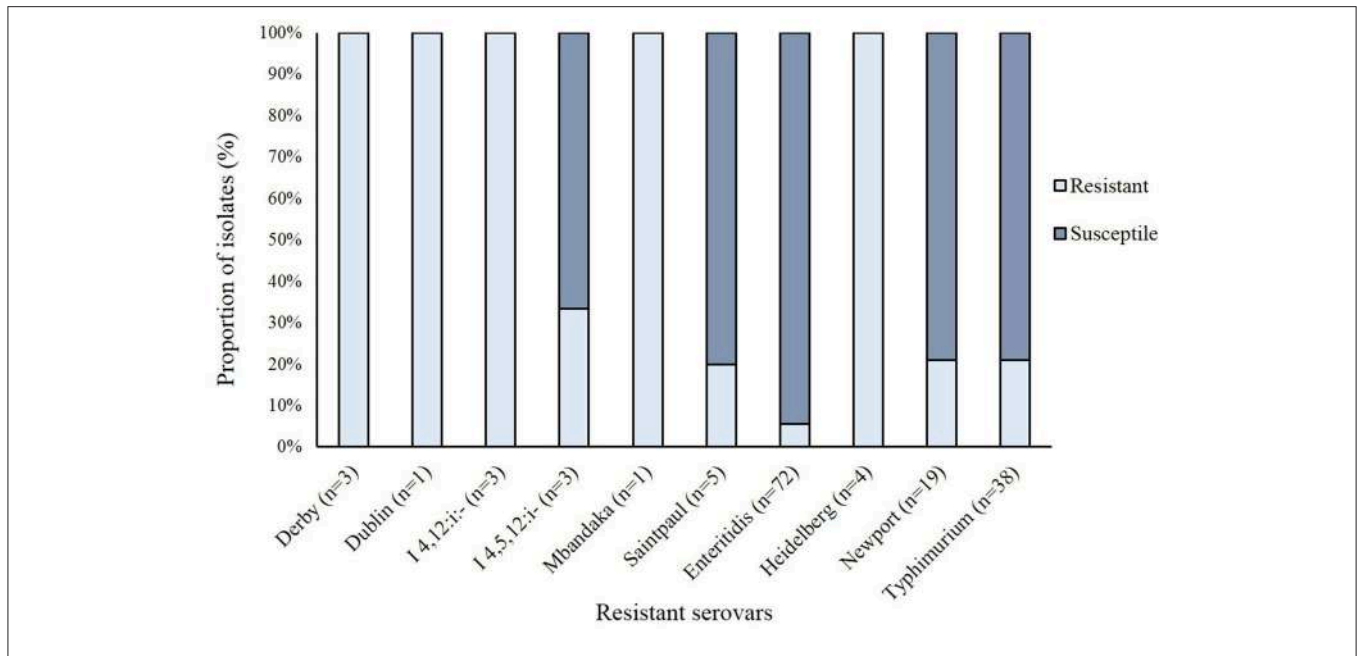
Important differences in resistance frequencies were also identified by year of isolation (Figure 4). Significant increases in resistance to tetracycline and cephalosporins, for example, were observed between 2011 and 2014 as were increases in multidrug resistance ( $p$ -value < 0.05). No significant difference in the frequency of resistance to trimethoprim-sulfamethoxazole or gentamicin were noted.



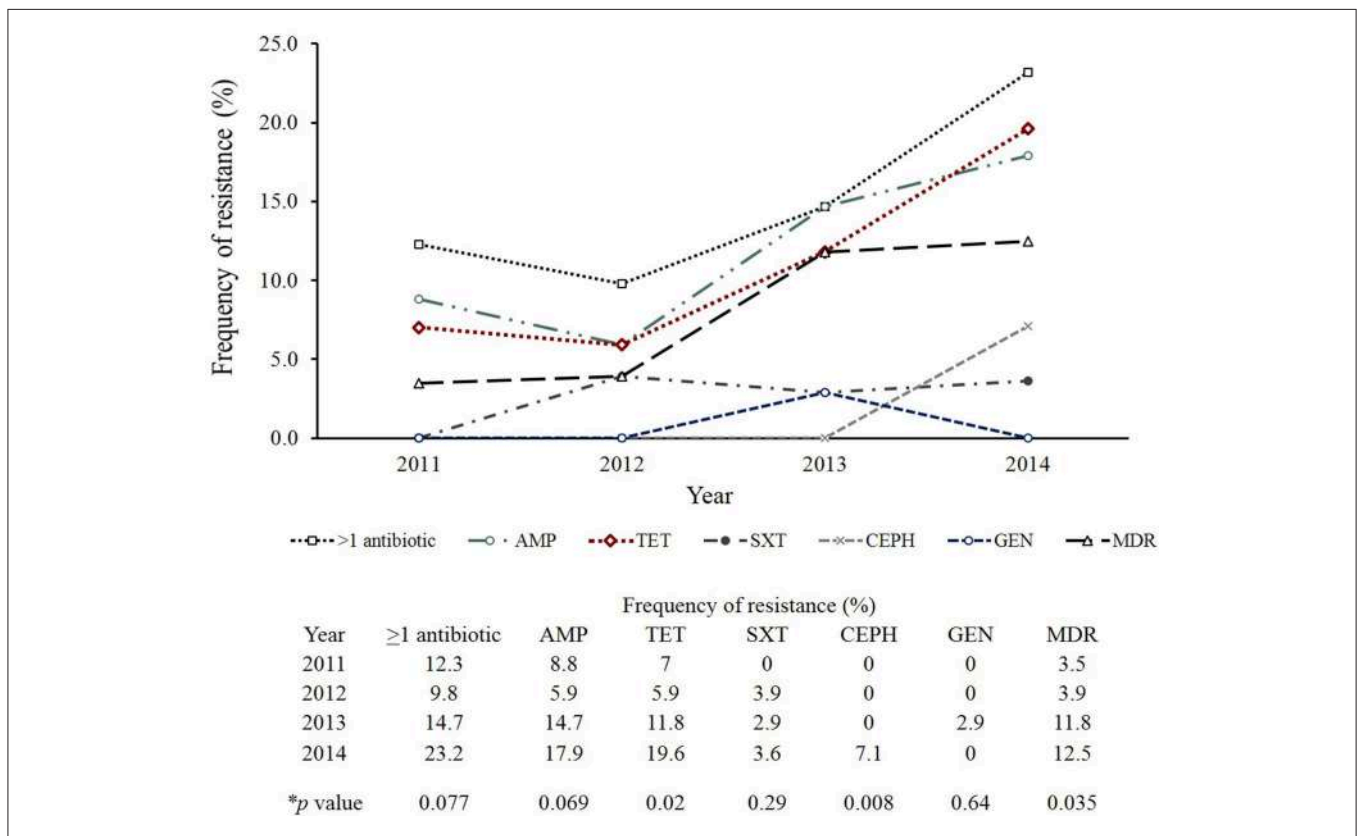
**FIGURE 2** | Antibiotic resistance frequencies in 198 non-typhoidal *Salmonella* (NTS) isolates from Michigan. TIM2, Ticarcillin / clavulanic acid constant 2; TET, Tetracycline; MIN, Minocycline; SXT, Trimethoprim / sulfamethoxazole; PIP, Piperacillin; GEN, Gentamicin; FAZ, Cefazolin; TAZ, Ceftazidime; A/S2, Ampicillin / sulbactam 2:1 ratio; AMP, Ampicillin; AXO, Ceftriaxone.

A comparison between all NTS isolates from Michigan to those tested by the National Antimicrobial Resistance Monitoring System (NARMS) (29) during the same time period also revealed slight differences in resistance frequencies by antibiotic (Figure 5A). None of these differences, however, were significant. For Enteritidis, tetracycline resistance was lower in Michigan ( $n = 1$ , 1.4%) than NARMS ( $n = 48$ , 3.0%) isolates (Figure 5B), while resistance to ampicillin and tetracycline was higher in Typhimurium isolates from NARMS than Michigan (Figure 5C). Resistance to trimethoprim-sulfamethoxazole was also higher in the Michigan Typhimurium isolates ( $n = 2$ , 5.3%) compared to the NARMS isolates ( $n = 21$ , 1.7%), yet none of the frequency differences

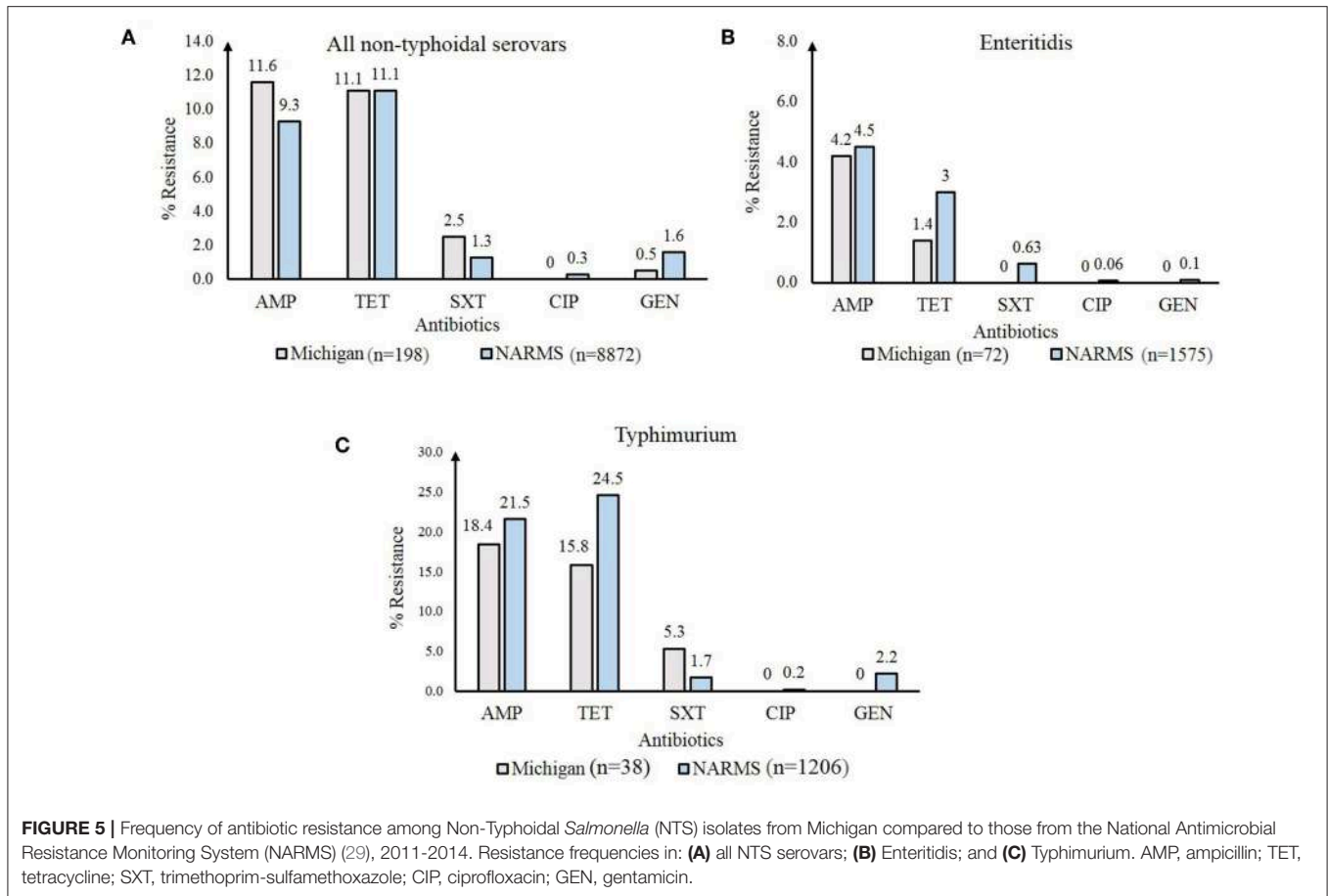




**FIGURE 3 |** Frequency of antibiotic resistance in 149 non-typhoidal *Salmonella* (NTS) isolates representing the 10 serovars with at least one resistant isolate.



**FIGURE 4 |** Trends in antibiotic resistance among clinical non-typhoidal *Salmonella* (NTS) isolates from Michigan over time. Mantel-Haenszel chi-square was used to identify trends over time and calculate *p*-values. AMP, Ampicillin; TET, Tetracycline; SXT, Trimethoprim/sulfamethoxazole; CEPH, Cephalosporin; GEN, Gentamicin; MDR, Multidrug resistance (resistance to ≥3 antimicrobial classes).



**FIGURE 5 |** Frequency of antibiotic resistance among Non-Typhoidal *Salmonella* (NTS) isolates from Michigan compared to those from the National Antimicrobial Resistance Monitoring System (NARMS) (29), 2011-2014. Resistance frequencies in: **(A)** all NTS serovars; **(B)** Enteritidis; and **(C)** Typhimurium. AMP, ampicillin; TET, tetracycline; SXT, trimethoprim-sulfamethoxazole; CIP, ciprofloxacin; GEN, gentamicin.

observed among Enteritidis and Typhimurium isolates were statistically significant.

## Epidemiological Associations With Antibiotic Resistant NTS Infections

To identify factors associated with resistant NTS infections, we conducted univariate and multivariate analyses using resistance to at least one ( $\geq 1$ ) antibiotic as the dependent variable. The univariate analysis demonstrated that the odds of resistance was significantly higher in Typhimurium isolates (OR: 4.5; 95% CI: 1.27-16.22) and other NTS serovars (OR: 4.6; 95% CI: 1.47-14.20) compared to Enteritidis isolates (**Table 1**). Higher resistance frequencies were also observed in counties with low antibiotic prescribing rates ( $n = 26$ , 16.9%) compared to those with high rates ( $n = 4$ , 10.3%), yet this difference was not statistically significant. Furthermore, frequencies of antibiotic resistant infections were higher in urban ( $n = 14$ , 16.7%) than rural ( $n = 16$ , 14.8%) areas and were lowest in the summer ( $n = 10$ , 10.3%) compared to winter, spring and fall ( $n = 20$ , 19.8%) (OR: 2.1; 95% CI: 0.95-4.86).

Notable differences in resistance frequencies were observed among the 59 patients who were hospitalized for one or more days. Among these 59 cases, the mean hospital stay was 5.9 days for the 39 patients hospitalized with resistant NTS

isolates compared to 4.0 days for the 48 patients infected with pansusceptible isolates (**Table S4**). Six of the 23 (26.1%) patients with hospital stays of  $\geq 5$  days had resistant infections compared to five of the 36 (13.9%) patients with stays between 1 and 4 days (Student's *t*-test  $p$ -value  $< 0.05$ ). Cases with tetracycline resistant and susceptible infections had mean hospital stays of 6.0 days and 4.2 days, respectively (Student's *t*-test  $p$ -value = 0.068), whereas the mean hospital stay was 6.2 days for patients infected with ampicillin-resistant NTS compared to 4.0 days for patients with ampicillin-susceptible infections (Student's *t*-test  $p$ -value  $< 0.05$ ). No association was observed between hospitalization and infection with either Enteritidis ( $n = 21$ , 30.9%) or Typhimurium ( $n = 11$ , 31.4%) when compared to all other serovars ( $n = 30$ , 36.6%).

Multivariate analysis using forward regression was performed to identify predictors of resistant infections. Because the frequency of resistance to  $\geq 1$  antibiotic was similar in isolates belonging to Typhimurium and the other NTS serovars except Enteritidis, they were grouped together for the multivariate analysis. After adjusting for sex and age, the model indicated that compared to Enteritidis, the remaining serovars were 3.8 times more likely to be resistant to at least one antibiotic (**Table 1**). Moreover, resistant NTS infections were significantly more likely to occur in fall (OR: 3.1; 95% CI: 1.22-7.60) than in the other

**TABLE 1 |** Univariate and multivariate analysis to identify factors associated with antibiotic resistance in 198 clinical non-typhoidal *Salmonella* in Michigan, 2011–2014.

Characteristic	Total isolates*	No (%) ≥1 resistance	OR (95% CI) <sup>†</sup>	p-value‡
<b>PATHOGEN FACTORS</b>				
<b>Serovar</b>				
Enteritidis	72	4 (5.6%)	–	0.008
Typhimurium	38	8 (21.1%)	–	
Other	85	18 (21.2%)	–	
<b>Outbreak associated</b>				
Yes	7	3 (42.9%)	–	0.06
No	39	4 (10.3%)	–	
<b>DEMOGRAPHIC FACTORS</b>				
<b>Residence</b>				
Urban	84	14 (16.7%)	1.1 (0.53–2.51)	0.72
Rural	108	16 (14.8%)	1.0	
<b>Age in years</b>				
0–10	44	7 (15.9%)	1.3 (0.35–4.97)	0.75
>10–59	122	19 (15.6%)	1.3 (0.41–4.10)	0.79
>59	32	4 (12.5%)	1.0	
<b>Sex</b>				
Male	104	17 (16.3%)	1.0	0.51
Female	92	12 (13.0%)	0.8 (0.34–1.71)	
<b>Race</b>				
Caucasian	125	19 (15.2%)	–	0.62
Other	44	5 (11.4%)	–	
<b>Antibiotic prescription rates by county</b>				
High	39	4 (10.3%)	–	0.46
Low	153	26 (16.9%)	–	
<b>EPIDEMIOLOGICAL AND OTHER FACTORS</b>				
<b>Length of hospital stay</b>				
No hospitalization	123	17 (13.8%)	1.0	
1–4 days	36	5 (13.9%)	–	1.0
≥5 days	23	6 (26.1%)	2.2 (0.76–6.37)	0.14
<b>Season</b>				
Fall	42	12 (28.6%)	3.5 (1.36–8.80)	0.0067
Winter	22	2 (9.1%)	–	1.0
Spring	37	6 (16.2%)	1.7 (0.57–5.03)	0.35
Summer	97	10 (10.3%)	1.0	
<b>Domestic travel in the past month</b>				
Yes	46	9 (19.6%)	1.7 (0.69–4.22)	0.25
No	120	15 (12.5%)	1.0	
<b>Animal contact</b>				
Yes	95	11 (11.6%)	0.6 (0.23–1.44)	0.24
No	60	11 (18.3%)	1.0	
<b>Chicken consumption</b>				
Yes	111	14 (12.6%)	0.7 (0.25–1.98)	0.50
No	87	6 (7.1%)	1.0	
<b>Water at home</b>				
Any municipal	103	14 (13.6%)	1.0	0.53
Any well	25	5 (20.0%)	1.6 (0.51–4.92)	0.52
Only bottled	22	4 (18.2%)	1.4 (0.42–4.79)	

(Continued)

**TABLE 1 |** Continued

Characteristic	Multivariate Analysis		
	OR	95% CI €	p-value‡
Sex: Female	0.7	0.31–1.75	0.76
Age in years: ≥ 60	0.7	0.20–2.74	0.82
Serovar: All serovars except Enteritidis	3.8	1.24–11.82	0.02
Season: Fall	3.0	c1.22–7.60	0.02
Hospitalization duration: ≥5 days	2.7	0.82–8.65	0.10

\* Depending on the variable examined, the number of isolates do not add up to the total (n = 198) because of missing data.

€ Wald 95% confidence intervals (CI) for odds ratio (OR).

‡ p-value was calculated by Chi square test and Fisher's exact test was used for variables < 5 in at least one cells; ORs were not calculated for variables with <5 per cell and the Mantel-Haenszel Chi square test was used for serogroup.

£ Logistic regression was performed using forward selection while controlling for variables that yielded significant (p-value ≤ 0.05) and strong (p-value ≤ 0.20) associations with in the univariate analysis and with a sufficient sample. Nineteen records were omitted from the analysis when hospitalization was added to the model, however, the associations between resistance and the other four variables remained the same with and without this variable. Hosmer and Lemeshow Goodness of Fit tests were >0.05 for both models with and without hospitalization. All variables were tested for collinearity.

three seasons. A strong association (OR: 2.7) was also observed between resistance and hospitalization stays longer than 5 days, however, it was not statistically significant while controlling for the other four variables.

## DISCUSSION

This study, which was conducted between 2011 and 2014 using data and isolates from an active surveillance system at four large, metropolitan hospital systems, indicated that most (64.1%) of the 198 cases were over the age of 19 and 16.2% were over 60 years of age. These data differ from those reported in a prior Michigan study of Enteritidis infections occurring between 1995 and 2001, which found children <4 years of age to have the greatest risk of infection (30). Although age was not significantly associated with Enteritidis infections or infections caused by any other serovars, these data suggest that the demographics of salmonellosis cases may have changed over time. Additional studies in different Michigan hospitals are therefore required.

Significantly more NTS infections occurred in Michigan during the summer and fall months consistent with a CDC report showing that most *Salmonella* infections occur between June and October in the U.S. (31). An increased frequency of infections caused by *S. Enteritidis* specifically (30) and other enteric pathogens has also been reported during the summer. Shiga toxin-producing *E. coli* (STEC) infections, for example, were highest in Michigan during the summer (37.3%) and fall (29.5%) over a 12-year period (2001–2012) (32). Such seasonal variation has been explained by recreational activities, inadequate cooking and suboptimal food storage temperatures

during outdoor picnics and barbecues (33) as well as visiting petting zoos and farms (34). Variation in the distribution of serovars by season was also observed and is consistent with data from a study of 690,479 *Salmonella* infections reported to the CDC. Specifically, this study found that the number of different *Salmonella* serotypes causing human infection, or the “serotype richness,” was greatest in the winter even though the greatest number of infections occurred during the summer (35).

Although salmonellosis frequencies were not significantly higher in patients residing in rural vs. urban areas ( $p$ -value = 0.083), urban residence was found to be a predictor of infection with *S. Enteritidis* using logistic regression. Intriguingly, urban residence was also associated with hospitalization due to any NTS infection, a finding that may be related to proximity of the health care facilities included in the study. The association between residence location and infection with specific serovars is supported by data from prior studies showing a lower prevalence of Enteritidis in the farm environment relative to other serovars. A Canadian study of urban and rural streams, for example, detected low frequencies of Enteritidis in the rural streams (36), while Enteritidis was rarely recovered from livestock and poultry in Alberta (37) or in the environment of commercial poultry farms in California (38). It is therefore possible that *Salmonella* serovars other than Enteritidis may be more widespread in the environment. An association was also observed between Typhimurium infections and history of animal contact, which has been reported in many prior studies. Indeed, one study indicated that living on a livestock farm was an independent risk factor for acquiring *S. Typhimurium* DT104 infections (13), while another study recovered indistinguishable *S. Typhimurium* DT104 isolates from a child and animals living on the same farm (39). The identification of animal contact as a risk factor for NTS infections in Michigan may be important as it highlights the need for additional studies to investigate this epidemiological association and develop more targeted prevention strategies. Indeed, we were only able to evaluate whether or not any animal contact was reported, which fails to adequately describe the level or duration of contact or even the well-being of the animals.

Importantly, a wide range of antibiotic resistance profiles in the 198 NTS isolates recovered from patients at four Michigan hospitals was observed. High frequencies of resistance to ampicillin and tetracycline were identified with an increasing trend in tetracycline resistance over the 4-year period; tetracycline resistance also contributed to the high frequency of MDR in the NTS isolates examined. It is notable that an increase in tetracycline resistance was not observed by NARMS for the same time period ( $p$ -value = 0.66) and hence, it is possible that Michigan harbors a unique population of resistant NTS. NARMS also reported an increased frequency of MDR in 2015 (12%) relative to 2008 (9.5%) (29). While tetracycline is not widely recommended for clinical use, antibiotics such as amoxicillin, penicillin, and sulfamethoxazole-trimethoprim are commonly prescribed to adults and children in Michigan (28). The high prescription rates of these antibiotics, among others, is likely to have an impact on resistance frequencies

in the state. Unfortunately, actual antibiotic usage data was not available for NTS cases in our study as these data are not collected by the MDHHS during case interviews. We also observed an increasing trend in the frequency of MDR in NTS over the 2011–2014 time period, however, the difference was not significant by year and could be due to our focused surveillance of only four hospitals. It is possible that increases in MDR frequencies over time could be linked to international travel or food imports as suggested previously (40, 41); however, travel was not associated with MDR infections in our study and import risk was not evaluated.

Although tetracyclines are not widely used in human medicine, they are among the most commonly used antibiotics in livestock and poultry worldwide (42). The FDA has estimated that 3,535,701 (kg)<sup>2</sup> of tetracyclines are used in food-producing animals in the U.S. each year representing 64% of all antibiotics used (43). While the use of tetracyclines in these animals decreased by 40% in 2016–2017 relative to the period between 2009 and 2017 (43), antibiotic residues and resistance determinants can persist in the environment (44) and animal reservoir, be transmitted to humans, and contribute to MDR in both gram-positive and -negative bacteria (45). Indeed, the emergence and spread of resistance between food animals and people has been documented. One historical study, for instance, found identical resistance patterns in *E. coli* isolates from livestock and farming families (46), while others have documented spread through food products and water (47–49). Since we have only examined resistance in clinical NTS isolates, additional studies are needed to quantify resistance frequencies in isolates from other sources to identify those strain types, virulence gene profiles, and resistance phenotypes that pose the highest risk of transmission to and infection in humans. A recent study, for example, documented different antibiotic resistance profiles among isolates from different sources and suggested that multiple sources in the food-chain are responsible for resistant *Salmonella* infections in humans (23).

As such, it is important to consider that the genetic and phenotypic diversity of NTS isolates in different geographical locations may play a role in human infections as specific NTS lineages circulating in Michigan may be more likely to carry resistance determinants. Support for this possibility comes from our finding that NTS serovars had varying resistance profiles. Notably, multivariate logistic regression identified serovar Enteritidis to be significantly less likely to be resistant to at least one antibiotic compared to all other NTS serovars. Serovar-dependent differences in resistance have been observed in NTS isolates in different geographic locations including Spain (50) and Brazil (51). The reason for serovar-specific differences is not clear, however, one study found that ciprofloxacin-resistant *S. Typhimurium* isolates were more competitive during growth *in vitro* with increasing concentrations of ciprofloxacin than the ciprofloxacin-resistant *S. Enteritidis* isolates (52). Other studies have shown that certain NTS serovars such as Kentucky, Typhimurium, and Heidelberg, were more likely to have MDR (53–55), whereas some serovars (e.g., Enteritidis, Montevideo, Infantis, and Mbandaka) were more commonly pansusceptible or were resistant to fewer antibiotics (56, 57).



Such differences could be due to the specificity of or ability to take up certain plasmids carrying resistance genes as some plasmids may be more commonly acquired across serovars and other bacterial species (58). Serovars such as Kentucky and Heidelberg have also been shown to have a mutation in the methyl mismatch repair (MMR) system, which may contribute to genetic heterogeneity (59). This genome plasticity has been offered as an explanation for higher frequencies of antibiotic resistance within these strain backgrounds (60). Differences in fitness between serovars, genetic plasticity and dissimilar resistance mechanisms could partly explain the varying frequencies of resistance in NTS serovars worldwide. Although serogrouping has been useful for differentiating NTS isolates for surveillance studies (61), future studies are needed to characterize the isolates using whole genome sequencing to identify bacterial features commonly associated with specific resistance phenotypes and carriage of specific resistance determinants. Having these data could help identify sources of resistant infections and identify whether some strains are epidemiologically linked.

Our study also identified season to be a predictor of resistant NTS infections, with fewer resistant infections occurring in the summer and more in the fall as is consistent with seasonal variation observed in prior studies. A study of fluoroquinolone resistance in *Campylobacter*, for example, observed higher frequencies in the winter and spring compared to the summer. This difference was attributed to higher consumption of poultry products containing resistant bacteria in the winter and more frequent exposure to susceptible *Campylobacter* through other sources in the summer (62). Our prior studies have also observed higher resistance frequencies in *C. jejuni* (63) and STEC (64) recovered from Michigan patients in the winter and/or spring and could be due, in part, to seasonal variation in antibiotic prescription rates (65, 66). Because prescribing rates may vary by the type of infection and geographic location given climate and other factors, additional studies are required to understand the most important factors that impact antibiotic resistance development and trends in Michigan.

While we did not identify antibiotic resistant NTS infections to be a significant predictor of hospitalization, we did observe a strong association between resistance in NTS and a longer duration ( $\geq 5$  days) of hospitalization. This finding is not surprising given that resistant infections take longer to clear than susceptible infections during antibiotic treatment and is consistent with other studies. Importantly, studies in other pathogens have identified associations between resistance and mortality, hospitalization, hospital stay duration, and the need for surgery (18, 64, 67, 68).

Because NTS pathogens are a leading cause of enteric infections worldwide and have been shown to frequently resist clinically important antibiotics, continuous surveillance, and monitoring is critical. NTS isolation and routine testing for resistance is imperative in order to help medical personnel and public health officials determine and modify the course of treatment for NTS infections. Furthermore, identifying risk

factors for NTS and resistant NTS infections may help in the development of disease management policies and antibiotic use standards aimed at curbing the spread of NTS and resistance determinants.

## DATA AVAILABILITY STATEMENT

All datasets generated for this study are included in the article/**Supplementary Material**.

## ETHICS STATEMENT

The studies involving human participants were reviewed and approved by Institutional Review Boards at Michigan State University (MSU; Lansing, MI, USA; IRB #10-736SM), the MDHHS (842-PHALAB), and the four participating hospitals. Written informed consent from the participants' legal guardian/next of kin was not required to participate in this study in accordance with the national legislation and the institutional requirements.

## AUTHOR CONTRIBUTIONS

SM performed the experiments with CA and RM organized samples and extracted the epidemiological data. SM and SDM managed the data, conducted the analyses, and drafted the manuscript. SM, SDM, JR, DN, HS, PL, and WK designed the study and organized sample collection at each site. All authors contributed and approved the manuscript content.

## FUNDING

This work was supported by the National Institutes of Health Enterics Research Investigational Network Cooperative Research Center (U19AI090872 to SDM), the Michigan State University (MSU) Foundation, and the United States Department of Agriculture (MICL02475). The Department of Microbiology and Molecular Genetics at MSU, the Ronald and Sharon Rogowski Fellowship and the MSU College of Natural Science provided student support to SM. A portion of these findings were included in SM dissertation from MSU (69).

## ACKNOWLEDGMENTS

We thank Ben Hutton and Jason Wholehan at the MDHHS and the laboratory staff at each participating hospital for help with specimen processing and culture as well as James Collins and Tiffany Henderson at the MDHHS Bureau of Epidemiology for help with MDSS.

## SUPPLEMENTARY MATERIAL

The Supplementary Material for this article can be found online at: <https://www.frontiersin.org/articles/10.3389/fmed.2019.00250/full#supplementary-material>

## REFERENCES

- Majowicz SE, Musto J, Scallan E, Angulo FJ, Kirk M, O'Brien SJ, et al. The global burden of nontyphoidal *Salmonella* gastroenteritis. *Clin Infect Dis.* (2010) 50:882–9. doi: 10.1086/650733
- Global Burden of Diseases Diarrhoeal Diseases Collaborators. Estimates of global, regional, and national morbidity, mortality, and aetiologies of diarrhoeal diseases: a systematic analysis for the Global Burden of Disease Study 2015. *Lancet Infect Dis.* (2017) 17:909–48. doi: 10.1016/S1473-3099(17)30276-1
- Crim SM, Iwamoto M, Huang JY, Griffin PM, Gilliss D, Cronquist AB, et al. Incidence and trends of infection with pathogens transmitted commonly through food—Foodborne Diseases Active Surveillance Network, 10 U.S. sites, 2006–2013. *Morb Mortal Wkly Rep.* (2014) 63:328–32.
- Gal-Mor O, Boyle EC, Grassl GA. Same species, different diseases: how and why typhoidal and non-typhoidal *Salmonella enterica* serovars differ. *Front Microbiol.* (2014) 5:391. doi: 10.3389/fmicb.2014.00391
- Murray CJ, Vos T, Lozano R, Naghavi M, Flaxman AD, Michaud C, et al. Disability-adjusted life years (DALYs) for 291 diseases and injuries in 21 regions, 1990–2010: a systematic analysis for the Global Burden of Disease Study 2010. *Lancet.* (2012) 380:2197–223. doi: 10.1016/S0140-6736(12)61689-4
- Scallan E, Hoekstra RM, Angulo FJ, Tauxe RV, Widdowson MA, Roy SL, et al. Foodborne illness acquired in the United States—major pathogens. *Emerg Infect Dis.* (2011) 17:7–15. doi: 10.3201/eid1701.P11101
- Hoffmann S, Maculloch B, Batz M. *Economic Burden of Major Foodborne Illnesses Acquired in the United States.* United States Department of Agriculture (2015). Available online at: [https://www.ers.usda.gov/webdocs/publications/43984/52807\\_eib140.pdf](https://www.ers.usda.gov/webdocs/publications/43984/52807_eib140.pdf)
- Galanis E, Lo Fo Wong DM, Patrick ME, Binsztein N, Cieslik A, Chalermchikit T, et al. Web-based surveillance and global *Salmonella* distribution, 2000–2002. *Emerg Infect Dis.* (2006) 12:381–8. doi: 10.3201/eid1205.050854
- Hoelzer K, Switt AIM, Wiedmann M. Animal contact as a source of human non-typhoidal salmonellosis. *Vet Res.* (2011) 42:34. doi: 10.1186/1297-9716-42-34
- Mermin J, Hutwagner L, Vugia D, Shallow S, Daily P, Bender J, et al. Reptiles, amphibians, and human *Salmonella* infection: a population-based, case-control study. *Clin Infect Dis.* (2004) 38 (Suppl. 3):S253–61. doi: 10.1086/381594
- Younus M, Wilkins MJ, Davies HD, Rahbar MH, Funk J, Nguyen C, et al. The role of exposures to animals and other risk factors in sporadic, non-typhoidal *Salmonella* infections in Michigan children. *Zoonoses Public Health.* (2010) 57:e170–6. doi: 10.1111/j.1863-2378.2010.01324.x
- Doorduyn Y, Van Den Brandhof WE, Van Duynhoven YT, Wannet WJ, Van Pelt W. Risk factors for *Salmonella* enteritidis and typhimurium (DT104 and non-DT104) infections in the Netherlands: predominant roles for raw eggs in enteritidis and sandboxes in Typhimurium infections. *Epidemiol Infect.* (2006) 134:617–26. doi: 10.1017/S0950268805005406
- Dore K, Buxton J, Henry B, Pollari F, Middleton D, Fyfe M, et al. Risk factors for *Salmonella* Typhimurium DT104 and non-DT104 infection: a Canadian multi-provincial case-control study. *Epidemiol Infect.* (2004) 132:485–93. doi: 10.1017/S0950268803001924
- Cherry WB, Hanks JB, Thomason BM, Murlin AM, Biddle JW, Croom JM. *Salmonellae* as an index of pollution of surface waters. *Appl Microbiol.* (1972) 24:334–40.
- Baudart J, Lemarchand K, Brisabois A, Lebaron P. Diversity of *Salmonella* strains isolated from the aquatic environment as determined by serotyping and amplification of the ribosomal DNA spacer regions. *Appl Environ Microbiol.* (2000) 66:1544–52. doi: 10.1128/AEM.66.4.1544-1552.2000
- Centers for Disease Control and Prevention (2013). *Antibiotic Resistance Threats in the United States, 2013.* Available online at: <https://www.cdc.gov/drugresistance/threat-report-2013/pdf/ar-threats-2013-508.pdf>
- Sanchez-Vargas FM, Abu-El-Haija MA, Gomez-Duarte OG. *Salmonella* infections: an update on epidemiology, management, and prevention. *Travel Med Infect Dis.* (2011) 9:263–77. doi: 10.1016/j.tmaid.2011.11.001
- Varma JK, Molbak K, Barrett TJ, Beebe JL, Jones TF, Rabatsky-Ehr T, et al. Antimicrobial-resistant nontyphoidal *Salmonella* is associated with excess bloodstream infections and hospitalizations. *J Infect Dis.* (2005) 191:554–61. doi: 10.1086/427263
- Helmis M, Ethelberg S, Molbak K, Group DTS. International *Salmonella* Typhimurium DT104 infections, 1992–2001. *Emerg Infect Dis.* (2005) 11:859–67. doi: 10.3201/eid1106.041017
- Yu CY, Chou SJ, Yeh CM, Chao MR, Huang KC, Chang YF, et al. Prevalence and characterization of multidrug-resistant (type ACSSuT) *Salmonella enterica* serovar Typhimurium strains in isolates from four gosling farms and a hatchery farm. *J Clin Microbiol.* (2008) 46:522–6. doi: 10.1128/JCM.00709-07
- Dos Reis EM, Rodrigues Ddos P, De Freitas-Almeida AC, Hofer E. Prevalence of R-type ACSSuT in strains of *Salmonella* serovar Typhimurium DT193 isolated from human infections in Brazil. *Rev Panam Salud Publica.* (2011) 29:387–92.
- Afema JA, Mather AE, Sischo WM. Antimicrobial resistance profiles and diversity in *Salmonella* from humans and cattle, 2004–2011. *Zoonoses Public Health.* (2015) 62:506–17. doi: 10.1111/zph.12172
- Wang X, Biswas S, Paudyal N, Pan H, Li X, Fang W, et al. Antibiotic resistance in *Salmonella* typhimurium isolates recovered from the food chain through national antimicrobial resistance monitoring system between 1996 and 2016. *Front Microbiol.* (2019) 10:985. doi: 10.3389/fmicb.2019.00985
- Association of Public Health Laboratories. *Salmonella Serotyping in US Public Health Laboratories.* (Silver Spring, MD) (2014). Available online at: [https://www.aphl.org/aboutAPHL/publications/Documents/FS\\_SalmonellaSustainabilityWhitePaper\\_Nov2014.pdf](https://www.aphl.org/aboutAPHL/publications/Documents/FS_SalmonellaSustainabilityWhitePaper_Nov2014.pdf)
- Singh P, Teal TK, Marsh TL, Tiedje JM, Mosci R, Jernigan K, et al. Intestinal microbial communities associated with acute enteric infections and disease recovery. *Microbiome.* (2015) 3:45. doi: 10.1186/s40168-015-0109-2
- Clinical Laboratory Standards Institute. *Performance Standards for Antimicrobial Susceptibility Testing: Twenty-Fourth Information Supplement.* (2014). Available online at: <https://clsi.org/standards/products/microbiology/documents/m100/>
- Ingram DD, Franco SJ. 2013 NCHS urban-rural classification scheme for counties. *Vital Health Stat.* (2014) 2:1–73.
- Kofke-Egger H, Udow-Phillips M. *Antibiotic Prescribing and Use.* University of Michigan, Center for Healthcare Research and Transformation, Ann Arbor, MI (2011). Available online at: <https://www.chrt.org/publication/antibiotic-prescribing-use/>
- Centers for Disease Control and Prevention (2018). *National Antimicrobial Resistance Monitoring System (NARMS) Now: Human Data.* Atlanta, GA. Available online at: <https://www.cdc.gov/narmsgnow>
- Younus M, Wilkins MJ, Arshad MM, Rahbar MH, Saeed AM. Demographic risk factors and incidence of *Salmonella* enteritidis infection in Michigan. *Foodborne Pathog Dis.* (2006) 3:266–73. doi: 10.1089/fpd.2006.3.266
- Centers for Disease Control and Prevention (2013). *National Enteric Disease Surveillance: Salmonella Annual Report, 2011.* Atlanta, GA. Available online at: <https://www.cdc.gov/ncezid/dfwed/PDFs/salmonella-annual-report-2011-508c.pdf>
- Tseng M, Sha Q, Rudrik JT, Collins J, Henderson T, Funk JA, et al. Increasing incidence of non-O157 Shiga toxin-producing *Escherichia coli* (STEC) in Michigan and association with clinical illness. *Epidemiol Infect.* (2016) 144:1394–405. doi: 10.1017/S0950268815002836
- Akil L, Ahmad HA, Reddy RS. Effects of climate change on *Salmonella* infections. *Foodborne Pathog Dis.* (2014) 11:974–80. doi: 10.1089/fpd.2014.1802
- Conrad CC, Stanford K, Narvaez-Bravo C, Callaway T, Mcallister T. Farm fairs and petting zoos: a review of animal contact as a source of zoonotic enteric disease. *Foodborne Pathog Dis.* (2017) 14:59–73. doi: 10.1089/fpd.2016.2185
- Judd MC, Hoekstra RM, Mahon BE, Fields PI, Wong KK. Epidemiologic patterns of human *Salmonella* serotype diversity in the USA, 1996–2016. *Epidemiol Infect.* (2019) 147:e187. doi: 10.1017/S0950268819000724
- Thomas JL, Slawson RM, Taylor WD. *Salmonella* serotype diversity and seasonality in urban and rural streams. *J Appl Microbiol.* (2013) 114:907–22. doi: 10.1111/jam.12079
- Guerin MT, Martin SW, Darlington GA, Rajic A. A temporal study of *Salmonella* serovars in animals in Alberta between 1990 and 2001. *Can J Vet Res.* (2005) 69:88–99. doi: 10.1007/BF03404039

38. Dailey N, Niemeier D, Elkhoraibi C, Senties-Cue CG, Pitesky M. Descriptive survey and *Salmonella* surveillance of pastured poultry layer farms in California. *Poult Sci.* (2017) 96:957–65. doi: 10.3382/ps/pew360
39. Hendriksen SW, Orsel K, Wagenaar JA, Miko A, Van Duijkeren E. Animal-to-human transmission of *Salmonella* Typhimurium DT104A variant. *Emerg Infect Dis.* (2004) 10:2225–7. doi: 10.3201/eid1012.040286
40. Aarestrup FM, Hendriksen RS, Lockett J, Gay K, Teates K, Mcdermott PF, et al. International spread of multidrug-resistant *Salmonella* Schwarzengrund in food products. *Emerg Infect Dis.* (2007) 13:726–31. doi: 10.3201/eid1305.061489
41. Williamson D, Lane C, Easton M, Valcanis M, Strachan J, Veitch M, et al. Increasing antimicrobial resistance in non-typhoidal *Salmonella* in Australia, 1979 - 2015. *Antimicrob. Agents Chemother.* (2017) 62:e02012-17. doi: 10.1128/AAC.02012-17
42. Chopra I, Roberts M. Tetracycline antibiotics: mode of action, applications, molecular biology, and epidemiology of bacterial resistance. *Microbiol Mol Biol Rev.* (2001) 65:232–60. doi: 10.1128/MMBR.65.2.232-260.2001
43. Food and Drug Administration. *Summary Report on Antimicrobials Sold or Distributed for Use in Food-Producing Animals.* (2011). Available online at: <https://www.fda.gov/media/119332/download>
44. Hamscher G, Sczesny S, Hoper H, Nau H. Determination of persistent tetracycline residues in soil fertilized with liquid manure by high-performance liquid chromatography with electrospray ionization tandem mass spectrometry. *Anal Chem.* (2002) 74:1509–18. doi: 10.1021/ac015588m
45. Levy SB. *The Antibiotic Paradox: How Miracle Drugs are Destroying the Miracle.* New York, NY: Plenum Press (1992). doi: 10.1007/978-1-4899-6042-9
46. Fein D, Burton G, Tsutakawa R, Blendon D. Matching of antibiotic resistance patterns of *Escherichia coli* of farm families and their animals. *J Infect Dis.* (1974) 130:274–9. doi: 10.1093/infdis/130.3.274
47. White DG, Zhao S, Sudler R, Ayers S, Friedman S, Chen S, et al. The isolation of antibiotic-resistant *Salmonella* from retail ground meats. *N Engl J Med.* (2001) 345:1147–54. doi: 10.1056/NEJMoa010315
48. Mackie RI, Koike S, Krapac J, Chee-Sanford J, Maxwell S, Aminov RI. Tetracycline residues and tetracycline resistance genes in groundwater impacted by swine production facilities. *Anim Biotechnol.* (2006) 17:157–76. doi: 10.1080/10495390600956953
49. Xi C, Zhang Y, Marrs CF, Ye W, Simon C, Foxman B, et al. Prevalence of antibiotic resistance in drinking water treatment and distribution systems. *Appl Environ Microbiol.* (2009) 75:5714–8. doi: 10.1128/AEM.00382-09
50. Soler P, Gonzalez-Sanz R, Bleda MJ, Hernandez G, Echeita A, Usera MA. Antimicrobial resistance in non-typhoidal *Salmonella* from human sources, Spain, 2001–2003. *J Antimicrob Chemother.* (2006) 58:310–4. doi: 10.1093/jac/dkl223
51. Voss-Rech D, Potter L, Vaz CS, Pereira DI, Sangioni LA, Vargas AC, et al. Antimicrobial resistance in nontyphoidal *Salmonella* isolated from human and poultry-related samples in Brazil: 20-year meta-analysis. *Foodborne Pathog Dis.* (2017) 14:116–24. doi: 10.1089/fpd.2016.2228
52. Zhang CZ, Ren SQ, Chang MX, Chen PX, Ding HZ, Jiang HX. Resistance mechanisms and fitness of *Salmonella*, Typhimurium and *Salmonella* Enteritidis mutants evolved under selection with ciprofloxacin *in vitro*. *Sci Rep.* (2017) 7:9113. doi: 10.1038/s41598-017-09151-y
53. Roy P, Dhillon AS, Lauerman LH, Schaberg DM, Bandli D, Johnson S. Results of *Salmonella* isolation from poultry products, poultry, poultry environment, and other characteristics. *Avian Dis.* (2002) 46:17–24. doi: 10.1637/0005-2086(2002)0460017:ROSIFFP2.0.CO;2
54. Berrang ME, Bailey JS, Altekruze SF, Shaw WK Jr, Patel BL, Meinersmann RJ, et al. Prevalence, serotype, and antimicrobial resistance of *Salmonella* on broiler carcasses postpick and postchill in 20 U.S. processing plants. *J Food Prot.* (2009) 72:1610–5. doi: 10.4315/0362-028X-72.8.1610
55. Han J, David DE, Deck J, Lynne AM, Kaldhone P, Nayak R, et al. Comparison of *Salmonella enterica* serovar Heidelberg isolates from human patients with those from animal and food sources. *J Clin Microbiol.* (2011) 49:1130–3. doi: 10.1128/JCM.01931-10
56. Edrington TS, Schultz CL, Bischoff KM, Callaway TR, Looper ML, Genovese KJ, et al. Antimicrobial resistance and serotype prevalence of *Salmonella* isolated from dairy cattle in the southwestern United States. *Microb Drug Resist.* (2004) 10:51–6. doi: 10.1089/107662904323047808
57. M'ikanatha N, M., Sandt CH, Localio AR, Tewari D, Rankin SC, et al. Multidrug-resistant *Salmonella* isolates from retail chicken meat compared with human clinical isolates. *Foodborne Pathog Dis.* (2010) 7:929–34. doi: 10.1089/fpd.2009.0499
58. Carattoli A. Resistance plasmid families in Enterobacteriaceae. *Antimicrob Agents Chemother.* (2009) 53:2227–38. doi: 10.1128/AAC.01707-08
59. Dhanani AS, Block G, Dewar K, Forgetta V, Topp E, Beiko RG, et al. Genomic comparison of non-typhoidal *Salmonella enterica* serovars Typhimurium, Enteritidis, Heidelberg, Hadar and Kentucky isolates from broiler chickens. *PLoS ONE.* (2015) 10:e0128773. doi: 10.1371/journal.pone.0128773
60. Shah DH, Paul NC, Sischo WC, Crespo R, Guard J. Population dynamics and antimicrobial resistance of the most prevalent poultry-associated *Salmonella* serotypes. *Poult Sci.* (2017) 96:687–702. doi: 10.3382/ps/pew342
61. Foley SL, Zhao S, Walker RD. Comparison of molecular typing methods for the differentiation of *Salmonella* foodborne pathogens. *Foodborne Pathog Dis.* (2007) 4:253–76. doi: 10.1089/fpd.2007.0085
62. Talsma E, Goetsch WG, Nieste HL, Schrijnemakers PM, Sprenger MJ. Resistance in *Campylobacter* species: increased resistance to fluoroquinolones and seasonal variation. *Clin Infect Dis.* (1999) 29:845–8. doi: 10.1086/520447
63. Cha W, Mosci R, Wengert SL, Singh P, Newton DW, Salimnia H, et al. Antimicrobial susceptibility profiles of human *Campylobacter jejuni* isolates and association with phylogenetic lineages. *Front Microbiol.* (2016) 7:589. doi: 10.3389/fmicb.2016.00589
64. Mukherjee S, Mosci RE, Anderson CM, Snyder BA, Collins J, Rudrik JT, et al. Antimicrobial drug-resistant Shiga toxin-producing *Escherichia coli* infections, Michigan, USA. *Emerg Infect Dis.* (2017) 23:1609–11. doi: 10.3201/eid2309.170523
65. Sun L, Klein EY, Laxminarayan R. Seasonality and temporal correlation between community antibiotic use and resistance in the United States. *Clin Infect Dis.* (2012) 55:687–94. doi: 10.1093/cid/cis509
66. Suda KJ, Hicks LA, Roberts RM, Hunkler RJ, Taylor TH. Trends and seasonal variation in outpatient antibiotic prescription rates in the United States, 2006 to 2010. *Antimicrob Agents Chemother.* (2014) 58:2763–6. doi: 10.1128/AAC.02239-13
67. Linden PK, Pasculle AW, Manez R, Kramer DJ, Fung JJ, Pinna AD, et al. Differences in outcomes for patients with bacteremia due to vancomycin-resistant *Enterococcus faecium* or vancomycin-susceptible *E. faecium*. *Clin Infect Dis.* (1996) 22:663–70. doi: 10.1093/clinids/22.4.663
68. Cosgrove S. The Relationship between antimicrobial resistance and patient outcomes: mortality, length of hospital stay, and health care costs. *Clin Infect Dis.* (2006) 42:S82–S89. doi: 10.1086/499406
69. Mukherjee S. *Epidemiology of antibiotic resistant Shiga toxin-producing Escherichia coli (STEC) and non-typhoidal Salmonella (NTS) in Michigan.* (Ph.D.) Michigan State University, East Lansing, MI (2018).

**Conflict of Interest:** The authors declare that the research was conducted in the absence of any commercial or financial relationships that could be construed as a potential conflict of interest.

Copyright © 2019 Mukherjee, Anderson, Mosci, Newton, Lephart, Salimnia, Khalife, Rudrik and Manning. This is an open-access article distributed under the terms of the Creative Commons Attribution License (CC BY). The use, distribution or reproduction in other forums is permitted, provided the original author(s) and the copyright owner(s) are credited and that the original publication in this journal is cited, in accordance with accepted academic practice. No use, distribution or reproduction is permitted which does not comply with these terms.



# Constructing and Characterizing Bacteriophage Libraries for Phage Therapy of Human Infections

Shelley B. Gibson<sup>1</sup>, Sabrina I. Green<sup>1</sup>, Carmen Gu Liu<sup>1</sup>, Keiko C. Salazar<sup>1</sup>, Justin R. Clark<sup>1</sup>, Austen L. Terwilliger<sup>1</sup>, Heidi B. Kaplan<sup>2</sup>, Anthony W. Maresso<sup>1\*</sup>, Barbara W. Trautner<sup>1,3,4\*</sup> and Robert F. Ramig<sup>1\*</sup>

<sup>1</sup> Department of Molecular Virology and Microbiology, Baylor College of Medicine, Houston, TX, United States, <sup>2</sup> Department of Microbiology and Molecular Genetics, McGovern Medical School, University of Texas Health Science Center at Houston, Houston, TX, United States, <sup>3</sup> Center for Innovations in Quality, Effectiveness and Safety, Michael E. DeBakey VA Medical Center, Houston, TX, United States, <sup>4</sup> Department of Medicine, Baylor College of Medicine, Houston, TX, United States

## OPEN ACCESS

### Edited by:

Rustam Aminov,  
University of Aberdeen,  
United Kingdom

### Reviewed by:

Paul Hyman,  
Ashland University, United States  
Pieter-Jan Ceyskens,  
Sciensano (Belgium), Belgium

### \*Correspondence:

Anthony W. Maresso  
maresso@bcm.edu  
Barbara W. Trautner  
trautner@bcm.edu  
Robert F. Ramig  
rramig@bcm.edu

### Specialty section:

This article was submitted to  
Antimicrobials, Resistance  
and Chemotherapy,  
a section of the journal  
Frontiers in Microbiology

**Received:** 25 May 2019

**Accepted:** 21 October 2019

**Published:** 12 November 2019

### Citation:

Gibson SB, Green SI, Liu CG, Salazar KC, Clark JR, Terwilliger AL, Kaplan HB, Maresso AW, Trautner BW and Ramig RF (2019) Constructing and Characterizing Bacteriophage Libraries for Phage Therapy of Human Infections. *Front. Microbiol.* 10:2537. doi: 10.3389/fmicb.2019.02537

Phage therapy requires libraries of well-characterized phages. Here we describe the generation of phage libraries for three target species: *Escherichia coli*, *Pseudomonas aeruginosa*, and *Enterobacter cloacae*. The basic phage characteristics on the isolation host, sequence analysis, growth properties, and host range and virulence on a number of contemporary clinical isolates are presented. This information is required before phages can be added to a phage library for potential human use or sharing between laboratories for use in compassionate use protocols in humans under eIND (emergency investigational new drug). Clinical scenarios in which these phages can potentially be used are discussed. The phages presented here are currently being characterized in animal models and are available for eINDs.

**Keywords:** phage libraries, phage therapy, host range, phage characteristics, killing spectrum, human infection

## INTRODUCTION

The crisis in clinical care imposed by the increasing resistance of bacterial infections to antibiotics threatens to return clinical practice to the pre-antibiotic era (Boucher et al., 2009; Centers for Disease Control [CDC], 2013; Bassetti et al., 2017; World Health Organization [WHO], 2017). The situation is particularly acute for infections caused by Gram-negative pathogens for which few new antibiotics are in the pipeline. The bacterial “mutagenic tetrasect” (mutation, transformation, transduction, and conjugation) is responsible for the rapid evolution of bacteria and suggests that bacteria are so flexible in their ability to adapt that production of antibiotics by pharmaceutical companies, will never be able to keep up with the evolution of resistance against that drug. Fortunately, a natural alternative to conventional chemical antibiotics (Ghosh et al., 2018; Stearns, 2019) exists in the form of bacteriophages (phages). Thus, phages can evolve to efficiently target specific bacteria and have been used to treat complex drug-resistant bacterial infections in a procedure termed phage therapy (Ghosh et al., 2018).

Although phage therapy has great potential as a treatment for antibiotic resistant infections, it is not without problems. Phage have a similar mutation rate to bacteria; the organisms reproduce



so rapidly that the high numbers lead to very large mutant populations on which selection can operate to enrich selected phenotypes. Host range expansion by evolution and selection has been achieved (Burrowes, 2011; Mapes et al., 2016; Burrowes et al., 2019) and is extremely rapid (unpublished data). In addition, phage ecologists have estimated the total number of phages on Earth to be greater than  $10^{31}$  (Suttle, 2005). This suggests that the environment is a plentiful resource for new phages; indeed, environmental phages to drug-resistant and pandemic *Escherichia coli* that have excellent efficacy in animal models of infection have been discovered, characterized, and tested in as short a time period as 14 days (Green et al., 2017).

Phages were discovered over a century ago, and phage therapy has a long history (Debarbieux et al., 2018; Gelman et al., 2018). However, the advent of chemical antibiotics led to virtual abandonment of phage therapy in most of the world, whereas in the countries of Eastern Europe phage therapy was continuously pursued (Chanishvili, 2016; Myelnikov, 2018). As the development of antibiotic resistance has grown, the interest in phage has been rekindled (Kutter et al., 2015). Studies with compassionate use investigational new drug (IND) have generated considerable excitement for use of phage therapy in human subjects (Wright et al., 2009; Schooley et al., 2017; Chan et al., 2018; Aslam et al., 2019). Recently the application of phage therapy to human infections was reviewed (El Haddad et al., 2018), and the majority of the studies analyzed showed efficacy (87%) and safety (67%), however only a few of the studies examined the development of phage-resistant bacteria during therapy. Bacteria become resistant to phage infection (phage-resistant) (Labrie et al., 2010), through mutational changes just as they become antibiotic-resistant upon treatment with antibiotics. The problem of phage-resistance is often overcome by [i] the use of single broad host range phages, [ii] phages for which development of phage-resistance carries high bacterial fitness costs (Chan et al., 2016; unpublished data), or [iii] mixtures (cocktails) of phages (generally recognizing different bacterial surface receptors). Others have argued that phage resistance is not a problem in phage therapy because phage resistant bacteria often have fitness defects and new environmental phages active on the resistant host can be isolated (Ormalala and Jalasvuori, 2013). Indeed it is likely that phages capable of infecting a resistant host can be isolated from the environment or evolved in the laboratory (Mapes et al., 2016, unpublished data). However, these operations are time consuming and best avoided. In addition, not all phage resistant hosts were found to have fitness defects, so that they could persist in the patient (Wei et al., 2010, our unpublished data).

The development of phages for use against human infections has been described as following two pipelines (Pirnay et al., 2011). The “*prêt à porter*” (ready-to-wear) is a method, in which a medicinal product of a single broad host range phage is developed and undergoes safety and efficacy testing. This is time consuming and costly but yields products that can be licensed by regulatory agencies. In contrast, in the “*sur-mesure*” (custom made) method many phages are isolated and characterized and can be combined as appropriate to treat the infection. This method is flexible, inexpensive, and can rapidly

respond to infections with phage- or antibiotic- resistant bacteria. However, *sur-mesure* approaches cannot currently be licensed, but therapeutic use of phage produced through this approach is under active discussion (Debarbieux et al., 2016; Pirnay et al., 2018). We have chosen the latter approach in which [i] libraries of well-characterized phages are generated and stored, [ii] as the clinical laboratory is assessing the antibiotic-resistance of the bacterial isolate (~48 h), it is also tested for sensitivity to phages from the library (<48 h), [iii] phages to which the clinical isolate is sensitive are selected for mono-phage-therapy or used to construct cocktails containing several individual phages. Two therapeutic options are available: the patient can be treated with the phage alone, or phage plus antibiotic.

Here, we describe the preparation of well-characterized libraries of *E. coli*-specific, *Pseudomonas aeruginosa*-specific, and *Enterobacter cloacae*-specific phages for use in a *sur-mesure* approach to phage therapy, which will ultimately result in a therapeutic that is personalized to the specific infection of the individual patient. We provide information on the phages including: descriptions of their sources, their efficacy against a panel of clinical strains, some basic infection characteristics (burst size and absorption rates), and their DNA sequence and annotation to determine if they harbor lysogenic, antibiotic resistance or toxin genes and their morphologic description; providing the means to select high quality phage(s) for use in therapy. Also described are the clinical scenarios for which these phage libraries have been developed, as their proposed use shaped the development of the libraries.

## MATERIALS AND METHODS

### Bacterial Strains

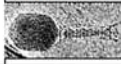
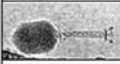


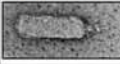

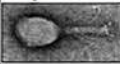

The laboratory strains used were *E. coli* (MG1655) and *P. aeruginosa* (PAO1 and BWT111). A collection of 13 *E. coli* ST131 strains (see **Supplementary Figures S1–S3**) was obtained from Dr. Jim Johnson (University of Minnesota). Two strains of *E. cloacae* were isolated from a phage therapy candidate with an infected hip prosthesis. One isolate was from a wound swab and other from the fluid exudate of the wound (collected at different times). De-identified clinical isolates of *E. coli*, *P. aeruginosa*, and *E. cloacae* and their antibiotic susceptibility data were obtained from the clinical microbiology laboratory at the Houston Veterans Administration Hospital or Baylor St. Luke’s Hospital. Collection of de-identified clinical isolates was approved by the Baylor College of Medicine Institutional Review Board (IRB). An isolated colony of each clinical isolate was streaked on LB agar and grown overnight. A single colony from the LB plate was grown overnight in LB medium, diluted 1:10 into LB medium containing 15% glycerol, and frozen at  $-80^{\circ}\text{C}$ . In cases where clinical isolates appeared to be mixed, the desired species was isolated from differential plates.

### Phages

Four *P. aeruginosa*-specific phages  $\phi\text{KMV}$ ,  $\phi\text{PA2}$ ,  $\phi\text{Paer4}$ , and  $\phi\text{E2005-24-39}$  (hereafter called  $\phi\text{E2005}$ ) were previously described (Mapes et al., 2016). These were the only *Pseudomonas*

wild type phages used in this work. All *E. coli*-specific and *E. cloacae* phages used here were isolated from environmental samples (see **Figures 1, 4A,B, 7** for source species) by plaque assay. Fecal samples were suspended to ~50% (w/v) in PBS,

shaken, and centrifuged to remove debris. The supernatant was filtered through a 0.22 micron filter, and 0.1 ml was plated with 0.8% LB top agar containing 100  $\mu$ l of an overnight culture of the desired isolation strain. After overnight incubation, well-isolated

Properties of <i>E. Coli</i> Phages								
Feature	<i>E. Coli</i> Phage							
	$\phi$ HP3	$\phi$ EC1	$\phi$ CF2	$\phi$ ES12	$\phi$ ES17	$\phi$ ES19	$\phi$ ES21	$\phi$ ES26
<b>Phage Characteristics</b>								
Source Species	Goose, & Duck	Dog	Chicken	Human	Human	Human	Human	Human
Source Location	Herman Park	E. Chew Dog Park	Rescue Farm	Raw* Sewage	Raw* Sewage	Raw* Sewage	Raw* Sewage	Raw* Sewage
Isolation Date	03/23/15	03/23/15		02/06/18	02/06/18	02/06/18	02/06/18	02/06/18
Isolation Strain	MG1655 $\pm$	MG1655 $\pm$	CP9 $\dagger$	JJ2050 $\dagger$	JJ2547 $\dagger$	DS104 $\#$	DS110 $\#$	DS182 $\#$
Plaque Size (mm)	0.5mm	0.5mm	1-2mm	0.5mm	0.5-1.0mm	0.5mm + halo	0.5mm + halo	0.5mm + halo
Plaque Morph.	Clear	Clear	Clear	Clear	Clear	Clear	Clear	Clear
Plate Stock (PFU/ml) $\approx$	3.00x10 <sup>9</sup>	4.20x10 <sup>9</sup>		7.40x10 <sup>8</sup>	9.80x10 <sup>9</sup>	2.00x10 <sup>9</sup>	9.20x10 <sup>9</sup>	2.00x10 <sup>7</sup>
CsCl Purified (PFU/ml)	1.90x10 <sup>12</sup>	5.80x10 <sup>11</sup>	2.4x10 <sup>10</sup>	2.85x10 <sup>11</sup>	4.85x10 <sup>11</sup>	3.10x10 <sup>11</sup>	1.80x10 <sup>11</sup>	1.43x10 <sup>11</sup>
EM Morphology	Myovirus	Myovirus	Myovirus	Myovirus	Podovirus	Myovirus	Myovirus	Myovirus
								
<b>Sequence</b>								
(Accession No.)	KY608976	KY608965	KY608966	MN508614	MN508615	MN508616	MN508617	MN508618
Genome (BP)	168,188	170,254	53,242	166,373	75,134	167,088	167,096	166,950
G + C (%)	35.4	37.6	45.9	35.37%	42.12	35.39	35.38	35.39%
ORFs	274	275	74	267	120	263	264	268
tRNAs	11	2	0	9	1	11	11	9
Toxin/Virulence Genes	None	None	None	None	None	None	None	None
Lysogeny Cassettes	None	None	None	None	None	None	None	None
Abx-Resistance Genes	None	None	None	None	None	None	None	None
Closest Relative	pSs-1	SHSML-52.1	BP63	slur07	PhiEco32	vB_Eco_HY01	vB_Eco_HY01	RB14
Genus	Tequatrovirus	Tequatrovirus	Unclassified	T4-like	PhiEco32-like	T4-like	T4-like	T4-like
<b>Growth Properties</b>								
Adsorption Constant (mL/min)	5.63x10 <sup>-9</sup>	5.94x10 <sup>-9</sup>	3.29x10 <sup>-9</sup>	3.49x10 <sup>-9</sup>	2.72x10 <sup>-9</sup>	6.48x10 <sup>-9</sup>	7.07x10 <sup>-9</sup>	1.68x10 <sup>-9</sup>
% Adsorbed (10 min)	98	61	65	93	32	96	90	16
Latent Period (Min)	22.5	22.0	40.0	26.0	33.0	28.5	23.0	25.0
Burst Size (PFU/cell)	60	57.4	>10	9.6	38.7	11	41	80.7
<b>Summary of Phage Killing Spectra – No. Lysed/No. Tested (% Lysed) see next three pages for details</b>								
<b>ST131 Strains<math>\dagger</math> (N=13)</b>								
(EOP > 0.1)	4/13 (31%)	2/13 (15%)	1/13 (8%)	7/13 (54%)	8/13 (62%)	7/13 (54%)	7/13 (54%)	7/13 (54%)
(EOP > 0.001)	9/13 (69%)	5/13 (38%)	4/13 (31%)	7/13 (54%)	9/13 (69%)	7/13 (54%)	9/13 (69%)	7/13 (54%)
<b>Clinical Isolates<math>\#</math> (N=76)</b>								
(EOP > 0.1)	39/76 (51%)	3/76 (4%)	8/76 (11%)	42/76 (55%)	34/76 (48%)	39/76 (51%)	43/76 (57%)	43/76 (57%)
(EOP > 0.001)	58/76 (76%)	6/76 (8%)	12/76 (16%)	44/76 (58%)	37/76 (49%)	42/76 (55%)	44/76 (58%)	45/76 (58%)
<b>Total Strains (N=89)</b>								
(EOP > 0.1)	43/89 (48%)	5/89 (6%)	8/89 (9%)	42/89 (47%)	34/89 (38%)	41/89 (46%)	43/89 (48%)	43/89 (48%)
(EOP > 0.001)	58/89 (65%)	6/89 (7%)	13/89 (15%)	44/89 (49%)	37/89 (42%)	42/89 (47%)	46/89 (52%)	45/89 (51%)
* Municipal Sewage Plant, Houston, Tx. $\pm$ <i>E. coli</i> K12 lab strain $\dagger$ <i>E. coli</i> ST131 strains (ExPEC) from Jim Johnson $\#$ <i>E. coli</i> clinical isolates from Houston VA Hospital $\approx$ Representative purified or plate stock								

**FIGURE 1** | Summary of characterization of *Escherichia coli* phages. The characteristics, DNA sequences, growth properties and a summary of phage killing spectra are presented for each phage.



plaques were picked into 1.0 ml phage storage buffer (Mapes et al., 2016), allowed to sit overnight for phage diffusion at 4°C, and 0.5 ml of suspended phage was used to prepare plate stocks using the isolation strain as host. Plate stocks were harvested and stored at 4°C.

### Host Range Determination/Efficiency of Killing (Virulence)

To determine phage host range a spot titration protocol was used that allowed us to determine both host range and relative phage killing (EOP). Five microliters of serial 10-fold dilutions of a CsCl purified phage stock ( $10^{10}$ – $10^{12}$  pfu/ml) were spotted on freshly seeded lawns of control, isolation, or clinical strains. The host range and titer were determined by formation of individual plaques within the area of the spot at terminal dilution. This avoided false positives by determining host range at dilutions where phenomena such as lysis from without (Abedon, 2011) or complementation between defective phages would not be expected. Phage virulence was determined as the efficiency of plating (EOP) (Mirzaei and Nilsson, 2015). EOP was calculated by dividing the titer of the phage at the terminal dilution on the test strain by the titer of the same phage on its isolation strain. On this basis, phages were classified as highly virulent ( $0.1 < \text{EOP} > 1.00$ ), moderately virulent ( $0.001 < \text{EOP} < 0.099$ ), avirulent but active ( $\text{EOP} < 0.001$ ), or avirulent (no plaques detected – see **Figures 2, 5, 8**).

### Host Range Expansion (HRE)

*Pseudomonas aeruginosa*-specific phages were subjected to the HRE protocol as described (Burrowes, 2011; Mapes et al., 2016; Burrowes et al., 2019). Briefly, in a 96 well plate, different host strains were placed in each of the eight rows at a dilution of 1:1000 of overnight culture. Serial 10-fold dilutions of phage (a single phage or a phage mixture) were placed in the 12 columns and the plate was incubated (37°C) with shaking (225 RPM) for 18 h. Following incubation, for each bacterial strain (row) the supernatant from the well with complete lysis and the adjacent well with higher phage dilution (partial lysis) were combined, into a single tube with the corresponding complete and partial lysis wells of the other bacterial strains. The pooled lysate was treated with  $\text{CHCl}_3$  and filtered through a 0.22 micron filter. The filtered lysate was the yield of the 1<sup>st</sup> cycle of HRE. This filtered lysate was serially diluted 10-fold, and the experiment was repeated using the pooled lysate as the phage and the same bacterial strains as host for cycle 2. The HRE was repeated up to 30 cycles, and yielded a mixture of phages that had replicated on at least one of the host bacterial strains. The heterogeneous mixture of phages in the lysate from any cycle of HRE can be assayed for plaque formers on a host refractory to the parental phage(s), plaques purified, and phage stocks with expanded host range produced (Mapes et al., 2016). The HRE protocol was also successfully applied to *E. coli*-specific phages (data not shown).

The HRE protocol exposes the lysate (including mutants) that arose during a cycle to new bacteria (unevolved) of the strains used in the previous cycle. Some of the mutations may allow phages to infect and replicate on bacterial strains that were

previously refractory to phage, thus amplifying the mutant that contained the host range expanding mutation.

### DNA Sequencing and Annotation of Phage Genomes

CsCl purified phages were submitted to the Center for Metagenomics and Microbiome Research at Baylor College of Medicine for DNA extraction, sequencing and assembly as described previously (Green et al., 2017). Briefly, DNA samples were constructed into Illumina paired-end libraries. The libraries had an average final size of 660 bp (including adapter and barcode sequences) and were pooled in equimolar amounts to achieve a final concentration of 10 nM. The library templates were prepared for sequencing on the Illumina MiSeq. After sequencing, the .bcl files were processed through Illumina's analysis software (CASAVA), which demultiplexes pooled samples and generates sequence reads and base-call confidence values (qualities). The average raw yield per sample was 802 Mbp. For analysis, the adapter sequences were removed, and the sequence was then assembled using SPAdes v3.5.0 (Bankevich et al., 2012) on careful mode, retaining only contigs longer than 1,000 bp and with an average coverage of 1000x or greater. This generated 1–2 contigs per sample, with an average of 74% of the original reads mapping with 100% identity to the final contigs. Genomes were analyzed using both PATRIC's comprehensive genome analysis service (Wattam et al., 2017) and EDGE Bioinformatic software (Li et al., 2017). Gene calling and genome annotation was performed using PROKKA (version 1.13) (Lo and Chain, 2014), RAST (Zerbino and Birney, 2008; Bankevich et al., 2012), GLIMMER3 (version 3.02) (Peng et al., 2010), and GeneMarkS (version 4.28) (Peng et al., 2012). **Figures 1, 4A,B, 7** show ORF predictions from the RAST pipeline and tRNA predictions from ARAGORN (version 1.2.36) (Seemann, 2014). ORFs were searched for virulence and antibiotic resistance genes by using BLAST (Aziz et al., 2008) to compare assembled genomes against the Virulence Factor Database (VFDB) (McNair et al., 2018), the PATRIC virulence factor database (Delcher et al., 2007), the Antibiotic Resistance Gene Database (ARDB) (Besemer, 2001) and the Comprehensive Antibiotic Resistance Database (CARD) (Laslett, 2004). ShortBRED (version 0.9.4M) (Johnson et al., 2008) was used for targeted searches of ORFs for genes in the VFDB, CARD, and the Resfam antibiotic resistance gene database (Chen et al., 2016). Genus was inferred from closest sequenced relatives identified by using BWA-Mem (version 0.7.9) (Mao et al., 2015) to aligning contigs to NCBI's RefSeq database and by ORF homology using PHAge Search Tool Enhanced Release (PHASTER) (Liu and Pop, 2009). Phage lifestyles were determined by classifying the genomes using PHACTs (McArthur et al., 2013), using PHASTER to predict integrases and attachment sites, and by parsing all versions of the annotated genome for "integrase." No virulence genes of known toxicity (viral or bacterial) or genes involved in lysogeny were detected. Thus it appears the phages examined here are devoid of any known lysogenic or toxic elements that would preclude their use in phage therapy.

Representative Antibiotic Sensitivity and Phage Killing of <i>E. coli</i> clinical isolates																								
Bacterial Group	Bacterial Pairs	Source:	Date Collected	Antibiotic Sensitivity										<i>E. coli</i> Clinical Isolate	Phage Killing (EOP)									
				Amikacin	Ampicillin	Cefepime	Gentamicin	Imipenem	Levofloxacin	Pip/Tazobacta	Amp/Sulbacta	Ceftriaxone	Cefazolin		Nitrofurantoin	Ertapenem	TMP/SMZ	φHP3 – AW *	φEC1 – CA †	φCF2 – AV ‡	φES12 – Hu #	φES17 – Hu #	φES19 – Hu #	φES21 – Hu #
Houston VA Isolates	-	U	10/28/16												DS218									
	-	U	10/28/16												DS217									
	-	U	10/28/16												DS216									
	-	U	10/24/16												DS215									
	-	U	10/23/18												DS452##									
	-	U	10/24/18												DS453##									
	-	U	11/01/18												DS454##									
	-	U	10/31/18												DS455##									
	-	U	11/05/18												DS456##									
	-	U	11/05/18												DS457##									
	-	U	11/13/18												DS458##									
	-	U	11/19/18												DS459##									
	-	U	12/05/18												DS460##									
	-	U	12/11/18												DS461##									
	-	U	12/17/18												DS462##									
	-	U	12/18/18												DS463##									
	-	L	03/15/19												BSL47a									

Footnotes	Key to Abx Sens.	Key to Phage Killing (EOP)
* Wild avian (goose)	Green Sensitive	+ EOP > 1.000
† Canine (dog)	Yellow Intermediate	EOP between 0.100 – 1.000
‡ Avian (chicken)	Red Resistant	EOP between 0.001 – 0.099
# Human (raw sewage)		EOP < 0.001; not useful
## From person with spinal cord injury		- No Growth
L=Left ventricular assist device driveline infection; U=Urine		Reference (EOP = 1.000)
		EOP = Titer X / Titer Reference

**FIGURE 2 |** Representative data for antibiotic sensitivity and phage killing (EOP) of clinical isolates of *E. coli*. Shown are the properties of the *E. coli* clinical isolates on the left, including: source, date of isolation and antibiotic sensitivity data (VITEK2). On the right are shown the killing spectra of the phages on the individual *E. coli* clinical isolates. The keys to antibiotic sensitivity and phage killing (EOP) are shown at the bottom of the figure.

## Phage Growth Parameters

The percentage of phage adsorbed in 10 min and the adsorption constant were determined for each phage on its isolation strain. Burst size and latent period (one-step growth curves) were also determined for each phage on its isolation strain (Kropinski, 2009, 2018).

## RESULTS

### *Escherichia coli* Phages

#### *E. coli* Phage Isolation

Our primary target for *E. coli* phage isolation was extraintestinal pathogenic *E. coli* (ExPEC) of the pandemic sequence type 131 (ST131). ExPEC are commonly associated with bacteremia and

urinary tract infections, and the ST131 lineage is characterized by multi-drug resistance and its high frequency of isolation over the past 10 years. Interestingly, a rapid screen of common laboratory *E. coli*-specific phages (T2, T4, T6, T7, λ<sup>vir</sup>) revealed that none of them formed plaques on the ST131 strains tested. As a result we began to isolate phages from the environment, concentrating on avian and canine species which are known reservoirs for *E. coli* ST131 (Johnson et al., 2001, 2017). Our first phage isolates were from mixed goose/duck feces collected at a local park (φHP3), canine feces from a dog park (φEC1) and chicken feces from a rehabilitation farm (φCF2). We subsequently isolated phages from raw sewage collected at a local sewage treatment plant (φES series; see Figure 1). All phages were plaque-purified three times prior to use.



## *E. coli* Phage Characteristics

The phage characteristics are summarized in **Figure 1**. The phages varied in plaque size, but plaques tended to be small and clear. Some produced halos around the plaques, suggesting enzymatic activity on the surrounding cells. Regardless of the small plaque sizes, reasonable titer plate stocks were obtained, and all phages could be CsCl purified to about  $10^{11}$  pfu/ml. Adsorption curves revealed that the phages ranged widely in adsorption (16–98%). For all the *E. coli* phages, one-step growth curves revealed the latent period was in the range of 22–40 min and burst sizes ranged from 9.6 to 80.7 pfu/cell. Sequence analysis revealed genome sizes ranging from (53,242 to 170,254 bp) with variable G + C content. The number of encoded ORFs and tRNAs identified was also variable. Notably, none of the sequences contained features that would preclude their use in phage therapy, such as genes to establish and maintain lysogeny, produce toxins or virulence factors, or confer antibiotic resistance (Merabishvili et al., 2018; Hyman, 2019). All of the *E. coli* phages had myovirus morphology except for  $\phi$ ES17 which was a podovirus with an elongated head. Phage ES17 also contained, at marginal statistical significance, an integrase gene when examined with PHACTs and PHASTER software. When colonies were isolated in the presence of excess  $\phi$ ES17, no phages were isolated following growth of those colonies in the presence of mitomycin C (data not shown). We concluded that  $\phi$ ES17 is a lytic phage, lacking an integrase.

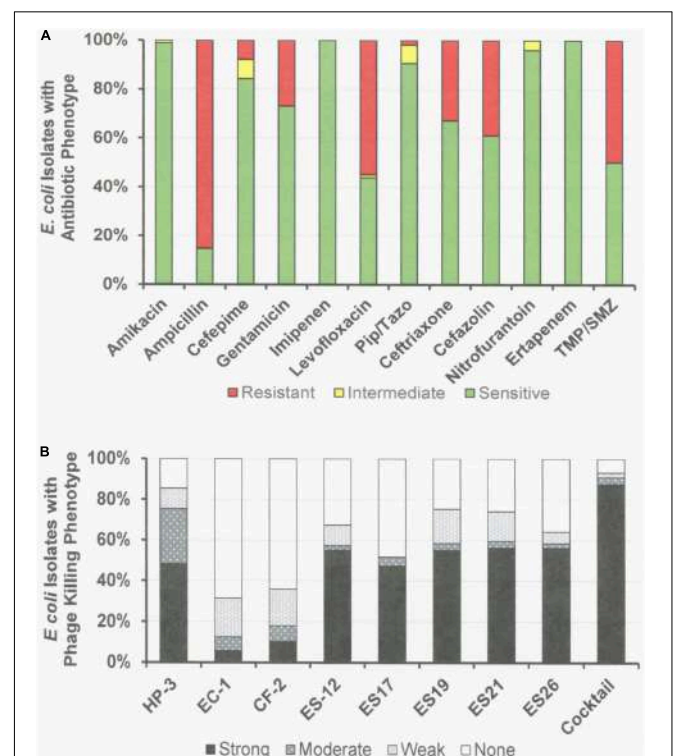
## Host Range of *E. coli* Phages

The host ranges of the phages was determined as described in Section “Materials and Methods” by spot testing serial 10-fold phage dilutions on the isolation strain and on other laboratory and clinical isolates. The virulence of the phage was determined by comparing the titer on a test strain with the titer on the isolation strain ( $EOP = \text{titer test}/\text{titer isolation}$ ). Phages with  $EOP > 0.1$  were considered highly virulent and most useful. Phages with  $EOP$  in the range of 0.001–0.099, were considered moderately virulent and may be useful if high titers can be produced. **Figure 2** shows the host range and virulence results for eight *E. coli* phages on a representative selection of *E. coli* clinical isolates. A complete determination of host range and virulence on (1) characterized ST131 strains, (2) a collection of paired clinical isolates from two sites (urine and blood) collected from the same patient on the same day, and (3) a set of clinical isolates collected between November 2015 and December 2018 is shown (**Supplementary Figures S1–S3**).

At least one of the *E. coli* phage isolates was able to kill each member of the ST131 collection, except for *E. coli* strain JJ1886 (**Supplementary Figures S1–S3**). For individual phages, 8–62% of ST131 strains were killed at  $EOP > 0.1$  and 31–69% were killed at  $EOP$ s in the range of 0.001–0.099 (**Supplementary Figures S1–S3**). A cocktail of as few as two *E. coli* phages ( $\phi$ HP3 and  $\phi$ ES17) was capable of killing 12/13 (92%) of ST131 strains (**Supplementary Figures S1–S3**).

Among the 76 *E. coli* clinical isolates (24 paired blood and urine isolates from the same patient on the same day; 40 single clinical isolates, mostly from patients with UTI; and 12 clinical isolates from urine of catheterized spinal cord injured [SCI]

patients) the eight *E. coli* phages killed from 4 to 57% at an  $EOP > 0.1$ . If  $EOP$ s between 0.001 and 0.099 (moderately virulent) were included very little increase in the number of clinical isolates killed was observed, except for  $\phi$ HP3 where the number killed was increased by 50% (**Figure 1**). For the 24 paired blood and urine isolates, a cocktail of as few as three of the *E. coli* phages ( $\phi$ CF2,  $\phi$ ES12, and  $\phi$ ES17) could be assembled that killed them all at  $EOP > 0.1$ . Among the 40 clinical isolates primarily of urinary origin, cocktails ( $\phi$ HP3,  $\phi$ ES17, and  $\phi$ ES19) capable of killing 35/40 (88%) of the isolates at  $EOP > 0.1$  could be made. Among 12 isolates originating from SCI patients, a cocktail of four phages ( $\phi$ HP3,  $\phi$ EC1,  $\phi$ ES12, and  $\phi$ ES17) could be made that killed 9/12 (75%) *E. coli* strains at  $EOP > 0.1$ . Among all 76 of the *E. coli* clinical isolates, we noted no correlation between killing at high efficiency and date of isolation (November 2015–December 2018) or antibiotic-sensitivity phenotype. A summary of the antibiotic sensitivity and phage killing of the 89 total *E. coli* isolates examined is shown in **Figure 3**. Although none of the individual phages killed more than 50–55% of the 76 bacterial strains at high efficiency, a three phage cocktail increased the high efficiency killing to nearly 90% (**Figure 3**).



**FIGURE 3** | Antibiotic Sensitivities and Phage Killing Phenotypes of *E. coli* Clinical Isolates ( $N = 89$ ). **(A)** Antibiotic sensitivities using cut off values used in the microbiology lab at the Houston VA Hospital. **(B)** The phage killing phenotypes were based on  $EOP$ . Strong killers,  $EOP > 0.1$ ; Moderate Killers,  $0.099 > EOP > 0.001$ ; Weak Killers,  $EOP < 0.00099$  but positive; None, no growth. Strong and moderate killers have  $EOP$  high enough to be useful in phage therapy. The phage cocktail consisted of equal titers of phages:  $\phi$ HP-3,  $\phi$ ES-12, and  $\phi$ ES17. Pip/Tazo, piperacillin/tazobactam; TMP/SMX, trimethoprim/sulfamethoxazole.

## ***Pseudomonas aeruginosa* Phages**

### **Origin of *P. aeruginosa* Phages**

Four *P. aeruginosa*-specific phages previously isolated and used by other laboratories were used here:  $\phi$ KMV (Lavigne et al., 2003; Chibeu et al., 2009),  $\phi$ PA2 (ATCC 14203-B1; McVay et al., 2007),  $\phi$ Paer4 (Fu et al., 2010), and  $\phi$ E2005 (Liao et al., 2012). All four phages as a mixture, or single phages, were used in the host range expansion protocol (HRE) as described (Mapes et al., 2016; see section “Materials and Methods”). The HRE protocol generates phage mutants able to infect and replicate on bacterial strains that were previously resistant to the phage (i.e., broadening their host range). The four parental phages subjected to HRE as a mixture lysed 38% of 16 bacterial strains (development strains) used. After 30 cycles of HRE 75% of the 16 development strains were lysed by the phage mixture. When 10 strains different from those used in the HRE process (test strains) were tested 100% of them were lysed by the phage mixture resulting from 30 HRE cycles (Mapes et al., 2016). During this directed evolution process all phages present are mixed, so that at any cycle the lysate is a heterogeneous mixture of phages. Individual plaques were picked after 20 and 30 cycles of HRE and plaque purified after plating on the desired host. For example, *P. aeruginosa* strain DS38 one of the development strains, was not lysed by the parental phage mixture. The heterogeneous phage mixture from HRE cycle 30 formed plaques on strain DS38 indicating that it contained phages with the host range expanded to DS38. Purified phage clones were generated on strain DS38 from 108 plaques picked from the 30 cycle lysate containing the heterogeneous mixture phages. Among the 108 phage clones that all lysed DS38, there were 30 different killing spectra when they were tested against the 16 development and 10 test strains (Mapes et al., 2016). Similarly,  $\phi$ KMV was subjected to five cycles of HRE, and was found have expanded host range phages in the lysate of cycle 5.

### ***P. aeruginosa* Phage Characteristics**

The characteristics of parental and host range expanded phages are shown in **Figures 4A,B**. The characteristics of the phages were variable and similar to those seen for *E. coli* phages (**Figure 1**). Importantly, DNA sequencing revealed that each of the phages derived from the HRE of the four phage mixture represented only mutants of one of the parental phages. This result indicated that recombination between parental phages did not contribute to expansion of host range in the progeny examined. Thus, the morphology of the HRE-derived clones was not determined but assumed to be like that of the parental phage (**Figures 4A,B**). Sequencing also revealed that none of the phages contained genes that would be detrimental to their use in phage therapy. The growth properties of the HRE-derived phages were also similar to the parental phages.

### **Host Range of *P. aeruginosa* Phages**

Host range and virulence of *P. aeruginosa* phages on representative *P. aeruginosa* clinical isolates is shown in **Figure 5**. Characterization of the host range and virulence on the complete set of *P. aeruginosa* clinical isolates tested is shown in the supplementary information (**Supplementary Figures S4, S5**). Compared to the parental phages, the HRE-derived phages

had expanded host range when tested against the development strains. They lysed, 19–69% of those strains compared to 12–31% for the parental phages. Likewise the HRE-derived phages had expanded host range when tested against the test strains; they lysed 20–90% of test strains compared to 1–10% for the parental phages (**Supplementary Figures S4, S5**). The parental and HRE-derived phages were then tested against a collection of 64 clinical isolates, which were mostly isolated from patient urine samples that were obtained between November 2015 and August 2017, and displayed a spectrum of antibiotic resistances. Examination of the killing activity (**Supplementary Figures S4, S5**) revealed the HRE-derived phages had expanded host range relative to the parental phages, although many of the phages were expanded at  $EOP < 0.001$ , an EOP too low to be useful. It is possible that additional rounds of HRE on some the clinical isolates could generate phage with an EOP in a useful range ( $EOP > 0.001$ ). Greater numbers of HRE cycles led to greater expansion of host range in the isolated phage clones (**Figures 5, 6** and **Supplementary Figures S4, S5**), both at highly efficient killing ( $EOP > 0.1$ ) and at useful levels of killing ( $EOP > 0.001$ ). This was observed for both HRE using four parental phages (compare 20 and 30 cycles) and for 5 cycles of HRE using a single parental phage  $\phi$ KMV (**Figure 5** and **Supplementary Figures S4, S5**).

**Figure 6** summarizes the antibiotic sensitivity and phage killing phenotypes of the phages on the 64 total *P. aeruginosa* clinical isolates examined. The increase in useful killing with cycles of the HRE protocol and with mixing of cocktails is shown in **Figure 6B**.

The lack of recombination in HRE-derived phages observed here, contrasts with the contribution of recombination reported by others (Burrowes et al., 2019). In retrospect, this finding is not surprising, since the four phages used were distant phylogenetically, making homology-driven recombination unlikely. The HRE-derived phage sequences contained mutations spread randomly across the genome, but all of them had mutations in the tail fiber gene as would be expected if the host range expansion was based on tail fiber-bacterial receptor interactions. In addition, the sequence analysis revealed no genes that would preclude the use of the HRE-derived phages in phage therapy. Thus, the HRE-derived *P. aeruginosa* phages are classified as variants of the parental phage to which they corresponded (**Figures 4A,B**).

## ***Enterobacter cloacae* Phages**

### ***E. cloacae* Phage Isolation**

*Enterobacter cloacae* phages were isolated from raw sewage collected on two different days by plaquing on a phage therapy candidate's isolates (**Figure 7**).

### ***E. cloacae* Phage Characteristics**

Sequence analysis of the phages revealed that the four phages were similar and T4-like (**Figure 7**). The growth properties of the *E. cloacae* phages were somewhat variable but had parameters within expected values (**Figure 7**). The *E. cloacae* phages contained no genes that would preclude their use in phage therapy (**Figure 7**).



### E. cloacae Phage Host Range and Virulence

The antibiotic sensitivity and phage killing phenotypes of four phages on *E. cloacae* clinical isolates are shown in **Figure 8**. The phages were strong killers, especially for *E. cloacae* isolates from LVAD infections where the original source of the infection may have been the skin. Only one phage strongly killed *E. cloacae* isolates from UTI. More isolates

from various sites must be examined to determine if site of origin of the bacteria affects the efficacy of phage killing. **Figure 9**, a summary of antibiotic sensitivity and phage killing of the isolates examined, shows > 70% of strains killed by all individual phages and only a small gain in killing by a cocktail composed of two phages when compared to the best single phage.


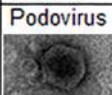


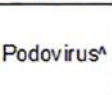
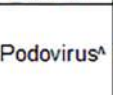
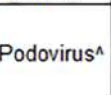
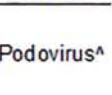
A Properties of <i>P. aeruginosa</i> Phages								
Feature	<i>P. aeruginosa</i> Phage							
	φKMV	φPa2	φPaer4	φE2005-24-39	4φC <sup>20</sup> -Clone 2	4φC <sup>20</sup> -Clone 5	4φC <sup>20</sup> -Clone 7	4φC <sup>20</sup> -Clone 9
<b>Phage Characteristics:</b>								
Source Species	?	?	?	Human	--	--	--	--
Source	Pond Water Moscow 2003 [1]	ATCC 14203-B1 ?	CDC ?	Sewage Dekalb, GA 2005 [2]	Lab-HRE 10/18/12	Lab-HRE 10/18/12	Lab-HRE 10/18/12	Lab-HRE 10/18/12
Isolation Date								
Isolation Strain	PAO1 <sup>+</sup>	PAO1 <sup>ref</sup>	Psa Strain Paer4	Psa Strain E2005-A	PAO1	PAO1	PAO1	PAO1
Plaque Size (mm)	4-5 mm + wide Halo	3-4 mm	2-3 mm	~1 mm	1.5mm	2.5mm	3.0mm	1.0mm
Plaque Morph.	Clear+Halo	Clear	Clear	Clear	Clear	Clear	Clear	Clear
Plate Stock (PFU/ml) <sup>a</sup>	4.8x10 <sup>9</sup>	2.1x10 <sup>10</sup>	1.2x10 <sup>10</sup>	5.7x10 <sup>8</sup>	4.0x10 <sup>8</sup>	2.0x10 <sup>10</sup>	1.8x10 <sup>11</sup>	1.4x10 <sup>8</sup>
CsCl Purified (PFU/ml) <sup>a</sup>	6.0x10 <sup>12</sup>	6.6x10 <sup>12</sup>	2.4x10 <sup>11</sup>	1.1x10 <sup>12</sup>	2.0x10 <sup>11</sup>	2.0x10 <sup>11</sup>	2.0x10 <sup>10</sup>	2.0x10 <sup>11</sup>
EM Morphology	 Podovirus	 Podovirus	 Podovirus	 Myovirus	 Podovirus <sup>A</sup>	 Podovirus <sup>A</sup>	 Podovirus <sup>A</sup>	 Podovirus <sup>A</sup>
<b>Sequence</b>								
Accession No.	AJ505558	NC027345	MN508619	MN508620	ND	MN553583	MN553584	MN553585
Genome (BP)	42,351	73,008	45,319	66,285	ND	72,601	72,474	42,232
G + C (%)	62.3%	54.9%	52.49%	55.25%	ND	54.89%	54.89%	62.25%
ORFs	49	91	70	97	ND	92	90	58
tRNAs	0	0	3	0	ND	0	0	0
Toxin/Virulence Genes	None	None	None	None	ND	None	None	None
Lysogeny Cassettes	None	None	None	None	ND	None	None	None
Abx-Resistance Genes	None	None	None	None	ND	None	None	None
Closest Relative	φKMV	φPa2	DL54	vB_Pae_PS44	ND	φPa2	φPa2	φKMV
Genus	φKMV-like	Lit1-like	Luz24-like	Pbunlike	ND	Lit1-like	Lit1-like	φKMV-like
<b>Growth Properties</b>								
Adsorption Const. (mL/min) [4]	4.07x10 <sup>-10</sup>	2.00x10 <sup>-9</sup>	8.01x10 <sup>-9</sup>	2.30x10 <sup>-9</sup>	2.18x10 <sup>-9</sup>	1.22x10 <sup>-10</sup>	6.28x10 <sup>-10</sup>	3.37x10 <sup>-10</sup>
% Adsorbed (10 min)	3.2%	63.3%	43.8%	84.9%	16.4%	13%	9%	22.4%
Latent Period [5]	32 min	41 min	30 min	36 min	28 min	44 min	40 min	22 min
Burst Size	184	25	17.9	102	100	127	153	198
<b>Summary of Phage Killing Spectra – # Lysed/# Tested (% lysed)</b>								
<b>HRE Development and Test Strains – EOP&gt;0.1 only</b>								
Develop. Strains N = 16	2/16 <sup>†</sup> (13%)	5/16 (31%)	2/16 (13%)	2/16 (13%)	3/16 (19%)	7/16 (44%)	7/16 (44%)	3/16 (19%)
Test strains N = 10	1/10 <sup>†</sup> (10%)	0/10 (0%)	1/10 (10%)	1/10 (10%)	2/10 (20%)	2/10 (20%)	2/10 (20%)	0/10 (0%)
<b>Clinical Isolates (N=64)</b>								
(EOP > 0.1)	3/64 <sup>‡</sup> (5%)	1/64 (2%)	7/64 (11%)	15/64 (23%)	0/64 (0%)	11/64 (17%)	13/64 (20%)	1/64 (2%)
Mean (EOP>0.1)	Parental φ: 10% Strains Killed				20 HRE cycle φ clones: 10% Strains Killed			
(EOP > 0.001)	7/64 <sup>‡</sup> (11%)	13/64 (20%)	13/64 (20%)	21/64 (33%)	6/64 (9%)	19/64 (29%)	19/64 (30%)	15/64 (23%)
Mean (EOP>0.001)	Parental φ: 21% Strains Killed				20 HRE cycle φ clones: 23% Strains Killed			
<sup>‡</sup> <i>P. aeruginosa</i> lab strain <sup>†</sup> No. killed/No. tested <i>P. aeruginosa</i> strains used for host range expansion (HRE) <sup>‡</sup> No. killed/No. tested <i>P. aeruginosa</i> clinical isolates tested <sup>a</sup> Representative purified or plate stock <b>Parental Phages</b> were φKMV, φPa2, φPaer4, φE2005-24-29. <b>Other phages</b> are clones from Host Range Expansion (HRE).								

FIGURE 4 | Continued



Feature	Properties of <i>P. aeruginosa</i> Phages							
	<i>P. aeruginosa</i> Phage							
	ϕKMVC <sup>S</sup> - (121)- Clone 4a	ϕKMVC <sup>S</sup> - (121)- Clone 13	ϕKMVC <sup>S</sup> - (111)- Clone 4	ϕKMVC <sup>S</sup> - (111)- Clone 12	4ϕC <sup>30</sup> - DS38- Clone 39	4ϕC <sup>30</sup> - DS38- Clone 57	4ϕC <sup>30</sup> - DS38- Clone 54	4ϕC <sup>30</sup> - DS38- Clone 20
<b>Phage Characteristics:</b>								
Source Species	--	--	--	--	--	--	--	--
Source	Lab- HRE	Lab- HRE	Lab- HRE	Lab- HRE	Lab- HRE	Lab- HRE	Lab- HRE	Lab- HRE
Isolation Date	2014	2014	2014	2014	2015	2015	2015	2015
Isolation Strain	PAO1	PAO1	BWT111	BWT111	DS38	DS38	DS38	DS38
Plaque Size (mm)	~3mm	~3mm	~3mm	~2mm	~2mm	~2mm	~2mm	~2mm
Plaque Morph.	Clear+Halo	Clear+Halo	Clear+Halo	Clear	Clear+halo	Clear+halo	Clear+halo	Clear+halo
Plate Stock (PFU/ml) <sup>a</sup>	1.6x10 <sup>10</sup>	3.0x10 <sup>10</sup>	2.6x10 <sup>10</sup>	9.0x10 <sup>9</sup>	1.7x10 <sup>9</sup>	1.4x10 <sup>9</sup>	1.1x10 <sup>9</sup>	1.8x10 <sup>9</sup>
CsCl Purified (PFU/ml) <sup>a</sup>	2.6x10 <sup>12</sup>	6.0x10 <sup>12</sup>	2.0x10 <sup>12</sup>	2.0x10 <sup>12</sup>	1.7x10 <sup>10</sup>	1.9x10 <sup>9</sup>	1.6x10 <sup>9</sup>	4.6x10 <sup>9</sup>
EM Morphology	Podovirus <sup>A</sup>	Podovirus <sup>A</sup>	Podovirus <sup>A</sup>	Podovirus <sup>A</sup>	ND	ND	ND	ND
<b>Sequence</b>								
Accession No.	MN553587	MN553589	MN553586	MN553588	ND	ND	ND	ND
Genome (BP)	42,231	42,231	45,446	42,432	ND	ND	ND	ND
G + C (%)	62.23	62.25	52.48	62.24	ND	ND	ND	ND
ORFs	59	58	71	59	ND	ND	ND	ND
tRNAs	0	0	3	0	ND	ND	ND	ND
Toxin/Virulence Genes	None	None	None	None	ND	ND	ND	ND
Lysogeny Cassettes	None	None	None	None	ND	ND	ND	ND
Abx-Resistance Genes	None	None	None	None	ND	ND	ND	ND
Closest Relative	ϕKMV	ϕKMV	DL54	ϕKMV	ND	ND	ND	ND
Genus	ϕKMV-like	ϕKMV-like	Luz24-like	ϕKMV-like	ND	ND	ND	ND
<b>Growth Properties</b>								
Adsorption Const. (mL/min) [4]	9.41x10 <sup>-10</sup>	5.54x10 <sup>-10</sup>	1.08x10 <sup>-9</sup>	1.05x10 <sup>-9</sup>	7.30x10 <sup>-10</sup>	1.30x10 <sup>-9</sup>	1.83x10 <sup>-9</sup>	1.64x10 <sup>-9</sup>
% Adsorbed (10 min)	50.7%	34.5%	63.3%	49.6%	51.4%	71.7%	87.9%	84.8%
Latent Period [5]	18 min	22 min	28 min	18 min	48 min	40 min	30 min	32 min
Burst Size	42	7	100	17.6	72	109	63.9	94.0
<b>Summary of Phage Killing Spectra – # Lysed/# Tested (% lysed)</b>								
<b>HRE Development and Test Strains – EOP&gt;0.1 only</b>								
Develop. Strains N = 16	4/16 <sup>†</sup> (25%)	9/16 (56%)	11/16 (69%)	8/16 (50%)	10/16 (63%)	10/16 (63%)	10/16 (63%)	8/16 (50%)
Test strains N = 10	2/10 <sup>†</sup> (20%)	4/10 (40%)	9/10 (90%)	3/10 (30%)	2/10 (20%)	5/10 (50%)	6/10 (60%)	2/10 (20%)
<b>Clinical Isolates (N=64)</b>								
(EOP > 0.1)	1/64 (2%)	5/64 (8%)	6/64 (9%)	18/64 (28%)	15/64 (23%)	19/64 (30%)	26/64 (41%)	28/64 (44%)
Mean (EOP>0.1)	5 HRE cycle ϕ clones: 12% Strains Killed				30 HRE cycle ϕ clones: 34% Strains Killed			
(EOP > 0.001)	7/64 (11%)	12/64 (19%)	12/64 (19%)	26/64 (41%)	20/64 (31%)	38/64 (59%)	37/64 (58%)	37/64 (58%)
Mean (EOP>0.001)	5 HRE cycle ϕ clones: 22% Strains Killed				30 HRE cycle ϕ clones: Strains Killed 52%			
<sup>a</sup> <i>P. aeruginosa</i> lab strain <sup>†</sup> No. killed/No. tested <i>P. aeruginosa</i> strains used for host range expansion (HRE) <sup>‡</sup> No. killed/No. tested <i>P. aeruginosa</i> clinical isolates tested <sup>*</sup> Representative purified or plate stock <b>Parental Phages</b> were ϕKMV, ϕPa2, ϕPaer4, ϕE2005-24-29. <b>Other phages</b> are clones from Host Range Expansion (HRE).								

**FIGURE 4 | (A,B)** Summary of characterization of *Pseudomonas aeruginosa* phages. The characteristics, DNA sequences, growth properties and a summary of phage killing spectra are presented for each phage.

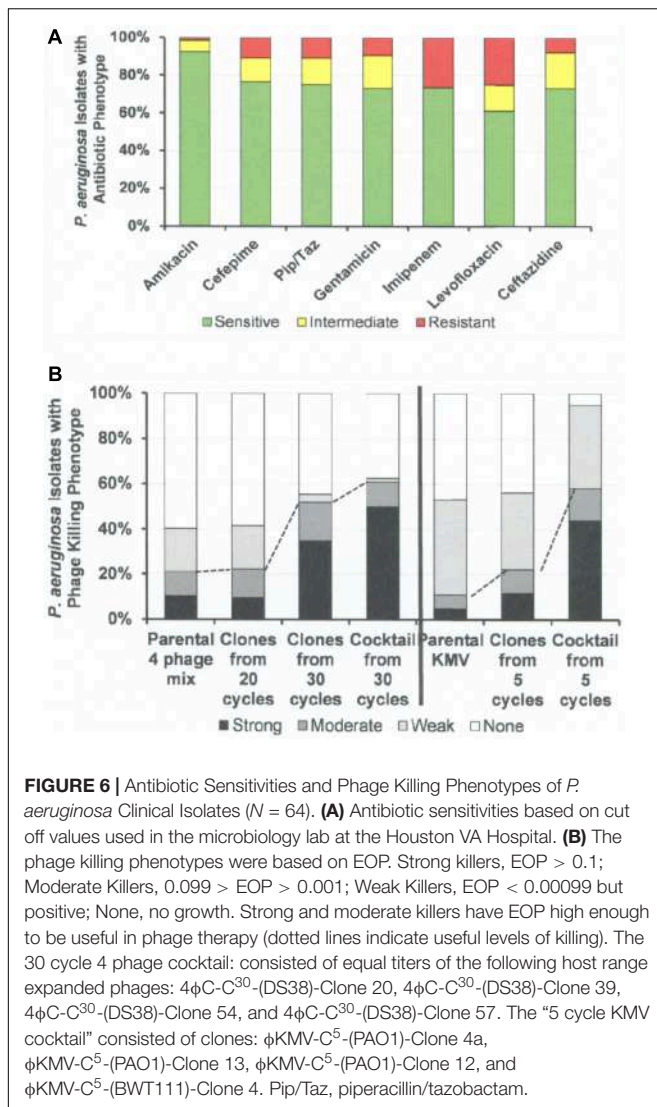
## DISCUSSION

This study presents a “*sur mesure*” approach to phage therapy (Pirnay et al., 2011). Here phage libraries were constructed, characterized, and prepared for use in preclinical or clinical situations. Specifically, we plan to concurrently test clinical isolates against phages from the appropriate library to identify phages for mono- or cocktail-based therapy while they are being characterized in the clinical microbiology laboratory. It

will then be the physician’s choice to treat the patient with phage alone, antimicrobials alone or the combination of the two. A broader interpretation of the “*sur mesure*” approach is to develop a phage library using the full spectrum of bacterial strains available in the clinical microbiology laboratory of a specific medical facility, so that the shelf-ready phage strains or cocktails can reasonably be expected to cover multidrug-resistant organisms that cause infections in patients in that facility. These libraries can be tested in the clinical laboratory of the hospital,







preventing clinical deterioration in sepsis (Kalil et al., 2017). Many patients are at high risk for sepsis caused by antibiotic resistant organisms, by virtue of prior healthcare exposures and/or known colonization with multidrug-resistant organisms. When such high-risk patients present with sepsis, a few early doses of a broad-spectrum phage cocktail used empirically, together with empiric antibiotics could act as a safety net, ensuring adequate coverage of the causative organisms, until the microbiology lab can identify the organism and determine its antibiotic sensitivities. In this scenario a “*sur mesure*” phage cocktail developed against the full panel of multidrug-resistant organisms isolated in the clinical microbiology laboratory of that specific institution would be used for initial treatment together with empiric antibiotics. Another example of a clinical scenario in which a single dose of phage might be very useful would be to temporarily sterilize a patient’s urine prior to an invasive urologic procedure. Phage cocktails mixed specifically for the organisms found in standard pre-procedure urine cultures at a given institution would offer a more targeted approach than our





current approach, which involves wiping out the bladder and much of the bowel flora with broad spectrum antibiotics.

In contrast, treatment of biofilm infections, such as those that cause life-threatening LVAD infections, would likely require a longer course of phage therapy, in part because of the longer clinical time frame given the chronicity of LVAD infections. New phage cocktails could be mixed to address phage-resistant bacterial pathogens that might develop during the course of therapy. Alternatively, treating these biofilm infections with phage and antibiotics simultaneously may allow for synergy, particularly if the phage is able to restore antibiotic susceptibility in the infecting pathogen (Comeau et al., 2007; Ryan et al., 2012; Chaudhry et al., 2017). This approach of re-mixing *sur-mesure* phage cocktails and using them together with an antibiotic to which the infecting organism is resistant was successful in treating a patient with disseminated *Acinetobacter* infection (Schooley et al., 2017).

To achieve these clinical goals, we have demonstrated that unmanipulated phages isolated from the environment on *E. coli* ST131, are capable of lysing as many as 58% of a collection of 76 *E. coli* clinical isolates. Cocktails of as few as three of the individual phages ( $\phi HP3$ ,  $\phi ES12$ , and  $\phi ES17$ ) were capable of lysing 92% of the 76 clinical isolates. These results indicate that environmental samples provide good reservoirs of phages capable of being used against *E. coli*, and that highly effective cocktails can be generated from them. In all cases the cocktails tested were highly effective against clinical isolates, killing at  $EOP > 0.1$ . The highly effective killing of the phages and the high titers obtained in the CsCl-purified preparations indicates that these phages should be useful in clinical therapy where a concentrated dose could be administered without fear of generating a septic response due to the presence of contaminating endotoxin (Figures 1, 4A,B, 7). Similar broad coverage was found for *E. cloacae* phages. In addition, we demonstrated that laboratory isolates of *P. aeruginosa*-specific phages can evolve to expand their host ranges to *P. aeruginosa* clinical isolates. A mixture of four parental phages subjected to 20 or 30 cycles of host range expansion was capable of killing 2–44% of the 64 clinical isolates tested, whereas the uncycled parental phages could lyse only 2–23% of the clinical isolates. However, cocktails containing as few as three individual HRE-derived phages were capable of killing 52 of the 64 clinical isolates tested (81%) (Figure 6). Additional cycles of HRE using the 12 clinical isolates not killed by any of the phages at useable EOP ( $> 0.001$ ), seems likely to further expand the host range among those isolates.

In addition to phage isolation for *E. coli*-, *P. aeruginosa*-, and *E. cloacae*-specific phage collections, a number of parameters were characterized that can be useful in choosing phages for phage therapy, making new phage isolates, and general work with the phages (Abedon, 2017). Our “phage master lists” (Figures 1, 4A,B, 7) contain information on the source of the phages, morphology, growth properties, DNA sequence, and host range much like a Physician’s Desk Reference provides useful parameters for chemical antibiotics. The DNA sequence analyses and morphologies of the phages are important to establish the relationship of the individual phage to other phages in the databases (Weber-Dabrowska et al., 2016;



Properties of <i>Enterobacter cloacae</i> Phages				
Feature	<i>E. cloacae</i> Phage			
	φEC-W1	φEC-W2	φEC-F1	φEC-F2
<i>Phage Characteristics</i>				
Source Species	Human	Human	Human	Human
Source Location (Houston)	Raw Sewage	Raw Sewage	Raw Sewage	Raw Sewage
Isolation Date	03/25/19	03/27/19	03/25/19	03/27/19
Isolation Strain	E.c -W*	E.c -W*	E.c -F*	E.c -F*
Plaque Size (mm)	1.0-1.5	1.0-1.5	1.0-1.5	1.0-1.5
Plaque Morph.	Clear	Clear	Clear	Clear
Plate Stock (PFU/ml) <sup>^</sup>	1.2x10 <sup>10</sup>	4.2x10 <sup>10</sup>	5.6x10 <sup>9</sup>	1.0x10 <sup>10</sup>
CsCl Purified (PFU/ml) <sup>^</sup>	2.2x10 <sup>11</sup>	7.2x10 <sup>11</sup>	1.0x10 <sup>11</sup>	8.6x10 <sup>12</sup>
EM Morphology	Myovirus 	Myovirus 	Myovirus 	Myovirus 
<i>Sequence</i>				
(Accession No.)	MN 508621	MN 508622	MN 508623	MN 508624
Genome (BP)	178,807	176,610	178,147	178,307
G + C (%)	44.79%	44.72%	44.74	44.73
ORFs	283	275	277	278
tRNAs	2	1	2	2
Toxin/Virulence Genes	None	None	None	None
Lysogeny Genes	None	None	None	None
Abx-Resistance Genes	None	None	None	None
Closest Relative	Margaery	vB_CsaM_GAP161	vB_CsaM_GAP161	vB_CsaM_GAP161
Genus	T4-like	T4-like	T4-like	T4-like
<i>Growth Properties</i>				
Adsorption Constant (mL/min)	9.52x10 <sup>-7</sup>	7.31x10 <sup>-8</sup>	4.51x10 <sup>-7</sup>	2.74x10 <sup>-7</sup>
% Adsorbed (10 min)	99.0	34.6	83.7	72.0
Latent Period (Min)	21	24	25	20
Burst Size (PFU/cell)	15.7	20.4	33.5	18.6
<i>Summary of Phage Killing Spectra – No. Lysed/No. Tested (% Lysed)</i>				
<b>E.c. SCI* isolates† (N=2)</b>				
(EOP > 0.1)	1/2 (50%)	0/2 (0%)	0/2 (0%)	0/2 (0%)
(EOP > 0.001)	1/2 (50%)	0/2 (0%)	0/2 (0%)	0/2 (0%)
<b>E.c. LVAD†† isolates# (N=10)</b>				
(EOP > 0.1)	9/10 (90%)	9/10 (90%)	9/10 (90%)	8/10 (80%)
(EOP > 0.001)	0/10 (0%)	0/10 (0%)	1/10 (10%)	2/10 (80%)
<b>Total Strains (N=14)</b>				
(EOP > 0.1)	12/14 (86%)	11/14 (78%)	12/14 (86%)	12/14 (86%)
(EOP > 0.001)	1/14 (7%)	0/14 (0%)	1/14 (7%)	2/14 (14%)
* <i>Enterobacter cloacae</i> isolated from a hip prosthesis. E.c.-W = isolate from wound E.c.-F = isolate from wound fluid (different date)				
† <i>Enterobacter cloacae</i> isolated from spinal cord injured patient urine (Houston VA Hospital)				
# <i>Enterobacter cloacae</i> isolated from left ventricular assist device driveline infection (Houston St. Luke's Hospital)				
<sup>^</sup> Titer of representative preparation				
* SCI = from patient with spinal cord injury				
†† LVAD = left ventricular assist device driveline				

**FIGURE 7 |** Summary of characterization of *Enterobacter cloacae* phages. The characteristics, DNA sequences, growth properties and a summary of phage killing spectra are presented for each phage.

Casey et al., 2018). In addition, DNA sequence analysis provides important information on the properties of the phage genome, ensuring that phages can be used as therapeutic agents because they do not encode genes to establish and maintain lysogeny, toxins, virulence factors, or antibiotic resistance. The data on adsorption constant, adsorption rate, latent period, and burst size all represent parameters that can affect the success of

phage therapy (Weber-Dabrowska et al., 2016). Finally, in our determinations of phage host range we examined EOP, a parameter that allows one to determine the relative killing power of a phage on a test strain compared to its killing power on the isolation strain. EOP has been shown to be an excellent method for estimating phage virulence on a given bacterial strain. Simple spot tests of high titer phage were found to overestimate

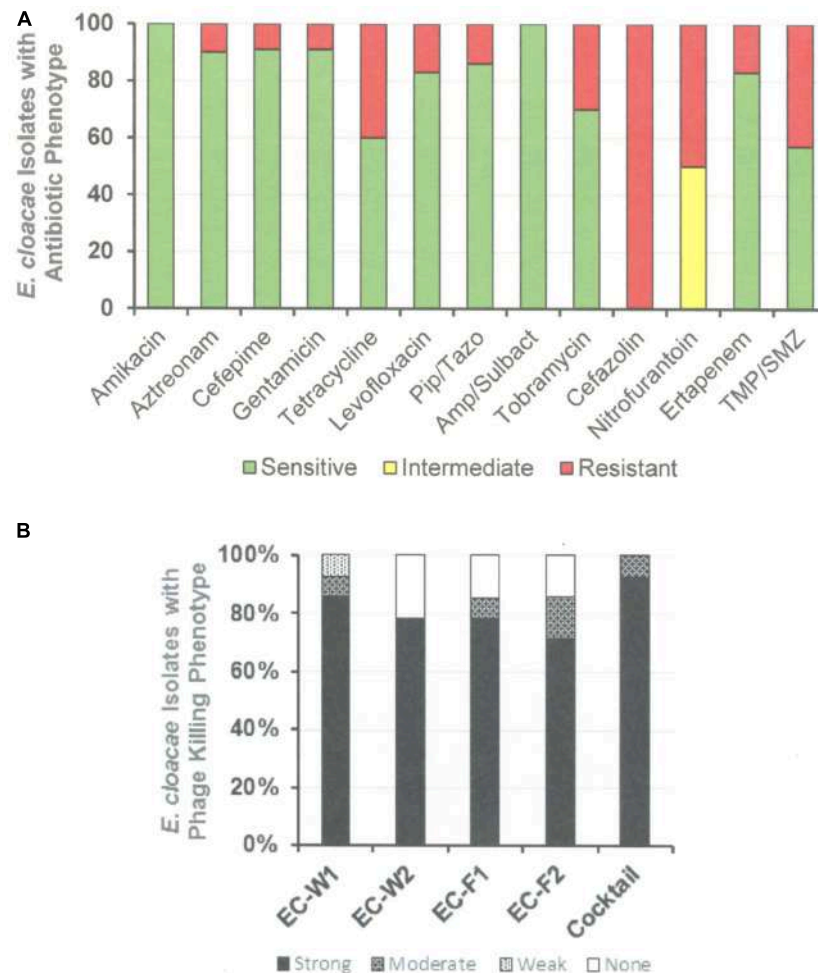
Antibiotic Sensitivity and Phage Killing of <i>Enterobacter cloacae</i> clinical Isolates																					
Bacterial Group	Source:*	Date Collected	Antibiotic Sensitivity											<i>E. cloacae</i> Clinical Isolate	Phage Killing (EOP)						
			Amikacin	Aztreonam	Cefepime	Gentamicin	Tetracycline	Levofloxacin	Pip/Tazobacta	Amp/Sulbacta	Tobramycin	Cefazolin	Nitrofurantoin		Ertapenem	TMP/SMZ	φEC-W1	φEC-W2	φEC-F1	φEC-F2	
Houston Clinical Isolates	W	Unk	NT	NT	NT	NT	NT	NT	NT	NT	NT	NT	NT	NT	NT	NT	E.c.Wound <sup>#</sup>	+	+	+	+
	F	Unk	NT	NT	NT	NT	NT	NT	NT	NT	NT	NT	NT	NT	NT	NT	E.c.Fluid <sup>#</sup>	-	-	-	-
	U	02/12/19	+	NT	+	+	NT	+	NT	NT	NT	+	+	+	+	+	DS464-SCI <sup>†</sup>	-	-	-	-
	U	04/09/19	+	NT	+	+	NT	+	NT	NT	NT	+	+	+	+	+	DS484-SCI <sup>†</sup>	-	-	-	-
	L	10/09/18	+	+	+	+	+	+	+	+	+	+	+	+	+	+	BSL11C	+	-	-	-
	L	10/23/18	+	+	+	+	+	+	+	+	+	+	+	+	+	+	BSL12A	-	-	-	-
	L	11/01/19	+	+	+	+	+	+	+	+	+	+	+	+	+	+	BSL14A	-	-	-	-
	L	11/01/18	+	+	+	+	+	+	+	+	+	+	+	+	+	+	BSL14B	-	-	-	-
	L	01/09/19	+	+	+	+	+	+	+	+	+	+	+	+	+	+	BSL25A	-	-	-	-
	L	01/09/19	+	+	+	+	+	+	+	+	+	+	+	+	+	+	BSL25C	-	-	-	-
	L	01/21/19	+	+	+	+	+	+	+	+	+	+	+	+	+	+	BSL29A	-	-	-	-
	L	01/21/19	+	+	+	+	+	+	+	+	+	+	+	+	+	+	BSL29B	-	-	-	-
	L	02/07/19	+	+	+	+	+	+	+	+	+	+	+	+	+	+	BSL40C	-	-	-	-
	L	02/07/19	+	+	+	+	+	+	+	+	+	+	+	+	+	+	BSL40G	-	-	-	-

Footnotes	Key to Abx Sens.	Key to Phage Killing (EOP)																		
* Source: W=wound; F=fluid; U=urine; L=LVAD infection † Spinal Cord Injury NT=Not Tested. # From hip prosthesis	<table border="1"> <tr><td>+</td><td>Sensitive</td></tr> <tr><td>+</td><td>Intermediate</td></tr> <tr><td>+</td><td>Resistant</td></tr> </table>	+	Sensitive	+	Intermediate	+	Resistant	<table border="1"> <tr><td>+</td><td>EOP &gt; 1.000</td></tr> <tr><td>+</td><td>EOP between 0.100 – 1.000</td></tr> <tr><td>+</td><td>EOP between 0.001 – 0.099</td></tr> <tr><td>+</td><td>EOP &lt; 0.001; not useful</td></tr> <tr><td>-</td><td>No Growth</td></tr> <tr><td>+</td><td>Reference (EOP = 1.000)</td></tr> </table>	+	EOP > 1.000	+	EOP between 0.100 – 1.000	+	EOP between 0.001 – 0.099	+	EOP < 0.001; not useful	-	No Growth	+	Reference (EOP = 1.000)
	+	Sensitive																		
	+	Intermediate																		
	+	Resistant																		
	+	EOP > 1.000																		
	+	EOP between 0.100 – 1.000																		
+	EOP between 0.001 – 0.099																			
+	EOP < 0.001; not useful																			
-	No Growth																			
+	Reference (EOP = 1.000)																			
EOP = Titer X / Titer Reference																				

**FIGURE 8 |** Representative data for antibiotic sensitivity and phage killing (EOP) of clinical isolates of *E. cloacae*. Shown are the properties of the *E. cloacae* clinical isolates on the left, including: source, date of isolation and antibiotic sensitivity data (VITEK2). On the right are shown the killing spectra of the phages on the individual *E. cloacae* clinical isolates. The keys to antibiotic sensitivity and phage killing (EOP) are shown at the bottom of the figure.





**FIGURE 9 |** Antibiotic Sensitivities and Phage Killing Phenotypes of *E. cloacae* Clinical Isolates (N=64). **(A)** Antibiotic sensitivities based on cut off values used in the microbiology lab at the Houston VA Hospital. **(B)** The phage killing phenotypes were based on EOP. Strong killers, EOP > 0.1; Moderate Killers, 0.099 > EOP > 0.001; Weak Killers, EOP < 0.00099 but positive; None, no growth. The cocktail was consisted of equal titers of  $\phi$ EC-W1 and  $\phi$ EC-W2. Pip/Tazo, piperacillin/tazobactam; TMA/SMZ, trimethoprim/sulfamethoxazole.

both the virulence and the host range of a phage (Mirzaei and Nilsson, 2015). Indeed, we have shown that phage virulence and bacterial susceptibility to the phage determined *in vitro* allowed us to predict the outcome of therapy *in vivo* (Green et al., 2017). While bacterial receptors for the phages were not identified here, that information is important for the rational mixing of phage cocktails. We are in the process of identifying receptors for phages in our libraries, and have identified the receptor for  $\phi$ HP3 as lipopolysaccharide in the *E. coli* JJ2528 host (unpublished data). Having all these parameters at hand aids in the selection of a phage for monotherapy, or a mixture of phages for cocktail therapy. Cesium chloride purified stocks of all phages described here exist and their endotoxin content has been reduced below clinically permissible levels, so that they can quickly be put to use. Our *E. coli*, *P. aeruginosa*, and *E. cloacae* phage libraries are now ready for rigorous *in vivo* studies in animal models of urinary tract infections and LVAD infections, as well as available for compassionate use protocols in humans.

## DATA AVAILABILITY STATEMENT

All datasets generated for this study are included in the article/Supplementary Material.

## ETHICS STATEMENT

The collection of de-identified clinical isolates was approved by the Baylor College of Medicine Institutional Review Board (IRB).

## AUTHOR CONTRIBUTIONS

AM, RR, HK, and BT conceived the experiments and guided their performance. SBG, SIG, CL, JC, AT, and KS performed the experiments and analyzed the results. BT arranged for collection

of clinical isolates and corresponding antibiotic sensitivity data. RR wrote the manuscript with editing from BT, HK, and AM. All authors contributed to manuscript revision, read and approved the submitted version.

## FUNDING

This work was supported by the following funding sources: 1R21AI121545 (RR), The Mike Hogg Fund (AM, RR, BT), The MacDonald General Research Fund (BT, AM, RR), Baylor College of Medicine seed funds (AM), and Veterans Administration RR&D I01 RX002595 (BT). The research reported here was supported in part by the U.S. Department of Veterans Affairs, Veterans Health Administration, Health Services Research and Development Service at the Center for Innovations in Quality, Effectiveness and Safety, Michael E. DeBakey VA Medical Center, Houston, TX, United States (CIN 13-413). The views expressed in this article are those

## REFERENCES

- Abedon, S. T. (2011). Lysis from without. *Bacteriophage* 1, 46–49. doi: 10.4161/bact.1.1.13980
- Abedon, S. T. (2017). Information phage therapy research should report. *Pharmaceuticals* 10:42. doi: 10.3390/ph10020043
- Aslam, S., Pretorius, V., Lehman, S. M., Morales, S., and Schooley, R. T. (2019). Novel bacteriophage therapy for treatment of left ventricular assist device infection. *J. Heart Lung Transplant.* 38, 475–476. doi: 10.1016/j.healun.2019.01.001
- Aziz, R. K., Bartels, D., Best, A. A., DeJongh, M., Disz, T., Edwards, R. A., et al. (2008). The RAST server: rapid annotations using subsystems technology. *BMC Genomics* 9:75. doi: 10.1186/1471-2164-9-75
- Bankevich, A., Nurk, S., Antipov, D., Gurevich, A. A., Dvorkin, M., Kulikov, A. S., et al. (2012). SPAdes: a new genome assembly algorithm and its applications to single-cell sequencing. *J. Comput. Biol.* 19, 455–477. doi: 10.1089/cmb.2012.0021
- Bassetti, M., Poulacou, G., Ruppe, E., Bouza, E., Van Hal, S. J., and Brink, A. (2017). Antimicrobial resistance in the next 30 years, humankind, bugs and drugs; a visionary approach. *Intensive Care Med.* 43, 1464–1475. doi: 10.1007/s00134-017-4878-x
- Besemer, J. (2001). GeneMarkS: a self-training method for prediction of gene starts in microbial genomes. Implications for finding sequence motifs in regulatory regions. *Nucleic Acids Res.* 29, 2607–2618. doi: 10.1093/nar/29.12.2607
- Boucher, H. W., Talbot, G. H., Bradley, J. S., Edwards, J. E., Gilbert, D., Rice, L. B., et al. (2009). Bad bugs, no drugs; no ESKAPE: an update from the infectious diseases society of America. *Clin. Infect. Dis.* 48, 1–12. doi: 10.1086/595011
- Burrowes, B. (2011). *Analysis of the Appelman protocol for the Generation of Therapeutic Bacteriophages*. Ph.D. thesis, Texas Tech Health Sciences center, Lubbock, TX.
- Burrowes, B. H., Molineux, I. J., and Fralick, J. A. (2019). Directed in vitro evolution of therapeutic bacteriophages: the Appelmans protocol. *Viruses* 11:241. doi: 10.3390/v11030241
- Casey, E., van Sinderen, D., and Mahoney, J. (2018). In vitro characteristics of phages to guide 'real life' phage therapy suitability. *Viruses* 10:163. doi: 10.3390/v10040163
- Centers for Disease Control [CDC] (2013). *Antibiotic Resistance Threats in the United States*. Available at: <https://www.cdc.gov/drugresistance/pdf/ar-threats-2013-508.pdf> (accessed May 10, 2018).
- Chan, B. K., Siström, M., Wertz, J. E., Kortright, K. E., Narayan, D., and Turner, P. E. (2016). Phage selection restores antibiotic sensitivity in MDR *Pseudomonas aeruginosa*. *Sci. Rep.* 6:26717. doi: 10.1038/srep26717

of the authors and do not necessarily reflect the position or policy of the Department of Veterans Affairs or the United States Government.

## ACKNOWLEDGMENTS

We thank Jim Johnson for providing well-characterized *E. coli* ST131 isolates from his collection. Laura Dillon and Dr. Faisal Cheema assisted in collecting clinical isolates from the hospital. Dr. Jason Kaelber and Kara Schoenemann performed electron microscopy.

## SUPPLEMENTARY MATERIAL

The Supplementary Material for this article can be found online at: <https://www.frontiersin.org/articles/10.3389/fmicb.2019.02537/full#supplementary-material>

- Chan, B. K., Turner, P. E., Kim, S., Mojibian, H. R., Elefteriades, J. A., and Narayan, D. (2018). Phage treatment of an aortic graft infected with *Pseudomonas aeruginosa*. *Evol. Med. Public Health* 2018, 60–66. doi: 10.1093/emph/eoy005
- Chanishvili, N. (2016). Phages as therapeutic and prophylactic means: summary of the soviet and post-soviet experience. *Curr. Drug Deliv.* 13, 309–323. doi: 10.2174/156720181303160520193946
- Chaudhry, W. N., Concepcion-Acevedo, J., Park, T., Andleeb, S., Bull, J. J., and Levin, B. R. (2017). Synergy and order effects of antibiotics and phages in killing *Pseudomonas aeruginosa* biofilms. *PLoS One* 12:e0168615. doi: 10.1371/journal.pone.0168615
- Chen, L., Zheng, D., Liu, B., Yang, J., and Jin, Q. (2016). VFDB 2016: hierarchical and refined dataset for big data analysis—10 years on. *Nucleic Acids Res.* 44, D694–D697. doi: 10.1093/nar/gkv1239
- Chibeu, A., Ceyssens, P. J., Hertveldt, K., Volckaert, G., Cornelis, P., Matthijs, S., et al. (2009). The adsorption of *Pseudomonas aeruginosa* bacteriophage phiKMV is dependent on expression regulation of type IV pili genes. *FEMS Microbiol. Lett.* 296, 210–218. doi: 10.1111/j.1574-6968.2009.01640.x
- Comeau, A. M., Tetart, F., Trojet, S. N., Prere, M. F., and Krisch, H. M. (2007). Phage-antibiotic synergy (PAS): beta-lactam and quinolone antibiotics stimulate virulent phage growth. *PLoS One* 2:e799. doi: 10.1371/journal.pone.0000799
- Debarbieux, L., Forterre, P., Krupovic, M., Kutateladze, M., and Prangishvili, D. (2018). Centennial celebration of bacteriophage research. *Res. Microbiol.* 169, 479–480. doi: 10.1016/j.resmic.2018.10.001
- Debarbieux, L., Pirnay, J. P., Verbeken, G., De Vos, D., Merabishvili, M., Huys, I., et al. (2016). A bacteriophage journey at the european medicines agency. *FEMS Microbiol. Lett.* 363:fnv225. doi: 10.1093/femsle/fnv225
- Delcher, A. L., Bratke, K. A., Powers, E. C., and Salzberg, S. L. (2007). Identifying bacterial genes and endosymbiont DNA with Glimmer. *Bioinformatics* 23, 673–679. doi: 10.1093/bioinformatics/btm009
- El Haddad, L., Harb, C. P., Gebara, M. A., Stibuch, M. A., and Chemaly, R. F. (2018). A systematic and critical review of phage therapy against multi-drug resistant ESKAPE organisms in humans. *Clin. Infect. Dis.* 69, 167–178. doi: 10.1093/cid/ciy947
- Fu, W., Forster, T., Mayer, O., Curtin, J. J., Lehman, S. M., and Donlan, R. M. (2010). Bacteriophage cocktail for the prevention of biofilm formation by *Pseudomonas aeruginosa* on catheters in an in vitro model system. *Antimicrob. Agents Chemother.* 54, 397–404. doi: 10.1128/AAC.00669-09
- Gelman, D., Eisenkraft, A., Chanishvili, N., Nachman, D., Copenhagen, G. S., and Hazan, R. (2018). The history and promising future of phage therapy in the military service. *J. Trauma Acute Care Surg.* 85(1S Suppl. 2), S18–S126. doi: 10.1097/TA.0000000000001809

- Ghosh, C., Sarkar, P., Issa, R., and Haldar, J. (2018). Alternatives to conventional antibiotics in the era of antimicrobial resistance. *Trends Microbiol.* 27, 323–338. doi: 10.1016/j.tim.2018.12.010
- Green, S. L., Kaelber, J. T., Ma, L., Trautner, B. W., Ramig, R. F., and Maresso, A. W. (2017). Bacteriophages from ExPEC reservoirs kill pandemic multidrug-resistant strains of clonal group ST131 in animal models of bacteremia. *Sci. Rep.* 7:46151. doi: 10.1038/srep46151
- Hargreaves, K. R., Otieno, J. R., Thanki, A., Blades, M. J., Millard, A. D., Browne, H. P., et al. (2015). As clear as mud? determining the diversity and prevalence of prophages in the draft genomes of estuarine isolates of *Clostridium difficile*. *Genome Biol. Evol.* 7, 1842–1855. doi: 10.1093/gbe/evv094
- Hyman, P. (2019). Phages for phage therapy: isolation, characterization, and host range breadth. *Pharmaceuticals* 12:35. doi: 10.3390/ph12010035
- Johnson, J. R., Porter, S. B., Johnston, B., Thuras, P., Clock, S., Crupain, M., et al. (2017). Extraintestinal pathogenic and antimicrobial-resistant *Escherichia coli*, including sequence type 131 (ST131), from retail chicken breasts in the United States in 2013. *Appl. Environ. Microbiol.* 83:e02956-16. doi: 10.1128/AEM.02956-16
- Johnson, J. R., Stell, A. L., and Delavari, P. (2001). Canine feces as reservoir of extraintestinal pathogenic *Escherichia coli*. *Infect. Immun.* 69, 1306–1314. doi: 10.1128/IAI.69.3.1306-1314.2001
- Johnson, M., Zaretskaya, I., Raytselis, Y., Merezuk, Y., McGinnis, S., and Madden, T. L. (2008). NCBI BLAST: a better web interface. *Nucleic Acids Res.* 36, W5–W9. doi: 10.1093/nar/gkn201
- Kalil, A. C., Johnson, D. W., Lisco, S. J., and Sun, J. (2017). Early goal-directed therapy for sepsis: a novel solution for discordant survival outcomes in clinical trials. *Crit. Care Med.* 45, 607–614. doi: 10.1097/CCM.0000000000002235
- Kropinski, A. M. (2009). “Measurement of the rate of attachment of bacteriophage to cells,” in *Bacteriophages, Methods and Protocols, Volume 1: Isolation, Characterization, and Interactions*, eds M. R. J. Clokie, and A. M. Kropinski, (New York, NY: Humana Press), doi: 10.1007/978-1-60327-164-6-15
- Kropinski, A. M. (2018). “Practical advice on the one-step growth curve,” in *Bacteriophages, Methods and Protocols*, eds M. R. J. Clokie, A. Kropinski, and R. Lavigne, (New York, NY: Humana Press), doi: 10.1007/978-1-4939-7343-9-3
- Kutter, E. M., Kuhl, S. J., and Abedon, S. T. (2015). Re-establishing a place for phage therapy in western medicine. *Future Microbiol.* 10, 685–688. doi: 10.4161/bact.1.2.15845
- Labrie, S. J., Samson, J. E., and Moineau, S. (2010). Bacteriophage resistance mechanisms. *Nat. Rev. Microbiol.* 8, 317–327. doi: 10.1038/nrmicro2315
- Laslett, D. (2004). ARAGORN, a program to detect tRNA genes and tmRNA genes in nucleotide sequences. *Nucleic Acids Res.* 32, 11–16. doi: 10.1093/nar/gkh152
- Latz, S., Wahida, A., Arif, A., Hafner, H., Hoss, M., Ritter, K., et al. (2016). Preliminary survey of local bacteriophages with lytic activity against multidrug resistant bacteria. *J. Basic Microbiol.* 56, 1117–1123. doi: 10.1002/jobm.201600108
- Lavigne, R., Burkal'tseva, M. V., Robben, J., Sykilinda, N. N., Kurochkina, L. P., Grymonprez, B., et al. (2003). The genome of bacteriophage phiKMV, a T7-like virus infecting *Pseudomonas aeruginosa*. *Virology* 312, 49–59. doi: 10.1016/S0042-6822(03)00123-5
- Li, P.-E., Lo, C.-C., Anderson, J. J., Davenport, K. W., Bishop-Lilly, K. A., Xu, Y., et al. (2017). Enabling the democratization of the genomics revolution with a fully integrated web-based bioinformatics platform. *Nucleic Acids Res.* 45, 67–80. doi: 10.1093/nar/gkw1027
- Liao, K. S., Lehman, S. M., Tweardy, D. J., Donlan, R. M., and Trautner, B. W. (2012). Bacteriophages are synergistic with bacterial interference for the prevention of *Pseudomonas aeruginosa* biofilm formation on urinary catheters. *J. Appl. Microbiol.* 113, 1530–1539. doi: 10.1111/j.1365-2672.2012.05432.x
- Liu, B., and Pop, M. (2009). ARDB—Antibiotic Resistance Genes Database. *Nucleic Acids Res.* 37, D443–D447. doi: 10.1093/nar/gkn656
- Lo, C.-C., and Chain, P. S. G. (2014). Rapid evaluation and quality control of next generation sequencing data with FaQCs. *BMC Bioinformatics* 15:366. doi: 10.1186/s12859-014-0366-362
- Mao, C., Abraham, D., Wattam, A. R., Wilson, M. J., Shukla, M., Yoo, H. S., et al. (2015). Curation, integration and visualization of bacterial virulence factors in PATRIC. *Bioinformatics* 31, 252–258. doi: 10.1093/bioinformatics/btu631
- Mapes, A. C., Trautner, B. W., Liao, K. S., and Ramig, R. F. (2016). Development of expanded host range phage active on multidrug-resistant *Pseudomonas aeruginosa*. *Bacteriophage* 6:e1096995. doi: 10.1080/21597081.2015.1096995
- Mattila, S., Ruotsalainen, P., and Jalasvuori, M. (2015). On-Demand isolation of bacteriophages against drug-resistant bacteria for personalized phage therapy. *Front. Microbiol.* 6:1271. doi: 10.3389/fmicb.2015.01271
- McArthur, A. G., Waglechner, N., Nizam, F., Yan, A., Azad, M. A., Baylay, A. J., et al. (2013). The comprehensive antibiotic resistance database. *Antimicrob. Agents Chemother.* 57, 3348–3357. doi: 10.1128/AAC.00419-413
- McNair, K., Aziz, R. K., Pusch, G. D., Overbeek, R., Dutilh, B. E., and Edwards, R. (2018). Phage genome annotation using the RAST pipeline. *Methods Mol. Biol.* 1681, 231–238. doi: 10.1007/978-1-4939-7343-9-17
- McVay, C. S., Velasquez, M., and Fralick, J. A. (2007). Phage therapy of *Pseudomonas aeruginosa* infection in a mouse burn model. *Antimicrob. Agents Chemother.* 51, 1934–1938. doi: 10.1128/AAC.01028-06
- Merabishvili, M., Pirnay, J.-P., and De Vos, D. (2018). Guidelines to compose an ideal bacteriophage cocktail. *Methods Mol. Biol.* 1693, 99–110. doi: 10.1007/978-1-4939-7395-8-9
- Mirzaei, M. K., and Nilsson, A. S. (2015). Isolation of phages for phage therapy: a comparison of spot tests and efficiency of plating analyses for determination of host range and efficacy. *PLoS One* 10:e0118557. doi: 10.1371/journal.pone.0118557
- Myelnikov, D. (2018). An alternative cure: the adoption and survival of phage therapy in the USSR, 1922–1955. *J. Hist. Med. Allied Sci.* 73, 385–411. doi: 10.1093/jhmas/jry024
- Ormla, A. M., and Jalasvuori, M. (2013). Phage therapy: should bacterial resistance to phages be a concern, even in the long run. *Bacteriophage* 3:e24219. doi: 10.4161/bact.24219
- Peng, Y., Leung, H. C. M., Yiu, S. M., and Chin, F. Y. L. (2010). IDBA – a practical iterative de bruijn graph de novo assembler. *Lecture Notes Comput. Sci.* 426–440. doi: 10.1007/978-3-642-12683-3-28
- Peng, Y., Leung, H. C. M., Yiu, S. M., and Chin, F. Y. L. (2012). IDBA-UD: a de novo assembler for single-cell and metagenomic sequencing data with highly uneven depth. *Bioinformatics* 28, 1420–1428. doi: 10.1093/bioinformatics/bts174
- Pirnay, J. P., De Vos, D., Verbeken, G., Merabishvili, M., Chanishvili, N., Vanechoutte, M., et al. (2011). The phage therapy paradigm: Prêt à Porter or Sur-mesure? *Pharm. Res.* 28, 934–937. doi: 10.1007/s11095-010-0313-5
- Pirnay, J. P., Merabishvili, M., Van Raemdonck, H., De Vos, D., and Verbeken, G. (2018). Phage production in compliance with regulatory requirements. *Meth. Mol. Biol.* 1693, 233–252. doi: 10.1007/978-1-4939-7395-8-18
- Ryan, E. M., Alkawareek, M. Y., Donnelly, R. F., and Gilmore, B. F. (2012). Synergistic phage-antibiotic combinations for the control of *Escherichia coli* biofilms in vitro. *Immunol. Med. Microbiol.* 65, 395–398. doi: 10.1111/j.1574-695X.2012.00977.x
- Schooley, R. T., Biswas, B., Gill, J. J., Hernandez-Morales, A., Lancaster, J., Lessor, L., et al. (2017). Development and use of personalized bacteriophage-based therapeutic cocktails to treat a patient with a disseminated resistant *Acinetobacter baumannii* infection. *Antimicrob. Agents Chemother.* 61:e00954-17. doi: 10.1128/AAC.00954-17
- Seemann, T. (2014). Prokka: rapid prokaryotic genome annotation. *Bioinformatics* 30, 2068–2069. doi: 10.1093/bioinformatics/btu153
- Stearns, S. C. (2019). Frontiers in molecular evolutionary medicine. *J. Mol. Evol.* [Epub ahead of print].
- Suttle, C. A. (2005). Viruses in the sea. *Nature* 437, 356–361. doi: 10.1038/nature04160
- Wattam, A. R., Davis, J. J., Assaf, R., Boisvert, S., Brettin, T., Bun, C., et al. (2017). Improvements to PATRIC, the all-bacterial bioinformatics database and analysis resource center. *Nucleic Acids Res.* 45, D535–D542. doi: 10.1093/nar/gkw1017
- Weber-Dabrowska, B., Jonczyk-Matysiak, E., Zaczek, M., Loocka, M., Lusiak-Szelachowska, M., and Gorski, A. (2016). Phage procurement for therapeutic purposes. *Front. Microbiol.* 12:2016. doi: 10.3389/fmicb.2016.01177
- Wei, Y., Ocampo, P., and Levin, B. R. (2010). An experimental study of the population and evolutionary dynamics of *Vibrio cholerae* O1 and the bacteriophage JSF4. *Proc. Biol. Sci.* 277, 3247–3254. doi: 10.1098/rspb.2010.0651

- World Health Organization [WHO] (2017). *Global Priority List of Antibiotic-Resistant Bacteria to Guide Research, Discovery, and Development of New Antibiotics*. Available at: <https://www.who.int/medicines/publications/global-priority-list-antibiotic-resistant-bacteria/en/> (accessed May 10, 2018).
- Wright, A., Hawkins, C. H., Anggard, E. E., and Harper, D. R. (2009). A controlled clinical trial of a therapeutic bacteriophage preparation in chronic otitis due to antibiotic-resistant *Pseudomonas aeruginosa*; a preliminary report of efficacy. *Clin. Otolaryngol.* 34, 349–357. doi: 10.1111/j.1749-4486.2009.01973.x
- Zerbino, D. R., and Birney, E. (2008). Velvet: algorithms for de novo short read assembly using de Bruijn graphs. *Genome Res.* 18, 821–829. doi: 10.1101/gr.074492.107
- Conflict of Interest:** The authors declare that the research was conducted in the absence of any commercial or financial relationships that could be construed as a potential conflict of interest.

Copyright © 2019 Gibson, Green, Liu, Salazar, Clark, Terwilliger, Kaplan, Maresso, Trautner and Ramig. This is an open-access article distributed under the terms of the Creative Commons Attribution License (CC BY). The use, distribution or reproduction in other forums is permitted, provided the original author(s) and the copyright owner(s) are credited and that the original publication in this journal is cited, in accordance with accepted academic practice. No use, distribution or reproduction is permitted which does not comply with these terms.





# Characterization of Lytic Bacteriophages Infecting Multidrug-Resistant Shiga Toxigenic Atypical *Escherichia coli* O177 Strains Isolated From Cattle Feces

Peter Kotsoana Montso<sup>1,2</sup>, Victor Mlambo<sup>3</sup> and Collins Njie Ateba<sup>1,2\*</sup>

<sup>1</sup> Bacteriophage Therapy and Phage Bio-Control Laboratory, Department of Microbiology, Faculty of Natural and Agricultural Sciences, North-West University, Mmabatho, South Africa, <sup>2</sup> Food Security and Safety Niche Area, North-West University, Mmabatho, South Africa, <sup>3</sup> Faculty of Agriculture and Natural Sciences, School of Agricultural Sciences, University of Mpumalanga, Mbombela, South Africa

## OPEN ACCESS

### Edited by:

Leonardo Neves de Andrade,  
University of São Paulo, Brazil

### Reviewed by:

Robert Czajkowski,  
University of Gdansk, Poland  
Kim Stanford,  
Alberta Ministry of Agriculture and  
Forestry, Canada  
Josefina Leon-Felix,  
Centro de Investigación en  
Alimentación y Desarrollo  
(CIAD), Mexico

### \*Correspondence:

Collins Njie Ateba  
collins.ateba@nwu.ac.za

### Specialty section:

This article was submitted to  
Infectious Diseases - Surveillance,  
Prevention and Treatment,  
a section of the journal  
Frontiers in Public Health

**Received:** 10 July 2019

**Accepted:** 07 November 2019

**Published:** 26 November 2019

### Citation:

Montso PK, Mlambo V and Ateba CN  
(2019) Characterization of Lytic  
Bacteriophages Infecting  
Multidrug-Resistant Shiga Toxigenic  
Atypical *Escherichia coli* O177 Strains  
Isolated From Cattle Feces.  
*Front. Public Health* 7:355.  
doi: 10.3389/fpubh.2019.00355

The increasing incidence of antibiotic resistance and emergence of virulent bacterial pathogens, coupled with a lack of new effective antibiotics, has reignited interest in the use of lytic bacteriophage therapy. The aim of this study was to characterize lytic *Escherichia coli* O177-specific bacteriophages isolated from cattle feces to determine their potential application as biocontrol agents. A total of 31 lytic *E. coli* O177-specific bacteriophages were isolated. A large proportion (71%) of these phage isolates produced large plaques while 29% produced small plaques on 0.3% soft agar. Based on different plaque morphologies and clarity and size of plaques, eight phages were selected for further analyses. Spot test and efficiency of plating (EOP) analyses were performed to determine the host range for selected phages. Phage morphotype and growth were analyzed using transmission electron microscopy and the one-step growth curve method. Phages were also assessed for thermal and pH stability. The spot test revealed that all selected phages were capable of infecting different environmental *E. coli* strains. However, none of the phages infected American Type Culture Collection (ATCC) and environmental *Salmonella* strains. Furthermore, EOP analysis (range: 0.1–1.0) showed that phages were capable of infecting a wide range of *E. coli* isolates. Selected phage isolates had a similar morphotype (an icosahedral head and a contractile tail) and were classified under the order Caudovirales, *Myoviridae* family. The icosahedral heads ranged from 81.2 to 110.77 nm, while the contractile tails ranged from 115.55 to 132.57 nm in size. The phages were found to be still active after 60 min of incubation at 37 and 40°C. Incremental levels of pH induced a quadratic response on stability of all phages. The pH optima for all eight phages ranged between 7.6 and 8.0, while at pH 3.0 all phages were inactive. Phage latent period ranged between 15 and 25 min while burst size ranged from 91 to 522 virion particles [plaque-forming unit (PFU)] per infected cell. These results demonstrate that lytic *E. coli* O177-specific bacteriophages isolated from cattle feces are highly stable and have the capacity to infect different *E. coli* strains, traits that make them potential biocontrol agents.

**Keywords:** atypical enterophagenic *E. coli* O177, bacteriophages, bacteriophage therapy, biocontrol, biological properties, multi-drug resistance, shiga-toxigenic *E. coli*

## INTRODUCTION

Bacteriophages (phages) are self-replicating viruses, which are capable of infecting and lysing their specific host bacteria (1). They are ubiquitous organisms on Earth estimated to number at  $10^{30}$ - $10^{32}$  (2). Phages are relatively safe, nontoxic, and harmless to animals, plants, and humans (3, 4). They are found in various environments related to their host such as in food, soil, sewage water, feces, and farm environments (2). Several bacterial species such as *Campylobacter*, *Escherichia coli*, *Listeria*, *Salmonella*, *Pseudomonas*, and *Vibrio* species are used as hosts to isolate their specific bacteriophages (5–7). Because of their host specificity and nontoxicity, lytic phages are considered to be an alternative solution to combat antimicrobial-resistant pathogens. Outbreaks of listeriosis and widespread occurrence of multidrug resistance in *E. coli*, *Salmonella*, and *Staphylococcus* species have been reported in South Africa (8–11). However, there has been no attempt to use bacteriophages to control antibiotic-resistant pathogens, in either hospital settings or food industry.

Antibiotic resistance in foodborne pathogens, particularly *E. coli* species, remains a public health concern. Antibiotic-resistant pathogens do not only increase economic and social costs but are also responsible for severe infections in humans (12). In 2014, foodborne infections caused an estimated 600 million illnesses and 420,000 deaths across the globe (13). In addition, 978 listeriosis cases were reported in South Africa from 2017 to 2018, resulting in 183 deaths (11). The leading pathogenic bacteria of concern are *E. coli* O157, *Campylobacter*, *Listeria*, and *Salmonella* species (14). Moreover, recent reports revealed that non-O157 strains, particularly O26, O45, O103, O111, O121, and O145, exhibit multidrug resistance and are among the leading causes of foodborne infection (15).

In view of the above, several interventions, such as physical, chemical, and biological methods, have been devised and implemented at all levels of the food chain to combat foodborne infection and the spread of antibiotic-resistant pathogens (16). However, these conventional methods have significant drawbacks such as corrosion of food processing plants, environmental pollution, change of food matrices, development of antibiotic resistance, and toxic effects of chemical residues (17). In addition, application of chemical agents coupled with a lack of effective enforcement regulations in food may hamper international trade and thus affect the economy of the exporting country (16, 18). Therefore, lack of new antibiotics and inefficacy of conventional strategies to combat multidrug-resistant bacterial pathogens necessitate the search for alternative control strategies such as the use of bacteriophages. Given their biological properties as explained above, lytic phages can be applied at all levels of the food chain, including preharvest application. Preharvest intervention has the advantage of preventing the transmission of foodborne pathogens from food-producing animals to human.

Considering the virulence and antibiotic resistance profiles of the *E. coli* O177 strain, coupled with the lack of new antibiotics and limitations of conventional strategies to mitigate antibiotic resistance, there is a need to expand the search for novel bacteriophages for biocontrol application. Therefore, the current study was designed to isolate and characterize lytic

*E. coli* O177-specific bacteriophages as potential biocontrol agents. Stability and viability of the phages were determined under temperature and pH ranges that would be obtained in a live ruminant to assess their stability for preharvest use in these animals.

## MATERIALS AND METHODS

### Bacterial Strain

Multidrug-resistant and virulent atypical enteropathogenic *E. coli* O177 strain was used to isolate *E. coli* O177-specific bacteriophages. The atypical enteropathogenic *E. coli* O177 isolates were obtained from cattle feces and confirmed through PCR analysis. The isolates were further screened for the presence of virulence and antimicrobial gene determinants. Prior to phage isolation, 40 *E. coli* O177 isolates stored at  $-80^{\circ}\text{C}$  were resuscitated on MacConkey agar and incubated at  $37^{\circ}\text{C}$  for 24 h. A single colony from each sample was transferred into 15-ml nutrient broth in 50-ml falcon tubes. The samples were incubated in a shaker (160 rpm) at  $37^{\circ}\text{C}$  for 3 h until the growth reached an optical density (OD) of 0.4–0.5 (600 nm).

### Enrichment and Isolation Purification of *E. coli* O177-Specific Bacteriophages

*Escherichia coli* O177-specific bacteriophages were isolated from cattle feces using *E. coli* O177 environmental strain following the enrichment method (19, 20) with some modifications. Twenty fecal samples were collected from two commercial feedlots and two dairy farms. Samples were collected directly from the rectum using arm-length rectal gloves, placed in a cooler box containing ice packs, and transported to the laboratory. Five grams of each fecal sample was dissolved in 20 ml of lambda diluent and vortexed to obtain a homogeneous mixture. The mixture was centrifuged at  $10,000 \times g$  for 10 min using Hi Centrifuge SR (model: Z300, Germany) to sediment fecal matter and other impurities. An aliquot of 10 ml from the supernatant was extracted and filter-sterilized using a 0.22- $\mu\text{m}$  pore-size syringe filter (GVS Filter Technology, USA) to obtain crude phage filtrates. For enrichment, 5 ml of each filtrate was added to 100  $\mu\text{l}$  of exponential-phase ( $\text{OD}_{600} = 0.4$ – $0.5$ ) culture of each of the 40 *E. coli* O177 host strains in 10 ml of double-strength tryptic soya broth (TSB) supplemented with 2 mM of calcium chloride ( $\text{CaCl}_2$ ). The samples were incubated in a shaking incubator (80 rpm) at  $37^{\circ}\text{C}$  for 24 h. After incubation, the samples were centrifuged at  $10,000 \times g$  for 10 min using Hi Centrifuge SR (Model: Z300, Germany) to remove bacterial cells and sample debris. The supernatant was filter-sterilized with a 0.22- $\mu\text{m}$  pore-size Acrodisc syringe filter (GVS Filter Technology, USA) to obtain crude phage filtrates.

Subsequently, a spot test was performed to determine the presence of phages as previously described (19). Briefly, 100  $\mu\text{l}$  of exponential-phase ( $\text{OD}_{600} = 0.4$ – $0.5$ ) culture of the bacterial host was mixed with 3 ml of soft agar (0.3% w/v agar) held at  $50^{\circ}\text{C}$ , then poured onto modified nutrient agar (MNA) plates so as to create a bacterial lawn, and allowed to solidify for 15 min. Ten microliters of each crude phage filtrate was spotted on bacterial lawn, and the plates were incubated at  $37^{\circ}\text{C}$  for 24 h. After

incubation, the plates were observed for the presence of clear zones or plaques at inoculated points. Plaques were picked using a sterile pipette tip and suspended in 1 ml of lambda diluent [10 mM of Tris Cl (pH 7.5), 8 mM of MgSO<sub>4</sub>·7H<sub>2</sub>O] in 2-μl Eppendorf tubes. The tubes were left at room temperature to allow phages to diffuse into the solution. The tubes were then centrifuged at 11,000 × g for 10 min, and the supernatant was filter-sterilized with a 0.22-μm pore-size Acrodisc syringe filter (GVS Filter Technology, Germany).

## Bacteriophage Purification and Propagation

Bacteriophages were purified from single plaque isolates using the soft agar overlay method (21, 22). Plaque assay was performed, and the plates were incubated at 37°C for 24 h. After incubation, single plaques from each plate were picked based on their sizes and clarity using a sterile pipette tip and were resuspended in 1 ml of lambda diluent in 2-μl Eppendorf tubes. The tubes were left at 4°C for 24 h to allow phage to diffuse into the buffer. The tubes were then centrifuged at 10,000 × g for 10 min, and the supernatant was filter-sterilized using a 0.22-μm pore-size Acrodisc syringe filter (GVS Filter Technology, Germany). The purification process was repeated three consecutive times until homogeneous plaques were obtained for each phage isolate. Purified phages were propagated using *E. coli* O177 host bacteria. One hundred microliters of pure phage stocks was mixed with 100 μl of exponential-phase (OD<sub>600</sub> = 0.4–0.5) culture of corresponding host(s) in a 50-ml falcon tube containing sterile 10-ml double-strength TSB supplemented with 2 mM of CaCl<sub>2</sub>. The mixture was incubated in a shaking incubator (150 rpm) at 37°C for 24 h. After incubation, the samples were centrifuged at 8,000 × g for 10 min at 4°C, and the supernatant was filter-sterilized using a 0.22-μm pore-size Acrodisc syringe filter (GVS Filter Technology, Germany). Ten-fold serial dilutions were prepared, phage titers were determined using plaque assay, and the titers were expressed as PFU per milliliter. The stock phages were stored at 4°C for further analysis.

## Characterization of Selected *E. coli* O177-Specific Bacteriophages Host Range and Cross Infectivity of the Phage Isolates

The host range of eight selected phage isolates was evaluated against 50 bacterial hosts [13 *E. coli* O177, 12 *E. coli* O157, 12 *E. coli* O26, and 10 *Salmonella* species (environmental strains), 1 *Pseudomonas aeruginosa* (ATCC 27853), 1 *Salmonella enterica* (ATCC 12325), and 1 *Salmonella typhimurium* (ATCC 14028)], and all environmental species were isolated from cattle feces. Phage isolates were selected based on different plaque morphologies and clarity of the plaques and sizes. The spot test technique was performed to determine lytic spectrum activity of each phage isolates as previously described (21). The bacterial lawns of all the selected bacterial hosts were prepared on MNA plates. Ten microliters of phage stock (10<sup>7</sup>–10<sup>9</sup> PFU/ml) was spotted on bacterial lawn and allowed to air-dry under laminar

airflow for 10 min. The plates were incubated at 37°C for 24 h. After incubation, the plates were observed for the presence of plaques at the point of application, and the phage lytic profiles were classified into three categories according to their clarity: clear, turbid, and no lysis (23). The test was performed in triplicates for each phage isolate.

## Efficiency of Plating of Phages

Efficiency of plating (EOP) was performed to determine lytic efficiency of the phage in comparison with their suitable host bacteria as previously described (24), with modification. Fifteen bacterial strains (five *E. coli* O177, five *E. coli* O26, and five *E. coli* O157) were selected based on their sensitivity against the phages. Ten-fold serial dilutions of phages were prepared to obtain single plaques. An aliquot of 100 μl of each phage (1 × 10<sup>4</sup> PFU/ml) was mixed with 100 μl of exponential-phase (OD<sub>600</sub> = 0.4–0.5) culture of each bacterium in 50-ml sterile falcon tubes and left for 10 min at room temperature to allow the phage to attach to the host. Then, 3 ml of soft agar (0.3% w/v) was added to the tube, and the mixture was poured onto MNA plates. Three independent assays were performed for each phage isolate. After solidifying, the plates were incubated at 37°C for 24 h. After incubation, the number of plaques per plate was counted. The EOP was calculated as the ratio between the average number of plaques on target host bacteria (PFUs) and average number of plaques of reference host bacteria (PFUs). The EOP was classified as high (EOP ≥ 0.5), moderate (EOP > 0.01 < 0.5), and low (EOP ≤ 0.1) based on the reproducible infection on the targeted bacteria (25). The following formula was used to calculate EOP values:

$$\text{Relative EOP} = \frac{\text{average number of plaques on targeted host bacteria (PFUs)}}{\text{average number of plaques on reference host bacteria (PFUs)}}$$

## Transmission Electron Microscopy Analysis

Eight phage isolates were subjected to transmission electron microscopy (TEM), and phage morphotype was determined using negative staining techniques as previously described (26), with some modifications. Briefly, phages were propagated to obtain high titer (10<sup>8</sup>–10<sup>11</sup> PFU/ml). Ten milliliters of each phage (10<sup>8</sup>–10<sup>11</sup> PFU/ml) was concentrated in 50-ml falcon tubes by adding 10% (w/v) PEG, and the mixture was incubated at 4°C overnight to allow precipitation of the phage particles. After incubation, phage particles were sedimented by centrifugation at 11,000 × g for 10 min at 4°C. The supernatant was discarded, and the pellet was washed three times with 0.1 M ammonium acetate (pH 7.0). The pellet was resuspended in 200 μl of ammonium acetate. Ten microliters of concentrated phage solution was deposited on 200-mesh copper grids with carbon-coated formvar films. The phage particles were allowed to adsorb for 2 min, and excess liquid was drained off with a sterile filter paper. The grid was allowed to air-dry. A drop of 1% (w/v) ammonium molybdate (aqueous, pH 6.5) was added to negatively stain the phage particles and allowed to air-dry for 10–15 min. The grid containing the specimen (phage particles)

was then loaded into a transmission electron microscope (model: FEI Tecnai; TEM, Czech Republic) and operated at 120 kV to scan and view phage images with a magnification range of 20,000–100,000. Micrographs were taken with a Gatan bottom-mounted camera using Digital Micrograph software at 80 kV and a magnification range of 20,000–250,000. The images were taken, and morphology characteristics were used to classify phage isolates as previously described (27).

## Effect of Different Temperatures and pH on the Stability and Viability of Phages

Phage stability and viability were evaluated across different temperatures (37 and 40°C) over a 60-min period in a temperature-controlled incubator. The concentration of the host bacteria and phage titers was standardized before starting the experiment. One hundred microliters of exponential-phase culture [ $10^5$  colony-forming unit (CFU)/ml] and 100  $\mu$ l of phages ( $10^5$  PFU/ml) was added to 10 ml of double-strength TSB supplemented with 2 mM of  $\text{CaCl}_2$ . The tubes were incubated in a preset shaking incubator at 37 and 40°C for 60 min, and samples were taken at 10, 30, and 60 min of incubation and assessed for viability and concentration using double-layer agar (22). Plaque assay was performed in triplicates for each sample, and the results were expressed as PFU per milliliter. For pH, phages were exposed to different pH levels (3.0, 4.5, 6.3, 7.0, 8.5, and 10.0) in a 48-h incubation period. Ten milliliters of sterile double-strength TSB (amended with 2 mM of  $\text{CaCl}_2$ ) was distributed into 50-ml falcon tubes to prepare different pH solutions. The pH was adjusted using hydrochloric acid (HCL, 6M) or sodium hydroxide (NaOH, 6M). One hundred microliters of each bacterial host ( $10^5$  CFU/ml) and their corresponding phage ( $10^5$  PFU/ml) isolates were added to 10 ml. The tubes were incubated in a preset shaking incubator (80 rpm) at 37°C for 48 h. Samples were taken at 24 and 48 h of incubation, and the phage titer for each sample was determined using the standard plaque assay. Plaque assay was performed in triplicates for each sample, and the results were expressed as PFU per milliliter.

## One-Step Growth Curve

A one-step growth curve experiment was performed to determine the latent period and burst size of the selected phages as previously described (21), with some modifications. Briefly, 5 ml of exponential-phase culture of each host was centrifuged at  $8,000 \times g$  for 5 min at 4°C. The pellet was resuspended in 10 ml of double-strength TSB supplemented with 2 mM of  $\text{CaCl}_2$  to obtain an OD of 0.4–0.5 (600 nm). The bacterial concentration was adjusted using sterile double-strength TSB to obtain  $1 \times 10^8$  CFU/ml. Each phage ( $10^8$  PFU/ml) was added to its respective host bacterial suspension to achieve multiplicity of infection (MOI) 1.0. The mixture was left at room temperature for 10 min to allow phages to adsorb to the host bacteria. After 10 min, 1.5  $\mu$ l of the mixture was transferred into 2- $\mu$ l Eppendorf tubes and centrifuged at  $11,000 \times g$  for 10 min to remove unadsorbed phage particles. The pellet was resuspended in 100  $\mu$ l of TSB supplemented with 10 mM of magnesium sulfate (mTSB) and transferred into 9.9 ml of prewarmed mTSB. The samples were incubated in a shaking incubator (160 rpm) at 37°C for 1 h.

Two hundred microliters was drawn from each sample at 5-min intervals for 60 min. Plaque assay was performed in triplicates for each samples to determine phage titer. The data generated were used to determine the latent period, burst time, and phage relative burst size per infected cell. The burst size was calculated as the ratio of the final count of released phage progeny to the initial count of infected bacterial host cell during the latent period using the following formula as previously described (28):

$$\text{Relative burst size} = \frac{\text{final titer (PFU)} - \text{initial titer (PFUs)}}{\text{initial titer (PFUs) (PFUs)}}$$

The relative burst size at different time points was plotted against time to determine the latent period and burst size of each phage isolate.

## Statistical Analysis

The viability and stability of phages were tested at different temperatures and pH levels. The data were converted to  $\log_{10}$  PFU per milliliter and analyzed using SAS (2010). The effect of temperature, time, and phage type on viability and stability of phages was analyzed using the general linear model (GLM) procedure of SAS (2010) for a 2 (temperature)  $\times$  3 (time)  $\times$  8 (phages) factorial treatment arrangement according to the following model:

$$Y_{ijkl} = \mu + T_i + S_j + V_k + (T \times S)_{ij} + (T \times V)_{ik} + (S \times V)_{jk} + (T \times S \times V)_{ijk} + E_{ijkl}$$

where  $Y_{ijkl}$  is the observation of the dependent variable  $ijkl$ ;  $\mu$  is the fixed effect of population mean for the variable;  $T_i$  is the effect of temperature;  $S_j$  is the effect of time;  $V_k$  is the effect of phages;  $(T \times S)_{ij}$  is the effect of interaction between temperature at level  $i$  and time at level  $j$ ;  $(T \times V)_{ik}$  is the effect of interaction between temperature at level  $i$  and phage at level  $k$ ;  $(S \times V)_{jk}$  is the effect of interaction between time at level  $j$  and phage at level  $k$ ;  $(T \times S \times V)_{ijk}$  is the effect of interaction between temperature at level  $i$ , time at level  $j$ , and phage at level  $k$ ; and  $E_{ijkl}$  is the random error associated with observation  $ijkl$ .

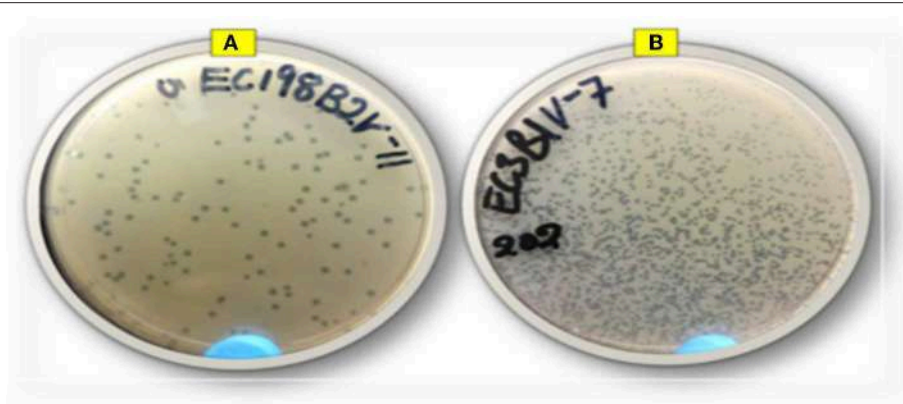
Phage viability and stability data in response to incremental levels of pH were evaluated for linear and quadratic effects using polynomial contrasts. Response surface regression analysis (Proc RSREG; SAS 2010) was applied to describe the responses to pH according to the following quadratic model:  $y = a + bx + cx^2$ , where  $y$  is the response variables,  $b$  and  $c$  are the coefficients of the quadratic equation,  $a$  is the intercept,  $x$  is the pH level, and  $-b/2c$  is the  $x$  value for maximum response. For all statistical tests, significance was declared at  $p \leq 0.05$ .

## RESULTS

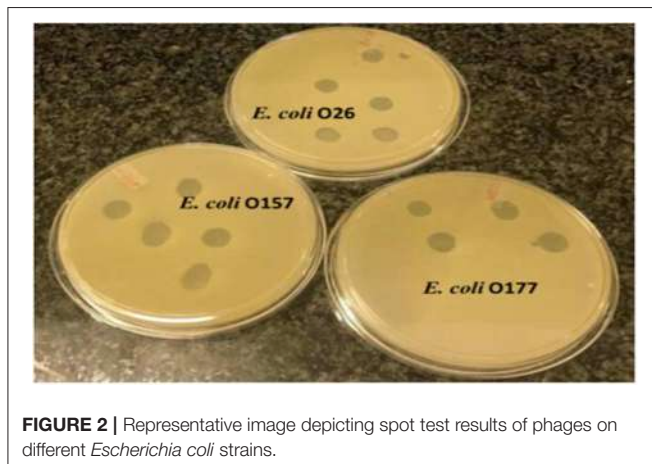
### Isolation, Purification, and Propagation of Bacteriophages

Thirty-one lytic *E. coli* O177-specific bacteriophages were isolated from cattle feces. Phages were able to infect 15% of the *E. coli* O177 isolates used for isolation. Phage isolates were designated as ECPV, according to the genus of the host bacteria,





**FIGURE 1** | Representative image of phage isolates depicting different plaque morphologies: **(A)** EC198B2PV (large plaques) and **(B)** EC3B1PV (small plaques).



**FIGURE 2** | Representative image depicting spot test results of phages on different *Escherichia coli* strains.

followed by the notation of phage virus and a numeric number as identity. Phage isolates revealed different plaque morphologies in terms of sizes, ranging from small to large (1–2 mm, respectively) plaques (Figure 1). A large proportion (71%) of the phage isolates revealed large plaques, while a small proportion (29%) showed small plaques on their preferred hosts. All the phages revealed clear (complete lysis) plaques, and no turbid plaques were observed. Phage titer after propagation ranged from  $6.2 \times 10^5$  to  $3.1 \times 10^{13}$  PFU/ml. Phage EC3A2PV had the lowest titer, while phage EC198B1PV had the highest titer compared to other phage isolates.

### Host Range of Phages and EOP Analysis Against Different *E. coli* Strains

A spot test was performed to determine the host range of eight selected lytic phage isolates against 50 bacterial hosts comprising different bacterial species. The results indicated that the phages were capable of infecting *E. coli* species (*E. coli* O177, *E. coli* O157, and *E. coli* O26 environmental strains) tested (Figure 2). All phage isolates produced clear plaques against all *E. coli* O177 and 83–100% of *E. coli* O26 strains (Table 1). Three phages

(EC10C3PV, EC11B2PV, and EC12A1PV) were able to infect *E. coli* O157 (75–83%; Table 2). None of the phages could infect ATCC strains and environmental *Salmonella* species. The EOP analysis was performed on 15 (five *E. coli* O177, five *E. coli* O26, and five *E. coli* O157) isolates that were susceptible to phages on the spot test. Although spot test results revealed clear plaques on *E. coli* O177, EOP results exhibited various lytic patterns of the phages. Even though EOP analysis revealed high (EOP  $\geq 0.5$ ) productive infection on *E. coli* O177, moderate infections were observed (Table 2). Four phages revealed high EOP values (0.5–0.8) on *E. coli* O177 isolates. On the other hand, EOP analysis exhibited moderate and low productive infections on *E. coli* O26 and *E. coli* O157 isolates (EOP values range from 0.0 to 0.4 and 0.0 to 0.3, respectively).

### Morphological Characterization of Phages Based on TEM

Eight selected phage isolates were subjected to TEM analysis to determine their morphotype. Transmission electron micrograph images of the phages and structural dimensions are shown in Figure 3 and Table 3, respectively. Phage isolates were classified as per the International Committee on Taxonomy of Virus (ICTV) classification based on the three-dimensional structure observed. All phage isolates showed similar morphotype on TEM analysis. Structurally, the phages had an icosahedral head and a neck attached to a long contractile tail, with tail fibers, and they were classified under the order Caudovirales, *Myoviridae* family. The phage icosahedral heads ranged from  $81.2 \pm 6$  to  $95.6 \pm 3$  nm while the contractile tails ranged from  $118.1 \pm 0.3$  to  $135 \pm 2$  nm. Phage EC10C2PV had the longest icosahedral head with a diameter of  $95.6 \pm 3$  nm and the longest contractile tail of  $135 \pm 2$  nm with fibers. Phage EC10C3PV had the smallest icosahedral head with a diameter of  $81.2 \pm 6$  nm and the shortest contractile tail of  $118.1 \pm 0.3$  nm with fibers.

### Phage Stability and Viability Against Different Temperatures

The results showed a significant ( $p < 0.001$ ) time  $\times$  temperature interaction effect on the stability and viability of the phages.

**TABLE 1 |** Host range infection of the phages.

Host bacteria	No.	Phage host range (%)							
		EC366VPV	EC11B2PV	EC10C2PV	EC12A1PV	EC3A1PV	EC118BPV	EC366BPV	EC10C3PV
<i>Pseudomonas aeruginosa</i> <sup>a</sup>	1	1 (0%)	1 (0%)	1 (0%)	1 (0%)	1 (0%)	1 (0%)	1 (0%)	1 (0%)
<i>Salmonella enterica</i> <sup>b</sup>	1	1 (0%)	1 (0%)	1 (0%)	1 (0%)	1 (0%)	1 (0%)	1 (0%)	1 (0%)
<i>Salmonella typhimurium</i> <sup>c</sup>	1	1 (0%)	1 (0%)	1 (0%)	1 (0%)	1 (0%)	1 (0%)	1 (0%)	1 (0%)
<i>Escherichia coli</i> O177 <sup>d</sup>	13	13 (100%)	13 (100%)	13 (100%)	13 (100%)	13 (100%)	13 (100%)	13 (100%)	13 (100%)
<i>E. coli</i> O26 <sup>d</sup>	12	12 (100%)	10 (83%)	11 (92%)	11 (92%)	10 (83%)	11 (92%)	11 (92%)	11 (92%)
<i>E. coli</i> O157 <sup>d</sup>	12	12 (0%)	9 (75%)	12 (0%)	10 (83%)	12 (0%)	12 (0%)	12 (0%)	10 (83%)
<i>Salmonella species</i> <sup>d</sup>	10	10 (0%)	10 (0%)	10 (0%)	10 (0%)	10 (0%)	10 (0%)	10 (0%)	10 (0%)

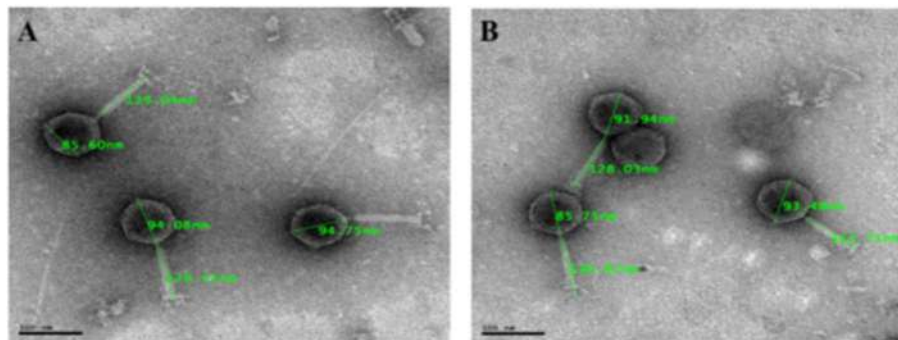
<sup>a,b,c,d</sup>ATCC 27853, ATCC 12325, ATCC 14028, and environmental strains, respectively.

**TABLE 2 |** Efficacy of plating of phages against different *Escherichia coli* serotypes.

Bacterial strain	Bacteria ID	EOP ratio of phage isolates							
		EC10C2PV	EC10C3PV	EC118BPV	EC11B2PV	EC12A1PV	EC366BPV	EC366VPV	EC3A1PV
<i>E. coli</i> O177	CF-D-D202	0.7	0.8	0.6	0.5	0.7	0.8	0.8	1.0 <sup>a</sup>
	CF-A27	0.5	0.6	0.7	0.7	1.0 <sup>a</sup>	0.8	0.7	0.6
	CF-H361	1.0 <sup>a</sup>	1.0 <sup>a</sup>	0.5	0.6	0.8	0.8	0.6	0.7
	CF-A28	0.4	0.7	0.5	1.0 <sup>a</sup>	0.5	0.5	1.0 <sup>a</sup>	0.8
	CF-D-D246	0.7	0.9	1.0 <sup>a</sup>	0.8	0.8	1.0	0.8	0.7
<i>E. coli</i> O26	2A	0.3	0.2	0.4	0.1	0.0	0.4	0.2	0.0
	4C	0.3	0.2	0.2	0.1	0.1	0.1	0.3	0.1
	17E	0.2	0.2	0.1	0.1	0.3	0.3	0.2	0.3
	21F	0.1	0.1	0.3	0.3	0.2	0.2	0.1	0.1
	25H	0.3	0.3	0.1	0.3	0.1	0.3	0.2	0.1
<i>E. coli</i> O157	1A	0.1	0.1	0.2	0.1	0.0	0.1	0.3	0.3
	3B	0.2	0.2	0.1	0.1	0.0	0.1	0.1	0.1
	5D	0.3	0.1	0.1	0.2	0.1	0.1	0.1	0.2
	7F	0.1	0.1	0.1	0.1	0.1	0.2	0.1	0.1
	8G	0.1	0.3	0.1	0.3	0.1	0.2	0.1	0.1

ID, identity.

<sup>a</sup>Reference host.



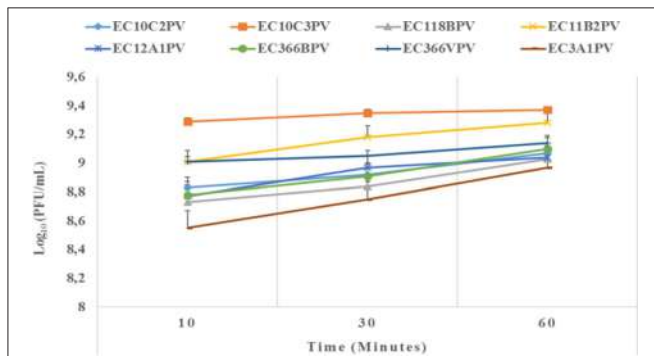
**FIGURE 3 |** Transmission electron micrograph images of representative phage isolates negatively stained with 1% ammonium molybdate. Both phages (**A**: EC11B2PV; **B**: EC118BPV) belong to the myoviridae family and are showing icosahedral capsid and long contractile tail with tail fibers. The bars indicate scale (100 nm).

Incubation of phages from 10 to 60 min resulted in significant phage growth at 37°C (**Figure 4**). The growth from 10 to 30 min ranged from 8.55 to 8.75 log<sub>10</sub> PFU/ml (at 37°C).

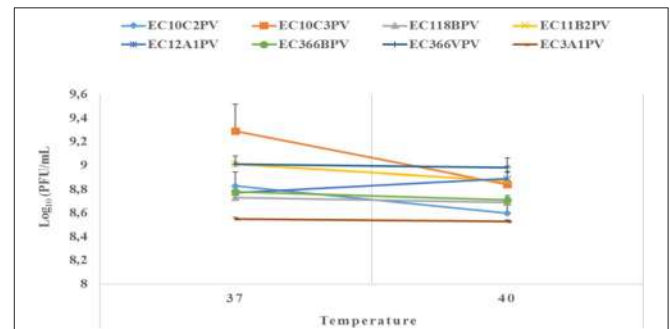
Phage EC3A1PV revealed the lowest growth rate, while phage EC10C3PV exhibited the fastest growth rate from 10 to 60 min. Phage growth at 40°C when incubated for 10 to 60 min is

**TABLE 3** | Phage dimensions based on transmission electron microscopy (TEM) analysis.

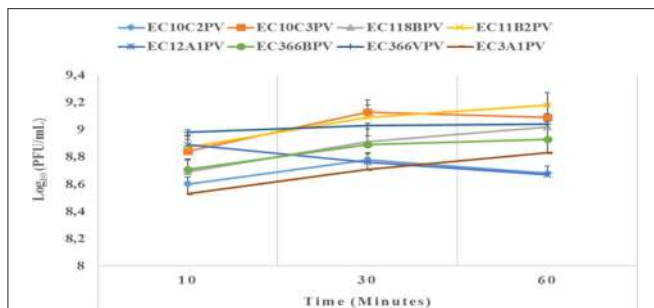
Phage ID	Phage morphotype				Order
	Head structure	Head dimensions (nm ± stdv)	Tail structure	Tail dimensions (nm ± stdv)	
EC366VPV	Icosahedral capsid	86.7 ± 2	Contractile sheath	120.3 ± 9	Caudovirales
EC11B2PV	Icosahedral capsid	91.5 ± 3	Contractile sheath	129.3 ± 0.2	
EC10C2PV	Icosahedral capsid	95.6 ± 3	Contractile sheath	135 ± 2	
EC366APV	Icosahedral capsid	88.5 ± 3	Contractile sheath	129.8 ± 3	
EC12APV	Icosahedral capsid	87.8 ± 2	Contractile sheath	121.9 ± 6	
EC118BPV	Icosahedral capsid	90.4 ± 3	Contractile sheath	123.9 ± 6	
EC3A1PV	Icosahedral capsid	85.6 ± 1	Contractile sheath	119.3 ± 1	
EC10C3PV	Icosahedral capsid	81.2 ± 6	Contractile sheath	118.1 ± 0.3	



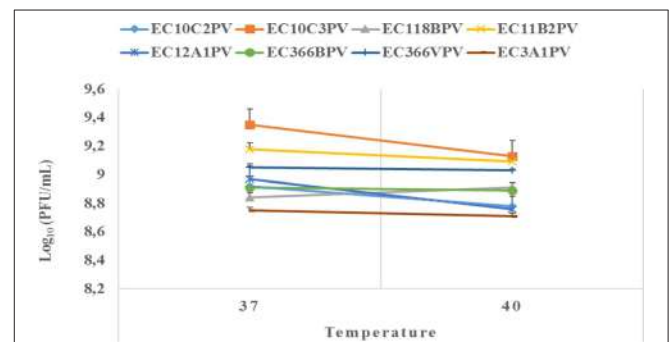
**FIGURE 4** | Effect of time on persistence (stability/survivability) of individual phages at 37°C. The error bars represent the standard deviation. PFU, plaque-forming unit.



**FIGURE 6** | Survival and stability of individual phages when exposed to different temperatures for 10 min. The error bars represent the standard deviation. PFU, plaque-forming unit.



**FIGURE 5** | Effect of time on persistence (stability/survivability) of individual phages at 40°C. The error bars represent the standard deviation. PFU, plaque-forming unit.

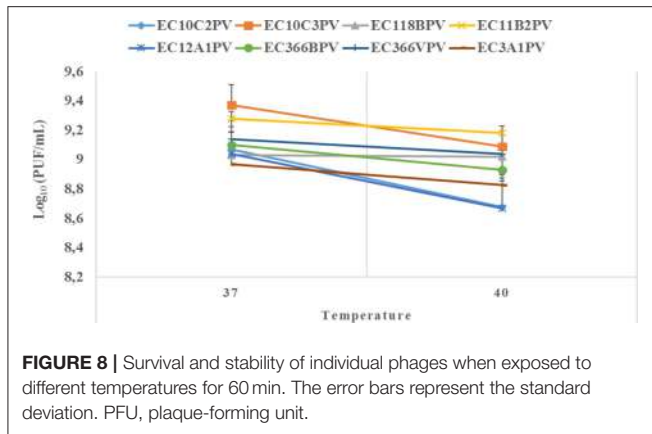


**FIGURE 7** | Survival and stability of individual phages when exposed to different temperatures for 30 min. The error bars represent the standard deviation. PFU, plaque-forming unit.

depicted in **Figure 5**. From 10 to 30 min, seven phages revealed significant growth rates (ranging from 8.71 to 9.13 log<sub>10</sub> PFU/ml). A decrease in phage EC12A1PV's growth rate was observed (from 10 to 60 min) while two phages (EC10C2PV and EC10C3PV) exhibited a decrease in growth rate from 30 to 60 min of incubation period.

An exposure of individual phages to 37°C for 10–30 min showed a significant increase in growth rate with time (0.4–2.3% growth rate at 37°C; **Figures 6, 7**). The average growth

rate of the phages increased from 0.2 to 0.17 log<sub>10</sub> PFU/ml at 37°C (10–30 min of incubation period). Phages revealed various responses when incubated at 40°C. A decline in growth rate in other phages was observed. When incubated for 10 min at 40°C, EC10C3PV's growth rate declined the most by 4.8%, while phage EC3A1PV's growth rate was the least affected, showing only a 0.2% decline. After 30 min of incubation, a decline in growth rate was observed in phages EC366BPV (0.2%), EC366VPV (0.2%), and EC10C3PV (2.4%) (**Figure 7**). When incubated for 60 min at 40°C, phages EC10C2PV (0.28 log<sub>10</sub> PFU/ml), EC10C3PV (0.39



log<sub>10</sub> PFU/ml), and EC12A1PV (0.37 log<sub>10</sub> PFU/ml) exhibited the greatest decline in growth rates when compared to their respective rates for 60 min at 37°C (Figure 8).

### Phage Stability and Viability Against Different pH Levels

Response surface regression analysis revealed quadratic effects ( $p < 0.0001$ ) of pH on phage stability when incubated for 24 and 48 h (Figures 9A–H, 10A1–H1, respectively). The pH optima for all the phages ranged from 7.6 to 8.0 with the  $R^2$  values ranging from 0.90 to 1.0 when incubated for 24 h (Figures 9A–H). Three phages showed maximum stability at pH 8.0 determined from the following quadratic equations:  $y = -13.9 (\pm 2.93) + 6.4 (\pm 0.98)x - 0.4 (\pm 0.07)x^2$  (EC10C2PV),  $y = -13.9 (\pm 3.04) + 6.4 (\pm 1.01)x - 0.4 (\pm 0.08)x^2$  (EC366BPV), and  $y = -13.9 (\pm 2.97) + 6.4 (\pm 0.99)x - 0.4 (\pm 0.08)x^2$  (EC366VPV). Phages EC10C3PV and EC11B2PV exhibited maximum stability at pH 7.6, which was determined from the following quadratic equations:  $y = -13.4 (\pm 2.87) + 6.1 (\pm 0.95)x - 0.4 (\pm 0.07)x^2$  and  $y = -13.5 (\pm 2.94) + 6.1 (\pm 0.98)x - 0.4 (\pm 0.07)x^2$ , respectively. When incubated for 48 h, pH optima for phage stability ranged from 7.9 to 8.0 with  $R^2$  values ranging from 0.90 to 1.0 (Figures 10A1–H1). Seven phages exhibited maximum stability at a higher (8.0) optimum pH while only one phage showed maximum stability at a lower (7.9) pH determined from the quadratic equation  $y = -13.8 (\pm 3.10) + 6.3 (\pm 1.03)x - 0.4 (\pm 0.08)x^2$ .

### One-Step Growth Curve Bacteriophages

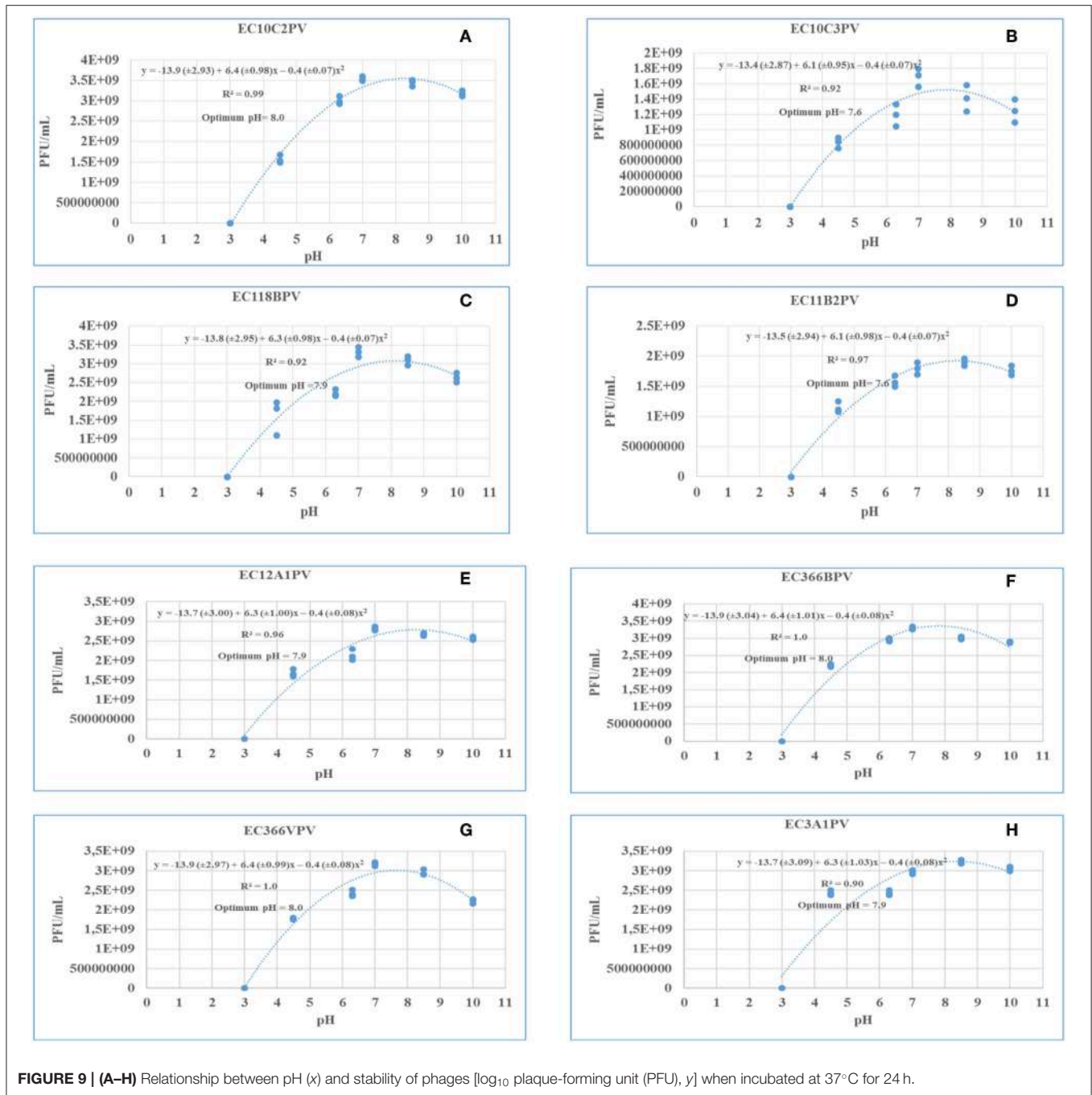
A one-step growth curve analysis for the eight phage isolates was performed to determine the latent period and relative burst size per infected bacterial cell. Data generated were analyzed and used to construct triphasic curves (Figures 5–11A–H). The latent period for all the phages ranged from 15 to 25 min (average =  $20 \pm 3.8$  min). Phages EC11B2PV and EC3A1PV had the longest latent period (25 min), while phages EC118BPV and EC366VPV had the shortest (15 min) latent period. The latent period for the other four phages was 20 min. In terms of burst size, phages EC10C3PV and EC12A1PV had the largest burst size per infected cell (522 and 367 PFUs, respectively), while phage EC366VPV had the smallest burst size (91 PFUs) per infected cell.

## DISCUSSION

The emergence of antibiotic resistance in foodborne pathogens has revitalized interest in the possible exploitation of lytic bacteriophages as an alternative biocontrol strategy. Because of their ability to lyse multidrug-resistant pathogens, lytic bacteriophages are considered as a natural and green technology for food preservation and safety (29). The isolation, identification, and full characterization of the bacterial host is a prerequisite for the successful isolation of suitable lytic bacteriophages intended for biocontrol of antimicrobial foodborne pathogens (30). Furthermore, reliable, reproducible, and efficient methods need to be employed for selection of suitable phage candidates for biocontrol application (31). In this study, 31 lytic *E. coli* O177-specific bacteriophage isolates were successfully isolated from cattle feces using multidrug-resistant atypical enteropathogenic *E. coli* O177 as a host. Since cattle are the main reservoirs of the atypical enteropathogenic *E. coli* O177 strain, this supports the idea that phages are present in every ecosystem where their hosts exist (4). The phages exhibited clear and discrete plaques with different sizes. The plaque size ranged between small and large (1–2 mm, respectively) sizes while phage titers ranged from  $6.2 \times 10^5$  to  $3.1 \times 10^{13}$  PFU/ml. Interestingly, a large proportion (71%) of phage isolates produced large and clear plaques on their preferred hosts. These characteristics were similar to those reported for *E. coli* O157-, *Listeria*-, *Pseudomonas*-, *Salmonella*-, and *Vibrio*-specific phages (23, 32, 33). From a biocontrol point of view, strictly lytic phages with high titers are considered as ideal candidates for biocontrol application (4, 34).

Host range is one of the most important criteria when selecting phages intended for biocontrol of antimicrobial foodborne pathogens (35). Eight phages were selected to determine phage host range. The selection criteria were based on the lytic profiles, plaque clarity, and size of the phages. A spot test revealed that the phages were capable of infecting different *E. coli* strains from two different categories [environmental atypical enteropathogenic *E. coli* O177 and Shiga toxin-producing *E. coli* (*E. coli* O26 and *E. coli* O157)]. Clear plaques were predominantly observed on *E. coli* O177 and *E. coli* O26 serotypes. Interestingly, three phages exhibited clear plaques on *E. coli* O177, *E. coli* O26, and *E. coli* O157 strains, suggesting that these phages were polyvalent, infecting strains from two different categories. Despite this, no phage could infect all the ATCC strains and environmental *Salmonella* species tested in this study. This could be attributed to the fact that ATCC strains and *Salmonella* species lack specific receptors for phage attachment. Based on EOP analysis, phages revealed high efficiency (EOP  $\geq 0.5$ ) on the *E. coli* O177 strain. Despite the fact that all the phages revealed clear plaques on *E. coli* O26 and O157 strains on the spot test, only three phages exhibited medium to low EOP (<0.5) on *E. coli* O26 and O157 serotypes. This suggested that phages were highly specific to the *E. coli* O177 strain. Moreover, host specificity is regarded as a desirable characteristic for potent phage application, particularly in live animals to ensure that they have little or no impact on the beneficial gut microflora (2, 6). Furthermore, infectivity variation might be due to the

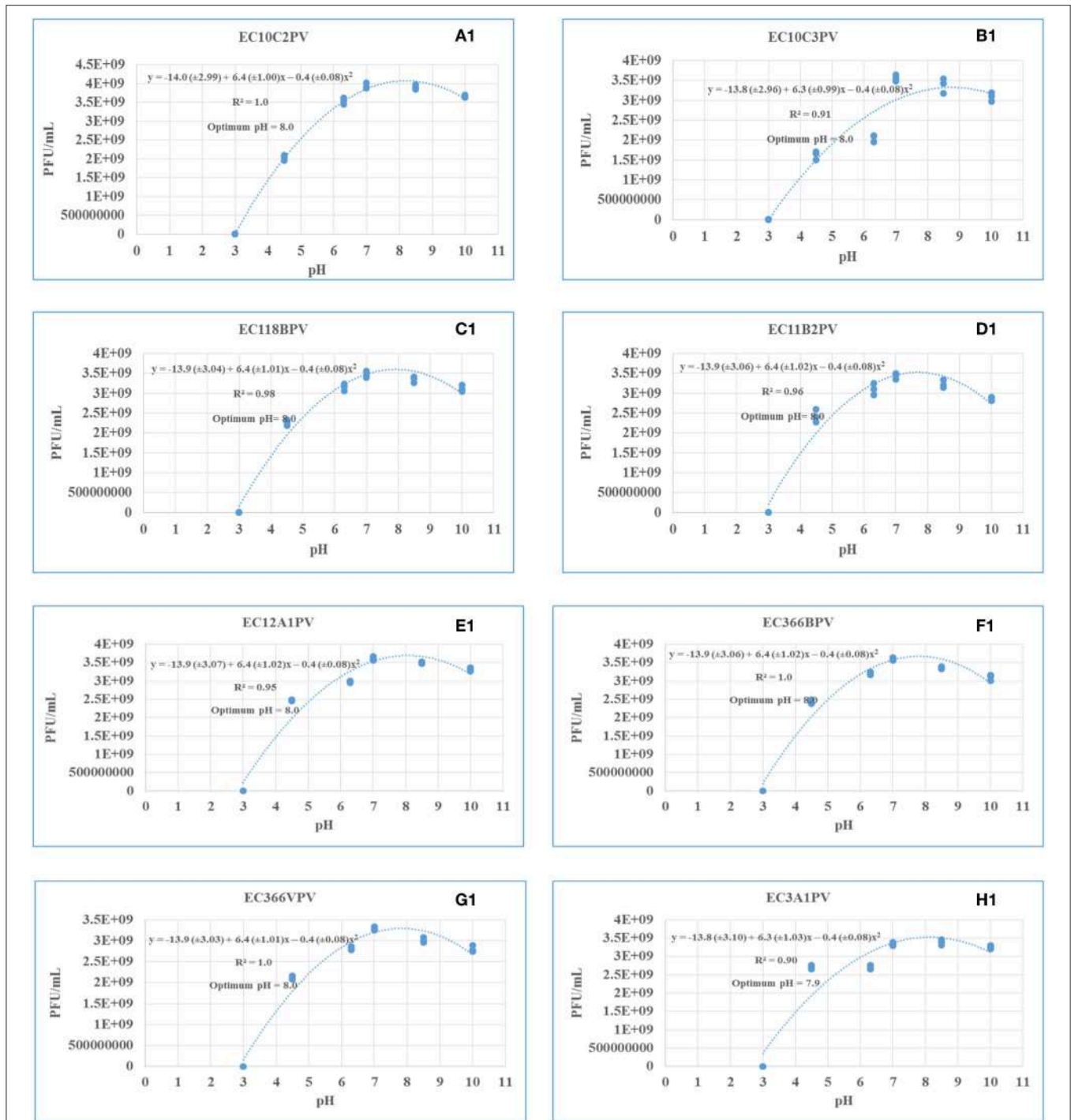




non-specific binding receptors on the host cell wall or the presence of phage-resistant strains (6).

A negative staining procedure was used for TEM analysis. Based on TEM results, all eight phage isolates revealed a similar morphotype. Structurally, the phages had an icosahedral head and a neck attached to a long contractile tail with tail fibers connected to the baseplate. The icosahedral head of the phages ranged from  $81.2 \pm 6$  to  $95.6 \pm 3$  nm in size while the contractile tails ranged from  $118.1 \pm 0.3$  to  $135 \pm 2$  nm. Based on these characteristics, phage isolates were classified under the

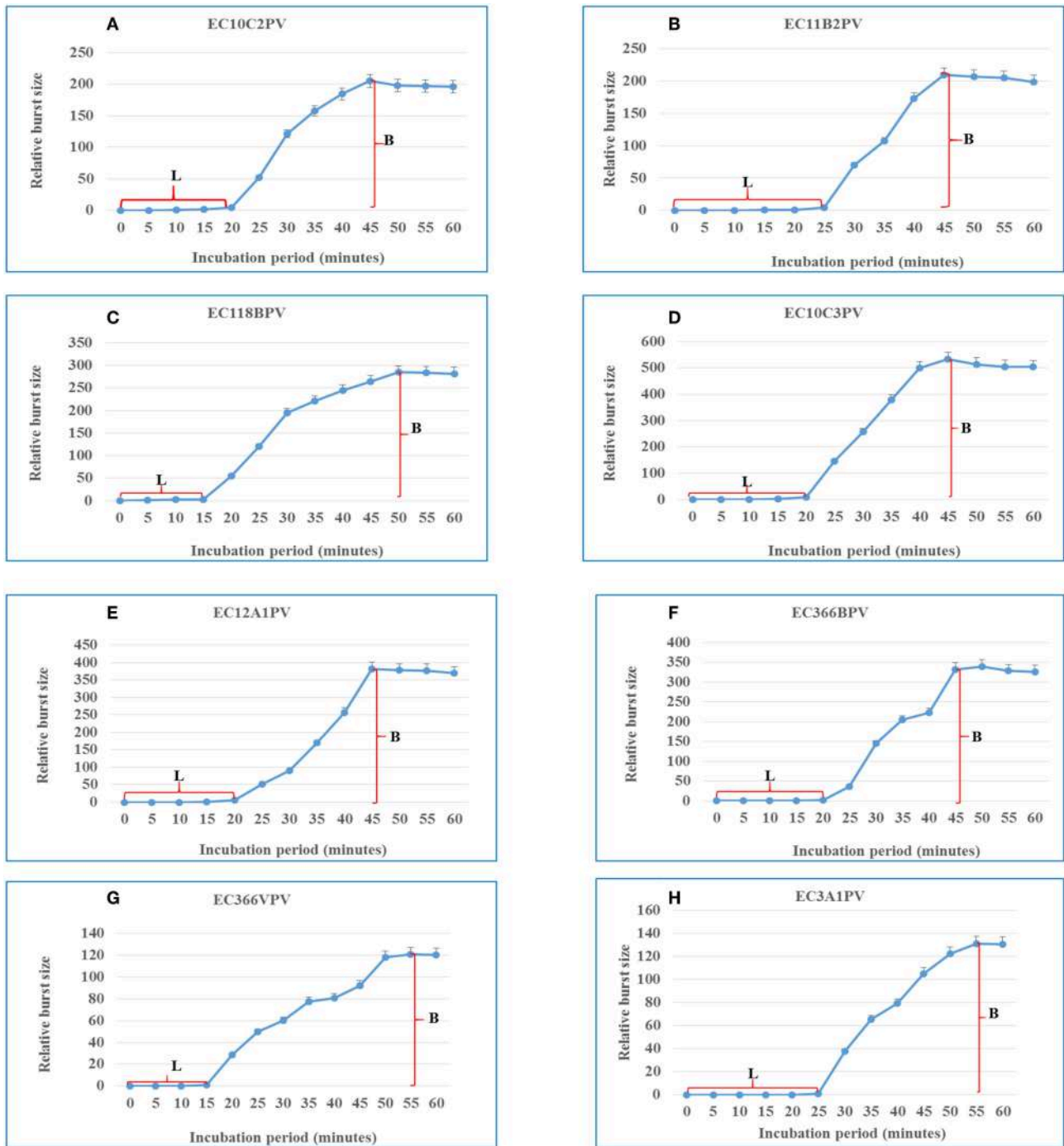
order Caudovirales and *Myoviridae* family (27). Moreover, these characteristics were similar to those of T1-7-like *E. coli* phages (4, 36). Given the fact that the *Myoviridae* family contains double-stranded DNA phages (4), all eight phages were presumptively classified under linear double-stranded DNA phages. The tail fibers contain proteins, which help the phage to recognize their specific receptors on the bacterial cell wall and thus restrict the phage from binding to non-specific bacterial cell (37). This explains the host specificity of the phages isolated in this study.



**FIGURE 10 | (A1–H1)** Relationship between pH (x) and stability of phages [ $\log_{10}$  plaque-forming unit (PFU), y] when incubated at 37°C for 48 h.

External factors such as pH and temperature may influence the stability and infectivity of the phages (7). These factors may fluctuate, particularly in live animals because of diet and/or ambient temperature. In view of this, phages intended for biocontrol application, particularly in live ruminants, must be tested against an appropriate range of pH and

temperature. For this reason, the effect of exposure to different temperatures (37 and 40°C) for different times on infectivity and stability of eight phages was evaluated. Given that complete bacterial lysis by phage takes 20–40 min (33), phage growth at different temperatures was monitored after 10, 30, and 60 min. Furthermore, the incubation temperatures were selected because



**FIGURE 11 | (A–H)** One-step growth curves for eight *Escherichia coli* O177-specific phage isolates. Latent period (L) and burst size (B). The error bars indicate standard deviation.

the temperature in the digestive system of the ruminant ranges from 37 to 40°C. The ability of phages to survive at these temperatures suggests that they can be applied in live animals as biocontrol agents. When incubated at 37°C, phages revealed a significant growth rate at each time point. Phages EC10C3PV, EC11B2PV, and EC366VPV revealed the fastest growth rates;

phage EC3A1PV showed the slowest growth rate from 10 to 60 min. These results are similar to those reported in previous studies (28).

Phages revealed variable growth patterns when exposed to 40°C. Generally, phages showed a decline in growth rate at 40°C when compared to their growth rate at 37°C. When exposed

to 40°C for 10–30 min, seven phages exhibited a significant growth rate. However, one phage revealed a decline in growth rate after 30 min while two phages, EC10C2PV and EC10C3PV, only exhibited a decline in growth from 30 to 60 min at 40°C. This demonstrates that these three phages were less stable at high temperature and, therefore, their application in live animals is limited because the rumen temperature is 39°C. Despite this, the other five phages were fairly stable at 40°C, suggesting they may be suitable for biocontrol application in live animals.

The response surface regression analysis revealed a significant relationship between pH and phage stability. The optimal pH for phages at different incubation times ranged from pH 7.6 to 8.0 (24 h) and pH 7.9 to 8.0 (48 h). When incubated for 24 and 48 h, all phages exhibited similar growth trends and survival over a wide range of pH (4.5–10.0). Despite this, all the phages were sensitive to low pH (3.0) with no activity being observed after 24 and 48 h of incubation at this pH. This is consistent with previous studies, which reported that exposure of phages to pH 3.0 and below significantly reduced the viability and stability of phages (38, 39). Although the optimum pH for all the phages is 7.6–8.0, phages revealed good stability even at lower pHs of 6.3 and 7.0, which encompasses rumen pH values (6.5–6.9). And this indicates their potential suitability for use in preharvest intervention strategies that may be designed for application in ruminants.

Phage latent period and burst size are important parameters to consider when selecting phages for biocontrol purposes (5, 31). Phages with a short latent period and large burst size are more effective in inactivating bacteria and are thus considered to be suitable for biocontrol application (35). One-step growth curves revealed that the eight phages have different patterns of growth, suggesting that they have distinct genotypes. They displayed outstanding characteristics such as short latent periods and large burst sizes, which make them attractive for the control of the *E. coli* O177 strain. The latent period of phages ranged from 15 to 25 min, while the burst size ranged from 91 to 522 PFU per host cell. In addition, the average latent period for all the phages was  $20 \pm 3.8$  min while the burst size was  $260 \pm 144$  PFU per host cell. These results were consistent with those reported previously (35). Two phages, EC118BPV and EC366VPV, had the shortest latent period (15 min) while EC11B2PV and EC3A1PV had the longest latent period (25 min). Phages EC10C3PV, EC118BPV, and EC12A1PV had the largest burst size per infected cell (522 and 367 PFU per host cell, respectively). Interestingly, these three phages also showed broad host range in the spot test. This demonstrates that these phages are better suited for biocontrol application (40).

## REFERENCES

- Akhtar M, Viazis S, Diez-Gonzalez F. Isolation, identification and characterization of lytic, wide host range bacteriophages from waste effluents against *Salmonella enterica* serovars. *Food Control*. (2014) 38:67–74. doi: 10.1016/j.foodcont.2013.09.064
- Huang C, Shi J, Ma W, Li Z, Wang J, Li J, et al. Isolation, characterization, and application of a novel specific *Salmonella* bacteriophage in different food matrices. *Food Res Int*. (2018) 111:631–41. doi: 10.1016/j.foodres.2018.05.071

In conclusion, lytic bacteriophages infecting the *E. coli* O177 environmental strain were successfully isolated in this study. Furthermore, phages were capable of infecting three *E. coli* strains from two different categories, atypical enteropathogenic *E. coli* (*E. coli* O177) and Shiga toxin-producing *E. coli* (*E. coli* O26 and *E. coli* O157). Despite this, no phage could infect ATCC strains and environmental *Salmonella* species tested. Considering strong lytic activity, broad spectrum, and stability at different temperatures and pH levels, phages isolated in this study are considered as potential candidates for *in vivo* control of the *E. coli* O177 strain. However, further studies using appropriate *in vitro* and *in vivo* models are required to evaluate the efficacy of *E. coli* O177-specific phages in reducing *E. coli* O177 in live animals and meat products. Moreover, whole-genome sequence analysis is also required to determine the presence of undesirable genes in these phages.

## DATA AVAILABILITY STATEMENT

The datasets generated for this study are available on request to the corresponding author.

## ETHICS STATEMENT

The statement, Ethical clearance was obtained from the Faculty of Natural and Agricultural Sciences Ethics committee, North West University prior to the commencement of the study. An ethics number NWU-01223-19-S9 was assigned to the study.

## AUTHOR CONTRIBUTIONS

VM and CA conceived and designed the experiments, contributed reagents, material, and analysis tools. PM performed the experiments. PM, VM, and CA wrote the paper and data analysis.

## FUNDING

This research was supported financially by the National Research Foundation (Grant Number: 112543) and the North-West University Postgraduate Bursary.

## ACKNOWLEDGMENTS

The authors wish to thank Dr. Anine Jordaan for her technical support during TEM analysis for bacteriophages and Mr. B. J. Morapedi for his assistance in sample collection.

- Sillankorva SM, Oliveira H, Azeredo J. Bacteriophages and their role in food safety. *Int J Microbiol*. (2012) 2012:863945. doi: 10.1155/2012/863945
- Harada LK, Silva EC, Campos WF, Del Fiol FS, Vila M, Dabrowska K, et al. Biotechnological applications of bacteriophages: state of the art. *Microbiol Res*. (2018) 212–3:38–58. doi: 10.1016/j.micres.2018.04.007
- Niu Y, Johnson R, Xu Y, McAllister T, Sharma R, Louie M, et al. Host range and lytic capability of four bacteriophages against bovine and clinical human isolates of Shiga toxin producing *Escherichia coli* O157: H7. *J Appl Microbiol*. (2009) 107:646–56. doi: 10.1111/j.1365-2672.2009.04231.x



6. Akhtar M, Viazis S, Christensen K, Kraemer P, Diez-Gonzalez F. Isolation, characterization and evaluation of virulent bacteriophages against *Listeria monocytogenes*. *Food Control*. (2017) 75:108–15. doi: 10.1016/j.foodcont.2016.12.035
7. Yin Y, Liu D, Yang S, Almeida A, Guo Q, Zhang Z, et al. Bacteriophage potential against *Vibrio parahaemolyticus* biofilms. *Food Control*. (2019) 98:156–63. doi: 10.1016/j.foodcont.2018.11.034
8. Ateba CN, Bezuidenhout CC. Characterisation of *Escherichia coli* O157 strains from humans, cattle and pigs in the North-West Province, South Africa. *Int J Food Microbiol*. (2008) 128:181–8. doi: 10.1016/j.ijfoodmicro.2008.08.011
9. Akindolire M, Babalola O, Ateba C. Detection of antibiotic resistant *Staphylococcus aureus* from milk: a public health implication. *Int J Environ Res Public Health*. (2015) 12:10254–75. doi: 10.3390/ijerph120910254
10. Dlamini BS, Montso PK, Kumar A, Ateba CN. Distribution of virulence factors, determinants of antibiotic resistance and molecular fingerprinting of *Salmonella* species isolated from cattle and beef samples: suggestive evidence of animal-to-meat contamination. *Environ Sci Pollut Res*. (2018) 5:32694–708. doi: 10.1007/s11356-018-3231-4
11. WHO. *Listeriosis – South Africa*. (2018). Available online at: <https://www.who.int/csr/don/28-march-2018-listeriosis-south-africa/en/> (accessed March 07, 2019).
12. Barilli E, Vismarra A, Villa Z, Bonilauri P, Bacci C. ESβL *E. coli* isolated in pig's chain: genetic analysis associated to the phenotype and biofilm synthesis evaluation. *Int J Food Microbiol*. (2019) 289:162–7. doi: 10.1016/j.ijfoodmicro.2018.09.012
13. WHO. *WHO's First Ever Global Estimates of Foodborne Diseases Find Children Under 5 Account for Almost One Third of Deaths*. (2015). Available online at: <http://www.who.int/mediacentre/news/releases/2015/foodborne-disease-estimates/en/> (accessed February 25, 2019).
14. Farrokh C, Jordan K, Auvray F, Glass K, Oppegaard H, Raynaud S, et al. Review of Shiga-toxin-producing *Escherichia coli* (STEC) and their significance in dairy production. *Int J Food Microbiol*. (2013) 162:190–212. doi: 10.1016/j.ijfoodmicro.2012.08.008
15. Gould LH, Mody RK, Ong KL, Clogher P, Cronquist AB, Garman KN, et al. Increased recognition of non-O157 Shiga toxin-producing *Escherichia coli* infections in the United States during 2000–2010: epidemiologic features and comparison with *E. coli* O157 infections. *Foodborne Pathog. Dis*. (2013) 10:453–60. doi: 10.1089/fpd.2012.1401
16. Hungaro HM, Mendonça RCS, Gouvêa DM, Vanetti MCD, De Oliveira Pinto CL. Use of bacteriophages to reduce *Salmonella* in chicken skin in comparison with chemical agents. *Food Res Int*. (2013) 52:75–81. doi: 10.1016/j.foodres.2013.02.032
17. Chen J, Ren Y, Seow J, Liu T, Bang W, Yuk H. Intervention technologies for ensuring microbiological safety of meat: current and future trends. *Compr Rev Food Sci Food Safety*. (2012) 11:119–32. doi: 10.1111/j.1541-4337.2011.00177.x
18. Boatema S, Barney M, Drimie S, Harper J, Korsten L, Pereira L. Awakening from the listeriosis crisis: food safety challenges, practices and governance in the food retail sector in South Africa. *Food Control*. (2019) 104:333–42. doi: 10.1016/j.foodcont.2019.05.009
19. Sambrook J, Fritsch EF, Maniatis T. *Molecular Cloning: A Laboratory Manual*. 2nd Edn. Cold Spring Harbor, NY: Cold Spring Harbor Laboratory Press (1989).
20. Van Twest R, Kropinski AM. Bacteriophage enrichment from water and soil. In: *Bacteriophages. Methods in Molecular Biology*<sup>TM</sup>. Humana Press (2009). p. 15–21. doi: 10.1007/978-1-60327-164-6\_2
21. Adams MH, editor. Methods of study of bacterial viruses. *Bacteriophages*. New York, NY: Interscience Publishers (1959). p. 443–522.
22. Sambrook J, Russell DW. *Molecular Cloning: A Laboratory Manual*. 3rd Edn. Cold Spring Harbor, NY: Cold Spring Harbor Laboratory Press (2001).
23. Zhang H, Yang Z, Zhou Y, Bao H, Wang R, Li T, et al. Application of a phage in decontaminating *Vibrio parahaemolyticus* in oysters. *Int J Food Microbiol*. (2018) 275:24–31. doi: 10.1016/j.ijfoodmicro.2018.03.027
24. Kutter E. Phage host range and efficiency of plating. In: Clokie MRJ, Kropinski AME, editors. *Bacteriophages. Methods in Molecular Biology*<sup>TM</sup>. New York, NY: Humana Press; Springer (2009). p. 501. doi: 10.1007/978-1-60327-164-6\_14
25. Manohar P, Stalsby Lundborg C, Tamhankar AJ, Nachimuthu, R. Therapeutic characterization and efficacy of bacteriophage cocktails infecting *Escherichia coli*, *Klebsiella pneumoniae* and *Enterobacter* species. *Front Microbiol*. (2019) 10:574. doi: 10.3389/fmicb.2019.00574
26. Brenner S, Horne R. A negative staining method for high resolution electron microscopy of viruses. *Biochim Biophys Acta*. (1959) 34:103–10. doi: 10.1016/0006-3002(59)90237-9
27. Ackermann HW. Phage classification and characterization. In: Clokie MRJ, Kropinski AM, editors. *Bacteriophages: Methods and Protocols, Volume 1: Isolation, Characterization, and Interactions*. Totowa, NJ: Humana Press; Springer (2009). p. 127–40. doi: 10.1007/978-1-60327-164-6\_13
28. El-DougDoug NK, Cucic S, Abdelhamid AG, Brovko L, Kropinski AM, Griffiths MW, et al. Control of *Salmonella* Newport on cherry tomato using a cocktail of lytic bacteriophages. *Int J Food Microbiol*. (2019) 293:60–71. doi: 10.1016/j.ijfoodmicro.2019.01.003
29. Moyo Z, Woolston J, Sulakvelidze A. Bacteriophage applications for food production and processing. *Viruses*. (2018) 10:205. doi: 10.3390/v10040205
30. Rao BM, Lalitha K. Bacteriophages for aquaculture: are they beneficial or inimical. *Aquaculture*. (2015) 437:146–54. doi: 10.1016/j.aquaculture.2014.11.039
31. Pereira C, Moreirinha C, Lewicka M, Almeida P, Clemente C, Cunha Â, et al. Bacteriophages with potential to inactivate *Salmonella* Typhimurium: use of single phage suspensions and phage cocktails. *Virus Res*. (2016) 220:179–92. doi: 10.1016/j.virusres.2016.04.020
32. Niu YD, McAllister TA, Nash JH, Kropinski AM, Stanford K. Four *Escherichia coli* O157: H7 phages: a new bacteriophage genus and taxonomic classification of T1-like phages. *PLoS ONE*. (2014) 9:e100426. doi: 10.1371/journal.pone.0100426
33. Perera MN, Abuladze T, Li M, Woolston J, Sulakvelidze A. Bacteriophage cocktail significantly reduces or eliminates *Listeria monocytogenes* contamination on lettuce, apples, cheese, smoked salmon and frozen foods. *Food Microbiol*. (2015) 52:42–8. doi: 10.1016/j.fm.2015.06.006
34. Snyder AB, Perry JJ, Yousef AE. Developing and optimizing bacteriophage treatment to control enterohemorrhagic *Escherichia coli* on fresh produce. *Int J Food Microbiol*. (2016) 36:90–7. doi: 10.1016/j.ijfoodmicro.2016.07.023
35. Duc HM, Son HM, Honjoh KI, Miyamoto T. Isolation and application of bacteriophages to reduce *Salmonella* contamination in raw chicken meat. *LWT*. (2018) 91:353–60. doi: 10.1016/j.lwt.2018.01.072
36. Truncaite L, Šimoliunas E, Zajančauskaite A, Kaliniene L, Mankevičiute R, Stanilius J, et al. Bacteriophage vB\_EcoM\_FV3: a new member of “rV5-like viruses”. *Arch Virol*. (2012) 157:2431–5. doi: 10.1007/s00705-012-1449-x
37. Singh A, Arya SK, Glass N, Hanifi-Moghaddam P, Naidoo R, Szymanski CM, et al. Bacteriophage tailspike proteins as molecular probes for sensitive and selective bacterial detection. *Biosens Bioelectron*. (2010) 26:131–8. doi: 10.1016/j.bios.2010.05.024
38. Hu Z, Meng XC, Liu F. Isolation and characterisation of lytic bacteriophages against *Pseudomonas* spp., a novel biological intervention for preventing spoilage of raw milk. *Int Dairy J*. (2016) 55:72–8. doi: 10.1016/j.idairyj.2015.11.011
39. Stalin N, Srinivasan P. Efficacy of potential phage cocktails against *Vibrio harveyi* and closely related *Vibrio* species isolated from shrimp aquaculture environment in the south east coast of India. *Vet Microbiol*. (2017) 207:83–96. doi: 10.1016/j.vetmic.2017.06.006
40. Kalatzis PG, Bastías R, Kokkari C, Katharios P. Isolation and characterization of two lytic bacteriophages, φSt2 and φGm1; phage therapy application for biological control of *Vibrio alginolyticus* in aquaculture live feeds. *PLoS ONE*. (2016) 11:e0151101. doi: 10.1371/journal.pone.0151101

**Conflict of Interest:** The authors declare that the research was conducted in the absence of any commercial or financial relationships that could be construed as a potential conflict of interest.

Copyright © 2019 Montso, Mlambo and Ateba. This is an open-access article distributed under the terms of the Creative Commons Attribution License (CC BY). The use, distribution or reproduction in other forums is permitted, provided the original author(s) and the copyright owner(s) are credited and that the original publication in this journal is cited, in accordance with accepted academic practice. No use, distribution or reproduction is permitted which does not comply with these terms.



# Is Meropenem as a Monotherapy Truly Incompetent for Meropenem-Nonsusceptible Bacterial Strains? A Pharmacokinetic/Pharmacodynamic Modeling With Monte Carlo Simulation

Xiangqing Song\*, Yi Wu, Lizhi Cao, Dunwu Yao and Minghui Long

Department of Pharmacy, Hunan Cancer Hospital, The Affiliated Cancer Hospital of Xiangya School of Medicine, Central South University, Changsha, China

## OPEN ACCESS

### Edited by:

Hemda Garelick,  
Middlesex University, United Kingdom

### Reviewed by:

Jozsef Soki,  
University of Szeged, Hungary  
César de la Fuente,  
University of Pennsylvania,  
United States

### \*Correspondence:

Xiangqing Song  
sxqmaster@163.com

### Specialty section:

This article was submitted to  
Antimicrobials, Resistance and  
Chemotherapy,  
a section of the journal  
Frontiers in Microbiology

Received: 04 July 2019

Accepted: 14 November 2019

Published: 29 November 2019

### Citation:

Song X, Wu Y, Cao L, Yao D and  
Long M (2019) Is Meropenem as a  
Monotherapy Truly Incompetent for  
Meropenem-Nonsusceptible  
Bacterial Strains? A  
Pharmacokinetic/Pharmacodynamic  
Modeling With Monte Carlo  
Simulation. *Front. Microbiol.* 10:2777.  
doi: 10.3389/fmicb.2019.02777

Infections due to meropenem-nonsusceptible bacterial strains (MNBSs) with meropenem minimum inhibitory concentrations (MICs)  $\geq 16$  mg/L have become an urgent problem. Currently, the optimal treatment strategy for these cases remains uncertain due to some limitations of currently available mono- and combination therapy regimens. Meropenem monotherapy using a high dose of 2g every 8h (q 8h) and a 3-h traditional simple prolonged-infusion (TSPI) has proven to be helpful for the treatment of infections due to MNBSs with MICs of 4–8 mg/L but is limited for cases with higher MICs of  $\geq 16$  mg/L. This study demonstrated that optimized two-step-administration therapy (OTAT, i.e., a new administration model of i.v. bolus plus prolonged infusion) for meropenem, even in monotherapy, can resolve this problem and was thus an important approach of suppressing such highly resistant bacterial isolates. Herein, a pharmacokinetic (PK)/pharmacodynamic (PD) modeling with Monte Carlo simulation was performed to calculate the probabilities of target attainment (PTAs) and the cumulative fractions of response (CFRs) provided by dosage regimens and 39 OTAT regimens in five dosing models targeting eight highly resistant bacterial species with meropenem MICs  $\geq 16$  mg/L, including *Acinetobacter baumannii*, *Acinetobacter* spp., *Enterococcus faecalis*, *Enterococcus faecium*, *Pseudomonas aeruginosa*, *Staphylococcus epidermidis*, *Staphylococcus haemolyticus*, and *Stenotrophomonas maltophilia*, were designed and evaluated. The data indicated that meropenem monotherapy administered at a high dose of 2g q 8h and as an OTAT achieved a PTA of  $\geq 90\%$  for isolates with an MIC of up to 128 mg/L and a CFR of  $\geq 90\%$  for all of the targeted pathogen populations when 50%  $fT > MIC$  (50% of the dosing interval during which free drug concentrations remain above the MIC) is chosen as the PD target, with *Enterococcus faecalis* being the sole exception. Even though 50%  $fT > 5 \times MIC$  is chosen as the PD target, the aforementioned dosage

regimen still reached a PTA of  $\geq 90\%$  for isolates with an MIC of up to 32 mg/L and a CFR of  $\geq 90\%$  for *Acinetobacter* spp., *Pseudomonas aeruginosa*, and *Klebsiella pneumoniae* populations. In conclusion, meropenem monotherapy displays potential competency for infections due to such highly resistant bacterial isolates provided that it is administered as a reasonable OTAT but not as the currently widely recommended TSPI.

**Keywords:** meropenem, monotherapy, meropenem-nonsusceptible bacteria, meropenem-resistant bacteria, pharmacokinetic/pharmacodynamics, Monte Carlo simulation

## INTRODUCTION

The increasing emergence of meropenem-nonsusceptible bacterial strains (MNBSs), such as *Enterobacteriaceae*, *Pseudomonas aeruginosa*, and *Acinetobacter* spp., which are defined as any isolate displaying minimum inhibitory concentration (MIC) of 2, 4, and 4 mg/L with meropenem, imipenem, and/or doripenem, respectively [Clinical and Laboratory Standards Institute (CLSI), 2019], has become a serious global health concern (Nordmann, 2014; Iovleva and Doi, 2017; Bulens et al., 2018; Moghnieh et al., 2018; Huang et al., 2019). The resulting infections, which have increasingly been identified not only in hospitals (Snitkin et al., 2012; Onori et al., 2015) but also in the community (Kelly et al., 2017; Salomão et al., 2017), result in excessive morbidity, mortality, and costs (Lemos et al., 2014; Bartsch et al., 2017) and severely limit treatment options.

Some traditional agents, such as polymyxins, tigecycline, fosfomycin, and aminoglycosides, etc. and currently relatively novel ones, such as ceftazidime-avibactam, meropenem-vaborbactam, and imipenem/cilastatin-relebactam, etc. in monotherapy exhibit good potency for MNBSs; however, these agents are unfortunately limited by either significant shortcomings for the traditional agents (e.g., nephrotoxicity for polymyxins and aminoglycosides, increased mortality for tigecycline, and insufficient blood concentration due to the oral dosage form and dosage for fosfomycin) or geographical availability restrictions or unlisting for the novel ones (Satlin and Walsh, 2017; Karaiskos et al., 2019). Likewise, meropenem-containing combination therapy (MCCT) with synergism, which is currently being widely studied and recommended for MNBSs, mostly for meropenem-nonsusceptible *Klebsiella pneumoniae*, is also limited for the following reasons: (i) it has not been satisfactorily investigated in large-scale randomized clinical

trials, despite the existence of sporadic controlled trials and *in vitro* studies on this form of therapy (Liu et al., 2016; Oliva et al., 2017; Satlin and Walsh, 2017; Paul et al., 2018), and (ii) the extrapolation of MCCT based on meropenem-nonsusceptible *K. pneumoniae* to other MNBSs with different resistance mechanisms lacks further investigation and verification; and importantly, (iii) its efficacy in certain situations remains controversial relative to monotherapy since some of them do not truly improve the clinical outcomes (Del Bono et al., 2017; Paul et al., 2018). Consequently, the choice of MCCT or monotherapy for the treatment of infections due to different MNBSs remains a matter of debate, and the optimal treatment for MNBSs remains uncertain.

Meropenem, at recommended optimal dosing conditions, is often included in treatment regimens for infections with a MNBS. Indeed, both theoretical and clinical studies have shown that an optimal regimen using a high dose of 2 g every 8 h (q 8h) and a 3-h prolonged infusion for meropenem as monotherapy improves its efficacy against MNBSs with MICs of 4–8 mg/L (Jaruratanasirikul et al., 2015; Tumbarello et al., 2015). However, the majority of these isolates often have meropenem MICs  $\geq 16$  mg/L (Tumbarello et al., 2015; Gomez-Simmonds et al., 2016; Cojutti et al., 2018), limiting the utility of this approach. However, to the best of our knowledge, this outcome occurs because traditional simple prolonged-infusion (TSPI) leads to both a decrease in the peak concentration and a delay in the peak time, resulting in an apparent incompetency for meropenem against the isolates with MICs  $\geq 16$  mg/L. For this reason, reoptimization of the method for administering meropenem in monotherapy may continue to show promise regarding the successful management of these problematic isolates, prompting us to design a theoretically optimized two-step-administration therapy (OTAT, see OTAT design in the part of Materials and Methods) for these problematic isolates. It is believed that this reoptimization will not only be crucial for maximizing microbiological outcomes but also be particularly important when better treatment options for these pathogens strains are absent.

Given that few attempts have been made to determine the optimal treatment for meropenem as a monotherapy against the increasing number of MNBSs with MICs  $\geq 16$  mg/L, this study focused on only these strains. An attempt was made to design OTAT regimens for meropenem to determine whether its use as a monotherapy can achieve an acceptable pharmacokinetic (PK)/pharmacodynamic (PD) exposure to illustrate whether meropenem monotherapy is incompetent for use with these

**Abbreviations:** MNBSs, meropenem-nonsusceptible bacterial strains; MIC, minimum inhibitory concentration; MCCT, meropenem-containing combination therapy; TSPI, traditional simple prolonged-infusion; OTAT, optimized two-step-administration therapy; PK, pharmacokinetic; PD, pharmacodynamic; EUCAST, European Committee on Antimicrobial Susceptibility Testing; PTAs, probabilities of target attainment; CFRs, cumulative fractions of response; IVB, i.v. bolus; AUC, area under the concentration-time curve; ELF, epithelial lining fluid;  $f_T > \text{MIC}$ , the time that the unbound (free) drug concentrations remain above the minimum inhibitory concentration;  $\%f_T > \text{MIC}$ , percentages of the dosing interval during which unbound (free) drug concentrations remain above the MIC; LRTIs, lower respiratory tract infections;  $f(C_{\text{min}})/\text{MIC}$ , ratio of the trough concentration of unbound (free) drug to the minimum inhibitory concentration;  $CL_{\text{cr}}$ , creatinine clearance; KPC, *Klebsiella pneumoniae* carbapenemase.

strains, with the intent of defining optimal dosage regimens for meropenem against such strains if possible.

## MATERIALS AND METHODS

### Study Design

Meropenem-specific serum PK parameters were obtained from published literature and microbiological susceptibility data for the targeted pathogens were obtained from the European Committee on Antimicrobial Susceptibility Testing (EUCAST); together with dosing parameters, such as the dose and infusion time, these data were incorporated into a PK/PD model. Monte Carlo simulation was used to calculate the probabilities of target attainment (PTAs) at different MICs and the cumulative fractions of response (CFRs) for the targeted bacteria population with a pooled MIC distribution provided by each dosage regimen against 8 targeted bacterial species with doubling MICs between 16 and 512 mg/L from the EUCAST database for a given PK/PD target. A PTA or CFR of  $\geq 90\%$  and the causal dosage regimens were considered optimal.

### OTAT Design

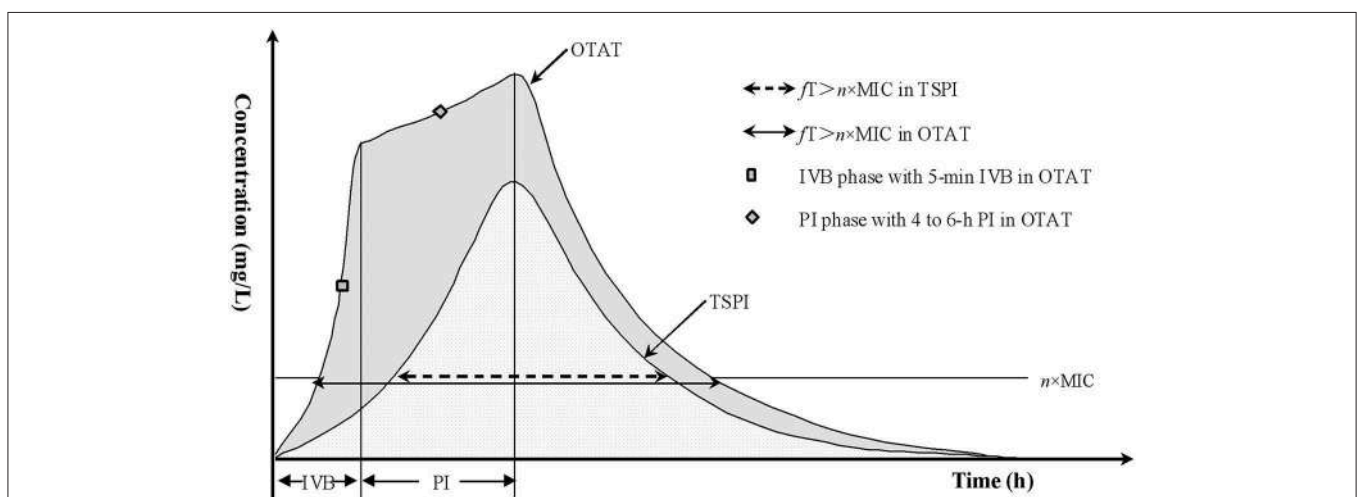
Considering that the i.v. bolus (IVB) administration mode can rapidly and maximally achieve the loading drug concentration for a given agent and that prolonged infusion can continuously maintain the efficacious drug exposure, using these two techniques in combination is speculated to be optimal and competent for coverage of highly resistant bacterial isolates for a given pathogen. Therefore, OTAT represents such an administration mode in this study in which a loading dose of the total amount of the tested drug is first administered via a rapid IVB, immediately followed by the remainder of the experiment via prolonged infusion after the first dose, as illustrated in **Figure 1**.

## Meropenem Dosage Regimens

Meropenem dosage regimens, including the injection method, were chosen based on the licensed and studied regimens used for infected adults with normal renal function, including 0.5 g every 8 h (q 8 h), 1 g q 8 h, and 2 g q 8 h. In addition, 0.75 g every 6 h (q 6 h) and 1.5 g q 6 h were also investigated as the modified dosage regimens of 1 g q 8 h and 2 g q 8 h, respectively. Since meropenem in solutions is stable for only  $\sim 6$  h at room temperature (Kuti et al., 2004), the remainder of the experiment can only be administered by prolonged infusion up to 6 h, and 4- to 6-h prolonged infusion for the remainder were thus simulated. In this study, the following 39 dosage regimens presented in **Table 1** were investigated.

## Meropenem Tissue PK Profiles and PD Model Associated With Clinical Response

Meropenem tissue penetration to the infection site is critical for obtaining a good clinical outcome in patients with different infection sites. Previous studies indicated that the mean meropenem tissue penetration (i.e., the mean tissue/concomitant serum concentration) after injection ranged from  $\sim 0.2$  to 1 for different tissues as follows:  $\sim 0.5$  for liver, lung, skin, uterus, ovaries, rectum, prostate, thyroid, trachea, and lymph nodes with the exception of a very small concentration in the brain and cerebrospinal fluid (Harrison et al., 1989), 0.95 for peritoneum (Hextall et al., 1991), 0.2 for bronchial secretions (Bergogne-Bérézin et al., 1994), 1.1 for skin exudate (Wise et al., 1990), and 0.85–0.87 for blister fluid (Mouton and Michel, 1991). However, Byl et al. (1999) reported it to be 0.17–0.43 for lung, 0.20–0.55 for bronchial mucosa, and 0.18–0.26 for pleural tissues. Regarding meropenem tissue penetration, especially for lung, a recent study conducted by Lodise et al. (2011) reported that the ratio of the area under the concentration-time curve (AUC) in epithelial lining fluid (ELF) to the AUC in plasma



**FIGURE 1** | Concentration-time profiles via TSPI and OTAT. IVB, i.v. bolus; PI, prolonged infusion; OTAT, optimized two-step-administration therapy; TSPI, traditional simple prolonged-infusion; MIC, minimum inhibitory concentration;  $f$ , fraction of unbound drug;  $fT > n \times \text{MIC}$ , the time that the unbound (free) drug concentrations remain above the MIC by  $n$ -fold.



**TABLE 1** | Simulated dosage regimens for meropenem.

Dosing model	Simulated dosage regimens	
	TSPI	OTAT
0.5 g q 8 h	0.5 g (4 h)	0.25 g (5-min IVB) + 0.25 g (4 h)
	0.5 g (5 h)	0.25 g (5-min IVB) + 0.25 g (5 h)
	0.5 g (6 h)	0.25 g (5-min IVB) + 0.25 g (6 h)
1 g q 8 h	1 g (4 h)	0.5 g (5-min IVB) + 0.5 g (4 h)
	1 g (5 h)	0.5 g (5-min IVB) + 0.5 g (5 h)
	1 g (6 h)	0.5 g (5-min IVB) + 0.5 g (6 h)
2 g q 8 h	2 g (4 h)	0.5 g (5-min IVB) + 1.5 g (4 h), 1 g (5-min IVB) + 1 g (4 h), 1.5 g (5-min IVB) + 0.5 g (4 h)
	2 g (5 h)	0.5 g (5-min IVB) + 1.5 g (5 h), 1 g (5-min IVB) + 1 g (5 h), 1.5 g (5-min IVB) + 0.5 g (5 h)
	2 g (6 h)	0.5 g (5-min IVB) + 1.5 g (6 h), 1 g (5-min IVB) + 1 g (6 h), 1.5 g (5-min IVB) + 0.5 g (6 h)
0.75 g q 6 h	0.75 g (4 h)	0.5 g (5-min IVB) + 0.25 g (4 h)
	0.75 g (5 h)	0.5 g (5-min IVB) + 0.25 g (5 h)
	0.75 g (6 h)	0.5 g (5-min IVB) + 0.25 g (6 h)
1.5 g q 6 h	1.5 g (4 h)	0.5 g (5-min IVB) + 1 g (4 h), 1 g (5-min IVB) + 0.5 g (4 h)
	1.5 g (5 h)	0.5 g (5-min IVB) + 1 g (5 h), 1 g (5-min IVB) + 0.5 g (5 h)
	1.5 g (6 h)	0.5 g (5-min IVB) + 1 g (6 h), 1 g (5-min IVB) + 0.5 g (6 h)

( $AUC_{ELF}/AUC_{plasma}$  ratio) for meropenem varied substantially between patients with ventilator-associated pneumonia, with the 10th and 90th percentile ELF exposures that were 3.7–178% of the plasma AUC values and with the mean and median AUC exposures that were 81.6 and 25.42% of the plasma values. Overall, these observations imply that logically, mean 1–2 times meropenem plasma concentrations or exposures would achieve the desired tissue concentration or exposure for most tissues if they increase proportionally, with the exception of ~5 times for lung, bronchial and pleural tissues. Theoretically, it would be more accurate to predict and establish a drug regimen based on the relationship between the tissue drug concentration and tissue exposure targets. However, to the best of our knowledge, penetration of meropenem in infected tissues to achieve the exposure targets has not been studied often, and drug concentrations in extracellular compartments are difficult to determine; thus, correlations between the PK/PD index in the tissue and antimicrobial effects are less well-understood (Nightingale and Mur, 2007). Therefore, serum PK parameters based on the plasma drug concentrations are most commonly used as surrogates for establishing and estimating the PK/PD indices in some studies (Kuti et al., 2003; Ikawa et al., 2011), and so it is with the present study.

Regarding the correlations between the PK/PD index and clinical response to meropenem therapy, Roberts et al. (2014) reported that 50 and 100% of the ratios of  $fT > MIC$  to a dosing interval are independent factors that influence the clinical outcome of patients receiving meropenem or other  $\beta$ -lactams and that a higher PK/PD index is associated with a higher likelihood of a positive clinical outcome. Likewise, Zhou et al. (2011) also found that  $fT > MIC$  is an independent influencing factor for predicting clinical success and that the cutoff value using  $fT > MIC$  based on serum concentrations in elderly patients with lower respiratory tract infections (LRTIs) is 76%.

However, Li et al. (2007) studied the indices of clinical PD for LRTIs through meropenem serum concentrations in 101 patients and considered that the minimum concentration of drug in serum  $f(C_{min})/MIC > 5$  rather than  $\%fT > MIC$  is the only significant predictor of clinical response since 100% of  $fT > MIC$  is achieved in the majority of LRTI patients. However, there is no consensus regarding which strategy ( $\%fT > MIC$  vs.  $f(C_{min})/MIC > 5$ ) is better. In the present study,  $\%fT > MIC$  is therefore used as the PD target associated with the clinical response of meropenem therapy.

Generally, 40–50% of  $fT > MIC$  for meropenem based on the serum concentration is usually used for predicting clinical and microbiological outcomes and for optimizing dosage regimens in most current meropenem PK/PD studies (Burgess et al., 2007; Watanabe et al., 2007; Ikawa et al., 2011; Kondo et al., 2014). However, given the profiles of meropenem tissue penetration described previously, we consider that (i) this exposure target in plasma may be underestimated when 40–50% of  $fT > MIC$  for meropenem is required in infected tissues; and (ii) it is reasonably speculated that a meropenem drug concentration of 1–2  $\times$  MIC in plasma for most types of infection but 5  $\times$  MIC in plasma for pulmonary, bronchial and pleural infection is sufficient to achieve the pathogen MIC without considering the influence of inflammation on meropenem tissue penetration. Based on all the abovementioned considerations, especially the profiles of meropenem tissue penetration, the targets of 50%  $fT > MIC$  (mainly for bacterial peritonitis or intraabdominal infections, bloodstream infections, skin and soft tissue infections, or urinary tract infections), 50%  $fT > 2 \times MIC$  (mainly for bacterial hepatitis, metritis, oophoritis, proctitis, or prostatitis, etc.), and 50%  $fT > 5 \times MIC$  (mainly for LRTIs, such as pneumonia, bronchitis, or pleural infections) based on the serum concentration were applied as the optimal PK/PD index in terms of obtaining adequate meropenem exposures regarding its

bacterial killing and clinical efficacy for various types of infection or infected sites in the present study.

The % $fT > MIC$  in OTAT was calculated using the following one-compartment intravenous infusion equation, as modified from a previously reported equation (Li et al., 2006):

- Meropenem was administered via TSPI;

$$fT > MIC = T_{inf} - \frac{V_d}{CL} \times \ln \left( \frac{R_0/CL}{R_0/CL - MIC} \right) + \frac{V_d}{CL} \times \ln \left( \frac{R_0/CL - R_0/CL \times e^{-CLT_{inf}/V_d}}{MIC} \right)$$

Then

$$fT > n \times MIC = T_{inf} - \frac{V_d}{CL} \times \ln \left( \frac{R_0/CL}{R_0/CL - n \cdot MIC} \right) + \frac{V_d}{CL} \times \ln \left( \frac{R_0/CL - R_0/CL \times e^{-CLT_{inf}/V_d}}{n \cdot MIC} \right)$$

- Meropenem was administered via OTAT, and prolonged infusion was started immediately following the completion of IVB (see **Figure 1**);

$$fT > n \times MIC = T_{inf} + \frac{V_d}{CL} \times \ln \left( \frac{f \cdot Dose_{bol} \cdot CL/V_d + f \cdot Dose_{inf} \cdot (1 - e^{-CL \cdot T_{inf}/V_d})/T_{inf}}{CL \cdot n \cdot MIC} \right)$$

and % $fT > n \times MIC = fT > n \times MIC \times 100/DI$ .

where  $f$  is the fraction of unbound drug,  $fT$  is the time that the drug is in unbound (free) form,  $MIC$  is the minimum inhibitory concentration,  $fT > MIC$  is the time that the unbound (free) drug concentrations remain above  $MIC$ ,  $fT > n \times MIC$  is the time that the unbound (free) drug concentrations remain above the  $MIC$  by  $n$ -fold,  $n$  is an integer set as 1, 2, or 5 in the present study, % $fT > n \times MIC$  is the percentage of the dosing interval during which unbound (free) drug concentrations remain above the  $MIC$  by  $n$ -fold,  $T_{inf}$  (h) is the infusion time,  $R_0$  (mg/h) is the zero-order infusion rate calculated as whole-dose  $\times f/T_{inf}$  in TSPI,  $Dose_{bol}$  (mg) is the dose administered via IVB in OTAT,  $Dose_{inf}$  (mg) is the dose administered via prolonged infusion in OTAT,  $CL$  (L/h) is the plasma clearance rate of the experiment,  $V_d$  (L) is the volume of distribution of the experiment at steady state,  $e$  is the exponent,  $Ln$  is the natural logarithm, and  $DI$  (h) is the dosing interval.

## Meropenem Population PK Parameters

Serum population PK parameters for meropenem were obtained from previously published studies documenting adult patients (preferably those describing infection studies when available) with normal renal function (i.e., creatinine clearance ( $CL_{cr}$ )  $\geq$

50 ml/min) or healthy volunteers (when the desired data from infected populations were unavailable). Meropenem population PK parameters were determined by the PK model established by Li et al. (2006) as follows:  $CL(L/h) = 14.6 \times (CL_{cr}/83)^{0.62} \times (AGE/35)^{-0.34}$ ,  $V_c(L) = 10.8 \times (WT/70)^{0.99}$ , and  $V_p(L) = 12.6$  where  $CL_{cr}$  (ml/min) is the creatinine clearance of the patient calculated according to the Cockcroft-Gault equation based on the patient's ideal body weight (Cockcroft and Gault, 1976),  $WT$  (kg) is the ideal body weight of the patient,  $V_c$  (L) is the central volume of distribution, and  $V_p$  (L) is the peripheral volume of distribution. The data in this study were chosen for our analysis because compared with other studies (Gonçalves-Pereira and Póvoa, 2011), this study had a relatively large number of patients ( $N = 79$ ), and all of the patients had various types of infections, including 52 patients with intra-abdominal infections, 21 patients with ventilator-associated pneumonia, and six patients with community-acquired pneumonia, and were treated with meropenem; therefore, the PK data obtained for meropenem are relatively representative. The meropenem population PK parameter estimates at steady state based on the demographic characteristics of the subjects in this study are summarized as follows:  $CL$   $14.97 \pm 4.13$  L/h and  $V_d$  ( $V_c + V_p$ )  $23.86 \pm 2.46$  L. The ranges of the unbound fraction ( $f$ ) were calculated from the protein binding data, and estimates of  $f$  for meropenem (0.85–0.98) were obtained from the package insert of the product (USP PACKAGE INSERT., 1996) and from the pharmacokinetic studies (Kuti et al., 2005), if measured.

## Microbiological Susceptibility Data

The microbiological susceptibility data, including the targeted bacterial species, the number of isolates with meropenem MICs  $\geq 16$  mg/L and the corresponding MIC frequency distributions (in **Table 2**), were derived from the EUCAST database [European Committee on Antimicrobial Susceptibility Testing (EUCAST), 2019]. This database was chosen for our analysis because it provided the most current and comprehensive collection of MIC data for the antibiotics and organisms modeled in the current study. Bacterial species with isolates having meropenem MICs  $\geq 16$  mg/L ( $\geq 100$  strains) include mainly *Acinetobacter baumannii* (763 strains), *Acinetobacter* spp. (1,209 strains), *Enterococcus faecalis* (1,317 strains), *Enterococcus faecium* (1,554 strains), *P. aeruginosa* (4,841 strains), *Staphylococcus epidermidis* (175 strains), *Staphylococcus haemolyticus* (103 strains), and *Stenotrophomonas maltophilia* (3,935 strains). These bacterial species will therefore be modeled as targets for investigating meropenem exposures in monotherapy against MNBSs with MICs  $\geq 16$  mg/L.

## Monte Carlo Simulation

A 5,000-subject simulation was performed by Crystal Ball software (version 7.2.2; Decisioneering, Inc., Denver, CO, USA) to calculate the probability of achieving the requisite PK/PD exposure (i.e., 50%  $fT > MIC$ , 50%  $fT > 2 \times MIC$ , and 50%  $fT > 5 \times MIC$ ) for each dosage regimen, referred to as the PTA against the isolates at a specific MIC and the CFR against a population of an organism with a pooled MIC distribution. Prior to the simulations, PK parameters were

**TABLE 2** | No. of targeted bacterial isolates and corresponding MIC frequency distributions at MICs  $\geq 16$  mg/L collected from the EUCAST database.

Organism	No. of isolates at an MIC of $\geq 16$ (mg/L, n)							Corresponding MIC frequency distributions ( $\mu\text{g/ml}$ , % of total isolates)						
	16	32	64	128	256	512	Total	16	32	64	128	256	512	Total
AB	570	62	59	54	8	10	763	74.71	8.13	7.73	7.08	1.05	1.31	100
AS	1198	10	1	0	0	0	1209	99.09	0.83	0.08	0	0	0	100
EFS	944	168	17	1	0	187	1317	71.68	12.76	1.29	0.08	0	14.20	100
EFM	483	912	5	13	141	0	1554	31.08	58.69	0.32	0.84	9.07	0	100
PA	3959	392	443	33	14	0	4841	81.78	8.10	9.15	0.68	0.29	0	100
SE	152	19	4	0	0	0	175	86.86	10.86	2.29	0	0	0	100
SHA	47	46	9	1	0	0	103	45.63	44.66	8.74	0.97	0	0	100
SM	3820	111	2	2	0	0	3935	97.08	2.82	0.05	0.05	0	0	100

AB, *Acinetobacter baumannii*; AS, *Acinetobacter* spp.; EFS, *Enterococcus faecalis*; EFM, *Enterococcus faecium*; PA, *Pseudomonas aeruginosa*; SE, *Staphylococcus epidermidis*; SHA, *Staphylococcus haemolyticus*; SM, *Stenotrophomonas maltophilia*.

assumed to follow log-normal distributions and the fraction unbound  $f$  followed a uniform distribution, whereby the probability was equal within the specified range. The PTA was determined by calculating the fraction of subjects who attained the target at a specific MIC and was determined for MICs between 16 and 512 mg/L. A regimen with a PTA of  $\geq 90\%$  against the isolates at this MIC was considered optimal. The overall expectation value for the PTA (i.e., CFR) is related to PD target attainment in that it expresses the probability of a given dosage regimen achieving the desired exposures against an entire population of pathogens. The CFR percentages for each organism were calculated by multiplying the PTA at each MIC by the percentage of isolates of each of the modeled organisms actually found at that MIC. A regimen with a CFR of  $\geq 90\%$  against an organism population of was considered optimal.

## RESULTS

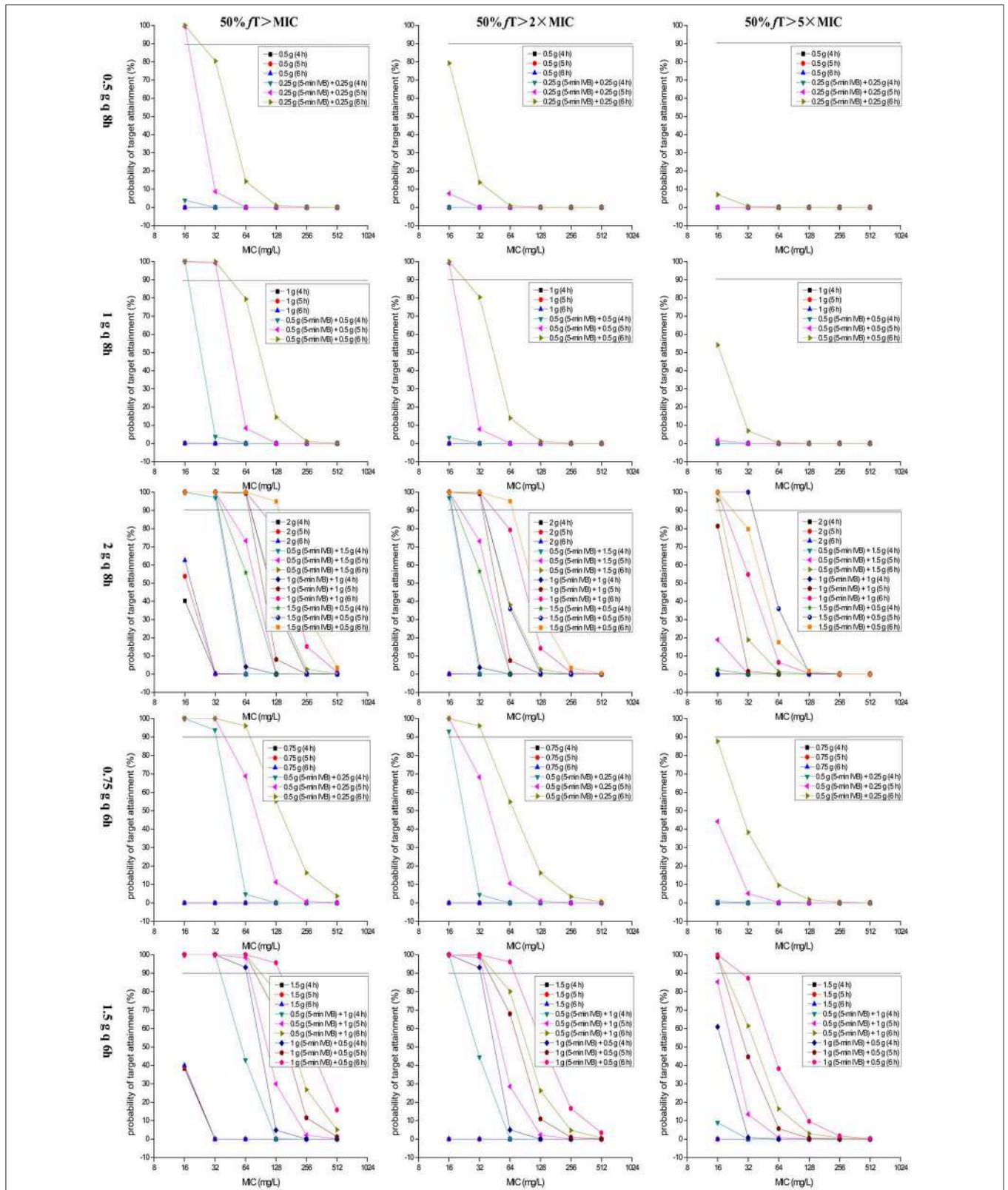
### Probability of Target Attainment

PTA vs. MIC profiles for simulations of different dosage regimens are presented in **Figure 2**. A PTA of  $\geq 90\%$  was considered satisfactory. For attainment of the classical PD target, i.e.,  $50\% fT > \text{MIC}$ , the dosage regimens of 0.5 g q 8 h, 1 g q 8 h, 2 g q 8 h, 0.75 g q 6 h, and 1.5 g q 6 h would be insufficient for the treatment of bacteria with MICs  $\geq 16$  mg/L if administered via 4- to 6-h TSPI, regardless of the MIC values and PD targets. However, they would be adequate if administered as a reasonable OTAT. Specifically, the dosage regimen of 0.5 g [e.g., 0.25 g (5-min IVB) + 0.25 g (5–6 h)] q 8 h for the isolates with MICs of 16 mg/L, 1 g [e.g., 0.5 g (5-min IVB) + 0.5 g (5 h)] q 8 h for the isolates with MICs of 32 mg/L, 0.75 g [e.g., 0.5 g (5-min IVB) + 0.25 g (6 h)] q 6 h for the isolates with MICs of 64 mg/L, 2 g [e.g., 1.5 g (5-min IVB) + 0.5 g (6 h)] q 8 h and 1.5 g [e.g., 1 g (5-min IVB) + 0.5 g (6 h)] q 6 h for the isolates with MICs of 128 mg/L produced sufficient PK/PD exposures when  $50\% fT > \text{MIC}$  was used as the PD target. However, the power of these dosage regimens was weakened by nearly half when  $50\% fT > 2 \times \text{MIC}$  was chosen as the PD target and substantially reduced when  $50\% fT > 5 \times \text{MIC}$  was chosen as the

PD target. Interestingly, the dosage regimen of 2 g [preferred 1.5 g (5-min IVB) + 0.5 g (5 h)] q 8 h still showed good antibacterial properties for the isolates with MICs of up to 32 mg/L even though the highest PD target of  $50\% fT > 5 \times \text{MIC}$  was used. Of note, as a modification of the dosage regimen of 2 g q 8 h, the dosage regimen of 1.5 g q 6 h produced a PTA of  $\geq 90\%$  for the isolates with MICs of 16 mg/L when  $50\% fT > 5 \times \text{MIC}$  was used as the PD target when it was administered as an OTAT [e.g., 1.5 g [1 g (5-min IVB) + 0.5 g (5 h)] q 6 h], suggesting a potentially useful dosage regimen for these isolates. **Table 3** summarizes the coverage of various dosage regimens for the pathogen isolates with meropenem MICs  $\geq 16$  mg/L in different types of infection at the condition of achieving  $\geq 90\%$  PTA.

### Cumulative Fraction of Response

CFR vs. various targeted pathogen populations for simulations of different dosage regimens are displayed in **Figure 3**. A CFR of  $\geq 90\%$  was considered optimal. Obviously, only regimens with OTAT achieved a CFR of  $\geq 90\%$  for the targeted pathogen population, regardless of the PD targets and dosing models. Based on currently pooled MIC distributions, when  $50\% fT > \text{MIC}$  was chosen as the PD target, the dosage regimen of 0.5 g [preferred 0.25 g (5-min IVB) + 0.25 g (6 h)] q 8 h yielded a CFR of  $\geq 90\%$  for only the *Acinetobacter* spp., *S. epidermidis*, and *S. maltophilia* populations; however, the dosage regimens of 1 g [preferred 0.5 g (5-min IVB) + 0.5 g (6 h)] q 8 h, 2 g [e.g., 0.5 g (5-min IVB) + 1.5 g (6 h)] q 8 h, 0.75 g [preferred 0.5 g (5-min IVB) + 0.25 g (6 h)] q 6 h, and 1.5 g [e.g., 0.5 g (5-min IVB) + 1 g (5 h)] q 6 h for all of the targeted pathogen populations achieved the requisite CFR, with *E. faecalis* being the sole exception. When using a higher PD target of  $50\% fT > 2 \times \text{MIC}$ , the majority of the simulated dosage regimens had decreased coverage of the targeted pathogens population at the condition of achieving  $\geq 90\%$  CFR. However, the dosage regimens of 2 g [preferred 1.5 g (5-min IVB) + 0.5 g (6 h)] q 8 h and 1.5 g [preferred 0.5 g (5-min IVB) + 1 g (6 h) or 1 g (5-min IVB) + 0.5 g (6 h)] q 6 h still covered the *A. baumannii*, *Acinetobacter* spp., *E. faecium*, *P. aeruginosa*, *S. epidermidis*, *S. haemolyticus*, and *S. maltophilia* populations at this condition.



**FIGURE 2** | PTAs of achieving 50%  $fT > MIC$ , 50%  $fT > 2 \times MIC$  and 50%  $fT > 5 \times MIC$  for meropenem with various dosage regimens simulated for MICs up to 512 mg/L. MIC, minimum inhibitory concentration; 50%  $fT > MIC$ , 50% of the dosing interval during which free drug concentrations remain above the MIC; 50%  $fT > 2 \times MIC$ , 50% of the dosing interval during which free drug concentrations remain above the MIC by two-fold; 50%  $fT > 5 \times MIC$ , 50% of the dosing interval during which free drug concentrations remain above the MIC by five-fold.



**TABLE 3 |** Summary of the coverage of various dosage regimens for the pathogen isolates with MICs of  $\geq 16$  mg/L at the condition of achieving  $\geq 90\%$  PTA and/or the targeted pathogen population with pooled MIC distributions between 16 and 512 mg/L at the condition of achieving  $\geq 90\%$  CFR in different types of infection.

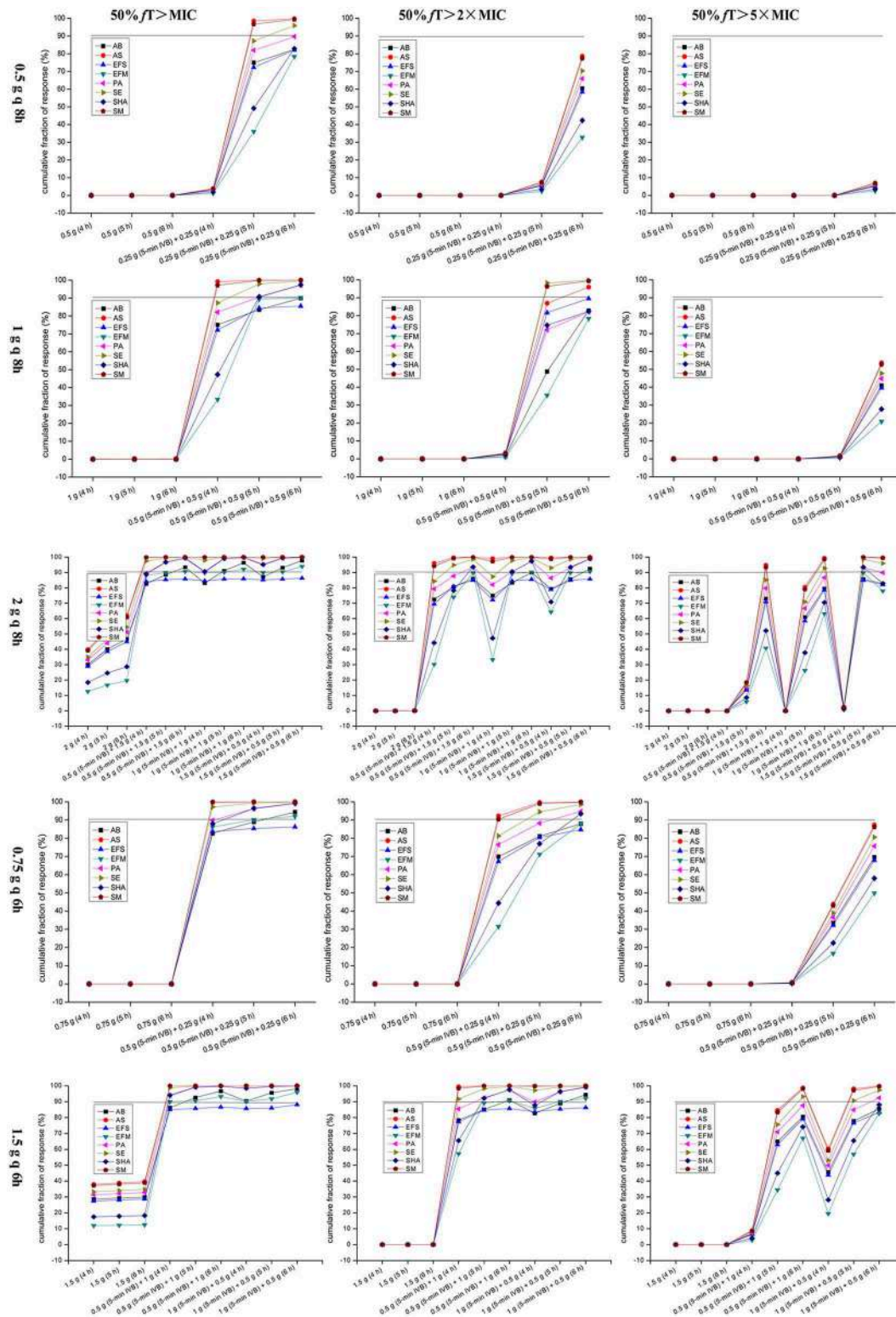
Dosing models	Dosage regimen	Covered pathogen isolates and/or populations in various types of the infection at different PD targets		
		50% fT > MIC	50% fT > 2 x MIC	50% fT > 5 x MIC
		<b>Mainly for bacterial peritonitis or intraabdominal infections, bloodstream infections, skin and soft tissue infections, or urinary tract infections</b>	<b>Mainly for bacterial hepatitis, metritis, oophoritis, proctitis, or prostatitis, etc.</b>	<b>Mainly for LRTIs, such as pneumonia, bronchitis, or pleural infections</b>
0.5 g q 8 h	0.5 g (4 h)	NA	NA	NA
	0.5 g (5 h)	NA	NA	NA
	0.5 g (6 h)	NA	NA	NA
	0.25 g (5-min IVB) + 0.25 g (4 h)	NA	NA	NA
	0.25 g (5-min IVB) + 0.25 g (5 h)	P <sub>16</sub> +(AS, SM)	NA	NA
	0.25 g (5-min IVB) + 0.25 g (6 h)	P <sub>16</sub> +(AS, SE, SM)	NA	NA
1 g q 8 h	1 g (4 h)	NA	NA	NA
	1 g (5 h)	NA	NA	NA
	1 g (6 h)	NA	NA	NA
	0.5 g (5-min IVB) + 0.5 g (4 h)	P <sub>16</sub> +(AS, SM)	NA	NA
	0.5 g (5-min IVB) + 0.5 g (5 h)	P <sub>32</sub> +(AS, PA, SE, SHA, SM)	P <sub>16</sub> +(SE, SM)	NA
	0.5 g (5-min IVB) + 0.5 g (6 h)	P <sub>32</sub> +(AB, AS, EFM, PA, SE, SHA, SM)	P <sub>16</sub> +(AS, SE, SM)	NA
2 g q 8 h	2 g (4 h)	NA	NA	NA
	2 g (5 h)	NA	NA	NA
	2 g (6 h)	NA	NA	NA
	0.5 g (5-min IVB) + 1.5 g (4 h)	P <sub>32</sub> +(AS, SE, SM)	P <sub>16</sub> +(AS, SM)	NA
	0.5 g (5-min IVB) + 1.5 g (5 h)	P <sub>32</sub> +(AS, EFM, PA, SE, SHA, SM)	P <sub>16</sub> +(AS, SE, SM)	NA
	0.5 g (5-min IVB) + 1.5 g (6 h)	P <sub>64</sub> +(AB, AS, EFM, PA, SE, SHA, SM)	P <sub>32</sub> +(AS, PA, SE, SHA, SM)	P <sub>16</sub> +(AS, SM)
	1 g (5-min IVB) + 1 g (4 h)	P <sub>32</sub> +(AS, PA, SE, SHA, SM)	P <sub>16</sub> +(AS, SM)	NA
	1 g (5-min IVB) + 1 g (5 h)	P <sub>64</sub> +(AB, AS, EFM, PA, SE, SHA, SM)	P <sub>32</sub> +(AS, PA, SE, SHA, SM)	NA
	1 g (5-min IVB) + 1 g (6 h)	P <sub>64</sub> +(AB, AS, EFM, PA, SE, SHA, SM)	P <sub>32</sub> +(AS, EFM, PA, SE, SHA, SM)	P <sub>16</sub> +(AS, SE, SM)
	1.5 g (5-min IVB) + 0.5 g (4 h)	P <sub>32</sub> +(AS, PA, SE, SHA, SM)	P <sub>16</sub> +(AS, SE, SM)	NA
0.75 g q 6 h	0.75 g (4 h)	NA	NA	NA
	0.75 g (5 h)	NA	NA	NA
	0.75 g (6 h)	NA	NA	NA
	0.5 g (5-min IVB) + 0.25 g (4 h)	P <sub>32</sub> +(AS, SE, SM)	P <sub>16</sub> +(AS, SM)	NA
	0.5 g (5-min IVB) + 0.25 g (5 h)	P <sub>32</sub> +(AS, EFM, PA, SE, SHA, SM)	P <sub>16</sub> +(AS, SE, SM)	NA
	0.5 g (5-min IVB) + 0.25 g (6 h)	P <sub>64</sub> +(AB, AS, EFM, PA, SE, SHA, SM)	P <sub>64</sub> +(AS, PA, SE, SHA, SM)	NA
	1.5 g q 6 h	1.5 g (4 h)	NA	NA
	1.5 g (5 h)	NA	NA	NA
	1.5 g (6 h)	NA	NA	NA
	0.5 g (5-min IVB) + 1 g (4 h)	P <sub>32</sub> +(AS, PA, SE, SHA, SM)	P <sub>16</sub> +(AS, SE, SM)	NA
0.5 g (5-min IVB) + 1 g (5 h)	P <sub>64</sub> +(AB, AS, EFM, PA, SE, SHA, SM)	P <sub>32</sub> +(AS, PA, SE, SHA, SM)	NA	
0.5 g (5-min IVB) + 1 g (6 h)	P <sub>64</sub> +(AB, AS, EFM, PA, SE, SHA, SM)	P <sub>32</sub> +(AB, AS, EFM, PA, SE, SHA, SM)	P <sub>16</sub> +(AS, SE, SM)	
1 g (5-min IVB) + 0.5 g (4 h)	P <sub>64</sub> +(AB, AS, EFM, PA, SE, SHA, SM)	P <sub>32</sub> +(AS, SE, SM)	NA	
1 g (5-min IVB) + 0.5 g (5 h)	P <sub>64</sub> +(AB, AS, EFM, PA, SE, SHA, SM)	P <sub>32</sub> +(AS, EFM, PA, SE, SHA, SM)	P <sub>16</sub> +(AS, SE, SM)	
1 g (5-min IVB) + 0.5 g (6 h)	P <sub>128</sub> +(AB, AS, EFM, PA, SE, SHA, SM)	P <sub>64</sub> +(AB, AS, EFM, PA, SE, SHA, SM)	P <sub>16</sub> +(AS, PA, SE, SM)	

AB, *Acinetobacter baumannii*; AS, *Acinetobacter* spp.; EFS, *Enterococcus faecalis*; EFM, *Enterococcus faecium*; PA, *Pseudomonas aeruginosa*; SE, *Staphylococcus epidermidis*; SHA, *Staphylococcus haemolyticus*; SM, *Stenotrophomonas maltophilia*.

NA, not applicable.

P<sub>16</sub>, P<sub>32</sub>, P<sub>64</sub>, P<sub>128</sub> signify the pathogen isolates with MICs of 16, 32, 64, and 128 mg/L, respectively.

Regimens with P<sub>x</sub> (x = 16, 32, 64 or 128) + (y) (y = AB, AS, EFM, PA, SE, SHA, SM, or a combination) signify that they are competent for the treatment of infections caused by the pathogen isolates actually found at that MIC if the exact MIC values are available and/or for the treatment of infections caused by the targeted pathogen population identified with only bacterial species if the exact MIC values are unavailable.



**FIGURE 3** | CFRs of achieving 50%  $fT > MIC$ , 50%  $fT > 2 \times MIC$ , and 50%  $fT > 5 \times MIC$  for meropenem with various dosage regimens simulated for the targeted bacteria populations with pooled MIC distributions between 16 and 512 mg/L. AB, *Acinetobacter baumannii*; AS, *Acinetobacter* spp.; EFS, *Enterococcus faecalis*; EFM, *Enterococcus faecium*; PA, *Pseudomonas aeruginosa*; SE, *Staphylococcus epidermidis*; SHA, *Staphylococcus haemolyticus*; SM, *Stenotrophomonas maltophilia*; 50%  $fT > MIC$ , 50% of the dosing interval during which free drug concentrations remain above the MIC; 50%  $fT > 2 \times MIC$ , 50% of the dosing interval during which free drug concentrations remain above the MIC by two-fold; 50%  $fT > 5 \times MIC$ , 50% of the dosing interval during which free drug concentrations remain above the MIC by five-fold.

However, when using an aggressive PD target of  $50\% fT > 5 \times \text{MIC}$ , these simulated dosage regimens had a drastically decreased coverages of the targeted pathogen populations at the condition of achieving  $\geq 90\%$  CFR. Surprisingly, however, the dosage regimen of 2 g [1.5 g (5-min IVB) + 0.5 g (5 h)] q 8 h still reached  $\geq 90\%$  CFR for the *Acinetobacter* spp., *P. aeruginosa*, *S. epidermidis*, *S. haemolyticus*, and *S. maltophilia* populations. **Table 3** summarizes the coverage of various dosage regimens for the targeted bacterial population with pooled MIC distributions between 16 and 512 mg/L in different types of infection at the condition of achieving  $\geq 90\%$  CFR.

## DISCUSSION

To the best of our knowledge, this study is the first to analyze meropenem as a monotherapy aimed at MNBSs with MICs  $\geq 16$  mg/L. In this study, we considered the tissue penetration profiles of meropenem for infections at different sites when establishing the PK/PD model associated with clinical response. We believe that this study is worthwhile because the PK/PD outcomes generated from our data could help clinicians treat these isolates more effectively through optimization of dosage regimens, especially when better treatment options are absent. Notably, our results support that meropenem as a monotherapy is still competent for isolates with MICs  $\geq 16$  mg/L provided that the drug is administered as a reasonable OTAT but not as the currently widely recommended TSPI.

### TSPI vs. OTAT for Meropenem Against Highly Resistant Bacterial Isolates

Currently, the optimal meropenem dosage is undergoing ardent evaluation to develop new strategies to overcome increasing meropenem resistance and maximally preserve the effectiveness of this drug. TSPI for meropenem has often been the preferred optimal mode. Indeed, TSPI for meropenem against central nervous system infections due to *P. aeruginosa* (Capitano et al., 2004) or *S. marcescens* (Nicasio et al., 2007) and ventilator-associated pneumonia due to gram-negative bacilli and for treating neutropenic patients with fever have resulted in successful clinical responses when compared with those resulting from intermittent infusion (Lorente et al., 2006; Fehér et al., 2014). However, the benefits of TSPI for meropenem reported by these studies were found using meropenem-susceptible bacterial strains. However, for infections due to MNBSs, especially those with MICs  $\geq 16$  mg/L, the benefit of this approach for improving clinical efficacy is unknown, and clinical data are limited.

Indeed, this approach is unfavorable for highly resistant bacterial isolates because it reduces the initial bactericidal effects due to both the decrease in meropenem peak concentration and the delay in its peak time, as demonstrated by Eguchi et al. (2010). It is therefore difficult for meropenem to achieve the MIC of highly resistant bacterial isolates, even at a high dose. This reduction in initial bactericidal effects may also be the reason why some studies found that meropenem, even at 3 g/day (e.g., 1 g q 8 h over a 3-h infusion or 0.5 g every 4 h (q 4 h) over a 4-h infusion), displayed poor PK/PD exposures for isolates with

MICs  $\geq 16$  mg/L but showed a relatively good effect for isolates with MICs  $\leq 8$  mg/L (Vourli et al., 2016; Zhao et al., 2017), thus inferring that TSPI for meropenem may be beneficial for isolates with low MICs. Likewise, our data confirmed this inference because using TSPI for meropenem, even at a high dose of 2 g q 8 h and using  $50\% fT > \text{MIC}$  as the PD target, did not yield a PTA  $\geq 90\%$  for isolates with MICs of 16 mg/L. Thus, this conventional approach of using TSPI to optimize PD exposure is rendered futile with the emergence of higher MICs (Avery and Nicolau, 2018). For the data obtained herein, OTAT is preferable because it provides a higher meropenem exposure relative to that of TSPI regardless of the MIC values, dosing models and PD targets. Additionally, meropenem administered via a loading dose of 0.5 g over a 30-min infusion followed immediately by 0.5 g q 4 h over a 4-h infusion [i.e., an OTAT regimen of 0.5 g (0.5 h) + 0.5 g (4 h)] reportedly achieved better outcomes than that administered intermittently against bacteria of intermediate susceptibility (Zhao et al., 2017), thus demonstrating the superiority of OTAT for meropenem against MNBSs.

### Competence of Meropenem in Monotherapy Against Highly Resistant Bacterial Isolates

Currently, clinical experience with meropenem monotherapy for MNBSs with MICs  $\geq 16$  mg/L is indeed limited because from a clinical point of view, determination of meropenem MICs  $\geq 8$  mg/L for the identified stains by susceptibility tests causes the vast majority of clinicians to switch to other better options. However, previous studies indicated that meropenem using a high dose and TSPI (e.g., 2 g q 8 h over a 2- to 3-h infusion) in monotherapy can provide some therapeutic benefit and therefore be considered to treat infections due to MNBSs with MICs  $\leq 4$  or even  $\leq 8$  mg/L based on the therapeutic efficacy of *K. pneumoniae* carbapenemase (KPC)-producing *K. pneumoniae* (Daikos and Markogiannakis, 2011; Tzouveleki et al., 2012; Hsu and Tamma, 2014; Tumbarello et al., 2015). Inconsistent with these findings, on a theoretical basis, our data indicated that even for the isolated *K. pneumoniae* strains with meropenem MICs of up to 32 mg/L and utilization of an aggressive PD target of  $50\% fT > 5 \times \text{MIC}$ , meropenem in monotherapy, even at the same daily dose used in the abovementioned studies, can still produce desired PK/PD exposures provided that it is administered using the dosage regimen of 2 g [1.5 g (5-min IVB) + 0.5 g (5 h)] q 8 h, as shown in **Figure 2**.

Regarding the treatment of infections due to MNBSs with MICs  $\geq 16$  mg/L, most reports currently focus on MCCT for meropenem-nonsusceptible *K. pneumoniae*. Joint guidelines prepared by the Working Party of the British Society for Antimicrobial Chemotherapy, the Healthcare Infection Society and the British Infection Association (Hawkey et al., 2018) considered that MCCT including a high dose and continuous infusion of meropenem would be appropriate for *K. pneumoniae* with MICs  $> 8$  and  $< 64$  mg/L. In addition, some studies have indicated that MCCT may grant a survival benefit relative to that of meropenem in monotherapy when the MIC of *K. pneumoniae* is  $< 16$  mg/L (Tumbarello et al., 2012; Daikos

et al., 2014). Moreover, even for strains with MICs  $\geq 16$  mg/L, MCCT including a high dose of 13.2 g/day and continuous infusion of meropenem with levels optimized by therapeutic drug monitoring were helpful in obtaining a favorable clinical outcome for infections due to KPC-producing *K. pneumoniae* with MICs of 16–64 mg/L (Pea et al., 2017). Another study also demonstrated the benefits of MCCT using a high dose of 6 g daily and 3-h extended infusion for meropenem for an infection due to meropenem-nonsusceptible *K. pneumoniae* strains with MICs  $\geq 16$  mg/L (Giannella et al., 2018).

Understandably, these reports imply that MCCT is preferable for treating meropenem-nonsusceptible *K. pneumoniae* infections arising from strains with MICs  $> 8$  or even  $\geq 16$  mg/L. Likewise, some retrospective, prospective observational cohort and multicentric studies have confirmed the superiority of MCCT over monotherapy for the treatment of infections due to KPC-producing *K. pneumoniae*, especially for bloodstream infections (Zarkotou et al., 2011; Qureshi et al., 2012; Tumbarello et al., 2012; Daikos et al., 2014). In contrast, another most recently retrospective study (Kuti et al., 2019), in which PD exposures of meropenem as an adjunctive treatment in plazomicin-based combination therapy (i.e., plazomicin plus meropenem) were evaluated to investigate its synergy in combination against meropenem-nonsusceptible *K. pneumoniae* with MICs  $\geq 64$  mg/L, showed PD exposures of 0% for meropenem at the target of  $\geq 40\%$   $fT > MIC$  when meropenem was administered as 2 g q 8 h over a 3-h infusion and therefore concluded that plazomicin monotherapy was sufficient and optimization of meropenem therapy was not required for the combination to achieve microbiological response and clinical efficacy against serious meropenem-nonsusceptible *K. pneumoniae* infections, including bloodstream infections, hospital acquired pneumonia or ventilator-associated pneumonia.

It should also be noted that because most conclusions on the superiority of MCCT reached from the abovementioned reports were derived based on meropenem-nonsusceptible *K. pneumoniae*, the extrapolation of MCCT using a high dose and prolonged infusion for meropenem to other MNBSs with different resistance mechanisms requires further investigation. Coincidentally, the recent Amsterdam Investigator-Initiated Absorb Strategy All-Comers trial (Paul et al., 2018), in which a randomized, controlled, superiority trial was conducted at six hospitals to investigate the superiority of MCCT (i.e., colistin plus meropenem) vs. colistin alone, showed no differences in the outcomes of patients treated with MCCT or colistin monotherapy for infections (including bloodstream infections, ventilator-associated pneumonia and/or hospital acquired pneumonia, and urinary tract infections) due to carbapenem-resistant *Acinetobacter* spp., *Enterobacteriaceae*, and *P. aeruginosa* in which 97% of the isolates had meropenem MICs  $> 8$  mg/L. This result supported that colistin monotherapy is equipotent to MCCT for such infections, and it is therefore unnecessary to use MCCT to treat infections due to these MNBSs. Overall, the choice of MCCT or monotherapy for the treatment of infections due to MNBSs remains a matter of debate. Also, it is important to note that co-administration of different antibiotics may lead to important concomitant adverse effects, including

*Clostridium difficile* infection, selection of further resistances, or nephrotoxicity (Petrosillo et al., 2013).

Inconsistent with these reports, our data supported that even meropenem monotherapy, rather than plazomicin monotherapy, colistin monotherapy, or MCCT, is sufficient for the treatment of such infections due to these pathogens (i.e., the abovementioned *Acinetobacter* spp., *P. aeruginosa*, and *Enterobacteriaceae*, including meropenem-nonsusceptible *K. pneumoniae*) and for situations in which meropenem exposures are not reduced relative to plasma exposures, such as bloodstream infections, skin and soft tissue infections, and urinary tract infections. Meropenem monotherapy, in which it must be administered at a high dose of 2 g q 8 h or 1.5 g q 6 h and as an OTAT, can achieve optimal PK/PD exposures for MNBSs with MICs of up to 128 mg/L and for pathogen populations with a pooled MIC distribution, as demonstrated by achieving a PTA of  $\geq 90\%$  at an MIC of 128 mg/L and a CFR of  $\geq 90\%$  for *Acinetobacter* spp., *P. aeruginosa*, and *Enterobacteriaceae* populations when using the dosage regimen of 2 g [1.5 g (5-min IVB) + 0.5 g (6h)] q 8 h or 1.5 g [1 g (5-min IVB) + 0.5 g (6h)] q 6 h and using 50%  $fT > MIC$  as the PD target for such types of infection.

However, meropenem monotherapy did not display acceptable PK/PD exposures for the isolates with MICs  $\geq 256$  mg/L in the present study regardless of the dosing models and PD targets. Interestingly, another PK/PD study (Del Bono et al., 2017) in which meropenem using a high dose of 2 g q 8 h and 3-h TSPI in MCCT (i.e., meropenem plus tigecycline or gentamicin or colistin, or meropenem plus tigecycline plus gentamicin or colistin) was used to treat bloodstream infections due to KPC-producing *K. pneumoniae* with actual meropenem MICs  $\geq 256$  mg/L also showed that meropenem did not achieve the PD target of  $T > 40\% \times MIC$  in these isolates based on the measured meropenem levels despite the MCCT used. Moreover, at this dosage condition, meropenem could have attained PTAs of only 68 and 32% at that PD target in isolates with hypothetical MICs of 16 and 32 mg/L, respectively, despite the MCCT used. Thus, no synergisms were concluded between meropenem and the co-administered agents in this study. This conclusion was confirmed by the study conducted by Kuti et al. (2019), in which meropenem administered as 2 g q 8 h over a 3-h infusion had no synergy on the co-administered plazomicin when used for the treatment of infections due to meropenem-nonsusceptible *K. pneumoniae* with meropenem MICs  $\geq 64$  mg/L. One reason why unsatisfactory meropenem exposures were observed in these studies may be that TSPI for meropenem reduced its AUC exposures above the MIC, especially for values  $> 16$  mg/L, due to both the decrease in its peak concentration and the delay in its peak time. Based on these observations and ours, when administered as a reasonable OTAT and used for bloodstream infections, meropenem monotherapy displayed equally discontented exposures against highly resistant bacterial isolates with MICs  $\geq 256$  mg/L but showed a superior effect against relatively lowly resistant bacterial isolates with MICs  $\leq 128$  mg/L when compared with that of MCCT including a high dose and TSPI of meropenem. This finding suggests a possible usefulness of meropenem monotherapy for the treatment of such infections caused by isolates with MICs of up to 128 mg/L.



High MICs often result in insufficient antimicrobial tissue exposures, especially when the drug is used in inappropriate dosage regimens and used for infected sites with poor drug penetration. Regarding this issue, our data provide very useful directions on whether meropenem at the optimal dosage regimens can be used as a monotherapy for the treatment of infections due to isolates with high MICs at different sites based on the exact MICs if available. Given the profiles of meropenem tissue penetration, for infections due to isolates with MICs  $\geq 16$  mg/L occurring in the liver, skin, uterus, ovaries, rectum, prostate, trachea, etc., meropenem monotherapy with at least a 3 g daily dose yields good outcomes, e.g., the dosage regimen of 1 g [preferred 0.5 g (5-min IVB) + 0.5 g (5–6 h)] q 8 h for isolates with MICs of 16 mg/L, the dosage regimen of 2 g [preferred 1.5 g (5-min IVB) + 0.5 g (6 h)] q 8 h, 0.75 g [preferred 0.5 g (5-min IVB) + 0.25 g (6 h)] q 6 h or 1.5 g [preferred 1 g (5-min IVB) + 0.5 g (6 h)] q 6 h for isolates with MICs of up to 64 mg/L, and is thus sufficient. Satisfactorily, for infections occurring in the peritoneum, the dosage regimen of 0.5 g [preferred 0.25 g (5-min IVB) + 0.25 g (5–6 h)] q 8 h would be sufficient for isolates with MICs of 16 mg/L, and the dosage regimen of 1 g [preferred 0.5 g (5-min IVB) + 0.5 g (5–6 h)] q 8 h, 0.75 g [preferred 0.5 g (5-min IVB) + 0.25 g (6 h)] q 6 h, 2 g [preferred 1.5 g (5-min IVB) + 0.5 g (6 h)] q 8 h or 1.5 g [preferred 1 g (5-min IVB) + 0.5 g (6 h)] q 6 h for isolates with MICs of up to 32, 64, and 128 mg/L would be adequate, respectively. Surprisingly, even for infections located in the lung, bronchus, and pleura, meropenem with the preferred regimen of 2 g [1.5 g (5-min IVB) + 0.5 g (5 h)] q 8 h still proved effective for isolates with MICs of up to 32 mg/L, suggesting that for LRTIs and pleural infections, meropenem monotherapy can still perform good bactericidal action on isolates with MICs of up to 32 mg/L.

However, the exact MIC values, especially those  $>16$  mg/L, are often unavailable because automated systems such as VITEK-2, which indicate MIC values as high as  $>16$  mg/L, are unable to determine the precise MIC. Regarding this problem, our data provided the CFR for the targeted bacterial population and summarized the treatment options (Table 3). As a potential monotherapy, meropenem with an aggressive dosage regimen of 2 g [preferred 1.5 g (5-min IVB) + 0.5 g (6 h)] q 8 h or 1.5 g [preferred 1 g (5-min IVB) + 0.5 g (6 h)] q 6 h may be the best choice and is worth trying in its empiric therapy, especially for critically ill patients, because even at a PD target of  $50\% fT > 2 \times \text{MIC}$ , these dosage regimens could produce

a CFR of  $\geq 90\%$  for all of the tested bacterial populations with MICs  $\geq 16$  mg/L, including *A. baumannii*, *Acinetobacter* spp., *E. faecium*, *P. aeruginosa*, *S. epidermidis*, *S. haemolyticus*, and *S. maltophilia*, with the sole exception of *E. faecalis*. This result suggests that in the empiric therapy of meropenem, these dosage regimens would be competent for the vast majority of infections (e.g., bloodstream infections, intraabdominal infections, skin, and soft tissue infections, and urinary tract infections) due to these pathogens based on the profiles of meropenem tissue penetration. However, for LRTIs and pleural infections, meropenem monotherapy with the most promising dosage regimen of 2 g [1.5 g (5-min IVB) + 0.5 g (5 h)] q 8 h would be sufficient for infections due to only *Acinetobacter* spp., *P. aeruginosa*, *S. epidermidis*, *S. haemolyticus*, and *S. maltophilia*. Table 4 summarizes some preferred dosage regimens in the empiric therapy of meropenem for different types of infection based on our analysis.

Of note, these optimal dosage regimens sufficient for MNBSs are also adequate for meropenem-susceptible bacterial strains since the regimens established at higher MICs generate higher PTAs and CFRs at low MICs. In addition, we need to monitor renal function regularly and adjust the meropenem dose as required, particularly for the high dose regimens, as the majority of the patients infected with meropenem-nonsusceptible *K. pneumoniae* are critically ill and have altered renal function (Daikos and Markogiannakis, 2011). Although meropenem monotherapy displays satisfactory PK/PD exposures against highly resistant bacterial isolates, especially when it is administered at a high dose of 2 g q 8 h in OTAT, the accompanying safety issues are also worthy of our attention, especially when a high dose is used. However, although the most frequent adverse events associated with meropenem use, such as diarrhea, rash, nausea, and vomiting, thrombocytosis, eosinophilia and changes in hepatic biochemistry and the possible episodes of seizures are reported, meropenem exhibits an acceptable safety profile with good central nervous system and gastrointestinal tolerability, even at a high dose of up to 6 g per day (2 g q 8 h), and shows also a favorable safety profile in a number of special patient populations, including elderly, renally impaired, pediatric, and neutropenic patients, patients with cystic fibrosis and those with meningitis (Norrby, 1995; Norrby et al., 1995; Norrby and Gildon, 1999; Linden, 2007). Therefore, the dosage regimens recommended herein for highly resistant bacterial strains should be safe and worthwhile to try.

**TABLE 4 |** Summary of preferred treatment option recommendations in the empiric therapy of meropenem for different types of infection based on our analysis.

Optimal PD target	Corresponding types of infection or infected sites	Preferred treatment option recommendations for MNBSs with MICs $\geq 16$ mg/L
50% $fT > \text{MIC}$	Bacterial peritonitis or intraabdominal infections, bloodstream infections, skin and soft tissue infections, or urinary tract infections	2 g [1.5 g (5-min IVB) + 0.5 g (6 h)] q 8 h or 1.5 g [(5-min IVB) + 0.5 g (6 h)] q 6 h
50% $fT > 2 \times \text{MIC}$	Bacterial hepatitis, metritis, oophoritis, proctitis, or prostatitis	2 g [1.5 g (5-min IVB) + 0.5 g (6 h)] q 8 h or 1.5 g [1 g (5-min IVB) + 0.5 g (6 h)] q 6 h
50% $fT > 5 \times \text{MIC}$	LRTIs, such as pneumonia, bronchitis, or pleural infections	2 g [1.5 g (5-min IVB) + 0.5 g (5 h)] q 8 h

## Study Limitations

The present study has some limitations. First, our data did not include meropenem concentrations in plasma or infected sites. Second, the results of simulation analysis were not validated by evaluating clinical outcomes, limiting the generalization of the conclusions. Third, the susceptibility data used in the modeling for our predictions of target attainment were obtained from the EUCAST database. As such, our findings should be interpreted and extrapolated while paying attention to the different or changing susceptibility profiles in one's own hospital. Fourth, a one-compartment model was used to calculate the meropenem PD exposures, whereas other studies have suggested that its *in vivo* pharmacokinetic disposition is best fitted using a two-compartment model. However, studies on its PK have been published using both one- and two-compartment models as well as non-compartmental analysis (Christensson et al., 1992; Leroy et al., 1992a,b).

Despite these limitations, our data are believable and instructive for prescribers because it considered the profiles of meropenem tissue penetration, used the more representative PK parameters, and integrated the most current and comprehensive MIC data. Importantly, even with  $f(C_{\min})/MIC > 5$  recommended by Li et al. (2007) as a PD target associated with clinical response, our data derived from  $50\% fT > 5 \times MIC$  also confirmed that meropenem monotherapy is competent for infections due to isolates with MICs of up to 32 mg/L, and importantly in the absence of alternative treatments, our data provide very useful directions on how to choose an optimal dosage regimen for meropenem monotherapy for the treatment of infections due to isolates with high MICs at different sites. To the best of our knowledge, this is the first PD analysis in which meropenem was used as a monotherapy aimed at MNBSs with MICs  $\geq 16$  mg/L and in which the profiles of meropenem tissue penetration were taken into account for setting the PD targets and calculating the PTAs and CFRs. In addition, we plan to perform a clinical trial to confirm our findings and to validate the optimal dosage by using the established equation for  $\%fT > MIC$  and the Monte Carlo simulation.

## REFERENCES

- Avery, L. M., and Nicolau, D. P. (2018). Investigational drugs for the treatment of infections caused by multidrug-resistant Gram-negative bacteria. *Expert Opin. Investig. Drugs* 27, 325–338. doi: 10.1080/13543784.2018.1460354
- Bartsch, S. M., McKinnell, J. A., Mueller, L. E., Miller, L. G., Gohil, S. K., Huang, S. S., et al. (2017). Potential economic burden of carbapenem-resistant *Enterobacteriaceae* (CRE) in the United States. *Clin. Microbiol. Infect.* 23, 48.e9–48.e16. doi: 10.1016/j.cmi.2016.09.003
- Bergogne-Bérézin, E., Muller-Serieys, C., Aubier, M., and Dombret, M. C. (1994). Concentration of meropenem in serum and in bronchial secretions in patients undergoing fiberoptic bronchoscopy. *Eur. J. Clin. Pharmacol.* 46, 87–88. doi: 10.1007/BF00195922
- Bulens, S. N., Yi, S. H., Walters, M. S., Jacob, J. T., Bower, C., Reno, J., et al. (2018). Carbapenem-nonsusceptible *Acinetobacter baumannii*, 8 US metropolitan areas, 2012–2015. *Emerg. Infect. Dis.* 24, 727–734. doi: 10.3201/eid2404.171461
- Burgess, D. S., Frei, C. R., Lewis II, J. S., Fiebelkorn, K. R., and Jorgensen, J. H. (2007). The contribution of pharmacokinetic-pharmacodynamic modelling with Monte Carlo simulation to the development of susceptibility breakpoints for *Neisseria meningitidis*. *Clin. Microbiol. Infect.* 13, 33–39. doi: 10.1111/j.1469-0691.2006.01617.x
- Byl, B., Jacobs, F., Roucloux, I., de Franquen, P., Cappello, M., and Thys, J. P. (1999). Penetration of meropenem in lung, bronchial mucosa, and pleural tissues. *Antimicrob. Agents Chemother.* 43, 681–682. doi: 10.1128/AAC.43.3.681
- Capitano, B., Nicolau, D. P., Potoski, B. A., Byers, K. E., Horowitz, M., Venkataramanan, R., et al. (2004). Meropenem administered as a prolonged infusion to treat serious gram-negative central nervous system infections. *Pharmacotherapy* 24, 803–807. doi: 10.1592/phco.24.8.803.36070
- Christensson, B. A., Nilsson-Ehle, I., Hutchison, M., Haworth, S. J., Oqvist, B., and Norrby, S. R. (1992). Pharmacokinetics of meropenem in subjects with various degrees of renal impairment. *Antimicrob. Agents Chemother.* 36, 1532–1537. doi: 10.1128/AAC.36.7.1532
- Clinical and Laboratory Standards Institute (CLSI) (2019). *Performance Standards for Antimicrobial Susceptibility Testing, 29th Edn*. Wayne, PA: Clinical and Laboratory Standards Institute.

## CONCLUSIONS

When faced with the daily challenge of infections due to MNBSs, we should try to reduce the gap between the available medical evidence for using meropenem against such infections and the dearth of alternative therapeutic options, some of which have not been sufficiently explored and/or whose efficacy in certain situations remains doubtful. Whether we can continue to use meropenem in the presence of MNBSs with high MICs remains controversial. The data analyses presented herein support the opinion that meropenem monotherapy can still be considered for use against MNBSs provided that (i) the MIC for the infecting pathogen isolates is  $\leq 32$  mg/L and (ii) a reasonable OTAT is used to drive the PK/PD profiles to acceptable exposures. However, in the absence of control trials, the continued appraisal of meropenem for use as a monotherapy, along with the optimal dosage regimens in clinical experience, will provide further important information on its utility against MNBSs.

## DATA AVAILABILITY STATEMENT

All datasets generated for this study are included in the manuscript.

## AUTHOR CONTRIBUTIONS

XS performed the model simulation and wrote the manuscript. YW, LC, DY, and ML conceptualized and supervised the manuscript. All authors approved the final version of the manuscript.

## ACKNOWLEDGMENTS

The authors are grateful to Profs. Lu and Shen for their directions on meropenem anti-infection therapy, and we thank all members of our hospital library for access to their information resources.

- Cockcroft, D. W., and Gault, M. H. (1976). Prediction of creatinine clearance from serum creatinine. *Nephron* 16, 31–41. doi: 10.1159/000180580
- Cojutti, P., Sartor, A., Bassetti, M., Scarparo, C., and Pea, F. (2018). Is meropenem MIC increase against KPC-producing *Klebsiella pneumoniae* correlated with increased resistance rates against other antimicrobials with Gram-negative activity? *J. Glob. Antimicrob. Resist.* 14, 238–241. doi: 10.1016/j.jgar.2018.05.005
- Daikos, G. L., and Markogiannakis, A. (2011). Carbapenemase-producing *Klebsiella pneumoniae*: (when) might we still consider treating with carbapenems? *Clin. Microbiol. Infect.* 17, 1135–1141. doi: 10.1111/j.1469-0691.2011.03553.x
- Daikos, G. L., Tsaousi, S., Tzouveleki, L. S., Anyfantis, I., Psychogiou, M., Argyropoulou, A., et al. (2014). Carbapenemase-producing *Klebsiella pneumoniae* bloodstream infections: lowering mortality by antibiotic combination schemes and the role of carbapenems. *Antimicrob. Agents Chemother.* 58, 2322–2328. doi: 10.1128/AAC.02166-13
- Del Bono, V., Giacobbe, D. R., Marchese, A., Parisini, A., Fucile, C., Coppo, E., et al. (2017). Meropenem for treating KPC-producing *Klebsiella pneumoniae* bloodstream infections: should we get to the PK/PD root of the paradox? *Virulence* 8, 66–73. doi: 10.1080/21505594.2016.1213476
- Eguchi, K., Kanazawa, K., Shimizudani, T., Kanemitsu, K., and Kaku, M. (2010). Experimental verification of the efficacy of optimized two-step infusion therapy with meropenem using an *in vitro* pharmacodynamic model and Monte Carlo simulation. *J. Infect. Chemother.* 16, 1–9. doi: 10.1007/s10156-009-0001-8
- European Committee on Antimicrobial Susceptibility Testing (EUCAST) (2019). *Antimicrobial Wild Type Distributions of Microorganisms, Version 5.26*. Available online at: <https://mic.eucast.org/Eucast2/SearchController/search.jsp?action=performSearch&BeginIndex=0&Midif=mic&NumberIndex=50&Antib=177&Specium=-1> (accessed April 12, 2019).
- Fehér, C., Rovira, M., Soriano, A., Esteve, J., Martínez, J. A., Marco, F., et al. (2014). Effect of meropenem administration in extended infusion on the clinical outcome of febrile neutropenia: a retrospective observational study. *J. Antimicrob. Chemother.* 69, 2556–2562. doi: 10.1093/jac/dku150
- Giannella, M., Trearicchi, E. M., Giacobbe, D. R., De Rosa, F. G., Bassetti, M., Bartoloni, A., et al. (2018). Effect of combination therapy containing a high-dose carbapenem on mortality in patients with carbapenem-resistant *Klebsiella pneumoniae* bloodstream infection. *Int. J. Antimicrob. Agents* 51, 244–248. doi: 10.1016/j.ijantimicag.2017.08.019
- Gomez-Simmonds, A., Nelson, B., Eiras, D. P., Loo, A., Jenkins, S. G., Whittier, S., et al. (2016). Combination regimens for treatment of carbapenem-resistant *Klebsiella pneumoniae* bloodstream infections. *Antimicrob. Agents Chemother.* 60, 3601–3607. doi: 10.1128/AAC.03007-15
- Gonçalves-Pereira, J., and Póvoa, P. (2011). Antibiotics in critically ill patients: a systematic review of the pharmacokinetics of  $\beta$ -lactams. *Crit Care* 15:R206. doi: 10.1186/cc10441
- Harrison, M. P., Moss, S. R., Featherstone, A., Fowkes, A. G., Sanders, A. M., and Case, D. E. (1989). The disposition and metabolism of meropenem in laboratory animals and man. *J. Antimicrob. Chemother.* 24(Suppl. A), 265–277. doi: 10.1093/jac/24.suppl\_A.265
- Hawkey, P. M., Warren, R. E., Livermore, D. M., McNulty, C. A. M., Enoch, D. A., Otter, J. A., et al. (2018). Treatment of infections caused by multidrug-resistant Gram-negative bacteria: report of the British Society for Antimicrobial Chemotherapy/Healthcare Infection Society/British Infection Association Joint Working Party. *J. Antimicrob. Chemother.* 73, iii2–iii78. doi: 10.1093/jac/dky027
- Hextall, A., Andrews, J. M., Donovan, I. A., and Wise, R. (1991). Intraperitoneal penetration of meropenem. *J. Antimicrob. Chemother.* 28, 314–316. doi: 10.1093/jac/28.2.314
- Hsu, A. J., and Tamma, P. D. (2014). Treatment of multidrug-resistant Gram-negative infections in children. *Clin. Infect. Dis.* 58, 1439–1448. doi: 10.1093/cid/ciu069
- Huang, Y., Zhou, Q., Wang, W., Huang, Q., Liao, J., Li, J., et al. (2019). *Acinetobacter baumannii* ventilator-associated pneumonia: clinical efficacy of combined antimicrobial therapy and *in vitro* drug sensitivity test results. *Front. Pharmacol.* 10:92. doi: 10.3389/fphar.2019.00092
- Ikawa, K., Nakashima, A., Morikawa, N., Ikeda, K., Murakami, Y., Ohge, H., et al. (2011). Clinical pharmacokinetics of meropenem and biapenem in bile and dosing considerations for biliary tract infections based on site-specific pharmacodynamic target attainment. *Antimicrob. Agents Chemother.* 55, 5609–5615. doi: 10.1128/AAC.00497-11
- Iovleva, A., and Doi, Y. (2017). Carbapenem-resistant *enterobacteriaceae*. *Clin. Lab. Med.* 37, 303–315. doi: 10.1016/j.cll.2017.01.005
- Jaruratanasirikul, S., Thengyai, S., Wongpoowarak, W., Wattanavijitkul, T., Tangkitwanitjaroen, K., Sukarnjanaset, W., et al. (2015). Population pharmacokinetics and Monte Carlo dosing simulations of meropenem during the early phase of severe sepsis and septic shock in critically ill patients in intensive care units. *Antimicrob. Agents Chemother.* 59, 2995–3001. doi: 10.1128/AAC.04166-14
- Karaiskos, I., Galani, I., Souli, M., and Giamarellou, H. (2019). Novel  $\beta$ -lactam- $\beta$ -lactamase inhibitor combinations: expectations for the treatment of carbapenem-resistant Gram-negative pathogens. *Expert Opin. Drug Metab. Toxicol.* 15, 133–149. doi: 10.1080/17425255.2019.1563071
- Kelly, A. M., Mathema, B., and Larson, E. L. (2017). Carbapenem-resistant *Enterobacteriaceae* in the community: a scoping review. *Int. J. Antimicrob. Agents* 50, 127–134. doi: 10.1016/j.ijantimicag.2017.03.012
- Kondo, N., Ikawa, K., Murakami, Y., Uemura, K., Sudo, T., Hashimoto, Y., et al. (2014). Clinical pharmacokinetics of meropenem in pancreatic juice and site-specific pharmacodynamic target attainment against Gram-negative bacteria: dosing considerations. *Pancreatolgy* 14, 95–99. doi: 10.1016/j.pan.2014.02.002
- Kuti, J. L., Dandekar, P. K., Nightingale, C. H., and Nicolau, D. P. (2003). Use of Monte Carlo simulation to design an optimized pharmacodynamic dosing strategy for meropenem. *J. Clin. Pharmacol.* 43, 1116–1123. doi: 10.1177/0091270003257225
- Kuti, J. L., Horowitz, S., Nightingale, C. H., and Nicolau, D. P. (2005). Comparison of pharmacodynamic target attainment between healthy subjects and patients for ceftazidime and meropenem. *Pharmacotherapy* 25, 935–941. doi: 10.1592/phco.2005.25.7.935
- Kuti, J. L., Kim, A., Cloutier, D. J., and Nicolau, D. P. (2019). Evaluation of plazomicin, tigecycline, and meropenem pharmacodynamic exposure against carbapenem-resistant *Enterobacteriaceae* in patients with bloodstream infection or hospital-acquired/ventilator-associated pneumonia from the CARE study (ACHN-490-007). *Infect. Dis. Ther.* 8, 383–396. doi: 10.1007/s40121-019-0251-4
- Kuti, J. L., Nightingale, C. H., Knauff, R. F., and Nicolau, D. P. (2004). Pharmacokinetic properties and stability of continuous-infusion meropenem in adults with cystic fibrosis. *Clin. Ther.* 26, 493–501. doi: 10.1016/S0149-2918(04)90051-3
- Lemos, E. V., de la Hoz, F. P., Einarsen, T. R., McGhan, W. F., Quevedo, E., Castañeda, C., et al. (2014). Carbapenem resistance and mortality in patients with *Acinetobacter baumannii* infection: systematic review and meta-analysis. *Clin. Microbiol. Infect.* 20, 416–423. doi: 10.1111/1469-0691.12363
- Leroy, A., Fillastre, J. P., Borsa-Lebas, F., Etienne, I., and Humbert, G. (1992a). Pharmacokinetics of meropenem (ICI 194,660) and its metabolite (ICI 213,689) in healthy subjects and in patients with renal impairment. *Antimicrob. Agents Chemother.* 36, 2794–2798. doi: 10.1128/AAC.36.12.2794
- Leroy, A., Fillastre, J. P., Etienne, I., Borsa-Lebas, F., and Humbert, G. (1992b). Pharmacokinetics of meropenem in subjects with renal insufficiency. *Eur. J. Clin. Pharmacol.* 42, 535–538. doi: 10.1007/BF00314864
- Li, C., Du, X., Kuti, J. L., and Nicolau, D. P. (2007). Clinical pharmacodynamics of meropenem in patients with lower respiratory tract infections. *Antimicrob. Agents Chemother.* 51, 1725–1730. doi: 10.1128/AAC.00294-06
- Li, C., Kuti, J. L., Nightingale, C. H., and Nicolau, D. P. (2006). Population pharmacokinetic analysis and dosing regimen optimization of meropenem in adult patients. *J. Clin. Pharmacol.* 46, 1171–1178. doi: 10.1177/0091270006291035
- Linden, P. (2007). Safety profile of meropenem: an updated review of over 6,000 patients treated with meropenem. *Drug Saf.* 30, 657–668. doi: 10.2165/00002018-200730080-00002
- Liu, X., Zhao, M., Chen, Y., Bian, X., Li, Y., Shi, J., et al. (2016). Synergistic killing by meropenem and colistin combination of carbapenem-resistant *Acinetobacter baumannii* isolates from Chinese patients in an *in vitro* pharmacokinetic/pharmacodynamic model. *Int. J. Antimicrob. Agents* 48, 559–563. doi: 10.1016/j.ijantimicag.2016.07.018
- Lodise, T. P., Sorgel, F., Melnick, D., Mason, B., Kinzig, M., and Drusano, G. L. (2011). Penetration of meropenem into epithelial lining fluid of patients



- with ventilator-associated pneumonia. *Antimicrob. Agents Chemother.* 55, 1606–1610. doi: 10.1128/AAC.01330-10
- Lorente, L., Lorenzo, L., Martín, M. M., Jiménez, A., and Mora, M. L. (2006). Meropenem by continuous versus intermittent infusion in ventilator-associated pneumonia due to gram-negative bacilli. *Ann. Pharmacother.* 40, 219–223. doi: 10.1345/aph.1G467
- Moghnieh, R. A., Kanafani, Z. A., Tabaja, H. Z., Sharara, S. L., Awad, L. S., and Kanj, S. S. (2018). Epidemiology of common resistant bacterial pathogens in the countries of the Arab League. *Lancet Infect. Dis.* 18, e379–e394. doi: 10.1016/S1473-3099(18)30414-6
- Mouton, J. W., and Michel, M. F. (1991). Pharmacokinetics of meropenem in serum and suction blister fluid during continuous and intermittent infusion. *J. Antimicrob. Chemother.* 28, 911–918. doi: 10.1093/jac/28.6.911
- Nicasio, A. M., Quintiliani, R., DeRyke, C. A., Kuti, J. L., and Nicolau, D. P. (2007). Treatment of Serratia marcescens meningitis with prolonged infusion of meropenem. *Ann. Pharmacother.* 41, 1077–1081. doi: 10.1345/aph.1K060
- Nightingale, C. H., and Mur (2007). “Pharmacodynamics of antimicrobials: general concepts and applications,” in *Antimicrobial Pharmacodynamics in Theory and Clinical Practice. 2nd Edn*, eds H. N. Charles, P. G. Ambrose, G. L. Drusano, and T. Murakawa (New York, NY: CRC Press), 28–29. doi: 10.3109/9781420017137
- Nordmann, P. (2014). Carbapenemase-producing *Enterobacteriaceae*: overview of a major public health challenge. *Med. Mal. Infect.* 44, 51–56. doi: 10.1016/j.medmal.2013.11.007
- Norrby, S. R. (1995). Carbapenems. *Med. Clin. North Am.* 79, 745–759. doi: 10.1016/S0025-7125(16)30037-2
- Norrby, S. R., and Gildon, K. M. (1999). Safety profile of meropenem: a review of nearly 5,000 patients treated with meropenem. *Scand. J. Infect. Dis.* 31, 3–10. doi: 10.1080/00365549950161808
- Norrby, S. R., Newell, P. A., Faulkner, K. L., and Lesky, W. (1995). Safety profile of meropenem: international clinical experience based on the first 3125 patients treated with meropenem. *J. Antimicrob. Chemother.* 36(Suppl. A), 207–223. doi: 10.1093/jac/36.suppl\_A.207
- Oliva, A., Scorzolini, L., Cipolla, A., Mascellino, M. T., Cancelli, F., Castaldi, D., et al. (2017). *In vitro* evaluation of different antimicrobial combinations against carbapenemase-producing *Klebsiella pneumoniae*: the activity of the double-carbapenem regimen is related to meropenem MIC value. *J. Antimicrob. Chemother.* 72, 1981–1984. doi: 10.1093/jac/dkx084
- Onori, R., Gaiarsa, S., Comandatore, F., Pongolini, S., Brisse, S., Colombo, A., et al. (2015). Tracking nosocomial *Klebsiella pneumoniae* infections and outbreaks by whole-genome analysis: small-scale Italian scenario within a single hospital. *J. Clin. Microbiol.* 53, 2861–2868. doi: 10.1128/JCM.00545-15
- Paul, M., Daikos, G. L., Durante-Mangoni, E., Yahav, D., Carmeli, Y., Benattar, Y. D., et al. (2018). Colistin alone versus colistin plus meropenem for treatment of severe infections caused by carbapenem-resistant Gram-negative bacteria: an open-label, randomised controlled trial. *Lancet Infect. Dis.* 18, 391–400. doi: 10.1016/S1473-3099(18)30099-9
- Pea, F., Della Siega, P., Cojutti, P., Sartor, A., Crapis, M., Scarparo, C., et al. (2017). Might real-time pharmacokinetic/pharmacodynamic optimisation of high-dose continuous-infusion meropenem improve clinical cure in infections caused by KPC-producing *Klebsiella pneumoniae*? *Int. J. Antimicrob. Agents* 49, 255–258. doi: 10.1016/j.ijantimicag.2016.10.018
- Petrosillo, N., Giannella, M., Lewis, R., and Viale, P. (2013). Treatment of carbapenem-resistant *Klebsiella pneumoniae*: the state of the art. *Expert Rev. Anti Infect. Ther.* 11, 159–177. doi: 10.1586/eri.12.162
- Qureshi, Z. A., Paterson, D. L., Potoski, B. A., Kilayko, M. C., Sandovsky, G., Sordillo, E., et al. (2012). Treatment outcome of bacteremia due to KPC-producing *Klebsiella pneumoniae*: superiority of combination antimicrobial regimens. *Antimicrob. Agents Chemother.* 56, 2108–2113. doi: 10.1128/AAC.06268-11
- Roberts, J. A., Paul, S. K., Akova, M., Bassetti, M., De Waele, J. J., Dimopoulos, G., et al. (2014). DALI: defining antibiotic levels in intensive care unit patients: are current  $\beta$ -lactam antibiotic doses sufficient for critically ill patients? *Clin. Infect. Dis.* 58, 1072–1083. doi: 10.1093/cid/ciu027
- Salomão, M. C., Guimarães, T., Duailibi, D. F., Perondi, M. B. M., Letaif, L. S. H., Montal, A. C., et al. (2017). Carbapenem-resistant *Enterobacteriaceae* in patients admitted to the emergency department: prevalence, risk factors, and acquisition rate. *J. Hosp. Infect.* 97, 241–246. doi: 10.1016/j.jhin.2017.08.012
- Satlin, M. J., and Walsh, T. J. (2017). Multidrug-resistant *Enterobacteriaceae*, *Pseudomonas aeruginosa*, and vancomycin-resistant Enterococcus: three major threats to hematopoietic stem cell transplant recipients. *Transpl. Infect. Dis.* 19:e12762. doi: 10.1111/tid.12762
- Snitkin, E. S., Zelazny, A. M., Thomas, P. J., Stock, F., NISC Comparative Sequencing Program Group, Henderson, D. K., et al. (2012). Tracking a hospital outbreak of carbapenem-resistant *Klebsiella pneumoniae* with whole-genome sequencing. *Sci. Transl. Med.* 4:148ra116. doi: 10.1126/scitranslmed.3004129
- Tumbarello, M., Trecarichi, E. M., De Rosa, F. G., Giannella, M., Giacobbe, D. R., Bassetti, M., et al. (2015). Infections caused by KPC-producing *Klebsiella pneumoniae*: differences in therapy and mortality in a multicentre study. *J. Antimicrob. Chemother.* 70, 2133–2143. doi: 10.1093/jac/dkv086
- Tumbarello, M., Viale, P., Viscoli, C., Trecarichi, E. M., Tumietto, F., Marchese, A., et al. (2012). Predictors of mortality in bloodstream infections caused by *Klebsiella pneumoniae* carbapenemase-producing *K. pneumoniae*: importance of combination therapy. *Clin. Infect. Dis.* 55, 943–950. doi: 10.1093/cid/cis588
- Tzouveleki, L. S., Markogiannakis, A., Psychogiou, M., Tassios, P. T., and Daikos, G. L. (2012). Carbapenemases in *Klebsiella pneumoniae* and other *Enterobacteriaceae*: an evolving crisis of global dimensions. *Clin. Microbiol. Rev.* 25, 682–707. doi: 10.1128/CMR.05035-11
- USP PACKAGE INSERT. (1996). *MEROPENEM For Injection (Approval: 1996)*. Available online at: <https://www.sagentpharma.com/wpcproduct/meropenem-for-injection-usp/> (accessed April 12, 2019).
- Vourli, S., Tsala, M., Kotsakis, S., Daikos, G. L., Tzouveleki, L., Miriagou, V., et al. (2016). Comparison of short versus prolonged infusion of standard dose of meropenem against carbapenemase-producing *Klebsiella pneumoniae* isolates in different patient groups: a pharmacokinetic-pharmacodynamic approach. *J. Pharm. Sci.* 105, 1513–1518. doi: 10.1016/j.xphs.2016.02.008
- Watanabe, A., Fujimura, S., Kikuchi, T., Gomi, K., Fuse, K., and Nukiwa, T. (2007). Evaluation of dosing designs of carbapenems for severe respiratory infection using Monte Carlo simulation. *J. Infect. Chemother.* 13, 332–340. doi: 10.1007/s10156-007-0562-3
- Wise, R., Logan, M., Cooper, M., Ashby, J. P., and Andrews, J. M. (1990). Meropenem pharmacokinetics and penetration into an inflammatory exudate. *Antimicrob. Agents Chemother.* 34, 1515–1517. doi: 10.1128/AAC.34.8.1515
- Zarkotou, O., Pournaras, S., Tselioti, P., Dragoumanos, V., Pitiriga, V., Ranellou, K., et al. (2011). Predictors of mortality in patients with bloodstream infections caused by KPC-producing *Klebsiella pneumoniae* and impact of appropriate antimicrobial treatment. *Clin. Microbiol. Infect.* 17, 1798–1803. doi: 10.1111/j.1469-0691.2011.03514.x
- Zhao, H.-Y., Gu, J., Lyu, J., Liu, D., Wang, Y.-T., Liu, F., et al. (2017). Pharmacokinetic and pharmacodynamic efficacies of continuous versus intermittent administration of meropenem in patients with severe sepsis and septic shock: a prospective randomized pilot study. *Chin. Med. J.* 130, 1139–1145. doi: 10.4103/0366-6999.205859
- Zhou, Q., He, B., Zhang, C., Zhai, S., Liu, Z., and Zhang, J. (2011). Pharmacokinetics and pharmacodynamics of meropenem in elderly chinese with lower respiratory tract infections: population pharmacokinetics analysis using nonlinear mixed-effects modelling and clinical pharmacodynamics study. *Drugs Aging* 28, 903–912. doi: 10.2165/11595960-000000000-00000

**Conflict of Interest:** The authors declare that the research was conducted in the absence of any commercial or financial relationships that could be construed as a potential conflict of interest.

Copyright © 2019 Song, Wu, Cao, Yao and Long. This is an open-access article distributed under the terms of the Creative Commons Attribution License (CC BY). The use, distribution or reproduction in other forums is permitted, provided the original author(s) and the copyright owner(s) are credited and that the original publication in this journal is cited, in accordance with accepted academic practice. No use, distribution or reproduction is permitted which does not comply with these terms.





# Multiple *Klebsiella pneumoniae* KPC Clones Contribute to an Extended Hospital Outbreak

Carolina Ferrari<sup>1</sup>, Marta Corbella<sup>1,2</sup>, Stefano Gaiarsa<sup>1</sup>, Francesco Comandatore<sup>3,4</sup>, Erika Scaltriti<sup>5</sup>, Claudio Bandi<sup>3,6</sup>, Patrizia Cambieri<sup>1</sup>, Piero Marone<sup>1</sup> and Davide Sasserà<sup>7\*</sup>

<sup>1</sup> Microbiology and Virology Unit, Fondazione IRCCS Policlinico San Matteo, Pavia, Italy, <sup>2</sup> Biometric and Medical Statistics Unit, Fondazione IRCCS Policlinico San Matteo, Pavia, Italy, <sup>3</sup> Pediatric Research Center Romeo ed Enrica Invernizzi, University of Milan, Milan, Italy, <sup>4</sup> Department of Biomedical and Clinical Sciences "L. Sacco", University of Milan, Milan, Italy, <sup>5</sup> Risk Analysis and Genomic Epidemiology Unit, Istituto Zooprofilattico Sperimentale della Lombardia e dell'Emilia Romagna (IZSLER), Brescia, Italy, <sup>6</sup> Department of Biosciences, University of Milan, Milan, Italy, <sup>7</sup> Department of Biology and Biotechnology "L. Spallanzani", University of Pavia, Pavia, Italy

## OPEN ACCESS

### Edited by:

Rustam Aminov,  
University of Aberdeen,  
United Kingdom

### Reviewed by:

Costas C. Papagiannitsis,  
University of Thessaly, Greece  
Philippe Glaser,  
Institut Pasteur, France  
Marco Maria D'Andrea,  
University of Rome Tor Vergata, Italy

### \*Correspondence:

Davide Sasserà  
davide.sassera@unipv.it

### Specialty section:

This article was submitted to  
Antimicrobials, Resistance  
and Chemotherapy,  
a section of the journal  
Frontiers in Microbiology

**Received:** 12 June 2019

**Accepted:** 13 November 2019

**Published:** 29 November 2019

### Citation:

Ferrari C, Corbella M, Gaiarsa S, Comandatore F, Scaltriti E, Bandi C, Cambieri P, Marone P and Sasserà D (2019) Multiple *Klebsiella pneumoniae* KPC Clones Contribute to an Extended Hospital Outbreak. *Front. Microbiol.* 10:2767. doi: 10.3389/fmicb.2019.02767

The circulation of carbapenem-resistant *Klebsiella pneumoniae* (CRKP) is a significant problem worldwide. In this work we characterize the isolates and reconstruct the spread of a multi-clone epidemic event that occurred in an Intensive Care Unit in a hospital in Northern Italy. The event took place from August 2015 to May 2016 and involved 23 patients. Twelve of these patients were colonized by CRKP at the gastrointestinal level, while the other 11 were infected in various body districts. We retrospectively collected data on the inpatients and characterized a subset of the CRKP isolates using antibiotic resistance profiling and whole genome sequencing. A SNP-based phylogenetic approach was used to depict the evolutionary context of the obtained genomes, showing that 26 of the 32 isolates belong to three genome clusters, while the remaining six were classified as sporadic. The first genome cluster was composed of multi-resistant isolates of sequence type (ST) 512. Among those, two were resistant to colistin, one of which indicating the insurgence of resistance during an infection. One patient hospitalized in this period was colonized by two strains of CRKP, both carrying the *blaKPC* gene (variant KPC-3). The analysis of the genome contig containing the *blaKPC* locus indicates that the gene was not transmitted between the two isolates. The second infection cluster comprised four other genomes of ST512, while the third one (ST258) colonized 12 patients, causing five clinical infections and resulting in seven deaths. This cluster presented the highest level of antibiotic resistance, including colistin resistance in all 17 analyzed isolates. The three outbreaking clones did not present more virulence genes than the sporadic isolates and had different patterns of antibiotic resistance, however, were clearly distinct from the sporadic ones in terms of infection status, being the only ones causing overt infections.

**Keywords:** KPC, genomic epidemiology, MDR, *Klebsiella pneumoniae*, nosocomial outbreak, colistin resistance

## INTRODUCTION

*Klebsiella pneumoniae* (*Kp*) is ubiquitous in the environment, part of the normal intestinal microbiota in humans and capable of colonizing the skin and nasopharynx of healthy individuals (Podschun and Ullmann, 1998; Broberg et al., 2014). *Kp* can persist on abiotic surfaces of different origin through the synthesis of biofilm, which can also make bacteria resistant to the action of antimicrobial agents (Di Martino et al., 2003). In immunocompromised or debilitated hospitalized patients with severe underlying diseases, *Kp* causes urinary tract, respiratory tract and bloodstream infections (Podschun and Ullmann, 1998) as well as other less frequent diseases, including osteomyelitis, arthritis (Ghorashi et al., 2011), and meningitis (Ko et al., 2002; Tumbarello et al., 2006; Nordmann et al., 2009). *Kp* is responsible for roughly 12% of Gram-negative infections in hospital intensive care units (ICUs) in Europe (European Centre for Disease Prevention and Control [ECDC], 2016). *Kp* invasive infections are associated with high rates of morbidity and mortality due to the high prevalence of resistance to most available antimicrobial agents (Patel et al., 2008; Borer et al., 2009). This is an emerging concern in clinical care resulting in an increase of mortality rates and costs.

The most commonly used class of antibiotics against nosocomial infections is  $\beta$ -lactams, which includes penicillin derivatives, cephalosporins, monobactams and the most recently developed carbapenems. Frequent use and abuse of these drugs, combined with the transmissibility of resistance determinants mediated by mobile elements (plasmids, transposons, and other integrative conjugative elements), has contributed to the spread of resistance to  $\beta$ -lactams by *Kp* (Mathers et al., 2015; Navon-Venezia et al., 2017). In the last 20 years, the emergence of isolates resistant to carbapenems has limited the efficacy of this last line treatment option hampering the use of this whole class of antibiotics, with few alternatives (Mathers et al., 2015; Navon-Venezia et al., 2017). One of the most common mechanism of resistance to carbapenems in *Kp* is the *K. pneumoniae* carbapenemase (KPC). This is an Ambler molecular class A serine enzyme that is able to hydrolyze a broad variety of  $\beta$ -lactams. KPC carbapenemases are plasmid-encoded, they have been originally associated with the *Kp* clonal group 258 (CG258) (Samuelsen et al., 2009; Breurec et al., 2013) but are not limited to it, as a number of occurrences of strains of other sequence types (ST) carrying the gene have been reported (Giakkoupi et al., 2010; Qi et al., 2010; Tzouveleki et al., 2013; Markovska et al., 2015; Oteo et al., 2016; Villa et al., 2016; Wei et al., 2016; Aires et al., 2017). KPC-carrying *Kp* strains have recently spread worldwide, with some countries, including Italy, being heavily affected. In Italy, in 2017, 33.9% of the *Kp* nosocomial infections were caused by KPC strains (Sabbatucci et al., 2017). Most of these strains belong to the CG258, which in Italy has been shown to have been imported on four occasions, giving rise to four Italian-subclades (Gaiarsa et al., 2015). The spread of carbapenem-resistant strains has led to the resurgence of the use of colistin, previously abandoned due to its nephrotoxicity and neurotoxicity (Javan et al., 2015; Velkov et al., 2018). This has however resulted in the emergence of colistin-resistant

strains, both due to the insurgence of chromosomal mutations (Cannatelli et al., 2014; Olaitan et al., 2014) and to the acquisition of plasmid-encoded resistance genes (Di Pilato et al., 2016; Liu et al., 2016).

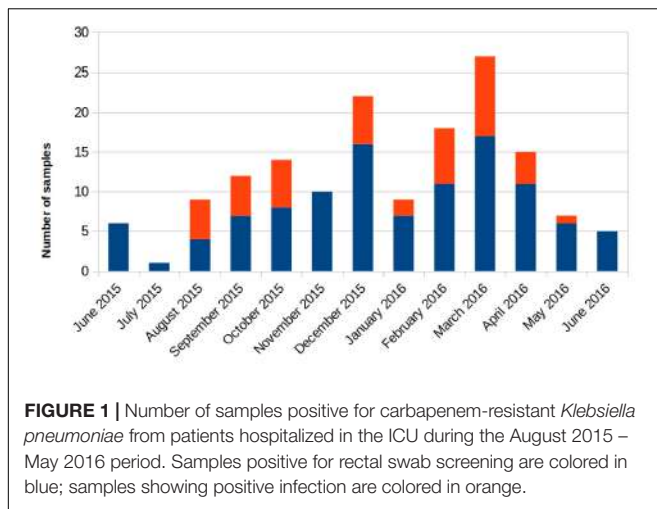
Whole genome sequencing (WGS) of bacterial isolates is increasingly used for epidemiological investigations (Sabat et al., 2013). The use of genomics in clinical settings as a routine tool could in the future be an important aid to the microbiologist to accurately identify and characterize outbreaks at early stages, and to identify transmission routes. However, only from the combination of typing data with clinical and demographic data the correct interpretation of the origin and evolution of an outbreak can be obtained (Van Belkum et al., 2007).

The present retrospective study analyzes a nosocomial outbreak, lasting 10 months (August 2015 – May 2016), caused by *K. pneumoniae* KPC, in an ICU and the period immediately before and after, for a total of 12 months. Thanks to the combination of genomic, microbiological and clinical data it was possible to reconstruct the epidemic event and to characterize the multiple unrelated strains that spread in mostly temporally non-overlapping periods.

## THE EVENT

At the Fondazione IRCCS Policlinico San Matteo in Pavia, a 900-bed hospital in Northern Italy, cardio-respiratory patients are admitted to a specific Cardiorespiratory ICU where preoperative assessment, anesthetic treatment and intensive post-operative treatment of the patients undergoing cardiac and thoracic surgery are performed. This ICU has eight beds and is managed by 37 staff members. All ICU patients are subjected to surveillance through rectal swab at admission and once a week during the stay in the ward, to monitor for carbapenem-resistant *Enterobacteriaceae* colonization. In case of positivity, additional contact precautions are applied, which are interrupted only after three consecutive negative surveillance samples and are resumed in case of a single new positive screening swab.

Retrospectively, an increase in the number of carbapenem-resistant *Klebsiella pneumoniae* (CRKP) colonizations and infections in the ICU was observed in the period from August 2015 to May 2016. The first infection was reported on 15th August 2015. After this event, the number of infected and colonized patients gradually increased and peaked twice, in December 2015 and March 2016. When the first increase in cases was detected (December 2015), additional surveillance measures were undertaken: increase in the training of health personnel and in the use of disposable devices, more accurate daily cleaning, and increased passive surveillance. Environmental screenings were performed in the ward after the second peak in cases in March 2016, all resulting negative. No cohorting or spatial isolation of individual patients were applied. The situation returned to the norm, with no clinical infections, in June 2016 (Figure 1). The period from June 2015 to May 2016 was thus analyzed to understand the characteristics of the observed prolonged outbreak. A total of 426 patients were hospitalized in the ICU during that period and the procedure for rectal swab screening



**FIGURE 1 |** Number of samples positive for carbapenem-resistant *Klebsiella pneumoniae* from patients hospitalized in the ICU during the August 2015 – May 2016 period. Samples positive for rectal swab screening are colored in blue; samples showing positive infection are colored in orange.

for Carbapenem-Resistant *Enterobacteriaceae* identified 23/426 CRKP-colonized patients (average age: 61.1 years; range: 27–80 years). Out of these 23 patients, 18 were negative at the admission time into the ICU. Two of the five patients (numbers 6 and 22) that were positive at admission at the ICU were previously hospitalized in other wards (respectively another ICU and Cardiac Surgery) were they became colonized. The remaining three patients (numbers 2, 4, and 7) were positive at the first swab, suggesting positivity before hospitalization. During the event 11/23 (47.8%) patients died, 2/23 (8.7%) were discharged for rehabilitation and 10/23 (43.5%) were transferred to other hospitalization facilities or hospital wards. Eleven of these 23 (47.8%) patients developed overt infections, with CRKP isolated from blood, respiratory tract, urine and wounds. Seven of the 11 infected patients died while at the ICU. The demographic and hospitalization characteristics of the 23 patients are reported in **Table 1**. During the same period, a total of eight other patients resulted infected by non-carbapenem resistant *Kp*, thus 58% of total *Kp* infections were CRKP.

## MATERIALS AND METHODS

### Ethics Statement

The study was designed and conducted in accordance with the Helsinki declaration and approved by the Ethics Committee of Fondazione IRCCS Policlinico San Matteo in Pavia, Italy.

### Bacterial Strain Identification and Susceptibility Testing

During the entirety of the event, all surveillance rectal swabs were sent to the Microbiology and Virology Unit and were directly plated on chromID CARBA Agar (BioMérieux, Marcy-l'Étoile, France) to screen for the presence of carbapenemase-producing *Enterobacteriaceae*. In the same period, all clinical specimens (blood samples, bronchial aspirates, bronchoalveolar wash, urine samples, and wound

swabs) were all cultured in parallel on all the following media: Columbia Blood Agar with 5% sheep blood, chocolate agar, selective media or on Schaedler agar and 5% sheep blood (BioMérieux SA, Marcy-l'Étoile, France) anaerobically and incubated at 37°C overnight. Colonies suspected to be *Kp* based on morphology were identified with the MALDI Biotyper 3.1 system based on Matrix-Assisted Laser Desorption Ionization time-of-flight (MALDI-TOF) (Bruker Daltonics, Bremen, Germany).

We selected a subset of the *Kp* isolates from surveillance and clinical samples based on sample type, collection date and resistance profile, to perform additional characterization. Antibiotic susceptibility testing and minimum inhibitory concentrations (MICs) determinations were performed using the BD Phoenix 100 automated system (Becton, Dickinson and Company, Franklin Lakes, NJ, United States) and interpreted following the clinical breakpoints of the version 6.0 of the European Committee on Antimicrobial Susceptibility Testing [EUCAST] (2016)<sup>1</sup>. Tigecycline and carbapenems MICs were confirmed by *E*-test strips (BioMérieux, Marcy-l'Étoile, France). As recommended by European Committee on Antimicrobial Susceptibility Testing [EUCAST] (2016)<sup>2</sup> and the European Centre for Disease Prevention and Control [ECDC] (2016)<sup>3</sup>, colistin MICs were confirmed performing the broth microdilution (MIC-Strip Colistin (MERLIN Diagnostika GmbH, Germany).

### DNA Extraction and Genome Sequencing

Total DNA extraction was performed for the selected isolates using the QIAamp DNA mini kit (Qiagen, Italy) according to manufacturer's instructions. DNA was sequenced using the Illumina MiSeq platform (Illumina Inc., San Diego, CA, United States), with paired-end runs of 2 × 250 bp, after Nextera XT library preparation.

### Genomic Analyses

Sequencing reads were quality checked using FastQC<sup>4</sup> and trimmed using the Trimmomatic software (Bolger et al., 2014). SPAdes-3.10.1 (Bankevich et al., 2012) was then used to assemble the pair-end reads using the accurate setting. Multilocus sequence typing (MLST) profiles and virulence/resistance gene variants were determined *in silico* using the Kleborate tool<sup>5</sup>. Presence of the *mcr* gene was tested using ResFinder Version 3.1.0 (database updated to February 20, 2019) (Zankari et al., 2012). Plasmid content was characterized using PlasmidFinder Version 2.0.1 (database updated to November 20, 2018) (Carattoli et al., 2014), while the contigs containing the *bla*KPC gene were

<sup>1</sup>[http://www.eucast.org/fileadmin/src/media/PDFs/EUCAST\\_files/Breakpoint\\_tables/v\\_6.0\\_Breakpoint\\_table.xls](http://www.eucast.org/fileadmin/src/media/PDFs/EUCAST_files/Breakpoint_tables/v_6.0_Breakpoint_table.xls)

<sup>2</sup>[http://www.eucast.org/fileadmin/src/media/PDFs/EUCAST\\_files/General\\_documents/Recommendations\\_for\\_MIC\\_determination\\_of\\_colistin\\_March\\_2016.pdf](http://www.eucast.org/fileadmin/src/media/PDFs/EUCAST_files/General_documents/Recommendations_for_MIC_determination_of_colistin_March_2016.pdf)

<sup>3</sup><https://ecdc.europa.eu/sites/portal/files/media/en/publications/Publications/enterobacteriaceae-risk-assessment-diseases-caused-by-antimicrobial-resistant-microorganisms-europe-june-2016.pdf>

<sup>4</sup>[www.bioinformatics.babraham.ac.uk/projects/fastqc/](http://www.bioinformatics.babraham.ac.uk/projects/fastqc/)

<sup>5</sup><https://github.com/katholt/Kleborate>

**TABLE 1** | Table showing the hospitalization characteristics of all patients admitted to the ICU in the examined period that resulted positive to carbapenem-resistant *Klebsiella pneumoniae* at least once.

Patient number	Admission date	Discharge date	Sample number		Outcome
			Surveillance	Clinical	
1	May 24, 2015	June 17, 2015	3	0	Transfer to another hospital ward
2	June 17, 2015	June 23, 2015	2	0	Transfer to another hospital ward
3	July 31, 2015	September 16, 2015	13	1	Death
4	June 29, 2015	June 30, 2015	2	0	Transfer to another hospital ward
5	August 21, 2015	March 04, 2016	28	15	Death
6	July 11, 2015	September 18, 2015	1	1	Transfer to another hospital ward
7	October 08, 2015	October 23, 2015	3	1	Transfer to another hospital ward
8	October 14, 2015	November 17, 2015	6	2	Death
9	October 22, 2015	December 28, 2015	10	0	Death
10	October 31, 2015	December 17, 2015	7	0	Discharge for rehabilitation
11	November 24, 2015	December 03, 2015	2	0	Transfer to another hospital ward
12	November 26, 2015	December 31, 2015	9	4	Death
13	December 30, 2015	January 25, 2016	4	1	Transfer to another hospital ward
14	January 07, 2016	February 12, 2016	6	0	Death
15	January 08, 2016	May 06, 2016	17	2	Death
16	January 15, 2016	March 22, 2016	11	10	Death
17	January 22, 2016	March 21, 2016	8	0	Death
18	February 06, 2016	March 20, 2016	6	0	Death
19	February 26, 2016	April 03, 2016	6	8	Death
20	March 01, 2016	March 15, 2016	3	0	Transfer to another hospital ward
21	March 31, 2016	May 25, 2016	5	1	Discharge for rehabilitation
22	April 04, 2016	April 08, 2016	1	0	Transfer to another hospital ward
23	April 11, 2016	April 26, 2016	3	0	Transfer to another hospital ward

compared using the BLASTn and the Mauve software (Darling et al., 2010) and subjected to Maximum Likelihood phylogeny using RAxML (Stamatakis, 2014) with the GAMMA substitution model, considering the Ascertainment bias and applying the Lewis correction (Lewis, 2001). The tree topology reliability was tested using 100 bootstrap replicates.

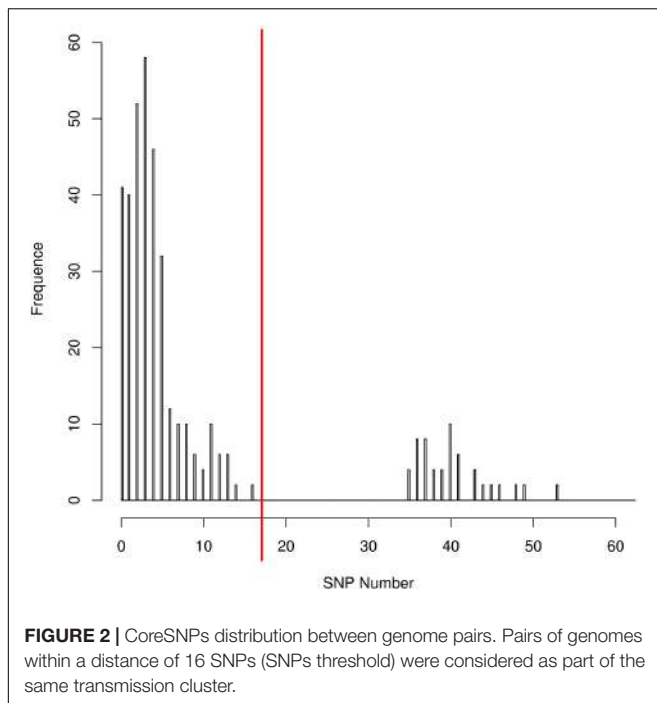
To estimate genomic variability, the obtained genome sequences were added to a selected dataset of *K. pneumoniae* genomes extracted from the PATRIC database (Wattam et al., 2016). PATRIC genomes were selected, using an in-house script, to be the closest in genomic distance to our strains. In detail, each genome was compared to all PATRIC database genomes using Mash (Ondov et al., 2016) and the 50 best hits were selected. All the obtained best hits lists were merged removing duplication, to obtain the final genomic dataset. CoreSNPs were extracted from the resulting dataset following a published method (Gaiarsa et al., 2015). Briefly, the Mauve software (Darling et al., 2010) was used to align all novel genomes and the similar PATRIC genomes to a well-characterized complete genome reference [NZ\_CP006923 (DeLeo et al., 2014)]. Individual alignments were merged using a Python script to obtain a multi-alignment file, allowing to extract coreSNPs (defined as variations of a single nucleotide flanked on each side by two nucleotides conserved in all the genomes analyzed).

The distribution of the coreSNPs distances among strains was visualized using the software R Version 3.2.3

(R Core Team, 2013) and the coreSNP cut-off threshold was determined manually by looking at the graph and finding that there were two groups of genome pairs, those with less than 15 SNPs and those with more than 35 SNPs (Figure 2). The distribution allowed us to safely infer that two genomes could be considered as part of the same transmission cluster if their distance in number of coreSNPs was lower than the 15 SNPs threshold value. The coreSNPs alignment was used to perform a phylogenetic analysis using the software RAxML (Stamatakis, 2014) with the GAMMA substitution model, considering the Ascertainment bias and applying the Lewis correction (Lewis, 2001). The tree topology reliability was tested using 100 bootstrap replicates.

The genomes of the epidemic clusters were investigated also in order to detect possible unique genomic characteristics. A SNP based phylogeny was generated for each cluster, using the same approach as the global phylogeny, and adding to each cluster the genome not part of the cluster that resulted the closest in the global phylogeny. The phylogenies and the genomic alignments of each cluster and their outgroup were used as inputs for a recombination analysis with the software ClonalFrameML (Didelot and Wilson, 2015). Furthermore, the presence and abundance of Insertion Sequences (IS) was tested using the software ISSeeker (Adams et al., 2016) against all IS retrieved from the Issaga database (Varani et al., 2011) using “*Klebsiella*” as organism keyword (on date July 17, 2019).





## RESULTS

An outbreak of CRKP occurred in the cardio-respiratory ICU from August 2015 to May 2016, involving 23 patients (12 colonized, 11 infected). In order to characterize the event, we retrieved all the CRKP strains isolated during the event and in the 2 months before. We obtained a total of 144 samples, 98/144 (68.1%) surveillance samples and 46/144 (31.9%) clinical samples (16 blood cultures, 12 bronchial aspirates, 1 bronchoalveolar wash, 8 urines, and 9 wound swabs). A total of 32/144 *K. pneumoniae* isolates, from 22 rectal swabs and 10 clinical specimens, were selected based on sample types and collection date, including at least one per each of the 23 positive patients, for antibiotic resistance characterization and genome sequencing (Table 2). The results of the antibiotic susceptibility tests are reported in Supplementary Table S1 and show that all the isolates are resistant to at least one carbapenem: 32/32 to Ertapenem, 31/32 to Meropenem, 29/32 to Imipenem. Moreover, 31 isolates are resistant to aminoglycosides (25 to Amikacin, 22 to Gentamicin, 28 to Tobramycin). Twenty isolates are resistant to Fosfomycin (MICs > 64 mg/L), 20 to Colistin (MICs ranging from 4 to >64 mg/L) and three are resistant to Tigecycline (MICs > 2 mg/L). Only one strain from a surveillance sample (genome ID: 1880), resulted to be resistant to all five classes of antibiotics.

Whole-genome sequences were obtained for the 32 selected strains using Illumina technology and assembled into draft genomes after read polishing. Genomes resulted to be of good quality (average N50: 191,110; average number for contigs above 500 bp = 116; average genome size (5,671,622 bp, see Supplementary Table S2 for complete genome characteristics).

Genomes have been submitted to EMBL and are accessible under accession PRJEB32609 (ERP115310). Genomes were characterized by calculating the MLST, detecting antibiotic resistance determinants and virulence factors (see Supplementary Tables S3, S4 for complete results). The most prevalent ST was ST258 ( $n = 19$ , 59.4%), followed by ST512 ( $n = 11$ , 34.4%). One isolate was found to belong to ST45 (3.1%). One new ST was found, a single-locus variant (-SLV) of ST940 (genome 1998 from patient 5, now registered as ST3985). Among the 5 patients with more than one isolate sequenced, one resulted to be colonized by isolates of different STs (patients 5).

Results of the antibiotic resistance factors analysis (Supplementary Table S3) were grouped in 12 drug classes according to the ARG-ANNOT database (Gupta et al., 2014), with  $\beta$ -lactamases divided into the six Lahey classes (Bush and Jacoby, 2010). All 32 analyzed isolates carried at least one ESBL gene (3.1% CTX-M-15, 3.1% SHV-1, 87.5% SHV-11, 6.3% SHV-12) and/or inhibitor-resistant  $\beta$ -lactamase genes (87.5% TEM-54 and 3.1% TEM-122). All the isolates were confirmed to be resistant to carbapenems (9.4% KPC-2 and 90.6% KPC-3). Kleborate identified colistin resistance as truncation or loss of *mcrB* gene in 20 isolates (62.5%), if less than 90% of the reference gene was covered by sequencing reads. Manual analysis allowed to detect the presence of an Insertion Sequence (IS5-like) interrupting *mcrB* in two resistant isolates (1880 and 1753). The interruption due to this mobile element has been previously reported (Cannatelli et al., 2014). All the other resistant isolates, belonging to cluster 3, exhibited a frameshift mutation in *mcrB* due to a 10 nucleotide insertion in position 109 of the gene. Presence of *mcr* genes was investigated with ResFinder, but they were never detected. Colistin antibiogram and genomic data resulted to be coherent for all clones, with two exceptions, clone 1760 indicated as resistant in Kleborate but resulting sensitive at the microdilution test and clone 1870 resistant to the phenotypic test but not to the genomic analysis.

Results of the virulence determinants presence show that only 4/32 strains (12.5%) contained the *ybt* locus, which encodes the biosynthesis pathway of the siderophore yersiniabactin (Lam et al., 2018). None of the strains were found to harbor other siderophores (aerobactin and salmochelin were screened). All the four *ybt* positive strains were isolated from surveillance rectal swabs of different patients and were sporadic cases. Two of them (genomes 1758 and 1760) showed *ybt* allele 13, carried by integrative conjugative element: ICEKp 2. The other two isolates (genomes 1826 and 1998) showed respectively the variants: *ybt* 10 (carried by ICEKp 4) and *ybt* 4 (plasmid-borne allele). The association between the mobile genetic elements found and the allelic variants of *ybt* gene is in agreement with previous observations (Lam et al., 2018). The biosynthetic pathway for the production of the toxin colibactin, as well as the virulence factor *rmpA/rmpA2* (responsible for the expression of the hypermucose-viscous phenotype) were absent from all 32 strains. Finally, using the Kleborate tool we identified three distinct K-loci. The most common K-locus was KL107 ( $n = 28$ , 90.3%), followed by KL106 ( $n = 2$ , 6.5%) and KL24 ( $n = 1$ , 3.2%). As expected from the literature (Shu et al., 2009), they were found to be associated with *wzi* alleles 154, 29, and 101,

**TABLE 2** | Description of the 32 *Klebsiella pneumoniae* KPC isolates selected for the genomic characterization.

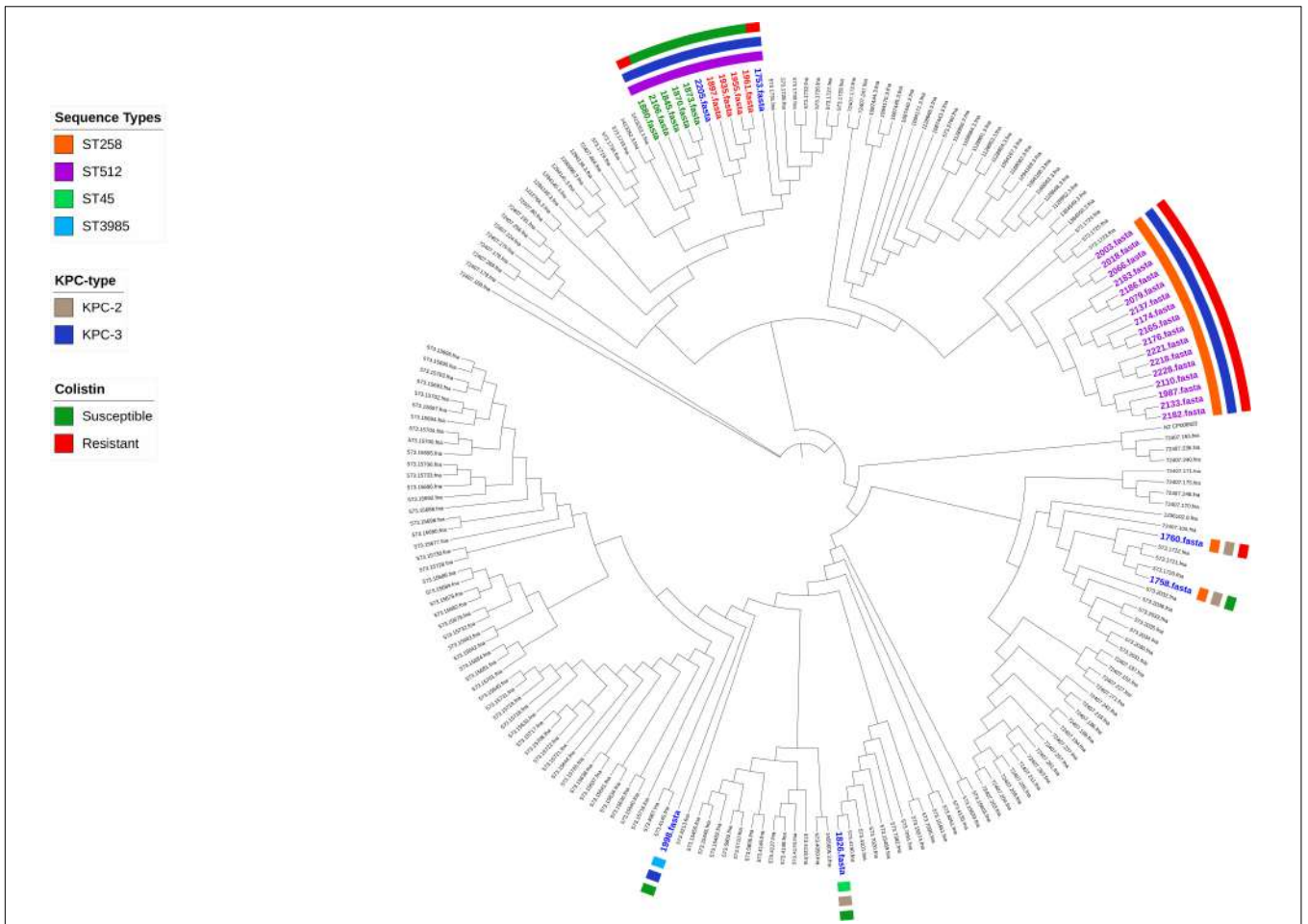
Genome ID	Patient number	Sample date	Sample type	Sequence type	KPC-type
1753	1	June 02, 2015	rectal swab	ST512	KPC-3
1758	2	June 23, 2015	rectal swab	ST258	KPC-2
1760	4	June 29, 2015	rectal swab	ST258	KPC-2
1826	3	August 11, 2015	rectal swab	ST45	KPC-2
1845	5	September 01, 2015	rectal swab	ST512	KPC-3
1870	5	September 14, 2015	wound swab	ST512	KPC-3
1873	5	August 31, 2015	blood	ST512	KPC-3
1880	6	September 15, 2015	rectal swab	ST512	KPC-3
1897	7	October 08, 2015	rectal swab	ST512	KPC-3
1935	8	October 26, 2015	bronchial aspirate	ST512	KPC-3
1955	9	November 10, 2015	rectal swab	ST512	KPC-3
1961	10	November 17, 2015	rectal swab	ST512	KPC-3
1987	11	December 01, 2015	rectal swab	ST258	KPC-3
1998	5	December 01, 2015	rectal swab	ST3985	KPC-3
2003	12	December 08, 2015	rectal swab	ST258	KPC-3
2018	12	December 29, 2015	bronchial aspirate	ST258	KPC-3
2066	13	January 15, 2016	bronchial aspirate	ST258	KPC-3
2079	16	January 26, 2016	rectal swab	ST258	KPC-3
2106	5	February 02, 2016	rectal swab	ST512	KPC-3
2110	14	February 02, 2016	rectal swab	ST258	KPC-3
2133	17	February 16, 2016	rectal swab	ST258	KPC-3
2137	16	February 07, 2016	blood	ST258	KPC-3
2165	19	March 01, 2016	bronchial aspirate	ST258	KPC-3
2174	19	March 14, 2016	blood	ST258	KPC-3
2176	20	March 08, 2016	rectal swab	ST258	KPC-3
2182	18	March 15, 2016	rectal swab	ST258	KPC-3
2183	15	March 15, 2016	rectal swab	ST258	KPC-3
2186	16	March 19, 2016	wound swab	ST258	KPC-3
2205	22	April 04, 2016	rectal swab	ST512	KPC-3
2218	23	April 19, 2016	rectal swab	ST258	KPC-3
2221	21	April 19, 2016	rectal swab	ST258	KPC-3
2228	21	April 24, 2016	blood	ST258	KPC-3

respectively. K-locus was not typable for one isolate (1998) (see **Supplementary Table S4** for full results).

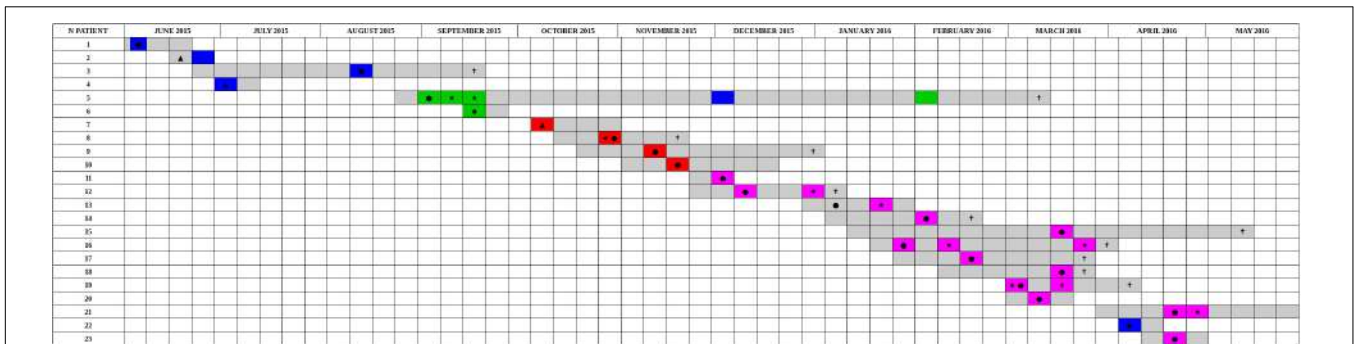
The distribution of the coreSNPs distances among the 32 sequenced genomes was calculated and plotted to determine a threshold cut-off indicating epidemiological relatedness. A clear threshold was detected at 16 coreSNPs (**Figure 2**), allowing to determine the presence of three clades of genomes. Within each clade, all genomes have reciprocal coreSNP distances lower than the calculated threshold. A global coreSNPs maximum-likelihood phylogeny was performed, including the 32 genomes investigated in this work and 172 related genomes extracted from the PATRIC database, in order to contextualize our strains within the surrounding *Kp* diversity. The genomes with coreSNPs distance below the threshold clustered in three monophyletic clades (**Figure 3** for the cladogram, see also **Supplementary Figure S1** that shows subtrees of the three clusters) and were thus considered part of three separate outbreak clusters (green, red, and violet clusters in **Figures 3, 4**). Five of the other six genomes do not cluster with other genomes of the outbreak and are thus considered sporadic cases. The last remaining genome (2205) is the

phylogenetic sister group of cluster 2, but presents a relatively high number of coreSNPs with the other genomes of the cluster (average 42 coreSNPs), and was thus considered as a separate, sporadic, case.

Comparative genomic analyses were performed within the three clades and to compare them to their nearest neighbor, showing very limited genomic variation. No recombination was detected at the origin of any of the three epidemic clades (**Supplementary Figure S2**). IS content of isolates of each of the three outbreaking clusters was compared using ISfinder. The IS content resulted to be stable within each cluster, while each cluster appears to have more ISs than the evolutionary closest sporadic isolates. Specifically, isolates of Cluster 1 have IS of families ISL3 and IS1 that are absent in the sporadic sister group. Isolates of cluster 2 present IS66 sequences, absent in the evolutionary closest sporadic isolate. Isolates of cluster 2 are also richer in ISL3 and IS6 sequences than their neighbor and those of cluster 3 are richer in IS5 and IS6. It must be noted however that the accuracy, especially quantitatively, of such an analysis on draft genomes is limited, due to the difficulties in assembling IS sequences (**Supplementary Figure S3**).



**FIGURE 3 |** Phylogenetic tree based on coreSNPs from 32 *Klebsiella pneumoniae* KPC strains isolated from the Intensive Care Unit and 172 related genomes retrieved from the PATRIC database. Sporadic strains are highlighted in blue; in green, red, and violet are the genomes belonging to three monophyletic clusters (distance in SNPs < 16).



**FIGURE 4 |** Timeline of the presence of carbapenem-resistant *Klebsiella pneumoniae* positive patients in the ICU in the period from June 2015 to May 2016. The periods of hospitalization are colored in gray. The other colors identify the sequenced samples based on genomic characterization. The colors green, red, and violet correspond to the three clusters identified based on SNPs distance, are reported sporadic cases in blue. Samples obtained from clinical infections (not surveillance swabs) are indicated by stars. The crosses indicate patients death. Black circles indicate the first positive CRKP rectal swab for each patient, negative (not at the admission). Black triangles indicate the first positive CRKP rectal swab for patients already CRKP-colonized at the admission time into the hospital. Black diamonds indicated the patients that became positive in other hospital wards.

## DISCUSSION

Here we present the results of the integrated characterization of the CRKP strains isolated during a 1-year period (10 months outbreak plus 2 months before) in the cardio-respiratory ICU of the San Matteo hospital in Pavia, Northern Italy. Retrospectively, starting in August 2015, we observed a strong increase in CRKP isolated from routine surveillance rectal swabs, taken from each ICU patient every week indicating a high number of colonized patients. We also observed an increase in CRKP isolations from clinical samples, indicating overt infections. This trend continued until June 2016, with a total of 23 colonized patients, among which 11 infected, prompting the investigation presented here. Antibiotic resistance characterization coupled with genome sequencing of 32 isolates from these 23 patients (Table 2), collected in the outbreak period and in the 2 months before, allowed the characterization of the extended outbreak. Most strains were found to belong to CG258, one of the most widespread KPC-bearing group in Italy and worldwide (Gaiarsa et al., 2015; Onori et al., 2015).

Performing a SNPs distance analysis (Figure 1) we found that twenty-six of the 32 isolates resulted to belong to three genome clusters (coreSNPs < 16) that appeared in the ICU, infected multiple patients, and then disappeared, with one single strain lasting for most of the event (Figure 4, see also Supplementary Figure S1 for phylogenetic reconstructions of the three clusters). The remaining six genomes resulted to be unrelated and were consequently classified as sporadic isolates, as they all showed more than 35 coreSNPs with all the other analyzed genomes. This result is coherent with a recent multicenter study that proposed to set a threshold for SNPs distance in *Kp* outbreak at 21 (David et al., 2019). Interestingly, four of the six sporadic isolates represent the strains characterized in the 2 months before the outbreak (June–August 2015, see Figure 4), indicating that multiple strains were present in the ICU, but they were only responsible for colonization, did not cause clinical infections, nor they spread to multiple patients. The six sporadic isolates are characterized by variable levels of antibiotic resistance (number of resistance classes determined with Kleborate ranging from 3 to 11). Two of them are resistant to colistin (genomes ID: 1753, 1760). In terms of virulence, the only isolates that present yersiniabactin are four of the six sporadic isolates, all isolated from colonized, not infected, patients. Most sporadic isolates belong to the CG258 ( $n = 4$ ), one belongs to ST45, already reported as a KPC-bearing strain in Italy (Cristina et al., 2016), and the final one to a novel ST, variant of ST940, now classified as ST3985. These sporadic isolates could be epidemiologically important, acting as a “reservoir” for the spread of the mobile element carrying *blaKPC*.

The strain responsible for the first cluster of isolations, belonging to ST512, was isolated from patient 5 from a screening sample in August 2015 and then from clinical samples in September. The patient remained colonized until his death in March. The isolates of this cluster are characterized by the resistance to 10 antibiotic classes, remaining susceptible to colistin, with two exceptions. The first one (genome ID: 1880) is

the only strain of the cluster, belonging to patient 6, which present a correspondence between phenotypic (MIC > 64 mg/L) and genotypic (loss/truncation of *mgrB* gene) colistin resistance. The other colistin-resistant strain of the cluster (genome ID: 1870) was the third of four in the temporal series isolated from patient 5 and resulted phenotypically colistin-resistant (MIC = 4 mg/L), even though no colistin-resistance mutation/gene was detected in the genome. In order to investigate the presence of other mutations potentially causing colistin resistance, the genomes of the isolates belonging to patient 5 were manually examined, detecting 2 SNPs unique to the colistin-resistant isolate. These SNPs are co-localized in an intergenic region upstream of the *pca* operon, potentially responsible for the  $\beta$ -ketoacid pathway. Understanding whether these SNPs could be related to colistin resistance would require additional investigations.

One additional CRKP was isolated from patient 5 on December 1st. This isolate was unrelated to those of cluster 1, belonging to ST3985 (a novel SLV of ST940). In order to evaluate whether this strain acquired the KPC plasmid from the ST512 strain co-present in patient 5, we compared the contigs harboring the KPC gene, performing a phylogenetic analysis including contigs from isolates of cluster 1, from the ST3985, and from another sporadic isolate (1753), as control. We found that the KPC-harboring contig from the ST3985 was divergent from all identical contigs retrieved from the ST512 isolates belonging to cluster 1, but also from the sporadic control, which resulted sister group of the isolates of the cluster (Supplementary Figure S4).

Four isolates were grouped in cluster 2, belonging again to ST512. This clone was short-lived but was transmitted from patient 7 to three other patients in the course of 6 weeks and caused one clinical infection. The isolates of this cluster are resistant to most antibiotics, retaining susceptibility to colistin and tigecycline. Two of four isolates resulted phenotypically sensitive to aminoglycosides, while genome analysis are only in partial agreement, indicating that all four strains carry the *aph3-Ia* gene, which should confer resistance to this class of antibiotics.

The largest of the clusters is represented by 17 strains, isolated from 12 patients during 5 months, causing five clinical infections and resulting in three deaths. The isolates of this cluster are those characterized by the highest level of resistance, retaining susceptibility only to tigecycline. Genomic analysis agrees with this result indicating the presence of resistance genes against 11 antibiotic classes, one more than the two other clusters. Indeed, all the isolates of this cluster resulted resistant to colistin with phenotypic tests, and the analysis of the genome content using Kleborate highlighted a possible resistance-causing truncation in the *mgrB* gene in all 17 strains. Manual analysis allowed to detect a frameshift mutation in *mgrB* due to a ten nucleotide insertion in position 109 of the gene.

## CONCLUSION

Over the course of 1 year, nine different strains of Carbapenem resistant *K. pneumoniae* were isolated in the ICU from 23 patients, 12 only colonized, 11 infected. Three strains colonized multiple patients, were the cause of all the seven clinical



infections reported in the ICU in this period and were responsible for the outbreak that lasted for 10 months. The three outbreaking strains did not present more virulence genes than the six sporadic isolates, four of which were actually the only ones exhibiting yersiniabactin. In terms of antibiotic resistance, both outbreaking and sporadic strains were phenotypically resistant to most classes, a result confirmed by strong repertoires of resistance genes. A clear correlation between antibiotic resistance profiles and number of colonizations or infections is thus not clearly evident. Our results highlight the importance of the overall environmental context, possibly more than the intrinsic characteristics of a strain, in determining the spread of different CRKP isolates.

## DATA AVAILABILITY STATEMENT

The genomes generated for this study can be found in the EMBL EBI repository, under the PRJEB32609 entry.

## ETHICS STATEMENT

Neither ethics committee approval, nor informed consent were required as all collected data were fully anonymized, there was no contact with patients and/or their families and no interventions or changes to treatment and management were made, in accordance with institutional guidelines.

## AUTHOR CONTRIBUTIONS

CF, CB, PM, and DS designed the project. MC and PC performed the microbiological analyses. ES performed the genome sequencing. CF, SG, and FC performed the bioinformatic analyses. CF, MC, and DS performed the epidemiological analyses. CF, MC, SG, and DS drafted the manuscript. CB, PM, and DS finalized the manuscript. All authors read and approved the final manuscript.

## REFERENCES

- Adams, M. D., Bishop, B., and Wright, M. S. (2016). Quantitative assessment of insertion sequence impact on bacterial genome architecture. *Microbial. Genom.* 18:e000062. doi: 10.1099/mgen.0.000062
- Aires, C. A. M., Aires, da Conceição-Neto, O. C., Tavares, E., Oliveira, T. R., Dias, C. F., et al. (2017). Emergence of the plasmid-mediated mcr-1 gene in clinical KPC-2-producing *Klebsiella pneumoniae* sequence type 392 in Brazil. *Antimicrob. Agents Chemother.* 61:e00317-17. doi: 10.1128/AAC.00317-17
- Bankevich, A., Nurk, S., Antipov, D., Gurevich, A. A., Dvorkin, M., Kulikov, A. S., et al. (2012). SPAdes: a new genome assembly algorithm and its applications to single-cell sequencing. *J. Comput. Biol.* 19, 455–477. doi: 10.1089/cmb.2012.0021
- Bolger, A. M., Lohse, M., and Usadel, B. (2014). Trimmomatic: a flexible trimmer for Illumina sequence data. *Bioinformatics* 30, 2114–2120. doi: 10.1093/bioinformatics/btu170
- Borer, A., Sidel-Odes, L., Riesenber, K., Eskira, S., Peled, N., Nativ, R., et al. (2009). Attributable mortality rate for carbapenem-resistant *Klebsiella pneumoniae* bacteremia. *Infect. Control Hosp. Epidemiol.* 30, 972–976. doi: 10.1086/605922

## FUNDING

This research was supported by the Italian Ministry of Education, University and Research (MIUR): Dipartimenti di Eccellenza Program (2018–2022) – Department of Biology and Biotechnology “L. Spallanzani”, University of Pavia to DS.

## SUPPLEMENTARY MATERIAL

The Supplementary Material for this article can be found online at: <https://www.frontiersin.org/articles/10.3389/fmicb.2019.02767/full#supplementary-material>

**FIGURE S1** | Recombination analysis of Cluster 1 (A), Cluster 2 (B) and Cluster 3 (C). The analysis was performed using the software ClonalFrameML and including the evolutionary closest sporadic genome as outgroup.

**FIGURE S2** | Insertion sequences (IS) content of the three epidemic clusters. The evolutionary closest sporadic genome was added as a reference, last in order in the figure for each cluster.

**FIGURE S3** | Phylogenetic trees of the three genomic clusters [Cluster 1 in panel (A), Cluster 2 in panel (B) and Cluster 3 in panel (C)], based on coreSNPs from the global alignment described in Figure 1, determined using RAxML, with 100 bootstrap, showing branch lengths and patients numbers. For each cluster, the sister group genome, as determined by the tree in Figure 1 was used as outgroup.

**FIGURE S4** | Phylogenetic comparison of the KPC-bearing contigs of the 32 isolates. The contig from isolate 1998, the ST3985 genome, is clearly distinct from the contigs from the ST512 strains belonging to Cluster 1 (1897, 1935, 1955, 1961).

**TABLE S1** | Antimicrobial susceptibility profiles determined using the BD Phoenix 100 System on the 32 investigated *Klebsiella pneumoniae* strains.

**TABLE S2** | Characteristics of the sequenced genomes.

**TABLE S3** | Predicted antimicrobial susceptibility profiles determined using the Kleborate tool on 32 *Klebsiella pneumoniae* KPC isolates.

**TABLE S4** | Factors of the 32 *Klebsiella pneumoniae* KPC isolates.

- Breurec, S., Guessennd, N., Timinouni, M., Le, T. T. H., Cao, V., Ngandjio, A., et al. (2013). *Klebsiella pneumoniae* resistant to third-generation cephalosporins in five African and two Vietnamese major towns: multiclonal population structure with two major international clonal groups CG15 and CG258. *Clin. Microbiol. Infect.* 19, 349–355. doi: 10.1111/j.1469-0691.2012.03805.x
- Broberg, C. A., Palacios, M., and Miller, V. L. (2014). *Klebsiella*: a long way to go towards understanding this enigmatic jet-setter. *F1000prime Rep.* 6:64. doi: 10.12703/P6-64
- Bush, K., and Jacoby, G. A. (2010). Updated functional classification of  $\beta$ -lactamases. *Antimicrob. Agents Chemother.* 54, 969–976. doi: 10.1128/AAC.01009-09
- Cannatelli, A., Giani, T., D'Andrea, M. M., Di Pilato, V., Arena, F., Conte, V., et al. (2014). *MgrB* inactivation is a common mechanism of colistin resistance in KPC-producing *Klebsiella pneumoniae* of clinical origin. *Antimicrob. Agents Chemother.* 58, 5696–5703. doi: 10.1128/AAC.03110-14
- Carattoli, A., Zankari, E., Garcia-Fernandez, A., Larsen, M. V., Lund, O., Villa, L., et al. (2014). In silico detection and typing of plasmids using PlasmidFinder and plasmid multilocus sequence typing. *Antimicrob. Agents Chemother.* 58, 3895–3903. doi: 10.1128/AAC.02412-14

- Cristina, M. L., Sartini, M., Ottria, G., Schinca, E., Cenderello, N., Crisalli, M. P., et al. (2016). Epidemiology and biomolecular characterization of carbapenem-resistant *Klebsiella pneumoniae* in an Italian hospital. *J. Prev. Med. Hyg.* 57, E149–E156.
- Darling, A. E., Mau, B., and Perna, N. T. (2010). progressiveMauve: multiple genome alignment with gene gain, loss and rearrangement. *PLoS One* 5:e11147. doi: 10.1371/journal.pone.0011147
- David, S., Reuter, S., Harris, S. R., Glasner, C., Feltwell, T., Argimon, S., et al. (2019). Epidemic of carbapenem-resistant *Klebsiella pneumoniae* in Europe is driven by nosocomial spread. *Nat. Microbiol.* 4, 1919–1929. doi: 10.1038/s41564-019-0492-8
- DeLeo, F. R., Chen, L., Porcella, S. F., Martens, C. A., Kobayashi, S. D., Porter, A. R., et al. (2014). Molecular dissection of the evolution of carbapenem-resistant multilocus sequence type 258 *Klebsiella pneumoniae*. *Proc. Natl. Acad. Sci. U.S.A.* 111, 4988–4993. doi: 10.1073/pnas.1321364111
- Di Martino, P., Cafferini, N., Joly, B., and Darfeuille-Michaud, A. (2003). *Klebsiella pneumoniae* type 3 pili facilitate adherence and biofilm formation on abiotic surfaces. *Res. Microbiol.* 154, 9–16. doi: 10.1016/S0923-2508(02)0004-9
- Di Pilato, V., Arena, F., Tascini, C., Cannatelli, A., De Angelis, L. H., Fortunato, S., et al. (2016). mcr-1.2, a new mcr variant carried on a transferable plasmid from a colistin-resistant KPC carbapenemase-producing *Klebsiella pneumoniae* strain of sequence type 512. *Antimicrob. Agents Chemother.* 60, 5612–5615. doi: 10.1128/AAC.01075-16
- Didelot, X., and Wilson, D. (2015). ClonalFrameML: efficient inference of recombination in whole bacterial genomes. *PLoS Comput. Biol.* 11:e1004041. doi: 10.1371/journal.pcbi.1004041
- European Centre for Disease Prevention and Control [ECDC], (2016). *Plasmid-Mediated Colistin Resistance in Enterobacteriaceae*. Solna Municipality: ECDC.
- European Committee on Antimicrobial Susceptibility Testing [EUCAST] (2016). *Recommendations for MIC Determination of Colistin (Polymyxin E) as Recommended by the Joint CLSI-EUCAST Polymyxin Breakpoints Working Group*. Växjö: European Committee on Antimicrobial Susceptibility Testing.
- Gaiarsa, S., Comandatore, F., Gaibani, P., Corbella, M., Dalla Valle, C., Epis, S., et al. (2015). Genomic epidemiology of *Klebsiella pneumoniae* in Italy and novel insights into the origin and global evolution of its resistance to carbapenem antibiotics. *Antimicrob. Agents Chemother.* 59, 389–396. doi: 10.1128/AAC.04224-14
- Ghorashi, Z., Nezami, N., Hoseinpour-feizi, H., Ghorashi, S., and Tabrizi, J. S. (2011). Arthritis, osteomyelitis, septicemia and meningitis caused by *Klebsiella* in a low-birth-weight newborn: a case report. *J. Med. Case Rep.* 5:241. doi: 10.1186/1752-1947-5-241
- Giakkoupi, P., Papagiannitsis, C. C., Miriagou, V., Pappa, O., Polemis, M., Tryfinopoulou, K., et al. (2010). An update of the evolving epidemic of bla KPC-2-carrying *Klebsiella pneumoniae* in Greece (2009–10). *J. Antimicrob. Chemother.* 66, 1510–1513. doi: 10.1093/jac/dkr166
- Gupta, S. K., Padmanabhan, B. R., Diene, S. M., Lopez-Rojas, R., Kempf, M., Landraud, L., et al. (2014). ARG-ANNOT, a new bioinformatic tool to discover antibiotic resistance genes in bacterial genomes. *Antimicrob. Agents Chemother.* 58, 212–220. doi: 10.1128/AAC.01310-13
- Javan, A. O., Shokouhi, S., and Sahraei, Z. (2015). A review on colistin nephrotoxicity. *Eur. J. Clin. Pharmacol.* 71, 801–810. doi: 10.1007/s00228-015-1865-4
- Ko, W. C., Paterson, D. L., Sagnimeni, A. J., Hansen, D. S., Von Gottberg, A., Mohapatra, S., et al. (2002). Community-acquired *Klebsiella pneumoniae* bacteremia: global differences in clinical patterns. *Emerg. Infect. Dis.* 8, 160–166. doi: 10.3201/eid0802.010025
- Lam, M. M., Wick, R. R., Wyres, K. L., Gorrie, C. L., Judd, L. M., Jenney, A. W., et al. (2018). Genetic diversity, mobilisation and spread of the yersiniabactin-encoding mobile element ICEKp in *Klebsiella pneumoniae* populations. *Microb. Genom.* 4:9. doi: 10.1099/mgen.0.000196
- Lewis, P. O. (2001). A likelihood approach to estimating phylogeny from discrete morphological character data. *Syst. Biol.* 50, 913–925. doi: 10.1080/106351501753462876
- Liu, Y. Y., Wang, Y., Walsh, T. R., Yi, L. X., Zhang, R., Spencer, J., et al. (2016). Emergence of plasmid-mediated colistin resistance mechanism MCR-1 in animals and human beings in China: a microbiological and molecular biological study. *Lancet Infect. Dis.* 16, 161–168. doi: 10.1016/S1473-3099(15)00424-7
- Markovska, R., Stoeva, T., Schneider, I., Boyanova, L., Popova, V., Dacheva, D., et al. (2015). Clonal dissemination of multilocus sequence type ST 15 KPC-2-producing *Klebsiella pneumoniae* in Bulgaria. *APMIS* 123, 887–894. doi: 10.1111/apm.12433
- Mathers, A. J., Peirano, G., and Pitout, J. D. D. (2015). The role of epidemic resistance plasmids and international high-risk clones in the spread of multidrug-resistant *Enterobacteriaceae*. *Clin. Microbiol. Rev.* 28, 565–591. doi: 10.1128/CMR.00116-14
- Navon-Venezia, S., Kondratyeva, K., and Carattoli, A. (2017). *Klebsiella pneumoniae*: a major worldwide source and shuttle for antibiotic resistance. *FEMS Microbiol. Rev.* 41, 252–275. doi: 10.1093/femsre/fux013
- Nordmann, P., Cuzon, G., and Naas, T. (2009). The real threat of *Klebsiella pneumoniae* carbapenemase-producing bacteria. *Lancet Infect. Dis.* 9, 228–236. doi: 10.1016/S1473-3099(09)70054-4
- Olaïtan, A. O., Morand, S., and Rolain, J. M. (2014). Mechanisms of polymyxin resistance: acquired and intrinsic resistance in bacteria. *Front. Microbiol.* 5:643. doi: 10.3389/fmicb.2014.00643
- Ondov, B. D., Treangen, T. J., Melsted, P., Mallonee, A. B., Bergman, N. H., Koren, S., et al. (2016). Mash: fast genome and metagenome distance estimation using MinHash. *Genome Biol.* 17:132. doi: 10.1186/s13059-016-0997-x
- Onori, R., Gaiarsa, S., Comandatore, F., Pongolini, S., Brisse, S., Colombo, A., et al. (2015). Tracking nosocomial *Klebsiella pneumoniae* infections and outbreaks by whole-genome analysis: small-scale Italian scenario within a single hospital. *J. Clin. Microbiol.* 53, 2861–2868. doi: 10.1128/JCM.00545-15
- Oteo, J., Pérez-Vázquez, M., Bautista, V., Ortega, A., Zamarrón, P., Saez, D., et al. (2016). The spread of KPC-producing *Enterobacteriaceae* in Spain: WGS analysis of the emerging high-risk clones of *Klebsiella pneumoniae* ST11/KPC-2, ST101/KPC-2 and ST512/KPC-3. *J. Antimicrob. Chemother.* 71, 3392–3399. doi: 10.1093/jac/dkw321
- Patel, G., Huprikar, S., Factor, S. H., Jenkins, S. G., and Calfee, D. P. (2008). Outcomes of carbapenem-resistant *Klebsiella pneumoniae* infection and the impact of antimicrobial and adjunctive therapies. *Infect. Control Hosp. Epidemiol.* 29, 1099–1106. doi: 10.1086/592412
- Podschun, R., and Ullmann, U. (1998). *Klebsiella* spp. as nosocomial pathogens: epidemiology, taxonomy, typing methods, and pathogenicity factors. *Clin. Microbiol. Rev.* 11, 589–603. doi: 10.1128/CMR.11.4.589
- Qi, Y., Wei, Z., Ji, S., Du, X., Shen, P., and Yu, Y. (2010). ST11, the dominant clone of KPC-producing *Klebsiella pneumoniae* in China. *J. Antimicrob. Chemother.* 66, 307–312. doi: 10.1093/jac/dkq431
- R Core Team. (2013). *R: A Language and Environment for Statistical Computing*. Vienna: R Foundation for Statistical Computing.
- Sabat, A. J., Budimir, A., Nashev, D., Sá-Leão, R., Van Dijk, J. M., Laurent, F., et al. (2013). Overview of molecular typing methods for outbreak detection and epidemiological surveillance. *Eurosurveillance* 18:20380.
- Sabbatucci, M., Iacchini, S., Iannazzo, C., Farfusola, C., Marella, A. M., Bizzotti, V., et al. (2017). *Sorveglianza nazionale delle batteriemie da enterobatteri produttori di carbapenemasi. Rapporto 2013–2016*. Rapporti ISTISAN 2017. Rome: Istituto Superiore di Sanità.
- Samuelsen, Ø., Naseer, U., Tofteland, S., Skutlaberg, D. H., Onken, A., Hjetland, R., et al. (2009). Emergence of clonally related *Klebsiella pneumoniae* isolates of sequence type 258 producing plasmid-mediated KPC carbapenemase in Norway and Sweden. *J. Antimicrob. Chemother.* 63, 654–658. doi: 10.1093/jac/dkp018
- Shu, H. Y., Fung, C. P., Liu, Y. M., Wu, K. M., Chen, Y. T., Li, L. H., et al. (2009). Genetic diversity of capsular polysaccharide biosynthesis in *Klebsiella pneumoniae* clinical isolates. *Microbiology* 155, 4170–4183. doi: 10.1099/mic.0.029017-0
- Stamatakis, A. (2014). RAxML version 8: a tool for phylogenetic analysis and post-analysis of large phylogenies. *Bioinformatics* 30, 1312–1313. doi: 10.1093/bioinformatics/btu033
- Tumbarello, M., Spanu, T., Sanguineti, M., Citton, R., Montuori, E., Leone, F., et al. (2006). Bloodstream infections caused by extended-spectrum-β-lactamase-producing *Klebsiella pneumoniae*: risk factors, molecular epidemiology, and clinical outcome. *Antimicrob. Agents Chemother.* 50, 498–504. doi: 10.1128/AAC.50.2.498-504.2006
- Tzouveleki, L. S., Miriagou, V., Kotsakis, S. D., Spyridopoulou, K., Athanasiou, E., Karagouni, E., et al. (2013). KPC-producing, multidrug-resistant *Klebsiella*

- pneumoniae* sequence type 258 as a typical opportunistic pathogen. *Antimicrob. Agents Chemother.* 57, 5144–5146. doi: 10.1128/AAC.01052-13
- Van Belkum, A., Tassios, P. T., Dijkshoorn, L., Haeggman, S., Cookson, B., Fry, N. K., et al. (2007). Guidelines for the validation and application of typing methods for use in bacterial epidemiology. *Clin. Microbiol. Infect.* 13, 1–46. doi: 10.1111/j.1469-0691.2007.01786.x
- Varani, A. M., Siguier, P., Gourbeyre, E., Charneau, V., and Chandler, M. (2011). ISSaga is an ensemble of web-based methods for high throughput identification and semi-automatic annotation of insertion sequences in prokaryotic genomes. *Genome Biol.* 12:R30. doi: 10.1186/gb-2011-12-3-r30
- Velkov, T., Dai, C., Ciccotosto, G. D., Cappai, R., Hoyer, D., and Li, J. (2018). Polymyxins for CNS infections: pharmacology and neurotoxicity. *Pharmacol. Ther.* 181, 85–90. doi: 10.1016/j.pharmthera.2017.07.012
- Villa, L., Feudi, C., Fortini, D., Iacono, M., Bonura, C., Endimiani, A., et al. (2016). Complete genome sequence of KPC-3-and CTX-M-15-producing *Klebsiella pneumoniae* sequence type 307. *Genome Announc.* 4:e00213-16. doi: 10.1128/genomeA.00213-16
- Wattam, A. R., Davis, J. J., Assaf, R., Boisvert, S., Brettin, T., Bun, C., et al. (2016). Improvements to PATRIC, the all-bacterial bioinformatics database and analysis resource center. *Nucleic Acids Res.* 45, D535–D542. doi: 10.1093/nar/gkw1017
- Wei, D. D., Wan, L. G., Deng, Q., and Liu, Y. (2016). Emergence of KPC-producing *Klebsiella pneumoniae* hypervirulent clone of capsular serotype K1 that belongs to sequence type 11 in Mainland China. *Diagn. Microbiol. Infect. Dis.* 85, 192–194. doi: 10.1016/j.diagmicrobio.2015.03.012
- Zankari, E., Hasman, H., Cosentino, S., Vestergaard, M., Rasmussen, S., Lund, O., et al. (2012). Identification of acquired antimicrobial resistance genes. *J. Antimicrob. Chemother.* 67, 2640–2644. doi: 10.1093/jac/dks261
- Conflict of Interest:** The authors declare that the research was conducted in the absence of any commercial or financial relationships that could be construed as a potential conflict of interest.
- Copyright © 2019 Ferrari, Corbella, Gaiarsa, Comandatore, Scaltriti, Bandi, Cambieri, Marone and Sasser. This is an open-access article distributed under the terms of the Creative Commons Attribution License (CC BY). The use, distribution or reproduction in other forums is permitted, provided the original author(s) and the copyright owner(s) are credited and that the original publication in this journal is cited, in accordance with accepted academic practice. No use, distribution or reproduction is permitted which does not comply with these terms.



# Over-Expression of IS*Aba1*-Linked Intrinsic and Exogenously Acquired OXA Type Carbapenem-Hydrolyzing-Class D- $\beta$ -Lactamase-Encoding Genes Is Key Mechanism Underlying Carbapenem Resistance in *Acinetobacter baumannii*

OPEN ACCESS

**Edited by:**

Leonardo Neves de Andrade,  
University of São Paulo, Brazil

**Reviewed by:**

Andres Felipe Opazo-Capurro,  
Universidad de Concepción, Chile  
Jitendraa Vashist,  
Jaypee University of Information  
Technology, India

**\*Correspondence:**

Sheng Chen  
shechen@cityu.edu.hk

†These authors have contributed  
equally to this work

**Specialty section:**

This article was submitted to  
Antimicrobials, Resistance  
and Chemotherapy,  
a section of the journal  
Frontiers in Microbiology

**Received:** 24 July 2019

**Accepted:** 19 November 2019

**Published:** 04 December 2019

**Citation:**

Wong MH-y, Chan BK-w,  
Chan EW-c and Chen S (2019)  
Over-Expression of IS*Aba1*-Linked  
Intrinsic and Exogenously Acquired  
OXA Type  
Carbapenem-Hydrolyzing-Class  
D- $\beta$ -Lactamase-Encoding Genes Is  
Key Mechanism Underlying  
Carbapenem Resistance  
in *Acinetobacter baumannii*.  
*Front. Microbiol.* 10:2809.  
doi: 10.3389/fmicb.2019.02809

Marcus Ho-yin Wong<sup>1†</sup>, Bill Kwan-wai Chan<sup>1†</sup>, Edward Wai-chi Chan<sup>1</sup> and Sheng Chen<sup>1,2\*</sup>

<sup>1</sup> State Key Laboratory of Chemical Biology and Drug Discovery, The Hong Kong Polytechnic University, Kowloon, Hong Kong, <sup>2</sup> Department of Infectious Diseases and Public Health, Jockey Club College of Veterinary Medicine and Life Sciences, City University of Hong Kong, Kowloon, Hong Kong

*Acinetobacter baumannii* is an important clinical pathogen which often causes fatal infections among seriously ill patients. Treatment options for managing infections caused by this organism have become limited as a result of emergence of carbapenem resistant strains. In the current study, whole genome sequencing, gene expression studies and enzyme kinetics analyses were performed to investigate the underlying carbapenem resistance mechanisms in fourteen clinical *A. baumannii* strains isolated from two hospitals, one each in Hong Kong and Henan Province, People's Republic of China. A large majority of the *A. baumannii* strains (11/14) were found to belong to the International Clone II (IC-II), among which six were ST208. Twelve of these strains were carbapenem resistant and found to either harbor *bla*<sub>OXA-23</sub>/*bla*<sub>OXA-72</sub>, or exhibit over-expression of the *bla*<sub>OXA-51</sub> gene upon IS*Aba1* insertion. Enzymatic assay confirmed that the OXA variants, including those of *bla*<sub>OXA-51</sub>, exhibited strong carbapenem-degrading activities. In terms of other intrinsic mechanisms, a weak correlation was observed between reduced production of outer membrane porin CarO/expression resistance-nodulation-division (RND) efflux AdeB and phenotypic resistance. This finding implied that over-production of carbapenem-hydrolyzing-class D- $\beta$ -lactamases (CHDLs), including the intrinsic *bla*<sub>OXA-51</sub> gene and the acquired *bla*<sub>OXA-23</sub> and *bla*<sub>OXA-24</sub> elements, is the key mechanism of carbapenem resistance in *A. baumannii*. This view is confirmed by testing the effect of NaCl, a known *bla*<sub>OXA</sub> inhibitor, which was found to cause reduction in carbapenem MIC by twofolds to eightfolds, suggesting that inhibiting OXA type carbapenemases represents the most effective strategy to control phenotypic carbapenem resistance in *A. baumannii*.

**Keywords:** *Acinetobacter baumannii*, carbapenem resistance, OXA-23, OXA-51, mechanisms



## INTRODUCTION

*Acinetobacter baumannii* is an important Gram-negative pathogen that often causes serious hospital infections, especially among immunocompromised patients in intensive care units (ICUs) (Bergogne-Berezin and Towner, 1996). The increasing mortality due to *A. baumannii* infections is of major concern as this pathogen exhibits the potential to evolve into carbapenem resistant variants through acquiring antibiotic resistance-encoding mobile genetic elements, which is often exacerbated by the intrinsic low membrane permeability of this organism. These features render *A. baumannii* one of the bacterial pathogens that exhibits the highest resistance rate in clinical settings (Pegel et al., 2008). In 2013, the United States Center for Disease Control and Prevention estimated that as many as 11,500 *A. baumannii* infections occurred annually, among which 63% were multidrug resistant, resulting in 500 deaths (Queenan et al., 2012). Likewise, *A. baumannii* is responsible for more than 1/5 of all clinical Gram-negative bacterial infections in Hong Kong and other Asia-Pacific regions, with a high portion being multidrug resistant (Liu et al., 2012). Recently, the World Health Organization has listed carbapenem-resistant *A. baumannii* to be “Priority 1: Critical” in its “Global Priority List of Antibiotic-Resistant Bacteria to Guide Research, Discovery and Development of New Antibiotics,” further highlighting the worsen situation caused by this pathogen (World Health Organisation, 2017).

Carbapenem resistance in *A. baumannii* has been attributed to intrinsic cellular mechanisms, including loss of outer membrane porins (OMP) and over-expression of efflux pumps, which could result in alteration of cytoplasmic antimicrobial drug concentration and hence its bactericidal effect (Magnet et al., 2001; Siroy et al., 2005). Several OMPs, including CarO, HMP-AB and OmpW, were found to be involved in transportation of  $\beta$ -lactams across cytoplasmic membrane of this bacterial pathogen (Gribun et al., 2003; Siroy et al., 2006). While OMPs are responsible for the uptake of antibiotics, the multi-drug efflux systems are believed to be involved in removal of drugs by pumping them out of the cell. In particular, the resistance-nodulation-division (RND) type efflux pumps, have long been hypothesized to play a role in rendering resistance toward various antibiotics. In *A. baumannii*, the most extensively studied RND efflux system is the *adeABC* gene product, which exhibits substrate specificity toward various  $\beta$ -lactams, including fluoroquinolones, aminoglycosides, tetracyclines and chloramphenicol (Higgins et al., 2004). Nevertheless, evidence confirming a direct linkage between carbapenem susceptibility and the presence/absence of these porin proteins and efflux systems in *A. baumannii* is currently not available.

Enzymatic mechanisms have been regarded as the key factors that mediate development of carbapenem resistance in Gram negative bacteria, including *A. baumannii*. Instead of *bla<sub>IMP</sub>*, *bla<sub>VIM</sub>* and *bla<sub>NDM</sub>* which are commonly identified in other bacterial pathogens, the carbapenem-hydrolyzing-class-D  $\beta$ -lactamases (CHDLs) are regarded as key determinants underlying the emergence of carbapenem-resistant *A. baumannii* (Poirel and Nordmann, 2006). CHDLs denote the OXA-type  $\beta$ -lactamases which exhibit carbapenem hydrolyzing activity.

There are various types of *bla<sub>OXA</sub>* genes which are known to be harbored by *A. baumannii*, including *bla<sub>OXA-51</sub>*, *bla<sub>OXA-23</sub>*, *bla<sub>OXA-24/40</sub>*, *bla<sub>OXA-58</sub>*, *bla<sub>OXA-143</sub>*, and *bla<sub>OXA-235</sub>* (Higgins et al., 2013; Evans and Amyes, 2014). A considerable number of studies have been conducted on enzymes encoded by these resistance genes due to their uniqueness in *A. baumannii*, particularly the *bla<sub>OXA-51</sub>*-like  $\beta$ -lactamases, the genetic determinant of which is inherent in *A. baumannii* chromosome and can be readily overexpressed as a result of promoter activation by insertion sequences such as *IS<sub>Aba1</sub>* (Turton et al., 2006). Apart from this chromosomal resistance gene, plasmid-borne *bla<sub>OXA-23</sub>*-like, *bla<sub>OXA-24/40</sub>*-like, and *bla<sub>OXA-58</sub>*-like elements are also frequently identified in resistant isolates. Among them, *bla<sub>OXA-23</sub>* is the most prevalent CHDL-encoding element in carbapenem-resistant *A. baumannii* worldwide (Mugnier et al., 2010). A previous study in China reported that 96.5% of carbapenem-resistant *A. baumannii* isolates carried *bla<sub>OXA-23</sub>*-like elements, and that over 96% of those isolates belonged to the Clonal Complex CC92 (Ji et al., 2014). In Hong Kong, the majority of carbapenem-resistant *A. baumannii* were *bla<sub>OXA-23</sub>*-like carrier that belonged to sequence type ST26 (Ho et al., 2010). Similarly, dissemination of *bla<sub>OXA-23</sub>*-bearing *A. baumannii* was also observed in other Asian countries, including Taiwan, Japan, and Korea (Pegel et al., 2008).

A comprehensive study was performed in 2013 to investigate the interplay between intrinsic and extrinsic mechanisms in mediating development of antimicrobial resistance in *A. baumannii*, including efflux systems, membrane porins, and production of CHDL  $\beta$ -lactamases (Rumbo et al., 2013). The study concluded that the *bla<sub>OXA-24</sub>* and *bla<sub>OXA-58</sub>* are the major determinants of carbapenem resistance in this organism, and that *bla<sub>OXA-51</sub>* and porin proteins were not involved in antimicrobial resistance of *bla<sub>OXA-24</sub>* and *bla<sub>OXA-58</sub>*-carrying isolates (Rumbo et al., 2013). Nevertheless, the exact role of intrinsic mechanisms in mediating carbapenem resistant phenotypes in *A. baumannii* strains carrying *bla<sub>OXA-23</sub>* and *bla<sub>OXA-51</sub>* remained unclear. In this work, we showed that intrinsic resistance mechanisms including RND-mediated efflux and reduced expression of porin proteins did not play a major role in mediating onset of carbapenem resistance in *A. baumannii*. Instead, the phenotype was mainly conferred by CHDL encoded by the *bla<sub>OXA-23</sub>*, *bla<sub>OXA-72</sub>*, and *bla<sub>OXA-51</sub>*-like genes. In addition, we identified several variants of *bla<sub>OXA-51</sub>*, which exhibited carbapenem-hydrolyzing activities that resemble those encoded by *bla<sub>OXA-23</sub>* in terms of substrate profile, as over-expression of these *bla<sub>OXA-51</sub>* variants in *A. baumannii* upon insertional activation by *IS<sub>Aba1</sub>* conferred the host strain a carbapenem resistant phenotype identical to *bla<sub>OXA-23</sub>*-carrying strains.

## MATERIALS AND METHODS

### Bacterial Isolates

A total of 14 representative *Acinetobacter baumannii* clinical strains were first included in the genome sequencing, gene expression study, and western blot analysis as described below. The strains were isolated from patients of two hospitals, one each

in Hong Kong and Henan Province, People's Republic of China, during the period between 2000 and 2013. These strains exhibited various carbapenem resistance phenotypes and genotypes. The genetic identity of these isolates was confirmed by the Vitek II bacterial identification system prior to further analysis. The ethic approval for this study was covered by human subject ethic approval, 2018-039, approved by the Second Affiliated Hospital of Zhejiang University, Zhejiang, China. An addition 453 clinical carbapenem-resistant *A. baumannii* strains isolated from four different regions of China, were included in the screening of *bla*<sub>OXA</sub> genes in the latter part of the study. The experimental flow is illustrated by **Supplementary Figure S1**.

## Antimicrobial Susceptibility Test

Minimal inhibitory concentration (MIC) of carbapenems was tested for the 14 *Acinetobacter baumannii* strains by using the microdilution method and interpreted according to CLSI guidelines (Clinical and Laboratory Standards Institute, 2016). Briefly, bacterial strains were grown on MH agar. Bacterial cell suspensions at a concentration equivalent to a 0.5 McFarland Standard were prepared and inoculated into microplate wells containing different concentrations of carbapenem. The final volume in each well was 150  $\mu$ L. The effect of the efflux pump inhibitor Phenylalanine-arginine  $\beta$ -naphthylamide (PA $\beta$ N) and CHDL inhibitor Sodium chloride on the susceptibility of the test strains to carbapenem was determined by adding the compounds to specific wells of the microtiter plate to produce a concentration of 30  $\mu$ g/ml and 200 mM, respectively. The MIC test was repeated twice to ensure the accuracy of the result.

## Whole Genome Sequencing and ST Typing of *Acinetobacter baumannii*

Whole genomic DNA was extracted from the strains using the Invitrogen™ PureLink™ Genomic DNA Mini kit, followed by sequencing with an Illumina® NextSeq 550 system. Raw reads generated in this study and the Illumina reads of 11 strains obtained from the NCBI database were trimmed or filtered to remove low-quality sequences and adaptors. Genome data were annotated with the RAST tool (Overbeek et al., 2014) and Prokka (Seemann, 2014). Scaffolds obtained were analyzed by Geneious 9.7. *A. baumannii* type strain ATCC19606 was used as reference throughout the analysis. ST profiles were determined according to the *A. baumannii* MLST (Oxford) database using sequences extracted from whole genome sequencing. Discrimination of International Clone II was based on analysis of the *bla*<sub>OXA-51</sub> gene as described previously (Matsui et al., 2013).

## qRT-PCR Analysis on Gene Expression

Overnight culture of *A. baumannii* isolate was inoculated into fresh LB broth until OD 0.6 was reached. Total RNA was extracted using the QIAGEN RNeasy® Mini Kit. The extracted RNA was further treated with the Invitrogen Turbo DNA-free™ Kit to remove any DNA contaminants. 1  $\mu$ g of purified mRNA samples were reverse-transcribed to cDNA by using the Invitrogen™ SuperScript™ III First-Strand Synthesis SuperMix kit for qRT-PCR. Real-time PCR was performed on a Roche

LightCycler® 480 System and PowerSYBR™ Green PCR Master Mix was used as the reaction medium. The parameters of PCR were as followed: the reaction mixture was first incubated at 95°C for 10 min for complete denaturation of template and activation of DNA polymerase; followed by 40 cycles of denaturation at 95°C for 10 s, annealing and polymerization at 60°C for 1 min. The melting temperature of PCR product was measured after completion of PCR to ensure the absent of non-specific PCR product. Expression level of endogenous genes was normalized with *gyrB* and *A. baumannii* ATCC19606 was used as control for comparison. The gene expression study was performed in triplicate. Primers used in this study are listed in **Supplementary Table S1**.

## Western Blot of *bla*<sub>OXA-51</sub>-Like Proteins

Cell lysates were solubilized by boiling with SDS running buffer for 10 min and subsequently separated by SDS-PAGE with 12% separating gel. Proteins were transferred to a PVDF membrane followed by blocking by skimmed milk for 1 h and incubated with mouse anti-OXA-51 antibody at 4°C overnight. The goat anti-mouse antibody was used as the secondary antibody. The signal was generated by HRP substrate and detected by chemiluminator. The broad range anti-GADPH (ABCAM) was used as loading control.

## Further Screening of Carbapenem-Resistant *Acinetobacter baumannii* Clinical Isolates

An addition 453 clinical carbapenem-resistant *A. baumannii* strains, isolated from four different regions of China, were further screened for the presence of *bla*<sub>OXA-23</sub>, presence of *ISAbal* in the promoter region of *bla*<sub>OXA-23</sub>, *bla*<sub>OXA-51</sub> and presence of *ISAbal* in the promoter region of *bla*<sub>OXA-51</sub>. The primers sequences are shown in **Supplementary Table S1**. To screen for the presence of *ISAbal* in the promoter region of *bla*<sub>OXA-23</sub> or *bla*<sub>OXA-51</sub>, PCR assay was performed using primer *ISAbal*-F was used together with reverse primer of *bla*<sub>OXA-23</sub> or *bla*<sub>OXA-51</sub>. Strains that did not contain *bla*<sub>OXA-23</sub> with insertion of *ISAbal* in the promoter region were selected for Western-blot analysis as mentioned above to check for the over-expression of OXA-51 in these strains.

## RESULTS AND DISCUSSION

### Antimicrobial Susceptibility and Sequence Analysis of *Acinetobacter baumannii* Strains

Fourteen clinical *A. baumannii* strains were first tested for their susceptibility toward carbapenems. Resistance toward imipenem and meropenem was observable in 12 of the 14 strains, with MIC ranging from 8 to  $\geq 64$   $\mu$ g/ml (**Table 1**). The fourteen strains were then subjected to whole-genome sequencing. Based on the sequences obtained, about half of the strains were found to belong to ST208 (6 out of 14), whereas three strains (AB2, AB5, and MH5) belonged to ST940. For the remaining five strains they belonged to different ST types. Only the three ST940 strains

**TABLE 1** | Genetic and phenotypic characteristics of 14 *Acinetobacter baumannii* clinical strains tested in this study.

Strain	Year/Origin	ST type (Oxford)	International clone	Presence of resistance determinants							MIC ( $\mu\text{g/ml}$ )				
				<i>carO</i>	<i>adeB</i>	<i>adeRS</i>	<i>bla</i> <sub>OXA-51</sub> variants	<i>ISAbal-1-bla</i> <sub>OXA-51</sub>	<i>bla</i> <sub>OXA-23/24/40</sub>	<i>ISAbal-1-bla</i> <sub>OXA23</sub>	IMP <sup>®</sup>	IMP/PABN	MER <sup>®</sup>	MER/PABN	COL
AB1	2004, HK	208	IC II	+	+	–	OXA-83	+	–	–	16 (4)	16	32 (8)	32	1
AB2	2008, HK	940	Non-IC II	+	+	+	OXA-99	–	OXA-23	+	16 (8)	16	32 (16)	16	2
AB3	2011, HK	208	IC II	+	–	–	OXA-66	+	OXA-23 <sup>#</sup>	+	32 (8)	32	$\geq 64$ (32)	32	2
AB4	2011, HK	253	IC II	+	+	+	OXA-66	–	OXA-23	+	$\geq 64$ (8)	$\geq 64$	$\geq 64$ (32)	$\geq 64$	2
AB5	2004, HK	940	Non-IC II	+	+	+	OXA-99	–	OXA-23	+	16 (4)	16	8 (8)	8	1
AB7	2011, HK	208	IC II	+	+	+	OXA-82	+	–	–	8 (4)	8	16 (16)	16	8
AB8	2003, HK	208	IC II	+	+	+	OXA-82	+	–	–	8 (8)	8	32 (16)	16	2
AB10	2000, HK	208	IC II	+	+	+	OXA-66	–	–	–	1 (0.25)	0.5	0.25 (0.25)	0.5	2
MH1	2000, HK	684	IC II	+	+	+	OXA-66	–	–	–	0.5 (0.5)	1	0.25 (0.125)	0.5	0.5
MH2	2010, HK	218	IC II	+	+	+	OXA-66	–	OXA-72	–	$\geq 64$ (64)	$\geq 64$	$\geq 64$ ( $\geq 64$ )	64	1
MH3	2011, HK	208	IC II	+	+	+	OXA-79	+	–	–	8 (4)	8	32 (8)	16	2
MH5	2006, HK	940	Non-IC II	+	–	–	OXA-99	–	OXA-23	+	32 (16)	16	32 (8)	4	1
MH6	2013, HN	195	IC II	+	+	+	OXA-66	–	OXA-23	+	32 (16)	16	32 (8)	8	2
MH7	2013, HN	369	IC II	+	+	+	OXA-66	–	OXA-23 <sup>#</sup>	+	$\geq 64$ (32)	$\geq 64$	$\geq 64$ (16)	32	2

Presence of endogenous genes and other resistance determinants were investigated by analysis of whole genome sequences.<sup>®</sup>MIC performed in the presence of NaCl.<sup>#</sup>Chromosome-based. HK, Hong Kong; HN, Henan province, China. IMP, imipenem; MER, meropenem; COL, colistin; PABN, Phenylalanine-arginine  $\beta$ -naphthylamide.

were found to belong to International Clone II (IC II) based on analysis on the intrinsic *bla<sub>OXA-51</sub>* gene harbored by these strains (Table 1 and Supplementary Figure S6). The findings corroborated with those in previous studies which reported the dissemination of *A. baumannii* Clonal Complex 92 strains within the Asia Pacific region, including Taiwan, South Korea and China (Kim et al., 2013). It has previously been demonstrated that the high genome plasticity of *A. baumannii* may result in sporadic loss of endogenous genes, altering the physiological status and hence antibiotic susceptibilities of the organism (Roca et al., 2012). In view of the possibility that resistance formation is due to loss of specific physiological functions, the relationship between presence of various intrinsic determinants of carbapenem sensitivity was determined; the determinants tested included the outer membrane porin-encoding genes *carO* and *ompA*, as well as the efflux gene *adeABC* and its regulator *adeRS*. It was found that all the test strains carried the intact *carO* and *ompA* genes without insertion of IS elements; this finding was consistent with that of a previous report (Rumbo et al., 2013). However, three strains (AB1, AB3, and MH5) were found to lack *adeRS*, with the latter two also lacking *adeB*. The intrinsic *bla<sub>OXA-51</sub>* gene was detectable in all test strains, among them, the three ST940 strains were found to carry the variant gene *bla<sub>OXA-99</sub>*, whereas the *bla<sub>OXA-66</sub>*, *bla<sub>OXA-79</sub>*, *bla<sub>OXA-82</sub>* and *bla<sub>OXA-83</sub>* variants were identified in the other strains. Interestingly, the *ISAbal* element was found to be inserted into the promoter region of *bla<sub>OXA-51</sub>* in five strains, all of which belonged to IC-II. Apart from carriage of various intrinsic CHDL genes, half of the strains were found to have acquired the *bla<sub>OXA-23</sub>* gene, two of which were located in the chromosome. One strain was also found to harbor the *bla<sub>OXA-72</sub>* element (a variant of *bla<sub>OXA-24</sub>*) (Table 1). It has been described that

alteration of amino acids of the *adeRS* gene product could result in change of expression level of *adeB* (Wen et al., 2017). Sequences of *carO*, *adeB* and *adeRS* were then analyzed and aligned in attempt to establish their relationship with carbapenem susceptibility. However, it was shown that the genetic differences detectable in these genes were linked closely to their genetic types (IC-II and non IC-II) rather than carbapenem sensitivity (Supplementary Figures S2–S5). Other known carbapenemase genes such as *bla<sub>NDM-1</sub>* were not detectable in the test strains. The combinational analysis of carbapenem resistance genotypes and their genetic characteristics showed that strains exhibiting carbapenem resistance were either carrying an additional CHDL gene (*bla<sub>OXA-23</sub>* and *bla<sub>OXA-24</sub>*) or having an *ISAbal* linked upstream region in their *bla<sub>OXA-51</sub>* element. Consistently, two carbapenem-susceptible isolates carried neither *bla<sub>OXA-23</sub>* or *bla<sub>OXA-24</sub>* nor insertion of *ISAbal* in the intrinsic *bla<sub>OXA-51</sub>* (Tables 1, 2).

### Efflux Pumps Did Not Mediate Carbapenem Resistance in *Acinetobacter baumannii*

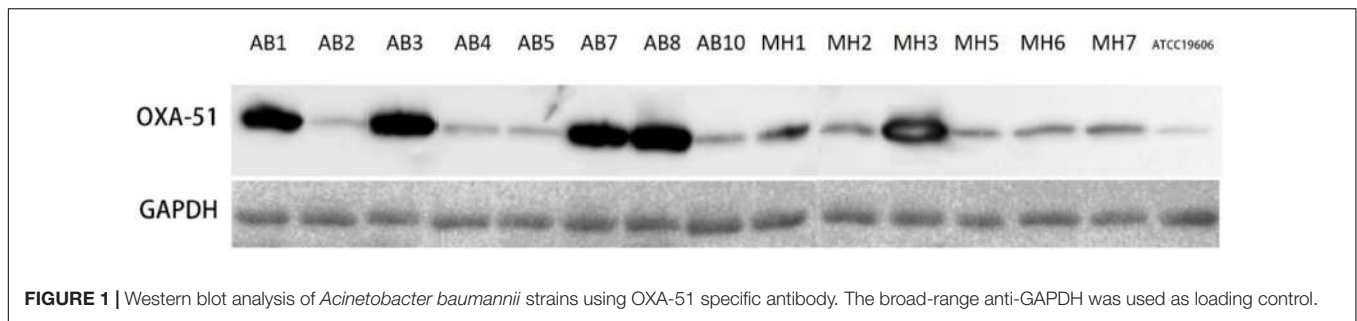
The effect of RND-efflux systems on carbapenem susceptibility in *A. baumannii* clinical strains was evaluated by supplementing Phenylalanine-arginine  $\beta$ -naphthylamide (PA $\beta$ N) at a concentration of 30  $\mu$ g/ml in determination of MIC toward carbapenem. As shown in Table 1, we found that addition of PA $\beta$ N exhibited minimal effect on altering carbapenem MIC except for two strains (Table 1). This finding demonstrated that RND efflux pumps only play a minimal role in mediating carbapenem resistance in *A. baumannii* strains of hospital origins and that the resistance phenotype is mainly conferred by the *bla<sub>OXA</sub>* enzymes.

**TABLE 2** | Expression level of genes related to carbapenem resistance in *A. baumannii* strains.

Strain	Relative expression level of different genes by qPCR				
	<i>carO</i>	<i>adeB</i>	<i>adeR</i>	<i>bla<sub>OXA-51</sub></i>	<i>bla<sub>OXA-23</sub></i>
ATCC19606	1	1	1	1	n.a
AB1	1.53 $\pm$ 0.10	0.07 $\pm$ 0.01	n.a	25.75 $\pm$ 2.85	n.a
AB2	0.79 $\pm$ 0.09	0 $\pm$ 0.00	0.91 $\pm$ 0.01	1.53 $\pm$ 0.21	3.93 $\pm$ 0.31
AB3	1.1 $\pm$ 0.05	n.a	n.a	25.09 $\pm$ 3.06	3.14 $\pm$ 0.11
AB4	0.54 $\pm$ 0.06	0.04 $\pm$ 0.00	1.37 $\pm$ 0.02	0.98 $\pm$ 0.32	2.24 $\pm$ 0.06
AB5	0.53 $\pm$ 0.06	0 $\pm$ 0.01	0.92 $\pm$ 0.01	1.8 $\pm$ 0.10	3.82 $\pm$ 0.39
AB7	2.86 $\pm$ 0.12	0.31 $\pm$ 0.01	2.74 $\pm$ 0.21	58.26 $\pm$ 4.87	n.a
AB8	2.29 $\pm$ 0.11	0.25 $\pm$ 0.02	2.16 $\pm$ 0.16	53.27 $\pm$ 4.03	n.a
AB10	0.74 $\pm$ 0.01	0.2 $\pm$ 0.02	3.63 $\pm$ 0.28	2.81 $\pm$ 0.26	n.a
MH1	0.27 $\pm$ 0.01	0.12 $\pm$ 0.01	1.04 $\pm$ 0.08	2.46 $\pm$ 0.57	n.a
MH2	1.39 $\pm$ 0.15	0.2 $\pm$ 0.02	2.84 $\pm$ 0.30	1.39 $\pm$ 0.13	n.a
MH3	2.33 $\pm$ 0.15	0.17 $\pm$ 0.01	2.89 $\pm$ 0.19	64.96 $\pm$ 5.07	n.a
MH5	1.18 $\pm$ 0.28	n.a	n.a	7.16 $\pm$ 0.65	4.37 $\pm$ 0.36
MH6	1.13 $\pm$ 0.13	0.15 $\pm$ 0.01	3.44 $\pm$ 0.36	2.99 $\pm$ 0.45	7.64 $\pm$ 0.72
MH7	1.43 $\pm$ 0.13	0.13 $\pm$ 0.01	3.27 $\pm$ 0.50	2.25 $\pm$ 0.22	5.10 $\pm$ 0.16

Expression levels were normalized with ATCC19606 for *carO*, *adeB*, *adeR* and *bla<sub>OXA-51</sub>*. Strains lacking the corresponding genes were depicted by "n.a." Expression of *adeB* was not detected in AB2 and AB5.





**TABLE 3** | Surveillance of mechanisms of carbapenem resistance in clinical carbapenem-resistant *A. baumannii* isolates from different regions of China.

Characteristics of <i>A. baumannii</i> isolates from different sources	Guangdong, China	Zhejiang, China	Henan, China	Hong Kong, China	Total
Total No of strains of each source	163	173	72	45	453
Average MICs					
MER	24.4	18.4	24.8	20.6	21.8
IMP	26.8	16.2	24.6	22.4	22.0
ERA	86.4	64.2	78.8	66.4	74.7
No of positive strains					
<i>bla</i> <sub>OXA-51</sub>	163	173	72	45	453
IS <i>Aba1</i> - <i>bla</i> <sub>OXA-51</sub>	18	19	4	8	49
<i>bla</i> <sub>OXA-23</sub>	145	154	68	37	404
IS <i>Aba1</i> - <i>bla</i> <sub>OXA-23</sub>	145	154	68	37	404
Overexpression of OXA-51 (WB) <sup>#</sup>	18	19	4	8	49

MER, meropenem; IMP, imipenem; ERA, ertapenem. <sup>#</sup>OXA-51 expression level was determined by Western-blot using OXA-51 specific antibody developed in our lab.

To further investigate the role of various host determinants in mediating changes in carbapenem susceptibility, the expression level of various putative resistance genes, including the RND efflux pump gene *adeB*, its regulator *adeR*, the outer membrane porin gene *carO*, as well as the *bla*<sub>OXA-23</sub> and *bla*<sub>OXA-51</sub>-like β-lactamase-encoding elements, were further analyzed by RT-qPCR. The expression level of each gene was normalized by the gene encoding the gyrase protein subunit B (*gyrB*) of the *A. baumannii* type strain ATCC19606. The results are shown in **Table 2** and **Supplementary Figures S7–S11**. For *carO*, varied expression level was observed among the test strains, with most isolates exhibiting a level similar to or lower than that of ATCC19606. For the two susceptible strains, AB10 and MH1, *carO* expression was lower than that of ATCC19606 and most of the other carbapenem-resistant counterparts. The result is in line with a previous study, in which a decreased expression of *carO* has been described in carbapenem susceptible isolates recovered from Brazil (Fonseca et al., 2013). It should be noted that although strains AB7, AB8, and MH3 exhibited elevated *carO* expression by an amplitude >twofolds, their contribution to carbapenem resistance was hard to be addressed due to the presence of other major resistance mechanism, presence of OXA types of carbapenemases (**Tables 1, 2**).

An unexpected phenomenon regarding the *adeB* expression level of the test strains was observed. It was proposed that elevated expression of *adeABC* might contribute to reduced carbapenem susceptibility, possibly due to enhanced extrusion of intracellular antibiotics through efflux activity (Kim et al., 2013). Nevertheless, except for the two test strains AB3 and

MH5, which lacked *adeB*, all other test strains exhibited a very low transcript level of this efflux gene, with a range of 0.07 to 0.31 compared to ATCC19606. Transcript of *adeB* was not detected in strains AB2 and AB5. Of note, *adeB* expression in the two carbapenem sensitive strains AB10 and MH1 was similar to most of their resistant counterparts. In order to evaluate whether decreased *adeABC* expression was due to effect of transcription regulation, expression level of *adeR* was also examined in an attempt to determine the degree of correlation between the two. Contrary to the data on *adeB*, similar or higher transcription level of *adeR* was observed among the majority of the test isolates, ranging from 0.91 to 3.63 folds when compared to ATCC19606 (**Table 2**). Correlation between expression of *adeB* and *adeR*, as well as *adeR* and carbapenem susceptibility, therefore could not be established. Taken together, the results suggest that the *adeABC* gene plays a negligible role in mediating changes in carbapenem susceptibility, particularly in strains which harbor additional CHDL genes such as *bla*<sub>OXA-23</sub> and *bla*<sub>OXA-24</sub>. Indeed, the results of genotypic analysis corroborated with those of the expression study in that a lack of *adeABC* efflux system was observed in several resistant strains.

### Overexpression of OXA-23 and Intrinsic OXA-51 Through IS*Aba1* Insertion Was the Major Mechanisms of Carbapenem Resistance

Antimicrobial susceptibility test revealed that all *bla*<sub>OXA-23</sub> carriers were resistant to imipenem and meropenem but

exhibited varied MIC values, presumably due to the fact that these strains carried various variants of *bla*<sub>OXA-23</sub> and *bla*<sub>OXA-51</sub>. Expression level of *bla*<sub>OXA-51</sub> and *bla*<sub>OXA-23</sub> was examined in an attempt to determine the degree of contribution of carbapenemases encoded by these genes to reduction in carbapenem susceptibility of the *A. baumannii* strains tested in this study. All *bla*<sub>OXA-23</sub> genes were found to carry insertion in the promoter region by *ISAbal*. Consistently, expression level of the *bla*<sub>OXA-23</sub> gene was found to be up-regulated 2.24 to 7.64 folds among the strains. Discrepancies between the effects of plasmid-borne and chromosome-based elements were not observed (Tables 1, 2). Among the 6 *bla*<sub>OXA-23</sub> carriers which lacked an over-expressed *bla*<sub>OXA-51</sub>, MIC values of imipenem and meropenem ranged from 16 to  $\geq 64$   $\mu\text{g/ml}$  and 8 to  $\geq 64$   $\mu\text{g/ml}$ , respectively. In particular, the higher transcript level of *bla*<sub>OXA-23</sub> did not necessarily confer higher resistance level toward carbapenems. Since identical *bla*<sub>OXA-23</sub> was harbored by all the strains, the possibility of varied activity toward carbapenem in individual variants can be ruled out. The lack of association between *bla*<sub>OXA-23</sub> expression and susceptibility might then be attributed to physiological status of individual *A. baumannii* strains. Result of *bla*<sub>OXA-51</sub> expression revealed consistency between *ISAbal* insertion and transcript level of this endogenous carbapenemase. For the five test strains which carried the IS element, *bla*<sub>OXA-51</sub> expression ranged from 25.09 to 64.96 folds compared to ATCC19606. To ensure that the overexpression of *bla*<sub>OXA-51</sub> was consistent with their protein production, we took advantage of the monoclonal antibody specific to OXA-51 variants that produced by our lab to examine the production level of these OXA-51 variants by western blotting (Figure 1). It was shown that protein production correlated well with the qRT-PCR data, and that the five strains apparently over-produced the OXA-51 enzymes. The result confirmed that the *ISAbal* insertion sequence is a key factor that promotes *bla*<sub>OXA-51</sub> expression. To summarize, although the physiological status of individual strain may affect carbapenem susceptibility to some extent, resistance was observed only among *A. baumannii* strains which carried either *ISAbal*-*bla*<sub>OXA-51</sub> or additional CHDL-encoding genes such as *bla*<sub>OXA23</sub> and *bla*<sub>OXA-72</sub>.

To confirm that overexpression of OXA-23 and intrinsic OXA-51 is the major mechanisms of carbapenem resistance in clinical *A. baumannii*, a total of 453 carbapenem-resistant clinical *A. baumannii* isolated from four different regions of China were screened for the presence of these two mechanisms (Table 3). Our results showed that 404/453 strains carried over-expressed OXA-23 with *ISAbal* in the promoter region of *bla*<sub>OXA-23</sub>, while the rest of 49 strains that did not carry *bla*<sub>OXA-23</sub> exhibited an insertion of *ISAbal* in the promoter region of *bla*<sub>OXA-51</sub> and over-expression of OXA-51, which was confirmed by Western-blot using specific antibody to OXA-51 (Table 3). These data suggested that mechanisms of carbapenem resistance in clinical *A. baumannii* were mediated by either over-production of OXA-23 or OXA-51 through insertion of *ISAbal* in their promoter region.

Correlation analysis of the enzymatic activity of OXA types carbapenemase and meropenem MIC of strains producing these enzymes indicated that: (1) *A. baumannii* strains that over-expressed OXA-23/OXA-24 regardless of the status of over-expression of OXA-51 variants generally displayed higher MIC of meropenem ( $\geq 16$   $\mu\text{g/ml}$ ); (2) *A. baumannii* strains that over-expressed OXA-51 variants only displayed relatively low MIC of meropenem, with OXA-83 (32  $\mu\text{g/ml}$ ) being higher than OXA-79/OXA-83 (8  $\mu\text{g/ml}$ ); and (3) Western-blot experiments indicated that OXA-51 variants exhibited base line expression without the insertion of *ISAbal*, which is probably true for extrinsic OXAs. OXA variants with lower activity like OXA51 variants are needed to be overexpressed to counter carbapenem resistance phenotype, while variants with high catalytic activity such as OXA-72 may not need to be overexpressed, its basic line expression might be enough to mediate high carbapenem resistance in *A. baumannii* in the case of MH2 in this study.

## CONCLUSION

*Acinetobacter baumannii* is an important pathogen that may cause fatal infections in nosocomial settings. It was thought that the interplay of multiple resistance mechanisms, including over-expression of endogenous efflux systems, suppression of expression of porin proteins, reduced membrane permeability and carriage of CHDL-encoding elements could lead to carbapenem resistance in this bacterial pathogen. In the current study, through systematic characterization of a set of clinical *A. baumannii* strains with different OXA-23 and MIC profiles, we demonstrated that the RND efflux system and membrane porin proteins were not the key factors that conferred carbapenem resistance in the *A. baumannii* strains tested. Instead the OXA-23 and OXA-24 enzymes (OXA-72 variant) were found to be the key elements underlying carbapenem resistance in *A. baumannii* strains as a result of insertion of the *ISAbal* element, which provides a promoter for over-expression of the *bla*<sub>OXA-23</sub> and *bla*<sub>OXA-23</sub> genes (Nigro and Hall, 2016). In *A. baumannii* strains lacking these genes, carbapenem resistance was mainly due to the over-expression of *bla*<sub>OXA-51</sub> variants, again through insertion of the promoter-bearing *ISAbal* elements. Findings in this study emphasized the role of *bla*<sub>OXA</sub> type enzymes in mediating carbapenem resistance in this major clinical pathogen. These data provided essential information for the design of new strategies to treat clinical infections caused by carbapenem-resistant *A. baumannii* strains.

## DATA AVAILABILITY STATEMENT

The whole genome shotgun sequences of isolates included in this study have been deposited in GenBank with the following accession numbers: AB1, SAMN09667770; AB2, SAMN09667771; AB3, SAMN09667772; AB4, SAMN09667773;

AB5, SAMN09667774; AB7, SAMN09667775; AB8, SAMN-09667776; AB10, SAMN09667777; MH1, SAMN09667778; MH2, SAMN09667779; MH3, SAMN09667780; MH5, SAMN09667781; MH6, SAMN09667782; and MH7, SAMN09667783.

## AUTHOR CONTRIBUTIONS

MW and BC designed and performed the research, and drafted the manuscript. EC edited the manuscript. SC supervised the study and edited the manuscript.

## REFERENCES

- Bergogne-Berezin, E., and Towner, K. J. (1996). *Acinetobacter* spp. as nosocomial pathogens: microbiological, clinical, and epidemiological features. *Clin. Microbiol. Rev.* 9, 148–165. doi: 10.1128/cmr.9.2.148
- Clinical and Laboratory Standards Institute (2016). *Performance Standards for Antimicrobial Susceptibility Testing: Twenty-sixth Informational Supplement M100-S26*. Wayne, PA: CLSI.
- Evans, B. A., and Amyes, S. G. (2014). OXA  $\beta$ -lactamases. *Clin. Microbiol. Rev.* 27, 241–263. doi: 10.1128/CMR.00117-113
- Fonseca, E. L., Scheidegger, E., Freitas, F. S., Cipriano, R., and Vicente, A. C. (2013). Carbapenem-resistant *Acinetobacter baumannii* from Brazil: role of carO alleles expression and blaOXA-23 gene. *BMC Microbiol.* 13:245. doi: 10.1186/1471-2180-13-245
- Gribun, A., Nitzan, Y., Pechatnikov, I., Hershkovits, G., and Katcoff, D. J. (2003). Molecular and structural characterization of the HMP-AB gene encoding a pore-forming protein from a clinical isolate of *Acinetobacter baumannii*. *Curr. Microbiol.* 47, 434–443.
- Higgins, P. G., Pérez-Llarena, F. J., Zander, E., Fernández, A., Bou, G., and Seifert, H. (2013). OXA-235, a novel class D  $\beta$ -lactamase involved in resistance to carbapenems in *Acinetobacter baumannii*. *Antimicrob. Agents Chemother.* 57, 2121–2126. doi: 10.1128/AAC.02413-2412
- Higgins, P. G., Wisplinghoff, H., Stefanik, D., and Seifert, H. (2004). Selection of topoisomerase mutations and overexpression of adeB mRNA transcripts during an outbreak of *Acinetobacter baumannii*. *J. Antimicrob. Chemother.* 54, 821–823. doi: 10.1093/jac/dkh427
- Ho, P. L., Ho, A. Y., Chow, K. H., Lai, E. L., Ching, P., and Seto, W. H. (2010). Epidemiology and clonality of multidrug-resistant *Acinetobacter baumannii* from a healthcare region in Hong Kong. *J. Hosp. Infect.* 74, 358–364. doi: 10.1016/j.jhin.2009.10.015
- Ji, S., Chen, Y., Ruan, Z., Fu, Y., Ji, J., Fu, Y., et al. (2014). Prevalence of carbapenem-hydrolyzing class D  $\beta$ -lactamase genes in *Acinetobacter* spp. isolates in China. *Eur. J. Microbiol. Infect. Dis.* 33, 989–997. doi: 10.1007/s10096-013-2037-z
- Kim, D. H., Choi, J.-Y. Y., Kim, H. W., Kim, S. H., Chung, D. R., Peck, K. R., et al. (2013). Spread of carbapenem-resistant *Acinetobacter baumannii* global clone 2 in Asia and AbaR-type resistance islands. *Antimicrob. Agents Chemother.* 57, 5239–5246. doi: 10.1128/AAC.00633-613
- Liu, Y.-M. M., Chen, Y.-S. S., Toh, H.-S. S., Huang, C.-C. C., Lee, Y.-L. L., Ho, C.-M. M., et al. (2012). In vitro susceptibilities of non-*Enterobacteriaceae* isolates from patients with intra-abdominal infections in the Asia-Pacific region from 2003 to 2010: results from the study for monitoring antimicrobial resistance trends (SMART). *Int. J. Antimicrob. Agents* 40(Suppl.), S11–S17. doi: 10.1016/S0924-8579(12)70004-3
- Magnet, S., Courvalin, P., and Lambert, T. (2001). Resistance-nodulation-cell division-type efflux pump involved in aminoglycoside resistance in *Acinetobacter baumannii* strain BM4454. *Antimicrob. Agents Chemother.* 45, 3375–3380. doi: 10.1128/AAC.45.12.3375-3380.2001

## FUNDING

This work was supported by the Health and Medical Research Fund of the Food and Health Bureau, Hong Kong (15141322) to SC.

## SUPPLEMENTARY MATERIAL

The Supplementary Material for this article can be found online at: <https://www.frontiersin.org/articles/10.3389/fmicb.2019.02809/full#supplementary-material>

- Matsui, M., Suzuki, S., Suzuki, M., Arakawa, Y., and Shibayama, K. (2013). Rapid discrimination of *Acinetobacter baumannii* international clone II lineage by pyrosequencing SNP analyses of bla(OXA-51-like) genes. *J. Microbiol. Methods* 94, 121–124. doi: 10.1016/j.mimet.2013.05.014
- Mugnier, P. D., Poirel, L., Naas, T., and Nordmann, P. (2010). Worldwide dissemination of the blaOXA-23 carbapenemase gene of *Acinetobacter baumannii*. *Emerg. Infect. Dis.* 16, 35–40. doi: 10.3201/eid1601.090852
- Nigro, S. J., and Hall, R. M. (2016). Structure and context of acinetobacter transposons carrying the oxa23 carbapenemase gene. *J. Antimicrob. Chemother.* 71, 1135–1147. doi: 10.1093/jac/dkv440
- Overbeek, R., Olson, R., Pusch, G. D., Olsen, G. J., Davis, J. J., Disz, T., et al. (2014). The SEED and the rapid annotation of microbial genomes using subsystems technology (RAST). *Nucleic Acids Res.* 42, D206–D214. doi: 10.1093/nar/gkt1226
- Peleg, A. Y., Seifert, H., and Paterson, D. L. (2008). *Acinetobacter baumannii*: emergence of a successful pathogen. *Clin. Microbiol. Rev.* 21, 538–582. doi: 10.1128/CMR.00058-07
- Poirel, L., and Nordmann, P. (2006). Carbapenem resistance in *Acinetobacter baumannii*: mechanisms and epidemiology. *Clin. Microbiol. Infect.* 12, 826–836. doi: 10.1111/j.1469-0691.2006.01456.x
- Queenan, A. M., Pillar, C. M., Deane, J., Sahn, D. F., Lynch, A. S., Flamm, R. K., et al. (2012). Multidrug resistance among acinetobacter spp. in the USA and activity profile of key agents: results from CAPITAL surveillance 2010. *Diagn. Microbiol. Infect. Dis.* 73, 267–270. doi: 10.1016/j.diagmicrobio.2012.04.002
- Roca, I., Espinal, P., Vila-Farres, X., and Vila, J. (2012). The *Acinetobacter baumannii* oxymoron: commensal hospital dweller turned pan-drug-resistant menace. *Front. Microbiol.* 3:148. doi: 10.3389/fmicb.2012.00148
- Rumbo, C., Gato, E., López, M., Ruiz de Alegría, C., Fernández-Cuenca, F., Martínez-Martínez, L., et al. (2013). Contribution of efflux pumps, porins, and  $\beta$ -lactamases to multidrug resistance in clinical isolates of *Acinetobacter baumannii*. *Antimicrob. Agents Chemother.* 57, 5247–5257. doi: 10.1128/AAC.00730-713
- Seemann, T. (2014). Prokka: rapid prokaryotic genome annotation. *Bioinformatics* 30, 2068–2069. doi: 10.1093/bioinformatics/btu153
- Siroy, A., Cosette, P., Seyer, D., Lemaitre-Guillier, C., Vallenet, D., Van Dorsselaer, A., et al. (2006). Global comparison of the membrane subproteomes between a multidrug-resistant *Acinetobacter baumannii* strain and a reference strain. *J. Proteome Res.* 5, 3385–3398. doi: 10.1021/pr060372s
- Siroy, A., Molle, V., Lemaitre-Guillier, C., Vallenet, D., Pestel-Caron, M., Cozzone, A. J., et al. (2005). Channel formation by CarO, the carbapenem resistance-associated outer membrane protein of *Acinetobacter baumannii*. *Antimicrob. Agents Chemother.* 49, 4876–4883. doi: 10.1128/AAC.49.12.4876-4883.2005
- Turton, J. F., Ward, M. E., Woodford, N., Kaufmann, M. E., Pike, R., Livermore, D. M., et al. (2006). The role of ISAbal in expression of OXA carbapenemase genes in *Acinetobacter baumannii*.

- FEMS Microbiol. Lett.* 258, 72–77. doi: 10.1111/j.1574-6968.2006.00195.x
- Wen, Y., Ouyang, Z., Yu, Y., Zhou, X., Pei, Y., Devreese, B., et al. (2017). Mechanistic insight into how multidrug resistant *Acinetobacter baumannii* response regulator AdeR recognizes an intercistronic region. *Nucleic Acids Res.* 45, 9773–9787. doi: 10.1093/nar/gkx624
- World Health Organisation (2017). *Global Priority List of Antibiotic-resistant Bacteria to Guide Research, Discovery, and Development of New Antibiotics*. Geneva: WHO Press.
- Conflict of Interest:** The authors declare that the research was conducted in the absence of any commercial or financial relationships that could be construed as a potential conflict of interest.
- Copyright © 2019 Wong, Chan, Chan and Chen. This is an open-access article distributed under the terms of the Creative Commons Attribution License (CC BY). The use, distribution or reproduction in other forums is permitted, provided the original author(s) and the copyright owner(s) are credited and that the original publication in this journal is cited, in accordance with accepted academic practice. No use, distribution or reproduction is permitted which does not comply with these terms.*





# Antibiotic Susceptibility, Virulence Pattern, and Typing of *Staphylococcus aureus* Strains Isolated From Variety of Infections in India

## OPEN ACCESS

### Edited by:

Raffaele Zarrilli,  
University of Naples Federico II, Italy

### Reviewed by:

Mohamamd Emaneini,  
Tehran University of Medical  
Sciences, Iran  
Morovat Taherikalani,  
Lorestan University of Medical  
Sciences, Iran

### \*Correspondence:

Durg Vijai Singh  
durg\_singh@yahoo.co.in;  
singhdv@ils.res.in;  
dvsingh@cusb.ac.in

† These authors have contributed  
equally to this work

### \* Present address:

Sasmita Panda,  
Department of Pathology  
and Microbiology, University  
of Nebraska Medical Center, Omaha,  
NE, United States

### Specialty section:

This article was submitted to  
Antimicrobials, Resistance  
and Chemotherapy,  
a section of the journal  
Frontiers in Microbiology

**Received:** 08 August 2019

**Accepted:** 12 November 2019

**Published:** 04 December 2019

### Citation:

Aggarwal S, Jena S, Panda S,  
Sharma S, Dhawan B, Nath G,  
Singh NP, Nayak KC and Singh DV  
(2019) Antibiotic Susceptibility,  
Virulence Pattern, and Typing  
of *Staphylococcus aureus* Strains  
Isolated From Variety of Infections  
in India. *Front. Microbiol.* 10:2763.  
doi: 10.3389/fmicb.2019.02763

Shifu Aggarwal<sup>1†</sup>, Smrutiti Jena<sup>1†</sup>, Sasmita Panda<sup>1†\*</sup>, Savitri Sharma<sup>2</sup>, Benu Dhawan<sup>3</sup>,  
Gopal Nath<sup>4</sup>, N. P. Singh<sup>5</sup>, Kinshuk Chandra Nayak<sup>6</sup> and Durg Vijai Singh<sup>1,7\*</sup>

<sup>1</sup> Infectious Disease Biology, Institute of Life Sciences, Bhubaneswar, India, <sup>2</sup> Jhaveri Microbiology Centre, LV Prasad Eye Institute, Brien Holden Eye Research Centre, Kallam Anji Reddy Campus, Hyderabad, India, <sup>3</sup> Department of Microbiology, All India Institute of Medical Sciences, New Delhi, India, <sup>4</sup> Department of Microbiology, Institute of Medical Sciences, Banaras Hindu University, Varanasi, India, <sup>5</sup> Department of Microbiology, Faculty of Medical Sciences, University of Delhi, New Delhi, India, <sup>6</sup> Institute of Life Sciences, Bhubaneswar, India, <sup>7</sup> Department of Biotechnology, Central University of South Bihar, Gaya, India

*Staphylococcus aureus* is one of the major causes of nosocomial infections. This organism produces powerful toxins and cause superficial lesions, systemic infections, and several toxemic syndromes. A total of 109 *S. aureus* strains isolated from a variety of infections like ocular diseases, wound infection, and sputum were included in the study. Minimum inhibitory concentration (MIC) was determined against 8 antimicrobials. PCR determined the presence of 16S rRNA, *nuc*, *mecA*, *czrC*, *qacA/B*, *pvl*, and toxin genes in *S. aureus* isolates. Pulse-field gel electrophoresis (PFGE), multi-locus sequence typing (MLST), SCC*mec*, *spa*-, and *agr*-typing and serotyping determined the diversity among them. All isolates of *S. aureus* were resistant to two or more than two antibiotics and generated 32 resistance patterns. These isolates were positive for 16S rRNA and *S. aureus*-specific *nuc* gene, but showed variable results for *mecA*, *czrC*, and *qacA/B* and *pvl* genes. Of the 32 methicillin-resistant *S. aureus* (MRSA), 13 strains carried SCC*mec* type V, seven type IV, two type III, and nine carried unreported type UT6. Of the 109 strains, 98.2% were positive for *hlg*, 94.5% for *hla*, 86.2% for *sei*, 73.3% for *efb*, 70.6% for *cna*, 30.2% for *sea*, and 12.8% for *sec* genes. Serotypes VII and VI were prevalent among *S. aureus* strains. PFGE analysis grouped the 109 strains into 77 clusters. MLST classified the strains into 33 sequence types (ST) and eight clonal complexes (CCs) of which 12 were singletons, and two belong to new allelic profiles. Isolates showed 46 *spa*-types that included two new *spa*-types designated as t14911 and t14912. MRSA and methicillin-susceptible *S. aureus* (MSSA) isolates were diverse in terms of antibiotic resistance pattern, toxin genotypes, SCC*mec* types, serotypes and PFGE, MLST, and *spa*-types. However, few isolates from eye infection and wound

infection belong to CC239, ST239, and *spa*-type t037/t657. The study thus suggests that *S. aureus* strains are multidrug resistant, virulent, and diverse irrespective of sources and place of isolation. These findings necessitate the continuous surveillance of multidrug-resistant and virulent *S. aureus* and monitoring of the transmission of infection.

**Keywords:** antibiotic susceptibility, virulence, MLST, *spa*-typing, PFGE, biofilm, *Staphylococcus aureus*

## INTRODUCTION

*Staphylococcus aureus* commensal to human skin and mucous membranes could cause nosocomial (Lindsay and Holden, 2004) and systemic infections (Jarraud et al., 2002). The isolation of methicillin-resistant *S. aureus* (MRSA) from ocular infections varies from 3 to 30% in a hospital in India and other countries (Shanmuganathan et al., 2005; Freidlin et al., 2007). MRSA strains belonging to ST5, ST72, and ST88 and isolated from severe eye infections in India were resistant to all antibiotics except tetracycline, chloramphenicol, and cefazolin (Nadig et al., 2012). Godebo et al. (2013) showed that 94.5% of *S. aureus* isolated from wound infection were resistant to penicillin, 91.8% to ampicillin, and 76.7% to oxacillin.

Several studies have shown the presence of toxin genes among MRSA. The presence of the *sea* gene in MRSA varies from country to country (Mehrotra et al., 2000; Kim et al., 2006; Wang et al., 2013). However, *hla* gene was present in all isolates (Shukla et al., 2010). MRSA isolated from conjunctivitis in Nigeria belonging to ST88 and SCCmec type IV were positive for *pvl* gene (Ghebremedhin et al., 2009). However, *pvl* gene positive methicillin-susceptible *S. aureus* (MSSA) strains belonged to ST30 (D'Souza et al., 2010). *S. aureus* carrying the *pvl* gene and belonging to ST239, ST5, and ST88 was reported from a teaching hospital in China (Liu et al., 2009). MSSA belonging to ST121 and *spa*-type 287 isolated from community-acquired pneumonia in young patients carried the virulence genes (*cna* and *bbp*) and *pvl* (Baranovich et al., 2010). The role of virulence genes in *S. aureus* pathogenesis may vary from one infection type to another type of infections. Dhawan et al. (2015) reported the isolation of SCCmec type IV and V clones of MRSA in an Indian hospital. Several other workers also showed a decrease in SCCmec III MRSA isolation but increased SCCmec IV and V MRSA isolation (Hsu et al., 2005; D'Souza et al., 2010). Multidrug-resistant isolates belonging to ST239 and SCCmec type III were slowly replaced by multidrug-susceptible ST22 (SCCmec type IV) and ST772 (SCCmec type V) in hospitals (D'Souza et al., 2010).

Several molecular biology techniques like multi-locus sequence typing (MLST), pulse-field gel electrophoresis (PFGE), SCCmec typing, and *spa*-typing have been used to study epidemiology and clonal diversity of *S. aureus* (Maslow et al., 1993; Norazah et al., 2001; Ghaznavi-Rad et al., 2011). However, not a single technique alone could discriminate the bacteria because of differences in the degree of typeability, reproducibility, and discriminatory power (Tenover et al., 1994). Overall analysis of different typing techniques can provide information on diversity of the isolates that can be useful for outbreak investigations. In India, *S. aureus* is rated as one of the major pathogen causing a variety of infections and showing

resistance to several antibiotics; however, not much information is available on their antibiotic susceptibility, virulence profile, and genomic diversity. In this study, our aim was to determine the antibiotic susceptibility pattern, virulence profiles, and genomic diversity among MRSA and MSSA isolated from patients with a variety of infections, including ocular diseases and collected from different parts of India from 2007 to 2015. Genetic, serotype, and phenotypic data were used to determine whether isolates from a variety of infections had similar characteristics.

## MATERIALS AND METHODS

### Bacterial Strains

A total of 109 *S. aureus* strains isolated from patients visited/admitted to hospitals with infections in different part of India between July 2007 and November 2015 were included in the study. These isolates were from LV Prasad Eye Institute, Bhubaneswar ( $n = 54$ ), comprised of microbial keratitis ( $n = 18$ ), eyelid abscess ( $n = 8$ ), endophthalmitis ( $n = 5$ ), Steven Johnson syndrome with bacterial keratitis ( $n = 9$ ), suture-related infections ( $n = 3$ ), and other ocular infection ( $n = 5$ ); LV Prasad Eye Institute, Hyderabad ( $n = 10$ ) comprised of cornea scrapping ( $n = 5$ ), pus from eye ( $n = 4$ ), and suture-related infections ( $n = 1$ ); Institute of Medical Sciences, Banaras Hindu University, Varanasi ( $n = 21$ ) comprised of wound infection ( $n = 16$ ) and unknown sources ( $n = 5$ ); All India Institute of Medical Sciences, New Delhi (wound infection  $n = 10$ ); and University College of Medical Sciences, Delhi (wound infection  $n = 9$ ). Also, five isolates were from the conjunctiva of the asymptomatic healthy volunteers LV Prasad Eye Institute, Bhubaneswar. We conducted the study following the guidelines mentioned in the Declaration of Helsinki. We identified all the 109 isolates by using biochemical tests including Gram staining, catalase production, fermentation of glucose and mannitol, and ID32 STAPH strips using ATB<sup>TM</sup> NEW v.1.0.0 software on an ATB<sup>TM</sup> reader (bioMérieux, France) (Panda et al., 2014). The amplification of the *S. aureus nuc* gene confirmed the identity of isolates (Hirotaki et al., 2011). We used *S. aureus* ATCC 25293 and *S. aureus* ATCC 29213 as quality control strains for antibiotic susceptibility testing, and *S. aureus* ATCC 25923 and ATCC 43300 as a reference for serotyping, PFGE, MLST, and *spa*-typing.

### Coagulase Gene Typing

Coagulation-inhibition test with coagulase type I–VIII-specific antisera (staphylococcal coagulase antiserum kit; Denka Seiken, Inc., Tokyo, Japan) was conducted to determine the coagulase type of *S. aureus* following the manufacturer's instructions (Goh et al., 1992). Briefly, a single colony for each test

strain was suspended in BHI broth (Becton Dickinson Co.) and incubated at 37°C for overnight. Then centrifuged the culture and 0.1 ml of the supernatant used as test antigen. Distributed an aliquot (0.1 ml) of the test antigen into ten tubes followed by addition of 0.1-ml aliquots of anticoagulase types I–VIII sera to first eight tubes, except 9th and 10th tubes which were used as positive and negative controls and incubated at 37°C for 1 h. After that, 0.2 ml of diluted rabbit plasma was added to each tube and incubated at 37°C for 1 h. Visual inspection judged the coagulation of plasma after 2, 4, 24, and 48 h and accordingly, strains were typed based on results obtained with staphylocoagulase reaction showing coagulation inhibition.

### Minimum Inhibitory Concentration (MIC) Determination

Minimum inhibitory concentrations (MICs) of oxacillin, chloramphenicol, vancomycin, tetracycline, gentamicin, erythromycin, clindamycin, and trimethoprim were determined by broth microdilution methodology as recommended by the CLSI breakpoints. The 96-well plates were incubated at 37°C and were read for turbidity after 24 h.

### Polymerase Chain Reaction (PCR) Assays

The presence of genes encoding for methicillin resistance (*mecA*), the nuclease (*nuc*), Panton-Valentine leukocidin (*pvl*), cadmium resistance (*czrC*), and quaternary ammonium resistance (*qacA/B*) was determined by hexaplex PCR (Panda et al., 2014). PCR identified the presence of *msrA*, *ermA*, *ermC* (erythromycin resistance), *tetK* (tetracycline resistance) genes (Duran et al., 2012). Also, PCR determined the presence of gene encoding for resistance to aminoglycosides [*aac* (6′)/*aph* (2), *aph* (3′-III)] by the method described earlier (Schmitz et al., 1999). The presence of *catpC221*, *catpC223*, and *catpC194* (chloramphenicol resistance) was determined by PCR as described by Argudín et al. (2011). The *mphC* (clindamycin resistance) gene was detected by PCR method described earlier (Panda et al., 2016).

### SCC<sub>mec</sub> Typing

Two PCRs, MPCR1 and MPCR2 were used to detect the presence of *mec* complex, *ccr* complex, and SCC<sub>mec</sub> type among *S. aureus* (Kondo et al., 2007).

### Virulence Gene Profile and Accessory Gene Regulator (*Agr*) Typing

PCR determined the presence of Staphylococcal enterotoxin (SE) genes encoding for *seA*, *seC*, and *seI* (Monday and Bohach, 1999; Jarraud et al., 2002). Also, the presence of hemolysin genes, *hla* and *hlG*, was determined by PCR (Mitchell et al., 2010; Paniagua-Contreras et al., 2012). PCR was used to detect the presence of collagen adhesion (*cna*) and extracellular fibrinogen binding protein (*efb*) among *S. aureus* strains (Zecconi et al., 2006). The presence of intracellular adhesion genes (*icaA*, *icaD*) was

determined by PCR as described by Arciola et al. (2001). PCR amplification was carried out to determine the presence of *agr* alleles using group-specific primers as described by Gilot et al. (2002).

### Pulsed-Field Gel Electrophoresis (PFGE)

Pulsed-field gel electrophoresis of *S. aureus* genomic DNA digested with *Sma*I (NEB) was carried out by the protocol described for *S. aureus* by Centre for Disease Control and Prevention. The dendrogram of similarity showing the clustering of the isolates according to banding patterns was generated with Bionumerics software, version 7.1 (Applied Maths, Belgium) using the Dice index and the un-weighted pair group method with arithmetic average (UPGMA) with 0.5% optimization and 1% position tolerance. Isolates showing similarity coefficient of up to 80% were considered belonging to similar pulsotype (Van Belkum et al., 2007).

### Multi-Locus Sequence Typing (MLST)

The internal fragments of seven housekeeping genes, viz., *arcC*, *gmk*, *aroE*, *glpF*, *pta*, *tpi*, and *yqil* were amplified by PCR method described earlier (Enright and Spratt, 1999). The amplified products were purified (ExoSAP; Affymetrix, Cleveland, OH, United States) and both strands sequenced using an ABI sequencer model 3500 (Life Technologies, Marsiling, Singapore) at the sequencing facility of the Institute of Life Sciences (Bhubaneswar, India). The nucleotide sequences were aligned using Mega 5.2 software. After manually comparing with reported alleles, STs were assigned accordingly. Sequencing was performed in biological duplicates to confirm the presence of novel alleles.

The advanced cluster analysis was performed to define the clonal complexes (CCs) by using Bionumerics software, version 7.1 (Applied Maths, Belgium). A minimum spanning tree (MST) was constructed using the MLST data and partitions were created to form clusters. The similarity in at least six alleles grouped isolates of *S. aureus* in one CC. The central ST of each separation was used to designate a CC.

### *Spa*-Typing

PCR amplified the polymorphic X region of *Staphylococcus* protein A (*spa*) gene following the conditions mentioned earlier (Nelson et al., 2007). Amplified products were purified, and both strands were sequenced using an ABI sequencer model 3500 (Life Technologies, Marsiling, Singapore) at the sequencing facility of the Institute of Life Sciences (Bhubaneswar, India). The nucleotide sequences were aligned using Mega 5.2 software. Repeat succession in the polymorphic X-region assigned the *spa*-types, and accordingly the MST was generated using Bionumerics 7 software (Applied Maths, Belgium) using gap creation cost 250%, gap extension cost 50%, duplicate production cost 25%, duplicate expansion cost 25%, and maximum duplication three repeats.



## Statistical Analysis

We performed principal coordinates analysis (PCoA) and discriminant analysis (DA) using PAST program v2.17 for the antibiotic resistance genes and virulence genes in MRSA and MSSA isolates with regard to sources of isolation (Hammer et al., 2001). We carried out the DA using default values to confirm the hypothesis of whether MRSA and MSSA isolates are different.

## RESULTS

### Hexaplex PCR

All the isolates of *S. aureus* were positive for 16S rRNA and *S. aureus*-specific *nuc* genes. Hexaplex PCR discriminates between MSSA and MRSA isolates. Thirty-one of 109 (29.4%) methicillin-resistant strains were positive for the *mecA* gene, and 77 (70.6%) methicillin sensitive isolates were negative for the *mecA* gene. One of the methicillin-resistant strains of *S. aureus* was negative for the *mecA* gene. Among 109 isolates, 43 (39.4%) isolates comprising 23 of the 77 (29.9%) MSSA and 20 of the 31 (64.5%) MRSA isolates were positive for *pvl* gene. Of the 31 MRSA isolates, two (6.5%) strains were positive for the *czrC* gene and four (12.9%) isolates were positive for *qacA/B* gene, and remaining isolates were negative for both *czrC* and *qacA/B* genes (data not shown).

### Coagulase Serotyping

Serotyping classified *S. aureus* isolates into I–VIII serotypes by using coagulase typing scheme. Twelve of the 109 (11%) strains belong to serotype I, 11 (10%) to serotype II, nine (8%) to serotype III, 14 (12.8%) to serotype IV, 12 (11%) to serotype V, 19 (17.4%) to serotype VI, 20 (18.3%) to serotype VII, and 12 (11%) to serotype VIII, respectively. Nine of 31 (29%) MRSA belong to serotype VI and 17 of 78 (21.8%) and MSSA isolates belong to serotype VII (Table 1). Nine of the 24 (37.5%) isolates from wound infection belong to serotype VI and 16 of 64 (25%) isolates from eye infection belonged to serotype VII.

### Antibiotic Resistance Genes

One hundred two of the 109 *S. aureus* isolates were multidrug resistant showing resistance to two or more antibiotics. All the strains were susceptible to vancomycin when tested by broth microdilution assay. Thirty-one isolates of *S. aureus* were resistant to oxacillin and carried the *mecA* gene; however, one isolate of *S. aureus* resistant to oxacillin was negative by PCR for the *mecA* gene. The remaining 77 isolates were sensitive to oxacillin and negative by PCR for the *mecA* gene (Table 1).

Ninety-five isolates of *S. aureus* resistant to chloramphenicol carried *cat: pC221* gene; however, 86 isolates carried *cat: pC223* and 37 isolates carried *cat: pC194* gene, respectively. Twenty isolates carried all the three genes tested; however, 83 isolates were positive for *cat: pC221* and *cat: pC223* and 37 isolates for *cat: pC221* and *cat: pC194* genes, respectively (Table 1). One of the isolates sensitive to chloramphenicol was negative by PCR for all three genes. In contrast, 15 strains of *S. aureus* susceptible to chloramphenicol were positive for *cat: pC221* and 14 for *cat: pC223* genes, respectively.

Twenty-nine isolates were phenotypically resistant to tetracycline of which 29 isolates were positive for *tetK*, 25 for *tetL*, and 28 for *tetM* genes. Twenty-five isolates carried all the three genes tested; however, three strains carried *tetK* and *tetM* genes and one isolate *tetL* and *tetM* genes. In contrast, 76 isolates sensitive to tetracycline were positive for the *tetM* gene, 66 for *tetL*, and 29 for *tetK* genes. Among them, 27 isolates carried all the three genes, six had *tetK* and *tetM*, and 39 strains had *tetL* and *tetM* genes, respectively. One isolate sensitive to tetracycline was negative by PCR for all three genes tested (Table 1).

A total of 54 isolates were resistant to gentamicin of which 45 isolates were positive for *aac(6′)/aph(2′)* and *aph (3′-III)* genes and nine isolates for *aph (3′-III)* gene only. In contrast, 43 gentamicin sensitive isolates showed positive results for *aac(6′)/aph(2′)* and *aph (3′-III)*, seven isolates for *aac(6′)/aph(2′)*, and two isolates for *aph (3′-III)* genes. However, 56 isolates sensitive to gentamicin were negative by PCR for *aac(6′)/aph(2′)* and *aph (3′-III)* genes (Table 1).

Of the 91 isolates of *S. aureus* showing resistance to macrolides carried erythromycin resistance genes. Twenty-eight isolates carried all the erythromycin resistance genes, namely, *msrA*, *ermA*, and *ermC*. Fifty-one isolates were positive for two genes, of which 30 isolates carried *msrA* and *ermC* genes, and 21 strains had *ermA* and *ermC* genes. Besides, 12 isolates were positive for a single gene of which five isolates carried the *ermC* gene, and seven isolates had *msrA* gene. In contrast, two of the 10 erythromycin sensitive isolates carried *msrA* and *ermC* genes, four strains possess *msrA* and *ermC* genes, and three isolates had the *ermC* gene. Of the 64 isolates carrying the *mphC* gene, 22 isolates were phenotypically resistant to clindamycin (Table 1). None of the 17 strains showing sensitivity to erythromycin carried any of the erythromycin resistance genes. One of the resistant isolate not carrying any of the erythromycin resistant genes is likely to be mediated by an as-yet-unknown mechanism.

Similarly, 74 isolates were resistant to trimethoprim of which 45 isolates were positive for *dfrA*, *dfrB*, and *dfrG* genes, 27 strains for *dfrB* and *dfrG* genes, and one isolate each for *dfrB* and *dfrG* genes, respectively. In contrast, 34 isolates sensitive to trimethoprim were also positive for *dfrA*, *dfrB*, and *dfrG* genes; however, one strain was positive for the *dfrG* gene (Table 1).

### D-Test and Macrolide Resistance

Ninety of 109 (89.9%) *S. aureus* isolates that exhibited erythromycin resistance were evaluated for MLSB resistance phenotype, namely, iMLSB, cMLSB and MSB. Seventy eight of 90 (79.5%) isolates were erythromycin-resistant but clindamycin susceptible were tested for D-test. We found 14 isolates (10 MRSA and four MSSA) showed iMLSB phenotype, and 12 (two MRSA and 10 MSSA) had MSB phenotype. Seven erythromycin-resistant isolates comprising six MRSA and one MSSA had cMLSB phenotype. The remaining 45 isolates (14 MRSA and 31 MSSA) did not show any MLSB phenotypes.

Among MRSA and MSSA showing cMLSB resistance phenotype, three of six MRSA isolates possessed the *ermA* and *ermC* genes and one each possessed *ermC* gene, *msrA*, *ermC*, *mphC* genes, and *ermC* and *mphC* genes. One MSSA isolate was positive for *msrA*, *ermA*, and *ermC* genes. On the hand, one



**TABLE 1** | Antibiotic resistance patterns and presence of antibiotic resistance genes in *Staphylococcus aureus* isolates from different parts of India.

Phenotypic antibiotic resistance pattern	Number of isolates showing presence of gene(s) encoding for																		
	MRSA	MSSA	<i>mecA</i>	<i>aac(6')</i> / <i>aph(2)</i>	<i>aph (3'III)</i>	<i>msrA</i>	<i>ermA</i>	<i>ermC</i>	<i>mphC</i>	<i>tetK</i>	<i>tetL</i>	<i>tetM</i>	<i>cat::pC221</i>	<i>cat::pC223</i>	<i>cat::pC194</i>	<i>dfrA</i>	<i>dfrB</i>	<i>dfrG</i>	
OX, CHL, TET, GEN, ERY, CL, TMP	10	0	10	<b>10</b>	<b>10</b>	–	<b>10</b>	<b>10</b>	<b>10</b>	<b>10</b>	<b>10</b>	<b>10</b>	<b>10 (3)</b>	–	<b>10</b>	<b>10</b>	<b>10</b>	<b>10</b>	
OX, CHL, ERY, TMP	0	1	–	1	–	<b>1</b>	–	<b>1 (1)</b>	<b>1</b>	–	–	1	<b>1 (1)</b>	–	<b>1</b>	–	–	<b>1</b>	
CHL, ERY, TMP	0	11	–	11	11	–	<b>11 (3)</b>	<b>11</b>	<b>11</b>	–	11	11	<b>11 (3)</b>	<b>11</b>	–	<b>11</b>	<b>11</b>	<b>11</b>	
CHL, TMP	0	6	–	6	–	–	–	+	–	–	6	6	<b>6 (2)</b>	–	<b>6</b>	–	<b>6</b>	<b>6</b>	
OX, CHL, TET, ERY, TMP	3	0	3	3	3	<b>3</b>	<b>3(1)</b>	<b>3</b>	<b>3</b>	<b>3</b>	<b>3</b>	<b>3</b>	<b>3 (1)</b>	–	–	–	<b>3</b>	<b>3</b>	
OX, CHL, GEN, ERY, TMP	11	0	11	<b>11</b>	<b>11</b>	<b>11</b>	<b>11 (5)</b>	<b>11</b>	<b>11</b>	–	<b>11</b>	<b>11</b>	<b>11 (2)</b>	<b>11</b>	<b>11</b>	–	<b>11</b>	<b>11</b>	
OX, CHL, TET, GEN, ERY, TMP	5	0	5	<b>5 (1)</b>	<b>5</b>	<b>5</b>	–	<b>5</b>	<b>5</b>	<b>5</b>	<b>5</b>	<b>5</b>	<b>5 (1)</b>	<b>5</b>	–	<b>5</b>	<b>5</b>	<b>5</b>	
ERY, CL, TMP	0	1	–	–	1	<b>1</b>	<b>1</b>	<b>1</b>	–	–	–	–	–	–	–	–	–	<b>1</b>	–
CHL, ERY, CL, TMP	0	2	–	2	2	–	–	<b>2(1)</b>	<b>2(1)</b>	–	–	2	<b>2 (1)</b>	<b>2</b>	–	<b>2</b>	<b>2</b>	<b>2</b>	<b>2</b>
CHL, ERY, <b>CL</b>	0	13	–	13	13	<b>13</b>	<b>13(9)</b>	<b>13</b>	<b>13(1)</b>	13	13	13	<b>13 (3)</b>	<b>13</b>	–	13	13	13	
CHL	0	3	–	–	–	3	–	3	–	3	3	3	<b>3 (1)</b>	<b>3</b>	–	3	3	3	
CHL, TET, GEN, ERY, <b>CL</b> , TMP	0	3	–	–	<b>3</b>	<b>3</b>	–	<b>3</b>	–(2)	<b>3</b>	–	<b>33</b>	<b>3</b>	–	–	<b>3</b>	<b>3</b>	<b>3</b>	
CHL, TET, GEN, TMP	0	1	–	<b>1</b>	<b>1</b>	–	–	1	–	<b>1</b>	–	–	<b>1 (1)</b>	–	–	–	–	–	
CHL, GEN, ERY, CL, TMP	0	2	–	<b>2 (1)</b>	<b>2</b>	–	–	<b>2(2)</b>	<b>2(2)</b>	2	2	2	<b>2</b>	<b>2</b>	–	–	<b>2</b>	<b>2</b>	
CHL, GEN, ERY, <b>CL</b> , TMP	0	7	–	<b>7 (2)</b>	<b>7</b>	<b>7(3)</b>	–	–	–(3)	7	7	7	<b>7</b>	<b>7</b>	<b>7</b>	<b>7</b>	<b>7</b>	<b>7</b>	
CHL, TET, GEN, ERY, CL, TMP	0	1	–	–	<b>1</b>	–	–	–	<b>1(1)</b>	<b>1</b>	–	–	<b>1</b>	<b>1(1)</b>	–	<b>1</b>	<b>1</b>	<b>1</b>	
CHL, GEN, ERY	0	3	–	<b>3</b>	<b>3</b>	<b>3 (1)</b>	–	<b>3 (1)</b>	–	–	3	3	<b>3</b>	<b>3</b>	–	3	3	3	
CHL, TET, GEN, ERY	0	3	–	<b>3 (2)</b>	<b>3</b>	<b>3</b>	–	<b>3(1)</b>	–	<b>3</b>	<b>3</b>	<b>3</b>	<b>3 (1)</b>	<b>3</b>	–	3	3	3	
GEN, ERY, CL, TMP	0	1	–	<b>1 (1)</b>	<b>1</b>	–	–	<b>1</b>	<b>1</b>	1	–	1	1	1	–	<b>1</b>	<b>1</b>	<b>1</b>	
GEN, ERY	0	2	–	–	<b>2(1)</b>	<b>2</b>	–	<b>2(1)</b>	–	–	2	2	2	2	–	2	2	2	
ERY	0	4	–	4	4	<b>4</b>	–	<b>4(2)</b>	–	4	–	4	4	4	–	4	4	4	
ERY, TMP	0	3	–	3	3	<b>3</b>	–	<b>3(3)</b>	–	–	3	3	3	3	–	<b>3</b>	<b>3</b>	<b>3</b>	
OX, CHL, GEN, <b>ERY</b>	1	0	1	–	<b>1</b>	–	–	–(1)	–	1	–	1	<b>1</b>	<b>1</b>	–	1	1	1	
CHL, TET, <b>ERY</b> , TMP	0	2	–	2	2	–	–	2 (1)	–	<b>2</b>	<b>2</b>	<b>2</b>	<b>2 (1)</b>	<b>2</b>	–	<b>2</b>	<b>2</b>	<b>2</b>	
CHL, ERY, CL	0	1	–	–	1	<b>1</b>	–	<b>1(1)</b>	<b>1</b>	–	1	1	<b>1</b>	<b>1</b>	–	1	1	1	
GEN, ERY, TMP, <b>CHL</b>	0	1	–	<b>1</b>	<b>1</b>	<b>1</b>	–	<b>1</b>	–	–	–	1	1 (1)	–	–	–	<b>1</b>	<b>1</b>	
CHL, CL, TMP	0	2	–	2	2	2	–	2	2	–	2	2	<b>2</b>	<b>2</b>	<b>2</b>	–	<b>2</b>	<b>2</b>	
TET, TMP	0	1	–	1	1	1	–	1	–	<b>1</b>	<b>1</b>	<b>1</b>	1	1	–	–	<b>11</b>		
ERY, CL, <b>CHL</b>	0	1	–	1	1	<b>1</b>	–	<b>1</b>	<b>1(1)</b>	1	1	1	1 (1)	1	–	1	1	1	
TET, GEN, <b>CL</b> , ERY	0	2	–	–	<b>2</b>	<b>2</b>	–	<b>2</b>	–(1)	–	–	<b>2</b>	2	2	–	2	2	2	
OX, CHL, ERY, <b>CL</b> , TMP	1	0	1	1	1	<b>1</b>	–	<b>1</b>	–(1)	1	1	1	<b>1</b>	<b>1</b>	–	–	<b>1</b>	<b>1</b>	
CHL, TET, GEN	0	1	–	<b>1</b>	<b>1</b>	–	–	–	–	–	<b>1 (1)</b>	<b>1</b>	<b>1</b>	<b>1</b>	–	–	–	<b>1</b>	

MRSA: methicillin-resistant *Staphylococcus aureus*; MSSA: methicillin-susceptible *Staphylococcus aureus*, OX: oxacillin, GEN: gentamicin, ERY: erythromycin, TET: tetracycline, CL: clindamycin; CHL: chloramphenicol; TMP: trimethoprim. Isolates showing phenotypic resistance to given antibiotic(s) are shown in bold. Number in brackets indicate phenotypic sensitive isolates.

**TABLE 2** | Result of D-test obtained with MRSA and MSSA isolates showing presence of erythromycin resistance genes and its correlation with MLSB phenotypes among *Staphylococcus aureus*.

Erythromycin resistance and MSB phenotypes	Phenotype (%)	Gene combinations									
		<i>msrA</i>	<i>ermA</i>	<i>ermC</i>	<i>mphC</i>	<i>msrA, ermC</i>	<i>ermA, ermC</i>	<i>ermC, mphC</i>	<i>msrA, ermA, ermC</i>	<i>msrA, ermC, mphC</i>	<i>msrA, ermA, ermC, mphC</i>
<b>MRSA (n=32)</b>											
ER-S, CL-S	10 (31.25%)	0	0	0	0	3 (30%)	0	1 (10%)	1 (10%)	3 (30%)	1 (10%)
ER-R, CL-S (MSB phenotype)	2 (6.25%)	0	0	0	0	1 (50%)	0	0	0	1 (50%)	0
ER-R, CL-R (cMLSB phenotype)	6 (18.75%)	0	0	1 (16.6%)	0	0	3 (50%)	1 (16.6%)	0	1 (16.6%)	0
ER-R, CL-D (iMLSB phenotype)	10 (31.25%)	0	0	6 (60%)	0	0	1 (10%)	0	1 (10%)	1 (10%)	0
<b>MSSA (n=77)</b>											
ER-S, CL-S	52 (67.5%)	3 (5.7%)	1 (1.9%)	16 (30.7%)	1 (1.9%)	20 (38.4%)	0	4 (7.6%)	0	4 (7.6%)	0
ER-R, CL-S (MSB phenotype)	12 (15.5%)	0	1 (8.3%)	1 (8.3%)	2 (16.6%)	6 (50%)	0	0	0	0	0
ER-R, CL-R (cMLSB phenotype)	1 (1.29%)	0	0	0	0	0	0	0	1 (100%)	0	0
ER-R, CL-D (iMLSB phenotype)	4 (5.19%)	0	0	1 (25%)	0	3 (75%)	0	0	0	0	0

S: sensitive; R: resistance; ER: erythromycin; CL: clindamycin.

**TABLE 3** | Distribution of SCCmec types among *S. aureus* strains isolated from wound and ocular infection.

Distribution of SCCmec types among <i>S. aureus</i> strains isolated from wound and ocular infection						
SCCmec type	Recombinase complex	<i>mecA</i> complex	Source of infection			Total no. of isolates (n = 109)
			Wound (n = 34)	Ocular (n = 69)	Unknown (n = 6)	
III	ccrC1, ccrAB3	Class A	2	0	0	2 (1.8%)
IV	ccrAB2	Class B	7	0	0	7 (6.4%)
V	ccrC1	Class C2	5	4	4	13 (11.9%)
UT6	ccrC1	Class A	5	3	1	9 (8.2%)
Untypable-1	ccrC1	–	1	0	0	1 (0.91%)
Untypable-2	ccrAB4	–	0	1	0	1 (0.91%)
Untypable-3	ccrAB1	–	0	14	0	14 (12.8%)
Untypable-4	ccrAB2	–	0	1	0	1 (0.91%)
Untypable-5	ccrAB3	–	0	1	0	1 (0.91%)

of the two MRSA isolates showing MSB phenotype had *msrA*, *ermC* genes and other strain had *msrA*, *ermC*, and *mphC* genes (Table 2). Of the 12 MSSA, six isolates contained *msrA* and *ermC* genes, one isolate each contained *ermC* and *ermA* genes, respectively, two strains had *mphC* gene. The remaining isolates did not carry any of the genes tested. Of the 10 MRSA, six isolates with iMLSB phenotype had *ermC* gene. One isolate each carried *msrA*, *ermA*, and *ermC* genes, *ermA*, *ermC* genes, *msrA*, *ermC*, and *mphC* genes, respectively. The remaining one isolate did not possess any of the resistance genes. Of the four MSSA isolates that showed iMLSB phenotype, three strains were positive for *msrA*, *ermC* genes, and one isolate was positive for *ermC* gene (Table 2).

Of the 109 *S. aureus* isolates tested for the presence of MLSB resistance genes, 102 isolates carried one or more *erm* genes. Three strains carried all the erythromycin resistance genes, namely, *msrA*, *ermA*, and *ermC*. Fifty-one isolates were positive for two genes, of which 46 isolates carried *msrA* and *ermC* genes, and five had *ermA* and *ermC* genes. Besides, 37 isolates were positive for a single gene of which 34 isolates carried the *ermC* gene, two isolates had *ermA* gene, and three isolates had the *msrA* gene (Table 2). In contrast, four of the 13 erythromycin-sensitive isolates carried *msrA* and *ermC* genes. One strain each had the *ermC* gene and *msrA* gene. The remaining isolates did not carry any resistance genes. Twelve of the 21 *mphC* gene-positive isolates showed phenotypic resistant to clindamycin. The remaining nine isolates were sensitive to clindamycin (Table 2). Eight erythromycin-resistant strains did not carry any of the erythromycin-resistant genes is likely to be mediated by an as-yet-unknown mechanism.

## SCCmec Typing

The presence of the *mec* complex and *ccr* complex classified *S. aureus* strains into different SCCmec types. Thirty-one MRSA isolates showed four known SCCmec types of which 13 (40.6%) belong to type V, nine (28.1) belong to type UT6, seven (21.9%) belong to type IV, and two (6.3%) belong to type III (Table 3). One isolate showing phenotypic resistance to methicillin but negative for *mecA* gene carried C1 type of *ccr* complex but lack *mec* complex. Of the 32 methicillin-sensitive isolates lacking the *mec* complex, 14 isolates carried *ccrA1B1*, one strain possesses

*ccrA4B4*, and 17 isolates had *ccrA3B3* and *ccrA4B4* type of *ccr* complex, respectively (Table 3).

## Toxin Gene Profiles

Of the 109 isolates, 34 (31.2%) isolates harbored *sea* gene, 14 (12.8%) isolates *sec* gene, 93 (85.3%) isolates *sei* gene, 76 (69.7%) *cna* gene, 101 (92.6%) isolates *hla* gene, 107 (98%) isolates *hlg* gene, and 84 (77%) isolates carried *efb* gene, respectively. All the isolates, except one isolate, was positive for the *hlg*, and carried multiple virulence genes (Table 4).

Ninety-one isolates comprising 26 MRSA and 65 MSSA were positive for both *icaA* and *icaD* genes, but five strains containing three MRSA and two MSSA were negative for both *icaA* and *icaD* genes. Two of the three MRSA isolates were positive for *icaA* gene, and another strain was positive for *icaD* gene. Similarly, nine of the 10 MSSA isolates were positive for *icaD* gene and one isolate for *icaA* gene, respectively (Table 4).

Also, a total of 25 toxin genes combinations was obtained with 109 strains belonging to 77 PFGE patterns, 32 sequence types (STs), 46 *spa*-types, and five *agr*-types. Twenty-three isolates belonging to five MRSA and 18 MSSA showed a toxin pattern comprising *sei-cna-hla-hlg-efb* genes. On the other hand, five MRSA and two MSSA showed another virulence pattern composed of *sea-sec-sei-cna-hla-hlg-efb* genes. The remaining isolates showed 23 different virulence gene patterns (Table 4).

## Agr-Typing

Of 109 *S. aureus* strains, 40 (36.7%) isolates belong to *agr*-I, 31 (28.4%) isolates to *agr*-III, 18 (16.5%) to *agr*-II, and seven (6.4%) belong to *agr*-IV; however, 13 (11.9%) isolates were not typeable by the method employed (Table 4). Of the 32 MRSA isolates, 20 (62.5%) belong to *agr*-I, five (15.6%) to *agr*-II, three (9.4%) to *agr*-III, and remaining isolates were untypeable. On the other hand, 28 of 77 (36.4%) MSSA isolates belong to *agr*-III, 20 (25.9%) to *agr*-I, 13 (16.9%) to *agr*-II, seven (9%) to *agr*-IV, and nine (11.7%) isolates were untypeable. There was a good correlation between virulence patterns and specific molecular types (Table 4). The *sea-sei-cna-hla-hlg-efb* was the dominant virulence pattern shown by MRSA belonged to SCCmec type UT6, and *agr* type I, followed by *sei-hla-hlg-efb* and *sei-cna-hla-hlg-efb* pattern showed

**TABLE 4 |** Source, clonal complex, sequence-, *spa*-, *SSCmec*-, and *agr*-types and virulence profiles of *S. aureus* isolated from different parts of India.

Source (isolate number)	CC/ST, <i>spa</i> -type	<i>SSCmec</i> type	<i>agr</i> type	<i>pvl</i> gene	<i>icaA/icaD</i>	Serotypes	Virulence pattern
<b>MRSA (n = 32)</b>							
Wound infection (2095)	239/239, t037	III	1	-	+ /+	II	<i>sei-cna-hla-hlg-efb</i>
Wound infection (2103)					+ /+	IV	<i>sea-sei-cna-hla-hlg-efb</i>
Wound infection (2656)	239/239,t037	UT6	1	-	+ /+	IV	<i>sea-sei-cna-hla-hlg-efb</i>
Wound infection (22/248)					+ /+	III	<i>sea-cna-hla</i>
Wound infection (UC650)					+ /+	IV	<i>sea-cna-hla-hlg-efb</i>
Wound infection (UC858)					-/-	V	<i>sea-hla-hlg-efb</i>
Wound infection (UC1079)	239/239,t2952	UT6	1	-	+ /+	I	<i>sea-sei-cna-hla-hlg-efb</i>
Wound infection (2658)	239/241,t037	UT6	1	-	+ /+	IV	<i>sei-cna-hlg-efb</i>
Eye infection (P844628, N307002)	239/239, t037	UT6	1	-	+ /+	IV	<i>sei-cna-hla-hlg</i>
					±		
Eye infection (P853836)	239/239, t037	UT6	1	-	±	V	<i>sea-cna-hla-hlg-efb</i>
Wound infection (2380,2452)	772/772, t657	V	None	+	+ /+	VI	<i>sea-sec-sei-cna-hla-hlg-efb</i>
					+ /+		
Wound infection (UC609)	772/772, t657	V	2	+	+ /+	VI	<i>sea-sec-sei-cna-hla-hlg-efb</i>
Wound infection (22/252)	772/Unk, t657	V	None	+	-/-	VI	<i>sea-sec-sei-cna-hla-hlg-efb</i>
Eye infection (845)	772/772, t345	V	3	+	-/+	I	<i>sea-sec-sei-cna-hla-hlg-efb</i>
Eye infection (1295)	2884/88, t2526	V	2	+	+ /+	III	<i>sei-hla-hlg-efb</i>
Eye infection (1690)	5/5, t442	V	1	-	+ /+	IV	<i>sei-hla-hlg-efb</i>
Eye infection (1820)	772/772, t657	V	1	+	+ /+	VII	<i>sea-sec-sei-cna-hla-hlg-efb</i>
Unknown (1189)	772/772, t657	V	2	+	+ /+	VI	<i>sec-sei-cna-hla-hlg-efb</i>
Unknown (1192,1249)	772/772, t345	V	2	+	+ /+	VII	<i>sea-sei-cna-hla-hlg-efb</i>
					+ /+	VI	<i>sec-sei-cna-hla-hlg-efb</i>
Unknown (2654)	772/772, t345	V	1	+	+ /+	VI	<i>sea-sei-cna-hla-hlg-efb</i>
Wound infection (284)	Singleton 4/2642, t064	V	1	-	+ /+	IV	<i>hla-hlg-efb</i>
Wound infection (221)	30/30, t012	IV	3	+	+ /+	VI	<i>sei-cna-hla-hlg-efb</i>
Wound infection (27/231)	30/503, t012	IV	3	+	+ /+	VII	<i>sei-cna-hla-hlg</i>
Wound infection (296)	22/22, t005	IV	1	+	+ /+	I	<i>sec-sei-cna-hla-hlg</i>
Wound infection (293)	22/1414, t1328	IV	1	+	+ /+	I	<i>sei-cna-hla-hlg</i>
Wound infection (UC104)	22/22, Unk	IV	1	+	+ /+	II	<i>sei-cna-hla-hlg-efb</i>
Wound infection (UC101)	22/22, t091				+ /+		
Wound infection (UC463)	22/22, t309	IV	1	+	-/-	III	<i>sec-sei-cna-hla-hlg-efb</i>
Wound infection (2518)*	121/120, t272		NT	+	+ /+	VI	<i>sea-sei-cna-hla-hlg-efb</i>
<b>MSSA (n = 77)</b>							
Wound infection (2130)	772/772, t345		2	+	+ /+	VI	<i>sec-cna-hla-hlg-efb</i>
Wound infection (2164)	772/772, t1839	UT*	None	+	+ /+	VI	<i>sea-sec-sei-cna-hla-hlg-efb</i>
Wound infection (2493)	772/1, t386		4	+	+ /+	VI	<i>sei-cna-hla-hlg-efb</i>
Eye infection (N309852)	772/1, t098		3	-	+ /+	VII	<i>sea-cna-hla-hlg</i>
Eye infection (518)	772/1, t693	UT*	3	-	+ /+	VII	<i>sea-sei-cna-hla-hlg-efb</i>
Eye infection (535,1636)	772/1, t127	UT*	3	-	+ /+	VII	<i>sea-sei-cna-hlg-efb</i>
					+ /+	V	
Eye infection (831)	772/1, t127	UT*	3	-	+ /+	II	<i>sea-sei-cna-hla-hlg-efb</i>
Eye infection (1361)	772/1, t128	UT*	3	-	+ /+	VII	<i>sea-sec-sei-hla-hlg-efb</i>
Eye infection (1321)	772/1, t177	UT*	3	-	+ /+	VII	<i>sea-sei-cna-hla-hlg-efb</i>
Eye infection (1476)	772/1, t127		3	-	+ /+	VIII	<i>sea-sei-cna-hla-hlg-efb</i>
Eye infection (1881)					+ /+	I	
Eye infection (1503)	772/1, t127		3	-	+ /+	VI	<i>sei-cna-hla-hlg-efb</i>
Eye infection (975)	772/1, t8078		3	-	+ /+	VI	<i>sei-hla-hlg-efb</i>
Eye infection (1214)	772/772, t657		3	+	+ /+	VI	<i>sea-sec-sei-cna-hla-hlg</i>
Healthy conjunctiva (N110D)	772/1, t948	UT*	None	-	+ /+	I	<i>sea-sei-cna-hla-hlg-efb</i>
Healthy conjunctiva (N120D)	772/1, t948		3	-	+ /+	IV	<i>sea-cna-hla-hlg-efb</i>
Wound infection (2151)	30/714, t021		3	+	+ /+	VI	<i>sei-cna-hla-hlg-efb</i>
Wound infection (2413)	30/1482, t386		3	+	+ /+	IV	<i>sei-cna-hla-hlg-efb</i>

(Continued)

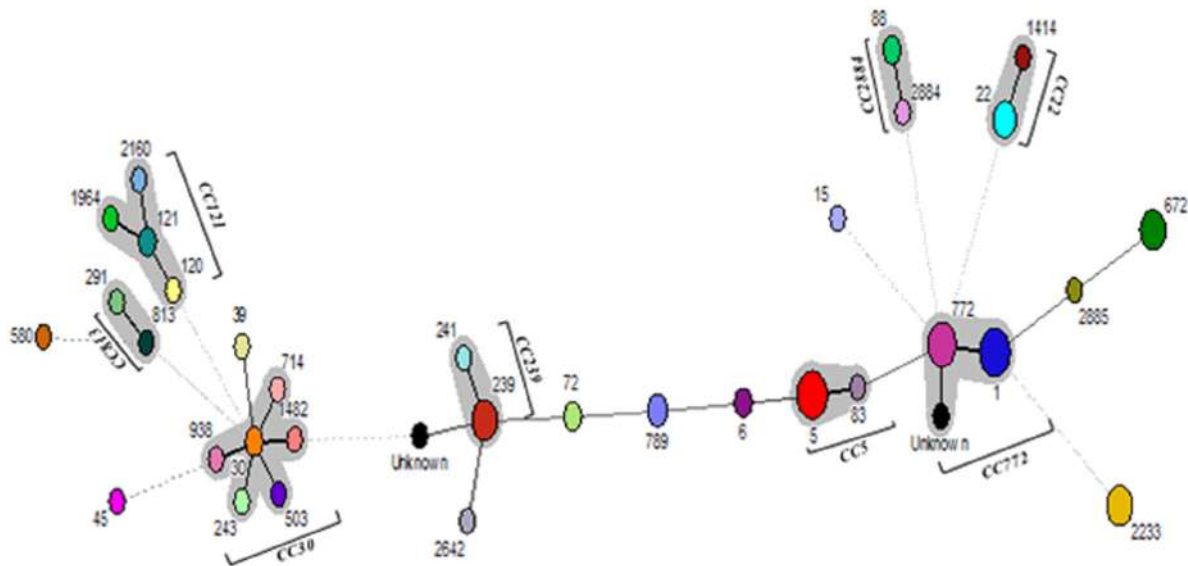


**TABLE 4 |** Continued

Source (isolate number)	CC/ST, spa-type	SCCmec type	agr type	pvl gene	icaA/icaD	Serotypes	Virulence pattern
Eye infection (1196)	30/938, t021		3	+	+/+	IV	<i>sei-cna-hla-hlg-efb</i>
Eye infection (1850)					+ / +	V	
Wound infection (2488)	121/121, t159		4	-	+ / +	II	<i>sei-cna-hla-hlg-efb</i>
Eye infection (P832812)	121/121, t3204		4	+	+/+	V	<i>cna-hla-hlg</i>
Eye infection (P706434)	121/1964, t272		4	-	+ / +	V	<i>sei-cna-hla-hlg</i>
Eye infection (917)	121/2160, t159		4	+	+/+	V	<i>cna-hla-hlg-efb</i>
Unknown (2657)	2884/2884, t4104		3	+	+/+	III	<i>hla-hlg-efb</i>
Eye infection (149)	2884/88, t5562		3	+	- / +	VI	<i>sei-hla-hlg-efb</i>
Eye infection (1764Y)	2884/88, t448		3	+	+/+	VIII	<i>sea-sei-hla-hlg-efb</i>
Eye infection (504, 1035, 1271)	5/5, t442		2	-	+ / +	II	<i>sei-cna-hla-hlg-efb</i>
					+ / +		<i>sei-hla-hlg-efb</i>
					+ / +		<i>sei-hlg</i>
Eye infection (N303284)			None	-	+ / +	I	<i>sei-cna-hla-hlg</i>
Eye infection (843)			2	-	+ / +	VIII	<i>sei-hlg-efb</i>
Eye infection (1042)			2	-	+ / +	VII	<i>sei-hla-hlg-efb</i>
Eye infection (1766, 1862)			1	-	+ / +	VIII	<i>sei-hla-hlg</i>
					+ / +		<i>sei-hla-hlg-efb</i>
Eye infection (1867)			1	-	+ / +	VII	<i>sei-hla-hlg-efb</i>
Eye infection (1103)	5/5, t14912		2	-	+ / +	V	<i>sei-hla-hlg-efb</i>
Eye infection (1306)	5/83, t442		2	-	+ / +	II	<i>sei-hla-hlg-efb</i>
Eye infection (1424)	5/5, 8179		2	-	- / +	VI	<i>sei-hla-hlg-efb</i>
Healthy conjunctiva (N9OD)	5/5, t010		2	-	+ / +	VII	<i>sei-hla-hlg-efb</i>
Wound infection (17/201)	813/813, t10579		1	-	+ / +	VII	<i>sei-cna-hla-hlg</i>
Wound infection (262)	813/291, t1149		1	-	+ / +	VII	<i>hlg</i>
Eye infection (186)	22/22, t310		1	+	+/+	II	<i>sei-cna-hla-hlg-efb</i>
Healthy conjunctiva (N61OD)	22/22, t948	UT*	1	+	+/+	VII	<i>sea-sei-hla-hlg-efb</i>
Eye infection (481)	Singleton 1/580, t14911		None	-	- / +	V	<i>sei-cna-hla-hlg-efb</i>
Eye infection (N297214)	Singleton 2/45, t302		1	-	+ / +	VII	<i>cna-hla-hlg</i>
Wound infection (2417)	Singleton 3/Unk, t021		None	-	- / -	VI	<i>sei-hla-hlg-efb</i>
Eye infection (1525, 1545)	Singleton 5/72, t148		1	-	- / +	VI	<i>sei-hla-hlg</i>
			None	-	- / +	V	<i>sei-cna-hla-hlg-efb</i>
Wound infection (1/229, 861)	Singleton 6/789, t091		1	-	- / -	III	<i>sei-cna-hla-hlg</i>
			None	-	+ / +	III	<i>sei-cna-hla-hlg-efb</i>
Wound infection (379)	Singleton 6/789, t2505		None	-	+ / +	III	<i>sei-cna-hla-hlg-efb</i>
Eye infection (1603)	Singleton 6/789, t091		1	-	+ / +	V	<i>sei-hla-hlg-efb</i>
Eye infection (1320)	Singleton 7/6, t657		1	-	+ / +	III	<i>sei-cna-hla-hlg-efb</i>
Eye infection (1428)	Singleton 7/6, t4285		1	-	- / +	VIII	<i>sea-sei-cna-hla-hlg-efb</i>
Eye infection (1698)	Singleton 7/6, t12406		1	-	+ / +	VIII	<i>sea-sei-cna-hla-hlg-efb</i>
Healthy conjunctiva (N21OS)	Singleton 8/15, t084		2	-	+ / +	IV	<i>sei-hla-efb</i>
Wound infection (2508)	Singleton 9/2885, t15579		4	+	+/+	III	<i>sei-cna-hla-hlg-efb</i>
Wound infection (2653)	Singleton 10/672, t3841		2	-	±	I	<i>sei-hla-hlg-efb</i>
Eye infection (N259615, N289378, 1049, 1506)	Singleton 10/672, t3841		1	-	+ / +	I	<i>sei-cna-hla-hlg</i>
			None	-	+ / +	I	<i>cna-hla-hlg</i>
			1	-	+ / +	VII	<i>sei-hla-hlg-efb</i>
			1	-	+ / +	VIII	<i>sei-hla-hlg-efb</i>
Eye infection (188, 1164, 1355, 1670)	Singleton 10/672, t1309		I	-	+ / +	I	<i>sei-hla-hlg-efb</i>
			I	-	- / +	II	<i>sei-hla-hlg-efb</i>
			I	-	+ / +	I	<i>sei-cna-hla-hlg-efb</i>
			1	-	+ / +	VIII	<i>sei-cna-hla-hlg</i>
Eye infection (884, 1333)	Singleton 11/2233, t2663		3	+	+ / +	VII	<i>sei-cna-hlg-efb</i>
					+ / +		
Eye infection (1716OD, 1758)			3	+	+ / +	IV	<i>sei-cna-hla-hlg</i>
					+ / +		

(Continued)





**FIGURE 2 |** Minimum spanning tree (MST) showing the relationship between different STs assigned by the analysis of MLST data. Each node represents one sequence type, and the corresponding ST is given beside the node. The size of each node is directly proportional to the number of isolates included in that ST. Bold lines connect types that are identical for six loci, solid lines connecting types identical for  $\geq$ four but  $\leq$ six locus, and dotted lines connecting STs differing from each other by  $\geq$ four genes out of seven gene locus.

t272, respectively. Moreover, one isolate each of 30 strains belong to single *spa*-types, namely, t15579, t8179, t14912, t010, t852, t005, t310, t309, t1328, t302, t1149, t10579, t007, t14911, t2952, t693, t2526, t8078, t5562, t448, t4104, t177, t098, t084, t2505, t3204, t1839, t064, t12406, and t4285 (Figure 1). Whereas 10 of 32 (31.2%) MRSA isolates belong to t037, 11 of 77 (14.3%) MSSA isolates belong to t442. *S. aureus* strain ATCC 25923 showed *spa*-type t948 along with three test isolates. We found two novel *spa*-types, namely, t14911 and t14912 among *S. aureus* strains after submission of nucleotide sequences to the Ridom *spa* server. *Spa*-type t14912 showed a close association with major *spa*-type t442, but t14911 *spa*-type was diverse and unrelated. One of the isolates was not assigned any *spa*-type (Figure 1).

### Multi-Locus Sequence Typing (MLST)

Multi-locus sequence typing of 109 *S. aureus* isolates showed 32 STs, eight CCs, and 12 singletons (Figure 2). The major ST comprised of ST1 (12.8%), ST5 (11.9%), ST772 (11%) followed by ST239 (9.2%), ST672 (8.3%), and ST2233 (8.3%). Also, we found two new allelic profiles designated as unknown not reported earlier among *S. aureus* strains (Supplementary Table S2). Of the eight CCs, CC5 contained 14 isolates, CC22 had eight isolates, CC30 had six isolates, CC121 had five isolates, CC239 had 11 isolates, CC772 had 26 isolates, CC813 had two isolates, and CC2884 contained four isolates, respectively. Of the major CCs, CC30 contained five STs, namely, ST30, ST503, ST714, ST938, and ST1482, CC121 contained four STs, namely, ST120, ST121, ST1964, ST2160, and CC772 had three STs, namely, ST772, ST1, and new unknown ST (Figure 2). Seven of the 32 (21.8%) of MRSA strains belong to ST239, *spa*-type t037, and SCC*mec* type UT6. However, 14 (18.2%) of MSSA strains possessing ST1

belong to different *spa*-types, namely, t127, t948, t177, t693, t098, and t386, of which few strains carry *ccr* complex but devoid of *mec* complex (Table 4). However, few isolates from eye infection and wound infection belong to CC239, ST239, and *spa*-type t037/t657. Reference strain of *S. aureus* ATCC25923 belonged to ST30 and CC30.

### Pulsed-Field Gel Electrophoresis

*Sma*I-digested genomic DNA of *S. aureus* yielded bands classifying the 109 strains into 77 pulsotypes that includes two identical pairs (12 and 19A), three major clusters (1, 3, and 19), 17 minor clusters (14, 15, 17, 19, 20, 22, 24, 25, 28, 32, 57, 58, 63, 67, 69, 71, and 73), and 56 singletons. Four isolates were untypeable by the method employed. We found a total of 24 PFGE patterns among 32 MRSA isolates, of which one isolate was untypeable. Similarly, 77 MSSA isolates showed 53 PFGE patterns, of which three MSSA isolates were untypeable (Figure 3). MSSA isolates belonging to the major pulsotype 19 contained seven subtypes 19A, 19B, 19C, 19D, 19E, 19F, and 19G. These isolates were mostly from ocular infection and belong to ST1, *agr* type III, except one subtype 19G which belongs to ST6 and *agr* type I. *S. aureus* strain ATCC 25923 showed pulsotype 14. A dendrogram was generated using Bionumerics 7 software and percentage similarity with a cut-off of 80% and dice coefficients.

### Statistical Analysis

Principal coordinates analysis segregates MRSA and MSSA isolates, except for few isolates with 25.75% of explained variance for antibiotic resistance genes (Figure 4A) and 26% for virulence genes (Figure 5A). We used axis one for the highest percentage

of representation. DA graph showed that MRSA isolates grouped within more positive values, whereas MSSA isolates grouped within negative values for both antibiotic resistance genes and virulence genes (Figures 4B, 5B). Predominant biomarkers were determined by calculating the coefficient of discriminant function and considered when the value was equal to 0.5 or >0.5. For antibiotic resistance genes, MRSA isolates are discriminating in the biomarker of resistance to *ermA* (0.8407), *mphC* (2.0167), *tetK* (2.3495), *tetL* (2.0604), and *dfrA* (1.3116), whereas the MSSA isolates were discriminating in resistance to *aac(6′)/aph(2)* (−0.351), *aph3* (−2.7179), *ermC* (−0.8473), *tetM* (−0.522), *cat:pC221* (−2.421), *cat:pC223* (−6.601), *dfrB* (−0.443), and *dfrG* (−0.603). For virulence genes, MRSA isolates are discriminating in the biomarker of resistance to *icaA* (0.67169), *seA* (0.68593), *seC* (2.3245), *cnA* (0.90744), and *hla* (0.54797). On the other hand, MSSA isolates were discriminating in resistance to *icaD* (−2.1945), *seI* (−0.58795), and *hlG* (−1.4999). PCoA and discriminant function of antibiotic resistance and virulence genes of *S. aureus* isolates with source and place of isolation was heterologous and complex (data not shown).

## DISCUSSION

We used hexaplex PCR for detection of MRSA and MSSA isolates along with the presence of *mecA*, *pvl*, *czrC*, and *qacA/B* genes. We found a good correlation between oxacillin resistance and the presence of the *mecA* gene. However, one isolate showing resistance to oxacillin and lack *mecA* gene indicate the occurrence of different mechanism of methicillin resistance. Twenty of 31 MRSA and 23 of 77 MSSA isolates were positive for *pvl* gene indicating the prevalence of *pvl* gene among MRSA strains from the wound and eye infections. This finding is in contrast to those who did not find such correlation among clinical isolates (Shittu et al., 2011); therefore, it cannot be used as a reliable marker for MRSA. The presence of *czrC* and *qacA/B* genes among the number of MRSA isolates indicates their possible association with the *mecA* gene; however, further investigation is required to authenticate these findings.

Coagulase gene typing has been used to characterize *S. aureus* strains. Hwang and Kim (2007) showed the presence of coagulase

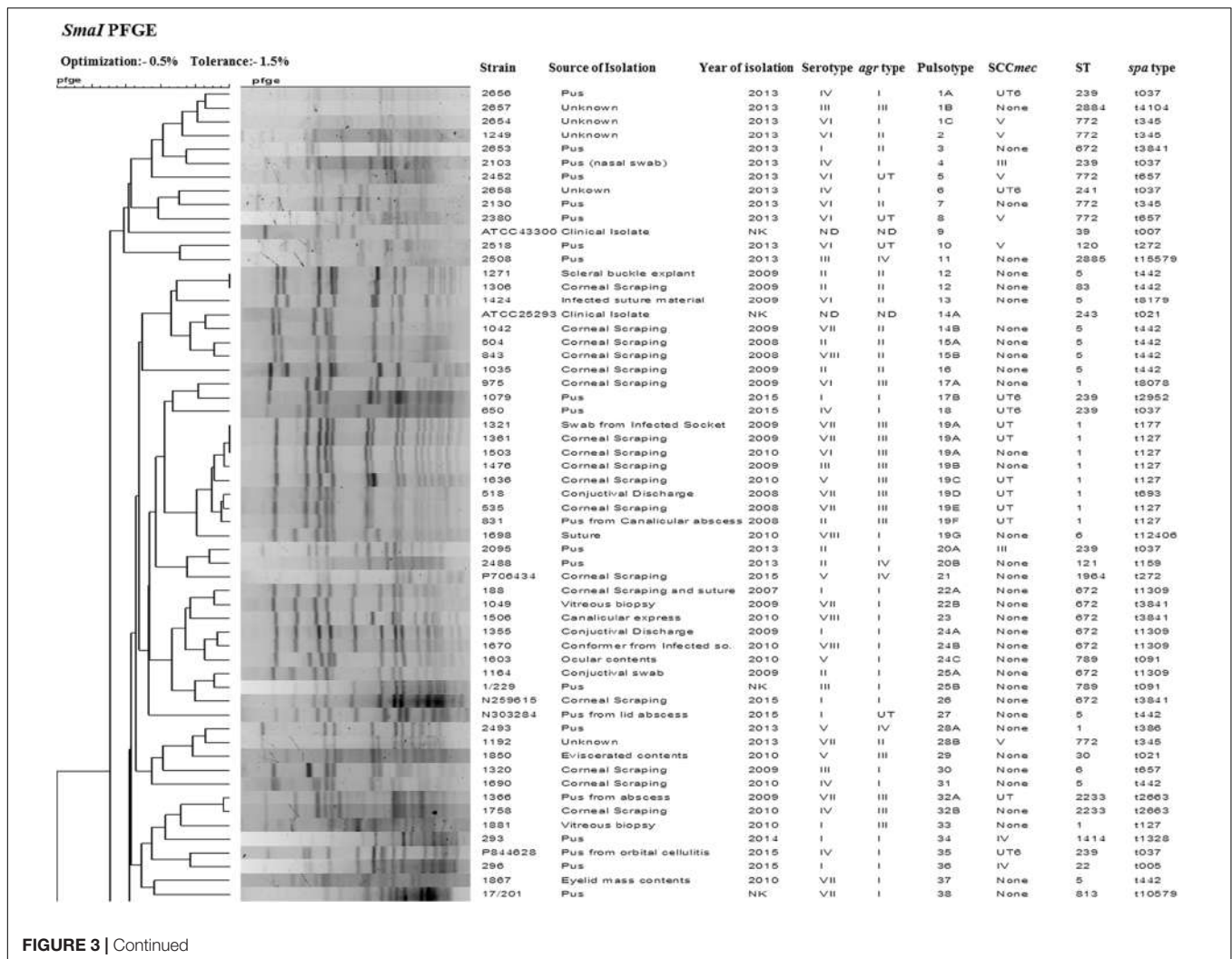
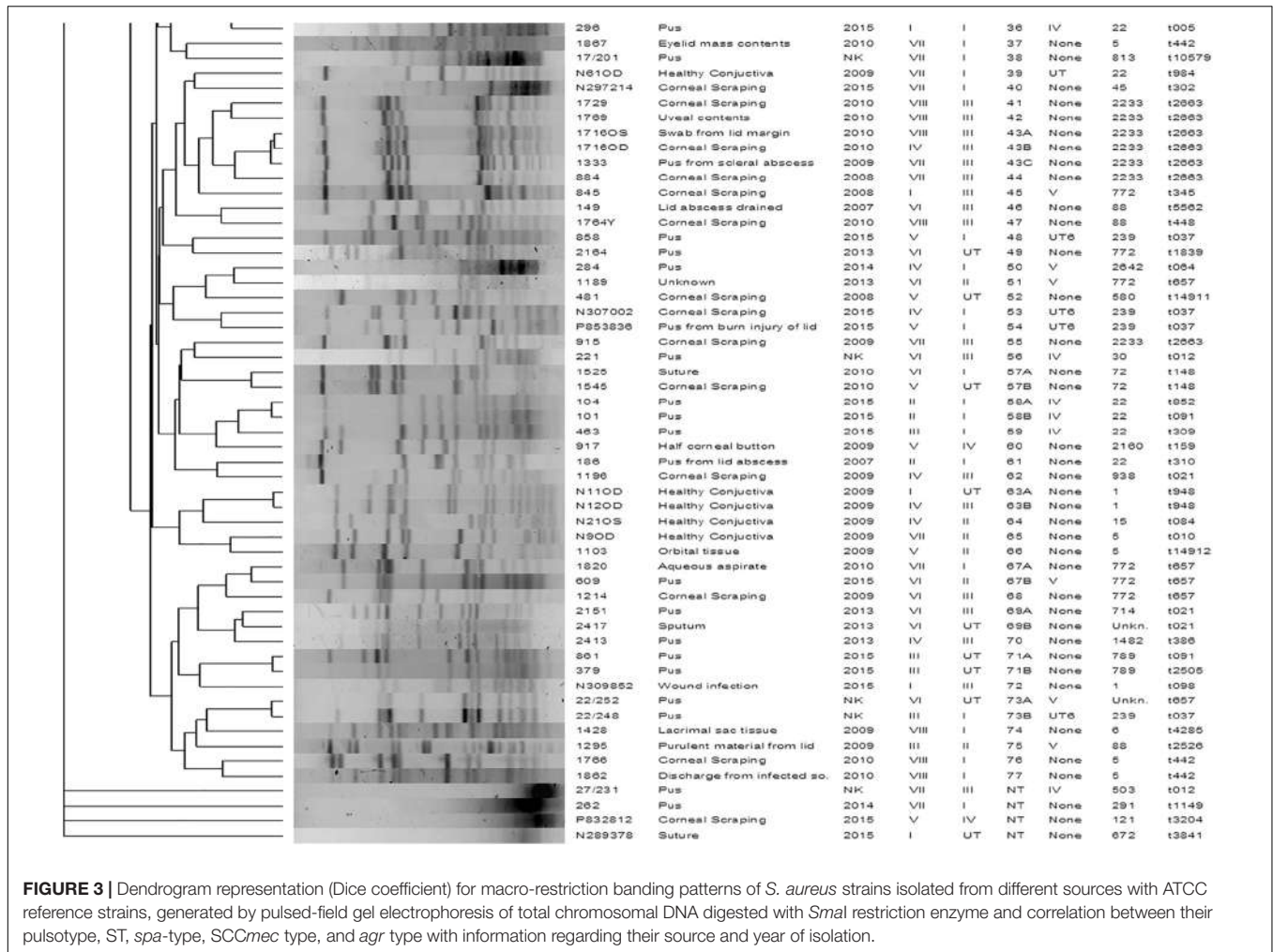


FIGURE 3 | Continued





**FIGURE 3 |** Dendrogram representation (Dice coefficient) for macro-restriction banding patterns of *S. aureus* strains isolated from different sources with ATCC reference strains, generated by pulsed-field gel electrophoresis of total chromosomal DNA digested with *Sma*I restriction enzyme and correlation between their pulsotype, ST, *spa*-type, SCCmec type, and *agr* type with information regarding their source and year of isolation.

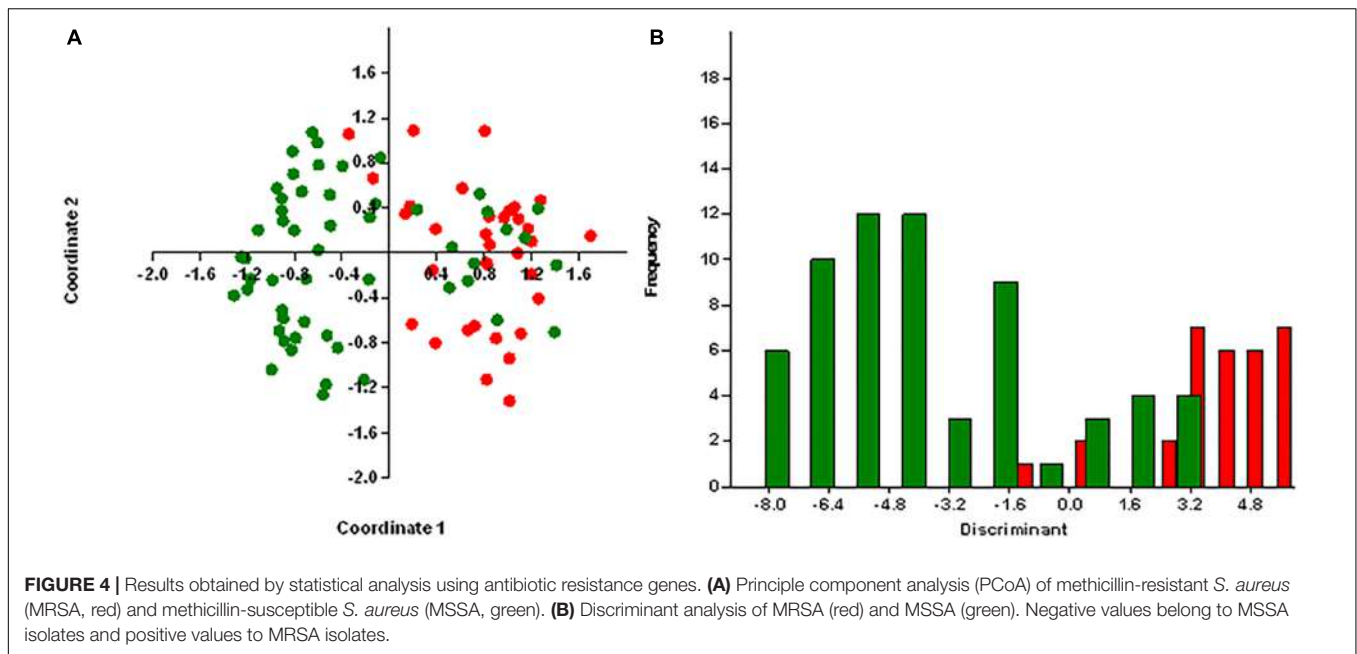
serotype II among 54.4% MRSA and serotype VII among 30.9% MSSA. In contrast, we found serotype VII was present among 22% of MSSA isolates and serotype VI in 28.1% of MRSA isolates. These observations thus suggest that there is a difference in the presence of serotypes with regard to MRSA and MSSA.

Genetic determinants study among *S. aureus* showed a good correlation between resistance to aminoglycosides, chloramphenicol, clindamycin, erythromycin, trimethoprim, and tetracycline, and the presence of corresponding resistance genes. In this study, we found 85.3% strains showing resistance to chloramphenicol carried the *pC221* gene; however, some of these strains also carried either *pC223* or *pC194* or both genes. Although one of 109 strains sensitive to chloramphenicol did not carry any of these genes, 13.8% strains showing sensitivity to chloramphenicol carried either *pC221* or *pC223* genes. These observations thus suggest that chloramphenicol sensitive strains carrying antibiotic resistance genes can develop resistance against this drug on exposure.

The aminoglycoside-modifying enzyme, encoded by *aac(6')-aph(2'')* gene, is responsible for resistance against aminoglycosides (Vanhoof et al., 1994). Besides, two other genes encoding for *aph(3.III)* and *ant(4, IV)* are accountable for

aminoglycoside resistance, but their frequency is less compared to *aac(6')-aph(2'')* among staphylococci (Busch-Sørensen et al., 1996). In this study, we found 41.3% *S. aureus* possesses both *aac(6')-aph(2'')* and *aph(3, III)* genes and 8.3% contained *aph(3, III)* gene and showed phenotypic resistance to gentamycin. These findings thus suggest that there are strains which harbor aminoglycoside resistance genes other than *aac(6')-aph(2'')* and few strains had *aph(3, III)* only. At least 47.7% strains of *S. aureus* that were sensitive to aminoglycosides contain either *aph(3, III)* or *aac(6')-aph(2'')* or both; however, three strains susceptible to gentamycin lack resistance genes. These findings are in contrast to those workers who reported that all aminoglycoside-resistant strains carried *aac(6')-aph(2'')* (Price et al., 1981; Lovering et al., 1988; Dornbusch et al., 1990; Vanhoof et al., 1994; Martineau et al., 2000). The presence of aminoglycoside resistance gene among gentamycin sensitive isolates of *S. aureus* indicates that there is likely hood development of aminoglycoside resistance among *S. aureus* upon exposure to these drugs.

Similarly, 83.4% strains of *S. aureus* resistant to erythromycin harbored any of the four genes, namely, *ermA*, *ermB*, *ermC*, and *msrA*; however, an strain sensitive to erythromycin did not



carry any of the genes. Previously, it was reported that the *ermA* gene is dominant among erythromycin resistance genes in *S. aureus* (Kaur and Chate, 2015). In contrast, we found the presence of the *ermC* gene in 83.4% strains compared to 49% of *ermA* gene. Kaur and Chate (2015) reported that majority of MRSA strains showed constitutive MLSB (cMLSB) resistance; however, two isolates had inducible MLSB (iMLSB) phenotype. In this study, 64.5% MRSA and 37.1% MSSA strains belong to iMLSB phenotype; however, 35.4% of MRSA and 43.5% of MSSA strains belong to cMLSB phenotype. This difference could be due to less number of MRSA isolates used in the study, and MSSA isolates were multidrug resistant. Seventeen strains showing sensitivity to erythromycin harbored one of the resistance genes, and one of the strains resistant to erythromycin did not possess any of the resistance genes to indicate that these strains are likely to develop resistance and mediated by an unknown mechanism.

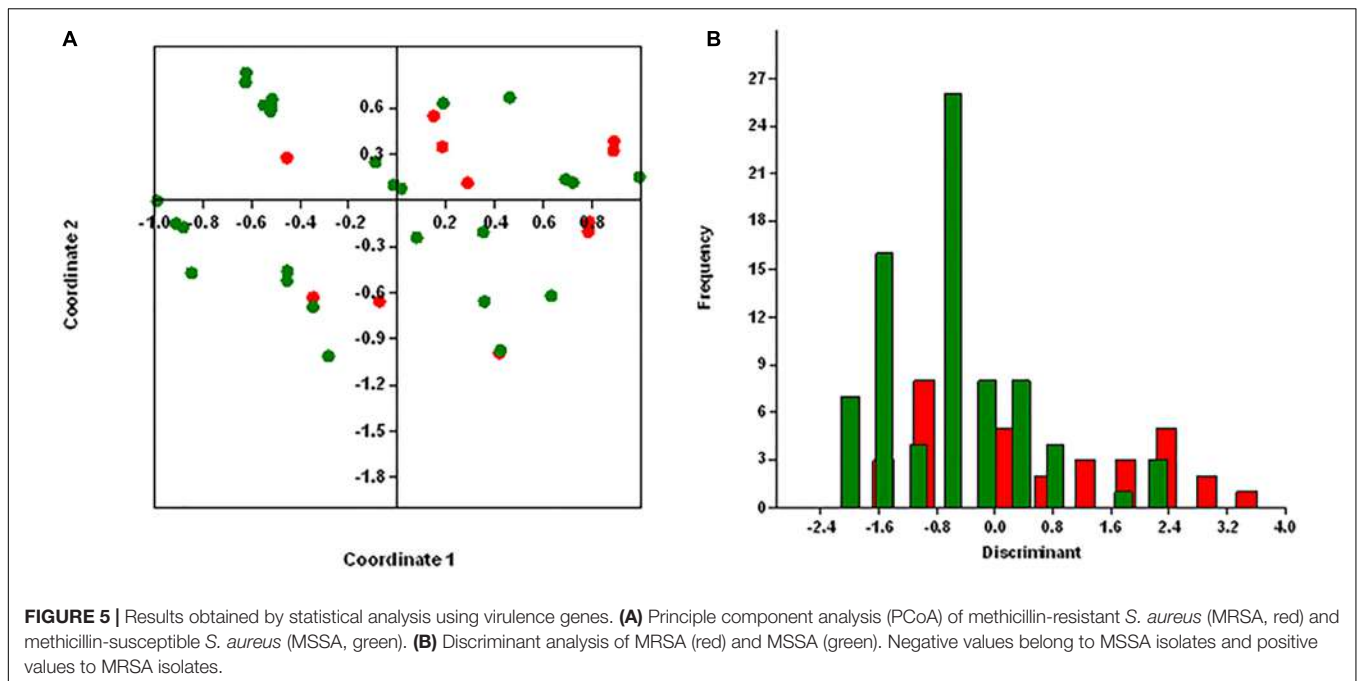
About trimethoprim resistance, 67.8% strains harbored any of the three genes, namely, *dfpA*, *dfpB*, and *dfpG*. The remaining strains showing sensitivity to trimethoprim also carried all or one of the three genes. In this study, 73 of 74 trimethoprim resistance strains possess *dfpG* and *dfpB* genes; 45 strains carried the *dfpA* gene. These findings are in contrast to those who reported the presence of the *dfpG* gene in 92% strains, *dfpA* in 7% strains, and one strain carried a *dfpB* among trimethoprim resistance strains in a travel-associated skin and soft tissue infection study in Europe (Nurjadi et al., 2015).

Like other antibiotic resistance, 26.6% phenotypic resistance strains carried one or all the three tetracycline resistance genes, namely, *tetK*, *tetL*, and *tetM*. One of the strains sensitive to tetracycline was devoid of carrying any genes. However, the majority (69.7%) strain showing sensitivity to tetracycline carried one or all three resistance genes indicating that these isolates could develop resistance after exposure to an antibiotic. From

this study, it is clear that erythromycin and gentamicin were least active; however, vancomycin and clindamycin were the most effective drugs. These results corroborate the finding of Pai et al. (2010), who also reported that vancomycin and clindamycin are the most effective drugs.

SCC*mec* type V was predominant type among MRSA strains followed by SCC*mec* type UT6, IV, and III, respectively. This finding is similar to Nadig et al. (2012), who also reported the prevalence of SCC*mec* type V among isolates from eye infections. To our knowledge, we are the first to inform of the presence of SCC*mec* type UT6 among *S. aureus* from India. The combination of SCC*mec* IV, V, and *pvl* gene was reported as the genetic markers for a community-associated MRSA (Bhutia et al., 2015). Similarly, our study showed the presence of SCC*mec* V (40.6%), IV (21.9%), and *pvl* (64.5%); therefore it can be used as a marker for hospital-associated infections. However, new UT6 SCC*mec* type is emerging in India. Many untypeable strains carried *ccr* complex but no *mec* complex. This observation thus suggests the ability of such strains to acquire *mec* complex and become a known or unknown SCC*mec* type.

A total of 25 unique toxin combination was found among *S. aureus* strains, of which at least one toxin gene was present in a given strain. Sotto et al. (2008) reported the presence of *sei* and *sea* genes in *S. aureus* isolated from diabetic foot ulcer. Similarly, we found the presence of *sei* and *sea* genes in both MRSA and MSSA strains. Although we noted the high percentage of *hlg* (98%) and *hla* (92.6%) among in *S. aureus* comprising both MSSA and MRSA, other workers reported the presence of these genes in mupirocin resistant in MRSA isolates in China (Liu et al., 2012). Moreover, the distribution of virulence genes with regards to source and place of isolation was complex. Gowrishankar et al. (2016) reported the isolation of 84% MRSA strains carrying *icaADBC* genes from patients with pharyngitis. Also, in this



study, 81.3% MRSA and 84.4% MSSA carrying *icaA/icaD* genes were isolated from the eye and wound infections (**Supplementary Table S3**). Absence of *icaA/icaD* genes in *S. aureus* strains was similar to those of the previous report (Agarwal and Jain, 2013).

Several molecular genotyping tools are used to trace the origin of the strain, and distribution of CC with regard to methicillin-resistant, methicillin-sensitive, sources and place of isolation. We determined the population structure of *S. aureus* isolated from ocular and wound infections from different parts of India using MLST, *agr*-typing, *spa*-typing, and PFGE.

Multi-locus sequence typing analysis showed the presence of six major ST(s) comprising ST1, ST5, ST772, ST239, ST672, and ST2233, respectively. While ST239-MRSA-UT6 was the typical type among MRSA isolates from wound infection, ST772-MRSA-V were from eye infections (Nadig et al., 2012). Similarly, ST772-SCC*mec*-V were reported slowly replacing multidrug resistant ST239-SCC*mec*-III in Asian studies (D'Souza et al., 2010). This finding is in contrast to Suzuki et al. (2012), who reported the presence of ST5 and ST764 among MRSA strains from the infected eye and healthy conjunctiva sacs. Also, Mohammadi et al. (2014) showed emergence of SCC*mec*-III with variable antimicrobial resistance profiles in Iran. We found ST772-MRSA-V with *spa*-type t345 and t657 belonging to dominant CC772 among wound infection isolates. Besides, we reported two new *spa*-types among *S. aureus* strains from India.

There were eight CCs, namely, CC30, CC121, CC772, CC813, CC239, CC28841, CC22, and CC5 present among *S. aureus* represents different PFGE clusters. CC30 and CC121 comprising different STs were almost equally distributed among MRSA and MSSA isolates. Whereas CC772-ST772 was dominant among MRSA, CC772-ST1 was prevalent among MSSA isolates. Similarly, CC239-ST239 and CC22-ST22 were prevalent among

MRSA isolates and CC5-ST5, CC813-ST813, and CC28841-ST28841 were more commonly found in MSSA isolates. The prevalent CC among Varanasi isolates (mostly wound infection) were CC772 followed by CC239 besides the presence of CC30, and CC121. However, isolates from wound infection from Delhi showed varied results. Whereas AIIMS isolates showed CC CC30, CC22, and CC813, UCMS isolates showed the presence of CC239 and CC22 CCs. Interestingly isolates from Hyderabad (eye infection) had CC239 but isolates from Bhubaneswar (eye infection) showed the presence of CC772, CC5, CC2884, and CC30.

Mobasherizadeh et al. (2019) reported the prevalence of CC5 and CC30 and other CCs among MRSA isolates isolated from nasal carriage in Iranian hospitals. Similarly, CC8, CC121, CC1, CC45, and CC5 were reported in MRSA isolates from Malaysia (Ghasemzadeh-Moghaddam et al., 2011). These observations indicate the existence of different CCs in India and Asian countries. MLST and *spa*-typing was better than PFGE and toxin genotyping a finding unusual from those who reported a good correlation between various typing schemes. Overall, there was diversity in genotypes, antimicrobial resistance, and virulence determinants among MRSA and MSSA strains.

From this study, it is clear that *S. aureus* strains sensitive to antibiotics but carried antibiotic resistance genes could develop resistance upon exposure to antibiotic(s), and vancomycin and clindamycin were the most effective drugs. ST239-SCC*mec* UT6/t035 were dominant clones among *S. aureus*. There was diversity in genotypes, antimicrobial resistance, and virulence determinants among MRSA and MSSA strains, therefore suggests continuous surveillance of multidrug-resistant strains circulating in the community/hospitals in India, to take adequate measures to control the infection.

## DATA AVAILABILITY STATEMENT

The raw data supporting the conclusions of this article will be made available by the authors, without undue reservation, to any qualified researcher.

## ETHICS STATEMENT

The studies involving human participants were reviewed and approved by the Institutional Review Board (IRB) of LV Prasad Eye Institute (LEC/08/110/2009) and by the Institute Ethics Sub-Committee (IESC) of All India Institute of Medical Sciences, New Delhi (IESC/T-34/2013), and the data were analyzed anonymously and reported. The patients/participants provided their written informed consent to participate in this study.

## AUTHOR CONTRIBUTIONS

SA, SJ, SS, and DS conceived the experiments. SA, SJ, and SP conducted the experiments. SA, SJ, SP, SS, BD, GN, NS, and DS analyzed the results. KN performed statistical analysis. SA, SJ, and DS wrote the manuscript. All authors reviewed and approved the manuscript.

## REFERENCES

- Agarwal, A., and Jain, A. (2013). Glucose & sodium chloride induced biofilm production & *ica* operon in clinical isolates of staphylococci. *Indian J. Med. Res.* 138:262.
- Arciola, C. R., Baldassarri, L., and Montanaro, L. (2001). Presence of *icaA* and *icaD* genes and slime production in a collection of *Staphylococcal* strains from catheter-associated infections. *J. Clin. Microbiol.* 39, 2151–2156. doi: 10.1128/JCM.39.6.2151-2156.2001
- Argudin, M., Tenhagen, B.-A., Fetsch, A., Sachsenröder, J., Käsohrer, A., Schroeter, A., et al. (2011). Virulence and resistance determinants of German *Staphylococcus aureus* ST398 isolates from nonhuman sources. *Appl. Environ. Microbiol.* 77, 3052–3060. doi: 10.1128/AEM.02260-10
- Baranovich, T., Zaraket, H., Shabana, I., Nevzorova, V., Turcutyuciov, V., and Suzuki, H. (2010). Molecular characterization and susceptibility of methicillin-resistant and methicillin-susceptible *Staphylococcus aureus* isolates from hospitals and the community in Vladivostok, Russia. *Clin. Microbiol. Infect.* 16, 575–582. doi: 10.1111/j.1469-0691.2009.02891.x
- Bhutia, K. O., Singh, T., Adhikari, L., and Biswas, S. (2015). Molecular characterization of community- & hospital-acquired methicillin-resistant & methicillin-sensitive *Staphylococcus aureus* isolates in Sikkim. *Indian J. Med. Res.* 142:330. doi: 10.4103/0971-5916.166600
- Busch-Sørensen, C., SØNmezoglu, M., Frimodt-Møller, N., Hojbjerg, T., Miller, G. H., and Espersen, F. (1996). Aminoglycoside resistance mechanisms in *Enterobacteriaceae* and *Pseudomonas* spp. from two Danish hospitals: correlation with type of aminoglycoside used. *Apmis* 104, 763–768. doi: 10.1111/j.1699-0463.1996.tb04940.x
- Dhawan, B., Rao, C., Udo, E., Gadepalli, R., Vishnubhatla, S., and Kapil, A. (2015). Dissemination of methicillin-resistant *Staphylococcus aureus* SCCmec type IV and SCCmec type V epidemic clones in a tertiary hospital: challenge to infection control. *Epidemiol. Infect.* 143, 343–353. doi: 10.1017/S095026881400065X
- Dornbusch, K., Miller, G., Hare, R., Shaw, K., and Group, E. S. (1990). Resistance to aminoglycoside antibiotics in gram-negative bacilli and staphylococci isolated from blood. Report from a European collaborative study. *J. Antimicrob. Chemother.* 26, 131–144. doi: 10.1093/jac/26.1.131

## FUNDING

This study was supported by the Department of Science and Technology (Grant No. SR/SO/HS-117 to DS). This study, in part, was also supported by the fund contributed by the Department of Biotechnology, New Delhi, to the Institute of Life Sciences, Bhubaneswar. The funder had no role in study design, data collection and analysis, decision to publish, or preparation of the manuscript.

## ACKNOWLEDGMENTS

SA and SJ are grateful to the Institute of Life Sciences, Bhubaneswar and Department of Science and Technology, New Delhi, respectively for providing Senior Research Fellowship.

## SUPPLEMENTARY MATERIAL

The Supplementary Material for this article can be found online at: <https://www.frontiersin.org/articles/10.3389/fmicb.2019.02763/full#supplementary-material>

- D'Souza, N., Rodrigues, C., and Mehta, A. (2010). Molecular characterization of methicillin-resistant *Staphylococcus aureus* with emergence of epidemic clones of sequence type (ST) 22 and ST 772 in Mumbai, India. *J. Clin. Microbiol.* 48, 1806–1811. doi: 10.1128/JCM.01867-09
- Duran, N., Ozer, B., Duran, G. G., Onlen, Y., and Demir, C. (2012). Antibiotic resistance genes & susceptibility patterns in staphylococci. *Indian J. Med. Res.* 135:389.
- Enright, M. C., and Spratt, B. G. (1999). Multilocus sequence typing. *Trends Microbiol.* 7, 482–487. doi: 10.1016/S0966-842X(99)01609-1
- Freidlin, J., Acharya, N., Lietman, T. M., Cevallos, V., Whitcher, J. P., and Margolis, T. P. (2007). Spectrum of eye disease caused by methicillin-resistant *Staphylococcus aureus*. *Am. J. Ophthalmol.* 144, 313–315. doi: 10.1016/j.ajo.2007.03.032
- Ghasemzadeh-Moghaddam, H., Ghaznavi-Rad, E., Sekawi, Z., Yun-Khoon, L., Aziz, M. N., Hamat, R. A., et al. (2011). Methicillin-susceptible *Staphylococcus aureus* from clinical and community sources are genetically diverse. *Int. J. Med. Microbiol.* 301, 347–353. doi: 10.1016/j.ijmm.2010.10.004
- Ghaznavi-Rad, E., Goering, R., Shamsudin, M. N., Weng, P., Sekawi, Z., Tavakol, M., et al. (2011). *mec*-associated *dru* typing in the epidemiological analysis of ST239 MRSA in Malaysia. *Eu. J. Clin. Microbiol. Infect. Dis.* 30, 1365–1369. doi: 10.1007/s10096-011-1230-1
- Ghebremedhin, B., Olugbosi, M., Raji, A., Layer, F., Bakare, R., König, B., et al. (2009). Emergence of a community-associated methicillin-resistant *Staphylococcus aureus* strain with a unique resistance profile in Southwest Nigeria. *J. Clin. Microbiol.* 47, 2975–2980. doi: 10.1128/JCM.00648-09
- Gilot, P., Lina, G., Cochard, T., and Poutrel, B. (2002). Analysis of the genetic variability of genes encoding the RNA III-activating components Agr and TRAP in a population of *Staphylococcus aureus* strains isolated from cows with mastitis. *J. Clin. Microbiol.* 40, 4060–4067. doi: 10.1128/JCM.40.11.4060-4067.2002
- Godebo, G., Kibru, G., and Tassew, H. (2013). Multidrug-resistant bacterial isolates in infected wounds at Jimma University Specialized Hospital, Ethiopia. *Annals Clin. Microbiol. Antimicrob.* 12:17. doi: 10.1186/1476-0711-12-17
- Goh, S.-H., Byrne, S., Zhang, J., and Chow, A. (1992). Molecular typing of *Staphylococcus aureus* on the basis of coagulase gene polymorphisms. *J. Clin. Microbiol.* 30, 1642–1645.



- Gowrishankar, S., Kamaladevi, A., Balamurugan, K., and Pandian, S. K. (2016). In vitro and in vivo biofilm characterization of methicillin-resistant *Staphylococcus aureus* from patients associated with pharyngitis infection. *Biomed. Res. Int.* 2016, 1–14. doi: 10.1155/2016/1289157
- Hammer, Ø, Harper, D., and Ryan, P. (2001). Paleontological statistics software: package for education and data analysis. *Palaeontol. Electron.* 4:9.
- Hirotsuki, S., Sasaki, T., Kuwahara-Arai, K., and Hiramatsu, K. (2011). Rapid and accurate identification of human-associated staphylococci by use of multiplex PCR. *J. Clin. Microbiol.* 49, 3627–3631. doi: 10.1128/JCM.00488-11
- Hsu, L.-Y., Koh, T.-H., Singh, K., Kang, M.-L., Kurup, A., and Tan, B.-H. (2005). Dissemination of multisusceptible methicillin-resistant *Staphylococcus aureus* in Singapore. *J. Clin. Microbiol.* 43, 2923–2925. doi: 10.1128/JCM.43.6.2923-2925.2005
- Hwang, S.-M., and Kim, T.-U. (2007). Changes in coagulase serotype of *Staphylococcus aureus* isolates in Busan, 1994–2005. *Korean J. Microbiol.* 43, 346–350.
- Jarraud, S., Mougél, C., Thioulouse, J., Lina, G., Meugnier, H., Forey, F., et al. (2002). Relationships between *Staphylococcus aureus* genetic background, virulence factors, *agr* groups (alleles), and human disease. *Infect. Immun.* 70, 631–641. doi: 10.1128/IAI.70.2.631-641.2002
- Kaur, D. C., and Chate, S. S. (2015). Study of antibiotic resistance pattern in methicillin resistant *Staphylococcus aureus* with special reference to newer antibiotic. *J. Glob. Infect. Dis.* 7, 78–84. doi: 10.4103/0974-777X.157245
- Kim, J.-S., Song, W., Kim, H.-S., Cho, H. C., Lee, K. M., Choi, M.-S., et al. (2006). Association between the methicillin resistance of clinical isolates of *Staphylococcus aureus*, their staphylococcal cassette chromosome *mec* (SCC*mec*) subtype classification, and their toxin gene profiles. *Diagn. Microbiol. Infect. Dis.* 56, 289–295. doi: 10.1016/j.diagmicrobio.2006.05.003
- Kondo, Y., Ito, T., Ma, X. X., Watanabe, S., Kreiswirth, B. N., Etienne, J., et al. (2007). Combination of multiplex PCRs for staphylococcal cassette chromosome *mec* type assignment: rapid identification system for *mec*, *ccr*, and major differences in junkyard regions. *Antimicrob. Agents Chemother.* 51, 264–274. doi: 10.1128/AAC.00165-06
- Lindsay, J. A., and Holden, M. T. (2004). *Staphylococcus aureus*: superbug, super genome? *Trends Microbiol.* 12, 378–385. doi: 10.1016/j.tim.2004.06.004
- Liu, Q., Han, L., Li, B., Sun, J., and Ni, Y. (2012). Virulence characteristic and MLST-*agr* genetic background of high-level mupirocin-resistant, MRSA isolates from Shanghai and Wenzhou, China. *PLoS One* 7:e37005. doi: 10.1371/journal.pone.0037005
- Liu, Y., Wang, H., Du, N., Shen, E., Chen, H., Niu, J., et al. (2009). Molecular evidence for spread of two major methicillin-resistant *Staphylococcus aureus* clones with a unique geographic distribution in Chinese hospitals. *Antimicrob. Agents Chemother.* 53, 512–518. doi: 10.1128/AAC.00804-08
- Lovering, A., Bywater, M., Holt, H., Champion, H., and Reeves, D. (1988). Resistance of bacterial pathogens to four aminoglycosides and six other antibiotics and prevalence of aminoglycoside modifying enzymes, in 20 UK centres. *J. Antimicrob. Chemother.* 22, 823–839. doi: 10.1093/jac/22.6.823
- Martineau, F., Picard, F. J., Lansac, N., Ménard, C., Roy, P. H., Ouellette, M., et al. (2000). Correlation between the resistance genotype determined by multiplex PCR assays and the antibiotic susceptibility patterns of *Staphylococcus aureus* and *Staphylococcus epidermidis*. *Antimicrob. Agents Chemother.* 44, 231–238. doi: 10.1128/aac.44.2.231-238.2000
- Maslow, J. N., Mulligan, M. E., and Arbeit, R. D. (1993). Molecular epidemiology: application of contemporary techniques to the typing of microorganisms. *Clin. Infect. Dis.* 17, 153–162. doi: 10.1093/clinids/17.2.153
- Mehrotra, M., Wang, G., and Johnson, W. M. (2000). Multiplex PCR for detection of genes for *Staphylococcus aureus* enterotoxins, exfoliative toxins, toxic shock syndrome toxin 1, and methicillin resistance. *J. Clin. Microbiol.* 38, 1032–1035.
- Mitchell, G., Séguin, D. L., Asselin, A.-E., Déziel, E., Cantin, A. M., Frost, E. H., et al. (2010). *Staphylococcus aureus* sigma B-dependent emergence of small-colony variants and biofilm production following exposure to *Pseudomonas aeruginosa* 4-hydroxy-2-heptylquinoline-N-oxide. *BMC Microbiol.* 10:33. doi: 10.1186/1471-2180-10-33
- Mobasherzadeh, S., Shojaei, H., Azadi, D., Havaei, A. A., and Rostami, S. (2019). Molecular characterization and genotyping of methicillin-resistant *Staphylococcus aureus* in nasal carriage of healthy Iranian children. *J. Med. Microbiol.* 68, 374–378. doi: 10.1099/jmm.0.000924
- Mohammadi, S., Sekawi, Z., Monjezi, A., Maleki, M.-H., Soroush, S., Sadeghifard, N., et al. (2014). Emergence of SCC*mec* type III with variable antimicrobial resistance profiles and *spa* types among methicillin-resistant *Staphylococcus aureus* isolated from healthcare- and community-acquired infections in the west of Iran. *Int. J. Infect. Dis.* 25, 152–158. doi: 10.1016/j.ijid.2014.02.018
- Monday, S. R., and Bohach, G. A. (1999). Use of multiplex PCR to detect classical and newly described pyrogenic toxin genes in staphylococcal isolates. *J. Clin. Microbiol.* 37, 3411–3414.
- Nadig, S., Velusamy, N., Lalitha, P., Kar, S., Sharma, S., and Arakere, G. (2012). *Staphylococcus aureus* eye infections in two Indian hospitals: emergence of ST772 as a major clone. *Clin. Ophthalmol.* 6, 165–173. doi: 10.2147/OPHT. S23878
- Nelson, J. L., Rice, K. C., Slater, S. R., Fox, P. M., Archer, G. L., Bayles, K. W., et al. (2007). Vancomycin-intermediate *Staphylococcus aureus* strains have impaired acetate catabolism: implications for polysaccharide intercellular adhesin synthesis and autolysis. *Antimicrob. Agents Chemother.* 51, 616–622. doi: 10.1128/AAC.01057-06
- Norazah, A., Liew, S., Kamel, A., Koh, Y., and Lim, V. (2001). DNA fingerprinting of methicillin-resistant *Staphylococcus aureus* by pulsed-field gel electrophoresis (PFGE): comparison of strains from 2 Malaysian hospitals. *Singapore Med. J.* 42, 015–019.
- Nurjadi, D., Schäfer, J., Friedrich-Jänicke, B., Mueller, A., Neumayr, A., Calvo-Cano, A., et al. (2015). Predominance of *dfgR* as determinant of trimethoprim resistance in imported *Staphylococcus aureus*. *Clin. Microbiol. Infect.* 21, 1095.e5–1095.e9. doi: 10.1016/j.cmi.2015.08.021
- Pai, V., Rao, V. I., and Rao, S. P. (2010). Prevalence and antimicrobial susceptibility pattern of methicillin-resistant *Staphylococcus aureus* [MRSA] isolates at a tertiary care hospital in Mangalore South India. *J. Lab. Physicians* 2:82. doi: 10.4103/0974-2727.72155
- Panda, S., Kar, S., Choudhury, R., Sharma, S., and Singh, D. V. (2014). Development and evaluation of hexaplex PCR for rapid detection of methicillin, cadmium/zinc and antiseptic-resistant staphylococci, with simultaneous identification of PVL-positive and negative *Staphylococcus aureus* and coagulase negative staphylococci. *FEMS Microbiol. Lett.* 352, 114–122. doi: 10.1111/1574-6968.12383
- Panda, S., Kar, S., Sharma, S., and Singh, D. V. (2016). Multidrug-resistant *Staphylococcus haemolyticus* isolates from infected eyes and healthy conjunctivae in India. *J. Glob. Antimicrob. Res.* 6, 154–159. doi: 10.1016/j.jgar.2016.05.006
- Paniagua-Contreras, G., Sáinz-Espuñes, T., Monroy-Pérez, E., Rodríguez-Moctezuma, J. R., Arenas-Aranda, D., Negrete-Abascal, E., et al. (2012). Virulence markers in *Staphylococcus aureus* strains isolated from hemodialysis catheters of Mexican patients. *Adv. Microbiol.* 2:476. doi: 10.4236/aim.2012.24061
- Price, K., Kresel, P., Farchione, L., Siskin, S., and Karpow, S. (1981). Epidemiological studies of aminoglycoside resistance in the USA. *J. Antimicrob. Chemother.* 8(Suppl. A), 89–105. doi: 10.1093/jac/8.suppl-A.89
- Schmitz, F.-J., Fluit, A. C., Gondolf, M., Beyrau, R., Lindenlauf, E., Verhoef, J., et al. (1999). The prevalence of aminoglycoside resistance and corresponding resistance genes in clinical isolates of staphylococci from 19 European hospitals. *J. Antimicrob. Chemother.* 43, 253–259. doi: 10.1093/jac/43.2.253
- Shanmuganathan, V., Armstrong, M., Buller, A., and Tullo, A. (2005). External ocular infections due to methicillin-resistant *Staphylococcus aureus* (MRSA). *Eye* 19, 284–291. doi: 10.1038/sj.eye.6701465
- Shittu, A. O., Okon, K., Adesida, S., Oyedara, O., Witte, W., Strommenger, B., et al. (2011). Antibiotic resistance and molecular epidemiology of *Staphylococcus aureus* in Nigeria. *BMC Microbiol.* 11:92. doi: 10.1186/1471-2180-11-92
- Shukla, S. K., Karow, M. E., Brady, J. M., Stemper, M. E., Kislow, J., Moore, N., et al. (2010). Virulence genes and genotypic associations in nasal carriage, community-associated methicillin-susceptible and methicillin-resistant USA400 *Staphylococcus aureus* isolates. *J. Clin. Microbiol.* 48, 3582–3592. doi: 10.1128/JCM.00657-10
- Sotto, A., Lina, G., Richard, J.-L., Combescure, C., Bourg, G., Vidal, L., et al. (2008). Virulence potential of *Staphylococcus aureus* strains isolated from diabetic foot ulcers: a new paradigm. *Diabetes Care* 31, 2318–2324. doi: 10.2337/dc08-1010
- Suzuki, T., Hayashi, S., and Ohashi, Y. (2012). Genotypic characterization of *Staphylococcus aureus* isolates from eyes with keratitis. *Invest. Ophthalmol. Vis. Sci.* 53, 6139–6139.

- Tenover, F. C., Arbeit, R., Archer, G., Biddle, J., Byrne, S., Goering, R., et al. (1994). Comparison of traditional and molecular methods of typing isolates of *Staphylococcus aureus*. *J. Clin. Microbiol.* 32, 407–415.
- Van Belkum, A., Tassios, P., Dijkshoorn, L., Haeggman, S., Cookson, B., Fry, N., et al. (2007). Guidelines for the validation and application of typing methods for use in bacterial epidemiology. *Clin. Microbiol. Infect.* 13, 1–46. doi: 10.1111/j.1469-0691.2007.01786.x
- Vanhoof, R., Godard, C., Content, J., and Nyssen, H. (1994). Detection by polymerase chain reaction of genes encoding aminoglycoside-modifying enzymes in methicillin-resistant *Staphylococcus aureus* isolates of epidemic phage types. *J. Med. Microbiol.* 41, 282–290. doi: 10.1099/00222615-41-4-282
- Wang, L., Hu, Z., Hu, Y., Tian, B., Li, J., Wang, F., et al. (2013). Molecular analysis and frequency of *Staphylococcus aureus* virulence genes isolated from bloodstream infections in a teaching hospital in Tianjin. *China Genet. Mol. Res.* 12, 646–654. doi: 10.4238/2013.March.11.12
- Zecconi, A., Cesaris, L., Liandris, E., Dapra, V., and Piccinini, R. (2006). Role of several *Staphylococcus aureus* virulence factors on the inflammatory response in bovine mammary gland. *Microb. Pathogen.* 40, 177–183. doi: 10.1016/j.micpath.2006.01.001

**Conflict of Interest:** The authors declare that the research was conducted in the absence of any commercial or financial relationships that could be construed as a potential conflict of interest.

Copyright © 2019 Aggarwal, Jena, Panda, Sharma, Dhawan, Nath, Singh, Nayak and Singh. This is an open-access article distributed under the terms of the Creative Commons Attribution License (CC BY). The use, distribution or reproduction in other forums is permitted, provided the original author(s) and the copyright owner(s) are credited and that the original publication in this journal is cited, in accordance with accepted academic practice. No use, distribution or reproduction is permitted which does not comply with these terms.



# Baicalin Inhibits Biofilm Formation and the Quorum-Sensing System by Regulating the MsrA Drug Efflux Pump in *Staphylococcus saprophyticus*

Jinli Wang<sup>1,2</sup>, Haihong Jiao<sup>3</sup>, Jinwu Meng<sup>1,2</sup>, Mingyu Qiao<sup>1,2</sup>, Hongxu Du<sup>1,2</sup>, Miao He<sup>1,2</sup>, Ke Ming<sup>1,2</sup>, Jiaguo Liu<sup>1,2\*</sup>, Deyun Wang<sup>1,2</sup> and Yi Wu<sup>1,2</sup>

<sup>1</sup> MOE Joint International Research Laboratory of Animal Health and Food Safety, College of Veterinary Medicine, Nanjing Agricultural University, Nanjing, China, <sup>2</sup> Institute of Traditional Chinese Veterinary Medicine, College of Veterinary Medicine, Nanjing Agricultural University, Nanjing, China, <sup>3</sup> Key Laboratory of Tarim Animal Husbandry Science and Technology of Xinjiang Production & Construction Corps, College of Animal Science, Tarim University, Alar, China

## OPEN ACCESS

### Edited by:

Raffaele Zarrilli,  
University of Naples Federico II, Italy

### Reviewed by:

Adline Princy Solomon,  
SASTRA University, India  
Mara Di Giulio,  
Università degli Studi "G. d'Annunzio"  
Chieti e Pescara, Italy

Iqbal Ahmad,  
Aligarh Muslim University, India

### \*Correspondence:

Jiaguo Liu  
liujiaguo@njau.edu.cn

### Specialty section:

This article was submitted to  
Antimicrobials, Resistance  
and Chemotherapy,  
a section of the journal  
Frontiers in Microbiology

Received: 23 September 2019

Accepted: 18 November 2019

Published: 10 December 2019

### Citation:

Wang J, Jiao H, Meng J, Qiao M,  
Du H, He M, Ming K, Liu J, Wang D  
and Wu Y (2019) Baicalin Inhibits  
Biofilm Formation  
and the Quorum-Sensing System by  
Regulating the MsrA Drug Efflux  
Pump in *Staphylococcus  
saprophyticus*.  
Front. Microbiol. 10:2800.  
doi: 10.3389/fmicb.2019.02800

*Staphylococcus saprophyticus* (*S. saprophyticus*) is one of the main pathogens that cause serious infection due to its acquisition of antibiotic resistance. The efflux pump decreases antibiotic abundance, and biofilm compromises the penetration of antibiotics. It has been reported that baicalin is a potential agent to inhibit efflux pumps, biofilm formation, and quorum-sensing systems. The purpose of this study was to investigate whether baicalin can inhibit *S. saprophyticus* biofilm formation and the quorum-sensing system by inhibiting the MsrA efflux pump. First, the mechanism of baicalin inhibiting efflux was investigated by the ethidium bromide (EtBr) efflux assay, measurement of ATP content, and pyruvate kinase (PK) activities. These results revealed that baicalin significantly reduced the efflux of EtBr, the ATP content, and the activity of PK. Moreover, its role in biofilm formation and the *agr* system was studied by crystal violet staining, confocal laser scanning microscopy, scanning electron microscopy, and real-time polymerase chain reaction. These results showed that baicalin decreased biofilm formation, inhibited bacterial aggregation, and downregulated mRNA transcription levels of the quorum-sensing system regulators *agrA*, *agrC*, RNAlII, and *sarA*. Correlation analysis indicated that there was a strong positive correlation between the efflux pump and biofilm formation and the *agr* system. We demonstrate for the first time that baicalin inhibits biofilm formation and the *agr* quorum-sensing system by inhibiting the efflux pump in *S. saprophyticus*. Therefore, baicalin is a potential therapeutic agent for *S. saprophyticus* biofilm-associated infections.

**Keywords:** baicalin, efflux pump, biofilm, quorum sensing (QS), *Staphylococcus saprophyticus*

## INTRODUCTION

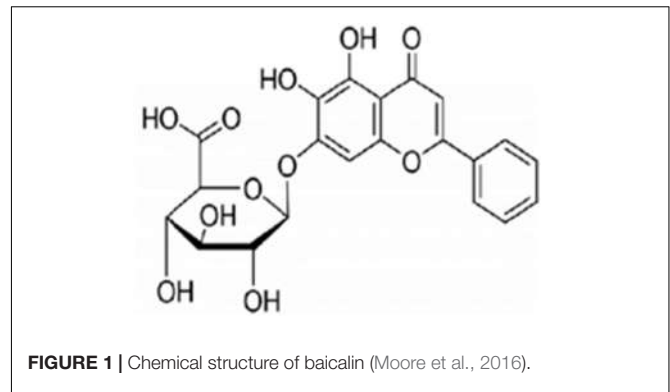
*Staphylococcus saprophyticus*, a member of the opportunistic coagulase-negative *Staphylococci* (CoNS), is a common pathogen of acute uncomplicated urinary tract infection, francolin ophthalmia, and bovine mastitis (Mahato et al., 2017; Mlaga et al., 2017; Wang J. et al., 2019). It has also been reported that *S. saprophyticus* is a common gastrointestinal flora in pigs and cows and

may thus be transferred to humans by eating these respective foods. The use of antibiotics to treat and prevent bacterial infections has made an unprecedented impact on improving human health. However, multidrug-resistant bacteria have seriously threatened people's health in recent decades. Wang et al. discovered that over 90% of *S. saprophyticus* isolated from ready-to-eat food displayed multiantibiotic resistance (Wang Y. et al., 2019). Bacteria are resistant to antibiotics due to target mutations, multidrug efflux pumps, drug-inactivating enzymes, biofilm formation, etc. Recently, *S. saprophyticus* has been shown to form biofilms in umbilical catheters (Martins et al., 2019).

Bacterial biofilms are adherent complex communities of bacteria encased within extracellular polymeric substances (EPSs), and they are considered intrinsically resistant to antibiotic treatment and host defenses (Thurlow et al., 2011; Paharik and Horswill, 2016). It has been estimated that nearly 60% of nosocomial infections in the human body are the result of biofilm formation on medical devices such as indwelling catheters and prostheses (Hou et al., 2012). The MIC of antibiotics toward bacteria biofilm is 1000-fold higher than that of planktonic counterparts (Costerton et al., 1987). Bacterial biofilms may represent an important barrier to the therapy of bacterial infections due to their lower sensitivity to antibiotic treatment. Therefore, the development of biofilm inhibitors based on a completely novel concept is urgently needed.

Recently, several studies have provided evidence to show that genetic inactivation and chemical inhibition of efflux pumps resulted in transcriptional inhibition of biofilm matrix components and a short biofilm formation (Baugh et al., 2014; Van Acker and Coenye, 2016; Sabatini et al., 2017). Biofilm formation is regulated by the quorum-sensing (QS) system. QS is a potential target for the therapy of bacterial biofilm infections. *Staphylococcus* uses a canonical Gram-positive two-component QS system encoded by the accessory gene regulator (*agr*) locus. Autoinducing peptide (AIP) is the signaling molecule of the *agr* system. When the cell density increases, the secretion of AIP is upregulated. In most Gram-positive QS bacteria, AIP is processed and exported by ABC transporters (Bassler, 1999). Our previous study indicated that azithromycin-resistant *S. saprophyticus* (ARSS) was resistant to macrolide antibiotics (Wang J. et al., 2019). The *ermA*, *ermB*, *ermC*, *mphC*, and *msrA* genes are the main resistance genes of macrolide antibiotics in *S. saprophyticus*, and the *msrA* gene is most prevalent in hospitals (Le Bouter et al., 2011). The MsrA efflux pump encoded by the *msrA* gene belongs to the ATP-binding cassette (ABC) transporters. We hypothesized that MsrA efflux pump inhibitors influence the *agr* system and biofilm formation.

Several natural plant products act as efflux pump inhibitors (Stavri et al., 2007). Baicalin (Figure 1; Moore et al., 2016), a type of flavonoid derived from the roots of *Scutellaria baicalensis* Georgi, exerts many biological activities and pharmacological effects, including remarkable antibiofilm, antibacterial (Sass et al., 2019), antiviral (Chen et al., 2018), and immune-enhancing ability (Ge et al., 2012). Our previous study has shown that baicalin possessed synergistic anti-ARSS with azithromycin (Azsm; Wang J. et al., 2019). Chen et al. elucidated that a sub-inhibitory concentration of baicalin can prevent biofilm



formation by inhibiting the *agr* system of *S. aureus* (Chen et al., 2016). Thus, we hypothesized that baicalin has the potential to be an effective therapeutic strategy against *S. saprophyticus* biofilm formation and the *agr* system by inhibiting efflux pumps.

Considering these aspects, this study evaluated whether baicalin could effectively inhibit the efflux pump, biofilm formation, and QS system in ARSS. We also tried to explain the relationship between the efflux pump and biofilm formation and the QS system. To our knowledge, there are no papers regarding the relationship between efflux and biofilm formation and the QS system in *S. saprophyticus*.

## MATERIALS AND METHODS

### Bacterial Strains and Culture Conditions

The azithromycin-resistant *S. saprophyticus* (ARSS) strain used in this experiment was isolated in 2016 from francolins suffering from ophthalmia in a francolin farm in Jiangsu Province, China. ARSS was coagulase negative and resistant to azithromycin with an MIC value of 1000 mg/L (Wang J. et al., 2019). *S. saprophyticus* ATCC 15305 was purchased from the China Center of Industrial Culture Collection (CICC). Strains were routinely cultured on brain heart infusion broth (BHI; Haibo, Qingdao, China) or nutrient broth (NB, Haibo, Qingdao, China) and incubated at 37°C.

### Determination of Growth Kinetics

For the growth kinetics assay, overnight ARSS cultures were prepared and cocultured with sub-inhibitory concentrations of baicalin or verapamil (an efflux pump inhibitor as a positive control compound). Normal saline containing up to 2% NaHCO<sub>3</sub> was used to prepare a 4000 mg/L baicalin solution. We have previously demonstrated that the MIC value of ARSS to baicalin was 500 mg/L (Wang J. et al., 2019). The sub-inhibitory concentrations of baicalin were used in this experiment, and the final concentrations of baicalin were 250, 125, 62.5, and 31.25 mg/L. The final concentration of verapamil was 250 mg/L. At the same time, the *S. saprophyticus* control group (SS group, not containing drug) was set. The cell densities based on the optical density at 600 nm in BHI were measured every 2 h from 0 h to 24 h.



## Efflux of Ethidium Bromide

The efflux of ethidium bromide (EtBr) by ARSS was implemented as previously described with some modifications (Smith and Blair, 2014): bacterial strains were grown to an OD<sub>600 nm</sub> of 0.6. The cells were pelleted by centrifuging at 4000 rpm for 10 min at room temperature, and the precipitation was washed twice with the same volume of phosphate buffer saline (PBS). Then, the OD<sub>600 nm</sub> of the bacterial suspension was adjusted to 0.3 with PBS containing 1 mM MgCl<sub>2</sub>. EtBr was added at a final concentration of 7.81 mg/L (1/2 MIC). Cultures were incubated at 37°C with shaking for 60 min. After centrifugation for 10 min at 4000 rpm, the supernatant was discarded, and the pellet was resuspended in PBS with 1 mM MgCl<sub>2</sub> and 5% glucose to energize the cells. Aliquots of 0.05 ml were put into each well of black, clear-bottom 96-well microplates that contained 0.05 ml baicalin or verapamil at sub-inhibitory concentrations prepared at 2-fold serial dilutions in PBS with 1 mM MgCl<sub>2</sub> and 5% glucose. Verapamil at 250 mg/L was used as a known efflux pump inhibitor, while the *S. saprophyticus* control (SS) group contained an equal volume of PBS with 1 mM MgCl<sub>2</sub> and 5% glucose. The fluorescence was measured over 60 min at excitation and emission wavelengths of 530 nm and 590 nm, respectively, in a Tecan Infinite 200 Pro (Switzerland).

## Measurement of the ATP Content and Pyruvate Kinase Activity

Overnight cultures were used to inoculate 4 ml of NB containing baicalin at concentrations of 250, 125, 62.5, and 31.25 mg/L and incubated at 37°C with shaking (180 rpm). The samples from each group were removed at 24 h. Then, the ATP content and pyruvate kinase (PK) activity were determined using an ATP assay kit (Beyotime, China) and a Pyruvate Kinase Assay Kit (Solarbio, Beijing, China) according to the manufacturer's instructions.

## Measuring Gene Transcription Levels via RT-PCR

Overnight cultures were used to inoculate 4 ml of NB containing baicalin at concentrations of 250, 125, 62.5, and 31.25 mg/L and incubated at 37°C with shaking (180 rpm). The samples used to detect the transcription level of the *msrA* gene from each group were removed at 24 h in the efflux mechanism experiment. Overnight cultures of ARSS were diluted into fresh BHI. Then, 0.5 ml of diluted cultures was applied to each well of sterile 96-well flat-bottom tissue culture plates that contained an equal volume of sub-inhibitory concentrations of baicalin (final concentrations of 250, 125, 62.5, and 31.25 mg/L) or verapamil (final concentration of 250 mg/L). The *S. saprophyticus* control (SS) group contained an equal volume of fresh BHI. The plates were incubated at 37°C without shaking. The samples from each group were removed at 24 h and 48 h post-inoculation for RNA extraction. These samples were used to detect the transcription levels of *msrA*, *agrA*, *agrC*, RNAIII, and *sarA* in biofilms. Then, total RNA was extracted by using a Bacteria RNA kit (Vazyme, Nanjing, China) as recommended in the manufacturer's instructions. The value of A260/A280 was

confirmed to be between 1.8 and 2.1. The reverse transcription assay took place in a PCR instrument (2720 Thermal Cycler PCR instrument, Applied Biosystems, America) by using a HiScript II 1st Strand cDNA Synthesis Kit (Vazyme, Nanjing, China). Reverse transcription was carried out at 50°C for 15 min and 85°C for 5 s. Real-time PCR was reacted in a PCR instrument (StepOnePlus™ Real Time PCR instrument, Applied Biosystems, United States) using ChamQ™ SYBR® qPCR Master Mix according to the manufacturer's instructions. The cycling parameters were as follows: holding stage of 95°C for 3 min; 40 cycles at the cycling stage of 95°C for 10 s and 60°C for 60 s; one melt curve stage of 95°C for 15 s, then 60°C for 60 s, and 95°C for 15 s. The 16S rRNA of ARSS was chosen as the housekeeping control gene. The sequences of primers used in this experiment are listed in Table 1.

## Semiquantitative Determination of Biofilm Formation

Semiquantitative biofilm assays were conducted as described previously with some modifications (Liu et al., 2017). Briefly, overnight cultures of ARSS or ATCC 15305 strains were diluted into fresh BHI. Then, 0.1 ml of diluted cultures was applied to each well of sterile 96-well plates that contained an equal volume of sub-inhibitory concentrations of baicalin (final concentrations of 250, 125, 62.5, and 31.25 mg/L) or verapamil (final concentration of 250 mg/L). The *S. saprophyticus* control (SS) group and the ATCC group contained equal volumes of fresh BHI. The negative control group contained only an equal volume of fresh BHI. Then, the plates were incubated at 37°C for 24 and 48 h without shaking. Culture supernatants were gently removed, and wells were washed with PBS twice to remove the floating cells, followed by fixation with 2.5% glutaraldehyde for 1.5 h and finally air-dried. The adherent bacteria in the wells were stained for 20 min with 1% (wt/vol) crystal violet and then rinsed thoroughly with PBS until the negative control wells (without biofilms) appeared colorless. To quantify biofilm formation, 0.2 ml of 33% glacial acetic acid was added to the wells of plates that were stained with crystal violet. Biofilm formation was measured with a Thermo™ Multiskan™ FC

TABLE 1 | Oligonucleotide primers used in this study.

Target gene	Primer	Sequence (5'–3')	Source
16S rRNA	16S rRNA-F	TGAAGAGTTTGATCATGGCTCAG	Hwang et al., 2011
	16S rRNA-R	ACCGCGGCTGCTGGCAC	
<i>msrA</i>	<i>msrA</i> -F	GCTCTACTGAATGATTCTGATG	This study
	<i>msrA</i> -R	TGGCATACTACTCGTCAACTT	
<i>agrA</i>	<i>agrA</i> -F	CCACTGCTGATCCTTATGA	This study
	<i>agrA</i> -R	GCGGCTACCTTATAGACAA	
<i>agrC</i>	<i>agrC</i> -F	GTCATTACACCACTGCTATTC	This study
	<i>agrC</i> -R	GTCCATCCATATCTTCTTCTCT	
<i>sarA</i>	<i>sarA</i> -F	ATTAGCGATGGTTACTTACG	This study
	<i>sarA</i> -R	CTGCTTTAACAACCTTGAGGT	
RNAIII	RNAIII-F	ACGACCTTCACTTGATCC	This study
	RNAIII-R	GCTACGGCATCTTCTTCTA	

enzyme-labeled instrument at 570 nm. The results are presented as the values in the experimental groups minus the values in the negative control group.

## CLSM Protocol Studies for Biofilm Inhibition

Biofilms were stained with the fluorescent LIVE/DEAD BacLight™ bacterial viability kit L7012 (Molecular Probes, Invitrogen) according to the manufacturer's instructions. Bacteria with damaged or intact cell membranes stain fluorescent green when SYTO 9 was used alone. Briefly, fluorescent green (SYTO 9) was used according to the product information manual supplied by the manufacturer. Afterward, 1 ml of overnight cultures that were diluted by BHI was used to grow biofilms on cover slides in 6-well microtiter plates containing 1 ml of baicalin at concentrations of 62.5, 125, 250, and 500 mg/L, verapamil (VP group) at a concentration of 500 mg/L or an equal volume of BHI (SS group) for 24 or 48 h at 37°C without shaking. Then, the supernatant was removed, and the adherent organisms were stained with dye at room temperature in the dark for 15 min. Finally, these carriers were rinsed three times with 0.85% NaCl and detected under CLSM (Nikon A1).

## Scanning Electron Microscope Studies for Biofilm Morphology

Biofilm morphology was observed using an S3400N scanning electron microscope (SEM; Hitachi, Japan). In this experiment, 0.5 ml of overnight cultures that were diluted with fresh BHI were used to grow biofilms on round cover slides in 24-well microtiter plates containing 0.5 ml of baicalin at a concentration of 500 mg/L or an equal volume of BHI (SS group) for 48 h at 37°C without shaking. Each biofilm slice was washed with PBS, fixed in 2.5% glutaraldehyde overnight at 4°C, and then rinsed thoroughly three times with fresh PBS (pH 7.4). The slices were passed through an ethanol gradient (e.g., 50, 70, 80, and 90%) for 15 min, passed through 100% ethanol (three times for 10 min) for dehydration, dried, and then coated with gold (Fujimura et al., 2008).

## Baicalin and Azithromycin Combined Efficacy *in vitro* on Mature Biofilm

In order to compare the combined effects of baicalin and Azm against ARSS biofilms, 48 h biofilms were prepared in 24-well plates. Briefly, overnight cultures of ARSS were diluted into fresh BHI. Then, 1 ml of diluted cultures was applied to each well of sterile 96-well flat-bottom tissue culture plates. The plates were incubated at 37°C for 48 h without shaking. Then, the culture supernatants were gently removed. The plates were gently washed twice with PBS. Baicalin and verapamil in the presence or absence of Azm were added to each well in BHI. The total volume per well was 1 ml. The final concentrations of verapamil and Azm were 250 and 7.8 mg/L, respectively. The final concentrations of baicalin were 250, 125, 62.5, and 31.25 mg/L. Finally, the plates with biofilms were cultured for 24 h at 37°C. After the treatment was completed, planktonic bacteria were discarded by washing with PBS, and clumps were disrupted by sonicating.

The bacterial CFU counts in biofilm were performed by plating serial dilutions on NB agar. This experiment was conducted three times in parallel.

## Correlation Analysis

Correlations among the relative expression of the efflux gene and the ability of biofilm formation and the relative expression of *agr* system-associated genes were determined using Pearson's correlation coefficient.

## Statistical Analysis

Relative gene expression data were analyzed by the  $2^{-\Delta\Delta CT}$  method. Duncan's Multiple Range Test was used to determine the differences among groups by the SPSS Software Package version 20.0 (IBM, Armonk, NY, United States). The results were expressed as the mean  $\pm$  standard deviation (SD). Differences were considered statistically significant at  $p < 0.05$ .

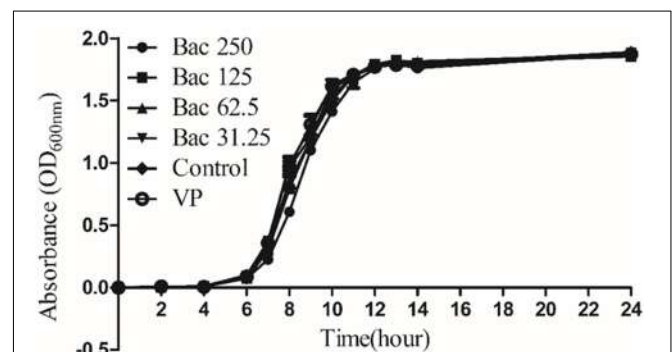
## RESULTS

### Sub-Inhibitory Concentrations of Baicalin and Verapamil Did Not Influence Bacterial Growth *in vitro*

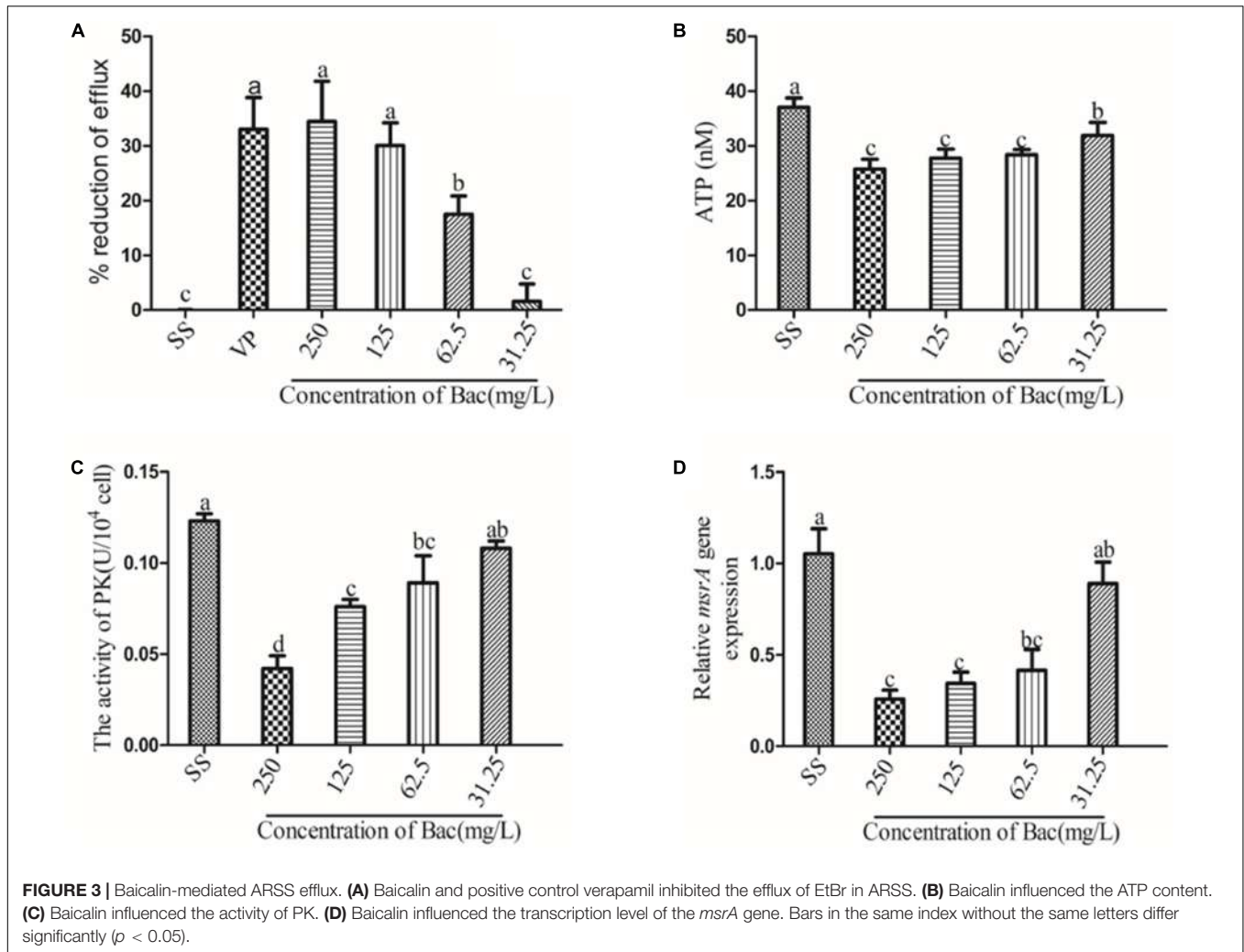
Our previous investigation indicated that the MICs of baicalin and azithromycin against ARSS were 500 and 1000 mg/L, respectively (Wang J. et al., 2019). The results of the growth kinetics assay showed that the growth kinetics of the ARSS under sub-inhibitory concentrations of baicalin and verapamil did not exhibit any difference from the control group when the bacteria were cultured in BHI, indicating that in a nutrient-rich environment, the sub-inhibitory concentrations of baicalin and verapamil may not affect *S. saprophyticus* growth (Figure 2).

### Baicalin Inhibited EtBr Efflux

The inhibitory effect of increasing concentrations of baicalin and the known efflux pump inhibitor verapamil (VP) on EtBr



**FIGURE 2 |** Growth kinetics of *Staphylococcus saprophyticus* strains in BHI under sub-inhibitory concentrations of baicalin or verapamil. OD<sub>600 nm</sub> values are the means  $\pm$  SD from three independent experiments. Sub-inhibitory concentrations of baicalin are 250, 125, 62.5, and 31.25 mg/L, and verapamil had no effect on bacterial growth.



efflux is shown in **Figure 3**. A concentration-dependent effect was observed for baicalin. In the presence of verapamil or 250, 125, or 62.5 mg/L baicalin, the rate of efflux reduction was significantly higher than that of the SS group, as presented in **Figure 3A** ( $p < 0.05$ ). Importantly, the rates of efflux reduction were not significantly different from that of the VP group when 250 or 125 mg/L baicalin was added. *MsrA* is an ATP-dependent efflux pump, suggesting that ATP is essential for *MsrA* efflux function (Hu et al., 2015). PK is associated with ATP production. Thus, the ATP content and PK activity were detected. Baicalin markedly decreased the content of ATP and the activity of PK (**Figures 3B,C**) ( $p < 0.05$ ). The *MsrA* efflux pump was encoded by the *msrA* gene. Baicalin significantly reduced the relative expression of the *msrA* gene at 250, 125, and 62.5 mg/L, as presented in **Figure 3D** ( $p < 0.05$ ). However, baicalin at 31.25 mg/L did not exert beneficial effects.

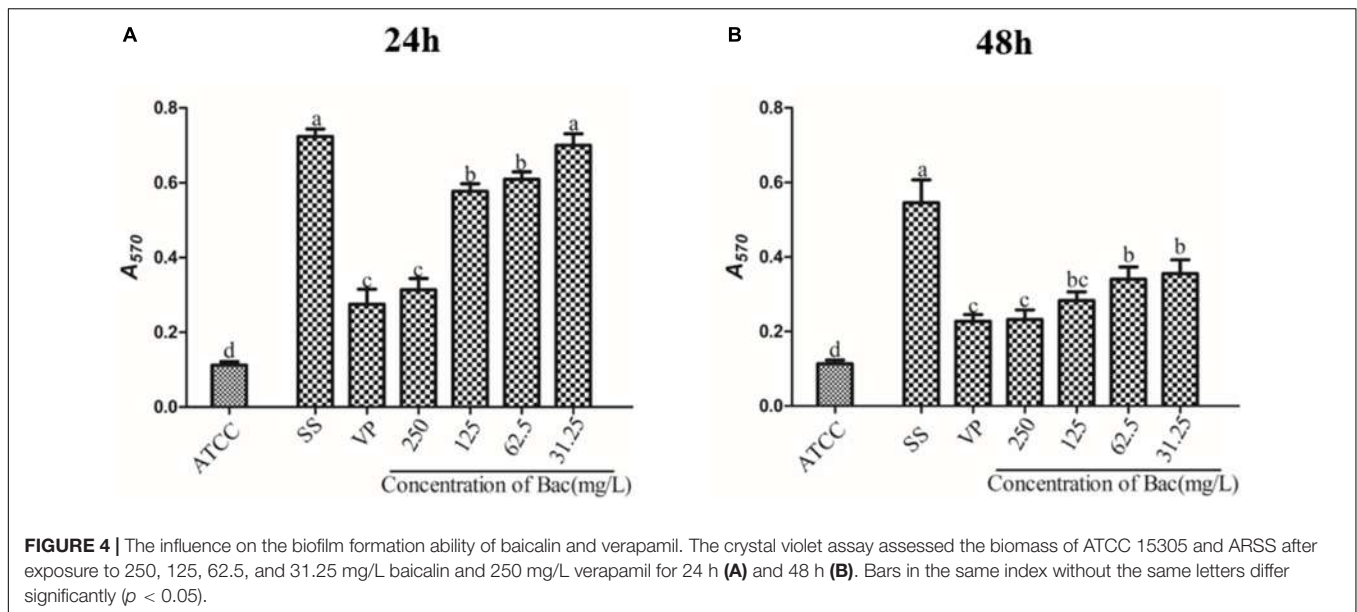
### Biofilm Formation Was Impeded by Baicalin and Verapamil

To examine whether baicalin or verapamil inhibited ARSS biofilm formation, the ability of biofilm formation was

investigated. These results reflected that the  $A_{570}$  values of ARSS biofilm in the SS group were significantly higher than those of the ATCC group for 24 and 48 h. We found that baicalin reduced biomass in a dose-dependent manner in spite of whether the cultures were grown for 24 or 48 h, while 31.25 mg/L baicalin had almost no effect at 24 h in ARSS (**Figures 4A,B**). Additionally, verapamil significantly decreased biofilm formation compared with that of the SS group (not containing drug). Interestingly, the  $A_{570}$  values were not different when verapamil or 250 mg/L baicalin was added for 24 or 48 h. Moreover, fluorescence microscopy revealed similar results (**Figure 5**). From **Figures 5, 6**, we find that many bacteria accumulated together and were enrolled in large amounts of extracellular matrix in the SS group. However, when baicalin was added, only a few bacteria adhered to the glass side and did not form mature biofilms.

### Combined Anti-ARSS Biofilm Efficacy of Baicalin Plus Azm

To determine whether baicalin was effective at disrupting ARSS biofilms combined with Azm, 48-h biofilms were treated with



baicalin and verapamil in the presence or absence of Azm. The results showed that Azm alone did not eradicate ARSS in the formed biofilms. However, combination treatment with verapamil + Azm or baicalin + Azm markedly reduced the counts of bacteria on plates in a concentration-dependent manner ( $p < 0.05$ ), while 31.25 mg/L baicalin had almost no effect. Furthermore, there was no significant difference between the 250 and 125 mg/L baicalin + Azm groups and the verapamil + Azm group (Figure 7).

### Baicalin Inhibited the Relative Expression Level of the *msrA* Efflux Gene in Biofilm

We measured the expression of the *msrA* gene in ARSS biofilm bacteria at 24 and 48 h by RT-PCR to detect the relationship between efflux and biofilm formation. As shown in Figure 8, the relative expression of the *msrA* gene was significantly decreased in a dose-dependent manner when baicalin was added compared with relative expression in the SS group ( $p < 0.05$ ). However, the transcript level of the *msrA* gene was not significantly affected by 31.25 mg/L baicalin at 24 h.

### In the ARSS Background, Baicalin and Verapamil Lowered the Activity of the *agr* System

In *Staphylococcus*, the two-component QS system *agr* is an important contributor to the establishment of biofilm and infection by this bacterium (Boles and Horswill, 2008). In order to detect the transcription levels of specific RNA in different samples, the levels of *agr* system-associated gene transcripts were measured using RT-PCR. After the bacterial biofilms were treated with either 250, 125, or 62.5 mg/L baicalin or 250 mg/L verapamil for 24 and 48 h, the transcription levels of *agrA*, *agrC*, *sarA*, and RNAIII genes significantly decreased in a dose-independent

manner ( $p < 0.05$ ). Treating the biofilms with 31.25 mg/L baicalin (24 or 48 h) did not change *agr* system-associated gene expression levels. More importantly, no significant difference in *agr* system-associated gene expression levels resulted from treatment with 250 mg/L baicalin and verapamil (Figure 9).

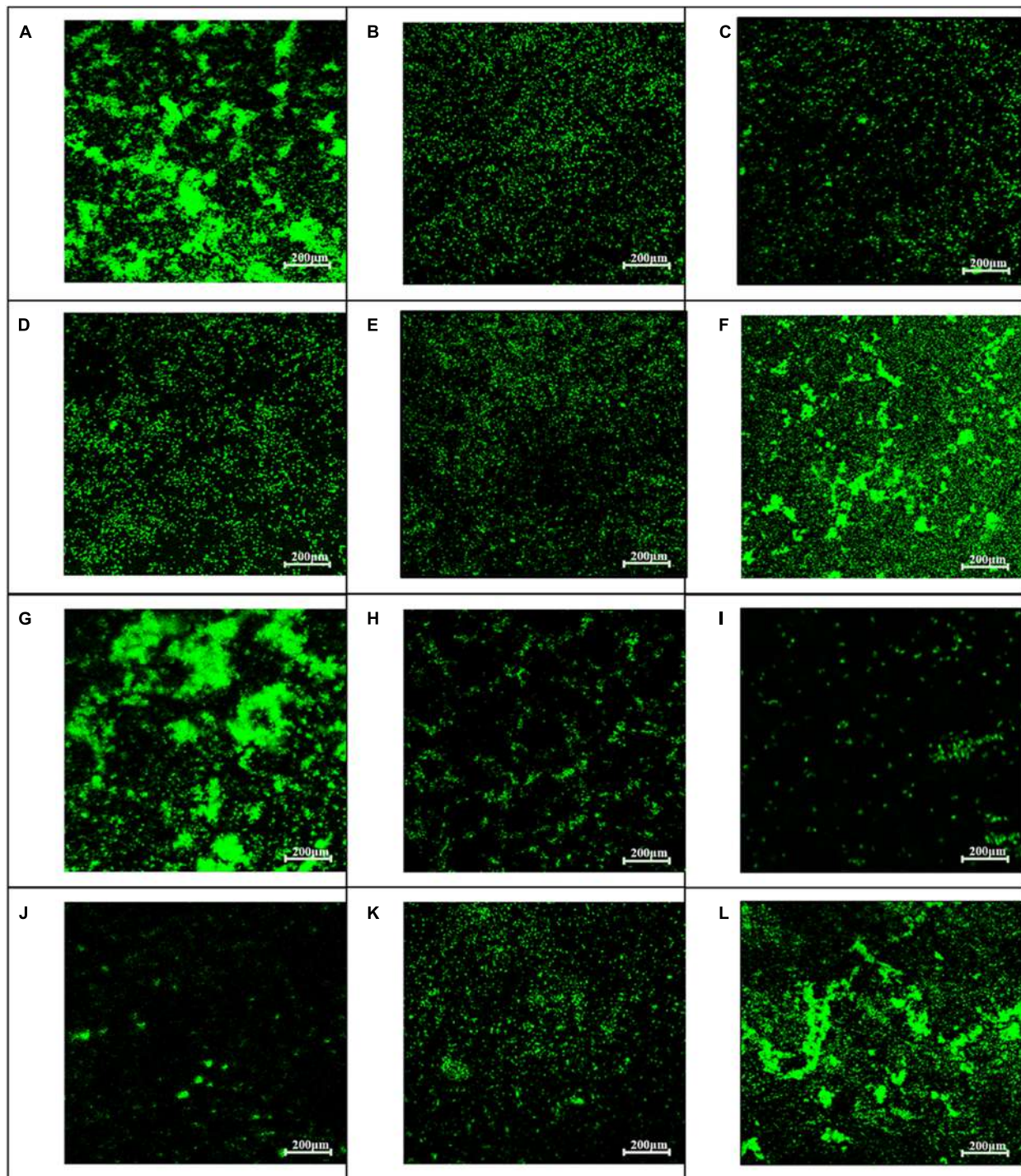
### Pearson's Correlation Coefficients Between the Relative Expression of the Efflux Gene and Biofilm Formation and the Transcript Levels of *agr* System-Associated Genes

The correlation coefficients among the measured indices of *msrA* efflux gene relative expression and biofilm formation and transcript levels of *agr*-associated genes are presented in Table 2. As shown in Table 2, the relative expression of the *msrA* efflux gene was positively correlated with the  $A_{570}$  values of biofilm ( $p < 0.01$ ) and the relative expression of *agr* system-associated genes ( $p < 0.01$ ). In particular, the relative expression of *agrA* and *agrC* was positively correlated with the relative expression of *sarA* and RNAIII.

## DISCUSSION

Efflux pumps, which are membrane-bound proteinaceous transporters, are in charge of transporting xenobiotics or chemotherapeutic agents that are otherwise harmful for bacterial survival. Many researchers have reported that multidrug-resistant (MDR) efflux pumps play a prominent role in the biology of bacteria and have roles in drug resistance, cell division, pathogenicity, and, as recently described, the formation of biofilms (Kvist et al., 2008; Buckley et al., 2006). MsrA is an MDR efflux pump of the ABC family. It was established to expel various macrolide antibiotics in *Staphylococcus*. The MsrA efflux



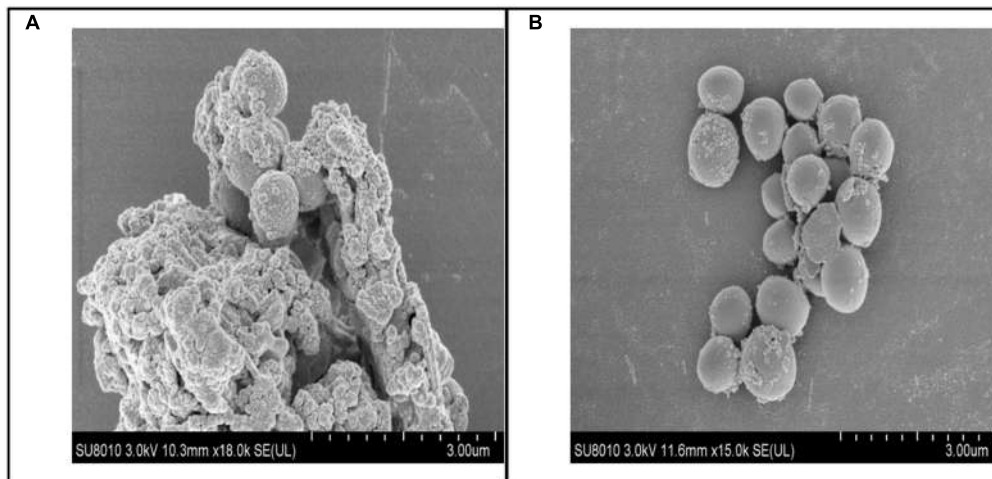


**FIGURE 5 |** Influence of baicalin on biofilm formation assessed by fluorescence microscopy (200 $\times$ ). Static biofilms after exposure to baicalin or verapamil for 24 h (A–F) and 48 h (G–L) were stained with SYTO 9. ARSS within biofilms on glass carriers display green fluorescence. Control group (A,G); verapamil group (B,H); 250 mg/L baicalin group (C,I); 125 mg/L baicalin group (D,J); 62.5 mg/L baicalin group (E,K); 31.25 mg/L baicalin group (F,L).

pump has been well established as a model system for studying efflux inhibition in *Staphylococcus* (Chan et al., 2013).

In the present study, baicalin was assessed for its MsrA efflux pump inhibitory activity in ARSS, which expresses the *msrA*

efflux gene and is resistant to Azm. Baicalin could inhibit 33% of the EtBr extrusion from ARSS. Importantly, there was no significant difference in the rate of efflux reduction resulting from treatment with either the positive control compound verapamil

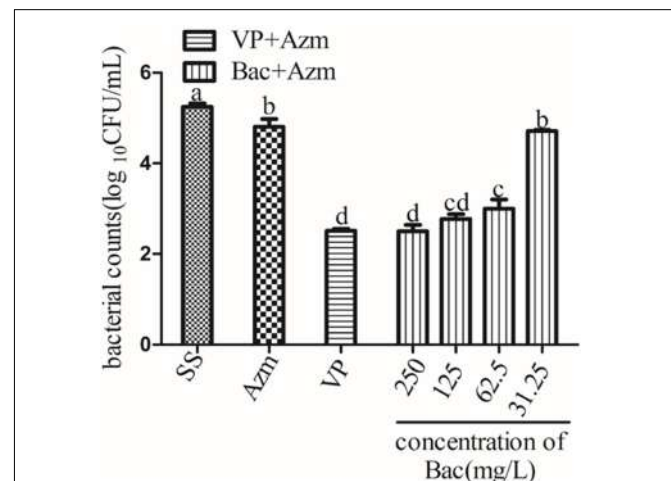


**FIGURE 6** | Biofilm scanning by SEM. **(A)** Bacteria control group, lots of bacteria aggregated together and enrolled by EPS. **(B)** 250 mg/L baicalin group, a small amount of bacteria aggregated.

or 250 mg/L baicalin (**Figure 3A**). These results suggested that baicalin could inhibit the MsrA efflux pump and has the potential to be an efflux pump inhibitor. MsrA is an ATP-dependent efflux pump, indicating that the inhibitory activities of baicalin against the ARSS efflux pump were more correlated with the ATP-dependent process in bacteria (Hu et al., 2015). In this study, our results indicated that baicalin significantly decreased the content of ATP compared with the SS group. PK, a final-stage enzyme in glycolysis, converts phosphoenolpyruvate (PEP) to pyruvate and ATP (Zoraghi et al., 2010). PK is critical for bacterial survival. Chan et al. proved that diosmetin could statistically reverse the resistance of MRSA to erythromycin possibly by inhibiting the MsrA efflux pump *in vitro* and MRSA-specific PK selectively, and they also confirmed that baicalin could inhibit the activity of PK (Chan et al., 2013; Chan et al., 2011). Because the chemical structure of diosmetin is similar to baicalin, it is interesting to detect whether baicalin has potential inhibitory actions on ARSS PK. In this study, our results revealed that the enzymatic activity of ARSS PK was inhibited by baicalin. It is possible that interfering with ATP production by baicalin may stop the function of the MsrA efflux pump and contribute to the synergistic action of baicalin and Azm against ARSS. We also elucidated that baicalin could dose-dependently inhibit the transcript level of the *msrA* gene. Taken together, these results indicated that baicalin interfered with ATP generation by inhibiting PK enzymatic activity and decreasing the relative expression of the *msrA* gene, ultimately inhibiting the MsrA efflux pump.

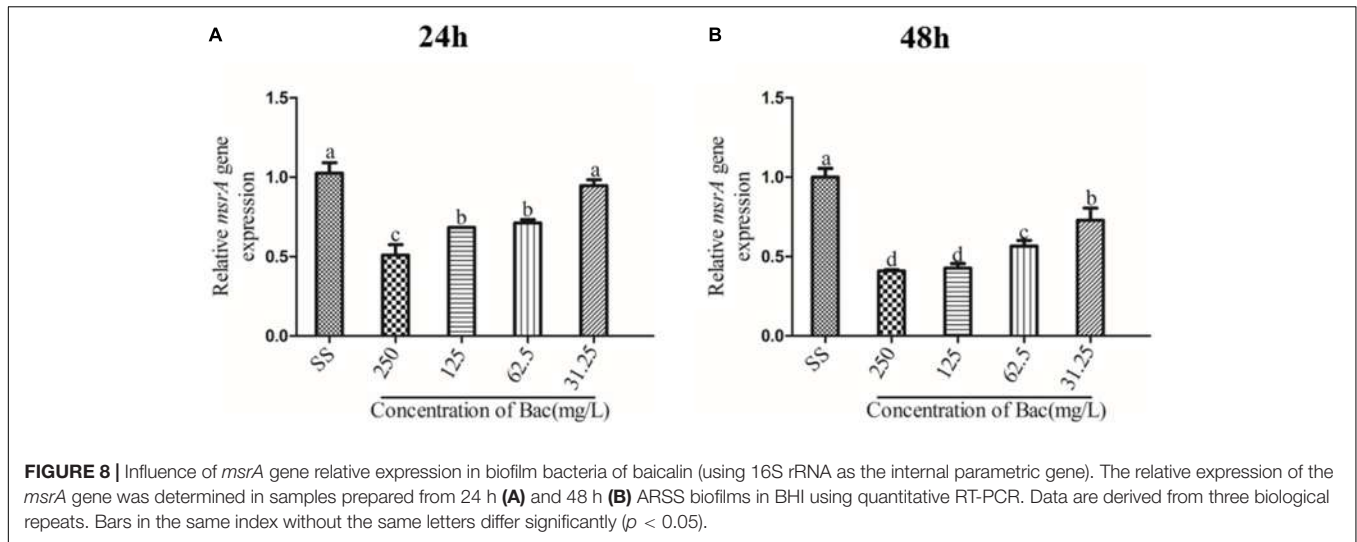
It has been reported that increasing resistance is associated with active efflux in bacterial biofilms (Van Acker and Coenye, 2016; Danquah et al., 2018). Baugh et al. demonstrated that numerous functional efflux pumps give rise to biofilm matrix expression in *Salmonella Typhimurium* and that the addition of a variety of efflux inhibitors inhibited biofilm formation (Baugh et al., 2012). Therefore, we hypothesized that the efflux inhibitor baicalin could be used as a biofilm formation inhibitor.

In the present study, sub-inhibitory concentrations of baicalin or positive control verapamil did not affect *S. saprophyticus* growth (**Figure 2**) but reduced the values of  $A_{570}$  measured by staining with crystal violet. ARSS was unable to form mature biofilms under baicalin or verapamil incubation conditions even after extended incubation times up to 48 h. These results indicated that baicalin and verapamil inhibited biofilm formation. Pearson's correlation coefficient analysis indicated that the relative expression of the efflux gene was positively correlated with biofilm formation ( $p < 0.01$ ). Therefore, baicalin can inhibit biofilm formation by inhibiting the MsrA efflux pump in ARSS. Evidently, biofilms render the cells less accessible to the defense

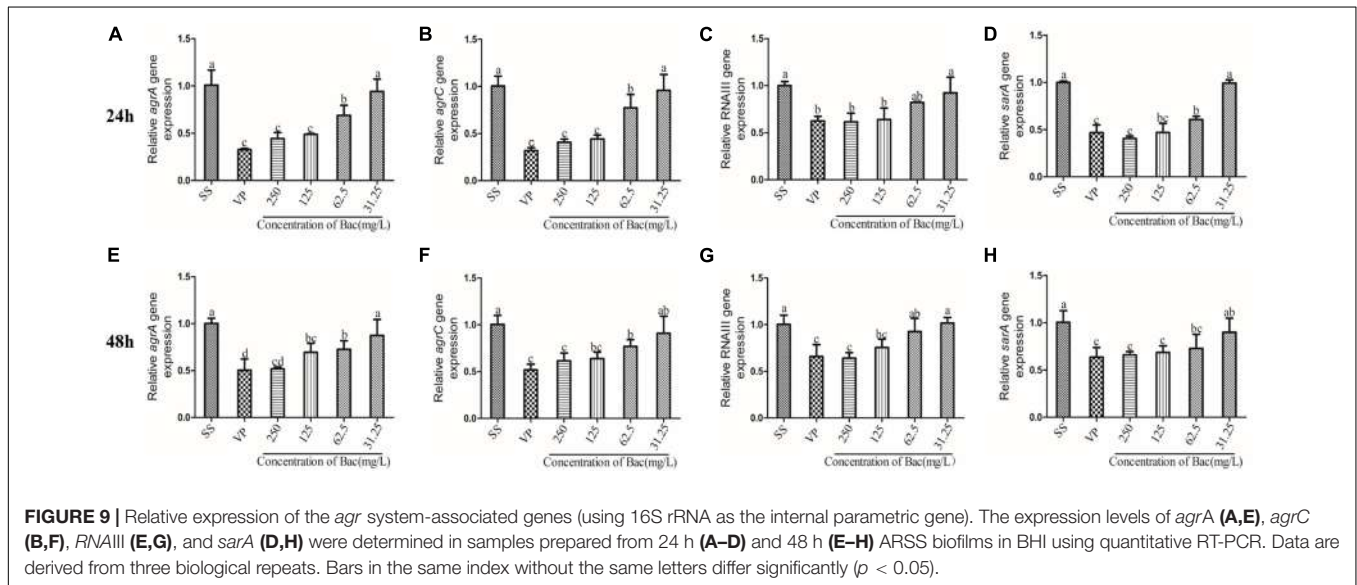


**FIGURE 7** | Viable bacterial counts of 48 h biofilms after exposure to agents for 24 h. Biofilms were formed on slices for 48 h by growing ARSS in BHI and then treated with Azm alone or in combination with 250, 125, 62.5, and 31.25 mg/L baicalin and 250 mg/L verapamil for 24 h. Bars in the same index without the same letters differ significantly ( $p < 0.05$ ).





**FIGURE 8 |** Influence of *msrA* gene relative expression in biofilm bacteria of baicalin (using 16S rRNA as the internal parametric gene). The relative expression of the *msrA* gene was determined in samples prepared from 24 h (A) and 48 h (B) ARSS biofilms in BHI using quantitative RT-PCR. Data are derived from three biological repeats. Bars in the same index without the same letters differ significantly ( $p < 0.05$ ).



**FIGURE 9 |** Relative expression of the *agr* system-associated genes (using 16S rRNA as the internal parametric gene). The expression levels of *agrA* (A,E), *agrC* (B,F), *RNAIII* (E,G), and *sarA* (D,H) were determined in samples prepared from 24 h (A–D) and 48 h (E–H) ARSS biofilms in BHI using quantitative RT-PCR. Data are derived from three biological repeats. Bars in the same index without the same letters differ significantly ( $p < 0.05$ ).

system of the organism and reduce antibiotic concentrations inside the target pathogen. The treatment of biofilm-related infections is a critical clinical problem in the current era. Because

of frequent reports on resistance to antimicrobials, the synergistic antibacterial method may be a better treatment strategy (Drugeon et al., 1999). The combined action of molecules was reported to eradicate the biofilms (Baugh et al., 2014). Overall, this evidence encouraged the investigation of the roles of baicalin in the prevention and eradication of biofilms. In this study, baicalin and Azm increased antibiotic permeability by disrupting the already-formed biofilms. Verapamil was used as a positive control compound to evaluate the combined effects of sub-inhibitory concentrations of baicalin with Azm on biofilms that were established for 48 h. *S. saprophyticus* could not be eradicated by Azm alone, and both baicalin + Azm and VP + Azm could significantly decrease the counts of bacteria compared with the counts for the SS group. Presumably, baicalin may be a potential agent for treating biofilm infections by either inhibiting biofilm formation or eradicating biofilms in combination with Azm.

**TABLE 2 |** Pearson’s correlation coefficients between the relative expression of *msrA* and biofilm formation ability and the expression of *agr* system-associated genes.

	BF formation	<i>msrA</i>	<i>agrA</i>	<i>agrC</i>	<i>sarA</i>	<i>RNAIII</i>
BF formation	1	0.850**	0.584	0.560	0.549	0.480
<i>msrA</i>		1	0.814**	0.769**	0.764*	0.723*
<i>agrA</i>			1	0.927**	0.937**	0.943**
<i>agrC</i>				1	0.924**	0.943**
<i>sarA</i>					1	0.803**
<i>RNAIII</i>						1

\*\* $p < 0.01$ , \* $p < 0.05$ . 0.8–1.0, extreme correlation; 0.6–0.8, strong correlation; 0.4–0.6, moderate correlation; 0.2–0.4, weak correlation; 0.0–0.2, very weak correlation or no correlation.

In addition, multidrug efflux pumps often secrete metabolites involved in QS (Polkade et al., 2016). QS is a process of

bacterial cell–cell communication that allows bacteria to sense cell density and change bacterial gene expression patterns to alter bacteria group behaviors at high cell numbers (Rutherford and Bassler, 2012; Camilli and Bassler, 2006). This cross-talk between bacteria is believed to be essential for the establishment of bacterial biofilms and bacterial biofilm infection (Danquah et al., 2018). QS regulates the expression of genes encoding virulence factors involved in a range of toxins, adhesion molecules, and compounds that influence immune function. Chen et al. (2016) prophage studies demonstrated that baicalein interfered with the QS system and affected bacterial virulence. Therefore, the potential target for the treatment of bacterial biofilm infection is the QS system. *Staphylococcus* biofilm is regulated by a Gram-positive two-component QS system encoded by the *agr* locus. An increase in cell density accounts for a prompt upsurge in the production, secretion, and detection of AIP. When AIP accumulates, it binds with *agrC*, which is a membrane-bound histidine kinase. Then, *agrC* autophosphorylates at a conserved histidine and transfers the phosphate group to an aspartate on the response regulator *agrA* (Lina et al., 1998). *AgrA* activates the divergently encoded P3 promoter, which controls the expression of RNAPIII (Novick et al., 1993). Most of the effects of QS regulating virulence in *Staphylococcus* are achieved by direct and indirect regulation of RNAPIII (Queck et al., 2008). Our results showed that 250, 125, and 62.5 mg/L baicalin and verapamil downregulated the transcript levels of *agrA*, *agrC*, RNAPIII, and *sarA* in a dose-dependent manner compared with that of the SS group. In most Gram-positive QS bacteria, AIP was processed and exported by ABC transporters (Bassler, 1999). The MsrA efflux pump belongs to the ABC transporters. We found that there was a significant correlation between the relative expression of *agr* system-associated genes and the efflux gene ( $p < 0.01$ , **Table 2**). Therefore, we inferred that baicalin may inactivate the *agr* system by inhibiting the efflux of AIP. Recent findings (Ge et al., 2012; Drugeon et al., 1999) have demonstrated that RNAPIII regulates biofilm formation and induces toxin production, such as plasma-coagulase, enterotoxin, and thermostable nuclease. Additionally, RNAPIII is a transcriptional regulator of the *Staphylococcal* accessory regulator A (*sarA*) family (Lewis, 2007). Recent evidence has elucidated that SarA, as a central regulatory element, controls the production of staphylococcus virulence factors (Van Acker and Coenye, 2016). Therefore, we inferred that baicalin may regulate virulence by inhibiting the *agr* system.

## REFERENCES

- Bassler, B. L. (1999). How bacteria talk to each other: regulation of gene expression by quorum sensing. *Curr. Opin. Microbiol.* 2, 582–587. doi: 10.1016/S1369-5274(99)00025-9
- Baugh, S., Ekanayaka, A. S., Piddock, L. J., and Webber, M. A. (2012). Loss of or inhibition of all multidrug resistance efflux pumps of *Salmonella enterica* serovar Typhimurium results in impaired ability to form a biofilm. *J. Antimicrob. Chemother.* 67, 2409–2417. doi: 10.1093/jac/dks228
- Baugh, S., Phillips, C. R., Ekanayaka, A. S., Piddock, L. J. V., and Webber, M. A. (2014). Inhibition of multidrug efflux as a strategy to prevent biofilm formation. *J. Antimicrob. Chemother.* 69, 673–681. doi: 10.1093/jac/dkt420
- Boles, B., and Horswill, A. (2008). *agr*-mediated dispersal of *Staphylococcus aureus* biofilms. *PLoS Pathog.* 4:e1000052. doi: 10.1371/journal.ppat.1000052

## CONCLUSION

In conclusion, baicalin effectively inhibited the MsrA efflux pump, biofilm formation and the *agr* system in ARSS. In addition, there is a significant positive correlation between efflux and biofilm formation and the *agr* system. Therefore, we believe that *S. saprophyticus* biofilm-related infections could be treated by baicalin combined with Azm. To our knowledge, we first elucidated the positive relationship between efflux and biofilm formation in *S. saprophyticus*.

## DATA AVAILABILITY STATEMENT

All datasets generated for this study are included in the article.

## AUTHOR CONTRIBUTIONS

JW, HJ, and JL conceived and designed the experiments. JW, JM, MQ, HD, MH, and KM performed the experiments. JW and HJ analyzed the data. DW and YW contributed to the reagents, materials, and analysis tools. JW wrote the manuscript. All authors read and made additions to the manuscript during revision stages.

## FUNDING

This work was supported by the Fundamental Research Funds for the Central Universities (Y0201700441 and KYYJ201803), the National Natural Science Foundation of China (Grant Nos. 31572557 and 31772784), the Special Fund for Agro-Scientific Research in the Public Interest (201303040 and 201403051), and the Project Funded by the Priority Academic Program Development of Jiangsu Higher Education Institutions (PAPD).

## ACKNOWLEDGMENTS

We thank all other staff at the Institute of Traditional Chinese Veterinary Medicine of Nanjing Agricultural University for their assistance with the experiments.

- Buckley, A. M., Webber, M. A., Cooles, S., Randall, L. P., Ragione, R. L., Woodward, M. J., et al. (2006). The AcrAB-TolC efflux system of *Salmonella enterica* serovar Typhimurium plays a role in pathogenesis. *Cell Microbiol.* 8, 847–856. doi: 10.1111/j.1462-5822.2005.00671.x
- Camilli, A., and Bassler, B. L. (2006). Bacterial small-molecule signaling pathways. *Science* 311, 1113–1116. doi: 10.1126/science.1121357
- Chan, B. C., Ip, M., Lau, C. B., Liu, S. L., Jolivald, C., Ganem-Elbaz, C., et al. (2011). Synergistic effects of baicalein with ciprofloxacin against NorA over-expressed methicillin-resistant *Staphylococcus aureus* (MRSA) and inhibition of MRSA pyruvate kinase. *J. Ethnopharmacol.* 137, 767–773. doi: 10.1016/j.jep.2011.06.039
- Chan, B. C. L., Margaret, I., Gong, H., Lui, S. L., See, R., Jolivald, C., et al. (2013). Synergistic effects of diosmetin with erythromycin against ABC transporter over-expressed methicillin-resistant *Staphylococcus aureus* (MRSA)



- RN4220/pUL5054 and inhibition of MRSA pyruvate kinase. *Phytomedicine* 20, 611–614. doi: 10.1016/j.phymed.2013.02.007
- Chen, Y., Liu, T., Wang, K., Hou, C., Cai, S., Huang, Y., et al. (2016). Baicalein inhibits *Staphylococcus aureus* biofilm formation and the quorum sensing system *In Vitro*. *PLoS One* 11:e153468. doi: 10.1371/journal.pone.0153468
- Chen, Y., Yuan, W., Yang, Y., Yao, F., Ming, K., and Liu, J. (2018). Inhibition mechanisms of baicalin and its phospholipid complex against DHAV-1 replication. *Poult. Sci.* 97, 3816–3825. doi: 10.3382/ps/pey255
- Costerton, J. W., Cheng, K. J., Geesey, G. G., Ladd, T. I., Nickel, J. C., Dasgupta, M., et al. (1987). Bacterial biofilms in nature and disease. *Annu. Rev. Microbiol.* 41, 435–464. doi: 10.1146/annurev.mi.41.100187.002251
- Danquah, C. A., Kakagianni, E., Khondkar, P., Maitra, A., Rahman, M., Evangelopoulos, D., et al. (2018). Analogues of disulfides from allium stipitatum demonstrate potent anti-tubercular activities through drug efflux pump and biofilm inhibition. *Sci. Rep.* 8:1150. doi: 10.1038/s41598-017-18948-w
- Druegeon, H. B., Juvin, M. E., and Bryskier, A. (1999). Relative potential for selection of fluoroquinolone-resistant *Streptococcus pneumoniae* strains by levofloxacin: comparison with ciprofloxacin, sparfloxacin and ofloxacin. *J. Antimicrob. Chemother.* 43(Suppl. C), 55–59. doi: 10.1093/jac/43.suppl\_3.55
- Fujimura, S., Sato, T., Mikami, T., Kikuchi, T., Gomi, K., and Watanabe, A. (2008). Combined efficacy of clarithromycin plus cefazolin or vancomycin against *Staphylococcus aureus* biofilms formed on titanium medical devices. *Int. J. Antimicrob. Agents* 32, 481–484. doi: 10.1016/j.ijantimicag.2008.06.030
- Ge, H. U., Xue, J. Z., Liu, J., Zhang, T., Dong, H., Duan, H., et al. (2012). Baicalin induces IFN- $\alpha/\beta$  and IFN- $\gamma$  expressions in cultured mouse pulmonary microvascular endothelial cells. *J. Integr. Agric.* 11, 646–654. doi: 10.1016/S2095-3119(12)60052-5
- Hou, W., Sun, X., Wang, Z., and Zhang, Y. (2012). Biofilm-forming capacity of *Staphylococcus epidermidis*, *Staphylococcus aureus*, and *Pseudomonas aeruginosa* from ocular infections. *Invest. Ophthalmol. Vis. Sci.* 53, 5624–5631. doi: 10.1167/iovs.11-9114
- Hu, Z., Zhou, Z., Hu, Y., Wu, J., Li, Y., and Huang, W. (2015). HZ08 reverse P-glycoprotein mediated multidrug resistance *In vitro* and *In vivo*. *PLoS One* 10:e116886. doi: 10.1371/journal.pone.0116886
- Hwang, S. M., Kim, M. S., Park, K. U., Song, J., and Kim, E. C. (2011). Tuf gene sequence analysis has greater discriminatory power than 16s rRNA sequence analysis in identification of clinical isolates of coagulase-negative staphylococci. *J. Clin. Microbiol.* 49, 4142–4149. doi: 10.1128/JCM.05213-11
- Kvist, M., Hancock, V., and Klemm, P. (2008). Inactivation of efflux pumps abolishes bacterial biofilm formation. *Appl. Environ. Microbiol.* 74, 7376–7382. doi: 10.1128/AEM.01310-08
- Le Bouter, A., Leclercq, R., and Cattoir, V. (2011). Molecular basis of resistance to macrolides, lincosamides and streptogramins in *Staphylococcus saprophyticus* clinical isolates. *Int. J. Antimicrob. Agents* 37, 118–123. doi: 10.1016/j.ijantimicag.2010.10.008
- Lewis, K. (2007). Persister cells, dormancy and infectious disease. *Nat. Rev. Microbiol.* 5, 48–56. doi: 10.1038/nrmicro1557
- Lina, G., Jarraud, S., Ji, G., Greenland, T., Pedraza, A., Etienne, J., et al. (1998). Transmembrane topology and histidine protein kinase activity of AgrC, the agr signal receptor in *Staphylococcus aureus*. *Mol. Microbiol.* 28, 655–662. doi: 10.1046/j.1365-2958.1998.00830.x
- Liu, Q., Wang, X., Qin, J., Cheng, S., Yeo, W., He, L., et al. (2017). The ATP-dependent protease ClpP inhibits biofilm formation by regulating Agr and cell wall hydrolase Sle1 in *Staphylococcus aureus*. *Front. Cell Infect. Microbiol.* 7:181. doi: 10.3389/fcimb.2017.00181
- Mahato, S., Mistry, H. U., Chakraborty, S., Sharma, P., Saravanan, R., and Bhandari, V. (2017). Identification of variable traits among the methicillin resistant and sensitive coagulase negative staphylococci in milk samples from mastitic cows in India. *Front. Microbiol.* 8:01446. doi: 10.3389/fmicb.2017.01446
- Martins, K. B., Ferreira, A. M., Pereira, V. C., Pinheiro, L., Oliveira, A. D., Ribeiro, M. L., et al. (2019). *In vitro* effects of antimicrobial agents on planktonic and biofilm forms of *Staphylococcus saprophyticus* isolated from patients with urinary tract infections. *Front. Microbiol.* 10:40. doi: 10.3389/fmicb.2019.00040
- Mlaga, K. D., Dubourg, G., Abat, C., Chaudet, H., Lotte, L., Diene, S. M., et al. (2017). Using MALDI-TOF MS typing method to decipher outbreak: the case of *Staphylococcus saprophyticus* causing urinary tract infections (UTIs) in Marseille, France. *Eur. J. Clin. Microbiol.* 36, 2371–2377. doi: 10.1007/s10096-017-3069-6
- Moore, O. A., Gao, H., Chen, A. Y., Brittain, R., and Chen, Y. C. (2016). The extraction, anticancer effect, bioavailability, and nanotechnology of Baicalin. *J. Nutr. Med. Diet Care* 2:11. doi: 10.23937/2572-3278.1510011
- Novick, R. P., Ross, H. F., Projan, S. J., Kornblum, J., Kreiswirth, B., and Moghazeh, S. (1993). Synthesis of staphylococcal virulence factors is controlled by a regulatory RNA molecule. *EMBO J.* 12, 3967–3975. doi: 10.1111/j.1365-2958.2004.04222.x
- Paharik, A. E., and Horswill, A. R. (2016). The staphylococcal biofilm: adhesins, regulation, and host response. *Microbiol. Spectr.* 4, 529–566. doi: 10.1128/microbiolspec.VMBF-0022-2015
- Polkade, A. V., Mantri, S. S., Patwekar, U. J., and Jangid, K. (2016). Quorum sensing: an under-explored phenomenon in the phylum actinobacteria. *Front. Microbiol.* 7:131. doi: 10.3389/fmicb.2016.00131
- Queck, S. Y., Jameson-Lee, M., Villaruz, A. E., Bach, T. H., Khan, B. A., Sturdevant, D. E., et al. (2008). RNAPIII-independent target gene control by the agr quorum-sensing system: insight into the evolution of virulence regulation in *Staphylococcus aureus*. *Mol. Cell.* 32, 150–158. doi: 10.1016/j.molcel.2008.08.005
- Rutherford, S. T., and Bassler, B. L. (2012). Bacterial quorum sensing: its role in virulence and possibilities for its control. *Cold Spring Harb. Perspect. Med.* 2:a12427. doi: 10.1101/cshperspect.a012427
- Sabatini, S., Piccioni, M., Felicetti, T., Marco, S. D., Manfroni, G., Pagiotti, R., et al. (2017). Investigation on the effect of known potent *S. aureus* NorA efflux pump inhibitors on the staphylococcal biofilm formation. *RSC Adv.* 7, 37007–37014. doi: 10.1039/c7ra03859c
- Sass, A., Schlachmuylders, L., Van Acker, H., Vandenbussche, I., Ostyn, L., Bové, M., et al. (2019). Various evolutionary trajectories lead to loss of the tobramycin-potentiating activity of the quorum sensing inhibitor baicalin hydrate in Burkholderia cenocepacia biofilms. *Antimicrob. Agents Chemother.* 63, e2092–e2018. doi: 10.1128/AAC.02092-18
- Smith, H. E., and Blair, J. M. A. (2014). Redundancy in the periplasmic adaptor proteins AcrA and AcrE provides resilience and an ability to export substrates of multidrug efflux. *J. Antimicrob. Chemother.* 69, 982–987. doi: 10.1371/journal.pone.0116886
- Stavri, M., Piddock, L. J., and Gibbons, S. (2007). Bacterial efflux pump inhibitors from natural sources. *J. Antimicrob. Chemother.* 59, 1247–1260. doi: 10.1093/jac/dkl460
- Thurlow, L. R., Hanke, M. L., Fritz, T., Angle, A., Aldrich, A., Williams, S. H., et al. (2011). *Staphylococcus aureus* biofilms prevent macrophage phagocytosis and attenuate inflammation in vivo. *J. Immunol.* 186, 6585–6596. doi: 10.4049/jimmunol.1002794
- Van Acker, H., and Coenye, T. (2016). The role of efflux and physiological adaptation in biofilm tolerance and resistance. *J. Biol. Chem.* 291, 12565–12572. doi: 10.1074/jbc.R115.707257
- Wang, J., Qiao, M., Zhou, Y., Du, H., Bai, J., Yuan, W., et al. (2019). *In vitro* synergistic effect of baicalin with azithromycin against *Staphylococcus saprophyticus* isolated from francolins with ophthalmia. *Poult. Sci.* 98, 373–380. doi: 10.3382/ps/pey356
- Wang, Y., Lin, Y., Wan, T., Wang, D., Lin, H., Lin, C., et al. (2019). Distribution of antibiotic resistance genes among *Staphylococcus* species isolated from ready-to-eat foods. *J. Food Drug Anal.* 27, 841–848. doi: 10.1016/j.jfda.2019.05.003
- Zoraghi, R., See, R. H., Gong, H., Lian, T., Swayze, R., Finlay, B. B., et al. (2010). Functional analysis, overexpression, and kinetic characterization of pyruvate kinase from methicillin-resistant *Staphylococcus aureus*. *Biochemistry* 49, 7733–7747. doi: 10.1021/bi100780t

**Conflict of Interest:** The authors declare that the research was conducted in the absence of any commercial or financial relationships that could be construed as a potential conflict of interest.

Copyright © 2019 Wang, Jiao, Meng, Qiao, Du, He, Ming, Liu, Wang and Wu. This is an open-access article distributed under the terms of the Creative Commons Attribution License (CC BY). The use, distribution or reproduction in other forums is permitted, provided the original author(s) and the copyright owner(s) are credited and that the original publication in this journal is cited, in accordance with accepted academic practice. No use, distribution or reproduction is permitted which does not comply with these terms.



# Increasing Prevalence of ESBL-Producing Multidrug Resistance *Escherichia coli* From Diseased Pets in Beijing, China From 2012 to 2017

Yanyun Chen<sup>1†</sup>, Zhihai Liu<sup>2,3†</sup>, Yaru Zhang<sup>1,4</sup>, Zhenbiao Zhang<sup>1</sup>, Lei Lei<sup>2</sup> and Zhaofei Xia<sup>1\*</sup>

## OPEN ACCESS

### Edited by:

Leonardo Neves de Andrade,  
University of São Paulo, Brazil

### Reviewed by:

Tiago Casella,  
Faculdade de Medicina de São José  
do Rio Preto, Brazil  
Nilton Lincopan,  
University of São Paulo, Brazil  
Rafael Antonio Casarin Penha Filho,  
São Paulo State University, Brazil

### \*Correspondence:

Zhaofei Xia  
zhaofeixiacau@126.com

† These authors have contributed  
equally to this work

### Specialty section:

This article was submitted to  
Antimicrobials, Resistance  
and Chemotherapy,  
a section of the journal  
Frontiers in Microbiology

Received: 23 August 2019

Accepted: 25 November 2019

Published: 10 December 2019

### Citation:

Chen Y, Liu Z, Zhang Y, Zhang Z,  
Lei L and Xia Z (2019) Increasing  
Prevalence of ESBL-Producing  
Multidrug Resistance *Escherichia coli*  
From Diseased Pets in Beijing, China  
From 2012 to 2017.  
Front. Microbiol. 10:2852.  
doi: 10.3389/fmicb.2019.02852

<sup>1</sup> Department of Veterinary Internal Medicine, College of Veterinary Medicine, China Agricultural University, Beijing, China, <sup>2</sup> College of Chemistry and Pharmaceutical Sciences, Qingdao Agricultural University, Qingdao, China, <sup>3</sup> Beijing Advanced Innovation Center for Food Nutrition and Human Health, College of Veterinary Medicine, China Agricultural University, Beijing, China, <sup>4</sup> The New Hope Liuhe Co., Ltd., Qingdao, China

We investigated antimicrobial resistance trends and characteristics of ESBL-producing *Escherichia coli* isolates from pets and whether this correlates with antibiotic usage in the clinic. Clinical samples containing *E. coli* from diseased cats and dogs were screened for antibiotic sensitivity and associated genotypic features. We identified 127 *E. coli* isolates from 1886 samples from dogs ( $n = 1565$ ) and cats ( $n = 321$ ) with the majority from urinary tract infections ( $n = 108$ , 85%). High rates of resistance were observed for  $\beta$ -lactams and fluoroquinolones and resistance to > 3 antibiotic classes (MDR) increased from 67% in 2012 to 75% in 2017 ( $P < 0.0001$ ). This was especially true for strains resistant to 6–9 antibiotics that increased from 26.67 to 60.71%. Increased rates in  $\beta$ -lactam use for clinical treatment accompanied these increasing resistance rates. Accordingly, the most frequently encountered subtypes were *bla*<sub>CTX-M</sub> ( $n = 44$ , 34.65%), *bla*<sub>CTX-M-65</sub> ( $n = 19$ ) and *bla*<sub>CTX-M-15</sub> ( $n = 18$ ) and *qnrB* ( $n = 119$ , 93.70%). The *bla*<sub>CTX-M</sub>-isolates possessed 36 unique pulsed field electrophoretic types (PFGEs) and 28 different sequence types (STs) in ST405 (7, 15.9%), ST131 (3, 6.8%), ST73, ST101, ST372, and ST827 (2, 4.5% each) were the most prevalent. This data demonstrated a high level of diversity for the *bla*<sub>CTX-M</sub>-positive *E. coli* isolates. Additionally, *bla*<sub>NDM-5</sub> was detected in three isolates ( $n = 3$ , 2.36%), comprised of two ST101 and one ST405 isolates, and *mcr-1* was also observed in three colistin-resistant *E. coli* with three different STs (ST6316, ST405, and ST46). Our study demonstrates an increasing trend in MDR and ESBL-producing *E. coli* and this correlated with  $\beta$ -lactam antibiotic usage for treatment of these animals. This data indicates that there is significant risk for the spread of resistant bacteria from pets to humans and antibiotic use for pets should be more strictly regulated.

**Keywords:** multidrug resistance, antimicrobial drug usage, companion animals, ESBL, *Escherichia coli*

## INTRODUCTION

Antimicrobial resistance has become one of the most challenging problems for public health and results in 700,000 deaths annually (O'Neill, 2016). Antibiotic misuse has led to the spread of antibiotic resistance genes (ARGs) in humans, food animals, pets, songbirds, water, and soil and even agricultural plants, and this represents a significant threat to public health security (Carter et al., 2018; Hartantyo et al., 2018; Anderson et al., 2019; Chen et al., 2019; Gros et al., 2019; Sanchez et al., 2019; Vikesland et al., 2019). However, novel ARGs have emerged that encode resistance to carbapenems (*bla*<sub>NDM</sub>, *bla*<sub>IMP</sub>, *bla*<sub>VIM</sub>, and *bla*<sub>KPC</sub>) (Perez and Bonomo, 2019) colistin (*mcr-1* to 9) and tigecycline (*tetX3* and *tetX4*) (Carroll et al., 2019; He et al., 2019; Wang et al., 2019). The current limited development of novel drugs and substitutes makes the use of ARGs monitoring even more important to develop comprehensive and integrative measures for antimicrobial resistance.

Over the past two decades, there has been a significant number of infections caused by bacteria expressing extended-spectrum- $\beta$ -lactamase (ESBL) and carbapenemases (Logan and Weinstein, 2017). In particular, ESBL isolates have been found in humans (Pitout and Laupland, 2008), animals, the environment (water and soil) (Runcharoen et al., 2017), meat and even vegetables (Yang et al., 2019). ESBL are becoming more common because this phenotype is being selected for by the use and exposure to  $\beta$ -lactams, especially the cephalosporins. This has generated a vicious cycle of drug resistance and decreased therapeutic effects. The increasing use of cephalosporin has been linked to *Escherichia coli* infections in pigs (Hammerum et al., 2014) and a high frequency of ESBL-producing *E. coli* was directly linked with a high consumption of third- or fourth- cephalosporins (Andersen et al., 2015).

One area that has not been thoroughly investigated is ARG presence in companion animals. This group comes in intimate contact with humans and pet contact can lead to bacterial spread to humans (Lloyd, 2007). In particular, *E. coli* is a common pathogenic agent isolated from pets (Mathers et al., 2015) and is often present in dogs and cats with urinary tract infections (UTIs), pyometra and respiratory tract infections (Karkaba et al., 2019; Moyaert et al., 2019). Multidrug resistance (MDR) *E. coli* isolates have emerged in companion animals in the United States and Europe (Morrissey et al., 2016), but data for China is lacking.

Here, we explored the effects of antibiotic dose on resistance phenotypes in pet bacterial isolates over a 6-year period. The aim of this study was to investigate the dissemination of ESBL-producing multidrug-resistant pathogens in diseased pets and the correlation between resistance rates and consumption of  $\beta$ -lactam antibiotics.

## MATERIALS AND METHODS

### Samples and Identification of Bacterial Isolates

Animal samples were collected at the Veterinary Teaching Hospital of China Agricultural University (VTH-CAU), between

January 2012 and June 2017. This study was approved by the China Agricultural University Animal Ethics Committee and the approval document (No. AW08104102-2) (see **Supplementary Information**). We collected 1886 samples from dogs (1565) and cats (321) and where some samples were gathered from different infections in the same pet. All samples consisted of urine (UTI) samples (1398, 74.1%) and samples from pyoderma (125, 6.7%), ear swabs (6.1%), effusions (115, 6.1%) and other specimens (132, 7.0%), which included pus from the uterus and soft tissue infections and several trachea lavage fluids.

Bacterial strains were recovered using blood agar and MacConkey agar plates that were incubated at 37°C for 24 h and single pink colonies were collected from each isolation plate. Subsequently, the DNA of individual clones was extracted by Fast Pure Bacteria DNA Isolation Mini Kit (Vazyme Biotech, Nanjing, China) and used as templates for PCR. PCR amplification of the 16S rDNA gene were performed for all isolates as previously described (Brianna et al., 2013), and amplicons were sequenced to confirm bacterial genus using the BLAST algorithm<sup>1</sup>.

### Antimicrobial Susceptibility Testing

Antimicrobial susceptibility of isolates was performed using the broth microdilution method according to Clinical and Laboratory Standards Institute guidelines (CLSI, 2015a). The breakpoints for other antimicrobials used the CLSI (M100-S25 or Vet01-A4/Vet01-S2) and EUCAST (CLSI, 2015b; EUCAST, 2019), where the breakpoints (R) for tigecycline, orbifloxacin, enrofloxacin, and marbofloxacin were recommended as  $\geq 0.5$ ,  $\geq 4$ ,  $\geq 4$ , and  $\geq 8$   $\mu\text{g/ml}$ , respectively. The screening panel consisted of 17 antibiotics that included ampicillin, cefazolin, cefotaxime, ceftriaxone, meropenem, amoxicillin-clavulanic acid, aztreonam, ciprofloxacin, enrofloxacin, marbofloxacin, orbifloxacin, chloramphenicol, amikacin, gentamicin, doxycycline, colistin, and tigecycline. Isolates with resistance to three or more categories of antimicrobial agents were classified as MDR (Magiorakos et al., 2012). *E. coli* ATCC 25922 was used as the quality control strain. Resistance was categorized according to Standardized International Terminology and our 17 test antibiotics were contained within nine categories (Magiorakos et al., 2012).

### Survey of Antimicrobial Drug Usage at the VTH-CAU

Antibiotic usage at VTH-CAU was recorded between January 2014 and September 2017 to correlate antibiotic usage and the resistance of *E. coli* isolates for each study animal.

### ARG Detection

Screening of *E. coli* isolates for ARG types was conducted using PCR for each isolate depending on the antibiotic resistance phenotype. The ARGs we examined were (1) carbapenemase genes *bla*<sub>NDM</sub>, *bla*<sub>IMP</sub>, *bla*<sub>KPC</sub>, *bla*<sub>VIM</sub>, *bla*<sub>OXA</sub>, *bla*<sub>AIM</sub>, *bla*<sub>BIC</sub>, *bla*<sub>DIM</sub>, *bla*<sub>GIM</sub>, *bla*<sub>SIM</sub>, and *bla*<sub>SPM</sub> including *bla*<sub>NDM</sub> and *bla*<sub>CTX-M</sub> subtyping (Poirel et al., 2011), (2)  $\beta$ -lactamase genes

<sup>1</sup><https://www.ncbi.nlm.nih.gov/>



*bla*<sub>SHV</sub>, *bla*<sub>TEM</sub>, and *bla*<sub>CTX-M</sub> (Casella et al., 2018), (3) plasmid-mediated AmpC  $\beta$ -lactamase genes *bla*<sub>MOX</sub>, *bla*<sub>CMY</sub>, *bla*<sub>LAT</sub>, *bla*<sub>DHA</sub>, *bla*<sub>ACC</sub>, *bla*<sub>MIR</sub>, *bla*<sub>ACT</sub>, and *bla*<sub>FOX</sub> (Perez-Perez and Hanson, 2002), (4) colistin resistance genes *mcr-1-8* (Rebelo et al., 2018; Wang X. et al., 2018; Yang et al., 2018; Carroll et al., 2019), and (5) plasmid-mediated quinolone resistance (PMQR) genes *qnrA*, *qnrB* and *qnrS* including whether the *gyrA* and *parC* genes in the quinolone resistance determining region (QRDR) were mutated (Komp et al., 2003; Kraychete et al., 2016; Onseedaeng and Ratthawongjirakul, 2016). PCR primers used for screening are shown in **Supplementary Table S1**. All PCR amplicons were sequenced to confirm gene identity.

## Transconjugation Assays and Whole Genome Sequencing

Conjugation assays were performed between clinical isolates and *E. coli* J53 to evaluate whether *bla*<sub>NDM</sub> and *mcr-1* were mobilizable. Transconjugants were selected on MacConkey agar containing 100 mg/L sodium azide and 1 mg/L meropenem or colistin. Presumptive transconjugants were identified using PCR screening for *bla*<sub>NDM</sub> and *mcr-1*.

Transconjugant DNA was extracted and used for whole genome sequencing (WGS). A library of 250-bp paired-end was constructed by using a NEXT Ultra DNA Library Prep kit (New England Biolabs, Beverly, MA, United States) and sequenced using an Illumina HiSeq 2500 system at Bionova Biotech (Beijing, China). Raw data was *de novo* assembled using the SPAdes algorithm v.3.10.0. ARGs and plasmid incompatibility groups were analyzed using ResFinder v.3.2<sup>2</sup>, RASTtk v.2.0<sup>3</sup> and PlasmidFinder 2.1<sup>4</sup>, respectively.

## PFGE and MLST Typing of *E. coli* Strains

The clonal relatedness of *bla*<sub>CTX-M</sub> positive was determined using pulsed-field gel electrophoresis (PFGE) typing conducted as previously described (Tenover et al., 1995). PFGE patterns were visually inspected and gel images were analyzed using InfoQuest FP software (Biorad, Hercules, CA, United States). Group analysis of PFGE profiles was performed using the Dice coefficient and the unweighted pair group method with arithmetic means. Simultaneously, multilocus sequence typing (MLST) analysis was conducted using the following *E. coli* gene set: *recA*, *adk*, *fumC*, *icd*, *mdh*, *purA*, and *gyrB*. The results were interpreted using the MLST database<sup>5</sup>. Sequence types (STs) of 131 clades in *E. coli* isolates were also screened using multiplex conventional PCR assays as previously described (Matsumura et al., 2017).

## Statistical Analysis

Tests of statistical significance was determined using Fisher's exact test with Yates continuity correction in GraphPad Prism 6 (San Diego, CA, United States) and the level of significance

was set at  $P < 0.05$ . All figures were designed by ggplot2<sup>6</sup> and GraphPad Prism 6.

## RESULTS

### Samples and *E. coli* Isolates

We isolated 127 *E. coli* strains that included 108 (85.0%) urine and 5 (3.9%) uterus, 4 (3.1%) abdominal fluid, 3 (2.4%) pyoderma, 2 (1.6%) soft tissue infectious sites, and 1 (0.8%) from synovial fluid. The *E. coli* isolation rate was 6.73% (127/1886) and ranged from 4.42 to 9.41% per year. Resistance to  $\beta$ -lactams was extremely high for these isolates and included resistance to ampicillin (77.9%), cefotaxime (58.3%) and ceftriaxone (58.3%) and cefazolin (65.35%) with the exception of amoxicillin + clavulanic acid (22.8%) (**Supplementary Tables S2, S3**).

The range of resistance rates was narrow for ampicillin (68.42–92.86%) compared with cefotaxime (36.67–72.73%), ceftriaxone and cefotaxime (36.67–72.73%), cefazolin (43.33–86.36%), and amoxicillin + clavulanic acid (10.00–27.27%). These data demonstrated a significant increase in resistance rates from 2012 to 2017 and the cefotaxime, ceftriaxone, cefazolin, and amoxicillin + clavulanic acid rates more than doubled (**Supplementary Figure S1** and **Supplementary Table S3**). The aztreonam resistance rate showed the greatest variability and was maximal in 2014 (71.43%) and minimal in 2012 (13.33%). We also found high rates of resistance to the four fluoroquinolones we tested (52.76–57.48%) except for 2013 (36.84%) (**Supplementary Table S3**). The other resistance groups we examined displayed irregular trends or slight increases over the 2012–2017 study period. Notably, almost all isolates showed high susceptibility to the “last-resort” antibiotics colistin, meropenem, and tigecycline and only 5 (3.94%) of our isolates were resistant to colistin and 3 (2.4%) to meropenem (**Figure 1** and **Supplementary Table S3**).

The MDR values for our isolates from these pets were high with an overall MDR rate that increased 73.2% from 2012 to 2017 ( $n = 93$ ). These MDR rates from 2012 to 2017 were 66.67, 68.42, 64.29, 85.71, 81.82, and 75.00% in 2017, respectively ( $P < 0.0001$ ) (**Supplementary Table S4**). Specifically, MDR prevalence in 6–9 antimicrobial categories exhibited an obvious increase (**Figure 1** and **Supplementary Table S4**). The MDR of our 44 CTX-M-producing *E. coli* was greater than for the non-CTX-M-expressing isolates (**Supplementary Figures S5a,b**). Moreover, all *bla*<sub>CTX-M</sub>-positive *E. coli* were MDR strains possessing resistance to the penicillins [ampicillin (AMP)], non-extended spectrum cephalosporins [cefazoline (CZO)], extended-spectrum cephalosporins [cefotaxime (CTX) and ceftriaxone (CRO)]. The most common MDR pattern was resistance to quinolones (ciprofloxacin, enrofloxacin, orbifloxacin, and marbofloxacin) and the tetracyclines (doxycycline) and aminoglycosides (gentamycin) +  $\beta$ -lactams (AMP, CZO, CTX, and CRO). When this data was viewed solely by the number of antibiotics per MDR isolate, resistance rates to 11–17 antibiotics

<sup>2</sup><https://cge.cbs.dtu.dk>

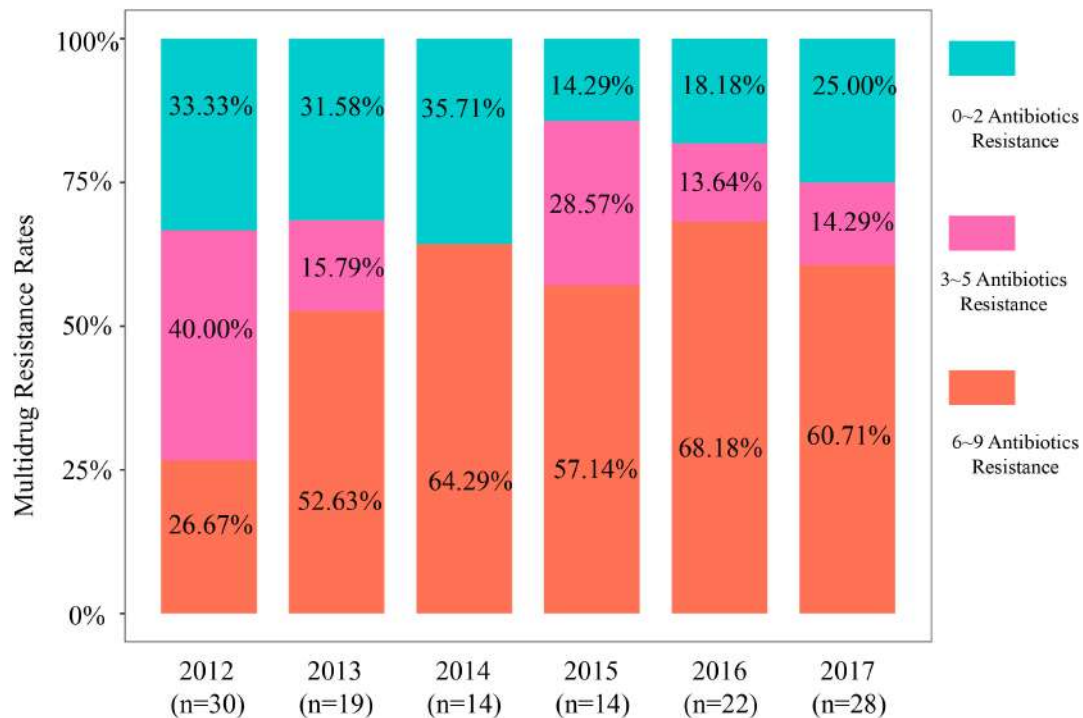
<sup>3</sup><http://rast.nmpdr.org/rast.cgi>

<sup>4</sup><https://cge.cbs.dtu.dk/services/PlasmidFinder/>

<sup>5</sup>[http://enterobase.warwick.ac.uk/species/ecoli/allele\\_st\\_search](http://enterobase.warwick.ac.uk/species/ecoli/allele_st_search)

<sup>6</sup><https://ggplot2.tidyverse.org/>





**FIGURE 1** | Multidrug resistance rates of 127 isolates based on antimicrobial category from 2012 to 2017.

increased significantly over the study period from 13.3, 31.6, 35.7, 35.7, 50.0, and 53.6% from 2012 to 2017, respectively (**Supplementary Figure S2** and **Supplementary Table S5**).

We performed a correlation analysis between antibiotic usage and the rate of antibiotic resistance between 2014 and 2017. Amoxicillin-clavulanic acid ( $1.3 \times 10^7$  mg/yr), doxycycline ( $5.7 \times 10^6$  mg/yr), ampicillin ( $1.9 \times 10^6$  mg/yr), and enrofloxacin ( $8.1 \times 10^5$  mg/yr) were the most widely used antibiotics at the animal facility. With the widespread use of FQs in VTH-CAU, >50% of the clinical *E. coli* isolates showed resistance to FQs since 2012. Interestingly, even though fluoroquinolone usage had decreased dramatically, resistance rates to this antibiotic class remained high. In addition, the use of  $\beta$ -lactams, including amoxicillin-clavulanic acid, ampicillin, and ceftriaxone, had increased over the study period and was positively correlated with an increase in  $\beta$ -lactam resistance that was also related to dosage. Meropenem and imipenem were not used at the facility and we found no resistance from 2012~2015 although three resistant *E. coli* were detected in 2016 (**Supplementary Figure S3**).

## ARG Prevalence and NDM Plasmid Characterization

In our study, we identified 10 ARG types and mutations in *gyrA* and *parC*. The *qnrB* gene was present in 119 (93.70%) of the isolates (**Supplementary Figure S4**). In the *gyrA* gene of 77 quinolone-resistant isolates, 38 carried the mutations S83L and D87N, 9 S83L and D87Y, 2 D87N, 3 D87G, and 14 S83L (**Supplementary Table S6**). In the *parC* gene we found the

mutations S80I (22 isolates), S80I and E84G (14 isolates) and S80I and E84V (8 strains). The ESBL and pAmpC-containing isolates harbored *bla*<sub>CTX-M</sub> ( $n = 44$ , 34.65%), *bla*<sub>SHV</sub> ( $n = 21$ , 16.55%), *bla*<sub>OXA</sub> ( $n = 9$ , 7.09%), *bla*<sub>CMY</sub> ( $n = 12$ , 9.45%), *bla*<sub>FOX</sub> ( $n = 4$ , 3.15%), and *bla*<sub>NDM</sub> ( $n = 3$ , 2.36%). CTX-M alleles were assigned to two main clusters; CTX-M-14 and -15 including seven CTX-M genotypes (-14, -15, -64, -65, -116, -127, and -174) where CTX-M-65 (43.18%,  $n = 19$ ) and CTX-M-5 (40.91%,  $n = 18$ ) predominated. All 44 *bla*<sub>CTX-M</sub>-positive isolates were resistant to cefotaxime and ceftriaxone and were classified as MDR. When compared with *bla*<sub>CTX</sub>-negative isolates, the *bla*<sub>CTX</sub>-positive isolates showed significantly greater resistance to second and third-generation cephalosporins, the fluoroquinolones, aztreonam, doxycycline, gentamicin, and chloramphenicol ( $P < 0.05$ ) (**Table 1** and **Supplementary Figure S5**). The only observed carbapenemase gene we identified was NDM-5 that was present in three isolates 16DU02, 16DF03, and 16XXI8 and all showed resistance to meropenem and all were collected from dogs in 2016. Of note, 16DU02 and 16DF03 were isolated from same dog but the samples were isolated from urine and an abdominal effusion, respectively, and they carried same genes *bla*<sub>NDM-5</sub>, *bla*<sub>TEM</sub>, *bla*<sub>CTX-M-65</sub>, and *qnrB*. The 16XXI8 isolate recovered from dog urine possessed *bla*<sub>NDM-5</sub>, *bla*<sub>TEM</sub>, *bla*<sub>CTX-M-15</sub>, *bla*<sub>OXA</sub>, and *qnrB*. Additionally, the colistin resistance gene *mcr-1* was detected in three *bla*<sub>CTX-M</sub> positive *E. coli* while other *mcr* variants were undetected.

We further examined our *mcr-1* and *bla*<sub>NDM</sub> isolates and tested whether these genes were present on mobile elements. In our conjugation tests, only *bla*<sub>NDM</sub> in three *E. coli* isolates

**TABLE 1** | Minimum inhibitory concentration (MIC) of antimicrobial agents for clinical *E. coli* isolates from cats and dogs in Beijing, China, 2012–2017 ( $n = 127$ )<sup>†</sup>.

Antimicrobial agents	<i>bla</i> <sub>CTX</sub> Positive <i>E. coli</i> ( $n = 44$ )			<i>bla</i> <sub>CTX</sub> Negative <i>E. coli</i> ( $n = 83$ )			P-value <sup>†</sup>
	MIC50 (μg/mL)	MIC90 (μg/mL)	Resistance, %	MIC50 (μg/mL)	MIC90 (μg/mL)	Resistance, %	
Ampicillin	>128	>128	100.0	>128	>128	63.8	<0.0001**
Cefazolin	>128	>128	100.0	8	>128	47.0	<0.0001**
Cefotaxime	>128	>128	100.0	≤0.125	>128	31.3	<0.0001**
Ceftriaxone	>128	>128	100.0	≤0.125	>128	31.3	<0.0001**
Meropenem	≤0.125	≤0.125	6.8	≤0.125	≤0.125	0.0	0.0397*
Amoxicillin-clavulanic acid	16/8	64/32	27.3	16/8	32/16	14.4	0.0972
Aztreonam	32	>128	75.0	≤0.125	>128	28.9	<0.0001**
Colistin	≤0.125	≤0.125	6.8	≤0.125	≤0.125	1.2	0.1195
Doxycycline	16	32	59.1	8	32	32.5	0.0048**
Tigecycline	≤0.125	≤0.125	0.0	≤0.125	≤0.125	0.0	1.0000
Gentamycin	>128	>128	77.3	8	>128	36.1	<0.0001**
Amikacin	8	>128	27.3	8	>128	13.2	0.0575
Chloramphenicol	16	>128	50.0	8	128	24.1	0.0052*
Ciprofloxacin	16	>128	81.8	0.25	64	37.3	<0.0001**
Enrofloxacin	32	128	81.8	0.25	64	39.7	<0.0001**
Orbifloxacin	128	>128	81.8	4	>128	38.6	<0.0001**
Marbofloxacin	16	64	81.8	0.5	32	37.3	<0.0001**

<sup>†</sup>The 127 isolates consisted of 107 isolates from urinary tract, 5 from uterus, 4 from abdominal fluid, 1 from synovial fluid, and 10 from pyoderma and soft tissue. <sup>†</sup>P-values were determined by Fisher's exact test. \* $P < 0.05$ ; \*\* $P < 0.01$ .

were successfully transferred at frequencies of  $4.86 \times 10^{-8}$ – $8.02 \times 10^{-7}$ . Two complete 46,161 bp *bla*<sub>NDM-5</sub>-harboring plasmids pP16NDM-502 (MN701974) and pP16NDM-503 (MN701975) were obtained from strains 16DU02 and 16DF03 transconjugants, respectively. The backbone sequences were assembled and contigs and gaps were identified by additional PCR and sequence analyses. The other NDM-1-carrying plasmid was unsuccessfully assembled because of fragmentary and short contigs (**Supplementary Figure S6**). The two completely assembled plasmids were all in the IncX3 replication group. In addition, *bla*<sub>NDM-5</sub> was contained within an insertion sequence (IS) cassette ( $\Delta$ IS<sub>Aba125</sub>-IS5-*bla*<sub>NDM</sub>-*ble*-*trpF*-*dsbC*-IS26). *bla*<sub>NDM-5</sub> and *ble*<sub>MBL</sub> were the only ARGs present in the two plasmids. Homology analysis revealed that pP16NDM-502 and pP16NDM-503 were ≥ 99% identical to the following IncX3 *bla*<sub>NDM</sub> plasmids: (i) pNDM\_MGR194 (KF220657) from a *Klebsiella pneumoniae* human isolate in India, (ii) p1079-NDM (MG825384) from a chicken *E. coli* isolate in China. (iii) pL65-9 (CP034744) from *E. coli* in goose in China, (iv) pZHDC40 (KY041843) from *E. coli* human isolate in China, (v) pQDE2-NDM (MH917280) from *K. pneumoniae* human isolate in China, (vi) pCRCB-101\_1 (CP024820) from a *Citrobacter freundii* human isolate in Korea (vii) p128379-NDM (MF344560) from *Enterobacter hormaechei* from a human sample in China and (viii) pAD-19R (KX833071) from a chicken *E. coli* isolate in China (**Supplementary Figure S6**). We were unable to transfer the *mcr-1* gene by conjugation in three separate tests and we could not assemble a complete plasmid sequence. However, no complete plasmid sequence of *mcr-1* was successfully assembled by using three clinical isolates genomes. Although the analysis of incompatibility group in three clinical isolates genomes by analyzed PlasmidFinder-2.0 Serve revealed they possessed

IncFIB, IncFIC, IncFII, and IncHI2 typical fragments, all *mcr-1* genes weren't located on those fragments (data not showed).

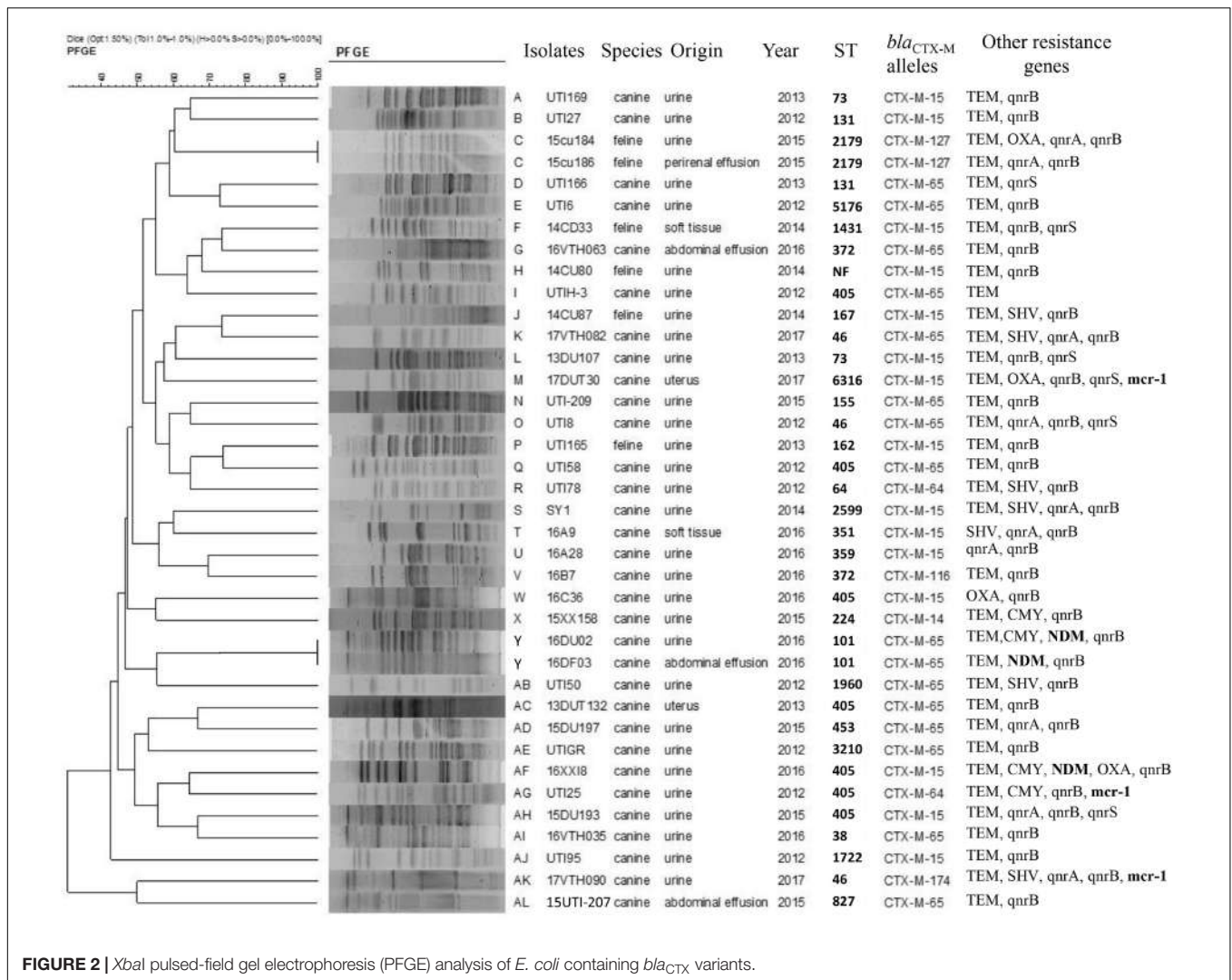
## PFGE and MLST Typing

In our group of 127 *E. coli* isolates, most ( $n = 109$ , 85.8%) were successfully characterized by PFGE typing and included 38/44 *bla*<sub>CTX-M</sub>-positive isolates. These 38 isolates were obtained from cats (6) and dogs (32) and could be subdivided into 36 unique PFGE patterns. Interestingly, two isolates obtained from urine (15cu184) and perirenal effusion (15cu186) samples showed identical PFGE patterns and carried the same *bla*<sub>CTX-M-127</sub> subtype but were recovered from different animals (**Figure 2**).

We also found universality in MLST types and identified 28 different STs although 1 isolate failed to type. The most prevalent were ST405 (7, 15.9%), ST131 (3, 6.8%) ST73, ST101, ST372, and ST827 (2, 4.5% each). All ST405 strains were collected from dogs but in different years. Three ST131 isolates (UTI-27, UTI-166, and DU40) belonged to clade C1, in which UTI-27 and DU40 were assigned as C1-nM27, and UTI-166 as C1-M27. The *bla*<sub>CTX-M-65</sub> and *bla*<sub>CTX-M-15</sub> positive *E. coli* exhibited the greatest ST diversity and contained 13 and 14 STs, respectively. Additionally, three *bla*<sub>NDM-5</sub>-positive isolates belonged to ST405 ( $n = 1$ ) and ST101 ( $n = 2$ ) and three carrying-*mcr-1* *E. coli* were classified as three different STs: ST6316, ST405, and ST46 (**Figure 3**).

## DISCUSSION

In this study, we investigated the antibiotic resistance profiles and trends in MDR *E. coli* isolates collected from diseased dogs and cats. We identified 127 *E. coli* isolates and most were



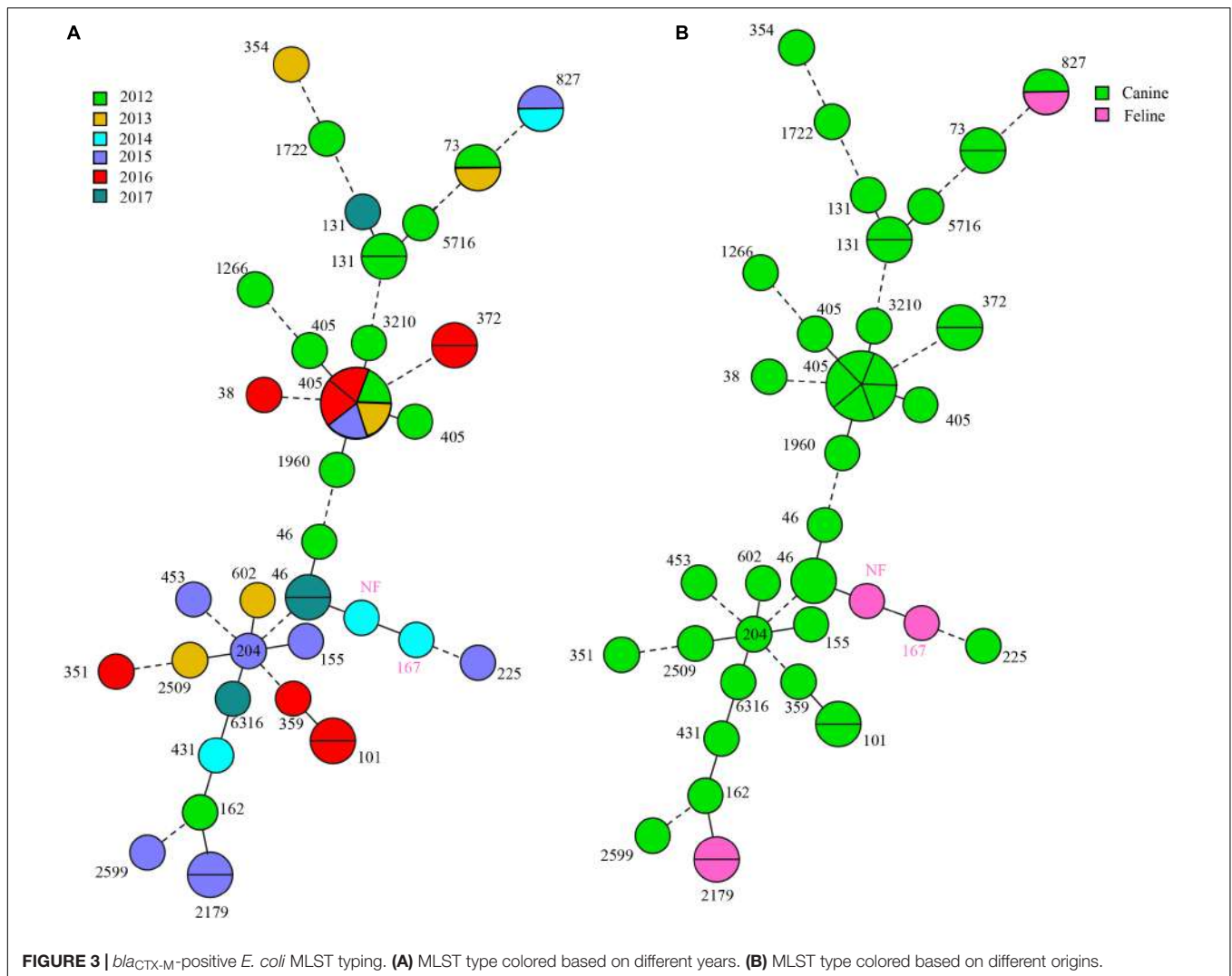
**FIGURE 2** | *Xba*I pulsed-field gel electrophoresis (PFGE) analysis of *E. coli* containing *bla*<sub>CTX</sub> variants.

associated with UTI (84.2%) accounting for 20.4% (108/529) of the confirmed bacterial UTI cases. In contrast, in the United States nearly 30% of UTI isolates from pets were *E. coli* (Ling et al., 2001; Hall et al., 2013). Previous studies in European countries based on 22,256 isolates from dogs and cats with UTI between 2008 and 2013 showed that *E. coli* was the most common pathogen in both dogs (59.50%) and cats (59.31%) (Marques et al., 2016). Isolation of *E. coli* from the respiratory tract is much less frequent and occurred in 10–15% of dog respiratory tract infections (Rheinwald et al., 2015; Morrissey et al., 2016).

Our 127 clinical *E. coli* isolates showed high prevalence rates of resistance to  $\beta$ -lactams (58.3–77.9%) and quinolones (52.8–57.4%). This pattern was quite different from the data of dog and cat *E. coli* isolates from United States that identified resistance to ampicillin at 40%, cephalexin 98% and doxycycline at 100% (Thungrat et al., 2015). An Australian study revealed that canine clinical *E. coli* isolates had low rates of resistance to quinolones (9.1–9.3%) and among 392 canine UTI isolates, 9.9–10.2% were resistant to third-generation cephalosporins (Saputra et al., 2017).

In the current study, the overall MDR frequency of 73.2% was higher than that observed in studies from the United States (52%) and Poland (66.8%) (Rzewuska et al., 2015; Thungrat et al., 2015). In contrast, a European multi-centre study on AMR of various bacteria isolated from companion animals with UTIs showed a much lower frequency of MDR among *E. coli* isolates (1.4–29.7%). The high MDR rates observed in the current study indicated that currently available antimicrobial treatment options for *E. coli* infections in companion animals are limited. We also identified an increase in *E. coli* MDR prevalence between 2012 and 2017 and increased rates of third-generation cephalosporins and amoxicillin-clavulanic acid usage was accompanied by increased AMR and MDR rates. Based on these findings, we speculate that the rising incidence of multidrug-resistant *E. coli* might be associated with the heavy use of these antibiotics in companion animals at the hospital.

Among the 44 CTX-M-producing *E. coli* isolates in this study, *bla*<sub>CTX-M-65</sub> (43.2%) and *bla*<sub>CTX-M-15</sub> (40.9%) were the most *bla*<sub>CTX-M</sub> variants. Currently, more than 220 CTX-M-lactamases have been reported and clustered into five subgroups, containing



CTX-M-1, -2, -8, -9, and -25 depending on amino acid sequence homology (Peirano and Pitout, 2019). CTX-M-15 (CTX-M-1) is the most frequent CTX-M variant worldwide (Karim et al., 2001) especially in South-East Asia, China, South Korea, and Japan (Peirano and Pitout, 2019). Since 2000, *bla*<sub>CTX-M-15</sub> has emerged worldwide and is the most prevalent ESBL globally (Peirano and Pitout, 2019). The spread of *bla*<sub>CTX-M-15</sub> contributed to the dissemination of MDR bacterial isolates in animals but also in humans; a significant public health concern (Mugnaioli et al., 2006; Canton et al., 2012; Liu et al., 2016b). While the *bla*<sub>CTX-M-15</sub> variant was also common in canine *E. coli* isolates from both Shanxi, China ( $n = 40$ ) and the United States ( $n = 50$ ), *bla*<sub>CTX-M-123</sub> predominated in those studies (Liu et al., 2016a,b). The *bla*<sub>CTX-M-65</sub> was the most prevalent subtype we found and is frequently detected in *Salmonella* isolates. In a previous study, the *bla*<sub>CTX-M-65</sub> gene ( $n = 131$ ) was identified among 153 ESBL-positive *Salmonella* isolates from poultry slaughterhouses ( $n = 121$ ) and humans ( $n = 10$ ) (Bai et al., 2016). Similarly, a study on chickens and pigs in China surveyed seven *bla*<sub>CTX-M-65</sub> among *Salmonella* isolates (Zhang et al., 2016). All these studies

indicated more frequent occurrences in China and is supported by data from 2005 to 2017 in another study (Bevan et al., 2017). Additionally, *bla*<sub>CTX-M-55</sub> prevalence has increased in recent years in China among animal and human isolates, although not in our present study. Conversely, *bla*<sub>CTX-M-14</sub> has a remarkable reduction based on data for China (Bevan et al., 2017). We found only one *bla*<sub>CTX-M-14</sub> isolate while this gene is globally present (Bevan et al., 2017). Although other *bla*<sub>CTX-M</sub> variants, such as *bla*<sub>CTX-M-64</sub>, -174, -116, and -127 rarely occur, their presence in diseased pets suggests that diversity and evolution of *bla*<sub>CTX-M</sub> had occurred in these companion animals.

All *bla*<sub>CTX</sub>-carrying isolates in the current study had MDR profiles and showed high resistance rates to  $\beta$ -lactams, quinolones, doxycycline, gentamycin, and chloramphenicol. This suggested that other resistance genes may be co-transferred with *bla*<sub>CTX</sub>, making it even more difficult to eliminate the spread of MDR. Most *bla*<sub>CTX-M</sub> positive strains in other studies were also resistant to quinolones due to topoisomerase modifications of *qnr* genes (Lahlaoui et al., 2014) as we found in the present study. Additionally, mutations in *gyrA*



and *parC* also can be responsible for quinolone resistance. Our results showed S83L and D87 alterations to N, Y, G generated in *gyrA* were commonly associated with resistance to fluoroquinolones and mostly generate high level resistance (Basu and Mukherjee, 2019).

Only three *E. coli* isolates containing *bla*<sub>NDM-5</sub> were identified in our study animals with UTI in late 2016. Five (3.94%) were colistin resistance and three carried *mcr-1*. Previous reports implied that the transmissible *bla*<sub>NDM</sub> and *mcr-1*-carrying plasmids play a major role in the dissemination of these genes (Wang et al., 2017). For example, *mcr-1*, initially named as mobile colistin resistance gene, was generally considered as mediating the rapid spread of bacterial colistin resistance worldwide due to its mobile plasmid association. In contrast, we found that *mcr-1* could not be mobilized by conjugation. In a previous study, 14/23 *mcr-1*-positive isolates were successfully transferred and six plasmids were non-transferable (Zhou et al., 2017). The *mcr-1* gene was located in the chromosome of *E. coli* from a goose isolate (Lu et al., 2019). Furthermore, IS*Apl1* transposon can mediate *mcr-1* transfer from chromosome to plasmids and this is the reason for its current global distribution (Wang R. et al., 2018). So, *mcr-1*-carried in a non-transferable plasmid or chromosome may be spread by IS*Apl1* or others transposons. In our study, we could not assemble a complete plasmid sequence for the *mcr-1* genomic data; and *mcr-1* genes were not present on those plasmid fragments and may be chromosomal. There are nine variants of *mcr* and we identified only *mcr-1* (Carroll et al., 2019). This gene is the most prevalent variant globally and has been detected in almost 40 countries/regions across five continents in both involving developed and non-developed countries. Moreover, the *mcr-1* gene was found in more than 11 bacterial species and in diverse locations such as rivers, public beaches, well water, wastewater, hospital sewage, foods (vegetables and meats), animals (wild birds, housefly/blowfly, cattle, pigs, poultry, and companion animals) (Feng, 2018). Our study provided new evidence for the above claim and we identified three *mcr-1* positive *E. coli* in diseased pets. Recently, carbapenem-resistant Enterobacteriaceae (CRE) have posed a threat to humans and animals because they exhibited resistance to most  $\beta$ -lactams including carbapenems, further compromising treatment of MDR infections (Gupta et al., 2011; Potter et al., 2016).

Carbapenem-resistant Enterobacteriaceae is mediated largely by the production of carbapenemase especially for NDM isolates. NDM-5, an NDM-1 variant, exhibited increased enzyme activity to carbapenems (Rogers et al., 2013) and its gene *bla*<sub>NDM-5</sub> has been reported worldwide (Khan et al., 2017) and is the most prevalent variant in China (Shen et al., 2018). In support of this, 84 (52%) NDM-5-producing *E. coli* were collected from 161 *bla*<sub>NDM</sub> carrying CRE in chickens (Wang et al., 2017). Our study revealed that pets have become a reservoir of NDM-5-producing *E. coli*. The *bla*<sub>NDM-5</sub> gene is also associated with different plasmids such as IncFIA/B, IncFII, IncN, and IncX3 (Sun et al., 2015; Tyson et al., 2019; Zhang et al., 2019) and IncX3 was the dominant type (Li et al., 2018; Zhang et al., 2019). Similarly, the *bla*<sub>NDM-5</sub>-harboring plasmid was assigned to the IncX3 type, and their transferability was

confirmed in our study indicating a risk of *bla*<sub>NDM-5</sub> plasmid transfer between bacteria. However, further studies should be conducted to determine the origins of *bla*<sub>NDM</sub> and *mcr-1* in the *E. coli* isolates from companion animals at the hospital. This will be helpful in designing measures to control the spread of MDR isolates.

All CTX-M-producing *E. coli* in our study displayed a diversity of PFGE patterns and STs demonstrating that *bla*<sub>CTX-M</sub> encoding ESBLs are present in diverse *E. coli*. Additionally, our diseased pet samples were from animals having no prior contact suggesting that clonal spread had a low frequency and it was not likely that clonal spread of *bla*<sub>CTX-M</sub>-positive *E. coli* occurred between the pets. But ESBL or other resistance genes can transfer between different *E. coli* by transferable genetic elements, as previously reported (Kim et al., 2019). However, two *E. coli* isolates (15cu184 and 15cu186) from same cat but different sample sources shared the same PFGE, ST, and *bla*<sub>CTX-M-127</sub> types, indicating that clonal spread may be occurring. It was reported that dissemination of Enterobacteriaceae can occur between pets and their owners by both horizontal transfer and clonal expansion (Yao et al., 2016).

In our study, ST405 *E. coli* ( $n = 7$ ) was the most prevalent isolates carrying *bla*<sub>CTX-M</sub>. They presented different *bla*<sub>CTX-M</sub> subtype genes including *bla*<sub>CTX-M-15</sub> ( $n = 3$ ), *bla*<sub>CTX-M-65</sub> ( $n = 3$ ), and *bla*<sub>CTX-M-64</sub> ( $n = 1$ ). In a clinical study from King Abdulaziz Medical City (KAMC) in Riyadh (Alghoribi et al., 2015), six ST405 *E. coli* harboring *bla*<sub>CTX-M</sub> were detected in UTI and ST405 ( $P \leq 0.02$ ) were significantly associated with ESBL production. ST405 extended-spectrum  $\beta$ -lactamase-producing *E. coli* (ESBL-EC) was also detected in animals, in which one ST405 ESBL-EC was screened in barbary macaques (*Macaca sylvanus*) in Algeria, notably, it held the *mcr-1*, *bla*<sub>TEM-1</sub>, and *qnrB19* genes and *bla*<sub>CTX-M-15</sub> (Bachiri et al., 2017). We observed a similar pattern and a UTI25 (ST405 ESBL-EC) isolate harbored *mcr-1*, *bla*<sub>TEM</sub>, *qnrB*, and *bla*<sub>CTX-M-64</sub>. Additionally, ST405 ESBL-EC (16XXI8) carried *bla*<sub>NDM-5</sub>, *bla*<sub>OXA</sub>, *bla*<sub>TEM</sub>, and *qnrB*. These data indicated ST405 ESBL-EC has become the vector of multiple resistance genes, containing carbapenem- and colistin-resistance genes. In a Sweden project, ST405 ESBL-EC was also found in UTI from a diseased cat (Bogaerts et al., 2015). We found seven ST405 ESBL-EC that were all recovered from dogs but in different years. Thus, companion animals already contain the hosts of ST405 ESBL-EC. In addition, except for ST405, we also identified two ST101 *E. coli* carrying *bla*<sub>NDM-5</sub> (16DU02 and 16DF03). They were from the same animal source and possessed the same ST, PFGE, plasmid type and *bla*<sub>NDM-5</sub>, suggesting a clonal origin. ST101 was reported to be strongly associated with the NDM genotype although most were NDM-1 rather than NDM-5. Recently, five *bla*<sub>NDM-5</sub>-positive *E. coli* were identified associated with ST101 and ST1196 (Ranjan et al., 2016; Aung et al., 2018). In contrast, only two ST101 NDM-5-producing *E. coli* were observed in another study and most were ST167 and ST410 but were clonally spread in a hospital (Sun et al., 2019). This was similar to our study and suggested that ST101 may be becoming the most important clone for dissemination of *bla*<sub>NDM-5</sub>, similar to ST167 and ST410.

The clone ST131 was observed in three *E. coli* isolates. This is the predominant *E. coli* lineage in extraintestinal pathogenic *E. coli* (ExPEC) isolates worldwide and are associated with global community and nosocomial dissemination (Marie-Hélène et al., 2014). Currently, ST131 is classified as three clades: A, B, and C (Peirano and Pitout, 2019). In our study, all ST131 belonged to clade C and ST131 is in clade C 80% of the time (Peirano and Pitout, 2019). Clade C evolved from clade B and further evolved into C1 and C2. Recently, a new C1 subclade C1-M27 was identified in animal and human (Matsumura et al., 2016), including companion animals (Melo et al., 2019), and we found one C1-M27 subclades that are rare in China, but prevalent in Europe (Ghosh et al., 2017; Merino et al., 2018). The other ST131 belonged to subclade C1-nM27. C1 is commonly associated with quinolone resistance, in agreement with our results. The ESBL-EC isolates were commonly associated with ST131, where 40–80% of ESBL ExPEC belong to ST131 *E. coli* (Marie-Hélène et al., 2014), and CTX-15 was the most prevalent ESBL enzyme in ST131 ESBL-EC (Alghoribi et al., 2015). Our study demonstrated that *bla*<sub>CTX-M-65</sub> was found in two ST131 ESBL-EC and one *bla*<sub>CTX-M-15</sub> isolate. Almost all ST131 isolates were resistant to fluoroquinolones, especially for ESBL CTX-M-15 isolates (Marie-Hélène et al., 2014). We found similar results that almost all CTX-M ESBL isolates (40/44) were resistant to quinolones. ST131 ESBL *E. coli* possessed more frequent resistance to amikacin than non-ST131 ESBL isolates, but showed more frequent susceptibility to gentamicin or trimoxazole. On the other hand, the non-ESBL isolates such as *E. coli* ST131 were more frequently resistant to fluoroquinolones than non-ST131 isolates. Therefore, the resistance to quinolones may be associated with ST131 rather than ESBL presence (Marie-Hélène et al., 2014). These findings indicated that quinolones resistance may have been the predecessor of ESBL enzymes. We found that ST131 and ST405 were correlated to ESBL production as previously found (Alghoribi et al., 2015). Other STs in our study occurred infrequently. Recently, a water sample study revealed that ESBL-producing *E. coli* isolates were present 15 different STs (ST10, ST46, ST48, ST58, ST69, ST101, ST117, ST131, ST141, ST288, ST359, ST399, ST405, ST617, ST4530) (Said et al., 2016). We detected ST46, ST101, ST131, ST359, and ST405 in our study. Multiple ST types (ST46, ST1286, ST10, ST29, ST101, and ST354) have also been found in chickens and they carried *mcr-1* and produced ESBLs (Wu et al., 2018). In our work, 28 diverse STs in ESBL-EC were found.

## CONCLUSION

We found a high prevalence of MDR *E. coli* isolates from diseased cats and dogs in Beijing and this rate has markedly

## REFERENCES

Alghoribi, M. F., Gibreel, T. M., Farnham, G., Al Johani, S. M., Balkhy, H. H., and Upton, M. (2015). Antibiotic-resistant ST38, ST131 and ST405 strains are the leading uropathogenic *Escherichia coli* clones in Riyadh, Saudi Arabia. *J. Antimicrob. Chemother.* 70, 2757–2762. doi: 10.1093/jac/dkv188

increased over the last 6 years. The widespread use of third-generation cephalosporins and amoxicillin-clavulanic acid at the veterinary teaching hospital has likely contributed to the increasing frequency of  $\beta$ -lactam resistance in these isolates. These strains carried *bla*<sub>CTX</sub>, *bla*<sub>NDM-5</sub>, and *mcr-1* and most possessed an MDR profile. Diversity analysis of the PFGE patterns and STs of these clinical *E. coli* isolates from different origins suggested that the dissemination of *bla*<sub>CTX</sub> have broad reservoirs of *E. coli*. Future studies should be undertaken to identify the MDR transmission mechanisms and establish national standards for the rational use of antibiotics in companion animals.

## DATA AVAILABILITY STATEMENT

All datasets generated for this study are included in the article/Supplementary Material.

## ETHICS STATEMENT

This study was approved by the Agricultural University Animal Ethics Committee, China. The animals were given the best practice veterinary care and informed consent was granted by the owners.

## AUTHOR CONTRIBUTIONS

ZX was responsible for the study design. YC, ZL, YZ, and ZZ assisted in the data collection. ZL, YC, and LL interpreted the data. ZL, YC, and ZX completed the report writing. All authors revised, reviewed, and approved the final report.

## FUNDING

This work was supported by the Beijing Science and Technology Plan Project (Z171100001517008) and the National Natural Science Foundation of China (31422055).

## SUPPLEMENTARY MATERIAL

The Supplementary Material for this article can be found online at: <https://www.frontiersin.org/articles/10.3389/fmicb.2019.02852/full#supplementary-material>

Anderson, M., Clift, C., Schulze, K., Sagan, A., Nahrgang, S., Ait Ouakrim, D., et al. (2019). *Averting the AMR Crisis: What are the Avenues for Policy Action for Countries in Europe?* Copenhagen: European Observatory on Health Systems and Policies.

Andersen, V. D., Jensen, V. F., Vigre, H., Andreasen, M., and Agersø, Y. (2015). The use of third and fourth generation cephalosporins affects the occurrence of

- extended-spectrum cephalosporinase-producing *Escherichia coli* in Danish pig herds. *Vet. J.* 204, 345–350. doi: 10.1016/j.tvjl.2015.03.014
- Aung, M. S., San, N., Maw, W. W., San, T., Urushibara, N., Kawaguchiya, M., et al. (2018). Prevalence of extended-spectrum beta-lactamase and carbapenemase genes in clinical isolates of *Escherichia coli* in Myanmar: dominance of blaNDM-5 and emergence of blaOXA-181. *Microb. Drug. Resist.* 24, 1333–1344. doi: 10.1089/mdr.2017.0387
- Bachiri, T., Lalaoui, R., Bakour, S., Allouache, M., Belkebla, N., Rolain, J. M., et al. (2017). First report of the plasmid-mediated colistin resistance gene *mcr-1* in *Escherichia coli* ST405 isolated from wildlife in Bejaia, Algeria. *Microb. Drug. Resist.* 24, 2017–2026. doi: 10.1089/mdr.2017.0026
- Bai, L., Zhao, J., Gan, X., Wang, J., Zhang, X., Cui, S., et al. (2016). Emergence and diversity of *Salmonella enterica* serovar indiana isolates with concurrent resistance to ciprofloxacin and cefotaxime from patients and food-producing animals in China. *Antimicrob. Agents. Chemother.* 60, 3365–3371. doi: 10.1128/AAC.02849-15
- Basu, S., and Mukherjee, M. (2019). Conjugal transfer of PMQR from uropathogenic *E. coli* under high ciprofloxacin selection pressure generates gyrA mutation. *Microbial. Pathog.* 132, 26–29. doi: 10.1016/j.micpath.2019.04.021
- Bevan, E. R., Jones, A. M., and Hawkey, P. M. (2017). Global epidemiology of CTX-M-beta-lactamases: temporal and geographical shifts in genotype. *J. Antimicrob. Chemother.* 72, 2145–2155. doi: 10.1093/jac/dkx146
- Bogaerts, P., Huang, T. D., Bouchahrouf, W., Bauraing, C., Berhin, C., El, G. F., et al. (2015). Characterization of ESBL- and AmpC-producing *Enterobacteriaceae* from diseased companion animals in Europe. *Microb. Drug. Resist.* 21:643. doi: 10.1089/mdr.2014.0284
- Brianna, L., Mihai, P., Martin, A., Walker, A. W., Volker, M., Ahmed, D., et al. (2013). Survey of culture, goldengate assay, universal biosensor assay, and 16s rRNA gene sequencing as alternative methods of bacterial pathogen detection. *J. Clin. Microbiol.* 51, 3263–3269. doi: 10.1128/JCM.01342-13
- Canton, R., Gonzalez-Alba, J. M., and Galan, J. C. (2012). CTX-M enzymes: origin and diffusion. *Front. Microbiol.* 3:110. doi: 10.3389/fmicb.2012.00110
- Carroll, L. M., Gaballa, A., Guldemann, C., Sullivan, G., Henderson, L. O., Wiedmann, M., et al. (2019). Identification of novel mobilized colistin resistance gene in a multidrug-resistant, colistin-susceptible *Salmonella enterica* serotype typhimurium isolate. *MBio* 10:e853-19. doi: 10.1128/mBio.00853-19
- Carter, D. L., Docherty, K. M., Gill, S. A., Baker, K., Teachout, J., and Vonhof, M. J. (2018). Antibiotic resistant bacteria are widespread in songbirds across rural and urban environments. *Sci. Total. Environ.* 627, 1234–1241. doi: 10.1016/j.scitotenv
- Casella, T., Haenni, M., Madela, N. K., Andrade, L. K. D., Pradela, L. K., Andrade, L. N. D., et al. (2018). Extended-spectrum cephalosporin-resistant *Escherichia coli* isolated from chickens and chicken meat in Brazil is associated with rare and complex resistance plasmids and pandemic ST lineages. *J. Antimicrob. Chemother.* 73, 3293–3297. doi: 10.1093/jac/dky335
- Chen, Q. L., Cui, H. L., Su, J. Q., Penuelas, J., and Zhu, Y. G. (2019). Antibiotic resistomes in plant microbiomes. *Trends. Plant. Sci.* 24, 530–541. doi: 10.1016/j.tplants.2019.02.010
- CLSI, (2015a). *Clinical and Laboratory Standards Institute. Performance Standards for Antimicrobial Susceptibility Testing: 25th Informational Supplement, M100-S25.* Wayne, PA: Clinical and Laboratory Standards Institute.
- CLSI, (2015b). *Performance Standards for Antimicrobial Disk and Dilution Susceptibility Tests for Bacteria Isolated From Animals. Approved Standard-Fourth Edition and Supplement. CLSI documents VET01A4E and VET01S3E.* Wayne, PA: Clinical and Laboratory Standards Institute.
- EUCAST, (2019). *Breakpoint Tables for Interpretation of MICs and Zone Diameters.* Växjö: The European Committee on Antimicrobial Susceptibility Testing.
- Feng, Y. (2018). Transferability of *mcr-1/2* polymyxin resistance: complex dissemination and genetic mechanism. *ACS. Infect. Dis.* 4, 291–300. doi: 10.1021/acscinfed.7b00201
- Ghosh, H., Dojjad, S., Falgenhauer, L., Fritzenwanker, M., Imirzalioglu, C., and Chakraborty, T. (2017). blaCTX-M-27—Encoding *Escherichia coli* sequence type 131 lineage C1-M27 clone in clinical isolates. Germany. *Emerg. Infect. Dis.* 23, 1754–1756. doi: 10.3201/eid2310.170938
- Gros, M., Marti, E., Balcázar, J. L., Boy-Roura, M., Busquets, A., Colón, J., et al. (2019). Fate of pharmaceuticals and antibiotic resistance genes in a full-scale on-farm livestock waste treatment plant. *J. Hazard. Mater.* 378:120716. doi: 10.1016/j.jhazmat.2019.05.109
- Gupta, N., Limbago, B. M., Patel, J. B., and Kallen, A. J. (2011). Carbapenem-resistant *Enterobacteriaceae*: epidemiology and prevention. *Clin. Infect. Dis.* 53, 60–67. doi: 10.1093/cid/cir202
- Hall, J. L., Holmes, M. A., and Baines, S. J. (2013). Prevalence and antimicrobial resistance of canine urinary tract pathogens. *Vet. Rec.* 173:549. doi: 10.1136/vr.101482
- Hammerum, A. M., Larsen, J., Andersen, V. D., Lester, C. H., Skovgaard Skytte, T. S., Hansen, F., et al. (2014). Characterization of extended-spectrum beta-lactamase (ESBL)-producing *E. coli* obtained from Danish pigs, pig farmers and their families from farms with high or no consumption of third- or fourth-generation cephalosporins. *J. Antimicrob. Chemother.* 69, 2650–2657. doi: 10.1093/jac/dku180
- Hartantyo, S. H. P., Chau, M. L., Fillon, L., Ariff, A. Z. B. M., Kang, J. S. L., Aung, K. T., et al. (2018). Sick pets as potential reservoirs of antibiotic-resistant bacteria in Singapore. *Antimicrob. Resist. Infect. Control.* 7:106. doi: 10.1186/s13756-018-0399-9
- He, T., Wang, R., Liu, D., Walsh, T. R., Zhang, R., Lv, Y., et al. (2019). Emergence of plasmid-mediated high-level tigecycline resistance genes in animals and humans. *Nat. Microbiol.* 4, 1450–1456. doi: 10.1038/s41564-019-0445-442
- Karim, A., Poirel, L., Nagarajan, S., and Nordmann, P. (2001). Plasmid-mediated extended-spectrum beta-lactamase (CTX-M-3 like) from India and gene association with insertion sequence ISEcp1. *FEMS. Microbiol. Lett.* 201, 237–241. doi: 10.1111/j.1574-6968.2001.tb10762.x
- Karkaba, A., Hill, K., Benschop, J., Pleydell, E., and Grinberg, A. (2019). Carriage and population genetics of extended spectrum  $\beta$ -lactamase-producing *E. coli* in cats and dogs in new zealand. *Vet. Microbiol.* 233, 61–67. doi: 10.1016/j.vetmic.2019.04.015
- Khan, A. U., Maryam, L., and Zarrilli, R. (2017). Structure, Genetics and worldwide spread of New Delhi Metallo-beta-lactamase (NDM): a threat to public health. *BMC. Microbiol.* 17:101. doi: 10.1186/s12866-017-1012-8
- Kim, K. G., Jeong, J., Kim, M. J., Park, D. W., Shin, J. H., Park, H. J., et al. (2019). Prevalence and molecular epidemiology of ESBLs, plasmid-determined AmpC-type  $\beta$ -lactamases and carbapenemases among diarrhoeagenic *E. coli* isolates from children in gwangju, korea: 2007-16. *J. Antimicrob. Chemother.* 74, 2181–2187. doi: 10.1093/jac/dkz175
- Komp, L. P., Karlsson, A. D., and Hughes, D. (2003). Mutation rate and evolution of fluoroquinolone resistance in *E. coli* isolates from patients with urinary tract infections. *Antimicrob. Agents. Chemother.* 47:3222. doi: 10.1128/AAC.47.10.3222-3232.2003
- Kraychete, G. B., Botelho, L. A. B., Campana, E. H., Picão, R. C., and Bonelli, R. R. (2016). Updated multiplex PCR for detection of all six plasmid-mediated *qnr* gene families. *Antimicrob. Agents. Chemother.* 60, 1416–1447. doi: 10.1128/AAC.01447-16
- Lahlou, H., Khalifa, A. B. H., and Moussa, M. B. (2014). Epidemiology of *Enterobacteriaceae* producing CTX-M type extended spectrum beta-lactamase (ESBL). *Med. Mal. Infect.* 44, 400–404. doi: 10.1016/j.medmal.2014.03.010
- Li, X., Fu, Y., Shen, M., Huang, D., Du, X., Hu, Q., et al. (2018). Dissemination of blaNDM-5 gene via an IncX3-type plasmid among non-clonal *E. coli* in China. *Antimicrob. Resist. Infect. Control.* 7:59. doi: 10.1186/s13756-018-0349-6
- Ling, G. V., Norris, C. R., Franti, C. E., Eisele, P. H., Johnson, D. L., Ruby, A. L., et al. (2001). Interrelations of organism prevalence, specimen collection method, and host age, sex, and breed among 8,354 canine urinary tract infections (1969-1995). *J. Vet. Intern. Med.* 15, 341–347. doi: 10.1111/j.1939-1676.2001.tb02327.x
- Liu, X., Liu, H., Li, Y., and Hao, C. (2016a). High prevalence of beta-lactamase and plasmid-mediated quinolone resistance genes in extended-spectrum cephalosporin-resistant *Escherichia coli* from dogs in shaanxi, china. *Front. Microbiol.* 7:1843. doi: 10.3389/fmicb.2016.01843
- Liu, X., Thungrat, K., and Boothe, D. M. (2016b). Occurrence of OXA-48 carbapenemase and other beta-lactamase genes in ESBL-producing multidrug resistant *Escherichia coli* from dogs and cats in the United States, 2009-2013. *Front. Microbiol.* 7:1057. doi: 10.3389/fmicb.2016.01057
- Lloyd, H. D. (2007). Reservoirs of antimicrobial resistance in pet animals. *Clin. Infect. Dis.* 45, 148–152. doi: 10.1086/519254



- Logan, L. K., and Weinstein, R. A. (2017). The epidemiology of carbapenem-resistant *Enterobacteriaceae*: the impact and evolution of a global menace. *J. Infect. Dis.* 215, S28–S36. doi: 10.1093/infdis/jiw282
- Lu, X., Xiao, X., Liu, Y., Li, Y., Li, R., and Wang, Z. (2019). Chromosome-mediated *mcr-1* in *E. coli* strain L73 from a goose. *Int. J. Antimicrob. Agents.* 54, 99–101. doi: 10.1016/j.ijantimicag.2019.03.003
- Magiorakos, A. P., Srinivasan, A., Carey, R. B., Carmeli, Y., Falagas, M. E., Giske, C. G., et al. (2012). Multidrug-resistant, extensively drug-resistant and pandrug-resistant bacteria: an international expert proposal for interim standard definitions for acquired resistance. *Clin. Microbiol. Infect.* 18, 268–281. doi: 10.1111/j.1469-0691.2011.03570
- Marie-Hélène, N. C., Xavier, B., and Jean-Yves, M. (2014). *E. coli* ST131, an intriguing clonal group. *Clin. Microbiol. Rev.* 27, 543–574. doi: 10.1128/CMR.00125-13
- Marques, C., Gama, L. T., Belas, A., Bergstrom, K., Beurlet, S., Briend-Marchal, A., et al. (2016). European multicenter study on antimicrobial resistance in bacteria isolated from companion animal urinary tract infections. *BMC. Vet. Res.* 12:213. doi: 10.1186/s12917-016-0840-3
- Mathers, A. J., Peirano, G., and Pitout, J. D. (2015). The role of epidemic resistance plasmids and international high-risk clones in the spread of multidrug-resistant *Enterobacteriaceae*. *Clin. Microbiol. Rev.* 28, 565–591. doi: 10.1128/CMR.00116-14
- Matsumura, Y., Pitout, J. D. D., Gomi, R., Matsuda, T., Noguchi, T., Yamamoto, M., et al. (2016). Global *Escherichia coli* sequence type 131 clade with *bla*CTX-M-27 gene. *Emerg. Infect. Dis.* 22:1900. doi: 10.3201/eid2211.160519
- Matsumura, Y., Pitout, J. D. D., Peirano, G., DeVinney, R., Noguchi, T., Yamamoto, M., et al. (2017). Rapid identification of different *Escherichia coli* sequence type 131 clades. *Antimicrob. Agents. Chemother.* 61:e179-17. doi: 10.1128/AAC.00179-17
- Melo, L. C., Haenni, M., Saras, E., Duprilot, M., Nicolas-Chanoine, M. H., and Madec, J. Y. (2019). Emergence of the C1-M27 cluster in ST131 *Escherichia coli* from companion animals in France. *J. Antimicrob. Chemother.* 74, 3111–3113. doi: 10.1093/jac/dkz304
- Merino, I., Hernández-García, M., Turrientes, M. C., Pérez-Viso, B., López-Fresneña, N., and Diaz-Agero, C. (2018). Emergence of ESBL-producing *Escherichia coli* ST131-C1-M27 clade colonizing patients in Europe. *J. Antimicrob. Chemother.* 73, 2973–2980. doi: 10.1093/jac/dky296
- Morrissey, I., Moyaert, H., de Jong, A., El, G. F., Klein, U., Ludwig, C., et al. (2016). Antimicrobial susceptibility monitoring of bacterial pathogens isolated from respiratory tract infections in dogs and cats across Europe: compath results. *Vet. Microbiol.* 191, 44–51. doi: 10.1016/j.vetmic.2016.05.020
- Moyaert, H., Jong, D. A., Simjee, S., Rose, M., Youala, M., Garch, E. F., et al. (2019). Survey of antimicrobial susceptibility of bacterial pathogens isolated from dogs and cats with respiratory tract infections in Europe: compath results. *J. Appl. Microbiol.* 127, 29–46. doi: 10.1111/jam.14274
- Mugnaioli, C., Luzzaro, F., De Luca, F., Brigante, G., Perilli, M., Amicosante, G., et al. (2006). CTX-M-type extended-spectrum beta-lactamases in Italy: molecular epidemiology of an emerging countrywide problem. *Antimicrob. Agents. Chemother.* 50, 2700–2706. doi: 10.1128/AAC.00068-06
- O'Neill, J. (2016). Tackling drug-resistant infections globally: final report and recommendations. The review on antimicrobial resistance. Available at: [http://amr-review.org/sites/default/files/160525\\_Final%20paper\\_with%20cover.pdf](http://amr-review.org/sites/default/files/160525_Final%20paper_with%20cover.pdf) (accessed August, 2019).
- Onseadaeng, S., and Rathawongjirakul, P. (2016). Rapid detection of genomic mutations in *gyrA* and *parC* genes of *E. coli* by multiplex allele specific polymerase chain reaction. *J. Clin. Lab. Anal.* 30, 947–955. doi: 10.1002/jcla.21961
- Peirano, G., and Pitout, J. D. (2019). Extended spectrum beta-lactamase-producing *Enterobacteriaceae*: update on molecular epidemiology and treatment options. *Drugs* 79, 1529–1541. doi: 10.1007/s40265-019-01180-3
- Perez, F., and Bonomo, R. A. (2019). Carbapenem-resistant *Enterobacteriaceae*: global action required. *Lancet. Infect. Dis.* 19:561. doi: 10.1016/S1473-3099(19)30210-5
- Perez-Perez, F. J., and Hanson, N. D. (2002). Detection of plasmid-mediated AmpC beta-lactamase genes in clinical isolates by using multiplex PCR. *J. Clin. Microbiol.* 40:2153. doi: 10.1128/JCM.40.6.2153-2162.2002
- Pitout, J. D., and Laupland, K. B. (2008). Extended-spectrum beta-lactamase-producing *Enterobacteriaceae*: an emerging public-health concern. *Lancet. Infect. Dis.* 8, 159–166. doi: 10.1016/S1473-3099(08)70041-0
- Poirel, L., Walsh, T. R., Cuvillier, V., and Nordmann, P. (2011). Multiplex PCR for detection of acquired carbapenemase genes. *Diagn. Microbiol. Infect. Dis.* 70, 119–123. doi: 10.1016/j.diagmicrobio.2010.12.002
- Potter, R. F., D'Souza, A. W., and Dantas, G. (2016). The rapid spread of carbapenem-resistant *Enterobacteriaceae*. *Drug. Resist. Updates.* 29, 30–46. doi: 10.1016/j.drug.2016.09.002
- Ranjan, A., Shaik, S., Mondal, A., Nandanwar, N., Hussain, A., Semmler, T., et al. (2016). Molecular epidemiology and genome dynamics of New Delhi Metallo-β-lactamase-producing extra intestinal pathogenic *Escherichia coli* strains from India. *Antimicrob. Agents. Chemother.* 60, 6795–6805. doi: 10.1128/AAC.01345-16
- Rebello, A. R., Bortolaia, V., Kjeldgaard, J. S., Pedersen, S. K., Leekitcharoenphon, P., Hansen, I. M., et al. (2018). Multiplex PCR for detection of plasmid-mediated colistin resistance determinants, *mcr-1*, *mcr-2*, *mcr-3*, *mcr-4* and *mcr-5* for surveillance purposes. *Eur. Surveill.* 23:17-00672. doi: 10.2807/1560-7917.ES.2018.23.6.17-00672672
- Rheinwald, M., Hartmann, K., Hahner, M., Wolf, G., Straubinger, R. K., and Schulz, B. (2015). Antibiotic susceptibility of bacterial isolates from 502 dogs with respiratory signs. *Vet. Rec.* 176:357. doi: 10.1136/vr.102694
- Rogers, B. A., Sidjabat, H. E., Anna, S., Anderson, T. L., Shalini, P., Jian, L., et al. (2013). Treatment options for New Delhi metallo-beta-lactamase-harboring *Enterobacteriaceae*. *Microb. Drug. Resist.* 19, 100–103. doi: 10.1089/mdr.2012.0063
- Runcharoen, C., Raven, K. E., Reuter, S., Kallonen, T., Paksanont, S., Thammachote, J., et al. (2017). Whole genome sequencing of ESBL-producing *Escherichia coli* isolated from patients, farm waste and canals in Thailand. *Genome. Med.* 9:81. doi: 10.1186/s13073-017-0471-8
- Rzewuska, M., Czopowicz, M., Kizerwetter-Swida, M., Chrobak, D., Blaszczyk, B., and Biniek, M. (2015). Multidrug resistance in *Escherichia coli* strains isolated from infections in dogs and cats in Poland (2007–2013). *Sci. World J.* 2015:408205. doi: 10.1155/2015/408205
- Said, L. B., Jouini, A., Alonso, C. A., Klibi, N., Dziri, R., Boudabous, A., et al. (2016). Characteristics of extended-spectrum beta-lactamase (ESBL)-and pAmpC beta-lactamase-producing *Enterobacteriaceae* of water samples in Tunisia. *Sci. Total. Environ.* 550, 1103–1109. doi: 10.1016/j.scitotenv.2016.01.042
- Sanchez, M. L., Vallina-Victorero, M. J., Bachiller, M. R., Arbizu, R., Llana, E., Rozada, S., et al. (2019). Variability in the community consumption of antibiotics: a problem in Europe. *Spain Asturias. Infez. Med.* 27, 134–140.
- Saputra, S., Jordan, D., Mitchell, T., Wong, H. S., Abraham, R. J., Kidsley, A., et al. (2017). Antimicrobial resistance in clinical *Escherichia coli* isolated from companion animals in Australia. *Vet. Microbiol.* 211, 43–50. doi: 10.1016/j.vetmic.2017.09.014
- Shen, Z., Hu, Y., Sun, Q., Hu, F., Zhou, H., Shu, L., et al. (2018). Emerging carriage of *bla*NDM-5 and *mcr-1* in *Escherichia coli* from healthy people in multiple regions in China: a cross sectional observational study. *EClinicalMedicine* 6, 11–20. doi: 10.1016/j.eclinm.2018.11.003
- Sun, P., Xia, W., Liu, G., Huang, X., Tang, C., Liu, C., et al. (2019). Characterization of *bla*NDM-5-positive *Escherichia coli* prevalent in a university hospital in eastern China. *Infect. Drug. Resist.* 12:3029. doi: 10.2147/IDR.S225546
- Sun, Y. C., Huh, H. J., Jin, Y. B., Na, Y. C., Ryu, J. G., Ki, C. S., et al. (2015). *Klebsiella pneumoniae* co-producing NDM-5 and OXA-181 carbapenemases, South Korea. *Emerg. Infect. Dis.* 21:1088. doi: 10.3201/eid2106.150048
- Tenover, F. C., Arbeit, R. D., Goering, R. V., Mickelsen, P. A., Murray, B. E., Persing, D. H., et al. (1995). Interpreting chromosomal DNA restriction patterns produced by pulsed-field gel electrophoresis: criteria for bacterial strain typing. *J. Clin. Microbiol.* 33, 2233–2239.
- Thungrat, K., Price, S. B., Carpenter, D. M., and Boothe, D. M. (2015). Antimicrobial susceptibility patterns of clinical *Escherichia coli* isolates from dogs and cats in the United States: January 2008 through January 2013. *Vet. Microbiol.* 179, 287–295. doi: 10.1016/j.vetmic.2015.06.012
- Tyson, G. H., Li, C., Ceric, O., Reimschuessel, R., Cole, S., Peak, L., et al. (2019). Complete genome sequence of a carbapenem-resistant *Escherichia coli* isolate



- with *bla*NDM-5 from a dog in the United States. *Microbiol. Resour. Announc.* 8:e00872-19. doi: 10.1128/MRA.00872-19
- Vikesland, P., Garner, E., Gupta, S., Kang, S., Maile-Moskowitz, A., and Zhu, N. (2019). Differential drivers of antimicrobial resistance across the world. *Acc. Chem. Res.* 52, 916–924. doi: 10.1021/acs.accounts.8b00643
- Wang, R., Van, D. L., Shaw, L. P., Bradley, P., Wang, Q., Wang, X., et al. (2018). The global distribution and spread of the mobilized colistin resistance gene *mcr-1*. *Nat. Commun.* 9:1179. doi: 10.1038/s41467-018-03205-z
- Wang, X., Wang, Y., Zhou, Y., Li, J., Yin, W., Wang, S., et al. (2018). Emergence of a novel mobile colistin resistance gene, *mcr-8*, in NDM-producing *Klebsiella pneumoniae*. *Emerg. Microbes. Infect.* 7:122. doi: 10.1038/s41426-018-0124-z
- Wang, X., Wang, Y., Zhou, Y., Wang, Z., Wang, Y., Zhang, S., et al. (2019). Emergence of colistin resistance gene and its variant in *Raoultella ornithinolytica*. *Front. Microbiol.* 10:228. doi: 10.3389/fmicb.2019.00228
- Wang, Y., Zhang, R., Li, J., Wu, Z., Yin, W., Schwarz, S., et al. (2017). Comprehensive resistome analysis reveals the prevalence of NDM and MCR-1 in Chinese poultry production. *Nat. Microb.* 2:16260. doi: 10.1038/nmicrobiol.2016.260
- Wu, C., Wang, Y., Shi, X., Wang, S., Ren, H., Shen, Z., et al. (2018). Rapid rise of the ESBL and *mcr-1* genes in *Escherichia coli* of chicken origin in China, 2008–2014. *Emerg. Microbes. Infect.* 7:30. doi: 10.1038/s41426-018-0033-1
- Yang, F., Zhang, K., Zhi, S., Li, J., Tian, X., Gu, Y., et al. (2019). High prevalence and dissemination of beta-lactamase genes in swine farms in northern China. *Sci. Total. Environ.* 651, 2507–2513. doi: 10.1016/j.scitotenv.2018.10.144
- Yang, Y., Li, Y., Lei, C., Zhang, A., and Wang, H. (2018). Novel plasmid-mediated colistin resistance gene *mcr-7.1* in *Klebsiella pneumoniae*. *J. Antimicrob. Chemother.* 73, 1791–1795. doi: 10.1093/jac/dky111
- Yao, H., Wu, D., Lei, L., Shen, Z., Wang, Y., and Liao, K. (2016). The detection of fosfomycin resistance genes in *Enterobacteriaceae* from pets and their owners. *Vet. Microbiol.* 193, 67–71. doi: 10.1016/j.vetmic.2016.07.019
- Zhang, Q., Lv, L., Huang, X., Huang, Y., Zhuang, Z., and Lu, J. (2019). Rapid increase in carbapenemase-producing *Enterobacteriaceae* in retail meat driven by the spread of the *bla*NDM-5-carrying IncX3 plasmid in China from 2016 to 2018. *Antimicrob. Agents. Chemother.* 63:e00573-19. doi: 10.1128/AAC.00573-19
- Zhang, W., Lin, X., Xu, L., Gu, X., Yang, L., and Li, W. (2016). CTX-M-27 producing *Salmonella enterica* serotypes typhimurium and indiana are prevalent among food-producing animals in China. *Front. Microbiol.* 7:436. doi: 10.3389/fmicb.2016.00436
- Zhou, H. W., Zhang, T., Ma, J. H., Fang, Y., Wang, H. Y., Huang, Z. X., et al. (2017). Occurrence of plasmid-and chromosome-encoded *mcr-1* in waterborne *Enterobacteriaceae* in China. *Antimicrob. Agents Chemother.* 61:17. doi: 10.1128/AAC.00017-17

**Conflict of Interest:** YZ was employed by the company of Shandong New Hope Liuhe Group Ltd.

The remaining authors declare that the research was conducted in the absence of any commercial or financial relationships that could be construed as a potential conflict of interest.

Copyright © 2019 Chen, Liu, Zhang, Zhang, Lei and Xia. This is an open-access article distributed under the terms of the Creative Commons Attribution License (CC BY). The use, distribution or reproduction in other forums is permitted, provided the original author(s) and the copyright owner(s) are credited and that the original publication in this journal is cited, in accordance with accepted academic practice. No use, distribution or reproduction is permitted which does not comply with these terms.



# Down-Regulation of Flagellar, Fimbriae, and Pili Proteins in Carbapenem-Resistant *Klebsiella pneumoniae* (NDM-4) Clinical Isolates: A Novel Linkage to Drug Resistance

## OPEN ACCESS

Divakar Sharma<sup>1†</sup>, Anjali Garg<sup>2</sup>, Manish Kumar<sup>2</sup>, Faraz Rashid<sup>3</sup> and Asad U. Khan<sup>1\*</sup>

### Edited by:

Raffaele Zarrilli,  
University of Naples Federico II, Italy

### Reviewed by:

Gokhlesh Kumar,  
University of Veterinary Medicine  
Vienna, Austria  
Rita Berisio,  
Italian National Research Council  
(CNR), Italy

### \*Correspondence:

Asad U. Khan  
asad.k@rediffmail.com

### † Present address:

Divakar Sharma,  
Central Research Facility, Mass  
Spectrometry Laboratory, Kusuma  
School of Biological Sciences, Indian  
Institute of Technology, New Delhi,  
India

### Specialty section:

This article was submitted to  
Antimicrobials, Resistance  
and Chemotherapy,  
a section of the journal  
Frontiers in Microbiology

Received: 17 August 2019

Accepted: 27 November 2019

Published: 17 December 2019

### Citation:

Sharma D, Garg A, Kumar M,  
Rashid F and Khan AU (2019)  
Down-Regulation of Flagellar,  
Fimbriae, and Pili Proteins  
in Carbapenem-Resistant *Klebsiella  
pneumoniae* (NDM-4) Clinical Isolates:  
A Novel Linkage to Drug Resistance.  
*Front. Microbiol.* 10:2865.  
doi: 10.3389/fmicb.2019.02865

<sup>1</sup> Interdisciplinary Biotechnology Unit, Aligarh Muslim University, Aligarh, India, <sup>2</sup> Department of Biophysics, University of Delhi, New Delhi, India, <sup>3</sup> SCIEX Pvt. Ltd., Gurgaon, India

The emergence and spread of carbapenem-resistant *Klebsiella pneumoniae* infections have worsened the current situation worldwide, in which totally drug-resistant strains (bad bugs) are becoming increasingly prominent. Bacterial biofilms enable bacteria to tolerate higher doses of antibiotics and other stresses, which may lead to the drug resistance. In the present study, we performed proteomics on the carbapenem-resistant NDM-4-producing *K. pneumoniae* clinical isolate under meropenem stress. Liquid chromatography coupled with mass spectrometry (LC-MS/MS) analysis revealed that 69 proteins were down-regulated ( $\leq 0.42$ -fold change) under meropenem exposure. Within the identified down-regulated proteome (69 proteins), we found a group of 13 proteins involved in flagellar, fimbriae, and pili formation and their related functions. Further, systems biology approaches were employed to reveal their networking pathways. We suggest that these down-regulated proteins and their interactive partners cumulatively contribute to the emergence of a biofilm-like state and the survival of bacteria under drug pressure, which could reveal novel mechanisms or pathways involved in drug resistance. These down-regulated proteins and their pathways might be used as targets for the development of novel therapeutics against antimicrobial-resistant (AMR) infections.

**Keywords:** *Klebsiella pneumoniae* (NDM-4), proteomics, bioinformatics, pathway enrichment, biofilm, carbapenem resistance

## INTRODUCTION

*Klebsiella pneumoniae* is a gram-negative bacteria of the family Enterobacteriaceae. In clinical settings, the emergence and spread of drug-resistant *K. pneumoniae* are worsening the medical situation worldwide. Carbapenems have been considered the last line of defense in the treatment of drug-resistant infections (Paterson, 2000; Paterson and Bonomo, 2005). Interrupted use of

**Abbreviations:** CLSI, Clinical and Laboratory Standards Institute; ESBLs, extended spectrum beta-lactamases; LB, Luria-Bertani; MIC, minimum inhibitory concentration; STRING, Search Tool for the Retrieval of Interacting Genes/Proteins.

carbapenem during the course of treatment leads to the emergence of carbapenem-resistant infections. Carbapenemases are produced that cleave or hydrolyze the carbapenem drugs and contribute to carbapenem resistance. Carbapenemase overproduction and porin deficiency are the two major causes of carbapenem resistance (Ambler et al., 1991; Martínez-Martínez et al., 1999; Jacoby et al., 2004; Loli et al., 2006). Several explanations have been put forward to explain the mechanisms of carbapenem resistance, but our information is as yet incomplete or fragmentary.

Biofilm formation is among the mechanisms known to be responsible for microbial drug resistance. During biofilm formation, bacteria first become sessile and then colonize and grow up from surfaces. The biofilm protects the bacteria from various stresses like altered pH, osmolarity, and nutrient scarcity (Costerton and Lewandowski, 1995; Fux et al., 2005; McCarty et al., 2012) and blocks the entry of drugs to the bacterial communities (Costerton et al., 1999; Stewart and William Costerton, 2001; Sharma et al., 2019c). In the first step of biofilm formation, bacteria lose their motility and become sessile. We assume that decreased expression of proteins related to motility could lead to biofilm formation and thus might contribute to the development of drug resistance. Comparative proteomics addressing the whole-cell proteins of drug-resistant microbes with or without drug pressures have been reported previously (Lata et al., 2015; Khan et al., 2017; Sharma et al., 2018a; Qayyum et al., 2019; Sharma et al., 2019a). However, little information is available regarding the bacterial proteome related to biofilm, and, to the best of our knowledge, no data has yet been reported related to the proteome of drug-resistant microbes, especially carbapenem-resistant *K. pneumoniae*, in relation to motility-mediated drug resistance.

In this study, we used comparative proteomics and systems biology-based approaches to investigate the correlation of the decreased expression of motility-related proteins (flagellar, fimbriae, and pili) with biofilm formation, which may lead to the development of drug resistance. Proteomics and systems biology approaches are both among the potential strategies for exploring biological problems such as the mechanisms of drug resistance. In the present study, we used liquid chromatography coupled with mass spectrometry (LC-MS/MS) to determine the expression of the motility-related proteome of a carbapenem-resistant *K. pneumoniae* (NDM-4) clinical isolate under meropenem stress. The results of this study could lead to the exploration of novel therapeutic targets against carbapenem resistance.

## MATERIALS AND METHODS

### Strain Selection and Drug Susceptibility Testing

An NDM-4-encoding carbapenem-resistant *K. pneumoniae* clinical isolate (AK-97) was selected for this study. This was reported in our earlier study, which showed its presence in the NICU of a northern Indian Hospital (Ahmad et al., 2018). Drug susceptibility testing (DST) against the drug meropenem was

carried out via the micro-dilution method according to CLSI guidelines (Wayne, 2014).

### Culture Scaling, Drug Induction, and Protein Sample Preparation

A single colony of *K. pneumoniae* was inoculated in LB broth and kept at 37°C at 220 rpm, and a sub-MIC (32 µg/ml) of meropenem was used for induction in a 200 ml culture flask. Bacteria were grown up to the exponential phase ( $OD_{600} = 0.8$ ), and cells were harvested by centrifugation at  $8000 \times g$  for 8 min at 4°C. The cells were washed with normal saline and re-suspended in a lysis buffer [50 mM Tris-HCl containing 10 mM MgCl<sub>2</sub>, 0.1% sodium azide, 1 mM phenyl-methyl-sulfonyl-fluoride (PMSF), and 1 mM ethylene glycol tetra-acetic acid (EGTA); pH 7.4] at a concentration of 1 g wet weight per 5 ml. Cell lysis was performed by intermittent sonication with a sonicator with the power at 35% amplitude (Sonics & Materials Inc., Newtown, CT, United States) for 10 min at 4°C. Further, the homogenate was centrifuged at  $12,000 \times g$  for 20 min at 4°C, and the supernatant was precipitated overnight at -20°C by adding cold acetone in excess (1:4) (Lata et al., 2015; Sharma and Bisht, 2016; Sharma et al., 2019a). The precipitated protein was collected by centrifugation ( $12,000 \times g$ , 20 min), allowed to air dry, and then suspended in an appropriate volume of protein-dissolving buffer. The protein concentration was estimated using the Bradford (1976) assay. All of the experiments were replicated biologically and technically.

### Separation and Identification of the Proteome by nanoLC-TripleTOF 5600 MS

Equal concentrations of protein samples were trypsinized, and digested proteins were analyzed using a TripleTOF 5600 MS (AB Sciex, Foster City, CA, United States) equipped with an Eksigent MicroLC 200 system (Eksigent, Dublin, CA, United States) with an Eksigent C18 reverse-phase column (150 × 0.3 mm, 3 µm, 120 Å) (Sharma et al., 2019a). For protein identification, spectral libraries were generated using information-dependent acquisition (IDA) mode after injecting 2 µg of tryptic digest on the column using an Eksigent NanoLC-Ultra™ 2D Plus system coupled with a SCIEX Triple TOF® 5600 system fitted with a NanoSpray III source. The samples were loaded on the trap (Eksigent Chrom XP 350 µm × 0.5 mm, 3 µm, 120 Å) and washed for 30 min at 3 µl/min. A 120 min gradient in multiple steps (ranging from 5 to 50% acetonitrile in water containing 0.1% formic acid) was set up to elute the peptides from the ChromXP 3-C18 (0.075 × 150 mm, 3 µm, 120 Å) analytical column. Technical replicates of the nanoLC-TripleTOF 5600 MS experiments were performed.

### Sequential Window Acquisition of all Theoretical Fragment Ion Spectra (SWATH) Analysis for Label-Free Quantification

For label-free quantification (SWATH analysis), data-dependent analysis (DDA) mode was applied for both samples to generate high-quality spectral ion libraries by operating the mass spectrometer with specific parameters (Sharma and Bisht, 2016).

In the SWATH acquisition method, the Q1 transmission window was set to 12 Da from the mass range 350–1250 Da. A total of 75 windows were acquired independently with an accumulation time of 62 ms, along with three technical replicates for each of the sets. The total cycle time was kept constant at <5 s. Protein Pilot™ v. 5.0 was used to generate the spectral library. For label-free quantification, peak extraction and spectral alignment were performed using PeakView® 2.2 Software with the parameters set as follows: number of peptides, 2; number of transitions, 5; peptide confidence, 95%; XIC width, 30 ppm; XIC extraction window, 3 min. The data were further processed in MarkerView software v. 1.3 (AB Sciex, Foster City, CA, United States) for statistical data interpretation. In MarkerView, the peak area under the curve (AUC) for the selected peptides was normalized by the internal standard protein (beta-galactosidase) spike during SWATH accumulation. The results were extracted as three output files containing the AUC of the ions, the summed intensity of peptides for protein, and the summed intensity of ions for the peptide. All SWATH acquisition data were processed using SWATH Acquisition MicroApp 2.0 in PeakView® Software.

## Data Analysis

Data were processed with Protein Pilot Software v. 5.0 (AB Sciex, Foster City, CA, United States) utilizing the Paragon and Progroup Algorithm. The analysis was done using the tools integrated into Protein Pilot at a 1% false discovery rate (FDR) with statistical significance. In brief, the UniProt database searched for the *K. pneumoniae* taxonomy, which was download from the database in July 2018. The download included total combined (reviewed and un-reviewed) entries of 409,060 proteins. We used cRAP analysis to identify the proteins commonly found in proteomics experiments (unavoidable contamination) of protein samples. *E. coli* beta-galactosidase (BGAL\_ECOLI-[P00722]) was used as a molecular weight marker to calibrate the system for sample acquisition.

The internal standard was used for the normalization of statistical parameters. We exported the label-free quantified data and imported them into MarkerView software V1.3 to obtain statistical data for further interpretation. Triplicate data for each sample were normalized using the internal protein (beta-galactosidase) area, which was initially spiked in the samples. After normalization, principal component analysis (PCA) was performed to check the possible correlated variables within the group. We plotted a volcano curve to determine the statistical significant fold change versus *p*-value for the control and test. Proteins with a significant fold change < 0.42 were considered down-regulated proteins. Peak extraction and spectral alignment were performed using PeakView software (v. 2.2, AB Sciex, Foster City, CA, United States) with the following parameter settings: number of peptides per protein, 5; number of transitions per peptide, 6; selected peptide confidence, 1% FDR; XIC width, 30 ppm; XIC extraction window, 3 min.

## Gene Ontology Term Assignment and Analysis

*Klebsiella pneumoniae* subsp. *pneumoniae* (strain ATCC 700721/MGH 78578) was used as a reference strain to carry out the functional studies. The proteins obtained from LC-MS/MS were firstly aligned to the reference strain proteome. Reference strain proteins that showed alignment identity of ≥50% over 80% of the sequence length of the reference strain protein were considered as homologs of the LC-MS/MS identified proteins. The Gene Ontology (GO) terms associated with the reference strain protein were used for the functional annotation. We used the slim version of GO terms, which were obtained from the Gene Ontology Consortium<sup>1</sup> (Camon et al., 2003).

<sup>1</sup><http://www.geneontology.org/>

**TABLE 1** | Details of the down-regulated proteome (flagella-, fimbriae-, and pili-related proteins) under meropenem stress in *Klebsiella pneumoniae* clinical isolates (NDM-4).

S. No.	Protein name	Log fold change vs. <i>p</i> -value	Accession number	Protein symbol	Matched organism strain
1	Flagellar motor switch protein FlIG	0.42	W1AYD1	FlIG	<i>K. Pneumoniae</i> IS22
2	Flagellar hook protein FlgE	0.32	W1AUQ1	FlgE	<i>K. Pneumoniae</i> IS22
3	Negative regulator of flagellin synthesis FlgM	0.23	W1AWJ3	FlgM	<i>K. Pneumoniae</i> IS22
4	Putative fimbriae major subunit StbA	0.23	A6T548	StbA	<i>K. pneumoniae</i> subsp. <i>pneumoniae</i> (strain ATCC 700721/MGH 78578)
5	Flagellar hook-associated protein 2	0.22	W1B018	.....	<i>K. Pneumoniae</i> IS22
6	FimC protein	0.17	W1AP20	FimC	<i>K. Pneumoniae</i> IS22
7	Chaperone FimC	0.15	W1BBF2	FimC	<i>K. Pneumoniae</i> IS22
8	Flagellar biosynthesis protein FlgN	0.09	W1ATC5	FlgN	<i>K. Pneumoniae</i> IS22
9	Flagellar basal body protein	0.08	W1AT19	.....	<i>K. Pneumoniae</i> IS22
10	Conjugal transfer protein TraC	0.06	W1B0W2	TraC	<i>K. Pneumoniae</i> IS22
11	Fimbrial subunit type 1	0.05	W1B9X4	FimA	<i>K. Pneumoniae</i> IS22
12	Chemotaxis regulator-transmits chemoreceptor signals to flagellar motor components CheY	0.04	W1BDF3	CheY	<i>K. Pneumoniae</i> IS22
13	Flagellin	0.01	W1AZS9	.....	<i>K. Pneumoniae</i> IS22



**TABLE 2 |** Functional analysis of down-regulated genes associated with *Klebsiella pneumoniae* subsp. *pneumoniae* (strain ATCC 700721/MGH 78578).

GO ID	Function	Gene name	No. of genes in which GO term was found
<b>(A) Biological functions</b>			
GO:0005975	Carbohydrate metabolic process	<i>deoC, dhaK, dhaL, glk, gmhB, gnd, lacZ2, malP, talB, treC, uxaC</i>	11
GO:0006091	Generation of precursor metabolites and energy	<i>aspA, fdhF, glk, gor</i>	4
GO:0006259	DNA metabolic process	<i>ung, uvrD</i>	2
GO:0006399	tRNA metabolic process	<i>gltX, pheS, thrS</i>	3
GO:0006412	Translation	<i>gltX, pheS, thrS</i>	3
GO:0006457	Protein folding	<i>fimC</i>	1
GO:0006461	Protein complex assembly	<i>hscB</i>	1
GO:0006464	Cellular protein modification process	<i>ppiD, ptsH</i>	2
GO:0006520	Cellular amino acid metabolic process	<i>aspA, gcvH, gcvP, gcvT, gltX, hisD, ilvC, pheS, thrS</i>	9
GO:0006629	Lipid metabolic process	<i>dxs, glpQ</i>	2
GO:0006790	Sulfur compound metabolic process	<i>dxs, gor</i>	2
GO:0006810	Transport	<i>artI, copA, pcoC, ptsH</i>	4
GO:0006950	Response to stress	<i>sodB, ung</i>	2
GO:0007155	Cell adhesion	<i>fimA</i>	1
GO:0007165	Signal transduction	<i>artI</i>	1
GO:0009056	Catabolic process	<i>deoC, gcvH, gcvP, gcvT, glk, glpA, treC, uxaC</i>	8
GO:0009058	Biosynthetic process	<i>dxs, hisD, hns, ilvC, nadE, pdxY, rmlD, rnk, sul, udp, uvrD</i>	11
GO:0034641	Cellular nitrogen compound metabolic process	<i>cpdB, dxs, glk, gnd, gor, hisD, hns, nadE, pdxY, rmlB, rmlD, rnk, sul, talB, udp</i>	15
GO:0034655	Nucleobase-containing compound catabolic process	<i>cdd, cpdB, deoC, udp</i>	4
GO:0042592	Homeostatic process	<i>Gor</i>	1
GO:0044281	Small molecule metabolic process	<i>aspA, cdd, cpdB, deoC, dhaK, dhaL, dxs, fdhF, glk, glpA, gnd, nadE, pdxY, sul, talB, udp, uxaC</i>	17
GO:0051186	Cofactor metabolic process	<i>glk, gnd, nadE, pdxY, sul, talB</i>	6
GO:0051276	Chromosome organization	<i>uvrD</i>	1
GO:0051604	Protein maturation	<i>hscB</i>	1
GO:0055085	Transmembrane transport	<i>copA</i>	1
GO:0071554	Cell wall organization or biogenesis	<i>fimC</i>	1
<b>(B) Molecular functions</b>			
GO:0003677	DNA binding	<i>hns, rnk, uvrD</i>	3
GO:0003723	RNA binding	<i>gltX, pheS, thrS</i>	3
GO:0004386	Helicase activity	<i>uvrD</i>	1
GO:0004871	Signal transducer activity	<i>artI</i>	1
GO:0008168	Methyltransferase activity	<i>gcvT</i>	1
GO:0016301	Kinase activity	<i>dhaK, dhaL, glk, pdxY, ptsH, rnk</i>	6
GO:0016491	Oxidoreductase activity	<i>KPN_02441, fdhF, gcvP, glpA, gnd, gor, hisD, ilvC, nfnB, nfsA, rmlD, sodB, ydgJ</i>	13
GO:0016746	Transferring acyl groups	<i>Maa</i>	1
GO:0016757	Transferring glycosyl groups	<i>malP, udp</i>	2
GO:0016765	Transferring alkyl or aryl (other than methyl) groups	<i>Sul</i>	1
GO:0016791	Phosphatase activity	<i>aphA, gmhB</i>	2
GO:0016798	Acting on glycosyl bonds	<i>lacZ2, rihC, treC, ung</i>	4
GO:0016810	Acting on carbon–nitrogen (but not peptide) bonds	<i>Cdd</i>	1
GO:0016829	Lyase activity	<i>acnA, aspA, deoC, rmlB, yhbL</i>	5
GO:0016853	Isomerase activity	<i>ppiD, uxaC</i>	2
GO:0016874	Ligase activity	<i>gltX, nadE, pheS, thrS</i>	4
GO:0016887	ATPase activity	<i>copA, uvrD</i>	2
GO:0019899	Enzyme binding	<i>Rnk</i>	1
GO:0022857	Transmembrane transporter activity	<i>artI, copA</i>	2
GO:0030234	Enzyme regulator activity	<i>hscB</i>	1

(Continued)

TABLE 2 | Continued

GO ID	Function	Gene name	No. of genes in which GO term was found
<b>(B) Molecular functions</b>			
GO:0043167	Ion binding	<i>KPN_pKPN3p05899, aphA, cdd, copA, cpdB, dxs, fdhF, glk, glpA, gltX, gmhB, gor, hisD, ilvC, lacZ2, malP, nadE, pcoC, pdxY, pheS, sodB, sul, thrS, uvrD, yjiM</i>	25
<b>(C) Cellular component</b>			
GO:0005622	Intracellular	<i>artI, copA, lacZ2, ppiD</i>	1
GO:0005623	Cell	<i>Hns</i>	6
GO:0005737	Cytoplasm	<i>aphA, artI, fimA, fimC, gor, pcoC</i>	15
GO:0005886	Plasma membrane	<i>deoC, gcvH, glk, glpA, gltX, gmhB, maf, pheS, ptsH, talB, thrS, treC, udp, ung, uvrD</i>	2

TABLE 3 | List of *Klebsiella pneumoniae* sp. proteins mapped on *E. coli* K12 substr.DH10B.

<i>K. pneumoniae</i> IS22 protein entry	Sequence length	<i>K. pneumoniae</i> protein name	<i>E. coli</i> K12 substr. DH10B protein entry	Sequence length	<i>E. coli</i> K12 substr. DH10B gene name	Identity (%)
W1AYD1	331	Flagellar motor switch protein FlIG	P0ABZ1	331	flIG	99.698
W1AUQ1	206	Flagellar hook protein FlgE	P75937	402	flgE	91.304
W1AWJ3	97	Negative regulator of flagellin synthesis	P0AEM4	97	flgM	100.000
W1B018	468	Flagellar hook-associated protein 2	P24216	97	flID	99.786
W1AP20	224	Chaperone FimC	No hit	–	–	–
W1ATC5	138	Flagellar biosynthesis protein FlgN	P43533	468	flgN	100.000
W1AT19	191	Flagellar basal body protein	P75937	138	flgE	95.812
W1BDF3	129	Chemotaxis regulator-transmits chemoreceptor signals to flagellar motor components CheY	P0AE67	129	cheY	100.000
W1B0W2	533	Conjugal transfer protein traC	No hit	–	–	–
W1AZS9	447	Flagellin	No hit	–	–	–
A6T548	178	Putative fimbriae major subunit StbA	No hit	–	–	–

## Protein–Protein Interaction Network Integration

To find the interaction partner(s) of down-regulated proteins, protein–protein interaction (PPI) information were obtained from the STRING database v10.0<sup>2</sup> and Cytoscape (version 3.6.1) (Shannon et al., 2003; Sharma and Bisht, 2017a,b,c; Sharma et al., 2018b, 2019b; Sharma and Khan, 2018). The PPI information provided by the STRING database has been established by experimental studies or by genomic analyses like domain fusion, phylogenetic profiling high-throughput experiments, co-expression studies, and gene neighborhood analysis. In the present study, only interactions with a score of  $\geq 0.4$  were used.

## RESULTS

### Identification of Proteins by LC–MS/MS

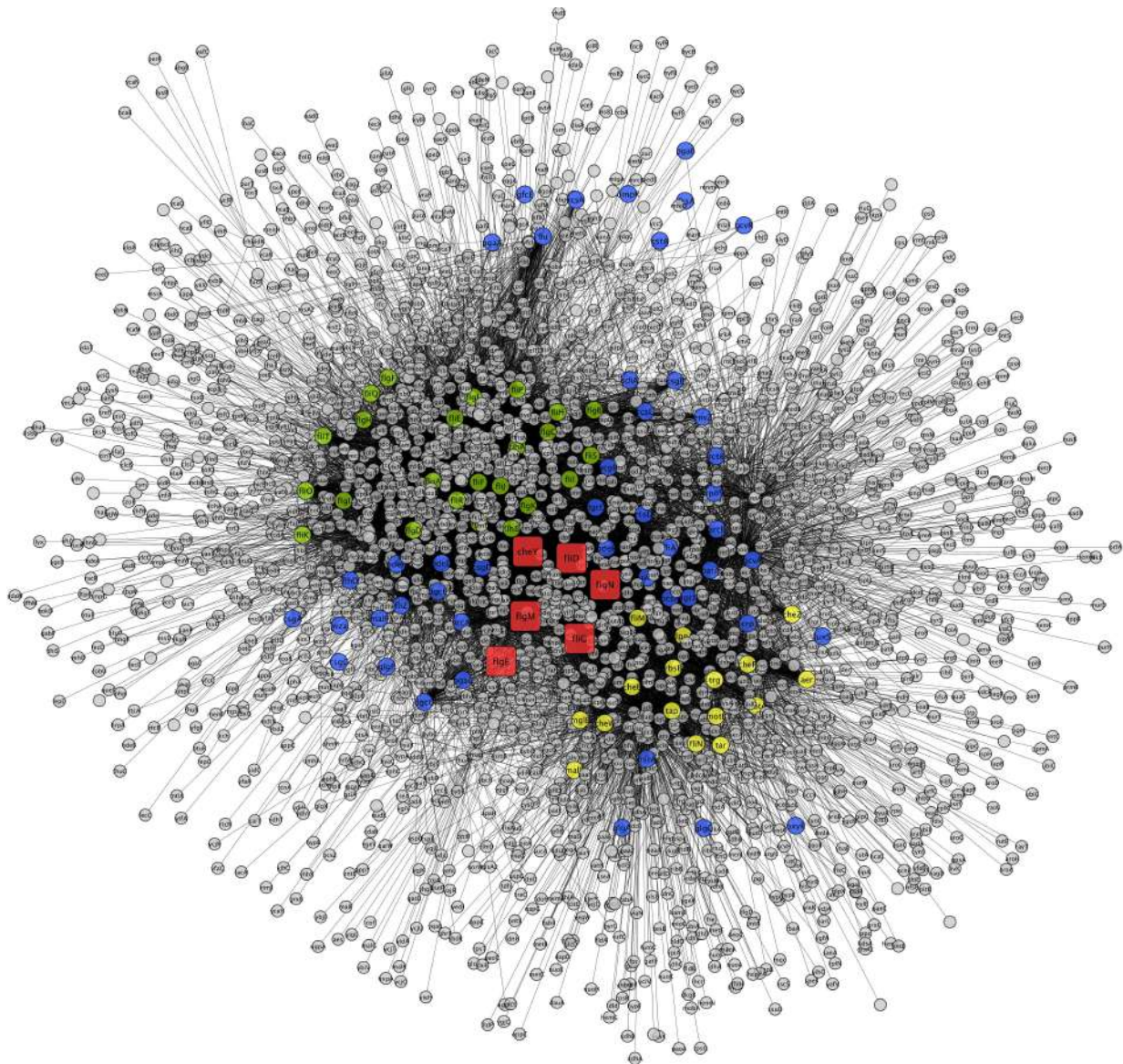
In this study, we grew the carbapenem-resistant isolate at meropenem sub-MIC 32 mg/L. Further, we identified the down-regulated proteome of the same bacteria by LC–MS/MS using a SWATH workflow; 1156 proteins

<sup>2</sup><http://www.string-db.org/>

were quantified at 1% FDR with statistical significance as per the log fold change vs. *p*-value. Among them, 69 proteins were down-regulated ( $< 0.42$  log fold change vs. *p*-value) and are tabulated in the **Supplementary Material (Supplementary Table S1)**.

In the present work, our main focus was on motility-related proteins. After critical analysis of the 69 down-regulated proteins, we found 13 proteins (around 19%) that belonged to the flagella-, fimbriae-, and pili-related protein functional groups (**Table 1**). These proteins are flagellar motor switch protein FlIG, flagellar hook protein FlgE, negative regulator of flagellin synthesis FlgM, putative fimbriae major subunit StbA, flagellar hook-associated protein 2, chaperone FimC protein, flagellar biosynthesis protein FlgN, flagellar basal body protein, conjugal transfer protein TraC, fimbrial subunit type 1, chemotaxis regulator-transmits chemoreceptor signals to flagellar motor components CheY, and flagellin, all of which are involved in motility and its supporting processes.

On the basis of the parameters described in the section “Materials and Methods,” we were able to map 67 out of the 69 down-regulated proteins on the proteome of the ATCC 700721/MGH 78578 strain of *K. pneumoniae* (**Supplementary Table S2**). Our GO results for down-regulated genes also show that most down-regulated proteins were involved in



**FIGURE 1 |** Interaction networks for down-regulated genes of *K. pneumoniae* using *E. coli* K12 substr. DH10B homologs. Interacting proteins were color coded by functions, biofilm formation (blue), chemotaxis proteins (yellow), and flagellar assembly (green). Square nodes in red color indicate down-regulated protein mapped on *E. coli*.

nitrogen and other small molecule metabolism, ion binding, and oxidoreductase activity (Table 2).

### Protein Network Analysis

To construct the PPI network, the down-regulated proteins with motility-related functions were annotated using *E. coli* K12 strain DH10B homologs, as tabulated in Table 3. Among them, few proteins showed no hits in *E. coli*, and the rest of the proteins interacted with other proteins to make an interactome; this was visualized through Cytoscape (version 3.6.1) (Figure 1). Interacting proteins were color-coded by their functions: biofilm formation, blue; chemotaxis proteins, yellow; flagellar assembly, green. Square red nodes indicate down-regulated proteins.

### DISCUSSION

The development of carbapenem-resistant *K. pneumoniae* has worsened the medical situation around the globe. The emergence of carbapenem resistance is usually due to the over-expression of carbapenemases and loss of porins. Recently, we reported a cluster of over-expressed proteins in carbapenem-resistant *K. pneumoniae* under meropenem pressure. These could be responsible for the drug resistance and belong to various categories such as the protein translational machinery complex, DNA/RNA modifying enzymes or proteins, proteins involved in carbapenem cleavage, modification, and transport, and energy metabolism- and intermediary metabolism-related



proteins (Sharma et al., 2019a). Therefore, we suggested that they could be potential targets for the development of novel therapeutics against this resistance. Biofilm formation is also one of the mechanisms that leads to the development of drug resistance. In the present study, we have found a group flagellar, fimbriae, and pili proteins that are down-regulated under meropenem stress (sub-MIC). We hypothesize that the down-regulation of these proteins under meropenem stress makes the bacteria sessile or non-motile, leading to the emergence of a biofilm-like state that could contribute to carbapenem resistance in *K. pneumoniae* (NDM-4). Earlier microarray analysis of *K. pneumoniae* also reported the down-regulation of genes related to nitrogen metabolism, porin genes, and some membrane-associated proteins in association with the antibiotic resistance phenomenon (Doménech-Sánchez et al., 2006). The significance of the aforementioned pathways in antibiotic-evading mechanisms is also highlighted in several other reports (Yeung et al., 2011; Piek et al., 2014).

## A Hub of Flagellar, Fimbriae, and Pili Proteins Could Regulate Resistance

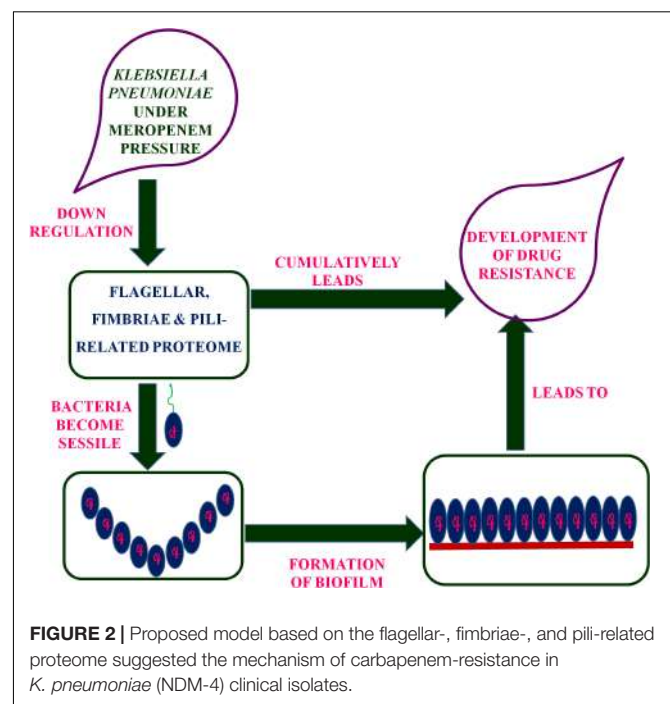
A group of flagellar, fimbriae, and pili proteins involved in the formation of the flagellar machinery complex and the regulation of motility processes were found to be down-regulated in meropenem-induced carbapenem-resistant *K. pneumoniae* clinical strains. These proteins are flagellar motor switch protein FliG, flagellar hook protein FlgE, negative regulator of flagellin synthesis FlgM, putative fimbriae major subunit StbA, flagellar hook-associated protein 2, chaperone FimC protein, flagellar biosynthesis protein FlgN, flagellar basal body protein FlgF, conjugal transfer protein TraC, fimbrial subunit type 1, chemotaxis regulator-transmits chemoreceptor signals to flagellar motor components CheY, and flagellin.

The observed expression down-regulation of flagella-, fimbriae-, and pili-related proteins provides clues to a novel mechanism of drug resistance. Flagellin, flagellar biosynthesis protein FlgN, and FlgM, respectively, cumulatively maintain equilibrium in the biosynthesis of flagella. Flagellin protein is part of the structural component of flagella, and biosynthesis of flagella is favored by flagellar biosynthesis protein FlgN (Bennett et al., 2001). FlgM is a negative regulator that switches off flagellar transport. FlgM can be exported from the cell via a flagellum, and the transport occurs only after the completion of hook formation (Hughes et al., 1993). This unique regulatory mechanism further postpones flagellin synthesis in the cell. Cumulatively, the expression of these proteins is involved in the flagella formation, regulation, and motility of the bacteria. Therefore, we suggest that, under meropenem pressure, down-regulation of these proteins might make the bacteria sessile, which is the first step in biofilm-formation. Therefore, we assume that down-regulation of these proteins could create a biofilm-like state, which ultimately leads to the drug resistance.

Flagella are composed of three different parts: a filament (helical and long), hook (a curved and short structure), and basal body (a complex structure with a central rod and a series of rings). Flagellar motor switch protein (FliG), flagellar hook

protein FlgE, flagellar hook-associated protein 2, and flagellar basal body protein FlgF together make up part of the flagellar motor switch complex (FliG, FliN, and FliM), which is involved in bacterial motility, after receipt and transduction of the signal by chemotaxis (Djordjevic and Stock, 1998). This is a complex apparatus that senses the signal from the chemotaxis sensory signaling system and is transduced into motility. Chemotaxis response regulator CheY transmits chemoreceptor signals to flagellar motor components and is believed to be the “on” switch that directly induces tumbles in the swimming pattern (Robinson et al., 2000). Physical interactions of CheY and switch proteins have not been reported. Chemotactic stimuli change the association of the CheY signal protein with the distal FliM<sub>NC</sub>FliN C ring (Dyer et al., 2009; Sarkar et al., 2010). In the present study, down-regulation of the chemotaxis response regulator (CheY) subsequently down-regulates signal transmission to the flagellar motor components, which may act as an “off” switch and make the bacteria sessile or non-motile. Further, it might lead to a biofilm-like state and could contribute to the drug resistance.

Putative fimbriae major subunit StbA, Fimbrial subunit type 1, conjugal transfer protein TraC, and chaperone FimC protein are involved in pillus organization, fimbriae formation, and their associated assemblies (Johnson and Clegg, 2010). FimC protein acts as a periplasmic pilin chaperone that not only protects the bacteria under stress through chaperone-mediated folding but is also involved in pillus formation (Klemm, 1992). In the periplasm, the FimC chaperone binds to the major and minor structural components and protects them from degradation. Conjugal transfer protein TraC, encoded by a gene, *traC*, presents on plasmid and is involved in the conjugation process as well as pili formation (Winans and Walker, 1985; Kado, 1994), leading



**FIGURE 2 |** Proposed model based on the flagellar-, fimbriae-, and pili-related proteome suggested the mechanism of carbapenem-resistance in *K. pneumoniae* (NDM-4) clinical isolates.



to the transfer of drug-resistant plasmid to bacteria. These down-regulated proteins (flagellar, fimbriae, and pili proteins) form a hub of proteins in the PPI network, which indicates their important role in flagellar, fimbriae, and pili assemblies, signaling through chemotaxis proteins, and biofilm formation (Figure 1). In this study, the down-regulation of fimbriae-, pili-, and conjugative-related proteins leads to the creation of the biofilm-like state, which may contribute to drug resistance. On the basis of the flagella-, fimbriae-, and pili-related proteome, we propose a model (Figure 2) that suggests the potential path or mechanism of carbapenem resistance in *K. pneumoniae* (NDM-4) clinical isolates. Overall this group of down-regulated proteins and their interactive protein partners cumulatively make a hub that leads to the formation of a biofilm-like scenario and could contribute to meropenem resistance.

## CONCLUSION

In brief, the present study focused on the down-regulated proteome of carbapenem-resistant *K. pneumoniae* clinical isolate (NDM-4) under meropenem pressure through proteomics and systems biology approaches. A group of down-regulated proteins was identified that belongs to the flagellar, fimbriae, and pili proteins. Therefore, we suggest that these proteins and their interactive protein partners cumulatively lead to the bacteria becoming sessile, which further creates a biofilm-like state and could contribute to the survival of bacteria under meropenem pressure, which might reveal a novel mechanism of drug resistance. Further research on these motility-related protein targets and their pathways may lead to the development of novel therapeutics against the worsening situation of drug resistance.

## REFERENCES

- Ahmad, N., Khalid, S., Ali, S. M., and Khan, A. U. (2018). Occurrence of blaNDM variants among Enterobacteriaceae from a neonatal intensive care unit in a northern India hospital. *Front Microbiol.* 9:407. doi: 10.3389/fmicb.2018.00407
- Ambler, R. P., Coulson, A. F., Frère, J. M., Ghuyssen, J. M., Joris, B., Forsman, M., et al. (1991). A standard numbering scheme for the class A beta-lactamases. *Biochem. J.* 276(Pt 1), 269–270. doi: 10.1042/bj2760269
- Bennett, J. C., Thomas, J., Fraser, G. M., and Hughes, C. (2001). Substrate complexes and domain organization of the *Salmonella flagellar* export chaperones FlgN and FliT. *Mol. Microbiol.* 39, 781–791. doi: 10.1046/j.1365-2958.2001.02268.x
- Bradford, M. M. (1976). A rapid and sensitive method for the quantification of microgram quantities of protein utilizing the principle of protein-dye binding. *Anal. Biochem.* 72, 248–254. doi: 10.1006/abio.1976.9999
- Camon, E., Barrell, D., Lee, V., Dimmer, E., and Apweiler, R. (2003). The Gene Ontology Annotation (GOA) database—an integrated resource of GO annotations to the UniProt Knowledgebase. *Silico Biol.* 4, 5–6.
- Costerton, J. W., and Lewandowski, Z. (1995). Microbial biofilms. *Annu. Rev. Microbiol.* 49, 711–745.
- Costerton, J. W., Stewart, P. S., and Greenberg, E. P. (1999). Bacterial biofilms: a common cause of persistent infections. *Science* 1999, 1318–1322. doi: 10.1126/science.284.5418.1318
- Djordjevic, S., and Stock, A. M. (1998). Structural analysis of bacterial chemotaxis proteins: components of a dynamic signaling system. *J. Struct. Biol.* 124, 189–200. doi: 10.1006/jsbi.1998.4034
- Doménech-Sánchez, A., Javier, Benedi V, Martínez-Martínez, L., and Alberti, S. (2006). Evaluation of differential gene expression in susceptible and resistant

## DATA AVAILABILITY STATEMENT

The raw data supporting the conclusions of this article will be made available by the authors, without undue reservation, to any qualified researcher.

## AUTHOR CONTRIBUTIONS

DS designed the concept, and experimented and wrote the manuscript. AG and MK carried out the systems biology analysis. FR provided support in the LC-MS experiments and analysis. AK designed and guided the study and finalized the manuscript. All authors approved the final manuscript.

## FUNDING

Science and Engineering Research Board (SERB) is gratefully acknowledged for providing fellowship and funds to DS (SERB-N-PDF/2016/001622) to work at IBU-AMU Aligarh. The authors also acknowledge SCIEX Pvt. Ltd., Gurgaon, India, for data acquisition and proteomics facility support.

## SUPPLEMENTARY MATERIAL

The Supplementary Material for this article can be found online at: <https://www.frontiersin.org/articles/10.3389/fmicb.2019.02865/full#supplementary-material>

- clinical isolates of *Klebsiella pneumoniae* by DNA microarray analysis. *Clin. Microbiol. Infect.* 12, 936–940. doi: 10.1111/j.1469-0691.01470.x
- Dyer, C. M., Vartanian, A. S., Zhou, H., and Dahlquist, F. W. (2009). A molecular mechanism of bacterial flagellar motor switching. *J. Mol. Biol.* 388, 71–84. doi: 10.1016/j.jmb.2009.02.004
- Fux, C. A., Costerton, J. W., Stewart, P. S., and Stoodley, P. (2005). Survival strategies of infectious biofilms. *Trends Microbiol.* 13, 34–40. doi: 10.1016/j.tim.2004.11.010
- Hughes, K. T., Gillen, K. L., Semon, M. J., and Karlinsey, J. E. (1993). Sensing structural intermediates in bacterial flagellar assembly by export of a negative regulator. *Science* 262, 1277–1280. doi: 10.1126/science.8235660
- Jacoby, G. A., Mills, D. M., and Chow, N. (2004). Role of beta-lactamases and porins in resistance to Ertapenem and other beta-lactams in *Klebsiella pneumoniae*. *Antimicrob. Agents Chemother.* 48, 3203–3206. doi: 10.1128/aac.48.8.3203-3206.2004
- Johnson, J. G., and Clegg, S. (2010). Role of MrkJ, a phosphodiesterase, in type 3 fimbrial expression and biofilm formation in *Klebsiella pneumoniae*. *J. Bacteriol.* 192, 3944–3950. doi: 10.1128/JB.00304-10
- Kado, C. I. (1994). Promiscuous DNA transfer system of *Agrobacterium tumefaciens*: role of the virB operon in sex pilus assembly and synthesis. *Mol. Microbiol.* 12, 17–22. doi: 10.1111/j.1365-2958.1994.tb00990.x
- Khan, A., Sharma, D., Faheem, M., Bisht, D., and Khan, A. U. (2017). Proteomic analysis of a carbapenem-resistant *Klebsiella pneumoniae* strain in response to meropenem stress. *J. Glob. Antimicrob. Resist.* 8, 172–178. doi: 10.1016/j.jgar.2016.12.010
- Klemm, P. (1992). FimC, a chaperone-like periplasmic protein of *Escherichia coli* involved in biogenesis of type 1 fimbriae. *Res. Microbiol.* 143, 831–838. doi: 10.1016/0923-2508(92)90070-5

- Lata, M., Sharma, D., Deo, N., Tiwari, P. K., Bisht, D., and Venkatesan, K. (2015). Proteomic analysis of ofloxacin-mono resistant *Mycobacterium tuberculosis* isolates. *J. Proteomics* 127, 114–121. doi: 10.1016/j.jprot.2015.07.031
- Loli, A., Tzouveleki, L. S., Tzelepi, E., Carattoli, A., Vatopoulos, A. C., Tassios, P. T., et al. (2006). Sources of diversity of carbapenem resistance levels in *Klebsiella pneumoniae* carrying blaVIM-1. *J. Antimicrob. Chemother.* 58, 669–672. doi: 10.1093/jac/dkl302
- Martínez-Martínez, L., Pascual, A., Hernández-Allés, S., Álvarez-Díaz, D., Suárez, A. I., Tran, J., et al. (1999). Roles of  $\beta$ -lactamases and porins in activities of carbapenems and cephalosporins against *Klebsiella pneumoniae*. *Antimicrob. Agents Chemother.* 43, 1669–1673. doi: 10.1128/aac.43.7.1669
- McCarty, S. M., Cochrane, C. A., Clegg, P. D., and Percival, S. L. (2012). The role of endogenous and exogenous enzymes in chronic wounds: a focus on the implications of aberrant levels of both host and bacterial proteases in wound healing. *Wound Repair Regen.* 20, 125–136. doi: 10.1111/j.1524-475X.2012.00763.x
- Paterson, D. L. (2000). Recommendation for treatment of severe infections caused by Enterobacteriaceae producing extended-spectrum beta-lactamases (ESBLs). *Clin. Microbiol. Infect.* 6, 460–463. doi: 10.1046/j.1469-0691.2000.00107.x
- Paterson, D. L., and Bonomo, R. A. (2005). Extended-spectrum beta-lactamases: a clinical update. *Clin. Microbiol. Rev.* 18, 657–686. doi: 10.1128/cmr.18.4.657-686.2005
- Piek, S., Wang, Z., Ganguly, J., Lakey, A. M., Bartley, S. N., Mowlaboccus, S., et al. (2014). The role of oxidoreductases in determining the function of the neisserial lipid A phosphoethanolamine transferase required for resistance to polymyxin. *PLoS One* 9:e106513. doi: 10.1371/journal.pone.0106513
- Qayyum, S., Sharma, D., Bisht, D., and Khan, A. U. (2019). Identification of factors involved in *Enterococcus faecalis* biofilm under quercetin stress. *Microb. Pathog.* 126, 205–211. doi: 10.1016/j.micpath.2018.11.013
- Robinson, V. L., Buckler, D. R., and Stock, A. M. (2000). A tale of two components: a novel kinase and a regulatory switch. *Nat. Struct. Biol.* 7, 626–633.
- Sarkar, M. K., Paul, K., and Blair, D. (2010). Chemotaxis signaling protein CheY binds to the rotor protein FliN to control the direction of flagellar rotation in *Escherichia coli*. *Proc. Natl. Acad. Sci. U.S.A.* 107, 9370–9375. doi: 10.1073/pnas.1000935107
- Shannon, P., Markiel, A., Ozier, O., Baliga, N. S., Wang, J. T., Ramage, D., et al. (2003). Cytoscape: a software environment for integrated models of biomolecular interaction networks. *Genome Res.* 13, 2498–2504. doi: 10.1101/gr.1239303
- Sharma, D., and Bisht, D. (2016). An efficient and rapid method for enrichment of lipophilic proteins from *Mycobacterium tuberculosis* H37Rv for two dimensional gel electrophoresis. *Electrophoresis* 37, 1187–1190. doi: 10.1002/elps.201600025
- Sharma, D., and Bisht, D. (2017a). M.tuberculosis hypothetical proteins and proteins of unknown function: hope for exploring novel resistance mechanisms as well as future target of drug resistance. *Front. Microbiol.* 8:465. doi: 10.3389/fmicb.2017.00465
- Sharma, D., and Bisht, D. (2017b). Role of bacterioferritin & ferritin in *M.tuberculosis* pathogenesis and drug resistance: a future perspective by interactomic approach. *Front. Cell. Infect. Microbiol.* 7:240. doi: 10.3389/fcimb.2017.00240
- Sharma, D., and Bisht, D. (2017c). Secretory proteome analysis of streptomycin resistant *Mycobacterium tuberculosis* clinical isolates. *SLAS Discov.* 22, 1229–1238. doi: 10.1177/2472555217698428
- Sharma, D., Bisht, D., and Khan, A. U. (2018a). Potential alternative strategy against drug resistant tuberculosis: a proteomics prospect. *Proteomes* 6:26. doi: 10.3390/proteomes6020026
- Sharma, D., Singh, R., Deo, N., and Bisht, D. (2018b). Interactome analysis of Rv0148 to predict potential targets and their pathways linked to aminoglycosides drug resistance: an insilico approach. *Microb. Pathog.* 121, 179–183. doi: 10.1016/j.micpath.2018.05.034
- Sharma, D., Garg, A., Kumar, M., and Khan, A. U. (2019a). Proteome profiling of carbapenem-resistant *K. pneumoniae* clinical isolate (NDM-4): exploring the mechanism of resistance and potential drug targets. *J. Proteomics* 200, 102–110. doi: 10.1016/j.jprot.2019.04.003
- Sharma, D., Lata, M., Faheem, M., Khan, A. U., Joshi, B., Venkatesan, K., et al. (2019b). Role of *M.tuberculosis* protein Rv2005c in the aminoglycosides resistance. *Microb. Pathog.* 132, 150–155. doi: 10.1016/j.micpath.2019.05.001
- Sharma, D., Misba, L., and Khan, A. U. (2019c). Antibiotics versus Biofilm: an emerging battleground in microbial communities. *Antimicrob. Resist. Infect. Control* 8:76. doi: 10.1186/s13756-019-0533-3
- Sharma, D., and Khan, A. U. (2018). Role of cell division protein divIVA in *Enterococcus faecalis* pathogenesis, biofilm and drug resistance: a future perspective by in silico approaches. *Microb. Pathog.* 125, 361–365. doi: 10.1016/j.micpath.2018.10.001
- Stewart, P. S., and William Costerton, J. (2001). Antibiotic resistance of bacteria in biofilms. *Lancet* 358, 135–138. doi: 10.1016/s0140-6736(01)05321-1
- Wayne, P. A. (2014). Performance standards for antimicrobial susceptibility testing: 24 informational supplement. *CLSI* 100, S24.
- Winans, S. C., and Walker, G. C. (1985). Conjugal transfer system of the IncN plasmid pKM101. *J. Bacteriol.* 161, 402–410.
- Yeung, A. T., Bains, M., and Hancock, R. E. (2011). The sensor kinase CbrA is a global regulator that modulates metabolism, virulence, and antibiotic resistance in *Pseudomonas aeruginosa*. *J. Bacteriol.* 15, 918–931. doi: 10.1128/JB.00911-10

**Conflict of Interest:** FR was employed by SCIEEX Pvt. Ltd.

The remaining authors declare that the research was conducted in the absence of any commercial or financial relationships that could be construed as a potential conflict of interest.

Copyright © 2019 Sharma, Garg, Kumar, Rashid and Khan. This is an open-access article distributed under the terms of the Creative Commons Attribution License (CC BY). The use, distribution or reproduction in other forums is permitted, provided the original author(s) and the copyright owner(s) are credited and that the original publication in this journal is cited, in accordance with accepted academic practice. No use, distribution or reproduction is permitted which does not comply with these terms.



# Effect of Dietary Copper on Intestinal Microbiota and Antimicrobial Resistance Profiles of *Escherichia coli* in Weaned Piglets

Yiming Zhang<sup>1,2</sup>, Jian Zhou<sup>2</sup>, Zhenglin Dong<sup>1,2</sup>, Guanya Li<sup>1,2</sup>, Jingjing Wang<sup>2</sup>, Yikun Li<sup>2</sup>, Dan Wan<sup>2\*</sup>, Huansheng Yang<sup>1</sup> and Yulong Yin<sup>1,2</sup>

<sup>1</sup> Hunan International Joint Laboratory of Animal Intestinal Ecology and Health, Laboratory of Animal Nutrition and Human Health, College of Life Sciences, Hunan Normal University, Changsha, China, <sup>2</sup> Hunan Province Key Laboratory of Animal Nutritional Physiology and Metabolic Process, Key Laboratory of Agro-ecological Processes in Subtropical Region, National Engineering Laboratory for Pollution Control and Waste Utilization in Livestock and Poultry Production, Institute of Subtropical Agriculture, Chinese Academy of Sciences, Changsha, China

## OPEN ACCESS

### Edited by:

Leonardo Neves de Andrade,  
University of São Paulo, Brazil

### Reviewed by:

Yulan Liu,  
Wuhan Polytechnic University, China  
Evelyne Forano,  
INRA Centre Auvergne –  
Rhône-Alpes, France

### \*Correspondence:

Dan Wan  
w.dan@isa.ac.cn

### Specialty section:

This article was submitted to  
Antimicrobials, Resistance  
and Chemotherapy,  
a section of the journal  
Frontiers in Microbiology

**Received:** 15 July 2019

**Accepted:** 19 November 2019

**Published:** 17 December 2019

### Citation:

Zhang Y, Zhou J, Dong Z, Li G,  
Wang J, Li Y, Wan D, Yang H and  
Yin Y (2019) Effect of Dietary Copper  
on Intestinal Microbiota  
and Antimicrobial Resistance Profiles  
of *Escherichia coli* in Weaned Piglets.  
*Front. Microbiol.* 10:2808.  
doi: 10.3389/fmicb.2019.02808

Copper is an essential microelement for animals, and not only it has been used as a feed additive at pharmacological doses in swine production to improve growth performance, but it also has an effect on intestinal microbes by enhancing host bacterial resistance. However, there are few reports on the effects of pharmacological doses of copper on intestinal microorganisms and the antimicrobial resistance profiles of pathogenic bacteria, such as *Escherichia coli*, in pigs. Therefore, this study aimed to investigate the effects of pharmacological doses of copper on the microbial communities in the hindgut and the antimicrobial resistance profiles of *E. coli* in weaned piglets. Twenty-four healthy weaned piglets aged  $21 \pm 1$  days and with an average weight of  $7.27 \pm 0.46$  kg were randomly divided into four groups. The control group was fed a basal diet, while the treatment groups were fed a basal diet supplemented with 20, 100, or 200 mg copper/kg feed, in the form of  $\text{CuSO}_4$ . Anal swabs were collected at 0, 21, and 42 days of the trial, and *E. coli* was isolated. Meanwhile, the contents of the ileum and cecum from the control and 200 mg copper/kg feed groups were collected at 21 and 42 days for microbial community analysis and *E. coli* isolation. All isolated *E. coli* strains were used for antimicrobial resistance profile analysis. A pharmacological dose of copper did not significantly change the diversity, but significantly affected the composition, of microbial communities in the ileum and cecum. Moreover, it affected the microbial metabolic functions of energy metabolism, protein metabolism, and amino acid biosynthesis. Specifically, copper treatment increased the richness of *E. coli* in the hindgut and the rates of *E. coli* resistance to chloramphenicol and ciprofloxacin. Moreover, the rate of *E. coli* resistance to multiple drugs increased in the ileum of pigs

fed a pharmacological dose of copper. Thus, a pharmacological dose of copper affected the composition of the microbial community, increased the antimicrobial resistance rates of intestinal *E. coli*, and was most likely harmful to the health of piglets at the early stage after weaning.

**Keywords:** copper, piglet, microbial community, *Escherichia coli*, antimicrobial resistance

## INTRODUCTION

Copper (Cu) is an essential trace element for animals, with many biological functions, including iron metabolism, immunity, protection from oxidative stress, and improvement in the activity of digestive enzymes (Gipp et al., 1967; Harris, 1991; Amachawadi et al., 2010; Braune et al., 2010; Huang et al., 2015). Feeding weaned piglets a high Cu diet, usually at pharmacological doses (150–250 mg Cu/kg feed) as CuSO<sub>4</sub>, Cu-AA, or Cu hydroxychloride, may improve their average daily weight gain and feed conversion ratio and reduce the frequency of diarrhea (Smith et al., 1997; Cromwell et al., 1998; Hill et al., 2000; Perez et al., 2011; Bikker et al., 2016; Espinosa et al., 2017).

However, as the Cu requirement of piglets is 4–6 mg Cu/kg feed (Okonkwo et al., 1979), the excess Cu results in an increase in the Cu content of pig slurry and, consequently, an accumulation of Cu in soils, which poses a high environmental risk (Jondreville et al., 2002). Meanwhile, excess amounts of Cu in the gut can affect the intestinal microbial community and result in reduced counts of streptococci, ureolytic bacteria, and total anaerobes in the feces (Fuller et al., 1960; Kellogg et al., 1966; Varel et al., 1987). Recently, it has been found that feeding piglets with 300 mg Cu/kg feed affected the abundance of *Clostridium* genera and decreased the relative abundance of butyrate-producing bacteria, such as *Acidaminococcus*, *Coprococcus*, and *Roseburia* in fecal microbiota (Zhang et al., 2019). It also altered the gut microbiota and decreased the counts of *Lactobacilli* and Enterobacteriaceae in the cecum and ileum of weaned piglets (Ole et al., 2005; Mei et al., 2010). However, the effects on gut microbiota composition and function when pharmacological amounts of Cu are added to feed have not been thoroughly investigated.

In pigs, enteric bacteria have been shown to develop Cu resistance by transferable tcrB in enterococci (Hasman and Aarestrup, 2005) or by the multicopper oxidase, PcoA, and the metal sponge, PcoE, in enterobacteria (Djoko et al., 2008; Zimmermann et al., 2012). Resistance to Cu in bacteria, particularly in enterococci, is often associated with resistance to antimicrobial drugs, such as macrolides and glycopeptides (Hasman et al., 2006; Yazdankhah et al., 2014), while Cu resistance in *Escherichia coli* is negatively associated with both tetA and bla (CMY-2) (Agga et al., 2014). Nevertheless, the potential connection between Cu resistance and antimicrobial drug resistance, particularly in the enterobacterium, *E. coli*, has not been fully elucidated. Therefore, the objective of the present study was to investigate the effects of different doses of Cu, including a pharmacological dose, on hindgut microbiota diversity, composition, and metabolic function in weaned piglets after 3 and 6 weeks of supplementation. Based on the results of microbiota analysis, *E. coli* was isolated from feces at 0, 21, and

42 days of the feeding period, and the drug resistance profile of the isolates was assessed for the first time.

## MATERIALS AND METHODS

### Animals, Feeding, and Sampling

Animal experiments were approved by the Animal Protocol Review Committee of the Institute of Subtropical Agriculture, Chinese Academy of Sciences (Changsha, China), and all experiments were performed according to the institutional animal welfare requirements. Forty-eight healthy weaned piglets, aged  $21 \pm 1$  days ( $8.26 \pm 0.17$  kg), were randomly assigned to four groups, with six barrows and six females in each group. The piglets were housed individually and given free access to drinking water and food. The control group was fed a basal diet (Table 1), and the treatment groups were fed a basal diet supplemented with 20, 100, or 200 mg Cu/kg feed, as CuSO<sub>4</sub>·5H<sub>2</sub>O, for 6 weeks. Anal swabs were collected from piglets at days 0, 21, and 42 of the experimental period, for *E. coli* isolation and antimicrobial drug resistance detection. At days 21 and 42, piglets ( $n = 6$ ) in the control and 200 mg Cu group were anesthetized with Zoletil (15 mg/kg BW, i.m.) and euthanized. The ileal and cecal contents were collected under sterile conditions, using a 15-ml sterile conical centrifuge tube and submitted for 16S rRNA sequencing, *E. coli* isolation, and antimicrobial drug resistance evaluation.

### 16S rDNA Sequencing

The ileal and cecal contents from piglets in the control (without Cu supplementation) group and the group receiving a pharmacological dose of Cu (200 mg Cu/kg feed,  $n = 6$  per treatment) were collected for microbiota analysis, as described previously (Zhou et al., 2018; Xiong et al., 2019). Briefly, total bacterial DNA was extracted using a QIAamp DNA Stool Mini Kit (Qiagen, Hilden, Germany), and the V3–V4 hypervariable region of the microbial 16S rRNA genes were sequenced using the primers, 341F: 5'-CCTAYGGGRBGCASCAG-3' and 806R: 5'-GGACTACNNGGTATCTAAT-3'; Illumina adaptors; and molecular barcodes. Libraries were prepared using a TruSeq DNA PCR-Free Sample Preparation Kit (Illumina Inc., San Diego, CA, United States) and were assessed using a Qubit 2.0 Fluorometer (Thermo Scientific, Madison, WI, United States) and a Bioanalyzer 2100 system (Agilent Technologies, Santa Clara, CA, United States). Libraries were sequenced on a HiSeq 2500 platform (Illumina Inc., San Diego, CA, United States). Raw 16S rDNA sequences were assembled using the QIIME (v1.9.0) and FLASH software packages. Operational taxonomic units (OTUs) were analyzed using UPARSE (v7.0.1001), and



**TABLE 1** | Formulation of basal diet (air-dry basis, %).

Ingredient	Content (%)	Analyzed nutrient levels <sup>a</sup>	Content
Corn	25	Dry matter (%)	87
Extruded corn	34	Digestible energy (kcal/kg)	3.40
Soymeal	2.5	CP (%)	20.00
Fermented soymeal	8	Ash (%)	7.84
Extruded soybean	5	Ether extract (%)	3.55
Fish meal	10	NDF (%)	22.16
Whey powder	4	ADF (%)	11.75
Glucose	5	Ca (%)	0.80
L-Thr (≥97.5%)	0.45	Total P (%)	0.45
L-Trp (≥98.0%)	0.05	Cu (control)	5.09 mg/kg
D,L-Met (≥98.5%)	0.2	Cu (20 mg/kg)	25.68 mg/kg
L-Lys-HCl (≥98.5%)	0.8	Cu (100 mg/kg)	81.80 mg/kg
Soybean oil	1.1	Cu (200 mg/kg)	176.58 mg/kg
Sodium chloride (≥91.0%)	0.74		
Calcium carbonate	0.4		
Calcium hydrophosphate	0.28		
Antioxidant	0.08		
Citric acid	1.3		
Mildew preventive	0.1		
Premix <sup>b</sup>	1		

<sup>a</sup>Feed analyses were performed according to the AOAC guidelines (2004). <sup>b</sup>The vitamin–mineral premix provided the following per kilogram of feed: 100 mg of antioxidant, 100 mg of preservatives, 100 mg of choline chloride, 6,000 IU of vitamin A, 3,000 IU of vitamin D<sub>3</sub>, 20 IU of vitamin E, 1.8 mg of vitamin K<sub>3</sub>, 2.0 mg of thiamine, 6.0 mg of riboflavin, 4.0 mg of pyridoxine, 0.02 mg of vitamin B<sub>12</sub>, 26.0 mg of niacin, 18.0 mg of pantothenic acid, 3.2 mg of folic acid, 0.4 mg of biotin, 100 mg of Fe as FeSO<sub>4</sub>·7H<sub>2</sub>O, 100 mg of Zn as ZnSO<sub>4</sub>·H<sub>2</sub>O, 50 mg of Mn as MnSO<sub>4</sub>·H<sub>2</sub>O, 1.2 mg of I as KI, and 0.30 mg of Se as Na<sub>2</sub>SeO<sub>3</sub>.

high-quality sequences were aligned against the SILVA reference database 1 and clustered into OTUs at a 97% similarity level using the UCLUST algorithm 2. Each OTU was assigned to a taxonomic level using the Ribosomal Database Project Classifier program v2.203. The assembled sequences were then submitted to the NCBI Sequence Read Archive (No. PRJNA551517) for open access.

## *E. coli* Isolation and Identification

Samples were collected with sterile swabs, and the swab sample was immediately inserted into a 15-ml sterile centrifuge tube containing 5 ml of phosphate-buffered saline. Then, 10 μl of each sample was swabbed onto MacConkey agar and incubated at 37°C for 18–24 h. Three red- or pink-colored colonies were picked per sample and inoculated on eosin methylene blue agar plates at 37°C for 18–24 h to obtain pure cultures. A single colony with a black metallic luster was picked and cultured in Luria–Bertani (LB) liquid medium at 37°C for 8–12 h. Bacterial smears were from the LB liquid culture, and Gram staining and microscopic examination were performed as described (Feyzioglu et al., 2014; Usaini et al., 2015). LB liquid cultures containing Gram-negative bacilli were swabbed onto

eosin methylene blue agar plates and incubated at 37°C for 18–24 h. A single colony with a black metallic luster was picked, inoculated on a nutrient agar plate, and cultured at 37°C for 12–18 h. Single colonies from the nutrient agar plate were inoculated in biochemical identification tubes (Hangzhou Microbial Reagent Co., Ltd., Hangzhou, China) for lactose fermentation, and indole and citrate utilization tests, according to the manufacturer's instructions. Isolates with a Lac+/Ind+/Cit– phenotype were identified as *E. coli*. Finally, the 16S rRNA gene of isolated *E. coli* was amplified by PCR. DNA extraction and PCR amplification were performed as previously described (Blyton et al., 2013). Three oligonucleotide primers, 16E1, 16E2, and 16E3, were designed and used in the PCR assays for the identification of *E. coli* isolates, as previously described (Tsen et al., 1998). The sequences and locations of these primers are shown in **Supplementary Table S1**. PCR products were analyzed by gel electrophoresis through a 2% agarose gel, as previously described (Tsen et al., 1998) and sequenced by Sangon Biotech Co., Ltd. (Shanghai, China). Homology analysis between the amplified sequences and the *E. coli* 16S rRNA gene sequences published in GenBank was performed to confirm that the isolates were *E. coli*. Repetitive element PCR with both ERIC and (CGG)<sub>4</sub> primers was also used to discriminate clonal isolates from the same samples (Adamus-Bialek et al., 2009). Isolates producing the same banding pattern were considered to be the same strain.

## Drug-Resistant Phenotype Identification

After PCR validation, the *E. coli* suspensions were subjected to antimicrobial susceptibility testing on Müller–Hinton agar using the Kirby–Bauer disk diffusion method, in accordance with the Clinical and Laboratory Standards Institute guidelines, using *E. coli* ATCC 25922 as an internal quality control. The antimicrobial disks used for the test included ampicillin (10 μg/disk), amoxicillin/clavulanic acid (20/10 μg/disk), ceftriaxone (30 μg/disk), meropenem (10 μg/disk), aztreonam (30 μg/disk), gentamicin (10 μg/disk), trimethoprim/sulfamethoxazole (1.25/23.75 μg/disk), amikacin (30 μg/disk), and ciprofloxacin (CIP) (5 μg/disk) (Oxoid Ltd., Hampshire, United Kingdom).

## Statistical Analysis

All statistical analyses were performed using SPSS 20.0 software (SPSS Inc., Chicago, IL, United States).  $\alpha$  and  $\beta$  diversity were analyzed using QIIME (v1.7.0). Data for microbial metabolic functions were analyzed by Student's *t*-test only, due to minor changes in the microbiome data. The differences in isolation rates and antimicrobial resistance of *E. coli* among the groups were analyzed by Chi-square test. A  $P < 0.05$  was considered statistically significant.

## RESULTS

### Bodyweight and Growth Performance

The average bodyweights of the weaned piglets at 21 ± 1 days in the control and Cu-supplemented groups were 8.13 ± 0.22 and 8.40 ± 0.26 kg, respectively. There were no significant differences

in average daily gain, average daily feed intake, or feed conversion ratio between the control and Cu-supplemented groups in early (1–3 weeks) and late postweaning stages (4–6 weeks, **Table 2**).

## Microbiota Diversity in Intestinal Contents

There were no significant differences between treatments for the indices of  $\alpha$  diversity, including observed\_species, Shannon, Simpson, Chao1, ACE, and PD\_whole\_tree indices, of ileal (**Supplementary Table S2**) and cecal microbiota (**Supplementary Table S3**). In addition, the weighted principal

**TABLE 2** | The effect of Cu levels on the growth performance of piglets during the first 3 weeks and the second 3 weeks of feeding.

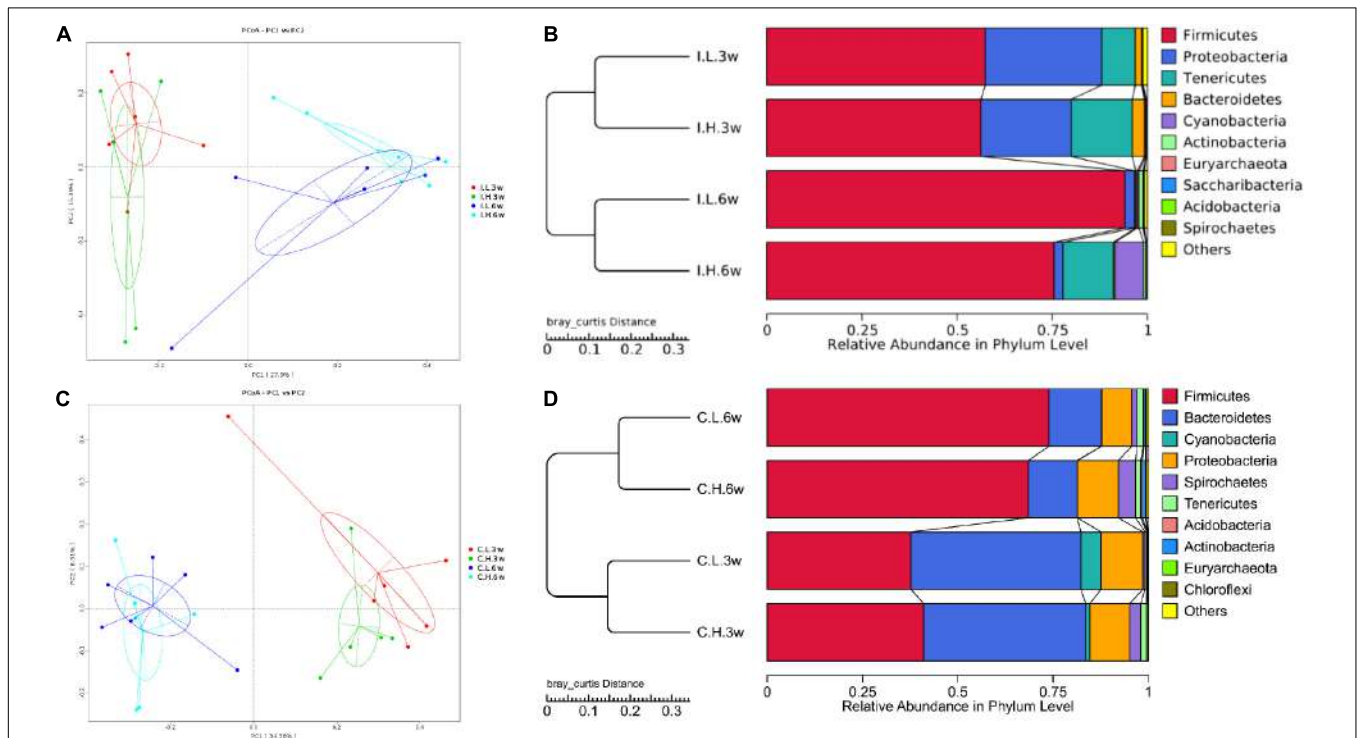
Time	Growth performance <sup>a</sup>	Control	High Cu	P-value
1–3 weeks	ADG (kg)	0.22 ± 0.01	0.25 ± 0.02	0.154
	ADFI (g)	405.58 ± 14.62	444.57 ± 21.58	0.157
	FCR	1.86 ± 0.04	1.80 ± 0.09	0.559
4–6 weeks	ADG (kg)	0.37 ± 0.02	0.42 ± 0.03	0.201
	ADFI (g)	787.41 ± 34.66	805.18 ± 40.89	0.743
	FCR	2.12 ± 0.08	1.95 ± 0.09	0.177

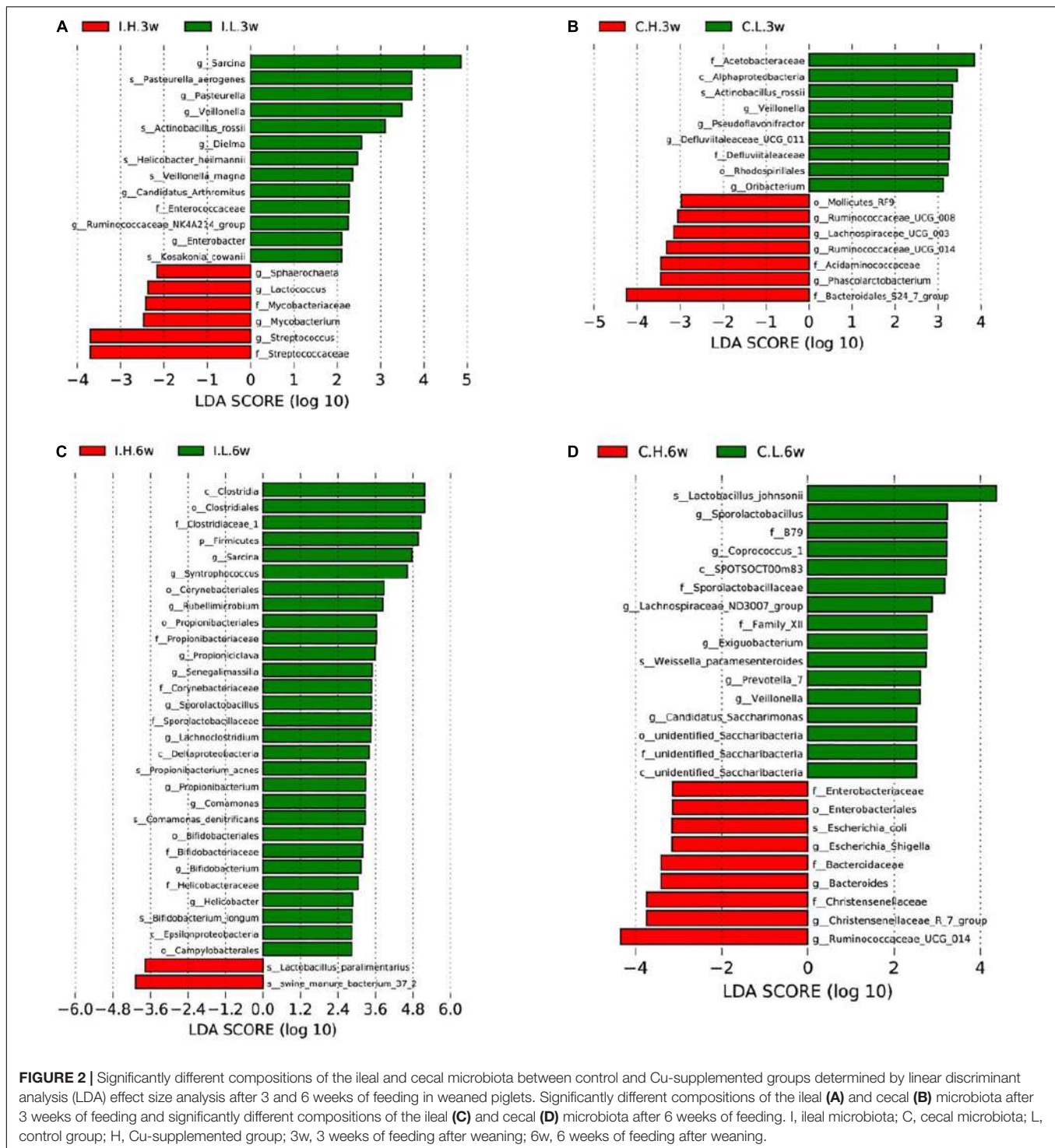
<sup>a</sup>ADG, average daily gain; ADFI, average daily feed intake; FCR, feed conversion ratio.

coordinate analysis plots of ileal (**Figure 1A**) and cecal microbiota (**Figure 1C**) verified that there were few differences in microbial communities between Cu treatments.

## Microbiota Composition of Intestinal Contents

Based on an unweighted pair-group method with arithmetic mean analysis, Firmicutes, Proteobacteria, Tenericutes, and Bacteroidetes were found to be the dominant bacteria in the ileal microbiome (**Figure 1B**), while Firmicutes, Bacteroidetes, Cyanobacteria, Proteobacteria, and Spirochaetes were the dominant bacteria in the cecal microbiome (**Figure 1D**). Furthermore, the linear discriminant analysis effect size method was used to determine the variation in microbial composition between groups. Minimal changes were observed after short-term feeding (3 weeks), with differences in abundance of the genera *Sarcina*, *Pasteurella*, *Veillonella*, *Streptococcus*, *Mycobacterium*, *Lactococcus*, and *Sphaerochaeta* in the ileal microbiome (**Figure 2A**) and in the family, Acetobacteraceae, and the genera, *Veillonella*, *Pseudoflavonifractor*, Defluviitaleaceae, *Oribacterium*, Ruminococcaceae (UCG008, 014), Lachnospiraceae (UCG003), and *Phascolarctobacterium* in the cecal microbiome (**Figure 2B**). Meanwhile, after a longer time of feeding (6 weeks) with Cu supplementation at a pharmacological dose, marked differences



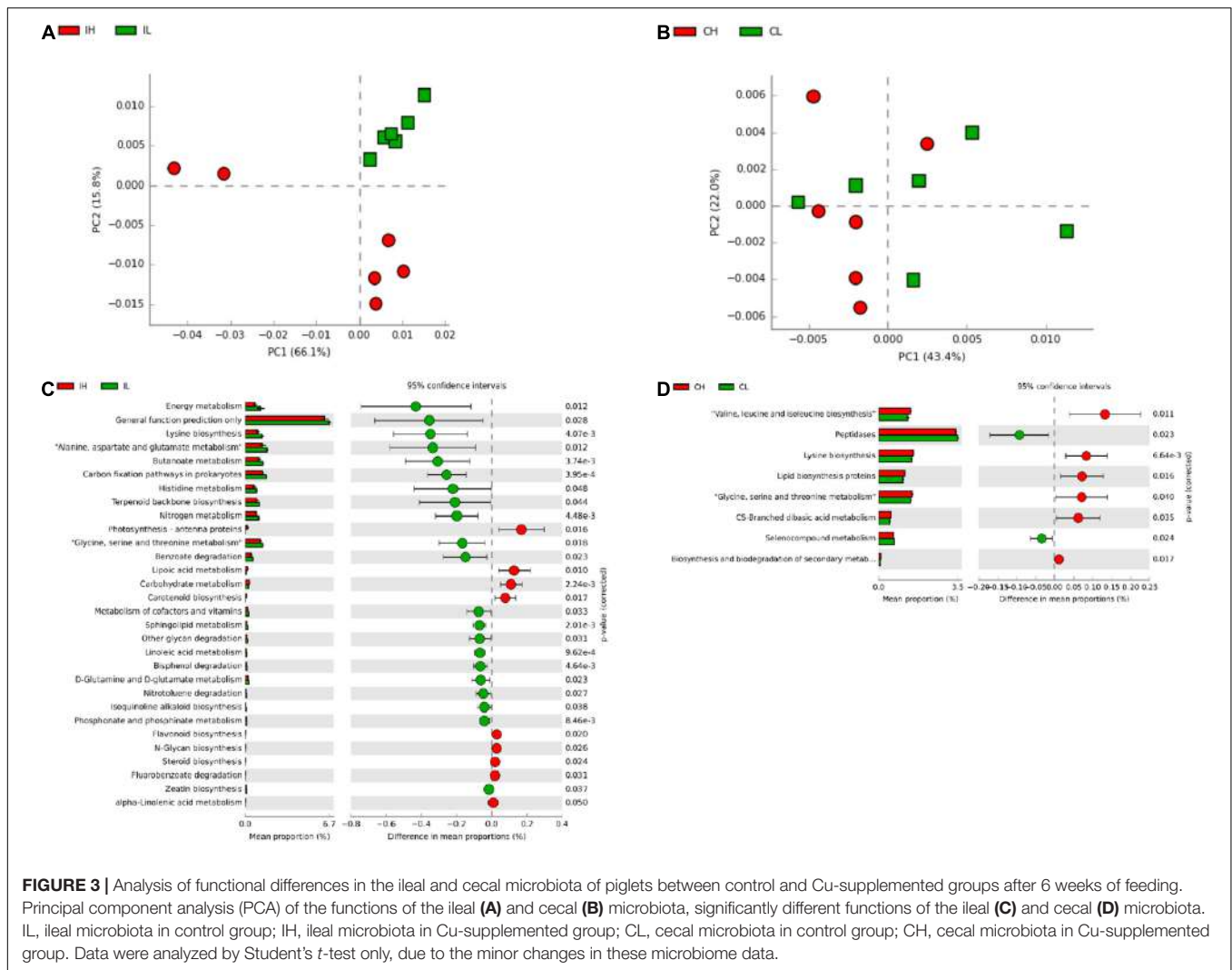


**FIGURE 2 |** Significantly different compositions of the ileal and cecal microbiota between control and Cu-supplemented groups determined by linear discriminant analysis (LDA) effect size analysis after 3 and 6 weeks of feeding in weaned piglets. Significantly different compositions of the ileal (A) and cecal (B) microbiota after 3 weeks of feeding and significantly different compositions of the ileal (C) and cecal (D) microbiota after 6 weeks of feeding. I, ileal microbiota; C, cecal microbiota; L, control group; H, Cu-supplemented group; 3w, 3 weeks of feeding after weaning; 6w, 6 weeks of feeding after weaning.

were found in the abundance of the family, Clostridiaceae, the phylum Firmicutes, the genus, *Sarcina*, *Lactobacillus paralimentarius*, and swine manure bacterium in the ileal microbiome (Figure 2C), and the genera, *Lactobacillus* and *Sporolactobacillus* and *E. coli* in the cecal microbiome (Figure 2D). A heat map of the 40 most different genera showed the taxonomic distributions among groups after 3 and 6 weeks

of treatment (Supplementary Figure S1). Next, the impact of Cu treatment on aerobic, anaerobic, mobile element-containing, facultatively anaerobic, biofilm-forming, Gram-negative, Gram-positive, potentially pathogenic, and stress-tolerant bacteria were predicted via BugBase (Zhou et al., 2019). No significant differences were found to occur as a result of Cu treatment (Supplementary Figure S3).





## Predicted Metabolic Functions in the Gut Microbiota

Subsequently, to further investigate the changes in the function of the gut microbiota, the metagenome was generated, based on 16S rDNA sequencing results, using Picrust. The Kyoto Encyclopedia of Genes and Genomes annotation results were then submitted for principal component analysis. Microbial metabolism-related pathways at Kyoto Encyclopedia of Genes and Genomes level 3 were specifically filtered. No obvious segregation of ileal and cecal microbiomes was found in the third week (Supplementary Figures S2A,B). Furthermore, a *t*-test showed that Cu supplementation (200 mg Cu/kg feed) increased the abundance of microbiota related to the transcriptional machinery and tuberculosis in the ileal microbiome, while an increase in the abundance of microbiota related to methane metabolism was observed in the cecal microbiome at the third week (Supplementary Figures S2C,D). An obvious segregation was found in the ileal microbiome in the sixth week (Figure 3A), but there was still no obvious segregation in the cecal microbiome at this time point (Figure 3B).

Cu supplementation decreased the abundance of microbiota related to energy metabolism, lysine biosynthesis, amino acid metabolism (alanine, aspartate, glutamate, histidine, glycine, serine, and threonine), butanoate metabolism, carbon-fixation pathways in prokaryotes, terpenoid backbone biosynthesis, nitrogen metabolism, benzoate degradation, and the metabolism of cofactors and vitamins in the ileal microbiome (Figure 3C). Meanwhile, Cu supplementation increased the abundance of microbiota related to amino acid biosynthesis (valine, leucine, isoleucine, and lysine), lipid biosynthesis protein, amino acid metabolism (glycine, serine, and threonine), and C5-branched dibasic acid metabolism and decreased the abundance of microbiota related to peptidases in the cecal microbiome (Figure 3D).

## Antimicrobial Resistance Profiles of *E. coli* Isolates From Intestinal Contents

Based on microbial composition analysis, we further determined the antimicrobial resistance profiles of *E. coli* isolated from the ileal and cecal contents. Isolates that were resistant to three



or more classes of antimicrobials were defined as multidrug-resistant strains. A total of 119 *E. coli* isolates from ileal ( $n = 50$ ) and cecal contents ( $n = 69$ ) were included in disk diffusion testing, with 20 ileal isolates and 34 cecal isolates from control pigs and 30 ileal isolates and 35 cecal isolates from pigs fed a pharmacological dose of Cu (**Supplementary Table S4**).

Of the 119 isolates, 10 (8.40%) were not resistant to any of the antimicrobial agents tested, 9 (7.56%) were resistant to one antimicrobial agent, and 21 (17.65%) were resistant to two antimicrobial agents. Furthermore, 79 (66.39%) were resistant to at least three antimicrobial agents, and 47 (39.50%) of these were isolated from pigs fed a pharmacological dose of Cu. In particular, seven isolates (5.88%) were resistant to more than six classes of antimicrobials, and six (5.04%) of these were isolated from pigs fed a pharmacological dose of Cu (**Table 3**). The antimicrobial resistance rates of *E. coli* in the ileum and cecum are summarized in **Table 4**. Resistance to CIP in ileal isolates and resistance to chloramphenicol (C) in cecal isolates were found to significantly respond to Cu dose.

On the basis of these results, anal swabs were collected from four groups of pigs and used for *E. coli* isolation to investigate the development of resistance in response to Cu dose and feeding period. No significant differences were found in the rate of *E. coli* response to Cu dosage or feeding period (**Supplementary Table S5**). However, a dose-dependent effect on resistance to C and CIP was found at day 42 ( $P < 0.05$ , **Table 5**).

## DISCUSSION

For many years, a pharmacological dose of Cu (150–250 mg/kg feed) has been added to animal diets to improve growth performance. However, as the Cu requirement of pigs is 4–6 mg/kg feed, the growth-promoting effect of dietary Cu is mostly attributed to the regulation of the composition and metabolism of the intestinal microbiota (Varel et al., 1987). Meanwhile, there are increasing concerns regarding the potential adverse effects of Cu accumulation on the intestinal microbiota, i.e., microbial drug resistance (Hasman and Aarestrup, 2005; Hasman et al., 2006; Djoko et al., 2008; Amachawadi et al., 2011; Zimmermann et al., 2012; Agga et al., 2014; Yazdankhah et al., 2014). The effects of Cu on the counts of coliforms and microbial drug resistance have previously been reported (Djoko et al., 2008;

Zimmermann et al., 2012; Zhang et al., 2019). Thus, the present research focused on microbial diversity, composition, and function, as well as the potential risks of *E. coli* resistance in the intestine of piglets after pharmacological doses of Cu.

$\alpha$  and  $\beta$  diversity are important features of microbial communities. In our study,  $\alpha$  diversity indices, including observed species, Shannon, Simpson, Chao1, ACE, and PD\_whole\_tree indices were not affected by dietary Cu. Our results were consistent with those of a previous study of high dietary Cu levels (300 mg/kg) in suckling piglets (Zhang et al., 2019) but in contrast to previous studies reporting that high dietary Cu levels (100–200 mg/kg, as  $\text{CuSO}_4$ ) significantly affect microbial species in the ileac, cecal, and colonic chyme of piglets (Varel et al., 1987; Hojberg et al., 2005; Namkung et al., 2006; Mei et al., 2010). A possible reason for these differences is that the method used to investigate the microbial

**TABLE 4** | Antimicrobial resistance rates (95% CI) of *Escherichia coli* in ileum and cecum<sup>1</sup>.

Antimicrobial agent <sup>a</sup>	Groups	Ileum <i>E. coli</i>	Cecum <i>E. coli</i>
AMC	Control	0.00 (0.00, 16.84)	0.00 (0.00, 10.28)
	High Cu	6.67 (0.82, 22.07)	5.71 (0.70, 19.16)
	<i>P</i> -value	0.510	0.493
CRO	Control	10.00 (1.24, 31.70)	11.76 (3.30, 27.45)
	High Cu	20.00 (7.71, 38.57)	14.29 (4.81, 30.26)
	<i>P</i> -value	0.450	1.000
C	Control	75.00 (50.90, 91.34)	47.06 (29.78, 64.87)
	High Cu	80.00 (61.43, 92.29)	74.29 (56.74, 87.51)
	<i>P</i> -value	0.736	0.027
CN	Control	20.00 (5.73, 43.66)	41.18 (24.65, 59.30)
	High Cu	20.00 (7.71, 38.57)	28.57 (14.64, 46.30)
	<i>P</i> -value	1.000	0.318
CIP	Control	15.00 (3.21, 37.89)	35.29 (19.75, 53.51)
	High Cu	46.67 (28.34, 65.67)	25.71 (12.49, 43.26)
	<i>P</i> -value	0.032	0.440
AMP	Control	50.00 (27.20, 72.80)	73.53 (55.64, 87.12)
	High Cu	73.33 (54.11, 87.72)	71.43 (53.70, 85.36)
	<i>P</i> -value	0.134	1.000
ATM	Control	0.00(0.00, 16.84)	2.94 (0.07, 15.33)
	High Cu	13.33(3.76, 30.72)	8.57(1.80, 23.06)
	<i>P</i> -value	0.140	0.614
MEM	Control	0.00 (0.00, 16.84)	2.94 (0.07, 15.33)
	High Cu	0.00 (0.00, 11.57)	5.71 (0.70, 19.16)
	<i>P</i> -value		1.000
AK	Control	0.00 (0.00, 16.84)	5.88 (0.72, 19.68)
	High Cu	13.33 (3.76, 30.72)	14.29 (4.81, 30.26)
	<i>P</i> -value	0.140	0.428
SXT	Control	80.00 (56.34, 94.27)	94.12 (80.32, 99.28)
	High Cu	80.00 (61.43, 92.29)	91.43 (76.94, 98.20)
	<i>P</i> -value	1.000	1.000

<sup>1</sup>The differences in antibiotic resistance of *E. coli* among groups were analyzed by Chi-square test. A  $P < 0.05$  was considered statistically significant.

<sup>a</sup>AMP, ampicillin; AMC, amoxicillin/clavulanic acid; CRO, ceftriaxone; MEM, meropenem; ATM, aztreonam; CN, gentamicin; AK, amikacin; CIP, ciprofloxacin; C, chloramphenicol; SXT, trimethoprim/sulfamethoxazole.

**TABLE 3** | Number of antimicrobial multiresistant *E. coli* isolates in ileum and cecum.

	Ileum		Cecum		Overall ( $n = 119$ )
	Control ( $n = 20$ )	High Cu ( $n = 30$ )	Control ( $n = 34$ )	High Cu ( $n = 35$ )	
0	3	4	2	1	10
1	0	1	3	5	9
2	10	1	4	6	21
3	3	6	11	8	28
$\geq 4$ and $\leq 6$	4	15	13	12	44
$> 6$	0	3	1	3	7

**TABLE 5** | Antimicrobial resistance rates (95% CI) of *Escherichia coli* from anal swabs<sup>1</sup>.

Antibiotic <sup>s</sup>	Time (weeks)	Copper treatments (mg Cu/kg feed)				P-value
		0	20	100	200	
C	0	53.33 (26.59, 78.73)	46.67 (21.27, 73.41)	53.33 (26.59, 78.73)	38.89 (17.30, 64.25)	0.812
	3	53.33 (26.59, 78.73)	29.41 (10.31, 55.96)	60.00 (32.29, 83.66)	66.67 (38.38, 88.18)	0.153
	6	19.05 (5.45, 41.91) <sup>a</sup>	23.81 (8.22, 47.17) <sup>a</sup>	46.67 (21.27, 73.41) <sup>a</sup>	78.26 (56.30, 92.54) <sup>b</sup>	0.000
CIP	0	29.41 (10.31, 55.96)	11.11 (1.38, 34.71)	40.00 (16.34, 67.71)	50.00 (26.02, 73.98)	0.063
	3	20.00 (4.33, 48.09)	11.76 (1.46, 36.44)	26.67 (7.79, 55.10)	13.33 (1.66, 40.46)	0.692
	6	14.29 (3.05, 36.34) <sup>a</sup>	4.76 (0.12, 23.82) <sup>a</sup>	26.67 (7.79, 55.10) <sup>ab</sup>	30.43 (13.21, 52.92) <sup>b</sup>	0.046

<sup>1</sup>The differences in antibiotic resistance of *E. coli* among groups were analyzed by Chi-square test. <sup>a,b</sup>Means in a row without a common superscript letter differ significantly for the same period. <sup>s</sup>CIP, ciprofloxacin; C, chloramphenicol.

flora is inconsistent among the different studies. As most bacterial species in the gut are yet to be cultured, 16S rRNA gene sequencing is recommended for the analysis of gut microbial communities. In the present study, unweighted pair-group method with arithmetic mean analysis showed that Firmicutes, Bacteroidetes, and Proteobacteria were the most abundant phyla in the ileum and cecum, which is similar to previous findings in piglets (Xiong et al., 2019; Zhang et al., 2019). Linear discriminant analysis effect size analysis also showed that the differences included, but were not limited to, the phylum Firmicutes, the family, Clostridiaceae, and the genera, *Streptococcus*, *Lactococcus*, and Ruminococcaceae, which were found to be affected in previous studies in which Cu was supplemented at high levels (200–300 mg/kg) as CuSO<sub>4</sub> (Fuller et al., 1960; Kellogg et al., 1966; Varel et al., 1987; Hojberg et al., 2005; Xia et al., 2005; Namkung et al., 2006; Mei et al., 2010; Wang et al., 2012; Song et al., 2013; Zhang et al., 2019). In addition, consistent with previous studies, the addition of high concentrations of Cu to the diet had no significant effect on the populations of aerobic, anaerobic, mobile element-containing, facultatively anaerobic, biofilm-forming, Gram-negative, Gram-positive, potentially pathogenic, or stress-tolerant bacteria (Varel et al., 1987; Hojberg et al., 2005; Mei et al., 2010; Zhang et al., 2019). Moreover, in accordance with the results of Zhang et al. (2019), carbohydrate metabolism by ileal microbes was significantly enhanced by high levels of dietary Cu.

Based on Picrust predictions, our study suggested that Cu supplementation affected the abundance of microbiota related to protein metabolism, amino acid synthesis and metabolism, and carbohydrate metabolism in the intestine. In accordance with this result, multiomics analysis showed that dietary Cu levels affected protein and carbohydrate metabolites and amino acid metabolism. The abundance of the genera, Lachnospiraceae and Ruminococcaceae, was positively correlated with energy metabolism pathways, and the abundance of the genus, *Streptococcus*, was negatively correlated with amino acid metabolism pathways (Zhang et al., 2019). Thus, the abundance of these species was also altered by Cu supplementation, resulting in effects on energy metabolism and amino acid biosynthesis and metabolism in piglets. In addition, we found that Cu supplementation affected the abundance of cecal microbiota related to

lipid metabolism, suggesting that Cu may affect lipid metabolism in the cecum by regulating the abundance of the cecal microbiota.

Specially, our results showed that the abundance of *E. coli* in ileal and cecal contents tended to increase with high levels of dietary Cu at 3 weeks, and its abundance significantly increased in the cecum after 6 weeks of a pharmacological dose of Cu. However, there was no significant difference in the rate of isolation of *E. coli* from anal swabs. This discrepancy may be due to the high abundance of *E. coli* in rectum. These results were of great interest, since *E. coli* is the main diarrhea-causing opportunistic pathogen in piglets and also has high a rate of drug resistance. Therefore, *E. coli* was isolated at the beginning, middle, and end of the trial. As *E. coli* is present at a high abundance in the intestine and feces, three clones were isolated from all samples for drug resistance analysis.

The Cu resistance system in *E. coli* mainly consists of the *cut* and *pco* systems (Brown et al., 1992, 1995). Other Cu resistance systems, such as the CusCFBA efflux system (Franke et al., 2003), have also been reported. The absorption, efflux, and distribution of Cu are controlled by these systems to balance the content of Cu inside and outside the cell and avoid excessive Cu in the cell (Harris, 1991; Bull and Cox, 1994). Under conditions of high Cu concentration, intestinal Cu-resistant *E. coli* were selected, and thus, the resistance of *E. coli* to Cu increased, resulting in an improvement in the adaptability to high levels of Cu and an increase in the abundance of *E. coli*. However, some previous studies have indicated that Cu inhibits the growth of *E. coli* in *in vitro* culture experiments (Ding et al., 2010; Reyes-Jara et al., 2016). This difference may be explained by the fact that the *E. coli* strain used for *in vitro* culturing did not possess a Cu resistance system, while the strains of *E. coli* in the intestinal tract varied, with some being resistant to Cu.

Copper promotes the selection of antibiotic resistance in *E. coli* (Page, 2003). Hölzel et al. (2012) found that high levels of Cu in liquid pig manure promoted the resistance of *E. coli* to  $\beta$ -lactam antibiotics. Our study showed that the addition of high levels of Cu in the diet also contributed to the resistance of *E. coli* to CIP and C in both the intestine and feces. The mechanism responsible for this increased antibiotic

resistance of *E. coli* after exposure to high levels of Cu was not clear. Previous studies have shown that the Cu-resistance gene (*tcrB*), the macrolides-resistance gene (*ERM*), and the glycopeptide-resistance gene (*vanA*) of *Enterococcus faecium* are located on the same plasmid. *E. faecium* isolates with *tcrB* have been shown to be resistant to macrolides (erythromycin) and glycopeptides (vancomycin) (Hasman and Aarestrup, 2002; Amachawadi et al., 2010, 2011, 2013). Therefore, Cu resistance may play a synergistic role in the development of antibiotic resistance, through coresistance, cross-resistance, or coregulatory resistance.

In addition, *E. coli* isolates in the present study were found to be highly multidrug resistant. A previous study has shown that >88% of *E. coli* isolates from pig feces are multidrug resistant, which is in agreement with the results of our study (Agga et al., 2014). In our study, of the 79 isolates (66.39%) that were resistant to at least three antimicrobial agents, 47 (39.50%) were from piglets treated with a pharmacological dose of Cu, and only 32 isolates (26.89%) were from piglets in the low-Cu group. In particular, six isolates from the group treated with a pharmacological dose of Cu were found to be resistant to six or more classes of antimicrobials, whereas only one isolate resistant to six or more classes of antimicrobials was found in the control group. Our results indicated that a high level Cu supplementation in the diet contributed to an increase in the rate of multidrug resistance of *E. coli*. The mechanism by which Cu promotes multiple drug resistance in *E. coli* remains unclear and should be the focus of future studies.

## DATA AVAILABILITY STATEMENT

The datasets generated for this study can be found in the <https://www.ncbi.nlm.nih.gov/sra/PRJNA551517>.

## REFERENCES

- Adamus-Bialek, W., Wojtasik, A., Majchrzak, M., Sosnowski, M., and Parniewski, P. (2009). (CGG) 4-based PCR as a novel tool for discrimination of uropathogenic *Escherichia coli* strains: comparison with enterobacterial repetitive intergenic consensus-PCR. *J. Clin. Microbiol.* 47, 3937–3944. doi: 10.1128/JCM.01036-09
- Agga, G. E., Scott, H. M., Amachawadi, R. G., Nagaraja, T. G., Vinasco, J., Bai, J., et al. (2014). Effects of chlortetracycline and copper supplementation on antimicrobial resistance of fecal *Escherichia coli* from weaned pigs. *Prev. Vet. Med.* 114, 231–246. doi: 10.1016/j.prevetmed.2014.02.010
- Amachawadi, R., Shelton, N., Shi, X., Vinasco, J., Dritz, S., Tokach, M., et al. (2011). Selection of fecal enterococci exhibiting *tcrB*-mediated copper resistance in pigs fed diets supplemented with copper. *Appl. Environ. Microbiol.* 77, 5597–5603. doi: 10.1128/AEM.00364-11
- Amachawadi, R. G., Scott, H. M., Alvarado, C. A., Mainini, T. R., Vinasco, J., Drouillard, J. S., et al. (2013). Occurrence of the transferable copper resistance gene *tcrB* among fecal enterococci of U.S. feedlot cattle fed copper-supplemented diets. *Appl. Environ. Microbiol.* 79, 4369–4375. doi: 10.1128/AEM.00503-13
- Amachawadi, R. G., Shelton, N. W., Jacob, M. E., Shi, X., Narayanan, S. K., Zurek, L., et al. (2010). Occurrence of *tcrB*, a transferable copper resistance gene, in fecal enterococci of swine. *Foodborne Pathog. Dis.* 7, 1089–1097. doi: 10.1007/s00780-003-0108-1

## ETHICS STATEMENT

The animal study was reviewed and approved by the Animal Protocol Review Committee of the Institute of Subtropical Agriculture, Chinese Academy of Sciences.

## AUTHOR CONTRIBUTIONS

YZ, DW, HY, and YY designed the study. YZ, JZ, ZD, GL, JW, and YL performed the animal feeding trial and sample analysis. YZ and DW wrote and revised the article.

## FUNDING

This work was supported by the National Key R&D Program of China (2016YFD0501201), the National Natural Science Foundation of China (31702127), the Young Elite Scientists Sponsorship Program by CAST (2018QNRC001), and the Hunan Province Key Laboratory of Animal Nutritional Physiology and Metabolic Process (2018TP1031).

## ACKNOWLEDGMENTS

The authors thank Beijing Novogene Bioinformatics Technology Co., Ltd. for microbiota analysis by 16S rRNA sequencing.

## SUPPLEMENTARY MATERIAL

The Supplementary Material for this article can be found online at: <https://www.frontiersin.org/articles/10.3389/fmicb.2019.02808/full#supplementary-material>

- Bikker, P., Jongbloed, A. W., and van Baal, J. (2016). Dose-dependent effects of copper supplementation of nursery diets on growth performance and fecal consistency in weaned pigs. *J. Anim. Sci.* 94, 181–186. doi: 10.2527/jas.2015-9874
- Blyton, M. D., Banks, S. C., Peakall, R., and Gordon, D. M. (2013). High temporal variability in commensal *Escherichia coli* strain communities of a herbivorous marsupial. *Environ. Microbiol.* 15, 2162–2172. doi: 10.1111/1462-2920.12088
- Braune, A., Bendrat, K., Rospert, S., and Buckel, W. (2010). The sodium ion translocating glutaconyl-CoA decarboxylase from *Acidaminococcus fermentans*: cloning and function of the genes forming a second operon. *Mol. Microbiol.* 31, 473–487. doi: 10.1046/j.1365-2958.1999.01189.x
- Brown, N. L., Barrett, S. R., Camakaris, J., Lee, B. T., and Rouch, D. A. (1995). Molecular genetics and transport analysis of the copper-resistance determinant (*pco*) from *Escherichia coli* plasmid pRJ1004. *Mol. Microbiol.* 17, 1153–1166. doi: 10.1111/j.1365-2958.1995.mmi\_17061153.x
- Brown, N. L., Rouch, D. A., and Lee, B. T. (1992). Copper resistance determinants in bacteria. *Plasmid* 27, 41–51. doi: 10.1016/0147-619X(92)90005-U
- Bull, P. C., and Cox, D. W. (1994). Wilson disease and Menkes disease: new handles on heavy-metal transport. *Trends Genet.* 10, 246–252. doi: 10.1016/0168-9525(94)90172-4
- Cromwell, G. L., Lindemann, M. D., Monegue, H. J., Hall, D. D., and Orr, D. E. (1998). Tribasic copper chloride and copper sulfate as copper sources for weaning pigs. *J. Anim. Sci.* 76, 118–123. doi: 10.2527/1998.761118x

- Ding, L., Li, X., Liu, P., Li, S., and Lv, J. (2010). Study of the action of Se and Cu on the growth metabolism of *Escherichia coli* by microcalorimetry. *Biol. Trace Elem. Res.* 137, 364–372. doi: 10.1007/s12011-009-8583-7
- Djoko, K. Y., Xiao, Z. G., and Wedd, A. G. (2008). Copper resistance in E-coli: the multicopper oxidase PcoA catalyzes oxidation of copper(I) in (CuCuII)-Cu-I-PcoC. *Chembiochem* 9, 1579–1582. doi: 10.1002/cbic.20080100
- Espinosa, C. D., Fry, R. S., Usry, J. L., and Stein, H. H. (2017). Copper hydroxychloride improves growth performance and reduces diarrhea frequency of weanling pigs fed a corn-soybean meal diet but does not change apparent total tract digestibility of energy and acid hydrolyzed ether extract. *J. Anim. Sci.* 95, 5447–5454. doi: 10.2527/jas2017.1702
- Feyzioglu, B., Dogan, M., Sanli, O. O., Ozdemir, M., and Baykan, M. (2014). Comparison of the performance of TK system with LJ and MGIT methods in the diagnosis of tuberculosis. *Int. J. Clin. Exp. Med.* 7, 1084–1088.
- Franke, S., Grass, G., Rensing, C., and Nies, D. H. (2003). Molecular analysis of the copper-transporting efflux system CusCFBA of *Escherichia coli*. *J. Bacteriol.* 185, 3804–3812. doi: 10.1128/JB.185.13.3804-3812.2003
- Fuller, R., Newland, L. G. M., Briggs, C. A. E., Braude, R., and Mitchell, K. G. (1960). The normal intestinal flora of the pig. IV. The effect of dietary supplements of penidillin, chlortetracycline or copper sulphate on the faecal flora. *J. Appl. Bact.* 23, 195–205. doi: 10.1111/j.1365-2672.1960.tb00197.x
- Gipp, W. F., Pond, W. G., and Smith, S. E. (1967). Effects of level of dietary copper molybdenum sulfate and zinc on bodyweight gain hemoglobin and liver copper storage of growing pigs. *J. Anim. Sci.* 26, 727–730. doi: 10.2527/jas1967.264727x
- Harris, E. D. (1991). Copper transport: an overview. *Proc. Soc. Exp. Biol. Med.* 196, 130–140. doi: 10.3181/00379727-196-43171b
- Hasman, H., and Aarestrup, F. M. (2002). tcrB, a gene conferring transferable copper resistance in *Enterococcus faecium*: occurrence, transferability, and linkage to macrolide and glycopeptide resistance. *Antimicrob. Agents Chemother.* 46, 1410–1416. doi: 10.1016/j.metabol.2009.05.029
- Hasman, H., and Aarestrup, F. M. (2005). Relationship between copper, glycopeptide, and macrolide resistance among *Enterococcus faecium* strains isolated from pigs in Denmark between 1997 and 2003. *Antimicrob. Agents Chemother.* 49, 454–456. doi: 10.1128/aac.49.1.454-456.2005
- Hasman, H., Kempf, I., Chidaine, B., Cariolet, R., Ersboll, A. K., Houe, H., et al. (2006). Copper resistance in *Enterococcus faecium*, mediated by the tcrB gene, is selected by supplementation of pig feed with copper sulfate. *Appl. Environ. Microbiol.* 72, 5784–5789. doi: 10.1128/AEM.02979-05
- Hill, G. M., Cromwell, G. L., Crenshaw, T. D., Dove, C. R., Ewan, R. C., Knabe, D. A., et al. (2000). Growth promotion effects and plasma changes from feeding high dietary concentrations of zinc and copper to weanling pigs (regional study). *J. Anim. Sci.* 78, 1010–1016. doi: 10.1046/j.1439-0396.2000.00263.x
- Hojberg, O., Canibe, N., Poulsen, H. D., Hedemann, M. S., and Jensen, B. B. (2005). Influence of dietary zinc oxide and copper sulfate on the gastrointestinal ecosystem in newly weaned piglets. *Appl. Environ. Microbiol.* 71, 2267–2277. doi: 10.1128/AEM.71.5.2267-2277.2005
- Hölzel, C. S., Müller, C., Harms, K. S., Mikolajewski, S., Schäfer, S., Schwaiger, K., et al. (2012). Heavy metals in liquid pig manure in light of bacterial antimicrobial resistance. *Environ. Res.* 113, 21–27. doi: 10.1016/j.envres.2012.01.002
- Huang, Y. L., Ashwell, M. S., Fry, R. S., Lloyd, K. E., Flowers, W. L., and Spears, J. W. (2015). Effect of dietary copper amount and source on copper metabolism and oxidative stress of weanling pigs in short-term feeding. *J. Anim. Sci.* 93, 2948–2955. doi: 10.2527/jas.2014-8082
- Jondreville, C., Revy, P. S., Jaffrezic, A., and Dourmad, J. Y. (2002). Copper in pig nutrition: essential trace element, growth promoter, and its potential adverse effects on human nutrition and environment. *Prod. Anim.* 15, 247–265.
- Kellogg, T. F., Hays, V. W., Catron, D. V., Quinn, L. Y., and Speer, V. C. (1966). Effect of dietary chemotherapeutics on the performance and fecal flora of baby pigs. *J. Anim. Sci.* 25, 1102–1106. doi: 10.2527/jas1966.2541102x
- Mei, S. F., Yu, B., Ju, C. F., Zhu, D., and Chen, D. W. (2010). Effect of different levels of copper on growth performance and cecal ecosystem of newly weaned piglets. *Ital. J. Anim. Sci.* 9, 378–381. doi: 10.4081/ijas.2010.e71
- Namkung, H., Gong, J., Yu, H., and Lange, C. F. M. D. (2006). Effect of pharmacological intakes of zinc and copper on growth performance, circulating cytokines and gut microbiota of newly weaned piglets challenged with coliform lipopolysaccharides. *Can. J. Anim. Sci.* 86, 511–522. doi: 10.4141/A05-075
- Okonkwo, A. C., Ku, P. K., Miller, E. R., Keahey, K. K., and Ullrey, D. E. (1979). Copper requirement of baby pigs fed purified diets. *J. Nutr.* 109, 939–948. doi: 10.1093/jn/109.6.939
- Ole, H. J., Nuria, C., Hanne Damgaard, P., Mette Skou, H., and Bent Borg, J. (2005). Influence of dietary zinc oxide and copper sulfate on the gastrointestinal ecosystem in newly weaned piglets. *Appl. Environ. Microbiol.* 71, 2267–2277. doi: 10.1128/AEM.71.5.2267-2277.2005
- Page, S. (2003). *The Role of Enteric Antibiotics in Livestock Production*. Canberra, ACT: Avcare Ltd.
- Perez, V. G., Waguespack, A. M., Bidner, T. D., Southern, L. L., Fakler, T. M., Ward, T. L., et al. (2011). Additivity of effects from dietary copper and zinc on growth performance and fecal microbiota of pigs after weaning. *J. Anim. Sci.* 89, 414–425. doi: 10.2527/jas.2010-2839
- Reyes-Jara, A., Cordero, N., Aguirre, J., Troncoso, M., and Figueroa, G. (2016). Antibacterial effect of copper on microorganisms isolated from bovine mastitis. *Front. Microbiol.* 7:626. doi: 10.3389/fmicb.2016.00626
- Smith, J. W., Tokach, M. D., Goodband, R. D., Nelssen, J. L., and Richert, B. T. (1997). Effects of the interrelationship between zinc oxide and copper sulfate on growth performance of early-weaned pigs. *J. Anim. Sci.* 75, 1861–1866. doi: 10.2527/1997.7571861x
- Song, J., Li, Y. L., and Hu, C. H. (2013). Effects of copper-exchanged montmorillonite, as alternative to antibiotic, on diarrhea, intestinal permeability and proinflammatory cytokine of weanling pigs. *Appl. Clay Sci.* 77–78, 52–55. doi: 10.1016/j.clay.2013.01.016
- Tsen, H. Y., Lin, C. K., and Chi, W. R. (1998). Development and use of 16S rRNA gene targeted PCR primers for the identification of *Escherichia coli* cells in water. *J. Appl. Microbiol.* 85, 554–560. doi: 10.1046/j.1365-2672.1998.853535.x
- Usaini, B., Taura, D., Mukhtar, M., Koki, Y., Adamu, S., Musa, A., et al. (2015). Studies on seasonal variations in the occurrences of schistosoma haematobium and bacterial urinary infections among school age Children in Kano, Nigeria. *J. Pharm. Pharmacol.* 10, 27–33. doi: 10.9790/3008-10132733
- Varel, V. H., Robinson, I. M., and Pond, W. G. (1987). Effect of dietary copper sulfate, Aureo SP250, or clinoptilolite on ureolytic bacteria found in the pig large intestine. *Appl. Environ. Microbiol.* 53, 2009–2012. doi: 10.1007/BF01569544
- Wang, M. Q., Du, Y. J., Wang, C., Tao, W. J., He, Y. D., and Li, H. (2012). Effects of copper-loaded chitosan nanoparticles on intestinal microflora and morphology in weaned piglets. *Biol. Trace Elem. Res.* 149, 184–189. doi: 10.1007/s12011-012-9410-0
- Xia, M. S., Hu, C. H., and Xu, Z. R. (2005). Effects of copper bearing montmorillonite on the growth performance, intestinal microflora and morphology of weanling pigs. *Anim. Feed Sci. Tech.* 118, 307–317. doi: 10.1016/j.anifeeds.2004.11.008
- Xiong, X., Zhou, J., Liu, H. N., Tang, Y. L., Tan, B., and Yin, Y. L. (2019). Dietary lysozyme supplementation contributes to enhanced intestinal functions and gut microflora of piglets. *Food Funct.* 10, 1696–1706. doi: 10.1039/C8FO02335B
- Yazdankhah, S., Rudi, K., and Bernhoft, A. (2014). Zinc and copper in animal feed - development of resistance and co-resistance to antimicrobial agents in bacteria of animal origin. *Microb. Ecol. Health Dis.* 25, 1–7. doi: 10.3402/mehd.v25.25862
- Zhang, F., Zheng, W. J., Xue, Y. Q., and Yao, W. (2019). Suhuai suckling piglet hindgut microbiome-metabolome responses to different dietary copper levels. *Appl. Microbiol. Biot.* 103, 853–868. doi: 10.1007/s00253-018-9533-0
- Zhou, J., Xiong, X., Wang, K. X., Zou, L. J., Ji, P., and Yin, Y. L. (2018). Ethanolamine enhances intestinal functions by altering gut microbiome and



- mucosal anti-stress capacity in weaned rats. *Br. J. Nutr.* 120, 241–249. doi: 10.1017/S0007114518001101
- Zhou, J., Xiong, X., Yin, J., Zou, L. J., Wang, K. X., Shao, Y. R., et al. (2019). Dietary lysozyme alters sow's gut microbiota, serum immunity and milk metabolite profile. *Front. Microbiol.* 10:177. doi: 10.3389/fmicb.2019.00177
- Zimmermann, M., Udagedara, S. R., Sze, C. M., Ryan, T. M., Howlett, G. J., Xiao, Z., et al. (2012). PcoE - a metal sponge expressed to the periplasm of copper resistance *E. coli*. Implication of its function role in copper resistance. *J. Inorg. Chem.* 115, 186–197. doi: 10.1016/j.jinorgbio.2012.04.009

**Conflict of Interest:** The authors declare that the research was conducted in the absence of any commercial or financial relationships that could be construed as a potential conflict of interest.

Copyright © 2019 Zhang, Zhou, Dong, Li, Wang, Li, Wan, Yang and Yin. This is an open-access article distributed under the terms of the Creative Commons Attribution License (CC BY). The use, distribution or reproduction in other forums is permitted, provided the original author(s) and the copyright owner(s) are credited and that the original publication in this journal is cited, in accordance with accepted academic practice. No use, distribution or reproduction is permitted which does not comply with these terms.



# Clinical Impact of Antibiotics for the Treatment of *Pseudomonas aeruginosa* Biofilm Infections

Elodie Olivares<sup>1,2\*</sup>, Stéphanie Badel-Berchoux<sup>3</sup>, Christian Provot<sup>2,3</sup>, Gilles Prévost<sup>1</sup>, Thierry Bernardi<sup>2,3</sup> and François Jehl<sup>1</sup>

<sup>1</sup> University of Strasbourg, CHRU Strasbourg, Fédération de Médecine Translationnelle de Strasbourg, EA7290, Institut de Bactériologie, Strasbourg, France, <sup>2</sup> BioFilm Pharma SAS, Saint-Beauzire, France, <sup>3</sup> BioFilm Control SAS, Saint-Beauzire, France

Bacterial biofilms are highly recalcitrant to antibiotic therapies due to multiple tolerance mechanisms. The involvement of *Pseudomonas aeruginosa* in a wide range of biofilm-related infections often leads to treatment failures. Indeed, few current antimicrobial molecules are still effective on tolerant sessile cells. In contrast, studies increasingly showed that conventional antibiotics can, at low concentrations, induce a phenotype change in bacteria and consequently, the biofilm formation. Understanding the clinical effects of antimicrobials on biofilm establishment is essential to avoid the use of inappropriate treatments in the case of biofilm infections. This article reviews the current knowledge about bacterial growth within a biofilm and the preventive or inducer impact of standard antimicrobials on its formation by *P. aeruginosa*. The effect of antibiotics used to treat biofilms of other bacterial species, as *Staphylococcus aureus* or *Escherichia coli*, was also briefly mentioned. Finally, it describes two *in vitro* devices which could potentially be used as antibiotic susceptibility testing for adherent bacteria.

**Keywords:** biofilms, antibiotic tolerance, biofilm-related infections, *Pseudomonas aeruginosa*, clinical laboratory technique, MBEC assay, antibiofilmogram

## OPEN ACCESS

### Edited by:

Fabian Cieplik,  
University Medical Center  
Regensburg, Germany

### Reviewed by:

Rodolfo García-Contreras,  
National Autonomous University  
of Mexico, Mexico  
Monique L. Van Hoek,  
George Mason University,  
United States

### \*Correspondence:

Elodie Olivares  
elodie.olivares@biofilmpharma.com

### Specialty section:

This article was submitted to  
Antimicrobials, Resistance  
and Chemotherapy,  
a section of the journal  
Frontiers in Microbiology

**Received:** 29 July 2019

**Accepted:** 02 December 2019

**Published:** 09 January 2020

### Citation:

Olivares E, Badel-Berchoux S,  
Provot C, Prévost G, Bernardi T and  
Jehl F (2020) Clinical Impact  
of Antibiotics for the Treatment  
of *Pseudomonas aeruginosa* Biofilm  
Infections. *Front. Microbiol.* 10:2894.  
doi: 10.3389/fmicb.2019.02894

## INTRODUCTION

Bacterial biofilm was defined for the first time in 1978 as a structured community of microorganisms adhering to a surface and producing an extracellular matrix of polysaccharides (Costerton et al., 1978). It represents a particular behavior of bacteria triggered by the proximity of a surface and involving complex signaling networks, including quorum sensing (QS). Its discovery was attributed to the microscope inventor, Antoni Van Leeuwenhoek who observed bacteria clusters on dental plaque in 1684. He wrote in a report for the Royal Society of London: “The number of these animalcules in the scurf of a man’s teeth are so many that I believe they exceed the number of men in a kingdom” (Biofilms: The Hypertextbook, 2011).

Nowadays, it is well-recognized that biofilms play an ecological role and have a significant impact in medicine by the development of healthcare-associated infections. The National Institutes of Health (NIH) estimated that bacterial biofilms are involved in 65% of microbial diseases and in more than 80% of chronic infections (Jamal et al., 2018). Sessile cells can colonize indwelling medical devices as any type of catheters, contact lenses, heart valves, and prostheses. Their presence on retrieved infected implants is easily detectable by laboratory methods. Indeed, bacterial colony outgrowths can be revealed by culturing techniques but can also be directly visualized by microscopy methodologies (Dibartola et al., 2017). Biofilm formation is equally involved in non-device-associated infections as periodontitis, osteomyelitis, and chronic infections (Srivastava and Bhargava, 2016). *Pseudomonas aeruginosa* biofilms are particularly deadly in cystic fibrosis (CF)

patients. They also have a relevant impact on clinical outcomes of patients with chronic wounds (Mulcahy et al., 2014). Relevant animal models are now available to study the involvement of *P. aeruginosa* sessile cells *in vivo* infections. Diabetic wounds were mimicked in mice by Watters et al. (2013) and a porcine model allowed replicating the development of bacterial infections in CF lungs (Pezzulo et al., 2012).

A specific feature of sessile cells is their inherent tolerance to antimicrobials. Despite this basic knowledge, classical antibiotic susceptibility testing, providing the minimal inhibitory concentration (MIC) of molecules, is performed on non-adherent bacteria. Results collected according to antibiogram methods cannot predict the therapeutic success of the corresponding antibiotic therapies against biofilms. Furthermore, it is now well-recognized that low doses of antibiotics, encountered during continuous and fluctuating treatments, can stimulate biofilm establishment and are partly responsible for biofilm-specific antimicrobial tolerance.

Currently, no guidelines exist to help clinicians treat this kind of infections, although they are involved in the majority of untreatable clinical cases. Therefore, it appears urgent to develop a susceptibility test specific to biofilm or to validate a new-existing method for a routine use in diagnostic labs.

This review summarizes the basic knowledge about the growth of bacteria within a biofilm and the main steps of its formation. The tolerance features of sessile microorganisms to antimicrobial molecules were also detailed as well as the beneficial or deleterious effects of antibiotics for biofilm treatment. Available diagnostic tools for the selection of appropriate therapies against adherent bacteria are discussed herein.

## THE BACTERIAL BIOFILM

### A Community Way of Life

The growth of bacteria within biofilms is a natural process. The entirety of microorganisms could be sessile and live attached to a surface. This community mode is different from the planktonic growth, in which bacteria are isolated and mobile in the environment. The sessile cells differ from the planktonic ones by their morphology, physiology, and gene expression. The ability to adhere and grow on a surface as a biofilm is a survival strategy allowing the colonization of the environment by microorganisms. Bacteria continuously switch from a planktonic phenotype to a sessile one. This state variation is strategic for the cell as it allows a rapid adaptation to environmental conditions (Lebeaux and Ghigo, 2012).

The use of microscope can highlight a specific mushroom-like structure, especially for *P. aeruginosa* biofilms. They are mainly composed of microorganism clusters, delimited by aqueous channels. These latter separate bacterial microcolonies and allow the flow of oxygen and nutriment in the deepest areas of the biofilm as well as the elimination of degradation products. Nevertheless, it appears hard to generalize the composition, structure and features of biofilms owing to the wide range of environments and bacterial species. External factors, as medium composition and/or genetic properties of bacteria, contribute to the perpetual structure variation of the sessile population.

The key step of biofilm development is the synthesis of the extracellular matrix. It incorporates all the elements apart the bacterial cells. By forming up to 90% of its total organic matter, the matrix is the main structural component of the bacterial biofilm. It is highly hydrated and mainly composed of exopolysaccharides, proteins, nucleic acids, and minerals (Limoli et al., 2015). Its composition depends on the bacterial species and growth conditions. It allows strengthening of the biofilm structure while keeping a high flexibility. It also plays a protective role as it enhances the tolerance of bacteria to antimicrobials by creating a physical barrier that limits their diffusion to other environmental factors (UV, pH, and osmotic pressure variations, desiccation, etc.).

During the early development of the bacterial structure, it has been highlighted that extracellular DNA (eDNA) is essential for the adhesion of microorganisms and for their intercellular cohesion (Whitchurch et al., 2002). Quantitatively, in the biofilm matrix of *P. aeruginosa*, eDNA is six times more abundant than proteins and eighteen times more abundant than carbohydrates. Its origin was confirmed as being genomic. Nucleic acids can arise either from the lysis of a part of sessile cells or from an active secretion by living bacteria through merging membrane vesicles (Okshevsky and Meyer, 2015).

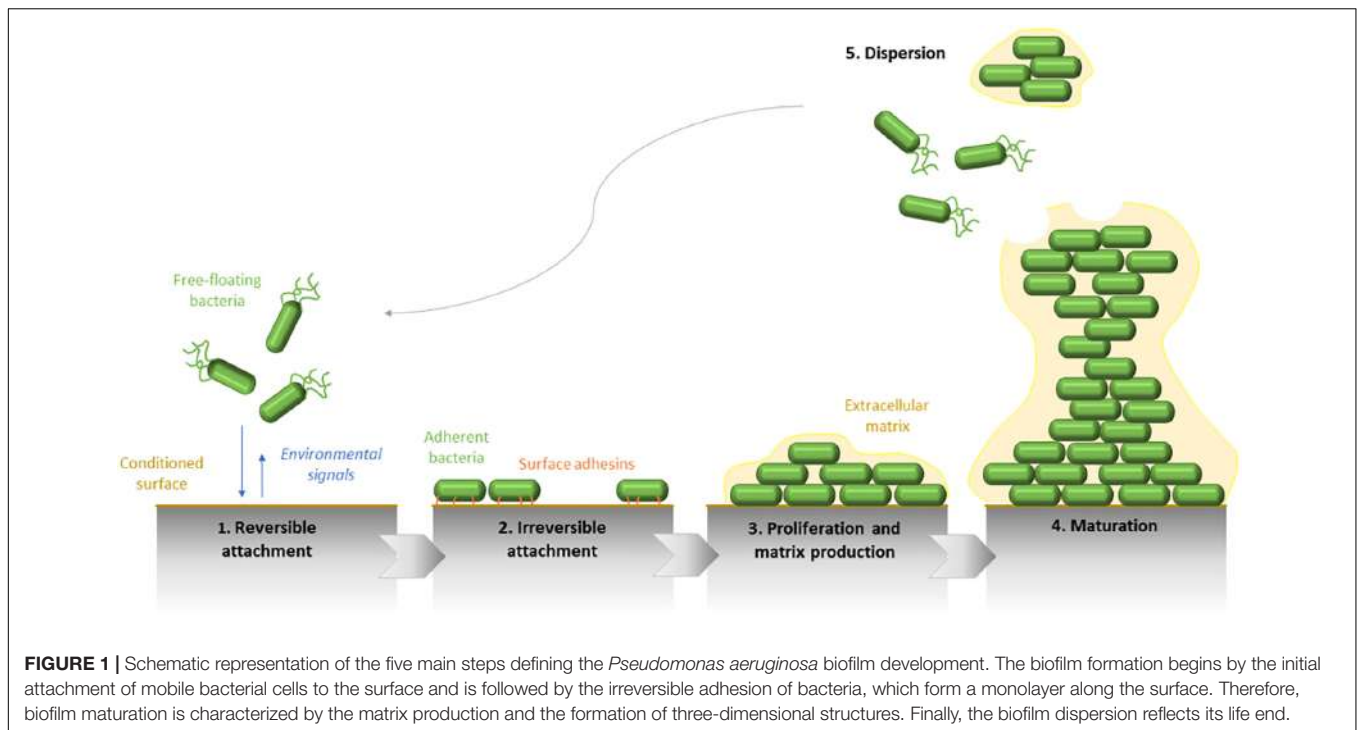
### Development of a Mixed Environment

Bacterial biofilm can be formed in a few hours. Its general development consists of five main steps (Dufour et al., 2010). Mobile free-floating bacteria detect an available conditioned surface through environmental signals as pH variation, oxygen and nutriment concentrations, temperature, and osmolarity, etc. They are transported by physical forces or bacterial appendages (i.e., flagella). The flagellum is as much required in the surface arrival as in the biofilm formation initiation since mutants defective in its synthesis are not able to adhere (O'Toole and Kolter, 1998). In the same way, a complete but inactive flagellum does not allow the establishment of the biofilm (Vallet et al., 2001).

The increasing proximity of the support, which is conditioned by the fluids and flows to where it is exposed, allows the initial adhesion of bacterial cells by physicochemical and electrostatic interactions. At this stage, the adhesion is reversible (**Figure 1**). Besides the environmental influence, this attachment is strongly influenced by the nature of the surface itself. A rough and/or hydrophobic surface boosts the adhesion of microorganisms, contrary to a smooth and/or hydrophilic support. Furthermore, the organic molecules, which are present at the surface, also condition the cell attachment.

Following this first step, which can occur few seconds after the initial contact with the surface, a second stage of adhesion happens, allowing the strengthening of the bacteria-surface bonds by the implication of bacterial compounds, such as type IV pili or more generally, surface adhesins. The surface binding, becoming irreversible, enables subsequently the multiplication of adherent bacteria, and the formation of microcolonies.

As for the flagella, *P. aeruginosa* mutants defective in the production of type IV pili adhere to a surface by the formation of a cell monolayer but are not able to gather in microcolonies. This data confirms that the microcolony formation is a process



requiring bacterial mobility and not only a clonal growth from a bacterial cell (O'Toole and Kolter, 1998). In general, bacterial structures involved in the mobility of microorganisms are needed for the initial step of biofilm formation. They allow the approach and the colonization of the surface. The use of DNA microarrays on biofilms formed by the PAO1 strain, on sterilized granite pebbles in a continuous-culture model, showed that genes required for the synthesis of bacterial surface structures are repressed as soon as biofilm formation is initiated (Whiteley et al., 2001). They are no longer necessary for biofilm development and move on to compounds allowing its structuring and differentiation. It was shown that QS is involved in the structural steps of the biofilm. Analysis of *P. aeruginosa* wild type and *lasI* mutant highlighted an architectural difference in both biofilms (thinner and less heterogeneous for the mutant one) (Davies et al., 1998).

The first maturation step of biofilm development is defined by the production of the extracellular matrix. It allows a mechanical cohesion between bacterial cells and favors the switch from a “free life” to a “static life.” Its composition fluctuates in space and time and determines the spatial configuration of the biofilm.

As for the gene inactivation of extracellular structures, studies on *P. aeruginosa* showed that bacteria have a “sense of touch,” namely the ability to detect the presence of a surface and to combine a specific gene expression. During the first stages of adhesion, the transcription of genes involved in the alginate synthesis is activated to organize the matrix production after the formation of microcolonies (Davies and Geesey, 1995). More recent works showed that this gene regulation is directly dependent on the cyclic di-GMP (c-di-GMP), a central messenger present in the cytoplasm of bacterial cells, which controls the transition between the planktonic life and biofilm

establishment and whose intracellular concentration is affected by environmental stimuli (Donné and Dewilde, 2015).

If growth conditions are optimal, a second phase of biofilm maturation occurs, defined by a growth in thickness. Therefore, the mature biofilm shows a complex 3D-structure. It can acquire a typical “mushroom-like” shape formed by bacterial columns on the basement of cells and in which bacteria are mobile. The whole biofilm is surrounded by an extracellular matrix. Through this structure, channels remain and allow the transfer of oxygen and nutrients required for the growth of sessile bacteria. Gradients of oxygen and pH also set up from the top to the bottom of the biofilm. These variations of concentrations within the biofilm lead to metabolic activity and growth differences of bacteria even in a monomicrobial community, their activity being increased at the surface and reduced at its center. These physicochemical differences lead to a physiological heterogeneity of microorganisms and generate the formation of environmental microniches constituted by bacterial subpopulations that are genetically identical but physiologically distinct (concerning the tolerance against antimicrobials for instance).

The final step of the biofilm formation cycle is its destructuring. Biofilm dispersion can be initiated by various factors as mechanical disruptions (abrasion), enzymatic degradations (enzyme secretion determined by QS) or even a lack in nutrients or an overpopulation (McDougald et al., 2011). Fractions of bacteria are removed from the community and are spread in the environment. Newly mobile and adherent individual cells will be able to explore and colonize new surfaces by the establishment of a new biofilm. A new cycle of adhesion/maturation can get back.

Biofilms must be considered as an elaborate and dynamic organization which constantly evolve to get used to its



environment. The passing through the sessile state to the planktonic one plays a considerable role in the transmission of bacteria from environmental reserves to the host and also in the transmission between hosts and in the infection propagation in the individual (biofilm metastasis).

## BACTERIA UNDER SHELTER

The main advantage of the sessile way of life is the modification of the adherent bacteria in regard to their susceptibility to mechanisms of immune defenses and antimicrobials. Indeed, a single planktonic cell is vulnerable to the action of antibodies or phagocytes and is fairly sensitive to antibiotics. Conversely, bacteria that are embedded in a biofilm structure can be tolerant to the host immune system, antimicrobials, and biocide molecules (Høiby et al., 2011). Indeed, we usually talk about biofilm tolerance to antibiotics rather than resistance.

The resistance can be defined as the ability of a microorganism to grow when an antimicrobial compound is present in the environment. Resistance mechanisms are heritable and avoid the antibiotic interaction with its target. On the contrary, the term tolerance must be used for bacteria, which are able to survive in high concentrations of antimicrobials, but with a suspended growth. This feature, specific to the sessile bacterial life, is reversible, phenotypical, and non-inherited. A bacterial cell from a biofilm, which is resuspended in liquid medium, will get back an *in vitro* susceptibility to antimicrobials.

## Inefficiency of Immune System

The size of the bacterial biofilm is the first brake to the phagocytosis process. Even in immunocompetent individuals, components of the immune system are seldom effective against biofilm infections. During the innate immune response, macrophages and neutrophils are rapidly activated following the direct contact with bacteria (i.e., through the O-antigen of the bacterial lipopolysaccharide (LPS) or the alginate for *P. aeruginosa*). Then, the immediate immune response triggers an important accumulation of neutrophils around the biofilm structure associated with an oxygen exhaustion, which is due to an active stimulation of the oxidative metabolism, as the molecular oxygen is reduced in superoxide (Watters et al., 2016).

The phagocytic cells penetrate with difficulty the extracellular matrix. They are slowed down and become more vulnerable to the inactivation by bacterial enzymes. Besides, the extended lysis of neutrophils leads to the overflow of harmful compounds in the medium, which are responsible for consecutive tissue damages. The host immune response is the main cause of the healthy tissue degradation surrounding the bacterial infection.

Concerning the memory of the immune system response, it has been reported that specific antibodies against bacterial compounds as the elastase, the LPS or the flagellum are secreted in CF patients. These data show that antigenic determinants were neutralized during chronic lung infection. Unfortunately, it has been demonstrated that these antibodies contribute to the formation of immune complexes, which are precipitated into the parenchyma and lead to complement activation and opsonization

of neutrophils, namely in an indirect way, to the nearby tissue degradation (Jensen et al., 2010).

## General Tolerance to Antimicrobials

Biofilm tolerance to external aggressions, notably to antibiotic treatments, is one of its exceptional features. It is well-known that the MIC of an antimicrobial, which is effective on sessile bacteria, is 10 to 1,000 times more concentrated than the one which would be active on their planktonic version (Schurek et al., 2012). This decreased antimicrobial susceptibility can have several causes. It can be inherent to the own organization of the biofilm (structure and functioning) but can also be acquired by transmission of resistance factors.

Given its complex architecture, the biofilm itself creates a protective environment for bacterial cells. It can be seen as an “innate” tolerance. As for compounds of the host immune system, the extracellular matrix forms a mechanical barrier limiting antibiotic diffusion within the biofilm and their access to microorganisms. The electrostatic charges or some matrix components bind antimicrobial molecules and trap them. The general high viscosity of the polymeric matrix can also prevent the antibiotics from reaching their effective concentrations in the deeper layers of the bacterial community. Consequently, bacteria in the outer layers of the biofilm die following an antimicrobial treatment, while those in the deeper layers have time to react (Paraje, 2011). This invasion delay should be enough to allow a progressive physiological adaptation of bacteria exposed to antimicrobials (expression of resistance genes, secretion of inactivating enzymes...). For instance, it has been demonstrated that alginate and eDNA in the biofilm matrix of *P. aeruginosa* could link aminoglycosides and play a role in the sessile bacterial tolerance to tobramycin (Hentzer et al., 2001). Similarly, an extracytoplasmic process of antibiotic sequestration by periplasmic glucans was highlighted. The locus *ndvB* was identified as being required for the production of cyclic glucans (Mah et al., 2003). The authors showed that polymers physically bound antimicrobial compounds in the periplasm, leading to the diffusion slowdown of antibiotics into the cells and preventing them from reaching their action sites. Nevertheless, this global diffusion barrier, specific of the biofilm matrix and the sessile cells, appears to be strain- and antibiotic-dependent. By itself, it cannot explain the radical tolerance of biofilms against antimicrobial agents.

In view of their own biofilm organization, bacterial metabolism plays an important part in antibiotic tolerance. The concentration gradients of metabolites, oxygen, and nutrients within the mature biofilm create bacterial niches that are less metabolically active. For example, in *P. aeruginosa* microcolonies, the oxygen is consumed faster at the surface than it diffuses into the deeper layers of the biofilm. Its graduated diffusion leads to the formation of hypoxic areas in the bacterial community (Serra and Hengge, 2014). Some of microorganisms could get back to a stationary phase in lowering their growth and multiplication rates as an induced stress response. This reduced metabolism of sessile cells is partly responsible for the tolerance associated with the biofilm, as the action mode of the majority of antimicrobials targets metabolic processes in growing

bacteria (replication, transcription, translation, or cell wall synthesis). Lots of works have validated the advantageous efficacy of antimicrobials on active bacteria, which are located in external areas of the biofilm. However, parallel studies showed that other types of molecules, such as SDS, EDTA, or chlorhexidine could conversely act on bacterial cells in stationary phase of growth, located in the internal niches (Ciofu et al., 2015).

The activation of efflux pumps by bacteria embedded in the extracellular matrix can also contribute to the inefficiency of antimicrobials in actively discharging them outside the biofilm structure before they can reach their target. These membrane transporters can be specific of a class of antibiotics or responsible for multidrug resistance. In Gram-negative bacteria as *P. aeruginosa*, efflux pumps are usually composed of a pump located in the inner membrane, an outer membrane factor, and a periplasmic fusion protein. The association of cell impermeability with the expression of the efflux system MexAB-OprM leads partly to the inherent resistance of the bacillus to antibiotics. The expression of some of them was demonstrated as being specific to the biofilm mode (Zhang and Mah, 2008).

The bacterial density and the spatial proximity of microorganisms within a mature biofilm promote the gene exchange and the resistance plasmid transmission. The horizontal gene transfer could be 1,000-fold more important in a bacterial community than between planktonic cells. Due to the starved local environment within the biofilm, bacteria are also subjected to random mutations and genetic rearrangements. This generation of bacterial variants, favored by natural selection, leads to a chromosomal resistance (Poole, 2012). The mutation frequency can be stimulated by environmental factors, as the presence of reactive oxygen species from the lung inflammatory response. These reagents, in damaging DNA, cause mutations in bacteria and lead to the diversity of bacterial phenotypes in the biofilm (Rodríguez-Rojas et al., 2012). Finally, by combination of several of these mechanisms, sessile bacteria rapidly became multiresistant.

It also demonstrated the existence of a “persister” bacterial population which could constitute a reserve allowing the infection relaunch after elimination of peripheral planktonic and sessile cells (Stewart, 2002).

## The “Persister Cells” Enigma

Persisters are regular cells exhibiting a specific non-growing phenotype, combined with an excessive tolerance to antibiotic concentrations. Their existence was firstly described in the 1940s (Bigger, 1944). The transcription downregulation of genes involved in motility and energy production was highlighted for these isolated bacteria. Consequently, as they are in a dormant state, antimicrobials are able to bind to their target molecules but not to impair their initial function (Lewis, 2005).

The presence of persisters can be easily detected in bacterial cultures by a process of biphasic death, further to an exposition to bactericidal antibiotic concentrations. Firstly, a lethal dose of antimicrobials will rapidly eradicate the sensitive bacterial population. A much slower second phase of death follows, reflecting the poor killing of persister cells. Finally, the end of antimicrobial treatment will allow the renewal of the

bacterial community by regeneration of persister survivors (Conlon et al., 2015).

Each bacterium shows the capacity to be differentiated in a persister cell, but few of them are really observed during the early exponential phase of growth. Indeed, the genuine persister population is formed during the mid-exponential phase and finally, they reach up to 1% of the overall population at the stationary phase. This phenotypic conversion can be induced by environmental stimuli or stresses, as antibiotic exposure, which are predictive of immediate threats for cells, or they may be preexisting in the bacterial population (Harms et al., 2016; Fisher et al., 2017). It is assumed that stochastic modifications in genes can lead to the phenotypic switch along with the over-expression of specific toxin-antitoxin (TA) module proteins. Typically, the toxin portions are neutralized by their antitoxins, but under cellular stresses, proteases must be over-expressed and degrade the antitoxin proteins. In that case, the toxin modules are free to exert their toxic action on bacteria. The expression of many other compounds implicated in the persister phenotype can be induced by environmental stimuli. The signaling pathway of the SOS response and the alarmone ppGpp, two stringent responses to stress, also appears to be associated with the persistence of bacteria (Del Pozo, 2018).

## EFFECTIVENESS OF CONVENTIONAL ANTIBIOTICS

Despite the intensive tolerance of the biofilm to antimicrobials, certain conventional antibiotics still demonstrate activity against bacterial cells growing in the biofilm state.

In a recent study, Otani et al. (2018) showed that sub-MICs of ceftazidime reduce biofilm volume, inhibit twitching motility, and repress gene expression involved in bacterial adhesion and matrix production of *P. aeruginosa* PAO1. Roudashti et al. (2017) had previously noticed this effect of cephalosporin on motility and biofilm formation for the same strain.

Similarly, other common antimicrobials were described as being effective on biofilm behavior of *P. aeruginosa*. Subinhibitory doses of piperacillin/tazobactam altered the pathogenic potential of various clinical and laboratory strains of *P. aeruginosa* in reducing bacterial adhesion, in decreasing biofilm formation, swimming, and twitching motility and conversely in increasing the susceptibility of cells to oxidative stress (Fonseca, 2004). Indeed, one early step of biofilm formation which can be targeted for the prevention of chronic infection is bacterial adhesion to a surface. The process of twitching motility contributes to this part of virulence of sessile microorganisms. Wozniak and Keyser (2004) noticed that clarithromycin substantially inhibited cell translocation of *P. aeruginosa* through its type IV pilus as well as altered its biofilm architecture at sub-MIC levels. Another control strategy against bacterial biofilm is QS disruption. Azithromycin, ceftazidime, and ciprofloxacin showed, at subinhibitory concentrations, QS-inhibitory activities in bacteria (Skindersoe et al., 2008). This beneficial effect of the macrolide was also emphasized in an experimental urinary tract infection model. Antibiotic

concentrations below the MIC could inhibit the production of QS molecules, leading to the complete clearance of *P. aeruginosa* from the mouse kidneys (Bala et al., 2011). Azithromycin was also described as being able to prevent PAO1 biofilm formation in a flow cell biofilm model (Gillis and Iglewski, 2004).

Continuous treatment of colistin (25  $\mu\text{g/ml}$ ) turned out to be effective against the non-dividing central part of a *P. aeruginosa* biofilm growing in a flow chamber for 4 days. Associated with ciprofloxacin (60  $\mu\text{g/ml}$ ), which can kill metabolically active cells in the surface layers, this combination therapy showed a clinical efficacy for the early eradication treatment of bacteria in CF patients (Høiby et al., 2010). In a more recent study, the association of minimal biofilm inhibitory concentrations (MBICs) of fosfomicin with tobramycin ( $\geq 1024$   $\mu\text{g/ml}$  and from 8 to 32  $\mu\text{g/ml}$ , respectively) has been demonstrated to be synergistic against CF isolates in *in vitro* models (Díez-Aguilar et al., 2018). Overall, the aminoglycosides usually prescribed in CF (amikacin and tobramycin) showed a preventive action on the early adhesion of clinical *P. aeruginosa* strains at various concentrations (sub-MICs, MICs, and so-called PK/PD doses) (Olivares et al., 2017).

The efficacy of antibiotic lock solution (meropenem, levofloxacin, and colistin) on *P. aeruginosa* clinical and reference strains was also confirmed. The antibiotic lock technique (ALT), using antimicrobial molecules, prevented bacterial regrowth in an *in vitro* antibiotic lock model. The efficacy of ALT to eliminate *P. aeruginosa* biofilms should be improved when the three antibiotics were used in combination with clarithromycin (Ozbek and Mataraci-Kara, 2016).

Finally, all the cited publications attest that some conventional molecules can still be active on *P. aeruginosa* in the context of chronic infections, in preventing its growth within the biofilm. Nevertheless, a lot of these studies were carried out on the reference PAO1 strain. To confirm the clinical effectiveness of antimicrobial treatments, antibiotic susceptibility testing must be performed on clinical isolates, and clinical trials must be planned.

Concerning the positive effect of classic antimicrobial therapies on other sessile pathogens, MICs and minimal bactericidal concentrations (MBCs) of rifampicin have demonstrated an activity against biofilms of *Staphylococcus epidermidis* and *Staphylococcus aureus* isolates associated with device infections, especially when it is used in association with other molecules as fusidic acid, vancomycin or ciprofloxacin in an *in vitro* biofilm model (Saginur et al., 2006). More recently, adherent staphylococci involved in skin and soft tissue infections were described as being more or less susceptible to multiples of tedizolid MICs and other comparator agents (vancomycin, linezolid, and daptomycin) (Delpech et al., 2018). The use of daptomycin-lock therapy (50 mg/ml) also showed a therapeutic advantage for the 24 h-treatment of a long-term catheter-related bloodstream infections by coagulase-negative *S. epidermidis* in a rabbit model (Basas et al., 2018). Similarly, subinhibitory concentrations of fluoroquinolones were able to reduce the number of sessile cells to prevent the adhesion of the corresponding *S. epidermidis* strains and to alter biofilm morphology (Szczyka et al., 2017).

This overall review of publications, dealing with the anti-biofilm property of conventional antimicrobials, can be

completed with studies using *Escherichia coli*, another bacterial specie well-characterized for its capacity to form biofilm structures. In a recent article, Klinger-Strobel et al. (2017) noticed that colistin concentrations from 4 to 16 mg/l could reduce the amount of adherent *E. coli* bacteria and exert a matrix-reducing effect on biofilms in formation. Similarly, Butini et al. (2018) investigated the anti-biofilm property of gentamicin-eluting bone graft substitute against bacterial species involved in bone and implant-associated infections. Calcium sulfate bone graft substitutes served as local antibiotic delivery carrier, and gentamicin is one of the most used molecules for the treatment of bone-related infections. Therefore, they demonstrated that 12  $\mu\text{g/ml}$  of released gentamicin were able to prevent *E. coli* adhesion and 23  $\mu\text{g/ml}$  of the molecule could eliminate a 24 h-old biofilm. These data are promising as the applied concentrations are achievable for local treatment in bone and soft tissues. In another recent publication, a mupirocin spray was formulated and tested against *E. coli* strains, in a context of wound and surgical site infections. Inhibition and disruption of formed biofilms were achieved with a single and a sub-actual dose of the antibiotic spray (1 mg per spray or 1 mg per 50 mg of ointment), compared to the commercialized mupirocin ointment (Bakkiyaraj et al., 2017). Results showed that both formulations had an anti-biofilm action on *E. coli* sessile cultures in tissue culture plates but microscope studies provided complementary evidences that it remained more individual adherent cells with ointment formulation than for treatment with the antibiotic spray. Authors concluded that this efficacy on biofilm prevention and disruption was comparable with that of the ointment. Nevertheless, the spray use seemed beneficial as it included an easy application: while the ointment was removed from the application site upon washing, the spray formulation significantly resisted removal after a single wash.

Finally, for the treatment of recurrent urinary tract infections (UTIs) associated with the presence of biofilm, the use of amikacin, ciprofloxacin, and third-generation cephalosporins could be recommended. Indeed, various concentrations of these molecules, selected according the bioavailability of antibiotics in human urine, showed the ability to significantly reduce biofilm biomass in a study of 116 *E. coli* strains of UTIs (González et al., 2017).

Even if it seems that antimicrobials can be effective on prematurely adherent bacteria, a small percentage of persister cells develop a high tolerance to antibiotics and are typically involved in infection relapses. Moreover, the biofilm must be considered as a single compartment with its own pharmacokinetic parameters. This will influence local antibiotic concentration and its metabolization in the biofilm (Cao et al., 2015). All these combined factors lead to the recommended use of high doses of antimicrobials for long periods, which cannot always be practicable in patients because of severe systemic side effects.

Biofilm tolerance to antimicrobials is complex and above all multifactorial. A now long list of studies demonstrate that low doses of antimicrobials at the infection site might increase the selection of mutagenesis and the risk of biofilm formation initiation induction (Ciofu et al., 2017).

## INDUCTION OF BIOFILM FORMATION BY ANTIMICROBIALS

At high concentrations, antibiotics appear to be perfect bacterial killers. Their original function in the environment is fighting and inhibiting the growth of competitors (Linares et al., 2006). The production of antimicrobials by bacteria themselves allows the killing of predators. This application of the classical Darwinian principle supports the idea that they allow the competing colonization of soil by microorganisms. However, antibiotic molecules constitute only a small part of organic compounds produced by bacteria. Consequently, it can be assumed that they can affect the general modulation metabolic function in bacteria, as other signaling analogous (rhamnolipids, peptides, and QS signals, etc.). Supporting this assumption, phylogenetic analyses revealed that antimicrobial resistant genes were present in bacterial genomes millions of years before the modern use of antibiotics. A similar example concerns the metagenomic study of Alaskan soils, which demonstrated the existence of an ancient and varied collection of  $\beta$ -lactamase genes, whereas this antimicrobial family is not detected in the environment (Aminov, 2009).

In activating specific gene transcription, antimicrobial compounds seem to act as signaling molecules, regulating the homeostasis of bacterial communities. As sessile cells are significantly less sensitive to antimicrobials, biofilm formation would be a strategic evolution of bacterial populations to counteract non-lethal doses of antibiotics produced by soil microorganisms. This implies that antimicrobials can also be beneficial for the survival of susceptible planktonic cells in nature. Therefore, they can permit a more efficient colonization of heterogeneous environments. Especially at subinhibitory levels, antibiotics modulate bacterial virulence, stress response, motility, and biofilm formation (Song et al., 2016).

The first report describing the ability of low doses of antibiotics to interfere with bacterial functions was made by Gardner (1940). In the presence of subinhibitory concentrations of penicillin, numerous gram-negative, and positive pathogens formed elongated filaments.

Since then, similar studies introducing the structure modification of bacterial cells by antibiotics were published. *P. aeruginosa* showed the most morphological changes as bacteria reacted to meropenem and biapenem in forming a “bulge” midway along them (Horii et al., 1998). The authors also described a relationship between the induction of a new morphology and the amount of endotoxin released by bacteria. The modification of the bacterial size and shape was explained by the fact that antibiotic molecules inhibit the Penicillin-Binding-Proteins 2 and 3 (PBP-2 and PBP-3). They are involved in the assembly of the bacterial cell wall by the catalysis of the terminal stages of the peptidoglycan network. These proteins are the primary target of  $\beta$ -lactam antibiotics in Gram-negative bacteria. The inactivation of PBP-1 leads to bacteria lysis, whereas the inhibition of PBP-2 and PBP-3 is associated with either spherical cells or filamentous bacteria. These effects of antimicrobials onto the bacterial morphology were also observed in experimental infections in mice (Yokochi et al., 2000).

More precisely, the authors highlighted a relationship between the shape of bacteria and their susceptibility to phagocytosis. Induced round bacteria were phagocytosed by peritoneal cells, whereas long filaments were not. Finally, it appeared that the morphological reorganization of bacteria is a reversible process as when antibiotics were no longer present, the induced spherical or filamentous population converts back to the normal bacillary form (Monahan et al., 2014). This transition is a strategy to survive antibiotic exposure as the biofilm formation.

Furthermore, exposure of *P. aeruginosa* strains to sub-MICs of ciprofloxacin leads to the selection of pre-existing mutants with high level resistance (Jørgensen et al., 2013). The analysis of the strains selected by subinhibitory doses of the fluoroquinolone showed phenotypic changes in bacteria, as decreased protease activity and swimming motility, down-regulation of the type III secretion system and higher levels of quorum-sensing signals (Wassermann et al., 2016). In some cases, this implies that antimicrobial therapies may expose patients to detrimental side-effects by accelerating pathogen adaptation and raising the risk of antimicrobial tolerance and spread in the commensal bacterial flora if bacteria are exposed to low antibiotic concentrations.

The first study demonstrating the real “inducer” property of antimicrobials on biofilm formation at subinhibitory concentrations dates back to 1988 (Schadow et al., 1988). The adherence of coagulase-negative staphylococci was increased to 65% after rifampicin treatment. Since then, numerous works focusing on the effect of low antibiotic doses on biofilm formation were published.

Although several studies have shown that aminoglycoside antibiotics act as antagonists of biofilm formation *in vitro* (see previous section of this paper), opposite data were collected and highlighted the ability of the same molecules to significantly induce the sessile growth of a variety of bacterial species. Hoffman et al. (2005) described the effect of subinhibitory doses of aminoglycosides in *P. aeruginosa* and *E. coli* biofilms. They showed that these antibiotics stimulated the expression of the *arr* gene, which encodes a phosphodiesterase whose substrate is the c-di-GMP. Reinforcing this idea, induction of biofilm formation after an exposure to sub-MICs of aminoglycosides was detected among half of a *P. aeruginosa* clinical isolate collection (Elliott et al., 2010).

Imipenem, a carbapenem molecule, was also able to substantially influence the expression of 34 genes in the common reference PAO1 strain. When subinhibitory concentrations of this antibiotic were applied to bacterial cultures, the alginate gene cluster, the main component of the biofilm matrix of *P. aeruginosa* was more than 10-fold induced (Bagge et al., 2004). The corresponding polysaccharide amount in biofilms was quantified by the authors and they found that the alginate level in the matrix of stimulated-biofilms was 20-fold higher than the one of the non-exposed controls.

Induction phenomenon of biofilm formation by antimicrobials was also described for other bacterial species. The use of  $\beta$ -lactam antibiotics at sub-MIC concentrations leads to the induction of the bacterial adhesion by a community-associated Methicillin-Resistant *S. aureus* (MRSA) strain and clinical isolates (Ng et al., 2014). All of the antimicrobial molecules tested



in this study exhibited a biphasic dose-response curve. Authors also described an inversely proportional relationship between the biofilm amount and the susceptibility of bacteria to methicillin: the more sensitive the strain to antibiotic, the lower is the concentration required to induced biofilm. Biofilm formation of a clinical isolate of *Enterococcus faecalis*, which commonly underlies prosthetic valve endocarditis and multiple device infections, was also significantly increased by low concentrations of ampicillin, ceftriaxone, oxacillin, and fosfomycin. This enhancement of biofilm establishment appeared to be specific of molecules inhibiting cell wall synthesis (Yu et al., 2017). Additionally, a collection of ninety-six clinical isolates of *S. epidermidis*, which originate from various samples as wounds, catheters, sputum, etc., was recovered by He et al. (2016). The authors described that 27% of erythromycin-resistant strains exhibited biofilm induction by 0.25 MIC of the molecule. The induction intensity ranged from 1.11-fold to more than twofold (He et al., 2016).

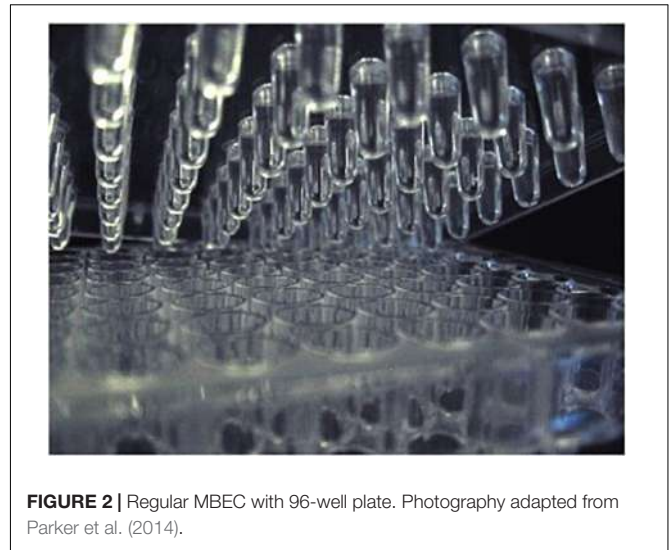
A more complete review article written by Kaplan (2011) gathers studies showing that subinhibitory concentrations of antimicrobial molecules can act as agonists of bacterial biofilms *in vitro*.

Biological responses of bacterial species are strain- and dose-dependent. Some molecules can promote the biofilm formation at high levels and conversely be antagonists and repress its establishment at lower doses. Nonetheless, this dose-response relationship cannot be generalized as it can be inverted, depending on the considered antibiotic, which is used in the treatment for a specific laboratory or clinical strain. The discovery of this ecological function of antibiotics is essential as, in a clinical context, the induction of biofilm formation by low concentrations of antibiotics would contribute to the failure of antimicrobial therapies in case of biofilm-related infections. It can be speculated that this is a common phenomenon as microorganisms are usually under fluctuating doses of antibiotics during a chemotherapy.

## Clinical Tools Available for the Diagnosis and Treatment of Biofilm Infections

Traditionally, clinical microbiology laboratories have focused on the culture of isolated bacterial strains and provide their susceptibility to antibiotics in defining the breakpoints and the PK/PD parameters under planktonic growth conditions. The corresponding antibiotic therapies, based on non-adherent microorganisms, are often associated with treatment failures and/or recurrence of the infection. No guidelines are offered to clinicians to successfully treat biofilm infections, which can result to false-negative data if the samples do not significantly represent the main infection.

Besides, there is still no available standardized tool to detect easily the presence of sessile cells in a clinical sample and allow determination of their specific antibiotic susceptibility. As biofilm bacteria are inherently more tolerant to antimicrobials, the establishment of the corresponding breakpoints to predict therapeutic success is needed. New methods monitoring the effect/response of biofilm cells to antibiotic therapy must

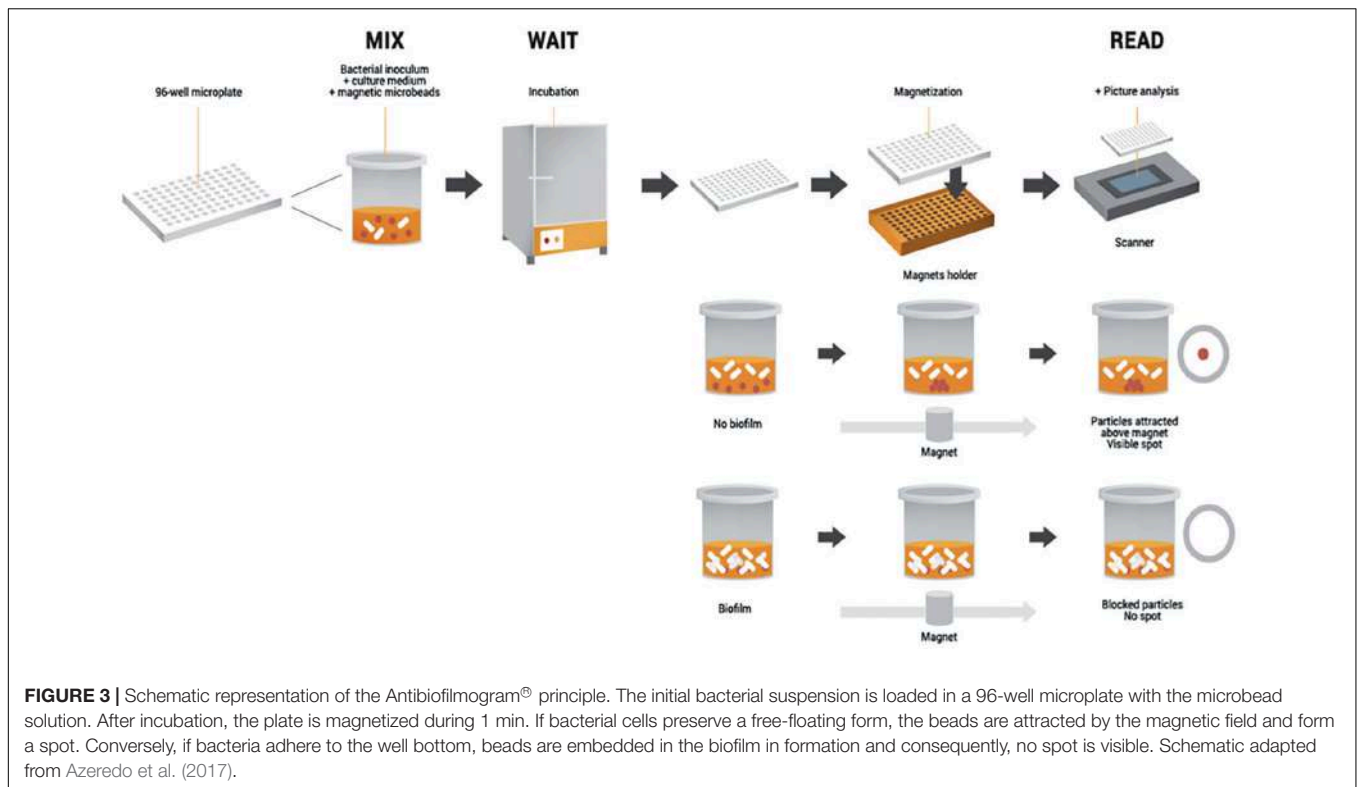


**FIGURE 2** | Regular MBEC with 96-well plate. Photography adapted from Parker et al. (2014).

be designed. Currently, two technologies were developed but not yet standardized for a rapid routine use in hospital laboratories: the Calgary device (also called MBEC assay) and the Antibiofilmogram®.

The Calgary biofilm device consists of a two-part reaction vessel (Ceri et al., 1999). A lid, composed of 96 pegs, forms the first and top component. The bottom component of the device is a standard 96-well plate, in which the pegs are designed to sit into each well. The microplate contains the medium allowing the growth of bacteria, which is set up in 96 equivalent biofilms at each peg site (Figure 2). Biofilm susceptibility testing is performed in transferring the lid with bacterial biofilms to a standard 96-well plate containing serial dilutions of antibiotics. The minimal biofilm eradication concentration (MBEC) is defined as the minimal concentration of antibiotic that prevents visible growth in the recovery medium used to collect sessile cells.

Moskowitz et al. (2004) evaluated the *in vitro* activity of twelve antimicrobials on a large number of CF sessile clinical isolates of *P. aeruginosa* using a modified Calgary device protocol. The MBECs of the antimicrobial agents were much higher than the corresponding conventional MICs. In a context of biofilm infections, this suggests that the use of broth microdilution susceptibility testing or other standard methods to guide therapy may not contribute to improve clinical outcomes. Quite the reverse, devices simulating biofilm growth conditions might guide therapy more effectively. To verify this hypothesis, clinical trials were already conducted. Unfortunately, no evidence that biofilm susceptibility testing performed with the Calgary device was more efficient than conventional techniques in terms of clinical outcomes was provided (Waters and Ratjen, 2017). Yau et al. (2015) introduced the first randomized controlled trial evaluating the utility of biofilm antimicrobial susceptibility testing in the treatment of CF pulmonary exacerbations. They concluded that the choice of antibiotic therapies based on biofilm behavior of bacteria did not improve clinical outcomes and did not decrease pulmonary bacterial loads. They explained the lack of Calgary method efficacy by an oversimplification



of the sessile growth conditions. Biofilm formation on a lid composed of 96 plastic pegs could not recreate the environment *in vivo*, in which sessile cells grow and express specific properties. Moreover, the determination of antimicrobial susceptibility of a selected isolate could underestimate the microbial diversity response to antibiotics.

The Antibiofilmogram® (ATBFG) method was specifically designed to investigate early steps of biofilm development, by rapidly screening antibiotic effective against sessile bacteria. Its functioning principle is based on the potential immobilization of magnetic microbeads by bacteria forming a biofilm in the well bottom of a microplate (Chavant et al., 2007).

Briefly, a given bacterial culture is mixed with the microbead suspension and loaded in the plate (Figure 3). Afterward, it is incubated and submitted to a magnetic field at a desired time point, without staining and/or washing stages. The formation of a brown spot in the bottom of wells reveals the free migration of beads during plate magnetization and so, the remaining-free state of bacteria. Conversely, the absence of visible spots reflects the bead blockage by a pre-forming biofilm (Olivares et al., 2016). The main advantage of this methodology is its capacity to collect data within a couple of hours, allowing comparison of antibiotic susceptibility of sessile bacteria to the results of classical antibiograms. But as for the Calgary method, the ATBFG is an *in vitro* assay, which does not provide information about structure or thickness of the mature biofilms.

Results of ATBFG performed on 29 clinical strains of *S. aureus* isolated from bone and joint infections (BIJs) were also published (Tasse et al., 2016). On the basis of antibiotic breakpoint values, the authors defined effective antimicrobial

molecules against adhesion of the majority of *S. aureus* strains (rifampicin, linezolid, clindamycin, and fusidic acid), others inefficient against bacterial adherence (fosfomycin, ofloxacin, daptomycin, and gentamicin) and some of them whose efficacy was strain-dependent (cloxacillin, vancomycin, and teicoplanin). Data validity was confirmed by *in vivo* assays (catheter-related infections in the mouse). Results showed that serum concentrations of cloxacillin, corresponding to the MBICs determined by ATBFG (either 2 or 4 µg/ml), allowed reduction to 3 log the bacterial biomasses colonizing the catheters for three clinical strains, whereas the simple MICs of the antibiotic were inefficient on biofilm formation.

In a CF context, the use of ATBFG on clinical *P. aeruginosa* strains also showed the capacity of two aminoglycosides (amikacin and tobramycin) to prevent bacterial adhesion at concentrations close to the MICs (Olivares et al., 2017). Only *in vitro* assays were performed in this study but an inter-method reproducibility was conducted through Crystal Violet staining and a tissue culture system, which validated the inhibitory effect of the antimicrobials on the early adhesion of *P. aeruginosa* isolates.

## CONCLUDING REMARKS

As demonstrated in previous sections, the treatment of bacterial infections with chemically distinct antibiotics can lead to a variety of responses from sessile bacteria. Despite the increased tolerance of microorganisms toward antimicrobials, some molecules are always effective against newly adherent bacteria. In clinical

practice, it is recommended that when possible, as for the diabetic foot for instance, to resort to topical administration to provide high local concentrations to the infection site without systemic side-effects.

Disappointingly, numerous studies have also described that low doses of antibiotics can significantly induce biofilm formation *in vitro* for a variety of bacterial species. The plausibility of this phenomenon *in vivo* must be considered as bacterial pathogens are exposed to sub-MIC concentrations of antimicrobials during a clinical therapy with fluctuating dosing regimens. More researches on antibiotic-induced biofilm formation are required to elucidate the involved mechanisms. Clinical trials that verify the relevance of this process in patients and the potential relationship with therapy failure will also be highly helpful. The prospect of complementary assays evaluating the susceptibility of free and sessile cells to antibiotics would also allow the optimization of the general use of antimicrobials in the treatment of biofilm-related infections.

## REFERENCES

- Aminov, R. I. (2009). The role of antibiotics and antibiotic resistance in nature. *Environ. Microbiol.* 11, 2970–2988. doi: 10.1111/j.1462-2920.2009.01972.x
- Azeredo, J., Azevedo, N. F., Briandet, R., Cerca, N., Coenye, T., Costa, A. R., et al. (2017). Critical review on biofilm methods. *Crit. Rev. Microbiol.* 43, 331–351. doi: 10.1080/1040841X.2016.1208146
- Bagge, N., Schuster, M., Hentzer, M., Ciofu, O., Givskov, M., Greenberg, E. P., et al. (2004). *Pseudomonas aeruginosa* biofilms exposed to imipenem exhibit changes in global gene expression and  $\beta$ -Lactamase and alginate production. *Antimicrob. Agents Chemother.* 48, 1175–1187. doi: 10.1128/AAC.48.4.1175-1187.2004
- Bakkiyaraj, D., Sritharadol, R., Padmavathi, A. R., Nakpheng, T., and Srichana, T. (2017). Anti-biofilm properties of a mupirocin spray formulation against *Escherichia coli* wound infections. *Biofouling* 33, 591–600. doi: 10.1080/08927014.2017.1337100
- Bala, A., Kumar, R., and Harjai, K. (2011). Inhibition of quorum sensing in *Pseudomonas aeruginosa* by azithromycin and its effectiveness in urinary tract infections. *J. Med. Microbiol.* 60, 300–306. doi: 10.1099/jmm.0.025387-0
- Basas, J., Palau, M., Ratia, C., Del Pozo, J. L., Martín-Gómez, M. T., Gomis, X., et al. (2018). High-dose daptomycin is effective as an antibiotic lock therapy in a rabbit model of *Staphylococcus epidermidis* catheter-related infection. *Antimicrob. Agents Chemother.* 62:e01777-17. doi: 10.1128/AAC.01777-17
- Bigger, J. W. (1944). Treatment of staphylococcal infections with penicillin by intermittent sterilisation. *The Lancet* 244, 497–500. doi: 10.1016/S0140-6736(00)74210-3
- Biofilms: The Hypertextbook (2011). Available at: <http://www.hypertextbookshop.com/biofilmbook/v004/r003Test/index.html> (accessed December 15, 2016).
- Butini, M. E., Cabric, S., Trampuz, A., and Di Luca, M. (2018). *In vitro* anti-biofilm activity of a biphasic gentamicin-loaded calcium sulfate/hydroxyapatite bone graft substitute. *Colloids Surf. B Biointerfaces* 161, 252–260. doi: 10.1016/j.colsurfb.2017.10.050
- Cao, B., Christophersen, L., Thomsen, K., Sønderholm, M., Bjarnsholt, T., Jensen, P. Ø, et al. (2015). Antibiotic penetration and bacterial killing in a *Pseudomonas aeruginosa* biofilm model. *J. Antimicrob. Chemother.* 70, 2057–2063. doi: 10.1093/jac/dkv058
- Ceri, H., Olson, M. E., Stremick, C., Read, R. R., Morck, D., and Buret, A. (1999). The calgary biofilm device: new technology for rapid determination of antibiotic susceptibilities of bacterial biofilms. *J. Clin. Microbiol.* 37, 1771–1776.
- Chavant, P., Gaillard-Martinie, B., Talon, R., Hébraud, M., and Bernardi, T. (2007). A new device for rapid evaluation of biofilm formation potential by bacteria. *J. Microbiol. Methods* 68, 605–612. doi: 10.1016/j.mimet.2006.11.010

## AUTHOR CONTRIBUTIONS

EO wrote the manuscript. All authors read and approved the submitted version.

## FUNDING

This study was received funding from the BioFilm Pharma SAS. The funder was not involved in the study design, collection, analysis, interpretation of data, and the writing of this article or the decision to submit it for publication. This study was supported by the 15th Fonds Unique Interministériel (FUI).

## ACKNOWLEDGMENTS

We thank BioFilm Pharma SAS for the financial support.

- Ciofu, O., Rojo-Molinero, E., Macià, M. D., and Oliver, A. (2017). Antibiotic treatment of biofilm infections. *APMIS* 125, 304–319. doi: 10.1111/apm.12673
- Ciofu, O., Tolker-Nielsen, T., Jensen, P. Ø, Wang, H., and Høiby, N. (2015). Antimicrobial resistance, respiratory tract infections and role of biofilms in lung infections in cystic fibrosis patients. *Adv. Drug Deliv. Rev.* 85, 7–23. doi: 10.1016/j.addr.2014.11.017
- Conlon, B. P., Rowe, S. E., and Lewis, K. (2015). Persister cells in biofilm associated infections. *Adv. Exp. Med. Biol.* 831, 1–9. doi: 10.1007/978-3-319-09782-4\_1
- Costerton, J. W., Geesey, G. G., and Cheng, K. J. (1978). How bacteria stick. *Sci. Am.* 238, 86–95. doi: 10.1038/scientificamerican0178-86
- Davies, D. G., and Geesey, G. G. (1995). Regulation of the alginate biosynthesis gene *algC* in *Pseudomonas aeruginosa* during biofilm development in continuous culture. *Appl. Environ. Microbiol.* 61, 860–867.
- Davies, D. G., Parsek, M. R., Pearson, J. P., Iglewski, B. H., Costerton, J. W., and Greenberg, E. P. (1998). The involvement of cell-to-cell signals in the development of a bacterial biofilm. *Science* 280, 295–298. doi: 10.1126/science.280.5361.295
- Del Pozo, J. L. (2018). Biofilm-related disease. *Expert Rev. Anti Infect. Ther.* 16, 51–65. doi: 10.1080/14787210.2018.1417036
- Delpech, P., ALeryan, M., Jones, B., Gemmel, C., and Lang, S. (2018). An *in vitro* evaluation of the efficacy of tedizolid: implications for the treatment of skin and soft tissue infections. *Diagn. Microbiol. Infect. Dis.* 91, 93–97. doi: 10.1016/j.diagmicrobio.2018.01.006
- Dibartola, A. C., Swearingen, M. C., Granger, J. F., Stoodley, P., and Dusane, D. H. (2017). Biofilms in orthopedic infections: a review of laboratory methods. *APMIS* 125, 418–428. doi: 10.1111/apm.12671
- Diez-Aguilar, M., Morosini, M. I., Köksal, E., Oliver, A., Ekkelenkamp, M., and Cantón, R. (2018). Use of calgary and microfluidic BioFlux systems to test the activity of fosfomycin and tobramycin alone and in combination against cystic fibrosis *Pseudomonas aeruginosa* biofilms. *Antimicrob. Agents Chemother.* 62:e01650-17. doi: 10.1128/AAC.01650-17
- Donné, J., and Dewilde, S. (2015). The challenging world of biofilm physiology. *Adv. Microb. Physiol.* 67, 235–292. doi: 10.1016/bs.ampbs.2015.09.003
- Dufour, D., Leung, V., and Lévesque, C. M. (2010). Bacterial biofilm: structure, function, and antimicrobial resistance. *Endod. Topics* 22, 2–16. doi: 10.1111/j.1601-1546.2012.00277.x
- Elliott, D., Burns, J. L., and Hoffman, L. R. (2010). Exploratory study of the prevalence and clinical significance of tobramycin-mediated biofilm induction in *Pseudomonas aeruginosa* isolates from cystic fibrosis patients. *Antimicrob. Agents Chemother.* 54, 3024–3026. doi: 10.1128/AAC.00102-10
- Fisher, R. A., Gollan, B., and Helaine, S. (2017). Persistent bacterial infections and persister cells. *Nat. Rev. Microbiol.* 15, 453–464. doi: 10.1038/nrmicro.2017.42



- Fonseca, A. P. (2004). Effect of subinhibitory concentration of piperacillin/tazobactam on *Pseudomonas aeruginosa*. *J. Med. Microbiol.* 53, 903–910. doi: 10.1099/jmm.0.45637-0
- Gardner, A. D. (1940). Morphological effects of penicillin on bacteria. *Nature* 146, 837–838. doi: 10.1038/146837b0
- Gillis, R. J., and Iglewski, B. H. (2004). Azithromycin retards *Pseudomonas aeruginosa* biofilm formation. *J. Clin. Microbiol.* 42, 5842–5845. doi: 10.1128/JCM.42.12.5842-5845.2004
- González, M. J., Robino, L., Iribarnegaray, V., Zunino, P., and Scavone, P. (2017). Effect of different antibiotics on biofilm produced by uropathogenic *Escherichia coli* isolated from children with urinary tract infection. *Pathog. Dis.* 75:ftx053. doi: 10.1093/femspd/ftx053
- Harms, A., Maisonneuve, E., and Gerdes, K. (2016). Mechanisms of bacterial persistence during stress and antibiotic exposure. *Science* 354:aaf4268. doi: 10.1126/science.aaf4268
- He, H.-J., Sun, F.-J., Wang, Q., Liu, Y., Xiong, L.-R., and Xia, P.-Y. (2016). Erythromycin resistance features and biofilm formation affected by subinhibitory erythromycin in clinical isolates of *Staphylococcus epidermidis*. *J. Microbiol. Immunol. Infect.* 49, 33–40. doi: 10.1016/j.jmii.2014.03.001
- Hentzer, M., Teitzel, G. M., Balzer, G. J., Heydorn, A., Molin, S., Givskov, M., et al. (2001). Alginate overproduction affects *Pseudomonas aeruginosa* biofilm structure and function. *J. Bacteriol.* 183, 5395–5401. doi: 10.1128/JB.183.18.5395-5401.2001
- Hoffman, L. R., D'Argenio, D. A., MacCoss, M. J., Zhang, Z., Jones, R. A., and Miller, S. I. (2005). Aminoglycoside antibiotics induce bacterial biofilm formation. *Nature* 436, 1171–1175. doi: 10.1038/nature03912
- Høiby, N., Bjarnsholt, T., Givskov, M., Molin, S., and Ciofu, O. (2010). Antibiotic resistance of bacterial biofilms. *Int. J. Antimicrob. Agents* 35, 322–332. doi: 10.1016/j.ijantimicag.2009.12.011
- Høiby, N., Ciofu, O., Johansen, H. K., Song, Z., Moser, C., Jensen, P. Ø, et al. (2011). The clinical impact of bacterial biofilms. *Int. J. Oral Sci.* 3, 55–65. doi: 10.4248/IJOS11026
- Horii, T., Kobayashi, M., Sato, K., Ichiyama, S., and Ohta, M. (1998). An *in vitro* study of carbapenem-induced morphological changes and endotoxin release in clinical isolates of gram-negative bacilli. *J. Antimicrob. Chemother.* 41, 435–442. doi: 10.1093/jac/41.4.435
- Jamal, M., Ahmad, W., Andleeb, S., Jalil, F., Imran, M., Nawaz, M. A., et al. (2018). Bacterial biofilm and associated infections. *J. Chin. Med. Assoc.* 81, 7–11. doi: 10.1016/j.jcma.2017.07.012
- Jensen, P. Ø, Givskov, M., Bjarnsholt, T., and Moser, C. (2010). The immune system vs. *Pseudomonas aeruginosa* biofilms. *FEMS Immunol. Med. Microbiol.* 59, 292–305. doi: 10.1111/j.1574-695X.2010.00706.x
- Jørgensen, K. M., Wassermann, T., Jensen, P. Ø, Hengzuang, W., Molin, S., Høiby, N., et al. (2013). Sublethal ciprofloxacin treatment leads to rapid development of high-level ciprofloxacin resistance during long-term experimental evolution of *Pseudomonas aeruginosa*. *Antimicrob. Agents Chemother.* 57, 4215–4221. doi: 10.1128/AAC.00493-13
- Kaplan, J. B. (2011). Antibiotic-induced biofilm formation. *Int. J. Artif. Organs* 34, 737–751. doi: 10.5301/ijao.5000027
- Klinger-Strobel, M., Stein, C., Forstner, C., Makarewicz, O., and Pletz, M. W. (2017). Effects of colistin on biofilm matrices of *Escherichia coli* and *Staphylococcus aureus*. *Int. J. Antimicrob. Agents* 49, 472–479. doi: 10.1016/j.ijantimicag.2017.01.005
- Lebeaux, D., and Ghigo, J.-M. (2012). Infections associées aux biofilms - Quelles perspectives thérapeutiques issues de la recherche fondamentale?? *Med. Sci.* 28, 727–739. doi: 10.1051/medsci/2012288015
- Lewis, K. (2005). Persistor cells and the riddle of biofilm survival. *Biochemistry* 70, 267–274. doi: 10.1007/s10541-005-0111-6
- Limoli, D. H., Jones, C. J., and Wozniak, D. J. (2015). Bacterial extracellular polysaccharides in biofilm formation and function. *Microbiol. Spectr.* 3, doi: 10.1128/microbiolspec.MB-0011-2014
- Linares, J. F., Gustafsson, I., Baquero, F., and Martinez, J. L. (2006). Antibiotics as intermicrobial signaling agents instead of weapons. *Proc. Natl. Acad. Sci. U.S.A.* 103, 19484–19489. doi: 10.1073/pnas.0608949103
- Mah, T.-F., Pitts, B., Pellock, B., Walker, G. C., Stewart, P. S., and O'Toole, G. A. (2003). A genetic basis for *Pseudomonas aeruginosa* biofilm antibiotic resistance. *Nature* 426, 306–310. doi: 10.1038/nature02122
- McDougald, D., Rice, S. A., Barraud, N., Steinberg, P. D., and Kjelleberg, S. (2011). Should we stay or should we go: mechanisms and ecological consequences for biofilm dispersal. *Nat. Rev. Microbiol.* 10, 39–50. doi: 10.1038/nrmicro2695
- Monahan, L. G., Turnbull, L., Osvath, S. R., Birch, D., Charles, I. G., and Whitchurch, C. B. (2014). Rapid conversion of *Pseudomonas aeruginosa* to a spherical cell morphotype facilitates tolerance to carbapenems and penicillins but increases susceptibility to antimicrobial peptides. *Antimicrob. Agents Chemother.* 58, 1956–1962. doi: 10.1128/AAC.01901-13
- Moskowitz, S. M., Foster, J. M., Emerson, J., and Burns, J. L. (2004). Clinically feasible biofilm susceptibility assay for isolates of *Pseudomonas aeruginosa* from patients with cystic fibrosis. *J. Clin. Microbiol.* 42, 1915–1922. doi: 10.1128/JCM.42.5.1915-1922.2004
- Mulcahy, L. R., Isabella, V. M., and Lewis, K. (2014). *Pseudomonas aeruginosa* biofilms in disease. *Microb. Ecol.* 68, 1–12. doi: 10.1007/s00248-013-0297-x
- Ng, M., Epstein, S. B., Callahan, M. T., Piotrowski, B. O., Simon, G. L., Roberts, A. D., et al. (2014). Induction of MRSA biofilm by low-dose  $\beta$ -Lactam antibiotics: specificity, prevalence and dose-response effects. *Dose Response* 12, 152–161. doi: 10.2203/dose-response.13-021.Kaplan
- Okshevsky, M., and Meyer, R. L. (2015). The role of extracellular DNA in the establishment, maintenance and perpetuation of bacterial biofilms. *Crit. Rev. Microbiol.* 41, 341–352. doi: 10.3109/1040841X.2013.841639
- Olivares, E., Badel-Berchoux, S., Provot, C., Jaulhac, B., Prévost, G., Bernardi, T., et al. (2016). The BioFilm ring test: a rapid method for routine analysis of *Pseudomonas aeruginosa* biofilm formation kinetics. *J. Clin. Microbiol.* 54, 657–661. doi: 10.1128/JCM.02938-15
- Olivares, E., Badel-Berchoux, S., Provot, C., Jaulhac, B., Prévost, G., Bernardi, T., et al. (2017). Tobramycin and amikacin delay adhesion and microcolony formation in *Pseudomonas aeruginosa* cystic fibrosis isolates. *Front. Microbiol.* 8:1289. doi: 10.3389/fmicb.2017.01289
- Otani, S., Hiramatsu, K., Hashinaga, K., Komiya, K., Umeki, K., Kishi, K., et al. (2018). Sub-minimum inhibitory concentrations of ceftazidime inhibit *Pseudomonas aeruginosa* biofilm formation. *J. Infect. Chemother.* 24, 428–433. doi: 10.1016/j.jiac.2018.01.007
- O'Toole, G. A., and Kolter, R. (1998). Flagellar and twitching motility are necessary for *Pseudomonas aeruginosa* biofilm development. *Mol. Microbiol.* 30, 295–304. doi: 10.1046/j.1365-2958.1998.01062.x
- Ozbek, B., and Mataraci-Kara, E. (2016). Comparative *in vitro* efficacies of various antipseudomonal antibiotics based catheter lock solutions on eradication of *Pseudomonas aeruginosa* biofilms. *J. Chemother.* 28, 20–24. doi: 10.1179/1973947814Y.0000000212
- Paraje, M. G. (2011). "Antimicrobial resistance in biofilms," in *Science Against Microbial Pathogens: Communicating Current Research and Technological Advances*, ed. A. Méndez-Vilas, (Badajoz: Formatex Research Center), 736–744.
- Parker, A. E., Walker, D. K., Goeres, D. M., Allan, N., Olson, M. E., and Omar, A. (2014). Ruggedness and reproducibility of the MBEC biofilm disinfectant efficacy test. *J. Microbiol. Methods* 102, 55–64. doi: 10.1016/j.mimet.2014.04.013
- Pezzulo, A. A., Tang, X. X., Hoegger, M. J., Abou Alaiwa, M. H., Ramachandran, S., Moninger, T. O., et al. (2012). Reduced airway surface pH impairs bacterial killing in the porcine cystic fibrosis lung. *Nature* 487, 109–113. doi: 10.1038/nature11130
- Poole, K. (2012). Stress responses as determinants of antimicrobial resistance in Gram-negative bacteria. *Trends Microbiol.* 20, 227–234. doi: 10.1016/j.tim.2012.02.004
- Rodríguez-Rojas, A., Oliver, A., and Blázquez, J. (2012). Intrinsic and environmental mutagenesis drive diversification and persistence of *Pseudomonas aeruginosa* in chronic lung infections. *J. Infect. Dis.* 205, 121–127. doi: 10.1093/infdis/jir690
- Roudashti, S., Zeighami, H., Mirshahabi, H., Bahari, S., Soltani, A., and Haghi, F. (2017). Synergistic activity of sub-inhibitory concentrations of curcumin with ceftazidime and ciprofloxacin against *Pseudomonas aeruginosa* quorum sensing related genes and virulence traits. *World J. Microbiol. Biotechnol.* 33:50. doi: 10.1007/s11274-016-2195-0
- Saginur, R., Stdenis, M., Ferris, W., Aaron, S. D., Chan, F., Lee, C., et al. (2006). Multiple combination bactericidal testing of staphylococcal biofilms from implant-associated infections. *Antimicrob. Agents Chemother.* 50, 55–61. doi: 10.1128/AAC.50.1.55-61.2006
- Shadow, K. H., Simpson, W. A., and Christensen, G. D. (1988). Characteristics of adherence to plastic tissue culture plates of coagulase-negative staphylococci



- exposed to subinhibitory concentrations of antimicrobial agents. *J. Infect. Dis.* 157, 71–77. doi: 10.1093/infdis/157.1.71
- Schurek, K. N., Breidenstein, E. B. M., and Hancock, R. E. W. (2012). “*Pseudomonas aeruginosa*: a persistent pathogen in cystic fibrosis and hospital-associated infections” in *Antibiotic Discovery and Development*, eds T. J. Dougherty, and M. J. Pucci, (New York, NY: Springer), 679–715. doi: 10.1007/978-1-4614-1400-1\_21
- Serra, D. O., and Hengge, R. (2014). Stress responses go three dimensional - the spatial order of physiological differentiation in bacterial macrocolony biofilms. *Environ. Microbiol.* 16, 1455–1471. doi: 10.1111/1462-2920.12483
- Skindersoe, M. E., Alhede, M., Phipps, R., Yang, L., Jensen, P. O., Rasmussen, T. B., et al. (2008). Effects of antibiotics on quorum sensing in *Pseudomonas aeruginosa*. *Antimicrob. Agents Chemother.* 52, 3648–3663. doi: 10.1128/AAC.01230-07
- Song, T., Dupertuy, M., and Wai, S. N. (2016). Sub-optimal treatment of bacterial biofilms. *Antibiotics* 5:E23. doi: 10.3390/antibiotics5020023
- Srivastava, S., and Bhargava, A. (2016). Biofilms and human health. *Biotechnol. Lett.* 38, 1–22. doi: 10.1007/s10529-015-1960-8
- Stewart, P. S. (2002). Mechanisms of antibiotic resistance in bacterial biofilms. *Int. J. Med. Microbiol.* 292, 107–113. doi: 10.1078/1438-4221-00196
- Szczuka, E., Jabłońska, L., and Kaznowski, A. (2017). Effect of subinhibitory concentrations of tigecycline and ciprofloxacin on the expression of biofilm-associated genes and biofilm structure of *Staphylococcus epidermidis*. *Microbiology* 163, 712–718. doi: 10.1099/mic.0.000453
- Tasse, J., Croisier, D., Badel-Berchoux, S., Chavanet, P., Bernardi, T., Provot, C., et al. (2016). Preliminary results of a new antibiotic susceptibility test against biofilm installation in device-associated infections: the antibiofilmogram. *Pathog. Dis.* 74: ftw057. doi: 10.1093/femspd/ftw057
- Vallet, I., Olson, J. W., Lory, S., Lazdunski, A., and Filloux, A. (2001). The chaperone/usher pathways of *Pseudomonas aeruginosa*: identification of fimbrial gene clusters (cup) and their involvement in biofilm formation. *Proc. Natl. Acad. Sci. U.S.A.* 98, 6911–6916. doi: 10.1073/pnas.111551898
- Wassermann, T., Meinike Jørgensen, K., Ivanyshyn, K., Bjarnsholt, T., Khademi, S. M. H., Jelsbak, L., et al. (2016). The phenotypic evolution of *Pseudomonas aeruginosa* populations changes in the presence of subinhibitory concentrations of ciprofloxacin. *Microbiology* 162, 865–875. doi: 10.1099/mic.0.000273
- Waters, V., and Ratjen, F. (2017). Standard versus biofilm antimicrobial susceptibility testing to guide antibiotic therapy in cystic fibrosis. *Cochrane Database Syst. Rev.* 10:CD009528. doi: 10.1002/14651858.CD009528.pub4
- Watters, C., DeLeon, K., Trivedi, U., Griswold, J. A., Lyte, M., Hampel, K. J., et al. (2013). *Pseudomonas aeruginosa* biofilms perturb wound resolution and antibiotic tolerance in diabetic mice. *Med. Microbiol. Immunol.* 202, 131–141. doi: 10.1007/s00430-012-0277-7
- Watters, C., Fleming, D., Bishop, D., and Rumbaugh, K. P. (2016). Host responses to biofilm. *Prog. Mol. Biol. Transl. Sci.* 142, 193–239. doi: 10.1016/bs.pmbts.2016.05.007
- Whitchurch, C. B., Tolker-Nielsen, T., Ragas, P. C., and Mattick, J. S. (2002). Extracellular DNA required for bacterial biofilm formation. *Science* 295:1487. doi: 10.1126/science.295.5559.1487
- Whiteley, M., Bangera, M. G., Bumgarner, R. E., Parsek, M. R., Teitzel, G. M., Lory, S., et al. (2001). Gene expression in *Pseudomonas aeruginosa* biofilms. *Nature* 413, 860–864. doi: 10.1038/35101627
- Wozniak, D. J., and Keyser, R. (2004). Effects of subinhibitory concentrations of macrolide antibiotics on *Pseudomonas aeruginosa*. *CHEST J.* 125, 62S–69S. doi: 10.1378/chest.125.2\_suppl.62s
- Yau, Y. C. W., Ratjen, F., Tullis, E., Wilcox, P., Freitag, A., Chilvers, M., et al. (2015). Randomized controlled trial of biofilm antimicrobial susceptibility testing in cystic fibrosis patients. *J. Cyst. Fibros.* 14, 262–266. doi: 10.1016/j.jcf.2014.09.013
- Yokochi, T., Narita, K., Morikawa, A., Takahashi, K., Kato, Y., Sugiyama, T., et al. (2000). Morphological change in *Pseudomonas aeruginosa* following antibiotic treatment of experimental infection in mice and its relation to susceptibility to phagocytosis and to release of endotoxin. *Antimicrob. Agents Chemother.* 44, 205–206. doi: 10.1128/aac.44.1.205-206.2000
- Yu, W., Hallinen, K. M., and Wood, K. B. (2017). Interplay between antibiotic efficacy and drug-induced lysis underlies enhanced biofilm formation at subinhibitory drug concentrations. *Antimicrob. Agents Chemother.* 62:e01603-17. doi: 10.1128/AAC.01603-17
- Zhang, L., and Mah, T.-F. (2008). Involvement of a novel efflux system in biofilm-specific resistance to antibiotics. *J. Bacteriol.* 190, 4447–4452. doi: 10.1128/JB.01655-07

**Conflict of Interest:** EO, CP, and TB were employed by the company BioFilm Pharma SAS, and SB-B, CP, and TB were employed by the company BioFilm Control SAS.

The remaining authors declare that the research was conducted in the absence of any commercial or financial relationships that could be construed as a potential conflict of interest.

Copyright © 2020 Olivares, Badel-Berchoux, Provot, Prévost, Bernardi and Jehl. This is an open-access article distributed under the terms of the Creative Commons Attribution License (CC BY). The use, distribution or reproduction in other forums is permitted, provided the original author(s) and the copyright owner(s) are credited and that the original publication in this journal is cited, in accordance with accepted academic practice. No use, distribution or reproduction is permitted which does not comply with these terms.



# Colistin Resistance Gene *mcr-1* Mediates Cell Permeability and Resistance to Hydrophobic Antibiotics

Baiyuan Li<sup>1</sup>, Fang Yin<sup>2</sup>, Xuanyu Zhao<sup>3,4</sup>, Yunxue Guo<sup>3</sup>, Weiquan Wang<sup>3,4</sup>, Pengxia Wang<sup>3</sup>, Honghui Zhu<sup>5</sup>, Yeshe Yin<sup>1</sup> and Xiaoxue Wang<sup>3,4\*</sup>

<sup>1</sup> Key Laboratory of Comprehensive Utilization of Advantage Plants Resources in Hunan South, College of Chemistry and Bioengineering, Hunan University of Science and Engineering, Yongzhou, China, <sup>2</sup> Department of Breast and Thyroid Surgery, The Fifth Affiliated Hospital, Sun Yat-sen University, Zhuhai, China, <sup>3</sup> Key Laboratory of Tropical Marine Bio-resources and Ecology, Guangdong Key Laboratory of Marine Materia Medica, RNAM Center for Marine Microbiology, South China Sea Institute of Oceanology, Chinese Academy of Sciences, Guangzhou, China, <sup>4</sup> University of the Chinese Academy of Sciences, Beijing, China, <sup>5</sup> State Key Laboratory of Applied Microbiology Southern China, Guangdong Provincial Key Laboratory of Microbial Culture Collection and Application, Guangdong Open Laboratory of Applied Microbiology, Guangdong Microbial Culture Collection Center, Guangdong Institute of Microbiology, Guangzhou, China

## OPEN ACCESS

### Edited by:

Raffaele Zarrilli,  
University of Naples Federico II, Italy

### Reviewed by:

Ximin Zeng,  
The University of Tennessee,  
Knoxville, United States  
Jian-Hua Liu,  
South China Agricultural University,  
China

### \*Correspondence:

Xiaoxue Wang  
xxwang@scsio.ac.cn

### Specialty section:

This article was submitted to  
Antimicrobials, Resistance  
and Chemotherapy,  
a section of the journal  
Frontiers in Microbiology

Received: 19 September 2019

Accepted: 16 December 2019

Published: 10 January 2020

### Citation:

Li B, Yin F, Zhao X, Guo Y,  
Wang W, Wang P, Zhu H, Yin Y and  
Wang X (2020) Colistin Resistance  
Gene *mcr-1* Mediates Cell  
Permeability and Resistance  
to Hydrophobic Antibiotics.  
*Front. Microbiol.* 10:3015.  
doi: 10.3389/fmicb.2019.03015

Colistin is considered the last-resort antibiotic used to treat multidrug resistant bacteria-related infections. However, the discovery of the plasmid-mediated colistin resistance gene, *mcr-1*, threatens the clinical utility of colistin antibiotics. In this study, the physiological function of MCR-1, which encodes an LPS-modifying enzyme, was investigated in *E. coli* K-12. Specifically, the impact of *mcr-1* on membrane permeability and antibiotic resistance of *E. coli* was assessed by constructing an *mcr-1* deletion mutant and by a complementation study. The removal of the *mcr-1* gene from plasmid pHNSHP45 not only led to reduced resistance to colistin but also resulted in a significant change in the membrane permeability of *E. coli*. Unexpectedly, the removal of the *mcr-1* gene increased cell viability under high osmotic stress conditions (e.g., 7.0% NaCl) and led to increased resistance to hydrophobic antibiotics. Increased expression of *mcr-1* also resulted in decreased growth rate and changed the cellular morphology of *E. coli*. Collectively, our results revealed that the spread of *mcr-1*-carrying plasmids alters other physiological functions in addition to conferring colistin resistance.

**Keywords:** *mcr-1*, colistin resistance, permeability, hydrophobic antibiotics, plasmid

## INTRODUCTION

Colistin is one of the primary classes of antibiotics with activity against most gram-negative bacteria and is considered the last resort antibiotic for the treatment of infections caused by carbapenem-resistant Enterobacteriaceae. In 2015, a plasmid-encoded colistin resistance gene named *mcr-1* was described in Enterobacteriaceae isolated from humans and livestock in China (Liu et al., 2016).

Since then, polymyxins have rightfully drawn renewed attention to colistin resistance, and plasmid-mediated colistin resistance by *mcr-1* has been reported worldwide in livestock, food and humans (Poirel et al., 2017; Li et al., 2018). The *mcr-1* gene confers colistin resistance by encoding a phosphoethanolamine transferase that catalyzes the addition of a phosphoethanolamine moiety to lipid A in the bacterial outer membrane (OM) (Gao et al., 2016; Hinchliffe et al., 2017), which may modify the structure of lipid A and then decrease the growth rate, cell viability, and competitive ability and shape cytoplasmic structures (Yang et al., 2017).

The OM of gram-negative bacteria plays a crucial role in protecting cells against an adverse environment and exchanging material (Costerton et al., 1974). To work effectively, antibiotics must pass across the OM barricade to reach the inhibitory concentration inside the bacterial cell (Vergalli et al., 2017). Bacterial OMs with low permeability have been identified as robust barriers that prevent many antibiotics from reaching their intracellular targets (Nikaido, 2003). Antibiotics usually traverse the OM by one of two mechanisms: the lipid-mediated pathway responsible for macrolides and hydrophobic antibiotics, such as aminoglycosides (gentamycin, kanamycin), and general diffusion porins for hydrophilic antibiotics such as  $\beta$ -lactams (Benz, 1988; Nikaido, 2003). The lipid and protein compositions of the OM have a major impact on the susceptibility of the microorganism to antibiotics, and drug resistance involving modifications of these macromolecules is common (Benz, 1988). For instance, several studies showed that alternations in the hydrophobic properties of the membrane or null mutations in porins create resistance to  $\beta$ -lactam antibiotics (Miller, 2016; Ghai and Ghai, 2018). MCR-1 is a membrane-bound enzyme consisting of five hydrophobic transmembrane helices and a soluble form located in the periplasmic space (Liu et al., 2016). A recent study reported that mutants with a high-level colistin resistance are more susceptible to most antibiotics compared with their respective parental strains (Yang et al., 2017). However, whether other antibiotic resistances could be affected by expression of *mcr-1* remain unclear. Since *mcr-1* encodes a phosphoethanolamine transferase that modifies the structure of LPS of the OM, it raises the possibility that MCR-1 may affect the susceptibility of bacteria to hydrophobic antibiotics by changing the membrane permeability. Therefore, we analyzed the impact of *mcr-1* expression on the membrane permeability of *E. coli* by constructing an *mcr-1* deletion mutant strain and by constructing a vector to overexpress *mcr-1*.

## MATERIALS AND METHODS

### Bacterial Strains, Plasmids, and Growth Conditions

The bacterial strains and plasmids used in this study are listed in Table 1, and the sequences of primers used in this study are listed in Supplementary Table S1. The *E. coli* strains were grown in Luria–Bertani (LB) broth or on LB agar plates (with 10 g NaCl per liter) at 37°C, except for *E. coli* carrying pKD46 or pCP20, which were grown at 30°C. Antibiotics and other chemicals were used

**TABLE 1** | Strains and plasmids used in this study.

Strains/Plasmids	Phenotypes	
<b>Strains</b>		
<i>E. coli</i> K12 BW25113	<i>lacI<sup>q</sup></i> <i>rrmB</i> <sub>T14</sub> $\Delta$ <i>lacZ</i> <sub>WJ16</sub> <i>hsdR</i> <sub>514</sub> $\Delta$ <i>araBAD</i> <sub>AH33</sub> $\Delta$ <i>rhaBAD</i> <sub>LD78</sub>	Baba et al. (2006)
<i>E. coli</i> C600	<i>F-thr-1</i> <i>leuB6</i> (Am) <i>fhuA21</i> <i>cyn-101</i> <i>lacY1</i> <i>glnX44</i> (AS) $\lambda^-$ <i>e14-rfbC1</i> <i>glpR200</i> ( <i>glp</i> <sup>c</sup> ) <i>thiE1</i>	Appleyard (1954)
Wild type	<i>E. coli</i> BW25113/pHNSHP45	This study
$\Delta$ <i>mcr-1</i> :cat	<i>E. coli</i> BW25113/pHNSHP45 $\Delta$ <i>mcr-1</i> Cm <sup>R</sup>	This study
$\Delta$ <i>mcr-1</i>	<i>E. coli</i> BW25113/pHNSHP45 $\Delta$ <i>mcr-1</i> $\Delta$ Cm <sup>R</sup>	This study
<b>Plasmids</b>		
pHNSHP45	<i>mcr-1</i> , GenBank accession no. KP347127	Liu et al. (2016)
pKD46	Amp <sup>R</sup> , $\lambda$ . Red recombinase expression	Datsenko and Wanner (2000)
pKD3	FRT-flanked <i>cat</i> gene (Cm <sup>R</sup> ) in <i>oriF<sub>y</sub></i> replicon requiring the <i>pir</i> gene product	Datsenko and Wanner (2000)
pCP20	Amp <sup>R</sup> and Cm <sup>R</sup> ; temperature-sensitive replication, thermal induction of FLP recombinase synthesis	Baba et al. (2006)
pCA24N	Cm <sup>R</sup> ; <i>lacI<sup>q</sup></i> , IPTG inducible expression vector in <i>E. coli</i>	Kitagawa et al. (2005)
pCA24N- <i>mcr-1</i>	Cm <sup>R</sup> ; <i>lacI<sup>q</sup></i> , P <sub>T5-lac</sub> : <i>mcr-1</i>	This study
pCA24N- <i>mcr-1-gfp</i>	Cm <sup>R</sup> ; <i>lacI<sup>q</sup></i> , P <sub>T5-lac</sub> : <i>mcr-1-gfp</i>	This study

at the following final concentrations: chloramphenicol, 30  $\mu$ g/ml; polymyxin B, 2  $\mu$ g/ml; ampicillin, 100  $\mu$ g/ml; isopropyl- $\beta$ -d-thiogalactopyranoside (IPTG), 0.5 mM; and arabinose, 1 mM. A total of 1 mM L-arabinose or 0.5 mM IPTG (Sigma) was used to induce *Para* or *Plac*, respectively.

### Construction of the Deletion Mutant

The coding region of the *mcr-1* gene was deleted from *E. coli* K12 BW25113 carrying plasmid pHNSHP45 (Liu et al., 2016) following a one-step inactivation method (Datsenko and Wanner, 2000). The primers used in this study are shown in Supplementary Table S1. PCR products containing chloramphenicol resistance cassettes flanked by 39 bp of homology to the 5' and 3' termini of *mcr-1* were electroporated into competent cells of parent strains carrying pKD46. To construct the *mcr-1* deletion mutant, PCR products that included 37-nt homology extensions and 20-nt priming sequences for the chloramphenicol resistance gene *cat*, bordered by FLP recombination target (FRT) sites, were amplified from plasmid pKD3 (*cat*) using primers pKD46-mcrF/pKD46-mcrR. Removal of the *mcr-1* gene from pHNSHP45 in *E. coli* was verified by PCR and DNA sequencing using the primer pair MCR-LF/MCR-LR. The FRT-flanked chloramphenicol cassette was removed after transformation with pCP20 as described previously (Datsenko and Wanner, 2000). pCP20 is a plasmid that carries ampicillin

and chloramphenicol resistance genes and exhibits temperature-sensitive replication and thermal induction of FLP synthesis (Cherepanov and Wackernagel, 1995). CmR mutants were transformed with pCP20, and ampicillin-resistant transformants were selected at 30°C, propagated non-selectively at 42°C and then tested for loss of all antibiotic resistances.

## Plasmid Constructs

The pCA24N vector was used to express target genes in *E. coli*. The coding region of *mcr-1* was PCR-amplified from genomic DNA of *E. coli* carrying pHNSHP45 using the primer pair pCA24N-mcrF/pCA24N-mcrR. PCR products were digested with *SalI* and *XbaI* and inserted into the corresponding sites of pCA24N. The correct constructs were verified by PCR with primer pair pCA24N-F/pCA24N-R and DNA sequencing. The same procedures were performed to fuse *gfp* before the stop codon of the *mcr-1* gene, as well as for the construction of the plasmid pCA24N-*mcr-1-gfp*. To generate pCA24N-*mcr-1-gfp*, the coding region of *mcr-1* without its stop codon was amplified with primers Mcr-1F(*sall*) and Mcr-1R(*xbaI*), and the coding region of *gfp* was amplified using pCA24N-*gfp* (Guo et al., 2017) as the template with primers Gfp-F(*xbaI*) and Gfp-R(*EcoRI*). The *mcr-1* fragment was digested with *SalI* and *XbaI*, the *gfp* fragment was digested *XbaI* and *RcoRI*, and inserted into the corresponding sites of pCA24N. pCA24N-based expression vectors were transferred into the *E. coli* BW25113 host.

## Antibiotics Susceptibility Testing

The antibiotics tested include ampicillin, polymyxin B (PB), ceftazidime, ciprofloxacin, gentamycin (GEN), kanamycin, chloramphenicol, tetracycline, rifampicin, nalidixic acid, and spectinomycin. The antibiotic resistance level was described by the minimum inhibitory concentrations (MICs) determined using a custom-made 96-well MIC panel (Flentie et al., 2019). The results were interpreted according to the criteria of the Clinical and Laboratory Standards Institute (CLSI) (Clinical and Laboratory Standards Institute, 2017).

## Microscopy Exam

To evaluate cell membrane integrity, the membrane-specific red-fluorescent dye FM4-64 (Thermo Fisher Scientific, Rockford, IL, United States) was used. Overnight cultures were diluted in 50 ml of fresh medium and cultured to an OD<sub>600 nm</sub> of 0.5, and cells were harvested by centrifugation (6000 × *g*, 2 min), washed and resuspended in phosphate buffered saline (PBS). Cells were then treated with 0.85% NaCl or 7.0% NaCl for 30 min followed by staining with 4 μg/ml FM 4-64 for 15 min in the dark at ambient temperature. Bacterial cells were imaged using a Zeiss Axiovert fluorescence microscope (Carl Zeiss Inc., Thornwood, NY, United States).

## Protein Localization

For localization of MCR-1 by GFP fusion, overnight cultures of BW25113 carrying pCA24N-*mcr-1-gfp* were inoculated into LB broth supplemented with chloramphenicol (30 μg/ml) to an OD<sub>600 nm</sub> of 0.1 and 0.5 mM IPTG was added to induce

MCR-1-GFP expression for 2 h before imaging. Cells were washed with PBS and imaged with fluorescence microscopy (Zeiss Axiophot) using an oil immersion objective (100×).

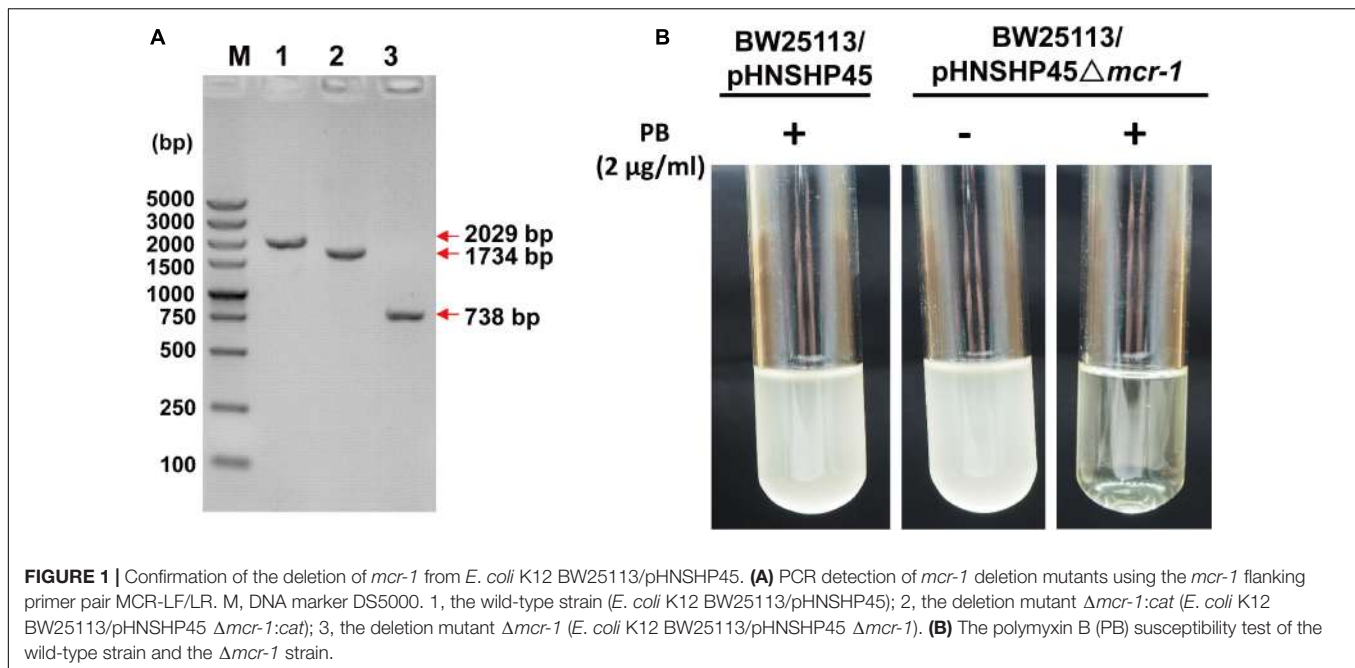
## RESULTS AND DISCUSSION

### The Expression of *mcr-1* Decreases Resistance to Hydrophobic Antibiotics

The plasmid pHNSHP45 was extracted from *E. coli* K12 C600/pHNSHP45 using the EZNA<sup>®</sup> plasmid mini kit I (Omega) and then electroporated into the *E. coli* K12 BW25113 host, which is susceptible to polymyxin B (MIC = 0.5 μg/ml). Positive clones were selected with 2 μg/ml polymyxin B and confirmed by PCR with the primer pair CLR5-F/R (Supplementary Table S1). To explore the impact of *mcr-1*, we deleted the *mcr-1* gene with a one-step inactivated method using a λ-red recombinase expression plasmid pKD46 as described by Datsenko and Wanner (2000). The replacement of the *mcr-1* gene with the *cat* cassette amplified from pKD3 (strain BW25113/pHNSHP45 Δ*mcr-1:cat*) and the elimination of the FRT-flanked *cat* cassette by using the FLP recombinase expression plasmid pCP20 to obtain strain BW25113/pHNSHP45 Δ*mcr-1* were confirmed by PCR and DNA sequencing (Figure 1). As expected, the deletion of *mcr-1* resulted in decreased resistance to polymyxin B (MIC = 0.5 μg/ml) (Figure 1B). The MIC value of PB for the *mcr-1* deletion mutant was 0.5 μg/ml compared to an 8 μg/ml for the wild type (Table 2).

The asymmetric lipopolysaccharide (LPS)-phospholipid bilayer of the OM provides a formidable permeability barrier for both hydrophilic and hydrophobic antibiotics (Nikaido, 2003; Zgurskaya et al., 2015). Previous studies have found that small hydrophilic drugs use the pore-forming porins to cross the OM, while hydrophobic drugs diffuse across the LPS-phospholipid bilayer (Vaara, 1992; Nikaido, 2003). To explore whether MCR-1 expression demonstrates differences in different families of antibiotics, we performed MIC tests of the Δ*mcr-1* and wild-type strains using a 96-well MIC panel test assay that contained 11 antibiotics. As expected, the Δ*mcr-1* strain showed increased resistance to gentamicin, kanamycin and rifampicin. However, no effect was found for resistance to ampicillin, nalidixic acid, spectinomycin, or ciprofloxacin (Table 2). Interestingly, gentamicin, kanamycin, and rifampicin are hydrophobic antibiotics, while ampicillin, nalidixic acid, spectinomycin, and ciprofloxacin are hydrophilic antibiotics. Thus, the deletion of *mcr-1* also increases resistance to hydrophilic antibiotics. *mcr-1* confers colistin resistance through the addition of cationic phosphoethanolamine (pEtN) to phosphate groups on the lipid A component of LPS, which reduces the net anionic charge of the cell surface (Jeannot et al., 2017). LPS modification in Gram-negative bacteria plays a significant role in resistance to antimicrobial factors (Gunn, 2001). Thus, we proposed that the expression of *mcr-1* resulted in the modification of LPS and disrupt the organization of the LPS-phospholipid bilayer, change its permeability, and therefore decrease the resistance to hydrophobic antibiotics, but the hydrophilic antibiotics traverse the OM through porin channels.





## The Expression of *mcr-1* Decreases Survival During High Salt Stress

Acquired antibiotic resistance by horizontal gene transfer tends to be related to a fitness cost for bacterial hosts (Andersson and Levin, 1999; Andersson and Hughes, 2010; Vogwill and MacLean, 2015). The osmotic stresses of *E. coli* strains with and without *mcr-1* were tested. The growth of the wild type strain was severely hindered in the presence of 7.0% NaCl in LB broth (total NaCl concentration was 7.0%) when compared with the  $\Delta mcr-1$  strain, while no growth defect was observed for the two strains in regular LB broth containing 1.0% NaCl (Figure 2A). In addition, the growth of *E. coli* with or without *mcr-1* in LB

broth with different NaCl concentration was tested and the cell density was measured by optical density at 600 nm. The results showed that the cell density of the *E. coli* was decreased with the increase of NaCl concentration, and *E. coli* without *mcr-1* was able to tolerance to higher NaCl concentration than *E. coli* with *mcr-1* (Supplementary Table S2). Furthermore, we examined cell integrity using the red membrane dye FM 4-64 (Life Technologies, United States), which specifically stains the cell membrane. Exponentially growing cells ( $OD_{600\text{ nm}} \sim 0.5$ ) were collected, washed and incubated with 0.85% NaCl or 7.0% NaCl for 30 min. Cells were then collected and imaged by fluorescence microscopy (Zeiss Axiophot) using an oil immersion objective (100 $\times$ ). The cell membranes appeared intact in the presence of low concentrations of NaCl, while membrane integrity of wild type strain was only severely reduced in the presence of 7% NaCl (The membrane defects of wild type strain was about 79.2% compared with  $\Delta mcr-1$  strain is 19.4%) (Figure 2B). Consistent with the above results, the  $\Delta mcr-1$  strain demonstrated 10-fold higher viability than the wild-type cells in the presence of 7% NaCl (Figure 2C). Taken together, these results showed that the expression of the *mcr-1* gene decreases tolerance to high salt stress. We proposed that the mechanism of the expression of the *mcr-1* gene decreases cell fitness under high salt conditions may be due to expression of the *mcr-1* gene affects the membrane permeability.

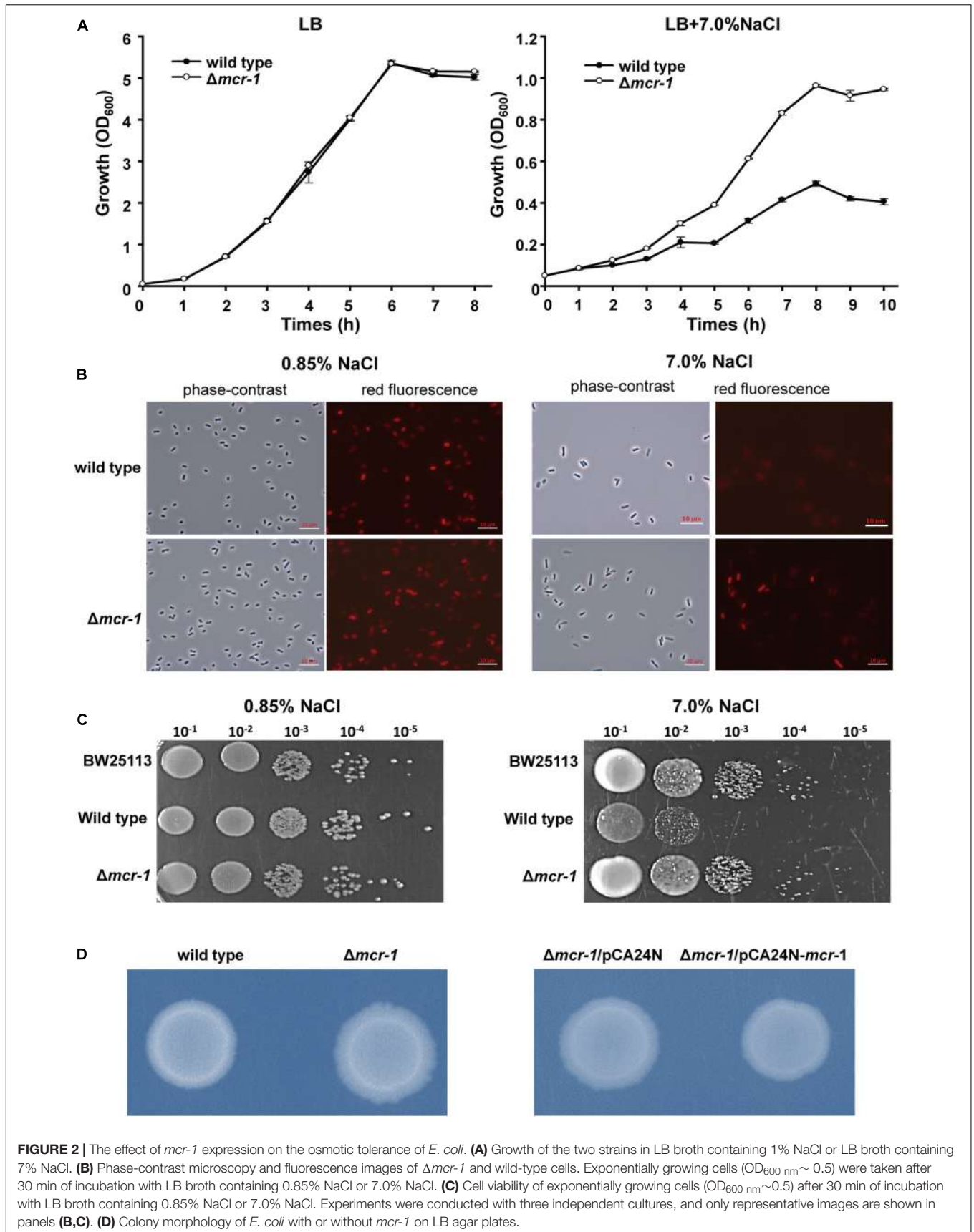
**TABLE 2** | Antimicrobial susceptibility of *E. coli* BW25113, the wild-type strain and the *mcr-1* deletion mutant.

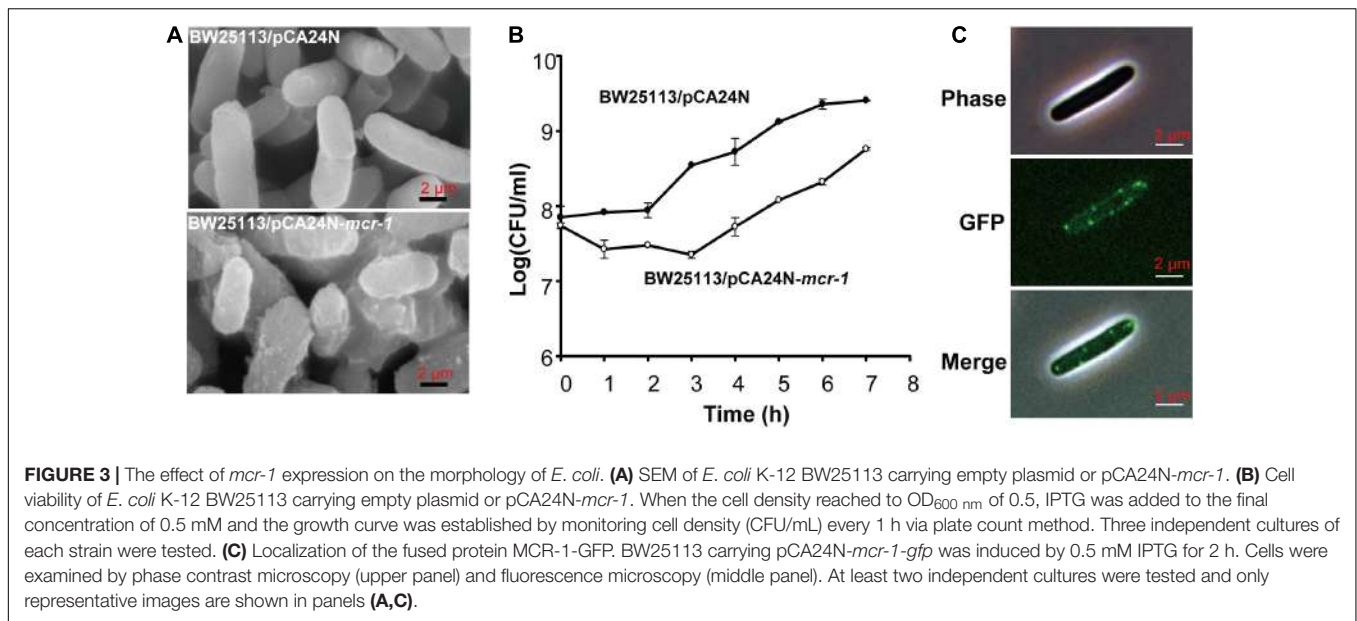
Antibiotics	MIC ( $\mu\text{g}/\text{mL}$ )		
	BW25113	Wild type	$\Delta mcr-1$
Polymyxin B	0.5	8	0.5
Gentamicin	16	8	16
Kanamycin	8	4	8
Rifampicin	16	8	16
Ampicillin	4	4	4
Ciprofloxacin	0.125	0.125	0.125
Ceftazidime	0.5	0.5	0.5
Chloramphenicol	8	8	8
Tetracycline	4	4	4
Nalidixic acid	4	4	4
Spectinomycin	32	32	32

MIC values ( $\mu\text{g}/\text{mL}$ ) of 11 antibiotics are listed. Three independent cultures of each strain were tested.

## The Expression of *mcr-1* Affects the Growth and Cell Morphology of *E. coli*

After prolonged incubation on LB agar plates for 24 h, the edge of the colonies formed by the  $\Delta mcr-1$  strain appeared more wrinkle compared with the wild-type strain (Figure 2D). Furthermore, the *mcr-1* coding region from pHNSHP45 was cloned into plasmid pCA24N to construct pCA24N-*mcr-1*. To





further check the cell morphology of *E. coli*, the complementation experiments were carried out. As expected, the edge of the colonies formed by the  $\Delta mcr-1/pCA24N$  strain appeared more wrinkle compared with the  $\Delta mcr-1/pCA24N-mcr-1$  (Figure 2D). Scanning electron microscopy (SEM) was then employed to study the cell morphology of *E. coli* K-12 BW25113/pCA24N-*mcr-1* with the addition of 0.5 mM IPTG. As shown in Figure 3A, cells overexpressing *mcr-1* via pCA24N-*mcr-1* had rougher cell envelopes than the cells carrying empty pCA24N. In addition, overexpression of *mcr-1* significantly reduced the cell growth rate (Figure 3B), which is consistent with a recent report indicating that increased expression of *mcr-1* results in decreased growth rate and cell viability (Yang et al., 2017). To further check the localization of MCR-1 in *E. coli*, the green fluorescence protein gene *gfp* was fused to the C-terminus of the *mcr-1* gene to express the fused protein MCR-1-GFP. As expected, MCR-1-GFP was located around the cellular membrane (Figure 3C), which further confirmed that MCR-1 is a membrane protein. As a control, the green fluorescence protein GFP was produced using pCA24N-*gfp* and the protein GFP was localized to the cytoplasm (Supplementary Figure S1). To further determine if the MCR-1-GFP fusion protein confers polymyxin resistance, we performed MIC tests of the BW25113/pCA24N and BW25113/pCA24N-*mcr-1-gfp* strains using a 96-well MIC panel test assay. The MIC value of PB for the BW25113/pCA24N-*mcr-1-gfp* was 8.0  $\mu\text{g/ml}$ , but BW25113/pCA24N was 0.5  $\mu\text{g/ml}$ , suggesting that GFP fused to the MCR-1 does not affect the polymyxin resistance of MCR-1. Thus, MCR-1 is localized at the membrane, and the expression of *mcr-1* affects cellular morphology and colony morphology.

## CONCLUSION

In this study, we demonstrated that MCR-1 is a membrane protein that localizes to the cellular membrane. Furthermore,

MCR-1 increases the loss of the cell membrane integrity and decreases the MICs of gentamicin, kanamycin and rifampicin. Evolving colistin resistance by acquiring *mcr-1* therefore challenges bacterial populations with an evolutionary trade-off: input of *mcr-1* protects the host against colistin but changes the membrane permeability and reduces resistance to hydrophobic antibiotics. This trade-off may further explain the balance between *mcr-1* expression and bacterial survival. Several studies have documented a link between antibiotic use and the development of antibiotic resistance (Goossens et al., 2005; Bergman et al., 2009). Our results provide a further possibility of *mcr-1* gene transfer, which was affected not only by colistin use but also by environmental cues, such as osmotic pressure conditions.

## DATA AVAILABILITY STATEMENT

All datasets generated for this study are included in the article/Supplementary Material.

## AUTHOR CONTRIBUTIONS

XW and BL conceptualized and designed the project. BL, XW, FY, XZ, YG, WW, HZ, PW, and YY did the investigation, and data curation and analysis. BL and XW did the supervision and visualization. BL and XW wrote, reviewed, and edited the original draft.

## FUNDING

This work was supported by the National Science Foundation of China (31290233, 41230962, 41406189, and 31470141), the Chinese Academy of Sciences (XDA11030402), the China

Postdoctoral Science Foundation (2017M622649), and the Science and Technology Innovation Leading Talent Program of Guangdong Province (2015TX01N036). XW is the recipient of the 1000-Youth Elite Program award (a program for the recruitment of global experts to China).

## REFERENCES

- Andersson, D. I., and Hughes, D. (2010). Antibiotic resistance and its cost: is it possible to reverse resistance? *Nat. Rev. Microbiol.* 8, 260–271. doi: 10.1038/nrmicro2319
- Andersson, D. I., and Levin, B. R. (1999). The biological cost of antibiotic resistance. *Curr. Opin. Microbiol.* 2, 489–493. doi: 10.1016/S1369-5274(99)00005-3
- Appleyard, R. K. (1954). Segregation of new lysogenic types during growth of a doubly lysogenic strain derived from *Escherichia coli* K12. *Genetics* 39, 440–452.
- Baba, T., Ara, T., Hasegawa, M., Takai, Y., Okumura, Y., Baba, M., et al. (2006). Construction of *Escherichia coli* K-12 in-frame, single-gene knockout mutants: the Keio collection. *Mol. Syst. Biol.* 2:2006.0008. doi: 10.1038/msb4100050
- Benz, R. (1988). Structure and function of porins from gram-negative bacteria. *Annu. Rev. Microbiol.* 42, 359–393. doi: 10.1146/annurev.mi.42.100188.002043
- Bergman, M., Nyberg, S. T., Huovinen, P., Paakkari, P., Hakonen, A. J., and Re, F. S. G. A. (2009). Association between antimicrobial consumption and resistance in *Escherichia coli*. *Antimicrob. Agents Chemother.* 53, 912–917. doi: 10.1128/AAC.00856-08
- Cherepanov, P. P., and Wackernagel, W. (1995). Gene disruption in *Escherichia coli*: TcR and KmR cassettes with the option of FLP-catalyzed excision of the antibiotic-resistance determinant. *Gene* 158, 9–14. doi: 10.1016/0378-1119(95)00193-a
- Clinical and Laboratory Standards Institute (2017). *Performance Standards for Antimicrobial Susceptibility Testing*, 26th Edn. Wayne, PA: CLSI.
- Costerton, J. W., Ingram, J. M., and Cheng, K. J. (1974). Structure and function of cell-envelope of gram-negative bacteria. *Bacteriol. Rev.* 38, 87–110.
- Datsenko, K. A., and Wanner, B. L. (2000). One-step inactivation of chromosomal genes in *Escherichia coli* K-12 using PCR products. *Proc. Natl. Acad. Sci. U.S.A.* 97, 6640–6645. doi: 10.1073/pnas.120163297
- Fleentie, K., Spears, B. R., Chen, F., Purmort, N. B., Daponte, K., Viveiros, E., et al. (2019). Microplate-based surface area assay for rapid phenotypic antibiotic susceptibility testing. *Sci. Rep.* 9:237. doi: 10.1038/s41598-018-35916-0
- Gao, R. S., Hu, Y. F., Li, Z. C., Sun, J., Wang, Q. J., Lin, J. X., et al. (2016). Dissemination and mechanism for the MCR-1 colistin resistance. *PLoS Pathog.* 12:e1005957. doi: 10.1371/journal.ppat.1005957
- Ghai, I., and Ghai, S. (2018). Understanding antibiotic resistance via outer membrane permeability. *Infect. Drug Resist.* 11, 523–530. doi: 10.2147/IDR.S156995
- Goossens, H., Ferech, M., Stichele, R. V., Elseviers, M., and Grp, E. P. (2005). Outpatient antibiotic use in Europe and association with resistance: a cross-national database study. *Lancet* 365, 579–587. doi: 10.1016/S0140-6736(05)17907-0
- Gunn, J. S. (2001). Bacterial modification of LPS and resistance to antimicrobial peptides. *J. Endotoxin. Res.* 7, 57–62. doi: 10.1177/09680519010070011001
- Guo, Y., Liu, X., Li, B., Yao, J., Wood, T. K., and Wang, X. (2017). Tail-anchored inner membrane protein elab increases resistance to stress while reducing persistence in *Escherichia coli*. *J. Bacteriol.* 199:e00057-17. doi: 10.1128/JB.00057-17
- Hinchliffe, P., Yang, Q. E., Portal, E., Young, T., Li, H., Tookey, C. L., et al. (2017). Insights into the mechanistic basis of plasmid-mediated colistin resistance from crystal structures of the catalytic domain of MCR-1. *Sci. Rep.* 7:39392. doi: 10.1038/srep39392
- Jeannot, K., Bolard, A., and Plesiat, P. (2017). Resistance to polymyxins in Gram-negative organisms. *Int. J. Antimicrob. Agents* 49, 526–535. doi: 10.1016/j.ijantimicag.2016.11.029
- Kitagawa, M., Ara, T., Arifuzzaman, M., Ioka-Nakamichi, T., Inamoto, E., Toyonaga, H., et al. (2005). Complete set of ORF clones of *Escherichia coli* ASKA library (A complete set of *E. coli* K-12 ORF archive): unique resources for biological research. *DNA Res.* 12, 291–299. doi: 10.1093/dnares/dsi012
- Li, B., Ke, B., Zhao, X., Guo, Y., Wang, W., Wang, X., et al. (2018). Antimicrobial resistance profile of mcr-1 positive clinical isolates of *Escherichia coli* in China from 2013 to 2016. *Front. Microbiol.* 9:2514. doi: 10.3389/fmicb.2018.02514
- Liu, Y. Y., Wang, Y., Walsh, T. R., Yi, L. X., Zhang, R., Spencer, J., et al. (2016). Emergence of plasmid-mediated colistin resistance mechanism MCR-1 in animals and human beings in China: a microbiological and molecular biological study. *Lancet Infect. Dis.* 16, 161–168. doi: 10.1016/S1473-3099(15)00424-7
- Miller, S. I. (2016). Antibiotic resistance and regulation of the gram-negative bacterial outer membrane barrier by host innate immune molecules. *mBio* 7:e01541-16. doi: 10.1128/mBio.01541-16
- Nikaido, H. (2003). Molecular basis of bacterial outer membrane permeability revisited. *Microbiol. Mol. Biol. Rev.* 67, 593–656. doi: 10.1128/mmb.67.4.593-656.2003
- Poirel, L., Jayol, A., and Nordmann, P. (2017). Polymyxins: antibacterial activity, susceptibility testing, and resistance mechanisms encoded by plasmids or chromosomes. *Clin. Microbiol. Rev.* 30, 557–596. doi: 10.1128/CMR.00064-16
- Vaara, M. (1992). Agents that increase the permeability of the outer-membrane. *Microbiol. Rev.* 56, 395–411.
- Vergalli, J., Dumont, E., Cinquin, B., Maigre, L., Pajovic, J., Bacque, E., et al. (2017). Fluoroquinolone structure and translocation flux across bacterial membrane. *Sci. Rep.* 7:9821. doi: 10.1038/s41598-017-08775-4
- Vogwill, T., and MacLean, R. C. (2015). The genetic basis of the fitness costs of antimicrobial resistance: a meta-analysis approach. *Evol. Appl.* 8, 284–295. doi: 10.1111/eva.12202
- Yang, Q., Li, M., Spiller, O. B., Andrey, D. O., Hinchliffe, P., Li, H., et al. (2017). Balancing *mcr-1* expression and bacterial survival is a delicate equilibrium between essential cellular defence mechanisms. *Nat. Commun.* 8:2054. doi: 10.1038/s41467-017-02149-0
- Zgurskaya, H. I., Lopez, C. A., and Gnanakaran, S. (2015). Permeability barrier of gram-negative cell envelopes and approaches to bypass it. *ACS Infect. Dis.* 1, 512–522. doi: 10.1021/acscinfed.5b00097

## SUPPLEMENTARY MATERIAL

The Supplementary Material for this article can be found online at: <https://www.frontiersin.org/articles/10.3389/fmicb.2019.03015/full#supplementary-material>

**Conflict of Interest:** The authors declare that the research was conducted in the absence of any commercial or financial relationships that could be construed as a potential conflict of interest.

Copyright © 2020 Li, Yin, Zhao, Guo, Wang, Wang, Zhu, Yin and Wang. This is an open-access article distributed under the terms of the Creative Commons Attribution License (CC BY). The use, distribution or reproduction in other forums is permitted, provided the original author(s) and the copyright owner(s) are credited and that the original publication in this journal is cited, in accordance with accepted academic practice. No use, distribution or reproduction is permitted which does not comply with these terms.





# CRISPR-Cas System in Antibiotic Resistance Plasmids in *Klebsiella pneumoniae*

Muhammad Kamruzzaman<sup>1\*</sup> and Jonathan R. Iredell<sup>1,2\*</sup>

<sup>1</sup> Centre for Infectious Diseases and Microbiology, The Westmead Institute for Medical Research, The University of Sydney, Westmead, NSW, Australia, <sup>2</sup> Westmead Hospital, Westmead, NSW, Australia

## OPEN ACCESS

### Edited by:

Luciene Andrade Da Rocha  
Minarini,

Federal University of São Paulo, Brazil

### Reviewed by:

Ørjan Samuelsen,

University Hospital of North Norway,

Norway

Edze Westra,

University of Exeter, United Kingdom

### \*Correspondence:

Muhammad Kamruzzaman

muhammad.kamruzzaman@

sydney.edu.au

Jonathan R. Iredell

jonathan.iredell@sydney.edu.au

### Specialty section:

This article was submitted to

Antimicrobials, Resistance

and Chemotherapy,

a section of the journal

Frontiers in Microbiology

**Received:** 02 October 2019

**Accepted:** 06 December 2019

**Published:** 10 January 2020

### Citation:

Kamruzzaman M and Iredell JR

(2020) CRISPR-Cas System

in Antibiotic Resistance Plasmids

in *Klebsiella pneumoniae*.

Front. Microbiol. 10:2934.

doi: 10.3389/fmicb.2019.02934

CRISPR-Cas (clustered regularly interspersed short palindromic repeats-CRISPR-associated protein) is a microbial adaptive immune system involved in defense against different types of mobile genetic elements. CRISPR-Cas systems are usually found in bacterial and archaeal chromosomes but have also been reported in bacteriophage genomes and in a few mega-plasmids. *Klebsiella pneumoniae* is an important member of the Enterobacteriaceae with which they share a huge pool of antibiotic resistance genes, mostly via plasmids. CRISPR-Cas systems have been identified in *K. pneumoniae* chromosomes, but relatively little is known of CRISPR-Cas in the plasmids resident in this species. In this study, we searched for CRISPR-Cas system in 699 complete plasmid sequences (>50-kb) and 217 complete chromosomal sequences of *K. pneumoniae* from GenBank and analyzed the CRISPR-Cas systems and CRISPR spacers found in plasmids and chromosomes. We found a putative CRISPR-Cas system in the 44 plasmids from *Klebsiella* species and GenBank search also identified the identical system in three plasmids from other Enterobacteriaceae, with CRISPR spacers targeting different plasmid and chromosome sequences. 45 of 47 plasmids with putative type IV CRISPR had IncFIB replicon and 36 of them had an additional IncHI1B replicon. All plasmids except two are very large (>200 kb) and half of them carried multiple antibiotic resistance genes including *bla*<sub>CTX-M</sub>, *bla*<sub>NDM</sub>, *bla*<sub>OXA</sub>. To our knowledge, this is the first report of multi drug resistance plasmids from Enterobacteriaceae with their own CRISPR-Cas system and it is possible that the plasmid type IV CRISPR may depend on the chromosomal type I-E CRISPRs for their competence. Both chromosomal and plasmid CRISPRs target a large variety of plasmids from this species, further suggesting key roles in the epidemiology of large plasmids.

**Keywords:** *Klebsiella pneumoniae*, Enterobacteriaceae, plasmid, CRISPR, antibiotic resistance

## INTRODUCTION

Acquisition of genetic material including virulence, fitness and antibiotic resistance genes by horizontal gene transfer (HGT) is an essential process in bacterial adaptation to different environments (Frost et al., 2005). In addition bacteria have acquired an adaptive immune system, clustered regularly interspaced short palindromic repeats and their associated Cas proteins

(CRISPR-Cas), which helps to limit the acquisition of genetic materials and defend against invasive bacteriophages and plasmids (Garneau et al., 2010; Barrangou, 2015; Samson et al., 2015).

A typical CRISPR-Cas locus is comprised of a CRISPR array, Cas genes and a leader sequence. A CRISPR array is comprised of nearly identical short (21 to 47 nucleotides) direct repeats, separated by unique DNA fragments (spacers) acquired from foreign DNA [mobile genetic elements (MGEs)]. The leader sequence is usually a (~100–500 bp) AT rich region believed to serve as a promoter for the transcription of the CRISPR array (Marraffini, 2015). The CRISPR-Cas defense mechanism can be considered as three steps. In an initial adaptation step foreign DNA fragments (protospacers) from infecting bacteriophages and plasmids are incorporated into the CRISPR array as new spacers. These spacers provide the sequence specific memory for a targeted defense against subsequent invasions by the same bacteriophage or plasmid. The CRISPR array transcript is then processed to matured CRISPR RNAs (crRNAs). After expression of the array, mature crRNAs, aided by Cas proteins, identify specific targets and cleave the nucleic acid strands of corresponding viruses or plasmids (van der Oost et al., 2009; Garneau et al., 2010; Makarova et al., 2011b, 2015; Barrangou, 2015).

CRISPR-Cas systems show a great deal of diversity in their Cas protein composition, structure of effector proteins complex, genetic organization and localization in the genome, mechanism of adaptation, crRNA processing and interference. Based on the effector complexes CRISPR-Cas systems can be divided into two classes and six types (Class 1, including types I, III, IV and class 2, including types II, V and VI), those can be subdivided into at least 34 sub-types (Makarova et al., 2011b, 2015, 2018; Koonin et al., 2017; Hille et al., 2018), Class 1 CRISPR-Cas system provides interference by using multi-Cas effector protein complex whereas Class 2 uses single effector protein for interference (Hille et al., 2018). Generally there are signature genes for each type of CRISPR-Cas system and those include *cas3* for type I, *cas9* for type II, *cas10* for type III, *csf1* (large subunit, *cas8*-like) for type IV, *cas12* for type V, and *cas13* for type VI (Makarova et al., 2018). Types I and II CRISPR-Cas systems provide immunity against DNA (Brouns et al., 2008; Gasiunas et al., 2012) whereas type III systems may target DNA or RNA (Tamulaitis et al., 2014). Types I–III are well-studied and are generally found in chromosomes of bacteria and archaea, whereas types IV, V, and VI are three putative new types. Type IV systems are usually localized on plasmids or other MGEs and lack apparent adaptation modules (*cas1* and *cas2*) and type V was identified in archaeal chromosome only (Makarova et al., 2011a, 2015). Type VI is another new type identified recently carrying HEPN-domain containing effector protein Cas13, which, unlike, other class II effector cleaves single stranded RNA (ssRNA) (Hille et al., 2018). HEPN RNase is a toxin domain of bacterial toxin-antitoxin module and suggests that type VI includes dedicated RNA-targeting CRISPR-Cas system (Makarova et al., 2011b, 2018; Koonin et al., 2017).

The classification, functions and mechanism of actions of all CRISPR-Cas systems are well-characterized except type IV.

A recent study demonstrated that the function of type IV system in the maturation of crRNAs and in the subsequent formation of a Cascade-like crRNA-guided effector complex (Ozcan et al., 2019). Type IV system can be classified as two sub-types, type IV-A and IV-B, based on the presence of DinG family helicase and type IV specific effector protein Csf5. Type IV-A encodes a DinG helicase (Csf4) and an effector protein Csf5 and whereas type IV-B lacks these proteins (Makarova et al., 2015, 2018; Koonin et al., 2017; Hille et al., 2018; Pinilla-Redondo et al., 2019) and usually, the type IV-A system carries CRISPR-array.

*Klebsiella pneumoniae*, a member of the bacterial family Enterobacteriaceae, is a common opportunistic hospital associated pathogen, accounting for about one third of total Gram-negative infections (Navon-Venezia et al., 2017). It causes a variety of infections including urinary tract infections, pneumonia, cystitis, wound infections, and life-threatening sepsis (Podschun and Ullmann, 1998). Occurrence of transmissible antibiotic resistance in this organism is a major problem worldwide. *K. pneumoniae* have a huge pool of antibiotic resistance genes that they share among other Enterobacteriaceae, mostly via self-transferrable plasmids (Navon-Venezia et al., 2017). Almost all modern antibiotic resistance (to carbapenems, cephalosporins, aminoglycosides, now even colistin) in these organisms is encoded on large (40–200 kb) low-copy (1–6 per cell) conjugative plasmids (Carattoli, 2009; Navon-Venezia et al., 2017). Plasmid-borne antibiotic resistance is acquired very quickly and, once acquired, could become fixed in the bacterial accessory genome by 'addiction systems' that poison cells from which the antibiotic resistance plasmid is lost (Hayes, 2003).

Several studies have identified CRISPR-Cas systems in *K. pneumoniae* chromosomes as I-E and I-E\* types (Ostria-Hernandez et al., 2015; Shen et al., 2017; Li et al., 2018) but little is known about CRISPR-Cas systems of plasmids in *K. pneumoniae* and other Enterobacteriaceae (Enas Newire et al., 2019). CRISPR-Cas systems are associated with relative antibiotic susceptibility in *Streptococcus pyogenes* and *E. coli* and the chromosomal CRISPR-Cas system is known to interfere with acquisition of antibiotic-resistant plasmids in *E. coli* (Zheng et al., 2014; Aydin et al., 2017). In this study, we examined 699 complete plasmid sequences from *K. pneumoniae* and 217 *K. pneumoniae* chromosomal sequences from the GenBank for the presence of CRISPR-Cas system and further analyzed the identified CRISPR-Cas systems and their spacers.

## MATERIALS AND METHODS

### Extraction of Complete Nucleotide Sequence of Plasmids and Chromosomes for *K. pneumoniae* From the GenBank

*Klebsiella pneumoniae* chromosome and plasmid sequences available in the GenBank database<sup>1</sup> were downloaded and

<sup>1</sup><https://www.ncbi.nlm.nih.gov/genome/?term=Klebsiella+pneumoniae>

subjected to CRISPR analysis. For complete *K. pneumoniae* chromosomal sequences, after opening the database link, we selected “genome assembly and annotation report” and chose complete sequences and then extracted all the complete nucleotide sequences individually and saved as FASTA format sequence file. For complete plasmid sequences, in the same link we selected “plasmid annotation report” and downloaded plasmid sequences > 50 kb and saved as separate FASTA files for individual plasmid sequences.

## Identification and Characterization of CRISPR-Cas in Plasmid and Chromosomal Sequences

CRISPR was identified with CRISPRFinder<sup>2</sup> (Grissa et al., 2007) software. This algorithm locates direct repeat sequences of 23–55 bp separated by variable sequences of a size no greater than 2.5 times or no less than 0.6 times the length of the repeated sequences (25–60 bp). When the algorithm detects at least three repeating regions that are exactly the same (in sequence and size), which are separated by variable sequences, it is considered a “confirmed CRISPR.” If the algorithm locates two repeats separated by a variable sequence, it establishes the status of a “questionable CRISPR.” For the present study we only considered those indicated by the program as “confirmed CRISPRs.” In addition, with this platform, we searched for *cas* genes in regions adjacent to CRISPR sequences. Fasta formatted complete nucleotide sequence of each individual plasmid or chromosome was uploaded in the CRISPRFinder and run the program by using a default setting parameters and outcomes provided the possible CRISPR-array (CRISPR repeats and spacers). Spacers sequences were collected from CRISPRFinder outputs and saved to use for further analysis. The CRISPR region identified by CRISPRFinder was then detected on the plasmid or chromosomal sequences and nearly 10 kb upstream and downstream regions were analyzed for putative *cas* genes. The CRISPR-array neighboring genes and their respective protein sequences were analyzed by BLASTn and BLASTp searches for the GenBank identity. For nucleotide sequence analysis, megablast was performed by using following parameters: (i) expectation threshold (e-values) less than or equal to 0.01 and a score greater than 40, (ii) maximum target sequence was set at 1000, (iii) automatically adjusted parameters for short input sequences, (iv) different match/mismatch scores were selected to identify highly conserved to low conserved sequences. BLASTp for protein sequences were performed against non-redundant protein sequence database and against reference proteins sequence database with expectation values (e-value) less than or equal to 0.01 were considered significant as well as a coverage percentage of more than or equal to 80%. The identified CRISPR-array and *cas* genes were further verified by using CRISPRone software<sup>3</sup> (Zhang and Ye, 2017). The individual fasta formatted nucleotide sequence of plasmid and chromosome was run through CRISPRone software by using default settings.

<sup>2</sup><https://crispr.i2bc.paris-saclay.fr/Server/>

<sup>3</sup><http://omics.informatics.indiana.edu/CRISPRone/>

## Search for Similar CRISPR-Cas System in GenBank Data

The *cas* genes identified in the putative type IV CRISPR-Cas systems in the plasmids of *K. pneumoniae* were used to fish similar type of CRISPR-Cas system in the GenBank data. Both the *cas* genes nucleotide sequences and amino acid sequences were used separately for BLASTn and BLASTp search in the GenBank data with the parameters mentioned earlier. The additional plasmid sequences identified with identical *cas* genes or Cas proteins were downloaded and analyzed for CRISPR-array and *cas* genes orientation by CRISPRFinder and CRISPRone software.

## Analysis of CRISPR Spacers and Identification of Spacers Protospacers Match

Spacers from respected plasmid CRISPR-Cas system were extracted from CRISPRFinder outputs and made a fasta formatted sequence file for all spacer pool by BioEdit software<sup>4</sup>. Each of the spacers sequence, their reverse complement sequence and both 3' and 5' truncated version were then searched against the spacer pool and identified all the unique spacers found in the plasmid CRISPRs and then plotted their distribution. Each of the unique spacer was then analyzed for their identity (match with protospacers) to GenBank sequences by nucleotide blast search (BLASTn) with parameters described earlier.

## Identification of Chromosomal CRISPR Type

Two different types of *cas1* and *cas3* alleles were found in *K. pneumoniae* genomes and CRISPR-Cas systems were further divided into types I-E or I-E\* (Li et al., 2018) on the basis of the *cas1* and *cas3* alleles and their localization in the chromosome.

## Plasmid Characterization

The presence of antibiotic resistance genes in sequenced plasmids were identified by ResFinder 3.2<sup>5</sup> and plasmid replicon types by PlasmidFinder 2.1<sup>6</sup> (Carattoli et al., 2014).

## RESULTS

### CRISPR-Cas System in *K. pneumoniae* Plasmids

A total of 699 complete plasmid sequences of > 50-kb in size found in *K. pneumoniae* were extracted from the GenBank database. CRISPR-arrays were identified in 5% (37 of 699; **Table 1** and **Supplementary Table S1**) of the plasmids. The identified CRISPR-arrays had direct repeats of 23–30 bp separated by a variable number (0–22) of spacer sequences of 25–57 bp and most of them are 30–33 bp long (**Supplementary Table S2**). Immediately upstream of the CRISPR-array an ~130 bp conserved AT rich region was present, which may act as a

<sup>4</sup><https://bioedit.software.informer.com/7.2/>

<sup>5</sup><https://cge.cbs.dtu.dk/services/ResFinder/>

<sup>6</sup><https://cge.cbs.dtu.dk/services/PlasmidFinder/>

**TABLE 1** | Characteristics of CRISPR-Cas positive plasmids.

SI no.	Plasmid	Species <sup>a</sup>	Accession no.	CRISPR-array position	DR-length (bp)	No. of spacers	Plasmid size (kb)	Replicon type <sup>b</sup>	Antibiotic resistance genes identified (annotation by ResFinder <sup>c</sup> )
1	pKPM501	<i>Kp</i>	CP031735.1	200609–201185	28	9	253	IncFIB <sub>k</sub> , IncFII <sub>k</sub>	<i>bla</i> <sub>CTX-M-15</sub> , <i>bla</i> <sub>TEM-1A</sub> , <i>aac</i> (6')-Ib, <i>aac</i> (6')-Ib-cr, <i>dfrA14</i>
2	unnamed_1	<i>Kp</i>	CP022612.1	313185–313943	29	12	335	IncHI1, IncHI1B, IncFIB, IncR	<i>bla</i> <sub>NDM-1</sub> , <i>bla</i> <sub>CTX-M-15</sub> , <i>bla</i> <sub>TEM-1A</sub> , <i>bla</i> <sub>OXA-9</sub> , <i>bla</i> <sub>SHV-13</sub> , <i>aph</i> (3')-VI, <i>armA</i> , <i>aadA2</i> , <i>aac</i> (6')-Ib, <i>aac</i> (6')-Ib-cr, <i>aac</i> (3)-IId, <i>aph</i> (6)-Id, <i>sul</i> 1,2,3; <i>dfrA12</i>
3	AR_0153 plasmid unnamed1	<i>Kp</i>	CP028929.1	62241–63001	29	12	283	IncHI1B, IncFIB	<i>bla</i> <sub>NDM-1</sub> , <i>bla</i> <sub>OXA-1</sub> , <i>aph</i> (3')-VI, <i>armA</i> , <i>aadA2</i> , <i>aac</i> (6')-Ib-cr, <i>qnrB1</i> , <i>sul</i> 1, <i>dfrA12</i> , <i>dfrA14</i>
4	pKPN528-1	<i>Kp</i>	CP020854.1	251737–252495	29	12	292	IncHI1B, IncFIB	<i>bla</i> <sub>NDM-1</sub> , <i>bla</i> <sub>OXA-1</sub> , <i>aph</i> (3')-VI, <i>armA</i> , <i>aadA2</i> , <i>aac</i> (6')-Ib-cr, <i>qnrB1</i> , <i>sul</i> 1, <i>dfrA12</i> , <i>dfrA14</i>
5	AR_0068 plasmid unitig_1	<i>Kp</i>	CP020068.1	136244–137004	29	12	276	IncHI1B, IncFIB	<i>bla</i> <sub>NDM-1</sub> , <i>bla</i> <sub>SHV-13</sub> , <i>aph</i> (3')-VI, <i>armA</i> , <i>aadA2</i> , <i>aac</i> (3)-IId, <i>aph</i> (6)-Id, <i>sul</i> 1,2; <i>dfrA12</i>
6	pIncHI1B_DHQP1300920	<i>Kp</i>	CP016921.1	229597–230357	29	12	283	IncHI1B, IncFIB	<i>bla</i> <sub>NDM-1</sub> , <i>bla</i> <sub>OXA-1</sub> , <i>aph</i> (3')-VI, <i>armA</i> , <i>aadA2</i> , <i>aac</i> (6')-Ib-cr, <i>qnrB1</i> , <i>sul</i> 1, <i>dfrA12</i> , <i>dfrA14</i>
7	KP617 plasmid KP-plasmid1	<i>Kp</i>	CP012754.1	114404–115164	29	12	273	IncHI1B, IncFIB	<i>bla</i> <sub>NDM-1</sub> , <i>aph</i> (3')-VI, <i>armA</i> , <i>aadA2</i> , <i>qnrB1</i> , <i>sul</i> 1, <i>dfrA12</i>
8	PittNDM01 plasmid1	<i>Kp</i>	CP006799.1	114132–114892	29	12	283	IncHI1B, IncFIB	<i>bla</i> <sub>NDM-1</sub> , <i>bla</i> <sub>OXA-1</sub> , <i>aph</i> (3')-VI, <i>armA</i> , <i>aadA2</i> , <i>aac</i> (6')-Ib-cr, <i>qnrB1</i> , <i>sul</i> 1, <i>dfrA12</i> , <i>dfrA14</i>
9	pKJNM10C3.2	<i>Kp</i>	CP030878.1	136256–137016	29	12	276	IncHI1B, IncFIB	<i>bla</i> <sub>NDM-7</sub> , <i>aph</i> (3')-VI, <i>armA</i> , <i>aadA2</i> , <i>aph</i> (3'')-Ib, <i>aph</i> (6)-Id, <i>aac</i> (3)-IIa, <i>sul</i> 1, 2; <i>dfrA12</i>
10	p18ES-342	<i>Kp</i>	CM008881	52979–53610	23	10	332	IncHI1B, IncFIB	<i>dfrA1</i>
11	unnamed1	<i>Kp</i>	CP031818	223392–224022	23	10	430	IncFIB	None
12	pKpvST147L	<i>Kp</i>	CM007852	167552–168555	29	16	343	IncHI1B, IncFIB	<i>armA</i> , <i>aph</i> (3')-Ia, <i>sul</i> 1, 2; <i>dfrA5</i>
13	KSB2_1B plasmid unnamed1	<i>Kp</i>	CP024507.1	41987–42747	29	12	310	IncFIB	None
14	pKp_Goe_414-1	<i>Kp</i>	CP018339.1	75291–76111	29	13	204	IncFIB	None
15	pKPN-3967	<i>Kp</i>	CP026186.1	221215–221302	27	1	373	IncFIB	None

(Continued)



TABLE 1 | Continued

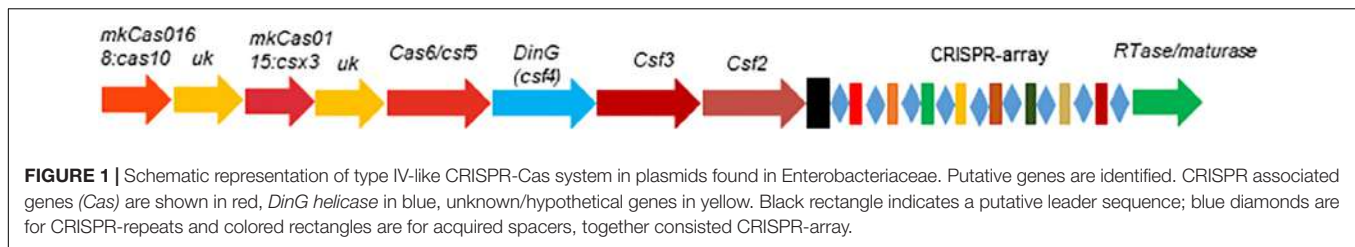
SI no.	Plasmid	Species <sup>a</sup>	Accession no.	CRISPR-array position	DR-length (bp)	No. of spacers	Plasmid size (kb)	Replicon type <sup>b</sup>	Antibiotic resistance genes identified (annotation by ResFinder <sup>c</sup> )
16	p44-1	<i>Kp</i>	CP025462.1	42604–43120	29	8	261	IncFIB	None
17	TVGHCRE225 plasmid unnamed1	<i>Kp</i>	CP023723.1	10881–11763	29	14	297	IncHI1B, IncFIB	None
18	pOXA1_020030	<i>Kp</i>	CP028791.1	30205–30843	29	10	288	IncFIB	<i>bla</i> <sub>OXA-1</sub> , <i>aac</i> (6')-Ib-cr, <i>sul1</i>
19	825795-1 plasmid unnamed1	<i>Kp</i>	CP017986.1	148524–149585	30	17	244	IncHI1B, IncFIB	None
20	pKp_Goe_304-1	<i>Kp</i>	CP018720.1	24563–25679	24	18	246	IncHI1B, IncFIB	None
21	pKp_Goe_021-1	<i>Kp</i>	CP018714.1	7697–8748	30	17	246	IncHI1B, IncFIB	None
22	pKp_Goe_026-1	<i>Kp</i>	CP018708.1	54661–55777	24	18	246	IncHI1B, IncFIB	None
23	pKp_Goe_024-1	<i>Kp</i>	CP018702.1	5006–6122	24	18	246	IncHI1B, IncFIB	None
24	pKp_Goe_832-1	<i>Kp</i>	CP018696.1	102143–103259	24	18	246	IncHI1B, IncFIB	None
25	pKp_Goe_473-1	<i>Kp</i>	CP018687.1	116666–117727	30	17	246	IncHI1B, IncFIB	None
26	pKp_Goe_579-1	<i>Kp</i>	CP018313.1	94773–95834	30	17	246	IncHI1B, IncFIB	None
27	AR_0363 plasmid unnamed4	<i>Kp</i>	CP027156.1	127062–128305	29	20	186	IncHI1B, IncFIB	<i>aac</i> (6')-Ib, <i>aac</i> (6')-Ib-cr
28	pKPN-edaa	<i>Kp</i>	CP026398.1	7401–8525	29	18	249	IncHI1B, IncFIB	<i>bla</i> <sub>NDM-1</sub> , <i>bla</i> <sub>OXA-1</sub> , <i>bla</i> <sub>DHA-1</sub> , <i>aph</i> (3'')-Ib, <i>aph</i> (6)-Id, <i>aac</i> (6')-Ib-cr, <i>qnrB4</i> , <i>sul1</i>
29	pKPN-bbef	<i>Kp</i>	CP026172.1	227283–228407	29	18	244	IncHI1B, IncFIB	None
30	pKpvST101_5	<i>Kp</i>	CP031372.1	144828–145262	25	10	210	IncHI1B, IncFIB	None
31	pKpn23412-362	<i>Kp</i>	CP011314.1	141865–142618	23	12	362	IncHI1B, IncFIB	<i>bla</i> <sub>OXA-1</sub> , <i>bla</i> <sub>CTX-M-15</sub> , <i>bla</i> <sub>TEM-1B</sub> , <i>bla</i> <sub>OXA-1</sub> , <i>aac</i> (3)-IIa, <i>aph</i> (3'')-Ib, <i>aph</i> (6)-Id, <i>aac</i> (6')-Ib-cr, <i>sul2</i> , <i>dfr1</i>
32	p1502320-3	<i>Kp</i>	CP031580.1	7608–8781	29	19	87	ND	None
33	pKP3301 DNA	<i>Kp</i>	AP018748.1	3677–4373	29	11	296	IncHI1B, IncFIB	<i>bla</i> <sub>NDM-1</sub> , <i>bla</i> <sub>CTX-M-15</sub> , <i>bla</i> <sub>TEM-1A</sub> , <i>bla</i> <sub>OXA-1</sub> , <i>aph</i> (3')-VI, <i>armA</i> , <i>aadA2</i> , <i>aac</i> (6')-Ib, <i>aac</i> (6')-Ib-cr
34	SKGH01 plasmid unnamed 1	<i>Kp</i>	CP015501.1	7545–7875	29	15	281	IncHI1B, IncFIB	None
35	Plasmid_A_Kpneumoniae_MS6671	<i>Kp</i>	LN824134.1	16764–17823	29	17	280	IncHI1B, IncFIB	None
36	pKJNM8C2.1	<i>Kp</i>	CP030858.1	10639–11155	30	8	304	IncHI1B, IncFIB	<i>bla</i> <sub>NDM-1</sub> , <i>bla</i> <sub>CTX-M-15</sub> , <i>bla</i> <sub>OXA-1</sub> , <i>armA</i> , <i>aadA2</i> , <i>aac</i> (6')-Ib-cr, <i>qnrB1</i> , <i>sul1</i> , <i>dfrA12</i>

(Continued)

TABLE 1 | Continued

SI no.	Plasmid	Species <sup>a</sup>	Accession no.	CRISPR-array position	DR-length (bp)	No. of spacers	Plasmid size (kb)	Replicon type <sup>b</sup>	Antibiotic resistance genes identified (annotation by ResFinder <sup>c</sup> )
37	pPMK1-NDM	<i>Kp</i>	CP008933.1	10628–11144	30	8	304	IncHI1B, IncFIB	<i>bla</i> <sub>NDM-1</sub> , <i>bla</i> <sub>CTX-M-15</sub> , <i>bla</i> <sub>OXA-1</sub> , <i>armA</i> , <i>aadA2</i> , <i>aac(6′)-Ib-cr</i> , <i>qnrB1</i> , <i>sul1</i> , <i>dfrA12</i>
38	pFB2.1	<i>Pg</i>	CP014776.1	56849–57852	29	16	242	IncFIB	None
39	pE20-HI3	<i>Kp</i>	MG288682.1	27978–29043	29	17	240	IncFIB	<i>bla</i> <sub>OXA-1</sub> , <i>armA</i> , <i>aac(6′)-Ib-cr</i> , <i>sul1</i>
40	pEC422_1	<i>Ec</i>	CP018961.1	276922–277868	29	15	290	IncHI1B, IncFIB	<i>bla</i> <sub>CTX-M-2</sub> , <i>bla</i> <sub>TEM-1B</sub> , <i>bla</i> <sub>OXA-1</sub> , <i>aac(6′)-Ib-cr</i> , <i>aac(3)-IIa</i> , <i>sul1</i>
41	pNDM-TJ03	<i>Kp</i>	MG845201.1	130378–131435	29	17	280	IncHI1B, IncFIB	<i>bla</i> <sub>NDM-1</sub> , <i>bla</i> <sub>OXA-1</sub> , <i>bla</i> <sub>SHV-12</sub> , <i>bla</i> <sub>DHA-1</sub> , <i>aph(3′′)-Ib</i> , <i>aph(6)-Id</i> , <i>aac(6′)-Ib-cr</i> , <i>qnrB4</i> , <i>sul1</i>
42	pNDM-TJ11	<i>Ko</i>	MG845200.1	130294–131351	29	17	275	IncHI1B, IncFIB	<i>bla</i> <sub>NDM-1</sub> , <i>bla</i> <sub>OXA-1</sub> , <i>bla</i> <sub>DHA-1</sub> , <i>aph(3′′)-Ib</i> , <i>aph(6)-Id</i> , <i>aac(6′)-Ib-cr</i> , <i>qnrB4</i> , <i>sul1</i>
43	pENVA	<i>Kp</i>	HG918041.1	99454–100629	23	19	254	IncHI1B, IncFIB	<i>bla</i> <sub>NDM-1</sub> , <i>bla</i> <sub>OXA-1</sub> , <i>bla</i> <sub>SHV-12</sub> , <i>bla</i> <sub>DHA-1</sub> , <i>aph(3′′)-Ib</i> , <i>aph(6)-Id</i> , <i>aac(6′)-Ib-cr</i> , <i>qnrB4</i> , <i>sul1</i>
44	pKP64477b	<i>Kp</i>	MF150122.1	84064–85428	29	22	205	IncHI1B, IncFIB	None
45	<i>Raoultella ornithinolytica</i> strain 18 plasmid 1	<i>Ro</i>	CP012556.1	115417–115897	29	7	216	ND	None
46	pKPN1481-1	<i>Kv</i>	CP020848.1	325794–326308	29	8	347	IncHI1B, IncFIB	<i>bla</i> <sub>NDM-1</sub> , <i>bla</i> <sub>CTX-M-15</sub> , <i>bla</i> <sub>OXA-1</sub> , <i>bla</i> <sub>TEM-1A</sub> , <i>bla</i> <sub>OXA-9</sub> , <i>aac(6′)-Ib</i> , <i>aac(6′)-Ib-cr</i> , <i>aadA1</i> , <i>qnrB1</i>
47	pK66-45-1	<i>Kp</i>	CP020902.1	None	0	0	338	IncFIB, IncFII, IncHI1B, IncR	<i>bla</i> <sub>NDM-1</sub> , <i>bla</i> <sub>CTX-M-15</sub> , <i>armA</i> , <i>aadA2</i> , <i>aph(3′′)-VI</i> , <i>qnrS1</i> , <i>sul1</i> , <i>dfrA12</i>

<sup>a</sup>*Kp*, *K. pneumoniae*; *Pg*, *Pluralibacter gergoviae*; *Ec*, *E. coli*; *Ko*, *Klebsiella oxytoca*; *Ro*, *Raoultella ornithinolytica*; *Kv*, *Klebsiella varicola*. <sup>b</sup>ND, not detected. <sup>c</sup>*aac(6′)-Ib* also commonly annotated as *aacA4*; *aph(3′′)-Ib*, *aph(6)-Id* also commonly annotated as *strA*, *strB*.



leader sequence of this CRISPR. We also identified *csf2*, *csf3*, *DinG* helicase (*csf4*), *cas6* (*csf5*), *csx3*, and *cas10* homologs upstream and a reverse transcriptase (*RTase*) or maturase gene downstream of the CRISPR-array (**Figure 1**). Two genes of unknown function were also present in the *Cas* genes locus, but we could not identify the adaptation genes *cas1* or *cas2*, or evident homologs, in these plasmids. The structure of the CRISPR-Cas array and organization of *cas* genes identified here is very close to that of the type IV CRISPR-Cas system previously identified in the mega-plasmid of *Aromatoleum aromaticum* EbN1, an aromatic-degrading betaproteobacteria found in freshwater and soil habitats (Ozcan et al., 2019), even though a large subunit (*Csf1*) that acts as the signature protein for this type (Makarova et al., 2015) is absent from the system identified here. The *Cas* genes and their orientations in identified CRISPR-Cas systems are very similar among the plasmids except for the presence of Insertion Sequences (ISs) insertion events in some. ISs were also identified between the CRISPR-array and *RTase* gene in a few plasmids.

## CRISPR-Cas System in Other Enterobacteriaceae Plasmids

A BLAST search identified identical CRISPR-Cas systems in 10 other plasmids in GenBank, in addition to the 37 plasmids identified in *K. pneumoniae* (**Table 1**). Five of these 10 plasmids were from *K. pneumoniae* and 1 each from *E. coli*, *K. oxytoca*, *Pluralibacter gergoviae*, *K. variicola*, and *Raoultella ornithinolytica*. One of the plasmids from *K. pneumoniae* has a *cas* locus without any CRISPR-array identified. No match was found in chromosomal sequences on GenBank.

## Characterization of CRISPR-Positive Plasmids

A total of 47 type IV CRISPR-positive plasmids were analyzed. All but two are very large (>200 kb) and the largest is 430 kb (**Table 1**). Almost all had an IncFIB replicon identified by PlasmidFinder except for two in which no replicon match was identified. Most plasmids (36/47) also have an IncHI1B replicon (**Table 1**). Interestingly, although most of the plasmids (44/47) were found in *Klebsiella* species, only one plasmid has the characteristic *Klebsiella* type IncFIB<sub>K</sub> replicon (Garcia-Fernandez et al., 2012). The %GC content of almost all CRISPR-negative plasmids is > 50% and lower (~44–46%) in CRISPR-positive plasmids (**Supplementary Table S1**). The only CRISPR-positive plasmid with an IncFIB<sub>K</sub> replicon had a GC content of ~52%, similar to other CRISPR-negative plasmids of *K. pneumoniae*.

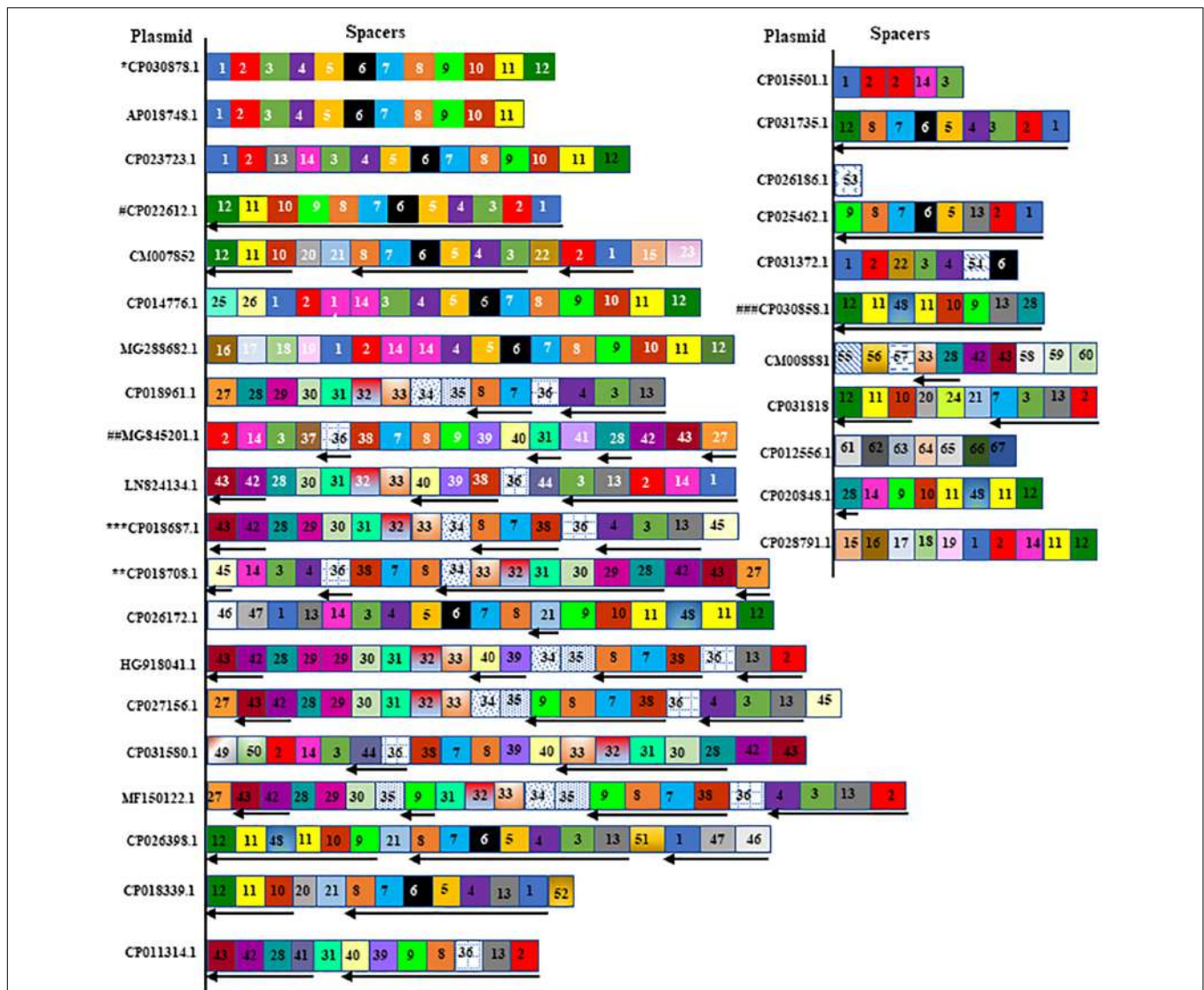
ResFinder identified multiple antibiotic resistance genes including *bla*<sub>CTX-M</sub>, *bla*<sub>NDM</sub>, *bla*<sub>OXA</sub>, *armA* and *qnr* genes, associated with resistance to β-lactam, carbapenem, aminoglycoside and quinolone antibiotics, in almost half the plasmids (24/47; **Table 1**).

## Analysis of Spacers From Plasmid CRISPRs

A total of 623 spacers from 46 CRISPR-positive plasmids were analyzed by BLASTn search, identifying 67 unique spacer sequences that made up the total pool of 623, including some repetition or reversed orientation of the same sequence, along with loss or gain of a few nucleotides (**Figure 2** and **Supplementary Table S2**). Spacer numbers varies without any relationship with plasmid size or the presence or absence of antibiotic resistance genes (**Table 1**). Five unique spacers (SP11, 36, 43, 55, 57) were found specific for plasmid sequences other than the match with CRISPR-array region and one of them (SP11) appears to match with the *traL* gene of 457 different CRISPR-negative plasmid sequences and another one (SP43) hits the *traN* gene of 260 different CRISPR-negative plasmid sequences in GenBank, mostly (>98%) from *K. pneumoniae* (**Table 2** and **Supplementary Table S2**). Both spacers are found in the CRISPR-array of 17 of the 46 CRISPR-positive plasmids we examined (**Table 2**). Spacers SP36, SP55, and SP57 have identity with plasmid *transposases*, *transcriptional regulator* and *traH* gene, respectively. Genes, *traL*, *traN*, and *traH* play an important role in plasmid transfer and are highly conserved among plasmids. Five unique spacers (SP8, 20, 42, 62, 63) were also found to match *K. pneumoniae* chromosomes but not those of their current host bacteria (**Table 2** and **Supplementary Table S2**). Two of them occurred in 17 of the 46 plasmids, targeting *DUF1367* family protein and *hypothetical protein* genes for 111 and 139 *K. pneumoniae* chromosomes, respectively. Another spacer, that occurred in one plasmid only, appears to recognize a *hypothetical protein* gene from 3 of the *K. pneumoniae* chromosomes (**Table 2**). Many spacers (18/67) did not have any match in GenBank (**Supplementary Table S2**).

## Analysis of CRISPR-Cas System in *K. pneumoniae* Chromosomes

A total of 217 *K. pneumoniae* complete chromosomal sequences were extracted from GenBank (June 2019) and we identified that 81 of these (37%) carried CRISPR-Cas system on the chromosome. Of these 81, 45 were I-E and 36 were I-E\* type (**Supplementary Table S3**), consistent with previous reports (Ostria-Hernandez et al., 2015; Shen et al., 2017; Li et al., 2018).



**FIGURE 2 |** A spacer map for the distribution of spacers in plasmid CRISPRs. Spacers are represented in box without repeats. Identical spacers are represented by same number and color or pattern. Spacers found in reverse orientation in the plasmid CRISPR are shown by reverse arrow at the bottom of the spacer. Exactly same spacers and their orientation are shared by a number of plasmids and are mentioned below in the brackets, and spacers from one of them were represented in the figure. Those plasmids are (\*CP030878.1, CP020068.1, CP0016921.1, CP028929.1, CP024507.1, CP020854.1), (\*\*CP018708.1, CP018702.1, CP018696.1, CP018720.1), (\*\*\*)CP018687.1, CP018714.1, CP017986.1), (#CP022612.1, CP012754.1, CP006799.1), (##MG845201.1, MG845200.1) and (###CP030858.1, CP008933.1) and marked with asterisk or hashtag were the representative from each group showed in the figure. The unique spacer sequences and their match with protospacers will be found in **Supplementary Table S2**.

### Relationship Between the Presence of Chromosomal CRISPR and Plasmid in *K. pneumoniae* Bacteria

We also gathered information about the presence of plasmids in those 217 *K. pneumoniae* isolates from GenBank. Most bacteria (185 of 217, 85%) carried plasmids, from 1 to 10 in number (Figure 3A and Supplementary Table S3) and 37% of these 217 had the putative CRISPR-Cas system. We found that the occurrence of chromosomal CRISPR is more in plasmid-free than plasmid-carrying strains (43 vs. 35%) (Figure 3B), a relationship that has been noted before

(Li et al., 2018). We found that bacteria with chromosomal type I-E CRISPR had more plasmids (from 1 to 7 in number, most with 4–5 plasmids) whereas bacteria with chromosomal type I-E\* CRISPR had less plasmids (from 0 to 4 in number, mostly only 1 or 2 plasmids or none) (Supplementary Table S3).

### Analysis of Spacers From *K. pneumoniae* Chromosomal CRISPRs

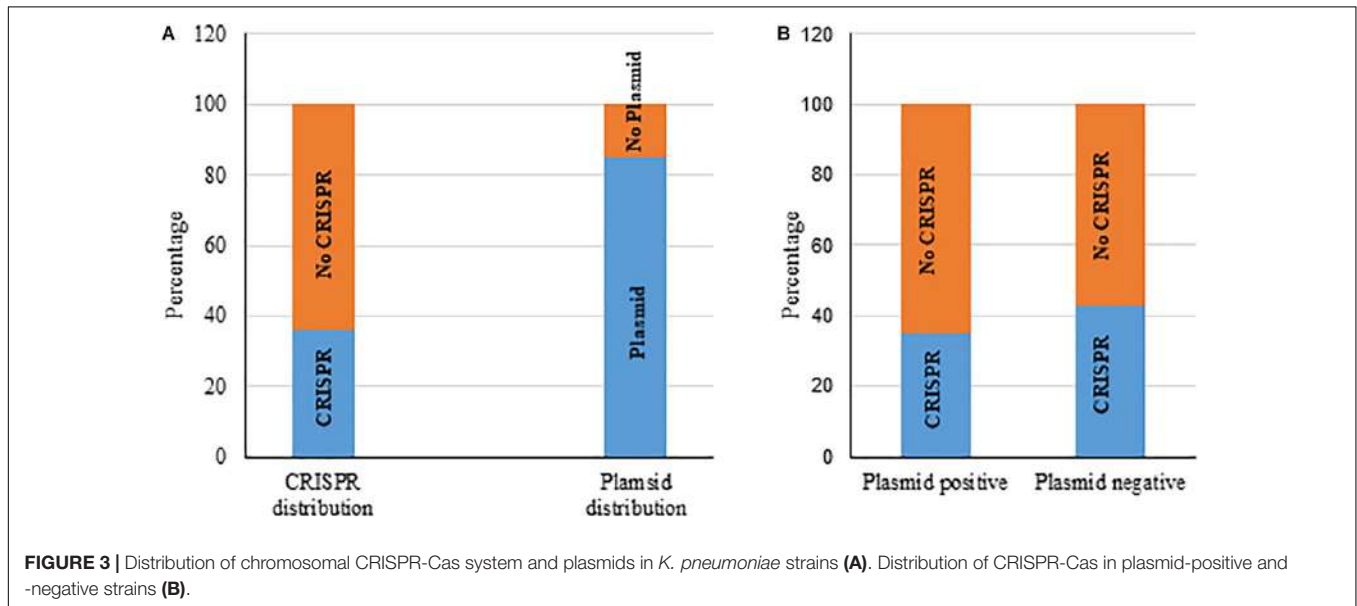
A total of 2,464 spacers were extracted from chromosomal CRISPR-positive strains. A BLASTn search with these spacers



**TABLE 2** | Spacers from plasmid mediated CRISPR specific to plasmids and *K. pneumoniae* chromosomes.

Spacer	Hits to	Target gene	No. of occurrence
CCGAGATTGAGTAAAGCAAAGTAACGGCGGTG	111 <i>Kp</i> strains chromosome	<i>DUF1367</i> family protein	17
TTCCGGACTCCTGTTTCCGGCAGTGGATAAA	457 CRISPR-negative plasmids	<i>traL</i>	17
CCGAGCTACCGATTACAGGAGAGCGCTCGC	139 <i>Kp</i> strains Chromosome	<i>hp</i>	17
CCGTTTCGGATTTTGCAGAACAGGTGCAGGGC	260 CRISPR-negative plasmids	<i>traN</i>	17
TTGGCGACCACCAGCGTTTTAGTGCAGGGAAC	3 <i>Kp</i> strains chromosome	<i>hp</i>	1
AAGTTATTATCATGTGCCATTACAGTCCGGCGCGTATT	62 CRISPR-negative plasmids	<i>traH</i>	1
TTCTCTCCGCCGGGCAGTGTGATGCCGGAGGGGTATTC	7 CRISPR-negative plasmids	<i>transcriptional regulator</i>	1
ATTTACAATGAAGATTTTTCCCATTTGGTAA	48 CRISPR-negative plasmids	IS200/IS605 family transposase	10
TTCCCTGCACTAAGACGCTGGTGGTCCGCCAC	17 <i>Kp</i> strains chromosome	<i>hp</i>	9
AGTTTGTATGAAAGCCTCATGTTTTGCACCTGTGCCGG	6 <i>Klebsiella</i> chromosome	<i>hp</i>	1
TGCATATCATCCTCAGAGC			

*hp*, hypothetical protein.



matched *K. pneumoniae* chromosomal sequences as well as different mobile elements including bacteriophages and plasmids. We identified 18 unique spacers matched sequences on plasmids (Table 3). Interestingly, 5 of these 18 spacers were from plasmid conjugative transfer region genes (*traH*, *traG*, *traT*, *traN*, *traF*) in several hundred different plasmid sequences in GenBank. Spacers matching *traH* and *traG* gene sequences from 413 and 401 different plasmids respectively were identified. One spacer matched the plasmid segregation gene *parM*, one matched the ubiquitous toxin antitoxin system gene *hok-sok* (Table 3), one matched the *SAM-methyl transferase* gene and another matched DNA sequence in a hypothetical gene located immediate upstream of *SAM-methyltransferase* on the plasmid. Three spacers matched different regions in the *DUF3560 domain-containing protein* gene, which was found in turn on ~1,000 plasmids in GenBank. One spacer matched *ydeA*, two matched a hypothetical protein and other three in intergenic regions of plasmid sequences; one spacer matched an intergenic region with identity to 524 different plasmids (Table 3) which, in a few cases, was present in multiple times in a single plasmid sequence.

## DISCUSSION

In this study we have identified a putative type IV CRISPR-Cas system in the plasmids of *K. pneumoniae*. To our knowledge, this is the first comprehensive report of type IV CRISPR-Cas system in plasmids of *K. pneumoniae*, specifically in antibiotic resistance plasmids.

Type IV CRISPR-Cas was previously identified in a mega-plasmid of *Aromatoleum aromaticum* species, an aromatic-degrading  $\beta$ -proteobacteria found in freshwater and soils. The CRISPR-positive plasmids we describe are also very large (200–430 kb; Table 1). Like the previously reported type IV CRISPR-Cas system (Makarova et al., 2015; Enas Newire et al., 2019; Pinilla-Redondo et al., 2019) homologs of *cas* region genes *csf2*, *csf3*, *DinG* helicase (*csf4*), *cas6* (*csf5*) were present, the organization of the *cas* genes was very similar and the adaptation genes *cas1* and *cas3* were absent, all typical of the previously reported type IV CRISPR-Cas. The large subunit *csf1* gene thought to be the signature gene for type IV system was absent in the CRISPR-Cas system reported here, but two additional *cas*

**TABLE 3** | Plasmid specific spacers in *K. pneumoniae* chromosomal CRISPR.

Spacers	Target gene on plasmid <sup>a</sup>	No. of plasmid matched	No. of occurrence in chromosome
TACTGCAGCAGGATGTCGTAGCCGATATAGTC	Conjugal transfer protein <i>traH</i>	413	1
ATAGAAAAGATGTGTATCGCATCTCGGTA	Conjugal transfer protein <i>traG</i>	401	1
TTTGGTATTTGTGCTGATTACCCGTTTCAGTA	Conjugal transfer protein <i>traT</i>	126	1
GAAATAACCGTCTTCATTTCCACCTCCCTCA	Type-F conjugative transfer system mating-pair stabilization protein <i>traN</i>	90	1
GATACAGAATGGCTTCGTACAGCGACCGTTTG	Type-F conjugative transfer system pilin assembly protein <i>traF</i>	20	1
GTGTTTGTACCGTGTGTGGCAAAAAGC	<i>hok-sok</i> toxin-antitoxin system	152	5
CGTGACCAATTGATACGCCAATATCAGGATTAC	Plasmid segregation protein <i>parM</i>	13	1
CGGCCGTTTAAATCGCGGTGATGATATCCGGCA	<i>SAM-dependent methyltransferase</i>	209	7
GTCTTCCCTGTTTGCTGCTGTGTCTGTCTG	<i>hp</i> , immediate upstream of <i>SAM-dependent methyltransferase</i>	405	29
GGGGACCTGCTGAACCTGCCCCCTGGTATTAA	<i>DUF3560</i> domain-containing protein	214	24
CGATAACCGGGCGTTTCGACTGAACTCACCTC	<i>DUF3560</i> domain-containing protein	351	24
TTGATACGGCGGTAACGCACATCCGGACGCTC	<i>DUF3560</i> domain-containing protein	425	1
CCGGCATCCGTCAGCTCGACGGCCAGCTGCAG	<i>ydeA</i> protein	19	24
TGATTGACGCGAAGCTGCGTTATCCCAACACC	<i>hp</i>	19	1
GCAGCATGAACGTTTCCCACTCGCCGTTCTCA	<i>hp</i>	93	1
GAGCAGGCACCCGCGCAACGACGAAGAGCGC	Intergenic region/ <i>hp</i> , (2–4 hits in same plasmid)	524	19
GAACGGAGGAATAAAGAACAAGCCCGCAG	Intergenic region	145	1
TCGTCTGAGTTCGGCTTACGCCGTGCCGACA	Intergenic region	178	5

<sup>a</sup>*hp* for hypothetical protein.

genes (*csx3* and *cas10* homologs) and two genes of unknown functions were identified in the *cas* gene locus, any of which may compensate for the absent *csf1*. The Cas1 protein of type IV CRISPR-Cas is a Zn-finger containing protein with a weak similarity to Zn-finger sequences of Cas10 and it has been suggested that Csf1 could be a highly divergent, inactivated and N-terminally truncated Cas10-like polymerase derivative (Makarova et al., 2011a). The presence of *DinG helicase* (*csf4*), only previously reported in type IV-A CRISPR-Cas (Koonin et al., 2017; Makarova et al., 2018; Pinilla-Redondo et al., 2019), further supports the designation of these plasmid systems as type IV-A CRISPR-Cas.

A preliminary study identified putative type IV CRISPR-Cas system in the IncH1B/IncFIB plasmids of Enterobacteriaceae (Enas Newire et al., 2019). In the present study most (45 of 47) of these very large CRISPR-carrying plasmids had an IncFIB replicon identified and most had an additional IncH1B replicon. We identified only one of the IncF replicons that are thought to be typical (i.e., IncFIB<sub>K</sub>) of *K. pneumoniae* (Garcia-Fernandez et al., 2012; Villa and Carattoli, 2020). This suggests that CRISPR-positive plasmids might have originated from some other species in Enterobacteriaceae and transferred into *K. pneumoniae*. Analysis of %GC content shows that almost all CRISPR-positive plasmids have lower %GC (44–46%) than CRISPR-negative plasmids (~50% or greater); we identified only one IncFIB<sub>K</sub> plasmid with CRISPR (pKPM501) and this had a 'normal' %GC of > 51%.

Plasmids have their own genetic modules that they can utilize to exist stably in certain bacterial host by competing with other plasmids. Plasmid incompatibility is one of the

such mechanism by which two plasmids with similar or related replication genes cannot co-exist in the same cell. By interfering with host replication system only one plasmid of similar type can be efficiently replicate and segregate to daughter cell and others lost from the system (Novick, 1987; Austin and Nordstrom, 1990). Acquiring antibiotic resistance genes also give plasmids the advantage to maintain over sensitive plasmids at antibiotic selection pressure (Carattoli, 2013). Plasmid mediated toxin-antitoxin (TA) module also provide another alternative to displace incompatible plasmid by toxin mediated killing of plasmid free cells (Hayes, 2003; Yamaguchi et al., 2011). For example, if a cell carries two incompatible plasmids and one plasmid encodes a TA system, then after segregation of these incompatible plasmids, only plasmid carrying TA system will be maintained into daughter cells and cells carrying the other plasmid are eliminated from the population. Similar to those systems, it was suggested that plasmid mediated type IV CRISPR-Cas system may involve in the competition between plasmids by acquiring spacers specifically targeting different plasmids (Pinilla-Redondo et al., 2019). Chromosomal CRISPR are known to acquire spacers against different MGEs (Samson et al., 2015) and many plasmid-borne CRISPR spacers we found were also directed against other plasmids, including three unique spacers targeting 100% identical sequences (the common and highly conserved *traN*, *traH*, and *traL* of conjugative plasmids) in more than 700 other plasmids in GenBank. Large potentially expensive plasmids such as these CRISPR-positive plasmids may need this competitive edge and may reduce the overall plasmid burden in their host bacteria. Plasmid CRISPR spacers

targeting heterologous *K. pneumoniae* chromosomes may also have a role in determining the epidemiology of plasmids in this species.

Acquisition of a new plasmid produces burden to the host by reducing growth rate and lessened competitiveness of plasmid-bearing hosts under conditions that do not select for plasmid genes (San Millan and MacLean, 2017). Although this fitness-cost can be mitigated over time through compensatory evolutions, however, the initial cost associated with plasmid carriage is one of the main barrier in the acquisition, maintenance and transfer of new plasmids (San Millan and MacLean, 2017; Dionisio et al., 2019). Multiple plasmids impose more fitness-cost related to single plasmid. Acquisition of plasmid mediated CRISPR spacers targeting other plasmids and host chromosome may provide advantage in the formation of plasmid co-integrate with other plasmids or integrated into the host chromosome by homologous recombination that might facilitate the stability and compatibility of the plasmids. CRISPR-Cas defense system not only identified in plasmids but also distributed in other MGEs including bacteriophages, T7-transposable elements and integrative conjugative elements (ICEs) (Faure et al., 2019; Koonin et al., 2019). The recruitment of CRISPR-Cas defense system by different MGEs may contribute to the evolution of both MGEs and defense systems.

Several previous studies identified and analyzed chromosomal CRISPR-Cas systems in *K. pneumoniae* by analyzing 52 (Ostria-Hernandez et al., 2015), 68 (Shen et al., 2017) and 97 (Li et al., 2018) complete and draft genome sequences. Here, we analyzed 217 complete *K. pneumoniae* chromosomes available in GenBank for the distribution of CRISPR-Cas systems, their types, acquired spacers and relationship between presence and absence of CRISPR and plasmids. Consistent with previous studies, we found type I-E and type I-E\* CRISPRs distributed in *K. pneumoniae* chromosomes. We found that chromosomal CRISPR-negative strains had more plasmids (Figure 3 and Supplementary Table S3) and that *K. pneumoniae* with type I-E\* chromosomal CRISPR appeared to have less plasmids than those with type I-E.

Spacer sequences from chromosomal CRISPR matched different MGEs including plasmids. A total of 18 unique spacers were acquired from plasmids and many from conjugative transfer region genes, plasmid partition (*parM*) and stability genes (*hok-sok*). Acquired plasmid-specific spacers in *K. pneumoniae* chromosomal CRISPR may provide immunity against plasmids and, it has been suggested, promote or select for mobilization of important plasmid-borne antibiotic resistance genes such as *bla<sub>CTX-M</sub>* and *bla<sub>KPC</sub>* onto the chromosome (Huang et al., 2017). Similar phenomena have been directly observed for *Streptococcus thermophilus* CRISPR-Cas systems (Garneau et al., 2010).

Type IV CRISPR-Cas systems on plasmids lack genes for target cleavage enzymes (*cas3* or *cas10*) (Makarova et al., 2015) but we have identified a putative *cas10-like* gene in these plasmid CRISPR-Cas system in Enterobacteriaceae. They also lack key adaptation modules (*cas1* and *cas2*) but

RNA processing and effector complex formation has been experimentally demonstrated for these systems in *Aromatoleum aromaticum*, in which a chromosomal type I-C CRISPR is also present (Ozcan et al., 2019). Importantly, we also noted that type IV CRISPR-Cas system-positive plasmids were found only in bacteria with chromosomal type I-E or I-E\* CRISPR-Cas, suggesting cross-talk between plasmid and chromosomal CRISPR which may compensate for the lack of adaptation and target cleavage functions encoded from plasmid mediated CRISPR.

Chromosomal CRISPR-Cas systems clearly protect some bacteria from horizontally acquired mobile elements (Palmer and Gilmore, 2010; Price et al., 2016). Multi-drug resistant *Enterococcus* lacking CRISPR-Cas (Palmer and Gilmore, 2010) more readily acquire new genes and adapt to new antibiotics (Price et al., 2016). *Vibrio cholerae* that acquired phage-inducible chromosomal islands (PICI) as a defense against bacteriophages (Novick et al., 2010; Seed, 2015) now must contend with bacteriophages that have acquired CRISPR-Cas with spacers directed against chromosomal PICI to inactivate that very defense system (Naser et al., 2017). We describe here a novel type IV CRISPR-Cas that is evidently circulating in Enterobacteriaceae plasmids, predominantly within *K. pneumoniae*, and appears to have a complementary relationship with chromosomal Type I-E/I-E\* CRISPRs. Plasmid CRISPR-Cas directed against other plasmids (and some *K. pneumoniae* chromosomes) provide another level of incompatibility in plasmid communities. Both plasmid and chromosomal CRISPR-Cas are evidently important determinants of the epidemiology of large antibiotic resistance plasmids in *K. pneumoniae*.

## DATA AVAILABILITY STATEMENT

All datasets generated for this study are included in the article/Supplementary Material.

## AUTHOR CONTRIBUTIONS

MK conceived and designed the study, and generated the data. MK and JI analyzed the data and wrote the manuscript.

## FUNDING

This work was funded by a grant G1145914, from the National Health and Medical Research Council (NHMRC), Australia.

## SUPPLEMENTARY MATERIAL

The Supplementary Material for this article can be found online at: <https://www.frontiersin.org/articles/10.3389/fmicb.2019.02934/full#supplementary-material>

## REFERENCES

- Austin, S., and Nordstrom, K. (1990). Partition-mediated incompatibility of bacterial plasmids. *Cell* 60, 351–354. doi: 10.1016/0092-8674(90)90584-2
- Aydin, S., Personne, Y., Newire, E., Laverick, R., Russell, O., Roberts, A. P., et al. (2017). Presence of Type I-F CRISPR/Cas systems is associated with antimicrobial susceptibility in *Escherichia coli*. *J. Antimicrob. Chemother.* 72, 2213–2218. doi: 10.1093/jac/dkx137
- Barrangou, R. (2015). Diversity of CRISPR-Cas immune systems and molecular machines. *Genome Biol.* 16:247. doi: 10.1186/s13059-015-0816-9
- Brouns, S. J., Jore, M. M., Lundgren, M., Westra, E. R., Slijkhuis, R. J., Snijders, A. P., et al. (2008). Small CRISPR RNAs guide antiviral defense in prokaryotes. *Science* 321, 960–964. doi: 10.1126/science.1159689
- Carattoli, A. (2009). Resistance plasmid families in *Enterobacteriaceae*. *Antimicrob. Agents Chemother.* 53, 2227–2238. doi: 10.1128/AAC.01707-8
- Carattoli, A. (2013). Plasmids and the spread of resistance. *Int. J. Med. Microbiol.* 303, 298–304. doi: 10.1016/j.ijmm.2013.02.001
- Carattoli, A., Zankari, E., Garcia-Fernandez, A., Voldby Larsen, M., Lund, O., Villa, L., et al. (2014). In silico detection and typing of plasmids using PlasmidFinder and plasmid multilocus sequence typing. *Antimicrob. Agents Chemother.* 58, 3895–3903. doi: 10.1128/AAC.02412-14
- Dionisio, F., Zilhao, R., and Gama, J. A. (2019). Interactions between plasmids and other mobile genetic elements affect their transmission and persistence. *Plasmid* 102, 29–36. doi: 10.1016/j.plasmid.2019.01.003
- Enas Newire, A. A., Samina, J., Virve, E., and Adam, R. (2019). Identification of a Type IV CRISPR-Cas system located exclusively on IncHI1B/IncFIB plasmids in *Enterobacteriaceae*. *bioRxiv[Preprints]* doi: 10.1101/536375
- Faure, G., Shmakov, S. A., Yan, W. X., Cheng, D. R., Scott, D. A., Peters, J. E., et al. (2019). CRISPR-Cas in mobile genetic elements: counter-defence and beyond. *Nat. Rev. Microbiol.* 17, 513–525. doi: 10.1038/s41579-019-0204-7
- Frost, L. S., Leplae, R., Summers, A. O., and Toussaint, A. (2005). Mobile genetic elements: the agents of open source evolution. *Nat. Rev. Microbiol.* 3, 722–732. doi: 10.1038/nrmicro1235
- Garcia-Fernandez, A., Villa, L., Carta, C., Venditti, C., Giordano, A., Venditti, M., et al. (2012). *Klebsiella pneumoniae* ST258 producing KPC-3 identified in Italy carries novel plasmids and OmpK36/OmpK35 porin variants. *Antimicrob. Agents Chemother.* 56, 2143–2145. doi: 10.1128/AAC.05308-11
- Garneau, J. E., Dupuis, M. E., Villion, M., Romero, D. A., Barrangou, R., Boyaval, P., et al. (2010). The CRISPR/Cas bacterial immune system cleaves bacteriophage and plasmid DNA. *Nature* 468, 67–71. doi: 10.1038/nature09523
- Gasiunas, G., Barrangou, R., Horvath, P., and Siksnys, V. (2012). Cas9-crRNA ribonucleoprotein complex mediates specific DNA cleavage for adaptive immunity in bacteria. *Proc. Natl. Acad. Sci. U.S.A.* 109, E2579–E2586. doi: 10.1073/pnas.1208507109
- Grissa, I., Vergnaud, G., and Pourcel, C. (2007). CRISPRFinder: a web tool to identify clustered regularly interspaced short palindromic repeats. *Nucleic Acids Res.* 35, W52–W57. doi: 10.1093/nar/gkm360
- Hayes, F. (2003). Toxins-antitoxins: plasmid maintenance, programmed cell death, and cell cycle arrest. *Science* 301, 1496–1499. doi: 10.1126/science.1088157
- Hille, F., Richter, H., Wong, S. P., Bratovic, M., Ressel, S., and Charpentier, E. (2018). The biology of CRISPR-Cas: backward and forward. *Cell* 172, 1239–1259. doi: 10.1016/j.cell.2017.11.032
- Huang, W., Wang, G., Sebra, R., Zhuge, J., Yin, C., Aguero-Rosenfeld, M. E., et al. (2017). Emergence and evolution of multidrug-resistant *Klebsiella pneumoniae* with both blaKPC and blaCTX-M integrated in the chromosome. *Antimicrob. Agents Chemother.* 61:e00076-17. doi: 10.1128/AAC.00076-17
- Koonin, E. V., Makarova, K. S., Wolf, Y. I., and Krupovic, M. (2019). Evolutionary entanglement of mobile genetic elements and host defence systems: guns for hire. *Nat. Rev. Genet.* 1:77. doi: 10.1038/s41576-019-0172-9
- Koonin, E. V., Makarova, K. S., and Zhang, F. (2017). Diversity, classification and evolution of CRISPR-Cas systems. *Curr. Opin. Microbiol.* 37, 67–78. doi: 10.1016/j.mib.2017.05.008
- Li, H. Y., Kao, C. Y., Lin, W. H., Zheng, P. X., Yan, J. J., Wang, M. C., et al. (2018). Characterization of CRISPR-Cas systems in clinical *Klebsiella pneumoniae* isolates uncovers its potential association with antibiotic susceptibility. *Front. Microbiol.* 9:1595. doi: 10.3389/fmicb.2018.01595
- Makarova, K. S., Aravind, L., Wolf, Y. I., and Koonin, E. V. (2011a). Unification of Cas protein families and a simple scenario for the origin and evolution of CRISPR-Cas systems. *Biol. Direct.* 6:38. doi: 10.1186/1745-6150-6-38
- Makarova, K. S., Haft, D. H., Barrangou, R., Brouns, S. J., Charpentier, E., Horvath, P., et al. (2011b). Evolution and classification of the CRISPR-Cas systems. *Nat. Rev. Microbiol.* 9, 467–477. doi: 10.1038/nrmicro2577
- Makarova, K. S., Wolf, Y. I., Alkhnbashi, O. S., Costa, F., Shah, S. A., Saunders, S. J., et al. (2015). An updated evolutionary classification of CRISPR-Cas systems. *Nat. Rev. Microbiol.* 13, 722–736. doi: 10.1038/nrmicro3569
- Makarova, K. S., Wolf, Y. I., and Koonin, E. V. (2018). Classification and nomenclature of CRISPR-Cas systems: where from here? *CRISPR J.* 1, 325–336. doi: 10.1089/crispr.2018.0033
- Marraffini, L. A. (2015). CRISPR-Cas immunity in prokaryotes. *Nature* 526, 55–61. doi: 10.1038/nature15386
- Naser, I. B., Hoque, M. M., Nahid, M. A., Tareq, T. M., Rocky, M. K., and Faruque, S. M. (2017). Analysis of the CRISPR-Cas system in bacteriophages active on epidemic strains of *Vibrio cholerae* in Bangladesh. *Sci. Rep.* 7:14880. doi: 10.1038/s41598-017-14839-2
- Navon-Venezia, S., Kondratyeva, K., and Carattoli, A. (2017). *Klebsiella pneumoniae*: a major worldwide source and shuttle for antibiotic resistance. *FEMS Microbiol. Rev.* 41, 252–275. doi: 10.1093/femsre/fux013
- Novick, R. P. (1987). Plasmid incompatibility. *Microbiol. Rev.* 51, 381–395.
- Novick, R. P., Christie, G. E., and Penades, J. R. (2010). The phage-related chromosomal islands of Gram-positive bacteria. *Nat. Rev. Microbiol.* 8, 541–551. doi: 10.1038/nrmicro2393
- Ostria-Hernandez, M. L., Sanchez-Vallejo, C. J., Ibarra, J. A., and Castro-Escarpulli, G. (2015). Survey of clustered regularly interspaced short palindromic repeats and their associated Cas proteins (CRISPR/Cas) systems in multiple sequenced strains of *Klebsiella pneumoniae*. *BMC Res. Notes* 8:332. doi: 10.1186/s13104-015-1285-7
- Ozcan, A., Pausch, P., Linden, A., Wulf, A., Schuhle, K., Heider, J., et al. (2019). Type IV CRISPR RNA processing and effector complex formation in *Aromatoleum aromaticum*. *Nat. Microbiol.* 4, 89–96. doi: 10.1038/s41564-018-0274-8
- Palmer, K. L., and Gilmore, M. S. (2010). Multidrug-resistant enterococci lack CRISPR-cas. *mBio* 1:e00227-10. doi: 10.1128/mBio.00227-10
- Pinilla-Redondo, R., Mayo-Muñoz, D., Russel, J., Garrett, R. A., Randau, L., and Sørensen, S. J. (2019). Type IV CRISPR-Cas systems are highly diverse and involved in competition between plasmids. *bioRxiv[Preprints]* doi: 10.1101/780106
- Podschun, R., and Ullmann, U. (1998). *Klebsiella* spp. as nosocomial pathogens: epidemiology, taxonomy, typing methods, and pathogenicity factors. *Clin. Microbiol. Rev.* 11, 589–603. doi: 10.1128/cmr.11.4.589
- Price, V. J., Huo, W., Sharifi, A., and Palmer, K. L. (2016). CRISPR-Cas and restriction-modification act additively against conjugative antibiotic resistance plasmid transfer in *Enterococcus faecalis*. *mSphere* 1:e00064-16. doi: 10.1128/mSphere.00064-16
- Samson, J. E., Magadan, A. H., and Moineau, S. (2015). The CRISPR-Cas immune system and genetic transfers: reaching an equilibrium. *Microbiol. Spectr.* 3:PLAS-0034–2014. doi: 10.1128/microbiolspec.PLAS-0034-2014
- San Millan, A., and MacLean, R. C. (2017). Fitness costs of plasmids: a limit to plasmid transmission. *Microbiol. Spectr.* 5:MTBP0016-2017. doi: 10.1128/microbiolspec.MTBP-0016-2017
- Seed, K. D. (2015). Battling phages: how bacteria defend against viral attack. *PLoS Pathog.* 11:e1004847. doi: 10.1371/journal.ppat.1004847
- Shen, J., Lv, L., Wang, X., Xiu, Z., and Chen, G. (2017). Comparative analysis of CRISPR-Cas systems in *Klebsiella* genomes. *J. Basic Microbiol.* 57, 325–336. doi: 10.1002/jobm.201600589



- Tamulaitis, G., Kazlauskienė, M., Manakova, E., Venclovas, C., Nwokeoji, A. O., Dickman, M. J., et al. (2014). Programmable RNA shredding by the type III-A CRISPR-Cas system of *Streptococcus thermophilus*. *Mol. Cell* 56, 506–517. doi: 10.1016/j.molcel.2014.09.027
- van der Oost, J., Jore, M. M., Westra, E. R., Lundgren, M., and Brouns, S. J. (2009). CRISPR-based adaptive and heritable immunity in prokaryotes. *Trends Biochem. Sci.* 34, 401–407. doi: 10.1016/j.tibs.2009.05.002
- Villa, L., and Carattoli, A. (2020). Plasmid typing and classification. *Methods Mol. Biol.* 2075, 309–321. doi: 10.1007/978-1-4939-9877-7\_22
- Yamaguchi, Y., Park, J. H., and Inouye, M. (2011). Toxin-antitoxin systems in bacteria and archaea. *Annu. Rev. Genet.* 45, 61–79. doi: 10.1146/annurev-genet-110410-132412
- Zhang, Q., and Ye, Y. (2017). Not all predicted CRISPR-Cas systems are equal: isolated cas genes and classes of CRISPR like elements. *BMC Bioinformatics* 18:92. doi: 10.1186/s12859-017-1512-4
- Zheng, P. X., Chiang-Ni, C., Wang, S. Y., Tsai, P. J., Kuo, C. F., Chuang, W. J., et al. (2014). Arrangement and number of clustered regularly interspaced short palindromic repeat spacers are associated with erythromycin susceptibility in emm12, emm75 and emm92 of group A streptococcus. *Clin. Microbiol. Infect.* 20, 516–523. doi: 10.1111/1469-0691.12379

**Conflict of Interest:** The authors declare that the research was conducted in the absence of any commercial or financial relationships that could be construed as a potential conflict of interest.

Copyright © 2020 Kamruzzaman and Iredell. This is an open-access article distributed under the terms of the Creative Commons Attribution License (CC BY). The use, distribution or reproduction in other forums is permitted, provided the original author(s) and the copyright owner(s) are credited and that the original publication in this journal is cited, in accordance with accepted academic practice. No use, distribution or reproduction is permitted which does not comply with these terms.



# Linezolid and Rifampicin Combination to Combat *cfr*-Positive Multidrug-Resistant MRSA in Murine Models of Bacteremia and Skin and Skin Structure Infection

Yu-Feng Zhou<sup>1,2†</sup>, Liang Li<sup>3†</sup>, Meng-Ting Tao<sup>1,2</sup>, Jian Sun<sup>1,2</sup>, Xiao-Ping Liao<sup>1,2</sup>, Ya-Hong Liu<sup>1,2,4\*</sup> and Yan Q. Xiong<sup>3,5</sup>

<sup>1</sup> National Risk Assessment Laboratory for Antimicrobial Resistance of Animal Original Bacteria, College of Veterinary Medicine, South China Agricultural University, Guangzhou, China, <sup>2</sup> Guangdong Provincial Key Laboratory of Veterinary Pharmaceutics Development and Safety Evaluation, South China Agricultural University, Guangzhou, China, <sup>3</sup> The Lundquist Institute for Biomedical Innovation at Harbor-UCLA Medical Center, Torrance, CA, United States, <sup>4</sup> Jiangsu Co-Innovation Center for the Prevention and Control of Important Animal Infectious Diseases and Zoonoses, Yangzhou University, Yangzhou, China, <sup>5</sup> David Geffen School of Medicine at UCLA, Los Angeles, CA, United States

## OPEN ACCESS

### Edited by:

Leonardo Neves de Andrade,  
University of São Paulo, Brazil

### Reviewed by:

Sandeep Sharma,  
Lovely Professional University, India  
Xiang-Dang Du,  
Henan Agricultural University, China

### \*Correspondence:

Ya-Hong Liu  
lyh@scau.edu.cn

†These authors have contributed  
equally to this work

### Specialty section:

This article was submitted to  
Antimicrobials, Resistance  
and Chemotherapy,  
a section of the journal  
Frontiers in Microbiology

Received: 09 September 2019

Accepted: 19 December 2019

Published: 14 January 2020

### Citation:

Zhou Y-F, Li L, Tao M-T, Sun J,  
Liao X-P, Liu Y-H and Xiong YQ (2020)  
Linezolid and Rifampicin Combination  
to Combat *cfr*-Positive  
Multidrug-Resistant MRSA in Murine  
Models of Bacteremia and Skin  
and Skin Structure Infection.  
*Front. Microbiol.* 10:3080.  
doi: 10.3389/fmicb.2019.03080

Linezolid resistance mediated by the *cfr* gene in MRSA represents a global concern. We investigated relevant phenotype differences between *cfr*-positive and -negative MRSA that contribute to pathogenesis, and the efficacy of linezolid-based combination therapies in murine models of bacteremia and skin and skin structure infection (SSSI). As a group, *cfr*-positive MRSA exhibited significantly reduced susceptibilities to the host defense peptides tPMPs, human neutrophil peptide-1 (hNP-1), and cathelicidin LL-37 ( $P < 0.01$ ). In addition, increased binding to fibronectin (FN) and endothelial cells paralleled robust biofilm formation in *cfr*-positive vs. -negative MRSA. *In vitro* phenotypes of *cfr*-positive MRSA translated into poor outcomes of linezolid monotherapy *in vivo* in murine bacteremia and SSSI models. Importantly, rifampicin showed synergistic activity as a combinatorial partner with linezolid, and the EC<sub>50</sub> of linezolid decreased 6-fold in the presence of rifampicin. Furthermore, this combination therapy displayed efficacy against *cfr*-positive MRSA at clinically relevant doses. Altogether, these data suggest that the use of linezolid in combination with rifampicin poses a viable therapeutic alternative for bacteremia and SSSI caused by *cfr*-positive multidrug resistant MRSA.

**Keywords:** MRSA, *cfr*, phenotype, biofilm, bacteremia, skin and skin structure infection, combination therapy

## INTRODUCTION

MRSA is particularly challenging due to its inherent pathogenicity and multidrug resistant phenotypes contributing to a variety of infectious diseases, ranging from skin and skin structure infection (SSSI) to bacteremia (Tong et al., 2015; Wang et al., 2019). An increased global incidence of MRSA infections associated with high mortality has been observed over the past decades (Bassetti et al., 2014; Hassoun et al., 2017). For example, in the United States, *S. aureus* is most often contracted as a nosocomial infection leading to more than 80,000 illnesses and 11,000 deaths yearly

(Lepak and Andes, 2016). Therefore, new alternative strategies for the treatment of such infections are urgently needed.

Linezolid has become an important drug for treating nosocomial infections due to MRSA, including those with reduced vancomycin susceptibility (e.g., VISA) (Dryden, 2011). However, linezolid resistance due to acquisition of the *cfr* (chloramphenicol and florfenicol resistance) gene has compromised MRSA treatment options (Long et al., 2006). The *cfr* gene encodes a 23S rRNA methyltransferase that confers combined resistance to phenicol, lincosamides, oxazolidinones, pleuromutilins, and streptogramin A (PhLOPS<sub>A</sub> phenotype) (Long et al., 2006; Witte and Cuny, 2011). In addition, there is only a low fitness cost to the host for *cfr* carriage and this facilitates its spread (LaMarre et al., 2011). Infections due to *cfr*-positive MRSA are increasing and pose a serious threat to the clinical success of oxazolidinone antibiotics (Witte and Cuny, 2011). Although the level of resistance to linezolid conferred by *cfr* is moderate, the ability of *cfr* to enhance bacterial survival in the presence of linezolid has been shown *in vivo* in a murine pneumonia model (Zhou et al., 2018). Linezolid-resistant MRSA strains carrying *cfr* were also associated with prolonged use of linezolid in patients (Endimiani et al., 2011). These data suggest that in addition to the *cfr*-mediated linezolid resistance, *cfr*-positive MRSA may possess phenotypes associated with pathogenesis that contribute to poor *in vivo* treatment outcomes.

In this study, we profiled relevant phenotype differences between *cfr*-positive and -negative MRSA that contribute to bacteremia and SSSI. We examined whether these MRSA were susceptible to host defense cationic peptides (HDP) and assayed their biofilm forming abilities and binding to fibronectin (FN) and endothelial cells. In addition, we correlated *in vitro* phenotypes to linezolid resistance *in vivo* in murine SSSI and bacteremia models to characterize *cfr*-positive and -negative MRSA.

## MATERIALS AND METHODS

### Bacterial Strains and Background Information

Ten well-characterized MRSA strains were used in this study (Li et al., 2018; Zhou et al., 2018). Human clinical MRSA strains (161402, 161400, 161494, and 161813) were kindly provided by the Third Affiliated Hospital of Sun Yat-sen University (Guangzhou, China) that obtained from hospitalized patients with pulmonary infections. MRSA strains of animal origin (N50, 6Y2C, HYP6, N4-2, HYXC4, and 2B3) were collected from blood and abscess cultures of sick animals at the Animal Diagnostic Laboratory of South China Agricultural University. All strains were identified by MALDI-TOF MS system (Ostergaard et al., 2015). Four MRSA strains of human origin were typed as ST 764 and *spa*-type t1081, and the remaining six strains were typed as ST 398 and ST 9 (Li et al., 2018; Zhou et al., 2018). The ST 764 MRSA has emerged as a novel hybrid variant of the ST 5 HA-MRSA lineage with the characteristics of CA-MRSA in Asia, causing invasive infections (necrotizing

fasciitis and bacteremia) in both hospital and community settings (Takano et al., 2013). The ST 398 MRSA has been reported in China and Europe that was responsible for zoonotic infections in patients with pneumonia and SSSIs (Stegger et al., 2010; van der Mee-Marquet et al., 2011).

### Linezolid-Based Combination Susceptibility Testing and Time-Kill Curves

The MICs of linezolid and other ten antibiotics (oxacillin, cefotaxime, amikacin, azithromycin, tetracycline, vancomycin, clindamycin, retapamulin, ciprofloxacin, and rifampicin) against clinical MRSA isolates were conducted by the broth microdilution method as recommended (CLSI, 2015). *S. aureus* ATCC 29213 served as the quality control strain. Fold reduction in MIC was determined by dividing the MIC of the antibiotic alone by its MIC in the presence of 0.5 mg/L linezolid. Three biological replicates were done for each combination and the means of fold reduction were used for generating heat maps. *In vitro* interactions between linezolid and rifampicin were evaluated by the checkerboard method, and a fractional inhibitory concentration index (FICI) of  $\leq 0.5$  was deemed synergistic (Zhou et al., 2018).

*In vitro* time-kill curves were performed to compare the activity of linezolid and rifampicin alone and in combination against two representative *cfr*-positive and -negative strain sets. In brief, a starting inoculum of  $\sim 10^6$  cfu/mL logarithmic phase MRSA cells was used to expose to linezolid (16 mg/L) with or without rifampicin (0.5 mg/L). The drug concentrations were chosen to mimic the free serum steady-state peak concentrations ( $fC_{max}$ ) at the usual clinical doses in human (i.e., 600 mg for linezolid, 300 mg for rifampicin) (Andes et al., 2002; Sirgel et al., 2005; Chik et al., 2010; Dryden, 2011). MRSA densities were determined by the serial viable counts collected over 24 h incubation and expressed as  $\log_{10}$  cfu/mL. Synergistic effect was defined as the combination caused  $\geq 2 \log_{10}$  cfu/mL reduction vs. the single drug.

### *In vitro* Concentration-Effect Relationship

Concentration-effect curves were used to evaluate linezolid potency against *cfr*-positive and -negative MRSA. Briefly, an overnight culture of MRSA cell was washed, adjusted to 0.5 McFarland units and diluted in cation-adjusted Mueller Hinton broth to a final density of  $10^6$  cfu/mL. The testing procedure consisted of two groups, and each group included tubes with two-fold increasing concentrations of linezolid from 0.015 to 32 mg/L, in the presence and absence of  $0.5 \times$  MIC rifampicin. After 16 h of incubation at 37°C, absorbance of each tube was measured at OD<sub>600nm</sub> to quantify bacterial growth and normalized with the no drug control. The relationship between linezolid concentrations and antibacterial potency was calculated using the Hill sigmoid  $E_{max}$  equation:  $E = E_{max} + (E_0 - E_{max}) / (1 + 10^{-(\log EC_{50} - C) \times \text{Hill slope}})$  using GraphPad Prism 8 software (Zhou et al., 2017).

## In vitro HDP Susceptibility

The tPMPs were prepared from thrombin-stimulated platelets isolated from fresh rabbit blood and their bioactivity was quantified using *Bacillus subtilis* ATCC 6633 as previously described (Yeaman et al., 1992). Human neutrophil peptide-1 (hNP-1) and cathelicidin LL-37 were purchased from Peptides International (Louisville, KY, United States) and Eurogentec (Fremont, CA, United States), respectively. *In vitro* HDP susceptibilities were assessed by adding tPMP (2 mg/L equivalent) to  $10^3$  cfu/mL MRSA cells and hNP-1 (5 mg/L) or LL-37 (20 mg/L) to  $10^5$  cfu/mL MRSA cells (Xiong et al., 2009; Seidl et al., 2011a). The HDP concentrations were selected to cover the peptide concentrations that did not rapidly kill MRSA cells over 2 h of incubation based on previous studies (Seidl et al., 2011a). Results were expressed as the percentage of the initial inoculum that survived exposure to HDPs.

## Adherence to Fibronectin and Endothelial Cells

Six-well tissue culture plates were coated using 50 mg/L purified human FN (Sigma Chemical, St. Louis, MO, United States) overnight at 4°C, and then treated with 3% bovine serum albumin for 3 h to prevent non-specific adhesion (Xiong et al., 2009). The human microvascular endothelial cell line (HMEC-1) was cultured as previously described (Seidl et al., 2012). Logarithmic-phase MRSA cells were added to FN-coated plates ( $5 \times 10^3$  cfu/mL) and endothelial cell monolayer-coated plates ( $5 \times 10^5$  cfu/mL; MOI = 1:1), and then incubated for 1 h at 37°C under static conditions. For FN binding assay, unbound bacteria were removed by washing the plates with PBS, and melted tryptic soy agar (TSA; 2 mL) was added into each well and allowed to solidify. For endothelial cell binding assay, unbound bacteria were removed by washing the plates with Hanks balanced salt solution (HBSS) and permeabilized using 1.0% Triton X-100 (Seidl et al., 2012), after which bacterial numbers per well were determined by serial dilutions and plating on TSA. Adherence was expressed as the percentage of the initial inoculum bound.

## Biofilm Formation, Extracellular Polysaccharide (EPS) and DNA Determinations

The ability of MRSA to form biofilm was determined as described previously (Seidl et al., 2011a). Briefly, overnight cultured MRSA at 0.5 McFarland units ( $\sim 10^8$  cfu/mL) was diluted 1:100 into brain heart infusion (BHI) broth supplemented with 0.5% glucose. 200  $\mu$ L of the suspension was transferred into 96-well plates and incubated for 18 h at 37°C. After incubation, the plates were washed with PBS, air dried and stained with 0.1% safranin. The adhering dye was dissolved in 30% acetic acid, and absorption was measured at OD<sub>490nm</sub> to quantify biofilm formation.

The water-soluble and -insoluble EPS synthesized by the biofilms was examined using the anthrone-sulfuric method (Chen et al., 2016). Briefly, 24 h biofilms were rinsed, removed and dispersed by sonication at 20 kHz for 5 s. The suspension was centrifuged at  $6000 \times g$  for 10 min at 4°C, and the supernatant

was collected for water-soluble EPS determinations. The pellets were resuspended in PBS, washed and air-dried to ensure all the water-soluble EPS was discarded. The dry weight of each biofilm was measured to adjust biomass differences between *cfr*-positive and -negative MRSA. The water-insoluble EPS was extracted using 1.0 M NaOH under agitation for 2 h at 37°C and quantified using an anthrone-sulfuric acid colorimetric assay (Chen et al., 2016).

Release of extracellular DNA (eDNA) was determined from 18 h MRSA biofilm using a microplate fluorescence assay with Hoechst dye 33258 (Leggate et al., 2006). Protocols for extraction and purification of eDNA from MRSA biofilms were described in detail elsewhere (Rice et al., 2007). The eDNA was quantified using an EnSight fluorescence plate reader at Ex<sub>350</sub>/Em<sub>460</sub> (PerkinElmer, Waltham, MA, United States). Purified salmon sperm DNA was used to generate a standard curve. To account for differences in biomass, the average OD<sub>490nm</sub> of each unwashed biofilm was determined to calculate the amount of eDNA per relative biomass.

## Hemolytic Activity and Nuclease Production

Hemolytic activity was evaluated by spotting 2  $\mu$ L of MRSA suspension ( $\sim 10^8$  cfu/mL) onto 5% sheep blood agar plates and incubated at 37°C for 24 h (Seidl et al., 2011b). The diameters of the zones of clearance (cm) indicating hemolytic activity were measured. Nuclease production was assessed by spotting 15  $\mu$ L of filtered culture supernatants of the strains into wells cut into DNase test agar (Beenken et al., 2010). Plates were incubated overnight at 37°C. Nuclease activity was then assessed by overlaying the agar with 1 M HCl to precipitate undigested DNA and define the zone diameters (cm) of clearance (Beenken et al., 2010).

## In vivo Murine Bacteremia and SSSI Models

Six-week-old, pathogen-free female ICR mice (25–27 g from Guangdong Medical Lab Animal Center, Guangzhou, China) were used in this study. All animal experimental procedures were approved by the South China Agricultural University (SCAU) Institutional Ethics Committee (2017B075 and 2017018) and performed in accordance with the SCAU Institutional Laboratory Animal Care and Use guidelines. For bacteremia model, mice were infected *via* the tail vein with a 0.5 mL bacterial suspension delivering  $\sim 10^{5.5-6.0}$  cfu/mouse (Thakker et al., 1998). For SSSI model, 0.1 mL of bacterial suspension consisting of  $\sim 10^{7.0}$  cfu was inoculated subcutaneously into the flanks of mice (Tseng et al., 2011). Four representative MRSA strains were selected for *in vivo* studies based on their *in vitro* phenotypes and MLST types that included *cfr*-positive and -negative MRSA.

To assess the therapeutic efficacy of linezolid and rifampicin alone and in combination, mice were randomized at 24 h (bacteremia model) and 48 h (SSSI model) post-infection to receive: (i) no therapy (control); (ii) linezolid at 100 mg/kg, orally twice daily; (iii) rifampicin at 5 mg/kg, orally twice daily; or (iv) a combination of linezolid and rifampicin. The linezolid and



rifampicin doses were selected to mimic the pharmacokinetic profiles of recommended human clinical doses (i.e., 600 mg and 300 mg, orally twice daily for linezolid and rifampicin, respectively) (Chik et al., 2010; Zhou et al., 2018). Treatments lasted for 3 and 5 days for the bacteremia and SSSI models, respectively. Groups of five or six mice were included at each dose regimen. Control and antibiotic-treated mice were sacrificed either at the beginning of treatment (untreated controls) or 12 h after the last antibiotic dose, respectively. At sacrifice, the target tissues (blood, spleen and kidney for bacteremia model, and skin abscess for SSSI model) were removed and quantitatively cultured. Bacterial densities in infected tissues were calculated as the mean  $\log_{10}$  cfu/g. of tissue and  $\log_{10}$  cfu/mL of blood ( $\pm$  SD). In addition, the mean areas of superficial skin lesions were quantitated for statistical comparisons in the SSSI model.

## Statistical Analysis

*In vitro* studies were performed with three biological replicates in triplicate. Two-tailed Student's *t*-test was used to compare relevant phenotype differences between *cfr*-positive and -negative MRSA groups. Mann-Whitney non-parametric test was used to analyze MRSA densities in target tissue among different groups.

## RESULTS

### Linezolid-Based Combination Potentiated Activity Against *cfr*-Positive MRSA

As expected, all the study MRSA isolates were resistant to oxacillin with MICs ranging from 8 to 128 mg/L. The MICs of linezolid were markedly higher in MRSA isolates harboring the *cfr* gene (1–8 mg/L) than in those lacking the *cfr* (0.5–2 mg/L; **Table 1**). Fold reductions in MICs of amikacin and

vancomycin were observed for part of *cfr*-positive MRSA isolates when combined with the sub-MIC levels of linezolid at 0.5 mg/L. However, the broad-spectrum antibiotics including cefotaxime and ciprofloxacin displayed a limited MIC reduction. Notably, in the presence of linezolid, rifampicin achieved the highest therapeutic potential as a combinatorial partner with a greater than 8-fold reduction in MIC against 8/10 MRSA isolates, and this was independent of *cfr* expression (**Figure 1A**). The combination of linezolid and rifampicin resulted in synergistic activity against 5/6 *cfr*-positive MRSA isolates and 2/4 *cfr*-negative MRSA isolates, with FICIs ranging from 0.375 to 0.5 (**Table 1**).

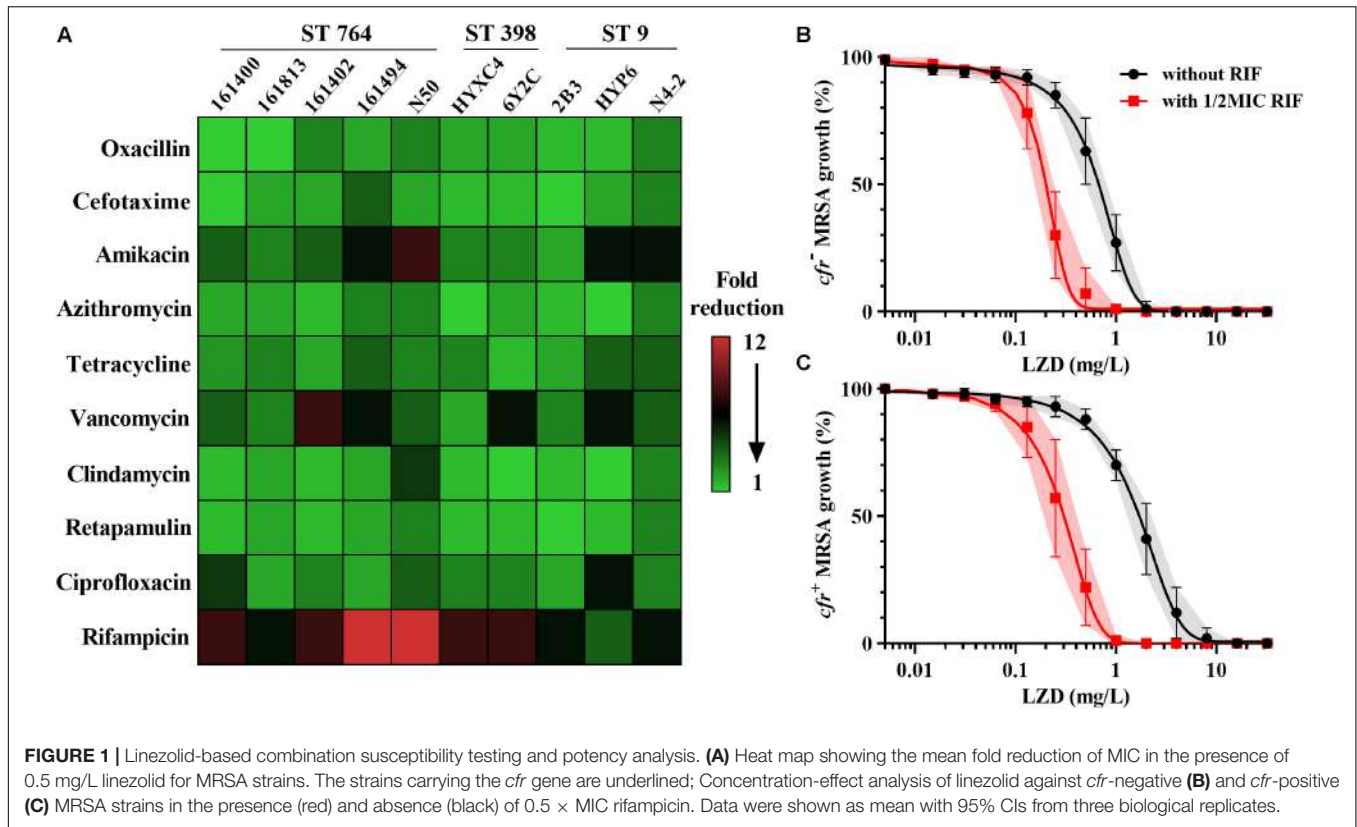
Control cultures increased  $\sim 3\text{-log}_{10}$  cfu/mL for both *cfr*-positive and -negative MRSA over a 24 h of incubation. Rifampicin alone had the similar bacterial growths vs. their control groups (**Supplementary Figure S1**). Of note, despite having the same MICs, linezolid alone at 16 mg/L resulted in greater bacterial killing for *cfr*-negative strain HYXC4 (1.70- $\log_{10}$  cfu/mL) vs. the *cfr*-positive strain 6Y2C (0.78- $\log_{10}$  cfu/mL; **Supplementary Figure S1**). Importantly, the combination of linezolid (16 mg/L) and rifampicin (0.5 mg/L) showed a synergistic bactericidal effect compared to each drug alone regardless of the presence of *cfr* gene (**Supplementary Figure S1**).

For *cfr*-negative MRSA group, the 50% maximal killing effect occurred at an average linezolid concentration of 0.71 mg/L (**Figure 1B**) and this decreased 3.4-fold to 0.21 mg/L in the presence of sub-MIC levels of rifampicin (**Supplementary Table S1**; paired *t*-test,  $P < 0.01$ ). Expression of the *cfr* gene increased linezolid concentrations required to achieve 50% maximal effect to 2.01 mg/L and were significantly higher than the *cfr*-negative test group (**Table 2**;  $P < 0.05$ ). However, when combined with rifampicin, the concentration of linezolid required to achieve 50% maximal effect was only 0.34 mg/L for *cfr*-positive MRSA group (**Figure 1C**). In fact, this level was comparable to the concentration required to potentiate rifampicin for *cfr*-negative

**TABLE 1** | Genotypic summary and MICs for study MRSA isolates.

MRSA strains	MLST	<i>spa</i> types	MIC (mg/L) <sup>a</sup>			FICI <sup>b</sup>
			OXA	LZD	RIF	
<b><i>cfr</i>-positive</b>						
161402	ST764	t1084	128	8	1	0.375
161494	ST764	t1084	128	4	1	0.5
N50	ST764	t899	32	2	8	0.25
6Y2C	ST398	t7829	16	2	8	0.5
HYP6	ST9	t899	64	1	0.12	0.5
N4-2	ST9	t899	32	1	16	0.75
<b><i>cfr</i>-negative</b>						
161400	ST764	t1084	32	1	0.5	0.5
161813	ST764	t1084	32	0.5	1	0.75
HYXC4	ST398	t7880	8	2	4	0.375
2B3	ST9	t899	64	1	0.25	0.625
<b>ATCC strain</b>						
29213	ST5	t002	0.25	1	0.008	0.5

<sup>a</sup>OXA, oxacillin; LZD, linezolid; RIF, rifampicin. <sup>b</sup>Interpreted as synergy (FICI  $\leq$  0.5), no interaction (0.5 < FICI  $\leq$  4) or antagonism (FICI > 4).



group (Table 2). Although the concentration of 0.34 mg/L linezolid was insufficient to inhibit growth of MRSA carrying the *cfr* gene, its combination with rifampicin provided a promising alternative to overcome MRSA infections irrespective of *cfr* expression.

### In vitro HDPs Susceptibility and Adherence to FN and Endothelial Cells

As a group, the *cfr*-positive MRSA exhibited significantly higher survival rates after exposure to 2 mg/L tPMP (73.8%) or 5 mg/L hNP-1 (78.5%) compared with the *cfr*-negative strain group (43.1 and 57.7%, respectively;  $P < 0.01$ ). Similarly, a markedly reduced LL-37 killing was observed in *cfr*-positive vs. *cfr*-negative MRSA group ( $P < 0.005$ ; Figure 2A). The *cfr*-positive MRSA

demonstrated significantly higher binding rates to FN (14.8%) compared with the *cfr*-negative MRSA (4.02%;  $P < 0.005$ ), despite a relatively low adherence to FN observed with the *cfr*-positive strain N4-2. Consistent with FN binding profiles, *cfr*-positive MRSA strain group bound substantially better to human endothelial cells than *cfr*-negative group (11.30 vs. 3.87%,  $P < 0.005$ ; Figure 2B).

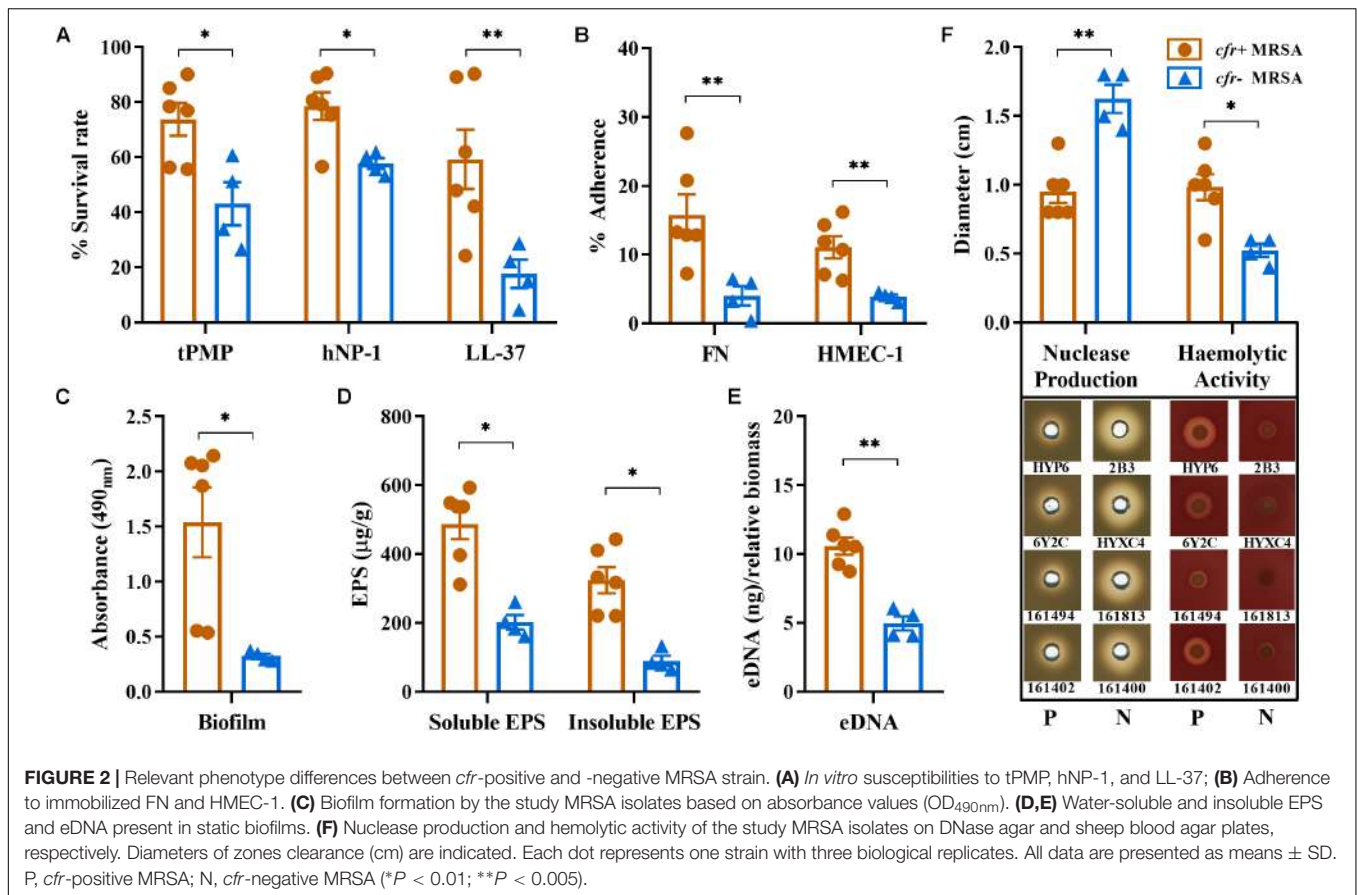
### Biofilm Formation, EPS and eDNA Determinations and Nuclease Productions

We compared *cfr*-positive and -negative MRSA strain groups with respect to *in vitro* biofilm capacity and composition. Overall, the *cfr*-positive MRSA group had a greater ability to form biofilms

**TABLE 2 |** Calculated EC<sub>50</sub> and Hill slope (*N*) values representing the antimicrobial potency of linezolid alone or with 0.5 × MIC rifampicin against *cfr*-positive and -negative MRSA strains.<sup>a</sup>

MRSA strains	Hill plot PD parameters					
	Linezolid alone			Linezolid + 0.5 × MIC rifampicin		
	EC <sub>50</sub> <sup>b</sup>	<i>N</i>	<i>R</i> <sup>2</sup>	EC <sub>50</sub> <sup>c</sup>	<i>N</i>	<i>R</i> <sup>2</sup>
<i>cfr</i> +	2.01 ± 0.53	3.95 ± 0.46	0.95 ± 0.02	0.34 ± 0.15	4.22 ± 0.54	0.96 ± 0.02
<i>cfr</i> -	0.71 ± 0.18	3.53 ± 0.87	0.94 ± 0.02	0.21 ± 0.05	3.66 ± 1.03	0.97 ± 0.02

<sup>a</sup>EC<sub>50</sub>, the linezolid concentration required to achieve 50% of maximal effect (*E*<sub>max</sub>); *N*, the Hill coefficient that described the slope of the dose-response curve. <sup>b</sup> $P < 0.05$  for EC<sub>50</sub> of linezolid alone in *cfr*-positive vs. -negative strains. <sup>c</sup> $P < 0.01$  for EC<sub>50</sub> of linezolid and rifampicin in combination vs. linezolid alone.



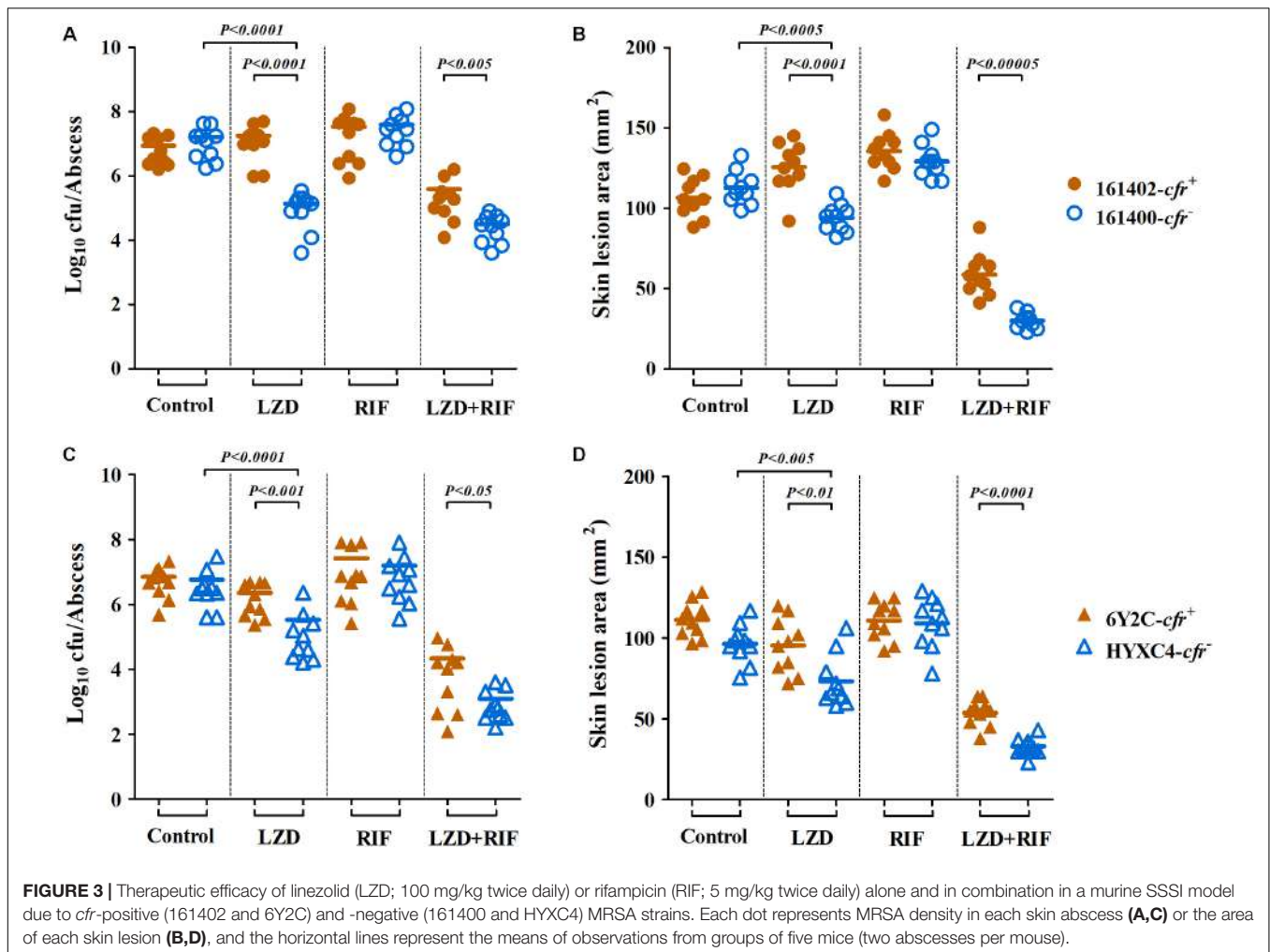
compared with the *cfr*-negative group (OD<sub>490nm</sub> 1.51 vs. 0.33, *P* < 0.01; **Figure 2C**). The production of the water-soluble EPS ranged from 161 to 593 μg/g, with the average production in *cfr*-positive group being considerably higher than that in *cfr*-negative group (487 μg/g vs. 202 μg/g, *P* < 0.01). A similar pattern was observed for the water-insoluble EPS between *cfr*-positive and -negative strain groups (*P* < 0.01; **Figure 2D**). Of note, the 24 h old MRSA biofilms showed increased production of the water-soluble EPS compared to water-insoluble EPS in both groups. In addition, the average amount of eDNA present in the *cfr*-positive MRSA biofilms (10.6 ± 1.37 ng) was 2.1-fold greater than that present in the *cfr*-negative MRSA biofilms (4.96 ± 0.88 ng), a statistically significant difference (*P* < 0.005; **Figure 2E**). These results were further corroborated by a significantly lower level of nuclease production in the *cfr*-positive MRSA group (*P* < 0.005; **Figure 2F**). In addition, except for strain 161494, the *cfr*-positive MRSA strain group possessed more α-hemolysin activity, compared with weak or non-detectable α-hemolysin production in *cfr*-negative MRSA group (**Figure 2F**).

### ***In vivo* Responsiveness to Linezolid and Rifampicin Alone and in Combination**

In the murine SSSI model, MRSA densities in skin abscesses and the areas of skin lesions in mice infected with *cfr*-negative MRSA isolates 161400 and HYXC4 were significantly reduced after

5 days of linezolid monotherapy as compared to their untreated controls (*P* < 0.005, **Figure 3**). In contrast, for *cfr*-positive MRSA isolates 161402 and 6Y2C, the mice did not respond to linezolid monotherapy and residual abscess-tissue MRSA densities and the areas of skin lesions similar to those in their respective controls (**Figure 3**). Of note, combination therapy with linezolid and rifampicin resulted in 1.5–3.6 log<sub>10</sub> cfu/abscess reductions in MRSA densities vs. linezolid monotherapy against both *cfr*-positive and -negative MRSA infections (**Figures 3A,C**). This result occurred despite the lower MRSA densities in skin abscesses observed in *cfr*-negative isolates (*P* < 0.05; **Figure 3**).

In the bacteremia model, we found the similar results. Linezolid monotherapy resulted in uniform and highly significant reductions of MRSA densities in all the target tissues of mice infected with *cfr*-negative MRSA isolates 161400 and HYXC4. For instance, a ≥2.0 log<sub>10</sub> cfu/mL reductions in blood density and ≥1.0 log<sub>10</sub> cfu/g reductions in spleen and kidney densities were observed with linezolid monotherapy as compared to their respective control mice infected with *cfr*-negative MRSA (*P* < 0.01). However, bacteremia caused by *cfr*-positive MRSA isolates showed the opposite results: (i) a ≥1.0 log<sub>10</sub> cfu/g increases in both spleen and kidney (161402, **Figures 4A,B**) or (ii) no response to linezolid monotherapy, with similar residual target-tissue MRSA densities compared with untreated controls (6Y2C; **Figures 4D–F**). Importantly, the combination of linezolid and rifampicin showed efficacies higher



than each monotherapy in mice infected with both *cfr*-positive and -negative MRSA ( $P < 0.001$ ; **Figure 4**).

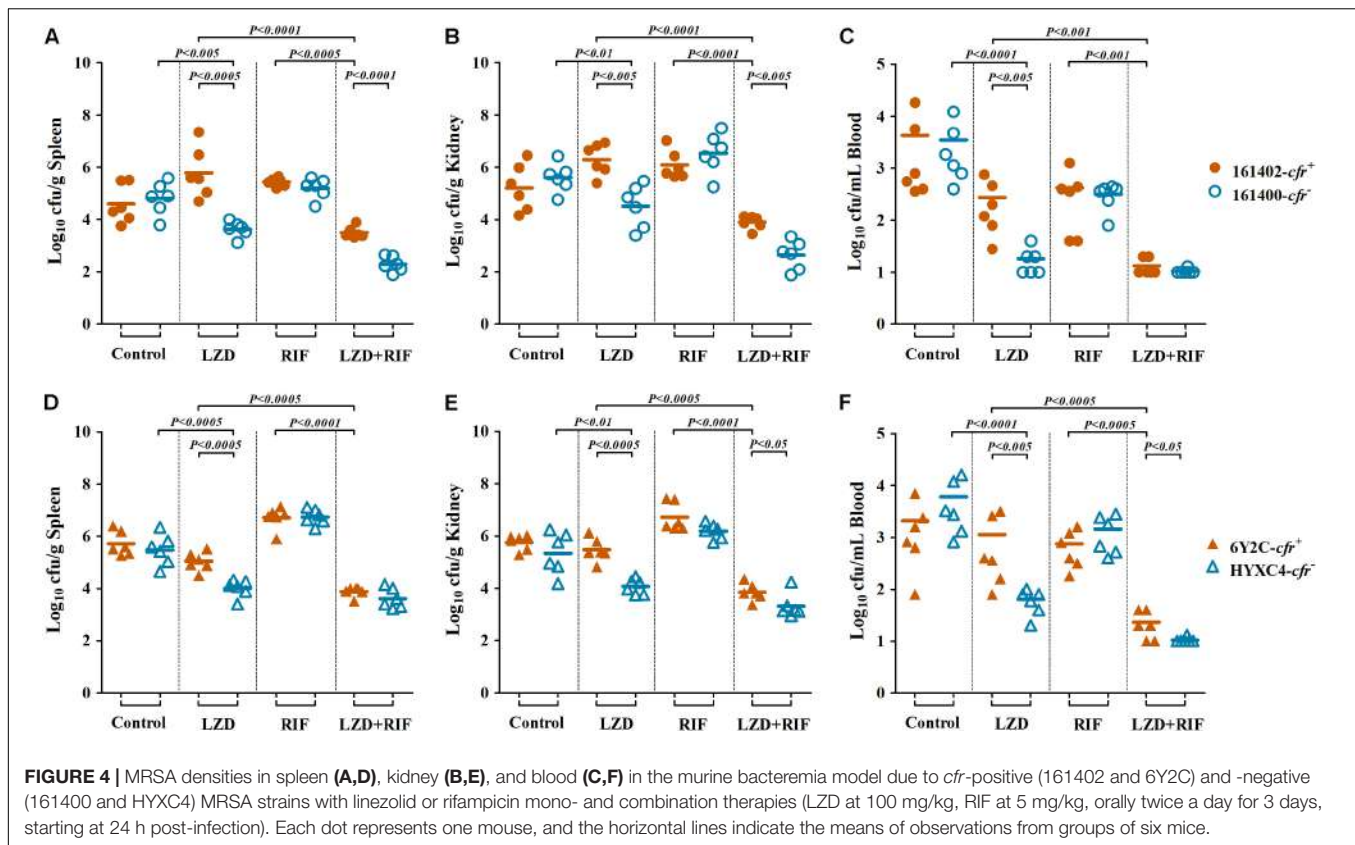
## DISCUSSION

*S. aureus* is a common opportunistic pathogen that causes a wide range of infections affecting skin and soft tissues as well as invasive infections that include bacteremia, endocarditis and pneumonia (Bassetti et al., 2014; Hassoun et al., 2017). In particular, bacteremia caused by MRSA is often associated with a high mortality rate, even with appropriate antibiotic treatments (Seidl et al., 2011a). Linezolid has been an important drug for therapy of MRSA infection. However, the emergence and rapid spread of horizontally transferable *cfr* determinant in MRSA has become a substantial concern (Witte and Cuny, 2011). The effective therapeutic alternatives were limited, especially for the vancomycin-intermediate and linezolid-resistant MRSA carrying *cfr* gene (Barber et al., 2016). Fortunately, unlike the chromosomally encoded resistance mechanisms, *cfr* has been shown to confer the low-level resistance to linezolid (Locke et al., 2014). Therefore, the combination

therapy is an appealing option for retaining the clinical utility of linezolid.

Linezolid is a valuable alternative to glycopeptide antibiotics (e.g., vancomycin) and an oral formulation allows a rapid intravenous to oral switch (Dryden, 2011; Bassetti et al., 2014). As described in previous clinical studies, linezolid achieved significantly greater efficacy (e.g., higher cure rates) and earlier discharges from hospital than vancomycin treatment in patients with MRSA-complicated SSSI (Sharpe et al., 2005). This clinical outcome may be ascribed to a good penetration into skin and soft tissues with almost 100% oral bioavailability (Bassetti et al., 2014). Furthermore, linezolid treatments for MRSA bacteremia had roughly equivalent clinical and microbiological outcomes compared with vancomycin (Shorr et al., 2005). In our previous pneumonia model, addition of rifampicin to linezolid significantly decreased fAUC/MIC targets in both plasma and lung epithelial lining fluid (Zhou et al., 2018). Here, we extended the effectiveness of linezolid and rifampicin combination to the clinically relevant murine models of SSSI and bacteremia due to *cfr*-positive and -negative MRSA. More importantly, rifampicin decreases *S. aureus* FN binding that is a further advantage of the combination therapy (Rasigade et al., 2011).





This is supported by other studies showing successful clinical outcomes with oral linezolid and rifampicin combination therapy in the management of recurrent and persistent MRSA bacteremia (Schwalm et al., 2004).

Indeed, we observed significant phenotype differences between *cfr*-positive and -negative MRSA that contribute to bacteremia and SSSI. The capability of *S. aureus* to circumvent clearance mediated by locally secreted HDPs is an important factor for its pathogenicity (Seidl et al., 2011a). In the current study, we demonstrated that *cfr*-positive MRSA isolates tended to be more resistant to key innate HDPs from neutrophils (hNP-1), platelets (tPMPs), and epithelial cells (LL-37), compared with the *cfr*-negative MRSA isolates. These findings suggested that *cfr*-positive MRSA might be more capable to survive in the bloodstream early in the course of skin infections. In particular, survival rates of >40% after 2 h of exposure to HDPs were positively correlated with the severity of endovascular infections and reduced responsiveness to antimicrobial therapy (Yeaman et al., 1992; Seidl et al., 2011a). Similarly, we observed a dramatic relationship between the reduced HDP killing *in vitro* and decreased efficacy of linezolid-based therapy in the murine bacteremia model.

Interestingly, *cfr*-positive MRSA group exhibited greater biofilm formation and higher EPS and eDNA productions compared with *cfr*-negative strain group. Biofilms enhance bacterial resistance to HDPs and antibiotics due to poor penetration past this barrier and this was the case for *cfr*-positive

MRSA (Donlan and Costerton, 2002). Cathelicidin LL-37 can protect against MRSA-induced skin infections but *cfr*-positive MRSA were also able to resist the adverse effects of LL-37 exposure (Haisma et al., 2014). The alterations may contribute to the poor outcomes of linezolid therapy in mice infected with *cfr*-positive MRSA isolates in the SSSI model.

Invasive *S. aureus* must attach to extracellular matrix ligands or surface proteins on host cells to enable adhesion and internalization (Xiong et al., 2009). Therefore, the ability to bind FN is necessary for inducing *S. aureus* infections (e.g., bacteremia) (Seidl et al., 2011a). Consistent with this, increased FN binding of *cfr*-positive MRSA correlated with worse outcomes of linezolid-based mono- and combination therapies in the murine bacteremia model. This observation is also in line with previous reports that the development of a hyper-adhesive FN binding phenotype contributed to persistent MRSA bacteremia and infective endocarditis (Xiong et al., 2009, 2015). In addition, we found that *cfr*-positive MRSA isolates adhered better than *cfr*-negative isolates to human endothelial cells, and this may facilitate MRSA colonization and provide an advantage in the pathogenesis of invasive MRSA infections.

The exact mechanisms how the presence of *cfr* correlates with the phenotypic characteristics remain to be fully elucidated. In the recent past, it was assumed that the development of antibiotic resistance was linked to virulence and fitness costs (Beceiro et al., 2013). However, the acquisition of *cfr* in *S. aureus* has been associated with low fitness cost that potentially facilitates the

growth rates, invasiveness and transmission capacity (LaMarre et al., 2011; Beceiro et al., 2013). In addition, in most of our study MRSA strains, *cfr* co-expressed with the *erm* gene (erythromycin resistance) that has a significant correlation with biofilm formations (Beceiro et al., 2013; Li et al., 2018). Previous studies in *Enterococcus* species exhibited that strong biofilm formation was more prevalent among linezolid-resistant compared with -sensitive isolates (Osman et al., 2020). *S. aureus* is a highly adaptable bacterium capable of dynamic changes in its virulence and resistance phenotypes when exposure to the host defenses or antibiotics (Abdelhady et al., 2015). Thus, additional unknown mechanisms likely contribute to the adaptive response phenotypes *in vitro* and linezolid-associated outcomes *in vivo*. Studies including comparative genomic and transcriptomic analysis are in progress in our laboratories to further determine other possible mechanisms.

Our investigation has several limitations. For example, we assessed a relatively small number of *cfr*-positive and -negative MRSA strains despite the different clonal types that raise the possibility of strain-dependent bias. In addition, some strains were isolated from animals and we only examined four representative MRSA strain sets in our animal models. Future studies should examine the phenotypic characteristics and usefulness of this combination in a larger population of strains from patients and in the clinical settings. Moreover, based on current findings, we do not know whether the relationship between the phenotypic profiles and the outcome of linezolid-based treatment is “*cfr* specific” or other unknown mechanisms. Although this is beyond the scope of the present study, future mechanism-based studies is warranted to better understand the precise factors responsible for this potential correlation.

Of note, the previous study reported that bacteriostatic-bactericidal antibiotic combinations could result in attenuation of bactericidal activity (Lobritz et al., 2015). However, our results showed the synergistic bactericidal effect for linezolid and rifampicin combination. This is supported by the previous observation that the combination of linezolid and rifampicin resulted in 3.1- $\log_{10}$  cfu/mL killing *in vitro* against staphylococcal biofilm (El Haj et al., 2018). Similarly, linezolid used in combination with rifampicin was more effective than their monotherapies, reducing the planktonic MRSA cells by  $>3.0$   $\log_{10}$  cfu/mL in the cage fluids of foreign-body infections (Baldoni et al., 2009). In light of the divergent effects that observed between our results and previous study, future investigation is warranted to better understand the precise mechanism of this combination.

In summary, our results indicated that increased FN and endothelial cell adhesion, reduced susceptibility to HDPs and robust biofilm formation all contributed to linezolid treatment outcomes we found *in vivo*. Combination therapy with linezolid and rifampicin significantly enhanced therapeutic efficacy against experimental bacteremia and SSSI due to *cfr*-positive and -negative MRSA isolates.

## DATA AVAILABILITY STATEMENT

The raw data supporting the conclusions of this article will be made available by the authors, without undue reservation, to any qualified researcher.

## ETHICS STATEMENT

This study was carried out in accordance with the recommendations of ethical guidelines of South China Agricultural University (SCAU). The protocol of *in vivo* studies and isolation procedures for animal-origin strains were approved by the SCAU Institutional Animal Ethics Committee (approval no. 2017B075). Individual written informed consent for the use of samples was obtained from all animal owners. Human-origin strains were kindly provided by the Third Affiliated Hospital of Sun Yat-sen University (Guangzhou, China), and isolation procedures were carried out in accordance with relevant guidelines with written informed consent from all subjects. The isolation and use protocols of human-origin strains were reviewed and approved by the Human Research Protection Office of SCAU Institutional Ethics Committee (approval no. 2017018).

## AUTHOR CONTRIBUTIONS

Y-HL, YX, and Y-FZ designed the study. Y-FZ, LL, and M-TT carried out the experiments. Y-FZ, JS, and X-PL analyzed the data. Y-FZ wrote the manuscript. LL and YX revised the manuscript. All authors read and approved the final manuscript.

## FUNDING

This study was supported by the National Key Research and Development Program of China (2016YFD0501300), the Program of Changjiang Scholars and Innovative Research Team in University of Ministry of Education of China (IRT\_17R39), and the Foundation for Innovation and Strengthening School Project of Guangdong, China (2016KCXTD010).

## ACKNOWLEDGMENTS

The authors thank the Third Affiliated Hospital of Sun Yat-sen University for providing the clinical *S. aureus* isolates.

## SUPPLEMENTARY MATERIAL

The Supplementary Material for this article can be found online at: <https://www.frontiersin.org/articles/10.3389/fmicb.2019.03080/full#supplementary-material>

## REFERENCES

- Abdelhady, W., Chen, L., Bayer, A. S., Seidl, K., Yeaman, M. R., Kreiswirth, B. N., et al. (2015). Early *agr* activation correlates with vancomycin treatment failure in multi-clonotype MRSA endovascular infections. *J. Antimicrob. Chemother.* 70, 1443–1452. doi: 10.1093/jac/dkv547
- Andes, D., Van Ogtrop, M. L., Peng, J., and Craig, W. A. (2002). *In vivo* pharmacodynamics of a new oxazolidinone (linezolid). *Antimicrob. Agents Chemother.* 46, 3484–3489. doi: 10.1128/aac.46.11.3484-3489.2002
- Baldoni, D., Haschke, M., Rajacic, Z., Zimmerli, W., and Trampuz, A. (2009). Linezolid alone or combined with rifampin against methicillin-resistant *Staphylococcus aureus* in experimental foreign-body infection. *Antimicrob. Agents Chemother.* 53, 1142–1148. doi: 10.1128/AAC.00775-08
- Barber, K. E., Smith, J. R., Raut, A., and Rybak, M. J. (2016). Evaluation of tedizolid against *Staphylococcus aureus* and *enterococci* with reduced susceptibility to vancomycin, daptomycin or linezolid. *J. Antimicrob. Chemother.* 71, 152–155. doi: 10.1093/jac/dkv302
- Bassetti, M., Baguneid, M., Bouza, E., Dryden, M., Nathwani, D., and Wilcox, M. (2014). European perspective and update on the management of complicated skin and soft tissue infections due to methicillin-resistant *Staphylococcus aureus* after more than 10 years of experience with linezolid. *Clin. Microbiol. Infect.* 20(Suppl. 4), 3–18. doi: 10.1111/1469-0691.12463
- Beceiro, A., Tomas, M., and Bou, G. (2013). Antimicrobial resistance and virulence: a successful or deleterious association in the bacterial world? *Clin. Microbiol. Rev.* 26, 185–230. doi: 10.1128/CMR.00059-12
- Beenken, K. E., Mrak, L. N., Griffin, L. M., Zielinska, A. K., Shaw, L. N., Rice, K. C., et al. (2010). Epistatic relationships between *sarA* and *agr* in *Staphylococcus aureus* biofilm formation. *PLoS One* 5:e10790. doi: 10.1371/journal.pone.0010790
- Chen, L., Ren, Z., Zhou, X., Zeng, J., Zou, J., and Li, Y. (2016). Inhibition of *Streptococcus* mutants biofilm formation, extracellular polysaccharide production, and virulence by an oxazole derivative. *Appl. Microbiol. Biotechnol.* 100, 857–867. doi: 10.1007/s00253-015-7092-1
- Chik, Z., Basu, R. C., Pendek, R., Lee, T. C., and Mohamed, Z. (2010). A bioequivalence comparison of two formulations of rifampicin (300- vs 150-mg capsules): an open-label, randomized, two-treatment, two-way crossover study in healthy volunteers. *Clin. Ther.* 32, 1822–1831. doi: 10.1016/j.clinthera.2010.09.006
- CLSI (2015). *Performance Standards for Antimicrobial Susceptibility Testing: Twenty-Fifth Informational Supplement. CLSI Document M100-S25*. Wayne, PA: Clinical and Laboratory Standards Institute.
- Donlan, R. M., and Costerton, J. W. (2002). Biofilms: survival mechanisms of clinically relevant microorganisms. *Clin. Microbiol. Rev.* 15, 167–193. doi: 10.1128/cmr.15.2.167-193.2002
- Dryden, M. S. (2011). Linezolid pharmacokinetics and pharmacodynamics in clinical treatment. *J. Antimicrob. Chemother.* 66(Suppl. 4), iv7–iv15. doi: 10.1093/jac/dkr072
- El Haj, C., Murillo, O., Ribera, A., Lloberas, N., Gomez-Junyent, J., Tubau, F., et al. (2018). Evaluation of linezolid or trimethoprim/sulfamethoxazole in combination with rifampicin as alternative oral treatments based on an *in vitro* pharmacodynamic model of staphylococcal biofilm. *Int. J. Antimicrob. Agents* 51, 854–861. doi: 10.1016/j.ijantimicag.2018.01.014
- Endimiani, A., Blackford, M., Dasenbrook, E. C., Reed, M. D., Bajaksouszian, S., Hujer, A. M., et al. (2011). Emergence of linezolid-resistant *Staphylococcus aureus* after prolonged treatment of cystic fibrosis patients in Cleveland, Ohio. *Antimicrob. Agents Chemother.* 55, 1684–1692. doi: 10.1128/AAC.01308-10
- Haisma, E. M., De Breijl, A., Chan, H., Van Dissel, J. T., Drijfhout, J. W., Hiemstra, P. S., et al. (2014). LL-37-derived peptides eradicate multidrug-resistant *Staphylococcus aureus* from thermally wounded human skin equivalents. *Antimicrob. Agents Chemother.* 58, 4411–4419. doi: 10.1128/AAC.02554-14
- Hassoun, A., Linden, P. K., and Friedman, B. (2017). Incidence, prevalence, and management of MRSA bacteremia across patient populations—a review of recent developments in MRSA management and treatment. *Crit. Care* 21:211. doi: 10.1186/s13054-017-1801-3
- LaMarre, J. M., Locke, J. B., Shaw, K. J., and Mankin, A. S. (2011). Low fitness cost of the multidrug resistance gene *cfr*. *Antimicrob. Agents Chemother.* 55, 3714–3719. doi: 10.1128/AAC.00153-11
- Leggatte, J., Allain, R., Isaac, L., and Blais, B. W. (2006). Microplate fluorescence assay for the quantification of double stranded DNA using SYBR Green I dye. *Biotechnol. Lett.* 28, 1587–1594. doi: 10.1007/s10529-006-9128-1
- Lepak, A. J., and Andes, D. R. (2016). *In Vivo* pharmacodynamic target assessment of delafloxacin against *Staphylococcus aureus*, *Streptococcus pneumoniae*, and *Klebsiella pneumoniae* in a murine lung infection model. *Antimicrob. Agents Chemother.* 60, 4764–4769. doi: 10.1128/AAC.00647-16
- Li, S. M., Zhou, Y. F., Li, L., Fang, L. X., Duan, J. H., Liu, F. R., et al. (2018). Characterization of the multi-drug resistance gene *cfr* in methicillin-resistant *Staphylococcus aureus* (MRSA) strains isolated from animals and humans in China. *Front. Microbiol.* 9:2925. doi: 10.3389/fmicb.2018.02925
- Lobritz, M. A., Belenky, P., Porter, C. B., Gutierrez, A., Yang, J. H., Schwarz, E. G., et al. (2015). Antibiotic efficacy is linked to bacterial cellular respiration. *Proc. Natl. Acad. Sci. U.S.A.* 112, 8173–8180. doi: 10.1073/pnas.1509743112
- Locke, J. B., Zuilli, D. E., Scharn, C. R., Deane, J., Sahm, D. F., Denys, G. A., et al. (2014). Linezolid-resistant *Staphylococcus aureus* strain 1128105, the first known clinical isolate possessing the *cfr* multidrug resistance gene. *Antimicrob. Agents Chemother.* 58, 6592–6598. doi: 10.1128/AAC.03493-14
- Long, K. S., Poehlsgaard, J., Kehrenberg, C., Schwarz, S., and Vester, B. (2006). The *Cfr* rRNA methyltransferase confers resistance to Phenicol, Lincosamides, Oxazolidinones, Pleuromutins, and Streptogramin A antibiotics. *Antimicrob. Agents Chemother.* 50, 2500–2505. doi: 10.1128/aac.00131-06
- Osman, K., Zolnikov, T. R., Badr, J., Naim, H., Hanafy, M., Saad, A., et al. (2020). Vancomycin and florfenicol resistant *Enterococcus faecalis* and *Enterococcus faecium* isolated from human urine in an Egyptian urban-rural community. *Acta Trop.* 201:105209. doi: 10.1016/j.actatropica.2019.105209
- Ostergaard, C., Hansen, S. G., and Moller, J. K. (2015). Rapid first-line discrimination of methicillin resistant *Staphylococcus aureus* strains using MALDI-TOF MS. *Int. J. Med. Microbiol.* 305, 838–847. doi: 10.1016/j.ijmm.2015.08.002
- Rasigade, J. P., Moulay, A., Lhoste, Y., Tristan, A., Bes, M., Vandenesch, F., et al. (2011). Impact of sub-inhibitory antibiotics on fibronectin-mediated host cell adhesion and invasion by *Staphylococcus aureus*. *BMC Microbiol.* 11:263. doi: 10.1186/1471-2180-11-263
- Rice, K. C., Mann, E. E., Endres, J. L., Weiss, E. C., Cassat, J. E., Smeltzer, M. S., et al. (2007). The *cidA* murein hydrolase regulator contributes to DNA release and biofilm development in *Staphylococcus aureus*. *Proc. Natl. Acad. Sci. U.S.A.* 104, 8113–8118. doi: 10.1073/pnas.0610226104
- Schwalm, J. D., El-Helou, P., and Lee, C. H. (2004). Clinical outcome with oral linezolid and rifampin following recurrent methicillin-resistant *Staphylococcus aureus* bacteremia despite prolonged vancomycin treatment. *Can. J. Infect. Dis.* 15, 97–100. doi: 10.1155/2004/768765
- Seidl, K., Bayer, A. S., Fowler, V. G. Jr., Mckinnell, J. A., Abdel Hady, W., Sakoulas, G., et al. (2011a). Combinatorial phenotypic signatures distinguish persistent from resolving methicillin-resistant *Staphylococcus aureus* bacteremia isolates. *Antimicrob. Agents Chemother.* 55, 575–582. doi: 10.1128/AAC.01028-10
- Seidl, K., Bayer, A. S., Mckinnell, J. A., Ellison, S., Filler, S. G., and Xiong, Y. Q. (2011b). *In vitro* endothelial cell damage is positively correlated with enhanced virulence and poor vancomycin responsiveness in experimental endocarditis due to methicillin-resistant *Staphylococcus aureus*. *Cell Microbiol.* 13, 1530–1541. doi: 10.1111/j.1462-5822.2011.01639.x
- Seidl, K., Solis, N. V., Bayer, A. S., Hady, W. A., Ellison, S., Klashman, M. C., et al. (2012). Divergent responses of different endothelial cell types to infection with *Candida albicans* and *Staphylococcus aureus*. *PLoS One* 7:e39633. doi: 10.1371/journal.pone.0039633
- Sharpe, J. N., Shively, E. H., and Polk, H. C. Jr. (2005). Clinical and economic outcomes of oral linezolid versus intravenous vancomycin in the treatment of MRSA-complicated, lower-extremity skin and soft-tissue infections caused by methicillin-resistant *Staphylococcus aureus*. *Am. J. Surg.* 189, 425–428. doi: 10.1016/j.amjsurg.2005.01.011
- Shorr, A. F., Kunkel, M. J., and Kollef, M. (2005). Linezolid versus vancomycin for *Staphylococcus aureus* bacteraemia: pooled analysis of randomized studies. *J. Antimicrob. Chemother.* 56, 923–929. doi: 10.1093/jac/dki355
- Sirgel, F. A., Fourie, P. B., Donald, P. R., Padayatchi, N., Rustomjee, R., Levin, J., et al. (2005). The early bactericidal activities of rifampin and rifapentine in pulmonary tuberculosis. *Am. J. Respir. Crit. Care Med.* 172, 128–135. doi: 10.1164/rccm.200411-1557oc

- Stegger, M., Lindsay, J. A., Sorum, M., Gould, K. A., and Skov, R. (2010). Genetic diversity in CC398 methicillin-resistant *Staphylococcus aureus* isolates of different geographical origin. *Clin. Microbiol. Infect.* 16, 1017–1019. doi: 10.1111/j.1469-0691.2009.03003.x
- Takano, T., Hung, W. C., Shibuya, M., Higuchi, W., Iwao, Y., Nishiyama, A., et al. (2013). A new local variant (ST764) of the globally disseminated ST5 lineage of hospital-associated methicillin-resistant *Staphylococcus aureus* (MRSA) carrying the virulence determinants of community-associated MRSA. *Antimicrob. Agents Chemother.* 57, 1589–1595. doi: 10.1128/AAC.01147-12
- Thakker, M., Park, J. S., Carey, V., and Lee, J. C. (1998). *Staphylococcus aureus* serotype 5 capsular polysaccharide is antiphagocytic and enhances bacterial virulence in a murine bacteremia model. *Infect. Immun.* 66, 5183–5189.
- Tong, S. Y., Davis, J. S., Eichenberger, E., Holland, T. L., and Fowler, V. G. Jr. (2015). *Staphylococcus aureus* infections: epidemiology, pathophysiology, clinical manifestations, and management. *Clin. Microbiol. Rev.* 28, 603–661. doi: 10.1128/cmr.00134-14
- Tseng, C. W., Sanchez-Martinez, M., Arruda, A., and Liu, G. Y. (2011). Subcutaneous infection of methicillin resistant *Staphylococcus aureus* (MRSA). *J. Vis. Exp.* 48:2528.
- van der Mee-Marquet, N., Francois, P., Domelier-Valentin, A. S., Coulomb, F., Decreux, C., Hombrock-Allet, C., et al. (2011). Emergence of unusual bloodstream infections associated with pig-borne-like *Staphylococcus aureus* ST398 in France. *Clin. Infect. Dis.* 52, 152–153. doi: 10.1093/cid/ciq053
- Wang, Q., Lv, Y., Pang, J., Li, X., Lu, X., Wang, X., et al. (2019). In vitro and in vivo activity of d-serine in combination with beta-lactam antibiotics against methicillin-resistant *Staphylococcus aureus*. *Acta Pharm. Sin.* B 9, 496–504. doi: 10.1016/j.apsb.2019.01.017
- Witte, W., and Cuny, C. (2011). Emergence and spread of *cfr*-mediated multiresistance in *Staphylococci*: an interdisciplinary challenge. *Future Microbiol.* 6, 925–931. doi: 10.2217/FMB.11.69
- Xiong, Y. Q., Fowler, V. G., Yeaman, M. R., Perdreau-Remington, F., Kreiswirth, B. N., and Bayer, A. S. (2009). Phenotypic and genotypic characteristics of persistent methicillin-resistant *Staphylococcus aureus* bacteremia in vitro and in an experimental endocarditis model. *J. Infect. Dis.* 199, 201–208. doi: 10.1086/595738
- Xiong, Y. Q., Sharma-Kuinkel, B. K., Casillas-Ituarte, N. N., Fowler, V. G. Jr., Rude, T., Dibartola, A. C., et al. (2015). Endovascular infections caused by methicillin-resistant *Staphylococcus aureus* are linked to clonal complex-specific alterations in binding and invasion domains of fibronectin-binding protein A as well as the occurrence of *fnbB*. *Infect. Immun.* 83, 4772–4780. doi: 10.1128/IAI.01074-15
- Yeaman, M. R., Puentes, S. M., Norman, D. C., and Bayer, A. S. (1992). Partial characterization and staphylocidal activity of thrombin-induced platelet microbicidal protein. *Infect. Immun.* 60, 1202–1209.
- Zhou, Y. F., Tao, M. T., Feng, Y., Yang, R. S., Liao, X. P., Liu, Y. H., et al. (2017). Increased activity of colistin in combination with amikacin against *Escherichia coli* co-producing NDM-5 and MCR-1. *J. Antimicrob. Chemother.* 72, 1723–1730. doi: 10.1093/jac/dkx038
- Zhou, Y. F., Xiong, Y. Q., Tao, M. T., Li, L., Bu, M. X., Sun, J., et al. (2018). Increased activity of linezolid in combination with rifampicin in a murine pneumonia model due to MRSA. *J. Antimicrob. Chemother.* 73, 1899–1907. doi: 10.1093/jac/dky129

**Conflict of Interest:** The authors declare that the research was conducted in the absence of any commercial or financial relationships that could be construed as a potential conflict of interest.

Copyright © 2020 Zhou, Li, Tao, Sun, Liao, Liu and Xiong. This is an open-access article distributed under the terms of the Creative Commons Attribution License (CC BY). The use, distribution or reproduction in other forums is permitted, provided the original author(s) and the copyright owner(s) are credited and that the original publication in this journal is cited, in accordance with accepted academic practice. No use, distribution or reproduction is permitted which does not comply with these terms.





# Topical Therapeutic Efficacy of Ebselen Against Multidrug-Resistant *Staphylococcus aureus* LT-1 Targeting Thioredoxin Reductase

Chuanjiang Dong<sup>1†</sup>, Jingxuan Zhou<sup>2†</sup>, Peng Wang<sup>1,2†</sup>, Tao Li<sup>1</sup>, Ying Zhao<sup>3</sup>, Xiaoyuan Ren<sup>4</sup>, Jun Lu<sup>3</sup>, Jun Wang<sup>2,5\*</sup>, Arne Holmgren<sup>4</sup> and Lili Zou<sup>1\*</sup>

## OPEN ACCESS

### Edited by:

Luciene Andrade Da Rocha  
Minarini,  
Federal University of São Paulo, Brazil

### Reviewed by:

Jianhua Wang,  
Chinese Academy of Agricultural  
Sciences, China  
David Leitsch,  
Medical University of Vienna, Austria  
Luigi Messori,  
University of Florence, Italy

### \*Correspondence:

Jun Wang  
wangjfox@gmail.com  
Lili Zou  
zoullili@ctgu.edu.cn;  
zoullili@mail3.sysu.edu.cn

†These authors have contributed  
equally to this work

### Specialty section:

This article was submitted to  
Antimicrobials, Resistance  
and Chemotherapy,  
a section of the journal  
Frontiers in Microbiology

Received: 19 July 2019

Accepted: 16 December 2019

Published: 15 January 2020

### Citation:

Dong C, Zhou J, Wang P, Li T,  
Zhao Y, Ren X, Lu J, Wang J,  
Holmgren A and Zou L (2020) Topical  
Therapeutic Efficacy of Ebselen  
Against Multidrug-Resistant  
*Staphylococcus aureus* LT-1  
Targeting Thioredoxin Reductase.  
*Front. Microbiol.* 10:3016.  
doi: 10.3389/fmicb.2019.03016

<sup>1</sup> The First College of Clinical Medical Science, China Three Gorges University, Yichang, China, <sup>2</sup> The Institute of Infection and Inflammation, Medical College, China Three Gorges University, Yichang, China, <sup>3</sup> Key Laboratory of Luminescent and Real-Time Analytical Chemistry (Southwest University), Ministry of Education, College of Pharmaceutical Sciences, Southwest University, Chongqing, China, <sup>4</sup> Division of Biochemistry, Department of Medical Biochemistry and Biophysics, Karolinska Institutet, Stockholm, Sweden, <sup>5</sup> Translational Neuroscience & Neural Regeneration and Repair Institute/Institute of Cell Therapy, The People's Hospital of China Three Gorges University, Yichang, China

As a thiol-dependent enzyme, thioredoxin reductase (TrxR) is a promising antibacterial drug target. Ebselen, an organo-selenium with well-characterized toxicology and pharmacology, was recently reported to have potent antibacterial activity against *Staphylococcus aureus*. In this paper, we demonstrated that ebselen has strong bactericidal activity against multidrug-resistant (MDR) *S. aureus* based on taking TrxR as a major target and disruption of the redox microenvironment. Further, the topical therapeutic efficacy of ebselen for staphylococcal skin infections was assessed in a rat model. Treatment with ebselen significantly reduced the bacterial load and the expression of pro-inflammatory cytokines tumor necrosis factor- $\alpha$  (TNF- $\alpha$ ), interleukin-6 (IL-6) and interleukin-1 beta (IL-1 $\beta$ ) in *S. aureus* skin lesions; further, wound healing and pathological changes were obvious improved in ebselen-treated rats compare to controls. Finally, ebselen was found to sensitize *S. aureus* to curcumin, which may be due to their synergistic effects in inhibiting bacterial TrxR. Altogether, ebselen is an effective topical antibacterial agent in animal model of MDR *S. aureus* LT-1 skin infection. This may lay the foundation for further analysis and development of ebselen as an antibacterial agent for topical treatment of MDR staphylococcal infections.

**Keywords:** ebselen, thioredoxin reductase, topical treatment, *Staphylococcus aureus*, curcumin

## INTRODUCTION

Novel antimicrobials and new bacterial cell targets are urgently needed to overcome the ever-increasing worldwide antimicrobial resistance (AMR), which is now widely accepted as a global health threat with leading causes of morbidity and mortality (Brown and Wright, 2016; Baptista et al., 2018). In May 2018, the World Health Organization (WHO), the Food and Agriculture Organization of the United Nations (FAO), and the World Organization for Animal Health (OIE) signed a Memorandum of Understanding (MoU) to support governments, health care workers, and stakeholders to engage and collaborate in the fight against AMR (Balkhy et al., 2018). Limiting the

emergence of AMR is critical to preserve our ability to treat bacterial and microbial infections not only in humans, but also in animal, plant, food, and environment circumstances (Bhatia, 2018).

*Staphylococcus aureus* is a highly adaptable, “Janus-faced” Gram-positive pathogen, for which humans are the only known reservoir (Kobayashi et al., 2015; Balasubramanian et al., 2017; Dweba et al., 2018). *S. aureus* is present in approximately 30% of the human population, and its presence has been linked to skin rashes, wound infections, pleuropulmonary, bacteremia, infective endocarditis, and device-related infections (Coates et al., 2014; Tong et al., 2015). In the pre-antibiotic era, the case fatality rate (CFR) for *S. aureus* was ~80%; it has since decreased and plateaued at 15~50% over the past several decades since the introduction of penicillin (van Hal et al., 2012). However, the adaptive evolution of *S. aureus* during the modern antibiotic era has enabled its acquisition of antibiotic resistance, thus increasing disease burden worldwide (Pantosti et al., 2007; McGuinness et al., 2017).

Ebselen or 2-phenyl-1,2 benzisoxaselenazol-3(2H)-one, an organo-selenium compound, is a clinical trial drug with well-characterized toxicology and pharmacology (Zou et al., 2017; Figure 1). Recent studies have shown that ebselen possesses bactericidal activity against Gram-positive, including multidrug-resistant (MDR) clinical isolates of *S. aureus*. Bacterial thioredoxin reductase (TrxR) was assessed to be a critical target, and the ebselen inhibition is through a reaction with the active site dithiol of TrxR to act as a competitive inhibitor (Lu et al., 2013; Thangamani et al., 2015; Zou et al., 2018). Bacterial TrxR transfers an electron from NADPH to Trx allowing it to regulate functions of various critical cellular proteins, including ribonucleotide reductase (RNR), methionine-S-sulfoxide reductase (Msr), thiol peroxidase (Tpx), bacterioferritin comigratory protein (Bcp) (Holmgren, 1985; Lu and Holmgren, 2012, 2014a; Leitsch, 2017). Bcp is critical in antioxidant defense and DNA synthesis and repair (Lu and Holmgren, 2012, 2014b). However, animal experiments testing antibacterial activity of ebselen are rare. Thus, the aim of this study was to evaluate the bactericidal activity of ebselen against MDR *S. aureus* *in vitro*, and to assess its topical therapeutic efficacy, anti-inflammatory properties, and potential clinical applications in staphylococcal skin infection rat model.

## RESULTS

### Antibacterial Activity of Ebselen Targeting *S. aureus* TrxR

*Staphylococcus aureus* LT-1 was isolated from patients with cutaneous infections in The first clinical hospital of Yichang (China), and identified as an MDR strain (Tables 1, 2 and Supplementary Figure S1). LT-1 cells with logarithmic growth were treated with different concentrations of ebselen for 16 h. The antibacterial effect of ebselen on the growth of *S. aureus* was investigated in microplates by a spectrophotometer, which estimated cell number. As shown in Figure 2A,

ebselen inhibited *S. aureus* growth with a minimal inhibition concentration (MIC) of 2.2  $\mu\text{g/ml}$  (8  $\mu\text{M}$ ). Meanwhile, the positive control gentamycin inhibited *S. aureus* growth with a MIC of 0.85  $\mu\text{g/ml}$  (1.08  $\mu\text{M}$ ). Further, the propidium iodide (PI) nuclear staining which represents the bacterial membrane permeability was performed after treatment with 22  $\mu\text{g/ml}$  ebselen. PI stains the nucleic acids inside dead cells, or those with damaged membranes. In agreement with the inhibitory effect on bacterial growth curve, when LT-1 cells were treated with ebselen, there was a significant increase in PI positive cells ( $P < 0.001$ , Figure 2B).

The effect of ebselen on the morphology of *S. aureus* was detected by transmission electron microscopy (Figures 2C–H). The morphology of *S. aureus* changed significantly when treated with ebselen compared to the control. Untreated *S. aureus* cells have a smooth surface and a complete cell membrane and cell wall (Figures 2C,D). After 20 min treatment with 22  $\mu\text{g/ml}$  ebselen, the *S. aureus* cell membrane and cell wall were ruptured, cytoplasmic material flowed out, and the cells eventually died (Figures 2E,F). In contrast, gentamycin-treated *S. aureus* cells showed no obvious morphological changes compared to untreated cells (Figures 2G,H).

The inhibitory effect of ebselen on *S. aureus* TrxR activity was detected by dithiobis nitrobenzoic acid (DTNB) assay. Interestingly, ebselen treatment significantly inhibited bacterial TrxR activity when compared with untreated cells ( $P < 0.001$ , Figure 2I). In addition, the mean fluorescent intensity (MFI) of reactive oxygen species (ROS) was detected by Flow cytometry, and showed that the ROS production level in ebselen-treated *S. aureus* cells was significantly upregulated compared to the control ( $P < 0.01$ , Figure 2J).

Altogether, these results shown that ebselen is an effective antibacterial compound that inhibits *S. aureus* TrxR *in vitro*, and that ROS production is one of the key virulent factors for its bactericidal activity.

### The Therapeutic Efficacy of Ebselen in Rat Model of Staphylococcal Skin Infections

Thirty rats were randomly divided into three groups: control group, ebselen-treated group, and gentamycin-treated group. Thick scalpel cuts were made into the dermis of the skin on the posterior upper back and neck of rats and inoculated with *S. aureus* LT-1 cells. Two days post-infection, the bacteria from the three groups showed no obvious difference in colony forming units (average of  $3.8 \pm 1.0$  ( $\text{Log}_{10}^3$ ) CFU/ml) ( $P < 0.05$ ). Rats were then treated topically with 25 mg/kg ebselen, 5 mg/kg gentamycin or PBS once per day for 5 days, respectively. The results are highlighted in Figure 3A. After 5 days post-treatment, the rats receiving ebselen had a significantly reduced mean bacterial count compared with the group receiving PBS ( $P < 0.05$ ). The ebselen-treated group had the highest reduction ( $43 \pm 26.4$  CFU/ml), followed by gentamycin ( $57 \pm 17.3$  CFU/ml) and control ( $403 \pm 130.1$  CFU/ml). There was no obvious difference between ebselen and gentamycin in their antibacterial activities ( $P > 0.05$ ).

**TABLE 1** | Biochemistry identification of clinical isolated *Staphylococcus aureus* LT-1.

2 AMY	-	16 BGAR	-	28 AlaA	-	44 NAG	+	57 dRAF	-
4 PIPLC	-	17 AMAN	-	29 TyrA	-	45 dMAL	+	58 O129R	+
5 DXY	-	19 dSOR	-	30 dSOR	+	46 BACI	+	59 SAL	-
8 ADH1	+	20 LeuA	-	31 URE	+	47 NOVO	-	60 SAC	+
9 BGAL	+	23 PROA	-	32 POLYB	-	50 NC6.5	+	62 dTRE	+
11 AGLU	+	24 BGURr	-	37 dGAL	+	52 dMAN	+	63 ADH2s	+
13 APPA	-	25 AGAL	-	38 dRIB	+	53 dMNE	+	64 OPTO	+
14 CDEX	-	26 PyrA	+	39 ILATK	+	54 MBdG	+		
15 AspA	-	27 BGUR	-	42 LAC	-	56 PUL	-		

AMY, amygdalin; PIPLC, phosphatidyl phosphatase C; dXYL, D-xylose; ADH1, arginine double hydrolase 1; BGAL,  $\beta$ -D-galactosidase; AGLU,  $\alpha$ -glucosidase; APPA, alanine-phenylalanine-proline aromaminase; CDEX, cyclodextrin; AspA, L-aspartate arylamine; BGAR,  $\beta$ -galactopyranosidase; AMAN,  $\alpha$ -Mannosidase; PHOS, phosphatase; LeuA, leucine aromaminase; ProA, proline aromaminase; BGURr,  $\beta$ -glucuronidase; AGAL,  $\alpha$ -galactosidase; PyrA, pyroglutaminase; BGUR,  $\beta$ -D-glucuronidase; AlaA, alanine aromatinase; TyrA, tyrosine aromaminase; dSOR, D-sorbitol; URE, urease; POLYB, polyclistin B tolerance; dGAL, D-galactose; dRIB, D-ribose; ILATK, lactate produces alkali; LAC, lactose; NAG, N-acetyl-D-glucosamine dMAL D-Maltose; BACI, bacillus peptide tolerance; NOVO, novomycin tolerance; NC6.5, 6.5% NaCl growth; dMAN, D-mannitol; dMNE, D-mannose; MBdG, methyl-B-D- glucopyranoside; PUL, pullulan; dRAF, D-raffinose; O129R, O/129 tolerant; SAL, salicin; SAC, saccharose; dTRE, D-trehalose; ADH2s, arginine double hydrolase 2; OPTO, optoxin tolerance.

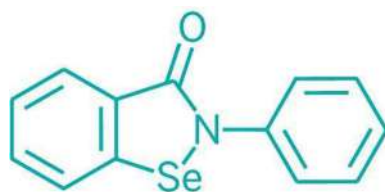
**TABLE 2** | Antimicrobial susceptibility test of *S. aureus* LT-1.

Antibiotics	Diameter (mm)	Cut-off	Sensitivity/resistance
Gentamicin	23	12–15	(S)
Levofloxacin	28	15–19	(S)
Ciprofloxacin	24	15–21	(S)
Selectin	30	10–16	(S)
Tetracycline	14	14–19	(R)
Penicillin	10	28–29	(R)
Oxacillin	6	10–13	(R)
Vancomycin	0.38	2–16	(S)
Erythromycin	6	13–23	(R)
Clindamycin	6	14–21	(R)
Rifampicin	31	16–20	(S)
Linezolid	31	20–21	(S)
Chloromycetin	26	12–18	(S)

gentamycin ( $42.43 \pm 5.54$ ), and PBS ( $33.56 \pm 6.12$ ). There was no difference in wound healing in rats treated with ebselen and gentamycin ( $P > 0.05$ ).

## Topical Effect of Ebselen on Inflammatory Cytokines of Staphylococcal Skin Infection

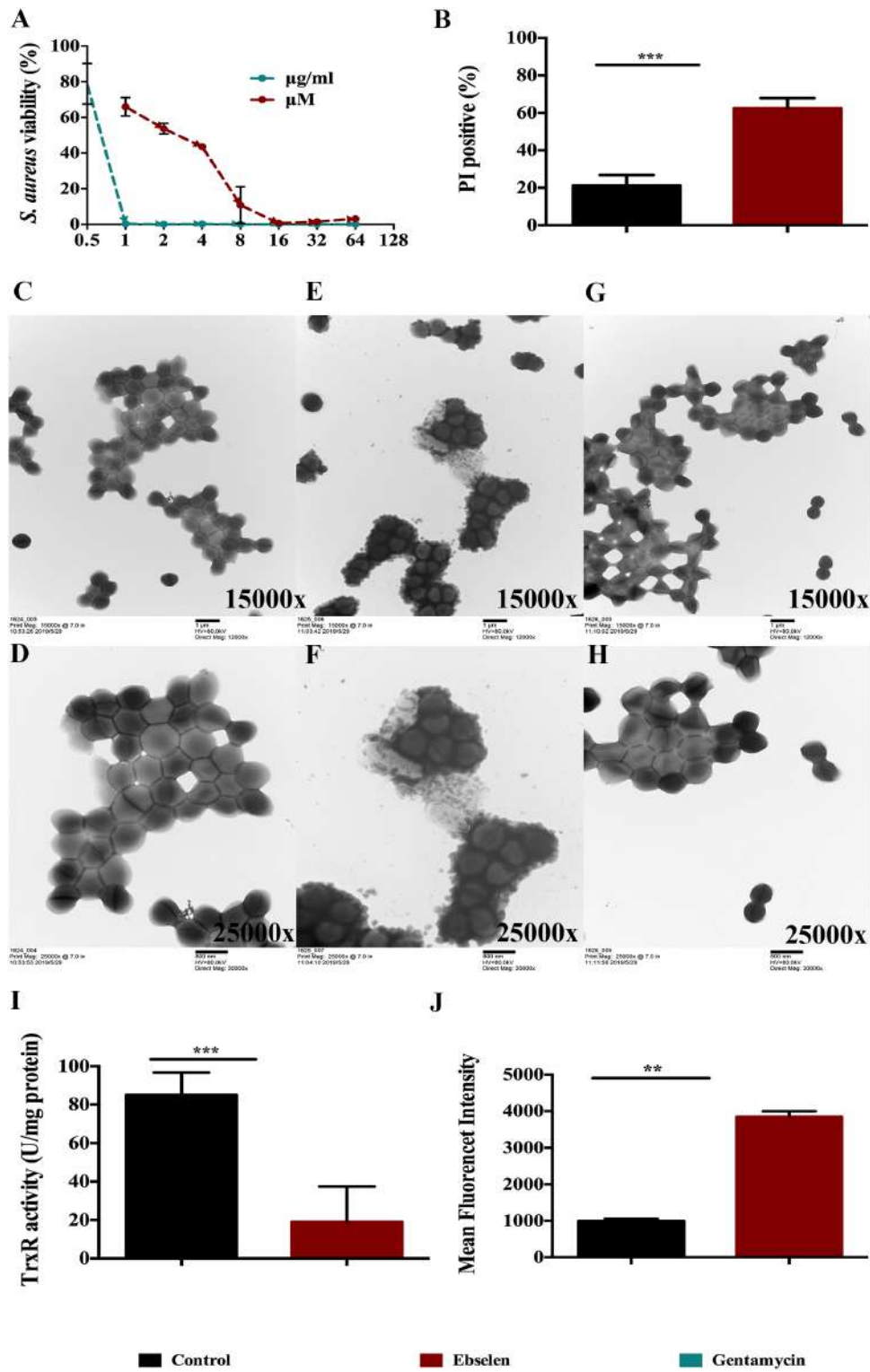
To study the immune-modulatory activity of ebselen in a topical application against *S. aureus* LT-1 skin infection, forty rats were randomly divided into 4 groups: A to D. Scalpel cuts were made in the dermis of the skin on the posterior upper back and neck of the rats. Rats from group A served as a control group and were not infected or treated. Rats from groups B to D were inoculated with the *S. aureus* strain LT-1 and further topically treated with 25 mg/kg ebselen, 5 mg/kg gentamycin, or PBS once per day for 5 days, respectively. An ELISA assay was used to measure the presence of pro-inflammatory cytokines, including tumor necrosis factor- $\alpha$  (TNF- $\alpha$ ), interleukin-6 (IL-6), and interleukin-1 beta (IL-1 $\beta$ ). As shown in **Figure 4**, ebselen significantly reduced the expression of all three tested pro-inflammatory cytokines compared to rats treated with PBS ( $P < 0.05$ ). For TNF- $\alpha$ , the group treated with ebselen had the highest reduction in expression ( $44.83 \pm 3.59$  pg/ml), followed by gentamycin ( $47.01 \pm 4.19$  pg/ml), and PBS ( $51.90 \pm 6.98$  pg/ml) (**Figure 4A**), while there was no difference between ebselen and gentamycin ( $P > 0.05$ ). For IL-1 $\beta$ , the group treated with ebselen had the highest reduction in expression ( $64.83 \pm 8.91$  pg/ml), followed by gentamycin ( $75.61 \pm 7.37$  pg/ml), and PBS ( $102.02 \pm 11.22$  pg/ml) (**Figure 4B**), while there was difference between ebselen and gentamycin ( $P < 0.05$ ). Finally, for IL-6, the group treated with ebselen had the highest reduction in expression ( $38.03 \pm 5.85$  pg/ml), followed by gentamycin ( $45.21 \pm 8.7$  pg/ml), and PBS ( $71.92 \pm 10.0$  pg/ml) (**Figure 4C**), while there was difference between ebselen and gentamycin ( $P < 0.05$ ). Overall, ebselen treatment had the greatest effect in reducing the expression of pro-inflammatory cytokines, and its anti-inflammatory activity was considerably higher than gentamycin.



**Ebselen**

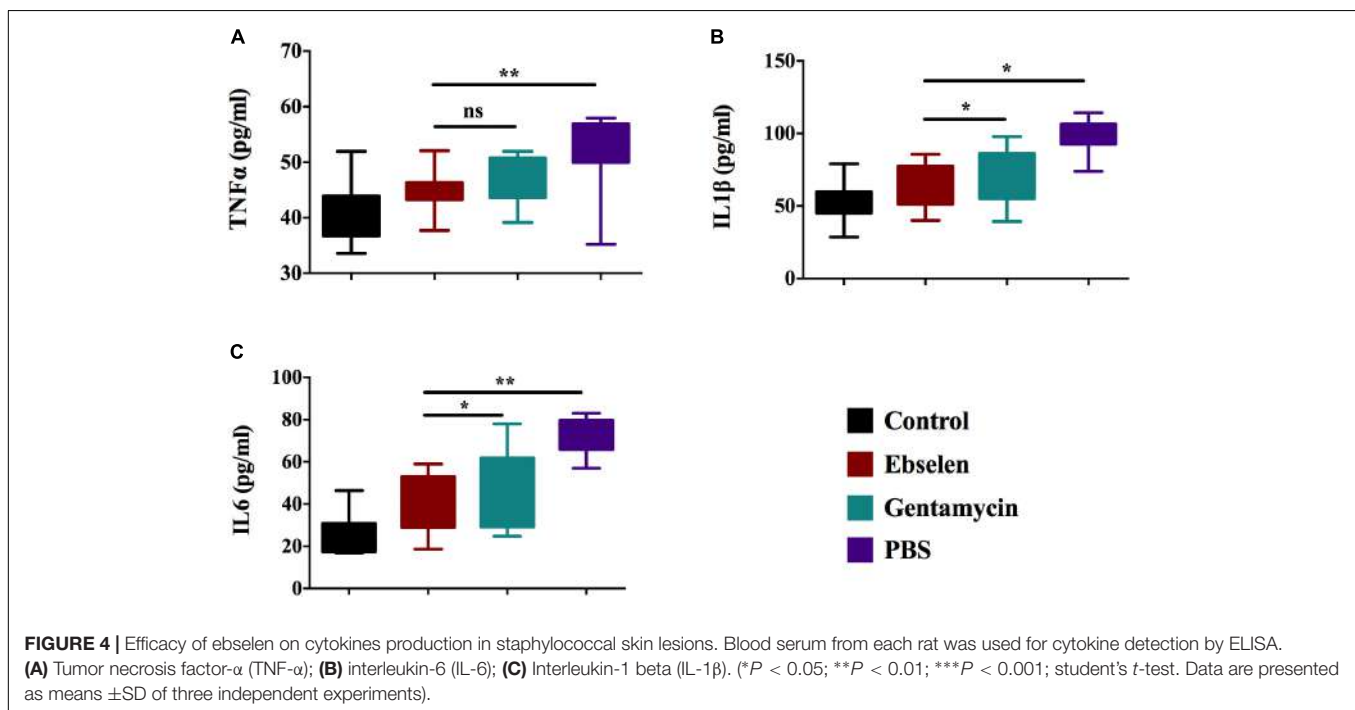
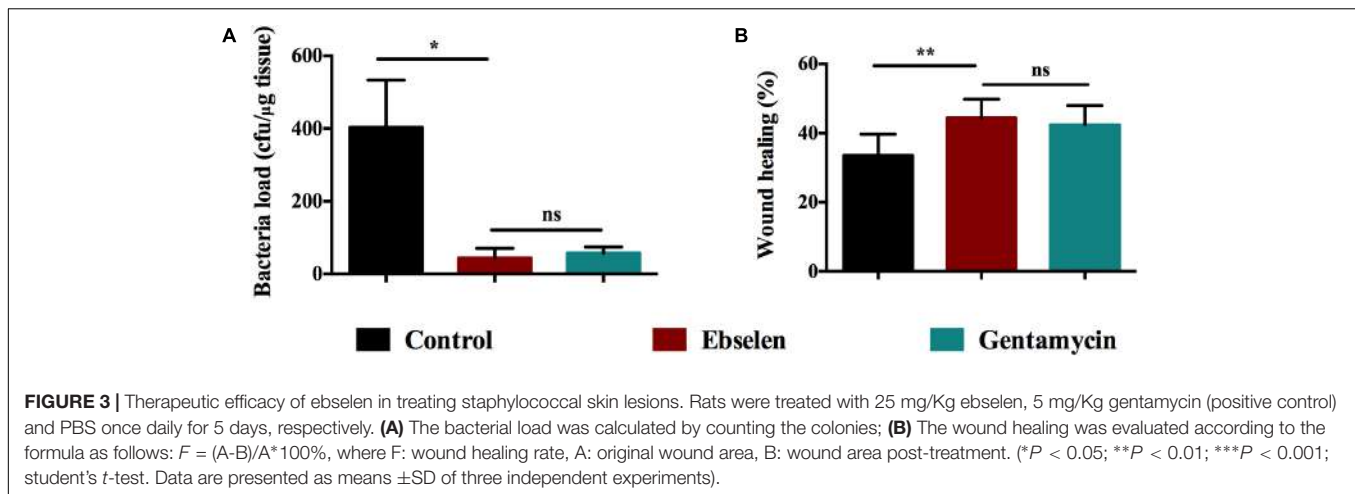
**FIGURE 1** | Chemical structure of ebselen.

Wound healing was also evaluated according to the formula as follows:  $F = (A - B) / A * 100\%$ , where F: wound healing rate, A: original wound area, and B: wound area post-treatment. As the results showed in **Figure 3B**, ebselen-treated rats had a wound healing rate that was significantly higher than the control ( $P < 0.01$ ). The group treated with ebselen had the highest healing rate in wound ( $44.43 \pm 5.41$ ), followed by



**FIGURE 2 |** Antibacterial effect of ebselen on *Staphylococcus aureus* through targeting bacterial TrxR. *S. aureus* LT-1 cells grown to DO 600 nm of 0.4 and diluted 100 times were treated with serial dilution of ebselen, and gentamycin was used as positive control. **(A)** Antibacterial effect of ebselen on the growth of *S. aureus*. Bacterial growth was presented by measuring OD<sub>600</sub> nm. *S. aureus* LT-1 cells grown to DO 600 nm of 0.4 and were treated with 22 μg/ml ebselen. **(B)** Mean ± SD of propidium iodide (PI)-stained *S. aureus* LT-1 by Flow cytometry; **(C–H)** Transmission electron microscopy of *S. aureus* treated with ebselen; **(C,D)** control; **(E,F)** 22 μg/ml ebselen; **(G,H)** 64 μg/ml gentamycin; **(C,E,G)** 15000x; **(D,F,H)** 25000x; **(I)** TrxR activity was assayed for DTNB reduction in the presence of Trx in *S. aureus* LT-1 extracts; **(J)** Mean fluorescent intensity (MFI) Means ±SD of H<sub>2</sub>DCF-DA-stained *S. aureus* LT-1 were detected to present ROS level. (\*\**P* < 0.01; \*\*\**P* < 0.001; student's *t*-test. Data are presented as means ±SD of three independent experiments).



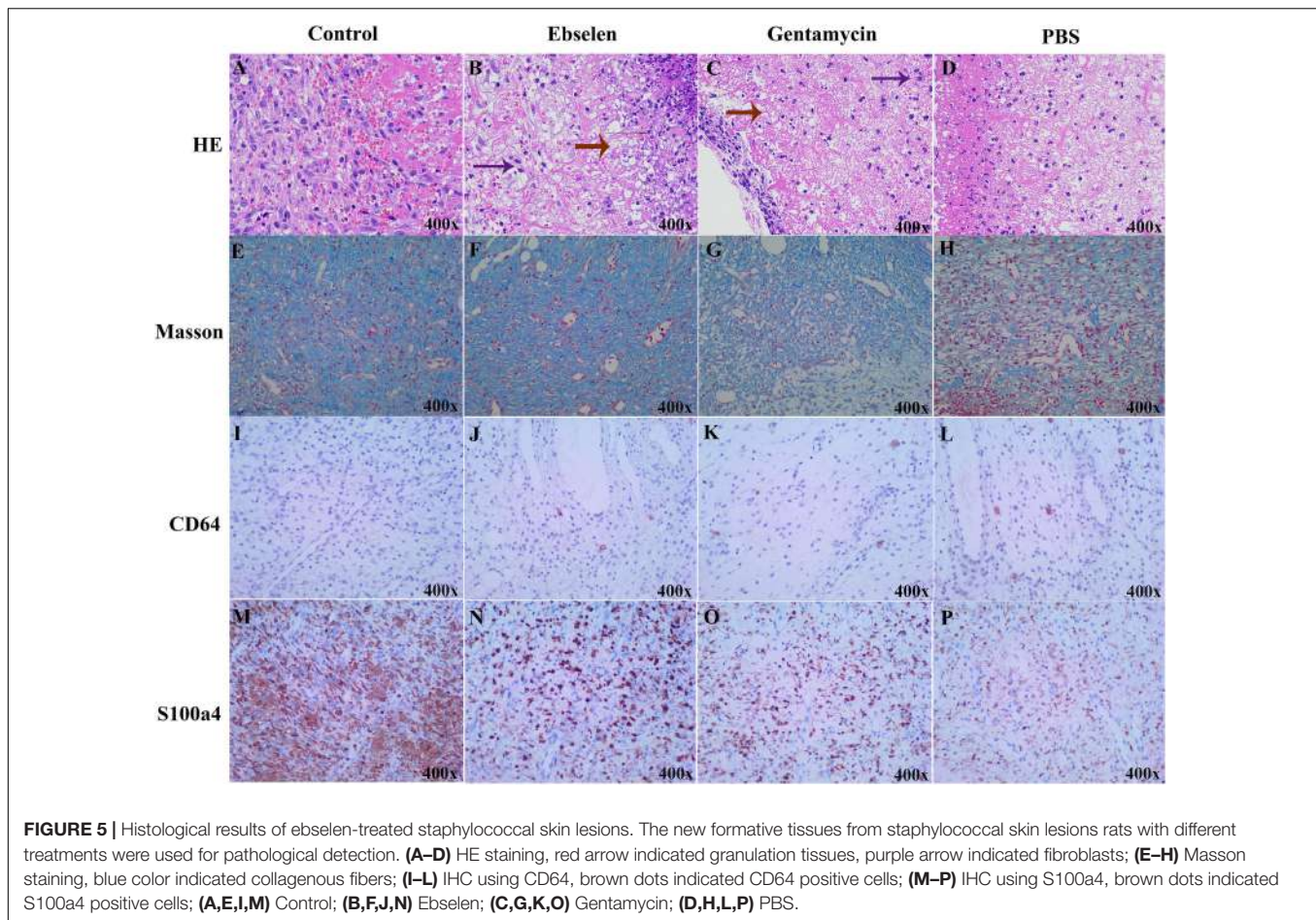


Further, hematoxylin and eosin (H&E) and Masson staining were performed using the new formative tissues. Staining revealed that PBS-treated rats had reduced number of fibroblasts and microvascular, and increased number of inflammatory cells and erythrocytes. Meanwhile, the ebselen or gentamycin-treated rats had dense granulation tissues and microvascular, and less scattered lymphocytes (Figures 5A–H). Anti-CD64 antibody was further used to detect activated mature neutrophil by Immunohistochemistry (IHC). Rats treated with ebselen had less infiltrative neutrophils than those treated with PBS (Figures 5I–L). Moreover, fibroblasts were detected by S100a4 antibody, also termed FSP-1 (fibroblast-specific protein-1). The results showed an increased number of fibroblasts in ebselen or gentamycin-treated rats compared to the PBS-treated group (Figures 5M–P).

Altogether, these results demonstrated that ebselen may influence the repair of damaged skin, and its efficacy to do so is considerably higher than that of gentamycin.

### Synergistic Activity of Ebselen With Curcumin Against *S. aureus* *in vitro*

As an important constituent of turmeric, curcumin, has various biological activities due to its antioxidant mechanism. Previous studies have shown that curcumin has antibacterial activity against various bacteria, including *S. aureus* (Song et al., 2012), and that it operates through blocking the assembly dynamics of filamentous temperature-sensitive protein Z (FtsZ) in the Z ring at the site of division in bacterial cells (Rai et al., 2008; Kaur et al., 2010), affecting biofilm initiation (Rudrappa and Bais, 2008). It may also have bacterial membrane lysing



properties (Tyagi et al., 2015), yet whether it targets bacterial TrxR remains unknown.

The synergistic inhibition effect of bacterial growth by ebselen and curcumin was tested on *S. aureus* ATCC25923. The growth of *S. aureus* was substantially inhibited by 5  $\mu\text{M}$  ebselen and 10  $\mu\text{M}$  curcumin in 96 well-plate 4 h post-incubation ( $P < 0.01$ , **Figure 6A**). Furthermore, as showed in **Figure 5B**, adding 5  $\mu\text{M}$  ebselen to 10  $\mu\text{M}$  curcumin-treated *S. aureus* could also significantly inhibit cells growth ( $P < 0.05$ , **Figure 6B**). In addition, the Bliss model of synergism against *S. aureus* was used, and the degree of synergy of 5  $\mu\text{M}$  ebselen and 10  $\mu\text{M}$  curcumin is 0.89 2 h post-incubation (**Supplementary Figure S2**).

To detect whether treatment with 5  $\mu\text{M}$  ebselen and 80  $\mu\text{M}$  curcumin affected bacterial membrane permeability, PI nuclear staining was performed. Consistent with the inhibitory effect on bacterial growth, treatment with ebselen and curcumin increased the number of PI positive *S. aureus* cells compared to that of ebselen or curcumin alone ( $P < 0.01$ , **Figure 6C**).

### The Inhibition Activity of Bacterial TrxR by Ebselen and Curcumin

Thioredoxin reductase activity in *S. aureus* was assessed following treatment with 5  $\mu\text{M}$  ebselen and 80  $\mu\text{M}$  curcumin. Although curcumin alone could inhibit TrxR activity, the combination

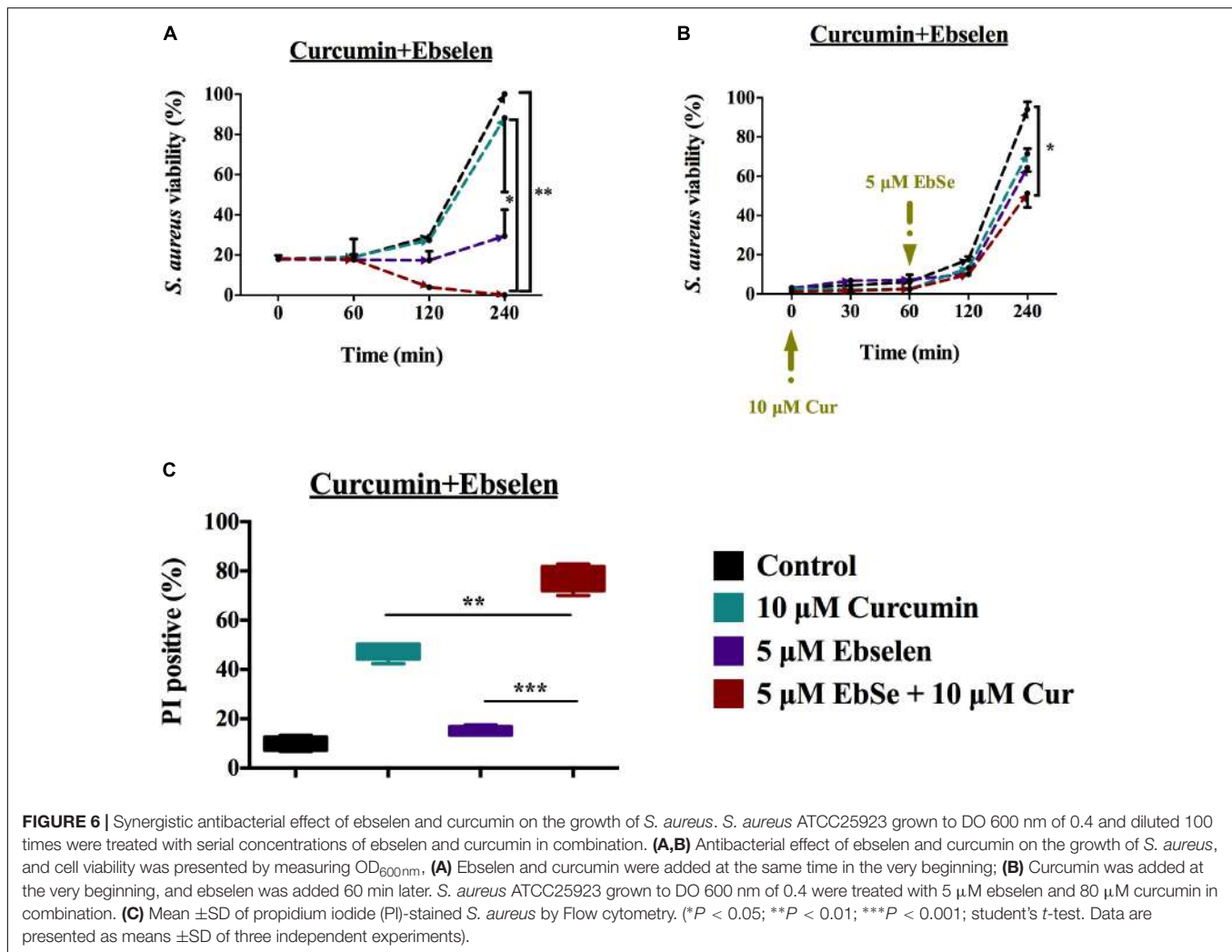
with ebselen exhibited a significantly stronger inhibitory effect ( $P < 0.01$ ) (**Figures 7A,B**).

Since the Trx system is the major mediator in redox balance, ROS production was assessed following treatment with 5  $\mu\text{M}$  ebselen and 80  $\mu\text{M}$  curcumin as detected with  $\text{H}_2\text{DCF-DA}$  by flow cytometry. When *S. aureus* cells were treated with curcumin alone, ROS production was increased ( $P < 0.05$ ); however, the effect of ebselen and curcumin in combination on ROS production was significantly higher ( $P < 0.001$ ) (**Figure 7C**).

Altogether, the above results demonstrated that targeting *S. aureus* TrxR is one of the antibacterial mechanisms of curcumin, and ebselen enhances its efficacy.

## DISCUSSION

The WHO stated that 1 in 10 patients suffer an infection while receiving medical care and that more than half of surgical site infections may be antibiotic-resistant (Odell, 2010). Meanwhile, skin infections caused by MDR *S. aureus* have been defined as a major public health threat worldwide (McCaig et al., 2006). Therefore, new and effective treatment strategies are warranted (Antonelou et al., 2011).

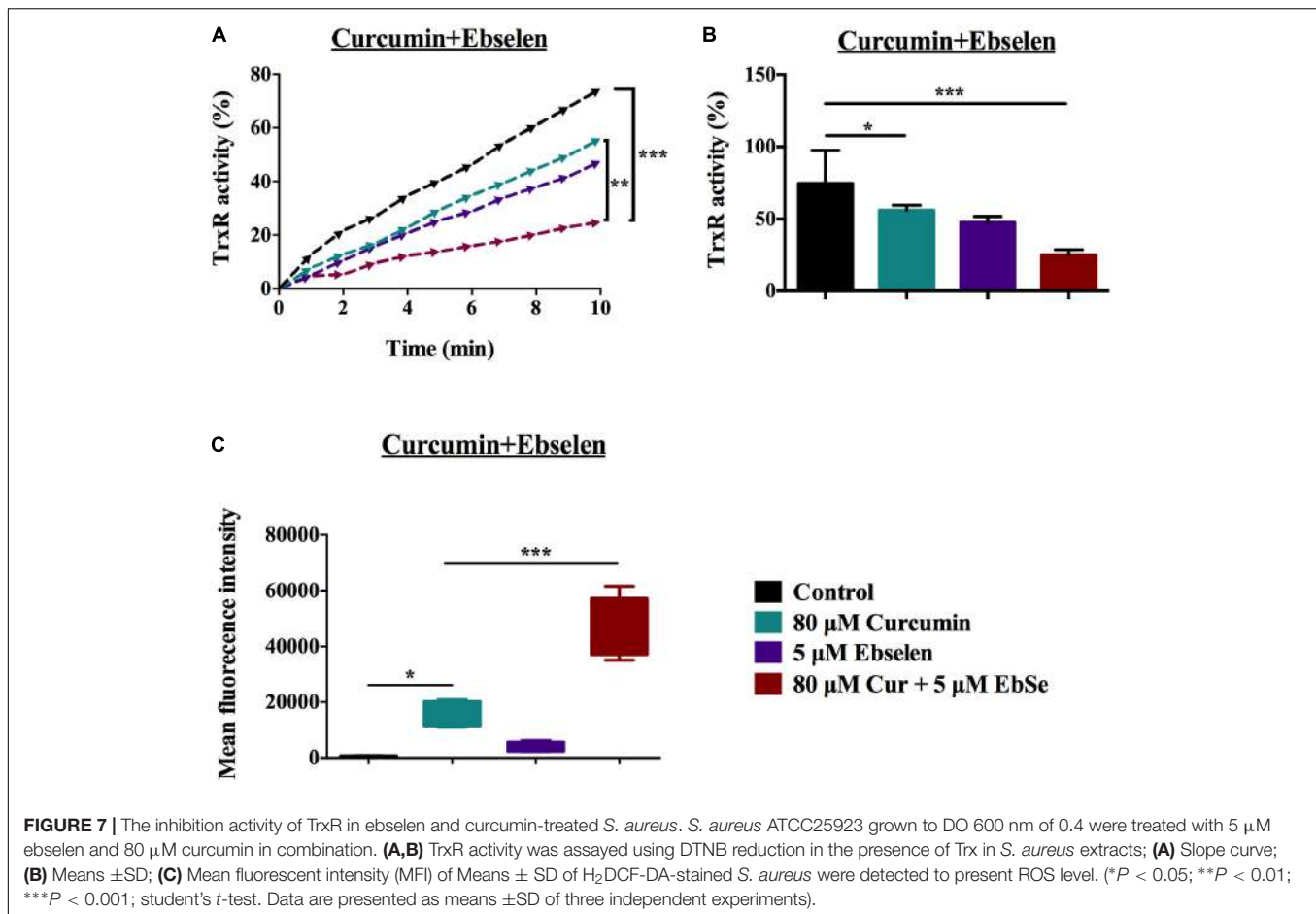


As a major thiol-dependent enzyme system exists in both mammalian and most Gram-positive bacteria, Trx system transfers electrons from NADPH to corresponding substrates via TrxR, which is critical for DNA synthesis, defense against oxidative stress, repair of oxidized proteins, and post-translational modifications (Lillig and Holmgren, 2007; Tejman-Yarden et al., 2013; Leitsch, 2017; Zou et al., 2017, 2018). Bacterial TrxR has notable differences in components, enzyme structure, and reaction mechanisms compared with corresponding mammalian host (Holmgren, 1989; Sandalova et al., 2001; Lu et al., 2013), which guaranteed it act as an appropriate target by specific antibiotics. We and other groups previously found that the selenazol drug ebselen was a lead compound for this antibiotic principle (Winterbourn and Hampton, 2008; Lu and Holmgren, 2014a; Thangamani et al., 2015). Briefly, mammalian TrxR is a large (55 kDa/subunit) selenium-containing enzyme, and ebselen react with it to form Se-Se bond to be a substrate for better redox homeostasis. Meanwhile, bacterial TrxR is a small enzyme (35 kDa/subunit) free from selenium, and ebselen react with it to form Se-Se

bond to act as a competitive inhibitor that could upregulate ROS production (Lu et al., 2013; Lu and Holmgren, 2014a; Zou et al., 2017).

In recent studies, we and other groups have shown that ebselen has potent antimicrobial activity against most Gram-positive bacteria including MDR *S. aureus* (Lu et al., 2013; Thangamani et al., 2015). As a well-known organo-selenium compound, ebselen is under phase II clinical trials for stroke, hearing loss, atherosclerosis, and other conditions, which guaranteed its safety and tolerance in human being (Pratta et al., 1998; Ishii et al., 2000; Zhang et al., 2002; Johnsen-Soriano et al., 2007). In this study, the bactericidal activity of ebselen was confirmed by visible spectrophotometer, transmission electron microscopy, DTNB assay, and Flow cytometry *in vitro*. These results verified the potent bactericidal activity of ebselen against MDR *S. aureus*, and demonstrated one of its ability to inhibit bacterial TrxR and disrupt the intracellular redox microenvironment.

The bacterial Trx system is important for reducing various cellular antioxidants, such as RNR, Msr, Tpx, Bcp. Thus, inhibition of TrxR is highly related to the excessive production



of ROS, which may disrupt many physiological processes and cause cellular damages or even cell death (Zou et al., 2017). In order to detect the intracellular ROS level, ebselen-treated cells were stained with H<sub>2</sub>DCFH-DA. FACS results confirmed that ebselen inhibited the electrons transfer from TrxR to its corresponding oxidized substrates, which greatly influences ROS removal. This result demonstrated that ROS elevation is a major player in determining the bacterial fates, which is consistent with previous reports showing that ROS produced by some clinically used antibiotics contribute to their bactericidal efficacy (Kohanski et al., 2007; Morones-Ramirez et al., 2013; Zou et al., 2018).

Further, the rat model with staphylococcal skin wound infection of *S. aureus* LT-1 strain was used to determine the therapeutic efficacy of ebselen on bacterial burden and infection-induced inflammation, *in vitro*. As this model represented a staphylococcus infection of open skin wounds, it provided the opportunity to evaluate the efficacy of topical ebselen treatment. Ebselen showed high therapeutic efficacy against MDR *S. aureus* LT-1 caused skin infection, including substantially reducing the bacterial burden by day 5 (10-fold), increasing fibroblasts and microvascular, and reducing scattered lymphocytes. Moreover, since increased host inflammatory cytokines are mediators for clinical severity of staphylococcal

skin infections, the expression of infection-induced inflammation cytokines was also evaluated (Montgomery et al., 2013; Sharma-Kuinkel et al., 2013). The results showed that TNF- $\alpha$ , IL-1 $\beta$ , and IL-6 all contributed to host defense during a *S. aureus* skin wound infection, whereas IL-1 $\beta$  was more critical during a deeper intradermal *S. aureus* infection. A similar study demonstrated that during the intradermal infection, the inducible IL-1 $\beta$  response of the bone-marrow-derived recruited cells of the abscess was a more critical determinant for host defense (Miller et al., 2007). Our results showed that ebselen dramatically decreased the infection-induced inflammation that provide a favorable outcome in wound healing, which might be highly related to its recognized immunomodulatory, anti-inflammatory, and anti-oxidant activities (Schewe, 1995; Ren et al., 2017, 2018). Together, the results demonstrated that ebselen has a higher skin repairing efficacy than gentamycin, which may make it a better antimicrobial than gentamycin, especially because it is predicted to have less severe side effects.

Moreover, we have investigated whether ebselen has the potential to act synergistically with the traditional polyphenol, curcumin, against *S. aureus*. The results showed that TrxR is one of the antibacterial targets of curcumin, and ebselen sensitized its ability.



Together, these results suggested that ebselen could serve as an alternative topical agent to gentamycin to treat Staphylococcal skin infections. The sensitivity of bacteria to ebselen is dependent on the antioxidant systems equipped in bacteria. Notably, ebselen increased the sensitivity of *S. aureus* to curcumin, which is a commonly used polyphenol antimicrobials component. Importantly, the combination of ebselen with other antimicrobials may help overcome the MDR in bacteria.

## MATERIALS AND METHODS

### Rat and Bacterial Strains

Sprague Dawley rats (male, 180–200 g) were purchased from China Three Gorges University, and approval from the Medical Animal Care & Welfare Committee of China Three Gorges University was obtained prior to using the animals for research. All rats were kept in individually cages under a constant dark-light cycle in a conventional SPF animal house and were free access to food and water.

*Staphylococcus aureus* LT-1 was isolated from the skin lesion of a clinical patient in the First Affiliated Hospital of Three Gorges University in Hubei Province, China, with an approval for research from the Ethics Committee of the First Affiliated Hospital of Three Gorges University and written informed consent of the patient. *S. aureus* LT-1 strain was thoroughly identified by biochemical, 16S rRNA PCR (5'-GATAACCTACCTATAAGACT-3' and 5'-TCCATCTATAAGTGACAG-3' as primers), and MALDI-TOF MS (bioMérieux VITEK MS), and stored in our laboratory (Tables 1, 2 and Supplementary Figure S2). *S. aureus* ATCC25923 was stored in our lab.

### Reagents

Bacteria cells were cultured in Luria Bertani (LB) medium (EMD millipore). 2-Phenyl-1, 2-benzisoxselenazol-3(2H)-one (ebselen) (Daiichi), protease inhibitor cocktails (Roche), *Escherichia coli* DHB4 Trx was from IMCO Corp. (Stockholm, Sweden)<sup>1</sup>, Rabbit anti-sheep IgG-HRP (Santa cruz), Curcumin (Selleck), all the other reagents were from Sigma-Aldrich.

### The Inhibition of *S. aureus* LT-1 Growth by Ebselen

The inhibition of *S. aureus* LT-1 growth by ebselen was measured by visible spectrophotometer. *S. aureus* LT-1 cells were grown (37°C, 220 rpm) till an OD<sub>600 nm</sub> of 0.4 and diluted 100 times to be treated with different concentrations of ebselen (gentamycin was used as positive control) for 16 h at 37°C in 96 wells plate, and the absorbance values at 600 nm were measured.

In addition, nuclear staining reagent propidium iodide (PI) was used to detect the inhibition efficiency of *S. aureus* LT-1 by ebselen. LT-1 cells were grown (37°C, 220 rpm) till an OD<sub>600 nm</sub> of 0.4 and treated with 22 µg/ml ebselen for 40 min at 37°C, and washed three times with PBS and the cells were collected by centrifugation (6,000 rpm, 5 min). Nuclei were

stained by 5 µg/ml PI for 30 min at 37°C, and were washed three times and re-suspended in PBS after the incubation, and the fluorescence measured by flow cytometry (BECKMAN COULTER, CytoFLEX).

### Effect of Ebselen on Bacterial Morphology

*Staphylococcus aureus* LT-1 was grown till an OD<sub>600 nm</sub> of 0.4 in LB medium, and treated with 22 µg/ml ebselen, 64 µg/ml gentamycin and PBS for 20 min, respectively. Cells were obtained by centrifuging (4°C, 13000 rpm, 15 min), and fixed with 2.5% glutaraldehyde. The morphology and structure of *S. aureus* cells were observed under transmission electron microscopy (Hitachi H-7500, Japan).

### The Inhibition of *S. aureus* LT-1 TrxR Activity by Ebselen

*Staphylococcus aureus* LT-1 cells were cultured till an OD<sub>600 nm</sub> of 0.4 and incubated with 22 µg/ml ebselen for 40 min. LT-1 cells were obtained by centrifugation (4°C, 5000 rpm, 5 min), which were washed three times and re-suspended in 50 mM Tris-EDTA buffer (pH 7.4), and the protein inhibitor cocktail was added to decrease the protease activity. Finally, the cells were disrupted with before sonication (240 W, 5 min). The cell supernatants were obtained by centrifugation (4°C, 12000 rpm, 10 min), and the protein concentration was measured by Bradford assay and used for TrxR activity assay.

The determination of TrxR activity was performed in 96 wells plate. 25 µg obtained cell lysate was incubated with 2 mM EDTA, 200 µM NADPH at 37°C for 5 min, and added 5 µM *E. coli* Trx, 2 mM DTNB. The absorbance at 412 nm was detected with a VERSA micro-wells plate reader for 5 min, and the slope was used to represent TrxR activity. The activity of the untreated group was considered as 100%.

### Determination of ROS Production in Ebselen Treated *S. aureus* LT-1

*Staphylococcus aureus* LT-1 was grown till an OD<sub>600 nm</sub> of 0.4 in LB medium, and incubated with 22 µg/ml ebselen for 40 min. The LT-1 cells were obtained by centrifugation (4°C, 5000 rpm, 5 min). The pellets were washed three times with PBS and stained with 10 µM H<sub>2</sub>DCFH-DA for 30 min at 37°C. After the incubation, cells were washed three times and re-suspended in PBS, and the ROS production was quantified by flow cytometry (BECKMAN COULTER, CytoFLEX).

### Rat Model of *S. aureus* LT-1 Skin Wound Infection

All experiments were performed in accordance with the relevant guidelines and regulations. Healthy male SD rats (body weight 180–200 g) were used for this study. Animals were housed adaptively for 1 week in SPF room and were free access to food and water. For bacterial load and wound healing tests, thirty rats were randomly divided into three groups: control group, ebselen-treated group, and gentamycin-treated group. Thick scalpel cuts were made into the dermis of

<sup>1</sup><http://www.imcocorp.se>

the skin on the posterior upper back and neck of rats and inoculated with 200  $\mu\text{l}$   $3.26 \times 10^9$  CFU/ml *S. aureus* LT-1 cells. Rats were then treated intradermal administered with 80  $\mu\text{l}$  25 mg/kg ebselen, 5 mg/kg gentamycin or PBS once per day for 5 days, respectively. Twenty-four hours after the last treatment, the wound was excised for bacteria load on *S. aureus* after homogenization. The wound healing was calculated by formula as follows:  $F = (A-B)/A \times 100\%$ , where F: wound healing rate, A: original wound area, and B: wound area post-treatment.

For inflammatory cytokines, pathological and IHC detection, forty rats were randomly divided into four groups: A to D, and the skin cuts were constructed as described above. Further, rats from group A served as a control group and were not infected or treated. Rats of groups B–D were inoculated with 200  $\mu\text{l}$  of *S. aureus* strain LT-1 ( $3.26 \times 10^9$ ). Group B was intradermal administered 80  $\mu\text{l}$  PBS; Group C and group D were administered 80  $\mu\text{l}$  25 mg/kg ebselen and 5 mg/kg gentamycin, respectively. All groups were treated once a day for 5 days. Blood serum was used to detect the cytokines level by ELISA. TNF- $\alpha$ , IL-6, and IL-1 $\beta$  ELISA Kits (Uscn Life Science, Inc.) were used for the quantification of cytokines. The experiment was carried out as the manufacture instructions.

## Histological Analysis

Rats from four groups were treated as described above, and were euthanized and lesional 8-mm punch biopsy (Acuderm) tissues specimens were bisected and fixed in formalin (10%) and embedded in paraffin. Paraffin sections (4  $\mu\text{m}$  thick) were cut and stained with hematoxylin and eosin and Masson stain.

Further, anti-CD64 antibody and anti-S100a4 antibody were used to present neutrophils and fibroblasts, respectively, by IHC.

## Synergistic Antibacterial Activity of Ebselen Combined With Curcumin

*Staphylococcus aureus* ATCC25923 cells were incubated till an  $\text{OD}_{600 \text{ nm}}$  of 0.4 and diluted 100 times in LB medium. In 96 wells plate, the diluted bacteria were incubated with serial concentrations of ebselen and curcumin for 16 h at 37°C and read the  $\text{OD}_{600 \text{ nm}}$  values by VERSA microplate reader. In addition, PI staining was used to identify whether cells were synergistically killed by 5  $\mu\text{M}$  ebselen and 80  $\mu\text{M}$  curcumin as described above.

Further, the TrxR activity and ROS production were performed by DTNB and flow cytometry, respectively, to detect the synergistically inhibition effect of 5  $\mu\text{M}$  ebselen and 80  $\mu\text{M}$  curcumin on *S. aureus* as described above.

## The Synergist Degree Measurement

The synergist degree was measured by Bliss independent model which described as previous study and the synergist degree S was calculated by the following formula (Hegreness et al., 2008):  $S = (f_{X0}/f_{00})(f_{0Y}/f_{00}) - (f_{XY}/f_{00})$ ,  $f_{XY}$  refers to the growth rate of bacteria under the two drugs in combination treatment, the concentration of one drug is X and the other is Y;  $f_{X0}$ ,  $f_{0Y}$  refers to the growth rate of bacteria just one drug treatment, the concentration of one drug is X and the other is Y;  $f_{00}$  refers to

the growth rate of bacteria without drug; S refers to the degree of synergy. The value of the combined degree S is between -1 and 1, and the value is closer to -1, indicating that the antagonism effect, and the value is closer to 1, indicating that the synergy efficient.

## Statistical Analyses

Statistical analyses were assessed by Graph Pad Prism 6.0 (Graph Pad Software, La Jolla, CA, United States). Statistical analysis was assessed between two groups using the Student's two-tailed *t*-test; among multiple groups comparisons, one-way ANOVA analysis was performed.  $P < 0.05$  was considered to indicate a statistically significant difference.  $P$ -values of  $< 0.05$  were considered as significant (\*\* $P < 0.01$ ; \*\*\* $P < 0.001$ ).

## DATA AVAILABILITY STATEMENT

The raw data supporting the conclusions of this article will be made available by the authors, without undue reservation, to any qualified researcher.

## ETHICS STATEMENT

The animal study was reviewed and approved by the Medical Animal Care & Welfare Committee of China Three Gorges University.

## AUTHOR CONTRIBUTIONS

CD, JZ, PW, TL, and YZ performed the experiments. JL and AH conceived the project. XR, JW, and LZ drafted the manuscript and analyzed the results.

## FUNDING

We are grateful for the support of the Swedish Research Council Medicine Grant (13x-3529), the National Natural Science Foundation of China (81903105), and Yichang Medical Treatment and Public Health Foundation (A19-301-50).

## SUPPLEMENTARY MATERIAL

The Supplementary Material for this article can be found online at: <https://www.frontiersin.org/articles/10.3389/fmicb.2019.03016/full#supplementary-material>

**FIGURE S1** | 16 S rRNA Identification of *Staphylococcus aureus* LT-1. *S. aureus* LT-1 cells was identified by 16 S rRNA PCR using primers as following: 5'-GATAACCTACCTATAAGACT-3' and 5'-TCCATCTATAAGTGACAG-3', and the predictive product is 115 bp. M, marker; 1–4, PCR products.

**FIGURE S2** | Synergistic activity of ebselen with curcumin. The Bliss Model for Synergy confirms a synergistic effect, between 5  $\mu\text{M}$  ebselen and 10  $\mu\text{M}$  curcumin. Degree of synergy was quantified after 2 h of treatment with ebselen in combination with curcumin.

## REFERENCES

- Antonelou, M., Knowles, J., Siddiqi, S., and Sharma, P. (2011). Recurrent cutaneous abscesses caused by PVL-MRSA. *BMJ Case Rep.* 2011:bcr0120113680. doi: 10.1136/bcr.01.2011.3680
- Balasubramanian, D., Harper, L., Shopsin, B., and Torres, V. J. (2017). *Staphylococcus aureus* pathogenesis in diverse host environments. *Pathog. Dis.* 75:ftx005. doi: 10.1093/femspd/ftx005
- Balkhy, H. H., Zowawi, H., Albatshan, H. A., Alshamrani, M. M., Aidara-Kane, A., Erlacher-Vindel, E., et al. (2018). Antimicrobial resistance: a round table discussion on the "One Health" concept from the gulf cooperation council countries. part one: a focus on leadership. *J. Infect. Public Health* 11, 771–777. doi: 10.1016/j.jiph.2018.05.007
- Baptista, P. V., McCusker, M. P., Carvalho, A., Ferreira, D. A., Mohan, N. M., Martins, M., et al. (2018). Nano-Strategies to fight multidrug resistant bacteria—“A battle of the titans”. *Front. Microbiol.* 9:1441. doi: 10.3389/fmicb.2018.01441
- Bhatia, R. (2018). Antimicrobial resistance: threat, consequences and options. *Natl. Med. J. India* 31, 133–135.
- Brown, E. D., and Wright, G. D. (2016). Antibacterial drug discovery in the resistance era. *Nature* 529, 336–343. doi: 10.1038/nature17042
- Coates, R., Moran, J., and Horsburgh, M. J. (2014). Staphylococci: colonizers and pathogens of human skin. *Future Microbiol.* 9, 75–91. doi: 10.2217/fmb.13.145
- Dweba, C. C., Zishiri, O. T., and El Zowalaty, M. E. (2018). Methicillin-resistant *Staphylococcus aureus*: livestock-associated, antimicrobial, and heavy metal resistance. *Infect. Drug Resist.* 11, 2497–2509. doi: 10.2147/IDRS.175967
- Hegreness, M., Shores, N., Damian, D., Hartl, D., and Kishony, R. (2008). Accelerated evolution of resistance in multidrug environments. *Proc. Natl. Acad. Sci. U.S.A.* 105, 13977–13981. doi: 10.1073/pnas.0805965105
- Holmgren, A. (1985). Thioredoxin. *Annu. Rev. Biochem.* 54, 237–271.
- Holmgren, A. (1989). Thioredoxin and glutaredoxin systems. *J. Biol. Chem.* 264, 13963–13966.
- Ishii, Y., Hashimoto, K., Hirano, K., Morishima, Y., Mochizuki, M., Masuyama, K., et al. (2000). Ebselen decreases ozone-induced pulmonary inflammation in rats. *Lung* 178, 225–234. doi: 10.1007/s0040800000026
- Johnsen-Soriano, S., Genovés, J. M., Romero, B., García-Delpech, S., Muriach, M., Sancho-Tello, M., et al. (2007). [Chronic ethanol feeding induces oxidative stress in the rat retina: treatment with the antioxidant ebselen]. *Arch. Soc. Esp. Ophthalmol.* 82, 757–762.
- Kaur, S., Modi, N. H., Panda, D., and Roy, N. (2010). Probing the binding site of curcumin in *Escherichia coli* and *Bacillus subtilis* FtsZ—a structural insight to unveil antibacterial activity of curcumin. *Eur. J. Med. Chem.* 45, 4209–4214. doi: 10.1016/j.ejmech.2010.06.015
- Kobayashi, S. D., Malachowa, N., and DeLeo, F. R. (2015). Pathogenesis of *Staphylococcus aureus* abscesses. *Am. J. Pathol.* 185, 1518–1527. doi: 10.1016/j.ajpath.2014.11.030
- Kohanski, M. A., Dwyer, D. J., Hayete, B., Lawrence, C. A., and Collins, J. J. (2007). A common mechanism of cellular death induced by bactericidal antibiotics. *Cell* 130, 797–810. doi: 10.1016/j.cell.2007.06.049
- Leitsch, D. (2017). Drug susceptibility testing in microaerophilic parasites: cysteine strongly affects the effectiveness of metronidazole and auranofin, a novel and promising antimicrobial. *Int. J. Parasitol. Drugs Drug Resist.* 7, 321–327. doi: 10.1016/j.ijpddr.2017.09.001
- Lillig, C. H., and Holmgren, A. (2007). Thioredoxin and related molecules—from biology to health and disease. *Antioxid. Redox. Signal.* 9, 25–47. doi: 10.1089/ars.2007.9.25
- Lu, J., and Holmgren, A. (2012). Thioredoxin system in cell death progression. *Antioxid. Redox. Signal.* 17, 1738–1747. doi: 10.1089/ars.2012.4650
- Lu, J., and Holmgren, A. (2014a). The thioredoxin antioxidant system. *Free Radic. Biol. Med.* 66, 75–87. doi: 10.1016/j.freeradbiomed.2013.07.036
- Lu, J., and Holmgren, A. (2014b). The thioredoxin superfamily in oxidative protein folding. *Antioxid. Redox. Signal.* 21, 457–470. doi: 10.1089/ars.2014.5849
- Lu, J., Vlamis-Gardikas, A., Kandasamy, K., Zhao, R., Gustafsson, T. N., Engstrand, L., et al. (2013). Inhibition of bacterial thioredoxin reductase: an antibiotic mechanism targeting bacteria lacking glutathione. *FASEB J.* 27, 1394–1403. doi: 10.1096/fj.12-223305
- McCaig, L. F., McDonald, L. C., Mandal, S., and Jernigan, D. B. (2006). *Staphylococcus aureus*-associated skin and soft tissue infections in ambulatory care. *Emerg. Infect. Dis.* 12, 1715–1723. doi: 10.3201/eid1211.060190
- McGuinness, W. A., Malachowa, N., and DeLeo, F. R. (2017). Vancomycin resistance in *Staphylococcus aureus*. *Yale J. Biol. Med.* 90, 269–281.
- Miller, L. S., Pietras, E. M., Uricchio, L. H., Hirano, K., Rao, S., Lin, H., et al. (2007). Inflammasome-mediated production of IL-1 $\beta$  is required for neutrophil recruitment against *Staphylococcus aureus* in vivo. *J. Immunol.* 179, 6933–6942. doi: 10.4049/jimmunol.179.10.6933
- Montgomery, C. P., Daniels, M. D., Zhao, F., Spellberg, B., Chong, A. S., and Daum, R. S. (2013). Local inflammation exacerbates the severity of *Staphylococcus aureus* skin infection. *PLoS One* 8:e69508. doi: 10.1371/journal.pone.0069508
- Morones-Ramirez, J. R., Winkler, J. A., Spina, C. S., and Collins, J. J. (2013). Silver enhances antibiotic activity against gram-negative bacteria. *Sci. Transl. Med.* 5:190ra181.
- Odell, C. A. (2010). Community-associated methicillin-resistant *Staphylococcus aureus* (CA-MRSA) skin infections. *Curr. Opin. Pediatr.* 22, 273–277. doi: 10.1097/MOP.0b013e328339421b
- Pantosti, A., Sanchini, A., and Monaco, M. (2007). Mechanisms of antibiotic resistance in *Staphylococcus aureus*. *Future Microbiol.* 2, 323–334.
- Pratta, M. A., Ackerman, N. R., and Arner, E. C. (1998). Effect of ebselen on IL-1-induced alterations in cartilage metabolism. *Inflamm. Res.* 47, 115–121. doi: 10.1007/s000110050296
- Rai, D., Singh, J. K., Roy, N., and Panda, D. (2008). Curcumin inhibits FtsZ assembly: an attractive mechanism for its antibacterial activity. *Biochem. J.* 410, 147–155. doi: 10.1042/bj20070891
- Ren, X., Zou, L., Lu, J., and Holmgren, A. (2018). Selenocysteine in mammalian thioredoxin reductase and application of ebselen as a therapeutic. *Free Radic. Biol. Med.* 127, 238–247. doi: 10.1016/j.freeradbiomed.2018.05.081
- Ren, X., Zou, L., Zhang, X., Branco, V., Wang, J., Carvalho, C., et al. (2017). Redox signaling mediated by thioredoxin and glutathione systems in the central nervous system. *Antioxid. Redox. Signal.* 27, 989–1010. doi: 10.1089/ars.2016.6925
- Rudrappa, T., and Bais, H. P. (2008). Curcumin, a known phenolic from *Curcuma longa*, attenuates the virulence of *Pseudomonas aeruginosa* PAO1 in whole plant and animal pathogenicity models. *J. Agric. Food Chem.* 56, 1955–1962. doi: 10.1021/jf072591j
- Sandalova, T., Zhong, L., and Lindqvist, Y. (2001). A. holmgren, G. schneider, three-dimensional structure of a mammalian thioredoxin reductase: implications for mechanism and evolution of a selenocysteine-dependent enzyme. *Proc. Natl. Acad. Sci. U.S.A.* 98, 9533–9538. doi: 10.1073/pnas.171178698
- Schewe, T. (1995). Molecular actions of ebselen—an antiinflammatory antioxidant. *Gen. Pharmacol.* 26, 1153–1169. doi: 10.1016/0306-3623(95)00003-j
- Sharma-Kuinkel, B. K., Zhang, Y., Yan, Q., Ahn, S. H., and Fowler, V. G. Jr. (2013). Host gene expression profiling and in vivo cytokine studies to characterize the role of linezolid and vancomycin in methicillin-resistant *Staphylococcus aureus* (MRSA) murine sepsis model. *PLoS One* 8:e60463. doi: 10.1371/journal.pone.0060463
- Song, J., Choi, B., Jin, E. J., Yoon, Y., and Choi, K. H. (2012). Curcumin suppresses *Streptococcus mutans* adherence to human tooth surfaces and extracellular matrix proteins. *Eur. J. Clin. Microbiol. Infect. Dis.* 31, 1347–1352. doi: 10.1007/s10096-011-1448-y
- Tejman-Yarden, N., Miyamoto, Y., Leitsch, D., Santini, J., Debnath, A., Gut, J., et al. (2013). A reprofiled drug, auranofin, is effective against metronidazole-resistant *Giardia lamblia*. *Antimicrob. Agents Chemother.* 57, 2029–2035. doi: 10.1128/AAC.01675-12
- Thangamani, S., Younis, W., and Seleem, M. N. (2015). Repurposing ebselen for treatment of multidrug-resistant staphylococcal infections. *Sci. Rep.* 5:11596. doi: 10.1038/srep11596
- Tong, S. Y., Davis, J. S., Eichenberger, E., Holland, T. L., and Fowler, V. G. Jr. (2015). *Staphylococcus aureus* infections: epidemiology, pathophysiology, clinical manifestations, and management. *Clin. Microbiol. Rev.* 28, 603–661. doi: 10.1128/cmr.00134-14
- Tyagi, P., Singh, M., Kumari, H., Kumari, A., and Mukhopadhyay, K. (2015). Bactericidal activity of curcumin I is associated with damaging of bacterial membrane. *PLoS One* 10:e0121313. doi: 10.1371/journal.pone.0121313

- van Hal, S. J., Jensen, S. O., Vaska, V. L., Espedido, B. A., Paterson, D. L., and Gosbell, I. B. (2012). Predictors of mortality in *Staphylococcus aureus* bacteremia. *Clin. Microbiol. Rev.* 25, 362–386. doi: 10.1128/CMR.05022-11
- Winterbourn, C. C., and Hampton, M. B. (2008). Thiol chemistry and specificity in redox signaling. *Free Radic Biol. Med.* 45, 549–561. doi: 10.1016/j.freeradbiomed.2008.05.004
- Zhang, M., Nomura, A., Uchida, Y., Iijima, H., Sakamoto, T., Iishii, Y., et al. (2002). Ebselen suppresses late airway responses and airway inflammation in guinea pigs. *Free Radic Biol. Med.* 32, 454–464. doi: 10.1016/s0891-5849(01)00825-5
- Zou, L., Lu, J., Wang, J., Ren, X., Zhang, L., Gao, Y., et al. (2017). Synergistic antibacterial effect of silver and ebselen against multidrug-resistant gram-negative bacterial infections. *EMBO Mol. Med.* 9, 1165–1178. doi: 10.15252/emmm.201707661
- Zou, L., Wang, J., Gao, Y., Ren, X., Rottenberg, M. E., Lu, J., et al. (2018). Synergistic antibacterial activity of silver with antibiotics correlating with the upregulation of the ROS production. *Sci. Rep.* 8:11131. doi: 10.1038/s41598-018-29313-w

**Conflict of Interest:** The authors declare that the research was conducted in the absence of any commercial or financial relationships that could be construed as a potential conflict of interest.

Copyright © 2020 Dong, Zhou, Wang, Li, Zhao, Ren, Lu, Wang, Holmgren and Zou. This is an open-access article distributed under the terms of the Creative Commons Attribution License (CC BY). The use, distribution or reproduction in other forums is permitted, provided the original author(s) and the copyright owner(s) are credited and that the original publication in this journal is cited, in accordance with accepted academic practice. No use, distribution or reproduction is permitted which does not comply with these terms.





# New Tetramic Acids Comprising of Decalin and Pyridones From *Chaetomium olivaceum* SD-80A With Antimicrobial Activity

Xinzhu Wang<sup>1</sup>, Liya Zhao<sup>2</sup>, Chao Liu<sup>3</sup>, Jun Qi<sup>2</sup>, Peipei Zhao<sup>2</sup>, Zhaoming Liu<sup>4</sup>, Chunlei Li<sup>2</sup>, Yingying Hu<sup>1</sup>, Xin Yin<sup>2</sup>, Xin Liu<sup>2</sup>, Zhixin Liao<sup>1\*</sup>, Lixin Zhang<sup>2,5\*</sup> and Xuekui Xia<sup>2\*</sup>

<sup>1</sup> Department of Pharmaceutical Engineering, School of Chemistry and Chemical Engineering, Southeast University, Nanjing, China, <sup>2</sup> Shandong Provincial Key Laboratory for Biosensor, Biology Institute, Qilu University of Technology (Shandong Academy of Sciences), Jinan, China, <sup>3</sup> Institute of Agro-Food Science and Technology, Shandong Academy of Agricultural Sciences, Jinan, China, <sup>4</sup> Guangdong Institute of Microbiology, Guangdong Academy of Sciences, Guangzhou, China, <sup>5</sup> State Key Laboratory of Bioreactor Engineering, East China University of Science and Technology, Shanghai, China

## OPEN ACCESS

### Edited by:

Raffaele Zarrilli,  
University of Naples Federico II, Italy

### Reviewed by:

Guojun Wang,  
Florida Atlantic University,  
United States  
Annalisa Guaragna,  
University of Naples Federico II, Italy

### \*Correspondence:

Zhixin Liao  
zxliao@seu.edu.cn;  
101010762@seu.edu.cn  
Lixin Zhang  
lxzhang@ecust.edu.cn  
Xuekui Xia  
xiaxk@sdas.org

### Specialty section:

This article was submitted to  
Antimicrobials, Resistance  
and Chemotherapy,  
a section of the journal  
Frontiers in Microbiology

Received: 31 August 2019

Accepted: 09 December 2019

Published: 15 January 2020

### Citation:

Wang X, Zhao L, Liu C, Qi J, Zhao P, Liu Z, Li C, Hu Y, Yin X, Liu X, Liao Z, Zhang L and Xia X (2020) New Tetramic Acids Comprising of Decalin and Pyridones From *Chaetomium olivaceum* SD-80A With Antimicrobial Activity. *Front. Microbiol.* 10:2958. doi: 10.3389/fmicb.2019.02958

Cycloaddition reactions such as intramolecular Diels–Alder (IMDA) are extremely important in constructing multicyclic scaffolds with diverse bioactivities. Using MycB as a biomarker, three new polyketides – Chaetolivacines A (**1**), B (**3**), and C (**4**) – with one known compound Myceliothermophin E (**2**) comprising of decalin and 4-hydroxy-2-pyridones were obtained from the culture of *Chaetomium olivaceum* SD-80A under the guidance of gene mining. The structures of these compounds were established using detailed 1D, 2D NMR, and high-resolution electron spray ionization mass spectroscopy (HRESIMS) analysis. The relative and absolute configurations of the compounds **1**, **3**, and **4** were elucidated by NOESY and ECD. The biosynthesis pathways of these compounds were proposed, which involves in three key genes *ChaA* [polyketide synthase-non-ribosomal peptide synthetases (PKS-NRPS)], *ChaB*, and *ChaC*. Compounds **1–4** were tested for their antimicrobial activities, and compounds **2** and **3** showed moderate bioactivity against *Staphylococcus aureus* (SA) and methicillin-resistant *S. aureus* (MRSA) with MIC values of 15.8 and 27.1  $\mu$ M. The results showed that configuration of C-21 in **3** and **4** is important for anti-SA and anti-MRSA activities. This study reveals the significant potential of the genus *Chaetomium* in producing new PKS-NRPS, therefore increasing the speed in the mining for new sources of antimicrobial agents.

**Keywords:** *Chaetomium olivaceum*, tetramic acids, isolation, anti-MRSA, biosynthesis pathway

## INTRODUCTION

The increasing resistance to drugs of bacteria like methicillin-resistant *Staphylococcus aureus* (MRSA) has become a major threat to public health (Coast et al., 1996; Stanton, 2013). The first strain of MRSA appeared in Cairo in 1961. Since then, the specific strain has spread to become a worldwide problem (Chapman et al., 2005). MRSA has increased in prevalence during the past decade due to the steady growth of elderly and immunocompromised patients and the

emergence of multidrug-resistant (MDR) bacterial strains. Because MRSA is one of the most common and problematic bacteria associated with increasing antimicrobial resistance, continuous efforts to discover compounds, develop alternative therapies, and create faster diagnostics methods are required (Kurosu et al., 2013). MRSA continues to be associated with significant morbidity and mortality rates. Vancomycin was the “gold standard” for treatment of serious MRSA infections; however, the emergence of less-susceptible strains, poor clinical outcomes, and increased nephrotoxicity associated with high-dose therapy have challenged vancomycin’s role as a first-line therapy. Linezolid is recommended for PO or IV treatments of skin and skin structure infections (SSSIs) and pneumonia caused by MRSA. Daptomycin (IV) should be considered for patients with MRSA bacteremia and right-sided endocarditis as well as for cases of complicated SSSIs; however, daptomycin should not be used to treat MRSA-related pneumonia. Tigecycline and telavancin are alternative (IV) treatments for SSSIs caused by MRSA; however, safety concerns have limited use of these agents (Rodvold and McConeghy, 2013). Recently, more and more attention has been devoted to fungi, which is an important resource to produce lead compounds for drug-resistant bacteria (Ghisalberti, 2003). *Chaetomium* sp. is a large fungal group (Royles, 1995) known for its secondary metabolites with physiological activity and is considered a potential biological control group (Hazuda et al., 1999; Kirk et al., 2001). A variety of secondary metabolites can be produced by the *Chaetomium* sp., such as decalinepolyketides containing a tetramic acid (2,4-pyrrolidine-2,4-dione) ring; it is one of the most important classes of metabolites (Yang et al., 2006, Yang S.W. et al., 2007). The tetramic acid (2,4-pyrrolidine-dione) ring system has been reported since the early 20th century (Osterhage et al., 2000) when the first simple derivative was prepared. Compounds containing this specific structural unit exhibit a diverse range of biological activities (Soytong et al., 2001). For instance, codinaeopsin (Kontnik and Clardy, 2008; Ramanathan et al., 2013) is active against *Plasmodium falciparum*, the causative agent for the most lethal form of malaria. Equisetin (Vesonder et al., 1979; Wheeler et al., 1999) suppresses germination or inhibits the growth of various monocotyledonous and dicotyledonous seeds. Additionally, it inhibits the growth of young seedlings and causes necrotic lesions on the roots, cotyledons, and coleoptiles of tested plant seedlings. Trichosetin (Marfori et al., 2002a, 2003b) is produced by the dual culture of *Trichoderma harzianum* and *Catharanthus roseus* callus and shows remarkable antimicrobial activity against the Gram-positive bacteria MRSA and *Bacillus subtilis*. UCS1025A (Nakai et al., 2000) exhibited antimicrobial and antiproliferative activities.

Many important compounds are produced by polyketide synthase-non-ribosomal peptide synthetase (PKS-NRPS) hybrid clusters, such as fusarin C (Song et al., 2004), equisetin (Kato et al., 2015), and decalinepolyketides (Han et al., 2017). This type of compounds exhibit a wide variety of biological activities (Boettger and Hertweck, 2012; Chooi and Tang, 2012). In recent years, with the development of whole genome sequencing technology, an increasing number

of genomes have been released. The separation of natural products, which were biosynthesized by the regulation of particular gene clusters, has become more efficient under the guidance of genome mining. According to recent studies, collecting and mining “Diels–Alderase” (DAases) from fungi may lead to the discovery of new decalin-containing natural products (Li et al., 2016). Based on the above literature, the *trans*-decalin tetramic acids structure is widely present in bioactive natural products isolated from fungi. In this study, under the guidance of biosynthesis gene cluster analysis of *C. olivaceum* SD-80A, four derived decalin-containing natural products were obtained. Apart from myceliothermophin E (2) (Yang Y.L. et al., 2007; Shionozaki et al., 2012), the compounds 1, 3, and 4 are new. Their activity against drug-resistant bacteria was tested for compounds 1–4. Compounds 2 and 3 showed moderate bioactivity against MRSA (MIC = 15.8 and 21.7  $\mu$ M, respectively). In conclusion, we report the detailed isolation, structural elucidation, biological activities, and possible biosynthesis pathways of these compounds. This is also the first time that these compounds have been found to exhibit anti-MRSA activity.

## MATERIALS AND METHODS

### Genome Mining of Biosynthetic Gene Clusters

The genome *C. olivaceum* SD-80A was firstly deciphered using *de novo* sequencing technology. As reported, DAases have many important biological functions (Zheng et al., 2016). The diversity of DAases have been found to simulate the discovery of certain structural features compounds (Li et al., 2016). In this work, MycB (NCBI Accession No. AEO57198), a kind of DAases used as a signature biosynthetic marker from *Myceliophthora thermophila* was used as probe for mining the homologous protein based on the *C. olivaceum* SD-80A genome. Gene cluster analysis was implemented using anti-SMASH 3.0 (Weber et al., 2015), and gene function was predicted by NCBI combined with reported references (Doroghazi et al., 2014). Amino acid sequence alignment was performed by BLAST<sup>1</sup>.

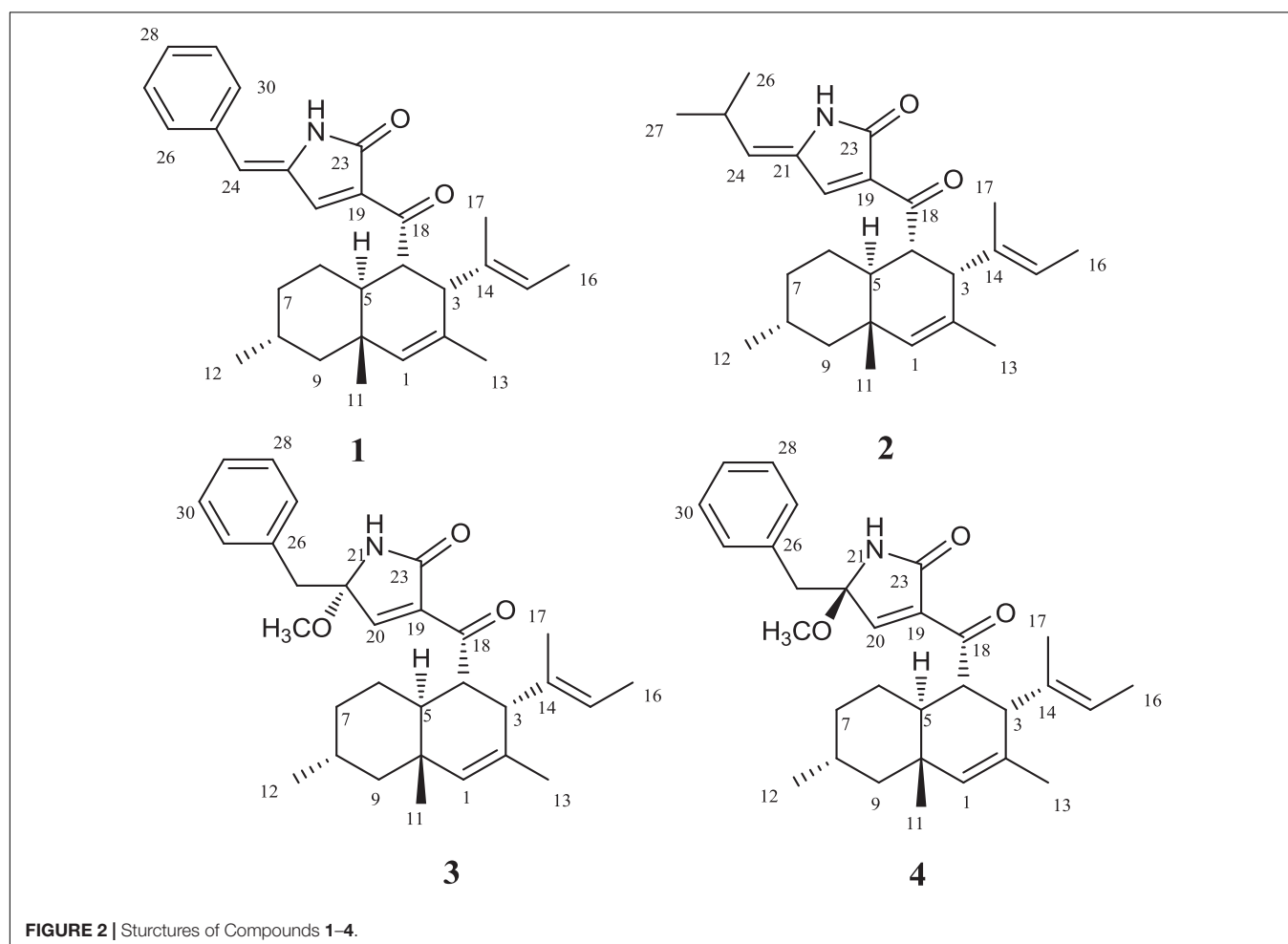
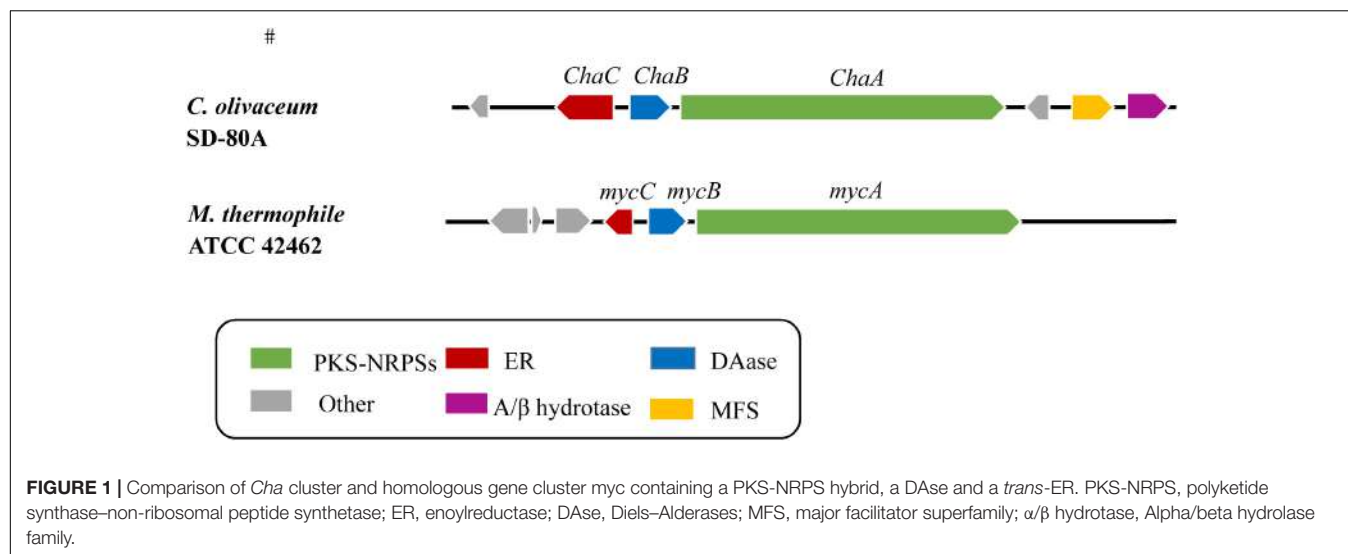
### Producing Fungus and Fermentation

The fungus *C. olivaceum* SD-80A was isolated from a feces of *Boselaphus tragocamelus* collected in New Delhi, India. The strain was grown on a PDA medium for 7 days in the dark at

<sup>1</sup><https://blast.ncbi.nlm.nih.gov/Blast.cgi>

**TABLE 1** | The features of the *Chaetomium olivaceum* SD-80A genome.

Features	<i>Chaetomium olivaceum</i> SD-80A
Sequencing technology	<i>De novo</i> Illumina HiSeq
Total size	34,782,639
Average G + C content	55.57%
Scaffolds	10658



28°C, then transferred to five 500 mL Erlenmeyer flasks with a PDB medium for 5 days at 28°C, with 120 rpm as the seed medium. After the seed medium grew well, the culture was evenly transplanted to 30 1 L Erlenmeyer flasks on an ultra-clean bench,

each containing 50 mL of water and 50 g of rice. Fermentation was conducted under stationary conditions for 30 days at 28°C. After the fermentation, we procured the fungus of *C. olivaceum* SD-80A.

**TABLE 2** |  $^1\text{H}$  and  $^{13}\text{C}$  NMR data of **1** and **2** ( $\delta_{\text{H}}$  in ppm,  $J$  in Hz).

Position	1 <sup>a</sup>		2 <sup>a</sup>	
	$\delta_{\text{C}}$	$\delta_{\text{H}}$ , mult. ( $J$ in Hz)	$\delta_{\text{C}}$	$\delta_{\text{H}}$ , mult. ( $J$ in Hz)
1	136.3	5.37, s	136.1	5.36, s
2	130.2		131.7	
3	51.1	3.23, d (7.2)	51.0	3.23 d (7.2)
4	49.7	3.89, dd (12, 7.2)	49.6	4.04, dd (12, 7.2)
5	40.0	1.86, td (12, 2)	39.8	1.84, td (12, 2)
6	24.3	0.98, m 1.69, m	24.2	0.99, m 1.68, m
7	35.8	0.98, m 1.70, m	35.8	0.98, m 1.70, m
8	27.5	1.69, m	28.3	1.69, m
9	48.6	0.95, m 1.47, m	48.5	0.95, m 1.47, m
10	35.2		35.3	
11	22.8	0.90, s	20.6	0.94, s
12	20.6	0.86, d (6.0)	22.8	0.86, d (6.0)
13	22.2	1.48, s	22.2	1.47, s
14	135.9		135.9	
15	123.4	5.08, d (6.8)	123.2	5.08, d (6.8)
16	13.3	1.43, s	13.3	1.44, s
17	14.0	1.46, s	14.2	1.45, s
18	196.6		197.1	
19	134.8		134.8	
20	143.9	7.61, d (2.0)	142.0	7.44 d (2.0)
21	134.2		134.0	
23	169.8		170.3	
24	119.5	6.34, s	130.3	5.48, d (10.0)
25	129.5		27.5	2.93, m
26, 30	129.4	7.50, d (7.2)	22.5	1.11, d (6.4)
27, 29	129.4	7.45, t (8.0)	22.4	1.14, d (6.4)
28	129.0	7.35, m		
NH		8.65, brs		10.65, brs

<sup>a</sup>Compounds **1** and **2** were measured at  $^1\text{H}$  NMR (400 MHz), and  $^{13}\text{C}$  NMR (100 MHz) with  $\text{CDCl}_3$  as solvent.

## Solvent Extraction and Purification of Secondary Metabolites

The fungus *C. olivaceum* SD-80A was extracted with ethyl acetate (5 × 2 L, 24 h each time) at 25°C to create a dark brown residue (12.0 g) after removal of the solvent *in vacuo*. The ethyl acetate extract (12.0 g) was subjected to a silica gel column using petroleum ether-EtOAc (100:0–0:100, v/v) as an eluent to create seven fractions (Fr. A–G). Fr. A (0.6 g) was separated with semi-preparative high-performance liquid chromatography (HPLC) using  $\text{CH}_3\text{OH}$ - $\text{H}_2\text{O}$  (60:40–100:0, v/v) as the mobile phase to create Fr. A.1 (306.7 mg). Fr. A.1 was further followed by semi-preparative HPLC by using  $\text{CH}_3\text{OH}$ - $\text{H}_2\text{O}$  (80:20–100:0, v/v) as the mobile phase to create **1** (22.5 mg) and **2** (48.6 mg). Fr. C (2.8 g) was subjected to a silica gel column using petroleum ether-EtOAc (15:85–0:100, v/v) to generate Fr. C.1–C.6. Fr. C.3 was separated by semi-preparative HPLC eluted by  $\text{CH}_3\text{OH}$ - $\text{H}_2\text{O}$  (80:20–100:0, v/v) to yield compounds **3** (8.1 mg,  $R_t$  = 15.0 min) and **4** (9.7 mg,  $R_t$  = 17.6 min) (Supplementary Figure S25).

## Antimicrobial Activity Assay of Fractions

All antimicrobial assays mentioned in the article were performed using Gram-positive bacteria pathogens *S. aureus* (SA, ATCC 6538) and MRSA (clinical strain from Chaoyang Hospital, Beijing, China) to which vancomycin was used as a positive control, and Gram-negative bacteria *Pseudomonas aeruginosa* strain 14 (PA14, ATCC 15692) to which ciprofloxacin was used as a positive control. For each organism, a loopful of glycerol stock was streaked on an LB-agar plate, which was incubated overnight at 37°C. The *Candida albicans* strains (type G5, 17#, ATCC 10231; type SC5314, ATCC MYA-2876) were grown on Sabouraud dextrose agar and incubated overnight at 28°C; Amphotericin B was used as a positive control.

The fresh (about 3 days old) single colony bacteria were removed from the YPD medium plate with an inoculating ring and mixed in 1 mL RPMI1640 medium. The concentration of bacterial solution was then properly adjusted. In a 96-well plate, an 80  $\mu\text{L}$  bacterial solution of the above concentration was added to each well; the first column was added with antibiotics as the positive control, and the last column was added with DMSO as the negative control. The compound was then added to be tested in the middle. During the operation, the concentration of a compound in the intermediate part was successively half diluted by the pipette. In this study, all isolated compounds (**1–4**) were screened for their antibacterial activity and antibiotic resistance bacteria activity toward a panel of bacteria using the MIC method.

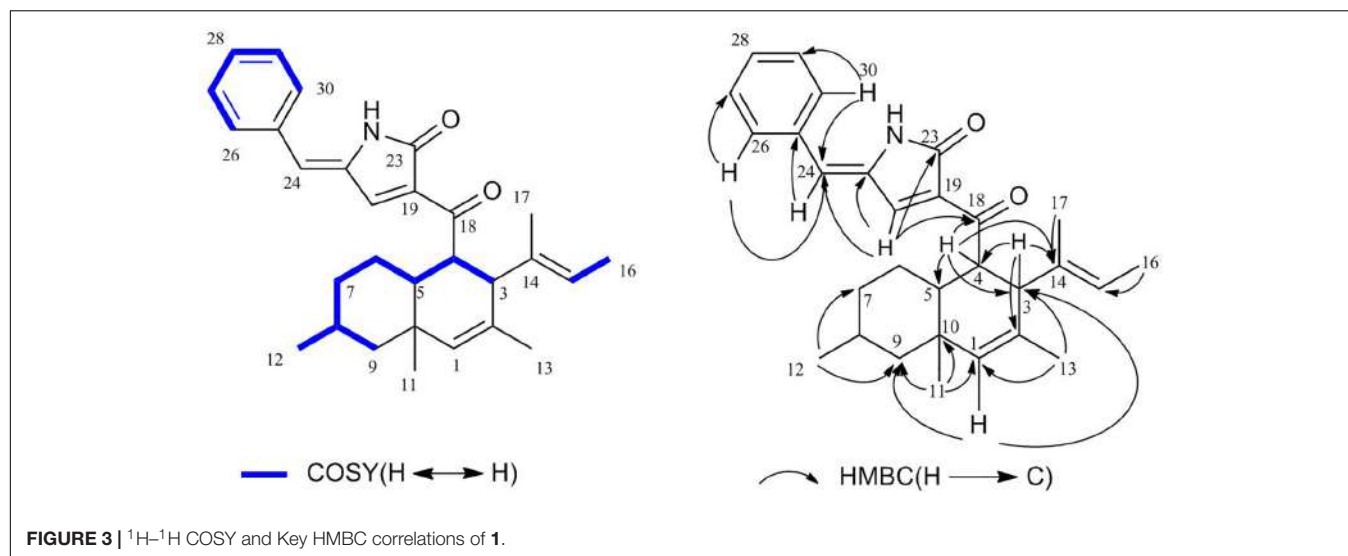
## Experimental Apparatus and Materials

The 1D and 2D NMR spectra were recorded in  $\text{CDCl}_3$  on a BRUKER ASCEND 400 AVANCE III HD spectrometer with tetramethylsilane as the internal standard. All NMR assignments were based on the  $^1\text{H}$ - $^1\text{H}$  COSY, HSQC, HMBC, and NOESY spectroscopic data. High-resolution electron spray ionization mass spectroscopy (HRESIMS) data were acquired on an Agilent 6520 Q-TOF mass spectrometer (Agilent Technologies, United States). ECD spectra were recorded on a JASCO J-815 spectropolarimeter using a Nicolet Magna-IR 750 spectrophotometer. Sephadex LH-20 (Pharmacia, Sweden), MCI gel (CHP20P, 75–150  $\mu\text{m}$ , Mitsubishi Chemical Industries Ltd.) and YMC ODS-AQ (S-50  $\mu\text{m}$ , 12 nm, YMC Co., Ltd., Japan). Thin-layer chromatography was performed on a precoated GF254 plate (Qingdao Marine Chemical Co., Ltd., China). Spots were detected under UV light followed by heating after spraying with a 10% vanillin/ $\text{H}_2\text{SO}_4$  solution. Semi-preparative HPLC was carried out on an Agilent 1260 Infinity instrument equipped with a DAD detector and a Waters Sunfire Prep C-18 column (10 × 250 mm, 5  $\mu\text{m}$ ).

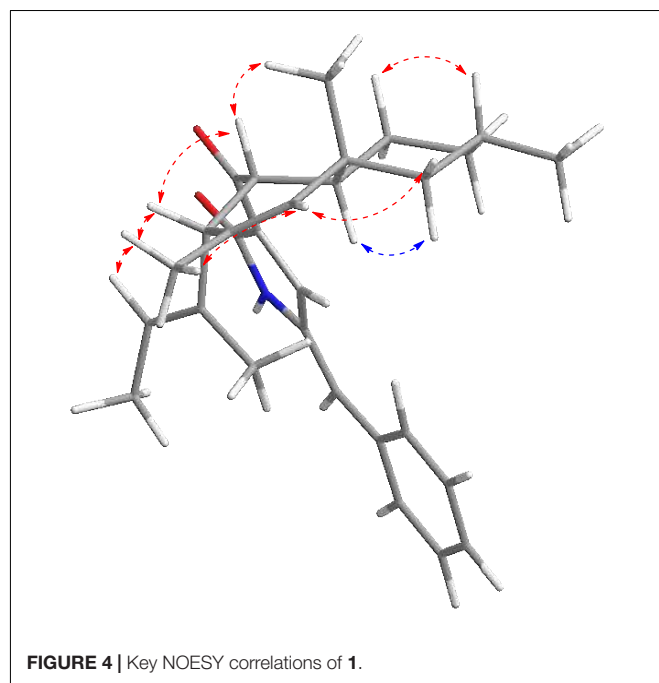
## Genome Analysis and Functional Assays

To get a genome of *Chaetomium olivaceum* SD-80A, *de novo* whole genome sequencing approach was used and a 500 bp library was sequenced on Illumina HiSeq 2500 platform. In this work, the total size of predicted assembly is 34782639 bp. The resulting 3.47 G of data were assembled to 10658 scaffolds using the SOAP *de novo* (v2.04) assembler (Luo et al., 2012). The





average G + C content is 55.57% (Table 1). The amino acid sequence of MycB (XP\_003662443.1) was used as a probe to blast the genome of *C. olivaceum* SD-80A. Four homologous gene sequences that were separately located at scaffold 1389, scaffold 1605, scaffold 647, and scaffold 1433 were mined with different levels of identities of 68, 32, 26, and 28%, respectively. Herein, the scaffold 1389 has a higher identity and the *E*-value is 0. Therefore, it is a likely candidate. Furthermore, the identity between the homologous protein encoded by the gene at scaffold 1389 and MycB was up to 68%. The corresponding gene was designated as *ChaB*. Combined with the gene cluster analysis results of the *C. olivaceum* SD-80A genome, *ChaB* and a PKS-NRPS gene located at scaffold 1389 were adjacent (Figure 1). This PKS-NRPS gene showed an identity of 68% with the myceliothermophin gene (MycA, XP\_003662442) from *M. thermophila* ATCC 42464 was named as *ChaA*. Through further sequence analysis, the MycC (XP\_003662444) from *M. thermophila* ATCC 42464 has a 55% identity sequence homology to *ChaC*, another adjacent gene of *ChaB*. The presence of these three genes in the *C. olivaceum* SD-80A genome suggests that the strain may produce decalin-containing compounds during secondary metabolism.



## Structural Analysis and Identification of Compounds

To verify our inferences, secondary metabolites of *C. olivaceum* SD-80A were accumulated through fermentation. Four decalin-containing compounds were obtained as follows (Figure 2): Compound **1** was obtained as yellow amorphous powder, and its molecular formula was designated as  $\text{C}_{29}\text{H}_{35}\text{NO}_2$  according to the ion peaks at  $m/z$  430.2266  $[\text{M} + \text{H}]^+$  under its HRESIMS (Supplementary Figure S1), which indicates that it contains 12 degrees of unsaturation. The formula was supported by the  $^1\text{H}$  NMR and  $^{13}\text{C}$  NMR data. The  $^1\text{H}$  NMR spectrum (Table 2 and Supplementary Figure S2) exhibited one active hydrogen at  $\delta_{\text{H}}$  8.65 (22-NH), five  $\text{CH}_3$  at  $\delta_{\text{H}}$  0.90 (H-11), 0.86 (H-12), 1.48 (H-13), 1.43 (H-16), and 1.46 (H-17), four

CH at  $\delta_{\text{H}}$  5.37 (H-1), 5.08 (H-15), 7.61 (H-20), and 6.34 (H-24), five benzene ring CH at  $\delta_{\text{H}}$  7.50 (H-26, H-30), 7.45 (H-27, H-29), and 7.35 (H-28). The  $^{13}\text{C}$  NMR data (Table 2 and Supplementary Figure S3) exhibited 29 signals consisting of five methyls, three methylenes, 13 methines, and eight quaternary carbon atoms, including two carbonyl atoms at  $\delta_{\text{C}}$  169.8 and 196.6. Furthermore,  $\delta_{\text{C}}$  134.8 (C-19), 143.9 (C-20), 134.2 (C-21), and 169.8 (C-23) with the N atom could be elucidated to a pyridine ring.

The  $^1\text{H}$ - $^1\text{H}$  COSY (Supplementary Figure S4) correlations of H-3, H-4, H-5, H-6, H-7, H-8, and H-9/12, correlations of H-15, H-16, correlations of H-26, H-27, H-28, H-29, and H-30 indicate three parts in blue color of **1** (Figure 3). The HMBC (HSQC and

**TABLE 3** |  $^1\text{H}$  and  $^{13}\text{C}$  NMR data of **3** and **4** ( $\delta_{\text{H}}$  in ppm,  $J$  in Hz).

No.	<b>3<sup>a</sup></b>		<b>4<sup>a</sup></b>	
	$\delta_{\text{C}}$	$\delta_{\text{H}}$ , mult. ( $J$ in Hz)	$\delta_{\text{C}}$	$\delta_{\text{H}}$ , mult. ( $J$ in Hz)
1	136.4	5.35, brs	136.4	5.35, brs
2	136.3		136.3	
3	51.0	3.17, d (7.2)	51.0	3.06, d (7.6)
4	50.9	3.80, dd (12.4, 7.6)	51.0	3.83, dd (12.4, 7.6)
5	39.9	1.81 (dt, covered)	39.9	1.81 (dt, covered)
6	24.2	1.62, m 0.94, m	24.2	1.62, m 0.94, mF
7	35.8	1.69, m 0.95, m	35.7	1.69, m 0.95, m
8	27.4	1.60, m	27.4	1.60, m
9	48.5	1.48, m 0.97, m	48.5	1.48, m 0.97, m
10	35.1		35.2	
11	22.8	0.91, s	20.5	0.91, s
12	20.5	0.86, d (6.4)	22.8	0.86, d (6.4)
13	22.1	1.45, s	22.1	1.45, s
14	129.8		129.8	
15	123.0	5.02, dd (6.4)	123.1	5.07, dd (6.4)
16	13.1	1.41, s	13.3	1.41, s
17	13.7	1.39, s	13.7	1.39, s
18	196.0		196.4	
19	138.6		138.8	
20	154.3	7.40, d (1.6)	153.7	7.33, d (1.6)
21	89.8		89.7	
23	167.8		167.7	
24- O-CH <sub>3</sub>	49.8	3.13, s	49.9	3.13, s
25	44.2	3.12 (d, 14.4) 3.02 (d, 13.6)	44.4	3.18 (d, 14) 2.95 (d, 13.6)
26	134.3		134.3	
27,31	130.6	7.23 (m)	130.5	7.23 (m)
28,30	128.4	7.28 (m)	128.5	7.28 (m)
29	127.4	7.30 (m)	127.4	7.30 (m)
NH		6.02, brs		5.86, brs

<sup>a</sup>Compounds **3** and **4** were measured at  $^1\text{H}$  NMR (400 MHz) and  $^{13}\text{C}$  NMR (100 MHz) with  $\text{CDCl}_3$  as solvent. Chaetolivacine A (**1**), yellow amorphous powder,  $[\alpha]_{\text{D}}^{20} = +18.6$  (c 0.1, MeOH); HRESIMS  $m/z$  430.2266  $[\text{M} + \text{H}]^+$  (calcd for  $\text{C}_{29}\text{H}_{36}\text{NO}_2$ , 430.2263). Myceliothermophin E (**2**), white amorphous powder, HRESIMS  $m/z$  396.2897  $[\text{M} + \text{H}]^+$  (calcd for  $\text{C}_{26}\text{H}_{38}\text{NO}_2$ , 396.2903) (Yang Y.L. et al., 2007). Chaetolivacine B (**3**), yellow amorphous powder,  $[\alpha]_{\text{D}}^{20} = +28.5$  (c 0.1, MeOH); HRESIMS  $m/z$  462.3036  $[\text{M} + \text{H}]^+$  (calcd for  $\text{C}_{30}\text{H}_{40}\text{NO}_3$ , 462.3033). Chaetolivacine C (**4**), yellow amorphous powder,  $[\alpha]_{\text{D}}^{20} = -18.8$  (c 0.1, MeOH); HRESIMS  $m/z$  462.2999  $[\text{M} + \text{H}]^+$  (calcd for  $\text{C}_{30}\text{H}_{40}\text{NO}_3$ , 462.3003).

HMBC see **Supplementary Figures S5, S6** correlations from H-1 to C-3, C-5, C-9, C-10, and C-13; from H-4 to C-3, C-5, and C-10; from 11-Me to C-1, C-5, and C-9, from 12-Me to C-7 and C-9; and from 13-Me to C-1 and C-3 revealed the presence of the decalin ring moiety. HMBC correlations from H-15 to C-16 and C-3 displayed a butene group linked to C-3. Furthermore, HMBC correlations of H-4, H-5, and H-20 to C-18 supported a tetramic acid moiety and the decalin ring joined with C-18. HMBC correlations of H-24 to C-29, C-21, C-26, and C-30 and correlations of H-26, H-20, and H-30 to C-24 indicate that the benzene connected to C-24.

A NOESY experiment (**Supplementary Figure S7**) combined with a coupling constant resulted in two 1,3-diaxial correlations.

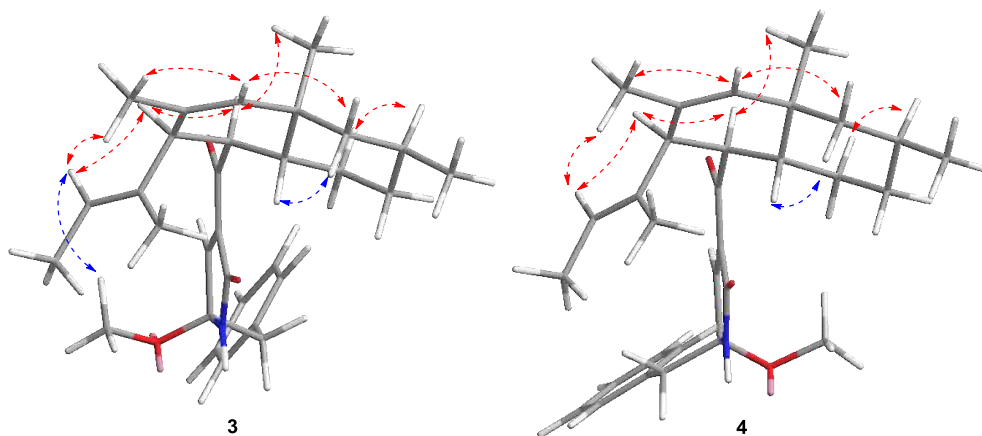
$J = 12.0$  Hz of H-4 and H-5 indicated the two protons are in an axial position. Additionally, H-4 was related to H-11 and H-5 was related to H-9 $\alpha$ , which indicates that **1** has a *trans*-decalin ring (H-4/H-11 and H-5/H-9 $\alpha$ ). The other NOESY correlations from H-11 to H-6 $\beta$ , from H-6 $\beta$  to H-8, suggest that the orientation of  $\text{CH}_3$ -12 is equatorial. In addition, it can also be elucidated from the NOESY correlation that H-3, H-4, H-8, and H-11 are  $\beta$  configurations, and H-5 is an  $\alpha$  configuration. Thus, the relative configurations of **1** is determined as  $3\text{S}^*4\text{R}^*5\text{R}^*8\text{R}^*10\text{S}^*$  (**Figure 4**).

To establish the absolute configuration, ECD calculations were carried out to compare with the experiment plot. At first, the search for conformers was carried out by Spartan'14 with a Molecular Merck Force Field (MMFF). As a result, two conformers with an energy  $<10$  kcal/mol were subjected to optimization to a minimum energy of b3lyp/6-31 + g(d, p), which consequently gave a Boltzmann distribution of 87.7 and 12.3%, respectively, based on their free energies ( $\delta G$ ). Secondly, the theoretical ECD plot in methanol was predicted at a b3lyp/6-311 + g(d, p) level and weighted with Boltzmann distribution. Solvent effects were taken into consideration using the self-consistent reaction field (SCRF) method with a polarizable continuum model (PCM). The calculated spectrum **1** showed an excellent fit with the experimental plot, suggesting that the absolute configuration should be 3S, 4R, 5R, 8R, and 10S. Finally, the overall characterization of compound **1** was elucidated and named as Chaetolivacine A. The experimental method is based on the experience of predecessors (Yang Y.L. et al., 2007).

The molecular formula of **2** was confirmed as  $\text{C}_{26}\text{H}_{37}\text{NO}_2$  through HRESIMS (**Supplementary Figure S8**), which has nine degrees of unsaturation. The  $^1\text{H}$  and  $^{13}\text{C}$  NMR data (**Table 2** and **Supplementary Figures S9, S10**) were very similar to that of **1**, except that the monosubstituted benzene ring connected to C-24 in **1** was replaced by the isopropyl in **2**. Comparing the  $^1\text{H}$  NMR and  $^{13}\text{C}$  NMR data (**Table 2**) with that reported data, compound **2** was determined as myceliothermophin E (Yang Y.L. et al., 2007).

Compound **3** was isolated as yellow amorphous powders. The molecular formula of **3** was designated as  $\text{C}_{30}\text{H}_{39}\text{NO}_3$  according to the ion peaks at  $m/z$  462.3036  $[\text{M} + \text{H}]^+$  in its HRESIMS (**Supplementary Figure S11**). The  $^1\text{H}$  NMR and  $^{13}\text{C}$  NMR data (**Table 3** and **Supplementary Figures S12, S13**) of **3** are similar to that of **1**, except that the signal of one double bond at C-21/C-24 in **1** ( $\delta_{\text{C}21}$  134.2,  $\delta_{\text{C}24}$  119.5,  $\delta_{\text{H}24}$  6.34, s) was reduced to C-21 ( $\delta_{\text{C}}$  89.8), C-24 ( $\delta_{\text{C}}$  44.2), H-24 ( $\delta_{\text{H}24}$  3.12, d,  $J = 14.4$  Hz, 3.02, d,  $J = 13.6$  Hz), and a methoxy group  $\text{OCH}_3$ -24 ( $\delta_{\text{C}}$  49.8) was connected to C-21. HMBC correlations from  $\text{OCH}_3$ -24 to C-20, C-21 confirmed the elucidation. Then, the structure of **3** was elucidated and named as Chaetolivacine B.

Compound **4** was also obtained as yellow amorphous powders. The molecular formula of **4** was designated as  $\text{C}_{30}\text{H}_{39}\text{NO}_3$  according to the ion peaks at  $m/z$  462.2999  $[\text{M} + \text{H}]^+$  in its HRESIMS (**Supplementary Figure S18**). The  $^1\text{H}$  and  $^{13}\text{C}$  NMR data of **4** (**Supplementary Figures S19, S20**) are highly similar to that of **3**, except for  $\delta_{\text{H}}$  7.40 (H-20) of **3** and  $\delta_{\text{H}}$  7.33 (H-20) of **4**. Compound **3**'s  $R_t = 15.0$  min is different from **4**'s  $R_t = 17.6$  min in HPLC (**Supplementary Figure S25**). The assignments of  $^1\text{H}$  and  $^{13}\text{C}$  signals of **4** are summarized in **Table 3**.



**FIGURE 5** | Key NOESY correlations of **3** and **4**.

Attentive analyses of HSQC,  $^1\text{H}$ - $^1\text{H}$  COSY, and HMBC spectra of **3** (Supplementary Figures S14–S16) and **4** (Supplementary Figures S21–S23) revealed that they have the same planar structures, which are proposed to be diastereomers. Spectral data indicated that **3** and **4** are a pair of isomers with different configurations. The observations also support the above deduction. However, based on the different chemical shifts of H-3, H-4, and the deoxy-tetramic acid moieties proposed, the configuration of C-21 in **3** and **4** is reversed (Yang Y.L. et al., 2007). In our situation, the NOESY correlation between H-15 and H-24 in **3** (Supplementary Figure S17) in the absence of the correlation in **4** (Supplementary Figure S24) suggests the relative configuration of C-21. Thus, the relative configurations of **3** and **4** were determined as  $3\text{S}^*4\text{R}^*5\text{R}^*8\text{R}^*10\text{S}^*21\text{S}^*$  and  $3\text{S}^*4\text{R}^*5\text{R}^*8\text{R}^*10\text{S}^*21\text{R}^*$ , respectively (Figure 5).

The absolute configuration of **3** and **4** was further elucidated by comparing the experimental ECD spectra with those calculated at the b3lyp/6-311 + g (d, p) and b3lyp/6-31 + g (d, p) levels. The results suggest that they were epimers at C-21 while both of them perform the absolute configuration in deoxy-tetramic acid moieties at 3S, 4R, 5R, 8R, 10S (Yang Y.L. et al., 2007).

## Antimicrobial Activity of Compounds

The isolated compounds **1**–**4** were evaluated for their antimicrobial properties, specifically their abilities against

drug-resistant bacteria. Their antimicrobial activity against SA, MRSA, G5, SC5314, 17#, and PA14 were evaluated. As shown in the results, compounds **1**–**4** exhibited weak inhibitive activity against SC5314, 17#, and G5 as well as PA14; however, compounds **2** and **3** showed inhibitive activity against SA and MRSA (Table 4). Compound **3** showed moderate anti-SA bioactivity with an MIC of 10.8  $\mu\text{M}$ . Compounds **2** and **3** showed potent inhibitory effects against MRSA with MIC values of 15.8 and 27.1  $\mu\text{M}$ . For the isomers 21R-3 and 21S-4, the MIC value of inhibition of SA and MRSA increased from 10.8 and 27.1  $\mu\text{M}$ , respectively, to over 100  $\mu\text{M}$ , implying that configurations of C-21 played a critical role in the biological activity toward SA and MRSA.

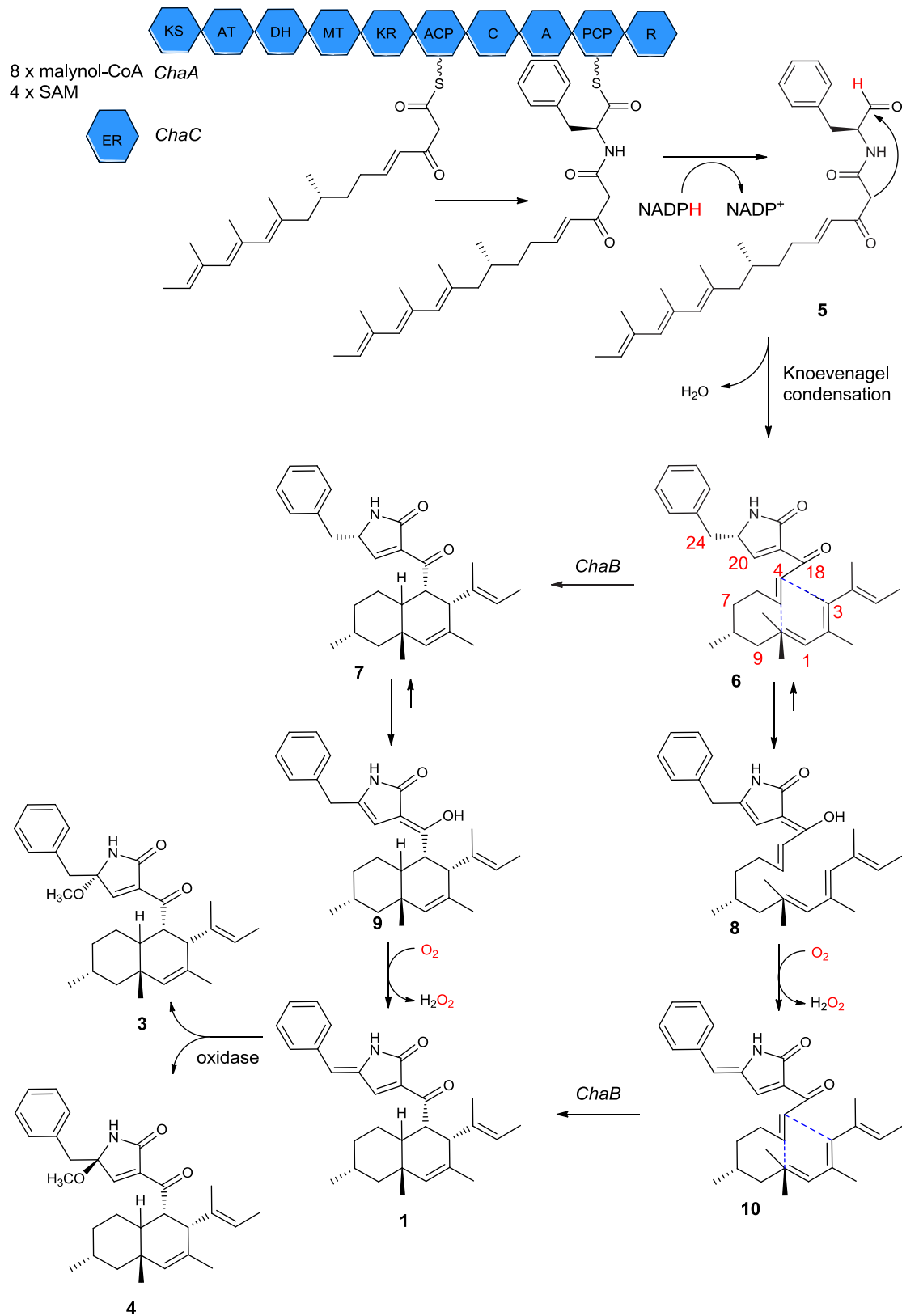
## Postulated Biogenetic Pathways

It has been reported that some secondary metabolites such as oteromycin (Singh et al., 1995; Uchiro et al., 2013), ZG-1494a (West et al., 1996), UCS1025 A and B (Agatsuma et al., 2002; Lambert and Danishefsky, 2005), trichosetin (Marfori et al., 2002), and talaroconvolutins A–D (Suzuki et al., 2000) have a subtle biogenetic pathway in the deoxy-tetramic acid ring system. Although the pathways of the newly isolated compounds **1**, **3**, and **4** remain unclear, a reasonable biological pathway could be assumed. The three genes *ChaA*, *ChaB*, and *ChaC* may play an important role in the synthesis of compounds **1**–**4** (Li et al., 2016). The proteins encoded by *ChaA* and *ChaC* functioned with

**TABLE 4** | Antimicrobial activity of compounds **1**–**4**.

Compound	SA (MIC/ $\mu\text{M}$ )	MRSA (MIC/ $\mu\text{M}$ )	G5 (MIC/ $\mu\text{M}$ )	SC5314 (MIC/ $\mu\text{M}$ )	17# (MIC/ $\mu\text{M}$ )	PA14 (MIC/ $\mu\text{M}$ )
1	>100	>100	>100	>100	>100	>100
2	>100	15.8	>100	>100	>100	>100
3	10.8	27.1	>100	>100	>100	>100
4	>100	>100	>100	>100	>100	>100

*Vancomycin* (McCormick et al., 1995) was positive control of SA and MRSA, MIC = 0.84  $\mu\text{M}$ . *Ciprofloxacin* as positive control of PA, MIC = 0.19  $\mu\text{M}$ ; *amphotericin B*, positive control for SC5314, 17#, and G5, MIC = 1.69  $\mu\text{M}$ .



**FIGURE 6** | Proposed biosynthetic pathway for compound **1** based on isolated natural products and biochemical characterization of *ChaB*.



aminoacyl polyketide aldehyde **5** from eight malonyl-CoAs and four *S*-adenosylmethionines (SAM). Following *ChaA*-catalyzed constructions and the release of aminoacyl polyketide aldehyde **5**, then Knoevenagel condensation yielded the intermediate ketone **6**; as a substrate, **6** could lead to the formation of the endo product **7** by *ChaB*, and **7** will be used as a substrate to get **9** through enolization. Finally, **9** would be oxidized to form **1**. Another possible biosynthesis pathway of **1** is the creation of **6** by tautomerization, oxidation, and cyclization (Figure 6). Compounds **3** and **4** could be formed by the hydroxyl attached to C-21 from different directions of the double bond planar and that are then methylated. The pathway involves leucine in **2** or phenylalanine in **1**, **3**, and **4** that participates in a polyketide reaction.

Drug-resistant bacteria are microorganisms that produce tolerance to corresponding antibiotics after a long period of antibiotic selection. MRSA has been recognized as one of the major pathogens that cause nosocomial infections (Imamura et al., 2001). *Chaetomium*, which belongs to the family of Chaetomiaceae, contains >100 species derived from marine and terrestrial environments. In previous investigations, *Chaetomium* producing >200 bioactive metabolites has been a valuable source for mining anti-MRSA compounds (Zhang et al., 2012). Our study clearly shows that *C. olivaceum* hosts rich genes, including I PKS, NRPS, PKS-NRPS, terpene, and other kinds. However, *trans*-decalin ring systems were found in *Chaetomium* for the first time. In this study, compounds **1–4** containing naphthalene type tetramic acid groups produced by *C. olivaceum* SD-80A were obtained. The terminal of the tetramic acid group in compounds **1**, **3**, and **4** were identical benzene rings. Compounds **3** and **4** were identified as isomers with different configurations of C-21. These compounds were tested against drug-resistant bacteria and revealed moderate activity, and the configuration of C-21 is important for anti-MRSA activity in these kind of compounds. As reported before, the configuration of C-21 in the two sets of diastereomers of myceliothermophins A–E also play a critical role in the biological toxicities toward cancer cells (Yang Y.L. et al., 2007). The results revealed the significant potential of the genus *Chaetomium* in producing new compounds with PKS-NRPS, which will speed the mining for new sources of antimicrobial agents.

Genome mining has recently been used for the discovery of new secondary metabolites. Cycloaddition reactions such as IMDA reactions are found to occur widely among fungal natural product pathways of PKS and NRPS (Minami and Oikawa, 2016), like lovastatin (Auclair et al., 2000) and cytochalasin (Scherlach et al., 2010). Therefore, using DAases (MycB) as biosynthesis marker to focus *C. olivaceum* SD-80A efficiently from our fungi library, then decalin-containing natural products **1–4** were obtained, and these compounds involved three proteins encoded by key genes *ChaA* responding to the synthesis of the acetate-derived portion, including the decalin. Concurrently, the NRPS adds the amino acid *ChaB*, which responds for a Diels–Alder reaction, and *ChaC*, an auxiliary enoyl reductase (ER) is created. The predicted biosynthesis pathway provided a theoretical basis for the future biosynthesis of these compounds using a heterologous expression. For compounds **1–4**, leucine in

**2** or phenylalanine in **1**, **3**, and **4** involved in the biosynthesis pathway **2** with isopropyl showed stronger bioactivity than **1** with phenyl against MRSA with an MIC of 15.8  $\mu$ M and over 100, respectively. Therefore, the different groups from amino acid as a precursor may play an important role in the antimicrobial activity of this kind of compound. The experiments for more novel bioactive compounds of this class using different amino acid as a precursor are ongoing.

## CONCLUSION

In this study, using genome mining and *ChaB* as a probe, compounds **1–4** were isolated as polyketones containing naphthalene-type tetramic acid groups produced by *C. olivaceum* SD-80A. This is the first report of this kind in regard to compounds generated from *Chaetomium*. The terminal of the tetramic acid group in compounds **1**, **3**, and **4** were identical benzene rings, and compounds **3** and **4** were identified as isomers with different configurations of C-21. These compounds were tested against drug-resistant bacteria and revealed moderate activity, and configurations of C-21 are important for anti-MRSA activity in this kind of compound. The biosynthetic pathway was proposed, which provides a theoretical basis for the future biosynthesis of these compounds in *C. olivaceum* SD-80A. This also presents an interesting potential application in food, feed, as well as pharmaceutical industries. The experiments for more novel bioactive compounds of this class using different amino acid as precursor are ongoing.

## DATA AVAILABILITY STATEMENT

All datasets generated for this study are included in the article/Supplementary Material.

## AUTHOR CONTRIBUTIONS

XX, ZXL, and LXZ conceived, designed, and coordinated the study, edited the manuscript, and critically revised the manuscript. XW contributed to the extraction and purification of the compounds, data acquisition, analysis, and interpretation, and manuscript drafting. LYZ did the bioinformatics, genome analysis, and helped in the manuscript writing. ZML did the chemical calculation. JQ and XL helped with the experimental assays and the manuscript revision. PZ, CLL, and XY helped with the antimicrobial experiments and verifying the identity of all the strains. CL and YH contributed to the manuscript preparation.

## FUNDING

We gratefully acknowledge the financial support of the 2016 Scientific Research Innovation Plan for Academic

Degree Postgraduates in Jiangsu Universities (KYLX16\_0264, Southeast University), the National Natural Science Foundation of China (Nos. 31320103911, 31430002, and 31770024), the Qinghai Key R&D and Transformation Project (Qinghai Science and Technology Department) (2017-NK-C25), the Open Project of Qinghai Key Laboratory of Qinghai-Tibet Plateau Biological Resources, Grant No. 2017-ZJ-Y10, the Priority Academic Program Development of Jiangsu Higher Education Institutions (No. 1107047002), the Natural Science Foundation from Shandong Province (Nos. ZR2017MH025 and ZR2017ZB0206), and the Taishan Scholar Project from Shandong Province to LXZ.

## REFERENCES

- Agatsuma, T., Akama, T., Nara, S., Matsumiya, S., Nakai, R., Ogawa, H., et al. (2002). UCS1025A and B, new antitumor antibiotics from the fungus *Acremonium* species. *Org. Lett.* 4, 4387–4390. doi: 10.1021/ol026923b
- Auclair, K., Sutherland, A., Kennedy, J., Witter, D. J., Van den Heever, J. P., Hutchinson, C. R., et al. (2000). Lovastatin nonaketide synthase catalyzes an intramolecular Diels-Alder reaction of a substrate analogue. *J. Am. Chem. Soc.* 122, 11519–11520. doi: 10.1021/ja003216
- Boettger, D., and Hertweck, C. (2012). Molecular diversity sculpted by fungal PKS-NRPS hybrids. *ChemBioChem* 14, 28–42. doi: 10.1002/cbic.201200624
- Chapman, A. L. N., Greig, J. M., and Innes, J. A. (2005). MRSA in the community. *N. Engl. J. Med.* 353, 530–532. doi: 10.1056/nejm200508043530521
- Chooi, Y. H., and Tang, Y. (2012). Navigating the fungal polyketide chemical space: from genes to molecules. *J. Org. Chem.* 77, 9933–9953. doi: 10.1021/jo301592k
- Coast, J., Smith, R. D., and Millar, M. R. (1996). Superbugs: should antimicrobial resistance be included as a cost in economic evaluation? *Health Econ.* 5, 217–226. doi: 10.1002/(SICI)1099-1050(199605)5:3<217::AID-HEC200<3.0.CO;2-S
- Dorghazi, J. R., Albright, J. C., Goering, A. W., Ju, K. S., Haines, R. R., Tchalukov, K. A., et al. (2014). A roadmap for natural product discovery based on large-scale genomics and metabolomics. *Nat. Chem. Biol.* 10, 963–968. doi: 10.1038/nchembio.1659
- Ghisalberti, E. L. (2003). “Bioactive tetramic acid metabolites,” in *Studies in Natural Products Chemistry*, ed. A. U. Rahman, (Amsterdam: Elsevier), 109–163. doi: 10.1016/S1572-5995(03)80140-0
- Han, J., Liu, C., Li, L., Zhou, H., Liu, L., Bao, L., et al. (2017). Decalin-containing tetramic acids and 4-hydroxy-2-pyridones with antimicrobial and cytotoxic activity from the fungus *Coniochaeta cephalothecoides* collected in Tibetan plateau (medog). *J. Org. Chem.* 82, 11474–11486. doi: 10.1021/acs.joc.7b02010
- Hazuda, D., Blau, C. U., Felock, P., Hastings, J., Pramanik, B., Wolfe, A., et al. (1999). Isolation and characterization of novel human immunodeficiency virus integrase inhibitors from fungal metabolites. *Antivir. Chem. Chemother.* 10, 63–70. doi: 10.1177/095632029901000202
- Imamura, H., Ohtake, N., Jona, H., Shimizu, A., Moriya, M., Sato, H., et al. (2001). Dicationic dithiocarbamate carbapenems with anti-MRSA activity. *Bioorg. Med. Chem.* 9, 1571–1578. doi: 10.1016/S0968-0896(01)00044-x
- Kato, N., Nogawa, T., Hirota, H., Jang, J. H., Takahashi, S., Ahn, J. S., et al. (2015). A new enzyme involved in the control of the stereochemistry in the decalin formation during equisetin biosynthesis. *Biochem. Biophys. Res. Commun.* 460, 210–215. doi: 10.1016/j.bbrc.2015.03.011
- Kirk, P. M., Cannon, P. F., and David, J. C. (2001). *Ainsworth & Bisby's dictionary of the fungi*. Wallingford: CABI Publishing, doi: 10.1590/S0036-46651996000400018
- Kontnik, R., and Clardy, J. (2008). Codinaeopsin, an antimalarial fungal polyketide. *Org. Lett.* 10, 4149–4151. doi: 10.1021/ol801726k
- Kurosu, M., Siricilla, S., and Mitachi, K. (2013). Advances in MRSA drug discovery: where are we and where do we need to be? *Expert. Opin. Drug Discov.* 8, 1095–1116. doi: 10.1517/17460441.2013.807246
- Lambert, T. H., and Danishefsky, S. J. (2005). Total synthesis of UCS1025A. *J. Am. Chem. Soc.* 128, 426–427. doi: 10.1021/ja0574567

## ACKNOWLEDGMENTS

We thank Zhang's Lab for their excellent technical assistance. We gratefully thank the Shandong Analysis and Test Center for NMR core facility (BRUKER).

## SUPPLEMENTARY MATERIAL

The Supplementary Material for this article can be found online at: <https://www.frontiersin.org/articles/10.3389/fmicb.2019.02958/full#supplementary-material>

- Li, L., Yu, P., Tang, M. C., Zou, Y., Gao, S. S., Hung, Y. S., et al. (2016). Biochemical characterization of a eukaryotic decalin-forming Diels-Alderase. *J. Am. Chem. Soc.* 138, 15837–15840. doi: 10.1021/jacs.6b10452
- Luo, R., Liu, B., Xie, Y., Li, Z., Huang, W., Yuan, J., et al. (2012). SOAPdenovo2: an empirically improved memory-efficient short-read *de novo* assembler. *GigaScience* 1, 1–6. doi: 10.1186/2047-217X-1-18
- Marfori, E. C., Bamba, T., Kajiyama, S., Fukusaki, E., and Kobayashi, A. (2002). Biosynthetic studies of the tetramic acid antibiotic trichosetin. *Tetrahedron* 58, 6655–6658. doi: 10.1016/S0040-4020(02)00689-0
- Marfori, E. C., Fukusaki, E., and Kobayashi, A. (2002a). Trichosetin, a novel tetramic acid antibiotic produced in dual culture of *Trichoderma harzianum* and *Catharanthus roseus* Callus. *Z. Naturforsch.* 57c, 465–470. doi: 10.1515/znc-2002-5-611
- Marfori, E. C., Kajiyama, S., Fukusaki, E., and Kobayashi, A. (2003b). Phytotoxicity of the tetramic acid metabolite trichosetin. *Phytochemistry* 62, 715–721. doi: 10.1016/S0031-9422(02)00629-5
- McCormick, M. H., Stark, W. M., Pittinger, G. E., and Mcguire, G. M. (1995). Vancomycin, a new antibiotic. I. Chemical and biologic properties. *Antibiot. Ann.* 3, 606–611.
- Minami, A., and Oikawa, H. (2016). Recent advances of Diels-Alderases involved in natural product biosynthesis. *J. Antibiot.* 69, 500–506. doi: 10.1038/ja.2016.67
- Nakai, R., Ogawa, H., Asai, A., Ando, K., Agatsuma, T., Matsumiya, S., et al. (2000). UCS1025A, a novel antibiotic produced by *Acremonium* sp. *J. Antibiot.* 53, 294–296. doi: 10.7164/antibiotics.53.294
- Osterhage, C., Kaminsky, R., König, G. M., and Wright, A. D. (2000). Ascosalipyrrolidinone A, an antimicrobial alkaloid, from the obligate marine fungus *Ascochyta Salicorniae*. *J. Org. Chem.* 65, 6412–6417. doi: 10.1021/jo000307g
- Ramanathan, M., Tan, C. J., Chang, W. J., Tsai, H. H., and Hou, D. R. (2013). Synthesis of the decalin core of codinaeopsin via an intramolecular Diels-Alder reaction. *Org. Biomol. Chem.* 11, 3846–3854. doi: 10.1039/c3ob40480c
- Rodvold, K. A., and McConeghy, K. W. (2013). Methicillin-resistant *staphylococcus aureus* therapy: past, present, and future. *Clin. Infect. Dis.* 58, S20–S27. doi: 10.1093/cid/cit614
- Royles, B. J. L. (1995). Naturally occurring tetramic acids: structure, isolation, and synthesis. *Chem. Rev.* 95, 1981–2001. doi: 10.1021/cr00038a009
- Scherlach, K., Boettger, D., Remme, N., and Hertweck, C. (2010). The chemistry and biology of cytochalasans. *Nat. Prod. Rep.* 27, 869–886. doi: 10.1039/b903913a
- Shionozaki, N., Yamaguchi, T., Kitano, H., Tomizawa, M., Makino, K., and Uchiro, H. (2012). Total synthesis of myceliothermophins A–E. *Tetrahedron Lett.* 53, 5167–5170. doi: 10.1016/j.tetlet.2012.07.058
- Singh, S. B., Goetz, M. A., Jones, E. T., Bills, G. F., Giacobbe, R. A., Herranz, L., et al. (1995). Oteromycin: a novel antagonist of endothelin receptor. *J. Org. Chem.* 60, 7040–7042. doi: 10.1021/jo00126a071
- Song, Z., Cox, R. J., Lazarus, C. M., and Simpson, T. J. (2004). Fusarin C biosynthesis in *Fusarium moniliforme* and *Fusarium venenatum*. *ChemBioChem* 5, 1196–1203. doi: 10.1002/cbic.200400138
- Soytong, K., Kanokmedhakul, S., Kukongviriyapan, V., and Isobe, M. (2001). Application of *Chaetomium* species as new broad spectrum biological fungicide for plant diseases control. *Fungal Divers.* 7, 1–15.

- Stanton, T. B. (2013). A call for antibiotic alternatives research. *Trends Microbiol.* 21, 111–113. doi: 10.1016/j.tim.2012.11.002
- Suzuki, S., Hosoe, T., Nozawa, K., Kawai, K., Yaguchi, T., and Udagawa, S. (2000). Antifungal substances against pathogenic fungi, Talaroconvolutins, from *Talaromyces Convolutus*. *J. Nat. Prod.* 63, 768–772. doi: 10.1021/np990371x
- Uchiro, H., Shionozaki, N., Tanaka, R., Kitano, H., Iwamura, N., and Makino, K. (2013). First total synthesis of oteromycin utilizing one-pot four-step cascade reaction strategy. *Tetrahedron Lett.* 54, 506–511.
- Vesonder, R. F., Tjarks, L. W., Rohwedder, W. K., Burmeister, H. R., and Laugal, J. A. (1979). Equisetin, an antibiotic from *Fusarium equiseti* NRRL 5537, identified as a derivative of n-methyl-2,4-pyrrolidone. *J. Antibiot.* 45, 759–761. doi: 10.7164/antibiotics.32.759
- Weber, T., Blin, K., Duddela, S., Krug, D., Kim, H. U., Bruccoleri, R., et al. (2015). AntiSMASH 3.0 - a comprehensive resource for the genome mining of biosynthetic gene clusters. *Nucleic Acids Res.* 43, W237–W243. doi: 10.1093/nar/gkv437
- West, R. R., Van Ness, J., Varming, A. M., Rassing, B., Biggs, S., Gasper, S., et al. (1996). ZG-1494 alpha, a novel platelet-activating factor acetyltransferase inhibitor from *Penicillium rubrum*, isolation, structure elucidation and biological activity. *J. Antibiot.* 49, 967–973. doi: 10.7164/antibiotics.49.967
- Wheeler, M. H., Stipanovic, R. D., and Puckhaber, L. S. (1999). Phytotoxicity of equisetin and epi-equisetin isolated from *Fusarium equiseti* and *F. pallidoroseum*. *Mycol. Res.* 103, 967–973. doi: 10.1017/s0953756298008119
- Yang, S. W., Mierzwa, R., Terracciano, J., Patel, M., Gullo, V., Wagner, N., et al. (2007). Sch 213766, a novel chemokine receptor CCR-5 inhibitor from *Chaetomium globosum*. *J. Antibiot.* 60, 524–528. doi: 10.1038/ja.2007.67
- Yang, S. W., Mierzwa, R. J., Patel, M., Gullo, V., Wagner, N., Baroudy, B., et al. (2006). Chemokine receptor CCR-5 inhibitors produced by *Chaetomium globosum*. *J. Nat. Prod.* 69, 1025–1028. doi: 10.1021/np060121y
- Yang, Y. L., Lu, C. P., Chen, M. Y., Chen, K. Y., Wu, Y. C., and Wu, S. H. (2007). Cytotoxic polyketides containing tetramic acid moieties isolated from the fungus *Myceliophthora thermophila*: elucidation of the relationship between cytotoxicity and stereoconfiguration. *Chem. Eur. J.* 13, 6985–6991. doi: 10.1002/chem.200700038
- Zhang, Q., Li, H., Zong, S., Gao, J., and Zhang, A. (2012). Chemical and bioactive diversities of the genus *Chaetomium* secondary metabolites. *Mini Rev. Med. Chem.* 12, 127–148. doi: 10.2174/138955712798995066
- Zheng, Q., Tian, Z., and Liu, W. (2016). Recent advances in understanding the enzymatic reactions of [4+2] cycloaddition and spiroketalization. *Curr. Opin. Chem. Biol.* 31, 95–102. doi: 10.1016/j.cbpa.2016.01.020

**Conflict of Interest:** The authors declare that the research was conducted in the absence of any commercial or financial relationships that could be construed as a potential conflict of interest.

Copyright © 2020 Wang, Zhao, Liu, Qi, Zhao, Liu, Li, Hu, Yin, Liu, Liao, Zhang and Xia. This is an open-access article distributed under the terms of the Creative Commons Attribution License (CC BY). The use, distribution or reproduction in other forums is permitted, provided the original author(s) and the copyright owner(s) are credited and that the original publication in this journal is cited, in accordance with accepted academic practice. No use, distribution or reproduction is permitted which does not comply with these terms.



# COL<sup>R</sup> *Acinetobacter baumannii* sRNA Signatures: Computational Comparative Identification and Biological Targets

Viviana Cafiso<sup>1\*</sup>, Stefano Stracquadanio<sup>1</sup>, Flavia Lo Verde<sup>1</sup>, Veronica Dovere<sup>2</sup>, Alessandra Zega<sup>1</sup>, Giuseppe Pigola<sup>3</sup>, Jesús Aranda<sup>4</sup> and Stefania Stefani<sup>1</sup>

<sup>1</sup> Department of Biomedical and Biotechnological Sciences, University of Catania, Catania, Italy, <sup>2</sup> Department of Translational Research and New Technology in Medicine and Surgery, Azienda Ospedaliero Universitaria Pisana, University of Pisa, Pisa, Italy, <sup>3</sup> Department of Clinical and Experimental Medicine, University of Catania, Catania, Italy, <sup>4</sup> Departament de Genètica i Microbiologia, Facultat de Biociències, Universitat Autònoma de Barcelona, Barcelona, Spain

## OPEN ACCESS

### Edited by:

Benjamin Andrew Evans,  
University of East Anglia,  
United Kingdom

### Reviewed by:

Younes Smani,  
Institute of Biomedicine of Seville  
(IBIS), Spain  
Margarita Poza,  
Biomedical Research Institute, Spain

### \*Correspondence:

Viviana Cafiso  
v.cafiso@unicat.it

### Specialty section:

This article was submitted to  
Antimicrobials, Resistance  
and Chemotherapy,  
a section of the journal  
Frontiers in Microbiology

**Received:** 29 October 2019

**Accepted:** 19 December 2019

**Published:** 17 January 2020

### Citation:

Cafiso V, Stracquadanio S,  
Lo Verde F, Dovere V, Zega A,  
Pigola G, Aranda J and Stefani S  
(2020) COL<sup>R</sup> *Acinetobacter*  
*baumannii* sRNA Signatures:  
Computational Comparative  
Identification and Biological Targets.  
*Front. Microbiol.* 10:3075.  
doi: 10.3389/fmicb.2019.03075

Multidrug-Resistant (MDR) and Extensively Drug Resistant (XDR) *Acinetobacter baumannii* (*Ab*) represent a serious cause of healthcare-associated infections worldwide. Currently, the available treatment options are very restricted and colistin-based therapies are last-line treatments of these infections, even though colistin resistant (COL<sup>R</sup>) *Ab* have rarely been isolated yet. In bacteria, small non-coding RNAs (sRNAs) have been implicated in regulatory pathways of different biological functions, however, no knowledge exists about the sRNA role on the biological adaptation in COL<sup>R</sup> *Ab*. Our study investigated two Italian XDR isogenic colistin-susceptible/resistant (COL<sup>S/R</sup>) *Ab* strain-pairs to discover new sRNA signatures. Comparative sRNA transcriptome (sRNAome) analyses were carried out by Illumina RNA-seq using both a Tru-Seq and a Short Insert library, whilst *Ab* ATCC 17978 and ACICU Reference Genome assembly, mapping, annotation and statistically significant differential expression ( $q$ -value  $\leq 0.01$ ) of the raw reads were performed by the Rockhopper tool. A computational filtering, sorting only similarly statistically significant differentially expressed (DE) sRNAs mapping on the same gene in both COL<sup>R</sup> *Ab* isolates was conducted. COL<sup>R</sup> vs. COL<sup>S</sup> sRNAome, analyzed integrating the DE sRNAs obtained from the two different libraries, revealed some statistically significant DE sRNAs in COL<sup>R</sup> *Ab*. In detail, we found: (i) two different under-expressed *cis*-acting sRNAs (*AbsRNA*<sub>1</sub> and *AbsRNA*<sub>2</sub>) mapping in antisense orientation the 16S rRNA gene A1S\_r01, (ii) one under-expressed *cis*-acting sRNA (*AbsRNA*<sub>3</sub>) targeting the A1S\_2505 gene (hypothetical protein), (iii) one under-expressed microRNA-size small RNA fragment (*AbsRNA*<sub>4</sub>) and its pre-micro*AbsRNA*<sub>4</sub> targeting the A1S\_0501 gene (hypothetical protein), (iv) as well as an over-expressed microRNA-size small RNA fragment (*AbsRNA*<sub>5</sub>) and its pre-micro*AbsRNA*<sub>5</sub> targeting the A1S\_3097 gene (signal peptide). Custom TaqMan<sup>®</sup> probe-based real-time qPCRs validated the expression pattern of the selected sRNA candidates shown by RNA-seq. Furthermore, analysis on sRNA  $\Delta$ A1S\_r01,  $\Delta$ A1S\_2505 as well as the over-expressed A1S\_3097 mutants revealed no effects on colistin resistance. Our study, for the



first time, found the sRNAome signatures of clinical COL<sup>R</sup> *Ab* with a computational prediction of their targets related to protein synthesis, host-microbe interaction and other different biological functions, including biofilm production, cell-cycle control, virulence, and antibiotic-resistance.

**Keywords:** XDR *Acinetobacter baumannii*, colistin resistance, small RNAs, Illumina RNA-seq, bioinformatics

## INTRODUCTION

The Multidrug-Resistant (MDR) Gram-negative pathogens included recently in the WHO black list (Tacconelli et al., 2018), i.e., *Acinetobacter*, *Pseudomonas*, and various *Enterobacterales* (including *Klebsiella*, *E. coli*, *Serratia*, and *Proteus*) represent a serious health problem worldwide. In particular, focusing on the *Acinetobacter baumannii* infections, the therapeutic options for their treatment are very limited and mainly draw on colistin-based therapies (Hancock and Chapple, 1999; Zavascki et al., 2007; Vila and Pachón, 2012). Therefore, the increasing use of colistin (COL) and the spread of colistin resistant (COL<sup>R</sup>) can consequently determine an increase in polymyxin resistance onset (Ko et al., 2007; Gales et al., 2011).

Small non-coding RNAs (sRNAs) [~30–300 nucleotides (nt) length] have been recognized as a major class of regulatory molecules in bacteria (Barquist and Vogel, 2015). They unroll a regulatory function affecting gene expression – by base pairing to their related target mRNA – modulating transcription, translation, mRNA stability, DNA maintenance, and silencing. Functionally, sRNAs are involved in the regulation of a wide range of physiological responses, reacting to environmental signals, such as pH or temperature shifts (Wassarman, 2002). They can help the modulation of changes in cellular metabolism to optimize use of available nutrients and improve the probability for survival, as well as contributing to virulence (Chabelskaya et al., 2010; Gottesman and Storz, 2011; Sayed et al., 2012; Álvarez-Fraga et al., 2017; Kröger et al., 2018).

sRNAs act in *trans* or *cis* depending on the transcription start position where the sRNA is transcribed with respect to their regulated gene. *Trans*-encoded sRNAs are transcribed at a genetic locus separated from the gene that they regulate and they often work via an imperfect base pairing with their target mRNAs. Conversely, *cis*-acting sRNAs are transcribed from the same genetic locus that they regulate even though in an antisense orientation to the target gene. Since transcribed proximally to their target, *cis*-antisense RNAs share a perfect match with their targets allowing duplex formation and a stringent regulation (Thomason and Storz, 2010; Chang et al., 2015; Georg and Hess, 2018).

A third class of small RNA, the microRNA-size small RNA fragments (~15–26 nt) have been identified in a few different species of bacteria by next generation sequencing (NGS). These molecules could originate from a cut of a longer precursor (pre-sRNA) in analogy with maturation of the eukaryotic microRNAs (Bloch et al., 2017).

Few mechanisms have been proposed to the underlying colistin resistance in *Ab* (Li et al., 2006; Adams et al., 2009; Falagas et al., 2010; Moffatt et al., 2010; Arroyo et al., 2011; Cai et al.,

2012; Hood et al., 2013; Parra-Millán et al., 2018; Cafiso et al., 2019), however, no investigations have been conducted so far on the role that sRNAs exert on the biological adaptations of colistin resistance acquisition. Few studies have analyzed the sRNA contribution to the *A. baumannii* biology and antimicrobial resistance. Weiss et al. (2016) offer a detailed view of the sRNA content of *Ab* and provide new insights into the evolution and role of these regulatory molecules. In detail, using RNA-seq, 78 *Ab* sRNAs were identified in the AB5075 background, grouped in six classes of similar sRNAs, with one particularly abundant and homologous to regulatory C4 antisense RNAs found in bacteriophages. Sharma et al. (2014) found three new sRNAs, namely AbsR11, AbsR25, and AbsR28, hypothesizing an sRNA involvement in the regulation of antibiotic resistance in bacteria, specifically in cryptic *A. baumannii*.

Our study aimed to gain new insight on the sRNA signature and biological target of clinical COL<sup>R</sup> *Ab* by high-throughput technology RNA-seq.

Our data define the distinctive signatures of COL<sup>R</sup> *Ab* sRNAs revealing computational predicted targets involved in the protein synthesis machinery, host-microbe interactions, pathways involved in biofilm production, cell cycle control, virulence, and antibiotic-resistance.

## MATERIALS AND METHODS

### Bacterial Strains

Two Italian Extensively Drug Resistant (XDR) isogenic colistin-susceptible/resistant (COL<sup>S/R</sup>) clinical *Ab* strain-pairs (1-S/R, 2-S/R) were investigated. *Ab* strain-pair source, antimicrobial susceptibility, molecular characterization, genomic epidemiology, and phylogeny were previously characterized (Cafiso et al., 2019).

### RNA-Seq

To optimize data, RNA-seq was carried out using the Illumina Mi-seq Standard pipeline on two biological replicates consisting of two different libraries of each strain i.e., a Single-end library with 50 bp reads (Short-Insert library) and a Paired-end Read library with 150 bp reads (Tru-Seq library).

For RNA extraction, a single colony of each *Ab* strain was grown in 10 ml of Cation-adjusted Mueller-Hinton broth (Ca-MHB) (Becton Dickinson) and incubated at 37°C overnight. The overnight cultures were then diluted 1:50 in 50 ml of Ca-MHB in a sterile 250 ml flask and incubated with shaking at 250 rpm at 37°C. Bacterial pellets were harvested at mid-log growth phase (OD<sub>600</sub> 0.6 ~1.5 × 10<sup>7</sup> CFU/ml, 18 h) according to the strain growth-curves (**Supplementary Figure S1**).

RNA extraction was performed using the NucleoSpin RNA kit (Macherey-Nagel, Düren, Germany) following the manufacturer's protocol with minor modifications according to the previously published protocols (Cafiso et al., 2019).

The total RNA quality was checked by the 2200 TapeStation RNA Screen Tape device (Agilent, Santa Clara, CA, United States) and the RNA concentrations were determined using an ND-1000 spectrophotometer (NanoDrop, Wilmington, DE, United States). RNA Integrity Number (RIN) values, ranging from 1 to 10 with 10 being the highest quality, was determined by the Agilent TapeStation 2200 system. Only RNAs with preserved 16S and 23S peaks and with RIN values >8 were used for library construction. The RIN values >8 indicated intact and high quality RNA samples usable for downstream applications as previously published (Fleige and Pfaffl, 2006).

## Library Preparation and Sequencing

The Tru-Seq library (TS) was an A Paired-end library with reads of 150 bp and average insert size of 350/400 bp. After sequencing, raw reads were processed using FastQC v0.11.2 to check data quality and, then, reads were trimmed by Trimmomatic v.0.33.2 to remove the adapters for Paired-end reads. A minimum base quality of 15 over a 4-bases sliding-window was required. Only trimmed reads with a length above 36 nucleotides were included in the downstream analysis (Cafiso et al., 2019).

The Short-Insert library (SI) was processed with an A Single-end stranded library with reads of 50 bp. After sequencing, raw reads were processed using FastQC v0.11.2 to evaluate data quality. Reads were then trimmed using Trimmomatic v.0.33.2 to remove sequencing adapters for Single-end reads, requiring a minimum base quality of 15 (Phred scale) and a minimum read length of 15 nucleotides. Only trimmed reads were included in the downstream analysis (Cafiso et al., 2019).

## Tru-Seq and Short-Insert Library Analysis

TS and SI RNA-seq reads were aligned on *Ab* ATCC 17978 (CP000521.1) and on *Ab* ACICU (CP000863.1) Reference Genomes, assembled and quantified using Rockhopper v.2.03 opportunely developed to investigate the bacterial gene structures and transcriptomes as well as validated to identify novel sRNAs (McClure et al., 2013; Tjaden, 2015; Cafiso et al., 2019).

To obtain the data, analyses were carried out with default parameters and verbose output. Rockhopper normalizes read counts for each sample using the upper quartile gene expression level. Starting from the *p*-values calculated according to the Anders and Huber approach, differentially expressed genes (DEGs) were selected as statistically significant by computing *q*-values  $\leq 0.01$  based on the Benjamini–Hochberg correction with a false discovery rate of <1%. In addition, Rockhopper is a tool using biological replicates when available and surrogates when biological replicates for two different conditions are unavailable, considering the two conditions under investigation surrogate replicates for each other (McClure et al., 2013).

## Comparative sRNA Prediction

A double computational filtering was carried out on the library analysis data outputs, first for the DE sRNAs in the COL<sup>R</sup> strains versus their COL<sup>S</sup> counterparts and, thus, to identify only those mapping on the same gene in both COL<sup>R</sup> *Ab* isolates with a statistically significant *q*-value  $\leq 0.01$ .

## Determination of Small RNA Functional Categories

Functional categories of small RNA target genes were investigated by different bioinformatic tools including BLAST, PANTHER (Protein ANalysis THrough Evolutionary Relationships) Classification System, Gene Ontology (GO) Consortium, ExpASy, and KEGG.

## RNA-Seq Data Accession Number

RNA-seq data of the two different libraries have been deposited in the NCBI GEO database under study accession no. GSE109951.

## I-Tasser *ab initio* Structure Modeling

For the I-Tasser (Iterative Threading asseMBLY Refinement) analysis (Zhang, 2009; Roy et al., 2010, 2012; Yang and Zhang, 2015), the first N-terminal 120 AA of the *Ab* ATCC 17978 *Abs*RNA<sub>2</sub> target (A1S\_2505) was selected as a target to obtain more significant predictions, as the C-terminal part of the A1S\_2505 protein was excluded because of its low coverage with threading templates identified from the PDB-library: MTYQYHDESIVTELPEDTVFVFGSNMAGQHSGAARVASQ HFGAVEGVGRGWAGQSFAPITLNEHIQQMPLSQIEHYVEDF KVVYAKNHPKMKYFVTALGCGIAGYKVFSEIAPLFKGIHNN.

For the analysis of the micro*Abs*RNA<sub>4</sub> target (A1S\_0501) the whole FASTA sequence of the protein was used as a template.

## Validation of sRNA-Seq Expression

*Abs*RNA<sub>3</sub> and micro*Abs*RNA<sub>5</sub> were selected to be validated since they are representative of under-expression and over-expression, respectively. Particularly, their RNA-seq expression levels were validated by Custom TaqMan® Small RNA Assays as follow: a single colony of each strain was grown in 10 ml of Ca-MHB (Becton Dickinson) and incubated at 37°C overnight. The overnight cultures were diluted 1:50 in 50 ml of Ca-MHB in a sterile 250 ml flask and incubated with shaking at 250 rpm under normal atmospheric conditions at 37°C. Bacterial pellets were harvested in mid-log growth phase, lysed by adding lysozyme (10 mg/ml) and incubated for 1 h at 37°C. Small RNA extraction was performed by using the *mirVana*<sup>TM</sup> miRNA Isolation Kit (Ambion, Austin, TX, United States) according to the manufacture's protocol following the enrichment procedure for small RNAs. Extracted sRNAs were quantified using Eppendorf BioPhotometer D30 to assess their quality and to properly dilute them to the amount suggested by Custom TaqMan® Small RNA Assays protocol (Applied Biosystems<sup>TM</sup>), then a stem-loop qRT-PCR was performed, one of the most commonly used real-time PCR approaches to quantify sRNAs. The quantification assay was divided into two steps: i) RNA was reverse-transcribed into cDNA using a stem-loop specific primer, and ii) the quantified RT

**TABLE 1** | Oligonucleotides used in this work.

Name	Sequence (5' to 3')	Application
A1S_r01intF	GTAGCTTGCTACTGGACC	Construction of the $\Delta$ A1S_r01 mutant
A1S_r01intR	AGTAAATCCGATTAACGC	Construction of the $\Delta$ A1S_r01 mutant
A1S_r01extF	CTTAACACATGCAAGTCG	Confirmation of the $\Delta$ A1S_r01 mutant
A1S_r01extR	ATAAGCCGCTACGCACG	Confirmation of the $\Delta$ A1S_r01 mutant
A1S_2505intF	GCACGTGTTGCCAGTCAG	Construction of the $\Delta$ A1S_2505 mutant
A1S_2505intR	TCACTGCCGTGATTGAAG	Construction of the $\Delta$ A1S_2505 mutant
A1S_2505extF	ATGGCTGGACAACATGGTAG	Confirmation of the $\Delta$ A1S_2505 mutant
A1S_2505extR	TTAACGGTTAATAGGGTG	Confirmation of the $\Delta$ A1S_2505 mutant
A1S_3097FXbal	ATCGTCTAGAATGGGTGTTGTTGCTGATAG	Overexpression of the A1S_3097 gene
A1S_3097RNcoI	ATCGCCATGGTTATGGTTGAACGTCGGC	Overexpression of the A1S_3097 gene
pETRAFW	TTCTTCGTGAAATAGTGATGATTTTT	Sequencing primer for pET-RA plasmid
pETRARV	CTGTTTCATATGATCTGGGTATC	Sequencing primer for pET-RA plasmid
M13FpUC	GTTTTCCAGTCACGAC	Sequencing primer for the pCR-BluntII-TOPO plasmid
M13RpUC	CAGGAACAGCTATGAC	Sequencing primer for the pCR-BluntII-TOPO plasmid

product was consequently used as a template for real-time qPCR with TaqMan<sup>®</sup> Fast Advanced Master Mix (Applied Biosystems). The stem-loop specific primer used for RT and the specific TaqMan<sup>®</sup> probes and primers used for real-time qPCR were provided by Custom TaqMan<sup>®</sup> Small RNA Assay Design Tool on the Applied Biosystems website<sup>TM</sup>. All real-time qPCRs were performed in triplicate, using Agilent AriaMx Real-Time PCR System, with three different biological replicates using one of the thermal profiles suggested by the Custom TaqMan<sup>®</sup> Small RNA Assays protocol, which provided a first enzymatic activation step of 95°C for 10 min, followed by 40 cycles of 95°C for 15 s and 60°C for 60 s (Salone and Rederstorff, 2015). The expression levels of *AbsRNA*<sub>3</sub> and *microAbsRNA*<sub>5</sub> are shown as the increment/decrement fold-change (FC) in COL<sup>R</sup> (1-R, 2-R) vs. COL<sup>S</sup> strains (1-S, 2-S) in RNA-seq and real-time qPCR.

## Statistics

*AbsRNA*<sub>3</sub> and *microAbsRNA*<sub>5</sub> expression levels found by Custom TaqMan<sup>®</sup> probe-based real-time qPCRs were expressed as means  $\pm$  standard deviations and analyzed by the one-way analysis of variance (ANOVA) using the on-line Free Statistics Calculators-DanielSoper (Soper, 2019) considering a *p*-value  $\leq$  0.01 as statistically significant.

## Ab ATCC 17978 Mutant Construction

Due to the difficult to manipulate the clinical *A. baumannii* strain-pairs related to the lack of antibiotic markers for the mutants selection, *A. baumannii* ATCC 17978 strain was used to generate  $\Delta$ A1S\_r01 and  $\Delta$ A1S\_2505 mutants as well as to overexpress the A1S\_3097 gene.

Gene inactivation was carried out as previously described (Aranda et al., 2010). Briefly, an internal fragment of the target gene was PCR-amplified from the *A. baumannii* ATCC 17978 genome, using the appropriated primers (listed in Table 1). The internal fragment was cloned into the pCR-BluntII-TOPO plasmid (Invitrogen), introduced by electroporation in *Escherichia coli* DH5 $\alpha$  (Clontech) and selected in kanamycin-containing LB plates. Purified plasmids

were then introduced by electroporation in *A. baumannii* ATCC 17978 strain and selected on kanamycin-containing plates. Recombinant clones were confirmed by sequencing (Macrogen) of the PCR products obtained by using the appropriate primers (Table 1). For overexpression, the A1S\_3097 gene was cloned, using the indicated primers (Table 1), into *Xba*I-*Nco*I sites of the pET-RA vector (Aranda et al., 2010). The recombinant plasmid was introduced in *E. coli* DH5 $\alpha$  and once correct construction was verified by both PCR and sequencing (Macrogen), in ATCC 17978. Finally, *A. baumannii* transformants overexpressing the A1S\_3097 gene were selected on rifampicin- and kanamycin-containing plates and confirmed by PCR with the pETRAFW and pETRARV primers (Table 1).

## RESULTS

### Comparative Transcriptome Analysis

To define the characterizing sRNA traits of the two COL<sup>R</sup> vs. COL<sup>S</sup> clinical *Ab* strains, a comparative analysis of the DE sRNAs was conducted by a computational double cross-filtering.

RNA-sequencing generated 1,307,792 – 1,175,327 – 1,173,332 – 1,270,020 total reads in 1-S, 1-R, 2-S, and 2-R, respectively, with 96, 96, 72, and 93% mapped reads on *Ab* ATCC 17978; as well as 97, 97, 76, and 95% reads aligned on *Ab* ACICU for the TS library, whilst 2,353,045 – 2,041,858 – 1,804,167 – 1,819,349 total reads in 1-S, 1-R, 2-S, and 2-R, respectively, with 57, 56, 53, and 56% mapped reads on *Ab* ATCC 17978 and 59, 58, 54, and 57% on *Ab* ACICU for the SI library. RNome structures were previously published (Cafiso et al., 2019).

As shown in Tables 2, 3 and Supplementary Table S1, the comparative statistically significant filtering-analysis of the sRNAome sorting for DE sRNAs of the COL<sup>R</sup> vs. COL<sup>S</sup> *Ab* parental strains returned two different under-expressed *cis*-acting sRNAs (*AbsRNA*<sub>1</sub> and *AbsRNA*<sub>2</sub>) mapping in antisense orientation the 16S rRNA gene A1S\_r01, one under-expressed *cis*-acting sRNA (*AbsRNA*<sub>3</sub>) targeting the A1S\_

TABLE 2 | sRNA nucleotide positions in *Ab* ATCC 17978 reference genome.

sRNA interaction mechanisms	Ab <sup>a</sup> ATCC 17978 Locus Tag				Strain-pair 1				Strain-pair 2			
	sRNA	RefGen <sup>*</sup> position (nt)	sRNA size (bp)	Library <sup>b</sup>	sRNA	RefGen <sup>*</sup> position (nt)	sRNA size (bp)	Library <sup>b</sup>	sRNA	RefGen <sup>*</sup> position (nt)	sRNA size (bp)	Library <sup>b</sup>
cis-acting	A1S_r01	194580	35	SI	AbsRNA <sub>1</sub>	194546	35	SI	AbsRNA <sub>2</sub>	193995	39	SI
cis-acting	A1S_2505	2904500	75	SI	AbsRNA <sub>3</sub>	2904426	75	SI	AbsRNA <sub>3</sub>	2904426	70	SI
microRNA-size small RNA fragment	A1S_0501	545842	21	SI	microAbsRNA <sub>4</sub>	545822	21	SI	pre-microAbsRNA <sub>4</sub>	545917	107	TS
microRNA-size small RNA fragment	A1S_3097	3577445	20	SI	microAbsRNA <sub>5</sub>	3577464	20	SI	pre-microAbsRNA <sub>5</sub>	3577563	228	SI

<sup>a</sup>*Ab*, *Acinetobacter baumannii*; <sup>b</sup>SI, Short-Insert Library; \*RefGen, Reference Genome.

2505/ACICU\_02783 gene (hypothetical protein), one under-expressed microRNA-size small RNA fragment (*AbsRNA*<sub>4</sub>) and its pre-micro*AbsRNA*<sub>4</sub> targeting the A1S\_0501 gene (hypothetical protein), as well as an over-expressed microRNA-size small RNA fragment (*AbsRNA*<sub>5</sub>) and its pre-micro*AbsRNA*<sub>5</sub> targeting the A1S\_3097 gene coding a signal peptide involved in the cytokinin biosynthesis. In detail, the two different *cis*-acting sRNAs – mapping on the *Ab* ATCC 17978 Reference Genome – targeted two different positions (Table 2) of the A1S\_r01 gene with a size of 35 bp in strain-pair 1 (*AbsRNA*<sub>1</sub>) and 39 bp in strain-pair 2 (*AbsRNA*<sub>2</sub>), no mapped regions were found on the *Ab* ACICU Reference Genome. The 70–75 nt *cis*-acting *AbsRNA*<sub>3</sub> mapped in an analog position both on *Ab* ATCC 17978 and *Ab* ACICU Reference Genomes targeting the A1S\_2505/ACICU\_02783 gene in both the *Ab* strain-pairs. The 107 nt pre-micro*AbsRNA*<sub>4</sub> covering the A1S\_0501 mapping on *Ab* ATCC 17978 Reference Genome and its smaller fragment of 21 bp (micro*AbsRNA*<sub>4</sub>) were found in *Ab* strain-pair 2 and in *Ab* strain-pair 1, respectively. Similarly, a 228 pre-micro*AbsRNA*<sub>5</sub> targeting the A1S\_3097 gene in *Ab* strain-pair 2 and its inner fragment of 20 nt in *Ab* strain-pair 1 were found. Furthermore, both *Ab* strain-pairs presented the same aforementioned sRNAs with similar expression profiles (over- or under-expression), though the *q*-value did not allow, in some cases, to return the same fragments in both strain-pairs, considering the two different genomic annotations. Moreover, the only sRNA with a statistically significant expression in *Ab* ACICU Reference Genome was ACICU\_02783 (*AbsRNA*<sub>3</sub>) in both strain-pairs (Supplementary Table S1).

The sRNA nucleotide positions (transcription start and stop) reported by Rockhopper tool were shown in Table 2. In addition, none of these sRNAs targeted the 5' or 3' untranslated regions (UTR) of their target genes.

## I-Tasser

To predict the putative role of *AbsRNA*<sub>2</sub>, an A1S\_2505/ACICU\_02783 conserved domain (CD) BLAST search and I-Tasser *ab initio* protein structure prediction were computationally investigated. The three-dimensional structure of a protein can be very informative and useful to understand functional characteristics of proteins with unknown functions. This is because the structure of a protein provides the precise molecular details that often facilitate experimental characterization of an expected function. In a case in which there is no expected function, the structure of a protein can be used to facilitate its functional predictions by using the structure as a search template for better-characterized proteins that share regions of structural similarity (Kemege et al., 2011). The CD-BLAST search provided a match with the PHA00684 super family (cl10259) domain related to a protein of unknown function. On the contrary, analyzing the concordances of the highest significant prediction of the I-Tasser TM-align structural alignment and the COACH Predicted biological function, we resolved the structure and biological function as similar to the Orphan Macrodomein Protein (human C6orf130) with O-Acyl-ADP-ribose deacylase activity. In particular, the closest structural similarity of



TABLE 3 | Comparative sRNAs of the *A. baumannii* strains.

AbsRNA	Ab <sup>a</sup> ATCC 17978 Locus Tag	Description	I-Tasser Ab Initio modeling prediction	COG <sup>b</sup>	GO number <sup>c</sup>	RPKM <sup>d</sup> of RNA-seq data annotated on Ab ATCC 17978 <sup>a</sup> q-value ≤ 0.01 <sup>e</sup>			Expression profile	
						1-R	1-S	2-R		2-S
AbsRNA <sub>1</sub>	A1S_r01	Antisense sRNA: 16S ribosomal RNA	–	–	–	105	523	19	780	↓
AbsRNA <sub>2</sub>	A1S_2505	Antisense sRNA: hypothetical protein	O-Acyl-ADP-ribose deacylase	–	–	187	647	6	352	↓
AbsRNA <sub>3</sub>	A1S_0501	Antisense sRNA: hypothetical protein	Bacterial actin MreB assembles in complex with cell shape protein RodZ	1426	GO:0016021	111	696	5	310	↓
microAbsRNA <sub>4</sub> pre-microAbsRNA <sub>4</sub>	A1S_3097	Antisense sRNA: signal peptide for cytochrome biosynthesis	–	R	GO:0009691	173	0	472	15	↑

<sup>a</sup>Ab, *Acinetobacter baumannii*; <sup>b</sup>R, general functional prediction only; 1426, Cytoskeletal protein RodZ, contains Xre-like HTH and DUF4115 domains; <sup>c</sup>GO numbers refer only to the biological process; <sup>d</sup>RPKM, Reads per kilo base per million mapped reads; <sup>e</sup>q-value ≤ 0.01 according to the Rockhopper guidelines were considered statistically significant.

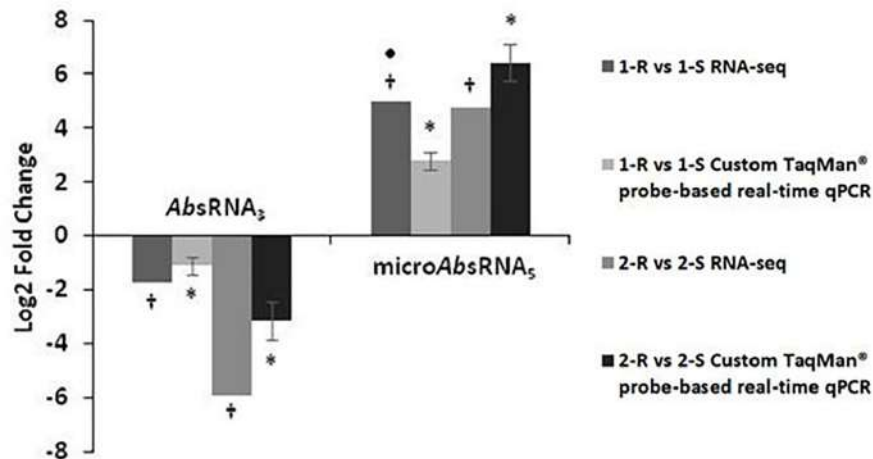
the targeted A1S\_2505 was the PDB-Hit 2lgrA (TM-score 0.925) matching the human protein C6orf130, previously published as an Orphan Macrodomain Protein (human C6orf130) with an O-Acyl-ADP-ribose deacylase activity, which catalyzes the deacylation of O-acetyl-ADP-ribose, O-propionyl-ADP-ribose, and O-butyryl-ADP-ribose to produce ADP-ribose (ADP-r) with acetate, propionate, and butyrate, respectively. Due to the structural similarity, we can speculate that A1S\_2505/ACICU\_02783 could have a function similar to O-Acyl-ADP-ribose deacylase. This structural prediction was also supported by the COACH Predicted biological function, 2l8rA, defining the human protein C6orf130 in complex with ADP-ribose (C-score 0.59), matching the O-acetyl-ADP-ribose deacylase receptor binding the ADP-ribose in the AA residues – G19 D20 L21 F22 H32 C33 I34 S35 R39 A42 I44 A45 L47 A87 P118 R119 I120 G121 C122 G123 L124 D125 Y150 L152- representing the binding sites. This ligand binding site (BL0101984) showed GO Molecular Functions of purine nucleoside binding (GO:0001883), hydrolase activity (GO:0016787) and deacylase activity (GO:0019213) as well as the GO Biological Process of the purine nucleoside metabolic process (GO:0042278). Regarding the computational prediction of the putative role of AbsRNA<sub>3</sub>, the A1S\_0501 hypothetical protein referred to an integral membrane component (GO:0016021), whilst the CD BLAST search provided a CD of the cytoskeletal protein RodZ containing Xre-like HTH and DUF4115 domains related to the cell-cycle control, cell division, and chromosome partitioning (cl34261 Superfamily). This result was also supported by the I-Tasser predictions. By LOMETS, the A1S\_0501 protein showed homology with the highest Norm Z-score (1.71) and 0.33 coverage with 2wus hit referred as a bacterial structural protein actin MreB that can be complexed with the cell shape protein RodZ. As regards the A1S\_0501 GO and the consensus prediction of GO term, obtained from I-Tasser, the A1S\_0501 protein showed a molecular function of DNA polymerase activity (GO:0034061) (GO-score 0.38) and DNA binding (GO:0003677) (GO-score 0.34) and the biological process of nucleic acid metabolism (GO:0090304) (GO-score 0.38).

## Validation of sRNA Expression Profile

Custom TaqMan<sup>®</sup> probe-based real-time qPCRs, dedicated for the analysis of bacterial sRNAs, validated and confirmed the RNA-seq expression profiles of two selected sRNA candidates: AbsRNA<sub>3</sub> and microAbsRNA<sub>5</sub> in both Ab strain-pairs, as shown in Figure 1. In detail, AbsRNA<sub>3</sub> had a statistically significant under-expression ( $p$ -value ≤ 0.01), whilst microAbsRNA<sub>5</sub> showed a statistically significant over-expression ( $p$ -value ≤ 0.01) in both COL<sup>R</sup> Ab strains compared with their COL<sup>S</sup> parents.

## sRNA Target Mutants

No COL MIC changes with respect to the wild-type Ab ATCC 17978 (COL-MIC 1 mg/L) were observed in the ΔA1S\_r01 Ab ATCC 17978 and ΔA1S\_2505 Ab ATCC 17978 mutants as well as in the WT + A1S\_3097 (Table 4).



**FIGURE 1** | Custom TaqMan probe-based real-time qPCR validation of RNA-seq expression data on colistin resistant (COL<sup>R</sup>) characterizing sRNAs. a value of 5-Fold Changes (FC) was indicated for incalculable FC due to the presence of a 0 value in one of the strains. \**p*-value  $\leq 0.01$  obtained by a Student's *T*-test and †*q*-value  $\leq 0.01$  according to the Rockhopper guidelines were considered statistically significant.

**TABLE 4** | COL MIC in *Ab* ATCC 17978 mutants.

Phenotype of wild type and derivative strains	Colistin MIC (mg/L)
Wild type (WT) <i>Ab</i> ATCC 17978	1
$\Delta$ A1S_r01	1
$\Delta$ A1S_2505	1
WT + clinical strain derived A1S_3097	1

## DISCUSSION

The comparative (sRNAome) integrated to bioinformatics, computational cross-double filtering and experimental validations of COL<sup>R</sup> versus COL<sup>S</sup> *Ab* strain-pair revealed distinctive small RNA signatures in COL<sup>R</sup> *Ab*.

Small non-coding RNAs have been identified so far as crucial regulatory elements in bacteria showing high structural diversity and molecular action mechanisms. The most intensively studied prokaryotic sRNA regulators are *cis*-acting sRNAs or *trans*-encoded sRNAs, however, the more recent discovery of microRNAs in prokaryotes represents a challenging field of investigation regarding bacterial regulatory mechanisms.

Our clinical COL<sup>R</sup> *Ab* were distinguished by 3 *cis*-acting sRNAs and 2 microRNA-size small RNA fragments involved in different biological networks. These distinctive features span a different area of bacterial biology involving protein synthesis apparatus, host-microbe interactions, biofilm production, cell-cycle control, virulence and antibiotic resistance that emerge as sRNA targets. Notably, they do not seem apparently related to colistin resistance mechanism as demonstrated by our preliminary data on  $\Delta$ A1S\_r01,  $\Delta$ A1S\_2505 and high expressed A1S\_3097 *Ab* ATCC 17978 mutants showing no COL MIC variations of mutants compared to the WT *Ab* ATCC 17978 – reflecting, however, the wide biological adaptations that the co-existence of colistin resistance and the XDR profile implies.

Regarding the novel *AbsRNA*<sub>1</sub>, *AbsRNA*<sub>2</sub> and *AbsRNA*<sub>3</sub>, we can speculatively assume that via a *cis*-antisense regulation mechanism they could post-transcriptionally regulate the target translation. On the contrary, no regulation appears at the transcriptional level as demonstrated by the lack of statistically significant differential expression in these *AbsRNA* targets according to previously published transcriptomic data (Cafiso et al., 2019). On top, in COL<sup>R</sup> strains, *AbsRNA*<sub>1</sub> and *AbsRNA*<sub>2</sub> under-expression could indicate that they are characterized by sRNAs modulating the protein synthesis machinery and the amount of active ribosomes in agreement with other previous findings (Fernández-Reyes et al., 2009). The occurrence of the under-expressed *AbsRNA*<sub>3</sub> – targeting the O-acetyl-ADP-ribose – provided evidence that COL<sup>R</sup> *Ab* are distinguished by an *AbsRNA*<sub>3</sub> involved in the RNase III inhibition previously associated with different biological functions, including biofilm production, virulence, and antibiotic resistance in Gram-negative bacteria (Chen et al., 2011; Kim et al., 2013; Song et al., 2014). In fact, the O-acetyl-ADP-ribose is a substrate for several related macrodomain proteins such as the human MacroD1, human MacroD2, *Escherichia coli* YmdB. In *E. coli*, YmdB is an RNase III inhibitor that modulates many different functions including biofilm formation (Kim et al., 2013), and *E. coli* adaptive resistance to aminoglycosides via an antibiotic stress-induced sequential modulation of the endoribonucleolytic activity of RNase III and RNase G (Song et al., 2014).

Regarding the microRNA-size small RNA fragments (*microAbsRNA*<sub>4</sub> and its pre-*microAbsRNA*<sub>4</sub> as well as the *microAbsRNA*<sub>5</sub> and its pre-*microAbsRNA*<sub>5</sub>), our data suggest that these sRNAs exist in a premature form (pre-*microAbsRNA*) that act as precursors of their mature form, *microAbsRNAs*, likely obtained cutting the premature form. Moreover, the under-expressed *microAbsRNA*<sub>4</sub> and its pre-*microAbsRNA*<sub>4</sub> targeting a gene coding a structural membrane protein with a CD similar to cytoskeletal protein RodZ related to the cell-cycle control,

cell division and chromosome partitioning, could speculatively address its regulation of these functions. In fact, the GO-term prediction highlighted two possible molecular functions, a DNA polymerase activity and a DNA-binding function. Furthermore, the microAbsRNA<sub>4</sub> target (A1S\_0501) was previously listed as a transcript that decreased significantly upon exposure to NaCl in *A. baumannii*, but no relationship with the mechanisms of antimicrobial tolerance in response to monovalent cations was previously found (Hood et al., 2010).

For the over-expressed microAbsRNA<sub>5</sub> and its pre-microAbsRNA<sub>5</sub>, targeting a signal peptide involved in the cytokinin biosynthetic process, we have to keep in mind that *A. baumannii* is a versatile pathogen that can adhere and invade numerous cell types displaying varying degrees of susceptibility to invasion, stimulating the pro-inflammatory immune response (Choi et al., 2008). The stimuli and signaling pathways implicated in cell death are not yet established; however, they involve imbalanced calcium homeostasis, pro-inflammatory cytokines, and oxidative stress, all traits related to strain virulence (Smani et al., 2011; Mortensen and Skaar, 2012). MicroAbsRNA<sub>5</sub> can regulate host-microbe *A. baumannii* interactions that shape the pathogenesis of *Ab* infection mediated by the host immune response.

In this study, we experimentally and computationally discovered five statistically significant DE sRNAs characterizing COL<sup>R</sup> *Ab* strains speculatively implicated, as *cis*-antisense sRNAs, in the regulation of protein synthesis machinery *via* under-expressed AbsRNA<sub>1</sub> and AbsRNA<sub>2</sub> and in different biological functions, including biofilm production, virulence and aminoglycoside-resistance *via* an under-expressed AbsRNA<sub>3</sub>. Likewise, we found two microAbsRNAs that may be involved in cell-cycle control *via* an under-expressed microAbsRNA<sub>4</sub> and in the host-microbe interaction *via* an over-expressed microAbsRNA<sub>5</sub>.

Colistin resistance onset in *A. baumannii* entails dissimilar biological adaptations – not exclusively related to colistin-resistance – supporting the extremely complex and dynamic nature of this life-threatening microorganism and the urgent need to elucidate the role of small RNAs, whose only the tip of the iceberg is known.

## REFERENCES

- Adams, M. D., Nickel, G. C., Bajaksouzian, S., Lavender, H., Murthy, A. R., Jacobs, M. R., et al. (2009). Resistance to colistin in *Acinetobacter baumannii* associated with mutations in the PmrAB two-component system. *Antimicrob. Agents Chemother.* 53, 3628–3634. doi: 10.1128/AAC.00284-09
- Álvarez-Fraga, L., Rumbo-Feal, S., Pérez, A., Gómez, M. J., Gayoso, C., Vallejo, J. A., et al. (2017). Global assessment of small RNAs reveals a non-coding transcript involved in biofilm formation and attachment in *Acinetobacter baumannii* ATCC 17978. *PLoS One* 12:e0182084. doi: 10.1371/journal.pone.0182084
- Aranda, J., Poza, M., Pardo, B. G., Rumbo, S., Rumbo, C., Parreira, J. R., et al. (2010). A rapid and simple method for constructing stable mutants of *Acinetobacter baumannii*. *BMC Microbiol.* 10:279. doi: 10.1186/1471-2180-10-279
- Arroyo, L. A., Herrera, C. M., Fernandez, L., Hankins, J. V., Trent, M. S., and Hancock, R. E. (2011). The *pmrCAB* operon mediates polymyxin resistance in *Acinetobacter baumannii* ATCC 17978 and clinical isolates through

This work offers a model for the identification of sRNA signatures and the prediction of their targets in *A. baumannii*. Although we do not have clear information on their functions yet, our bioinformatic analysis may provide indications regarding the cellular roles of these new sRNAs.

## DATA AVAILABILITY STATEMENT

The datasets generated for this study can be found in the NCBI GEO Database: GSE109951.

## AUTHOR CONTRIBUTIONS

VC and SSt conceived and designed the study. VC, SSt, FL, VD, and AZ performed the genomics, transcriptomics, real time qPCR, and bioinformatics. GP contributed to the bioinformatics analysis. JA carried out the mutant construction. All authors analyzed the data and contributed and approved the manuscript.

## FUNDING

This study was supported by a research grant PRIN 2017SFBFER from MIUR, Italy. This study was also supported by grant BIO2016-77011-R from the Ministerio de Economía y Competitividad. JA is a Serra Hünter Fellow, Generalitat de Catalunya, Barcelona, Spain.

## ACKNOWLEDGMENTS

We wish to thank the Scientific Bureau of the University of Catania (Italy) for language support.

## SUPPLEMENTARY MATERIAL

The Supplementary Material for this article can be found online at: <https://www.frontiersin.org/articles/10.3389/fmicb.2019.03075/full#supplementary-material>

- phosphoethanolamine modification of lipid A. *Antimicrob. Agents Chemother.* 55, 3743–3751. doi: 10.1128/AAC.00256-11
- Barquist, L., and Vogel, J. (2015). Accelerating discovery and functional analysis of small RNAs with new technologies. *Annu. Rev. Genet.* 49, 367–394. doi: 10.1146/annurev-genet-112414-054804
- Bloch, S., Węgrzyn, A., Węgrzyn, G., and Nejman-Faleńczyk, B. (2017). Small and smaller-sRNAs and MicroRNAs in the regulation of toxin gene expression in prokaryotic cells: a mini-review. *Toxins* 30:9. doi: 10.3390/toxins9060181
- Cafiso, V., Stracquadiano, S., Lo Verde, F., Gabriele, G., Mezzatesta, M. L., Caio, C., et al. (2019). Colistin resistant *A. baumannii*: genomic and transcriptomic traits acquired under colistin therapy. *Front. Microbiol.* 9:3195. doi: 10.3389/fmicb.2018.03195
- Cai, Y., Chai, D., Wang, R., Liang, B., and Bai, N. (2012). Colistin resistance of *Acinetobacter baumannii*: clinical reports, mechanisms and antimicrobial strategies. *J. Antimicrob. Chemother.* 67, 1607–1615. doi: 10.1093/jac/dks084
- Chabelskaya, S., Gaillot, O., and Felden, B. (2010). A *Staphylococcus aureus* small RNA is required for bacterial virulence and regulates the expression of an

- immune-evasion molecule. *PLoS Pathog.* 6:e1000927. doi: 10.1371/journal.ppat.1000927
- Chang, H., Replogle, J. M., Vather, N., Tsao-Wu, M., Mistry, R., and Liu, J. M. (2015). A cis-regulatory antisense RNA represses translation in *Vibrio cholerae* through extensive complementarity and proximity to the target locus. *RNA Biol.* 12, 136–148. doi: 10.1080/15476286.2015.1017203
- Chen, D., Vollmar, M., Rossi, M. N., Phillips, C., Kraehenbuehl, R., Slade, D., et al. (2011). Identification of macrodomain proteins as novel O-acetyl-ADP-ribose deacetylases. *J. Biol. Chem.* 286, 13261–13271. doi: 10.1074/jbc.M110.206771
- Choi, C. H., Lee, J. S., Lee, Y. C., Park, T. I., and Lee, J. C. (2008). *Acinetobacter baumannii* invades epithelial cells and outer membrane protein A mediates interactions with epithelial cells. *BMC Microbiol.* 10:216. doi: 10.1186/1471-2180-8-216
- Falagas, M. E., Rafailidis, P. I., and Matthaïou, D. K. (2010). Resistance to polymyxins: mechanisms, frequency and treatment options. *Drug Resist Updat.* 13, 132–138. doi: 10.1016/j.drug.2010.05.002
- Fernández-Reyes, M., Rodríguez-Falcón, M., Chiva, C., Pachón, J., Andreu, D., and Rivas, L. (2009). The cost of resistance to colistin in *Acinetobacter baumannii*: a proteomic perspective. *Proteomics* 9, 1632–1645. doi: 10.1002/pmic.200800434
- Fleige, S., and Pfaffl, M. W. (2006). RNA integrity and the effect on the real-time qRT-PCR performance. *Mol. Aspects Med.* 27, 126–139. doi: 10.1016/j.mam.2005.12.003
- Gales, A. C., Jones, R. N., and Sader, H. S. (2011). Contemporary activity of colistin and polymyxin B against a worldwide collection of gram-negative pathogens: results from the SENTRY antimicrobial surveillance program (2006–09). *J. Antimicrob. Chemother.* 66, 2070–2074. doi: 10.1093/jac/dkr239
- Georg, J., and Hess, W. R. (2018). Widespread antisense transcription in prokaryotes. *Microbiol. Spectr.* 6. doi: 10.1128/microbiolspec.RWR-0029-2018
- Gottesman, S., and Storz, G. (2011). Bacterial small RNA regulators: versatile roles and rapidly evolving variations. *Cold Spring Harb. Perspect. Biol.* 3:a003798. doi: 10.1101/cshperspect.a003798
- Hancock, R. E., and Chapple, D. S. (1999). Peptide antibiotics. *Antimicrob. Agents Chemother.* 43, 1317–1323.
- Hood, M. I., Becker, K. W., Roux, C. M., Dunman, P. M., and Skaar, E. P. (2013). Genetic determinants of intrinsic colistin tolerance in *Acinetobacter baumannii*. *Infect Immun.* 81, 542–551. doi: 10.1128/IAI.00704-12
- Hood, M. I., Jacobs, A. C., Sayood, K., Dunman, P. M., and Skaar, E. P. (2010). *Acinetobacter baumannii* increases tolerance to antibiotics in response to monovalent cations. *Antimicrob. Agents Chemother.* 54, 1029–1041. doi: 10.1128/AAC.00963-09
- Kemege, K. E., Hickey, J. M., Lovell, S., Battaile, K. P., Zhang, Y., and Hefty, P. S. (2011). Ab initio structural modeling of and experimental validation for chlamydia trachomatis protein CT296 reveal structural similarity to Fe(II) 2-oxoglutarate-dependent enzymes. *J. Bacteriol.* 193, 6517–6528. doi: 10.1128/JB.05488-11
- Kim, T., Lee, J., and Kim, K. S. (2013). *Escherichia coli* YmdB regulates biofilm formation independently of its role as an RNase III modulator. *BMC Microbiol.* 24:266. doi: 10.1186/1471-2180-13-266
- Ko, K. S., Suh, J. Y., Kwon, K. T., Jung, S. I., Park, K. H., and Kang, C. I. (2007). High rates of resistance to colistin and polymyxin B in subgroups of *Acinetobacter baumannii* isolates from Korea. *J. Antimicrob. Chemother.* 60, 1163–1167. doi: 10.1093/jac/dkm305
- Kröger, C., MacKenzie, K. D., Alshabib, E. Y., Kirzinger, M. W. B., Suchan, D. M., Chao, T. C., et al. (2018). The primary transcriptome, small RNAs and regulation of antimicrobial resistance in *Acinetobacter baumannii* ATCC 17978. *Nucleic Acids Res.* 12, 9684–9698. doi: 10.1093/nar/gky603
- Li, J., Rayner, C. R., Nation, R. L., Owen, R. J., Spelman, D., Tan, K. E., et al. (2006). Heteroresistance to colistin in multidrug-resistant *Acinetobacter baumannii*. *Antimicrob. Agents Chemother.* 50, 2946–2950. doi: 10.1128/AAC.00103-06
- McClure, R., Balasubramanian, D., Sun, Y., Bobrovskyy, M., Sumbly, P., Genco, C. A., et al. (2013). Computational analysis of bacterial RNA-seq data. *Nucleic Acids Res.* 41:e140. doi: 10.1093/nar/gkt444
- Moffatt, J. H., Harper, M., Harrison, P., Hale, J. D., Vinogradov, E., Seemann, T., et al. (2010). Colistin resistance in *Acinetobacter baumannii* is mediated by complete loss of lipopolysaccharide production. *Antimicrob. Agents Chemother.* 54, 4971–4977. doi: 10.1128/AAC.00834-10
- Mortensen, B. L., and Skaar, E. P. (2012). Host-microbe interactions that shape the pathogenesis of *Acinetobacter baumannii* infection. *Cell Microbiol.* 14, 1336–1344. doi: 10.1111/j.1462-5822.2012.01817.x
- Parra-Millán, R., Vila-Farrés, X., Ayerbe-Algaba, R., Varese, M., Sánchez-Encinales, V., Bayó, N., et al. (2018). Synergistic activity of an OmpA inhibitor and colistin against colistin-resistant *Acinetobacter baumannii*: mechanistic analysis and in vivo efficacy. *J. Antimicrob. Chemother.* 73, 3405–3412. doi: 10.1093/jac/dky343
- Roy, A., Kucukural, A., and Zhang, Y. (2010). I-TASSER: a unified platform for automated protein structure and function prediction. *Nat. Protoc.* 5, 725–738. doi: 10.1038/nprot.2010.5
- Roy, A., Yang, J., and Zhang, Y. (2012). COFACTOR: an accurate comparative algorithm for structure-based protein function annotation. *Nucleic Acids Res.* 40, W471–W477. doi: 10.1093/nar/gks372
- Salone, V., and Rederstorff, M. (2015). Stem-loop RT-PCR based quantification of small non-coding RNAs. *Methods Mol. Biol.* 2015, 103–108. doi: 10.1007/978-1-4939-2547-6-1
- Sayed, N., Jousselin, A., and Felden, B. (2012). A cis-antisense RNA acts in trans in *Staphylococcus aureus* to control translation of a human cytolytic peptide. *Nat. Struct. Mol. Biol.* 19, 105–112. doi: 10.1038/nsmb.2193
- Sharma, R., Arya, S., Patil, S. D., Sharma, A., Jain, P. K., Navani, N. K., et al. (2014). Identification of novel regulatory small RNAs in *Acinetobacter baumannii*. *PLoS One* 9:e93833. doi: 10.1371/journal.pone.0093833
- Smani, Y., Docobo-Perez, F., McConnell, M. J., and Pachon, J. (2011). *Acinetobacter baumannii*-induced lung cell death: role of inflammation, oxidative stress and cytosolic calcium. *Microb. Pathog.* 50, 224–232. doi: 10.1016/j.micpath.2011.01.008
- Song, W., Kim, Y. H., Sim, S. H., Hwang, S., Lee, J. H., Lee, Y., et al. (2014). Antibiotic stress-induced modulation of the endoribonucleolytic activity of RNase III and RNase G confers resistance to aminoglycoside antibiotics in *Escherichia coli*. *Nucleic Acids Res.* 42, 4669–4681. doi: 10.1093/nar/gku093
- Soper, D. S. (2019). *Analysis of Variance (ANOVA) Calculator - One-Way ANOVA from Summary Data [Software]*. Available from <http://www.danielsooper.com/statcalc> (accessed September 18, 2019).
- Tacconelli, E., Magrini, N., Carmeli, Y., Harbarth, S., Kahlmeter, G., Kluytmans, J., et al. (2018). Discovery, research, and development of new antibiotics: the WHO priority list of antibiotic-resistant bacteria and tuberculosis. *Lancet Infect Dis.* 18, 318–327. doi: 10.1016/S1473-3099(17)30753-3
- Thomason, M. K., and Storz, G. (2010). Bacterial antisense RNAs: how many are there, and what are they doing? *Annu. Rev. Genet.* 44, 167–188. doi: 10.1146/annurev-genet-102209-163523
- Tjaden, B. (2015). *De novo* assembly of bacterial transcriptomes from RNA-seq data. *Genome Biol.* 13:1. doi: 10.1186/s13059-014-0572-2
- Vila, J., and Pachón, J. (2012). Therapeutic options for *Acinetobacter baumannii* infections: an update. *Expert. Opin. Pharmacother.* 13, 2319–2336. doi: 10.1517/14656566.2012.729820
- Wassarman, K. M. (2002). Small RNAs in bacteria: diverse regulators of gene expression in response to environmental changes. *Cell.* 19, 109, 141–144. doi: 10.1016/s0092-8674(02)00717-1
- Weiss, A., Broach, W. H., Lee, M. C., and Shaw, L. N. (2016). Towards the complete small RNome of *Acinetobacter baumannii*. *Microb. Genom.* 2:e000045. doi: 10.1099/mgen.0.000045
- Yang, J., and Zhang, Y. (2015). I-TASSER server: new development for protein structure and function predictions. *Nucleic Acids Res.* 43, W174–W181. doi: 10.1093/nar/gkv342
- Zavascki, A. P., Goldani, L. Z., Li, J., and Nation, R. L. (2007). Polymyxin B for the treatment of multidrug-resistant pathogens: a critical review. *J. Antimicrob. Chemother.* 60, 1206–1215. doi: 10.1093/jac/dkm357
- Zhang, Y. (2009). I-TASSER: fully automated protein structure prediction in CASP8. *Proteins* 77(Suppl. 9), 100–113. doi: 10.1002/prot.22588

**Conflict of Interest:** The authors declare that the research was conducted in the absence of any commercial or financial relationships that could be construed as a potential conflict of interest.

Copyright © 2020 Cafiso, Stracquadanio, Lo Verde, Dovere, Zega, Pigola, Aranda and Stefani. This is an open-access article distributed under the terms of the Creative Commons Attribution License (CC BY). The use, distribution or reproduction in other forums is permitted, provided the original author(s) and the copyright owner(s) are credited and that the original publication in this journal is cited, in accordance with accepted academic practice. No use, distribution or reproduction is permitted which does not comply with these terms.





# Reducing the Consumption of Antibiotics: Would That Be Enough to Slow Down the Dissemination of Resistances in the Downstream Environment?

Christophe Merlin\*

Université de Lorraine, CNRS, LCPME, Nancy, France

**Keywords:** antibiotic resistance dissemination, antibiotic consumption, collateral antibiotic effect, resistance gene transfer, downstream environment

## CONTROLLING THE CONSUMPTION OF ANTIBIOTICS

### OPEN ACCESS

#### Edited by:

Luciene Andrade Da Rocha Minarini,  
Federal University of São Paulo, Brazil

#### Reviewed by:

Diamantis Plachouras,  
European Centre for Disease  
Prevention and Control  
(ECDC), Sweden  
Martina Barchitta,  
University of Catania, Italy

#### \*Correspondence:

Christophe Merlin  
christophe.merlin@univ-lorraine.fr

#### Specialty section:

This article was submitted to  
Antimicrobials, Resistance and  
Chemotherapy,  
a section of the journal  
Frontiers in Microbiology

**Received:** 17 October 2019

**Accepted:** 09 January 2020

**Published:** 28 January 2020

#### Citation:

Merlin C (2020) Reducing the  
Consumption of Antibiotics: Would  
That Be Enough to Slow Down the  
Dissemination of Resistances in the  
Downstream Environment?  
Front. Microbiol. 11:33.  
doi: 10.3389/fmicb.2020.00033

The emergence and dissemination of antibiotic resistance is now understood as an unavoidable aspect of bacterial evolution following the consumption of antibiotics (Courvalin, 2005). This dramatic phenomenon is well illustrated by the relationship existing between the occurrence of resistances and the consumption of antibiotics (Furuya and Lowy, 2006; Davies, 2007; Davies and Davies, 2010). Mechanistically speaking, the increasing occurrence of antibiotic resistant bacteria (ARB) has been widely attributed to the selection of resistant variants that pre-exist in susceptible communities (Andersson and Hughes, 2014). Such resistant bacteria are supposedly outcompeting the rest of the microbial communities in a context where antibiotics are administrated at relatively high levels, which means that local concentrations are well-over the Minimum Inhibitory Concentrations (MICs). Despite the fact that the increasing occurrence of antibiotic resistances among bacteria has been recognized decades ago as resulting from antimicrobial drug consumption, only recently has the seriousness of the situation been considered by international, national and local health organizations/agencies. This awareness led to series of reports and recommendations intending to educate and improve practices of health professionals and consumers, in order to preserve the effectiveness of our therapeutic potential (MSS, 2011; World Health Organization, 2015; O'Neil Report, 2016; EUR-Lex, 2018). Considering the correlation between antibiotic consumption and occurrence of resistances in bacteria (Davies, 2007), most recommendations proposed to take action in the public health and veterinary/farming domains by limiting the inappropriate exposure of bacteria to antibiotics in order to slow down a natural evolution toward resistance and its spread in the downstream environment in a One Health context (World Health Organization, 2015, 2017). Limiting the inappropriate exposure of bacteria to antibiotics implicitly means (i) reducing the need for antibiotics, which can be achieved with infection control measures that would limit the epidemic spread of resistant bacteria, and (ii) a better usage of antibiotics so as to reduce our overall antibiotic consumption when unnecessary.

Even if there is a great disparity between countries regarding the consumption of antibiotics (European Centre for Disease Prevention and Control (ECDC), 2017), change in practice remains difficult to implement when public health is concerned. In any case, taking action to reduce antibiotic resistance requires a coordinated and multi-sectorial approach combining political commitment, resources, specific governance mechanisms, and practical managements, as recently reported by World Health Organization (2018). In its 2018 reports, the ECDC indicated that the overall consumption of antibiotics in the EU did not significantly change in the community

and the hospital sectors, while a few decreasing and increasing trends were observed for some countries over the 2013–2017 period. Changes in consumption were probably more visible in veterinary medicine. In a report covering the 2011–2016 period on veterinary antibiotics sale, the European Surveillance of Veterinary Antimicrobial Consumption related an overall decrease of 20% aggregated for 25 countries (European Surveillance of Veterinary Antimicrobial Consumption (ESVAC), 2018). This was tentatively explained by the implementation of policies and measures aiming at reducing the misuse of antibiotics. Even if the studied period is too short yet to draw robust conclusion, the first effects of such responsible-use campaigns start to be visible. In France for instance, an unprecedented national plan to reduce the antibiotic consumption in the animal sector has been initiated (Ecoantibio, 2017). This led to a drastic 39% reduction of antibiotic prescription in veterinary medicine in 6 years, all animals considered. The reduction was even stronger for critical antibiotics such as fluoroquinolones (81% reduction) and last generation cephalosporin (75% reduction). According to the French surveillance network of antimicrobial resistance in pathogenic bacteria of animal origin, these measures were followed by a net diminution of pathogenic ARBs (RESAPATH, 2016). As reported by the French National Public Health Agency (Santé Publique France, 2018), using data also presented by the European Food Safety Agency, the proportion of resistant *E. coli* for C3G went down from 16% to <2% in poultry between 2010 and 2017, which was dramatically increasing before 2010 (Bourély et al., 2018; European Food Safety Agency (EFSA), 2018; Santé Publique France, 2018). Although more results are necessary to comfort these results, they tend to demonstrate that a better use leading to a reduced consumption of antibiotics can rapidly result in a sensible decrease of the relative occurrence of ARBs. If several other reports are rather encouraging to pursue in that direction (Seppala et al., 1997; Aarestrup et al., 2001; Dutil et al., 2010), the relationship between occurrence of resistance and antibiotic consumption does not always follow this trend. Indeed, even if it is not the vast majority of the reported cases, stopping or increasing the consumption of a given antibiotic does not always result in the concomitant decrease or increase of the corresponding resistances, and this may vary according to the studied environment, the public/animal concerned, and the antibiotic and bacteria considered. For instance, Lai et al. (2011) reported a negative correlation between a decreasing consumption of cefotaxime and the rate of cefotaxime resistant-*Escherichia coli* pathogens isolated in a Taiwanese university hospital. Similar trends were reported for the consumption of ceftriaxone and ceftriaxone-resistant *E. coli* and *Klebsiella* spp. in a Turkish hospital setting (Altunsoy et al., 2011). Negative correlations between antibiotic consumptions and development of resistances can also work the other way around, and may depend on the bacterial species considered. In a Korean study covering six university hospitals, Kim et al. (2018) observed contrasted results following an increased consumption of fluoroquinolones, where the resistance rate for ciprofloxacin in *E. coli*, *Klebsiella pneumoniae*, and *Pseudomonas aeruginosa*, either increased,

remained stable or decreased, respectively over an 8-years period. Surprisingly, the same authors also found negative correlation between decreasing consumptions of aminoglycosides and the resistance rate for third generation cephalosporins and ciprofloxacin, thus disconnecting a given drug consumption from its effect on the corresponding antibiotic resistance, at least for a few documented cases. To go further, it is worth noting that carbapenem-resistant *P. aeruginosa* could be isolated from animals that have not been previously treated with carbapenems. In this case, the resistance to carbapenem was attributed to an efflux pump dysregulation (rather than a carbapenemase) resulting from mutations possibly selected by disinfectants and other antibiotics in veterinary practices (Haenni et al., 2017), thus showing that resistant phenotypes can emerge independently from the presence of the corresponding antibiotics. On the other hand, the identification of antibiotic resistance genes in metagenomes from 30,000-years old sediments reminds us that resistance phenotypes and their corresponding genes probably existed before the so-called antibiotic era (D'Costa et al., 2011). Taken together, these observations clearly indicate that the emergence and the dissemination of antibiotic resistances in bacteria cannot solely be explained by a simple selective process occurring during antibiotics therapy, even if the latter is an important driving parameter in many instances.

## THE ANTIBIOTIC COLLATERAL EFFECTS

Tackling the spread of antibiotic resistance will surely require a better usage of antibiotics in order to slow down the emergence of resistant variants associated to antibiotic therapies. But, considering the indispensability of antibiotics in modern medicine, antibiotic resistances will continue to be released in anthropogenically-impacted environments where ARBs can persist, accumulate, transfer their resistant genes (ARGs) to indigenous microbes, and finally re-enter the food chain and contaminate human and animal guts for a new round of selection (Davies and Davies, 2010). It should be noted here that the environment has been described as a reservoir of ARGs in several occasions (Berendonk et al., 2015). Considering that the dissemination of antibiotic resistances lies on the acquisition of resistance but also implies a transmission, and therefore a contact, between people, or with wastewater, or manure, or animals, tackling the dissemination of ARB and ARGs will surely require controlling both the usage of antibiotics but also the route of transmission, especially at the environmental level. With that respect, Collignon et al. (2018) recently proposed that the transmission of ARB and ARGs was probably the dominant contributor to consider for controlling antibiotic resistance, which implies to act at other levels than the antibiotic consumption as well.

The global reduction of consumption is not the sole important measure implemented by national and international organizations for better usage antibiotics. The classification of antimicrobial agents as critically important molecules for human health (WHO classification list), the restriction of their availability/delivery, and the confinement of particular

antibiotic usages to human medicine are important measures aiming at preventing the emergence of particular resistances in the animal husbandry sector and their dissemination in the human health sector (EUR-Lex, 2018; OIE: World Organisation for Animal Health, 2018; World Health Organization, 2019). Nevertheless, confining the usage of a given antibiotic is likely to be of limited impact if collateral effects were to be observed between antibiotics of different nature on the emergence and the dissemination of unrelated ARGs. Lately, Scornec et al. (2017) demonstrated that *Tn916*, a mobile genetic element involved in the dissemination of an ARG for tetracycline, could exhibit a 1,000-fold increase of its transfer frequency when exposed to sub-inhibitory concentrations of tetracyclines, but also macrolides, lincosamides, and streptogramins. This means that not only sub-inhibitory concentrations of an antibiotic could stimulate the dissemination of its corresponding resistant gene, but that collateral stimulation by other antibiotics is also possible. This tends to rule out the effectiveness, at least partially, of any measure that would be based on confining the usage of cross-reacting antibiotics. On another ground, the use of trace metal elements such as zinc oxide or copper sulfate, is frequently used as an antibiotic alternative to promote growth of livestock and poultry. Consequently to such practices, several authors reported a concomitant increase of ARB and ARGs that are likely to result from co-selective processes, as ARGs and metal resistance genes can collocate on the same genetic entities (mobile genetic elements) (Hasman et al., 2006; Yin et al., 2017; van Aalen et al., 2018).

## CONCLUSION

Collateral effects of antibiotics at sub-inhibitory concentrations and trace metal elements clearly highlight the fact that the

## REFERENCES

- Aarestrup, F. M., Seyfarth, A. M., Emborg, H.-D., Pedersen, K., Hendriksen, R. S., and Bager, F. (2001). Effect of abolishment of the use of antimicrobial agents for growth promotion on occurrence of antimicrobial resistance in fecal enterococci from food animals in Denmark. *Antimicrob. Agents Chemother.* 45, 2054–2059. doi: 10.1128/AAC.45.7.2054-2059.2001
- Altunsoy, A., Aypak, C., Azap, A., Ergönül, Ö., and Balik I. (2011). The impact of a nationwide antibiotic restriction program on antibiotic usage and resistance against nosocomial pathogens in Turkey. *Int. J. Med. Sci.* 8, 339–44. doi: 10.7150/ijms.8.339
- Andersson, D. I., and Hughes, D. (2014). Microbiological effects of sublethal levels of antibiotics. *Nat. Rev. Microbiol.* 12, 465–478. doi: 10.1038/nrmicro3270
- Berendonk, T. U., Manaia, C. M., Merlin, C., Fatta-Kassinos, D., Cytryn, E., Walsh, F., et al. (2015). Tackling antibiotic resistance: the environmental framework. *Nat. Rev. Microbiol.* 13, 310–317. doi: 10.1038/nrmicro3439
- Bourély, C., Chauvin, C., Jouy, É., Cazeau, G., Jarrige, N., Leblond, A., et al. (2018). Comparative epidemiology of *E. coli* resistance to third-generation cephalosporins in diseased food-producing animals. *Vet. Microbiol.* 223, 72–78. doi: 10.1016/j.vetmic.2018.07.025
- Collignon, P., Beggs, J. J., Walsh, T. R., Gandra, S., and Laxminarayan, R. (2018). Anthropological and socioeconomic factors contributing to global antimicrobial resistance: a univariate and multivariable analysis. *Lancet Planetary Health* 2, e398–e405. doi: 10.1016/S2542-5196(18)30186-4

antibiotic resistance risk should not be associated with the sole antibiotic therapy practices, and should rather be considered as a multifactorial problem where co-selection and stimulation of horizontal gene transfer also fully applies. Further in depth epidemiological studies should allow determining the extent of such collateral effects outside the context of a Petri dish, and may explain why some antibiotic resistances escape any reduction of occurrence while reducing the corresponding antibiotic consumption. On the other hand determining exhaustively which antibiotic molecules exhibit collateral effects, and at which concentrations, would be an additional step toward antibiotic risk assessment, whether for therapeutic practices or for the effect of antibiotics once diluted in the downstream environments.

## AUTHOR CONTRIBUTIONS

CM wrote this opinion paper.

## FUNDING

The author wishes to thank the French National Agency for Research (ANR) (Project ReguloMobile, No. ANR-13-ADAP-0009) and the French Agency for Food, Environmental and Occupational Health & Safety (Project AquaResist, PNREST Anses, 2018/1/052) for research funding.

## ACKNOWLEDGMENTS

This article was based upon work carried out in the framework of the COST Action ES1403: New and emerging challenges and opportunities in wastewater reuse (NEREUS), supported by COST (European Cooperation in Science and Technology). The author also wishes to thank Sandrine Baron for fruitful discussion during the preparation of the manuscript.

- Courvalin, P. (2005). Antimicrobial drug resistance: “prediction is very difficult, especially about the future”. *Emerg. Infect. Dis.* 11, 1503–1506. doi: 10.3201/eid1110.051014
- Davies, J. (2007). Microbes have the last word. A drastic re-evaluation of antimicrobial treatment is needed to overcome the threat of antibiotic-resistant bacteria. *EMBO Rep.* 8, 616–621. doi: 10.1038/sj.embor.7401022
- Davies, J., and Davies, D. (2010). Origins and evolution of antibiotic resistance. *Microbiol. Mol. Biol. Rev.* 74, 417–433. doi: 10.1128/MMBR.00016-10
- D’Costa, V. M., King, C. E., Kalan, L., Morar, M., Sung, W. W., Schwarz, C., et al. (2011). Antibiotic resistance is ancient. *Nature.* 477, 457–461. doi: 10.1038/nature10388
- Dutil, L., Irwin, R., Finley, R., Ng, L. K., Avery, B., Boerlin, P., et al. (2010). Ceftiofur resistance in *Salmonella enterica* serovar Heidelberg from chicken meat and humans, Canada. *Emerg. Infect. Dis.* 16, 48–54. doi: 10.3201/eid1601.090729
- Ecoantibio (2017). *Écoantibio 2: The French National Plan for the Reduction of the Risks of Antimicrobial Resistance in Veterinary Medicine*. Available online at: <https://agriculture.gouv.fr/le-plan-ecoantibio-2-2017-2021> (accessed October 15, 2019).
- EUR-Lex (2018). *European Parliament Legislative Resolution of 25 October 2018 on the Proposal for a Regulation of the European Parliament and of the Council on Veterinary Medicinal Products (Document P8\_TA(2018)0421)*. Available online at: [https://eur-lex.europa.eu/legal-content/FR/TXT/?uri=EP%3AP8\\_TA%282018%290421](https://eur-lex.europa.eu/legal-content/FR/TXT/?uri=EP%3AP8_TA%282018%290421) (accessed October 14, 2019).

- European Centre for Disease Prevention and Control (ECDC) (2017). *Antimicrobial consumption - Annual Epidemiological Report for 2017*. Available online at: <https://www.ecdc.europa.eu/en/publications-data/antimicrobial-consumption-annual-epidemiological-report-2017> (accessed October 15, 2019).
- European Food Safety Agency (EFSA) (2018). *The European Union Summary Report on Antimicrobial Resistance in Zoonotic and Indicator Bacteria from Humans, Animals and Food in 2016*. Available online at: <https://efsa.onlinelibrary.wiley.com/doi/epdf/10.2903/j.efsa.2018.5182> (accessed October 15, 2019).
- European Surveillance of Veterinary Antimicrobial Consumption (ESVAC) (2018). *Sales of Veterinary Antimicrobial Agents in 30 European Countries in 2016*. Available online at: [https://www.ema.europa.eu/en/documents/report/sales-veterinary-antimicrobial-agents-30-european-countries-2016-trends-2010-2016-eighth-esvac\\_en.pdf](https://www.ema.europa.eu/en/documents/report/sales-veterinary-antimicrobial-agents-30-european-countries-2016-trends-2010-2016-eighth-esvac_en.pdf) (accessed October 15, 2019).
- Furuya, E. Y., and Lowy, F. D. (2006). Antimicrobial-resistant bacteria in the community setting. *Nat. Rev. Microbiol.* 4, 36–45. doi: 10.1038/nrmicro1325
- Haenni, M., Bour, M., Châtre, P., Madec, J.-Y., Plésiat, P., and Jeannot, K. (2017). Resistance of animal strains of *Pseudomonas aeruginosa* to carbapenems. *Front. Microbiol.* 8:1847. doi: 10.3389/fmicb.2017.01847
- Hasman, H., Kempf, I., Chidaïne, B., Cariolet, R., Ersbøll, A. K., Houe, H., et al. (2006). Copper resistance in *Enterococcus faecium*, mediated by the *tcrB* gene, is selected by supplementation of pig feed with copper sulfate. *Appl. Environ. Microbiol.* 72, 5784–5789. doi: 10.1128/AEM.02979-05
- Kim, B., Kim, Y., Hwang, H., Kim, J., Kim, S. W., Bae, I. G., et al. (2018). Trends and correlation between antibiotic usage and resistance pattern among hospitalized patients at university hospitals in Korea, 2004 to 2012: a nationwide multicenter study. *Medicine* 97:e13719. doi: 10.1097/MD.00000000000013719
- Lai, C.-C., Wang, C.-Y., Chu, C.-C., Tan, C.-K., Lu, C.-L., Lee, Y.-C., et al. (2011). Correlation between antibiotic consumption and resistance of Gram-negative bacteria causing healthcare-associated infections at a university hospital in Taiwan from 2000 to 2009. *J. Antimicrob. Chemother.* 66, 1374–1382. doi: 10.1093/jac/dkr103
- MSS, Ministère des Solidarités et de la Santé/French Ministry of Health (2011). *Plan national d'alerte sur les antibiotiques 2011-2016/National Antibiotic Alert Plan 2011-2016*. Available online at: [https://solidarites-sante.gouv.fr/IMG/pdf/Plan\\_antibiotiques\\_2011-2016\\_.pdf](https://solidarites-sante.gouv.fr/IMG/pdf/Plan_antibiotiques_2011-2016_.pdf) (accessed October 14, 2019).
- OIE: World Organisation for Animal Health (2018). *OIE List of Antimicrobial Agents of Veterinary Importance*. Available online at: [https://www.oie.int/fileadmin/Home/eng/Our\\_scientific\\_expertise/docs/pdf/AMR/A\\_OIE\\_List\\_antimicrobials\\_May2018.pdf](https://www.oie.int/fileadmin/Home/eng/Our_scientific_expertise/docs/pdf/AMR/A_OIE_List_antimicrobials_May2018.pdf) (accessed October 15, 2019).
- O'Neil Report (2016). *Tackling Drug-Resistant Infections Globally: Final Report and Recommendations*. Available online at: [https://amr-review.org/sites/default/files/160518\\_Final%20paper\\_with%20cover.pdf](https://amr-review.org/sites/default/files/160518_Final%20paper_with%20cover.pdf) (accessed October 14, 2019).
- RESAPATH (2016). RESAPATH: French surveillance network for antimicrobial resistance in pathogenic bacteria of animal origin (2016). *2016 Annual Report*. Available online at: <https://www.anses.fr/en/system/files/LABO-Ra-Resapath2016EN.pdf> (accessed October 15, 2019).
- Santé Publique France (2018) *Consommation d'antibiotiques et résistance aux antibiotiques en France : une infection évitée, c'est un antibiotique préservé!* Available online at: <https://www.santepubliquefrance.fr/maladies-et-traumatismes/infections-associees-aux-soins-et-resistance-aux-antibiotiques/resistance-aux-antibiotiques/documents/rapport-synthese/consommation-d-antibiotiques-et-resistance-aux-antibiotiques-en-france-une-infection-evitee-c-est-un-antibiotique-preserve> (accessed October 15, 2019).
- Scornec, H., Bellanger, X., Guilloteau, H., Groshenry, G. and Merlin, C. (2017). Inducibility of Tn916 conjugative transfer in *Enterococcus faecalis* by subinhibitory concentrations of ribosome-targeting antibiotics. *J. Antimicrob. Chemother.* 72, 2722–2728. doi: 10.1093/jac/dkx202
- Seppala, H., Klaukka, T., Vuopio-varkila, J., Muotiala, A., Helenius, H., Lager, K., et al. (1997). The effect of changes in the consumption of macrolide antibiotics on erythromycin resistance in group A streptococci in Finland. *N. Engl. J. Med.* 337, 441–446. doi: 10.1056/NEJM199708143370701
- van Alen, S., Kaspar, U., Idelevich, E. A., Köck, R., and Becker, K. (2018). Increase of zinc resistance in German human derived livestock-associated MRSA between 2000 and 2014. *Vet. Microbiol.* 214, 7–12. doi: 10.1016/j.vetmic.2017.11.032
- World Health Organization (2015). *Global Action Plan on Antimicrobial Resistance*. Available online at: <http://www.emro.who.int/health-topics/drug-resistance/global-action-plan.html> (accessed October 14, 2019).
- World Health Organization (2017). *Global Framework for Development & Stewardship to Combat Antimicrobial Resistance*. Available online at: [http://www.who.int/antimicrobial-resistance/global-action-plan/UpdatedRoadmap-Global-Framework-for-Development-Stewardship-to-combatAMR\\_2017\\_11\\_03.pdf?ua=1](http://www.who.int/antimicrobial-resistance/global-action-plan/UpdatedRoadmap-Global-Framework-for-Development-Stewardship-to-combatAMR_2017_11_03.pdf?ua=1) (accessed October 14, 2019).
- World Health Organization (2018). *Tackling Antimicrobial Resistance Together. Working paper 1.0: Multisectoral coordination*. Available online at: <https://www.who.int/antimicrobial-resistance/publications/workingpaper1multisectoralcoordinationAMR/en/> (accessed October 15, 2019).
- World Health Organization (2019). *WHO Model List of Essential Medicines, 21st List*. Available online at: <https://www.who.int/medicines/publications/essentialmedicines/en/> (accessed October 15, 2019).
- Yin, Y., Gu, J., Wang, X., Song, W., Zhang, K., Sun, W., et al. (2017). Effects of copper addition on copper resistance, antibiotic resistance genes, and *intl1* during swine manure composting. *Front. Microbiol.* 8:344. doi: 10.3389/fmicb.2017.00344

**Conflict of Interest:** The author declares that the research was conducted in the absence of any commercial or financial relationships that could be construed as a potential conflict of interest.

Copyright © 2020 Merlin. This is an open-access article distributed under the terms of the Creative Commons Attribution License (CC BY). The use, distribution or reproduction in other forums is permitted, provided the original author(s) and the copyright owner(s) are credited and that the original publication in this journal is cited, in accordance with accepted academic practice. No use, distribution or reproduction is permitted which does not comply with these terms.





# Evaluation of Machine Learning Models for Predicting Antimicrobial Resistance of *Actinobacillus pleuropneumoniae* From Whole Genome Sequences

Zhichang Liu<sup>1,2,3,4</sup>, Dun Deng<sup>1,2,3,4</sup>, Huijie Lu<sup>1,2,3,4</sup>, Jian Sun<sup>5</sup>, Luchao Lv<sup>5</sup>, Shuhong Li<sup>1,2,3,4</sup>, Guanghui Peng<sup>1,2,3,4</sup>, Xianyong Ma<sup>1,2,3,4</sup>, Jiazhou Li<sup>1,2,3,4</sup>, Zhenming Li<sup>1,2,3,4</sup>, Ting Rong<sup>1,2,3,4\*</sup> and Gang Wang<sup>1,2,3,4\*</sup>

## OPEN ACCESS

### Edited by:

Luciene Andrade Da Rocha Minarini,  
Federal University of São Paulo, Brazil

### Reviewed by:

Denise Mara Soares Bazzoli,  
Universidade Federal de Viçosa, Brazil  
Quêzia Moura,  
Federal University of Grande Dourados, Brazil

### \*Correspondence:

Ting Rong  
rongting@gdaas.cn  
Gang Wang  
wanggang@gdaas.cn

### Specialty section:

This article was submitted to Antimicrobials, Resistance and Chemotherapy, a section of the journal *Frontiers in Microbiology*

Received: 28 May 2019

Accepted: 10 January 2020

Published: 06 February 2020

### Citation:

Liu Z, Deng D, Lu H, Sun J, Lv L, Li S, Peng G, Ma X, Li J, Li Z, Rong T and Wang G (2020) Evaluation of Machine Learning Models for Predicting Antimicrobial Resistance of *Actinobacillus pleuropneumoniae* From Whole Genome Sequences. *Front. Microbiol.* 11:48. doi: 10.3389/fmicb.2020.00048

<sup>1</sup> Institute of Animal Science, Guangdong Academy of Agricultural Sciences, Guangzhou, China, <sup>2</sup> State Key Laboratory of Livestock and Poultry Breeding, Guangzhou, China, <sup>3</sup> Key Laboratory of Animal Nutrition and Feed Science of Ministry of Agriculture (South China), Guangzhou, China, <sup>4</sup> Guangdong Engineering Technology Research Center of Animal Meat Quality and Safety Control and Evaluation, Guangzhou, China, <sup>5</sup> National Veterinary Microbiological Drug Resistance Risk Assessment Laboratory, College of Veterinary Medicine, South China Agricultural University, Guangzhou, China

Antimicrobial resistance (AMR) is becoming a huge problem in countries all over the world, and new approaches to identifying strains resistant or susceptible to certain antibiotics are essential in fighting against antibiotic-resistant pathogens. Genotype-based machine learning methods showed great promise as a diagnostic tool, due to the increasing availability of genomic datasets and AST phenotypes. In this article, Support Vector Machine (SVM) and Set Covering Machine (SCM) models were used to learn and predict the resistance of the five drugs (Tetracycline, Ampicillin, Sulfisoxazole, Trimethoprim, and Enrofloxacin). The SVM model used the number of co-occurring k-mers between the genome of the isolates and the reference genes to learn and predict the phenotypes of the bacteria to a specific antimicrobial, while the SCM model uses a greedy approach to construct conjunction or disjunction of Boolean functions to find the most concise set of k-mers that allows for accurate prediction of the phenotype. Five-fold cross-validation was performed on the training set of the SVM and SCM model to select the best hyperparameter values to avoid model overfitting. The training accuracy (mean cross-validation score) and the testing accuracy of SVM and SCM models of five drugs were above 90% regardless of the resistant mechanism of which were acquired resistant or point mutation in the chromosome. The results of correlation between the phenotype and the model predictions of the five drugs indicated that both SVM and SCM models could significantly classify the resistant isolates from the sensitive isolates of the bacteria ( $p < 0.01$ ), and would be used as potential tools in antimicrobial resistance surveillance and clinical diagnosis in veterinary medicine.

**Keywords:** machine learning, Support Vector Machine, Set Covering Machine, antimicrobial resistance, *Actinobacillus pleuropneumoniae*, genomics

## INTRODUCTION

Antimicrobial resistance (AMR) in bacteria from humans and food-producing animals is becoming an urgent threat to the control of bacterial infections. Identification of strains resistant or susceptible to certain antibiotics is essential in fighting against antibiotic-resistant pathogens. Typically, the determination of antimicrobial susceptibility is done either by disk diffusion or minimum inhibitory concentration (MIC) assays. Identification of resistance-specific markers by PCR or microarray hybridization not only corroborates phenotypic results but is also useful for epidemiological purposes, as there are often multiple different genes that can confer resistance to a given antimicrobial agent (Bossé et al., 2017). With the increasing throughput and decreasing cost of DNA sequencing, whole genome sequencing (WGS) may be an alternative for routine surveillance of resistance profiles and for identification of emerging resistances (Mahé and Tournoud, 2018).

*Actinobacillus pleuropneumoniae* causes porcine pleuropneumonia, which is present in almost all the countries of the world. Pleuropneumonia can affect all ages of pigs and may result in great economic losses in pig production particularly as it causes serious respiratory distress and death. *A. pleuropneumoniae* is divided into 15 serotypes based on the antigenic properties of capsular polysaccharides and cell wall lipopolysaccharides. None of the serotype provides a cross-immune response for another serotype and therefore restricts the application of vaccine (Kim et al., 2016). *A. pleuropneumoniae* can be killed by using effective antimicrobials. However, resistant mutants increased gradually due to the misuse of antimicrobials (Zhang et al., 2018). Knowledge of resistance profiles for *A. pleuropneumoniae* is required to inform treatment decisions.

The presence or absence of specific resistance genes must be associated with resistance (and susceptibility) to particular antibiotics, and then the resistance profiles for all genes in a particular isolate must be added together to provide the predicted susceptibility profile for that organism. The routine studies make genotype-to-phenotype predictions based on identifying the AMR genes in the draft genomes via web servers like ResFinder (Zankari et al., 2012), the Comprehensive Antibiotic Resistance Database (CARD) (McArthur et al., 2013), and Resfams (Gibson et al., 2015).

With the help of computational tools, reference-based or reference-free machine-learning algorithms have been used increasingly to build models that correlate genomic variations with phenotypes. In supervised learning, each example consists of an input and an expected outcome. The goal of the algorithm is to learn a model that accurately maps any input to the correct outcome.

In this study, we propose to apply the Support Vector Machine (SVM) and Set Covering Machine (SCM) algorithm to accurately predict their phenotype against five antimicrobial agents (Tetracycline, Ampicillin, Sulfisoxazole, Trimethoprim, and Enrofloxacin) from the whole genomes of 96 isolates of *A. pleuropneumoniae*.

## MATERIALS AND METHODS

### Data

The WGS reads and binary resistance phenotypes of 5 antimicrobial agents (tetracycline, ampicillin, sulfisoxazole, trimethoprim, and enrofloxacin) of 96 isolated strains of *A. pleuropneumoniae* data were obtained from Bossé et al. (2017). The WGS reads were downloaded from the European Nucleotide Archive (Study: PRJEB2343<sup>1</sup>) and the phenotypes of the isolates against the antimicrobial agents were downloaded from the **Supplementary Material** of the same study<sup>2</sup>. Acquired resistance genes of the antimicrobial agents were downloaded from ResFinder Database as reference genes<sup>3</sup>.

For enrofloxacin, even though resistance might be mediated by the acquired *qnr* genes, resistance to fluoroquinolones in the *A. pleuropneumoniae* is most often mediated by mutations in the target genes *gyrA*, *parC*, and *parE* (Wang et al., 2010; Pesesky et al., 2016; Zhang et al., 2018). Therefore, gene sequences of the quinolone resistance determining regions (QRDR) of *gyrA* (residues 68–106), *parC* (residues 68–106), and *parE* (residue 425–478) of all the isolates were translated into amino acid and aligned with the same regions of the reference *gyrA* (GenBank accession number ABN73394), *parC* (GenBank accession number ABN73680) and *parE* (GenBank accession number ABN74341), respectively. All the DNA sequences of QRDR with no mutation in amino acid were appended into a FASTA file as reference genes (see **Supplementary Material**).

The WGS reads were further assembled using Velvet 1.2.08 (Zerbino and Birney, 2008). The contigs of the strains along with the AMR genes downloaded from ResFinder Database and the gene sequences of QRDR for recognition of enrofloxacin point mutation were subsequently split into k-mers (sequence of k nucleotides) of length 31 using the Ray Surveyor tool (Déraspe et al., 2017).

### Reference-Based SVM Model

With the input of resistance genes of interest as reference genes, the matrix of the co-occurring k-mers in the genome of the strains and the reference genes were simultaneously built by the Ray Surveyor tool during the splitting process. Support Vector Machine (SVM; radial basis function kernel) used the number of co-occurring k-mers of the strain and the reference genes of the specific antimicrobial to learn and predict the phenotypes of each isolate. The SVM was implemented in the Python sklearn package<sup>4</sup>.

The dataset was randomly divided into three subsets of equal size by the ID of the strains, and two subsets were used for training while the other one was used for testing. The training and testing process repeated three times so that every subset of the strains could be used to evaluate the performance of the model.

<sup>1</sup><https://www.ebi.ac.uk/ena/data/view/PRJEB2343>

<sup>2</sup><https://www.frontiersin.org/article/10.3389/fmicb.2017.00311/full#supplementary-material>

<sup>3</sup>[https://bitbucket.org/genomicepidemiology/resfinder\\_db/downloads/](https://bitbucket.org/genomicepidemiology/resfinder_db/downloads/)

<sup>4</sup><http://scikit-learn.org/>

## Reference-Free SCM Model

Unlike the SVM model which included k-mers of reference genes in the dataset, the SCM used to learn sparse and interpretable models of phenotypes by reference-free k-mers comparisons are performed implemented in Kover, an open-source software implemented in the Python and C programming languages<sup>5</sup>. Kover automates the machine learning analysis (e.g., dataset splitting, model selection, and model evaluation) without making assumptions about the underlying genetic mechanisms. The k-mers and phenotypic data of all the strains were used and packaged into a Kover dataset, and then split the dataset into a training set (2/3 of the Kover data) and a testing set (1/3 of the Kover data) according to the same ID of the datasets of the SVM model. The training set was used to learn a model containing combination rules of both conjunction (logical-AND) and disjunction (logical-OR) at most 5 rules, the testing dataset was used for testing the accuracy of the model.

## Model Selection and Performance Evaluation

In order to minimize the waste of the training dataset and avoid overfitting, five-fold cross-validation was performed on the training set of the SVM and SCM model to select the best hyperparameter values. The best hyperparameter values selected from the five-folds cross-validation were then averaged and chosen to evaluate the performance of the model.

The performances of the SVM and SCM model were evaluated in terms of sensitivity, specificity, accuracy, and precision. They were defined as: sensitivity =  $TP/(TP + FN)$ , specificity =  $TN/(TN + FP)$ , accuracy =  $(TP + TN)/(TP + FP + TN + FN)$ , and precision =  $TP/(TP + FP)$ . Where TP was the number of resistant strains predicted to be resistant, TN was the number of sensitive strains predicted to be sensitive, FP was the number of sensitive strains predicted to be resistant, and FN was the number of resistant strains predicted to be sensitive.

## RESULTS

A total of 96 clinical *A. pleuropneumoniae* isolates were included in the study, with 58, 19, 46, 16, 6 of the isolates resistant to Tetracycline, Ampicillin, Sulfisoxazole, Trimethoprim, and Enrofloxacin, respectively. There were 8 isolates were resistant to four kinds of antimicrobials (Tetracycline, Ampicillin, Sulfisoxazole, and Trimethoprim); 17 isolates were resistant to 3 kinds of antimicrobials, 10 of them were resistant to Tetracycline, Ampicillin, and Sulfisoxazole, 7 of them were resistant to Tetracycline, Ampicillin, and Trimethoprim, respective; 22 isolates were resistant to 2 kinds of antimicrobials, 20 of them were resistant to Tetracycline and Sulfisoxazole, one of them was resistant to Tetracycline and Ampicillin, one of them was resistant to Sulfisoxazole and Trimethoprim, respectively; 18 isolates were resistant to single antimicrobial, 12 and 6 of them

were resistant to Tetracycline and Enrofloxacin, respectively; and 31 were sensitive to all kinds of the five antimicrobials (**Figure 1**).

The *gyrA* QRDR DNA fragments of all the 90 Enrofloxacin sensitive isolates were the same as that region of the reference *gyrA*, while part of the isolates contained the same QRDR DNA fragments as the reference *parC* or *parE* genes. And including those fragments, there were 5 and 2 DNA fragments in the 90 Enrofloxacin sensitive isolates that code the same amino acid as reference *parC* and *parE*, respectively.

A total of 4,299,871 distinct k-mers of length 31 were obtained from the 96 genomes of *A. pleuropneumoniae*. By comparing the k-mers of the genes downloaded from ResFinder, a range of 509~607 k-mers of *tet(B)* gene were found in the genome of 50 strains, 540~613 k-mers of *tet(H)* gene in 5 strains, 454~463 k-mers of *blaROB-1* gene in 19 strains, 299~402 k-mers of *sul2* gene in 46 strains, and 172~236 k-mers of *dfrA14* gene together with 13 k-mers of *dfrA30* gene in 16 strains of the bacteria, respectively. For enrofloxacin, 53 and 84 k-mers of *gyrA* QRDR in the genomes of 7 and 89 isolates, 84 and 126 k-mers of *parC* and *parE* QRDR in 96 isolates, respectively (**Figure 2**). No k-mer of *qnr* genes were found in the genomes of the isolates.

The training accuracy (mean cross-validation score) and the testing accuracy of SVM and SCM models of five drugs were above 90% (**Figure 3**), indicating that both of the SVM and SCM models were not overfitted. Average and standard deviation of the sensitivity, specificity, accuracy, and precision measured on the 3 randomly partition testing sets representing the whole 96 unduplicated strains of the bacteria were provided in **Table 1**. The accuracies of Ampicillin, Sulfisoxazole, Trimethoprim, and Enrofloxacin were  $1.00 \pm 0.00$ , indicating that no false positive and no false-negative strain of bacteria were predicted by both of the models.

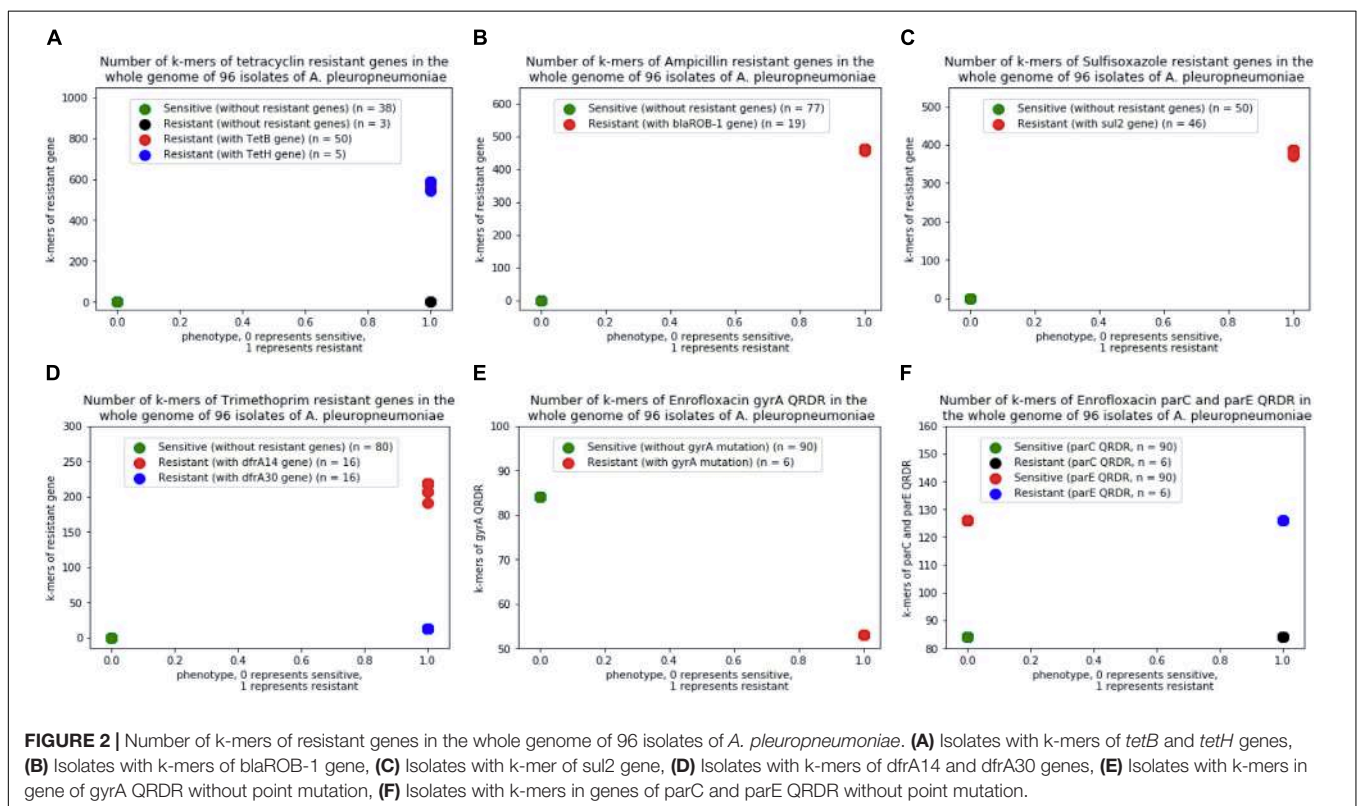
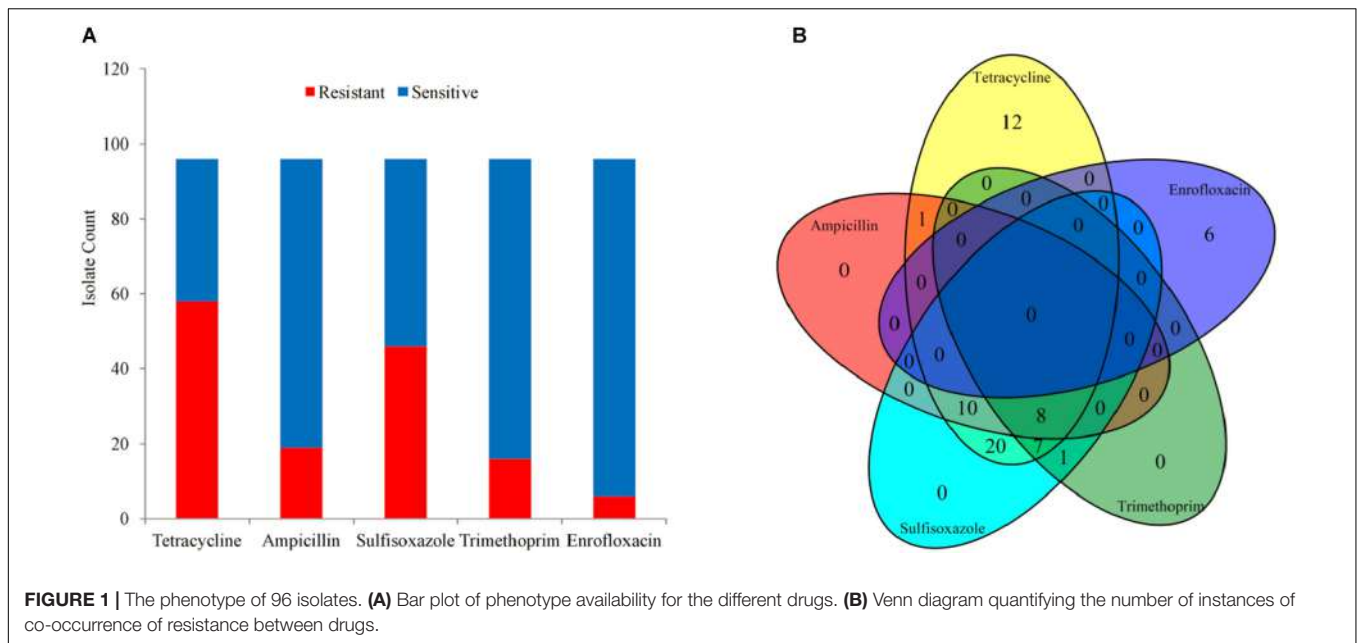
Even though 3 and 8 out of 58 phenotype resistant strains were predicted to be sensitive for tetracycline from SVM and SCM model, respectively, the sensitivity and accuracy of both of the models were still high enough for prediction. Of the 3 false-negative isolates (MIDG3342, MIDG3352, and MIDG3356) predicted by SVM and SCM, no acquired tetracycline-resistant genes were found in the genome of those isolates. Of the other 5 false negative isolates predicted by SCM, all of them were found to carry the *tetH* gene and predicted to be true positive by SVM.

Correlations between the phenotype and the model predictions of 3 subsets of testing datasets represented 96 unduplicated strains of *A. pleuropneumoniae* isolates were shown in **Table 2**. The results indicated that both SVM and SCM models could significantly classify the resistant isolates from the sensitive isolates of the bacteria ( $p < 0.01$ ).

## DISCUSSION

Support Vector Machine (SVM) has been applied to several biological problems such as prediction of protein-protein interactions, homology detection, gene expression analysis, drug discovery, and drug resistance analysis (Cui et al., 2012; Li et al., 2016; Kouchaki et al., 2018). To our knowledge, it's the first time to use the SVM model to predict the drug resistance

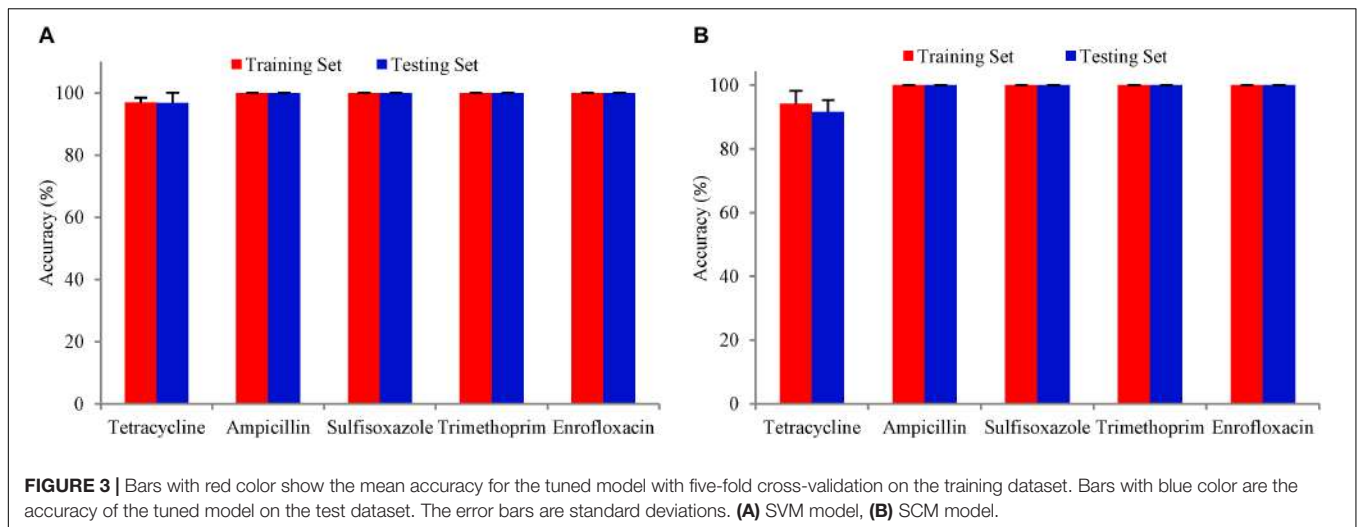
<sup>5</sup><https://github.com/aladro61/kover/>



based on the counts of co-occurring k-mers between the genome and the reference resistance genes. Using the reference gene fragments of QRDR built by the authors could cover the deficit that no point mutation databases provide the reference genes specific for *A. pleuropneumoniae*. And this new method could be used for phenotype prediction of the other genes or bacteria with point mutation.

Unlike the KmerResistance, which uses the “winner takes all strategy” (Clausen et al., 2016), the exact number of co-occurring k-mers between the genome and the reference resistance genes were counted. The supervised machine learning itself can learn from the situation where k-mers not being able to match due to the mismatch, indel, non-perfect assembly, or genomic rearrangements in the query genome from the training dataset





**TABLE 1** | Prediction metrics on test datasets using the best performing SVM and SCM models.

	SVM				SCM			
	Sensitivity	Specificity	Accuracy	Precision	Sensitivity	Specificity	Accuracy	Precision
Tetracycline	0.95 ± 0.05	1.00 ± 0.00	0.97 ± 0.03	1.00 ± 0.00	0.86 ± 0.08	1.00 ± 0.00	0.92 ± 0.04	1.00 ± 0.00
Ampicillin	1.00 ± 0.00	1.00 ± 0.00	1.00 ± 0.00	1.00 ± 0.00	1.00 ± 0.00	1.00 ± 0.00	1.00 ± 0.00	1.00 ± 0.00
Sulfisoxazole	1.00 ± 0.00	1.00 ± 0.00	1.00 ± 0.00	1.00 ± 0.00	1.00 ± 0.00	1.00 ± 0.00	1.00 ± 0.00	1.00 ± 0.00
Trimethoprim	1.00 ± 0.00	1.00 ± 0.00	1.00 ± 0.00	1.00 ± 0.00	1.00 ± 0.00	1.00 ± 0.00	1.00 ± 0.00	1.00 ± 0.00
Enrofloxacin	1.00 ± 0.00	1.00 ± 0.00	1.00 ± 0.00	1.00 ± 0.00	1.00 ± 0.00	1.00 ± 0.00	1.00 ± 0.00	1.00 ± 0.00

**TABLE 2** | Correlation of phenotype and model predictions of SVM and SCM models.

Antimicrobial agent	Number of isolates classified by phenotype (R, S)	SVM		SCM	
		Number of isolates predicted to be TP and TN (TP, TN)	Correlation of phenotype to the model prediction	Number of isolates predicted to be TP and TN (TP, TN)	Correlation of phenotype to the model prediction
Tetracycline	(58, 38)	(55, 38)	$p < 2.2e-16$	(50, 38)	$p < 2.2e-16$
Ampicillin	(19, 77)	(19, 77)	$p < 2.2e-16$	(19, 77)	$p < 2.2e-16$
Sulfisoxazole	(46, 50)	(46, 50)	$p < 2.2e-16$	(46, 50)	$p < 2.2e-16$
Trimethoprim	(16, 80)	(16, 80)	$p < 2.3e-16$	(16, 80)	$p < 2.3e-16$
Enrofloxacin	(6, 90)	(6, 90)	$p < 1.1e-09$	(6, 90)	$p < 1.1e-09$

R resistant, S sensitive. Correlation between phenotype and model predictions were calculated using Fisher's exact test in python.

and predict the correct answer while the same situation happened in the test dataset.

The Set Covering Problem is a classical question in combinatorics, computer science, operations research, and complexity theory. As of now, one of the most relevant applications of SCP is given by crew scheduling problems in railway and mass-transit transportation companies, where a given set of trips has to be covered by a minimum-cost set of pairings (Caprara et al., 2000). In this study, The SCM algorithm uses a greedy approach to construct conjunction (logical-AND) or disjunction (logical-OR) of Boolean functions to find the most concise set of genomic features (k-mers) that allows for accurate prediction of the phenotype. A conjunction model assigns the positive class to a genome if all the rules output true,

whereas a disjunction model does the same if at least one rule outputs true. The method was validated by generating models that predict the antibiotic resistance of *C. difficile*, *M. tuberculosis*, *P. aeruginosa*, and *S. pneumoniae* for 17 antibiotics (Drouin et al., 2016). The obtained models, implemented in Kover, were proven to be accurate, faithful to the biological pathways targeted by the antibiotics, and they provide insight into the process of resistance acquisition.

The numbers of isolates predicted to be sensitive or resistant by SVM was exactly the same as the result predicted by mapping the reference resistant genes against the assembly of the WGS data (Bossé et al., 2017). This indicated that the SVM model is excellent in classifying the phenotype of the bacteria. In general, reference-based SVM model should be equally successful whether

they are applied to a small or large set of pathogens since the accuracy of the prediction rely mainly on whether there were reference resistant genes in the reference databases like ResFinder or other built-in databases.

Until now, no point mutation was reported in the amino acid of GyrB QRDR of *A. pleuropneumoniae*. Of the amino acid of *parE* QRDR (residues 440–479) of 96 isolates in this study, 29 sensitive isolates had substitutions of D479E in the *parE* protein. The other 61 sensitive isolates and the 6 resistant isolates did not have substitutions of D479E comparing with the amino acid of reference *parE* gene. The finding indicated that mutation of D479E in the *parE* gene might not be related to the resistant of the bacteria against Enrofloxacin. So, DNA sequences of QRDRs of *gyrA* (residues 68–106), *parC* (residues 68–106), and *parE* (residue 425–478) of sensitive isolates were chosen and appended to a FASTA file as reference genes for the SVM model to learn and predict the phenotypes of the bacteria against Enrofloxacin.

The SCM model, regardless of the resistant mechanism of which were acquired AMR genes or point mutation in the chromosome, by comparing the difference of the k-mers between the resistant strains and the sensitive strains, finds the most concise set of equivalent k-mers that allows for accurate prediction of the phenotype.

Any approach that uses machine learning models requires adequate input data to form a “training set” to train the machine learning model and a “testing set” to assess the performance of the model (Macesic et al., 2017). Among the five antimicrobial agents, the resistant background of *A. pleuropneumoniae* against tetracycline is more complicated than the others. There were 58 phenotype resistant strains, with 50 isolates carrying *tet(B)*, 5 isolates carrying *tet(H)*, and 3 isolates did not have any tetracycline resistance genes detected. And up to now, we still could not able to collect the whole genome of the *A. pleuropneumoniae* with *tet(H)* genes publicly, therefore, after randomly split the limited data into training set or testing set, the SCM model did not have enough sample to learn from the training dataset and therefore lead to a relative lower accuracy while predicting the testing set of the model.

Both models have advantages and shortcuts. The reference-based SVM model performs well at classifying resistance from sensitive isolates regardless of the sample size of the training set since the counts of co-occurring k-mers between the genome and the reference resistance genes of the resistant isolates are significantly different from that of the sensitive isolates (Figure 2). But this method relies mainly on the database

and therefore cannot be used for predictions where resistance mechanisms have yet to be identified. The SCM model should need enough proportion of true phenotype data against false phenotype data as input to form a “training set” to train the model, but it provides a unique approach for deciphering, *de novo*, new biological mechanisms without the need for prior information (Drouin et al., 2016).

Even though both of the models can use raw reads to learn and predict the phenotype of the bacteria, it is recommended to use the assembled contigs as input data, since the genome assembly can increase the quality of the k-mer representation, reduces the number of unique k-mers and thus makes the process of splitting the genome into k-mers and building the matrix encoding the presence or absence of all k-mers by Ray Surveyor tool much faster (Drouin et al., 2016; Mahé and Tournoud, 2018).

## DATA AVAILABILITY STATEMENT

The raw data supporting the conclusions of this article will be made available by the authors, without undue reservation, to any qualified researcher.

## AUTHOR CONTRIBUTIONS

ZCL, TR, and GW designed the study and machine learning algorithm. DD, HL, JS, and LL analyzed the data and evaluated the biological relevance of the models. SL, GP, XM, JL, and ZML acquired the data and prepared it for analysis. ZCL wrote the manuscript.

## FUNDING

This work was financially supported by the Guangdong Modern Agro-industry Technology Research System (2018LM1080 and 2018LM2153), Science and Technology Program of Guangzhou (201707010217), and the Science and Technology Program of Guangdong Province (2014A070713026 and 2014A010107032).

## SUPPLEMENTARY MATERIAL

The Supplementary Material for this article can be found online at: <https://www.frontiersin.org/articles/10.3389/fmicb.2020.00048/full#supplementary-material>

## REFERENCES

- Bossé, J. T., Li, Y., Rogers, J., Fernandez Crespo, R., Li, Y., Chaudhuri, R. R., et al. (2017). Whole genome sequencing for surveillance of antimicrobial resistance in *Actinobacillus pleuropneumoniae*. *Front. Microbiol.* 8:311. doi: 10.3389/fmicb.2017.00311
- Caprara, A., Toth, P., and Fischetti, M. (2000). Algorithms for the set covering problem. *Ann. Oper. Res.* 98, 353–371. doi: 10.1023/a:1019225027893
- Clausen, P. T., Zankari, E., Aarestrup, F. M., and Lund, O. (2016). Benchmarking of methods for identification of antimicrobial resistance genes in bacterial whole genome data. *J. Antimicrob. Chemother.* 71, 2484–2488. doi: 10.1093/jac/dkw184
- Cui, G., Fang, C., and Han, K. (2012). Prediction of protein-protein interactions between viruses and human by an SVM model. *BMC Bioinform.* 13(Suppl. 7):S5. doi: 10.1186/1471-2105-13-s7-s5
- Déraspe, M., Raymond, F., Boisvert, S., Culley, A., Roy, P. H., Laviolette, F., et al. (2017). Phenetic comparison of prokaryotic genomes using k-mers. *Mol. Biol. Evol.* 34, 2716–2729. doi: 10.1093/molbev/msx200
- Drouin, A., Giguere, S., Déraspe, M., Marchand, M., Tyers, M., Loo, V. G., et al. (2016). Predictive computational phenotyping and biomarker discovery using

- reference-free genome comparisons. *BMC Genom.* 17:754. doi: 10.1186/s12864-016-2889-6
- Gibson, M. K., Forsberg, K. J., and Dantas, G. (2015). Improved annotation of antibiotic resistance determinants reveals microbial resistomes cluster by ecology. *ISME J.* 9, 207–216. doi: 10.1038/ismej.2014.106
- Kim, B., Hur, J., Lee, J. Y., Choi, Y., and Lee, J. H. (2016). Molecular serotyping and antimicrobial resistance profiles of *Actinobacillus pleuropneumoniae* isolated from pigs in South Korea. *Vet. Q.* 36, 137–144. doi: 10.1080/01652176.2016.1155241
- Kouchaki, S., Yang, Y., Walker, T. M., Walker, A. S., Wilson, D. J., Peto, T. E. A., et al. (2018). Application of machine learning techniques to tuberculosis drug resistance analysis. *Bioinformatics* 35, 2276–2282. doi: 10.1093/bioinformatics/bty949
- Li, Y., Kong, Y., Zhang, M., Yan, A., and Liu, Z. (2016). Using support vector machine (SVM) for classification of selectivity of H1N1 neuraminidase inhibitors. *Mol. Inform.* 35, 116–124. doi: 10.1002/minf.20150107
- Macesic, N., Polubriaginof, F., and Tatonetti, N. P. (2017). Machine learning: novel bioinformatics approaches for combating antimicrobial resistance. *Curr. Opin. Infect. Dis.* 30, 511–517. doi: 10.1097/QCO.0000000000000406
- Mahé, P., and Tournoud, M. (2018). Predicting bacterial resistance from whole-genome sequences using k-mers and stability selection. *BMC Bioinform.* 19:383. doi: 10.1186/s12859-018-2403-z
- McArthur, A. G., Wagglechner, N., Nizam, F., Yan, A., Azad, M. A., Baylay, A. J., et al. (2013). The comprehensive antibiotic resistance database. *Antimicrob. Agents Chemother.* 57, 3348–3357. doi: 10.1128/AAC.00419-13
- Pesesky, M. W., Hussain, T., Wallace, M., Patel, S., Andleeb, S., Burnham, C. D., et al. (2016). Evaluation of machine learning and rules-based approaches for predicting antimicrobial resistance profiles in gram-negative bacilli from whole genome sequence data. *Front. Microbiol.* 7:1887. doi: 10.3389/fmicb.2016.01887
- Wang, Y. C., Chan, J. P., Yeh, K. S., Chang, C. C., Hsuan, S. L., Hsieh, Y. M., et al. (2010). Molecular characterization of enrofloxacin resistant *Actinobacillus pleuropneumoniae* isolates. *Vet. Microbiol.* 142, 309–312. doi: 10.1016/j.vetmic.2009.09.067
- Zankari, E., Hasman, H., Cosentino, S., Vestergaard, M., Rasmussen, S., Lund, O., et al. (2012). Identification of acquired antimicrobial resistance genes. *J. Antimicrob. Chemother.* 67, 2640–2644. doi: 10.1093/jac/dks261
- Zerbino, D. R., and Birney, E. (2008). Velvet: algorithms for de novo short read assembly using de Bruijn graphs. *Genom. Res.* 18, 821–829. doi: 10.1101/gr.074492.107
- Zhang, L., Kang, Z., Yao, L., Gu, X., Huang, Z., Cai, Q., et al. (2018). Pharmacokinetic/pharmacodynamic integration to evaluate the changes in susceptibility of *Actinobacillus pleuropneumoniae* after repeated administration of Danofloxacin. *Front. Microbiol.* 9:2445. doi: 10.3389/fmicb.2018.02445

**Conflict of Interest:** The authors declare that the research was conducted in the absence of any commercial or financial relationships that could be construed as a potential conflict of interest.

Copyright © 2020 Liu, Deng, Lu, Sun, Lv, Li, Peng, Ma, Li, Li, Rong and Wang. This is an open-access article distributed under the terms of the Creative Commons Attribution License (CC BY). The use, distribution or reproduction in other forums is permitted, provided the original author(s) and the copyright owner(s) are credited and that the original publication in this journal is cited, in accordance with accepted academic practice. No use, distribution or reproduction is permitted which does not comply with these terms.



# Ectopic Expression of Rv0023 Mediates Isoniazid/Ethionamide Tolerance via Altering NADH/NAD<sup>+</sup> Levels in *Mycobacterium smegmatis*

Shailesh Kumar Gupta<sup>1,2†</sup>, Rajendra Kumar Angara<sup>1†</sup>, Suhail Yousuf<sup>†</sup>, Chilakala Gangi Reddy<sup>1,3†</sup> and Akash Ranjan<sup>1\*</sup>

<sup>1</sup> Computational and Functional Genomics Group, Centre for DNA Fingerprinting and Diagnostics, Hyderabad, India,

<sup>2</sup> Graduate Studies, Manipal Academy of Higher Education, Manipal, India, <sup>3</sup> Regional Centre for Biotechnology, Faridabad, India

## OPEN ACCESS

### Edited by:

Mattias Collin,  
Lund University, Sweden

### Reviewed by:

Yu-Min Chuang,  
Yale University, United States  
Diana Machado,  
NOVA University Lisbon, Portugal

### \*Correspondence:

Akash Ranjan  
akash@cdfd.org.in;  
dr.akash.ranjan@gmail.com

<sup>†</sup> These authors have contributed  
equally to this work

### Specialty section:

This article was submitted to  
Antimicrobials, Resistance  
and Chemotherapy,  
a section of the journal  
Frontiers in Microbiology

Received: 19 July 2019

Accepted: 03 January 2020

Published: 07 February 2020

### Citation:

Gupta SK, Angara RK, Yousuf S,  
Reddy CG and Ranjan A (2020)  
Ectopic Expression of Rv0023  
Mediates Isoniazid/Ethionamide  
Tolerance via Altering NADH/NAD<sup>+</sup>  
Levels in *Mycobacterium smegmatis*.  
Front. Microbiol. 11:3.  
doi: 10.3389/fmicb.2020.00003

Tuberculosis (TB) caused by *Mycobacterium tuberculosis* (*Mtb*) accounts for nearly 1.2 million deaths per annum worldwide. Due to the emergence of multidrug-resistant (MDR) *Mtb* strains, TB, a curable and avertable disease, remains one of the leading causes of morbidity and mortality. Isoniazid (INH) is a first-line anti-TB drug while ethionamide (ETH) is used as a second-line anti-TB drug. INH and ETH resistance develop through a network of genes involved in various biosynthetic pathways. In this study, we identified Rv0023, an *Mtb* protein belonging to the xenobiotic response element (XRE) family of transcription regulators, which has a role in generating higher tolerance toward INH and ETH in *Mycobacterium smegmatis* (*Msmeg*). Overexpression of Rv0023 in *Msmeg* leads to the development of INH- and ETH-tolerant strains. The strains expressing Rv0023 have a higher ratio of NADH/NAD<sup>+</sup>, and this physiological event is known to play a crucial role in the development of INH/ETH co-resistance in *Msmeg*. Gene expression analysis of some target genes revealed reduction in the expression of the *ndh* gene, but no direct interaction was observed between Rv0023 and the *ndh* promoter region. Rv0023 is divergently expressed to Rv0022c (*whiB5*) and we observed a direct interaction between the recombinant Rv0023 protein with the upstream region of Rv0022c, confirmed using reporter constructs of *Msmeg*. However, we found no indication that this interaction might play a role in the development of INH/ETH drug tolerance.

**Keywords:** XRE family of protein, *whiB5*, isoniazid resistance, ethionamide resistance, transcription regulation

## INTRODUCTION

Tuberculosis (TB) remains a major cause of death worldwide and the leading cause by a single infectious agent (World Health Organisation, 2018). Even though the disease can be cured and managed by several multidrug regimens, the emergence of multidrug-resistant (MDR) TB is proving to be a major challenge for complete eradication of the disease. Worldwide, MDR TB constitutes 3.5% of new TB cases and 18% of previously treated cases (World Health Organisation, 2018). To overcome these challenges and to better counter resistance in *Mycobacterium tuberculosis* (*Mtb*), understanding the mechanisms and deciphering the pathways majorly responsible for generating resistance are greatly required.



Isoniazid (INH), in combination with rifampicin (RIF), ethambutol (EMB), and pyrazinamide (PZA), forms the first-line therapy for TB. Cycloserine, ethionamide (ETH), and amikacin/capreomycin are used as second-line drugs<sup>1</sup>. INH was first used as an anti-TB drug in 1952 and shortly the first INH-resistant *Mtb* (INHr) clinical isolates were reported (Bernstein et al., 1952; Fox, 1952; Middlebrook and Cohn, 1953). INH and ETH are prodrugs that are converted into their active forms by proteins encoded by *katG* (catalase peroxidase KatG) and *ethA* (monooxygenase EthA), respectively (Johnsson and Schultz, 1994; Johnsson et al., 1997; Baulard et al., 2000; DeBarber et al., 2000; Vannelli et al., 2002; Fraaije et al., 2004). Although *katG* and *inhA* (encoding an NADPH-dependent enoyl-ACP reductase) are the main genes involved in INH resistance, clinical isolates with mutations in the *ndh* gene have been identified in INH-resistant *Mtb* strains (Lee et al., 2001). While in the study by Lee et al. (2001), INH resistance mutations were observed only in the *ndh* gene, in other studies, *ndh* mutations occur simultaneously with mutations in other genes (Hazbón et al., 2006; Cardoso et al., 2007). The role of the *ndh* gene mutations in INH and ETH co-resistance in *Mycobacterium smegmatis* (*Msmeg*) and *Mycobacterium bovis* (*Mbovis*) has been shown (Vilcheze et al., 2005), while the role of *ndh* in conferring resistance in *Mtb* is yet to be determined. The gene *ndh* encodes the type II NADH dehydrogenase and its ortholog in *Escherichia coli* (*E. coli*) has been characterized. In *E. coli*, it exists in a monomeric state bound to the membrane, where it oxidizes NADH, reduces quinone, and catalyzes the transfer of electrons from reduced flavin to quinone (Jaworowski et al., 1981; Matsushita et al., 1987; Yagi, 1993; Gennis and Stewart, 1996; Kerscher, 2000). In *Msmeg*, mutations in *ndh* lead to an increase in NADH cellular concentration and inhibition of INH-NAD and ETH-NAD adducts formation (Vilcheze et al., 2005).

Xenobiotic response element (XRE) family of transcription factors are one of the most frequently occurring families of regulators in bacteria. Among the well-studied members of the XRE family are the lambda and Cro repressors, from lambda bacteriophage, and the prophage repressor Xre from *Bacillus subtilis*. The XRE family of regulators share a conserved N-terminal helix-turn-helix (HTH) DNA binding domain, while the C-terminal regulatory region is highly variable. The XRE family of regulators control diverse metabolic functions; e.g., SinR regulates developmental process in *B. subtilis* (Gaur et al., 1991), ClgR regulates *Streptomyces* growth and controls Clp proteolytic complex (Bellier and Mazodier, 2004), PuuR regulates putrescine utilization pathway in *E. coli* K-12 (Nemoto et al., 2012), and BzdR is involved in the anaerobic catabolism of benzoate in the denitrifying *Azoarcus* sp. strain CIB (Barragán et al., 2005). There are seven members of the XRE family of transcription regulators in *Mtb*: Rv0023, Rv0465c, Rv0474, Rv1129, Rv2017, Rv2021, and EspR (*Rv3849*). Except for EspR, which positively regulates the ESX-1 protein secretion system, the principal virulence determinant of *Mtb* (Raghavan et al., 2008), the remaining XRE transcription regulators in *Mtb* are uncharacterized.

Rv0023 is a regulator from the XRE family of transcriptional regulators, known to induce 488 genes and repress 404 genes (Rustad et al., 2014). Rv0023 regulon is enriched for the regulation of NAD reductases (Rustad et al., 2014). *Rv0023* is transcribed in an operon together with *Rv0024*, a gene that codes for an NLPC/p60 family protein and is transcribed divergently from *whiB5*, belonging to the WhiB family of transcriptional regulators. The *whiB5* gene product is a positive regulator of transcription and contributes to *Mtb* virulence and reactivation (Casonato et al., 2012). At present, very little is known about Rv0023 functions and its effect on *Mtb* physiology.

Here, we studied the effects of Rv0023 overexpression in *Msmeg*. The results show that ectopic expression of Rv0023 confers enhanced INH and ETH tolerance in *Msmeg*. Rv0023 ectopic expression downregulates the expression of the *ndh* gene and increases NADH/NAD<sup>+</sup> levels, which are known to be mediators of INH and ETH resistance in *Msmeg* (Miesel et al., 1998; Vilcheze et al., 2005). We further studied the regulation of the *whiB5-Rv0023* locus and identified Rv0023 as a negative regulator of *whiB5*. We have characterized its binding site and identified the promoters of *Rv0023* and *whiB5*.

## MATERIALS AND METHODS

### Bacterial Strains and Growth Condition

A complete list of strains used in this study is mentioned in **Table 1**. Cloning and plasmid propagation were done using *E. coli* strain DH5α. For protein expression, *E. coli* BL21 (DE3) was used. Both strains were grown in Luria Bertani (LB) medium at 37°C. *Mbovis* BCG Pasteur 1173P2, *Msmeg* mc<sup>2</sup>155, and the recombinant strains were grown in Middlebrook 7H9 (Himedia) broth supplemented with 10% OADC (oleic albumin dextrose catalase) (Himedia), 0.2% glycerol, and 0.05% Tween80 (20% stock) or on 7H10 agar without Tween80 at 37°C. Kanamycin (50 μg/ml) (Sigma-Aldrich), ampicillin (100 μg/ml) (Sigma-Aldrich), and hygromycin (50 μg/ml) (Invitrogen) were used as and when required.

### Plasmids and DNA Manipulation

Cloning, genomic, and plasmid DNA isolations were done as per standard molecular biology procedures (Sambrook et al., 1989). The plasmids and primers used in this study are listed in **Tables 2, 3**, respectively. Overlapping extension PCR was performed to generate site-directed mutations for promoter and critical residues studies. Sequences of all clones generated were confirmed by Sanger sequencing.

### Protein Expression and Purification

pET23a-0023 plasmid containing *Rv0023* ORF was used to transform *E. coli* BL21 (DE3) strain. Cells were grown in LB broth at 37°C till mid-log phase, and then 1 mM IPTG (isopropyl 1-thio-β-D-galactopyranoside) was added to induce the expression of protein. Cells were grown for another 4 h at 37°C, after which cells were harvested and purified using Ni-NTA affinity chromatography as described earlier (Yousuf et al., 2018). The purity of recombinant protein was analyzed

<sup>1</sup><https://www.cdc.gov/tb/education/corecurr/>

**TABLE 1** | List of strains used in this study.

Strain	Chromosomal genotype	Source
<i>E. coli</i> DH5 $\alpha$	F- $\Phi$ 80 <i>lacZ</i> $\Delta$ M15 $\Delta$ ( <i>lacZYA-argF</i> ) U169 <i>recA1 endA1 hsdR17</i> (rK-, mK+) <i>phoA supE44</i> $\lambda$ - <i>thi-1 gyrA96 relA1</i>	Lab repository
<i>E. coli</i> BL21 (DE3)	<i>fhuA2</i> [ <i>lon</i> ] <i>ompT gal</i> ( $\lambda$ DE3) [ <i>dcm</i> ] $\Delta$ <i>hsdS</i> $\lambda$ DE3 = $\lambda$ sBamHlo $\Delta$ EcoRI-B int:( <i>lacI</i> :PlacUV5:T7 gene1) i21 $\Delta$ <i>nin5</i>	Lab repository
<i>M. smegmatis</i> mc <sup>2</sup> 155		Lab repository
<i>Msmegp</i> VV16	<i>M. smegmatis</i> mc <sup>2</sup> 155 harboring pVV16 plasmid	This study
<i>Msmegp</i> VV0023	<i>M. smegmatis</i> mc <sup>2</sup> 155 harboring pVV0023 plasmid	This study
<i>MsmegpEJwhiB5</i> WT	<i>M. smegmatis</i> mc <sup>2</sup> 155 harboring pEJwhiB5 plasmid	This study
<i>MsmegpEJwhiB5</i> MUT	<i>M. smegmatis</i> mc <sup>2</sup> 155 harboring pEJwhiB5MUT plasmid	This study
<i>MsmegpEJ0023</i> WT	<i>M. smegmatis</i> mc <sup>2</sup> 155 harboring pEJ0023 plasmid	This study
<i>MsmegpEJ0023</i> MUT	<i>M. smegmatis</i> mc <sup>2</sup> 155 harboring pEJ0023MUT plasmid	This study
<i>MsmegpEJwhiB5</i> -pVV16	<i>M. smegmatis</i> mc <sup>2</sup> 155 harboring pEJwhiB5 and pVV16 plasmids	This study
<i>MsmegpEJwhiB5</i> -pVV0023	<i>M. smegmatis</i> mc <sup>2</sup> 155 harboring pEJwhiB5 and pVV0023 plasmids	This study
<i>MsmegpEJ0023</i> -pVV16	<i>M. smegmatis</i> mc <sup>2</sup> 155 harboring pEJ0023 and pVV16 plasmids	This study
<i>MsmegpEJ0023</i> -pVV0023	<i>M. smegmatis</i> mc <sup>2</sup> 155 harboring pEJ0023 and pVV0023 plasmids	This study
<i>Msmegp</i> VV0494	<i>M. smegmatis</i> mc <sup>2</sup> 155 harboring pVV0494 plasmid	Yousuf et al., 2015

**TABLE 2** | List of plasmids used in this study.

Plasmid	Features	Source/reference
pET23a0023	pET21b carrying Rv0023 gene	This study
pEJ414	km <sup>r</sup> and lacZ reporter vector	Papavinasundaram et al., 2001
pEJ0023WT	pEJ414 carrying 400bp upstream and 50bp downstream of <i>Rv0023</i> start codon	This study
pEJ0023MUT	Derivative of pEJ0023 where TCATAG is mutated to CCAGAG	This study
pEJwhiB5WT	pEJ414 carrying 250 bp upstream and 50 bp downstream of <i>whiB5</i> start codon	This study
pEJwhiB5MUT	Derivative of pEJwhiB5 where ATACGCTT is mutated to GCACGCGG	This study
pVV16	Hsp60 promoter, Km <sup>r</sup> and Hyg <sup>r</sup>	Korduláková et al., 2002
pVV0023	pVV16 carrying <i>Rv0023</i> gene	This study
pVV0494	pVV16 carrying <i>Rv0494</i> gene	Yousuf et al., 2015

**TABLE 3** | List of primers used for cloning.

Clone name	Primer	Sequence	Restriction site
pET0023	0023FP	GGGAATTCATATGAGCCGTGAGTCGGCCGGCGCGGCC	<i>Nde</i> I
	0023RP	CCGCTCGAGCTGCTGCCCTCATCCGCGTCTGTG	<i>Pst</i> I
pEJ0023WT	UP0023FP	CTAGTCTAGAAAGCTGTTCCGCGCTTTCGGTACTGGC	<i>Xba</i> I
	UP0023RP	CCCAAGCTTCGCGAAGTGC GCGAATGGCCGC	<i>Hind</i> III
pEJ0023MUT	UP0023SDMFP	TGGCCGACCGCGCAGCGGGCGCGTGCCT	<i>Xba</i> I
	UP0023SDMRP	AGGCACGCGCCGCTGCGCGGTCCGGCCA	<i>Hind</i> III
pEJwhiB5WT	UPwhiB5FP	CTAGTCTAGAGAGCTGTGCTTCGGCGTAGC	<i>Xba</i> I
	UPwhiB5RP	CCCAAGCTTATCGGGGTACCGGAACC	<i>Hind</i> III
pEJwhiB5MUT	UPwhiB5SDMFP	CACAGACATGCACGCGGTTGCCTATGTTTCGTTCAACAA GGAGGCCGGCACAAGCTTGGG	<i>Xba</i> I
	UPwhiB5SDMRP	CCCAAGCTTGTGCCGCTCCTGTTGAACGAAACATAGG CAA <b>CCGCGTGC</b> ATGTCTGTG	<i>Hind</i> III
pVV0023	pw0023FP	GGGAATTCATATGAGCCGTGAGTCGGCCGGCGCGGCC	<i>Nde</i> I
	pw0023RP	AAA <b>ACTGCAG</b> CTGCTGCCCTCATCCGCGTCTGTG	<i>Hind</i> III
pEJUF1	UF1FP	GGCCTGAGCTATCTGGAGCGCG	
	UF1RP	CGCGCTCCAGATAGCTCAGGCC	
pEJUF2	UF2FP	CTGTGCTTTTGTGTGGCTTGC	
	UF2RP	CGCAAGCCACACAAAAGCACAG	

Restriction site in the primer was underlined. The point mutations incorporated in SDM primers were highlighted in bold.

by 12% SDS-PAGE and protein concentration was measured by Bradford assay.

## $\beta$ -Galactosidase Assay

*Mycobacterium smegmatis* mc<sup>2</sup>155 strain was transformed with various constructs as required and grown in 7H9 media. The cultures were grown to mid-log phase and  $\beta$ -galactosidase activity was measured in Miller Units (MU) and all experiments were done in triplicate (Miller, 1972).

## Electrophoretic Mobility Shift Assay

To verify the interaction between Rv0023 and the upstream region of *whiB5*, electrophoretic mobility shift assay (EMSA) was performed. The 500-bp upstream region and the 50-bp downstream region of *whiB5* were PCR amplified and labeled with  $\gamma$ -<sup>32</sup>P ATP (3000 Ci mmol<sup>-1</sup>) using T4 polynucleotide kinase as per manufacturer's instructions (New England Biolabs). Labeled DNA was purified using nucleotide purification kit (Qiagen). Purified labeled DNA was then incubated with increasing concentrations of recombinant Rv0023 protein in an EMSA reaction buffer (25 mM HEPES, pH 7.9, 0.1 mM EDTA, 10 mM MgCl<sub>2</sub>, 20 mM KCl, and 5% glycerol) with 50 ng/ $\mu$ l poly(dI-dC) as a non-specific DNA competitor. The protein-DNA complex was incubated for 45 min and was resolved on a 6% non-denaturing polyacrylamide gel in 0.5  $\times$  tris-borate (TBE) buffer. The gel was run for 3–4 h to allow sufficient resolution of protein-DNA complex.

Electrophoretic mobility shift assay with commercially synthesized overlapping oligonucleotide and motifs was performed to identify the exact binding region of Rv0023.

## Primer Extension

To map the (+1) transcription start site (TSS), primer extension was performed as described earlier and in Cold Spring Harbor protocols (Carey et al., 2013; Angara et al., 2018). As the ORFs and intergenic region of *whiB5-Rv0023* locus are 100% conserved between *Mtb* and *Mbovis*, we used *Mbovis* RNA for primer extension studies. RNA was isolated with the Qiagen RNeasy kit as per manufacturer's instructions. SuperScript III reverse transcriptase (Invitrogen) was used to transcribe cDNA from total RNA (10–15  $\mu$ g) using 5'-end labeled  $\gamma$ -<sup>32</sup>P ATP primers (Table 4). Primer extension products were resolved on 6% polyacrylamide/8 M urea gel in TBE buffer. The size of primer extension product was determined by generating a dideoxy sequencing ladder using pUC19 plasmid as template and M13 universal primer (USB; 70140 KT).

## Stress Assay

To check the sensitivity of *Msmeg* toward various stress conditions, *Msmeg*WT, *Msmeg*VV16, and *Msmeg*VV0023

cells were grown in complete 7H9 media (supplemented with 10% OADC, 0.2% glycerol, and 0.05% Tween80) at 37°C overnight. Then, the cells were centrifuged and washed with PBS. The cells were then suspended in 7H9 media and the cell concentration was adjusted to 0.02 OD at 600 nm. The sensitivity of bacterial cultures toward 0.1% SDS (Sigma Aldrich) and 5 mM hydrogen peroxide (Merck) was measured at 37°C for 6 h. Sensitivity to 250  $\mu$ g/ml lysozyme (Sigma Aldrich) was measured at 37°C for 24 h. Susceptibility of *Msmeg* toward the antibiotics (Sigma Aldrich) INH (10  $\mu$ g/ml, MIC of 5  $\mu$ g/ml), RIF (10  $\mu$ g/ml, MIC of 1  $\mu$ g/ml), and ETH (2.5  $\mu$ g/ml, MIC of 10  $\mu$ g/ml) was determined at 37°C for 24 h. For determining CFU numbers for each stress condition and antibiotics, the cells were serially diluted (10-fold) and plated onto 7H10 agar plates.

Further, the strains *Msmeg*WT, *Msmeg*VV16, and *Msmeg*VV0023 were serially diluted (10-fold) and spotted on the 7H10 agar plates containing increasing concentrations of INH (0, 5, 10, and 15  $\mu$ g/ml) and ETH (0, 2.5, and 5  $\mu$ g/ml). The plates were incubated at 37°C for 48 h.

## qRT-PCR

Total RNA from *Msmeg*VV16 (vector control) and *Msmeg*VV0023 (Rv0023 protein overexpressed) cultures were isolated using Qiagen RNeasy kit. SuperScript III reverse transcriptase (Invitrogen) was used to generate cDNA using random hexamers. Real-time PCR was carried on the BioRad CFX96 system using gene-specific primers (Table 5) and EvaGreen qPCR mastermix (Applied Biological Materials Inc.) as per standard protocol. The fold change in expression relative to *Msmeg*VV16 (vector control) was calculated after normalizing to *sigA*. The 2<sup>- $\Delta\Delta$ CT</sup> method was used to calculate relative changes in gene expression (Livak and Schmittgen, 2001).

## NADH/NAD<sup>+</sup> Cellular Concentration

To measure the cellular concentration of NADH and NAD<sup>+</sup>, *Msmeg*VV16 and *Msmeg*VV0023 cells were grown to an OD<sub>600</sub> of 0.8–1.2. Cells were collected (1 ml) by centrifugation (11,000 rpm for 2 min). The supernatant was removed and 300  $\mu$ l of 0.2 M HCl (for NAD<sup>+</sup> extraction) or 0.2 M NaOH (for NADH extraction) was added to the cells. The cells were resuspended and incubated at 50°C for 10 min after which extracts were cooled to 0°C. The bacterial suspensions were neutralized by adding 0.1 M HCl (for NADH extraction) or

TABLE 4 | List of primers used in primer extension.

Primer	Sequence
0023PE1	CTCACGGCTCACCGCACGCTCCG
0023PE2	CGCGAAGTGCGC GAATGGCCGC

TABLE 5 | List of primers used in real-time PCR.

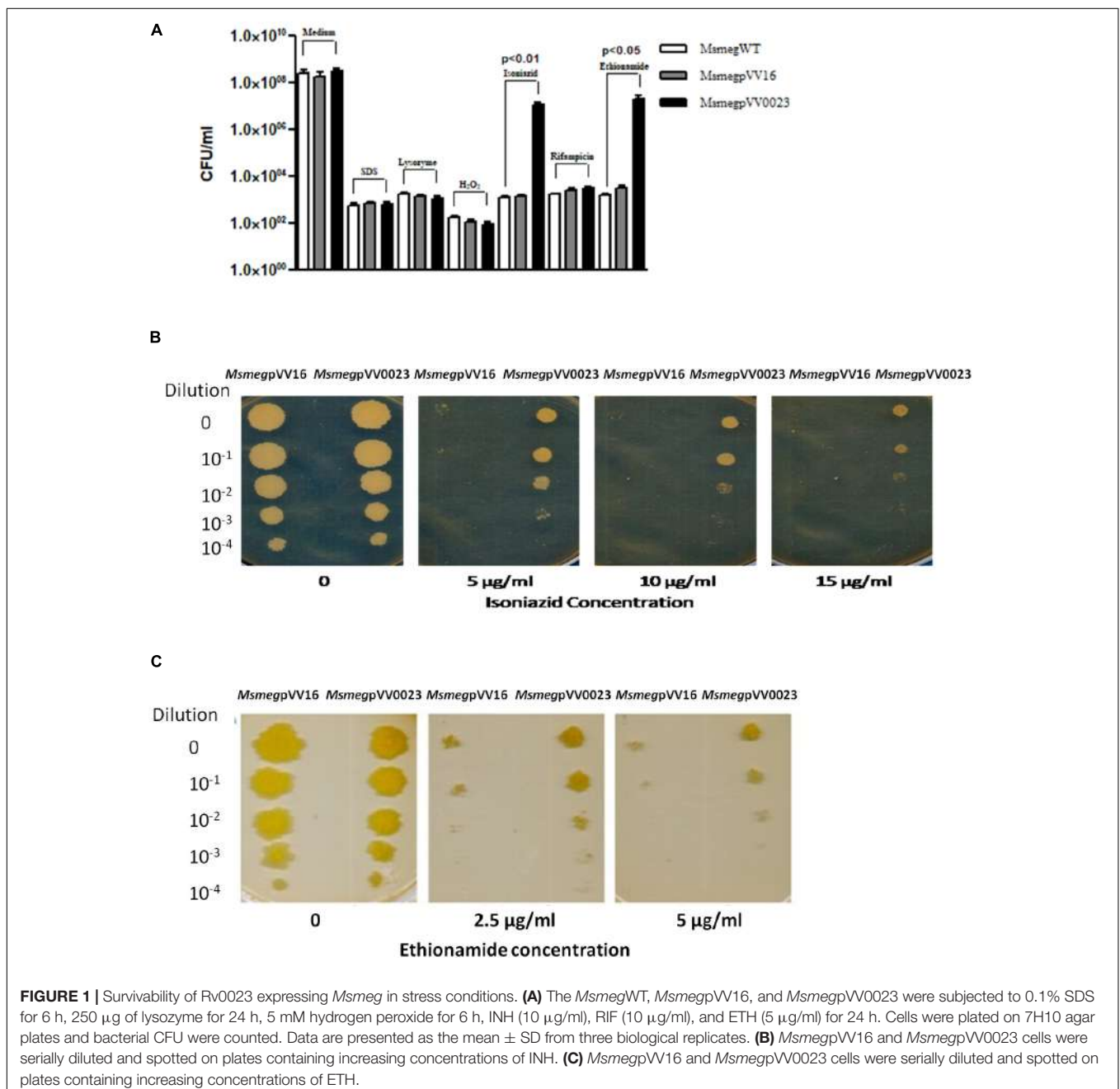
Primer	Sequence
inhARTFP	GTGAGGGCAACAAGATCGAC
inhARTRP	GTACGAGTACGCCGAGATGT
ndhRTFP	CGGGTTCAAGACGAAGATCG
ndhRTRP	CTTTCTCGGTGTCTCTGCAC
katGFP	CCAAGTGGGACAACAGCTTC
katGRP	GAGATCCGAGGTCAGCATCG
ethAFP	CGCCGAGAAGACCAACAAT
ethARP	AATGCTTCTGCACGTCGAAA

0.1 M NaOH (for NAD<sup>+</sup> extraction) dropwise while vortexing at high speed. Centrifugation was done to remove the cell debris and supernatant was transferred to a new tube and used immediately. NADH and NAD<sup>+</sup> concentrations were obtained by spectrophotometrically measuring the rate of MTT [3-(4,5-dimethylthiazol-2-yl)-2,5-diphenyl tetrazolium bromide, 4.2 mM] (Amresco), reduction by yeast alcohol dehydrogenase II (Sigma Aldrich) in the presence of PES (phenazine ethosulfate, 16.6 mM) (Sigma Aldrich) at 570 nm (Leonardo et al., 1996; San et al., 2002; Vilcheze et al., 2005). The concentration of nucleotide (NADH/NAD<sup>+</sup>) is proportional to the rate of MTT reduction.

## Bioinformatics

Rv0023 protein sequence (UniProt P9WMI3) was used as a query in the SynTax web server<sup>2</sup> for synteny analysis within the *Mycobacteriaceae* family (Oberto, 2013); a conserved domain database search was performed to identify HTH\_3 and XRE domains (Marchler-Bauer et al., 2015). Orthologous sequences of the *whiB5-Rv0023* intergenic region from different mycobacterial species were retrieved from KEGG genome database and aligned using CLUSTAL OMEGA (Sievers et al., 2011).

<sup>2</sup><http://archaea.u-psud.fr/SyntTax>





## Statistical Analysis

Data were presented as mean  $\pm$  SD. Student's *t*-test and one-way ANOVA were used to determine the statistical significance between groups and values with  $p < 0.05$  were considered to be significant. GraphPad Prism software version 5.02 was used for the statistical analysis.

## RESULTS

### Overexpression of Rv0023 Confers Increased INH and ETH Tolerance in *Msmeg*

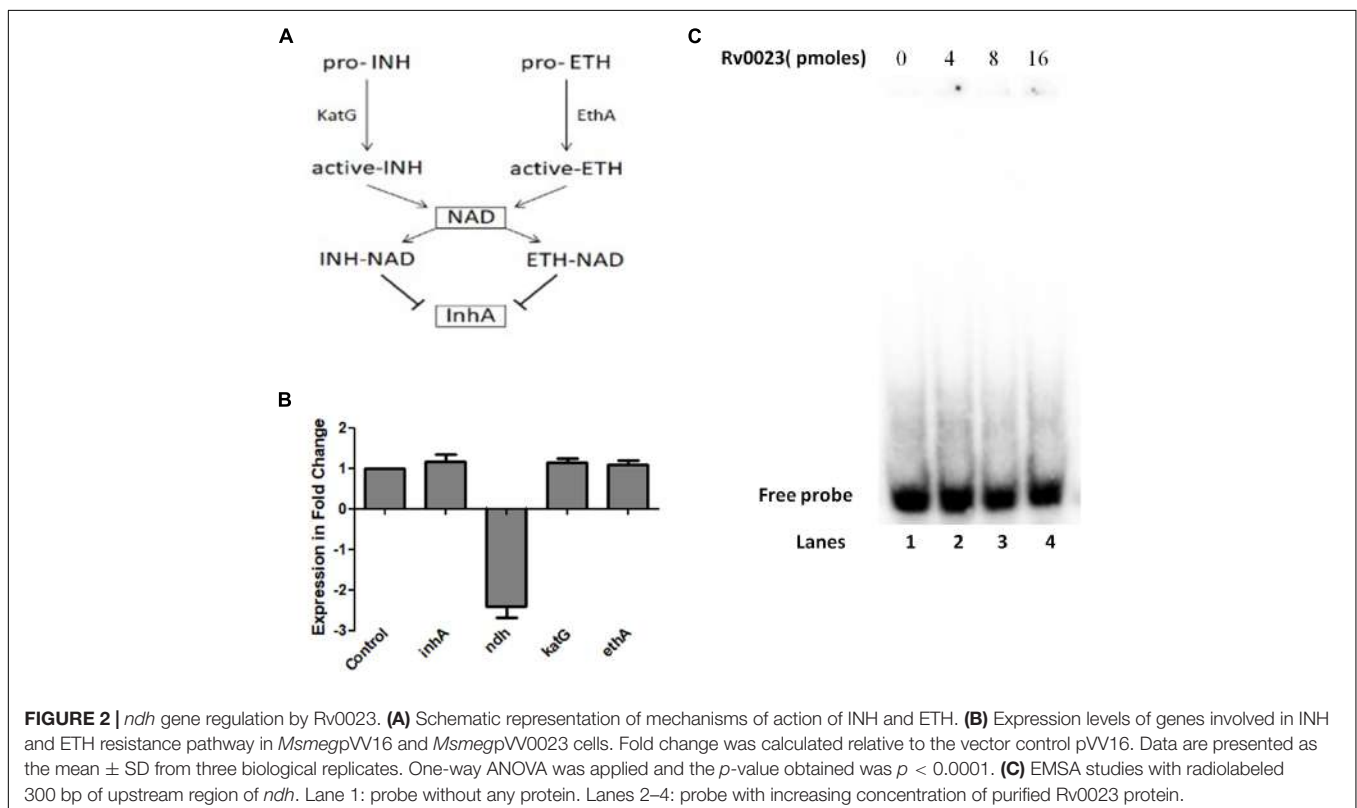
*Rv0023* is a non-essential gene in *Mtb*, yet it regulates a high number of genes in the genome (Sasseti et al., 2003; Rustad et al., 2014). *Msmeg* genome does not harbor the ortholog of Rv0023 and hence serves as a good model to study the function of Rv0023. To ascertain the role of *Rv0023*, we constructed an overexpressing strain of Rv0023 in *Msmeg*, *MsmegpVV0023*. The wild-type *MsmegWT*, vector control *MsmegpVV16*, and *MsmegpVV0023* strains were subjected to acid fast staining to rule out the effect of vector insertion on cellular integrity. The cells were found to be intact and acid fast (**Supplementary Figure 1**). To further study the role of Rv0023 in cellular physiology, *MsmegWT*, *MsmegpVV16*, and *MsmegpVV0023* were subjected to different stress conditions as depicted in **Figure 1A**, and tolerance was measured in terms of CFU. The CFU was counted for all conditions and we observed that overexpression of Rv0023 leads

to increased tolerance with regard to INH and ETH, and no effect was observed with any other stress conditions. Tolerance to INH and ETH was not seen either on the wild type or in vector control strains (**Figure 1A**).

The role of Rv0023 in generating tolerant strains was further confirmed via spotting the wild type, vector control, and Rv0023 overexpressed strains in the presence of increasing concentrations of INH and ETH. *MsmegWT*, *MsmegpVV16*, and *MsmegpVV0023* cells were serially diluted and spotted on plates containing 5, 10, and 15  $\mu\text{g/ml}$  of INH and 2.5 and 5  $\mu\text{g/ml}$  of ETH. Even at higher concentrations, *MsmegpVV0023* showed tolerance toward INH and ETH (**Figures 1B,C** and **Supplementary Figure 2**). The results indicate that Rv0023 expression specifically contributes toward the higher tolerance of INH and ETH in *Msmeg*.

### Rv0023 Expression in *Msmeg* Alters the NADH/NAD<sup>+</sup> Levels

Isoniazid and ethionamide are both prodrugs and they are activated by the protein catalase–peroxidase KatG and the NADPH-specific flavin adenine dinucleotide-containing monooxygenase, EthA, respectively. After activation, they react with NAD<sup>+</sup> to form INH-NAD and ETH-NAD adduct. This species then inhibits the enoyl ACP reductase *InhA*, which leads to the inhibition of mycolic acid biosynthesis and eventual mycobacterial cell death (**Figure 2A**). The major common genes to both pathways are the *ndh* (maintains NADH/NAD<sup>+</sup> ratio) and *inhA*. *Msmeg* orthologs of these and other important genes



**TABLE 6** | Cellular concentration of NADH and NAD<sup>+</sup>.

Strain	NADH ( $\mu\text{M}$ )	NAD <sup>+</sup> ( $\mu\text{M}$ )	NADH/NAD <sup>+</sup>
MsmegpVV16	8.29	9.93	0.83
MsmegpVV0023	11.27	9.44	1.19

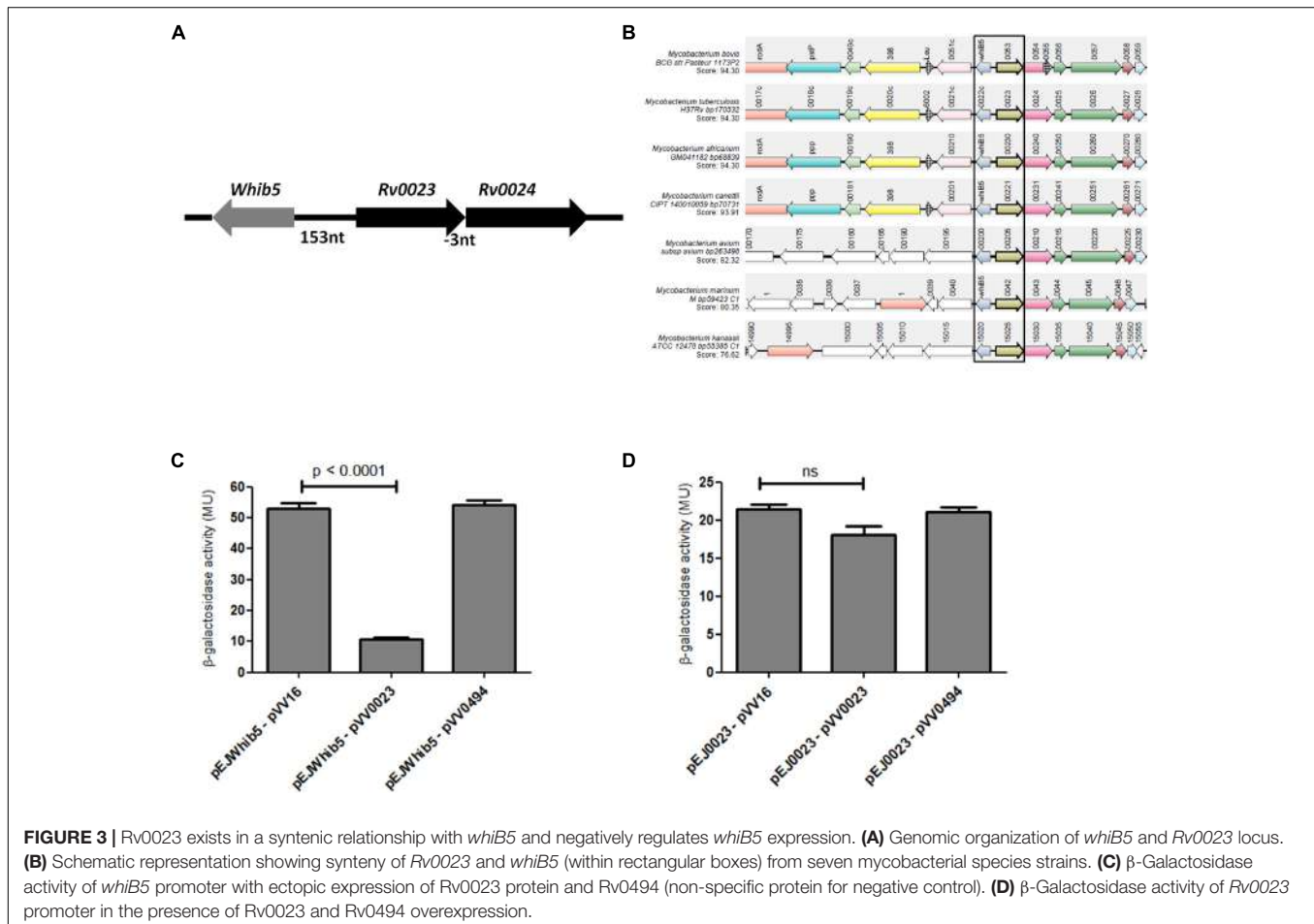
involved in INH and ETH resistance were subjected to qRT-PCR quantification. Total RNA was isolated from *MsmegpVV16* and *MsmegpVV0023* and the expression levels compared between the two strains. We found that the expression level of *ndh* (MSMEG\_3621) in *MsmegpVV0023* was approximately twofold lower than that of *MsmegpVV16*. No changes in the expression levels were observed in *inhA* (MSMEG\_3151), *katG* (MSMEG\_6384), and *ethA* (MSMEG\_6440) between both strains (**Figure 2B**). As *ndh* encodes NdhII, which oxidizes NADH to NAD<sup>+</sup>, we reasoned that the ratio of NADH/NAD<sup>+</sup> might be altered in *MsmegpVV0023* strain. So, we measured the cellular ratio of NADH and NAD<sup>+</sup> in *MsmegpVV16* and *MsmegpVV0023* strains and found that the ratio of NADH/NAD<sup>+</sup> is increased in *MsmegpVV0023* (**Table 6**). These results indicate that Rv0023 expression alters both the transcript levels of *ndh* gene and NADH/NAD<sup>+</sup> levels. To find out whether these effects are directly mediated by Rv0023 or through some

indirect means, we studied the interaction of recombinant Rv0023 with the upstream region of *ndh* (MSMEG\_3261) gene. However, under the experimental conditions mentioned, we did not observe any such positive interaction (**Figure 2C**).

## Rv0023 Negatively Regulates *whiB5*

*Rv0023* is in operon with *Rv0024* and is transcribed divergently from *whiB5* (**Figure 3A**). *Rv0023* and *whiB5* are absent from the non-pathogenic, fast-growing *Msmeg* but are present in *Mtb*. So, we tried to find the co-occurrence of these two genes in other mycobacterial species. Synteny analysis of *Rv0023* and *whiB5* was performed for important species of the *Mycobacterium* genus using the “SynTax” web server (**Figure 3B**). It was observed that *whiB5* is in synteny with *Rv0023* and that both are present only in pathogenic species of mycobacteria (**Supplementary Table 1**).

The syntenic relationship of the two regulators prompted us to probe the regulation of the *whiB5*-*Rv0023* locus. To identify the regulatory elements at this locus, upstream regions of *whiB5* and *Rv0023* were cloned in the promoter-less vector pEJ414 and named pEJ*whiB5* and pEJ0023, respectively. The coding region of *Rv0023* was cloned in the pVV16 vector to obtain pVV0023. *Msmeg* was transformed with pEJ*whiB5* or pEJ0023. The strains were again transformed with pVV0023

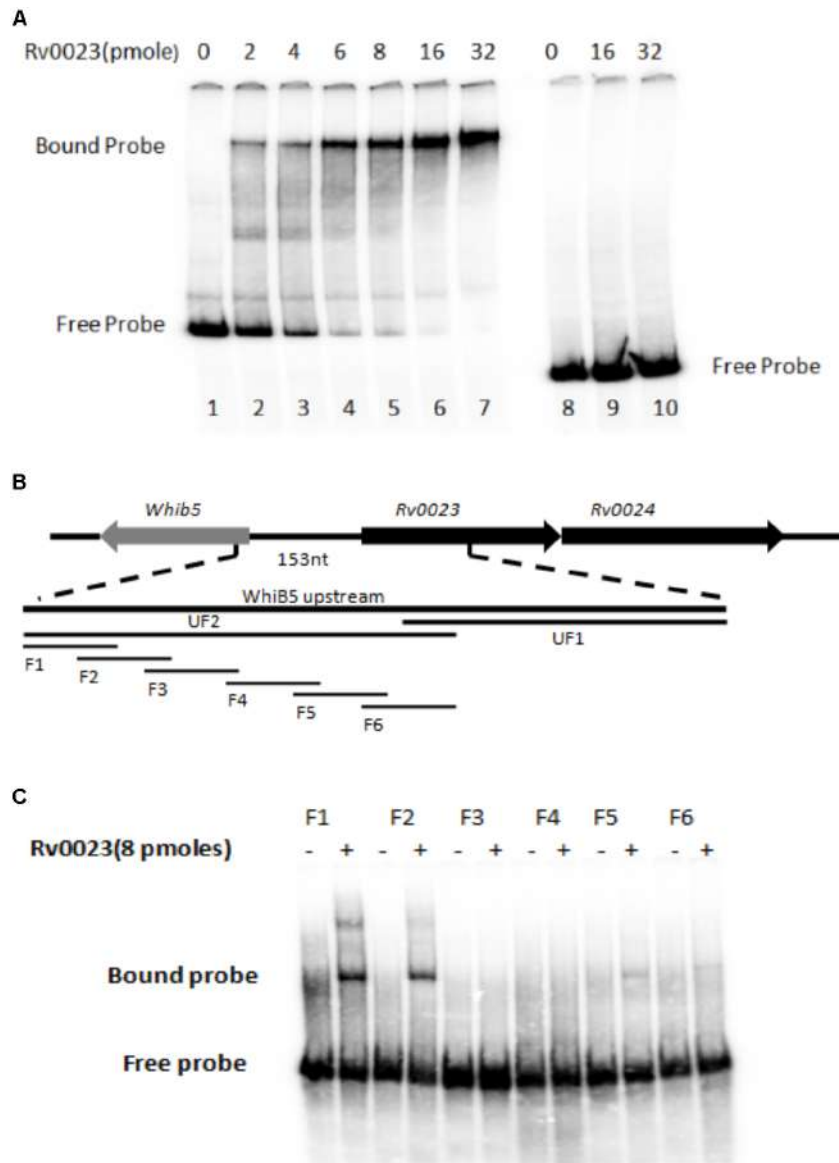


to obtain *MsmegpEJwhiB5*-pVV0023 and *MsmegpEJ0023*-pVV0023 double transformants. Promoter activities were measured in double transformants (*MsmegpEJwhiB5*-pVV0023, *MsmegpEJwhiB5*-pVV16, *MsmegpEJ0023*-pVV0023, and *MsmegpEJ0023*-pVV16). Overexpression of Rv0023 caused approximately fivefold decrease in *whiB5* promoter activity (Figure 3C), whereas no significant change in the promoter activity of *Rv0023* was noted (Figure 3D). Rv0494, a FadR transcriptional regulator, was used as a negative control, which did not affect the promoter activities of any of these genes. These

data suggest that Rv0023 negatively regulates the expression of *whiB5*, but it is not auto-regulatory.

### Rv0023 Binds to *whiB5* in vitro

As we have observed that Rv0023 expression represses the promoter activity of *whiB5* in *Msmeg*, it prompted us to further test whether Rv0023 interacts with *whiB5* promoter or not. Five hundred base pairs upstream and 50 bp downstream of *whiB5* gene containing the promoter were radiolabeled and EMSA was performed with the recombinant Rv0023.



**FIGURE 4 |** Rv0023 interaction with *whiB5* upstream. **(A)** Rv0023 binding to *whiB5* upstream in EMSA. Lane 1: radiolabeled *whiB5* upstream with no protein. Lanes 2–7: *whiB5* upstream with increasing concentration of Rv0023 protein. Lane 8: upstream region of Rv0494, a non-specific DNA, with no protein. Lanes 9–10: upstream region of Rv0494, a non-specific DNA, with increasing concentration of Rv0023 protein. **(B)** Six overlapping fragments (F1–F6) covering *whiB5* and *Rv0023* locus. **(C)** EMSA for overlapping fragments of *whiB5* upstream with purified Rv0023 protein. Lanes F1–F6: fragments with (+) and without (–) Rv0023 (8 pmol) protein.

**TABLE 7** | List of overlapping fragments used in **Figure 4**.

Overlapping fragment	Sequence
F1	AGAGCCCGCCACAGACATATACGCTTTTGC CTATGTTTCGTTCAACAAGGAGGCCGGCAC
F2	CACCCCTTATGTATATACGTTTTTATCGCG ATTCTCTTGCAGAGCCCGCCACAGACATAT
F3	CCATAAGCCGGATACTACCGGATACGACT CGGCCGCGGCCACCCCTTATGTATATACGT
F4	TGGCCGCGCCGGCCGACTCACGGCTCACCG CACGCTCCGGCCATAAGCCGGATACTACCC
F5	TCCGCGAGGGACCAGTCACGCGACTCGCGA AGTGCGCAATGGCCGCGCCGGCCGACTCA
F6	GCTCAGGCCATGGTGCTTACGCCAGTGGC GGCCGCCAGGTCCGCGAGGGACCAGTCACG

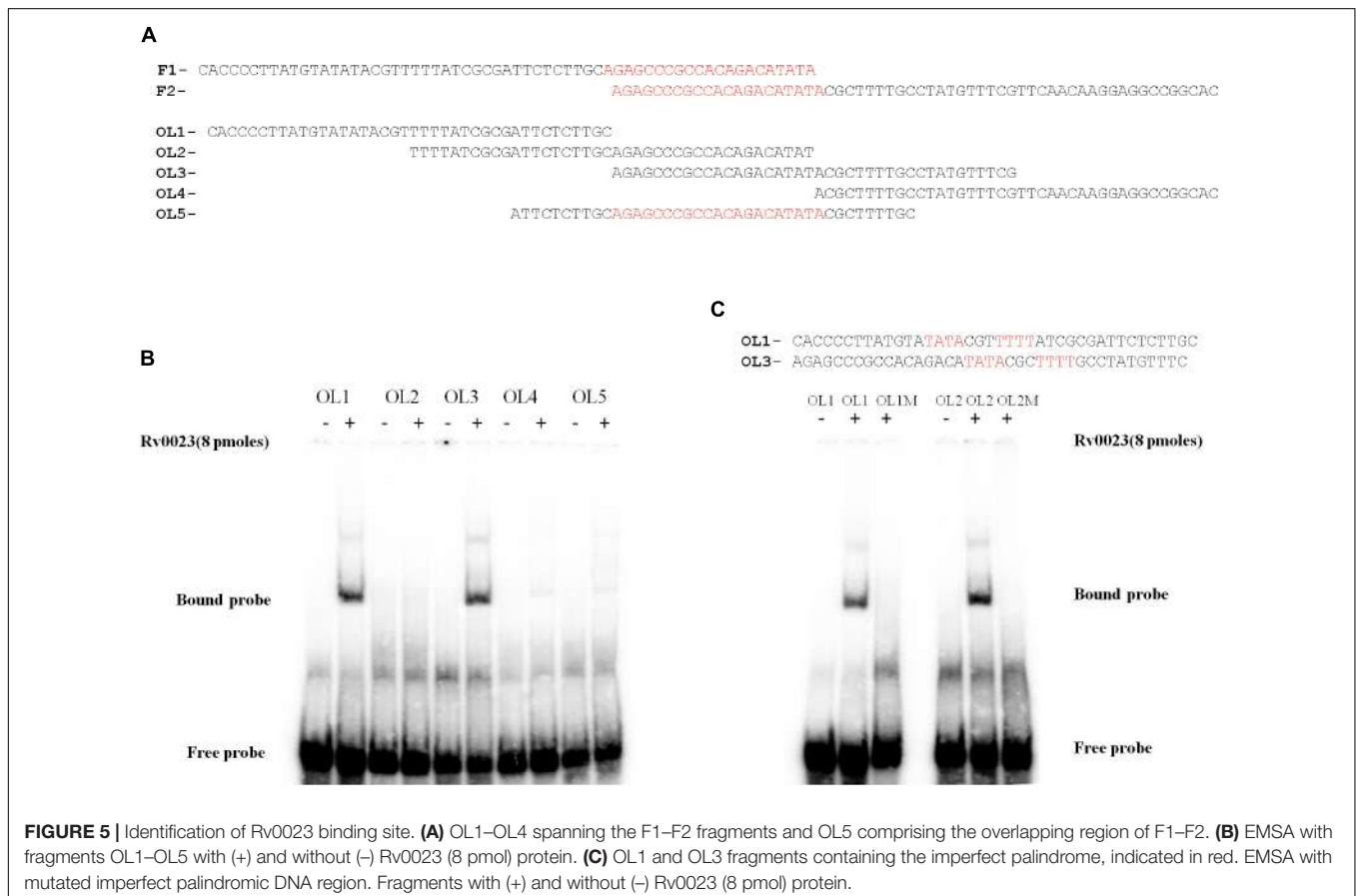
The radiolabeled upstream region of *whiB5* interacted with the purified recombinant Rv0023 in a dose-dependent manner. No interaction of Rv0023 was observed with non-specific DNA (**Figure 4A**).

Both EMSA and  $\beta$ -galactosidase assays confirmed that Rv0023 interacts with *whiB5* upstream and negatively regulates *whiB5* expression. In order to find the exact binding site of Rv0023, the 550 bp upstream of *whiB5* was divided into two fragments: UF1 of 340 bp and UF2 of 250 bp (**Figure 4B**). We observed that only the UF2 fragment binds to Rv0023 (**Supplementary Figure 3**).

The UF2 fragment was further divided into six overlapping fragments, F1–F6 (**Figure 4B** and **Table 7**). Purified Rv0023 binds to fragments F1 and F2, whereas no binding was observed with other fragments (**Figure 4C**). So, we looked for a binding site at the overlapping region of F1 and F2. We generated new oligonucleotides (OL1–OL5) covering the F1–F2 overlapping region (**Figure 5A** and **Table 8**). EMSA with these radiolabeled fragments showed that Rv0023 binds to OL1 and OL3 fragments whereas no binding was observed with other fragments (**Figure 5B**). Close examination of these fragments revealed the presence of an imperfect palindrome present in both sequences, TATAcgtTTTT in OL1 and TATAcgcTTTT in OL3 (**Figure 5C**). To confirm the binding sites identified, we mutated TATAcgtTTTT to TGTGcgtTGTG in OL1 and TATAcgcTTTT to TGTGcgcTGTG in OL3 to obtain OL1M and OL3M, respectively (**Table 8**). Binding studies have shown that Rv0023 binds to the native OL1 and OL3 fragments, but not to the mutant fragments, OL1M and OL3M (**Figure 5C**). We conclude that there are two binding sites (TATAcgtTTTT and TATAcgcTTTT) of Rv0023 in the upstream region of *whiB5* comprising an 11-bp imperfect palindromic sequence with a 3-bp spacer region.

### Analysis of Rv0023 Binding Site

The importance of each residue within the Rv0023 binding site was determined by generating 39 bp probes (M0–M12)





**TABLE 8** | List of overlapping fragments used in **Figure 5**.

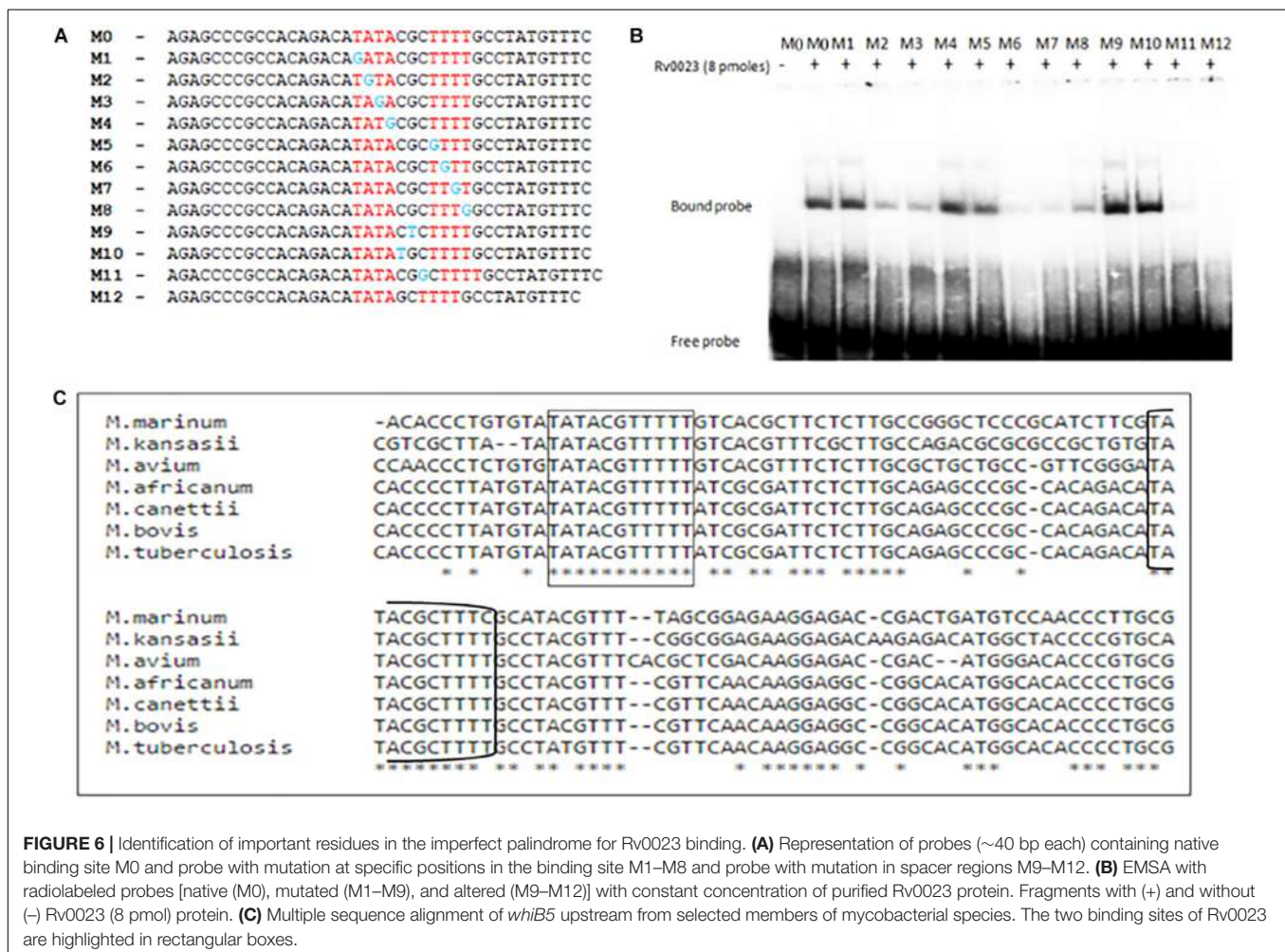
Overlapping fragment	Sequence
OL1	CACCCCTTATGTATATACGTTTTTATCGCGATTCTCTTGC
OL2	TTTTATCGCGATTCTCTTGACAGAGCCCGCCACAGACATAT
OL3	AGAGCCCGCCACAGACATATACGCTTTTGCCTATGTTTCG
OL4	ACGCTTTTGCCTATGTTTTCGTTCAACAAGGAGGCCGGCAC
OL5	ATTCTCTTGACAGAGCCCGCCACAGACATATACGCTTTTGC
OL1M	CACCCCTTATGTAGAGACGTGTGTATCGCGATTCTCTTGC
OL3M	AGAGCCCGCCACAGACAGAGACGCGTGTGCCTATGTTTCG

containing specific point mutations on each half of the imperfect palindrome and in the spacer region (**Figure 6A**). The probes were radiolabeled and were used in binding studies with recombinant Rv0023. The binding was observed with probes M0 (unaltered), M1, M4, and M5, and significant loss of binding was observed with M2, M3, M6, M7, and M8 fragments, suggesting the importance of these residues in Rv0023 binding. Changing the residues in the spacer region (M9–M10) did not affect Rv0023 binding; however,

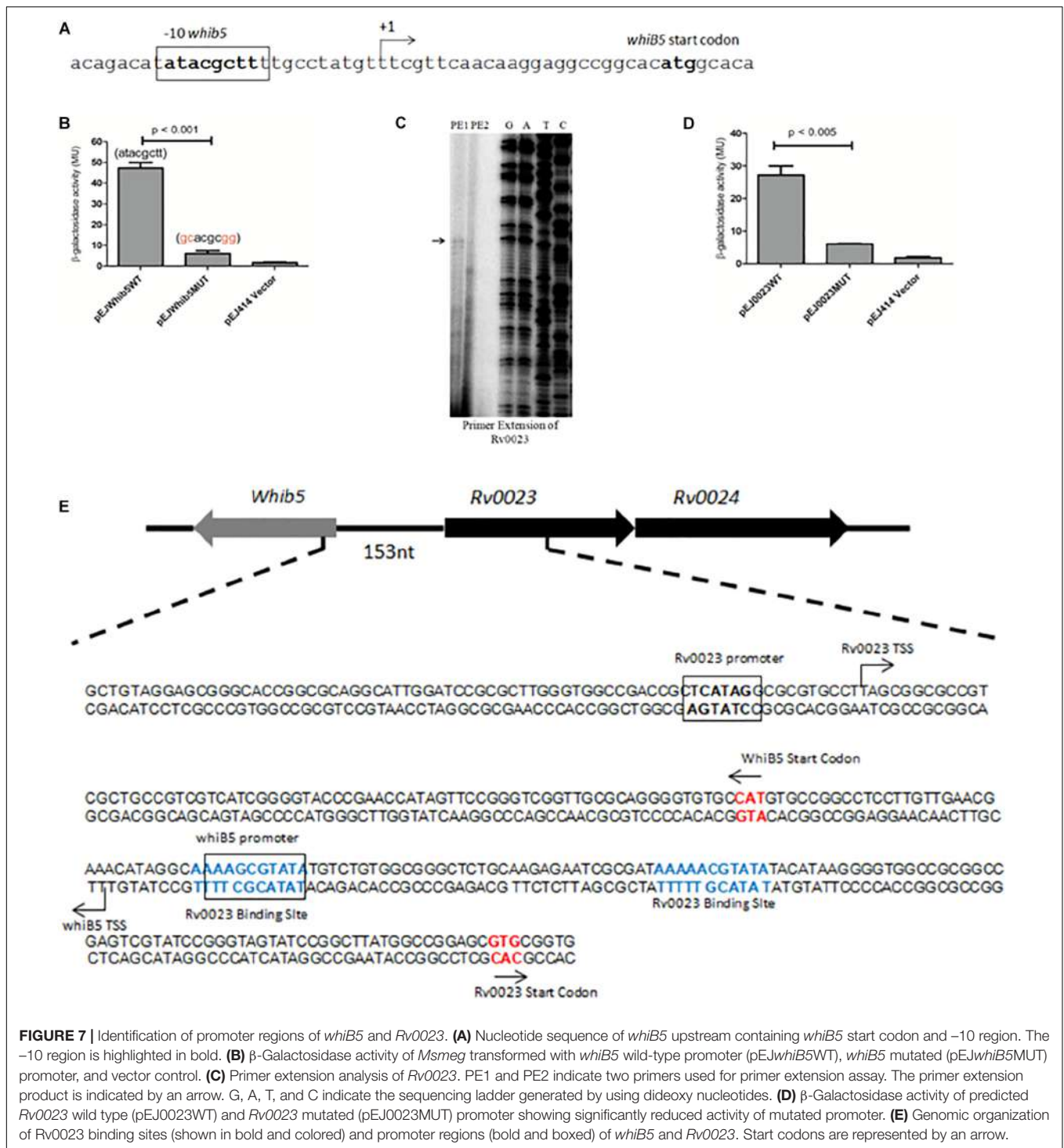
changing the length of spacer region by one base lead to significant loss of Rv0023 binding (M11–M12) (**Figure 6B**). As mentioned earlier, the organization of *Rv0023* and *whiB5* is conserved across pathogenic mycobacterial species. Therefore, we looked into the conservation of identified Rv0023 binding sites across the conserved genomes. For this, we aligned the upstream region of *whiB5* orthologs from different pathogenic mycobacterial species strains and found that the two binding sites of Rv0023 are conserved across the analyzed mycobacterial species (**Figure 6C**). These results highlight the important residues for Rv0023 binding and its conservation across mycobacterial species.

## Rv0023 Binding Site Overlaps With the *whiB5* Promoter Region

In order to understand the mechanism of Rv0023-mediated repression of *whiB5*, the TSSs of *whiB5* and *Rv0023* were mapped. The putative –10 region of *whiB5* was identified earlier by RACE (Casonato et al., 2012) (**Figure 7A**). To test the functionality of the putative –10 region, we cloned the 250 bp upstream of *whiB5* into lacZ reporter vector (pEJ*whiB5*WT). The promoter activity was measured using the



**FIGURE 6** | Identification of important residues in the imperfect palindrome for Rv0023 binding. **(A)** Representation of probes (~40 bp each) containing native binding site M0 and probe with mutation at specific positions in the binding site M1–M8 and probe with mutation in spacer regions M9–M12. **(B)** EMSA with radiolabeled probes [native (M0), mutated (M1–M9), and altered (M9–M12)] with constant concentration of purified Rv0023 protein. Fragments with (+) and without (–) Rv0023 (8 pmol) protein. **(C)** Multiple sequence alignment of *whiB5* upstream from selected members of mycobacterial species. The two binding sites of Rv0023 are highlighted in rectangular boxes.



**FIGURE 7 |** Identification of promoter regions of *whiB5* and *Rv0023*. **(A)** Nucleotide sequence of *whiB5* upstream containing *whiB5* start codon and -10 region. The -10 region is highlighted in bold. **(B)**  $\beta$ -Galactosidase activity of *Msmeg* transformed with *whiB5* wild-type promoter (pEJwhiB5WT), *whiB5* mutated (pEJwhiB5MUT) promoter, and vector control. **(C)** Primer extension analysis of *Rv0023*. PE1 and PE2 indicate two primers used for primer extension assay. The primer extension product is indicated by an arrow. G, A, T, and C indicate the sequencing ladder generated by using dideoxy nucleotides. **(D)**  $\beta$ -Galactosidase activity of predicted *Rv0023* wild type (pEJ0023WT) and *Rv0023* mutated (pEJ0023MUT) promoter showing significantly reduced activity of mutated promoter. **(E)** Genomic organization of *Rv0023* binding sites (shown in bold and colored) and promoter regions (bold and boxed) of *whiB5* and *Rv0023*. Start codons are represented by an arrow.

$\beta$ -galactosidase assay in *Msmeg*. Mutations in the putative -10 region of *whiB5* (atacgcctt to gcacgcgg) abolished the promoter activity, confirming the -10 region of *whiB5* (Figure 7B). To identify the promoter region of *Rv0023*, primer extension was performed. We identified the TSS at 228 bp upstream of *Rv0023* start codon (Figure 7C). A -10-like hexamer sequence TCATAG was identified upstream of TSS. To validate the

functionality of the -10 region of *Rv0023*, 400 bp upstream of *Rv0023* was cloned into a lacZ reporter vector (pEJ0023WT).  $\beta$ -Galactosidase assay with WT promoter and mutated promoter (pEJ0023MUT) indicated significant decrease in the promoter activity of the mutant strain compared to WT (Figure 7D). Mapping the promoters of *whiB5* and *Rv0023* with *Rv0023* binding site revealed that *Rv0023* binding site overlaps with

the promoter of *whiB5* but not of the *Rv0023* promoter region (Figure 7E).

## DISCUSSION

In this study, Rv0023, a member of the XRE family of transcriptional regulators, has been characterized, and its role in INH and ETH drug tolerance has been explored. The first part of our study concerns the role of Rv0023 in the physiology of mycobacteria. For our study, we used *Msmeg* as a surrogate model to study the effects of various stress conditions on wild type and Rv0023-expressing strains. It was observed that overexpression of Rv0023 confers higher tolerance toward INH and ETH in *Msmeg*. It was seen that the ectopic expression of Rv0023 alters the NADH/NAD<sup>+</sup> ratio, thereby increasing drug tolerance. In the second part of the manuscript, we identified Rv0023 as a transcriptional regulator and studied the regulatory effect at *whiB5-Rv0023* locus and observed that Rv0023 negatively regulates *whiB5* expression but is not auto-regulatory. Rv0023 regulates *whiB5* expression by binding to specific sequences in the upstream region of *whiB5*. Our data indicate that there are two binding sites for Rv0023 upstream of *whiB5* and one of the sites overlaps with the *whiB5* promoter, thereby possibly occluding the binding of RNA polymerase. The binding site of Rv0023 is conserved across mycobacterial species as confirmed by multiple sequence alignment. Apart from this, we have also characterized the binding site of Rv0023 and found important bases for binding. While analyzing the spacer region, it was found that the length of the spacer region is important for proper binding.

Isoniazid, isonicotinic acid hydrazide, is a synthetic drug and the occurrence of INH-resistant strains is significantly more frequent than other drug-resistant *Mtb* clinical strains (Nachega and Chaisson, 2003). ETH, 2-ethylthioisonicotinamide, is a structural analog of INH and was first synthesized in 1956 (Grumbach et al., 1956). Many genes have been found to be associated with INH and ETH resistance in clinical isolates, but the role of transcription factors regulating INH and ETH co-resistance is poorly understood. Rv0023, a transcriptional regulator, conferring higher tolerance toward INH and ETH in *Msmeg*, provided us a chance to explore the role of transcription factors in INH and ETH co-resistance in *Mtb*. To elucidate the mechanism by which Rv0023 confers drug tolerance, we investigated two main genes known to be involved in INH and ETH co-resistance, *inhA* (enzyme involved in the synthesis of cell wall mycolic acid) (Banerjee et al., 1994) and *ndh* (NADH dehydrogenase maintains the NADH/NAD<sup>+</sup> ratio) (Miesel et al., 1998). We checked their expression levels in the vector control and Rv0023-expressing *Msmeg* strains and differential expression was only observed in the *ndh* gene. The *ndh* gene oxidizes NADH to NAD<sup>+</sup>, which maintains the ratio of NADH/NAD<sup>+</sup> in mycobacterial cells (Jaworowski et al., 1981). Loss of *ndh* function leads to higher levels of NADH in the cytosol. Previous studies have shown that the higher NADH/NAD<sup>+</sup> levels interfere with activation of INH/ETH drugs by competitive inhibition with the formation of INH-NAD and ETH-NAD and thus confer resistance to INH/ETH in *Msmeg*

and BCG (Miesel et al., 1998; Vilcheze et al., 2005). So, we further measured the NADH/NAD<sup>+</sup> ratio in vector control and Rv0023-expressing *Msmeg* strains. The NADH/NAD<sup>+</sup> ratio was found to be increased in the Rv0023-overexpressed *Msmeg* strain, suggesting that negative regulation of *ndh* gene by Rv0023 is probably the mechanism by which Rv0023 confers INH and ETH tolerance in *Msmeg*. Our results were supported by previous studies where it was shown that Rv0023 regulon is enriched for NAD reductases (Rustad et al., 2014). Rv0023 did not bind to the upstream region of *ndh*, indicating that the regulation occurs possibly through indirect means, which may involve multiple intermediate gene products. Further studies are required to completely decipher this mechanism.

Synteny analysis has shown that *whiB5-Rv0023* locus is present mainly in pathogenic species of mycobacteria. The gene *whiB5* belongs to the WhiB family of transcriptional regulators, which are exclusive to actinomycetes, such as *Mycobacterium* and *Streptomyces* spp. (Soliveri et al., 2000). Earlier studies have shown that *whiB5* is a global transcriptional regulator, regulating 58 genes of diverse functions, including *sigM* and genes encoding for Type VII secretion systems such as *esx-2* and *esx-4*. It was shown that *whiB5* has a role in *Mtb* virulence and reactivation (Casonato et al., 2012). As the whole locus of *whiB5-Rv0023-Rv0024* is absent in *Msmeg*, it is difficult to gauge the true effect of Rv0023 in the physiology of *Mtb*. Further investigation in *Mtb* may reveal important aspects of Rv0023 regulation and its effects. Hence, taking into account the earlier studies and our current data, we surmise that Rv0023 plays a significant role in modulating genes associated with NADH/NAD<sup>+</sup> levels, which further influences mycobacterial physiology.

In conclusion, our work shows, for the first time, that Rv0023 has a role in conferring INH and ETH tolerance in *Msmeg*. Understanding the role of transcriptional factors in the development of drug resistance will open new avenues in the field of drug discovery and may provide important insights into *Mtb* physiology.

## DATA AVAILABILITY STATEMENT

The datasets generated for this study are available on request to the corresponding author.

## AUTHOR CONTRIBUTIONS

AR, SG, RA, and SY conceived the hypothesis and rationale of the study, analyzed the results, and wrote the manuscript. SG performed all the experiments. CR contributed in cloning of constructs and recombinant protein purification.

## FUNDING

SG was supported by a Centre for DNA Fingerprinting and Diagnostics fellowship. RA was supported earlier by a Department of Biotechnology fellowship. SY was supported earlier by a Council of Scientific and Industrial Research



fellowship at the Computational and Functional Genomics Group. CR was supported by a Centre for DNA Fingerprinting and Diagnostics fellowship.

## ACKNOWLEDGMENTS

We thank Dr. Roger Buxton (MRC, London, United Kingdom) for pEJ414 plasmid. Research in the AR laboratory was supported

## REFERENCES

- Angara, R. K., Yousuf, S., Gupta, S. K., and Ranjan, A. (2018). An IclR like protein from mycobacteria regulates leuCD operon and induces dormancy-like growth arrest in *Mycobacterium smegmatis*. *Tuberculosis* 108, 83–92. doi: 10.1016/j.tube.2017.10.009
- Banerjee, A., Dubnau, E., Quemard, A., Balasubramanian, V., Um, K. S., Wilson, T., et al. (1994). inhA, a gene encoding a target for isoniazid and ethionamide in *Mycobacterium tuberculosis*. *Science* 263, 227–230. doi: 10.1126/science.8284673
- Barragán, M. J., Blázquez, B., Zamarro, M. T., Mancheño, J. M., García, J. L., Díaz, E., et al. (2005). BzdR, a repressor that controls the anaerobic catabolism of benzoate in *Azoarcus* sp. CIB, is the first member of a new subfamily of transcriptional regulators. *J. Biol. Chem.* 280, 10683–10694. doi: 10.1074/jbc.m412259200
- Baulard, A. R., Betts, J. C., Engohang-Ndong, J., Quan, S., McAdam, R. A., Brennan, P. J., et al. (2000). Activation of the pro-drug ethionamide is regulated in mycobacteria. *J. Biol. Chem.* 275, 28326–28331.
- Bellier, A., and Mazodier, P. (2004). ClgR, a novel regulator of clp and lon expression in *Streptomyces*. *J. Bacteriol.* 186, 3238–3248. doi: 10.1128/jb.186.10.3238-3248.2004
- Bernstein, J. W., Lott, A., Steinberg, B. A., and Yale, H. L. (1952). Chemotherapy of experimental tuberculosis. *Am. Rev. Tuberc.* 65, 357–374.
- Cardoso, R. F., Cardoso, M. A., Leite, C. Q. F., Sato, D. N., Mamizuka, E. M., Hirata, R. D. C., et al. (2007). Characterization of *ndh* gene of isoniazid resistant and susceptible *Mycobacterium tuberculosis* isolates from Brazil. *Mem. Instit. Oswaldo Cruz* 102, 59–61. doi: 10.1590/s0074-02762007000100009
- Carey, M. F., Peterson, C. L., and Smale, S. T. (2013). The primer extension assay. *Cold Spring Harb. Protoc.* 8, 164–173.
- Casonato, S., Sánchez, A. C., Haruki, H., González, M. R., Provvedi, R., Dainese, E., et al. (2012). *WhiB5*, a transcriptional regulator that contributes to *Mycobacterium tuberculosis* virulence and reactivation. *Infect. Immun.* 80, 3132–3144. doi: 10.1128/IAI.06328-11
- DeBarber, A. E., Mdluli, K., Bosman, M., Bekker, L. G., and Barry, C. E. III (2000). Ethionamide activation and sensitivity in multidrug-resistant *Mycobacterium tuberculosis*. *Proc. Natl. Acad. Sci. U.S.A.* 97, 9677–9682. doi: 10.1073/pnas.97.17.9677
- Fox, H. H. (1952). The chemical approach to the control tuberculosis. *Science* 116, 129–134. doi: 10.1126/science.116.3006.129
- Fraaije, M. W., Kamerbeek, N. M., Heidekamp, A. J., Fortin, R., and Janssen, D. B. (2004). The prodrug activator EtaA from *Mycobacterium tuberculosis* is a Baeyer-Villiger monooxygenase. *J. Biol. Chem.* 279, 3354–3360. doi: 10.1074/jbc.m307770200
- Gaur, N. K., Oppenheim, J., and Smith, I. (1991). The Bacillus subtilis sin gene, a regulator of alternate developmental processes, codes for a DNA-binding protein. *J. Bacteriol.* 173, 678–686. doi: 10.1128/jb.173.2.678-686.1991
- Gennis, R. B., and Stewart, V. (1996). “Respiration,” in *Escherichia coli and Salmonella: Cellular and Molecular Biology*, Vol. 1, eds F. C. Neidhardt, R. Curtiss, III, J. L. Ingraham, E. C. C. Lin, K. B. Low, B. Magasanik, et al. (Washington, DC: ASM Press), 217–261.
- Grumbach, F., Rist, N., Libermann, D., Moyeux, M., Cals, S., and Clavel, S. (1956). Experimental antituberculous activity of certain isonicotinic thioamides substituted on the nucleus. *CR Hebd. Seances Acad. Sci.* 242, 2187–2189.
- Hazbón, M. H., Brimacombe, M., Del Valle, M. B., Cavatore, M., Guerrero, M. I., Varma-Basil, M., et al. (2006). Population genetics study of isoniazid resistance

by the Centre for DNA Fingerprinting and Diagnostics and Department of Biotechnology, Government of India.

## SUPPLEMENTARY MATERIAL

The Supplementary Material for this article can be found online at: <https://www.frontiersin.org/articles/10.3389/fmicb.2020.00003/full#supplementary-material>

- mutations and evolution of multidrug-resistant *Mycobacterium tuberculosis*. *Antimicrob. Agents Chemother.* 50, 2640–2649. doi: 10.1128/aac.00112-06
- Jaworowski, A., Mayo, G., Shaw, D. C., Campbell, H. D., and Young, I. G. (1981). Characterization of the respiratory NADH dehydrogenase of *Escherichia coli* and reconstitution of NADH oxidase in *ndh* mutant membrane vesicles. *Biochemistry* 20, 3621–3628. doi: 10.1021/bi00515a049
- Johnsson, K., Froland, W. A., and Schultz, P. G. (1997). Overexpression, purification, and characterization of the catalase-peroxidase KatG from *Mycobacterium tuberculosis*. *J. Biol. Chem.* 272, 2834–2840. doi: 10.1074/jbc.272.5.2834
- Johnsson, K., and Schultz, P. G. (1994). Mechanistic studies of the oxidation of isoniazid by the catalase peroxidase from *Mycobacterium tuberculosis*. *J. Am. Chem. Soc.* 116, 7425–7426. doi: 10.1021/ja00095a063
- Kerscher, S. J. (2000). Diversity and origin of alternative NADH:ubiquinone oxidoreductases. *Biochim. Biophys. Acta* 1459, 274–283. doi: 10.1016/s0005-2728(00)00162-6
- Korduláková, J., Gilleron, M., Mikuová, K., Puzo, G., Brennan, P. J., Gicquel, B., et al. (2002). Definition of the first mannosylation step in phosphatidylinositol mannoside synthesis: PimA is essential for growth of mycobacteria. *J. Biol. Chem.* 277, 31335–31344. doi: 10.1074/jbc.m204060200
- Lee, A. S., Teo, A. S., and Wong, S. Y. (2001). Novel mutations in *ndh* in isoniazid-resistant *Mycobacterium tuberculosis* isolates. *Antimicrob. Agents Chemother.* 45, 2157–2159. doi: 10.1128/aac.45.7.2157-2159.2001
- Leonardo, M. R., Dailly, Y., and Clark, D. P. (1996). Role of NAD in regulating the adhE gene of *Escherichia coli*. *J. Bacteriol.* 178, 6013–6018. doi: 10.1128/jb.178.20.6013-6018.1996
- Livak, K. J., and Schmittgen, T. D. (2001). Analysis of relative gene expression data using real-time quantitative PCR and the 2<sup>-</sup>ΔΔCT method. *Methods* 25, 402–408. doi: 10.1006/meth.2001.1262
- Marchler-Bauer, A., Derbyshire, M. K., Gonzales, N. R., Lu, S., Chitsaz, F., Geer, L. Y., et al. (2015). CDD: NCBI’s conserved domain database. *Nucleic Acids Res.* 43, D222–D226. doi: 10.1093/nar/gku1221
- Matsushita, K., Ohnishi, T., and Kaback, H. R. (1987). NADH-ubiquinone oxidoreductases of the *Escherichia coli* aerobic respiratory chain. *Biochemistry* 26, 7732–7737. doi: 10.1021/bi00398a029
- Middlebrook, G., and Cohn, M. L. (1953). Some observations on the pathogenicity of isoniazid-resistant variants of tubercle bacilli. *Science* 118, 297–299. doi: 10.1126/science.118.3063.297
- Miesel, L., Weisbrod, T. R., Marcinkeviciene, J. A., Bittman, R., and Jacobs, W. R. (1998). NADH dehydrogenase defects confer isoniazid resistance and conditional lethality in *Mycobacterium smegmatis*. *J. Bacteriol.* 180, 2459–2467. doi: 10.1128/jb.180.9.2459-2467.1998
- Miller, J. H. (1972). *Experiments in Molecular Genetics*. Cold Spring Harbor, NY: Cold Spring Harbor Press.
- Nachega, J. B., and Chaisson, R. E. (2003). Tuberculosis drug resistance: a global threat. *Clin. Infect. Dis.* 36(Suppl. 1), S24–S30.
- Nemoto, N., Kurihara, S., Kitahara, Y., Asada, K., Kato, K., and Suzuki, H. (2012). Mechanism for regulation of the putrescine utilization pathway by the transcription factor PuuR in *Escherichia coli* K-12. *J. Bacteriol.* 194, 3437–3447. doi: 10.1128/JB.00097-12
- Oberto, J. (2013). SyntTax: a web server linking synteny to prokaryotic taxonomy. *BMC Bioinf.* 14.4. doi: 10.1186/1471-2105-14-4
- Papavinasundaram, K. G., Anderson, C., Brooks, P. C., Thomas, N. A., Movahedzadeh, F., Jenner, P. J., et al. (2001). Slow induction of RecA by



- DNA damage in *Mycobacterium tuberculosis*. *Microbiology* 147, 3271–3279. doi: 10.1099/00221287-147-12-3271
- Raghavan, S., Manzanillo, P., Chan, K., Dovey, C., and Cox, J. S. (2008). Secreted transcription factor controls *Mycobacterium tuberculosis* virulence. *Nature* 454:717. doi: 10.1038/nature07219
- Rustad, T. R., Minch, K. J., Ma, S., Winkler, J. K., Hobbs, S., Hickey, M., et al. (2014). Mapping and manipulating the *Mycobacterium tuberculosis* transcriptome using a transcription factor overexpression-derived regulatory network. *Genome Biol.* 15:502.
- Sambrook, J., Fritsch, E. F., and Maniatis, T. (1989). *Molecular Cloning: a Laboratory Manual*. Cold Spring Harbor, NY: Cold Spring Harb Lab press.
- San, K. Y., Bennett, G. N., Berrios-Rivera, S. J., Vadali, R. V., Yang, Y. T., Horton, E., et al. (2002). Metabolic engineering through cofactor manipulation and its effects on metabolic flux redistribution in *Escherichia coli*. *Metab. Eng.* 4, 182–192. doi: 10.1006/mben.2001.0220
- Sasseti, C. M., Boyd, D. H., and Rubin, E. J. (2003). Genes required for mycobacterial growth defined by high density mutagenesis. *Mol. Microbiol.* 48, 77–84. doi: 10.1046/j.1365-2958.2003.03425.x
- Sievers, F., Wilm, A., Dineen, D., Gibson, T. J., Karplus, K., Li, W., et al. (2011). Fast, scalable generation of high-quality protein multiple sequence alignments using Clustal Omega. *Mol. Syst. Biol.* 7:539. doi: 10.1038/msb.2011.75
- Soliveri, J. A., Gomez, J., Bishai, W. R., and Chater, K. F. (2000). Multiple paralogous genes related to the *Streptomyces coelicolor* developmental regulatory gene *whiB* are present in *Streptomyces* and other actinomycetes. *Microbiology* 146, 333–343. doi: 10.1099/00221287-146-2-333
- Vannelli, T. A., Dykman, A., and Ortiz de Montellano, P. R. (2002). The antituberculosis drug ethionamide is activated by a flavoprotein monooxygenase. *J. Biol. Chem.* 277, 12824–12829. doi: 10.1074/jbc.m110751200
- Vilcheze, C., Weisbrod, T. R., Chen, B., Kremer, L., Hazbón, M. H., Wang, F., et al. (2005). Altered NADH/NAD<sup>+</sup> ratio mediates coresistance to isoniazid and ethionamide in mycobacteria. *Antimicrob. Agents Chemother.* 49, 708–720. doi: 10.1128/aac.49.2.708-720.2005
- World Health Organisation (2018). *Global Tuberculosis Report*. Geneva: WHO.
- Yagi, T. (1993). The bacterial energy-transducing NADH-quinone oxidoreductases. *Biochim. Biophys. Acta* 1141, 1–17. doi: 10.1016/0005-2728(93)90182-f
- Yousuf, S., Angara, R., Vindal, V., and Ranjan, A. (2015). Rv0494 is a starvation-inducible, autoregulatory FadR-like regulator from *Mycobacterium tuberculosis*. *Microbiology* 161, 463–476. doi: 10.1099/mic.0.000017
- Yousuf, S., Angara, R. K., Roy, A., Gupta, S. K., Misra, R., and Ranjan, A. (2018). Mce2R/Rv0586 of *Mycobacterium tuberculosis* is the functional homologue of FadR *E. coli*. *Microbiology* 164, 1133–1145. doi: 10.1099/mic.0.00686

**Conflict of Interest:** The authors declare that the research was conducted in the absence of any commercial or financial relationships that could be construed as a potential conflict of interest.

Copyright © 2020 Gupta, Angara, Yousuf, Reddy and Ranjan. This is an open-access article distributed under the terms of the Creative Commons Attribution License (CC BY). The use, distribution or reproduction in other forums is permitted, provided the original author(s) and the copyright owner(s) are credited and that the original publication in this journal is cited, in accordance with accepted academic practice. No use, distribution or reproduction is permitted which does not comply with these terms.



# Radezolid Is More Effective Than Linezolid Against Planktonic Cells and Inhibits *Enterococcus faecalis* Biofilm Formation

Jinxin Zheng<sup>1,2†</sup>, Zhong Chen<sup>1,2†</sup>, Zhiwei Lin<sup>2†</sup>, Xiang Sun<sup>1,2†</sup>, Bing Bai<sup>2</sup>, Guangjian Xu<sup>1,2</sup>, Junwen Chen<sup>2</sup>, Zhijian Yu<sup>2\*</sup> and Di Qu<sup>1\*</sup>

<sup>1</sup> Key Laboratory of Medical Molecular Virology of Ministries of Education and Health, School of Basic Medical Science and Institutes of Biomedical Sciences, Shanghai Medical College of Fudan University, Shanghai, China, <sup>2</sup> Department of Infectious Diseases and the Key Laboratory of Endogenous Infection, Shenzhen Nanshan People's Hospital, The 6th Affiliated Hospital of Shenzhen University Health Science Center, Shenzhen, China

## OPEN ACCESS

### Edited by:

Ilana L. B. C. Camargo,  
University of São Paulo, Brazil

### Reviewed by:

Lara Mendes Almeida,  
Federal University of Alagoas, Brazil  
Ali Al-Ahmad,  
Freiburg University Medical Center,  
Germany  
Daria Van Tyne,  
University of Pittsburgh, United States

### \*Correspondence:

Zhijian Yu  
yuzhijiansmu@163.com  
Di Qu  
dqu@fudan.edu.cn

† These authors have contributed  
equally to this work

### Specialty section:

This article was submitted to  
Antimicrobials, Resistance  
and Chemotherapy,  
a section of the journal  
Frontiers in Microbiology

Received: 20 August 2019

Accepted: 28 January 2020

Published: 14 February 2020

### Citation:

Zheng J, Chen Z, Lin Z, Sun X,  
Bai B, Xu G, Chen J, Yu Z and Qu D  
(2020) Radezolid Is More Effective  
Than Linezolid Against Planktonic  
Cells and Inhibits *Enterococcus  
faecalis* Biofilm Formation.  
*Front. Microbiol.* 11:196.  
doi: 10.3389/fmicb.2020.00196

The aim of this study was to compare the effects of radezolid and linezolid on planktonic and biofilm cells of *Enterococcus faecalis*. A total of 302 *E. faecalis* clinical isolates were collected, and the minimum inhibitory concentrations (MICs) of radezolid and linezolid were determined by the agar dilution method. Changes in the transcriptome of a high-level, *in vitro*-induced linezolid-resistant isolate were assessed by RNA sequencing and RT-qPCR, and the roles of efflux pump-related genes were confirmed by overexpression analysis. Biofilm biomass was evaluated by crystal violet staining and the adherent cells in the biofilms were quantified according to CFU numbers. The MIC<sub>50</sub>/MIC<sub>90</sub> values of radezolid (0.25/0.50 mg/L) against the 302 *E. faecalis* clinical isolates were eightfold lower than those of linezolid (2/4 mg/L). The radezolid MICs against the high-level linezolid-resistant isolates (linezolid MICs  $\geq$  64 mg/L) increased to  $\geq$  4 mg/L with mutations in the four copies of the V domain of the 23S rRNA gene. The mRNA expression level of *OG1RF\_12220* (*mdlB2*, multidrug ABC superfamily ATP-binding cassette transporter) increased in the high-level linezolid-resistant isolates, and radezolid and linezolid MICs against the linezolid-sensitive isolate increased with overexpression of *OG1RF\_12220*. Radezolid (at 1/4 or 1/8  $\times$  the MIC) inhibited *E. faecalis* biofilm formation to a greater extent than linezolid, which was primarily achieved through the inhibition of *ahrC*, *esp*, *relA*, and *relQ* transcription in *E. faecalis*. In conclusion, radezolid is more effective than linezolid against planktonic *E. faecalis* cells and inhibits biofilm formation by this bacterium.

**Keywords:** *Enterococcus faecalis*, radezolid, linezolid, resistance, biofilm, efflux pump

## INTRODUCTION

*Enterococcus faecalis* is a prominent example of a human pathogen that rapidly evolves and becomes refractory to a wide range of antimicrobials. In addition to the intrinsic and acquired resistance to many individual antimicrobials, the spread of multidrug-resistant (MDR) enterococci, especially those resistant to vancomycin (VRE), has further narrowed the choices for anti-infective

therapy (Ahmed and Baptiste, 2018). Linezolid (LZD), an important member of the oxazolidinone class of antibiotics, has proven to be highly effective against most gram-positive bacteria and is recommended as the first-line choice for the remedial

treatment of VRE and other MDR enterococci infections (Whang et al., 2013). However, widespread LZD application has led to the rapid, global emergence of LZD-resistant clinical isolates, including *Staphylococcus aureus*, *Staphylococcus*

**TABLE 1 |** The distribution of radezolid and linezolid minimum inhibitory concentrations (MICs) in 302 *Enterococcus faecalis* clinical isolates.

Antimicrobials	RZD MIC distribution (mg/L)					LZD MIC distribution (mg/L)					
	≤ 0.125	0.25	0.5	≥ 1	MIC <sub>50</sub> /MIC <sub>90</sub>	≤ 1	2	4	≥ 8	MIC <sub>50</sub> /MIC <sub>90</sub>	
<b>Ampicillin</b>	<b>S</b>	83	163	53	1	0.25/0.5	80	168	42	10	2/4
	<b>R</b>	1	1	0	0	≤0.125/0.25	1	1	0	0	1/2
<b>Doxycycline</b>	<b>S/I</b>	19	35	11	0	0.25/0.5	23	35	6	1	2/2
	<b>R</b>	66	128	42	1	0.25/0.5	57	135	36	9	2/4
<b>Vancomycin</b>	<b>S/I</b>	85	163	53	1	0.25/0.5	80	170	42	10	2/4
	<b>R</b>	0	0	0	0	–	0	0	0	0	–
<b>Erythromycin</b>	<b>S/I</b>	22	31	9	0	0.25/0.5	10	42	10	0	2/4
	<b>R</b>	63	132	44	1	0.25/0.5	70	128	32	10	2/4
<b>Ciprofloxacin</b>	<b>S/I</b>	64	129	37	1	0.25/0.5	60	140	26	5	2/4
	<b>R</b>	21	33	17	0	0.25/0.5	19	31	16	5	2/4
<b>Nitrofurantoin</b>	<b>S/I</b>	83	162	53	1	0.25/0.5	77	170	42	10	2/4
	<b>R</b>	2	1	0	0	≤0.125/0.25	3	0	0	0	1/1
<b>Rifampin</b>	<b>S/I</b>	15	25	8	1	0.25/0.5	13	25	9	2	2/4
	<b>R</b>	70	138	45	0	0.25/0.5	67	145	33	8	2/4
<b>Amikacin</b>	<b>S/I</b>	17	27	7	1	0.25/0.5	18	23	9	2	2/4
	<b>R</b>	67	137	46	0	0.25/0.5	61	148	33	8	2/4

RZD, radezolid; LZD, linezolid; S, sensitive; I, intermediate; R, resistant.

**TABLE 2 |** High-level linezolid resistance leads to the decreased sensitivity of *Enterococcus faecalis* to radezolid.

Isolates	MIC (mg/L)		23S rRNA mutations			
	LZD	RZD	R1	R2	R3	R4
ATCC29212-0	2	0.25	–	–	–	–
ATCC29212-6	8	0.25	C2424U	–	–	G2576U
ATCC29212-10	16	0.5	C2424U	–	–	G2576U
ATCC29212-18	64	1	C2424U	–	G2576U	G2576U
ATCC29212-22	128	1	C2424U	–	G2576U	G2576U
ATCC29212-27	256	4	C2424U	G2576U	G2576U	G2576U
ATCC29212-47	256	8	C2424U	G2576U	G2576U	G2576U
OG1RF-0	2	0.25	–	–	–	–
OG1RF-5	8	0.25	G2576U	–	G2505A	–
OG1RF-8	16	1	G2576U	–	G2505A	G2576U
OG1RF-18	64	4	G2576U, C2610A	G2576U, C2610A	G2505A	G2576U, C2610A
OG1RF-25	128	4	G2576U, C2610A	G2576U, C2610A	G2505A	G2576U, C2610A
OG1RF-30	256	4	G2576U, C2610A	G2576U, C2610A	G2505A	G2576U, C2610A
OG1RF-55	256	8	G2576U, C2610A	G2576U, C2610A	G2505A	G2576U, C2610A

RZD, radezolid; LZD, linezolid; MIC, minimum inhibitory concentration.

*epidermidis*, *E. faecalis*, *E. faecium*, *Mycobacterium tuberculosis*, and *Mycobacterium abscessus* (Balandin et al., 2016; Zimenkov et al., 2017; Chen et al., 2018; Silva et al., 2019; Ye et al., 2019). The consequent renewed interest in the optimization of oxazolidinones led to the development of new antimicrobials such as radezolid (RZD, RX-1741) (Lemaire et al., 2010b), which showed greater potency than LZD against a broad range of gram-positive bacteria, including VRE (Lemaire et al., 2010a; Wu et al., 2018, 2019). However, whether RZD is also effective against linezolid-resistant *E. faecalis* isolates remains unclear.

Numerous studies have demonstrated that LZD resistance is associated with mutations in domain V of the 23S rRNA gene and L3 and L4 ribosomal proteins, as well as with the acquisition of the *cfr*, *cfr(B)*, or *optrA* genes (Sadowy, 2018). Recently, the ABC-F subfamily ATP-binding cassette protein PoxTA was also found to play a role in the decreased susceptibility of *S. aureus* and *E. faecalis* to oxazolidinones (Antonelli et al., 2018; Elghaieb et al., 2019; Hasman et al., 2019; Lei et al., 2019). Nevertheless, the extent to which RZD exerts enhanced antibacterial activity against *E. faecalis* when compared with LZD is still not known. Additionally, LZD has been reported to have good inhibitory effects on *E. faecalis* biofilms (Holmberg et al., 2012); however, it is also unclear whether RZD shows greater efficacy than LZD against *E. faecalis* biofilms. To address these questions, in this study, we compared the antibacterial effects of RZD and LZD against biofilm and planktonic cells of *E. faecalis*.

## MATERIALS AND METHODS

### Bacterial Strains and Antimicrobials

A total of 302 non-duplicate *E. faecalis* isolates were collected from different inpatients at Shenzhen Nanshan People's Hospital (Grade A, level III Hospital, 1500 beds), Shenzhen University, China, between January 1, 2011, and December 31, 2016. These *E. faecalis* isolates were obtained from urine (135 isolates), blood (37 isolates), pus or secretions (86 isolates), bile (25 isolates), and other clinical sources (19 isolates). Based on a previous study, the dominant multilocus sequence types (MLSTs) of these isolates were ST16 and ST179 (Zheng et al., 2017). The isolates were identified by the Phoenix 100 automated microbiology system (BD, Franklin Lakes, NJ, United States), following which two subcultured generations of all the 302 isolates were re-identified with matrix-assisted laser desorption ionization time-of-flight mass spectrometry (IVD MALDI Biotyper, Bruker, Bremen, Germany). *E. faecalis* strains ATCC29212 and OG1RF (ATCC47077) were used as reference strains.

Chloramphenicol (catalog no. HY-B0239), linezolid (catalog no. HY-10394), and radezolid (catalog no. HY-14800) were purchased from MedChemExpress (MCE, Shanghai, China).

### Antimicrobial Susceptibility Test and Detection of LZD Resistance Genes

The susceptibilities of *E. faecalis* isolates to clinically relevant antimicrobials were tested by the Phoenix 100 automated microbiology system. The minimum inhibitory concentrations

(MICs) of LZD and RZD were determined by the agar dilution method according to Clinical and Laboratory Standards Institute (CLSI) guidelines. While no CLSI interpretive criteria existed for RZD against enterococci, the MICs of RZD for the quality control strain ATCC29212 were observed to range from 0.06 to 0.5 mg/L. Therefore, to analyze the distribution of MICs for RZD in these clinical isolates, the MICs were categorized into the following four levels:  $\leq 0.125$ , 0.25, 0.5, and  $\geq 1$  mg/L. The four copies of the V domain of the 23S rRNA gene, as well as the *rplC* and *rplD* genes, were amplified by PCR and sequenced. The *cfr*, *cfr(B)*, *optrA*, and *poxTA* genes were also amplified by PCR. The primers used for PCR are listed in **Supplementary Table S1**.

### *In vitro* Induction of High-Level LZD-Resistant Isolates and Efflux Inhibition Assay

The ATCC29212-0 and OG1RF (ATCC47077)-0 strains (LZD-sensitive, linezolid MIC: 2 mg/L) were serially subcultured in Mueller–Hinton Broth (MHB) containing LZD. The initial inducing concentration of LZD was 0.5 $\times$  the MIC, which was then successively increased to 1, 2, 4, 8, 16, 32, 64, and 128 $\times$  the MIC. Strains were cultured at each concentration for 3–5 passages before their exposure to the next concentration. Isolates from the final passage of each concentration were identified by matrix-assisted laser desorption ionization time-of-flight mass spectrometry (IVD MALDI Biotyper, Bruker, Bremen, Germany), and the MICs of RZD and LZD were determined by the agar dilution method according to CLSI guidelines.

The efflux pump activities in LZD-resistant isolates were detected using the efflux pump inhibitor Phe-Arg- $\beta$ -naphthylamide (PA $\beta$ N, Sigma, Shanghai, China). MICs for RZD and LZD were determined in the presence or absence of

**TABLE 3** | Radezolid and linezolid minimum inhibitory concentrations (MICs) decreased in the presence of PA $\beta$ N.

Isolates	MIC (mg/L)			
	LZD	LZD + PA $\beta$ N	RZD	RZD + PA $\beta$ N
ATCC29212-0	2	2	0.25	0.25
ATCC29212-6	8	4	0.25	0.25
ATCC29212-10	16	4	0.5	0.25
ATCC29212-18	64	8	1	0.25
ATCC29212-22	128	32	1	0.5
ATCC29212-27	256	32	1	0.5
ATCC29212-47	256	64	8	2
OG1RF-0	2	2	0.25	0.25
OG1RF-5	8	2	0.25	0.25
OG1RF-8	16	4	1	0.25
OG1RF-18	64	8	4	0.5
OG1RF-25	128	16	4	1
OG1RF-30	256	16	4	1
OG1RF-55	256	32	8	2

RZD, radezolid; LZD, linezolid; PA $\beta$ N, Phe-Arg- $\beta$ -naphthylamide (20 mg/L).



PAβN (20 mg/L) (Kothary et al., 2013). This assay was performed at least in triplicate.

## RNA Isolation and Sequencing

Total RNA isolation and RNA sequencing (RNA-seq) of the *E. faecalis* OG1RF wild-type isolate (OG1RF-0, LZD- and RZD-sensitive) and the high-level LZD-resistant isolate OG1RF-55 (linezolid MIC: 256 mg/L; radezolid MIC: 8 mg/L) were performed as previously described (Wang et al., 2017). Briefly, planktonic *E. faecalis* cells were homogenized using 0.1-mm zirconia-silica beads in a mini-BeadBeater and the total RNA in the supernatant was purified using an RNeasy Mini Kit (Qiagen, Hilden, Germany). RNA-seq was performed according to the Illumina RNA sequencing sample preparation guide. Total RNA samples were treated with RNase-free DNase I (TaKaRa Biotechnology, Dalian, China). cDNA libraries were prepared using an RNA-seq sample preparation kit (Illumina, San Diego, CA, United States), and sequencing was performed with an Illumina HiSeq 2500 sequencer for 50 cycles. All these procedures were performed according to the manufacturers' protocols. Raw sequencing data were processed using the data collection software provided by Illumina. RNA-seq was performed in three independent experiments.

## RNA-Seq Data Analysis and RT-qPCR

Raw sequencing reads were preprocessed by filtering out rRNA reads, sequencing adapters, short fragment reads, and

other low-quality reads. The remaining reads were mapped to the *E. faecalis* OG1RF reference genome (CP002621.1) at the National Center for Biotechnology Information (NCBI) website using Bowtie2 software (version 2.0.5) based on the local alignment algorithm. The alignments reported using Bowtie2 software were further processed with BED Tools software to determine transcript expression levels and their differential expression between each two of the three samples. Differential expression of all the transcripts was quantified using DEGseq software (version 2.16.1), and then the fold-change values were presented. For validation of the RNA-seq results, RT-qPCR was performed using the SYBR Premix Ex Taq II Kit (TaKaRa Biotechnology, Dalian, China) on a Mastercycler ep realplex system (Eppendorf, Hamburg, Germany) as previously described (Zheng et al., 2017). The primers used for RT-qPCR are listed in **Supplementary Table S2**. RT-qPCR was performed in triplicate at least three times.

## Overexpression of Efflux Pump-Related Genes in *E. faecalis*

The *OG1RF\_12220* gene (multidrug ABC superfamily ATP-binding cassette transporter, *mdlB2*) and three ABC superfamily ATP-binding cassette transporter genes (*OG1RF\_10126*, *OG1RF\_10665*, and *OG1RF\_10495*) were amplified by PCR. The amplicons were purified and digested with endonucleases, and then cloned into the pIB166 plasmid for gene overexpression. Correct cloning was verified by PCR

**TABLE 4** | Differential RNA levels of efflux pump-related genes in a high-level linezolid-resistant isolate.

Gene_ID	Gene locus_tag (gene name)	Function/description	RNA levels of OG1RF-55/OG1RF-0	
			RNA-seq	RT-qPCR
OG1RF_RS11380	OG1RF_12220 ( <i>mdlB2</i> )	Multidrug ABC superfamily ATP-binding cassette transporter, ABC protein	9.046	8.073
OG1RF_RS00635	OG1RF_10126	ABC superfamily ATP-binding cassette transporter, ABC protein	6.334	4.813
OG1RF_RS03455	OG1RF_10665	ABC superfamily ATP-binding cassette transporter, ABC protein	5.449	6.538
OG1RF_RS02620	OG1RF_10495	ABC superfamily ATP-binding cassette transporter, ABC protein	4.349	3.452
OG1RF_RS13115	OG1RF_12562 ( <i>odaA</i> )	Oxaloacetate decarboxylase	3.422	1.698
OG1RF_RS00860	OG1RF_10171 ( <i>secY</i> )	Preprotein translocase subunit SecY	2.998	0.913
OG1RF_RS07425	OG1RF_11442 ( <i>mdlB</i> )	Multidrug ABC superfamily ATP-binding cassette transporter, ABC protein	2.678	1.544
OG1RF_RS07430	OG1RF_11443 ( <i>mdlA</i> )	Multidrug ABC superfamily ATP-binding cassette transporter, ABC protein	2.595	1.948
OG1RF_RS03320	OG1RF_10638 ( <i>oppD</i> )	ABC superfamily ATP-binding cassette transporter, ABC protein	2.537	1.478
OG1RF_RS08840	OG1RF_11726	ABC superfamily ATP-binding cassette transporter, ABC protein	2.532	1.582
OG1RF_RS04005	OG1RF_10775	Drug: H <sup>+</sup> antiporter-1 family protein	2.383	1.841
OG1RF_RS04550	OG1RF_10869	von Willebrand factor type A domain protein	2.331	1.745
OG1RF_RS05865	OG1RF_11131	ABC superfamily ATP-binding cassette transporter, ABC protein	2.296	2.205
OG1RF_RS11385	OG1RF_12221	ABC superfamily ATP-binding cassette transporter, ABC/membrane protein	2.145	1.672
OG1RF_RS04555	OG1RF_10870	Cell wall surface anchor family protein	2.127	1.021
OG1RF_RS03325	OG1RF_10639 ( <i>oppF</i> )	ABC superfamily ATP-binding cassette transporter, ABC protein	2.004	1.969
OG1RF_RS05110	OG1RF_10982	Response regulator	0.357	0.527
OG1RF_RS03235	OG1RF_10620	ABC superfamily ATP-binding cassette transporter, ABC protein	0.222	0.369
OG1RF_RS11320	OG1RF_12207	ABC superfamily ATP-binding cassette transporter, ABC protein	0.200	0.047

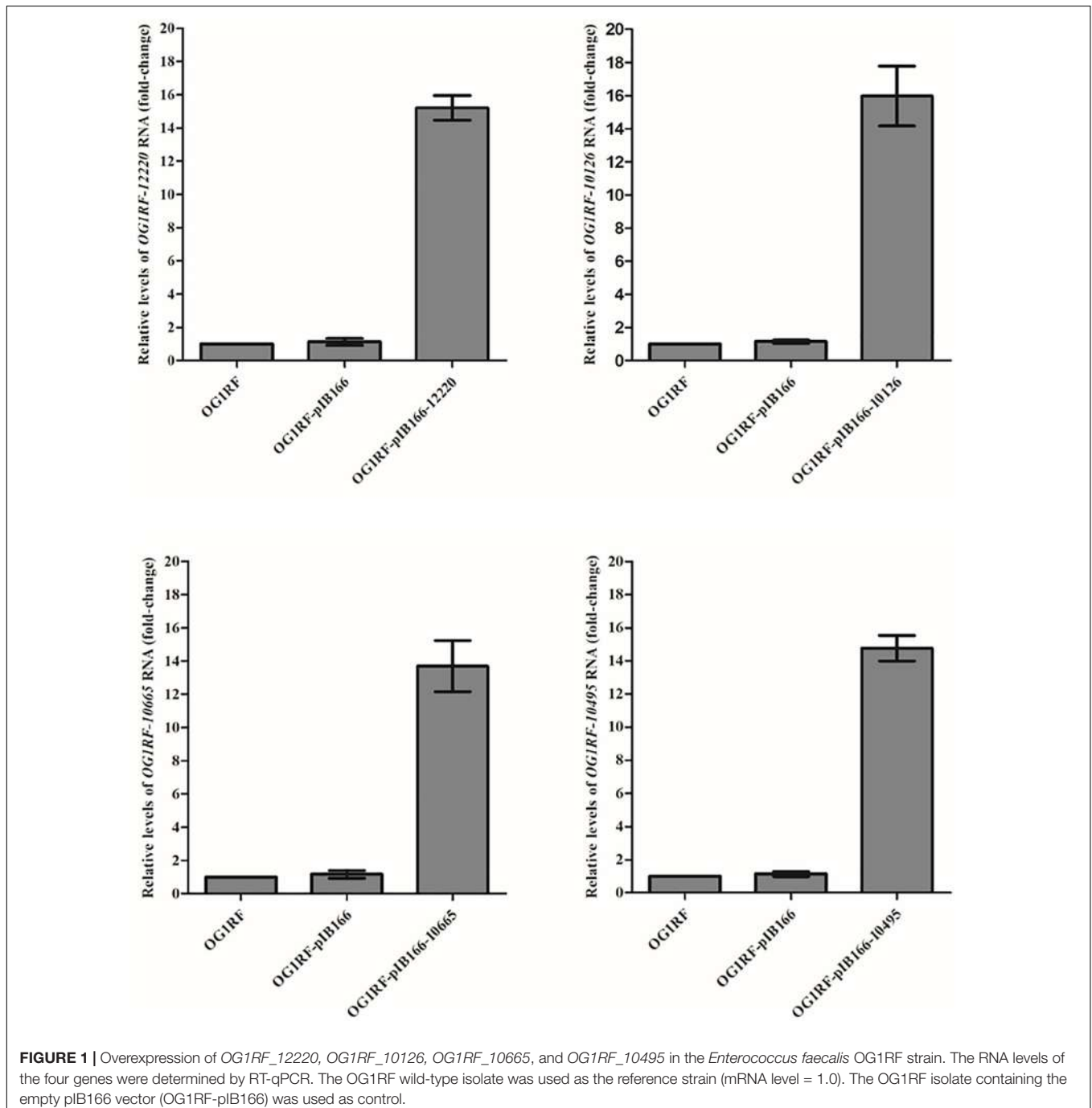
The *Enterococcus faecalis* OG1RF wild-type isolate (OG1RF-0, linezolid- and radezolid-sensitive) and the high-level linezolid-resistant isolate (OG1RF-55, linezolid MIC: 256 mg/L; radezolid MIC: 8 mg/L) were inoculated and grown to the logarithmic phase (4 h), total RNA was isolated and sequenced by Illumina HiSeq 2500 sequencer. Data are the means of the results from three independent experiments.

and sequencing. Verified loaded plasmids were introduced into the *E. faecalis* OG1RF strain. All strains, plasmids, and primers used for overexpression analysis are listed in **Supplementary Tables S3, S4**.

## Biofilm Biomass Assay and Adherent Cell Detection

The biofilm biomass of 13 *E. faecalis* clinical isolates (16C1, 16C35, 16C51, 16C102, 16C106, 16C124, 16C138, 16C152,

16C166, 16C201, 16C289, 16C350, and 16C353) was detected by crystal violet staining as previously described (Zheng et al., 2019). For analysis of the eradication potential of RZD or LZD against established *E. faecalis* biofilms, *E. faecalis* isolates were inoculated into 96-well polystyrene microtiter plates with TSBG (tryptic soy broth with 0.25% glucose) for formation of mature biofilms. After 24 h of static incubation, the supernatants were discarded and plates were washed with 0.9% saline to remove unattached cells, following which fresh TSBG containing RZD or LZD was added. After 48 h of static incubation, with the medium replaced daily,



the remaining biofilm biomass was determined by crystal violet staining. The numbers of adherent cells remaining in biofilms formed in 24-well polystyrene microtiter plates were determined

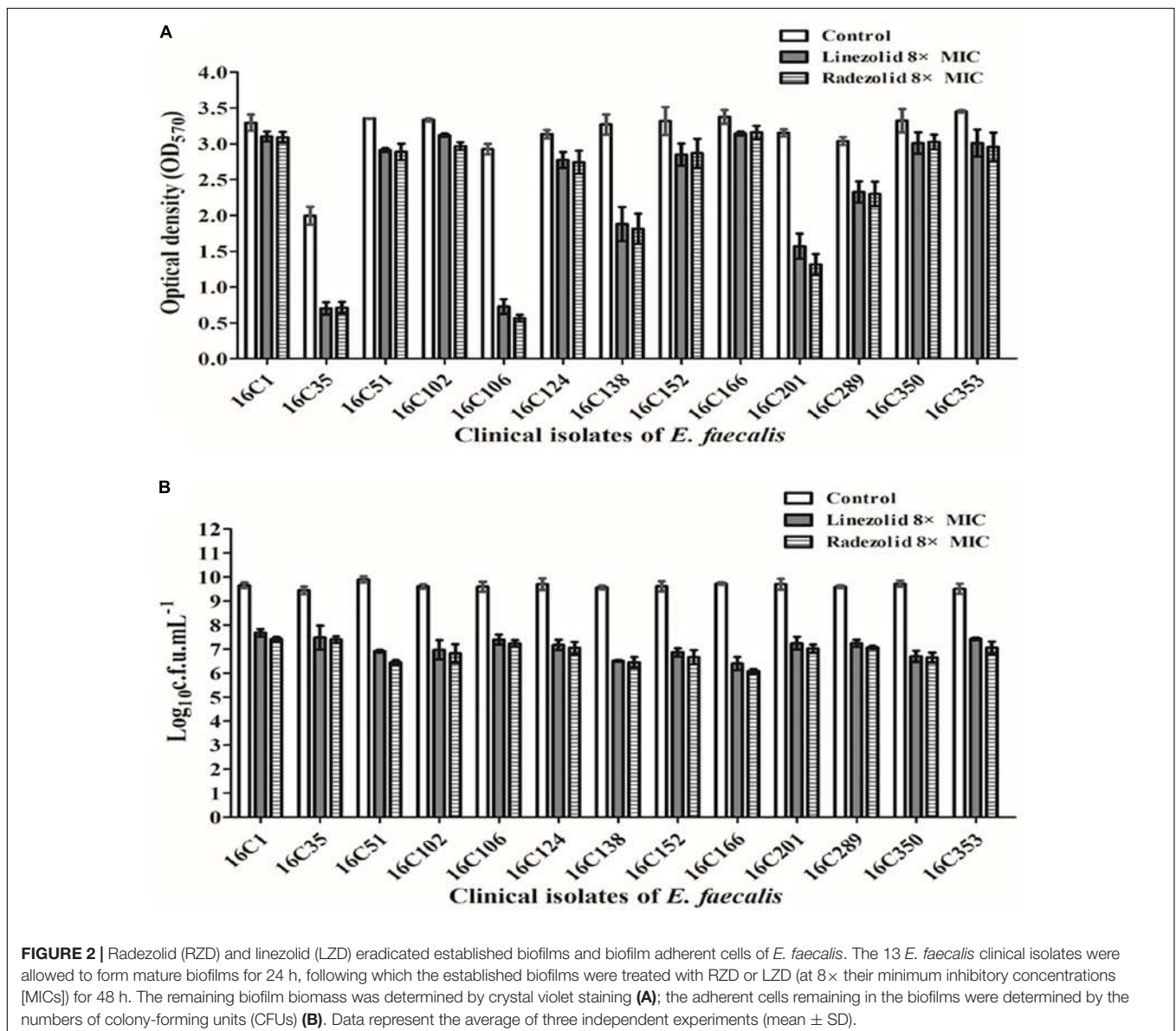
by counting the number of colony-forming units (CFUs), as previously described (Zheng et al., 2019). To investigate whether RZD or LZD could inhibit *E. faecalis* biofilm formation, *E. faecalis* isolates were inoculated into 96-well polystyrene microtiter plates with TSBG containing RZD or LZD (at sub-MICs). After 24 h of static incubation, biofilm biomass was determined by crystal violet staining. Each assay was performed in triplicate at least three times.

**TABLE 5** | Radezolid and linezolid minimum inhibitory concentrations (MICs) increased with *OG1RF\_12220* overexpression in the *Enterococcus faecalis* OG1RF strain.

Strains	MIC (mg/L)	
	Linezolid	Radezolid
OG1RF	2	0.25
OG1RF-12220	4	0.5
OG1RF-10126	2	0.25
OG1RF-10665	2	0.25
OG1RF-10495	2	0.25

## RT-qPCR to Determine the RNA Levels of *E. faecalis* Biofilm Formation-Related Genes

The RNA levels of 16 biofilm formation-related genes of the above 13 *E. faecalis* clinical isolates were determined by RT-qPCR based on published reports (Tendolkar et al., 2005;



Nallapareddy et al., 2006; Guiton et al., 2009; Chavez de Paz et al., 2012; Soares et al., 2014; Dale et al., 2015; Frank et al., 2015; Akbari Aghdam et al., 2017; Zheng et al., 2018). The *E. faecalis* clinical isolates were inoculated into 100 mm × 20 mm non-pyrogenic polystyrene cell culture dishes with TSBG containing RZD or LZD (at 1/4× the MIC). After 6, 12, or 24 h of static incubation, total RNA was extracted from planktonic and biofilm *E. faecalis* cells for RT-qPCR. The primers used for RT-qPCR are listed in **Supplementary Table S2**. Each assay was performed in triplicate at least three times.

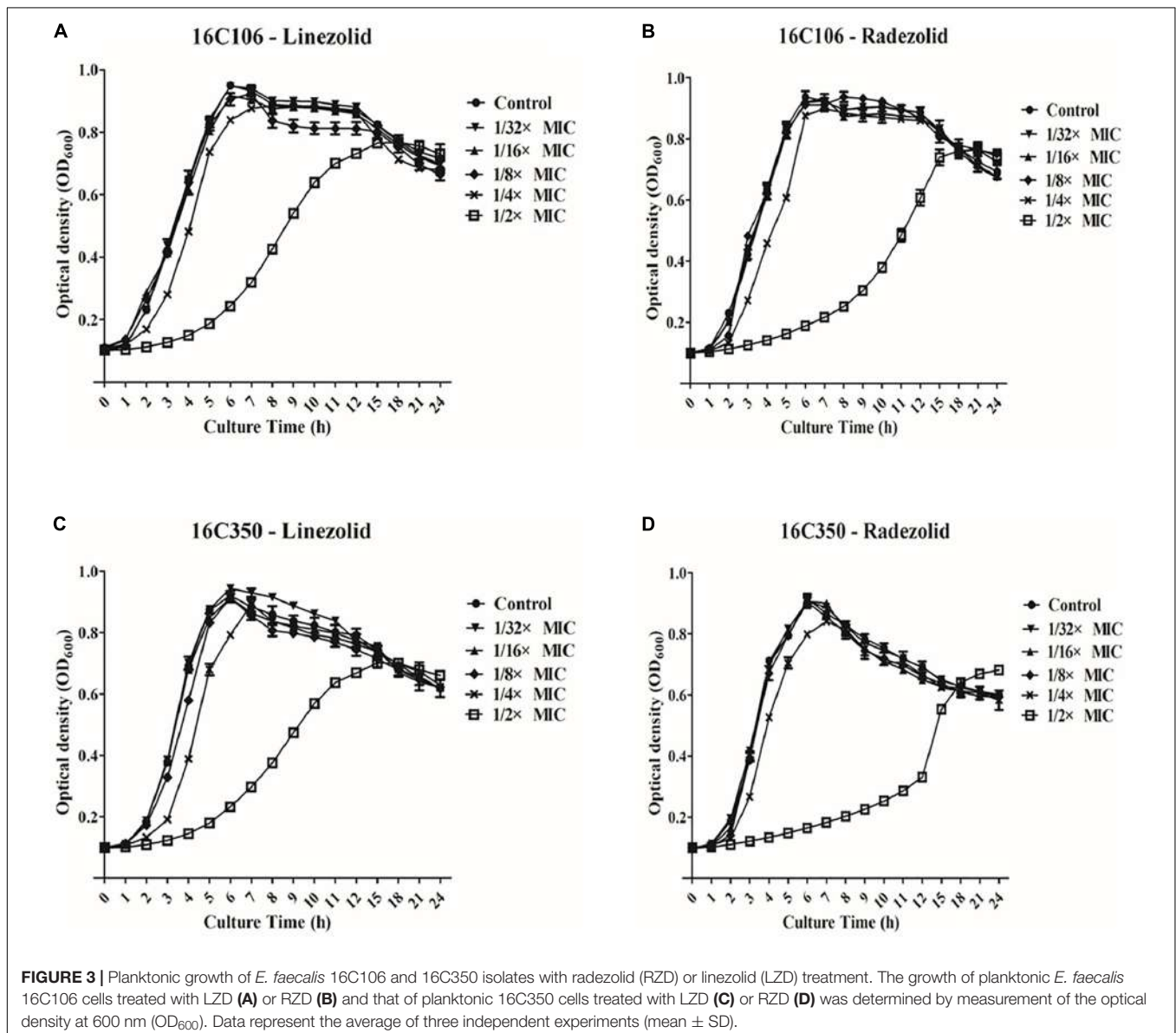
## Statistical Analysis

The data were analyzed using the Student's *t*-test. *P*-values < 0.05 were considered significant. All data were analyzed in SPSS version 16.0 (SPSS, Inc., Chicago, IL, United States).

## RESULTS

### RZD Was More Effective Than LZD Against *E. faecalis* Clinical Isolates

The distribution of MICs for RZD and LZD and their relationship with the susceptibilities for some other conventional antimicrobials are shown in **Table 1**. The data show that the MIC<sub>50</sub>/MIC<sub>90</sub> of RZD was eightfold lower than that of LZD, suggesting that the *in vitro* activity of RZD against the 302 *E. faecalis* clinical isolates was substantially higher than that of LZD. Moreover, the MICs of RZD against the 52 LZD-non-susceptible *E. faecalis* clinical isolates were also lower (**Supplementary Table S5**). Twenty-one LZD-non-susceptible clinical isolates presented mutations in domain V of the 23S rRNA gene, but only four isolates contained the *optRA* gene. As





shown in **Supplementary Table S5**, only two of the four *optrA*-carrying isolates (16C112 and 16C154) harbored mutations in the V domain of the 23S rRNA gene. No mutations were detected in ribosomes L3 and L4, or in the *cfr*, *cfr(B)*, *poxtA* genes in these isolates (data not shown).

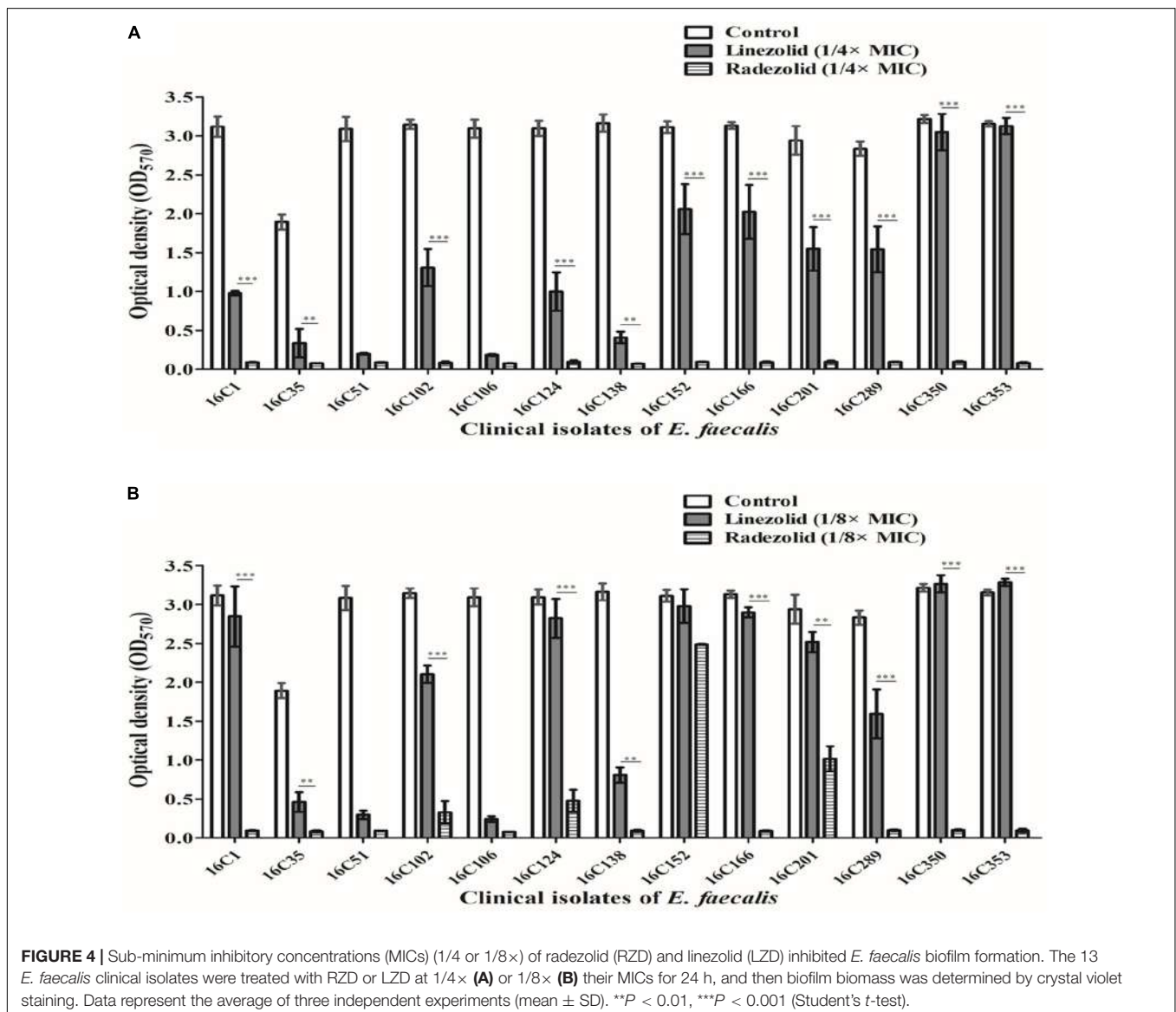
## Effects of RZD on High-Level LZD-Resistant *E. faecalis* Isolates

To evaluate the effect of RZD on the high-level LZD-resistant *E. faecalis* isolates and explore the extent to which RZD overcame LZD-related resistance mechanisms, high-level resistance to LZD was induced in the *E. faecalis* ATCC29212 and OG1RF strains. **Table 2** shows the primary mutation loci in the 23S rRNA gene in the high-level LZD-resistant G2576U isolates. Mutations in ribosomes L3 and L4, and in the *cfr*, *cfr(B)*, *optrA*, and *poxtA* genes were not detected in these isolates (data not shown). The

MICs for RZD increased sharply to  $\geq 4$  mg/L if the isolates presented with LZD-induced mutations in the four copies of domain V of the 23S rRNA gene (linezolid MICs  $\geq 64$  mg/L).

## Efflux Pumps Are Involved in *E. faecalis* Resistance to RZD and LZD

The MICs for LZD or RZD showed a two- to eight-fold decrease in the presence of PA $\beta$ N (**Table 3**). Thus, to explore the role of efflux pumps in RZD and LZD resistance, we assessed the changes occurring in the transcriptome of the high-level LZD-resistant OG1RF isolate (OG1RF-55, linezolid MIC: 256 mg/L; radezolid MIC: 8 mg/L) by RNA-seq (**Supplementary Figure S1** and **Supplementary Table S6**). Subsequently, we evaluated the RNA expression levels of efflux pump-related genes by RT-qPCR, and found that the transcriptional levels of four ABC superfamily ATP-binding cassette transporter



genes (*OG1RF\_12220*, *OG1RF\_10126*, *OG1RF\_10665*, and *OG1RF\_10495*) were increased in the high-level LZD-resistant OG1RF-55 isolate (Table 4). Finally, to confirm that the four genes were involved in the resistance to RZD and LZD, we overexpressed these genes in the LZD- and RZD-sensitive OG1RF isolate (Figure 1 and Supplementary Tables S3, S4). As indicated in Table 5, the MICs for LZD and RZD increased only with overexpression of *OG1RF\_12220* (*mdlB2*).

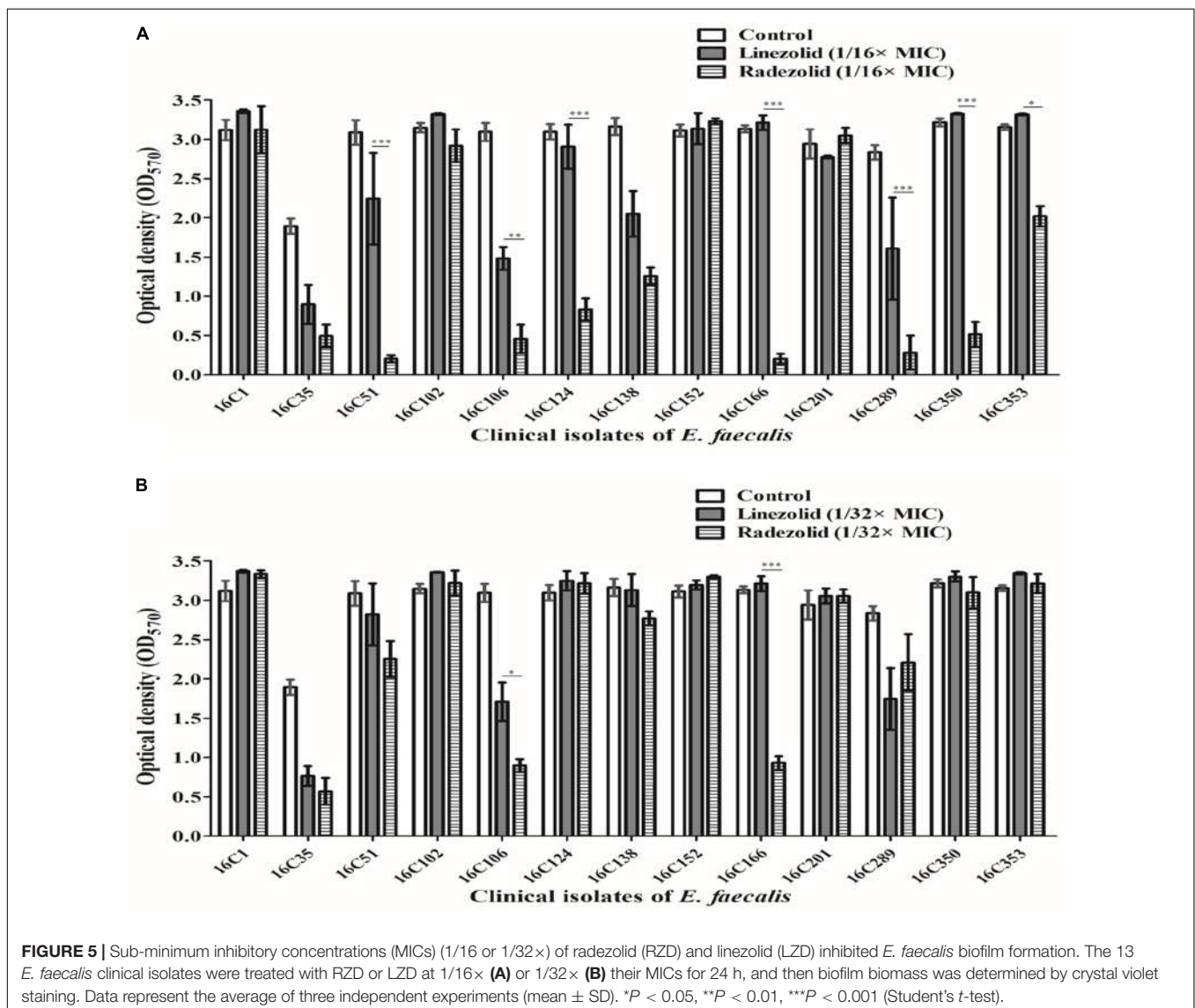
## RZD Inhibited *E. faecalis* Biofilm Formation to a Greater Extent Than LZD

Thirteen *E. faecalis* clinical isolates (biofilm-positive) were selected to compare the differential effects of RZD and LZD on *E. faecalis* biofilms (Supplementary Table S7). First, we compared the eradicating potential of RZD and LZD (at 8× their MICs) on established *E. faecalis* biofilms, and found no difference between them (Figure 2). Both drugs also elicited similar effects

on adherent cells of established biofilms. We also compared the sub-MICs at which RZD and LZD inhibited *E. faecalis* biofilm formation. Based on a previous study (Mlynek et al., 2016) and our preliminary results, 1/4, 1/8, 1/16, and 1/32× MICs were used in this study. The 1/2× MIC was not used because the planktonic growth of *E. faecalis* was markedly affected under this concentration of both RZD and LZD (Figure 3). As shown in Figure 4, the RZD at 1/4 or 1/8× its MIC efficiently inhibited *E. faecalis* biofilm formation and to a greater extent than LZD. This trend was also observed in several of the 13 clinical isolates at MICs of 1/16 or 1/32× (Figure 5).

## RZD Treatment Reduced the RNA Levels of Biofilm Formation-Related Genes

Isolates 16C106 and 16C350 were selected for RT-qPCR to evaluate the RNA expression levels of 16 *E. faecalis* biofilm formation-related genes at different stages of biofilm formation.



The RNA levels of *ahrC*, *cylA*, *esp*, *relA*, and *relQ* markedly decreased when the isolates were treated with RZD or LZD at 1/4× their MICs for 6 h (Table 6). The RNA levels of these 16 genes in the other 11 *E. faecalis* clinical isolates were also determined, and, as indicated in Table 7, the transcriptional levels of *ahrC*, *esp*, *relA*, and *relQ* showed a significant decrease, especially in isolates treated with RZD.

## DISCUSSION

Radezolid, a novel biaryl analog of LZD, exhibits excellent activity against gram-positive bacteria, including methicillin-resistant *Staphylococcus aureus* (MRSA) and LZD-resistant staphylococci (Lemaire et al., 2010a; Locke et al., 2010). The results of this study further indicate that RZD also exerts stronger effects than LZD against several *E. faecalis* clinical isolates. One study demonstrated that, in LZD-resistant *S. aureus* isolates (linezolid MICs ranging from 8 to 32 mg/L), the MICs of RZD against these isolates were two- to eight-fold lower (from 1 to 4 mg/L) than those of LZD (Locke et al., 2010). In this study, we also focused on LZD-non-susceptible *E. faecalis* clinical isolates (linezolid MICs ranging from 4 to 32 mg/L); however, we found that the MICs of RZD for these isolates (from 0.25 to 1 mg/L) were 8- to 32-fold lower than those of LZD. We also showed that when high-level resistance to LZD was induced in *E. faecalis* (linezolid MICs  $\geq$  64 mg/L), the MICs of RZD increased from 1 to 8 mg/L. This result indicated that cross-resistance to RZD and LZD was emerging in these isolates, and that this was mainly due to mutations in the four copies of domain V of the 23S rRNA gene.

The oxazolidinone class of antimicrobials, which includes LZD, exhibited excellent effects against gram-positive bacteria, but showed poor activity against gram-negative bacteria such as *Escherichia coli*, primarily due to the enhanced activity of AcrB, a RND-type efflux pump (Schumacher et al., 2007; Schuster et al., 2019). However, whether efflux pumps have a role in the resistance of gram-positive bacteria to LZD or RZD remains uncertain. In the present study, we found that the MICs of LZD and RZD decreased in the presence of PA $\beta$ N, an efflux pump inhibitor, indicating that efflux pumps are involved in *E. faecalis* resistance to LZD and RZD. We also found that the enhanced activity of *OG1RF-12220* (*mdlB2*) led to increases in the MICs of both LZD and RZD. The expression of the efflux pump gene *mdlB* was reported to be substantially increased among fluoroquinolone-resistant isolates of *Salmonella enterica* (Chen et al., 2007). Both *mdlB* and *mdlB2* belong to the efflux transport system of the ATP-binding cassette (ABC) superfamily, which plays an important role in antimicrobial resistance (Iannelli et al., 2018). We found that *mdlB2*, but not *mdlB*, was involved in the resistance to LZD and RZD. However, this result requires further experimental confirmation, especially in high-level LZD-resistant *E. faecalis* clinical isolates.

Several studies have indicated that LZD affects the biofilms of *E. faecalis*, both when administered alone or in combination with rifampicin or gentamicin (Bayston et al., 2012; Holmberg et al., 2012; Luther et al., 2014). In this study, we found that RZD had a significantly greater effect than LZD on planktonic *E. faecalis* cells. We further investigated whether this was also true for *E. faecalis* biofilm formation, but we did

**TABLE 6** | Changes in the RNA expression levels of biofilm formation-related genes of isolates 16C106 and 16C350 with radezolid or linezolid treatment.

Biofilm formation-related genes	16C106						16C350					
	Radezolid			Linezolid			Radezolid			Linezolid		
	6 h	12 h	24 h	6 h	12 h	24 h	6 h	12 h	24 h	6 h	12 h	24 h
<i>Agg</i>	0.457	0.793	1.373	0.633	0.916	1.577	–	–	–	–	–	–
<i>ahrC</i>	0.194	0.694	2.658	0.211	1.401	2.217	0.110 <sup>c</sup>	0.603	1.434	0.421	1.655	1.779
<i>asa1</i>	0.662	1.256	2.662	0.778	1.764	2.178	1.528	1.413	1.850	0.800	1.056	1.455
<i>Atn</i>	1.065	1.351	2.572	1.490	2.073	1.818	2.212	1.332	1.766	1.613	2.509	1.429
<i>cylA</i>	0.186 <sup>a</sup>	0.397	1.675	0.481	0.569	0.952	0.175 <sup>c</sup>	0.415	0.839	0.516	1.567	1.180
<i>Eep</i>	–	–	–	–	–	–	0.943	2.068	0.536	1.735	5.138	1.485
<i>ebpA</i>	0.772	1.516	4.725	0.685	7.799	3.691	2.658	5.318	1.690	1.880	3.193	1.185
<i>epal</i>	0.693	1.467	3.154	0.638	3.976	3.389	2.095	6.424	1.218	3.472	6.235	1.843
<i>epaOX</i>	0.859	2.729	4.933	1.035	1.662	4.324	2.939	4.336	0.943	2.669	4.403	1.765
<i>Esp</i>	0.089 <sup>b</sup>	0.806	2.550	0.178	1.405	2.597	0.196 <sup>c</sup>	0.993	1.456	0.517	2.896	1.562
<i>fsrA</i>	2.083	2.281	6.663	2.546	3.004	2.802	1.895	1.627	1.878	1.893	1.812	2.138
<i>gelE</i>	–	–	–	–	–	–	–	–	–	–	–	–
<i>hyl</i>	–	–	–	–	–	–	1.554	1.526	2.365	1.859	2.019	2.398
<i>relA</i>	0.103 <sup>b</sup>	0.567	1.966	0.246	1.565	3.965	0.218 <sup>d</sup>	2.528	2.385	0.520	2.299	3.269
<i>relQ</i>	0.182 <sup>b</sup>	0.624	3.098	0.314	1.487	4.562	0.241 <sup>c</sup>	2.839	2.260	0.611	4.613	4.400
<i>srtA</i>	0.687	1.660	3.819	0.726	1.724	3.755	0.572	2.573	4.572	0.895	3.276	4.295

Radezolid and linezolid were used at 1/4× their minimum inhibitory concentrations (MICs). RNA levels were detected by RT-qPCR, with untreated isolate as the reference strain (mRNA level = 1.0). –, not detected. <sup>a</sup>16C106: Radezolid (6 h) vs. Linezolid (6 h),  $P < 0.01$ ; <sup>b</sup>16C106: Radezolid (6 h) vs. Linezolid (6 h),  $P < 0.05$ ; <sup>c</sup>16C350: Radezolid (6 h) vs. Linezolid (6 h),  $P < 0.01$ ; <sup>d</sup>16C350: Radezolid (6 h) vs. Linezolid (6 h),  $P < 0.05$ .

**TABLE 7** | Changes in RNA expression levels of biofilm formation-related genes in 11 clinical isolates with radezolid or linezolid treatment.

	Biofilm formation-related genes															
	<i>agg</i>	<i>ahrC</i>	<i>asa1</i>	<i>atn</i>	<i>cylA</i>	<i>eep</i>	<i>ebpA</i>	<i>epal</i>	<i>epaOX</i>	<i>esp</i>	<i>fsrA</i>	<i>gelE</i>	<i>hyl</i>	<i>relA</i>	<i>relQ</i>	<i>srtA</i>
<b>16C1</b>																
RZD	0.578	0.108 <sup>a</sup>	0.784	1.358	0.388 <sup>c</sup>	–	0.864	0.897	1.062	0.113 <sup>d</sup>	1.234	0.687	1.657	0.218 <sup>f</sup>	0.359	0.687
LZD	0.864	0.368	0.895	1.295	0.664	–	1.234	1.065	1.364	0.268	1.498	0.892	1.552	0.458	0.487	0.734
<b>16C35</b>																
RZD	0.854	0.169 <sup>b</sup>	1.285	1.069	0.295	0.965	0.937	1.298	1.118	0.165 <sup>d</sup>	0.931	0.885	–	0.311 <sup>f</sup>	0.365	1.058
LZD	1.068	0.293	1.154	1.035	0.431	1.262	1.364	1.105	0.997	0.378	0.854	1.158	–	0.524	0.487	1.364
<b>16C51</b>																
RZD	0.814	0.167	1.025	1.168	0.505	–	1.035	0.954	1.548	0.075 <sup>d</sup>	0.875	–	–	0.309 <sup>f</sup>	0.224	0.564
LZD	0.962	0.208	1.132	0.864	0.598	–	1.125	1.264	1.068	0.119	0.965	–	–	0.524	0.368	0.635
<b>16C102</b>																
RZD	–	0.263 <sup>b</sup>	–	0.864	–	0.597	0.824	0.954	0.931	0.138 <sup>d</sup>	0.768	0.687	–	0.269 <sup>f</sup>	0.218 <sup>h</sup>	0.694
LZD	–	0.597	–	1.126	–	0.854	0.789	1.158	0.865	0.367	0.895	0.885	–	0.486	0.531	0.954
<b>16C124</b>																
RZD	–	0.597	1.164	1.106	0.167 <sup>c</sup>	0.364	0.764	0.854	0.954	0.107 <sup>e</sup>	0.964	0.989	–	0.208	0.497	1.065
LZD	–	0.631	0.965	1.357	0.284	0.543	0.805	0.762	1.035	0.485	1.165	1.164	–	0.294	0.551	1.321
<b>16C138</b>																
RZD	–	0.156	0.881	1.265	0.464	–	1.068	0.924	1.268	0.255 <sup>d</sup>	1.123	–	–	0.368 <sup>f</sup>	0.305 <sup>h</sup>	1.246
LZD	–	0.198	1.098	1.067	0.657	–	1.267	1.157	0.954	0.495	1.065	–	–	0.542	0.687	1.098
<b>16C152</b>																
RZD	0.954	0.468	1.065	1.196	0.365 <sup>c</sup>	1.354	0.854	1.094	1.354	0.073 <sup>e</sup>	0.882	0.724	–	0.097 <sup>g</sup>	0.267 <sup>h</sup>	0.769
LZD	1.367	0.598	1.298	0.932	0.697	1.158	1.063	1.265	1.165	0.396	0.854	0.658	–	0.264	0.576	0.854
<b>16C166</b>																
RZD	–	0.097 <sup>b</sup>	0.854	1.267	–	0.862	0.962	1.164	1.264	–	0.931	–	–	0.168 <sup>f</sup>	0.186 <sup>h</sup>	0.367
LZD	–	0.167	0.801	1.065	–	1.065	1.264	0.938	1.129	–	1.095	–	–	0.291	0.367	0.431
<b>16C201</b>																
RZD	–	0.157 <sup>b</sup>	0.652	0.597	–	–	0.531	0.789	0.631	–	0.934	–	–	0.103 <sup>g</sup>	0.158	0.687
LZD	–	0.269	0.896	0.786	–	–	0.764	0.894	0.835	–	1.264	–	–	0.324	0.263	1.357
<b>16C289</b>																
RZD	0.764	0.298	1.068	1.267	0.368 <sup>c</sup>	0.714	0.965	1.158	0.958	0.085 <sup>e</sup>	0.867	0.534	2.674	0.208 <sup>f</sup>	0.296 <sup>h</sup>	0.974
LZD	0.878	0.367	1.165	1.152	0.587	1.257	1.247	1.036	1.168	0.298	0.906	0.738	1.687	0.593	0.687	1.265
<b>16C353</b>																
RZD	–	0.394	1.267	0.954	0.464	–	0.854	0.964	1.068	0.069 <sup>e</sup>	0.768	–	–	0.082 <sup>g</sup>	0.158 <sup>i</sup>	0.875
LZD	–	0.485	1.597	1.264	0.568	–	0.834	1.167	0.915	0.468	0.934	–	–	0.368	0.497	1.068

RZD, radezolid; LZD, linezolid. Radezolid and linezolid were used at 1/4× their minimum inhibitory concentrations (MICs). The RNA levels were detected by RT-qPCR, with untreated isolate as the reference strain (mRNA level = 1.0). –, not detected. <sup>a</sup>*ahrC*: RZD vs. LZD,  $P < 0.01$ ; <sup>b</sup>*ahrC*: RZD vs. LZD,  $P < 0.05$ ; <sup>c</sup>*cylA*: RZD vs. LZD,  $P < 0.05$ ; <sup>d</sup>*esp*: RZD vs. LZD,  $P < 0.05$ ; <sup>e</sup>*esp*: RZD vs. LZD,  $P < 0.01$ ; <sup>f</sup>*relA*: RZD vs. LZD,  $P < 0.05$ ; <sup>g</sup>*relA*: RZD vs. LZD,  $P < 0.01$ ; <sup>h</sup>*relQ*: RZD vs. LZD,  $P < 0.05$ ; <sup>i</sup>*relQ*: RZD vs. LZD,  $P < 0.01$ .

not find any difference between RZD and LZD in eradicating established biofilms or adherent cells in the biofilms of *E. faecalis*. Interestingly, we found that RZD (at 1/4 or 1/8× the MIC) strongly inhibited *E. faecalis* biofilm formation, and more effectively than LZD. This result was similar to that of a previous study, in which Wu et al. (2014) found that another oxazolidinone, FYL-67, could more strongly inhibit *S. aureus* biofilm formation than LZD.

In the present study, we also explored the reasons for the RZD-mediated reduction in *E. faecalis* biofilm formation, and found that the mRNA levels of *ahrC*, *esp*, *relA*, and *relQ* were significantly decreased with RZD treatment. Several studies have demonstrated that the Esp virulence factor, which has been found to support *E. faecalis* cell adherence, colonization, and persistence

in the urinary tract, also plays an important role in *E. faecalis* biofilm formation (Toledo-Arana et al., 2001; Tendolkar et al., 2004; Zheng et al., 2017). The *ahrC* gene, which encodes a transcriptional regulator of the ArgR family, was found to be critical for *E. faecalis* attachment to polystyrene *in vitro*, and porcine heart valve surfaces *ex vivo*, during the early stages of biofilm formation (Frank et al., 2013). The hydrolase RelA and the small alarmone synthetase RelQ, encoded by the *relA* and *relQ* genes, respectively, have also been found to control (p)ppGpp metabolism and sustain biofilm formation in *E. faecalis* (Chavez de Paz et al., 2012). Our study indicated that the transcriptional levels of *ahrC*, *esp*, *relA*, and *relQ* were greatly decreased when *E. faecalis* clinical isolates were treated with RZD for 6 h, resulting in a significant reduction in biofilm formation by *E. faecalis*.



## CONCLUSION

We showed that radezolid was more effective than linezolid against planktonic *E. faecalis* cells. Additionally, this study is the first to report that the *mdlB2* gene is important for *E. faecalis* resistance to both RZD and LZD. We also found that RZD was more effective than LZD at inhibiting *E. faecalis* biofilm formation, which was mainly achieved through inhibition of the transcription of *ahrC*, *esp*, *relA* and *relQ* in *E. faecalis*.

## DATA AVAILABILITY STATEMENT

The datasets generated for this study can be found in the Sequence Read Archive (SRA) database under accession number PRJNA505107 (<https://www.ncbi.nlm.nih.gov/bioproject/PRJNA505107>).

## ETHICS STATEMENT

All procedures involving human participants were performed in accordance with the ethical standards of Shenzhen University School of Medicine and with the 1964 Helsinki Declaration and its later amendments, and this study was approved by the Ethics Committee of the Shenzhen University School of Medicine. For this type of study, formal consent is not required.

## AUTHOR CONTRIBUTIONS

JZ designed the study, performed gene manipulation, analyzed and interpreted the RNA-seq data, performed the biofilm assay, and drafted the manuscript. ZC performed gene manipulation, MIC detection, mRNA extraction, and RNA-seq and RT-qPCR data analysis. ZL conducted the LZD *in vitro* induction, MIC detection, and analyses of RNA-seq and overexpression data. XS performed MIC detection, gene manipulation, RT-qPCR, biofilm assay, and bacteria counting in the biofilm assay. BB, GX, and JC performed MIC detection, LZD *in vitro* induction, RT-qPCR, biofilm assay, and bacteria counting in the biofilm assay. ZY and DQ designed the study, analyzed the data, and critically revised the manuscript for important intellectual content.

## REFERENCES

- Ahmed, M. O., and Baptiste, K. E. (2018). Vancomycin-resistant enterococci: a review of antimicrobial resistance mechanisms and perspectives of human and animal health. *Microb. Drug Resist.* 24, 590–606. doi: 10.1089/mdr.2017.0147
- Akbari Aghdam, M., Soroush Barhaghi, M. H., Aghazadeh, M., Jafari, F., Beomide Hagh, M., Haghdoost, M., et al. (2017). Virulence genes in biofilm producer *Enterococcus faecalis* isolates from root canal infections. *Cell Mol. Biol.* 63, 55–59. doi: 10.14715/cmb/2017.63.5.11
- Antonelli, A., D'Andrea, M. M., Brenciani, A., Galeotti, C. L., Morroni, G., Pollini, S., et al. (2018). Characterization of *poxtA*, a novel phenicol-oxazolidinone-tetracycline resistance gene from an MRSA of clinical origin. *J. Antimicrob. Chemother.* 73, 1763–1769. doi: 10.1093/jac/dky088
- Balandin, B., Lobo, B., Orden, B., Roman, F., Garcia, E., Martinez, R., et al. (2016). Emergence of linezolid-resistant coagulase-negative staphylococci in

## FUNDING

This work was supported by grants from the National Science and Technology Major Projects for “Major New Drugs Innovation and Development” (grant number 2019ZX09721001); the Sanming Project of Medicine in Shenzhen (grant number SMGC201705029); Science, Technology and Innovation Commission of Shenzhen Municipality key funds (JCYJ20170412143551332 and JCYJ20180508162403996); and basic research funds (JCYJ20180302144721183 and JCYJ20180302144431923).

## ACKNOWLEDGMENTS

The authors thank Prof. Jingren Zhang (Center for Infectious Disease Research, School of Medicine, Tsinghua University, Beijing, China) for generously providing the pIB166 plasmid.

## SUPPLEMENTARY MATERIAL

The Supplementary Material for this article can be found online at: <https://www.frontiersin.org/articles/10.3389/fmicb.2020.00196/full#supplementary-material>

**FIGURE S1** | The volcano plot of all the genes measured by RNA-seq.

**TABLE S1** | PCR primers used for the detection of linezolid resistance genes.

**TABLE S2** | RT-qPCR primers used for the detection of the RNA levels of the efflux pump-related genes and the biofilm formation-related genes.

**TABLE S3** | Strains and plasmids used for the overexpression of *OG1RF\_12220*, *OG1RF\_10126*, *OG1RF\_10665*, and *OG1RF\_10495* in *E. faecalis* OG1RF strain.

**TABLE S4** | PCR primers used for the overexpression of *OG1RF\_12220*, *OG1RF\_10126*, *OG1RF\_10665*, and *OG1RF\_10495* in *E. faecalis* OG1RF strain.

**TABLE S5** | Radezolid against 52 linezolid-nonsusceptible *E. faecalis* clinical isolates.

**TABLE S6** | Differential RNA levels of the genes in a high-level linezolid-resistant isolate.

**TABLE S7** | Radezolid and linezolid minimum inhibitory concentrations (MICs) in 13 biofilm positive *E. faecalis* clinical isolates.

- an intensive care unit. *Infect. Dis.* 48, 343–349. doi: 10.3109/23744235.2015.1122225
- Bayston, R., Ullas, G., and Ashraf, W. (2012). Action of linezolid or vancomycin on biofilms in ventriculoperitoneal shunts *in vitro*. *Antimicrob. Agents Chemother.* 56, 2842–2845. doi: 10.1128/aac.06326-11
- Chavez de Paz, L. E., Lemos, J. A., Wickstrom, C., and Sedgley, C. M. (2012). Role of (p)ppGpp in biofilm formation by *Enterococcus faecalis*. *Appl. Environ. Microbiol.* 78, 1627–1630. doi: 10.1128/aem.07036-11
- Chen, M., Pan, H., Lou, Y., Wu, Z., Zhang, J., Huang, Y., et al. (2018). Epidemiological characteristics and genetic structure of linezolid-resistant *Enterococcus faecalis*. *Infect. Drug Resist.* 11, 2397–2409. doi: 10.2147/idr.s181339
- Chen, S., Cui, S., McDermott, P. F., Zhao, S., White, D. G., Paulsen, I., et al. (2007). Contribution of target gene mutations and efflux to decreased susceptibility of *Salmonella enterica* serovar *typhimurium* to fluoroquinolones and other

- antimicrobials. *Antimicrob. Agents Chemother.* 51, 535–542. doi: 10.1128/aac.00600-06
- Dale, J. L., Cagnazzo, J., Phan, C. Q., Barnes, A. M., and Dunny, G. M. (2015). Multiple roles for *Enterococcus faecalis* glycosyltransferases in biofilm-associated antibiotic resistance, cell envelope integrity, and conjugative transfer. *Antimicrob. Agents Chemother.* 59, 4094–4105. doi: 10.1128/aac.00344-15
- Elghaieb, H., Freitas, A. R., Abbassi, M. S., Novais, C., Zouari, M., Hassen, A., et al. (2019). Dispersal of linezolid-resistant enterococci carrying *poxtA* or *optrA* in retail meat and food-producing animals from Tunisia. *J. Antimicrob. Chemother.* 74, 2865–2869. doi: 10.1093/jac/dkz263
- Frank, K. L., Guiton, P. S., Barnes, A. M., Manias, D. A., Chuang-Smith, O. N., Kohler, P. L., et al. (2013). *AhrC* and *Eep* are biofilm infection-associated virulence factors in *Enterococcus faecalis*. *Infect. Immun.* 81, 1696–1708. doi: 10.1128/iai.01210-12
- Frank, K. L., Vergidis, P., Brinkman, C. L., Greenwood Quaintance, K. E., Barnes, A. M., Mandrekar, J. N., et al. (2015). Evaluation of the *Enterococcus faecalis* biofilm-associated virulence factors *AhrC* and *Eep* in rat foreign body osteomyelitis and in vitro biofilm-associated antimicrobial resistance. *PLoS One* 10:e0130187. doi: 10.1371/journal.pone.0130187
- Guiton, P. S., Hung, C. S., Kline, K. A., Roth, R., Kau, A. L., Hayes, E., et al. (2009). Contribution of autolysin and Sortase A during *Enterococcus faecalis* DNA-dependent biofilm development. *Infect. Immun.* 77, 3626–3638. doi: 10.1128/iai.00219-09
- Hasman, H., Clausen, P., Kaya, H., Hansen, F., Knudsen, J. D., Wang, M., et al. (2019). LRE-Finder, a Web tool for detection of the 23S rRNA mutations and the *optrA*, *cfr*, *cfr(B)* and *poxtA* genes encoding linezolid resistance in enterococci from whole-genome sequences. *J. Antimicrob. Chemother.* 74, 1473–1476. doi: 10.1093/jac/dkz092
- Holmberg, A., Morgelin, M., and Rasmussen, M. (2012). Effectiveness of ciprofloxacin or linezolid in combination with rifampicin against *Enterococcus faecalis* in biofilms. *J. Antimicrob. Chemother.* 67, 433–439. doi: 10.1093/jac/dkr477
- Iannelli, F., Santoro, F., Santagati, M., Docquier, J. D., Lazzeri, E., Pastore, G., et al. (2018). Type M resistance to macrolides is due to a two-gene efflux transport system of the ATP-Binding Cassette (ABC) Superfamily. *Front. Microbiol.* 9:1670. doi: 10.3389/fmicb.2018.01670
- Kothary, V., Scherl, E. J., Bosworth, B., Jiang, Z. D., Dupont, H. L., Harel, J., et al. (2013). Rifaximin resistance in *Escherichia coli* associated with inflammatory bowel disease correlates with prior rifaximin use, mutations in *rpoB*, and activity of Phe-Arg-beta-naphthylamide-inhibitable efflux pumps. *Antimicrob. Agents Chemother.* 57, 811–817. doi: 10.1128/aac.02163-12
- Lei, C. W., Kang, Z. Z., Wu, S. K., Chen, Y. P., Kong, L. H., and Wang, H. N. (2019). Detection of the phenicol-oxazolidinone-tetracycline resistance gene *poxtA* in *Enterococcus faecium* and *Enterococcus faecalis* of food-producing animal origin in China. *J. Antimicrob. Chemother.* 74, 2459–2461. doi: 10.1093/jac/dkz198
- Lemaire, S., Kosowska-Shick, K., Appelbaum, P. C., Verween, G., Tulkens, P. M., and Van Bambeke, F. (2010a). Cellular pharmacodynamics of the novel biarylloxazolidinone radezolid: studies with infected phagocytic and nonphagocytic cells, using *Staphylococcus aureus*, *Staphylococcus epidermidis*, *Listeria monocytogenes*, and *Legionella pneumophila*. *Antimicrob. Agents Chemother.* 54, 2549–2559. doi: 10.1128/aac.01724-09
- Lemaire, S., Tulkens, P. M., and Van Bambeke, F. (2010b). Cellular pharmacokinetics of the novel biarylloxazolidinone radezolid in phagocytic cells: studies with macrophages and polymorphonuclear neutrophils. *Antimicrob. Agents Chemother.* 54, 2540–2548. doi: 10.1128/aac.01723-09
- Locke, J. B., Finn, J., Hilgers, M., Morales, G., Rahawi, S., Kedar, G. C., et al. (2010). Structure-activity relationships of diverse oxazolidinones for linezolid-resistant *Staphylococcus aureus* strains possessing the *cfr* methyltransferase gene or ribosomal mutations. *Antimicrob. Agents Chemother.* 54, 5337–5343. doi: 10.1128/aac.00663-10
- Luther, M. K., Arvanitis, M., Mylonakis, E., and LaPlante, K. L. (2014). Activity of daptomycin or linezolid in combination with rifampin or gentamicin against biofilm-forming *Enterococcus faecalis* or *E. faecium* in an in vitro pharmacodynamic model using simulated endocardial vegetations and an in vivo survival assay using *Galleria mellonella* larvae. *Antimicrob. Agents Chemother.* 58, 4612–4620. doi: 10.1128/aac.02790-13
- Mlynek, K. D., Callahan, M. T., Shimkevitch, A. V., Farmer, J. T., Endres, J. L., Marchand, M., et al. (2016). Effects of low-dose amoxicillin on *Staphylococcus aureus* USA300 Biofilms. *Antimicrob. Agents Chemother.* 60, 2639–2651. doi: 10.1128/aac.02070-15
- Nallapareddy, S. R., Singh, K. V., Sillanpaa, J., Garsin, D. A., Hook, M., Erlandsen, S. L., et al. (2006). Endocarditis and biofilm-associated pili of *Enterococcus faecalis*. *J. Clin. Invest.* 116, 2799–2807. doi: 10.1172/jci29021
- Sadowy, E. (2018). Linezolid resistance genes and genetic elements enhancing their dissemination in enterococci and streptococci. *Plasmid* 99, 89–98. doi: 10.1016/j.plasmid.2018.09.011
- Schumacher, A., Trittler, R., Bohnert, J. A., Kummerer, K., Pages, J. M., and Kern, W. V. (2007). Intracellular accumulation of linezolid in *Escherichia coli*, *Citrobacter freundii* and *Enterobacter aerogenes*: role of enhanced efflux pump activity and inactivation. *J. Antimicrob. Chemother.* 59, 1261–1264. doi: 10.1093/jac/dkl380
- Schuster, S., Vavra, M., and Kern, W. V. (2019). Efflux-mediated resistance to new oxazolidinones and pleuromutilin derivatives in *Escherichia coli* with class specificities in the RND-type drug transport pathways. *Antimicrob. Agents Chemother.* 63:e001041-19. doi: 10.1128/aac.01041-19
- Silva, V., Almeida, F., Silva, A., Correia, S., Carvalho, J. A., Castro, A. P., et al. (2019). First report of linezolid-resistant *cfr*-positive methicillin-resistant *Staphylococcus aureus* in humans in Portugal. *J. Glob. Antimicrob. Resist.* 17, 323–325. doi: 10.1016/j.jgar.2019.05.017
- Soares, R. O., Fedi, A. C., Reiter, K. C., Caierao, J., and d’Azevedo, P. A. (2014). Correlation between biofilm formation and *gelE*, *esp*, and *agg* genes in *Enterococcus* spp. clinical isolates. *Virulence* 5, 634–637. doi: 10.4161/viru.28998
- Tendolkar, P. M., Baghdayan, A. S., Gilmore, M. S., and Shankar, N. (2004). Enterococcal surface protein, *Esp*, enhances biofilm formation by *Enterococcus faecalis*. *Infect. Immun.* 72, 6032–6039. doi: 10.1128/iai.72.10.6032-6039.2004
- Tendolkar, P. M., Baghdayan, A. S., and Shankar, N. (2005). The N-terminal domain of enterococcal surface protein, *Esp*, is sufficient for *Esp*-mediated biofilm enhancement in *Enterococcus faecalis*. *J. Bacteriol.* 187, 6213–6222. doi: 10.1128/jb.187.17.6213-6222.2005
- Toledo-Arana, A., Valle, J., Solano, C., Arrizubieta, M. J., Cucarella, C., Lamata, M., et al. (2001). The enterococcal surface protein, *Esp*, is involved in *Enterococcus faecalis* biofilm formation. *Appl. Environ. Microbiol.* 67, 4538–4545. doi: 10.1128/aem.67.10.4538-4545.2001
- Wang, X., Han, H., Lv, Z., Lin, Z., Shang, Y., Xu, T., et al. (2017). PhoU2 but Not PhoU1 as an important regulator of biofilm formation and tolerance to multiple stresses by participating in various fundamental metabolic processes in *Staphylococcus epidermidis*. *J. Bacteriol.* 199:e00219-17. doi: 10.1128/jb.00219-17
- Whang, D. W., Miller, L. G., Partain, N. M., and McKinnell, J. A. (2013). Systematic review and meta-analysis of linezolid and daptomycin for treatment of vancomycin-resistant enterococcal bloodstream infections. *Antimicrob. Agents Chemother.* 57, 5013–5018. doi: 10.1128/aac.00714-13
- Wu, S., Yang, T., Luo, Y., Li, X., Zhang, X., Tang, J., et al. (2014). Efficacy of the novel oxazolidinone compound FYL-67 for preventing biofilm formation by *Staphylococcus aureus*. *J. Antimicrob. Chemother.* 69, 3011–3019. doi: 10.1093/jac/dku240
- Wu, Y., Ding, X., Ding, L., Zhang, Y., Cui, L., Sun, L., et al. (2018). Synthesis and antibacterial activity evaluation of novel biarylloxazolidinone analogues containing a hydrazone moiety as promising antibacterial agents. *Eur. J. Med. Chem.* 158, 247–258. doi: 10.1016/j.ejmech.2018.09.004
- Wu, Y., Ding, X., Xu, S., Yang, Y., Zhang, X., Wang, C., et al. (2019). Design and synthesis of biarylloxazolidinone derivatives containing a rhodanine or thiohydantoin moiety as novel antibacterial agents against Gram-positive bacteria. *Bioorg. Med. Chem. Lett.* 29, 496–502. doi: 10.1016/j.bmcl.2018.12.012
- Ye, M., Xu, L., Zou, Y., Li, B., Guo, Q., Zhang, Y., et al. (2019). Molecular analysis of linezolid-resistant clinical isolates of *Mycobacterium abscessus*. *Antimicrob. Agents Chemother.* 63:e001842-18. doi: 10.1128/aac.01842-18
- Zheng, J. X., Bai, B., Lin, Z. W., Pu, Z. Y., Yao, W. M., Chen, Z., et al. (2018). Characterization of biofilm formation by *Enterococcus faecalis* isolates derived from urinary tract infections in China. *J. Med. Microbiol.* 67, 60–67. doi: 10.1099/jmm.0.000647
- Zheng, J. X., Sun, X., Lin, Z. W., Qi, G. B., Tu, H. P., Wu, Y., et al. (2019). In vitro activities of daptomycin combined with fosfomycin or rifampin on

- planktonic and adherent linezolid-resistant isolates of *Enterococcus faecalis*. *J. Med. Microbiol.* 68, 493–502. doi: 10.1099/jmm.0.000945
- Zheng, J. X., Wu, Y., Lin, Z. W., Pu, Z. Y., Yao, W. M., Chen, Z., et al. (2017). Characteristics of and virulence factors associated with biofilm formation in clinical *Enterococcus faecalis* isolates in China. *Front. Microbiol.* 8:2338. doi: 10.3389/fmicb.2017.02338
- Zimenkov, D. V., Nosova, E. Y., Kulagina, E. V., Antonova, O. V., Arslanbaeva, L. R., Isakova, A. I., et al. (2017). Examination of bedaquiline- and linezolid-resistant *Mycobacterium tuberculosis* isolates from the Moscow region. *J. Antimicrob. Chemother.* 72, 1901–1906. doi: 10.1093/jac/dkx094

**Conflict of Interest:** The authors declare that the research was conducted in the absence of any commercial or financial relationships that could be construed as a potential conflict of interest.

Copyright © 2020 Zheng, Chen, Lin, Sun, Bai, Xu, Chen, Yu and Qu. This is an open-access article distributed under the terms of the Creative Commons Attribution License (CC BY). The use, distribution or reproduction in other forums is permitted, provided the original author(s) and the copyright owner(s) are credited and that the original publication in this journal is cited, in accordance with accepted academic practice. No use, distribution or reproduction is permitted which does not comply with these terms.



# Analysis of Identification Method for Bacterial Species and Antibiotic Resistance Genes Using Optical Data From DNA Oligomers

Ryan L. Wood<sup>1</sup>, Tanner Jensen<sup>2</sup>, Cindi Wadsworth<sup>2</sup>, Mark Clement<sup>2</sup>, Prashant Nagpal<sup>3</sup> and William G. Pitt<sup>1\*</sup>

<sup>1</sup> Chemical Engineering, Brigham Young University, Provo, UT, United States, <sup>2</sup> Computer Science, Brigham Young University, Provo, UT, United States, <sup>3</sup> Chemical and Biological Engineering, University of Colorado Boulder, Boulder, CO, United States

## OPEN ACCESS

### Edited by:

Rustam Aminov,  
University of Aberdeen,  
United Kingdom

### Reviewed by:

Nabil Karah,  
Umeå University, Sweden  
Allison Hsiang,  
Ludwig Maximilian University  
of Munich, Germany  
Jason Sahl,  
Northern Arizona University,  
United States

### \*Correspondence:

William G. Pitt  
pitt@byu.edu

### Specialty section:

This article was submitted to  
Antimicrobials, Resistance  
and Chemotherapy,  
a section of the journal  
Frontiers in Microbiology

**Received:** 09 September 2019

**Accepted:** 03 February 2020

**Published:** 20 February 2020

### Citation:

Wood RL, Jensen T,  
Wadsworth C, Clement M, Nagpal P  
and Pitt WG (2020) Analysis  
of Identification Method for Bacterial  
Species and Antibiotic Resistance  
Genes Using Optical Data From DNA  
Oligomers. *Front. Microbiol.* 11:257.  
doi: 10.3389/fmicb.2020.00257

Bacterial antibiotic resistance is becoming a significant health threat, and rapid identification of antibiotic-resistant bacteria is essential to save lives and reduce the spread of antibiotic resistance. This paper analyzes the ability of machine learning algorithms (MLAs) to process data from a novel spectroscopic diagnostic device to identify antibiotic-resistant genes and bacterial species by comparison to available bacterial DNA sequences. Simulation results show that the algorithms attain from 92% accuracy (for genes) up to 99% accuracy (for species). This novel approach identifies genes and species by optically reading the percentage of A, C, G, T bases in 1000s of short 10-base DNA oligomers instead of relying on conventional DNA sequencing in which the sequence of bases in long oligomers provides genetic information. The identification algorithms are robust in the presence of simulated random genetic mutations and simulated random experimental errors. Thus, these algorithms can be used to identify bacterial species, to reveal antibiotic resistance genes, and to perform other genomic analyses. Some MLAs evaluated here are shown to be better than others at accurate gene identification and avoidance of false negative identification of antibiotic resistance.

**Keywords:** antibiotic resistance, machine learning, DNA sequencing, Raman spectroscopy, biomedical diagnostic

## INTRODUCTION

Novel DNA sequencing technologies have proliferated over the past two decades. Continual improvements in “next-generation sequencing” (NGS) and “third-generation sequencing” (TGS) have increased the fidelity and rate of sequencing, but it still takes hours or days to obtain complete sequences (van Dijk et al., 2018). Sequencing plays an essential role in biological classification, cell biology, forensic analysis, and gene manipulation for medical and research purposes. Furthermore, there are some diagnostic applications in which very rapid identification of a particular gene or genetic species becomes essential, while identification of all genes is not necessary. For example, in patients with septic shock from bacterial infections, identification of antibiotic-resistance genes is essential because the mortality rate increases 7.6% per hour of delay in administering correct



antibiotics (Kumar et al., 2006). Unfortunately, it takes more than 24 h to grow up the bacteria recovered from the blood of an infected patient, identify the species, and then determine to which antibiotics the organism is resistant, leading to a very high mortality rate for such infections (Kumar et al., 2009). Carbapenem resistance is one of the most concerning antibiotic resistances, as infections with carbapenem-resistant bacteria have a 48% mortality rate (Patel et al., 2008) caused in part by the good reluctance of physicians to initially prescribe carbapenem antibiotics without verifying resistance because of the severe side effects of carbapenems. The attending clinician wants to know the bacterial species and needs to know any resistance to antibiotics, with confidence that the diagnostic technique has a very low error rate of false negatives. As genome and plasmid sequencing can identify the species and previously identified resistance genes, it would be tremendously useful to perform bacterial sequencing in an hour or less. However, current and proposed NGS and TGS techniques still require much more time.

Herein we present a novel approach that is useful when the diagnostic objective is to rapidly identify the species of bacteria or the presence of an antibiotic resistance gene in the bacteria. Our approach employs a genomic analysis technique that has some data compression and data loss, but compensates by very rapid analysis of very short reads of DNA—sufficiently short length and suitably fast analysis that the species and resistance genes can be identified in about an hour. Such a process has been proposed and demonstrated for the identification of resistance genes in bacteria associated with bloodstream infections (Sagar et al., 2018; Korshoj and Nagpal, 2019). This technique employs a block optical sequencing (BOS) method using surface-enhanced Raman spectroscopy (SERS) to obtain a spectrum of short DNA oligomers of length  $k$ , called  $k$ -mers (Sagar et al., 2018; Korshoj and Nagpal, 2019). Because the Raman spectrum of each A, T, G and C base is known, the overall ATGC content of a single  $k$ -mer can be calculated by mathematical analysis of the  $k$ -mer spectrum. Sequence information is lost, but the base content—called block optical content (BOC)—is preserved. For example, the 10 bp DNA segment ATATGGCCTT would become a BOC datum of A<sub>2</sub>T<sub>4</sub>G<sub>2</sub>C<sub>2</sub>. For very rapid analysis, this BOC technique can be multiplexed by creating an array of 1000s of pyramidal peaks on a silicon wafer whose entire peak field can be imaged by a sensitive CCD camera. Using band-pass filters at discrete spectral windows, optical intensity at specific wavelengths can be obtained simultaneously from all peaks. Finally the optical spectra are processed to obtain the ATGC content of the DNA on each pyramid peak. The size of the tips is such that 10 bases, but not any longer length, fit within the SERS electromagnetic field “hot-spot” (Sagar et al., 2018). It is estimated that using a 1,000 × 1,000 array of SERS pyramids on a silicon wafer, 1,000,000 reads of DNA 10-mers can be done in about 100 s, using high-throughput Raman spectroscopy using quantum dot optical filters (Bao and Bawendi, 2015) and digital processing of the resulting spectra.

Such a technique is ideally suited for genomic identification of bacteria, as a typical bacterial genome is about 5,000,000 bp, or 10 Mbase of single-stranded DNA (ssDNA). Clipping this genome into 10-mer lengths would provide enough ssDNA from a single

bacterium to cover the SERS pyramids on a 1,000 × 1,000 array. Bloodstream infections contain very low counts of bacteria, often on the order of 10 colony forming units (CFU) per mL of blood. Thus a 10 mL sample of blood would provide 100-fold more DNA than needed to place a 10-mer on each pyramid. Bacteria (and their DNA) can be collected from blood in minutes (Pitt et al., 2016; Alizadeh et al., 2017; Pitt et al., 2019), and the SERS analysis can commence immediately, followed by computations for identification of species and antibiotic resistance.

Compared to species identification, analysis of resistance genes on plasmids is more challenging since those genes are usually contained within 500 to 1,000 bases while an average plasmid is roughly 200,000 bases in length. Thus, there is a much smaller signal to background ratio, making detection of resistance genes more difficult. Nevertheless, we show herein that our technique can still identify specific genes.

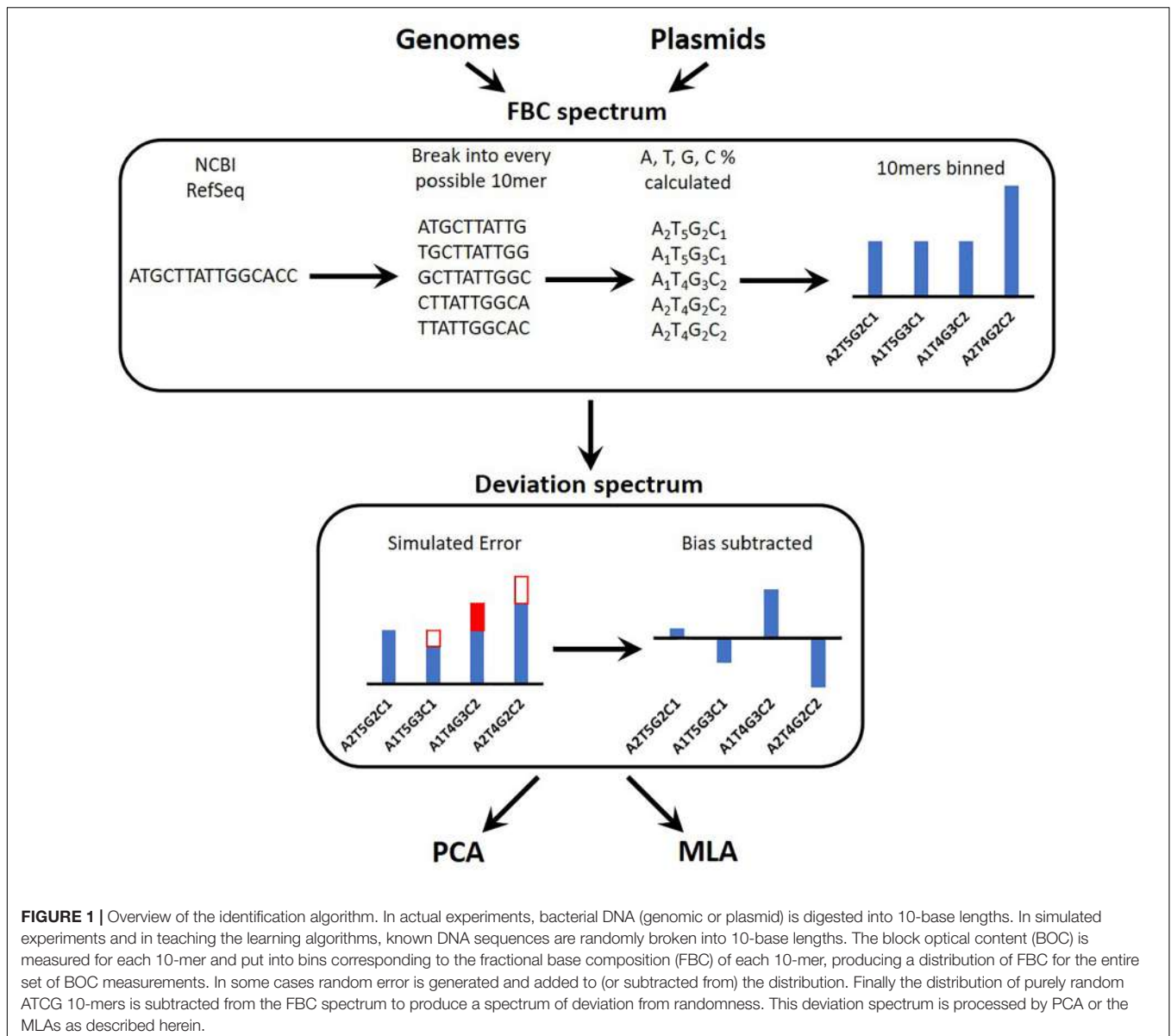
While such technology seems promising, a working device with many 1000s of pyramid tips is still in development, thus leaving some experimental questions unanswered for now. While we wait, however, many of the theoretical questions can be answered, the largest of which is whether the loss of sequence data (the BOC reads give only content, not sequence) will make it difficult to uniquely identify a bacterial species or state unequivocally whether a known resistance gene is present. Another theoretical question is whether random mutations in the bacterial genomes will compromise correct identification, or whether random noise from the experimental optical measurements will reduce accuracy.

The main goal of this study was to determine whether data produced in 10-mer blocks could be used in a diagnostic device, meaning that the data could correctly identify species and antibiotic resistance genes with a realistic number of pyramid tips ( $\leq 1,000,000$  tips). To answer this question, this study addressed four main objectives: (1) to determine how many BOC reads are needed for species identification; (2) to determine how many BOC reads are needed for single gene detections (such as an antibiotic resistance gene of around 800 bp); (3) to analyze how accuracy is affected by noise from the detecting instrument and from random gene mutations; (4) to identify which learning algorithms are best at accurately identifying the species and genes.

The present study answers these and other questions to show that only  $10^4$  BOC reads, even in the presence of mutations or experimental noise, are sufficient to identify bacterial species. The presence of resistance genes can be identified with an accuracy of 80% up to 95% using  $10^5$  BOC reads. Both of these results are well below the proposed  $10^6$  BOC reads, even when large error is present, showing that the algorithm could be used with high accuracy in a diagnostic device.

## MATERIALS AND METHODS

**Figure 1** provides an overview of the process for simulating the experimental data reads, converting these into a spectrum, and testing the machine learning algorithms (MLAs). A brief outline follows: a sequence is obtained (see section “DNA Sequences”); the sequence is broken into every possible 10-mer



for both strands of DNA (see section “Generating Sequence-Specific FBC Spectrum”); the 10-mers are binned according to the percent A, T, G, and C, resulting in the sequence-specific fractional base content (FBC) spectrum (see section “Generating Sequence-Specific FBC Spectrum”); experimental noise is simulated by introducing random errors into the sequence-specific FBC spectrum resulting in the simulated experimental FBC spectrum (see section “Simulating Gene Mutations and Experimental Errors”); the spectrum from a purely random sequence (bias) is subtracted from the simulated experimental FBC spectrum, producing a deviation spectrum (see section “Bias FBC Spectrum”); the FBC deviation spectra from many DNA samples are then analyzed by both principal component analysis (PCA) (see section “Principal Component Analysis”) and the MLAs (see section “Testing the MLAs”); the MLAs are trained and cross-validated on one set of FBC deviation

spectra and then tested against another set of never-before-seen FBC deviation spectra (see section “Testing the MLAs”).

## DNA Sequences

While awaiting experimental data from the SERS instrument, simulated SERS BOC data were generated to determine the feasibility of the device in identifying bacterial species and antibiotic resistance genes. Reference genomes for 12 bacterial species, 728 plasmids containing 4 different types of carbapenem antibiotic-resistant genes, and 600 control plasmids not containing any carbapenem resistance genes were collected from the National Center of Biotechnology Information’s reference sequence (NCBI RefSeq; see **Supplementary Material** for NCBI reference IDs for each genome and plasmid) (O’Leary et al., 2016). The DNA sequences were separated into genomic and plasmid DNA (gDNA and

pDNA, respectively) and studied separately using PCA and several MLAs.

Of the gDNA sequences, 10 of the 12 species are common organisms producing bloodstream infections (*Bacteroides fragilis*, *Campylobacter jejuni*, *Enterococcus hirae*, *Escherichia coli*, *Escherichia fergusonii*, *Klebsiella pneumoniae*, *Salmonella enterica*, *Staphylococcus aureus*, *Streptococcus pneumoniae*, and *Streptococcus pyogenes*) and were used in both training and testing (different genomic sequences were used for training and testing); and two additional species (*Klebsiella aerogenes* and *Mycobacterium tuberculosis*) were only used in testing (for taxonomy testing). Median GC% contents for the chosen species are included in **Supplementary Table 4**. One NCBI RefSeq genome was used for each species in the training set and one NCBI RefSeq genome was used for each species in the testing set. Only one was used because 1000 genomes are generated from each genome using the original genome FBC spectrum as the probability distribution for creating new genomes (see sections “Generating Sequence-Specific FBC Spectrum” and “Simulating Gene Mutations and Experimental Errors”). This means that no 2 simulated genomes are identical, even in the absence of error, and that the MLAs see the original genome and 999 variations for both the training and testing sets for each species, resulting in a similar analysis to one made with multiple NCBI RefSeq genomes per species.

For the pDNA, all sequenced plasmids from the NCBI RefSeq for the four carbapenem resistance plasmids [imipenemase 4 (IMP-4), *Klebsiella pneumoniae* carbapenemase 2 (KPC-2), New Delhi metallo-beta-lactamase 1 (NDM-1), and Verona integron-encoded metallo-beta-lactamase 1 (VIM-1)] were used in either training or testing (see **Table 1** for specific number used in training and testing). No variant plasmid data were used (a variant being KPC-4 or VIM-2), and all control plasmids were checked to make sure they did not contain the four carbapenem resistance plasmids or any variants. Two different tests were performed on the pDNA: the first test investigated whether the MLAs are able to identify the particular type of resistance (out of four types) or identify that none of these are present; the second test grouped the carbapenem resistance plasmids together and investigated whether the MLAs are able to identify the presence (or not) of any carbapenem resistance.

**TABLE 1** | Carbapenemase-gene-containing plasmids used in this study.

Plasmid type	Number of plasmids used in training set	Number of plasmids in test set (not seen in training set)
KPC-2	100	98
NDM-1	100	99
VIM-1	100	99
IMP-4	100	33
No-resistance plasmids	100 (or 400 for 2-group set) <sup>a</sup>	500 (or 200 for 2-group set) <sup>a</sup>

<sup>a</sup>Plasmids were tested against individual resistant types and not resistant (five groups), or as a resistant vs. non-resistant grouping (two groups).

## Generating Sequence-Specific FBC Spectrum

The physical optical instrument reads the BOC of each DNA  $k$ -mer bound to  $r$  number of SERS pyramids on a silicon chip in the instrument (Sagar et al., 2018). Since the size (i.e.,  $k$  bases) of each read is known, these base fractions are converted into specific integer counts of nucleotides for each  $k$ -mer. BOC reads are written in the form  $A_wT_xG_yC_z$  where  $0 \leq w, x, y, z \leq k$ , and  $w + x + y + z = k$ . For traditional sequencing, there are  $4^k$  possible reads for a single  $k$ -mer; however, there are only  $(k + 3)!/(k!3!)$  BOC reads corresponding to the different ways of assigning the variables  $w$ ,  $x$ ,  $y$ , and  $z$ , given the previous constraints. The distribution of BOC reads, hereafter called the FBC spectrum, is defined as the probability distribution function of sampling any BOC read of a specific base composition (see **Figure 2**).

In order to create the FBC spectrum for each gDNA and pDNA sequences of interest, each sequence is decomposed into every possible 10-mer block using both complementary strands of DNA, since both strands will be present in a physical system and a 10-mer block from either strand has the same probability of adhering to the pyramid tip for the BOC reads. Therefore, in creating the FBC spectrum, the  $k$ -mers from both complementary strands of DNA are used. These blocks are then assigned to their corresponding bins to produce the FBC spectrum. Once all blocks are binned for the given sequence, each bin count is divided by the total 10-mer count of all 286 bins for that DNA sequence to get the sequence-specific probability distribution function, or FBC spectrum.

To simulate BOC reads on a multi-pyramid chip, the FBC spectrum for the selected plasmid or genome is randomly sampled 2.5 million times, using the sequence-specific probability distribution. This represents having more than one copy of the DNA sequence present in a physical experiment. From this 2.5-million-value array, the first  $r$  number of values are selected and distributed into bins to produce a simulated experimental FBC spectrum, where  $r$  represents the number of pyramid tips on the SERS-BOC device. This is done for both the training and testing sets.

## Simulating Gene Mutations and Experimental Errors

Due to mutations present in bacteria, any given bacteria species or plasmid will not have a perfectly identical FBC spectrum as that of the corresponding NCBI reference sequence. These natural gene mutations, which are on the order of  $5 \times 10^{-4}$  to  $5 \times 10^{-9}$  in bacteria (Denamur et al., 2002; Denamur and Matic, 2006), are expected to be overwhelmed by the experimental errors produced during experimental BOC reads and assignments. There are several sources for error in the optical sequencing reads. A few examples are under-digestion and/or over-digestion which results in non-uniform length  $k$ -mer sequences,  $k$ -mer sequences adhering to the pyramid tips such that not all bases can be read, portions of multiple  $k$ -mer sequences adhering to the same pyramid tip, and optical noise from the instrumentation (Sagar et al., 2018). While creating more realistic training and test

samples, a single error rate parameter was introduced to modify the BOC read that accounts for both the expected bacterial mutations and the instrument errors, producing FBC spectra with various levels of random error.

We define an error rate  $m$  (where  $0 \leq m \leq 1$ ) to be the fraction of bases in the reference sequence that are expected to contain an error. Assuming that the errors are randomly distributed throughout the reference sequence, the number of errors in a randomly selected 10-mer is the same as the number of errors in 10 randomly selected bases. The probability of selecting a 10-mer without any errors is therefore determined by a binomial distribution in which the number of trials is the same as the number of pyramid tips,  $r$ , and the probability of being errorless is one minus the error rate,  $1-m$ . To simulate errors, a value of either  $[0,1]$  is sampled from the binomial distribution  $B(r,m)$ . If a 0 is chosen, then a value is chosen from the sequence-specific FBC spectrum (the 2.5-million-value array described above in Section “Generating Sequence-Specific FBC Spectrum”). If a 1 is chosen, then a random value from the bias spectrum (see section “Bias FBC Spectrum” for details) is chosen. This is repeated until a list of values is created that is  $r$  in length; next, the list is distributed into bins to produce the “noisy” FBC bins. The resulting FBC 10-mer bin counts are divided by  $r$  to obtain the “noisy” FBC spectrum for the given plasmid or genome.

## Bias FBC Spectrum

We discovered that a key to enhancing the differences in the FBC spectra of various DNA sequences is to subtract from each FBC spectrum the spectrum of totally random ATGC, leaving a spectrum of deviations from randomness. The resulting spectrum is called the “deviation spectrum” for a particular sequence.

Because the  $k$ -mer size is given, a purely random spectrum (called the bias spectrum) can be generated by including every possible  $k$ -mer once. Since there are  $4^k$  possible sequential  $k$ -mers, and given that any BOC read ( $A_wT_xG_yC_z$ ) has  $k!/(w!x!y!z!)$  ways of permuting the base counts to create nucleotide-specific  $k$ -mers, the bias spectrum can be calculated as:

$$\text{bias}(A_wT_xG_yC_z) = \frac{1}{4^k} \cdot \frac{k!}{w!x!y!z!}$$

This bias spectrum is subtracted from the FBC spectrum of the particular DNA sequence to yield a unique-DNA-sequence FBC deviation spectrum. This unique-DNA-sequence deviation spectrum is the deviation from pure randomness and should oscillate around zero.

For our given  $k$ -mer size of 10, there are 286 bins in the FBC spectrum. The FBC spectrum for a sequence can be visualized by plotting the frequency of a 10-mer in the bins of the spectrum, as shown in **Figure 2**. **Figure 2A** shows the corresponding FBC spectrum for *E. coli*, *K. pneumoniae*, *K. aerogenes*, and the bias spectrum. **Figure 2B** shows the resulting deviation spectra for *E. coli*, *K. pneumoniae*, and *K. aerogenes* produced by subtracting the bias spectrum. In **Figure 2A**, the commonness of the sequence is indicated by the height of the peak, with taller peaks being more common, such as  $A_3T_2G_3C_2$  and  $A_3T_3G_2C_2$ . A few of these peaks are labeled for easy comparison with **Figure 2B**. As

seen in **Figure 2B**, some FBC 10-mers appear more often than expected from a random sequence and some FBC 10-mers appear less than expected from a random sequence. While obvious that these bacteria do not have random sequences, it is useful and informative to observe that randomly breaking their DNA into all possible 10-mers does not produce a random FBC spectrum; in fact, unique features appear that suggest a species may be identified by its deviation spectrum.

To test the robustness of identification of species or genes by deviation spectra in the presence of real experimental noise and random mutations in the DNA sequence, random errors are introduced into the FBC spectra (see section “Simulating Gene Mutations and Experimental Errors” for details) and then the resulting noisy data are divided by  $r$  and the bias spectrum is subtracted to obtain a simulated FBC deviation spectrum (with noise) for the given plasmid or genome. For each gDNA and pDNA sequence (22 bacterial genomes and 1329 plasmids), 1000 simulated FBC deviation spectra were created from each specific sequence for both the training set and testing set.

## Principal Component Analysis

Principal component analysis is useful analysis is useful for reducing data dimensions data dimensions while retaining trends and patterns (Lever et al., 2017). This technique, which can reduce computational expense, is often used with biological data. For these reasons, PCA was used to investigate whether a simple data reduction analysis could easily identify the different species and antibiotic resistance genes using the noiseless and noisy FBC deviation spectra. As seen in **Figures 3, 4**, visualizing the first two principal components allows for some of the data to be easily classified into the correct groups, while other data are unclassifiable. Adding a third principal component may help cluster the data, but information is not easily retrieved from three dimensional plots, especially with 1000s of data points. From this initial result, MLAs were subsequently examined to determine if supervised learning methods could classify the data.

## Testing the MLAs

After creating the FBC deviation spectra from noiseless and noisy DNA BOC reads, the data sets were split into a training set and a never-before-seen test set (both sets of FBC spectra are created through the process detailed by Sections “Generating Sequence-Specific FBC Spectrum,” “Simulating Gene Mutations and Experimental Errors,” and “Bias FBC Spectrum”) and run through several MLAs to classify the bacterial species or the carbapenem resistance status of plasmids based on their FBC deviation spectra. The attributes used in the classification model were the values corresponding to the probability distribution from each FBC deviation spectrum. The training set was then randomly split into 900 and 100 deviation spectra for each DNA sequence for running 10-fold cross-validation. The MLAs were trained on the 900 deviation spectra from each DNA sequence and then tested against the remaining 100 deviation spectra from each DNA sequence of the training set and then tested against all of the never-before-seen sequences. For the gDNA, that meant that the MLAs were trained on 9,000 training deviation spectra (900 FBC spectra for each of the 10 training genome



sequences) and validated against the remaining 1,000 training deviation spectra from the training set and then tested against all the 12,000 testing deviation spectra (1,000 FBC spectra for each of the 12 testing genome sequences). The MLAs were trained and tested similarly for the pDNA. For the gDNA, the labels used for classifying were: *B. fragilis*, *C. jejuni*, *E. hirae*, *E. coli*, *E. fergusonii*, *K. pneumoniae*, *S. enterica*, *S. aureus*, *S. pneumoniae*, and *S. pyogenes*. The other two species, *K. aerogenes*, and *M. tuberculosis* are used to investigate how the MLAs group unknown species. For the pDNA, the labels used for the individual classification tests were: KPC, NDM, VIM, IMP and No Resistance; and the labels used for the group classification tests were: Resistance and No Resistance.

For both the gDNA and pDNA, the FBC deviation spectra were created with the following parameters:  $k = 10$ ;  $r = [10^2; 10^3; 10^4; 10^5; 10^6]$ ;  $m = [0, 0.01, 0.05, 0.1, 0.25, 0.33, 0.5, 0.75, 0.9, 1]$ ; and  $s = 1000$ ; where  $k$  is the size of the  $k$ -mer,  $r$  is the number of pyramid tips for generating the sample FBC spectra,  $m$  is the fractional error rate, and  $s$  is the number of FBC deviation spectra created per DNA sequence (genome or plasmid). All 50 combinations of  $r$  and  $m$  were tested.

From the machine learning python package, Sci-kit learn (version 0.20.3) (Pedregosa et al., 2011), 11 different MLAs were tested from the following categories: linear MLAs, decision tree learning algorithms, Naïve Bayes learning algorithms, discriminant analyses, and a neural network. For this initial study, default parameters were used for all of these algorithms. Each of these classification models were chosen for their ability to fit data with positive and negative values and to fit data to the model using out-of-core fitting, except for the discriminant analyses (see **Supplementary Material** for further details). Presented in the results is the best algorithm from each category; the results of the other algorithms are in the **Supplementary Material**.

## Model Performance Testing and Statistical Analysis

The robustness of each classification model was studied by measuring the predictive accuracy as a function of the parameters of the simulated BOC data. For each optical sequencing read number ( $r$ ) and each error rate ( $m$ ), the performance of the model was quantified by the predictive accuracy and a confusion matrix, which keeps track of the true positives, true negatives, false positives, and false negatives for the sample (Powers, 2011). The accuracies and confusion matrix presented for each MLA are the average of 10 trials ( $n = 10$ ) for the given  $r$  and  $m$ . Three different cutoff accuracies (95% for species, 90% for group plasmid, and 75% for individual plasmid) for the never-before-seen sequences were chosen as criteria for assessing the effects of the different error rates and sequencing read numbers.

## Simulation

To generate large amounts of simulated experimental data on which to test the different MLAs, the data were produced using code written in Python 3.7 as described above. Reference genomes were downloaded directly from the NCBI RefSeq

database. All code used for running the simulation is available at: <https://github.com/rlwphd/DNAFingerprints>. While these simulations were tested only on plasmids having a carbapenem antibiotic resistance gene, the simulation will work for any set of antibiotic resistance genes in which the full sequence of the gene-containing plasmid is known.

## RESULTS

### Principal Component Analysis

**Figures 3, 4** visually display the first two principal components for the deviation spectra of the species and resistance genes. For species, the PCA data are visually distinct, even when significant noise is added to the BOC data. For resistance gene detection, the PCA could not produce a clear distinction. Details are discussed below.

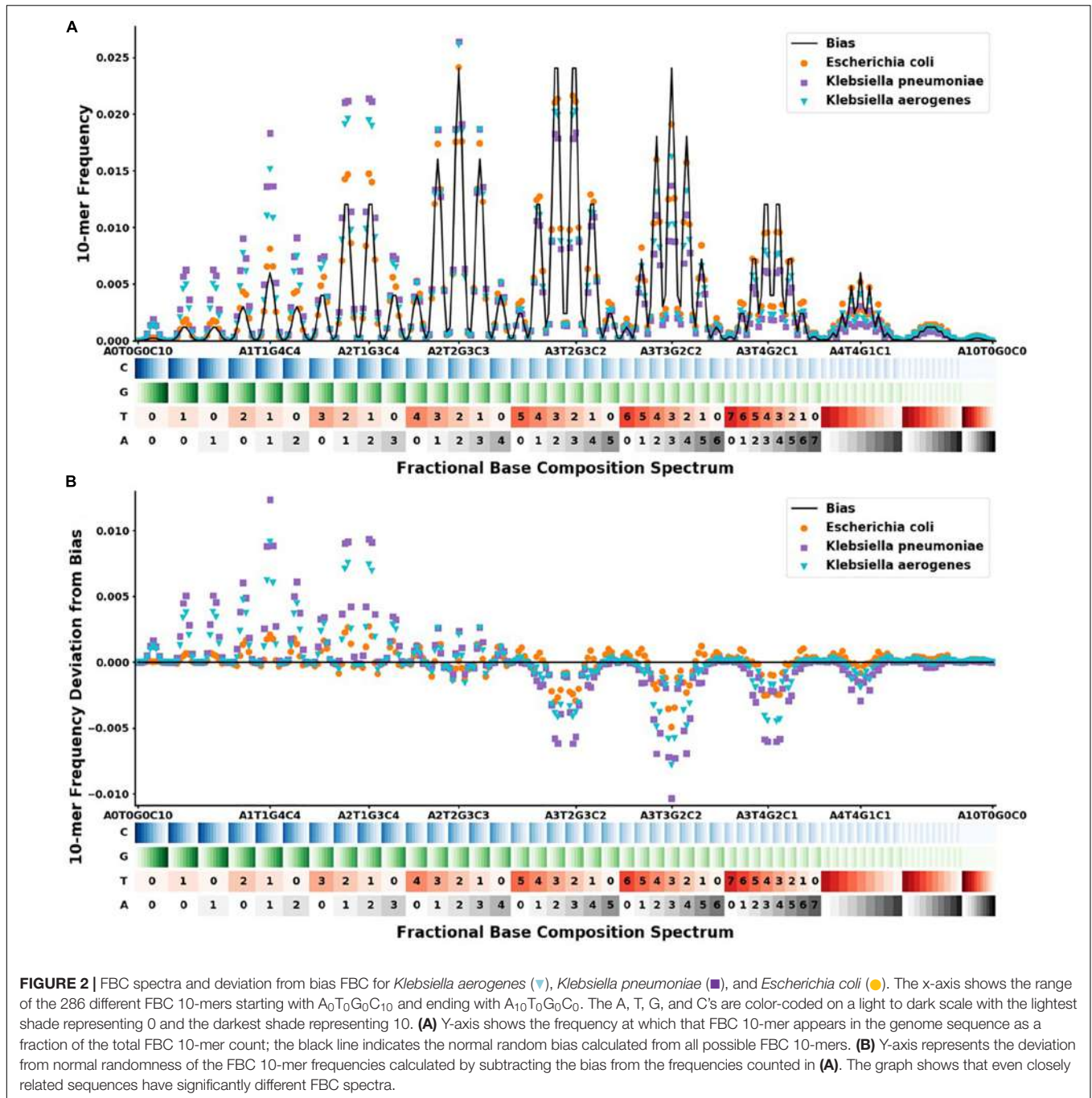
For both bacterial species and antibiotic resistance gene identification, it is noted that the PCA produced in all cases contains an arch effect, which indicates that the principal components are not completely independent of each other and are thus not completely orthogonal to each other (Morton et al., 2017). Since the PCA assumes independence and orthogonality between the principal components, it is not completely reliable as a means of identification without first adjusting for the arch effect. However, PCA was used here to reveal the extent of differences that might be learned by the MLAs.

### Bacterial Species

For the bacterial species, we found that the PCA revealed significant differences between the various species, even with a 90% error rate for  $10^6$  reads. As a control, using a 100% error rate produced no differences (data not shown) because the PCA yields the same value for all species, regardless of the number of reads. We selected *E. coli* and *E. fergusonii*, two genetically very similar bacteria, as a stringent test for sensitivity and discrimination. Because of the similarity of *E. coli* and *E. fergusonii*, the graphical plot can only reveal the difference between these two species for error rates of 0–33% for  $10^5$  reads and 0–90% for  $10^6$  reads (see difference between **Figures 3A,B**). **Figure 3** contains an example of a non-overlapping (significantly different) PCA (A) and an overlapping (some difference to no difference) PCA (B). **Figure 3** shows the PCA of the FBC deviation spectra data for the bacteria species for 25% error at  $10^6$  reads (A) and at  $10^4$  reads (B) (see **Supplementary Material** for additional PCA figures). This figure shows that with enough BOC reads even in the presence of error, there exists significant differences between the species when using only the first two principal components. This indicates that the FBCs of each of these 12 species are distinct enough that the MLAs should be able to easily classify each species, potentially perfectly, even in the presence of noise, even differentiating very similar species such as *E. coli* and *E. fergusonii*.

### Antibiotic Resistance Genes

For the plasmids, the PCA revealed that there is a greater spread across the plasmid sequences with no clear differences using only two principal components for any number of

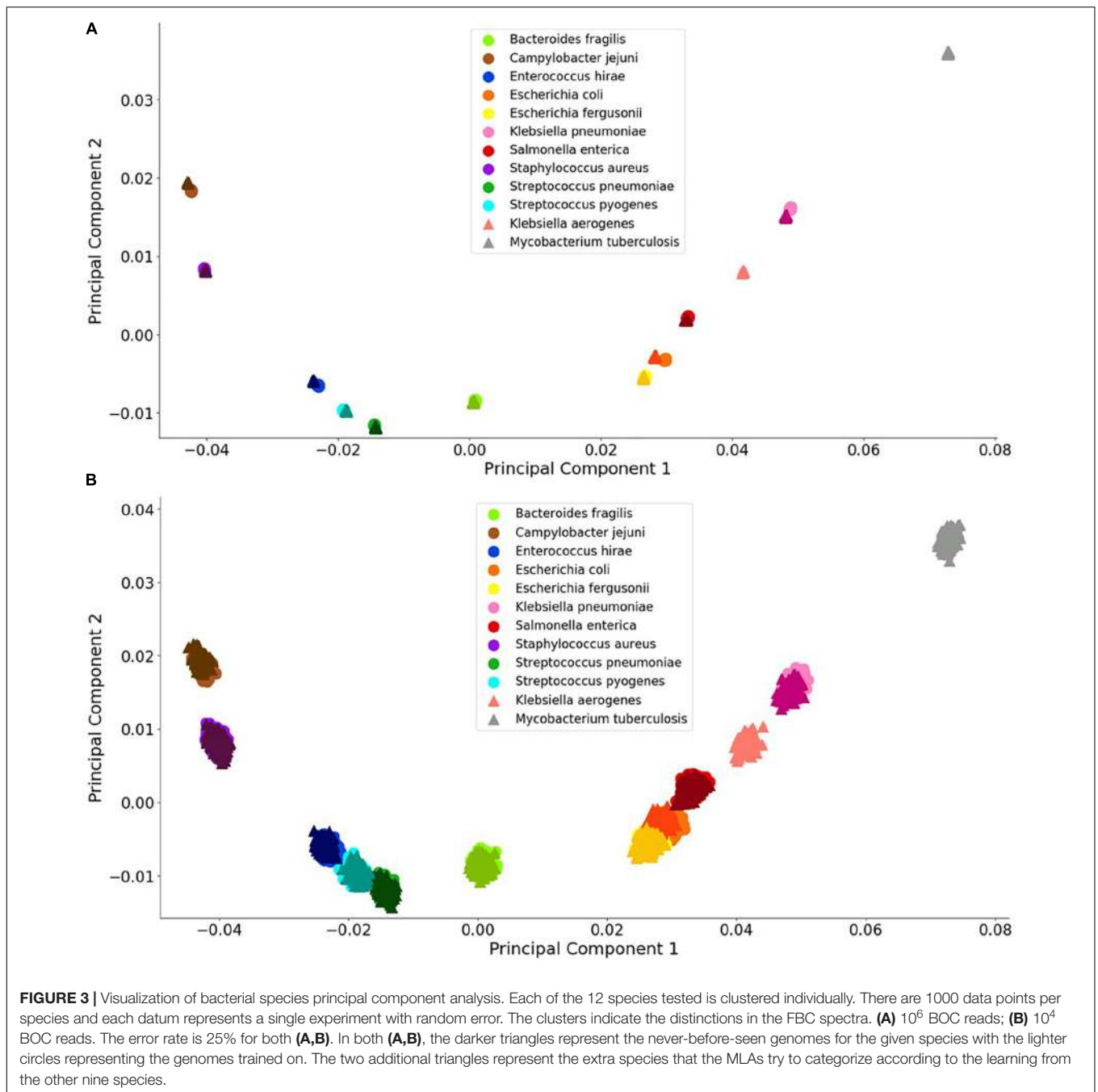


reads, even with no error. This is not surprising because the antibiotic resistant gene content could be affecting less than 1% of the FBC deviation spectrum (800 bases on a 200,000-base plasmid) for some of the samples. This indicates that the MLAs will need to detect the small resistance gene signal from a dominating background. In addition to a low signal competing with a strong background, there is a wide range of different DNA signatures in plasmids, increasing the complexity of the task. **Figure 4** highlights this varying range of DNA signatures; both control plasmids and plasmids containing resistance genes span the entire space of the PCA plot. Neither the

individual resistance categorization (**Figures 4A,B**) nor the group resistance categorization (**Figures 4C,D**) provided any insights into clustering or separation. **Figure 4** shows the PCA of the FBC spectra data for the plasmids for 0% error at  $10^6$  reads (A&C) and at  $10^4$  reads (B&D) (see **Supplementary Material** for additional PCA figures).

### Classification Using MLAs

The outputs from 1000s of simulated SERS-BOC experiments were produced to examine a wide range of combinations of error rates and the number of reads from pyramid tips. The simulation



creates hypothetical BOC reads from different bacterial genomes or plasmids which are then converted to FBC deviation spectra and handed to the different MLAs for categorizing. Simulating the experiments allows us to show feasibility and test the robustness of the algorithm in the presence of noise and genetic variation, and to examine the device as a diagnostic tool for bacteria classification and resistance profiling.

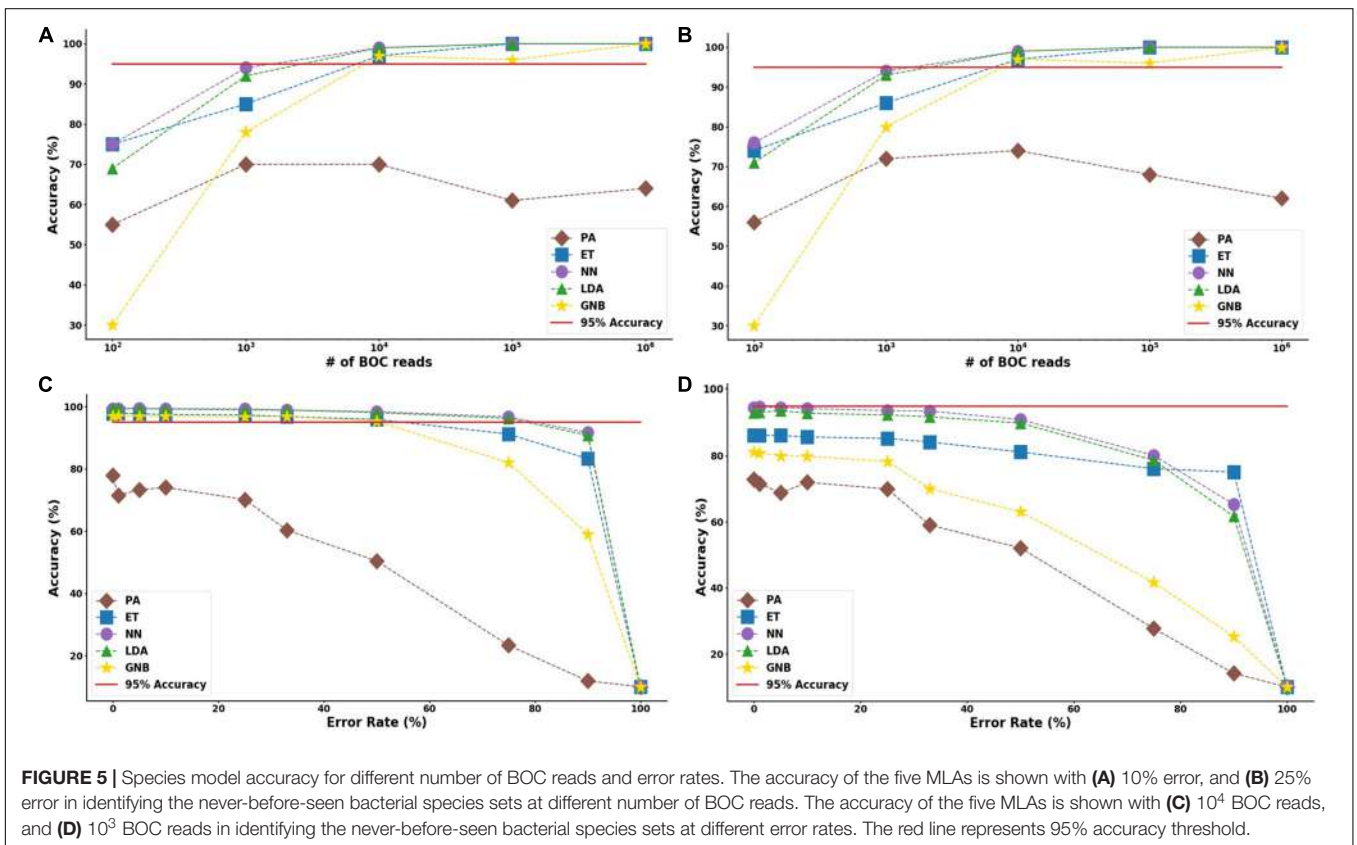
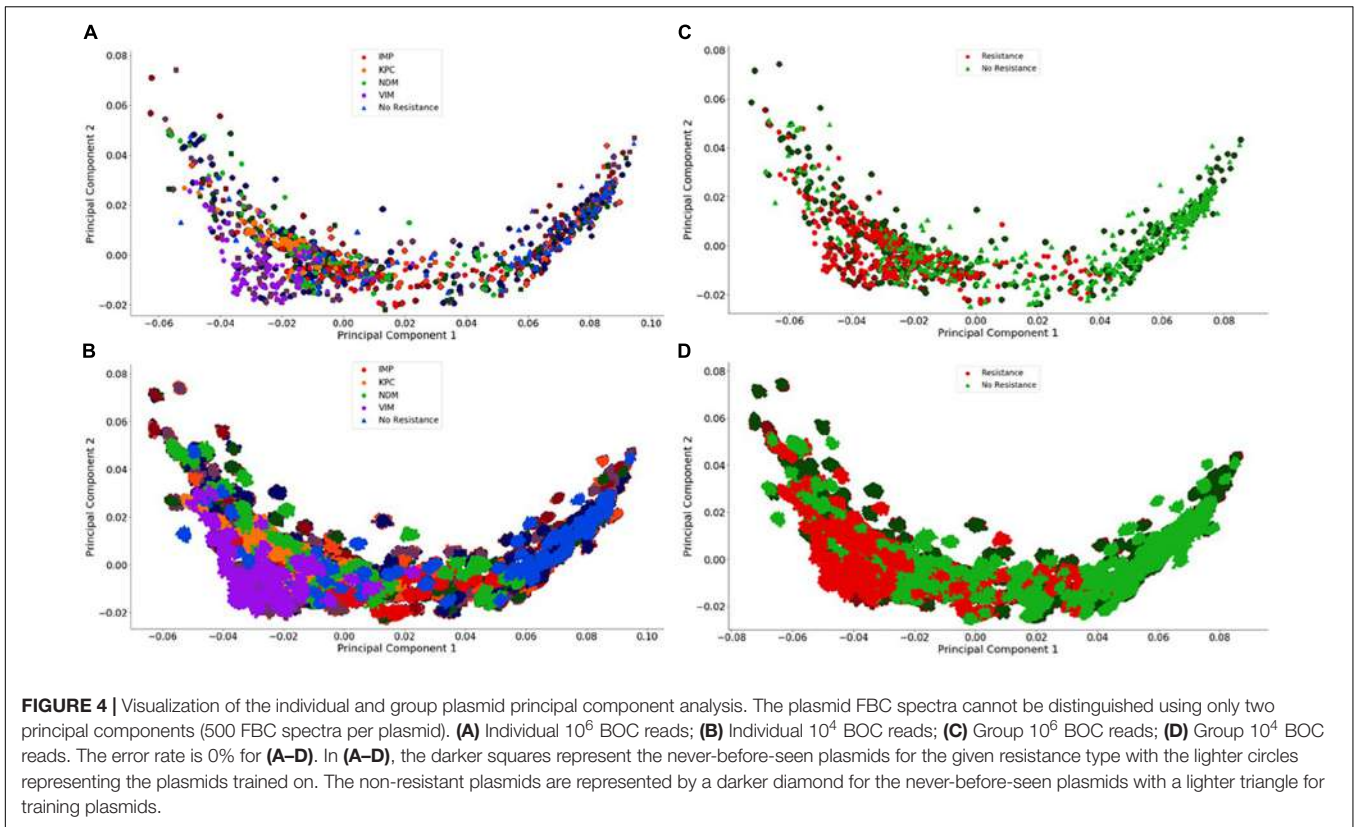
The results detailed below showed that the best algorithms from each category are: Passive-Aggressive Classifier (PA, linear machine learning algorithm); Extra Trees Classifier (ET, decision tree algorithm); Gaussian Naïve Bayes (GNB, Naïve Bayes

algorithm); Linear Discriminant Analysis (LDA, discriminant analysis algorithm); and the neural network (NN, whose default is 100 layers and the number of nodes determined by the number of input features). The results for each of these MLAs are presented below and the results for the other MLAs can be found in **Supplementary Tables 1–3**.

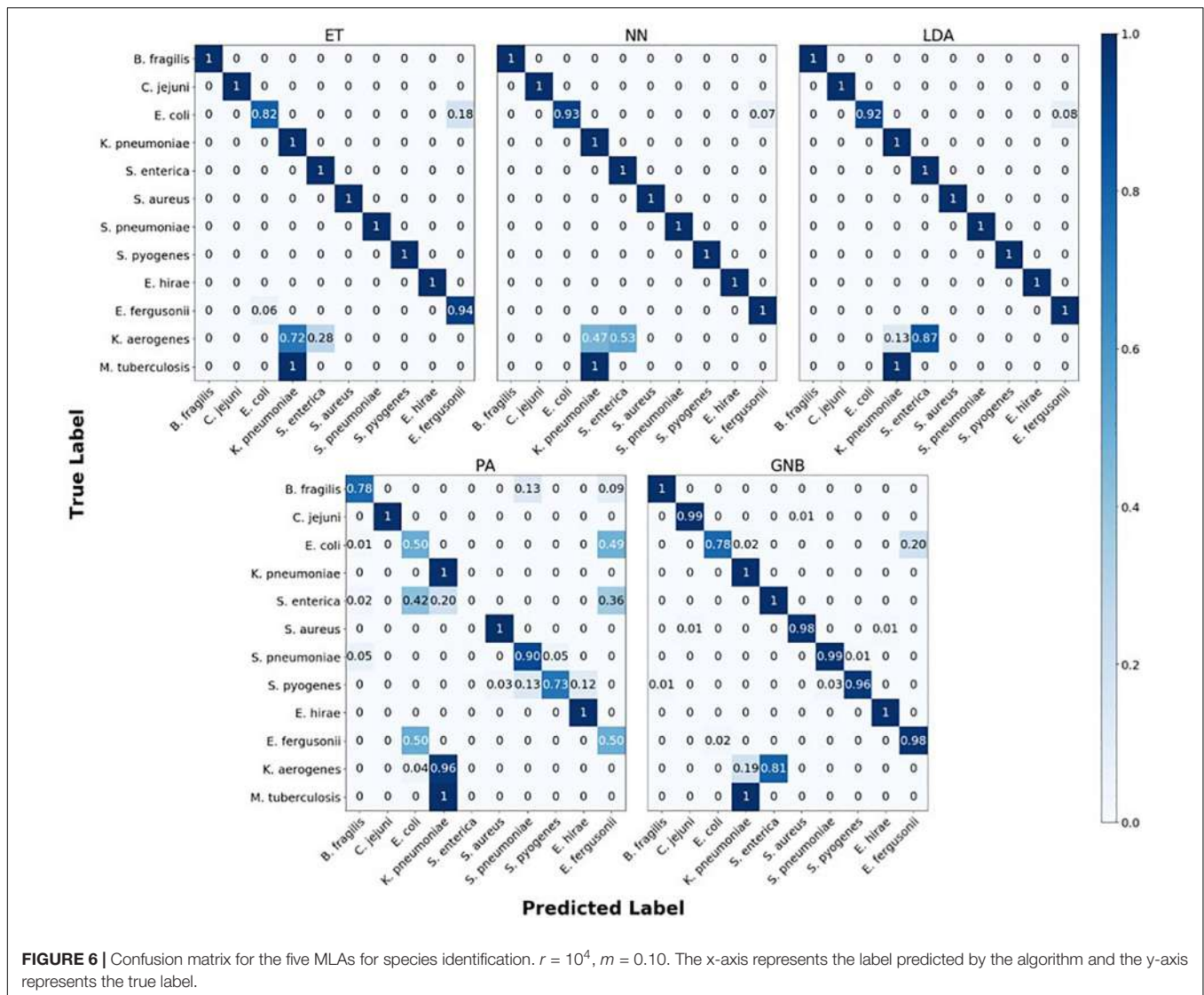
### Bacterial Species

The MLA analysis showed that we were able to accurately classify greater than 96% of the simulated unseen bacterial genome data sets (1000 samples per species) using the ET, LDA and NN MLAs









**FIGURE 6** | Confusion matrix for the five MLAs for species identification.  $r = 10^4$ ,  $m = 0.10$ . The x-axis represents the label predicted by the algorithm and the y-axis represents the true label.

employing as low as  $10^4$  BOC reads and up to 50% error. The PA MLA was the worst algorithm and never got better than 78% accuracy (see **Supplementary Material** for detailed table). As for the best algorithms, even at 90% error, the LDA and NN could accurately classify greater than 98% of the bacterial species at  $10^5$  BOC reads. This surprising result at very high noise levels is postulated to occur because random error added to the BOC generates random noise in the FBC spectrum, but the deviation spectrum has the bias spectrum subtracted out which removes random noise. Thus, the MLA models working on the FBC deviation spectra operate on data with a good signal-to-noise level, even up through 90% random error in the original BOC data.

The results suggest that a SERS-BOC device only needs a  $100 \times 100$  pyramid array ( $\sim 10^4$  reads per experiment) to accurately identify bacterial species. **Figure 5** shows the MLA accuracy for an error rate of 10% (A) and 25% (B) for all of the BOC reads. This figure shows that greater than 97% accuracy is

maintained at  $10^4$  BOC reads for both 10 and 25% error. **Figure 5** also shows how the various MLAs hold up to error for  $10^4$  BOC reads (C) and  $10^3$  BOC reads (D).

The confusion matrix for the MLAs shows how the models mislabel the species they were trained on, and how they label the two species which are not defined in the model. **Figure 6** shows the species confusion matrix for the five MLAs for  $10^4$  BOC reads and 10% error. While most of the species in this study are not closely related (see **Supplementary Material** for details), the best three MLAs only had problems distinguishing between *E. coli* and *E. fergusonii*, which are genetically very similar (same genus). The ET had a sensitivity rate of 82% for *E. coli* and a specificity rate of 94% for *E. fergusonii* when comparing the two genomes. The LDA had a sensitivity rate of 92% for *E. coli* and a specificity rate of 100% for *E. fergusonii* when comparing the two genomes; meaning that the LDA could correctly identify *E. fergusonii* but not *E. coli*. The NN had a sensitivity rate of 93% for *E. coli* and a specificity rate of

100% for *E. fergusonii* when comparing the two genomes. All other genomes trained on had 100% identification for the ET, LDA, and NN MLAs. As for the classification of the two extra species (*K. aerogenes* and *M. tuberculosis*), all three MLAs identify *M. tuberculosis* as *K. pneumoniae* (unrelated) 100% of the time. *K. aerogenes* was identified as both *K. pneumoniae* (same genus) and *S. enterica* (same family) by all three MLAs. Other details are found in **Figure 6**.

### Antibiotic Resistance Genes

In the study of the individual resistance categorization (distinguishing four carbapenem resistance genes), the MLAs had difficulty achieving better than 75% accuracy. Only with  $10^5$  BOC reads (or more) did the ET algorithm attain better than 75% accuracy, and even this algorithm only achieved 80% accuracy at best. The LDA and ET algorithms had similar accuracy at  $10^4$  reads (see **Figure 7D**) but the LDA did not perform as well at  $10^5$  reads (**Figure 7C**). The GNB and PA MLAs were the worst but were still able to achieve 64% accuracy (see **Figure 7** and **Supplementary Material** for a detailed table). **Figure 7** shows the MLA accuracy for an error rate of 10% (A) and 25% (B) for all of the BOC reads for the individual scenarios. **Figures 7A,B** show that greater than 75% accuracy is maintained at  $10^5$  BOC reads for both 10 and 25% error. **Figure 7** also shows how the MLAs hold up to error for  $10^5$  BOC reads (C) and  $10^4$  BOC reads (D).

For the group resistance categorization, the MLA analysis was able to accurately classify 90% of the simulated unseen data set using the ET, LDA and NN MLAs down to  $10^4$  BOC reads and up to 50% error. The GNB MLA performed the worst of those examined but was still able to achieve 86% accuracy (see **Figure 8** and **Supplementary Material** for detailed table). **Figure 8** shows the MLA accuracy for an error rate of 10% (A) and 25% (B) for all of the BOC reads for the group scenario. **Figure 8** shows that greater than 90% accuracy is maintained at  $10^4$  BOC reads for both 10 and 25% error. **Figure 8** also shows how the MLAs hold up to error for  $10^5$  BOC reads (C) and  $10^4$  BOC reads (D).

The ET MLA model for the individual resistance categorization maintains 74% accuracy for up to 25% error for  $10^4$  BOC reads and maintains 80% accuracy for up to 25% error for  $10^6$  BOC reads. The individual results suggest that a SERS-BOC device would need to be at least a  $100 \times 100$  pyramid array ( $10^4$  reads per experiment), but a  $1,000 \times 1,000$  pyramid array ( $10^6$  reads per experiment) would be optimal for the best results to accurately identify antibiotic resistance genes on plasmids. For the group resistance categorization, the three best MLA models maintain good signal-to-noise levels up through 50% error. The group results suggest that a SERS-BOC device with a  $100 \times 100$  pyramid array would be sufficient to accurately identify whether any carbapenem resistance gene was present in the presence of 50% experimental noise.

The confusion matrix for the MLAs shows how the models mislabel the plasmids, which allows us to calculate the false-negative rate for the antibiotic-resistant plasmids as a group, as well as the sensitivity of each individual plasmid. The false-negative rate metric is clinically important as it is incorrectly labeling resistant plasmids as not being resistant, which could result in the wrong (ineffective) antibiotics being given to the

patient, possibly leading to death. The sensitivity metric shows which type of resistance gene is harder to identify. **Figure 9** shows the confusion matrix for the five MLAs for  $10^5$  BOC reads and 10% error for the plasmid sets for individual identification. **Figure 10** shows the confusion matrix for the five MLAs for  $10^5$  BOC reads and 10% error for the plasmid sets for group identification.

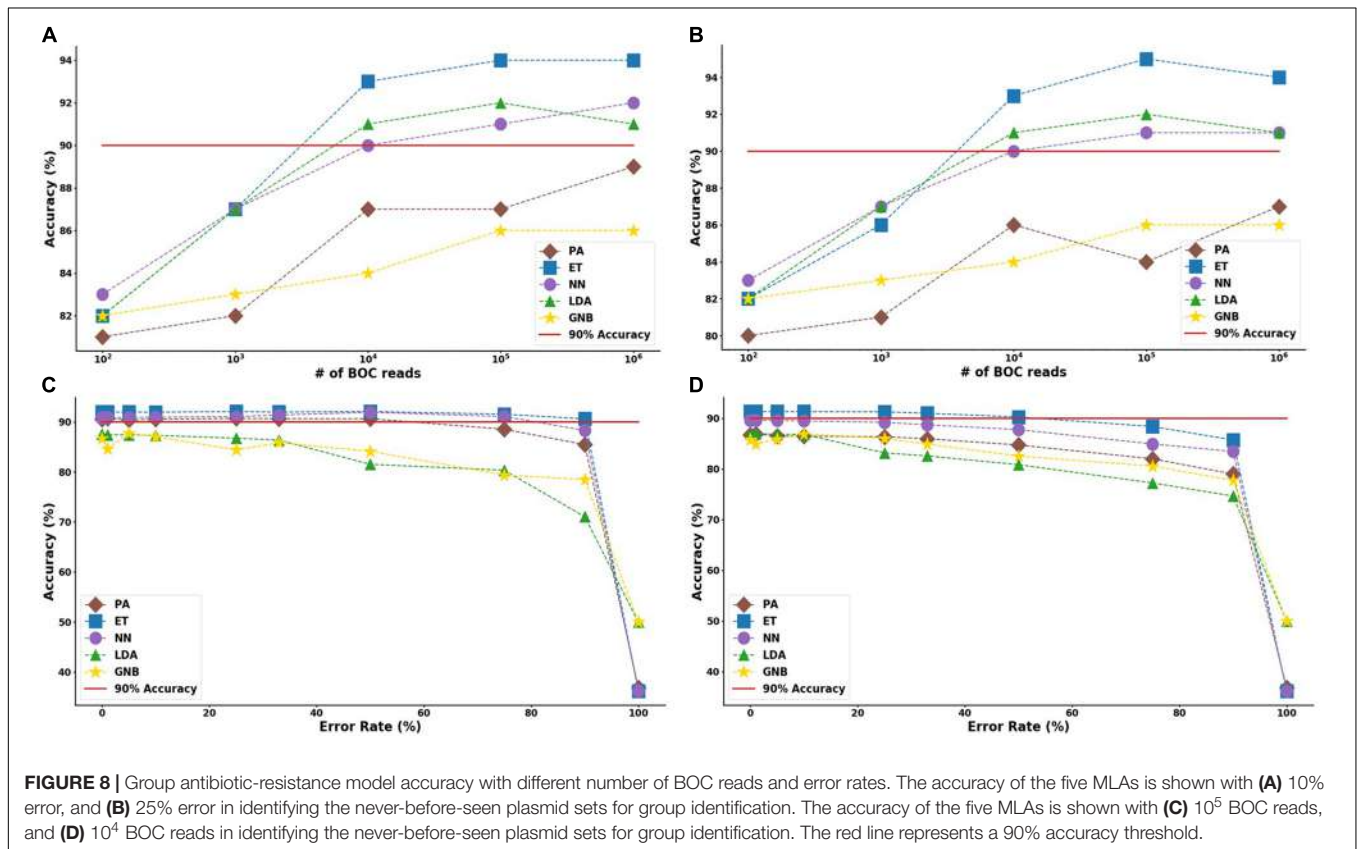
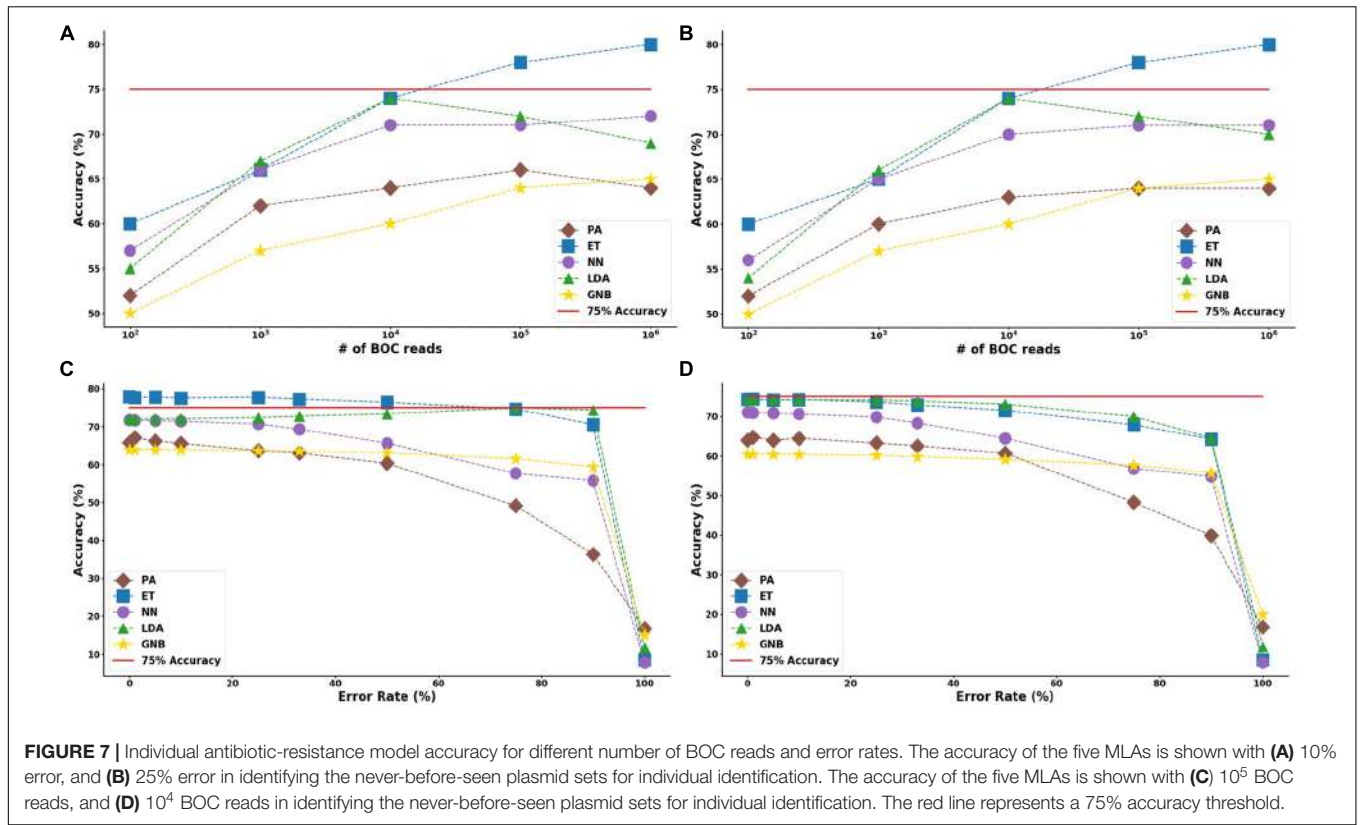
The sensitivity rate at  $10^5$  BOC reads and 10% error is the values on the diagonal on the confusion matrices shown in **Figures 9, 10**. The clinically important false negative rates at  $10^5$  BOC reads with 10% error from the individual carbapenem resistance identification are 0.50% for LDA, 1.00% for ET, 1.25% for NN, 2.50% for PA, and 4.75% for GNB. The false-negative rates at  $10^5$  BOC reads with 10% error from the grouped carbapenem resistance identification are 2.6% for LDA, 4.5% for ET, 5.4% for NN, 5.9% for GNB, and 8.2% for PA. Thus, the LDA MLA appears best at avoiding false-negative errors when identifying resistance genes on plasmids, while the ET most accurately identifies the resistance genes.

## DISCUSSION

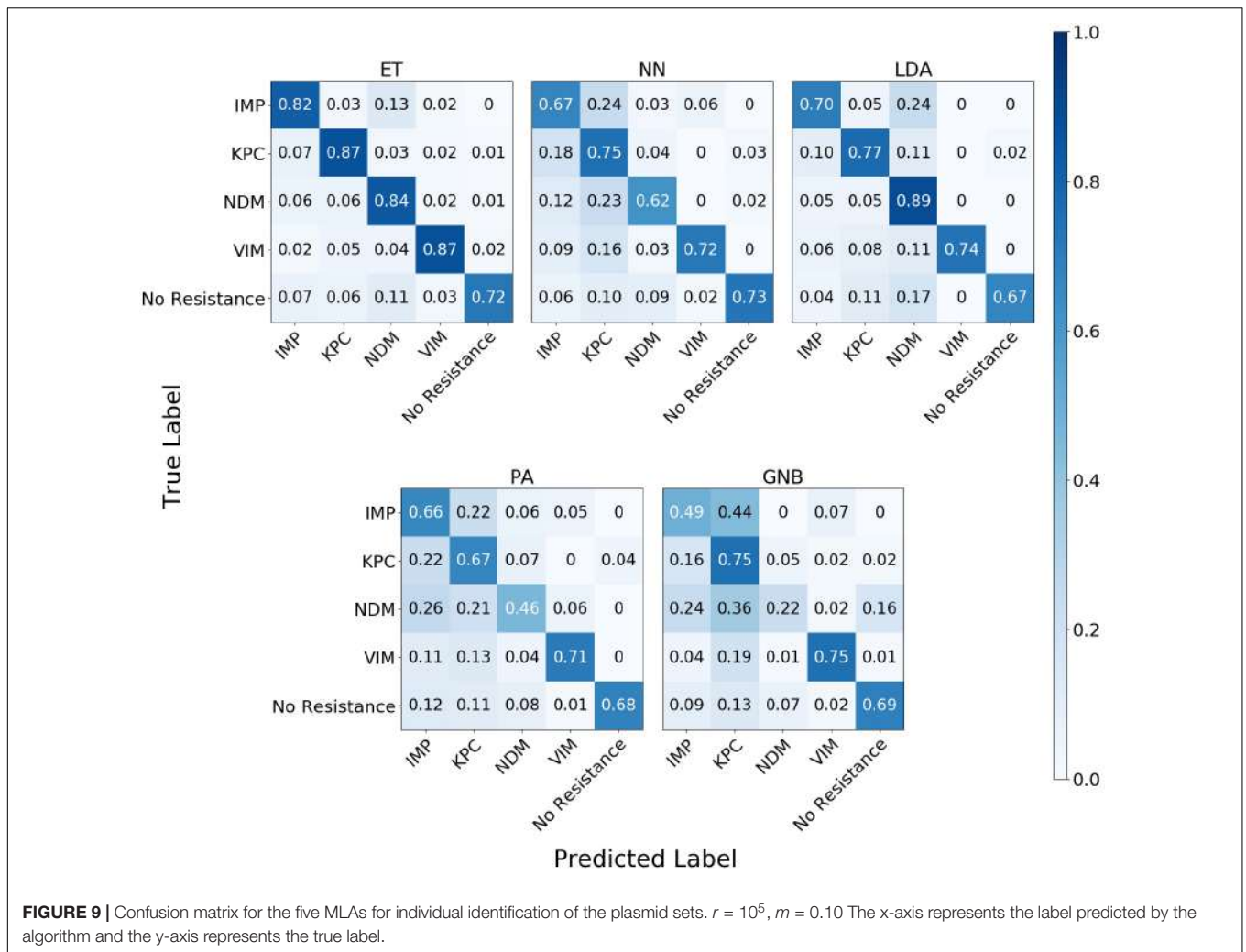
This research is the first of its kind and validates the SERS-BOC instrument (currently in development) as an excellent predictor of genetic signatures, even in the presence of genetic mutations and experimental noise. The use of FBC deviation spectra was able to achieve greater than 99% accuracy in classifying bacterial species using several types of MLAs.

We were able to detect individual antibiotic resistance genes on plasmids from their FBC deviation spectra with 80% accuracy and to detect the presence of a carbapenem resistance gene with 94% accuracy using MLAs. The implications of our research suggest that the use of MLA classifiers on fractional base composition data generated from a SERS-BOC type instrument (Sagar et al., 2018) has tremendous potential in accurately identifying both bacterial species and antibiotic resistance genes. With respect to bloodstream infection diagnosis, the creation of FBC models has the potential to help determine the bacterial species and the antibiotic-resistance profile associated with a bloodstream infection in a cost-efficient and time-efficient way, thus improving the outcomes for patients. Of most import, the false negative evaluations for carbapenem resistance genes were less than 3% using the LDA algorithm with  $10^5$  BOC reads.

We note with surprise the lack of spread within a species data cluster in PCA analysis even when introducing a 25% error rate. This indicates that the inclusion of error does not introduce enough variance to cause these species to have overlap in the principal component space until the number of BOC reads get low ( $10^2$  and  $10^3$  reads). Because we are sampling at least a million different *k*-mers to generate the FBC spectrum, the distribution of any single training sample does not deviate significantly from the FBC of the non-mutated genome. The high number of reads available on a 1-million-pyramid SERS array would enable this high predictive ability, and may be more than necessary. Even with experimental error causing deviation from the reference FBC, the FBCs of different species are distinct







enough that the simulated experimental noise had no negative effect on clustering in principal component space. The random error in BOC data from genomic mutation and experimental noise in the FBC spectra are subtracted out since we know what the random spectrum looks like. Thus, random errors reduce the signal levels but have little effect on noise levels.

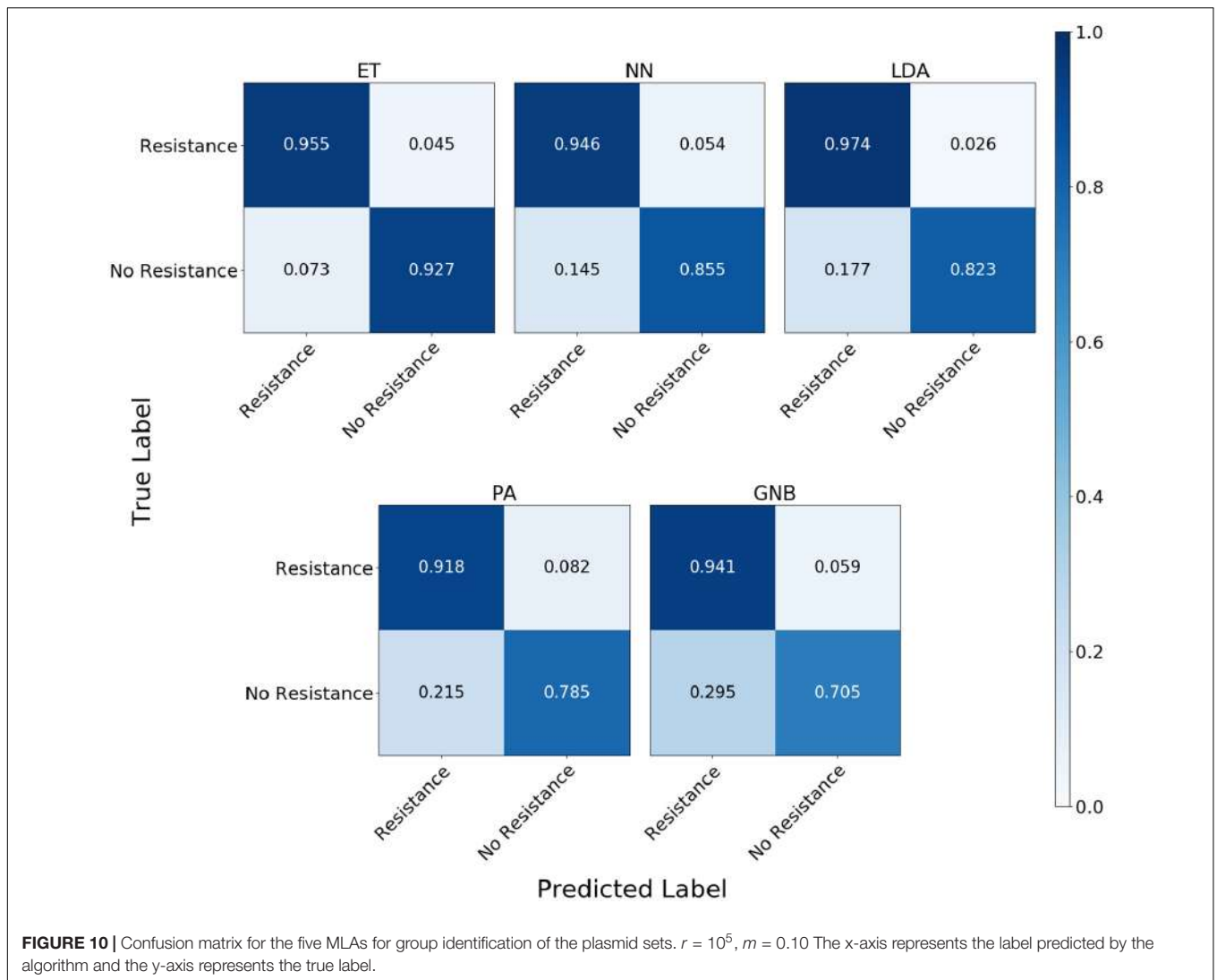
The MLA analysis shows how robust the species model is at handling experimental noise in the FBC, allowing for substantial error rates while maintaining its predictive power. Again, one reason why the model can still accurately classify species even with high error rates is that the experimental noise mimics the random bias distribution. Since we subtract out this random bias before running the machine learning classifier, we are essentially “subtracting out” the effects of the mutation or noise, and what is left is a smaller size of the accurate FBC, which the MLA can still use to accurately classify the species of bacteria. For example,  $10^6$  BOC reads with 90% random errors still leaves  $10^5$  good reads once the randomness is subtracted.

This study challenged the algorithms with much more random error in the data than expected in actual experiments. The largest source of error is anticipated to be wrong assignment of the

BOC values due to spectroscopic noise. Currently the accuracy of calling correct BOC is about 90% (Sagar et al., 2018), but accuracy is improving with time and experience and optical quality. Thus 25% error is probably a gross overestimate of actual experimental error, which we anticipate will be on the order of 10% or less. Random point mutations in bacteria are far less than 0.1% and have no bearing on the accuracy of species identification.

Plasmids come in all different sizes ranging from 2,000 to 200,000 bp long (and longer), and the carbapenem-resistant genes are about 800 bp. This means that the FBC that comes from the resistant genes has varying weight upon the FBC spectrum of the entire plasmid, which would explain why there is so much spread from one resistant plasmid to another in the PCA analysis. The ability for the MLAs to learn from that 800-bp region amongst all of the other data and noise shows great promise for this type of antibiotic resistance gene identification. Overall, the never-before-seen results show that the good performance of the models is not a result of overfitting; rather, the models are actually learning how to recognize the characteristic signatures in an FBC deviation spectrum when a specific target gene is included. Of course the application of the algorithm for antibiotic resistance





identification requires knowledge of an antibiotic resistance gene sequence, so this technique would not identify novel antibiotic resistance evolved by mutations.

In a real-world application, these models would need to be tuned to perform optimally, but the low sensitivity of the accuracy to error rates ranging from 0 to 90% proves the robustness of the models in dealing with noise. As previously stated, we postulate that this robustness stems from the subtraction of randomness from within the data set. A high number of BOC reads with high random error is similar to a model having less SERS-BOC readings, which our results show is still effective down to the  $10^4$  BOC reads. Additional sources of error in a real-world setting could include DNA contamination (human or bacterial), lack of good separation between plasmids and genomes (which would make the resistant genes on plasmids less distinguishable), and untested or new bacterial species causing the blood infections. We anticipate the continued development of the SERS-BOC instrument that will provide real BOC data from which FBC data can be created to further test our assumptions and postulates.

Further application of this method could go beyond analyzing bacterial bloodstream infections into other clinical scenarios that need fast and reliable analysis of only a few key genes of known sequence.

There are known limitations to this study. The first and foremost is that all of the data had to be simulated because a large enough device to produce experimental data are still being developed. Another limitation is that only a single group of antibiotic resistance genes (carbapenem resistant genes) was tested. Therefore, the results cannot be broadcasted to other groups of resistance genes or to identifying other genes. Also, this technique can only identify antibiotic resistance through known DNA sequences. Another limitation is the limited number of bacterial species used. Because of the focus on testing the technology for clinical use in bloodstream infections, a select group of bacterial species was used for this initial study. Future studies will test the ability of this technique to identify between all species. This study also did not tune the MLAs or perform a cost-benefit analysis to identify the factors influencing the accuracy of

the MLAs. However, this study provides the initial groundwork for further exploration in using a SERS-BOC device to identify species and genes based on 10-mer DNA sequences.

## DATA AVAILABILITY STATEMENT

All datasets generated for this study are included in the article/**Supplementary Material**.

## AUTHOR CONTRIBUTIONS

RW contributed to the concept, ran the simulations, and contributed to the writing. TJ and CW contributed to the concept and ran initial simulations. MC advised the simulations and contributed to the writing. PN contributed to

the concept and contributed to the writing. WP contributed to the concept, advised the simulations, and contributed to the writing.

## ACKNOWLEDGMENTS

RW acknowledges some graduate student stipend from NIH grant R01AI116989 and the Chemical Engineering Department at Brigham Young University.

## SUPPLEMENTARY MATERIAL

The Supplementary Material for this article can be found online at: <https://www.frontiersin.org/articles/10.3389/fmicb.2020.00257/full#supplementary-material>

## REFERENCES

- Alizadeh, M., Wood, R. L., Buchanan, C. M., Bledsoe, C. G., Wood, M. E., McClellan, D. S., et al. (2017). Rapid separation of bacteria from blood - Chemical aspects. *Colloids Surf. B Biointerfaces* 154, 365–372. doi: 10.1016/j.colsurfb.2017.03.027
- Bao, J., and Bawendi, M. G. (2015). A colloidal quantum dot spectrometer. *Nature* 523, 67–70. doi: 10.1038/nature14576
- Denamur, E., Bonacorsi, S., Giraud, A., Duriez, P., Hilali, F., Amorin, C., et al. (2002). High frequency of mutator strains among human uropathogenic *Escherichia coli* isolates. *J. Bacteriol.* 184, 605–609. doi: 10.1128/jb.184.2.605-609.2002
- Denamur, E., and Matic, I. (2006). Evolution of mutation rates in bacteria. *Mol. Microbiol.* 60, 820–827. doi: 10.1111/j.1365-2958.2006.05150.x
- Korshoj, L. E., and Nagpal, P. (2019). BOCS: DNA k-mer content and scoring for rapid genetic biomarker identification at low coverage. *Comput. Biol. Med.* 110, 196–206. doi: 10.1016/j.combiomed.2019.05.022
- Kumar, A., Ellis, P., Arabi, Y., Roberts, D., Light, B., Parrillo, J. E., et al. (2009). Initiation of inappropriate antimicrobial therapy results in a fivefold reduction of survival in human septic shock. *Chest* 136, 1237–1248. doi: 10.1378/chest.09-0087
- Kumar, A., Roberts, D., Wood, K. E., Light, B., Parrillo, J. E., Sharma, S., et al. (2006). Duration of hypotension before initiation of effective antimicrobial therapy is the critical determinant of survival in human septic shock. *Crit. Care Med.* 34, 1589–1596. doi: 10.1097/01.CCM.0000217961.75225.E9
- Lever, J., Krzywinski, M., and Atman, N. (2017). Principal component analysis. *Nature Methods* 14, 641–642. doi: 10.1038/nmeth.4346
- Morton, J. T., Toran, L., Edlund, A., Metcalf, J. L., Lauber, C., and Knight, R. (2017). Uncovering the horseshoe effect in microbial analyses. *mSystems* 2:e00166-e16. doi: 10.1128/mSystems.00166-16
- O'Leary, N. A., Wright, M. W., Brister, J. R., Ciufu, S., Haddad, D., McVeigh, R., et al. (2016). Reference sequence (RefSeq) database at NCBI: current status, taxonomic expansion, and functional annotation. *Nucleic Acids Res.* 44, D733–D745. doi: 10.1093/nar/gkv1189
- Patel, G., Huprikar, S., Factor, S. H., Jenkins, S. G., and Calfee, D. P. (2008). Outcomes of carbapenem-resistant *Klebsiella pneumoniae* infection and the impact of antimicrobial and adjunctive therapies. *Infect Control Hosp. Epidemiol.* 29, 1099–1106. doi: 10.1086/592412
- Pedregosa, F., Varoquaux, G., Gramfort, A., Michel, V., Thirion, B., Grisel, O., et al. (2011). Scikit-learn: machine learning in python. *J. Mach. Learn. Res.* 12, 2825–2830.
- Pitt, W. G., Alizadeh, M., Blanco, R., Hunter, A. K., Bledsoe, C. G., McClellan, D. S., et al. (2019). Factors affecting sedimentational separation of bacteria from blood. *Biotechnol. Prog.* 19, e2892. doi: 10.1002/btpr.2892
- Pitt, W. G., Alizadeh, M., Husseini, G. A., McClellan, D. S., Buchanan, C. M., Bledsoe, C. G., et al. (2016). Rapid separation of bacteria from blood-review and outlook. *Biotechnol. Prog.* 32, 823–839. doi: 10.1002/btpr.2299
- Powers, D. M. W. (2011). Evaluation: from precision, recall and f-measure to roc, informedness, markedness & correlation. *J. Mach. Learn. Technol.* 2, 37–63. doi: 10.9735/2229-3981
- Sagar, D. M., Korshoj, L. E., Hanson, K. B., Chowdhury, P. P., Otoupal, P. B., Chatterjee, A., et al. (2018). High-throughput block optical DNA sequence identification. *Small* 14:1703165 doi: 10.1002/smll.201703165
- van Dijk, E. L., Jaszczyszyn, Y., Naquin, D., and Thermes, C. (2018). The third revolution in sequencing technology. *Trends Genet.* 34, 666–681. doi: 10.1016/j.tig.2018.05.008

**Conflict of Interest:** The authors declare that the research was conducted in the absence of any commercial or financial relationships that could be construed as a potential conflict of interest.

Copyright © 2020 Wood, Jensen, Wadsworth, Clement, Nagpal and Pitt. This is an open-access article distributed under the terms of the Creative Commons Attribution License (CC BY). The use, distribution or reproduction in other forums is permitted, provided the original author(s) and the copyright owner(s) are credited and that the original publication in this journal is cited, in accordance with accepted academic practice. No use, distribution or reproduction is permitted which does not comply with these terms.



# Essential Metabolic Routes as a Way to ESKAPE From Antibiotic Resistance

Angélica Luana C. Barra<sup>1</sup>, Livia de Oliveira C. Dantas<sup>1</sup>, Luana Galvão Morão<sup>1</sup>, Raíssa F. Gutierrez<sup>1</sup>, Igor Polikarpov<sup>1</sup>, Carsten Wrenger<sup>2\*</sup> and Alessandro S. Nascimento<sup>1\*</sup>

<sup>1</sup> São Carlos Institute of Physics, University of São Paulo, São Carlos, Brazil, <sup>2</sup> Department of Parasitology, Institute of Biomedical Sciences, University of São Paulo, São Paulo, Brazil

## OPEN ACCESS

### Edited by:

Filipa Grosso,  
University of Porto, Portugal

### Reviewed by:

Roberto Contestabile,  
Sapienza University of Rome, Italy  
Andrea Mozzarelli,  
University of Parma, Italy

### \*Correspondence:

Carsten Wrenger  
cwrenger@icb.usp.br  
Alessandro S. Nascimento  
asnascimento@ifsc.usp.br

### Specialty section:

This article was submitted to  
Infectious Diseases - Surveillance,  
Prevention and Treatment,  
a section of the journal  
Frontiers in Public Health

**Received:** 28 October 2019

**Accepted:** 27 January 2020

**Published:** 28 February 2020

### Citation:

Barra ALC, Dantas LOC, Morão LG, Gutierrez RF, Polikarpov I, Wrenger C and Nascimento AS (2020) Essential Metabolic Routes as a Way to ESKAPE From Antibiotic Resistance. *Front. Public Health* 8:26. doi: 10.3389/fpubh.2020.00026

Antibiotic resistance is a worldwide concern that requires a concerted action from physicians, patients, governmental agencies, and academia to prevent infections and the spread of resistance, track resistant bacteria, improve the use of current antibiotics, and develop new antibiotics. Despite the efforts spent so far, the current antibiotics in the market are restricted to only five general targets/pathways highlighting the need for basic research focusing on the discovery and evaluation of new potential targets. Here we interrogate two biosynthetic pathways as potentially druggable pathways in bacteria. The biosynthesis pathway for thiamine (vitamin B1), absent in humans, but found in many bacteria, including organisms in the group of the ESKAPE pathogens (*Enterococcus faecium*, *Staphylococcus aureus*, *Klebsiella pneumoniae*, *Acinetobacter baumannii*, *Pseudomonas aeruginosa*, and *Enterobacter* sp.) and the biosynthesis pathway for pyridoxal 5'-phosphate and its vitamers (vitamin B6), found in *S. aureus*. Using current genomic data, we discuss the possibilities of inhibition of enzymes in the pathway and review the current state of the art in the scientific literature.

**Keywords:** ESKAPE pathogens, thiamine, pyridoxal 5'-phosphate, antibiotic resistance, vitamin biosynthesis

## INTRODUCTION

Antibiotic resistance is an urgent threat to human health and requires urgent actions from physicians, patients, industries, governmental agencies, and the academic community worldwide. According to the last document from the Centers for Disease Control and Prevention (CDC) regarding antibiotic resistance in the United States, from 2013, the number of people with serious infections caused by resistant bacteria reaches 2 million every year, with at least 23,000 deaths per year directly caused by these infections (1). The situation is similarly warning in Europe, where 25,100 deaths were reported from the European Center for Disease Prevention and Control in 2007 (2). Globally, 700,000 deaths are estimated every year as a consequence of antibiotic resistance (3). The same CDC document lists four general action lines to address antibiotic resistance: (i) preventing infections and the spread of resistance; (ii) tracking resistant bacteria; (iii) improving the use of current antibiotics; and (iv) developing new antibiotics (1).

Since bacteria have a short doubling time and efficient mechanisms for plasmid sharing, the development of antibiotic resistance is a very efficient defense mechanism. So, as previously said by Walsh and Wencewicz, the development of resistance is not a matter of *if*, but rather a matter of

when (4), and despite the title of this paper (which is rather provocative), there is no way we can escape from it (5). On the contrary, the development/discovery of new antibiotics will tend to be a continuous goal to be achieved in drug discovery pipelines.

Interestingly, even after what has been named as the “golden age” of antibiotic development, the drugs currently in the market are restricted to only five molecular targets and/or pathways (4): (i) the peptidoglycan/cell wall biosynthesis, site of action of beta-lactam antibiotics, for example; (ii) the protein biosynthesis, where the ribosome is an important target; (iii) DNA replication and RNA transcription; (iv) the folate biosynthesis pathway, and (v) the disruption of the bacterial membrane. Given the relevance of antibiotic therapy and the emergence of antibiotic resistance, the available choices of current drugs are very narrow in the context of the mechanism of action restricted to only five molecular/pathway targets.

Antibiotic resistance, as a threat to human health, should be addressed in multiple and simultaneous ways. For the academia, an interesting way to address antibiotic resistance is the discovery and validation of new targets/pathways that could be specifically targeted by new antibiotic candidates. It is worthy of note that, according to Kelly and Davies (3), no new class of antibiotics was discovered and released for routine treatment since the 1980s, highlighting the outstanding role that the academia can have in the preliminary research for discovery and validation of druggable targets/pathways.

About 7% of the *Escherichia coli* genome, 303 genes, were shown to be composed of essential genes (5, 6). Under stress conditions caused by a limited medium, additional 119 genes show some condition-dependent essentiality, including several genes related to the metabolism and synthesis of essential molecules such as amino acids and nucleotides (5), and obviously, some of these targets/pathways can be interesting choices for the development of new antibiotic candidates. A promising approach to screen compounds for their activity in metabolic pathways was shown by Zlitni et al. (7). The authors searched for antibacterial compounds under poor nutrient media and found three potential compounds in this screening strategy (7). Worthy of note, the metabolic profile of existing antibiotics showed that the supplementation of vitamins B5, B6, B1, and B2 did not significantly reverse the antimicrobial effect of any of the 24 inhibitors assayed (7), suggesting that the current antibiotics do not explore these essential pathways.

In this context, the enzymatic routes for the biosynthesis of vitamins are very interesting pathways to be explored as potential targets for the discovery of new antibiotic candidates. Vitamin B1, for example, cannot be synthesized by humans, although several microorganisms can synthesize this vitamin, including pathogens. In the absence of thiamin (vitamin B1), the activity of several carbohydrate metabolism enzymes is impaired, including pyruvate dehydrogenase, which connects glycolysis and the citric acid cycle (8). Other thiamin-dependent enzymes are transketolase,  $\alpha$ -ketoacid decarboxylase,  $\alpha$ -ketoacid dehydrogenase, and acetolactate synthase (9). A very similar scenario was observed for pyridoxal 5'-phosphate (vitamin B6) in the model Gram-positive organism *Bacillus subtilis* (10).

The pathways involved in the synthesis of vitamins, in particular, vitamin B1 (thiamin) and B6 (pyridoxal), seem to be of great relevance, since they are involved in central processes in the metabolism of carbohydrates and amino acids, and the corresponding enzymes are found in most bacteria, fungi, and plants but not in humans (8), favoring the development of specific drugs with minimal side effects due to the interaction with the host. However, a few questions still stand: (i) How feasible are the targets involved in the pathways for the biosynthesis of thiamin and pyridoxal for the microorganisms with a higher emergency in terms of resistance, or ESKAPE (*Enterococcus faecium*, *Staphylococcus aureus*, *Klebsiella pneumoniae*, *Acinetobacter baumannii*, *Pseudomonas aeruginosa*, and *Enterobacter* sp.)? (ii) What enzymes are present, and what do we know about them?

Here we used the available genomic and proteomic data to address these questions focusing on the ESKAPE pathogens. Vitamins B1 and B6 were chosen for this analysis, since the biosynthetic pathways for these enzymes have already been validated as molecular targets for some human pathogens, such as thiamin for *Plasmodium falciparum* (11), or pyridoxal for *P. falciparum* (12) or *Trypanosoma brucei* (13), for example.

## METHODS

The analyses provided here are the result of the interrogation of the enzymes in the biosynthesis pathways for thiamin and pyridoxine phosphate or pyridoxal phosphate using the KEGG database (14, 15). For this purpose, the KEGG pathway for thiamin metabolism (map 00730) was listed for the ESKAPE pathogens using, whenever possible, commercial strains rather than specific or antibiotic-resistant strains. Briefly, for each pathogen (*E. faecium*, *S. aureus*, *K. pneumoniae*, *A. baumannii*, *P. aeruginosa*, and *Enterobacter* species), a KEGG search for the maps of thiamin and pyridoxal metabolism was done, looking for the existing genes in commercial strains for each of the ESKAPE organisms. For the sake of comparison, some additional resistant strains were listed, with no differences in the observed genes for the pathways under study. A similar search was carried out for vitamin B6 metabolism (map 00750) in KEGG, interrogating the existing enzymes for the ESKAPE pathogens in comparison with humans. The analysis was focused in the enzymes in the biosynthesis of B1 and B6 vitamins in an attempt to identify the most promising targets for future medicinal chemistry studies. Finally, a table listing the existing genes for each pathogen was compiled and is presented in the following sections.

Using the existing literature, we sought to identify whenever possible the cases of enzymes with functional redundancy with another enzyme for the same organism. The identified cases were discussed as less promising targets for medicinal chemistry campaigns. Additionally, the existing data for enzyme inhibition using natural or synthetic compounds was compiled to provide initial proof-of-concept clues about the *druggability* of the identified promising targets.

When necessary, the sequence of an enzyme of the pathway was used to search for homologs using BLAST (16) searches



against the PDB (17) or the non-redundant database of proteins using BLAST default parameters, i.e., minimum expected threshold of 10, a word size of 6, and the BLOSUM62 substitution matrix.

## RESULTS AND DISCUSSION

### Thiamin Biosynthesis

The biosynthesis pathway for thiamin involves two branches, as shown in **Figure 1**. In summary, thiamin is synthesized from 4-amino-5-hydroxymethyl-2-methylpyrimidine (HMP) (superior branch in **Figure 1**) and 5-(2-hydroxyethyl)-4-methylthiazole (THZ, inferior branch). Both compounds are phosphorylated by ThiD and ThiM, respectively. Finally, the enzyme ThiE, central to the pathway, is responsible for synthesizing thiamine phosphate (TMP) by merging the two branches (18). Thiamin phosphate can be dephosphorylated to thiamine and then pyrophosphorylated to thiamin diphosphate (TPP) by TPK. Alternatively, thiamin can be degraded to HMP and THZ by TenA, a thiaminase II enzyme.

According to the KEGG pathway database, humans lack many of the enzymes of this pathway, but not all of them. In humans, a TPK (TPK1) enzyme is found, with UNIPROT ID Q9H3S4. Other than that, the remaining enzymes in the biosynthetic pathway for thiamin are missing in humans, making them very attractive for the design of chemical probes that could be used as proof-of-concept compounds.

The analysis of the thiamin pathway for *E. faecium* (ATCC 8459) in the KEGG database did not identify genes for ThiE, ThiM, and TenA. For this species, only ThiD and TPK were positively identified. However, a BLAST search for TenA homologous within the non-redundant database restricted to *E. faecium* (TAXID 1352) identified a single result for thiaminase II (GenBank: SAM74984.1), four results for ThiE (SAZ10134.1, WP\_086323306.1, WP\_010732763.1, and WP\_072538983.1), and two results for ThiM (SAZ10238.1, EJY48288.1). The small number of hits in the BLAST search may suggest some issues in the annotation.

Interestingly, when the *Enterococcus faecalis* thiamin pathway is compared with the pathway observed for *E. faecium*, many differences are found. The KEGG pathway for *E. faecalis* (ATCC 29212) shows that the entire pathway, as described in **Figure 1**, is found: ThiD, ThiM, ThiE, TPK, and TenA, in contrast with *E. faecium*. Additionally, there is no change in the repertoire of enzymes in the pathway for the Vancomycin-resistant strain V583 compared to the ATCC 29121 strain.

For *S. aureus* (NCTC 8325) and *K. pneumoniae* (subsp. pneumoniae ATCC 43816 KPPR1), the KEGG pathway indicates that all the enzymes in the pathway are observed, with no changes to an *S. aureus*-resistant strain such as COL (MRSA) compared to the NCTC 8325. For *A. baumannii* (ATCC 14978), all enzymes are observed but TPK. Instead, thiamin phosphate may be converted directly to thiamin diphosphate by a thiamin-monophosphate kinase, and then converted to thiamin triphosphate by an adenylate kinase. In the case of *P. aeruginosa* (NCGM 1900), some enzymes are missing: ThiD, TenA, TPK.

Finally, *Enterobacter* sp. (638) has ThiD, ThiE, ThiM and misses TenA and TPK.

The overall panel of enzymes for the thiamin pathway for the ESKAPE pathogens is summarized in **Table 1**.

TenA was shown to play a dual role in thiamine synthesis and salvage (19): beyond its function to hydrolyze thiamin, TenA also deaminates aminopyrimidine to form 4-amino-5-hydroxymethyl-2-methylpyrimidine (HMP), with the latter activity being about 100 times faster than the former (19, 20). In some organisms, such as *Bacillus subtilis*, the deaminase activity is somewhat redundant with the ThiC (ThiA) activity, since both activities provide HMP or HMP phosphate, which can be further phosphorylated by ThiD (9).

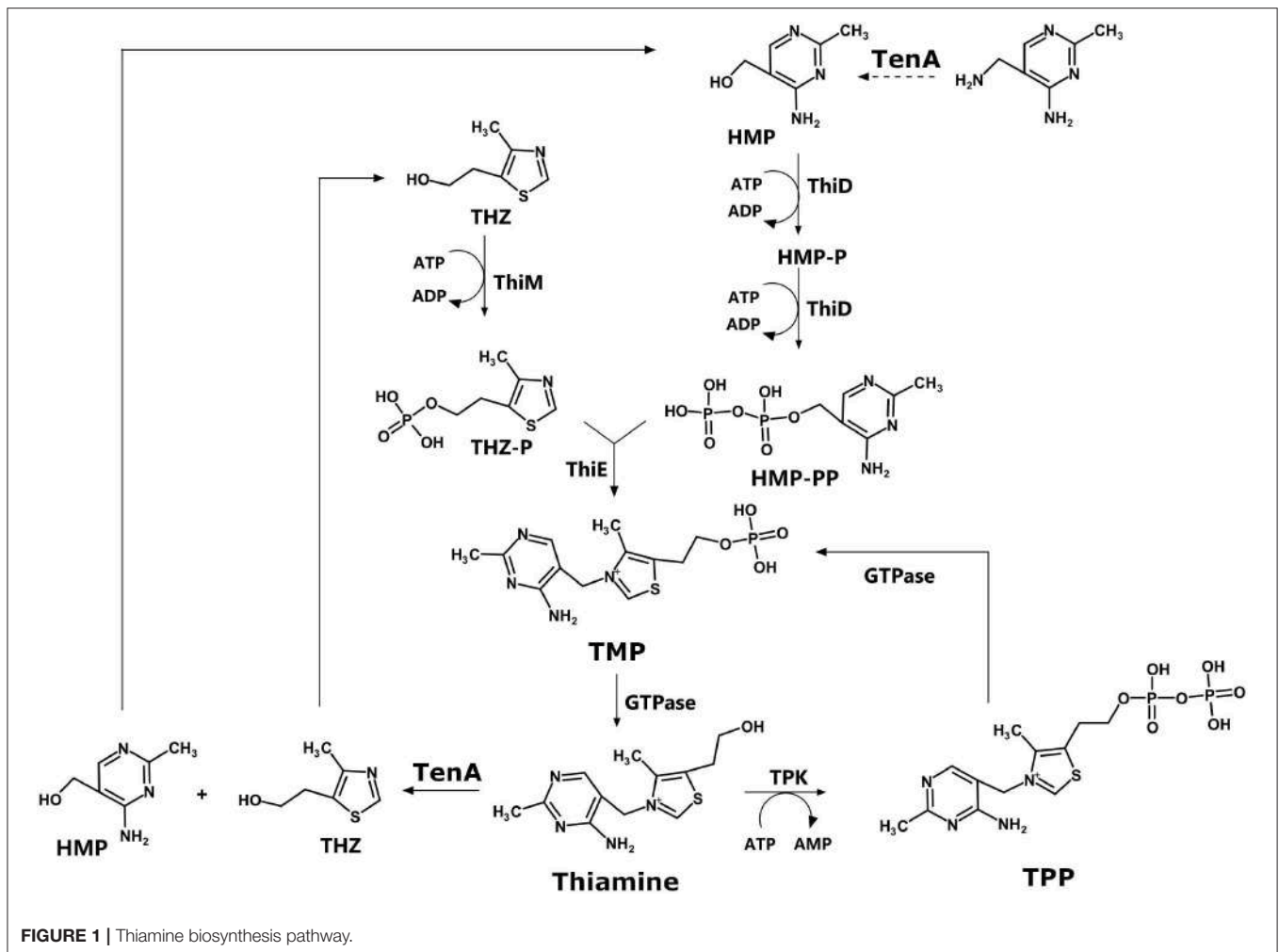
In the other branch of the thiamin biosynthesis pathway, thiazole phosphate can be generated from thiazole alcohol incorporated from the medium and phosphorylated by ThiM, or it can be synthesized in a series of enzymatically catalyzed reactions using amino acids such as glycine or tyrosine as substrates (9). In this context, according to Begley and coworkers (9), lesions in the ThiM gene were observed to be prototrophic. In contrast, selective mutations of ThiD and ThiE led to the requirement of externally provided thiamin (9).

ThiE is central to the pathway since the enzyme merges the two branches to finally synthesize thiamin phosphate (**Figure 1**). It is important to highlight that many of the mutational analysis was carried out in *E. coli*, and as **Table 1** shows, there is significant variance among bacterial species.

Taking together, the analysis of the literature suggests that ThiD and ThiE may represent interesting targets for the development of chemical probes to further evaluate their function. TPK is expressed in humans, and the inhibition of this enzyme could lead to harmful effects on the human host. TenA inhibition could be overcome by the somewhat functional redundancy with thiC (thiA), and ThiM function can be dispensable since thiazole phosphate can be synthesized *de novo*.

ThiD and ThiE are found in most ESKAPE organisms. Exceptions are *P. aeruginosa*, which lacks ThiD, and *E. faecium*, which lacks ThiE, according to the KEGG data. For ThiE, in particular, it was reported that 4-amino-2-trifluoromethyl-5-hydroxymethylpyrimidine (CF<sub>3</sub>-HMP), an HMP analog, can be converted by ThiD to CF<sub>3</sub>-HMP pyrophosphate, which in turn inhibits ThiE (8, 21). This enzymatic inhibition culminated with the inhibition of *E. coli* growth (8), suggesting that this strategy might be promising for the development of new inhibitors.

In terms of structural biology, some crystal structures of ThiD are available by the time of writing of this paper, including the enzymes from *Salmonella enterica* [PDB ID 1JXH (22)], *Clostridioides difficile* (PDB ID 4JJP), *B. subtilis* [PDB ID 2I5B (23)], *Thermus thermophilus* (PDB ID 1UB0), *A. baumannii* (PDB ID 4YL5), *Bacteroides thetaiotaomicron* (PDB ID 3MBH), and the bifunctional enzyme from *Saccharomyces cerevisiae* (PDB ID 3RM5). Typically, ThiDs are folded as typical ribokinases, with a central eight-stranded  $\beta$ -sheet surrounded by eight  $\alpha$ -helices, and structural studies suggest that some surface loops may have a structural change based on the presence of the nucleotide (23).



**TABLE 1 |** Panel of observed enzymes for the thiamine pathway in ESKAPE pathogens.

Enzyme	<i>Enterococcus faecium</i> (ATCC 8459)	<i>Staphylococcus aureus</i> (NCTC 8325)	<i>Klebsiella pneumoniae</i> (subsp. <i>pneumoniae</i> ATCC 43816 KPPR1)	<i>Acinetobacter baumannii</i> (ATCC 17978)	<i>Pseudomonas aeruginosa</i> (NCGM 1900)	<i>Enterobacter</i> sp. (638)
ThiD	✓	✓	✓	✓	×	✓
ThiM	×	✓	✓	✓	✓	✓
ThiE	×	✓	✓	✓	✓	✓
TPK	✓	✓	✓	×	×	×
TenA	×	✓	✓	✓	×	×

Interestingly, the *S. aureus* pyridoxal kinase enzyme (*SaPdxK*) has a dual role, phosphorylating pyridoxal and pyridoxine in the pyridoxal *de novo* biosynthesis pathway as well as HMP in the thiamin biosynthesis pathway, with a  $K_M$  almost 20 times greater for HMP than for pyridoxal and  $k_{cat}$  values three times faster for pyridoxal (24). So, *SaPdxK* has some redundancy with *S. aureus* ThiD (*SaThiD*), with less efficiency, though.

*SaThiD* was shown to be potentially inhibited by Rugulactone (Ru0), a natural product, as well as by its derivatives Ru1 and Ru2, with  $IC_{50}$  values ranging from 14 to 32  $\mu M$  (25). In the

absence of thiamine in the medium, the MIC observed for Ru1 was four times lower than in the presence of thiamine for *Listeria monocytogenes* (25), suggesting that the inhibitory effect of Rugulactone is due to ThiD inhibition, although Rugulactone also inhibits other kinases.

For ThiE, the crystal structures of a few enzymes are available, including the enzyme from *Pyrococcus furiosus* (PDB ID 1XI3), *B. subtilis* [PDB IDs 1G4T, 3O15, 3O16, 1G69, 1G4E, 1G67, 1G4P, 1YAD (26)], *Mycobacterium tuberculosis* (3O63), and for the bifunctional enzyme from *Candida glabrata* [PDB IDs 3NL2

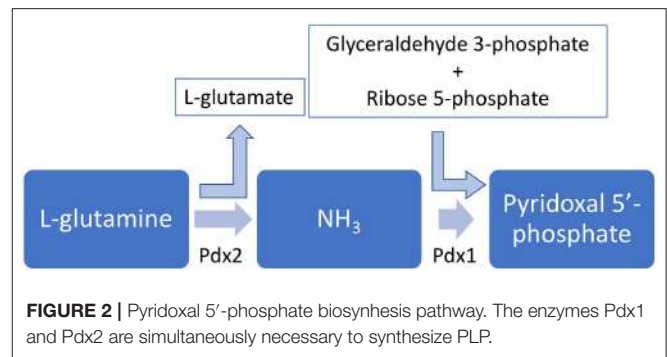
and 3NM1 (27)]. No crystal structure of an ESKAPE pathogen, ThiE, is available to date. From the structural point of view, ThiE is typically folded as an  $\alpha/\beta$  TIM barrel, with thiamine binding at the top of the barrel, as elegantly shown in the set of crystal structures determined for the *B. subtilis* zymase (26).

At this point, an important question has to be addressed: can the blockade of thiamine *de novo* biosynthesis pathway be overcome by internalization of the vitamin? In principle, several microorganisms can import thiamine from the environment (28). So, how effective can the inhibition of ThiD and ThiE be particularly for pathogenic bacteria? This question can be addressed in several levels. On the first level, the essentiality of ThiD, for example, has been shown some pathogenic microorganisms (23), such as *Streptococcus pneumoniae* (29), *Haemophilus influenzae* (30), and *M. tuberculosis* (31). This is not the case for other bacteria. For *B. subtilis*, for example, ThiD gene was shown to be dispensable (23). Whether ThiD and ThiE are essential for the ESKAPE pathogens is still an open question to be addressed by further investigation. On a second level, Nodwell et al. showed that *L. monocytogenes*, which is known to uptake thiamine from the environment, is still sensible to Rugulactone and its derivatives Ru1 and Ru2 (25). When grown in a chemical defined media without thiamine, the inhibitory effects of Rugulactone are potentiated with a 4-fold reduction in the MIC (25). However, the inhibitory effect observed even in the presence of thiamine highlights that the blockade of the *de novo* biosynthesis pathway is still a promising strategy. As a third level, the natural compound bacimethrin, isolated from *Bacillus megaterium* and from *Streptomyces albus* is known to be toxic for bacteria with MIC at a low micromolar range (32, 33). The mechanism of action of bacimethrin is based on the formation of 2'-methoxy-thiamine where bacimethrin is used by ThiD instead of HMP. 2'-Methoxy-thiamine pyrophosphate inhibits *E. coli* growth at concentrations 15 times lower than bacimethrin (32). Interestingly, some *Salmonella enterica* thiD mutants were shown to be bacimethrin resistant (34). Together, these data suggest that a very promising approach can be devised by the design of suicide drugs, i.e., compounds that are recognized by the enzymes in the pathway but lead to final compounds that cannot be used as thiamine substituents. Bacimethrin is a good example of a suicide inhibitor, and although its effects can be reverted by increased thiamine concentrations, the vitamin concentration that pathogens are exposed to is usually defined within a narrow range.

## Pyridoxal Biosynthesis

Pyridoxal, pyridoxine, and pyridoxamine, together with their respective phosphate esters, compose the six vitamers for vitamin B6 and can be interconverted (35). There are two biosynthetic routes for pyridoxal 5'-phosphate: a deoxyxylulose 5-phosphate-dependent pathway found in some bacteria and a deoxyxylulose 5-phosphate-independent pathway found in all kingdoms (35, 36). This second and widespread pathway, curiously, depends on only two enzymes, as shown in **Figure 2**.

In this pathway, the enzyme Pdx2 converts L-glutamine into L-glutamate and an ammonium molecule. The latter is thought to



**FIGURE 2** | Pyridoxal 5'-phosphate biosynthesis pathway. The enzymes Pdx1 and Pdx2 are simultaneously necessary to synthesize PLP.

diffuse to the Pdx1 active site, which also uses glyceraldehyde 3-phosphate and D-ribose 5-phosphate to synthesize pyridoxal 5'-phosphate (35, 37). Interestingly, in order to properly synthesize pyridoxal 5'-phosphate, a complex involving 12 Pdx1 molecules and 12 Pdx2 molecules has to be assembled (38–40), and this assembly is further stabilized by the interaction with L-glutamine (41).

Similar to what is observed to the thiamine biosynthesis pathway, humans lack the genes for Pdx1 and Pdx2, making the development of specific antibiotic candidates an attracting strategy. In the same direction, for some pathogenic organisms such as *Helicobacter pylori* (42), *M. tuberculosis* (43), and *Streptococcus pneumoniae* (44), the depletion in vitamin B6 resulted in reduced virulence, indicating that the biosynthesis of this vitamin may be a good strategy for the design of new antibiotic candidates.

Very interestingly and in contrast to what was observed for the thiamine pathways, from the ESKAPE pathogens, *S. aureus* is the only microorganism that has the ribose 5-phosphate-dependent pathway for the biosynthesis of pyridoxal 5'-phosphate, as shown in **Table 2**. A single enzyme (Pdx1 or Pdx2 alone) is never observed for these organisms (**Table 2**).

A comparison between the pyridoxal/pyridoxine phosphate pathways for *E. faecium* and *E. faecalis* shows that both pathogens miss the Pdx enzymes. On the other hand, some other pathogenic organisms, including organisms with high antibiotic resistance rates, have already been identified as susceptible to modulations of the pyridoxal phosphate biosynthesis pathway. Some organisms that have been the focus of basic research include *P. falciparum* and *Plasmodium vivax*, the malaria pathogens (45–48).

In terms of the structural biology of the enzymes in the vitamin B6 biosynthesis pathway, the *S. aureus* Pdx1 enzyme (UNIPROT ID Q2G0Q1) is a close homolog of *Bacillus subtilis* Pdx1 [81% identity, PDB ID 2NV1 (40)], *Geobacillus stearothermophilus* Pdx1 [78% identity, PDB ID 1ZNN (49)], and *T. thermophilus* enzyme (67% identity, PDB ID 2ZBT). *S. aureus* Pdx2 has *Geobacillus kaustophilus* [PDB ID 4WXY (38)], *G.s stearothermophilus* (PDB ID 1Q7R), and *B. subtilis* [PDB IDs 2NV0 and 2NV2 (40)] enzymes as its close homologs, with 60, 60, and 58% identity in sequence similarity, respectively.

In terms of its structure, the Pdx1 enzyme has a typical ( $\beta/\alpha$ )<sub>8</sub> barrel fold with a central eight-stranded  $\beta$ -barrel surrounded

**TABLE 2** | Panel of observed enzymes for the pyridoxal 5'-phosphate pathway in ESKAPE pathogens.

Enzyme	<i>Enterococcus faecium</i> (ATCC 8459)	<i>Staphylococcus aureus</i> (NCTC 8325)	<i>Klebsiella pneumoniae</i> (subsp. <i>pneumoniae</i> ATCC 43816 KPPR1)	<i>Acinetobacter baumannii</i> (ATCC 17978)	<i>Pseudomonas aeruginosa</i> (NCGM 1900)	<i>Enterobacter</i> sp. (638)
Pdx1	×	✓	×	×	×	×
Pdx2	×	✓	×	×	×	×

by eight  $\alpha$ -helices (49). The most impressive feature in the Pdx1 enzyme structure is its quaternary arrangement, where six Pdx1 enzymes interact with each other to form a “donut-like” arrangement with about 100 Å in diameter. For Pdx2, a Rossman fold is observed with an  $\alpha/\beta/\alpha$  sandwich topology (40). Curiously, in the active PLP synthase complex, 12 Pdx1 molecules (a two-layer donut) interact with 12 Pdx2 enzymes. However, Pdx2 molecules do not interact with each other in this complex (40).

Using a structural homology model, Reeksting et al. identified some ribose 5'-phosphate analogs with interesting *in vitro* inhibitory effects on the enzyme Pdx1 from *P. falciparum* (12). The compounds were identified in a structure-based computational screening campaign and were shown to have inhibitory effects *in vivo*, as well as the *in vitro* effect. The authors also showed that the *in vivo* effects could be at least partially suppressed in a mutant strain overexpressing Pdx1 and Pdx2, in a clear indication that the effect of the analogs was due to their inhibition of the pyridoxal 5'-phosphate biosynthesis pathway (12).

The inhibition of the Pdx2 activity by the glutamine analog acivicin was also demonstrated to be a feasible strategy for the inhibition of the vitamin B6 biosynthesis pathway (50). Raschle et al. showed that when inhibited by acivicin, Pdx2 is incapable of interacting with Pdx1, thus disrupting the pyridoxal 5'-phosphate synthase activity. Interestingly, acivicin is a covalent inhibitor that binds to a cysteine residue. So, it seems that multiple strategies may be available for the design of new binders, including the inhibition of Pdx2 (covalent and non-covalent), the inhibition of Pdx1, and possibly the inhibition of the assembly of the 24-mer complex with Pdx1/Pdx2. Another possibility to address the inhibition of PLP biosynthesis might be at the level of the Pdx1 transcription, which was shown to be regulated by PdxR (44). In principle, if PdxR action could be regulated by an exogenous chemical probe, the PLP synthase activity would be regulated as well. However, a proof-of-concept experimental validation is still necessary.

Finally, a salvage pathway for vitamin B6 is found in many bacteria, as well as in humans. In *E. coli*, it involves two enzymes: PdxK and PdxY. These kinases act by phosphorylating the vitamers pyridoxal, pyridoxine, and pyridoxamine into their phosphorylated forms (23, 35, 51). Interestingly, in some organisms, including pathogenic microorganisms such as *S. aureus*, the PdxK activity is carried out by the HMP kinase ThiD, showing some functional convergence between the vitamin B6 and B1 pathways (24). Not surprisingly, this enzyme has also been shown to be a validated druggable target for

some pathogens, such as *Trypanosoma brucei*, for example (13), although specificity may be an important issue, since humans also have genes for PdxK known to be inhibited by drugs like theophylline, for example, with known neurotoxic effects (52).

Again, the same question asked for the thiamine biosynthesis pathway can be asked here: How can the microbial uptake of vitamin B6 overcome the blockade of the biosynthetic pathway? Some evidence suggested that the blockade might be effective. For example, in *S. pneumoniae*, the deletion of Pdx1 resulted in defective growth of the bacteria. The growth was shown to be restored under increased concentrations of vitamin B6 (44). A similar scenario was also observed for *M. tuberculosis* (43), suggesting that the uptake might not be enough to meet the pathogen's requirement of the vitamin.

In conclusion, the biosynthesis pathways for vitamin B1 (thiamine) and B6 (pyridoxal 5'-phosphate) may be interesting molecular targets for the development of new chemical probes aiming to inhibit the synthesis of these essential cofactors in pathogenic organisms. Model compounds, mainly based on substrate analogs showed that inhibition of the vitamin B1 biosynthetic enzymes, ThiD and ThiE, as well as Pdx1, Pdx2, and PdxK in the pyridoxal 5'-phosphate biosynthesis pathway have shown an initial proof of concept for the model, and it is up to the scientific community and/or researcher in the industry to explore these targets further.

## DATA AVAILABILITY STATEMENT

The datasets generated for this study are available on request to the corresponding authors.

## AUTHOR CONTRIBUTIONS

CW, IP, and AN conceived the project. LM and RG analyzed the thiamine pathway, while AB and LD analyzed the pyridoxal pathway. All authors wrote and approved the manuscript.

## FUNDING

Financial support was provided by Fundação de Amparo à Pesquisa do Estado de São Paulo (FAPESP) through grants 2017/18173-0, 2015/26722-8, and 2015/13684-0 and by Conselho Nacional de Desenvolvimento Científico e Tecnológico (CNPq), through grants 303165/2018-9 and 406936/2017-0.



## ACKNOWLEDGMENTS

The authors thank the funding agencies FAPESP and CNPq. We are also indebted to Maria Auxiliadora M.

Santos, Lívia Regina M. Margarido, Josimar Sartori, and João Fernando Possatto for their technical support. This manuscript has been released as a Pre-Print at BioRxiv (53).

## REFERENCES

- CDC. *Antibiotic Resistance Threats in the USA*. Atlanta, GA: CDC (2013).
- WHO. *Prioritization of Pathogens to Guide Discovery, Research and Development of New Antibiotics for Drug-Resistant Bacterial Infections, Including Tuberculosis*. Geneva: WHO (2017).
- Kelly R, Davies SC. Tackling antimicrobial resistance globally. *Med J Aust.* (2017) 207:371–3.e1. doi: 10.5694/mja17.00865
- Walsh CT, Wenczewicz TA. Prospects for new antibiotics: a molecule-centered perspective. *J Antibiot.* (2013) 67:7–22. doi: 10.1038/ja.2013.49
- Brown ED, Wright GD. Antibacterial drug discovery in the resistance era. *Nature.* (2016) 529:336–43. doi: 10.1038/nature17042
- Baba T, Ara T, Hasegawa M, Takai Y, Okumura Y, Baba M, et al. Construction of *Escherichia coli* K-12 in-frame, single-gene knockout mutants: the Keio collection. *Mol Syst Biol.* (2006) 2:2006.0008. doi: 10.1038/msb4100050
- Zlitni S, Ferruccio LF, Brown ED. Metabolic suppression identifies new antibacterial inhibitors under nutrient limitation. *Nat Chem Biol.* (2013) 9:796–804. doi: 10.1038/nchembio.1361
- Du Q, Wang H, Xie J. Thiamin (vitamin B1) biosynthesis and regulation: a rich source of antimicrobial drug targets? *Int J Biol Sci.* (2011) 7:41–52. doi: 10.7150/ijbs.7.41
- Begley TP, Downs DM, Ealick SE, McLafferty FW, Van Loon APGM, Taylor S, et al. Thiamin biosynthesis in prokaryotes. *Arch Microbiol.* (1999) 171:293–300. doi: 10.1007/s002030050713
- Richts B, Rosenberg J, Commichau FM. A survey of pyridoxal 5'-phosphate-dependent proteins in the gram-positive model bacterium *Bacillus subtilis*. *Front Mol Biosci.* (2019) 6:32. doi: 10.3389/fmolb.2019.00032
- Chan XWA, Wrenger C, Stahl K, Bergmann B, Winterberg M, Müller IB, Saliba KJ. Chemical and genetic validation of thiamine utilization as an antimalarial drug target. *Nat Commun.* (2013) 4:2060. doi: 10.1038/ncomms3060
- Reeksting SB, Müller IB, Burger PB, Burgos ES, Salmon L, Louw AI, et al. Exploring inhibition of Pdx1, a component of the PLP synthase complex of the human malaria parasite *Plasmodium falciparum*. *Biochem J.* (2013) 449:175–87. doi: 10.1042/BJ20120925
- Jones DC, Alphey MS, Wyllie S, Fairlamb AH. Chemical, genetic and structural assessment of pyridoxal kinase as a drug target in the African trypanosome. *Mol Microbiol.* (2012) 86:51–64. doi: 10.1111/j.1365-2958.2012.08189.x
- Kanehisa M. KEGG: Kyoto Encyclopedia of Genes and Genomes. *Nucleic Acids Res.* (2000) 28:27–30. doi: 10.1093/nar/28.1.27
- Kanehisa M, Furumichi M, Tanabe M, Sato Y, Morishima K. KEGG: new perspectives on genomes, pathways, diseases and drugs. *Nucleic Acids Res.* (2017) 45:D353–61. doi: 10.1093/nar/gkw1092
- Camacho C, Coulouris G, Avagyan V, Ma N, Papadopoulos J, Bealer K, et al. BLAST+: architecture and applications. *BMC Bioinformatics.* (2009) 10:1–9. doi: 10.1186/1471-2105-10-421
- Berman HM, Battistuz T, Bhat TN, Bluhm WF, Bourne PE, Burkhardt K, et al. The protein data bank. *Acta Crystallogr Sect D-Biological Crystallogr.* (2002) 58:899–907. doi: 10.1107/S0907444902003451
- Backstrom AD, McMordie RAS, Begley TP. Biosynthesis of thiamin i: the function of the thiE gene product. *J Am Chem Soc.* (1995) 117:2351–2. doi: 10.1021/ja00113a025
- Begum A, Drebes J, Kikhney A, Müller IB, Perbandt M, Svergun D, et al. *Staphylococcus aureus* thiaminase II: Oligomerization warrants proteolytic protection against serine proteases. *Acta Crystallogr Sect D Biol Crystallogr.* (2013) 69:2320–29. doi: 10.1107/S0907444913021550
- Jenkins AH, Schyns G, Potot S, Sun G, Begley TP. A new thiamin salvage pathway. *Nat Chem Biol.* (2007) 3:492–7. doi: 10.1038/nchembio.2007.13
- Reddick JJ, Nicewonger R, Begley TP. Mechanistic studies on thiamin phosphate synthase: evidence for a dissociative mechanism<sup>†</sup>. *Biochemistry.* (2001) 40:10095–102. doi: 10.1021/bi010267q
- Cheng G, Bennett EM, Begley TP, Ealick SE. Crystal structure of 4-amino-5-hydroxymethyl-2-methylpyrimidine phosphate kinase from *Salmonella typhimurium* at 2.3 Å resolution. *Structure.* (2002) 10:225–35. doi: 10.1016/S0969-2126(02)00708-6
- Newman JA, Das SK, Sedelnikova SE, Rice DW. The crystal structure of an ADP complex of *Bacillus subtilis* pyridoxal kinase provides evidence for the parallel emergence of enzyme activity during evolution. *J Mol Biol.* (2006) 363:520–30. doi: 10.1016/j.jmb.2006.08.013
- Nodwell MB, Koch MF, Alte F, Schneider S, Sieber SA. A subfamily of bacterial ribokinases utilizes a hemithioacetal for pyridoxal phosphate salvage. *J Am Chem Soc.* (2014) 136:4992–9. doi: 10.1021/ja411785r
- Nodwell MB, Menz H, Kirsch SE, Sieber SA. Rugulactone and its analogues exert antibacterial effects through multiple mechanisms including inhibition of thiamine biosynthesis. *ChemBioChem.* (2012) 13:1439–46. doi: 10.1002/cbic.201200265
- Peapus DH, Chiu HJ, Campobasso N, Reddick JJ, Begley TP, Ealick SE. Structural characterization of the enzyme-substrate, enzyme-intermediate, and enzyme-product complexes of thiamin phosphate synthase. *Biochemistry.* (2001) 40:10103–114. doi: 10.1021/bi0104726
- Paul D, Chatterjee A, Begley TP, Ealick SE. Domain organization in *Candida glabrata* THI6, a bifunctional enzyme required for thiamin biosynthesis in Eukaryotes. *Biochemistry.* (2010) 49:9922–34. doi: 10.1021/bi101008u
- Manzetti S, Zhang J, van der Spoel D. Thiamin function, metabolism, uptake, and transport. *Biochemistry.* (2014) 53:821–35. doi: 10.1021/bi401618y
- Hava DL, Camilli A. Large-scale identification of serotype 4 *Streptococcus pneumoniae* virulence factors. *Mol Microbiol.* (2002) 45:1389–406. doi: 10.1046/j.1365-2958.2002.t01-1-03106.x
- Akerley BJ, Rubin EJ, Novick VL, Amaya K, Judson N, Mekalanos JJ. A genome-scale analysis for identification of genes required for growth or survival of *Haemophilus influenzae*. *Proc Natl Acad Sci USA.* (2002) 99:966–71. doi: 10.1073/pnas.012602299
- Sasseti CM, Boyd DH, Rubin EJ. Comprehensive identification of conditionally essential genes in mycobacteria. *Proc Natl Acad Sci USA.* (2001) 98:12712–17. doi: 10.1073/pnas.231275498
- Reddick JJ, Saha S, Lee J, Melnick JS, Perkins J, Begley TP. The mechanism of action of bacimethrin, a naturally occurring thiamin antimetabolite. *Bioorg Med Chem Lett.* (2001) 11:2245–48. doi: 10.1016/S0960-894X(01)00373-0
- Breiding-Mack S, Zeeck A, Zahner H. Metabolic products of microorganisms. 239 bacimethrin isolated from *Streptomyces albus* identification, derivatives, synthesis and biological properties. *J Antibiot.* (1987) 40:1431–39. doi: 10.7164/antibiotics.40.1431
- Zilles JL, Croal LR, Downs DM. Action of the thiamine antagonist bacimethrin on thiamine biosynthesis. *J Bacteriol.* (2000) 182:5606–10. doi: 10.1128/JB.182.19.5606-5610.2000
- Mukherjee T, Hanes J, Tews I, Ealick SE, Begley TP. Pyridoxal phosphate: biosynthesis and catabolism. *Biochim Biophys Acta.* (2011) 1814:1585–96. doi: 10.1016/j.bbapap.2011.06.018
- Ehrenshaft M, Bilski P, Li M, Chignell CF, Daub ME. A highly conserved sequence is a novel gene involved in *de novo* vitamin B6 biosynthesis. *Proc Natl Acad Sci USA.* (1999) 96:9374–8. doi: 10.1073/pnas.96.16.9374
- Neuwirth M, Strohmeier M, Windeisen V, Wallner S, Deller S, Rippe K, et al. X-ray crystal structure of *Saccharomyces cerevisiae* Pdx1 provides insights into the oligomeric nature of PLP synthases. *FEBS Lett.* (2009) 583:2179–86. doi: 10.1016/j.febslet.2009.06.009
- Smith AM, Brown WC, Harms E, Smith JL. Crystal structures capture three states in the catalytic cycle of a pyridoxal phosphate (PLP) Synthase. *J Biol Chem.* (2015) 290:5226–39. doi: 10.1074/jbc.M114.626382

39. Guédez G, Hipp K, Windeisen V, Derrer B, Gengenbacher M, Böttcher B, et al. Assembly of the eukaryotic PLP-synthase complex from Plasmodium and activation of the Pdx1 enzyme. *Structure*. (2012) 20:172–84. doi: 10.1016/j.str.2011.11.015
40. Strohmeier M, Raschle T, Mazurkiewicz J, Rippe K, Sinning I, Fitzpatrick TB, et al. Structure of a bacterial pyridoxal 5'-phosphate synthase complex. *Proc Natl Acad Sci USA*. (2006) 103:19284–89. doi: 10.1073/pnas.0604950103
41. Neuwirth M, Flicker K, Strohmeier M, Tews I, Macheroux P. Thermodynamic characterization of the protein-protein interaction in the heteromeric *Bacillus subtilis* pyridoxal phosphate synthase. *Biochemistry*. (2007) 46:5131–39. doi: 10.1021/bi602602x
42. Grubman A, Phillips A, Thibonnier M, Kaparakis-Liaskos M, Johnson C, Thiberge JM, et al. Vitamin B6 is required for full motility and virulence in *Helicobacter pylori*. *MBio*. (2010) 1:1–9. doi: 10.1128/mBio.00112-10
43. Dick T, Manjunatha U, Kappes B, Gengenbacher M. Vitamin B6 biosynthesis is essential for survival and virulence of *Mycobacterium tuberculosis*. *Mol Microbiol*. (2010) 78:980–88. doi: 10.1111/j.1365-2958.2010.07381.x
44. Qaidi S El, Yang J, Zhang JR, Metzger DW, Bai G. The vitamin B6 biosynthesis pathway in streptococcus pneumoniae is controlled by pyridoxal 5'-phosphate and the transcription factor PdxR and has an impact on ear infection. *J Bacteriol*. (2013) 195:2187–96. doi: 10.1128/JB.00041-13
45. Wrenger C, Knöckel J, Walter RD, Müller IB. Vitamin B1 and B6 in the malaria parasite: Requisite or dispensable? *Brazilian J Med Biol Res*. (2008) 41:82–8. doi: 10.1590/S0100-879X2008005000006
46. Kronenberger T, Lindner J, Meissner KA, Zimbres FM, Coronado MA, Sauer FM, et al. Vitamin B6-dependent enzymes in the human malaria parasite plasmodium falciparum: a druggable target? *Biomed Res Int*. (2014) 2014:108516. doi: 10.1155/2014/108516
47. Kronenberger T, Schetter I, Wrenger C. Targeting the vitamin biosynthesis pathways for the treatment of malaria. *Future Med Chem*. (2013) 5:769–79. doi: 10.4155/fmc.13.43
48. Wrenger C, Eschbach ML, Müller IB, Warnecke D, Walter RD. Analysis of the vitamin B6 biosynthesis pathway in the human malaria parasite Plasmodium falciparum. *J Biol Chem*. (2005) 280:5242–8. doi: 10.1074/jbc.M412475200
49. Zhu J, Burgner JW, Harms E, Belitsky BR, Smith JL. A new arrangement of ( $\beta/\alpha$ )8 barrels in the synthase subunit of PLP synthase. *J Biol Chem*. (2005) 280:27914–23. doi: 10.1074/jbc.M503642200
50. Raschle T, Amrhein N, Fitzpatrick TB. On the two components of pyridoxal 5'-phosphate synthase from *Bacillus subtilis*. *J Biol Chem*. (2005) 280:32291–300. doi: 10.1074/jbc.M501356200
51. Newman JA, Das SK, Sedelnikova SE, Rice DW. Cloning, purification and preliminary crystallographic analysis of a putative pyridoxal kinase from *Bacillus subtilis*. *Acta Crystallogr Sect F Struct Biol Cryst Commun*. (2006) 62:1006–9. doi: 10.1107/S1744309106035779
52. Gandhi AK, Desai JV, Ghatge MS, di Salvo ML, Di Biase S, Danso-Danquah R, et al. Crystal structures of human pyridoxal kinase in complex with the neurotoxins, ginkgotoxin and theophylline: insights into pyridoxal kinase inhibition. *PLoS ONE*. (2012) 7:e40954. doi: 10.1371/journal.pone.0040954
53. Barra ALC, Dantas L de OC, Morão LG, Gutierrez RF, Polikarpov I, Wrenger C, et al. Essential metabolic routes as a way to ESKAPE from antibiotic resistance. *bioRxiv*. (2019) 817015. doi: 10.1101/817015

**Conflict of Interest:** The authors declare that the research was conducted in the absence of any commercial or financial relationships that could be construed as a potential conflict of interest.

Copyright © 2020 Barra, Dantas, Morão, Gutierrez, Polikarpov, Wrenger and Nascimento. This is an open-access article distributed under the terms of the Creative Commons Attribution License (CC BY). The use, distribution or reproduction in other forums is permitted, provided the original author(s) and the copyright owner(s) are credited and that the original publication in this journal is cited, in accordance with accepted academic practice. No use, distribution or reproduction is permitted which does not comply with these terms.



# *In vitro* Activity of a New Fourth-Generation Cephalosporin, Cefoselis, Against Clinically Important Bacterial Pathogens in China

## OPEN ACCESS

### Edited by:

Ilana L. B. C. Camargo,  
University of São Paulo, Brazil

### Reviewed by:

Norma Margarita de la Fuente Salcido,  
Universidad Autónoma de Coahuila,  
Mexico  
Helio S. Sader,  
JMI Laboratories, United States

### \*Correspondence:

Qi-Wen Yang  
yangqiwen81@vip.163.com  
Ying-Chun Xu  
xycpumch@139.com

† These authors have contributed equally to this work

### Specialty section:

This article was submitted to Antimicrobials, Resistance and Chemotherapy, a section of the journal *Frontiers in Microbiology*

**Received:** 07 August 2019

**Accepted:** 24 January 2020

**Published:** 28 February 2020

### Citation:

Cheng J-W, Su J-R, Xiao M, Yu S-Y, Zhang G, Zhang J-J, Yang Y, Duan S-M, Kudinha T, Yang Q-W and Xu Y-C (2020) *In vitro* Activity of a New Fourth-Generation Cephalosporin, Cefoselis, Against Clinically Important Bacterial Pathogens in China. *Front. Microbiol.* 11:180. doi: 10.3389/fmicb.2020.00180

Jing-Wei Cheng<sup>1,2†</sup>, Jian-Rong Su<sup>2†</sup>, Meng Xiao<sup>1,3</sup>, Shu-Ying Yu<sup>1,3,4</sup>, Ge Zhang<sup>1,3</sup>, Jing-Jia Zhang<sup>1,3</sup>, Yang Yang<sup>1,3</sup>, Si-Meng Duan<sup>1,3</sup>, Timothy Kudinha<sup>5,6</sup>, Qi-Wen Yang<sup>1,3\*</sup> and Ying-Chun Xu<sup>1,3\*</sup>

<sup>1</sup> Department of Clinical Laboratory, Peking Union Medical College Hospital, Peking Union Medical College, Chinese Academy of Medical Sciences, Beijing, China, <sup>2</sup> Center of Clinical Laboratory, Beijing Friendship Hospital, Capital Medical University, Beijing, China, <sup>3</sup> Beijing Key Laboratory for Mechanisms Research and Precision Diagnosis of Invasive Fungal Diseases (BZ0447), Beijing, China, <sup>4</sup> Graduate School, Peking Union Medical College, Chinese Academy of Medical Sciences, Beijing, China, <sup>5</sup> School of Biomedical Science, Charles Sturt University, Orange, NSW, Australia, <sup>6</sup> Centre for Infectious Diseases and Microbiology Laboratory Services, ICPMR – Pathology West, Westmead Hospital, The University of Sydney, Sydney, NSW, Australia

The objective of this study was to systematically evaluate the *in vitro* activity of cefoselis and other comparators against common bacterial pathogens collected from 18 hospitals across China. Minimum inhibitory concentrations (MICs) were determined by the broth microdilution method following Clinical and Laboratory Standards Institute (CLSI) guidelines. Cefoselis showed poor activity against extended-spectrum  $\beta$ -lactamase (ESBL)-producing *Escherichia coli*, *Klebsiella pneumoniae*, and *Proteus mirabilis*, with susceptibility rates of < 10% each, while the susceptibility rates of this antibiotic against non-ESBL-producing strains of these organisms were 100%, 94.3%, and 97.0%, respectively. Cefoselis exhibited susceptibility rates of 56.7–83.3% against other tested Enterobacteriaceae isolates. For *Acinetobacter baumannii* and *Pseudomonas aeruginosa* isolates, the susceptibility rates to cefoselis were 18.7% and 73.3%, respectively. All methicillin-resistant *Staphylococcus aureus* (MRSA) strains were resistant to cefoselis, while all methicillin-sensitive *S. aureus* (MSSA) strains were susceptible to this antibiotic. In conclusion, cefoselis showed good activity against non-ESBL-producing *E. coli*, *K. pneumoniae*, and *P. mirabilis*, MSSA, and was also potent against Enterobacteriaceae, *P. aeruginosa*, and *Streptococcus*.

**Keywords:** cefoselis, cefepime, antimicrobial resistance, *in vitro* activity, China

## INTRODUCTION

Multidrug-resistant (MDR) pathogens, especially the ESKAPE pathogens (*Enterococcus faecium*, *Staphylococcus aureus*, *Klebsiella pneumoniae*, *Acinetobacter baumannii*, *Pseudomonas aeruginosa*, and *Enterobacter* species), are the leading cause of nosocomial infections throughout the world, which is usually caused by excessive drug usage or prescription and inappropriate use of antimicrobials. Understanding the mechanisms, developing novel antimicrobial agents, and knowing the latest antimicrobial resistance patterns of bacterial pathogens are crucial to combat these public health challenges (Santajit and Indrawattana, 2016; Sheu et al., 2018; Gajdacs, 2019).

Cefoselis is a member of the fourth-generation cephalosporins which exhibit a wider antibacterial spectrum activity than the third-generation cephalosporins to both Gram-negative and Gram-positive bacteria (King et al., 1995). The wide antibacterial spectrum of cefoselis is attributed to the resistance to hydrolysis by the chromosomal  $\beta$ -lactamases and the rapid penetration through the bacterial cell wall (Giamarellos-Bourboulis et al., 2000). However, few reports have been published in China on the antimicrobial activity of cefoselis against common bacterial pathogens. The objective of this study was to better understand the *in vitro* activity of cefoselis against common Gram-positive and Gram-negative bacterial pathogens in China.

## MATERIALS AND METHODS

### Ethics

The protocol was approved by the Human Research Ethics Committee of Peking Union Medical College Hospital (no. S-K262). Peking Union Medical College Hospital did not require written informed consent from participants because this was an *in vitro* study on bacteria isolates without any private data of the human participants.

### Clinical Isolates

A total of 1188 bacterial isolates derived from 18 hospitals in China (January 2014–December 2016) were studied. The bacterial species distribution is shown in **Table 1**. The isolates from each of the participating hospitals were re-identified by matrix-assisted laser desorption/ionization time-of-flight mass spectrometry (MALDI-TOF MS) (Bruker Daltonics GmbH, Bremen, Germany) at the Central Lab, Peking Union Medical College Hospital (Beijing), China.

### Antimicrobial Susceptibility Test Method

Minimum inhibitory concentrations (MICs) were determined by the broth microdilution method following Clinical and Laboratory Standards Institute (CLSI) guidelines. Thirty-two antimicrobial agents were tested against the isolates, among which 17 agents were against Gram-negative organisms, 24 agents against *Staphylococcus* spp., and 19 agents against *Streptococcus* spp. Cefoselis was obtained from Hansoh Pharma, and the other agents were

**TABLE 1** | Distribution of bacterial species.

Organisms	Number	Percentage
<i>E. coli</i> (ESBL+)	134	11.3
<i>E. coli</i> (ESBL–)	107	9.0
<i>K. pneumoniae</i> (ESBL+)	118	9.9
<i>K. pneumoniae</i> (ESBL–)	106	8.9
<i>P. mirabilis</i> (ESBL+)	33	2.8
<i>P. mirabilis</i> (ESBL–)	33	2.8
<i>C. freundii</i>	30	2.5
<i>E. aerogenes</i>	30	2.5
<i>E. cloacae</i>	30	2.5
<i>S. marcescens</i>	30	2.5
<i>P. vulgaris</i>	30	2.5
<i>A. baumannii</i>	198	16.7
<i>P. aeruginosa</i>	30	2.5
MRSA	97	8.2
MSSA	100	8.4
PSSP	25	2.1
PRSP	15	1.3
Beta-hemolytic streptococci	27	2.3
Viridans group streptococci	15	1.3
Total	1,188	100.0

ESBL, extended-spectrum  $\beta$ -lactamase; MRSA, methicillin-resistant *S. aureus*; MSSA, methicillin-sensitive *S. aureus*; PSSP, penicillin-susceptible *S. pneumoniae*; PRSP, penicillin-resistant *S. pneumoniae*.

provided by AstraZeneca. Interpretation of the antimicrobial testing results was based on CLSI M100-S28 (CLSI, 2018). *Escherichia coli* ATCC 25922, *P. aeruginosa* ATCC 27853, *K. pneumoniae* ATCC 700603, *S. aureus* ATCC 29213, and *Streptococcus pneumoniae* ATCC 49619 were used as the quality control strains.

### Extended-Spectrum $\beta$ -Lactamase Detection

Phenotypic identification of extended-spectrum  $\beta$ -lactamase (ESBL) production in *E. coli*, *K. pneumoniae*, and *Proteus mirabilis*, was carried out using CLSI-recommended methods. If the cefotaxime or ceftazidime MICs were  $\geq 2$   $\mu\text{g/ml}$ , the MICs of cefotaxime + clavulanic acid (4  $\mu\text{g/ml}$ ) or ceftazidime + clavulanic acid (4  $\mu\text{g/ml}$ ) were comparatively determined. ESBL production was defined as an eightfold or greater decrease in MICs for cefotaxime or ceftazidime tested in combination with clavulanic acid compared to their MICs without clavulanic acid.

## RESULTS

### *In vitro* Activity of Antimicrobial Agents Against Enterobacteriaceae

Against ESBL-producing *E. coli*, *K. pneumoniae*, and *P. mirabilis* isolates, cefoselis, cefepime, cefotaxime, and ceftriaxone showed relatively low susceptibility rates, with drug resistance rates of  $> 87\%$ . Against non-ESBL-producing strains, most



**TABLE 2** | In vitro activity of antimicrobial agents against ESBL-positive and ESBL-negative *Escherichia coli*, *Klebsiella pneumoniae* and *Proteus mirabilis* strains.

Antimicrobial agents	<i>E. coli</i> (ESBL+) (134)		<i>E. coli</i> (ESBL-) (107)		<i>K. pneumoniae</i> (ESBL+) (118)		<i>K. pneumoniae</i> (ESBL-) (106)		<i>P. mirabilis</i> (ESBL+) (33)		<i>P. mirabilis</i> (ESBL-) (33)	
	%R	%S	%R	%S	%R	%S	%R	%S	%R	%S	%R	%S
Piperacillin/tazobactam	12.7	84.3	1.9	97.2	23.7	65.3	2.8	97.2	3.0	93.9	3.0	93.9
Ceftazidime	55.2	30.6	0	100.0	59.3	30.5	1.9	97.2	9.1	90.9	0	100.0
Ceftriaxone	99.3	0.7	0	99.1	94.9	4.2	2.8	94.3	100.0	0.0	0	100.0
Cefotaxime	99.3	0.7	0	100.0	94.9	5.1	3.8	95.3	97.0	0.0	0	100.0
Cefoselis	97.8	2.2	0	100.0	93.2	6.8	0.9	94.3	97.0	3.0	3.0	97.0
Cefepime	91.0	3.7	0	100.0	90.7	6.8	0	100.0	87.9	3.0	0	97.0
Cefoxitin	20.9	58.2	1.9	93.5	18.6	78.0	12.3	84.0	3.0	93.9	0	100.0
Aztreonam	83.6	8.2	0	100.0	81.4	14.4	0.9	99.1	41.4	58.6	21.2	78.8
Ertapenem	0	92.5	0	100.0	0	92.4	0	100.0	0	97.0	0	100.0
Imipenem	0	97.8	0	100.0	0	94.9	0	96.2	15.2	27.3	9.1	45.5
Meropenem	0	100.0	0	100.0	0	100.0	0	100.0	0	100.0	0	100.0
Amikacin	3.0	95.5	0	100.0	7.6	91.5	0.9	99.1	6.1	90.9	0	100.0
Ciprofloxacin	78.4	20.1	29.0	69.2	55.9	40.7	11.3	87.7	90.9	9.1	48.5	48.5
Levofloxacin	72.4	20.9	27.1	71.0	46.6	47.5	10.4	87.7	69.7	27.3	27.3	63.6
Minocycline	47.0	40.3	28.0	54.2	44.1	38.1	21.7	69.8	–	–	–	–
Tetracycline	87.3	12.7	84.1	15.0	66.1	32.2	25.5	67.9	–	–	–	–
Tigecycline	0.7	92.5	0	98.1	3.4	82.2	0.9	90.6	–	–	–	–

ESBL, extended-spectrum  $\beta$ -lactamase; R, resistant; S, sensitive.

**TABLE 3** | In vitro activity of antimicrobial agents against Enterobacteriaceae strains.

Antimicrobial agents	<i>C. freundii</i> (30)		<i>E. aerogenes</i> (30)		<i>E. cloacae</i> (30)		<i>S. marcescens</i> (30)		<i>P. vulgaris</i> (30)	
	%R	%S	%R	%S	%R	%S	%R	%S	%R	%S
Piperacillin/tazobactam	20.0	73.3	20.0	63.3	26.7	60.0	13.3	83.3	0	93.3
Ceftazidime	30.0	63.3	33.3	60.0	43.3	46.7	3.3	93.3	0	100.0
Ceftriaxone	50.0	43.3	40.0	53.3	60.0	36.7	23.3	73.3	53.3	3.3
Cefotaxime	50.0	43.3	50.0	43.3	60.0	33.3	30.0	60.0	46.7	16.7
Cefoselis	30.0	56.7	10.0	83.3	33.3	56.7	20.0	80.0	3.3	83.3
Cefepime	26.7	70.0	10.0	90.0	13.3	70.0	16.7	80.0	0	100.0
Cefoxitin	63.3	23.3	90.0	3.3	93.3	3.3	80.0	0.0	13.3	73.3
Aztreonam	43.3	56.7	36.7	63.3	56.7	43.3	13.3	86.7	0	96.7
Ertapenem	6.7	90.0	10.0	90.0	16.7	60.0	13.3	86.7	6.7	93.4
Imipenem	6.7	86.7	6.7	50.0	6.7	83.3	16.7	56.7	66.7	6.7
Meropenem	6.7	93.3	3.3	96.7	6.7	93.3	13.3	83.3	3.3	96.7
Amikacin	3.3	90.0	0	100.0	0	100.0	3.3	93.3	3.3	96.7
Ciprofloxacin	26.7	70.0	10.0	83.3	40.0	53.3	23.3	73.3	30.0	66.7
Levofloxacin	26.7	66.7	6.7	90.0	30.0	60.0	13.3	73.3	6.7	80.0
Minocycline	16.7	70.0	10.0	66.7	30.0	63.3	6.7	86.7	–	–
Tetracycline	36.7	60.0	43.3	56.7	36.7	63.3	60.0	10.0	–	–
Tigecycline	0	100.0	0	96.7	0	93.3	0	93.3	–	–

R, resistant; S, sensitive.

antibiotics revealed good activity, of which cefoselis, cefepime, showed > 94% antimicrobial susceptibility rates. For *Citrobacter freundii*, *Enterobacter aerogenes*, *Enterobacter cloacae*, *Serratia marcescens*, and *Proteus vulgaris* isolates, the susceptibility rates for cefoselis ranged from 56.7% to 83.3%, which were slightly lower than that of cefepime, with susceptibility rates ranging from 70% to 100%. Meropenem and amikacin exhibited high activity against all the Enterobacteriaceae strains (Tables 2, 3).

### In vitro Activity of Antimicrobial Agents Against Non-fermentative Gram-Negative Organisms

The most active agents against *A. baumannii* were tigecycline and minocycline, with susceptibility rates of 58.6% and 45.5%, respectively. The other analyzed agents were less effective, with susceptibility rates of < 30%. Furthermore, against *P. aeruginosa*

**TABLE 4** | In vitro activity of antimicrobial agents against *Acinetobacter baumannii* and *Pseudomonas aeruginosa* strains.

Antimicrobial agents	<i>A. baumannii</i> (198)		<i>P. aeruginosa</i> (30)	
	%R	%S	%R	%S
Piperacillin/tazobactam	75.3	23.2	13.3	80.0
Ceftazidime	76.8	20.7	20.0	73.3
Ceftriaxone	78.8	7.1	96.7	0
Cefotaxime	78.8	14.6	100.0	0
Cefoselis	80.8	18.7	26.7	73.3
Cefepime	75.8	19.7	20.0	73.3
Cefoxitin	96.5	2.5	96.7	0
Aztreonam	84.3	5.1	20	73.3
Ertapenem	–	–	–	–
Imipenem	75.3	24.7	20.0	80.0
Meropenem	75.3	24.2	10.0	76.7
Amikacin	69.7	29.8	6.7	93.3
Ciprofloxacin	76.8	21.2	16.7	76.7
Levofloxacin	59.6	23.2	16.7	76.7
Minocycline	28.3	45.5	–	–
Tetracycline	81.3	16.2	–	–
Tigecycline	22.7	58.6	96.7	3.3

R, resistant; S, sensitive.

isolates, amikacin exhibited the highest *in vitro* activity, with a susceptibility rate of 93.3%. The susceptibility rates for cefoselis, cefepime, and ceftazidime were all 73.3% each for this organism (Table 4).

### In vitro Activity of Antimicrobial Agents Against MRSA and MSSA

Against methicillin-resistant *S. aureus* (MRSA) strains, linezolid, vancomycin, and teicoplanin exhibited a susceptibility rate of 100% each, followed by tigecycline (97.9%), and trimethoprim–sulfamethoxazole (TMP–SMX) (94.8%). All strains were resistant to ceftazidime, ceftriaxone, cefoselis, and cefepime. Against 100 methicillin-sensitive *S. aureus* (MSSA) strains, most antibiotics showed good activity, except for ampicillin, tetracycline, and erythromycin. All strains were susceptible to ceftazidime, ceftriaxone, cefoselis, and cefepime (Table 5).

### In vitro Activity of Antimicrobial Agents Against *Streptococcus* Strains

For the penicillin-susceptible *S. pneumoniae* (PSSP), beta-hemolytic *Streptococcus* strains, and viridans group *Streptococcus* strains, cefoselis and cefepime both showed very high antimicrobial activities, with susceptibility rates of > 90%. Against 15 penicillin-resistant *S. pneumoniae* (PRSP) strains, the susceptibility rate of cefoselis was higher than that of cefepime (60.0% vs. 40.0%). Linezolid, vancomycin, and tigecycline exhibited 100% antimicrobial activity against all the *Streptococcus* strains (Table 6).

**TABLE 5** | In vitro activity of antimicrobial agents against MRSA and MSSA strains.

Antimicrobial agents	MRSA (97)		MSSA (100)	
	%R	%S	%R	%S
Ampicillin	100.0	0	90.0	10
Oxacillin	100.0	0	0	100.0
Amoxicillin/clavulanate	100.0	0	0	100.0
Piperacillin/tazobactam	100.0	0	0	100.0
Ceftaroline	4.1	35.1	0	95.0
Ceftazidime	100.0	0	0	100.0
Ceftriaxone	100.0	0	0	100.0
Cefoselis	100.0	0	0	100.0
Cefepime	100.0	0	0	100.0
Doripenem	100.0	0	0	100.0
Meropenem	100.0	0	0	100.0
Gentamicin	49.5	38.1	18.0	81.0
Levofloxacin	79.4	20.6	23.0	75.0
Moxifloxacin	77.3	19.6	15.0	77.0
Trimethoprim–sulfamethoxazole	5.2	94.8	2.0	98.0
Clindamycin	47.4	50.5	21.0	78.0
Daptomycin	0	99	0	99.0
Erythromycin	82.5	8.2	38.0	60.0
Linezolid	0	100.0	0	100.0
Vancomycin	0	100.0	0	100.0
Teicoplanin	0	100.0	0	100.0
Minocycline	0	88.7	0	100.0
Tetracycline	60.8	36.1	43.0	52.0
Tigecycline	2.1	97.9	0	100.0

MRSA, methicillin-resistant *S. aureus*; MSSA, methicillin-sensitive *S. aureus*; R, resistant; S, sensitive.

### Comparison of Cefoselis and Cefepime Against Common Clinical Pathogens

Cefoselis exhibited a slightly lower antimicrobial activity than cefepime against Enterobacteriaceae and non-fermentative Gram-negative organisms, but a little higher activity than cefepime against MRSA, MSSA, PSSP, beta-hemolytic *Streptococcus*, and viridans group *Streptococcus* strains. The cumulative percentage MIC distributions of cefoselis and cefepime against common clinical pathogens are shown in Table 7.

## DISCUSSION

The Enterobacteriaceae family is a major group of pathogens causing several community- and hospital-acquired infections, among which the ESBL rates in *E. coli* and *K. pneumoniae* in China have been reported as high as 60–70% and 30–40%, respectively (Yang et al., 2010, 2013). According to our previous study, the genotype distribution of ESBL-producing strains among bacterial species was diverse, and *bla*CTX-M was the major ESBL gene, with occurrences in 99.5% of *E. coli*, 91.1% of *K. pneumoniae*, and 97.5% of *P. mirabilis* strains (Yang et al., 2015). In the present

**TABLE 6** | In vitro activity of antimicrobial agents against *Streptococcus* strains.

Antimicrobial agents	PSSP (25)		PRSP (15)		Beta-hemolytic streptococci (27)		Viridans group streptococci (15)	
	%R	%S	%R	%S	%R	%S	%R	%S
Penicillin	0	100.0	100.0	0	0	100.0	0	100.0
Amoxicillin/clavulanate	0	100.0	40.0	40.0	–	–	–	–
Ceftaroline	0	100.0	0	100.0	0	92.6	0	100.0
Ceftazidime	4.0	92.0	86.7	0	7.4	92.6	13.3	86.7
Ceftriaxone	0	96.0	40.0	53.3	0	92.6	6.7	91.7
Cefoselis	4.0	96.0	0	60.0	7.4	92.6	0	100.0
Cefepime	4.0	96.0	20.0	40.0	7.4	92.6	6.7	93.3
Doripenem	0	100.0	0	100.0	0	92.6	0	100.0
Meropenem	4.0	92.0	40.0	6.7	0	92.6	0	100.0
Levofloxacin	4.0	96.0	0	100.0	46.2	53.8	6.7	80.0
Moxifloxacin	32.0	68.0	0	100.0	–	–	–	–
Clindamycin	100.0	0	100.0	0	74.1	22.2	66.7	33.3
Daptomycin	–	–	–	–	–	92.7	–	93.3
Erythromycin	76.0	24.0	100.0	0	48.1	51.9	80.0	13.3
Linezolid	0	100.0	0	100.0	0	100.0	0	100.0
Vancomycin	0	100.0	0	100.0	0	100.0	0	100.0
Minocycline	12.0	48.0	6.7	73.3	33.3	48.1	6.7	80.0
Tetracycline	88.0	8.0	93.3	6.7	74.1	22.2	66.7	33.3
Tigecycline	0	100.0	0	100.0	0	100.0	0	100.0

PSSP, penicillin-susceptible *S. pneumoniae*; PRSP, penicillin-resistant *S. pneumoniae*; R, resistant; S, sensitive.

study, cefoselis and cefepime both showed poor activities against ESBL-producing *E. coli*, *K. pneumoniae*, and *P. mirabilis*, which may be attributed to the specific ESBL genes present in China, albeit further studies are needed for confirmation.

Against other Enterobacteriaceae strains, cefoselis exhibited a slightly lower antimicrobial activity than cefepime, but a higher activity than third-generation cephalosporins. The relatively high activities of fourth-generation cephalosporins against Enterobacteriaceae may be attributed to the low affinity for chromosome-mediated AmpC  $\beta$ -lactamases (D'Angelo et al., 2016), which are the common  $\beta$ -lactamases in Enterobacteriaceae isolates from China. A multicenter, double-blind, randomized clinical trial in China revealed equal clinical efficacy and safety of intravenous cefoselis and cefepime injection for the treatment of acute, moderate, and severe bacterial infections (Liu et al., 2014).

*Acinetobacter baumannii* was one of the bacteria considered to be of maximum resistance and is classified as a priority category according to the bacterial groups classified by priority categories of need for new antibiotics (Tacconelli and Magrini, 2017). In this study, *A. baumannii* exhibited low susceptibility to most of the tested antibiotics, with susceptibility rates ranging from 5.1 to 58.6%. Against *P. aeruginosa*, cefoselis and cefepime showed equal antimicrobial activities for this organism, with susceptibility rates of 73.3% each, which are slightly higher than those in a previous study in China; thus, these two antibiotics could be used to treat infections caused by *P. aeruginosa*, in combination with other antibiotics (Zhang et al., 2016).

Although the prevalence of MRSA in China showed a markedly decreasing trend from 69.0% in 2005 to 35.3% in 2017, as per the China Antimicrobial Surveillance Network (CHINET) program, MRSA remains a major pathogen responsible for nosocomial infections (Hu et al., 2018). No isolates were found to be resistant to vancomycin, linezolid, and teicoplanin in this study. Tigecycline and TMP-SMX also showed good activities, which were similar to previous studies (Zhao et al., 2012; Zhang et al., 2015). Vancomycin, linezolid, and TMP-SMX were recommended by the Infectious Diseases Society of America (IDSA) to treat MRSA infections (Liu et al., 2011).

Teicoplanin can be an effective alternative to vancomycin for treating patients infected by MRSA as the two therapies are similar in both efficacy and safety (Peng et al., 2013). Tigecycline was often recommended as a second- or third-line agent for MRSA infections when alternative agents cannot be used (Rodvold and McConeghy, 2014). Ceftaroline fosamil was the first FDA-approved cephalosporin with any activity against MRSA, but the low susceptibility among MRSA isolates in China needs attention (Lodise and Low, 2012; Zhang et al., 2015).

The bacterial isolates were collected from 2014 to 2016, and the susceptibility has certainly changed in the last 5 years for most organisms. More recently collected strains should be involved in further studies. This is a limitation of the study. In conclusion, cefoselis exhibited good antimicrobial activity against non-ESBL-producing *E. coli*, *K. pneumoniae*, *P. mirabilis*, and MSSA and was also potent against other Enterobacteriaceae, *P. aeruginosa*, and *Streptococcus*.

**TABLE 7** | Cumulative percentage MIC distributions of cefoselis and cefepime against common clinical pathogens collected in China.

Species (n) and drug		Cumulative% isolates at or below various MICs ( $\mu\text{g/ml}$ ) <sup>a</sup>															
		$\leq 0.015$	0.03	0.06	0.12	0.25	0.5	1	2	4	8	16	32	64	128	256	> 256
<i>E. coli</i> (ESBL+) (134)	Cefoselis			1.5	2.2	2.2	2.2	2.2	2.2	2.2	2.2	3.7	8.2	11.9	20.1	20.9	<b>100</b>
	Cefepime			0.7	1.5	2.2	2.2	2.2	3.7	5.2	9.0	18.7	26.9	32.8	36.6	40.3	<b>100</b>
<i>E. coli</i> (ESBL-) (107)	Cefoselis	1.9	17.8	71.0	<b>92.5</b>	98.1	98.1	98.1	100								
	Cefepime	0.9	16.8	66.4	<b>94.4</b>	97.2	100										
<i>K. pneumoniae</i> (ESBL+) (118)	Cefoselis		0.8	4.2	5.1	5.9	5.9	6.8	6.8	6.8	6.8	6.8	6.8	12.7	16.1	16.9	<b>100</b>
	Cefepime		0.8	4.2	5.1	5.1	5.1	6.8	6.8	6.8	9.3	11.9	17.8	21.2	26.3	31.4	<b>100</b>
<i>K. pneumoniae</i> (ESBL-) (106)	Cefoselis	1.9	30.2	60.4	81.1	<b>91.5</b>	93.4	93.4	94.3	97.2	99.1	99.1	100				
	Cefepime	3.8	46.2	67.9	82.1	<b>91.5</b>	92.5	96.2	100								
<i>P. mirabilis</i> (ESBL+) (33)	Cefoselis							3.0	3.0	3.0	3.0	3.0	6.1	9.1	9.1	9.1	<b>100</b>
	Cefepime					3.0	3.0	3.0	3.0	3.0	12.1	12.1	21.2	30.3	30.3	30.3	<b>100</b>
<i>P. mirabilis</i> (ESBL-) (33)	Cefoselis	3.0	39.4	48.5	60.6	66.7	75.8	81.8	<b>97.0</b>	97.0	97.0	100					
	Cefepime		42.4	45.5	51.5	57.6	69.7	87.9	<b>97.0</b>	97.0	100						
<i>C. freundii</i> (30)	Cefoselis	26.7	43.3	46.7	50.0	53.3	53.3	56.7	56.7	60.0	70.0	70.0	73.3	80.0	83.3	83.3	<b>100</b>
	Cefepime	30.0	46.7	53.3	56.7	60.0	63.3	63.3	70.0	73.3	73.3	83.3	83.3	83.3	<b>90.0</b>	93.3	100
<i>E. aerogenes</i> (30)	Cefoselis	10.0	33.3	43.3	50.0	63.3	70.0	73.3	83.3	<b>90.0</b>	90.0	90.0	90.0	90.0	90.0	93.3	100
	Cefepime	6.7	43.3	46.7	63.3	76.7	86.7	<b>90.0</b>	90.0	90.0	90.0	93.3	96.7	96.7	96.7	96.7	100
<i>E. cloacae</i> (30)	Cefoselis	3.3	30.0	36.7	36.7	43.3	46.7	46.7	56.7	60.0	66.7	66.7	83.3	86.7	<b>93.3</b>	93.3	100
	Cefepime	10.0	30.0	33.3	43.3	50.0	56.7	63.3	70.0	76.7	86.7	<b>93.3</b>	96.7	96.7	96.7	100	
<i>S. marcescens</i> (30)	Cefoselis	30.0	70.0	73.3	76.7	76.7	76.7	76.7	80.0	80.0	80.0	80.0	80.0	80.0	80.0	80.0	<b>100</b>
	Cefepime	10.0	66.7	73.3	76.7	76.7	76.7	76.7	80.0	80.0	83.3	86.7	86.7	86.7	86.7	86.7	<b>100</b>
<i>P. vulgaris</i> (30)	Cefoselis		3.3	30.0	46.7	60.0	70.0	76.7	83.3	<b>93.3</b>	96.7	96.7	96.7	96.7	96.7	96.7	100
	Cefepime		10.0	36.7	50.0	76.7	86.7	<b>100</b>									
<i>A. baumannii</i> (198)	Cefoselis	1.5	2.5	3.5	5.1	6.6	8.6	16.2	18.7	18.7	18.7	19.2	21.2	26.3	40.4	71.2	<b>100</b>
	Cefepime	1.0	2.0	3.5	4.5	5.6	6.6	12.1	16.2	18.7	19.7	24.2	36.9	52.0	84.3	<b>93.9</b>	100
<i>P. aeruginosa</i> (30)	Cefoselis						3.3	36.7	50.0	63.3	73.3	73.3	73.3	76.7	<b>96.7</b>	96.7	100
	Cefepime						3.3	53.3	56.7	70.0	73.3	80.0	80.0	<b>96.7</b>	100		
MRSA (97)	Cefoselis							2.1	3.1	18.6	27.8	32.0	<b>96.9</b>	100			
	Cefepime								1.0	2.1	5.2	13.4	18.6	25.8	28.9	28.9	<b>100</b>
MSSA (100)	Cefoselis	3.0	3.0	3.0	3.0	3.0	4.0	64.0	82.0	87.0	<b>90.0</b>	92.0	100				
	Cefepime	3.0	3.0	3.0	3.0	3.0	3.0	5.0	57.0	78.0	83.0	87.0	88.0	89.0	<b>90.0</b>	93.0	100
PSSP (25)	Cefoselis	32.0	72.0	80.0	84.0	<b>92.0</b>	92.0	96.0	96.0	96.0	96.0	96.0	100				
	Cefepime	4.0	72.0	76.0	80.0	88.0	<b>92.0</b>	96.0	96.0	96.0	96.0	96.0	100				
PRSP (15)	Cefoselis						6.7	40.0	40.0	86.7	<b>100</b>						
	Cefepime							20.0	60.0	<b>100</b>							
Beta-hemolytic streptococci (27)	Cefoselis	40.7	85.2	88.9	<b>92.6</b>	92.6	92.6	92.6	92.6	92.6	92.6	92.6	92.6	92.6	92.6	92.6	100
	Cefepime	37.0	40.7	85.2	<b>92.6</b>	92.6	92.6	92.6	92.6	92.6	92.6	92.6	92.6	92.6	92.6	92.6	100
Viridans group streptococci (15)	Cefoselis	26.7	46.7	93.3	<b>100</b>												
	Cefepime	26.7	33.3	40.0	53.3	<b>93.3</b>	93.3	93.3	93.3	93.3	100						

ESBL, extended-spectrum  $\beta$ -lactamase; MRSA, methicillin-resistant *S. aureus*; MSSA, methicillin-sensitive *S. aureus*; PSSP, penicillin-susceptible *S. pneumoniae*; PRSP, penicillin-resistant *S. pneumoniae*; MIC, minimum inhibitory concentration. <sup>a</sup>MIC90 values are in boldface.



## DATA AVAILABILITY STATEMENT

The datasets generated for this study are available on request to the corresponding author.

## AUTHOR CONTRIBUTIONS

J-WC, J-RS, and TK wrote the manuscript. S-YY, GZ, J-JZ, YY, and S-MD collaborated the strains and performed the antimicrobial susceptibility tests. MX, Q-WY, and Y-CX designed and supervised the study.

## FUNDING

This work was supported by the National Key Research and Development Program of China (2018YFE0101800,

2018YFC1200100, and 2018YFC1200105), Chinese Academy of Medical Sciences (CAMS) Initiative for Innovative Medicine (Grant No. 2016-I2M-3-014), CAMS Innovation Fund for Medical Sciences (Grant No. 2016-I2M-1-014), Beijing Innovation Base Cultivation and Development Special Fund (Z171100002217068), Outstanding Talents Training Funding Project of Dongcheng District, Beijing (2017), Graduate Innovation Fund of Peking Union Medical College (Grant No. 2017-1002-1-21), and the National Natural Science Foundation of China (Grant No. 81101287). The funders had no role in the study design, data collection and analysis, decision to publish, or in the preparation of the manuscript.

## ACKNOWLEDGMENTS

We thank all the 18 hospitals for providing the study strains.

## REFERENCES

- CLSI (2018). *Performance Standards for Antimicrobial Susceptibility Testing*. 28th Ed. CLSI Supplement M100. Wayne, PA: Clinical and Laboratory Standards Institute.
- D'Angelo, R. G., Johnson, J. K., Bork, J. T., and Heil, E. L. (2016). Treatment options for extended-spectrum beta-lactamase (ESBL) and AmpC-producing bacteria. *Expert Opin. Pharmacother.* 17, 953–967. doi: 10.1517/14656566.2016.1154538
- Gajdacs, M. (2019). The continuing threat of methicillin-resistant *Staphylococcus aureus*. *Antibiotics* 8:E52. doi: 10.3390/antibiotics8020052
- Giamarellos-Bourboulis, E. J., Grecka, P., Tsitsika, A., Tympanidou, C., and Giamarellou, H. (2000). In-vitro activity of FK 037 (Cefoselis), a novel 4(th) generation cephalosporin, compared to cefepime and ceftazidime on nosocomial staphylococci and gram-negative isolates. *Diagn. Microbiol. Infect. Dis.* 36, 185–191. doi: 10.1016/s0732-8893(99)00131-5
- Hu, F., Zhu, D., Wang, F., and Wang, M. (2018). Current status and trends of antibacterial resistance in China. *Clin. Infect. Dis.* 67, S128–S134. doi: 10.1093/cid/ciy657
- King, A., Bethune, L., and Phillips, I. (1995). The comparative *In Vitro* activity of FK-037 (Cefoselis), a new broad-spectrum cephalosporin. *Clin. Microbiol. Infect.* 1, 13–17. doi: 10.1111/j.1469-0691.1995.tb00018.x
- Liu, C., Bayer, A., Cosgrove, S. E., Daum, R. S., Fridkin, S. K., Gorwitz, R. J., et al. (2011). Clinical practice guidelines by the infectious diseases society of america for the treatment of methicillin-resistant *Staphylococcus aureus* infections in adults and children. *Clin. Infect. Dis.* 52, e18–e55. doi: 10.1093/cid/ciq146
- Liu, Y. B., Lv, X. J., Yu, R. J., Qiu, H. M., Bai, J. L., Jiang, N., et al. (2014). Multicenter, double-blind, randomized clinical trial of parenterally administered Cefoselis versus Cefepime for the treatment of acute bacterial infections. *Eur. Rev. Med. Pharmacol. Sci.* 18, 2006–2012.
- Lodise, T. P., and Low, D. E. (2012). Ceftazidime fosamil in the treatment of community-acquired bacterial pneumonia and acute bacterial skin and skin structure infections. *Drugs* 72, 1473–1493. doi: 10.2165/11635660-000000000-00000
- Peng, Y., Ye, X., Li, Y., Bu, T., Chen, X., Bi, J., et al. (2013). Teicoplanin as an effective alternative to vancomycin for treatment of MRSA infection in Chinese population: a meta-analysis of randomized controlled trials. *PLoS One* 8:e79782. doi: 10.1371/journal.pone.0079782
- Rodvold, K. A., and McConeghy, K. W. (2014). Methicillin-resistant *Staphylococcus aureus* therapy: past, present, and future. *Clin. Infect. Dis.* 58(Suppl. 1), S20–S27. doi: 10.1093/cid/cit614
- Santajit, S., and Indrawattana, N. (2016). Mechanisms of antimicrobial resistance in ESKAPE pathogens. *Biomed. Res. Int.* 2016:2475067. doi: 10.1155/2016/2475067
- Sheu, C. C., Lin, S. Y., Chang, Y. T., Lee, C. Y., Chen, Y. H., and Hsueh, P. R. (2018). Management of infections caused by extended-spectrum beta-lactamase-producing *Enterobacteriaceae*: current evidence and future prospects. *Expert Rev. Anti Infect. Ther.* 16, 205–218. doi: 10.1080/14787210.2018.1436966
- Taccconelli, E., and Magrini, N. (2017). *Global Priority List of Antibiotic-Resistant Bacteria to Guide Research, Discovery, and Development of New Antibiotics*. Geneva: WHO.
- Yang, Q., Wang, H., Chen, M., Ni, Y., Yu, Y., Hu, B., et al. (2010). Surveillance of antimicrobial susceptibility of aerobic and facultative Gram-negative bacilli isolated from patients with intra-abdominal infections in China: the 2002–2009 study for monitoring antimicrobial resistance trends (SMART). *Int. J. Antimicrob. Agents* 36, 507–512. doi: 10.1016/j.ijantimicag.2010.09.001
- Yang, Q., Zhang, H., Cheng, J., Xu, Z., Xu, Y., Cao, B., et al. (2015). In vitro activity of flomoxef and comparators against *Escherichia coli*, *Klebsiella pneumoniae* and *Proteus mirabilis* producing extended-spectrum beta-Lactamases in China. *Int. J. Antimicrob. Agents* 45, 485–490. doi: 10.1016/j.ijantimicag.2014.11.012
- Yang, Q., Zhang, H., Wang, Y., Xu, Y., Chen, M., Badal, R. E., et al. (2013). A 10 year surveillance for antimicrobial susceptibility of *Escherichia coli* and *Klebsiella pneumoniae* in community- and hospital-associated intra-abdominal infections in China. *J. Med. Microbiol.* 62, 1343–1349. doi: 10.1099/jmm.0.059816-0
- Zhang, H., Xiao, M., Kong, F., O'sullivan, M. V., Mao, L. L., Zhao, H. R., et al. (2015). A multicentre study of methicillin-resistant *Staphylococcus aureus* in acute bacterial skin and skin-structure infections in China: susceptibility to ceftaroline and molecular epidemiology. *Int. J. Antimicrob. Agents* 45, 347–350. doi: 10.1016/j.ijantimicag.2014.12.014
- Zhang, H., Yang, Q., Liao, K., Ni, Y., Yu, Y., Hu, B., et al. (2016). Antimicrobial susceptibilities of aerobic and facultative gram-negative Bacilli from intra-abdominal infections in patients from seven regions in China in 2012 and 2013. *Antimicrob. Agents Chemother.* 60, 245–251. doi: 10.1128/AAC.00956-15
- Zhao, C. J., Sun, H. L., Wang, H., Liu, Y. D., Hu, B. J., Yu, Y. S., et al. (2012). Antimicrobial resistance trends among 5608 clinical Gram-positive isolates in China: results from the gram-positive CocciResistance surveillance program (2005–2010). *Diagn. Microbiol. Infect. Dis.* 73, 174–181. doi: 10.1016/j.diagmicrobio.2012.03.003

**Conflict of Interest:** The authors declare that the research was conducted in the absence of any commercial or financial relationships that could be construed as a potential conflict of interest.

Copyright © 2020 Cheng, Su, Xiao, Yu, Zhang, Zhang, Yang, Duan, Kudinha, Yang and Xu. This is an open-access article distributed under the terms of the Creative Commons Attribution License (CC BY). The use, distribution or reproduction in other forums is permitted, provided the original author(s) and the copyright owner(s) are credited and that the original publication in this journal is cited, in accordance with accepted academic practice. No use, distribution or reproduction is permitted which does not comply with these terms.



# Metadata Analysis of *mcr-1*-Bearing Plasmids Inspired by the Sequencing Evidence for Horizontal Transfer of Antibiotic Resistance Genes Between Polluted River and Wild Birds

## OPEN ACCESS

### Edited by:

Raffaele Zarrilli,  
University of Naples Federico II, Italy

### Reviewed by:

Ruichao Li,  
Yangzhou University, China  
Stefano Gaiarsa,  
San Matteo Hospital Foundation  
(IRCCS), Italy

### \*Correspondence:

Kun Yang  
cookyoung@scu.edu.cn

†These authors have contributed  
equally to this work

### Specialty section:

This article was submitted to  
Antimicrobials, Resistance  
and Chemotherapy,  
a section of the journal  
Frontiers in Microbiology

**Received:** 15 September 2019

**Accepted:** 18 February 2020

**Published:** 10 March 2020

### Citation:

Lin Y, Dong X, Wu J, Rao D,  
Zhang L, Faraj Y and Yang K (2020)  
Metadata Analysis of *mcr-1*-Bearing  
Plasmids Inspired by the Sequencing  
Evidence for Horizontal Transfer  
of Antibiotic Resistance Genes  
Between Polluted River and Wild  
Birds. *Front. Microbiol.* 11:352.  
doi: 10.3389/fmicb.2020.00352

Yufei Lin<sup>†</sup>, Xiaohong Dong<sup>†</sup>, Jiao Wu<sup>†</sup>, Dawei Rao, Lihua Zhang, Yousef Faraj and  
Kun Yang\*

Department of Pharmaceutical and Biological Engineering, School of Chemical Engineering, Sichuan University, Chengdu, China

We sequenced the whole genomes of three *mcr-1*-positive multidrug-resistant *E. coli* strains, which were previously isolated from the environment of egret habitat (polluted river) and egret feces. The results exhibit high correlation between antibiotic-resistant phenotype and genotype among the three strains. Most of the mobilized antibiotic resistance genes (ARGs) are distributed on plasmids in the forms of transposons or integrons. Multidrug-resistant (MDR) regions of high homology are detected on plasmids of different *E. coli* isolates. Therefore, horizontal transfer of resistance genes has facilitated the transmission of antibiotic resistance between the environmental and avian bacteria, and the transfer of ARGs have involved multiple embedded genetic levels (transposons, integrons, plasmids, and bacterial lineages). Inspired by this, systematic metadata analysis was performed for the available sequences of *mcr-1*-bearing plasmids. Among these plasmids, IncHI2 plasmids carry the most additional ARGs. The composition of these additional ARGs varies according to their geographical distribution. The phylogenetic reconstruction of IncI2 and IncX4 plasmids provides the evidence for their multiregional evolution. Phylogenetic analysis at the level of mobile genetic element (plasmid) provides important epidemiological information for the global dissemination of *mcr-1* gene. Highly homologous *mcr-1*-bearing IncI2 plasmids have been isolated from different regions along the East Asian-Australasian Flyway, suggesting that migratory birds may mediate the intercontinental transportation of ARGs.

**Keywords:** antibiotic resistance, intercontinental dissemination, migratory birds, antibiotic resistance gene, horizontal gene transfer

## INTRODUCTION

Horizontal gene transfer (HGT) plays an important role in the global dissemination of antibiotic resistance, while the mobilization of ARGs is the first and also the most important evolutionary step for their horizontal transfer. The discovery of any new mobilized resistance gene always attracts great attention of the researchers. As evidenced by a number of studies, these mobilized resistance genes have been increasingly spreading all over the world (Stokes and Gillings, 2011). Typical cases include the discovery of *bla*<sub>KPC</sub>, *bla*<sub>NDM</sub>, and *mcr-1* genes. The *bla*<sub>KPC</sub> gene was first identified in 1996, and now it can be detected in many regions of the world (Munoz-Price et al., 2013). Its mobilization is related to a 10 kb Tn3-based mobile transposon Tn4401 (Naas et al., 2008; Cuzon et al., 2011). The *bla*<sub>NDM</sub> gene was first identified in 2008 in a *K. pneumoniae* isolate recovered from a Swedish patient, who had previously been hospitalized in New Delhi, India (Yong et al., 2009). Thereafter, this resistance gene was detected in different regions of the world (Dortet et al., 2014). Its mobilization is associated with an IS*Aba125* composite transposon Tn125 (Poirel et al., 2012). The *mcr-1* gene was first discovered in China (Liu et al., 2016), and the same ARG was then reported in various regions of the world (Wang et al., 2018). Its mobilization is mediated by an IS*Apl1* composite transposon Tn6330 (Snesrud et al., 2016; Li et al., 2017).

Although the effect of HGT on the dissemination of antibiotic resistance has been realized, the spread of specific resistant bacterial clones is also widely concerned (Munoz-Price et al., 2013; Matamoros et al., 2017). In early 1990s, it was found that the moving of transposons between carrier replicons (plasmids) resulted in the spread of ARGs between bacterial species (Liebert et al., 1999). Recently, it has been described as a nested Russian doll-like mobility of ARGs, which once again drew the attention of researchers (Sheppard et al., 2016; Wang et al., 2018; Hernando-Amado et al., 2019). These studies clearly explain the mechanism of the horizontal transfer of resistance genes at multiple genetic levels (transposons, integrons, plasmids, bacterial lineages and bacterial species) (Wang et al., 2018). In our previous study (Wu et al., 2018), we demonstrated that wild birds could transport antibiotic resistance from contaminated river to the surrounding environment, and the spread of antibiotic resistance was not mainly due to the transfer of resistant bacterial clones. Among those resistant *E. coli* isolates in the aforementioned work, no strong correlation was observed between strain genotypes (repetitive-element PCR genotyping) and their drug-resistance patterns. Therefore, we concluded that the horizontal transfer of resistance genes was the main mechanism of resistance transmission in that process. Nonetheless, there was no direct sequencing evidence at the time. In this study, we sequenced the whole genomes of three *mcr-1*-positive multidrug-resistant *E. coli* strains isolated in the previous work to pursue the evidence for horizontal transfer of resistance genes. Inspired by the sequencing results, we systematically analyzed *mcr-1*-bearing plasmid sequences downloaded from GenBank database. We tried to obtain epidemiological information of the *mcr-1* gene by analyzing its global dissemination at

multiple levels of mobile genetic elements (MGEs), especially at the plasmid level.

## MATERIALS AND METHODS

### *mcr-1*-Positive Strains

In our previous study, we found that the wild birds (egrets) could mediate the environmental transmission of antibiotic resistance in local area, from the polluted Jin River to birds' nightly habitat, Wangjianglou Park (Wu et al., 2018). Some of the *E. coli* strains isolated in that work exhibited colistin resistance ( $n = 6$ ), among which three isolates were proved to be *mcr-1*-positive and multidrug-resistant. Two of the three strains were isolated from the river (Jin River) polluted by antibiotic-resistant bacteria and the third one was isolated from egret feces. Three *E. coli* isolates were respectively labeled as W5-6, W2-5, and BE2-5.

### Antibiotic Susceptibility Testing

The minimum inhibitory concentrations (MICs) of 10 antibiotics against the three *E. coli* isolates has previously been determined (Wu et al., 2018) via a modified broth micro-dilution method as per ISO 20776-1:2006 CLSI using 96-well microtiter plates (Clinical and Laboratory Standards Institute [CLSI], 2019). The only modification in our method is in the step of inoculum preparation. Typically, the *E. coli* isolates were first grown in LB-broth-loaded 96 well plate at 37°C overnight to reach the stationary phase. The cell cultures were then 10<sup>3</sup> fold diluted and used as inoculum. When inoculating the testing 96-well plates containing antibiotics of different concentrations, a 48-pin replicator was used to improve the efficiency of experimental operation. The MIC endpoints were determined as the lowest concentration, at which there was no visible growth after 20 h of incubation at 37°C. Duplicate tests for each antibiotic concentration were conducted. Positive and negative controls were conducted in antibiotic-free LB to ensure the growth of environmental *E. coli* isolates under lab conditions and sterility of the assay, respectively. Quality control of the procedure was conducted by using the susceptible *E. coli* standard strain ATCC 25922.

### Bacteria Culture and Whole Genomic DNA Extraction

The whole genome DNA was extracted from fresh bacterial cell mass recovered from 100 mL LB pure culture containing colistin of 4 µg/mL with the FastDNA<sup>®</sup> Spin Kit for Soil (MP Biomedicals, France). About 1.2 mL of high-quality DNA was obtained for each *E. coli* strain. A small amount of each DNA sample was used for the amplification and sequencing of 16S rRNA gene to ensure that the DNA sample was obtained from a pure culture. The presence of *mcr-1* gene in the DNA sample was also verified via PCR. The primer pair for amplifying 16S rRNA gene was 27F (5'-AGAGTTTGATCCTGGCTCAG-3') and 1522R (5'-AAGGAGGTGATCCANCCRCA-3') and that for *mcr-1* was CLR5-F (5'-CGGTCAGTCCGTTTGTTC-3') and CLR5-R (5'-CTTGGTCGGTCTGTAGGG-3') (Liu et al., 2016).

Thereafter, the remaining bacterial DNA samples were kept frozen ( $-40^{\circ}\text{C}$ ) until sequencing.

## Whole Genome Sequencing for Three *E. coli* Isolates

The bacterial genome DNA was detected by agarose gel electrophoresis and quantified by Qubit. The genomes of the three isolates were sequenced using Single Molecule, Real-Time (SMRT) technology performed at Beijing Novogene Bioinformatics Technology Co., Ltd. The low quality reads were filtered by the SMRT 2.3.0 (Berlin et al., 2015), and the filtered reads were *de novo* assembled to generate contigs without gaps (Koren and Phillippy, 2015). All genome sequences (chromosome and plasmid sequences) of the three *E. coli* isolates were deposited into GenBank database under the BioProject PRJNA495707 with BioSample numbers SAMN10230266 to SAMN10230268 and accession numbers CP032986 to CP032995.

The strain types (STs) of the three *E. coli* isolates were determined from their assembled genomes using online MLST service provided by the Center for Genomic Epidemiology<sup>1</sup> according to Achtman's MLST scheme (Wirth et al., 2006; Larsen et al., 2012).

## Prediction of Open Reading Frames (ORFs) and Gene Functions

We used GeneMarks to predict ORFs for the three *E. coli* isolates (Besemer et al., 2001). We used seven databases to predict gene functions. They were GO (Gene Ontology) (Ashburner et al., 2000), KEGG (Kyoto Encyclopedia of Genes and Genomes) (Kanehisa et al., 2004, 2006), COG (Clusters of Orthologous Groups) (Tatusov et al., 2003), NR (Non-Redundant Protein Database) (Li et al., 2002), TCDB (Transporter Classification Database) (Saier et al., 2014), Swiss-Prot (Bairoch and Apweiler, 2000), and TrEMBL (Magrane and UniProt, 2011), respectively. A whole genome BLAST search (*E*-value less than  $10^{-5}$ , minimal alignment length percentage larger than 40%) was performed against above seven databases (Altschul et al., 1990). ARGs were annotated via BLAST searching the ORFs against the Comprehensive Antibiotic Resistance Database (CARD) (Liu and Pop, 2009; McArthur et al., 2013). We set the thresholds of *e*-value and "best identity" at  $10^{-5}$  and 80%, respectively.

## Epidemiological and Phylogenetic Analysis of the *mcr-1*-Bearing Plasmids

The discovery of the mobilized colistin resistance gene, *mcr-1*, is in the era of rapid development of next-generation sequencing technology. During only 4 years, hundreds of sequences of *mcr-1*-bearing plasmids have been uploaded to the database, which provides a good chance for metadata analysis of these plasmids. We retrieved the GenBank database with keywords "*mcr-1*" (or *mcr1*) and "plasmid" in June 2018. From the hit entries, the circular sequences were manually picked and recorded the metadata. Identification of the plasmid incompatibility group was performed for downloaded plasmid sequences via the CGE online

services PlasmidFinder v1.3<sup>2</sup> (Carattoli et al., 2014). ResFinder<sup>3</sup> was used to determine other acquired resistance genes on these plasmids (Zankari et al., 2012).

Most of the published *mcr-1*-bearing plasmids belong to three main incompatibility groups, IncHI2, IncI2, and IncX4 (Li et al., 2017; Matamoros et al., 2017). According to the respective characteristics of the three incompatibility plasmid groups, we performed a targeted analysis. The analysis routine is illustrated in **Supplementary Figure S1**.

## RESULTS AND DISCUSSION

### Genome Assembly and Annotation for Three *E. coli* Isolates

The original sequencing data obtain more than  $50 \times$  coverage of the whole genome for the three *E. coli* isolates. Chromosomes and plasmids of the three isolates are all assembled in circular contigs with no gaps. Three *E. coli* isolates are of different strain types (**Table 1**). The number, size and Inc-types of plasmids are also different among the three isolates (**Table 1**). *E. coli* W5-6 contains 3 plasmids. The other two isolates both carry 2 plasmids. The plasmid pMCR\_W5-6 gives the biggest size (241 kbp) among all plasmids. The numbers of genes predicted by GeneMarks are 4898, 4834, and 4576 for W5-6, W2-5, and BE2-5, respectively. The annotation of the three genomes with the COG database clusters these genes into 23 classes with annotation rate of 89.6, 90.7, and 93.8%, respectively (**Supplementary Figure S2**). Genomes of all the three *E. coli* strains, especially the strain W5-6, contain a considerable number of MGEs (Mobilome in **Supplementary Figure S2**).

### Antibiotic-Resistant Phenotype and Genotype of Three *E. coli* Isolates

All the three strains show multidrug resistance. The *E. coli* W5-6 demonstrates the highest level of drug resistance among the three isolates. It shows resistance against 9 out of 10 tested antibiotics. The other two *E. coli* isolates of lower resistance levels are resistant to 7 antibiotics (**Table 2**).

Eighty-five putative ARGs (via BLAST against the CARD database) are annotated in the whole genome of *E. coli* W5-6, 20 of which are on plasmids. The numbers of ARGs on chromosomes of *E. coli* W2-5 and BE2-5 are 65 and 66, respectively. The numbers of ARGs on plasmids of these two isolates are 3 and 11, respectively (**Table 3**). Fifty-two ARGs are common among all the three *E. coli* isolates. However, most of these shared ARGs ( $n = 44$ , 84.6%) are efflux pump genes, and they are distributed on their chromosomes, which implies that efflux pump genes are highly conserved in the same bacterial species. These efflux pump genes do not appear to be significantly associated with the antibiotic-resistant phenotype of the three strains. Although these efflux pump genes may be just involved in some detoxification process (Martinez et al., 2009), we still list them below (**Table 3**) for reference. The

<sup>1</sup><https://cge.cbs.dtu.dk/services/MLST/>

<sup>2</sup><https://cge.cbs.dtu.dk/services/PlasmidFinder/>

<sup>3</sup><https://cge.cbs.dtu.dk/services/ResFinder/>



**TABLE 1** | Genome assembly results for three *E. coli* isolates.

Isolates	Type	Contig ID	Size (bp)	GC%	Circular?	ST or Inc <sup>c</sup>	Accession
W5-6	Chromosome	W5-6Chr	4,638,901	50.7	Circular	ST2	CP032992
	Plasmid	pMCR_W5-6 <sup>a,b</sup>	241,043	46.42	Circular	IncHI2 (IncHI2A)	CP032993
	Plasmid	p2_W5-6	44,779	44.83	Circular	IncX1	CP032994
	Plasmid	p3_W5-6	72,717	51.52	Circular	IncN (IncFIA, IncFIB)	CP032995
W2-5	Chromosome	W2-5Chr	4,914,512	50.56	Circular	ST355	CP032989
	Plasmid	pMCR_W2-5 <sup>a</sup>	66,380	42.92	Circular	IncI2	CP032990
	Plasmid	p2_W2-5	83,867	51.13	Circular	IncN (IncFII)	CP032991
BE2-5	Chromosome	BE2-5Chr	4,677,021	50.76	Circular	ST532	CP032986
	Plasmid	pMCR_BE2-5 <sup>a</sup>	51,622	46.91	Circular	IncP1	CP032987
	Plasmid	p2_BE2-5 <sup>b</sup>	84,688	50.74	Circular	IncR (IncX1)	CP032988

<sup>a</sup>The plasmids bearing *mcr-1* gene. <sup>b</sup>The plasmids with MDR region of similar structure. <sup>c</sup>Strain type (ST) or incompatibility replicon type of plasmids (Inc). Multiple replicons on the same plasmid are indicated in bracket.

only non-efflux-pump common ARG with a definite resistant phenotype among the three isolates is the colistin resistance gene *mcr-1*. The *mcr-1* gene is located on the plasmids of different Inc-types in the three *E. coli* strains. The plasmids pMCR\_W5-6, pMCR\_W2-5, and pMCR\_BE2-5 are of the IncHI2, IncI2, and IncP1-type, respectively (Table 1). The *mcr-1* sequence on plasmid pMCR\_W2-5 lost the downstream IS*Apl1* (Supplementary Figure S3).

For Aminoglycosides, resistance genes encoding three types of antibiotic inactivation enzymes are detected among the three *E. coli* isolates, aminoglycoside acetyltransferases [*aac(3)-IV*], phosphotransferase [*aph(3')-Ia*, *aph(4)-Ia*, *aph(3'')-Ib* and *aph(6)-Id*] and nucleotidyltransferase [*aadA1* and *aadA2*] genes. *E. coli* W5-6 possesses all the three kinds of resistance genes (Table 2), and exhibits the highest resistance level to aminoglycosides. It is resistant to three out of four tested aminoglycosides: kanamycin A, gentamicin and streptomycin (Table 2). *E. coli* W2-5 has the ARGs, which render resistance to streptomycin [*aph(3'')-Ib* and *aph(6)-Id*], and exhibits resistance to this antibiotic. *E. coli* BE2-5 does not have these two ARGs, while it has *aph(3')-Ia*, which enables it to resist against kanamycin A (McArthur et al., 2013). For tetracycline, we detected corresponding ARGs in the genomes of all the three *E. coli* isolates either on chromosome [*tet(A)*, *tet(B)* and *tet(D)*] or on plasmid [*tet(A)*], which is in good agreement with their resistance to this antibiotic (Tables 2, 3). For  $\beta$ -lactams, different  $\beta$ -lactamase genes are detected on the plasmids of *E. coli* W5-6 (*bla*<sub>CTX-M-14</sub> on pMCR\_W5-6 and *bla*<sub>TEM-1</sub> on p2\_W5-6) and W2-5 (*bla*<sub>CTX-M-55</sub> on p2\_W2-5), while no  $\beta$ -lactamase gene is detected for *E. coli* BE2-5, as it is susceptible to ceftriaxone (Table 2). For quinolones, genes encoding subunits of efflux pump complex conferring resistance to fluoroquinolone (*oqxA* and *oqxB*) (Kim et al., 2009) are detected on the plasmid (pMCR\_W5-6) of *E. coli* W5-6. Point mutations in *gyrA* and *parC* genes conferring resistance to fluoroquinolones are detected in *E. coli* W5-6 and W2-5 (Oram and Fisher, 1991; Tankovic et al., 1996). In *E. coli* BE2-5, *qnrS2* gene is detected on its plasmid (p2\_BE2-5), which confers it weak resistance to ciprofloxacin and nalidixic acid (Gay et al., 2006; Table 2). Besides above ARGs conferring resistance to the tested antibiotics, resistance

genes against sulfonamides (*sul2* etc.), chloramphenicol (*cmlA1*), fosfomycin (*fosA3*), and trimethoprim (*drfA12*) are also detected among the three *E. coli* isolates. Point mutation in *glpT* gene conferring resistance to fosfomycin is detected in all three *E. coli* isolates (Takahata et al., 2010; Table 3). Overall, the antibiotic-resistant genotype is in good agreement with the resistant phenotype among the three *E. coli* isolates. The only exception is that no corresponding resistance gene is detected to explain the unexpected resistance of *E. coli* BE2-5 against ampicillin.

## Evidence for the Horizontal Transfer of ARGs Between Environmental and Avian *E. coli*

Almost all the ARGs detected in the avian *E. coli* (BE2-5) are found in two other environmental strains (W2-5 and W5-6, Table 3), which is consistent with our previous view that the antibiotic resistance (resistant bacteria or resistance genes) is mainly transferred from the polluted river (Jin River) to the wild bird (egret) (Wu et al., 2018). Most importantly, highly homologous MDR regions are detected on two plasmids of different Inc-types (pMCR\_W5-6 and p2\_BE2-5) in *E. coli* W5-6 and BE2-5, respectively (Figures 1A,B). The sizes of the MDR regions are around 12,800 bp (Figure 1D). Although the size and overall structure of the two plasmids are different (Figures 1A,B), the composition of the ARGs and MGE sequences (gene sequences encoding transposase and integrase) and their arrangement in the MDR regions are almost the same (Figure 1C and Supplementary Figure S4). The only difference is that the MDR region on the plasmid pMCR\_W5-6 missing an efflux pump gene *mef(B)* in comparison to the plasmid p2\_BE2-5. On the plasmid pMCR\_W5-6, there even remains a 33 nt 3' fragment of the *mef(B)* gene. This provides sequencing evidence for gene deletion and recombination during the evolution of the MDR region. The shared ARGs includes the genes conferring resistance to aminoglycosides [*aadA1*, *aadA2* and *aph(3')-Ia*], sulfonamides (*sul3*), trimethoprim (*drfA12*) and chloramphenicols (*cmlA1*). The shared MGE sequences, especially the IS26 sequences that are detected more than 5 copies on both plasmids (Figures 1A,B and Supplementary Figure S4),

**TABLE 2** | Antibiotic-resistant phenotype and corresponding resistance genes or genetic mutations in three *E. coli* isolates.

Isolates (Origin)	Phenotype and genotype	Aminoglycosides		Tetracyclines	Cephalosporins	Penicillins	Polypeptides	Quinolones	
		Kan	Ami					Gen	Str
W5-6 (Jin River)	AR (MIC)	R (> 128)	S (8)	R (> 128)	R (> 6.4)	R (> 128)	R (> 16)	R (> 6.4)	R (> 128)
	Gene	<i>aph(3')-Ia aph(4)-Ia</i>	<i>aac(3)-IV</i>	<i>aph(3')-Ib aadA1 aadA2 aph(6)-Id</i>	<i>bla<sub>CTX-M-14</sub></i>	<i>bla<sub>TEM-1</sub> bla<sub>CTX-M-14</sub></i>	<i>mcr-1</i>	<i>oqxA oqxB gyrA<sup>a</sup> parC<sup>a</sup></i>	<i>gyrA<sup>a</sup> parC<sup>a</sup></i>
W2-5 (Jin River)	AR (MIC)	S (16)	S (8)	S (4)	R (> 6.4)	R (> 128)	R (> 16)	R (> 6.4)	R (> 128)
	Gene			<i>aph(3')-Ib aph(6)-Id</i>	<i>bla<sub>CTX-M-55</sub></i>	<i>bla<sub>CTX-M-55</sub></i>	<i>mcr-1</i>	<i>gyrA<sup>a</sup> parC<sup>a</sup></i>	<i>gyrA<sup>a</sup> parC<sup>a</sup></i>
BE2-5 (Egret feces)	AR (MIC)	R (> 128)	S (8)	S (8)	S (0.025)	R (> 128)	R (16)	R (1.6)	R (16)
	Gene	<i>aph(3')-Ia</i>		<i>aadA1 aadA2</i>			<i>mcr-1</i>	<i>qnrS2</i>	<i>qnrS2</i>

AR, Antibiotic resistance; MIC, Minimum inhibitory concentration, µg/mL; Kan, kanamycin A; Ami, amikacin; Str, streptomycin; Tet, tetracycline; Cef, ceftriaxone; Amp, ampicillin; Col, colistin; Cip, ciprofloxacin; Nal, nalidixic acid; S, means susceptible; R, means resistant. <sup>a</sup>Point mutations in these genes confer resistance to fluoroquinolones. For specific details, please refer to Table 3.

should play an important role during the formation of the MDR regions, and provide conditions for the relocation of these ARGs. Since the highly homologous MDR regions are detected on the plasmids of different Inc-types and in the *E. coli* of different strain types, the evolution of the MDR regions must have involved the process of HGT.

The identical drug-resistant transposon containing *aph(3')-Ia* gene is also found on the chromosome (W5-6Chr) and plasmids (pMCR\_W5-6 and p2\_BE2-5) of different bacteria. Similarly, the resistance gene [*aph(3')-Ia*] is also flanked with transposase genes (*tnpA* IS26) on both sides (Supplementary Figure S5). The ARGs on other plasmids are illustrated in Supplementary Figure S6. Most of these ARGs also show close correlation with MGEs.

The spread of antibiotic resistance is closely related to the horizontal transfer of resistance genes, regardless in the clinical or in a natural environment, which is highly polluted with antibiotics or antibiotic resistant bacteria (Stokes and Gillings, 2011). In our case, Jin River (an urban river in Chengdu, Sichuan, China) is highly polluted with antibiotic resistant bacteria, and the avian inhabitants (egrets) there are also highly affected. The resistance genes conferring antibiotic-resistant phenotype in the three *E. coli* isolates are mainly distributed on plasmids or on chromosome, but in forms of transposons (Supplementary Figure S5). The resistance genes on plasmids are also closely related to MGE sequences (transposase and integrase genes on plasmids as shown in Figure 1 and Supplementary Figure S6). From environmental (polluted river water) and avian (egret) *E. coli* of different strain types, we have detected almost identical MDR regions on the plasmids of different incompatibility types. ARGs, which are flanked by MGE sequences, present as transposons or integrons in the MDR regions. Identical drug-resistance transposon [IS26-*aph(3')-Ia*-IS26] is also found on chromosome and plasmids of these host bacteria. These results indicate that HGT plays a crucial role in the environmental dissemination of antibiotic resistance, and the transfer of ARGs must involve multiple embedded genetic levels (transposons, integrons, plasmids, and bacterial lineages), which is so-called the nested “Russian doll” model of genetic mobility (Sheppard et al., 2016).

### Global Dissemination and Multiregional Evolution of *mcr-1* Plasmids

The metadata of 228 circular *mcr-1*-bearing plasmids were collected, as shown in Supplementary Table S1. The geographical distribution of plasmids of different incompatibility groups is depicted in Supplementary Figure S7. It is worth noting that the map outlines only the types of plasmid replicons on different continents. Some plasmids carry two or more (up to five) replicons (Supplementary Table S1). Therefore, a plasmid may have been counted more than once. The result still reflects the local diversity of plasmid types. Asia contributes the most types of *mcr-1*-bearing plasmids (13 out of 16). The other two continents in the Northern Hemisphere, Europe and North America also exhibit high diversity of plasmid types, 9 and 6, respectively. On the contrary, the regions in the Southern Hemisphere show poor plasmid

**TABLE 3** | CARD database annotated ARGs in three *E. coli* isolates.

Isolates	Location	Resistance mechanism					
		Efflux pump	Antibiotic inactivation	Target replacement/protection	Altering cell wall charge	Gene variant/mutant	Others (molecular bypass, absence, modulating permeability etc.)
W5-6	Chromosome	<i>A<sup>a</sup>, acrF, mdtB, tet(B)<sup>b</sup>, tet(D)<sup>b</sup></i>	<i>aph(3')-Ia, aph(6)-IId, aph(3')-Ib, catI</i>	<i>mfd, sul2</i>	<i>arnA, pmrC, pmrE, pmrF</i>	<i>glpT</i> (E448K) <sup>c</sup> ; <i>gyrA</i> (S83L, D87N) <sup>c</sup> ; <i>parC</i> (A56T, S80L, A620V) <sup>c</sup>	<i>bacA, lamB</i>
	pMCR_W5-6	<i>cmlA1, floR, qacH, oqxA, oqxB</i>	<i>aac(3)-IV, aadA1, aadA2, aph(3')-Ia, aph(4)-Ia, bla<sub>CTX-M-14</sub>, fosA3, bla<sub>TEM-1</sub></i>	<i>dfrA12, sul1, sul2, sul3</i>	<i>mcr-1</i>		
	p2_W5-6 p3_W5-6	<i>floR, vgaC</i>					
W2-5	Chromosome	<i>A<sup>a</sup>, floR, mdtF<sup>b</sup>, muxB, tet(A)</i>	<i>aph(3')-Ib, aph(6)-IId</i>	<i>mfd<sup>b</sup>, sul2</i>	<i>arnA, pmrC, pmrE, pmrF</i>	<i>glpT</i> (E448K) <sup>c</sup> ; <i>gyrA</i> (S83L, D87N) <sup>c</sup> ; <i>parC</i> (S80) <sup>c</sup>	<i>bacA, lamB</i>
	pMCR_W2-5				<i>mcr-1</i>		
	p2_W2-5	<i>vgaC</i>	<i>bla<sub>CTX-M-55</sub></i>				
BE2-5	Chromosome	<i>A<sup>a</sup>, mdtF<sup>b</sup>, muxB, tet(A)</i>		<i>mfd</i>	<i>arnA, pmrC, pmrE, pmrF</i>	<i>glpT</i> (E448K) <sup>c</sup>	<i>bacA, lamB</i>
	pMCR_BE2-5				<i>mcr-1</i>		
	p2_BE2-5	<i>cmlA1, mef(B), qacH, tet(A)</i>	<i>aadA1, aadA2, aph(3')-Ia</i>	<i>dfrA12, qnrS2, sul3</i>			

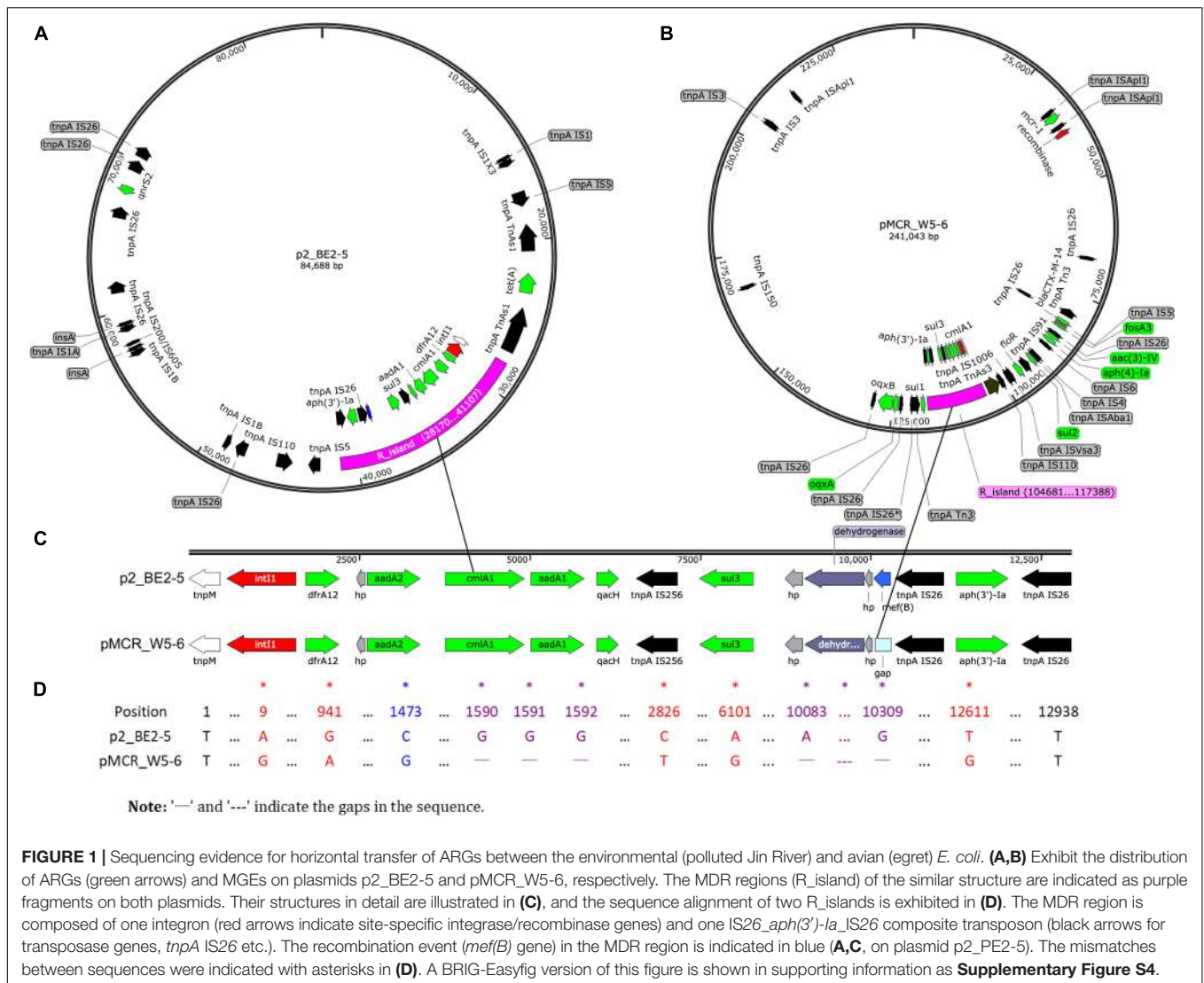
<sup>a</sup>*A* represents the common efflux pump genes in all three *E. coli* isolates, which include *acrA, acrB, acrE, acrR, acrS, baeR, baeS, cpxA, cpxR, crp, emrA, emrB, emrD, emrE, emrK, emrR, emrY, evgA, evgS, gadW, gadX, hns, kdpE, leuO, marA, mdfA, mdtA, mdtE, mdtF<sup>b</sup>, mdtG, mdtH, mdtL, mdtM, mdtN, mdtO, mdtP, mexN, msbA, msrB, patA, rob, tolC, yojI*. <sup>b</sup>There are two copies of *mdtF* on the chromosome of W5-6, three copies of *mdtF* on both chromosomes of W2-5 and BE2-5, two copies of *mfd* on the chromosome of W2-5, and two copies of *tet(B)* and *tet(D)* on the chromosome of W5-6. <sup>c</sup>Specific point mutations in each gene are listed in the bracket. The reference sequences are from the genome of *E. coli* K-12 MG1655 (Accession No. NC\_000913.3).

diversity (Supplementary Figure S7). Sampling bias may have led to this discrepancy. However, twenty-eight *mcr-1*-bearing plasmids recovered from South America give only two plasmid types, IncX4 and IncI2. Up to some extent it reflects that the Southern Hemisphere (at least South America) suffers fewer invasions of various *mcr-1*-bearing plasmids. Among these *mcr-1*-bearing plasmids, the numbers of IncI2, IncX4 and IncHI2 plasmids are ranked at the top 3. Their detection rates in various *Enterobacteriaceae* hosts on different continents are illustrated in Figure 2A. IncI2 plasmids exhibit the most diverse bacterial hosts (in 6 unique host species of *Enterobacteriaceae*) and the most extensive geographical distribution (in all continents).

The IncHI2-type plasmid is the most diverse plasmid and harbors a large MDR region (Li et al., 2017). Therefore, it is considered as a genetic element mediating the transmission of MDR genes. A wide range of resistance genes and MGEs can be found in a Mosaic MDR region of IncHI2-type plasmids (Li et al., 2017). We recorded the additional ARGs on each IncHI2 plasmid (Supplementary Table S1). Co-occurrence network analysis, showing the correlation between these ARGs and their geographic distribution, was performed in Matlab\_R2016a. The composition of ARGs in this MDR region varies according to their geographical distribution (Figure 2B). Such an MDR region is also discovered in our sequenced IncHI2-type plasmid, pMCR\_W5-6 (Figure 1B). Unlike other ARGs concentrated in such an MDR region, *mcr-1* gene is located in another location

on the plasmid away from the MDR region (Supplementary Table S1 also lists the interval between *mcr-1* and other ARGs). It has a unique transposon structure, IS*AplI*-*mcr-1*-orf-IS*AplI* (Snesrud et al., 2016; Li et al., 2017). The insertion of *mcr-1*-bearing transposon in such type of plasmid should be a late independent event. The exact time of the insertion event is hard to be determined, but the backbone structure of the IncHI2-type plasmid at the time of *mcr-1* insertion can be speculated. The ARGs with high occurrence frequency should be the original backbone structure of this type of plasmids (Figure 2B). Besides *mcr-1*, two other ARGs, *floR* and *aadA2*, are common all over the world on this type of plasmids. It has been reported that the resistance (*floR*) to florfenicol – a veterinary drug – is commonly associated with *mcr-1* (Matamoros et al., 2017; Shen et al., 2018), which supports the animal origin of the mobilized *mcr-1* gene (Matamoros et al., 2017; Wang et al., 2018). The *mcr-1*-bearing IncHI2 plasmids recovered from Asia (mainly from China) possess the most diverse ARGs (Figure 2C), which must be due to the extensive use of antibiotics in this area (Zhang et al., 2015). The three unique ARGs on European IncHI2 plasmids are *aadA12*, *bla<sub>TEM1A</sub>* and *catA1*. This may be attributed to regional evolution events in Europe.

The IncX4-type plasmids are the most conserved and the smallest (mostly around 33 kb) ones among all types of *mcr-1*-bearing plasmids (Li et al., 2017). The sequences of IncX4-type plasmids were adjusted from the same start point and



**FIGURE 1 |** Sequencing evidence for horizontal transfer of ARGs between the environmental (polluted Jin River) and avian (egret) *E. coli*. **(A,B)** Exhibit the distribution of ARGs (green arrows) and MGEs on plasmids p2\_BE2-5 and pMCR\_W5-6, respectively. The MDR regions (R\_island) of the similar structure are indicated as purple fragments on both plasmids. Their structures in detail are illustrated in **(C)**, and the sequence alignment of two R\_islands is exhibited in **(D)**. The MDR region is composed of one integron (red arrows indicate site-specific integrase/recombinase genes) and one IS26\_aph(3)-la\_IS26 composite transposon (black arrows for transposase genes, *tnpA* IS26 etc.). The recombination event (*mef(B)* gene) in the MDR region is indicated in blue **(A,C)**, on plasmid p2\_BE2-5. The mismatches between sequences were indicated with asterisks in **(D)**. A BRIG-Easyfig version of this figure is shown in supporting information as **Supplementary Figure S4**.

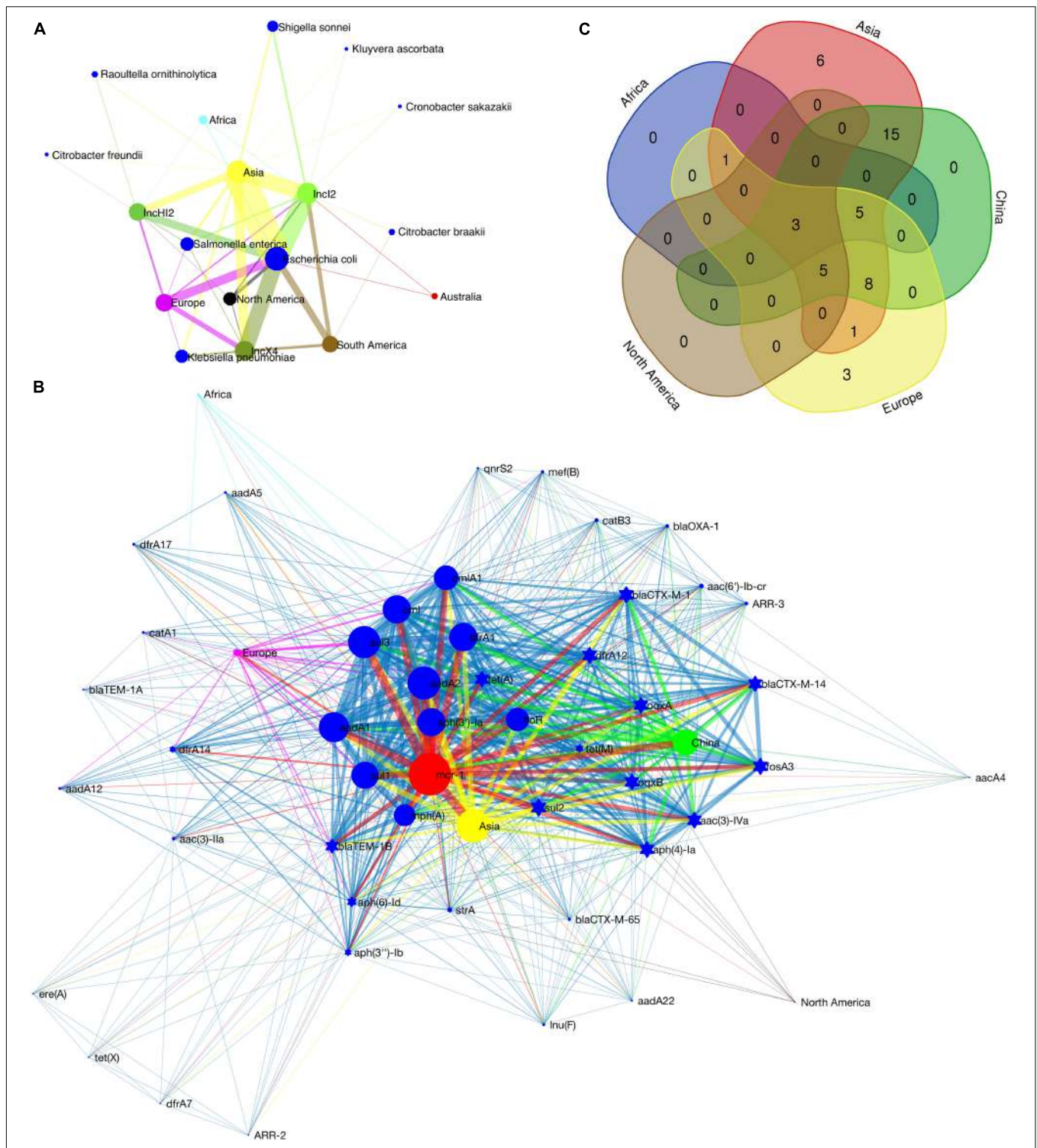
aligned with the multiple sequence alignment program MAFFT<sup>4</sup> (Katoh et al., 2017). The aligned sequences were used to construct a phylogenetic tree in MEGA7 (Kumar et al., 2016). The IncI2-type plasmids contain a site-specific recombination system, the shufflon. The shufflon generates variants of the PilV protein, a minor component of the thin pilus. The shufflon is one of the most difficult regions for *de novo* genome assembly, because of its structural diversity even in a single bacterial colony (Sekizuka et al., 2017). Therefore, the shufflon structure affects the alignment of the plasmid sequences, and thus affects the phylogenetic reconstruction. For this type of plasmid ( $n = 92$ ), we excised the shufflon region from each plasmid sequence and used the remaining part for phylogenetic analysis as we did for IncX4-type plasmids. From the phylogenetic trees of the two types of plasmid (**Supplementary Figures S8, S9A**), we detected the genotypic clusters of a single geographical origin. Typically, the plasmid clusters of South America are

observed in both phylogenetic trees, which indicates relatively seldom exchange of *mcr-I*-bearing plasmids between South America and other geographical regions. Geographical barriers may result in such a regional evolution. Meanwhile, Asia shows the closest communication with other geographical regions, and the interconnection between Europe and North America is relatively high. In addition, according to the phylogenetic trees of the two types of plasmids, the intercontinental exchange of IncI2 plasmids seems more frequent than that of IncX4 plasmids. The diversity of bacterial hosts of IncI2 plasmids (**Figure 2A**) may have facilitated their transportation among different continents, which can also explain why IncI2 plasmids occupy the largest share of the *mcr-I*-bearing plasmids (41% of 229 *mcr-I*-bearing plasmids).

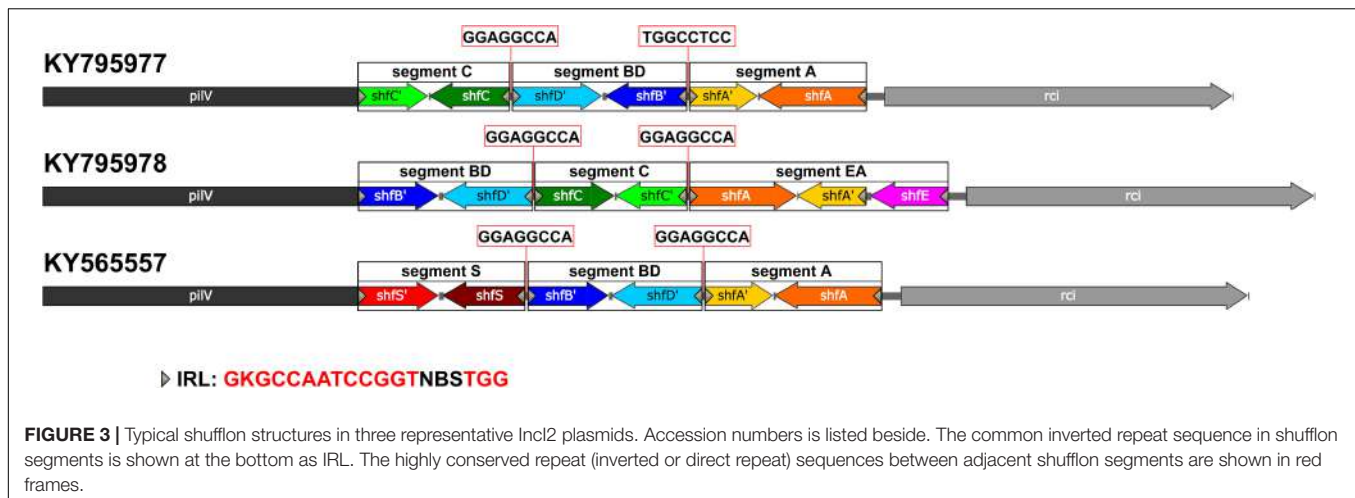
The shufflons extracted from IncI2 plasmids were carefully annotated the structure. Typical shufflon structures are illustrated in **Figure 3**. There is a pair of inverted *sfx* repeats (IRL: **GKGGCAATCCGGTNBSTGG** and IRR: **CCASVNACCGGATTGGCMC**) at both ends of each shufflon

<sup>4</sup><https://mafft.cbrc.jp/alignment/server/>





**FIGURE 2 |** Detection rate of *mcr-1*-bearing plasmids in various bacterial host species on different continents **(A)**, co-occurrence network of *mcr-1* with additional ARGs on IncHI2 plasmids **(B)** and Venn diagram showing the numbers of shared and unique additional ARGs on IncHI2 plasmids at different regions **(C)**. In **(A)**, the size of the nodes (plasmid type, bacterial species or continent) is proportional to their detection rate (log-transformed), and the width of the edge between two nodes is proportional to the detection rate of one node (plasmid type or bacterial species) from another (bacterial species and/or continent). Blue nodes indicate bacterial species, green of different saturations the plasmid types and the nodes of other colors the continents. In **(B)**, the size of the nodes (ARG or geographical region) indicates the frequency of their occurrence, and the width of the edges is proportional to the co-occurrence rate between two nodes (between two ARGs or between an ARG and its location). Blue nodes indicate additional ARGs, red the *mcr-1* gene and the nodes of other colors the geographical regions. Ten most frequently occurred ARGs are shown as blue circles.



segment, and also a highly conserved inverted or direct repeat sequence (GGAGGCCA) between adjacent shufflon segments. The shufflon structure also exhibits regional disparity (**Supplementary Table S2**), which is in good agreement with the clustering mode of IncI2 plasmids in the phylogenetic tree (**Supplementary Figure S9B**). IncI2-type plasmids isolated from Asia contain almost all kinds of shufflon structures. The shufflon rearrangement is closely related to plasmid transmission to a broad range of the Enterobacteriaceae (Ishiwa and Komano, 2003, 2004). This can explain why the most diverse Enterobacteriaceae hosts bearing *mcr-1*-positive IncI2 plasmids are detected in Asia (**Figure 2A**). The IncI2 plasmids isolated from Europe and North America commonly contain the shufflon segment E (except those plasmids with only one shufflon segment), while, to date (June 2018), no IncI2 plasmid from South America has been detected with definite structure of shufflon segment E (**Supplementary Table S2**). The *mcr-1*-bearing IncI2 plasmids in Europe and North America may mainly be derived from a plasmid with shufflon segment E, while those in South America may have been originated from one without the segment. Geographical barriers retain this original mark.

Some shufflon sequences cannot be annotated as accurate segmental structure, which could be due to sequencing/assembly mistakes (**Supplementary Table S2**). We also found an unnoticed shufflon segment structure that had never been annotated in the database. It is common and highly conserved in several IncI2 type plasmids (**Supplementary Table S2**, KY565557, CM008278, CP028153, CP006264, CP007134, FR851304, and CP030766), which cannot be accidental events. Thus we assigned the segment as segment S (**Figure 3**, KY565557).

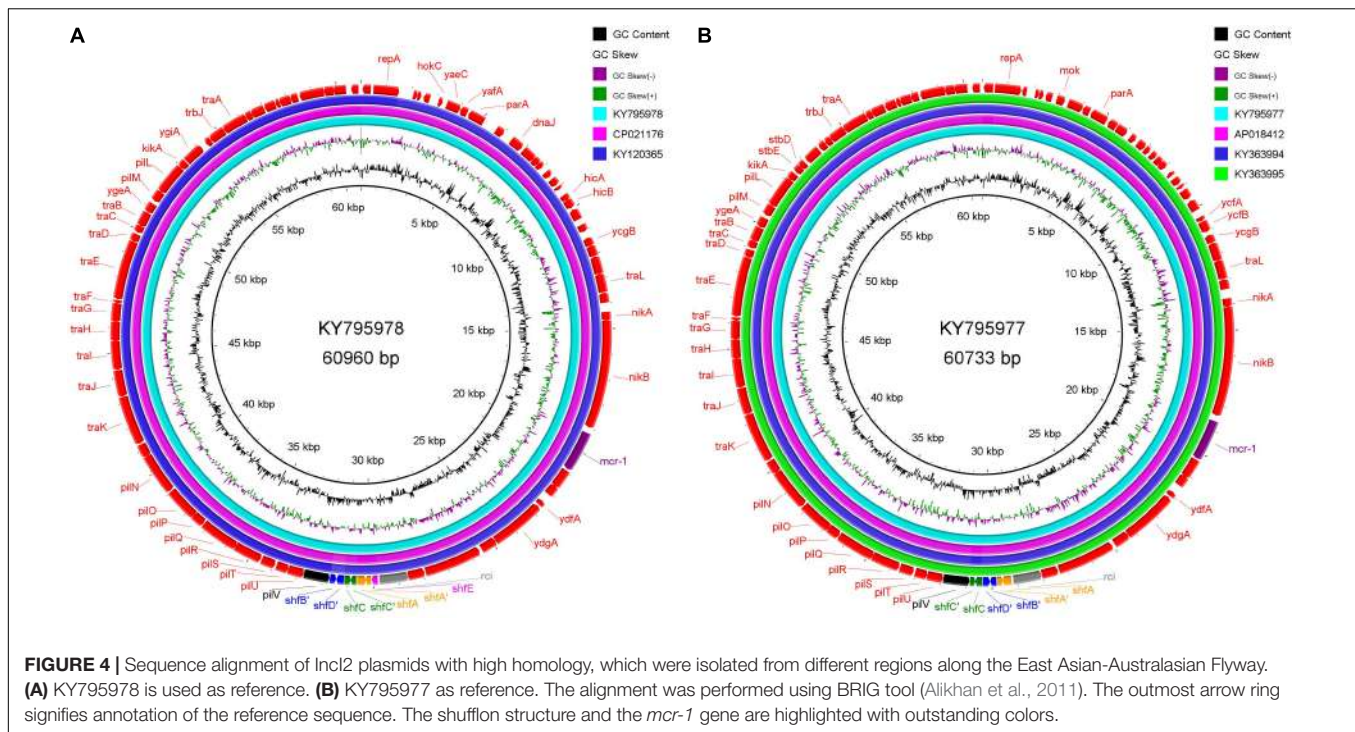
The mechanism of Nested Russian Doll-like genetic mobility must be common for the worldwide dissemination of various mobilized ARGs (Dortet et al., 2014; Sheppard et al., 2016; Wang et al., 2018). The *bla*<sub>NDM</sub> and *bla*<sub>KPC</sub> genes are mainly located on conjugative plasmids of several different incompatibility groups (Dortet et al., 2014; Sheppard et al., 2016), which is similar to the behavior of *mcr-1* gene. ARGs may be flanked by different MGE sequences at their mobilization, and exhibit different

characteristics in their relocation process. The transfer of *mcr-1* is mediated by the insertion sequence *ISAp11*. The high activity of this MGE enables *mcr-1* gene to jump flexibly between different plasmids and between different bacterial species (**Supplementary Table S1**). At bacterial genome level, no genotypic clustering by geographical origin and isolation source has been observed (Matamoros et al., 2017). While at the transposon level, scientists have predicted the time of the initial mobilization of *mcr-1* (Wang et al., 2018). In this work, at the plasmid level (one important genetic level involved in HGT) and according to the analysis routine illustrated in **Supplementary Figure S1**, we have found that the global spread of *mcr-1*-bearing plasmids is accompanied by their multiregional evolution. Based on the intrinsic mechanism of HGT, we believe that the analysis of mobilized ARGs at multiple levels of MGEs (transposons, integrons, and plasmids) can give important epidemiological information about their dissemination.

## Possible Intercontinental Transportation of Resistance Plasmids

Since we have found sequencing evidence for the horizontal transfer of ARGs between the environmental and avian bacteria, it is possible that migratory birds mediate the intercontinental transportation of the resistance plasmid. Two typical cases were noted at the analysis of IncI2 plasmids. First, the IncI2 plasmid, pJIE3685-1 (KY795978), isolated from Australia is of almost the same size (~60960 bp) with two plasmids isolated from China (Taiwan), p5CRE51-MCR-1 (CP021176 from a human *E. coli*), and pP111 (KY120365, from a porcine *Salmonella enterica* subsp.). The position and the segment composition of the shufflon structure is also the same in the three plasmids (**Supplementary Table S2**), which indicates that the shufflon of the three plasmids is equivalent. Alignment of the remaining parts of the three plasmids after shufflon excision shows high identity among them with mismatches of only several (~7 nts out of 59,042 nts) nucleotides (**Figure 4A**). In addition, another IncI2 plasmid from Australia, pJIE2288-1 (KY795977), is also highly identical (~8 nts mismatches out of 59,081 nts)





to the three plasmids from Asia (**Figure 4B**), pRYU2912C-1 (AP018412, Japan, from a *E. coli*), pSh113-m4 (KY363994, Shanghai, China, from a human *Shigella sonnei*) and pSh069-m6 (KY363995, Shanghai, China, from a human *Shigella sonnei*). Such close genetic relationships between these plasmids suggest that they do not seem to originate from a common evolutionary ancestor, but rather are duplicate offspring of the same plasmid. Two Australian plasmids are from *E. coli* strains that were isolated from two clinical patients at New South Wales. Neither patients had ever gone abroad or had taken colistin/polymyxin antimicrobial drugs during hospitalization (Ellem et al., 2017). We noticed that these highly homologous IncI2 plasmids were all found on the same flyway of migratory shorebirds, i.e., the East Asian-Australasian Flyway (**Supplementary Figure S7**). Many species of migratory shorebirds take extreme long-distance migration between eastern Russia and Oceania. During the migration, they stage once in Eastern Asia (typically the Yellow Sea region) for around 40 days, resting and refueling for the subsequent flight (Battley et al., 2012). There is continental-scale pollution of ARGs at the estuaries along the east coast of China, where the migratory shorebirds pass by Zhu et al. (2017). Migratory shorebirds can be an option for tracking the source of the resistance plasmids.

During the outbreak of avian influenza, migratory birds as potential global spreaders had attracted the attention of scientists (Liu et al., 2005; Normile, 2006; Olsen et al., 2006). However, according to a number of previously reported studies, the risk of migratory birds mediating intercontinental exchange of influenza virus, especially those highly pathogenic ones, is fairly low (Krauss et al., 2007; Langstaff et al., 2009). A sick bird can hardly accomplish the arduous task of long-distance (intercontinental)

migration. Nevertheless, migratory shorebirds carrying drug-resistant symbiotic bacteria can cross the **Wallace Line** and bring ARGs from Asia to Australia (**Supplementary Figure S7**). Since the discovery of the mobilized colistin resistance gene, several studies have reported the detection of *mcr-1*-positive *E. coli* in migratory birds (Liakopoulos et al., 2016; Mohsin et al., 2016; Ruzauskas and Vaskeviciute, 2016; Sellera et al., 2017). Salt tolerant *mcr-1*-positive *E. coli* strains have also been isolated from recreational waters of public urban beaches (Fernandes et al., 2017). Therefore, *mcr-1*-bearing plasmids may be transported, via avian migration, from Eastern Asia to Australia, where the usage of antibiotics is under strict control but is definitely affected by migratory shorebirds. In fact, *mcr-1*-positive *E. coli* has recently been isolated from wild bird (silver gull) in Australia (Mukerji et al., 2019). In view of limited data available for bacterial ARGs of migratory birds, it is difficult to discuss the global dissemination of ARGs in the context of avian ecology. Our analysis does not imply that avian migration is the main route for the global dissemination of antibiotic resistance. In today's highly globalized world, global population mobility and international trade, especially the trade of food animal, must be the main channels (Matamoros et al., 2017; Shen et al., 2018; Hernando-Amado et al., 2019). Even so, the large number of migratory birds and their fixed migration path will have a lasting impact on the receptor environment. In particular, different countries execute different strategies for using antibiotics. Antibiotics used for human in one country may be used as animal feed additives in another. If migratory birds transport antibiotic resistance from the latter environment to the former, the cause originated in one country may have a devastating consequence in another.

Nowadays, with the global dissemination of antibiotic resistance, no country can be immune from it. The application of antibiotics should follow the strategy of global unification.

## DATA AVAILABILITY STATEMENT

Publicly available datasets were analyzed in this study. This data can be found in GenBank database under the accession numbers CP032986 to CP032995.

## AUTHOR CONTRIBUTIONS

KY and JW designed the study. DR isolated the *E. coli* strains and evaluated their drug resistance. JW and YL prepared the DNA samples for sequencing and analyzed the sequencing data. XD and LZ performed the metadata analysis of the *mcr-1*-bearing

plasmids. YL, JW, and KY constructed the manuscript. YF edited the manuscript and put forward constructive suggestions on it. All authors reviewed, revised, and approved the final report.

## FUNDING

We gratefully acknowledge the financial support from the Initiating Research Fund for Talent Introduction of Sichuan University (YJ201355) and the Natural Science Foundation of China (21677104).

## SUPPLEMENTARY MATERIAL

The Supplementary Material for this article can be found online at: <https://www.frontiersin.org/articles/10.3389/fmicb.2020.00352/full#supplementary-material>

## REFERENCES

- Alikhan, N. F., Petty, N. K., Ben Zakour, N. L., and Beatson, S. A. (2011). BLAST ring image generator (BRIG): simple prokaryote genome comparisons. *BMC Genomics* 12:402. doi: 10.1186/1471-2164-12-402
- Altschul, S. F., Gish, W., Miller, W., Myers, E. W., and Lipman, D. J. (1990). Basic local alignment search tool. *J. Mol. Biol.* 215, 403–410. doi: 10.1016/S0022-2836(05)80360-2
- Ashburner, M., Ball, C. A., Blake, J. A., Botstein, D., Butler, H., Cherry, J. M., et al. (2000). Gene ontology: tool for the unification of biology. The gene ontology consortium. *Nat. Genet.* 25, 25–29. doi: 10.1038/75556
- Bairoch, A., and Apweiler, R. (2000). The SWISS-PROT protein sequence database and its supplement TrEMBL in 2000. *Nucleic Acids Res.* 28, 45–48. doi: 10.1093/nar/21.13.3093
- Battley, P. F., Warnock, N., Tibbitts, T. L., Gill, R. E., Piersma, T., Hassell, C. J., et al. (2012). Contrasting extreme long-distance migration patterns in bar-tailed godwits *Limosa lapponica*. *J. Avian Biol.* 43, 21–32. doi: 10.1111/j.1600-048X.2011.05473.x
- Berlin, K., Koren, S., Chin, C. S., Drake, J. P., Landolin, J. M., and Phillippy, A. M. (2015). Assembling large genomes with single-molecule sequencing and locality-sensitive hashing. *Nat. Biotechnol.* 33, 623–630. doi: 10.1038/nbt.3238
- Besemer, J., Lomsadze, A., and Borodovsky, M. (2001). GeneMarkS: a self-training method for prediction of gene starts in microbial genomes. Implications for finding sequence motifs in regulatory regions. *Nucleic Acids Res.* 29, 2607–2618. doi: 10.1371/journal.pone.0017473
- Carattoli, A., Zankari, E., Garcia-Fernandez, A., Voldby Larsen, M., Lund, O., Villa, L., et al. (2014). In silico detection and typing of plasmids using PlasmidFinder and plasmid multilocus sequence typing. *Antimicrob. Agents Chemother.* 58, 3895–3903. doi: 10.1128/AAC.02412-14
- Clinical and Laboratory Standards Institute [CLSI], (2019). *Performance Standards for Antimicrobial Susceptibility Testing—Twenty-Ninth Edition: M100*. Wayne, PA: CLSI.
- Cuzon, G., Naas, T., and Nordmann, P. (2011). Functional characterization of Tn4401, a Tn3-based transposon involved in blaKPC gene mobilization. *Antimicrob. Agents Chemother.* 55, 5370–5373. doi: 10.1128/AAC.05202-11
- Dortet, L., Poirel, L., and Nordmann, P. (2014). Worldwide dissemination of the NDM-type carbapenemases in Gram-negative bacteria. *Biomed. Res Int.* 2014:249856. doi: 10.1155/2014/249856
- Ellem, J. A., Ginn, A. N., Chen, S. C., Ferguson, J., Partridge, S. R., and Iredell, J. R. (2017). Locally acquired *mcr-1* in *Escherichia coli*, Australia, 2011 and 2013. *Emerg. Infect. Dis.* 23, 1160–1163. doi: 10.3201/eid2307.161638
- Fernandes, M. R., Sellera, F. P., Esposito, F., Sabino, C. P., Cerdeira, L., and Lincopan, N. (2017). Colistin-resistant *mcr-1*-positive *Escherichia coli* on public beaches, an infectious threat emerging in recreational waters. *Antimicrob Agents Chemother.* 61:e00234-17. doi: 10.1128/AAC.00234-17
- Gay, K., Robicsek, A., Strahilevitz, J., Park, C. H., Jacoby, G., Barrett, T. J., et al. (2006). Plasmid-mediated quinolone resistance in non-Typhi serotypes of *Salmonella enterica*. *Clin. Infect. Dis.* 43, 297–304. doi: 10.1086/505397
- Hernando-Amado, S., Coque, T. M., Baquero, F., and Martinez, J. L. (2019). Defining and combating antibiotic resistance from One Health and Global Health perspectives. *Nat. Microbiol.* 4, 1432–1442. doi: 10.1038/s41564-019-0503-9
- Ishiwa, A., and Komano, T. (2003). Thin pilus PilV adhesins of plasmid R64 recognize specific structures of the lipopolysaccharide molecules of recipient cells. *J. Bacteriol.* 185, 5192–5199. doi: 10.1128/jb.185.17.5192-5199.2003
- Ishiwa, A., and Komano, T. (2004). PilV adhesins of plasmid R64 thin pili specifically bind to the lipopolysaccharides of recipient cells. *J. Mol. Biol.* 343, 615–625. doi: 10.1016/j.jmb.2004.08.059
- Kanehisa, M., Goto, S., Hattori, M., Aoki-Kinoshita, K. F., Itoh, M., Kawashima, S., et al. (2006). From genomics to chemical genomics: new developments in KEGG. *Nucleic Acids Res.* 34, D354–D357. doi: 10.1093/nar/gkj102
- Kanehisa, M., Goto, S., Kawashima, S., Okuno, Y., and Hattori, M. (2004). The KEGG resource for deciphering the genome. *Nucleic Acids Res.* 32, D277–D280. doi: 10.1093/nar/gkh063
- Katoh, K., Rozewicki, J., and Yamada, K. D. (2017). MAFFT online service: multiple sequence alignment, interactive sequence choice and visualization. *Brief. Bioinform.* 20, 1160–1166. doi: 10.1093/bib/bbx108
- Kim, H. B., Wang, M., Park, C. H., Kim, E. C., Jacoby, G. A., and Hooper, D. C. (2009). oqxAB encoding a multidrug efflux pump in human clinical isolates of *Enterobacteriaceae*. *Antimicrob. Agents Chemother.* 53, 3582–3584. doi: 10.1128/AAC.01574-08
- Koren, S., and Phillippy, A. M. (2015). One chromosome, one contig: complete microbial genomes from long-read sequencing and assembly. *Curr. Opin. Microbiol.* 23, 110–120. doi: 10.1016/j.mib.2014.11.014
- Krauss, S., Obert, C. A., Franks, J., Walker, D., Jones, K., Seiler, P., et al. (2007). Influenza in migratory birds and evidence of limited intercontinental virus exchange. *PLoS Pathog.* 3:e167. doi: 10.1371/journal.ppat.0030167
- Kumar, S., Stecher, G., and Tamura, K. (2016). MEGA7: molecular evolutionary genetics analysis version 7.0 for bigger datasets. *Mol. Biol. Evol.* 33, 1870–1874. doi: 10.1093/molbev/msw054
- Langstaff, I. G., McKenzie, J. S., Stanislawek, W. L., Reed, C. E., Poland, R., and Cork, S. C. (2009). Surveillance for highly pathogenic avian influenza in migratory shorebirds at the terminus of the East Asian-Australasian flyway. *N. Z. Vet. J.* 57, 160–165. doi: 10.1080/00480169.2009.36896
- Larsen, M. V., Cosentino, S., Rasmussen, S., Friis, C., Hasman, H., Marvig, R. L., et al. (2012). Multilocus sequence typing of total-genome-sequenced bacteria. *J. Clin. Microbiol.* 50, 1355–1361. doi: 10.1128/JCM.06094-11
- Li, R., Xie, M., Zhang, J., Yang, Z., Liu, L., Liu, X., et al. (2017). Genetic characterization of *mcr-1*-bearing plasmids to depict molecular mechanisms



- underlying dissemination of the colistin resistance determinant. *J. Antimicrob. Chemother.* 72, 393–401. doi: 10.1093/jac/dkw411
- Li, W. Z., Jaroszewski, L., and Godzik, A. (2002). Tolerating some redundancy significantly speeds up clustering of large protein databases. *Bioinformatics* 18, 77–82. doi: 10.1093/bioinformatics/18.1.77
- Liakopoulos, A., Mevius, D. J., Olsen, B., and Bonnedahl, J. (2016). The colistin resistance *mcr-1* gene is going wild. *J. Antimicrob. Chemother.* 71, 2335–2336. doi: 10.1093/jac/dkw262
- Liebert, C. A., Hall, R. M., and Summers, A. O. (1999). Transposon Tn21, flagship of the floating genome. *Microbiol. Mol. Biol. Rev.* 63, 507–522. doi: 10.1128/mmbr.63.3.507-522.1999
- Liu, B., and Pop, M. (2009). ARDB—antibiotic resistance genes database. *Nucleic Acids Res.* 37, D443–D447. doi: 10.1093/nar/gkn656
- Liu, J., Xiao, H., Lei, F., Zhu, Q., Qin, K., Zhang, X. W., et al. (2005). Highly pathogenic H5N1 influenza virus infection in migratory birds. *Science* 309:1206. doi: 10.1126/science.1115273
- Liu, Y. Y., Wang, Y., Walsh, T. R., Yi, L. X., Zhang, R., Spencer, J., et al. (2016). Emergence of plasmid-mediated colistin resistance mechanism MCR-1 in animals and human beings in China: a microbiological and molecular biological study. *Lancet Infect. Dis.* 16, 161–168. doi: 10.1016/S1473-3099(15)00424-7
- Magrane, M., and UniProt, C. (2011). UniProt knowledgebase: a hub of integrated protein data. *Database* 2011:bar009. doi: 10.1093/database/bar009
- Martinez, J. L., Sanchez, M. B., Martinez-Solano, L., Hernandez, A., Garmendia, L., Fajardo, A., et al. (2009). Functional role of bacterial multidrug efflux pumps in microbial natural ecosystems. *FEMS Microbiol. Rev.* 33, 430–449. doi: 10.1111/j.1574-6976.2008.00157.x
- Matamoros, S., van Hattem, J. M., Arcilla, M. S., Willemse, N., Melles, D. C., Penders, J., et al. (2017). Global phylogenetic analysis of *Escherichia coli* and plasmids carrying the *mcr-1* gene indicates bacterial diversity but plasmid restriction. *Sci. Rep.* 7:15364. doi: 10.1038/s41598-017-15539-7
- McArthur, A. G., Wagelchner, N., Nizam, F., Yan, A., Azad, M. A., Baylay, A. J., et al. (2013). The comprehensive antibiotic resistance database. *Antimicrob. Agents Chemother.* 57, 3348–3357. doi: 10.1128/AAC.00419-13
- Mohsin, M., Raza, S., Roschanski, N., Schaufler, K., and Guenther, S. (2016). First description of plasmid-mediated colistin-resistant extended-spectrum beta-lactamase-producing *Escherichia coli* in a wild migratory bird from Asia. *Int. J. Antimicrob. Agents* 48, 463–464. doi: 10.1016/j.ijantimicag.2016.07.001
- Mukerji, S., Stegger, M., Truswell, A. V., Laird, T., Jordan, D., Abraham, R. J., et al. (2019). Resistance to critically important antimicrobials in Australian silver gulls (*Chroicocephalus novaehollandiae*) and evidence of anthropogenic origins. *J. Antimicrob. Chemother.* 74, 2566–2574. doi: 10.1093/jac/dkz242
- Munoz-Price, L. S., Poirel, L., Bonomo, R. A., Schwaber, M. J., Daikos, G. L., Cormican, M., et al. (2013). Clinical epidemiology of the global expansion of *Klebsiella pneumoniae* carbapenemases. *Lancet Infect. Dis.* 13, 785–796. doi: 10.1016/S1473-3099(13)70190-7
- Naas, T., Cuzon, G., Villeges, M. V., Lartigue, M. F., Quinn, J. P., and Nordmann, P. (2008). Genetic structures at the origin of acquisition of the beta-lactamase bla(KPC) gene. *Antimicrob. Agents Chemother.* 52, 1257–1263.
- Normile, D. (2006). Avian influenza. Evidence points to migratory birds in H5N1 spread. *Science* 311:1225. doi: 10.1126/science.311.5765.1225
- Olsen, B., Munster, V. J., Wallensten, A., Waldenstrom, J., Osterhaus, A. D., and Fouchier, R. A. (2006). Global patterns of influenza A virus in wild birds. *Science* 312, 384–388. doi: 10.1126/science.1122438
- Oram, M., and Fisher, L. M. (1991). 4-Quinolone resistance mutations in the DNA gyrase of *Escherichia coli* clinical isolates identified by using the polymerase chain reaction. *Antimicrob. Agents Chemother.* 35, 387–389. doi: 10.1128/aac.35.2.387
- Poirel, L., Bonnin, R. A., Boulanger, A., Schrenzel, J., Kaase, M., and Nordmann, P. (2012). Tn125-related acquisition of blaNDM-like genes in *Acinetobacter baumannii*. *Antimicrob. Agents Chemother.* 56, 1087–1089. doi: 10.1128/AAC.05620-11
- Ruzauskas, M., and Vaskeviciute, L. (2016). Detection of the *mcr-1* gene in *Escherichia coli* prevalent in the migratory bird species *Larus argentatus*. *J. Antimicrob. Chemother.* 71, 2333–2334. doi: 10.1093/jac/dkw245
- Saier, M. H. Jr., Reddy, V. S., Tamang, D. G., and Vastermark, A. (2014). The transporter classification database. *Nucleic Acids Res.* 42, D251–D258. doi: 10.1093/nar/gkt1097
- Sekizuka, T., Kawanishi, M., Ohnishi, M., Shima, A., Kato, K., Yamashita, A., et al. (2017). Elucidation of quantitative structural diversity of remarkable rearrangement regions, shufflons, in IncI2 plasmids. *Sci. Rep.* 7:928. doi: 10.1038/s41598-017-01082-y
- Sellera, F. P., Fernandes, M. R., Sartori, L., Carvalho, M. P., Esposito, F., Nascimento, C. L., et al. (2017). *Escherichia coli* carrying IncX4 plasmid-mediated *mcr-1* and blaCTX-M genes in infected migratory Magellanic penguins (*Spheniscus magellanicus*). *J. Antimicrob. Chemother.* 72, 1255–1256. doi: 10.1093/jac/dkw543
- Shen, Y., Zhou, H., Xu, J., Wang, Y., Zhang, Q., Walsh, T. R., et al. (2018). Anthropogenic and environmental factors associated with high incidence of *mcr-1* carriage in humans across China. *Nat. Microbiol.* 3, 1054–1062. doi: 10.1038/s41564-018-0205-8
- Sheppard, A. E., Stoesser, N., Wilson, D. J., Sebra, R., Kasarskis, A., Anson, L. W., et al. (2016). Nested Russian doll-like genetic mobility drives rapid dissemination of the carbapenem resistance gene blaKPC. *Antimicrob. Agents Chemother.* 60, 3767–3778. doi: 10.1128/AAC.00464-16
- Snesrud, E., He, S., Chandler, M., Dekker, J. P., Hickman, A. B., McGann, P., et al. (2016). A model for transposition of the colistin resistance gene *mcr-1* by ISAp1. *Antimicrob. Agents Chemother.* 60, 6973–6976. doi: 10.1128/AAC.01457-16
- Stokes, H. W., and Gillings, M. R. (2011). Gene flow, mobile genetic elements and the recruitment of antibiotic resistance genes into Gram-negative pathogens. *FEMS Microbiol. Rev.* 35, 790–819. doi: 10.1111/j.1574-6976.2011.00273.x
- Takahata, S., Ida, T., Hiraishi, T., Sakakibara, S., Maebashi, K., Terada, S., et al. (2010). Molecular mechanisms of fosfomycin resistance in clinical isolates of *Escherichia coli*. *Int. J. Antimicrob. Agents* 35, 333–337. doi: 10.1016/j.ijantimicag.2009.11.011
- Tankovic, J., Perichon, B., Duval, J., and Courvalin, P. (1996). Contribution of mutations in *gyrA* and *parC* genes to fluoroquinolone resistance of mutants of *Streptococcus pneumoniae* obtained *in vivo* and *in vitro*. *Antimicrob. Agents Chemother.* 40, 2505–2510. doi: 10.1128/aac.40.11.2505
- Tatusov, R. L., Fedorova, N. D., Jackson, J. D., Jacobs, A. R., Kiryutin, B., Koonin, E. V., et al. (2003). The COG database: an updated version including eukaryotes. *BMC Bioinformatics* 4:41. doi: 10.1186/1471-2105-4-41
- Wang, R., van Dorp, L., Shaw, L. P., Bradley, P., Wang, Q., Wang, X., et al. (2018). The global distribution and spread of the mobilized colistin resistance gene *mcr-1*. *Nat. Commun.* 9:1179. doi: 10.1038/s41467-018-03205-z
- Wirth, T., Falush, D., Lan, R., Colles, F., Mensa, P., Wieler, L. H., et al. (2006). Sex and virulence in *Escherichia coli*: an evolutionary perspective. *Mol. Microbiol.* 60, 1136–1151. doi: 10.1111/j.1365-2958.2006.05172.x
- Wu, J., Huang, Y., Rao, D., Zhang, Y., and Yang, K. (2018). Evidence for environmental dissemination of antibiotic resistance mediated by wild birds. *Front. Microbiol.* 9:745. doi: 10.3389/fmicb.2018.00745
- Yong, D., Toleman, M. A., Giske, C. G., Cho, H. S., Sundman, K., Lee, K., et al. (2009). Characterization of a new metallo-beta-lactamase gene, bla(NDM-1), and a novel erythromycin esterase gene carried on a unique genetic structure in *Klebsiella pneumoniae* sequence type 14 from India. *Antimicrob. Agents Chemother.* 53, 5046–5054. doi: 10.1128/AAC.00774-09
- Zankari, E., Hasman, H., Cosentino, S., Vestergaard, M., Rasmussen, S., Lund, O., et al. (2012). Identification of acquired antimicrobial resistance genes. *J. Antimicrob. Chemother.* 67, 2640–2644. doi: 10.1093/jac/dks261
- Zhang, Q. Q., Ying, G. G., Pan, C. G., Liu, Y. S., and Zhao, J. L. (2015). Comprehensive evaluation of antibiotics emission and fate in the river basins of China: source analysis, multimedia modeling, and linkage to bacterial resistance. *Environ. Sci. Technol.* 49, 6772–6782. doi: 10.1021/acs.est.5b0729
- Zhu, Y. G., Zhao, Y., Li, B., Huang, C. L., Zhang, S. Y., Yu, S., et al. (2017). Continental-scale pollution of estuaries with antibiotic resistance genes. *Nat. Microbiol.* 2:16270. doi: 10.1038/nmicrobiol.2016.270

**Conflict of Interest:** The authors declare that the research was conducted in the absence of any commercial or financial relationships that could be construed as a potential conflict of interest.

Copyright © 2020 Lin, Dong, Wu, Rao, Zhang, Faraj and Yang. This is an open-access article distributed under the terms of the Creative Commons Attribution License (CC BY). The use, distribution or reproduction in other forums is permitted, provided the original author(s) and the copyright owner(s) are credited and that the original publication in this journal is cited, in accordance with accepted academic practice. No use, distribution or reproduction is permitted which does not comply with these terms.



# Molecular Analysis of Selected Resistance Determinants in Diarrheal Fecal Samples Collected From Kolkata, India Reveals an Abundance of Resistance Genes and the Potential Role of the Microbiota in Its Dissemination

Rituparna De\*, Asish Kumar Mukhopadhyay and Shanta Dutta

Division of Bacteriology, National Institute of Cholera and Enteric Diseases, Kolkata, India

## OPEN ACCESS

### Edited by:

Inge C. Gyssens,  
Radboud University Nijmegen Medical  
Centre, Netherlands

### Reviewed by:

Veranja Chathurani Liyanapathirana,  
University of Peradeniya, Sri Lanka  
Ellen Stobberingh,  
National Institute  
Public Health, Netherlands

### \*Correspondence:

Rituparna De  
rituparna26@gmail.com

### Specialty section:

This article was submitted to  
Infectious Diseases - Surveillance,  
Prevention and Treatment,  
a section of the journal  
Frontiers in Public Health

**Received:** 29 June 2019

**Accepted:** 18 February 2020

**Published:** 11 March 2020

### Citation:

De R, Mukhopadhyay AK and Dutta S  
(2020) Molecular Analysis of Selected  
Resistance Determinants in Diarrheal  
Fecal Samples Collected From  
Kolkata, India Reveals an Abundance  
of Resistance Genes and the Potential  
Role of the Microbiota in Its  
Dissemination.  
Front. Public Health 8:61.  
doi: 10.3389/fpubh.2020.00061

Twenty-five diarrheal fecal samples from Kolkata were examined to determine the relative abundance of antimicrobial resistance genes (ARGs) against eight common classes of antibiotics with polymerase chain reaction (PCR) and Sanger sequencing. Relative abundance of an ARG was calculated as the percentage of fecal samples showing the presence of that particular ARG. The frequency of occurrence of resistance marker against each class of antibiotic was calculated as the percentage of fecal samples carrying at least one resistance marker for that particular class of antimicrobials. Antibiogram of *Vibrio cholerae* (*V. cholerae*) O1 strains isolated from four of these samples was obtained by disc diffusion method and was compared with the ARG profile of corresponding fecal samples from which the strains were isolated. A 464 bp amplicon of the V3-V4 region of bacterial 16S rDNA was obtained by PCR from 9 of these 25 samples using the primer pair *S-D-Bact-0341-b-S-17* and *S-D-Bact-0785-a-A-21* and sequenced to determine the major operational taxonomic unit (OTU). These 9 samples represented diarrhea due to diverse etiology and also unresolved etiology as determined by culture method. We conclude that the diarrheal intestinal microbiome has a common gene pool of ARGs against the major classes of antibiotics and may be serving as a reservoir of ARG dissemination. ARG profile of cholera stool showed that ARGs present in the gut of cholera patients may be transferred to the *V. cholerae* genome and pose a serious threat to the treatment of cholera by triggering resistance against potential drugs to which contemporary strains of *V. cholerae* were found to be sensitive in the present study. Fecal samples which were culture negative for diarrheal pathogens we tested also carried ARGs and OTU. Abundance of resistance markers against macrolides, tetracyclines, and aminoglycosides was the highest. Phylum Proteobacteria was the most abundant OTU suggesting proteobacterial blooms characteristic of disturbed gut microflora. Our study is the first comparative

study of ARG profile of diarrheal samples with varying etiologic agent revealing the presence of ARGs against the most important classes of antibiotics in the gut of diarrheal patients by common, robust molecular methods, which are easily accessible by molecular epidemiological laboratories worldwide.

**Keywords:** antimicrobial resistance, antimicrobial resistance genes, microbiota, microbiome, metagenomics, diarrhea, pathogen, commensal

## INTRODUCTION

Antimicrobial resistance (AMR) among diarrheal pathogens has emerged as a critical threat to the clinical management of diarrheal cases. Oral rehydration therapy (ORT) is the primary treatment for diarrhea and antibiotic therapy is used as a supplementary treatment to reduce severity and morbidity. Pathogens have developed resistance to multiple antibiotics which were used for controlling these infections giving rise to multi-drug resistance (MDR) which is leading to higher number of deaths. These are extremely difficult to treat with known chemotherapeutic agents in diarrheal patients for whom primary treatment with oral rehydration solution (ORS) is insufficient.

Common enteric pathogens like *Klebsiella pneumoniae* and *Escherichia coli* have developed resistance against last resort antimicrobials like carbapenem and these are, in turn, serving as potential agents for transmission of ARGs into the environment and the community<sup>1</sup> (1). Resistome analysis to understand the antimicrobial resistance (AMR) profile in pathogens is urgently required in order to discern divisive methods to prevent the transmission and spread of genetic determinants of AMR. The members of the microbiota in the environment and in humans are the primary sources of ARGs. These serve as potential reservoirs for the persistence and transmission of ARGs. The indiscriminate use of antibiotics in farm and for clinical and veterinary practices has led to the emergence of antimicrobial resistance as a critical threat. In this study we have attempted to report about the profile of selected resistance determinants obtained from fecal samples using simple polymerase chain reaction (PCR) with specific primers to detect a spectrum of antimicrobial resistance determinants that are involved in diverse antimicrobial resistance mechanisms in bacteria and which are associated with the most common classes of antibiotics advocated for diarrheal treatment. These include tetracyclines, macrolides, amphenicol, aminoglycosides, carbapenem, trimethoprim, sulfamethoxazole, and quinolones. The antimicrobial genetic determinants selected to serve as markers for these classes of antimicrobial resistance include those encoding enzymes, efflux proteins, and proteins which are involved in diverse mechanisms like cell wall degradation of bacteria and inhibition of protein synthesis. The presence of these genetic determinants was further confirmed by sequencing these genes where standard positive control DNA was not available. The results revealed the existence of antimicrobial resistance determinants against major classes of antibiotics in fecal DNA samples. The study helped us to forebode the possibility of

ARGs being transmitted in the near future from the microbiota into pathogens. Our study suggests that major members of the gut community are serving as reservoirs of ARGs as samples from which pathogens could not be isolated by conventional culture methods also presented an ARG profile. We also report the relative abundance of different ARGs in the diarrheal gut microbiota in Kolkata and the suburban areas. Our study is the first addressing the relative abundance of ARGs of different classes of antimicrobials with the help of common and economic laboratory tools in the gut microbiome of the local diarrheal patients in Kolkata and the suburban areas. The study would provide valuable understanding about the threat posed by the presence of ARGs in the gut of diarrheal patients in parts of the world where the economically backward population is under perpetual threat of diarrheal diseases due to lack of sanitation and for whom antimicrobial therapy is of utmost importance to reduce severity and mortality due to diarrhea along with ORS administration. Therefore, understanding the distribution of ARGs is important to reduce their transmission from their reservoir with interceptive methods.

## MATERIALS AND METHODS

### Sample Collection and Ethical Clearance

Twenty-five diarrheal stool samples were collected from the Bacteriology Division laboratory of National Institute of Cholera and Enteric Diseases (NICED), which routinely receives stool samples from the adjoining Infectious Diseases Hospital (IDH) and the B. C. Roy Hospital (BCH) for systematic screening and isolation of enteric pathogens from stool of diarrheal patients from Kolkata and the suburban areas. Thus, these 25 samples represented diverse etiology and the diarrheal population of Kolkata and the suburbs. These patients eliminated loose watery stool more than three times in a day and suffered mild to severe dehydration. Stool samples included in the study were from patients of age 2 months and above and were from male and female patients. Twenty-four of these samples were from patients who were admitted to IDH for 1–4 days for treatment of acute diarrhea and in these patients diarrhea lasted for 1–5 days. One sample KOL18B2-6 was collected at the outpatient ward of BCH from the patient who had symptoms of mild diarrhea. In this patient diarrhea lasted for 2 days. After collection, each stool sample was given a unique identity number for the study. All stool samples were collected and handled in a manner conforming to ethical rules and regulations of the local governing bodies and the institute (NICED). **Table 1** presents a description of the stool samples used for the study.

<sup>1</sup><https://www.who.int/news-room/fact-sheets/detail/antimicrobial-resistance>

**TABLE 1** | Stool samples used in the study, their description and AMR profile.

Stool sample	Description	Age of patient; Sex; Location*	AMR profile of fecal sample by ARG profile	Pathogen isolated
KOL18B2-1	Greenish yellow liquid	29y;M;S	<i>tetAB,cat1,sul2,ant,dfrA12,aac(3),aac(6'),aadA1,strAB,mefA,mphA,tnpA,int1,int4</i>	VC O1 <i>Inaba</i>
KOL18B2-2	Off-white liquid	16y;M;K	<i>tetABM,cat1,floR,sul2,dhfr1,ant,dfrA12,dfr1,aac(3),aac(6'),aadA1,strAB,mphA,tnpA,int1,int2,int4,sxt</i>	VC O1 <i>Ogawa+C.jejuni</i>
KOL18B2-3	Pale yellow liquid	55y;M;K	<i>tetABCDEM,cat1,floR,sul2,ant,dfrA12,dfrA15,dfr1,aac(3),aac(6'),aadA1,strAB,mphA,mefA,tnpA,int1,int2,int4,sxt</i>	TCBS(Y)OX + String-PCR-
KOL18B2-4	White liquid	23;M;S	<i>tetABM,cat1,sul2,ant,dfrA12,aac(3),aac(6'),aadA1,strAB,aph,mefA,mphA,tnpA,int1,int4</i>	VC O1 <i>Inaba+Campylobacter sp.</i>
KOL18B2-5	Bloody liquid	22y;F;K	<i>tetABM,sul2,ant,aac(3),aac(6'),aadA1,strAB,aph,mefA,mphA,tnpA,int1,int4</i>	VC Non-O1 nonO139
KOL18B2-6	Gray liquid	3.6y;F;S	<i>tetABM,sul2,aadA1,strAB,mefA,mphA</i>	No pathogen
KOL18B2-7	Green liquid	60y;M;K	<i>tetABDM,sul2,dfr1,ant,aac(3),aac(6'),aadA1,strAB,mefA,mphA,tnpA,int1,int2</i>	No pathogen(MAC LF)
KOL18B3-1	Off-white liquid	35y;F;K	<i>tetABM,cat1,floR,ant,dfrA12,dfr1,aac(3),aac(6'),aadA1,strAB,mphA,mefA,tnpA,int1,int2,int4,sxt</i>	VC O1 <i>Ogawa</i>
KOL18B3-2	Greenish yellow liquid	70y;M;K	<i>tetABM,cat1,ant,dfrA12,aac(6'),aadA1,strAB,mphA,mefA,int1,int4</i>	No pathogen
KOL18B3-3	Whitish-green liquid	1y;M;S	<i>tetEM,ant,aadA1,strAB,mphA,mefA,tnpA,int1</i>	EAEC
KOL18B3-4	Bloody, mucoid, liquid	4y;M;K	<i>tetAB,cat1,sul2,ant,dfr1,aac(3),aac(6'),aadA1,strAB,mefA,mphA,tnpA,int1,int2</i>	HEA (Green)TSI(k/A+G)
KOL18B3-5	Brown liquid	55y;F;S	<i>tetABM,sul2,dfr1,aac(6'),aadA1,strAB,mefA,mphA,tnpA,int1</i>	<i>S.flexeneri</i> 2a, <i>C.coli</i>
KOL18B3-6	Brown liquid	65y;M;K	<i>tetAB,cat1,sul2,ant,dfr1,aadA1,strAB,mefA,mphA,tnpA,int1,int2</i>	<i>S.flexeneri</i> 2a
KOL18B3-7	Yellowish liquid	25y;M;K	<i>tetABM,dfr1,aac(3),strAB,mefA,mphA,tnpA,int2</i>	No pathogen(MAC LF)
KOL18B3-8	Bloody, mucoid, liquid	53y;M;S	<i>tetAB,dfr1,sul2,aac(3),strAB,mefA,mphA,int2</i>	<i>Aeromonas sp.</i>
KOL18B3-9	Greenish yellow liquid	65y;M;K	<i>tetABM,sul2,ant,dfrA12,aac(3),aac(6'),aadA1,strAB,mefA,mphA,tnpA</i>	HEA (Green)TSI(k/A+G)
KOL18B3-10	Bloody liquid	30y;F;K	<i>tetABM,sul2,strAB,mefA,mphA,tnpA</i>	Mac (NLF)TSI(k/A+G)
KOL18B3-11	Yellowish liquid	9m;M;S	<i>tetM,strAB,mefA,mphA</i>	<i>Aeromonas sp.</i>
KOL18B3-12	Gray liquid	50y;F;K	<i>tetABDEM,sul2,ant,dfr1,aph,aac(3),aadA1,strAB,mefA,mphA,tnpA</i>	<i>Aeromonas sp.</i>
KOL18B3-13	Transparent liquid	2m;M;S	<i>dfr1,mefA,int2</i>	<i>S.sonnei</i>
KOL18B3-14	Greenish white semi-solid	7m;M;S	<i>tetA,ant,dfr1,aac6,strAB,mefA,mphA,tnpAint2</i>	EAEC
KOL18B3-15	Bloody, mucoid semi-solid	40y;M;K	<i>tetABM,cat1,sul2,ant,dfr1,aac(3),aac(6'),aadA1,strAB,mefA,mphA,tnpA,int2,int4</i>	<i>S.flexeneri</i>
KOL18B3-16	Brown liquid	45y;F;K	<i>tetA,sul2,aac(3),aac(6'),strAB,mefA,mphA,tnpA</i>	No pathogen(MAC LF/NLF)
KOL18B3-17	White liquid	7m;M;K	<i>tetABM,sul2,aac(3),aac(6'),strAB,mefA,mphA,tnpA</i>	No pathogen(MAC LF/NLF)
KOL18B3-18	Off-white mucoid liquid	7y;M;S	<i>tetABM,sul2,ant,dfr1,aac(3),aac(6'),strAB,mefA,mphA,tnpA</i>	<i>S.flexeneri</i>

Location\*: K, Kolkata; S, Suburban area.

Age: y, years; m, months.

Sex: M, Male; F, Female.

## Isolation of Genomic DNA From Standard Laboratory Strains

Standard laboratory strains N16961 (*V. cholerae* O1, El Tor), O395 *V. cholerae* O1, classical) and MO10 (*V. cholerae* O139) served as control for this study. The strains were obtained from the NICED strain repository and initially grown overnight at 37°C on TCBS (thiosulphate- citrate- bile salts-sucrose) (BD Difco™, U.S.A) plates followed by sub-culturing on Luria agar (BD Difco™, U.S.A) plates containing 1% NaCl (sodium chloride) (Merck-Millipore, U.S.A). A loopful of culture was

dissolved in TE (Tris-EDTA) buffer (pH 8) (Sigma Aldrich, USA) followed by extracting DNA using phenol-chloroform-isoamyl alcohol mixture in the ratio 25:24:1 and alkaline pH and finally eluting DNA in nuclease-free water.

## Isolation of Genomic DNA From Stool Samples

Microbial genomic DNA was isolated from stool samples using QIAampUCP Pathogen Mini Kit (cat.no. 50214, Qiagen Inc., MD, USA), using the protocol provided by the manufacturer,



for isolation of ultra-clean DNA. Accordingly, stool samples were subject to mechanical lysis using glass beads in a mini vortex-mixer (3020 Spinix, Tarsons) followed by enzymatic lysis using buffer containing pre-mixed bacterial cell-wall degrading enzyme cocktail under highly denaturing conditions at elevated temperatures of 70°C and protein removal and nuclease inactivation using a combination of Proteinase K (20 mg/ml) and buffer APL2 using spin columns (QIAamp UCP Mini Column, Qiagen Inc., MD, USA) wherein microbial nucleic acid is adsorbed on the silica membrane by centrifugation at 8,000 g for 1 min and washing with buffer containing ethanol followed by final elution using elution buffer containing Tris-EDTA (Ethylenediaminetetraacetic acid). The concentration of DNA from each sample was quantified using the NanoDrop Lite UV-Vis Spectrophotometer (Thermo Fisher Scientific, MA, USA) and diluted to obtain a uniform concentration of 25ng/ul for all samples using ultra-pure water obtained by purification with the Milli-Q® Integral Water Purification System (Merck-Millipore, USA) followed by autoclaving at 121°C for 15 min at 15psi. The DNA was used as template for PCR and Sanger sequencing. In the method described above salt and pH conditions help in the complete removal of proteins and other contaminants, which can inhibit downstream enzymatic reactions.

## AMR Profiling

AMR profile of each sample was obtained by PCR using specific primer set consisting of forward and reverse primers to amplify the gene of interest involved in antimicrobial resistance mechanism (Table 2). PCR was performed in a final reaction volume of 25 µl containing 1x GoTaq® Green master mix (cat.no. M7123, Promega Corporation, WI, USA), 0.4uMupstream and downstream primers and 1 ng/µl DNA template using a 96-well thermalcycler (GeneAmp® PCR system 9700, Applied Biosystems, Thermo Fisher Scientific, MA, USA). A list of genes and their corresponding primer sequences, annealing temperatures and size of the amplified fragment has been presented in Table 3. The PCR products were run on 1–1.5% agarose gel (depending on amplicon size) prepared using 1X TAE (Tris-acetic acid-EDTA) buffer followed by staining in ethidium bromide solution (10 mg/ml) and visualized in a UV-transilluminator (BioRad) and the results documented. For experimental control standard laboratory strains N16961, O395, and MO10 were used as template for the amplification of ARGs pre-documented as present or missing in these strains by previous reports archived in the public database NCBI. The amplicon size was determined using 100 bp and 1 kb DNA ladder (NEB, MA, USA and GeNetBio Corp., Korea).

## Sanger Sequencing for Confirmation of ARGs

PCR products obtained above and containing the amplicon of interest was purified using the Wizard® SV Gel and PCR Clean-Up System (cat. no. A9281, Promega Corporation, WI, USA) that can purify 100 bp to 10 kb DNA fragments with Wizard® SV Minicolumns. DNA quantity and quality was adjusted to fulfill the requirements for Sanger sequencing. Purified PCR products with optimum absorbance ratios ( $A_{260/280}$ ) between 1.8

**TABLE 2 |** The eight major classes of antibiotics and Mobile Genetic Elements (MGEs) and their corresponding ARGs whose presence or mutations were determined in the study.

ARG against class of antibiotic	ARG
Tetracycline	<i>tetABCDEMG</i>
Macrolide	<i>ereAB, ermABC, mefABC, mphABCG, msrA</i>
Sulfamethoxazole	<i>sul2</i>
Aminoglycoside	<i>aadA1, aad2, aac(3), aac(6), strAB, aph</i>
Trimethoprim	<i>dhfr1, dfrA1, dfrA12, dfrA15, dfrA27, tmpC</i>
Amphenicol	<i>cat1, floR</i>
Carbapenemase	<i>ndm1, bla-vcc1</i>
Quinolones	<i>qnrVC, gyrA, gyrB, parC, parE</i>
MGEs	<i>Sxt-int, int1, int2, int4, trpA, repA</i>

and 2.0 were selected to serve as template. Cycle sequencing was carried out with the BigDye™ Terminator v3.1 cycle sequencing kit (cat. no. 4337455, Applied Biosystems, Thermo Fisher Scientific, MA, USA) using 10 µl reaction mixture containing BigDye™ Terminator v3.1 Ready Reaction Mix, BigDye™ Terminator v3.1 Sequencing Buffer, final concentration of 3.2 pMol of either forward or reverse primer and DNA template quantity of 1–5 ng depending on the size of the fragment being sequenced. Cycling conditions consisted of denaturation at 96°C for 1 min and 25 cycles of denaturation, annealing, and extension at 96°C for 10 s, 50°C for 5 s, and 60°C for 4 min, respectively. The cycle sequencing product was purified using 3M sodium acetate solution (pH 4.8) and absolute ethanol (Emsure, Merck, Germany) and washed with 70% ethanol and finally vacuum dried. The dried pellet was resuspended in 10 µl Hi-Di™ Formamide and loaded onto the Applied Biosystems™ 48-capillary DNA Analyzer 3730 (Thermo Fisher Scientific, MA, USA) for sequencing and collection of data using the recommended signal to noise ratio. Accordingly, unambiguous clear curves with sharp peaks indicating clear base-calling and low background noise were considered. Curves with minimum signal 300 for all the bases and maximum noise 20 were set as the threshold for accepting raw data. Chromatograms considered for analysis had maximum signal in the range of  $G = 964-4,176$ ;  $A = 518-2,967$ ;  $T = 537-2,435$ ;  $C = 662-4,186$ . Noise was confined to baseline (signals 0–50) and did not interfere with data interpretation. Raw data was viewed and analyzed using SeqMan™ II (version Windows 32 SeqMan 5.01) software (DNASTAR Inc., WI, USA) and assembled sequence data in the clear range was accepted and considered. This was subject to local alignment using Megablast program of Nucleotide BLAST (Basic Local Alignment Search Tool) on the NCBI (National Center for Biotechnology Information) server.

## Calculation of Relative Abundance and Frequency of ARGs

Relative abundance of ARGs present in fecal samples was calculated. For each ARG it was represented as the percentage of fecal samples found to be carrying that particular ARG. This can be represented by the formula:

**TABLE 3** | Primers (5'-3') used in the study.

Primer	Gene/Description	Sequence	Annealing	Amplicon	References
<b>Carbapenemase</b>					
<i>bla<sub>VCC</sub>-1F</i>	<i>bla<sub>VCC</sub>1</i>	ATCTCTACTTCAACAGCTCG	55°C	755 bp	(2)
<i>bla<sub>VCC</sub>-1R</i>		CCTAGCTGCTTTAGCAATCC			
<i>ndm1-F</i>	<i>ndm1</i>	CAATATTATGCACCCGGTG	55°C	292 bp	(3)
<i>ndm1-R</i>		GTGATTGCGGCGCGGCTAC			
<b>Quinolones</b>					
<i>qnrVC-RD-F</i>	<i>qnr-VC</i>	GGGGGCAAATTGCTTTGGTA	60°C	220 bp	This study
<i>qnrVC-RD-R</i>		TGAAGCGCCTCGAAGATTTG			
<b>Aminoglycosides</b>					
<i>ant-F</i>	<i>ant(3'')-Ia / (add2)</i>	GCCTGAAGCCACACAGTGATA	51°C	660 bp	(4)
<i>ant-B</i>		CTACCTTGGTGATCTCGCCTT			
<i>aac(6')-Ib-cr-Fw</i>	<i>6'-N-acetyltransferase</i>	GGCGAATGCATCACAACCTGG	60°C	205 bp	This study
<i>aac(6')-Ib-cr-Rev</i>		AACCATGTACACGGCTGGAC			
<i>aac(3)-FRD</i>	<i>aminoglycoside 3-N-</i>	TGGCACTGTGATGGGATACG	60°C	448 bp	This study
<i>aac(3)-RRD</i>	<i>acetyltransferase/aac(3)-I</i>	CGTTTTCCAGGCGACTTCAC			
<i>aadA1Fw-RD</i>	<i>Aminoglycoside</i>	TTGGAAACTTCGGCTTCCCC	60°C	101 bp	This study
<i>aadA1Rev-RD</i>	<i>adenyltransferase/aadA1</i>	TTAGCTGGATAACGCCACGG			
<i>strB-F</i>	<i>strB</i>	GGCACCCATAAGCGTACGCC	60°C	470 bp	(5)
<i>strB-R</i>		TGCCGAGCACGGCGACTACC			
<i>strA-F</i>	<i>strA</i>	TTGATGTGGTGTCGCCAATGC	60°C	383 bp	(5)
<i>strA-B</i>		CCAATCGCAGATAGAAGGCAA			
<b>Trimethoprim</b>					
<i>dfrA15-F</i>	<i>dfrA15</i>	CAATGGGGGCTTTACCCAAC	60°C	153 bp	This study
<i>dfrA15-R</i>		CACCACCACCAGACACAATC			
<i>dfrA12-F</i>	<i>dfrA12</i>	CACGCTATCGCTTTGGCATC	60°C	146 bp	This study
<i>dfrA12-R</i>		ATTGGGAAGAAGCGTCACC			
<i>dhfr1 F</i>	<i>dhfr1</i>	CTGATATTCATGGAGTGCCA	57°C	434 bp	(4)
<i>dhfr1 B</i>		CGTTGCTGCCACTTGTTAACC			
<i>tmp-F</i>	<i>dfr18</i>	TGGGTAAGACACTCGTCATGGG	60°C	389 bp	(6)
<i>tmp-B</i>		ACTGCCGTTTTCGATAATGTGG			
<i>dfr1-F</i>	<i>dfr18</i>	CGAAGAATGGAGTTATCGGG	60°C	372 bp	(7)
<i>dfr1-B</i>		TGCTGGGGATTTCAAGAAAG			
<i>dfrA27-F</i>	<i>dfrA27</i>	TGGGGGCTCTCCCAAATAGA	60°C	192 bp	This study
<i>dfrA27-R</i>		TATGTAGCGTGTGGCATGG			
<b>Sulfamethoxazole</b>					
<i>sul2-F</i>	<i>sul2</i>	AGGGGGCAGATGTGATCGAC	60°C	625 bp	(6)
<i>sul2-B</i>		TGTGCGGATGAAGTCAGCTCC			
<b>Amphenicol</b>					
<i>floR-F</i>	<i>floR</i>	TTATCTCCCTGTGCT TCCAGCG	54°C	584 bp	(7)
<i>fLOR-2</i>		CCTATGAGCACACGGGGAGC			
<i>cat1-F</i>	<i>cat1</i>	GGCATTTCAGTCAGTTG	55°C	627 bp	(5)
<i>cat1-B</i>		CCGCCCTGCCACTCATC			
<b>Macrolide</b>					
<i>msrA-F</i>	<i>msrA</i>	GCACTTATTGGGGTAATGG	58°C	384 bp	(8)
<i>msrA-R</i>		GTCTATAAGTGCTCTATCGTG			
<i>mefA-F</i>	<i>mefA</i>	AGTATCATTAACTACTAGTGC	54°C	345 bp	(8)
<i>mefA-R</i>		TTCTTCTGGTACTAAAAGTGG			
<i>mefB-F</i>	<i>mefB</i>	ATGAACAGAATAAAAAATTG	45°C	1,255 bp	(9)

(Continued)

TABLE 3 | Continued

Primer	Gene/Description	Sequence	Annealing	Amplicon	References
<i>mefB-R</i>		AAATTATCATCAACCCGGTC			
<i>mefC-F</i>	<i>mefC</i>	ATGGAAAACCGTAAATGGTT	55°C	885 bp	(9)
<i>mefC-R</i>		TTAAATATTTTTGATTTTAC			
<i>mphA-F</i>	<i>mphA</i>	GTGAGGAGGAGCTTCGCGAG	60°C	403 bp	(8)
<i>mphA-R</i>		TGCCGCAGGACTCGGAGGTC			
<i>mphB-F</i>	<i>mphB</i>	GATATTAACAAGTAATCAGAATAG	58°C	494 bp	(8)
<i>mphB-R</i>		GCTCTTACTGCATCCATACG			
<i>mphG-F</i>	<i>mphG</i>	ATGAAAAATAGAGATATTCA	55°C	1,224 bp	(9)
<i>mphG-R</i>		CTACTCAACACCTAACTGTA			
<i>ermA-F</i>	<i>ermA</i>	TCTAAAAAGCATGTAAAAGAAA	52°C	533 bp	(8)
<i>ermA-R</i>		CGATACTTTTTGTAGTCCTTC			
<i>ermB-F</i>	<i>ermB</i>	GAAAAAGTACTCAACCAAATA	45°C	639 bp	(8)
<i>ermB-R</i>		AATTTAAGTACCGTTACT			
<i>ermC-F</i>	<i>ermC</i>	TCAAAACATAATATAGATAAA	45°C	642 bp	(8)
<i>ermC-R</i>		GCTAATATTGTTTAAATCGTCAAT			
<i>ereA-F</i>	<i>ereA</i>	GCCGGTGCTCATGAACCTTGAG	60°C	420 bp	(8)
<i>ereA-R</i>		CGACTCTATTCGATCAGAGGC			
<i>ereB-F</i>	<i>ereB</i>	TTGGAGATACCCAGATTGTAG	55°C	537 bp	(8)
<i>ereB-R</i>		GAGCCATAGCTTCAACGC			
Aph F	<i>aphA</i>	GGCAATCAGGTGCGACAAT	52°C	484 bp	(5)
Aph R		GTGACGACTGAATCCGGTGA			
<b>Tetracyclines</b>					
<i>tetA-F</i>	<i>tetA</i>	GTAATTCTGAGCACTGTCCG	62°C	957 bp	(10)
<i>tetA-R</i>		CTGCCTGGACAACATTGCTT			
<i>tetB-F</i>	<i>tetB</i>	CTCAGTATTCCAAGCCTTTG	57°C	436 bp	(10)
<i>tetB-R</i>		CTAAGCACTTGCTCCTGT			
<i>tetC-F</i>	<i>tetC</i>	TCTAACAATGCGCTCATCGT	62°C	589 bp	(10)
<i>tetC-R</i>		GGTTGAAGGCTCTCAAGGGC			
<i>tetD-F</i>	<i>tetD</i>	ATTACACTGCTGGACGCGAT	57°C	1,124 bp	(10)
<i>tetD-R</i>		CTGATCAGCAGACAGATTGC			
<i>tetE-F</i>	<i>tetE</i>	GTGATGATGGCACTGGTCAT	62°C	1,199 bp	(10)
<i>tetE-R</i>		CTCTGCTGTACATCGCTCTT			
<i>tetG-F</i>	<i>tetG</i>	TTTCGGATTCTTACGGTC	55°C	856 bp	(11)
<i>tetG-R</i>		TCCTGCGATAGAGCTTAGA			
<i>tetM-F</i>	<i>tetM</i>	GTRAYGAACTTTACCGAATC	55°C	634 bp	(11)
<i>tetM-R</i>		ATCGYAGAAGCGGRTCACT			
<b>MGEs</b>					
<i>sxt-F</i>	SXT Integrase	TTATCGTTTCGATGGC	50°C	800 bp	(10)
<i>sxt-B</i>		GCTCTTCTGTCCGTTT			
<i>int-1U</i>	Integron class 1	GTTCCGGTCAAGGTTCTG	50°C	923 bp	(5)
<i>int-1D</i>		GCCAACTTTCAGCACATG			
<i>int-2U</i>	Integron class 2	ATGTCTAACAGTCCATTTT	50°C	450 bp	(5)
<i>int-2D</i>		AAATCTTTAACCCGCAAAC			
<i>int-4U</i>	Integron class 4	GTGTTCCGGAATTTATGC	50°C	936 bp	(5)
<i>int-4D</i>		ACGGGATAATGGGCTTAA			
<i>tnpA-F</i>	<i>tnpA</i>	GAATCTCAGCAGGCAATGCG	55°C	545 bp	This study
<i>tnpA-R</i>		GCCAAAYTTGCCAGACTGGTG			
<i>repA-F</i>	<i>repA</i>	CGTTGGGGTTTCATCAATG	55°C	1,000 bp	(12)
<i>repA-R</i>		GACTCACCGCAAATGAGC			

(Continued)

TABLE 3 | Continued

Primer	Gene/Description	Sequence	Annealing	Amplicon	References
<b>Sequencing</b>					
130	16S rDNA C1-C9	GGCGGATCCAAGGAGGTGTCCAGCCGC	55°C	1,500 bp	(13)
139		GGCCTCGAGAGAGTTTGATCCTGGCTCAGG			
S-D-Bact-0341-b-S-17	16S rDNA V3-V4	CCTACGGGNGGCWGCAG	55°C	464 bp	(14)
S-D-Bact-0785-a-A-21		GACTACHVGGGTATCTAATCC			
gyrA_seqFOR2	gyrA	TCTTCCTGATGTGCGTGATG	55°C	771 bp	This study
gyrA_seqREV2		GCACTGATCCCTTCGACTTT			
gyrB_seqFOR	gyrB	TGAAAGTGCCGGATCCTAAAT	55°C	662 bp	This study
gyrB_seqREV		GTACTGCTCTTGTTCCTTTTC			
parC_seqFOR	parC	CGCAAATTTACTGAAGACGCTTATC	55°C	729 bp	This study
parC_seqREV		CACGATATCCGAGCCTTCTTTG			
parE_seqFOR	parE	TGCTGGCCAAACCAAAGA	55°C	640 bp	This study
parE_seqREV		CTGATCATCGAGTGCGTAGAAC			

**For ARG A**

(Number of fecal samples positive by PCR for ARG A/ n)\* 100

Where ARG A is any ARG which has been included in the study and PCR positive and n is the total number of fecal samples used in the study. Here, n is 25.

Frequency of occurrence of resistance marker was calculated by the formula:

**For any particular class of antibiotic:**

(Number of fecal isolates found positive for at least one ARG marker against that class / n)\* 100

Where, n is the total number of fecal samples used in the study. Here, n is 25.

On the basis of these two parameters described above we concluded which group of antibiotics has the highest abundance of resistance marker.

## 16S Conserved and Variable Region Amplification

PCR amplification for confirming the presence of bacterial DNA in the DNA isolated from fecal specimens was carried out for the conserved regions C1-C9 and variable regions V3-V4 of 16S rDNA using standard primer sets targeting these regions. PCR amplification was carried out in 25 µl final reaction volume using the same reagents described above. The cycling conditions for PCR using primer sets 130–139 and S-D-Bact-0341-b-S-17-S-D-Bact-0785-a-A-21 were described by Bag et al. (13) and Klindworth et al. (14), respectively.

## Sanger Sequencing of 16s rDNA Variable Region

For representative samples the 464 bp fragment obtained by PCR amplification of variable region V3-V4 of 16S rDNA with

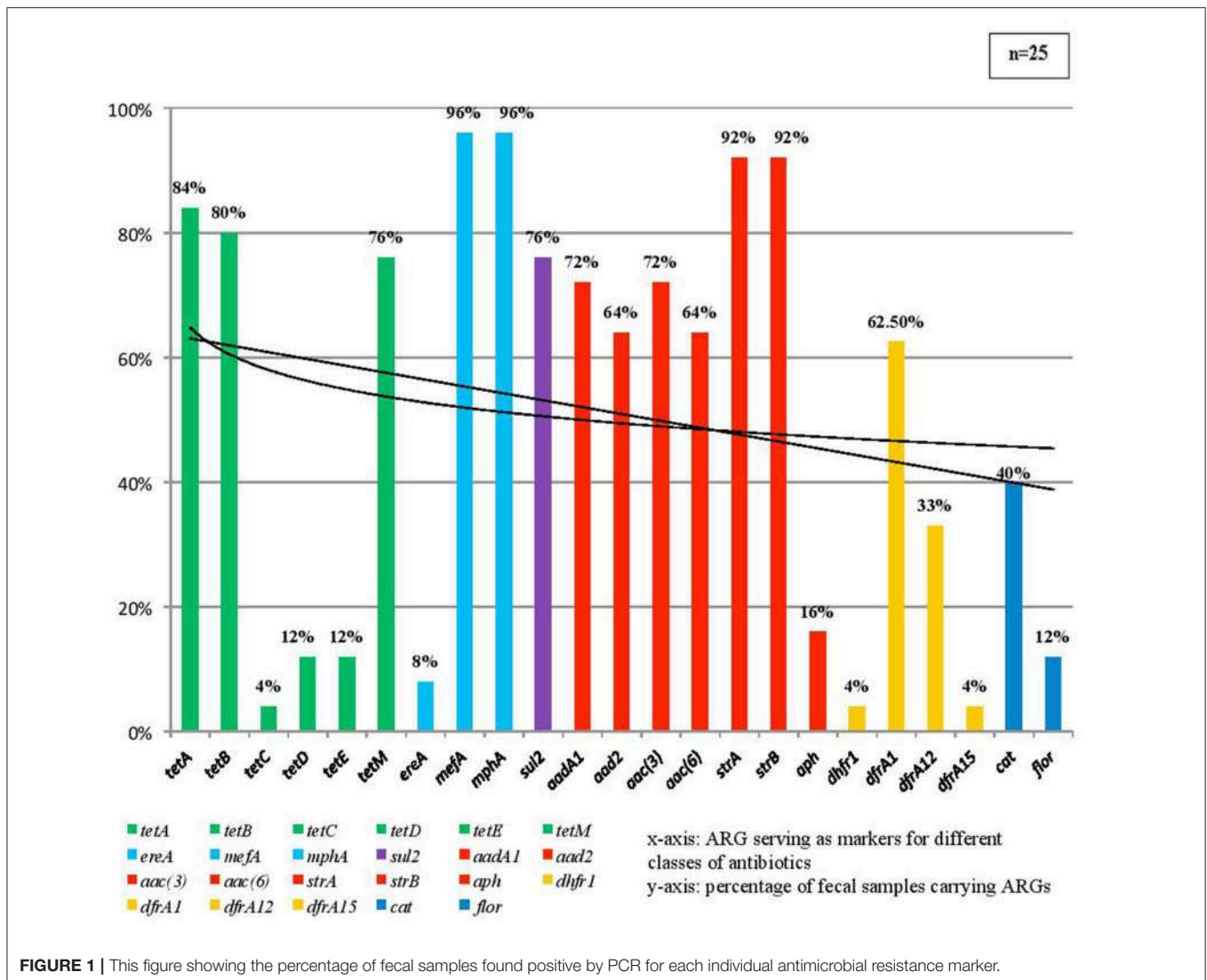
primer set S-D-Bact-0341-b-S-17- S-D-Bact-0785-a-A-21 was subject to Sanger sequencing. The PCR product was purified and subject to cycle sequencing reaction and finally sequenced using the 48-capillary DNA Analyzer 3730 (Thermo Fisher Scientific, MA, USA) following the same procedure described above. Sequence assembly and analysis was done using SeqManII software (DNASTAR Inc., WI, USA) and the assembled sequence data in the clear range was accepted and considered. With the help of the Megablast program of the local alignment tool Nucleotide BLAST on the NCBI server the sequenced data was matched with archived and annotated 16S rDNA sequences available in GenBank, the NIH genetic sequence database.

## Routine Isolation, Laboratory Culture, and Antibiotic Susceptibility Test of Diarrheal Pathogens

The enteric pathogen associated with diarrheal etiology in each fecal sample was isolated using enrichment technique. Accordingly, the samples were streaked onto selective and differential media plates for the detection of common diarrheal pathogens, *Vibrio* sp., *E. coli*, *Salmonella* sp., *Shigella* sp., *Aeromonas* sp., *Campylobacter* sp. in the Bacteriology Division Laboratory at NICED. Accordingly, bacterial culture plates TCBS, HEA (Hektoen enteric agar), XLD (Xylose Lysine Deoxycholate), MacConkey, Blood agar were used for each fecal specimen. Culture plates were incubated overnight at 37°C (3–5 days for *Campylobacter* sp.) and colonies from the plates were subject to biochemical test using Triple Sugar Iron Agar for identification of acid (lactose/sucrose fermenting and non-fermenting), gas, and hydrogen sulfide producing organisms. Single colonies from TCBS plates were subjected to oxidase and string test for the confirmation of *V. cholerae*.

Confirmed *V. cholerae* strains were further tested for antibiotic susceptibility by Kirby-Bauer Disc Diffusion method. The strains were grown on LA (Luria agar) plates overnight at 37°C and a loopful of culture was taken from the plate and inoculated into Luria broth and OD of this culture suspension was adjusted to obtain OD of 0.5 McFarland. With the help of autoclaved





swab stick bacterial culture from this broth was spread onto Mueller-Hinton Agar (MHA) plates and allowed to dry in a biosafety cabinet. Antibiotic discs (BD BBL™, NJ, U.S.A.) were placed on the surface of MHA plates with sterile forceps to test sensitivity toward common antibiotics, namely, ampicillin (10 µg), ceftriaxone (30 µg) chloramphenicol (30 µg), ciprofloxacin (5 µg), gentamicin (30 µg), ofloxacin (5 µg), imipenem (10 µg), azithromycin (15 µg), gentamicin (10 µg), norfloxacin (10 µg), nalidixic acid (30 µg), streptomycin (10 µg), SXT (trimethoprim-sulfamethoxazole) (1.25, 23.75 µg), and tetracycline (30 µg). The plates were incubated overnight at 37°C. The diameter of the clear zone (zone of inhibition) around each disc was measured, recorded and compared with the zone diameter interpretive chart provided by the manufacturer and which follows CLSI (Clinical and Laboratory Standards Institute) guidelines<sup>2</sup>. Accordingly, the strains were categorized as resistant, intermediate or susceptible.

<sup>2</sup>www.clsi.org

### Sanger Sequencing for Detecting Single Nucleotide Polymorphisms (SNPs) in Genes Involved in Quinolone Sensitivity

Four primer sets *gyrA\_seqFOR2-Rev2*, *gyrB\_seqFOR-Rev*, *parC\_seqFOR-Rev*, *parE\_seqFOR-Rev* (Table 2) were designed to amplify regions of genes encoding Topoisomerase II subunits A and B (*gyrA* and *gyrB*) and Topoisomerase IV subunits A and B (*parC* and *parE*). Sequencing was carried out to study SNPs in quinolone resistance determining regions (QRDR) in fecal DNA from representative samples. Amplification of fragments of *gyrA*, *gyrB*, *parC*, and *parE* was carried out by PCR with primers *gyrA\_seqFOR2-Rev2*, *gyrB\_seqFOR-Rev*, *parC\_seqFOR-Rev*, *parE\_seqFOR-Rev* which were designed from the N16961 sequence (reference sequence ID. NC\_002505; Gene ID: 2615137) to amplify 771 bp fragment of *gyrA*, 662 bp fragment of *gyrB*, 729 bp fragment of *parC* and 640 bp fragment of *parE* which were purified using the Wizard® SV Gel and PCR Clean-Up System (cat. no. A9281, Promega Corporation,

WI, USA) and used as template for cycle sequencing reaction with the BigDye™ Terminator v3.1 cycle sequencing kit (cat. no. 4337455, Applied Biosystems, ThermoFisher Scientific, MA, USA) and were sequenced on the Applied Biosystems™ 48-capillary DNA Analyzer 3730 (Thermo Fisher Scientific, MA, USA) in the same manner as already described in the preceding section (Sanger Sequencing for confirmation of ARGs). Sequence data was assembled with SeqMan II software (DNASTAR Inc., WI, USA) and the sequence identity was matched by global alignment with the corresponding genomic regions of standard *V. cholerae* O1 El Tor strain N16961 to map single nucleotide polymorphisms (SNPs).

## RESULT

### 16S Conserved Region PCR

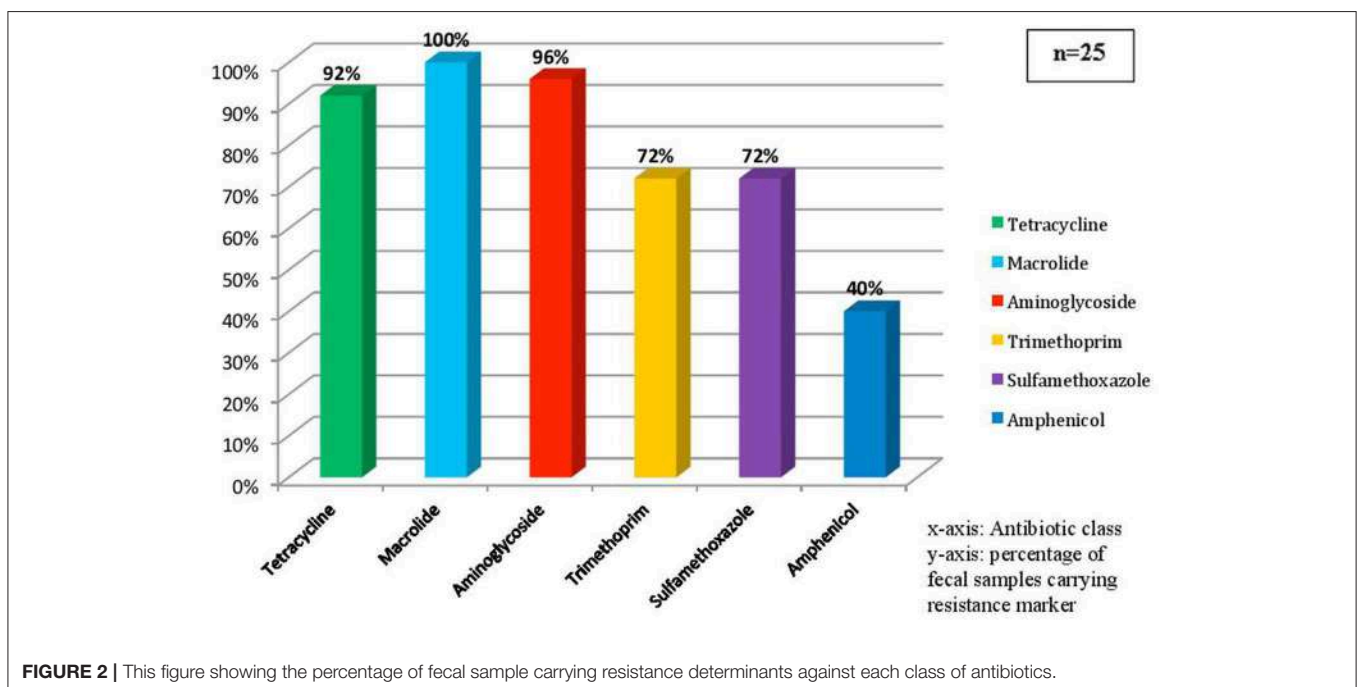
A 1,500 bp amplicon of conserved region of 16S rDNA was obtained spanning the C1-C9 region of bacterial genomic DNA in fecal samples on PCR amplification with primer set 130–139. The results confirmed the presence of bacterial DNA (Figure S1).

### AMR Profile

PCR was performed targeting a group of 49 genes associated with 8 different classes of common antibiotics like carbapenem, tetracycline, quinolones, aminoglycosides, macrolide, trimethoprim, sulfamethoxazole, amphenicol, and components of mobilome like transposase, SXT integrase, and markers of classes 1, 2, and 4 integron. PCR results showed amplification of genes *aadA1*, *aad2*, *strAB*, *aac(2)*, *aac(6′)-Ib-cr*, *tetABCDEM*, *SXT integrase*, *floR*, *dhfr1*, *dfrA1*, *dfrA12*, *dfrA15*, *cat1*, *sul2*, *aph*, *ereA*, *mefA*, *mphA*, *tnpA*, *int1*, *int2*, *int4*. This revealed that the microbial genomic DNA bore ARG markers against

aminoglycoside, tetracycline, macrolide, chloramphenicol, trimethoprim, sulfamethoxazole, and mobile genetic elements (MGEs). Table 1 shows the results obtained on screening for ARGs and the different classes of antibiotics against which they are active. All of the 25 samples tested for the presence of ARGs, showed genetic determinants associated with resistance against at least two classes of these broad-spectrum antibiotics. Where standard control strains were not available to compare and confirm the results, PCR products were sequenced using Sanger Sequencing to determine and confirm the identity of the gene. Accordingly, genes *tetABCDEM*, *aph*, *dhfr1*, *mphA*, *mefA*, *dfrA12*, *tnpA*, *aadA1*, *aad2*, *aac(3)/(aacC)*, *aac(6′)-Ib-cr*, *ereA*, *int1*, *int2* were sequenced and the assembled sequence on local alignment using Megablast program of Nucleotide BLAST confirmed the identity of these genes thereby confirming their presence in the fecal samples of diarrheal patients in Kolkata and suburban areas. Representative gel pictures showing the results of ARG profiling are available in Figures S2–S4. The assembled sequences and the results obtained on alignment of these sequences using BLAST are available as Supplementary Material S5.

The relative abundance of different ARGs (Figure 1) and the frequency of occurrence of resistance marker against each class of antibiotic (Figure 2) were calculated. It was found that 96% samples carried *mphA* and *mefA* genes encoding resistance against macrolide and hence these two genes were found to have highest occurrence followed by 92% occurrence of *strA* and *strB* encoding aminoglycoside resistance followed by tetracycline resistance due to the occurrence of 84% isolates with *tetA* gene, 80% isolates with *tetB* gene and 76% isolates with *tetE* gene. Other genes with high occurrence rate are *cat1* for chloramphenicol resistance (40%), *dfrA1* (62.5%), *dfrA12* (33%)



**TABLE 4** | Comparison of ARG profile of fecal cholera stool and antibiogram of *V. cholerae* isolated from it.

Stool sample	Pathogen isolated	AMR profile of fecal isolate by ARG profile	Resistance profile by antibiogram of pathogen
KOL18B2-1	VC O1 <i>Inaba</i>	<i>tetAB</i> , <i>cat1</i> , <i>sul2</i> , <i>ant</i> , <i>dfrA12</i> , <i>aac(3)</i> , <i>aac6'</i> , <i>aadA1</i> , <i>strAB</i> , <i>mefA</i> , <i>mphA</i> , <i>tnpA</i> , <i>int1</i> , <i>int4</i>	Tetracycline, SXT, nalidixic acid, streptomycin
KOL18B2-2	VC O1 <i>Ogama</i> , <i>C. jejuni</i>	<i>tetABM</i> , <i>cat1</i> , <i>floR</i> , <i>sul2</i> , <i>dhfr1</i> , <i>ant</i> , <i>dfrA12</i> , <i>dfr1</i> , <i>aac(3)</i> , <i>aac6'</i> , <i>aadA1</i> , <i>strAB</i> , <i>mphA</i> , <i>tnpA</i> , <i>int1</i> , <i>int2</i> , <i>int4</i> , <i>sxt</i>	*SXT, nalidixic acid, streptomycin, chloramphenicol
KOL18B2-4	VC O1 <i>Inaba</i> , <i>Campylobacter</i> sp.	<i>tetABM</i> , <i>cat1</i> , <i>sul2</i> , <i>ant</i> , <i>dfrA12</i> , <i>aac(3)</i> , <i>aac6'</i> , <i>aadA1</i> , <i>strAB</i> , <i>aph</i> , <i>mefA</i> , <i>mphA</i> , <i>tnpA</i> , <i>int1</i> , <i>int4</i>	*Ampicillin, tetracycline, SXT, nalidixic acid, streptomycin
KOL18B3-1	VC O1 <i>Ogama</i>	<i>tetABM</i> , <i>cat1</i> , <i>floR</i> , <i>ant</i> , <i>dfrA12</i> , <i>dfr1</i> , <i>aac(3)</i> , <i>aac6'</i> , <i>aadA1</i> , <i>strAB</i> , <i>mphA</i> , <i>mefA</i> , <i>tnpA</i> , <i>int1</i> , <i>int2</i> , <i>int4</i> , <i>sxt</i>	SXT, nalidixic acid, streptomycin, chloramphenicol

VC, *V. cholerae*. Antibiogram for VC\*.

both encoding trimethoprim resistance, *aad2* (64%), *aadA1* (72%), *aac(3)* (72%), *aac6'* (64%) all encoding resistance against aminoglycosides. Lower rate of occurrence was seen among *tetC* (4%), *ereA* (8%), *tetD* and *tetE* (12% each), *floR* (12%), *dhfr1* and *dfrA15* (4% each), and *aph* (16%).

In addition 3 isolates showed the presence of SXT integrase, 19 isolates showed the presence of *tnpA* encoding transposase and 21 isolates carried integron class1, 11 isolates carried integron class 2 and 8 isolates carried integron class 4 and 4 isolates were found to carry all the three classes of integrons showing the presence of MGEs and signatures associated with MGEs.

### Isolation of Diarrheal Pathogens by Conventional Culture and Antibiotic Sensitivity Test of *V. cholerae*

Pathogens responsible for causing diarrhea in the patients were isolated from the fecal samples by conventional culture method and confirmed using routine biochemical tests. **Table 1** shows pathogens isolated from each fecal sample. *V. cholerae* O1 strains were subject to antibiotic sensitivity test by Kirby-Bauer Disc Diffusion method. The antibiogram results were compared with results of PCR AMR profile of corresponding fecal sample from which the strain was isolated (**Table 4**). On comparison of ARG profile of feces with the antibiogram of its corresponding pathogen it was clear that fecal samples carried ARGs which were not always being expressed by pathogens. At the same time even the pathogen's antibiogram revealed resistance against those classes of antibiotics against which resistance markers were not detected by PCR. Fecal sample KOL18B3-1 carried the following genes *tetABM*, *cat1*, *floR*, *ant*, *dfrA12*, *dfr1*, *aac(3)*, *aac6'*, *aadA1*, *strAB*, *mphA*, *mefA*, *tnpA*, *int1*, *int2*, *int4*, *sxt* but the antibiogram of the *V. cholerae* strain isolated from this fecal sample showed that the strain was not resistant against tetracycline and macrolides. Similarly, *V. cholerae* strains isolated from fecal samples KOL18B2-1 and KOL18B2-4 were sensitive to chloramphenicol but the samples showed the presence of gene *cat1*, which affords resistance against chloramphenicol.

KOL18B2-6, KOL18B2-7, KOL18B3-2, KOL18B3-4, KOL18B3-7, KOL18B3-9, KOL18B3-10, KOL18B3-16, KOL18B3-17 failed to produce conclusive results by culture

method for the identification of any pathogen that we routinely test for diagnosis. However, from all of these samples, resistance determinants were detected successfully by PCR indicating the presence of bacterial DNA and ARGs (**Table 5**).

### 16S Variable Region Sequencing

Four hundred sixty-four bp amplicon from the V3-V4 region of 16S rDNA of representative samples was obtained by PCR and subject to Sanger sequencing. Accordingly DNA from nine samples namely, KOL18B2-1, KOL18B2-2, KOL18B3-1, KOL18B3-2, KOL18B3-3, KOL18B3-9, KOL18B3-10, KOL18B3-11, KOL18B3-12 and genomic DNA from two laboratory strains of *V. cholerae* namely O395 and N16961 were used for the amplification of 464 bp amplicon which was subject to nucleotide sequencing on the ABI platform and the sequence data was subject to pairwise alignment using local alignment software Nucleotide BLAST on the NCBI server. From KOL18B3-2, KOL18B3-3, and KOL18B3-10 no pathogen had been isolated by culture but they carried ARGs as revealed by PCR. The assembled sequence data obtained from sequencing of DNA from all of the above fecal samples could be successfully aligned with known annotated 16S ribosomal DNA sequences archived in the GenBank public database (**Table 6**). The results revealed significant information by indicating the presence of phyla *Bacteroidetes*, *Firmicutes*, and *Proteobacteria* (classes  $\beta$ -*proteobacteria* and  $\gamma$ -*proteobacteria*) in the fecal samples from Kolkata. The 16S variable region DNA sequencing revealed that a majority of fecal samples carried DNA from family *Enterobacteriaceae* as 16S rDNA amplicons from KOL18B2-1, KOL18B3-9, and KOL18B3-12 aligned 92–100% with 16S rDNA of *Escherichia* sp. and KOL18B3-2, matched 99% to uncultured *Escherichia* sp. KOL18B2-2 contained DNA that matched 89% with *Bacteroidetes* DNA. KOL18B3-3 and KOL18B3-10 matched up to 98% with DNA from *Bifidobacteriaceae* and KOL18B3-11 carried DNA from *Streptococcus* sp. revealing the presence of *Firmicutes* in KOL18B3-3, KOL18B3-10, and KOL18B3-11. KOL18B3-1 carried DNA that matched with uncultured  $\beta$ -*proteobacterium* and uncultured *Firmicutes* (*Clostridium* sp.). 5 out of 9 representatives and therefore >55% carried DNA from phylum *Proteobacteria*, 4 out of 9 samples and hence

**TABLE 5** | Fecal samples with resistome but no culturable pathogen.

Stool sample	Pathogen isolated	ARG profile
KOL18B2-6	No pathogen	<i>tetABM,sul2,aadA1,strAB,mefA,mphA</i>
KOL18B2-7	No pathogen(MAC LF)	<i>tetABDM,sul2,df1,ant,aac(3),aac(6'),aadA1,strAB,mefA,mphA,tnpA,int1,int2</i>
KOL18B3-2	No pathogen	<i>tetABM,cat1,ant,df1A12,aac(6'),aadA1,strAB,mphA,mefA,int1,int4</i>
KOL18B3-4	HEA (Green)TSI(k/A+G)	<i>tetAB,cat1,sul2,ant,df1,aac(3),aac(6'),aadA1,strAB,mefA,mphA,tnpA,int1,int2</i>
KOL18B3-7	No pathogen(MAC LF)	<i>tetABM,df1,aac(3),strAB,mefA,mphA,tnpA,int2</i>
KOL18B3-9	HEA (Green)TSI(k/A+G)	<i>tetABM,sul2,ant,df1A12,aac(3),aac(6'),aadA1,strAB,mefA,mphA,tnpA</i>
KOL18B3-10	Mac (NLF)TSI(k/A+G)	<i>tetABM,sul2,strAB,mefA,mphA,tnpA</i>
KOL18B3-16	No pathogen(MAC LF/NLF)	<i>tetA,sul2,aac(3),aac(6'),strAB,mefA,mphA,tnpA,</i>
KOL18B3-17	No pathogen(MAC LF/NLF)	<i>tetABM,sul2,aac(3),aac(6'),strAB,mefA,mphA,tnpA,</i>

**TABLE 6** | 16S rDNA V3-V4 region sequence identity of OTU obtained using Megablast.

Stool Sample	Pathogen isolated	16S rDNA V3-V4 identity (BLAST)
KOL18B2-1	VC O1 <i>Inaba</i>	100% to <i>Escherichia</i> sp.
KOL18B2-2	VC O1 <i>Ogawa</i> + <i>C.jejuni</i>	89% to uncultured bacterium and uncultured Bacteroidetes
KOL18B3-1	VC O1 <i>Ogawa</i>	88-90% to uncultured $\beta$ -proteobacterium, uncultured <i>Clostridium</i> sp.
KOL18B3-2	No pathogen	99% to uncultured <i>Escherichia</i> sp.
KOL18B3-3	EAEC	98% to <i>B. breve</i> , <i>B. longum</i> , <i>B. fecale</i> , <i>B. adolescentis</i> , uncultured <i>Bifidobacterium</i>
KOL18B3-9	HEA (Green)TSI(k/A+G)	92% to <i>E. coli</i> , uncultured <i>Enterobacteriaceae</i>
KOL18B3-1	Mac (NLF)TSI(k/A+G)	88% to uncultured <i>Bifidobacteriaceae</i> and 90% to uncultured bacterium clone
KOL18B3-11	<i>Aeromonas</i> sp.	93% to <i>Streptococcus thermophilus</i> , uncultured <i>Streptococcus</i> sp., uncultured organism
KOL18B3-12	<i>Aeromonas</i> sp.	99% to <i>Escherichia coli</i>

>44% carried DNA from phylum Firmicutes and 1 out of 9 fecal DNA samples and hence 11% revealed the presence of DNA from phylum Bacteroidetes. These results are available in **Figure S6**. The assembled sequences from O395 and N16961 used as experimental control matched 100% with *V. cholerae* 16S rDNA. The assembled sequences are available as **Supplementary Material S7**.

## Mutations in Quinolone Resistance Determining Regions (QRDR) of Topoisomerase II and IV Genes

Quinolone resistance develops due to mutations in the genes encoding topoisomerase II and IV. Twelve samples were subject to SNP analysis. From these fecal samples different diarrheal pathogens had been isolated by culture method. Accordingly, KOL18B2-1, KOL18B2-2, KOL18B2-4, KOL18B2-5, KOL18B3-1, KOL18B3-2, KOL18B3-3, KOL18B3-5, KOL18B3-12, KOL18B3-13, KOL18B3-14, and KOL18B3-15 were included for studying SNPs in the QRDRs. Clear amplification results showing presence of Topoisomerase II and IV genes of *V. cholerae* origin was obtained (for gel picture refer to **Figure S8**) by PCR using primers *gyrA\_seqFOR2-Rev2*, *gyrB\_seqFOR-Rev*, *parC\_seqFOR-Rev*, *parE\_seqFOR-Rev* which were designed from the N16961 sequence (reference sequence ID: NC\_002505.1) Samples used were KOL18B2-1 for *gyrB*, KOL18B2-2, and KOL18B3-1 for *gyrAB*, *parCE*. These were the samples from which *V. cholerae* was isolated as the diarrheal

pathogen. Amplified fragments of *gyrAB*, *parCE* from KOL18B2-2 and KOL18B3-1 were subject to SNP analysis by Sanger sequencing. Accordingly 771 bp fragment of *gyrA*, 662 bp fragment of *gyrB*, 729 bp fragment of *parC* and 640 bp fragment of *parE* were sequenced on the ABI platform. The assembled data obtained using the SeqMan II software was subject to pairwise alignment with the nucleotide sequence of the corresponding regions in the N16961 genome available in GenBank on NCBI (NC\_002505.1) The result of pairwise alignment revealed 100% pairwise match of nucleotide sequence between the assembled 586 bp *gyrA* fragment of KOL18B3-1 with that of N16961 (NC\_002505.1) corresponding to positions 1754436 to 1755021 at the locus VCO1597. The assembled fragment of *gyrB* subunit from KOL18B2-2 was of length 626 bp and it showed 99.84% identity to the corresponding 626 bp region of gene *gyrB* at the locus VC00005 positions 4668–5295 of the reference sequence *V. cholerae* strain N16961 (NC\_002505.1) chromosome 1 (accession no. CP028827.1). The alignment presented a gap showing a deletion at the 16th position of the aligned fragment which corresponded to position 5280 from the 3' end in the reference sequence that has an "A." The assembled and edited fragments of *parC* and *parE* from the same sample were of length 322 and 594 bp. These showed 100% identity to 322 bp fragment of *parC* gene at locus VC00463 and to 594 bp fragment of *parE* gene at locus VC00462 in the N16961 sequence (accession no. CP028827.1) on pairwise alignment using BLAST. The assembled and edited 420 bp fragment of *parE* gene from KOL18B3-1 was aligned



with reference sequence N16961 (accession no. CP028827.1) and also with *parE* sequence from KOL18B2-2. The pairwise alignment showed this region corresponded to positions 476083–476502 in the reference sequence. This 420 bp fragment of *parE* from KOL18B3-1 showed 99.76% sequence identity to both. A single base substitution was observed at position corresponding to position 476151 of reference sequence where in “A” in the reference sequence had been replaced by “T” in the fecal DNA sequence. The same difference was noticed in KOL18B3-1 when its nucleotide sequence of the same genomic region of 420 bp was compared with that of KOL18B2-2 that lacked this SNP. The nucleotide change was not observed in KOL18B2-2 and it bore 100% identity to reference sequence over this genomic region.

## DISCUSSION

AMR due to MDR has emerged as a critical obstacle to the treatment of enteric infections like diarrhea. Therefore, research directed toward leveraging this problem is an urgent need of the hour. The study described here has provided crucial insights into the gut microbiota composition and its resistome to understand transmission of ARGs between pathogens and microbiota. For a complete understanding of the microbiome, metagenomic analysis by next-generation sequencing (NGS) is the key that enables intensive analysis. However, it is an expensive technique and may not be within the affordability and outreach of a majority of laboratories, particularly in developing countries. In such situations, common molecular tools like PCR and Sanger sequencing, used decisively can produce far fetching outcome.

We have used these simple yet useful and robust methods to study the ARG composition in diarrheal fecal samples and to identify major members of the intestinal microbiota of diarrheal patients from Kolkata and the suburban areas. The QIAamp UCP Pathogen Mini Kit is a high quality kit for microbial DNA extraction and purification from small volumes of body fluids in only two hours. This kit provides high yield of DNA, requires no downstream purification and is compatible with Sanger Sequencing and deep sequencing techniques. In addition, since this kit is used for microbial DNA extraction from body fluids and urine, it is perfectly suitable for diarrheal stool which is liquid too. Fecal samples contain DNA from different members of the fecal microbiota and in such a polymicrobial community it is most likely that the most abundant member will be identified on the basis of Sanger sequencing of its 16S ribosomal DNA marker. This technique has been used for more than two decades for identification of bacterial taxa and also of unculturable bacteria for phylogenetic study (15–17). However, this is also one limitation of phylogenetic analysis by Sanger Sequencing of 16S rDNA. Since one of the major goals of the study was to identify the most abundant phylum present in the samples and to detect the presence of bacterial DNA in samples which were found to be devoid of any culturable bacterial pathogen which we tested using pure culture technique 16S rDNA Sanger Sequencing method was the method of choice as an alternative to NGS and was applied to achieve our goal.

The variety of taxonomic entities identified in a sample depends largely on the primers selected for amplification of 16S rDNA. The efficiency of different primers has been scrutinized by several groups who have attempted to select the one with the best coverage of bacterial taxa (14–16). The primers we used in the study to examine OTUs have been reported to be the most suitable for bacterial identification up to the group and genus levels and in identifying the most abundant groups (14) thereby serving our purpose of identification of the most abundant phyla. Diarrhea like other enteric infectious diseases is accompanied with dysbiosis of the microbiome. Our study indicates that in majority of diarrheal patients proteobacteria is the dominant phylum followed by firmicutes suggesting a dysbiotic microbiota with proteobacterial “blooms” which is a characteristic of an abnormal microbiota (18). Detection of a spectrum of 49 ARGs was carried out to study resistance against major classes of antibiotics recommended for the treatment of diarrhea. Primers used for the study were selected or designed from whole genome sequences of different organisms archived in GenBank, NCBI for different classes of antibiotics based on information provided by previous published reports of other workers indicating the source or origin of these genes. ARGs involved in resistance against tetracyclines, macrolides, and aminoglycosides were found to be the major components of the resistome irrespective of the diarrheal pathogen isolated or the major operational taxonomic unit (OTU) present in any particular fecal isolate. The ARGs *mphA* and *mefA* encode phosphotransferase and efflux pump, respectively. The phosphotransferase is involved as a modifying enzyme which inactivates macrolides. These genes are active against erythromycin and azithromycin (8). Both these genes have been found to be abundantly present in gram negative bacteria according to published reports by other groups (8). Primers used to amplify these genes were designed from *Enterobacteriaceae* nucleotide sequences (8). These genes have been reported to be plasmid-borne and have been found to be transferred from *E. coli* to *Shigella* sp. (8). In our study we found from the antibiogram of *V. cholerae* strains that these were sensitive toward macrolides. These were isolated from samples KOL18B2-1, KOL18B2-2, KOL18B2-4, KOL18B3-1. However, in these samples these genes were found to be present. The study helped us to predict the future possibility that these ARGs present in the gene pool may at any point of time be transferred into organisms like *Vibrio cholerae* which come in contact with them and confer resistance upon these pathogens and contribute to the spread of resistance of macrolide drugs which are recommended last resort drugs for treatment of diarrheal diseases like cholera. *mefC* and *mphG* which were examined using primers designed from genomic sequence of *Photobacterium damsela* subsp. *damsela* strain 04Ya311 (accession no. AB571865) (9), representing ARGs from marine bacteria, were not detected in any fecal sample. Our results demonstrated that among tetracycline resistance determinants classes A and B were widespread among the clinical samples, which were examined. KOL18B2-3, KOL18B2-7, and KOL18B3-12 were found to carry class D tetracycline resistance gene and KOL18B2-3, KOL18B3-3, and KOL18B3-12 were found to carry class E tetracycline resistance gene. Classes D and E tetracycline resistance gene

have been reported to be widespread among environmental gram-negative bacteria from marine sediment and fish intestine (19, 20) and are not often isolated from clinical strains. Tetracycline resistance gene was first isolated from *Shigella dysenteriae* (21). Latter studies showed they were widespread among families of class  $\gamma$ -Proteobacteria like *Enterobacteriaceae*, *Vibrionaceae*, *Aeromonadaceae*, and *Moraxellaceae*. They have been reported in clinical and environmental isolates of these classes and have been isolated from *Acinetobacter* sp., *Vibrio* sp., and *Aeromonas* sp. in addition to *E. coli* and *Salmonella* sp. (11, 22). The tetracycline resistance determinants are found on MGEs like plasmids and transposons and have been found to be effectively transferred among bacterial species by conjugation. The resistance determinants selected for this study are involved in efflux of tetracyclines except class M which may have a function in protection of bacterial ribosomes against tetracycline action. Class M appeared in a number of samples used in this study and has been previously reported in a number of gram-positive and gram-negative genera (21). The primers used in this study for the detection of all these genes were designed from members of family *Enterobacteriaceae* like *E. coli* and *S. Ordonez* and were of plasmid or transposon origin (11).

The human intestine is an optimum environment for conjugal transfer of genetic components among bacterial members. ARGs present in feces and representing the intestinal resistome may be easily transferred to pathogen genome and contribute to AMR development against those drugs in the future. From the presence of components of mobilome (SXT integrase, three different classes of integrons and transposase) one can forebode that ARGs present in the fecal microbiome are prone to dissemination by HGT, which is a common phenomenon in bacteria.

In the context of cholera, which is a common diarrheal illness in poverty-stricken parts of the world, predominantly in the low and middle income countries, the presence of a gene pool rich in ARGs in cholera stool against the most potential classes of antimicrobials namely, macrolides, tetracyclines, and aminoglycosides which are the drugs of choice in the treatment of cholera is highly alarming. The strains of *V. cholerae* used for antibiogram analysis were found to be sensitive to these drugs. However, the presence of resistance markers against these antimicrobials in the corresponding fecal resistome and in the population on the whole can admonish of grave danger lurking in the near future when these ARGs can well find their way into the genome of *V. cholerae* and contribute to resistance. HGT is a common occurrence in *V. cholerae*, which occurs when the organism passes through the human gut and also in the environment (23). It is a bacteria with dual lifestyle and can be an important agent in the transmission of ARGs between the gut and the environment (24).

Another significant finding of our study is the coexistence of 16S rDNA signature of *Bifidobacteria* sp. and ARGs in KOL18B3-3 and KOL18B3-10. *Bifidobacteria* sp. is an early intestinal

colonizer and commensal which impacts the development of newborns in multiple beneficial ways and have been developed as probiotics for the prevention and treatment of diseases (25). Recent work by Bag et al. (26) and Duranti et al. (27) demonstrated the existence of ARGs in whole-genome sequence (WGS) of *Bifidobacteria* sp. Bag et al. showed the physical linkage of these ARGs against different classes of antimicrobials to MGEs in the WGS of a strain of *Bifidobacterium longum indica* that was isolated from feces of a healthy Indian adult (26). Duranti et al. found interspecies variation in breakpoint levels for antibiotics like streptomycin and tetracycline indicating the role of HGT in the evolution of AMR in *Bifidobacteria* sp. (27). Acquisition of ARGs by *Bifidobacteria* sp. has led to its emergence as MDR and these in turn will serve as vehicles of transmission of ARGs.

This is the first study addressing the frequency and distribution of different classes of ARGs of diverse origin in the local intestinal milieu of diarrheal patients in Kolkata and the suburban areas. The structure and composition of microbiome is influenced by geography, ethnicity, and cultural practices. The study is distinct. It has been conducted using fecal samples from a discrete population. The study helped us to compare ARG profile between fecal samples from diarrheal patients afflicted with diarrhea due to different diarrheal pathogens. It helped us to conclude that fecal samples may share many ARGs in common, irrespective of the etiologic agent isolated from it. This is suggestive of a common gene pool acting as ARG reservoir and aiding in frequent lateral and vertical genetic exchange in pathogens and commensals. The study demonstrated that fecal samples from which routinely diagnosed pathogens were not isolated by conventional culture method also presented a resistome. These stool samples might have been harboring viral or eukaryotic diarrheal pathogens or any other enteric bacterial pathogen which was not tested for as it is beyond our scope. Further, it is difficult to obtain information from patients regarding self administration of antibiotics prior to their admission to the hospital. Self-administration of antibiotics is quite common in India due to over-the-counter sale of antibiotics and slack rules governing their purchase. The 16S rDNA sequence alignment from these fecal samples indicated that commensals and other members of the disturbed gut microflora or undiagnosed diarrheal agent may be contributing to the resistome. Although, metagenomics is the ultimate answer to the complex question about the structural and functional diversity of the microbiome, our findings obtained using common molecular methods is a highly significant pilot study indicating the presence and involvement of culturable and culture-resistant organisms in the development of AMR without the use of deep sequencing techniques and whole-genome sequence analysis. These findings are of immense importance for public health. It has enabled us to understand which resistant markers associated with different classes of antibiotics are present in the contemporary diarrheal microbiome and the relative abundance and frequency of the resistant markers will serve as parameters to understand and predict the potential threat that

each of these classes of antibiotics will encounter leading to AMR crisis. Finally, our study will help in devising research strategies to intervene the transmission route of these genes to alleviate the problem of AMR.

## DATA AVAILABILITY STATEMENT

All relevant data is contained within the article. All datasets generated for this study are included in the article/**supplementary material**.

## ETHICS STATEMENT

The study was conducted with the approval of the funding bodies and fecal samples were collected with the approval of the Institutional Ethics Committee, NICED. Informed consent was obtained from the participants of the study. Information obtained from the study participants was kept confidential. Information was kept locked in office. Any personal information was never passed to the third party.

## REFERENCES

- Luo Y, Luo R, Ding H, Ren X, Luo H, Zhang Y, et al. Characterization of carbapenem-resistant *Escherichia coli* isolates through the whole-genome sequencing analysis. *Microb Drug Resist.* (2018) 24:175–80. doi: 10.1089/mdr.2017.0079
- Hammerl JA, Jäckel C, Bortolaia V, Schwartz K, Bier N, Hendriksen RS, et al. Carbapenemase VCC-1–producing *Vibrio cholerae* in coastal waters of Germany. *Emerg Infect Dis.* (2017) 23:1735–37. doi: 10.3201/eid2310.161625
- Liu W, Zou D, Li Y, Wang X, He X, Wei X, et al. Sensitive and rapid detection of the New Delhi metallo-beta-lactamase gene by loop-mediated isothermal amplification. *J Clin Microbiol.* (2012) 50:1580–5. doi: 10.1128/JCM.06647-11
- Schmidt AS, Bruun MS, Larsen JL, Dalsgaard I. Characterization of class 1 integrons associated with R-plasmids in clinical *Aeromonas salmonicida* isolates from various geographical areas. *J Antimicrob Chemother.* (2001) 47:735–43. doi: 10.1093/jac/47.6.735
- Ceccarelli D, Salmia AM, Sami J, Cappuccinelli P, Colombo MM. New cluster of plasmid-located class 1 integrons in *Vibrio cholerae* O1 and a *dfrA15* cassette-containing integron in *Vibrio parahaemolyticus* isolated in Angola. *Antimicrob Agents Chemother.* (2006) 50:2493–99. doi: 10.1128/AAC.01310-05
- Hochhut B, Lotfi Y, Mazel D, Faruque SM, Woodgate R, Waldor MK. Molecular analysis of antibiotic resistance gene clusters in *Vibrio cholerae* O139 and O1 SXT constains. *Antimicrob Agents Chemother.* (2001) 45:2991–3000. doi: 10.1128/AAC.45.11.2991-3000.2001
- Iwanaga M, Toma C, Miyazato T, Insiengmay S, Nakasone N, Ehara M. Antibiotic resistance conferred by a class I integron and SXT constin in *Vibrio cholerae* O1 strains isolated in Laos. *Antimicrob Agents Chemother.* (2004) 48:2364–9. doi: 10.1128/AAC.48.7.2364-2369.2004
- Nguyen MCP, Woerther PL, Bouvet M, Andreumont A, Leclercq R, Canu A. *Escherichia coli* as reservoir for macrolide resistance genes. *Emerg Infect Dis.* (2009) 15:1648–50. doi: 10.3201/eid1510.090696
- Nonaka L, Maruyama F, Suzuki S, Masuda M. Novel macrolide-resistance genes, *meff(C)* and *mph(G)*, carried by plasmids from *Vibrio* and *Photobacterium* isolated from sediment and seawater of a coastal aquaculture site. *Lett Appl Microbiol.* (2015) 61:1–6. doi: 10.1111/lam.12414
- Dalsgaard A, Forslund A, Sandvang D, Arntzen L, Keddy K. *Vibrio cholerae* O1 outbreak isolates in Mozambique and South Africa in 1998 are multiple-drug resistant, contain the SXT element and the *aadA2* gene located on class 1 integrons. *J Antimicrob Chemother.* (2001) 48:827–38. doi: 10.1093/jac/48.6.827
- Guardabassi L, Dijkshoorn L, Collard JM, Olsen JE, Dalsgaard A. Distribution and *in-vitro* transfer of tetracycline resistance determinants in clinical and aquatic *Acinetobacter* strains. *J Med Microbiol.* (2000) 49:929–36. doi: 10.1099/0022-1317-49-10-929
- Wang R, Li J, Kan B. Sequences of a co-existing SXT element, a chromosomal integron (CI) and an IncA/C plasmid and their roles in multidrug resistance in a *Vibrio cholerae* O1 El Tor strain. *Int J Antimicrob Agents.* (2016) 48:305–9. doi: 10.1016/j.ijantimicag.2016.05.020
- Bag S, Saha B, Mehta O, Anbumani D, Kumar N, Dayal M, et al. An improved method for high quality metagenomics DNA extraction from human and environmental samples. *Sci Rep.* (2016) 6:26775. doi: 10.1038/srep26775
- Klindworth A, Pruesse E, Schweer T, Peplies J, Quast C, Horn M, et al. Evaluation of general 16S ribosomal RNA gene PCR primers for classical and next-generation sequencing-based diversity studies. *Nucleic Acids Res.* (2013) 41:e1. doi: 10.1093/nar/gks808
- Weisburg WG, Barns SM, Pelletier DA, Lane DJ. 16S ribosomal DNA amplification for phylogenetic study. *J Bacteriol.* (1991) 173:697–703. doi: 10.1128/jb.173.2.697-703.1991
- Wilson KH, Blitchington RB, Greene RC. Amplification of bacterial 16S ribosomal DNA with polymerase chain reaction. *J Clin Microbiol.* (1990) 28:1942–6.
- Wilson KH. Detection of culture-resistant bacterial pathogens by amplification and sequencing of ribosomal DNA. *Clin Infect Dis.* (1994) 18:958–62. doi: 10.1093/clinids/18.6.958
- Stecher B. The roles of inflammation, nutrient availability and the commensal microbiota in enteric pathogen infection. *Microbiol Spectr.* (2015) 3:3. doi: 10.1128/microbiolspec
- Andersen SR, Sandaa RA. Distribution of tetracycline resistance determinants among gram-negative bacteria isolated from polluted and unpolluted marine sediments. *Appl Environ Microbiol.* (1994) 60:908–12.
- DePaola A, Roberts MC. Class D and E tetracycline resistance determinants in gram-negative bacteria from catfish ponds. *Mol Cell Probes.* (1995) 9:311–3.
- Roberts MC. Tetracycline resistance determinants: mechanisms of action, regulation of expression, genetic mobility, and distribution. *FEMS Microbiol Rev.* (1996) 19:1–24. doi: 10.1111/j.1574-6976.1996.tb00251.x
- Schmidt AS, Bruun MS, Dalsgaard I, Larsen JL. Incidence distribution, and spread of tetracycline resistance determinants and integron-associated antibiotic resistance genes among motile *Aeromonads* from a

## AUTHOR CONTRIBUTIONS

RD planned, designed and executed experiments, analyzed the data, and wrote the paper. AM executed the experiments and analyzed the data. SD analyzed the data and wrote the paper.

## ACKNOWLEDGMENTS

The authors would like to thank the Department of Health Research and the Indian Council of Medical Research, Govt. of India for financial support for this research (Grant number R.12015/01/2018-HR). We would like to thank Dr. G. Balakrish Nair, for his inspiration and support for this work.

## SUPPLEMENTARY MATERIAL

The Supplementary Material for this article can be found online at: <https://www.frontiersin.org/articles/10.3389/fpubh.2020.00061/full#supplementary-material>

- fish farming environment. *Appl Environ Microbiol.* (2001) 67:5675–82. doi: 10.1128/AEM.67.12.5675-5682.2001
23. Stine OC, Morris JG Jr. Circulation and transmission of clones of *Vibrio cholerae* during cholera outbreaks. *Curr Top Microbiol Immunol.* (2014) 379:181–93. doi: 10.1007/82\_2013\_360
24. Faruque SM, Nair GB. Molecular Ecology of Toxigenic *Vibrio cholerae*. *Microbiol Immunol.* (2002) 46:59–66. doi: 10.1111/j.1348-0421.2002.tb02659.x
25. Hidalgo-Cantabrana C, Delgado S, Ruiz L, Ruas-Madiedo P, Sánchez B, Margolles A. *Bifidobacteria* and their health-promoting effects. *Microbiol Spec.* (2017) 5:3. doi: 10.1128/microbiolspec.BAD-0010-2016
26. Bag S, Ghosh TS, Banerjee S, Mehta O, Verma J, Dayal M, et al. Molecular insights into antimicrobial resistance traits of commensal human gut microbiota. *Microb Ecol.* (2019) 77:546–557. doi: 10.1007/s00248-018-1228-7
27. Duranti S, Lugli GA, Mancabelli L, Turrone F, Milani C, Mangifesta M, et al. Prevalence of antibiotic resistance genes among human gut-derived *Bifidobacteria*. *Appl Environ Microbiol.* (2017) 17:83:e02894-16. doi: 10.1128/AEM.02894-16

**Conflict of Interest:** The authors declare that the research was conducted in the absence of any commercial or financial relationships that could be construed as a potential conflict of interest.

Copyright © 2020 De, Mukhopadhyay and Dutta. This is an open-access article distributed under the terms of the Creative Commons Attribution License (CC BY). The use, distribution or reproduction in other forums is permitted, provided the original author(s) and the copyright owner(s) are credited and that the original publication in this journal is cited, in accordance with accepted academic practice. No use, distribution or reproduction is permitted which does not comply with these terms.





# *In vitro* Activity of Apramycin Against Carbapenem-Resistant and Hypervirulent *Klebsiella pneumoniae* Isolates

Mingju Hao<sup>1†</sup>, Xiaohong Shi<sup>1†</sup>, Jingnan Lv<sup>2†</sup>, Siqiang Niu<sup>3</sup>, Shiqing Cheng<sup>4</sup>, Hong Du<sup>2</sup>, Fangyou Yu<sup>5</sup>, Yi-Wei Tang<sup>6</sup>, Barry N. Kreiswirth<sup>7</sup>, Haifang Zhang<sup>2\*</sup> and Liang Chen<sup>7</sup>

<sup>1</sup> Department of Laboratory Medicine, Shandong Provincial Qianfoshan Hospital, The First Hospital Affiliated With Shandong First Medical University, Jinan, China, <sup>2</sup> Department of Clinical Laboratory, The Second Affiliated Hospital of Soochow University, Suzhou, China, <sup>3</sup> Department of Laboratory Medicine, The First Affiliated Hospital of Chongqing Medical University, Chongqing, China, <sup>4</sup> Department of Laboratory Medicine, Shandong Provincial Hospital Affiliated to Shandong University, Jinan, China, <sup>5</sup> Department of Clinical Laboratory, Shanghai Pulmonary Hospital, Tongji University School of Medicine, Shanghai, China, <sup>6</sup> Department of Laboratory Medicine, Memorial Sloan Kettering Cancer Center; Department of Pathology and Laboratory Medicine, Weill Medical College of Cornell University, New York, NY, United States, <sup>7</sup> Hackensack-Meridian Health Center for Discovery and Innovation, Nutley, NJ, United States

## OPEN ACCESS

### Edited by:

Luciene Andrade Da Rocha  
Minarini,

Federal University of São Paulo, Brazil

### Reviewed by:

Qi Wang,

Peking University People's Hospital,  
China

Willames M. B. S. Martins,

Federal University of São Paulo, Brazil

Ana Paula D'Alincourt

Carvalho-Assef,

Oswaldo Cruz Foundation (Fiocruz),

Brazil

### \*Correspondence:

Haifang Zhang

haifangzhang@sina.com

†These authors have contributed  
equally to this work

### Specialty section:

This article was submitted to  
Antimicrobials, Resistance  
and Chemotherapy,  
a section of the journal  
Frontiers in Microbiology

Received: 14 September 2019

Accepted: 27 February 2020

Published: 13 March 2020

### Citation:

Hao M, Shi X, Lv J, Niu S,  
Cheng S, Du H, Yu F, Tang Y-W,  
Kreiswirth BN, Zhang H and Chen L  
(2020) *In vitro* Activity of Apramycin  
Against Carbapenem-Resistant  
and Hypervirulent *Klebsiella  
pneumoniae* Isolates.  
Front. Microbiol. 11:425.  
doi: 10.3389/fmicb.2020.00425

**Objective:** The emergence of carbapenem-resistant and hypervirulent *Klebsiella pneumoniae* (CR-hvKp) strains poses a significant public threat, and effective antimicrobial therapy is urgently needed. Recent studies indicated that apramycin is a potent antibiotic with good activity against a range of multi-drug resistant pathogens. In this study, we evaluated the *in vitro* activity of apramycin against clinical CR-hvKp along with carbapenem-resistant non-hvKp (CR-non-hvKp) isolates.

**Methods:** Broth microdilution method was used to evaluate the *in vitro* activities of apramycin, gentamicin, amikacin, imipenem, meropenem, doripenem, ertapenem and other comparator “last-resort” antimicrobial agents, including ceftazidime-avibactam, colistin and tigecycline, against eighty-four CR-hvKp and forty CR-non-hvKp isolates collected from three Chinese hospitals. Multilocus Sequence typing (MLST), molecular capsule typing (*wzi* sequencing) and antimicrobial resistance genes were examined by PCR and Sanger sequencing. Pulsed-field gel electrophoresis and next generation sequencing were conducted on selected isolates.

**Results:** Among the 84 CR-hvKp isolates, 97.6, 100, 97.6, and 100% were resistant to imipenem, meropenem, doripenem and ertapenem, respectively. Apramycin demonstrated an MIC<sub>50</sub>/MIC<sub>90</sub> of 4/8 μg/mL against the CR-hvKp isolates. In contrast, the MIC<sub>50</sub>/MIC<sub>90</sub> for amikacin and gentamicin were >64/>64 μg/mL. All CR-hvKp isolates were susceptible to ceftazidime-avibactam, colistin and tigecycline with the MIC<sub>50</sub>/MIC<sub>90</sub> values of 0.5/1, 0.25/0.5, 1/1, respectively. For CR-non-hvKp, The MIC<sub>50/90</sub> values for apramycin, gentamicin and amikacin were 2/8, >64/>64, and >64/>64 μg/mL, respectively. There were no statistical significance in the resistance rates of antimicrobial agents between CR-hvKp and CR-non-hvKp groups (*p* > 0.05). Genetic analysis revealed that all CR-hvKp isolates harbored *bla*<sub>KPC-2</sub>, and 94% (*n* = 79) belong to the ST11 high-risk clone. 93.6% (44/47) of amikacin or gentamicin resistant strains carried 16S rRNA methyltransferases gene *rmtB*.

**Conclusion:** Apramycin demonstrated potent *in vitro* activity against CR-hvKp isolates, including those were resistant to amikacin or gentamicin. Further studies are needed to evaluate the applicability of apramycin to be used as a therapeutic antibiotic against CR-hvKp infections.

**Keywords:** apramycin, susceptibility, carbapenem resistance, hypervirulent *Klebsiella pneumoniae*, aminoglycoside

## INTRODUCTION

*Klebsiella pneumoniae* is a clinically important pathogen, causing a wide range of diseases including pneumonia, urinary tract infections (UTIs), bloodstream infections, in hospital settings among neonates, elderly and immunocompromised individuals (Paczosa and Meccas, 2016; Bengoechea and Sa Pessoa, 2019). Hypervirulent *K. pneumoniae* (hvKp) is an increasing recognized pathotype that is more virulent than classical *K. pneumoniae* (cKp), which showed the propensity to cause serious, life-threatening infections in otherwise healthy individuals in the community (Shon et al., 2013; Gu et al., 2018).

Historically, hvKp isolates are susceptible to most antibiotics, however, multidrug-resistant hvKp, especially carbapenem-resistant strains, are increasingly reported in the past few years (Cejas et al., 2014; Li et al., 2014; Siu et al., 2014). The emergence of carbapenem-resistant and hypervirulent *K. pneumoniae* (CR-hvKp) was either due to the acquisition of a pLVPK-like virulence plasmid by classic carbapenem-resistant *K. pneumoniae* strains (Gu et al., 2018) or through acquisition of a carbapenemase-encoding plasmid by hvKp isolates (Shon et al., 2013). The *rmpA*, *rmpA2*, *iutA*, *iucABCD* and *iroBCDN* genes harbored by pLVPK-like virulence plasmid is responsible for the virulence phenotype (Yang et al., 2019). A recent study from China reported a fatal outbreak of ventilator associated pneumonia caused by ST11 CR-hvKp strains (Gu et al., 2018). More recently, one hypermucoviscous isolate with KPC-3 carbapenemase-encoding plasmid was firstly described in the United States, which also exhibited colistin heteroresistance (Wozniak et al., 2019). The rapid dissemination of CR-hvKp strains in different global regions underscores the urgent need of appropriate antibiotic therapy against these life-threatening pathogens.

Aminoglycosides including amikacin, gentamicin and tobramycin, which belong to the 4,6-disubstituted deoxystreptamine (DOS) subclass, are among the few drugs that retain certain *in vitro* activity against CRE (Livermore et al., 2011). However, the acquisition of 16S rRNA methylases confer high level resistance to the 4,6-disubstituted DOS aminoglycosides, which imposes serious challenge for clinical management (Hu et al., 2017). Apramycin is of the 4-monosubstituted DOS subclass, markedly different in its chemical structure from other clinically used aminoglycoside antibiotics. Its unique structure makes apramycin molecules inherently resilient to almost all resistance determinants commonly found in multi-drug resistant strains (Juhás et al., 2019). Indeed, recent studies indicated that apramycin is a potent antibiotic with good activity against a range of clinical pathogens, including multidrug-resistant *Mycobacterium tuberculosis*, carbapenem-resistant

*Enterobacteriaceae*, spectinomycin-resistant *Neisseria gonorrhoeae* and *Staphylococcus aureus* (Smith and Kirby, 2016; Hu et al., 2017; Truelson et al., 2018; Galani et al., 2019; Riedel et al., 2019). In order to evaluate whether apramycin can be served as an alternative antibiotic to treat the CR-hvKp infections, we examined the *in vitro* activity of apramycin against a collection of CR-hvKp isolates collected from three different hospitals in China. Its *in vitro* activity was compared with the results from other aminoglycosides (amikacin and gentamicin) and some “last resort” antibiotics, including colistin, tigecycline and ceftazidime-avibactam.

## MATERIALS AND METHODS

### Bacterial Isolates

Eighty-four unique (one isolate per patient) CR-hvKp isolates, including 65 isolates from our previous study (Yu et al., 2018a), were included. They were collected from three hospitals across different regions in China (Shandong, Jiangsu and Shanghai) between 2014 and 2019. These isolates were obtained from sputum (53.6%, 45/84), urine (14.3%, 12/84), blood (14.3%, 12/84), pus (4.8%, 4/84), ascites (3.6%, 3/84) and other sources (9.5%, 8/84). In this study, we defined an hvKp strain based upon demonstration of a positive string test (hypermucoviscosity) and co-harboring the genes *rmpA* (*rmpA* or *rmpA2*) and *iutA* as previously (Yu et al., 2018a). All 84 isolates were hypermucoviscous (string test >5 mm) and were positive for the *rmpA/rmpA2* and *iutA* by PCR analysis (Yu et al., 2018b). In addition, 40 unique strains of carbapenem resistant non-hypervirulent *K. pneumoniae* (CR-non-hvKp) isolates, with negative hypermucoviscous phenotype and negative *rmpA/rmpA2* and *iutA* PCR results, were collected from the same three hospitals, and were included to compare with the susceptibility results of CR-hvKp.

### Antibiotic Susceptibility Assay

The antimicrobial susceptibility was assessed *via* a minimum inhibitory concentration (MIC) broth microdilution method. Results were interpreted using Clinical Laboratory Standards Institute (CLSI) breakpoints (Clinical and Laboratory Standards Institute, 2019) with the exception of tigecycline and polymyxin B, which were interpreted using EUCAST breakpoints (The European Committee on Antimicrobial Susceptibility Testing, 2019). National Antimicrobial Resistance Monitoring System (NARMS) breakpoints for enteric bacteria were used for the interpretation of apramycin susceptibility, in which strains were classified as susceptible (MIC ≤ 8 μg/mL), intermediate (MIC = 16~32 μg/mL), or resistant

(MIC  $\geq$  64  $\mu\text{g}/\text{mL}$ ) (National Antibiotic Resistance Monitoring System [NARMS], 2002). MICs were performed in duplicate on two separate days. *Escherichia coli* ATCC 25922 and *Pseudomonas aeruginosa* ATCC 27853 were used as the quality control strains in each experiment. *K. pneumoniae* ATCC 700603 was used as quality control strain for ceftazidime-avibactam which was tested against ceftazidime-avibactam and ceftazidime alone to confirm the activity of avibactam in the combination.

## Molecular Typing and Screening of Antibiotic Resistance Genes

All CR-Kp isolates including CR-hvKp and CR-non-hvKp were genotyped by multilocus Sequence Typing (MLST) and *wzi* sequencing (Brisse et al., 2013). Pulsed-field gel electrophoresis (PFGE) of XbaI-digested genomic DNA samples of 15 selected CR-hvKp isolates was performed with a CHEF MAPPER XA apparatus (Bio-Rad, United States). PFGE patterns were analyzed using GelJ software 2.0v (Heras et al., 2015).

A multiplex PCR was used to detect KPC, NDM, VIM, IMP, and OXA-48-like carbapenemase genes, followed by Sanger sequencing (Chen et al., 2011; Chavda et al., 2016; Evans et al., 2016). Common aminoglycoside modifying enzyme (AME) and RMT-encoding genes were determined by PCR and Sanger sequencing. AME coding genes, including *aac(3′)-IIa*, *aac(3′)-IIc*, *aac(3′)-IV*, *aac(6′)-IIa*, *aph(3′)-Ia*, *aph(3′)-Ib*, *ant(2′)-Ia* and *ant(3′)-Ia*, and ARM/RMT methyltransferases coding genes, including *armA*, *rmtA*, *rmtB*, *rmtC*, *rmtD* and *npmA* (Wu et al., 2009), were examined. The primers used in this study were listed in **Supplementary Table S1**.

The apramycin resistant isolate, KpApr172, was subject to next generation sequencing using the Illumina HiSeq system (Illumina, San Diego, CA, United States). Genomic DNA was isolated using a Wizard<sup>®</sup> Genomic DNA Purification Kit (Promega, Madison, WI, United States). Sequencing reads were *de novo* assembled using Spades 3.12.0 (Bankevich et al., 2012). *In silico* multi-locus sequence typing was performed using MLST 2.0 (Larsen et al., 2012) while the acquired antimicrobial resistance genes were identified using ResFinder 3.0 (Zankari et al., 2012). The plasmid replicons in the sequenced isolates were identified using PlasmidFinder 2.0 (Carattoli et al., 2014). The whole-genome sequence of KpApr172 was deposited in the GenBank database under accession number WUJI00000000.

## Statistical Analysis

Chi-square and Fisher's exact analysis were employed to compare resistance rate of antimicrobial agents between CR-hvKp and CR-non-hvKp groups. Statistical analyses were performed using GraphPad Prism 6.0 (GraphPad Software, La Jolla, CA, United States). *P* value of  $<0.05$  was considered to indicate statistically significant differences.

## RESULTS

### Susceptibility Testing

The *in vitro* activities of apramycin and other antimicrobials against 84 clinical isolates CR-hvKp and 40 CR-non-hvKp strains

were summarized in **Table 1**. The CR-hvKp isolates showed high-level resistance to four tested carbapenems, with MIC<sub>50/90</sub> values 128/ $>$ 256, 128/ $>$ 256, 64/128 and 128/ $>$ 256  $\mu\text{g}/\text{mL}$  for meropenem, imipenem, doripenem, and ertapenem, respectively, 97.6, 100, 97.6, and 100% of the isolates were resistant to imipenem, meropenem, doripenem and ertapenem. All isolates were resistant to ceftazidime and 97.6% ( $n = 82$ ) isolates were resistant to aztreonam. Apramycin exhibited significantly better antimicrobial activity than the clinical standard-of-care aminoglycosides gentamicin and amikacin, with MIC<sub>50/90</sub> values 4/8  $\mu\text{g}/\text{mL}$ . The MIC ranged from 1 to 16  $\mu\text{g}/\text{mL}$  (**Figure 1**). By contrast, the MIC<sub>50/90</sub> values for gentamicin and amikacin were both  $>64/>64$   $\mu\text{g}/\text{mL}$ .

For CR-non-hvKp, 2.5, 55, and 57.5% of the isolates were resistant to apramycin, gentamicin and amikacin, respectively. The MIC<sub>50/90</sub> values for apramycin, gentamicin and amikacin were 2/8,  $>64/>64$ , and  $>64/>4$   $\mu\text{g}/\text{mL}$ , respectively. One isolate was resistant to all three aminoglycosides including apramycin (MIC  $>$  128  $\mu\text{g}/\text{mL}$ ). Five NDM producing CR-non-hvKp isolates were resistant to ceftazidime-avibactam (MIC  $>$  128  $\mu\text{g}/\text{mL}$ ), but they remained susceptible to colistin and tigecycline. There were no statistical significance in the resistance rates of antimicrobial agents between CR-hvKp and CR-non-hvKp groups ( $p > 0.05$ ).

## Molecular Typing and *wzi* Genes Sequencing

Multilocus sequence typing showed that most clinical CR-hvKp strains (94%, 79/84) belong to ST11, the most prevalent CR-Kp ST in China (Gu et al., 2018), while the remaining five isolates were from ST268 ( $n = 2$ ), ST65 ( $n = 1$ ), ST412 ( $n = 1$ ), and ST595 ( $n = 1$ ). Among the 79 ST11 isolates, 44 have the capsular polysaccharide *wzi* allele 64 (*wzi64*) (corresponding with capsular type KL64), and the other 35 isolates carry *wzi209* (corresponding with capsular KL47). For CR-non-hvKp strains, 70% (28/40) of the isolates were identified as ST11, carrying *wzi64* ( $n = 18$ ) and *wzi209* ( $n = 10$ ), respectively. The other 12 CR-non-hvKp isolates were from ST2407 ( $n = 3$ ), ST1308 ( $n = 3$ ), ST25 ( $n = 2$ ), ST307 ( $n = 1$ ), ST1308 ( $n = 1$ ), ST412 ( $n = 1$ ), and ST48 ( $n = 1$ ). To further explore the relatedness of individual CR-hvKp strains, we randomly selected 15 ST11 CR-hvKp strains from the three hospitals for PFGE analysis (**Supplementary Figure S1**). The results showed these isolates generally clustered by hospitals and capsular KL types, but displayed various PFGE profiles. Our results suggested that apramycin is actively against CR-hvKp and CR-non-hvKp isolates most prevalent STs from different geographical regions (Jiangsu, Shanghai, and Shandong) in China.

## Genotyping of Carbapenemase and Aminoglycoside Resistance Genes

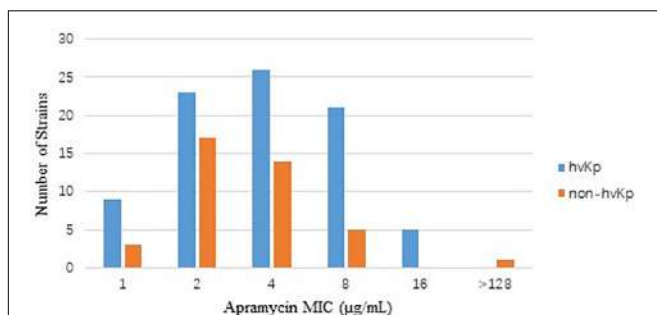
The distribution of carbapenemase and aminoglycoside resistance genes were summarized in **Table 2**. All CR-hvKp isolates and 72.5% (29/40) of CR-non-hvKp isolates harbored *bla*<sub>KPC-2</sub>. Five CR-non-hvKp strains harbored *bla*<sub>NDM-1</sub> ( $n = 4$ ) and *bla*<sub>NDM-5</sub> ( $n = 1$ ). 93.6% (44/47) of the CR-hvKp and 95.6%

**TABLE 1** | *In vitro* susceptibility of different antibiotics against 84 CR-hvKp and 40 CR-non-hvKp isolates.

Antimicrobial agents	MIC (range) ( $\mu\text{g/mL}$ )	Resistance n (%)	MIC <sub>50</sub> ( $\mu\text{g/mL}$ )	MIC <sub>90</sub> ( $\mu\text{g/mL}$ )
<b>CR-hvKp isolates (n = 84)</b>				
Meropenem	4 to >256	84 (100)	128	>256
Imipenem	2 to >256	82 (97.6)	128	>256
Doripenem	1 to >256	82 (97.6)	64	128
Ertapenem	2 to >256	84 (100)	128	>256
Aztreonam	8 to >64	82 (97.6)	>64	>64
Ceftazidime	16 to >256	84(100)	>256	>256
Ceftazidime-avibactam	<0.125 to 0.25	0 (0)	0.5	1
Colistin	<0.125 to 1	0 (0)	0.25	0.5
Tigecycline	0.5 to 1	0 (0)	1	1
Gentamicin	<0.5 to >64	47(55.9)	>64	>64
Amikacin	1 to >64	46 (54.8)	>64	>64
Apramycin	1 to 16	0 (0)	4	8
<b>CR-non-hvKp isolates (n = 40)</b>				
Meropenem	2 to >256	39 (97.5)	128	>256
Imipenem	2 to >256	39 (97.5)	128	>256
Doripenem	1 to >256	39 (97.5)	128	128
Ertapenem	16 to >256	40 (100)	256	>256
Aztreonam	>64	40(100)	>64	>64
Ceftazidime	32 to >256	40(100)	>256	>256
Ceftazidime-avibactam	< 0.125 to >128	5 (12.5)	0.5	>128
Colistin	<0.125 to 1	0 (0)	0.25	0.5
Tigecycline	0.5 to 1	0 (0)	1	1
Gentamicin	<0.5 to >64	22(55)	>64	>64
Amikacin	2 to >64	23 (57.5)	>64	>64
Apramycin	1 to >128	1 (2.5)	2	8

**TABLE 2** | Prevalence of carbapenemase and aminoglycoside resistance genes in CR-hvKp and CR-non-hvKp isolates.

Resistance genes		CR-hvKp (n = 84)	CR-non-hvKp (n = 40)
Carbapenemase	KPC-2	84 (100%)	29 (72.5%)
	NDM	0 (0%)	5 (12.5%)
	IMP	0 (0%)	0 (0%)
	VIM	0 (0%)	0 (0%)
	OXA-48	0 (0%)	0 (0%)
Aminoglycoside modifying enzyme (AME)	<i>Aac(3')-IIa</i>	1 (1.2%)	2 (5%)
	<i>Aac(3')-IId</i>	1 (1.2%)	0 (0%)
	<i>Aac(3')-IV</i>	0 (0%)	1 (2.5%)
	<i>Aac(6')-Ib</i>	6 (7.14%)	3 (7.5%)
	<i>Aac(6')-IIa</i>	0 (0%)	0 (0%)
	<i>Aph(3')-Ia</i>	4 (4.76%)	9 (22.5%)
	<i>Aph(3')-Ib</i>	0 (0%)	1 (2.5%)
	<i>Ant(2'')-Ia</i>	0 (0%)	0 (0%)
	<i>Ant(3'')-Ia</i>	0 (0%)	0 (0%)
	rRNA	<i>ArmA</i>	0 (0%)
methyltransferases (RMT)	<i>RmtA</i>	0 (0%)	0 (0%)
	<i>RmtB</i>	44 (52.4%)	22 (55%)
	<i>RmtC</i>	0 (0%)	0 (0%)
	<i>RmtD</i>	0 (0%)	0 (0%)
	<i>NpmA</i>	0 (0%)	0 (0%)

**FIGURE 1** | Distribution of apramycin MIC in CR-hvKp (n = 84) and CR-non-hvKp (n = 40) isolates. hvKp: hypervirulent *Klebsiella pneumoniae*, non-hvKp: non-hypervirulent *Klebsiella pneumoniae*.

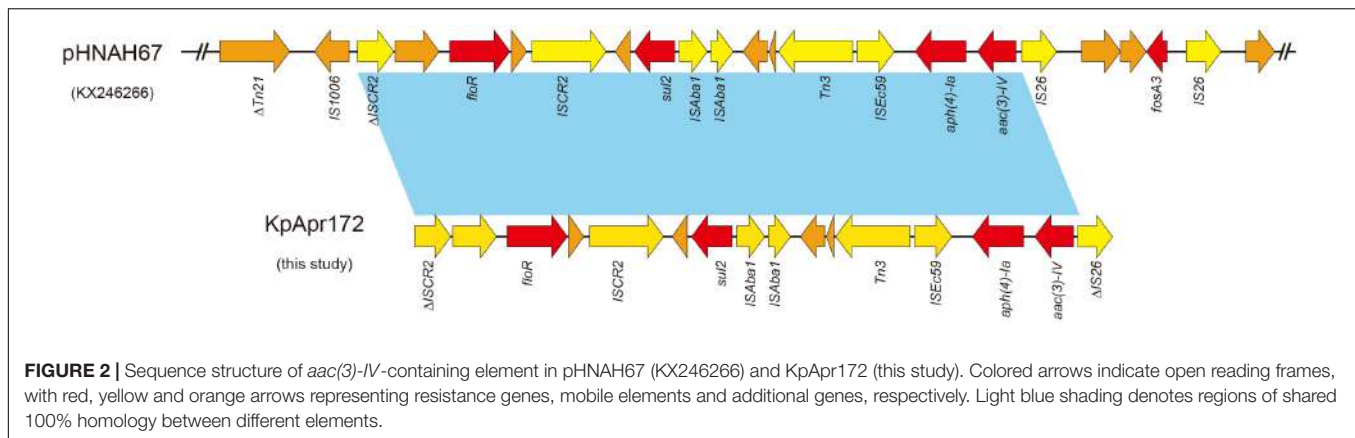
(22/23) of the CR-non-hvKp isolates that were resistant to amikacin or gentamicin carried the RMT gene *rmtB*.

Notably, one CR-non-hvKp isolate (KpApr172) was resistant to apramycin. PCR showed that it contains the aminoglycoside acetyltransferase 3-IV gene *aac(3)-IV*, which encodes resistance to apramycin, gentamicin, netilmicin and tobramycin. Further next generation sequencing revealed that KpApr172 was a strain ST11 and harbored the KL47 capsular type. Resistance gene mining indicated that KpApr172 harbored 17 antimicrobial resistance genes encoding resistance

to  $\beta$ -lactams (*bla*<sub>KPC-2</sub>, *bla*<sub>NDM-5</sub>, *bla*<sub>CTX-M-3</sub>, and *bla*<sub>SHV-12</sub>), aminoglycosides [*armA*, *aadA2*, *aac(3)-IId*, *aac(3)-IV* and *aph(4)-Ia*], macrolid [*msr(E)* and *mph(E)*], bleomycin (*ble*), florfenicol (*floR*), quaternary ammonium compound (*qacE $\Delta$ 1*) and sulfonamide-trimethoprim (*sul1*, *sul2* and *dfrA12*). The quinolone resistance-determining region (QRDR) genes *gyrA*, *gyrB*, *parC* and *parE* were further examined, and we observed mutations encoding amino acid substitutions at Ser83-Ile and Asp87-Gly within the QRDR regions of GyrA, and Ser80-Ile in ParC. Examination of the outer membrane protein *OmpK35* and *OmpK36* genes revealed a premature stop codon at AA63 in *OmpK35*, due to an adenine (A) deletion mutation at nt 82, and the glycine and aspartic acid insertion at AA134. *In silico* plasmid replicon typing identified five plasmid groups in KpApr172, belonging to incompatibility groups X3, R, FII and ColE-like (n = 2), respectively.

In order to further characterize the transferability of apramycin resistance gene *aac(3)-IV*, we attempted to transfer them via conjugation to a recipient *E. coli* J53 AzR strain (data not shown), however, we were not able to transfer the *aac(3)-IV* by conjugation, suggesting the gene may be harbored by a non-conjugative plasmid or on the chromosome. Examination of the *aac(3)-IV*-containing contig from the genome assemblies revealed that *aac(3)-IV* was located on a 13,397 bp segment, along with the resistance genes, *floR*, *sul2* and *aph(4)-Ia* (Figure 2). BLASTn analysis showed that the sequences of this contig were identical (100% query coverage and 100% identities) to the corresponding regions in some plasmids, including pHNAH67 (KX246266, from *E. coli* of chicken), pCFSA122-1 (CP033224, from *Salmonella enterica* of pork), pSH16G4466 (MK477617,





from *Salmonella enterica* in human), pXGE1mcr (KY990887, from *E. coli* of cow feces), pHNSHP45-2 (KU341381, from *E. coli* of pig feces), and chromosome of *E. coli* YSP8-1 (CP037910, from pig feces) from animal or human sources in China.

## DISCUSSION

Aminoglycosides resistance is mostly due to the chemical modification by aminoglycoside-modifying enzymes (AMEs), including acetyltransferases (AACs), phosphotransferases (APHs) and nucleotidyltransferases (ANTs) (Ramirez and Tolmasky, 2010). Some studies had shown AAC(6′)-Ib is one of the most prevalent and clinically relevant AMEs, which confers the resistance to amikacin and other aminoglycosides (Ramirez et al., 2013). A Greek study showed more than 70% of carbapenemase-producing Enterobacteriaceae strains carry *aac(6′)-Ib* gene (Galani et al., 2019). However, only 7.14% of CR-hvKp and 7.5% of CR-non-hvKp isolates were found to carry this gene in our study. By contrast, we found a high frequency of ARM/RMT methyltransferases gene in our study. ARM/RMT methyltransferases were found to confer high levels of resistance to most aminoglycosides other than apramycin (Galimand et al., 2003). ARM/RMT genes *armA* and *rmt* had been frequently described in clinical isolates throughout America, Europe and India (Fritsche et al., 2008). Our study showed 93.6% (44/47) CR-hvKp and 95.6% (22/23) CR-non-hvKp amikacin or gentamycin resistant strains contained the 16S rRNA methylase gene *rmtB*. These results suggested that gentamycin and amikacin have limited activities against clinical CRKp isolates, including CR-hvKp, in Chinese hospitals.

In comparison, our results showed that all CR-hvKp isolates were susceptible to apramycin, whereas ~ 50% of them were resistant to amikacin or gentamycin. Similarly, almost all CR-non-hvKp strains (39/40) were susceptible to apramycin irrespective of the presence of KPC-2 or NDM carbapenemase genes. In addition, our results were in accordance with previous studies that apramycin is not be inactivated by general AMEs and methylases (Livermore et al., 2011), making it an potential antibiotic against clinical amikacin or gentamycin resistant strains.

Nevertheless, apramycin resistance has also been described in clinical isolates worldwide (Threlfall et al., 1986; Chaslus-Dancla et al., 1989, 1991; Hunter et al., 1993; Johnson et al., 1995; Mathew et al., 2003; Zhang et al., 2009). Production of the acetylase *aac(3′)-IV* was the major mechanism underlying apramycin resistance in clinical isolates. The *aac(3′)-IV* gene encoding apramycin resistance was usually harbored by a mobile plasmid (Chaslus-Dancla et al., 1989; Zhang et al., 2009). In this study, we identified one *aac(3′)-IV*-harboring apramycin resistant isolate KpApr172 in CR-non-hvKp with a high MIC value of >128 μg/ml. Genomic analysis showed that KpApr172 belonged to the epidemic CRKp ST11 clone, while the *aac(3′)-IV*-harboring contigs showed highly identity to plasmid or chromosome sequences of isolates from animal sources. Since apramycin is only licensed for use in farm animals in China, we suspected that horizontal transfer of apramycin resistant genes from animals to human might be responsible for the dissemination of apramycin resistance (Yates et al., 2004). Therefore, *aac(3′)-IV* gene should be preferably screened for apramycin resistant isolates in clinical settings.

In this study no CR-hvKp isolates were found to be resistant to the “last resort” antimicrobial agents, including ceftazidime-avibactam, colistin and tigecycline, however, the treatment arsenal for CR-hvKp could be easily compromised by the spread of mobile resistant genes. Plasmid-mediated colistin and tigecycline resistance mechanisms, MCR-1 and Tet(x), have been described in China (Liu et al., 2016; He et al., 2019; Sun et al., 2019). In addition, the FDA approved ceftazidime-avibactam is ineffective against metallo-β-lactamase (e.g., NDM) producers. Furthermore, the original KPC-2 ST11 CR-hvKp outbreak study showed that despite being *in vitro* susceptible to tigecycline and colistin, long-term treatment with colistin or tigecycline (alone or in combination with several other antibiotics) was not able to eradicate KPC-2-producing ST11 CR-hvKp isolates, resulting in fatal outcomes (Gu et al., 2018). This convergence of increased resistance and hypervirulence of CR-hvKp underscores the need for the improvement of the antimicrobial treatment choices.

Our study showed apramycin had a potent *in vitro* activity to CR-hvKp irrespective of most commonly occurring carbapenemases and aminoglycoside modifying enzymes. In addition, recent studies had showed that apramycin was

associated with fewer ototoxic and nephrotoxic side effects in comparison with other human use aminoglycosides antibiotics (Perzynski et al., 1979; Matt et al., 2012; Ishikawa et al., 2019). These findings suggested apramycin and apramycin-derivative compounds could be a promising antibiotic for the treatment of CR-hvKp infections.

To our knowledge, this is the first study to examine the activities of apramycin against CR-hvKp clinical isolates. Our results indicate that apramycin remain highly active against CR-hvKp. These data support a possible role for apramycin in the treatment of infections due to this hypervirulent and multidrug-resistant strains. A further clinical evaluation of apramycin treatment efficacy is warranted.

## DATA AVAILABILITY STATEMENT

The whole-genome sequence of KpApr172 was deposited in the GenBank database under accession number WUJI00000000.

## AUTHOR CONTRIBUTIONS

MH, XS, and JL contributed to work, data analysis, and manuscript preparation. SN, SC, HD, and FY analyzed the data. Y-WT and BK prepared the manuscript. HZ and LC contributed to study design, data analysis, and manuscript preparation.

## REFERENCES

- Bankevich, A., Nurk, S., Antipov, D., Gurevich, A. A., Dvorkin, M., Kulikov, A. S., et al. (2012). SPAdes: a new genome assembly algorithm and its applications to single-cell sequencing. *J. Comput. Biol.* 19, 455–477. doi: 10.1089/cmb.2012.0021
- Bengoechea, J. A., and Sa Pessoa, J. (2019). *Klebsiella pneumoniae* infection biology: living to counteract host defences. *FEMS Microbiol. Rev.* 43, 123–144. doi: 10.1093/femsre/fuy043
- Brisse, S., Passet, V., Haugaard, A. B., Babosan, A., Kassis-Chikhani, N., Struve, C., et al. (2013). wzi Gene sequencing, a rapid method for determination of capsular type for *Klebsiella* strains. *J. Clin. Microbiol.* 51, 4073–4078. doi: 10.1128/JCM.01924-13
- Carattoli, A., Zankari, E., Garcia-Fernandez, A., Voldby Larsen, M., Lund, O., Villa, L., et al. (2014). In silico detection and typing of plasmids using PlasmidFinder and plasmid multilocus sequence typing. *Antimicrob. Agents Chemother.* 58, 3895–3903. doi: 10.1128/AAC.02412-14
- Cejas, D., Fernandez Canigia, L., Rincon Cruz, G., Elena, A. X., Maldonado, I., Gutkind, G. O., et al. (2014). First isolate of KPC-2-producing *Klebsiella pneumoniae* sequence type 23 from the Americas. *J. Clin. Microbiol.* 52, 3483–3485. doi: 10.1128/JCM.00726-14
- Chaslus-Dancla, E., Glupczynski, Y., Gerbaud, G., Lagorce, M., Lafont, J. P., and Courvalin, P. (1989). Detection of apramycin resistant *Enterobacteriaceae* in hospital isolates. *FEMS Microbiol. Lett.* 52, 261–265. doi: 10.1016/0378-1097(89)90208-5
- Chaslus-Dancla, E., Pohl, P., Meurisse, M., Marin, M., and Lafont, J. P. (1991). High genetic homology between plasmids of human and animal origins conferring resistance to the aminoglycosides gentamicin and apramycin. *Antimicrob. Agents Chemother.* 35, 590–593. doi: 10.1128/aac.35.3.590
- Chavda, K. D., Satlin, M. J., Chen, L., Manca, C., Jenkins, S. G., Walsh, T. J., et al. (2016). Evaluation of a Multiplex PCR assay to rapidly detect *Enterobacteriaceae* with a broad range of beta-lactamases directly from perianal swabs. *Antimicrob. Agents Chemother.* 60, 6957–6961. doi: 10.1128/AAC.01458-16

## FUNDING

This study was supported by the Jiangsu Overseas Visiting Scholar Program for University Prominent Young and Middle-aged Teachers and Presidents, the Natural Science Foundation of Jiangsu Province (BK20181173), the grant from the Medicine and Health Science Technology Development Project of Shandong Province, China (2017WS007), Key Research and Development Project of Jiangsu Provincial Science and Technology Department (BE2017654), Gusu Health Youth Talent of Suzhou, Jiangsu Youth Medical Talents Program (QN-866 and 867), and the Cultivate Fund from Shandong Provincial Qianfoshan Hospital (No. QYPY2019NSFC0623). This work was in part supported by the grants from the National Institutes of Health (R01AI090155 to BK).

## SUPPLEMENTARY MATERIAL

The Supplementary Material for this article can be found online at: <https://www.frontiersin.org/articles/10.3389/fmicb.2020.00425/full#supplementary-material>

**FIGURE S1** | Dendrogram of PFGE patterns of 15 CR-hvKp isolates from hospitals in Shanghai (a), Suzhou (b), and Jinan (c), respectively. PFGE typing revealed most of the CR-hvKp strains not belong to the same clone.

**TABLE S1** | Primers used in this study.

- Chen, L., Mediavilla, J. R., Endimiani, A., Rosenthal, M. E., Zhao, Y., Bonomo, R. A., et al. (2011). Multiplex real-time PCR assay for detection and classification of *Klebsiella pneumoniae* carbapenemase gene (bla KPC) variants. *J. Clin. Microbiol.* 49, 579–585. doi: 10.1128/JCM.01588-10
- Clinical and Laboratory Standards Institute (2019). *Performance Standards for Antimicrobial Susceptibility Testing. M100 standard*, 29th ed.
- Evans, S. R., Hujer, A. M., Jiang, H., Hujer, K. M., Hall, T., Marzan, C., et al. (2016). Rapid molecular diagnostics, antibiotic treatment decisions, and developing approaches to inform empiric therapy: PRIMERS I and II. *Clin. Infect. Dis.* 62, 181–189. doi: 10.1093/cid/civ837
- Fritsche, T. R., Castanheira, M., Miller, G. H., Jones, R. N., and Armstrong, E. S. (2008). Detection of methyltransferases conferring high-level resistance to aminoglycosides in *Enterobacteriaceae* from Europe, North America, and Latin America. *Antimicrob. Agents Chemother.* 52, 1843–1845. doi: 10.1128/AAC.01477-07
- Galani, I., Nafplioti, K., Adamou, P., Karaiskos, I., Giamarellou, H., Souli, M., et al. (2019). Nationwide epidemiology of carbapenem resistant *Klebsiella pneumoniae* isolates from Greek hospitals, with regards to plazomicin and aminoglycoside resistance. *BMC Infect. Dis.* 19:167. doi: 10.1186/s12879-019-3801-1
- Galimand, M., Courvalin, P., and Lambert, T. (2003). Plasmid-mediated high-level resistance to aminoglycosides in *Enterobacteriaceae* due to 16S rRNA methylation. *Antimicrob. Agents Chemother.* 47, 2565–2571. doi: 10.1128/aac.47.8.2565-2571.2003
- Gu, D., Dong, N., Zheng, Z., Lin, D., Huang, M., Wang, L., et al. (2018). A fatal outbreak of ST11 carbapenem-resistant hypervirulent *Klebsiella pneumoniae* in a Chinese hospital: a molecular epidemiological study. *Lancet Infect. Dis.* 18, 37–46. doi: 10.1016/S1473-3099(17)30489-9
- He, T., Wang, R., Liu, D., Walsh, T. R., Zhang, R., Lv, Y., et al. (2019). Emergence of plasmid-mediated high-level tigecycline resistance genes in animals and humans. *Nat. Microbiol.* 4, 1450–1456. doi: 10.1038/s41564-019-0445-2

- Heras, J., Dominguez, C., Mata, E., Pascual, V., Lozano, C., Torres, C., et al. (2015). GelJ—a tool for analyzing DNA fingerprint gel images. *BMC Bioinformatics* 16:270. doi: 10.1186/s12859-015-0703-0
- Hu, Y., Liu, L., Zhang, X., Feng, Y., and Zong, Z. (2017). In vitro activity of neomycin, streptomycin, paromomycin and apramycin against carbapenem-resistant *Enterobacteriaceae* clinical strains. *Front. Microbiol.* 8:2275. doi: 10.3389/fmicb.2017.02275
- Hunter, J. E., Hart, C. A., Shelley, J. C., Walton, J. R., and Bennett, M. (1993). Human isolates of apramycin-resistant *Escherichia coli* which contain the genes for the AAC(3)IV enzyme. *Epidemiol. Infect.* 110, 253–259. doi: 10.1017/s0950268800068175
- Ishikawa, M., Garcia-Mateo, N., Cusak, A., Lopez-Hernandez, L., Fernandez-Martinez, M., Muller, G., et al. (2019). Lower ototoxicity and absence of hidden hearing loss point to gentamicin C1a and apramycin as promising antibiotics for clinical use. *Sci. Rep.* 9:2410. doi: 10.1038/s41598-019-38634-3
- Johnson, A. P., Malde, M., Woodford, N., Cunney, R. J., and Smyth, E. G. (1995). Urinary isolates of apramycin-resistant *Escherichia coli* and *Klebsiella pneumoniae* from Dublin. *Epidemiol. Infect.* 114, 105–112. doi: 10.1017/s0950268800051955
- Juhas, M., Widlake, E., Teo, J., Huseby, D. L., Tyrrell, J. M., Polikanov, Y. S., et al. (2019). In vitro activity of apramycin against multidrug-, carbapenem- and aminoglycoside-resistant *Enterobacteriaceae* and *Acinetobacter baumannii*. *J Antimicrob Chemother.* 74, 944–952. doi: 10.1093/jac/dky546
- Larsen, M. V., Cosentino, S., Rasmussen, S., Friis, C., Hasman, H., Marvig, R. L., et al. (2012). Multilocus sequence typing of total-genome-sequenced bacteria. *J. Clin. Microbiol.* 50, 1355–1361. doi: 10.1128/JCM.06094-11
- Li, W., Sun, G., Yu, Y., Li, N., Chen, M., Jin, R., et al. (2014). Increasing occurrence of antimicrobial-resistant hypervirulent (hypermutoviscous) *Klebsiella pneumoniae* isolates in China. *Clin. Infect. Dis.* 58, 225–232. doi: 10.1093/cid/cit675
- Liu, Y. Y., Wang, Y., Walsh, T. R., Yi, L. X., Zhang, R., Spencer, J., et al. (2016). Emergence of plasmid-mediated colistin resistance mechanism MCR-1 in animals and human beings in China: a microbiological and molecular biological study. *Lancet Infect. Dis.* 16, 161–168. doi: 10.1016/S1473-3099(15)00424-7
- Livermore, D. M., Mushtaq, S., Warner, M., Zhang, J. C., Maharjan, S., Doumith, M., et al. (2011). Activity of aminoglycosides, including ACHN-490, against carbapenem-resistant *Enterobacteriaceae* isolates. *J. Antimicrob. Chemother.* 66, 48–53. doi: 10.1093/jac/dkq408
- Mathew, A. G., Arnett, D. B., Cullen, P., and Ebner, P. D. (2003). Characterization of resistance patterns and detection of apramycin resistance genes in *Escherichia coli* isolated from swine exposed to various environmental conditions. *Int. J. Food Microbiol.* 89, 11–20. doi: 10.1016/s0168-1605(03)00124-7
- Matt, T., Ng, C. L., Lang, K., Sha, S. H., Akbergenov, R., Shcherbakov, D., et al. (2012). Dissociation of antibacterial activity and aminoglycoside ototoxicity in the 4-monosubstituted 2-deoxystreptamine apramycin. *Proc. Natl. Acad. Sci. U.S.A.* 109, 10984–10989. doi: 10.1073/pnas.1204073109
- National Antibiotic Resistance Monitoring System [NARMS] (2002). *National Antibiotic Resistance Monitoring System (NARMS) Working Group. Annual Report.* Available at: <https://www.cdc.gov/narms/annual/2002/2002ANNUALREPORTFINAL.pdf> (accessed May 2019).
- Paczosa, M. K., and Meccas, J. (2016). *Klebsiella pneumoniae*: going on the offense with a strong defense. *Microbiol. Mol. Biol. Rev.* 80, 629–661. doi: 10.1128/MMBR.00078-15
- Perzyski, S., Cannon, M., Cundliffe, E., Chahwala, S. B., and Davies, J. (1979). Effects of apramycin, a novel aminoglycoside antibiotic on bacterial protein synthesis. *Eur. J. Biochem.* 99, 623–628. doi: 10.1111/j.1432-1033.1979.tb13295.x
- Ramirez, M. S., Nikolaidis, N., and Tolmasky, M. E. (2013). Rise and dissemination of aminoglycoside resistance: the aac(6′)-Ib paradigm. *Front. Microbiol.* 4:121. doi: 10.3389/fmicb.2013.00121
- Ramirez, M. S., and Tolmasky, M. E. (2010). Aminoglycoside modifying enzymes. *Drug Resist. Updat* 13, 151–171. doi: 10.1016/j.drug.2010.08.003
- Riedel, S., Vijayakumar, D., Berg, G., Kang, A. D., Smith, K. P., and Kirby, J. E. (2019). Evaluation of apramycin against spectinomycin-resistant and -susceptible strains of *Neisseria gonorrhoeae*. *J. Antimicrob. Chemother.* 74, 1311–1316. doi: 10.1093/jac/dkz012
- Shon, A. S., Bajwa, R. P., and Russo, T. A. (2013). Hypervirulent (hypermutoviscous) *Klebsiella pneumoniae*: a new and dangerous breed. *Virulence* 4, 107–118. doi: 10.4161/viru.22718
- Siu, L. K., Huang, D. B., and Chiang, T. (2014). Plasmid transferability of KPC into a virulent K2 serotype *Klebsiella pneumoniae*. *BMC Infect. Dis.* 14:176. doi: 10.1186/1471-2334-14-176
- Smith, K. P., and Kirby, J. E. (2016). Evaluation of apramycin activity against carbapenem-resistant and -susceptible strains of *Enterobacteriaceae*. *Diagn. Microbiol. Infect. Dis* 86, 439–441. doi: 10.1016/j.diagmicrobio.2016.09.002
- Sun, J., Chen, C., Cui, C. Y., Zhang, Y., Liu, X., Cui, Z. H., et al. (2019). Plasmid-encoded tet(X) genes that confer high-level tigecycline resistance in *Escherichia coli*. *Nat. Microbiol.* 4, 1457–1464. doi: 10.1038/s41564-019-0496-4
- The European Committee on Antimicrobial Susceptibility Testing (2019). *Breakpoint Tables for Interpretation of MICs and Zone Diameters, version 9.0.*
- Threlfall, E. J., Rowe, B., Ferguson, J. L., and Ward, L. R. (1986). Characterization of plasmids conferring resistance to gentamicin and apramycin in strains of *Salmonella typhimurium* phage type 204c isolated in Britain. *J. Hyg.* 97, 419–426. doi: 10.1017/s00222172400063609
- Truelson, K. A., Brennan-Krohn, T., Smith, K. P., and Kirby, J. E. (2018). Evaluation of apramycin activity against methicillin-resistant, methicillin-sensitive, and vancomycin-intermediate *Staphylococcus aureus* clinical isolates. *Diagn. Microbiol. Infect. Dis.* 92, 168–171. doi: 10.1016/j.diagmicrobio.2018.05.018
- Wozniak, J. E., Band, V. I., Conley, A. B., Rishishwar, L., Burd, E. M., Satola, S. W., et al. (2019). A nationwide screen of carbapenem-resistant *Klebsiella pneumoniae* reveals an isolate with enhanced virulence and clinically undetected colistin heteroresistance. *Antimicrob. Agents Chemother.* 63, 107–119. doi: 10.1128/AAC.00107-19
- Wu, Q., Zhang, Y., Han, L., Sun, J., and Ni, Y. (2009). Plasmid-mediated 16S rRNA methylases in aminoglycoside-resistant *Enterobacteriaceae* isolates in Shanghai China. *Antimicrob. Agents Chemother.* 53, 271–272. doi: 10.1128/AAC.00748-08
- Yang, X., Wai-Chi Chan, E., Zhang, R., and Chen, S. (2019). A conjugative plasmid that augments virulence in *Klebsiella pneumoniae*. *Nat. Microbiol.* 4, 2039–2043. doi: 10.1038/s41564-019-0566-7
- Yates, C. M., Pearce, M. C., Woolhouse, M. E., and Amyes, S. G. (2004). High frequency transfer and horizontal spread of apramycin resistance in calf faecal *Escherichia coli*. *J. Antimicrob. Chemother.* 54, 534–537. doi: 10.1093/jac/dkh353
- Yu, F., Lv, J., Niu, S., Du, H., Tang, Y. W., Bonomo, R. A., et al. (2018a). In vitro activity of Ceftazidime-Avibactam against carbapenem-resistant and Hypervirulent *Klebsiella pneumoniae* Isolates. *Antimicrob. Agents Chemother.* 62, 1031–1018. doi: 10.1128/AAC.01031-18
- Yu, F., Lv, J., Niu, S., Du, H., Tang, Y. W., Pitout, J. D. D., et al. (2018b). Multiplex PCR analysis for rapid detection of *Klebsiella pneumoniae* carbapenem-resistant (Sequence Type 258 [ST258] and ST11) and Hypervirulent (ST23, ST65, ST86, and ST375) strains. *J. Clin. Microbiol.* 56:JCM.00731-18. doi: 10.1128/JCM.00731-18
- Zankari, E., Hasman, H., Cosentino, S., Vestergaard, M., Rasmussen, S., Lund, O., et al. (2012). Identification of acquired antimicrobial resistance genes. *J. Antimicrob. Chemother.* 67, 2640–2644. doi: 10.1093/jac/dks261
- Zhang, X. Y., Ding, L. J., and Fan, M. Z. (2009). Resistance patterns and detection of aac(3)-IV gene in apramycin-resistant *Escherichia coli* isolated from farm animals and farm workers in northeastern of China. *Res. Vet. Sci.* 87, 449–454. doi: 10.1016/j.rvsc.2009.05.006

**Conflict of Interest:** The authors declare that the research was conducted in the absence of any commercial or financial relationships that could be construed as a potential conflict of interest.

Copyright © 2020 Hao, Shi, Lv, Niu, Cheng, Du, Yu, Tang, Kreiswirth, Zhang and Chen. This is an open-access article distributed under the terms of the Creative Commons Attribution License (CC BY). The use, distribution or reproduction in other forums is permitted, provided the original author(s) and the copyright owner(s) are credited and that the original publication in this journal is cited, in accordance with accepted academic practice. No use, distribution or reproduction is permitted which does not comply with these terms.



# Gastrointestinal Carriage of Vancomycin-Resistant Enterococci and Carbapenem-Resistant Gram-Negative Bacteria in an Endemic Setting: Prevalence, Risk Factors, and Outcomes

Alexandra Vasilakopoulou<sup>1</sup>, Polyxeni Karakosta<sup>1</sup>, Sophia Vourli<sup>1,2</sup>, Aikaterini Tarpatzi<sup>1,2</sup>, Paraskevi Varda<sup>2</sup>, Maria Kostoula<sup>2</sup>, Anastasia Antoniadou<sup>2,3</sup> and Spyros Pournaras<sup>1,2\*</sup>

<sup>1</sup> Clinical Microbiology Laboratory, Medical School, Attikon University General Hospital, National and Kapodistrian University of Athens, Athens, Greece, <sup>2</sup> Infection Control Committee, Attikon University General Hospital, Athens, Greece, <sup>3</sup> 4th Department of Internal Medicine, Medical School, Attikon University General Hospital, National and Kapodistrian University of Athens, Athens, Greece

## OPEN ACCESS

### Edited by:

Raffaele Zarrilli,  
University of Naples Federico II, Italy

### Reviewed by:

Martina Barchitta,  
University of Catania, Italy  
Stephan Göttig,  
University Hospital Frankfurt, Germany

### \*Correspondence:

Spyros Pournaras  
spournaras@med.uoa.gr

### Specialty section:

This article was submitted to  
Infectious Diseases—Surveillance,  
Prevention and Treatment,  
a section of the journal  
Frontiers in Public Health

**Received:** 31 October 2019

**Accepted:** 14 February 2020

**Published:** 18 March 2020

### Citation:

Vasilakopoulou A, Karakosta P, Vourli S, Tarpatzi A, Varda P, Kostoula M, Antoniadou A and Pournaras S (2020) Gastrointestinal Carriage of Vancomycin-Resistant Enterococci and Carbapenem-Resistant Gram-Negative Bacteria in an Endemic Setting: Prevalence, Risk Factors, and Outcomes. *Front. Public Health* 8:55. doi: 10.3389/fpubh.2020.00055

**Background:** Gastrointestinal carriage of vancomycin-resistant enterococci (VRE) and carbapenem-resistant Gram-negative bacteria (CRGN) constitutes a major public health concern as it may be followed by clinical infection development or lead to intra-hospital dissemination. Detection of carriers and implementation of infection control measures are essential in every hospital. In this study we determined the point prevalence of VRE and CRGN in the fecal flora of the inpatients of a tertiary university hospital in Greece. We determined risk factors for carriage and examined the impact of carriage on hospital outcomes.

**Materials/Methods:** A point prevalence study of VRE/CRGN rectal carriage of inpatients was conducted on March 2018. Specimens were selectively cultured for VRE/CRGN, microorganisms were biochemically identified, submitted to antibiotic susceptibility testing, and tested for carbapenemase production. Data on potential risk factors and hospital outcomes were collected at the time of culture and until hospital discharge. Multivariable logistic and linear regression models were used, adjusting for confounders.

**Results:** Four hundred ninety-one patients were enrolled in the study. Of them, 64 (13.0%) were positive for VRE carriage, 40 (8.2%) for CRGN, and 10 patients (2.1%) for both VRE and CRGN. VRE carriage was independently associated with age over 65 years (adjusted OR: 2.4 [95%CI: 1.3, 4.5]) and length of stay (LOS) before rectal sampling (OR: 1.1 [95%CI: 1.0, 1.1]). Carriage of CRGN was associated with 11 days increase of LOS after rectal sampling ( $\beta$ -coef: 11.4 [95%CI: 1.6, 21.2]), with a 3.5-fold increased risk of acquiring a resistant pathogen after rectal swabbing (RR: 3.5 [95%CI 1.2, 9.9]) and with a 6-fold increased risk of mortality (RR: 6.1 [95%CI: 2.1, 17.9]), after adjusting for sex, age, and comorbidity index.



**Conclusions:** High prevalence rates were found for VRE and CRGN carriage among the inpatients of our hospital. Prolonged hospitalization and age were independent risk factors for VRE carriage, while CRGN carriage was associated with increased risk of acquiring a resistant pathogen, prolonged hospital stay, and increased mortality.

**Keywords:** vancomycin-resistant enterococci, carbapenem-resistance, carriage, risk-factors, mortality, length of stay

## INTRODUCTION

The wide dissemination of carbapenem-resistant Gram-negative bacteria (CRGN) and vancomycin-resistant enterococci (VRE) limits therapeutic alternatives and represents a global public health threat (1). The consequences of multidrug-resistant (MDR) bacterial infections include high morbidity and mortality and considerable economic loss (2). A recent study estimated the impact of infections caused by antimicrobial-resistant bacteria in countries within the EU and the European Economic Area for 2015. It was estimated that ~670,000 infections with resistant bacteria were documented in EARS-Net data, with these infections accounting for ~33,000 attributable deaths and 870,000 disability-adjusted life-years (DALYs). Notably, Greece and Italy contributed the highest burden among all participating countries and, for Greece, most of the infections were due to carbapenem- or colistin-resistant bacteria (3). The hospital environment seems to serve as the breeding grounds for MDR organisms (MDRO) (4). Asymptomatic rectal carriage of these organisms may precede infection and constitutes a reservoir for transmission that may remain unidentified in hospitals that do not implement active surveillance testing (5).

While Greece is considered one of the most common countries in Europe for antimicrobial resistance (6), only a limited number of studies have focused on MDRO rectal carriage and colonization to assess their prevalence, risk factors, and associated adverse outcomes (7–11). A previous study from our hospital has reported a prevalence of 14.3% of VRE carriage among hospitalized patients, identified invasive devices and duration of antimicrobial treatment as risk factors, and found that VRE carriage was not an independent predictor of mortality (12). Similar studies from other regions have reported VRE carriage rates ranging from 2 to 37% (13–15), while prevalence rates for CRGN rectal carriage ranged from 5.3 to 52% (16–18). At the same time, there is an increased risk of carbapenem-resistant enterobacteriaceae (CRE) infection and mortality in patients who test positive for carriage of CRE (19, 20). To the best of our knowledge, there is no previous study from Greece focusing on both VRE and CRGN rectal carriage, exploring respective risk factors and adverse outcomes.

The primary objective of the present study was: (i) to determine the prevalence of rectal carriage of VRE and CRGN, (ii) to identify risk factors for VRE/CRGN rectal carriage, and (iii) to examine the impact of VRE/CRGN rectal carriage on hospital outcomes in inpatients of a University General Hospital in Greece.

## MATERIALS AND METHODS

### Subjects

The University Hospital “Attikon” in Athens is a modern tertiary care teaching hospital and is the largest in the West Attica region (2,000,000 population), with 750 beds in total and >71,000 admissions/year. The hospital attends to cases of high complexity in internal medicine and surgery.

The first part of the present project was a point prevalence study of VRE/CRGN rectal carriage of hospital patients that was conducted on March 22nd and 23rd, 2018. Adult patients hospitalized in all surgical and internal medicine departments were surveyed by obtaining rectal swab cultures. In total, 17 medical and surgical wards participated in the study: general internal medicine, cardiology, dermatology, neurology, respiratory medicine, obstetrics/gynecology, cardiothoracic surgery, neurosurgery, urology, otorhinolaryngology, orthopedics, vascular surgery, hematology, oncology, nephrology, gastroenterology, and general surgery. The special and intensive care units were not included in the study, as they were already on active surveillance for VRE/CRGN carriage. The psychiatric ward was also excluded because patients lacked the mental competency necessary to participate. The second part of the project was a cohort study that included all participants from the first part and followed them from the time of rectal swab culture until death or discharge from the hospital. Face-to-face completed questionnaires together with medical records and communication with physicians were used to obtain information on potential risk factors at the time of rectal swabbing, while all examined outcomes were extracted from medical records retrospectively. The study was approved by the institutional review board of the hospital (62,17/10/2017) and all patients provided informed consent after a complete description of the study.

### Culture, Identification, and Susceptibility Testing

A rectal swab was obtained from every consenting hospitalized patient. The swabs were transferred by using transport swabs in Amies transport medium (Biomedics, Madrid, Spain) and were transported to the microbiology laboratory for selective culture of VRE and CRGN. Bile-esculin agar with vancomycin (6 mg/L) and MacConkey agar with meropenem (1 mg/L) were used for selective cultivation. Microorganisms were biochemically identified by Phoenix automated microbiology system (BD Diagnostic Systems, Sparks, MD) and submitted to antibiotic susceptibility testing, according to EUCAST 2018 guidelines and breakpoints. The combination disk test was used for screening

carbapenemase production using meropenem 10 µg disks (BIO-RAD, Marnes-la-Coquette, France) with or without inhibitors [phenyl boronic acid (PBA), ethylenediaminetetraacetic acid (EDTA)] (21). The guidelines of the European Committee on Antimicrobial Susceptibility Testing (EUCAST) were applied for detection of resistance mechanisms and specific resistances of clinical and/or epidemiological importance (22). A meropenem disk with PBA and EDTA was also included to detect double carbapenemase producers (KPC and VIM), which have been found in Greek hospitals since 2009 (21, 23). The immunochromatographic assay, NG-test CARBA 5 (NG Biotech, 35480 Guipry, France) that discriminates KPC, IMP, VIM, NDM, and OXA-48-like producers, was also used.

## Rectal Carriage of VRE/CRGN

All patients that tested positive for VRE and/or CRGN in the rectal swab culture were defined as carriers. Standard infection control measures to reduce transmission were used in these cases. The health personnel had to implement contact precautions (gloves, gowns) for all encounters with the carriers. The wards focused on thorough cleaning of the environment surrounding the positive patient, especially the patient care equipment. Whenever it was possible, the patient was isolated in a single room (24, 25).

## Risk Factors for VRE/CRGN Rectal Carriage

Following informed consent and after obtaining the rectal swab, every hospitalized patient completed a face-to-face questionnaire which was captured in a standardized form. These data, along with parameters retrieved from the patients' records, included information on age, gender, ward, length of stay (LOS) before rectal swabbing, transfer from another hospital, comorbidities, presence of indwelling medical devices, chronic immobilization, last year hospitalization or ICU admission, and specific therapies, such as immunosuppressive therapy, antineoplastic, or antimicrobial chemotherapy.

Comorbidities included: chronic kidney disease, diabetes, dermatologic lesions, hematological malignancy, solid organ malignancy, metastatic disease, neurologic disease, heart failure, coronary artery disease, chronic liver disease, cerebrovascular disease, peripheral vascular disease, and chronic obstructive pulmonary disease. A slightly modified Charlson comorbidity index (CCI) (26) that predicts the 10-years mortality for a patient having a range of 17 comorbid conditions was also calculated. Each condition is assigned with a score of 1, 2, 3, or 6, depending on the risk of death associated with this condition; the scores are then summed up and give a total score which predicts mortality. The clinical conditions and scores are as follows: One for each: myocardial infarct, heart failure, peripheral vascular diseases, dementia, cerebrovascular disease, chronic lung diseases, connective tissue diseases, ulcer, and mild chronic liver diseases. Two for each: hemiplegia, moderate or severe kidney diseases, diabetes with or without complications, tumor, leukemia, lymphoma. Three for each: moderate or severe liver disease. Six for each: metastatic solid tumor, AIDS. In our modified version of CCI (modified CCI), we used chronic

immobilization instead of hemiplegia and we did not use data on mild chronic liver diseases, since they were not present in any patient.

Indwelling medical devices included central lines, urinary catheters, pacemakers, and other devices, such as external wound drains, enteral feeding tubes, endotracheal tubes, and tracheostomies.

Chronic immobilization is defined as loss of anatomical movement due to alteration of physiological function, which in daily practice is commonly defined as more than three-day-bed rest or inability to perform mobile activity on a bed, transfer, or ambulation (27, 28).

Last year, hospitalization or ICU admission included hospitalization in an acute care hospital (ward or ICU, respectively) for two or more days in the past 1 year.

Previous antibiotic therapy was defined as prescription of antibiotics for at least 2 days within the past 1 year. Immunosuppressive therapy included administration of steroids, cyclophosphamide, azathioprine, methotrexate, mycophenolate mofetil, and calcineurin inhibitors during the last year.

## Hospital Outcomes

Hospital outcomes were collected prospectively during hospitalization and included: (i) Mortality: death from any cause during hospitalization, (ii) Hospital LOS, (iii) LOS after rectal swabbing, and (iv) Isolation of a resistant pathogen [VRE, methicillin-resistant *Staphylococcus aureus* (MRSA), carbapenem-resistant Gram-negative bacteria and Gram-negative bacteria resistant to three or more of: beta-lactams, aminoglycosides, quinolones, co-trimoxazole]. from: (a) any clinical culture, and (b) blood, after rectal swabbing.

## Statistical Analysis

Statistical analysis was performed using the statistical package STATA, version 13 (StataCorp, College Station, TX). Univariate associations between background characteristics and VRE/CRGN rectal carriage were studied using Pearson's chi-square test for categorical variables (with Fisher's exact test for groups with <5 subjects expected in a cell) and non-parametric Kruskal-Wallis tests for continuous non-normally distributed variables (tested by the Shapiro-Wilk normality test). Since potential risk factors and VRE/CRGN rectal carriage were measured in a cross-sectional design, associations of potential risk factors with VRE/CRGN rectal carriage were estimated with univariate logistic regression models. Estimated associations were described as odds ratios (OR) with 95% confidence intervals. All variables with a  $p \leq 0.050$  in univariate analysis were included in a multiple regression model to examine independent risk factors for VRE/CRGN rectal carriage. In the prospective part of our study and in order to estimate the risk of VRE/CRGN rectal carriage on hospital outcomes, we used multivariable log-binomial or log-Poisson (if convergence failed) regression models to estimate relative risks (RRs) with 95% CIs for categorical outcomes (resistant pathogen in any culture and in blood after rectal swabbing, mortality) and multivariable linear regression models to estimate  $\beta$  coefficients with 95% CIs for continuous outcomes (hospital LOS, LOS after rectal

swab). Modified Charlson Comorbidity Index, age, and sex were included as confounders *a priori* in all analyses. All association testing was conducted assuming a  $p \leq 0.050$  significance level.

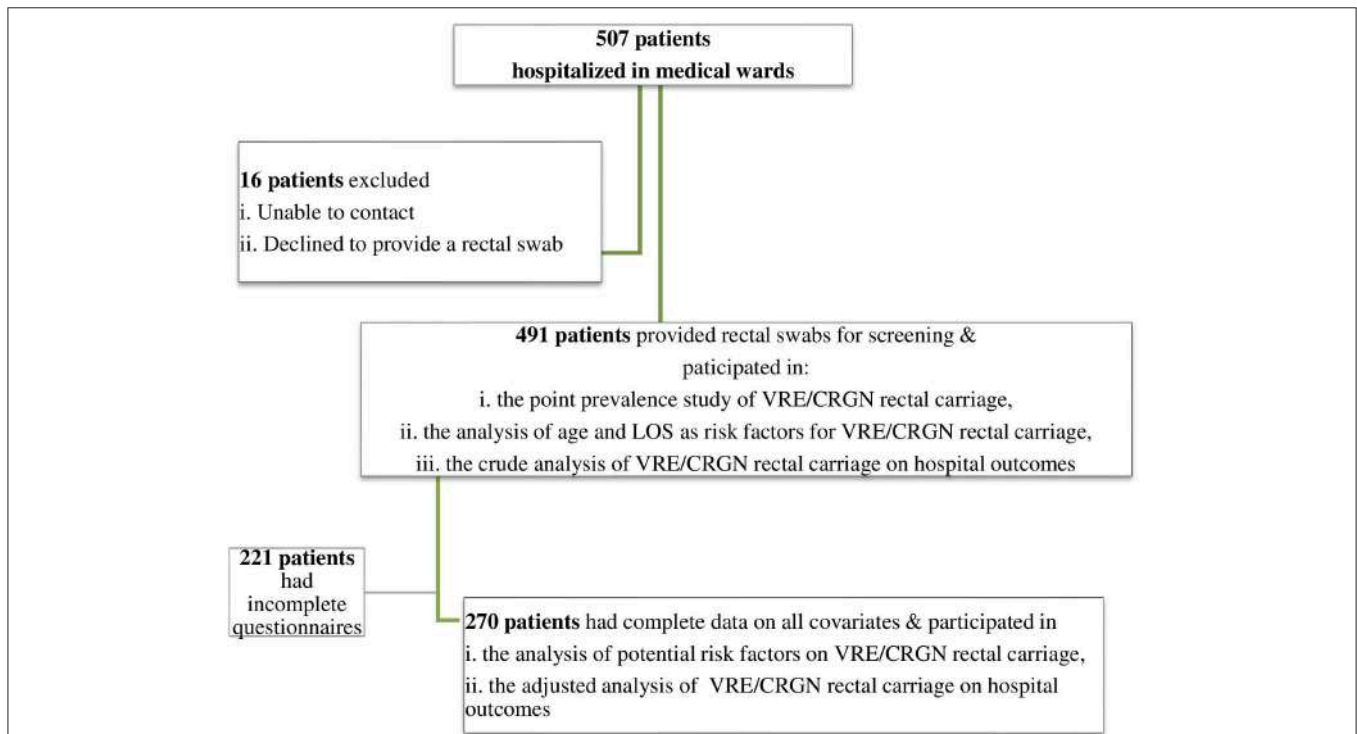
## RESULTS

In total, 507 adult patients hospitalized in medical wards were contacted to participate and 491 provided rectal swabs were included in the analysis (participation rate: 96.6%) (Figure 1). Baseline characteristics of the study population according to rectal carriage of CRGN and VRE are presented in Table 1. Forty patients were identified as CRGN carriers (prevalence: 8.2%) and 64 as VRE carriers (prevalence: 13.0%). Of the carrier patients, 30% were hospitalized in single rooms. All VRE isolates were identified as VanA-phenotype *E. faecium* (high level resistance to vancomycin and teicoplanin). Molecular detection of *van* genes was not performed. The respective prevalence for carbapenem-resistant (CR) enterobacteriaceae (CRE), CR-*Acinetobacter spp.*, and CR-*Pseudomonas spp.* carriers was 5.9, 1.8, and 1.2%, respectively. Four different types of carbapenemases were detected in CRE colonized patients: KPC, 65.5% ( $n = 19$ ); NDM, 24.1% ( $n = 7$ ); VIM, 6.9% ( $n = 2$ ); and OXA-48, 3.5% ( $n = 1$ ). Patients colonized with VRE tended to be older (>65 years) compared to non-colonized patients. Regarding CRGN carriers, they were characterized by a higher modified CCI, were more likely to have a urine catheter, and to have been hospitalized in a medical ward/ICU or to have received antibiotics during the last year, compared

with non-carriers. Moreover, both groups of CRGN and VRE carriers tended to have longer LOS before rectal swabbing. Mortality for non-carriers was 4.8% ( $n = 19$ ), lower than that for CRGN (40%,  $p < 0.001$ ) and VRE carriers (15.9%,  $p < 0.001$ ). Hospital outcomes, such as hospital LOS and subsequent resistant pathogens isolated from blood, were also more frequent in both subgroups of CRGN and VRE carriers, compared to non-colonized patients (Table 1).

Table 2 presents the results of the univariable analysis on the association between potential risk factors and CRGN and VRE carriage. The detection of VRE carriage was associated with age over 65 years (OR: 1.9 [95%CI: 1.1, 3.4]) and LOS before rectal swab (OR: 1.1 [95%CI: 1.0, 1.1]). In a multivariate logistic regression model, these variables were also independently associated with VRE carriage [adjusted OR: 2.4 [95%CI: 1.3, 4.5] and 1.1 [95%CI: 1.0, 1.1], respectively]. CRGN carriage was associated with LOS before rectal swab [OR: 1.1 (95%CI: 1.0, 1.1)], hospitalization [OR: 10.4 (95%CI: 1.3, 82.3)] and ICU admission during the past 1 year [OR: 9.3 (95%CI: 2.4, 36.0)], presence of a urinary catheter [OR: 3.5 (95%CI: 1.0, 12.4)] and pacemaker [OR: 6.0 (95%CI: 1.1, 32.6)], metastatic disease [OR: 4.9 (95%CI: 1.2, 20.4)], and high modified CCI [OR: 1.2 (95%CI: 1.0, 1.3)]. When these variables were included in the multivariable model, none of them were identified as an independently associated risk factor for CRGN carriage.

Table 3 shows the multivariable analysis estimating the effect of CRGN and VRE rectal carriage on hospital outcomes, after



**FIGURE 1** | Flow diagram depicting the patients that participated in: (i) the point prevalence study of VRE/CRGN rectal carriage, (ii) the analysis of potential risk factors on VRE/CRGN rectal carriage, (iii) the analysis of VRE/CRGN rectal carriage on hospital outcomes.

**TABLE 1** | Comparison of baseline characteristics between MDRO carriers and non-carriers.

	Non carriers (n = 397)	CRGN carriers (n = 40)	p-value	VRE carriers (n = 64)	p-value
Age (years); median (IQR)	68 (27)	72 (24.5)	0.341	72.5 (20)	0.120
Age ≥65 years; n (%)	220 (55.4)	27 (67.5)	0.142	45 (70.3)	<b>0.025</b>
Males; n (%)	214 (53.9)	19 (47.5)	0.439	35 (54.7)	0.907
LOS before rectal swabbing (days); median (IQR)	6 (8)	12.5 (20)	<b>&lt;0.001</b>	10 (16.5)	<b>&lt;0.001</b>
Ward type; n (%)					
• Internal medicine	230 (57.9)	19 (47.5)	0.204	44 (68.8)	0.102
• Surgery	167 (42.1)	21 (52.5)		20 (31.3)	
• Transfer from other hospital; n (%)	23 (10.1)	3 (27.3)	0.075	5 (17.9)	0.217
Indwelling medical devices; n (%)					
• Central line	16 (7.1)	1 (9.1)	0.808	4 (13.8)	0.212
• Urine catheter	75 (33.2)	7 (63.6)	<b>0.038</b>	9 (31.0)	0.816
• Pacemaker	8 (3.6)	2 (18.2)	<b>0.019</b>	1 (3.5)	0.977
• Other prosthetic material	40 (17.7)	2 (18.2)	0.967	7 (24.1)	0.400
• Chronic immobilization; n (%)	14 (6.2)	2 (18.2)	0.122	1 (3.5)	0.554
Last year; n (%)					
• Hospitalization	109 (48.2)	10 (90.9)	<b>0.007</b>	14 (50.0)	0.930
• ICU admission	13 (5.8)	4 (36.4)	<b>&lt;0.001</b>	0 (0.0)	0.192
• Chemotherapy	32 (14.2)	4 (36.4)	<b>0.045</b>	6 (20.7)	0.353
• Immunosuppressive therapy	22 (9.7)	2 (18.2)	0.364	4 (13.8)	0.497
• Antibiotic treatment	132 (58.7)	11 (100.0)	<b>0.006</b>	15 (53.6)	0.606
Comorbidities; n (%)					
• Chronic kidney disease	23 (10.2)	1 (9.1)	0.907	5 (17.9)	0.221
• Diabetes	57 (25.3)	4 (36.4)	0.415	11 (39.3)	0.116
• Dermatologic lesions	41 (18.1)	3 (27.3)	0.447	1 (3.5)	<b>0.045</b>
• Hematological malignancies	11 (4.9)	1 (9.1)	0.533	1 (3.5)	0.734
• Solid organ malignancy	34 (15.0)	4 (36.4)	0.060	8 (27.6)	0.086
• Metastatic disease	16 (7.1)	3 (27.3)	<b>0.016</b>	5 (17.2)	0.061
• Neurologic disease	35 (15.5)	0 (0.0)	0.157	3 (10.3)	0.464
• Heart failure	30 (13.3)	2 (18.2)	0.642	7 (25.0)	0.097
• Myocardial infarct	26 (11.5)	2 (18.8)	0.503	4 (14.3)	0.667
• Chronic liver disease	8 (3.5)	0 (0.0)	0.526	1 (3.5)	0.980
• Cerebrovascular disease	22 (9.8)	1 (9.1)	0.937	0 (0.0)	0.077
• Peripheral vascular disease	32 (14.2)	2 (18.2)	0.710	5 (17.3)	0.657
• Chronic obstructive pulmonary disease	30 (13.3)	3 (27.3)	0.193	4 (14.3)	0.889
• Modified CCI; median (IQR)	2 (4)	4 (8)	<b>0.049</b>	2 (6)	0.352
Outcomes					
• Resistant pathogen in blood after rectal swabbing; n (%)	8 (2.0)	4 (10.0)	<b>0.003</b>	5 (7.8)	<b>0.009</b>
• Resistant pathogen in clinical culture after rectal swabbing; n (%)	28 (7.1)	12 (30.0)	<b>&lt;0.001</b>	7 (10.9)	0.276
• Hospital LOS (days); median (IQR)	12 (13)	25 (38.5)	<b>&lt;0.001</b>	20.5 (21)	<b>&lt;0.001</b>
• LOS after rectal swabbing (days); median (IQR)	5 (10)	7 (13.5)	0.089	5 (12)	0.436
Mortality; n (%)	19 (4.8)	16 (40.0)	<b>&lt;0.001</b>	10 (15.9)	<b>&lt;0.001</b>

IQR, interquartile range; LOS, length of stay; ICU, intensive care unit; CCI, Charlson comorbidity index; CRGN, carbapenem-resistant Gram-negative bacteria; VRE, vancomycin-resistant enterococci.

Bold indicates significant differences ( $p \leq 0.050$ ) of ANOVA for continuous variables and  $\chi^2$  analysis for categorical variables.

Numbers may not correspond to the total due to missing numbers.

(n = 491).

adjusting for sex, age, and modified CCI. Carrying CRGN was associated with 38 days increased hospital LOS ( $\beta$ -coef: 38.0, [95%CI: 22.6, 53.4]) and 11 days increase in LOS after rectal swabbing ( $\beta$ -coef: 11.4, [95%CI: 1.6, 21.2]). More importantly,

it is associated with a 3.5-fold increased risk for acquiring a resistant pathogen after rectal swabbing (RR: 3.5, [95%CI 1.2, 9.9]) and with a 6-fold increase risk for mortality (RR: 6.1, [95%CI: 2.1, 17.9]). We then separately examined different



**TABLE 2 |** Associations between potential risk factors and carriage of CRGN and VRE.

	CRGN carriers			VRE carriers		
	n*	OR (95% CI)	p-value	n*	Crude OR (95% CI)	p-value
Age ≥65 years	437	1.7 (0.8, 3.3)	0.145	<b>461</b>	<b>1.9 (1.1, 3.4)</b>	<b>0.027</b>
LOS before rectal swabbing	<b>437</b>	<b>1.1 (1.0, 1.1)</b>	<b>&lt;0.001</b>	<b>461</b>	<b>1.1 (1.0, 1.1)</b>	<b>&lt;0.001</b>
<b>Indwelling medical devices</b>						
• Urine catheter	<b>237</b>	<b>3.5 (1.0, 12.4)</b>	<b>0.050</b>	255	0.9 (0.1, 2.1)	0.817
• Pacemaker	<b>236</b>	<b>6.0 (1.1, 32.6)</b>	<b>0.037</b>	254	1.0 (0.1, 8.0)	0.977
<b>Last year</b>						
Hospitalization	<b>237</b>	<b>10.4 (1.3, 82.3)</b>	<b>0.027</b>	254	1.1 (0.5, 2.4)	0.930
• ICU admission	<b>236</b>	<b>9.3 (2.4, 36.0)</b>	<b>0.001</b>	240	NA	NA
• Chemotherapy	237	3.5 (1.0, 12.5)	0.058	255	1.6 (0.6, 4.2)	0.356
• Antibiotic treatment	143	NA	NA	253	0.8 (0.4, 1.8)	0.607
<b>Comorbidities</b>						
• Chronic kidney disease	237	0.9 (0.1, 7.2)	0.907	254	1.9 (0.7, 5.5)	0.228
• Diabetes	236	1.7 (0.5, 6.0)	0.419	253	1.9 (0.8, 4.3)	0.121
• Dermatologic lesions	237	1.7 (0.4, 6.7)	0.452	255	0.2 (0.0, 1.2)	0.077
• Hematological malignancies	237	2.0 (0.1, 16.7)	0.540	255	0.7 (0.1, 5.6)	0.735
• Solid organ malignancy	237	3.2 (0.9, 11.6)	0.073	255	2.2 (0.9, 5.3)	0.092
• Metastatic disease	<b>237</b>	<b>4.9 (1.2, 20.4)</b>	<b>0.028</b>	255	2.7 (0.9, 8.1)	0.070
• Neurologic disease	202	NA	NA	255	0.6 (0.2, 2.2)	0.468
• Heart failure	237	1.5 (0.3, 7.1)	0.644	254	2.2 (0.9, 5.6)	0.104
• Myocardial infarct	237	1.7 (0.4, 8.3)	0.508	254	1.3 (0.4, 4.0)	0.668
• Chronic liver disease	229	NA	NA	255	1.0 (0.1, 8.1)	0.980
• Cerebrovascular disease	235	0.9 (0.1, 7.5)	0.937	231	NA	NA
• Peripheral vascular disease	237	1.4 (0.3, 6.5)	0.711	255	1.3 (0.4, 3.6)	0.658
• Chronic obstructive pulmonary disease	236	2.4 (0.6, 9.7)	0.206	253	1.1 (0.4, 3.3)	0.889
Modified CCI	<b>237</b>	<b>1.2 (1.0, 1.3)</b>	<b>0.037</b>	255	1.1 (1.0, 1.2)	0.069

OR, odds ratio; CI, confidence interval; LOS, length of stay; ICU, intensive care unit; CCI, Charlson comorbidity index; NA, not applicable. Bold indicates significant differences ( $p \leq 0.050$ ). \*Numbers do not correspond to the total in every risk factor, due to missing data.

**TABLE 3 |** Risk of CRGN and VRE carriage for hospital outcomes.

	CRGN carriers				VRE carriers			
	n	Crude β-coef (95% CI)	n	Adjusted β-coef (95% CI)	n	Crude β-coef (95% CI)	n	Adjusted β-coef (95% CI)
<b>HOSPITAL LOS (DAYS)</b>								
• Total	437	<b>25.0 (17.6, 32.4)</b>	237	<b>38.0 (22.6, 53.4)</b>	<b>437</b>	<b>9.9 (4.8, 15.1)</b>	<b>237</b>	4.7 (-3.2, 12.7)
• After rectal swabbing		<b>7.2 (2.4, 12.1)</b>		<b>11.4 (1.6, 21.2)</b>		1.3 (-2.3, 5.0)		0.4 (-6.1, 5.3)
	n	Crude RR (95% CI)	n	Adjusted RR (95% CI)	n	Crude RR (95% CI)	n	Adjusted RR (95% CI)
<b>RESISTANT PATHOGEN AFTER RECTAL SWABBING</b>								
• In blood	437	<b>5.0 (1.6, 15.8)</b>	237	NA	437	<b>3.9 (1.3, 11.5)</b>	237	1.7 (0.2, 15.1)
• In clinical culture		<b>4.3 (2.4, 7.7)</b>		<b>3.5 (1.2, 9.9)</b>		1.6 (0.7, 3.4)		0.9 (0.2, 3.7)
<b>Mortality</b>		<b>8.4 (4.7, 14.9)</b>		<b>6.1 (2.1, 17.9)</b>		<b>3.3 (1.6, 6.8)</b>		0.5 (0.1, 3.3)

RR, relative risk; β-coef, beta coefficients; CI, confidence interval; LOS, length of stay; CR, carbapenem-resistant; VRE, vancomycin-resistant enterococci; NA, not applicable. Models were adjusted for sex, age and modified Charlson comorbidity index. The values in bold are statistically significant.

CRGN subgroups in order to identify the specific pathogen underlying the observed associations; sample size was marginal for firm conclusions in some cases, but CR-enterobacteriaceae carriage was predictive of all outcomes (**Supplementary Table 1**).

Regarding VRE carriers, although a statistical significant risk was found for hospital LOS, resistant pathogen in blood after rectal swabbing, and mortality in the crude model (RR: 9.9, [95%CI: 4.8, 15.1], RR: 3.9, [95%CI: 1.3, 11.5] and RR: 3.3, [95%CI: 1.6,

6.8] respectively), statistical significance was in all circumstances not shown after adjusting for confounders.

## DISCUSSION

In the present study, we calculated simultaneously, for the first time, prevalence rates for VRE and CRGN carriage among inpatients of a Greek tertiary hospital and recognized prolonged hospitalization and age as independent risk factors for VRE carriage. We also showed that CRGN carriage is associated with increased risk of acquiring a resistant pathogen after rectal swabbing, prolonged hospital stays, and increased mortality.

The present study revealed a high prevalence of VRE and CRGN carriage among inpatients of our hospital (13.0 and 8.2% respectively). A previous study from the same hospital had determined a VRE carriage rate of 14.3% (29). Other studies have reported carriage rates that varied with geographic location and the general condition of patients (critically ill or not) (16, 17, 30–33). Greece is regularly regarded as an environment with high-selection pressure for the emergence of extensively drug-resistant Gram-negative bacilli in Europe, due to the over-consumption of antimicrobials both in the community and in the hospitals (34).

The multivariable analysis of potential risk factors showed that prolonged hospitalization and advanced age represent independent risk factors for VRE carriage. VRE can survive on environmental surfaces for a long time, and environmental contamination has been identified as a potential risk factor for VRE transmission to healthcare workers' hands and gloves and, subsequently, to patients (35, 36). Hand hygiene compliance rates in Greek hospitals have been reported to range from 22 to 43% (37–39). Since Greece is currently in the midst of a financial crisis, all Greek hospitals suffer from reductions in nursing and cleaning personnel, which may lead to compromises in infection control practices (40–42). All these factors might play a role in the further spread of VRE, especially in cases of prolonged hospitalization. In addition, long hospital stay may be associated with increased antibiotic consumption, which can also contribute to VRE selection and carriage (43). Moreover, the association of old age with VRE carriage may be attributed to several factors, such as alterations of the immune system, malnutrition, and social and economic factors (32, 44–46).

The univariate analysis revealed several risk factors for CRGN carriage: presence of indwelling devices (urinary catheter, pacemaker), CCI, metastatic disease, prolonged hospitalization before the fecal swab sampling, last year hospitalization, and ICU admission. Although none of these factors were independently associated with CRGN carriage in the multivariable logistic regression model, they all deserve to be considered. Indwelling devices are related to disease severity (47) and are recognized risk factors for healthcare-associated carriage and infection with MDR pathogens (48). Furthermore, serious underlying disease as a risk factor for CRGN carriage has been previously described (49) and can be explained by the patients' exposure to invasive procedures, as well as from impaired host defenses and extensive use of antibiotics. Almost invariably, these patients have longer hospitalization than patients with less severe illnesses (4). Also, previous hospitalization was identified as a risk factor for CRGN carriage. Our hospital is a referral center, where

patients from all over the country are admitted for treatment. The majority of these patients have complex medical diseases, prolonged exposure to a healthcare setting, and an extensive use of antibiotics.

Gut carriage of CRGN was independently associated with increased hospital LOS, risk of acquiring a resistant pathogen after rectal swabbing, and mortality. Several studies have demonstrated that gut carriage and subsequent colonization by *K. pneumoniae* in hospitalized patients is associated with a greater risk of infection by the colonizing strains (50, 51). Little is known, though, about the mechanisms that promote progression from carriage to infection. Increased total LOS among CRE carriers has been previously described (19, 49), as well as the association with increased rate of CRE infections and high mortality (19, 20). Previous research has demonstrated that CRE infections are associated more often with sepsis and increased early mortality rate (52), particularly in vulnerable patients such as pediatric, geriatric, immunosuppressed, hospitalized, and chronically ill (53, 54).

Our study has some limitations. We might have underestimated the prevalence of OXA-48 producers that weakly hydrolyze carbapenems (MIC for meropenem lower than 1 mg/L) because of the selective media we used for the culture (55). Moreover, our study lacks enough power to establish a causal relationship between possible risk factors and MDRO carriage, since the study design was cross-sectional. We were also not able to gather detailed information regarding previous exposure to antibiotics such as carbapenems and vancomycin or to assess their impact on MDRO carriage. In addition, we didn't collect subsequent rectal samples in order to differentiate between transient carriage and colonization. More importantly, we did not collect the required data in order to define specific types of infections from resistant pathogens; instead, we collected data on isolation of a subsequent resistant pathogen from a clinical sample. Our analysis was limited to all-cause, rather than attributable, mortality. Thus, we are unable to determine whether the mortality rates of CRGN carriers were directly attributable to infection or were more likely to occur in patients with other fatal illnesses. Furthermore, although statistically significant conclusions were produced, confidence intervals were wide due to the relatively small sample size. Finally, although we tried to incorporate all known potential risk factors for carriage, infection, and mortality, we acknowledge that residual confounding from unmeasured covariates is still possible.

Nevertheless, the results of this study provide valuable information about the CRGN and VRE carriage burden in our hospital and can be used for improving our infection control strategy. After this study, the infection control team has been reinforced with more personnel. The health care employees of our hospital have been informed about the findings of the study and further educational activities on effective infection control practices have been provided. A new point prevalence study of MDRO carriage is scheduled for the first trimester of 2020 in order to compare results and assess the impact of the intensified infection control effort.

In conclusion, VRE and CRGN represent a serious public health problem and carrier patients represent a silent threat

for hospitals. Efforts to limit the spread of MDRO need to be optimized.

## DATA AVAILABILITY STATEMENT

The datasets generated for this study are available on request to the corresponding author.

## ETHICS STATEMENT

The studies involving human participants were reviewed and approved by Institutional Review Board, University General Hospital Attikon. The patients/participants provided their written informed consent to participate in this study.

## REFERENCES

- Solomon SL, Oliver KB. Antibiotic resistance threats in the United States: stepping back from the brink. *Am Fam Physician*. (2014) 89:938–41.
- Sheng WH, Chie WC, Chen YC, Hung CC, Wang JTCS. Impact of nosocomial infections on medical costs, hospital stay, and outcome in hospitalized patients. *J Formos Med Assoc*. (2005) 104:318–26.
- Cassini A, Högberg LD, Plachouras D, Quattrocchi A, Hoxha A, Simonsen GS, et al. Attributable deaths and disability-adjusted life-years caused by infections with antibiotic-resistant bacteria in the EU and the European Economic Area in 2015: a population-level modelling analysis. *Lancet Infect Dis*. (2019) 19:56–66. doi: 10.1016/S1473-3099(18)30708-4
- Safdar N, Dennis G. Maki. Review the commonality of risk factors for nosocomial colonization and infection with antimicrobial-resistant *Staphylococcus aureus*, enterococcus, gram-negative bacilli, *Clostridium difficile*, and *Candida*. *Ann Intern Med*. (2002) 136:834–44. doi: 10.7326/0003-4819-136-11-200206040-00013
- Akova M, Daikos GL, Tzouveleki L, Carmeli Y. Interventional strategies and current clinical experience with carbapenemase-producing Gram-negative bacteria. *Clin Microbiol Infect*. (2012) 18:439–48. doi: 10.1111/j.1469-0691.2012.03823.x
- ECDC. *Annual Epidemiological Report: Antimicrobial Resistance and Healthcare-Associated Infections 2014*. Stockholm: ECDC (2015).
- Kontopoulou K, Iosifidis E, Antoniadou E, Tasioudis P, Petinaki E, Malli E, et al. The clinical significance of carbapenem-resistant *Klebsiella pneumoniae* rectal colonization in critically ill patients: from colonization to bloodstream infection. *J Med Microbiol*. (2019) 68:326–35. doi: 10.1099/jmm.0.000921
- Papadimitriou-Oliveris M, Christofidou M, Fligou F, Bartzavali C, Vretos T, Filos KS, et al. The role of colonization pressure in the dissemination of colistin or tigecycline resistant KPC-producing *Klebsiella pneumoniae* in critically ill patients. *Infection*. (2014) 42:883–90. doi: 10.1007/s15010-014-0653-x
- Papadimitriou-Oliveris M, Drougka E, Fligou F, Kolonitsiou F, Liakopoulos A, Dodou V, et al. Risk factors for enterococcal infection and colonization by vancomycin-resistant enterococci in critically ill patients. *Infection*. (2014) 42:1013–22. doi: 10.1007/s15010-014-0678-1
- Metallidis S, Chatzidimitriou M, Tsona A, Bisiklis A, Lazaraki G, Koumentaki E, et al. Vancomycin-resistant enterococci, colonizing the intestinal tract of patients in a university hospital in Greece. *Brazilian J Infect Dis*. (2006) 10:179–84. doi: 10.1590/S1413-86702006000300005
- Kofteridis DP, Valachis A, Dimopoulou D, Maraki S, Christidou A, Mantadakis E, et al. Risk factors for carbapenem-resistant *Klebsiella pneumoniae* infection/colonization: a case-control study. *J Infect Chemother*. (2014) 20:293–7. doi: 10.1016/j.jiac.2013.11.007
- Sakka V, Tsioutras S, Galani L, Antoniadou A, Souli M, Galani I, et al. Risk-factors and predictors of mortality in patients colonised with vancomycin-resistant enterococci. *Clin Microbiol Infect*. (2008) 14:14–21. doi: 10.1111/j.1469-0691.2007.01840.x

## AUTHOR CONTRIBUTIONS

SP, AA, and SV contributed to the study design and reviewed the manuscript. AV and PK contributed to the data analysis and manuscript preparation. SV and AT contributed to the data analysis. PV and MK collected and reviewed patients' data and contributed to the data analysis.

## SUPPLEMENTARY MATERIAL

The Supplementary Material for this article can be found online at: <https://www.frontiersin.org/articles/10.3389/fpubh.2020.00055/full#supplementary-material>

- Endtz HP, Van Den Braak N, Van Belkum A, Kluytmans JAJW, Koeleman JGM, Spanjaard L, et al. Fecal carriage of vancomycin-resistant enterococci in hospitalized patients and those living in the community in the Netherlands. *J Clin Microbiol*. (1997) 35:3026–31. doi: 10.1128/JCM.35.12.3026-3031.1997
- Tokars JI, Satake S, Rimland D, Carson L, Miller ER, Killum E, et al. The prevalence of colonization with vancomycin-resistant *Enterococcus* at a Veterans' Affairs institution. *Infect Control Hosp Epidemiol*. (1999) 20:171–5. doi: 10.1086/501606
- Gambarotto K, Ploy MC, Turlure P, Grélaud C, Martin C, Bordessoule D, et al. Prevalence of vancomycin-resistant enterococci in fecal samples from hospitalized patients and nonhospitalized controls in a cattle-rearing area of France. *J Clin Microbiol*. (2000) 38:620–4. doi: 10.1128/JCM.38.2.620-624.2000
- Vidal-Navarro L, Pfeiffer C, Bouziges N, Sotto A, Lavigne JP. Faecal carriage of multidrug-resistant Gram-negative bacilli during a non-outbreak situation in a French university hospital. *J Antimicrob Chemother*. (2010) 65:2455–8. doi: 10.1093/jac/dkq333
- Wiener-Well Y, Rudensky B, Yinnon AM, Kopuit P, Schlesinger Y, Broide E, et al. Carriage rate of carbapenem-resistant *Klebsiella pneumoniae* in hospitalised patients during a national outbreak. *J Hosp Infect*. (2010) 74:344–9. doi: 10.1016/j.jhin.2009.07.022
- Tran DM, Larsson M, Olson L, Hoang NTB, Le NK, Khu DTK, et al. High prevalence of colonisation with carbapenem-resistant Enterobacteriaceae among patients admitted to Vietnamese hospitals: risk factors and burden of disease. *J Infect [Internet]*. (2019) 79:115–22. doi: 10.1016/j.jinf.2019.05.013
- Tischendorf J, De Avila RA, Safdar N. Risk of infection following colonization with carbapenem-resistant Enterobacteriaceae: a systematic review. *Am J Infect Control*. (2016) 44:539–43. doi: 10.1016/j.ajic.2015.12.005
- McConville TH, Sullivan SB, Gomez-Simmonds A, Whittier S, Uhlemann AC. Carbapenem-resistant Enterobacteriaceae colonization (CRE) and subsequent risk of infection and 90-day mortality in critically ill patients, an observational study. *PLoS ONE*. (2017) 12:1–14. doi: 10.1371/journal.pone.0186195
- Pournaras S, Poulou A, Tsakris A. Inhibitor-based methods for the detection of KPC carbapenemase-producing Enterobacteriaceae in clinical practice by using boronic acid compounds. *J Antimicrob Chemother*. (2010) 65:1319–21. doi: 10.1093/jac/dkq124
- European Committee on Antimicrobial Susceptibility Testing EUCAST. *EUCAST Guidelines for Detection of Resistance Mechanisms and Specific Resistances of Clinical and/or Epidemiological Importance Version 2.0*. Basel.
- Giakkoupi P, Pappa O, Polemis M, Vatopoulos AC, Miriagou V, Zioga A, et al. Emerging *Klebsiella pneumoniae* isolates coproducing KPC-2 and VIM-1 carbapenemases. *Antimicrob Agents Chemother*. (2009) 53:4048–50. doi: 10.1128/AAC.00690-09
- Tacconelli E, Cataldo MA, Dancer SJ, Angelis GDe, Falcone M, Frank U, et al. ESCMID guidelines for the management of the infection control measures to reduce transmission of multidrug-resistant Gram-negative

- bacteria in hospitalized patients. *Clin Microbiol Infect.* (2013) 20:1–55. doi: 10.1111/1469-0691.12427
25. Morris-downes M, Smyth EG, Moore J, Thomas T, Fitzpatrick F, Walsh J, et al. Surveillance and endemic vancomycin-resistant enterococci : some success in control is possible. *J Hosp Infect.* (2010) 75:228–33. doi: 10.1016/j.jhin.2010.01.004
  26. Charlson ME, Pompei P, Ales KLMC. A new method of classifying prognostic comorbidity in longitudinal studies: development and validation. *J Chronic Dis.* (1987) 40:373–83. doi: 10.1016/0021-9681(87)90171-8
  27. Laksmi PW, Harimurti K, Setiati S, Soejono CH, Aries W, Roosheroe AG. Management of immobilization and its complication for elderly. *Acta Med Indones.* (2008) 40:233–40.
  28. Anderson CL CN. Principles of geriatric medicine and gerontology. In: Hazzard WR, BlassJP, Ettinger HW, Halter JB, editor. New York, NY: McGraw-Hill (1999). p. 1565–75.
  29. Souli M, Sakka V, Galani I, Antoniadou A, Galani L, Siafakas N, et al. Colonisation with vancomycin- and linezolid-resistant *Enterococcus faecium* in a university hospital: molecular epidemiology and risk factor analysis. *Int J Antimicrob Agents.* (2009) 33:137–42. doi: 10.1016/j.ijantimicag.2008.08.017
  30. Torres-Gonzalez P, Cervera-Hernandez ME, Niembro-Ortega MD, Leal-Vega F, Cruz-Hervert LP, Garcia-García L, et al. Factors associated to prevalence and incidence of carbapenem-resistant enterobacteriaceae fecal carriage: a cohort study in a Mexican tertiary care hospital. *PLoS ONE.* (2015) 10:1–13. doi: 10.1371/journal.pone.0139883
  31. Swaminathan M, Sharma S, Blash SP, Patel G, Banach DB, Phillips M, et al. Prevalence and risk factors for acquisition of carbapenem-resistant enterobacteriaceae in the setting of endemicity. *Infect Control Hosp Epidemiol.* (2013) 34:809–17. doi: 10.1086/671270
  32. Kim HS, Kim DH, Yoon HJ, Lee WJ, Woo SH, Choi SP. Factors associated with vancomycin-resistant enterococcus colonization in patients transferred to emergency departments in Korea. *J Korean Med Sci.* (2018) 33:1–7. doi: 10.3346/jkms.2018.33.e295
  33. Karki S, Houston L, Land G, Bass P, Kehoe R, Borrell S, et al. Prevalence and risk factors for VRE colonisation in a tertiary hospital in Melbourne, Australia: a cross sectional study. *Antimicrob Resist Infect Control.* (2012) 1:31. doi: 10.1186/2047-2994-1-31
  34. Souli M, Galani I, Giamarellou H. Emergence of extensively drug-resistant pandrug-resistant Gram-negative bacilli. *Eurosurveillance.* (2008) 13:1–11.
  35. Duckro AN, Blom DW, Lyle EA, Weinstein RA, Hayden MK. Transfer of vancomycin-resistant enterococci via health care worker hands. *Arch Intern Med.* (2005) 165:302–7. doi: 10.1001/archinte.165.3.302
  36. Boyce JM. Environmental contamination makes an important contribution to hospital infection. *J Hosp Infect.* (2007) 65 (Suppl. 2):50–4. doi: 10.1016/S0195-6701(07)60015-2
  37. Astrinaki E, Messaritaki A, Mourtou E, Niakas D. Hand hygiene compliance in a Greek university hospital. *Arch Hell Med.* (2016) 33:639–44.
  38. Poulou A, Voulgari E, Vrioni G, Xidopoulos G, Pliagkos A, Chatzipantazi V, et al. Imported *Klebsiella pneumoniae* carbapenemase-producing *K. pneumoniae* clones in a Greek hospital: impact of infection control measures for restraining their dissemination. *J Clin Microbiol.* (2012) 50:2618–23. doi: 10.1128/JCM.00459-12
  39. Kouni S, Kourlaba G, Mougkou K, Maroudi S, Chavela B, Nteli C, et al. Assessment of Hand hygiene resources and practices at the 2 children's hospitals in Greece. *Pediatr Infect Dis J.* (2014) 33:e247–51. doi: 10.1097/INF.0000000000000376
  40. Hugonnet S, Harbarth S, Sax H, Duncan RA, Pittet D. Nursing resources: a major determinant of nosocomial infection? *Curr Opin Infect Dis.* (2004) 17:329–33. doi: 10.1097/01.qco.0000136931.83167.d2
  41. Economou C, Kaitelidou D, Kentikelenis A, Sissouras A, Maresso A. The Impact of the Financial Crisis on the Health System and Health in Greece. Copenhagen: WHO; European Observatory on Health Systems and Policies (2014). Available online at: [http://www.euro.who.int/\\_data/assets/pdf\\_file/0007/266380/The-impact-of-the-financial-crisis-on-the-health-system-and-health-in-Greece.pdf](http://www.euro.who.int/_data/assets/pdf_file/0007/266380/The-impact-of-the-financial-crisis-on-the-health-system-and-health-in-Greece.pdf) (accessed March 8, 2020).
  42. Kousouli E, Zarkotou O, Politi L, Polimeri K, Vrioni G, Themeli-Digalaki K, et al. Infection control interventions affected by resource shortages: impact on the incidence of bacteremias caused by carbapenem-resistant pathogens. *Eur J Clin Microbiol Infect Dis.* (2018) 37:43–50. doi: 10.1007/s10096-017-3098-1
  43. McKinnell JA, Kunz DF, Moser SA, Vangala S, Tseng CH, Shapiro M, et al. Patient-level analysis of incident vancomycin-resistant enterococci colonization and antibiotic days of therapy. *Epidemiol Infect.* (2016) 144:1748–55. doi: 10.1017/S0950268815003118
  44. Tacconelli E, De Angelis G, Cataldo MA, Mantengoli E, Spanu T, Pan A, et al. Antibiotic usage and risk of colonization and infection with antibiotic-resistant bacteria: a hospital population-based study. *Antimicrob Agents Chemother.* (2009) 53:4264–9. doi: 10.1128/AAC.00431-09
  45. High KP. Infection as a cause of age-related morbidity and mortality. *Ageing Res Rev.* (2004) 3:1–14. doi: 10.1016/j.arr.2003.08.001
  46. McEvoy SP, Plant AJ, Pearman JW. Risk factors for the acquisition of vancomycin-resistant enterococci during a single-strain outbreak at a major Australian teaching hospital. *J Hosp Infect.* (2006) 62:256–8. doi: 10.1016/j.jhin.2005.06.
  47. Zhao ZC, Xu XH, Liu MB, Wu J, Lin J, Li B. Fecal carriage of carbapenem-resistant Enterobacteriaceae in a Chinese university hospital. *Am J Infect Control.* (2014) 42:e61–4. doi: 10.1016/j.ajic.2014.01.024
  48. Rosenthal VD, Maki DG, Salomao R, Álvarez-Moreno C, Mehta Y, Higuera F, et al. Device-associated nosocomial infections in 55 intensive care units of 8 developing countries. *Ann Intern Med.* (2006) 145:582–91. doi: 10.7326/0003-4819-145-8-200610170-00007
  49. Asai N, Sakanashi D, Suematsu H, Kato H, Hagihara M, Nishiyama N, et al. The epidemiology and risk factor of carbapenem-resistant enterobacteriaceae colonization and infections: case control study in a single institute in Japan. *J Infect Chemother.* (2018) 24:505–9. doi: 10.1016/j.jiac.2018.02.005
  50. Martin RM, Cao J, Brisse S, Passet V, Wu W, Zhao L, et al. Molecular epidemiology of colonizing and infecting isolates of *Klebsiella pneumoniae*. *mSphere.* (2016) 1:1–12. doi: 10.1128/mSphere.00261-16
  51. Gorrie CL, Mirceta M, Wick RR, Edwards DJ, Nicholas R, Strugnell RA, et al. Gastrointestinal carriage is a major reservoir of *Klebsiella pneumoniae* infection in intensive care patients. *Clin Infect Dis.* (2017) 65:208–15. doi: 10.1093/cid/cix270
  52. Tumbarello M, Viale P, Viscoli C, Trecarichi EM, Tumietto F, Marchese A, et al. Predictors of mortality in bloodstream infections caused by *Klebsiella pneumoniae* carbapenemase-producing *K. pneumoniae*: Importance of combination therapy. *Clin Infect Dis.* (2012) 55:943–50. doi: 10.1093/cid/cis588
  53. Kalpoe JS, Sonnenberg E, Factor SH, del Rio Martin J, Schiano T, Patel G, et al. Mortality associated with carbapenem-resistant *Klebsiella pneumoniae* infections in liver transplant recipients. *Liver Transplant.* (2012) 18:468–74. doi: 10.1002/lt.23374
  54. Wang Z, Qin RR, Huang L, Sun LY. Risk factors for carbapenem-resistant *Klebsiella pneumoniae* infection and mortality of *Klebsiella pneumoniae* infection. *Chin Med J.* (2018) 131:56–62. doi: 10.4103/0366-6999.221267
  55. Bakthavatchalam YD, Anandan S VB. Laboratory detection and clinical implication of oxacillinase-48 like carbapenemase: the hidden threat. *J Glob Infect Dis.* (2016) 8:41–50. doi: 10.4103/0974-777X.176149

**Conflict of Interest:** The authors declare that the research was conducted in the absence of any commercial or financial relationships that could be construed as a potential conflict of interest.

Copyright © 2020 Vasilakopoulou, Karakosta, Vourli, Tarpatzi, Varda, Kostoula, Antoniadou and Pournaras. This is an open-access article distributed under the terms of the Creative Commons Attribution License (CC BY). The use, distribution or reproduction in other forums is permitted, provided the original author(s) and the copyright owner(s) are credited and that the original publication in this journal is cited, in accordance with accepted academic practice. No use, distribution or reproduction is permitted which does not comply with these terms.





# Inactivation of Glutamine Synthetase-Coding Gene *glnA* Increases Susceptibility to Quinolones Through Increasing Outer Membrane Protein F in *Salmonella enterica* Serovar Typhi

Ana R. Millanao<sup>1,2,3</sup>, Aracely Y. Mora<sup>1</sup>, Claudia P. Saavedra<sup>4,5</sup>, Nicolás A. Villagra<sup>6,7</sup>, Guido C. Mora<sup>8</sup> and Alejandro A. Hidalgo<sup>1\*</sup>

<sup>1</sup> Escuela de Química y Farmacia, Facultad de Medicina, Universidad Andres Bello, Santiago, Chile, <sup>2</sup> Instituto de Farmacia, Facultad de Ciencias, Universidad Austral de Chile, Valdivia, Chile, <sup>3</sup> Facultad de Ciencias Químicas y Farmacéuticas, Universidad de Chile, Santiago, Chile, <sup>4</sup> Laboratorio de Microbiología Molecular, Departamento de Ciencias Biológicas, Facultad de Ciencias de la Vida, Universidad Andres Bello, Santiago, Chile, <sup>5</sup> Millennium Institute on Immunology and Immunotherapy, Departamento de Ciencias Biológicas, Facultad de Ciencias de la Vida, Universidad Andres Bello, Santiago, Chile, <sup>6</sup> Escuela de Tecnología Médica, Universidad Andres Bello, Santiago, Chile, <sup>7</sup> Departamento de Laboratorios Clínicos, Escuela de Medicina, Pontificia Universidad Católica de Chile, Santiago, Chile, <sup>8</sup> Instituto de Investigación Interdisciplinar en Ciencias Biomédicas SEK, Facultad de Ciencias de la Salud, Santiago, Universidad SEK, Santiago, Chile

## OPEN ACCESS

### Edited by:

Kunihiko Nishino,  
Osaka University, Japan

### Reviewed by:

Ricardo Oropeza,  
National Autonomous University  
of Mexico, Mexico  
Xiangmin Lin,  
Fujian Agriculture and Forestry  
University, China

### \*Correspondence:

Alejandro A. Hidalgo  
alejandro.hidalgo@unab.cl

### Specialty section:

This article was submitted to  
Antimicrobials, Resistance  
and Chemotherapy,  
a section of the journal  
Frontiers in Microbiology

Received: 30 July 2019

Accepted: 27 February 2020

Published: 20 March 2020

### Citation:

Millanao AR, Mora AY,  
Saavedra CP, Villagra NA, Mora GC  
and Hidalgo AA (2020) Inactivation  
of Glutamine Synthetase-Coding  
Gene *glnA* Increases Susceptibility  
to Quinolones Through Increasing  
Outer Membrane Protein F  
in *Salmonella enterica* Serovar Typhi.  
Front. Microbiol. 11:428.  
doi: 10.3389/fmicb.2020.00428

Ciprofloxacin is the choice treatment for infections caused by *Salmonella* Typhi, however, reduced susceptibility to ciprofloxacin has been reported for this pathogen. Considering the decreased approbation of new antimicrobials and the crisis of resistance, one strategy to combat this problem is to find new targets that enhances the antimicrobial activity for approved antimicrobials. In search of mutants with increased susceptibility to ciprofloxacin; 3,216 EZ-Tn5 transposon mutants of *S. Typhi* were screened. *S. Typhi* zxx::EZ-Tn5 mutants susceptible to ciprofloxacin were confirmed by agar diffusion and MIC assays. The genes carrying EZ-Tn5 transposon insertions were sequenced. Null mutants of interrupted genes, as well as inducible genetic constructs, were produced using site-directed mutagenesis, to corroborate phenotypes. SDS-PAGE and Real-time PCR were used to evaluate the expression of proteins and genes, respectively. Five mutants with increased ciprofloxacin susceptibility were found in the screening. The first confirmed mutant was the glutamine synthetase-coding gene *glnA*. Analysis of outer membrane proteins revealed increased OmpF, a channel for the influx of ciprofloxacin and nalidixic acid, in the *glnA* mutant. Expression of *ompF* increased four times in the *glnA* null mutant compared to WT strain. To understand the relationship between the expression of *glnA* and *ompF*, a strain with the *glnA* gene under control of the tetracycline-inducible P<sup>tet</sup> promoter was created, to modulate *glnA* expression. Induction of *glnA* decreased expression of *ompF*, at the same time that reduced susceptibility to ciprofloxacin. Expression of sRNA MicF, a negative regulator of OmpF was reduced to one-fourth in the *glnA* mutant, compared to WT strain. In addition, expression of *glnL* and *glnG* genes (encoding the two-component system NtrC/B that may positively regulate OmpF) were increased in the *glnA* mutant. Further

studies indicate that deletion of *glnG* decreases susceptibility to CIP, while deletion of *micF* gene increases susceptibility CIP. Our findings indicate that *glnA* inactivation promotes *ompF* expression, that translates into increased OmpF protein, facilitating the entry of ciprofloxacin, thus increasing susceptibility to ciprofloxacin through 2 possible mechanisms.

**Keywords:** *glnA*, ciprofloxacin, OmpF, *S. Typhi*, transposon

## INTRODUCTION

*Salmonella Typhi* is the etiological agent of typhoid fever, endemic in many developing countries worldwide. This disease is exclusive of humans with a mortality rate of 10%. The emergence of the extensively drug-resistant *S. Typhi* H58 strains in Pakistan, which are resistant to the first-line drugs (ampicillin, chloramphenicol, and cotrimoxazole), fluoroquinolones, and third-generation cephalosporin, is a real threat with potential to become typhoid fever untreatable (Cabello, 2018; Johnson et al., 2018; Klemm et al., 2018). Thus, typhoid fever requires alternative pharmacological treatment, including new antimicrobials and development of new combined therapies to revitalize existing antibiotics to prolong its useful life and slow down the emergence of resistance (Cottarel and Wierzbowski, 2007; Fajardo et al., 2008; Liu et al., 2010; Rodas et al., 2010; Sabbagh et al., 2012; González-Bello, 2017).

To find mutants with increased susceptibility to Ciprofloxacin (CIP), a screening was performed over 3,216 insertional mutants of *S. Typhi* STH2370 with the EZ-Tn5<sup>TM</sup> transposon exposed to sub-MIC concentrations of CIP. We identified both: a small number of known and new genetic determinants of resistance to quinolones. One such mutant in the *glnA* gene that encodes for glutamine synthetase (GS) was further characterized. GS produces glutamine from glutamate and ammonia and has a crucial role in nitrogen metabolism. The internal concentration of glutamine is the main intracellular signal for regulating nitrogen availability in enteric bacteria (Zimmer et al., 2000; Switzer et al., 2018). Nitrogen is essential for the biosynthesis of macromolecules in bacteria; thus, the adaptive response to metabolic stress induced by starvation of nitrogen (as it is the case of glutamine auxotrophic bacteria) could affect bacterial physiology, including the susceptibility to antimicrobials which today is known to be modulated by metabolism (Maria-Neto et al., 2012; Peng et al., 2015; Vestergaard et al., 2017; Cui et al., 2019).

One example that relates nitrogen metabolism and susceptibility to antimicrobials is the observation of *Escherichia coli* strains resistant to magainin I (a cationic peptide) which overexpress GS (Maria-Neto et al., 2012). In *Streptococcus pneumoniae* it was demonstrated that *glnA* was repressed in the presence of penicillin, as well as, the inhibition of GS enhanced susceptibility to penicillin. Hence, glutamine conferred a protective role against penicillin when added to the culture medium (El Khoury et al., 2017). In the same line, methicillin-resistant *Staphylococcus aureus* and methicillin-susceptible *S. aureus* with lower expression of GS decreased their level of methicillin resistance (Gustafson et al., 1994). It is proposed that

in *S. aureus* GS participates in the production of constituents of the cell envelope, therefore maintaining the cell wall thickness and the level of crosslinking on peptidoglycan (Gustafson et al., 1994; Lima et al., 2013). In *Mycobacterium tuberculosis*, GS plays a crucial role in the cell wall biosynthesis; therefore, inhibition of GS in *M. tuberculosis* with the inhibitor L-methionine-SR-sulfoximine increases susceptibility to isoniazid. Again, this study concludes that inhibition of GS activity affects the synthesis of peptidoglycan layers of the cell wall, changing susceptibility (Harth and Horwitz, 2003).

In this work, we describe that *glnA* mutants of *S. Typhi* increase their susceptibility to quinolones. Interestingly OmpF, a porin forming a homotrimer channel for the influx of CIP and nalidixic acid, was augmented in the *S. Typhi glnA* mutant. Further studies using a tetracycline-inducible system, revealed an inverse correlation between *glnA* and *ompF* expression. Our findings suggested that *glnA* inactivation increases the susceptibility of *S. Typhi* to CIP through increasing OmpF.

## MATERIALS AND METHODS

### Bacterial Strains and Growth Conditions

*Salmonella Typhi* SHT2370 an antibiotic-sensitive virulent clinical strain was obtained from the Infectious Diseases Hospital Lucio Cordova, Santiago, Chile (Valenzuela et al., 2014). Mutants used in this study were derived from *S. Typhi* STH2370 and are shown in **Table 1**. Bacteria were grown in LB medium (1% peptone, 0.5% yeast extract, 0.5% NaCl) at 37°C with aeration. When required, the medium was supplemented with Kanamycin (KAN) 50 mg/L, Ampicillin (AMP) 100 mg/L, Chloramphenicol (CAM), CIP (at different concentrations) or Chlortetracycline (CTET at different concentrations). Media were solidified with agar (15 g/L) as required. Mutants in genes *glnL* and *glnG* were produced by P22 transducing null mutations with the KAN<sup>R</sup> cassette from *S. Typhimurium*.

### Transposon Insertional Mutagenesis and Screening

Mutagenesis with the commercial transposon EZ-Tn5<sup>TM</sup> (Epicentre, CA, United States) was performed as indicated by the provider (protocols available at <https://www.lucigen.com/docs/manuals/MA155E-EZ-Tn5-r6kg-Ori-KAN-2-Transposome-Kit.pdf> at February 17, 2020) with minor modifications. In brief, *S. Typhi* STH2370 was grown to OD<sub>600</sub> 0.4, 5 mL were washed six times with sterile water, resuspended in 100 μL of sterile water and electroporated with

**TABLE 1** | Strains and plasmids used in this work.

Strain	Genotype/relevant features	Source
STH2370	<i>Salmonella</i> Typhi strain	Lab. stock
STH2370 <i>glnA</i> ::EZ-Tn5	<i>glnA</i> ::EZ-Tn5	This study
STH2370 <i>glnA</i> :: <i>kan</i>	$\Delta$ <i>glnA</i> :: <i>kan</i>	This study
STH2370 <i>glnA</i> ::FRT	$\Delta$ <i>glnA</i> ::FRT	This study
SHT2370 <i>glnA</i> <sup>TD</sup>	$\Delta$ P <sup><i>glnA</i></sup> ::[ <i>tetR</i> -P <sup><i>tet</i></sup> - $\Delta$ <i>tetA</i> ::FRT]	This study
STH2370 <i>glnG</i> :: <i>kan</i>	$\Delta$ <i>glnG</i> :: <i>kan</i>	This study
STH2370 <i>glnL</i> :: <i>kan</i>	$\Delta$ <i>glnL</i> :: <i>kan</i>	This study
STH2370 <i>micF</i> :: <i>cam</i>	$\Delta$ <i>micF</i> :: <i>cam</i>	This study
STH2370 <i>ompF</i> :: <i>kan</i>	$\Delta$ <i>ompF</i> :: <i>kan</i>	This study
STH2370 <i>ompF</i> <sup>TD</sup>	$\Delta$ P <sup><i>ompF</i></sup> ::[ <i>tetR</i> -P <sup><i>tet</i></sup> - $\Delta$ <i>tetA</i> ::FRT]	This study
STH2370 STY4173 <sup>TD</sup>	$\Delta$ P <sup>4173</sup> ::[ <i>tetR</i> -P <sup><i>tet</i></sup> - $\Delta$ <i>tetA</i> ::FRT]	This study
<i>E. coli</i> DH5 $\alpha$ $\lambda$ pir	encodes pir protein of phage lambda, used for propagation of plasmids with R6K replication origin	Lab. stock
Plasmid		
pKD4	AMP <sup>R</sup> , KAN <sup>R</sup> , FRT-KAN <sup>R</sup> -FRT	Datsenko and Wanner, 2000
pKD46	AMP <sup>R</sup> , $\lambda$ Red Recombination System	Datsenko and Wanner, 2000
pCP20	AMP <sup>R</sup> , Flp expression	Datsenko and Wanner, 2000

1  $\mu$ L of EZ-Tn5 transposome at a concentration of 0.1 pmol/ $\mu$ L. Electroporated bacteria were recovered in 1 mL of LB broth, and incubated with aeration for 40 min before plating on LB-agar containing KAN 50 mg/L and overnight incubation. Mutants *S. Typhi* mutants STH2370 *zxx*::EZ-Tn5 were organized on a 6  $\times$  8 pattern in 67 lots creating a collection of 3,216 mutants. The primary screening was performed by transferring colonies to LB plates with CIP 0.05 mg/L using a 48-pins microplate replicator. Mutants with increased susceptibility were selected by visual examination and confirmed by disk diffusion assay. The susceptibility of confirmed mutants was quantified by MICs assays before proceeding with cloning and sequencing of interrupted genes.

## Cloning and Sequencing

The mutants with at least two-fold-change in the MIC were subjected to cloning. Briefly, genomic DNA of mutants was extracted, digested with *EcoRV* and ligated with T4 DNA ligase. Ligated DNA was electroporated in *E. coli* DH5 $\alpha$  $\lambda$ pir, recovered in 1 mL of LB broth, and incubated with aeration for 40 min at 37°C before plating on LB-agar containing KAN 50 mg/L. KAN<sup>R</sup> colonies were grown, and plasmidial DNA was column-purified to perform Sanger sequencing. Sequences were analyzed using the Basic Local Alignment Search Tool available at <http://www.ncbi.nlm.nih.gov>.

## Disk Diffusion Test

The antibiotic susceptibility tests were performed by Kirby-Bauer disk diffusion method according to CLSI guidelines (CLSI, 2012a). Suspensions of 2 mL of microorganism were grown overnight in liquid culture using LB medium with aeration.

The bacterial suspensions were diluted 1:1000 in 0.9% NaCl and 100  $\mu$ L of this suspension were seeded on Mueller Hinton (MH) agar plates pH 7.3. CIP susceptibilities tests were performed with 5  $\mu$ g CIP disks onto seeded plates incubated at 37°C for 16–18 h. Halos were recorded as the average of 2-crossed diameters in biological triplicate assays.

## Determination of MIC

MIC was determined using broth microdilution susceptibility testing according to CLSI guidelines (CLSI, 2012b). Briefly, 0.9% NaCl was used to prepare inoculum until turbidity McFarland 0.5, with an equivalent density to 1–2  $\times$  10<sup>8</sup> CFU/mL. The inoculum was then diluted to reach a concentration of 5  $\times$  10<sup>4</sup> CFU/well. Antibiotics were serially diluted in base-2 and each well-inoculated with 50  $\mu$ L of diluted bacteria. The plates were incubated at 37°C for 16 h and read at 600 nm. The MIC was determined as the concentration that allowed less than 50% growth density compared to the non-antibiotic control.

## Construction of *S. Typhi* Site-Directed Mutants

Site-directed mutants of *S. Typhi* STH2370 were constructed by allelic exchange facilitated by the Red/Swap Technique (Datsenko and Wanner, 2000). Briefly, PCR product, with a resistance cassette flanked by regions with homology to the target DNA sequences, was electroporated into strains carrying pKD46, recovered in 1 mL of LB broth and incubated for 1 h at 37°C with aeration before plating onto plates with the corresponding antibiotic to select mutants. When needed the resistance cassette was eliminated to produce FRT scar mutants by introducing pCP20 which encodes the Flippase recombinase that promotes scission from FRT sequences flanking the resistance cassette. The primers used for these constructions are in **Supplementary Table 1**.

## Construction of Tetracycline-Dependent Mutants

Construction of the tetracycline-dependent (TD) mutants *S. Typhi glnA*<sup>TD</sup>, *S. Typhi ompF*<sup>TD</sup> and *S. Typhi STY4173*<sup>TD</sup>, was carried out using a modification of the Red-Swap method for promoter mutation of target genes as described by Hidalgo et al. (2016). The primers used for these constructions are in **Supplementary Table 1**.

## Preparation of Outer Membrane Proteins (OMPs) and SDS-PAGE

The OMPs fraction of protein was obtained by a method previously described (Lobos and Mora, 1991). Two mL of bacteria were centrifuged at 10,000 g for 10 min. The pellet obtained was resuspended in 10 mM Tris Hydrochloride pH 8, sonicated for 100 s and centrifuged at 7,000 g for 5 min. The supernatant obtained was centrifuged at 13,000 g for 45 min, and the pellet was resuspended in 10 mM Tris Hydrochloride pH 8 with 2% Triton X-100. The suspension was incubated at 37°C for 30 min with occasional stirring and centrifuged at 13,000 g for 45 min. The pellet containing OMPs was resuspended in 100 mM Tris

Hydrochloride pH 8, 2% SDS and quantified using BCA protein assay kit. Next, 50 µg of protein were heated at 98°C for 5 min and resolved in an SDS-PAGE at 100 V. The gels were rinsed with water, pre-treated for 60 min with 40% ethanol and 10% acetic acid, washed twice for 10 min and stained in 0.1% acid Coomassie blue R250, 2% orthophosphoric acid, 10% ammonium sulfate, and 20% methanol overnight. Finally, gels were washed with 1% acetic until all Coomassie particles were removed. High resolution pictures of gels were open in the ImageJ software. Using the area selection tool, a horizontal line was traced to cut pick that were then analyzed by their density, which was compared to density of WT strain for the bands corresponding to OmpF (Gallo-Oller et al., 2018).

## RNA Isolation, Reverse Transcription, and Real-Time PCR (RT-qPCR)

For extraction of RNA, overnight cultures were diluted 100 times and cultured in fresh LB or LB + CTET as appropriate, until reaching OD<sub>600</sub> 0.5. RNA was extracted using the Trizol method according to the provider instructions. Briefly, 20 mL of bacterial cell was harvested, washed twice with ice-cold water and treated with lysozyme at RT before adding Trizol™ (Invitrogen). The samples were mixed before adding ice-cold chloroform, centrifugation and recovering the supernatant. RNA was precipitated with isopropanol, washed with 70% v/v ethanol and resuspended in nuclease-free water before treatment with DNase I. Reverse transcriptions of samples were performed with 1 µg of DNase-treated RNA using SuperScript™ II Reverse Transcriptase (Invitrogen) with Random Hexamers (Invitrogen). Primers for the genes *dnaN* and *lon* were used to normalize the expression of target genes. Although *dnaN* and *lon* are both good expression controls, *dnaN* was preferred for assays that used tetracyclines to minimize distortion of results as *dnaN* remained unchanged compared to *lon*, in presence of CTet. Quantification was carried out in an Eco™ Real-Time PCR System using Brilliant II SYBR™ Master Mixes. The fold change was calculated as described by Pfaffl (Pfaffl, 2001). The primers used for these assays are listed in **Supplementary Table 1**.

## Statistical Analysis

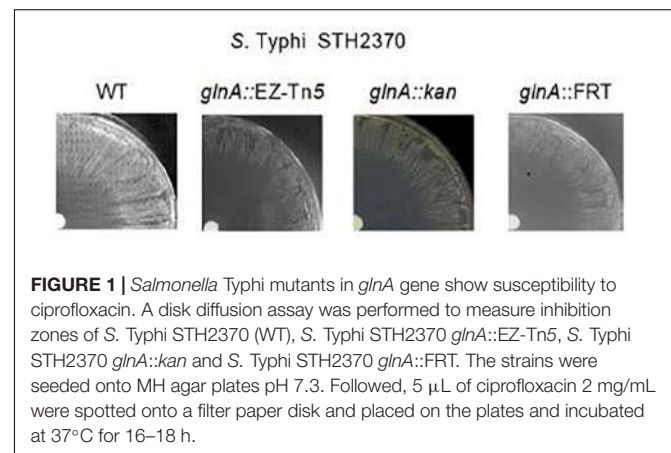
Student's *t*-test was realized if samples obtained of different experiments have passed Shapiro–Wilk test for normality. The data are presented as mean ± SD of at least biological triplicates. Statistical analyses of results from RT-qPCR were calculated using the paired Student's *t*-test (GraphPad Prism version 8.0, San Diego, CA, United States).

## RESULTS

### Screening of *S. Typhi* *zxx::EZ-Tn5* to Identify Mutants With Increased Susceptibility to Ciprofloxacin

We screened 3,216 *S. Typhi* STH2370 *zxx::EZ-Tn5* mutants on MH-agar plates with CIP 0.05 mg/L. A total of 43 susceptible mutants with poor or not growth were selected by visual

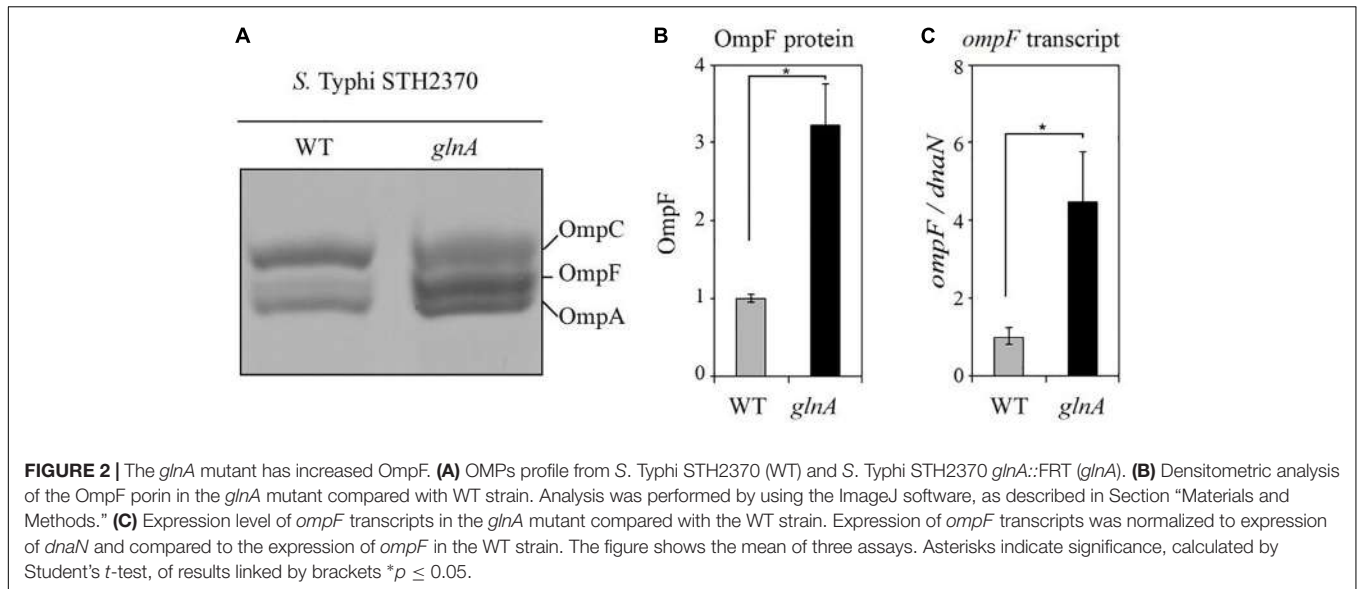
analysis of the colonies. Confirmation of CIP susceptible mutants was performed by using disk diffusion assay. From this test, 10 mutants were confirmed, as their inhibition halos were 6 mm greater compared with WT control and were subjected to MIC assays. Eight mutants were twice as sensitive, one mutant was four-times more sensitive, and one mutant was eight-times more sensitive to CIP, compared with the WT counterpart. These mutants were set for cloning and further sequencing of the interrupted genes. All selected mutants that were sent to sequencing had one transposon insertion only. An extensive search was performed for information linking the mutated genes to antibiotics resistance. Five mutants, *recC::EZ-Tn5*, *cysE::EZ-Tn5*, *aefA::EZ-Tn5*, *dacC::EZ-Tn5* and *glnA::EZ-Tn5*, resulted of especial interest after considering two criteria: (i) the level of susceptibility of the mutant and (ii) the relevance/novelty of the interrupted gene. **Supplementary Figure 1** shows the screening workflow to identify genes leading to susceptibility. Subsequently, a secondary screening was performed, over the five mutants of interest, to determine whether observed susceptibility was general or specific for one antimicrobial or a family of them. Diameters of inhibition haloes for the five insertional mutants selected with different antimicrobials were recorded (**Supplementary Table 2**). After discarding the best candidate (*S. Typhi aefA::EZ-Tn5*) whose increased susceptibility was product of polar effects produced by the transposon over the *acrAB* locus upstream of *aefA* gene, we began the characterization of mutant *S. Typhi* STH2370 *glnA::EZ-Tn5* that showed increased susceptibility to NAL and CIP in the screening (**Supplementary Table 2**). While the other three mutants were not further characterized.



**TABLE 2 |** Susceptibility to ciprofloxacin of WT *S. Typhi* and null mutants in *glnA*.

Strain	Inhibition haloes (mm ± SD)	MIC mg/L ± SD	MIC compared to control
<i>S. Typhi</i> STH2370	37.3 ± 1.25	0.078 ± 0	Control
<i>glnA::EZ-Tn5</i>	47.8 ± 0.76	0.039 ± 0	1/2 CIM
<i>glnA::kan</i>	48.0 ± 0.50	0.039 ± 0	1/2 CIM
<i>glnA::FRT</i>	48.2 ± 0.29	0.039 ± 0	1/2 CIM





**TABLE 3** | Induction of *glnA* in *glnA<sup>TD</sup>* mutant decreases the susceptibility to ciprofloxacin (CIP).

CTET	Diameter of inhibition haloes in presence of CIP (mm) ± SD				
	<i>glnA<sup>TD</sup></i>	<i>ompF<sup>TD</sup></i>	STY4173 <sup>TD</sup>	WT	<i>glnA::FRT</i>
vehicle (water)	46.0 ± 0.10	31.9 ± 0.25	40.1 ± 0.12	37.0 ± 0.17	48.0 ± 0.17
0.025 μg/mL	41.9 ± 0.17	37.3 ± 0.00	40.0 ± 0.10	38.9 ± 0.42	49.1 ± 0.25
0.050 μg/mL	38.1 ± 0.42	41.0 ± 0.17	40.0 ± 0.10	39.1 ± 0.5	48.8 ± 0.44

## S. Typhi *glnA* Mutants Are More Susceptible to Ciprofloxacin

To rule out polar effects that might modulate antimicrobial susceptibility, in the *S. Typhi* *glnA::EZ-Tn5*, we constructed mutant *S. Typhi* STH2370 *glnA::kan* and *S. Typhi* STH2370 *glnA::FRT* (Supplementary Figure 2). All mutants in *glnA* gene (*glnA::EZ-Tn5*, *glnA::kan*, and *glnA::FRT*) presented the same range of increased susceptibility to CIP with a diameter of inhibition haloes ~11 mm larger and a MIC twice as sensitive compared to the WT strain (Figure 1 and Table 2). The observation that *S. Typhi* *glnA::FRT* (as well as all null mutants in *glnA* gene) shows the same level of susceptibility, rule out any possible polar effect governing the observed phenotype, as *FRT* sequence is by far less invasive than resistance cassettes.

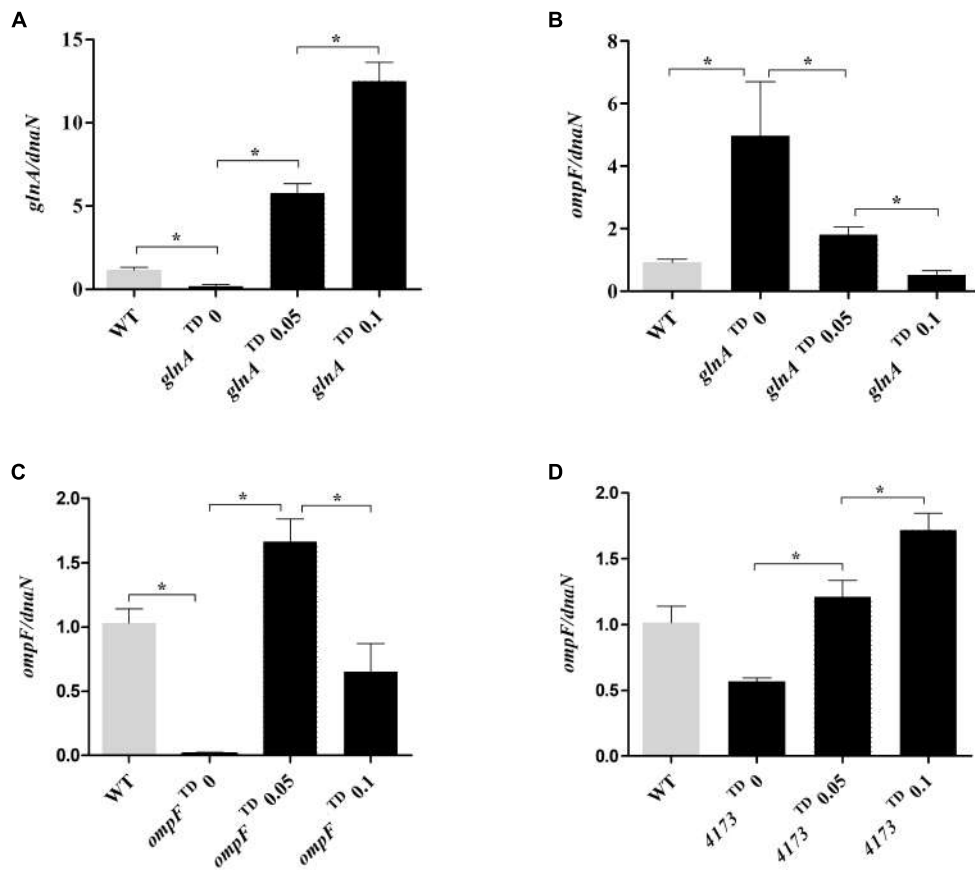
## Inactivation of *glnA* Gene Increases the Expression of OmpF

Because inactivating *glnA* gene increases susceptibility to CIP, we searched for information regarding determinants of susceptibility to this antibiotic. As outer membrane proteins may be implicated in antibacterial entry through the cell envelope (Nikaido, 2003), we decided to study the profiles of OMPs in the *glnA::FRT*. SDS-PAGE profile of OMPs, showed a threefold increase of OmpF in *S. Typhi* STH2370 *glnA::FRT*, compared with WT (Figures 2A,B). Same result was observed for all *glnA* null

mutants in *S. Typhi*, the results for *S. Typhi* *glnA::FRT* and *S. Typhi* *glnA::kan* are shown in Supplementary Figure 3, compared to *S. Typhi* WT and a *S. Typhi* *ompF* mutant. Interestingly, deletion of *ompF* produces changes in the OMPs pattern, at the level of making OMPs unrecognizable by simple Coomassie staining. Previous observation reported changes on the amount of OMPs in an *ompF* null mutant of a clinical isolate of *S. Typhi*. However, in this mutant main porins, such as *ompC* and *ompA* did not change their migration pattern (Villarreal et al., 2014). It could be the case that the extend of changes produced after *ompF* is mutated differs between isolates of *S. Typhi*. Despite that, abundance of OmpF would be the responsible of increased susceptibility to CIP, as *ompF* is also augmented in the *ompF* inducible mutant, but not other porins, as shown in further experiments. Next, RT-qPCR was performed to measure *ompF* expression in *glnA::FRT* mutant. As shown in Figure 2C, the expression of *ompF* gene was at least four-times higher in the *glnA::FRT* mutant compared with WT strain.

## Induction of *glnA* Inversely Correlates With Susceptibility to Ciprofloxacin

To confirm how changes in *glnA* expression cause changes in *ompF* expression and susceptibility to CIP, we modulated the expression of *glnA* by using a tetracycline-inducible system as previously described (Hidalgo et al., 2016). For that purpose, we successfully replaced the *glnA* gene promoter with



**FIGURE 3 |** Expression of *ompF* and its dependency in *glnA* expression. Expression level of *glnA* transcripts in the mutant *glnA<sup>TD</sup>* (A) and expression of *ompF* transcripts in the mutant *glnA<sup>TD</sup>* (B), *ompF<sup>TD</sup>* (C) and *4173<sup>TD</sup>* (D). The mRNA was extracted from tetracycline-dependent mutants under induced (0.05–0.1  $\mu\text{g/mL}$  CTET) and uninduced conditions. Expression of *glnA* or *ompF* was normalized to expression of *dnaN* and compared to expression of *glnA* or *ompF* in the WT strain without induction. Results are average of at least three biological replicates. Asterisks indicate significance, calculated by Student's *t*-test, of results linked by brackets. \* $p \leq 0.05$ .

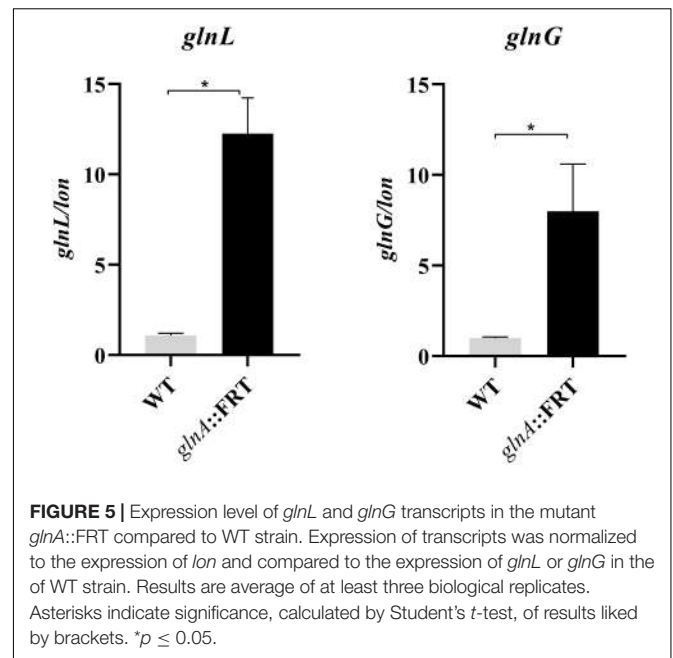
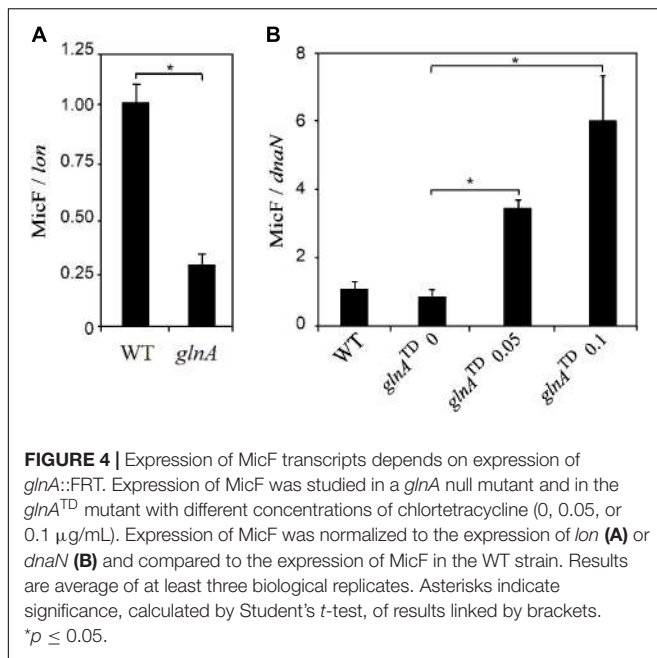
the *tetRA* cassette (Supplementary Figure 4). This mutant allows modulation of *glnA* expression by using tetracyclines, to study *ompF* expression and susceptibility to CIP as a function of *glnA* expression. Because both OmpF and TetA (the efflux pump for tetracyclines) participate in transport through membranes, we excised *tetA* gene, from the *tetRA* cassette, to reduce interferences, caused by the presence of TetA in the inner membrane. This last strain was named as the tetracycline-dependent *glnA* mutant (or simply *glnA<sup>TD</sup>*), as shown in Supplementary Figure 4. Using the same strategy, we constructed the tetracycline-dependent *ompF* mutant (*ompF<sup>TD</sup>*), and the same inducible construct was produced for the unrelated gene STY4173 (*4173<sup>TD</sup>*) that encodes for a putative protein, as a control. Details regarding these mutants are shown in Supplementary Figure 5. Using the *S. Typhi* *glnA<sup>TD</sup>* mutant, we observed that inhibition haloes in the presence of CIP decreased, as the concentration of CTET increases in the plates, to values comparable to the inhibition diameters observed for the WT strain (from 46.0 mm without induction to 38.1 mm with 0.05  $\mu\text{g/mL}$  of CTET). In addition, in uninduced conditions, the *glnA<sup>TD</sup>* mutant shows an inhibition diameter

closer to *glnA::FRT* null mutant, 46.0 mm and 48.0 mm, respectively (Table 3).

In contrast, using the *ompF<sup>TD</sup>* mutant, the inhibition haloes in the presence of CIP increased as the concentration of CTET increases in the plates, to values close to the inhibition diameters observed for the WT strain (from 31.9 mm without induction to 41.0 mm in the plates with 0.05  $\mu\text{g/mL}$  of CTET). Induction of STY4173<sup>TD</sup> expression did not cause significant changes in the inhibition halo to CIP (Table 3). The treatment with CTET did not produce significant changes in susceptibility of either WT or *glnA::FRT* strain to CIP.

### Expression of *glnA* Inversely Correlates With *ompF* Expression

In the view of the decreased susceptibility to CIP when *glnA* is induced with CTET, we decided to assess the expression of *glnA* and *ompF* transcripts in the tetracycline-dependent mutants by RT-qPCR. Expression of *glnA* was increased as CTET concentrations increased (Figure 3A). Next, we investigated the expression of *ompF* in the *glnA<sup>TD</sup>* with and without



**TABLE 4 |** Susceptibility to ciprofloxacin of *S. Typhi* null mutants in genes *glnL*, *glnG*, *micF*, and *ompF*.

<i>S. Typhi</i> STH2370	Inhibition haloes (mm ± SD)
Wild type	36.4 ± 0.4
Δ <i>glnL</i> ::kan	36.2 ± 0.0
Δ <i>glnG</i> ::kan	32.6 ± 0.8
Δ <i>micF</i> ::cam	39.1 ± 0.3
Δ <i>ompF</i> ::kan	27.7 ± 0.3

CTET induction. We found that in the *glnA*<sup>TD</sup> mutant without induction, *ompF* is overexpressed close to five-times compared with WT strain (Figure 3B), the expression of *ompF* in the *glnA*<sup>TD</sup> mutant without induction, is similar to the expression of *ompF* observed in *S. Typhi* *glnA*::FRT null mutant (Figure 2C). When *glnA* expression was induced with CTET we observed a significant decrease in *ompF* expression. Using the *ompF*<sup>TD</sup> mutant, we found that without induction, expression of *ompF* is dramatically reduced compared to WT strain. Induction of *ompF*<sup>TD</sup> mutant with 0.05 μg/mL of CTET significantly induced expression of *ompF* over 150-times compared to uninduced condition and over 1.5-times compared to the WT strain. Higher concentration (0.1 μg/mL) induced *ompF* only 50 times compared to uninduced condition and produces only half the expression of *ompF* observed in WT strain (Figure 3C). As a control, we measured the induction of *ompF* after inducing the unrelated gene STY4173 (Figure 3D). The presence of CTET induced expression of *ompF* two to threefold compared to uninduced condition and was slightly higher compared to WT strain in the presence of 0.1 μg/mL CTET. The results indicate that expression of *glnA* inversely correlates with expression of *ompF*, while increased expression of *ompF* may be responsible of increased susceptibility to CIP.

## Inactivation of *glnA* Reduces Expression of MicF

MicF is a small RNA that promotes degradation of *ompF* transcript and blocks translation by interacting with the Shine-Dalgarno sequence (Morillon, 2018). Because of this direct effect of MicF over *OmpF*, expression of MicF sRNA was studied in the *glnA* mutant and in the *glnA*<sup>TD</sup> mutant with different levels of *glnA* expression. As observed in the Figure 4A, the *S. Typhi* *glnA*::FRT null mutant expresses around one-fourth of MicF, compared to the *S. Typhi* WT. To corroborate this result, MicF expression was studied in the *S. Typhi* *glnA*<sup>TD</sup> mutant. Increased expression of *glnA* with 0.05 and 0.1 μg/mL CTET (as shown in Figure 3A) parallel with increased expression of MicF (Figure 4B). It is also observed that in uninduced conditions, MicF levels are slightly reduced compared with WT strain, probably MicF expression is sensitive to low levels of GlnA that transcribes even in the absence of induction with CTET. Conversely, deletion of *micF* gene slightly increased susceptibility to CIP in *S. Typhi* (Table 4). MicF is a well-described sRNA that negatively regulates transcript levels of *ompF*. Whether the induction of MicF by GlnA is direct or through other factors is unknown.

## The Deletion of *glnA* Activates Transcription of NtrBC Two-Component System

In *E. coli* previous findings indicate that *ompF* is under the control of NtrBC two-component system encoded by *glnL* and *glnG*, as observed in microarray assays (Zimmer et al., 2000). In enterobacteria, these genes are found downstream of *glnA* and are involved in the stress response of enteric bacteria to nitrogen-limited growth (Bhagirath et al., 2019) (Supplementary Figure 2). The deletion of *glnA* increases the





Importantly, it was found that expression of *ompF* is controlled by NtrC in *E. coli* (Zimmer et al., 2000). Therefore, this increase in the expression of *glnL* and *glnG* may explain the increased OmpF and increased susceptibility when *glnA* expression is suppressed or reduced as we illustrate in **Figure 6**. Indeed, mutation of *glnG* (encoding for NtrC transcriptional regulator) produces moderate resistance to CIP. This observation is consistent with increased *glnLG* expression in the *glnA* mutants, which may trigger *ompF* expression, finally allowing entry of CIP through OmpF porin.

Other mechanisms, modulating antimicrobial resistance were studied including regulators MarA, MarR, and RamA; efflux-system components AcrB and TolC and porin OmpC. We found no differences in the expression of the genes encoding for such antimicrobial's resistance factors (**Supplementary Figure 6**). Thus, enhanced susceptibility to quinolones observed in the *glnA* mutants could be linked to the increase of OmpF and associated with nutritional stress due to the decrease of glutamine and lower expression of MicF.

## CONCLUSION

The experimental results show that the inactivation of *glnA* gene drives to increased susceptibility to CIP in *S. Typhi*, through increasing outer membrane protein OmpF. The finding that genes implicated in nitrogen metabolism, such as *glnA*, modulate susceptibility to antimicrobials can be useful in search of potential targets to combat antimicrobial resistance.

## DATA AVAILABILITY STATEMENT

The datasets generated for this study are available on request to the corresponding author.

## REFERENCES

- Baquero, F., and Martínez, J.-L. (2017). Interventions on metabolism: making antibiotic-susceptible bacteria. *MBio* 8:e01950-17. doi: 10.1128/mbio.01950-17
- Bhagirath, A. Y., Li, Y., Patidar, R., Yerex, K., Ma, X., Kumar, A., et al. (2019). Two component regulatory systems and antibiotic resistance in gram-negative pathogens. *Int. J. Mol. Sci.* 20:781. doi: 10.3390/ijms20071781
- Cabello, F. (2018). Typhoid fever in Chile. *Am. J. Trop. Med. Hyg.* 99, 1649–1650. doi: 10.4269/ajtmh.18-0677
- CLSI, (2012a). *Methods for Dilution Antimicrobial Susceptibility Tests for Bacteria That Grow Aerobically: Approved Standard*, 9th Edn. Wayne, PA: CLSI.
- CLSI, (2012b). *Performance Standards for Antimicrobial Disk Susceptibility Tests: Approved Standard*. Wayne, PA: CLSI.
- Cottarel, G., and Wierzbowski, J. (2007). Combination drugs, an emerging option for antibacterial therapy. *Trends Biotechnol.* 25, 547–555. doi: 10.1016/j.tibtech.2007.09.004
- Cui, W.-Q., Qu, Q.-W., Wang, J.-P., Bai, J.-W., Bello-Onaghise, G., Li, Y.-A., et al. (2019). Discovery of potential anti-infective therapy targeting glutamine synthetase in *Staphylococcus xylosum*. *Front. Chem.* 7:381. doi: 10.3389/fchem.2019.00381
- Datsenko, K. A., and Wanner, B. L. (2000). One-step inactivation of chromosomal genes in *Escherichia coli* K-12 using PCR products. *Proc. Natl. Acad. Sci. U.S.A.* 97, 6640–6645. doi: 10.1073/pnas.120163297

## AUTHOR CONTRIBUTIONS

ARM and AH participated in the conception of ideas, performed the experiments, analyzed and interpreted the data, and participated in the drafting of manuscript. AYM performed experiments, collected and analyzed the data, and revised the draft. CS, NV, and GM collected and analyzed the data and participated in drafting of manuscript.

## FUNDING

This work was supported by the Fondo Nacional de Ciencia y Tecnología (FONDECYT, Government of Chile) Grants 11150588 (AH), 1151393 (GM), and 1160315 (CS); UNAB Regular Grants DI-15-19/RG (AH) and DI-4-17/RG (NV); and ECOS-CONICYT grant C16B04 (AH). ARM has been a predoctoral fellow at Comisión Nacional de Ciencia y Tecnología grant 21120035 (CONICYT, Government of Chile).

## ACKNOWLEDGMENTS

We thank Dr. Lionello Bossi, Dr. Nara Figueroa-Bossi, and Dr. Felipe Cabello for valuable comments on the manuscript. We thank Mr. Víctor Ahumada for technical assistant. Part of the results included in this manuscript were presented during the XXXVIII Meeting of the Chilean Society for Microbiology 2016, Valdivia, Chile.

## SUPPLEMENTARY MATERIAL

The Supplementary Material for this article can be found online at: <https://www.frontiersin.org/articles/10.3389/fmicb.2020.00428/full#supplementary-material>

- El Khoury, J. Y., Boucher, N., Bergeron, M. G., Leprohon, P., and Ouellette, M. (2017). Penicillin induces alterations in glutamine metabolism in *Streptococcus pneumoniae*. *Sci. Rep.* 7:14587. doi: 10.1038/s41598-017-15035-y
- Fajardo, A., Martínez-Martin, N., Mercadillo, M., Galán, J. C., Ghysels, B., Matthijs, S., et al. (2008). The neglected intrinsic resistome of bacterial pathogens. *PLoS One* 3:e1619. doi: 10.1371/journal.pone.0001619
- Gallo-Oller, G., Ordoñez, R., and Dotor, J. (2018). A new background subtraction method for Western blot densitometry band quantification through image analysis software. *J. Immunol. Methods* 457, 1–5. doi: 10.1016/j.jim.2018.03.004
- González-Bello, C. (2017). Antibiotic adjuvants – A strategy to unlock bacterial resistance to antibiotics. *Bioorganic Med. Chem. Lett.* 27, 4221–4228. doi: 10.1016/j.bmcl.2017.08.027
- Gustafson, J., Strassle, A., Hachler, H., Kayser, F. H., and Berger-Bachi, B. (1994). The femC locus of *Staphylococcus aureus* required for methicillin resistance includes the glutamine synthetase operon. *J. Bacteriol.* 176, 1460–1467. doi: 10.1128/jb.176.5.1460-1467.1994
- Harth, G., and Horwitz, M. A. (2003). Inhibition of *Mycobacterium tuberculosis* glutamine synthetase as a novel antibiotic strategy against tuberculosis: demonstration of efficacy in vivo. *Infect. Immun.* 71, 456–464. doi: 10.1128/IAI.71.1.456-464.2003
- Hidalgo, A. A., Villagra, N. A., Jerez, S. A., Fuentes, J. A., and Mora, G. C. (2016). A conditionally lethal mutant of *Salmonella Typhimurium* induces a

- protective response in mice. *Biochem. Biophys. Res. Commun.* 470, 313–318. doi: 10.1016/j.bbrc.2016.01.058
- Ikeda, T. P., Shauger, A. E., and Kustu, S. (1996). *Salmonella typhimurium* apparently perceives external nitrogen limitation as internal glutamine limitation. *J. Mol. Biol.* 259, 589–607. doi: 10.1006/jmbi.1996.0342
- Johnson, R., Mylona, E., and Frankel, G. (2018). Typhoidal *Salmonella*: distinctive virulence factors and pathogenesis. *Cell. Microbiol.* 20:e12939. doi: 10.1111/cmi.12939
- Klemm, E. J., Shakoor, S., Page, A. J., Qamar, F. N., Judge, K., Saeed, D. K., et al. (2018). Emergence of an extensively drug-resistant *Salmonella enterica* serovar typhi clone harboring a promiscuous plasmid encoding resistance to fluoroquinolones and third-generation cephalosporins. *MBio* 9:e00105-18. doi: 10.1128/mbio.00105-18
- Lima, T. B., Pinto, M. F. S., Ribeiro, S. M., Lima, L. A., De, Viana, J. C., et al. (2013). Bacterial resistance mechanism: what proteomics can elucidate. *FASEB J.* 27, 1291–1303. doi: 10.1096/fj.12-221127
- Liu, A., Tran, L., Becket, E., Lee, K., Chinn, L., Park, E., et al. (2010). Antibiotic sensitivity profiles determined with an *Escherichia coli* gene knockout collection: generating an antibiotic bar code. *Antimicrob. Agents Chemother.* 54, 1393–1403. doi: 10.1128/AAC.00906-09
- Lobos, S. R., and Mora, G. C. (1991). Alteration in the electrophoretic mobility of OmpC due to variations in the ammonium persulfate concentration in sodium dodecyl sulfate–polyacrylamide gel electrophoresis. *Electrophoresis* 12, 448–450. doi: 10.1002/elps.1150120615
- Maria-Neto, S., Cândido, E., de, S., Rodrigues, D. R., de Sousa, D. A., da Silva, E. M., et al. (2012). Deciphering the magainin resistance process of *Escherichia coli* strains in light of the cytosolic proteome. *Antimicrob. Agents Chemother.* 56, 1714–1724. doi: 10.1128/aac.05558-11
- Morillon, A. (2018). “Non-coding RNA, its history and discovery timeline,” in *Long Non-coding RNA*, ed. M. R. S. Rao, (Amsterdam: Elsevier), 1–24. doi: 10.1016/b978-1-78548-265-6.50001-0
- Murima, P., McKinney, J. D., and Pethe, K. (2014). Targeting bacterial central metabolism for drug development. *Chem. Biol.* 21, 1423–1432. doi: 10.1016/j.chembiol.2014.08.020
- Nikaido, H. (2003). Molecular basis of bacterial outer membrane permeability revisited. *Microbiol. Mol. Biol. Rev.* 67, 593–656. doi: 10.1128/mmbr.67.4.593-656.2003
- Peng, B., Su, Y., Bin, Li, H., Han, Y., Guo, C., et al. (2015). Exogenous alanine and/or glucose plus kanamycin kills antibiotic-resistant bacteria. *Cell Metab.* 21, 249–262. doi: 10.1016/j.cmet.2015.01.008
- Pfaffl, M. W. (2001). A new mathematical model for relative quantification in real-time RT-PCR. *Nucleic Acids Res.* 29, e45.
- Rodas, P. I., Contreras, I., and Mora, G. C. (2010). *Salmonella enterica* serovar Typhi has a 4.1 kb genetic Island inserted within the sapABCDF operon that causes loss of resistance to the antimicrobial peptide protamine. *J. Antimicrob. Chemother.* 65, 1624–1630. doi: 10.1093/jac/dkq197
- Sabbagh, S. C., Lepage, C., McClelland, M., and Daigle, F. (2012). Selection of *salmonella enterica* serovar typhi genes involved during interaction with human macrophages by screening of a transposon mutant library. *PLoS One* 7:e36643. doi: 10.1371/journal.pone.0036643
- Shimizu, K. (2013). Metabolic regulation of a bacterial cell system with Emphasis on *Escherichia coli* metabolism. *ISRN Biochem.* 2013:645983. doi: 10.1155/2013/645983
- Switzer, A., Brown, D. R., and Wigneshweraraj, S. (2018). New insights into the adaptive transcriptional response to nitrogen starvation in *Escherichia coli*. *Biochem. Soc. Trans.* 46, 1721–1728. doi: 10.1042/bst20180502
- Valenzuela, C., Ugalde, J. A., Mora, G. C., Alvarez, S., Contreras, I., and Santiviago, C. A. (2014). Draft genome sequence of *Salmonella enterica* serovar typhi strain STH2370. *Genome Announc.* 2, e104–e114. doi: 10.1128/genomeA.00104-14
- van Heeswijk, W. C., Westerhoff, H. V., and Boogerd, F. C. (2013). Nitrogen assimilation in *Escherichia coli*: putting molecular data into a systems perspective. *Microbiol. Mol. Biol. Rev.* 77, 628–695. doi: 10.1128/mmbr.00025-13
- Vestergaard, M., Nøhr-Meldgaard, K., Bojer, M. S., Krogsgård Nielsen, C., Meyer, R. L., Slavetinsky, C., et al. (2017). Inhibition of the ATP synthase eliminates the intrinsic resistance of staphylococcus aureus towards polymyxins. *MBio* 8:e01114-17. doi: 10.1128/mbio.01114-17
- Villarreal, J. M., Becerra-Lobato, N., Rebollar-Flores, J. E., Medina-Aparicio, L., Carbajal-Gómez, E., Zavala-García, M. L., et al. (2014). The *Salmonella enterica* serovar Typhi ltrR-ompR-ompC-ompF genes are involved in resistance to the bile salt sodium deoxycholate and in bacterial transformation. *Mol. Microbiol.* 92, 1005–1024. doi: 10.1111/mmi.12610
- Zimmer, D. P., Soupene, E., Lee, H. L., Wendisch, V. F., Khodursky, A. B., Peter, B. J., et al. (2000). Nitrogen regulatory protein C-controlled genes of *Escherichia coli*: scavenging as a defense against nitrogen limitation. *Proc. Natl. Acad. Sci. U.S.A.* 97, 14674–14679. doi: 10.1073/pnas.97.26.14674

**Conflict of Interest:** The authors declare that the research was conducted in the absence of any commercial or financial relationships that could be construed as a potential conflict of interest.

Copyright © 2020 Millanao, Mora, Saavedra, Villagra, Mora and Hidalgo. This is an open-access article distributed under the terms of the Creative Commons Attribution License (CC BY). The use, distribution or reproduction in other forums is permitted, provided the original author(s) and the copyright owner(s) are credited and that the original publication in this journal is cited, in accordance with accepted academic practice. No use, distribution or reproduction is permitted which does not comply with these terms.



# Confronting Tigecycline-Resistant *Acinetobacter baumannii* via Immunization Against Conserved Resistance Determinants

## OPEN ACCESS

Ming-Hsien Chiang<sup>1,2†</sup>, Ya-Sung Yang<sup>3†</sup>, Jun-Ren Sun<sup>4</sup>, Yung-Chih Wang<sup>3</sup>, Shu-Chen Kuo<sup>5</sup>, Yi-Tzu Lee<sup>6,7</sup>, Yi-Ping Chuang<sup>8</sup> and Te-Li Chen<sup>2,9\*</sup>

### Edited by:

Rustam Aminov,  
University of Aberdeen,  
United Kingdom

### Reviewed by:

Maria Bagattini,  
University of Naples Federico II, Italy  
Hua Zhou,  
Zhejiang University, China  
Weiwei Huang,  
Chinese Academy of Medical  
Sciences and Peking Union Medical  
College, China

### \*Correspondence:

Te-Li Chen  
tecklayyy@gmail.com

†These authors have contributed  
equally to this work

### Specialty section:

This article was submitted to  
Antimicrobials, Resistance  
and Chemotherapy,  
a section of the journal  
Frontiers in Microbiology

**Received:** 20 August 2019

**Accepted:** 12 March 2020

**Published:** 31 March 2020

### Citation:

Chiang M-H, Yang Y-S, Sun J-R,  
Wang Y-C, Kuo S-C, Lee Y-T,  
Chuang Y-P and Chen T-L (2020)  
Confronting Tigecycline-Resistant  
*Acinetobacter baumannii* via  
Immunization Against Conserved  
Resistance Determinants.  
*Front. Microbiol.* 11:536.  
doi: 10.3389/fmicb.2020.00536

<sup>1</sup> Department and Graduate Institute of Biology and Anatomy, National Defense Medical Center, Taipei, Taiwan, <sup>2</sup> Graduate Institute of Life Sciences, National Defense Medical Center, Taipei, Taiwan, <sup>3</sup> Division of Infectious Diseases and Tropical Medicine, Department of Internal Medicine, Tri-Service General Hospital, National Defense Medical Center, Taipei, Taiwan, <sup>4</sup> Institute of Preventive Medicine, National Defense Medical Center, Taipei, Taiwan, <sup>5</sup> National Institute of Infectious Diseases and Vaccinology, National Health Research Institutes, Zhunan, Taiwan, <sup>6</sup> School of Medicine, National Yang-Ming University, Taipei, Taiwan, <sup>7</sup> Department of Emergency Medicine, Taipei Veterans General Hospital, Taipei, Taiwan, <sup>8</sup> Department and Graduate Institute of Microbiology and Immunology, National Defense Medical Center, Taipei, Taiwan, <sup>9</sup> Institute of Clinical Medicine, National Yang-Ming University, Taipei, Taiwan

Antimicrobial-resistant (AMR) bacterial infections, including those caused by *Acinetobacter baumannii*, have emerged as a clinical crisis worldwide. Immunization with AMR determinants has been suggested as a novel approach to combat AMR bacteria, but has not been validated. The present study targeted tigecycline (TGC) resistance determinants in *A. baumannii* to test the feasibility of this approach. Using bioinformatic tools, four candidates, AdeA, Adel, AdeK, and TolC, belonging to the resistance-nodulation-division (RND) efflux pump were identified as highly conserved and exposed antigens from 15 *A. baumannii* genomes. Antisera generated from recombinant proteins showed the capability to reserve Hoechst 33342, a substrate of the efflux pump, in bacterial cells. The rTolC antisera had the highest complement-dependent killing and opsonophagocytosis effect compared to the sera from phosphate-buffered saline immunized mice. Among the antisera, anti-rAdeK-specific antisera decreased the minimal inhibitory concentration of TGC in 26.7% of the tested isolates. Immunization with rAdeK significantly potentiated TGC efficacy in treating TGC-resistant *A. baumannii* pneumonia in the murine model. The bacterial load ( $7.5 \times 10^5$  vs.  $3.8 \times 10^7$ ,  $p < 0.01$ ) and neutrophil infiltration in the peri-bronchial vasculature region of immunized mice was significantly lower compared to the PBS-immunized mice when TGC was administered concomitantly. Collectively, these results suggest that active immunization against resistance determinants might be a feasible approach to combat multidrug-resistant pathogens in high risk population.

**Keywords:** immunization, resistant determinant, *Acinetobacter*, tigecycline, efflux pump

## INTRODUCTION

Antimicrobial-resistant (AMR) bacterial infections have emerged as a serious problem in clinical settings worldwide. By 2050, 10 million people may die annually from AMR infections (Jansen et al., 2018). Unfortunately, the launch of new antibiotics is rapidly compromised by the emergence of resistance (Aleksun and Levy, 2007). Therefore, the development of new strategies to combat AMR bacteria is urgently needed.

Recently, vaccine development has been increasingly advocated as a new solution to AMR bacteria (McConnell et al., 2011; Huang et al., 2014; Jansen et al., 2018), especially for those with high risk of acquired infection (Gagneux-Brunon et al., 2018). Vaccine candidates often target capsule polysaccharides and virulent factors that are responsible for disease pathogenesis (Rappuoli et al., 2019). Unfortunately, AMR bacteria-targeting vaccines have not been very successful until now due to the heterogeneity in the expression levels of vaccine antigens in different circulating strains of the target pathogen (Garcia-Quintanilla et al., 2016; Rappuoli et al., 2019). Moreover, the immunity induced by single or multiple antigens, which is usually obtained both *in vitro* or *in vivo*, might be ineffective in protecting the host because the pathobiology in human infection is more complicated and remains obscure (Perez and Bonomo, 2014).

Antibiotic resistance determinants could be considered as potential vaccine candidates (Ni et al., 2017). Although there are variations in these resistance determinants in clinical isolates, this vaccination strategy might still be effective in eradicating resistant strains by means of replacing these strains which have reduced fitness with susceptible strains when vaccination coverage is high (Joice and Lipsitch, 2013; Niewiadomska et al., 2019). This approach has an advantage when the resistance determinants are consistently present *in vitro* and *in vivo* and also possess less selection pressure on bacteria (Niewiadomska et al., 2019). However, this approach has not been validated yet.

The present study tested this idea in *Acinetobacter baumannii*. *A. baumannii* is considered one of the most problematic bacteria by the Infectious Disease Society of America (IDSA) (Boucher et al., 2009) because of the rapid evolution of multidrug and pan-drug resistant strains. Currently, only few strains of this bacteria are still susceptible to last-line antibiotics such as, carbapenem and tigecycline (TGC) (Sun et al., 2013; Ni et al., 2016). In order to maximize the coverage of immunization, the antibiotic resistance determinants used for the vaccine candidate should be the major resistance mechanism of the antibiotic of interest in particular bacterial species. These determinants should be universal in different strains, conserved in sequence homology, and accessible by the immune system. In this aspect, carbapenem resistance determinants are not suitable vaccine candidates, as its major resistance mechanism is production of different classes of carbapenemases (Nordmann and Poirel, 2019), which are very diverse in their protein sequences and structures. On the contrary, the major mechanism for TGC resistance is overexpression of efflux pumps (Sugawara and Nikaido, 2014). These are universal and are conserved in *A. baumannii* strains (Ardehali et al., 2019), and therefore, might

be good vaccine candidates to test this immunization approach. The present study utilized bioinformatics tools to identify conserved and surface-exposed antigens of the chromosomal-encoded resistome of *A. baumannii*. Several protein components of the resistance-nodulation-division (RND) efflux system were identified, which have been associated with TGC resistance in *A. baumannii*. We propose an immunization approach using TGC resistance determinants in a murine pneumonia model to combat multidrug-resistant *A. baumannii*.

## MATERIALS AND METHODS

### Bioinformatic Tools

Microbial Genome Database (MBGD) was used for comparative analysis of completely sequenced microbial genomes to identify core genes that are universal from 15 *A. baumannii* genomes (Supplementary Table S1; Uchiyama et al., 2014). PSORTb 3.0.2 (Yu et al., 2010), CELLO2GO (Yu et al., 2014), or SOSUI-GramN (Imai et al., 2008) were applied to predict the conserved residues and sub-cellular localization of these proteins. Comprehensive Antibiotic Resistance Database (CARD) was used to predict the resistome from raw genome sequence using Resistance Gene Identifier (RGI) software (Jia et al., 2017).

### Bacterial Strain Preparation

*A. baumannii* ATCC17978 reference strain was purchased from the American Type Culture Collection (ATCC). TGC-resistant clinical *A. baumannii* isolates were obtained from Tri-Service General Hospital in Taiwan (Sun et al., 2014). All isolates were identified using conventional biochemical and genomic methods as previously described (Sun et al., 2014).

### Construction and Purification of Antigens

Recombinant AdeA (A1S\_1751), AdeI (A1S\_2735), AdeK (A1S\_2737), and TolC (A1S\_0255) from ATCC17978 were amplified (the primers are listed in Supplementary Table S2) and cloned into a pET-29a expression vector (Vovagen, Darmstadt, Germany) with a 6× polyhistidine tag fused to the C-terminus of the recombinant protein. The resulting plasmids were expressed and purified as described in our previous study (Chiang et al., 2015). Purified proteins were digested with trypsin for subsequent liquid chromatography–mass spectrometry/mass spectrometry (LC-MS/MS) analysis and protein identification was conducted by Mission Biotech Co., Ltd., Taiwan. Sequence similarity comparison of *adeA*, *adeI*, *adeK*, and *tolC* from ATCC17978 and all isolates were analyzed using MEGA7 (Kumar et al., 2016).

### Mouse Immunogenicity Assessment and Pneumonia Models

All animal studies were approved by the National Defense Medical Center Institutional Animal Care and Use Committee (NDMC IACUC-17-206). Female C57BL/6 mice (6 weeks old) were bred in a barrier facility under specific pathogen-free conditions. C57BL/6 mice ( $n = 10$ /group) were subcutaneously



(sc.) immunized with 10  $\mu$ g of individual recombinant antigens formulated with Complete Freund's Adjuvant/Incomplete Freund's Adjuvant (CFA/IFA) (Invivogen, Hong Kong), on days 0, 14, and 28. Blood samples were collected before the last immunization and tested against each immunogen. Immunoglobulin G (IgG) antibody titers were determined using antigen-specific enzyme-linked immunosorbent assays (ELISAs).

For conducting efficacy studies, immunized mice were challenged intra-tracheally (IT) on day 42 with a lethal dose [ $3 \times 10^7$  colony-forming units (CFUs)] of mid-log phase AB247 strain mixed with 10% porcine mucin (Sigma-Aldrich, MO, United States). The use of porcine mucin is to enhance the infectivity of *A. baumannii* (McConnell et al., 2011). TGC (10 mg/kg/d, q12h., sc.) treatment regimen was adopted from that used in a previous study (Pichardo et al., 2010). After 24 h therapy, the blood, lung, spleen, and kidney were homogenized and plated to evaluate for the CFUs. For histological analysis, the excised lungs were placed in vials containing 4% formaldehyde. The lungs were placed under vacuum overnight, paraffin-embedded, and stained with hematoxylin and eosin (HE). Histological scores were assigned by independent pathologists by evaluating 3–5 fields, according to the following criteria (Noto et al., 2017): 0, no pathology; 1, minimal infiltrates of neutrophils in alveolar spaces; 2, low numbers of neutrophils in alveoli; 3, moderate numbers of neutrophils and hemorrhage in alveoli with occasional lobar involvement and focal necrosis of alveolar-wall neutrophils in bronchioles; 4, marked numbers of neutrophils, consolidation, and widespread alveolar necrosis.

## Flow Cytometry

ATCC17978 and clinical isolates from late-log-phase growth ( $OD_{600} \approx 1.8$ ) in Luria-Bertani (LB) cultures were diluted in PBS containing 0.5% (w/v) bovine serum albumin (BSA) as a blocking buffer to an  $OD_{600}$  of 0.03. Each specific antiserum was added at a 1:100 dilution with the bacterium. Unbound antibody was removed by washing twice, then fixed by incubating with 4% formaldehyde/PBS for 10 min on ice. A secondary antibody, goat anti-mouse IgG-PE (Invitrogen Corp., Carlsbad, CA, United States) at 0.1 mL per well, was added at a 1:100 dilution and incubated for 30 min. The bacteria were analyzed using a FACSCalibur flow cytometer (BD, Franklin Lakes, NJ, United States). Wash buffer, secondary antibody, or PBS Immunize serum were used as negative controls.

## Hoechst 33342 (H33342) Accumulation Assay

H33342 accumulation assays were carried out as described by Richmond et al. (2013). Strains were grown to an  $OD_{600}$  of 0.4 and resuspended in PBS at room temperature, and the suspension was adjusted to an  $OD_{600}$  of 0.1. Centrifugation steps were carried out at 2500 g. The wells of a black microtiter plate (Corning, Amsterdam, Netherlands) were inoculated with 176  $\mu$ L of bacterial suspension and 20  $\mu$ L of 10  $\mu$ g/mL H33342. After 5 min equilibration, 4  $\mu$ L of the efflux pump inhibitor, phenylalanine-arginine- $\beta$ -naphthylamide (PA $\beta$ N), or specific antisera were added. The fluorescence intensity was recorded every 1 min for

60 min on a SPECTRAmax5 fluorometer (Molecular Devices, Sunnyvale, CA, United States) at excitation and emission wavelengths of 355 and 460 nm, respectively.

## Complement and Opsonophagocytosis Bactericidal Assays

ATCC17978 was freshly grown to a final bacterial cell concentration of  $10^6$  CFU/mL, and aliquoted into 96 well microtiter plates (10  $\mu$ L,  $10^4$  cells/well). For complementary studies, 10  $\mu$ L heat-inactivated or immune sera were mixed with 80  $\mu$ L of undiluted human complement and added to the wells for 1 h at 37°C. The samples were plated for bacterial enumeration. Bacteriolysis activity was defined as  $[1 - (\text{CFU immune sera at 60 min}/\text{CFU of PBS-immunized antisera at 60 min})] \times 100$ .

For the opsonophagocytic kill assay, RAW 264.7 macrophages were cultured in RPMI 1640 (Irvine Scientific, Santa Ana, CA, United States) with 10% fetal bovine serum (FBS), 1% penicillin/streptomycin, and glutamine (Gemini BioProducts), and 50  $\mu$ M  $\beta$ -mercaptoethanol (Sigma-Aldrich, St. Louis, MO, United States). RAW 264.7 cells were stimulated with 100 nM PMA (Sigma-Aldrich) for 3 days. RAW 264.7 macrophages ( $2 \times 10^5$ /well) and ATCC17978 ( $1 \times 10^4$ CFU/well) were added into the wells along with the heat-inactivated or immune sera (5%). After a 1 h incubation with gentle shaking, the samples were serially diluted and plated. Serum killing rates were counted by comparing the number of reduced CFUs with those observed using PBS-immunized antisera.

## RNA Isolation and Quantitative Reverse Transcriptase – PCR

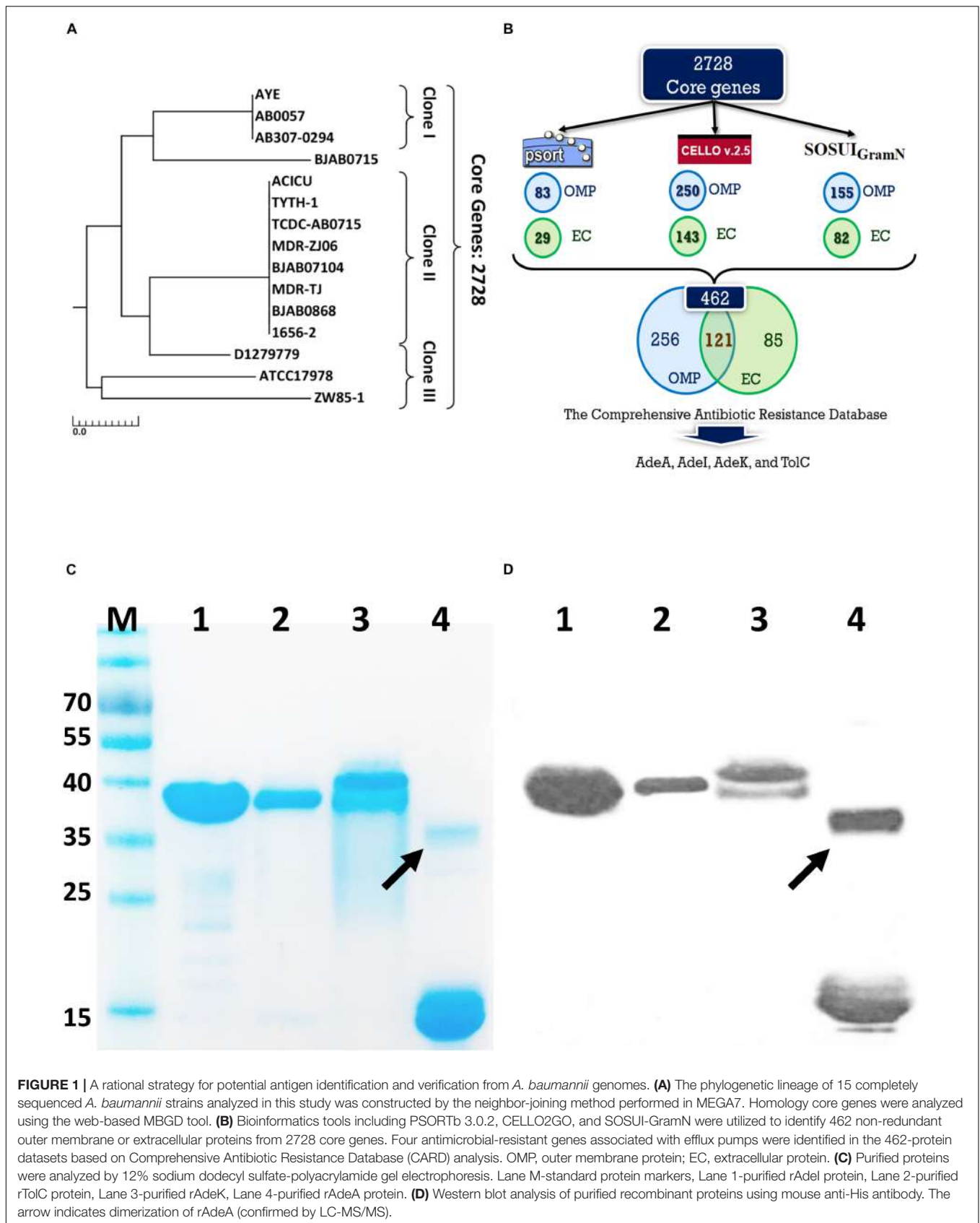
The expression level of *adeA*, *adeI*, *adeK*, and *tolC* were measured by quantitative real-time polymerase chain reaction (PCR) assays as described previously (Rosenfeld et al., 2012). The mRNA expression of *rpoB* from ATCC17978 was used for normalization with specific primers (Supplementary Table S2). The relative gene expression was expressed as fold-change calculated by the  $\Delta\Delta C_t$  method. Gene expression levels  $\geq 2$ -fold compared to that for the reference strain, ATCC17978, were considered significant overexpression. Each experiment was performed in duplicates and at least twice independently.

## Minimal Inhibitory Concentration (MIC) Determination by Broth Microdilution Method

The MICs of TGC were determined by broth microdilution methods in Mueller Hilton broth and interpreted according to the Clinical and Laboratory Standards Institute guidelines (CLSI, 2017). Since MIC breakpoints are not established for TGC in *Acinetobacter* spp., we used the Food and Drug Administration breakpoints set for *Enterobacteriaceae* (Pillar et al., 2008). Each experiment was performed in triplicate.

## Statistical Analysis

Statistical analyses were performed using GraphPad Prism 7 software. All graphical values were represented as means  $\pm$  standard error of the mean (SEM). Tests of statistical



significance were performed using one-way analysis of variance and Kruskal–Wallis tests with *post hoc* analysis. Differences were considered significant for  $p < 0.05$ .

## RESULTS

### *In silico* Screening of Conserved Outer Membrane Efflux Pump Proteins and Generation of Recombinant Proteins

Fifteen *A. baumannii* genomes included 12 multidrug resistant strains were used for analysis. The antibiotic susceptibility profiles of these isolates are listed in **Supplementary Table S1**. These strains were grouped by multilocus sequence typing (MLST) (Laure et al., 2010) and three strains belonged to international clone I (IC I), eight to IC II, three to IC III, and the last strain was unclassified, indicating a wide coverage of *A. baumannii* strains (**Figure 1A**). A total of 2728 core genes were identified; among them, 462 non-redundant proteins were predicted to be outer membrane or extracellular proteins. CARD predicted that among the 462 conserved and surface-exposed proteins, four were associated with antibiotic resistance, including AdeA (A1S\_1751), AdeI (A1S\_2735), AdeK (A1S\_2737), and TolC (A1S\_0255) and were selected as vaccine candidates (**Figure 1B**). All the proteins belonged to the chromosomally encoded RND efflux pump family and had been associated with resistance to multiple antibiotics, including TGC (Sun et al., 2013). The four recombinant proteins were expressed and purified (**Figure 1C**). The proteins were identified and confirmed by immunoblotting (**Figure 1D**) and LC-MS/MS analysis (**Table 1**).

### Polyclonal Antibody Production and Functional Analysis

We then produced antigen-specific polyclonal antibodies from C57BL/6 mice using immunization (**Figure 2A**). All recombinant antigens (rTolC, rAdeK, rAdeI, rAdeA) formulated with CFA/IFA induced strong antigen-specific IgG antibody responses (IgG titers  $> 10^5$ , **Figure 2B**) on day 42 after immunization. The results indicated that all four antigens are highly immunogenic. Antigen-specific antisera were used to verify the location of these proteins in the outer surface of bacteria by flow cytometry (**Figure 2C**). Data confirmed that all the antisera could bind on the surface of ATCC17978, with significantly higher intensities than that for the PBS control antisera (**Figure 2D**). *In vitro* complement-dependent and opsonophagocytosis bactericidal

assays were used to assess the potential bacteria-killing activity of each antiserum. The results showed that 2–79% of ATCC17978 were inhibited by these antisera (**Figures 2E,F**). Among them, rTolC-specific antisera had the highest killing efficacy compared to the sera from PBS-immunized mice.

The accumulation of bis-benzamide H33342 dye provides a reliable method to evaluate the effect of agents that can block efflux pumps (Richmond et al., 2013). The fold-change of fluorescence intensity dramatically increased after adding PAβN and specific antisera, except for the PBS antisera control (**Figure 3A**,  $p < 0.001$ ). Notably, fluorescence intensities were slightly decreased after 40 min of antisera treatment.

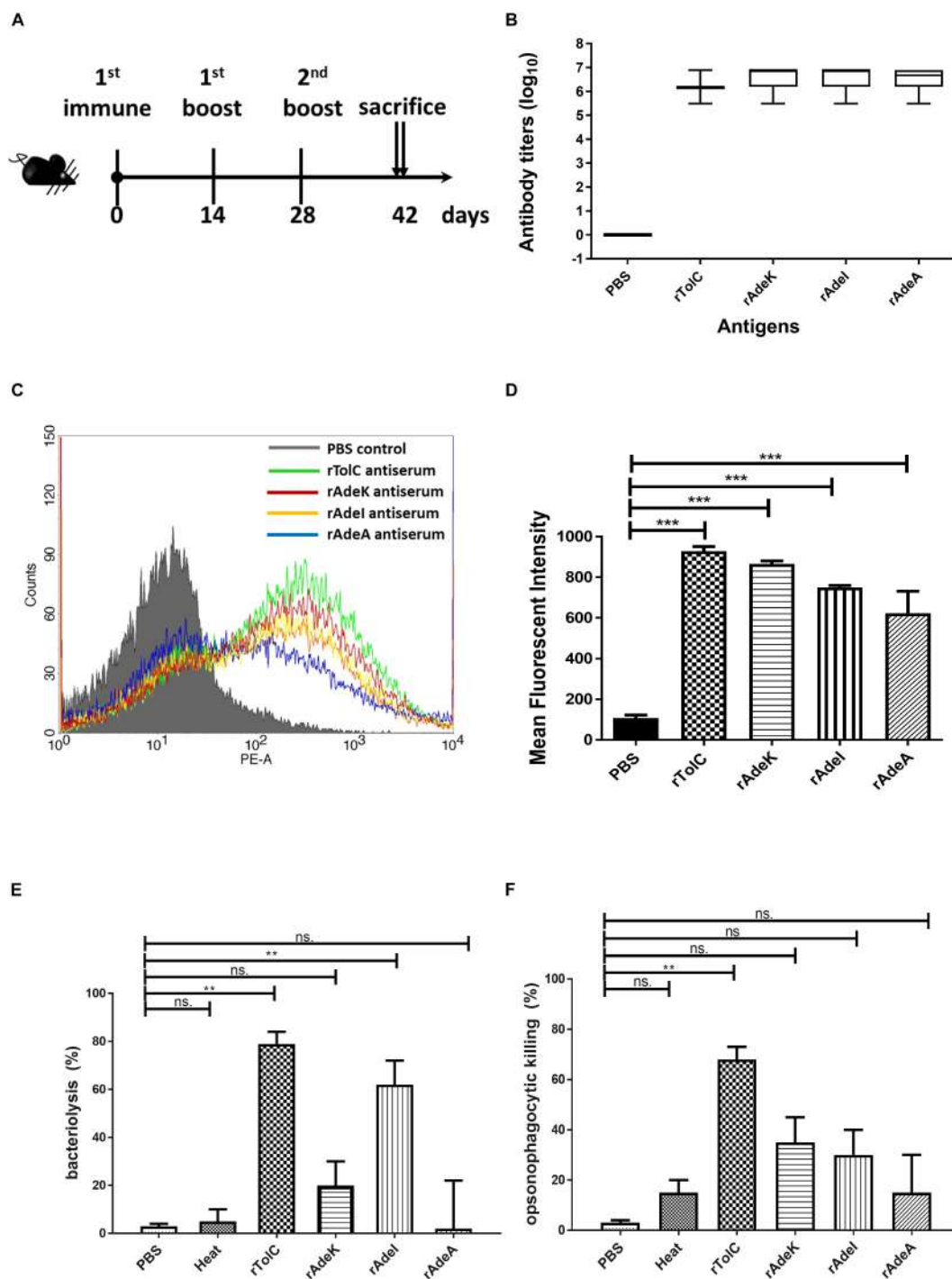
To examine the synergistic effect of antisera in the MICs range for TGCs in *A. baumannii*, 15 clinical TGC-R *A. baumannii* isolates were tested (**Table 2**). The TGC MICs of all isolates were  $> 4$  mg/L. The sequence similarities of *adeA*, *adeI*, *adeK*, and *tolC* were determined (**Table 3**) and the similarities were very high among the isolates (98.2–100%), compared to the ATCC17978 sequence. The quantitative expression levels of *adeA*, *adeI*, *adeK*, and *tolC* were also determined. In general, all strains showed more than one pump overexpression phenotype. TGC MICs were significantly reduced after a combination with rAdeK antisera was used (**Figure 3B**), and five of the tested isolates (AB099, AB247, AB294, AB304, AB347) revealed more than fourfold reduction in TGC MICs (**Table 2**), and all five strains had *adeA* overexpression, and similarities in *adeA* sequences was 100% in 4 of the isolates. The similarity in *adeA* sequence of AB099 was 99.8%, with only a single amino-acid substitution (N295T). However, no significant differences were found among the responses of strains to anti-rAdeK antisera regarding their sequence homology (**Table 3**), gene expression level (**Table 2**) and binding ability of antisera to bacterial cells (**Figure 3C**). Furthermore, we examined the synergistic effect of anti-AdeK serum and four antibiotics including amikacin, meropenem, colistin and ampicillin/sulbactam, remained active against different portions of *A. baumannii* isolates. We found that only two isolates demonstrated a twofold reduction in the ampicillin-sulbactam MIC value from 64/32 to 32/16 μg/mL in the presence of anti-AdeK (**Supplementary Table S3**).

### TGC Activity Potentiation by rAdeK Immunization in a Mouse Pneumonia Model

According to the *in vitro* data, rAdeK antisera showed the highest capability to potentiate the effect of TGC against TGC-R *A. baumannii*, and also had an addition role to in

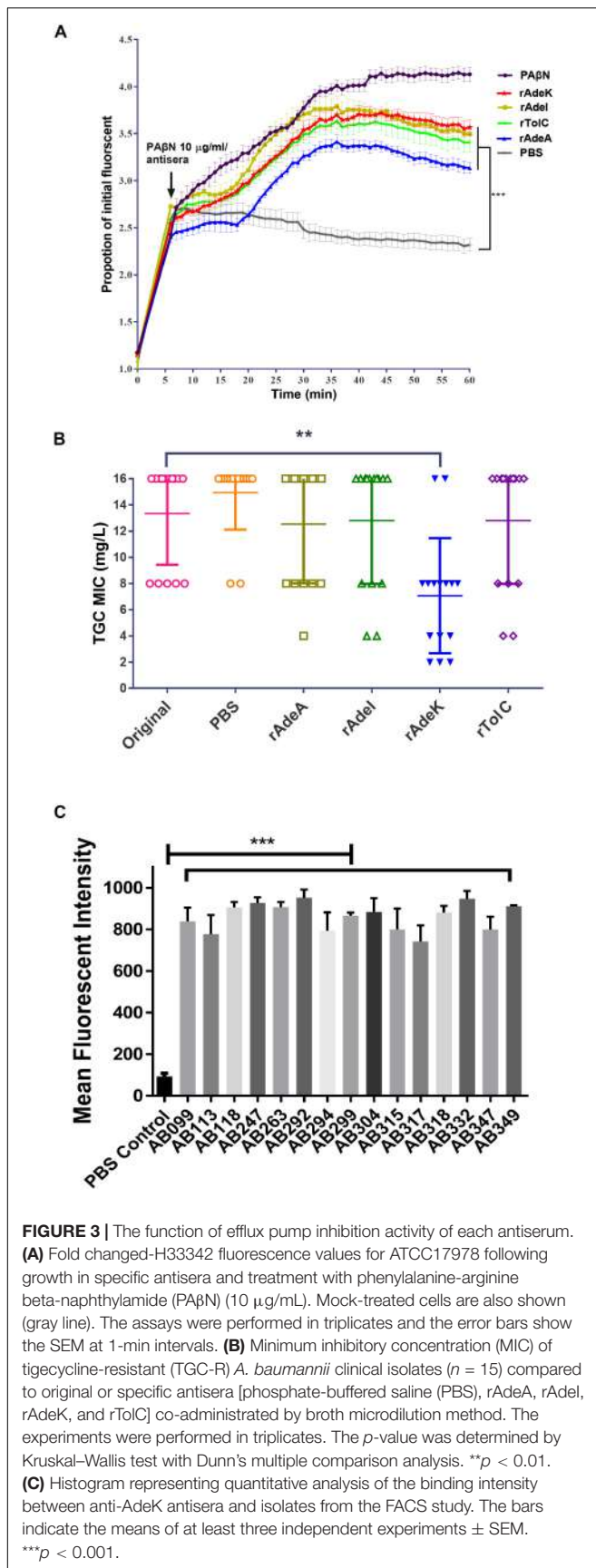
**TABLE 1** | Confirmation of the purified recombinant proteins by liquid chromatography–mass spectrometry/mass spectrometry (LC-MS/MS).

Sample name	Protein name	Accession number	pI	MW (KDa)	Sequence coverage
AdeA	Multidrug RND transporter [ <i>A. baumannii</i> ]	gi  500174963	5.46	15.714	76%
AdeI	Multidrug RND transporter [ <i>A. baumannii</i> ]	gi  500185983	9.04	39.778	83%
AdeK	adeC/adeK/oprM family multidrug efflux complex outer membrane factor [ <i>A. baumannii</i> ]	gi  691007736	9.12	52.770	83%
TolC	RND transporter [ <i>A. baumannii</i> ]	gi  500183799	9.21	44.273	78%



**FIGURE 2 |** Polyclonal mouse antisera production and characterization. **(A)** Groups of C57BL/6 mice ( $n = 10$ ) were subcutaneously immunized with either 10  $\mu$ g of individual antigen (rAdel, rToIC, rAdeK, and rAdeA) or phosphate-buffered saline (PBS) formulated with Complete Freund's Adjuvant/Incomplete Freund's Adjuvant (CFA/IFA) on days 0, 14, and 28. Blood samples were collected before sacrifice and tested against each antigen. **(B)** Serum IgG antibody titers against each antigen as indicated by enzyme-linked immunosorbent assay. **(C)** Flow cytometry (FACS) analysis demonstrating the surface accessibility of the antigen-specific antisera. Cells from late-log-phase cultures were probed with a control non-specific antibody (shaded histograms) or individual antisera (unshaded histograms). Each histogram shows the fluorescence intensity distribution of  $>20,000$  flow cytometry events. **(D)** Histogram representing quantitative analysis of the binding intensity from FACS studies. Bars indicate the means of at least three independent experiments  $\pm$  SEM. **(E)** Bacteria inhibition by each antigen-specific mouse antisera at 1:10 dilution, used in the presence of human complement and ATCC17978. **(F)** The complement-dependent opsonophagocytosis assays were performed with mouse antisera (1:10), ATCC17978 and RAW 264.7 macrophages. The results represent the percentage of bacterial survival in the assay after 1 h of incubation at 37°C compared to that in phosphate-buffered saline (PBS)-immunized antisera. Bars indicate the means of at least three independent experiments  $\pm$  SEM. ns., non-significance.  $**p < 0.01$ , Heat, complement replaced with a heat-inactivated complement.





antibody mediated killing, so rAdeK was selected as a vaccine candidate. The protocol for murine pneumonia model is shown in **Figure 4A**. An intratracheal challenge with a clinical isolate of AB247 was performed. AB247 was selected because of its high TGC-resistant phenotype (MIC 16 mg/L) and its significant response in broth microdilution evaluation. The results showed that TGC administration in rAdeK-immunized mice significantly reduced the bacterial load in the lungs compared to that in mice without immunization (**Figure 4B**,  $p < 0.001$ ). The bacterial load was also reduced in the kidney, spleen, and blood, but without statistical significance (**Figures 4C–E**). The histopathology of lung tissues showed that neutrophil infiltration in the peribronchial vasculature region was lower in rAdeK-immunization and TGC-treated mice (**Figure 5**) compared to that in other groups. More importantly, there was no evidence of morbidity or mortality among mice during the immunization course, which suggested that rAdeK is safe and suitable for immunization.

## DISCUSSION

AMR bacterial infection have been increasing dramatically in recent decades and account for about 80% of all severe bacterial infections (Du et al., 2018). Resistant phenotypes can arise from overexpression of intrinsic efflux activity to effectively respond to antibiotic or toxin related challenges (Du et al., 2018). Inhibition of antimicrobial determinants, such as efflux pump inhibitors (EPIs) is a feasible approach to preserve and improve the clinical performance of antituberculosis agents and overcome crucial drug-resistance challenges (Song and Wu, 2016). The use of EPIs could facilitate the revival of antibiotics and could be suitable for clinical applications. Unfortunately, no EPIs are yet available for clinical use (Abdali et al., 2017). We developed an alternative vaccine strategy targeting an antibiotic efflux pump. We tested this idea in TGC-resistant *A. baumannii*. We found that immunization with the RND efflux pump outer membrane protein, AdeK, interfered with the efflux activity of bacteria and, also induced antibodies with bactericidal effects (**Figure 6**). When co-administrated with TGC therapy, this strategy efficiently attenuated TGC-R *A. baumannii* pneumonia infection. A recent study showed that the combined treatment of anti-outer membrane vesicle serum and antibiotics could increase the intracellular aggregation of antibiotics by affecting porin function (Huang et al., 2019). The strategy significantly improved the antibiotic susceptibility of drug-resistant *A. baumannii* and strengthened the feasibility of combination therapy with vaccine and antibiotics. Accordingly, predominant resistance determinants with high homology, such as *MecA*, that confer resistance to methicillin in *Staphylococcus aureus* might also be good candidates for this approach.

Efflux-mediated TGC resistance has been extensively investigated in *A. baumannii*, especially in RND efflux pumps such as AdeABC, AdeFGH, AdeIJK, and AcrAB-TolC, in which overexpression leads to a TGC-resistant phenotype (Sugawara and Nikaido, 2014). Moreover, mutations in the *adeR* and *adeS* regulatory genes have been detected in TGC-R clinical isolates with efflux pump overexpression (Sun et al., 2014). Therefore,

**TABLE 2** | Minimum inhibitory concentrations (MICs) of clinical isolates and synergistic effects of antigen-specific antisera on tigecycline (TGC) MICs<sup>a</sup>.

Strains	Original	rAdeA		rAdeI		rAdeK		rToIC	
	TGC MIC	OE <sup>b</sup>	MIC	OE	MIC	OE	MIC	OE	MIC
AB099	8	+	8	+	4	+	<b>2</b>	+	4
AB113	16	+	16	+	16	+	8	+	16
AB118	8	+	8	+	16	-	4	-	8
AB247	16	+	16	+	<b>4</b>	+	<b>2</b>	-	8
AB263	16	+	16	+	16	+	8	-	16
AB292	8	+	16	+	16	-	16	+	16
AB294	8	+	4	+	4	+	<b>2</b>	-	8
AB299	8	+	16	+	8	+	8	-	16
AB304	16	+	8	-	8	+	<b>4</b>	+	16
AB315	16	+	8	+	16	-	8	+	16
AB317	16	+	16	+	16	+	8	+	16
AB318	16	+	16	+	16	+	16	-	16
AB332	16	+	8	+	16	-	8	+	16
AB347	16	+	16	+	16	+	<b>4</b>	+	<b>4</b>
AB349	16	+	16	+	16	-	8	-	16

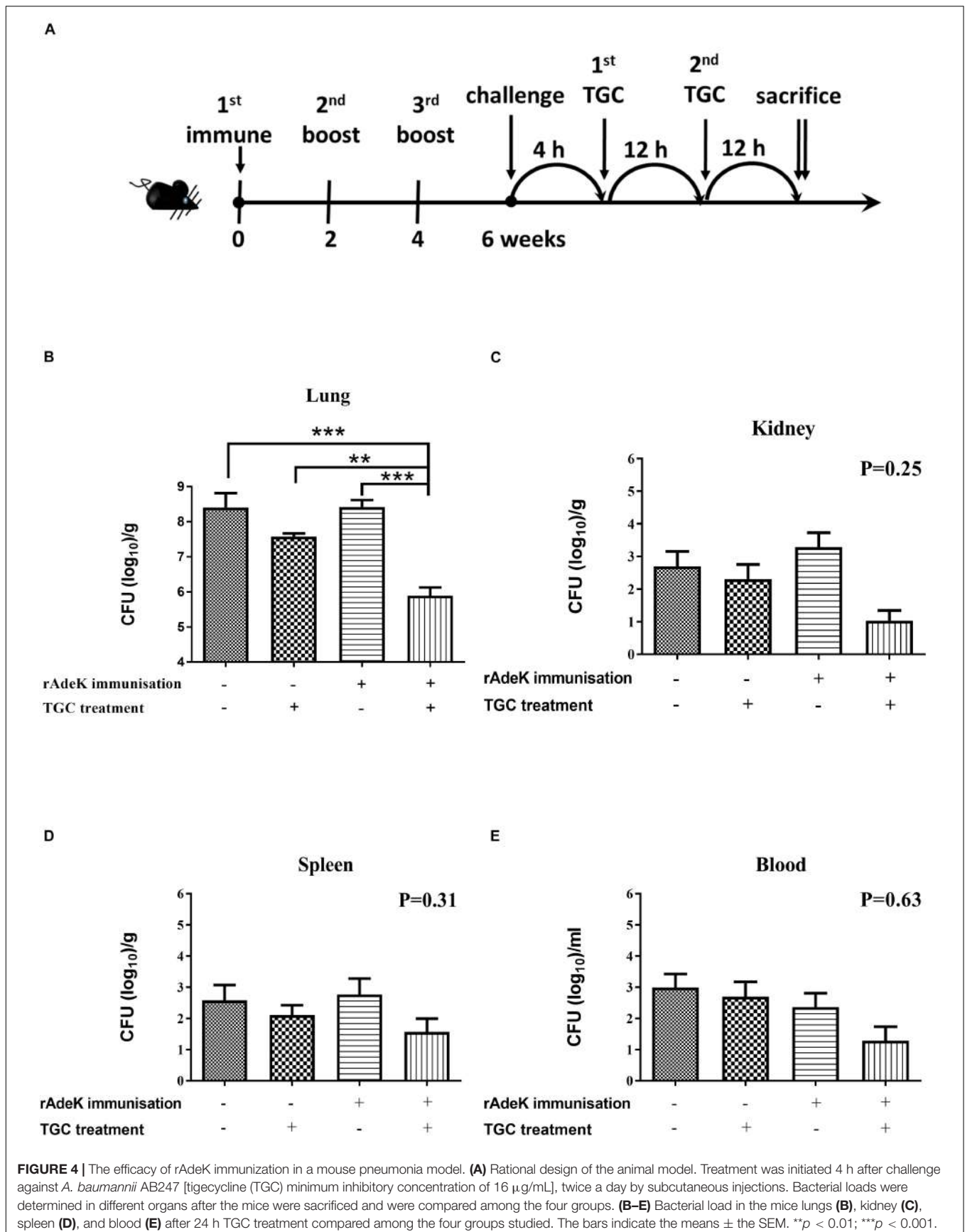
<sup>a</sup>Bold font indicates a fourfold reduction in MIC value. Experiments were performed in triplicate and repeated three times, with similar results. <sup>b</sup>OE: overexpression, gene expression level  $\geq$  twofold compared to that of the ATCC17978 reference strain was considered significant overexpression; +, Yes; -, No.

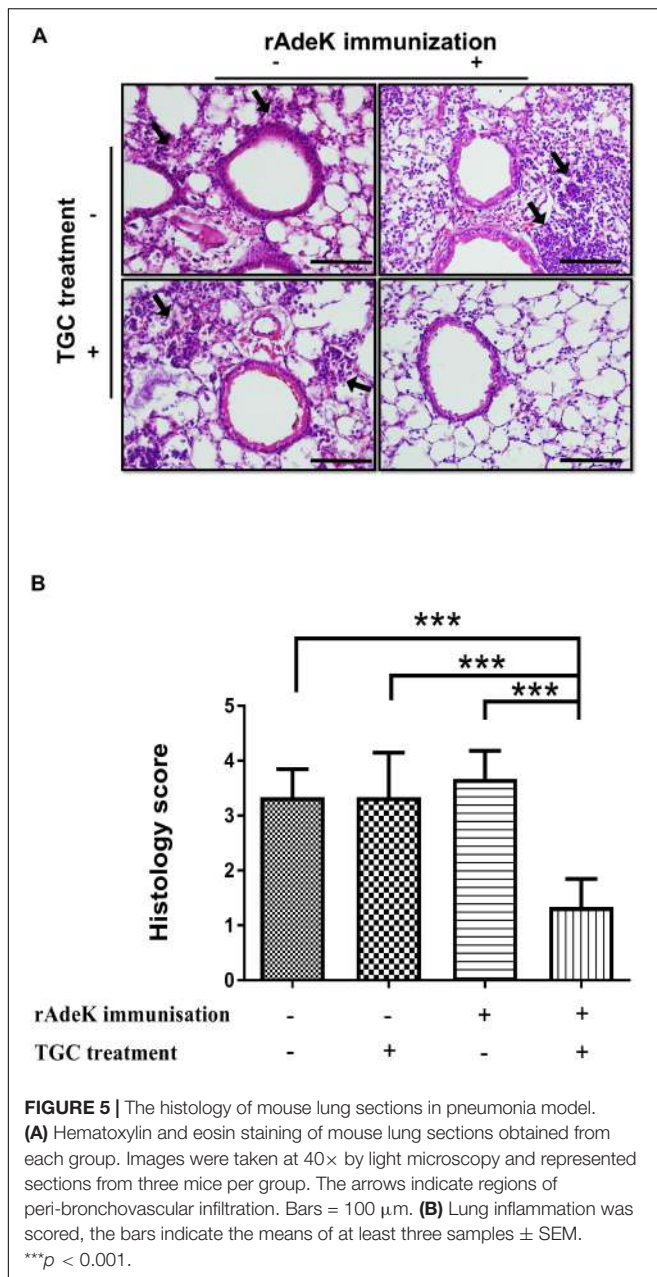
**TABLE 3** | Comparisons of efflux pump protein sequence similarities to *A. baumannii* ATCC 17978.

Strain ID	<i>adeA</i>	<i>adel</i>	<i>adeK</i>	<i>toIC</i>
AB099	100%	100%	99.80% (N295T)	99.60% (Q85H, K180T)
AB113	99.30% (T138A)	100%	99.80% (G212L)	100%
AB118	99.30% (T138A)	100%	100%	100%
AB247	99.30% (T138A)	100%	100%	100%
AB263	99.30% (T138A)	100%	99.80% (G212C)	100%
AB292	99.30% (T138A)	100%	100%	100%
AB294	99.30% (T138A)	100%	100%	99.60% (E219V, Y220F)
AB299	99.30% (T138A)	100%	100%	100%
AB304	99.30% (T138A)	100%	100%	100%
AB315	99.30% (T138A)	100%	99.80% (L296S)	100%
AB317	99.30% (T138A)	100%	99.80% (Q193H)	99.10% (T293I, R325G, T326S, S327Y)
AB318	99.30% (T138A)	100%	100%	100%
AB332	99.30% (T138A)	100%	100%	100%
AB347	99.30% (T138A)	100%	100%	98.20% (Q163R, N193C, Q195H, Y196D, A201T, A205E, N207D, A213T)
AB349	99.30% (T138A)	100%	100%	100%

inhibition of efflux activity is a promising approach to restore TGC susceptibility. RND efflux systems usually comprise three different components assembling into a functional complex, including outer membrane protein, middle periplasmic protein and inner membrane protein (Du et al., 2018). AdeA and AdeI belonged to the inner membrane protein of the system, whereas AdeK and TolC belonged to the outer membrane protein of the system. The results of kinetic accumulation study in the present study showed that all the antisera could potentially attenuate bisbenzimidazole H33342 efflux activity in ATCC strains, indicating

H33342 is the substrate of these efflux systems. Decreased accumulation of H33342 after 40 min of antisera treatment (**Figure 3A**) might indicate the activation of the redundant efflux system to extrude H33342. Compared to other antisera, rAdeK antisera efficiently reduced TGC MIC levels in the clinical isolates; this result might indicate the major contribution of AdeIJK in TGC resistance in *A. baumannii* (Rosenfeld et al., 2012). It is interesting that when targeting the same RND system (AdeIJK), different components of the system could have different effects. For example, antisera against AdeK could





potentiate TGC effects but antisera against *AdeI* could not. This result indicated that the outer membrane component might be a better vaccine candidate than inner membrane protein when combined with antibiotic use. As demonstrated in **Figure 3C**, antisera against rAdeK derived from ATCC17978 could cross-react with all fifteen clinical isolates by flow cytometry assay. The *in vivo* study also demonstrated a good response in AdeK-vaccinated and TGC-treated mice, as they demonstrated less lung inflammation and reduced bacterial load in the lung. The bacteria load in other tissues was also lower in the AdeK-vaccinated and TGC-treated mice, but the difference was not significant. This might be due to the lower bacterial load (about  $10^3$  CFU/g) in the no treatment or single treatment arms

(rAdeK vaccinated or TGC-treated group), as *A. baumannii* is a bacterium with low virulence.

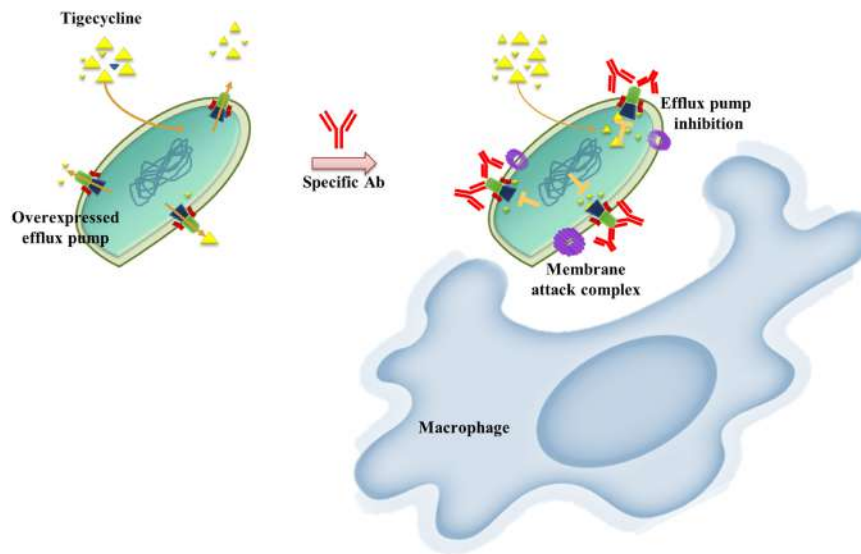
In addition to the potentiation of antibiotic treatment, the antisera had other roles as it could enhance the antibody mediated killing of bacteria. In the *in vivo* study, the effect of AdeK immunization might come from two aspects, one is antagonizing the efflux pump against antibiotic extrusion, another is through antibody mediated killing. It is unknown how the antisera of the efflux pump could reverse the antibiotic resistance. It is reported that antibodies may affect the function of specific antigens via conformation changes (Roguin and Retegui, 2003), or that this effect could be a result of blocking the channel of antibiotic extrusion. Some efflux pumps are associated with bacterial virulence and biofilm formation, which are responsible for host cell adhesion and invasion (Du et al., 2018). For example, TolC is a virulence factor associated with toxin translocation in *E. coli* (Lee et al., 2012). In our study, antisera derived from immunization with rTolC conferred significant complement-dependent bactericidal and opsonophagocytic activity. It is worth to determine whether rTolC could be an ideal vaccine candidate in future studies.

The non-responding strains also had similar *adeK* sequence and overexpression level of the gene. Unknown mechanisms for TGC resistance may have been present in the non-responding strains. Li et al. (2016) identified > 50 possible drug efflux pumps that could contribute to multidrug resistance from over 1000 genomes of *A. baumannii* strains. In addition, the antibody might need to be optimized to more effectively block the most critical epitope of the efflux protein. Future research should focus on physical data in three-dimensional structures of efflux pumps and specific antibodies need to be elucidated to understand the structure-function relationships in these pumps (Roguin and Retegui, 2003). Although only 26.7% of strains had reduced TGC MIC after adding antisera, low coverage of the bacteria population (even 1–4%) by immunization with resistant determinants might still be effective in eradicating the resistant population (Niewiadomska et al., 2019).

We examined the effect of the anti-AdeK antisera on amikacin, meropenem, colistin, and ampicillin/sulbactam (**Supplementary Table S3**). These results showed no significant synergistic effect to reverse the resistance against these antibiotics. These was not unexpected, as the major resistant mechanisms of these antibiotics are not through efflux pump. Instead, the major resistance mechanism for amikacin, meropenem and ampicillin/sulbactam is the production of antibiotic modifying or degrading enzymes (Lee et al., 2017), whereas modification or loss of lipopolysaccharide confers colistin resistance in *A. baumannii*.

It is important to note that efflux pumps are conserved not only in *A. baumannii* but also in different bacterial genera. The AdeK protein has sequence homology to efflux proteins in other nosocomial “bad bugs” listed by the Infectious Diseases Society of America (Boucher et al., 2009; **Supplementary Table S4**), thus having the potential of broader coverage and application in the near future. A recent report also supported that AdeK and other 24 resistant determinants are predicted as vaccine candidates to strengthen antibiotic treatments (Ni et al., 2017).





**FIGURE 6 |** Schematic representation of the proposed mechanism of anti-efflux antibodies-mediated tigecycline efflux inhibition and bactericidal activity. Under overexpressed conditions, activated efflux pumps efficiently remove tigecycline to attenuate antibiotic activity (**left**). These phenomena might be restored by using an anti-rAdeK antibody as an efflux pump inhibitor. Bactericidal effects might also be induced via complement-mediated lytic membrane attack complex pores and opsonophagocytic activity (**right**).

## CONCLUSION

In conclusion, our results demonstrate that active immunization with antibiotic-resistant determinants may be a promising approach to combat multidrug-resistant pathogens in high-risk population.

## DATA AVAILABILITY STATEMENT

The raw data supporting the conclusions of this article will be made available by the authors, without undue reservation, to any qualified researcher.

## ETHICS STATEMENT

The animal study was reviewed and approved by National Defense Medical Center Institutional Animal Care and Use Committee (NDMC IACUC-17-206).

## AUTHOR CONTRIBUTIONS

M-HC, T-LC, and Y-PC contributed to the conception and design of the studies. M-HC, Y-SY, S-CK, and Y-PC contributed to the execution of the animal vaccination studies. M-HC, Y-TL, and J-RS carried out the laboratory *in vitro* assays. M-HC, Y-SY, Y-CW, S-CK, Y-TL, Y-PC, and T-LC were involved in the drafting, revision, and approval of the final version of the manuscript.

## FUNDING

This work was supported by the Ministry of Science and Technology (Grant Nos. MOST 105-2628-B-016-003-MY2, MOST 105-2314-B-016-039-MY3, MOST 107-2314-B-016-051-MY3, MOST 107-2320-B-016-003, MOST 108-2314-B-016-029, and MOST 109-2320-B-016-002-MY2), Tri-Service General Hospital (Grant Nos. TSGH-C107-098 and TSGH-C108-137). The funders had no role in the study design, data collection and analysis, decision to publish, or preparation of the manuscript.

## ACKNOWLEDGMENTS

This study was supported by the ACTION study group. The members of the ACTION study group include Yea-Yuan Chang (National Yang-Ming University Hospital, Yilan, Taiwan), Yuag-Meng Liu (Changhua Christian Hospital, Changhua, Taiwan), S-CK (National Institute of Infectious Diseases and Vaccinology, National Health Research Institute, Miaoli County, Taiwan), Chang-Pan Liu (MacKay Memorial Hospital, Taipei, Taiwan), T-LC (Graduate Institute of Life Sciences, National Defense Medical Center, Taipei, Taiwan), Y-TL (Taipei Veterans General Hospital, Taipei, Taiwan), and Y-SY (National Defense Medical Center, Taipei, Taiwan).

## SUPPLEMENTARY MATERIAL

The Supplementary Material for this article can be found online at: <https://www.frontiersin.org/articles/10.3389/fmicb.2020.00536/full#supplementary-material>

## REFERENCES

- Abdali, N., Parks, J. M., Haynes, K. M., Chaney, J. L., Green, A. T., Wolloscheck, D., et al. (2017). Reviving antibiotics: efflux pump inhibitors that interact with AcrA, a membrane fusion protein of the AcrAB-TolC multidrug efflux pump. *ACS Infect. Dis.* 3, 89–98. doi: 10.1021/acsinfecdis.6b01067
- Alekshun, M. N., and Levy, S. B. (2007). Molecular mechanisms of antibacterial multidrug resistance. *Cell* 128, 1037–1050. doi: 10.1016/j.cell.2007.03.004
- Ardehali, S. H., Azimi, T., Fallah, F., Owrang, M., Aghamohammadi, N., and Azimi, L. (2019). Role of efflux pumps in reduced susceptibility to tigecycline in *Acinetobacter baumannii*. *New Microbes. New Infect.* 30:100547. doi: 10.1016/j.nmni.2019.10.0547
- Boucher, H. W., Talbot, G. H., Bradley, J. S., Edwards, J. E., Gilbert, D., Rice, L. B., et al. (2009). Bad bugs, no drugs: no ESCAPE! an update from the infectious diseases society of America. *Clin. Infect. Dis.* 48, 1–12. doi: 10.1086/595011
- Chiang, M. H., Sung, W. C., Lien, S. P., Chen, Y. Z., Lo, A. F., Huang, J. H., et al. (2015). Identification of novel vaccine candidates against *Acinetobacter baumannii* using reverse vaccinology. *Hum. Vaccin. Immunother.* 11, 1065–1073. doi: 10.1080/21645515.2015.1010910
- CLSI (2017). *M100-S27: Performance Standards for Antimicrobial Susceptibility Testing: 27th Informational Supplement*. Wayne, PA: Clinical and Laboratory Standards Institute.
- Du, D., Wang-Kan, X., Neuberger, A., Van Veen, H. W., Pos, K. M., Piddock, L. J. V., et al. (2018). Multidrug efflux pumps: structure, function and regulation. *Nat. Rev. Microbiol.* 16, 523–539.
- Gagneux-Brunon, A., Lucht, F., Launay, O., Berthelot, P., and Botelho-Nevers, E. (2018). Vaccines for healthcare-associated infections: present, future, and expectations. *Expert Rev. Vaccin.* 17, 421–433. doi: 10.1080/14760584.2018.1470507
- García-Quintanilla, M., Pulido, M. R., Carretero-Ledesma, M., and McConnell, M. J. (2016). Vaccines for antibiotic-resistant bacteria: possibility or pipe dream? *Trends Pharmacol. Sci.* 37, 143–152. doi: 10.1016/j.tips.2015.10.003
- Huang, W., Yao, Y., Long, Q., Yang, X., Sun, W., Liu, C., et al. (2014). Immunization against multidrug-resistant *Acinetobacter baumannii* effectively protects mice in both pneumonia and sepsis models. *PLoS One* 9:e100727. doi: 10.1371/journal.pone.0100727
- Huang, W., Zhang, Q., Li, W., Chen, Y., Shu, C., Li, Q., et al. (2019). Anti-outer membrane vesicle antibodies increase antibiotic sensitivity of pan-drug-resistant *Acinetobacter baumannii*. *Front. Microbiol.* 10:1379. doi: 10.3389/fmicb.2019.01379
- Imai, K., Asakawa, N., Tsuji, T., Akazawa, F., Ino, A., Sonoyama, M., et al. (2008). SOSUI-GRAMN: high performance prediction for sub-cellular localization of proteins in gram-negative bacteria. *Bioinformatics* 2, 417–421. doi: 10.6026/97320630002417
- Jansen, K. U., Knirsch, C., and Anderson, A. S. (2018). The role of vaccines in preventing bacterial antimicrobial resistance. *Nat. Med.* 24, 10–19. doi: 10.1038/nm.4465
- Jia, B., Raphenya, A. R., Alcock, B., Waglechner, N., Guo, P., Tsang, K. K., et al. (2017). CARD 2017: expansion and model-centric curation of the comprehensive antibiotic resistance database. *Nucleic Acids Res.* 45, D566–D573. doi: 10.1093/nar/gkw1004
- Joice, R., and Lipsitch, M. (2013). Targeting imperfect vaccines against drug-resistance determinants: a strategy for countering the rise of drug resistance. *PLoS One* 8:e68940. doi: 10.1371/journal.pone.0068940
- Kumar, S., Stecher, G., and Tamura, K. (2016). MEGA7: molecular evolutionary genetics analysis version 7.0 for bigger datasets. *Mol. Biol. Evol.* 33, 1870–1874. doi: 10.1093/molbev/msw054
- Laure, D., Virginie, P., Alexandr, N., Lenie, D., and Sylvain, B. (2010). The population structure of *Acinetobacter baumannii*: expanding multiresistant clones from an ancestral susceptible genetic pool. *PLoS One* 5:e10034. doi: 10.1371/journal.pone.0010034
- Lee, C. R., Lee, J. H., Park, M., Park, K. S., Bae, I. K., Kim, Y. B., et al. (2017). Biology of *Acinetobacter baumannii*: pathogenesis, antibiotic resistance mechanisms, and prospective treatment options. *Front. Cell Infect. Microbiol.* 7:55. doi: 10.3389/fcimb.2017.00055
- Lee, M., Jun, S. Y., Yoon, B. Y., Song, S., Lee, K., and Ha, N. C. (2012). Membrane fusion proteins of type I secretion system and tripartite efflux pumps share a binding motif for TolC in gram-negative bacteria. *PLoS One* 7:e40460. doi: 10.1371/journal.pone.0040460
- Li, L., Hassan, K. A., Brown, M. H., and Paulsen, I. T. (2016). Rapid multiplexed phenotypic screening identifies drug resistance functions for three novel efflux pumps in *Acinetobacter baumannii*. *J. Antimicrob. Chemother.* 71, 1223–1232. doi: 10.1093/jac/dkv460
- McConnell, M. J., Domínguez-Herrera, J., Smani, Y., López-Rojas, R., Docobo-Pérez, F., and Pachón, J. (2011). Vaccination with outer membrane complexes elicits rapid protective immunity to multidrug-resistant *Acinetobacter baumannii*. *Infect. Immun.* 79, 518–526. doi: 10.1128/IAI.00741-10
- Ni, W., Han, Y., Zhao, J., Wei, C., Cui, J., Wang, R., et al. (2016). Tigecycline treatment experience against multidrug-resistant *Acinetobacter baumannii* infections: a systematic review and meta-analysis. *Int. J. Antimicrob. Agents* 47, 107–116. doi: 10.1016/j.ijantimicag.2015.11.011
- Ni, Z., Chen, Y., Ong, E., and He, Y. (2017). Antibiotic resistance determinant-focused *Acinetobacter baumannii* vaccine designed using reverse vaccinology. *Int. J. Mol. Sci.* 18:458. doi: 10.3390/ijms18020458
- Niewiadomska, A. M., Jayabalasingham, B., Seidman, J. C., Willem, L., Grenfell, B., Spiro, D., et al. (2019). Population-level mathematical modeling of antimicrobial resistance: a systematic review. *BMC Med.* 17:81. doi: 10.1186/s12916-019-1314-9
- Nordmann, P., and Poirel, L. (2019). Epidemiology and diagnostics of carbapenem resistance in gram-negative bacteria. *Clin. Infect. Dis.* 69, S521–S528. doi: 10.1093/cid/ciz824
- Noto, M. J., Becker, K. W., Boyd, K. L., Schmidt, A. M., and Skaar, E. P. (2017). RAGE-mediated suppression of interleukin-10 results in enhanced mortality in a murine model of *Acinetobacter baumannii* sepsis. *Infect. Immun.* 85, e954–e916. doi: 10.1128/IAI.00954-16
- Perez, F., and Bonomo, R. A. (2014). Vaccines for *Acinetobacter baumannii*: thinking “out of the box”. *Vaccine* 32, 2537–2539. doi: 10.1016/j.vaccine.2014.03.031
- Pichardo, C., Pachon-Ibanez, M. E., Docobo-Perez, F., Lopez-Rojas, R., Jimenez-Mejias, M. E., Garcia-Curiel, A., et al. (2010). Efficacy of tigecycline vs. *imipenem* in the treatment of experimental *Acinetobacter baumannii* murine pneumonia. *Eur. J. Clin. Microbiol. Infect. Dis.* 29, 527–531. doi: 10.1007/s10096-010-0890-6
- Pillar, C. M., Draghi, D. C., Dowzicky, M. J., and Sahn, D. F. (2008). In vitro activity of tigecycline against gram-positive and gram-negative pathogens as evaluated by broth microdilution and Etest. *J. Clin. Microbiol.* 46, 2862–2867. doi: 10.1128/JCM.00637-08
- Rappuoli, R., Black, S., and Bloom, D. E. (2019). Vaccines and global health: in search of a sustainable model for vaccine development and delivery. *Sci. Transl. Med.* 11:eaaw2888. doi: 10.1126/scitranslmed.aaw2888
- Richmond, G. E., Chua, K. L., and Piddock, L. J. (2013). Efflux in *Acinetobacter baumannii* can be determined by measuring accumulation of H33342 (bis-benzamide). *J. Antimicrob. Chemother.* 68, 1594–1600. doi: 10.1093/jac/dk1052
- Roguin, L. P., and Retegui, L. A. (2003). Monoclonal antibodies inducing conformational changes on the antigen molecule. *Scand. J. Immunol.* 58, 387–394. doi: 10.1046/j.1365-3083.2003.01320.x
- Rosenfeld, N., Bouchier, C., Courvalin, P., and Perichon, B. (2012). Expression of the resistance-nodulation-cell division pump AdeIJK in *Acinetobacter baumannii* is regulated by AdeN, a TetR-type regulator. *Antimicrob. Agents Chemother.* 56, 2504–2510. doi: 10.1128/AAC.06422-11
- Song, L., and Wu, X. (2016). Development of efflux pump inhibitors in antituberculosis therapy. *Int. J. Antimicrob. Agents* 47, 421–429. doi: 10.1016/j.ijantimicag.2016.04.007
- Sugawara, E., and Nikaido, H. (2014). Properties of AdeABC and AdeIJK efflux systems of *Acinetobacter baumannii* compared with those of the AcrAB-TolC

- system of *Escherichia coli*. *Antimicrob. Agents Chemother.* 58, 7250–7257. doi: 10.1128/AAC.03728-14
- Sun, J. R., Perng, C. L., Lin, J. C., Yang, Y. S., Chan, M. C., Chang, T. Y., et al. (2014). AdeRS combination codes differentiate the response to efflux pump inhibitors in tigecycline-resistant isolates of extensively drug-resistant *Acinetobacter baumannii*. *Eur. J. Clin. Microbiol. Infect. Dis.* 33, 2141–2147. doi: 10.1007/s10096-014-2179-7
- Sun, Y., Cai, Y., Liu, X., Bai, N., Liang, B., and Wang, R. (2013). The emergence of clinical resistance to tigecycline. *Int. J. Antimicrob. Agents* 41, 110–116. doi: 10.1016/j.ijantimicag.2012.09.005
- Uchiyama, I., Mihara, M., Nishide, H., and Chiba, H. (2014). MGD update 2015: microbial genome database for flexible ortholog analysis utilizing a diverse set of genomic data. *Nucleic Acids Res.* 43, D270–D276. doi: 10.1093/nar/gku1152
- Yu, C. S., Cheng, C. W., Su, W. C., Chang, K. C., Huang, S. W., Hwang, J. K., et al. (2014). CELLO2GO: a web server for protein subCELLular LOcalization prediction with functional gene ontology annotation. *PLoS One* 9:e99368. doi: 10.1371/journal.pone.0099368
- Yu, N. Y., Wagner, J. R., Laird, M. R., Melli, G., Rey, S., Lo, R., et al. (2010). PSORTb 3.0: improved protein subcellular localization prediction with refined localization subcategories and predictive capabilities for all prokaryotes. *Bioinformatics (Oxford, England)* 26, 1608–1615. doi: 10.1093/bioinformatics/btq249

**Conflict of Interest:** The authors declare that the research was conducted in the absence of any commercial or financial relationships that could be construed as a potential conflict of interest.

Copyright © 2020 Chiang, Yang, Sun, Wang, Kuo, Lee, Chuang and Chen. This is an open-access article distributed under the terms of the Creative Commons Attribution License (CC BY). The use, distribution or reproduction in other forums is permitted, provided the original author(s) and the copyright owner(s) are credited and that the original publication in this journal is cited, in accordance with accepted academic practice. No use, distribution or reproduction is permitted which does not comply with these terms.



# Prevalence, Characterization, and Drug Resistance of *Staphylococcus Aureus* in Feces From Pediatric Patients in Guangzhou, China

Xiaolan Ai<sup>1†</sup>, Fei Gao<sup>1†</sup>, Shuwen Yao<sup>2</sup>, Bingshao Liang<sup>1</sup>, Jialiang Mai<sup>1</sup>, Zhile Xiong<sup>1</sup>, Xiantang Chen<sup>3</sup>, Zhuwei Liang<sup>1</sup>, Hongling Yang<sup>1</sup>, Zhiying Ou<sup>1</sup>, Sitang Gong<sup>1</sup>, Yan Long<sup>1\*</sup> and Zhenwen Zhou<sup>1\*</sup>

<sup>1</sup> Clinical Laboratory, Guangzhou Women and Children's Medical Center, Guangzhou Medical University, Guangzhou, China, <sup>2</sup> Clinical Laboratory, Guangzhou Children's Hospital, Guangzhou Medical University, Guangzhou, China, <sup>3</sup> Clinical Laboratory, Zengcheng Maternity and Children's Health Care Center, Guangzhou Medical University, Guangzhou, China

## OPEN ACCESS

### Edited by:

Ilana L. B. C. Camargo,  
University of São Paulo, Brazil

### Reviewed by:

Rima Abdallah Moghnieh,  
Makassed General Hospital, Lebanon  
Honghu Chen,  
Zhejiang Center for Disease Control  
and Prevention, China

### \*Correspondence:

Yan Long  
longyangmc@163.com  
Zhenwen Zhou  
zzw6248@126.com

<sup>†</sup>These authors have contributed  
equally to this work and share first  
authorship

### Specialty section:

This article was submitted to  
Infectious Diseases - Surveillance,  
Prevention and Treatment,  
a section of the journal  
Frontiers in Medicine

Received: 10 November 2019

Accepted: 23 March 2020

Published: 24 April 2020

### Citation:

Ai X, Gao F, Yao S, Liang B, Mai J,  
Xiong Z, Chen X, Liang Z, Yang H,  
Ou Z, Gong S, Long Y and Zhou Z  
(2020) Prevalence, Characterization,  
and Drug Resistance of  
*Staphylococcus Aureus* in Feces From  
Pediatric Patients in Guangzhou,  
China. *Front. Med.* 7:127.  
doi: 10.3389/fmed.2020.00127

**Background:** *Staphylococcus aureus* (*S. aureus*) is a major pathogen of human infections. Its fecal carriage serves as a risk factor for nosocomial transmission and disease development. However, the rate of *S. aureus* fecal carriage among Chinese children has not yet been reported. Therefore, we sought to investigate the prevalence, characterization, and drug resistance of *S. aureus* isolated from pediatric patients' feces in Southern China.

**Methods:** Fecal samples (2059) from pediatric patients in three centers in Guangzhou were cultured. From which, 412 *S. aureus* isolates were identified via selective mediums and automated VITEK Mass Spectrometer analysis. Antibiotic susceptibility was determined and DNA sequencing of seven housekeeping genes were used for multilocus sequence typing analysis.

**Results:** The fecal carriage rates were 20.0% for *S. aureus* and 4.5% for methicillin-resistant *S. aureus* (MRSA). Moreover, *S. aureus* fecal carriage was positively correlated with outpatient status and gastroenteritis diagnosis. Moreover, age-related patterns were observed with respect to prevalence of *S. aureus*. Besides, a total of 76 sequence types (STs) were identified, including 25 newly assigned STs and 28 clonal complexes (CCs). ST188, ST6, and ST15 were the most prevalent methicillin-sensitive *S. aureus* (MSSA) clones, while ST59 and ST45 were the major MRSA clones. *S. aureus* isolates also exhibited high rates of penicillin (84.2%), erythromycin (38.8%), and clindamycin (35.9%) resistance. Specifically, all ST30 and ST338 isolates were resistant to erythromycin and clindamycin, 61% of ST7 were resistant to tetracycline, and 84% of ST45 exhibited resistance and intermediate resistance to rifampicin. Also, CC59 (ST338 and ST59) and CC45 exhibited different antibiotic resistance patterns.

**Conclusion:** These results demonstrate the colonization dynamics and molecular epidemiology of *S. aureus* in child feces in Southern China. Further, they suggest an urgency for strengthening the surveillance programs in China and provide important information for the prevention and treatment of *S. aureus* infection.

**Keywords:** *Staphylococcus aureus*, prevalence, characterization, drug resistance, child fecal carriage



## INTRODUCTION

*Staphylococcus aureus* (*S. aureus*) is a major pathogen of human infection that causes diseases ranging from minor skin infections to severe bacteremia, necrotizing pneumonia, and life-threatening sepsis (1–3), and thus is a major global threat to human health. *S. aureus* can colonize multifarious body regions, including the anterior nares (4), skin (5), intestinal tract (6), oropharynx (7), and so on. Colonization is a crucial risk factor for the subsequent development of infections (8). Specifically, the importance of *S. aureus* fecal colonization was described as early as 1960 (9), in a study that demonstrated rectal carriage of *S. aureus* earlier than from the nose or throat. Subsequently, several studies have confirmed the clinical importance of *S. aureus* fecal carriage (10, 11). Additionally, *S. aureus* fecal carriage may contribute to environmental contamination (12), which can lead to nosocomial transmission and infection. Previous studies have reported fecal carriage of *S. aureus* in adults from Nigeria (13) and India (14), and a recent study investigated intestinal colonization by *S. aureus* and *Clostridium difficile* in healthy adult fecal samples from China (15), and a few studies have reported on *S. aureus* isolated from pediatric patients' feces samples in China.

Multilocus sequence typing (MLST) has become one of the most popular methods for evaluating *S. aureus* strains; however, only limited MLST studies of *S. aureus* from stool samples are available. Methicillin-sensitive (MSSA) strains ST30, ST398, and ST133 were detected from 100 healthy human fecal samples in Spain (16), while ST15, ST188, and ST59 were identified in six *S. aureus* isolates from stool specimens of diarrheal infants (17). Unfortunately, the diversity of molecular *S. aureus* types in these studies was limited due to the relatively small population size, which may have led to misinterpretation or inaccurate conclusions to be drawn regarding *S. aureus* colonization in fecal samples.

In addition to molecular characterization, antibiotic resistance, notably regarding the emergence and evolution of multi-drug-resistant (MDR) *S. aureus*, has become a major focal point in research across the world. Methicillin-resistant *S. aureus* (MRSA), which begins with resistance to methicillin or most  $\beta$ -lactam antibiotics and gradually develops co-resistance to vancomycin (18, 19), limits the use of alternative anti-infective drugs and threatens patient's health. Hence, drug resistance should be closely monitored to provide the basis for clinical antibacterial infection treatment, including exploring antibiotic resistance of *S. aureus* isolated from fecal samples.

Thus, the aims of this investigation were to evaluate the prevalence, molecular genotyping and antibiotic resistance of *S. aureus* isolated from pediatric patients' fecal samples in Southern China.

## MATERIALS AND METHODS

### Ethics

All patients were recruited voluntarily and provided informed consent from the participants or the guardians. The study was approved by the research ethics committee of the

Guangzhou women and children's medical center (registration no. 2016081029).

### Bacterial Isolates and Data Collection

This study enrolled children from three medical centers in Southern China between August and November 2018, including Guangzhou Women and Children's Medical Center (Tianhe District, central Guangzhou), Guangzhou Children's Hospital (Yuexiu District, western Guangzhou), and Zengcheng Maternity and Children's Health Care Center (Zengcheng District, northern Guangzhou). A total of 2059 non-duplicate pediatric stool samples (1308 outpatients and 751 inpatients) were collected. Approximately 20 mg of stool sample was streaked onto a selective mannitol salt agar medium (Hope Bio-technology, Qingdao, China) within 4 h of sample collection, and incubated in a humidified atmosphere at 37°C with 5% CO<sub>2</sub> for 24 h. Suspected *S. aureus* colonies from each sample were evaluated based on morphology and sub-cultured on Columbia Blood Agar Medium (Detgerm Microbiology Technology, Guangzhou, China) (20). All isolates were further identified for their species assignment by the automated VITEK MS (bioMérieux, Marcy-l'Étoile, France). Identified *S. aureus* was further confirmed by detecting *femB* (21). We also collected a range of clinical information from the laboratory information system, including gender, age, types, diagnosis, and fecal occult blood test (FOBT). Accordingly, the patients were classified into six age groups: 0–28 days, newborn; 28 days–3 months, young infant; 3 months–1 year, older infant; 1–3 years, child; 3–6 years, pre-school age; 6–18 years, school age and puberty (22, 23). Among these patients, the oldest was 17 years old, the youngest was 1 day, and the median age was 10 months and 23 days.

### Antibiotic Susceptibility Tests

Antibiotic susceptibility for 15 antibiotics (penicillin, oxacillin, gentamicin, rifampicin, levofloxacin, ciprofloxacin, trimethoprim/sulfamethoxazole, clindamycin, erythromycin, macrodantin, linezolid, vancomycin, quinoputin/dafutin, tetracycline, and tigecycline) was detected by VITEK 2 AST-GP67 cards (bioMérieux) using the automated VITEK2 compact system (bioMérieux). Antibiotic minimum inhibitory concentration (MIC) was determined according to the published guidelines (24). The quality control strain used in antibiotic susceptibility analysis was *S. aureus* ATCC 29213. MRSA was defined as an oxacillin-resistant isolate, and multidrug-resistant (MDR) isolates were identified as isolates with resistance to three or more non- $\beta$ -lactam antibiotics (25).

### DNA Extraction

Total DNA was extracted from 1.0 ml of nutrient broth medium culture grown overnight. After centrifugation, the supernatant was discarded and the *S. aureus* isolates were resuspended in 200  $\mu$ l of enzymatic lysis buffer (Sangon Biotech, Shanghai, China). Subsequently, *S. aureus* solution was incubated at 37°C for 30 min with 3  $\mu$ l of lysostaphin (Sigma-Aldrich, Shanghai, China), mixed with 200  $\mu$ l of Buffer BD (Sangon Biotech), and 200  $\mu$ l of 100% ethanol (Guangzhou Chemical Reagent Factory, Guangzhou, China), and then transferred to an absorbing

column (Sangon Biotech). Next, the Ezup Column Bacterial Genomic DNA Extraction Kit (Sangon Biotech) was used in accordance with the manufacturer's instructions.

## PCR Detection of *femB* and *mecA*

The *femB* gene plays an important role in formatting the pentaglycine bridges that stabilize peptidoglycan chains in *S. aureus*, while the *mecA* gene is the most important cause of *S. aureus* resistance to oxacillin (26). Thus, to further confirm the presence *S. aureus* and MRSA, we detected the expression of *femB* and *mecA* by PCR. The primers used for *femB* and *mecA* genes were described previously (27), and extracted DNA was amplified using TaqTM (Takara, Tokyo, Japan) following the manufacturer's instructions. Following amplification and extension, the PCR amplicons were separated on 1% agarose gels stained with ethidium bromide and visualized under UV illumination (TEX-20 M, Life Technologies, Carlsbad, USA).

## MLST Typing

All isolates were analyzed by multilocus sequence typing (MLST) according to a previously published procedure (28). The PCR products were purified and sequenced by a commercial sequencing company (Beijing Genomics Institute, Shenzhen, China). DNA sequencing of seven housekeeping genes (*arcC*, *aroE*, *glpF*, *gmk*, *pta*, *tpi*, and *yqiL*) was used for MLST analysis. Sequence types (STs) were determined by searching the *S. aureus* MLST database (<https://pubmlst.org/saureus/>), which included new emerging MLST alleles and MLST types. Clonal complex (CC) analysis was conducted using the eBURST v.3 programme (<https://www.mlst.net/eburst/>) according to our previously described protocol (27). Based on STs, a UPGMA dendrogram was constructed with START2.

## Statistical Analysis

Statistical analyses were carried out with SPSS software 20 (SPSS Inc., Chicago, USA). The chi-square ( $\chi^2$ ) test or Fisher's exact test were applied to dichotomous or categorical variables, which were described as frequencies and proportions.  $P < 0.05$  was considered statistically significant.

## RESULTS

### Prevalence of *S. aureus* and MRSA Was Associated With Clinical Features

A total of 2059 fecal samples were collected from pediatric patients in three hospitals, from which 412 *S. aureus* and 93 MRSA isolates were identified. The overall colonization prevalence of *S. aureus* and MRSA were 20.0 and 4.5%, respectively. Accordingly, we classified the 2059 patients into two groups consisting of those that were *S. aureus* positive ( $n = 412$ ) and negative ( $n = 1,647$ ), to analyze the correlation of *S. aureus* fecal carriage with different clinical features. As shown in **Table 1**, the fecal carriage of *S. aureus* was not associated with patient gender ( $P = 0.149$ ); however, it was positively correlated with outpatient status and gastroenteritis diagnosis ( $P < 0.01$ ). We also observed a positive relationship between *S. aureus* and different age groups. The minimum *S. aureus* carriage rate was

**TABLE 1** | Correlation of fecal carriage of *S. aureus* in pediatric patients with different clinical features.

Variable	Group	N	<i>S. aureus</i>		$\chi^2$	P
			+ N (%)	-N (%)		
Total patients		2059	412 (20.0)	1647 (80.0)		
Gender	Males	1215	256 (21.1)	959 (78.9)	2.082	0.149
	Females	844	156 (18.5)	688 (81.5)		
Status	Outpatients	1308	344 (26.3)	964 (73.7)	88.643	<0.001**
	Inpatients	751	68 (9.1)	683 (90.9)		
Diagnosis	Gastroenteritis	1242	319 (25.7)	923 (74.3)	62.974	<0.001**
	Others	817	93 (11.4)	724 (88.6)		
Age	0–28 days	205	15 (7.3)	190 (92.7)	55.629	<0.001**
	28 days–3 months	241	64 (26.6)	177 (73.4)		
	3 months–1 year	726	191 (26.3)	535 (73.7)		
	1–3 years	484	85 (17.6)	399 (82.4)		
FOBT	3–6 years	240	35 (14.6)	205 (85.7)	36.319	<0.001**
	6–18 years	163	22 (13.5)	141 (86.5)		
	Positive	784	210 (26.8)	574 (73.2)		
	Negative	1275	202 (15.8)	1073 (84.2)		

+ : *S. aureus*-positive group; - : *S. aureus*-negative group. Clinicopathological features were assessed using the chi-square test, \*\* $P < 0.01$ .

in newborn patients (7.3%), while the maximum rate was in infant patients (young infants, 26.6% and older infants 26.3%), after which the carriage rate gradually descended with increasing age of the patients (**Table 1**). In addition, we observed a positive correlation between FOBT results and *S. aureus* carriage ( $P < 0.01$ , **Table 1**).

Subsequently we divided the 412 positive *S. aureus* patients into two groups, MRSA ( $n = 93$ ) and MSSA ( $n = 319$ ), to explore the relationship of MRSA and clinical features. However, we found that MRSA was significantly correlated with inpatient status ( $P = 0.002$ ), and not gender, age, or FOBT results (**Table 2**).

### Antibiotic Susceptibility of *S. aureus* and MRSA

The antibiotic susceptibility results for the 412 *S. aureus* isolates according to MLST are presented in **Table 3**. All 93 MRSA strains were resistant to cefoxitin screening and carried the *mecA* gene. The *S. aureus* strains exhibited highest rate of resistance to penicillin (PEN, 84.2%), followed by erythromycin (ERY, 38.8%), clindamycin (CLI, 35.9%), tetracycline (TE, 14.6%), and sulfamethoxazole-trimethoprim (SXT, 6.1%). The resistance rates of antibiotics were lower for gentamicin (GEN, 2.7%), levofloxacin (LEV, 1.9%), ciprofloxacin (CIP, 1.9%), and rifampicin (RIF, 0.7%); however, all isolates were susceptible to macrodantin, linezolid, vancomycin, dalbapristin/quinupristin (QDA), and tigecycline. Compared to the MSSA group, the MRSA group had significantly higher rates of resistance to PEN ( $P < 0.01$ ), ERY ( $P < 0.01$ ), CLI ( $P < 0.01$ ), and TE ( $P = 0.03$ ) and intermediate resistance to RIF ( $P < 0.01$ ). Although 22.8% of all strains exhibited MDR, the MRSA group had a

significantly higher rate (74.2%) compared to that of the MSSA group (7.8%) ( $P < 0.01$ ).

### Molecular Characterization of *S. aureus*

According to the results of the MLST method, 76 unique STs were identified among 412 *S. aureus* isolates, including 25 novel STs. Based on eBURST analysis, the 76 STs were classified into 28 CCs, including 14 groups and 14 singletons (Figures 1, 2). The three most abundant STs among all *S. aureus* isolates were ST188

(12.9%), ST45 (12.1%), and ST59 (10.0%), comprising 35% of all isolates. Among the MRSA group, the three most abundant STs were ST59 (37.6%), ST45 (35.5%), and ST1 (5.4%), comprising 78.5% of all strains. Among MSSA group, ST188 (16.0%), ST6 (9.7%), and ST15 (8.5%) were the three prevalent STs. Further, the most common CCs among all strains were CC188, CC45, and CC59, representing 39.6% of all clones. Specifically, within the MRSA group, CC59 (41.9%), CC45 (35.5%), and CC1 (6.5%) were the three most abundant CCs, while in the MSSA group, the most common clone was CC188 (17.9%), followed by CC5 (11.6%) and CC6 (11.0%) (Table 4).

As shown in Figure 2, there were 25 newly assigned STs (ST5307 to ST5330, and ST5353) in this study, of which many were single-locus variants (SLVs). Among the 25 novel STs, 26 strains were identified, including 2 MRSA and 24 MSSA isolates; both MRSA isolates belonged to CC59, and the most abundant CC in the MSSA groups was CC188. Finally, we identified 18 novel SLVs in seven housekeeping genes, which were subsequently assigned as new alleles (Table S1).

### Association of Antibiotic Resistance With Specific *S. aureus* Sequence Types

When analyzing the correlation between antibiotic resistance profiles and unique sequence types (STs) in genotypes of the *S. aureus* isolates, 16 STs each had more than three strains that were selected in this study. Some specific STs were determined to be closely associated with certain antibiotic resistance patterns, while some exhibited high sensitivity. As shown in Figure 2 and Figure S1, all ST338, ST25, ST30, and ST1281 isolates were resistant to PEN, while ST72, ST950, and ST965 showed high sensitivity to PEN. However, ST950 and ST965 showed high resistance to CLI and ERY, yet were sensitive to all other antibiotics, with an MDR rate of 0%, similar to the MDR rate

**TABLE 2 |** Correlation of MRSA in pediatric patients' fecal samples with different clinical features.

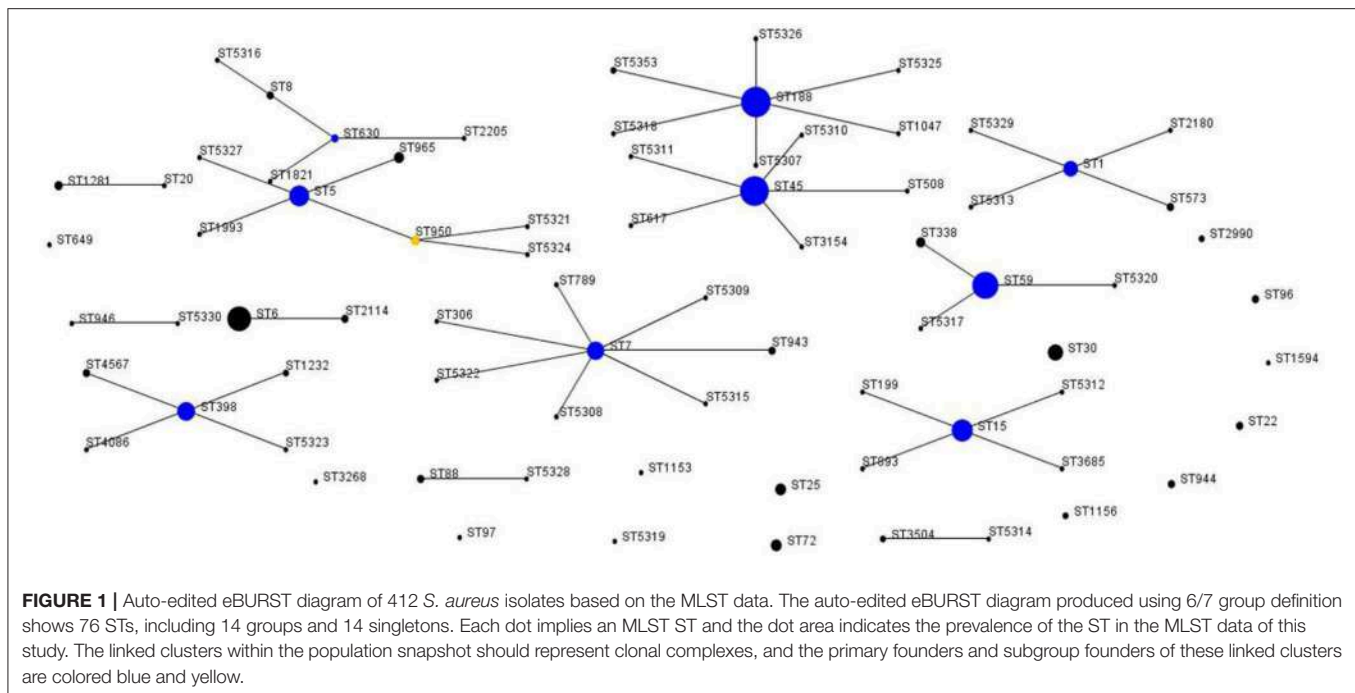
Variable	Groups	<i>S. aureus</i>	MRSA	MSSA	$\chi^2$	<i>P</i>
Total patients		412	93 (22.6)	319 (77.4)		
Gender	Males	256	60 (23.4)	196 (76.6)	0.289	0.591
	Females	156	33 (21.2)	123 (78.8)		
Status	Outpatients	344	68 (19.8)	276 (80.2)	9.385	0.002**
	Inpatients	68	25 (36.8)	43 (63.2)		
Age	0–28 days	15	5 (33.3)	10 (66.7)	1.763	0.881
	28 days–3 months	64	15 (23.4)	49 (76.6)		
	3 months–1 year	191	39 (20.4)	152 (79.6)		
	1–3 years	85	20 (23.5)	65 (76.5)		
	3–6 years	35	8 (22.9)	27 (77.1)		
FOBT	6–18 years	22	6 (27.3)	16 (72.7)		
	Positive	210	40 (19.0)	170 (81.0)	3.045	0.081
	Negative	202	53 (26.2)	149 (73.8)		

MRSA, methicillin-resistant *S. aureus*; MSSA, methicillin-susceptible *S. aureus*. Clinicopathological features were assessed using the chi-square test, \*\* $P < 0.01$ .

**TABLE 3 |** Antibiotic susceptibility of *S. aureus* and MRSA isolates from pediatric patients' feces.

Antibiotic	<i>S. aureus</i> (n = 412)		MRSA (n = 93)		MSSA (n = 319)		<i>P</i> <sup>a</sup>
	R, n (%)	I, n (%)	R, n (%)	I, n (%)	R, n (%)	I, n (%)	
Penicillin	347 (84.2)	0 (0.0)	93 (100)	0 (0.0)	254 (79.6)	0 (0.0)	<0.01**
Gentamicin	11 (2.7)	4 (1.0)	2 (2.2)	2 (2.2)	9 (2.8)	2 (0.6)	1.00
Rifampicin	3 (0.7)	43 (10.4)	2 (2.2)	27 (29.0)	1 (0.3)	17 (5.3)	<0.01 <sup>b</sup> **
Levofloxacin	8 (1.9)	0 (0.0)	4 (4.3)	0 (0.0)	4 (1.3)	0 (0.0)	0.148
Ciprofloxacin	8 (1.9)	1 (0.2)	4 (4.3)	0 (0.0)	4 (1.3)	1 (0.3)	0.149
SXT	25 (6.1)	0 (0.0)	2 (2.2)	0 (0.0)	23 (7.2)	0 (0.0)	0.072
Clindamycin	148 (35.9)	0 (0.0)	67 (72)	0 (0.0)	81 (25.4)	0 (0.0)	<0.01**
Erythromycin	160 (38.8)	1 (0.2)	67 (72)	0 (0.0)	93 (29.2)	1 (0.3)	<0.01**
Macrodantin	0 (0.0)	0 (0.0)	0 (0.0)	0 (0.0)	0 (0.0)	0 (0.0)	NA
Linezolid	0 (0.0)	0 (0.0)	0 (0.0)	0 (0.0)	0 (0.0)	0 (0.0)	NA
Vancomycin	0 (0.0)	0 (0.0)	0 (0.0)	0 (0.0)	0 (0.0)	0 (0.0)	NA
QDA	0 (0.0)	0 (0.0)	0 (0.0)	0 (0.0)	0 (0.0)	0 (0.0)	NA
Tetracycline	60 (14.6)	0 (0.0)	20 (21.5)	0 (0.0)	40 (12.5)	0 (0.0)	0.03*
Tigecycline	0 (0.0)	0 (0.0)	0 (0.0)	0 (0.0)	0 (0.0)	0 (0.0)	NA

SXT, trimethoprim/sulfamethoxazole; QDA, dalbapristin/quinupristin. R, Resistant; I, Intermediate; NA, not applicable. <sup>a</sup>Antibiotic resistance of MRSA vs. MSSA by chi-squared test (two-sided); <sup>b</sup>Rifampicin intermediate of MRSA vs. MSSA by chi-squared test (two-sided), \*\* $P < 0.01$ , \* $P < 0.05$ .



of ST1281 and ST15. Similarly, ST188, with the largest number of strain types and largest antibiotic resistance coverage, had a very low MDR rate (3.8%). All ST30 and ST338 isolates were resistant to ERY and CLI. ST59, which belongs to CC59 with ST338, also showed a high resistance rate (78%) to ERY and CLI. Additionally, ST59 and ST338 had a higher rate of resistance to TE, with the two highest MDR rates of 75.6 and 60.0%, respectively. In addition to the STs mentioned above, ST7 exhibited the highest resistance rate (61.1%) to TE, while ST45, another predominant ST in the MRSA isolate group, had the highest resistance and intermediate resistance rate (84.0%) to RIF (Figure 2 and Figure S1).

## DISCUSSION

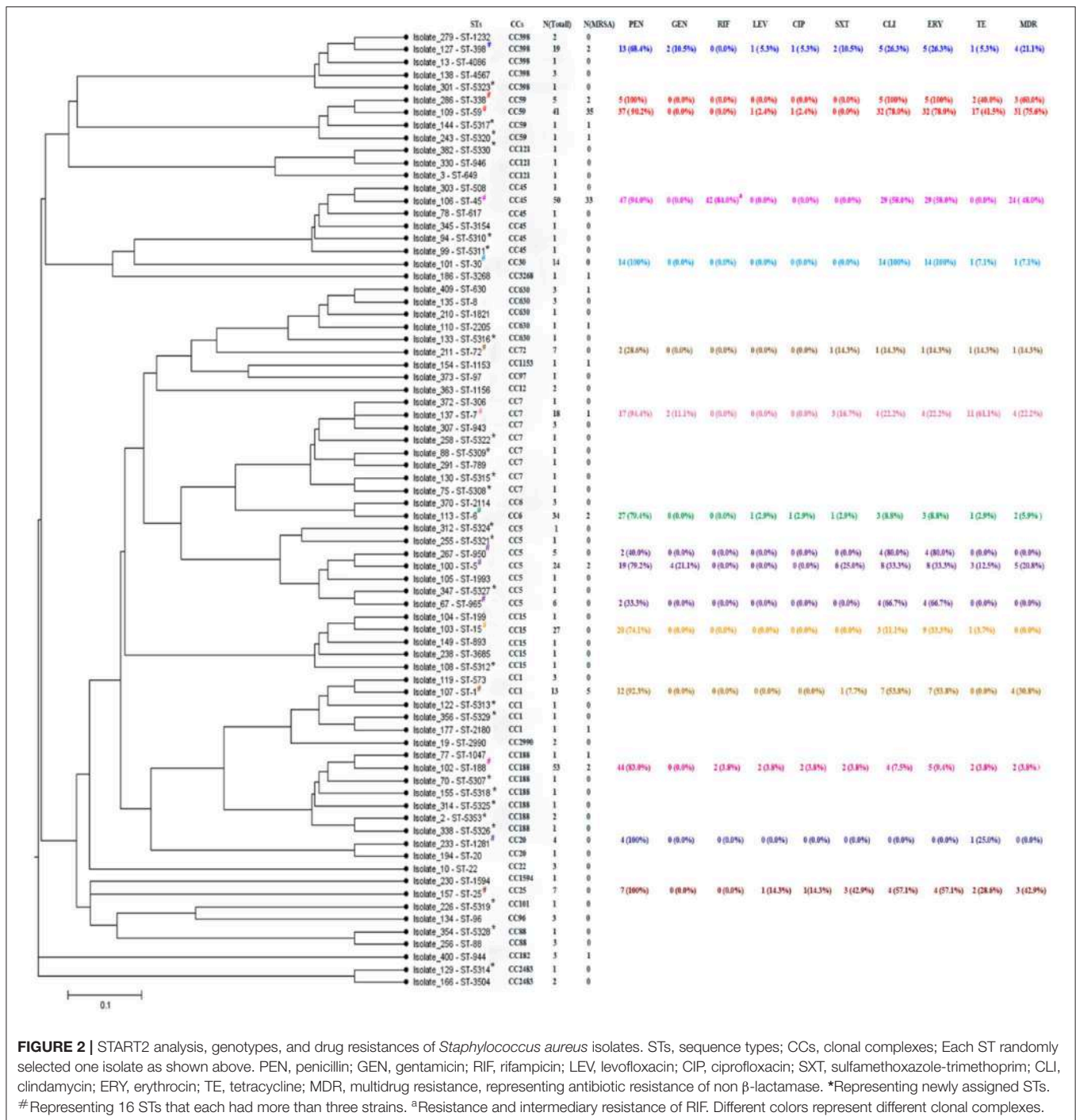
*S. aureus* fecal carriage may contribute to environmental contamination, facilitate nosocomial transmission, and promote human disease development. Moreover, fecal carriage of *S. aureus* among children is more likely to cause disease infection due to their immature and underdeveloped immune system (29). Since *S. aureus* fecal colonization has been identified as a risk factor for infection disease development (30), our findings may serve to advance the current understanding regarding *S. aureus* fecal colonization dynamics and prevention of *S. aureus* infection.

In this study, the *S. aureus* fecal carriage rate was determined to be 20.0% in pediatric patients from Guangzhou, while the MRSA carriage rate was 4.5%. These results agree with the reported prevalence of pooled estimates for *S. aureus* and MRSA fecal carriage rates (16.8–36.3%, 0.7–27.0%, respectively) (30). However, the prevalence of *S. aureus* in this study was higher than that reported from participants with nosocomial diarrhea in

Germany (7%) (31) compared to healthy adults in China (3.51%) (15), but was lower than that reported in a previous Nigerian study (31.7%) (13). Moreover, in China, the prevalence of MRSA nasal colonization in children between 2005 and 2015 was 4.4% (32), similar to the 4.5% carriage rate detected in our study, but slightly higher than a previous study in American children with cancer (2.9%) (33). Although the prevalence of *S. aureus* and MRSA is dynamic due to differences in geographical regions, age, gender, and health status, future studies continue to be warranted to better characterize the cause of these differences.

In our study, the fecal carriage of *S. aureus* was positively correlated with outpatient status and gastroenteritis diagnosis. Pediatric gastroenteritis primarily manifests as abdominal pain, diarrhea, and vomiting, and these patients comprise the majority of outpatients. Moreover, *S. aureus* has been described as the most common global causative pathogen of food-borne illness, while studies have reported it to be associated with infantile diarrhea (17), corresponding with our observed positive correlation between *S. aureus* fecal carriage and gastroenteritis in children. In addition, our study found that fecal *S. aureus* colonization was lowest during the first 4 weeks of life, after which it increased rapidly during the first year, followed by a gradual decline until 17 years of age. This may be explained by the underdeveloped intestinal function and microbiota composition in newborn patients. With improved intestinal function and increased diversity of intestinal microbes, *S. aureus* colonization increased within the following year. Further, human milk oligosaccharides have been suggested to be a strong contributor to bacterial reproduction in the infant gut and to stimulate *S. aureus* growth (34), providing an important function for breastfeeding in early life. Subsequently, with the consumption of a comprehensive diet and enhanced immune function, the fecal





carriage of *S. aureus* decreases with increasing age. Additionally, within this study, *S. aureus* fecal carriage was higher in patients that tested FOBT positive, which may be explained by virulence factors, especially staphylococcal enterotoxins, produced by *S. aureus*, causing intestinal damage that leads to intestinal bleeding. However, this hypothesis requires further validation.

We also determined that fecal carriage of MRSA was positively associated with inpatients status as hospitalized

patients are more likely to be infected with MRSA (35). Interestingly, 7 of the 68 hospitalized patients with *S. aureus* in their stool also had it within in their sputum or alveolar lavage fluid, demonstrating similar antibiotic susceptibility patterns, including 2 MRSA and 5 MSSA isolates (data not shown). This may suggest that the *S. aureus* isolated from stool sample was consistent with the source in the sputum or alveolar lavage fluid, and fecal carriage of *S.*

**TABLE 4** | Genotype ranking of *S. aureus* isolated from pediatric patients.

Rank	<i>S. aureus</i> (n = 412)				MRSA (n = 93)				MSSA (n = 319)			
	MLST	N (%)	CCs	N (%)	MLST	N (%)	CCs	N (%)	MLST	N (%)	CCs	N (%)
1	ST188	53 (12.9)	CC188	60 (14.6)	ST59	35 (37.6)	CC59	39 (41.9)	ST188	51 (16.0)	CC188	57 (17.9)
2	ST45	50 (12.1)	CC45	55 (13.3)	ST45	33 (35.5)	CC45	33 (35.5)	ST6	31 (9.7)	CC5	37 (11.6)
3	ST59	41 (10.0)	CC59	48 (11.7)	ST1	5 (5.4)	CC1	6 (6.5)	ST15	27 (8.5)	CC6	35 (11.0)
4	ST6	34 (8.3)	CC5	39 (9.5)	ST188	2 (2.2)	CC188	3 (3.2)	ST5	22 (6.9)	CC15	31 (9.7)
5	ST15	27 (6.6)	CC6	37 (9.0)	ST6	2 (2.2)	CC5	2 (2.2)	ST45	17 (5.3)	CC7	26 (8.2)
6	ST5	24 (5.8)	CC15	31 (7.5)	ST5	2 (2.2)	CC6	2 (2.2)	ST398	17 (5.3)	CC398	24 (7.5)
7	ST398	19 (4.6)	CC7	27 (6.6)	ST398	2 (2.2)	CC398	2 (2.2)	ST7	17 (5.3)	CC45	22 (6.9)
8	ST7	18 (4.4)	CC398	26 (6.3)	ST338	2 (2.2)	CC630	2 (2.2)	ST30	14 (4.4)	CC30	14 (4.4)
Total		266 (64.6)		323 (78.4)		83 (89.2)		89 (95.7)		196 (61.4)		246 (77.1)

*aureus* may be associated with infection in other parts of the body.

Based on the MLST results, 412 *S. aureus* isolates were divided into 76 STs, with fewer MRSA isolates (14 STs) than MSSA isolates (69 STs), indicating that MRSA isolates were more genetically stable than MSSA isolates. The most commonly reported *S. aureus* isolates in China are diverse and include ST1 (36), ST6 (20), ST5 (37), and ST188 (38) according to different regions, ages, and resources. Similarly, many different MSSA isolates have been identified throughout China, including ST7 and ST188 (39). In our study, ST188, ST6, and ST15 were the most frequently observed STs in the MSSA group. ST188 was reported as a major cause of childhood infections in China, due to its high adhesion and biofilm formation ability (38). In addition, ST15 and ST188 were the two most prevalent clones isolated from infantile diarrhea fecal samples (17). Although the types of MSSA strains are diverse, the most abundant ones have not changed significantly among children in China.

MRSA strains demonstrated strong homology with the prevalent clones in this study, which were determined to be ST59 (37.6%) and ST45 (35.5%). This result was consistent with a previous study reported by Ding et al. in Chinese children (40). ST59, a predominant MRSA clone causing CA-MRSA infections among children (41), was not only predominant in Chinese cities, including Shanghai (39), Sichuan (42), and Taiwan (43), but also is considered to be a prevalent isolate throughout the Asia-Pacific region (44). It is worth noting that ST45, the second most prevalent MRSA strain, has an increased carriage rate in children, compared to 18.8% for the MRSA isolated in our previous study (27). ST45, known as a Berlin clone, was also a common isolate throughout European countries, and has now spread to Australia (45), Singapore (46), and China (41). Further, previous studies from Shanghai have shown that ST239 was the most frequent MRSA clone between 2005 and 2010 (47), which was replaced by the increasingly abundant ST5, ST59, and ST398 clones between 2008 and 2017 (48). However, ST239 was not identified in our study, and ST5 and ST398 only accounted for 2.2% of MRSA isolates. Alternatively, ST45 and ST59 were not only the two dominant clones in the MRSA group, but also the second and the third most abundant clones in all *S. aureus* isolates. ST45-MRSA

is attributed to the acquisition of *mecA* by a MSSA clone in the community (49). Therefore, our results suggest that ST45 would alter the MRSA clone structure in this region of China, allowing for the development of additionally prominent clones in Chinese children, such as ST59.

The drug resistance of *S. aureus* has attracted great attention worldwide, especially in China, due to the abuse of antibiotics and the recent emergence of MDR bacteria. Consistent with a previous report (50), we show that *S. aureus* isolates exhibited a high rate of resistance to PEN, ERY, and CLI, which may be the result of the excessive use of PEN and macrolides (51). The current study demonstrated that *S. aureus* was more susceptible to vancomycin and linezolid, and displayed 100% sensitivity to vancomycin, linezolid, macrodantin, and QDA. Similarly, relatively low rates of resistance to CIP and LEV were observed in *S. aureus* isolates, which may be a result from the infrequent use of fluoroquinolones in pediatric patients due to their reported cartilage toxicity. In addition, *S. aureus* strains can differ in their antibiotic resistance patterns with specific STs. CC59 (ST59 and ST338) exhibited the highest MDR rate and a specific antibiotic resistance pattern (ERY-CLI-TE), while another common clone, CC45 (ST45), exhibited a different antibiotic resistance pattern (ERY-CLI-RIF). ST45 resistance or intermediate resistance to RIF is caused by *rpoB* mutations (52). However, strains assigned to the same cluster seemed to have similar resistance patterns, suggesting that further genotyping of the *S. aureus* strains may assist in designing more effective clinical treatment regimens.

Certain limitations were noted within this study. Firstly, more detailed clinical information was difficult to obtain, especially for outpatients, which account for the majority of patients; therefore, the study was limited in its ability to analyze the effect of additional risk factors for *S. aureus* carriage or MRSA colonization, including premature birth, duration of hospital stay, mother carriage status, history of antibiotic intake, etc. Secondly, inpatient status is strongly correlated with the carriage of MRSA; however, due to the diversity of the hospital environment, we were unable to differentiate MRSA strains based on the various areas in which the inpatients were admitted to; the source of

MRSA is worth exploring further. Lastly, we only applied a single method for *S. aureus* typing, which limited access to more specific and detailed prevalent molecular characterization of *S. aureus*.

In summary, the *S. aureus* carriage rate in pediatric feces in Southern China was as high as 20%. MSSA and MRSA exhibited significant differences in genotyping and antimicrobial susceptibility, with ST59 and ST45 emerging as two major MRSA clones and ST188 as the most prevalent MSSA clone. Antibiotic resistance patterns of *S. aureus* were also found to be closely associated with specific STs. These findings clarify the colonization dynamics and molecular epidemiology of *S. aureus* from child feces in Southern China and suggest an urgent need to strengthen the surveillance programs in this region, while also providing important information regarding the prevention and treatment of *S. aureus* infection.

## DATA AVAILABILITY STATEMENT

The datasets generated for this study can be found in the [https://pubmlst.org/bigsub?db=pubmlst\\_saureus\\_seqdef&page=downloadProfiles&scheme\\_id=1](https://pubmlst.org/bigsub?db=pubmlst_saureus_seqdef&page=downloadProfiles&scheme_id=1).

## ETHICS STATEMENT

The studies involving human participants were reviewed and approved by the research ethics committee of the Guangzhou women and children's medical center (registration no. 2016081029). Written informed consent to participate in this study was provided by the participants' legal guardian/next of kin.

## REFERENCES

1. Lowy FD. *Staphylococcus aureus* infections. *N Engl J Med.* (1998) 339:520–32. doi: 10.1056/NEJM199808203390806
2. Abrahamian FM, Moran GJ. Methicillin-resistant *Staphylococcus aureus* infections. *N Engl J Med.* (2007) 357:2090. doi: 10.1056/NEJMc072407
3. Yasmin M, El Hage H, Obeid R, El Haddad H, Zaarour M, Khalil A. Epidemiology of bloodstream infections caused by methicillin-resistant *Staphylococcus aureus* at a tertiary care hospital in New York. *Am J Infect Control.* (2016) 44:41–6. doi: 10.1016/j.ajic.2015.08.005
4. Millar EV, Chen WJ, Schlett CD, Cui T, Crawford KB, Lanier JB, et al. Frequent use of chlorhexidine-based body wash associated with a reduction in methicillin-resistant *Staphylococcus aureus* nasal colonization among military trainees. *Antimicrob Agents Chemother.* (2015) 59:943–9. doi: 10.1128/AAC.03993-14
5. Paharik AE, Parlet CP, Chung N, Todd DA, Rodriguez EI, Van Dyke MJ, et al. Coagulase-negative Staphylococcal strain prevents *Staphylococcus aureus* colonization and skin infection by blocking Quorum sensing. *Cell Host Microbe.* (2017) 22:746–56.e5. doi: 10.1016/j.chom.2017.11.001
6. Gagnaire J, Verhoeven PO, Grattard F, Rigault J, Lucht F, Pozzetto B, et al. Epidemiology and clinical relevance of *Staphylococcus aureus* intestinal carriage: a systematic review and meta-analysis. *Expert Rev Anti Infect Ther.* (2017) 15:767–85. doi: 10.1080/14787210.2017.1358611

## AUTHOR CONTRIBUTIONS

ZZ and YL initiated and designed the study. XA, FG, SY, BL, JM, ZX, XC, and ZL performed the experiments and/or analyzed the data. XA wrote the draft. HY, ZO, SG, ZZ, and YL revised the manuscript. All authors have approved the final version.

## FUNDING

This work was supported by grants from the Natural Science Foundation of Guangdong (Nos. 8451012001001570 and 9151012001000009), Guangdong Science and Technology Department (Nos. 2014A020212013 and 2016A020215013), Medical Health Science and Technology Foundation of Guangzhou (Nos. 20171A010267, and 20181A011039), Paediatric Institute Foundation of Guangzhou Women and Children's Medical Center (Nos. Pre-NSFC-2019-014 and IP-2019-022), and Guangzhou Science Technology and Innovation Commission (No. 201707010010).

## ACKNOWLEDGMENTS

We would like to thank all the patients who provided their specimens and clinical data for this study.

## SUPPLEMENTARY MATERIAL

The Supplementary Material for this article can be found online at: <https://www.frontiersin.org/articles/10.3389/fmed.2020.00127/full#supplementary-material>

**Figure S1** | Antibiotic resistance of *S. aureus* isolates from pediatric feces linked to sequence types, as illustrated by the tri-color scale.

7. Petersen IS, Larsen PL, Brandelev BL, Hald J, Praetorius C, Welinder R, et al. Close association between oropharyngeal and rhinopharyngeal colonization with *Staphylococcus aureus* - clues to new insight of MRSA colonization of the oropharynx. *J Hosp Infect.* (2013) 84:259–62. doi: 10.1016/j.jhin.2013.04.007
8. Bradley SE, Terpenning MS, Ramsey MA, Zarins LT, Jorgensen KA, Sottile WS, et al. Methicillin-resistant *Staphylococcus aureus*: colonization and infection in a long-term care facility. *Ann Intern Med.* (1991) 115:417–22. doi: 10.7326/0003-4819-115-6-417
9. Hurst V. Transmission of hospital staphylococci among newborn infants. II. Colonization of the skin and mucous membranes of the infants. *Pediatrics.* (1960) 25:204–14.
10. Bhalla A, Aron DC, Donskey CJ. *Staphylococcus aureus* intestinal colonization is associated with increased frequency of *S. aureus* on skin of hospitalized patients. *BMC Infect Dis.* (2007) 7:105. doi: 10.1186/1471-2334-7-105
11. Efuntoye MO, Adetosoye AI. Enterotoxigenicity and drug sensitivity of staphylococci from children aged five years and below with sporadic diarrhoea. *East Afr Med J.* (2003) 80:656–9. doi: 10.4314/eamj.v80i1.2.8784
12. Boyce JM, Havill NL, Otter JA, Adams NM. Widespread environmental contamination associated with patients with diarrhea and methicillin-resistant *Staphylococcus aureus* colonization of the gastrointestinal tract. *Infect Control Hosp Epidemiol.* (2007) 28:1142–7. doi: 10.1086/520737
13. Onanuga A, Temedie TC. Multidrug-resistant intestinal *Staphylococcus aureus* among self-medicated healthy adults in Amassoma, South-South,

- Nigeria. *J Health Popul Nutr.* (2011) 29:446–53. doi: 10.3329/jhpn.v29i5.8898
14. Vandana KE, Varghese G, Krishna S, Mukhopadhyay C, Kamath A, Ajith V. Screening at admission for carrier prevalence of multidrug-resistant organisms in resource-constrained settings: a hospital-based observational study. *J Hosp Infect.* (2010) 76:180–1. doi: 10.1016/j.jhin.2010.04.015
  15. Dong D, Ni Q, Wang C, Zhang L, Li Z, Jiang C, et al. Effects of intestinal colonization by *Clostridium difficile* and *Staphylococcus aureus* on microbiota diversity in healthy individuals in China. *BMC Infect Dis.* (2018) 18:207. doi: 10.1186/s12879-018-3111-z
  16. Benito D, Lozano C, Gomez-Sanz E, Zarazaga M, Torres C. Detection of methicillin-susceptible *Staphylococcus aureus* ST398 and ST133 strains in gut microbiota of healthy humans in Spain. *Microb Ecol.* (2013) 66:105–11. doi: 10.1007/s00248-013-0240-1
  17. Chen Z, Pan WG, Xian WY, Cheng H, Zheng JX, Hu QH, et al. Identification of infantile Diarrhea caused by breast milk-transmitted *Staphylococcus aureus* infection. *Curr Microbiol.* (2016) 73:498–502. doi: 10.1007/s00284-016-1088-7
  18. Kumar M. Multidrug-resistant *Staphylococcus aureus*, India, 2013–2015. *Emerg Infect Dis.* (2016) 22:1666–7. doi: 10.3201/eid2209.160044
  19. Tran KN, Rybak MJ.  $\beta$ -Lactam combinations with vancomycin show synergistic activity against vancomycin-susceptible *Staphylococcus aureus*, vancomycin-intermediate S. aureus (VISA), and heterogeneous VISA. *Antimicrob Agents Chemother.* (2018) 62:e00157–18. doi: 10.1128/AAC.00157-18
  20. Chen Z, Han C, Huang X, Liu Y, Guo D, Ye X. A molecular epidemiological study of methicillin-resistant and methicillin-susceptible *Staphylococcus aureus* contamination in the airport environment. *Infect Drug Resist.* (2018) 11:2363–75. doi: 10.2147/IDR.S178584
  21. Jonas D, Grundmann H, Hartung D, Daschner FD, Towner KJ. Evaluation of the *mecA* femB duplex polymerase chain reaction for detection of methicillin-resistant *Staphylococcus aureus*. *Eur J Clin Microbiol Infect Dis.* (1999) 18:643–7. doi: 10.1007/s100960050365
  22. Zhao XX, Zhang GQ, Li ZY. Clinical features and etiology of abdominal distension in children. *Zhongguo Dang Dai Er Ke Za Zhi.* (2019) 21:1022–7.
  23. Baraff LJ. Management of fever without source in infants and children. *Ann Emerg Med.* (2000) 36:602–14. doi: 10.1067/mem.2000.110820
  24. CLSI. Performance standards for antimicrobial susceptibility testing. In: *28th Edn CLSI supplement M100*. Wayne, PA: Clinical and Laboratory Standards Institute (2018).
  25. Lee GC, Dallas SD, Wang Y, Olsen RJ, Lawson KA, Wilson J, et al. Emerging multidrug resistance in community-associated *Staphylococcus aureus* involved in skin and soft tissue infections and nasal colonization. *J Antimicrob Chemother.* (2017) 72:2461–8. doi: 10.1093/jac/dkx200
  26. Giannouli S, Labrou M, Kyritsis A, Ikonomidis A, Pournaras S, Stathopoulos C, et al. Detection of mutations in the FemXAB protein family in oxacillin-susceptible *mecA*-positive *Staphylococcus aureus* clinical isolates. *J Antimicrob Chemother.* (2010) 65:626–33. doi: 10.1093/jac/dkq039
  27. Liang B, Mai J, Liu Y, Huang Y, Zhong H, Xie Y, et al. Prevalence and characterization of *Staphylococcus aureus* isolated from women and children in Guangzhou, China. *Front Microbiol.* (2018) 9:2790. doi: 10.3389/fmicb.2018.02790
  28. Feil EJ, Li BC, Aanensen DM, Hanage WP, Spratt BG. eBURST: inferring patterns of evolutionary descent among clusters of related bacterial genotypes from multilocus sequence typing data. *J Bacteriol.* (2004) 186:1518–30. doi: 10.1128/JB.186.5.1518-1530.2004
  29. Pedro Tda C, Morcillo AM Baracat EC. Etiology and prognostic factors of sepsis among children and adolescents admitted to the intensive care unit. *Rev Bras Ter Intensiva.* (2015) 27:240–6. doi: 10.5935/0103-507X.20150044
  30. Claassen-Weitz S, Shittu AO, Ngwarai MR, Thabane L, Nicol MP, Kaba M. Fecal carriage of *Staphylococcus aureus* in the hospital and community setting: a systematic review. *Front Microbiol.* (2016) 7:449. doi: 10.3389/fmicb.2016.00449
  31. Flemming K, Ackermann G. Prevalence of enterotoxin producing *Staphylococcus aureus* in stools of patients with nosocomial diarrhea. *Infection.* (2007) 35:356–8. doi: 10.1007/s15010-007-6268-8
  32. Lin J, Peng Y, Xu P, Zhang T, Bai C, Lin D, et al. Methicillin-resistant *Staphylococcus aureus* nasal colonization in Chinese children: a prevalence meta-analysis and review of influencing factors. *PLoS ONE.* (2016) 11:e0159728. doi: 10.1371/journal.pone.0159728
  33. Srinivasan A, Seifried SE, Zhu L, Srivastava DK, Perkins R, Shenep JL, et al. Increasing prevalence of nasal and rectal colonization with methicillin-resistant *Staphylococcus aureus* in children with cancer. *Pediatr Blood Cancer.* (2010) 55:1317–22. doi: 10.1002/psc.22815
  34. Hunt KM, Preuss J, Nissan C, Davlin CA, Williams JE, Shafiq B, et al. Human milk oligosaccharides promote the growth of staphylococci. *Appl Environ Microbiol.* (2012) 78:4763–70. doi: 10.1128/AEM.00477-12
  35. Milstone AM, Goldner BW, Ross T, Shepard JW, Carroll KC, Perl TM. Methicillin-resistant *Staphylococcus aureus* colonization and risk of subsequent infection in critically ill children: importance of preventing nosocomial methicillin-resistant *Staphylococcus aureus* transmission. *Clin Infect Dis.* (2011) 53:853–9. doi: 10.1093/cid/cir547
  36. Wu S, Huang J, Wu Q, Zhang J, Zhang F, Yang X, et al. *Staphylococcus aureus* isolated from retail meat and meat products in China: incidence, antibiotic resistance and genetic diversity. *Front Microbiol.* (2018) 9:2767. doi: 10.3389/fmicb.2018.02767
  37. Li X, Fang F, Zhao J, Lou N, Li C, Huang T, Li Y. Molecular characteristics and virulence gene profiles of *Staphylococcus aureus* causing bloodstream infection. *Braz J Infect Dis.* (2018) 22:487–94. doi: 10.1016/j.bjid.2018.12.001
  38. Wang Y, Liu Q. Phylogenetic analysis and virulence determinant of the host-adapted *Staphylococcus aureus* lineage ST188 in China. *Emerg Microbes Infect.* (2018) 7:45. doi: 10.1038/s41426-018-0048-7
  39. Wang X, Liu Q, Zhang H, Li X, Huang W, Fu Q, et al. Molecular characteristics of community-associated *Staphylococcus aureus* isolates from pediatric patients with bloodstream infections between 2012 and 2017 in Shanghai, China. *Front Microbiol.* (2018) 9:1211. doi: 10.3389/fmicb.2018.01211
  40. Ding YL, Fu J, Chen J, Mo SF, Xu S, Lin N, et al. Molecular characterization and antimicrobial susceptibility of *Staphylococcus aureus* isolated from children with acute otitis media in Liuzhou, China. *BMC Pediatr.* (2018) 18:388. doi: 10.1186/s12887-018-1366-6
  41. Wang L, Liu Y, Yang Y, Huang G, Wang C, Deng L, et al. Multidrug-resistant clones of community-associated methicillin-resistant *Staphylococcus aureus* isolated from Chinese children and the resistance genes to clindamycin and mupirocin. *J Med Microbiol.* (2012) 61:1240–7. doi: 10.1099/jmm.0.042663-0
  42. Tan S, Wan C, Wang H, Zhou W, Shu M. Relationship between nasal carrier isolates and clinical isolates in children with *Staphylococcus aureus* infections. *Microb Pathog.* (2019) 127:233–8. doi: 10.1016/j.micpath.2018.11.032
  43. Yao K, Wang L, Liu Y, Dong F, Song W, Zhen J, et al. Nasal methicillin-resistant *Staphylococcus aureus* colonization among otherwise healthy children aged between 2 months and 5 years in northern Taiwan, 2005–2010. *BMC Infect Dis.* (2018) 51:756–62. doi: 10.1016/j.jmii.2017.07.014
  44. Huh K, Chung DR. Changing epidemiology of community-associated methicillin-resistant *Staphylococcus aureus* in the Asia-Pacific region. *Expert Rev Anti Infect Ther.* (2016) 14:1007–22. doi: 10.1080/14787210.2016.1236684
  45. Dotel R, O'Sullivan MVN, Davis JS, Newton PJ, Gilbert GL. Molecular epidemiology of methicillin-resistant *Staphylococcus aureus* isolates in New South Wales, Australia, 2012–2017. *Infect Dis Health.* (2019) 24:134–40. doi: 10.1016/j.idh.2019.04.002
  46. Htun HL, Kyaw WM, de Sessions PF, Low L, Hibberd ML, Chow A. Methicillin-resistant *Staphylococcus aureus* colonisation: epidemiological and molecular characteristics in an acute-care tertiary hospital in Singapore. *Epidemiol Infect.* (2018) 146:1785–92. doi: 10.1017/S0950268818001966
  47. Song Y, Du X, Li T, Zhu Y, Li M. Phenotypic and molecular characterization of *Staphylococcus aureus* recovered from different clinical specimens of inpatients at a teaching hospital in Shanghai between 2005 and 2010. *J Med Microbiol.* (2013) 62:274–82. doi: 10.1099/jmm.0.050971-0
  48. Dai Y, Liu J, Guo W, Meng H, Huang Q, He L, et al. Decreasing methicillin-resistant *Staphylococcus aureus* (MRSA) infections is attributable to the disappearance of predominant MRSA ST239 clones, Shanghai, 2008–2017. *Emerg Microbes Infect.* (2019) 8:471–8. doi: 10.1080/22221751.2019.1595161
  49. Witte W. Antibiotic resistance in gram-positive bacteria: epidemiological aspects. *J Antimicrob Chemother.* (1999) 44(Suppl. A), 1–9. doi: 10.1093/jac/44.suppl\_1.1
  50. Qin Y, Wen F, Zheng Y, Zhao R, Hu Q, Zhang R. Antimicrobial resistance and molecular characteristics of methicillin-resistant *Staphylococcus aureus*



- isolates from child patients of high-risk wards in Shenzhen, China. *Jpn J Infect Dis.* (2017) 70:479–84. doi: 10.7883/yoken.JJID.2016.328
51. Chen B, Dai X, He B, Pan K, Li H, Liu X, et al. Differences in *Staphylococcus aureus* nasal carriage and molecular characteristics among community residents and healthcare workers at Sun Yat-Sen University, Guangzhou, Southern China. *BMC Infect Dis.* (2015) 15:303. doi: 10.1186/s12879-015-1032-7
  52. Bongiorno D, Mongelli G, Stefani S, Campanile F. Burden of Rifampicin- and methicillin-resistant *Staphylococcus aureus* in Italy. *Microb Drug Resist.* (2018) 24:732–8. doi: 10.1089/mdr.2017.0299

**Conflict of Interest:** The authors declare that the research was conducted in the absence of any commercial or financial relationships that could be construed as a potential conflict of interest.

Copyright © 2020 Ai, Gao, Yao, Liang, Mai, Xiong, Chen, Liang, Yang, Ou, Gong, Long and Zhou. This is an open-access article distributed under the terms of the Creative Commons Attribution License (CC BY). The use, distribution or reproduction in other forums is permitted, provided the original author(s) and the copyright owner(s) are credited and that the original publication in this journal is cited, in accordance with accepted academic practice. No use, distribution or reproduction is permitted which does not comply with these terms.



# Resistance of *Klebsiella pneumoniae* Strains Carrying *bla*<sub>NDM-1</sub> Gene and the Genetic Environment of *bla*<sub>NDM-1</sub>

Tianxin Xiang<sup>1†</sup>, Chuanhui Chen<sup>2†</sup>, Jiangxiong Wen<sup>3</sup>, Yang Liu<sup>1</sup>, Qi Zhang<sup>1</sup>, Na Cheng<sup>3</sup>, Xiaoping Wu<sup>3</sup> and Wei Zhang<sup>2\*</sup>

<sup>1</sup> Department of Hospital Infection Control, The First Affiliated Hospital of Nanchang University, Nanchang, China,

<sup>2</sup> Department of Respiratory and Critical Care, The First Affiliated Hospital of Nanchang University, Nanchang, China,

<sup>3</sup> Department of Infectious Disease, The First Affiliated Hospital of Nanchang University, Nanchang, China

## OPEN ACCESS

### Edited by:

Ilana L. B. C. Camargo,  
University of São Paulo, Brazil

### Reviewed by:

Zhi Ruan,  
Zhejiang University, China  
Andres Felipe Opazo-Capurro,  
University of Concepción, Chile

### \*Correspondence:

Wei Zhang  
ndzhangwei2016@126.com

† These authors have contributed  
equally to this work

### Specialty section:

This article was submitted to  
Antimicrobials, Resistance  
and Chemotherapy,  
a section of the journal  
Frontiers in Microbiology

Received: 26 September 2019

Accepted: 25 March 2020

Published: 30 April 2020

### Citation:

Xiang T, Chen C, Wen J, Liu Y,  
Zhang Q, Cheng N, Wu X and  
Zhang W (2020) Resistance  
of *Klebsiella pneumoniae* Strains  
Carrying *bla*<sub>NDM-1</sub> Gene  
and the Genetic Environment  
of *bla*<sub>NDM-1</sub>. *Front. Microbiol.* 11:700.  
doi: 10.3389/fmicb.2020.00700

**Objective:** Regional dissemination is the major cause of the widespread prevalence of a plasmid-encoding NDM-1 enzyme. We investigated the drug resistance, joint efficiency, and gene environment of a *Klebsiella pneumoniae* strain carrying *bla*<sub>NDM-1</sub> gene.

**Materials and Methods:** Carbapenem-non-susceptible strains were analyzed using the VITEK 2 Compact. Strains carrying *bla*<sub>NDM-1</sub> were identified using polymerase chain reaction and sequencing. Antimicrobial susceptibility testing and plasmid conjugation experiments were then conducted. Strains carrying *bla*<sub>NDM-1</sub> were subjected to Southern blot analysis. After the gene mapping of *bla*<sub>NDM-1</sub>, library construction, and sequencing, plasmids were subsequently spliced and genotyped using the software Glimmer 3.0, and then analyzed using Mauve software.

**Results:** Among 1735 carbapenem-non-susceptible strains, 54 strains of *bla*<sub>NDM-1</sub>-positive bacteria were identified, which consisted of 44 strains of *K. pneumoniae*, 8 strains of *Acinetobacter baumannii* and 2 strains of *Escherichia coli*. Strains carrying *bla*<sub>NDM-1</sub> had a resistance rate of more than 50% in most antibiotics. Plasmid conjugation between strains carrying *bla*<sub>NDM-1</sub> and *E. coli* strain J53 had a success rate of 50%. Southern blot analysis indicated that each strain had multiple plasmids containing *bla*<sub>NDM-1</sub>. Among the five plasmids containing *bla*<sub>NDM-1</sub> in *K. pneumoniae* for sequencing, two plasmids with complete sequences were obtained. The findings were as follows: (i) The p11106 and p12 plasmids were highly similar to pNDM-BTR; (ii) the p11106 and p12 plasmids showed differences in the 20–30 kb region (orf00032–orf00043) from the other six plasmids; and (iii) *bla*<sub>NDM-1</sub> was located at orf00037, while *ble* was found at orf00038. Two *tnpA* genes were located in the upstream region, and orf00052 (*tnpA*) in the 36 kb region was in the downstream sequence.

**Conclusion:** *bla*<sub>NDM-1</sub>-containing bacteria exhibit multidrug resistance, which rapidly spreads and is transferred through efficient plasmid conjugation; the multidrug

resistance of these bacteria may be determined by analyzing their drug-resistant plasmids. The presence of *ble* and *tnpA* genes suggests a possible hypothesis that *bla*<sub>NDM-1</sub> originates from *A. baumannii*, which is retained in *K. pneumoniae* over a long period by transposition of mobile elements.

**Keywords:** carbapenem resistance, NDM-1, *Klebsiella pneumoniae*, plasmid, genetic characteristics

## INTRODUCTION

The clinical application of sulfa drugs can be traced back to the 1930s, which marked a new era of antimicrobial therapy. Once exposed to antibacterial drugs, bacteria spontaneously change their metabolic pathways or produce corresponding inactivating substances to resist antibiotics, exhibiting drug resistance. Notably, the abuse of antibiotics poses selective pressure of bacteria, conferring a survival advantage on drug-resistant bacteria. Consequently, numerous drug-resistant bacteria are spread in different pathogens.

New Delhi metallo- $\beta$ -lactamase1 (NDM-1), also known as metallo- $\beta$ -lactamase or metal- $\beta$ -lactamase, was first isolated from a highly infectious and pathogenic multidrug-resistant strain of *Klebsiella pneumoniae* in 2009 (Yong et al., 2009). Cases of infection with the *bla*<sub>NDM-1</sub> gene have subsequently been reported in more than 20 countries and regions worldwide, including the United Kingdom and India (Kumarasamy et al., 2010). The therapeutic efficacy of multiple antibiotic treatments for bacteria carrying *bla*<sub>NDM-1</sub> is usually unsatisfactory. Therefore, bacterial strains carrying *bla*<sub>NDM-1</sub> are also called superbugs. With a prolonged length of stay, bacteria-carrying *bla*<sub>NDM-1</sub> have a higher probability of being isolated from stool samples. However, infection with *bla*<sub>NDM-1</sub> cannot be determined from clinical symptoms and signs (Bush and Fisher, 2011). Superbugs pose a serious challenge to antibiotic therapy.

The *bla*<sub>NDM-1</sub> gene is mainly distributed in plasmids and occasionally in the chromosomes of *Escherichia coli*, *Pseudomonas aeruginosa*, and *Proteus mirabilis* (Girlich et al., 2015; Rahman et al., 2015; Shen et al., 2017). In clinical practice, *bla*<sub>NDM-1</sub> plasmids from different bacterial species isolated from the same patient typically have a similar structure, suggesting the significance of plasmids in the spread of *bla*<sub>NDM-1</sub>. Plasmids containing *bla*<sub>NDM-1</sub> vary in size from 30–300 kb, and exist in different types, such as IncA/C, IncL/M, and IncR (Carattoli et al., 2015; Gamal et al., 2016). Specifically, IncA/C has a wide range of hosts and can exist in multiple strains, such as *Enterobacteriaceae*, *Pseudomonas*, *Acinetobacter*, and *Vibrio cholerae*, providing convenience for *bla*<sub>NDM-1</sub> in different species of bacterial hosts (Wailan and Paterson, 2014).

The sequences and genetic modes of *bla*<sub>NDM-1</sub> have been identified in previous studies. However, the *bla*<sub>NDM-1</sub> gene environment is yet to be determined. In addition, studies mostly focus on *bla*<sub>NDM-1</sub> in *Acinetobacter* (Bontron et al., 2016; Wang et al., 2017) and rarely on *bla*<sub>NDM-1</sub> carried by *K. pneumoniae*. In the present study, 1735 carbapenem-non-susceptible bacteria were collected from The First Affiliated Hospital of Nanchang University. These strains were sequenced,

conjugated, and compared with the corresponding plasmids. This study aimed to analyze the differences in the *bla*<sub>NDM-1</sub> gene environment and provide directions in clarifying the origin and propagation of the *bla*<sub>NDM-1</sub> gene.

## MATERIALS AND METHODS

### Sample Collection and Identification

Approval was obtained from the Medical Ethics Committee of The First Affiliated Hospital of Nanchang University and informed consent was obtained from each subject. Carbapenem-non-susceptible bacteria were then collected from The First Affiliated Hospital of Nanchang University from January 2013 to December 2016. A total of 1735 carbapenem-non-susceptible bacteria were isolated and then identified using VITEK 2 Compact (Pioneering Diagnostics, France) at the Microbiology Laboratory at The First Affiliated Hospital of Nanchang University.

### Polymerase Chain Reaction and Sequencing

Polymerase chain reaction (PCR) templates were prepared by boiling. Fresh bacteria were harvested and diluted in 500  $\mu$ L ddH<sub>2</sub>O for 10 min in a boiling water bath. The supernatant was collected as PCR templates. Subsequently, a PCR system with a total volume of 50  $\mu$ L was prepared, consisting of 25  $\mu$ L of Taq Mix (Takara, Dalian), 2  $\mu$ L of forward primer, 2  $\mu$ L of reverse primer, 2  $\mu$ L of template, and 19  $\mu$ L of ddH<sub>2</sub>O. Subsequently, 29 cycles of PCR were conducted. The *bla*<sub>NDM-1</sub> primer sequences were forward 5'-GGCGGAAGGCTCATCACGA-3' and reverse 5'-CGCAACACAGCCTGACTTTC-3'. The amplified product was 287 bp.

The PCR products were analyzed using electrophoresis with 1% agarose gel and 1  $\times$  TAE at 120 V for 25 min. Strains verified by sequencing to contain *bla*<sub>NDM-1</sub> were used as markers. Electrophoresis results were obtained using an ultraviolet (UV) transilluminator. Positive PCR products were sequenced (Synbio Technology, Suzhou, China), and the sequencing results were compared using the software BLAST. Strains that were positive for PCR and matched the sequencing results were identified as those containing *bla*<sub>NDM-1</sub>.

### Antimicrobial Susceptibility Testing

Antimicrobial susceptibility testing was conducted using the zone of inhibition test, and the comprehensive drug resistance of each antibiotic was determined using the E-test. The antibiotics screened in this study included imipenem,

meropenem, ertapenem, amikacin, amoxicillin/clavulanic acid, aztreonam, ceftriaxone, ceftazidime, cephalosporins, cefoxitin, cefazolin, ciprofloxacin, gentamicin, levofloxacin, piperacillin/tazobactam, trimethoprim/sulfamethoxazole, tetracycline, ticarcillin/clavulanic acid, and tobramycin.

## Plasmid Conjugation

The receptor strain was sodium azide-resistant *E. coli* strain J53. The donor and receptor strains were implanted in the Mueller-Hinton plate and cultured at 37°C for 16–18 h. Strains in appropriate amounts were inoculated in a glass tube containing 5 mL of LB medium and then cultured at 37°C for 16–18 h. Subsequently, 400 µL of the donor strain and 200 µL of the receptor strain were added to a glass tube containing 800 µL of LB broth medium and then cultured at 37°C for 16–18 h. Meanwhile, the donor strain, screened in 180 µg/mL sodium azide, and the receptor strain, screened in 0.5 µg/mL of imipenem, were used as blank controls. Exactly 100 µL of the aforementioned mixture was added to the Mueller-Hinton plate and cultured at 37°C for 16–18 h. Conjugation strains in good condition were ultimately identified using the VITEK 2 compact automatic microbial identification instrument.

## Southern Blot Analysis

Southern blot analysis was conducted using 1% agarose gel with 1 × TAE and run on 120 V electrophoresis for 40 min. The gel was incubated in 0.25 mol/L HCl for 15 min, 0.5 mol/L NaOH for 20 min twice, and 0.1 mol/L phosphate buffer for 15 min twice. Membrane transfer was conducted in a 20 × saline-sodium citrate buffer. The membrane was washed in a 2 × saline-sodium citrate buffer and then dried in a baking oven at 80°C for 2 h. PCR products carrying bla<sub>NDM-1</sub> were labeled using the DIG High Prime DNA Labeling and Detection Starter Kit I (Roche, United States). DIG-labeled DNA products were prepared and examined using Southern blot analysis, and images were obtained using a UV transilluminator.

## Plasmid Sequencing

Five qualified plasmids containing bla<sub>NDM-1</sub> were used to construct a sequencing library. These 5 vectors were from 4 strains, which showed high resistance to the antibiotics and successfully conjugated with *E. coli* J53. The data are provided as **Supplementary Material** and **Supplementary Table S2**. Briefly, 1 µg of plasmid was placed in a Covaris tube, and the DNA was separated into 400 bp fragments using Covaris S2 (Covaris, United States). Small DNA fragments were generated for library construction using the NEXTflex DNA Sequencing Kit compatible with Biomek FXp (Bio Scientific, United States). The library fragments were subjected to paired-end sequencing (2 × 150 bp) on the HiSeq2500 Sequencing System (Illumina, United States).

Clean reads after pre-processing were assembled using Velvetver.1.2.03 software. Gene prediction and annotation analyses were performed using Glimmer 3.0 software. The p11106 and p12 plasmids were compared with the plasmid sequences without bla<sub>NDM-1</sub> of the seven species. Similarities in

the plasmid sequences were depicted using Mauve software. Gene functions in different regions were annotated and analyzed.

## RESULTS

### Screening and Identification of Strains Carrying bla<sub>NDM-1</sub>

Among the 1735 carbapenem-non-susceptible strains harvested in this experiment, 54 strains (3.1%) were bla<sub>NDM-1</sub>-positive. These strains consisted of 44 strains of *K. pneumoniae*, 8 strains of *A. baumannii*, and 2 strains of *E. coli*. The bla<sub>NDM-1</sub> gene was not found in *P. aeruginosa*, *Enterobacter cloacae*, *Bacillus*, *Maltophilia*, or *Pseudomonas cepacia*. All sequencing results of the 54 strains were consistent with the NCBI database<sup>1</sup>. The positive rates of each strain are listed in **Table 1**.

These 54 multidrug-resistant strains were obtained from 43 patients at The First Affiliated Hospital of Nanchang University from January 2013 to December 2016. The patients were from different cities and provinces. Temporal and regional differences suggested that the same strains could not be causing the outbreak. Patient records are shown in **Supplementary Table S1**.

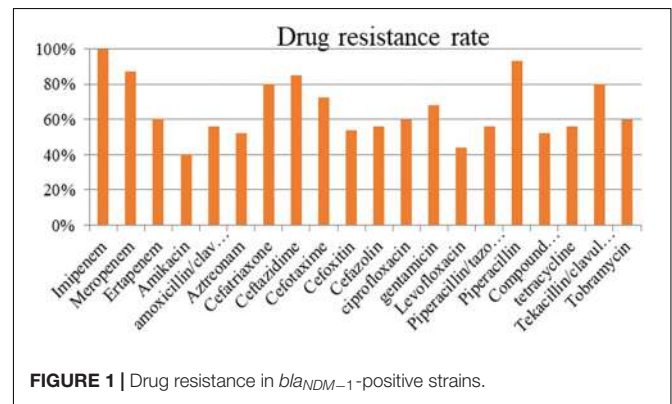
### Determination of Drug Resistance

The resistance rate of the strains carrying bla<sub>NDM-1</sub> exceeded 50% in most antibiotics (**Figure 1**). The tested antibiotics exhibited nearly 100% resistance to imipenem and more than

<sup>1</sup><http://blast.ncbi.nlm.nih.gov/Blast.cgi>

**TABLE 1** | Positive rate of the bla<sub>NDM-1</sub> gene in each strain.

Strain name	Sample size	Positive number	Positive rate
<i>Klebsiella pneumoniae</i>	935	44	4.7%
<i>Acinetobacter baumannii</i>	546	8	1.5%
<i>Escherichia coli</i>	92	2	2.1%
<i>Pseudomonas aeruginosa</i>	83	0	0
<i>Bacillus</i>	40	0	0
<i>Maltophilia</i>	20	0	0
<i>Pseudomonas cepacia</i>	19	0	0
Total	1735	54	3.1%



**FIGURE 1** | Drug resistance in bla<sub>NDM-1</sub>-positive strains.



90% resistance to meropenem and piperacillin. Meanwhile, the bla<sub>NDM-1</sub>-positive strains showed the lowest resistance (40%) to amikacin.

## Plasmid Conjugation

The plasmid conjugation experiment was conducted on all bla<sub>NDM-1</sub>-positive strains and J53. A total of 27 strains (21, *K. pneumoniae* strains; 5, *A. baumannii* strains; and 1, *E. coli* strain) successfully conjugated their plasmids containing the bla<sub>NDM-1</sub> gene (Table 2). The success rate of plasmid conjugation was 50%.

## Location of the bla<sub>NDM-1</sub> Gene

Bla<sub>NDM-1</sub>-positive strains that were successfully conjugated were subjected to Southern blot analysis to detect the location of

bla<sub>NDM-1</sub>. The results further demonstrated the conjugation of bla<sub>NDM-1</sub> in *E. coli* strain J53 (Figure 2).

## Sequencing of Plasmids

Plasmid libraries were constructed from genomic DNA. Qualified plasmid DNAs were sequenced, and the results suggested excellent qualifications for library construction and sequencing (Table 3). After removal of DNA from host genes and other plasmid DNAs, approximately 20% of the reads were extracted from target plasmid DNAs with over 2000× coverage.

Subsequently, the clean reads of each plasmid were synthesized using Velvet. Large-fragment sequence assembly is presented in Table 4. Although coverage was sufficiently high (>2000×), the synthesis was not satisfactory, with the contigs between 33 and 161. Thus, artificial gap closing with the KU862632.1 strain was conducted using the Cytoscape platform, and two complete plasmid (p12 and p11106) sequences were generated. Synthesis of p243323, p32, and p7-1973 failed (Table 4).

The size of p12 was the same as that of p11106 (58757 bp). Cytosine was located on 50396 bp of p11106, thymine was located in p12, and the remaining regions were the same. In the following gene prediction and annotation analysis, p12 was used as an example. As

TABLE 2 | Plasmid conjugation of strains.

Strain name	Number of bla <sub>NDM-1</sub> strains	Number conjugated	Rate of successful conjugation
<i>Klebsiella pneumoniae</i>	44	21	47.7%
<i>Acinetobacter baumannii</i>	8	5	62.5%
<i>Escherichia coli</i>	2	1	50.0%
Total	54	27	50.0%

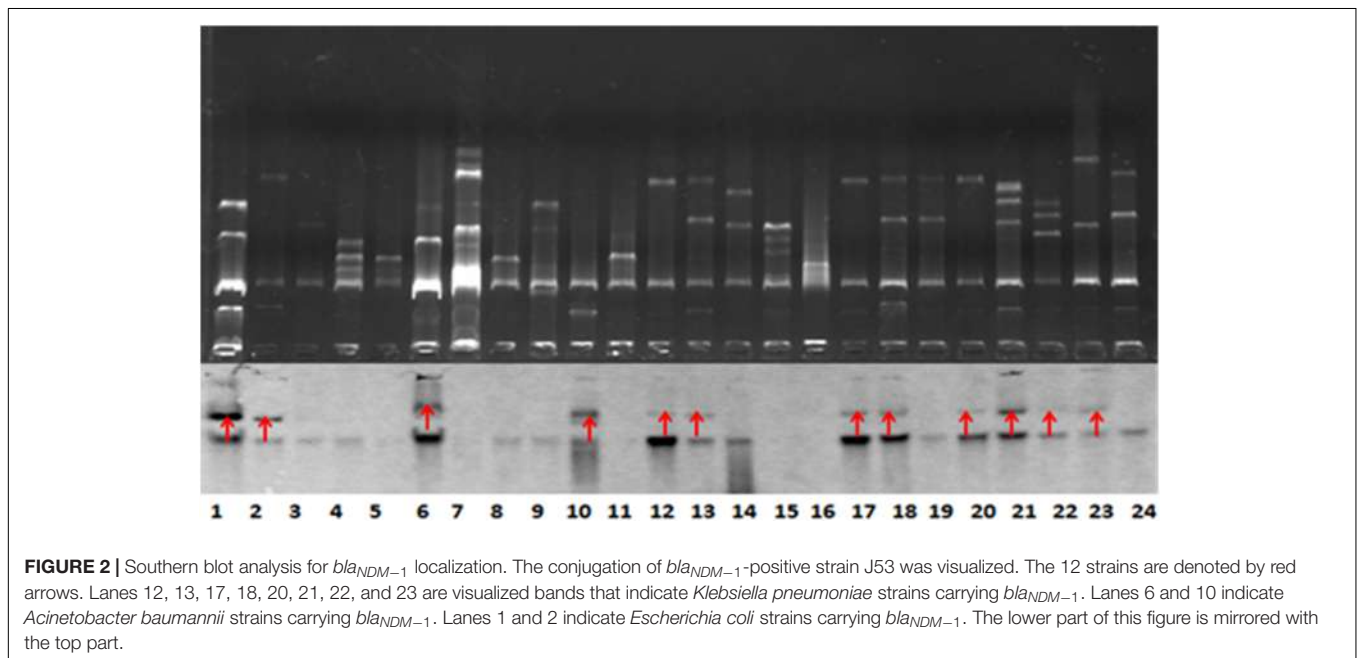


TABLE 3 | Quality and coverage statistics of plasmid genome sequencing.

Plasmid	Raw reads (pair)	Clean reads (pair)	Q20 (%)	Q30 (%)	Target plasmid reads (pair)	Coverage
p11106	5,581,280	5,567,524	95.94	91.06	1,523,524 (27.3%)	7,109
p12	4,562,335	4,551,783	95.05	89.62	1,157,414 (25.4%)	5,401
p243323	4,707,263	4,695,911	96.24	91.56	967,971 (20.6%)	4,517
p32	7,672,469	7,653,464	96.09	91.27	1542,915 (20.1%)	7,200
p7-1973	3,549,640	3,541,667	93.99	87.93	909,991 (25.6%)	2,316

**TABLE 4** | Statistics of plasmid synthesis.

Plasmid	Initial contigs	N50	Synthesis	Completed	GC (%)
p11106	68	4,477	9	Yes	51.99
p12	161	2,403	16	Yes	51.99
p243323	42	7,920	19	No	51.72
p32	33	15,996	16	No	51.74
p7-1973	146	2,914	25	No	53.23

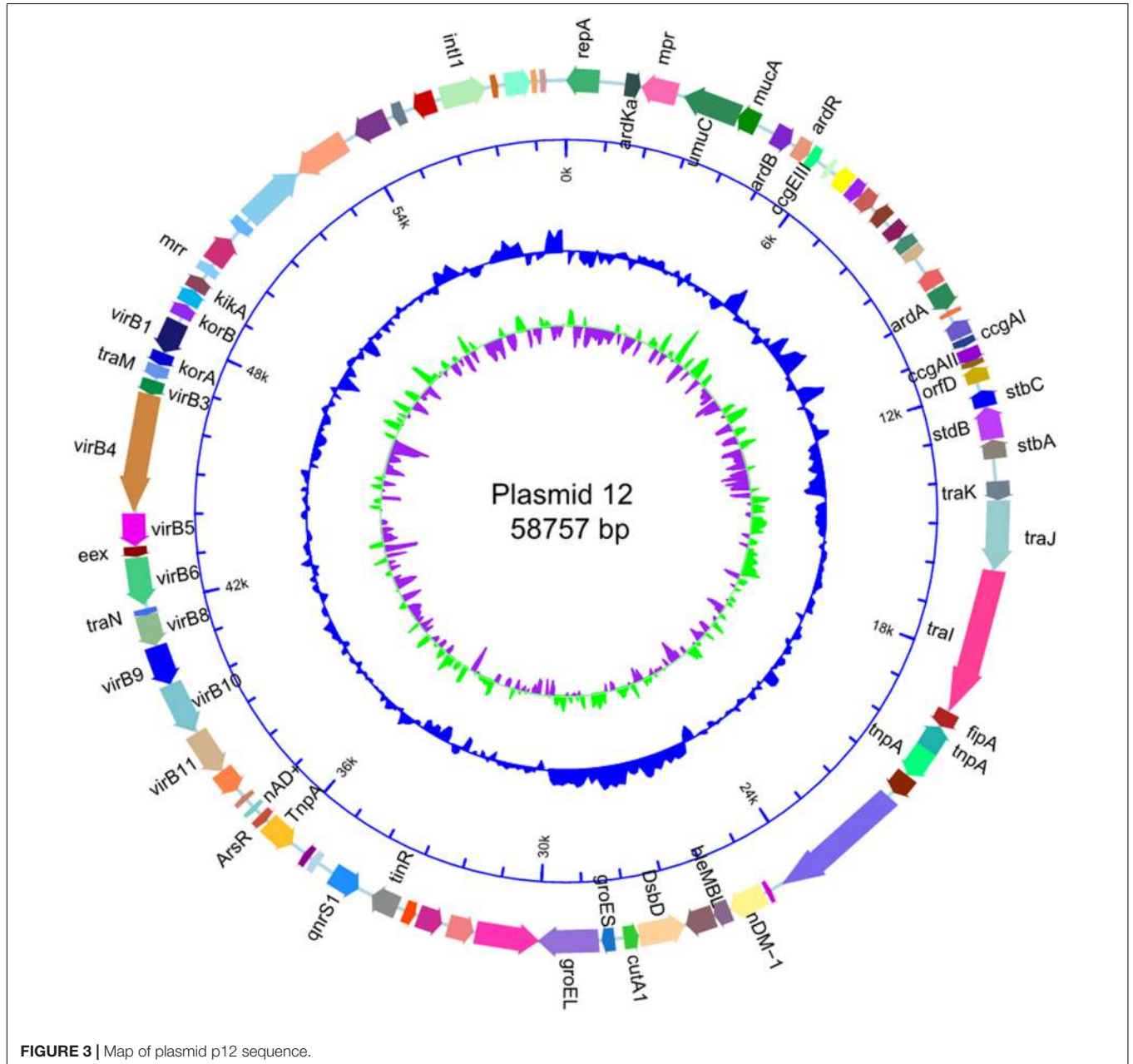
depicted in **Figure 3**, 46 genes were reverse transcribed, and 39 were forward transcribed without chain specificity ( $p = 0.627$ ). We uploaded the sequencing data to the NCBI

database under the SRA (Sequence Read Archive) accession number PRJNA596354.

### Comparative Analysis of the bla<sub>NDM-1</sub> Gene Environment

Plasmid sequences from seven species were subjected to similarity analysis using Mauve software. The baseline characteristics of the selected plasmids are listed in **Table 5**. p11106 and p12 were compared with the aforementioned plasmids, and their similarity information is depicted in **Figure 4** and **Table 6**.

In addition to the plasmid pNDM-BTR, differences between p11106 and p12, and the remaining seven plasmids were



**TABLE 5** | Plasmid information.

ID	Species
KF534788.1	<i>Escherichia coli</i> plasmid pNDM-BTR, complete sequence
CP017725.1	<i>Salmonella enterica</i> subsp. <i>enterica</i> serovar Stanleyville str. CFSAN000624 strain SARB61 plasmid pSARB26_02, complete sequence
HM126016.1	<i>Klebsiella oxytoca</i> plasmid pKOX105, complete sequence
KM660724.1	<i>Morganella morganii</i> strain MRSN22709 plasmid pMR3-OXA181, complete sequence
KT989598.1	<i>Enterobacter cloacae</i> strain CRE1506 plasmid pIMP-SH1506, complete sequence
KU051710.1	<i>Citrobacter freundii</i> strain CRE1503 plasmid pIMP-FJ1503, complete sequence
KU862632.1	<i>Klebsiella pneumoniae</i> strain CRE1495 plasmid pIMP-KP1495, complete sequence

mainly enriched in the 20–30 kb region. Although the plasmid pMR3-OXA181 was not absent in this region, it exhibited a considerably low homology to p11106 and p12. The corresponding genes mapping this 10 kb region were orf00032–orf00043. Moreover, gene annotation showed that two genes (*TnpA* and a mobile element protein) with similar functions were located in the upstream sequences of this region. *Bla*<sub>NDM-1</sub> was also located in these sequences (orf00037). *IMP-4* and  $\beta$ -lactamase were absent in this region. The gene annotations of orf00032–orf00043 are presented in **Table 7**.

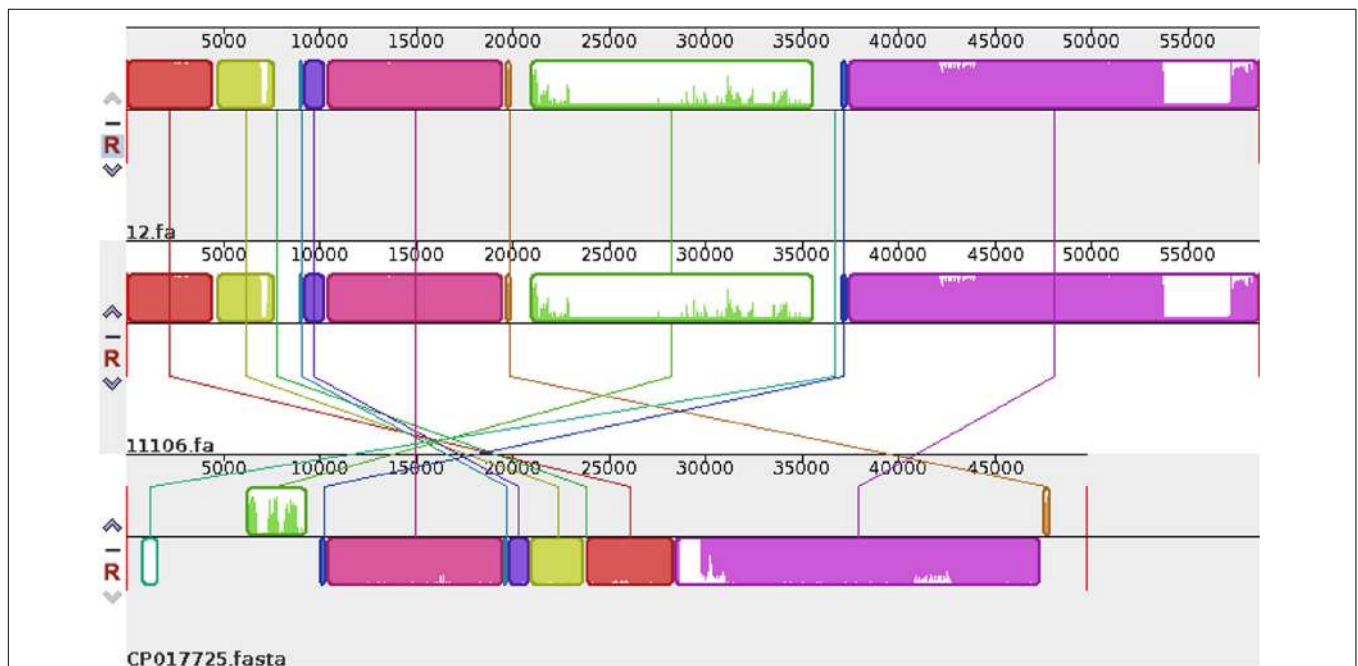
As shown in **Table 7**, (i) the p11106 and p12 plasmids were highly similar to pNDM-BTR; (ii) the p11106 and p12 plasmids showed differences in the 20–30 kb region (orf00032–orf00043) from the other six plasmids; and (iii) *bla*<sub>NDM-1</sub> was located in the middle of the orf00032–orf00043 region, whereas *ble* was found nearby. Two *tnpA* genes were on the top, and orf00052 (*tnpA*) in the 36 kb region was in the downstream sequence.

## DISCUSSION

Among the 1735 carbapenem-non-susceptible strains, 54 (3.1%) of *bla*<sub>NDM-1</sub>-positive bacteria were identified, consisting of 44

**TABLE 6** | Comparison of differential plasmids.

Plasmid	Inserted region (Gene)	Deleted region (Gene)
pNDM-BTR	38 kb ( <i>TnpA</i> )	
pSARB26_02	/	20–37 kb (orf00032–orf00052) 53–57.5 kb (orf00078–orf00082)
pKOX105	/	7–10 kb (orf00012–orf00017) 21–29 kb (orf00035–orf00042)
pMR3-OXA181	24.5–30 kb (orf00036–orf00043)	/
pIMP-SH1506	27–30 kb, 48–51 kb, and 52–53 kb	19.5–30 kb (orf00032–orf00043)
pIMP-FJ1503	45–47.5 kb, 48.5–49 kb	19.5–30 kb (orf00032–orf00043)
pIMP-KP1495	45–48 kb	21–30 kb (orf00034–orf00043)



**FIGURE 4** | Comparison between p12 and p11106 with pSARB26\_02. Differences between p12 and p11106 with pSARB26\_02 (CP017725) were mainly enriched in the 20–37 kb region (green region), with orf00032–orf00052 in p11106 and p12. Two *TnpA* transposases are located in this region (orf00032 mapped 20169–19597 bp, negative strand; orf00033 mapped 20160–20864 bp, positive strand), indicating that gene insertion is highly possible in this region of p11106 and p12. Similarly, additional 3.5 kb sequences present in the 3' UTR of p11106 and p12 were mapped orf00078–orf00082. This may also be explained by gene transposition or insertion.

**TABLE 7** | Gene annotation of orf00032–orf00042.

Gene	Start	End	Strand	Protein length	Function
orf00032	20169	19597	–	190	<i>tnpA</i>
orf00033	20160	20864	+	234	<i>tnpA</i>
orf00034	20870	21352	+	160	Mobile element protein
orf00035	21485	24502	+	1005	Mobile element protein
orf00036	24873	24757	–	38	Multispecies: hypothetical protein
orf00037	24931	25743	+	270	NDM-1
orf00038	25747	26112	+	121	<i>ble</i> <sub>MBL</sub>
orf00039	26117	26755	+	212	Phosphoribosylanthranilate isomerase
orf00040	27797	26766	–	343	DsbD
orf00041	28131	27802	–	109	<i>cutA</i> <sub>1</sub>
orf00042	28325	28615	+	96	<i>groES</i>

strains (4.7%) of *K. pneumoniae*, 8 strains (1.5%) of *A. baumannii*, and 2 strains (2.1%) of *E. coli*. Our findings are consistent with previous studies showing that *bla*<sub>NDM-1</sub> is mainly carried by *K. pneumoniae*, *E. coli*, *A. baumannii*, and *E. cloacae* (Deshpande et al., 2010; Rolain et al., 2010; Zarfel et al., 2011; Dongmei et al., 2017). Among the collected strains carrying *bla*<sub>NDM-1</sub> in our hospital, *K. pneumoniae* (4.7%) had the highest positive rate, which was inconsistent with other reports that identified *Acinetobacter* and *Klebsiella* as the major *bla*<sub>NDM-1</sub>-positive bacteria (Chen et al., 2014; Zhang et al., 2014; Shengshu et al., 2015). Both *Acinetobacter* and *Klebsiella* are significant in the regional dissemination of *bla*<sub>NDM-1</sub>-positive bacteria. *K. pneumoniae* could be the vital preservation host of *bla*<sub>NDM-1</sub>.

Antimicrobial susceptibility testing indicated that NDM-1-resistant bacteria exhibited strong resistance to most antibiotics (except for amikacin), with a total resistance rate above 50%. The drug resistance of NDM-1 to aminoglycosides,  $\beta$ -lactam antibiotics/ $\beta$ -lactamase inhibitors, and carbapenems are relatively high (Shengshu et al., 2015). NDM-1 has a drug resistance of up to 100% for dolipenem, ampicillin, furadantin, cefazolin, cefuroxime, cefotaxime, ceftriaxone sodium, ceftazidime, and ceftoxitin. Its drug resistance rates to some carbapenems are as follows: meropenem, 97.30%; imipenem, 97.30%; and ertapenem, 92.00%. However, the drug resistance rates of NDM-1 to polymyxin B (37.93%), amikacin (32.65%), tigecycline (7.69%), and polymyxin E (2.33%) are significantly lower, compared with other antibiotics. NDM-1-resistant bacteria might be mostly multidrug-resistant, and plasmids containing *bla*<sub>NDM-1</sub> can perform multiple drug-resistant gene transfers (Barguigua et al., 2015; Sarkar et al., 2015; Villa et al., 2015; Liu et al., 2016).

Our experiment obtained 27 successfully conjugated J53 strains resistant to sodium azide, which is consistent with previous studies (Wailan et al., 2015; Kocsis et al., 2016). Conjugation with *K. pneumoniae*, *A. baumannii*, and *E. coli* as donor plasmids containing *bla*<sub>NDM-1</sub> achieved a success

rate of approximately 50%. Southern blot analysis confirmed that *bla*<sub>NDM-1</sub> was mainly expressed in plasmids, and each drug-resistant strain carrying *bla*<sub>NDM-1</sub> could contain multiple *bla*<sub>NDM-1</sub>-positive plasmids. The *bla*<sub>NDM-1</sub>-positive plasmids exhibited a relatively strong ability for conjugation transfer. Specifically, IncA/C showed adaptation to a wide range of hosts. It can be found in *Enterobacteriaceae*, *Pseudomonas*, *Aeromonas*, *Vibrio cholera*, and other bacterial genera, and can be transmitted within or between strains through conjugation (Wailan and Paterson, 2014; Carattoli et al., 2015; Gamal et al., 2016).

Sequencing of five plasmids obtained from the collected *K. pneumoniae* strains was highly qualified (coverage >2000 $\times$ ). Regardless, the synthesis of p243323, p32, and p7-1973 failed; only p11106 and p12 were successfully synthesized. This result could be explained by the complexity of the plasmid structure and interruption of the host genome and other plasmids during plasmid extraction. Among the sequencing reads, only 20–30% of the plasmids were identified to carry the *bla*<sub>NDM-1</sub> gene, significantly increasing the difficulty of synthesis. The only difference between p11106 and p12 was the 50396 bp (orf00074 was mapped) region, where c.587T > C occurred in p11106 and thus resulted in p.196Ile > Thr. A total of 85 genes were contained in the p11106 sequence, and most of them had functions that could be identified using BLAST.

The structures of plasmids p11106 and p12 were similar, and their strains *Kp.11* and *Kp.12* were also similar in resistance (Supplementary Table S2). This finding suggests that resistant plasmids are a key factor in determining the drug resistance of strains.

The genetic environment of a certain gene helps reveal the origin and genetic characteristics of the gene. Poirel et al. (2011) uncovered the full-length or truncated IS*Aba125* sequences in the upstream region of *bla*<sub>NDM-1</sub> and conserved bleomycin (*ble*) resistance genes in the downstream region. They hypothesized that IS*Aba125* sequences are carried by *bla*<sub>NDM-1</sub> when it transfers from the original host, and the *bla*<sub>NDM-1</sub> and *ble* genes come from the same original host strain (Poirel et al., 2011). In 2012, Toleman analyzed all available *bla*<sub>NDM-1</sub>-associated sequences and found that IS*Aba125* sequences are always present in the 100 bp upstream region of *bla*<sub>NDM-1</sub>, and demonstrated that *bla*<sub>NDM-1</sub> is a chimera. The chimeric process occurs in *A. baumannii* and is mediated by IS*Aba125* (Jones et al., 2014, 2015; Toleman et al., 2015). Our sequencing results identified certain differences in the 20–30 kb region between p11106, p12, and the compared plasmids, except for pNDM-BTR. On the basis of the aforementioned findings, we propose the following: (a) p11106 and p12 are structurally similar to pNDM-BTR, indicating that p11106 and p12 may present characteristics of pNDM-BTR (McGann et al., 2015); (b) the differences in the 20–30 kb region between p11106, p12, and the compared plasmids support the theory of gene polymorphism (Potron et al., 2011; Mata et al., 2012; Datta et al., 2017); (c) the existence of *ble* indicates that *bla*<sub>NDM-1</sub> may originate from *A. baumannii*; and (d) the presence of two *TnpA* in the upstream region of *bla*<sub>NDM-1</sub> and orf00052 (*TnpA*) in the 36 kb downstream region suggests that *bla*<sub>NDM-1</sub> is acquired from plasmid



transposition and long-term preservation (Campos et al., 2015; An et al., 2016; Khong et al., 2016).

This experiment screened drug-resistant strains carrying *bla*<sub>NDM-1</sub> gene from carbapenem-non-susceptible bacteria collected from The First Affiliated Hospital of Nanchang University between January 2013 and December 2016. We assessed their drug resistance and plasmid conjugation transfer ability. Two complete plasmid sequences were obtained after sequencing analysis of five *bla*<sub>NDM-1</sub>-positive plasmids isolated from *K. pneumoniae* and compared with *bla*<sub>NDM-1</sub>-negative plasmids with known sequences. However, data on abundance were limited owing to the small sample size of drug-resistant strains as well as complexity and interferences during plasmid synthesis. In addition, the conclusion drawn from sequencing in this study is yet to be verified by molecular experiments. Gene deletion (*IMP-4* and  $\beta$ -lactamase) occurred in p11106 and p12. The presence of a potential relationship between gene deletion and *bla*<sub>NDM-1</sub> requires further study.

## CONCLUSION

In conclusion, NDM-1-resistant bacteria exhibit multidrug resistance and spread to a certain extent in the hospital via efficient plasmid conjugation transfer. *K. pneumoniae* may be an important intermediate retention host in the dissemination process. Nosocomial *bla*<sub>NDM-1</sub>-carrying bacteria are of concern.

Drug-resistant plasmids may be a key factor in determining drug resistance. The p11106 and p12 plasmids containing the *bla*<sub>NDM-1</sub> gene isolated from *K. pneumoniae* exhibit the characteristics of the pNDM-BTR plasmid and have a polymorphic gene environment. The existence of *ble* in the surrounding environment of *bla*<sub>NDM-1</sub> suggests that *bla*<sub>NDM-1</sub> is derived from *A. baumannii*. Meanwhile, the presence of *TnpA* in both the upstream and downstream regions of *bla*<sub>NDM-1</sub> indicates that *bla*<sub>NDM-1</sub> may be acquired from gene transposition and persists over a long period in *K. pneumoniae* strains.

## REFERENCES

- An, J., Guo, L., Zhou, L., Ma, Y., Luo, Y., Tao, C., et al. (2016). NDM-producing *Enterobacteriaceae* in a Chinese hospital, 2014–2015: identification of NDM-producing *Citrobacter werkmanii* and acquisition of bla<sub>NDM-1</sub>-carrying plasmid in vivo in a clinical *Escherichia coli* isolate. *J. Med. Microbiol.* 65, 1253–1259. doi: 10.1099/jmm.0.000357
- Barguigua, A., Zerouali, K., Katfy, K., El Otmani, F., Timinouni, M., and Elmdaghri, N. (2015). Occurrence of OXA-48 and NDM-1 carbapenemase-producing *Klebsiella pneumoniae* in a Moroccan university hospital in Casablanca, Morocco. *Infect. Genet. Evol.* 31, 142–148. doi: 10.1016/j.meegid.2015.01.010
- Bontron, S., Nordmann, P., and Poirel, L. (2016). Transposition of Tn125 Encoding the NDM-1 Carbapenemase in *Acinetobacter baumannii*. *Antimicrob. Agents Chemother.* 60, 7245–7251. doi: 10.1128/AAC.01755-16
- Bush, K., and Fisher, J. F. (2011). Epidemiological expansion, structural studies, and clinical challenges of new beta-lactamases from gram-negative bacteria. *Annu. Rev. Microbiol.* 65, 455–478. doi: 10.1146/annurev-micro-090110-102911
- Campos, J. C., da Silva, M. J., dos Santos, P. R., Barros, E. M., Pereira Mde, O., Seco, B. M., et al. (2015). Characterization of Tn3000, a Transposon Responsible for bla<sub>NDM-1</sub> Dissemination among *Enterobacteriaceae* in Brazil, Nepal, Morocco,

## DATA AVAILABILITY STATEMENT

The datasets generated for this study are available from the corresponding author upon reasonable request.

## ETHICS STATEMENT

Written informed consent was obtained from all participants, and the purpose and procedures of the study were explained to them. Ethical approval for this study was obtained from the Institutional Review Board of The First Affiliated Hospital of Nanchang University.

## AUTHOR CONTRIBUTIONS

TX and CC designed the study, collected and analyzed the data, and drafted the manuscript. TX, CC, JW, YL, and QZ contributed to the performance of the experiment and data collection. NC and XW reviewed the study design. WZ contributed to the review of data analysis and data interpretation. All authors have approved the final version of the manuscript.

## FUNDING

This work was supported by the Fund Project of Jiangxi Health and Family Planning Commission (20181058) and the Natural Science Foundation of Jiangxi Province (20181BAB215033).

## SUPPLEMENTARY MATERIAL

The Supplementary Material for this article can be found online at: <https://www.frontiersin.org/articles/10.3389/fmicb.2020.00700/full#supplementary-material>

- and India. *Antimicrob. Agents Chemother.* 59, 7387–7395. doi: 10.1128/aac.01458-15
- Carattoli, A., Seiffert, S. N., Schwendener, S., Perreten, V., and Endimiani, A. (2015). Differentiation of IncL and IncM Plasmids associated with the spread of clinically relevant antimicrobial resistance. *PLoS One* 10:e0123063. doi: 10.1371/journal.pone.0123063
- Chen, C. J., Wu, T. L., Lu, P. L., Chen, Y. T., Fung, C. P., Chuang, Y. C., et al. (2014). Closely related NDM-1-encoding plasmids from *Escherichia coli* and *Klebsiella pneumoniae* in Taiwan. *PLoS One* 9:e104899. doi: 10.1371/journal.pone.0104899
- Datta, S., Mitra, S., Chattopadhyay, P., Som, T., Mukherjee, S., and Basu, S. (2017). Spread and exchange of bla<sub>NDM-1</sub> in hospitalized neonates: role of mobilizable genetic elements. *Eur. J. Clin. Microbiol. Infect. Dis.* 36, 255–265. doi: 10.1007/s10096-016-2794-6
- Deshpande, P., Rodrigues, C., Shetty, A., Kapadia, F., Hedge, A., and Soman, R. (2010). New Delhi Metallo-beta lactamase (NDM-1) in *Enterobacteriaceae*: treatment options with carbapenems compromised. *J. Assoc. Physicians India* 58, 147–149.
- Dongmei, N., Wanqing, Z., and Zhang, Z. (2017). Distribution of NDM-1 gene in strains of *Acinetobacter* sp. *J. Clin. Transfus Lab. Med.* 19, 364–367. doi: 10.1093/jac/dkr174

- Gamal, D., Fernandez-Martinez, M., Salem, D., El-Defrawy, I., Montes, L. A., Ocampo-Sosa, A. A., et al. (2016). Carbapenem-resistant *Klebsiella pneumoniae* isolates from Egypt containing bla<sub>NDM-1</sub> on IncR plasmids and its association with rmtF. *Int. J. Infect. Dis.* 43, 17–20. doi: 10.1016/j.ijid.2015.12.003
- Girlich, D., Dortet, L., Poiriel, L., and Nordmann, P. (2015). Integration of the bla<sub>NDM-1</sub> carbapenemase gene into Proteus genomic island 1 (PGI1-PmPEL) in a *Proteus mirabilis* clinical isolate. *J. Antimicrob. Chemother.* 70, 98–102. doi: 10.1093/jac/dku371
- Jones, L. S., Carvalho, M. J., Toleman, M. A., White, P. L., Connor, T. R., Mushtaq, A., et al. (2015). Characterization of plasmids in extensively drug-resistant acinetobacter strains isolated in India and Pakistan. *Antimicrob. Agents Chemother.* 59, 923–929. doi: 10.1128/aac.03242-14
- Jones, L. S., Toleman, M. A., Weeks, J. L., Howe, R. A., Walsh, T. R., and Kumarasamy, K. K. (2014). Plasmid carriage of bla<sub>NDM-1</sub> in clinical *Acinetobacter baumannii* isolates from India. *Antimicrob. Agents Chemother.* 58, 4211–4213. doi: 10.1128/aac.02500-14
- Khong, W. X., Xia, E., Marimuthu, K., Xu, W., Teo, Y. Y., Tan, E. L., et al. (2016). Local transmission and global dissemination of New Delhi Metallo-Beta-Lactamase (NDM): a whole genome analysis. *BMC Genomics* 17:452. doi: 10.1186/s12864-016-2740-0
- Kocsis, E., Guzvinec, M., Butic, I., Kresic, S., Crnek, S. S., Tambic, A., et al. (2016). bla<sub>NDM-1</sub> carriage on IncR plasmid in *Enterobacteriaceae* strains. *Microb. Drug Resist.* 22, 123–128. doi: 10.1089/mdr.2015.0083
- Kumarasamy, K. K., Toleman, M. A., Walsh, T. R., Bagaria, J., Butt, F., Balakrishnan, R., et al. (2010). Emergence of a new antibiotic resistance mechanism in India, Pakistan, and the UK: a molecular, biological, and epidemiological study. *Lancet Infect. Dis.* 10, 597–602. doi: 10.1016/s1473-3099(10)70143-2
- Liu, Y. Y., Wang, Y., Walsh, T. R., Yi, L. X., Zhang, R., Spencer, J., et al. (2016). Emergence of plasmid-mediated colistin resistance mechanism MCR-1 in animals and human beings in China: a microbiological and molecular biological study. *Lancet Infect. Dis.* 16, 161–168. doi: 10.1016/s1473-3099(15)00424-7
- Mata, C., Miro, E., Alvarado, A., Garcillan-Barcia, M. P., Toleman, M., Walsh, T. R., et al. (2012). Plasmid typing and genetic context of AmpC beta-lactamases in *Enterobacteriaceae* lacking inducible chromosomal ampC genes: findings from a Spanish hospital 1999–2007. *J. Antimicrob. Chemother.* 67, 115–122. doi: 10.1093/jac/dkr412
- McGann, P., Snesrud, E., Ong, A. C., Appalla, L., Koren, M., Kwak, Y. I., et al. (2015). War wound treatment complications due to transfer of an IncN plasmid harboring bla(OXA-181) from *Morganella morganii* to CTX-M-27-producing sequence type 131 *Escherichia coli*. *Antimicrob. Agents Chemother.* 59, 3556–3562. doi: 10.1128/aac.04442-14
- Poiriel, L., Dortet, L., Bernabeu, S., and Nordmann, P. (2011). Genetic features of bla<sub>NDM-1</sub>-positive *Enterobacteriaceae*. *Antimicrob. Agents Chemother.* 55, 5403–5407. doi: 10.1128/aac.00585-11
- Potron, A., Poiriel, L., and Nordmann, P. (2011). Plasmid-mediated transfer of the bla(NDM-1) gene in gram-negative rods. *FEMS Microbiol. Lett.* 324, 111–116. doi: 10.1111/j.1574-6968.2011.02392.x
- Rahman, M., Prasad, K. N., Pathak, A., Pati, B. K., Singh, A., Ovejero, C. M., et al. (2015). RmtC and RmtF 16S rRNA methyltransferase in NDM-1-Producing *Pseudomonas aeruginosa*. *Emerg. Infect. Dis.* 21, 2059–2062. doi: 10.3201/eid2111.150271
- Rolain, J. M., Parola, P., and Cornaglia, G. (2010). New Delhi metallo-beta-lactamase (NDM-1): towards a new pandemic? *Clin. Microbiol. Infect.* 16, 1699–1701. doi: 10.1111/j.1469-0691.2010.03385.x
- Sarkar, A., Pazhani, G. P., Chowdhury, G., Ghosh, A., and Ramamurthy, T. (2015). Attributes of carbapenemase encoding conjugative plasmid pNDM-SAL from an extensively drug-resistant *Salmonella enterica* serovar senftenberg. *Front. Microbiol.* 6:969. doi: 10.3389/fmicb.2015.00969
- Shen, P., Yi, M., Fu, Y., Ruan, Z., Du, X., Yu, Y., et al. (2017). Detection of an *Escherichia coli* sequence type 167 strain with two tandem copies of bla<sub>NDM-1</sub> in the chromosome. *J. Clin. Microbiol.* 55, 199–205. doi: 10.1128/jcm.01581-16
- Shengshu, W., Jinzhu, S., Wenli, S., Zhi, H., Jianpeng, Y., and Wang, Y. (2015). Epidemiological analysis of NDM-1-positive bacteria in China. *Mil. Med. Sci.* 39, 825–830. doi: 10.1128/AAC.00165-11
- Toleman, M. A., Bugert, J. J., and Nizam, S. A. (2015). Extensively drug-resistant New Delhi metallo-beta-lactamase-encoding bacteria in the environment, Dhaka, Bangladesh, 2012. *Emerg. Infect. Dis.* 21, 1027–1030. doi: 10.3201/eid2106.141578
- Villa, L., Guerra, B., Schmoger, S., Fischer, J., Helmuth, R., Zong, Z., et al. (2015). IncA/C Plasmid Carrying bla(NDM-1), bla(CMY-16), and fosA3 in a *Salmonella enterica* Serovar Corvallis Strain Isolated from a Migratory Wild Bird in Germany. *Antimicrob. Agents Chemother.* 59, 6597–6600. doi: 10.1128/aac.00944-15
- Wailan, A. M., and Paterson, D. L. (2014). The spread and acquisition of NDM-1: a multifactorial problem. *Expert Rev. Anti Infect. Ther.* 12, 91–115. doi: 10.1586/14787210.2014.856756
- Wailan, A. M., Sartor, A. L., Zowawi, H. M., Perry, J. D., Paterson, D. L., and Sidjabat, H. E. (2015). Genetic contexts of bla<sub>NDM-1</sub> in patients carrying multiple NDM-Producing strains. *Antimicrob. Agents Chemother.* 59, 7405–7410. doi: 10.1128/aac.01319-15
- Wang, Y., Zhang, R., Li, J., Wu, Z., Yin, W., Schwarz, S., et al. (2017). Comprehensive resistome analysis reveals the prevalence of NDM and MCR-1 in Chinese poultry production. *Nat. Microbiol.* 2:16260. doi: 10.1038/nmicrobiol.2016.260
- Yong, D., Toleman, M. A., Giske, C. G., Cho, H. S., Sundman, K., Lee, K., et al. (2009). Characterization of a new metallo-beta-lactamase gene, bla(NDM-1), and a novel erythromycin esterase gene carried on a unique genetic structure in *Klebsiella pneumoniae* sequence type 14 from India. *Antimicrob. Agents Chemother.* 53, 5046–5054. doi: 10.1128/aac.00774-09
- Zarfel, G., Hoenigl, M., Leitner, E., Salzer, H. J., Feierl, G., Masoud, L., et al. (2011). Emergence of New Delhi metallo-beta-lactamase, Austria. *Emerg. Infect. Dis.* 17, 129–130. doi: 10.3201/eid1701.101331
- Zhang, R., Hu, Y. Y., Yang, X. F., Gu, D. X., Zhou, H. W., Hu, Q. F., et al. (2014). Emergence of NDM-producing non-baumannii *Acinetobacter* spp. isolated from China. *Eur. J. Clin. Microbiol. Infect. Dis.* 33, 853–860. doi: 10.1007/s10096-013-2024-4

**Conflict of Interest:** The authors declare that the research was conducted in the absence of any commercial or financial relationships that could be construed as a potential conflict of interest.

Copyright © 2020 Xiang, Chen, Wen, Liu, Zhang, Cheng, Wu and Zhang. This is an open-access article distributed under the terms of the Creative Commons Attribution License (CC BY). The use, distribution or reproduction in other forums is permitted, provided the original author(s) and the copyright owner(s) are credited and that the original publication in this journal is cited, in accordance with accepted academic practice. No use, distribution or reproduction is permitted which does not comply with these terms.



# Prevalence, Genetic Diversity, and Temporary Shifts of Inducible Clindamycin Resistance *Staphylococcus aureus* Clones in Tehran, Iran: A Molecular–Epidemiological Analysis From 2013 to 2018

Mehdi Goudarzi<sup>1\*</sup>, Nobumichi Kobayashi<sup>2</sup>, Masoud Dadashi<sup>3</sup>, Roman Pantůček<sup>4</sup>, Mohammad Javad Nasiri<sup>1</sup>, Maryam Fazeli<sup>5</sup>, Ramin Pouriran<sup>6</sup>, Hossein Goudarzi<sup>1</sup>, Mirmohammad Miri<sup>7</sup>, Anahita Amirpour<sup>8</sup> and Sima Sadat Seyedjavadi<sup>9</sup>

## OPEN ACCESS

### Edited by:

Ilana L. B. C. Camargo,  
University of São Paulo, Brazil

### Reviewed by:

Kiyyukia Matthews Ciira,  
Mount Kenya University, Kenya  
Artur J. Sabat,  
University Medical Center Groningen,  
Netherlands

### \*Correspondence:

Mehdi Goudarzi  
goudarzim@yahoo.com;  
m.goudarzi@sbm.ac.ir

### Specialty section:

This article was submitted to  
Antimicrobials, Resistance  
and Chemotherapy,  
a section of the journal  
Frontiers in Microbiology

**Received:** 22 August 2019

**Accepted:** 23 March 2020

**Published:** 30 April 2020

### Citation:

Goudarzi M, Kobayashi N,  
Dadashi M, Pantůček R, Nasiri MJ,  
Fazeli M, Pouriran R, Goudarzi H,  
Miri M, Amirpour A and  
Seyedjavadi SS (2020) Prevalence,  
Genetic Diversity, and Temporary  
Shifts of Inducible Clindamycin  
Resistance *Staphylococcus aureus*  
Clones in Tehran, Iran:  
A Molecular–Epidemiological Analysis  
From 2013 to 2018.  
*Front. Microbiol.* 11:663.  
doi: 10.3389/fmicb.2020.00663

<sup>1</sup> Department of Microbiology, School of Medicine, Shahid Beheshti University of Medical Sciences, Tehran, Iran,

<sup>2</sup> Department of Hygiene, School of Medicine, Sapporo Medical University, Sapporo, Japan, <sup>3</sup> Department of Microbiology, School of Medicine, Alborz University of Medical Sciences, Karaj, Iran, <sup>4</sup> Department of Experimental Biology, Faculty of Science, Masaryk University, Brno, Czechia, <sup>5</sup> Department of Virology, Pasteur Institute of Iran, Tehran, Iran, <sup>6</sup> School of Medicine, Shahid Beheshti University of Medical Sciences, Tehran, Iran, <sup>7</sup> Department of Critical Care and Anesthesiology, Imam Hossein Hospital, Shahid Beheshti University of Medical Sciences, Tehran, Iran, <sup>8</sup> Department of Internal Medicine, Shahid Beheshti University of Medical Sciences, Tehran, Iran, <sup>9</sup> Department of Mycology, Pasteur Institute of Iran, Tehran, Iran

The prevalence of *Staphylococcus aureus* as an aggressive pathogen resistant to multiple antibiotics causing nosocomial and community-acquired infections is increasing with limited therapeutic options. Macrolide-lincosamide streptogramin B (MLS<sub>B</sub>) family of antibiotics represents an important alternative therapy for staphylococcal infections. This study was conducted over a period of five years from August 2013 to July 2018 to investigate the prevalence and molecular epidemiology in Iran of inducible resistance in *S. aureus*. In the current study, 126 inducible methicillin-resistant *S. aureus* (MRSA) ( $n = 106$ ) and methicillin-sensitive *S. aureus* (MSSA) ( $n = 20$ ) isolates were characterized by *in vitro* susceptibility analysis, resistance and virulence encoding gene distribution, phenotypic and genotypic analysis of biofilm formation, prophage typing, *S. aureus* protein A locus (*spa*) typing, staphylocoagulase (SC) typing, staphylococcal cassette chromosome *mec* (SCC*mec*) typing, and multilocus sequence typing. Of the 126 isolates, 76 (60.3%) were classified as hospital onset, and 50 (39.7%) were classified as community onset (CO). Biofilm formation was observed in 97 strains (77%). A total of 14 sequence types (STs), 26 *spa* types, 7 coagulase types, 9 prophage types, 3 *agr* types (no *agr* IV), and 9 clonal complexes (CCs) were identified in this study. The prevalence of the inducible MLS<sub>B</sub> (iMLS<sub>B</sub>) *S. aureus* increased from 7.5% (25/335) to 21.7% (38/175) during the study period. The iMLS<sub>B</sub> MRSA isolates were distributed in nine CCs, whereas the MSSA isolates were less diverse, which mainly belonged to CC22 (7.95%) and CC30 (7.95%). High-level mupirocin-resistant strains belonged to ST85-SCC*mec* IV/t008 ( $n = 4$ ), ST5-SCC*mec* IV/t002 ( $n = 4$ ), ST239-SCC*mec* III/t631 ( $n = 2$ ), and ST8-SCC*mec* IV/t064 ( $n = 2$ ) clones, whereas low-level mupirocin-resistant

strains belonged to ST15-SCC*mec* IV/t084 ( $n = 5$ ), ST239-SCC*mec* III/t860 ( $n = 3$ ), and ST22-SCC*mec* IV/t790 ( $n = 3$ ) clones. All the fusidic acid-resistant iMLSB isolates were MRSA and belonged to ST15-SCC*mec* IV/t084 ( $n = 2$ ), ST239-SCC*mec* III/t030 ( $n = 2$ ), ST1-SCC*mec* V/t6811 ( $n = 1$ ), ST80-SCC*mec* IV/t044 ( $n = 1$ ), and ST59-SCC*mec* IV/t437 ( $n = 1$ ). The CC22 that was predominant in 2013–2014 (36% of the isolates) had almost disappeared in 2017–2018, being replaced by the CC8, which represented 39.5% of the 2017–2018 isolates. This is the first description of temporal shifts of iMLSB *S. aureus* isolates in Iran that identifies predominant clones and treatment options for iMLSB *S. aureus*-related infections.

**Keywords:** methicillin-resistant *S. aureus*, methicillin-susceptible *S. aureus*, inducible resistance, staphylocoagulase, SCC*mec*, agr allotype, MLST

## INTRODUCTION

*Staphylococcus aureus* is one of the most common aggressive pathogen that causes many diseases in humans and animals such as skin and soft tissue infections, osteomyelitis, bacteremia, and endocarditis (Gordon and Lowy, 2008). The expression of virulence factors promoting adhesion needs nutrients, and evasion of host immunologic responses including cell surface components (collagen-binding protein, clumping factor, fibronectin-binding protein, and elastin-binding protein), secreted factors (staphylokinase toxic shock syndrome toxin-1), hemolysin, exfoliative toxins (ETA and ETB), staphylococcal enterotoxins (SEs), and lipase and Panton–Valentine leukocidin (PVL), besides the presence of antibiotic resistance genes, turns *S. aureus* into a very pathogenic microorganism (Gordon and Lowy, 2008; Gould et al., 2012).

In addition to the aforementioned, the biofilm-forming of *S. aureus* strains can play a key role in pathogenesis and resistance to antimicrobials (Luther et al., 2018). The rate of infections due to *S. aureus*, especially the antibiotic-resistant strains, has dramatically increased recently, which is becoming a serious problem all over the world (Gould et al., 2012). Emerging simultaneous resistance to multiple antibacterial agents underscores the necessity for therapeutic alternatives for the treatment of bacterium-related infections (Pantosti et al., 2007; Dadashi et al., 2018). Although the use of effective antibiotics such as vancomycin, linezolid, and quinupristin–dalfopristin is considered appropriate for therapy, widespread utilization of these antibiotics has made the current usage of these therapeutic options often unsuccessful (Pantosti et al., 2007; Gould et al., 2012; Wang et al., 2012; Dadashi et al., 2018). In recent years, the use of macrolide–lincosamide–streptogramin group B (MLSB) antibiotics has been favored, which is regarded as an alternative approach to treating such infections (Patel et al., 2006). Clindamycin, a member of MLSB family, serves as one such effective therapeutic alternative for treating *S. aureus* infections, because of its proven efficacy, safety, convenience of administration (parenteral and oral), and excellent pharmacokinetic properties. However, one important issue in clindamycin administration is the potential emergence of inducible clindamycin resistance, which may increase the risk of clinical failure (Chavez-Bueno et al., 2005; Adhikari et al., 2017).

Recent published data indicate that there has been a concurrent worldwide increase in the prevalence of inducible clindamycin resistance in different areas (Abimanyu et al., 2012; Wang et al., 2012). Evidence of epidemiological researches has revealed that iMLSB *S. aureus* strains are mostly genetically distinct from each other. One of the most prevalent iMLSB *S. aureus* strains in the United States belongs to sequence type 8 (ST8) strains, whereas in European countries, the majority of iMLSB *S. aureus* strains circulating was affiliated with the clonal complexes CC5 and CC8 (Ilczyszyn et al., 2016). Many studies across the world have focused on molecular epidemiology and analysis of iMLSB *S. aureus* strains isolated from the clinic (Lewis and Jorgensen, 2005; Patel et al., 2006; Adhikari et al., 2017). In our country, data on the prevalence or genetic diversity of inducible clindamycin resistance among *S. aureus* are very unknown, and there have been no published data on the molecular epidemiological characterization of the inducible clindamycin-resistant *S. aureus* strains in Iran. Here we provide molecular characterization of iMLSB *S. aureus* strains. With this aim, phenotypic and genotypic resistance patterns, presence of different classes of prophages, biofilm-forming ability, presence of the *icaABCD*, adhesion genes, and virulence factors were assessed. Then, multilocus sequence typing (MLST), staphylococcal cassette chromosome *mec* (SCC*mec*), *agr*, *coa*, and *spa* typing methods were used to characterize the genotype of the iMLSB *S. aureus* strains. To the best of our knowledge, this is the first report on the molecular characterization of the inducible clindamycin-resistant *S. aureus* strains from Iran.

## MATERIALS AND METHODS

### Study Population, Bacterial Isolation, and Inducible Clindamycin Resistance Screening

A total of 1,161 non-duplicated clinical *S. aureus* isolates were obtained from different clinical specimens including wound, blood, pus, urine, sputum, conjunctivitis, and body fluids from both genders and all age groups of patients, over a period of 5 years from August 2013 to July 2018. This cross-sectional study was conducted in four hospitals affiliated to Shahid Beheshti



University of Medical Sciences (Loghman, Shohada, Taleghani, Emam Hossein). The processing of all samples was done in 2 h. Among these isolates, 126 *S. aureus* isolates were identified with iMLSB phenotype based on the routine biochemical techniques such as Gram staining; colony morphology comprising shape, size, color, and hemolysis patterns; catalase test; tube coagulase test; growth on mannitol salt agar; and DNase. Polymerase chain reaction (PCR) assay targeting the *S. aureus*-specific *nuc* gene was applied to verify the isolates (Goudarzi et al., 2016b). *Staphylococcus aureus* strains were studied to identify inducible resistance phenotypes according to the Clinical and Laboratory Standard Institute (CLSI) D-zone test. The D-zone test was performed by placing 15 µg erythromycin and 2 µg clindamycin disks at a spaced 15 to 26 mm apart from center to center on the Mueller–Hinton agar (Merck, Darmstadt, Germany) plate inoculated with a 0.5 McFarland-equivalent bacterial suspension. The results also were read at 16 to 18 h incubation at 37°C and ambient air, using transmitted and reflected light; inducible clindamycin resistance was verified if the clindamycin zone of inhibition adjacent to the erythromycin disk (D-shape) was flattened. A confirmatory microdilution broth test was done on all isolates for further confirmation. Briefly, any growth in the same well that contained 4 µg/mL erythromycin and 0.5 µg/mL clindamycin was set as a positive test and vice versa. *Staphylococcus aureus* ATCC 25923 was used to perform routine quality control of antibiotic disks. Confirmed isolates were kept into tryptic soy broth (TSB; Merck) with 20% glycerol at –70°C for molecular testing.

Hospital-onset (HO) *S. aureus* was set if the positive culture of *S. aureus* was obtained on or after 96 h of admission to a hospital. Community-onset (CO) *S. aureus* was set if the culture was obtained prior to 4 days of hospitalization with one or more of the following criteria: (1) a history of hospitalization, surgery, dialysis, or residence in a long-term care facility in 12 months prior to culture date or (2) the presence of a central vascular catheter within 2 days before *S. aureus* culture. Invasive *S. aureus* infection was defined according to the Centers for Disease Control and Prevention defining isolation of *S. aureus* from typically sterile body sites such as the blood, bone, fluids (pericardial, joint/synovial, peritoneal, cerebrospinal, and pleural), internal body sites (brain, lymph node, pancreas, ovary, liver, spleen, heart, and kidney), or other normally sterile sites (Goudarzi et al., 2016a). The Ethics Committee of the Shahid Beheshti University of Medical Sciences in Tehran, Iran, certified the protocol of this project (IR.SBMU. MSP.REC.1396.412).

## Determining Resistance Pattern

Phenotypic methicillin resistance screening was performed by placing the cefoxitin disk (30 µg) on Mueller–Hinton agar (Merck), previously inoculated with a 0.5 McFarland-equivalent bacterial suspension. *In vitro* susceptibility of the isolates to kanamycin, ciprofloxacin, penicillin, quinupristin–dalfopristin, rifampin, tetracycline, linezolid, teicoplanin, amikacin, tobramycin, gentamicin, and trimethoprim–sulfamethoxazole (Mast; Merseyside, United Kingdom) was done according to the modified Kirby–Bauer disk diffusion method on Mueller–Hinton agar plates, as per CLSI recommendation. The European

Committee for Antimicrobial Susceptibility Testing (EUCAST) breakpoint was used for interpreting the results of fusidic acid and ceftriaxone disks. As specified by the CLSI guidelines, the broth microdilution method was applied for determining the minimum inhibitory concentration (MIC) of vancomycin and mupirocin. Minimum inhibitory concentration values of 8 to 256 and  $\geq 512$  µg/mL were established to show low-level and high-level mupirocin resistance (LLMUPR, HLMUPR) of the strains, in the respective order. As specified by the CLSI guidelines, MIC breakpoints for vancomycin were set as follows: susceptible,  $\leq 2$  µg/mL; intermediate, 4–8 µg/mL; and resistant,  $\geq 16$  µg/mL. Fusidic acid MICs were specified by the broth microdilution method and interpreted based on EUCAST guidelines. Minimum inhibitory concentration breakpoints were set as follows: susceptible,  $\leq 1$  µg/mL; and resistant,  $> 1$  µg/mL. The *S. aureus* ATCC 25923 and ATCC 29213 strains were put to test as control strains. Sigma Chemical Co. (St. Louis, MO, United States) provided the study with the powders of antibiotics.

## DNA Extraction

To extract DNA, overnight cultures of *S. aureus* strains on 5% sheep blood agar (Merck) were used by applying the InstaGene Matrix kit (Bio-Rad, Hercules, CA, United States) following the manufacturer's instructions and adding lysostaphin (Sigma-Aldrich; St. Louis, United States) for bacterial lysis. Gel electrophoresis and NanoDrop 2000 spectrophotometer (Thermo, Wilmington, Delaware, United States) were applied, respectively, to test the quality and quantity of isolated *S. aureus* DNA (Goudarzi et al., 2016a,b). Seemingly, if the purity were appropriated, it would be applied as the template for PCR. Two hundred microliters of elution buffer [10 mM Tris–Cl, 0.5 mM EDTA (pH 9.0)] was applied to elute the extracted DNA, which was then kept at –20°C until use.

## Detecting Antimicrobial Resistance Determinants and Virulence Factors

Polymerase chain reaction method was used for genotypic amplification of the *mecA* gene (Goudarzi et al., 2016a,b). Isolates exhibiting phenotypic resistance to particular antimicrobial agents were put to test for the presence of resistance genes [*mecA*, *vanA*, *vanB*, *mupB*, *mupA*, *fusA*, *fusB*, *fusC*, *erm(A)*, *erm(B)*, *erm(C)*, *tet(M)*, *ant* (4')-Ia, *aac* (6')-Ie/aph (2''), *aph* (3')-IIIa] (Castanheira et al., 2010a; Nezhad et al., 2017). Virulence factors involved SE genes (*sea*, *seb*, *etb*, *sec*, *sed*, *see*, *seg*, *seh*, *sei*, and *sej*) (Monday and Bohach, 1999), exfoliative toxin genes (*eta* and *etb*), Panton–Valentine leukotoxin genes *lukS*-PV and *lukF*-PV (*pvl*), and toxic shock syndrome toxin genes (*tst*) (Goudarzi et al., 2016a; Nezhad et al., 2017).

## Phenotypic Analysis of Biofilm Formation

Slime production assay or Congo red agar (CRA) method and microtiter plate (MtP) assay were recruited as *in vitro* methods for the detection of phenotypic biofilm formation. In CRA method, briefly, after preparation of CRA by adding 0.8 g of CR (Sigma-Aldrich; St. Louis, United States) to 1 L of brain heart infusion agar (Merck) and autoclaving it, filters used for

add saccharose (36 g) (Sigma-Aldrich; St. Louis, United States) to CRA. Bacteria were inoculated on CRA and incubated at 37°C for 24 h and then overnight at room temperature. Biofilm formation was categorized in four levels based on colony color that strains appeared: (i) strong biofilm producer strains (very black colonies), (ii) moderate biofilm producer strains (black colonies), (iii) weak biofilm producer strains (gray colonies), and (iv) biofilm non-producer strains (red colonies) (Arciola et al., 2002; Yousefi et al., 2016).

The MtP assay as a quantitative method for biofilm detection was carried out as described previously. Concisely, an overnight culture of bacterial isolates in TSB (Merck) containing 1% glucose was diluted to 1:100 with fresh medium. Sterile MtP with flat-bottomed 96-well polystyrene was filled with 200 µL of the diluted culture and incubated at 37°C for 24 h. After incubation, wells were washed three times with 200 µL of phosphate-buffered saline (pH 7.2) to remove planktonic bacteria. Afterward, wells were fixed by 99% methanol, dried at room temperature, and then stained with 0.1% safranin. Safranin dye bound to the adherent cells was dissolved with 1 mL of 95% ethanol per well. As a negative control, 200 µL of TSB-1% glucose was used. The optical density (OD) of each well was measured using an enzyme-linked immunosorbent assay reader at a wavelength of 490 nm. Optical density cutoff defined as average OD of negative control + 3 × standard deviation of the negative control. Biofilm formation of strains was analyzed according to the absorbance of the safranin-stained attached cells and interpreted as per the criteria described by Stepanović et al. (2007). Accordingly, the degree of biofilm production was categorized into strong, moderate, weak, or without biofilm. For quality control, *Staphylococcus epidermidis* ATCC 35984 strain was used in each run.

## Genetic Analysis of Biofilm Formation

Polymerase chain reaction assays for the detection of *icaABCD*, *cna*, *ebp*, *fnbB*, *fnbA*, *clfB*, *clfA*, and *bap* genes were performed as described previously (Nemati et al., 2009; Yousefi et al., 2016). Detection of arginine catabolic mobile elements for definitive confirmation of USA300 was performed as previously described by Diep et al. (2008).

## Prophage Typing

iMLSB-positive *S. aureus* were characterized by prophage typing by using multiplex-PCR assay and oligonucleotide primers SGA, SGB, SGF (SGFa and SGFb), SGD, and SGL prophages as explained previously by Pantůček et al. (2004) and Rahimi et al. (2012).

## *Staphylococcus aureus* Protein A Locus (*spa*) Typing

*Staphylococcus aureus* isolates underwent *spa* typing as recommended by Harmsen et al. (2003); all PCR products were Sanger sequenced in both directions. The sequences obtained were edited using the Chromas software (version 1.45;

Technelysium, Tewantin, Australia). Ridom SpaServer database<sup>1</sup> was applied in order to assign the *spa* type.

## Staphylocoagulase Typing

Four sets of multiplex PCR reactions were used for assigning staphylocoagulase (SC) types (I–X) according to the procedure of Hirose et al. (2010). Set A contained primers for identifying SC types I, II, III, IVa, IVb, Va, and VI, whereas set B contained primers for identifying SC types VII, VIII, and X. Set 3 was used for identifying SC types IX and Vb. SC types IVa and IVb were distinguished using a set of four primers.

## SCCmec Typing

The multiplex PCR amplification was done with specific primers for SCCmec typing, as recommended by Boye et al. (2007). The prototype strains applied as control strains for typing were *S. aureus* ATCC 10442 (type I), *S. aureus* N315 (type II), *S. aureus* 85/2082 (type III), *S. aureus* MW2 (type IV), *S. aureus* WIS 173 (type V), and *S. aureus* HDE288 (type VI).

## agr Typing

Multiplex PCR was performed for *agr*-type detection using primer set comprising a common forward primer (pan-*agr*) and reverse primers (*agr1*, *agr2*, *agr3*, and *agr4*) specific to each *agr* group (Gilot et al., 2002).

## Multilocus Sequence Typing

All the 126 *S. aureus* isolates with iMLSB phenotype were further characterized by MLST as described by Enright et al. (2000) by sequencing an internal fragment of seven unlinked housekeeping genes to identify the following allelic profiles: phosphate acetyltransferase (*pta*), carbamate kinase (*arcC*), triosephosphate isomerase (*tpi*), shikimate dehydrogenase (*aroE*), guanylate kinase (*gmk*), acetyl-coenzyme A acetyltransferase (*yqiL*), and glycerol kinase (*glp*). The purification of PCR products was done by performing the Qiagen PCR purification kit. In addition, the two strands were sequenced on the ABI Prism 377 automated sequencer (Applied Biosystems, Perkin-Elmer Co., Foster City, CA, United States). Finally, STs were submitted to the online MLST website through the submission of DNA sequences<sup>2</sup>.

## Ethics Statement

The current study protocol was approved by the Ethics Committee of the Shahid Beheshti University of Medical Sciences in Tehran, Iran (IR.SBMU.MSP.REC.1396.700). Written informed consent was obtained from participants.

## RESULTS

### Isolation and Identification of *S. aureus*

A total of 126 *S. aureus* isolates with inducible resistance phenotype were identified, including 106 methicillin-resistant

<sup>1</sup><http://www.spaserver.ridom.de>

<sup>2</sup><https://pubmlst.org/>

*S. aureus* (MRSA) and 20 methicillin-sensitive *S. aureus* (MSSA) isolates representing 84.1 and 15.9% of isolates, respectively. Precisely, of 126 iMLSB *S. aureus* isolates, 41 were collected from female patients (32.6%), and the rest were collected from male patients (85, 67.4%). In the present study, 43 strains (34.1%) were isolated from wound, 32 (25.4%) from blood, 15 (11.9%) from body fluids, 14 (11.1%) from pus, 12 (9.5%) from urine, 7 (5.6%) from sputum, and 3 (2.4%) from conjunctiva. Of the 126 isolates, 76 (60.3%) were classified as HO, and 50 (39.7%) were classified as CO. According to the case notes, the rates of invasive and non-invasive *S. aureus* with iMLSB phenotype were found to be 37.3 and 62.7%, respectively. The patients' average age was 38 years. The patients were distributed in four age groups: 21 patients  $\leq 20$  years (16.7%), 60 patients between 21 and 45 years (47.6%), 30 patients between 46 and 65 years (23.8%), and 15 patients  $\geq 65$  years (11.9%). Regarding the occurrence of inducible resistance in *S. aureus* strains, data exhibited that most cases belonged to the age groups of 21 to 45 years between 2013 and 2017, whereas in 2018, more than half of the cases were found to be in the age group between 46 and 65 years. Patients with invasive infections and HO were older. Of 21 patients aged  $\leq 20$  years, 12 (57.1%) of 60 patients were between 21 and 45 years, 28 (46.7%) of 30 patients were between 46 and 65 years, and 9 (30%) had CO infections. However, among 15 patients aged  $\geq 65$  years, only 1 (6.7%) had CO infections. There were also trends toward an increasing incidence of HO infections in elderly patients.

### Antimicrobial Susceptibility

The highest and lowest rates of resistance in 126 *S. aureus* isolates tested were related to penicillin (91.3%) and fusidic acid (5.6%), respectively. The entire strains were susceptible to teicoplanin, linezolid, and vancomycin. Resistance to tested antibiotics was higher in MRSA than in MSSA. The rate of resistance to the tested antibiotics, with the exception of ciprofloxacin, was higher among HO *S. aureus* strains across CO *S. aureus* strains. The frequency of resistance rate among MRSA and MSSA strains to antimicrobial agents is presented in **Table 1**.

The entire *S. aureus* isolates were susceptible to vancomycin such that 15 isolates (11.9%) had MIC  $\geq 0.5$   $\mu\text{g/mL}$ , 38 (30.2%) had MIC  $\geq 1$   $\mu\text{g/mL}$ , and 73 (57.9%) exhibited MIC  $\geq 2$   $\mu\text{g/mL}$ . The data of the microbroth dilution method illustrated that 23 isolates (18.3%) were mupirocin-resistant; of these, 11 (8.7%) and 12 (9.6%) were LLMUPR and HLMUPR, respectively. Of the 126 isolates of *S. aureus* with iMLSB phenotype, seven (5.6%) were fusidic acid-resistant. In total, 80.2% of isolates (101/126) were multidrug resistance (MDR), and the MDR rate for MRSA isolates (85.8%) was significantly higher than that for MSSA (50%). Information about simultaneous resistance patterns and distribution of clinical samples is presented in **Table 2**.

### agr and SCCmec Typing

By using *agr* typing method, all 126 *S. aureus* isolates with iMLSB phenotype could be typed *agr* I–III. Of these isolates tested, 77 (10 MSSA and 67 MRSA) were *agr* I, 20 (MRSA) were *agr* II, and 29 (10 MSSA and 19 MRSA) were *agr* III. Staphylococcal cassette chromosome *mec* typing for MRSA isolates indicated that type

IV was the predominant SCC*mec* type (57.6%, 61/106), followed by SCC*mec* III (33%, 35/106), SCC*mec* V (7.5%, 8/106), and SCC*mec* II (1.9%, 2/106). In addition, no MRSA isolates harbored SCC*mec* type I.

### Determination of Adhesion and Biofilm Production Ability

Biofilm formation was observed in 97 strains (77%) using the CRA and MtP methods, whereas 29 strains (23%) were confirmed as non-biofilm producer strains. Of the total MRSA isolates, MtP detected 18 (17%) as weak, 23 (21.7%) as moderate, and 42 (39.6%) as strong biofilm producers. By CRA, 20 isolates (18.9%) were able to produce biofilm weakly, and 26 (24.5%) and 37 (34.9%) isolates presented moderate and potent biofilm formation, respectively. In MSSA isolates, MtP indicated weak biofilm production in five isolates (25), moderate biofilm production in three (15%), and strong biofilm production in six isolates (30%), whereas CRA detected four isolates (20%) as weak, five (25%) as moderate, and five (25%) as strong biofilm producers. The analysis of *icaA-D* genes among tested *S. aureus* strains showed that the most frequently detected gene was *icaD* ( $n = 92$ , 73%), followed by *icaA* ( $n = 90$ , 71.4%), *icaB* ( $n = 76$ , 60.3%), and *icaC* ( $n = 67$ , 53.2%). Overall, six different biofilm patterns were identified. **Figure 1** presents the distribution of *icaABCD* among tested strains. Regarding the presence of adhesion genes, the seven most frequent adhesion-related genes were *clfA* (93.7%, 118/126) followed by *clfB* (87.3%, 110/126), *fnbB* (61.9%, 78/126), *cna* (57.9%, 73/126), *fnbA* (54%, 68/126), *ebp* (50%, 63/126), and *bap* (3.2%, 8/126), respectively. The adhesion profiles are shown in **Figure 1**. None of the MSSA strains carried the *bap* gene. In MSSA strains, three different adhesion patterns including *clfA* + *clfB* + *fnbB* (50%, 10/20), *clfA* + *clfB* + *fnbB* + *fnbA* + *ebp* + *cna* (25%, 5/20), and *fnbB* + *fnbA* + *cna* (25%, 5/20) were observed. Apparently, higher diversity among the adhesion patterns from MRSA (six patterns) than those from MSSA (three patterns) was noticed.

### Determination of Prophage Types and Toxin and Enterotoxin Encoding Genes

A total of 103 strains (81.7%) of the 126 inducible resistant *S. aureus* strains tested had one or more virulence genes. The most frequently attained virulence genes were *pvl* (23.8%, 30/126), followed by *sea* (19.8%, 25/126), *tst* (19%, 24/126), *sec* (11.1%, 14/126), *sed* (9.5%, 12/126), *seg* (4.8%, 6/126), *seb* (4%, 5/126), *see* (3.2%, 4/126), and *eta* (2.4%, 3/126), but *she*, *sei*, and *sej* encoding genes were detected in any of the total number of 126 isolates tested. In this analysis, six prophage types were grouped into seven separate prophage profiles. **Figure 1** provides a summary data of the number and frequency of prophage profiles among isolates tested.

The data for antibiotic resistance genes in *S. aureus* strains studied revealed that the most common gene was *mecA* in 106 strains (84.1%), followed by *erm(A)* in 43 strains (34.1%), *erm(B)* in 41 (32.5%), *erm(C)* in 361 (28.6%), *ant* (4')-Ia in 35 (27.8%), *tet(M)* in 32 (25.4%), *aac* (6')-Ie/aph (2'') in 29 (23%), *aph* (3')-IIIa in 17 (13.5%), *mupA* in 12 (9.5%), *fusB* in 6 (4.8%) strains,

**TABLE 1** | Antimicrobial resistance pattern of MRSA and MSSA isolates with iMLS phenotype.

Antibiotic	106 MRSA isolates <i>n</i> (%)		20 MSSA isolates <i>n</i> (%)		Total <i>n</i> (%)
	Hospital onset	Community onset	Hospital onset	Community onset	
Penicillin	67(53.2)	39(31)	9(7.1)	—	115(91.3)
Gentamicin	76(60.3)	21(16.6)	5(4)	4(3.2)	106(84.1)
Tetracycline	45(35.7)	29(23)	9(7.1)	6(4.8)	89(70.6)
Kanamycin	34(27)	19(15.1)	8(6.3)	5(4)	66(52.4)
Ceftriaxone	41(32.5)	11(8.7)	7(5.6)	4(3.2)	63(50)
Amikacin	31(24.6)	17(13.5)	10(7.9)	1(0.8)	59(46.8)
Ciprofloxacin	23(18.2)	29(23)	5(4)	—	57(45.2)
Tobramycin	39(31)	5(4)	7(5.5)	—	51(40.5)
Rifampin	25(19.8)	9(7.1)	3(2.4)	2(1.6)	39(30.9)
Trimethoprim–sulfamethoxazole	17(13.5)	11(8.7)	5(4)	2(1.6)	35(27.8)
Quinupristin–dalbopristin	18(14.3)	9(7.1)	—	3(2.4)	30(23.8)
Mupirocin	13(10.3)	4(3.2)	5(4)	1(0.8)	23(18.3)
Fusidic acid	7(5.6)	—	—	—	7(5.6)

**TABLE 2** | Resistant pattern and distribution of samples in 126 *S. aureus* strains isolated from clinical sources.

Simultaneous resistance to antibiotics	Resistance profile	Resistance pattern <sup>a</sup>	Type of samples <sup>b</sup> (n;%)	Number of isolates (%)
Nine	A	PG, GM, T, K, CIP, TN, SYN, RI, TS	W (6; 40), B (3; 20), BF (2; 13.3), U (4; 26.7)	15 (11.9)
Eight	B	PG, GM, T, K, CRO, AK, CIP, TN	W (9; 52.9), B (6; 29.4), P (3; 17.7)	17 (13.5)
	C	PG, GM, T, K, CRO, RI, TS, MUP	W (4; 33.3), B (3; 25), P (2; 16.7), BF (2; 16.7), S (1; 8.3)	12 (9.5)
	D	PG, GM, T, CRO, AK, RI, MUP, TS	W (3; 37.5), BF (1; 12.5), P (4; 50)	8 (6.3)
Seven	E	PG, GM, T, K, CRO, AK, CIP	W (4; 26.8), B (3; 20), BF (2; 13.3), U (2; 13.3), P (2; 13.3), S (2; 13.3)	15 (11.9)
	F	PG, GM, T, CRO, AK, TN, FC	B (5; 100)	5 (4)
Six	G	PG, GM, T, AK, CIP, SYN	W (5; 50), BF (3; 30), U (2; 20)	10 (7.9)
Five	H	PG, GM, T, K, TN	W (3; 42.9), B (3; 42.9), C (1; 14.2)	7 (5.6)
	I	PG, GM, CRO, TN, SYN	BF (2; 40), C (1; 20), P (1; 20), U (1; 20)	5 (4)
	J	PG, GM, TN, MUP, FC	W (2; 100)	2 (1.6)
Four	K	PG, GM, AK, RI	B (2; 50), BF (1; 25), P (1; 25)	4 (3.2)
	L	PG, GM, CRO, MUP	C (1; 100)	1 (0.8)
Two	M	PG, GM	S (4; 80), U (1; 20)	5 (4)
One	N	PG	W (5; 55.6), B (4; 44.4)	9 (7.1)
Without	O	—	W (2; 18.2), B (4; 36.3), U (2; 18.2), P (1; 9.1), BF (2; 18.2)	11 (8.7)

<sup>a</sup>PG, penicillin; CRO, ceftriaxone; GM, gentamicin; K, kanamycin; AK, amikacin; TN, tobramycin; T, Tetracycline; CIP, ciprofloxacin; TS, trimethoprim–sulfamethoxazole; RI, rifampicin; MUP, mupirocin; FC, fusidic acid; SYN, quinupristin–dalbopristin. <sup>b</sup>B, blood; W, wound; P, pus; BF, body fluid; U, urine; S, sputum; C, conjunctiva.

and *fusC* in 1 strain. *vanB*, *mupB*, and *fusA* genes were not detected in none of experimented isolates.

## SC Typing

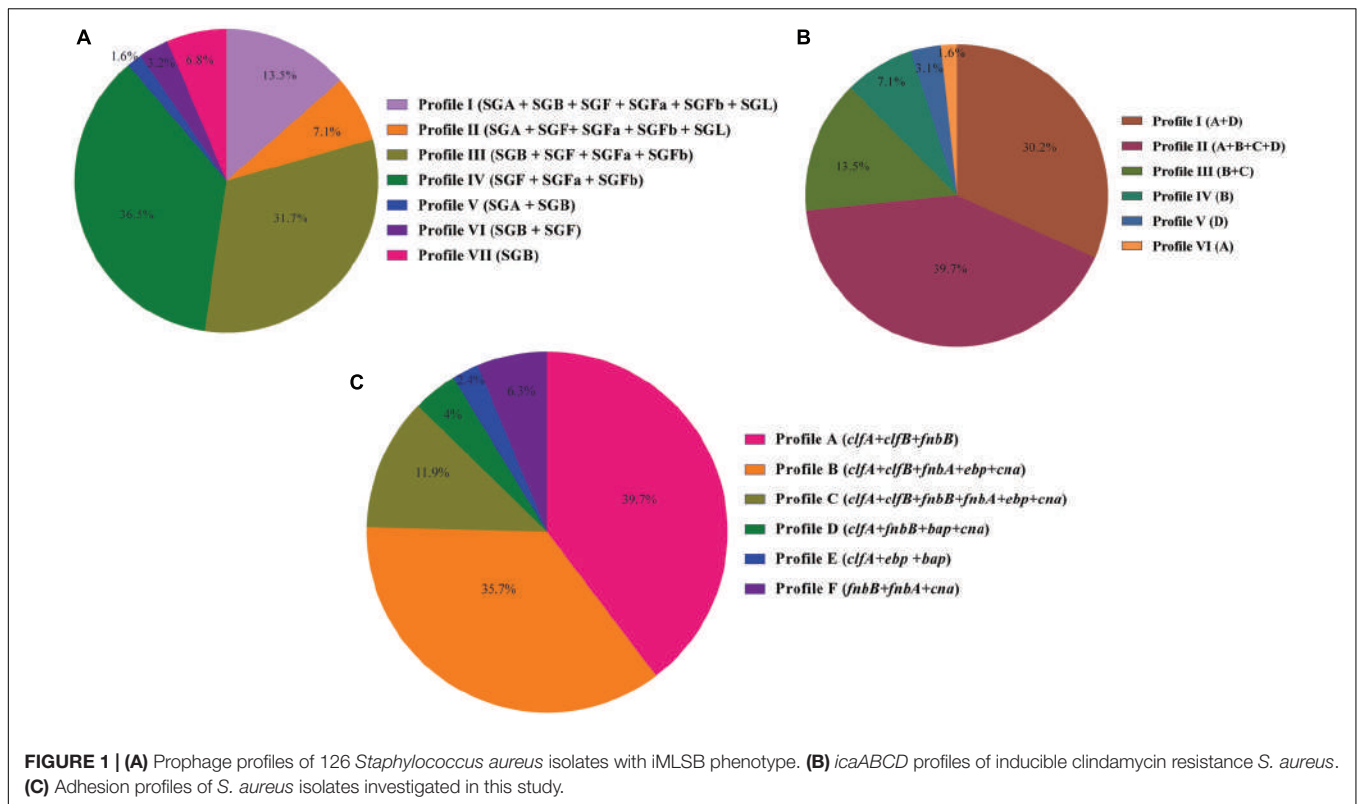
In the present study, all isolates could be typed by SC typing method. These isolates were distinguished into seven SC types (I–VI). The predominant SC type was III and included 56 isolates (44.4%), followed by II (28.6%, 36/126), IVa (9.5%, 12/126),

VI (7.9%, 10/126), I (4%, 5/126), V (4%, 5/126), and IVb (1.6%, 2/126). A total of seven SC types and two types (II and IVa) were detected in MSSA isolates.

## MLST and *spa* Typing

All the isolates were typed by *spa* and MLST. A total of 26 *spa* types were attained in the entire 126 *S. aureus*. The isolates identified as invasive *S. aureus* were assigned to particular t790,





t002, t008, t064, t030, t037, and t631 *spa* types. For CO, the isolates were assigned to *spa* types t005, t1869, t019, t021, t10795, t6811, t002, t045, t008, t065, t030, and t037. Among MSSA isolates, the most common *spa* types were t021, t005, t1869, and t318 representing 35 (7/20), 25 (5/20), 25 (5/20), and 15% (3/20), and among MRSA isolates, the top four *spa* types were t037, t437, t030, and t008 representing 10.4 (11/106), 9.4 (10/106), 8.5 (9/106), and 7.5% (8/106) of isolates. Multilocus sequence typing identified 14 ST types in both MRSA and MSSA isolates, namely, ST22 (14.3%, 18/126), ST30 (11.9%, 15/126), ST1 (1.6%, 2/126), ST772 (4.8%, 6/126), ST8 (10.3%, 13/126), ST239 (23%, 29/126), ST585 (1.6%, 2/126), ST5 (5.63%, 7/126), ST225 (1.6%, 2/126), ST80 (9.5%, 12/126), ST59 (4.8%, 6/126), ST338 (3.2%, 4/126), ST15 (4%, 5/126), and ST45 (4%, 5/126), which were further grouped into nine CCs including CC1, 5, 8, 15, 22, 30, 45, 59, and 80. Among MSSA, CC22 and CC30 were the dominant clones, each clone with 50% (10/20) of the isolates being assigned to these genotypes, and all were recovered from non-invasive *S. aureus* and both CO (55%, 11/20) and HO (45%, 9/20) cases. CC8 (41.5%, 44/106), CC80 (11.3%, 124/106), and CC5 (8.5%, 9/106) were the top three CCs in MRSA isolates. **Table 3** represents the analysis of *S. aureus* clones obtained from patients based on invasive and non-invasive infections.

## Temporal Changes in Inducible Resistant *S. aureus* Genotypes

**Table 4** gives information about the percentage of inducible resistant *S. aureus* strains assigned to each CC for each year

between 2013 and 2018. The prevalence of inducible resistance *S. aureus* isolates elevated in the experiment from 19.8% in 2013–2014 to 30.2% in 2017–2018. Apart from 2013 to 2014 in which CC22 genotype was the most prevalent CC among inducible resistance isolates (36%, 9/25), in the remaining years of study (2014–2018), the CC8 isolates were the most predominant genotype. The CC8, as a predominate genotype, was at its most prevalent in 2016–2017 (41.6%, 10/24). Its prevalence increased during the study period from 20% in 2013–2014 (5/25) to 39.5% (15/38) in 2017–2018. By contrast, the prevalence rate of CC22 decreased from 36% in 2013–2014 to 0% in 2017–2018. The CC30, the third predominated CC among our clinical isolates, had its most prevalence in 2017–2018 (18.4%, 7/38). The prevalence of this type varied dramatically each year during 2013–2018; despite a decrease to 8% (2/25) in 2013–2014, a slight increase in the prevalence of this type was noted during 2014–2015 (9.5%, 2/21) and 2015–2016 (16.7%, 3/18), followed by an overall decrease to 4.2% (1/24) in 2016–2017. The prevalence of this type increased to 18.4% (7/38) in 2017–2018.

The first CC45 isolates were found in 2015–2016. The prevalence of this genotype diminished during the study period from 22.2% (4/18) in 2015–2016 to 4.2% (1/24) in 2016–2017 apart from 2017–2018 when no CC45 was detected. The CC45 was the second predominant genotype in 2015–2016 (22.2%, 4/18). The CC15, absent during 2013–2016, was detected during 2016–2017 (8.3%, 2/24), but remained at relatively low prevalence (7.9%, 3/38) in 2017–2018.

**TABLE 3** | Analysis of *S. aureus* clones obtained from patients based on invasive and non-invasive infections.

Clonal complex (CC)	Molecular types	Invasive <i>S. aureus</i>		Non-invasive <i>S. aureus</i>		Total, n (%)
		Community onset, n (%)	Hospital onset, n (%)	Community onset, n (%)	Hospital onset, n (%)	
CC22	ST22-SCCmec IV/t852	0(0)	0(0)	0(0)	2(100)	2(1.6)
	ST22-SCCmec IV/t790	0(0)	3(60)	0(0)	2(40)	5(4)
	ST22-SCCmec IV/t005	0(0)	0(0)	0(0)	1(100)	1(0.7)
	ST22/t005	0(0)	0(0)	2(40)	3(60)	5(4)
	ST22/t1869	0(0)	0(0)	4(80)	1(20)	5(4)
CC30	ST30-SCCmec IV/t605	0(0)	0(0)	0(0)	2(100)	2(1.6)
	ST30-SCCmec IV/t019	0(0)	0(0)	3(100)	0(0)	3(2.4)
	ST30/t318	0(0)	0(0)	0(0)	3(100)	3(2.4)
	ST30/t021	0(0)	0(0)	5(71.4)	2(28.6)	7(5.5)
CC1	ST772-SCCmec IV/t10795	0(0)	0(0)	3(60)	2(40)	5(4)
	ST772-SCCmec IV/t657	0(0)	0(0)	0(0)	1(100)	1(0.7)
	ST1-SCCmec IV/t6811	0(0)	0(0)	1(50)	1(50)	2(1.6)
CC5	ST5-SCCmec IV/t002	2(28.6)	3(42.8)	1(14.3)	1(14.3)	7(5.5)
	ST225-SCCmec II/t045	0(0)	0(0)	1(50)	1(50)	2(1.6)
CC8	ST8-SCCmec IV/t008	1(12.5)	3(37.5)	4(50)	0(0)	8(6.3)
	ST8-SCCmec IV/t064	2(40)	2(40)	1(20)	0	5(4)
	ST585-SCCmec III/t713	0(0)	0(0)	0(0)	2(100)	2(1.6)
	ST239-SCCmec III/t030	0	4(44.4)	1(11.2)	4(44.4)	9(7.1)
	ST239-SCCmec III/t037	7(63.6)	1(9.1)	0(0)	3(27.3)	11(8.7)
	ST239-SCCmec III/t631	0(0)	1(25)	0(0)	3(75)	4(3.2)
	ST239-SCCmec III/t860	0(0)	0(0)	0(0)	3(100)	3(2.4)
	ST239-SCCmec III/t388	0(0)	0(0)	0(0)	2(100)	2(1.6)
CC80	ST80-SCCmec IV/t044	0(0)	6(75)	0(0)	2(25)	8(6.3)
	ST80-SCCmec IV/t131	0(0)	0(0)	2(50)	2(50)	4(3.2)
CC59	ST59-SCCmec IV/t437	3(50)	2(33.3)	0(0)	1(16.7)	6(4.8)
	ST338-SCCmec III/t437	0(0)	0(0)	0(0)	4(100)	4(3.2)
CC15	ST15-SCCmec IV/t084	2(40)	1(20)	0(0)	2(40)	5(4)
CC45	ST45-SCCmec IV/t038	4(80)	0(0)	1(20)	0(0)	5(4)

**TABLE 4** | Distribution of characterized *S. aureus* isolates with iMLSB phenotype by year.

<i>S. aureus</i> clones	2013–2014, n (%)	2014–2015, n (%)	2015–2016, n (%)	2016–2017, n (%)	2017–2018, n (%)	Total, n (%)
CC8	5(11.4)	8(18.2)	6(13.6)	10(22.7)	15(34.1)	44(34.9)
CC22	9(50)	5(27.8)	1(5.6)	3(16.6)	0(0)	18(14.3)
CC30	2(13.3)	2(13.3)	3(20)	1(6.7)	7(46.7)	15(11.9)
CC80	3(25)	0(0)	0(0)	4(33.3)	5(41.7)	12(9.5)
CC59	0(0)	1(10)	0(0)	2(20)	7(70)	10(7.9)
CC5	2(22.2)	3(33.4)	2(22.2)	1(11.1)	1(11.1)	9(7.1)
CC1	4(50)	2(25)	2(25)	0(0)	0(0)	8(6.4)
CC45	0(0)	0(0)	4(80)	1(20)	0(0)	5(4)
CC15	0(0)	0(0)	0(0)	2(40)	3(60)	5(4)
Total	25(19.8)	21(16.7)	18(14.3)	24(19)	38(30.2)	126(100)

The CC59 isolates were not detected between 2013–2014 and 2015–2016. The CC59 isolates were detected for the first time in 2014–2015 (4.8%, 1/21), and increased to 8.3% (2/24) in 2016–2017. This genotype was present at its greatest prevalence in 2017–2018, accounting for 18.4% (7/38) of inducible resistance strains. The prevalence of CC80 varied dramatically during the 5-year period, this genotype was not identified among any of

the 2014–2015 and 2015–2016 tested strains. In 2013–2014, only 12% (3/25) of isolates exhibited this genotype. An increase in the prevalence of this genotype was noted between 2016 and 2017 to 16.7% (4/24), followed by a decline to 13.2% (5/38) in 2017–2018. The CC5 genotype was present in each year between 2013 and 2018. The highest prevalence of this genotype occurred in 2014–2015 (14.3%, 3/21), followed by 11.1% (2/18) between 2015 and

2016. Overall, the prevalence of this genotype diminished during the study period from 8% (2/25) in 2013–2014 to 2.6% (1/38) in 2017–2018. The CC1 isolates were not identified between 2016 and 2018. It was the third predominant genotype in 2013–2014, accounting for 16% (4/25) of examined isolates, but it dropped to 9.5% (2/21) in 2014–2015 and then indicated an increase in 2015–2016 (11.1%, 2/18).

## Observations on Inducible Clindamycin-Resistant *S. aureus* Clones

The molecular characteristics of the isolates related to each genotype of inducible resistance MRSA and MSSA are shown in **Table 5**. Meanwhile, the details of each clonal lineage are explained below.

### CC1

In this study, most of the isolates identified as CC1/ST772-MRSA-V were represented by *spa* type t10795 (83.3%, 5/6). Among the CC1/ST772-MRSA-V isolates, resistance to aminoglycosides encoded by *aac* (6')-Ie/*aph* (2'') and *aph* (3')-IIIa, and tetracycline encoded by *tet*(M) was common. Three isolates (60%) were able to produce biofilm strongly. The finding indicated that *fnbB* gene was present in all of the CC1 isolates. *icaA* and *icaD* were the most prevalent biofilm-related genes. More than half of the isolates (60%) carried *pvl* genes. The one remaining CC1/ST772-MRSA-V isolate was assigned to *spa* type t657 and *coa* type IVa. This isolate exhibited resistance to multiple antibiotics and harbored resistance genes *mecA* and *erm*(C); meanwhile, enterotoxin genes *sea* + *seb* carried simultaneously. The CC1/ST1-MRSA-V isolates exhibited *spa* type, t6811. One isolate carried *fusc* and exhibited resistance to fusidic acid at MIC 32 µg/mL. MDR pattern was detected among these isolates. Both isolates were identified to be biofilm producers albeit weakly. Toxin gene differs from those detected in CC1/ST772-MRSA-V found among the CC1/ST1-MRSA-V isolates, namely, *sec*. All the isolates exhibited erythromycin resistance encoded by *erm*(C).

### CC5

All CC5/ST5-MRSA-IV isolates were assigned to single *spa* type t002. This isolates carried the enterotoxin genes *sea* (42.9%, 3/7) and *sed* + *seg* (42.9%, 3/7) and the toxin *tst* (42.9%, 3/7). Among the CC5/ST5-MRSA-IV isolates, resistance to erythromycin encoded by *erm*(A), tetracycline encoded by *tet*(M), and mupirocin encoded by *mupA* was common. Five of HLMUPR strains, which harbored the *mupA* gene, belonged to this CC (41.7%, 5/12). Nearly 60% of all isolates that occurred in these clones showed moderate biofilm formation. The remaining 40% were not able to produce biofilm. The top three adhesion-related genes among CC5 isolates were *clfA* (100%, 9/9), *clfB* (77.8%, 7/9), *ebp* (75%, 6/9), and *cna* (75%, 6/9). Of nine CC5 isolates, *icaA* and *icaD* were found in seven isolates, whereas *icaB* and *icaC* were detected in six isolates. The other CC5 genotypes identified (CC5/ST225-MRSA-II) were assigned to *spa* type t045, which exhibited resistance to multiple antibiotics including aminoglycosides resistance encoded by *ant* (4')-Ia (2) and *aac* (6')-Ie/*aph* (2'') genes. *tst* encoding gene

was detected in all isolates. All CC5/ST225-MRSA-II showed strong biofilm formation. The predominant prophage profile was SGF + SGFa + SGFb.

### CC8

In this study, CC8 was represented by ST8-MRSA-IV (29.6%, 13/44), ST239-MRSA-III (65.9%, 29/44), and ST585-MRSA-III (4.5%, 4/44). *spa* types t008 (61.5%, 8/13) and t064 (38.5%, 5/13) predominated among the CC8/ST8-MRSA-IV isolates. Among 13 ST8-MRSA-IV strains, 8 isolates harbored the *arcA* and *opp3AB* genes and confirmed as USA300. The majority of CC/ST8-MRSA-IV (USA300), as a major global epidemic clone that has been noticed for its rapidity dissemination within the community and hospitals isolates, exhibited resistance to aminoglycosides encoded by *aph* (3')-IIIa (61.5%, 8/13). Resistance to erythromycin encoded by *erm*(C) (38.5%, 5/13) and tetracycline encoded by *tet*(M) (38.5%, 5/13) was also detected in this genotype. Six strains belonging to CC/ST8-MRSA-IV clone demonstrated the HLMUPR phenotype and carried *mupA* gene. The findings showed that the majority of the isolates (77%, 10/13) was able to produce biofilm, although at different intensities. Nine isolates in this clone harbored the *pvl* genes (69.2%); the rest of four isolates carried the *sed* gene (30.8%).

The majority of CC8/ST239-MRSA-III isolates were assigned to *spa* type t037 (37.9%, 11/29), followed by t030 (31.1%, 9/29), t631 (13.8%, 4/29), t860 (10.3%, 3/29), and t388 (6.9%, 2/29). Resistance to multiple antibiotics simultaneously was identified in this genotype. Fusidic acid resistance encoded by *fusc* (6.9%, 2/29); tetracycline resistance encoded by *tet*(K) (41.4%, 12/29); aminoglycoside resistance encoded by *ant* (4')-Ia (58.6%, 17/29), *aac* (6')-Ie/*aph* (2'') (37.9%, 11/29), and *aph* (3')-IIIa (6.9%, 2/29); and mupirocin resistance encoded by *mupA* (6.9%, 2/29) were also noted. Almost more than half of the isolates carried *sea* (55.2%, 16/29), 48.3% (14/29) carried *tst*, and 17.2% (5/29) carried *sec* only three isolates harboring *seg* gene. All three ST239-SCC*mec* III/t860 isolates carried *eta* and demonstrated the LLMUPR phenotype. The CC8/ST239-MRSA-III isolates displayed high levels of biofilm production (86.2%, 25/29). Regarding the biofilm-related genes, the *icaD* (70.5%, 31/44) was common, followed by *icaA* (68.2%, 30/44), *icaB* (68.2%, 30/44), and *icaC* (61.4%, 27/44). The top three adhesion-related genes among CC8 isolates were *clfA* (100%, 44/44), *clfB* (86.4%, 38/44), and *cna* (86.4%, 38/44).

Two remaining CC8/ST585-MRSA-III isolates were assigned to *spa* type t713 and carried multiple resistance genes, that is, *tet*(M), *erm*(C), and enterotoxin genes *see*. Both of these strains indicated strong biofilm formation. The majority of the CC8 isolates was found to harbor SGF + SGFa + SGFb prophages.

### CC15

The five CC15/ST15 MRSA-IV isolates identified revealed the same *spa*, *coa*, *agr*, and prophage profile. Fewer than half of the isolates were resistant to fusidic acid encoded by *fusB*. All CC15/ST15 MRSA-IV isolates carried *pvl* genes. More than half of the isolates were biofilm producers. All CC15 isolates were positive for *fnbB* gene, and 80% of the isolates were found to carry all of the biofilm-related genes (*icaA-D*). One isolate was found

**TABLE 5 |** Phenotypic and genotypic typing data for inducible resistance MRSA ( $n = 106$ ) and MSSA ( $n = 20$ ) isolates studied in Tehran, Iran, between 2013 and 2018.

CC	Genotype	Typing category results (n)								
		MRSA	MSSA	<i>spa</i>	<i>agr</i>	<i>coa</i>	Phenotype profiles <sup>a</sup> (% indicated when not 100%)	Genotype (%)	Virulence genes (% indicated when not 100%)	Biofilm status <sup>b</sup> (% indicated when not 100%)
22	ST22-MRSA-IV (8)		t852 (2), t790 (5)	I	III	A (14.2), B (42.9), D (42.9)	<i>mecA</i> (100), <i>ant</i> (4')- <i>la</i> (28.6), <i>aac</i> (6')- <i>le/aph</i> (2'') (42.9), <i>erm</i> (C) (57.1), <i>erm</i> (B) (42.9)	<i>pvl</i> (28.6), <i>tst</i> (42.9), <i>sea</i> (14.2)	W (57.1), S (42.9)	I (28.6), IV (71.4)
			t005 (1)	I	IVa	H	<i>mecA</i> , <i>erm</i> (A), <i>erm</i> (B)	<i>pvl</i>	S	I
30	ST22-MSSA (10)		t005 (5), t1869 (5)	I	IVa	N (40), K (30), H (30)	<i>erm</i> (A) (50), <i>aac</i> (6')- <i>le/aph</i> (2'') (20), <i>ant</i> (4')- <i>la</i> (30), <i>tet</i> (M) (50), <i>erm</i> (B) (50)	<i>sec</i> (30)	N (50), W (30), S (20)	III (50), IV (50)
	ST30-MRSA-IV (5)		t605 (2), t019 (3)	III	II	A(40), B (20), E (40)	<i>mecA</i> (100), <i>erm</i> (C) (60), <i>aac</i> (6')- <i>le/aph</i> (2'') (40), <i>aph</i> (3')-IIIa (20), <i>tet</i> (M) (20)	<i>pvl</i> (60), <i>sea</i> (40)	N (20), W (40), S (40)	I (60), V (40)
1	ST30-MSSA (10)		t021 (7), t318 (3)	III	II	G (30), N (10), I (10), O (40), L (10)	<i>erm</i> (A) (10), <i>erm</i> (B) (20), <i>erm</i> (C) (50), <i>ant</i> (4')- <i>la</i> (30), <i>aph</i> (3')-IIIa (10), <i>erm</i> (B) (60)	<i>sed</i> (40), <i>pvl</i> (30)	N (10), W (20), M (30), S (40)	VI (10), VII (30), III (30), IV (30)
	ST1-MRSA-IV (2)		t6811 (2)	III	IVb	E (50), F (50)	<i>mecA</i> (100), <i>erm</i> (A) (100), <i>fusc</i> (50)	<i>sec</i>	W	III
8	ST772-MRSA-IV (6)		t10795 (5)	II	III	B (60), E (40)	<i>mecA</i> (100), <i>aac</i> (6')- <i>le/aph</i> (2'') (40), <i>aph</i> (3')-IIIa (60), <i>tet</i> (M) (60), <i>erm</i> (B) (100)	<i>pvl</i> (60), <i>sea</i> (40)	N (20), W (20), S (60)	I (40), IV (60)
			t657 (1)	II	IVa	I	<i>mecA</i> , <i>erm</i> (C)	<i>sea</i> + <i>seb</i>	S	VII
	ST8-MRSA-IV (13)		t008 (8), t064 (5)	I	III	C (30.8), D (23.1), O (38.5), M (7.6)	<i>mecA</i> (100), <i>mupA</i> (46.1), <i>aph</i> (3')-IIIa (61.5), <i>erm</i> (C) (38.5), <i>tet</i> (M) (38.5), <i>erm</i> (B) (30.8)	<i>pvl</i> (69.2), <i>sed</i> (30.8)	N (23.1), W (38.4), M (23.1), S (15.4)	I (69.2), IV (30.8)
5	ST239-MRSA-III (29)		t030 (9), t037 (11), t631 (4), t860 (3), t388 (2)	I	III	A (20.7), B (13.8), C (10.4), D (3.4), E (17.3), F (6.9), G (13.8), I (6.9), K (3.4), O (3.4)	<i>mecA</i> (100), <i>mupA</i> (6.9), <i>fusB</i> (6.9), <i>erm</i> (A) (51.7), <i>erm</i> (B) (17.3), <i>erm</i> (C) (44.8), <i>ant</i> (4')- <i>la</i> (58.6), <i>aac</i> (6')- <i>le/aph</i> (2'') (37.9), <i>aph</i> (3')-IIIa (6.9), <i>tet</i> (M) (41.3)	<i>tst</i> (48.3), <i>sea</i> (55.1), <i>sec</i> (17.3), <i>seg</i> (10.4), <i>eta</i> (10.4)	N (13.8), W (13.8), M (10.4), S (62)	III (41.4), IV (44.8), VII (13.8)
	ST585-MRSA-III (2)		t713 (2)	I	III	I (50), E (50)	<i>mecA</i> (100), <i>tet</i> (M) (50), <i>erm</i> (C) (50)	<i>see</i>	S	IV
80	ST5-MRSA-IV (7)		t002 (7)	II	II	C (42.9), D (14.2), H (42.9)	<i>mecA</i> (100), <i>mupA</i> (57.1), <i>erm</i> (A) (57.1), <i>tet</i> (M) (71.4)	<i>tst</i> (42.9), <i>sea</i> (42.9), <i>sed</i> + <i>seg</i> (42.9)	N (42.9), M (57.1)	IV
	ST225-MRSA-II (2)		t045 (2)	II	II	G	<i>mecA</i> (100), <i>ant</i> (4')- <i>la</i> (100), <i>aac</i> (6')- <i>le/aph</i> (2'') (100), <i>erm</i> (B) (50)	<i>tst</i> (100), <i>sed</i> (50)	S	VI
59	ST80-MRSA-IV (12)		t044 (8), t131 (4)	III	II	B (50), E (25), F (8.3), M (16.7)	<i>mecA</i> (100), <i>fusB</i> (8.3), <i>ant</i> (4')- <i>la</i> (41.7), <i>aac</i> (6')- <i>le/aph</i> (2'') (33.3), <i>erm</i> (A) (83.3)	<i>pvl</i> (33.3)	N (25), M (41.7), S (33.3)	III (58.4), VI (8.3), II (33.3)
15	ST59-MRSA-IV (6)		t437 (6)	I	VI	E (16.7), F (16.7), N (66.6)	<i>mecA</i> (100), <i>fusB</i> (16.7), <i>erm</i> (B) (33.3), <i>erm</i> (C) (66.7)	<i>seb</i> (66.7)	N (50), M (33.3), S (16.7)	III
	ST338-MRSA-III (4)		t437 (4)	I	VI	A (50), M (50)	<i>mecA</i> (100), <i>ant</i> (4')- <i>la</i> (75), <i>aph</i> (3')-IIIa (50), <i>erm</i> (B) (75)	<i>see</i> (50)	N (25), M (25), S (50)	III
45	ST15-MRSA-IV (5)		t084 (5)	II	I	C (40), J (40), O (20)	<i>mecA</i> (100), <i>fusB</i> (40), <i>erm</i> (B) (80)	<i>pvl</i> (100)	N (40), M (40), S (20)	II
	ST45-MRSA-IV (5)		t038 (5)	I	V	A (80), G (20)	<i>mecA</i> (100), <i>erm</i> (A) (100), <i>aac</i> (6')- <i>le/aph</i> (2'') (60)	<i>tst</i> (40), <i>sec</i> (80)	N (40), M (60)	III (20), IV (80)

<sup>a</sup>Phenotypic profile are presented in **Table 2**. <sup>b</sup>W, weak producer; M, moderate producer; S, strong producer; N, non-producer. <sup>c</sup>Prophage profiles are presented in **Figure 1A**.



to carry none of the tested *ica* genes. All of the CC15 isolates possessed SGA + SGF + SGFa + SGFb + SGL prophage profile.

### CC22

Three *spa* types t852, t790, and t005 and two *spa* types t005, t1869 predominated among the CC22/ST22-MRSA-IV isolates (44.4%, 8/18) and CC22/ST22-MSSA (55.6%, 10/18) isolates. Among the MRSA isolates, resistance to erythromycin encoded by *erm(C)* and aminoglycosides encoded by *aac* (6′)-*Ie/aph* (2′′) were prevalent, whereas in MSSA isolates resistance to tetracycline encoded by *tet(M)* and that to aminoglycosides encoded by *ant* (4′)-*Ia* (3) were common. All the MRSA isolates were biofilm producers, whereas in MSSA isolates half of the isolates were able to produce biofilm. The results indicated that adhesion genes *clfA* and *clfB* were detected in all of the MRSA strains, and the most common *ica* genes were *icaA* and *icaB*. All the MSSA isolates carried *clfA*, *clfB*, and *fnbB* simultaneously, and *icaA* and *icaD* were the most prevalent biofilm-related genes. The isolates identified as CC22/ST22-MRSA-IV isolates showed a prevalence of 37.5% (3/8) for the *pvl* and *tst* genes. One isolate carried *sea* gene (12.5%, 1/8). The *sec* gene (30%, 3/10) was the only toxin gene detected among CC22/ST22-MSSA isolates. The carriage of *pvl* genes was more common among MRSA isolates than among MSSA isolates. The SGB + SGF + SGFa + SGFb prophage profile was detected in the majority of CC22 isolates.

### CC30

CC/ST30 isolates were found in both MRSA and MSSA isolates. Among MRSA isolates, the most predominant *spa* types were t605 and t019, representing 40% (2/5) and 60% (3/5) of isolates. Multiple resistance genes including *erm(C)*, *aac* (6′)-*Ie/aph* (2′′), *aph* (3′)-*IIIa*, and *tet(M)* were identified among tested isolates. More than half of the CC/ST30-MRSA-IV isolates carried *pvl*, whereas isolates harboring *sea* were at a relatively low frequency. All CC/ST30-MRSA-IV isolates displayed *agr* type III and *coa* type II. Four isolates (80%) were able to produce biofilm, and the remaining 20% were non-biofilm producers. All the MRSA isolates carried biofilm (*icaA*, *icaB*, *icaC*, and *icaD*) and adhesion (*clfA*, *clfB*, and *fnbB*) related genes. In all the MSSA strains, *fnbA*, *cna*, and *icaA* genes were detected. Among MSSA isolates, *spa* types t021 and t318 represented 70% (7/10) and 30% (3/10) of isolates. Nearly 90% (9/10) of the CC/ST30-MSSA isolates could form biofilm at different intensities. Various prophage patterns with the majority of SGB (60%, 6/10) were identified among MSSA isolates. The majority of CC/ST30-MSSA isolates exhibited erythromycin resistance encoded by *erm(B)* (80%, 8/10), and *erm(C)* (50%, 5/10). The *pvl* and *sed* encoding genes were the only toxins produced by this genotype. The SGA + SGB + SGF + SGFa + SGFb + SGL was found as the most predominant prophage profile among CC/ST30-MRSA-IV isolates.

### CC45

All ST45-MRSA-IV isolates were assigned a *spa* type t038, *agr* I, and *coa* V. The isolates that exhibited resistance to multiple antibiotics were confirmed among these isolates. More than half of them (60%) were biofilm producers. All of these isolates carried

*icaB*, *clfA*, *clfB*, and *fnbB* encoding genes simultaneously. All ST45-MRSA-IV isolates possessed *erm(A)* gene. The carriage of *aac* (6′)-*Ie/aph* (2′′) gene was found in 60% of isolates. The enterotoxin gene *sec* was present in 80% of isolates. Among prophage patterns, the SGF + SGFa + SGFb was common.

### CC59

Two CC5 MRSA isolates were detected as one with ST59 and another one with ST338. All CC59 isolates indicated a single *spa* type, t437, *coa* type VI, and SGB-SGF-SGFa-SGFb phage pattern. All CC59/ST59 isolates were discriminated into SCC*mec* types IV. Two-thirds of ST59-MRSA-IV isolates carried *seb* gene; however, no other toxin genes were identified. Three isolates accounting for half (50%) of the entire ST59-MRSA-IV isolates were non-biofilm producers, and only one isolate showed strong biofilm formation. Results also demonstrated that the *icaA*, *icaD*, *clfA*, and *clfB* genes were detected in all of the CC59 isolates. Almost one-fifth of these isolates were resistant to fusidic acid encoded by *fusB* gene. Four and two ST59-MRSA-IV isolates carried *erm(C)* (66.7%) and *erm(B)* (33.3%), respectively. All CC59/ST338 isolates were assigned into an SCC*mec* type III. Half of CC59/ST338-MRSA-III isolates harbored *see* encoding gene. Other toxin-encoding genes were not noticed. The predominant isolates carried *erm(B)* (75%, 3/4), and aminoglycoside resistance encoded by *aph* (3′)-*IIIa* was also common among these isolates (50%, 2/4). All of the CC59 isolates possessed SGB + SGF + SGFa + SGFb prophage profile.

### CC80

The CC80 isolates exhibited different *spa* types including t044 (66.7%, 8/12), t131 (33.3%, 4/12). All the ST80-MRSA-IV isolates assigned *agr* III and *coa* II. One-fourth of isolates were categorized as non-biofilm producers. The results exhibited that the *clfA* and *clfB* genes were explored in the entire CC80 isolates. The gene encoding for *icaD* (91.7%, 11/12) was the most prevalent biofilm-related gene among isolates.

The carriage of *pvl* genes was confirmed in one-third of tested isolates. Resistances to aminoglycosides encoded by *ant* (4′)-*Ia* (41.7) and *aac* (6′)-*Ie/aph* (2′′) (33.3), erythromycin encoded by *erm(A)*, and fusidic acid encoded by *fusB* were common. The most prevalent prophage pattern was SGA + SGB + SGF + SGFa + SGFb + SGL.

## DISCUSSION

This cross-sectional study provided several novel findings regarding the prevalence and genetic diversity of iMLSB-positive *S. aureus* strains isolated from clinical samples. It was observed that there was approximately a threefold increase in the prevalence of iMLSB *S. aureus* strains, from 7.5 to 21.7%, between 2013 and 2018. In contrast, Chavez-Bueno et al. (2005) suggested a significant decline in the trend for the prevalence of iMLSB phenotype from 93% in 1999 to 7% in 2002. Although our results markedly exhibited an increase in the prevalence of the inducible resistance among clinical *S. aureus* isolates in Iran, enhanced clinical and laboratory awareness of inducible resistance may

also be responsible for this rise. Molecular epidemiology and prevalence of inducible resistance among *S. aureus* strains change geographically and dynamically (Monecke et al., 2011; Boswihi et al., 2016). In this experiment, the prevalence of iMLS<sub>B</sub> among *S. aureus* was found to be 10.9% with 84.1% MRSA and 15.9% MSSA isolates exhibiting iMLS<sub>B</sub>. This prevalence was lower than the rates reported from Nepal (21%) (Adhikari et al., 2017) and Jordan (76.7%) (Aqel et al., 2017), whereas it was higher than Brazil (7.9%) (Bottega et al., 2014). However, variable rates of iMLS<sub>B</sub> among *S. aureus* isolates have been reported in previously published data from Iran ranging from 4.1 to 20.7% (Memariani et al., 2009; Khashei et al., 2018). Regarding the increasing incidence of inducible resistance, our study suggests the necessity to revise the prescription of macrolides, which could cause a decline in resistance patterns. The investigated population and the prevalence of different clones in across various regions of the world could likely explain the striking differences in inducible clindamycin resistance.

In the present experiment, 18.3% of isolates tested were found to be resistant to mupirocin. This prevalence is higher than that reported rate in Jordan (5%) (Aqel et al., 2012) and other reports in France (2.2%) (Desroches et al., 2013) and Greece (1.6%) (Petinaki et al., 2004). A research performed by Abbasi-Montazeri et al. (2013) in Iran notified that 6% of *S. aureus* strains obtained from burn patients were detected as mupirocin-resistant. A high prevalence of resistance to mupirocin in this experiment indicates that there are unrestricted policies in the use of mupirocin for long periods and/or increasing trends of mupirocin prescription in our setup. Furthermore, we observed that 9.6 and 8.7% isolates had HLMUPR and LLMUPR phenotypes, respectively, which are higher than the rate stated in France (0.8%) (Desroches et al., 2013) and Korea (5%) (Yun et al., 2003). Different prevalence rates of HLMUPR *S. aureus* were reported from other researchers in Iran, 25% by Shahsavan et al. (2012) and 17% by Abbasi-Montazeri et al. (2013). We found that 9.5% of the examined isolates carried *mupA* gene, and all of them exhibited an HLMUPR phenotype. Researches from Spain (González-Domínguez et al., 2016) (27.2%) and Iran (Abbasi-Montazeri et al., 2013) (34%) revealed a higher rate of this gene among their *S. aureus* strains. Contrary to the study of Shahsavan et al. (2012), reporting *mupA* gene only in MRSA strains with cMLS<sub>B</sub> phenotype, the present data showed the existence of *mupA* gene in inducible resistance MRSA strains.

This study indicated that of 126 inducible clindamycin-resistant *S. aureus* isolates, 5.6% were fusidic acid-resistant, which was similar to those in Canada (7%) and Australia (7%); nonetheless, it was far lower than the values previously reported in Greece (62.4%) and Ireland (19.9%) (Castanheira et al., 2010a,b). In a multicenter experiment performed from 2007 to 2011 in three referral hospitals in Tehran, Iran, of 726 tested *S. aureus* isolates, 3% of isolates were found to be resistant to fusidic acid (Deotale et al., 2010). In our collections, we found that *fusB* and *fusC* were present in six strains and one strain, respectively. A previously studied experiment from China noted a higher rate of *fusB* gene (10.5%); on the other hand, *fusC* and *fusA* genes were not present in any of tested isolates (Yu et al., 2015). These data highlighted that *fusB* is the predominant determinant

responsible for resistance to fusidic acid among *S. aureus* in Iran. According to previously published data, different fusidic acid resistance rates were reported in both MRSA and MSSA strains. Notably, this study showed that fusidic acid resistance was only seen among MRSA isolates, which were in line with a report of China indicating that the prevalence of fusidic acid resistance among MRSA isolates was significantly higher than that among MSSA isolates (Yu et al., 2015).

According to the evidence, the ability to produce biofilm among *S. aureus* is diverse, with data ranging within 43 to 88% (Luther et al., 2018). Our results showed that, of the 126 isolates under investigation, 77% of strains could produce biofilm, whereas 23% were confirmed as non-biofilm producer strains. This finding is similar to those in Egypt (83.3%) (Gad et al., 2009), whereas based on a study of Iran biofilm production reported rate was 38.7% (a twofold decrease) (Mirzaee et al., 2014). In this study, the biofilm formability of MRSA isolates (78.3%) was higher than that of MSSA isolates (70%). Apparently, high capability of biofilm formation among MRSA strains was described by conducted studies from India (57.6%) (Mathur et al., 2006), China (66%) (Wang et al., 2010), and South Africa (37.8%) (Samie and Shivambu, 2011).

Data obtained from different studies suggest that the ability of biofilm formation in *S. aureus* strains is attributed to the expression of a wide range of virulence and adhesion factors of this bacterium (Nemati et al., 2009; Samie and Shivambu, 2011; Luther et al., 2018), but the correlation between the existence of specific virulence factor and biofilm production has been controversial. Researches has shown that *ica ABCD* and adhesion genes can affect the biofilm formation ability in *S. aureus*. In this study, the most frequent *ica* genes were *icaD* (73%), followed by *icaA* (71.4%), *icaB* (60.3%), and *icaC* (53.2%). According to an analysis by Mirzaee et al. (2014) on 31 clinical *S. aureus* isolates, *icaD*, *icaA*, and *icaC* genes with the exception of *icaB* were found in more than half of the isolates tested. In the study of Yousefi et al. (2016), of 39 isolates of *S. aureus* recovered from UTI patients, 69.2% were biofilm producers, and it was notable that all isolates carried *icaA*, *fnbA*, and *clfA* genes. In the current study, a high percentage of *ica ABCD* genes made up 39.7% of the overall sample, which was close to a recent report in Iran (38.7%) (Mirzaee et al., 2014). The correlation between biofilm formation and the presence of adhesion genes is well established. In present survey, the most prevalent gene was *clfA* (93.7%), followed by *clfB* (87.3%), *fnbB* (61.9%), *cna* (57.9%), *fnbA* (54%), *ebp* (50%), and *bap* (3.2%), respectively. The attained data are consistent with a previous finding from Iran, which has displayed the role of the *bap* gene in biofilm production rarely. Our findings indicated that isolates with more adhesion and *ica* encoding genes were strictly associated with biofilm formation. Overall, our data confirmed the high ability of biofilm formation among inducible resistance *S. aureus* strains, which helps *S. aureus* to persist in infections. This scenario draws attention from clinicians to use treatment protocols in patients potentially infected with these bacteria.

Based on the results of *coa* typing, the top three *coa* types were III (44.4%), II (28.6%), and IVa (9.5%). This result was in contrast with the previous report by Hirose et al. (2010) in Japan, which indicated that *coa* types II, VII, and I accounted for 91.9%, 3.9%,

and 1.7% of isolates. We detected seven SC types (I–VI) among iMLSB *S. aureus* strains suggesting diverse genetic backgrounds of tested isolates in this region of Iran. In a research involving 157 *S. aureus* strains from clinical specimens, nine different patterns of *coa* gene were detected (Afrough et al., 2013). These findings were confirmed by results in Thailand (Janwithayanuchit et al., 2006) and Egypt (Omar et al., 2014) reported previously. Genetic variability in *coa* gene among studied isolates indicated that it could not be a predictor for specific iMLSB *S. aureus* strains.

In the present study, the findings revealed that seven different prophage profiles were identified in the isolates studied. A high diversity of prophage patterns among *S. aureus* isolates has been reported from the United States (Workman et al., 2006), Czech Republic (Pantůček et al., 2004) and Iran (Rahimi et al., 2012). Our data exhibited that SGFa-SGFb (36.5%) and SGB-SGFa-SGFb (31.7%) were the major prophage profiles, which was in accordance with the study of Rahimi et al. (2012). SGF-type prophages are associated with the immune evasion cluster typical for *S. aureus* isolated from humans (Kahánková et al., 2010). SGA has been reported to be common among *pvl*-positive MRSA-IV isolates. This finding was consistent with previous research, revealing that all the *pvl*-positive isolates harbored SGA prophage type (Rahimi et al., 2012). Notably, the PVL was the most frequently encoded toxin in the tested isolates (23.8%). Previously published data from England and the United States (Holmes et al., 2005) indicated that the prevalence of *pvl* encoding genes among *S. aureus* was low (1.6%). Nevertheless, previous reports all over the world had shown a high prevalence of *pvl* among *S. aureus* strains (Monecke et al., 2011; Boswihi et al., 2016; Goudarzi et al., 2016a). In Iran, the *pvl*-positive rate ranged from 7.4 to 55.6% in *S. aureus* isolates. In our research, a relatively low but increasing prevalence of *pvl*-positive *S. aureus* strains was noted. According to our report, a recent study from Ireland showed an ascending trend of *pvl* among MRSA strains (from 0.2 to 8.8%), whereas this trend was diminishing for MSSA strains (20–2.5%) (Shore et al., 2014). Although this difference can, to some extent, reflect the origin of isolates and the type of sample, this could also be because of different *pvl*-encoding phages among *S. aureus* strains.

Considering the genes encoding enterotoxins, the data analysis of the current study exhibited that 54.8% of isolates carried one or more SE genes, with the *sea* (19.8%) and *sec* (11.1%) genes being the most commonly found. The attained data are consistent with the reports previously obtained from Iran and Turkey estimating enterotoxigenic *S. aureus* strains in 45 and 62.6% of isolates tested, respectively (Imanifooladi et al., 2007; Aydin et al., 2011). Based on earlier studies, the *she*, *sei*, and *sej* encoding genes were rarely present in *S. aureus* isolated from clinical samples, and similarly, these genes were not detected in the present survey either.

The present study displayed diversity in the numbers and the molecular types of iMLSB *S. aureus* clones identified in our health care settings. According to the current results, CC8 was the most prevalent clone in both CO and HO *S. aureus* isolates. The prevalence of CC8 was increased from 2013–2014 (20%) to 2017–2018 (39.5%). These strains were found in association with *pvl*-encoding bacteriophage and HLMUPR,

which carried *mupA* gene, which is similar to those reported in Iran (Azimian et al., 2014), Kuwait (Boswihi et al., 2016), and Ireland (Shore et al., 2014). According to evidence, phenotypic and genotypic resistance pattern in the ST8-IV isolates was found to be varied. In accordance with our research, high resistance to aminoglycosides and low resistance to tetracycline in ST8-MRSA isolates were described previously by researchers (Shore et al., 2014; Boswihi et al., 2016). The enterotoxin gene *sed* was the solo toxin gene detected among the ST8-IV isolates. Variability in the enterotoxin genes within ST8-IV isolates was reported by several investigators (Shore et al., 2014; Boswihi et al., 2016). The detection of the ST8-IV isolates in our study is of concern and highlights transmissibility and rapidity of its spread as an international epidemic MRSA clone in Iran.

ST239-MRSA-III, one of the most successful and persistent clones, was the most predominant genotype in CC8. Multiresistant ST239 clone was previously reported in South American, European, and some Asian countries, including Kuwait and Saudi Arabia (Shore et al., 2014; Boswihi et al., 2016). In this study, ST239 had five important *spa* types (t030, t037, t631, t860, and 388). The data in this experiment indicated that half of ST239-SCC*mec* III/t631 strains exhibited HLMUPR phenotype and harbored *mupA* gene. These findings are in parallel with previous reports from Iran (Goudarzi et al., 2016a) and those reported in India and Kuwait (Abimanyu et al., 2012; Boswihi et al., 2016). All ST239-SCC*mec* III/t860 strains exhibited the LLMUPR phenotype, which was similar to findings in other countries including China and Kuwait (Boswihi et al., 2016; Liang et al., 2018). According to the molecular typing results, ST239-SCC*mec* III/030 with 20.5% and ST239-SCC*mec* III/037 with 25% were recognized as the most common multiresistant ST239-MRSA-III type. These results were consistent with previous research performed by Li et al. (2018), who demonstrated multiresistant ST239-SCC*mec* III/030 as the most predominant genotype in China from 2005 to 2013, which decreased significantly in 2016. During a 12-year period in Norway, Fossum and Bukholm (2006) indicated ST239 as the most prevalent MRSA clones, which became endemic in hospital environments in Norway. However, molecular characteristics, especially antibiotic resistance gene and virulence factors, of our ST239-MRSA-III strains were similar to those of ST239 strains reported in Kuwait, China, and Saudi Arabia (Lewis and Jorgensen, 2005; Boswihi et al., 2016). The emergence of ST239-MRSA-III may be due to the import of this clone from neighboring countries.

Increasing prevalence rate of CC8 and disappearance of CC22 between 2013 and 2018 highlighted replacement and the changing clonal structure of MRSA in this region of Iran. As summarized in **Table 5**, *pvl* encoding genes were detected in two isolates of ST22-SCC*mec* IV/t852 and one isolate of ST22-SCC*mec* IV/t005. These *pvl*-positive genotypes were mainly distributed at some geographic area including England, Australia, Ireland, Kuwait, Iran, Germany, Saudi Arabia, and Nepal (Monecke et al., 2011; Shore et al., 2014; Boswihi et al., 2016). Of note, the majority of the ST22-SCC*mec* IV/t790 isolates was related to the *tst* gene, demonstrated LLMUPR phenotype, and could exhibit multiresistance. A recent report in Ireland



also displayed that most of *pvl*-positive ST22-MRSA-IV isolates were associated with resistance to gentamicin, trimethoprim, and ciprofloxacin and carried the *erm(C)*, *lnu(A)*, *aacA-aphD*, *aadD*, and *mupA* genes (Shore et al., 2014).

The ST22-MSSA isolates exhibited different antimicrobial resistance patterns including resistance to penicillin, gentamicin, tetracycline, kanamycin, rifampin, tobramycin, and amikacin. Our data are in concordance with a study conducted in Ireland, which reported the prevalence of low frequency of ST22-MSSA/t005 and ST22-MSSA/t1869 strains during the study period from 2002 to 2011. They indicated that ST22-MSSA was resistant to amikacin, ampicillin, fusidic acid, gentamycin, kanamycin, and tobramycin with multiple resistance genes *blaZ*, *aacA-aphD*, and *dfrS1* detected among these isolates (Shore et al., 2014).

Our data showed that 40% of the CC/ST30 isolates carried *pvl*, which belonged to MRSA and MSSA strains. PVL-positive CC30/ST30-IV strains have been described in Iran (Goudarzi et al., 2016a,b), Kuwait (Boswihi et al., 2016), and Ireland (Shore et al., 2014). Importantly, the prevalence of CC30/ST30 increased from 8% in 2013 to 18.4% in 2018 in our country. In this connection, Boswihi et al. exhibited ST30 as the second dominant MRSA genotypes in Kuwait hospitals, which decreased from 30% in 2001–2003 to 22% in 2006. They also showed a low prevalence of ST30-IV-MRSA among tested isolates (2.9%) (Boswihi et al., 2016). Surprisingly, all MRSA isolates carried biofilm and adhesion-related genes, and approximately 90% of the MSSA isolates were able to form biofilm at different intensities. In line with our study, Chamon et al. (2015) from Brazil showed biofilm production ability among ST30 strains. They also found *bbp* gene as a possible marker of this lineage. Congruent with the previous observations (Shore et al., 2014; Boswihi et al., 2016), all of our ST30 isolates belonged to *agr* type III, with different toxin and antimicrobial resistance patterns noted for this genotype.

As aforementioned, fewer than half of the CC/ST80-MRSA-IV isolates showed aminoglycoside resistance encoded by *ant* (4')-Ia, *aac* (6')-Ie/*aph* (2''). Resistance to fusidic acid encoded by *fusB* was detected in one isolate. These results were different from a previous study conducted in Ireland, which exhibited all CC/ST80-MRSA-IV isolates were resistant to kanamycin and neomycin, encoded by *aph* (3')-IIIa. In addition, our data revealed that resistances to tetracycline, fusidic acid, and erythromycin encoded by *tet(K)*, *fusB*, and *erm(C)*, respectively, were frequent among tested isolates (Shore et al., 2014). The variations could be a result of differences in the genetic backgrounds of the *S. aureus* strains. The prevalence of CC/ST80-MRSA-IV increased from 12% in 2013 to 13.2% in 2018. This increasing rate of ST80-IV raises the concern that this strain is becoming endemic in our hospitals.

Based on the evidence, ST80-IV is acknowledged as a toxigenic virulent isolate. In the present study, *pvl*-positive CC/ST80-SCCmec/t044 isolates were confirmed by approximately half of the isolates. ST80-MRSA-MRSA isolates harboring the *pvl* genes

were previously reported from Kuwait, Malaysia, Singapore, and Ireland (Shore et al., 2014; Boswihi et al., 2016).

According to previously published data, CC/ST59 has limited geographical spread. In the present research CC/ST59 was present in 10 isolates, accounting for 7.9%. This clone was previously reported in Australia, Ireland, United Kingdom, Korea, Kuwait, and Taiwan (Monecke et al., 2011; Boswihi et al., 2016). In this study, the results revealed that our isolates carried resistance genes at a relatively low level, but *erm(C)* encoding resistance to erythromycin was noted in more than half of the isolates. Conversely, high frequencies of multiple resistance genes including *erm(B)*, *aph* (3')-IIIa, and *tet(K)* were identified among tested isolates of a study performed in Ireland (Shore et al., 2014). Notably, resistance to fusidic acid encoded by *fusB* was also detected in one isolate, which was similar to the previous report from Ireland (Shore et al., 2014). According to this experiment, 66.7% of the isolates were positive for *seb* (60.4%) gene. This is inconsistent with the research conducted in Ireland showing that *seb* gene could be a possible marker of this lineage. The observed frequency of CC59/ST338-SCCmecIII/t437 isolates was in accordance with previous reports, as this genotype is infrequently isolated (Li et al., 2013).

Another clone found among inducible resistance *S. aureus* strains was ST5-SCCmec IV/t002 (7.1%). Recent studies have shown the presence of CC/ST5- SCCmecIV/t002 clones in Asian and European countries, such as Iran, Japan, Korea, the United Arab Emirates, Kuwait, Ireland, and Australia (Monecke et al., 2011; Boswihi et al., 2016). The present data indicated that the prevalence of CC/ST5- SCCmecIV/t002 diminished during the study from 8% in 2013–2014 to 2.6% in 2017–2018. Conversely, a recent cross-sectional study performed in New Zealand on 3,323 patients from 2005 to 2011 documented seven most frequent MRSA clones. This study also indicated an ST5-SCCmecIV clone, which rapidly displaced ST30-SCCmecIV as the dominant CA-MRSA clone (Williamson et al., 2013). It was also observed that nearly half of ST5-SCCmecIV/t002 isolates were confirmed as HLMUPR strains. The finding of CC/ST5-SCCmecIV/t002 isolates in our screening indicated that resistance was observed for erythromycin encoded by *erm(A)*, tetracycline encoded by *tet(M)*, and mupirocin encoded by *mupA*. In an experiment conducted in 2010 in China, Song et al. (2013) revealed a different result. They showed a high prevalence of ST5-SCCmecIV/t002 among their clinical *S. aureus* isolates.

As shown in **Table 5**, the CC1 isolates belonged to two STs (ST772 and ST1). *spa* types t10795 and t657 pertained to ST772, whereas *spa* type t6811 was identified in ST1 isolates. ST772- SCCmecV, which is known as Bengal Bay clone, emerged in Bangladesh and was reported in New Zealand, Nepal, Italy, the United Arab Emirates, Malaysia, the United Kingdom, Ireland, Saudi Arabia, India, Australia, and Kuwait (Monecke et al., 2011; Shore et al., 2014; Boswihi et al., 2016). This clone was found in 6.4% of the examined isolates. All isolates were multiresistant and carried *aac* (6')-Ie/*aph* (2''), *aph* (3')-IIIa, *tet(M)*, and



*erm(B)*. The attained data are in accordance to results of the study of Shore et al. (2014), which reported MDR pattern and carriage of *ant (4')-Ia*, *aac (6')-Ie/aph (2'')*, and *tet(M)* genes among CC1/ST772-SCC*mecV* isolates. The study demonstrated similarities in genetic characteristics including susceptibility to antibiotics and toxin-encoding genes of our ST772-SCC*mecV* isolates recently reported in Kuwait (Boswihi et al., 2016). Of two CC1/ST1-SCC*mecV*/t6811 isolates, one isolate carried *fusc* and exhibited resistance to fusidic acid at MIC 32 µg/mL. Boswihi et al. (2016) previously reported ST1-SCC*mecV*/t6811 carrying *fusc* gene from Kuwait.

In contrast to our study, which reported a low prevalence of ST15 (4%), a recent multicenter study performed in 25 European countries documented a relatively high prevalence of ST15 and reported it as the second most frequent clone across most of the European countries (Grundmann et al., 2014). In a study of 568 *S. aureus* isolates in 11 European countries, researchers reported a low level of this type among the tested isolates (Rolo et al., 2012). Our data demonstrated that all the ST15 isolates were *pvl*-positive and displayed the LLMUPR phenotype. The analysis of our previous study indicated that the most common mupirocin-resistant MRSA isolates belonged to ST15-SCC*mec IV*/t084 (Goudarzi et al., 2017), which is in line with the present data. Although ST15 is more frequently detected in MRSA, there are reports that indicate the high distribution of this type among MSSA strains (Monecke et al., 2011; Boswihi et al., 2016). It was notable that all ST15 isolates harbored SCC*mec IV*, *agr* type II, and *coa* type I and belonged to *spa* type t084. Different antimicrobial resistance patterns were noted among these isolates, which is in accordance with previous studies (Rolo et al., 2012; Grundmann et al., 2014; Goudarzi et al., 2017).

In contrast to a study conducted in Kuwait, which reported CC45 as one of the most epidemics MRSA isolates with different antimicrobial resistance patterns, in the current research, a low frequency of the CC45 (4%) was observed among examined isolates. In a study conducted in the South of Poland, 26.1% of *S. aureus* isolates were found to be related to CC45 (Ilczyszyn et al., 2016). This ST was at its most prevalent in 2015, when it accounted for 22.2% (4/18) of inducible resistance isolates, reduced to 4.2% (1/24) in 2016, and disappeared in 2017–2018.

The strengths of our research included examining the prevalence and temporal differences in iMLSB *S. aureus* strains. It was the first study on the molecular characterization of inducible clindamycin-resistant *S. aureus* strains from Iran. However, the present research had limitations. One limitation of our study was the modest sample size and the impossibility of using typing methods such as pulsed-field gel electrophoresis (PFGE). It was not possible either to correlate demographics data with circulating clones owing to a lack of data linking patient characteristics. Another important limitation of our study was *clfA*- and *clfB*-negative *S. aureus* strains, which were unusual and required further analysis using whole-genome sequencing and microarray system.

## CONCLUSION

This was the first report of monitoring the prevalence and characterization of *S. aureus* isolates with the inducible resistance phenotype in Iran. Our investigation supports a detailed epidemiological survey on the prevalence and temporal differences in iMLSB *S. aureus* strains. It was ultimately attained that there is a considerable increasing trend for CC8 versus a decreasing trend for CC22. However, we revealed a shift in the clonal composition of MRSA isolates over time with the emphasis on a progressive replacement of CC22 clone by CC8 clones between 2013 and 2018. Indeed, our research indicated that iMLSB *S. aureus* isolates with similar genetic backgrounds exhibited specific virulence gene profiles, antimicrobial resistance patterns, and biofilm patterns. Increase in *S. aureus* with inducible resistance phenotype harboring SCC*mecIV* during the 5-year period makes sense that there is a shift in the iMLSB population from our community to hospital. Therefore, we conclude that there is a need for ongoing and nationwide surveillance studies to further evaluate of *S. aureus* with inducible resistance phenotype and to prevent these strains from becoming endemic in the Iranian hospitals.

## DATA AVAILABILITY STATEMENT

The datasets generated for this study are available on request to the corresponding author.

## ETHICS STATEMENT

The current study protocol was approved by the Ethics Committee of the Shahid Beheshti University of Medical Sciences in Tehran, Iran (IR.SBMU.MSP.REC.1396.700). Written informed consent was obtained from participants.

## AUTHOR CONTRIBUTIONS

MG and HG conceived, designed, and supervised the study. MD, RaP, MN, MF, MM, SS, and AA performed the experiments. NK, RoP, and MG analyzed and interpreted the data. MG, HG, NK, SS, and RoP drafted and written the manuscript. All authors approved the final version of manuscript.

## FUNDING

This study was supported financially by the grant (No. 12688) from Research Deputy of Shahid Beheshti University of Medical Sciences, Tehran, Iran.

## ACKNOWLEDGMENTS

We are indebted to Dr. Edet E. Udo (Kuwait University) and Dr. Agnes Marie Sá Figueiredo (Universidade Federal do Rio de Janeiro) for providing reference strains of the *S. aureus*.

## REFERENCES

- Abbasi-Montazeri, E., Khosravi, A. D., Feizabadi, M. M., Goodarzi, H., Khoramrooz, S. S., Mirzaii, M., et al. (2013). The prevalence of methicillin resistant *Staphylococcus aureus* (MRSA) isolates with high-level mupirocin resistance from patients and personnel in a burn center. *Burns* 39, 650–654. doi: 10.1016/j.burns.2013.02.005
- Abimanyu, N., Murugesan, S., and Krishnan, P. (2012). Emergence of methicillin-resistant *Staphylococcus aureus* ST239 with high-level mupirocin and inducible clindamycin resistance in a tertiary care center in Chennai. *South India. J. Clin. Microbiol.* 50, 3412–3413. doi: 10.1128/JCM.01663-12
- Adhikari, R., Shrestha, S., Barakoti, A., and Amatya, R. (2017). Inducible clindamycin and methicillin resistant *Staphylococcus aureus* in a tertiary care hospital. Kathmandu, Nepal. *BMC. Infect. Dis.* 17:483. doi: 10.1186/s12879-017-2584-5
- Afrough, P., Pourmand, M. R., Sarajian, A. A., Saki, M., and Saremy, S. (2013). Molecular investigation of *Staphylococcus aureus*, *coa* and *spa* genes in Ahvaz hospitals, staff nose compared with patients clinical samples. *Jundishapur. J. Microbiol.* 6:e5377.
- Aqel, A., Alzoubi, H., and Al-Zereini, W. (2017). Prevalence of inducible clindamycin resistance in methicillin-resistant *Staphylococcus aureus*: the first study in Jordan. *J. Infect. Dev. Ctries.* 11, 350–354. doi: 10.3855/jidc.8316
- Aqel, A., Ibrahim, A., and Shehabi, A. (2012). Rare occurrence of mupirocin resistance among clinical *Staphylococcus aureus* isolates in Jordan. *Acta Microbiol. Immun. Hung* 59, 239–247. doi: 10.1556/AMic.59.2012.2.8
- Arciola, C. R., Campoccia, D., Gamberini, S., Cervellati, M., Donati, E., and Montanaro, L. J. B. (2002). Detection of slime production by means of an optimised Congo red agar plate test based on a colourimetric scale in *Staphylococcus epidermidis* clinical isolates genotyped for *ica* locus. *Biomaterials* 23, 4233–4239. doi: 10.1016/S0142-9612(02)00171-0
- Aydin, A., Sudagidan, M., and Muratoglu, K. (2011). Prevalence of staphylococcal enterotoxins, toxin genes and genetic-relatedness of foodborne *Staphylococcus aureus* strains isolated in the Marmara Region of Turkey. *Int. J. Food. Microbiol.* 148, 99–106. doi: 10.1016/j.ijfoodmicro.2011.05.007
- Azimian, A., Havaei, S. A., Ghazvini, K., Khosrojerdi, M., Naderi, M., and Samiee, S. M. (2014). Isolation of PVL/ACME-positive, community acquired, methicillin-resistant *Staphylococcus aureus* (USA300) from Iran. *J. Med. Microbiol.* 2, 100–104.
- Boswihi, S. S., Udo, E. E., and Al-Sweih, N. (2016). Shifts in the clonal distribution of methicillin-resistant *Staphylococcus aureus* in Kuwait hospitals: 1992–2010. *PLoS One* 11:e0162744. doi: 10.1371/journal.pone.0162744
- Bottega, A., Rodrigues, M. D. A., Carvalho, F. A., Wagner, T. F., Leal, I. A. S., Santos, S. O. D., et al. (2014). Evaluation of constitutive and inducible resistance to clindamycin in clinical samples of *Staphylococcus aureus* from a tertiary hospital. *Rev. Soc. Bras. Med. Trop.* 47, 589–592. doi: 10.1590/0037-8682-0140-2014
- Boye, K., Bartels, M. D., Andersen, I. S., Moeller, J. A., Westh, H. (2007). A new multiplex PCR for easy screening of methicillin-resistant *Staphylococcus aureus* SCCmec types I–V. *J. Clin. Microbiol.* 13, 725–727. doi: 10.1111/j.1469-0691.2007.01720.x
- Castanheira, M., Watters, A. A., Bell, J. M., Turnidge, J. D., and Jones, R. N. (2010a). Fusidic acid resistance rates and prevalence of resistance mechanisms among *Staphylococcus* spp. isolated in North America and Australia, 2007–2008. *Antimicrob. Agents. Chemother.* 54, 3614–3617. doi: 10.1128/AAC.01390-09
- Castanheira, M., Watters, A. A., Mendes, R. E., Farrell, D. J., and Jones, R. N. (2010b). Occurrence and molecular characterization of fusidic acid resistance mechanisms among *Staphylococcus* spp. from European countries (2008). *J. Antimicrob. Chemother.* 65, 1353–1358. doi: 10.1093/jac/dkq094
- Chamon, R. C., Iorio, N. L. P., da Silva Ribeiro, S., Cavalcante, F. S., and dos Santos, K. R. N. (2015). Molecular characterization of *Staphylococcus aureus* isolates carrying the Pantone-Valentine leukocidin genes from Rio de Janeiro hospitals. *Diagn. Microbiol. Infect. Dis.* 83, 331–334. doi: 10.1016/j.diagmicrobio.2015.09.004
- Chavez-Bueno, S., Bozdogan, B., Katz, K., Bowlware, K. L., Cushion, N., Cavuoti, D., et al. (2005). Inducible clindamycin resistance and molecular epidemiologic trends of pediatric community-acquired methicillin-resistant *Staphylococcus aureus* in Dallas. *Texas. Antimicrob. Agents. Chemother.* 49, 2283–2288. doi: 10.1128/AAC.49.6.2283-2288.2005
- Dadashi, M., Nasiri, M. J., Fallah, F., Owlia, P., Hajikhani, B., Emameini, M., et al. (2018). Methicillin-resistant *Staphylococcus aureus* (MRSA) in Iran: a systematic review and meta-analysis. *J. Glob. Antimicrob. Resist.* 12, 96–103. doi: 10.1016/j.jgar.2017.09.006
- Deotale, V., Mendiratta, D., Raut, U., and Narang, P. (2010). Inducible clindamycin resistance in *Staphylococcus aureus* isolated from clinical samples. *Indian. J. Med. Microbiol.* 28:124. doi: 10.4103/0255-0857.62488
- Desroches, M., Potier, J., Laurent, F., Bourrel, A.-S., Doucet-Populaire, F., Decousser, J.-W., et al. (2013). Prevalence of mupirocin resistance among invasive coagulase-negative staphylococci and methicillin-resistant *Staphylococcus aureus* (MRSA) in France: emergence of a mupirocin-resistant MRSA clone harbouring *mupA*. *J. Antimicrob. Chemother.* 68, 1714–1717. doi: 10.1093/jac/dkt085
- Diep, B. A., Stone, G. G., Basuino, L., Graber, C. J., Miller, A., des Etages, S. A., et al. (2008). The arginine catabolic mobile element and staphylococcal chromosomal cassette *mec* linkage: convergence of virulence and resistance in the USA300 clone of methicillin-resistant *Staphylococcus aureus*. *J. Infect. Dis.* 197, 1523–1530. doi: 10.1086/587907
- Enright, M. C., Day, N. P., Davies, C. E., Peacock, S. J., and Spratt, B. G. (2000). Multilocus sequence typing for characterization of methicillin-resistant and methicillin-susceptible clones of *Staphylococcus aureus*. *J. Clin. Microbiol.* 38, 1008–1015.
- Fossum, A., and Bukholm, G. (2006). Increased incidence of methicillin-resistant *Staphylococcus aureus* ST80, novel ST125 and SCCmecIV in the south-eastern part of Norway during a 12-year period. *J. Clin. Microbiol.* 12, 627–633. doi: 10.1111/j.1469-0691.2006.01467.x
- Gad, G. F. M., El-Feky, M. A., El-Rehewy, M. S., Hassan, M. A., Abolella, H., and El-Baky, R. M. A. (2009). Detection of *icaA*, *icaD* genes and biofilm production by *Staphylococcus aureus* and *Staphylococcus epidermidis* isolated from urinary tract catheterized patients. *J. Infect. Dev. Countr.* 3, 342–351. doi: 10.3855/jidc.241
- Gilot, P., Lina, G., Cochard, T., and Poutrel, B. (2002). Analysis of the genetic variability of genes encoding the RNA III-activating components Agr and TRAP in a population of *Staphylococcus aureus* strains isolated from cows with mastitis. *J. Clin. Microbiol.* 40, 4060–4067. doi: 10.1128/jcm.40.11.4060-4067.2002
- González-Domínguez, M., Seral, C., Potel, C., Sáenz, Y., Álvarez, M., Torres, C., et al. (2016). Genotypic and phenotypic characterization of methicillin-resistant *Staphylococcus aureus* (MRSA) clones with high-level mupirocin resistance. *Diagn. Microbiol. Infect. Dis.* 85, 213–217. doi: 10.1016/j.diagmicrobio.2016.02.021
- Gordon, R. J., and Lowy, F. D. (2008). Pathogenesis of methicillin-resistant *Staphylococcus aureus* infection. *Clin. Infect. Dis.* 46(Suppl. 5), S350–S359. doi: 10.1086/533591
- Goudarzi, M., Bahramian, M., Tabrizi, M. S., Udo, E. E., Figueiredo, A. M. S., Fazeli, M., et al. (2017). Genetic diversity of methicillin resistant *Staphylococcus aureus* strains isolated from burn patients in Iran: ST239-SCCmec III/t037 emerges as the major clone. *Microb. Pathog.* 105, 1–7. doi: 10.1016/j.micpath.2017.02.004
- Goudarzi, M., Goudarzi, H., Figueiredo, A. M. S., Udo, E. E., Fazeli, M., Asadzadeh, M., et al. (2016a). Molecular characterization of methicillin resistant *Staphylococcus aureus* strains isolated from intensive care units in Iran: ST22-SCCmec IV/t790 emerges as the major clone. *PLoS One* 11:e0155529. doi: 10.1371/journal.pone.0155529
- Goudarzi, M., Seyedjavadi, S. S., Azad, M., Goudarzi, H., and Azimi, H. (2016b). Distribution of *spa* types, integrons and associated gene cassettes in *Staphylococcus aureus* strains isolated from intensive care units of hospitals in Tehran, Iran. *Arch. Clin. Infect. Dis.* 11, 1–11.
- Gould, I. M., David, M. Z., Esposito, S., Garau, J., Lina, G., Mazzei, T., et al. (2012). New insights into methicillin-resistant *Staphylococcus aureus* (MRSA) pathogenesis, treatment and resistance. *Int. J. Antimicrob. Agents* 39, 96–104. doi: 10.1016/j.ijantimicag.2011.09.028
- Grundmann, H., Schouls, L. M., Aanensen, D. M., Pluister, G. N., Tami, A., Chlebowicz, M., et al. (2014). The dynamic changes of dominant clones of *Staphylococcus aureus* causing bloodstream infections in the European region: results of a second structured survey. *Euro. Surveill.* 19:20987. doi: 10.2807/1560-7917.es2014.19.49.20987
- Harmen, D., Claus, H., Witte, W., Rothgänger, J., Claus, H., Turnwald, D., et al. (2003). Typing of methicillin-resistant *Staphylococcus aureus* in a university

- hospital setting by using novel software for spa repeat determination and database management. *J. Clin. Microbiol.* 41, 5442–5448. doi: 10.1128/jcm.41.12.5442-5448.2003
- Hirose, M., Kobayashi, N., Ghosh, S., Paul, S. K., Shen, T., Urushibara, N., et al. (2010). Identification of Staphylocoagulase Genotypes I-X and Discrimination of Type IV and V Subtypes by Multiplex PCR Assay for Clinical Isolates of *Staphylococcus aureus*. *Jpn. J. Infect. Dis.* 63, 257–263.
- Holmes, A., Ganner, M., McGuane, S., Pitt, T., Cookson, B., and Kearns, A. (2005). *Staphylococcus aureus* isolates carrying Panton-Valentine leucocidin genes in England and Wales: frequency, characterization, and association with clinical disease. *J. Clin. Microbiol.* 43, 2384–2390. doi: 10.1128/JCM.43.5.2384-2390.2005
- Iłczyszyn, W. M., Sabat, A. J., Akkerboom, V., Szkarlat, A., Klepacka, J., Sowa-Sierant, I., et al. (2016). Clonal structure and characterization of *Staphylococcus aureus* strains from invasive infections in paediatric patients from South Poland: association between age, spa types, clonal complexes, and genetic markers. *PLoS One* 11:e0151937. doi: 10.1371/journal.pone.0151937
- Imanifooladi, A., Sattari, M., Peerayeh, S. N., Hassan, Z., and Hossainidoust, S. (2007). Detection the *Staphylococcus aureus* producing enterotoxin isolated from skin infections in hospitalized patients. *Pak. J. Biol. Sci.* 10, 502–505.
- Janwithayanuchit, I., Ngam-Ululert, S., Paungmoung, P., and Rangspanuratan, W. (2006). Epidemiologic study of methicillin-resistant *Staphylococcus aureus* by coagulase gene polymorphism. *Scienceasia* 32, 127–132. doi: 10.2306/scienceasia1513-1874.2006.32.127
- Kahánková, J., Pantůček, R., Goerke, C., Růžicková, V., Holochová, P., and Doškař, J. (2010). Multilocus PCR typing strategy for differentiation of *Staphylococcus aureus* siphoviruses reflecting their modular genome structure. *Environ. Microbiol.* 12, 2527–2538. doi: 10.1111/j.1462-2920.2010.02226.x
- Khashei, R., Malekzadegan, Y., Sedigh Ebrahim-Saraie, H., and Razavi, Z. (2018). Phenotypic and genotypic characterization of macrolide, lincosamide and streptogramin B resistance among clinical isolates of staphylococci in southwest of Iran. *BMC. Res. Notes* 11:711. doi: 10.1186/s13104-018-3817-4
- Lewis, J. S., and Jorgensen, J. H. (2005). Inducible clindamycin resistance in staphylococci: should clinicians and microbiologists be concerned? *Clin. Infect. Dis.* 40, 280–285. doi: 10.1086/426894
- Li, J., Wang, L., Ip, M., Sun, M., Sun, J., Huang, G., et al. (2013). Molecular and clinical characteristics of clonal complex 59 methicillin-resistant *Staphylococcus aureus* infections in Mainland China. *PLoS One* 8:e70602. doi: 10.1371/journal.pone.0070602
- Li, S., Sun, S., Yang, C., Chen, H., Yin, Y., Li, H., et al. (2018). The changing pattern of population structure of *Staphylococcus aureus* from bacteremia in China from 2013 to 2016: ST239-030-MRSA replaced by ST59-t437. *Front. Microbiol.* 9:332. doi: 10.3389/fmicb.2018.00332
- Liang, B., Mai, J., Liu, Y., Huang, Y., Zhong, H., Xie, Y., et al. (2018). Prevalence and Characterization of *Staphylococcus aureus* isolated from women and Children in Guangzhou. *China. Front. Microbiol.* 9:2790. doi: 10.3389/fmicb.2018.02790
- Luther, M. K., Parente, D. M., Caffrey, A. R., Daffinee, K. E., Lopes, V. V., Martin, E. T., et al. (2018). Clinical and genetic risk factors for biofilm-forming *Staphylococcus aureus*. *Antimicrob. Agents Chemother.* 62, e2252–e2217. doi: 10.1128/AAC.02252-17
- Mathur, T., Singhal, S., Khan, S., Upadhyay, D., Fatma, T., and Rattan, A. (2006). Detection of biofilm formation among the clinical isolates of staphylococci: an evaluation of three different screening methods. *Indian J. Med. Microbiol.* 24:25. doi: 10.4103/0255-0857.19890
- Memariani, M., Pourmand, M., Shirazi, M., Dallal, M., Abdossamadi, Z., and Mardani, N. (2009). The importance of inducible clindamycin resistance in enterotoxin positive *S. aureus* isolated from clinical samples. *Tehran. Univ. Med. J.* 67, 250–256.
- Mirzaee, M., Najar-Peerayeh, S., Behmanesh, M., Forouzandeh-Moghadam, M., and Ghasemian, A.-M. (2014). Detection of intracellular adhesion (ica) gene and biofilm formation *Staphylococcus aureus* isolates from clinical blood cultures. *J. Med. Bacteriol.* 3, 1–7.
- Monday, S. R., and Bohach, G. A. (1999). Use of multiplex PCR to detect classical and newly described pyrogenic toxin genes in staphylococcal isolates. *J. Clin. Microbiol.* 37, 3411–3414.
- Monecke, S., Coombs, G., Shore, A. C., Coleman, D. C., Akpaka, P., Borg, M., et al. (2011). A field guide to pandemic, epidemic and sporadic clones of methicillin-resistant *Staphylococcus aureus*. *PLoS One* 6:e17936. doi: 10.1371/journal.pone.0017936
- Nemati, M., Hermans, K., Devriese, L. A., Maes, D., and Haesebrouck, F. (2009). Screening of genes encoding adhesion factors and biofilm formation in *Staphylococcus aureus* isolates from poultry. *Avian. Pathol.* 38, 513–517. doi: 10.1080/03079450903349212
- Nezhad, R. R., Meybodi, S. M., Rezaee, R., Goudarzi, M., and Fazeli, M. (2017). Molecular characterization and resistance profile of methicillin resistant *Staphylococcus aureus* strains isolated from hospitalized patients in intensive care unit. *Tehran-Iran. Jundishapur. J. Microbiol.* 10:e41666. doi: 10.5812/jjm.41666
- Omar, N. Y., Ali, H. A. S., Harfoush, R. A. H., and El Khayat, E. H. (2014). Molecular typing of methicillin resistant *Staphylococcus aureus* clinical isolates on the basis of protein A and coagulase gene polymorphisms. *Int. J. Microbiol.* 2014:650328. doi: 10.1155/2014/650328
- Pantosti, A., Sanchini, A., and Monaco, M. (2007). Mechanisms of antibiotic resistance in *Staphylococcus aureus*. *Future Microbiol.* 2, 323–334. doi: 10.2217/17460913.2.3.323
- Pantůček, R., Doškař, J., Růžicková, V., Kašpárek, P., Oráčová, E., Kvardova, V., et al. (2004). Identification of bacteriophage types and their carriage in *Staphylococcus aureus*. *Arch. Virol.* 149, 1689–1703. doi: 10.1007/s00705-004-0335-6
- Patel, M., Waites, K. B., Moser, S. A., Cloud, G. A., and Hoesley, C. J. (2006). Prevalence of inducible clindamycin resistance among community- and hospital-associated *Staphylococcus aureus* isolates. *J. Clin. Microbiol.* 44, 2481–2484. doi: 10.1128/JCM.02582-05
- Petinaki, E., Spiliopoulou, I., Kontos, F., Mianati, M., Bersos, Z., Stakias, N., et al. (2004). Clonal dissemination of mupirocin-resistant staphylococci in Greek hospitals. *J. Antimicrob. Chemother.* 53, 105–108. doi: 10.1093/jac/dkh028
- Rahimi, F., Bouzari, M., Katouli, M., and Pourshafie, M. R. (2012). Prophage and antibiotic resistance profiles of methicillin-resistant *Staphylococcus aureus* strains in Iran. *Arch. Virol.* 157, 1807–1811. doi: 10.1007/s00705-012-1361-4
- Rolo, J., Miragaia, M., Turlej-Rogacka, A., Empel, J., Bouchami, O., Faria, N. A., et al. (2012). High genetic diversity among community-associated *Staphylococcus aureus* in Europe: results from a multicenter study. *PLoS One* 7:e34768. doi: 10.1371/journal.pone.0034768
- Samie, A., and Shivambu, N. (2011). Biofilm production and antibiotic susceptibility profiles of *Staphylococcus aureus* isolated from HIV and AIDS patients in the Limpopo Province, South Africa. *Afr. J. Biotechnol.* 10, 14625–14636. doi: 10.5897/AJB11.1287
- Shahsavani, S., Emaneini, M., Khoshnab, B. N., Khoramian, B., Asadollahi, P., Aligholi, M., et al. (2012). A high prevalence of mupirocin and macrolide resistance determinant among *Staphylococcus aureus* strains isolated from burnt patients. *Burns* 38, 378–382. doi: 10.1016/j.burns.2011.09.004
- Shore, A. C., Tecklenborg, S. C., Brennan, G. I., Ehrlich, R., Monecke, S., and Coleman, D. C. (2014). Panton-Valentine leukocidin-positive *Staphylococcus aureus* in Ireland from 2002 to 2011: 21 clones, frequent importation of clones, temporal shifts of predominant methicillin-resistant *S. aureus* clones, and increasing multidrug resistance. *J. Clin. Microbiol.* 52, 859–870. doi: 10.1128/JCM.02799-13
- Song, Y., Du, X., Li, T., Zhu, Y., and Li, M. (2013). Phenotypic and molecular characterization of *Staphylococcus aureus* recovered from different clinical specimens of inpatients at a teaching hospital in Shanghai between 2005 and 2010. *J. Med. Microbiol.* 62, 274–282. doi: 10.1099/jmm.0.050971-0
- Stepanović, S., Vuković, D., Hola, V., Bonaventura, G. D., Djukić, S., Ćirković, I., et al. (2007). Quantification of biofilm in microtiter plates: overview of testing conditions and practical recommendations for assessment of biofilm production by staphylococci. *APMIS* 115, 891–899. doi: 10.1111/j.1600-0463.2007.apm\_630.x
- Wang, L., Liu, Y., Yang, Y., Huang, G., Wang, C., Deng, L., et al. (2012). Multidrug-resistant clones of community-associated methicillin-resistant *Staphylococcus aureus* isolated from Chinese children and the resistance genes to clindamycin and mupirocin. *J. Med. Microbiol.* 61, 1240–1247. doi: 10.1099/jmm.0.042663-0
- Wang, L., Yu, F., Yang, L., Li, Q., Zeng, X. Z., and Xu, Y. (2010). Prevalence of virulence genes and biofilm formation among *Staphylococcus aureus* clinical

- isolates associated with lower respiratory infection. *Afr. J. Microbiol. Res.* 4, 2566–2569.
- Williamson, D. A., Roberts, S. A., Ritchie, S. R., Coombs, G. W., Fraser, J. D., and Heffernan, H. (2013). Clinical and molecular epidemiology of methicillin-resistant *Staphylococcus aureus* in New Zealand: rapid emergence of sequence type 5 (ST5)-SCCmec-IV as the dominant community-associated MRSA clone. *PLoS One* 8:e62020. doi: 10.1371/journal.pone.0062020
- Workman, M., Nigro, O. D., and Steward, G. F. (2006). Identification of prophagein Hawaiian coastal water isolate of *Staphylococcus Aureus*. *J. Young. Investig.* 15, 1–8.
- Yousefi, M., Pourmand, M. R., Fallah, F., Hashemi, A., Mashhadi, R., and Nazari-Alam, A. (2016). Characterization of *Staphylococcus aureus* biofilm formation in urinary tract infection. *Iran J. Public Health* 45:485.
- Yu, F., Liu, Y., Lu, C., Jinnan, L., Qi, X., Ding, Y., et al. (2015). Dissemination of fusidic acid resistance among *Staphylococcus aureus* clinical isolates. *BMC Microbiol.* 15:210. doi: 10.1186/s12866-015-0552-z
- Yun, H.-J., Lee, S. W., Yoon, G. M., Kim, S. Y., Choi, S., Lee, Y. S., et al. (2003). Prevalence and mechanisms of low-and high-level mupirocin resistance in staphylococci isolated from a Korean hospital. *J Antimicrob. Chemother.* 51, 619–623. doi: 10.1093/jac/dkg140

**Conflict of Interest:** The authors declare that the research was conducted in the absence of any commercial or financial relationships that could be construed as a potential conflict of interest.

Copyright © 2020 Goudarzi, Kobayashi, Dadashi, Pantůček, Nasiri, Fazeli, Pouriran, Goudarzi, Miri, Amirpour and Seyedjavadi. This is an open-access article distributed under the terms of the Creative Commons Attribution License (CC BY). The use, distribution or reproduction in other forums is permitted, provided the original author(s) and the copyright owner(s) are credited and that the original publication in this journal is cited, in accordance with accepted academic practice. No use, distribution or reproduction is permitted which does not comply with these terms.





# Exploring the Potential of CRISPR-Cas9 Under Challenging Conditions: Facing High-Copy Plasmids and Counteracting Beta-Lactam Resistance in Clinical Strains of *Enterobacteriaceae*

## OPEN ACCESS

### Edited by:

Rustam Aminov,  
University of Aberdeen,  
United Kingdom

### Reviewed by:

Yahong Liu,  
South China Agricultural University,  
China  
Sheng Chen,  
Army Medical University, China

### \*Correspondence:

Hans-Peter Horz  
jhorz@ukaachen.de  
Simone Gonçalves dos Santos  
simonesantoskey@ufmg.br  
Tiago Antônio de Oliveira Mendes  
tiagoaomendes@ufv.br

†These authors share last authorship

### Specialty section:

This article was submitted to  
Antimicrobials, Resistance  
and Chemotherapy,  
a section of the journal  
Frontiers in Microbiology

Received: 13 November 2019

Accepted: 16 March 2020

Published: 30 April 2020

### Citation:

Tagliaferri TL, Guimarães NR,  
Pereira MPM, Vilela LFF, Horz H-P,  
Santos SG and Mendes TAO (2020)  
Exploring the Potential  
of CRISPR-Cas9 Under Challenging  
Conditions: Facing High-Copy  
Plasmids and Counteracting  
Beta-Lactam Resistance in Clinical  
Strains of *Enterobacteriaceae*.  
Front. Microbiol. 11:578.  
doi: 10.3389/fmicb.2020.00578

Thaysa Leite Tagliaferri<sup>1,2</sup>, Natália Rocha Guimarães<sup>1</sup>,  
Marcella de Paula Martins Pereira<sup>1</sup>, Liza Figueiredo Felicori Vilela<sup>3</sup>, Hans-Peter Horz<sup>2\*†</sup>,  
Simone Gonçalves dos Santos<sup>1\*†</sup> and Tiago Antônio de Oliveira Mendes<sup>4\*†</sup>

<sup>1</sup> Department of Microbiology, Institute of Biological Sciences, Universidade Federal de Minas Gerais, Belo Horizonte, Brazil,

<sup>2</sup> Institute of Medical Microbiology, RWTH Aachen University Hospital, Aachen, Germany, <sup>3</sup> Department of Biochemistry and Immunology, Institute of Biological Sciences, Universidade Federal de Minas Gerais, Belo Horizonte, Brazil, <sup>4</sup> Department of Biochemistry and Molecular Biology, Universidade Federal de Viçosa, Viçosa, Brazil

The antimicrobial resistance (AMR) crisis urgently requires countermeasures for reducing the dissemination of plasmid-borne resistance genes. Of particular concern are opportunistic pathogens of *Enterobacteriaceae*. One innovative approach is the CRISPR-Cas9 system which has recently been used for plasmid curing in defined strains of *Escherichia coli*. Here we exploited this system further under challenging conditions: by targeting the *bla*<sub>TEM-1</sub> AMR gene located on a high-copy plasmid (i.e., 100–300 copies/cell) and by directly tackling *bla*<sub>TEM-1</sub>-positive clinical isolates. Upon CRISPR-Cas9 insertion into a model strain of *E. coli* harboring *bla*<sub>TEM-1</sub> on the plasmid pSB1A2, the plasmid number and, accordingly, the *bla*<sub>TEM-1</sub> gene expression decreased but did not become extinct in a subpopulation of CRISPR-Cas9 treated bacteria. Sequence alterations in *bla*<sub>TEM-1</sub> were observed, likely resulting in a dysfunction of the gene product. As a consequence, a full reversal to an antibiotic sensitive phenotype was achieved, despite plasmid maintenance. In a clinical isolate of *E. coli*, plasmid clearance and simultaneous re-sensitization to five beta-lactams was possible. Reusability of antibiotics could be confirmed by rescuing larvae of *Galleria mellonella* infected with CRISPR-Cas9-treated *E. coli*, as opposed to infection with the unmodified clinical isolate. The drug sensitivity levels could also be increased in a clinical isolate of *Enterobacter hormaechei* and to a lesser extent in *Klebsiella variicola*, both of which harbored additional resistance genes affecting beta-lactams. The data show that targeting drug resistance genes is encouraging even when facing high-copy plasmids. In clinical isolates, the simultaneous interference with multiple genes mediating overlapping drug resistance might be the clue for successful phenotype reversal.

**Keywords:** CRISPR-Cas9, antimicrobial resistance, *bla*<sub>TEM</sub>, re-sensitization, resistance reduction, plasmid maintenance

## INTRODUCTION

Antimicrobial resistant microorganisms have become a public health concern due to their impact on human morbidity and mortality in recent decades. The reality of ineffective drugs allied to the insufficient launching of new antimicrobials may result in about 10 million deaths caused by multidrug-resistant organism infections in 2050 (O'Neil, 2016). The costs involved in the development of a new drug amount to around 800 million dollars and it can take up to 12 years until its commercialization (Adams and Brantner, 2006; Van Norman, 2016). Of particular concern is antimicrobial resistance (AMR) evolving in and spreading across species from the *Enterobacteriaceae* family, which includes plasmid encoded extended-spectrum beta-lactamases and carbapenemases as the main mechanism to disrupt antimicrobials (Savard and Perl, 2012).

Plasmids are well known for facilitating bacterial adaptation by their vertical and horizontal transmission. More specifically, small (<10 kb) multicopy plasmids have an important role in counteracting antimicrobial stressors. Multiple copies of a resistance gene increase the probability of mutational adaptation, thereby rapidly generating allele variations (Hall and Harrison, 2016). In addition, the repeated exposure to beta-lactams and high levels of beta-lactam resistance have been shown to be associated with an increase of plasmid copy number, reaching values higher than 100 copies/cell (San Millan et al., 2015, 2016). Hence, the increase of plasmid copy numbers can lead to maximum levels of AMR (San Millan et al., 2015, 2016; Hall and Harrison, 2016; Schechter et al., 2018).

Considering the capacity of plasmid-based resistance dispersal and the global public health impact of resistant bacteria, studies are needed for developing new technologies that could impede this progression. In recent years, CRISPR-Cas9 [clustered regularly interspaced short palindromic repeats (CRISPR)-CRISPR-associated protein 9 (Cas9)] has been demonstrated as an effective tool to cleave double-stranded DNA with accuracy (Ceasar et al., 2016). First studies have already successfully employed the CRISPR-Cas technology for genetically targeting AMR in different bacteria (Bikard et al., 2014; Citorik et al., 2014; Yosef et al., 2015). For instance, Yosef et al. (2015), not only reverted AMR but also eliminated the transfer of plasmids encoding two different beta-lactamases among *Escherichia coli* strains. Bikard et al. (2014) and Citorik et al. (2014) achieved plasmid curing and observed a CRISPR-Cas9 mediated cytotoxicity after specifically editing AMR genes in *Staphylococcus aureus* and in *E. coli*, respectively.

Given the importance of plasmid copy number variation in a cell (San Millan et al., 2015) and the overall complexity of AMR mechanisms within clinical isolates (Blair et al., 2015) we here investigated the potential of the CRISPR-Cas9 system under two challenging conditions. First, the CRISPR-Cas9 system was used to specifically target the *bla*<sub>TEM-1</sub> gene, located on the small high-copy plasmid pSB1A2, with 100–300 copies/cell (Yang et al., 2013;

Registry of Standard Biological Parts, 2019), using a model *E. coli* strain. The *bla*<sub>TEM</sub> gene codifies for one of the most frequently encountered beta-lactamase in *Enterobacteriaceae* (Lachmayr et al., 2009; Rawat and Nair, 2010). Subsequently, we investigated the re-sensitization effect when targeting the same gene in clinical isolates of *E. coli* and related *Enterobacteriaceae* species.

## MATERIALS AND METHODS

### *Escherichia coli* Model Strain and Plasmids Used

The *E. coli* strain BL21 (Studier and Moffatt, 1986; Kim et al., 2017) was used in this study to validate the CRISPR-Cas9 system when targeting a high-copy plasmid. Bacteria were cultivated in LB medium at 37°C and supplemented with ampicillin, 100 µg/ml; chloramphenicol, 30 µg/ml; and kanamycin, 50 µg/ml, depending on the plasmids harbored by the strains (Table 1). Three plasmids were used in this study, pSB1C3, pSB1A2, and pSB1K3, which are available at the Registry of Standard Biological Parts<sup>1</sup> under the accession numbers BBa\_K1218011, BBa\_J04450, and BBa\_I20260, respectively.

The pSB1C3 plasmid contains a constitutively expressed *Streptococcus pyogenes* derived CRISPR-Cas9 system. The sequence of the sgRNA responsible for the specificity of Cas9 cleavage was designed by indoor scripts using Pearl language based on public available sequences of the 861 bp-long *bla*<sub>TEM-1</sub> gene and its variants *bla*<sub>TEM-1a-d</sub> (Supplementary Figure S1A), including members of the *Enterobacteriaceae*. The sliding window method was used to find all 20-nucleotide length sequences with NGG flanking the 3-prime end. The conserved region most closely located at the 5'-end of the gene was selected (AGATCAGTTGGGTGCACGAGTGG). After synthesis of the 5'-located sgRNA, it was phosphorylated using a polynucleotide kinase (Thermo Fischer Scientific, MA, United States) and inserted into the plasmid pSB1C3 containing the CRISPR-Cas9 locus.

### Clinical Isolates

*Escherichia coli* 189A, *Enterobacter hormaechei* 4962 and *Klebsiella variicola* 68AI were isolated from patients with bacteremia in two different hospitals of Belo Horizonte, Brazil (Supplementary Table S2). Clinical strain collection was approved by the Human Research Ethics Committee from Universidade Federal de Minas Gerais (Brazil) under the protocol number ETIC 614/08 and written informed consent was obtained from each participant. *E. hormaechei* belongs to the *Enterobacter cloacae* complex and *K. variicola* is a member of the *Klebsiella pneumoniae* complex, as they share some biochemical and phenotypical features with *E. cloacae* and *K. pneumoniae*, respectively (Hoffmann et al., 2005; Barrios-Camacho et al., 2019). Because of this similarity, the species are frequently misclassified and the worldwide

<sup>1</sup><http://parts.igem.org/>

**TABLE 1** | Plasmids used in this study, their relevant features and associated strains.

Plasmid features			
Plasmid name	Size	Relevant features	References
pSB1A2	3148 bp	Amp <sup>R</sup> mediated via <i>bla</i> <sub>TEM-1</sub> gene (sgRNA target); red fluorescent protein (RFP) gene.	(Yang et al., 2013; Registry of Standard Biological Parts, 2019)
pSB1K3	3123 bp	Km <sup>R</sup> ; green fluorescent protein (GFP) gene.	(Registry of Standard Biological Parts, 2019)
pSB1C3	7150 bp	Cm <sup>R</sup> ; contains the <i>Streptococcus pyogenes</i> CRISPR-Cas9 loci (sgRNA targeting the <i>bla</i> <sub>TEM-1</sub> gene was added in this study).	(Registry of Standard Biological Parts, 2019)

<i>E. coli</i> BL21 strains containing the plasmids			
Strain number	Name	Description	References
1	BL21 <sup>-</sup>	<i>E. coli</i> BL21	(Studier and Moffatt, 1986; Kim et al., 2017)
2	CRISPR <sup>+</sup>	<i>E. coli</i> BL21 with the plasmid pSB1C3	This study
3	TEM <sup>+</sup>	<i>E. coli</i> BL21 with the plasmids pSB1A2 and pSB1K3	This study
4	TEM <sup>+</sup> /CRISPR <sup>+</sup>	<i>E. coli</i> BL21 with the plasmids pSB1A2, pSB1K3 and pSB1C3	This study

Cm<sup>R</sup>, chloramphenicol resistance as selective marker; Amp<sup>R</sup>, ampicillin resistance as selective marker; Km<sup>R</sup>, kanamycin resistance as selective marker.

presence of these bacteria in human infections may be underestimated, although their relevance as clinical pathogens has been demonstrated (Long et al., 2017; Beyrouthy et al., 2018; Barrios-Camacho et al., 2019; Rodríguez-Medina et al., 2019). The selection criteria of the isolates were the absence of a natural chloramphenicol-resistant phenotype, since the antibiotic was used as a selective marker of the pSB1C3 plasmid; the presence of the *bla*<sub>TEM-1</sub> gene and the absence of carbapenemase genes.

## Plasmid Transformation

Chemically competent *E. coli* BL21 were prepared using 0.1M MgCl<sub>2</sub>-CaCl<sub>2</sub> and competent cells were then transformed with plasmids by the heat-shock method (Chan et al., 2013; Lim et al., 2015). The clinical isolates used in this study received the CRISPR-Cas9 plasmid pSB1C3 by electroporation (Gonzales et al., 2013).

## Polymerase Chain Reactions

All primers used for polymerase chain reactions (PCRs), as well as the reaction conditions are provided in **Supplementary Table S1**. Cas9 functionality and *bla*<sub>TEM-1</sub> expression were assessed by reverse transcription quantitative polymerase chain reaction (RT-qPCR), which were performed based on cDNA from reverse transcription of total RNA. The 16S rRNA served as endogenous transcript for an internal control. Total bacterial RNA was extracted using TRIzol reagent and DNA was removed using DNase (both from Thermo Fischer Scientific, MA, United States). Integrity of extracted RNA was evaluated by agarose gel electrophoresis. Reverse transcription was performed with 1 µg of total RNA according to the iScript cDNA Synthesis Kit protocol (Bio-Rad, CA, United States). RT-qPCR was performed based on the CFX 96 Real Time PCR Detection System using the SYBR Green Master Mix (both from Bio-Rad, CA, United States). The analyses were performed by the relative standard curve method using a serial dilution of total cDNA pool as previously described (Larionov et al., 2005).

For determination of total plasmid copy number, the *bla*<sub>TEM-1</sub> gene was selected as a plasmid target. The amplified products of the chromosomal 16S rRNA gene and the *bla*<sub>TEM-1</sub> gene were cloned into TOPO vector (Thermo Fischer Scientific, MA, United States) for subsequent construction of the standard curves and absolute quantification. Determination of bacterial cell numbers was based on 16S rRNA gene quantification under consideration of the average 16S copy numbers per cell in strains (Klappenbach et al., 2000; Větrovský and Baldrian, 2013). Establishment of standards with defined amounts of DNA was performed as previously described (Vianna et al., 2008).

## Growth Curves

Overnight bacterial cultures were adjusted to an OD<sub>600 nm</sub> of 0.1 and re-grown in LB medium with and without ampicillin. The growth kinetics were recorded every hour for 24 h similarly described in Jansen et al. (2018). Each assay was performed in triplicate and the whole experiment, starting from the pSB1C3 transformation, was performed three times on different days, accounting for technical and biological replicates.

## Disk Diffusion Test and Minimum Inhibitory Concentration

The disk diffusion test was performed in duplicate according to the Change to Clinical and Laboratory Standards Institute and the European Committee on Antimicrobial Susceptibility Testing (CLSI) protocol (Clinical and Laboratory Standards Institute, 2019). In total, 12 antibiotics were selected, namely chloramphenicol (CHL), ampicillin (AMP), ampicillin/sulbactam (SAM), amoxicillin/clavulanic acid (AMC), cefazolin (CFZ), cefoxitin, cefuroxime (CXM), ceftriaxone (CRO), ceftazidime (CAZ), cefotaxime (CTX), cefepime (FEP), and aztreonam (ATM). Measurements of diameter of the inhibition zones were performed in duplicate. For the *Galleria mellonella* assay, the minimum inhibitory concentration (MIC) of the clinical isolate of *E. coli* 189A was determined using the microdilution protocol (Clinical and Laboratory Standards Institute and Weinstein, 2012).

## Fluorescence Measurement

Fluorescence microscopy was performed using the EVOS® FL microscope (Life Technology, CA, United States). Cells were analyzed at the bright field and with the green fluorescent protein (GFP) (ex:470 nm/em:524 nm) and red fluorescence protein (RFP) (ex:530 nm/em:593 nm) fixed filters. For an overall analysis of RFP and GFP intensity, fluorescence was quantified using the Cytation 5 Cell Imaging Multi-Mode Reader (BioTeck, VT, United States). Fluorescence experiments were performed in triplicate and the whole experiment, starting from the pSB1C3 transformation, was performed three times on different days, accounting for technical and biological replicates.

Fluorescence-activated cell sorting (FACS) (BD FACS Canto II, BD, NJ, United States) was employed to distinguish between RFP positives and negative cells upon CRISPR-Cas9 treatment. Each measurement analyzed 30,000 events at a low flow rate. The following settings were used: an SSC voltage of 473; a FSC voltage of 398; and a PerCP-Cy5-5-A of 445 V.

## Sequencing Analyses

Sanger sequencing of purified PCR products was performed by Myleus Biotechnology (Minas Gerais, Brazil) and Eurofins Genomics (Luxembourg, Luxembourg). Sanger sequence analyses were performed using the Phred/Phrap pipeline and the Degenerate Sequence Decode program (DSDDecodeM) (Liu et al., 2015). Deep sequencing of the genomes was performed using the Miseq platform (Illumina, CA, United States). Reads were trimmed to Phred15 using the Trimmomatic program (Bolger et al., 2014). The *de novo* assembly of the contigs was performed via the St. Petersburg genome assembler (SPAdes) (Bankevich et al., 2012) and resistance genes were detected via ResFinder (Zankari et al., 2012). Genome sequences were submitted to GenBank (accession number: *E. coli* SAMN12872130, *E. hormaechei* SAMN12872875 and *K. variicola* SAMN10216245).

## Galleria mellonella Infection Model

Larvae of the great wax moth *G. mellonella* were selected according to their length (2–3 cm, instar stage), weight (150–250 mg), and excluded in case of dark coloration or limited activity. They were subsequently placed in the dark without food supply for 24-h acclimation prior to the infection assay (Harding et al., 2013). Larvae were challenged with *E. coli* 189A treated or untreated with CRISPR-Cas9 ( $\sim 4.0 \times 10^6$  CFU/ml). After 1-h of infection, either ceftriaxone (16 mg/kg) or sterile distilled water was administered in the front larvae proleg with a 10  $\mu$ l syringe (Hamilton, NV, United States). Each group contained ten larvae sorted randomly, and the experiment was performed in triplicate ( $n = 30$ ). Larvae were incubated at 37°C, monitored after 24, 48, and 72 h and death was determined by absence of movement and unresponsiveness to touch.

## Statistical Analysis

Statistical analyses were performed using the GraphPad Prism (version 6, GraphPad Software, CA, United States), the VassarStats (NY, United States), as well as the BD FACSDiva and FlowJo softwares.

## RESULTS

### Resistance Reversal in a Model Strain of *E. coli*

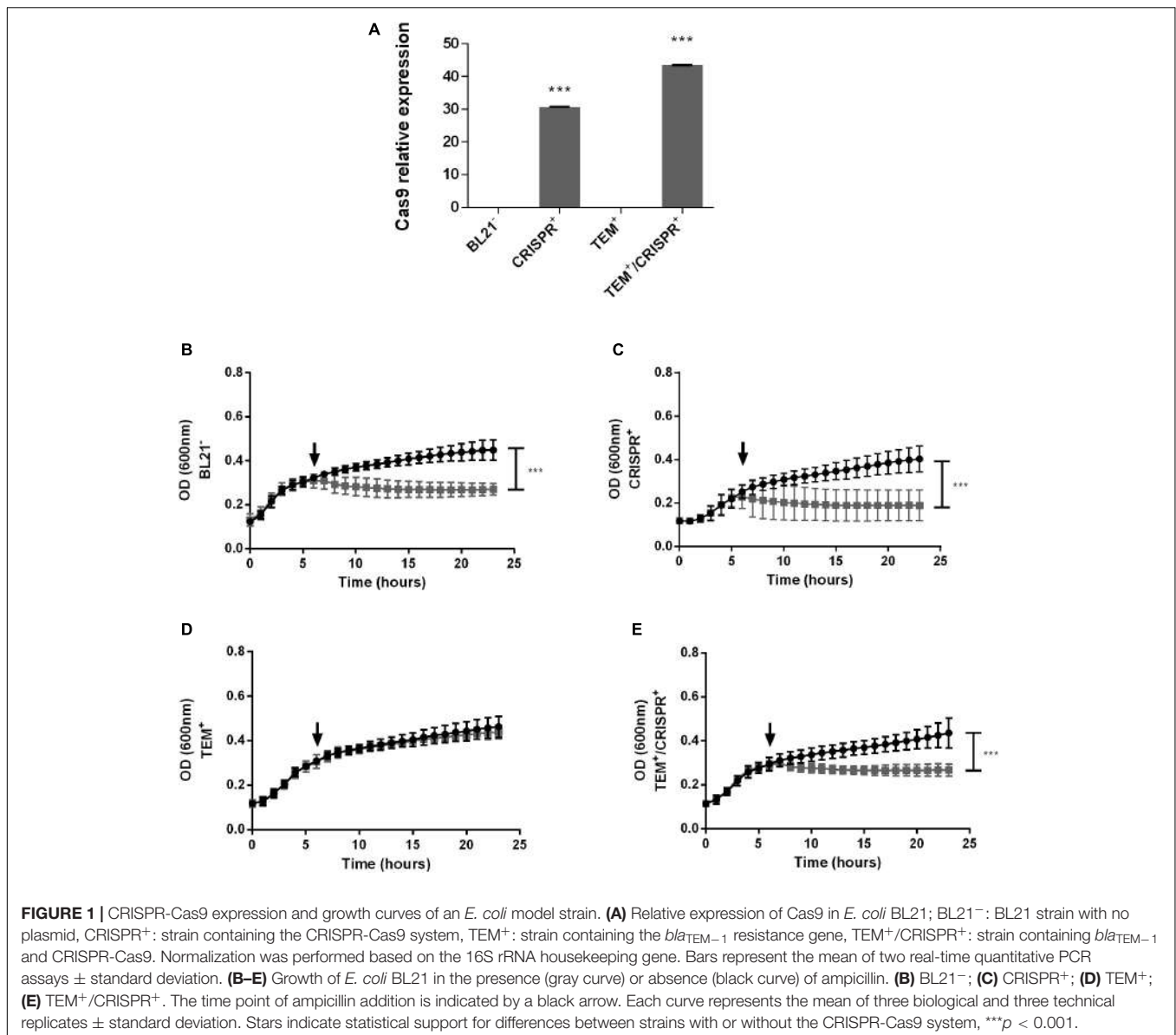
Initially, the *bla*<sub>TEM-1</sub> gene located on the small high-copy plasmid pSB1A2 was introduced into the *E. coli* strain BL21, which was otherwise devoid of AMR. Located on this plasmid was also the RFP gene, as a marker, to verify the integrity of pSB1A2 upon CRISPR-Cas9 insertion. A second plasmid, pSB1K3, which contained the GFP gene, but no CRISPR-Cas9 target was also introduced into BL21. This plasmid served as an independent and indirect measurement of plasmid stability. The two plasmids pSB1A2 and pSB1K3 were chosen because of their high-copy number (i.e., 100–300 copies/cell) (Yang et al., 2013; Registry of Standard Biological Parts, 2019). For the design of a proper sgRNA, the conserved region most closely located at the 5'-end of the *bla*<sub>TEM-1</sub> gene was selected (Supplementary Figure S1A) in order to maximize the likelihood of an early stop codon generated during an eventual bacterial DNA repair mechanism (Chayot et al., 2010). Basic features of the three plasmids used in this study and associated strains are given in Table 1.

The presence and expression of Cas9 could be confirmed in CRISPR<sup>+</sup> and TEM<sup>+</sup>/CRISPR<sup>+</sup>, but not in BL21<sup>-</sup> or TEM<sup>+</sup> (Figure 1A), as expected. Growth curve analyses in the presence or absence of ampicillin confirmed antibiotic sensitivity of BL21<sup>-</sup> and CRISPR<sup>+</sup> (Figures 1B,C, respectively). In contrast, TEM<sup>+</sup> grew in the presence of ampicillin demonstrating the effectiveness of the introduced beta-lactamase gene (Figure 1D). The targeted re-sensitization to ampicillin was achieved in TEM<sup>+</sup>/CRISPR<sup>+</sup> (Figure 1E). Disk diffusion tests confirmed resistance of TEM<sup>+</sup> and sensitivity of TEM<sup>+</sup>/CRISPR<sup>+</sup> strains (Supplementary Figure S1B).

We observed a 100-fold lower RFP signal in TEM<sup>+</sup>/CRISPR<sup>+</sup>, compared to TEM<sup>+</sup> ( $p < 0.001$ ) indicating a strong but not entire reduction of pSB1A2 (Figures 2A,C) upon CRISPR-Cas9 insertion. FACS results confirmed that only 0.005% of cells were RFP positive (Figures 2D, plot D.1 and D.3), which represents an around 150-fold reduction compared to the TEM<sup>+</sup> cells (Figure 2D, plot D.2). A control experiment with the pSB1C3 vector lacking the sgRNA led to a high percentage of RFP-positive cells (85.2%), similar to TEM<sup>+</sup> cells, confirming that the plasmid reduction was due to the presence of the sgRNA. This result combined with quantitative PCR analysis (qPCR) of the *bla*<sub>TEM</sub> gene indicated, that on average, the 0.005% persistent RFP positive TEM<sup>+</sup>/CRISPR<sup>+</sup> cells carried around 48 pSB1A2 copies/cell. In contrast, TEM<sup>+</sup> cells harbored around 100 copies/cell of pSB1A2. Since the GFP signals did not decrease (Figures 2A,B), pSB1A2 reduction was the result of CRISPR-Cas9 activity rather than any unspecific plasmid clearance by the cell.

In keeping with the RFP and plasmid reduction, the expression of the *bla*<sub>TEM-1</sub> gene was significantly reduced (by more than 2.5-fold,  $p < 0.05$ ) in TEM<sup>+</sup>/CRISPR<sup>+</sup>, again confirming reduction but not entire plasmid loss (Figure 2E). Since those persistent gene expression levels did not confer ampicillin resistance (Figure 1E and Supplementary Figure S1B), it is likely





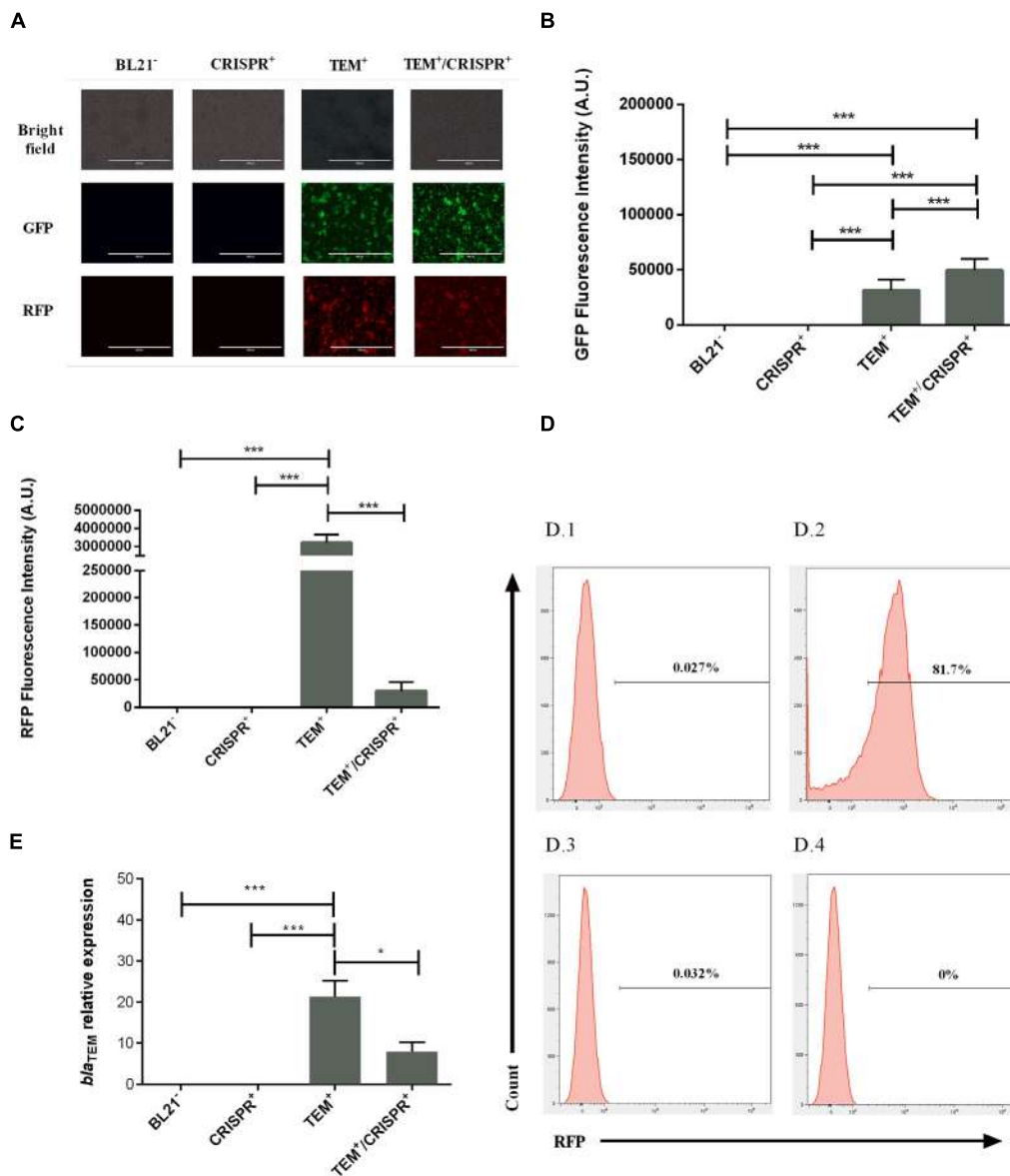
that gene defects occurred. In fact, deletions could be seen in the sequence data of the *bla*<sub>TEM-1</sub> resistance gene (**Supplementary Figure S2A**). This means, that any possible transmission of the remaining plasmid, vertically or horizontally, would not necessarily lead to the spread of *bla*<sub>TEM-1</sub>-based AMR, because of the non-functional resistance gene.

However, cases where the CRISPR-Cas9 was able to completely eradicate the high-copy plasmid pSB1A2 were also achieved, as evident by FACS analysis (**Figures 2D**, plot D.4) and confirmed by qPCR.

## Resistance Reversal in the Clinical Isolate of *E. coli* 189A

We next tested a *bla*<sub>TEM-1</sub> positive clinical isolate of *E. coli* 189A. Principally, considering that *bla*<sub>TEM</sub> variants potentially confer resistance to many beta-lactam antibiotics

(Rawat and Nair, 2010), targeting this gene might restore the usability of several antibiotics. In fact, after CRISPR-Cas9 insertion into the clinical isolate of *E. coli* 189A, a re-sensitization was observed to AMP, CFZ, CXM, CRO, and CTX (**Figures 3A,B** and **Supplementary Figure S2B**), along with an introduced resistance against chloramphenicol co-mediated via pSB1C3. Based on qPCR, the *bla*<sub>TEM-1</sub> harboring plasmid was found to occur in low-copy numbers, as on average less than a single copy per bacterial cell was detected, indicating that some bacteria might be already plasmid free. After the CRISPR-Cas9 insertion, the *bla*<sub>TEM</sub> gene was not detectable anymore, indicating complete eradication of the plasmid (**Figure 3C**). The achieved plasmid clearance also resulted in the extinction of other resistance genes conferring resistance to beta-lactams and other classes of antibiotics. Genome sequencing identified the *sul2* (sulfonamide), *aph*(3'')-Ib and *aph*(6)-Id (both confer resistance



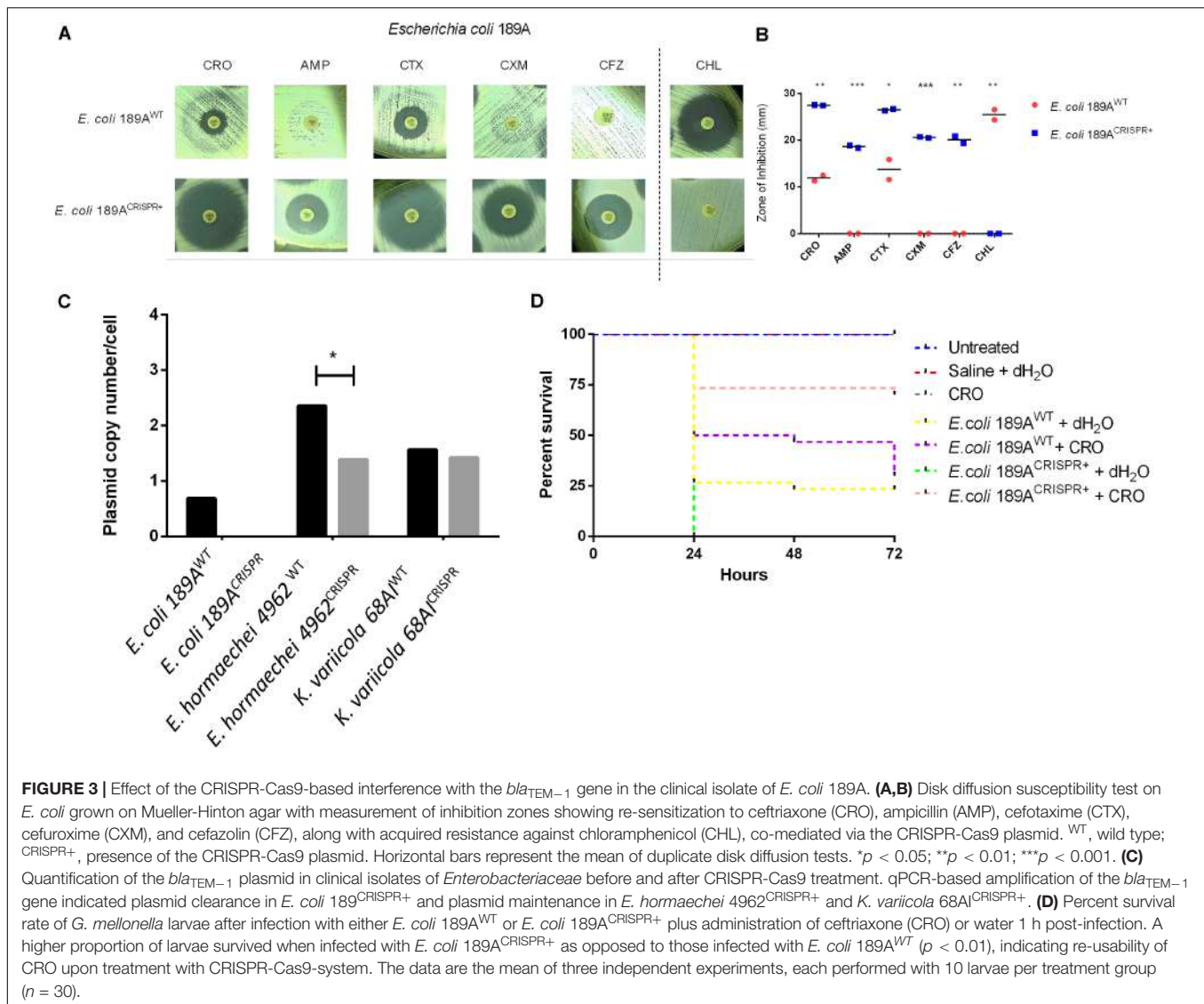
**FIGURE 2 |** Effect of the CRISPR-Cas9 transformation on plasmid maintenance and *bla*<sub>TEM-1</sub> gene expression in *E. coli* BL21<sup>-</sup>; BL21<sup>-</sup>: BL21 strain with no plasmid, CRISPR<sup>+</sup>: strain containing the CRISPR-Cas9 system, TEM<sup>+</sup>: strain containing the *bla*<sub>TEM-1</sub> resistance gene, TEM<sup>+</sup>/CRISPR<sup>+</sup>: strain containing *bla*<sub>TEM-1</sub> and CRISPR-Cas9 **(A)** Fluorescence microscopy indicating bacterial viability and maintenance of the plasmids pSB1A2 and pSB1K3 based on the RFP/GFP signals. For each strain, pictures were taken at the same microscopy field (40 $\times$  objective). **(B)** GFP fluorescence intensity indicating the continued presence of plasmid pSB1K3 (thus no natural causes of plasmid reduction) in strain TEM<sup>+</sup>/CRISPR<sup>+</sup>. A.U., arbitrary units. **(C)** RFP fluorescence intensity indicating a significant reduction of the plasmid pSB1A2 (but no entire plasmid loss) in strain TEM<sup>+</sup>/CRISPR<sup>+</sup> compared to TEM<sup>+</sup>. Bars represent the mean of three biological and three technical replicates  $\pm$  standard deviation. A.U., arbitrary units. **(D)** Histograms of negative (D.1) and the positive controls (D.2) of FACS analysis used to demarcate the gate areas. The plot (D.3) represents the colony with higher RFP percentage (0.032%), while (D.4) demonstrates the colony with no RFP signal (0%). When analyzing all retrieved colonies, 0.005% of RFP positive cells were present upon CRISPR-Cas9 insertion. A control experiment with the pSB1C3 vector lacking the sgRNA led to a high percentage of RFP-positive cells (85.2%), similar to TEM<sup>+</sup> cells, confirming the sgRNA-dependant plasmid reduction. **(E)** Relative expression of the *bla*<sub>TEM-1</sub> gene confirming plasmid presence and gene functioning in the cells. Bars represent average and standard deviation of two replicate assays. The results were normalized with the 16S rRNA housekeeping gene. \* $p < 0.05$ ; \*\*\* $p < 0.001$ .

to aminoglycoside), as well as *bla*<sub>CTX-M-9</sub> (beta-lactam) genes before, but not after the CRISPR-Cas9 insertion.

To further investigate the meaningfulness of the re-sensitization approach, the reusability of CRO as one representative antibiotic was verified by infecting larvae of

the great wax moth *G. mellonella* either with the CRISPR-Cas9 treated *E. coli* 189A (*E. coli* 189A<sup>CRISPR+</sup>) or with the *E. coli* 189A wild type (*E. coli* 189A<sup>WT</sup>).

Upon administration of CRO, 70% of larvae infected with *E. coli* 189A<sup>CRISPR+</sup> survived the time period of 72 h, as opposed



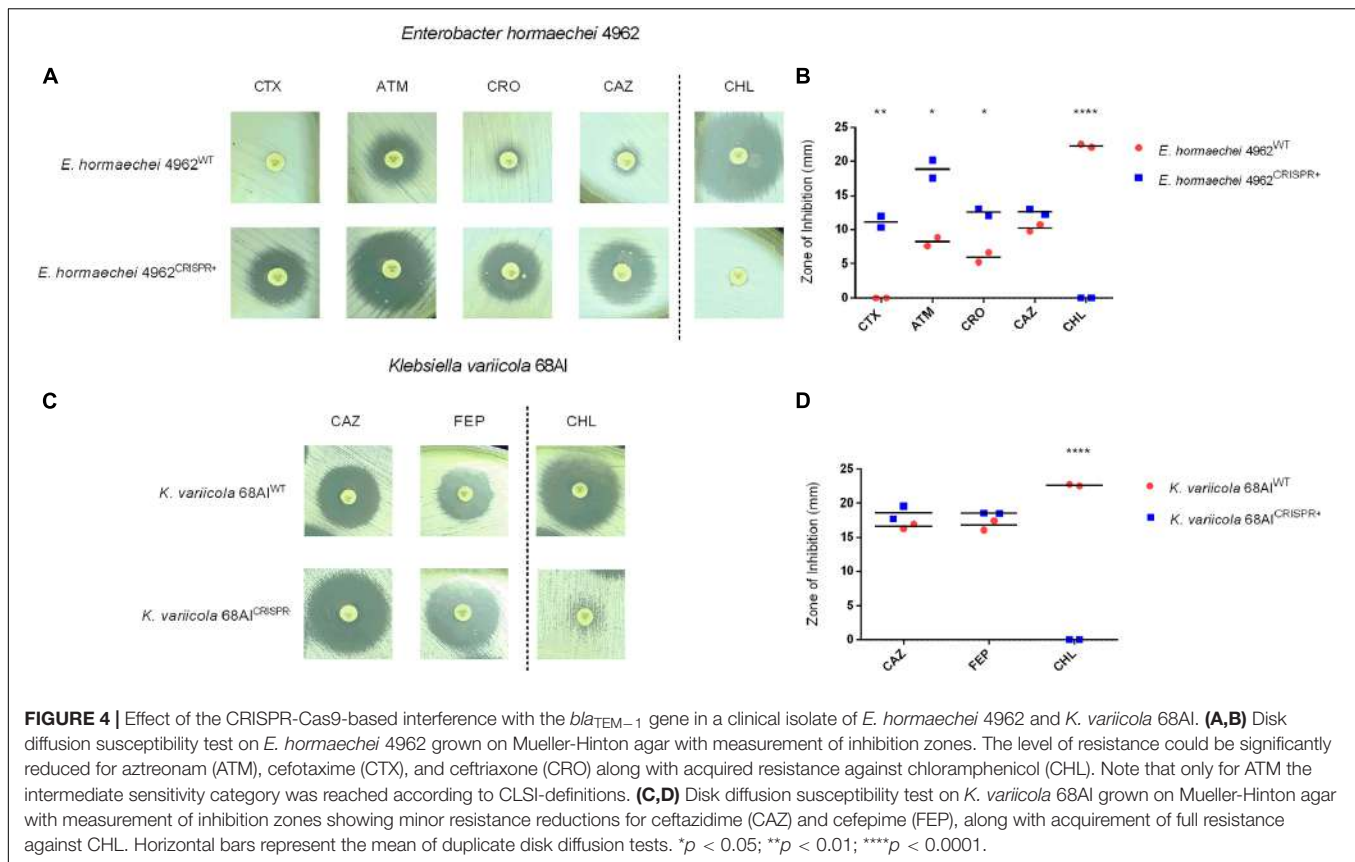
to only 30% of larvae infected with *E. coli* 189A<sup>WT</sup> (log-rank test, *p* < 0.01) (Figure 3D). No significant difference was seen between the CRO-treated larvae challenged with *E. coli* 189A<sup>CRISPR+</sup> and larvae used as controls (i.e., mock-infection with saline or administration of antibiotic only, or no treatment at all. Log-rank test, *p* > 0.05). Conversely, it made no difference whether *E. coli* 189A<sup>WT</sup> infected larvae were treated with antibiotic or with water (log-rank test, *p* > 0.3) (Figure 3D). The outcome of this experiment indicates that antibiotic-treated larvae had a 5.44 times higher chance of survival, when challenged with *E. coli* 189A<sup>CRISPR+</sup> rather than with *E. coli* 189A<sup>WT</sup> (*p* < 0.01).

## Resistance Reduction in Clinical Isolates of *E. hormaechei* 4962 and *K. variicola* 68AI

A more complex situation was encountered when targeting the *bla*<sub>TEM-1</sub> gene of *E. hormaechei* 4962 and *K. variicola*

68AI. Upon CRISPR-Cas9 insertion, significant increases in the inhibition zones were observed for ATM, CTX, and CRO in the case of *E. hormaechei* (Figures 4A,B and Supplementary Figure S2B). However, the CLSI-defined threshold levels for an intermediate sensitivity was only reached for ATM. In some disk diffusion assays, a few colonies grew within the inhibition zones which were, however, not further analyzed (Figure 4A). For *K. variicola*, only non-significant increases in the inhibition zones were observed for CAZ and FEP (Figures 4C,D and Supplementary Figure S2B).

Further analysis revealed the continued presence of the *bla*<sub>TEM-1</sub> gene in *E. hormaechei* 4962 and *K. variicola* 68AI, in contrast to what was observed with the clinical isolate of *E. coli* 189A, which could be re-sensitized for several antibiotics. qPCR-based detection of the *bla*<sub>TEM-1</sub> gene showed that a substantial plasmid reduction had occurred in *E. hormaechei* 4962, as opposed to only a negligible fraction of plasmid reduction in *K. variicola* 68AI (Figure 3C). Since both *E. hormaechei* 4962



**FIGURE 4 |** Effect of the CRISPR-Cas9-based interference with the *bla*<sub>TEM-1</sub> gene in a clinical isolate of *E. hormaechei* 4962 and *K. variicola* 68AI. **(A,B)** Disk diffusion susceptibility test on *E. hormaechei* 4962 grown on Mueller-Hinton agar with measurement of inhibition zones. The level of resistance could be significantly reduced for aztreonam (ATM), cefotaxime (CTX), and ceftriaxone (CRO) along with acquired resistance against chloramphenicol (CHL). Note that only for ATM the intermediate sensitivity category was reached according to CLSI-definitions. **(C,D)** Disk diffusion susceptibility test on *K. variicola* 68AI grown on Mueller-Hinton agar with measurement of inhibition zones showing minor resistance reductions for ceftazidime (CAZ) and cefepime (FEP), along with acquisition of full resistance against CHL. Horizontal bars represent the mean of duplicate disk diffusion tests. \**p* < 0.05; \*\**p* < 0.01; \*\*\*\**p* < 0.0001.

and *K. variicola* 68AI were found to harbor the *bla*<sub>TEM-1</sub> gene on a low-copy number plasmid (Figure 3C), we expected to achieve plasmid clearance. However, damages on the CRISPR-Cas9 loci after insertion were observed in both strains, affecting the expected CRISPR-Cas9-based outcome (Supplementary Figure S3). These findings explain the lower efficiency of re-sensitization when compared to the clinical strain of *E. coli* 189A.

Importantly, other genes conferring resistance to beta-lactams could be identified by genome sequencing in both strains. In *E. hormaechei* 4962, the intrinsic AmpC-type resistance gene was present (*bla*<sub>ACT-7</sub>), as well as the beta-lactamases *bla*<sub>CTX-M-9</sub> and *bla*<sub>OXA-9</sub>. The same *bla*<sub>CTX-M-9</sub> was also detected in *K. variicola* 68AI, along with the *bla*<sub>LEN16</sub> and *bla*<sub>LEN19</sub> genes conferring resistance to beta-lactams. Since these resistance genes were not targeted by the sgRNA, failure to achieve fully reverted phenotypes was likely due to their presence in the bacteria, in addition to the damages in the CRISPR-Cas9 plasmid region.

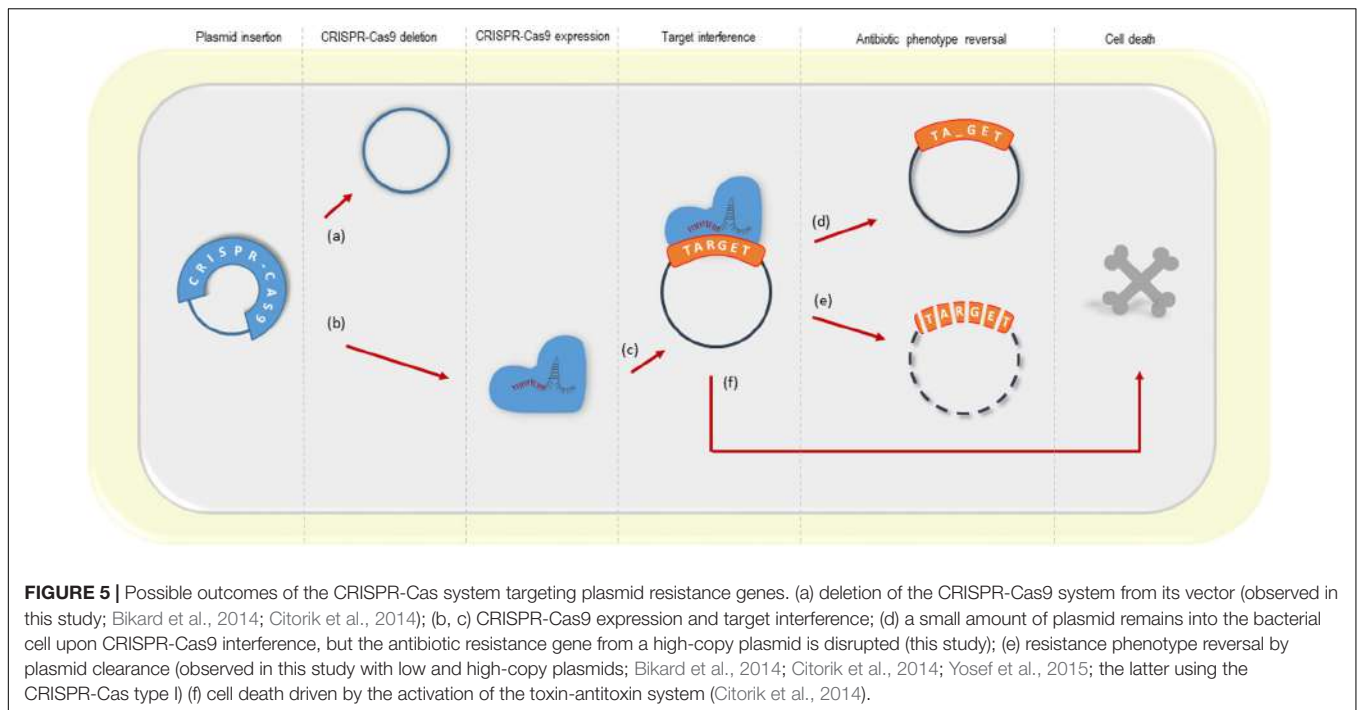
## DISCUSSION

In this study, we investigated the potential of the CRISPR-Cas9 system to counteract antibiotic resistance mediated by the *bla*<sub>TEM-1</sub> gene harbored either in the high-copy plasmid pSB1A2 or when present in clinical isolates. In a model strain of *E. coli* having received the *bla*<sub>TEM-1</sub> gene on a high-copy plasmid (i.e., 100–300 copies/cell) the phenotype could be clearly reversed.

However, an entire elimination of the plasmid and the target gene did not occur in some retrieved colonies. This outcome is likely linked with the initial high overall abundance of the vector, since CRISPR-Cas9 is able to completely clear a resistance gene plasmid, when the copy number per cell ranges between 50 and 70 (Citorik et al., 2014). Those remaining plasmid-positive cells, could be considered “persister cells” in an analogy to bacteria persisting antibiotic treatment (Van den Bergh et al., 2017), given their low fraction within the whole population, and their endurance in the presence of CRISPR-Cas9 concomitant with an otherwise re-sensitized phenotype (Wood et al., 2013; Van den Bergh et al., 2017). However, even facing high-copy plasmids, CRISPR-Cas9 demonstrated the potential to completely clear the vector from some bacterial colonies, indicating its promising application under this challenging condition. Optimization of the system may be required for a complete clearance of high-copy plasmids carrying resistance genes in the whole population.

The reason why a bacterial subpopulation maintains the plasmid while being attacked by CRISPR-Cas9 remains unknown. However, laboratorial and pathogenic *E. coli* strains possess an end-joining repair mechanism to bridge broken DNA ends (Chayot et al., 2010). Named as alternative end-joining (A-EJ), this restoration attempt typically leads to microdeletions in the sgRNA region (affecting regions of 1–10 bp), similar to those observed in this study (Supplementary Figure S2A; Chayot et al., 2010; Chen et al., 2019). Although the deletions lead to a non-functional *bla*<sub>TEM-1</sub> gene, the possible existence of





CRISPR-Cas9-persisters in the context of clinical isolates, could still result in therapeutic failure, because other intact resistance genes might still reside on the plasmid. Therefore, the detection and knowledge of CRISPR-Cas9-persisters may be important for devising strategies to minimize their potential clinical impact.

The deleterious effects on plasmids and bacterial cells of CRISPR-Cas9 targeting other resistance genes have been previously reported. Bikard et al. (2014) interfered with the kanamycin and the methicillin resistant genes *aph-3* and *mecA*, in *S. aureus* (MRSA), while Citorik et al. (2014) re-sensitized *E. coli* that possessed the *bla<sub>NDM-1</sub>* and *bla<sub>SHV-18</sub>* genes. In both studies, a cytotoxicity of the CRISPR-Cas9 system was apparent with episomal and chromosomal targets. In the first situation, bacteria were killed because plasmid clearance led to the loss of the toxin-antitoxin genes. As the antitoxin is less stable than the toxin, its faster degradation results in cell toxicity as a consequence (Citorik et al., 2014). When the target was a chromosomal gene, the lethality was due to irreparable chromosomal damages (Bikard et al., 2014; Citorik et al., 2014). Conversely, no cytotoxicity was observed when CRISPR-Cas9 eliminated a resistance plasmid in bacteria lacking a toxin-antitoxin system (Bikard et al., 2014; Citorik et al., 2014). Plasmid clearance was also achieved in another model strain of *E. coli* in which the *bla<sub>NDM-1</sub>* and *bla<sub>CTX-M-15</sub>* resistance genes were targeted (Yosef et al., 2015). The authors went one step further and simultaneously conferred resistance against the lytic phage T7, thereby providing the re-sensitized bacteria a selective advantage in the presence of the phage. Using this approach, antibiotic treatment along with administration of T7 should robustly oppress the re-emergence of resistant variants.

With the successful reversal of drug resistance in *E. coli* model strains, the consecutive step would be to test clinical

isolates. In fact, in our study, plasmid clearance was achieved in the clinical strain of *E. coli* 189A when tackling the *bla<sub>TEM-1</sub>* gene present in a low-copy plasmid. Importantly, CRISPR-Cas9 activity led to a simultaneous re-sensitization to several beta-lactam antibiotics including CRO. This is particularly encouraging, given that third generation cephalosporins are “critically important antimicrobials,” which need to be preserved as last resource treatments (Collignon et al., 2016). Re-sensitization effectiveness could be verified *in vivo* by rescuing *E. coli* 189A infected larvae with CRO, confirming the benefit of CRISPR-Cas9 for controlling drug resistant clinical isolates.

Both pSB1C3 vectors harbored by the clinical isolates of *K. variicola* 68AI and *E. hormaechei* 4962 demonstrated deletions in the CRISPR-Cas9 locus, and subsequent maintenance of the *bla<sub>TEM-1</sub>*-carrying low-copy plasmid. This is similar to what has been described by Bikard et al. (2014), who found that survival of *S. aureus* was due to the lack of the Cas9 region after CRISPR-Cas9 delivery, impeding DNA cleavage. Apart from this, plasmid maintenance with the presence of at least one other resistance gene not covered by our CRISPR-Cas9 system might explain why the re-sensitization in *E. hormaechei* 4962 and *K. variicola* 68AI was only partially successful. Given that clinical strains frequently harbor different resistance genes on plasmids (Bennett, 2009; Blair et al., 2015), this signifies that multiple sgRNA for potentially targeting different AMR genes need to be employed, for re-gaining full susceptibility to traditional antibiotics.

Even though the resistance reversal was not completely achieved to the sensitive category in *E. hormaechei* 4962, the intermediate sensitivity may still imply therapeutic success.

After all, according to the latest guidelines of the CLSI (2019) and The European Committee on Antimicrobial Susceptibility Testing [EUCAST] (2019), intermediate levels are to be interpreted as persisting clinical efficacy under elevated drug exposure.

Clearly, impediment of re-sensitization can also stem from overexpression of efflux pumps, or from reduction of permeability. Those intrinsic resistance mechanisms contribute to increased levels of resistance against cephalosporins and are typically found in clinical strains of *Enterobacteriaceae* (Blair et al., 2015). Nonetheless, overexpression of efflux pumps or alterations in porins in the clinical isolate of *E. coli*, if having occurred, did not prevent phenotype reversal. Furthermore, despite the versatile challenges imposed by clinical isolates, the interference with the *bla*<sub>TEM-1</sub> gene led after all to minor but clear resistance reductions in the other two clinical isolates.

Our findings support multiple aspects of the previous studies and complement the possible outcomes of the CRISPR-Cas9-based interference with plasmid-borne resistance genes, summarized in **Figure 5**.

When translating the use of the CRISPR-Cas9 system into clinical settings, phages might be an elegant approach for targeted delivery of the system into the bacterial pathogens. Successful application in mice and larvae using bio-engineered phages (Bikard et al., 2014; Citorik et al., 2014) pave the way for a possible future utilization in humans. Alternatively, phage-mediated CRISPR-Cas9 systems could be dispersed on surfaces to serve as preventive disinfection and cleansing procedures along with elaborate selection mechanisms that ensure stability of the CRISPR-Cas systems in bacterial cells, as demonstrated previously (Yosef et al., 2015). Importantly, cases in which CRISPR-Cas9 maintenance in the bacterial cell is intended, resistance genes commonly used as plasmid selective markers should be removed from the CRISPR-Cas9 vector in order to prevent further AMR spread. The possibility to restore sensitivity to traditional antibiotics might be superior to searching for new antimicrobials and potentially could deaccelerate the crisis that we are currently facing with AMR carrying bacteria.

## REFERENCES

- Adams, C. P., and Brantner, V. V. (2006). Estimating the cost of new drug development: is it really \$802 Million? *Health Affairs* 25, 420–428. doi: 10.1377/hlthaff.25.2.420
- Bankevich, A., Nurk, S., Antipov, D., Gurevich, A. A., Dvorkin, M., Kulikov, A. S., et al. (2012). SPAdes: a new genome assembly algorithm and its applications to single-cell sequencing. *J. Comput. Biol.* 19, 455–477. doi: 10.1089/cmb.2012.0021
- Barrios-Camacho, H., Aguilar-Vera, A., Beltran-Rojel, M., Aguilar-Vera, E., Duran-Bedolla, J., Rodriguez-Medina, N., et al. (2019). Molecular epidemiology of *Klebsiella variicola* obtained from different sources. *Sci. Rep.* 9:10610. doi: 10.1038/s41598-019-46998-9
- Bennett, P. M. (2009). Plasmid encoded antibiotic resistance: acquisition and transfer of antibiotic resistance genes in bacteria: plasmid-encoded antibiotic resistance. *Br. J. Pharmacol.* 153, S347–S357. doi: 10.1038/sj.bjp.0707607
- Beyrouthy, R., Baretts, M., Marion, E., Dananché, C., Dauwalder, O., Robin, F., et al. (2018). Novel *Enterobacter* lineage as leading cause of nosocomial outbreak

## DATA AVAILABILITY STATEMENT

The genomic dataset generated for this study can be found in the Genbank (accession number: *E. coli* SAMN12872130, *E. hormaechei* SAMN12872875, and *K. variicola* SAMN10216245).

## ETHICS STATEMENT

Clinical strain collection was approved by the Human Research Ethics Committee from Universidade Federal de Minas Gerais (Brazil) under the protocol number ETIC 614/08 and written informed consent was obtained from each participant.

## AUTHOR CONTRIBUTIONS

TT, TM, SS, and H-PH designed the study. TT, NG, and MP performed the research. H-PH, LV, TM, and SS contributed with new reagents. TT, TM, and H-PH analyzed the data. TT, H-PH, SS, and TM wrote the manuscript.

## FUNDING

This work was supported by the Conselho Nacional de Desenvolvimento Científico e Tecnológico (CNPq); Coordenação de Aperfeiçoamento de Pessoal de Nível Superior (CAPES); Fundação de Amparo à Pesquisa do Estado de Minas Gerais (FAPEMIG); and Fundação Arthur Bernardes and Bill and Melinda Gates Foundation (grant number OPP1193112). TT was supported by CNPq Scholarship - Brazil (grant number 203319/2016-6).

## SUPPLEMENTARY MATERIAL

The Supplementary Material for this article can be found online at: <https://www.frontiersin.org/articles/10.3389/fmicb.2020.00578/full#supplementary-material>

- involving carbapenemase-producing strains. *Emerg. Infect. Dis.* 24, 1505–1515. doi: 10.3201/eid2408.180151
- Bikard, D., Euler, C. W., Jiang, W., Nussenzweig, P. M., Goldberg, G. W., Duportet, X., et al. (2014). Exploiting CRISPR-Cas nucleases to produce sequence-specific antimicrobials. *Nat. Biotechnol.* 32, 1146–1150. doi: 10.1038/nbt.3043
- Blair, J. M. A., Webber, M. A., Baylay, A. J., Ogbolu, D. O., and Piddock, L. J. V. (2015). Molecular mechanisms of antibiotic resistance. *Nat. Rev. Microbiol.* 13, 42–51. doi: 10.1038/nrmicro3380
- Bolger, A. M., Lohse, M., and Usadel, B. (2014). Trimmomatic: a flexible trimmer for Illumina sequence data. *Bioinformatics* 30, 2114–2120. doi: 10.1093/bioinformatics/btu170
- Ceasar, S. A., Rajan, V., Prykhodzhiy, S. V., Berman, J. N., and Ignacimuthu, S. (2016). Insert, remove or replace: A highly advanced genome editing system using CRISPR/Cas9. *Biochim. Biophys. Acta Mol. Cell Res.* 1863, 2333–2344. doi: 10.1016/j.bbamcr.2016.06.009
- Chan, W., Verma, C. S., Lane, D. P., and Gan, S. K. (2013). A comparison and optimization of methods and factors affecting the transformation of *Escherichia coli*. *Biosci. Rep.* 33, 931–937. doi: 10.1042/BSR20130098

- Chayot, R., Montagne, B., Mazel, D., and Ricchetti, M. (2010). An end-joining repair mechanism in *Escherichia coli*. *Proc. Natl. Acad. Sci. U.S.A.* 107, 2141–2146. doi: 10.1073/pnas.0906355107
- Chen, W., McKenna, A., Schreiber, J., Haeussler, M., Yin, Y., Agarwal, V., et al. (2019). Massively parallel profiling and predictive modeling of the outcomes of CRISPR/Cas9-mediated double-strand break repair. *Nucleic Acids Res.* 47, 7989–8003. doi: 10.1093/nar/gkz487
- Citorik, R. J., Mimee, M., and Lu, T. K. (2014). Sequence-specific antimicrobials using efficiently delivered RNA-guided nucleases. *Nat. Biotechnol.* 32, 1141–1145. doi: 10.1038/nbt.3011
- Clinical and Laboratory Standards Institute, and Weinstein, M. P. (2012). *Methods for Dilution Antimicrobial Susceptibility Tests for Bacteria that Grow Aerobically*. Wayne, PA: Committee for Clinical Laboratory Standards.
- Clinical and Laboratory Standards Institute, (2019). *Performance Standards for Antimicrobial Susceptibility Testing*, 27th Edn. Wayne, PA: Committee for Clinical Laboratory Standards.
- Collignon, P. C., Conly, J. M., Andrement, A., McEwen, S. A., and Aidara-Kane, A. (2016). World health organization ranking of antimicrobials according to their importance in human medicine: a critical step for developing risk management strategies to control antimicrobial resistance from food animal production. *Clin. Infect. Dis.* 63, 1087–1093. doi: 10.1093/cid/ciw475
- Gavin, L., Lum, D., Ng, B., and Sam, C. (2015). Differential transformation efficiencies observed for pUC19 and pBR322 in *E. coli* may be related to calcium chloride concentration. *J. Exp. Microbiol. Immunol.* 20, 1–6.
- Gonzales, M. F., Brooks, T., Pukatzki, S. U., and Provenzano, D. (2013). Rapid Protocol for Preparation of Electrocompetent *Escherichia coli* and *Vibrio cholerae*. *J. Vis. Exp.* 80:50684. doi: 10.3791/50684
- Hall, J. P. J., and Harrison, E. (2016). Bacterial evolution: resistance is a numbers game. *Nat. Microbiol.* 1:16235. doi: 10.1038/nmicrobiol.2016.235
- Harding, C. R., Schroeder, G. N., Collins, J. W., and Frankel, G. (2013). Use of galleria mellonella as a model organism to study *Legionella pneumophila* infection. *JoVE* 81:e50964. doi: 10.3791/50964
- Hoffmann, H., Stindl, S., Ludwig, W., Stumpf, A., Mehlen, A., Monget, D., et al. (2005). Enterobacter hormaechei subsp. oharae subsp. nov., E. hormaechei subsp. hormaechei comb. nov., and E. hormaechei subsp. steigerwaltii subsp. nov., three new subspecies of clinical importance. *J. Clin. Microbiol.* 43, 3297–3303. doi: 10.1128/JCM.43.7.3297-3303.2005
- Jansen, M., Wahida, A., Latz, S., Krüttgen, A., Häfner, H., Buhl, E. M., et al. (2018). Enhanced antibacterial effect of the novel T4-like bacteriophage KARL-1 in combination with antibiotics against multi-drug resistant *Acinetobacter baumannii*. *Sci. Rep.* 8:14140. doi: 10.1038/s41598-018-32344-y
- Kim, S., Jeong, H., Kim, E.-Y., Kim, J. F., Lee, S. Y., and Yoon, S. H. (2017). Genomic and transcriptomic landscape of *Escherichia coli* BL21(DE3). *Nucleic Acids Res.* 45, 5285–5293. doi: 10.1093/nar/gkx228
- Klappenbach, J. A., Dunbar, J. M., and Schmidt, T. M. (2000). rRNA operon copy number reflects ecological strategies of bacteria. *Appl. Environ. Microbiol.* 66, 1328–1333. doi: 10.1128/AEM.66.4.1328-1333.2000
- Lachmayr, K. L., Kerkhof, L. J., DiRienzo, A. G., Cavanaugh, C. M., and Ford, T. E. (2009). Quantifying nonspecific TEM -lactamase (blaTEM) genes in a wastewater stream. *Appl. Environ. Microbiol.* 75, 203–211. doi: 10.1128/AEM.01254-08
- Larionov, A., Krause, A., and Miller, W. (2005). A standard curve based method for relative real time PCR data processing. *BMC Bioinformatics* 6:62. doi: 10.1186/1471-2105-6-62
- Lim, G., Lum, D., Ng, B., and Sam, C. (2015). Differential transformation efficiencies observed for pUC19 and pBR322 in *E. coli* may be related to calcium chloride concentration. *J. Exp. Microbiol. Immunol.* 20, 1–6.
- Liu, W., Xie, X., Ma, X., Li, J., Chen, J., and Liu, Y.-G. (2015). DSDecode: a web-based tool for decoding of sequencing chromatograms for genotyping of targeted mutations. *Mol. Plant* 8, 1431–1433. doi: 10.1016/j.molp.2015.05.009
- Long, S. W., Linson, S. E., Ojeda Saavedra, M., Cantu, C., Davis, J. J., Brettin, T., et al. (2017). Whole-genome sequencing of human clinical *Klebsiella pneumoniae* isolates reveals misidentification and misunderstandings of *Klebsiella pneumoniae*, *Klebsiella variicola*, and *Klebsiella quasipneumoniae*. *mSphere* 2:e00290-17. doi: 10.1128/mSphereDirect.00290-17
- O’Neil, J. (2016). Tackling Drug-Resistant Infections Globally: Final Report And Recommendations. Available online at: <http://amr-review.org> (accessed November, 2019).
- Rawat, D., and Nair, D. (2010). Extended-spectrum  $\beta$ -lactamases in gram negative bacteria. *J. Glob. Infect. Dis.* 2:263. doi: 10.4103/0974-777X.68531
- Registry of Standard Biological Parts, (2019). *Plasmid Backbones/Assembly - Parts.igem.org*. Available at: [http://parts.igem.org/Plasmid\\_backbones/Assembly](http://parts.igem.org/Plasmid_backbones/Assembly) (Accessed September 10, 2018).
- Rodríguez-Medina, N., Barrios-Camacho, H., Duran-Bedolla, J., and Garza-Ramos, U. (2019). *Klebsiella variicola*: an emerging pathogen in humans. *Emerg. Microbes Infect.* 8, 973–988. doi: 10.1080/22221751.2019.1634981
- San Millan, A., Escudero, J. A., Gifford, D. R., Mazel, D., and MacLean, R. C. (2016). Multicopy plasmids potentiate the evolution of antibiotic resistance in bacteria. *Nat. Ecol. Evol.* 1:10. doi: 10.1038/s41559-016-0010
- San Millan, A., Santos-Lopez, A., Ortega-Huedo, R., Bernabe-Balas, C., Kennedy, S. P., and Gonzalez-Zorn, B. (2015). Small-plasmid-mediated antibiotic resistance is enhanced by increases in plasmid copy number and bacterial fitness. *Antimicrob. Agents Chemother.* 59, 3335–3341. doi: 10.1128/AAC.00235-15
- Savard, P., and Perl, T. M. (2012). A call for action: managing the emergence of multidrug-resistant *Enterobacteriaceae* in the acute care settings. *Curr. Opin. Infect. Dis.* 25, 371–377. doi: 10.1097/QCO.0b013e3283558c17
- Schechter, L. M., Creely, D. P., Garner, C. D., Shortridge, D., Nguyen, H., Chen, L., et al. (2018). Extensive gene amplification as a mechanism for piperacillin-tazobactam resistance in *Escherichia coli*. *mBio* 9:e00583-18. doi: 10.1128/mBio.00583-18
- Studier, F. W., and Moffatt, B. A. (1986). Use of bacteriophage T7 RNA polymerase to direct selective high-level expression of cloned genes. *J. Mol. Biol.* 189, 113–130. doi: 10.1016/0022-2836(86)90385-2
- The European Committee on Antimicrobial Susceptibility Testing [EUCAST], (2019). *New definitions of S, I and R*. Available online at: <http://www.eucast.org/newsiandr/> (accessed July, 2019).
- Van den Bergh, B., Fauvart, M., and Michiels, J. (2017). Formation, physiology, ecology, evolution and clinical importance of bacterial persisters. *FEMS Microbiol. Rev.* 41, 219–251. doi: 10.1093/femsrev/fux001
- Van Norman, G. A. (2016). Drugs, devices, and the FDA: Part 1. *JACC* 1, 170–179. doi: 10.1016/j.jacpts.2016.03.002
- Větrovský, T., and Baldrian, P. (2013). The variability of the 16S rRNA gene in bacterial genomes and its consequences for bacterial community analyses. *PLoS One* 8:e57923. doi: 10.1371/journal.pone.0057923
- Vianna, M. E., Holtgraewe, S., Seyfarth, I., Conrads, G., and Horz, H. P. (2008). Quantitative analysis of three hydrogenotrophic microbial groups, methanogenic archaea, sulfate-reducing bacteria, and acetogenic bacteria, within plaque biofilms associated with human periodontal disease. *J. Bacteriol.* 190, 3779–3785. doi: 10.1128/JB.01861-07
- Wood, T. K., Knabel, S. J., and Kwan, B. W. (2013). Bacterial persister cell formation and dormancy. *Appl. Environ. Microbiol.* 79, 7116–7121. doi: 10.1128/AEM.02636-13
- Yang, S., Sleight, S. C., and Sauro, H. M. (2013). Rationally designed bidirectional promoter improves the evolutionary stability of synthetic genetic circuits. *Nucleic Acids Res.* 41:e33. doi: 10.1093/nar/gks972
- Yosef, I., Manor, M., Kiro, R., and Qimron, U. (2015). Temperate and lytic bacteriophages programmed to sensitize and kill antibiotic-resistant bacteria. *Proc. Natl. Acad. Sci. U.S.A.* 112, 7267–7272. doi: 10.1073/pnas.1500107112
- Zankari, E., Hasman, H., Cosentino, S., Vestergaard, M., Rasmussen, S., Lund, O., et al. (2012). Identification of acquired antimicrobial resistance genes. *J. Antimicrob. Chemother.* 67, 2640–2644. doi: 10.1093/jac/dks261

**Conflict of Interest:** The authors declare that the research was conducted in the absence of any commercial or financial relationships that could be construed as a potential conflict of interest.

Copyright © 2020 Tagliaferri, Guimarães, Pereira, Vilela, Horz, dos Santos and Mendes. This is an open-access article distributed under the terms of the Creative Commons Attribution License (CC BY). The use, distribution or reproduction in other forums is permitted, provided the original author(s) and the copyright owner(s) are credited and that the original publication in this journal is cited, in accordance with accepted academic practice. No use, distribution or reproduction is permitted which does not comply with these terms.



# Characterization of KPC-Producing *Serratia marcescens* in an Intensive Care Unit of a Brazilian Tertiary Hospital

Roumayne L. Ferreira<sup>1†</sup>, Graziela S. Rezende<sup>1†</sup>, Marcelo Silva Folhas Damas<sup>1†</sup>, Mariana Oliveira-Silva<sup>2</sup>, André Pitondo-Silva<sup>2</sup>, Márcia C. A. Brito<sup>3</sup>, Eduardo Leonardecz<sup>1</sup>, Fabiana R. de Góes<sup>4</sup>, Emeline Boni Campanini<sup>1</sup>, Iran Malavazi<sup>1</sup>, Anderson F. da Cunha<sup>1</sup> and Maria-Cristina da Silva Pranchevicius<sup>1\*</sup>

<sup>1</sup> Departamento de Genética e Evolução, Universidade Federal de São Carlos, São Carlos, Brazil, <sup>2</sup> Programas de Pós-graduação em Odontologia e Tecnologia Ambiental, Universidade de Ribeirão Preto, Ribeirão Preto, Brazil, <sup>3</sup> Laboratório Central de Saúde Pública do Tocantins, Palmas, Brazil, <sup>4</sup> Instituto de Ciências Matemáticas e de Computação, Universidade de São Paulo, São Carlos, Brazil

## OPEN ACCESS

### Edited by:

Filipa Grosso,  
University of Porto, Portugal

### Reviewed by:

Martina Barchitta,  
University of Catania, Italy  
Daria Van Tyne,  
University of Pittsburgh, United States

### \*Correspondence:

Maria-Cristina da Silva  
Pranchevicius  
mcspranc@gmail.com

†These authors have contributed  
equally to this work

### Specialty section:

This article was submitted to  
Antimicrobials, Resistance  
and Chemotherapy,  
a section of the journal  
Frontiers in Microbiology

Received: 28 October 2019

Accepted: 21 April 2020

Published: 20 May 2020

### Citation:

Ferreira RL, Rezende GS,  
Damas MSF, Oliveira-Silva M,  
Pitondo-Silva A, Brito MCA,  
Leonardecz E, Góes FR,  
Campanini EB, Malavazi I,  
da Cunha AF and Pranchevicius  
M-CS (2020) Characterization  
of KPC-Producing *Serratia  
marcescens* in an Intensive Care Unit  
of a Brazilian Tertiary Hospital.  
Front. Microbiol. 11:956.  
doi: 10.3389/fmicb.2020.00956

*Serratia marcescens* has emerged as an important opportunistic pathogen responsible for nosocomial and severe infections. Here, we determined phenotypic and molecular characteristics of 54 *S. marcescens* isolates obtained from patient samples from intensive-care-unit (ICU) and neonatal intensive-care-unit (NIUC) of a Brazilian tertiary hospital. All isolates were resistant to beta-lactam group antibiotics, and 92.6% (50/54) were not susceptible to tigecycline. Furthermore, 96.3% showed intrinsic resistance to polymyxin E (colistin), a last-resort antibiotic for the treatment of infections caused by MDR (multidrug-resistant) Gram-negative bacteria. In contrast, high susceptibility to other antibiotics such as fluoroquinolones (81.5%), and to aminoglycosides (as gentamicin 81.5%, and amikacin 85.2%) was found. Of all isolates, 24.1% were classified as MDR. The presence of resistance and virulence genes were examined by PCR and sequencing. All isolates carried KPC-carbapenemase (*bla<sub>KPC</sub>*) and extended spectrum beta-lactamase *bla<sub>TEM</sub>* genes, 14.8% carried *bla<sub>OXA-1</sub>*, and 16.7% carried *bla<sub>CTX-M-1</sub>* group genes, suggesting that bacterial resistance to  $\beta$ -lactam antibiotics found may be associated with these genes. The genes *SdeB/HasF* and *SdeY/HasF* that are associated with efflux pump mediated drug extrusion to fluoroquinolones and tigecycline, respectively, were found in 88.9%. The *aac(6')-Ib-cr* variant gene that can simultaneously induce resistance to aminoglycoside and fluoroquinolone was present in 24.1% of the isolates. Notably, the virulence genes to (i) pore-forming toxin (*ShIA*); (ii) phospholipase with hemolytic and cytolytic activities (*PhIA*); (iii) flagellar transcriptional regulator (*FlhD*); and (iv) positive regulator of prodigiosin and serratamolide production (*PigP*) were present in 98.2%. The genetic relationship among the isolates determined by ERIC-PCR demonstrated that the vast majority of isolates were grouped in a single cluster with 86.4% genetic similarity. In addition, many isolates showed 100% genetic similarity to each other, suggesting that the *S. marcescens* that circulate in this ICU are closely related. Our results suggest that the antimicrobial resistance to many drugs



currently used to treat ICU and NIUC patients, associated with the high frequency of resistance and virulence genes is a worrisome phenomenon. Our findings emphasize the importance of active surveillance plans for infection control and to prevent dissemination of these strains.

**Keywords:** *Serratia marcescens*, intensive care units, KPC, virulence and resistance genes, ERIC-PCR

## INTRODUCTION

*Serratia marcescens* is a Gram-negative bacillus that naturally resides in the soil and water and produces a red pigment at room temperature. Although previously considered non-pathogenic, this species has emerged as a prominent opportunistic pathogen found in nosocomial outbreaks in neonatal intensive care Units (NICUs), intensive care units (ICUs) and other hospital units over the last few decades (Enciso-Moreno et al., 2004; Moradigaravand et al., 2016; Ghaith et al., 2018).

The true occurrence of *S. marcescens* is still underestimated (Zingg et al., 2017). In NICUs, studies have shown that infected newborns are a potential source of *S. marcescens* (Cristina et al., 2019), although there is a constant increase of *S. marcescens* bacteremia across all age groups (Vetter et al., 2016; Phan et al., 2018). *S. marcescens* increasingly adapts to hospital environments (Yoon et al., 2005; Gastmeier, 2014). It accounts for 15% of all isolates from nosocomial infections (Raymond and Aujard, 2000). Although it is difficult to identify the source of *S. marcescens* during outbreaks, it is the third most frequent pathogen identified (Gastmeier et al., 2007), and more than one clone can be usually identified (David et al., 2006; Montagnani et al., 2015; Dawczynski et al., 2016).

*Serratia marcescens* associated with hospital outbreaks or epidemic events are commonly resistant to several antibiotics (Moradigaravand et al., 2016; Cristina et al., 2019). In fact, one important feature of *S. marcescens* is its resistance to narrow-spectrum penicillins and cephalosporins; nitrofurantoin; tetracycline; macrolides; cefuroxime; cephamycins; fluoroquinolone, and colistin (Stock et al., 2003; Liou et al., 2014; Moradigaravand et al., 2016; Sandner-Miranda et al., 2018). The resistance to some of these molecules may be intrinsic to this specie and is explained by either the presence of resistance genes on the chromosome or by the acquisition of such genes via horizontal transfer. It is noteworthy that the latter mechanism is considered the most important event that leads to multiple antibiotic resistance (von Wintersdorff et al., 2016; Sandner-Miranda et al., 2018).

Extended-spectrum  $\beta$ -lactamases (ESBLs) are a group of bacterial enzymes that can be rapidly transferred via plasmid exchange (Rawat and Nair, 2010) causing resistance to a broad range of  $\beta$ -lactams (Naas et al., 2008). Carbapenemases are the most versatile family of  $\beta$ -lactamases able to hydrolyze carbapenems and many other  $\beta$ -lactams (Jeon et al., 2015) including penicillins, cephalosporins, and monobactams (Anderson et al., 2007; Marschall et al., 2009). In general, bacteria carrying the *bla*<sub>KPC</sub> and/or ESBLs genes usually harbor other resistance genes associated with several classes of antimicrobials (Tzouveleakis et al., 2012; Cao et al., 2014; Ribeiro et al., 2016).

Since *S. marcescens* has been acquiring a range of ESBLs and commonly exhibit co-resistance to many other classes of antibiotics, the infections caused by these multidrug-resistant (MDR) isolates impair therapy and limit treatment options (Yu et al., 1998; Mostatabi et al., 2013; Herra and Falkiner, 2018).

In this study, we investigated the phenotypic characteristics regarding antimicrobial resistance and the genotypic traits of *S. marcescens* isolated from a tertiary care hospital's ICUs including the search for resistance and virulence genes as well as the genetic relationship among the isolates. Our report describes MDR profile and KPC-producing *S. marcescens* isolates and highlight the importance of monitoring *S. marcescens* infection and the need of constant surveillance to support continuous and effective measures to prevent the spread of these strains.

## MATERIALS AND METHODS

### Study Design and Bacterial Isolates

From February 2014 to June 2015, a total of 54 *S. marcescens* were isolated of clinical specimens collected from 45 patients admitted to intensive-care-unit (ICU) and neonatal intensive care unit (NICU) of a tertiary care government hospital in Palmas, Tocantins, Brazil. Since 2013, there has been an increase in detection of *S. marcescens* isolates from hospital inpatients, and in 2015, the hospital reported an apparent *S. marcescens* outbreak that occurred from July to August 2015. Appropriate intervention measures were established, such as reviewing the infection control policies, hand antisepsis practices and determination of trends of isolation of *S. marcescens* over time. To trace the source of the infection, bacteria were isolated from various samples obtained from clinical indications of infections during the patients' ICU stay.

As part of the control measures, surveillance cultures were obtained from tracheal aspirate and rectal swabs from all ICU patients, on admission (within the first 24 h) and during the stay (once a week). Blood, wound, catheter tip, drain, sputum, urine, rectal swab, and tracheal aspirate samples were primarily sent to the hospital's laboratory, processed and cultured by standard microbiological techniques. The blood samples were inoculated first in blood culture bottles (Hemoprov-NewProv, Brazil). All clinical samples, including blood culture bottles giving positive signals were cultured onto MacConkey agar (Probac, Brazil), blood agar (Probac, Brazil), and chocolate blood agar (Probac, Brazil). Plates were incubated at 37°C for up to 48 h. *S. marcescens* were identified by Gram staining, cultural characteristics in MacConkey agar (Probac, Brazil), blood agar (Probac, Brazil), and biochemical tests (Bactray I, II,III; Laborclin, Brazil). The antimicrobial susceptibility profile

was determined by Kirby-Bauer disk diffusion method. All *S. marcescens* isolates and the microbiological reports prepared at the hospital were sent to the Central Laboratory of Public Health of Tocantins (LACEN-TO) for further phenotypic validations.

## Bacterial Identification and Antimicrobial Susceptibility Test

Once samples were received at LACEN, bacterial identification and antimicrobial susceptibility tests were performed by the Vitek 2 system (Biomerieux, France), according to Clinical and Laboratory Standards Institute guidelines (CLSI, 2019). All 54 *S. marcescens* isolates were screened for susceptibility against 16 antimicrobial agents: ampicillin (AMP), ampicillin/sulbactam (SAM), piperacillin/tazobactam (TZP), cefuroxime (CXM), ceftazidime (CAZ), ceftriaxone (CRO), cefepime (FEP), ertapenem (ETP), imipenem (IPM), meropenem (MEM), amikacin (AMK), gentamicin (GEN), ciprofloxacin (CIP), tigecycline (TGC), and colistin (CST). Broth microdilution method was performed to determine tigecycline and colistin minimum inhibitory concentration (MICs) and results were interpreted based on the European Committee on Antimicrobial Susceptibility Testing (EUCAST, 2018) criteria, available at [https://www.eucast.org/fileadmin/src/media/PDFs/EUCAST\\_files/Breakpoint\\_tables/v\\_8.1\\_Breakpoint\\_Tables.pdf](https://www.eucast.org/fileadmin/src/media/PDFs/EUCAST_files/Breakpoint_tables/v_8.1_Breakpoint_Tables.pdf). All isolates were tested for carbapenemase production by Modified Hodge test, synergy test and ethylenediaminetetraacetic acid (EDTA) test under the CLSI guidelines (CLSI, 2019) as described elsewhere (Miriagou et al., 2010; Nordmann et al., 2011; Okoche et al., 2015; Ferreira et al., 2019). Multidrug-resistance *S. marcescens* isolates were classified by non-susceptibility to at least one agent of three or more antimicrobial categories (Magiorakos et al., 2012). *S. marcescens* is intrinsically resistant to AMP, SAM, CXM, FOX, and CST; therefore, these antibiotics were not included in the MDR classification (Magiorakos et al., 2012).

## Genomic DNA Extraction

Isolates of *S. marcescens* were subcultured on Brain Heart Infusion (BHI) agar (Oxoid, United Kingdom) and incubated for 24 h at 37°C. All samples were submitted to genomic DNA extraction using the Wizard Genomic DNA Purification Kit (Promega, Madison, WI, United States), according to manufacturer's instructions.

## Detection of Antibiotic-Resistance

Polymerase chain reaction (PCR) was performed for detection of  $\beta$ -lactamase genes (*bla*<sub>TEM</sub>, *bla*<sub>SHV</sub> variants, *bla*<sub>OXA-1, 4 and 30</sub>, *bla*<sub>CTX-M-1group</sub>), carbapenemase genes (*bla*<sub>KPC</sub>, *bla*<sub>IMP</sub>, *bla*<sub>VIM</sub>, *bla*<sub>NDM</sub>, *bla*<sub>OXA-48</sub>) (Ferreira et al., 2019), plasmid mediated quinolone resistance (PMQR) gene (*aac*(6')-Ib-cr) (Wong et al., 2014; Mitra et al., 2019), resistance-nodulation-division (RND) efflux pumps (*SdeB*, *SdeY*), and outer membrane gene (*HasF*, a *TolC* homolog) involved in energy-dependent efflux of antimicrobial agents (Kumar and Worobec, 2005b). The genes were amplified using specific primers designed to follow the conditions described in the references from **Table 1**. All primers were synthesized by Exxtend (Brazil). Amplicons were

analyzed by gel electrophoresis in 1.0% agarose and visualized under ultraviolet (UV) light.

## Virulence Gene Detection

The presence of four virulence genes were assessed by PCR: genes *PigP*, a positive regulator of prodigiosin and serratamolide production; *FlhD*, a flagellar transcriptional regulator; *ShlA*, a pore-forming toxin with hemolytic activity; *PhlA*, a phospholipase A with hemolytic activity. The primers sequences amplicon sizes and annealing temperatures are listed in **Table 1**. Amplicons were analyzed by gel electrophoresis in 1.0% agarose and visualized under ultraviolet (UV) light.

## Sequence Analysis of Antibiotic-Resistance Markers and Virulence Genes

One amplicon of each studied gene was randomly selected for confirmation of identity by DNA sequencing using an automated sequencer (ABI 3500xL Genetic Analyzer; Applied Biosystems, Foster City, CA, United States). After amplification, we extracted the PCR products from agarose gels using the Illustra GFX PCR DNA (GE Healthcare), which were purified using the Gel Band Purification Kit (GE Healthcare), both according to manufacturer's instructions. Obtained sequences were edited with Bioedit v7.0.5 (Hall, 1999), compared with the nr database using the Blastn tool<sup>1</sup> and submitted to the GenBank database. Genes and their respective accession numbers: *bla*<sub>CTX</sub> – MK576103; *bla*<sub>KPC</sub> – MK576104; *bla*<sub>OXA</sub> – MK576105; *bla*<sub>TEM</sub> – MK576106; *SdeB* – MN583232; *SdeY* – MN583233; *HasF* – MN583234; *aac*(6')-Ib-cr – MN583235; *FlhD* – MN583236; *PigP* – MN583237; *ShlA* – MN583238; *PhlA* – MN583239. Access to genetic heritage was approved by the National System for the Management of Genetic Heritage (SisGen n° AFF27ED).

## Enterobacterial Repetitive Intergenic Consensus Polymerase Chain Reaction

Enterobacterial repetitive intergenic consensus PCR (ERIC-PCR) analysis was performed to evaluate the genetic similarity among the 54 *S. marcescens* isolates using the primers and conditions previously described by Versalovic et al. (1994). PCR reactions were performed using the enzyme TaKaRa Ex Taq DNA Polymerase (Takara Bio, Kusatsu, Japan). The BioNumerics program version 5.1 (AppliedMaths, Keistraat, Belgium) was used to construct the unweighted pair group mean method (UPGMA) similarity dendrogram with Dice's similarity coefficient, following Ferreira et al. (2019).

## Statistical Analyses

In the analysis of contingency tables, we used Fisher's exact test and/or Barnard's exact test. Maximum likelihood did not present superior efficiency in relation to the previous methods (data not show). It was used logistic regression model with two predictor variables  $x_1$  and  $x_2$ . Statistical software R was used in all data analysis.

<sup>1</sup><https://blast.ncbi.nlm.nih.gov/>

**TABLE 1** | Sequences of primers used for detection of resistance markers.

Gene	Sequence (5'-3'), F/R	TM (°C)	Amplicon size (bp)	References
<i>bla<sub>KPC</sub></i>	CGTCTAGTTCTGCTGTCTTG CTTGTTCATCCTTGTAGGCG	61.3	797	Poirel et al., 2011
<i>bla<sub>TEM</sub></i>	TGCGGTATTATCCCGTGTG TCGTGCTTTGGTATGGCTTC	63	296	Xiong et al., 2007
<i>bla<sub>CTX-M-1group</sub></i>	ACAGCGATAACGTGGCGATG TCGCCAATGCTTTACCCAG	64	216	Li and Li, 2005
<i>bla<sub>SHV</sub>variants</i>	AGCCGCTTGAGCAAATTAAC ATCCCGCAGATAAATCACCAC	55.6	712	Dallenne et al., 2010
<i>bla<sub>OXA-1</sub></i>	GGCACCAGATCAACTTTCAAG GACCCCAAGTTTCTGTAAGTG	63	563	Dallenne et al., 2010
<i>bla<sub>OXA-48</sub></i>	GCGTGGTTAAGGATGAACAC CATCAAGTTCAACCCAACCG	55	438	Poirel et al., 2011
<i>bla<sub>IMP</sub></i>	CTACCGCAGCAGACTTTTGC ACAACCAGTTTTGCCTTACC	55	587	Martins et al., 2007
<i>bla<sub>VIM</sub></i>	AAAGTTATGCCGCACTCACC TGCAACTTCATGTTATGCCG	55	865	Yan et al., 2001
<i>bla<sub>NDM</sub></i>	GCAGCTTGTGCGCCATGCGGGC GGTCGCGAAGCTGAGCACCGCAT	60	782	Doyle et al., 2012
<i>mcr-1</i>	CGGTCAGTCCGTTTGTTC CTGGTGGTCTGTAGGG	51.6	309	Liu et al., 2015
<i>aac(6)-Ib-cr</i>	ATGACTGAGCATGACCTTGC TTAGGCATCACTGCGTGTTC	55.4	519	Platell et al., 2011
<i>SdeB</i>	AGATGGCCGATAAGCTGTTG CAGCGTCCAGCTTTCATACA	55.4	200	Hornsey et al., 2010
<i>SdeY</i>	TCCATCAACGAAGTGGTGAA GTTTATCGAGAAGCCGAACG	55.5	200	Hornsey et al., 2010
<i>HasF</i>	CATGTGCAAATGGCGCCAAC TTGTAGGCGTTGATGCTGCT	57.5	785	Hornsey et al., 2010
<i>PigP</i>	GAACATGTTGGCAATGAAAA ATGTAACCCAGGAATTGCAC	53.4	207	Srinivasan et al., 2017
<i>FliH</i>	TGTCGGGATGGGAATATGG CGATAGCTCTTGCAAGTAAATGG	57	307	Salini and Pandian, 2015
<i>ShlA</i>	AGCGTGATCCTCAACGAAGT TGCGATTATCCAGAGTGCTG	55.4	217	Aggarwal et al., 2017
<i>PhlA</i>	GGGGACAACAATCTCAGGA ACGCCAACAACATACTGCTTG	55.4	207	Aggarwal et al., 2017

## Ethical Considerations

In our study, we did not use/collect human genetic material and biological samples. Strains were part of the collection of the Central Laboratory of Public Health, (LACEN-TO), a health-care facility that is a reference in diagnosis in the state of Tocantins, Brazil. It was a retrospective study, and epidemiological data were obtained from a database or similar, which will be kept confidential in accordance with the with the terms of Resolution 466/12 of the National Health Council. These epidemiological data were also provided by LACEN-TO. Informed consent was not required according to resolution 466/12 concerning research involving humans of the National Health Council (Conselho Nacional de Saúde/Ministério da Saúde, Brasília, Brazil, 2012). The study was approved by the Committee of Ethics in Human Research of the Federal University of São Carlos (no. 1.088.936). Permission to conduct the study was also obtained from the

Health Department of the State of Tocantins (Secretaria de Saúde do Estado do Tocantins – SESAU) and LACEN/TO.

## RESULTS

### *Serratia marcescens* Isolates

A total of 54 *S. marcescens* strains were isolated from 39 ICU and 6 NICU patients' samples at a tertiary hospital located in city of Palmas, Tocantins state. In six patients, 5 from ICU and 1 from NICU, *S. marcescens* was isolated in more than one infection site. The prevalence of *S. marcescens* strains by age group was the following: 0–1 day (12.96%;  $n = 7$ ), 18–59 years (38.89%,  $n = 21$ ), 60 years or more (48.15%,  $n = 26$ ). The median age of patients was 57.0 years (range, 0–93 years). *S. marcescens* strains were more frequently found in male (68.5%,  $n = 37$ )

than in female (31.5%,  $n = 17$ ) patients (**Figure 1A**). Forty-three samples (79%) were from tracheal aspirate (33%,  $n = 18$ ), rectal swab, (22%,  $n = 12$ ), and blood (24%,  $n = 13$ ) cultures, while 11 (21%) came from wound (9%,  $n = 5$ ), catheter tip (4%,  $n = 2$ ), surgical drain (4%,  $n = 2$ ), sputum (2%,  $n = 1$ ), and urine (2%,  $n = 1$ ) cultures (**Figure 1B**). Antibiotic resistance profiles of *S. marcescens* isolated from the abovementioned different sites showed that all strains were resistant to  $\beta$ -lactams antibiotics. In addition, colistin (CST) and tigecycline (TGC) non-susceptibility pattern of *S. marcescens* per site of isolation was statistically significant ( $p < 0.01$ ) in several organs (tracheal aspirate, blood, rectal swab, and wound) when compared with amikacin (AMK), gentamicin (GEN), and ciprofloxacin (CIP) antibiotics (**Figure 1C**).

## Antimicrobial Resistance Profile and Genetic Markers for Antibiotic-Resistance and Virulence Patterns

*Serratia marcescens* strains showed high-levels of resistance to all  $\beta$ -lactams (100%,  $n = 54$ ) (TZP, CAZ, CRO, FEP, ETP, IPM, MEM), including high-levels of intrinsic resistance to  $\beta$ -lactams (AMP, SAM, CXM, FOX) (100%,  $n = 54$ ) and colistin (CST) (96.3%,  $n = 52$ ). Resistance to tigecycline (TGC) *S. marcescens* was found in nearly all isolates (92.6%;  $n = 50$ ). However, for the antibiotics classes fluoroquinolones (CIP) (81.5%,  $n = 44$ ) and aminoglycosides such as gentamicin (GEN) (81.5%,  $n = 44$ ), amikacin (AMK) (85.2%,  $n = 46$ ) (**Figure 2A**), high susceptibility profile was detected. In contrast, MDR was observed in 24.1% ( $n = 13$ ) of the isolates, and the most common MDR profile was related to  $\beta$ -lactams-glycylcycline-aminoglycosides-quinolone (14.8%,  $n = 8$ ), followed by  $\beta$ -lactams-glycylcycline-quinolone (5.6%,  $n = 3$ ), and ( $\beta$ -lactams-glycylcycline-aminoglycosides 3.7%,  $n = 2$ ).

All 54 tested isolates harbored KPC-carbapenemase (*bla*<sub>KPC</sub>) and ESBL (*bla*<sub>TEM</sub>) genes. The ESBL-encoding genes *bla*<sub>OXA-1</sub> was detected in 14.8% (8/54), and the *bla*<sub>CTX-M-1group</sub> in 16.7% (9/54). However, the *bla*<sub>SHV</sub> variants, *bla*<sub>IMP</sub>, *bla*<sub>OXA-48</sub>, *bla*<sub>NDM</sub>, *bla*<sub>VIM</sub>, and *mcr-1* genes were not detected. The *aac*(6)-Ib-cr variant gene that can induce simultaneous resistance against aminoglycoside and fluoroquinolone was found in 13 (24.1%) strains. The RND pump efflux encoding genes *SdeY* and *SdeB* were identified in all strains while the outer membrane component gene (*HasF*) was present in 48 (88.9%). Thus, the coexistence of *SdeY/HasF* genes and *SdeB/HasF* was observed in 49 (88.9%) strains (**Figure 2B**). Finally, with the exception of one strain (*Sm40*), the virulence-associated genes *PigP*, *FlhD*, *ShlA*, and *PhlA* were regularly distributed among *S. marcescens* strains, which were detected in 98.2% of all strains (**Figure 2B**).

## Resistance Phenotype-Genotype Correlation and Genetic Markers for Virulence Factors

The correlation between the results of phenotypic and genotypic detection and the presence of virulence genes is shown in **Figure 3**.

All isolates carried *bla*<sub>KPC</sub> and conferred resistance to all beta-lactam, including carbapenem antibiotics. Furthermore, all detectable *bla* genes in *bla*<sub>CTX-M-1</sub>, *bla*<sub>OXA-1</sub>, and *bla*<sub>TEM</sub> group presented ESBL phenotype. Of the 13 isolates with *aac*(6)-Ib-cr gene, 9 (69.2%) were non-susceptible to gentamicin, 7 (53.9%) to amikacin, and 8 (61.5%) to ciprofloxacin. Among the 49 (88.9%) *HasF*-positive isolates, 44 (81.5%) were non-susceptible to tigecycline.

## ERIC-PCR

The ERIC-PCR results indicated that the majority of the isolates presented a rate of genetic similarity above 85% (**Figure 4**). Almost all strains (96.3%) were grouped into a large cluster named B cluster, sharing 86.4% of genetic similarity. In addition, the B cluster was separated into two sub-clusters named B1, with 21 isolates, and B2, with 31 isolates, sharing a genetic similarity of 96.1% and 100%, respectively. Although the cluster B1 presented two subgroups with 4 and 17 isolates, they showed 100% genetic similarity in each one. Interestingly, two strains (*Sm38* and *Sm40*) were grouped separately within the A cluster and presented 71.4% of genetic similarity (**Figure 4**).

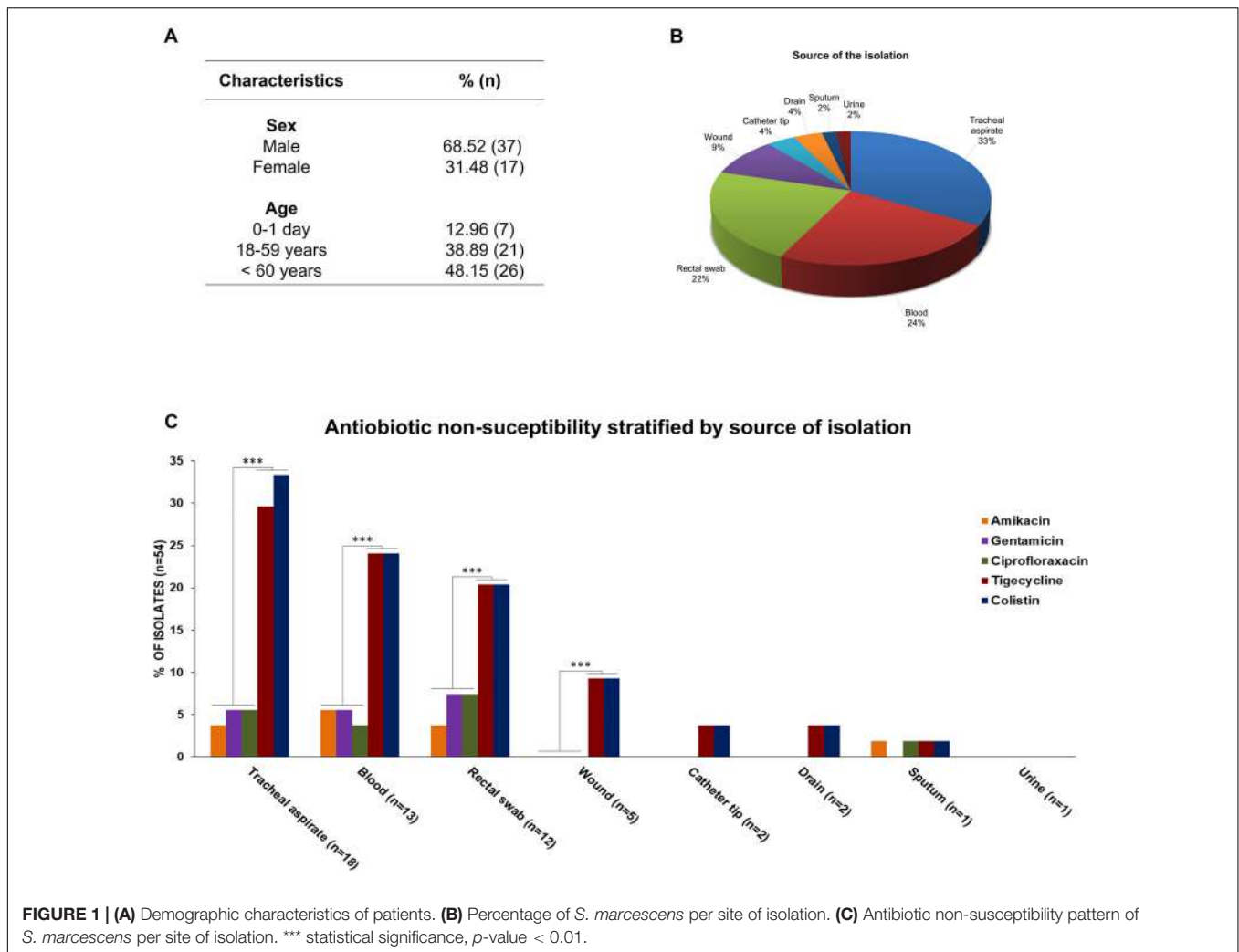
## DISCUSSION

*Serratia marcescens* is a prominent opportunistic pathogen that frequently causes infections in intensive care, surgical and dialysis units (Krishnan et al., 1991; Martineau et al., 2018). In Brazil, there are only few studies on *S. marcescens* (Ribeiro et al., 2013; Silva et al., 2015). Therefore, we here describe the presence of MDR *S. marcescens* isolates producing KPC-carbapenemase (*bla*<sub>KPC</sub>) and extended spectrum beta-lactamase (*bla*<sub>TEM</sub>, *bla*<sub>CTX-M-1group</sub> e *bla*<sub>OXA-1</sub>, 4 and 30) in the state of Tocantins, Brazil. Tocantins, located southeast of the Northern Region, is the newest state of Brazil and shares borders with six states presenting intensive migration flow.

*Serratia marcescens* were isolated mainly from male patients with 60 or more years of age, similarly to previous studies that demonstrated advanced age male patients as presenting a higher risk of contracting *S. marcescens* infections (Ulu-Kilic et al., 2013; Kim et al., 2015; O'Horo et al., 2017). Samples with higher amounts of *S. marcescens* were those from tracheal aspirate, followed by blood, rectal swab, and wounds. Our findings corroborate studies by Kim et al. (2015) and Liou et al. (2014) that reported the respiratory tract as the main route of infection for *S. marcescens*. Other studies have also reported *S. marcescens* in other sites as bloodstream (Seeyave et al., 2006) and wounds (Us et al., 2017), demonstrating the versatility of these strains in colonizing the host and affecting a wide variety of physiological system.

In addition to the intrinsic resistance to the antibiotics AMP, SAM, CXM, FOX, and CST, we found multidrug-resistant (MDR) *S. marcescens* isolates to beta-lactam, glycylcycline, and/or aminoglycoside and quinolone group antibiotics. This is in line with other studies that have also reported MDR *S. marcescens* mainly to beta-lactam, aminoglycoside, and quinolone antibiotics groups (Stock et al., 2003), in hospital



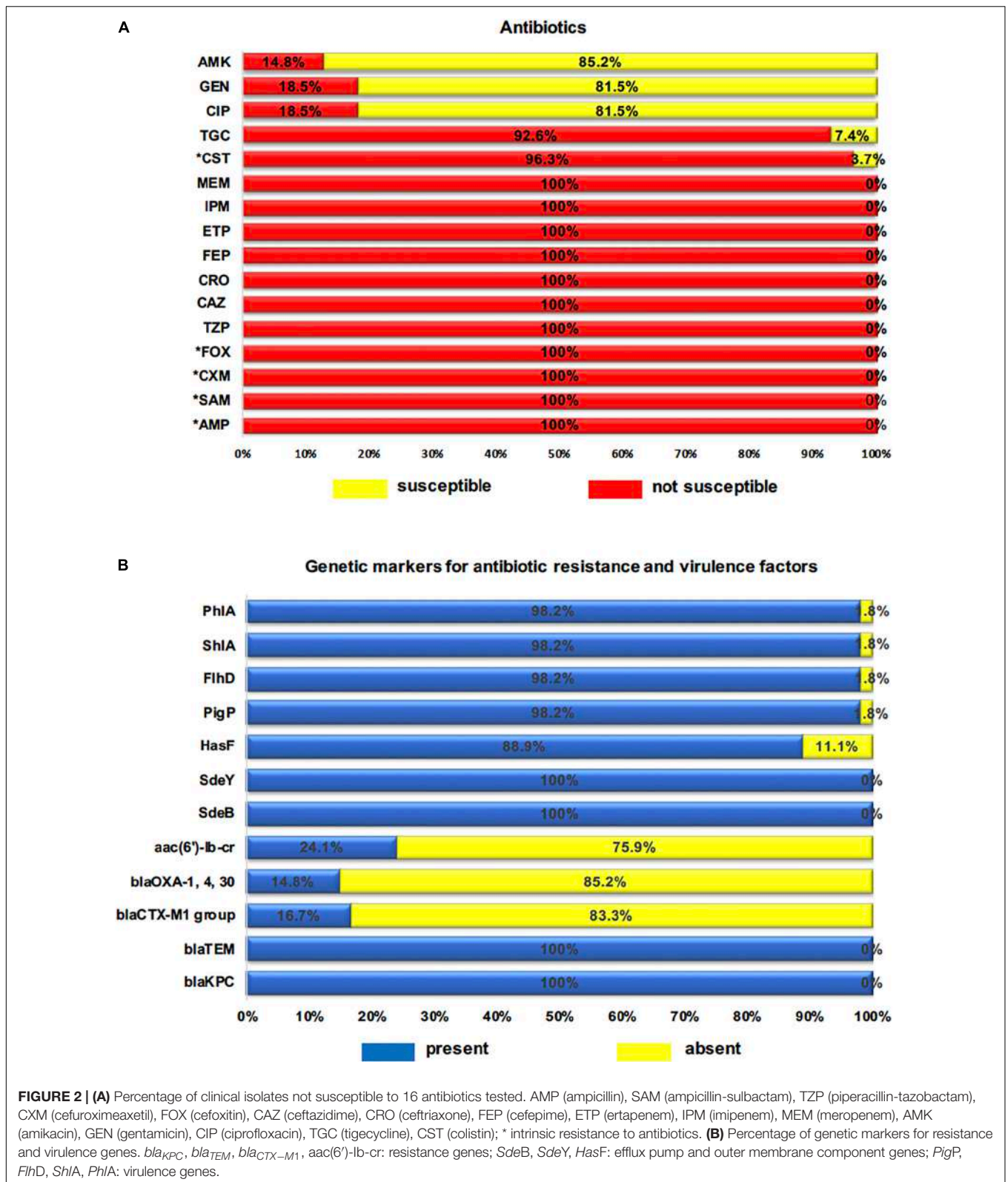


environment (Merkier et al., 2013), and particularly in critically ill patients and neonatal intensive care units (Maragakis et al., 2008). We also observed a significant resistance to colistin and tigecycline in several colonization sites, as shown by a previous study (Silva et al., 2017).

All the *S. marcescens* strains tested here were resistant to  $\beta$ -lactams, including carbapenems antibiotics. Resistance to carbapenems used to be uncommon among *Serratia* species (Stock et al., 2003), but many resistant strains have now emerged throughout the world (Lin et al., 2016). Although few studies have related resistance to carbapenems in *S. marcescens* in Brazil (Milisavljevic et al., 2004; da Costa Guimarães et al., 2013; Ribeiro et al., 2013), Silva et al. (2015) obtained similar results. They have isolated *S. marcescens* resistant to imipenem, meropenem and ertapenem in samples from different infection sites of ICU patients in another Brazilian locality. Both results are troubling. Infections caused by carbapenem-resistant bacteria often do not respond to conventional treatment (Okoche et al., 2015), as produced carbapenemases hydrolyze not only carbapenems but also penicillins, cephalosporins and monobactams

(Queenan and Bush, 2007). The most common carbapenem resistance of *S. marcescens* in Brazil is due to the production of carbapenemases, especially the KPC-2 type (da Costa Guimarães et al., 2013; Ribeiro et al., 2013), that is encoded by the gene *bla*<sub>KPC-2</sub>.

*Enterobacteriaceae*, such as *S. marcescens*, have the genes *bla*<sub>TEM-1</sub> and *bla*<sub>SHV-1</sub>; these genes express classical class A beta-lactamases, encoded by plasmid that hydrolyze first generation penicillins and cephalosporins (Bush, 2010). We found gene *bla*<sub>TEM</sub> in all isolates while gene *bla*<sub>SHV</sub> variants was not detected. It is noteworthy that even though *S. marcescens* also carries the gene *bla*<sub>CTX-M</sub> (Yu et al., 2003; Kim et al., 2005; Tenover et al., 2013), few of our strains had the gene. Some strains also carried the genes *bla*<sub>OXA-1</sub>, 4 and 30, that have been reported in few studies in Brazil or in other countries, either alone or associated with extended spectrum beta-lactamases genes (ESBL) (*bla*<sub>TEM</sub>, *bla*<sub>SHV</sub> e *bla*<sub>CTX-M</sub>) in *S. marcescens* strains. Although there are discrepancies in frequency rate and in genotyping of ESBL-producing *S. marcescens* (Cheng et al., 2006), the observed beta-lactam antibiotic resistance may have also been caused by the genes *bla*<sub>TEM</sub>, *bla*<sub>CTX-M</sub>, and



*bla<sub>OXA</sub>*, since the production of broad-spectrum beta-lactamases enzymes (TEM-1, TEM-2, SHV-1, OXA-1) generate resistant to ampicillin, ticarcillin, piperacillin, piperacillin/tazobactam

and cephalosporin antibiotics, and the enzymes CTX-M have hydrolytic activity against cefotaxime (Levy and Marshall, 2004; Sugumar et al., 2014).



**FIGURE 3 |** Phenotyping and genotyping of *Serratia marcescens* isolates. Sm represents *Serratia marcescens* and numbers represent identifications of strains. \*Sm is classified as multidrug resistant (MDR) strains. AMP (ampicillin), SAM (ampicillin-sulbactam), TZP (piperacillin-tazobactam), CXM (cefuroximeaxetil), FOX (cefotaxim), CAZ (ceftazidime), CRO (ceftriaxone), FEP (cefepime), ETP (ertapenem), IPM (imipenem), MEM (meropenem), AMK (amikacin), GEN (gentamicin), CIP (ciprofloxacin). *Serratia marcescens* are intrinsically resistant to TGC (tigecycline) and CST (colistin). AMP, SAM, CXM, FOX, and CST antibiotics were not included in the MDR classification. The *bla<sub>IMP</sub>*, *bla<sub>OXA-48</sub>*, *bla<sub>NDM</sub>*, *bla<sub>VIM</sub>*, *bla<sub>SHV</sub>* variants and *mcr-1* genes were not detected. Blue box correlates with AMP, SAM, TZP, CXM, FOX, CAZ, CRO, FEP, ETP, IPM, MEM. Green boxes correlate with AMK, GEN, CIP. Multicolored box (*HasF*) correlates with CIP and TGC. Brown box shows number of *S. marcescens* carrying virulence genes.

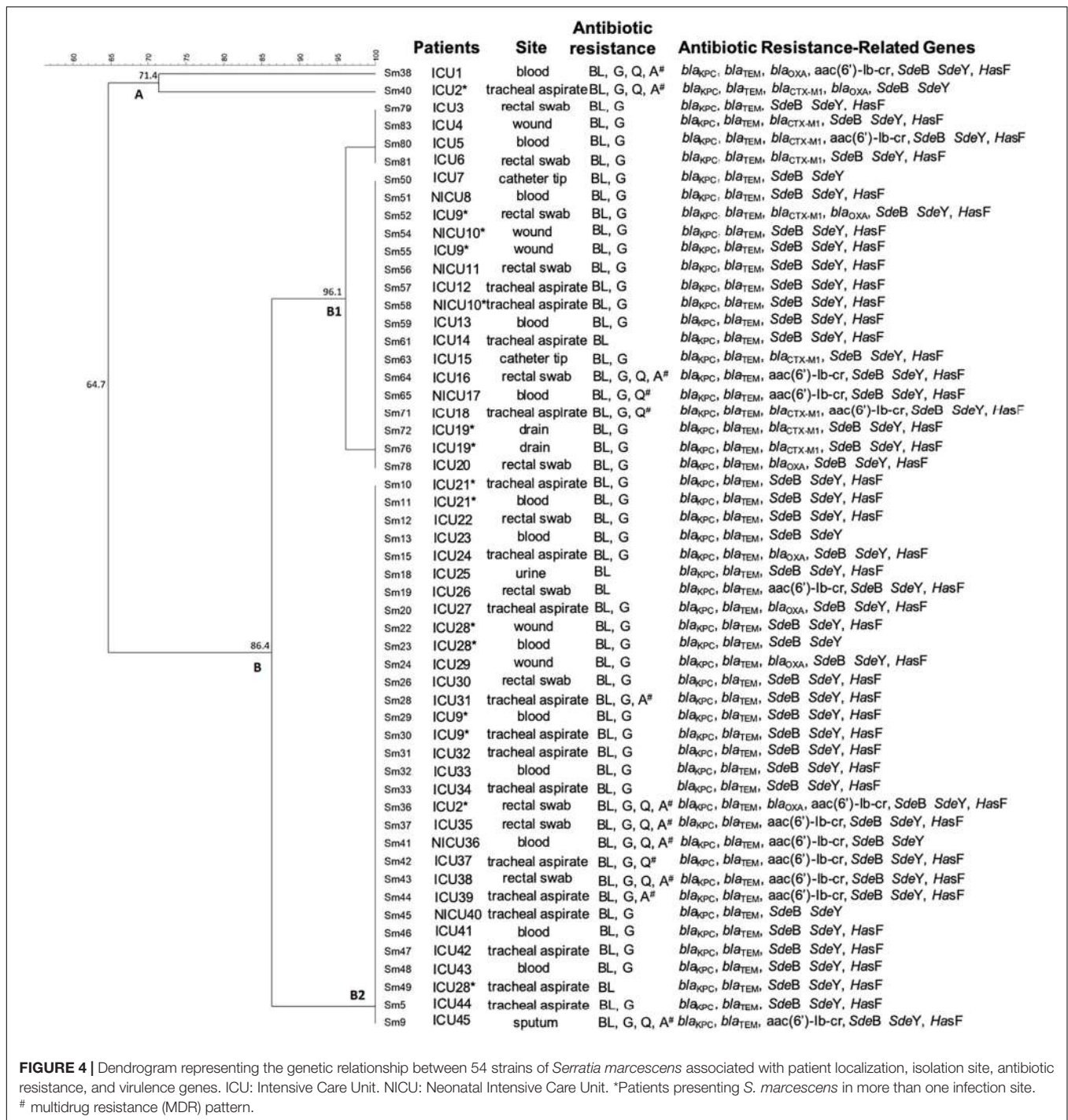
In our study, most strains of *S. marcescens* were only sensitive to aminoglycosides (gentamicin and amikacin) and fluoroquinolone (ciprofloxacin). Aminoglycosides are the oldest antibiotics that have been used less frequently in the last years, thus possibly preserving activity against some resistant bacteria that cause difficult to cure infections (Falagas et al., 2008; Gad et al., 2011). The observed low resistance to ciprofloxacin (18.18%) is in agreement with the results obtained by Sheng et al. (2002) who observed 20–30% resistance to quinolone in *S. marcescens* isolates. However, it is important to consider that *S. marcescens* is highly adaptable, so rates of resistance to fluoroquinolones diverge considerably among institutions (Young et al., 1980; Mahlen, 2011; Sader et al., 2014), including within Brazilian ones.

Resistance to fluoroquinolones may be caused by alterations in the target enzymes DNA gyrase and topoisomerase IV, and

by acquisition of the transferable plasmid-mediated quinolone resistance (PMQR) determinants *qnr*, *qepA*, *aac(6′)-Ib-cr*, and *oqxAB* (Veldman et al., 2011; Poirel et al., 2012; Moradigaravand et al., 2016). The gene *aac(6′)-Ib-cr*, a variant gene of the aminoglycoside acetyltransferase, was also present in most of strains that presented fluoroquinolone and/or aminoglycoside resistance. This finding is consistent with others studies that have shown that *aac(6′)-Ib-cr* may be associated with antibacterial resistance against fluoroquinolone and aminoglycoside (Kim et al., 2009, 2011) antibiotics.

Three RND-type efflux have been reported in *S. marcescens*, namely *SdeAB* (Kumar and Worobec, 2005a), *SdeCDE* (Kumar and Worobec, 2005a; Begic and Worobec, 2008), and *SdeXY* (Chen et al., 2003). *SdeAB* and *SdeXY* interact with *HasF* (an outer membrane component, *TolC* homolog gene) contributing to resistance against a wide variety of antimicrobial agents





**FIGURE 4 |** Dendrogram representing the genetic relationship between 54 strains of *Serratia marcescens* associated with patient localization, isolation site, antibiotic resistance, and virulence genes. ICU: Intensive Care Unit. NICU: Neonatal Intensive Care Unit. \*Patients presenting *S. marcescens* in more than one infection site. # multidrug resistance (MDR) pattern.

(Begic and Worobec, 2008; Hornsey et al., 2010). Although we did not analyze the genes *SdeA* e *SdeX*, the genes *SdeB* and *SdeX* were present in all strains and the gene *HasF* was also found in most strains. Drug extrusion by efflux pumps as *SdeAB-HasF* comprises one of the main mechanisms for fluoroquinolones antibiotic resistance (Dalvi and Worobec, 2012). Additionally, Hornsey et al. (2010) has shown the intrinsic activity of the *SdeXY-HasF* efflux pump is responsible for the lower

susceptibility to ciprofloxacin. Thus, in addition to the presence of the genes *aac*(6′)-Ib-cr [associated with plasmid-mediated quinolone resistance (PMQR)], the genes *SdeB*, *SdeY*, and *HasF* that encode RND-type efflux pump may have contributed to the observed ciprofloxacin resistance.

Our data shows high prevalence of tigecycline-resistant *S. marcescens* strains and *SdeY* and *HasF* genes. The reduced sensitivity of *S. marcescens* to tigecycline may be related to the



up-regulation of the *SdeXY-HasF* efflux pump (Hornsey et al., 2010). Although the gene *SdeX* was not analyzed, our findings strongly suggest that these genes may be responsible for the high tetracycline resistance.

Many bacteria produce virulence factors as hydrolytic enzymes and toxins that enable host invasion, bacterial proliferation and inhibit host defense mechanisms, sometimes resulting in host death (Aggarwal et al., 2017). *S. marcescens* strains were also evaluated for the presence of toxin genes *ShlA* and *phlA*, and all but the *Sm40* strain carried these genes. Our findings are in agreement with other studies that reported the presence these genes in *S. marcescens* (strain SEN) (Aggarwal et al., 2017). *FlhDC* has been proposed as a regulator controlling flagellum biogenesis, biofilm formation, cell septation and expression of virulence factors during swarming (Givskov et al., 1995; Fraser and Hughes, 1999; Chilcott and Hughes, 2000; Lin et al., 2010). In our study, the presence of *FlhC* was not analyzed but the gene *FlhD* was present in almost all isolates. *S. marcescens* produces biosurfactant serrawettin and red pigment prodigiosin used in surfaces colonization (Hejazi and Falkiner, 1997). *PigP* is a positive regulator of prodigiosin production that regulates swarming and hemolysis through serratamolide production (Fineran et al., 2005; Shanks et al., 2013). In our study, *PigP* gene was found in almost all isolates (98.15%). Overall, our results suggest that the combination of these virulence genes could have contributed to the pathogenicity of *S. marcescens* strains.

The dendrogram based on ERIC-PCR fingerprint analysis demonstrated that the vast majority of isolates are closely related, sharing a genetic similarity of 86.4% (except for two strains). In addition, many isolates showed 100% similarity to each other. A study conducted by Ferreira-Firmo et al. (2019) evaluated nine *S. marcescens* from different clinical sources and three hospitals in Northeast Brazil showed a greater genetic diversity among the studied strains. Lin et al. (2016) studied 83 carbapenem-resistant *S. marcescens* isolates recovered from Zhejiang Provincial 501 People's Hospital, China, from which they found 63 blaKPC-2 positive strains sharing nine different profiles. Our results demonstrate the predominance of few genetic profiles grouped together, with similarity above 85%, indicating that, although bacteria have been isolated from different patients and devices, the circulating *S. marcescens* in this hospital is highly genetically related.

Our study has some limitations worth noting. There was a high number of *S. marcescens* isolated from rectal swabs and tracheal aspirate, and both cultures are recommended for surveillance in ICU and NICU patients. However, microbiological reports sent to LACEN were not clear regarding how many of these samples were analyzed for both clinical and surveillance purposes. This study was further limited by the duration of the research, which was relatively short (2014–2015), and by conventional phenotypic and genotypic techniques, that have their own particular strengths and limitations in detecting MDR strains. Nonetheless, we intend to extend the analysis period of *S. marcescens* isolates, and

whole genome sequencing to type relevant MDR strains must be performed. We expect that this study broadens our understanding on epidemiology, antibiotic resistance, and putative virulence factors of these strains, and provides relevant information for the prevention and management of *S. marcescens* infections.

In conclusion, *S. marcescens* represents a problem for public health (Kurz et al., 2003) and the resistance pattern exhibited by clinical isolates along with the transmission to other clones show the importance of researching factors associated with the increase in frequency and/or emergence of infections caused by *S. marcescens* in Brazilian hospitals. The occurrence of antibiotic-resistant bacteria considerably varies according to country, region and susceptible population, and the mitigation of this problem in ICUs is especially associated with actions to control the spreading of such drug-resistant bacteria (Ko et al., 2002; Hou et al., 2015). Thus, it is crucial to eliminate sources of resistance development and associated reservoirs as well as to overtake standardized sanitation and enforce mandatory notification to gather important data for continuous risk assessment evaluation and effective decision making to control these species in hospital environments.

## DATA AVAILABILITY STATEMENT

The datasets generated for this study can be found in the GenBank database. Genes and their respective accession numbers: blaCTX – MK576103; blaKPC – MK576104; blaOXA – MK576105; blaTEM – MK576106; SdeB – MN583232; SdeY – MN583233; HasF – MN583234; aac(6′)-Ib-cr – MN583235; FlhD – MN583236; PigP – MN583237; ShlA – MN583238; PhlA – MN583239. Access to genetic heritage was approved by the National System for the Management of Genetic Heritage (SisGen n° AFF27ED).

## ETHICS STATEMENT

The studies involving human participants were reviewed and approved by the Committee of Ethics in Human Research of the Federal University of São Carlos (no. 1.088.936). In this work, all *Serratia marcescens* and the anonymous archival data related patient age, gender, and sample type were obtained from the Central Laboratory of Public Health of Tocantins (LACEN/TO, data's owner). Permission to conduct the present study was obtained from the Health Department of the State of Tocantins (Secretaria da Saúde do Estado do Tocantins – SESAU) and LACEN/TO. Patient consent was not required, since the data presented in this study do not relate to any specific person or persons. Written informed consent from the participants' legal guardian/next of kin was not required to participate in this study in accordance with the national legislation and the institutional requirements.

## AUTHOR CONTRIBUTIONS

RF, GR, MD, MO-S, MB, and M-CP performed the experiments. FG and EL aided with statistical analysis. EC aided with the sequencing analysis and the sequence submission to the NCBI platform. M-CP conceived and supervised the study. M-CP, AC, IM, and AP-S wrote the manuscript and analyzed the data. MO-S performed ERIC-PCR.

## FUNDING

This work was supported by the Fundação de Amparo a Pesquisa do Estado de São Paulo (FAPESP grants 2020/05699-6 to M-CP and FAPESP grant 2013/22581-5 to AP-S) and Conselho Nacional de Desenvolvimento Científico e Tecnológico (CNPq, grant 2013/485873 to M-CP). This study was partially financed by the Fundação de Amparo à Pesquisa do Estado de São Paulo-Brazil (FAPESP) as a fellowship to MD (FAPESP fellowship 2018/24213-7), and by

## REFERENCES

- Aggarwal, C., Paul, S., Tripathi, V., Paul, B., and Khan, M. A. (2017). Characterization of putative virulence factors of *Serratia marcescens* strain SEN for pathogenesis in *Spodoptera litura*. *J. Invertebr. Pathol.* 143, 115–123. doi: 10.1016/j.jip.2016.12.004
- Anderson, K. F., Lonsway, D. R., Rasheed, J. K., Biddle, J., Jensen, B., McDougal, L. K., et al. (2007). Evaluation of methods to identify the *Klebsiella pneumoniae* Carbapenemase in *Enterobacteriaceae*. *J. Clin. Microbiol.* 45, 2723–2725. doi: 10.1128/JCM.00015-07
- Begic, S., and Worobec, E. A. (2008). Characterization of the *Serratia marcescens* SdeCDE multidrug efflux pump studied via gene knockout mutagenesis. *Can. J. Microbiol.* 54, 411–416. doi: 10.1139/w08-019
- Bush, K. (2010). The coming of age of antibiotics: discovery and therapeutic value. *Ann. N. Y. Acad. Sci.* 1213, 1–4. doi: 10.1111/j.1749-6632.2010.05872.x
- Cao, X., Xu, X., Zhang, Z., Shen, H., Chen, J., and Zhang, K. (2014). Molecular characterization of clinical multidrug-resistant *Klebsiella pneumoniae* isolates. *Ann. Clin. Microbiol. Antimicrob.* 13:16. doi: 10.1186/1476-0711-13-16
- Chen, J., Kuroda, T., Huda, M. N., Mizushima, T., and Tsuchiya, T. (2003). An RND-type multidrug efflux pump SdeXY from *Serratia marcescens*. *J. Antimicrob. Chemother.* 52, 176–179. doi: 10.1093/jac/dkg308
- Cheng, K., Chuang, Y., Wu, L., Huang, G., and Yu, W. (2006). Clinical experiences of the infections caused by extended-spectrum beta-lactamase-producing *Serratia marcescens* at a medical center in Taiwan. *Jpn. J. Infect. Dis.* 59, 147–152.
- Chilcott, G. S., and Hughes, K. T. (2000). Coupling of flagellar gene expression to flagellar assembly in *Salmonella enterica* serovar typhimurium and *Escherichia coli*. *Microbiol. Mol. Biol. Rev.* 64, 694–708. doi: 10.1128/mmr.64.4.694-708.2000
- CLSI (2019). *Performance Standards for Antimicrobial Susceptibility Testing. CLSI Supplement M100*, 29th Edn. Wayne, PA: Clinical and Laboratory Standards Institute.
- Cristina, M. L., Sartini, M., and Spagnolo, A. M. (2019). *Serratia marcescens* Infections in Neonatal Intensive Care Units (NICUs). *Int. J. Environ. Res. Public Health* 16:E610. doi: 10.3390/ijerph16040610
- da Costa Guimarães, A. C., Almeida, A. C. S., Nicoletti, A. G., Vilela, M. A., Gales, A. C., and Morais, M. M. C. (2013). Clonal spread of carbapenem-resistant *Serratia marcescens* isolates sharing an IncK plasmid containing blaKPC-2. *Int. J. Antimicrob. Agents* 42, 369–370. doi: 10.1016/j.ijantimicag.2013.05.017
- Dallenne, C., Da Costa, A., Decre, D., Favier, C., and Arlet, G. (2010). Development of a set of multiplex PCR assays for the detection of genes encoding important

the Coordenação de Aperfeiçoamento de Pessoal de Nível Superior – Brazil (CAPES) – Finance Code 001 as a fellowship to GR, FG, and EC.

## ACKNOWLEDGMENTS

The authors thank the Laboratório Central de Saúde Pública do Tocantins, Palmas, TO, Brazil (LACEN-TO) who kindly provided the *S. marcescens* strains, and to Secretaria de Saúde do Estado do Tocantins (SESAU-TO) for facilitating the development of project.

## SUPPLEMENTARY MATERIAL

The Supplementary Material for this article can be found online at: <https://www.frontiersin.org/articles/10.3389/fmicb.2020.00956/full#supplementary-material>

- $\beta$ -lactamases in *Enterobacteriaceae*. *J. Antimicrob. Chemother.* 65, 490–495. doi: 10.1093/jac/dkp498
- Dalvi, S. D., and Worobec, E. A. (2012). Gene expression analysis of the SdeAB multidrug efflux pump in antibiotic-resistant clinical isolates of *Serratia marcescens*. *Indian J. Med. Microbiol.* 30, 302–307. doi: 10.4103/0255-0857.99491
- David, M. D., Weller, T. M., Lambert, P., and Fraise, A. P. (2006). An outbreak of *Serratia marcescens* on the neonatal unit: a tale of two clones. *J. Hosp. Infect.* 63, 27–33. doi: 10.1016/j.jhin.2005.11.006
- Dawczynski, K., Proquitté, H., Roedel, J., Edel, B., Pfeifer, Y., Hoyer, H., et al. (2016). Intensified colonisation screening according to the recommendations of the German Commission for Hospital Hygiene and Infectious Diseases Prevention (KRINKO): identification and containment of a *Serratia marcescens* outbreak in the neonatal intensive care unit, Jena, Germany, 2013–2014. *Infection* 44, 739–746. doi: 10.1007/s15010-016-0922-y
- Doyle, D., Peirano, G., Lascols, C., Lloyd, T., Church, D. L., and Pitout, J. D. (2012). Laboratory detection of *Enterobacteriaceae* that produce carbapenemases. *J. Clin. Microbiol.* 50, 3877–3880. doi: 10.1128/JCM.02117-12
- Enciso-Moreno, J. A., Pernas-Buitrón, N., Ortiz-Herrera, M., and Coria-Jiménez, R. (2004). Identification of *Serratia marcescens* populations of nosocomial origin by RAPD-PCR. *Arch. Med. Res.* 35, 12–17. doi: 10.1016/j.armed.2003.07.005
- EUCAST (2018). The European Committee on Antimicrobial Susceptibility Testing. 2018. Breakpoint tables for Interpretation of MICs and Zone Diameters. Available online at: [https://www.eucast.org/fileadmin/src/media/PDFs/EUCAST\\_files/Breakpoint\\_tables/v\\_8.1\\_Breakpoint\\_Tables.pdf](https://www.eucast.org/fileadmin/src/media/PDFs/EUCAST_files/Breakpoint_tables/v_8.1_Breakpoint_Tables.pdf)
- Falagas, M. E., Grammatikos, A. P., and Michalopoulos, A. (2008). Potential of old-generation antibiotics to address current need for new antibiotics. *Expert Rev. Anti Infect. Ther.* 6, 593–600. doi: 10.1586/14787210.6.5.593
- Ferreira, R. L., Silva, B. C. M., Rezende, G. S., Nakamura-Silva, R., Pitondo-Silva, A., Campanini, E. B., et al. (2019). High prevalence of multidrug-resistant *Klebsiella pneumoniae* harboring several virulence and  $\beta$ -Lactamase encoding genes in a Brazilian intensive care unit. *Front. Microbiol.* 9:3198. doi: 10.3389/fmicb.2018.03198
- Ferreira-Firmo, E., Beltrão, E. M. B., da Silva, F. R. F., Alves, L. C., Brayner, F. A., Veras, D. L., et al. (2019). Association of blaNDM-1 with blaKPC-2 and aminoglycoside-modifying enzymes genes among *Klebsiella pneumoniae*, *Proteus mirabilis* and *Serratia marcescens* clinical isolates in Brazil. *J. Glob. Antimicrob. Resist.* doi: 10.1016/j.jgar.2019.08.026 [Epub ahead of print].
- Fineran, P. C., Slater, H., Everson, L., Hughes, K., and Salmond, G. P. (2005). Biosynthesis of tripyrrole and beta-lactam secondary metabolites in *Serratia*: integration of quorum sensing with multiple new regulatory

- components in the control of prodigiosin and carbapenem antibiotic production. *Mol. Microbiol.* 56, 1495–1517. doi: 10.1111/j.1365-2958.2005.04660.x
- Fraser, G. M., and Hughes, C. (1999). Swarming motility. *Curr. Opin. Microbiol.* 2, 630–635.
- Gad, G. F., Heba, A., Mohamed, and Hossam, M. A. (2011). aminoglycoside resistance rates, phenotypes, and mechanisms of Gram-negative bacteria from infected patients in upper Egypt. *PLoS One* 6:e17224. doi: 10.1371/journal.pone.0017224
- Gastmeier, P. (2014). *Serratia marcescens*: an outbreak experience. *Front. Microbiol.* 5:81. doi: 10.3389/fmicb.2014.00081
- Gastmeier, P., Loui, A., Stamm-Balderjahn, S., Hansen, S., Zuschneid, I., Sohr, D., et al. (2007). Outbreaks in neonatal intensive care units—they are not like others. *Am. J. Infect. Control* 35, 172–176. doi: 10.1016/j.ajic.2006.07.007
- Ghaith, D. M., Zafer, M. M., Ismail, D. K., Al-Agamy, M. H., Bohol, M. F. F., Al-Qahtani, A., et al. (2018). First reported nosocomial outbreak of *Serratia marcescens* harboring bla IMP-4 and bla VIM-2 in a neonatal intensive care unit in Cairo, Egypt. *Infect. Drug Resist.* 11, 2211–2217. doi: 10.2147/IDR.S174869
- Givskov, M., Eberl, L., Christiansen, G., Benedik, M. J., and Molin, S. (1995). Induction of phospholipase- and flagellar synthesis in *Serratia liquefaciens* is controlled by expression of the flagellar master operon flhD. *Mol. Microbiol.* 15, 445–454. doi: 10.1111/j.1365-2958.1995.tb02258.x
- Hall, T. A. (1999). BioEdit: a user-friendly biological sequence alignment editor and analysis program for Windows 95/98/NT. *Nucleic Acids Symp. Ser.* 41, 95–98.
- Hejazi, A., and Falkiner, F. R. (1997). *Serratia marcescens*. *J. Med. Microbiol.* 46, 903–912.
- Herra, C., and Falkiner, F. R. (2018). *Serratia marcescens*. In: *Antimicrobe Microbes*. Available online at: <http://www.antimicrobe.org/b26.asp> (accessed June 8, 2019).
- Hornsey, M., Ellington, M. J., Doumith, M., Hudson, S., Livermore, D. M., and Woodford, N. (2010). Tigecycline resistance in *Serratia marcescens* associated with up-regulation of the SdeXY-HasF efflux system also active against ciprofloxacin and cefpirome. *J. Antimicrob. Chemother.* 65, 479–482. doi: 10.1093/jac/dkp475
- Hou, X. H., Song, X. Y., Ma, X. B., Zhang, S. Y., and Zhang, J. Q. (2015). Molecular characterization of multidrug-resistant *Klebsiella pneumoniae* isolates. *Braz. J. Microbiol.* 46, 759–768. doi: 10.1590/S1517-838246320140138
- Jeon, J., Lee, J., Lee, J., Park, K., Karim, A., Lee, C., et al. (2015). Structural basis for carbapenem-hydrolyzing mechanisms of carbapenemases conferring antibiotic resistance. *Int. J. Mol. Sci.* 16, 9654–9692. doi: 10.3390/ijms16059654
- Kim, E. S., Jeong, J. Y., Jun, J. B., Choi, S. H., Lee, S. O., Kim, M. N., et al. (2009). Prevalence of aac(6)-Ib-cr encoding a ciprofloxacin-modifying enzyme among *Enterobacteriaceae* blood isolates in Korea. *Antimicrob. Agents Chemother.* 53, 2643–2645. doi: 10.1128/AAC.01534-08
- Kim, J., Lim, Y.-M., Jeong, Y.-S., and Seol, S.-Y. (2005). Occurrence of CTX-M-3, CTX-M-15, CTX-M-14, and CTX-M-9 Extended-Spectrum  $\beta$ -Lactamases in *Enterobacteriaceae* Clinical Isolates in Korea. *Antimicrob. Agents Chemother.* 49, 1572–1575. doi: 10.1128/AAC.49.4.1572-1575.2005
- Kim, S. B., Jeon, Y. D., Kim, J. H., Kim, J. K., Ann, H. W., Choi, H., et al. (2015). Risk factors for mortality in patients with *Serratia marcescens* bacteremia. *Yonsei Med. J.* 56:348. doi: 10.3349/yjm.2015.56.2.348
- Kim, Y. T., Jang, J. H., Kim, H. C., Kim, H., Lee, K. R., Park, K. S., et al. (2011). Identification of strain harboring both aac(6)-Ib and aac(6)-Ib-cr variant simultaneously in *Escherichia coli* and *Klebsiella pneumoniae*. *BMB Rep.* 4, 262–266. doi: 10.5483/BMBRep.2011.44.4.262
- Ko, W. C., Paterson, D. L., Sagnimeni, A. J., Hansen, D. S., Von Gottberg, A., Mohapatra, S., et al. (2002). Community-acquired *Klebsiella pneumoniae* bacteremia: global differences in clinical patterns. *Emerg. Infect. Dis.* 8, 160–166. doi: 10.3201/eid0802.010025
- Krishnan, P. U., Pereira, B., and Macaden, R. (1991). Epidemiological study of an outbreak of *Serratia marcescens* in a haemodialysis unit. *J. Hosp. Infect.* 18, 57–61. doi: 10.1016/0195-6701(91)90093-n
- Kumar, A., and Worobec, E. A. (2005a). Cloning, sequencing, and characterization of the SdeAB multidrug efflux pump of *Serratia marcescens*. *Antimicrob. Agents Chemother.* 49, 1495–1501. doi: 10.1128/AAC.49.4.1495-1501.2005
- Kumar, A., and Worobec, E. A. (2005b). HasF, a TolC-homolog of *Serratia marcescens*, is involved in energy-dependent efflux. *Can. J. Microbiol.* 51, 497–500. doi: 10.1139/w05-029
- Kurz, C. L., Chauvet, S., Andrès, E., Aurouze, M., Vallet, I., Michel, G. P., et al. (2003). Virulence factors of the human opportunistic pathogen *Serratia marcescens* identified by in vivo screening. *EMBO J.* 22, 1451–1460. doi: 10.1093/emboj/cdg159
- Levy, S. B., and Marshall, B. (2004). Antibacterial resistance worldwide: causes, challenges and responses. *Nat. Med.* 10, S122–S129. doi: 10.1038/nm1145
- Li, H., and Li, J. B. (2005). Detection of five novel CTX-M-type extended spectrum  $\beta$ -lactamases with one to three CTX-M-14 point mutations in isolates from Hefei, Anhui province, China. *J. Clin. Microbiol.* 43, 4301–4302. doi: 10.1128/JCM.43.8.4301-4302.2005
- Lin, C. S., Horng, J. T., Yang, C. H., Tsai, Y. H., Su, L. H., Wei, C. F., et al. (2010). RssAB-FlhDC-ShlBA as a major pathogenesis pathway in *Serratia marcescens*. *Infect. Immun.* 78, 4870–4881. doi: 10.1128/IAI.00661-10
- Lin, X., Hu, Q., Zhang, R., Hu, Y., Xu, X., and Lv, H. (2016). Emergence of *Serratia marcescens* isolates possessing carbapenem-hydrolysing  $\beta$ -lactamase KPC-2 from China. *J. Hosp. Infect.* 94, 65–67. doi: 10.1016/j.jhin.2016.04.006
- Liou, B. H., Duh, R. W., Lin, Y. T., Lauderdale, T. L., and Fung, C. P. (2014). Taiwan surveillance of antimicrobial resistance (TSAR) hospitals. *J. Microbiol. Immunol. Infect.* 47, 387–393. doi: 10.1016/j.jmii.2013.04.003
- Liu, Y. Y., Wang, Y., Walsh, T. R., Yi, L. X., Zhang, R., Spencer, J., et al. (2015). Emergence of plasmid mediated colistin resistance mechanism MCR-1 in animals and human beings in China: a microbiological and molecular biological study. *Lancet Infect. Dis.* 16, 161–168. doi: 10.1016/S1473-3099(15)00424-7
- Magiorakos, A.-P., Srinivasan, A., Carey, R. B., Carmeli, Y., Falagas, M. E., Giske, C. G., et al. (2012). Multidrug-resistant, extensively drug-resistant and pandrug-resistant bacteria: an international expert proposal for interim standard definitions for acquired resistance. *Clin. Microbiol. Infect.* 18, 268–281. doi: 10.1111/j.1469-0691.2011.03570.x
- Mahlen, S. D. (2011). *Serratia* infections: from military experiments to current practice. *Clin. Microbiol. Rev.* 24, 755–791. doi: 10.1128/CMR.00017-11
- Maragakis, L. L., Winkler, A., Tucker, M. G., Cosgrove, S. E., Ross, T., Lawson, E., et al. (2008). Outbreak of multidrug-resistant *Serratia marcescens* infection in a neonatal intensive care unit. *Infect. Control Hosp. Epidemiol.* 29, 418–423. doi: 10.1086/587969
- Marschall, J., Tibbetts, R. J., Dunne, W. M., Frye, J. G., Fraser, V. J., and Warren, D. K. (2009). Presence of the KPC carbapenemase gene in *Enterobacteriaceae* causing bacteremia and its correlation with in vitro carbapenem susceptibility. *J. Clin. Microbiol.* 47, 239–241. doi: 10.1128/JCM.02123-08
- Martineau, C., Li, X., Lalancette, C., Perreault, T., Fournier, E., Tremblay, J., et al. (2018). *Serratia marcescens* outbreak in a neonatal intensive care unit: new insights from next-generation sequencing applications. *J. Clin. Microbiol.* 56:e00235-18. doi: 10.1128/JCM.00235-18
- Martins, A. F., Zavascki, A. P., Gaspareto, P. B., and Barth, A. L. (2007). Dissemination of *Pseudomonas aeruginosa* producing SPM-1-like and IMP-1-like metallo- $\beta$ -lactamases in hospitals from southern Brazil. *Infection* 35, 457–460. doi: 10.1007/s15010-007-6289-3
- Merkier, A. K., Rodríguez, C., Togneri, A., Brengi, S., Osuna, C., and Pichel, M. (2013). Outbreak of a cluster with epidemic behavior due to *Serratia marcescens* after colistin administration in a hospital setting. *J. Clin. Microbiol.* 51, 2295–2302. doi: 10.1128/JCM.03280-12
- Milislavjevic, V., Wu, F., Larson, E., Rubenstein, D., Ross, B., Drusin, L. M., et al. (2004). Molecular epidemiology of *Serratia marcescens* outbreaks in two neonatal intensive care units. *Infect. Control Hosp. Epidemiol.* 25, 719–721. doi: 10.1086/502466
- Miriagou, V., Cornaglia, G., Edelstein, M., Galani, I., Giske, C. G., Gniadkowski, M., et al. (2010). Acquired carbapenemases in Gram-negative bacterial pathogens: detection and surveillance issue. *Clin. Microbiol. Infect.* 16, 112–122. doi: 10.1111/j.1469-0691.2009.03116.x
- Mitra, S., Mukherjee, S., Naha, S., Chattopadhyay, P., Dutta, S., and Basu, S. (2019). Evaluation of co-transfer of plasmid-mediated fluoroquinolone resistance genes and bla NDM gene in *Enterobacteriaceae* causing neonatal septicaemia. *Antimicrob. Resist. Infect. Control* 8:46. doi: 10.1186/s13756-019-0477-7
- Montagnani, C., Cocchi, P., and Lega, L. (2015). *Serratia marcescens* outbreak in a neonatal intensive care unit: crucial role of implementing hand hygiene among external consultants. *BMC Infect. Dis.* 15:11. doi: 10.1186/s12879-014-0734-6
- Moradigaravand, D., Boinett, C. J., Martin, V., Peacock, S. J., and Parkhill, J. (2016). Recent independent emergence of multiple multidrug-resistant *Serratia*



- marcescens* clones within the United Kingdom and Ireland. *Genome Res.* 26, 1101–1109. doi: 10.1101/gr.205245.116.Freely
- Mostatabi, N., Farshad, S., and Ranjbar, R. (2013). Molecular evaluations of extended spectrum  $\beta$ -lactamase producing strains of *Serratia* isolated from blood samples of the patients in Namazi Hospital, Shiraz, Southern Iran. *Iran. J. Microbiol.* 5, 328–333.
- Naas, T., Cuzon, G., Villegas, M.-V., Lartigue, M.-F., Quinn, J. P., and Nordmann, P. (2008). Genetic structures at the origin of acquisition of the beta-lactamase bla KPC gene. *Antimicrob. Agents Chemother.* 52, 1257–1263. doi: 10.1128/AAC.01451-07
- Nordmann, P., Naas, T., and Poirel, L. (2011). Global Spread of Carbapenemase-producing *Enterobacteriaceae*. *Emerg. Infect. Dis.* 17, 1791–1798. doi: 10.3201/eid1710.110655
- O'Horo, J., Mahler, S. B., Gardner, B., and Barbari, E. F. (2017). *Serratia* and Surgical Site Infections: risk factors and Epidemiology. *Open Forum Infect. Dis.* 4, S650–S650. doi: 10.1093/ofid/ofx163.1730
- Okoche, D., Asimwe, B. B., Katabazi, F. A., Kato, L., and Najjuka, C. F. (2015). Prevalence and characterization of carbapenem-resistant *Enterobacteriaceae* Isolated from Mulago National Referral Hospital, Uganda. *PLoS One* 10:e0135745. doi: 10.1371/journal.pone.0135745
- Phan, H. T. T., Stoesser, N., Maciucă, I. E., Toma, F., Szekele, E., Flonta, M., et al. (2018). Illumina short-read and MinION long-read WGS to characterize the molecular epidemiology of an NDM-1 *Serratia marcescens* outbreak in Romania. *J. Antimicrob. Chemother.* 73, 672–679. doi: 10.1093/jac/dkx456
- Platell, J. L., Cobbold, R. N., Johnson, J. R., Heisig, A., Heisig, P., Clabots, C., et al. (2011). Commonality among fluoroquinolone-resistant sequence type ST131 extraintestinal *Escherichia coli* isolates from humans and companion animals in Australia. *Antimicrob. Agents Chemother.* 55, 3782–3787. doi: 10.1128/AAC.00306-11
- Poirel, L., Cattoir, V., and Nordmann, P. (2012). Plasmid-mediated quinolone resistance; interactions between Human, Animal, and Environmental Ecologies. *Front. Microbiol.* 3:24.
- Poirel, L., Dortet, L., Bernabeu, S., and Nordmann, P. (2011). Genetic features of blaNDM-1-Positive *Enterobacteriaceae*. *Antimicrob. Agents Chemother.* 55, 5403–5407. doi: 10.1128/AAC.00585-11
- Queenan, A. M., and Bush, K. (2007). Carbapenemases: the Versatile betalactamases. *Clin. Microbiol. Rev.* 20, 440–458. doi: 10.1128/CMR.00001-07
- Rawat, D., and Nair, D. (2010). Extended-spectrum  $\beta$ -lactamases in gram negative bacteria. *J. Glob. Infect. Dis.* 2, 263–274. doi: 10.4103/0974-777X.68531
- Raymond, J., and Aujard, Y. (2000). Nosocomial infections in pediatric patients: a European, multicenter prospective study. European study group. *Infect. Control Hosp. Epidemiol.* 21, 260–263. doi: 10.1086/501755
- Ribeiro, P. C. S., Monteiro, A. S., Marques, S. G., Monteiro, S. G., Monteiro-Neto, V., Coqueiro, M. M. M., et al. (2016). Phenotypic and molecular detection of the blaKPC gene in clinical isolates from inpatients at hospitals in São Luis, MA, Brazil. *BMC Infect. Dis.* 16:737. doi: 10.1186/s12879-016-2072-3
- Ribeiro, V. B., Andrade, L. N., Linhares, A. R., Barin, J., Darini, A. L. D. C., Zavascki, A. P., et al. (2013). Molecular characterization of *Klebsiella pneumoniae* carbapenemase-producing isolates in southern Brazil. *J. Med. Microbiol.* 62, 1721–1727. doi: 10.1099/jmm.0.062141-0
- Sader, H. S., Farrell, D. J., Flamm, R. K., and Jones, R. N. (2014). Antimicrobial susceptibility of Gram-negative organisms isolated from patients hospitalized in intensive care units in United States and European hospitals (2009–2011). *Diagn. Microbiol. Infect. Dis.* 78, 443–448. doi: 10.1016/j.diagmicrobio.2013.11.025
- Salini, R., and Pandian, S. K. (2015). Interference of quorum sensing in urinary pathogen *Serratia marcescens* by *Anethum graveolens*. *Pathog. Dis.* 73:ftv038. doi: 10.1093/femspd/ftv038
- Sandner-Miranda, L., Vinuesa, P., Cravioto, A., and Morales-Espinosa, R. (2018). The genomic basis of intrinsic and acquired antibiotic resistance in the genus *Serratia*. *Front. Microbiol.* 9:828. doi: 10.3389/fmicb.2018.00828
- Seeyave, D., Desai, N., Miller, S., Rao, S. P., and Piecuch, S. (2006). Fatal delayed transfusion reaction in a sickle cell anemia patient with *Serratia marcescens* sepsis. *J. Natl. Med. Assoc.* 98, 1697–1699.
- Shanks, R. M. Q., Lahr, R. M., Stella, N. A., Arena, K. E., Brothers, K. M., Kwak, D. H., et al. (2013). A *Serratia marcescens* PigP homolog controls prodigiosin biosynthesis, swarming motility and hemolysis and is regulated by cAMP-CRP and HexS. *PLoS One* 8:e57634. doi: 10.1371/journal.pone.0057634
- Sheng, W. H., Chen, Y. C., Wang, J. T., Chang, S. C., Luh, K. T., and Hsieh, W. C. (2002). Emerging fluoroquinolone-resistance for common clinically important gram-negative bacteria in Taiwan. *Diagn. Microbiol. Infect. Dis.* 43, 141–147. doi: 10.1016/S0732-8893(02)00381-4
- Silva, D. D. C., Rampelotto, R. F., Lorenzoni, V. V., Santos, S. O. D., Damer, J., Hörner, M., et al. (2017). Phenotypic methods for screening carbapenem-resistant *Enterobacteriaceae* and assessment of their antimicrobial susceptibility profile. *Rev. Soc. Bras. Med. Trop.* 50, 173–178. doi: 10.1590/0037-8682-0471-2016
- Silva, K. E., Cayó, R., Carvalhaes, C. G., Sacchi, F. P. C., Rodrigues-Costa, F., Da Silva, A. C. R., et al. (2015). Coproduction of KPC-2 and IMP-10 in Carbapenem-Resistant *Serratia marcescens* isolates from an outbreak in a Brazilian teaching hospital. *J. Clin. Microbiol.* 53, 2324–2328. doi: 10.1128/JCM.00727-15
- Srinivasan, R., Mohankumar, R., Kannappan, A., Karthick Raja, V., Archunan, G., Karutha Pandian, S., et al. (2017). Exploring the anti-quorum sensing and antibiofilm efficacy of phytol against *Serratia marcescens* associated acute pyelonephritis infection in Wistar rats. *Front. Cell. Infect. Microbiol.* 7:498. doi: 10.3389/fcimb.2017.00498
- Stock, I., Grueger, T., and Wiedemann, B. (2003). Natural antibiotic susceptibility of strains of *Serratia marcescens* and the *S. liquefaciens* complex: *S. liquefaciens* sensu stricto, *S. proteamaculans* and *S. grimesii*. *Int. J. Antimicrob. Agents* 22, 35–47. doi: 10.1016/s0924-8579(02)00163-2
- Sugumar, M., Kumar, K. M., Manoharan, A., Anbarasu, A., and Ramaiah, S. (2014). Detection of OXA-1  $\beta$ -lactamase gene of *Klebsiella pneumoniae* from blood stream infections (BSI) by conventional PCR and in-silico analysis to understand the mechanism of OXA mediated resistance. *PLoS One* 9:e91800. doi: 10.1371/journal.pone.0091800
- Tenover, F. C., Canton, R., Kop, J., Chan, R., Ryan, J., Weir, F., et al. (2013). Detection of Colonization by Carbapenemase-Producing Gram-Negative Bacilli in Patients by Use of the Xpert MDRO Assay. *J. Clin. Microbiol.* 51, 3780–3787. doi: 10.1128/JCM.01092-13
- Tzouveleki, L. S., Markogiannakis, A., Psychogiou, M., Tassios, P. T., and Daikos, G. L. (2012). Carbapenemases in *Klebsiella pneumoniae* and Other *Enterobacteriaceae*: an Evolving Crisis of Global Dimensions. *Clin. Microbiol. Rev.* 25, 682–707. doi: 10.1128/CMR.05035-11
- Ulu-Kilic, A., Parkan, O., Ersoy, S., Koc, D., Percin, D., Onal, O., et al. (2013). Outbreak of postoperative empyema caused by *Serratia marcescens* in a thoracic surgery unit. *J. Hosp. Infect.* 85, 226–229. doi: 10.1016/j.jhin.2013.07.008
- Us, E., Kutlu, H. H., Tekeli, A., Ocal, D., Cirpan, S., and Memikoglu, K. O. (2017). Wound and soft tissue infections of *Serratia marcescens* in patients receiving wound care: a health care-associated outbreak. *Am. J. Infect. Control* 45, 443–447. doi: 10.1016/j.ajic.2016.11.015
- Veldman, K., Cavaco, L. M., Mevius, D., Battisti, A., Franco, A., Botteldoorn, N., et al. (2011). International collaborative study on the occurrence of plasmid-mediated quinolone resistance in *Salmonella enterica* and *Escherichia coli* isolated from animals, humans, food and the environment in 13 European countries. *J. Antimicrob. Chemother.* 66, 1278–1286. doi: 10.1093/jac/dk084
- Versalovic, J., Schneider, M., De Bruijn, F. J., and Lupski, J. R. (1994). Genomic fingerprinting of bacteria using repetitive sequence-based polymerase chain reaction. *Meth. Mol. Cell. Biol.* 5, 25–40. doi: 10.1128/JCM.43.1.199-207.2005
- Vetter, L., Schuepfer, G., Kuster, S. P., and Rossi, M. (2016). A Hospital-wide Outbreak of *Serratia marcescens*, and Ishikawa's "Fishbone" Analysis to Support Outbreak Control. *Qual. Manag. Health Care* 25, 1–7. doi: 10.1097/QMH.0000000000000078
- von Wintersdorff, C. J., Penders, J., van Niekerk, J. M., Mills, N. D., Majumder, S., van Alphen, L. B., et al. (2016). Dissemination of antimicrobial resistance in microbial ecosystems through horizontal gene transfer. *Front. Microbiol.* 19:173. doi: 10.3389/fmicb.2016.00173
- Wong, M. H., Chan, E. W., Liu, L. Z., and Chen, S. (2014). PMQR genes *oxqAB* and *aac(6)Ib-cr* accelerate the development of fluoroquinolone resistance in *Salmonella typhimurium*. *Front. Microbiol.* 5:521. doi: 10.3389/fmicb.2014.00521
- Xiong, S., Li, T., Xu, Y., and Li, J. (2007). Detection of CTX-M-14 extended-spectrum  $\beta$ -lactamase in *Shigella sonnei* isolates from China. *J. Infect.* 55, e125–e128. doi: 10.1016/j.jinf.2007.07.017



- Yan, B. C., Westfall, B. A., and Orlean, P. (2001). Ynl038wp (Gpi15p) is the *Saccharomyces cerevisiae* homologue of human Pig-Hp and participates in the first step in glycosylphosphatidylinositol assembly. *Yeast* 18, 1383–1389. doi: 10.1002/yea.783
- Yoon, H. J., Choi, J. Y., Park, Y. S., Kim, C. O., Kim, J. M., Yong, D. E., et al. (2005). Outbreaks of *Serratia marcescens* bacteriuria in a neurosurgical intensive care unit of a tertiary care teaching hospital: a clinical, epidemiologic, and laboratory perspective. *Am. J. Infect. Control* 33, 595–601. doi: 10.1016/j.ajic.2005.01.010
- Young, V. M., Moody, M. R., and Morris, M. J. (1980). Distribution of *Serratia marcescens* serotypes in cancer patients. *J. Med. Microbiol.* 13, 333–339. doi: 10.1099/00222615-13-2-333
- Yu, W. L., Lin, C. W., and Wang, D. Y. (1998). *Serratia marcescens* bacteremia: clinical features and antimicrobial susceptibilities of the isolates. *J. Microbiol. Immunol. Infect.* 31, 171–179.
- Yu, W. L., Wu, L. T., Pfaller, M. A., Winokur, P. L., and Jones, R. N. (2003). Confirmation of extended-spectrum beta-lactamase-producing *Serratia marcescens*: preliminary report from Taiwan. *Diagn. Microbiol. Infect. Dis.* 45, 221–224. doi: 10.1016/s0732-8893(02)00539-4
- Zingg, W., Soulake, I., Baud, D., Huttner, B., Pfister, R., Renzi, G., et al. (2017). Management and investigation of a *Serratia marcescens* outbreak in a neonatal unit in Switzerland - the role of hand hygiene and whole genome sequencing. *Antimicrob. Resist. Infect. Control* 6:125. doi: 10.1186/s13756-017-0285-x

**Conflict of Interest:** The authors declare that the research was conducted in the absence of any commercial or financial relationships that could be construed as a potential conflict of interest.

Copyright © 2020 Ferreira, Rezende, Damas, Oliveira-Silva, Pitondo-Silva, Brito, Leonardez, Góes, Campanini, Malavazi, da Cunha and Pranchevicius. This is an open-access article distributed under the terms of the Creative Commons Attribution License (CC BY). The use, distribution or reproduction in other forums is permitted, provided the original author(s) and the copyright owner(s) are credited and that the original publication in this journal is cited, in accordance with accepted academic practice. No use, distribution or reproduction is permitted which does not comply with these terms.



# Prediction of Antimicrobial Resistance in Gram-Negative Bacteria From Whole-Genome Sequencing Data

Pieter-Jan Van Camp<sup>1,2</sup>, David B. Haslam<sup>3,4</sup> and Aleksey Porollo<sup>2,4,5\*</sup>

<sup>1</sup> Department of Biomedical Informatics, University of Cincinnati, Cincinnati, OH, United States, <sup>2</sup> Division of Biomedical Informatics, Cincinnati Children's Hospital Medical Center, Cincinnati, OH, United States, <sup>3</sup> Division of Infectious Diseases, Cincinnati Children's Hospital Medical Center, Cincinnati, OH, United States, <sup>4</sup> Department of Pediatrics, University of Cincinnati, Cincinnati, OH, United States, <sup>5</sup> Center for Autoimmune Genomics and Etiology, Cincinnati Children's Hospital Medical Center, Cincinnati, OH, United States

## OPEN ACCESS

### Edited by:

Leonardo Neves de Andrade,  
University of São Paulo, Brazil

### Reviewed by:

Brock Aaron Arivett,  
Middle Tennessee State University,  
United States  
Zhi Ruan,  
Zhejiang University, China

### \*Correspondence:

Aleksey Porollo  
Aleksey.Porollo@cchmc.org

### Specialty section:

This article was submitted to  
Antimicrobials, Resistance  
and Chemotherapy,  
a section of the journal  
Frontiers in Microbiology

**Received:** 30 January 2020

**Accepted:** 24 April 2020

**Published:** 25 May 2020

### Citation:

Van Camp P-J, Haslam DB and  
Porollo A (2020) Prediction  
of Antimicrobial Resistance  
in Gram-Negative Bacteria From  
Whole-Genome Sequencing Data.  
*Front. Microbiol.* 11:1013.  
doi: 10.3389/fmicb.2020.01013

**Background:** Early detection of antimicrobial resistance in pathogens and prescription of more effective antibiotics is a fast-emerging need in clinical practice. High-throughput sequencing technology, such as whole genome sequencing (WGS), may have the capacity to rapidly guide the clinical decision-making process. The prediction of antimicrobial resistance in Gram-negative bacteria, often the cause of serious systemic infections, is more challenging as genotype-to-phenotype (drug resistance) relationship is more complex than for most Gram-positive organisms.

**Methods and Findings:** We have used NCBI BioSample database to train and cross-validate eight XGBoost-based machine learning models to predict drug resistance to cefepime, cefotaxime, ceftriaxone, ciprofloxacin, gentamicin, levofloxacin, meropenem, and tobramycin tested in *Acinetobacter baumannii*, *Escherichia coli*, *Enterobacter cloacae*, *Klebsiella aerogenes*, and *Klebsiella pneumoniae*. The input is the WGS data in terms of the coverage of known antibiotic resistance genes by shotgun sequencing reads. Models demonstrate high performance and robustness to class imbalanced datasets.

**Conclusion:** Whole genome sequencing enables the prediction of antimicrobial resistance in Gram-negative bacteria. We present a tool that provides an *in silico* antibiogram for eight drugs. Predictions are accompanied with a reliability index that may further facilitate the decision making process. The demo version of the tool with pre-processed samples is available at <https://vancampn.shinyapps.io/wgs2amr/>. The stand-alone version of the predictor is available at <https://github.com/pieterjanvc/wgs2amr/>.

**Keywords:** antimicrobial resistance, antibiotic resistance, whole-genome sequencing, machine learning, prediction, genotype-phenotype relationship

**Abbreviations:** AB, antibiotic; ABR, antibiotic resistance; ARG, antibiotic resistance gene; ARGc, antibiotic resistance gene cluster; MCC, Matthew's correlation coefficient; MIC, minimum inhibitory concentration; WGS, whole genome sequencing.

## INTRODUCTION

Since the discovery and widespread use of antibiotics (AB) in the early 20th century, resistance to those same AB has generally developed rapidly; often even within the first years of introduction (Marston et al., 2016). As a consequence, many bacteria have developed antibiotic resistance (ABR) to most of the major classes of AB, often seen in the Gram-negatives (Centers for Disease Control and Prevention, 2018). Effective treatment of these infections requires knowledge of the organism's susceptibility to the various AB, currently obtained by culturing bacteria in the clinical laboratory and subsequent testing for commonly used AB. Depending on the pathogen, this process may require 72 h or more. Drug susceptibility is usually reported to the clinician as either resistant or susceptible (sometimes intermediate is also used) with cut-offs based on the minimum inhibitory concentration (MIC) of an AB needed to halt growth or kill the pathogen in the lab. In serious systemic infections, early treatment with an effective antibiotic is paramount as unexpected resistance may lead to treatment failure, while fear of inadequate therapy may drive overly broad antibiotic use which contributes to extensively resistant and potentially untreatable bacteria (Marston et al., 2016).

With decreasing cost and increasing speed of high-throughput sequencing technology such as whole genome sequencing (WGS), in-depth analysis of pathogens is increasingly used in clinical decision-making. Studies already showed the potential of these techniques in ABR prediction in single, Gram-positive pathogens like *Staphylococcus aureus* and *Mycobacterium tuberculosis*. An example is the Mykrobe predictor that maps DNA sequencing data to a reference genome and a set of plasmid genes conferring ABR (Bradley et al., 2015). The model also accounts for polymorphism in select loci when predicting drug resistance. Data analysis and prediction is rapid, enabling it as a practical tool for clinical care during the decision-making process. PhyResSE is another tool that follows a similar strategy but may process data in minutes to a few days, attributing such time extension to more careful variant calling (Feuerriegel et al., 2015). Both tools report high accuracy of ABR prediction. However, their application to other pathogens like Gram-negative bacteria has not been described.

The prediction of ABR in Gram-negative bacteria, often the cause of serious systemic infections, is more challenging as the source of drug resistance is more complicated. For example, Gram-negative pathogens may possess one or more  $\beta$ -lactamases with similar amino acid sequences but various activity against  $\beta$ -lactam-based AB (Livermore, 1998). They are also more likely to develop mutations that result in lower membrane permeability, or increase the expression of a variety of genes for excreting xenobiotics (efflux pumps) and for inactivating  $\beta$ -lactam-targeting drugs (Marston et al., 2016). There have been a few clinical predictors reported for assessing the risk of infection with resistant Gram-negative bacteria but they solely rely on data from the electronic health record and just predict the likelihood of infection with a resistant strain rather than individual drug resistance (Martin et al., 2013; Vasudevan et al., 2014). Thus far, only a handful of studies were published

on the prediction of Gram-negative resistance using WGS data. These models were built for individual species, such as *Neisseria gonorrhoeae* or *Klebsiella pneumoniae*, and were based on small sample sizes resulting in poor predictive accuracy (Eyre et al., 2017; Nguyen et al., 2018). A more extensive study recently published by Drouin et al. (2019) utilizes 107 machine-learning-based models, trained on WGS data, to predict ABR in 12 bacterial species, including six Gram-negatives, against a variety of AB with generally high accuracy. These models were trained without incorporating prior ABR knowledge as they were based on nucleotide k-mers from sequenced genomes of these pathogens, thus utilizing information from non-coding regions and polymorphism. Furthermore, their methodology produced small, human-interpretable decision trees, when the k-mers are mapped back to the respective genomes to make decisions interpretable (provided that k-mers belong to annotated genomic regions). However, the study was performed on heavily imbalanced datasets, while reporting only two-class accuracy, which could overestimate the real performance. Finally, isolates with intermediate resistance were excluded from the final predictors making the performance estimates on such samples uncertain. For more details on the bioinformatics approaches to the AMR analysis and prediction, the reader can refer to a recent review (Van Camp et al., 2020).

In this work, we present a machine learning-based method for the fast estimation of ABR in 5 Gram-negative species for 8 AB. The models were trained on WGS data and laboratory confirmed drug susceptibility. All isolates were assigned to either of two classes (susceptible or resistant) and subsequently used in the training and validation of binary predictors. Each model was evaluated using multiple performance measures. The presented workflow could inform early clinical decision-making on the choice of AB therapy (within a day) while waiting for the final antibiogram (typically 2–4 days) thereby decreasing the time to start effective therapy. A web-based demo application to show the potential clinical implementation is publicly available at <https://vancampn.shinyapps.io/wgs2amr/>. The stand-alone tool can be freely downloaded from <https://github.com/pieterjanvc/wgs2amr/>.

## MATERIALS AND METHODS

### Pathogens and Antibiotics of Interest

This study focused on five common nosocomial Gram-negative organisms that can cause sepsis (Vincent, 2003; Couto et al., 2007): *Acinetobacter baumannii*, *Escherichia coli*, *Enterobacter cloacae*, *Klebsiella aerogenes*, and *Klebsiella pneumoniae*. These specific Gram-negative pathogens were chosen because, in addition to clinical relevance, they are the most represented in terms of DNA-sequenced and AMR annotated samples available at NCBI. For machine learning, the larger the dataset to train on, the more accurate and generalized model can be achieved. *E. cloacae* is the major representative of *Enterobacter* species and therefore part of ESKAPE pathogens. Their antibiotic susceptibility was evaluated for cefepime, cefotaxime, ceftriaxone, ciprofloxacin, gentamicin, levofloxacin, meropenem,

and tobramycin. This panel of AB covers those most commonly used to treat Gram-negative bacterial infections. Consequently, these AB are most frequently tested for susceptibility against bacterial isolates.

## Public Data Collection

Meta-data for 6564 bacterial samples (isolates) were retrieved from the NCBI BioSample database using the “antibiogram” keyword filter. Of these, 4933 samples had the required information, such as bacterium name, antibiogram, and sequencing data accession number. For this work, all “intermediate” ABR levels were converted to “resistant” to project data to a binary classification problem (i.e., resistant versus susceptible). The list was subsequently refined to only include the bacteria and AB of interest (see section “Pathogens and antibiotics of interest”) resulting in 2516 samples. Given the resistance to AB was highly imbalanced in the data (mostly skewed toward resistant phenotype), the samples were randomly chosen so that the number of susceptible, and resistant isolates for each antibiotic was as equal as possible in order to balance the input for machine learning models. This resulted in a final total of 946 samples (**Supplementary Table S1**). Of these, 3% of samples available for each species (total  $n = 31$ ) were set aside to create a demo dataset to showcase the online application (see section “Preliminary pipeline implementation and evaluation” for details). The remaining 915 samples were used to build and evaluate eight XGBoost-based models, where available data for each antibiotic were randomly split in 70% training and 30% testing subsets. The overall flow of data collection is summarized in **Figure 1**. The counts of samples per species include: *A. baumannii* – 256; *E. cloacae* – 67; *E. coli* – 330; *K. aerogenes* – 51; and *K. pneumoniae* – 211. Of note, we did not stratify samples by different bacterial species during the model training as we intended our models to be species independent. **Table 1** shows the distribution of the 915 samples through the AB of interest.

Whole genome sequencing data for all samples were retrieved from the NCBI Sequence Read Archive (SRA) using the SRA toolkit (SRA Toolkit Development Team, 2019). In case multiple runs (SRR) of a sample (SRS) were available (e.g., sample was run through different sequencers or with different settings), the file

**TABLE 1** | Summary of the 915 samples used to build and evaluate antimicrobial resistance prediction models.

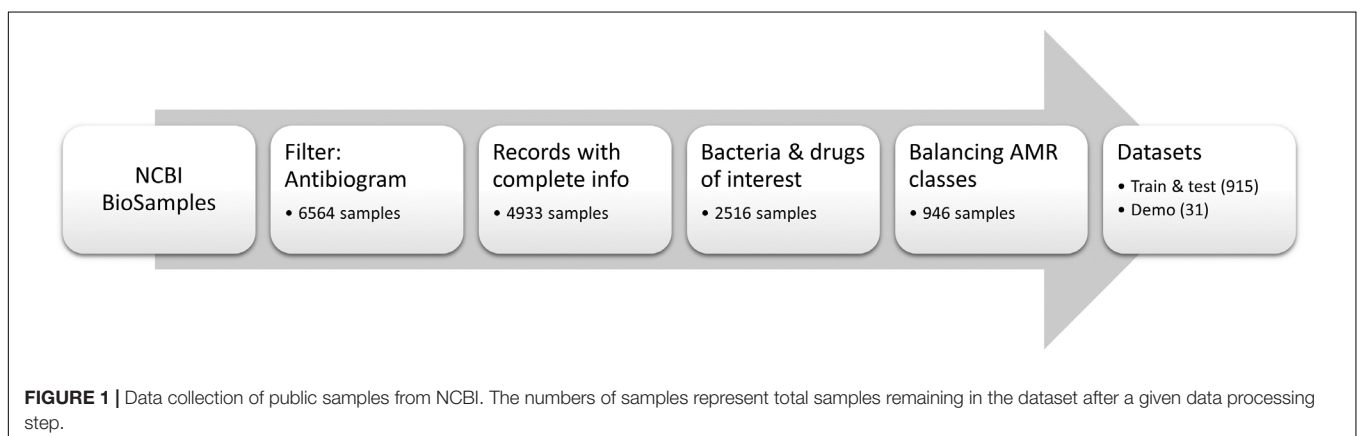
Antibiotic	Resistant	Susceptible	Total
Cefepime	442	275	717
Cefotaxime	437	50	487
Ceftriaxone	671	133	804
Ciprofloxacin	577	335	912
Gentamicin	351	542	893
Levofloxacin	471	258	729
Meropenem	332	420	752
Tobramycin	354	320	674

\*Note that not all samples were tested for every antibiotic, thus the counts per AB do not add up to 915.

with the smallest size was selected. Smaller file size may frequently be attributed to lower sequencing depth and/or shorter shotgun reads. We reasoned that, if a model is able to make predictions on smaller sequence files, it will most likely be applicable to larger files with better gene coverage. List of all samples used can be found in **Supplementary Table S1**.

## In-House Dataset of Samples

Gram-negative bacterial pathogens were collected from blood or urine of patients hospitalized at Cincinnati Children’s Hospital Medical Center (CCHMC), 19 samples total. Organisms were identified to the species level and antimicrobial susceptibility testing was performed using the VITEK® 2 machine (Biomérieux) in the Diagnostic Infectious Diseases Testing Laboratory at CCHMC. Samples represent *A. baumannii* ( $n = 1$ ), *E. coli* ( $n = 11$ ), *K. aerogenes* ( $n = 2$ ), and *K. pneumoniae* ( $n = 3$ ). No in-house samples are available with *E. cloacae*. Two available samples of *Klebsiella oxytoca* are included. DNA was extracted from overnight liquid broth cultures using the QIAamp PowerFecal DNA Kit (Qiagen Inc, Germantown, MD, United States). Sequencing libraries were generated using the Nextera XT kit (Illumina Corporation, San Diego, CA, United States). Pooled libraries were sequenced on a NextSeq 500 (Illumina Corporation, San Diego, CA, United States) in the Microbial Genomics and Metagenomics Laboratory at





CCHMC using paired 150 bp reads to a depth of approximately 5 million reads per sample. Sample collection was approved by the Institutional Review Board (IRB) at CCHMC (IRB approval # 2016–9424: Molecular Epidemiology of Bacterial Infections). The in-house samples are available at the NCBI BioSample database (BioProject ID: PRJNA587095), where detailed metadata can be found (see **Supplementary Table S1** for sample IDs). Of note, the antimicrobial susceptibility testing with VITEK takes at least 72 h and generally requires a pure isolate, whereas sequencing preparation followed by the WGS data analysis can be completed under 48 h and does not rely on a pure colony (Scaggs Huang et al., 2019).

## Analysis of WGS Data

The sequencing files in the FASTQ format were aligned to 4579 antibiotic resistance genes (ARG) found in the NCBI Bacterial Antimicrobial Resistance Reference Gene Database (NCBI Accession: PRJNA313047, version as of September 26, 2018) using DIAMOND (Buchfink et al., 2015), a greatly improved version of BLASTx (Altschul et al., 1990) with regards to speed, and on par sensitivity. Given the same ARG can be present in multiple species (e.g., plasmid DNA), no filtering was performed based on original bacterium in which the ARG was sequenced. The default settings of DIAMOND were used to map shotgun reads to ARGs.

Antibiotic resistance genes coverage ( $C$ ) within a sample was quantified as follows. First, reads aligned by DIAMOND were discarded if the alignment to the gene covered <90% of the read's length or yielded <90% sequence identity. Second, a gene was discarded if all aligned reads covered <90% of its length (i.e., protein sequence). The cutoff was chosen as being suboptimal after probing 70, 80, 90, and 100% coverage (**Supplementary Table S2**). If a gene was retained in the hit list, the number of alignments ( $n$ ) was adjusted for gene length (i.e., the number of amino acids,  $L$ ), and sequencing depth (i.e., total number of reads in the file divided by  $10^7$ ,  $D$ ). Such scaled data (Eq. 1) are better suitable for the machine learning.

$$C = \frac{n}{L \times D} \quad (1)$$

## Clustering Similar Antibiotic Resistance Genes

Many of the ARG in the NCBI database have a high sequence similarity (e.g., polymorphism in strains or sequences derived from closely related species) that cannot be discriminated by the alignment techniques used in this study. Therefore, antibiotic resistance gene clusters (ARGC) were created using the cluster\_fast module of the USEARCH algorithm (Edgar, 2010) to group genes with  $\geq 90\%$  sequence identity together, naming them after the most representative gene as defined by USEARCH (i.e., cluster centroid). This threshold for grouping was chosen as a suboptimal compromise between balancing the number of genes per cluster, performance of the model, and the biological relevance of the genes grouped together (**Supplementary Table S3**). For cutoffs lower 85%, genes from different ABR classes started to group together, hence such cutoffs

were excluded from consideration. The clustering resulted in the reduction of the potential input space for the machine learning models from 4579 ARG to 1027 ARGC, with 410 clusters (40%) consisting of just a single gene. To represent the coverage of each ARGC, the average coverage (Eq. 1) of all ARG detected in this ARGC was taken. Finally, of the 1027 ARGC, only 152 were found in our data and thereby used for subsequent machine learning.

## Building and Evaluating Machine Learning Models

Regression models are less stable on datasets where the input space is large, sparse, and the features are correlated (e.g., in the context of this work, drug resistance may be exerted by multiple ARGC; Farrar and Glauber, 1967; Devika et al., 2016). Using penalized regression (e.g., LASSO and Ridge regression) to reduce both the input space and select most important features can help increase performance of the model, but it still operates on the premise that input features are uncorrelated. In correlated datasets, feature selection will be distorted in this process resulting in less reliable model interpretation. Decision trees, on the other hand, inherently perform better in such cases as correlation does not influence the feature selection process (Piramuthu, 2008). In random forest models, hundreds to thousands of these trees are built, each with different subset of the input space, resulting in a more robust reporting of important features. Neural networks (NN), especially their currently popular application to deep learning, and require much larger training data-sets (tens of thousands to millions of input vectors/samples) than currently available for antimicrobial resistance (hundreds of samples) in order to demonstrate benefits of deep learning. Moreover, the resulting NN-based models represent a black box that would be difficult to dissect in order to see the decision making rules and factors influencing the decision (Van Camp et al., 2020).

XGBoost is an extreme gradient booster for decision trees that is capable of handling correlated inputs. It has innate support for sparse datasets (in our case, only a handful of ARGC are present in each sample) and can extract important features to provide additional insights in the decision-making process (Chen and Guestrin, 2016). Although XGBoost supports multi-class classification (i.e., model can choose between more than two classes), our samples can have resistance to multiple AB at the same time (i.e., multi-labeling classification), which is not supported and thus a separate, independent binomial model (resistance versus susceptible) was created for each antibiotic of interest (8 models total).

The input for each model was the list of ARGC and their presence ( $C > 0$ ) or absence ( $C = 0$ ) in each sample (Eq. 1). The output was binomial with label *resistant* ( $= 1$ ) or *susceptible* ( $= 0$ ) to the antibiotic of interest. The XGBoost models were trained with a learning rate of 0.1, maximum tree depth of 2, training subsampling of 0.8, and column subsampling of 0.8. All other parameters were kept default. The algorithm was run for a maximum of 300 iterations, but early stopping was done when no improvement was seen in 50 consecutive iterations using 10-fold cross-validation.

Despite the efforts to balance the number of samples with susceptible and resistant phenotypes per drug the final distributions on individual AB remained unbalanced (**Table 1**) because each sample was not tested for all drugs of interest. For two most imbalanced drugs, cefotaxime and ceftriaxone, an under-sampling was performed to reach 3:1 ratio and prevent the model overfitting toward the over-represented class. For heavily class-imbalanced data, standard performance measures like sensitivity or 2-class accuracy could overestimate the true performance. The Matthew's correlation coefficient (MCC) was therefore used as a more stringent performance statistic (Eq. 2). MCC measures binary classification in unbalanced datasets with range from -1 (inverse prediction) through 0 (random prediction) to 1 (perfect prediction).

$$\text{MCC} = \frac{TP * TN - FP * FN}{\sqrt{(TP + FP)(TP + FN)(TN + FP)(TN + FN)}} \quad (2)$$

where *TP*, *TN*, *FP*, and *FN* are true positive, true negative, false positive, and false negative instances, respectively.

For complete performance evaluation, two-class accuracy (*Acc*, Eq. 3), sensitivity (recall, *R*), precision (*P*), specificity (*Sp*), areas under ROC (*AUC*), and precision-recall (*PR-AUC*) curves are also provided.

$$\text{Acc} = \frac{TP + TN}{TP + FP + TN + FN} \quad (3)$$

where *Acc* is a two-class accuracy; *TP*, *TN*, *FP*, and *FN* are the same as in Eq. 2.

## Reliability Index

To provide an additional assessment how certain the prediction is by a given model, we introduce a reliability index (RI). The RI is based on the observation that in classification models values closer to extremes (0 or 1) are more likely to yield a correct prediction compared to values hovering around 0.5. Using adjusted model output (AMO, Eq. 4), we computed a misclassification rate (MR, Eq. 5) for every AMO in the test subset of each model, defined as the percentage of incorrect predictions in test cases with AMO equal or higher than a given cutoff (Eq. 5). A regression model was fit to this MR distribution for each drug and then was used to calculate the MR for new model outputs (**Supplementary Figure S1**). The RI is the inverse of the MR and simply defined as 1 - MR.

$$\text{AMO}(x) = \begin{cases} x & , x \geq 0.5 \\ 1 - x & , x < 0.5 \end{cases} \quad (4)$$

$$\text{MR}(c) = \frac{\text{fp} + \text{fn}}{\text{tp} + \text{fp} + \text{tn} + \text{fn}} \quad (5)$$

where *tp*, *fp*, *tn*, and *fn* are the number of true positive, false positive, true negative, and false negative instances, respectively, predicted with  $\text{AMO} \geq c$ .

## Feature Importance

XGBoost, being a random forest-based algorithm, can provide important features from the model once it has been built in order

to evaluate the individual feature impact in the decision-making process. In our case, XGBoost lists the most important ARGC for each model. By design, random-forest-based algorithms ignore strongly correlated features while using only one in the model, as adding redundant features will not provide extra discrimination capabilities (see section "Building and evaluating machine learning models"). From a biology standpoint, however, it is interesting to know all the ARGC that occur in high frequency. Thus, when the most important features are extracted from the models, we reviewed the correlated features ARGC as well.

In consideration that organism(s)/strain(s) composition in the sample should not be known *a priori*, whereas *de novo* genome assembly may be inefficient and inaccurate, no genome assembly from WGS data is conducted in this work. Therefore, the prediction model is agnostic to the source of the detected antimicrobial gene, as to whether it is inherent to an organism or acquired via mobile genetic element (plasmid). Hence, no weighting scheme for plasmid-derived genes was considered for the model.

## Preliminary Pipeline Implementation and Evaluation

The long term goal of this project is to build a platform where prediction models like the ones presented here can be used in research or clinical practice to quickly estimate a bacterium's antibiogram from WGS data with sufficient accuracy, in order to inform early decisions about the correct AB use while awaiting the final antibiogram.

For illustration of developed models, an R-Shiny web-based application was developed where pre-processed samples from two datasets unseen in training (31 public, demo dataset, and 19 in-house samples, sections "Public data collection" and "In-house dataset of samples") can be individually submitted to the prediction models and subsequently compared to their actual ABR status. Furthermore, the application allows the user to explore the performance of the current ABR models in more detail, and review the important genes used in the decision-making process.

## RESULTS

### Data Collection and Pre-processing

After the processing and filtering (sections "Analysis of WGS data" and "Clustering similar antibiotic resistance genes"), of the 4579 ARG in the NCBI database 2605 (57%) were detected in at least one of the 946 samples. When clustered, only 152 ARGC (15%) were detected in the whole dataset. The median number of ARGC present in any sample is 10 resulting in a very sparse dataset. **Table 2** lists the most frequently found ARGC per species.

To review correlation between the 152 ARGC, a hierarchical clustering using Ward's algorithm (Ward, 1963) was performed (**Figure 2A**). An example of the strong correlation between several specific ARGC can be seen in **Figure 2B**. Even though some of the clusters have similar names, they represent different subtypes of the same gene (i.e., different enough in sequence to be placed in separate clusters, section "Clustering

**TABLE 2** | Most common antibiotic resistance gene clusters per species detected from the WGS data.

Species (Total samples)	Most common gene (% occurrence)	Second most common gene (% occurrence)
<i>A. baumannii</i> (264)	Class C beta-lactamase ADC-98 (98.5)	OXA-51 family carbapenem-hydrolyzing class D beta-lactamase OXA-561 (98.5)
<i>E. coli</i> (341)	Class C extended-spectrum beta-lactamase EC-18 (99.4)	Aminoglycoside O-phosphotransferase APH(3'')-Ib (51.3)
<i>E. cloacae</i> (70)	Multidrug efflux RND transporter permease subunit OqxB21 (92.2)	Fosfomycin resistance glutathione transferase FosA2 (78.6)
<i>K. aerogenes</i> (53)	Multidrug efflux RND transporter permease subunit OqxB21 (100.0)	FosA family fosfomycin resistance glutathione transferase (100.0)
<i>K. pneumoniae</i> (218)	FosA family fosfomycin resistance glutathione transferase (100.0)	Class A beta-lactamase SHV-200 (96.3)

\*The occurrence refers to the percentage of samples, stratified by species, where a given ARG is found in the WGS data.

similar antibiotic resistance genes"). The full table with all ARG pairwise correlation values can be found in supplements (Supplementary Table S4).

## XGBoost Model Training and Testing

Since sparse input in machine learning models can bias performance (both under- or overestimating) depending on the split in training and testing data (Wu et al., 2013), we trained 51 independent models for each antibiotic (polling isolates of all species together). Each model was trained and validated with a different split in order to see the performance distribution (refer to Supplementary Figure S2 for the overall flow of model training). Figure 3 shows the distribution of AUC based on the testing subset for each individual split. The model with the median performance over all 51 splits for each antibiotic (represented by the thick line in the boxplots) is assumed to be the closest to real-life performance (i.e., the least biased) and was chosen as the final model. The performance of these final models are detailed in Table 3 and Figure 4 (see Supplementary Table S5 for the performance of all other models).

## Feature Importance

Regardless of fluctuations in model performance based on split in training and testing, the important features ARG extracted from the models appeared to be largely the same per antibiotic prediction. Table 4 shows the 5 most important ARG (on average over the 51 models) for each ABR prediction model. The full table can be found in the supplements (Supplementary Table S6).

As mentioned in section "Feature importance", once a feature is chosen for the use in the decision-making, random forest-based methods often ignore other highly correlated features as they do not contribute to class discrimination. However, in the context of this study, when unused ARG may provide additional biological

**TABLE 3** | Performance of final ABR prediction models.

Antibiotic	Acc	R	P	Sp	MCC	AUC	PR-AUC
Cefepime	0.82	0.86	0.86	0.77	0.62	0.89	0.92
Cefotaxime	0.83	0.93	0.86	0.53	0.52	0.80	0.92
Ceftriaxone	0.84	0.93	0.87	0.56	0.55	0.88	0.96
Ciprofloxacin	0.81	0.86	0.85	0.73	0.60	0.89	0.94
Gentamicin	0.91	0.90	0.89	0.93	0.82	0.96	0.95
Levofloxacin	0.81	0.87	0.84	0.70	0.58	0.89	0.94
Meropenem	0.89	0.82	0.92	0.94	0.78	0.94	0.94
Tobramycin	0.95	0.92	0.98	0.98	0.90	0.97	0.98

insights, we list all ARG, chosen by the models and those correlated, in supplemental materials (Supplementary Table S4).

## Comparison With Other Algorithms

XGBoost models were compared with those based on LASSO and Ridge regression, which also can deal with data sparsity and have built-in feature selection (Supplementary Table S7). In 6–7 (depending on the metric to compare) out of 8 AB, XGBoost models appear to be slightly better than linear regression models. The real advantage of XGBoost over the linear regression algorithms is the robustness in the important feature selection. Table 5 in conjunction with Supplementary Table S6 demonstrate that XGBoost yields the best consistency in selecting top informative features compared to LASSO and Ridge regression models.

## Reliability Indexes

Figure 5 shows distributions of the RI for each final model based on the corresponding testing set. While there is no unified cut-off for RI across all models, there is a clear trend that correct predictions tend to have a higher RI.

## Practical Implementation of Models

Demo dataset (section "Preliminary pipeline implementation and evaluation") is used to illustrate how new unseen samples could be run through the pipeline of preprocessing and subsequent prediction by the 8 models (Figure 6). For a given sample, each antibiotic is assigned a binary resistance prediction with a confidence (reliability index). For demonstration purposes, current implementation retrieves meta-data information for a given sample, such as species name (a header of the table), and known drug resistance status (last colored column).

Figure 6 shows how prediction results on novel samples could be presented to the clinician in the format of an antibiogram. The online application provides a more intuitive way to explore the results and use of this pipeline. The predicted antibiograms from all extra samples (the Demo set based on public samples and the In-house dataset) can be explored in detail, and an additional tab (not shown) provides more information about the models and the important features. The summary of all predictions for Demo and In-house datasets can be found in Figure 7. The web-based demonstration and stand-alone versions of the application can be found at <https://vancampn.shinyapps.io/wgs2amr/> and <https://github.com/pieterjanvc/wgs2amr/>, respectively.

## DISCUSSION

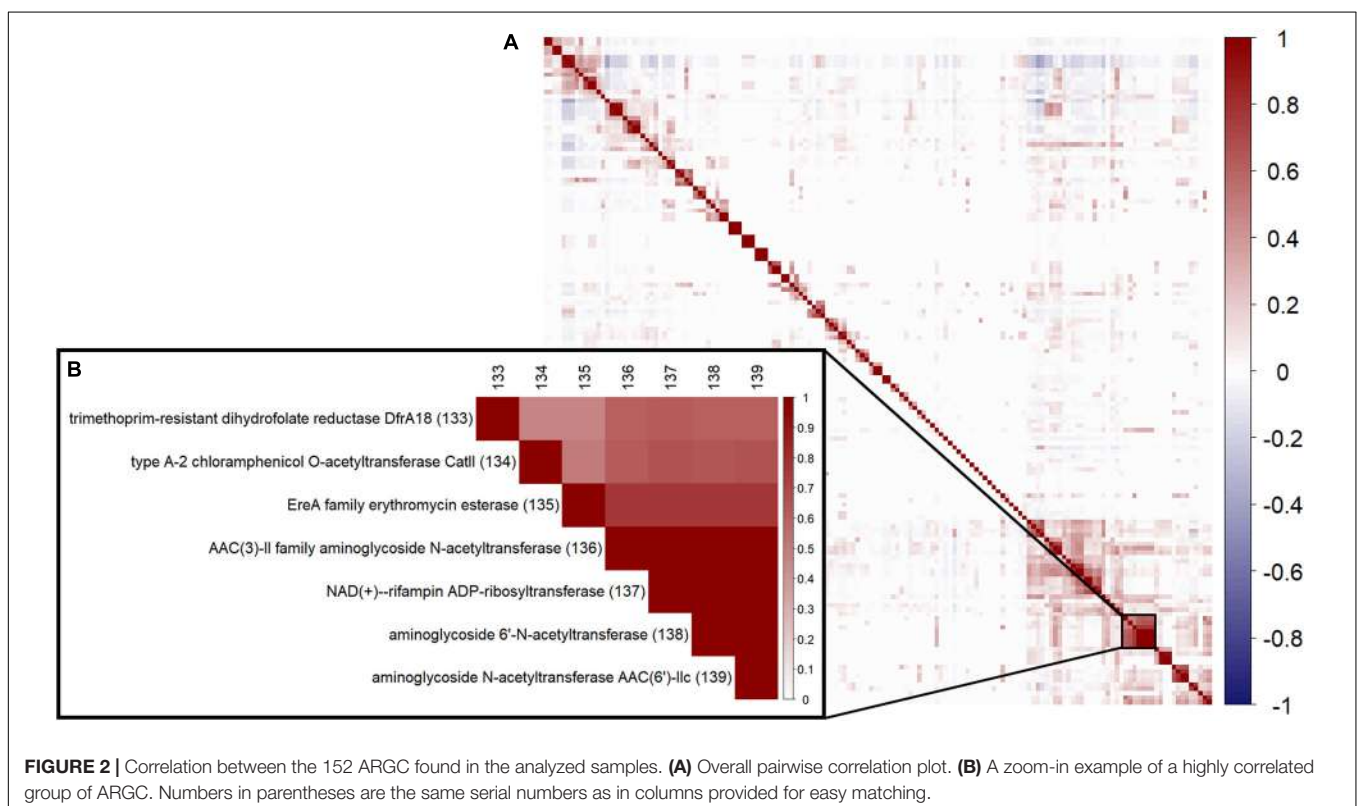
This work provides a framework wherein bacterial samples can be tested quickly to obtain a preliminary antibiogram to guide initial antibiotic selection for treatment. Culturing bacteria and getting a full antibiogram can take 2–4 days, whereas WGS and the computational pipeline presented here only takes around a day. At present, sequencing is taking up the majority of time but is likely to decrease significantly with the improvements in sequencing technologies.

Presenting the results as an early antibiogram estimate (**Figure 6**) instead of just individual predictions, provides clinicians with a clear and intuitive way to inform the choice of the otherwise empiric initial AB. The general resistance pattern of the whole antibiogram can be informative in itself, even if there may still be errors in individual predictions. The latter is further aided by the addition of the RI that indicates how certain the models are on individual predictions. While there is not a single clear cut for the RI, **Figures 5, 7** suggest that the majority of samples assessed with a high RI appear to have correct predictions. All of this helps early, informed AB choice that can decrease the time to start effective AB therapy while limiting the use of empiric broad-spectrum AB and slowing the development of new resistant strains. The predictions could become especially helpful in settings where resources do not permit the use of a full microbiology lab (e.g., in developing countries). Upcoming technologies, like the Nanopore MinION, (Z) (2019), will allow clinicians in the near future to sequence pathogens with smaller

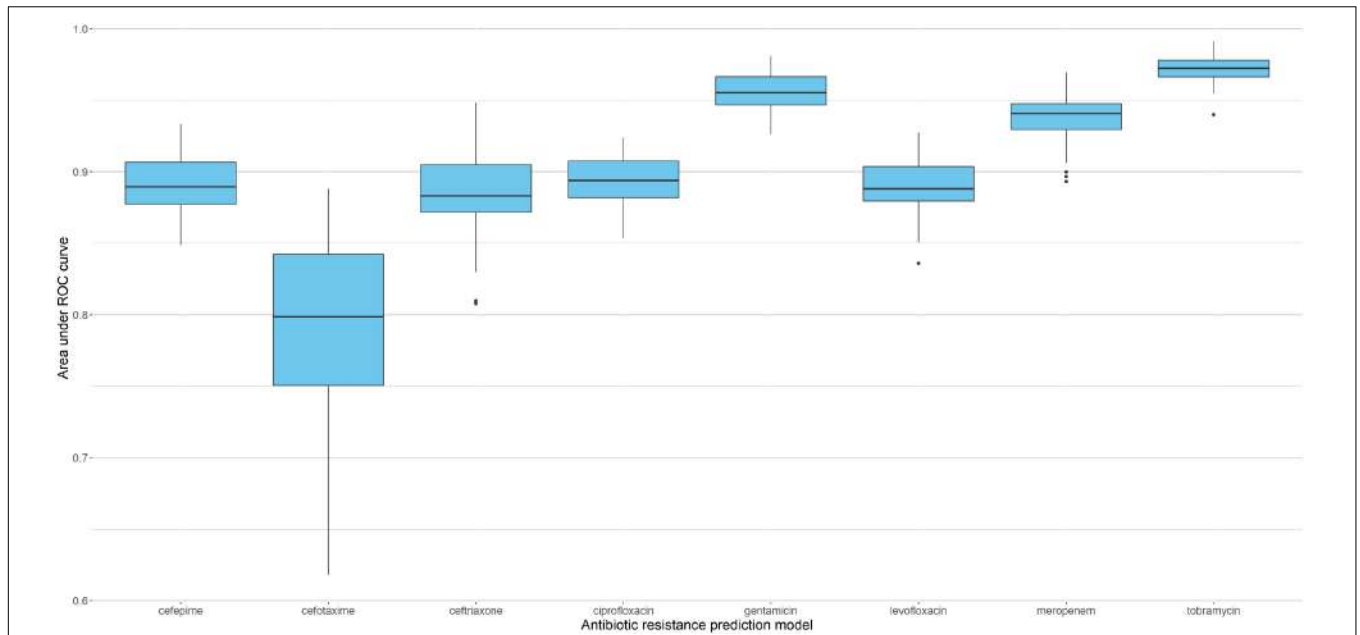
portable devices. This, coupled with analytical pipelines like the one presented here, could provide valuable information on pathogen resistance that would otherwise not be available. Regardless, the results will require clinical judgment.

All pathogens have several ARGC that are found in nearly every sample, regardless of its resistance status to the tested AB (e.g., *class C extended-spectrum beta-lactamase EC-18* cluster was detected in 99% of *E. coli* isolates, **Table 2**). This underlines that Gram-negatives have no easy one-to-one genotype-phenotype relationship for some ARG as their presence does not equal resistance *per se*. A well-studied example of this is the *AmpC* gene, which is expressed in many species or strains, even those fully susceptible to AB (Bajaj et al., 2016). The complex relationships between the ARG and phenotype dictated the application of more complex machine learning algorithms, such as random forest (the basis of XGBoost). An additional advantage of XGBoost is that it provides a glimpse into its decision-making process by reporting the list of features ARGC most often used when building the model as a proxy for key decisions. The downside of this simplification is that caution is warranted when interpreting these features. Finally, given that the datasets are sparse, models are prone to having to rely on different features depending on the split in training and testing. The higher the consistency in selecting important features across different independent models, the more robust the final model is anticipated to be (**Table 5**).

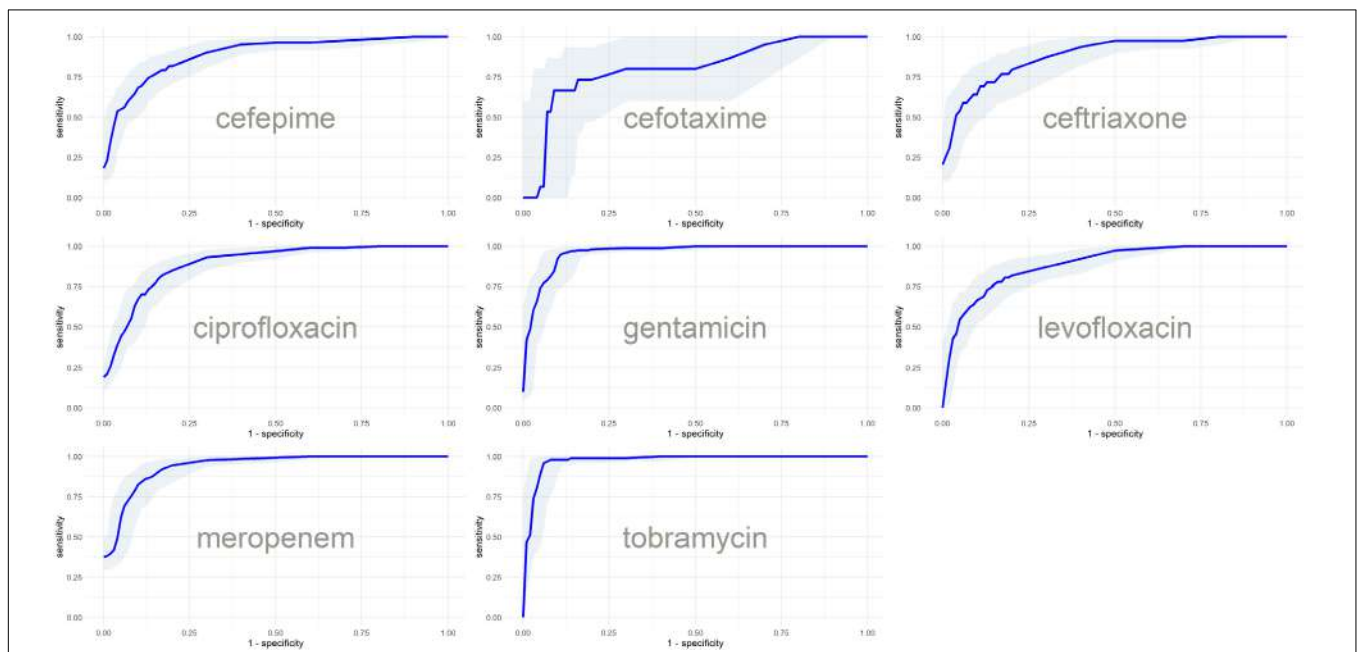
An intuitive example is the *class A extended-spectrum beta-lactamase* cluster as an important feature in the cephalosporin prediction models (**Table 4**). Other ARGs seem less relevant







**FIGURE 3 |** Performance of XGBoost models based on 51 different splits of the data. Boxplots represent distribution of AUC for the corresponding testing subsets, with thick lines indicating the median performance.



**FIGURE 4 |** ROC curves with confidence intervals of the final models based on the predictions of test subsets.

at first glance but might make more sense when interpreted in a broader context. *AAC(6′)-Ib family aminoglycoside 6′-N-acetyltransferase* is an aminoglycoside resistance gene, but apart from being important in the tobramycin model (an aminoglycoside), it is also found to be important in the models predicting cephalosporin and levofloxacin resistance. This is where a more careful interpretation of important features is

warranted as the non-linearity of XGBoost models is starting to provide less intuitive connections. For example, this gene is found in a variety of Gram-negative species and is known to be present in many different plasmids, genomic islands and integrons that carry other genetic resistance genes. It could be that this gene is a proxy for other, more relevant genes or even other genetic factors in the genome associated with resistance

**TABLE 4 |** Top 5 most important features for each antibiotic model.

ARGC	Gain
<b>Cefepime</b>	
AAC(6′)-Ib family aminoglycoside 6′-N-acetyltransferase	18.90 ± 3.27
Class A extended-spectrum beta-lactamase CTX-M-222	7.84 ± 1.07
Aminoglycoside O-phosphotransferase APH(3′′)-Ib	6.44 ± 1.91
Class C extended-spectrum beta-lactamase EC-18	5.49 ± 1.30
Carbapenem-hydrolyzing class A beta-lactamase KPC-33	5.14 ± 1.32
<b>Cefotaxime</b>	
Aminoglycoside nucleotidyltransferase ANT(3′′)-IIa	17.09 ± 7.27
AAC(6′)-Ib family aminoglycoside 6′-N-acetyltransferase	13.75 ± 7.65
Class C extended-spectrum beta-lactamase EC-18	13.16 ± 4.84
Multidrug efflux RND transporter permease subunit OqxB21	9.74 ± 4.27
OXA-51 family carbapenem-hydrolyzing class D beta-lactamase OXA-561	8.26 ± 3.86
<b>Ceftriaxone</b>	
AAC(6′)-Ib family aminoglycoside 6′-N-acetyltransferase	15.52 ± 4.35
Class C beta-lactamase CMY-163	8.76 ± 1.79
Class A extended-spectrum beta-lactamase CTX-M-222	8.37 ± 2.17
Class C extended-spectrum beta-lactamase EC-18	8.10 ± 1.99
Multidrug efflux RND transporter permease subunit OqxB21	7.00 ± 3.20
<b>Ciprofloxacin</b>	
AAC(6′)-Ib family aminoglycoside 6′-N-acetyltransferase	23.44 ± 4.94
Sulfonamide-resistant dihydropteroate synthase Sul1	10.29 ± 3.20
Tetracycline efflux MFS transporter Tet(B)	4.99 ± 1.71
Class A beta-lactamase TEM-219	4.93 ± 1.14
Aminoglycoside O-phosphotransferase APH(3′′)-Ib	4.47 ± 1.63
<b>Gentamicin</b>	
Aminoglycoside N-acetyltransferase AAC(3)-IIc	28.79 ± 3.10
ANT(3′′)-Ia family aminoglycoside nucleotidyltransferase AadA1	20.98 ± 2.52
Aminoglycoside nucleotidyltransferase ANT(2′′)-Ia	17.79 ± 2.03
OXA-24 family carbapenem-hydrolyzing class D beta-lactamase OXA-25	4.15 ± 1.59
Mph(E) family macrolide 2′-phosphotransferase Levofloxacin	2.07 ± 1.10
AAC(6′)-Ib family aminoglycoside 6′-N-acetyltransferase	25.11 ± 6.17
Sulfonamide-resistant dihydropteroate synthase Sul1	7.72 ± 3.73
Tetracycline efflux MFS transporter Tet(B)	5.92 ± 1.67
Class A beta-lactamase TEM-219	5.89 ± 1.74
Class C extended-spectrum beta-lactamase EC-18	4.97 ± 1.73
<b>Meropenem</b>	
Carbapenem-hydrolyzing class A beta-lactamase KPC-33	30.09 ± 5.21
Bleomycin binding protein Ble-MBL	9.55 ± 2.02
OXA-23 family carbapenem-hydrolyzing class D beta-lactamase OXA-483	8.58 ± 3.25
Class C extended-spectrum beta-lactamase EC-18	5.79 ± 2.05
Class A beta-lactamase SHV-200	5.59 ± 2.74
<b>Tobramycin</b>	
AAC(6′)-Ib family aminoglycoside 6′-N-acetyltransferase	60.50 ± 5.02
Aminoglycoside nucleotidyltransferase ANT(2′′)-Ia	17.91 ± 1.98
Aminoglycoside N-acetyltransferase AAC(3)-IIc	6.54 ± 1.24
Aminoglycoside 6′-N-acetyltransferase AAC(6′)-Iq	4.62 ± 1.51
ArmA family 16S rRNA [guanine(1405)-N(7)]-methyltransferase	1.89 ± 0.97

\*Gain is the relative importance of the ARGC in a prediction model, reported here as mean with standard deviation computed over 51 independent models for the same AB.

**TABLE 5 |** Counts of unique features found among top 5 across 51 independent models for each AB.

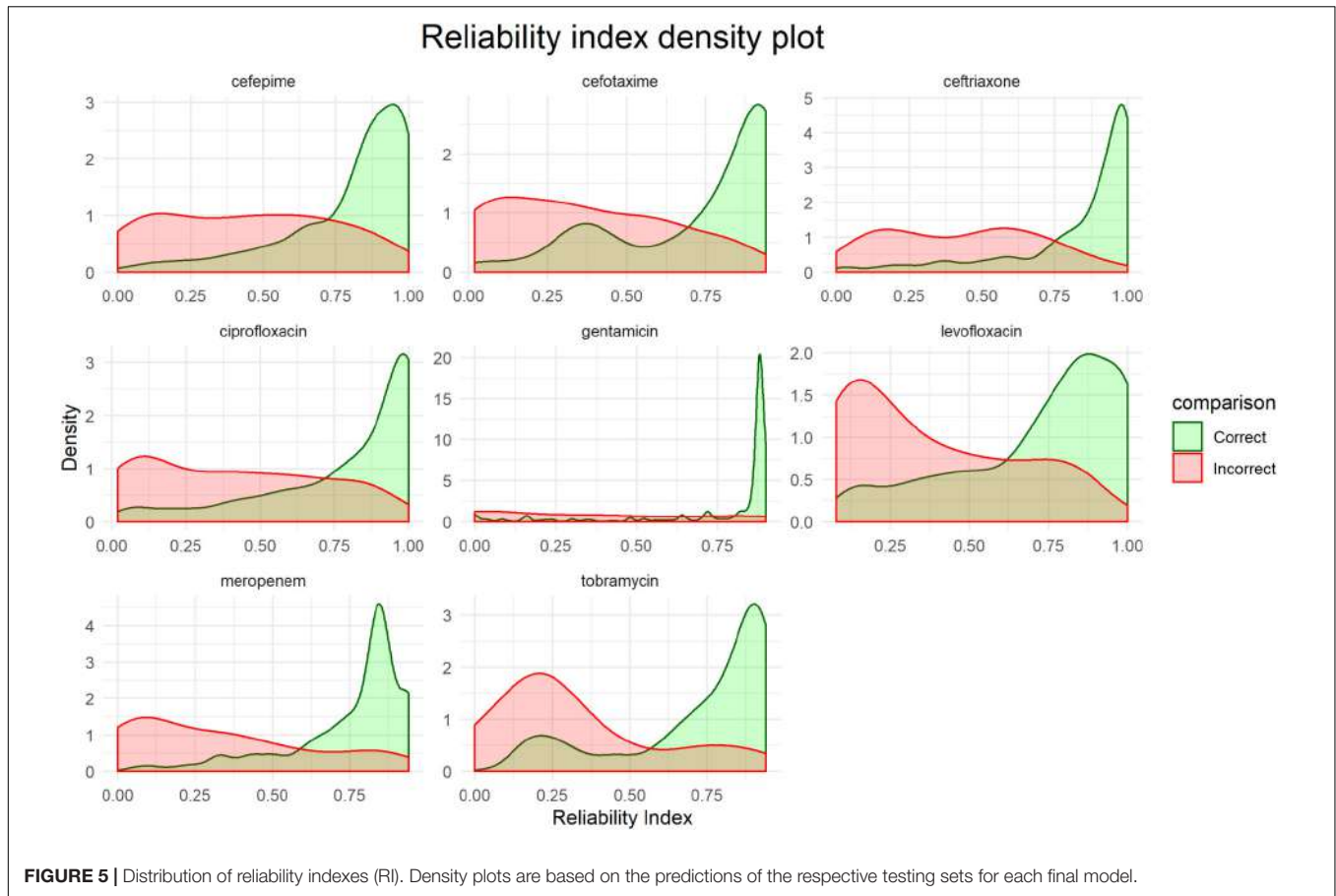
Antibiotic model	LASSO	Ridge	XGBoost
Cefepime	28	13	11
Cefotaxime	38	38	12
Ceftriaxone	25	29	12
Ciprofloxacin	30	16	13
Gentamicin	16	12	18
Levofloxacin	24	17	11
Meropenem	25	18	11
Tobramycin	14	16	14

\*The lower number signifies the more consistent feature selection across data resampling.

(Wilson et al., 2016; Lehtinen et al., 2017). Furthermore, this gene is prominent in *Klebsiella* species which could be used during decision-making to take advantage of innate differences in resistance between species. The fact that our prediction models are species independent could make them more powerful when focusing on resistance patterns in contaminated, mixed, and metagenomic samples. The latter is part of the future goals of this work. To show that the presence of ARG only could easily predict species, a model with the same input, but trained on predicting species instead of ABR, was built and had a near perfect accuracy (**Supplementary Table S8**).

The most striking discordance between an antibiotic and its model's important ARGC features was observed for levofloxacin. None of the most important ARGC picked up by the model are directly related to quinolone resistance. This is likely because levofloxacin resistance is largely based on mutations or small variations (e.g., gyrase gene; Chen and Lo, 2003). Given our models do not incorporate such information (section “Clustering similar antibiotic resistance genes”), all important ARGC in the levofloxacin resistance model appear to be proxies for these mutations. This illustrates both the strength and limitations of models like XGBoost. It can make accurate predictions (**Table 3**) on correlated and complex data by using non-linear logic, but the interpretation of such models can be obscure and could limit biological understanding of the underlying processes.

As any other previous work in this early-stage field of predicting ABR based on the WGS data, our study has several limitations. One of the main challenges was the sparsity of the model input, which may result in biased performance depending on the split in training and testing data. Even after clustering highly similar ARG in ARGC (hence no account for polymorphism), we still ended up with some ARGC only seen once in the whole dataset (median presence of 10 out of 152 clusters per sample). The sparsity is likely because some genes are rare, or the dataset is not fully representative of all evaluated resistances (limitation of using publicly available data). If we would only have used the genes originally sequenced in the bacteria of interest, we might have had less sparsity, but would likely be underestimating the presence of resistance as many species have developed similar resistance genes or exchanged them in processes like horizontal gene transfer. The



**FIGURE 5 |** Distribution of reliability indexes (RI). Density plots are based on the predictions of the respective testing sets for each final model.

**Escherichia coli**

antibiotic	prediction	reliability	reference
cefepime	Susceptible	0.24	Incorrect
cefotaxime	Resistant	0.86	Unknown
ceftriaxone	Resistant	0.86	Correct
ciprofloxacin	Resistant	0.96	Correct
gentamicin	Susceptible	0.88	Correct
levofloxacin	Resistant	1	Correct
meropenem	Susceptible	0.86	Correct
tobramycin	Resistant	0.66	Correct

**FIGURE 6 |** Example of the predicted antibiogram. An illustration of the output from the *R* shiny app using the sample SAMN07450853 from the Demo set. Other samples from the Demo and In-house datasets can be accessed through the app. The “reference” column compares the predicted resistance to the one confirmed in the clinical laboratory. This would normally not be present at the time the models do their prediction for *de novo* samples. Color coding used: green – correct, red – incorrect, and blue – unknown.

second reason performance suffered in some cases is the class imbalance between available susceptible and resistant samples, e.g., cefotaxime only has 50 susceptible samples (Table 1), and also the lowest performance (Table 3). By creating many

independent models for each antibiotic and selecting the one with median performance, we ensured that the final model would be the closest estimate of the real-life performance (section “XGBoost model training and testing”). This technique is not to



be confused with model cross-validation, where different splits of data are used to enhance one final model, and additional validation data is needed to estimate the performance.

Other limitations are that the models cannot predict the level of resistance (i.e., as regression) as they were trained on a binary data (resistant versus susceptible). Using the MIC values as input could help in this case, but the data is not always available or may be inconsistent. Also, the

current predictor accounts for presence or absence of certain known drug resistance genes and hence cannot detect the presence of previously unseen genes conferring new drug resistance. In other words, the prediction of a sample being resistant has higher confidence than being susceptible. Furthermore, due to the nature of sequencing data (DNA-seq), the models cannot incorporate resistance originating from the over-expression of genes targeted



by inhibitors. RNA-seq potentially could mitigate this problem but presents additional challenges. (Meta-)transcriptomics data, unfortunately, and remains mostly within research realm. Complexity of reference database, inference of organisms/strains, and their relative abundance data (Cox et al., 2017), dynamic gene expression profile upon different drug treatments, and overall complexity of data preparation/generation impede the application of meta-transcriptomics data for real-time predictions (Van Camp et al., 2020).

Finally, the models use sequencing data derived from isolates, but it remains to be seen how they would perform on contaminated or mixed (e.g., metagenomic) samples. All limitations will be further addressed in future studies. Nevertheless, this study has shown a great potential of sequencing data as a basis for the prediction of antimicrobial resistance in Gram-negative bacteria. We additionally focused on the more practical implementation of resistance prediction models by presenting the end-users (medical practitioners) with an easy to use and interpret interface where novel predictions on different AB are shown together as in a traditional antibiogram but with an additional RI to further assist during the decision making process.

To summarize, this work demonstrates that whole-genome sequencing coupled with modern machine-learning methods has great potential to deliver early estimations of the antibiogram for Gram-negative bacteria. The generated models, being trained solely on the presence-absence of the clusters of ARG, demonstrate promising performance and robustness to heavily class-imbalanced data. RI are introduced to provide further assessment of predictions and may be used in subsequent machine learning models to improve accuracy further. By presenting the results in the form of an antibiogram, we provide an intuitive way for the clinician to interpret predictions and guide the initial empiric antibiotic choice before the laboratory

results are available. This may help in shortening the time to start effective AB treatment.

## DATA AVAILABILITY STATEMENT

The datasets generated for this study can be found in the NCBI BioSample database (BioProject ID: PRJNA587095).

## AUTHOR CONTRIBUTIONS

P-JV did the data collection and curation, model training and validation, developed the R shiny app, and stand-alone analytical pipeline. DH and AP conceived of the study, evaluated results, and supervised the project. DH provided clinical samples for the In-house dataset. AP provided computational resources. All authors participated in writing the manuscript.

## FUNDING

This work was supported by the Centers for Disease Control (Contract Number OADS BAA 2016-N-17812) and funding from the Academic Research Committee at Cincinnati Children's Hospital Medical Center.

## SUPPLEMENTARY MATERIAL

The Supplementary Material for this article can be found online at: <https://www.frontiersin.org/articles/10.3389/fmicb.2020.01013/full#supplementary-material>

## REFERENCES

- Altschul, S. F., Gish, W., Miller, W., Myers, E. W., and Lipman, D. J. (1990). Basic local alignment search tool. *J. Mol. Biol.* 215, 403–410. doi: 10.1016/S0022-2836(05)80360-2
- Bajaj, P., Singh, N. S., and Virdi, J. S. (2016). *Escherichia coli*  $\beta$ -Lactamases: what really matters. *Front. Microbiol.* 7:417. doi: 10.3389/fmicb.2016.00417
- Bradley, P., Gordon, N. C., Walker, T. M., Dunn, L., Heys, S., Huang, B., et al. (2015). Rapid antibiotic-resistance predictions from genome sequence data for *Staphylococcus aureus* and *Mycobacterium tuberculosis*. *Nat. Commun.* 6:10063. doi: 10.1038/ncomms10063
- Buchfink, B., Xie, C., and Huson, D. H. (2015). Fast and sensitive protein alignment using DIAMOND. *Nat. Methods* 12, 59–60. doi: 10.1038/nmeth.3176
- Centers for Disease Control and Prevention (2018). *Antibiotic / Antimicrobial Resistance*. Available online at: <https://www.cdc.gov/drugresistance/index.html> (accessed March 20, 2019).
- Chen, F.-J., and Lo, H.-J. (2003). Molecular mechanisms of fluoroquinolone resistance. *J. Microbiol. Immunol. Infect.* 36, 1–9.
- Chen, T., and Guestrin, C. (2016). XGBoost: a scalable tree boosting system. *Proc. Int. Conf. Knowl. Discov. Data Min.* 16, 785–794. doi: 10.1145/2939672.2939785
- Couto, R. C., Carvalho, E. A. A., Pedrosa, T. M. G., Pedroso, E. R., Neto, M. C., and Biscione, F. M. (2007). A 10-year prospective surveillance of nosocomial infections in neonatal intensive care units. *Am. J. Infect. Control* 35, 183–189. doi: 10.1016/j.ajic.2006.06.013
- Cox, J. W., Ballweg, R. A., Taft, D. H., Velayutham, P., Haslam, D. B., and Porollo, A. (2017). A fast and robust protocol for metataxonomic analysis using RNAseq data. *Microbiome* 5:7. doi: 10.1186/s40168-016-0219-5
- Devika, S., Jeyaseelan, L., and Sebastian, G. (2016). Analysis of sparse data in logistic regression in medical research: a newer approach. *J. Postgrad. Med.* 62, 26–31. doi: 10.4103/0022-3859.173193
- Drouin, A., Letarte, G., Raymond, F., Marchand, M., Corbeil, J., and Laviolette, F. (2019). Interpretable genotype-to-phenotype classifiers with performance guarantees. *Sci. Rep.* 9:4071. doi: 10.1038/s41598-019-40561-2
- Edgar, R. C. (2010). Search and clustering orders of magnitude faster than BLAST. *Bioinformatics* 26, 2460–2461. doi: 10.1093/bioinformatics/btq461
- Eyre, D. W., De Silva, D., Cole, K., Peters, J., Cole, M. J., Grad, Y. H., et al. (2017). WGS to predict antibiotic MICs for *Neisseria gonorrhoeae*. *J. Antimicrob. Chemother.* 72, 1937–1947. doi: 10.1093/jac/dkx067
- Farrar, D. E., and Glauber, R. R. (1967). Multicollinearity in regression analysis: the problem revisited. *Rev. Econ. Stat.* 49, 92–107. doi: 10.2307/1937887
- Feuerriegel, S., Schleusener, V., Beckert, P., Kohl, T. A., Miotto, P., Cirillo, D. M., et al. (2015). PhyResSE: a web tool delineating *Mycobacterium tuberculosis* antibiotic resistance and lineage from whole-genome sequencing data. *J. Clin. Microbiol.* 53, 1908–1914. doi: 10.1128/JCM.00025-15
- Lehtinen, S., Blanquart, F., Croucher, N. J., Turner, P., Lipsitch, M., and Fraser, C. (2017). Evolution of antibiotic resistance is linked to any genetic mechanism affecting bacterial duration of carriage. *Proc. Natl. Acad. Sci. U.S.A.* 114, 1075–1080. doi: 10.1073/pnas.1617849114

- Livermore, D. M. (1998). Beta-lactamase-mediated resistance and opportunities for its control. *J. Antimicrob. Chemother.* 41(Suppl. D), 25–41. doi: 10.1093/jac/41.suppl\_4.25
- Marston, H. D., Dixon, D. M., Knisely, J. M., Palmore, T. N., and Fauci, A. S. (2016). Antimicrobial resistance. *JAMA* 316, 1193–1204. doi: 10.1001/jama.2016.11764
- Martin, E. T., Tansek, R., Collins, V., Hayakawa, K., Abreu-Lanfranco, O., Chopra, T., et al. (2013). The carbapenem-resistant *Enterobacteriaceae* score: a bedside score to rule out infection with carbapenem-resistant *Enterobacteriaceae* among hospitalized patients. *Am. J. Infect. Control* 41, 180–182. doi: 10.1016/j.ajic.2012.02.036
- MinION (2019). *Oxford Nanopore Technologies*. Available online at: <http://nanoporetech.com/products/minion> (accessed May 16, 2019).
- Nguyen, M., Brettin, T., Long, S. W., Musser, J. M., Olsen, R. J., Olson, R., et al. (2018). Developing an in silico minimum inhibitory concentration panel test for *Klebsiella pneumoniae*. *Sci. Rep.* 8, 1–11. doi: 10.1038/s41598-017-18972-w
- Piramuthu, S. (2008). Input data for decision trees. *Expert Syst. Appl.* 34, 1220–1226. doi: 10.1016/j.eswa.2006.12.030
- Scaggs Huang, F. A., Mortensen, J., Skoch, J., Andersen, H., Staat, M. A., Schaffzin, J. K., et al. (2019). Successful whole genome sequencing-guided treatment of *Mycoplasma hominis* *Ventriculitis* in a preterm infant. *Pediatr. Infect. Dis. J.* 38, 749–751. doi: 10.1097/INF.0000000000002306
- SRA Toolkit Development Team (2019). *SRA Toolkit NCBI - National Center for Biotechnology Information/NLM/NIH*. Available online at: <https://github.com/ncbi/sra-tools> (accessed March 15, 2019).
- Van Camp, P.-J., Haslam, D. B., and Porollo, A. (2020). Bioinformatics approaches to the understanding of molecular mechanisms in antimicrobial resistance. *Int. J. Mol. Sci.* 21:1363. doi: 10.3390/ijms21041363
- Vasudevan, A., Mukhopadhyay, A., Li, J., Yuen, E. G. Y., and Tambyah, P. A. (2014). A prediction tool for nosocomial multi-drug resistant gram-negative *Bacilli* infections in critically ill patients - prospective observational study. *BMC Infect. Dis.* 14:615. doi: 10.1186/s12879-014-0615-z
- Vincent, J.-L. (2003). Nosocomial infections in adult intensive-care units. *Lancet* 361, 2068–2077. doi: 10.1016/S0140-6736(03)13644-6
- Ward, J. H. (1963). Hierarchical grouping to optimize an objective function. *J. Am. Stat. Assoc.* 58, 236–244. doi: 10.2307/2282967
- Wilson, B. A., Garud, N. R., Feder, A. F., Assaf, Z. J., and Pennings, P. S. (2016). The population genetics of drug resistance evolution in natural populations of viral, bacterial and eukaryotic pathogens. *Mol. Ecol.* 25, 42–66. doi: 10.1111/mec.13474
- Wu, W., May, R. J., Maier, H. R., and Dandy, G. C. (2013). A benchmarking approach for comparing data splitting methods for modeling water resources parameters using artificial neural networks. *Water Resour. Res.* 49, 7598–7614. doi: 10.1002/2012WR012713

**Conflict of Interest:** The authors declare that the research was conducted in the absence of any commercial or financial relationships that could be construed as a potential conflict of interest.

Copyright © 2020 Van Camp, Haslam and Porollo. This is an open-access article distributed under the terms of the Creative Commons Attribution License (CC BY). The use, distribution or reproduction in other forums is permitted, provided the original author(s) and the copyright owner(s) are credited and that the original publication in this journal is cited, in accordance with accepted academic practice. No use, distribution or reproduction is permitted which does not comply with these terms.



# Hospital-Associated Multidrug-Resistant MRSA Lineages Are Trophic to the Ocular Surface and Cause Severe Microbial Keratitis

Paulo J. M. Bispo<sup>1,2</sup>, Lawson Ung<sup>1,2</sup>, James Chodosh<sup>1,2</sup> and Michael S. Gilmore<sup>1,2,3\*</sup>

<sup>1</sup> Department of Ophthalmology, Massachusetts Eye and Ear, Harvard Medical School, Boston, MA, United States,

<sup>2</sup> Infectious Disease Institute, Harvard Medical School, Boston, MA, United States, <sup>3</sup> Department of Microbiology and Immunobiology, Harvard Medical School, Boston, MA, United States

## OPEN ACCESS

### Edited by:

Filipa Grosso,  
University of Porto, Portugal

### Reviewed by:

Tingtao Chen,  
Nanchang University, China  
Edet E. Udo,  
Kuwait University, Kuwait

### \*Correspondence:

Michael S. Gilmore  
michael\_gilmore@meei.harvard.edu

### Specialty section:

This article was submitted to  
Infectious Diseases - Surveillance,  
Prevention and Treatment,  
a section of the journal  
Frontiers in Public Health

Received: 01 November 2019

Accepted: 05 May 2020

Published: 03 June 2020

### Citation:

Bispo PJM, Ung L, Chodosh J and  
Gilmore MS (2020)  
Hospital-Associated  
Multidrug-Resistant MRSA Lineages  
Are Trophic to the Ocular Surface and  
Cause Severe Microbial Keratitis.  
Front. Public Health 8:204.  
doi: 10.3389/fpubh.2020.00204

Methicillin-resistant *Staphylococcus aureus* (MRSA) is a common cause of severe and difficult to treat ocular infection. In this study, the population structure of 68 ocular MRSA isolates collected at Massachusetts Eye and Ear between January 2014 and June 2016 was assessed. By using a combination of multilocus sequence typing (MLST) analysis, SCCmec typing and detection of the panton-valentine leukocidin (PVL) gene, we found that the population structure of ocular MRSA is composed of lineages with community and hospital origins. As determined by eBURST analysis of MLST data, the ocular MRSA population consisted of 14 different sequence types (STs) that grouped within two predominant clonal complexes: CC8 (47.0%) and CC5 (41.2%). Most CC8 strains were ST8, harbored type IV SCCmec and were positive for the PVL-toxin (93.7%). The CC5 group was divided between strains carrying SCCmec type II (71.4%) and SCCmec type IV (28.6%). Remaining isolates grouped in 6 different clonal complexes with 3 isolates in CC6 and the other clonal complexes being represented by a single isolate. Interestingly, major MRSA CC5 and CC8 lineages were isolated from discrete ocular niches. Orbital and preseptal abscess/cellulitis were predominantly caused by CC8-SCCmec IV PVL-positive strains. In contrast, infections of the cornea, conjunctiva and lacrimal system were associated with the MDR CC5 lineage, particularly as causes of severe infectious keratitis. This niche specialization of MRSA is consistent with a model where CC8-SCCmec IV PVL-positive strains are better adapted to cause infections of the keratinized and soft adnexal eye tissues, whereas MDR CC5 appear to have greater ability in overcoming innate defense mechanisms of the wet epithelium of the ocular surface.

**Keywords:** MRSA, Ocular infection, Molecular Epidemiology, Tissue tropism, biogeography of infections

## INTRODUCTION

Antimicrobial resistance in human infections has reached alarming levels and has become one of the major public health threats of the twenty first Century (1). Methicillin-resistant *Staphylococcus aureus* (MRSA) remains a leading cause of antibiotic-resistant infections at many anatomical sites (2, 3). MRSA initially were confined to the hospital environment, but in the mid 1990s began to

proliferate in the community (4), and are now leading causes of antibiotic-resistant infections in both settings (5). In US, strains within lineages that constitute clonal complex 5 (CC), notably the USA100 clone, are most commonly hospital-associated (5). USA300, a representative of CC8, has emerged as the most prevalent CA-MRSA clone in the US (5, 6). USA300 has also invaded the hospital setting where it is now a common cause of MRSA infections in American hospitals (7).

Ocular infections caused by MRSA have become increasingly common in the last two decades (8–11). These infections have been associated with serious ocular damage and permanent vision loss (12, 13), including bilateral blindness (14). Despite the growing importance of MRSA in ophthalmology, little is known about the population structure of MRSA causing the most common eye infections, or the microbial and host features that dictate this structure. The eye has extensive defenses for protection of vital structures from constant environmental exposure. These include mechanical barriers (e.g., lids, lashes), a polarized wet epithelium, a secreted tear film containing immunoglobulins and various other antimicrobial factors, mucins (secreted MUC5AC and shed epithelial cell surface-associated transmembrane mucins MUC1, MUC4, and MUC16), and cells of the innate immune system (15–17).

This unique environment of the ocular wet mucosa and its components are expected to act as selective forces that can shape the spatial distribution of microorganisms colonizing and infecting this ocular niche. The study of these ecological and geographical forces, as classically applied in ecology to study the biogeography of life in the natural world can now be combined with refined genetic and genomic epidemiology data to advance our understanding of community structures and distribution of microbes in different body sites (18, 19). We previously reported the genomic characteristics of a divergent cluster of unencapsulated *Streptococcus pneumoniae* strains that are uniquely tropic and adapted to the conjunctiva (20). These strains carry a set of genes that are absent or substantially different from those encoded within the genomes of encapsulated respiratory strains, which appear to be important for the pathogenesis of epidemic conjunctivitis. We have demonstrated that a unified model of microbial biogeography that incorporates classic ecological principles to explain community assemblage and dynamics can be applied to the understanding of this radical bifurcation in phylogeny and niche subspecialization of the unencapsulated *S. pneumoniae* conjunctivitis cluster (21). Because MRSA now rank among leading causes of a variety of ocular infections, to gain insight into particular features of importance in the pathogenesis of infection, it was of interest to determine the microscale biogeography of MRSA eye infections, whether dominant genetic lineages were associated with all sites of infection, or if there was evidence of a tissue tropism that would drive a specific population structure. We report that the population structure of ocular MRSA strains isolated at Massachusetts Eye and Ear (MEE) is dominated by the two major clonal complexes that cause infections at other body sites, but exhibit a distinct distribution in the types of infection they cause.

## METHODS

### Bacterial Strains

Protocols for obtaining bacterial isolates collected for infection diagnosis were approved by the MEE Institutional Review Board (IRB). Since this study only included discarded bacterial isolates that were frozen in our pathogen repository, written informed consent was waived by the MEE IRB. In total, 68 consecutive MRSA isolates recovered from January 2014 to June 2016 were analyzed for this study. For patients from whom multiple isolates from the same eye were obtained for infection diagnosis within a period of 6 months, only the first isolate was included. Specimens were obtained by the attending ophthalmologist or resident physician following institutional guidelines and submitted to the clinical laboratory for processing. Suspected *S. aureus* colonies were routinely identified using a combination of phenotypic methods including detection of coagulase and protein A by latex agglutination, followed by confirmation of species and antimicrobial susceptibility testing using the MicroScan Walkaway 40 Plus System (Beckman Coulter, Brea, CA). Isolates were stored at  $-80^{\circ}\text{C}$  in Microbank™ cryopreservative tubes (ProLab Diagnostics). Frozen isolates were cultured twice on blood agar before further testing.

### Clinical Data Collection and Statistical Analyses

Demographic data and risk factors for MRSA infection were collected using the IRB-approved Research Electronic Data Capture (REDCap) tool, hosted by MEE and Harvard Medical School (22). General demographic data included age, sex and ethnicity. Ocular comorbidities, including any ophthalmic surgical history, ocular surface disease, eyelid disease, lacrimal system dysfunction, atopy, contact lens use and trauma were collected (see **Table 2** legend for full definitions). Patient systemic comorbidities and previous healthcare exposures were also captured. To identify possible healthcare exposures which may potentiate selective pressures for antibiotic-resistant infection, we identified these following groups in our data: patients residing in nursing homes and/or residential facilities; those requiring chronic ambulatory care such as renal replacement therapy (dialysis) and hospital-based infusions; and patients who had either inpatient hospital admission and/or day admission for eye surgery within the preceding 3 prior to developing an MRSA infection. For patients with MRSA keratitis, we recorded the presenting features of the ulcers according to an institution-wide clinical algorithm which mandates the collection of corneal cultures for lesions meeting any of the following criteria:  $\geq 1+$  cells in the anterior chamber;  $\geq 2$  mm infiltrate and/or the presence of  $\geq 2$  satellite lesions; or infiltrate located  $\leq 3$  mm from the corneal center (23). Simple 2 by 2 tests of proportion (Fischer's exact test) were used to compare CC5 and CC8 groups according to collected categorical variables, while age was compared using the non-parametric Wilcoxon rank-sum test.

### Antimicrobial Susceptibility Testing

*In vitro* susceptibility to ciprofloxacin (Fluka), ofloxacin, levofloxacin (TCI America), moxifloxacin, and besifloxacin



(Sigma-Aldrich) was performed by broth microdilution methods according to the Clinical and Laboratory Standards Institute (CLSI) (24). Quality control was performed by testing the *S. aureus* ATCC 29213 control strain. The interpretative criteria for each antimicrobial agent tested were those published by CLSI (25).

## DNA Extraction

DNA extraction was performed using Chelex 100 molecular biology resin (Bio-Rad) as previously described (26). Purified genomic DNA was diluted 1:10, and was assessed for purity and DNA concentration using a Synergy 2 Multi-Mode Plate Reader and Take3 software system (BioTek).

## SCCmec Typing

PCR-based genotyping of the chromosomal cassette recombinase (*ccr*) and *mec* complexes comprising the SCCmec was determined by a combination of multiplex PCR designed to classify the *mec* complex and *ccr* complex using a previously published protocol (27). For each multiplex PCR assay, reference MRSA strains for SCCmec types II (USA100) and IV (USA800), provided by the Network of Antimicrobial Resistance in *Staphylococcus aureus* (NARSA) were included. SCCmec was considered nontypeable if *mec* and/or *ccr* complex gave no amplification results, if the isolate carried more than one *ccr* or *mec* complex, or if there was a *mec/ccr* complex combination not previously described.

## PVL Detection

The presence or absence of the Panton-Valentine Leukocidin (PVL) toxin gene was determined by PCR amplification of the *LukS-PV-lukF-PV* genes as previously described (28). Reference MRSA strains (provided by NARSA) USA300 and USA100 served as positive and negative controls, respectively.

## MLST

Multilocus sequence typing (MLST) was performed for all MRSA isolates using a scheme based on the sequencing of internal fragments of seven *S. aureus* housekeeping genes (*arcC*, *aroE*, *glpF*, *gmk*, *pta*, *tpi*, and *yqiL*). The PCR products were purified (QIAquick PCR purification kit; Qiagen), and both strands were sequenced by Genewiz Incorporated (South Plainfield, NJ). The sequences obtained were edited using Geneious R8 and sequence types (STs) were assigned using the *S. aureus* MLST database (<https://pubmlst.org/saureus/>). Clonal complexes (CC) were determined using the go eBURST algorithm (<http://www.phylviz.net/goeburst/>).

## Statistics

Descriptive statistics were calculated using SPSS software (version 25, IBM, Armonk, New York), and proportions were compared by  $\chi^2$  or Fisher exact test, as appropriate. A *P* value of <0.05 was considered statistically significant.

## RESULTS

A total of 75 MRSA were identified from 281 *S. aureus* recovered from ocular sites at MEE from January 2014 to June 2016 (overall

rate of 26.7%). The proportion of ocular MRSA isolates did not change considerably in 2014 (25.9%) compared to 2015 (22.3%), but was substantially higher during the sampling period of 2016 (37.7%). Of those, 7 MRSA were obtained from second cultures of the same patient eye, and were excluded from further study. The remaining 68 non-duplicate MRSA isolates were then analyzed. Sites of infection from which MRSA were isolated included orbital and preseptal abscess/cellulitis (*n* = 27), keratitis (*n* = 14), conjunctivitis (*n* = 9), lacrimal system infection (*n* = 8), eyelid margin infections (*n* = 4), endophthalmitis (*n* = 2), and miscellaneous (*n* = 4).

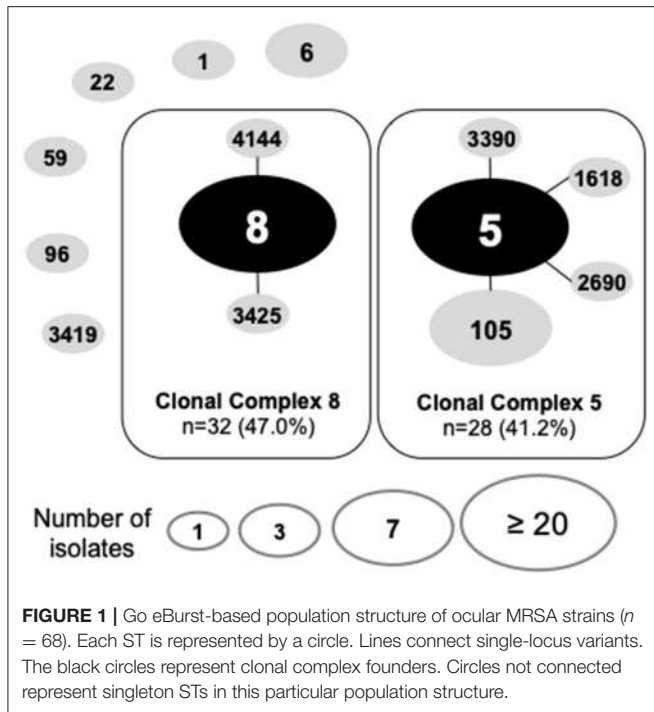
## Two Major Clonal Complexes Dominate the Ocular MRSA Population

Despite the clinical importance of MRSA, much remains to be learned about the pathogenesis of infection at different anatomical sites on and around the eye. Because the tissues of the eye and adnexa differ widely in host defenses (e.g., wet epithelium vs. keratinized epithelium and soft tissues), it was of interest to know whether some MRSA lineages were enriched in pathogenic features that select for one MRSA lineage over another. By using a combination of multilocus sequence typing analysis, SCCmec typing and detection of the PVL-toxin encoding gene, we found that the population structure of ocular MRSA is diverse, but dominated by the CC5 and CC8 lineages associated with infection at other anatomical sites (4, 5). As determined by eBURST analysis of MLST data (Figure 1), 14 different sequence types (STs) were identified, with most belonging to clonal clusters CC8 (47.0%, *n* = 32) and CC5 (41.2%, *n* = 28). The clonal cluster CC6 encompassed 3 strains (4.4%), and 5 strains represented single sequence types. Most CC8 strains (93.7%, *n* = 30) were ST8, harbored a SCCmec type IV and were positive for the PVL-toxin, common features of the USA300 strain. The CC5 group could be divided into those carrying a SCCmec type II (71.4%, *n* = 20), which includes isolates with the characteristics of the USA100 clone, and (28.6%, *n* = 8) SCCmec type IV, typical of the USA800 clone (Table 1).

Age at presentation ranged from 2 to 102 years (median 53.08) with CC5-infected patients being significantly older (median age, 68.05 vs. 35.9, *p* < 0.001) (Table 2). CC5-infected patients were more frequently subjected to eye surgery (66.7 vs. 16.7%, *p* < 0.001), especially cataract surgery with implantation of intraocular lenses (44.4 vs. 10%, *p* = 0.006). Healthcare exposure was more common among patients infected with CC5 strains, including higher rates of topical antibiotic use at presentation (55.6 vs. 10.0%, *p* < 0.001) and prior to presentation (48.5 vs. 16.7%, *p* = 0.02). There was also a higher proportion of patients known to require non-acute clinical care and/or residents of aged care facilities in the CC5 group (22.2 vs. 3.3%, *p* = 0.05).

## Distribution of MRSA Lineages Across Different Ocular Niches

Although *S. aureus* causes a wide range of human infections, patterns of association of distinct genotypes have been noted with



**FIGURE 1 |** Go eBurst-based population structure of ocular MRSA strains ( $n = 68$ ). Each ST is represented by a circle. Lines connect single-locus variants. The black circles represent clonal complex founders. Circles not connected represent singleton STs in this particular population structure.

**TABLE 1 |** SCCmec typing and PVL detection according to the clonal complex.

Clonal complex (No.)	SCCmec typing		No. PVL positive
	Type	No. (% of total)	
CC8 (32)	IV	31 (45.6)	30
	V	1 (1.5)	1
CC5 (28)	II	20 (29.4)	–
	IV	8 (11.7)	–
CC6 (3)	IV	3 (4.4)	–
CC1 (1)	IV	1 (1.5)	1
CC15 (1)	II	1 (1.5)	1
CC22 (1)	IV	1 (1.5)	1
CC59 (1)	IV	1 (1.5)	1
CC96 (1)	NT	1 (1.5)	–

specific types of infection (29–32). The most well documented example is community-acquired skin and soft-tissue infection (SSTI) in the US, where a large majority of cases are caused by the CC8/USA300 lineage (29, 32). In agreement, ocular SSTIs including mainly orbital and preseptal abscess/cellulitis were found in this study to be caused mainly by CC8 SCCmec IV PVL-positive strains, characteristics of the USA300 clone ( $p < 0.001$ ; Table 3). Interestingly, infections of the wet epithelial tissues of the ocular surface were substantially enriched in the CC5 lineage, which was particularly pronounced for infectious keratitis cases ( $p < 0.001$ ; Table 3). Keratitis patients frequently presented with potentially sight-threatening corneal ulcers (85.7%) according to the 1,2,3 rule (23) for categorization of the severity of bacterial keratitis (Table 5).

**TABLE 2 |** Demographic and clinicopathologic data for patients with culture-positive MRSA ocular infections at MEE, 2014–2016 ( $n = 58$ ).<sup>a</sup>

Patient characteristics	MRSA clonal group		P value
	CC5 ( $n = 27$ )	CC8 ( $n = 30$ )	
<b>DEMOGRAPHIC DATA</b>			
Age (years, median)	68.05	35.4	<b>&lt; 0.001</b>
<b>Gender</b>			
Male	6 (22.2)	13 (43.4)	0.16
Female	21 (77.8)	17 (56.7)	
<b>Ethnicity</b>			
Caucasian	22 (81.5)	23 (76.7)	0.75
Non-Caucasian	5 (18.5)	7 (23.3)	
<b>OCULAR HISTORY</b>			
History of contact lens wear	8 (29.6)	5 (16.7)	0.35
History of eye trauma	3 (11.1)	4 (13.3)	1
Prior eye surgery	18 (66.7)	5 (16.7)	<b>&lt; 0.001</b>
Previous intraocular lens insertion	12 (44.4)	3 (10.0)	<b>0.006</b>
Ocular surface disease*	9 (33.3)	5 (16.7)	0.22
Dry eye syndrome	4 (14.8)	4 (13.3)	1
Atopic eye disease	1 (3.7)	1 (3.3)	1
Lid disease**	9 (33.3)	6 (20.0)	0.37
Lacrimal system dysfunction***	5 (18.5)	5 (16.7)	1
Glaucoma	6 (22.2)	1 (3.3)	<b>0.05</b>
Glaucoma drainage device	1 (3.7)	0 (0)	0.47
<b>HEALTHCARE EXPOSURES</b>			
Use of topical antibiotic at presentation	15 (55.6)	3 (10.0)	<b>&lt; 0.001</b>
Use of topical antibiotic within the last week preceding presentation	13 (48.5)	5 (16.7)	<b>0.02</b>
Use of topical steroids at presentation	11 (40.7)	5 (16.7)	0.08
Use of topical steroids within the last week preceding presentation	10 (37.0)	5 (16.7)	0.13
Known inpatient hospital admission in the last 3 months	4 (14.8)	3 (10.0)	0.7
Admission for eye surgery in the last 3 months <sup>†</sup>	5 (18.5)	2 (6.7)	0.24
Non-acute clinical care <sup>††</sup>	6 (22.22)	1 (3.3)	<b>0.05</b>
Healthcare worker <sup>†††</sup>	4 (14.8)	5 (16.7)	1

<sup>a</sup>Out of 68 isolates included, 66 patient records were reviewed. One patient had two separate MRSA episodes (caused by different clones) and for one patient the record was not available.

\*includes corneal degenerative disease, bullous keratopathy, exposure keratopathy, dry eye syndrome, atopy, Stevens-Johnson syndrome and toxic epidermal necrolysis.

\*\*including blepharitis, trichiasis, floppy eyelid syndrome, ectropion and entropion, and lagophthalmos.

\*\*\*including dacryocystitis and dacryoadenitis.

<sup>†</sup>including day-only procedures and overnight stays.

<sup>††</sup>includes long-term care residents, nursing home care, chronic ambulatory care.

<sup>†††</sup>includes professions in close working contact with patients (e.g., nursing and allied health).

Bold values are represent statistically significant.

### CC5 Strains Preferentially Associated With Infection of the Wet Epithelial Ocular Surface Are Multidrug Resistant

To compare rates of antibiotic resistance among ocular MRSA of various lineages and from the different ocular sites, we tested the sensitivities of all isolates to a panel of clinically

relevant antibiotics using an automated microbiology system (MicroScan WalkAway). Overall, moderate to high rates of resistance to erythromycin (88.2%), levofloxacin (54.4%), and clindamycin (42.6%) was found among this MRSA collection. Resistance to gentamycin (2.9%) and tetracycline (1.5%) was rare (**Figure 2B**). Stratified analysis by clonal complex showed that CC5 strains are significantly more likely to be multidrug resistant (resistance to  $\geq 3$  non-beta-lactam antimicrobial classes) than CC8 strains (78.8 vs. 6.1%;  $p < 0.0001$ ; **Figure 2A**). Ocular CC5-SCCmec II strains, which include isolates resembling the hospital-adapted clone USA100, were all resistant to erythromycin, clindamycin and levofloxacin (**Figure 2B**). CC5-SCCmec IV strains, including isolates with the characteristics of the USA800 clone, were frequently resistant to erythromycin (62.5%), levofloxacin (62.5%), and clindamycin (25.0%). While CC5 strains were frequently resistant to  $\geq 3$  non-beta-lactam antibiotics, CC8 isolates were usually resistant to only one antibiotic class in addition to beta-lactams, most often to the macrolide erythromycin (**Figures 2A,B**).

Because topical fluoroquinolone is widely used for empirical treatment of ocular infection, we assessed the *in vitro* susceptibility of the main ocular MRSA clonal complexes for the most commonly used fluoroquinolones (**Table 4**). The minimum inhibitory concentrations (MICs) for these agents were determined by reference broth microdilution (24, 25). CC5 isolates were in general highly resistant to the older fluoroquinolones ciprofloxacin, ofloxacin and levofloxacin. All canonical CC5-SCCmec II strains were resistant to oxifloxacin, levofloxacin, ofloxacin and ciprofloxacin with MIC<sub>90</sub> values  $>256 \mu\text{g/mL}$ . Among CC5-SCCmec IV strains, the MIC<sub>90</sub> values ranged from  $64 \mu\text{g/mL}$  for moxifloxacin to  $>256 \mu\text{g/mL}$  for levofloxacin, ofloxacin and ciprofloxacin (% of non-susceptible = 62.5% for the 3 drugs). Remarkably, many CC5 isolates were also highly resistant to the newer 8-methoxyfluoroquinolone moxifloxacin (MIC<sub>90</sub>  $64 \mu\text{g/mL}$ , 62.5% non-susceptible for CC5-SCCmec IV; MIC<sub>90</sub>  $32 \mu\text{g/mL}$ , 100% non-susceptible for CC5-SCCmec II).

## DISCUSSION

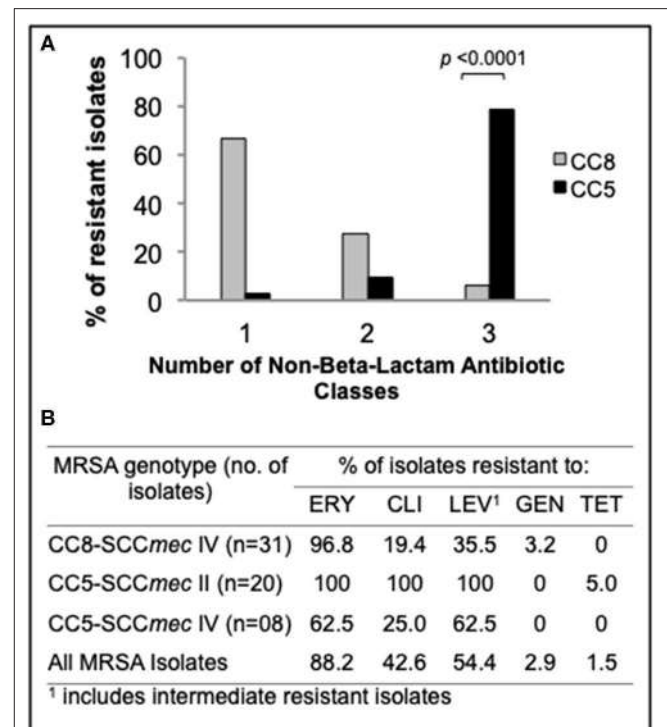
The population structure of *S. aureus* isolates from human infections is highly diverse (33). However, only a small proportion of these lineages have become successful MRSA clones that are now widely disseminated in both community and hospital settings (5). These epidemic lineages cause a variety of human infections, with some showing strong tropisms for specific body niches (29–32).

The eye has developed unique mechanisms to protect its delicate and exceptionally important structures against constant external disturbance (15–17). Because of this, we postulated that the uniqueness of this environment could be a driving force shaping the population structure of ocular MRSA infections, in a similar manner as reported for *Streptococcus pneumoniae* (20). To begin testing this hypothesis, we selected a collection of consecutive and non-duplicate MRSA strains prospectively isolated from a variety of eye infections, representing two major

**TABLE 3** | Distribution of the main ocular MRSA clones across different infections.

Eye infection	Total no. of cases	No. of eyes infected by			Fisher's test (CC5 vs. CC8)
		CC5	CC8	Others	
Abscess/Cellulitis	27	1	22	4	<b>e&lt;0.001</b>
Keratitis	14	12	1	1	<b>&lt;0.001</b>
Conjunctivitis	9	6	2	1	0.1300
Lacrimal system	8	5	2	1	0.2349
Eyelids	4	–	4	–	–
Endophthalmitis	2	2	–	–	–
Miscellaneous	4	2	1	1	–

*Bold values are represent statistically significant.*



**FIGURE 2** | Antimicrobial susceptibility profile of the main ocular MRSA clonal complexes. **(A)** Frequency (%) of CC5 and CC8 strains resistant to additional non-beta-lactam antibiotic classes. **(B)** Resistance rates for common antibiotics representing 5 different classes. Statistical significance was determined using Fisher's exact test.

and distinct localizations: (i) the ocular surface and (ii) the ocular adnexal soft tissues. We found that the ocular MRSA population was dominated by two major clonal complexes that are also common causes of MRSA infections in other body sites: CC8 (47.0%) and CC5 (41.2%). The distribution of lineages within these clonal complexes followed a pattern of enrichment that was split into the main ocular niches tested, with preseptal and orbital abscess/cellulitis being predominantly associated to CC8, while ocular surface infections were frequently caused by CC5 strains, with a significant enrichment in keratitis (**Table 3**).

**TABLE 4** | *In vitro* susceptibility profile for topically used fluorquinolones among ocular MRSA isolates according to the clonal group.

Antimicrobial agent	CC8-SCCmec IV (n = 31)		CC5-SCCmec II (n = 20)		CC5-SCCmec IV (n = 08)	
	MIC <sub>90</sub>	%NS <sup>a</sup>	MIC <sub>90</sub>	%NS <sup>a</sup>	MIC <sub>90</sub>	%NS <sup>a</sup>
Moxifloxacin	2	35.5	32	100	64	62.5
Levofloxacin	8	35.5	>256	100	>256	62.5
Ofloxacin	16	38.7	>256	100	>256	62.5
Ciprofloxacin	32	42.0	>256	100	>256	62.5

<sup>a</sup>includes intermediate resistant isolates.

**TABLE 5** | Molecular typing and antimicrobial resistances of MRSA keratitis cases.

Patient	Year	Sequence type	Clonal complex	SCCmec type	PVL	Resembles clonal lineage	Antimicrobial resistances	Number of 1, 2, 3 criteria met on presentation*	Topical ATBs at time of culture
1	2014	ST5	CC5	II	Negative	USA100	OXA, CLIN, ERY, CIP, LEV, OFLX, MOX	3	Vigamox
2	2014	ST105	CC5	II	Negative	SLV of ST5	OXA, CLIN, ERY, CIP, LEV, OFLX, MOX	3	None
3	2014	ST5	CC5	IV	Negative	USA800	OXA	1	UKN
4	2014	ST5	CC5	II	Negative	USA100	OXA, CLIN, ERY, CIP, LEV, OFLX, MOX	0	None
5	2014	ST5	CC5	II	Negative	USA100	OXA, CLIN, ERY, CIP, LEV, OFLX, MOX	2	UKN
6	2015	ST5	CC5	IV	Negative	USA800	OXA, CLIN, ERY, CIP, LEV, OFLX, MOX	2	Polytrim + Erythromycin
7	2015	ST5	CC5	II	Negative	USA100	OXA, CLIN, ERY, CIP, LEV, OFLX, MOX	1	UKN
8	2015	ST5	CC5	II	Negative	USA100	OXA, CLIN, ERY, CIP, LEV, OFLX, MOX	3	None
9	2015	ST96	CC96	NT	Negative	NA	OXA, ERY	3	None
10	2015	ST8	CC8	IV	Positive	USA300	OXA, CLIN, ERY, CIP, LEV, OFLX, MOX	2	None
11	2015	ST105	CC5	II	Negative	SLV of ST5	OXA, CLIN, ERY, CIP, LEV, OFLX, MOX	2	Eythromycin and Ofloxacin
12	2016	ST5	CC5	II	Negative	USA100	OXA, CLIN, ERY, CIP, LEV, OFLX, MOX	0	Vigamox + Tobramycin
13	2016	ST3390	CC5	II	Negative	SLV of ST5	OXA, CLIN, ERY, CIP, LEV, OFLX, MOX	3	Vigamox
14	2016	ST5	CC5	II	Negative	USA100	OXA, CLIN, ERY, CIP, LEV, OFLX, MOX	3	None

\*The “1, 2, 3-Rule,” originally conceived by Vital et al. (23), was formally implemented across MEE on July 1, 2015 as a means of identifying patients at greatest risk of developing sight-threatening complications. It is composed of three simple features on clinical examination, and the presence of any of these warrants the collection of corneal cultures and treatment with topical fortified antibiotics. These rules are: ≥1+ anterior chamber cells; ≥2mm infiltrate and/or ≥2 satellite lesions; edge of lesion within 3mm of the corneal center.

The basis for the discernable tropism of CC5 strains for the ocular surface is unknown, but viewed in light of the findings of others, we can develop a testable model. Strains grouped within CC5, notably the USA100 and USA800, are well established as major causes of healthcare-related infections in the US (5). CC5 strains are often replete with acquired antibiotic resistances (34, 35), and were implicated in the first 12 cases of frank vancomycin resistant *S. aureus* stemming from independent acquisitions of the *vanA* gene from *Enterococcus* spp. (36). Despite their hospital association, CC5-MRSA strains also occur in the community, potentially bridged by long-term

care facilities. The nasal reservoir of MRSA of long-term care facility residents mirrors the molecular epidemiology of US hospitals, with CC5-related strains being predominant (37). Data from national surveillance programs show that CC5 lineages USA100 and USA800 are now widely disseminated in the community, even among noninstitutionalized individuals with no known risk factors for nasal colonization with these hospital-adapted clones (38). Although CC5 strains are frequently found among carriers in the community, they are only occasionally associated with community-acquired infection (32). In our population, despite the community origins of the patients in



which ocular infections occurred, CC5 strains predominated as causes of infection of the wet epithelial surface of the eye. Keratitis in our series was predominantly caused by strains resembling the USA100 lineage, and mostly presented as severe and potentially sight-threatening infections as determined the “1, 2, 3-Rule” (23). The severity of CC5-caused keratitis points toward the possible existence of virulence factors that could be particularly associated with corneal damage. In addition to carrying a variety of antimicrobial resistance genes, CC5 strains also possess a constellation of virulence genes (35). Of particular interest is the enterotoxin gene cluster (*egc*), which represents a unique group of enterotoxins with superantigen activities, and seems to be particularly enriched among CC5 strains (35), while being completely absent in CC8 strains (36, 39). Epidemiological observations have found an association of *egc*-encoded enterotoxins in the development of corneal ulcer in patients with atopic keratoconjunctivitis (40). Whether this locus is associated with exacerbation of the ocular surface inflammatory response and aggravation of the corneal damage is yet to be fully elucidated.

Empirical use of topical broad-spectrum antibiotics remains the first-line treatment for bacterial keratitis (41) and is commonly initiated with a topical newer fluoroquinolone ophthalmic solution (e.g., moxifloxacin 0.5%) (42). CC5 strains display generally higher fluoroquinolone MICs (non-susceptibility rate for moxifloxacin of 89.3%, MIC<sub>90</sub> 64 µg/mL) (Table 4). However, CC8-SCC*mec* IV strains associated with ocular infections at other sites were also often resistant to the commonly used fourth-generation fluoroquinolone, moxifloxacin (non-susceptibility rate using systemic breakpoints of 35.5%, MIC<sub>90</sub> 2 µg/mL). The influence of degrees of resistance on population structure is unclear. In light of its pharmacokinetics on the ocular surface, neither CC5 nor CC8 would be predicted to respond to topical moxifloxacin therapy. Based on pharmacokinetic data for topical moxifloxacin in the cornea of pigmented rabbits (43), we calculated PK/PD (AUC<sub>0–24h</sub>/MIC<sub>90</sub> ratio) indices for the main MRSA lineages examined in our study (Figure S1). Although the index was higher for CC8 strains compared to CC5, all the indices were far below the PK/PD target that predicts clinical efficacy as determined for systemic infections (44) and also for keratitis treated with fluoroquinolone (45). In addition, a review of the medical records of 14 patients with MRSA keratitis included in this study showed that only 4/14 had prior exposure to a fluoroquinolone (Vigamox, *n* = 2; erythromycin plus ofloxacin, *n* = 1; and Vigamox plus tobramycin, *n* = 1), with no information available for 3 patients (Table 5). Together, the data on prior topical antibiotic use and the calculated PK/PD indices for the ocular MRSA lineages discounts the role of direct fluoroquinolone selection as the driver of the CC5 predominant population structure associated with keratitis.

Our results are consistent with a report of 30 cases of *S. aureus* keratitis in Japan, that also found CC5 strains to be the predominant cause of MRSA-infected ulcers (46). CC8 isolates were more frequently isolated from the healthy conjunctival sac (46). Together, these findings suggest an enhanced ability of CC5 to endure selective pressures and colonize the cornea

and adjacent tissues. Lactoferrin, one the most abundant tear proteins with antimicrobial activity is inhibitory for *S. aureus*, including MRSA, but this activity varies among clinical isolates from different sites of isolation (47, 48). In one study, clinical *S. aureus* isolates causing bloodstream infections (50%) were frequently resistant to lactoferrin concentrations  $\geq 20$  µM, while isolates from conjunctivitis (33%) and SSTI (13%) were less often resistant (47). Since these infections are caused by distinct MRSA lineages, with CC5 strains being commonly associated to bloodstream infections (49), variations across different genotypes may contribute to increased resistance to this tear antimicrobial compound, especially among CC5. Similarly, the antimicrobial activity of phospholipase A2 (PLA<sub>2</sub>), an enzyme that has been found to be the major tear molecule with bactericidal activity against staphylococci, varies against methicillin-susceptible and -resistant isolates, with MRSA being more resistant to its action following short incubations (50), pointing toward a variance of this enzyme in its ability to kill *S. aureus* according to the genetic background. Further, previous reports have demonstrated that *S. aureus* strains may be differently equipped to bind to and invade ocular tissues *in vitro* and in a rabbit model of conjunctivitis and keratitis (51, 52), suggesting the existence of specific sets of adhesive surface proteins that enhance *S. aureus* ability to bind and invade the ocular tissues in a strain-specific manner.

A recent study of *S. aureus* keratitis in South Florida (53) found both CC5 (40%) and CC8 (37.3%) MRSA among isolates, clearly showing that although CC5 strains are most common, CC8 strains in other circumstances are also capable of causing keratitis. Among our patients, 12 out of 14 (85.7%), were classified as potentially sight-threatening MRSA keratitis cases according to an institution-wide grading system based on the “1, 2, 3” rule (23). For these patients, corneal cultures were unequivocally positive at diagnostic levels for the pathogen. We do not yet know whether the differences between studies stem from levels of disease severity, or other factors such as association with contact lens wear. Larger studies with well-defined criteria for enrollment will be important for determining conditions that favor infection by various pathogenic, antibiotic resistant lineages of *S. aureus*.

In contrast to the wet epithelial surface of the eye, CC8 MRSA strains, typified by the USA300 lineage, predominate as causes of infections of the keratinized epithelium and eye soft tissues. Lineage enrichment has been also reported in patients with bloodstream infection with haematogenous complications (30) infective endocarditis (31) and respiratory tract infections (54). Among our patients, CC8 strains were the predominant causes of preseptal and orbital abscess/cellulitis (22 out of 27 cases), consistent with their known tropism for infecting keratinized epithelium and soft tissues (29, 32). Among the remaining abscess/cellulitis cases, only one was caused by a CC5 isolate and 3 by other lineages (Table 3). In the early 2000s, the USA300 clone appeared in outbreaks of community-acquired SSTIs in otherwise healthy people (55, 56). Because of its ability to rapidly spread through person-to-person contact and readily compete with commensal skin flora (56), the USA300 lineage quickly predominated as the main cause of SSTIs (29, 32), and a significant cause of severe invasive infections (6). USA300 is

generally more virulent, causing infections of greater severity and associated with worse outcome compared to other MRSA clones (57, 58). The aggressiveness of USA300 type strains is thought to be associated to the carriage of a variety of virulence factors, including the pore-forming toxin PVL, which is predominantly found in CC8 strains (59), and has been linked to the ability of this strain to cause necrotizing infections (60).

Orbital and preseptal abscesses are SSTIs commonly caused by *Staphylococcus aureus* (61, 62), and MRSA rates appear to be rising (63). Severe cases have been reported, including orbital and periorbital necrotizing fasciitis (64–66), necrotizing conjunctivitis with orbital invasion (12) and orbital cellulitis with bilateral involvement that progressed to blindness (14). A prospective study (2012–2015) of children and adolescents presenting with staphylococcal periorbital and orbital cellulitis in Houston found that most of the *S. aureus* isolates in their population were methicillin-resistant (67%) and were genetically related to the USA300 clone (78%) (67). Similarly, in a series of 11 patients presenting with culture-positive MRSA infections of the eye and orbit in San Francisco, most (82%) were caused by USA300 (13). Preseptal and orbital abscess/cellulitis were among the most common manifestations in these cases, some presenting with extensive necrosis of the eyelid and orbital tissues.

Collectively, these results are consistent with various MRSA lineages being enriched for properties that enhance their ability to resist defenses and competitive pressures, and colonize and infect either the wet epithelial surface or the ocular adnexal tissues. We propose that many of the features that have allowed CC5-type MRSA to adapt and be transmitted in the hospital environment, and readily acquire antibiotic resistances, endows them with properties that enhance their ability to resist robust ocular surface defenses and infect the cornea. In a comparative analysis of the genomes of the CC5 strains that had acquired vancomycin resistance from enterococci, we identified a constellation of traits with the *S. aureus* pathogenicity island as likely involved with their ability to persist in a mixed infection and acquire resistances by horizontal gene transfer (36). These same traits may well enhance their survival despite the defenses of the wet epithelial surface. In contrast, CC8-SCC*mec* IV PVL-positive strains are already well known to have features that enhance their ability to colonize the skin and compete effectively for that niche with coagulase negative strains, including the ACME locus (68). We believe these features account for their association with infection of the keratinized surfaces of the ocular adnexa. Direct testing of isogenic mutants will be required to identify the major contributors to pathogenesis of various anatomical sites of the eye by MRSA, and to develop new approaches for

mitigating that common threat. It is important to note that these findings represent the population structure of a relatively small ocular MRSA population isolated at the Massachusetts Eye and Ear, and validation of our results using a larger bacterial collection and isolates from other locations would be warranted.

## DATA AVAILABILITY STATEMENT

The datasets generated for this study are available on request to the corresponding author.

## AUTHOR CONTRIBUTIONS

PB, LU, JC, and MG contributed conception and design of the study and wrote sections of the manuscript. PB and LU organized the database and performed the statistical analysis. PB wrote the first draft of the manuscript. All authors contributed to manuscript revision, read and approved the submitted version.

## FUNDING

This work was supported in part by NEI grant EY024285, and the Harvard-wide Program on Antibiotic Resistance NIAID grant AI083214. Funding agencies had no role in study design, data analysis, decision to publish or preparation of the manuscript.

## ACKNOWLEDGMENTS

The authors thank Rick Body, James Cadorette and other medical technologists from the Clinical Microbiology Laboratory at MEE for their support in creating a microbial repository of strains isolated from ocular and otolaryngology infections.

## SUPPLEMENTARY MATERIAL

The Supplementary Material for this article can be found online at: <https://www.frontiersin.org/articles/10.3389/fpubh.2020.00204/full#supplementary-material>

**Figure S1** | PK/PD ( $AUC_{0-24h}/MIC_{90}$  ratio) indices for the main MRSA clones isolated in our study.  $AUC_{0-24h}$  data was derived from pharmacokinetic studies of topical moxifloxacin in the cornea of pigmented rabbits (43). Dashed line indicates the PK/PD target that predicts clinical efficacy in keratitis patients treated with topical fluoroquinolone (45).

## REFERENCES

- World Health Organization (WHO). *Antimicrobial Resistance: Global Report on Surveillance*. (2014).
- Klein EY, Mojica N, Jiang W, Cosgrove SE, Septimus E, Morgan DJ, et al. Trends in methicillin-Resistant staphylococcus aureus hospitalizations in the united states, 2010–2014. *Clin Infect Dis*. (2017) 65:1921–3. doi: 10.1093/cid/cix640
- Kourtis AP, Hatfield K, Baggs J, Mu Y, See I, Epton E, et al. Vital signs: epidemiology and recent trends in methicillin-Resistant and in methicillin-Susceptible staphylococcus aureus bloodstream infections - united states. *MMWR Morb Mortal Wkly Rep*. (2019) 68:214–9. doi: 10.15585/mmwr.mm6809e1
- van Duin D, Paterson DL. Multidrug-Resistant bacteria in the community: trends and lessons learned. *Infect Dis Clin North Am*. (2016) 30:377–90. doi: 10.1016/j.idc.2016.02.004

5. DeLeo FR, Chambers HF. Reemergence of antibiotic-resistant staphylococcus aureus in the genomics era. *J Clin Invest.* (2009) 119:2464–74. doi: 10.1172/JCI38226
6. David MZ, Daum RS. Community-associated methicillin-resistant staphylococcus aureus: epidemiology and clinical consequences of an emerging epidemic. *Clin Microbiol Rev.* (2010) 23:616–87. doi: 10.1128/CMR.00081-09
7. Diekema DJ, Richter SS, Heilmann KP, Dohrn CL, Riahi F, Tendolkar S, et al. Continued emergence of uSA300 methicillin-resistant staphylococcus aureus in the united states: results from a nationwide surveillance study. *Infect Control Hosp Epidemiol.* (2014) 35:285–92. doi: 10.1086/675283
8. Asbell PA, Colby KA, Deng S, McDonnell P, Meisler DM, Raizman MB, et al. Ocular tRUST: nationwide antimicrobial susceptibility patterns in ocular isolates. *Am J Ophthalmol.* (2008) 145:951–8. doi: 10.1016/j.ajo.2008.01.025
9. Asbell PA, Sahm DF, Shaw M, Draghi DC, Brown NP. Increasing prevalence of methicillin resistance in serious ocular infections caused by staphylococcus aureus in the united states: 2000 to 2005. *J Cataract Refract Surg.* (2008) 34:814–8. doi: 10.1016/j.jcrs.2008.01.016
10. Asbell PA, Sanfilippo CM, Pillar CM, DeCory HH, Sahm DF, Morris TW. Antibiotic resistance among ocular pathogens in the united states: five-Year results from the antibiotic resistance monitoring in ocular microorganisms (ARMOR) surveillance study. *JAMA Ophthalmol.* (2015) 133:1445–54. doi: 10.1001/jamaophthalmol.2015.3888
11. Cavuoto K, Zutshi D, Karp CL, Miller D, Feuer W. Update on bacterial conjunctivitis in south florida. *Ophthalmology.* (2008) 115:51–6. doi: 10.1016/j.ophtha.2007.03.076
12. Brown SM, Rafflo GT, Fanning WL. Transconjunctival orbital invasion by methicillin-resistant staphylococcus aureus. *Arch Ophthalmol.* (2009) 127:941–2. doi: 10.1001/archophthalmol.2009.144
13. Rutar T, Chambers HF, Crawford JB, Perdreau-Remington F, Zwick OM, Karr M, et al. Ophthalmic manifestations of infections caused by the uSA300 clone of community-associated methicillin-resistant staphylococcus aureus. *Ophthalmology.* (2006) 113:1455–62. doi: 10.1016/j.ophtha.2006.03.031
14. Rutar T, Zwick OM, Cockerham KP, Horton JC. Bilateral blindness from orbital cellulitis caused by community-acquired methicillin-resistant staphylococcus aureus. *Am J Ophthalmol.* (2005) 140:740–2. doi: 10.1016/j.ajo.2005.03.076
15. Mantelli F, Argueso P. Functions of ocular surface mucins in health and disease. *Curr Opin Allergy Clin Immunol.* (2008) 8:477–83. doi: 10.1097/ACI.0b013e32830e6b04
16. McClellan KA. Mucosal defense of the outer eye. *Surv Ophthalmol.* (1997) 42:233–46. doi: 10.1016/S0039-6257(97)00090-8
17. Sack RA, Nunes I, Beaton A, Morris C. Host-defense mechanism of the ocular surfaces. *Biosci Rep.* (2001) 21:463–80. doi: 10.1023/A:1017943826684
18. Costello EK, Stagaman K, Dethlefsen L, Bohannan BJ, Relman DA. The application of ecological theory toward an understanding of the human microbiome. *Science.* (2012) 336:1255–62. doi: 10.1126/science.1224203
19. Martiny JB, Bohannan BJ, Brown JH, Colwell RK, Fuhrman JA, Green JL, et al. Microbial biogeography: putting microorganisms on the map. *Nat Rev Microbiol.* (2006) 4:102–12. doi: 10.1038/nrmicro1341
20. Valentino MD, McGuire AM, Rosch JW, Bispo PJ, Burnham C, Sanfilippo CM, et al. Encapsulated streptococcus pneumoniae from conjunctivitis encode variant traits and belong to a distinct phylogenetic cluster. *Nat Commun.* (2014) 5:5411. doi: 10.1038/ncomms6411
21. Ung L, Bispo PJM, Bryan NC, Andre C, Chodosh J, Gilmore MS. The best of all worlds: streptococcus pneumoniae conjunctivitis through the lens of community ecology and microbial biogeography. *Microorganisms.* (2019) 8:46. doi: 10.3390/microorganisms8010046
22. Harris PA, Taylor R, Thielke R, Payne J, Gonzalez N, Conde JG. Research electronic data capture (REDCap)—a metadata-driven methodology and workflow process for providing translational research informatics support. *J Biomed Inform.* (2009) 42:377–81. doi: 10.1016/j.jbi.2008.08.010
23. Vital MC, Belloso M, Prager TC, Lanier JD. Classifying the severity of corneal ulcers by using the “1, 2, 3” rule. *Cornea.* (2007) 26:16–20. doi: 10.1097/ICO.0b013e31802b2e47
24. Clinical and Laboratory Standard Institute. *Methods for Dilution Antimicrobial Susceptibility Tests for Bacteria That Grow Aerobically; Approved Standard-Ninth Edition.* CLSI document M07-A9. Wayne, PA: Clinical and Laboratory Standard Institutes. (2012).
25. Clinical and Laboratory Standard Institute. *Performance Standards for Antimicrobial Susceptibility Testing.* 28th ed. CLSI supplement M100. Wayne, PA: Clinical and Laboratory Standards Institute (2018).
26. Bispo P, Höfling-Lima A, Pignatari A. Characterization of ocular methicillin-resistant staphylococcus epidermidis isolates belonging predominantly to clonal complex 2 subcluster ii. *J Clin Microbiol.* (2014) 52:1412–7. doi: 10.1128/JCM.03098-13
27. Kondo Y, Ito T, Ma X, Watanabe S, Kreiswirth B, Etienne J, et al. Combination of multiplex pCRs for staphylococcal cassette chromosome mec type assignment: rapid identification system for mec, ccr, and major differences in junkyard regions. *Antimicro Agents Chem.* (2007) 51:264–74. doi: 10.1128/AAC.00165-06
28. David MZ, Boyle-Vavra S, Zychowski DL, Daum RS. Methicillin-susceptible staphylococcus aureus as a predominantly healthcare-associated pathogen: a possible reversal of roles? *PLoS ONE.* (2011) 6:e18217. doi: 10.1371/journal.pone.0018217
29. Albrecht VS, Limbago BM, Moran GJ, Krishnadasan A, Gorwitz RJ, McDougal LK, et al. Staphylococcus aureus colonization and strain type at various body sites among patients with a closed abscess and uninfected controls at US Emergency Departments. *J Clin Microbiol.* (2015) 53:3478–84. doi: 10.1128/JCM.01371-15
30. Fowler VG, Jr, Nelson CL, McIntyre LM, Kreiswirth BN, Monk A, Archer GL, et al. Potential associations between hematogenous complications and bacterial genotype in staphylococcus aureus infection. *J Infect Dis.* (2007) 196:738–47. doi: 10.1086/520088
31. Nienaber JJ, Sharma Kuinkel BK, Clarke-Pearson M, Lamlerthton S, Park L, Rude TH, et al. Methicillin-susceptible staphylococcus aureus endocarditis isolates are associated with clonal complex 30 genotype and a distinct repertoire of enterotoxins and adhesins. *J Infect Dis.* (2011) 204:704–13. doi: 10.1093/infdis/jir389
32. Talan DA, Krishnadasan A, Gorwitz RJ, Fosheim GE, Limbago B, Albrecht V, et al. Comparison of staphylococcus aureus from skin and soft-tissue infections in uS emergency department patients, 2004 and 2008. *Clin Infect Dis.* (2011) 53:144–9. doi: 10.1093/cid/cir308
33. Wurster JJ, Bispo PJM, Van Tyne D, Cadorette JJ, Boody R, Gilmore MS. Staphylococcus aureus from ocular and otolaryngology infections are frequently resistant to clinically important antibiotics and are associated with lineages of community and hospital origins. *PLoS ONE.* (2018) 13:e0208518. doi: 10.1371/journal.pone.0208518
34. Aanensen DM, Feil EJ, Holden MT, Dordel J, Yeats CA, Fedosejev A, et al. Whole-Genome sequencing for routine pathogen surveillance in public health: a population snapshot of invasive staphylococcus aureus in europe. *MBio.* (2016) 7:16. doi: 10.1128/mBio.00444-16
35. Monecke S, Coombs G, Shore AC, Coleman DC, Akpaka P, Borg M, et al. A field guide to pandemic, epidemic and sporadic clones of methicillin-resistant staphylococcus aureus. *PLoS ONE.* (2011) 6:e17936. doi: 10.1371/journal.pone.0017936
36. Kos VN, Desjardins CA, Griggs A, Cerqueira G, Van Tonder A, Holden MT, et al. Comparative genomics of vancomycin-resistant staphylococcus aureus strains and their positions within the clade most commonly associated with methicillin-resistant S. aureus hospital-acquired infection in the United States. *MBio.* (2012) 3:12. doi: 10.1128/mBio.00112-12
37. Hudson LO, Reynolds C, Spratt BG, Enright MC, Quan V, Kim D, et al. Diversity of methicillin-resistant staphylococcus aureus strains isolated from residents of 26 nursing homes in orange county, california. *J Clin Microbiol.* (2013) 51:3788–95. doi: 10.1128/JCM.01708-13
38. Tenover FC, McAllister S, Fosheim G, McDougal LK, Carey RB, Limbago B, et al. Characterization of staphylococcus aureus isolates from nasal cultures collected from individuals in the united states in 2001 to 2004. *J Clin Microbiol.* (2008) 46:2837–41. doi: 10.1128/JCM.00480-08
39. van Belkum A, Melles DC, Snijders SV, van Leeuwen WB, Wertheim HF, Nouwen JL, et al. Clonal distribution and differential occurrence of the enterotoxin gene cluster, egc, in carriage- versus bacteremia-associated isolates of *Staphylococcus aureus*. *J Clin Microbiol.* (2006) 44:1555–7. doi: 10.1128/JCM.44.4.1555-1557.2006



40. Fujishima H, Okada N, Dogru M, Baba F, Tomita M, Abe J, et al. The role of staphylococcal enterotoxin in atopic keratoconjunctivitis and corneal ulceration. *Allergy*. (2012) 67:799–803. doi: 10.1111/j.1398-9995.2012.02818.x
41. Austin A, Lietman T, Rose-Nussbaumer J. Update on the management of infectious keratitis. *Ophthalmology*. (2017) 124:1678–89. doi: 10.1016/j.ophtha.2017.05.012
42. Hsu HY, Nacke R, Song JC, Yoo SH, Alfonso EC, Israel HA. Community opinions in the management of corneal ulcers and ophthalmic antibiotics: a survey of 4 states. *Eye Contact Lens*. (2010) 36:195–200. doi: 10.1097/ICL.0b013e3181e3ef45
43. Proksch JW, Ward KW. Ocular pharmacokinetics/pharmacodynamics of besifloxacin, moxifloxacin, and gatifloxacin following topical administration to pigmented rabbits. *J Ocul Pharmacol Ther*. (2010) 26:449–58. doi: 10.1089/jop.2010.0054
44. Segreti J, Jones RN, Bertino JS, Jr. Challenges in assessing microbial susceptibility and predicting clinical response to newer-generation fluoroquinolones. *J Ocul Pharmacol Ther*. (2012) 28:3–11. doi: 10.1089/jop.2011.0072
45. Wilhelmus KR. Evaluation and prediction of fluoroquinolone pharmacodynamics in bacterial keratitis. *J Ocul Pharmacol Ther*. (2003) 19:493–9. doi: 10.1089/108076803322473042
46. Hayashi S, Suzuki T, Yamaguchi S, Inoue T, Ohashi Y. Genotypic characterization of *Staphylococcus aureus* isolates from cases of keratitis and healthy conjunctival sacs. *Cornea*. (2014) 33:72–6. doi: 10.1097/ICO.0b013e3182a4810f
47. Aguila A, Herrera AG, Morrison D, Cosgrove B, Perojo A, Montesinos I, et al. Bacteriostatic activity of human lactoferrin against staphylococcus aureus is a function of its iron-binding properties and is not influenced by antibiotic resistance. *FEMS Immunol Med Microbiol*. (2001) 31:145–52. doi: 10.1111/j.1574-695X.2001.tb00511.x
48. Chen PW, Jheng TT, Shyu CL, Mao FC. Synergistic antibacterial efficacies of the combination of bovine lactoferrin or its hydrolysate with probiotic secretion in curbing the growth of methicillin-resistant staphylococcus aureus. *J Med Microbiol*. (2013) 62(Pt 12):1845–51. doi: 10.1099/jmm.0.052639-0
49. Chua T, Moore CL, Perri MB, Donabedian SM, Masch W, Vager D, et al. Molecular epidemiology of methicillin-resistant staphylococcus aureus bloodstream isolates in urban detroit. *J Clin Microbiol*. (2008) 46:2345–52. doi: 10.1128/JCM.00154-08
50. Qu XD, Lehrer RI. Secretory phospholipase a2 is the principal bactericide for staphylococci and other gram-positive bacteria in human tears. *Infect Immun*. (1998) 66:2791–7. doi: 10.1128/IAI.66.6.2791-2797.1998
51. McCormick CC, Caballero AR, Balzli CL, Tang A, Weeks A, O'Callaghan RJ. Diverse virulence of staphylococcus aureus strains for the conjunctiva. *Curr Eye Res*. (2011) 36:14–20. doi: 10.3109/02713683.2010.523194
52. Tang A, Balzli CL, Caballero AR, McCormick CC, Taylor SD, O'Callaghan RJ. Staphylococcus aureus infection of the rabbit cornea following topical administration. *Curr Eye Res*. (2012) 37:1075–83. doi: 10.3109/02713683.2012.716485
53. Peterson JC, Durkee H, Miller D, Maestre-Mesa J, Arboleda A, Aguilar MC, et al. Molecular epidemiology and resistance profiles among healthcare- and community-associated staphylococcus aureus keratitis isolates. *Infect Drug Resist*. (2019) 12:831–43. doi: 10.2147/IDR.S190245
54. Booth MC, Pence LM, Mahareshti P, Callegan MC, Gilmore MS. Clonal associations among staphylococcus aureus isolates from various sites of infection. *Infect Immun*. (2001) 69:345–52. doi: 10.1128/IAI.69.1.345-352.2001
55. Begier EM, Frenette K, Barrett NL, Mshar P, Petit S, Boxrud DJ, et al. A high-morbidity outbreak of methicillin-resistant staphylococcus aureus among players on a college football team, facilitated by cosmetic body shaving and turf burns. *Clin Infect Dis*. (2004) 39:1446–53. doi: 10.1086/425313
56. Kazakova SV, Hageman JC, Matava M, Srinivasan A, Phelan L, Garfinkel B, et al. A clone of methicillin-resistant staphylococcus aureus among professional football players. *N Engl J Med*. (2005) 352:468–75. doi: 10.1056/NEJMoa042859
57. Kempker RR, Farley MM, Ladson JL, Satola S, Ray SM. Association of methicillin-resistant staphylococcus aureus (MRSA) uSA300 genotype with mortality in mRSA bacteremia. *J Infect*. (2010) 61:372–81. doi: 10.1016/j.jinf.2010.09.021
58. Kreisel KM, Stine OC, Johnson JK, Perencevich EN, Shardell MD, Lesse AJ, et al. USA300 methicillin-resistant staphylococcus aureus bacteremia and the risk of severe sepsis: is uSA300 methicillin-resistant staphylococcus aureus associated with more severe infections? *Diagn Microbiol Infect Dis*. (2011) 70:285–90. doi: 10.1016/j.diagmicrobio.2011.03.010
59. Brown ML, O'Hara FP, Close NM, Mera RM, Miller LA, Suaya JA, et al. Prevalence and sequence variation of panton-valentine leukocidin in methicillin-resistant and methicillin-susceptible staphylococcus aureus strains in the united states. *J Clin Microbiol*. (2012) 50:86–90. doi: 10.1128/JCM.05564-11
60. Chi CY, Lin CC, Liao IC, Yao YC, Shen FC, Liu CC, et al. Pantone-Valentine leukocidin facilitates the escape of staphylococcus aureus from human keratinocyte endosomes and induces apoptosis. *J Infect Dis*. (2014) 209:224–35. doi: 10.1093/infdis/jit445
61. Carniciu AL, Chou J, Leskov I, Freitag SK. Clinical presentation and bacteriology of eyebrow infections: the massachusetts eye and ear infirmary experience (2008–2015). *Ophthalmic Plast Reconstr Surg*. (2017) 33:372–5. doi: 10.1097/IOP.0000000000000797
62. McKinley SH, Yen MT, Miller AM, Yen KG. Microbiology of pediatric orbital cellulitis. *Am J Ophthalmol*. (2007) 144:497–501. doi: 10.1016/j.ajo.2007.04.049
63. Amato M, Pershing S, Walvick M, Tanaka S. Trends in ophthalmic manifestations of methicillin-resistant staphylococcus aureus (MRSA) in a northern california pediatric population. *J AAPOS*. (2013) 17:243–7. doi: 10.1016/j.jaapos.2012.12.151
64. Gurdal C, Bilkan H, Sarac O, Seven E, Yenidunya MO, Kutluhan A, et al. Periorbital necrotizing fasciitis caused by community-associated methicillin-resistant staphylococcus aureus periorbital necrotizing fasciitis. *Orbit*. (2010) 29:348–50. doi: 10.3109/01676831003697509
65. Shield DR, Servat J, Paul S, Turbin RE, Moreau A, de la Garza A, et al. Periocular necrotizing fasciitis causing blindness. *JAMA Ophthalmol*. (2013) 131:1225–7. doi: 10.1001/jamaophthalmol.2013.4816
66. Singam NV, Rusia D, Prakash R. An eye popping case of orbital necrotizing fasciitis treated with antibiotics, surgery, and hyperbaric oxygen therapy. *Am J Case Rep*. (2017) 18:329–33. doi: 10.12659/AJCR.902535
67. Foster CE, Yarotsky E, Mason EO, Kaplan SL, Hulten KG. Molecular characterization of staphylococcus aureus isolates from children with periorbital or orbital cellulitis. *J Pediatric Infect Dis Soc*. (2018) 7:205–9. doi: 10.1093/jpids/pix036
68. Planet PJ, LaRussa SJ, Dana A, Smith H, Xu A, Ryan C, et al. Emergence of the epidemic methicillin-resistant staphylococcus aureus strain uSA300 coincides with horizontal transfer of the arginine catabolic mobile element and speG-mediated adaptations for survival on skin. *MBio*. (2013) 4:e00889–13. doi: 10.1128/mBio.00889-13

**Conflict of Interest:** The authors declare that the research was conducted in the absence of any commercial or financial relationships that could be construed as a potential conflict of interest.

Copyright © 2020 Bispo, Ung, Chodosh and Gilmore. This is an open-access article distributed under the terms of the Creative Commons Attribution License (CC BY). The use, distribution or reproduction in other forums is permitted, provided the original author(s) and the copyright owner(s) are credited and that the original publication in this journal is cited, in accordance with accepted academic practice. No use, distribution or reproduction is permitted which does not comply with these terms.





# Amoxicillin Increased Functional Pathway Genes and Beta-Lactam Resistance Genes by Pathogens Bloomed in Intestinal Microbiota Using a Simulator of the Human Intestinal Microbial Ecosystem

## OPEN ACCESS

### Edited by:

Leonardo Neves de Andrade,  
University of São Paulo, Brazil

### Reviewed by:

Rosa Del Campo,  
Ramón y Cajal Institute for Health  
Research, Spain  
Pallavi Singh,  
Northern Illinois University,  
United States

### \*Correspondence:

Daqing Mao  
maodq@nankai.edu.cn  
Yi Luo  
luoy@nankai.edu.cn

† These authors have contributed  
equally to this work

### Specialty section:

This article was submitted to  
Antimicrobials, Resistance  
and Chemotherapy,  
a section of the journal  
Frontiers in Microbiology

**Received:** 22 October 2019

**Accepted:** 12 May 2020

**Published:** 04 June 2020

### Citation:

Liu L, Wang Q, Lin H, Das R,  
Wang S, Qi H, Yang J, Xue Y, Mao D  
and Luo Y (2020) Amoxicillin  
Increased Functional Pathway Genes  
and Beta-Lactam Resistance Genes  
by Pathogens Bloomed in Intestinal  
Microbiota Using a Simulator of the  
Human Intestinal Microbial  
Ecosystem.  
Front. Microbiol. 11:1213.  
doi: 10.3389/fmicb.2020.01213

Lei Liu<sup>1†</sup>, Qing Wang<sup>1,2†</sup>, Huai Lin<sup>1</sup>, Ranjit Das<sup>1</sup>, Siyi Wang<sup>1</sup>, Hongmei Qi<sup>1</sup>, Jing Yang<sup>1</sup>,  
Yingang Xue<sup>3</sup>, Daqing Mao<sup>4\*</sup> and Yi Luo<sup>1\*</sup>

<sup>1</sup> College of Environmental Science and Engineering, Ministry of Education Key Laboratory of Pollution Processes and Environmental Criteria, Nankai University, Tianjin, China, <sup>2</sup> Hebei Key Laboratory of Air Pollution Cause and Impact (preparatory), College of Energy and Environmental Engineering, Hebei University of Engineering, Handan, China, <sup>3</sup> Key Laboratory of Environmental Protection of Water Environment Biological Monitoring of Jiangsu Province, Changzhou Environmental Monitoring Center, Changzhou, China, <sup>4</sup> School of Medicine, Nankai University, Tianjin, China

Antibiotics are frequently used to treat bacterial infections; however, they affect not only the target pathogen but also commensal gut bacteria. They may cause the dysbiosis of human intestinal microbiota and consequent metabolic alterations, as well as the spreading of antibiotic resistant bacteria and antibiotic resistance genes (ARGs). *In vitro* experiments by simulator of the human intestinal microbial ecosystem (SHIME) can clarify the direct effects of antibiotics on different regions of the human intestinal microbiota, allowing complex human microbiota to be stably maintained in the absence of host cells. However, there are very few articles added the antibiotics into this *in vitro* model to observe the effects of antibiotics on the human intestinal microbiota. To date, no studies have focused on the correlations between the bloomed pathogens caused by amoxicillin (AMX) exposure and increased functional pathway genes as well as ARGs. This study investigated the influence of 600 mg day<sup>-1</sup> AMX on human intestinal microbiota using SHIME. The impact of AMX on the composition and function of the human intestinal microbiota was revealed by 16S rRNA gene sequencing and high-throughput quantitative PCR. The results suggested that: (i) AMX treatment has tremendous influence on the overall taxonomic composition of the gut microbiota by increasing the relative abundance of *Klebsiella* [linear discriminant analysis (LDA) score = 5.26] and *Bacteroides uniformis* (LDA score = 4.75), as well as taxonomic diversity (Simpson,  $P = 0.067$ ,  $T$ -test; Shannon,  $P = 0.061$ ,  $T$ -test), and decreasing the members of *Parabacteroides* (LDA score = 4.18), *Bifidobacterium* (LDA score = 4.06), and *Phascolarctobacterium* (LDA score = 3.95); (ii) AMX exposure significantly enhanced the functional pathway genes and beta-lactam resistance genes, and the bloomed pathogens were strongly correlated with the metabolic and immune system diseases

gene numbers ( $R = 0.98$ ,  $P < 0.001$ ) or *bl2\_jen* and *bl2be\_shv2* abundance ( $R = 0.94$ ,  $P < 0.001$ ); (iii) the changes caused by AMX were “SHIME-compartment” different with more significant alteration in ascending colon, and the effects were permanent, which could not be restored after 2-week AMX discontinuance. Overall results demonstrated negative side-effects of AMX, which should be considered for AMX prescription.

**Keywords:** amoxicillin, antibiotic resistance genes (ARGs), functional pathway genes, human intestinal microbiota, simulator of the human intestinal microbial ecosystem (SHIME)

## INTRODUCTION

Human intestinal microbiota co-exists in symbiosis with human beings and comprises with about 150 times more genes than the human genome, which makes intestinal microbiota become “another” genome of human beings (Qin et al., 2010). Moreover, human intestinal microbiota has been demonstrated to provide numerous important functions for the human health, including fermentation of indigestible dietary polysaccharides, synthesis of essential amino acids, and vitamins, modulation of the immune function and protection from the pathogens, as well as metabolism of the xenobiotic drugs (Chow et al., 2010; Yatsunenkov et al., 2012; Cabreiro et al., 2013). Both human and veterinary antibiotics were detected in the collective gut of the Chinese population through our previous research (Wang et al., 2020). The antibiotics in our gut would kill or prevent the growth of commensal beneficial bacteria, which would cause the dysbiosis of intestinal microbiota, resulting multiple human diseases (Blaser, 2016; Ianiro et al., 2016; Flandroy et al., 2018; Kho and Lal, 2018). Antibiotics may also promote the spreading of antibiotic resistant bacteria (ARB) and antibiotic resistance genes (ARGs) in the human gut (Stecher et al., 2013; Barraud et al., 2018). One of the most commonly prescribed antibiotic in clinical and residential applications is amoxicillin (AMX), an inexpensive oral penicillin-type, beta-lactam antibiotic that kills a broad spectrum of bacteria by interfering with the synthesis of bacterial cell wall peptidoglycan layer (Zapata and Quagliarello, 2015; Zhang et al., 2015). The influence of AMX on human intestinal microbiota by *in vivo* research has been well studied and recorded, including human (Ladirat et al., 2014a; Pallav et al., 2014; Vrieze et al., 2014; Zaura et al., 2015; Oh et al., 2016) and human microbiota associated-animal models (Barc et al., 2008; Collignon et al., 2008; Collignon et al., 2010). Oh et al. (2016) noticed that AMX increased the abundance of *Klebsiella* in human intestinal microbiota. As a typical Gram-negative bacterial pathogen, *K. pneumoniae* is ubiquitous in the environment and symbioses in the human gut (Rock et al., 2014). However, the bloom of *K. pneumoniae* in human gut is often related to unhealthy status (Pena et al., 1997; Wiener-Well et al., 2010; Gorrie et al., 2017). Furthermore, no studies have suggested the bloom of *K. pneumoniae* caused by AMX exposure contributed to the increase of functional pathway genes and beta-lactam resistance genes.

Previous reports have revealed that changes of intestinal microbiota by AMX exposure are region-dependent and more significant effects were observed in the proximal colon than in the

distal colon (Ladirat et al., 2014b; Marzorati et al., 2017). *In vivo* experiments detected the fecal samples that generally stand for the distal intestinal microbiota, which could not reveal the impacts of antibiotics on different gut regions. Moreover, *in vitro* experiment using simulator of the human intestinal microbial ecosystem (SHIME) can elucidate the direct effects of medicines on different regions of the human intestinal microbiota, which allows the complex human microbiota to be stably maintained in the absence of host cells (Van de Wiele et al., 2015). The SHIME model is known to be a useful tool for the *in vitro* study, which has already been used to identify the influence of bacteria and compounds on the colon microbiota, including probiotics such as *Clostridium cluster XIVa* and *Bifidobacterium longum* (Van den Abbeele et al., 2013; Truchado et al., 2015), prebiotics and prebiotics like compounds such as inulin, polyphenols and orange juice (Kemperman et al., 2013; Duque et al., 2016; Selak et al., 2016), and other toxic compounds such as Chlorpyrifos and Arsenic (Reygner et al., 2016; Yu et al., 2016). However, to the best of our knowledge, there are very few research that applied antibiotics into the SHIME model (Van den Abbeele et al., 2012; Bussche et al., 2015; Marzorati et al., 2017; Ichim et al., 2018; El Hage et al., 2019; Liu et al., 2020). These articles focused on the benefit of the mucosal environment, high-fiber diets, probiotic, and propionate-producing consortium in human intestinal microbiota. The effects of antibiotics, including AMX and other antibiotics mixture, vancomycin, and clindamycin, were limited on microbiota composition and metabolite. Also, there was little information available to demonstrate the link between the bloomed pathogens and functional pathway genes or ARGs. Hence, there is a need to study the influence of AMX on human intestinal microbiota in the SHIME model that integrates the entire gastrointestinal tract and maintains microbiome stability over an extended timeframe (Van de Wiele et al., 2015).

Since the reasonable dosage of AMX for the adult human study is about 750 to 1,500 mg day<sup>-1</sup>, and only half volume of the adult gut can be simulated in the SHIME model, here the direct effects of 600 mg day<sup>-1</sup> of AMX on the composition and function of the human fecal microbiota were followed by the previous studies (Pallav et al., 2014; Reijnders et al., 2016). Three reactors (representing the ascending, transverse, and descending colon, respectively) that inoculated with human intestinal microbiota were studied for the three groups: immediately before AMX administration during 0 to 21 days (a control group), AMX-exposure during 22 to 28 days (an AMX treated group), and after the AMX discontinuance during 29 to 42 days (a recovery

group). The 16S rRNA gene sequencing and high-throughput quantitative PCR (HT-qPCR) results revealed that AMX exposure caused a tremendous impact on the overall taxonomic composition of the gut microbiota, and increased functional pathway genes as well as ARGs. The changes were “SHIME-compartment” different with more significant modulation in the ascending colon, which could not be restored after 2-week AMX discontinuance. Therefore, the results of our research demonstrated a severe impact and a negative side-effect of AMX related to health problems, which should be considered as a fundamental aspect of the cost-benefit equation for its prescription.

## MATERIALS AND METHODS

### The SHIME Model Experimental Setup and Sampling

The SHIME set up was formed by five double-jacketed reactors designated as the stomach, small intestine, ascending colon, transverse colon, and descending colon, respectively (**Supplementary Figure S1**). The last three reactors were inoculated with a mixture of fecal microbiota from a healthy adult volunteer, who did not suffer from gastrointestinal diseases or take antibiotics in the previous 6 months according to previous classic studies (Yu et al., 2016; Wang et al., 2018). And the differences between individuals may be alleviated by same culture condition (Van den Abbeele et al., 2013). The study was approved by the Biomedical Ethics Committees of Nankai University. The participant has given written informed consent to understand the study purpose, procedures, risks, benefits, and rights. The details of the SHIME system and the startup process are summarized in the **Supplementary Material**.

As shown in **Supplementary Figure S1**, during the first 2 weeks (0 to 14 days) of the experiment, control nutritional medium was added into the reactors to stabilize the microbial community. After this period, the SHIME was sequentially exposed to nutritious medium (15 to 21 days), and nutritious medium + 600 mg day<sup>-1</sup> AMX (22 to 28 days), each time system was maintained for 1-week. Then a nutritious medium was added and observed for another 2-weeks (29 to 42 days). Samples were collected and analyzed at six time points of 14, 21, 24, 28, 35, and 42 days from the ascending colon, transverse colon and descending colon, respectively. Each of the 18 samples is a mixture of three samples collected at specific time intervals in a day (Liu et al., 2020), and AMX was added after samples (C-A2, C-T2, and C-D2) had been collected in 22 days and discontinued after samples (AMX-A2, AMX-T2, and AMX-D2) had been collected in 29 days. Therefore, these samples were divided into three groups: before AMX administration during 0 to 21 days (control group), AMX exposure during 22 to 28 days (AMX treatment group) and after the AMX discontinuance during 29 to 42 days (recovery group), which were according to previous classic studies (Yu et al., 2016; Wang et al., 2018). Specifically, during each sampling time, three sterilized centrifuge tubes (50 ml) were used to collect

the samples (10 ml) flow out from each colon vessel of the SHIME, respectively, and these samples were initially stored at -4°C (Van de Wiele et al., 2010; Yu et al., 2016). After all the samples were collected in each sampling day, three samples from the same vessel were mixed into one sterilized centrifuge tube (50 ml), which was operated in a super-clean bench. Then the samples were centrifuged at 10,400 g for 10 min, and the separated supernatants and pellets were stored at -80°C for further analyses.

### 16S rRNA Gene Sequencing and Analysis

Total DNA was extracted from the samples using the E.Z.N.A. stool DNA Kit (Omega, United States) according to the manufacturer's protocols. The V3-V4 region of the bacterial 16S rRNA gene was amplified by polymerase chain reaction (PCR) using primers 341F 5'-CCTAYGGGRBGCASCAG-3' and 806R 5'-GGACTACNNGGGTATCTAAT-3' (95°C for 2 min, followed by 27 cycles at 95°C for 30 s, 55°C for 30 s, and 72°C for 30 s, and a final extension at 72°C for 5 min). Amplicons were paired-end sequenced (PE250) on Illumina HiSeq2500 platform. In the end, a total of 651,502 tags were obtained. The raw reads were deposited into the NCBI Sequence Read Archive (SRA) database under the accession number of SRR9330193-SRR9330210. The details of bacterial DNA extraction and PCR amplification of the 16S rRNA gene are described in the **Supplementary Material**.

Raw Illumina fastq files were de-multiplexed, quality-filtered, and analyzed using Quantitative Insights Into Microbial Ecology (QIIME) (Caporaso et al., 2010). The 16S rRNA gene sequences were classified taxonomically using the Ribosomal Database Project (RDP), and classifier 2.0.1 (Wang et al., 2007). The AMX exposure on alpha diversity was further measured by the taxon richness (Chao1 index), evenness (Simpson index), and diversity index (Shannon index) using all recommended samples. Besides, beta diversity of microbiota communities at baseline and after antibiotics were portrayed by nonmetric multidimensional scaling (NMDS) and principal coordinate analysis (PCoA) of weighted and unweighted UniFrac distances. Linear discriminant analysis effect size (LEfSe) analysis was performed to determine the bacterial taxa that significantly differed between the control and AMX exposure group using Galaxy application tool (Segata et al., 2011). Functional predictions of microbial community were performed to visualize the distribution of functional pathway genes in the three parts of the colon with different treatments using Phylogenetic Investigation of Communities by Reconstruction of Unobserved States (PICRUSt) (Langille et al., 2013). The accuracy of PICRUSt for the detection of these more challenging functional groups was good (minimum accuracy = 0.82), suggesting that their inference of gene abundance across various types of functions was reliable, and PICRUSt predictions had high agreement with metagenome sample abundances across all body sites (Spearman  $r = 0.82$ ,  $P < 0.001$ ). PICRUSt has been successfully manipulated in many previous research for predicting microbial function of human intestinal microbiota (McHardy et al., 2013; Bunyavanich et al., 2016; Labus et al., 2017; Puri et al., 2018). The details of taxonomical classification, LEfSe analysis, and functional predictions are described in the **Supplementary Material**.

## High-Throughput Quantitative PCR (HT-qPCR) and Analysis

High-throughput quantitative PCR reactions were performed to visualize the variation of ARGs during the treatment using Wafergen SmartChip Real-time PCR system, conducted by Anhui MicroAnaly Gene Technologies Co., Ltd. (Anhui, China). A total of 108 primer sets were used (Excel S1), including 102 primer sets to target the almost all major classes of ARGs found in the Chinese human gut microbiota (Hu et al., 2013), five mobile genetic elements (MGEs), and one 16S rRNA gene. The results were analyzed with SmartChip qPCR Software by excluding the wells with multiple melting peaks or amplification efficiency beyond the range (90–110%). Then data were screened with the conditions that a threshold cycle (CT) must be <31 and positive samples should have three replicates simultaneously. The details of HT-qPCR analysis are described in the **Supplementary Material**.

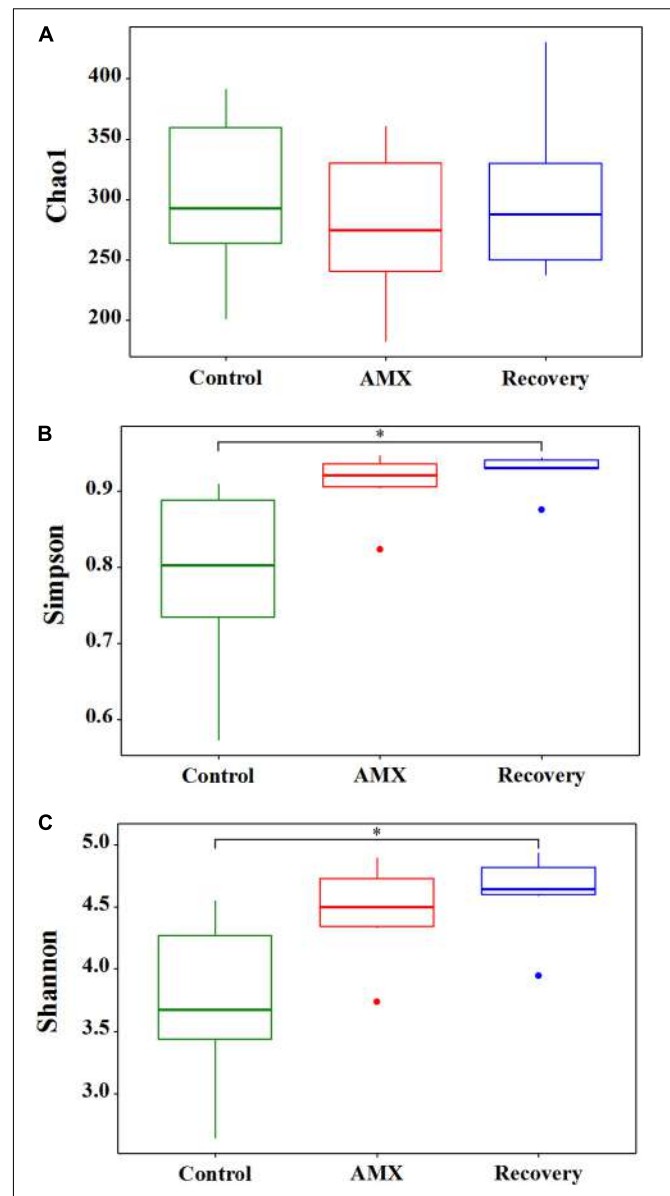
## Data Analysis

All the results were expressed as mean values and standard deviations. The statistical analysis was performed with SPSS 17.0 software (SPSS Inc., Chicago, IL, United States). The *T*-test was conducted to compare the differences between the groups, and all the statistical tests were two-tailed. The statistical significance was set at three different levels (\* $P < 0.05$ , \*\* $P < 0.01$ , and \*\*\* $P < 0.001$ ). Spearman test, Mantel test, and Procrustes test for correlation analysis between the microbiota and the functional pathway genes or ARGs were performed in *R* with the vegan package. Correlations between the pairs of variables were considered to be significant at  $R > 0.6$ , and  $P$  values were <0.05. The Gephi (V 0.9.1) software was used to visualize the bipartite network graphs using the Force Atlas algorithm.

## RESULTS

### AMX Exposure Increased Microbiota Diversity

The effects of 600 mg day<sup>-1</sup> AMX treatment on the gut bacterial community were revealed by the 16S rRNA gene sequencing of fecal samples collected from three different vessels designated as ascending, transverse, and descending colon. The vessels were set up for three groups: before AMX administration during 0 to 21 days (control group), AMX exposure during 22 to 28 days (AMX treatment group) and after the AMX discontinuance during 29 to 42 days (recovery group). The alpha diversity of the fecal microbiota was assessed in each group. The taxon richness (Chao1 index), evenness (Simpson index), and diversity index (Shannon index) of the three groups are shown in **Figure 1**. As compared with the control group, a substantially rising in the evenness (Simpson,  $P = 0.067$ , *T*-test) and diversity (Shannon,  $P = 0.061$ , *T*-test) was observed in the AMX treatment groups; however, no change occurred in the microbiota richness (Chao1,  $P = 0.564$ , *T*-test). Moreover, data displayed that an increasing of microbiota evenness and diversity caused by the AMX treatments

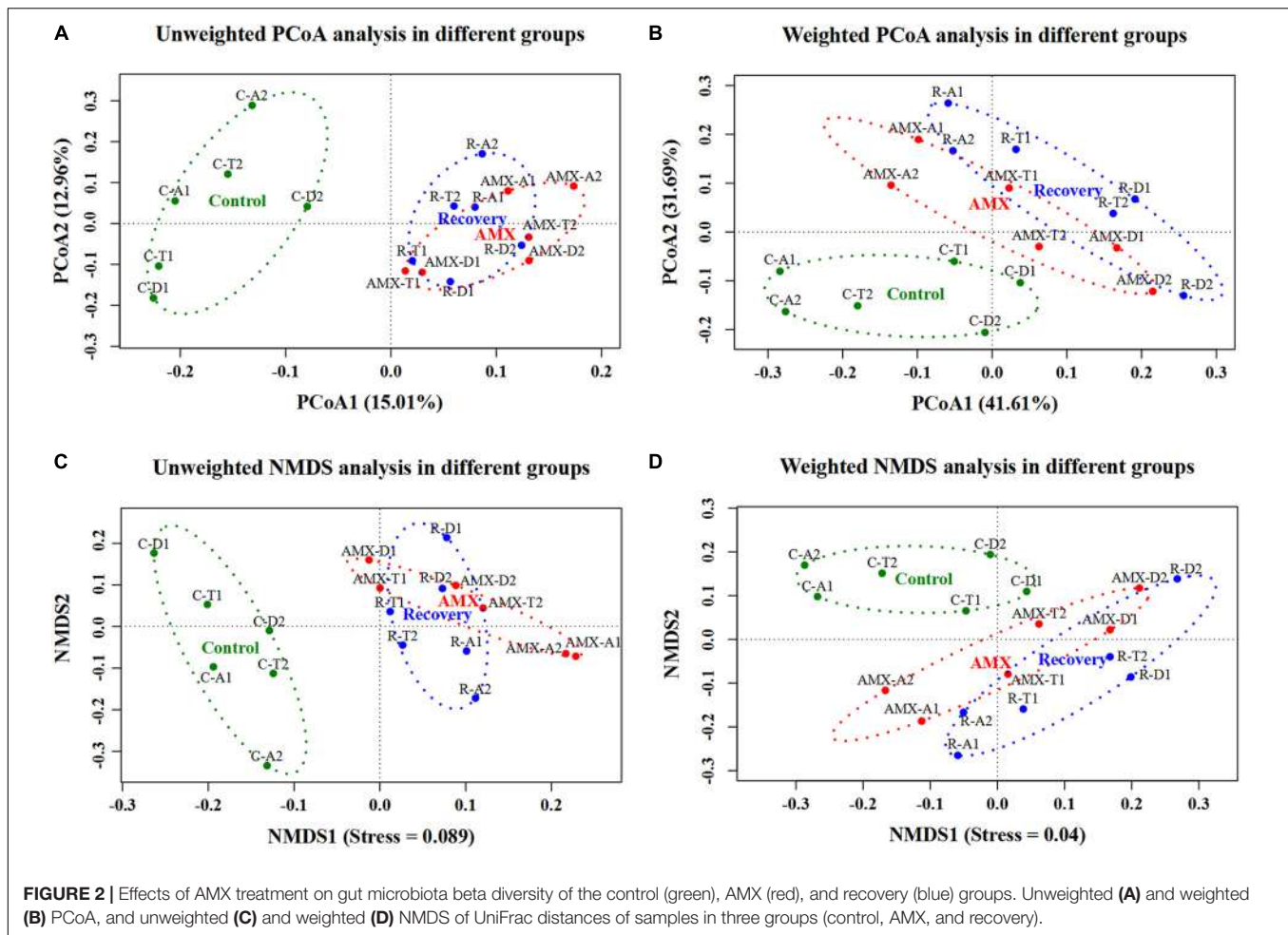


**FIGURE 1** | Effects of AMX treatment on gut microbiota alpha diversity of the control (green), AMX (red), and recovery (blue) groups. The Chao1 index (A) was used to calculate the community richness, Simpson index (B) was used to calculate the community evenness, and Shannon index (C) was used to calculate the community diversity within each of the three groups (control, AMX, and recovery). Statistical significance between each of the three groups were analyzed using the *T* test at a significance level of 0.05.

was continued after two weeks of AMX discontinuance (Simpson,  $P = 0.044$ , *T*-test; Shannon,  $P = 0.028$ , *T*-test).

In addition, the beta diversity of the microbial communities and weighted UniFrac distance was also affected by AMX treatment. As shown in **Figure 2** and **Supplementary Figure S2**, the samples collected after the AMX treatment were differed from the control group, because the two groups clustered far away from each other in both UniFrac NMDS and PCoA analyses. The average weighted UniFrac distance between the AMX treatment





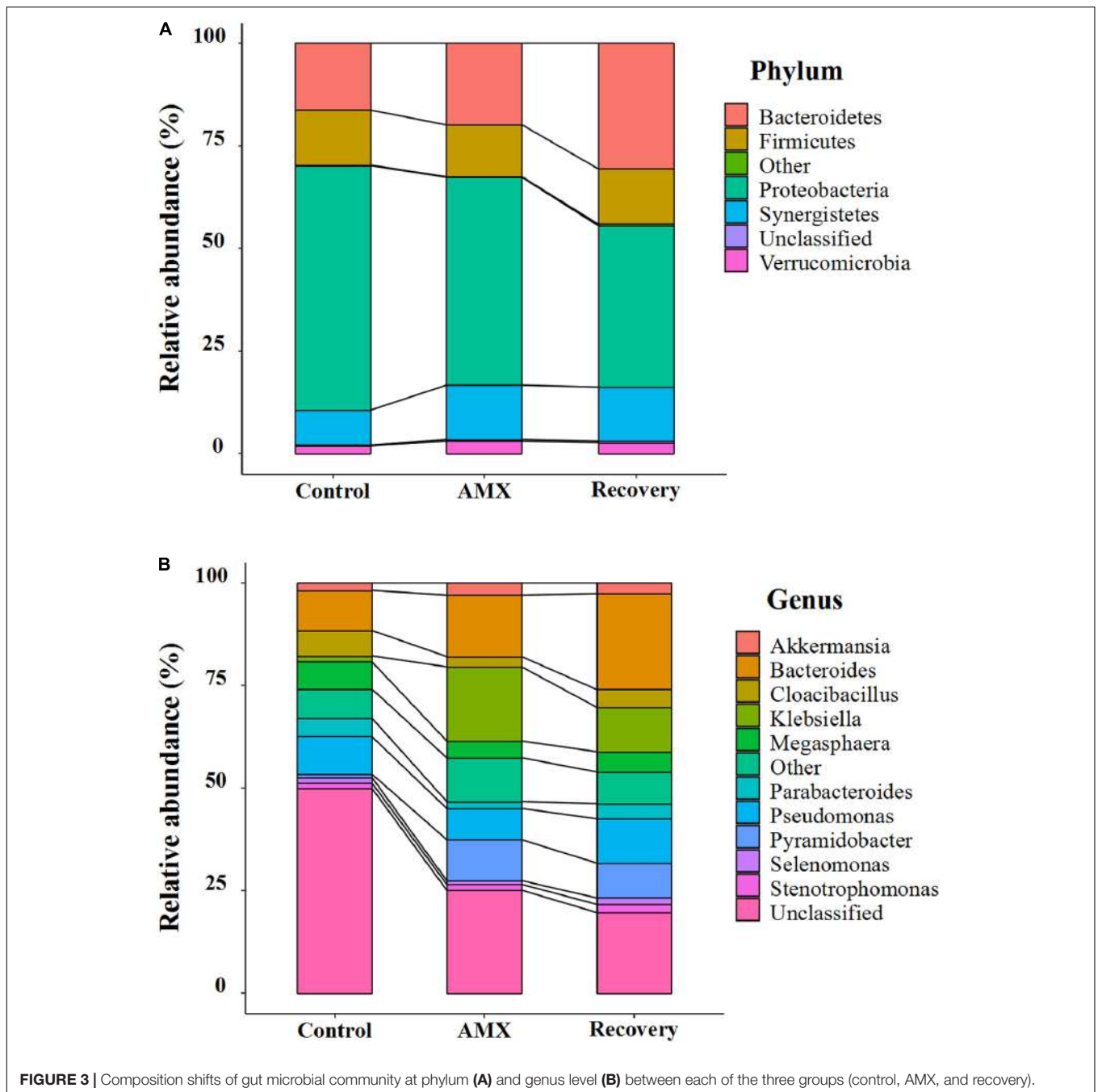
group and control group (AMX vs control) was significantly higher ( $P < 0.001$ ,  $T$ -test) than that within the control group (control vs control). Similarly, the beta diversity results showed that the gut microbial composition remained comparable after 2-week of AMX discontinuance because these samples were clustered together with the AMX treatment groups observed in both UniFrac NMDS and PCoA analyses. The average weighted UniFrac distance between the recovery group and the control group (recovery vs control) was also significantly higher ( $P < 0.001$ ,  $T$ -test) than the control group (control vs control).

## AMX Exposure Changed Microbiota Community Composition

The bacterial community compositions and their shifts at the phylum and genus levels after AMX exposure are shown in **Figure 3** and **Supplementary Figure S3**. Based on the 16S rRNA gene analysis, the taxonomic assignment was related to most four dominant phyla such as *Bacteroidetes*, *Firmicutes*, *Proteobacteria*, and *Synergistetes*, which accounted for 96.5 to 97.9% of the total community (**Figure 3A**). However, a noticeable increase in abundance of *Bacteroidetes* (from 16.3 to 19.9%) and *Synergistetes* (from 8.6 to 13.2%), and decrease of *Proteobacteria* (from 59.6 to 50.7%) were seen after AMX treatment. The shifted

phenomena (*Bacteroidete* from 13.3 to 23.2%; *Proteobacteria* from 68.8 to 57.8%) were more prominent in the ascending colon than the transverse and descending colons (**Supplementary Figure S3A**). A significant alteration in the communities was also observed at the phylum level (*Bacteroidetes* from 19.9 to 30.5%; *Proteobacteria* from 50.7 to 39.4%) after 2-week of AMX discontinued.

At the genus level, the *Bacteroides*, *Klebsiella*, *Megasphaera*, and *Pseudomonas* were predominant (**Figure 3B**). The antibiotic-treated subjects were shown to be substantially overgrown by *Bacteroides* (from 9.8 to 15.0%), *Klebsiella* (from 1.5 to 18.1%) and *Pyramidobacter* (from 0.8 to 10.0%), and declined in the percentage of *Cloacibacillus* (from 6.2 to 2.5%) and *Parabacteroides* (from 4.5 to 1.7%). Similarly, the changes of *Bacteroides* (from 8.4 to 20.5%) and *Klebsiella* (from 1.6 to 32.9%) were more evident in the ascending colon (**Supplementary Figure S3B**). As shown in **Figure 3B**, during the recovery period, it observed that the gut microbiota was not fully recuperated. Only, *Bacteroides* was inclined by abundance from 15.0 to 23.4%; however, all others were less retrieved (*Klebsiella* from 18.1% to 10.9%; *Pyramidobacter* from 10.0 to 8.5%; *Cloacibacillus* from 2.5 to 4.3%; *Parabacteroides* from 1.7 to 3.7%).

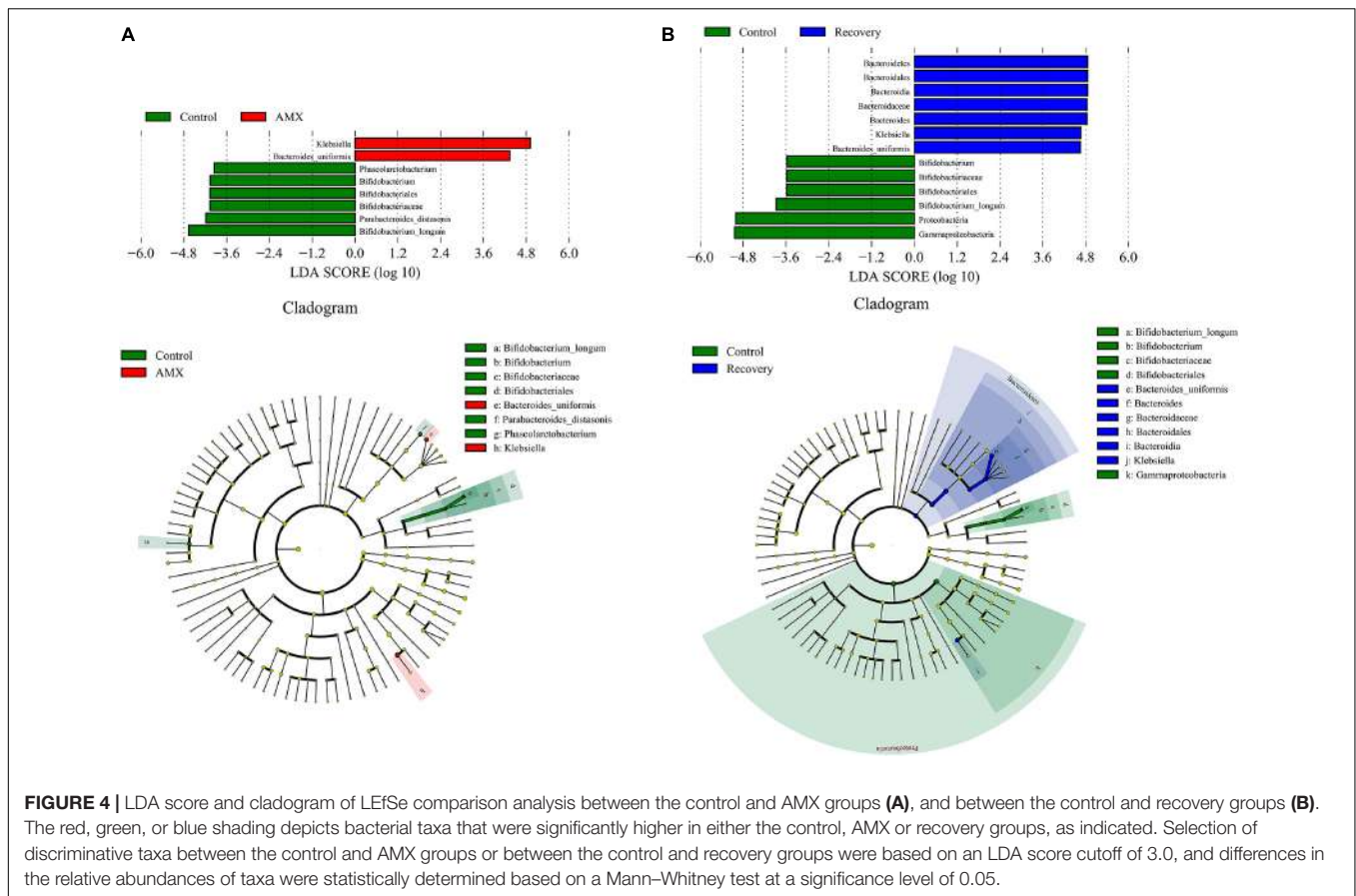


The LEfSe showed that the AMX exposure caused an obvious decrease in several taxa, including the members of *Parabacteroides* [linear discriminant analysis (LDA) score = 4.18], *Bifidobacterium* (LDA score = 4.06), and *Phascolarctobacterium* (LDA score = 3.95) (Figure 4A). The variation was accompanied by significant increases in the relative abundances of *Klebsiella* (LDA score = 5.26), and *Bacteroides uniformis* (LDA score = 4.75). However, after 2-week of AMX discontinuance, the decrease of *Bifidobacterium* (LDA score = 3.88), and increase of *Klebsiella* (LDA score = 4.67) and *Bacteroides uniformis*

(LDA score = 4.65) were still recognizable as compare with the control group (Figure 4B).

### AMX Exposure Increased Functional Pathway Genes

The hierarchy cluster heatmap analysis using metagenomic 16S rRNA gene sequencing was predicted by PICRUSt. Results showed that functional pathway genes, which included cellular processes, environmental information processing, genetic information processing, human diseases, metabolism, and



organismal systems were more abundant in the antibiotic exposure group than in the control group that represented by the ascending colon (Figure 5). For instance, as compared to the AMX-free sample C-A2, collected from the ascending colon before AMX administration, the gene numbers of human diseases related-pathways were 2.4–3.8 times enriched in the AMX exposed sample AMX-A2 that obtained after AMX treatment for 7 days. Similarly, the numbers of genes respect to functional pathways, for examples, membrane transport, transcription, xenobiotics biodegradation, metabolism, and excretory system were nearly 4.6–5.3 folds enriched in the AMX-A2 sample than C-A2. Moreover, these pathways were still maintained at a higher level (approximately 2.2–2.5 times enhanced than the control group) after the recovery phase.

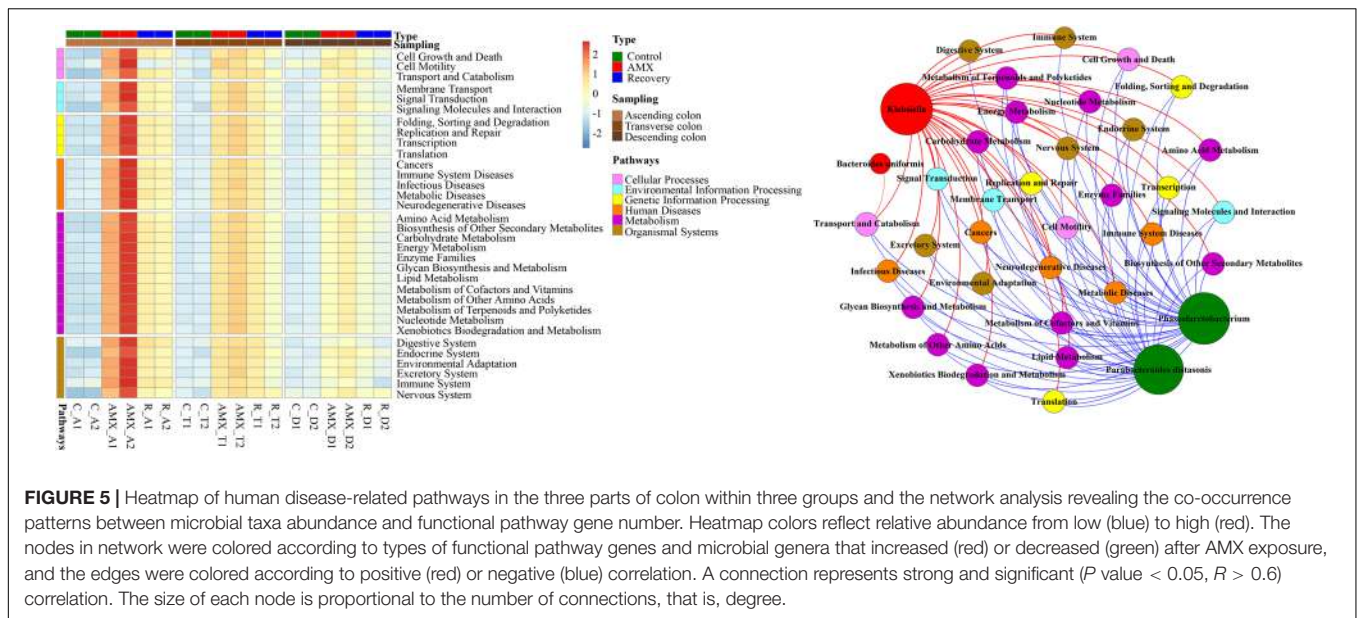
To investigate whether the OTUs correlated with the functional pathway genes, the Mantel test and Procrustes analysis were used. The results showed that OTUs from the ascending, transverse, and descending colons were moderately correlated with the numbers of functional pathway genes (Mantel test,  $R = 0.743$ ,  $P < 0.001$ ). The Procrustes analysis indicated that OTUs obtained from the 16S rRNA gene data and the functional genes could be clustered according to the type of sample, which further exhibited a goodness-of-fit test ( $R = 0.669$ ,  $P < 0.001$ , and 9,999 permutations) based on the Bray–Curtis dissimilarity metrics (Supplementary Figure S4A). As shown in Figure 5, the results demonstrated the co-occurrence

patterns of significantly shifted microbial taxa and functional pathway genes during AMX-treatment. It can be seen that the abundances of most imminent bacteria after AMX exposure such as *Bacteroides uniformis* and *Klebsiella* were positively associated with the gene numbers of functional pathways; however, the suppressed bacteria like *Phascolarctobacterium* and *Parabacteroides* were negatively associated (Figure 5). Specifically, the correlation coefficients of *Klebsiella* with the gene numbers of the digestive system, immune system, and metabolic diseases were about 0.98 ( $P < 0.001$ ) and the correlation coefficients of *Phascolarctobacterium* abundance with gene numbers of signaling molecules and interaction, transport and catabolism, endocrine system, cell growth, and death were about  $-0.77$  ( $P < 0.01$ ).

### AMX Exposure Increased the Abundance of Beta-Lactam and Tetracycline Resistance Genes

The relative abundances of ARGs such as beta-lactam and tetracycline resistance genes were substantially higher in the AMX exposure group as compared to the control group, while the multidrug-resistant ARGs and transposase were lower in the AMX exposure group (Figure 6). Notably, the relative log abundance of *bl2\_len*, *bl2b\_tem1*, and *bl2be\_ctxm* (aminoglycoside) were about 1.6–2.4 log units higher after AMX





treatment (AMX-A2) than in control (C-A2). Similarly, the *tetB*, *tetC*, and *tetR* (tetracycline) were about 1.4–2.5 log units higher than the control group. Besides, the reductions of relative log abundance in the ARGs such as *mdte* and *tolc* (multidrug) were about 1.2 log units after AMX treatment (AMX-A2) than control (C-A2), and *Tn22* (transposase) was 3.0 log units. Similarly, these ARGs were unable to return at the baseline level following the recovery procedure with about 0.6 to 3.2 log units change of relative abundance compared with the control group.

To investigate whether the OTUs correlated with the resistome composition, Mantel test and Procrustes analysis were also performed to correlate the OTUs with the resistome using ascending, transverse and descending colons' samples. Our results showed that OTUs were strongly correlated to the ARG profiles (Mantel test,  $R = 0.895$ ,  $P < 0.001$ ). The Procrustes analysis demonstrated that the bacterial OTUs and the ARGs in HT-qPCR data could be clustered by the type of sample and exhibited a goodness-of-fit-test ( $R = 0.941$ ,  $P < 0.001$ , and 9,999 permutations) by Bray-Curtis dissimilarity metrics (Supplementary Figure S4B). The network analyses of co-occurrence patterns between the significantly changed microbial taxa after AMX treatment and ARG subtypes were shown in Figure 6. Interestingly, a very similar pattern of results was observed between the microbial taxa and functional pathway genes. The abundance of bacteria that significantly decreased after AMX treatment was positively associated with multidrug ARGs, while the abundance of increased bacteria was positively associated with beta-lactam resistance genes. For example, the moderate correlation coefficient of *Bifidobacterium longum* with *acra* abundance was 0.70 ( $P < 0.05$ ), and for *Phascolarctobacterium* with *acrb* and *mdte* were 0.67 ( $P < 0.05$ ). The strong correlations were found in the abundance of *Klebsiella* with the abundances of *bl2\_len*, *bl2b\_tem1*, and *bl2be\_shv2* ( $R = 0.9$ ,  $P < 0.001$ ), and in *Bacteroides uniformis* with *bl2\_len* and *bl2be\_shv2* ( $R = 0.8$ ,  $P < 0.01$ ).

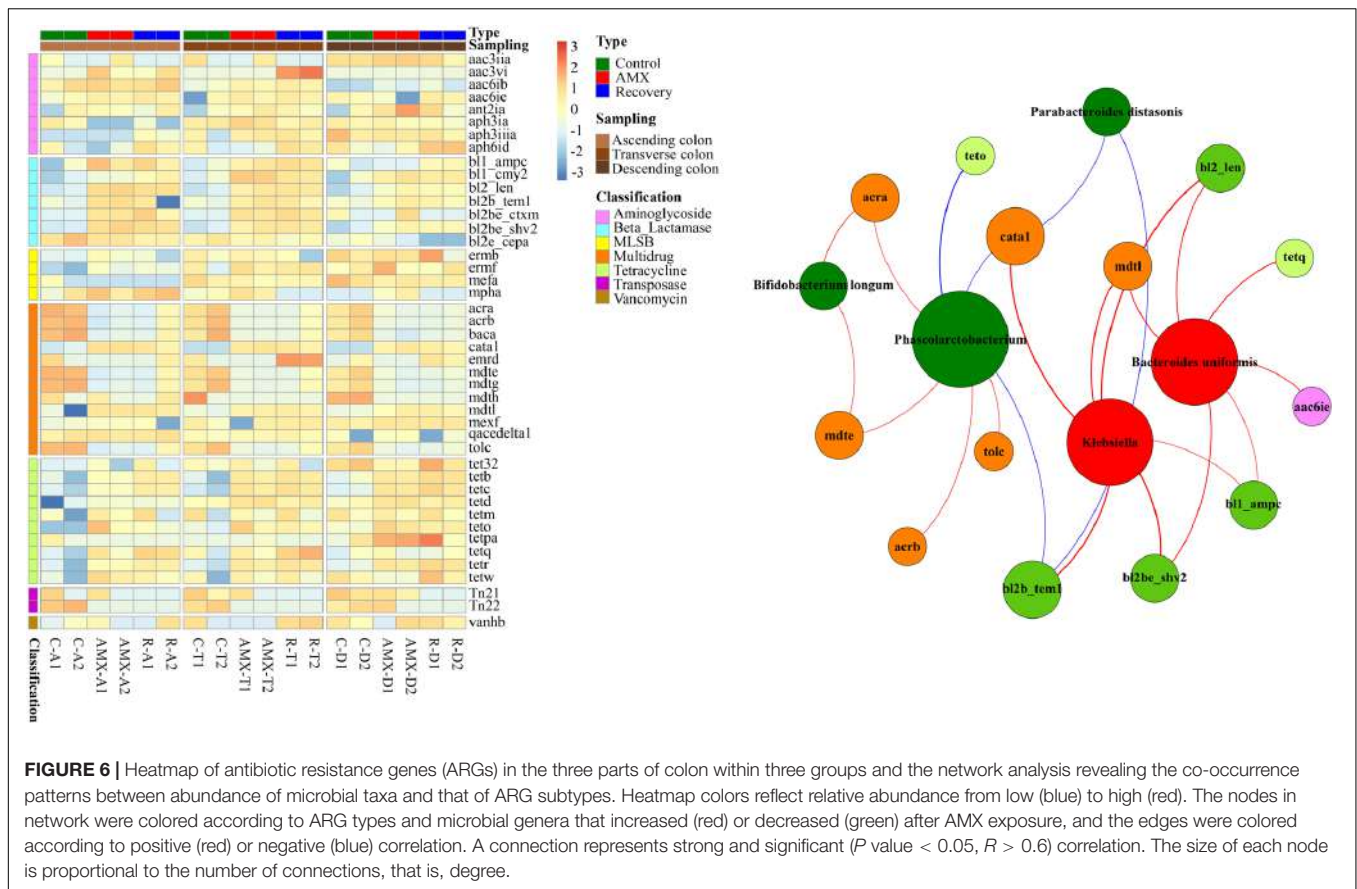
## DISCUSSION

### AMX Treatment Has a Tremendous Influence on the Overall Taxonomic Composition and Biodiversity

The SHIME model was stably operated in this study because the predominant phyla of *Bacteroidetes*, *Proteobacteria*, *Synergistetes*, and *Firmicutes* in the gut microbiome was previously demonstrated Yu et al. (2016). *Firmicutes* and *Bacteroidetes* are usually dominate in the microbiota of a healthy subject, however in the control microbiota of SHIME, *Proteobacteria* is majoritarian. For *in vivo* studies, highest percentage of *Proteobacteria* had also been observed in fecal samples from healthy human and animals (Gao et al., 2015; Li et al., 2015). Our previous *in vitro* study also discovered this phenomenon (Liu et al., 2020).

It has been reported that *in vivo* experiments of AMX caused by tiny effects on human gut microbiota composition (Vrieze et al., 2014; Reijnders et al., 2016). However, a definite shift in the phylum level in our research may attribute to the absence of disturbances from neurohumoral regulation, the individual differences, dietary habits, and physiological status using *in vitro* SHIME (Karl et al., 2018). The decrease of *Proteobacteria* shown in our study may also attribute to AMX is more effective for sensitive Gram-negative bacteria that belonging to *Proteobacteria* by interfering with the synthesis of bacterial cell wall peptidoglycan layer (Zapata and Quagliarello, 2015). And *Bacteroides uniformis* belonging to *Bacteroidetes* may be resistant to AMX to make them survive, because of the strong correlations were found in their abundance with *bl2\_len* and *bl2be\_shv2* ( $R = 0.8$ ,  $P < 0.01$ ). Some studies even showed the opposite phenomena like increasing of *Proteobacteria* and decreasing of *Bacteroidetes*, which might be caused by the combined effects with other antibiotics





**FIGURE 6 |** Heatmap of antibiotic resistance genes (ARGs) in the three parts of colon within three groups and the network analysis revealing the co-occurrence patterns between abundance of microbial taxa and that of ARG subtypes. Heatmap colors reflect relative abundance from low (blue) to high (red). The nodes in network were colored according to ARG types and microbial genera that increased (red) or decreased (green) after AMX exposure, and the edges were colored according to positive (red) or negative (blue) correlation. A connection represents strong and significant ( $P$  value < 0.05,  $R$  > 0.6) correlation. The size of each node is proportional to the number of connections, that is, degree.

such as clarithromycin, fosfomycin, and metronidazole (Oh et al., 2016; Ishikawa et al., 2017). However, at the genus level, the blooming of intestinal microbiota such as *Bacteroides uniformis* and *Klebsiella* and decrease of *Bifidobacterium* occurred following AMX administration. These data were further supported by earlier reports (Ladirat et al., 2014a; Oh et al., 2016; Marzorati et al., 2017), while an increase of *Parabacteroides* was found in another study (Kabbani et al., 2017).

Amoxicillin treatment affected a vast number of sensitive intestinal bacterial species that directly engrossed their corresponding functions. As a result, the functionally redundant resistant intestinal bacterial species were initially present at low levels and became more abundant. Thus, to compensate this loss of function to maintain community function, and species with closer evolutionary relationship usually have more similar functions (Moya and Ferrer, 2016). For example, Van den Abbeele et al. (2012) have found that during antibiotic treatment, the abundance of antibiotic-resistant *Pediococcus acidilactici* was enlarged, while the amount of sensitive *Lactobacillus mucosae* was declined. Similarly, in this study, a reduction of sensitive *Parabacteroides* might be replaced by resistant *Bacteroides* species. Although the metabolic function of the intestinal microbiota could recover quickly, the unrestored composition of the intestinal microbiota was supported by increasing ARB,

which may pose a significant therapeutic challenge and that needs more attention.

As demonstrated by several studies that administration of antibiotics is significantly associated with decrease in microbial community diversity and richness, our results that AMX exposure increased the microbial diversity seems counterintuitive (Dethlefsen et al., 2008). The study by Vrieze et al. (2014) discovered a trend toward increased taxonomic diversity after AMX exposure, which was in accordance with our study. However, in some other studies no significant effect on microbiome diversity was found, which were opposed to our study (Pallav et al., 2014; Zaura et al., 2015; Reijnders et al., 2016). For this phenomenon, the possible reason was that AMX resistant intestinal bacterial species could bloom and compensate for or even surpassed the loss of AMX sensitive species. Intestinal microbiota with higher biodiversity was usually more resistant to the perturbation and colonization by pathogens, which might help in maintaining the intestinal homeostasis (Li et al., 2016). However, the improved biodiversity by AMX exposure that discovered in our study is mainly caused by increased abundance of AMX resistant intestinal bacterial species, which included opportunistic pathogen of the human intestine. This phenomenon may not be considered healthy for people because the increasing of opportunistic pathogens may be related to some human diseases that may cause the transmission and diffusion of ARGs.

## Pathogen Contribute to the Increased Human Disease Pathway Genes and Beta-Lactam Resistance Genes

Some research articles have not mentioned the significant alteration of metabolic functions of the gut microbiota after AMX treatment (Vrieze et al., 2014; Reijnders et al., 2016), while the disruption of the metabolic activity of microbiota (increased in succinate and monosaccharide and oligosaccharide levels) in the fecal samples were found elsewhere (Ladirat et al., 2014a). Moreover, this study found that *Klebsiella* was positively associated with the gene numbers of functional pathways including cancer, metabolic and immune diseases, and other human diseases, which have not been reported yet in other research articles. *K. pneumoniae* is a typical Gram-negative bacterial pathogen, which frequently colonizes in the human gut and processes to infection diseases (Pena et al., 1997; Wiener-Well et al., 2010; Gorrie et al., 2017). The increase of the relative abundance of intestinal *Klebsiella* genus has been reported to associate with diverse human diseases such as pneumonia, inflammation, Crohn's disease, colitis, cystitis, liver abscess, and wound infections (Schneditz et al., 2014; Atarashi et al., 2017). All above findings suggested that *Klebsiella* might contribute to increase the pathway genes, including cancer, immune system diseases, infectious diseases, metabolic diseases, and neurodegenerative diseases.

It is also known from the literature that frequent use of antibiotics such as AMX may cause the transmission and proliferation of ARB and ARGs (Canton and Morosini, 2011; Zaura et al., 2015; Lenart-Boron et al., 2016). This study further demonstrated that the beta-lactamase resistance genes and the potential co-selected ARGs were increased after AMX exposure. The co-occurrence patterns between abundance of microbial taxa and that of ARG subtypes (Figure 6) showed that *Bacteroides uniformis* and *Klebsiella* might contributed to the increasing of ARGs including beta-lactam, tetracycline, and multidrug resistance. Therefore, treatment with AMX increases the number of resistance genes, even those not directly related to the antibiotic ingested. *Bacteroides uniformis* and *Klebsiella* are ubiquitous in the environment and are commensal in the human gut, notably the increased of their population, especially for *Klebsiella* is not usually considered as healthy. Moreover, resistance to beta-lactams via beta-lactamase production has mostly been described in *Klebsiella* spp. (Madhi et al., 2013; Marco et al., 2017). *Bifidobacterium* and *Parabacteroides* are most common or novel probiotics (Pinto-Sanchez et al., 2017; Wu et al., 2019), and the decreasing of these probiotics may cause dysbiosis of gut microbiota, which also leads to human health problem (Wischmeyer et al., 2016; George Kerry et al., 2018).

## AMX Caused "SHIME-Compartment" Different and Permanent Alterations

In this study, *Klebsiella* and *Bacteroides uniformis* were found to be more significantly enriched in the ascending colon than other two colonic-regions, which was in keeping with the previous reports of the alteration in intestinal microbiota by exposure of antibiotics mixture and other toxic compounds like chlorpyrifos

and arsenic (Reygner et al., 2016; Yu et al., 2016; Marzorati et al., 2017). These studies revealed the "SHIME-compartment" specific effects that could be due to the inconsistent biodegradation of multiple compounds, gut microbiome community, and pH in different colon regions (Reygner et al., 2016; Yu et al., 2016; Marzorati et al., 2017). Moreover, a large number of functional pathways related genes was also shown to be increased in the ascending colon after AMX exposure, which further clarified that the primary effect observed at the level of the microbiota could also be identified at the genomic and metabolic levels (Garcia-Villalba et al., 2017; Wang et al., 2018). The intestinal microbiota is a key "organ" for the individual's health, and its response to AMX is started from the proximal colon and hence observed more obvious shifts there. This phenomenon suggested that more studies should focus on the proximal colon; however, it may be challenging to study by *in vivo* experiments that usually analysis the feces standing for the distal intestinal microbiota.

Furthermore, these AMX effects were still evident for at least 2 weeks after the AMX discontinuance, although the resilient tendency of microbial composition, functional pathway genes and ARGs were also observed. Pallav et al. (2014) revealed that AMX mediated opportunistic pathogen such as *Escherichia/Shigella* persisted up to 42 days after the interruption of antibiotic therapy. Similar phenomenon was also reported by Zwitterink et al. (2018), whose work primarily discovered a 5 days treatment with combined of AMX and ceftazidime allowed *Enterococcus* to thrive and remain dominant up to 2 weeks, while the abundance of *Bifidobacterium* remained decreased till postnatal of 6 weeks after antibiotic treatment discontinuation. Therefore, our results demonstrated a serious negative side-effect of AMX, which could be persistent and different in the specific colon region and should be considered as an essential aspect of the risk assessment for AMX prescription.

## PERSPECTIVES

Typical antibiotics have been detected in the collective gut of the Chinese population in our previous research, which provided a reference for this study of the effects of AMX on human gut microbiota (Wang et al., 2020). This study provides the originality of being able to control the effect of antibiotics in the different parts of the colon, evaluating *in situ* the alterations of the microbiota. Although SHIME has been successfully manipulated according to previous classic studies (Van den Abbeele et al., 2013; Yu et al., 2016; Wang et al., 2018), there were still three limitations of this study. First, AMX could not be absorbed by SHIME on the small intestine nor interact with the upper microbiota, which make the burden reaching the colon in the SHIME is much higher comparing to practical exposure to human colon. Considering that about 77 to 93% AMX is absorbed by the gastrointestinal tract and their interaction with the upper microbiota, the putative exposure dosage of AMX in colon is about 10% of the original oral dosage (Spyker et al., 1977; Arancibia et al., 1980; Huttner et al., 2019). This model is better to include the interaction with the human cell to get a closer result to *in vivo*, which is also a very good suggestion. Therefore, we would like to use 60 mg day<sup>-1</sup> AMX (10% of this study) and include interaction with the human cell in our

future work, with which the results would be close to *in vivo*. Second, this study lack of biological replicates and appropriate controls, which makes it difficult to interpret the results in relation to the microbial community variations and changes observed. Therefore, we would collect biological replicates and run a parallel experiment with blank medium at T0 and other timelines in our future study to negate any background noise and make the research scientifically reasonable. Another limitation is that the composition of the microbiota from the donor has not been analyzed before introducing it into the simulator. The composition of the initial microbiota from the donor may affect the stabilized microbiota in SHIME. Therefore, we would analyze the composition of the microbiota from the donor before introducing it into the simulator and compare the stabilized microbiota in SHIME that using multiple donors either by mixing their fecal samples or adding individually to explore the effects of initial microbiota composition in our future work, which would make this study more interesting. Although our work has these limitations, our findings would be valuable for directing future work. The findings in this study suggested several numbers of opportunities for additional study. One avenue is to expand the analysis to incorporate multi-omics approaches of the metagenome, metatranscriptome, and metabolome. Functional and metabolite analysis by multi-omics approaches would refine the results of predicting microbial function. Including interaction with the human cell in the fermentation vessels or manipulate *in vivo* study is also a good avenue to confirm the actual AMX's effects on cancers, metabolic and immune diseases, and other human diseases that found in our *in vitro* experiments. On the other hand, the studies of virome and fungome may exert the substantial influences on the intestinal microbiome. Thus, an expanded analysis of other microorganisms will also be necessary. It is of interest to investigate the impacts of different kinds of antibiotics and a mixture of them on the gut microbiota. Moreover, research on the restoration effects of some prebiotics, probiotics, and synbiotics during and after antibiotic therapy is promising, which may help to discover several clinical strategies and restore side effects caused by antibiotics. As the increasing of opportunistic pathogens, functional genes and ARGs by antibiotics exposure may pose a significant therapeutic challenge, it should be more critical to take some efficient measures to reduce or even eliminate the effects caused by antibiotic treatment.

## CONCLUSION

Exposure to AMX had significantly altered the overall taxonomic composition of the gut microbiota with increasing taxonomic richness, functional pathway genes, and beta-lactam resistance genes. The changes were "SHIME-compartment" different and more substantial effect was observed in the ascending colon. The shifted human gut microbiota could not be restored after 2 weeks' of AMX discontinued. Importantly, most of the functional pathway genes and quantified beta-lactam resistance genes are positively associated with bacteria that increased after AMX exposure. Our results may open up new perspectives for

the assessing of direct effects by antibiotics on the intestinal microbiota – a key "organ" in individual health. The results demonstrated the negative side-effects of AMX and should be considered for AMX prescription.

## DATA AVAILABILITY STATEMENT

The datasets generated for this study can be found in the NCBI SRA database, SRR9330193–SRR9330210.

## ETHICS STATEMENT

The study was approved by the Biomedical Ethics Committees of Nankai University. The participant has given written informed consent to confirm they understand the study purpose, procedures, risks, benefits, and rights.

## AUTHOR CONTRIBUTIONS

LL carried out the laboratory work, analyzed the data, and wrote the manuscript. QW provided suggestions in the manuscript preparation and revised this manuscript. RD edited the language and improved the clarity of this manuscript. HL, SW, HQ, and JY carried out the laboratory work. YX provided funding support. DM and YL guided the laboratory work and revised this manuscript. All authors read and approved the final manuscript.

## FUNDING

This study was sponsored by the Key projects of the National Natural Science Foundation of China (41831287), China National Funds for Distinguished Young Scientists (41525013), National Natural Science Foundation of China (31870351, 41703088, 31670509, and 21607016), Key projects of Research and Development of Hebei Province (19273707D), and Key projects of Tianjin Natural Science Foundation (19JCZDJC40800).

## ACKNOWLEDGMENTS

The authors express the sincerest thanks to Professor Bing Wu at Nanjing University for the guidance of constructing SHIME model, and Guangzhou Gene Denovo Co., Ltd. and Anhui MicroAnaly Gene Technologies Co., Ltd. for genome sequencing and analysis.

## SUPPLEMENTARY MATERIAL

The Supplementary Material for this article can be found online at: <https://www.frontiersin.org/articles/10.3389/fmicb.2020.01213/full#supplementary-material>



## REFERENCES

- Arancibia, A., Guttman, J., Gonzalez, G., and Gonzalez, C. (1980). Absorption and disposition kinetics of amoxicillin in normal human subjects. *Antimicrob. Agents Chemother.* 17, 199–202. doi: 10.1128/aac.17.2.199
- Atarashi, K., Suda, W., Luo, C., Kawaguchi, T., Motoo, I., Narushima, S., et al. (2017). Ectopic colonization of oral bacteria in the intestine drives TH1 cell induction and inflammation. *Science* 358, 359–365. doi: 10.1126/science.aan4526
- Barc, M. C., Charrin-Sarnel, C., Rochet, V., Bourliou, F., Sandre, C., Boureau, H., et al. (2008). Molecular analysis of the digestive microbiota in a gnotobiotic mouse model during antibiotic treatment: influence of *Saccharomyces boulardii*. *Anaerobe* 14, 229–233. doi: 10.1016/j.anaerobe.2008.04.003
- Barraud, O., Peyre, M., Couve-Deacon, E., Chainier, D., Bahans, C., Guignon, V., et al. (2018). Antibiotic resistance acquisition in the first week of life. *Front. Microbiol.* 9:1467. doi: 10.3389/fmicb.2018.01467
- Blaser, M. J. (2016). Antibiotic use and its consequences for the normal microbiome. *Science* 352, 544–545. doi: 10.1126/science.aad9358
- Bunyavanich, S., Shen, N., Grishin, A., Wood, R., Burks, W., Dawson, P., et al. (2016). Early-life gut microbiome composition and milk allergy resolution. *J. Allergy Clin. Immunol.* 138, 1122–1130. doi: 10.1016/j.jaci.2016.03.041
- Bussche, J. V., Marzorati, M., Laukens, D., and Vanhaecke, L. (2015). Validated high resolution mass spectrometry-based approach for metabolomic fingerprinting of the human gut phenotype. *Anal. Chem.* 87, 10927–10934. doi: 10.1021/acs.analchem.5b02688
- Cabreiro, F., Au, C., Leung, K. Y., Vergara-Irigaray, N., Cocheme, H. M., Noori, T., et al. (2013). Metformin retards aging in *C. elegans* by altering microbial folate and methionine metabolism. *Cell* 153, 228–239. doi: 10.1016/j.cell.2013.02.035
- Canton, R., and Morosini, M. I. (2011). Emergence and spread of antibiotic resistance following exposure to antibiotics. *FEMS Microbiol. Rev.* 35, 977–991. doi: 10.1111/j.1574-6976.2011.00295.x
- Caporaso, J. G., Kuczynski, J., Stombaugh, J., Bittinger, K., Bushman, F. D., Costello, E. K., et al. (2010). QIIME allows analysis of high-throughput community sequencing data. *Nat. Methods* 7, 335–336. doi: 10.1038/nmeth.f.303
- Chow, J., Lee, S. M., Shen, Y., Khosravi, A., and Mazmanian, S. K. (2010). Host-bacterial symbiosis in health and disease. *Adv. Immunol.* 107, 243–274. doi: 10.1016/S0065-2776(10)07001-X
- Collignon, A., Bouttier, S., Lambert, S., Hoys, S., and Barc, M.-C. (2008). Gnotobiotic mouse model to study the effect of antibiotics on human faecal microbiota. *Microb. Ecol. Health Dis.* 20, 204–206. doi: 10.1080/08910600802408137
- Collignon, A., Sandre, C., and Barc, M. C. (2010). *Saccharomyces boulardii* modulates dendritic cell properties and intestinal microbiota disruption after antibiotic treatment. *Gastroenterol. Clin. Biol.* 34, S71–S78. doi: 10.1016/S0399-8320(10)70024-5
- Dethlefsen, L., Huse, S., Sogin, M. L., and Relman, D. A. (2008). The pervasive effects of an antibiotic on the human gut microbiota, as revealed by deep 16S rRNA sequencing. *PLoS Biol.* 6:e280. doi: 10.1371/journal.pbio.0060280
- Duque, A. L. R. F., Monteiro, M., Adorno, M. A. T., Sakamoto, I. K., and Sivieri, K. (2016). An exploratory study on the influence of orange juice on gut microbiota using a dynamic colonic model. *Food Res. Int.* 84, 160–169. doi: 10.1016/j.foodres.2016.03.028
- El Hage, R., Hernandez-Sanabria, E., Calatayud Arroyo, M., Props, R., and Van de Wiele, T. (2019). Propionate-producing consortium restores antibiotic-induced dysbiosis in a dynamic *in vitro* model of the human intestinal microbial ecosystem. *Front. Microbiol.* 10:1206. doi: 10.3389/fmicb.2019.01206
- Flandroy, L., Poutahidis, T., Berg, G., Clarke, G., Dao, M. C., Deceaestecker, E., et al. (2018). The impact of human activities and lifestyles on the interlinked microbiota and health of humans and of ecosystems. *Sci. Total Environ.* 627, 1018–1038. doi: 10.1016/j.scitotenv.2018.01.288
- Gao, Z., Guo, B., Gao, R., Zhu, Q., and Qin, H. (2015). Microbiota dysbiosis is associated with colorectal cancer. *Front. Microbiol.* 6:20. doi: 10.3389/fmicb.2015.00020
- García-Villalba, R., Vissenaekens, H., Pitart, J., Romo-Vaquero, M., Espin, J. C., Grootaert, C., et al. (2017). Gastrointestinal simulation model TWIN-SHIME shows differences between human urolithin-metabotypes in gut microbiota composition, pomegranate polyphenol metabolism, and transport along the intestinal tract. *J. Agric. Food Chem.* 65, 5480–5493. doi: 10.1021/acs.jafc.7b02049
- George Kerry, R., Patra, J. K., Gouda, S., Park, Y., Shin, H. S., and Das, G. (2018). Benefaction of probiotics for human health: a review. *J. Food Drug Anal.* 26, 927–939. doi: 10.1016/j.jfda.2018.01.002
- Gorrie, C., Mirceta, M., Wick, R., Edwards, D., Thomson, N., Strugnell, R., et al. (2017). Gastrointestinal carriage is a major reservoir of *Klebsiella pneumoniae* infection in intensive care patients. *Clin. Infect. Dis.* 65, 208–215. doi: 10.1093/cid/cix270
- Hu, Y., Yang, X., Qin, J., Lu, N., Cheng, G., Wu, N., et al. (2013). Metagenome-wide analysis of antibiotic resistance genes in a large cohort of human gut microbiota. *Nat. Commun.* 4, 2151–2249. doi: 10.1038/ncomms3151
- Huttner, A., Bielicki, J., Clements, M. N., Frimodt-Møller, N., Müller, A. E., Paccaud, J. P., et al. (2019). Oral amoxicillin and amoxicillin-clavulanic acid: properties, indications and usage. *Clin. Microbiol. Infect.* doi: 10.1016/j.cmi.2019.11.028 [Epub ahead of print].
- Ianiro, G., Tilg, H., and Gasbarrini, A. (2016). Antibiotics as deep modulators of gut microbiota: between good and evil. *Gut* 65, 1906–1915. doi: 10.1136/gutjnl-2016-312297
- Ichim, T. E., Kesari, S., and Shafer, K. (2018). Protection from chemotherapy- and antibiotic-mediated dysbiosis of the gut microbiota by a probiotic with digestive enzymes supplement. *Oncotarget* 9, 30919–30935. doi: 10.18632/oncotarget.25778
- Ishikawa, D., Sasaki, T., Osada, T., Kuwahara-Arai, K., Haga, K., Shibuya, T., et al. (2017). Changes in intestinal microbiota following combination therapy with fecal microbial transplantation and antibiotics for ulcerative colitis. *Inflamm. Bowel Dis.* 23, 116–125. doi: 10.1097/MIB.0000000000000975
- Kabbani, T. A., Pallav, K., Dowd, S. E., Villafuerte-Galvez, J., Vanga, R. R., Castillo, N. E., et al. (2017). Prospective randomized controlled study on the effects of *Saccharomyces boulardii* CNCM I-745 and amoxicillin-clavulanate or the combination on the gut microbiota of healthy volunteers. *Gut Microbes* 8, 17–32. doi: 10.1080/19490976.2016.1267890
- Karl, J. P., Hatch, A. M., Arcidiacono, S. M., Pearce, S. C., Pantoja-Feliciano, I. G., Doherty, L. A., et al. (2018). Effects of psychological, environmental and physical stressors on the gut microbiota. *Front. Microbiol.* 9:2013. doi: 10.3389/fmicb.2018.02013
- Kemperman, R. A., Gross, G., Mondot, S., Possemiers, S., Marzorati, M., Van de Wiele, T., et al. (2013). Impact of polyphenols from black tea and red wine/grape juice on a gut model microbiome. *Food Res. Int.* 53, 659–669. doi: 10.1016/j.foodres.2013.01.034
- Kho, Z. Y., and Lal, S. K. (2018). The human gut microbiome - a potential controller of wellness and disease. *Front. Microbiol.* 9:1835. doi: 10.3389/fmicb.2018.01835
- Labus, J. S., Hollister, E. B., Jacobs, J., Kirbach, K., Oezgen, N., Gupta, A., et al. (2017). Differences in gut microbial composition correlate with regional brain volumes in irritable bowel syndrome. *Microbiome* 5:49. doi: 10.1186/s40168-017-0260-z
- Ladirat, S. E., Schoterman, M. H. C., Rahaoui, H., Mars, M., Schuren, F. H. J., Gruppen, H., et al. (2014a). Exploring the effects of galacto-oligosaccharides on the gut microbiota of healthy adults receiving amoxicillin treatment. *Br. J. Nutr.* 112, 536–546. doi: 10.1017/S0007114514001135
- Ladirat, S. E., Schuren, F. H. J., Schoterman, M. H. C., Nauta, A., Gruppen, H., and Schols, H. A. (2014b). Impact of galacto-oligosaccharides on the gut microbiota composition and metabolic activity upon antibiotic treatment during *in vitro* fermentation. *FEMS Microbiol. Ecol.* 87, 41–51. doi: 10.1111/1574-6941.12187
- Langille, M. G., Zaneveld, J., Caporaso, J. G., McDonald, D., Knights, D., Reyes, J. A., et al. (2013). Predictive functional profiling of microbial communities using 16S rRNA marker gene sequences. *Nat. Biotechnol.* 31, 814–821. doi: 10.1038/nbt.2676
- Lenart-Boron, A., Wolny-Koladka, K., Stec, J., and Kasprówic, A. (2016). Phenotypic and molecular antibiotic resistance determination of airborne coagulase negative *Staphylococcus* spp. strains from healthcare facilities in Southern Poland. *Microb. Drug Resist.* 22, 515–522. doi: 10.1089/mdr.2015.0271
- Li, D. T., Wang, P., Wang, P. P., Hu, X. S., and Chen, F. (2016). The gut microbiota: a treasure for human health. *Biotechnol. Adv.* 34, 1210–1224. doi: 10.1016/j.biotechadv.2016.08.003



- Li, S., Zhang, C., Gu, Y., Chen, L., Ou, S., Wang, Y., et al. (2015). Lean rats gained more body weight than obese ones from a high-fibre diet. *Br. J. Nutr.* 114, 1188–1194. doi: 10.1017/S0007114515002858
- Liu, L., Wang, Q., Wu, X., Qi, H., Das, R., Lin, H., et al. (2020). Vancomycin exposure caused opportunistic pathogens bloom in intestinal microbiome by simulator of the human intestinal microbial ecosystem (SHIME). *Environ. Pollut.* doi: 10.1016/j.envpol.2020.114399 [Epub ahead of print].
- Madhi, F., Biscardi, S., Bingen, E., Jaby, O., Epaud, R., and Cohen, R. (2013). Combined relay therapy with oral cefixime and clavulanate for febrile urinary tract infection caused by extended-spectrum beta-lactamase-producing *Escherichia coli*. *Pediatr. Infect. Dis. J.* 32, 96–97. doi: 10.1097/INF.0b013e318271f369
- Marco, R. H., Olmos, E. G., Breton-Martinez, J. R., Perez, L. G., Sanchez, B. C., Fajkova, J., et al. (2017). Community-acquired febrile urinary tract infection caused by extended-spectrum beta-lactamase-producing bacteria in hospitalised infants. *Enferm. Infecc. Microbiol. Clin.* 35, 287–292. doi: 10.1016/j.eimc.2016.01.012
- Marzorati, M., Vilchez-Vargas, R., Bussche, J. V., Truchado, P., Jauregui, R., El Hage, R. A., et al. (2017). High-fiber and high-protein diets shape different gut microbial communities, which ecologically behave similarly under stress conditions, as shown in a gastrointestinal simulator. *Mol. Nutr. Food Res.* 61, 1600150. doi: 10.1002/mnfr.201600150
- McHardy, I. H., Goudarzi, M., Tong, M., Ruegger, P. M., Schwager, E., Weger, J. R., et al. (2013). Integrative analysis of the microbiome and metabolome of the human intestinal mucosal surface reveals exquisite inter-relationships. *Microbiome* 1:17. doi: 10.1186/2049-2618-1-17
- Moya, A., and Ferrer, M. (2016). Functional redundancy-induced stability of gut microbiota subjected to disturbance. *Trends Microbiol.* 24, 402–413. doi: 10.1016/j.tim.2016.02.002
- Oh, B., Kim, B. S., Kim, J. W., Kim, J. S., Koh, S. J., Kim, B. G., et al. (2016). The effect of probiotics on gut microbiota during the *Helicobacter pylori* eradication: randomized controlled trial. *Helicobacter* 21, 165–174. doi: 10.1111/hel.12270
- Pallav, K., Dowd, S. E., Villafuerte, J., Yang, X., Kabbani, T., Hansen, J., et al. (2014). Effects of polysaccharopeptide from *Trametes versicolor* and amoxicillin on the gut microbiome of healthy volunteers: a randomized clinical trial. *Gut Microbes* 5, 458–467. doi: 10.4161/gmic.29558
- Pena, C., Pujol, M., Ricart, A., Ardanuy, C., Ayats, J., Linares, J., et al. (1997). Risk factors for faecal carriage of *Klebsiella pneumoniae* producing extended spectrum beta-lactamase (ESBL-KP) in the intensive care unit. *J. Hosp. Infect.* 35, 9–16. doi: 10.1016/s0195-6701(97)90163-8
- Pinto-Sanchez, M. I., Hall, G. B., Ghajar, K., Nardelli, A., Bolino, C., Lau, J. T., et al. (2017). Probiotic *Bifidobacterium longum* NCC3001 reduces depression scores and alters brain activity: a pilot study in patients with irritable bowel syndrome. *Gastroenterology* 153, 448–459. doi: 10.1053/j.gastro.2017.05.003
- Puri, P., Liangpunsakul, S., Christensen, J. E., Shah, V. H., Kamath, P. S., Gores, G. J., et al. (2018). The circulating microbiome signature and inferred functional metagenomics in alcoholic hepatitis. *Hepatology* 67, 1284–1302. doi: 10.1002/hep.29623
- Qin, J. J., Li, R. Q., Raes, J., Arumugam, M., Burgdorf, K. S., Manichanh, C., et al. (2010). A human gut microbial gene catalogue established by metagenomic sequencing. *Nature* 464, 59–65. doi: 10.1038/nature08821
- Reijnders, D., Goossens, G. H., Hermes, G. D., Neis, E. P., van der Beek, C. M., Most, J., et al. (2016). Effects of gut microbiota manipulation by antibiotics on host metabolism in obese humans: a randomized double-blind placebo-controlled trial. *Cell Metab.* 24, 63–74. doi: 10.1016/j.cmet.2016.06.016
- Reygnier, J., Joly Condet, C., Bruneau, A., Delanaud, S., Rhazi, L., Depeint, F., et al. (2016). Changes in composition and function of human intestinal microbiota exposed to chlorpyrifos in oil as assessed by the SHIME® model. *Int. J. Environ. Res. Public Health* 13:1088. doi: 10.3390/ijerph13111088
- Rock, C., Thom, K. A., Masnick, M., Johnson, J. K., Harris, A. D., and Morgan, D. J. (2014). Frequency of *Klebsiella pneumoniae* carbapenemase (KPC)-producing and non-KPC-producing *Klebsiella* species contamination of healthcare workers and the environment. *Infect. Control Hosp. Epidemiol.* 35, 426–429. doi: 10.1086/675598
- Schneditz, G., Rentner, J., Roier, S., Pletz, J., Herzog, K. A., Bucker, R., et al. (2014). Enterotoxigenicity of a nonribosomal peptide causes antibiotic-associated colitis. *Proc. Natl. Acad. Sci. U.S.A.* 111, 13181–13186. doi: 10.1073/pnas.1403274111
- Segata, N., Izard, J., Waldron, L., Gevers, D., Miropolsky, L., Garrett, W. S., et al. (2011). Metagenomic biomarker discovery and explanation. *Genome Biol.* 12:R60. doi: 10.1186/gb-2011-12-6-r60
- Selak, M., Riviere, A., Moens, F., Van den Abbeele, P., Geirnaert, A., Rogelj, I., et al. (2016). Inulin-type fructan fermentation by bifidobacteria depends on the strain rather than the species and region in the human intestine. *Appl. Microbiol. Biotechnol.* 100, 4097–4107. doi: 10.1007/s00253-016-7351-9
- Spyker, D. A., Rugloski, R. J., Vann, R. L., and O'Brien, W. M. (1977). Pharmacokinetics of amoxicillin: dose dependence after intravenous, oral, and intramuscular administration. *Antimicrob. Agents Chemother.* 11, 132–141. doi: 10.1128/aac.11.1.132
- Stecher, B., Maier, L., and Hardt, W. D. (2013). 'Blooming' in the gut: how dysbiosis might contribute to pathogen evolution. *Nat. Rev. Microbiol.* 11, 277–284. doi: 10.1038/nrmicro2989
- Truchado, P., Van den Abbeele, P., Riviere, A., Possemiers, S., De Vuyst, L., and Van de Wiele, T. (2015). *Bifidobacterium longum* D2 enhances microbial degradation of long-chain arabinoxylans in an *in vitro* model of the proximal colon. *Beneficial Microbes* 6, 849–860. doi: 10.3920/Bm2015.0023
- Van de Wiele, T., Gallawa, C. M., Kubachka, K. M., Creed, J. T., Basta, N., Dayton, E. A., et al. (2010). Arsenic metabolism by human gut microbiota upon *in vitro* digestion of contaminated soils. *Environ. Health Perspect.* 118, 1004–1009. doi: 10.1289/ehp.0901794
- Van de Wiele, T., Van den Abbeele, P., Ossieur, W., Possemiers, S., and Marzorati, M. (2015). "The simulator of the human intestinal microbial ecosystem (SHIME®)," in *The Impact of Food Bioactives on Health: In Vitro and Ex Vivo Models*, eds K. Verhoeckx, P. Cotter, I. López-Expósito, C. Kleiveland, T. Lea, A. Mackie, et al. (Cham: Springer International Publishing), 305–317. doi: 10.1007/978-3-319-16104-4\_27
- Van den Abbeele, P., Belzer, C., Goossens, M., Kleerebezem, M., De Vos, W. M., Thas, O., et al. (2013). Butyrate-producing *Clostridium cluster* XIVa species specifically colonize mucins in an *in vitro* gut model. *ISME J.* 7, 949–961. doi: 10.1038/ismej.2012.158
- Van den Abbeele, P., Roos, S., Eeckhaut, V., MacKenzie, D. A., Derde, M., Verstraete, W., et al. (2012). Incorporating a mucosal environment in a dynamic gut model results in a more representative colonization by *Lactobacilli*. *Microb. Biotechnol.* 5, 106–115. doi: 10.1111/j.1751-7915.2011.00308.x
- Vrieze, A., Out, C., Fuentes, S., Jonker, L., Reuling, I., Kootte, R. S., et al. (2014). Impact of oral vancomycin on gut microbiota, bile acid metabolism, and insulin sensitivity. *J. Hepatol.* 60, 824–831. doi: 10.1016/j.jhep.2013.11.034
- Wang, Q., Duan, Y. J., Wang, S. P., Wang, L. T., Hou, Z. L., Cui, Y. X., et al. (2020). Occurrence and distribution of clinical and veterinary antibiotics in the faeces of a Chinese population. *J. Hazard. Mater.* 383, 121129. doi: 10.1016/j.jhazmat.2019.121129
- Wang, Q., Garrity, G. M., Tiedje, J. M., and Cole, J. R. (2007). Naive Bayesian classifier for rapid assignment of rRNA sequences into the new bacterial taxonomy. *Appl. Environ. Microbiol.* 73, 5261–5267. doi: 10.1128/Aem.00062-07
- Wang, Y., Rui, M., Nie, Y., and Lu, G. (2018). Influence of gastrointestinal tract on metabolism of bisphenol A as determined by *in vitro* simulated system. *J. Hazard. Mater.* 355, 111–118. doi: 10.1016/j.jhazmat.2018.05.011
- Wiener-Well, Y., Rudensky, B., Yinnon, A. M., Kopuit, P., Schlesinger, Y., Broide, E., et al. (2010). Carriage rate of carbapenem-resistant *Klebsiella pneumoniae* in hospitalised patients during a national outbreak. *J. Hosp. Infect.* 74, 344–349. doi: 10.1016/j.jhin.2009.07.022
- Wischmeyer, P. E., McDonald, D., and Knight, R. (2016). Role of the microbiome, probiotics, and 'dysbiosis therapy' in critical illness. *Curr. Opin. Crit. Care* 22, 347–353. doi: 10.1097/MCC.0000000000000321
- Wu, T. R., Lin, C. S., Chang, C. J., Lin, T. L., Martel, J., Ko, Y. F., et al. (2019). Gut commensal *Parabacteroides goldsteinii* plays a predominant role in the anti-obesity effects of polysaccharides isolated from *Hirsutella sinensis*. *Gut* 68, 248–262. doi: 10.1136/gutjnl-2017-315458
- Yatsunenko, T., Rey, F. E., Manary, M. J., Trehan, I., Dominguez-Bello, M. G., Contreras, M., et al. (2012). Human gut microbiome viewed across age and geography. *Nature* 486, 222–227. doi: 10.1038/nature11053
- Yu, H., Wu, B., Zhang, X., Liu, S., Yu, J., Cheng, S., et al. (2016). Arsenic metabolism and toxicity influenced by ferric iron in simulated gastrointestinal tract and the roles of gut microbiota. *Environ. Sci. Technol.* 50, 7189–7197. doi: 10.1021/acs.est.6b01533

- Zapata, H. J., and Quagliariello, V. J. (2015). The microbiota and microbiome in aging: potential implications in health and age-related diseases. *J. Am. Geriatr. Soc.* 63, 776–781. doi: 10.1111/jgs.13310
- Zaura, E., Brandt, B. W., Teixeira de Mattos, M. J., Buijs, M. J., Caspers, M. P., Rashid, M. U., et al. (2015). Same exposure but two radically different responses to antibiotics: resilience of the salivary microbiome versus long-term microbial shifts in feces. *mBio* 6:e01693-15. doi: 10.1128/mBio.01693-15
- Zhang, Q., Ying, G., Pan, C., Liu, Y., and Zhao, J. (2015). Comprehensive evaluation of antibiotics emission and fate in the river basins of China: source analysis, multimedia modeling, and linkage to bacterial resistance. *Environ. Sci. Technol.* 49, 6772–6782. doi: 10.1021/acs.est.5b00729
- Zwittink, R. D., Renes, I. B., van Lingen, R. A., van Zoeren-Grobbe, D., Konstanti, P., Norbruis, O. F., et al. (2018). Association between duration of intravenous antibiotic administration and early-life microbiota development in late-preterm infants. *Eur. J. Clin. Microbiol. Infect. Dis.* 37, 475–483. doi: 10.1007/s10096-018-3193-y
- Conflict of Interest:** The authors declare that the research was conducted in the absence of any commercial or financial relationships that could be construed as a potential conflict of interest.
- Copyright © 2020 Liu, Wang, Lin, Das, Wang, Qi, Yang, Xue, Mao and Luo. This is an open-access article distributed under the terms of the Creative Commons Attribution License (CC BY). The use, distribution or reproduction in other forums is permitted, provided the original author(s) and the copyright owner(s) are credited and that the original publication in this journal is cited, in accordance with accepted academic practice. No use, distribution or reproduction is permitted which does not comply with these terms.



OPEN ACCESS

**Edited by:**

Eliana De Gregorio,  
University of Naples Federico II, Italy

**Reviewed by:**

Ajay Kumar Sharma,  
Institute of Nuclear Medicine & Allied  
Sciences (DRDO), India  
A. Gnanamani,  
Central Leather Research Institute  
(CSIR), India  
Giovanni Di Bonaventura,  
Università degli Studi G. d'Annunzio  
Chieti e Pescara, Italy

**\*Correspondence:**

Myunghee Kim  
foodtech@ynu.ac.kr  
Natarajan Devarajan  
natarajpu@gmail.com

†These authors have contributed  
equally to this work

**Specialty section:**

This article was submitted to  
Infectious Diseases - Surveillance,  
Prevention and Treatment,  
a section of the journal  
Frontiers in Public Health

**Received:** 25 April 2019

**Accepted:** 21 April 2020

**Published:** 10 June 2020

**Citation:**

Murugan N, Srinivasan R, Murugan A,  
Kim M and Natarajan D (2020)  
*Glycosmis pentaphylla* (Rutaceae): A  
Natural Candidate for the Isolation of  
Potential Bioactive Arborine and  
Skimmianine Compounds for  
Controlling Multidrug-Resistant  
*Staphylococcus aureus*.  
*Front. Public Health* 8:176.  
doi: 10.3389/fpubh.2020.00176

# *Glycosmis pentaphylla* (Rutaceae): A Natural Candidate for the Isolation of Potential Bioactive Arborine and Skimmianine Compounds for Controlling Multidrug-Resistant *Staphylococcus aureus*

Natarajan Murugan<sup>1†</sup>, Ramalingam Srinivasan<sup>1,2,3†</sup>, Athiappan Murugan<sup>4</sup>, Myunghee Kim<sup>2\*</sup> and Devarajan Natarajan<sup>1\*</sup>

<sup>1</sup> Natural Drug Research Laboratory, Department of Biotechnology, School of Biosciences, Periyar University, Salem, India,

<sup>2</sup> Department of Food Science and Technology, Yeungnam University, Gyeongsan-si, South Korea, <sup>3</sup> Department of Biotechnology, K. S. Rangasamy College of Arts and Science, Namakkal, India, <sup>4</sup> Department of Microbiology, School of Biosciences, Periyar University, Salem, India

Several multidrug-resistant organisms have emerged, which increases the threat to public health around the world and a limited number of therapeutics were available to counteract these issues. Thus, researchers are trying to find out novel antimicrobials to overcome multidrug-resistant issues. The present study aimed to isolate antibacterial principles against the clinical isolates of multidrug-resistant (MDR) *Staphylococcus aureus* from the ethyl acetate extract of *Glycosmis pentaphylla*. The isolation and structural characterization of bioactive compounds were carried out using various chromatographic techniques (TLC, column, HPLC, and LC-MS) and spectral studies such as FT-IR, CHNS analysis, <sup>1</sup>H-NMR, and <sup>13</sup>C-NMR. The antimicrobial potential of isolated compounds was assessed according to the standard methods. The isolated compounds were identified as arborine and skimmianine, which exhibited a significant antibacterial effect with the lowest MIC and MBC values against MDR *S. aureus* and *in vitro* kinetic and protein leakage assays supported the antimicrobial activity. Significant morphological changes such as uneven cell surfaces and morphology, cell shrinkage, and cell membrane damages were observed in the MDR *S. aureus* upon the treatment of arborine and skimmianine. The present investigation concludes that the isolated arborine and skimmianine compounds from *G. pentaphylla* harbor a strong antibacterial activity against MDR *S. aureus* and may be used as alternative natural drugs in the treatment of MDR *S. aureus*.

**Keywords:** *Glycosmis pentaphylla*, antibacterial compounds, chromatography, spectral study, MDR *Staphylococcus aureus*, arborine, skimmianine

## INTRODUCTION

*Staphylococcus aureus* is a Gram-positive bacterium that belongs to the family Staphylococaceae and is often found at a commensal on the skin, skin glands, and mucous membranes, particularly in the nose of a healthy individual (1). It is causing infections ranging from relatively mild skin and soft tissue infections to life-threatening sepsis, pneumonia, osteomyelitis, endocarditis, as well as toxin-mediated syndromes such as toxic shock syndrome and food poisoning (2). Multidrug resistant *S. aureus* (MRSA) is resistant to two or more antimicrobial agents like penicillin, oxacillin, ampicillin, and methicillin. In general, MRSA infections have been categorized into four groups based on their sources: healthcare-associated hospital-onset MRSA (HAHO-MRSA), community-associated MRSA (CA-MRSA), healthcare-associated MRSA with community-onset (HACO-MRSA), and livestock-associated MRSA (LA-MRSA) (3). Although MRSA infections mainly occur in hospitals, the human illness caused by community-associated MRSA (CA-MRSA) is increasing considerably (4).

In recent years, drug-resistant human pathogenic bacteria have been frequently reported (5). The drug-resistant Enterotoxigenic *Escherichia coli* pathogenic bacteria demand the development of new antimicrobial drugs with a novel mode of action, targeting either the cell membrane or intracellular targets (6). Increasing the bacterial resistance is prompting a resurgence in the research on the antimicrobial role of herbs available in nature as effective combinations against antibiotic-resistant bacteria (7). Moreover, using natural products also help to diminish the toxicity of the drugs when they are used on humans (8).

Since ancient times, plants have been the primary sources of many therapeutic agents that possess several secondary metabolites with significant physiological effects. Recently, many active ingredients have been isolated from plants and those are used to develop synthetic analogs for the treatment of ailments. There are 300 plant species frequently used in 7,800 drug-manufacturing units around India, which consume more than 2,000 tons of herbs annually (9). Generally, bioactive principles are isolated from different parts of plants such as leaves, bark, roots, seeds, etc. based on folklore usage. According to WHO, medicinal plants would be the best source to obtain a variety of drugs (10), and ~20% of the known plants were subjected to biological tests and a sustainable number of new antibiotics were introduced into the market (11). Concurrently, the characterizations of antimicrobial compounds from medicinal plants have been very challenging to the researchers (12). Hence, a systemic screening of plants for the identification of antimicrobial compounds to act against microbial pathogens needs an hour. Recently, many researchers have been focused on the isolation of potential bioactive compounds from medicinal plants to produce high-quality and potential secondary metabolites responsible for the control of microorganisms (13, 14). With this background, the present study was aimed to isolate antibacterial principles from *Glycosmis pentaphylla*.

## MATERIALS AND METHODS

### Isolation and Identification of MDR *S. aureus*

About 500 specimens [wound (138), pus (122), blood (119), sputum (70), and urine (51)] were collected from patients suspected to have *S. aureus* infections from private and government hospitals in and around Salem and Namakkal Districts, Tamil Nadu, India. The present study has ethical clearance from the institutional ethical committee (reference no.: PU/IEC/HR/2014/008 dated: 31/06/2014), Periyar University, Salem, Tamil Nadu. The methods of isolation and identification of the selected MDR *S. aureus* strains were described in our previous published data (15, 16). The isolation and identification of MDR *S. aureus* were carried out by the standard methods such as colony morphology on differential media, microscopic observations, and biochemical tests, and confirmed by molecular analysis like 16s rRNA sequencing. The antibiotic-resistant potential of isolated *S. aureus* was identified using the standard antimicrobial susceptibility test and identification of antibiotic-resistant marker genes such as *MecA*, *blaZ*, *Aph (III)*, etc. The 16s rRNA sequence of isolated MDR *S. aureus* (101, 270, 315, 319, and 410) strains used in the present study is deposited in GenBank and GenBank accession nos. are KU198419 (*S. aureus* 101), KX290715.1 (*S. aureus* 270), KX454514 (*S. aureus* 315), KX447584 (*S. aureus* 319), and KX447585 (*S. aureus* 410).

### Plant Material and Extraction

The healthy and young leaves of *G. pentaphylla* (Figure 1) were collected from Vellimalai village (Latitude 11° 47' 55.6836" N, longitude 78° 41' 58.0056" E), Villupuram district, Tamil Nadu, India. The taxonomic identification of collected plant material was done by the Botanical Survey of India (Southern Circle), Tamil Nadu Agricultural University, Coimbatore, Tamil Nadu, India (reference letter No BSI/SRC/5/26/2016/402). The voucher specimen of collected plant material was deposited (No. PU/BT/NDRL/2016/09) in the Natural Drug Research Laboratory, Department of Biotechnology, Periyar University, Salem, Tamil Nadu, India. The collected plant materials were washed twice in running tap water and shade dried at room temperature for 3 weeks. The air-dried plant leaves were pulverized, using an electric blender to make a fine powder. A total of 3 kg of powdered *G. pentaphylla* leaves was sequentially extracted with different organic solvents (1:10 solvent ratio) in an increasing polarity (hexane, chloroform, ethyl acetate, acetone, and methanol) using a Soxhlet apparatus until the efflux solvents become colorless. All extracts were filtered through filter paper (Whatman No. 1) and dried under vacuum at 40°C. The dried crude solvent extracts were stored in a freezer at -4°C for further study (17).

### Isolation of Antibacterial Principles

The preliminary antibacterial activity results of various crude extracts of *G. pentaphylla* (15) revealed that the crude ethyl acetate of *G. pentaphylla* possesses a significant high antibacterial





**FIGURE 1** | A close view of *Glycosmis pentaphylla* (Rutaceae).

potential; thus, the ethyl acetate extract was selected for isolation of active principles. The selected ethyl acetate extract was subjected to different chromatography techniques and the structure of isolated bioactive compounds were identified using various spectral studies.

## Separation of Active Compounds by Chromatography

The ethyl acetate extracts (in both low and high concentration) were spotted on the TLC plate (TLC Silica gel F254, Merck, Germany,  $10 \times 10 \text{ cm}^2$ ) origin and kept in a TLC chamber containing the desired solvent system. The solvent traveled to the top of the TLC plate by capillary action until it reached the solvent front. The TLC plate was taken out of the solvent tank. The dried TLC plate was viewed by iodine vapor and visualized under UV light (low and high wavelength). The same method was followed to find the optimal solvent system with other TLC plates in various solvent systems like hexane:ethyl acetate, ethyl acetate:methanol, chloroform:ethyl acetate, and chloroform:methanol in 100:0 to 0:100 ratios by increasing 10% more polar solvents used in the solvent system until a good resolution was noticed (18). The selected bioactive extract of *G. pentaphylla* was subjected to column chromatography to obtain fractions by increasing polarity of eluents using different solvent systems (chosen from the TLC trials) of chloroform:methanol 100:0, 80:20, 70:30, 60:40, and 50:50 ratios by increasing 10–20% more polar solvent used in the solvent system. The column ( $120 \times 4 \text{ cm}$ ) was packed with a solution of silica gel (60–120 mesh) with ethyl acetate using the wet slurry method. This involves preparing a solution of silica gel, with chloroform filled in the column up to one-third (about 40 cm) length. A significant amount of chloroform was added to the column and allowed to drain for silica gel setting in the column and the volume of the solvent collected was again poured back into the column.

The ethyl acetate extract (60 g) was absorbed into silica gel (100–200 mesh) by triturating in a mortar and left for 1 h to dry. The dried plant extract coated with silica gel was loaded on the prepared column by adding gently into the column filled with chloroform without any air bubbles and eluted with the desired solvent system. A total of 60 fractions was obtained and tested for their antibacterial potential against MDR *S. aureus* strains (clinical isolates) according to the method of Srinivasan et al. (19). The *G. pentaphylla* leaf ethyl acetate extract 9.7:0.3 chloroform:methanol ratio fraction (GPLCM-58F) showed significant antibacterial activity against *S. aureus* strains, which selected for further purification of bioactive compounds. The selected fraction was again monitored by TLC (pre-coated plate, 0.02 mm thick) to determine the optimal solvent system for further purification in column chromatography. Another small size column chromatography ( $60 \times 2 \text{ cm}$ ) was employed for further purification of selected fractions as per the abovementioned procedures. The fractions were eluted with chloroform:methanol (9:1–9.8:0.2 ratio) solvent system by increasing 0.1% of the volume of the polar solvents used in the solvent system. All the collected column fractions were again examined for antimicrobial activity and purity by TLC (pre-coated plate, 0.02 mm thick) for the single spot and the  $R_f$  values were calculated.

A total of two fractions (GPSC-55SF and GPSC-73SF) exhibited considerable antibacterial activity; these fractions again were subjected to preparative TLC purification (20). The preparative TLC plate was performed based on the noted  $R_f$  values. The fractions were scraped with silica powder using the sterile scoop and the collected UV-active pure compounds were dissolved in ethyl acetate solvent, and it can allow stirring with a magnetic stirrer for 1 h. After the pure fraction of active compounds was separated in the solvent, it was collected and concentrated under vacuum conditions. The UV-active pure fractions of the compound (GP-1 and GP-2) with similar  $R_f$  value was pooled together and subjected to the antimicrobial activity and spectral studies.

## Structural Identification of Isolated Compounds

### Liquid Chromatography–Mass Spectroscopy (LC-MS) Analysis

LC-MS analyses of the two isolated compounds were carried out according to the method of Natarajan et al. (21) using a Thermo/Finnigan Surveyor System consisting of a degasser, binary pump, autosampler, and column heater. The LC was coupled with the Ion Trap mass spectrometer (ThermoFleet, LCQ-Fleet) supported with an ESI ion source. Data acquisition and mass spectrometric evaluation were carried out in a personal computer with Data Analysis software (Qual Browser; Thermo Electron, San Jose, CA). For the chromatographic separation, Acquity BEC 1.7- $\mu\text{m}$  C18 column ( $2.1 \times 50 \text{ mm}$ ) was used. The column was programmed to run 95% of 0.1% acetic acid in water and 5% acetonitrile for both compounds 1 and 2. The final, elution program was operated at the linear gradient level of acetonitrile from 100 to 5% for a minimum 2 min. The flow rate

was 1 ml/min and the injection volume was 1  $\mu$ l. The capillary voltage, column temperature, nebulizer pressure, and gas flow rate were set to 20 V, 300°C, 40 psi, and 15 ml/min, respectively, for the entire MS analysis.

### Nuclear Magnetic Resonance (NMR) Spectroscopy Analysis

The structures of the isolated compounds were elucidated primarily by homonuclear ( $^1\text{D}$ ) NMR (22).  $^1\text{D}$  NMR experiments included  $^1\text{H}$  and  $^{13}\text{C}$  NMR, which used to locate atom positions and fragment units. NMR spectra were recorded on a Bruker Avance 300-MHz and/or Bruker Avance 600-MHz spectrometers coupled with Topsis acquisition software. Samples were dissolved in 500–600  $\mu$ l of suitable deuterated solvent. An NMR experiment on samples with very little mass was carried out using Shigemi NMR tubes (100–200  $\mu$ l sample). Signals were recorded in chemical shifts ( $\delta$ ) and expressed in parts per million (ppm), with coupling constants ( $J$ ) calculated in hertz (Hz).

### Fourier Transform Infrared Spectroscopy (FT-IR) Analysis

The UV-active pure compounds (GP-1 and GP-2) of fraction samples were used for FT-IR analysis. The dried compounds (each 3 mg) were encapsulated in 100 mg of KBr pellet, to prepare translucent sample discs. The compounds were loaded in an FTIR spectroscope (Shimadzu, Japan), measured from 400 to 4,000  $\text{cm}^{-1}$  and at a resolution of 4  $\text{cm}^{-1}$ .

### High-Performance Liquid Chromatography (HPLC) Analysis

The HPLC analysis of active compounds isolated from *G. pentaphylla* ethyl acetate extract was performed using the modified method of Hawry et al. (23). About 1 mg of concentrated sample was dissolved in 1 ml of chloroform:methanol (9.8:0.2) and 20  $\mu$ l was injected to determine the purity of compounds.

### Antibacterial Activity of Isolated Compounds

The selected MDR *S. aureus* strain suspension culture was prepared by growing a single colony overnight in Luria-Bertani (LB) broth with a turbidity of 0.5 McFarland standards. The antibacterial activity of isolated compounds was evaluated against MDR *S. aureus* strains using the agar well diffusion method (24). The isolated compounds (10  $\mu\text{g/ml}$ ) were added into the corresponding wells using a micropipette. Commercial antibiotic (amoxicillin) was used as a positive control, whereas DMSO served as a negative control. The plates were incubated at 37°C for 24 h and the diameter of the growth inhibition zone was measured.

### MIC and MBC Test

Minimum inhibitory concentration (MIC) of the isolated compounds was carried out using the microdilution method (25), using LB broth (Hi-media, India), and inoculum was adjusted to  $2.5 \times 10^5$  CFU/ml. In brief, 10  $\mu$ l ( $2.5 \times 10^5$  CFU/ml) of each MDR *S. aureus* strains was added individually in 1 ml of

LB broth. Different concentrations (0.5, 1, and 2  $\mu\text{g/ml}$ ) of the isolated compounds were mixed with test tubes containing the MDR *S. aureus* strains. After 24-h incubation, the MIC values were obtained by visual observation of bacterial growth. The minimum bactericidal concentration (MBC) value of the isolated compounds was evaluated using the method of Natarajan et al. (25). The MBC values were determined by sub-culturing (10  $\mu$ l) the MIC dilutions into the sterile Müller Hinton agar plates and incubated at 37°C for 24 h, and the results were observed.

### Mechanism of Action of Isolated Compounds Against MDR *S. aureus* Protein Leakage Assay

The impact of the isolated compounds on the MDR *S. aureus* cells was measured in the terms of leakage of intracellular protein materials. The MDR *S. aureus* were treated with the isolated compounds at 37°C for 120 min; each cell suspension was centrifuged at 7,000 RPM. About 100  $\mu$ l of each sample supernatant was mixed with 900  $\mu$ l of Bradford reagent and then incubated for 10 min. The optical density was measured at 595 nm. Bovine serum albumin was used as a standard protein and the experiment was done in triplicate (26).

### In vitro Killing Kinetic Assay

The time-kill kinetic assays were performed in five test tubes (two sets) containing an initial inoculum of  $1 \times 10^6$  CFU/ml in tryptic soy broth with isolated compounds according to the modified method of García et al. (27). Changes in the bacterial count during exposure of the isolated compounds to the bacteria were monitored in five test tubes. MDR *S. aureus* culture alone served as a control. The bacterial counts of the treated samples were determined in 3-h intervals up to 12-h periods (0, 3, 6, 9, and 12 h) of incubation. One hundred microliters of treated samples was diluted and 10  $\mu$ l of each sample was spread on Baird–Parker agar plates and incubated at 37°C overnight, and the control samples were incubated under the same conditions. The number of viable cells in each tube was estimated after counting bacterial colonies on plates and by multiplying the appropriate dilution factor (28). All the experiments were conducted in triplicate, and mean values were measured.

### SEM Analysis

The effect of isolated compounds on the morphology of MDR *S. aureus* strains was observed under scanning electron microscopy (SEM) after the bacterial cells were treated with the isolated compounds (arborine and skimmianine) for 6 h. After the treatment, 1 ml of each test bacterial strain was collected, centrifuged, and washed three times with phosphate buffer saline and incubated for 30 min at 4°C and fixed with 2.5% glutaraldehyde. The MDR *S. aureus* cells were dehydrated in ethanol, freeze-dried under vacuum condition, coated with an ion sputtering apparatus, and observed through SEM (Hitachi S-3400N). All strains of MDR *S. aureus* cells that are not exposed to the isolated compounds and a standard reference strain of *S. aureus* (MTCC 96) [procured from Microbial Type Culture Collection and Gene Bank (MTCC), Institute of Microbial

Technology, Chandigarh, India] cells were similarly processed and used as controls (29).

## RESULTS

### Isolation of Bioactive Compounds

Chloroform and methanol were used in various proportions as mobile phases. After elution, the purity of each fraction was tested by analytical TLC using chloroform:methanol in the ratio 9.7:0.3, which showed clear separation of fractions. The TLC containing nine major active compounds with different  $R_f$  values and similar  $R_f$  value fractions were scraped and pooled together (Figure S1) for further analysis. The ethyl acetate solvent extract of *G. pentaphylla* leaves (60 g) was applied to a silica gel column for isolation of the bioactive compounds. The column was eluted with a linear gradient solvent system consisting of chloroform:methanol, by increasing 10% polarity (100:0 to 0:100) of the solvents and the fractions were collected in a glass container. The similar  $R_f$  value fractions were pooled together according to the TLC profile and serially numbered (GP1, GP2, GP3, etc.) and all those fractions were kept at room temperature to allow condensation. After solvent evaporation, all collected fractions were tested for their antibacterial activity against the MDR *S. aureus* strains.

### Spectroscopic Analysis

The structural characterization of the isolated compounds was identified using NMR, LC-MS mass spectrometry, and HPLC analysis. UV and IR spectroscopy along with the determination melting point was carried out as they required for both the physical and structural characterization of isolated compounds.

### HPLC Analysis

The purity of isolated compounds was checked by HPLC analysis. The isolated active compound shows a separation peak at a retention time of 3.212 and 3.434 min for active compounds 1 and 2 respectively. In both the solvent system used, the purity of the active compounds was indicated as a single sharp peak (Figure S2).

## Structural Elucidation of Bioactive Compounds

### Physical Properties of Isolated Compounds

Compound 1 (arborine) was a yellowish-green color and soluble in ethyl acetate, methyl chloride, and DMSO, and insoluble in water. The melting point of the compound was 160–161°C and the yield was 120 mg. The  $R_f$  value of compound 1 was 0.98 mm in analytical TLC using a chloroform:methanol 9.8:0.2 solvent system as the mobile phase, whereas compound 2 (skimmianine) appeared as yellow color powder, soluble in ethyl acetate, methyl chloride, and DMSO. The yield of the isolated compound was 150 mg and the melting point was 180°C. The  $R_f$  value of compound 2 was 0.5 mm in analytical TLC using a chloroform:methanol 9.8:0.2 solvent system as the mobile phase.

**TABLE 1** | FT-IR spectrum of arborine and skimmianine compounds.

Compound name	$\nu_{\max}$ (cm <sup>-1</sup> )	Functional groups
Arborine	2,925	Aromatic C–H Stretch
	2,855	Aliphatic C–H Stretch
	1,602	C=O
	1,264	C–N Stretch
	1,402	Methyl bend
	765	Aromatic C–H bend out of the plane
Skimmianine	3,116	Aromatic C–H Stretch
	2,937, 2,839	Aliphatic C–H Stretch
	1,616	C=N Stretch
	1,266, 1,056	Phenyl ether C–O
	1,390	Methyl bend
	1,056, 1,192	Furan C–O
	736	C–H bend out of the plane

### FT-IR Spectrum Analysis of Compounds

The FT-IR spectrum of arborine shows a broad peak at 1,602 cm<sup>-1</sup>, which corresponds to the carbonyl group. The aromatic C–H stretching peak was observed at 2,925 cm<sup>-1</sup> while aliphatic C–H stretching frequency was found at 2,853 cm<sup>-1</sup>. The absorption band at 1,264 and 1,402 cm<sup>-1</sup> corresponds to the C=N stretch of amide and CH<sub>3</sub> bend, respectively. The aromatic C–H out of the plane bending vibration was detected at 765 cm<sup>-1</sup> (Figure S3, Table 1). The FT-IR analysis of skimmianine showed an absorption band at 1,616 cm<sup>-1</sup> due to the C=N group and characteristic phenyl ether C–O stretching vibration observed at 1,266 and 1,056 cm<sup>-1</sup>. The C–H stretching vibration corresponding to aromatic was observed at 3,116 cm<sup>-1</sup> while aliphatic C–H stretching vibration was identified at 2,937 and 2,839 cm<sup>-1</sup>. The characteristic methyl bend and aromatic C–H bend out of plane vibrations were seen at 1,390 cm<sup>-1</sup> and 739 cm<sup>-1</sup>, respectively. The stretching frequency of C–O in the furan ring was observed at 1,056 and 1,192 cm<sup>-1</sup> (Figure S7, Table 1).

### LC-MS and Elemental Analysis of Compounds

The mass spectra of arborine showed a molecular ion peak at  $m/z$  251 ( $M+1$ )<sup>+</sup> corresponding to the molecular formula C<sub>16</sub>H<sub>14</sub>N<sub>2</sub>O. The molecular weight was exactly matching with expected structure arborine (Figure S6). The result of the CHNS/O analysis of arborine showed carbon 76.22%, hydrogen 5.48%, nitrogen 10.96%, and oxygen 6.39%, which is in agreement with theoretical values (Table 2). The mass spectra of skimmianine showed a molecular ion peak at  $m/z$  260 ( $M+1$ )<sup>+</sup> corresponding to the molecular formula C<sub>14</sub>H<sub>13</sub>NO<sub>4</sub>. The molecular weight of the compound exactly matched the expected structure of skimmianine (Figure S10). The result of the CHNS/O analysis of skimmianine showed carbon 63.36%, hydrogen 4.98%, nitrogen 5.02%, and oxygen 24.96%, which is in agreement with theoretical values. The elemental analysis result was interpreted with molecular mass, which revealed the molecular formula of the GP-2 compound as C<sub>14</sub>H<sub>13</sub>NO<sub>4</sub> (Table 2).

**TABLE 2** | Elemental analysis of arborine and skimmianine compounds.

Compound name	Elements	Theoretical value (%)	Observed value (%)
Arborine	Carbon	76.78	76.22
	Hydrogen	5.67	5.48
	Nitrogen	11.19	10.96
	Oxygen	6.39	6.23
Skimmianine	Carbon	64.86	63.36
	Hydrogen	5.05	4.98
	Nitrogen	5.40	5.02
	Oxygen	24.68	24.96

**TABLE 3** | NMR (<sup>1</sup>H-NMR and <sup>13</sup>C-NMR) spectral data of arborine compound.

Chemical shift (δ ppm)	Proton/carbon numbered	Splitting pattern	Nature of the proton/carbon
<b><sup>1</sup>H-NMR</b>			
3.63	5	Singlet	N-methyl proton
4.29	6	Singlet	Benzylic proton
7.28–7.36	7, 8, 9, 10, 11, 12, 13, 14	Multiplet	Aromatic (benzene ring)
7.46	2, 3	Triplet	Aromatic (quinazoline ring)
7.71	1	Doublet	Aromatic (quinazoline ring)
8.37	4	Doublet	Aromatic (quinazoline ring)
<b><sup>13</sup>C-NMR</b>			
34.8	7	Singlet	N-methyl carbon
43.4	10	Singlet	Benzylic carbon
114.4	1	Singlet	Aromatic (Quinazoline ring)
120.0	8	Singlet	Aromatic (Quinazoline ring)
125.9	3	Singlet	Aromatic (Quinazoline ring)
127.3	14	Singlet	Aromatic (Benzene ring)
128.2	13, 15	Singlet	Aromatic (Benzene ring)
128.5	4	Singlet	Aromatic (Quinazoline ring)
129.0	12, 16	Singlet	Aromatic (Benzene ring)
133.7	2	Singlet	Aromatic (Quinazoline ring)
134.5	11	Singlet	Aromatic (Benzene ring)
141.4	9	Singlet	Aromatic (Quinazoline ring)
162.2	6	Singlet	C=N (Quinazoline ring)
169.0	5	Singlet	Amide C=O

### <sup>1</sup>H-NMR and <sup>13</sup>C-NMR Analysis of Compounds

The <sup>1</sup>H-NMR spectrum of arborine revealed a total of 14 protons present in the compound. The characteristic N-methyl proton was observed at δ 3.63 ppm as a singlet. The benzylic protons present in the arborine was seen at δ 4.29 ppm as singlet (Figure S4). In the downfield aromatic region, eight aromatic protons were observed between δ 7.28 and δ 7.36 ppm as a multiplet. The quinazoline fused aromatic ring protons numbered 3, 1, and 4 were observed at δ 7.46 ppm (triplet), δ 7.71 ppm (doublet), and δ 8.37 ppm (doublet), respectively (Figure S4, Table 3).

In the <sup>13</sup>C-NMR of arborine, N-methyl and benzylic carbons are observed at δ 34.8 and δ 43.4 ppm, respectively. The highest

**TABLE 4** | NMR (<sup>1</sup>H-NMR and <sup>13</sup>C-NMR) spectral data of skimmianine compound.

Chemical shift (δ ppm)	Proton/carbon numbered	Splitting pattern	Nature of the proton/carbon
<b><sup>1</sup>H-NMR</b>			
4.03	3	Singlet	Methoxy
4.11	6	Singlet	Methoxy
4.41	7	Singlet	Methoxy
7.02	2	Doublet	C–H (Furan ring)
7.23	5	Doublet	C–H (Aromatic ring)
7.56	1	Doublet	C–H (Furan ring)
7.99	4	Doublet	C–H (Aromatic ring)
<b><sup>13</sup>C-NMR</b>			
56.7	8	Singlet	Methoxy carbon
58.8	9	Singlet	Methoxy carbon
61.5	10	Singlet	Methoxy carbon
101.9	11	Singlet	Aromatic-fused ring carbon
104.4	2	Singlet	Furan-fused ring carbon
112.2	4	Singlet	Aromatic ring carbon
114.8	13	Singlet	Aromatic-fused ring carbon
117.9	5	Singlet	Aromatic ring carbon
141.4	14	Singlet	Aromatic-fused ring carbon
142.1	12	Singlet	Furan-fused ring carbon
142.8	1	Singlet	Furan ring carbon
152.0	6	Singlet	Aromatic ring carbon
157.0	7	Singlet	Aromatic ring carbon
164.2	3	Singlet	Aromatic ring carbon

carbon chemical shift δ 169.0 ppm was observed for amide carbonyl carbon. The chemical shift for imine carbon (C=N) was seen at δ 162.2 ppm. The aromatic carbon chemical shifts were observed between δ 114.4 and δ 141.4 ppm (Figure S5, Table 3). Three methoxy groups present in skimmianine showed chemical shift values between δ 4.03 and δ 4.49 ppm. All the methoxy protons in the upfield showed a clear singlet pattern. The two protons correspond to the furan ring observed at δ 7.02 and δ 7.56 ppm, respectively, and those protons show a doublet splitting pattern. The other aromatic protons are seen at δ 7.23 and δ 7.99 ppm, which also showed a doublet splitting pattern (Figure S8, Table 4). In the <sup>13</sup>C-NMR of skimmianine, the characteristic three methoxy carbons were seen at δ 56.7, δ 58.8, and δ 61.5 ppm. The highest carbon chemical shift δ 164.2 ppm was observed for the methoxy group-attached carbon, which is present in the pyridine ring part of skimmianine. The other methoxy-attached carbons are seen at δ 152.0 and δ 157.0 ppm. The characteristic imine carbon C=N was observed at δ 142.1 ppm. All aromatic magnetically non-equivalent carbons are observed between δ 101.9 and δ 142.8 ppm (Figure S9, Table 4).

### Antibacterial Activity of Isolated Compounds

Arborine and skimmianine compounds showed significant antibacterial activity against clinical isolated MDR *S. aureus*



**TABLE 5** | Anti-bacterial activity of arborine and skimmianine compounds against MDR *S. aureus*.

S. no.	MDR Strains	Arborine	Skimmianine	Amoxicillin	DMSO
1	<i>S. aureus</i> 101	28 ± 0.58	27 ± 0.24	23 ± 0.58	00 ± 0.00
2	<i>S. aureus</i> 270	26 ± 0.00	25 ± 0.58	26 ± 0.58	00 ± 0.00
3	<i>S. aureus</i> 315	27 ± 0.58	28 ± 0.08	29 ± 0.58	00 ± 0.00
4	<i>S. aureus</i> 319	25 ± 0.15	26 ± 0.73	25 ± 0.58	00 ± 0.00
5	<i>S. aureus</i> 410	28 ± 0.39	25 ± 0.08	27 ± 0.58	00 ± 0.00

**TABLE 6** | MIC and MBC values of arborine and skimmianine compounds against MDR *S. aureus*.

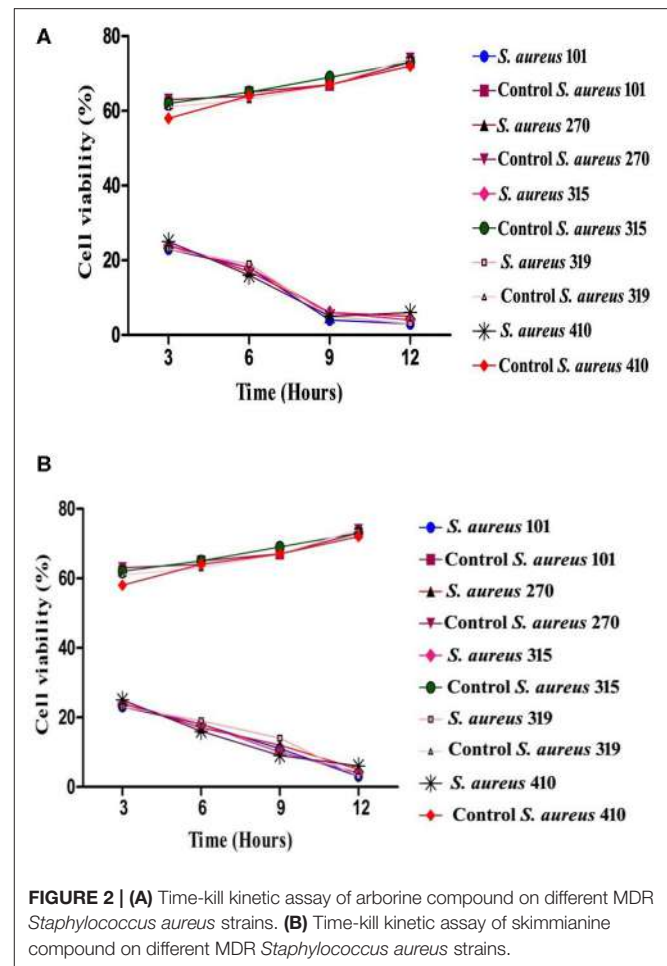
S. no.	MDR strains	MIC and MBC values (μg/ml)					
		Arborine		Skimmianine		Amoxicillin	
		MIC	MBC	MIC	MBC	MIC	MBC
1	<i>S. aureus</i> 101	0.2	0.2	0.2	1	>2	>2
2	<i>S. aureus</i> 270	1	2	2	>2	2	>2
3	<i>S. aureus</i> 315	1	1	0.2	0.2	1	2
4	<i>S. aureus</i> 319	1	>2	1	1	>2	>2
5	<i>S. aureus</i> 410	0.2	0.2	2	>2	2	>2

strains reported that 25 mm to 28mm of growth inhibition zones (Table 5). The results of the antibacterial activity of arborine and skimmianine clearly showed a dose-dependent effect (Table 6). The antibacterial activity results of arborine indicated that MDR *S. aureus* 101 and 410 strain was highly susceptible to the isolated compounds with the maximum inhibition of growth zone (28 mm) and lower MIC (0.2 μg/ml) and MBC (0.2 μg/ml) values. Similarly, skimmianine compound exhibit the highest antibacterial activity against the MDR *S. aureus* 315 strain (28 mm) with the lowest MIC (0.2 μg/ml) and MBC (0.2 μg/ml) values. The antibacterial activity was noticed in low concentration with stronger inhibitory potential. The results indicated that arborine and skimmianine exhibit a strong growth inhibition effect on all tested pathogens. The overall results indicated that the arborine and skimmianine possess better antibacterial activity than commercial antibiotics. Even a low MIC and MBC concentration of isolated compounds expressed a remarkable amount of bactericidal activity against the tested MDR *S. aureus* strains.

## Bacterial Mechanism Study of Compounds

### Time Kill Kinetic Assay

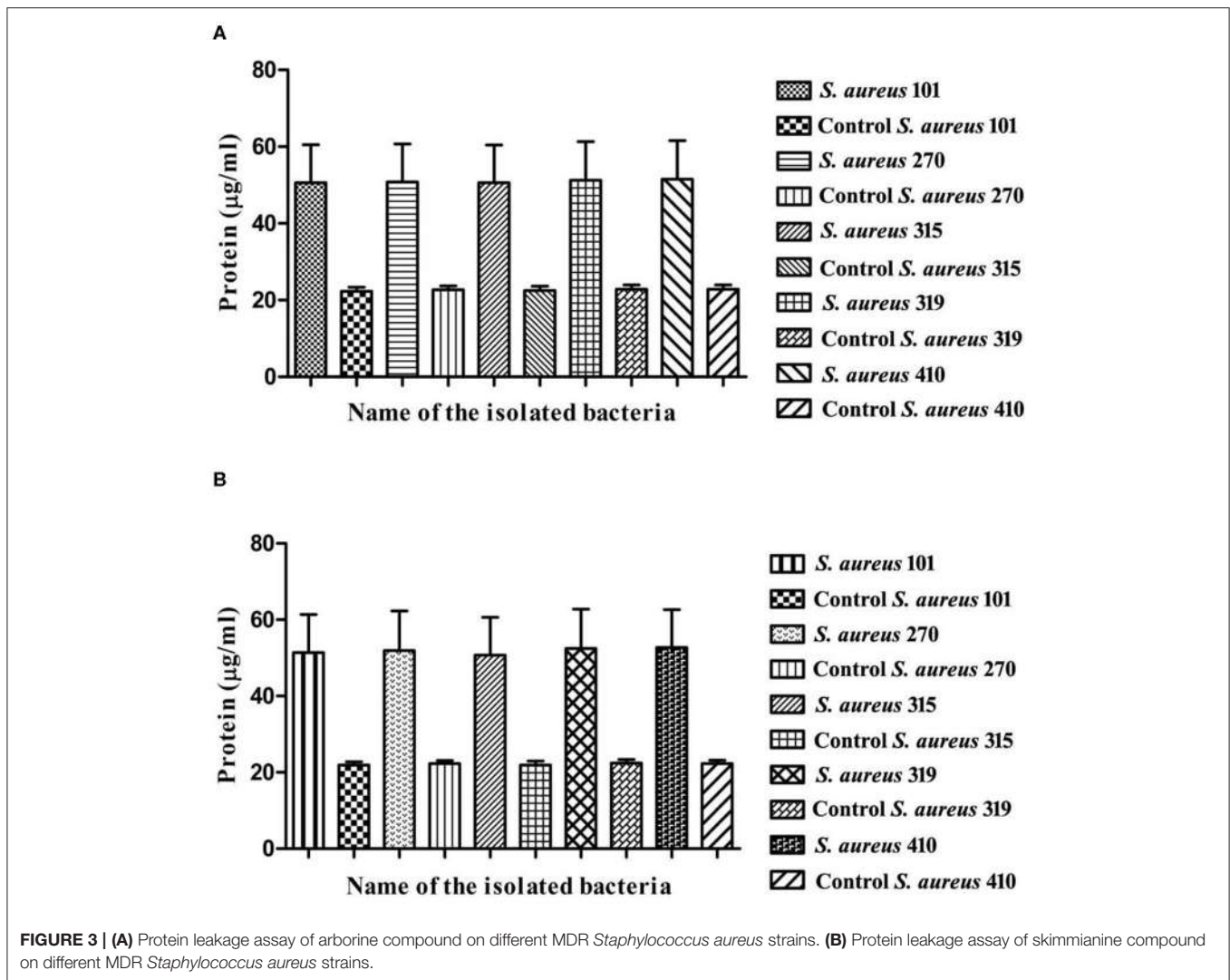
The time-killing kinetic assay was used to analyze the post-treatment bacterial viability and to define the minimum time required to obtain the bactericidal effect. Both arborine and skimmianine compounds show similar time-killing kinetic patterns of bactericidal effect on the MDR *S. aureus* strains (Figures 2A,B). Bactericidal activity was gradually increased by the time up to 12 h exposure of the MDR *S. aureus* strains against arborine and skimmianine compounds at their respective MBC concentration for both the strains and the MDR *S. aureus* strains



were killed within this period. The arborine and skimmianine compounds expressed a time-dependent and prompt bactericidal potential against the tested MDR *S. aureus* strains, which leads to bacterial death at the early stationary phase, as shown in time-kill curves (Figures 2A,B) compared with the control cells.

### Protein Leakage Assay

Arborine and skimmianine compounds are known to enhance protein leakage by increasing the membrane permeability in MDR *S. aureus* strains. To determine the impact of arborine and skimmianine compounds alone on protein leakage, the cells were treated with arborine for 75 μg/ml, resulting in all strains exhibiting 54% protein leakage, and skimmianine compounds were treated for 100 μg/ml and the leakage of proteins was 55%. When the cells were treated with arborine and skimmianine compounds, the amount of protein released from the cells was increased compared to control (commercial antibiotics with recommended doses) (Figures 3A,B).



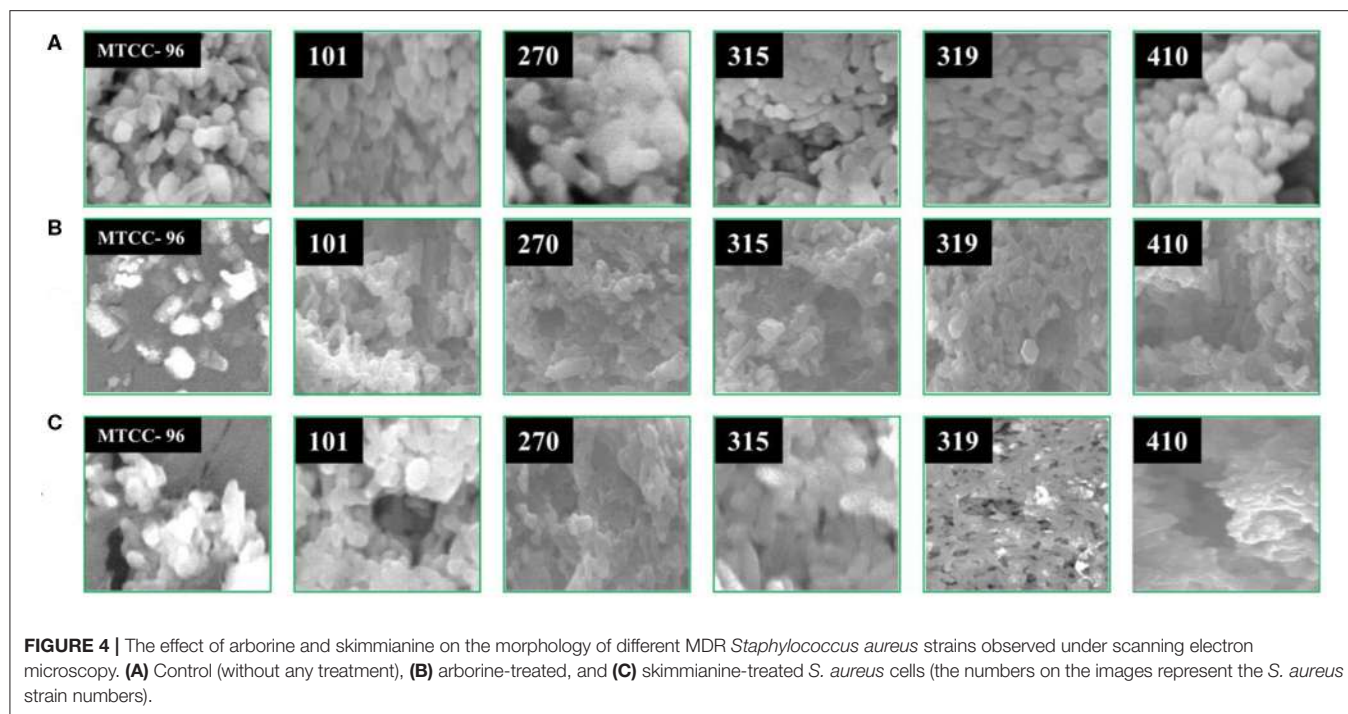
### Morphological Changes of MDR *S. aureus*

In order to have a better understanding of the antibacterial mechanism, arborine and skimmianine compounds were further studied for their effects on bacterial cell surfaces. Using SEM analysis, the present study observed the morphological changes in all MDR *S. aureus* strains and the reference standard *S. aureus* MTCC-96 strain, upon treatment with the antibacterial effect of arborine and skimmianine compounds (Figure 4). In MDR *S. aureus*, the untreated bacterial cells (control strains) appeared as grape-shaped (cocci), and the surfaces of the cells were intact with no damage observed. The *S. aureus* cells treated with arborine and skimmianine compounds, was not able to maintain the cocci (grape) shaped characteristics. Moreover, uneven fragments were observed, which indicated the damages induced on bacterial cell membranes. Moreover, the treated *S. aureus* cell surfaces were uneven, the size of cells were reduced, and the cells seemed to be damaged. Through the SEM analysis, the present study confirmed that the MDR

*S. aureus* membrane surfaces were damaged, upon the treatment with arborine and skimmianine compounds isolated from *G. pentaphylla*.

### DISCUSSION

Medicinal plants have been the major source for innumerable therapeutic agents, which are of great importance to the health of an individual as well as communities (30). *G. pentaphylla* ethyl acetate crude extract was separated into nine fractions by thin-layer chromatography. Only two fractions showed excellent antibacterial property. This fraction was composed of two compounds that were visualized in TLC under the UV chamber. This study clearly shows that the active fractions obtained from column chromatographic separation are found to be mixtures of compounds. The purity of the fractions was obtained by column chromatography. The column purified compounds were



**FIGURE 4 |** The effect of arborine and skimmianine on the morphology of different MDR *Staphylococcus aureus* strains observed under scanning electron microscopy. **(A)** Control (without any treatment), **(B)** arborine-treated, and **(C)** skimmianine-treated *S. aureus* cells (the numbers on the images represent the *S. aureus* strain numbers).

characterized by  $^1\text{H}$  NMR,  $\text{C}^{13}$  NMR, FT-IR, HPLC, and LC-MS. The compounds GP-1 and GP-2 exactly matched the structure of arborine and skimmianine compounds with the molecular formula  $\text{C}_{16}\text{H}_{14}\text{N}_2\text{O}$  and  $\text{C}_{14}\text{H}_{13}\text{NO}_4$ , respectively. The  $^{13}\text{C}$  NMR also supports the presence of the N-methyl and benzylic group. The characteristic functional groups found at  $1602\text{ cm}^{-1}$  ( $\text{C}=\text{O}$ ) and  $1402\text{ cm}^{-1}$  ( $\text{C}-\text{N}$ ) in the FT-IR spectra confirmed the arborine structure. Finally, the LC-MS also complies with the mass of arborine (MW 250), which is observed as an M+1 peak (251).

Similarly, Chakravarti et al. (31) have isolated the alkaloid arborine compound from the leaves of *Glycosmis arborea*, and its structure was further confirmed as 2-benzyl-1-methylquinazol-4-one based on UV, FT-IR, and  $^1\text{H}$ NMR analysis. The present findings correlated with the observations of the arborine compound isolated from the stem of *G. pentaphylla*, which was already reported by Chakravarti et al. (32), Govindachari et al. (33), and Muthukrishnana et al. (34). Ghani (35) reported that the *G. pentaphylla* leaves contain alkaloids arborine, arborinine, skimmianine, glycorine, glycophyminine, glycophyminoline, glycosmicine, and glycomide.

The structure of skimmianine was confirmed by  $^1\text{H}$  NMR,  $^{13}\text{C}$  NMR, FT-IR, and LC-MS. In  $^{13}\text{C}$  NMR, three methoxy carbons were observed at  $\delta$  56.7, 58.8, and 61.5 ppm. The FT-IR values of about  $1,616\text{ cm}^{-1}$  ( $\text{C}=\text{N}$ ),  $1,266$ ,  $1,056\text{ cm}^{-1}$  ( $\text{C}-\text{O}$ , ether), and  $1,056$ ,  $1,192\text{ cm}^{-1}$  ( $\text{C}-\text{O}$ , Furan) confirmed the structure of skimmianine. The LC-MS also confirmed the molecular weight of skimmianine, which was observed as M+1 peak (MW 260). The findings were in good agreement with earlier reports of Sreelekha (36) who isolated the skimmianine from *Zanthoxylum rhetsa*. Desai et al. (37) have isolated arborinine, cycleanine, isochondrodendrine, and skimmianine

from the leaves of *G. pentaphylla*. Similarly, Sinhababu and Takur (38) have reported alkaloids arborine, arborinine, skimmianine, glycorine, glycosmicine, and an amide that was isolated from the flower heads of *G. pentaphylla*. On the other hand, Chakravarty et al. (39) isolated a skimmianine compound from *G. arborea*. Another study was done by Mester (40) and Greger et al. (41) isolated well-known alkaloids, arborine, and skimmianine compounds from *G. parviflora*.

The isolated arborine and skimmianine compounds show significant antibacterial activity against multidrug-resistant *S. aureus* isolates. Similar findings were reported by Bowen et al. (42), Chakravarti et al. (31), and Chakravarty et al. (39) who carried out the antibacterial activity of arborine and skimmianine compounds against both Gram-positive bacteria (*S. aureus* and MRSA) and Gram-negative bacteria (*E. coli* and *S. typhimurium*), which were inactive against *S. aureus*. Previously, Jeyachandran et al. (43) have reported that the plumbagin bioactive compound was isolated from the root extract of *Plumbago zeylanica*, exhibiting more toxic potential against *S. aureus*. The *in vitro* time-kill assay is one of the most commonly used experimental models to assess the antibacterial activity, efficiently characterizing the rate, extent, and timing of bacterial killing and regrowth (44). The time-kill test finds out the differences in the rate and extent of antibacterial activity over time, and it can also provide growth kinetics information (45). The overall result of this assay revealed a stronger bactericidal effect in arborine and skimmianine compounds against *S. aureus* than in a laboratory medium. The evaluation of protein leakage of the arborine and skimmianine showed a significant strong effect on the tested MDR *S. aureus* strains. A similar kind of protein leakage when treated with oil compounds from medicinal plants supports the findings of the present study (46).



The SEM result of the present study shows that bacterial cell membranes were significantly affected by the activity of arborine and skimmianine compounds. It is indicated that arborine and skimmianine bioactive compounds disturb the bacterial membrane and death to cells. Similar findings were reported by Campos et al. (47) who identified that the *S. aureus* and *E. coli* bacterial membranes and cytoplasm were highly affected due to the passive diffusion of plant metabolites into the cells that caused consequent cell disruption. These changes in bacteria cells may be due to the lysis of membrane and transformation caused by the damage on the permeability and integrity of membrane from arborine and skimmianine compounds. Consequently, the changes can lead to loss of inner cell materials (48, 49). The results of SEM were in good agreement with other findings of Paul et al. (50) and Sharma et al. (51) reported that other antimicrobials treated cells. Shen et al. (29) have reported that *S. aureus* damaged cell membrane affects the cell permeability, and outflow of cellular components that lead to cell death which supported the present study.

## CONCLUSION

The present study indicated that *G. pentaphylla* is a good source of arborine and skimmianine, which acts as potent antibacterial agents against MDR *S. aureus* clinical isolates. Besides, these compounds induced significant strong bactericidal effects on the MDR *S. aureus* such as intracellular molecular imbalance and cell membrane disturbances that caused cell death. Hence, this study recommends that the isolated compounds can be used as a template molecule for pharmaceutical drug design for the treatment of diseases caused by MDR *S. aureus*.

## REFERENCES

- Plata K, Rosato AE, Wegrzyn G. *Staphylococcus aureus* as an infectious agent: overview of biochemistry and molecular genetics of its pathogenicity. *Acta Biochim Pol.* (2009) 56:597–612. doi: 10.18388/abp.2009\_2491
- Shittu AO, Lin J, Kolawole DO. Antimicrobial susceptibility patterns of *Staphylococcus aureus* and characterization of MRSA in Southwestern Nigeria. *Wounds.* (2006) 18:77–84.
- Price LB, Stegger M, Hasman H, Aziz M, Larsen J. *Staphylococcus aureus* CC398: host adaptation and emergence of methicillin resistance in livestock. *Am Soc Microbiol.* (2012) 52:139–46. doi: 10.1128/mBio.00305-11
- Deleo FR, Kennedy AD, Chen L. Molecular differentiation of historic phage-type 80/81 and contemporary epidemic *Staphylococcus aureus*. *Proc Natl Acad Sci USA.* (2011) 108:18091–6. doi: 10.1073/pnas.1111084108
- World Health Organization. Antimicrobial resistance: global report on surveillance 2014. (2014). Available online at: [https://apps.who.int/iris/bitstream/handle/10665/112642/9789241564748\\_eng.pdf;jsessionid=E8D8B96F2905D8AFBDCBDE65C4D0D825?sequence=1](https://apps.who.int/iris/bitstream/handle/10665/112642/9789241564748_eng.pdf;jsessionid=E8D8B96F2905D8AFBDCBDE65C4D0D825?sequence=1)
- Xie X, Wong WW, Tang Y. Improving simvastatin bioconversion in *Escherichia coli* by deletion of bioH. *Metab Eng.* (2007) 9:379–86. doi: 10.1016/j.jymben.2007.05.006
- Alviano DS, Alviano CS. Plant extracts: search for new alternatives to treat microbial diseases. *Curr Pharm Biotechnol.* (2009) 10:106–21. doi: 10.2174/138920109787048607
- Junio HA, Sy-Cordero AA, Ettefagh KA, Burns JT, Micko KT, Graf TN et al. (2011). Synergy-directed fractionation of botanical medicines: a case study with goldenseal (*Hydrastis canadensis*). *Nat Prod.* 74:1621–9. doi: 10.1021/np200336g

## DATA AVAILABILITY STATEMENT

All datasets generated for this study are included in the article/**Supplementary Material**.

## AUTHOR CONTRIBUTIONS

NM and RS equally contributed to the experiments and wrote the manuscript. AM, MK, and DN designed the research work and carry out the corrections in the article.

## ACKNOWLEDGMENTS

The authors acknowledge the Department of Biotechnology, Periyar University, Salem, Tamil Nadu, India, for providing necessary laboratory facilities, Tamil Nadu State Council for Science and Technology for financial support under the S&T Project Scheme (TNSCST/S&T Projects/RJ/BS/2013-2014), and DST-FIST (SR/FIST/LSI-673/2016) for strengthening the instrumentation facility of the Biotechnology Department of Periyar University. We thank Dr. S. Gnanavel, Department of Chemistry, Government Engineering College, Salem, for his technical assistance in the isolation of compounds and Dr. G. Ramkumar, ICAR-Indian Institute of Horticultural Research, for his suggestions on the manuscript.

## SUPPLEMENTARY MATERIAL

The Supplementary Material for this article can be found online at: <https://www.frontiersin.org/articles/10.3389/fpubh.2020.00176/full#supplementary-material>

- Choi J, Choi J, Mun S, Kang O, Preeti B, Dong-Won S, et al. Antimicrobial activity and synergism of Sami-Hyanglyun-Hwan with ciprofloxacin against methicillin-resistant *Staphylococcus aureus*. *Asian Pac J Trop Med.* (2008) 8:538–42. doi: 10.1016/j.apjtm.2015.06.010
- Santos PRV, Oliveira ACX, Tomassini TCB. Controle microbiológico de produtos fitoterápicos. *Rev Farm Bioquím.* (1995) 31:35–8.
- Suganya A, Murugan K, Kovendan K, Mahesh Kumar P, Hwang JS. Green synthesis of silver nanoparticles using *Murraya koenigii* leaf extract against *Anopheles stephensi* and *Aedes aegypti*. *Parasitol Res.* (2013) 112:1385–97. doi: 10.1007/s00436-012-3269-z
- Kuzel S, Vydra J, Triska J, Vrchatova N, Hruby Mand Cigler P. Elicitation of pharmacologically active substances in an intact medical plant. *J Agri Food Chem.* (2009) 57:7907–11. doi: 10.1021/jf9011246
- Taware AS, Mukadam DS, Chavan AM, Taware SD. Comparative studies of *in vitro* and *in vivo* grown plants and callus of *Stevia rebaudiana* (Bertoni). *Int J Integr Biol.* (2010) 9:10–5.
- Dakah A, Suleiman M, Zaid S. Effect of some Environmental stress in tissue culture media on *in vitro* propagation and antioxidant activity of medicinal plant *Ziziphora canescens* Benth. *Adv Nat Appl Sci.* (2014) 8:224–32.
- Murugan N, Natarajan D. Phytochemical, antioxidant and antibacterial activities of *Glycosmis pentaphylla* (Rutaceae) leaf extracts against selected multi-drug resistant bacteria. *J Chem Pharm Res.* (2016) 8:737–44.
- Murugan N. *Antibacterial activity of Glycosmis Pentaphylla plant against clinically isolated multi drug resistant Staphylococcus aureus and their in silico analysis* (Ph.D Thesis). Periyar University, Salem, Tamil Nadu (2016). p. 97–110.
- Srinivasan R. *Bioactivity guided isolation and structural elucidation of antimicrobial, antioxidant and larvicidal compounds from Elaeagnus indica*



- and *Memecylon edule* and their molecular docking studies (Ph.D Thesis). Periyar University, Salem, Tamil Nadu (2014). p. 20–43.
18. Srinivasan R, Natarajan D, Shivakumar MS, Vinuchakkaravarthy T, Velmurugan D. Bioassay-guided isolation of mosquito larvicidal compound from acetone leaf extract of *Elaeagnus indica* Servett Bull and its *in-silico* study. *Ind Crops Prod.* (2015) 76:394–401. doi: 10.1016/j.indcrop.2015.07.032
  19. Srinivasan R, Natarajan D, Shivakumar MS. Spectral characterization and antibacterial activity of an isolated compound from *Memecylon edule* leaves. *J. Photochem Photobiol B Biol.* (2017) 168:20–4. doi: 10.1016/j.jphotobiol.2017.01.019
  20. Srinivasan R, Natarajan D, Shivakumar MS, Nagamurugan N. Isolation of fisetin from *Elaeagnus indica* Servett. Bull. (Elaeagnaceae) with antioxidant and antiproliferative activity. *Free Radic Antioxid.* (2016) 6:145–50. doi: 10.5530/fra.2016.2.3
  21. Natarajan D, Srinivasan R, Shivakumar MS. Gas chromatography mass spectroscopy chromatogram and antimicrobial activity of leaf extracts of *Blepharis maderaspatensis* and *Maesa indica*. *J Herbs Spices Med Plants.* (2015) 21:267–82. doi: 10.1080/10496475.2014.960637
  22. Parsons HM, Ludwig C, Gunther UL, Viant MR. Improved classification accuracy in 1- and 2-dimensional NMR metabolomics data using the variance stabilising generalised logarithm transformation. *BMC Bioinform.* (2007) 8:234. doi: 10.1186/1471-2105-8-234
  23. Hawry MA, Soczewinski E, Dzido TH. Separation of coumarins from *Archangelica officinalis* in high-performance liquid chromatography and thin-layer chromatography system. *J. Chromatogr A.* (2000) 366:75–81. doi: 10.1016/S0021-9673(00)00321-6
  24. Srinivasan R, Natarajan D, Shivakumar MS. Antimicrobial and GC-MS analysis of *Memecylon edule* leaf extracts. *Int J Curr Pharma. Rev Res.* (2014) 5:1–13. doi: 10.5530/fra.2015.1.6
  25. Natarajan D, Srinivasan R, Shivakumar MS. *Phyllanthus wightianus* Müll. Arg - a potential source for natural antimicrobial agents. *Biomed Res Int.* (2014) 2014:135082. doi: 10.1155/2014/135082
  26. Balakumaran MD, Ramachandran R, Balashanmugam P, Mukeshkumar DJ, Klaichelvan PT. Mycosynthesis of silver and gold nanoparticles: optimization, characterization and antimicrobial activity against human pathogens. *Microb Res.* (2016) 182:8–20. doi: 10.1016/j.micres.2015.09.009
  27. García P, Martínez B, Rodríguez L, Rodríguez A. Synergy between the phage endolysin LysH5 and nisin to kill *Staphylococcus aureus* in pasteurized milk. *Int. Food Microbiol.* (2010) 141:151–5. doi: 10.1016/j.ijfoodmicro.2010.04.029
  28. Dos Santos AO, Ueda-Nakamura T, Dias BP, Veiga VF, Pinto AC, Nakamura CV. Antimicrobial activity of Brazilian copaiba oils obtained from different species of the *Copaifera* genus. *Mem Inst Oswaldo Cruz.* (2008) 103:277–81. doi: 10.1590/S0074-02762008005000015
  29. Shen SX, Zhang TH, Yuan Y, Lin SY, Xu JY, Ye HQ. Effects of cinnamaldehyde on *Escherichia coli* and *Staphylococcus aureus* membrane. *Food Control.* (2015) 47:196–202. doi: 10.1016/j.foodcont.2014.07.003
  30. Ganesan, S. Traditional oral care medicinal plant survey of Tamilnadu. *Nat Prod. Radiance.* (2008). p. 7:166–72.
  31. Chakravarti D, Chakravarti RN, Cohen LA, Dasgupta B, Datta S, Miller HK. Alkaloids of *Glycosmis arborea*-II. Structure of arborine. *Tetrahedron.* (1961) 16:224–50. doi: 10.1016/0040-4020(61)80074-4
  32. Chakravarti D, Chakravarti RN, Chakravarti SC. Alkaloids of *Glycosmis arborea*. Part I Isolation of arborine and arborinine: the structure of arborine. *J Chem Soc.* (1953) 3337. doi: 10.1039/jr9530003337
  33. Govindachari TR, Jadhav SJ, Joshi BS, Kamat VN, Mohamed PA, Parthasarathy PC, et al. Chemical investigation of some Indian Plants. *Indian J Chem.* (1969) 7:308–9.
  34. Muthukrishnana J, Seifert K, Homann KH, Lorenz MW. Inhibition of juvenile hormone biosynthesis in *Gryllus bimaculatus* by *Glycosmis pentaphylla* leaf compounds. *Phytochemistry.* (1999) 50:249–54. doi: 10.1016/S0031-9422(98)00537-8
  35. Ghani A. Medicinal plants of Bangladesh. *Asiatic Soc.* (2003) 430:502–4.
  36. Sreelekha, M. (2012). *Studies on secondary plant metabolites and their biological properties.* (Ph.D thesis). Department of Chemistry, University of Calicut, Tirur, Kerala.
  37. Desai PD, Dutta MD, Ganguly AI, Govindachary TR, Joshi BS, Kamat VN, et al. Chemical investigation of some Indian plants: Part III. *Indian J Chem.* (1967) 5:523–4.
  38. Sinhababu A, Thakur S. Constituents of flower of *Glycosmis pentaphylla* (Retz) Correa. *Asian J Chem.* (1995) 7:221–2.
  39. Chakravarty AK, Sarkar T, Masuda K, Shiojima K. Carbazole alkaloids from root of *Glycosmis arborea*. *Phytochemistry.* (1999) 50:1263–6. doi: 10.1016/S0031-9422(98)00666-9
  40. Mester I. Structural diversity and distribution of alkaloids in the Rutales. In: Waterman PG, Grundon ML, editors. *Chemistry and Chemical Taxonomy of the Rutales.* New York, NY; London: Academic Press (1983). p. 31–96.
  41. Greger H, Zechner G, Hofer O, Hadacek F, Wurz G. Sulphur-containing amides from *Glycosmis* species with different antifungal activity. *Phytochemistry.* (1993) 34:175–9. doi: 10.1016/S0031-9422(00)90802-1
  42. Bowen IH, Perera CKPW, Lewis JR. Alkaloids of the leaves of *Glycosmis bilocularis*. *Phytochemistry.* (1978) 17:2125–7. doi: 10.1016/S0031-9422(00)89294-8
  43. Jeyachandran R, Mahesh A, Cindrella L, Sudhakar S, Pazhanichamy K. Antibacterial activity of plumbagin and root extracts of *Plumbago zeylanica* L. *Acta Biol Cracoviensis Ser Bot.* (2009) 51:17–22.
  44. Cheahe D, Zhang Y, Gao D, Zhang H. Antibacterial and anti-inflammatory activities of extract and fractions from *Pyrrosia petiolosa* (Christ et Bar.) Ching. *J Ethnopharmacol.* (2015) 155:1300–05. doi: 10.1016/j.jep.2014.07.029
  45. Lewis S, Tarrier N, Haddock G, Lewis S, Tarrier N, Haddock G. Randomised controlled trial of cognitive-behavioural therapy in early schizophrenia: acute-phase outcomes. *Br J Psychiatry.* (2002) 181:s91–7. doi: 10.1192/bjp.181.43.s91
  46. Lattaoui N, Tantaoui-Elaraki A. Individual and combined antibacterial activity of the main components of three thyme essential oils. *Riv Ital EPPOS.* (1994) 13:13–9.
  47. Campos FM, Couto JA, Figueiredo AR, Tóth IV, Rangel AOSS, Hogg TA. Cell membrane damage induced by phenolic acids on wine lactic acid bacteria. *Int J Food Microbiol.* (2009) 135:144–51. doi: 10.1016/j.ijfoodmicro.2009.07.031
  48. Bajpai VK, Al-Reza SM, Choi UK, Lee JH, Kang SC. Chemical composition, antibacterial and antioxidant activities of leaf essential oil and extracts of *Metasequoia glyptostroboides* Miki ex Hu. *Food Chem Toxicol.* (2009) 47:1876–83. doi: 10.1016/j.fct.2009.04.043
  49. Shin SY, Bajpai VK, Kim HR, Kang SC. Antibacterial activity of bioconverted eicosapentaenoic (EPA) and docosahexaenoic acid (DHA) against foodborne pathogenic bacteria. *Int J Food Microbiol.* (2007) 113:233–6. doi: 10.1016/j.ijfoodmicro.2006.05.020
  50. Paul S, Dubey RC, Maheswari DK, Kang S. *Trachyspermum ammi* (L.) fruit essential oil influencing on membrane permeability and surface characteristics in inhibiting food-borne pathogens. *Food Control.* (2011) 22:725–31. doi: 10.1016/j.foodcont.2010.11.003
  51. Sharma A, Bajpai VK, Baek K. Determination of antibacterial mode of action of *Allium sativum* essential oil against foodborne pathogens using membrane permeability and surface characteristic parameters. *J Food Saf.* (2013) 33:197–208. doi: 10.1111/jfs.12040

**Conflict of Interest:** The authors declare that the research was conducted in the absence of any commercial or financial relationships that could be construed as a potential conflict of interest.

Copyright © 2020 Murugan, Srinivasan, Murugan, Kim and Natarajan. This is an open-access article distributed under the terms of the Creative Commons Attribution License (CC BY). The use, distribution or reproduction in other forums is permitted, provided the original author(s) and the copyright owner(s) are credited and that the original publication in this journal is cited, in accordance with accepted academic practice. No use, distribution or reproduction is permitted which does not comply with these terms.



# Extended-Spectrum Beta-Lactamase-Producing *Escherichia coli* in Drinking Water Samples From a Forcibly Displaced, Densely Populated Community Setting in Bangladesh

Zahid Hayat Mahmud<sup>1\*</sup>, Mir Himayet Kabir<sup>1</sup>, Sobur Ali<sup>1</sup>, M. Moniruzzaman<sup>1</sup>, Khan Mohammad Imran<sup>1</sup>, Tanvir Noor Nafiz<sup>1</sup>, Md. Shafiqul Islam<sup>1</sup>, Arif Hussain<sup>1</sup>, Syed Adnan Ibna Hakim<sup>2</sup>, Martin Worth<sup>2</sup>, Dilruba Ahmed<sup>1</sup>, Dara Johnston<sup>2</sup> and Niyaz Ahmed<sup>1</sup>

## OPEN ACCESS

### Edited by:

Ilana L. B. C. Camargo,  
University of São Paulo, Brazil

### Reviewed by:

Rebecca Ashley Gladstone,  
University of Oslo, Norway  
Sebastian Guenther,  
University of Greifswald, Germany

### \*Correspondence:

Zahid Hayat Mahmud  
zhmahmud@icddr.org

### Specialty section:

This article was submitted to  
Infectious Diseases - Surveillance,  
Prevention and Treatment,  
a section of the journal  
Frontiers in Public Health

**Received:** 31 October 2019

**Accepted:** 14 May 2020

**Published:** 18 June 2020

### Citation:

Mahmud ZH, Kabir MH, Ali S, Moniruzzaman M, Imran KM, Nafiz TN, Islam MS, Hussain A, Hakim SAI, Worth M, Ahmed D, Johnston D and Ahmed N (2020) Extended-Spectrum Beta-Lactamase-Producing *Escherichia coli* in Drinking Water Samples From a Forcibly Displaced, Densely Populated Community Setting in Bangladesh. *Front. Public Health* 8:228. doi: 10.3389/fpubh.2020.00228

<sup>1</sup> International Centre for Diarrhoeal Disease Research, Dhaka, Bangladesh, <sup>2</sup> WASH Division, UNICEF Bangladesh, Dhaka, Bangladesh

**Introduction:** Community-acquired infections due to extended-spectrum beta-lactamase (ESBL) producing *Escherichia coli* are rising worldwide, resulting in increased morbidity, mortality, and healthcare costs, especially where poor sanitation and inadequate hygienic practices are very common.

**Objective:** This study was conducted to investigate the prevalence and characterization of multidrug-resistant (MDR) and ESBL-producing *E. coli* in drinking water samples collected from Rohingya camps, Bangladesh.

**Methods:** A total of 384 *E. coli* isolates were analyzed in this study, of which 203 were from household or point-of-use (POU) water samples, and 181 were from source water samples. The isolates were tested for virulence genes, ESBL-producing genes, antimicrobial susceptibility by VITEK 2 assay, plasmid profiling, and conjugal transfer of AMR genes.

**Results:** Of the 384 *E. coli* isolates tested, 17% (66/384) were found to be ESBL producers. The abundance of ESBL-producers in source water contaminated with *E. coli* was observed to be 14% (27/181), whereas, 19% (39/203) ESBL producers was found in household POU water samples contaminated with *E. coli*. We detected 71% (47/66) ESBL-*E. coli* to be MDR. Among these 47 MDR isolates, 20 were resistant to three classes, and 27 were resistant to four different classes of antibiotics. Sixty-four percent (42/66) of the ESBL producing *E. coli* carried 1 to 7 plasmids ranging from 1 to 103 MDa. Only large plasmids with antibiotic resistance properties were found transferrable via conjugation. Moreover, around 7% (29/384) of *E. coli* isolates harbored at least one of 10 virulence factors belonging to different *E. coli* pathotypes.

**Conclusions:** The findings of this study suggest that the drinking water samples analyzed herein could serve as an important source for exposure and dissemination of MDR, ESBL-producing and pathogenic *E. coli* lineages, which therewith pose a health risk to the displaced Rohingya people residing in the densely populated camps of Bangladesh.

**Keywords:** ESBL-producing *E. coli*, multidrug-resistant, drinking water, Rohingya camps, Bangladesh

## INTRODUCTION

Extended-spectrum beta-lactamase (ESBL)-producing *E. coli* have been recognized as a major multidrug-resistant bacteria implicated in serious hospital and community-acquired infections worldwide, especially in places where poor sanitation, and inadequate hygienic practices are very common (1–4). Infections caused by MDR-*E. coli* incur huge medical costs and limit treatment options (5–7).

Multidrug-resistant *E. coli* has been detected in different ecological niches in the community and environment (8, 9). For instance, ESBLs and New Delhi Metallo beta-lactamase 1 (NDM-1) producing *E. coli* were detected in drinking water and retail meat, respectively (10, 11). In Bangladesh, ESBL producing-*E. coli* were reported from drinking water as well as from river water samples (12, 13). Though *E. coli* has had a significant role in water microbiology as an indicator of fecal pollution, it is of greater public health concern when these *E. coli* isolates turn out to be multidrug-resistant pathogens (14). Detection of ESBL-producing *E. coli* in drinking water samples is important to recognize the risk of transmission of antimicrobial resistance (AMR) and gastrointestinal diseases. Transmission of ESBL-encoding genes among bacteria is often plasmid-mediated (15), and aquatic environments provide ideal settings for horizontal transfer of AMR genes encoded on various forms of mobile genetic elements (16).

Though the majority of *E. coli* are typically innocuous, some *E. coli* variants are virulent and may inflict varying severity of enteric infections. Currently, there are six different *E. coli* pathotypes that have been documented to cause intestinal infections, they include, enterotoxigenic *E. coli* (EPEC), enteroinvasive *E. coli* (EIEC), enteropathogenic *E. coli* (EPEC), shiga toxin-producing *E. coli* (STEC), enteroaggregative *E. coli* (EAEC), and diffusely adhering *E. coli* (DAEC) (17). In Bangladesh, following rotavirus, the second most leading cause of diarrheal infections are caused by pathogenic *E. coli* (18). Several virulence genes such as *st*, *lt* (EPEC); *bfp*, *eae* (EPEC); *aat*, *aai* (EAEC) are associated with diarrheagenic *E. coli* pathotypes (19), which can be used to detect these pathotypes using PCR based gene amplification. Watery diarrhea is caused by the secretion of heat-labile (LT) and/or heat-stable (ST) enterotoxins from EPEC. Shiga toxin (Stx) expression is the unique feature of EHEC where systemic absorption of this toxin leads to possibly life-threatening complications. Multiple putative virulence factors expression for typical EAEC strains, containing the aggregative adherence fimbriae (AAF), dispersin, the dispersin translocator Aat, and the Aai type VI secretion system directs to adherence and triggering

diarrhea. EPEC adhesion is associated with attaching and effacing adhesion and intestinal colonization, which also include bundle-forming pili (BFP), EspA filaments and intimin (19, 20).

The contaminated drinking water was found to be responsible for a number of waterborne gastroenteritis outbreaks due to diarrheagenic *E. coli* (21–23). Therefore, it is pertinent to analyze the prevalence and properties of ESBL-*E. coli* from drinking waters in community settings, particularly, from human habitations that are projected to pose exceptionally high risks of waterborne diseases due to overcrowding, scarcity of safe drinking water, and unhygienic living conditions. In Bangladesh, the displaced Rohingya people are one such community with a population of ~1.16 million who are living in 32 congested camps in a challenging hilly landscape of Cox's Bazar district (290,000 persons per square kilometer). This displacement, of a large population are facing compounding problems, particularly related to water, sanitation, hygiene and health care (24–27). Water from hand-pumped tube wells is the primary water supply for the people in Rohingya camps. Around 6057 water points and 50087 emergency latrines have been built (during the study in 2018). Moreover, in the absence of efficient community sanitation, insufficient sewage disposal, and treatment facilities, the risks of transmission of enteric pathogens become extremely high, and the community as a whole face serious public health concerns (28–30).

In our previous study, we analyzed source water (tubewell) samples, as well as POU drinking water samples, from Rohingya camps and found 10.5% source water and 34.7% POU water samples were contaminated with *E. coli*, which could cause waterborne diseases in the camps (26). An outbreak of ESBL-producing *E. coli* might create a medical emergency in a large congested habitation like Rohingya camps because of limited treatment options. The AMR surveillance, especially with regard to ESBL-producing *E. coli* has never been carried out in these camps. Therefore, this study aims to determine the prevalence of ESBL-producing, MDR, and virulent *E. coli* in drinking water samples. Furthermore, plasmid profiling and horizontal transfer of resistant gene analyses of isolated ESBL-producing *E. coli* will provide important insights in understanding the dissemination of resistance determinants.

## MATERIALS AND METHODS

### Bacterial Isolates

We employed drinking water samples from Rohingya camps collected in our previous study to culture *E. coli* isolates (26). From a total of 2512 *E. coli* contaminated water samples, 421

water samples were randomly selected for the present study. One random *E. coli* isolate was taken as a representative from each sample, which was further tested using the API-20E test kit (Biomerieux SA, Marcy-l'Étoile, France), and 384 API-20E confirmed *E. coli* were stored at  $-70^{\circ}\text{C}$  in 30% LB glycerol-broth for downstream analysis. Out of 384 *E. coli* isolates, 203 isolates were from the household water samples and 181 from source water samples. In brief, for each sample, 100 ml water was filtered through a  $0.22\ \mu\text{m}$  membrane filter (Sartorius Stedim, Goettingen, Germany), the membrane filter paper was then firmly laid on the mTEC agar plate. Later, the culture plate was incubated for 2 h at  $35 \pm 0.5^{\circ}\text{C}$ , followed by further incubation for  $22 \pm 2$  h at  $44.5 \pm 0.2^{\circ}\text{C}$ . After incubation, red to magenta-colored colonies, typical of *E. coli* colony was picked and subcultured on MacConkey agar plate and incubated at  $35 \pm 2^{\circ}\text{C}$  for 18 h to 24 h. After incubation, the characteristics of dark pink colonies typical of *E. coli* were obtained and confirmed using API-20E kit.

### Isolation and Confirmation of ESBL-Producing and Carbapenem-Resistant *E. coli* Using Chromagar

All 384 confirmed *E. coli* isolates were cultured on CHROMagar ESBL and CHROMagar KPC media at  $37^{\circ}\text{C}$  for 18–24 h. The production of extended-spectrum beta-lactamases and carbapenemase was confirmed by observing the growth and characteristic colony morphology on respective culture media. Dark pink to reddish colonies on CHROMagar ESBL plate indicate ESBL producing *E. coli* whereas pink to reddish colonies on CHROMagar KPC media suggest carbapenem-resistant *E. coli*.

### Confirmation of *E. coli* by VITEK 2

ESBL positive *E. coli* isolated from the ESBL CHROMagar plate were further confirmed by the VITEK 2 system (bioMérieux, Marcy l'Étoile, France) using VITEK 2 GN ID card. *Enterobacter hormacchi* (ATCC-700323) was used as a positive control for the identification in this system. For VITEK 2 assays, pure isolates were streaked on MacConkey agar plates and incubated at  $35^{\circ}\text{C}$  overnight. One to three isolated colonies were selected from each MacConkey agar plate and suspended in saline for preparation of inoculum to obtain an absorbency of  $\sim 0.5$  McFarland Units before being subjected to VITEK 2 analysis.

### Detection of Diarrheagenic and ExPEC Associated Virulence Genes

Several virulence genes such as *st*, *lt* (EPEC); *bfp*, *eae* (EPEC); *aat*, *aai* (EAEC) are associated with diarrheagenic *E. coli* pathotypes (19) are used to detect the pathotypes using PCR based gene amplification. In the present study, PCR based screening of diarrheagenic virulence genes was carried out for all 384 *E. coli* isolates. Gene-specific primers entailing heat-labile (*lt*), heat-stable (*st*), attaching and effacing (*eae*), anti-aggregation protein transporter (*aat*), bundle forming pilus (*bfp*) and aggR-activated island (*aaiC*) were used to detect the respective genes employing a multiplex PCR setup (31–34). The boiling lysis method was used

to obtain the DNA template (35). A  $3\ \mu\text{l}$  template DNA was taken for a  $25\ \mu\text{l}$  PCR reaction containing  $12.5\ \mu\text{l}$  of 2X GoTaq G2 Green Master Mix (Promega, USA) with  $0.44\ \mu\text{l}$  of *eae* primer, the primers *lt*, *st*, *aaiC*, *aat*, *bfp* were taken in  $0.4\ \mu\text{l}$  volume each. The PCR was carried out at standard cycling conditions with an annealing temperature of  $57^{\circ}\text{C}$  for 20 s. A separate PCR was performed for Shiga toxin genes (*stx1* and *stx2*), which was described previously (36, 37). PCR for invasion plasmid antigen H (*ipaH*) and the invasion associated locus (*ial*) was performed according to the procedure described elsewhere (38–41). Primer details are tabulated in **Supplementary Table 1**.

To examine the presence of seven ExPEC associated virulence factors, we performed two multiplex PCRs on 55 non diarrheagenic ESBL-*E. coli* isolates (42). Among these, the first one was done to screen the presence of *kpsMIII* (group II capsule), *papA* (pilus-associated protein A), *sfaS* (S-fimbrial adhesine), and *focG* (F1C fimbriae protein) genes; whereas the second multiplex was performed to detect *hlyD* (haemolysin D), *afa* (afimbrial adhesine), and *iutA* genes (aerobactin siderophore ferric receptor protein).

### Antibiotic Susceptibility by VITEK 2

Antibiotic susceptibility testing (AST) was performed using VITEK 2 system with VITEK 2 cards (AST-N280) for 19 antimicrobial agents according to the CLSI guidelines and manufacturer's recommendations; two additional antimicrobial agents (cefixime and ceftazidime) were also incorporated. *E. coli* ATCC 25922, susceptible to all drugs, was used for AST in each VITEK testing step as quality control. The 21 antibiotics tested included amikacin, amoxicillin/clavulanic acid, ampicillin, cefepime, cefixime, cefoperazone/sulbactam, ceftazidime, ceftriaxone, cefuroxime, cefuroxime axetil, ciprofloxacin, colistin, ertapenem, gentamicin, imipenem, meropenem, nalidixic acid, nitrofurantoin, piperacillin, tigecycline, and trimethoprim/sulfamethoxazole. Minimum inhibitory concentrations (MIC) were determined, and the isolates were classified into resistant, intermediate and susceptible as per CLSI criteria. The raw MIC data from the VITEK 2 assay are shown in **Supplementary Table 2**.

### Detection of ESBL, Quinolone, and Carbapenemase Resistance Genes by PCR

All CHROMagar confirmed ESBL-producing *E. coli* isolates were screened for molecular determinants of ESBL and carbapenem resistance comprising of *bla*<sub>SHV</sub>, *bla*<sub>TEM</sub>, *bla*<sub>CTX-M-15</sub> and all CTX-M-groups (*bla*<sub>CTX-M-1</sub>-group, *bla*<sub>CTX-M-2</sub>-group, *bla*<sub>CTX-M-8</sub>-group, *bla*<sub>CTX-M-9</sub>-group) including, *bla*<sub>OXA-1</sub>-group, *bla*<sub>OXA-47</sub>, and *bla*<sub>NDM-1</sub> were screened (34, 43–48). The gene *bla*<sub>CMY-2</sub> encoding for AmpC  $\beta$ -lactamase was also screened by PCR as per a published protocol (12, 49). Besides, all 66 isolates were tested for the three *qnr* (quinolone) resistance genes; *qnrA*, *qnrB*, and *qnrS* according to the methods described by others (50–52).

### Plasmid Profiling and Conjugal Transfer

Plasmids from ESBL-*E. coli* isolates were extracted employing the Kado alkaline lysis method (53) and visualized after separation in low percent agarose gel (0.7%) electrophoresis. The size of



extracted plasmids was determined comparing with size standard plasmids ran alongside. The following plasmids were used as size standards; Sa (23 MDa), RP4 (34 MDa), R1 (62 MDa), pDK9 (140 MDa), and *E. coli* V517 plasmids (1.4, 1.8, 2.0, 2.6, 3.4, 3.7, 4.8, and 35.8 MDa) (54). ESBL-producing *E. coli* were used as donors, and the sodium azide resistant strain *E. coli*-J53 was employed as a recipient for conjugation using broth mating assays at 30°C for 19 ± 1 h. Transconjugants obtained were plated on MacConkey plates prepared with cefotaxime (20 µg/L) and sodium azide (100 mg/L), transconjugants were selected observing their growth and colony morphology. Transconjugants were analyzed for antibiotic susceptibility tests using VITEK 2 assay, plasmid profiling and presence of ESBL genes (53).

## Phylogenetic Analysis

As per the method described by Clermont and colleagues, the distribution of phylogenetic groups among ESBL- *E. coli* isolates was determined by performing multiplex PCRs after DNA extraction by boiling lysis (55).

## RESULTS

### ESBL-Positive but Carbapenem Sensitive *E. coli* Recovered From Drinking Water

To screen for ESBL-producing *E. coli*, 384 isolates were cultured on ESBL CHROMagar. The typical growth of pink colonies on the CHROMagar plate was considered as ESBL positive *E. coli*. Of the 384 isolates tested, 17.2% ( $n = 66$ ) were found to be ESBL-producing *E. coli* (Table 1). About 15% (27/181), and 19% (39/203) ESBL producing *E. coli* originated from *E. coli* contaminated source water and POU water samples, respectively. Further, the ESBL producing *E. coli* was investigated for carbapenem resistance on CHROMagar KPC media, and none of the isolates was able to grow on CHROMagar KPC media. Therefore, we did not detect any carbapenem-resistance in our collection of ESBL-*E. coli* isolates.

### High Prevalence of MDR in ESBL-Producing *E. coli*

Antimicrobial susceptibility of 66 ESBL-*E. coli* isolates (Supplementary Table 3) were tested against 21 different antibiotics (Supplementary Table 4) using VITEK 2 assay. All 66 CHROMagar confirmed ESBL positive *E. coli* isolates demonstrated resistance against ampicillin, ceftriaxone, ceftazidime, cefixime, cefuroxime, and cefuroxime axetil (Figure 1). About 70% (46/66) of the isolates were found to be resistant to nalidixic acid, 37.9% (25/66) isolates were resistant to trimethoprim/sulfamethoxazole, whereas 22.7% (15/66) and 19.7% (13/66) isolates were resistant for cefepime and ciprofloxacin, respectively. However, no resistance was detected in any of the tested strains to the antibiotics used of aminoglycosides (amikacin and gentamicin), cefoperazone/sulbactam, glycylicycline, carbapenem, and polymyxins groups. It was found that 71% (47/66) of *E. coli* isolates were MDR that were resistant to at least three classes of antibiotics. Among the 47 MDR isolates, 20 were resistant

to three different classes, and 27 were resistant to four different classes of antibiotics.

### bla<sub>CTX-M-1</sub> Group Is the Predominant ESBL Gene Detected

The presence of molecular determinants of ESBLs was tested on all ESBL-producing *E. coli* isolates. Out of the 66 ESBL-*E. coli* isolates, 59% (39/66) isolates harbored both bla<sub>CTX-M-1</sub> group and bla<sub>CTX-M-15</sub> gene. However, 4.5% (3/66) isolates harbored either bla<sub>CTX-M-1</sub>group or bla<sub>CTX-M-15</sub> gene. The bla<sub>TEM</sub> β-lactamase gene was present in 35% (23/66) of isolates, and none of the isolates harbored other β-lactamase genes such as bla<sub>SHV</sub>, bla<sub>CTX-M-2</sub>-group, bla<sub>CTX-M-8</sub>-group, and bla<sub>CTX-M-9</sub>-group. The two genes, bla<sub>OXA-1</sub>-group and bla<sub>OXA-47</sub> were screened among 66 ESBL- *E. coli* isolates, but none of the isolates was found to be positive. In addition, the New Delhi metallo-β-lactamase gene, bla<sub>NDM-1</sub> as well as plasmid-mediated ampC-type β-lactamase gene the bla<sub>CMY-2</sub> was not present in any of the isolates. The quinolone resistance gene; qnrS, and qnrB were found in 34% (22/66) and 5% (3/66) of the ESBL-*E. coli* isolates, respectively (Figure 2, Supplementary Table 5).

### Distribution of *E. coli* Pathotypes

Screening for the presence of virulence factors demonstrated that 7% (29/384) of *E. coli* isolates were positive for at least one virulence factor out of the 10 *E. coli* pathotype-specific virulence genes tested. Ten isolates were positive for only *aaiC* gene and five isolates were positive for both *aaiC* and *aat*; whereas four isolates were positive for both *bfp* and *eae* genes. Heat labile (*lt*) gene was present in 7 isolates, whereas the heat stable (*st*) gene was found in 2 isolates and a single isolate was found positive for *stx1*. None of the isolates was positive for *ipaH* and *iaa* genes. Among the 29 pathogenic *E. coli* isolates detected; 52% (15/29) were EAEC, 31% (9/29) were ETEC, 14% (4/29) were EPEC and 4% (1/29) were EHEC (Figure 3).

When the ExPEC virulence genes were screened only three out of the seven virulence factors were detected that comprised of *KpsMII*, *sfaS*, and *iutA* genes, their prevalence rates were, 21.8% (12/55), 5.4% (3/55), and 16.4% (9/55), respectively. Most of isolates (12/18) harboring ExPEC genes were affiliated to phylogenetic group D. However, out of the 55 isolates tested, only 6 isolates qualify as ExPEC as per the inclusion criteria (strains harboring at least two ExPEC associated virulence factors) 5 out of these 6 isolates were from phylogroup D.

The potential pathogenic (diarrheagenic and ExPEC) *E. coli* isolates showed high resistance rates 83% (39/47) to ampicillin, followed by 74% (35/47) to nalidixic acid, 68% (32/47) to cefuroxime, cefuroxime axetil, 61% (29/47) to cefixime, ceftazidime, and 51% (24/47) to sulfonamides. Out of 29 pathogenic *E. coli* 11 were found to be ESBL producing in this study (Table 2). Of note, all the pathogenic isolates detected were found to be susceptible to carbapenems, aminoglycosides (amikacin and gentamicin), and polymyxin.

**TABLE 1 |** Antibiotic resistance pattern, presence of antibiotic resistance genes and plasmid patterns of ESBL-producing *Escherichia coli* isolated from water sample.

Serial no	Isolates ID	Antibiotic resistance Pattern <sup>a</sup>	Presence of antibiotic resistant genes	Plasmid size in MDa
1	05095B	Amp, Cro, Cxm, Cfa, Caz, Cfm, NA	<i>bla</i> <sub>CTX-M-1</sub> , <i>bla</i> <sub>CTX-M-15</sub> , <i>bla</i> <sub>TEM</sub> , <i>qnrS</i>	75, 54, 4.5, 2.8, 2.6, 2
2	09036H2	Amp, Cro, Cxm, Cfa, Caz, Cfm, NA	<i>bla</i> <sub>CTX-M-1</sub> , <i>bla</i> <sub>CTX-M-15</sub> , <i>qnrS</i>	No plasmid
3	34022A	Amp, Fep, Cro, Cxm, Cfa, NA, Sxt, Caz, Cfm	<i>bla</i> <sub>CTX-M-1</sub> , <i>bla</i> <sub>CTX-M-15</sub> , <i>bla</i> <sub>TEM</sub>	90
4	34008B	Amp, Fep, Cro, Cxm, Cfa, Caz, Cfm	<i>bla</i> <sub>CTX-M-1</sub> , <i>bla</i> <sub>CTX-M-15</sub> , <i>qnrS</i>	No plasmid
5	34012H2	Amp, Fep, Cro, Cxm, Cfa, NA, Caz, Cfm		No plasmid
6	05080H2	Amp, Fep, Cro, Cxm, Cfa, Cip, NA, Sxt, Caz, Cfm	<i>bla</i> <sub>CTX-M-1</sub> , <i>bla</i> <sub>TEM</sub>	No plasmid
7	11023H2	Amp, Cro, Cxm, Cfa, Caz, Cfm	<i>bla</i> <sub>CTX-M-1</sub> , <i>bla</i> <sub>CTX-M-15</sub> , <i>qnrS</i>	No plasmid
8	34022H1	Amp, Cro, Cxm, Cfa, NA, Caz, Cfm	<i>bla</i> <sub>CTX-M-1</sub> , <i>bla</i> <sub>CTX-M-15</sub>	94
9	5375B	Amp, Cro, Cxm, Cfa, NA, Tzp, Caz, Cfm	<i>bla</i> <sub>CTX-M-1</sub> , <i>bla</i> <sub>CTX-M-15</sub> , <i>bla</i> <sub>TEM</sub> , <i>qnrS</i>	22
10	5095H2	Amc, Amp, Cro, Cxm, Cfa, NA, Caz, Cfm	<i>bla</i> <sub>CTX-M-1</sub> , <i>bla</i> <sub>CTX-M-15</sub> , <i>qnrS</i>	3.1, 2.04, 1.9
11	1109H1	Amp, Cro, Cxm, Cfa, Caz, Cfm	<i>bla</i> <sub>CTX-M-1</sub> , <i>bla</i> <sub>CTX-M-15</sub> , <i>qnrS</i>	6.5, 4.6, 4.3, 3.4, 2.7
12	8E756H2	Amp, Cro, Cxm, Cfa, Cip, NA, Caz, Cfm	<i>bla</i> <sub>CTX-M-1</sub> , <i>bla</i> <sub>CTX-M-15</sub>	77, 56, 6.5, 4.6, 4.3, 3.4, 2.8
13	9125B	Amc, Amp, Cro, Cxm, Cfa, Sxt, Caz, Cfm	<i>bla</i> <sub>TEM</sub>	85, 57, 49, 37
14	8E285B	Amc, Amp, Cro, Cxm, Cfa, Caz, Cfm	<i>bla</i> <sub>CTX-M-1</sub>	No plasmid
15	11269H1	Amp, Cro, Cxm, Cfa, Cip, NA, Caz, Cfm		29, 2.5
16	9736H2	Amc, Amp, Cro, Cxm, Cfa, Cip, NA, Tzp, Caz, Cfm		37, 3.3
17	11597A	Amp, Cro, Cxm, Cfa, NA, Sxt, Caz, Cfm	<i>bla</i> <sub>CTX-M-1</sub> , <i>bla</i> <sub>CTX-M-15</sub>	68
18	11611H1	Amp, Cro, Cxm, Cfa, NA, Sxt, Caz, Cfm	<i>bla</i> <sub>CTX-M-1</sub> , <i>bla</i> <sub>CTX-M-15</sub>	65
19	04584H2	Amp, Cro, Cxm, Cfa, Caz, Cfm	<i>bla</i> <sub>CTX-M-1</sub> , <i>bla</i> <sub>CTX-M-15</sub> , <i>qnrS</i>	No plasmid
20	8W645H2	Amp, Cro, Cxm, Cfa, Caz, Cfm	<i>bla</i> <sub>CTX-M-1</sub> , <i>bla</i> <sub>CTX-M-15</sub> , <i>qnrS</i>	No plasmid
21	8W390H1	Amp, Cro, Cxm, Cfa, Caz, Cfm	<i>bla</i> <sub>CTX-M-1</sub> , <i>bla</i> <sub>CTX-M-15</sub> , <i>qnrS</i>	42, 3.2, 2.6
22	8W803H2	Amp, Cro, Cxm, Cfa, NA, Sxt, Caz, Cfm	<i>bla</i> <sub>CTX-M-1</sub> , <i>bla</i> <sub>CTX-M-15</sub>	103, 4.9, 2.9, 2.6
23	8W454H1	Amp, Fep, Cro, Cxm, Cfa, Cip, NA, Sxt, Caz, Cfm	<i>bla</i> <sub>CTX-M-1</sub> , <i>bla</i> <sub>CTX-M-15</sub>	No plasmid
24	18544A	Amp, Cro, Cxm, Cfa, NA, Fd, Caz, Cfm		No plasmid
25	18162H2	Amp, Cro, Cxm, Cfa, NA, Fd, Caz, Cfm		No plasmid
26	18544B	Amp, Cro, Cxm, Cfa, NA, Fd, Caz, Cfm		No plasmid
27	12224H1	Amp, Cro, Cxm, Cfa, NA, Caz, Cfm	<i>bla</i> <sub>CTX-M-1</sub> , <i>bla</i> <sub>CTX-M-15</sub> , <i>qnrS</i>	97, 39, 2
28	11448B	Amp, Cro, Cxm, Cfa, Caz, Cfm	<i>qnrB</i>	34, 2.3
29	9441H2	Amp, Cro, Cxm, Cfa, NA, Caz, Cfm	<i>bla</i> <sub>CTX-M-1</sub> , <i>bla</i> <sub>CTX-M-15</sub>	No plasmid
30	1E181H2	Amp, Fep, Cro, Cxm, Cfa, NA, Sxt, Caz, Cfm	<i>bla</i> <sub>CTX-M-1</sub> , <i>bla</i> <sub>CTX-M-15</sub>	67, 52
31	2W242H2	Amp, Cro, Cxm, Cfa, Cip, NA, Sxt, Caz, Cfm	<i>bla</i> <sub>CTX-M-1</sub> , <i>bla</i> <sub>CTX-M-15</sub> , <i>bla</i> <sub>TEM</sub>	63, 6.4
32	2W246A	Amp, Cro, Cxm, Cfa, NA, Sxt, Caz, Cfm	<i>bla</i> <sub>CTX-M-1</sub> , <i>bla</i> <sub>CTX-M-15</sub> , <i>bla</i> <sub>TEM</sub>	89, 4.4
33	1E365B	Amp, Cro, Cxm, Cfa, Caz, Cfm	<i>bla</i> <sub>CTX-M-1</sub> , <i>bla</i> <sub>CTX-M-15</sub> , <i>qnrS</i>	55
34	1E07H2	Amp, Cro, Cxm, Cfa, Caz, Cfm	<i>bla</i> <sub>TEM</sub>	71, 33, 30
35	2W150H2	Amp, Cro, Cxm, Cfa, Caz, Cfm	<i>bla</i> <sub>TEM</sub>	No plasmid
36	2W047H2	Amp, Cro, Cxm, Cfa, NA, Caz, Cfm	<i>bla</i> <sub>CTX-M-1</sub> , <i>bla</i> <sub>CTX-M-15</sub> , <i>bla</i> <sub>TEM</sub> , <i>qnrS</i>	42, 8.3
37	2W246B	Amp, Cro, Cxm, Cfa, NA, Caz, Cfm	<i>bla</i> <sub>CTX-M-1</sub> , <i>bla</i> <sub>CTX-M-15</sub> , <i>qnrS</i>	92, 74, 55
38	1E391A	Amp, Cro, Cxm, Cfa, Caz, Cfm	<i>bla</i> <sub>CTX-M-15</sub> , <i>qnrS</i>	92, 74, 56
39	1E424H2	Amp, Fep, Cro, Cxm, Cfa, Caz, Cfm	<i>bla</i> <sub>CTX-M-1</sub> , <i>bla</i> <sub>CTX-M-15</sub> , <i>qnrS</i>	53
40	2E218H1	Amp, Cro, Cxm, Cfa, Caz, Cfm		No plasmid
41	2E219A	Amp, Cro, Cxm, Cfa, Caz, Cfm	<i>qnrS</i>	83
42	2E179H2	Amp, Fep, Cro, Cxm, Cfa, NA, Caz, Cfm	<i>bla</i> <sub>CTX-M-1</sub> , <i>bla</i> <sub>CTX-M-15</sub> , <i>bla</i> <sub>TEM</sub>	No plasmid

(Continued)

TABLE 1 | Continued

Serial no	Isolates ID	Antibiotic resistance pattern <sup>a</sup>	Presence of antibiotic resistant genes	Plasmid size in MDa
43	2E0280B	Amp, Fep, Cro, Cxm, Cfa, NA, Caz, Cfm	<i>bla</i> <sub>CTX-M-1</sub> , <i>bla</i> <sub>CTX-M-15</sub> , <i>bla</i> <sub>TEM</sub>	No plasmid
44	1E345A	Amc, Amp, Cro, Cxm, Cfa, Cip, NA, Tzp, Sxt, Caz, Cfm	<i>bla</i> <sub>TEM</sub>	32, 1.9
45	1E370H2	Amp, Cro, Cxm, Cfa, Cip, NA, Fd, Tzp, Sxt, Caz, Cfm	<i>bla</i> <sub>CTX-M-1</sub> , <i>bla</i> <sub>CTX-M-15</sub> , <i>bla</i> <sub>TEM</sub>	81, 19, 7.6
46	2W241H2	Amp, Cro, Cxm, Cfa, NA, Sxt, Caz, Cfm	<i>bla</i> <sub>CTX-M-1</sub> , <i>bla</i> <sub>CTX-M-15</sub> , <i>bla</i> <sub>TEM</sub>	4.2
47	2W146H2	Amp, Cro, Cxm, Cfa, NA, Sxt, Caz, Cfm	<i>bla</i> <sub>CTX-M-1</sub> , <i>bla</i> <sub>CTX-M-15</sub> , <i>bla</i> <sub>TEM</sub>	No plasmid
48	1E336H2	Amp, Cro, Cxm, Cfa, NA, Sxt, Caz, Cfm	<i>bla</i> <sub>CTX-M-15</sub> , <i>bla</i> <sub>TEM</sub>	No plasmid
49	1E414A	Amp, Cro, Cxm, Cfa, NA, Sxt, Caz, Cfm	<i>qnrB</i>	74, 45, 36, 3.5
50	1E586A	Amp, Cro, Cxm, Cfa, NA, Caz, Cfm	<i>bla</i> <sub>TEM</sub>	No plasmid
51	11512H2	Amp, Fep, Cro, Cxm, Cfa, Caz, Cfm	<i>bla</i> <sub>CTX-M-1</sub> , <i>bla</i> <sub>CTX-M-15</sub> , <i>qnrS</i>	56, 44.7, 4.4, 3.8
52	18433H2	Amp, Cro, Cxm, Cfa, NA, Sxt, Caz, Cfm	<i>bla</i> <sub>CTX-M-1</sub> , <i>bla</i> <sub>CTX-M-15</sub> , <i>qnrS</i>	52, 42.7, 4.3, 3.6
53	1E286H2	Amc, Amp, Cro, Cxm, Cfa, Cip, NA, Sxt, Caz, Cfm	<i>bla</i> <sub>TEM</sub>	No plasmid
54	C-2WH4	Amp, Cro, Cxm, Cfa, Caz, Cfm		91, 37
55	18441A	Amp, Fep, Cro, Cxm, Cfa, Cip, NA, Sxt, Caz, Cfm	<i>bla</i> <sub>CTX-M-1</sub> , <i>bla</i> <sub>CTX-M-15</sub> , <i>qnrS</i>	81
56	1E499H1	Amp, Cro, Cxm, Cfa, NA, Caz, Cfm	<i>bla</i> <sub>CTX-M-15</sub> , <i>qnrS</i>	2.8, 1.9
57	07137A	Amp, Cro, Cxm, Cfa, Cip, NA, Sxt, Caz, Cfm	<i>bla</i> <sub>CTX-M-1</sub> , <i>bla</i> <sub>CTX-M-15</sub>	84, 2.2, 1.7
58	34034B	Amp, Fep, Cro, Cxm, Cfa, NA, Sxt, Caz, Cfm	<i>bla</i> <sub>CTX-M-1</sub> , <i>bla</i> <sub>CTX-M-15</sub> , <i>bla</i> <sub>TEM</sub>	82
59	410H2	Amp, Cro, Cxm, Cfa, Caz, Cfm	<i>bla</i> <sub>CTX-M-1</sub> , <i>bla</i> <sub>CTX-M-15</sub> , <i>qnrS</i>	No plasmid
60	192B	Amp, Cro, Cxm, Cfa, NA, Caz, Cfm		No plasmid
61	2W147H2	Amp, Cro, Cxm, Cfa, Caz, Cfm	<i>qnrB</i>	56, 37, 2.8, 2.5, 2
62	2W158B	Amp, Cro, Cxm, Cfa, Cip, NA, Sxt, Caz, Cfm	<i>bla</i> <sub>CTX-M-1</sub> , <i>bla</i> <sub>CTX-M-15</sub>	49, 4.1, 1.9, 1.4
63	2W160H2	Amp, Cro, Cxm, Cfa, Cip, NA, Caz, Cfm	<i>bla</i> <sub>TEM</sub> , <i>qnrS</i>	No plasmid
64	266B	Amp, Fep, Cro, Cxm, Cfa, NA, Sxt, Caz, Cfm	<i>bla</i> <sub>CTX-M-1</sub> , <i>bla</i> <sub>CTX-M-15</sub>	49, 4, 1.9, 1.4
65	31029B	Amp, Fep, Cro, Cxm, Cfa, NA, Sxt, Caz, Cfm	<i>bla</i> <sub>CTX-M-1</sub> , <i>bla</i> <sub>TEM</sub>	84
66	35001H1	Amp, Fep, Cro, Cxm, Cfa, NA, Sxt, Caz, Cfm	<i>bla</i> <sub>TEM</sub>	75, 54, 4.5, 2.8, 2.6, 2

<sup>a</sup>Ak, Amikacin; Amc, Amoxicillin/Clavulanic Acid; Amp, Ampicillin; Fep, Cefepime; Scf, Cefoperazone/Sulbactam; Cro, Ceftriaxone; Cxm, Cefuroxime; Cfa, Cefuroxime Axetil; Cip, Ciprofloxacin; Cl, Colistin; Etp, Ertapenem; Cn, Gentamicin; Imp, Imipenem; Men, Meropenem; NA, Nalidixic Acid; Fd, Nitrofurantoin; Tzp, Piperacillin-Tazobactam; Tgc, Tigecycline; Sxt, Sulphamethoxazoletrimethoprim; Cfm, Cefixime; Caz, Ceftazidime.

## Phylogrouping

Among the ESBL-*E. coli* isolates, all phylogenetic groups were represented except for phylogroup F. The predominant phylogenetic group identified was B1 (23/66; 34.8%), followed by D (22/66; 33.3%), E (17/66; 25.7%), B2 and C (2/66; each 3%). Among the 47 multidrug resistant ESBL-*E. coli* (20/47) were of phylogroup D followed by A (13/47), B1 (12/47), C (2/47). Majority of isolates carrying diarrheagenic virulence genes were from B1(14/29; 48%) followed by A(6/29; 20.6%), B2, C, and unknown groups (2/29; each 7%) (Figure 4).

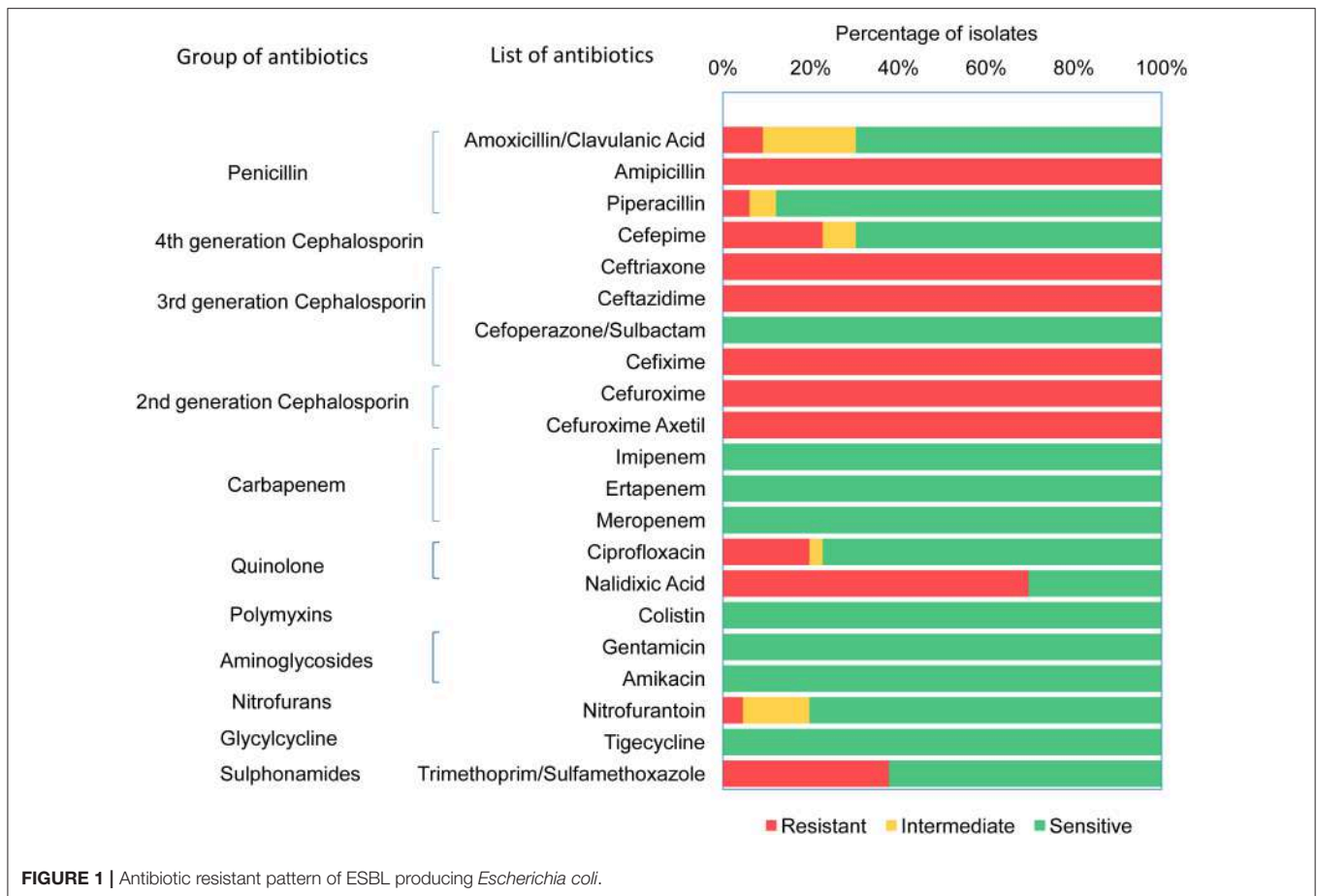
## Plasmid Analysis of ESBL-Producing *E. coli*

Plasmid profiling and conjugation analysis were performed to see whether the antibiotic-resistance genes of the 66 ESBL producing isolates were plasmid-mediated and can they be horizontally transferred. Plasmid number and size were determined using conventional lysis and agarose gel electrophoresis. About 63% ( $n = 42$ ) isolates carried 1 to 7 plasmids ranging in size from

~1 to 103 MDa (Figure 5), and the distribution of plasmids was heterogeneous (Table 1). Further, the plasmid containing isolates that showed the ESBL phenotype were tested for their ability to transfer the ESBL determinant by conjugation experiments. Nine isolates were able to transfer the cefotaxime resistance marker to a susceptible *E. coli* recipient with transfer rates ranging from  $4.75 \times 10^{-6}$  to  $1.19 \times 10^{-4}$  per donor cell (Table 3). Large plasmids (30–103 MDa) were transferred to the sodium azide resistant *E. coli*-J53 recipient. Whereas, the smaller plasmids (<30 MDa) were not seen to be transferred during conjugation. Among the nine donor isolates, two were able to transfer two plasmids each whereas seven isolates transferred single plasmids (Table 3).

## DISCUSSION

In our previous study, we investigated the occurrence of *E. coli* and fecal coliforms in source and household drinking water samples in Rohingya camps, wherein 10.5% tubewell water and



**FIGURE 1 |** Antibiotic resistant pattern of ESBL producing *Escherichia coli*.

34.7% POU water samples were found to be contaminated with *E. coli* (26). In the current study, the ESBL-producing *E. coli* isolates from the contaminated drinking water samples of our previous study were characterized concerning antimicrobial susceptibility, dissemination of drug resistance, and pathogenic potential to comprehend the extent of public health threat due to the exposure of contaminated drinking water in Rohingya camps of Bangladesh.

ESBL-producing *E. coli* has been increasingly reported globally, it is not only restricted to clinical settings but also recovered from environmental niches like livestock, wildlife and particularly water (56–58). The pandemic spread of ESBL-producing Gram-negative bacteria is a serious health concern. Human habitation and the surrounding environment in Bangladesh are reportedly contaminated by antimicrobial-resistant bacteria (59, 60). Reports emanating from developing countries like Bangladesh indicated a high prevalence of ESBL-producing *E. coli* in hospital and community drinking water samples (34, 61).

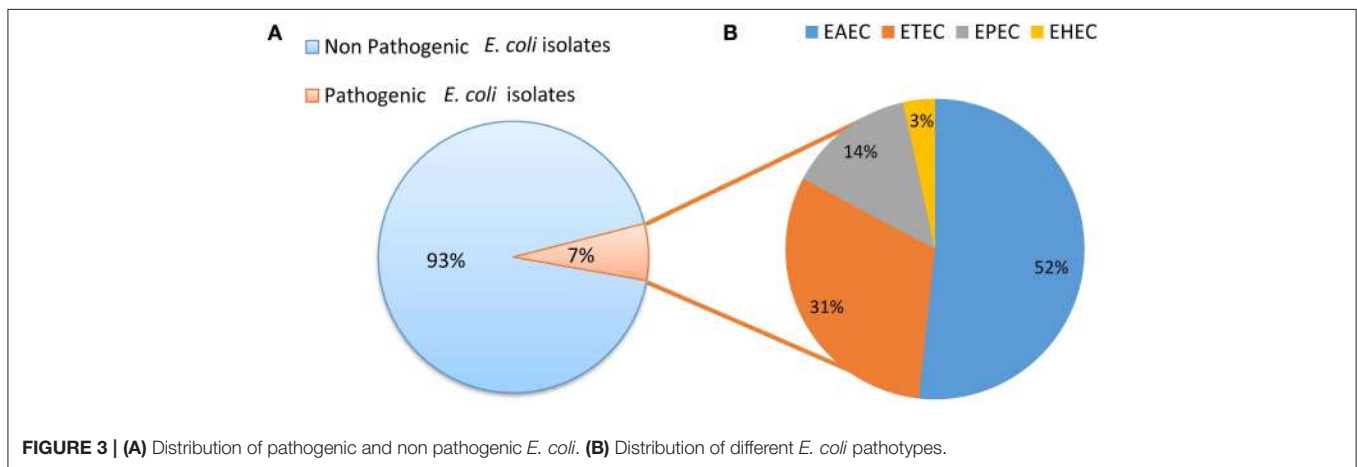
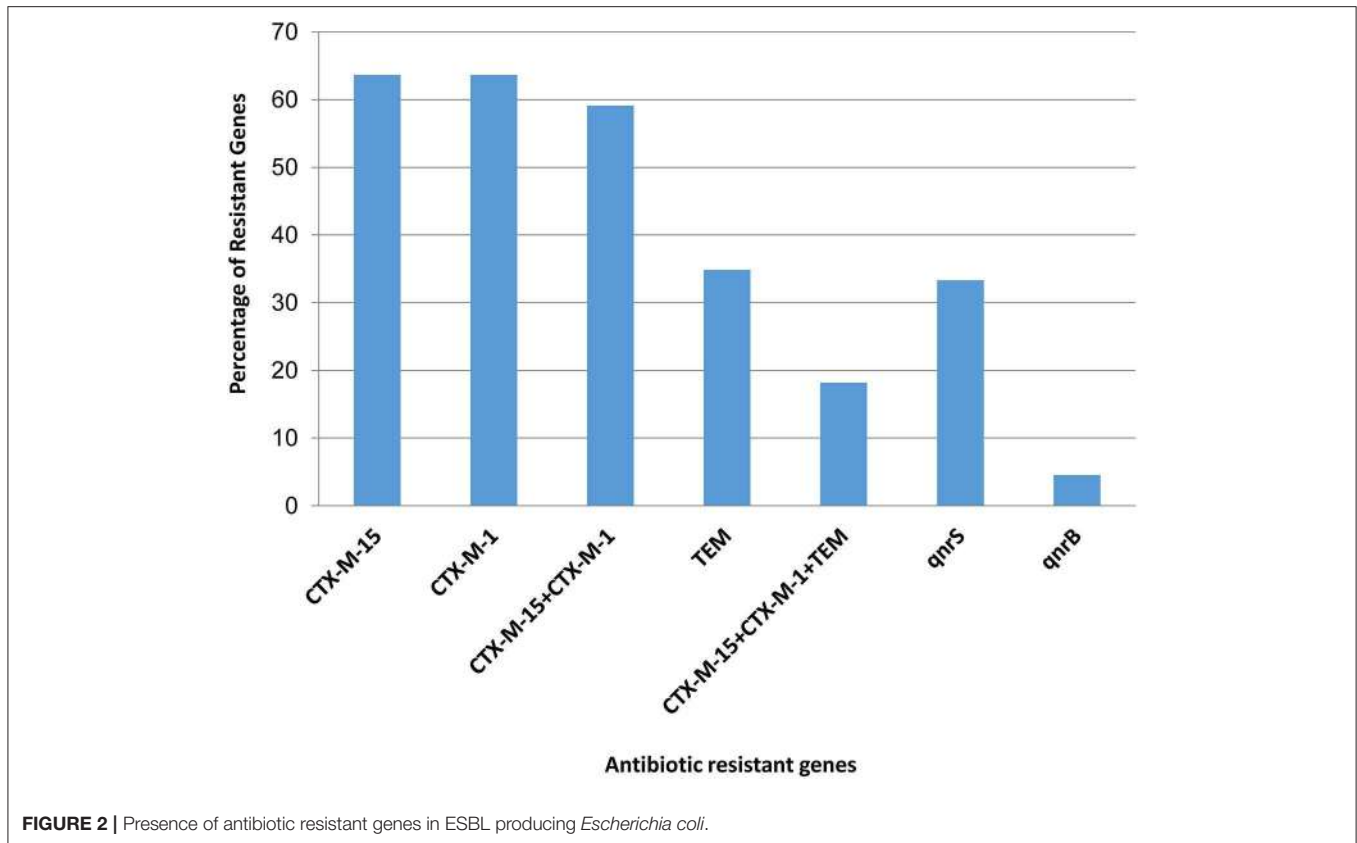
In the current study, we detected 17.2% (66/384) ESBL-producing *E. coli*, of which 71% (47/66) was multidrug-resistant. The high prevalence of multidrug-resistant *E. coli* among the ESBL-producing isolates implies that not only  $\beta$ -lactam antibiotics but resistance to other classes of antibiotics is being

co-selected. In Bangladesh, cephalosporins and penicillins are the most commonly used antibiotics (62), which explain why all the 66 ESBL-producing isolates are found to be resistant to both the classes of antibiotics. Besides, the majority of ESBL-producing isolates were found to be resistant to the quinolone class of antibiotics (46 to nalidixic acid). This may reflect the overuse and misuse of antibiotics (63) as these drugs are often sold and distributed over the counter (64). The uncontrolled and unregulated use of antibiotics severely limits the therapeutic options as well as aids the rapid dissemination of resistance in such overpopulated Rohingya camps.

We found ESBL-producing *E. coli* isolates are 100% susceptible to the antibiotics tested of carbapenem, aminoglycoside (amikacin and gentamicin), glycylcycline, and polymyxin groups. This finding was similar to a study in Jordan, where all the *E. coli* isolates from drinking water were sensitive to carbapenem and glycylcycline (65). There might be several factors responsible for susceptibility, such as these drugs are rarely prescribed in Bangladesh (64) and are not readily available in the hard to reach hilly terrain like Rohingya camps.

In this study, most of the isolates were positive for *bla*<sub>CTX-M-1</sub> group and *bla*<sub>CTX-M-15</sub>, genes that concur the previous reports from Bangladesh (59, 60, 66). All *bla*<sub>CTX-M-1</sub>



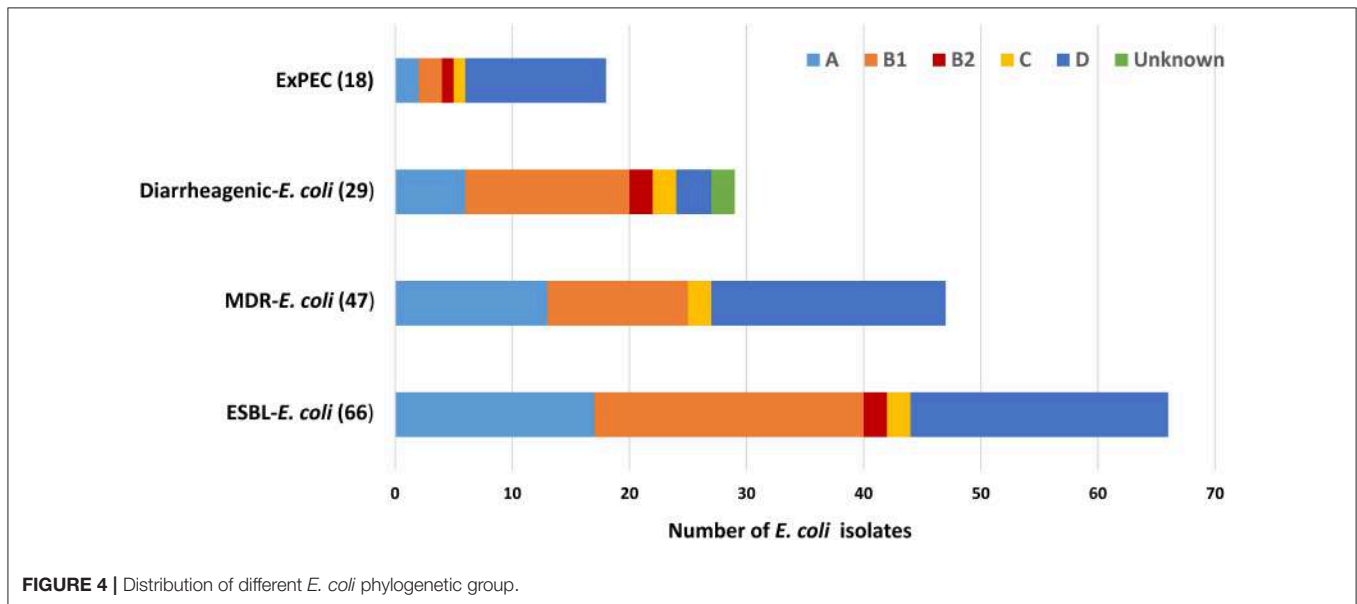


group, *bla*<sub>CTX-M-15</sub> and *bla*<sub>TEM</sub> ESBL-positive *E. coli* isolates showed MDR phenotype ranging from 3 to 4 classes of antibiotics. Similar to our observation, a previous study from Bangladesh showed a high prevalence of CTX-M-15 in ESBL-producing *E. coli* cultured from drinking water samples from different households (34). The CTX-M group of beta-lactamases are a group of rapidly emerging ESBL genes globally, which has been predominantly detected in *E. coli* and *Klebsiella* spp. (56, 67–70). The NDM-1 producing bacteria have been reported in clinical isolates from Bangladesh (71), but in the current study, no NDM-1-producing *E. coli* was detected in the water samples.

The gene *qnrB* has been recognized in various enterobacterial species, such as *E. coli* and *Klebsiella* spp. (72–74). Plasmid-mediated quinolone resistance is intervened by the genes (*qnr*) encoding proteins that protect DNA gyrase and topoisomerase IV against quinolone compounds (75). Among the nonclinical sources, *qnr* gene was reported in *E. coli* isolated from swine, livestock and poultry (76, 77). In the present study, 25 isolates harbored plasmid-mediated *qnr* genes comprising of 22 isolates positive for *qnrS* and 3 isolates for *qnrB* genes. Isolates harboring *qnrS* gene also demonstrated co-existence of *bla*<sub>CTX-M-15</sub> and *bla*<sub>CTX-M-1</sub> group gene. Additionally, they were resistant to a

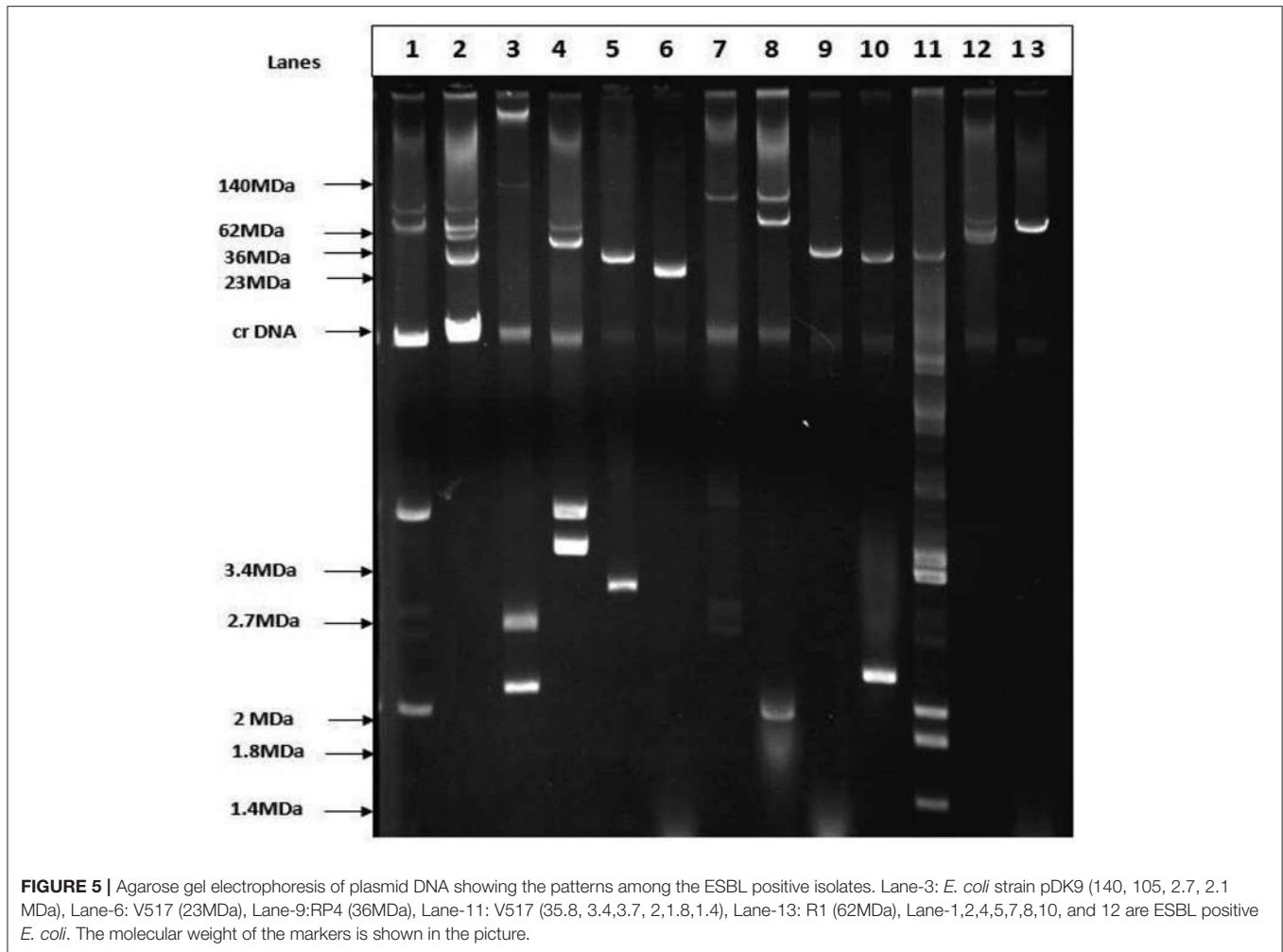
**TABLE 2** | ESBL-producing pathogenic *E. coli*.

Serial no.	Isolates ID	Antibiotic resistance pattern	ESBL genes	Virulent genes	Pathotypes
1	34012H2	Amp, Fep, Cro, Cxm, Cfa, NA, Caz, Cfm		<i>st</i>	ETEC
2	05080H2	Amp, Fep, Cro, Cxm, Cfa, Cip, NA, Sxt, Caz, Cfm	<i>bla</i> <sub>CTX-M-1</sub> , <i>bla</i> <sub>TEM</sub>	<i>aaiC</i>	EAEC
3	8E285B	Amc, Amp, Cro, Cxm, Cfa, Caz, Cfm	<i>bla</i> <sub>CTX-M-1</sub>	<i>aaiC</i>	EAEC
4	8W454H1	Amp, Fep, Cro, Cxm, Cfa, Cip, NA, Sxt, Caz, Cfm	<i>bla</i> <sub>CTX-M-1</sub> , <i>bla</i> <sub>CTX-M-15</sub>	<i>aaiC</i> , <i>aat</i>	EAEC
5	18544A	Amp, Cro, Cxm, Cfa, NA, Fd, Caz, Cfm		<i>aaiC</i>	EAEC
6	18162H2	Amp, Cro, Cxm, Cfa, NA, Fd, Caz, Cfm		<i>aaiC</i>	EAEC
7	18544B	Amp, Cro, Cxm, Cfa, NA, Fd, Caz, Cfm		<i>aaiC</i>	EAEC
8	1E181H2	Amp, Fep, Cro, Cxm, Cfa, NA, Sxt, Caz, Cfm	<i>bla</i> <sub>CTX-M-1</sub> , <i>bla</i> <sub>CTX-M-15</sub>	<i>aaiC</i>	EAEC
9	1E370H2	Amp, Cro, Cxm, Cfa, Cip, NA, Fd, Tzp, Sxt, Caz, Cfm	<i>bla</i> <sub>CTX-M-1</sub> , <i>bla</i> <sub>CTX-M-15</sub> , <i>bla</i> <sub>TEM</sub>	<i>aaiC</i>	EAEC
10	2W241H2	Amp, Cro, Cxm, Cfa, NA, Sxt, Caz, Cfm	<i>bla</i> <sub>CTX-M-1</sub> , <i>bla</i> <sub>CTX-M-15</sub> , <i>bla</i> <sub>TEM</sub>	<i>aaiC</i> , <i>aat</i>	EAEC
11	192B	Amp, Cro, Cxm, Cfa, NA, Caz, Cfm		<i>aaiC</i>	EAEC



range of 7–11 antibiotics, including ciprofloxacin and nalidixic acid. In contrast, all isolates containing *qnrS* gene also harbored the two ESBL genes, *bla*<sub>CTX-M-1group</sub> and *bla*<sub>CTX-M-15</sub>; they were resistant to 8 different antibiotics; most interestingly, they were susceptible to ciprofloxacin. Hence, the presence of *qnrS* gene alone may not be indicative of the isolate being resistant to fluoroquinolones as also been observed in a previous study (78). Using PCR for virulence genes, 29 (7%) was found to be pathogenic out of 384 isolates from drinking water. The most prevalent pathotype was EAEC, accountable for 52% of

the pathogenic isolates; followed by ETEC, EPEC, and EHEC responsible for 31, 14, and 4% of the pathogenic isolates, respectively. In addition to the diarrheagenic *E. coli* around 22% of *E. coli* isolates were at least positive for 1 ExPEC associated virulence genes, moreover 11% (6/55) of the isolates were detected to be potential ExPEC strains. This indicates that the drinking water samples present potential risk of disease epidemic particularly, the diarrheal disease, this assumes more important as in this particular setting where the drinking water is not treated before consumption. Though the reservoir for



**FIGURE 5 |** Agarose gel electrophoresis of plasmid DNA showing the patterns among the ESBL positive isolates. Lane-3: *E. coli* strain pDK9 (140, 105, 2.7, 2.1 MDa), Lane-6: V517 (23MDa), Lane-9:RP4 (36MDa), Lane-11: V517 (35.8, 3.4,3.7, 2,1.8,1.4), Lane-13: R1 (62MDa), Lane-1,2,4,5,7,8,10, and 12 are ESBL positive *E. coli*. The molecular weight of the markers is shown in the picture.

**TABLE 3 |** Results of conjugation assays between antibiotic resistant *E. coli* isolates obtained from water samples and the recipient *E. coli* J53 strain.

Isolates ID	Parent Strains		Transconjugants		Transfer Rate
	Resistant pattern	Plasmid pattern	Resistant pattern	Plasmid pattern	
9125B	Amc, Amp, Cro, Cxm, Cfa, Sxt, Caz, Cfm	85, 57, 49, 37	Amc, Amp, Cxm, Cfa	57	$3.33 \times 10^{-5}$
8W390H1	Amp, Cro, Cxm, Cfa, Caz, Cfm	42, 3.2, 2.6	Amp, Cro, Cxm, Cfa, Caz, Cfm	42	$3.37 \times 10^{-6}$
8W803H2	Amp, Cro, Cxm, Cfa, NA, Sxt, Caz, Cfm	103, 4.9, 2.9, 2.6	Amp,Cro, Cxm, Cfa, NA, Caz, Cfm	103	$1.8 \times 10^{-5}$
8W454H1	Amp, Fep, Cro, Cxm, Cfa, Cip, NA, Sxt, Caz, Cfm	82, 44, 37	Amp, Fep, Cro, Cxm, Cfa, Sxt, Caz, Cfm	44	$1.57 \times 10^{-6}$
12224H1	Amp, Cro, Cxm, Cfa, NA, Caz, Cfm	97, 39, 2	Amp, Cro, Cxm, Cfa, Caz, Cfm	39	$3.6 \times 10^{-4}$
1E07H2	Amp, Cro, Cxm, Cfa Caz, Cfm	71, 33, 30	Amp, Cro, Cxm, Cfa, Caz, Cfm	33, 30	$5.26 \times 10^{-5}$
1E391A	Amp, Cro, Cxm, Cfa, Caz, Cfm	92, 74, 56	Amp, Cro, Cxm, Cfa, Caz, Cfm	56	$5.17 \times 10^{-6}$
C-2WH4	Amp, Cro, Cxm, Cfa, Caz, Cfm	91, 37	Amp, Cro, Cxm, Cfa, Caz, Cfm	91	$1.19 \times 10^{-4}$
2W147H2	Amp, Cro, Cxm, Cfa, Caz, Cfm	56,37, 2.8, 2.5, 2	Amp, Cro, Cxm, Cfa, Caz, Cfm	56, 37	$4.75 \times 10^{-6}$

EAEC is still unclear, it is generally considered to be human (79–81). The transmission of EAEC is often described as waterborne or foodborne; therefore, it is assumed to be transmitted by the fecal-oral route (82). The presence of ETEC in drinking water and environmental water has been reported previously in Bangladesh; viability after long term water incubation and capacity of biofilm formation might imply that the water is

an important transmission route of ETEC (83–85). From the 29 pathogenic isolates, 11 were found to be ESBL positive and surprisingly, 10 of them were of EAEC pathotype. In recent studies of Iran and China, a high prevalence of ESBL in EAEC was also reported (86, 87). The alarming rate of ESBL-producing EAEC isolates recommends strict infection control policies to prevent additional spreading of the virulent and

resistant EAEC strains. All phylogenetic groups were represented in the *E. coli* isolates indicating that they were not homogenous in their population structure instead they belonged to diverse phylogenetic backgrounds, mainly the phylogenetic groups that are associated with commensal (group B1) as well as pathogenic and antimicrobial resistant *E. coli* lineages (group D) were detected. The presence of ESBL producing *E. coli* among the phylogenetic group D strains represents major public health risks due to the spread of such strains via drinking water.

In this study, 64% of the isolates were observed to harbor plasmids ranging from 1 to 103 MDa and a negligible similarity of plasmids pattern among the isolates inferred their clonal diversity due to heterogenous people of diverse geographical origin. Conjugation experiments are important to understand the transfer potential of plasmids conferring extended-spectrum- $\beta$ -lactamase resistance. It is reported that only plasmids above 35 MDa contain and transfer antibiotic resistance genes via conjugation (18, 88), and In line with other studies, we have also observed plasmid-mediated transfer of antibiotic resistance genes (18, 88). Conjugative plasmids, carrying cefotaxime resistance phenotype among different isolates, ranged from 42 to 103 MDa in size. These findings imply that horizontal gene transfer might worsen the existing antibiotic resistance scenario by speeding up the spread of antimicrobial resistance (AMR) within heterogeneous bacterial communities in environment (89).

Lack of proper sanitation and hygiene in a densely-populated area like Rohingya camps (26) might play a key role in the development and dissemination of AMR. Open defecation with poor personal hygiene, poor community sanitation and lack of controlled antibiotic usage has been reported to exacerbate the transmission of AMR infections (90). A previous study in four middle-income countries, Brazil, Indonesia, India, and Nigeria showed that improvement in water quality and sanitation alone could lead to reduction in antibiotic usage (90). The contamination of drinking water with ESBL-producing *E. coli*, as observed in this study could be due to poor sanitation and hygiene, including, open defecation, inappropriate fecal sludge management, etc. This study has shown that the environmental *E. coli* pose public health threat by being carriers of ESBL-genes. Moreover, these ESBL-producing *E. coli* were harboring virulence factors corresponding to major *E. coli* pathotypes. Limitations of this study include lack of genetic fingerprinting analysis of the antibiotic-resistant *E. coli* from drinking water, lack of exhaustive antimicrobial resistance gene, and extraintestinal pathogenic *E. coli* (ExPEC) virulence gene screening.

In conclusion, the findings of this study suggest that the drinking water samples analyzed herein could serve as an important source for exposure and dissemination of MDR, ESBL-producing and pathogenic *E. coli* variants, which also pose a

health risk to the displaced Rohingya population residing in the densely populated camps in Cox's Bazar. Based on the results of this work we recommend that the policymakers should make considerable efforts in implementing strong infection control strategies by focusing on providing good quality water and ensuring water quality monitoring programs in the Rohingya camps.

## DATA AVAILABILITY STATEMENT

All datasets generated for this study are included in the article/**Supplementary Material**.

## ETHICS STATEMENT

The Ethical Review Committee of International Centre for Diarrhoeal Disease Research, Bangladesh has approved the study.

## AUTHOR CONTRIBUTIONS

ZM, MI, SH, MW, KI, DJ, and NA planned and organized the study. ZM, MI, SA, MK, MM, TN, SH, MW, DJ, DA, and NA were involved to implement the study. ZM, SA, MK, KI, DA, and NA carried out laboratory work. ZM, MM, MI, SH, DA, and NA were involved to interpret the data. ZM, MK, SA, MM, MI, and NA had a major contribution in writing the manuscript. All authors contributed in proofreading the manuscript.

## FUNDING

This research study was funded by United Nations International Children's Emergency Fund (unicef), grant number BCO/PCA/2017/035-2018/001. International Centre for Diarrhoeal Disease Research, Bangladesh (icddr,b) acknowledges with gratitude the commitment of unicef to its research efforts. icddr,b is also grateful to the Government of Bangladesh, Canada, Sweden and the UK for providing core/unrestricted support. The authors are grateful to Frederic Geser of unicef Bangladesh for his constructive input and cooperation during the study. The authors are also grateful to Department of Public Health Engineering (DPHE) Cox's Bazar and unicef Cox's Bazar, Bangladesh for their valuable guidance and cooperation during the study.

## SUPPLEMENTARY MATERIAL

The Supplementary Material for this article can be found online at: <https://www.frontiersin.org/articles/10.3389/fpubh.2020.00228/full#supplementary-material>

## REFERENCES

1. Aruna K, Mobashshera T. Prevalence of extended spectrum beta-lactamase production among uropathogens in south Mumbai and its antibiogram pattern. *EXCLI J*. (2012) 11:363–72.

2. Hussain A, Shaik S, Ranjan A, Nandanwar N, Tiwari SK, Majid M, et al. Risk of transmission of antimicrobial resistant *Escherichia coli* from commercial broiler and free-range retail chicken in India. *Front Microbiol*. (2017) 8:2120. doi: 10.3389/fmicb.2017.02120



3. Hussain A, Shaik S, Ranjan A, Suresh A, Sarker N, Semmler T, et al. Genomic and functional characterization of poultry *Escherichia coli* from India revealed diverse Extended-spectrum  $\beta$ -lactamase-producing lineages with shared virulence profiles. *Front Microbiol.* (2019) 10:2766. doi: 10.3389/fmicb.2019.02766
4. Pitout JDD, Nordmann P, Laupland KB, Poirel L. Emergence of Enterobacteriaceae producing extended-spectrum beta-lactamases (ESBLs) in the community. *J Antimicrob Chemother.* (2005) 56:52–9. doi: 10.1093/jac/dki166
5. Cantón R, Akóva M, Carmeli Y, Giske CG, Glupczynski Y, Gniadkowski M, et al. Rapid evolution and spread of carbapenemases among Enterobacteriaceae in Europe. *Clin Microbiol Infect.* (2012) 18:413–31. doi: 10.1111/j.1469-0691.2012.03821.x
6. Harris PNA, Tambyah PA, Paterson DL.  $\beta$ -lactam and  $\beta$ -lactamase inhibitor combinations in the treatment of extended-spectrum  $\beta$ -lactamase producing Enterobacteriaceae: time for a reappraisal in the era of few antibiotic options? *Lancet Infect Dis.* (2015) 15:475–85. doi: 10.1016/S1473-3099(14)70950-8
7. Paterson DL, Bonomo RA. Extended-spectrum beta-lactamases: a clinical update. *Clin Microbiol Rev.* (2005) 18:657–86. doi: 10.1128/CMR.18.4.657-686.2005
8. Muñoz-Miguel J, Roig-Sena J, Saa-Casal A, Salvador-Aguilá M, Bediaga-Collado A. Multidrug-resistant *E. coli* in the community: assessment and proposal of a feasible indicator. *Eur J Public Health.* (2018) 28:cky213.709. doi: 10.1093/eurpub/cky212.709
9. Odonkor ST, Addo KK. Prevalence of multidrug-resistant *Escherichia coli* isolated from drinking water sources. *Int J Microbiol.* (2018) 2018:7204013. doi: 10.1155/2018/7204013
10. Overdeest I, Willemsen I, Rijnsburger M, Eustace A, Xu L, Hawkey P, et al. Extended-spectrum  $\beta$ -lactamase genes of *Escherichia coli* in chicken meat and humans, The Netherlands. *Emerg Infect Dis.* (2011) 17:1216. doi: 10.3201/eid1707.110209
11. Walsh TR, Weeks J, Livermore DM, Toleman MA. Dissemination of NDM-1 positive bacteria in the New Delhi environment and its implications for human health: an environmental point prevalence study. *Lancet Infect Dis.* (2011) 11:355–62. doi: 10.1016/S1473-3099(11)70059-7
12. Islam MA, Talukdar PK, Hoque A, Huq M, Nabi A, Ahmed D, et al. Emergence of multidrug-resistant NDM-1-producing Gram-negative bacteria in Bangladesh. *Eur J Clin Microbiol Infect Dis.* (2012) 31:2593–600. doi: 10.1007/s10096-012-1601-2
13. Rashid M, Rakib MM, Hasan B. Antimicrobial-resistant and ESBL-producing *Escherichia coli* in different ecological niches in Bangladesh. *Infect Ecol Epidemiol.* (2015) 5:26712. doi: 10.3402/iee.v5.26712
14. Hunter PR. Drinking water and diarrhoeal disease due to *Escherichia coli*. *J Water Health.* (2003) 1:65–72. doi: 10.2166/wh.2003.0008
15. Sirot D. Extended-spectrum plasmid-mediated beta-lactamases. *J Antimicrob Chemother.* (1995) 36:19–34. doi: 10.1093/jac/36.suppl\_A.19
16. Taylor NGH, Verner-Jeffreys DW, Baker-Austin C. Aquatic systems: maintaining, mixing and mobilising antimicrobial resistance? *Trends Ecol Evol.* (2011) 26:278–84. doi: 10.1016/j.tree.2011.03.004
17. Levine MM. *Escherichia coli* that cause diarrhea: enterotoxigenic, enteropathogenic, enteroinvasive, enterohemorrhagic, and enteroadherent. *J Infect Dis.* (1987) 155:377–89. doi: 10.1093/infdis/155.3.377
18. Talukder KA, Islam Z, Dutta DK, Islam MA, Khajanchi BK, Azmi IJ, et al. Antibiotic resistance and genetic diversity of *Shigella sonnei* isolated from patients with diarrhoea between 1999 and 2003 in Bangladesh. *J Med Microbiol.* (2006) 55:1257–63. doi: 10.1099/jmm.0.46641-0
19. Nataro JP, Kaper JB. Diarrheagenic *Escherichia coli*. *Clin Microbiol Rev.* (1998) 11:142–201. doi: 10.1128/CMR.11.1.142
20. Kaper JB, Nataro JP, Mobley HLT. Pathogenic *Escherichia coli*. *Nat Rev Microbiol.* (2004) 2:123–40. doi: 10.1038/nrmicro818
21. Coleman BL, Louie M, Salvadori MI, McEwen SA, Neumann N, Sibley K, et al. Contamination of Canadian private drinking water sources with antimicrobial resistant *Escherichia coli*. *Water Res.* (2013) 47:3026–36. doi: 10.1016/j.watres.2013.03.008
22. Park J, Kim JS, Kim S, Shin E, Oh K-H, Kim Y, et al. A waterborne outbreak of multiple diarrhoeagenic *Escherichia coli* infections associated with drinking water at a school camp. *Int J Infect Dis.* (2018) 66:45–50. doi: 10.1016/j.ijid.2017.09.021
23. Swerdlow DL, Woodruff BA, Brady RC, Griffin PM, Tippen S, Donnell HDJ, et al. A waterborne outbreak in Missouri of *Escherichia coli* O157:H7 associated with bloody diarrhea and death. *Ann Intern Med.* (1992) 117:812–9. doi: 10.7326/0003-4819-117-10-812
24. Chan EYY, Chiu CP, Chan GKW. Medical and health risks associated with communicable diseases of Rohingya refugees in Bangladesh 2017. *Int J Infect Dis.* (2018) 68:39–43. doi: 10.1016/j.ijid.2018.01.001
25. Islam MM, Nuzhath T. Health risks of Rohingya refugee population in Bangladesh: a call for global attention. *J Glob Health.* (2018) 8:20309. doi: 10.7189/jogh.08.020309
26. Mahmud ZH, Islam MS, Imran KM, Ibna Hakim SA, Worth M, Ahmed A, et al. Occurrence of *Escherichia coli* and faecal coliforms in drinking water at source and household point-of-use in Rohingya camps, Bangladesh. *Gut Pathog.* (2019) 11:52. doi: 10.1186/s13099-019-0333-6
27. Rahman MR. Rohingya Crisis—Health issues. *Delta Med Coll J.* (2018) 6:1–3. doi: 10.3329/dmcj.v6i1.35960
28. Finley R, Glass-Kaasta SK, Hutchinson J, Patrick DM, Weiss K, Conly J. Declines in outpatient antimicrobial use in Canada (1995–2010). *PLoS ONE.* (2013) 8:e76398. doi: 10.1371/journal.pone.0076398
29. Levy S. *The Antibiotic Paradox: How Misuse of Antibiotics Destroys Their Curative Powers* (Perseus Cambridge, 2002).
30. WHO. *Antimicrobial Resistance: Global Report on Surveillance.* World Health Organization (2014).
31. Mohamed JA, DuPont HL, Jiang Z-D, Flores J, Carlin LG, Belkind-Gerson J, et al. A single-nucleotide polymorphism in the gene encoding osteoprotegerin, an anti-inflammatory protein produced in response to infection with diarrheagenic *Escherichia coli*, is associated with an increased risk of nonsecretory bacterial diarrhea in North Ame. *J Infect Dis.* (2009) 199:477–85. doi: 10.1086/596319
32. Nguyen TV, Le Van P, Le Huy C, Gia KN, Weintraub A. Detection and characterization of diarrheagenic *Escherichia coli* from young children in Hanoi, Vietnam. *J Clin Microbiol.* (2005) 43:755–60. doi: 10.1128/JCM.43.2.755-760.2005
33. Oswald E, Schmidt H, Morabito S, Karch H, Marches O, Caprioli A. Typing of intimin genes in human and animal enterohemorrhagic and enteropathogenic *Escherichia coli*: characterization of a new intimin variant. *Infect Immun.* (2000) 68:64–71. doi: 10.1128/IAI.68.1.64-71.2000
34. Talukdar PK, Rahman M, Rahman M, Nabi A, Islam Z, Hoque MM, et al. Antimicrobial resistance, virulence factors and genetic diversity of *Escherichia coli* isolates from household water supply in Dhaka, Bangladesh. *PLoS ONE.* (2013) 8:e61090. doi: 10.1371/journal.pone.0061090
35. Mahmud ZH, Shirazi FF, Hossainy MRH, Islam MI, Ahmed MA, Nafiz TN, et al. Presence of virulence factors and antibiotic resistance among *Escherichia coli* strains isolated from human pit sludge. *J Infect Dev Ctries.* (2019) 13:195–203. doi: 10.3855/jidc.10768
36. Heuvelink AE, Van de Kar N, Meis J, Monnens LAH, Melchers WJG. Characterization of verocytotoxin-producing *Escherichia coli* O157 isolates from patients with haemolytic uraemic syndrome in Western Europe. *Epidemiol Infect.* (1995) 115:1–3. doi: 10.1017/S0950268800058064
37. Islam MA, Heuvelink AE, De Boer E, Sturm PD, Beumer RR, Zwietering MH, et al. Shiga toxin-producing *Escherichia coli* isolated from patients with diarrhoea in Bangladesh. *J Med Microbiol.* (2007) 56:380–5. doi: 10.1099/jmm.0.46916-0
38. Frankel G, Giron JA, Valmassoi J, Schoolnik GK. Multi-gene amplification: simultaneous detection of three virulence genes in diarrhoeal stool. *Mol Microbiol.* (1989) 3:1729–34. doi: 10.1111/j.1365-2958.1989.tb00158.x
39. Lüscher D, Altwegg M. Detection of shigellae, enteroinvasive and enterotoxigenic *Escherichia coli* using the polymerase chain reaction (PCR) in patients returning from tropical countries. *Mol Cell Probes.* (1994) 8:285–90. doi: 10.1006/mcpr.1994.1040
40. Talukder KA, Islam MA, Khajanchi BK, Dutta DK, Islam Z, Safa A, et al. Temporal shifts in the dominance of serotypes of *Shigella dysenteriae* from 1999 to 2002 in Dhaka, Bangladesh. *J Clin Microbiol.* (2003) 41:5053–8. doi: 10.1128/JCM.41.11.5053-5058.2003
41. Thong KL, Hoe SLL, Puthuchery SD, Yasin RM. Detection of virulence genes in Malaysian *Shigella* species by multiplex PCR assay. *BMC Infect Dis.* (2005) 5:8. doi: 10.1186/1471-2334-5-8

42. Johnson JR, Kuskowski MA, Smith K, O'Bryan TT, Tatini S. Antimicrobial-resistant and extraintestinal pathogenic *Escherichia coli* in retail foods. *J Infect Dis.* (2005) 191:1040–9. doi: 10.1086/428451
43. Ahmed AM, Motoi Y, Sato M, Maruyama A, Watanabe H, Fukumoto Y, et al. Zoo animals as reservoirs of gram-negative bacteria harboring integrons and antimicrobial resistance genes. *Appl Environ Microbiol.* (2007) 73:6686–90. doi: 10.1128/AEM.01054-07
44. Guessennd N, Bremont S, Gbonou V, Kacou-Ndouba A, Ekaza E, Lambert T, et al. Qnr-type quinolone resistance in extended-spectrum beta-lactamase producing enterobacteria in Abidjan, Ivory Coast. *Pathol Biol.* (2008) 56:439–46. doi: 10.1016/j.patbio.2008.07.025
45. Jouini A, Vinué L, Slama K, Ben SY, Klibi N, Hammami S, et al. Characterization of CTX-M and SHV extended-spectrum  $\beta$ -lactamases and associated resistance genes in *Escherichia coli* strains of food samples in Tunisia. *J Antimicrob Chemother.* (2007) 60:1137–41. doi: 10.1093/jac/dkm316
46. Leflon-Guibout V, Jurand C, Bonacorsi S, Espinasse F, Guelfi MC, Duportail F, et al. Emergence and spread of three clonally related virulent isolates of CTX-M-15-producing *Escherichia coli* with variable resistance to aminoglycosides and tetracycline in a French geriatric hospital. *Antimicrob Agents Chemother.* (2004) 48:3736–42. doi: 10.1128/AAC.48.10.3736-3742.2004
47. Muzahheed YD, Adams-Haduch JM, Endimiani A, Sidjabat HE, Gaddad SM, Paterson DL. High prevalence of CTX-M-15-producing *Klebsiella pneumoniae* among inpatients and outpatients with urinary tract infection in Southern India. *J Antimicrob Chemother.* (2008) 61:1393. doi: 10.1093/jac/dkn109
48. Nordmann P, Poirel L, Carrère A, Toleman MA, Walsh TR. How to detect NDM-1 producers. *J Clin Microbiol.* (2011) 49:718–21. doi: 10.1128/JCM.01773-10
49. Zhao S, White DG, McDermott PF, Friedman S, English L, Ayers S, et al. Identification and expression of cephamycinasebla CMY Genes in *Escherichia coli* and *Salmonella* Isolates from food animals and ground meat. *Antimicrob Agents Chemother.* (2001) 45:3647–50. doi: 10.1128/AAC.45.12.3647-3650.2001
50. Jacoby GA, Chow N, Waites KB. Prevalence of plasmid-mediated quinolone resistance. *Antimicrob Agents Chemother.* (2003) 47:559–62. doi: 10.1128/AAC.47.2.559-562.2003
51. Jacoby GA, Walsh KE, Mills DM, Walker VJ, Oh H, Robicsek A, et al. qnrB, another plasmid-mediated gene for quinolone resistance. *Antimicrob Agents Chemother.* (2006) 50:1178–82. doi: 10.1128/AAC.50.4.1178-1182.2006
52. Pu X-Y, Pan J-C, Wang H-Q, Zhang W, Huang Z-C, Gu Y-M. Characterization of fluoroquinolone-resistant *Shigella flexneri* in Hangzhou area of China. *J Antimicrob Chemother.* (2009) 63:917–20. doi: 10.1093/jac/dkp087
53. Kado C, Liu S. Rapid procedure for detection and isolation of large and small plasmids. *J Bacteriol.* (1981) 145:1365–73. doi: 10.1128/JB.145.3.1365-1373.1981
54. Macrina FL, Kopecko DJ, Jones KR, Ayers DJ, McCowen SM. A multiple plasmid-containing *Escherichia coli* strain: convenient source of size reference plasmid molecules. *Plasmid.* (1978) 1:417–20. doi: 10.1016/0147-619X(78)90056-2
55. Clermont O, Christenson JK, Denamur E, Gordon DM. The C lermont *Escherichia coli* phylo-typing method revisited: improvement of specificity and detection of new phylo-groups. *Environ Microbiol Rep.* (2013) 5:58–65. doi: 10.1111/1758-2229.12019
56. Bradford PA. Extended-spectrum  $\beta$ -lactamases in the 21st century: characterization, epidemiology, and detection of this important resistance threat. *Clin Microbiol Rev.* (2001) 14:933–51. doi: 10.1128/CMR.14.4.933-951.2001
57. Ensor VM, Shahid M, Evans JT, Hawkey PM. Occurrence, prevalence and genetic environment of CTX-M  $\beta$ -lactamases in Enterobacteriaceae from Indian hospitals. *J Antimicrob Chemother.* (2006) 58:1260–3. doi: 10.1093/jac/dkl422
58. Kamruzzaman M, Shoma S, Bari SMN, Ginn AN, Wiklendt AM, Partridge SR, et al. Genetic diversity and antibiotic resistance in *Escherichia coli* from environmental surface water in Dhaka City, Bangladesh. *Diagn Microbiol Infect Dis.* (2013) 76:222–6. doi: 10.1016/j.diagmicrobio.2013.02.016
59. Hasan B, Drobni P, Drobni M, Alam M, Olsen B. Dissemination of NDM-1. *Lancet Infect Dis.* (2012) 12:99–100. doi: 10.1016/S1473-3099(11)70333-4
60. Hasan B, Melhus Å, Sandegren L, Alam M, Olsen B. The gull (*Chroicocephalus brunnicephalus*) as an environmental bioindicator and reservoir for antibiotic resistance on the coastlines of the Bay of Bengal. *Microb Drug Resist.* (2014) 20:466–71. doi: 10.1089/mdr.2013.0233
61. Rahman MM, Haq JA, Hossain MA, Sultana R, Islam F, Islam AHMS. Prevalence of extended-spectrum  $\beta$ -lactamase-producing *Escherichia coli* and *Klebsiella pneumoniae* in an urban hospital in Dhaka, Bangladesh. *Int J Antimicrob Agents.* (2004) 24:508–10. doi: 10.1016/j.ijantimicag.2004.05.007
62. Choudhuri AU, Biswas M, Haque MU, Arman MSI, Uddin N, Kona N, et al. Cephalosporin-3G, highly prescribed antibiotic to outpatients in Rajshahi, Bangladesh: prescription errors, carelessness, irrational uses are the triggering causes of antibiotic resistance. *J Appl Pharm Sci.* (2018) 8:105–12. doi: 10.7324/JAPS.2018.8.614
63. Ahmed I, Rabbi MB, Sultana S. Antibiotic resistance in Bangladesh: a systematic review. *Int J Infect Dis.* (2019) 80:54–61. doi: 10.1016/j.ijid.2018.12.017
64. Biswas M, Roy DN, Tajmim A, Rajib SS, Hossain M, Farzana F, et al. Prescription antibiotics for outpatients in Bangladesh: a cross-sectional health survey conducted in three cities. *Ann Clin Microbiol Antimicrob.* (2014) 13:15. doi: 10.1186/1476-0711-13-15
65. Swedan S, Abu Alrub H. Antimicrobial resistance, virulence factors, and pathotypes of *Escherichia coli* isolated from drinking water sources in Jordan. *Pathogens.* (2019) 8:86. doi: 10.3390/pathogens8020086
66. Hasan B, Islam K, Ahsan M, Hossain Z, Rashid M, Talukder B, et al. Fecal carriage of multi-drug resistant and extended spectrum beta-lactamases producing *E. coli* in household pigeons, Bangladesh. *Vet Microbiol.* (2014) 168:221–4. doi: 10.1016/j.vetmic.2013.09.033
67. Bonnet R. Growing group of extended-spectrum  $\beta$ -lactamases: the CTX-M enzymes. *Antimicrob Agents Chemother.* (2004) 48:1–14. doi: 10.1128/AAC.48.1.1-14.2004
68. Doublet B, Granier SA, Robin F, Bonnet R, Fabre L, Brisabois A, et al. Novel plasmid-encoded ceftazidime-hydrolyzing CTX-M-53 extended-spectrum  $\beta$ -lactamase from *Salmonella enterica* serotypes Westhampton and Senftenberg. *Antimicrob Agents Chemother.* (2009) 53:1944–51. doi: 10.1128/AAC.01581-08
69. Liu W, Chen L, Li H, Duan H, Zhang Y, Liang X, et al. Novel CTX-M  $\beta$ -lactamase genotype distribution and spread into multiple species of Enterobacteriaceae in Changsha, Southern China. *J Antimicrob Chemother.* (2009) 63:895–900. doi: 10.1093/jac/dkp068
70. Radice M, Power P, Di Conza J, Gutkind G. Early dissemination of CTX-M-derived enzymes in South America. *Antimicrob Agents Chemother.* (2002) 46:602–4. doi: 10.1128/AAC.46.2.602-604.2002
71. Islam MA, Huq M, Nabi A, Talukdar PK, Ahmed D, Talukder KA, et al. Occurrence and characterization of multidrug-resistant New Delhi metallo- $\beta$ -lactamase-1-producing bacteria isolated between 2003 and 2010 in Bangladesh. *J Med Microbiol.* (2013) 62:62–8. doi: 10.1099/jmm.0.048066-0
72. Kao C-Y, Wu H-M, Lin W-H, Tseng C-C, Yan J-J, Wang M-C, et al. Plasmid-mediated quinolone resistance determinants in quinolone-resistant *Escherichia coli* isolated from patients with bacteremia in a university hospital in Taiwan, 2001–2015. *Sci Rep.* (2016) 6:32281. doi: 10.1038/srep32281
73. Poirel L, Cattoir V, Nordmann P. Is plasmid-mediated quinolone resistance a clinically significant problem? *Clin Microbiol Infect.* (2008) 14:295–7. doi: 10.1111/j.1469-0691.2007.01930.x
74. Takasu H, Suzuki S, Reungsang A, Viet PH. Fluoroquinolone (FQ) contamination does not correlate with occurrence of FQ-resistant bacteria in aquatic environments of Vietnam and Thailand. *Microbes Environ.* (2011) 26:135–43. doi: 10.1264/jsme2.me10204
75. Strahilevitz J, Jacoby GA, Hooper DC, Robicsek A. Plasmid-mediated quinolone resistance: a multifaceted threat. *Clin Microbiol Rev.* (2009) 22:664–89. doi: 10.1128/CMR.00016-09
76. Ma J, Zeng Z, Chen Z, Xu X, Wang X, Deng Y, et al. High prevalence of plasmid-mediated quinolone resistance determinants qnr, aac(6')-Ib-cr, and qepA among ceftiofur-resistant Enterobacteriaceae isolates from companion and food-producing animals. *Antimicrob Agents Chemother.* (2009) 53:519–24. doi: 10.1128/AAC.00886-08
77. Yue L, Jiang H-X, Liao X-P, Liu J-H, Li S-J, Chen X-Y, et al. Prevalence of plasmid-mediated quinolone resistance qnr genes in poultry and swine

- clinical isolates of *Escherichia coli*. *Vet Microbiol.* (2008) 132:414–20. doi: 10.1016/j.vetmic.2008.05.009
78. Cattoir V, Poirel L, Aubert C, Soussy C-J, Nordmann P. Unexpected occurrence of plasmid-mediated quinolone resistance determinants in environmental *Aeromonas* spp. *Emerg Infect Dis.* (2008) 14:231. doi: 10.3201/eid1402.070677
  79. Beutin L, Martin A. Outbreak of Shiga toxin-producing *Escherichia coli* (STEC) O104: H4 infection in Germany causes a paradigm shift with regard to human pathogenicity of STEC strains. *J Food Prot.* (2012) 75:408–18. doi: 10.4315/0362-028X.JFP-11-452
  80. Huppertz HI, Rutkowski S, Aleksic S, Karch H. Acute and chronic diarrhoea and abdominal colic associated with enteroaggregative *Escherichia coli* in young children living in western Europe. *Lancet.* (1997) 349:1660–2. doi: 10.1016/S0140-6736(96)12485-5
  81. Oundo JO, Kariuki SM, Boga HI, Muli FW, Iijima Y. High incidence of enteroaggregative *Escherichia coli* among food handlers in three areas of Kenya: a possible transmission route of travelers' diarrhea. *J Travel Med.* (2008) 15:31–8. doi: 10.1111/j.1708-8305.2007.00174.x
  82. Jiang Z-D, Greenberg D, Nataro JP, Steffen R, DuPont HL. Rate of occurrence and pathogenic effect of enteroaggregative *Escherichia coli* virulence factors in international travelers. *J Clin Microbiol.* (2002) 40:4185–90. doi: 10.1128/JCM.40.11.4185-4190.2002
  83. Ahmed D, Islam MS, Begum YA, Janzon A, Qadri F, Sjöling Å. Presence of enterotoxigenic *Escherichia coli* in biofilms formed in water containers in poor households coincides with epidemic seasons in Dhaka. *J Appl Microbiol.* (2013) 114:1223–9. doi: 10.1111/jam.12109
  84. Begum YA, Talukder KA, Nair GB, Qadri F, Sack RB, Svennerholm A-M. Enterotoxigenic *Escherichia coli* isolated from surface water in urban and rural areas of Bangladesh. *J Clin Microbiol.* (2005) 43:3582–3. doi: 10.1128/JCM.43.7.3582-3583.2005
  85. Lothigius Å, Janzon A, Begum Y, Sjöling Å, Qadri F, Svennerholm A, et al. Enterotoxigenic *Escherichia coli* is detectable in water samples from an endemic area by real-time PCR. *J Appl Microbiol.* (2008) 104:1128–36. doi: 10.1111/j.1365-2672.2007.03628.x
  86. Mansour Amin MS, Javaherizadeh H, Motamedifar M, Saki M, Veisi H, Ebrahimi S, et al. Antibiotic resistance pattern and molecular characterization of extended-spectrum  $\beta$ -lactamase producing enteroaggregative *Escherichia coli* isolates in children from southwest Iran. *Infect Drug Resist.* (2018) 11:1097. doi: 10.2147/IDR.S167271
  87. Zhang R, Gu D, Huang Y, Chan EW-C, Chen G-X, Chen S. Comparative genetic characterization of Enterotoxigenic *Escherichia coli* strains recovered from clinical and non-clinical settings. *Sci Rep.* (2016) 6:24321. doi: 10.1038/srep24321
  88. Talukder KA, Islam MA, Dutta DK, Hassan F, Safa A, Nair GB, et al. Phenotypic and genotypic characterization of serologically atypical strains of *Shigella flexneri* type 4 isolated in Dhaka, Bangladesh. *J Clin Microbiol.* (2002) 40:2490–7. doi: 10.1128/JCM.40.7.2490-2497.2002
  89. Dionisio F, Matic I, Radman M, Rodrigues OR, Taddei F. Plasmids spread very fast in heterogeneous bacterial communities. *Genetics.* (2002) 162:1525–32.
  90. O'Neill J. Tackling drug-resistant infections globally: Final report and recommendations. 2016. *HM Gov. Wellcome Trust UK* (2018).

**Conflict of Interest:** The authors declare that the research was conducted in the absence of any commercial or financial relationships that could be construed as a potential conflict of interest.

Copyright © 2020 Mahmud, Kabir, Ali, Moniruzzaman, Imran, Nafiz, Islam, Hussain, Hakim, Worth, Ahmed, Johnston and Ahmed. This is an open-access article distributed under the terms of the Creative Commons Attribution License (CC BY). The use, distribution or reproduction in other forums is permitted, provided the original author(s) and the copyright owner(s) are credited and that the original publication in this journal is cited, in accordance with accepted academic practice. No use, distribution or reproduction is permitted which does not comply with these terms.



# Molecular Mechanisms and Epidemiology of Fosfomycin Resistance in *Staphylococcus aureus* Isolated From Patients at a Teaching Hospital in China

Wenya Xu<sup>1</sup>, Tao Chen<sup>1</sup>, Huihui Wang<sup>1</sup>, Weiliang Zeng<sup>2</sup>, Qing Wu<sup>1</sup>, Kaihang Yu<sup>2</sup>, Ye Xu<sup>1</sup>, Xiucai Zhang<sup>1</sup> and Tielu Zhou<sup>1\*</sup>

<sup>1</sup> Department of Clinical Laboratory, The First Affiliated Hospital of Wenzhou Medical University, Wenzhou, China, <sup>2</sup> School of Laboratory Medicine and Life Science, Wenzhou Medical University, Wenzhou, China

## OPEN ACCESS

### Edited by:

Eliana De Gregorio,  
University of Naples Federico II, Italy

### Reviewed by:

Que Chi Truong-Bolduc,  
Massachusetts General Hospital and  
Harvard Medical School,  
United States  
Hong-Ning Wang,  
Sichuan University, China

### \*Correspondence:

Tielu Zhou  
wyztlj@163.com

### Specialty section:

This article was submitted to  
Antimicrobials, Resistance  
and Chemotherapy,  
a section of the journal  
Frontiers in Microbiology

Received: 28 November 2019

Accepted: 20 May 2020

Published: 26 June 2020

### Citation:

Xu W, Chen T, Wang H, Zeng W,  
Wu Q, Yu K, Xu Y, Zhang X and  
Zhou T (2020) Molecular Mechanisms  
and Epidemiology of Fosfomycin  
Resistance in *Staphylococcus aureus*  
Isolated From Patients at a Teaching  
Hospital in China.  
Front. Microbiol. 11:1290.  
doi: 10.3389/fmicb.2020.01290

*Staphylococcus aureus* is a major cause of hospital- and community-acquired infections placing a significant burden on the healthcare system. With the widespread of multidrug-resistant bacteria and the lack of effective antibacterial drugs, fosfomycin has gradually attracted attention as an “old drug.” Thus, investigating the resistance mechanisms and epidemiology of fosfomycin-resistant *S. aureus* is an urgent requirement. In order to investigate the mechanisms of resistance, 11 fosfomycin-resistant *S. aureus* isolates were analyzed by PCR and sequencing. The genes, including *fosA*, *fosB*, *fosC*, *fosD*, *fosX*, and *tet38*, as well as mutations in *murA*, *glpT*, and *uhpT* were identified. Quantitative real-time PCR (qRT-PCR) was conducted to evaluate the expression of the target enzyme gene *murA* and the efflux pump gene *tet38* under the selection pressure of fosfomycin. Furthermore, multilocus sequence typing (MLST) identified a novel sequence type (ST 5708) of *S. aureus* strains. However, none of the resistant strains carried *fosA*, *fosB*, *fosC*, *fosD*, and *fosX* genes in the current study, and 12 distinct mutations were detected in the *uhpT* (3), *glpT* (4), and *murA* (5) genes. qRT-PCR revealed an elevated expression of the *tet38* gene when exposed to increasing concentration of fosfomycin among 8 fosfomycin-resistant *S. aureus* strains and reference strain ATCC 29213. MLST analysis categorized the 11 strains into 9 STs. Thus, the mutations in the *uhpT*, *glpT*, and *murA* genes might be the primary mechanisms underlying fosfomycin resistance, and the overexpression of efflux pump gene *tet38* may play a major role in the fosfomycin resistance in these isolates.

**Keywords:** fosfomycin, *Staphylococcus aureus*, resistance mechanism, mutation, *tet38*

## INTRODUCTION

*Staphylococcus aureus* is a kind of facultative anaerobe pathogenic Gram-positive coccus with strong resistance and tolerance to harsh environments (Wang et al., 2020). At present, *S. aureus* has become a significant pathogen of nosocomial infections, such as deep-seated skin and soft tissue infections (SSTI), endocarditis, and other life-threatening severe infections (Mehraj et al., 2016). In



recent years, with the widespread use of antibiotics, the emergence of multidrug-resistant (MDR) *S. aureus* has become a major concern (Gatadi et al., 2019). In addition, the lack of effective clinical treatments against MDR *S. aureus* has rekindled the interest of clinicians in fosfomycin. It is an antimicrobial agent that was discovered in *Streptomyces* sp. It exhibits broad-spectrum activity against both Gram-positive and Gram-negative bacteria by inhibiting the peptidoglycan synthesis pathway, which is essential for the synthesis of the cell walls (Shorr et al., 2017). However, the number of fosfomycin-resistant *S. aureus* strains is increasing rapidly (Etienne et al., 1991).

Several mechanisms of fosfomycin resistance have been proposed, including the plasmid-encoded fosfomycin-modifying enzymes (FosA, FosB, FosC, FosD, and FosX) and the acquisition of chromosomal mutations (Nakaminami et al., 2008; Liu et al., 2017; Silver, 2017). Mutations in the MurA target enzyme and transporters (GlpT and UhpT) have been shown to be responsible for fosfomycin resistance (Michalopoulos et al., 2011). Additionally, the overexpression of target enzymes, MurA and Tet38 efflux pump, also contributes to fosfomycin resistance in *S. aureus* (Truong-Bolduc et al., 2018). Notably, there are no reports yet suggesting that fosfomycin can stimulate the expression of the efflux pump gene and mediate drug resistance. However, a few studies on *S. aureus* have described the drug sensitivity and resistance mechanism of fosfomycin in *S. aureus*, although they are not fully understood.

In the present study, we focus on the mutations of the target enzyme MurA, which catalyzes the initial step in the biosynthesis of peptidoglycan and transporters (GlpT and UhpT), as well as the overexpression of *murA* and *tet38* efflux pump in 11 fosfomycin-resistant *S. aureus*. In addition, a strong correlation was established between fosfomycin resistance and efflux pump gene *tet38* overexpression that has not been reported previously. The results of quantitative real-time PCR (qRT-PCR) indicated that the Tet38 efflux pump plays a vital role in fosfomycin resistance by pumping out the drug.

## MATERIALS AND METHODS

### Bacterial Strains

In 2018, a total of 200 *S. aureus* isolates were obtained from the First Affiliated Hospital of Wenzhou Medical University, a comprehensive teaching hospital in China. The bacteria were identified by matrix-assisted laser desorption/ionization time of flight mass spectrometry (MALDI-TOF MS; BioMérieux, Lyons, France). *S. aureus* ATCC 29213 (American Type Tissue Culture Collection, Manassas, VA, United States) was used as an endogenous control strain in antimicrobial susceptibility testing experiments. The study and consent procedure were approved by the Ethics Committee of the hospital.

### Antimicrobial Susceptibility Testing

The minimum inhibitory concentration (MIC) of fosfomycin for each clinical strain was determined using the agar

dilution method, wherein the media were supplemented with glucose-6-phosphate (25 mg/L), according to the recommendations of the Clinical and Laboratory Standards Institute [CLSI], 2018 (Ushanov et al., 2020). The data were interpreted according to the European Committee on Antimicrobial Susceptibility Testing criteria (available at [http://www.eucast.org/clinical\\_breakpoints/](http://www.eucast.org/clinical_breakpoints/)) (susceptible,  $\leq 32$  mg/L; resistant,  $\geq 64$  mg/L), and the fosfomycin-resistant isolates were selected for further investigation. In addition, the MICs of fosfomycin-resistant *S. aureus* to other classes of antibiotics, including oxacillin, erythromycin, ciprofloxacin, levofloxacin, gentamicin, rifampicin, linezolid, vancomycin, and teicoplanin, were detected using the broth microdilution method.

### Detection of Fosfomycin-Resistant Genes

The DNA of fosfomycin-resistant and fosfomycin-susceptible *S. aureus* isolates was extracted using a Biospin Bacterial Genomic DNA Extraction Kit (Bioflux, Tokyo, Japan) and was utilized as the template for PCR amplification of the *fosA*, *fosB*, *fosC*, *fosD*, *fosX*, *glpT*, *uhpT*, *murA*, and *tet38* genes; the primers are listed in **Table 1**. The PCR products were sequenced by Beijing Genomics Institute Technology Co., Ltd. (Shanghai, China), and the sequences were aligned by BLAST on the NCBI platform<sup>1</sup>. The PCR products of *uhpT*, *glpT*, and *murA* were sequenced to scan for mutations.

### Fosfomycin Treatment and Total RNA Isolation

Actively growing *S. aureus* specimens were treated with increasing concentrations of fosfomycin (1/8 MIC, 1/4 MIC, and 1/2 MIC) for 2 h, after which the cells were harvested, and total RNA was extracted using a Bacterial RNA Miniprep Kit (Biomiga, Shanghai, China) according to the manufacturer's instructions. Then, 1000 ng RNA was used as the template for reverse transcription using a RevertAid First Strand cDNA Synthesis Kit (Thermo Scientific, Waltham, MA, United States) to obtain cDNA.

### Quantitative Real-Time PCR (qRT-PCR)

qPCR was performed on a CFX-96 Touch<sup>TM</sup> Real-Time PCR system (Bio-Rad, Hercules, CA, United States) using TB Green Premix Ex Taq II (Tli RNase H Plus) (2 $\times$ ) (Takara, Japan), specific primers (**Table 1**), and 100 ng cDNA as the template. Cycling conditions were as follows: 95°C for 30 s, followed by 40 cycles of 95°C for 5 s and 60°C for 20 s. A melting curve was performed after each run (raising the temperature by 0.5°C/s, from 65 to 95°C). Each sample was run in triplicate, and the means of the Ct values were used for analysis. The relative expression levels of *tet38* and *murA* genes were normalized to the *gmk* reference gene (Chen and Hooper, 2018). The quantification of the target genes was analyzed using the comparative threshold cycle  $2^{-\Delta\Delta Ct}$  method. All experiments

<sup>1</sup><http://blast.ncbi.nlm.nih.gov/Blast.cgi>

**TABLE 1** | Primers used in this study.

Gene	Primer sequences (5' → 3')	Product size (bp)	References
<b>PCR primers</b>			
<i>fosA</i>	F:GCTGCACGCCCGCTGGAATA R:CGACGCCCCCTCGCTTTTGT	217	Chen et al., 2014
<i>fosB</i>	F:CAGAGATATTTTAGGGGCTGACA R:CTCAATCTATCTTCTAAACTTCCTG	312	Chen et al., 2014
<i>fosC</i>	F:GGGTTACATGCCCTTGCTCA R:AACCCGCACAACGACAGATG	354	Chen et al., 2014
<i>fosD</i>	F: AACTCTAACTTGTGTCCGTGAC R: GTGGCTTATGGGTTGCGTTA	220	Liu et al., 2017
<i>fosX</i>	F: ATGATCAGTCATATGACATTTATCG R: ATTTAGCCCCTTGTGCGATAACG	243	Zhang et al., 2020
<i>murA</i>	F:GCCCTTGAAAGAATGGTTGCT R:GTTACAATACTCGACGCGAGGT	1600*	NC_002745.2**
<i>glpT</i>	F:TGAATAAAACAGCAGGGCAA R:CACAGCTAGTATGTATAACGAC	1699*	NC_002745.2**
<i>uhpT</i>	F:TGTGTTTATGTTTCTGATTTTGGGA R:TCTTTCATCTCTTACGAC	1571*	NC_002745.2**
<i>tet38</i>	F:GCGGATACAACGCGAGTGA R:TCGACGCACCTAATGGGAAT	1353	Truong-Bolduc et al., 2005
<b>qRT-PCR primers</b>			
<i>gmk</i>	F:ACTAGGGATGCGTTTGAAGC R:TCATGACCTTCGTCATTGT	122	Chen and Hooper, 2018
<i>tet38</i>	F:TGACAGGTGTGGCTATTGGT R:TTGCCTGGGAAATTAATGC	112	Chen and Hooper, 2018
<i>murA</i>	F:TGTGCACCTTGCAATTGACT R:CCGTTTTATGCATGTTGCAG	102	G et al., 2019

\*PCR product including surrounding sequences adjacent to the target gene. \*\*GenBank-EMBL-DDBL accession number.

were repeated in triplicate independently. The relative expression of the mRNA of the target gene was normalized to that of *S. aureus* ATCC 29213.

## Multilocus Sequence Typing (MLST)

Isolates were screened using a previously described method to detect the following seven housekeeping genes: carbamate kinase (*arcC*), shikimate dehydrogenase (*aroE*), glycerol kinase (*glp*), guanylate kinase (*gmk*), phosphate acetyltransferase (*pta*), triosephosphate isomerase (*tpi*), and acetyl coenzyme A acetyltransferase (*yqiL*) (Enright and Spratt, 1999). The sequences of the PCR products were compared with those available from the MLST website<sup>2</sup> for *S. aureus*. Also, the allelic number was determined for each sequence.

## Planktonic Growth Assay

The planktonic growth rates of 8 *tet38*-overexpressed *S. aureus* isolates were determined as described previously (Wijesinghe et al., 2019), with some modifications. Briefly, 8 *tet38*-overexpressed isolates and ATCC 29213 standard cell suspensions were prepared by adjusting the turbidity of suspension to 0.5 McFarland standard in sterile saline. Then, 200  $\mu$ L of each suspension was inoculated in 20 mL sterile LB

broth containing fosfomycin in 0, 1/8 MIC, 1/4 MIC, and 1/2 MIC, respectively, for growth at 37°C and 180 rpm for 24 h. The growth rate of the planktonic bacteria was determined by measuring the optical density (OD) of the suspension in each well of the 96-well plate at 600 nm at 2-h intervals for 24 h using a microtiter plate reader (BioTek, United States). The growth curve was generated in triplicate for each experiment. ATCC 29213 served as the control strain.

## Statistical Analysis

The relative expression of *murA* and *tet38* was compared using Student's *t*-test, and *P*-value < 0.05 was considered to be statistically significant.

## RESULTS

### Susceptibility to Fosfomycin and Other Types of Antibiotics

The susceptibility to fosfomycin of 200 *S. aureus* isolates was determined by the agar dilution method using glucose-6-phosphate (25 mg/L). The results showed that 5.5% (11/200) of the isolates were resistant to fosfomycin. Also, resistance to other antibiotics was determined (Table 2); 81.8% (9/11) of the

<sup>2</sup><http://www.mlst.net>

**TABLE 2** | Characteristics and resistance spectrum of fosfomycin-resistant *S. aureus* strains.

Isolates	ST type	FOM	OXA	ERY	CIP	LVX	GEN	RIF	LNZ	VAN	TEC
JP3187	5	256 <sup>R</sup>	> 128 <sup>R</sup>	32 <sup>R</sup>	> 256 <sup>R</sup>	32 <sup>R</sup>	4	<0.03	2	2	4
JP3189	4539	64 <sup>R</sup>	> 128 <sup>R</sup>	64 <sup>R</sup>	64 <sup>R</sup>	32 <sup>R</sup>	16 <sup>R</sup>	> 16 <sup>R</sup>	1	1	4
JP3212	5	256 <sup>R</sup>	> 128 <sup>R</sup>	64 <sup>R</sup>	128 <sup>R</sup>	32 <sup>R</sup>	4	<0.03	2	2	8
JP3235	5708	64 <sup>R</sup>	> 128 <sup>R</sup>	1	128 <sup>R</sup>	32 <sup>R</sup>	64 <sup>R</sup>	> 16 <sup>R</sup>	2	1	4
JP3244	7	128 <sup>R</sup>	0.5	64 <sup>R</sup>	0.25	0.25	<0.125	<0.03	2	1	0.5
JP3505	4739	512 <sup>R</sup>	0.5	1	2	1	<0.125	<0.03	4	2	0.5
JP3535	5	64 <sup>R</sup>	> 128 <sup>R</sup>	16 <sup>R</sup>	128 <sup>R</sup>	16 <sup>R</sup>	0.25	<0.03	4	1	2
JP3539	59	64 <sup>R</sup>	8 <sup>R</sup>	64 <sup>R</sup>	0.5	0.25	0.25	<0.03	4	2	1
JP3589	1	64 <sup>R</sup>	0.25	64 <sup>R</sup>	2	1	2	<0.03	2	2	1
JP3592	239	256 <sup>R</sup>	> 128 <sup>R</sup>	64 <sup>R</sup>	128 <sup>R</sup>	64 <sup>R</sup>	<0.125	> 8 <sup>R</sup>	4	1	1
JP3600	965	64 <sup>R</sup>	0.5	64 <sup>R</sup>	4 <sup>R</sup>	1	0.5	<0.03	2	2	2

FOM, fosfomycin; OXA, oxacillin; ERY, erythromycin; CIP, ciprofloxacin; LVX, levofloxacin; GEN, gentamicin; RIF, rifampicin; LNZ, linezolid; VAN, vancomycin; TEC, teicoplanin. Superscript “R” indicates resistance.

**TABLE 3** | Characteristics and amino acid substitutions in fosfomycin-resistant and fosfomycin-sensitive *S. aureus*.

Strains	Type	tet38	fos					Amino acid substitution		
			fosA	fosB	fosC	fosD	fosX	uhpT	glpT	murA
JP3187	R	+	-	-	-	-	-	None	TypeA <sub>glpT</sub>	TypeI <sub>murA</sub>
JP3189	R	+	-	-	-	-	-	None	None	TypeC <sub>murA</sub>
JP3212	R	+	-	-	-	-	-	TypeA <sub>uhpT</sub>	None	TypeI <sub>murA</sub>
JP3235	R	+	-	-	-	-	-	None	None	TypeI <sub>murA</sub> TypeC <sub>murA</sub>
JP3244	R	+	-	-	-	-	-	None	None	TypeI <sub>murA</sub> TypeC <sub>murA</sub>
JP3505	R	+	-	-	-	-	-	None	TypeI <sub>glpT</sub>	TypeA <sub>murA</sub> TypeI <sub>murA</sub>
JP3535	R	+	-	-	-	-	-	None	TypeI <sub>glpT</sub> TypeB <sub>glpT</sub>	TypeI <sub>murA</sub>
JP3539	R	+	-	-	-	-	-	None	TypeA <sub>glpT</sub> TypeI <sub>glpT</sub>	TypeI <sub>murA</sub> TypeII <sub>murA</sub>
JP3589	R	+	-	-	-	-	-	None	None	TypeI <sub>murA</sub> TypeB <sub>murA</sub>
JP3592	R	+	-	-	-	-	-	None	None	TypeI <sub>murA</sub> TypeC <sub>murA</sub>
JP3600	R	+	-	-	-	-	-	TypeII <sub>uhpT</sub>	TypeI <sub>glpT</sub>	TypeI <sub>murA</sub>
JP3200	S	+	-	-	-	-	-	None	None	None
JP3203	S	+	-	-	-	-	-	TypeI <sub>uhpT</sub>	None	None
JP3277	S		-	-	-	-	-	None	None	None
JP3230	S	+	-	-	-	-	-	None	None	None
JP3240	S	+	-	-	-	-	-	TypeII <sub>uhpT</sub>	TypeI <sub>glpT</sub> TypeII <sub>glpT</sub>	None
JP3245	S	+	-	-	-	-	-	None	None	None
JP3502	S	+	-	-	-	-	-	None	None	TypeI <sub>murA</sub> TypeII <sub>murA</sub>
JP3512	S	+	-	-	-	-	-	None	None	None
JP3518	S	+	-	-	-	-	-	None	None	TypeI <sub>murA</sub>
JP3520	S	+	-	-	-	-	-	None	TypeI <sub>glpT</sub>	TypeI <sub>murA</sub>
JP3522	S	+	-	-	-	-	-	None	None	TypeI <sub>murA</sub>

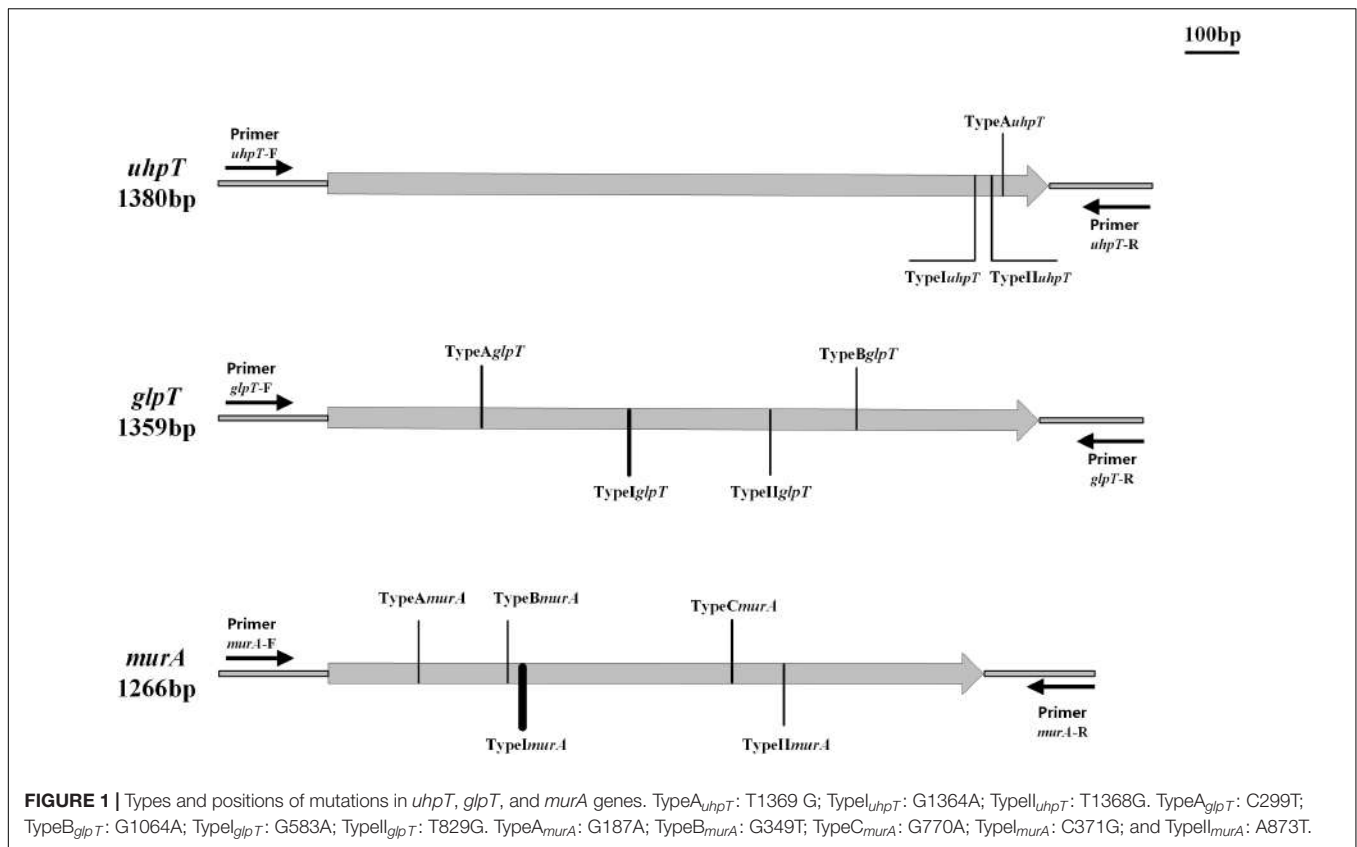
+, carries the corresponding gene; -, does not carry the corresponding gene; None: nonsense mutation; TypeA<sub>uhpT</sub>: T1369 G; TypeI<sub>uhpT</sub>: G1364A; TypeII<sub>uhpT</sub>: T1368G; TypeA<sub>glpT</sub>: C299T; TypeB<sub>glpT</sub>: G1064A; TypeI<sub>glpT</sub>: G583A; TypeII<sub>glpT</sub>: T829G; TypeA<sub>murA</sub>: G187A; TypeB<sub>murA</sub>: G349T; TypeC<sub>murA</sub>: G770A; TypeI<sub>murA</sub>: C371G; TypeII<sub>murA</sub>: A873T.

isolates displayed resistance to erythromycin, while 72.7% (8/11) belonged to MDR *S. aureus*.

### Molecular Mechanisms of Fosfomycin-Resistant Isolates

Strains carrying the *fosA*, *fosB*, *fosC*, *fosD*, or *fosX* gene were not found in the current study (Table 3). Based on the classification method of Fu et al. (2015) we named the sense mutations as TypeA, TypeB, and TypeC according to

the amino acid sequence, and the nonsense mutations were named as TypeI, TypeII, and TypeIII; the subscripts represent different genes (Fu et al., 2015). Three distinct mutations were detected in the *uhpT* gene of the 11 fosfomycin-resistant *S. aureus* isolates and the corresponding sensitive strains. Mutation TypeA<sub>uhpT</sub>, found in JP3212, resulted in an amino acid substitution at position 457 (Leu457Val) of UhpT. Conversely, the other two mutations (TypeI-II<sub>uhpT</sub>), which resulted in distinct amino acid substitutions within the UhpT protein, were identified in fosfomycin-sensitive isolates, although one mutation



(TypeII<sub>uhpT</sub>) was also found in fosfomycin-resistant *S. aureus* (Figure 1 and Table 3).

Moreover, four different mutations were detected in the *glpT* gene (TypeA–B<sub>glpT</sub> and TypeI–II<sub>glpT</sub>). Notably, TypeB<sub>glpT</sub>, found in the fosfomycin-resistant isolates JP3535, produced a premature stop codon within the *glpT* coding sequence at position 355 (Trp335Ter), thereby resulting in truncated proteins. In addition, TypeII<sub>glpT</sub> was detected only in the fosfomycin-sensitive isolates (Figure 1 and Table 3).

Of the 11 fosfomycin-resistant isolates, 6 contained one of the three different mutations (TypeA–C<sub>murA</sub>) in the *murA* gene. TypeA–C<sub>murA</sub>, which resulted in distinct amino acid substitutions within the MurA protein at positions 63 (Ala63Thr), 117 (Gly117Trp), and 257 (Gly257Asp), could only be found in fosfomycin-resistant isolates, and two mutations (TypeI–II<sub>murA</sub>) could be found in both fosfomycin-resistant and fosfomycin-susceptible *S. aureus* (Figure 1 and Table 3). Moreover, only one sense mutation was present in each fosfomycin-resistant *S. aureus* isolate.

### Expression Analysis of *murA* and *tet38*

qRT-PCR revealed significant differences in the expression of *murA* between resistant and susceptible groups of *S. aureus* as compared with *S. aureus* ATCC 29213 ( $P < 0.05$ ) (Table 4). The data showed that the average expression level of *murA* gene decreased by 0.7-fold in fosfomycin-resistant and fosfomycin-susceptible *S. aureus* isolates. In addition, compared with the

fosfomycin-susceptible *S. aureus*, the expression of *murA* in the resistance isolates was not significantly higher.

However, the results (Table 4) indicated that compared with that in ATCC29213 and susceptible isolates, the expression level of efflux pump gene *tet38* in JP3212, JP3535, JP359, and JP3600 was elevated. Notably, the level of the *tet38* gene in JP3212, JP3535, JP3592, and JP3600 was altered markedly (21.60-, 2.74-, 143.36-, and 24.59-fold) as compared with that in ATCC29213 (Table 4).

### Exposure to Fosfomycin Resulted in Increased Expression of *tet38* Efflux Pump Genes Among Some Resistant Isolates

The expression of *tet38* in the presence of increasing amounts of fosfomycin with 0, 1/8 MIC, 1/4 MIC, and 1/2 MIC concentrations was determined by qRT-PCR. Notably, the expression of the *tet38* gene in JP3187, JP3212, JP3244, JP3505 JP3535, JP3539, P3589, JP3592, and ATCC 29213 was upregulated with the increase in fosfomycin concentration as compared with the 0 MIC strains (Figure 2 and Table 4). Also, 4.63-fold and 6.42-fold increases were noted in the expression of *tet38* in JP3505 cells treated with 1/8 MIC (64 mg/L) and 1/4 MIC (128 mg/L) fosfomycin, respectively, as compared with that in cells that were not treated with fosfomycin (Table 5). A further 8.46-fold increase was observed in those treated with 1/2 MIC (256 mg/L) fosfomycin.



**TABLE 4** | Relative expression of target enzyme gene *murA* and efflux pump gene *tet38* in fosfomycin-susceptible and fosfomycin-resistant *S. aureus*.

Strains	Relative expression level of <i>murA</i> <sup>a</sup> (mean ± SD)	Relative expression level of <i>tet38</i> <sup>a</sup> (mean ± SD)
S1	0.77 ± 0.15	0.77 ± 0.13
S2	1.45 ± 0.10	1.48 ± 1.02
S3	0.40 ± 0.05	0.71 ± 0.21
S4	0.48 ± 0.01	1.55 ± 0.33
S5	0.48 ± 0.06	0.98 ± 0.35
JP3187	0.75 ± 0.09	1.71 ± 0.93
JP3189	0.35 ± 0.01	0.71 ± 0.25
JP3212	0.47 ± 0.01	<b>21.6 ± 5.75</b>
JP3235	1.47 ± 0.14	0.92 ± 0.34
JP3244	0.21 ± 0.04	1.24 ± 0.15
JP3505	0.23 ± 0.04	<b>2.65 ± 1.04</b>
JP3535	0.34 ± 0.03	<b>2.74 ± 0.37</b>
JP3539	0.39 ± 0.05	1.71 ± 0.48
JP3589	0.42 ± 0.08	0.54 ± 0.23
JP3592	0.40 ± 0.07	<b>143.36 ± 2.05</b>
JP3600	1.52 ± 0.23	<b>24.59 ± 0.17</b>

S1–S5 represent the 5 fosfomycin-susceptible *S. aureus* strains. ATCC 29213 served as the control strain. <sup>a</sup>The relative gene expression with more than 2-fold change compared with ATCC 29213 after fosfomycin induction is shown in bold.

### Molecular Typing

The 11 fosfomycin-resistant *S. aureus* specimens were categorized into 9 STs (Table 2): ST1 (*n* = 1), ST5 (*n* = 3), ST59 (*n* = 1), ST7 (*n* = 1), ST239 (*n* = 1), ST965 (*n* = 1), ST4539 (*n* = 1), ST4739 (*n* = 1), and a new ST that was found in the current study (ST 5708) (*n* = 1).

### Growth Rate

In order to gain quantitative insight into the fitness cost imposed by *tet38*-overexpressed isolates, the growth curves of

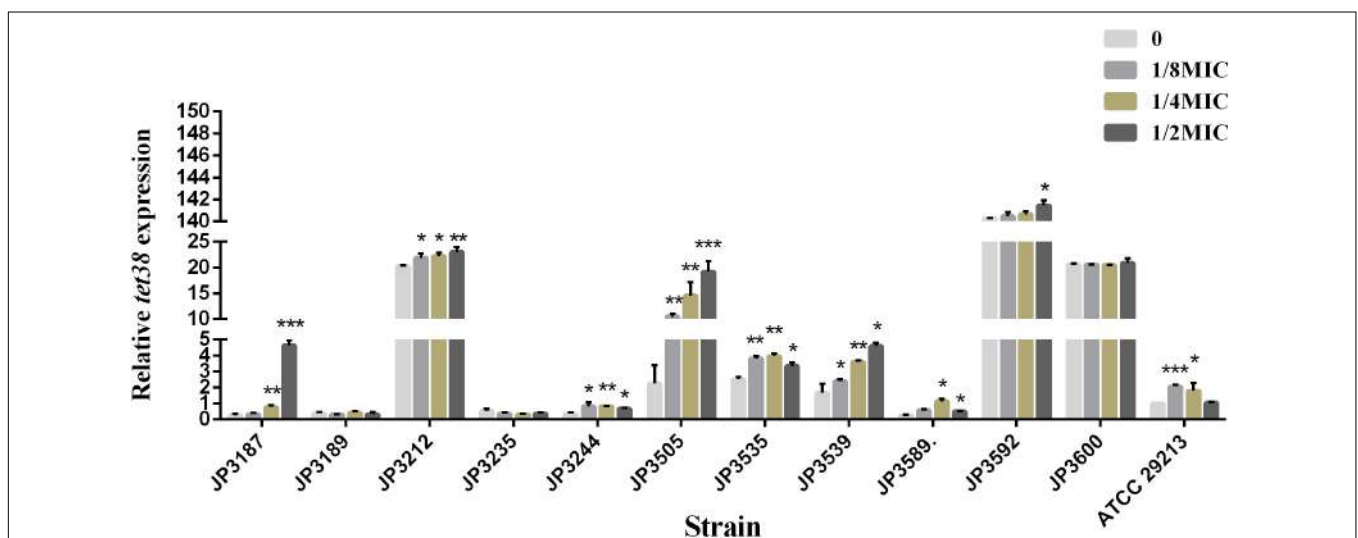
8 *tet38*-overexpressed *S. aureus* were recorded. We identified a fitness cost after fosfomycin induction. The growth of 8 *tet38*-overexpression strains was inhibited in LB at a subinhibitory concentration of fosfomycin (Figure 3).

## DISCUSSION

Due to the unique mechanisms of action, fosfomycin exhibits significant antimicrobial activity against a broad spectrum of pathogens, including *S. aureus* (Goto, 1977). A review described that the susceptibility of *S. aureus* to fosfomycin ranged from 33.2% to 100% in the nine available studies [odds ratio (OR) = 91.7%, 95% confidence interval (CI): 88.7–94.9%] (Vardakas et al., 2016). In the current study, the susceptibility rate of fosfomycin in *S. aureus* was 94.5% (189/200). However, the prevalence of fosfomycin resistance in clinical isolates of *S. aureus* has been reported with increasing frequency in many areas (Del Rio et al., 2014; Mihailescu et al., 2014; Shi et al., 2014).

The resistance mechanism of fosfomycin in Gram-negative bacteria has been widely reported; also, in a previous study, we reported the resistance of fosfomycin in ESBL-producing *Escherichia coli* (Bi et al., 2017). Fosfomycin enters the cell via two transporters, GlpT and UhpT, and mutations or insertions in *glpT* and/or *uhpT* genes result in the loss of function (Takahata et al., 2010). According to the study by Castaneda-Garcia et al. (2009), *glpT* inactivation played an essential role in the resistance to fosfomycin in *Pseudomonas aeruginosa* (Castaneda-Garcia et al., 2009). The *murA* gene is also closely related to fosfomycin resistance (Takahata et al., 2010; Couce et al., 2012). In addition, fosfomycin activity can be inhibited via the catalytic activity of FosA, FosB, and FosC, respectively (Garcia et al., 1995; Lee et al., 2012).

Among Gram-positive bacteria, the resistance mechanism of fosfomycin is rarely reported. In the current study, none of

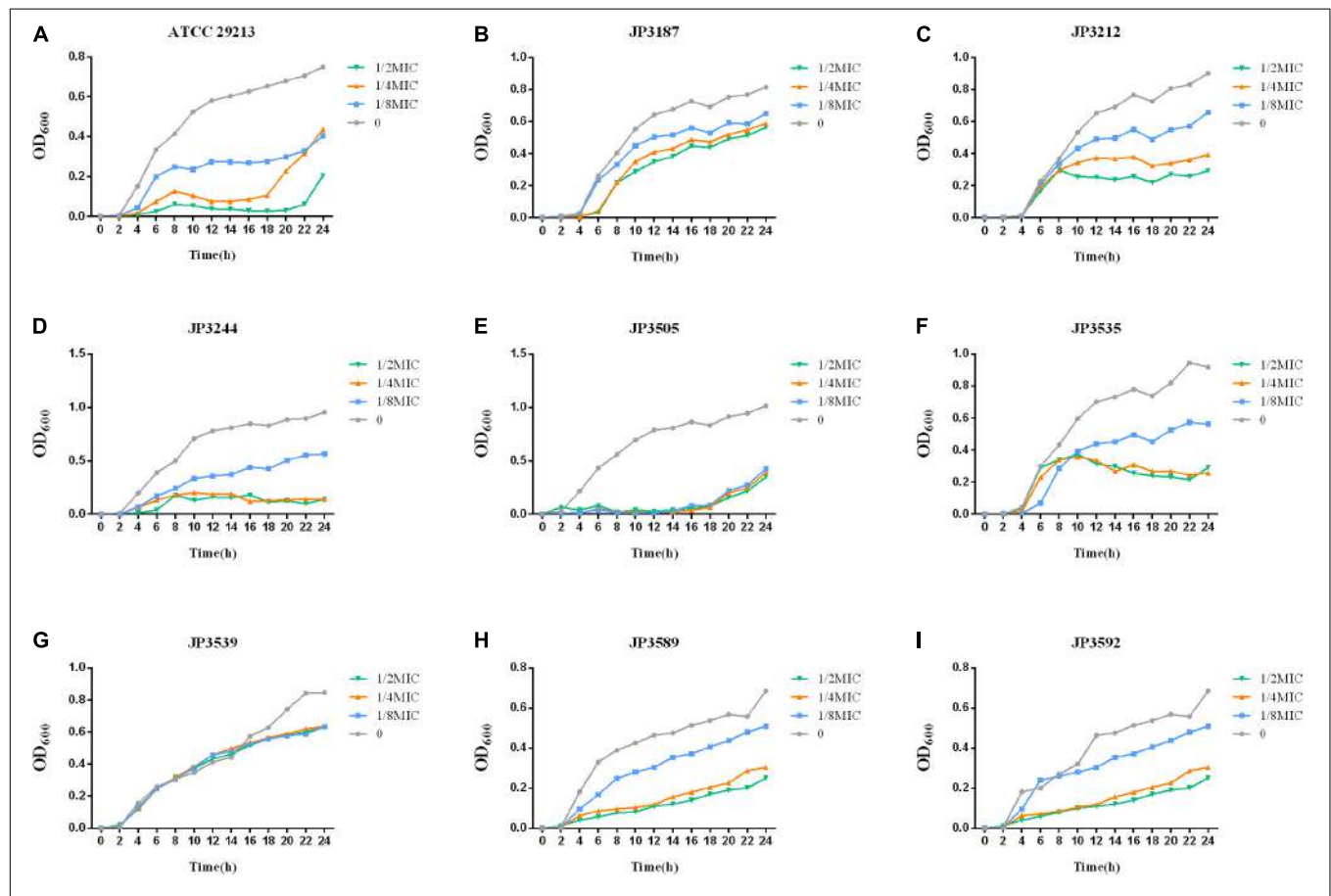


**FIGURE 2** | The relative expression of efflux pump gene *tet38* in fosfomycin-resistant *S. aureus* exposed to 0, 1/8 MIC, 1/4 MIC, and 1/2 MIC concentrations. Bars indicate the mean values, and asterisks denote the significant difference of expression (*P* < 0.05).

**TABLE 5** | Relative expression of efflux pump gene *tet38* in fosfomicin-resistant *S. aureus* exposed to different concentrations of fosfomicin.

Strains	The relative expression level of <i>tet38</i> <sup>a</sup> (mean ± SD)			
	0 MIC	1/8 MIC	1/4 MIC	1/2 MIC
JP3187	0.25 ± 0.09	0.32 ± 0.08	<b>0.77 ± 0.10</b>	<b>4.64 ± 0.25</b>
JP3189	0.38 ± 0.08	0.32 ± 0.01	0.43 ± 0.07	0.32 ± 0.13
JP3212	20.32 ± 0.10	21.89 ± 0.69	22.22 ± 0.56	23.02 ± 0.8
JP3235	0.53 ± 0.12	0.36 ± 0.08	0.33 ± 0.03	0.37 ± 0.06
JP3244	0.35 ± 0.06	<b>0.81 ± 0.20</b>	<b>0.83 ± 0.01</b>	0.68 ± 0.03
JP3505	2.27 ± 0.91	<b>10.51 ± 0.38</b>	<b>14.57 ± 2.12</b>	<b>19.21 ± 1.65</b>
JP3535	2.50 ± 0.12	3.82 ± 0.12	3.95 ± 0.14	3.34 ± 0.17
JP3539	1.67 ± 0.45	2.40 ± 0.08	<b>3.60 ± 0.08</b>	<b>4.60 ± 0.14</b>
JP3589	0.27 ± 0.02	<b>0.57 ± 0.06</b>	<b>1.13 ± 0.14</b>	0.51 ± 0.01
JP3592	140.27 ± 0.05	140.48 ± 0.30	140.65 ± 0.23	141.47 ± 0.36
JP3600	20.58 ± 0.20	20.62 ± 0.04	20.47 ± 0.08	20.93 ± 0.72

<sup>a</sup>The relative gene expression with more than 2-fold change compared with 0 MIC after fosfomicin induction is shown in bold.



**FIGURE 3** | Growth curves at different fosfomicin concentrations in *tet38*-overexpression *S. aureus*. The values shown are the average of three independent experiments. Different colors of lines represent different concentrations of fosfomicin. (A) Growth of control strain ATCC 29213. (B–I) Growth of 8 *tet38*-overexpression isolates.

the resistant strains carried the *fosA*, *fosB*, *fosC*, *fosD*, or *fosX* gene, indicating that these genes might not be the primary factors mediating the resistance of *S. aureus* against fosfomicin. Other studies have shown that the prevalence of fosfomicin

resistance genes (*fosA*, *fosB*, and *fosC*) was not the predominant factor contributing to resistance in *S. aureus* (Xu et al., 2017). In addition, a total of 12 mutations were found in 11 strains of fosfomicin-resistant *S. aureus* by sequencing analysis. Of

these, 3 were detected in *uhpT*, and TypeA<sub>*uhpT*</sub> was carried only by fosfomycin-resistant strain JP3212, while TypeI<sub>*uhpT*</sub> and TypeII<sub>*uhpT*</sub> were found in both fosfomycin-resistant and fosfomycin-sensitive strains, which likely did not contribute to fosfomycin resistance. Within the *glpT* gene of 11 drug-resistant strains, 2 mutations TypeA–B<sub>*glpT*</sub> were observed only in the drug-resistant strains. On the other hand, mutation TypeI<sub>*glpT*</sub> was widely detected in both drug-resistant and susceptible strains. Intriguingly, TypeB<sub>*glpT*</sub>, which generated a stop codon (TA<sub>1064</sub>G) at position 335 (Figure 1), was harbored in JP3535. Also, we found a mutation (TypeII<sub>*glpT*</sub>) merely in the fosfomycin-sensitive strains. Of the five *murA* gene mutations found in the drug-resistant strains, TypeI<sub>*murA*</sub> and TypeII<sub>*murA*</sub> could also be found in susceptible strains, and the remaining three mutations (TypeA–C<sub>*murA*</sub>) were found only in drug-resistant strains (TypeA<sub>*murA*</sub>: JP3505; TypeB<sub>*murA*</sub>: JP3589; TypeC<sub>*murA*</sub>: JP3189, JP3235, JP3244; JP3592). In addition, TypeI<sub>*murA*</sub> was also found in fosfomycin-resistant strains (10/11). Among the above mutations, four mutation sites, TypeA<sub>*glpT*</sub>, TypeB<sub>*glpT*</sub>, TypeC<sub>*murA*</sub>, and TypeII<sub>*murA*</sub>, were consistent with those reported (Fu et al., 2015). We also found that the frequency of *murA* mutation in *S. aureus* was high, which might play a major role in mediating fosfomycin resistance, which needs an in-depth investigation.

Although several studies have mentioned that the overexpression of the *murA* gene can greatly increase the MICs of fosfomycin, the difference in *murA* expression between fosfomycin-sensitive and fosfomycin-resistant *S. aureus* has not been reported (Garcia et al., 1995; Olesen et al., 2014). In the current study, the results of qRT-PCR revealed a significant difference between the fosfomycin-resistant and fosfomycin-susceptible *S. aureus* with respect to the expression of *murA* as compared with that of *S. aureus* ATCC 29213. However, statistical differences could not be detected between two types of strains (Table 4), indicating that the overexpression of target gene *murA* has no role in conferring fosfomycin resistance in the strains identified in this study. Interestingly, some resistant strains showed a downward trend in the expression of *murA*, suggesting that the role of the *murA* gene in fosfomycin needs to be studied further.

Recent studies have shown that the *tet38* gene exerts a specific effect on fosfomycin resistance. According to the study by Truong-Bolduc, the overexpression of *tet38* resulted in a fourfold increase in the MIC of fosfomycin compared with that of the parent strain (Truong-Bolduc et al., 2018). The results of the current study showed that the expression of the *tet38* efflux pump gene in fosfomycin-resistant strains JP3212, JP3535, JP3592, and JP3600 was significantly higher than that in the control strain ATCC29213 and the susceptible strains ( $P = 0.007$ ,  $P = 0.002$ ,  $P < 0.001$ ,  $P < 0.001$ , respectively). Furthermore, under the treatment of 0, 1/8 MIC, 1/4 MIC, and 1/2 MIC with fosfomycin, we found that the expression of efflux pump gene *tet38* was upregulated in most resistant isolates, even in the reference strain ATCC 29213. Although nonsense mutation was detected in *uhpT*, *glpT*, and *murA* genes, the level of *tet38* in JP3600 was high even without the drug, which might explain the resistance to fosfomycin. This phenomenon suggests that the

*tet38* efflux pump plays a critical role in mediating fosfomycin resistance. Reportedly, abscess and other factors can promote the expression of *tet38* (Chen and Hooper, 2018), and the current study has shown that the stimulation of the drug also enhances the expression of the efflux pump, albeit the specific mechanism remains to be studied further. Moreover, the overexpression of *tet38* can also lead to changes in the cost of bacterial fitness. Some studies have demonstrated that the global regulator MgrA functions as a direct regulator of *tetR21*, which is a TetR-like regulator of the *tet38* efflux pump gene. TetR21 acts as a repressor of *tet38* expression and may also regulate the expression of other bacterial resistance determinants (Truong-Bolduc et al., 2005, 2015). We speculated that the high expression of the *tet38* gene in *S. aureus* might be related to the regulation of TetR-like regulator TetR21 and the global regulator MgrA. We will also continue to focus on these phenomena in other bacteria in future studies.

MLST analyses designated three fosfomycin-resistant *S. aureus* isolated to ST5. Combined with drug sensitivity, we found that the ST5 resistant strains were resistant to at least five antibiotics. Among 11 fosfomycin-resistant strains, 72.7% were MDR strains, and further follow-up treatment was essential. Wu et al. (2018) reported that ST5 and ST239 strains were usually resistant to fosfomycin and constituted the predominant HA-MRSA clones in China. The new sequence type found in the resistant strain has been submitted to the repository (see text footnote 2).

## CONCLUSION

A total of 11 fosfomycin-resistant strains were screened out from 200 *S. aureus* isolates, and the mechanism was explored. Our findings indicated that *fosA*, *fosB*, *fosC*, *fosD*, and *fosX* genes might not be the major resistant mechanism of *S. aureus* to fosfomycin. The mutations within the *glpT*, *uhpT*, and *murA* genes might play a critical role in conferring fosfomycin resistance. However, the role of overexpression of *murA* in fosfomycin resistance needs to be discussed further in *S. aureus*. Also, the phenomenon of overexpression in the *tet38* gene under a subinhibitory concentration of fosfomycin needs to be investigated further.

## DATA AVAILABILITY STATEMENT

The datasets generated for this study are available on request to the corresponding author.

## AUTHOR CONTRIBUTIONS

WX conducted the experiments, analyzed the data, and wrote the manuscript. TC participated in experiments and writing. HW and WZ provided fosfomycin-resistant strains and participated

in the analysis of results. KY and QW participated in the analysis of the results. TZ helped to design the study. YX and XZ designed the study and corrected the manuscript. All authors read and approved the manuscript.

## REFERENCES

- Bi, W., Li, B., Song, J., Hong, Y., Zhang, X., Liu, H., et al. (2017). Antimicrobial susceptibility and mechanisms of fosfomycin resistance in extended-spectrum beta-lactamase-producing *Escherichia coli* strains from urinary tract infections in Wenzhou, China. *Int. J. Antimicrob. Agents* 50, 29–34. doi: 10.1016/j.ijantimicag.2017.02.010
- Castaneda-Garcia, A., Rodriguez-Rojas, A., Guelfo, J. R., and Blazquez, J. (2009). The glycerol-3-phosphate permease GlpT is the only fosfomycin transporter in *Pseudomonas aeruginosa*. *J. Bacteriol.* 191, 6968–6974. doi: 10.1128/jb.00748-09
- Chen, C., and Hooper, D. C. (2018). Effect of *Staphylococcus aureus* Tet38 native efflux pump on in vivo response to tetracycline in a murine subcutaneous abscess model. *J. Antimicrob. Chemother.* 73, 720–723. doi: 10.1093/jac/dkx432
- Chen, C., Xu, X., Qu, T., Yu, Y., Ying, C., Liu, Q., et al. (2014). Prevalence of the fosfomycin-resistance determinant, fosB3, in *Enterococcus faecium* clinical isolates from China. *J. Med. Microbiol.* 63, 1484–1489. doi: 10.1099/jmm.0.077701-0
- Clinical and Laboratory Standards Institute [CLSI] (2018). *Performance Standards For Antimicro-Bial Susceptibility Testing: Twenty Eighth Informational Supplement M100-S28*. Wayne, PA: CLSI.
- Couce, A., Briaies, A., Rodriguez-Rojas, A., Costas, C., Pascual, A., and Blazquez, J. (2012). Genomewide overexpression screen for fosfomycin resistance in *Escherichia coli*: MurA confers clinical resistance at low fitness cost. *Antimicrob. Agents Chemother.* 56, 2767–2769. doi: 10.1128/aac.06122-11
- Del Rio, A., Gasch, O., Moreno, A., Pena, C., Cuquet, J., Soy, D., et al. (2014). Efficacy and safety of fosfomycin plus imipenem as rescue therapy for complicated bacteremia and endocarditis due to methicillin-resistant *Staphylococcus aureus*: a multicenter clinical trial. *Clin. Infect. Dis.* 59, 1105–1112. doi: 10.1093/cid/ciu580
- Enright, M. C., and Spratt, B. G. (1999). Multilocus sequence typing. *Trends Microbiol.* 7, 482–487.
- Etienne, J., Gerbaud, G., Fleurette, J., and Courvalin, P. (1991). Characterization of staphylococcal plasmids hybridizing with the fosfomycin resistance gene fosB. *FEMS Microbiol. Lett.* 68, 119–122. doi: 10.1111/j.1574-6968.1991.tb04580.x
- Fu, Z., Ma, Y., Chen, C., Guo, Y., Hu, F., Liu, Y., et al. (2015). Prevalence of Fosfomycin Resistance and Mutations in murA, glpT, and uhpT in Methicillin-Resistant *Staphylococcus aureus* strains isolated from blood and cerebrospinal fluid samples. *Front. Microbiol.* 6:1544. doi: 10.3389/fmicb.2015.01544
- G, C. B., Sahukhal, G. S., and Elaris, M. O. (2019). Role of the msAABC Operon in Cell Wall Biosynthesis, Autolysis, Integrity, and Antibiotic Resistance in *Staphylococcus aureus*. *Antimicrob. Agents Chemother.* 63:e00680-19.
- Garcia, P., Arca, P., and Evaristo Suarez, J. (1995). Product of fosC, a gene from *Pseudomonas syringae*, mediates fosfomycin resistance by using ATP as cosubstrate. *Antimicrob. Agents Chemother.* 39, 1569–1573. doi: 10.1128/aac.39.7.1569
- Gatadi, S., Madhavi, Y. V., Chopra, S., and Nanduri, S. (2019). Promising antibacterial agents against multidrug resistant *Staphylococcus aureus*. *Bioorg. Chem.* 92:103252. doi: 10.1016/j.bioorg.2019.103252
- Goto, S. (1977). Fosfomycin, antimicrobial activity in vitro and in vivo. *Chemotherapy* 23(Suppl. 1), 63–74. doi: 10.1159/000222028
- Lee, S. Y., Park, Y. J., Yu, J. K., Jung, S., Kim, Y., Jeong, S. H., et al. (2012). Prevalence of acquired fosfomycin resistance among extended-spectrum beta-lactamase-producing *Escherichia coli* and *Klebsiella pneumoniae* clinical isolates in Korea and IS26-composite transposon surrounding fosA3. *J. Antimicrob. Chemother.* 67, 2843–2847. doi: 10.1093/jac/dks319
- Liu, B. H., Lei, C. W., Zhang, A. Y., Pan, Y., Kong, L. H., Xiang, R., et al. (2017). Colocation of the Multiresistance Gene cfr and the Fosfomycin Resistance Gene fosD on a Novel Plasmid in *Staphylococcus arlettae* from a Chicken Farm. *Antimicrob. Agents Chemother.* 61:e01388-17.
- Mehraj, J., Witte, W., Akmatov, M. K., Layer, F., Werner, G., and Krause, G. (2016). Epidemiology of *Staphylococcus aureus* nasal carriage patterns in the community. *Curr. Top. Microbiol. Immunol.* 398, 55–87.
- Michalopoulos, A. S., Livaditis, I. G., and Gougoutas, V. (2011). The revival of fosfomycin. *Int. J. Infect. Dis.* 15, e732–e739. doi: 10.1016/j.ijid.2011.07.007
- Mihailescu, R., Furustrand Tafin, U., Corvec, S., Oliva, A., Betrisey, B., Borens, O., et al. (2014). High activity of Fosfomycin and Rifampin against methicillin-resistant *Staphylococcus aureus* biofilm in vitro and in an experimental foreign-body infection model. *Antimicrob. Agents Chemother.* 58, 2547–2553. doi: 10.1128/aac.02420-12
- Nakaminami, H., Noguchi, N., Nishijima, S., Kurokawa, I., and Sasatsu, M. (2008). Characterization of the pTZ2162 encoding multidrug efflux gene qacB from *Staphylococcus aureus*. *Plasmid* 60, 108–117. doi: 10.1016/j.plasmid.2008.04.003
- Olesen, S. H., Ingles, D. J., Yang, Y., and Schonbrunn, E. (2014). Differential antibacterial properties of the MurA inhibitors terreic acid and fosfomycin. *J. Basic Microbiol.* 54, 322–326. doi: 10.1002/jobm.201200617
- Shi, J., Mao, N. F., Wang, L., Zhang, H. B., Chen, Q., Liu, H., et al. (2014). Efficacy of combined vancomycin and fosfomycin against methicillin-resistant *Staphylococcus aureus* in biofilms in vivo. *PLoS One* 9:e113133. doi: 10.1371/journal.pone.0113133
- Shorr, A. F., Pogue, J. M., and Mohr, J. F. (2017). Intravenous fosfomycin for the treatment of hospitalized patients with serious infections. *Expert Rev. Anti Infect. Ther.* 15, 935–945. doi: 10.1080/14787210.2017.1379897
- Silver, L. L. (2017). Fosfomycin: mechanism and resistance. *Cold Spring Harb. Perspect. Med.* 7:a025262. doi: 10.1101/cshperspect.a025262
- Takahata, S., Ida, T., Hiraishi, T., Sakakibara, S., Maebashi, K., Terada, S., et al. (2010). Molecular mechanisms of fosfomycin resistance in clinical isolates of *Escherichia coli*. *Int. J. Antimicrob. Agents* 35, 333–337. doi: 10.1016/j.ijantimicag.2009.11.011
- Truong-Bolduc, Q. C., Bolduc, G. R., Medeiros, H., Vyas, J. M., Wang, Y., and Hooper, D. C. (2015). Role of the Tet38 Efflux Pump in *Staphylococcus aureus* internalization and survival in epithelial cells. *Infect. Immun.* 83, 4362–4372. doi: 10.1128/iai.00723-15
- Truong-Bolduc, Q. C., Dunman, P. M., Strahilevitz, J., Projan, S. J., and Hooper, D. C. (2005). MgrA is a multiple regulator of two new efflux pumps in *Staphylococcus aureus*. *J. Bacteriol.* 187, 2395–2405. doi: 10.1128/jb.187.7.2395-2405.2005
- Truong-Bolduc, Q. C., Wang, Y., and Hooper, D. C. (2018). Tet38 efflux pump contributes to fosfomycin resistance in *Staphylococcus aureus*. *Antimicrob. Agents Chemother.* 62:e00927-18.
- Ushanov, L., Lasareishvili, B., Janashia, I., and Zautner, A. E. (2020). Application of *Campylobacter jejuni* phages: challenges and perspectives. *Animals* 10:279. doi: 10.3390/ani10020279
- Vardakas, K. Z., Legakis, N. J., Triarides, N., and Falagas, M. E. (2016). Susceptibility of contemporary isolates to fosfomycin: a systematic review of the literature. *Int. J. Antimicrob. Agents* 47, 269–285. doi: 10.1016/j.ijantimicag.2016.02.001
- Wang, Y., Lin, J., Zhang, T., He, S., Li, Y., Zhang, W., et al. (2020). Environmental contamination prevalence, antimicrobial resistance and molecular characteristics of methicillin-resistant *Staphylococcus aureus* and *Staphylococcus epidermidis* isolated from secondary schools in Guangzhou, China. *Int. J. Environ. Res. Public Health* 17:623. doi: 10.3390/ijerph17020623
- Wijesinghe, G., Dilhari, A., Gayani, B., Kottegoda, N., Samaranyake, L., and Weerasekera, M. (2019). Influence of laboratory culture media on in vitro growth, adhesion, and biofilm formation of *Pseudomonas aeruginosa* and *Staphylococcus aureus*. *Med. Princ. Pract.* 28, 28–35. doi: 10.1159/000494757

## FUNDING

This study was supported by a research grant from the National Natural Science Foundation of China (no. 81171614).



- Wu, D., Chen, Y., Sun, L., Qu, T., Wang, H., and Yu, Y. (2018). Prevalence of Fosfomycin Resistance in Methicillin-Resistant *Staphylococcus aureus* isolated from patients in a University Hospital in China from 2013 to 2015. *Jpn. J. Infect. Dis.* 71, 312–314. doi: 10.7883/yoken.jiid.2018.013
- Xu, S., Fu, Z., Zhou, Y., Liu, Y., Xu, X., and Wang, M. (2017). Mutations of the Transporter Proteins GlpT and UhpT confer fosfomycin resistance in *Staphylococcus aureus*. *Front. Microbiol.* 8:914. doi: 10.3389/fmicb.2017.00914
- Zhang, X., Bi, W., Chen, L., Zhang, Y., Fang, R., Cao, J., et al. (2020). Molecular mechanisms and epidemiology of fosfomycin resistance in enterococci isolated from patients at a teaching hospital in China, 2013-2016. *J. Glob. Antimicrob. Resist.* 20, 191–196. doi: 10.1016/j.jgar.2019.08.006

**Conflict of Interest:** The authors declare that the research was conducted in the absence of any commercial or financial relationships that could be construed as a potential conflict of interest.

Copyright © 2020 Xu, Chen, Wang, Zeng, Wu, Yu, Xu, Zhang and Zhou. This is an open-access article distributed under the terms of the Creative Commons Attribution License (CC BY). The use, distribution or reproduction in other forums is permitted, provided the original author(s) and the copyright owner(s) are credited and that the original publication in this journal is cited, in accordance with accepted academic practice. No use, distribution or reproduction is permitted which does not comply with these terms.



# Alternative Therapeutic Options to Antibiotics for the Treatment of Urinary Tract Infections

Paul Loubet<sup>1</sup>, Jérémy Ranfaing<sup>2</sup>, Aurélien Dinh<sup>3</sup>, Catherine Dunyach-Remy<sup>2</sup>, Louis Bernard<sup>4,5</sup>, Franck Bruyère<sup>4,6</sup>, Jean-Philippe Lavigne<sup>2\*</sup> and Albert Sotto<sup>1</sup>

<sup>1</sup> VBMI, INSERM U1047, Université de Montpellier, Service des Maladies Infectieuses et Tropicales, CHU Nîmes, Nîmes, France, <sup>2</sup> VBMI, INSERM U1047, Université de Montpellier, Service de Microbiologie et Hygiène Hospitalière, CHU Nîmes, Nîmes, France, <sup>3</sup> Service des Maladies Infectieuses, AP-HP Raymond-Poincaré, Garches, France, <sup>4</sup> PRES Centre Val de Loire, Université François Rabelais de Tours, Tours, France, <sup>5</sup> Service des Maladies Infectieuses, CHU Tours, Tours, France, <sup>6</sup> Service d'Urologie, CHU Tours, Tours, France

## OPEN ACCESS

### Edited by:

Ilana L. B. C. Camargo,  
University of São Paulo, Brazil

### Reviewed by:

Nina Chanishvili,  
George Eliava Institute  
of Bacteriophage, Microbiology  
and Virology, Georgia  
Jason John Paxman,  
La Trobe University, Australia  
Saeid Bouzari,  
Pasteur Institute of Iran (PII), Iran

### \*Correspondence:

Jean-Philippe Lavigne  
jean.philippe.lavigne@chu-nimes.fr

### Specialty section:

This article was submitted to  
Antimicrobials, Resistance  
and Chemotherapy,  
a section of the journal  
Frontiers in Microbiology

Received: 27 November 2019

Accepted: 10 June 2020

Published: 03 July 2020

### Citation:

Loubet P, Ranfaing J, Dinh A, Dunyach-Remy C, Bernard L, Bruyère F, Lavigne J-P and Sotto A (2020) Alternative Therapeutic Options to Antibiotics for the Treatment of Urinary Tract Infections. *Front. Microbiol.* 11:1509. doi: 10.3389/fmicb.2020.01509

Urinary tract infections (UTIs) mainly caused by Uropathogenic *Escherichia coli* (UPEC), are common bacterial infections. Many individuals suffer from chronically recurring UTIs, sometimes requiring long-term prophylactic antibiotic regimens. The global emergence of multi-drug resistant uropathogens in the last decade underlines the need for alternative non-antibiotic therapeutic and preventative strategies against UTIs. The research on non-antibiotic therapeutic options in UTIs has focused on the following phases of the pathogenesis: colonization, adherence of pathogens to uroepithelial cell receptors and invasion. In this review, we discuss vaccines, small compounds, nutraceuticals, immunomodulating agents, probiotics and bacteriophages, highlighting the challenges each of these approaches face. Most of these treatments show interesting but only preliminary results. *Lactobacillus*-containing products and cranberry products in conjunction with propolis have shown the most robust results to date and appear to be the most promising new alternative to currently used antibiotics. Larger efficacy clinical trials as well as studies on the interplay between non-antibiotic therapies, uropathogens and the host immune system are warranted.

**Keywords:** urinary tract infection, alternative therapeutics, vaccines, nutraceuticals, immunomodulating agents, probiotics, cranberry, bacteriophages

## INTRODUCTION

Urinary Tract Infections (UTIs) are frequent bacterial infections (Silverman et al., 2013) especially in women, estimated to affect more than one in every two women at least once in her lifetime (Foxman, 2014; McLellan and Hunstad, 2016). Uropathogenic *Escherichia coli* (UPEC) is the main pathogen isolated from patients with UTIs (>85%) (Flores-Meireles et al., 2015), while other Gram-negative rods (e.g., *Proteus mirabilis*, *Klebsiella pneumoniae*) and Gram-positive cocci (e.g., *Staphylococcus saprophyticus*, *Enterococcus faecalis*) are responsible for the remaining cases (Flores-Meireles et al., 2015). UTI recurrence is defined by the occurrence of more than two episodes in 6 months, or three in 12 months (Professionals, 2019). The annual incidence of UTI in women is estimated to be 30 per 1000 subjects (Laupland et al., 2007), with approximately

20–40% experiencing recurrence within 6–12 months (Ikähelmo et al., 1996; Foxman, 2014). The epidemiology of UTI changes significantly in the healthcare environment. Urethral catheterization is strongly associated with UTI, and the risk of infection increases with the length of catheterization (Suetens et al., 2018). Catheter-associated UTI (CAUTI) is the most common nosocomial infection (Suetens et al., 2018). CAUTI affects both sexes, with long-term urinary catheterization of both men and women almost invariably leading to detection of bacteria in the urine (bacteriuria). Long-term catheterization carries a daily risk of 3–7% for the development of symptomatic CAUTI (Saint et al., 2009).

The urinary tract is normally sterile, with the exception of the flora of the distal urethra which is diverse and reflects both the digestive flora, the cutaneous flora and genital flora (*Lactobacilli* in women). There are several physiological mechanisms to prevent the host from the development of an ascending infection. First, the urethra itself, which is an obstacle to the intravesical inoculation; second, the physicochemical characteristics of normal urine (osmolarity, pH, organic acid content) that makes growth of most of the bacteria colonizing the urethra difficult; third urination that eliminates most of the bacterial population; fourth the presence in the urine of glycoproteins and oligosaccharides acting as soluble receptors to capture bacteria and enhance their clearance. Finally, in case of bacterial colonization, three factors contribute to avoid the invasion of the mucous membrane (Sobel, 1997): (i) the presence of inhibitors of bacterial adhesion to the surface of urothelial cells (Tamm-Horsfall protein, mucopolysaccharides); (ii) the existence of a local bactericidal effect (independent of inflammatory response or immune response); (iii) a process of exfoliation of the infected urothelial cells. The occurrence of UTI implies either a flaw in these defense mechanisms or the development in the urethral flora of a virulent bacteria, termed uropathogenic. Only a minority of *E. coli* strains, are endowed with uropathogenicity by the production of one or more adhesins (fimbriae): (i) type 1 allowing low urinary tract colonization, (ii) type P inducing pyelonephritis by modification of ureteral peristalsis in binding to glomerulus and endothelial cells of vessel walls helping *E. coli* to cross the epithelial barrier to enter the bloodstream and causing hemagglutination of erythrocytes and by decreasing the renal filtrate flow due to the formation of dense bacterial communities within the tubular lumen (Roberts, 1991; Melican et al., 2011), and (iii) non-fimbrial adhesins such as UpaB that facilitate *E. coli* adherence to extracellular matrix proteins and colonization of the urinary tract (Paxman et al., 2019). An increased adherence of *E. coli* to uroepithelial cells is observed in patients with recurrent UTIs compared to healthy controls (Schaeffer et al., 1981). Moreover, it has been demonstrated that UPEC can invade and replicate within the bladder cells to form intracellular bacterial communities (Mulvey et al., 2001), which can be frequently found in urothelial cells in women with symptomatic UTIs (Rosen et al., 2007) and may act as a source of recurrence in women with same-strain recurrent UTIs (Beerepoot et al., 2012a). Finally, biofilm formation is a critical aspect of CAUTI (Soto et al., 2006; Beerepoot et al., 2012a). Mechanisms of recurrence in UTIs are not fully characterized.

Besides pathogen virulence factors, an impaired mucosal immune response (with urinary IgA involved in the UPEC clearance from the bladder mucosa) of the urogenital tract may have a role in the host-pathogen process (Ingersoll and Albert, 2013; Abraham and Miao, 2015).

Long-term low dose antibiotic use is currently the keystone of the preventive treatment for UTI recurrence. Indeed, prophylactic antibiotics have been shown to decrease UTI recurrence by 85% compared to patients with placebo (relative risk (RR) 0.15, 95% confidence interval (95%CI) 0.08 to 0.28) (Albert et al., 2004). Moreover, with regard to urinary tract conditions such as neurogenic bladder, it has been suggested that weekly cycling of antibiotics could be the most optimal preventative strategy (Salomon et al., 2006; Dinh et al., 2019). Indeed, this original strategy seems effective with only a limited ecological effect on native gut microbiota according to long-term follow-up (Poirier et al., 2015). However, prolonged antibiotic use often results in the emergence of multidrug-resistant organisms (Beerepoot et al., 2012b) and increases the cost of care. Consequently, the development of new therapeutic options to prevent and treat UTIs, and most particularly recurrent UTIs, are of interest.

This review aims to describe all the existing non-antibiotic treatment options in UTI (Table 1 and Figure 1).

## VACCINES

Vaccines have been studied to prevent recurrent UTI in the aim not to kill infectious pathogens but to protect the host against infection by priming the immune response to uropathogens. Different vaccine strategies have considered the use of both surface antigen or inactivated whole bacterium, from uropathogens, to generate protective antibodies as a preventive strategy for recurrent UTIs. An ideal vaccine will target factors critical for establishment of bladder colonization (O'Brien et al., 2016). In this way, vaccines containing O antigens (important virulence factors that are targets of both the innate and adaptive immune systems), fimbrial subunits (responsible for the attachment to host cells, the first step of UTI),  $\alpha$ -hemolysin (a membrane-active protein exotoxin leading to serious tissue damage), siderophores and a variety of outer membrane siderophore receptors (allowing the sequestration of iron, the main source of bacterial growth) have been developed.

## Current Vaccine Solutions

There are currently four available vaccines with established results from randomized control trials (RCT): Uro-Vaxom<sup>®</sup>, Urovac<sup>®</sup>, ExPEC4V and Uromune<sup>®</sup> (Azimonia et al., 2019).

- Uro-Vaxom<sup>®</sup>, also known as OM-89, is comprised of bacterial extracts from 18 UPEC strains that mediated its effect by the ability of bacterial component pathogen-associated molecular patterns to non-specifically stimulate cells of the innate immune systems (Huber et al., 2000). This effect was shown in mouse models inducing an immunological defense response within the bladder.

**TABLE 1** | Non-antibiotic therapeutic options for the treatment of urinary tract infections.

Therapeutic options	References	Mechanism	Benefits	Drawbacks
<b>Vaccine</b>				
Targeting adhesion	(O'Hanley et al., 1985; De Ree and Van den Bosch, 1987; Riegman et al., 1988; Wizemann et al., 1999; Langermann et al., 2000; Roberts et al., 2004; Poggio et al., 2006; Habibi et al., 2016)	<ul style="list-style-type: none"> <li>Block the liaison adhesin-host cell receptor (pili vaccine)</li> <li>Reduction of adhesion and protection against cystitis (FimH vaccine)</li> </ul>	<ul style="list-style-type: none"> <li>Decrease the bacterial colonization</li> <li>Protection of the bladder and the kidneys</li> </ul>	<ul style="list-style-type: none"> <li>Heterogeneity of the proteins of the bacterial membrane</li> </ul>
Targeting capsule	(Kajiser et al., 1983; Roberts et al., 1993; Kumar et al., 2005; Stenutz et al., 2006)		<ul style="list-style-type: none"> <li>Promising animal model results</li> </ul>	<ul style="list-style-type: none"> <li>No human studies</li> <li>Great heterogeneity in antigen used making creation of a vaccine with broad protection difficult</li> </ul>
Targeting toxins	(O'Hanley et al., 1991; Ellis and Kuehn, 2010)	<ul style="list-style-type: none"> <li>Reduction of renal injury</li> </ul>	<ul style="list-style-type: none"> <li>Decrease virulence</li> </ul>	<ul style="list-style-type: none"> <li>No long-term protection</li> </ul>
Targeting iron metabolism	(Alteri et al., 2009; Brumbaugh et al., 2013)	<ul style="list-style-type: none"> <li>Effective immunologic reaction against specific molecules</li> </ul>	<ul style="list-style-type: none"> <li>Protection of the bladder and the kidneys</li> <li>Reduce UTI recurrence</li> </ul>	<ul style="list-style-type: none"> <li>Cannot target all UPEC strains (heterogeneity of the targets)</li> </ul>
<b>Small compounds</b>				
Pillicide	(Åberg and Almqvist, 2007; Greene et al., 2014; Pinkner et al., 2006; Svensson et al., 2001)	<ul style="list-style-type: none"> <li>Prevent the formation of pili</li> <li>Decrease the expression of genes related to fimbriae</li> </ul>	<ul style="list-style-type: none"> <li>Reduce adhesion, virulence and biofilm formation of UPEC</li> </ul>	<ul style="list-style-type: none"> <li>No <i>in vivo</i> experiments</li> </ul>
Mannoside	(Cusumano et al., 2011; Klein et al., 2010)	<ul style="list-style-type: none"> <li>Diminution of bladder colonization</li> <li>Orally bioavailable</li> </ul>	<ul style="list-style-type: none"> <li>Reduction of the adhesion</li> </ul>	<ul style="list-style-type: none"> <li>Clinical study in progress</li> </ul>
Hydroxamic acid	(Griffith et al., 1978, 1988, 1991; Munakata et al., 1980; Bailie et al., 1986; Benini et al., 2000; Amtul et al., 2002; Xu et al., 2017)	<ul style="list-style-type: none"> <li>Prevent urine alkalization</li> </ul>	<ul style="list-style-type: none"> <li>Prevent the formation of urinary stones</li> <li>Decrease bladder inflammation</li> </ul>	<ul style="list-style-type: none"> <li>Side effects (mutagenic power)</li> </ul>
Phenyl phosphoramidates	(Texier-Maugein et al., 1987; Faraci et al., 1995; Morris and Stickler, 1998; Pope et al., 1998)	<ul style="list-style-type: none"> <li>Prevent urine alkalization</li> </ul>	<ul style="list-style-type: none"> <li>Prevent the formation of urinary stones</li> <li>Decrease bladder inflammation</li> </ul>	<ul style="list-style-type: none"> <li>Poor stability</li> </ul>
Capsule inhibitor	(Roberts, 1995, 1996; Lobet et al., 2008; Varki, 2008; Anderson et al., 2010; Goller et al., 2014)	<ul style="list-style-type: none"> <li>Reduce biofilm formation</li> </ul>	<ul style="list-style-type: none"> <li>Affects a large proportion of UPEC strains</li> </ul>	<ul style="list-style-type: none"> <li>Antigenicity in human</li> <li>Poor bioavailability</li> <li>Conflicting results</li> </ul>
<b>Nutraceutical</b>				
Cranberry	(Ahuja et al., 1998; Howell et al., 2005; Freitas et al., 2006; Liu et al., 2006, 2019; AFSSA, 2007; Jepson and Craig, 2008; Pereira et al., 2011; Ermel et al., 2012; Jepson et al., 2012; Stapleton et al., 2012; Chan et al., 2013; Boonsai et al., 2014; Olczyk et al., 2014; Ulrey et al., 2014; Rafsanjany et al., 2015; Rodríguez-Pérez et al., 2016; Wojnicz et al., 2016; Pasupuleti et al., 2017; Ranfaing et al., 2018a,b; Anger et al., 2019; Bruyère et al., 2019)	<ul style="list-style-type: none"> <li>Reduction of adhesion, motility, and biofilm formation</li> </ul>	<ul style="list-style-type: none"> <li>Impacts UPEC strains and also <i>P. aeruginosa</i>, <i>P. mirabilis</i> and <i>E. faecalis</i></li> <li>Could be used in prophylaxis</li> </ul>	<ul style="list-style-type: none"> <li>Conflicting results</li> </ul>
Hyaluronic acid	(Constantinides et al., 2004; Birder and de Groat, 2007; Cicione et al., 2014; Ciani et al., 2016; Torella et al., 2016; Goddard and Janssen, 2018)	<ul style="list-style-type: none"> <li>Reduction of adhesion</li> </ul>	<ul style="list-style-type: none"> <li>Promising results in humans</li> </ul>	<ul style="list-style-type: none"> <li>Only retrospective studies</li> </ul>

(Continued)



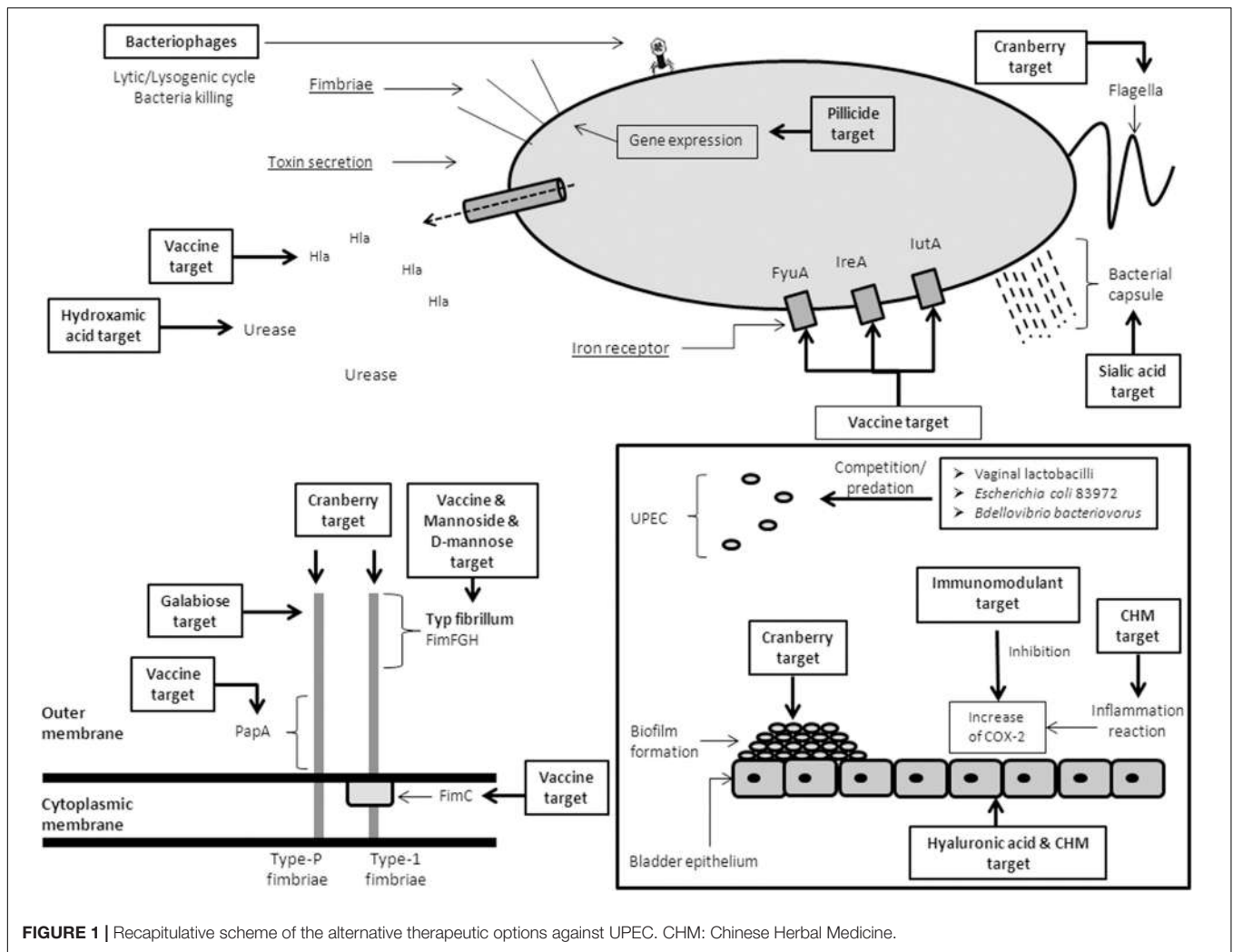
TABLE 1 | Continued

Therapeutic options	References	Mechanism	Benefits	Drawbacks
D-mannose	(Hills et al., 2001; Klein et al., 2010; Cusumano et al., 2011; Kranjčec et al., 2014; Domenici et al., 2016)	• Reduction of adhesion	• Fast effect after oral administration	• Conflicting results
Galabiose	(Strömberg et al., 1990; Sung et al., 2001; Larsson et al., 2003)	• Reduction of adhesion	• Diminution of kidney infections	• Not enough <i>in vivo</i> results
Chinese Medical Herb and other plants	(Banu and Kumar, 2009; Gu et al., 2011; Issac Abraham et al., 2011; Tong et al., 2011; Zhao et al., 2011; Flower et al., 2015; Meng et al., 2015; Hou and Wang, 2016; Pu et al., 2016; Sharifi-Rad et al., 2016; Mazarei et al., 2017; Jaiswal et al., 2018; Mickymaray and Al Aboody, 2019)	• Reduction of adhesion	• Reduction of UTI recurrences	• Small size studies • Little safety data
<b>Immunomodulant agents</b>				
COX-2 inhibitor	(Bleidorn et al., 2010; Hannan et al., 2014; Moore et al., 2019)	• Reduction of inflammation linked to cystitis	• Substantial reduction of UTI recurrences	• No significant results in clinical trials
Green Tea Extract	(Hoshino et al., 1999; Arakawa et al., 2004; Cooper et al., 2005a,b; Reygaert and Jusufi, 2013; Bae et al., 2015)	• Reduction of inflammation	• Reduction of UTI recurrences	• Mechanisms of action unclear • Not proved in humans
<b>Probiotics</b>				
Vaginal lactobacilli	(Isolauri et al., 2001; Galdeano and Perdigon, 2006; De Vuyst and Leroy, 2007; Cribby et al., 2008; Cadieux et al., 2009; Riaz et al., 2010; Hardy et al., 2013; Kemgang et al., 2014; Di Cerbo et al., 2016; Chikindas et al., 2018; Ng et al., 2018; Koradia et al., 2019)	• Competition, reduction of adhesion and virulence	• Natural production of antimicrobial compounds • No known side effects	• Not enough <i>in vivo</i> results
<i>E. coli</i> 83972	(Hull et al., 2000; Darouiche et al., 2001, 2005; Dashiff et al., 2011; Roos et al., 2006; Trautner et al., 2007; Prasad et al., 2009; Sundén et al., 2010)	• Colonization of the bladder by avirulent strain	• Reduction of UPEC colonization	• Not enough inclusions in clinical studies
Predatory bacteria	(Stolp and Starr, 1963; Kadouri and O'Toole, 2005; Sockett, 2009; Dashiff et al., 2011; Shatzkes et al., 2015; Gupta et al., 2016)	• Decrease of bacterial number and biofilm formation	• Efficient against Gram-negative bacteria	• Not yet tested to treat UTIs
<b>Bacteriophages</b>	(Dufour et al., 2016; Sybesma et al., 2016; Leitner et al., 2017; Ferry et al., 2018; Ujmajuridze et al., 2018; Jault et al., 2019; Kuipers et al., 2019)	• Direct bacteria killing	• Interesting animal models and human case reports.	• More human studies are required

However, its use in human trials has shown conflicting results. Four placebo controlled studies (Tammen, 1990; Schulman et al., 1993; Magasi et al., 1994; Bauer et al., 2005) showed that taking one Uro-Vaxom® tablet daily for 3 months significantly reduced the number of UTIs in the treatment group, with a RR = 0.61 (95%CI 0.48–0.78) of developing a UTI in the treatment group during an observation ranging from 3 to 12 months.

However, a recent multicenter double-blind control trial of 451 patients showed no significant difference in UTI rates between Uro-Vaxom® and the placebo (Wagenlehner et al., 2015).

- Urovac® is a mucosal vaccine in the form of a vaginal suppository containing 10 different strains of heat-inactivated uropathogenic bacteria (six serotypes of *E. coli* strains, *P. vulgaris*, *Morganella morganii*, *E. faecalis* and



**FIGURE 1** | Recapitulative scheme of the alternative therapeutic options against UPEC. CHM: Chinese Herbal Medicine.

*K. pneumoniae* (Yang and Foley, 2019). The aim of this vaccine preparation was to incorporate a broader range of commonly implicated uropathogens and thus provide broad protection. Overall, Urovac<sup>®</sup> has been shown to reduce the risk of recurrence (RR 0.75, 95% CI 0.63–0.89) (Uehling et al., 1997, 2003; Hopkins et al., 2007). This effect was more pronounced in the group that received a follow-up booster vaccination (Azimonia et al., 2019).

- ExPEC4V is composed of O-antigens of four *E. coli* serotypes (O1A, O2, O6A, and O25B) delivered as a single intra-muscular injection. These serotypes are a key immune evasion strategy used by the bacterium. This vaccine has shown good safety and immunogenicity in several phase 1 and 2 trials (Hopkins et al., 2007; Huttner et al., 2017; Huttner and Gambillara, 2018; Frenck et al., 2019).
- Uromune<sup>®</sup> is a new sublingual vaccine composed of inactivated *E. coli*, *K. pneumoniae*, *Proteus vulgaris* and *E. faecalis*. This vaccine has been evaluated in three large retrospective Spanish studies and showed a 70–90% reduction of recurrence when compared to

antibiotic prophylaxis (Lorenzo-Gómez et al., 2013, 2015). A prospective observational study showed that 59 out of 75 women (78%) which received 3 months of Uromune<sup>®</sup> treatment as a sub-lingual spray once a day, had no new UTIs during both the treatment and the one year of follow-up period (Yang and Foley, 2018). Another recent larger prospective study showed that 65% of 784 women had 0 or 1 UTI after 6 months of daily sub-lingual administration of Uromune<sup>®</sup> (Ramirez Sevilla et al., 2019).

This interesting result should be confirmed in a larger study with a control group. It has to be noted that the need for a 3-month daily administration raises questions on the immunogenicity and the expected compliance to this treatment. One international multicenter phase III RCT is currently underway.

A recent meta-analysis noted that the use of vaccines appeared to reduce UTI recurrence compared to placebo. However, the heterogeneity amongst studies renders interpretation and recommendation for routine clinical use difficult at present (Prattley et al., 2020). Further randomized controlled trials are

warranted to assess the efficiency and the safety of the existing vaccines against UTIs.

## New Candidates

Several bacterial virulence factors involved in UTI are promising vaccine targets.

### Vaccines Targeting Adhesion

Bacterial adhesion to urothelium represents a crucial step in the pathogenesis of UTIs. It permits bacteria to resist mechanical elimination by the flow of urine and bladder and increases persistence of *E. coli*. One large family of adhesive organelles are pili assembled by the chaperone-usher pathway (CUP) pili. These pili are critical virulence factors in a wide range of pathogenic bacteria, including *E. coli*. CUP pili mediate adhesion to host and environmental surfaces, facilitate invasion of host tissues, and promote interaction of bacteria with each other to form biofilms (Sauer et al., 2004). The most studied of the CUP pili are the Type 1, P, and S pili, present in UPEC and allowing the colonization of mucosal surfaces. They promote both irreversible bacterial attachment and invasion of uroepithelial cell membrane within the bladder. Interactions mediated by these adhesins can stimulate a number of host responses that can directly influence the outcome of a UTI (Mulvey, 2002). They are thus promising vaccine candidates because of the importance of this adhesion. The potential exists to develop antibodies that block the adhesin-host cell receptor interaction and thus decrease bacterial colonization (Wizemann et al., 1999).

FimH is a major determinant of the adhesive subunit of Type 1 fimbriae, which has high tropism for urinary tract receptors. It binds to mono-mannose. Lack of this compound on renal epithelia has suggested a limited role in pyelonephritis. It has been targeted as a good candidate for a vaccine because of its critical role in cystitis pathogenesis (Figure 1). A FimCH vaccine protected cynomolgus monkeys from cystitis (Langermann et al., 2000). Another study on mice with an intranasal and intramuscular administration also showed a protection against cystitis, but the intranasal method produced a stronger immune response (Poggio et al., 2006). In a more recent study, a recombinant protein MrpH.FimH (consisting of a combination between two adhesins, FimH from UPEC and MrpH from *P. mirabilis*) was injected with a transurethral instillation and the authors demonstrated a high immune response and a protection against *E. coli* and *P. mirabilis* (Habibi et al., 2016).

By comparison the Type P pilus is more involved in pyelonephritis due to the presence of globoseries glycosphingolipids (the receptor of this pilus) in kidney. This P fimbria helps to cross the epithelial barrier to enter the bloodstream and can cause hemagglutination of erythrocytes (Riegman et al., 1988). Approximately 1,000 of subunits form a P fimbria. Among them the major constituent is the protein subunit PapA, and minor subunits are PapD, PapE, PapF, and PapG. So subunit vaccines based on this pilus have been developed to block renal colonization. Attempts on using the major subunit PapA as a vaccine, although initially favorable in mice (O'Hanley et al., 1985), failed due to the poor generation

of protective antibodies most probably due to natural variation in the PapA pilus subunit (Figure 1; De Ree and Van den Bosch, 1987). A new vaccine based on purified PapDG protein demonstrated a good efficiency to prevent colonization of kidney on cynomolgus monkeys (Roberts et al., 2004).

### Vaccines Targeting Capsule

The main role of a capsule is to cover and protect *E. coli* from the host immune system. It provides protection against engulfment and complement-mediated bactericidal effect in the host (Johnson, 1991). Based on this implication in virulence strategy, capsules represent a promising vaccine target. In this way, conjugate UTI vaccines against UPEC capsule and lipopolysaccharide (LPS) components have shown protection in animal models after same-strain challenge. In early studies, intraperitoneal, subcutaneous or bladder injection of O-antigen from *E. coli* of different serotypes (O6, O8 and K13) protected rats and rhesus monkeys from pyelonephritis (Kaijser et al., 1983; Roberts et al., 1993; Kumar et al., 2005). A considerable challenge in formulating a vaccine targeting capsule or O-antigen, the most exposed component of LPS, is the great heterogeneity of serotypes among *E. coli* isolates. Indeed, six different O serotypes account for only 75% of UPEC isolates (Stenutz et al., 2006), making the formulation of a broadly protective conjugate vaccine impractical. Furthermore, some capsule serotypes, such as K1 and K5, are thought to evade the host immune response by molecular mimicry, potentially making them poor vaccine candidates. No studies on these vaccines have been conducted in humans yet.

### Vaccines Targeting Toxins

Several toxins secreted by UPEC play a consequential role as virulence factors in UTI. They have the ability to alter the host cell signaling cascade and modulate inflammatory responses. They also contribute to the stimulation of the host cell death and the ability to access deeper tissues. Many toxins have been reported including  $\alpha$ -hemolysin (HlyA) or cytotoxic necrotizing factor 1 (CNF1).  $\alpha$ -hemolysin is a pore-forming toxin, it can lyse erythrocytes, and induces the apoptosis of target host cells promoting the exfoliation of bladder epithelial cells (Johnson, 1991). CNF1 stimulates actin stress fiber formation and membrane ruffle formation resulting in the entry of *E. coli* into the cells. This protein interferes with polymorphonuclear phagocytosis and provokes apoptotic death of bladder epithelial cells (Asadi Karam et al., 2019). Following their importance in virulence, the toxins produced by UPEC have been used to develop vaccines to protect the bladder and kidney during a UTI. However, as they are secreted and thus removed from the bacteria, they do not make ideal vaccine candidates. Indeed, a purified  $\alpha$ -hemolysin toxoid vaccine prevented renal injury, but not colonization, in mice after challenge with a hemolytic UPEC strain (Figure 1; O'Hanley et al., 1991). Of note, rather than being secreted as "naked" proteins,  $\alpha$ -hemolysin and CNF1 are associated with outer membrane vesicles (OMVs), which bleb from the surface of Gram-negative bacteria during all stages of growth (Ellis and Kuehn, 2010). OMVs also contain adhesins, enzymes, and non-protein antigens like LPS. OMVs are intriguing vaccine candidates, and because they contain LPS

and other pro-inflammatory virulence factors, they should not require adjuvants to stimulate the immune system. However, no UPEC OMV vaccines have yet been tested.

### Vaccines Targeting Iron Metabolism

The acquisition of iron is crucial for bacteria life and *E. coli* uses iron for transporting and storing oxygen, DNA synthesis, electron transport and metabolism peroxides. However, the amount of iron availability is reduced in host. In response, *E. coli* produces siderophores, molecules that mediate iron uptake. Four siderophore systems have been identified such as yersiniabatin, aerobactin, enterobacterin, and salmochelin (Johnson, 1991).

Some studies have targeted siderophore, heme receptors and other functional molecules involved in iron acquisition. In one study, the authors tested six iron receptors and found that the antibodies against the yersiniabactin receptor, FyuA, conferred kidney protection in mice (Brumbaugh et al., 2013). In another mouse model, instead of targeting iron receptors, the same authors targeted molecules involved in iron metabolism. Of the six candidates, two conferred a protection to the bladder (IreA and IutA) and one protected the kidneys (Hma) after an intranasal immunization (Alteri et al., 2009).

## SMALL COMPOUNDS

In the current setting small compounds are low molecular weight molecules that are typically bacterial substrates or products or mimics thereof. They can act as inhibitors by binding active sites and substrate binding sites of proteins involved in pathogenicity and so impact bacterial infections.

### Small Compounds Targeting Adhesion

As previously noted, one of the critical mechanisms for the pathogenesis of the uropathogenic bacteria is its adhesion to uroepithelium (Beerepoot and Geerlings, 2016), due to fimbriae (specially the Type 1 and the P-fimbriae), playing a role in both cystitis and pyelonephritis (Beerepoot and Geerlings, 2016; Muenzner et al., 2016). The very conserved structure of the adhesive organelles makes them good candidates to develop antibacterial agents (Piatek et al., 2013). The small molecules targeting adhesion can be classified into two categories: those inhibiting the capacity of adhesion of the fimbriae, and those targeting fimbriae assembly.

#### Pilicide

The main action of these molecules is to prevent the formation of UPEC pili by decreasing the levels of Type 1 and P piliation (Åberg and Almquist, 2007). Pilicides are small molecules which have a ring-fused 2-pyridone backbone. Some pilicides act directly on pili assembly chaperones, through adhering to their hydrophobic substrate binding sites (Svensson et al., 2001; Pinkner et al., 2006). Others interfere with the transcription of pili genes and some cases genes involved in flagella biogenesis such as the pilicide ec240, the most potent inhibitor of Type 1 piliation and of type 1 pilus-dependent biofilm formation to date (Greene et al., 2014).

*In vitro* studies testing the potential of pilicides have shown promising results. These compounds decreased (i) the adhesion of UPEC strains on cells by a strong reduction (70–80%) of fimbriae density (Piatek et al., 2013), and (ii) the ability to form Type 1 pilus dependent biofilms (Pinkner et al., 2006). In a mouse study, the pilicide had a strong impact on adhesion and biofilm formation and also reduced the virulence *in vivo*. It is also interesting to note that it reduced the biofilm formation on abiotic surface (Cegelski et al., 2010).

To develop this compound into a therapeutic, further studies are needed to assess its pharmacokinetics and pharmacodynamics and to determine the concentration at which it accumulates in the bladder or other potential sites of infection.

### Small Compounds Targeting Urease

Urease, an enzyme which catalyzes the hydrolysis of urea, is crucial in the pathogenesis of several uropathogenic bacteria such as *P. mirabilis*, *Klebsiella* sp., *Pseudomonas* sp. and *Staphylococcus* sp. (Mobley and Hausinger, 1989). This enzyme leads to the alkalization of the urine and the production of struvite and carbonate apatite that make up the major component of urinary stones (Burne and Chen, 2000). These conditions lead to the inflammation of the urogenital epithelia thus increasing the risk of catheter-associated biofilm formation that may contribute to pyelonephritis (Musher et al., 1975; Jacobsen et al., 2008), mainly due to both bacterial and host cysteine protease (Xu et al., 2017).

The most studied inhibitors of urease are hydroxamic acids (Amtul et al., 2002; **Figure 1**). These molecules have a high inhibitory activity against urease, by bonding to the two nickel ions in the urease active site (Benini et al., 2000). Initially, these molecules were used to treat UTIs by preventing urine alkalization (Griffith et al., 1978, 1988). However, because of the growing evidence of side effects such as mutagenic power, they were progressively phased out (Munakata et al., 1980; Bailie et al., 1986; Griffith et al., 1991).

Through similarly interacting with nickel ions in the urease active site, the phenyl phosphoramidates were found to have the highest inhibitory activity (Faraci et al., 1995). Studies testing these molecules in an *in vitro* model (Morris and Stickler, 1998) and in a rat model (Texier-Maugein et al., 1987) found promising results. Since then, no *in vivo* studies or clinical trials have been developed, probably due to the poor hydrolytic stability of these molecules which leads to a very short half-life (Pope et al., 1998).

Other molecules that possess inhibitory activity against bacterial urease have been developed, but they are not fully adapted to treat UTIs. One of them is the quinones, a class of active compounds with a high oxidizing potency (Zaborska et al., 2002). These molecules had not been evaluated *in vivo* models due to their cytotoxic and cancerogenic properties.

### Small Compounds Targeting Bacterial Capsule

Polysaccharide capsule biogenesis plays an important role in UPEC virulence. Like other pathogens, the capsule is used as a defense against opsonophagocytosis and complement-mediated killing (Roberts, 1995, 1996). The capsule is also involved in the



formation of biofilm and the formation of intracellular bacterial communities (Llobet et al., 2008; Anderson et al., 2010). Until now, the human use of small-molecule inhibitors of UPEC capsule biogenesis was not available because of their antigenicity and poor bioavailability (Varki, 2008). Nevertheless, mouse studies identified two active agents (DU003 and DU01), that caused significant bacterial death (Goller et al., 2014; **Figure 1**).

## NUTRACEUTICALS

Nutraceuticals are pharmaceutical alternatives, consisting of all the foods or food products which provide medical benefits and can be delivered under medical form. They provide health benefits in addition to their basic nutritional value.

### Cranberry (*Vaccinium macrocarpon*)

Cranberry (*Vaccinium macrocarpon* Ait.) is a berry that grows in North America. In recent years, the use of cranberry has increased in the prophylactic approach of recurrent UTI (Howell et al., 2005). Although, its mechanism of action is unclear, there are several possible targets of cranberry (**Figure 1**).

The main efficacy is related to the antiadherence properties of cranberry (Ahuja et al., 1998; Liu et al., 2006) due to the A-type proanthocyanidin (PAC-A) that has been shown to be an important inhibitor of Type-I fimbriae *E. coli* adhesion to uroepithelial cells. Some *in vitro* and *in vivo* studies demonstrated the capacity of the cranberry to reduce the adhesion of bacteria to the cells (Ermel et al., 2012; Rafsanjany et al., 2015; Liu et al., 2019). Cranberry has also shown convincing results on motility and biofilm formation. Indeed, it has a negative impact on the swarming of *Pseudomonas aeruginosa* and *P. mirabilis* (Chan et al., 2013) and on the biofilm formation of *E. faecalis*, *P. aeruginosa* and *E. coli* (Ulrey et al., 2014; Rodríguez-Pérez et al., 2016; Wojnicz et al., 2016).

The use of cranberry has been associated with a decrease in the incidence of UTIs, although some conflicting results have been reported in the literature. Although cranberry products have been shown to significantly reduce the incidence of UTIs at 12 months (RR 0.65, 95% CI 0.46–0.90) compared with placebo/control in women with recurrent UTIs in a Cochrane review from 2008 (Jepson and Craig, 2008), in an updated review concluded that cranberry products did not show any significant reduction in the occurrence of symptomatic UTI in the same population (Jepson et al., 2012).

A placebo controlled trial, published after the last review, showed that women randomized to cranberry juice had a non-significant reduction in numbers of P-fimbriated *E. coli* in urine and in the rate of symptomatic UTIs (Stapleton et al., 2012).

Because dosage, concentration and formulation of PAC-A are not well defined, the conflicting results may be explained by the difference in PAC-A concentration between cranberry formulations (juice, beverage, tablets) in the different studies making it difficult to choose one formulation over another (Anger et al., 2019).

It must be noted that many of the products containing cranberry used in studies are only for research purposes, limiting

the prophylactic application of cranberries beyond research (Stapleton et al., 2012).

Finally, a recent publication showed that the cranberry proanthocyanidins had a variable effect on a collection of *E. coli* strains that could explain the discordant results observed in the clinical studies (Ranfaing et al., 2018a).

In order to enhance the effectiveness of cranberry, combinations of cranberry and other natural products with antimicrobial properties could be used, such as propolis. Propolis is a resinous material collected by bees from plants then mixed with wax and bee enzymes (AFSSA, 2007). Propolis has antimicrobial, anti-inflammatory, anti-tumoral, immunomodulatory and anti-oxidant activities (Boonsai et al., 2014). It has been used for several years to treat gastrointestinal disorders (food supplement) (Freitas et al., 2006), to promote oral health (mouthwash) (Pereira et al., 2011) and in dermatological care (creams and ointments) (Olczyk et al., 2014; Pasupuleti et al., 2017; Ranfaing et al., 2018b). *In vitro* studies showed that propolis potentiated the effect of cranberry proanthocyanidins on adhesion, motility (swarming and swimming), biofilm formation (early formation and fully-formed biofilm), iron metabolism and stress response of UPEC (Olczyk et al., 2014; Pasupuleti et al., 2017; Ranfaing et al., 2018a,b). Moreover, this association was active in all the *E. coli* strains studied, ruling out the variable effect observed with the cranberry used alone (Ranfaing et al., 2018a).

A recent RCT versus placebo in 85 women with recurrent UTIs showed a slight reduction in the number of cystitis events in the first 3 months in the propolis and cranberry group after adjustment on water consumption (0.7 vs. 1.3,  $p = 0.02$ ), but no difference in the mean number of infections in women with at least one infection. Of note, the mean time to onset of the first cystitis episode was significantly longer in the propolis + cranberry group (70 vs. 43 days,  $p = 0.03$ ) and tolerance to the treatment was similar in both groups (Bruyère et al., 2019).

### Hyaluronic Acid

The urinary bladder epithelium is composed of urothelial cells which carry specific sensors and properties as well as forming the first barrier to pathogens (Birder and de Groat, 2007). To maintain this capacity to fight infections, these cells produce sulfated polysaccharide glycosaminoglycan (GAG) which covers the epithelium and forms a non-specific anti-adherence factor. A major proportion of the GAG layer of the bladder is composed of hyaluronic acid (HA) and chondroitin sulfate (CS). Virulence factors (secreted by *E. coli* for example) damage the GAG layer to prepare its adhesion (Constantinides et al., 2004; **Figure 1**). One strategy for the management of UTI is based on the re-establishment of the GAG layer of the bladder epithelium with intravesical instillations of HA alone or in combination with CS. Various randomized and non-randomized studies have been performed.

A study investigated the impact of HA and CS on recurrent UTIs on 276 women (aged 18–75 years). The intravesical administration of HA and CS was given to 181 women and the standard treatment against recurrent UTIs was given to 95

women. There was a 49% reduction in the rate of recurrence (defined as one bacteriologically confirmed UTI in the year following the treatment initiation) in patients treated with HA + CS compared with standard care [adjusted OR 0.51 (95%CI 0.27–0.96)]. However, no significant difference was found when considering the number of recurrences or the median time to first recurrence (Ciani et al., 2016).

Another retrospective study in 157 women found similar results with a significant reduction in UTI recurrence and an increased time-to-recurrence between UTIs (Cicione et al., 2014).

It has to be noted that the administration protocol (different between participating centers) of weekly instillation for one month followed by monthly instillations may be a limiting factor for patients.

A synergy might exist between HA + CS and estrogen. This association has been explored in 145 postmenopausal women with mild-to-moderate urogenital atrophy and a history of recurrent UTI. Participants were divided into three groups: vaginal estrogen, oral HA, and oral HA + CS and vaginal estrogen. Oral treatments were effective in preventing recurrent UTI (number of patients with fewer than two infective episodes in the 6-month follow-up and fewer than three episodes in the 12-month follow-up), especially if administered with vaginal estrogen therapy. A slight effect on the HA alone but also a significant impact of the estrogen and the HA + CS on the recurrence of UTIs in postmenopausal women was observed (Torella et al., 2016).

Recently a meta-analysis suggested that HA ± CS decreased the rate of UTI recurrence and increased the time to recurrence (Goddard and Janssen, 2018). Moreover the authors noted the safety of HA therapy even if the intravesical instillation is more invasive than other administrations (usually *per os*). The combination therapy was more performant than the use of HA alone. It seems essential to perform a well-designed, randomized, controlled clinical trials with larger population.

## D-mannose

As seen above, CUP pili are important virulence factors and represent optimal targets for antivirulence compound development. *E. coli* binds to mannosylated host cells via their mannose-binding lectin domains of FimH.

Two developments have been proposed to prevent this interaction:

- D-mannose is a monosaccharide closely related to glucose. It blocks the adhesion by high affinity binding to the FimH, thus preventing FimH from binding host mannose on urinary tract surfaces. Absorption after oral administration is fast (30 min to reach the organs) and it is eliminated via the urinary tract (Hills et al., 2001).
- The structure of the FimH adhesin bound to mannosilable proteins has been used to design mannosides, These molecules block FimH function by binding in the FimH mannose-binding pocket (Pinkner et al., 2006; Domenici et al., 2016). Mannosides are also potent inhibitors of biofilm formation *in vitro*. Some mouse models

demonstrated a decrease in bladder colonization after an oral administration of mannosides and a prevention of acute and chronic UTI (Klein et al., 2010; Cusumano et al., 2011; **Figure 1**). In this way, an exogenous intake of D-mannose competitively blocks the interaction between the bacterial fimbriae and host cells (Cusumano et al., 2011; **Figure 1**). One RCT compared the recurrence of UTIs in a group of patients taking daily nitrofurantoin to a group treated with daily D-mannose powder. The risk of recurrence was similar between groups, whilst there was a reduction of the side effects in the D-mannose group (Kranjčec et al., 2014).

## Galabiose

Type P fimbriae adhere to the galabiose-like receptor via PapG (Larsson et al., 2003). As previously noted, this kind of fimbriae is essential for the pathogenesis of UTIs in helping the bacteria to reach the kidneys (Strömberg et al., 1990). Better understanding of the structure of the different variants of PapG (mostly PapG II and PapG III) might lead to drugs designed to target this adhesin (Sung et al., 2001; **Figure 1**). No *in vivo* studies on the impact of this sugar on UTIs have yet been performed. Evaluation on the most prevalent uropathogenic bacteria is essential to clearly evaluate the potential of galabiose to reduce UTI.

## Vitamin C

Vitamin C (ascorbic acid) is known to possess antioxidant and antimicrobial activities. As microbial infections cause reactive oxygen species (ROS) release by phagocytes, it is helpful in the limitation of infection through deactivation of microorganism killing. ROS may also cause damage to the host cells, therefore the level of ROS released by phagocytes should be reduced directly after infection (Liu et al., 2018). Vitamin C is an essential co-enzyme in the oxidative stress pathways, capable of ROS removal. Habash et al. (1999) suggested that vitamin C decreased the adhesion and microorganisms colonization of the biomaterials used in diagnostic/treatment procedures involving the urinary tract.

Moreover, two trials have studied the use of vitamin C to prevent UTIs. In a single-blind randomized study in thirteen spinal cord injury patients randomized to placebo or 500 mg ascorbic acid four times daily, there was no clinical benefit on urinary infection from the use of ascorbic acid (Castelló et al., 1996). In a second single-blind randomized trial in 110 pregnant women, participants taking a vitamin regimen with 100 mg ascorbic acid per day for 3 months showed a reduction in symptomatic UTIs incidence from 29.1 to 12.7% compared to participants following a vitamin regimen without ascorbic acid (Ochoa-Brust et al., 2007).

To date, there is no evidence of vitamin C action in the prevention of UTI.

## Chinese Herbal Medicine (CHM)

Chinese Herbal Medicine (CHM) is the ancient art of compiling complex herbal formulae usually comprising up to 15 herbs. CHM has been historically used to treat UTI. Some frequently used Chinese herbs are known to have significant diuretic,

antibiotic, immune enhancing, antipyretic, anti-inflammatory and pain relieving activities. Some of these herbs have shown an *in vitro* inhibitory activity against several uropathogens, especially against *E. coli* in decreasing its adherence to bladder epithelial cells (Tong et al., 2011). In an antibacterial test against mice, it was found that Sanjin tablets (composed by five kinds of CHM) have strong bacteriostasis activity (Hou and Wang, 2016). This product is used to treat acute uncomplicated lower UTI (Meng et al., 2015) and to reduce the symptoms of chronic UTI by reducing the secretory level of some urinary cytokines (Hou and Wang, 2016). A first meta-analysis of three RCTs including 282 women suggested that CHM significantly reduced recurrent UTI rates compared to antibiotics (RR 0.28, 95%CI [0.09 to 0.82]) (Flower et al., 2015). The second one has concluded that the current evidence is insufficient to support the efficacy and safety of Sanjin tablets for acute uncomplicated lower UTI (Pu et al., 2016). Only two of these RCTs reported adverse events (Gu et al., 2011; Zhao et al., 2011). Neither found any liver or renal impairment. Further studies are needed to definitively evaluate the potential of CHM on prevention/treatment of UTI.

### Other Phytochemicals

For centuries, plants have been used as alternative and traditional medicine around the world notably as therapies for infectious diseases (Banu and Kumar, 2009; Sharifi-Rad et al., 2016). Plants and their secondary metabolic derivatives are a major resource of antioxidants due to the presence of phenolic compounds including flavonoids, phenolic acids, or tannins. Different extracts from plants and spices have demonstrated anti-inflammatory, antimicrobial and diuretic activities (Mickymaray and Al Aboody, 2019). They also exhibited anti-quorum sensing and anti-biofilm potentials (Issac Abraham et al., 2011; Mazarei et al., 2017). One of the main mechanism of action is the antiadhesive action due to the formation of H-bonds between the FimH protein ligand and the plant compounds (Jaiswal et al., 2018). Future clinical trials must be done after complete pharmacokinetic/pharmacodynamic analyses.

## IMMUNOMODULANT AGENTS

The innate immune system activation through the secretion of cytokines and the recruitment of macrophages and neutrophils rapidly occurs after the onset of UTI (Duell et al., 2012). Even in the absence of an effective antibiotic treatment, this immune reaction might be enough to counter the infection. In the case of the persistence of several bacterial strains in the bladder, persistent acute immune response and tissue inflammation can be observed. Moreover, multiple infections can lead to chronic inflammation that increases the risk of developing recurrent UTIs (Ferry et al., 2004; Hannan et al., 2010). There is an increase in the expression of cyclooxygenase (COX)-2 after an infection of the bladder epithelial cells by UPEC. Moreover, there is a correlation between the severity of the inflammation and the increase of COX-2 expression (Chen et al., 2011; **Figure 1**). COX-2 inhibition prevents urothelial transmigration by neutrophils and damage to the urothelial barrier and facilitates the innate

responses (Hannan et al., 2014). A double-blind RCT on 79 women with uncomplicated UTI showed equivalent symptoms at Day 4, when taking ibuprofen (200 mg t.i.d) compared to ciprofloxacin (Bleidorn et al., 2010).

A recent 2 × 2 factorial placebo RCT evaluating ibuprofen in 382 women demonstrated a substantial reduction in antibiotic use in patients taking ibuprofen without differences in terms of symptom relief or speed of recovery (Moore et al., 2019).

Plant-based immunomodulants such as Green Tea Extract (GTE) have also shown promise (Bae et al., 2015). GTE contains an array of polyphenolic compounds, especially catechins. The biological properties of catechins are antioxidant, antiangiogenesis, antiproliferative activity, and antineoplastic (Cooper et al., 2005a,b). Some *in vitro* studies showed an antibacterial impact of GTE against UPEC (Hoshino et al., 1999; Arakawa et al., 2004; Reygaert and Jusufi, 2013) and in a rat model of cystitis, catechins significantly decreased inflammation and uroepithelium edema (Noormandi and Dabaghzadeh, 2015). These results are promising even though the mechanisms of action are still unclear.

## PROBIOTICS

A probiotic is a live microorganism that confers a health benefit.

### Vaginal Lactobacilli

*Lactobacilli* are frequently dominant microorganisms in vaginal flora (Mendling, 2016). Different observations can be done: (i) they have the ability to interfere with the adherence, growth and colonization of UPEC (Falagas et al., 2006); (ii) a change in the normal vaginal flora has been shown to facilitate the recurrence of UTIs (Cribby et al., 2008); and (iii) the use of commensal bacteria (such as *Lactobacilli*) reduces the proportion of uropathogens and thus restores bacterial homeostasis (Hardy et al., 2013). Although their exact mechanisms of action are still unknown, lactobacilli strains seem to have at least three different modes of action (Ng et al., 2018; **Figure 1**):

- The first one is the bacteriostatic effect due to the direct competition of probiotics with uropathogens in terms of nutrient and attachment sites (Di Cerbo et al., 2016).
- The second is the impact of probiotics on uropathogens virulence through the ability of *Lactobacillus* byproducts (such as lactic acid and hydrogen peroxide) to downregulate the expression of virulence genes. This has been illustrated in an *in vitro* study in which *Lactobacillus* byproducts inhibited the expression of Type 1- and P-fimbriae-encoding genes in *E. coli*, disrupting adhesion and invasion capacity (Cadieux et al., 2009).
- The third is the bactericidal effect of *Lactobacillus* on uropathogens. This effect can be achieved through the production of antimicrobial peptides known as bacteriocins. These bacteriocins reduce the number of uropathogens (Chikindas et al., 2018) in a strain-specific manner (De Vuyst and Leroy, 2007). *Lactobacillus* species that produce bacteriocins against *E. coli* have been identified (Riaz et al., 2010).



Probiotics can also modulate the immune system. In addition, bacterial strains secreting “immunomodulins” and cytokines are able to reduce infection by pathogenic bacteria (Galdeano and Perdígón, 2006; Kemgang et al., 2014). *Lactobacillus* species have these anti-inflammatory and immune-regulatory actions (Isolauri et al., 2001).

A non-inferiority randomized trial compared antibiotic prophylaxis and *Lactobacillus* prophylaxis in 252 postmenopausal women with recurrent UTIs who received 12 months of prophylaxis with trimethoprim-sulfamethoxazole (TMP-SMX), 480 mg once daily or oral capsules containing  $10^9$  CFU of *Lactobacillus rhamnosus* GR-1 and *Lactobacillus reuteri* RC-14 twice daily (Beerepoot et al., 2012b). The *Lactobacillus* treatment did not demonstrate non-inferiority, with an average number of symptomatic UTIs during the year of follow-up of 2.9 in the antibiotic group versus 3.3 in the lactobacilli group. The benefit of Lactobacilli was that it had no impact on antibiotic resistance compared to trimethoprim-sulfamethoxazole.

A reduction in the recurrence rate of UTI with the use of lactobacilli products (pooled RR = 0.68, 95%CI 0.44 to 0.93,  $p < 0.001$ ) (Ng et al., 2018) was underlined in a meta-analysis including 620 patients. In this study, two intravaginal suppositories (containing *Lactobacillus crispatus* CTV05, *Lactobacillus rhamnosus* GR1 and *Lactobacillus reuteri* RC14) had the highest efficacy (Ng et al., 2018).

A recent randomized, double-blind, placebo-controlled pilot study in 81 premenopausal women showed that the administration of Bio-Kult Pro-Cyan (a commercially available product containing probiotic strains (*Lactobacillus acidophilus* PXN 35, *Lactobacillus plantarum* PXN 47) and cranberry extract (36 mg/d PACs) twice-daily for 26 weeks, led to significantly lower number of recurrent UTIs compared to placebo (9.1 vs. 33.3%;  $P = 0.0053$ ) (Koradia et al., 2019).

## Bacterial Interference: *Escherichia coli* Strain 83972

The intentional colonization of the bladder with a non-virulent strain, also called bacterial interference, has been studied among patients with neurogenic bladder. *E. coli* 83972 is a clinical strain, isolated from a woman with chronic urinary colonization and which has naturally lost its capacity to develop Type 1 and Type P fimbriae. This strain has been used for prophylactic purposes to deliberately colonized the bladders with this bacterium to prevent colonization/infection by pathogenic species.

In a mouse model of UTI, *E. coli* 83972 demonstrated a better fitness than a virulent strain of UPEC. In a poor environment, like the bladder, this difference in fitness is a crucial advantage for the competition between bacteria. The 83972 strain could reduce the impact of UTIs by a monopolization of resources and space (Roos et al., 2006).

Seven clinical studies are available: three are RCT, one of which is a crossover designed study; and four are prospective cohorts (Hull et al., 2000; Darouiche et al., 2001, 2005; Dashiff et al., 2011; Trautner et al., 2007; Prasad et al., 2009; Sundén et al., 2010). Sample sizes were small and varied from 12 to 44 patients.

Clinical endpoints were the interval before first recurrence or the incidence of UTI during follow up.

Despite this heterogeneity, all studies demonstrated the ability of non-virulent strain to protect patients from UTI. One limit is the difficulty to achieve bladder colonization with the non-virulent strain (only 38% of patients in one of the RCT) (Darouiche et al., 2011).

## Predatory Bacteria

Predatory bacteria are small, motile, deltaproteobacteria that are a predatory invader of other Gram-negative bacteria (Figure 1). They occupy an intraperiplasmic niche and kill, digest and lyse their host, the prey cell. *Bdellovibrio* and *Micavibrio* are the most studied predatory bacteria (Stolp and Starr, 1963). *Bdellovibrio bacteriovorus* uses its type IV pilus to adhere and penetrate the outer membrane (bdelopast) of its prey. Inside the bacteria, *B. bacteriovorus* modifies the membrane of its prey to allow its growth until it uses all the nutrients. This entire process takes only 2–3 h (Sockett, 2009). Several Gram-negative human pathogenic bacteria such as *E. coli*, *Klebsiella* spp. and *Pseudomonas* spp. can be targeted by these predatory bacteria (Dashiff et al., 2011). Furthermore, it has been showed *in vitro* that *B. bacteriovorus* significantly reduced the quantity of biofilm (Kadouri and O’Toole, 2005).

*In vitro* and mouse model studies have underlined the fact that the predatory bacteria have no negative impact on human cell lines (Gupta et al., 2016) nor on animals (Shatzkes et al., 2015). *B. dellovibrio* is thus a potential therapeutic agent, but has not been yet applied in this way. No studies have investigated *B. bacteriovorus* to treat UTIs to date. However, these bacteria offer an exciting path for further research where *in vivo* studies should be the focus.

## BACTERIOPHAGES

Bacteriophages are viruses that parasitize a bacterium by infecting it and reproducing inside it and can act as bactericidal agents. Bacteriophage therapy is currently applied in different areas of medical research. Indeed, it has been recognized as an alternative treatment in localized infections such as otitis, infected burns and osteoarticular infections (Ferry et al., 2018; Jault et al., 2019). However, its use in UTI is scarce.

One research team has studied the combination of transurethral resection of prostate with bacteriophage therapy used instead of per operative antibiotics. They first demonstrated the *in vitro* lytic activity of commercial bacteriophage cocktails on 41 *E. coli* and 9 *K. pneumoniae* strains. The lytic activity of the bacteriophage cocktails varied between 66% and 93%. They also showed the potential of bacteriophage adaptation experiments to increase the lytic activity, leading to an increase from 66 to 93% for one of the cocktails (Sybesma et al., 2016).

In an animal model, Dufour et al. (2016) showed the ability of phage to treat an *E. coli* UTI. The administration of the same bacteriophage cocktail showed a significant reduction of the bacterial load in the *E. coli* kidney infection model as well as in the *E. coli* pneumonia model, but not in an *E. coli* sepsis model.



*In vivo* studies were performed with a commercial preparation called Pyo bacteriophage, composed of bacteriophage lines active against a broad spectrum of uropathogenic bacteria: *S. aureus*, *E. coli*, *Streptococcus* spp. (including *Enterococcus* spp.), *P. aeruginosa*, and *Proteus* spp. in nine patients planned for transurethral resection. Bacteria load decreased in two-thirds of the patients (6/9), without any associated adverse events (Ujmajuridze et al., 2018).

One case report described the treatment of a recurrent *P. aeruginosa* UTI associated with a bilateral ureteral stent. A phage cocktail containing phages with activity against *Streptococcus pyogenes*, *S. aureus*, *E. coli*, *P. aeruginosa*, *P. vulgaris*, and *P. mirabilis* was administered. After 6 days of treatment, meropenem and colistin were started for 30 days. The results showed a 10-fold reduction of bacteria load in the urine after the first 5 days of phage treatment. The bacterial load was undetectable after 2 days of subsequent antibiotic treatment. Urine samples remained sterile until 1 year after the end of the antibiotic treatment.

Another case report showed the treatment of a recurrent UTI with an ESBL-producing *K. pneumoniae* in a renal transplant patient whose infection evolved into an epididymitis. The patient was definitively cured after an oral and intravesical bacteriophage treatment of 10 days following 6-week meropenem treatment (Kuipers et al., 2019).

One randomized, double-blind trial versus placebo in patients planned for transurethral resection of the prostate with UTI is ongoing. Patients will be randomized in a 1:1:1 ratio to receive 7 days of either: (i) bacteriophage (Pyo bacteriophage) solution, (ii) placebo solution, or (iii) antibiotic treatment (Leitner et al., 2017).

More human studies are warranted to further define the role of this treatment option in UTIs.

## CONCLUSION

Although prophylactic antibiotics remain the preferred preventive treatment in recurrent UTIs, the emergence of antimicrobial resistance worldwide has made the development of non-antibiotics strategies a priority. The better understanding of UTI mechanisms will help direct future research on the topic. Indeed, recent studies have revealed that infection with UPEC and a number of other Gram-negative uropathogens proceeds through dynamic intracellular and extracellular host niches during the course of acute and chronic infection.

Several targets such as uropathogenic adhesins, toxins, urease, iron metabolism and motility have been explored. Although

non-antibiotic prophylactic agents appear to be well tolerated and do not seem to increase the antimicrobial resistance of the commensal flora, most of therapeutic options displayed in this review are still preliminary.

Other approaches have also been evaluated in prevention of CAUTI. In case of prolonged utilization of catheter, some techniques have been developed to prevent bacterial growth and biofilm formation. These techniques, including the devices with antimicrobial coatings such as silver, peptides, enzymes or bacteriophages, provide minimal reduction in infection incidence and will need further assessment (Percival et al., 2015; Al-Qahtani et al., 2019).

While *Lactobacillus*-containing products appear to be the most promising new alternative to currently used antibiotics, cranberry products combined with propolis would need further investigations. Studies should now be designed to investigate the interaction between non-antibiotic therapies, uropathogens and the host immune system. Importantly, clinical trials must use standardized definitions of UTI (infection versus colonization based on urinary symptoms), treatment regimens and control groups as well as an assessment of the risk/benefit ratio especially on tolerance and antibiotic resistance and an economic evaluation of the reviewed therapeutics versus prolonged antibiotic treatments. Likewise, further research is needed for vaccines, which have shown potential in initial trials.

## AUTHOR CONTRIBUTIONS

PL, JR, J-PL, and AS wrote the manuscript. AD, CD-R, LB, and FB critically reviewed the manuscript. All authors contributed to the article and approved the submitted version.

## FUNDING

This work was supported by CHU Nîmes (Grant Thématiques phares).

## ACKNOWLEDGMENTS

PL, CD-R, AS and J-PL belong to the FHU INCh (Federation Hospitalo Universitaire Infections Chroniques, Aviesan). We thank the Nîmes University hospital for its structural, human and financial support through the award obtained by our team during the internal call for tenders Thématiques phares. We also thank Sarah Kabani for her editing assistance.

## REFERENCES

- Åberg, V., and Almqvist, F. (2007). Pilicides—small molecules targeting bacterial virulence. *Org. Biomol. Chem.* 5, 1827–1834. doi: 10.1039/b702397a
- Abraham, S. N., and Miao, Y. (2015). The nature of immune responses to urinary tract infections. *Nat. Rev. Immunol.* 15, 655–663. doi: 10.1038/nri3887
- AFSSA (2007). *Saisine n° 2007*. Available online at: <https://www.anses.fr/fr/system/files/DIVE2007sa0209.pdf> (accessed January 13, 2009).

- Ahuja, S., Kaack, B., and Roberts, J. (1998). Loss of fimbrial adhesion with the addition of *Vaccinium macrocarpon* to the growth medium of P-fimbriated *Escherichia coli*. *J. Urol.* 159, 559–562. doi: 10.1016/s0022-5347(01)63983-1
- Albert, X., Huertas, I., Pereiro, I., Sanfélix, J., Gosalbes, V., and Perrotta, C. (2004). Antibiotics for preventing recurrent urinary tract infection in non-pregnant women. *Cochrane Database Syst. Rev.* 3:CD001209.
- Al-Qahtani, M., Safan, A., Jassim, G., and Abadla, S. (2019). Efficacy of antimicrobial catheters in preventing catheter associated urinary tract infections

- in hospitalized patients: a review on recent updates. *J. Infect. Public Health* 12, 760–766. doi: 10.1016/j.jiph.2019.09.009
- Alteri, C. J., Hagan, E. C., Sivick, K. E., Smith, S. N., and Mobley, H. L. T. (2009). Mucosal immunization with iron receptor antigens protects against urinary tract infection. *PLoS Pathog.* 5:e1000586. doi: 10.1371/journal.ppat.1000586
- Amtul, Z., Rahman, A.-U., Siddiqui, R. A., and Choudhary, M. I. (2002). Chemistry and mechanism of urease inhibition. *Curr. Med. Chem.* 9, 1323–1348. doi: 10.2174/0929867023369853
- Anderson, G. G., Goller, C. C., Justice, S., Hultgren, S. J., and Seed, P. C. (2010). Polysaccharide capsule and sialic acid-mediated regulation promote biofilm-like intracellular bacterial communities during cystitis. *Infect. Immun.* 78, 963–975. doi: 10.1128/iai.00925-09
- Anger, J., Lee, U., Ackerman, A. L., Chou, R., Chughtai, B., Clemens, J. Q., et al. (2019). Recurrent uncomplicated urinary tract infections in women: AUA/CUA/SUFU guideline. *J. Urol.* 202, 282–289. doi: 10.1097/ju.0000000000000296
- Arakawa, H., Maeda, M., Okubo, S., and Shimamura, T. (2004). Role of hydrogen peroxide in bactericidal action of catechin. *Biol. Pharm. Bull.* 27, 277–281. doi: 10.1248/bpb.27.277
- Asadi Karam, M. R., Habibi, M., and Bouzari, S. (2019). Urinary tract infection: pathogenicity, antibiotic resistance and development of effective vaccines against Uropathogenic *Escherichia coli*. *Mol. Immunol.* 108, 56–67. doi: 10.1016/j.molimm.2019.02.007
- Aziminia, N., Hadjipavlou, M., Philippou, Y., Pandian, S. S., Malde, S., and Hammadeh, M. Y. (2019). Vaccines for the prevention of recurrent urinary tract infections: a systematic review. *BJU Int.* 123, 753–768. doi: 10.1111/bju.14606
- Bae, W.-J., Ha, U.-S., Kim, S., Kim, S.-J., Hong, S.-H., Lee, J.-Y., et al. (2015). Reduction of oxidative stress may play a role in the anti-inflammatory effect of the novel herbal formulation in a rat model of hydrochloric acid-induced cystitis. *Neurourol. Urodyn.* 34, 86–91. doi: 10.1002/nau.22507
- Baillie, N. C., Osborne, C. A., Leininger, J. R., Fletcher, T. F., Johnston, S. D., Ogburn, P. N., et al. (1986). Teratogenic effect of acetohydroxamic acid in clinically normal beagles. *Am. J. Vet. Res.* 47, 2604–2611.
- Banu, G. S., and Kumar, G. (2009). Preliminary screening of endophytic fungi from medicinal plants in India for antimicrobial and antitumor activity. *Int. J. Pharma. Sci. Nanotechnol.* 2, 566–571.
- Bauer, H. W., Alloussi, S., Egger, G., Blümlein, H.-M., Cozma, G., Schulman, C. C., et al. (2005). A long-term, multicenter, double-blind study of an *Escherichia coli* extract (OM-89) in female patients with recurrent urinary tract infections. *Eur. Urol.* 47, 542–548. doi: 10.1016/j.eururo.2004.12.009
- Beerepoot, M., and Geerlings, S. (2016). Non-antibiotic prophylaxis for urinary tract infections. *Pathogens* 5:36. doi: 10.3390/pathogens5020036
- Beerepoot, M. A. J., den Heijer, C. D. J., Penders, J., Prins, J. M., Stobberingh, E. E., and Geerlings, S. E. (2012a). Predictive value of *Escherichia coli* susceptibility in strains causing asymptomatic bacteriuria for women with recurrent symptomatic urinary tract infections receiving prophylaxis. *Clin. Microbiol. Infect.* 18, E84–E90.
- Beerepoot, M. A. J., ter Riet, G., Nys, S., van der Wal, W. M., de Borgie, C. A. J. M., de Reijke, T. M., et al. (2012b). Lactobacilli vs antibiotics to prevent urinary tract infections: a randomized, double-blind, noninferiority trial in postmenopausal women. *Arch. Intern. Med.* 172, 704–712.
- Benini, S., Rypniewski, W. R., Wilson, K. S., Miletto, S., Ciarli, S., and Mangani, S. (2000). The complex of *Bacillus pasteurii* urease with acetohydroxamate anion from X-ray data at 1.55 Å resolution. *J. Biol. Inorg. Chem.* 5, 110–118. doi: 10.1007/s007750050014
- Birder, L. A., and de Groat, W. C. (2007). Mechanisms of disease: involvement of the urothelium in bladder dysfunction. *Nat. Clin. Pract. Urol.* 4, 46–54. doi: 10.1038/ncpuro0672
- Bleidorn, J., Gágyor, I., Kochen, M. M., Wegscheider, K., and Hummers-Pradier, E. (2010). Symptomatic treatment (ibuprofen) or antibiotics (ciprofloxacin) for uncomplicated urinary tract infection?—results of a randomized controlled pilot trial. *BMC Med.* 8:30. doi: 10.1186/1741-7015-8-30
- Boonsai, P., Phuwapraisirisan, P., and Chanchao, C. (2014). Antibacterial activity of a cardanol from Thai *Apis mellifera* propolis. *Int. J. Med. Sci.* 11, 327–336. doi: 10.7150/ijms.7373
- Brumbaugh, A. R., Smith, S. N., and Mobley, H. L. T. (2013). Immunization with the yersiniabactin receptor, FyuA, protects against pyelonephritis in a murine model of urinary tract infection. *Infect. Immun.* 81, 3309–3316. doi: 10.1128/iai.00470-13
- Bruyère, F., Azzouzi, A. R., Lavigne, J.-P., Droupy, S., Coloby, P., Game, X., et al. (2019). A multicenter, randomized, placebo-controlled study evaluating the efficacy of a combination of propolis and cranberry (*Vaccinium macrocarpon*) (DUAB®) in preventing low urinary tract infection recurrence in women complaining of recurrent cystitis. *Urol. Int.* 103, 41–48. doi: 10.1159/000496695
- Burne, R. A., and Chen, Y. Y. M. (2000). Bacterial ureases in infectious diseases. *Microbes Infect.* 2, 533–542. doi: 10.1016/s1286-4579(00)00312-9
- Cadieux, P. A., Burton, J., Devillard, E., and Reid, G. (2009). Lactobacillus by-products inhibit the growth and virulence of uropathogenic *Escherichia coli*. *J. Physiol. Pharmacol.* 60, 13–18.
- Castelló, T., Girona, L., Gómez, M. R., Mena Mur, A., and García, L. (1996). The possible value of ascorbic acid as a prophylactic agent for urinary tract infection. *Spinal Cord.* 34, 592–593. doi: 10.1038/sc.1996.105
- Cegelski, L., Pinkner, J. S., Hammer, N. D., Cusumano, C. K., Hung, S., Chorell, E., et al. (2010). Small-molecule inhibitors target *Escherichia coli* amyloid biogenesis and biofilm formation. *Natl. Inst. Health* 5, 913–919. doi: 10.1038/nchembio.242
- Chan, M., Hidalgo, G., Asadishad, B., Almeida, S., Muja, N., Mohammadi, M. S., et al. (2013). Inhibition of bacterial motility and spreading via release of cranberry derived materials from silicone substrates. *Colloids Surf. B Biointerfaces* 110, 275–280. doi: 10.1016/j.colsurfb.2013.03.047
- Chen, T.-C., Tsai, J.-P., Huang, H.-J., Teng, C.-C., Chien, S.-J., Kuo, H.-C., et al. (2011). Regulation of cyclooxygenase-2 expression in human bladder epithelial cells infected with type I fimbriated uropathogenic *E. coli*. *Cell. Microbiol.* 13, 1703–1713. doi: 10.1111/j.1462-5822.2011.01650.x
- Chikindas, M. L., Weeks, R., Drider, D., Chistyakov, V. A., and Dicks, L. M. (2018). Functions and emerging applications of bacteriocins. *Curr. Opin. Biotechnol.* 49, 23–28. doi: 10.1016/j.copbio.2017.07.011
- Ciani, O., Arendsen, E., Romancik, M., Lunik, R., Costantini, E., Di Biase, M., et al. (2016). Intravesical administration of combined hyaluronic acid (HA) and chondroitin sulfate (CS) for the treatment of female recurrent urinary tract infections: a European multicentre nested case-control study. *BMJ Open* 6:e009669. doi: 10.1136/bmjopen-2015-009669
- Cicione, A., Cantello, F., Ucciero, G., Salonia, A., Torella, M., De Sio, M., et al. (2014). Intravesical treatment with highly-concentrated hyaluronic acid and chondroitin sulphate in patients with recurrent urinary tract infections: results from a multicentre survey. *J. Can. Urol. Assoc.* 8, E721–E727.
- Constantinides, C., Manousakas, T., Nikolopoulos, P., Stanitsas, A., Haritopoulos, K., and Giannopoulos, A. (2004). Prevention of recurrent bacterial cystitis by intravesical administration of hyaluronic acid: a pilot study. *BJU Int.* 93, 1262–1266. doi: 10.1111/j.1464-410x.2004.04850.x
- Cooper, R., Morré, D. J., and Morré, D. M. (2005a). Medicinal benefits of green tea: Part I. Review of noncancer health benefits. *J. Altern. Complement. Med.* 11, 521–528. doi: 10.1089/acm.2005.11.521
- Cooper, R., Morré, D. J., and Morré, D. M. (2005b). Medicinal benefits of green tea: Part II. Review of anticancer properties. *J. Altern. Complement. Med.* 11, 639–652. doi: 10.1089/acm.2005.11.639
- Cribby, S., Taylor, M., and Reid, G. (2008). Vaginal microbiota and the use of probiotics. *Interdiscip. Perspect. Infect. Dis.* 2008:256490.
- Cusumano, C. K., Pinkner, J. S., Han, Z., Greene, S. E., Ford, B. A., Crowley, J. R., et al. (2011). Treatment and prevention of urinary tract infection with orally active FimH inhibitors. *Sci. Transl. Med.* 3:109ra115. doi: 10.1126/scitranslmed.3003021
- Darouiche, R. O., Donovan, W. H., Del Terzo, M., Thornby, J. I., Rudy, D. C., and Hull, R. A. (2001). Pilot trial of bacterial interference for preventing urinary tract infection. *Urology* 58, 339–344. doi: 10.1016/s0090-4295(01)01271-7
- Darouiche, R. O., Green, B. G., Donovan, W. H., Chen, D., Schwartz, M., Merritt, J., et al. (2011). Multicenter randomized controlled trial of bacterial interference for prevention of urinary tract infection in patients with neurogenic bladder. *Urology* 78, 341–346. doi: 10.1016/j.urology.2011.03.062
- Darouiche, R. O., Thornby, J. I., Stewart, C. C., Donovan, W. H., and Hull, R. A. (2005). Bacterial Interference for prevention of urinary tract infection: a prospective, randomized, placebo-controlled, double-blind pilot trial. *Clin. Infect. Dis.* 41, 1531–1534. doi: 10.1086/497272
- Dashiff, A., Junka, R. A., Libera, M., and Kadouri, D. E. (2011). Predation of human pathogens by the predatory bacteria *Micavibrio aeruginosavorus* and

- Bdellovibrio bacteriovorus*. *J. Appl. Microbiol.* 110, 431–444. doi: 10.1111/j.1365-2672.2010.04900.x
- De Ree, J. M., and Van den Bosch, J. F. (1987). Serological response to the P fimbriae of uropathogenic *Escherichia coli* in pyelonephritis. *Infect. Immun.* 55, 2204–2207. doi: 10.1128/iai.55.9.2204-2207.1987
- De Vuyst, L., and Leroy, F. (2007). Bacteriocins from lactic acid bacteria: production, purification, and food applications. *J. Mol. Microbiol. Biotechnol.* 13, 194–199. doi: 10.1159/000104752
- Di Cerbo, A., Palmieri, B., Aponte, M., Morales-Medina, J. C., and Iannitti, T. (2016). Mechanisms and therapeutic effectiveness of lactobacilli. *J. Clin. Pathol.* 69, 187–203. doi: 10.1136/jclinpath-2015-202976
- Dinh, A., Hallouin-Bernard, M. C., Davido, B., Lemaigen, A., Bouchand, F., Duran, C., et al. (2019). Weekly sequential antibioprophyllaxis for recurrent UTI among patients with neurogenic bladder: a randomized controlled trial. *Clin. Infect. Dis.* ciz1207. doi: 10.1093/cid/ciz1207. [Epub ahead of print].
- Domenici, L., Monti, M., Bracchi, C., Giorgini, M., Colagiovanni, V., Muzii, L., et al. (2016). D-mannose: a promising support for acute urinary tract infections in women. A pilot study. *Eur. Rev. Med. Pharmacol. Sci.* 20, 2920–2925.
- Duell, B. L., Carey, A. J., Tan, C. K., Cui, X., Webb, R. I., Totsika, M., et al. (2012). Innate transcriptional networks activated in bladder in response to uropathogenic *Escherichia coli* drive diverse biological pathways and rapid synthesis of IL-10 for defense against bacterial urinary tract infection. *J. Immunol.* 188, 781–792. doi: 10.4049/jimmunol.1101231
- Dufour, N., Clermont, O., La Combe, B., Messika, J., Dion, S., Khanna, V., et al. (2016). Bacteriophage LM33\_P1, a fast-acting weapon against the pandemic ST131-O25b:H4 *Escherichia coli* clonal complex. *J. Antimicrob. Chemother.* 71, 3072–3080. doi: 10.1093/jac/dkw253
- Ellis, T. N., and Kuehn, M. J. (2010). Virulence and immunomodulatory roles of bacterial outer membrane vesicles. *Microbiol. Mol. Biol. Rev.* 74, 81–94. doi: 10.1128/mmr.00031-09
- Ermel, G., Georgeault, S., Inisan, C., and Besnard, M. (2012). Inhibition of adhesion of uropathogenic *Escherichia coli* Bacteria to uroepithelial cells by extracts from cranberry. *J. Med. Food* 15, 126–134. doi: 10.1089/jmf.2010.0312
- Falagas, M. E., Betsi, G. I., Tokas, T., and Athanasiou, S. (2006). Probiotics for prevention of recurrent urinary tract infections in women: a review of the evidence from microbiological and clinical studies. *Drugs* 66, 1253–1261. doi: 10.2165/00003495-200666090-00007
- Faraci, W. S., Yang, B. V., O'Rourke, D., and Spencer, R. W. (1995). Inhibition of *Helicobacter pylori* urease by phenyl phosphorodiamidates: mechanism of action. *Bioorg. Med. Chem.* 3, 605–610. doi: 10.1016/0968-0896(95)00043-g
- Ferry, S. A., Holm, S. E., Stenlund, H., Lundholm, R., and Monsen, T. J. (2004). The natural course of uncomplicated lower urinary tract infection in women illustrated by a randomized placebo controlled study. *Scand. J. Infect. Dis.* 36, 296–301. doi: 10.1080/00365540410019642
- Ferry, T., Boucher, F., Fevre, C., Perpoint, T., Chateau, J., Petitjean, C., et al. (2018). Innovations for the treatment of a complex bone and joint infection due to XDR *Pseudomonas aeruginosa* including local application of a selected cocktail of bacteriophages. *J. Antimicrob. Chemother.* 73, 2901–2903. doi: 10.1093/jac/dky263
- Flores-Meireles, A., Walker, J., Caparon, M., and Hultgren, S. (2015). Urinary tract infections: epidemiology, mechanisms of infection and treatment options. *Nat. Rev. Microbiol.* 13, 269–284. doi: 10.1038/nrmicro3432
- Flower, A., Wang, L.-Q., Lewith, G., Liu, J. P., and Li, Q. (2015). Chinese herbal medicine for treating recurrent urinary tract infections in women. *Cochrane Database Syst. Rev.* 2015:CD010446.
- Foxman, B. (2014). Urinary tract infection syndromes: occurrence, recurrence, bacteriology, risk factors, and disease burden. *Infect. Dis. Clin. North Am.* 28, 1–13. doi: 10.1016/j.idc.2013.09.003
- Freitas, S. F., Shinohara, L., Sforzin, J. M., and Guimarães, S. (2006). In vitro effects of propolis on *Giardia duodenalis* trophozoites. *Phytomedicine* 13, 170–175. doi: 10.1016/j.phymed.2004.07.008
- Frenck, R. W., Ervin, J., Chu, L., Abbanat, D., Spiessens, B., Go, O., et al. (2019). Safety and immunogenicity of a vaccine for extra-intestinal pathogenic *Escherichia coli* (ESTELLA): a phase 2 randomised controlled trial. *Lancet Infect. Dis.* 19, 631–640. doi: 10.1016/s1473-3099(18)30803-x
- Galdeano, C. M., and Perdigón, G. (2006). The probiotic bacterium *Lactobacillus casei* induces activation of the gut mucosal immune system through innate immunity. *Clin. Vaccine Immunol.* 13, 219–226. doi: 10.1128/cvi.13.2.219-226.2006
- Goddard, J. C., and Janssen, D. A. W. (2018). Intravesical hyaluronic acid and chondroitin sulfate for recurrent urinary tract infections: systematic review and meta-analysis. *Int. Urogynecol. J.* 29, 933–942. doi: 10.1007/s00192-017-3508-z
- Goller, C. C., Arshad, M., Noah, J. W., Ananthan, S., Evans, C. W., Nebane, N. M., et al. (2014). Lifting the mask: identification of new small molecule inhibitors of uropathogenic *Escherichia coli* group 2 capsule biogenesis. *PLoS One* 9:e96054. doi: 10.1371/journal.pone.0096054
- Greene, S. E., Pinkner, J. S., Chorell, E., Dodson, K. W., Shaffer, C. L., Conover, M. S., et al. (2014). Pilicide ec240 disrupts virulence circuits in uropathogenic *Escherichia coli*. *mBio* 5:14.
- Griffith, D. P., Gibson, J. R., Clinton, C. W., and Musher, D. M. (1978). Acetohydroxamic acid: clinical studies of a urease inhibitor in patients with staghorn renal calculi. *J. Urol.* 119, 9–15. doi: 10.1016/s0022-5347(17)57366-8
- Griffith, D. P., Gleeson, M. J., Lee, H., Longuet, R., Deman, E., and Earle, N. (1991). Randomized, double-blind trial of Lithostat (acetohydroxamic acid) in the palliative treatment of infection-induced urinary calculi. *Eur. Urol.* 20, 243–247. doi: 10.1159/000471707
- Griffith, D. P., Khonsari, F., Skurnick, J. H., and James, K. E. (1988). A randomized trial of acetohydroxamic acid for the treatment and prevention of infection-induced urinary stones in spinal cord injury patients. *J. Urol.* 140, 318–324. doi: 10.1016/s0022-5347(17)41592-8
- Gu, X. C., Xu, Z., Chen, M., and Wang, M. (2011). Study of erding erxian decoction compared with sanjin tablet in treating recurrent urinary tract infection. *Zhongguo Zhongxiyi Jiehe Shenbing Zazhi.* 12, 623–624.
- Gupta, S., Tang, C., Tran, M., and Kadouri, D. E. (2016). Effect of predatory bacteria on human cell lines. *PLoS One* 11:e0161242. doi: 10.1371/journal.pone.0161242
- Habash, M. B., Van der Mei, H. C., Busscher, H. J., and Reid, G. (1999). The effect of water, ascorbic acid, and cranberry derived supplementation on human urine and uropathogen adhesion to silicone rubber. *Can. J. Microbiol.* 45, 691–694. doi: 10.1139/w99-065
- Habibi, M., Asadi Karam, M. R., and Bouzari, S. (2016). Transurethral instillation with fusion protein MrpH.FimH induces protective innate immune responses against uropathogenic *Escherichia coli* and *Proteus mirabilis*. *APMIS* 124, 444–452. doi: 10.1111/apm.12523
- Hannan, T. J., Mysorekar, I. U., Hung, C. S., Isaacson-Schmid, M. L., and Hultgren, S. J. (2010). Early severe inflammatory responses to uropathogenic *E. coli* predispose to chronic and recurrent urinary tract infection. *PLoS Pathog.* 6:e1001042. doi: 10.1371/journal.ppat.1001042
- Hannan, T. J., Roberts, P. L., Riehl, T. E., van der Post, S., Binkley, J. M., Schwartz, D. J., et al. (2014). Inhibition of cyclooxygenase-2 prevents chronic and recurrent cystitis. *EBioMedicine* 1, 46–57. doi: 10.1016/j.ebiom.2014.10.011
- Hardy, H., Harris, J., Lyon, E., Beal, J., and Foey, A. D. (2013). Probiotics, prebiotics and immunomodulation of gut mucosal defences: homeostasis and immunopathology. *Nutrients* 5, 1869–1912. doi: 10.3390/nu5061869
- Hills, A. E., Patel, A., Boyd, P., and James, D. C. (2001). Metabolic control of recombinant monoclonal antibody N-glycosylation in GS-NS0 cells. *Biotechnol. Bioeng.* 75, 239–251. doi: 10.1002/bit.10022
- Hopkins, W. J., Elkahwaji, J., Beierle, L. M., Levenson, G. E., and Uehling, D. T. (2007). Vaginal mucosal vaccine for recurrent urinary tract infections in women: results of a phase 2 clinical trial. *J. Urol.* 177, 1349–1353. doi: 10.1016/j.juro.2006.11.093
- Hoshino, N., Kimura, T., Yamaji, A., and Ando, T. (1999). Damage to the cytoplasmic membrane of *Escherichia coli* by catechin-copper (II) complexes. *Free Radic. Biol. Med.* 27, 1245–1250. doi: 10.1016/s0891-5849(99)00157-4
- Hou, X., and Wang, L. X. (2016). Research progress of sanjin tablets. *Eval. Anal. Drug Chin. Hosp.* 16, 1148–1151.
- Howell, A. B., Reed, J. D., Krueger, C. G., Winterbottom, R., Cunningham, D. G., and Leahy, M. (2005). A-type cranberry proanthocyanidins and uropathogenic bacterial anti-adhesion activity. *Phytochemistry* 66, 2281–2291. doi: 10.1016/j.phytochem.2005.05.022
- Huber, M., Ayoub, M., Pfannes, S. D., Mittenbühler, K., Weis, K., Bessler, W. G., et al. (2000). Immunostimulatory activity of the bacterial extract OM-8. *Eur. J. Med. Res.* 5, 101–109.
- Hull, R., Rudy, D., Donovan, W., Svanborg, C., Wieser, I., Stewart, C., et al. (2000). Urinary tract infection prophylaxis using *Escherichia coli* 83972 in spinal cord injured patients. *J. Urol.* 163, 872–877. doi: 10.1016/s0022-5347(05)67823-8



- Huttner, A., and Gambillara, V. (2018). The development and early clinical testing of the ExPEC4V conjugate vaccine against uropathogenic *Escherichia coli*. *Clin. Microbiol. Infect.* 24, 1046–1050. doi: 10.1016/j.cmi.2018.05.009
- Huttner, A., Hatz, C., van den Dobbelsteen, G., Abbanat, D., Hornacek, A., Frölich, R., et al. (2017). Safety, immunogenicity, and preliminary clinical efficacy of a vaccine against extraintestinal pathogenic *Escherichia coli* in women with a history of recurrent urinary tract infection: a randomised, single-blind, placebo-controlled phase 1b trial. *Lancet Infect. Dis.* 17, 528–537. doi: 10.1016/s1473-3099(17)30108-1
- Ikähelmo, R., Siitonen, A., Heiskanen, T., Kärkkäinen, U., Kuosmanen, P., Lipponen, P., et al. (1996). Recurrence of urinary tract infection in a primary care setting: analysis of a 1-year follow-up of 179 women. *Clin. Infect. Dis.* 22, 91–99. doi: 10.1093/clinids/22.1.91
- Ingersoll, M. A., and Albert, M. L. (2013). From infection to immunotherapy: host immune responses to bacteria at the bladder mucosa. *Mucosal Immunol.* 6, 1041–1053. doi: 10.1038/mi.2013.72
- Isolauri, E., Sütas, Y., Kankaanpää, P., Arvilommi, H., and Salminen, S. (2001). Probiotics: effects on immunity. *Am. J. Clin. Nutr.* 73, 444S–450S.
- Issac Abraham, S. V., Palani, A., Ramaswamy, B. R., Shunmugiah, K. P., and Arumugam, V. R. (2011). Antiquorum sensing and antibiofilm potential of *Capparis spinosa*. *Arch. Med. Res.* 42, 658–668. doi: 10.1016/j.arcmed.2011.12.002
- Jacobsen, S. M., Stickler, D. J., Mobley, H. L. T., and Shirtliff, M. E. (2008). Complicated catheter-associated urinary tract infections due to *Escherichia coli* and *Proteus mirabilis*. *Clin. Microbiol. Rev.* 21, 26–59. doi: 10.1128/cmr.00019-07
- Jaiswal, S. K., Sharma, N. K., Bharti, S. K., Krishnan, S., Kumar, A., Prakash, O., et al. (2018). Phytochemicals as uropathogenic *Escherichia coli* FimH antagonist: in vitro and in silico approach. *Curr. Mol. Med.* 18, 640–653. doi: 10.2174/1566524019666190104104507
- Jault, P., Leclerc, T., Jennes, S., Pirnay, J. P., Que, Y.-A., Resch, G., et al. (2019). Efficacy and tolerability of a cocktail of bacteriophages to treat burn wounds infected by *Pseudomonas aeruginosa* (PhagoBurn): a randomised, controlled, double-blind phase 1/2 trial. *Lancet Infect. Dis.* 19, 35–45. doi: 10.1016/s1473-3099(18)30482-1
- Jepson, R. G., and Craig, J. C. (2008). Cranberries for preventing urinary tract infections. *Cochrane Database Syst. Rev.* CD001321. doi: 10.1002/14651858.CD001321.pub4
- Jepson, R. G., Williams, G., and Craig, J. C. (2012). Cranberries for preventing urinary tract infections. *Cochrane Database Syst. Rev.* 10:CD001321.
- Johnson, J. R. (1991). Virulence factors in *Escherichia coli* urinary tract infection. *Clin. Microbiol. Rev.* 4, 80–128. doi: 10.1128/cmr.4.1.80
- Kadouri, D., and O'Toole, G. A. (2005). Susceptibility of biofilms to *Bdellovibrio bacteriovorus* attack. *Appl. Environ. Microbiol.* 71, 4044–4051. doi: 10.1128/aem.71.7.4044-4051.2005
- Kajiser, B., Larsson, P., Olling, S., and Schneerson, R. (1983). Protection against acute, ascending pyelonephritis caused by *Escherichia coli* in rats, using isolated capsular antigen conjugated to bovine serum albumin. *Infect. Immun.* 39, 142–146. doi: 10.1128/iai.39.1.142-146.1983
- Kemgang, T. S., Kapila, S., Shanmugam, V. P., and Kapila, R. (2014). Cross-talk between probiotic lactobacilli and host immune system. *J. Appl. Microbiol.* 117, 303–319. doi: 10.1111/jam.12521
- Klein, T., Abgottspon, D., Wittwer, M., Rabbani, S., Herold, J., Jiang, X., et al. (2010). FimH antagonists for the oral treatment of urinary tract infections: from design and synthesis to in vitro and in vivo evaluation. *J. Med. Chem.* 53, 8627–8641. doi: 10.1021/jm101011y
- Koradia, P., Kapadia, S., Trivedi, Y., Chanchu, G., and Harper, A. (2019). Probiotic and cranberry supplementation for preventing recurrent uncomplicated urinary tract infections in premenopausal women: a controlled pilot study. *Exp. Rev. Anti Infect. Ther.* 17, 733–740. doi: 10.1080/14787210.2019.1664287
- Kranjčec, B., Papes, D., and Altarac, S. (2014). D-mannose powder for prophylaxis of recurrent urinary tract infections in women: a randomized clinical trial. *World J. Urol.* 32, 79–84. doi: 10.1007/s00345-013-1091-6
- Kuipers, S., Ruth, M. M., Mientjes, M., de Sévaux, R. G. L., and van Ingen, J. A. (2019). Dutch case report of successful treatment of chronic relapsing urinary tract infection with bacteriophages in a renal transplant patient. *Antimicrob. Agents Chemother.* 64:e01281-19.
- Kumar, V., Ganguly, N., Joshi, K., Mittal, R., Harjai, K., Chhibber, S., et al. (2005). Protective efficacy and immunogenicity of *Escherichia coli* K13 diphtheria toxoid conjugate against experimental ascending pyelonephritis. *Med. Microbiol. Immunol.* 194, 211–217. doi: 10.1007/s00430-005-0241-x
- Langermann, S., Möllby, R., Burlein, J. E., Palaszynski, S. R., Auguste, C. G., DeFusco, A., et al. (2000). Vaccination with FimH adhesin protects cynomolgus monkeys from colonization and infection by uropathogenic *Escherichia coli*. *J. Infect. Dis.* 181, 774–778. doi: 10.1086/315258
- Larsson, A., Ohlsson, J., Dodson, K. W., Hultgren, S. J., Nilsson, U., and Kihlberg, J. (2003). Quantitative studies of the binding of the class II PapG adhesin from uropathogenic *Escherichia coli* to oligosaccharides. *Bioorg. Med. Chem.* 11, 2255–2261. doi: 10.1016/s0968-0896(03)00114-7
- Laupland, K. B., Ross, T., Pitout, J. D. D., Church, D. L., and Gregson, D. B. (2007). Community-onset urinary tract infections: a population-based assessment. *Infection* 35, 150–153. doi: 10.1007/s15010-007-6180-2
- Leitner, L., Sybesma, W., Chanishvili, N., Goderdzishvili, M., Chkhotua, A., Ujmajuridze, A., et al. (2017). Bacteriophages for treating urinary tract infections in patients undergoing transurethral resection of the prostate: a randomized, placebo-controlled, double-blind clinical trial. *BMC Urol.* 17:90. doi: 10.1186/s12894-017-0283-6
- Liu, H., Howell, A. B., Zhang, D. J., and Khoo, C. (2019). A randomized, double-blind, placebo-controlled pilot study to assess bacterial anti-adhesive activity in human urine following consumption of a cranberry supplement. *Food Funct.* 10, 7645–7652. doi: 10.1039/c9fo01198f
- Liu, Y., Black, M. A., Caron, L., and Comesano, T. A. (2006). Role of cranberry juice on molecular-scale surface characteristics and adhesion behavior of *Escherichia coli*. *Biotechnol. Bioeng.* 93, 297–305. doi: 10.1002/bit.20675
- Liu, Z., Ren, Z., Zhang, J., Chuang, C. C., Kandaswamy, E., Zhou, T., et al. (2018). Role of ROS and nutritional antioxidants in human diseases. *Front. Physiol.* 9:477. doi: 10.3389/fphys.2018.00477
- Llobet, E., Tomás, J. M., and Bengoechea, J. A. (2008). Capsule polysaccharide is a bacterial decoy for antimicrobial peptides. *Microbiol. Read. Engl.* 154, 3877–3886. doi: 10.1099/mic.0.2008/022301-0
- Lorenzo-Gómez, M. F., Padilla-Fernández, B., García-Cenador, M. B., Virseda-Rodríguez, ÁJ., Martín-García, I., Sánchez-Escudero, A., et al. (2015). Comparison of sublingual therapeutic vaccine with antibiotics for the prophylaxis of recurrent urinary tract infections. *Front. Cell. Infect. Microbiol.* 5:50. doi: 10.3389/fcimb.2015.00050
- Lorenzo-Gómez, M. F., Padilla-Fernández, B., García-Criado, F. J., Mirón-Canelo, J. A., Gil-Vicente, A., Nieto-Huertos, A., et al. (2013). Evaluation of a therapeutic vaccine for the prevention of recurrent urinary tract infections versus prophylactic treatment with antibiotics. *Int. Urogynecology J.* 24, 127–134. doi: 10.1007/s00192-012-1853-5
- Magasi, P., Pánovics, J., Illés, A., and Nagy, M. (1994). Uro-Vaxom and the management of recurrent urinary tract infection in adults: a randomized multicenter double-blind trial. *Eur. Urol.* 26, 137–140. doi: 10.1159/000475363
- Mazarei, F., Jooyandeh, H., Noshad, M., and Hojjati, M. (2017). Polysaccharide of caper (*Capparis spinosa* L.) Leaf: extraction optimization, antioxidant potential, and antimicrobial activity. *Int. J. Biol. Macromol.* 95, 224–231. doi: 10.1016/j.ijbiomac.2016.11.049
- McLellan, L. K., and Hunstad, D. A. (2016). Urinary tract infection: pathogenesis and outlook. *Trends Mol. Med.* 22, 946–957. doi: 10.1016/j.molmed.2016.09.003
- Melican, K., Sandoval, R. M., Kader, A., Josefsson, L., Tanner, G. A., Molitoris, B. A., et al. (2011). Uropathogenic *Escherichia coli* P and Type 1 fimbriae act in synergy in a living host to facilitate renal colonization leading to nephron obstruction. *PLoS Pathog.* 7:e1001298. doi: 10.1371/journal.ppat.1001298
- Mendling, W. (2016). Vaginal microbiota. *Adv. Exp. Med. Biol.* 902, 83–93.
- Meng, J., Zou, Z., and Lu, C. (2015). Identification and characterization of bioactive compounds targeting uropathogenic *Escherichia coli* from Sanjin tablets. *J. Chem.* 2015, 789809.
- Mickymaray, S., and Al Aboody, M. S. (2019). In vitro antioxidant and bactericidal efficacy of 15 common spices: novel therapeutics for urinary tract infections? *Medicina (Kaunas)* 55:E289.
- Mobley, H. L., and Hausinger, R. P. (1989). Microbial ureases: significance, regulation, and molecular characterization. *Microbiol. Rev.* 53, 85–108. doi: 10.1128/mmbr.53.1.85-108.1989



- Moore, M., Trill, J., Simpson, C., Webley, F., Radford, M., Stanton, L., et al. (2019). Uva-ursi extract and ibuprofen as alternative treatments for uncomplicated urinary tract infection in women (ATAFUTI): a factorial randomized trial. *Clin. Microbiol. Infect.* 25, 973–980. doi: 10.1016/j.cmi.2019.01.011
- Morris, N. S., and Stickler, D. J. (1998). The effect of urease inhibitors on the encrustation of urethral catheters. *Urol. Res.* 26, 275–279. doi: 10.1007/s002400050057
- Muenzner, P., Tchoupa, A. K., Klausner, B., Brunner, T., Putze, J., Dobrindt, U., et al. (2016). Uropathogenic *E. coli* exploit CEA to promote colonization of the urogenital tract mucosa. *PLoS Pathog.* 12:e1005608. doi: 10.1371/journal.ppat.1005608
- Mulvey, M. A. (2002). Adhesion and entry of uropathogenic *Escherichia coli*. *Cell. Microbiol.* 4, 257–271. doi: 10.1046/j.1462-5822.2002.00193.x
- Mulvey, M. A., Schilling, J. D., and Hultgren, S. J. (2001). Establishment of a persistent *Escherichia coli* reservoir during the acute phase of a bladder infection. *Infect. Immun.* 69, 4572–4579. doi: 10.1128/iai.69.7.4572-4579.2001
- Munakata, K., Mochida, H., Kondo, S., and Suzuki, Y. (1980). Mutagenicity of N-acylglycinohydroxamic acids and related compounds. *J. Pharmacobiodyn.* 3, 557–561. doi: 10.1248/bpb1978.3.557
- Musher, D. M., Griffith, D. P., Yawn, D., and Rossen, R. D. (1975). Role of urease in pyelonephritis resulting from urinary tract infection with *Proteus*. *J. Infect. Dis.* 131, 177–181. doi: 10.1093/infdis/131.2.177
- Ng, Q. X., Peters, C., Venkatanarayanan, N., Goh, Y. Y., Ho, C. Y. X., and Yeo, W.-S. (2018). Use of *Lactobacillus* spp. to prevent recurrent urinary tract infections in females. *Med. Hypotheses* 114, 49–54. doi: 10.1016/j.mehy.2018.03.001
- Noormandi, A., and Dabaghzadeh, F. (2015). Effects of green tea on *Escherichia coli* as a uropathogen. *J. Tradit. Complement. Med.* 5, 15–20. doi: 10.1016/j.jtcm.2014.10.005
- O'Brien, V. P., Hannan, T. J., Nielsen, H. V., and Hultgren, S. J. (2016). Drug and vaccine development for the treatment and prevention of urinary tract infections. *Microbiol. Spectr.* 4:10.1128/microbiolsec.UTI-0013-2012.
- Ochoa-Brust, G. J., Fernández, A. R., Villanueva-Ruiz, G. J., Velasco, R., Trujillo-Hernández, B., and Vásquez, C. (2007). Daily intake of 100 mg ascorbic acid as urinary tract infection prophylactic agent during pregnancy. *Acta Obstet. Gynecol. Scand.* 86, 783–787. doi: 10.1080/00016340701273189
- O'Hanley, P., Lalonde, G., and Ji, G. (1991). Alpha-hemolysin contributes to the pathogenicity of pilated digalactoside-binding *Escherichia coli* in the kidney: efficacy of an alpha-hemolysin vaccine in preventing renal injury in the BALB/c mouse model of pyelonephritis. *Infect. Immun.* 59, 1153–1161. doi: 10.1128/iai.59.3.1153-1161.1991
- O'Hanley, P., Lark, D., Falkow, S., and Schoolnik, G. (1985). Molecular basis of *Escherichia coli* colonization of the upper urinary tract in BALB/c mice. *J. Clin. Invest.* 75, 347–360. doi: 10.1172/jci111707
- Olczyk, P., Komosińska-Vassev, K., Wisowski, G., Mencner, L., Stojko, J., and Kozma, E. M. (2014). Propolis modulates fibronectin expression in the matrix of thermal injury. *BioMed Res. Int.* 2014:748101.
- Pasupuleti, V. R., Sammugam, L., Ramesh, N., and Gan, S. H. (2017). Honey, propolis, and royal jelly: a comprehensive review of their biological actions and health benefits. *Oxid. Med. Cell. Longev.* 2017, 1–21. doi: 10.1155/2017/1259510
- Paxman, J. J., Lo, A. W., Sullivan, M. J., Panjkar, S., Kuiper, M., Whitten, A. E., et al. (2019). Unique structural features of a bacterial autotransporter adhesin suggest mechanisms for interaction with host macromolecules. *Nat. Comm.* 10:1967.
- Percival, S. L., Suleman, L., Vuotto, C., and Donelli, G. (2015). Healthcare-associated infections, medical devices and biofilms: risk, tolerance and control. *J. Med. Microbiol.* 64, 323–334. doi: 10.1099/jmm.0.000032
- Pereira, E. M. R., da Silva, J. L. D. C., Silva, F. F., De Luca, M. P., Ferreira, E. F. E., Lorentz, T. C. M., et al. (2011). Clinical evidence of the efficacy of a mouthwash containing propolis for the control of plaque and gingivitis: a phase II study. *Evid.-based complement. Altern. Med.* 2011:750249.
- Piatek, R., Zalewska-Piatek, B., Dzierzbicka, K., Makowiec, S., Pilipczuk, J., Szemiako, K., et al. (2013). Pilicides inhibit the FGL chaperone/usher assisted biogenesis of the Dr fimbrial polyadhesin from uropathogenic *Escherichia coli*. *BMC Microbiol.* 13:131. doi: 10.1186/1471-2180-13-131
- Pinkner, J. S., Remaut, H., Buelens, F., Miller, E., Aberg, V., Pemberton, N., et al. (2006). Rationally designed small compounds inhibit pilus biogenesis in uropathogenic bacteria. *Proc. Natl. Acad. Sci. U.S.A.* 103, 17897–17902. doi: 10.1073/pnas.0606795103
- Poggio, T. V., La Torre, J. L., and Scodeller, E. A. (2006). Intranasal immunization with a recombinant truncated FimH adhesin adjuvanted with CpG oligodeoxynucleotides protects mice against uropathogenic *Escherichia coli* challenge. *Can. J. Microbiol.* 52, 1093–1102. doi: 10.1139/w06-065
- Poirier, C., Dinh, A., Salomon, J., Grall, N., Andremont, A., and Bernard, L. (2015). Antibiotic cycling prevents urinary tract infections in spinal cord injury patients and limits the emergence of multidrug resistant organism. *J. Infect.* 71, 491–493. doi: 10.1016/j.jinf.2015.06.001
- Pope, A. J., Toseland, C. D., Rushant, B., Richardson, S., McVey, M., and Hills, J. (1998). Effect of potent urease inhibitor, fluorofamide, on *Helicobacter* sp. in vivo and in vitro. *Dig. Dis. Sci.* 43, 109–119.
- Prasad, A., Cevallos, M. E., Riosa, S., Darouiche, R. O., and Trautner, B. W. (2009). A bacterial interference strategy for prevention of UTI in persons practicing intermittent catheterization. *Spinal Cord.* 47, 565–569. doi: 10.1038/sc.2008.166
- Prattley, S., Geraghty, R., Moore, M., and Somani, B. K. (2020). Role of vaccines or recurrent urinary tract infections: a systematic review. *Eur. Urol. Focus* 6, 593–604. doi: 10.1016/j.euf.2019.11.002
- Professionals, S.-O. (2019). *EAU Guidelines: Urological Infections [Internet]. Uroweb [cité 2019 juill 9].* Available online at: <https://uroweb.org/guideline/urological-infections/> (accessed July 9, 2019).
- Pu, X., Zhang, L. Y., and Zhang, J. H. (2016). A systemic review of Sanjin tablets in the treatment of simple urinary tract infection: a randomized controlled trial. *Lishizhen Med. Mat. Med. Res.* 27, 1012–1014.
- Rafsanjany, N., Senker, J., Brandt, S., Dobrindt, U., and Hensel, A. (2015). In vivo consumption of cranberry exerts ex Vivo antiadhesive activity against FimH-dominated uropathogenic *Escherichia coli*: a combined in vivo, ex vivo, and in vitro study of an extract from *Vaccinium macrocarpon*. *J. Agric. Food Chem.* 63, 8804–8818. doi: 10.1021/acs.jafc.5b03030
- Ramirez Sevilla, C., Gómez Lanza, E., Manzanera, J. L., Martin, J. A. R., and Sanz, M. A. B. (2019). Active immunoprophylaxis with uromune® decreases the recurrence of urinary tract infections at three and six months after treatment without relevant secondary effects. *BMC Infect. Dis.* 19:901. doi: 10.1186/s12879-019-4541-y
- Ranfaing, J., Dunyach-Remy, C., Lavigne, J.-P., and Sotto, A. (2018a). Propolis potentiates the effect of cranberry (*Vaccinium macrocarpon*) in reducing the motility and the biofilm formation of uropathogenic *Escherichia coli*. *PLoS One* 13:e0202609. doi: 10.1371/journal.pone.0202609
- Ranfaing, J., Dunyach-Remy, C., Louis, L., Lavigne, J.-P., and Sotto, A. (2018b). Propolis potentiates the effect of cranberry (*Vaccinium macrocarpon*) against the virulence of uropathogenic *Escherichia coli*. *Sci. Rep.* 8:10706.
- Reygaert, W., and Jusufi, I. (2013). Green tea as an effective antimicrobial for urinary tract infections caused by *Escherichia coli*. *Front. Microbiol.* 4:162. doi: 10.3389/fmicb.2013.00162
- Riaz, S., Kashif Nawaz, S., and Hasnain, S. (2010). Bacteriocins produced by *L. fermentum* and *L. acidophilus* can inhibit cephalosporin resistant *E. coli*. *Braz. J. Microbiol.* 41, 643–648. doi: 10.1590/s1517-83822010000300015
- Riegman, N., van Die, I., Leunissen, J., Hoekstra, W., and Bergmans, H. (1988). Biogenesis of F71 and F72 fimbriae of uropathogenic *Escherichia coli*: influence of the FsoF and FstFG proteins and localization of the Fso/FstE protein. *Mol. Microbiol.* 2, 73–80. doi: 10.1111/j.1365-2958.1988.tb00008.x
- Roberts, I. S. (1995). Bacterial polysaccharides in sickness and in health. *Microbiology* 141, 2023–2031. doi: 10.1099/13500872-141-9-2023
- Roberts, I. S. (1996). The biochemistry and genetics of capsular polysaccharide production in bacteria. *Annu. Rev. Microbiol.* 50, 285–315. doi: 10.1146/annurev.micro.50.1.285
- Roberts, J. A. (1991). Etiology and pathophysiology of pyelonephritis. *Am. J. Kidney Dis.* 17, 1–9. doi: 10.1016/s0272-6386(12)80242-3
- Roberts, J. A., Kaack, M. B., Baskin, G., Chapman, M. R., Hunstad, D. A., Pinkner, J. S., et al. (2004). Antibody responses and protection from pyelonephritis following vaccination with purified *Escherichia coli* PapDG protein. *J. Urol.* 171, 1682–1685. doi: 10.1097/01.ju.0000116123.05160.43
- Roberts, J. A., Kaack, M. B., Baskin, G., and Svenson, S. B. (1993). Prevention of renal scarring from pyelonephritis in nonhuman primates by vaccination with a synthetic *Escherichia coli* serotype O8 oligosaccharide-protein conjugate. *Infect. Immun.* 61, 5214–5218. doi: 10.1128/iai.61.12.5214-5218.1993
- Rodríguez-Pérez, C., Quirantes-Piné, R., Uberos, J., Jiménez-Sánchez, C., Peña, A., and Segura-Carretero, A. (2016). Antibacterial activity of isolated phenolic

- compounds from cranberry (*Vaccinium macrocarpon*) against *Escherichia coli*. *Food Funct.* 7, 1564–1573. doi: 10.1039/c5fo01441g
- Roos, V., Ulett, G. C., Schembri, M. A., and Klemm, P. (2006). The asymptomatic bacteriuria *Escherichia coli* strain 83972 outcompetes uropathogenic *E. coli* strains in human urine. *Infect. Immun.* 74, 615–624. doi: 10.1128/iai.74.1.615-624.2006
- Rosen, D. A., Hooton, T. M., Stamm, W. E., Humphrey, P. A., and Hultgren, S. J. (2007). Detection of intracellular bacterial communities in human urinary tract infection. *PLoS Med.* 4:e329. doi: 10.1371/journal.pmed.0040329
- Saint, S., Meddings, J. A., Calfee, D., Kowalski, C. P., and Krein, S. L. (2009). Catheter-associated urinary tract infection and the medicare rule changes. *Ann. Intern. Med.* 150, 877–884.
- Salomon, J., Denys, P., Merle, C., Chartier-Kastler, E., Perronne, C., Gaillard, J.-L., et al. (2006). Prevention of urinary tract infection in spinal cord-injured patients: safety and efficacy of a weekly oral cyclic antibiotic (WOCA) programme with a 2 year follow-up—an observational prospective study. *J. Antimicrob. Chemother.* 57, 784–788. doi: 10.1093/jac/dkl010
- Sauer, F. G., Remaut, H., Hultgren, S. J., and Waksman, G. (2004). Fiber assembly by the chaperone-usher pathway. *Biochim. Biophys. Acta.* 1694, 259–267. doi: 10.1016/j.bbamcr.2004.02.010
- Schaeffer, A. J., Jones, J. M., and Dunn, J. K. (1981). Association of in vitro *Escherichia coli* adherence to vaginal and buccal epithelial cells with susceptibility of women to recurrent urinary-tract infections. *N. Engl. J. Med.* 304, 1062–1066. doi: 10.1056/nejm198104303041802
- Schulman, C. C., Corbusier, A., Michiels, H., and Taenzer, H. J. (1993). Oral immunotherapy of recurrent urinary tract infections: a double-blind placebo-controlled multicenter study. *J. Urol.* 150, 917–921. doi: 10.1016/s0022-5347(17)35648-3
- Sharifi-Rad, J., Mnyer, D., Roointan, A., Shahri, F., Ayatollahi, S. A., Sharifi-Rad, M., et al. (2016). Antibacterial activities of essential oils from Iranian medicinal plants on extended-spectrum  $\beta$ -lactamase-producing *Escherichia coli*. *Cell. Mol. Biol.* 62, 75–82.
- Shatzkes, K., Chae, R., Tang, C., Ramirez, G. C., Mukherjee, S., Tsenova, L., et al. (2015). Examining the safety of respiratory and intravenous inoculation of *Bdellovibrio bacteriovorus* and *Micavibrio aeruginosavorus* in a mouse model. *Sci. Rep.* 5:12899.
- Silverman, J. A., Schreiber, H. L. IV, Hooton, T. M., and Hultgren, S. J. (2013). From physiology to pharmacy: developments in the pathogenesis and treatment of recurrent urinary tract infections. *Curr. Urol. Rep.* 14, 448–456. doi: 10.1007/s11934-013-0354-5
- Sobel, J. D. (1997). Pathogenesis of urinary tract infection. Role of host defenses. *Infect. Dis. Clin. North Am.* 11, 531–549.
- Sockett, R. E. (2009). Predatory Lifestyle of *Bdellovibrio bacteriovorus*. *Annu. Rev. Microbiol.* 63, 523–539.
- Soto, S. M., Smithson, A., Horcajada, J. P., Martinez, J. A., Mensa, J. P., and Vila, J. (2006). Implication of biofilm formation in the persistence of urinary tract infection caused by uropathogenic *Escherichia coli*. *Clin. Microbiol. Infect.* 12, 1034–1036. doi: 10.1111/j.1469-0691.2006.01543.x
- Stapleton, A. E., Dziura, J., Hooton, T. M., Cox, M. E., Yarova-Yarova, Y., Chen, S., et al. (2012). Recurrent urinary tract infection and urinary *Escherichia coli* in women ingesting cranberry juice daily: a randomized controlled trial. *Mayo Clin. Proc.* 87, 143–150. doi: 10.1016/j.mayocp.2011.10.006
- Stenutz, R., Weintraub, A., and Widmalm, G. (2006). The structures of *Escherichia coli* O-polysaccharide antigens. *FEMS Microbiol. Rev.* 30, 382–403.
- Stolp, H., and Starr, M. P. (1963). *Bdellovibrio bacteriovorus* gen. et sp. n., a predatory, ectoparasitic, and bacteriolytic microorganism. *Antonie Van Leeuwenhoek* 29, 217–248. doi: 10.1007/bf02046064
- Strömberg, N., Marklund, B. I., Lund, B., Ilver, D., Hamers, A., Gaastra, W., et al. (1990). Host-specificity of uropathogenic *Escherichia coli* depends on differences in binding specificity to Gal alpha 1-4Gal-containing isoreceptors. *EMBO J.* 9, 2001–2010. doi: 10.1002/j.1460-2075.1990.tb08328.x
- Suetens, C., Latour, K., Kärki, T., Ricchizzi, E., Kinross, P., Moro, M. L., et al. (2018). Prevalence of healthcare-associated infections, estimated incidence and composite antimicrobial resistance index in acute care hospitals and long-term care facilities: results from two European point prevalence surveys, 2016 to 2017. *Euro Surveill.* 23:1800516.
- Sundén, F., Håkansson, L., Ljunggren, E., and Wullt, B. (2010). *Escherichia coli* 83972 bacteriuria protects against recurrent lower urinary tract infections in patients with incomplete bladder emptying. *J. Urol.* 184, 179–185. doi: 10.1016/j.juro.2010.03.024
- Sung, M. A., Fleming, K., Chen, H. A., and Matthews, S. (2001). The solution structure of PapGII from uropathogenic *Escherichia coli* and its recognition of glycolipid receptors. *EMBO Rep.* 2, 621–627. doi: 10.1093/embo-reports/kve133
- Svensson, A., Larsson, A., Emténäs, H., Hedenström, M., Fex, T., Hultgren, S. J., et al. (2001). Design and evaluation of plicides: potential novel antibacterial agents directed against uropathogenic *Escherichia coli*. *ChemBiochem* 2, 915–918. doi: 10.1002/1439-7633(20011203)2:12<915::aid-cbic915>3.0.co;2-m
- Sybesma, W., Zbinden, R., Chanishvili, N., Kutateladze, M., Chkhotua, A., Ujmajuridze, A., et al. (2016). Bacteriophages as potential treatment for urinary tract infections. *Front. Microbiol.* 7:465. doi: 10.3389/fmicb.2016.00465
- Tammen, H. (1990). Immunobiotherapy with Uro-vaxom in recurrent urinary tract infection. The German urinary tract infection study group. *Br. J. Urol.* 65, 6–9. doi: 10.1111/j.1464-410x.1990.tb14649.x
- Texier-Maugein, J., Clerc, M., Vekris, A., and Bebear, C. (1987). *Ureaplasma urealyticum*-induced bladder stones in rats and their prevention by flurofamide and doxycycline. *Isr. J. Med. Sci.* 23, 565–567.
- Tong, Y., Wu, Q., Zhao, D., Liu, Y., Cao, M., Zhang, L., et al. (2011). Effects of Chinese herbs on the hemagglutination and adhesion of *Escherichia coli* strain in vitro. *Afr. J. Tradit. Complement. Altern. Med.* 8, 82–87.
- Torella, M., Del Deo, F., Grimaldi, A., Iervolino, S. A., Pezzella, M., Tammaro, C., et al. (2016). Efficacy of an orally administered combination of hyaluronic acid, chondroitin sulfate, curcumin and quercetin for the prevention of recurrent urinary tract infections in postmenopausal women. *Eur. J. Obstet. Gynecol. Reprod. Biol.* 207, 125–128. doi: 10.1016/j.ejogrb.2016.10.018
- Trautner, B. W., Hull, R. A., Thornby, J. I., and Darouiche, R. O. (2007). Coating urinary catheters with an avirulent strain of *Escherichia coli* as a means to establish asymptomatic colonization. *Infect. Control Hosp. Epidemiol.* 28, 92–94. doi: 10.1086/510872
- Uehling, D. T., Hopkins, W. J., Balish, E., Xing, Y., and Heisey, D. M. (1997). Vaginal mucosal immunization for recurrent urinary tract infection: phase II clinical trial. *J. Urol.* 157, 2049–2052. doi: 10.1097/00005392-199706000-00004
- Uehling, D. T., Hopkins, W. J., Elkahwaji, J. E., Schmidt, D. M., and Levenson, G. E. (2003). Phase 2 clinical trial of a vaginal mucosal vaccine for urinary tract infections. *J. Urol.* 170, 867–869. doi: 10.1097/01.ju.0000075094.54767.6e
- Ujmajuridze, A., Chanishvili, N., Goderdzishvili, M., Leitner, L., Mehnert, U., Chkhotua, A., et al. (2018). Adapted bacteriophages for treating urinary tract infections. *Front. Microbiol.* 9:1832. doi: 10.3389/fmicb.2018.01832
- Ulrey, R. K., Barksdale, S. M., Zhou, W., and van Hoek, M. L. (2014). Cranberry proanthocyanidins have anti-biofilm properties against *Pseudomonas aeruginosa*. *BMC Complement. Altern. Med.* 14:499. doi: 10.1186/1472-6882-14-499
- Varki, A. (2008). Sialic acids in human health and disease. *Trends Mol. Med.* 14, 351–360. doi: 10.1016/j.molmed.2008.06.002
- Wagenlehner, F. M. E., Ballarini, S., Pilatz, A., Weidner, W., Lehr, L., and Naber, K. G. (2015). A randomized, double-blind, parallel-group, multicenter clinical study of *Escherichia coli*-Lyophilized lysate for the prophylaxis of recurrent uncomplicated urinary tract infections. *Urol. Int.* 95, 167–176. doi: 10.1159/000371894
- Wizemann, T. M., Adamou, J. E., and Langermann, S. (1999). Adhesins as targets for vaccine development. *Emerg. Infect. Dis.* 5, 395–403. doi: 10.3201/eid0503.990310
- Wojnicz, D., Tichaczek-Goska, D., Korzekwa, K., Kicia, M., and Hendrich, A. B. (2016). Study of the impact of cranberry extract on the virulence factors and biofilm formation by *Enterococcus faecalis* strains isolated from urinary tract infections. *Int. J. Food Sci. Nutr.* 67, 1005–1016. doi: 10.1080/09637486.2016.1211996
- Xu, W., Flores-Mireles, A. L., Cusumano, Z. T., Takagi, E., Hultgren, S. J., and Caparon, M. G. (2017). Host and bacterial proteases influence biofilm formation and virulence in a murine model of enterococcal catheter-associated urinary tract infection. *NPJ Biofilms Microbiomes.* 3:28.
- Yang, B., and Foley, S. (2018). First experience in the UK of treating women with recurrent urinary tract infections with the bacterial vaccine Uromune®. *BJU Int.* 121, 289–292. doi: 10.1111/bju.14067

- Yang, B., and Foley, S. (2019). Urinary tract infection vaccines – the ‘burning’ issue. *BJU Int.* 123, 743–744. doi: 10.1111/bju.14678
- Zaborska, W., Kot, M., and Superata, K. (2002). Inhibition of jack bean urease by 1,4-benzoquinone and 2,5-dimethyl-1,4-benzoquinone. Evaluation of the inhibition mechanism. *J. Enzyme Inhib. Med. Chem.* 17, 247–253. doi: 10.1080/1475636021000011670
- Zhao, K., Liu, B., Wei, W., Ma, Q., Zhao, W., and Zhang, S. (2011). Clinical study of clearing liver fire, removing dampness, strengthening spleen and tonifying kidney methods in treating middle-aged and old woman with chronic urinary tract infection. *Int. J. Tradit. Chin. Med.* 33, 976–978.

**Conflict of Interest:** The authors declare that the research was conducted in the absence of any commercial or financial relationships that could be construed as a potential conflict of interest.

Copyright © 2020 Loubet, Ranfaing, Dinh, Dunyach-Remy, Bernard, Bruyère, Lavigne and Sotto. This is an open-access article distributed under the terms of the Creative Commons Attribution License (CC BY). The use, distribution or reproduction in other forums is permitted, provided the original author(s) and the copyright owner(s) are credited and that the original publication in this journal is cited, in accordance with accepted academic practice. No use, distribution or reproduction is permitted which does not comply with these terms.



# Coexistence of the Oxazolidinone Resistance–Associated Genes *cfr* and *optrA* in *Enterococcus faecalis* From a Healthy Piglet in Brazil

Lara M. Almeida<sup>1,2\*</sup>, Anthony Gaca<sup>3</sup>, Paulo M. Bispo<sup>3</sup>, François Lebreton<sup>3</sup>, Jose T. Saavedra<sup>3</sup>, Rafael A. Silva<sup>1</sup>, Irinaldo D. Basílio-Júnior<sup>1</sup>, Felipe M. Zorzi<sup>4</sup>, Pedro H. Filsner<sup>4</sup>, Andrea M. Moreno<sup>4</sup> and Michael S. Gilmore<sup>3</sup>

<sup>1</sup> Institute of Pharmaceutical Sciences, Federal University of Alagoas, Maceió, Brazil, <sup>2</sup> Department of Clinical and Toxicological Analyses, Faculty of Pharmaceutical Sciences, University of São Paulo, São Paulo, Brazil, <sup>3</sup> Department of Ophthalmology and Department of Microbiology, Harvard Medical School, Boston, MA, United States, <sup>4</sup> School of Veterinary Medicine and Animal Science, University of São Paulo, São Paulo, Brazil

## OPEN ACCESS

### Edited by:

Filipa Grosso,  
University of Porto, Portugal

### Reviewed by:

Yeshi Yin,  
Hunan University of Science and  
Engineering, China  
Amira Awad Moawad,  
Friedrich Loeffler Institute, Germany

### \*Correspondence:

Lara M. Almeida  
larameal@gmail.com

### Specialty section:

This article was submitted to  
Infectious Diseases – Surveillance,  
Prevention and Treatment,  
a section of the journal  
Frontiers in Public Health

Received: 04 April 2020

Accepted: 11 August 2020

Published: 24 September 2020

### Citation:

Almeida LM, Gaca A, Bispo PM, Lebreton F, Saavedra JT, Silva RA, Basílio-Júnior ID, Zorzi FM, Filsner PH, Moreno AM and Gilmore MS (2020) Coexistence of the Oxazolidinone Resistance–Associated Genes *cfr* and *optrA* in *Enterococcus faecalis* From a Healthy Piglet in Brazil. *Front. Public Health* 8:518. doi: 10.3389/fpubh.2020.00518

Oxazolidinones are one of the most important antimicrobials potentially active against glycopeptide- and  $\beta$ -lactam-resistant Gram-positive pathogens. Linezolid—the first oxazolidinone to be approved for clinical use in 2000 by the US Food and Drug Administration—and the newer molecule in the class, tedizolid, inhibit protein synthesis by suppressing the formation of the 70S ribosomal complex in bacteria. Over the past two decades, transferable oxazolidinone resistance genes, in particular *cfr* and *optrA*, have been identified in Firmicutes isolated from healthcare-related infections, livestock, and the environment. Our goals in this study were to investigate the genetic contexts and the transferability of the *cfr* and *optrA* genes and examine genomic features, such as antimicrobial resistance genes, plasmid incompatibility types, and CRISPR-Cas defenses of a linezolid-resistant *Enterococcus faecalis* isolated in feces from a healthy pig during an antimicrobial surveillance program for animal production in Brazil. The *cfr* gene was found to be integrated into a transposon-like structure of 7,759 nt flanked by IS1216E and capable of excising and circularizing, distinguishing it from known genetic contexts for *cfr* in *Enterococcus* spp., while *optrA* was inserted into an Inc18 broad host-range plasmid of >58 kb. Conjugal transfer of *cfr* and *optrA* was shown by filter mating. The coexistence of *cfr* and *optrA* in an *E. faecalis* isolated from a healthy nursery pig highlights the need for monitoring the use of antibiotics in the Brazilian swine production system for controlling spread and proliferation of antibiotic resistance.

**Keywords:** oxazolidinones, resistance, *Enterococcus faecalis*, *cfr* gene, *optrA* gene, livestock

## INTRODUCTION

Few drugs remain available for treating infections caused by antibiotic-resistant bacteria. Oxazolidinone antimicrobials, including linezolid and tedizolid, are among the few last-line therapies effective for multidrug-resistant (MDR) Gram-positive pathogens. Linezolid inhibits protein synthesis by targeting the peptidyl transferase center of the 50S subunit of bacterial ribosomes, blocking the binding of aminoacyl-tRNA to the A-site of the peptidyl transferase center



(PTC), and also affecting the positioning of fMet-tRNA at the P-site, which prevents formation of the initiation complex (1–4). Over the past two decades, however, mutations in domain V of the 50S ribosomal subunit of 23S rRNA or in the ribosomal proteins L3 and L4 (5, 6) and the transferable resistance genes *cf*, *optrA*, and *poxTA* (7–9) have driven the spread of oxazolidinone resistance in Gram-positive bacteria in healthcare and animal agriculture settings.

The spread of the multiresistance gene *cf* has raised concern since its first report in a bovine *Staphylococcus sciuri* isolate (10). The *cf* gene initially reported occurred in *Enterococcus* spp. from healthcare-related infections in Thailand (11) and from livestock in China (12). So far, a BLASTn search of the GenBank database identifies 3 *cf* homologs in enterococci. While *cf* has been found in both human and animal isolates of *Enterococcus faecalis* (Thailand, China) (11–13), *Enterococcus faecium* (Italy, Ireland, U.S.) (14–16), *Enterococcus casseliflavus*, and *Enterococcus thailandicus* (China) (17), the *cf*(B) variant has been detected only in clinical isolates of *E. faecalis* (Japan) (18) and *E. faecium* (U.S., Germany, Netherlands) (19, 20). The most recently described *cf*(D) variant has only four entries so far recorded in NCBI's databases, all *E. faecium* (France, Ireland, Netherlands) (21).

A Cfr-mediated adenosine modification A2503 in the PTC of 23S rRNA, which confers resistance to the oxazolidinone, phenicol, lincosamide, pleuromutilin, streptogramin A, and 16-member-ring macrolide antimicrobials (22), was until 2015 the only known transferable oxazolidinone resistance mechanism. Since then, the ATP-binding cassette (ABC)-F protein *OptrA* (23) has also been identified as conferring resistance to oxazolidinones, including the newer molecule in the class, tedizolid (24). *optrA* was identified in both *E. faecalis* and *E. faecium* of human and animal origins (8, 25, 26), as well as in *E. thailandicus* and *Enterococcus gallinarum* isolated from hospitals in China (27). Elsewhere in Asia (18, 28), Europe (29, 30), and America (16, 31), *optrA* has been found in *E. faecalis* and *E. faecium* of both human and animal origins. In Africa, *optrA*-positive *E. faecalis* isolated from humans (32), urban wastewater (33), and food-producing animals (34) were also reported. The *cf* and *optrA* genes can be either plasmid or chromosomally encoded, and the co-location of both in the same plasmid has already been described in a porcine *Staphylococcus sciuri* isolate in China (35) and in *E. faecium* and *E. faecalis* recovered from hospitalized patients and livestock from Europe and the US (14–16).

In this study, we investigated the genetic contexts and the transferability of the *cf* and *optrA* genes from the linezolid-resistant (LR) *E. faecalis* strain L9 (CP018004.1), which was isolated from a rectal swab collected from a healthy piglet in a surveillance study of antimicrobial susceptibility in Brazil's swine production system (36). Antimicrobial resistance genes, plasmid incompatibility types, epidemiology, and CRISPR-Cas (Clustered Regularly Interspaced Short Palindromic Repeat) defenses of LR *E. faecalis* L9 were also examined. Whole-genome sequencing (WGS) analysis revealed the presence of *cf* associated with a transposable element capable of excision and formation of an intracellular circular intermediate flanked

by IS1216E (CP041775.1), which is different from all previously known genetic contexts in *Enterococcus* spp. from human and animal sources. Further, the core *araC*-hp-*optrA* was found to be inserted into a conjugative Inc18 broad host-range plasmid of >58 kb (CP041776.1) in LR *E. faecalis* L9.

## MATERIALS AND METHODS

### Bacterial Isolation

LR *E. faecalis* L9 comes from a collection of 13 LR *E. faecalis* (linezolid MIC of 8 mg/L) that were screened from 245 MDR *E. faecalis* isolated from rectal swabs from healthy piglets (45 days old) in different states of Brazil (36). These 13 *optrA*-positive *E. faecalis*, epidemiologically unrelated (ST29, ST330, ST591, ST710, ST711), were recovered from different pigs found to be distributed in 6 out of the 7 states chosen for sample collection. Three LR *E. faecalis* isolated in the same state (DF) harbored both *optrA* and *cf* (ST591 and ST29), but conjugal transfer of these resistance genes to an enterococcal recipient was achieved only using the ST29 *E. faecalis* strain L9 as donor in our previous filter mating assays. Therefore, here we investigated the mobile element types that enabled horizontal transfer of *cf* and *optrA*.

### Whole-Genome Sequencing and Data Analysis

LR *E. faecalis* L9 was grown in brain heart infusion (BHI) broth at 37°C (24 h). Genomic DNA was isolated using the QIAGEN DNeasy Blood & Tissue Kit, and quantified using Qubit dsDNA HS. Sequencing libraries were prepared with the Illumina Nextera XT DNA kit and sequenced on a MiSeq instrument (Illumina Inc., USA) at the Massachusetts Eye and Ear Infirmary (MEEI) Ocular Genomics Institute, as 250 nt paired-end reads. *De novo* assembling was performed using CLC Genomics Workbench 8.0.3. For genome annotations, both the RAST server (Rapid Annotation using Subsystem Technology) and the Prokaryotic Genome Annotation Pipeline (NCBI PGAP) were used. Genome data analysis was performed using BLAST (<http://blast.ncbi.nlm.nih.gov/Blast.cgi>) and Center for Genomic Epidemiology (<http://www.genomicepidemiology.org>) online tools. ResFinder (<https://cge.cbs.dtu.dk/services/ResFinder/>) was used to identify acquired antimicrobial resistance genes, and PlasmidFinder (<https://cge.cbs.dtu.dk/services/PlasmidFinder/>) was used to determine plasmid incompatibility types. For detection of the oxazolidinone resistance determinants, LRE-Finder (<https://cge.cbs.dtu.dk/services/LRE-finder/>) was used as well. Multilocus sequence typing (MLST) loci were assigned by the MLST database (<https://pubmlst.org/efaecalis/>), and the presence of CRISPR-*cas* defenses was identified by CRISPRfinder (<https://crisprcas.i2bc.paris-saclay.fr>).

### Filter Mating Assay

Conjugation by filter mating as described previously by Jaworski and Clewell (37) was performed using LR *E. faecalis* L9 as donor, and the *E. faecalis* strain OG1RF as recipient. Donor and recipient were grown overnight in BHI broth at 37°C. One milliliter from donor culture plus 1 ml from recipient culture were inoculated in 3 ml of phosphate buffered saline (PBS) solution, filtered through

a sterile 25-mm-diameter, 0.22- $\mu$ m-pore-size membrane filter, and subsequently incubated on BHI agar at 37°C for 24–48 h. PBS (5 ml) was used to wash the filters, and 500  $\mu$ l of this solution was spread on BHI agar plates (100  $\times$  15 mm Petri plates) containing 25  $\mu$ g/ml of fusidic acid, 25  $\mu$ g/ml of rifampicin to select for the OG1RF chromosomal markers, and 25 or 10  $\mu$ g/ml of chloramphenicol (CHL) to select for oxazolidinone and phenicol resistance genes; linezolid (LZD) (4  $\mu$ g/ml) instead of chloramphenicol was also tested to select for *cfr* and *optrA*. Conjugation efficiency (CFU/ml of transconjugants per CFU/ml of donors) was calculated as previously described (38). PCR using primer sets specific for *optrA*, *cfr*, *poxtA*, *fexA*, and *cat* genes (36) and Sanger sequencing were carried out to detect these resistances in OG1RF transconjugants. Minimum inhibitory concentrations (MIC's) of chloramphenicol, florfenicol, linezolid, and tedizolid were determined by broth microdilution testing according to the guidelines of the Clinical Laboratory Standards Institute (CLSI). *E. faecalis* ATCC 29212 was used as a control for antimicrobial susceptibility testing.

## RESULTS AND DISCUSSION

*Enterococcus faecalis* is a commensal bacterium of the gut microbiota of humans and various animal species and also a cause of infections in critically ill patients (39, 40). Besides being an important hospital pathogen, *E. faecalis* has emerged as a potential reservoir of oxazolidinone resistance genes in animal agriculture settings worldwide (8, 31, 34, 36, 41). It is of substantial concern that antibiotics used in food-producing animals may be selecting for the proliferation of MDR *E. faecalis* lineages in which *cfr* and *optrA* coexist. Cfr rRNA methyltransferase confers resistance to six important antimicrobial classes that target the 50S ribosomal subunit (22), while the ATP-binding cassette (ABC)-F protein OptrA confers resistance to phenicol and oxazolidinone, including resistance to the new oxazolidinone tedizolid (23). The spread of *cfr* and *optrA* inter-species/genera has been driven by plasmids containing other important resistance determinants (14–16, 35). Therefore, oxazolidinone resistance can be co-selected by antimicrobials that have been largely used in swine production, such as phenicol, macrolide, lincosamide, and pleuromutilin.

### Antimicrobial Resistance Determinants of LR *E. faecalis* L9

ResFinder identified that LR *E. faecalis* L9 carries the *lsa(A)* gene, which is responsible for intrinsic LS<sub>A</sub>P resistance in *E. faecalis*, and acquired resistance genes for aminoglycoside (*str*), phenicol *fex(A)*, phenicol and oxazolidinone (*optrA*), and tetracycline [*tet(L)*, *tet(M)*, *tet(S)*], in addition to the multiresistance gene *cfr*. LRE-Finder confirmed the presence of *cfr* and *optrA* (CP041775.1 and CP041776.1, respectively), but the phenicol–oxazolidinone–tetracycline resistance gene *poxtA* was not found. 23S rRNA mutations were not detected in LR *E. faecalis* L9, nor were they identified in ribosomal protein genes *rplC*, *rplD*, and *rplV* (L3, L4, and L22, respectively).

### Genetic Context of *cfr* in the Porcine LR *E. faecalis* Isolate L9

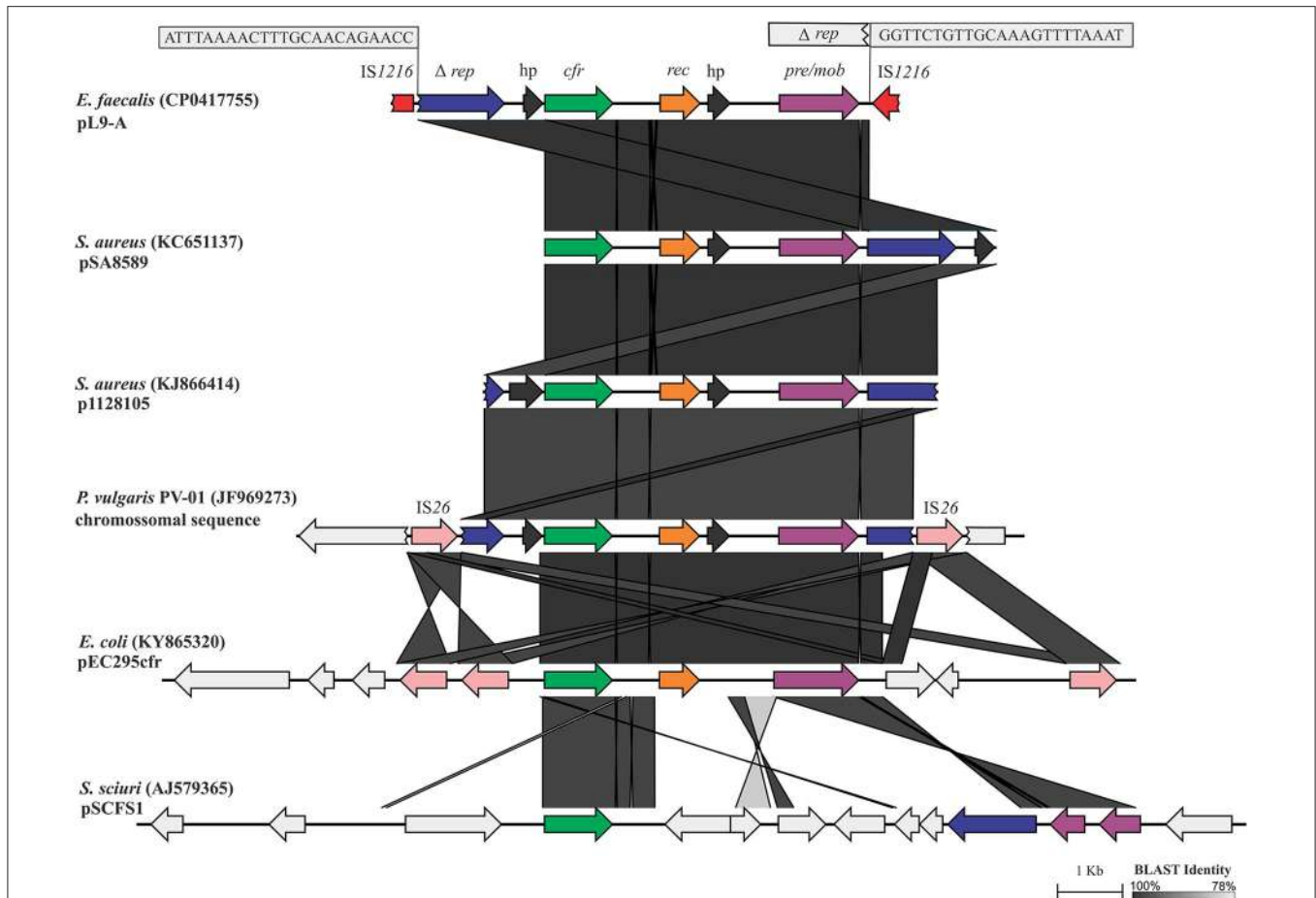
A *cfr*-carrying DNA segment of 7,759 nt, pL9-A (CP041775.1), was found to be inserted into LR *E. faecalis* L9 (Figure 1). The *cfr* gene was flanked upstream by the Tn554-related  $\Delta$ *tnpB* gene. Further upstream of  $\Delta$ *tnpB*, a gene coding for RepUS18 was detected that was disrupted by the integration of an IS1216E. The *repUS18* gene is often found in Inc18 broad host-range plasmids, which have been related to antimicrobial resistance gene transfer in enterococci. Downstream, the *cfr* gene was flanked by a recombinase *rec* gene, a gene coding for a hypothetical protein, and a plasmid recombination/mobilization *pre/mob* gene. *In silico* predictions indicated that the IS1216E-flanked segment pL9-A could excise and exist within the cell as a non-replicating circular intermediate in LR *E. faecalis* L9, which was confirmed by PCR and Sanger sequencing using the primers 5'AGGTTTAGAATAATCTCCCGA3' and 5'GCTGACAACATATCTAATATCTCAA3'.

pL9-A possesses 100% DNA identity over 93% of its length to a chromosomal DNA sequence from *Proteus vulgaris* PV-01 (JF969273) isolated from a pig nasal swab in China (42), and 99.98% and 99.83% DNA identity to the pSA8589 and p1128105 from *Staphylococcus aureus* 1900 (43) and *S. aureus* 1128105 (44) of human origin in the US (KC561137 and KJ866414, respectively), highlighting its very broad-range horizontal transfer capabilities. IS6 insertion sequence family elements, which have been commonly associated with antibiotic resistance genes, appear to be also involved in transposition events of the core *cfr-rec-pre/mob* in Gram-positive and Gram-negative bacteria.

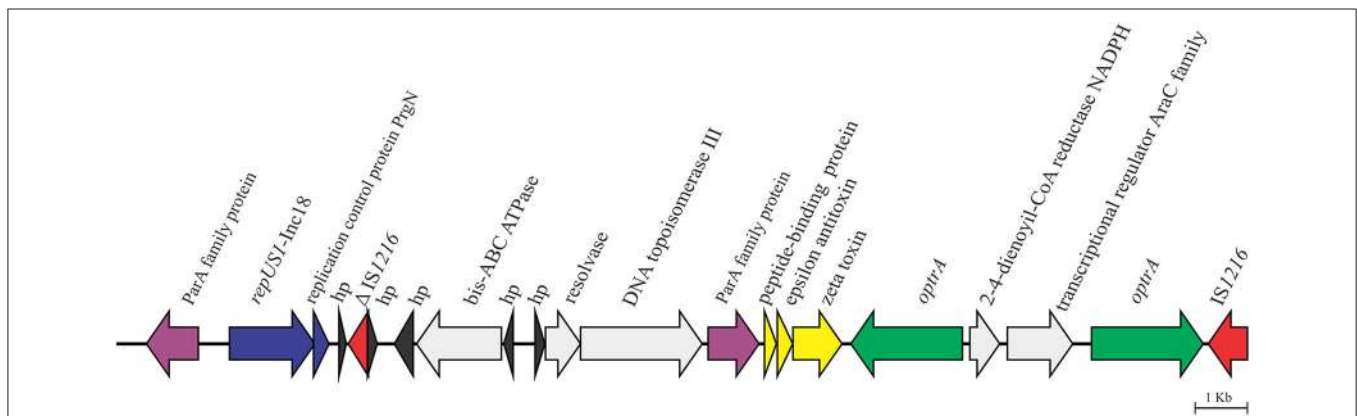
The *cfr*-carrying mobile element pL9-A was distinctly different from all known genetic contexts of *cfr* in *Enterococcus* spp. from human and animal sources. The similarity of pL9-A to the *cfr*-carrying segments previously identified in bacteria of other genera indicates that it has most likely been acquired horizontally from other bacteria or, alternatively, could be intrinsic in some lineages of *E. faecalis* and then transferred to other bacteria. The IS1216E element appears to be involved in the acquisition and dispersal of pL9-A in LR *E. faecalis* L9. In Brazil, the *cfr* gene has been reported to date only in an ST398 MSSA strain of human origin (45) in a genetic context other than that observed in the porcine LR *E. faecalis* isolate L9.

### Plasmid-Borne *optrA*-Carrying Partial Sequence (pL9) in the Porcine LR *E. faecalis* Isolate L9

We recently reported that the core *araC*-hp-*optrA* of 3,453 nt in length, which was composed of genes coding for a hypothetical protein and an AraC family transcriptional regulator at the 5' of *optrA*, was inserted upstream of an IS1216E element into a plasmid of >58 kb, which was not closed during *de novo* assembly of the high quality draft sequence (CP041776.1) (36). On the flank 5' of the core *araC*-hp-*optrA*, LR *E. faecalis* L9 showed *in silico* a duplication of *optrA*, which was confirmed by PCR and Sanger sequencing using the primers 5'TTGAGTGAAATACCTGTGCG3' and



**FIGURE 1** | Linear comparison of the 7,759-bp *cfr*-carrying DNA segment pL9-A (CP041775.1) generated by EasyFig. The boxes zoom in on the 23-bp inverted repeats (IR) at the ends of an IS1216 that was inserted into *repUS18*. The 6,956-bp segment between the IRs shows high DNA identity to the corresponding stretches in pSA8589 (KC651137), p1128105 (KJ866414), and *P. vulgaris* PV-01 chromosomal sequence (JF969273). Alignment of these sequences revealed only a deletion of 7 bp in *repUS18* from pL9-A and an insertion of 10 bp in the hypothetical protein on the flank 5' of *cfr* in p1128105, which is represented by the slightly lighter shade of identity over this region.



**FIGURE 2** | Genetic context of the 58,593-bp *optrA*-carrying partial sequence pL9 (CP041776.1) in the porcine LR *E. faecalis* isolate L9.

5'TGATGGTAATATGGTGGTGGAA3'. Further analysis of pL9 showed the presence of genes coding for the zeta-epsilon-delta ( $\omega$ - $\epsilon$ - $\zeta$ ) toxin-antitoxin (TA) system upstream of the

duplication of *optrA* (Figure 2). The  $\omega$ - $\epsilon$ - $\zeta$  TA module, a post-segregational killing system which acts at cell division eliminating progeny that fails to inherit plasmid copy, has



been found in various MDR Gram-positive bacteria, including the *cfr*-carrying conjugative plasmids pW9-2 from *E. faecalis*, and pW3 and p3-38 from *E. thailandicus* isolated from sewage in swine farm contexts in China (12) and pEF12-0805 from *E. faecium* isolated from human blood in Italy (14). pL9 harbored a gene coding for the plasmid replication protein *repUS1*, which is found in Inc18 broad host-range plasmids. On the 5' flank of *repUS1*, a 912-nt open reading frame (ORF) for the partitioning protein ParA which mediates plasmid segregation was found. These mechanisms ensure the maintenance of plasmids that exist in low-copy numbers in a bacterial population, such as Inc18 family plasmids. At the 3' flank of *repUS1*, a 288-nt ORF for the replication control protein PrgN is present. Upstream to this region, an 1,494-nt ORF for ATP-binding cassette domain-containing protein came to our attention due to the very few entries so far recorded in NCBI's databases, as it only matches nucleotide sequences from 6 *Lactococcus garvieae*, which causes fatal hemorrhagic septicaemia in fish (South Korea and Japan), and 1 *Lactococcus petauri* isolated from human feces in China. This ORF codes for the ATP-binding cassette domain-containing protein (*E. faecalis* WP\_155282194.1), which has 81.74% DNA identity over 99% of its length to the *Lactococcus* ABC-F-type ribosomal protection protein (WP\_019291880.1).

pL9 was found to be inserted into a conjugative Inc18 plasmid of >58 kb. Inc18 broad host-range plasmids have been associated with a variety of antibiotic resistances in enterococci, including the high-level *vanA* glycopeptide resistance carried by Tn1546, which can be transferred to MRSA lineages (46). Inc18 plasmids can play a crucial role in the oxazolidinone resistance emergence, as they are widespread in enterococci, streptococci, and staphylococci in both clinical and environmental settings (47, 48). Moreover, most Inc18 plasmids carry locus coding for stabilization systems, such as the post-segregation killing (PSK) system (49), which has already been implicated in the persistence of the Tn1546-mediated *vanA* resistance in *E. faecium* (50). The presence of ORFs adjacent to *optrA* in pL9 that matched few or no DNA sequences available in GenBank indicates that further investigation is required to understand how new conjugative Inc18 plasmid mosaics are evolving and how that might favor the spread of oxazolidinone resistance in animal agriculture settings.

## Transferability of *cfr*, *optrA*, and Other Resistance Determinants in LR *E. faecalis* L9

Filter mating assays were carried out to determine the potential for conjugal transfer of *cfr* and *optrA* at different CHL and LZD concentrations (Table 1). *optrA/fexA/tet(S)*-carrying OG1RF-L9 transconjugants were selected at a frequency of  $4 \times 10^{-7}$  transconjugant cells per donor cell using 25 µg/ml CHL, but conjugation experiments failed to transfer *cfr* at 25 µg/ml CHL. Decreasing CHL concentration from 25 to 10 µg/ml, countless small colonies of *optrA/cfr/fexA/tet(S)*-carrying OG1RF-L9 transconjugants could be selected. Linezolid could select only countless small colonies of

*optrA*-positive OG1RF-L9 transconjugants; no *cfr*-positive OG1RF-L9 transconjugant was obtained, indicating that *optrA* is responsible for linezolid resistance, and *cfr*, for a lower-level chloramphenicol resistance phenotype in LR *E. faecalis* L9.

Tn558, which harbors the chloramphenicol/florfenicol efflux MFS transporter *fexA* gene and the tetracycline resistance ribosomal protection gene *tet(S)*, was also transferred to OG1RF-L9 in a yet to be determined genetic context, as pL9 could not be closed during *de novo* assembly. A 204-nt fragment of a gene for a conjugal transfer protein 5' of *tet(S)* that appears to be involved in its mobilization is identical to homologs occurring in Firmicutes as identified in a BLASTn search. A 210 nt ORF 3' flank to Tn558 matched a gene coding for the replication-associated protein RepB identified in *Listeria monocytogenes* (KY613776.1 and KY613741.1) isolated from food in Canada, in *Carnobacterium divergens* (LT984411.1) from beef carpaccio in France, and in an *optrA*-carrying conjugative plasmid from the *Enterococcaceae* strain E508 (MK425645.1) in China. Another 606-nt ORF encoding a hypothetical protein at the extreme 3' end of *repB* also matched ORFs from the *L. monocytogenes*, *C. divergens*, and *Enterococcaceae* isolates mentioned above, and the *optrA*-carrying *Enterococcus avium* isolate C674 (MH018573.1) from an asymptomatic healthy human in China. At 5', Tn558 is flanked by a 210-nt ORF for a hypothetical protein that only matches sequences from the *optrA* gene cluster from *E. avium* C674 and pStrcfr from *Streptococcus suis* S10 (KF129409.1). Further upstream, a 1,272-nt ORF for a Y-family DNA polymerase is present, but no match was found for this nucleotide sequence.

## Bacterial Immunity of *cfr/optrA*-Carrying *E. faecalis* L9

Genome defenses for porcine LR *E. faecalis* L9 were investigated using CRISPRfinder. Clustered, regularly interspaced short palindromic repeat (CRISPR) loci provide an important defense against parasitic mobile element entry. MDR, hospital-adapted enterococcal lineages lack CRISPR defenses, which are thought to enhance the facility with which they acquire antibiotic resistances on mobile elements (39, 51). A CRISPR-related loci consisting of 9 spacers and direct repeat sequences of 36 bp was found in the L9 chromosome (1,708,044 to 1,708,673 bp), but genes coding for Cas proteins were not identified. A BLASTn search revealed that the L9 CRISPR-related loci possess 95.12% DNA identity over 100% of its length to the corresponding chromosomal DNA sequence from *E. faecalis* SGAir0397 (CP039434.1), which was recovered from air in Singapore. L9 CRISPR spacer sequences only matched to sequences from *E. faecalis* FDAARGOS\_324 (CP028285.1) isolated from a human eye in the US, and the cyanobacterium *Geminocystis* sp. isolate NIES-3708 (AP014815.1) from Japan, besides *E. faecalis* SGAir0397. LR *E. faecalis* L9 lacked the *E. faecalis* CRISPR1 locus (a CAS-TypeIIA cluster consisting of Csn2\_0\_IIA, Cas2\_0\_I-II-III, Cas1\_0\_II, Cas9\_1\_II) typically located between genes EF0672 and EF0673 (51).



**TABLE 1** | Conjugation efficiency of *cfr* and *optrA* from *E. faecalis* L9 to *E. faecalis* OG1RF transconjugants.

Recipient strain <sup>a</sup>	Conjugation efficiency <sup>b</sup>	Resistance genes <sup>c</sup>	MIC (μg/ml)			
			LZD	TZD	CHL	FFC
OG1RF-L9 (25 μg/ml CHL)	4 × 10 <sup>-7</sup>	<i>optrA</i> , <i>fex(A)</i> , <i>tet(S)</i>	8	0.5	128	64
OG1RF-L9 (10 μg/ml CHL)	ND	<i>optrA</i> , <i>fex(A)</i> , <i>tet(S)</i> , <i>cfr</i>	8	0.5	128	64
OG1RF-L9 (8 μg/ml LZD)	ND	<i>optrA</i> , <i>fex(A)</i> , <i>tet(S)</i>	8	0.5	128	64
OG1RF-L9 (4 μg/ml LZD)	ND	<i>optrA</i> , <i>fex(A)</i> , <i>tet(S)</i>	8	0.5	128	64

<sup>a</sup>Graded levels of CHL and LZD were tested to select for oxazolidinone and phenicol resistance genes, in addition to 25 μg/ml fusidic acid, and 25 μg/ml rifampicin to select for the OG1RF chromosomal markers.

<sup>b</sup>Conjugation efficiency corresponds to the number of CFU transconjugants per CFU donors; ND (not determined): only small bacterial colonies (countless) were obtained, all *optrA/fexA*-positive.

<sup>c</sup>*optrA* could be efficiently transferred by conjugation at a frequency of 4 × 10<sup>-7</sup> per donor cell using 25 μg/ml of CHL as previously reported (36), and also decreasing CHL concentration or using LZD instead of CHL.

To the best of our knowledge, this is the first report of the coexistence of *optrA* and *cfr* in a bacterial isolate in Brazil. The fact that LR *E. faecalis* L9 came from a pool of 13 LR *E. faecalis* collected from healthy piglets in swine herds distributed across 7 Brazilian States highlights the need for monitoring the use of antibiotics in the country's swine production system in order to preserve the few remaining last-line antibiotics to treat infections caused by MDR pathogens.

## DATA AVAILABILITY STATEMENT

The datasets presented in this study can be found in online repositories. The names of the repository/repositories and accession number(s) can be found below: <https://www.ncbi.nlm.nih.gov/genbank/>, CP018004.1, <https://www.ncbi.nlm.nih.gov/genbank/>, CP041775.1, <https://www.ncbi.nlm.nih.gov/genbank/>, CP041776.1.

## REFERENCES

- Long KS, Munck C, Andersen TMB, Schaub MA, Hobbie SN, Böttger EC, et al. Mutations in 23S rRNA at the peptidyl transferase center and their relationship to linezolid binding and cross-resistance. *Antimicrob Agents Chemother.* (2010) 54:4705–13. doi: 10.1128/AAC.00644-10
- Long KS, Vester B. Resistance to linezolid caused by modifications at its binding site on the ribosome. *Antimicrob Agents Chemother.* (2012) 56:603–12. doi: 10.1128/AAC.05702-11
- Ippolito JA, Kanyo ZF, Wang D, Franceschi FJ, Moore PB, Steitz TA, et al. Crystal structure of the oxazolidinone antibiotic linezolid bound to the 50S ribosomal subunit. *J Med Chem.* (2008) 51:3353–6. doi: 10.1021/jm800379d
- Wilson DN, Schluenzen F, Harms JM, Starosta AL, Connell SR, Fucini P. The oxazolidinone antibiotics perturb the ribosomal peptidyl-transferase center and effect tRNA positioning. *Proc Natl Acad Sci USA.* (2008) 105:13339–44. doi: 10.1073/pnas.0804276105
- Mendes RE, Hogan PA, Streit JM, Jones RN, Flamm RK. Zyvox® Annual Appraisal of Potency and Spectrum (ZAAPS) program: report of linezolid activity over 9 years (2004–12). *J Antimicrob Chemother.* (2014) 69:1582–8. doi: 10.1093/jac/dkt541
- Pfaller MA, Mendes RE, Streit JM, Hogan PA, Flamm RK. Five-year summary of *in vitro* activity and resistance mechanisms of linezolid against clinically

## ETHICS STATEMENT

The study was approved by the Ethics Committee of Faculdade de Medicina Veterinária e Zootecnia- Universidade de São Paulo, under number CEUA N.8026060214.

## AUTHOR CONTRIBUTIONS

LA and MG planned the study and wrote the manuscript with suggestions from AG, PB, and FL. PF and AM provided a collection of 245 MDR *E. faecalis* strains isolated from swine. LA, JS, RS, and IB-J carried out the experimental work and genome sequencing. LA, FZ, AG, PB, and FL contributed to the bioinformatic analyses. All authors contributed to the article and approved the submitted version.

## FUNDING

This project has been funded by the Harvard-wide Program on Antibiotic Resistance NIH/NIAID AI083214, and FAPESP scholarship 2014/ 27267-0.

- important gram-positive cocci in the United States from the LEADER surveillance program (2011 to 2015). *Antimicrob Agents Chemother.* (2017) 61:e00609–17. doi: 10.1128/AAC.00609-17
- Shen J, Wang Y, Schwarz S. Presence and dissemination of the multiresistance gene *cfr* in gram-positive and gram-negative bacteria. *J Antimicrob Chemother.* (2013) 68:1697–706. doi: 10.1093/jac/dkt092
- Wang Y, Lv Y, Cai J, Schwarz S, Cui L, Hu Z, et al. A novel gene, *optrA*, that confers transferable resistance to oxazolidinones and phenicols and its presence in *Enterococcus faecalis* and *Enterococcus faecium* of human and animal origin. *J Antimicrob Chemother.* (2015) 70:2182–90. doi: 10.1093/jac/dkv116
- Antonelli A, D'Andrea MM, Brenciani A, Galeotti CL, Morroni G, Pollini S, et al. Characterization of *poxtA*, a novel phenicol-oxazolidinone-tetracycline resistance gene from an MRSA of clinical origin. *J Antimicrob Chemother.* (2018) 73:1763–9. doi: 10.1093/jac/dky088
- Schwarz S, Werckenthin C, Kehrenberg C. Identification of a plasmid-borne chloramphenicol-florfenicol resistance gene in *Staphylococcus sciuri*. *Antimicrob Agents Chemother.* (2000) 44:2530–3. doi: 10.1128/AAC.44.9.2530-2533.2000
- Diaz L, Kiratisin P, Mendes RE, Panesso D, Singh KV, Arias CA. Transferable plasmid-mediated resistance to linezolid due to *cfr* in a human clinical isolate

- of *Enterococcus faecalis*. *Antimicrob Agents Chemother.* (2012) 56:3917–22. doi: 10.1128/AAC.00419-12
12. Liu Y, Wang Y, Schwarz S, Li Y, Shen Z, Zhang Q, et al. Transferable multiresistance plasmids carrying *cfr* in *Enterococcus* spp. from swine and farm environment *Antimicrob Agents Chemother.* (2013) 57:42–8. doi: 10.1128/AAC.01605-12
  13. Fang LX, Duan JH, Chen MY, Deng H, Liang HQ, Xiong YQ, et al. Prevalence of *cfr* in *Enterococcus faecalis* strains isolated from swine farms in China: predominated *cfr*-carrying pCPPF5-like plasmids conferring “non-linezolid resistance” phenotype. *Infect Genet Evol.* (2018) 62:188–92. doi: 10.1016/j.meegid.2018.04.023
  14. Morroni G, Brenciani A, Antonelli A, D’Andrea MM, Di Pilato V, Fioriti S, et al. Characterization of a multiresistance plasmid carrying the *optrA* and *cfr* resistance genes from an *Enterococcus faecium* clinical isolate. *Front Microbiol.* (2018) 9:2189. doi: 10.3389/fmicb.2018.02189
  15. Lazaris A, Coleman DC, Kearns AM, Pichon B, Kinnevey PM, Earls MR, et al. Novel multiresistance *cfr* plasmids in linezolid-resistant methicillin-resistant *Staphylococcus epidermidis* and vancomycin-resistant *Enterococcus faecium* (VRE) from a hospital outbreak: co-location of *cfr* and *optrA* in VRE. *J Antimicrob Chemother.* (2017) 72:3252–7. doi: 10.1093/jac/dkx292
  16. Tyson GH, Sabo JL, Hoffmann M, Hsu C-H, Mukherjee S, Hernandez J, et al. Novel linezolid resistance plasmids in *Enterococcus* from food animals in the USA. *J Antimicrob Chemother.* (2018) 73:3254–8. doi: 10.1093/jac/dky369
  17. Liu Y, Wang Y, Dai L, Wu C, Shen J. First report of multiresistance gene *cfr* in *Enterococcus* species *casseliflavus* and *gallinarum* of swine origin. *Vet Microbiol.* (2014) 170:352–7. doi: 10.1016/j.vetmic.2014.02.037
  18. Kuroda M, Sekizuka T, Matsui H, Suzuki K, Seki H, Saito M, et al. Complete genome sequence and characterization of linezolid-resistant *Enterococcus faecalis* clinical isolate KUB3006 carrying a *cfr*(B)-transposon on its chromosome and *optrA*-Plasmid. *Front Microbiol.* (2018) 9:2576. doi: 10.3389/fmicb.2018.02576
  19. Deshpande LM, Ashcraft DS, Kahn HP, Pankey G, Jones RN, Farrell DJ, et al. Detection of a new *cfr*-Like Gene, *cfr*(B), in *Enterococcus faecium* isolates recovered from human specimens in the United States as part of the SENTRY antimicrobial surveillance program. *Antimicrob Agents Chemother.* (2015) 59:6256–61. doi: 10.1128/AAC.01473-15
  20. Bender JK, Fleige C, Klare I, Fiedler S, Mischnik A, Mutters N, et al. Detection of a *cfr*(B) variant in German *Enterococcus faecium* Clinical Isolates and the impact on linezolid resistance in *Enterococcus* spp. *PLoS ONE.* (2016) 11:e0167042. doi: 10.1371/journal.pone.0167042
  21. Guerin F, Sassi M, Dejoies L, Zouari A, Schutz S, Potrel S, et al. Molecular and functional analysis of the novel *cfr*(D) linezolid resistance gene identified in *Enterococcus faecium*. *J Antimicrob Chemother.* (2020) 75:1699–703. doi: 10.1093/jac/dkaa125
  22. Long KS, Poehlsgaard J, Kehrenberg C, Schwarz S, Vester B. The Cfr rRNA methyltransferase confers resistance to Phenicol, Lincosamides, Oxazolidinones, Pleuromutilins, and Streptogramin A antibiotics. *Antimicrob Agents Chemother.* (2006) 50:2500–5. doi: 10.1128/AAC.00131-06
  23. Sharkey LKR, O’Neill AJ. Antibiotic resistance ABC-F proteins: bringing target protection into the limelight. *ACS Infect Dis.* (2018) 4:239–46. doi: 10.1021/acsinfecdis.7b00251
  24. Fala L. Sivextro (Tedizolid Phosphate) approved for the treatment of adults with acute bacterial skin and skin-structure infections. *Am Health Drug Benefits.* (2015) 8:111–5.
  25. Zhang Y, Dong G, Li J, Chen L, Liu H, Bi W, et al. A high incidence and coexistence of multiresistance genes *cfr* and *optrA* among linezolid-resistant enterococci isolated from a teaching hospital in Wenzhou, China. *Eur J Clin Microbiol Infect Dis.* (2018) 37:1441–8. doi: 10.1007/s10096-018-3269-8
  26. Shang Y, Li D, Shan X, Schwarz S, Zhang S-M, Chen Y-X, et al. Analysis of two pheromone-responsive conjugative multiresistance plasmids carrying the novel mobile *optrA* locus from *Enterococcus faecalis*. *Infect Drug Resist.* (2019) 12:2355–62. doi: 10.2147/IDR.S206295
  27. Cai J, Wang Y, Schwarz S, Lv H, Li Y, Liao K, et al. Enterococcal isolates carrying the novel oxazolidinone resistance gene *optrA* from hospitals in Zhejiang, Guangdong, and Henan, China, 2010–2014. *Clin Microbiol Infect.* (2015) 21:1095.e1–4. doi: 10.1016/j.cmi.2015.08.007
  28. Chien J-Y, Mendes RE, Deshpande LM, Hsueh P-R. Empyema thoracis caused by an *optrA*-positive and linezolid-intermediate *Enterococcus faecalis* strain. *J Infect.* (2017) 75:182–4. doi: 10.1016/j.jinf.2017.05.003
  29. Sassi M, Guérin F, Zouari A, Beyrouthy R, Auzou M, Fines-Guyon M, et al. Emergence of *optrA*-mediated linezolid resistance in enterococci from France, 2006–16. *J Antimicrob Chemother.* (2019) 74:1469–72. doi: 10.1093/jac/dkz097
  30. Bender JK, Fleige C, Lange D, Klare I, Werner G. Rapid emergence of highly variable and transferable oxazolidinone and phenicol resistance gene *optrA* in German *Enterococcus* spp. *clinical isolates Int J Antimicrob Agents.* (2018) 52:819–27. doi: 10.1016/j.ijantimicag.2018.09.009
  31. Cavaco LM, Bernal JF, Zankari E, León M, Hendriksen RS, Perez-Gutierrez E, et al. Detection of linezolid resistance due to the *optrA* gene in *Enterococcus faecalis* from poultry meat from the American continent (Colombia). *J Antimicrob Chemother.* (2017) 72:678–83. doi: 10.1093/jac/dkw490
  32. Said HS, Abdelmegeed ES. Emergence of multidrug resistance and extensive drug resistance among enterococcal clinical isolates in Egypt. *Infect Drug Resist.* (2019) 12:1113–25. doi: 10.2147/IDR.S189341
  33. Freitas AR, Elghaieb H, León-Sampedro R, Abbassi MS, Novais C, Coque TM, et al. Detection of *optrA* in the African continent (Tunisia) within a mosaic *Enterococcus faecalis* plasmid from urban wastewaters. *J Antimicrob Chemother.* (2017) 72:3245–51. doi: 10.1093/jac/dkx321
  34. Elghaieb H, Freitas AR, Abbassi MS, Novais C, Zouari M, Hassen A, et al. Dispersal of linezolid-resistant enterococci carrying *poxtA* or *optrA* in retail meat and food-producing animals from Tunisia. *J Antimicrob Chemother.* (2019) 74:2865–9. doi: 10.1093/jac/dkz263
  35. Li D, Wang Y, Schwarz S, Cai J, Fan R, Li J, et al. Co-location of the oxazolidinone resistance genes *optrA* and *cfr* on a multiresistance plasmid from *Staphylococcus sciuri*. *J Antimicrob Chemother.* (2016) 71:1474–8. doi: 10.1093/jac/dkw040
  36. Almeida LM, Lebreton F, Gaca A, Bispo PM, Saavedra JT, Calumby RN, et al. Transferable resistance gene *optrA* in *Enterococcus faecalis* from Swine in Brazil. *Antimicrob Agents Chemother.* (2020) 64:e00142–20. doi: 10.1128/AAC.00142-20
  37. Jaworski DD, Clewell DB. Evidence that coupling sequences play a frequency-determining role in conjugative transposition of Tn916 in *Enterococcus faecalis*. *J Bacteriol.* (1994) 176:3328–35. doi: 10.1128/JB.176.11.3328-3335.1994
  38. Jett BD, Hatter KL, Huycke MM, Gilmore MS. Simplified agar plate method for quantifying viable bacteria. *BioTechniques.* (1997) 23:648–50. doi: 10.2144/97234bm22
  39. Gilmore MS, Lebreton F, van Schaik W. Genomic transition of enterococci from gut commensals to leading causes of multidrug-resistant hospital infection in the antibiotic era. *Curr Opin Microbiol.* (2013) 16:10–6. doi: 10.1016/j.mib.2013.01.006
  40. Van Tyne D, Gilmore MS. Friend turned foe: evolution of enterococcal virulence and antibiotic resistance. *Annu Rev Microbiol.* (2014) 68:337–56. doi: 10.1146/annurev-micro-091213-113003
  41. Morroni G, Brenciani A, Simoni S, Vignaroli C, Mingoia M, Giovanetti E. Commentary: nationwide surveillance of novel oxazolidinone resistance gene *optrA* in *Enterococcus* isolates in China from 2004 to 2014. *Front Microbiol.* (2017) 8:1631. doi: 10.3389/fmicb.2017.01631
  42. Wang Y, Wang Y, Wu CM, Schwarz S, Shen Z, Zhang W, et al. Detection of the staphylococcal multiresistance gene *cfr* in *Proteus vulgaris* of food animal origin. *J Antimicrob Chemother.* (2011) 66:2521–6. doi: 10.1093/jac/dkr322
  43. Mendes RE, Deshpande LM, Bonilla HF, Schwarz S, Huband MD, Jones RN, et al. Dissemination of a pSCFS3-like *cfr*-carrying plasmid in *Staphylococcus aureus* and *Staphylococcus epidermidis* clinical isolates recovered from hospitals in Ohio. *Antimicrob Agents Chemother.* (2013) 57:2923–8. doi: 10.1128/AAC.00071-13
  44. Locke JB, Zuill DE, Scharn CR, Deane J, Sahn DF, Denys GA, et al. Linezolid-resistant *Staphylococcus aureus* strain 1128105, the first known clinical isolate possessing the *cfr* multidrug resistance gene. *Antimicrob Agents Chemother.* (2014) 58:6592–8. doi: 10.1128/AAC.03493-14
  45. Gales AC, Deshpande LM, de Souza AG, Pignatari ACC, Mendes RE. MSSA ST398/t034 carrying a plasmid-mediated Cfr and Erm(B) in Brazil. *J Antimicrob Chemother.* (2015) 70:303–5. doi: 10.1093/jac/dku366

46. Kohler V, Vaishampayan A, Grohmann E. Broad-host-range Inc18 plasmids: occurrence, spread and transfer mechanisms. *Plasmid*. (2018) 99:11–21. doi: 10.1016/j.plasmid.2018.06.001
47. Freitas AR, Coque TM, Novais C, Hammerum AM, Lester CH, Zervos MJ, et al. Human and swine hosts share vancomycin-resistant *Enterococcus faecium* CC17 and CC5 and *Enterococcus faecalis* CC2 clonal clusters harboring Tn1546 on indistinguishable plasmids. *J Clin Microbiol*. (2011) 49:925–31. doi: 10.1128/JCM.01750-10
48. Zhu W, Murray PR, Huskins WC, Jernigan JA, McDonald LC, Clark NC, et al. Dissemination of an *Enterococcus* Inc18-Like *vanA* plasmid associated with vancomycin-resistant *Staphylococcus aureus*. *Antimicrob Agents Chemother*. (2010) 54:4314–20. doi: 10.1128/AAC.00185-10
49. Meinhart A, Alonso JC, Sträter N, Saenger W. Crystal structure of the plasmid maintenance system epsilon/zeta: functional mechanism of toxin zeta and inactivation by epsilon 2 zeta 2 complex formation. *Proc Natl Acad Sci USA*. (2003) 100:1661–6. doi: 10.1073/pnas.0434325100
50. Sletvold H, Johnsen PJ, Hamre I, Simonsen GS, Sundsfjord A, Nielsen KM. Complete sequence of *Enterococcus faecium* pVEF3 and the detection of an omega-epsilon-zeta toxin-antitoxin module and an ABC transporter. *Plasmid*. (2008) 60:75–85. doi: 10.1016/j.plasmid.2008.04.002
51. Palmer KL, Gilmore MS. Multidrug-resistant enterococci lack CRISPR-cas. *mBio*. (2010) 1:e00227–10. doi: 10.1128/mBio.00227-10

**Conflict of Interest:** The authors declare that the research was conducted in the absence of any commercial or financial relationships that could be construed as a potential conflict of interest.

Copyright © 2020 Almeida, Gaca, Bispo, Lebreton, Saavedra, Silva, Basilio-Júnior, Zorzi, Filsner, Moreno and Gilmore. This is an open-access article distributed under the terms of the Creative Commons Attribution License (CC BY). The use, distribution or reproduction in other forums is permitted, provided the original author(s) and the copyright owner(s) are credited and that the original publication in this journal is cited, in accordance with accepted academic practice. No use, distribution or reproduction is permitted which does not comply with these terms.

# Advantages of publishing in Frontiers



## OPEN ACCESS

Articles are free to read for greatest visibility and readership



## FAST PUBLICATION

Around 90 days from submission to decision



## HIGH QUALITY PEER-REVIEW

Rigorous, collaborative, and constructive peer-review



## TRANSPARENT PEER-REVIEW

Editors and reviewers acknowledged by name on published articles

## Frontiers

Avenue du Tribunal-Fédéral 34  
1005 Lausanne | Switzerland

Visit us: [www.frontiersin.org](http://www.frontiersin.org)

Contact us: [info@frontiersin.org](mailto:info@frontiersin.org) | +41 21 510 17 00



## REPRODUCIBILITY OF RESEARCH

Support open data and methods to enhance research reproducibility



## DIGITAL PUBLISHING

Articles designed for optimal readership across devices



## FOLLOW US

[@frontiersin](https://www.instagram.com/frontiersin)



## IMPACT METRICS

Advanced article metrics track visibility across digital media



## EXTENSIVE PROMOTION

Marketing and promotion of impactful research



## LOOP RESEARCH NETWORK

Our network increases your article's readership